10th International Conference on Acid Rock Drainage & IMWA Annual Conference

EDITORS

Adrian Brown Charles Bucknam Joanna Burgess Manuel Carballo Devin Castendyk
Linda Figueroa Lisa Kirk Virginia McLemore James McPhee Mike O'Kane Robert Seal
Jacques Wiertz David Williams Ward Wilson Christian Wolkersdorfer

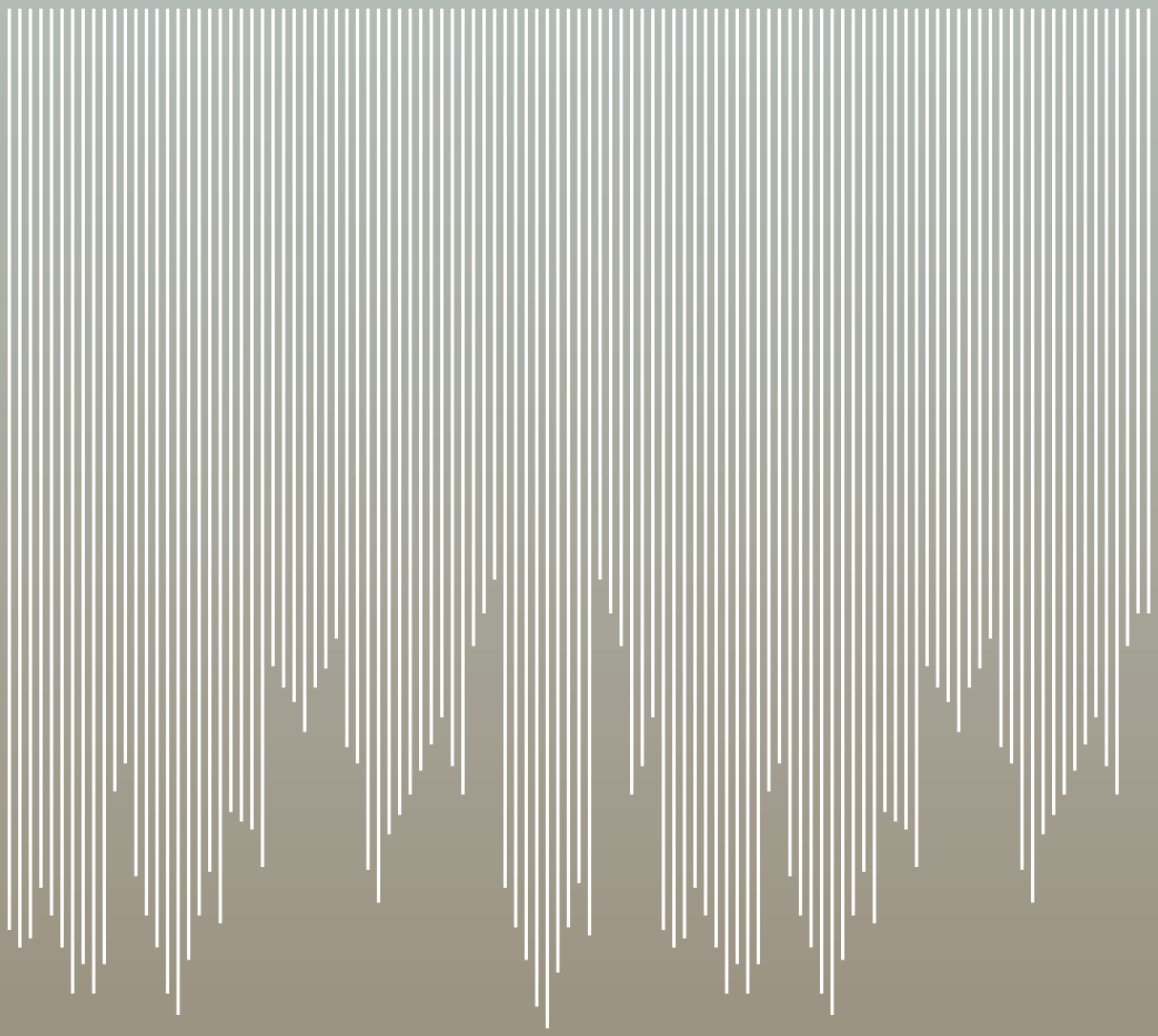

10th ICARD - IMWA 2015

10th International Conference on Acid Rock Drainage & IMWA Annual Conference

EDITORS

Adrian Brown Charles Bucknam Joanna Burgess Manuel Carballo Devin Castendyk
Linda Figueroa Lisa Kirk Virginia McLemore James McPhee Mike O'Kane Robert Seal
Jacques Wiertz David Williams Ward Wilson Christian Wolkersdorfer

APRIL 21-24

Santiago, Chile

10th ICARD - IMWA 2015

Author's disclaimer
Any views and opinions presented in the articles published
in these proceedings are solely those of the authors and do
not necessarily represent those of Gecamin. The authors take
full and exclusive responsibility for technical content, style,
language and accuracy of the information published herein.
This information is not intended nor implied to be a substitute
for professional advice. The editors are not responsible for
any damage to property or persons that may occur as a
result of use of the information contained in this volume.

I.S.B.N. 978-956-9393-28-0

Gecamin
Paseo Bulnes 197, Piso 6
Santiago, Chile
Postcode: 833 0336
Telephone: +56 2 2652 1500
www.gecamin.com

Contents

CHAPTER 2
APPLIED MINERALOGY AND GEOENVIRONMENTAL UNITS

CHAPTER 3

PREDICTION OF DRAINAGE FLOW

CHAPTER 4

PREDICTION OF DRAINAGE CHEMISTRY

ORGANIZERS

The ICARD-IMWA 2015 was organized by SANAP and Gecamin, Chile.

South American Network for Acid Prevention (SANAP)

SANAP was created in 2008 in Brazil by a group of professionals and academics interested in the problems of acid rock drainage and in identifying solutions to prevent its impact.

Active primarily in Brazil, the main objectives are to develop training activities, information exchange amongst professionals, and support research in the prediction, prevention and control of acid rock drainage in the context of South America. SANAP is currently in a development phase and national chapters are being established, further strengthening the South American network within the already formed national networks in countries concerned.

SANAP is a member of the Global Alliance which brings together varying networks that have developed around the issue of Acid Rock Drainage.

Gecamin

Powering professional development for sustainable mining

Gecamin is a Chilean company with 17 years of experience organizing technical and international conferences for the mining industry. Our conferences aim to inform and inspire professionals from all over the world, fostering the exchange of best practices and innovative experiences.

Over 20,000 professionals have attended our events and have been trained in areas fundamental to the mining industry. These areas include: Geology and Mining, Mineral Processing, Hydrometallurgy, Sustainability and Environment, Water and Energy, Maintenance and Automation, and Human Capital.

Gecamin seeks to contribute to the sustainable development of the mining industry by openly addressing its most pressing concerns and by offering a platform for knowledge exchange that aims at identifying the most sustainable solutions.

In 2014, Gecamin organized 11 conferences and 12 courses, with a total of 922 technical presentations, gathering 2,947 delegates from 54 countries. Additionally, a total of 734 delegates from mining sites attended, and a book with the proceedings was published for each conference.

Learn more about Gecamin conferences by visiting

www.gecamin.com

COMMITTEES

Organizing Committee

Executive Committee

CHAIR

Robert Mayne-Nicholls, CEO, Minera Los Pelambres, Antofagasta Minerals, Chile

CO-CHAIRS

Terrence Chatwin, Technical Manager, INAP, USA
Adrian Brown, Past-President IMWA, USA

EXECUTIVE DIRECTOR

Carlos Barahona, General Manager, Gecamin, Chile

TECHNICAL COORDINATOR

Jacques Wiertz, Professor, University of Chile

CONFERENCE COORDINATOR

Rebekah Zale, Gecamin, Chile

Directing Members

Guillermo Aguirre, Environmental Manager, Teck Resources, Chile
Stephen Foot, Water Resources Manager, Antofagasta Minerals, Chile
Caius Priscu, Head of Mineral Residue Management, Anglo American, Chile
Flávio Vasconcelos, Geoquímico Ambiental, Brazil

Editorial Committee

APPLIED MINERALOGY AND GEOENVIRONMENTAL UNITS

Manuel Caraballo, University of Chile
Robert Seal, US Geological Survey

COVERS

Mike O'Kane, O'Kane Consultants, Australia
Ward Wilson, University of Alberta, Canada

GEOMICROBIOLOGY, BIOGEOCHEMICAL CYCLES AND BIOMINING

Lisa Kirk, Montana State University, USA

MINE DEWATERING

Adrian Brown, Adrian Brown Consultants, Inc., USA

MINE WATER GEOCHEMISTRY

Virginia McLemore, New Mexico Bureau of Geology and Mineral Resources, New Mexico Institute of Mining and Technology, USA

MINE WATER AND DRAINAGE COLLECTION AND TREATMENT

Jo Burgess, Water Research Commission, South Africa
Linda Figueroa, Colorado School of Mines, USA

MINE WATER MANAGEMENT FOR CLOSURE

Jacques Wiertz, University of Chile

PIT LAKES

Devin Castendyk, State University of New York, USA

PREDICTION OF DRAINAGE CHEMISTRY

David Williams, Bureau of Land Management, USA

PRECITION OF DRAINAGE FLOW

James McPhee, University of Chile

RELIABLE MINE WATER OPERATION

Christian Wolkersdorfer, Tshwane University of Technology, South Africa & Lappenranta University of Technology, Finland

SCALING FROM LABORATORY TO FIELD STUDIES

Charles Bucknam, Newmont Metallurgical Technologies, USA

Technical Reviewers

William Albright, Desert Research Institute, USA • **Richard Amos**, Carleton University, Canada • **Felipe Aravena**,

Ecopreneur, Chile • **Steven Atkin**, Golder Associates, Canada • **Bernard Aubé**, AMEC Foster Wheeler, Canada • **Mike Aziz**, Goldcorp, Canada • **Mattias Bäckström**, Örebro University, Sweden • **Jeff Bain**, University of Waterloo, Canada • **Kashi Banerjee**, Veolia Water Technologies, USA • **Andre Banning**, Ruhr University Bochum, Germany • **Scott Benowitz**, Water Engineering Technologies Inc., USA • **Valerie Bertrand**, Golder Associates, Canada • **Nico Bezuidenhout**, Golder Associates, South Africa • **David Bird**, SRK Consulting, USA • **David Blowes**, University of Waterloo, Canada • **Rudy Boer**, Ferret Mining and Environmental Services, South Africa • **Colin Booth**, Northern Illinois University, USA • **Lauren Bozeman**, Enviromin, USA • **Jennifer Broadhurst**, University of Cape Town, South Africa • **Paul Brown**, Rio Tinto, Australia • **Bruno Bussière**, RIME UQAT-Polytechnique, Canada • **Nuria Castro**, Centre for Mineral Technology, Brazil • **Virginia Ciminelli**, Federal University of Minas Gerais, Brazil • **Jude Cobbing**, SLR Consulting, South Africa • **Alan Cook**, Latona Consulting Pty Ltd., South Africa • **Don Cowan**, University of Pretoria, South Africa • **Ewa Cukrowska**, University of the Witwatersrand, South Africa • **Linda Daniell**, University of Chile • **Stephen Day**, SRK Consulting, Canada • **Ingrid Dennis**, North-West University, South Africa • **Lore-Mari Deysel**, University of the Free State, South Africa • **Sharon Diehl**, U. S. Geological Survey • **Enrico Dinelli**, University of Bologna, Italy • **Bonnie Dobchuk**,O'Kane Consultants, Canada • **Bernhard Dold**, SUMIRCO, Chile • **Ted Eary**, Hatch, USA • **Amparo Edwards**, Golder Associates, Chile • **Scott Effner**, Whetstone Associates Inc., USA • **Jenny Ellerton**, SLR Consulting, South Africa • **Nils Erickson**, Zitro Works, Spain • **Skya Fawcett**, Golder Associates, Canada • **Jim Fricke**, Resource Environmental Management Consultants, USA • **Philippe Garneau**, O'Kane Consultants, Australia • **Richard Garner**, Independent Sustainability Consultant, South Africa • **Massimo Gasparon**, University of Queensland, Australia • **Robel Gebrekristos**, Digby Wells & Associates, South Africa • **Martin Ginster**, Sasol, South Africa • **Cleber Jose Baldoni Gomes**, Brazil • **Nandha Govender**, Primary Energy Division Eskom Holdings Ltd.,South Africa • **Mike Gunsinger**, Golder Associates, Canada • **Peter Günther**, Anglo American, South Africa • **James Gusek**, Sovereign Consulting Inc., USA • **Kevin Hallberg**, Bangor University, United Kingdom • **Terry Harck**, Solution [H+], South Africa • **Kevin Harding**, University of the Witwatersrand, South Africa • **Shameer Hareeparsad**, Sasol Technology, South Africa • **Sue Harrison**, University of Cape Town, South Africa • **Ralph Heath**, Golder Associates, South Africa • **Bob Hedin**, Hedin Environmental, USA • **Philip Hobbs**, Council for Scientific and Industrial Research, South Africa • **Martin Holland**, Delta-H Water Systems Modeling Pty Ltd., South Africa • Jennifer Huang, Sasol Technology Research and Development, South Africa • **Amy Hudson**, Tetra Tech, United States • **Wolfie Jahn**, Exxaro Resources, South Africa • **Adam Jarvis**, Newcastle University, United Kingdom • **Walter Johannes**, Aurencon Group, South Africa • **David Jones**, DR Jones Environmental Excellence, Australia • **Margarete Kalin**, Boojum Research Ltd., Switzerland • **Robert Kleinmann**, CH2M Hill, Inc., USA • **Frans Knops**, X-Flow BV / Pentair Water Process Technology BV, The Netherlands • **Kim Lapakko**, Minnesota Department of Natural Resources, Division of Lands and Minerals, USA • **Alison Lewis**, University of Cape Town, South Africa • **Charles Linström**, Exxaro Resources, South Africa • **Patrick Littlejohn**, BioteQ Environmental Technologies, Canada • **Mark Logsden**, Geochimica Inc., USA • **David Love**, Golder Associates, South Africa • **Karen Mackenzie**, Golder Associates, Australia • **Greg Maddocks**, RGS Environmental Pty Ltd ATF, Australia • **Jannie Maree**, Tshwane University of Technology, South Africa • **Richard Marton**, BHP Billiton Iron Ore, Australia • **Rob McCrindle**, Tshwane University of Technology, South Africa • **Clint McCullough**, Golder Associates, Australia • **Matthew McGann**, Newmont Mining Corporation, Peru • Jean Carlos Menezes, Brazil • **Tom Meuzelaar**, Golder Associates, USA • **Wendy Mey**, BHP Billiton, South Africa • **Patsy Moran**, Arcadis, USA • **Ritva Mühlbauer**, Anglo American, South Africa • **Kevin Myers**, New Mexico Office of the State Engineer, USA • **Thubendran Naidu**, Mondi Group, South Africa • **Jeeten Nathoo**, NuWater, South Africa • **Ron Nicholson**, EcoMetrix Incorporated, Canada • **Charl Nolte**, Independent Consultant, South Africa • **Gail Nussey**, Sasol Mining, South Africa • **Meera Ormea**, Eskom, South Africa • **Eric Perry**, US Office of Surface

Mining • **Leslie Petrik**, University of the Western Cape, South Africa • **Brent Peyton**, Montana State University, USA • **Raymond Phillipe**, MWH, Chile • **Sarushen Pillay**, Sasol, South Africa • **Caius Priscu**, Anglo American, Chile • William Pulles, Pulles Howard & De Lange Inc., South Africa • **Cristhian Quezada**, VAIGS, Chile • **Sashnee Raja**, University of the Witwatersrand, South Africa • **Bruce Randell**, iLanda Water Services CC, South Africa • **Alan Robertson**, RGS Environmental Pty Ltd ATF, Australia • **Marcos Rodriquez-Pascual**, Crystallization and Precipitation Research Unit, South Africa • **Henry Roman**, Department of Science and Technology, South Africa • **Cheryl Ross**, Golder Associates, USA • **Pierre Rousseau**, WAFE Pty Ltd., Australia • **David Salmon**, Golder Associates, Australia • **Kristin Salzsauler**, Golder Associates, Canada • **Martin Schultz**, Helmholtz Centre for Environmental Research, Germany • **Giles Searby**, Anglo American, South Africa • **Katharine Seipel**, Enviromin Inc., USA • **Vicki Shaw**, Glencore SA, South Africa • **Shannon Shaw**, pHase Geochemistry Inc., Canada • **Mei Shelp**, Barrick Gold, Canada • **Craig Sheridan**, University of the Witwatersrand, South Africa • **Robert Shurniak**, O'Kane Consultants, Canada • **Steve Sibbick**, AMEC Environment & Infrastructure, Canada • **Alison Sinclair**, Office of the Supervising Scientist, Australia • **Kerry Slatter-Christie**, Kalao Solutions, South Africa • **Kathleen Smith**, U.S. Geological Survey • **Lianna Smith**, Lianna Smith Consulting, University of Waterloo, Canada • **Heidi Snyman**, Golder Associates, South Africa • **Andre Sobolewski**, Clear Coast Consulting Inc., Canada • **Diksha Somai,** Exxaro Resources, South Africa • **Russell Staines**, Klohn Crippen Berger, Australia • **Frank Stapelfeldt**, Independent Consultant, Brazil • **Gideon Steyl**, Golder Associates, Australia • **Justin Stockwell**, Lorax Environmental, Canada • **Surya Sunkavalli**, Geomega, USA • **Phil Tanner**, DWE/GMIRM, South Africa • **Andrew Tanner**, Independent Consultant, South Africa • **Jeff Taylor**, Earth Systems, Australia • **Luiz Teixeira**, Pontifical Catholic University of Rio de Janeiro, Brazil • **David Thomson**, Golder Associates, Australia • **Annalien Toerien**, Golder Associates, South Africa • **Ester Torres Sanchez**, Université Montpellier and Centre Nationale de la Recherche Scientifique, France • **Jorge Tovar**, HydroGeo Inc., Peru • **Graham Trusler**, Digby Wells & Associates, South Africa • **Wayne Truter**, University of Pretoria, South Africa • **Brent Usher**, Klohn Crippen Berger, Australia • **Piet Van Deventer**, Envirogreen, South Africa • **Esta van Heerden**, University of the Free State, South Africa • **Rob van Hille**, University of Cape Town, The Moss Group, South Africa • **Josef Van Hooydonck**, Artois Consulting, Chile • **Andre van Niekerk**, Golder Associates, South Africa • **Gerrit van Tonder**, Institute for Groundwater Studies, South Africa • **Dirk van Zyl**, University of British Columbia, Canada • **Jerry Vandenberg**, Golder Associates, Canada • **Flávio Vasconcelos**, HIDROGEO, Brazil • **Rens Verbug**, Golder Associates, USA • **Danie Vermeulen**, Institute for Groundwater Studies, South Africa • **Germán Vinueza**, Vale Institute of Technology, Brazil • Harro von Blottnitz, University of Cape Town, South Africa • **Wolf von Igel**, ICLASS, Chile • **Jacob Waples**, Golder Associates, USA/Chile • **Ian Watson**, Coal Authority, United Kingdom • **Elmien Webb**, Glencore, South Africa • **Paul Weber**, O'Kane Consultants, New Zealand • **Björn Weeks**, Golder Associates, Chile • **Cristopher Weisener**, University of Windsor, Canada • **Phillip Whittle**, Hydrobiology, Australia • **Patrick Williamson**, SRK Consulting, Mexico • **Christian Wisskirchen**, Golder Associates, Chile • **Achim Wurster**, Independent Consultant, South Africa • **Jorge Zafra**, Amphos 21, Peru • **Johnny Zhan**, Barrick Gold, USA • **Janice Zinck**, Natural Resources Canada

FOREWORD

On behalf of the ICARD-IMWA 2015 Organizing Committee, I am pleased to welcome all authors and participants to Santiago, Chile. For the first time in history, the International Conference on Acid Rock Drainage, ICARD, is being held in South America, a fact that demonstrates the interest of the local mining sector and its growing approach to responsibly address the problem of acid rock drainage. The issue is very important in Chile, especially in the context of the new mine closure regulation whose main objective is to guarantee the physical and chemical stability of closed mining facilities and waste deposits.

The decision to organize the conference together with the IMWA (International Mine Water Association) annual meeting is another important fact; illustrating that beyond the specific issue of acid drainage, responsible water management in the mining environment is of the upmost importance for the industry.

We hope that ICARD-IMWA 2015 will provide participants with an opportunity to exchange success stories but also to examine industry failures in the search of solutions for more sustainable mine water management. This is a fairly unique gathering in terms of a mix of academia, government and industry and allows for constructive analysis and discussions through in-depth research presentations. All papers have been peer-reviewed and we hope to have gathered the highest quality knowledge that embraces both applied research examples and case studies which might otherwise not find a place at conventional academic conferences. This convergence of research and practice was a key mandate for the Organizing Committee and I hope that these proceedings reflect the effort of both the authors and reviewers. I am confident that these proceedings will prove to be a useful tool in the daily lives of mining professionals.

Thank you for joining us in this conference.

Robert Mayne-Nicholls

CHAIR

10th International Conference on Acid Rock Drainage

and IMWA Annual Conference

PREFACE

ICARD-IMWA 2015, held from April 21-24, 2015 at the Grand Hyatt Hotel in Santiago, Chile, is the 10th International Conference on Acid Rock Drainage, organized this year in conjunction with the International Mine Water Association annual meeting. The Conference is hosted by the South American Network on Acid Prevention, SANAP, and by Gecamin, Chile.

Acid rock drainage and mine water management are now widely recognized by the mining industry as priority issues that should be addressed throughout the entire life of a mine; specifically, paying special attention to the long-term impacts. The main focus of ICARD and IMWA conferences has moved from prediction, analyzing and describing the different mechanisms involved, and developing models, to prevention and control, proposing and developing engineering solutions for reducing environmental impacts and minimizing risks. The conference slogan "Agreeing on solutions for more sustainable mine water management" reflects the effort undertaken to provide reliable solutions to the different problems related with water management in the mining environment.

ICARD-IMWA 2015 is organized to provide an international forum where mining professionals, operators, researchers and suppliers can meet to exchange, interact, analyze and discuss experiences and recent innovations in the area of sound and responsible mine water and effluent management. The objectives of the congress are to:

- Discuss the most recent advances and developments related to prediction, prevention and control of acid mine drainage.
- Bring together professionals committed to improving water management and minimizing mining impacts on surface and underground water.

These proceedings contain 220 abstracts of papers and posters written by authors from 24 countries.

The main topics addressed by the abstracts included in these proceedings are:

Geomicrobiology, biogeochemical cycles and biomining; Applied mineralogy and geoenvironmental units; Prediction of drainage flow; Prediction of drainage chemistry; Mine water and drainage collection and treatment; Cover design and performance; Scaling from laboratory to field studies; Reliable mine waste management; Reliable mine water operation; Mine dewatering; Mine water management for closure; Mine water geochemistry and Pit lakes.

The full version of the papers can be found on *gecaminpublications.com*

All papers published in these conference proceedings have been peer-reviewed by experts from around the world, whom we thank for their contribution by dedicating their time in reviewing, correcting and commenting on the articles.

We believe that these conference proceedings, as well as the conference program, will be of great interest to mine water and industry professionals.

Jacques Wiertz

TECHNICAL COORDINATOR

10th International Conference on Acid Rock Drainage and IMWA Annual Conference

All papers published in these conference proceedings have been peer-reviewed by experts from around the world, whom we thank for their contribution by dedicating their time in reviewing, correcting and commenting on the articles.

We believe that these conference proceedings, as well as the conference program, will be of great interest to mine water and industry professionals.

Jacques Wiertz

TECHNICAL COORDINATOR

10th International Conference on Acid Rock Drainage

and IMWA Annual Conference

ACKNOWLEDGEMENTS

The Executive Organizing Committee acknowledges with gratitude the efforts of all the authors for contributing a large variety of high quality, detailed and innovative papers to the technical program. We also would like to thank the reviewers, the employees from Gecamin, and all those involved in the creation of these proceedings for their assistance. The support of the Organizing, Editorial and Technical Committees has been greatly appreciated, as has been the support of the ICARD-IMWA 2015 Chair, Co-Chairs and the Chairs of technical sessions.

The Executive Organizing Committee also wishes to thank the following sponsors (as of March 23, 2015 in the order in which they were confirmed) for their generous support:

Platinum: O'Kane Consultants

Gold: SRK Consulting

Silver: GEO-SLOPE International, Amphos 21, Andritz Ritz GmbH and GeoSystems Analysis

Proceedings: Minera Los Pelambres

Social: INAP and Golder Associates

Official Material: Hatch

Wi-Fi: Tetra Tech

Students: Minera Los Pelambres

Other: Miwatek

Institutional Partners: Fundación Chile, Sociedad Nacional de Minería (SONAMI), Chile; Consejo Minero, Chile; Servicio Nacional de Geología y Minería (SERNAGEOMIN), Chile; Instituto de Ingenieros de Minas del Perú (IIMP), and The Brazilian Mining Association (IBRAM)

Official Media: Nueva Minería & Energía, Chile

Media Partner: AreaMinera, Chile

Finally, we would like to thank all the delegates who attended the conference and exchanged their valuable knowledge and expertise, thus contributing to the great success of this 10th edition of the International Conference on Acid Rock Drainage and the Annual Conference of the International Mine Water Association, ICARD-IMWA 2015.

Executive Organizing Committee
10th International Conference on Acid Rock Drainage
and IMWA Annual Conference

PROCEEDINGS SPONSOR

We proudly acknowledge Minera Los Pelambres as the Proceedings Sponsor of the 10th International Conference on Acid Rock Drainage and The IMWA Annual Conference.

PLENARY PRESENTATIONS

International Network for Acid Prevention's Path Forward

Terrence Chatwin
International Network for Acid Prevention (INAP), USA

ABSTRACT

Expanded populations increase potable and agriculture water use, as well as all other needs for clean water including mining. These pressures have focused International Network for Acid Prevention's (INAP's) efforts to foster best practice to maintain water quality throughout the mining industry. In addition, INAP is committed to assist in building capacity of all stakeholders whether they be large or small operators, regulators or communities through relevant research, information transfer and continuous improvement of operational and remedial practice.

INAP is recognized for its effort in the prevention and mitigation of acid-rock drainage (ARD) through the publication of the GARD Guide, a global best practice guide for ARD prevention. A key element to the success of INAP has been their partnership and support by the Global Alliance, a network of regional orgainzation committed ARD prevention and sustainable mining. To increase INAP's influence and further promote these best practices, we are commited to expanding our partnerships not only with the Global Alliance; but with other like organizations including governmental and non-governmental agencies to educate stakeholders through short courses and on-line presentations. To support its use, we are producing an on-line PDF file of the GARD Guide to allow users to print hard copies of the document. We are also continually updating the GARD Guide with new and relevant information and best practice.

Recognizing the value of inputs from all partners and stakeholders, INAP hosted a "Path Forward Symposium" at the 9th ICARD, where excellent recommendations were proposed and compiled into a report that was used by INAP in its strategic planning process. We look forward to further outstanding suggestions from all stakeholders to assist INAP in its path forward in supporting the mining industry in its sustainable development.

Keywords: ARD, acid drainage, INAP, GARD Guide

INTRODUCTION

With the expansion of human population, the need for increased food, water, material and energy have increased. Each of these required resources places its own specific requirements on clean water. This rapid growth of and competition for water usage, as well as, unexpected drought in certain regions have raised water costs and forced many water users to focus on availability and true value of water. This increased demand combined with inadequate mine closure actions have resulted in an adverse perception of mining's impact on present and future water quality, which in turn has resulted in increased regulatory and societal pressures on the mining industry. INAP and its member companies have raised their review of water resource issues to the highest levels.

Some forms that these pressures on the mining industry have taken are lower water discharge levels for dissolved metals and other contaminates. They have also resulted in higher bond requirements for mine closures and more stringent financial assurances for final closure options. Also in the United States (USA), there are limitations to how mine discharges can be treated post closure. Two states in the USA will not accept perpetual water treatment as a final closure option (Kempton et al., 2010).

Combining these pressures for clean water with the potential adverse impacts of acid rock drainage (ARD) and metal leaching can create significant problems for the mining industry. ARD is one of the most serious and potentially enduring environmental problems of the mining industry, as indicated by the high liability cost carried by many mining companies to cover potential liabilities of ARD and metal leaching. Effective prevention of acid drainage is a formidable challenge, to which INAP, the mining industry and its stakeholders have committed a strong effort to foster best practice to enhance water quality within its member's operations and throughout the mining industry. In addition, INAP is committed to assist in building capacity of all stakeholders whether they be large or small operators, regulators or communities through relevant research, information transfer and continuous improvement of operational, remedial and waste management practice.

Who is INAP?

INAP is an international network of mining companies dedicated to the prevention and mitigation of acid rock, saline and neutral drainage (ARD), (SD) or (ND) and metal leaching in the support of sustainable mining. INAP was formed in 1998 to coordinate and facilitate global research, information transfer and capacity building on the management of sulfide mine wastes, acid rock drainage and metal leaching (www.inap.com.au, 2014). Since then, INAP has grown into a proactive, global leader in the field

We have also organized workshops that address technical, economic, and societal and policy issues. These workshops provide a discussion forum of issues and result in identifying research needs and opportunities. Within these workshops, INAP works to link these issues with interested parties to develop possible solutions and initiatives.

INAP plays a strong supporting role in major ARD events. The International Conference on Acid Rock Drainage (ICARD) is sponsored by INAP every 3 years. At this time, I would like to

recognize the International Mine Water Association, who is partnering with INAP and the Global Alliance in sponsoring the Tenth ICARD/IMWA 2015 Conference. Our close relationship with IMWA is based on our shared objectives and our commitment to sustainable mining. We are pleased to share this venue with our "kindred spirits".

ICARD is a key platform for information transfer and discussion of ARD prevention and mitigation processes, mine waste management methodologies, developments in geochemistry, characterization, modeling and prediction and innovative treatment techniques. This forum is open to all mining industry stakeholders. Through this conference and focused workshop, INAP indentifies and promotes best practice in ARD prevention, supporting continuous improvement in mine waste management and closure, and seeking innovative solutions to critical ARD issues.

A major element of INAP is the identification and promotion of ARD prevention best practice. The most effective best practice tool INAP has produced is the Global Acid Rock Drainage Guidance Document (GARD Guide). The GARD Guide is a compilation and update of all of the ARD, AMD, ND and SD documents and compendia from across the globe. It includes information from not only hard-rock mining but coal mining as well. The GARD Guide was rolled out in 2009 at the Eighth ICARD as a web-based guidance document located at (www.gardguide.com), which is available and free for all to use. The original publication was compiled by an international team lead by Golder and Associates with many external academic and consulting authors. The web-based format was designed to facilitate updating and expanding the document, and it is readily available for those users connected to the web.

INAP's partners

There are eight regional partners that support INAP's goal of preventing ARD and metal leaching, which form the Global Alliance (GA). These organizations represent significant technical and regional expertise on ARD and metal leaching prevention, mitigation and mine waste management. These regional partners are listed below:

- Australia - The Sustainable Minerals Institute–Knowledge Transfer (SMIKT)
- Canada – The Mine Environmental Neutral Drainage Program (MEND)
- China – The Chinese Network for Acid and Metalliferous Drainage (CNAMD)
- Europe – The Partnership for Acid Drainage Remediation in Europe (PADRE)
- Indonesia - The Indonesian Network for Acid Drainage (INAD)
- South Africa – The Water Research Commission (WRC)
- South America – The South American Network for Acid Prevention (SANAP)
- United States – The Acid Drainage Technology initiative (ADTI)

INAP is also keen to engage other regional organizations focused on prevention and treatment of ARD and encourage them to join the GA.

A major activity of the GA members is to host or to assist in the planning of the ICARD. Each ICARD is hosted by a GA member or its associate. The Eighth ICARD held in Skelleftea, Sweden and was hosted by the Swedish Association of Mines (SveMin) and supported by PADRE. The Ninth ICARD was hosted by MEND, in Ottawa, Canada. The Tenth and current ICARD is being

hosted by Gecamin with support from SANAP. GA members in Australia (SMIKT) and in the United States (ADTI) have also hosted the ICARD.

In recognition of the strength of the GA, INAP hosts a reception at the ICARD for the GA where they can network and update one another on their regional activities. During this reception each member organization has an opportunity to inform the Alliance on their efforts and successes. INAP would also like to recognize recent relevant reports that have been published by Global Alliance members. In 2014, MEND published an excellent report on mining-impacted waters entitled, *Study to Identify BATEA for the Management and Control of Effluent Quality from Mines, MEND Report 3.50.1* (MEND 2014). The Water Research Commission of South Africa has published many articles and report that are available at their website (www.wrc.org.za).

Over the past six years, ADTI has been working on a set of five workbooks that have been published through the Society of Mining, Metallurgy and Exploration (SME). These volumes include:

- Basics of Metal Mining Influenced Water
- Mitigation of Metal Mining Influence Water
- Mine Pit Lakes: Characteristics, Predictive Modeling and Sustainability
- Techniques for Predicting Metal Mining Influenced Water
- Sampling and Monitoring for the Mine Life Cycle

All of the editors and many of the authors of these volumes are members of ADTI. This is an outstanding accomplishment for an organization that is composed totally of volunteers and is self-sustaining.

As well as the Global Alliance, INAP partners with many consultants, service providers, governmental, non-governmental organizations as well as local communities and other mining industry stakeholders. The next section of the paper will illustrate how INAP partners with many organizations with common interests to build capacity and transfer information to a broad range of mining industry stakeholders.

INAP'S CURRENT ACTIVITIES

We believe that the role INAP performs in its current activities not only demonstrates its commitment to the prevention and mitigation of ARD, but it also shows our willingness to be a transparent partner to achieve strong communications with and build capacity within our stakeholders. We also seek to foster best practice throughout the mining industry's waste and drainage management plans and continually improve operations and prevent ARD.

Research

In this paper, actions that INAP and its partners have organized and implemented to prevent and mitigated ARD and metal leaching will be presented. These actions have included a gap-driven research project that focused on a key industry need, mine-waste management. Typically, these

efforts concentrate on large-scale projects that require large collaborative efforts or large scale demonstration. An example of this large-scale project is the Diavik country rock instrumentation study in Northern Canada performed by the University of Waterloo, the University of British Columbia and the University of Alberta. Whereas, INAP's financial funding commitment was small compared to the total funding, we did represent a consortium of international mining companies, who assisted technical planning and review from its inception. INAP has supported this project for almost a decade. The lessons learned from this large-scale, long-term project has been very rewarding and valuable and has resulted in a substantial mine-waste management bond reduction for Diavik.

INAP is currently working with O'Kane Consulting and a group of international experts from Canada, Australia, and the USA to prepare a "Global Soil Cover System Design Guidance Document." The planning and organization of this project goes back to 2011 at the Seventh Acid and Metalliferous Drainage Workshop in Darwin. At a plenary session, Dr. Bruce Kelley, formally the Global Practice Leader - Environment at Rio Tinto Limited spoke on the management of mine wastes. As he pointed out, the biggest job of most mining companies is to manage their waste, since over 98% of the materials they handle consist of overburden, low-grade ore, mine waste and tailings. He described managing this waste as the elephant in the room. The discussion following that presentation resulted in an ad-hoc group of about 40 who stayed for an hour after the meeting discussing approaches to address this issue. By the next, morning a group had been formed to prepare and submit a proposal to INAP. The INAP Operating Committee welcomed the proposal and requested further review. Further discussion was carried on at the INAP Path Forward Symposium held at the Ninth ICARD in Ottawa in May 2012.

In 2013, INAP entered into an agreement with O'Kane Consulting (OKC) to prepare a guidance document on the design and construction of soil cover systems. In organizing the technical team, O'Kane Consulting and INAP felt the need for global input for this document. Consequently, a global technical advisory group (TAG) was formed to review and advise O'Kane on this project. Not unexpectedly, some of that original Australian Ad hoc committee are on this TAG. INAP has reviewed the first draft of the document and O'Kane and the TAG have responded to our suggestions and comments. This document is schedule for presentation at the Tenth ICARD in Santiago in 2015.

Capacity Building

A key element of INAP's strategy to prevent and mitigate ARD is to support the enhancement and development of technical and leadership capacity of mining stakeholders including regulators, small operators and exploration companies and communities, particularly in developing regions where training and experience is less available to stakeholders.

Since its publication, the GARD Guide has become such an integral part of INAP capacity building program. To promote the GARD Guide and train stakeholders in its use, INAP and its Global Alliance partners have sponsored and organized short courses across the globe. A GARD Guide short course was presented prior to the Tenth ICARD/IMWA meeting here in Santiago, Chile.

Those presenting include a member of the ADTI Steering Committee and another who was a supporter of the SANAP organization. INAP has been very pleased with outcome of these GARD Guide short courses. For example a few years ago, a GARD Guide short course was organized and presented in Turkey (Personal Communications Rens Verburg, 2013). Resulting from this short course, a committee was organized to translate the GARD Guide Executive Summary into Turkish. In addition to the GARD Guide Executive Summary being translated into Turkish, it has been translated into Spanish, French and German as well.

To assure that there are global opportunities for short courses on the GARD Guide in remote locations, INAP has also entered into an agreement with EduMine for an internet GARD Guide course which is presented within the EduMine web-based educational program.

Since its roll-out in 2009, the GARD Guide has been updated three times. The original version of the GARD Guide was compiled by an international team of consultants and academics lead by Golder and Associates. Since that first version, the following organizations and consulting firms have participated in additions and upgrades to the GARD Guide:

- Natural Resources Canada - Canada
- Environmental Geochemistry International - Australia
- Earth Systems - Australia
- EcoMetrix Inc. - Canada
- Knight Piesold / Sovereign Consulting Inc - USA

As you will note from this list, they are geographically diverse, and they were not part of the original GARD Guide production team. INAP desires that the entire mining consulting and service community recognize and support the best practices compiled in the GARD Guide. If there are best practices or relevant case studies that have not been include in the GARD Guide, let us know, so together, we can correct the oversight.

One of the modifications that GARD Guide users have requested is the addition of more case studies of actual mining operations. Many of the recent upgrading editors and reviewers were requested to include brief case studies that would focus on specific best practices and illustrate how they can upgrade the operations or express lessons learned from less effective actions. Numerous case studies have been added from a variety of climatic and geochemical regimes. INAP thanks these consulting firms and governmental agencies for their efforts to broaden the GARD Guide perspective and strengthen its value to our stakeholders.

INAP has received numerous requests for a GARD Guide hard copy. Consequently, INAP and its service providers have formatted the GARD Guide as a printable PDF file thus allowing users to print all or sections of the GARD Guide has a hard copy. This printable version of the GARD Guide is found at www.gardguide.com and is presently available to all stakeholders.

Many organizations use and reference the GARD Guide. INAP was pleased that the U.S. Environmental Protection Agency (US EPA) translated to Spanish and appended the executive summary of the GARD Guide to the Central American Free Trade Act *EIA Technical Review Guideline: Non-Metal and Metal Mining* (US EPA, 2012). The GARD Guide is also referenced in the

US EPA CLU-IN webinar on mining – resources and is linked and referenced in the Interstate Technology and Regulatory Council (ITRC) web page on mining waste treatment technology selection (www.itrcweb.org/miningwaste-guidance/other_resources.htm) (ITRC viewed 2014). The GARD Guide will also be referenced in future mining guidance documents prepared by International Finance Corporation (IFC) (Personal communication, John Middleton, IFC, 2013).

I also met with Dr Anthony Hodge, the president of International Council for Mining and Metals (ICMM) and we discussed how INAP and ICMM could team to support our joint water management and conservation programs.

Another key partnership that INAP is seeking to enhance is teaming with universities and research centers. These centers of learning and research train future miners, engineers, planners, managers and regulators for the mining industry and develop innovative ARD mitigation methods.

In a recent discussion with a mining engineering professor, it became apparent how important it is emphasize sustainable mining and ARD prevention to all technical disciplines including those that explore, develop, construct, operate and close a mining operation. To achieve this shared responsibility of preventing ARD and maintain clean mining discharges, requires the engagement of all mining industry stakeholders.

Not only do our academics train the students, but they are on the cutting edge of innovative research to produce the new tools to prevent, model, predict and mitigate ARD. Hence, it is important that INAP and our collaborative partners are teaming with universities and research centers. I know ADTI has had a university consortium as a key element of their program. I believe that this should be implemented in all Global Alliance organizations to engage universities in our programs and objectives and to keep us informed of new and relevant tools and programs that are being developed within the academic community. This connection is of particular interest in the field of biogeochemistry where new tools are developing on a regular basis.

One activity that INAP and the Global Alliance is implementing to strengthen its ties with the academic community is the new program to recognize brief (four to five page) case study based on published work of current investigations or operations. As discussed earlier, case studies are a very effective tool to illustrate best practice principles. By limiting the length of the case study, we believe that they can be focused on a specific practice relevant to ARD prevention, and that they can be harvested from the current literature describing current operations or research activities. Students can seek out mentors in either academic or operational venues and create lasting relationships. In addition, these case studies will be useful for illustrating best practice and lessons learned for future students. The results of the first Case Study Competition will be presented at the Tenth ICARD in Santiago. We believe that it will be successful in not only developing useful and relevant case studies, but it will also develop lasting inter-generational relationship that will strengthen the mining industry.

Sulfate Treatment Workshop

Through INAP and ADTI members, a Sulfate Treatment Workshop was organized and presented in Salt Lake City on February, 27-28, 2014. One hundred and ten delegates from five different countries attended this meeting. The program included a broad ranging panel discussion with six separate presentations. An additional twenty-one presentations or case studies and innovative processes were given. At the conclusion of the program, five breakout sessions were held to discuss future efforts. Following the technical program, a field tour of the Kennecott reverse osmosis plant, which treats sulfate-bearing groundwater, was held. As well as recognizing ADTI's crucial support, I would also like to recognize the workshop's sponsors – Veolia Water, Golder Associates and Arcadis, US.

Path Forward Symposium

Recognizing the value of inputs from all partners and stakeholders, INAP hosted a "Path Forward Symposium" prior to the Ninth ICARD. The INAP path forward symposium was attended by over 70 ARD experts from across the globe. The program consisted of seventeen presentations on innovative ARD technologies and other ideas relevant to ARD prevention. The symposium format allowed each presenter five minutes to present his/her idea followed by two minutes for questions and answers. Needless to say, a lot of information was disseminated in a short period of time. It was like an extended "elevator presentation." These talks were then followed by detailed discussion by focus groups. The themes of the four discussion groups included: 1) Biogeochemical processes and tools, 2) Mine-waste management, 3) Innovative treatment technologies and 4) Stakeholder engagement. Following the breakout sessions, a short summary meeting was held to organize and compile the discussion points and findings. These findings were disseminated to the attendees. A second summary session was convened following the ICARD to focus on some of the salient points made at the symposium. At this session many excellent recommendations were proposed and compiled into a report that was discussed at the INAP Strategic Planning Meeting held in November 2013. This strategic planning meeting was facilitated by Dr. Dirk van Zyl, a well respected consultant and professor at the University of British Columbia.

INAP PATH FORWARD

Based on the suggestions made at the Path Forward Symposium and inputs and recommendations by INAP Operating Committee members at the INAP Strategic Planning Meeting in Vancouver, BC a strategic plan was developed to facilitate our planning and future programs. This plan focus on four themes 1) building capacity within INAP, its partners and industry stakeholders, 2) strengthening our communication links with our member companies, our Global Alliance and other stakeholder partners; 3) implementing ARD prevention best practice throughout the entire mining industry; and 4) maintaining continuous improvement. For INAP to be successful in meeting these goals, we need to develop closer ties with our existing and future partners.

Good communications is critical to maintaining quality partnerships and accomplishing our goals. Superior communication combines a well designed message with focused listening and understanding by both parties. Comprehending concerns and desires are often crucial to successful project implementation. Because of the importance of the ARD prevention concept, we often focus

on the message. But to assure successful projects, INAP will work on understanding the needs of our partners as strongly as we focus on project implementation. I believe this approach will lead to stronger partnerships and more shared successes.

Sharing information and experience was a theme that was heard consistently within the planning meeting and path forward symposium. This concept has been exemplified by INAP members as they hosted our Operating Committee (OpCom) meetings. Our last OpCom meeting was hosted by Freeport McMoRan Copper and Gold and held in Tucson, AZ. Following the meeting, we toured the Sierrita and the Bisbee mining sites. During the tour, we observed three water-treatment pilot-plants that were treating discharges from the Sierrita operations. We also toured an innovative water management operation located on the Bisbee tailings management facility. At the end of the tour, one of our experienced OpCom members expressed, "I learned a lot from this tour."

At a separate OpCom meeting, INAP heard a presentation on the Rio Tinto ARD Risk Management Protocol. This program has been operating at Rio Tinto's mining and processing facilities over the past decade and it is based on Rio's corporate-wide review and audit program. The design and implementation of this ARD review program was first presented at the 7th ICARD in 2008. Since that time, the experiences of nearly one hundred audits have been included in the risk management data base covering facilities in a variety of commodities and operating units. Many INAP members have similar programs, and we believe that these resulting discussions on ARD risk management will be informative and valuable to all and help promote the mission of INAP.

Other topics we are looking forward to discussing are developing and implementing ARD management plans throughout the mine-life cycle, working with exploration groups and junior companies to develop early waste characterization data and engaging communities to address their concerns and develop sustainable mining.

CONCLUSIONS

ARD management and prevention is critical to the success and reputation of the mining industry. To achieve these goals, measurement and ongoing improvement of the ARD management plan are necessary throughout the life of mine. Successful implementation of the ARD management plan relies on commitment from company management and the systematic use of ARD management tools including partnering with all stakeholders. We believe that by partnering with all mining industry stakeholders, we will be more successful in achieving our joint goals of preventing ARD and supporting sustainable mining.

Finally, the prevention and mitigation of ARD is becoming more technically viable and more widely applied through the efforts of all mining stakeholders including mining operators, consultants, researchers and suppliers; regulatory agencies; NGOs and the environmental community. We would like to thank all of INAP's partners in this important endeavor to prevent ARD and metal leaching in mining-impacted waters resulting in more clean water for all of us.

REFERENCES

Kempton, H., Bloomfield, T. A., Hanson, J.L., and Limerick, P., (2010) Environmental Science & Policy, vol. 1, pp. 558–566.

www.gardguide.com. viewed September 16, 2014.

Hatch, (2014) Study to Identify BATEA for the management and control of effluent quality from mines, MEND Report 3.50.1, pp. 1-614.

CAFTA DR and US Country EIA, (2011) EIA Technical review guideline: non-metal and metal mining, vol. 2, appendix E. GARD Guide (Acid rock drainage) pp. 93-114.

www,itrcweb.org/miningwaste-guidance/other_resources.htm viewed September 16, 2014.

Richard, D. G., Borden, R. K., et. al., (2008) Design and Implementation of a Strategic Review of ARD Risk in Rio Tinto, Proceeding of the 7th International Conference on Acid Rock Drainage (ICARD), March 26-30, 2006, St. Louis , MO, pp. 1657-1672.

Acid Rock Drainage Best Management Practices: A Great Success Story at the Margajita River, Pueblo Viejo Gold Mine, Dominican Republic

Carlos Tamayo, Rodolfo Espinel, Tim Kahl, Benoit Bissonnette and Jorge Lobato
Barrick Gold Corporation, Dominican Republic

ABSTRACT

The Margajita River is about six kilometers long, skirting Barrick's Pueblo Viejo mine before winding its way into Hatillo reservoir, one of the largest fresh water bodies in Dominican Republic.

As far back as most people in the communities could remember the waters of the Margajita River were colored a dark, ominous red – a product of acid rock drainage (ARD) from the old waste rock dumps and facilities from previous mining operations. The local inhabitants called it 'blood' river.

For decades, the stream was highly acidic (pH below 3) and metal concentrations exceeded Dominican water quality standards by orders of magnitude.

Pueblo Viejo Dominicana Corporation (PVDC), a joint venture between Barrick Gold Corporation (60%) and Goldcorp (40%), started commercial operations at this gold mine in January 2013. PVDC efforts to clean-up the Margajita water were an extraordinary challenge. A comprehensive approach for ARD management throughout the mine-life cycle was planned and is currently being executed. This approach follows management principles for ARD mitigation and prevention as described at the Global ARD Guide developed by the International Network of Acid Prevention (INAP).

PVDC spent lots of effort to clean-up this brownfield mining site and in implementing best industry management practices. ARD water is collected in two different areas on site and used as much as possible as high pressure cooling water for the autoclave process. ARD water is treated at the onsite Effluent Treatment Plant (ETP) prior to final discharge into Margajita. Approximately 40,000 cubic meters of water is treated daily. Management practices and careful operation of the ETP have brought dramatic improvements to Margajita River. Communities now see evidence and extraordinary results of high quality water being returned into the river. Also, fishing has returned upstream at the confluence of the river to Hatillo reservoir.

**There is no full article associated with this abstract.*

Conga Mining Project (Cajamarca, Peru). International Expertise of the Water Component

Rafael Fernández-Rubio[1], Luis López García[2] and José Martins Carvalho[3]

1. *School of Mines, Madrid Polytechnic University. FRASA Consulting Engineers, Spain*
2. *Consultant in Water Resources, Spain*
3. *Porto Institute of Engineering, Portugal*

ABSTRACT

Given the social conflicts that arose around Conga mining project (gold-copper), the Presidency of the Council of Ministers of Peru commissioned an independent international expert's report, to analyze all hydrological aspects included in the Environmental Impact Study and in the responses to the presented allegations.

The studies have addressed surface water and groundwater, in terms of possible interference with the quality and quantity, from the pre-mine situation, through the mining operation and after mine closure.

The hydro-climatology of the Andean area where the project is located has been reviewed concluding that the interference conditions would be significant only during the dry seasons due to a structural deficit of water outside the mining project. The mitigation measures have been studied and completed. Mitigation is acheived mainly through construction of surface water storage reservoirs, for replacement of affected volumes, with the possibility of ensuring higher low water flows, and with the implementation of collecting boreholes to ensure water supply to surrounding community users.

The designed water storage will allow increasing the availability of water in the required period and better management of water resources for the affected users. The loss of four existing small lakes as a consequence of the project implementation does not affect existing area water supplies.

There are no aquifers in entity that may be affected by the project, and there are well known hydrogeological disconnects between permeable materials. It is for these reasons that the groundwater is not considered as significant alternative for water supply, while sub-surface water, captured by sub horizontal bore-holes can be improved.

From the bacteriological point of view, the quality of groundwater in pre mine conditions is often deficient, as a result of livestock and lack of sanitary controls contamination. Groundwater exceeds the maximum level of heavy metals in some analyses as well.

The international expert's report recommends a set of participatory water management controls, to ensure compliance with provisions and proposals.

Keywords: Conga Mining Project; Peru; international expert report; water quality and quantity interference.

CONTEXT

In January 2012 the Presidency of the Council of Ministers of Peru commissioned an independent international expert report to the authors of this paper. The objective was to analyze the water component of the Environmental Impact Study (EIS) of the Conga Mining Project whose approval had been questioned by different groups opposed to it.

The Conga Mining Project is located at the Andes range, with an average elevation over 4000 m above sea level, east of Yanacocha Mine and 73 km northeast of the city of Cajamarca (Fernández Rubio, López García, Martins Carvalho, 2012). The owner of the project is Minera Yanacocha S.R.L. (MYSRL) (Figure 1).

Figure 1 Location of Minas Conga near Cajamarca, Peru

The geology of the area includes Cretaceous sedimentary rocks, Miocene's volcanic rocks, Eocene/Miocene sub-volcanic and plutonic formation and alluvial, and Quaternary fluvio-glacial and moraines sediments.

Mineralization was found in two cupriferous porphyry deposits (Chailhuagon and Perol) with 0.28% copper and 0.72 grams per ton gold grade. Mining operations are planned for 14 and 19 years, respectively with projections for extraction of 504 Tm of mineral and 581 Tm of low grade mineral and waste rocks.

The project is located within the Marañón river basin, a major watershed of the Amazonian basin and extends over a minor percentage of the headwaters surface of five microwatersheds: Alto Jadibamba (9%), Chugurmayo (0.4%), Alto Chirimayo (8%), Chailhuagón (2%) and Toromacho

(2%). The area affected by the project is minimal as compared to that apportioned to agriculture, the activity that produces the largest negative impact on the biodiversity.

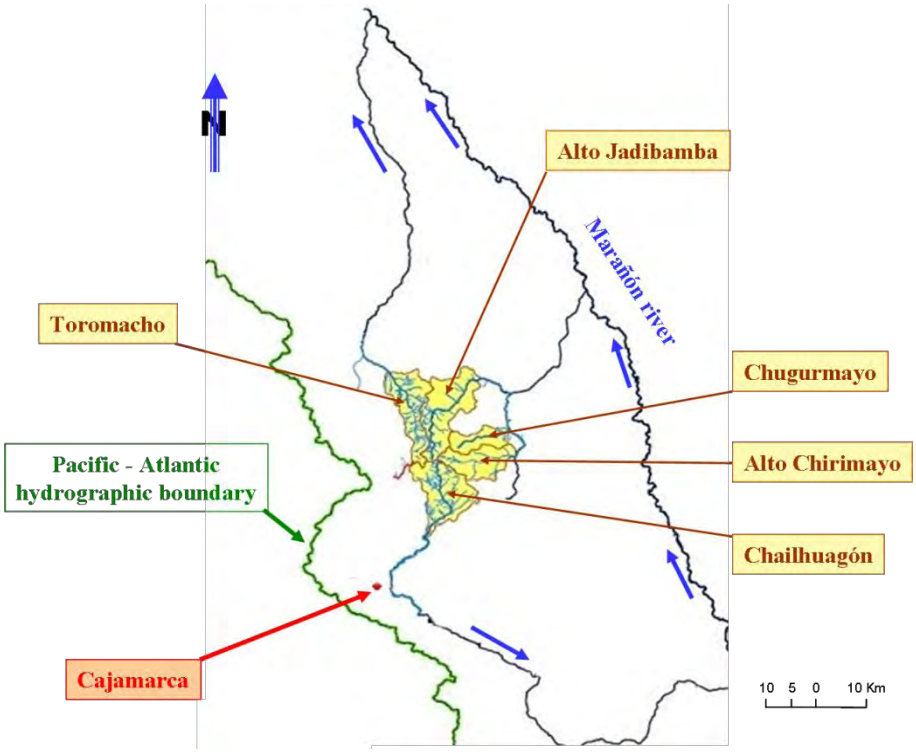

Figure 2 Conga Project footprints and micro-watersheds

SCOPE OF THE EXPERT REPORT

The basis of the report focuses on four major tasks: analysis of the available information; evaluation of the proposed prevention; mitigation and compensation measures; and, finally, proposal of complementary solutions to increase water availability to the downstream users. The report was completed, as expected, in forty days of intensely dedicated work.

The basic groundwork was the analysis of the 18 volumes of the EIS (Knight Piésold Consulting, 2010a) plus the 15 volumes of response to the observations received (Knight Piésold Consulting, 2010b), for a total of around 27,000 pages. These analyses were complemented with on-site surveys and studies, helicopter flights and multiple meetings with technical staff from public and private institutions that provided invaluable additional information as well as with social groups, associations and local residents. The product of these tasks was a 261 page expert report formally submitted to the Presidency of the Council of Ministers of Peru on April 13th, 2012.

The authors greatly appreciate the support provided by David Lorca Fernández, Project Manager of FRASA Consulting Engineers (Spain) and Tiago Carvalho, Production Assistant at TARH – Terra, Ambiente e Recursos Hídricos, Lda. (Portugal).

THE CONGA PROJECT INFRASTRUCTURE

The Conga project includes a number of facilities and specific infrastructures, extending over an area of less than 2,000 has (Figure 3).

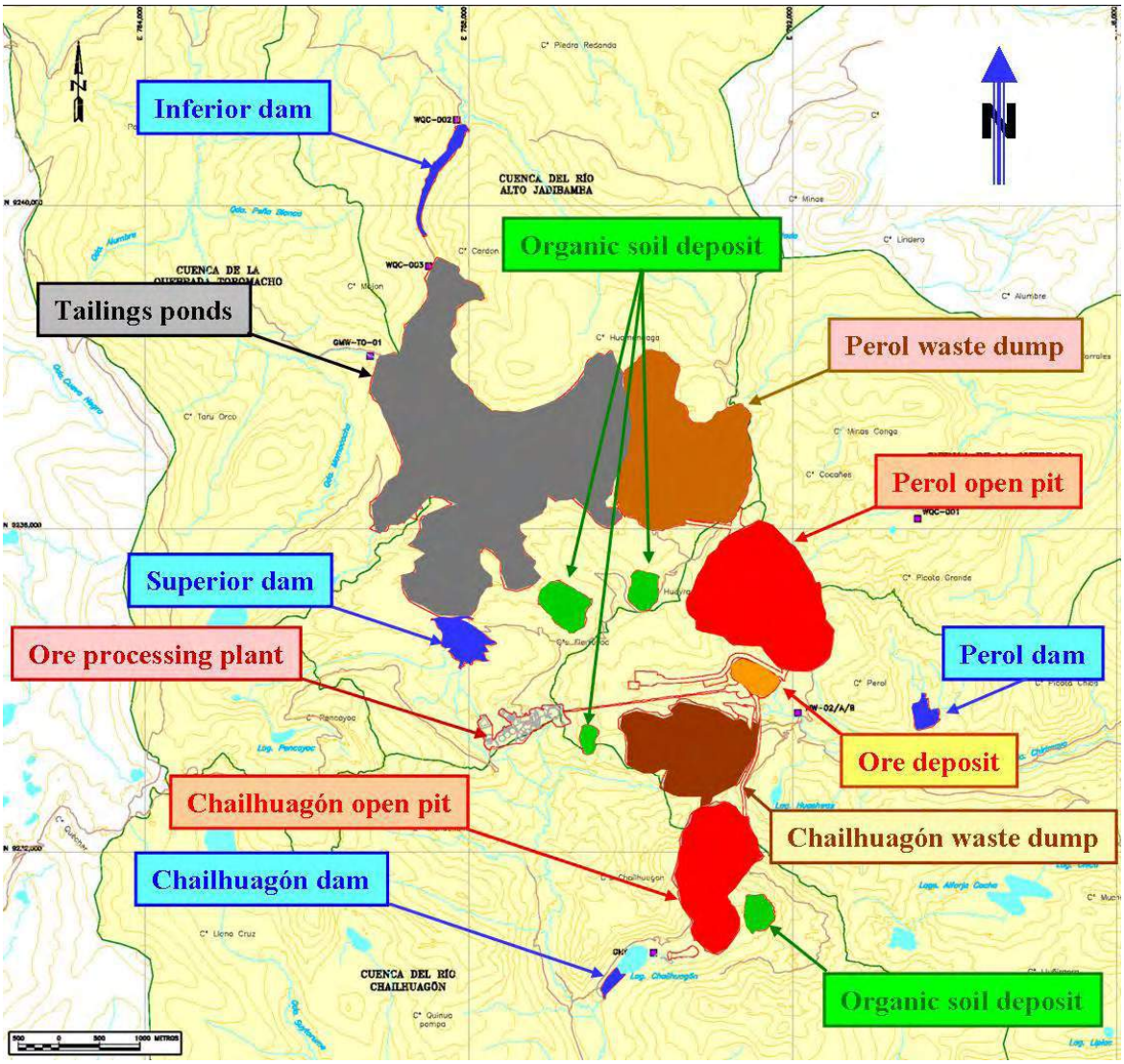

Figure 3 Main infrastructures of the Conga project

In addition to the two open mining pits (Perol and Chailhuagon), two wastes and low grade rocks dumps are provided. Chailhuagon waste dump is expected to not produce acidity, given the presence of abundant carbonate rocks; so its drainage, after passing through control and settling sediments facilities, would be released without issue. Perol is anpotential acidic water producing deposit, will be built upon relatively low permeability materials, but if necessary, a secondary system of interception and collection of water, or waterproofing work will be installed. In any case the natural drainage waters will be discharged by runoff to the tailings deposit, and pumped to the designed water treatment plant.

The planned thickened tailings are stored in sub-aerial conditions, under the protection of two dams (Figure 4), with planned capacity for 315 Mm^3, occupying an area of around 700 has. These dams will rise gradually, as required by the volume of waste; the upper dam will be permeable to retain the solid tailings, and filter the water; the downstream will be waterproof, to retain the effluents that will be pumped to the acid water treatment plant, designed for a flow of 850 m^3/h. Treated, good quality water, will contribute to the Inferior reservoir, to meet the demand of affected users in the months of drought, while the sediments of the treatment (4.45 Tm/h of mud) will be stored in the tailings deposit.

The planned infrastructure also includes: organic soil stockpiles for use in rehabilitation work; ore stockpile to be processed; and the ore processing concentrator plant (with capacity to 92,000 Tm/day), with no use of mercury and cyanide. Natural runoff waters will be directed to solids sedimentation pools or to the tailings deposit, used in the concentrator plant or the grinding, or pumped for their treatment and temporary storage in the reservoirs, in the case of low quality water.

It should be noted that it is necessary to remove two lagoons (Perol and Mala), for excavation of the open pits (Figure 4), and two others (Azul and Chica) which will be covered by a waste dump.

Figure 4 International Experts Team of the Conga Project water component in the Perol lagoon (from left to right: Luis López García, Dr. Civil Engineer; José Martins Carvalho, Dr. European Geologist; Rafael Fernández-Rubio, Dr. Mining Engineer).

As compensation has projected the construction of four regulating reservoirs, of which three (Inferior, Perol and Chailhuagon) will be used to store runoff in rainy period, which compensate for affections that can cause the mining project in the surrounding micro-basins. The fourth reservoir (Superior) will serve the needs of the project and, once finished the mining operation, will supply water to the surrounding users.

Table 1 Storage capacity, current and future, of the water bodies associated with the mining project

Original lagoon	Capacity (Mm^3)	Reservoir	Capacity (Mm^3)
Perol	0.8	Perol	0.8
Chica	0.1	Superior	7.6
Azul	0.4		
Mala	0.1	Chailhuagón*	1.6
Chailhuagón	1.2		
		Inferior	1.0
Total	**2.6**		**11.0**

* Originally: 1.43 Mm^3

In any case, the water runoff decrease will be small, given the low dimension of the subtracted area, and taking into account the decrease in rainfall above the elevation of the "optimum rain" (Fernández Rubio, Lorca Fernández & Novo Negrillo, 2014).

SURFACE WATER ON THE CONGA PROJECT

As expected, the surface water component of the Conga project is extensively analyzed in the EIS. The database used is correct but, as usual in undeveloped, small, isolated high mountain areas, is somewhat limited. The methods used are generally adequate, although some minor discrepancies on the procedure or the analysis of results, without significant influence on the conclusions of the EIS, were detected and should be accounted for in future updates. The impact of the project on the surface water is properly assessed and the mitigation measures proposed are correct, even if the expert report recommends some additional complementary improvements.

The mitigation measures are based on the construction of four reservoirs, three to recover the low flow loss derived from the occupation of part of the collecting watersheds and one to insure the availability of water for the mining operations that will also serve to increase water availability in the area after the mine closure. The reservoirs will store excess water runoff during the humid season and make controlled releases of mitigation flows during the dry season. It has been proved that the current estimated low flows can be fully recovered and even supplementary water to downstream irrigation users could be provided by the reservoirs. Therefore, the project will certainly not negatively affect the downstream users. It may however positively affect users, since the excess water of the humid season can be stored and used to fulfill their dry season needs (Figure 5).

The report points out that if the reservoirs are used to increase water availability downstream and not only to release mitigation flows, they must be operated by a participative management board where all stakeholders are represented: mining company, water authorities and water users, basically agricultural. In this way, the two-fold objective of providing mitigation flows and

increasing water availability to improve local agricultural output could be achieved with minimum conflicts.

The report points out that if the reservoirs are used to increase water availability downstream and not only to release mitigation flows, they must be operated by a participative management board where all stakeholders are represented: mining company, water authorities and water users, basically agricultural. In this way, the two-fold objective of providing mitigation flows and increasing water availability to improve local agricultural output could be achieved with minimum conflicts.

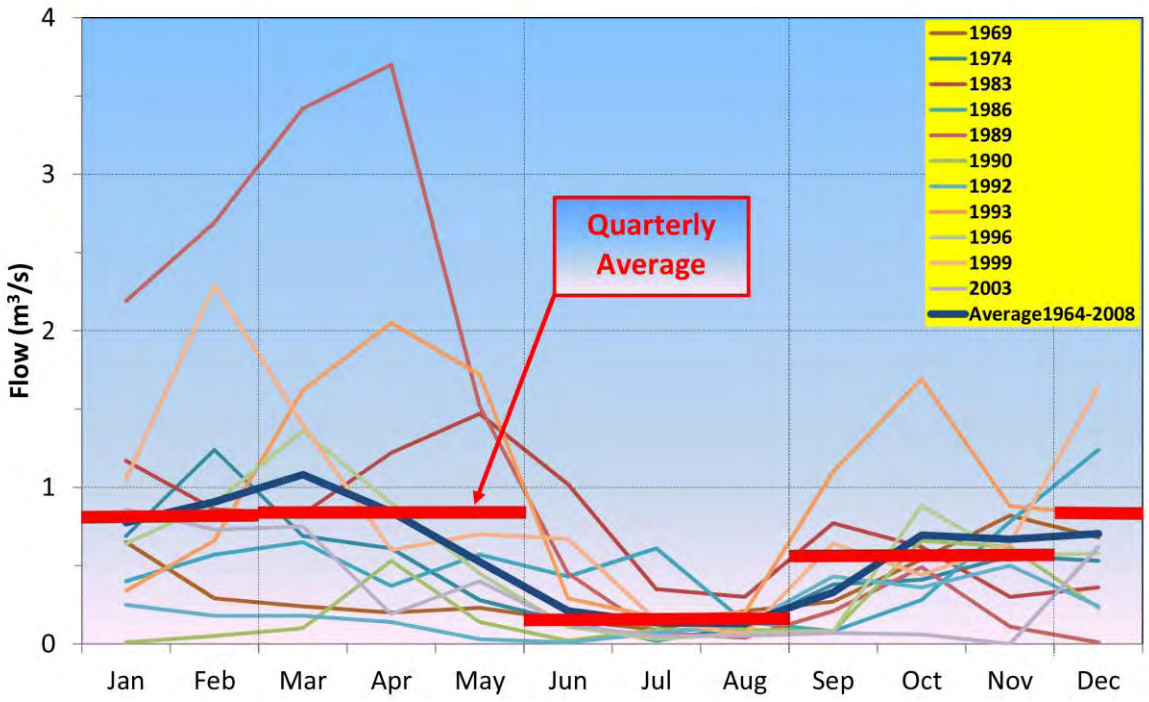

Figure 5 Monthly flow in selected years of the 1964-2008 period in Alto Jadibamba river.

Reservoir capacity must be adequate according to the hydrological characteristics of the microwatersheds that receive moderate rainfall but show a significant runoff excess in humid periods, and must take into account an eventual agricultural water demand. Therefore, it is recommended to update the hydrological studies using the data collected at the local hydrometeorological stations built by the project after publication of the EIS. It should be based on a revision of the rainfall – runoff model and, if possible, develop specific models for each microwatershed. Thus, the mitigation flows required could be adjusted and the availability of supplementary water for agricultural users would be a function of reservoir capacity as defined.

Recommendations of the expert report emphasize the need for future real time control of the evolution of the hydrologic variables and the application of the actions proposed on the EIS. Thus, the institutions with responsibility on water resources administration —basically the Ministry of Mines and Energy and the Ministry of Agriculture through the National Water Authority— can verify the degree of compliance with the proposals of the EIS and insure that correcting measures

are employed, if necessary. This systematic control will improve the hydrological knowledge of the area and provide transparent information to the local population and institutions.

Therefore, it will be necessary to build and operate a complementary hydrometeorological observation network and design adequate protocols for the collection and analysis of data and the drafting of monitoring reports.

This network should include continuous river flow gauging stations at the outlet of the five microwatersheds, since the stations installed in 2004 were destroyed in vandalistic attacks. The information obtained will be critical for the improvement of the rainfall – runoff models discussed prior. Moreover, it is recommended that at least one unaffected watershed is also gauged, in order to define the natural changes that might take place in the hydrologic regime of the area, not attributable to the mining operation.

Again, these various controls must be participative, involving institutions of the administration, local universities and communities and social groups implicated in the management of the water resources and especially the users of water for irrigation, primary consumers of the area.

The protocols for systematic handling and information must define the frequency and extent of the analysis and reports to be executed, the warning thresholds for emergencies and their associated actions. Dissemination procedures for the information obtained should be established based on the need for transparency and simplicity.

The EIS concluded that the proposed reservoirs, designed to provide only the mitigation flow, would generally be at full capacity, either during mining operations or after closure. Therefore, they are undersized in their capability for regulation of the natural runoff, so any technical and economical feasible capacity increase would augment the availability of water during the dry season and, consequently, the positive impact of the project. This is not the objective of a mining operation but, if properly managed, it would greatly improve the relations with the local population.

GROUND WATER ON THE CONGA PROJECT

A conceptual hydrogeological model and a numerical model were carried out within the EIS. These models have to be recalibrated and validated with the suggestions arising from the Expertise including also the new data to be supplied by the hydrogeological monitoring to update the ground water resource management. With this approach a better estimation of the qualitative and quantitative impacts on the existing micro basins will be achieved.

A complete integration of all data of the hydrogeological inventory is recommended, including its geo-referentiated location, defining the water points to be considered in a future monitoring network (springs and wells) down gradient of the main mining installations. This the future monitoring network will include controlling measurements in adjacent basins not affected by the project.

The deep ground water circulation is quite low in the volcanic rocks and even in the existing limestone units as they are confined between aquitards. The investigations carried out in the EIS and our field investigations did not demonstrate the occurrence of karst aquifers and fissured deep systems. The occurrence of fissured semi confined or confined aquifers are possible in limited sectors but they can allow the propagation of influenced levels, and mass transport over considerable distances after the closure and flooding of the main mining excavations. However, the hydraulic continuity between aquifers is not significant or is not present.

The available information allows for the conclusion that area ground water are mainly present in cutaneous (skin) aquifers and in alluvial and fluvioglacial deposits, all located at shallow depths and only following the seasonal precipitation. This ground water temporally feeds lagoons and the surface water runoff of ravines, gorges and rivers (Figure 6). Ground water recharge was estimated at about 34 mm/years, approximately 3% of the average annual rainfall.

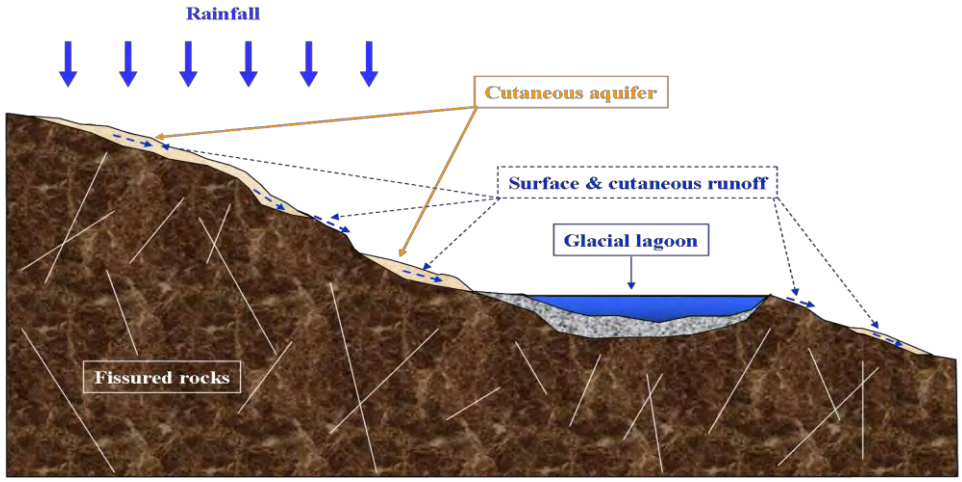

Figure 6 Hydrogeological context.

The main groundwater resources are located inside cutaneous shallow aquifers and its management shall be done in conjunction with surface water. Ground water resource is small and does not allow its systematic utilization for irrigation.

Additionally to the prevention, mitigation and compensation measures adopted by the EIS, the Experts suggested the execution of an appropriate vulnerability to contamination mapping to support technically the protection and mitigation activities for the future waste dumps and tailings dam. The design of wellhead protection zones for ground water sources used for public supply, considering chemical and biological contamination, is also suggested.

The Expertise also proposes the exploitation of the numerical model as a management tool considering the main mining project structures operation and its closing. The conclusions must be taken in account to the wise management of water resources and on the design of preventing and corrective activities, even considering that the Expertise classified the impacts as marginal over the discontinuous hydrogeological units ("aquifers") of the volcanic basement and of the interbedded limestone.

Among the mitigation and compensation measures, in addition to the surface reservoirs to be constructed, alternate water exploitation structures should be considered, such as sub-horizontal boreholes. This, offers better water management capabilities than springs, and the "rain sowing water" (managed aquifer recharge, MAR) in the cutaneous (skin) hydrogeological units using recharge channels (the well-known "acequias amunadoras" of the San Andrés de Tupicocha in the Peruvian Andes), very efficient and with great social acceptance.

WATER QUALITY

Comprehensive information on water quality, from analysis of accredited laboratories, from Cajamarca, Lima and Ontario (Canada), using standard process control and quality assurance is included in the EIS. According to these data we can highlight the following subjects.

Quality of surface waters in the pre-mine state

The water quality in lakes, streams, rivers and canals is studied in the EIS from historical data, for the five micro-watersheds located in the area, including various studies and controls developed for the Conga project, since 2003 until 2009.

The general characterization achieved, concerning composition of surface water, is considered adequate and its extension to more control points is recommended, for better knowledge of the pre-mining state, keeping track of spatial-temporal quality during the mining operation. It is also recommended to select referential points in similar basins unaffected by proposed mining activities.

In the EIS, analytical data are considered in the framework of national environmental quality standards for water (ECA), established by the Ministry of Environment and specifically, with Category 3, corresponding to irrigating high and low stem vegetables and to animal drink, as this is the primary use of these surface waters.

As for the quality of superficial water in the pre-mining state, the following could be highlighted:

- The major chemical facies is calcium bicarbonate, correspondent to low salinity waters, as a result of the low solubility of lithological materials where these waters flow; although some samples are calcium bicarbonate-sulfated and others are calcium sulfated.
- The pH measured in the field, for most samples, is higher than 7, even reaching 9; occasionally there are values between 6.5 and 7, and in wetlands ("bofedales") pH becomes very low (from 3.0 to 6.4 with medium values of 3.1 to 4.2).
- The total dissolved solids range from less than 3 mg/L to 302 mg/L, values that can be classified as low.
- The minimum alkalinity values were recorded in wetlands (<1.0 to 12 $CaCO_3$ / L, with a mean value of 1.3), which shows the poor quality of these waters. In the remaining tests, variable values were observed, surpassing 202 equivalents of $CaCO_3$ / L. In some ponds and irrigation canals values below 20 were measured, reflecting its poor quality for maintenance of animal life.
- The sulfate content may be considered low (<0.5 and 42.9 mg/L), although the presence of pyrite (especially in mineralized rocks), confirms its no-reactiveness, as a result of being under water and, therefore, without oxygen.
- In general, the recorded concentrations of heavy metals (Al, As, Cd, Cu, Fe, Mn, Ni, Pb, Sb and Zn), are low (sometimes even below detection limits) without values exceeding ECA´s Category 3, although in some analysis relatively high contents are observed, deriving from the presence of particulates, either in suspension or settled.

- In relation to the biological quality, content in fecal and total coliforms often exceed the limits set by the ECA for Category 3, especially in rivers, but also in channels, and samples exceeding the limits of these pathogens are frequent in water for human consumption, resulting in ill conditions for livestock and human activity.

Groundwater quality in the pre-mine state

EIS discusses the composition and quality of groundwater in the project area and its surroundings, from periodic analyzes by several laboratories, especially since 2009.

Since these waters are used primarily for human consumption, its quality was evaluated using the ECA standards, established by the Ministry of Environment for Category 1 - Subcategory A1 (water which may be turned potable with simple disinfection). The results were processed using statistical techniques and graphical displays, also using standard geochemical modeling programs. The results provide a good contribution to the knowledge of the characteristics, composition and behavior of groundwater quality.

Among the notable aspects, these can be highlighted:

- The majority chemical facies are calcium bicarbonate, although there are sodium-potassium calcium, and other chemical facies.
- The pH is generally neutral to alkaline, although there were analysis with very high values (over 11), possibly due to grouting additives used in drilling holes.
- Total dissolved solids is usually very low to low, but there are values higher than 4,000 mg/L.
- Most metals regulated for human consumption are below the maximum established values; however, in a series of water samples from wells the values were exceeded regarding the contents of Al, As, Fe, Hg, Pb and Mn in different sampling campaigns, a situation attributable to natural geochemical background, from a geological area that has received deep mineralized fluids.
- Values for total and fecal coliforms are generally low, although in some groundwater were obtained values that exceed the limits established by ECA regarding fecal coliforms, which highlight the human or animal influence.
- In terms of dissolved oxygen, DBO and DQO, some samples do not meet the ECA standards.

Quality of contact water in the mining and post-mine stage

Forecast for water quality that could be drained on a mining operation, always has a degree of uncertainty, especially for water in contact with reactive rocks (presence of pyrite and oxygen).

For an approximated value, a number of studies and hydro-geochemical leaching tests (including tests in humidity cells) were conducted in the EIS, to predict future water quality. For safety reasons, it is planned in the EIS to submit to water treatment all potentially quality-affected water. These changes in water quality are expected to be higher in waters in contact with rocks from the Perol open pit, as it presents pyrite and marcasite that, when exposed to this environment, would

be the main generating source of acidity, having little material to support natural neutralization except from Chailhuagón open pit where limestone is present.

Regarding the reactivity of the tailings in the presence of water and oxygen, and given its small grain size, no doubt they will be acid generating materials, which may incorporate: As, Cu, Mo, Sb and Zn . Therefore, an operating facility of acidic water treatment in the long term is included in the project design.

The process plant for mineral treatment will not use cyanide nor mercury, and reagents used for the differential flotation of targeted metals, will be in part, recovered and reused in the process, in a closed circuit. Another portion of reagent content will be incorporated into the produced concentrates, destined for export and transported by truck; and a third fraction will remain in the deposit, designed with zero discharge.

In the EIS it is proposed a sub-aerial disposal for the thickened tailings. To avoid the need for a very prolonged treatment of acidic waters, alternatives such as underwater tailings storage exist, avoiding the generation of acid waters and dramatically reducing the need for treatment, but requiring water, while it reduces the storage volume, which would require having a second tailings storage area.

RECOMMENDATIONS

The expert report proposes some improvements related to the infrastructures planned, whose feasibility must be confirmed after the necessary detailed studies. If proven possible, they could reduce the negative impacts identified in the EIS and increase the positive impact of hydrologic and environmental measures.

Moreover, the report emphasizes the opportunities to improve the expertise on the hydrologic behavior of high altitude Andean systems provided by the project. It would also enhance the environmental and hydrologic management practices in such areas.

Accordingly, the expert report recommends starting investigation, as soon as possible, of several aspects that could environmentally improve the design of some infrastructures:

- Optimize the conservation conditions of organic soils recovered from different areas of facilities in the provided storage (piles), for better preservation of its seed bank.
- Properly maintain humic materials from the dismantling of wetlands (“bofedales”), for later use in rehabilitation work.
- Evaluate technical and economically alternative relocation or displacement of the wastes and low grade Perol rocks dumps, to avoid cover the Lagoons Chica and Azul.
- Study the possibility of encapsulating residues from the treatment of acidic waters, in a secure deposit.
- Analyze the suitability of employing biotechnological passive methods of treatment of acid water, and in particular wetlands with planting of reeds (“totoras”) (Fernández Rubio, 1991).
- Analyze the possibilities for the increase in capacity of the designed reservoirs, in order to optimize the management of the water resources generated in the project area by. More specifically:

  - Expand the capacity of the Inferior reservoir to increase the availability of water during the dry season.
  - Expand the capacity of the Perol reservoir, if there is evidence of the need for supplementary water to the downstream users.
  - Expand the capacity of the Chailhuagón reservoir, to its feasible maximum to benefit downstream users (MYSRL has already undertaken this proposal). Thus it would happen in a current capacity of the lagoons of 1.2 Mm^3 to a current availability of reservoirs of 11 Mm^3.
- Build or improve intake structures for water supply of small urban populations that currently use natural springs, through sub-horizontal boreholes allowing control of the outflow.
- Systematically implement the "Water Earth Technology" (WET), or "rain sowing water" using recharge channels (the well known "acequias amunadoras" of the Peruvian Andes), to "collect water" through the "water harvesting" downstream during the dry season.

However, the need for a realistic framework that avoids the creation of false hopes must be emphasized. There is a strong risk of encouraging the misleading idea that a mining project has to solve the structural shortages of water during the dry season.

The recommended actions could be a first step towards the development of the water resources management system of the microwatersheds that should be complemented by the Peruvian National Water Authority through the Watershed Management Plans currently being drafted.

AKNOWLEDGMENTS

To the members of the various institutions that made our work easier by providing all the required means: Óscar Valdés Dancuart (President of the Council of Ministers); Jorge Humberto Merino Tafur (Minister of Energy and Mines); Manuel Pulgar Vidal (Minister of the Environment); Luis Ginocchio Balcázar (Minister of Agriculture); Mariano Castro S.M. (Deputy Minister for Environmental Management, Ministry of the Environment); Gabriel Quijandría Acosta (Deputy Minister for Development Strategic of the Natural Resources, Ministry of the Environment); Manuel Castro Baca (Director General of Mining Environmental Affairs, Ministry of Energy and Mines); Hugo E. Jara Facundo (Chief National Water Authority, Ministry of Agriculture); Jorge Luis Montenegro Chavesta (Director of Water National Authority, Ministry of Agriculture); Susana G. Vilca Achata (President Board of Directors, Geological Mining and Metallurgical Institute (INGEMMET)); Gustavo Adolfo Luyo Velit, Víctor Santiago Carlotto Caillaux and Flucker Peña Laureano (Geological Mining and Metallurgical Institute, Ministry of Energy and Mines); Milagros Verastegui Salazar (Ministry of Environment); Roque Vargas Huamán (Ministry of Energy and Mines); Amelia Díaz Pabló (President of the National Service of Meteorology and Hydrology of Peru (SENAMHI)); Julio Ordóñez Gálvez, Oscar Felipe Obando, Juan Fernando Arboleda Orozco y Waldo Sven Lavado Casimiro (Directors of the SENAMHI).

To those that provided liaison, coordination and logistical support: María Elena Juscamaita Arangüena (General Secretary, Presidency of the Council of Ministers); Tábata Dulce Vivanco del Castillo (General Secretary, Ministry of Energy and Mines); Marina Vilca Tasayco (Director of the General Administration Office of the Presidency of the Council of Ministers); Víctor E. Caballero Martín (Chief of the Office of Management of Social Conflicts, of the Presidency of the Council of Ministers); Walter Obando Licera (Adviser of the Office of Management of Social Conflicts, of the Presidency of the Council of Ministers; Technical Coordinator of the Expert Team); Martín Carbajal Zegarra (Adviser to the Office of Management of Social Conflicts, of the Presidency of the Council

of Ministers); Rodrigo Prada Vargas (Adviser to the Office of Management of Social Conflicts, of the Presidency of the Council of Ministers); Luis Alberto León Flores (Head of the Office of Administrative Affairs, the Presidency of the Council of Ministers); Lourdes de Souza Ferreyra Odar (Secretariat of the Office of Management of Social Conflicts, of the Presidency of the Council of Ministers); Michael Acosta Arce (Environmental Engineer of the Ministry of Energy and Mines); Miluska Eran Bodero (Assistant of the Ministry of Energy and Mines); Wendy Alfaro Wall (Assistant of Technical Support, Ministry of Energy and Minas); Raúl González Neira (Technical Support Engineer of the Ministry of Energy and Mines); and Sofía Mescua (Photographer).

To the technical staff of consulting companies that worked at the EIS, who provided complementary information and handled our requests for clarification (alphabetically ordered): Carlos Aguilera M. (Process Engineer. Fluor); Michael K. Herrel (Geochemist. Golder Associates); Alfredo Híjar (Environmental Consultant); Rafael S. Dávila (Principal, General Manager. Golder Associates); Simon Mansell (Senior Project Manager, Schlumberger Water Services); Mayra Medina (Consulting. Metis Gaia Consultores); Nathan Nadramija (General Manager. Metis Gaia Consultores); Xavier G. Panozo M. (Project Manager. Knight Piésold Consulting); Roberto Parra (Environmental Consultant); Abelardo de la Torre Villanueva (Asesores Técnicos Asociados, S.A.); Javier Torrealva (Lider Grupo Hidrotecnia. Golder Associates); and Mario Villavisencio (General Manager. Knight Piésold Consulting).

Finally, to all those who answered to our call for meetings both in Cajamarca and Lima, to incorporate their invaluable information to the expert report (alphabetically ordered): Narda Alarcón Rojas (UPAGU); Hugo Arévalo Escaró (PROESMIN); Nicole Bernex (Pontificia Universidad Católica del Perú); Luis Céspedes Ortiz (General Manager. Chamber of Commerce and Production of Cajamarca); Antenor Floríndez Díaz (ONG CUENCAS); Cristian H. Gálvez Ruiz (Director. Chamber of Commerce and Production of Cajamarca); Héctor Garay Montáñez (Universidad Particular Antonio Guillermo Urrelo (UPAGU); Ever Glicerio Hernández Cervera (Regional Governor Cajamarca Region); José J. Huamán Mantilla (PSI SIERRA – MINAG); José Carmelo Martínez Lázaro (Bishop of Cajamarca); Mirco H. Miranda Sotil (Advisor to the High Direction of High Water Authority); Rosa Olivera González (AGRORURAL – MINAG); Telmo Ramón Rojas Alcalde (ONG CUENCAS); Hugo Loli Salomón (Director of Committees. Chamber of Commerce and Production of Cajamarca); Francisca Torres Hernández (Josemar Consultores EIRL).

OFFER

Those interested in obtaining further information, not for commercial use, may ask for the complete expert report (in Spanish) and a power point presentation (rfrubio@gmail.com).

REFERENCES

Fernández Rubio, R. (1991). Tratamiento biológico de aguas en pantanales. Tecno Ambiente 1: 37-44. Madrid.

Fernández Rubio, R.; López García, L.; Martins Carvalho, J. (2012). Dictamen pericial internacional. Componente hídrico del estudio de impacto ambiental del proyecto minero Conga (Cajamarca - Perú). Elaborado para la Presidencia del Consejo de Ministros de Perú. 261 pp. Lima.

Fernández Rubio, R.; Lorca Fernández, D. & Novo Negrillo, J. (2014). Mitos y realidades de las cabeceras de cuencas andinas peruanas. El Ingeniero de Minas. Col. Ing. del Perú. 20-26. Lima.

Knight Piésold Consulting. (2010a) Proyecto Conga. Estudio de Impacto Ambiental. Informe Final. Realizado para Minera Yanacocha S.R.L. 20.467 pp. Lima.

Knight Piésold Consulting. (2010b). Levantamiento de Observaciones. Ministerio de Energía y Minas. 6.919 pp. Lima.

MINAM. (2006). ECA para el agua, con alrededor de 80 parámetros agrupados por uso en cuatro categorías. Art. 81º y 82º del Reglamento de la LGA. Aprobado por D.S. Nº 002- 2008. Lima.

Mine Planning and Acid Rock Management

Dean Williams[1], Jim Fowler[1] and Dirk van Zyl[2]

1. *Kinross Gold, USA*
2. *University of British Columbia, Canada*

ABSTRACT

Mine planners face a number of obstacles to good management of acid generating materials. Too often the consequence of these obstacles is the generation of acid drainage, long-term water treatment, and possibly environmental impact. This paper reviews leading practice approaches to mine waste characterization drawing on the GARD Guide and mine planning from Kinross Gold Corporation's G4 resource characterization approach. Key obstacles to mine waste characterization and planning are discussed and solutions suggested.

Keywords: Mine planning, acid rock, management, characterization, life cycle

INTRODUCTION

Acid mine drainage and the need to manage acid generating materials is a well-documented problem of which mine planners are well aware. Nevertheless success in avoiding acid mine drainage through good management from start to finish of a project is mixed. Mine planners face a number of obstacles to good management of these materials, which this paper will discuss.

Mine planning is used in this paper to indicate the task of converting resources to economic reserves. This is a complex task that includes a large amount of information of variable detail and accuracy. The information includes metal content, processing costs, capital requirements, metallurgical properties, geotechnical characteristics, hydrogeological characteristics, as well as geochemical properties, etc. Mine planners are generally judged on their ability to optimize the economic value of a mineral deposit to allow the company to evaluate the overall feasibility of proceeding with a project. This task is often associated with very tight time schedules that require quick decision-making, in many cases with incomplete data or interpretations.

This paper explores the obstacles that mine planners face in developing good management strategies for acid generating materials. It focuses on the following three aspects:

- Incomplete geochemical characterization
- Integration of geochemical characterization into mine planning
- Long-term ARD management

Leading practice approaches will be identified as well as the obstacles faced by the mine planner to implement these practices. Recommendations will be made of how the practices can be improved.

LEADING PRACTICE

GARD Guide

Much has been written on the topic of geochemical characterization during the mine life-cycle. The Global Acid Rock Drainage Guide (GARD Guide, www.gardguide.com) provides a description of ARD characterization and prediction techniques (in Chapters 4 and 5) that can be used in developing the information required for mine planning and evaluation. A phased assessment approach is promoted that provides sufficient data at all stages of the mine life-cycle (exploration, pre-feasibility, feasibility, construction, operation, closure and post closure). Leading practice environmental management requires that the potential for acid drainage be identified early in the mine life-cycle. The overall characterization aims to identify the distribution and variability of key geochemical parameters, including sulfur content, acid neutralizing capacity and elemental composition and their influence on acid generation and element leaching.

The components of the characterization include (the information below draws on the GARD Guide, refer to it for more details):

- Sample selection from each geological material that will be mined and exposed and from each waste type. Selection of representative samples should consider material type, spatial

representation, compositional representation, and focused vs. random sampling. Standard operating procedures should be developed for the geological logging and the collection and documentation of sample selection. The GARD Guide recommends that the number of samples depends on the amount of disturbance, the compositional variability within each material type and the statistical degree of confidence that is required for the assessment.

- Laboratory and field testing to characterize the acid generating and metal leaching potential of mine materials, including static and kinetic tests:
    - Static tests:
        - Chemical composition (whole rock and elemental analysis)
        - Mineralogical analysis
        - Acid base accounting (ABA)
        - Net acid generation (NAG)
        - Water extraction (batch extraction) tests with solution assay
    - Kinetic tests:
        - Humidity cell leach testing
        - Column leach testing
        - Field column or rock pile testing to obtain information about material reactivity under ambient site conditions

The results from these tests, together with climatic, hydrologic, and hydrogeologic information for the site, provide a basis for predicting the potential for acid generation and metals leaching. With this information mine plans, including management strategies and environmental impact assessment, can be developed. This geochemical characterization process is depicted in Figure 1 from the GARD Guide (Figure 5.5).

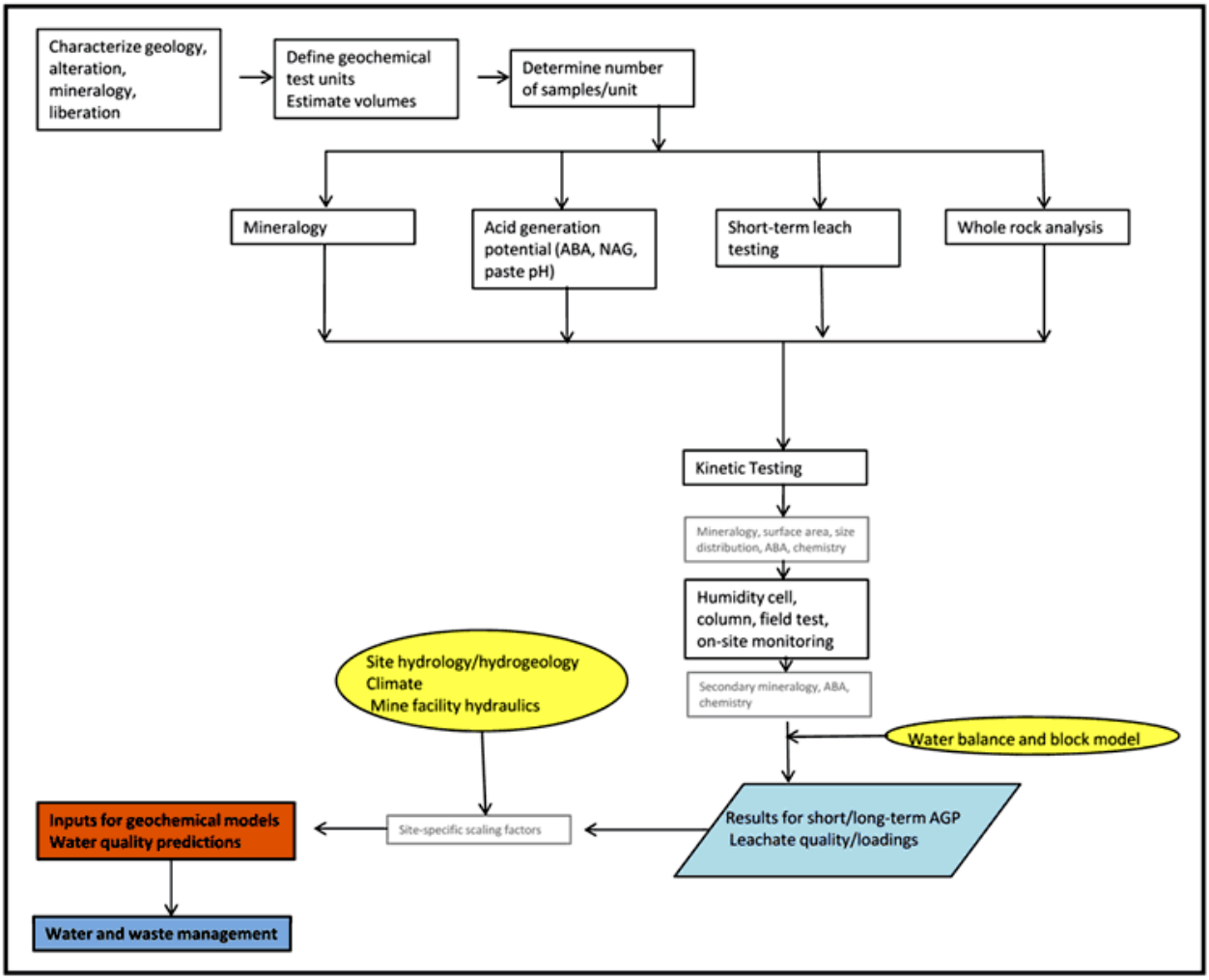

Figure 1 Geochemical Characterization Program

Kinross G4 Approach

An example of how geochemical information can be considered in mine planning is Kinross Gold Corporation's (KGC) in-house system for resource modeling referred to as G4 (Sims, 2014). Resource modeling using G4 draws from a database that includes four components:

- Geologic (G1)
- Geochemical (G2)
- Geometallurgical (G3)
- Geotechnical (G4)

Detailed correlation analysis is used to assess the 'G' components and populate the resource model with key variables. These variables; in addition to density, grade, and process characteristics; include elemental characteristics, acid base accounting, and hydrogeologic information. Scorecards are used to measure the maturity of all data bases with respect to project maturity. Target Maturity stages are:

- Initial Project Setup

- Initial Drilling
- Infill Drilling
- Scoping Study
- Pre-Feasibility Study
- Feasibility Study
- Operations

Figure 2 illustrates how the G4 feeds into the Resource Block Model and Mine Optimization

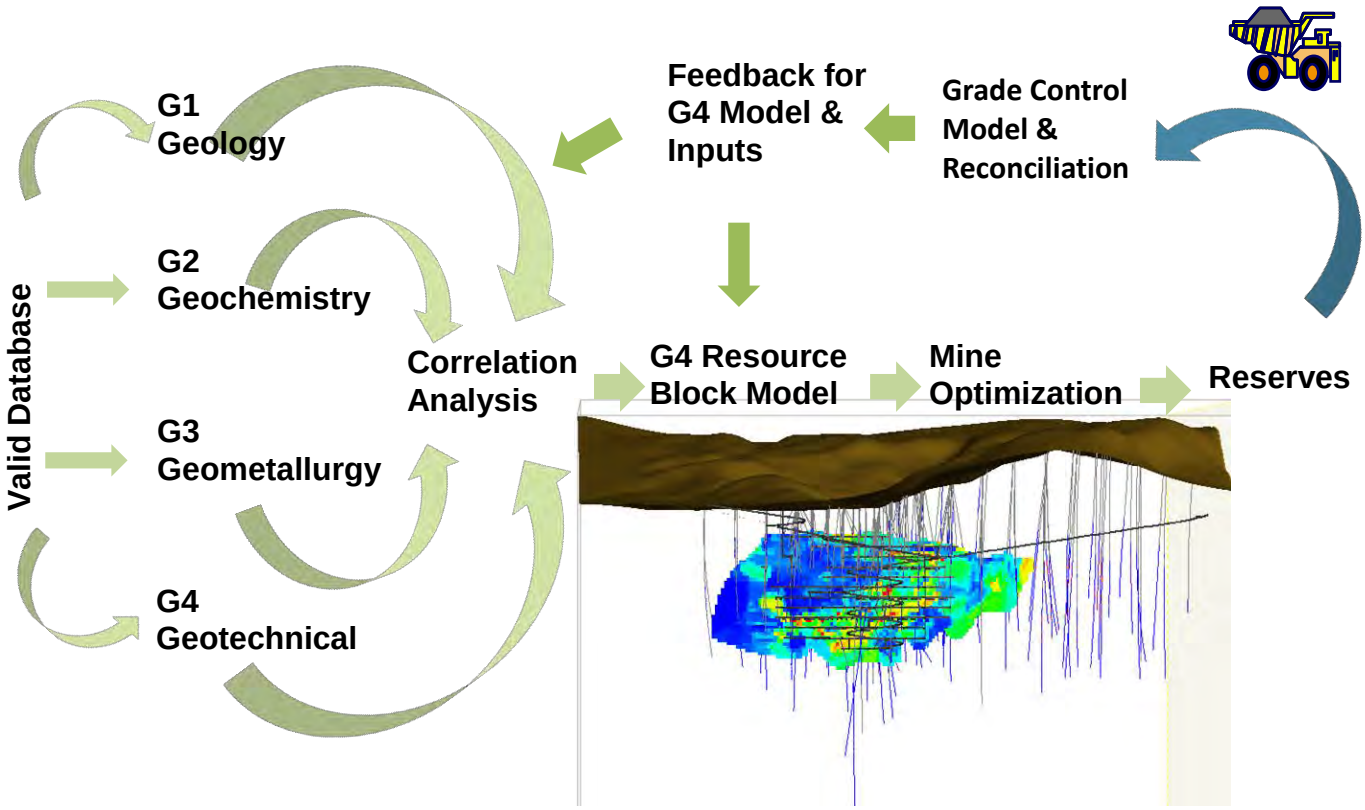

Figure 2 KGC G4 Process for Developing Resource Block Model and Mine Optimization

THE MINE PLANNER'S DILEMMA

INADEQUATE GEOCHEMICAL CHARACTERIZATION

Good management of acid generating materials often begins with initial geochemical characterization efforts. Geochemical characterization is a typical component of baseline studies and factored into mining plans, impact assessment and permitting. Unfortunately too often geochemical characterization begins when an orebody is determined to be economic. At this point in mine feasibility planning, time is money and the pressure to obtain necessary approvals is high. Because sampling, analysis, interpretation and reporting require time, there is a tendency to manage the scope of characterization efforts to stay on schedule. While statistical analysis of test

results is advisable to confirm that a representative data set has been obtained, this may be ignored in deference to pre-established schedules.

Additionally, kinetic testing is required to assess the relative rates of acid generation and metals leaching reactions and to provide information on the evolution of potential acid drainage over time. Because kinetic testing requires time, and time is often in short supply, the mine planner or project team may feel considerable pressure to limit the extent or duration of kinetic testing.

These obstacles can of course be overcome. Sulfur analysis should begin with initial exploration and should be performed on all samples analyzed for target elements. As the geology of a mineral target becomes known, static testing of representative samples from each material type should be performed. Additional static testing, kinetic testing and water quality characterization should follow. With an early start and progressively expanded, it is possible to characterize geologic materials and develop appropriate management strategies for inclusion in mine plans without delay to feasibility and project development schedules.

Acid base accounting (ABA) evaluates the acid generation potential of the various geologic units present at a site. As part of ABA, the bulk quantities of acid generating minerals (e.g., sulfide minerals) and acid neutralizing minerals (e.g., carbonate minerals) are measured to assess whether the materials tested will have sufficient capacity to neutralize the acid potential, or if the materials have the potential to generate acidity. Acid generation potential is commonly interpreted by the ratio of neutralizing potential over acid generating potential (NP/AP) or NPR ratio. Unfortunately, all-too-often, there are geologic units that are quite geochemically variable. In addition, because geochemical weathering rates are dependent upon oxygen, water and temperature, the timeframes for the onset of acid drainage can be quite delayed or difficult to estimate. The mine planner, confronted with these unknowns, is challenged to select the "right" management approach or even, in some cases, to understand if there is a "real" problem.

Of course it can be argued that the mine planner should always exercise the "precautionary principle" when it comes to potential acid rock management, but that is in many cases an overly simplistic, costly, and conservative approach. Support from environmental and geochemical advisors is recommended to ensure that management requirements for various geochemical domains are understood and incorporated into the mine plan.

Because few ore bodies are fully characterized prior to mine development, ultimate geochemistry and mine planning options may not be fully understood. In too many cases, following initial permitting and approvals, ongoing monitoring of geochemical characteristics of wastes is not continued. Further, changes in geochemical domains within the same geologic unit are common, and the need for expanded geochemical characterization, are often not recognized. Failure to recognize these changes can result in the construction of acid generating dumps, tailings facilities, or use of acid generating materials for construction, roads, etc. In the end, mitigation of the consequences of failure to recognize these types of changes can be time consuming, costly, and damaging to the social license of a company.

To reduce the potential that the mine planner is working with inadequate information, geochemical characterization efforts need to continue as the ore body continues to be developed. Plans must include procedures to recognize new geochemical domains and the requirement for more extensive characterization to ensure that these materials are properly recognized and managed.

Integration of characterization in mine planning

Possibly an even more significant obstacle is that geochemistry is commonly not fully integrated into block models. Acid generating potential must be correlated with geology type to create geochemical domains. This information is input to the block model along with metallurgical, geotechnical, and hydrogeological information. At the end of the day, the mine planner is working with a very complex data set. Failure to achieve strong correlations with geology type or to fully understand the potential for acid generation and the management options available can result in the mine planner deciding to ignore the data, as "it is not clear what it means".

The mine planner should be provided support by a geochemist to ensure that initial characterization is well done and correlations with geology are strong. Additional support may also be appropriate to ensure that management strategies for different geochemical domains are well conceived.

As mine plans develop and more information becomes available regarding recovery, grade, geochemistry, etc., mine planners and operators seek management solutions that have minimal impacts on reserve estimate and economic performance. Mine planners are judged on their ability to convert resource to economic reserves and this unfortunately may mean that issues, especially where the impacts are not clear or will only manifest over time, may not be entirely addressed. This focus on positive results can mean that more environmentally acceptable options may not be fully considered as they would mean lower reserve estimates and lower short-term economics. For mines with relatively long lives, e.g. greater than 15 years, the economic tradeoff between avoidance or isolation of potentially acid generating materials and ultimate treatment of acid drainage often favors the selection of water treatment as the preferred alternative.

Corporate policies on full-cost analysis and environmental protection are required in order to limit the potential for this obstacle to result in unacceptable environmental performance. Corporate environmental departments along with independent reviewers of block models and mine plans must be diligent and engaged. More recently, capital approval systems (CAS) which have been adopted by many companies, include more detailed outlines of what is required at each evaluation step, from scoping through feasibility studies, helping ensure that the correct environmental parameters are collected.

Another obstacle, hinted to previously, is that geochemistry and acid rock management are typically not core competence areas for the mine planner. Due to the unique knowledge requirements, planning and management input is typically provided by outside experts who may not fully understand the geotechnical, metallurgical, or economic factors that are critical for planning. The planner's ability to incorporate this information into the mine plan will vary by individual and level of experience. Clearly the ability of geochemical and environmental advisors to understand what is involved in mine planning and to support the mine planning process can be invaluable. Environmental advisors must have a good understanding of the management practices available and the ability to effectively communicate with the mine planning team.

DISCUSSION

Responsible acid rock management involves a host of leading practices of which mine planning, highlighted in this paper, is an important consideration. It is essential that obstacles to responsible acid rock management be identified and overcome. Because many of the obstacles involve the availability of data and its interpretation, it is critical that data base maturity be clearly defined for

all stages of project maturity. Table 1 provides a general summary of critical analyses relative to project maturity/life cycle.

Table 1. Critical geochemical analyses related to project life cycle

Data or Analysis	**Lead**	**Initial**	**Infil l**	**Scopin g**	**PF S**	**FS**	**Ops**
Design/review of data collection strategy (selection of analytical method and sampling density and distribution)	Expl	●	→	→	→	→	→
Total sulphur and carbon	Expl	◔	●	→	→	→	→
Multi-element data	Expl	◔	●	→	→	→	→
ABA, NAG, water extraction	Expl/ Env		◗	●	→	→	→
Kinetic Investigations	Env		◔	◕	●	→	→
Identification of materials management requirements	Env/M-Planner		◔	◗	◕	●	→
Monitoring data collection strategy (sampling frequency, distribution, analysis)	Env/M-Planner						●

Progressively more detailed/advanced 

Full implementation 

Use/maintain/update as necessary 

The mine planner cannot be expected to solve the mine waste characterization and management dilemmas described above alone. Geochemical and environmental advisors must provide support and assistance to the mine planning process including the identification of management options, costs and their expected effectiveness. Strategies for more effective planning for acid generating materials should include:

- Statistical analysis and other modelling to integrate basic geochemical information, including a clear understanding of ARD potential, into the overall mine block model. This process may be done in a number of steps of refinement to expedite the overall mine planning process.
- Development of inventories of effective management strategies for various types of ore bodies, acid generating potentials, and climates.
- On-going monitoring of the geochemical behavior of mine materials and the effectiveness of management strategies. Every effort should be made to identify the potential range of uncertainty/variability that may exist. Likewise management strategy performance must be monitored and where necessary updated over the mine life-cycle to maximize the potential for success.

When mine planning is done with a complete set of data, confidence in the results, as required by processes such as NI 43-101, is more likely. When geochemical characterization is not well defined it is suggested that comments be provided to indicate the approach that was used, potential uncertainties and their possible implications. This would provide important information for investors. It is recommended that this be further considered by the ARD community, INAP, and others to support the development of more standardized definition of data and planning requirements for project maturity stages.

CONCLUSION

The mine planner faces a number of obstacles to good management of acid generating materials. Inclusion of 'screening analyses', such as total sulphur and carbon in early analysis of drill holes provides a foundation for subsequent static and kinetic testing. As discussed, this information provides a basis for understanding geochemical weathering, management requirements, and potential environmental impact. Begun early in the process, it is possible to minimize or avoid planning and permitting delays.

Data base and management strategies must advance with project maturity stage. Most mining companies have project stage gates, with well described requirements, that must be met before a project can be advanced. Geochemical characterization and management strategies are important components of the stage gate process and must be defined.

Environmental advisors must provide input on management options, costs and their effectiveness. On-going monitoring of management effectiveness is required to recognize problems early and make adjustments as required.

On-going monitoring data collection and interpretation aims to recognize changes in geochemical domains that may require new management strategies. Collaboration between mine planners and environmental personnel is critical to ensure that management strategies are embedded in mine plans and environmental protection requirements are achieved.

ACKNOWLEDGEMENTS

The authors acknowledge the many individual contributions that have been made to the development of the GARD Guide and acid rock management practices. As this paper points out, the tools for management of acid rock have been developed, it is simply a matter of their utilization.

NOMENCLATURE

ABA	Acid base accounting
ARD	Acid Rock Drainage
Env	Environmental (includes geochemistry)
Expl	Exploration
G4	Kinross Gold Corporation's standard for resource characterization
M-Planner	Mine planner
NAG	Net acid generation potential
NPR	Ratio of neutralizing potential over acid generating potential (NP/AP)

REFERENCES

INAP (International Network for Acid Prevention), 2010 GARD Guide

Sims, John, 2014 Kinross Standards for Resource Characterization – G4, Version 1.4

A Global Mining Industry Perspective on Water Stewardship

Ross Hamilton
International Council on Mining and Metals (ICMM), United Kingdom

ABSTRACT

In recent years water has risen to become one of the most significant issues facing the mining industry. Water is not only a critical resource for mining operations, but also for other industries, communities and the natural environment. Inadequate consideration of water and its other users has resulted in costly project delays, cancellation of licenses, community conflicts and reputational damage. Such experiences have led the industry to acknowledge that its approach has to shift from simply management of operational water supplies to one in which the needs and priorities of other users are considered. In response to this challenge the International Council of Mining and Metals developed a Water Stewardship Framework in 2014, and launched a *Practical Guide to Catchment-based Water Management* for the industry, this year. The new guidance sets out a comprehensive and systematic approach for identifying, evaluating and responding to water-related risks for the mining and metals industry. The document is structured as an interactive and informative prompt to guide companies in the development of their water strategies and plans in accordance with the local context and hydrology in which mining and metals operations take place. Implementation of a catchment-based approach at the operational level is a fundamental step towards mining companies becoming effective water stewards.

**There is no full article associated with this abstract.*

Acid Rock Drainage Treatment (TADA) at Codelco Andina

Jorge Lobos
Codelco, Andina Division, Chile

ABSTRACT

The Andina Division of Codelco Chile has a copper operation which combines surface and underground mining. The first requires prestripping which needs to be deposited in waste dumps. These dumps, with a limited authorized capacity, need to be replaced at the end of their lives. For this reason, the Division carried out studies to identify mid and long term alternatives to support current production and future expansions. The Norte Waste Dump (NWD) -located in the upper basin close to the open pit- was chosen as the best alternative to replace the actual dumps once they are depleted.

Precipitation and oxygen in the environment cause chemical reactions over low grade materials with sulfur contents deposited in the dumps, acidifying waters and promoting the growth and development of bacteria. These can accelerate the generation of acidic drainage which contains copper, iron, manganese and sulfates among others.

The purpose of the TADA (acid water treatment) Project is to offer a solution to the acid drainage resulting from the NWD. The plant captures and diverts clean water, avoiding contact with these dumps. It also captures water drained by the NWD and treats it in a High Density Sludge Plant (HDS technology). Treated waters are then returned to natural courses or to the production processes, according to water permissions and environmental regulations.

In order to comply with environmental requirements and meet investment criteria, the TADA Project was constructed stage by stage. The waste dump construction, as well as the treatment plants, was constructed using this mode.

**There is no full article associated with this abstract.*

10th ICARD IMWA 2015 | 10th International Conference on Acid Rock Drainage & IMWA Annual Conference

Control of Water Pressure in Mine Slopes

Adrian Brown
Adrian Brown Consultants, Inc., USA

ABSTRACT

Water pressure degrades the performance of slopes, causing reduced slope angles, reduced slope safety, and slope movement leading to catastrophic slope failure. The additional mining costs associated with these slope water pressure effects are significant, and catastrophic failure can be enterprise threatening. Accordingly, for cost-effective large-scale surface mining, elimination of water pressure in slopes is required.

Water pressure exists in slopes for two fundamental reasons. First, water pressure is present throughout slope rockmasses due to normal flow of infiltrating and stored water. Second, water pressure spikes can occur in mining-destressed fractures and faults due to infiltration from rainstorms, flooding, or snowmelt, causing elevated water pressures to propagate deep into the slope rockmass, resulting in water-driven slope movement and, in the extreme, catastrophic failure.

Water pressure in mine slopes is traditionally controlled by dewatering wells, horizontal drains, or drainage galleries. These methods reduce but do not eliminate long-term slope water pressures on failure surfaces. More importantly, they do not significantly reduce sudden pressure spikes in the fracture system. The only reliable method to prevent both of these stability-reducing and failure-inducing conditions is prevention of ingress of water to the mine surface and to the mine crest area, together with conventional pressure mitigation.

This paper reviews the theory of slope stabilization, examines methods of improving the effectiveness of the "standard" pressure control strategies by control of infiltration, evaluates methods of infiltration prevention in large surface mines, determines the effectiveness of infiltration prevention in achieving maximal slope performance, and makes the business case for infiltration control to achieve maximum slope angles, maximum slope safety, and maximum profitability.

**There is no full article associated with this abstract.*

Challenges Following the Transitional Phase of Implementing the New Mine Closure Law in Chile

Lilian Valdebenito
SERNAGEOMIN, Chile

ABSTRACT

The Mine Closure Law (N°20.551) and its Regulations (DS 41/2012) took effect in November 2012, and with it the transitional phase began. The law applies to companies that were in operation with a mineral extraction rate or benefit of over 10,000 tons per month. The transitional law was applied for two years and aimed to ensure that all companies had a valued closure plan and would present the State with a Financial Guarantee proposal. The deadline for these companies to submit their closure plan proposals was November 11, 2014.

The question then becomes; what happens now? The mine closure law states that companies must audit their closure plans every five years in order to ensure that the stipulated plans align with the operational reality and comply with the essential requirement of ensuring the chemical and physical stability of mining facilities. The reassessment therefore serves to determine if closure costs and financial guarantees are appropriate. This requirement "forces" companies to internally evaluate if the closures measures that were valued in the transitional phase are really needed to reach the target of physical and chemical stability of the mining facility.

Now is when the real challenge begins for mining operations in relation to the mine closure regulation and how to incorporate these concepts from the earliest stages of projects. By assessing risk and constantly monitoring operations, mine sites can determine which closure measures and activities are really necessary to control these risks.

To achieve this objective, the mining operation needs to make itself present. An appropriate control of mining operations (operating according to design) lowers the risks during closure.

From the physical stability point of view, a permanent geotechnical control of the mining facilities is necessary. This way, one can fix deviations produced during operation, and not when operation will be ending, which certainly will be much complex and expensive. In the same way, to achieve chemical stability, it is necessary to establish a chemical stabilization program for the mining facility to identify the potential sources of mine drainage and to work on them to finally ensure that a non-significant risk could exist once the operations have ceased.

CHAPTER 1

GEOMICROBIOLOGY, BIOGEOCHEMICAL CYCLES AND BIOMINING

10th ICARD IMWA 2015 | 10th International Conference on Acid Rock Drainage & IMWA Annual Conference

Chemical Transformations of Metals Leaching from Gold Tailings

Bronwyn Camden-Smith, Nicole Pretorius, Anthony Turton, Peter Camden-Smith and Hlanganani Tutu
Molecular Sciences Institute, University of the Witwatersrand, South Africa

ABSTRACT

Chemical reactions that follow the release of metals from gold mine tailings in the Witwatersrand Goldfields were assessed through a combination of analytical techniques and geochemical modeling. A flow path for metal pollutants which consisted of a tailings storage facility (TSF), a rainwater runoff pond, a pollutant control dam and a wetland was considered. Water and solid samples from these features were collected and analyzed. Sequential extractions of solids were conducted to assess the chemical partitioning of metals within them. Metal content was partitioned into water and acid-soluble (readily soluble salt phases), reducible (associated with iron and manganese oxides), oxidizable (bound to organic or sulfide minerals) and residual (silicate minerals) fractions. The change in metal partitioning with increasing distance from the tailings storage facilities was found to be correlated to changes in the chemistry of water which in turn was correlated to the change in the geochemistry of solids along the flow path. Speciation-solubility, inverse and forward modeling using the PHREEQC modeling code were combined with sequential extractions and used to characterize the chemical reactions that transform the metals.

Keywords: Chemical partitioning, sequential extraction, geochemical modeling, inverse modeling

INTRODUCTION

Environmental impacts of the decant of metal-rich, sulfate-rich, low pH water from gold mine tailings around Johannesburg, South Africa have been a cause for concern for some time now (Förstner & Wittmann, 1979; Naicker, Cukrowska & McCarthy, 2003; Tutu, McCarthy & Cukrowska, 2008).

The release of metals from gold mine tailings into the environment is dependent on the mineralogy of the tailings and the association of metals with that mineralogy. Knowledge of bulk mineralogy alone does not provide an accurate indication of the potential release of metal pollutants from the tailings. Metal pollutants could exist in minor minerals that are below standard powder X-ray diffraction (PXRD) detection limits. The chemical behavior of the minerals hosting metal contaminants affects their release and mobility. A metal ion of interest, for instance, can be associated with a single mineral phase or a combination of mineral phases. Such mineral hosts include water-soluble salts, ion-exchange sites on clay minerals, carbonate minerals, adsorption on or inclusion into amorphous or crystalline iron (Fe) oxides, sulfide minerals and silicate minerals (Leinz et al., 2000). Leaching and sequential extraction techniques have been used to characterize the phase association of metals in contaminated sediments and solid waste (Rao et al., 2008). The most commonly used sequential extraction methods have been the Tessier method (Tessier, Campbell & Bisson, 1979) and the Communities Bureau of Reference method (BCR) (Rauret et al., 1999).

In this paper, the use of sequential extractions was combined with speciation-solubility and inverse modeling in order to better understand the partitioning and transport of metals emanating from gold mine tailings at a site in the West Rand of the Witwatersrand Goldfields, South Africa.

METHODOLOGY

Sampling and analysis

The study site comprised a tailings storage facility (TSF) that was undergoing reprocessing; a tailings pond which collected rainwater runoff from the TSF; a pollution control dam that encroached partially onto a reprocessed TSF and collected water from the TSF in the study; and a wetland which is adjacent to the pollution control dam wall.

Water samples were collected during the rainy season (January and March 2014). Water sampling was conducted using acid-washed and deionised water rinsed polypropylethylene bottles. Measurements of temperature, pH, Eh, electrical conductivity (EC) and dissolved oxygen were conducted in the field using calibrated field electrodes. A portion of each sample was filtered in the field using a syringe mounted with 0.45 µm polytetrafluoroethylene (PTFE) filters and acidified prior to metal analysis using inductively coupled plasma-optical emission spectrometry (ICP-OES). A separate portion was filtered in the same manner without acidification and analyzed for anion content using chemically-suppressed ion chromatography (IC). The remaining portion of sample was not filtered and was used for alkalinity determination. Alkalinity was determined using titrations with standard HCl solutions to pH 4.5 using bromocresol green and a calibrated pH electrode to detect the end-point (ASTM International, 2010).

Sediment samples were collected at the same time as water samples in March 2014. Samples with a high water content were centrifuged to extract pore water. Sediment samples were collected at the same points where water samples were collected. In the pollution control dam, there were two distinct layers in the shallow sediments that were sampled as separate samples.

The samples were dried at 35 °C. Samples were ground using a mortar and pestle to particle size <10 μm. Sequential extractions to determine metal partitioning were performed using the Communities Bureau of Reference method (BCR) (Rauret et al., 1999). Leaching solutions were shaken on an elliptical shaker for the duration recommended by the method. The BCR-701 certified reference material was used for assessment of leaching accuracy. The leaching protocol was used to determine the following environmentally important or environmentally extractable metal fractions: 1) water soluble, acid soluble and exchangeable; 2) reducible (metals associated with Fe and manganese (Mn) oxyhydroxides); 3) oxidizable (metals associated with organic matter or sulfide minerals). Acidic microwave digestion of the residues after the third leach step and of the unleached material was conducted using hydrochloric, nitric and hydrofluoric acids to dissolve the silicate matrix. Inductively coupled plasma-optical emission spectrometry was used to determine metal content in the resulting leachates and acidic solutions.

Geochemical modeling

Speciation-solubility, inverse and forward modeling were conducted using the United States Geological Survey (USGS) software PHREEQC combined with the Lawrence Livermore National Laboratory database (llnl.dat) (Parkhurst & Appelo, 1999; Charlton & Parkhurst, 2002). Speciation-solubility models are used to define the distribution of stable species in the system and to determine the saturation states of minerals within the system. In forward modeling, the final composition of a solution after a reaction or equilibration is calculated. Inverse modeling is also known as mass balance modeling and can provide a set of possible reactions that occur between two known solutions along the same flow path (Zhu & Anderson, 2002).

RESULTS AND DISCUSSION

Overview of water analysis

Table 1 summarizes the electrode measurements of the water samples taken during the two sampling sessions. The first sampling took place in the middle of the rainy season, before major thundershowers. The tailings pond samples had lower pH, elevated Eh and EC than samples taken from the same pond two months later towards the end of rainy season. The effect of pH on metal mobility was obvious for the tailings pond samples collected in January that had an average Fe concentration of 54 $mg.L^{-1}$ whereas samples collected in March had an average of 4.2 $mg.L^{-1}$. The same dilution effects are less evident in the pollution control dam samples. The results for percentage electrical charge balance (calculated using PHREEQC) are also presented in Table 1. The charge balance is a common indication of the quality of water analysis (Zhu & Anderson, 2002). Large percentage errors can indicate that a cation or anion was not analyzed for, analyzed incorrectly or that the sample was altered during transport or storage (for example, precipitation of analytes can occur). The charge balances presented in Table 1 are below 20%, with the largest deviations observed in the pollution control dam. The dam has a number of tributaries that could be contributing to various chemical processes occurring in it. Cyanide and organic matter were not

quantified in this study, but their contribution to charge balance may be significant if they are present in high concentrations. Even though the samples were filtered with 0.45 µm filter paper, several colloids are smaller than this and would be analyzed as dissolved species. This would contribute to a positive error. Colloidal aluminum (Al) is known for such behavior and the studied samples contained elevated Al concentrations.

Table 1 Summary of field measurements and PHREEQC-determined charge balance for water samples.

Location	Sample	Month	Temperature (°C)	pH	Eh (mV)	Conductivity (mS/cm)	Dissolved oxygen (mg/L)	Charge Balance (%)
Tailings Pond	TP 1	January	23.8	2.68	625	3.14	6.53	-9.9
	TP 2	January	23.8	2.67	611	3.17	6.51	-7.5
	TP 3	March	25.6	3.43	448	1.67	5.60	9.6
	TP 4	March	23.8	3.36	454	1.74	6.96	1.0
	TP 5	March	22.4	3.36	461	1.78	7.17	-8.0
Pollution Control Dam Inlet	PCDI 1	March	25.8	3.50	550	3.79	3.64	1.4
	PCDI 2	March	25.1	3.02	538	2.79	4.69	-7.5
	PCDI 3	March	24.3	2.72	607	3.11	6.41	6.3
Pollution Control Dam	PCD 1	January	24.4	2.31	660	7.37	6.73	-18.8
	PCD 2	January	24.4	2.31	667	7.55	6.82	-18.5
	PCD 3	March	26.5	2.67	682	3.21	6.69	-3.8
	PCD 4	March	26.6	2.70	672	3.17	6.75	10.6
	PCD 5	March	25.8	2.74	642	3.19	6.58	-14.7
Wetland	W 1	March	28.1	2.59	648	6.76	4.00	1.3

Sequential extractions and speciation-solubility modeling

Water and sediment samples from the rainwater runoff pond adjacent to the TSF were analyzed. Speciation-modeling was conducted on water samples in Table 1. Saturation indices (SI) are an indication of a solution's saturation with respect to a mineral (Zhu & Anderson, 2002). A positive SI indicates that the mineral is supersaturated in the system and a negative SI indicates that the mineral is undersaturated. Generally, the water samples showed that most minerals dissolved in them are undersaturated with the exception of gypsum, alunite and jarosite. Gypsum ($CaSO_4.2H_2O$) was close to saturation in TP 1 and TP 2 (SI of -0.03), close to saturation in PCD 1 (SI of 0.02),

supersaturated in PCD 1 and PCD 2 (average SI of 0.10) and supersaturated in W 1 (SI of 0.11). In all other samples, gypsum was undersaturated (SI of < -0.20). Jarosite ($KFe_3(SO_4)_2(OH)_6$) was undersaturated in all of the tailings pond samples and PCDI 2, was close to saturation in PCDI 3 (SI of -0.06) and was supersaturated in all of the pollution control dam samples, PCDI 1 and wetland sample. Alunite ($KAl_3(SO_4)_2(OH)_6$) was undersaturated in all of the samples except for PCDI 1 (SI of 1.5).

The results for BCR extractions of the tailings pond sediments are presented in Figure 1. Over 90% of the total Al, calcium (Ca), potassium (K), magnesium (Mg) and sodium (Na) content is held within silicates that are in the residual phase of the extraction protocol. The residual fraction has been omitted from Figure 1 in order to clarify the partitioning of the environmentally extractable fraction (Figure 1). A significant proportion of Ca and sulfur (S) is held in the water soluble, acid soluble or exchangeable phase. This relates well with the gypsum being near to saturation within the pond (from modeling results). The environmentally extractable Al (from the first three leach steps) is equally distributed in the sediment. Most of the environmentally extractable Fe is present as a reducible phase, that is, ferric oxyhydroxides. The majority of Fe in the tailings pond water samples was speciated as dissolved ferrous iron (Fe(II)). The water samples were found to be close to saturation with atmospheric oxygen. This meant that Fe(II) in solution was oxidized by atmospheric oxygen and converted to Fe(III) which is insoluble and precipitates from solution as ferric hydroxide. The partitioning of trace elements is presented in Figure 1. Cobalt (Co), copper (Cu), Mn and zinc (Zn) were found to be largely held in the water soluble, acid soluble or exchangeable phase. This phase is likely associated with sulfate salts owing to the abundance of sulfates due to AMD. From modeling results, the sulfate salts of these elements were undersaturated in the pond water samples. The saturation indices are calculated for pure end members (Zhu & Anderson, 2002). The minerals present in the system are likely to be solid solutions and will have different thermodynamic properties. Less than 10% of the environmentally extractable fraction of Cd, Co, Mn, U and Zn was associated with reducible Fe oxyhydroxides. There was a strong association of Cr, Cu and Li with the reducible Fe oxyhydroxides (greater than 18%), likely through adsorption on the surface or through incorporation of solid solutions within the lattice. A significant proportion (> 40%) of the trace metals cadmium (Cd), Co, Cu, uranium (U) and Zn extracted from the first three leaches were associated with oxidizable phases. These phases could include organic material, sulfide minerals and possibly strong cyanide complexes.

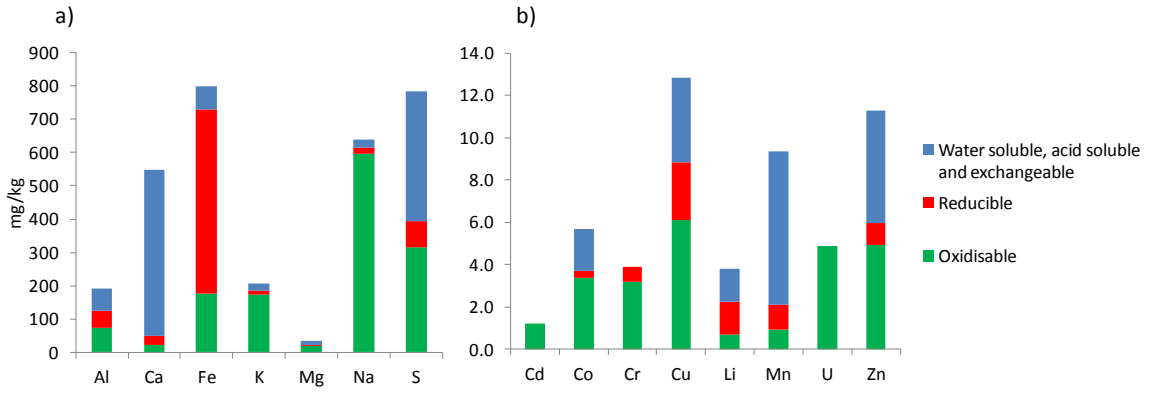

Figure 1 a) Major metal and sulfur partitioning within tailings pond sample. b) Minor metal partitioning within tailings pond sample.

Sequential extractions and inverse modeling

The pollution control dam will be used an example of how the use of sequential extractions can help in mineral selection for inverse modeling.

Modeling results showed that water sample PCD 3 was almost saturated with gypsum (SI of -0.27). Iron was found to be in ferrous (85%) and ferric (15%) form at the measured Eh. The presence of soluble ferric phases led to higher saturation indices of these phases. For instance, $Fe(OH)_3$ had an SI of -2.2; goethite was supersaturated; Na jarosite ($NaFe_3(SO_4)_2(OH)_6$) was saturated (SI of 0.0); and K jarosite ($KFe_3(SO_4)_2(OH)_6$) was supersaturated (SI of 3.4). The results for partitioning of elements in sediments collected at the pollution control dam are presented in Figure 2. The results showed elevated concentrations of Fe in the reducible phase (largely Fe oxyhydroxides), and this corresponded with the characteristic reddish-orange color of the sediments. A large proportion of Cd, Cr, Cu and Mn were associated with the reducible phase in these sediments (Figure 2). In the rainwater runoff pond, Mn and Cu were associated with the water soluble acid soluble or exchangeable phase; Cd, Co and a small proportion of Cu were associated with the oxidizable phase; and Cr was associated with the residual phase (Figure 1). These results suggest that the metals could be readily released from the runoff pond, adsorbing onto Fe oxyhydroxides along the flow path and deposited in the pollution control dam. The contribution of leachates from a municipal waste site is not apparent as sampling at that site could not be conducted.

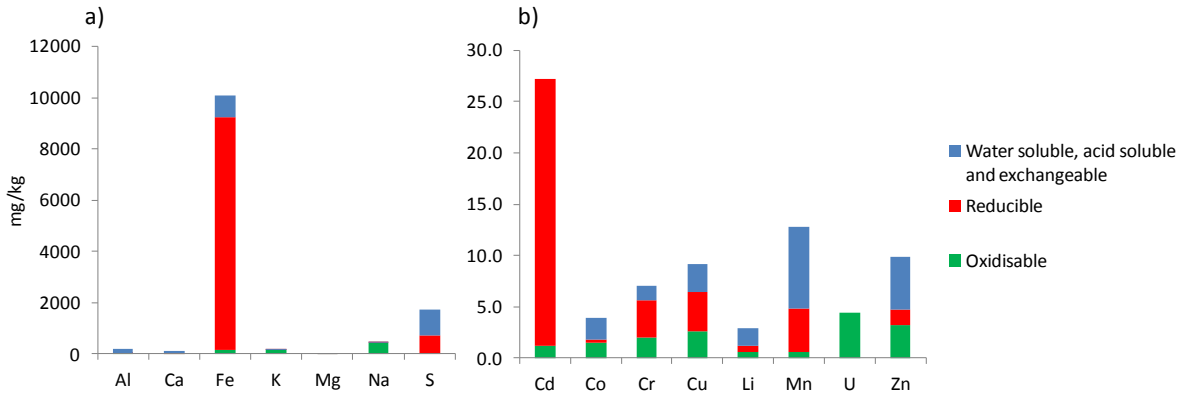

Figure 2 a) Major metal and sulfur partitioning within upper pollution control dam sediments. B) Minor metal partitioning within upper pollution control dam sediments.

To gain further insight into metal partitioning in the sediments, some inverse models were used. One such model generated the pollution control dam sample (PCD 3) from mixing the three incoming water types. The main aim was to identify minerals that would precipitate from this process and correlate these to the phases observed in sequential extractions. The minerals that were chosen as phases of interest were selected from the sequential extraction results of the upper sediments sample presented in Figure 2. The following minerals were selected as phases: $Fe(OH)_3$, gypsum ($CaSO_4.2H_2O$), $Mn(OH)_2$, epsomite ($MgSO_4$), $NiSO_4$, $ZnSO_4$ and bieberite ($CoSO_4.7H_2O$). Chloride and Na were regarded as conservative elements while water vapor was used in the simulation to allow for the impact of evaporation. Several potential models were generated. The

general trend in the models was a large contribution from PCDI 3, a smaller contribution from PCDI 1 and a negligible contribution from PCDI 2. A minimal phase model is presented in Table 2. The solution mixing fractions were: PCDI 1 (0.340), PCDI 2 (0.069) and PCDI 3 (0.840). The mixing of the different solutions generated a solution with a mass of 1.25 kg. An amount of 250 g of water vapor was allowed to exit the system, resulting in 1.00 kg remaining. The negative sign for gypsum in Table 2 indicates that the mineral precipitated out of the solution while a positive sign as in the case of $Fe(OH)_3$ indicates that the mineral dissolved into the solution. Thus, the pollution control dam sample was undersaturated with respect to $Fe(OH)_3$. Given the high concentration of ferric oxyhydroxide in the upper sediments of the dam, it is possible that $Fe(OH)_3$ was in the process of being released from the sediments.

Table 2 Phase mole transfers between a mixture of pollution control dam inlet streams and pollution control dam water.

Phase	Mole transfer
$Fe(OH)_3$	3.04×10^{-4}
Gypsum	-2.35×10^{-3}
$Mn(OH)_2$	-4.01×10^{-4}
Epsomite	-3.43×10^{-3}
NiSO4	-6.56×10^{-5}
ZnSO4	-3.38×10^{-5}
Bieberite	-2.61×10^{-5}
$H_2O(g)$	-138

Since inverse models are based on mass balance principles only and do not take into account mass action principles, forward modeling can be used to test whether the results from an inverse model are thermodynamically possible. The inverse model presented above was tested using non-equilibrium and equilibrium approaches. The non-equilibrium approach forces the precipitation and dissolution of minerals (by disregarding their saturation indices). The equilibrium approach only dissolves minerals that are undersaturated in solution and only precipitates minerals that are supersaturated. A comparison of the final modeled results with the experimental solution is presented in Table 3. In the equilibrium model, no minerals precipitated as they remain undersaturated in solution. Therefore, there are higher elemental concentrations and a correspondingly higher ionic strength than for the other two solutions.

Table 3 Comparison of an experimental solution, non-equilibrium and equilibrium forward-modeled solutions.

Parameter	Experimental solution	Non-equilibrium model	Equilibrium model
pH	2.7	2.78	2.92
pe	11.4	12.5	12.4
Ionic strength	0.065	0.068	0.079
Elemental concentrations (mol.kg^{-1})			
Al	6.68×10^{-3}	5.58×10^{-3}	5.57×10^{-3}
Ca	1.02×10^{-2}	0.90×10^{-2}	1.14×10^{-2}
Cl	1.02×10^{-3}	1.14×10^{-3}	1.14×10^{-3}
Co	6.49×10^{-5}	6.48×10^{-5}	9.09×10^{-5}
Cu	3.38×10^{-5}	2.85×10^{-5}	2.85×10^{-5}
Fe	2.30×10^{-3}	1.95×10^{-3}	1.94×10^{-3}
K	2.49×10^{-4}	3.02×10^{-4}	3.02×10^{-4}
Mg	3.60×10^{-3}	3.47×10^{-3}	6.90×10^{-3}
Mn	3.30×10^{-4}	3.30×10^{-4}	7.31×10^{-4}
Na	1.27×10^{-3}	1.28×10^{-3}	1.28×10^{-3}
Ni	1.27×10^{-4}	1.27×10^{-4}	1.92×10^{-4}
S	2.47×10^{-2}	2.91×10^{-2}	3.50×10^{-2}
U	5.63×10^{-6}	4.61×10^{-6}	4.60×10^{-6}
Zn	1.19×10^{-4}	1.19×10^{-4}	1.53×10^{-4}

CONCLUSION

This study has shown that partitioning of metals within various mineralogical phases in gold mine wastes exerts control over their release and transport to the surroundings. From sequential extraction and geochemical modeling, processes such as dissolution, precipitation, ligand complexation, adsorption and desorption were shown to be important. These processes were apparent when metals in the runoff pond were shown to be essentially in oxidizable phases while a short distance further in the pollution control dam they were found to be held in reducible phases. Combining sequential extractions with geochemical modeling provides insight into the water-solid interactions. Model simulations depicted elemental speciation (through speciation-solubility models) and the likely partitioning within the mineral phases (through inverse models). The simulations were also useful in predicting minerals that would precipitate when various water types are mixed.

ACKNOWLEDGEMENTS

The authors would like to thank the South African National Research Foundation, National Academy of Science (through the PEER Program) and the University of the Witwatersrand for financial support.

REFERENCES

ASTM International (2010) D1067-06: Standard test Methods for Acidity or Alkalinity of Water. In Annual Book of ASTM Standards Section 11 Water and Environmental Technology (Vol. 11.01), Baltimore: ASTM International.

Charlton, S & Parkhurst, D (2002) PHREEQCI—A Graphical User Interface to the Geochemical Model PHREEQC, Retrieved May 20, 2012, from ftp://brrftp.cr.usgs.gov/pub/dlpark/geochem/pc/phreeqc/PhreeqcI.FactSheet.pdf

Förstner, U & Wittmann, G (1979) Metal accumulations in acidic waters from gold mines in South Africa, Geoforum , 7 (1), 41-49.

Leinz, R, Sutley, S, Desborough, G & Briggs, P (2000) An Investigation of the Partitioning of Metals in Mine Wastes Using Sequential Extractions, In Proceedings from the Fifth International Conference on Acid Rock Drainage (pp. 1489-1499). Littleton, Colorado: The Society for Mining, Metallurgy, and Exploration Inc.

Naicker, K, Cukrowska, E & McCarthy, T.S (2003) Acid mine drainage arising from gold mining activity in Johannesburg, South Africa and environs, Environmental Pollution , 29-40.

Parkhurst, D & Appelo, C (1999) User's guide to PHREEQC (Version2)—A computer program for speciation, batch-reaction, one-dimensional transport, and inverse geochemical calculations.

Rao, C, Sahuquillo, A & Lopez Sanchez, J. (2008) A Review of the Different Methods Applied in Environmental Geochemistry For Single and Sequential Extraction of Trace Elements in Soils and Related Materials, Water, Air & Soil Pollution (189), 291–333.

Rauret, G, Lopez-Sanchez, J, Sahuquillo, A, Rubio, R, Davidson, C, Ure, A & Quevauviller, P (1999) Improvement of the BCR three step sequential extraction procedure prior to the certification of new sediment and soil reference materials, Journal of Environmental Monitoring, , 1 (1), 57-61.

Reeder, R, Schoonen, M & Lanzirotti, A (2006) Metal Speciation and Its Role in Bioaccessibility and Bioavailability, Reviews in Mineralogy and Geochemistry , 64, 59-113.

Tessier, A, Campbell, P & Bisson, M (1979) Sequential Extraction Procedure for the Speciation of Particulate Trace Metals, Analytical Chemistry , 51 (7), 844-851.

Tutu, H, McCarthy, T. S & Cukrowska, E (2008) The chemical characteristics of acid mine drainage with particular reference to sources, distribution and remediation: The Witwatersrand Basin, South Africa as a case study, Applied Geochemistry , 3666-3684.

Zhu, C & Anderson, G (2002) Environmental Applications of Geochemical Modeling, Cambridge, United Kingdom: The Press Syndicate of the University of Cambridge.

Characterization of Uranium and Rare Earth Element Mobility Downstream of a Tailings Impoundment Near Bancroft, Ontario

Allison Laidlow[1*], Michael Parsons[2] and Heather Jamieson[1]

1. *Department of Geological Sciences and Geological Engineering, Queen's University, Canada*
2. *Natural Resources Canada, Geological Survey of Canada (Atlantic)*

** Now at Golder Associates, Canada*

ABSTRACT

Attenuation of uranium (U) and rare earth elements (REEs) has been observed in stream and wetland sediments, but the geochemical and mineralogical processes involved in sequestering these elements in natural systems are not fully understood. The decommissioned Bicroft Uranium Mine near Bancroft, ON, operated from 1957 to 1963, and processed approximately 2,284,421 tonnes of low-grade, disseminated U ore hosted by pegmatite dykes in amphibolite gneiss. During operations, the mine used two tailings impoundments and a modified stream and wetland system to reduce the concentrations of U, other metals, and radionuclides in tailings effluent to levels below the Provincial Water Quality Objectives. Since mine closure, the streams and wetland have continued to operate as a passive treatment system for tailings effluent, demonstrating the potential viability and longevity of natural attenuation to sequester U and REEs. In this study, we used tangential flow filtration, ICP-ES/MS, scanning electron microscopy, and synchrotron techniques (bulk- and micro-XANES, -XRF, and -XRD) to characterize processes controlling U and REE mobility and attenuation in tailings, sediment, and colloid samples. Results of this study indicate that Fe- and Mn-(oxyhydr)oxides, including goethite [α-FeO(OH)] and birnessite (δ-MnO_2), are the main mineral hosts for U and REEs in colloids and sediments. In addition, detrital grains of U- and REE-bearing minerals were found >200 m downstream in colloids and sediments, showing the potential for long-range transport of colloids and fine particulates in the stream system. While natural attenuation exhibits great potential to reduce U- and REE- concentrations, seasonal influences on the stability of trace metals in sediments were observed and may demonstrate the limitations of streams and wetlands as a viable method of attenuation. The results of this study are intended to aid development of more effective passive treatment systems and improve environmental monitoring strategies for U and REEs.

Keywords: Uranium, rare earth elements, synchrotron micro-analysis, colloids, passive attenuation

INTRODUCTION

The decommissioned Bicroft Uranium Mine is located 19 km southwest of Bancroft, Ontario, Canada in granitic pegmatites (ca. 1020 to 1050 Ma) of the Grenville Geological Province (Evans 1962; Lentz 1996), (Lat. 44°59'30.39"N, Long. 78°2'16.83"W). Since the closure of the mine in 1963, following seven years of operation, the Bicroft site has acted as a passively attenuating stream and wetland system to achieve below-Provincial Water Quality Objectives (PWQOs) for uranium (U) and other trace metals (MOE 2003). The two decommissioned tailings impoundments at the Bicroft Mine, Auger Lake and South Tailings Basin, drain through an approximately 1 km tributary stream and wetland system, to Deer Creek, before being discharged to Paudash Lake where the waters are required to meet PWQOs (MOE 2003). The environmental conditions and geochemical processes that control the mobility of metals and radionuclides at the Bicroft site are poorly understood. Specifically, the methods by which U and rare earth elements (REEs) are released from the tailings basins and then partially sequestered in the stream and wetland system are unknown.

In effluent released from mine tailings, trace metals and other contaminants are generally partitioned between particulate matter, colloids, and dissolved phases. In most studies of natural water systems colloidal material is considered part of the dissolved fraction (<0.45 μm), and any particles unable to pass through a 0.45 μm filter are considered to be suspended particulate matter. Colloids, in aqueous systems, are any suspended material with a single linear dimension between 0.001 μm and 1 μm. Colloids have large surface-area-to-volume ratios due to their small size, which provides increased sites for reactivity and heightened surface charge allowing for high adsorption capacity (Klaine *et al.* 2008). The large surface area of colloidal particles relative to their mass allows for particles to overcome gravitational forces and to remain in suspension in waters of varying velocities, and travel significant distances (1 km to >500 km), until flocculation of colloidal material results from changes in the solution chemistry and the colloids settle from solution (Kersting *et al.* 1999; Kretzschmar and Schäfer 2005; Wigginton *et al.* 2007).

The natural attenuation of U from mine wastes has been observed in other studies of stream and wetland sediments by Schöner *et al.* (2009) in Germany, Veselic *et al.* (2001) in Slovenia, Groudev *et al.* (1999) in Bulgaria, and Lottermoser and Ashley (2005) in Australia. These studies suggest that U is primarily attenuated in Fe- and Mn-oxyhydroxides and natural organic matter; however, the host mineralogy of U was undetermined. The natural attenuation of REEs has been observed in other studies that focused on the use of REEs as a tracer for geochemical processes by relating the absolute and relative concentrations of REEs to a variety of environments (Goldberg *et al.* 1963; Quinn *et al.* 2006). However, the release of lanthanides from mine waste through weathering processes, and their environmental impacts and toxicity once released into aqueous solution, have not been fully characterized. Previous studies have determined that REEs are mobilized under acidic conditions, and precipitated or otherwise sequestered at high pH conditions (Brookins 1989; Verplanck *et al.* 2004). In addition, REEs are known to readily complex with various ligands in the aqueous environment and are often associated with particulate matter and organics in shallow surface waters (Cantrell and Byrne 1987). Critical gaps remain in our knowledge of the host mineralogy and the processes involved in sequestering U and REEs in complex field systems (Brookins 1989; Schöner *et al.* 2009).

This study focuses on understanding the mineralogical and geochemical controls that influence the mobilization, sequestration, and stability of U and REEs (specifically, cerium (Ce) and lanthanum (La)) in sediments of a stream and wetland system sourced by effluent from a U tailings

impoundment at the Bicroft Mine. The passive treatment system has been in operation for over 50 years and thus provides an ideal natural laboratory to study the processes involved in attenuating these trace elements and the long-term effectiveness of this method of pollution control (Parsons *et al.* 2014). Detailed characterization of tailings, colloids, and stream and wetland sediments through field observations, bulk chemistry, and mineralogical observations from scanning electron microscopy and synchrotron micro-analyses were used to identify the main sources for U and REE within the tailings and their attenuation and stability in downstream environments. The results of this study will help to develop better monitoring strategies for U tailings sites and should reduce the impacts of future U and REE mining operations.

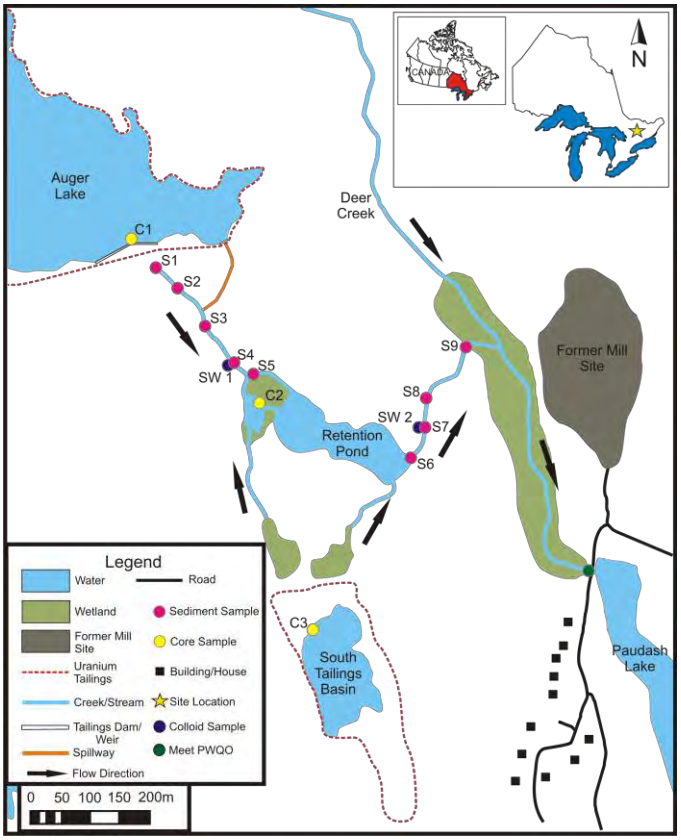

Figure 1 Bicroft Mine site map with field sampling locations of bulk sediment (pink), core (yellow) samples, and surface water (blue) samples. All samples were collected in October 2011, with the exception of a second set of surface water samples in July 2012. PWQOs are to be met at the discharge point of Deer Creek to Paudash Lake (green).

METHODOLOGY

To characterize the chemical and mineralogical controls by which U, La, and Ce are sequestered, 15 bulk samples of hardpan, pebbles, streambed sediments (S1-S9), and tailings were collected in October 2011 from the tributary stream and wetland system, and tailings basins (Figure 1). In addition, two sediment cores were collected in the Auger Lake tailings basin (C1) and Retention Pond (C2) to examine the effect of redox conditions on the mobility and attenuation of U (Figure 1). Surface water sampling was conducted in October 2011 and July 2012 to account for any seasonal changes in water composition. Two water samples were collected in each field season, with a

sample both upstream and downstream of the Retention Pond, identified as SW1 and SW2 respectively, to determine whether this pond was removing colloids from solution. Tangential flow filtration (TFF) was applied to analyze the colloid fraction from the stream waters at the two locations, using a Millipore Prep/Scale Spiral Wound Ultrafiltration Cartridge. Within 48 hours of collection, the water samples were filtered through a 0.557 m^2 (6 ft^2) TFF cartridge with a 10 kdalton (0.005 μm) filter cut off. The <10 kdalton permeate from the TFF system is assumed to represent the dissolved fraction of the sample (Guegon *et al.*, 2002). The retentate, with a size fraction between 0.45 μm and 10 kdaltons, contains the colloid fraction from the water (Guegon *et al.*, 2002). For further information regarding sample collection and preparation please refer to Laidlow (2013).

Bulk chemistry and X-Ray diffraction (XRD)

Ultra-trace analysis for a 43-element suite plus 12 REEs by inductively coupled plasma-mass spectrometry (ICP-MS) (package 1T-MS), following 4-acid digestion, was completed at ACME Analytical Laboratories on all bulk sediments and sub-samples from sediment cores. Additionally, two samples were re-analyzed by inductively coupled plasma-emission spectrometry (ICP-ES) after 4-acid digestion (package 7TD) to determine the percent-level concentrations of manganese (Mn). To identify the major crystalline phases present in the samples, X-ray diffraction (XRD) was completed using the Philips X-Pert diffractometer at Queen's University.

Petrographic analyses and synchrotron micro-analysis

Thin sections were examined optically under the petrographic microscope and characterized using a scanning electron microscope at Queen's University. Two hard X-ray microprobe synchrotron beamlines were used for trace element micro-analysis: X26A at the National Synchrotron Light Source in Upton, New York and Sector 20-ID beamline at the Argonne Photon Source in Argonne, Illinois. Micro X-ray radiation fluorescence (μXRF) mapping and micro X-ray diffraction (μXRD) analyses were conducted at both beamlines, and bulk- and micro-X-ray absorption near edge structure (XANES and μXANES) were conducted at the Sector 20-ID beamline.

RESULTS AND DISCUSSION

Characterization of U and REEs in colloids

During the process of TFF, orange-yellow staining of the ultrafiltration cell was observed for upstream (SW1) water samples. Calculated filter losses are shown in Figure 2. In both the October and July sampling, there were significant losses of iron (Fe) and aluminium (Al), as well as all REEs in the SW1 samples (Figure 2). This demonstrates that these waters were not fully oxidized when sampled and were further oxidized during the filtration process, causing Fe and Al phases to precipitate onto the filter along with their associated REEs.

In Figure 3 it can be seen that U and Mn were present mainly in the dissolved phase, Ce, La, Fe, and Al were present in both the colloidal and dissolved phases, with high proportions of Ce and La in the colloidal phase. This diagram also shows the importance of documenting seasonal variations at sample locations.

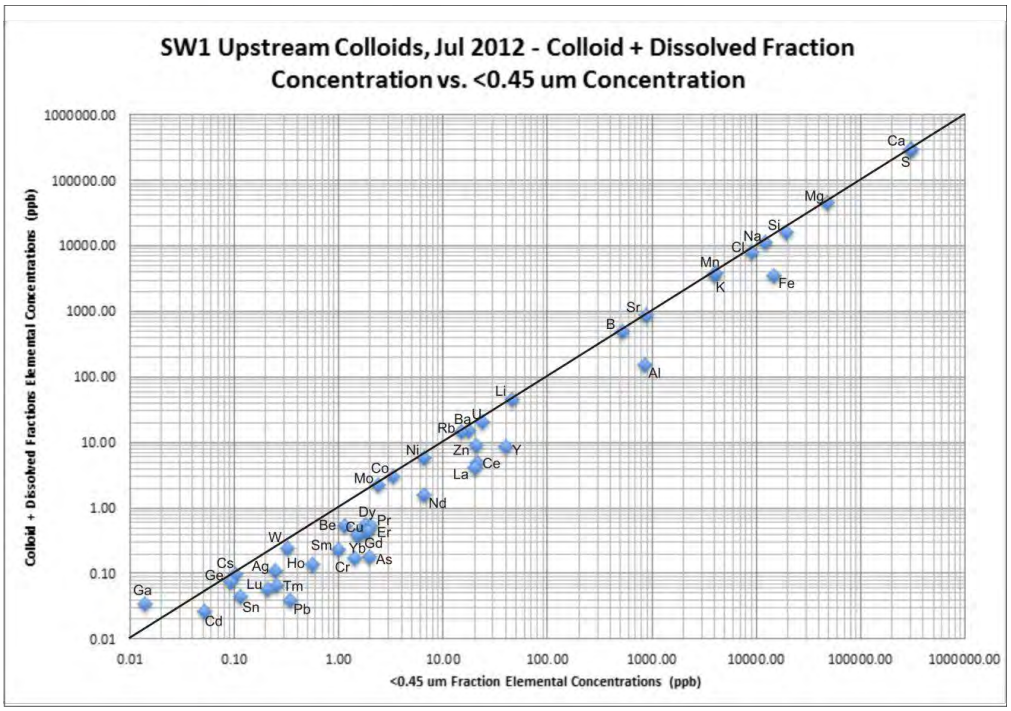

Figure 2 Correlation plot of calculated colloid + dissolved fraction elemental concentrations (ppb) vs. <0.45 µm elemental concentrations (ppb) for SW1 surface water sample from July 2012. Black line represents a 1:1 ratio of concentrations and no element retention on the filter. Elements plotting below the line show greater concentrations in the initial <0.45 µm water sample than in the combined colloid + dissolved aliquots suggesting a loss due to retention on the filter cartridge. Precision is within 5% for most samples, which is represented by the size of each point on the graph.

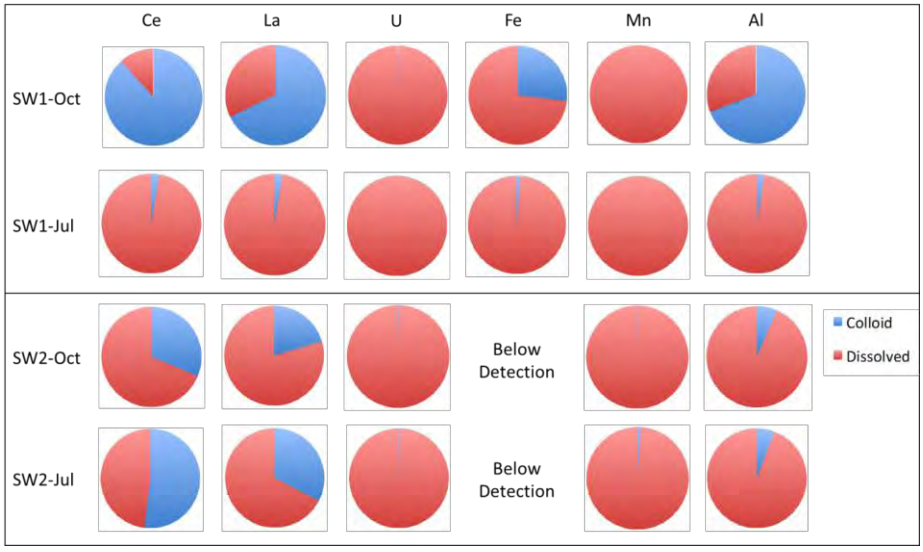

Figure 3 Relative % of Ce, La, U, Fe, Mn, and Al in colloid (blue) and dissolved (red) fractions from TFF.

Lanthanum and Ce were present in both the colloid and dissolved phases, with the greatest relative percent of colloids observed in the SW1-October 2011 sample (Figure 3). Uranium, however, was

predominantly found in the dissolved phase, with less than 1% of its total concentration in the colloid fraction for all samples. This observation is consistent with the results of aqueous speciation modeling by Parsons *et al*. (2014), which demonstrated that >95% of U in the tailings effluent at the Bicroft site occurs as calcium-uranyl-carbonato complexes, which are known to diminish the sorption of U to mineral surfaces and suppress the reduction of U(VI) to the less soluble U(IV).

In the SW1 samples, Al and La showed similar relative percentages in the colloid and dissolved fractions. Concentrations of U and Mn in the dissolved and colloidal fractions showed little variation between the October and July samples. The variance between the SW1 results in October 2011 and July 2012 may be explained in part by dilution of the July 2012 sample by heavy rainfall the day before sampling occurred (Laidlow 2013).

Iron and Mn-oxyhydroxides

Good correlations between Fe and REEs, and Mn and REEs, were observed in the XRF maps (Figure 4), and Fe XANES results suggest a strong association with Fe-oxyhydroxides. At the SW1 (upstream) location, goethite and lepidocrocite dominated the mineralogical composition of the colloids, and at the SW2 (downstream) location, hematite, ferrihydrite and lepidocrocite were the dominant REE-hosting minerals (Figure 5). The observed change in mineralogical composition between SW1 and SW2 may reflect kinetic controls on the formation of Fe-oxyhydroxide minerals in the stream. Hematite is kinetically unlikely to form in solution, but may have formed through dehydration and recrystallization of goethite and ferrihydrite.

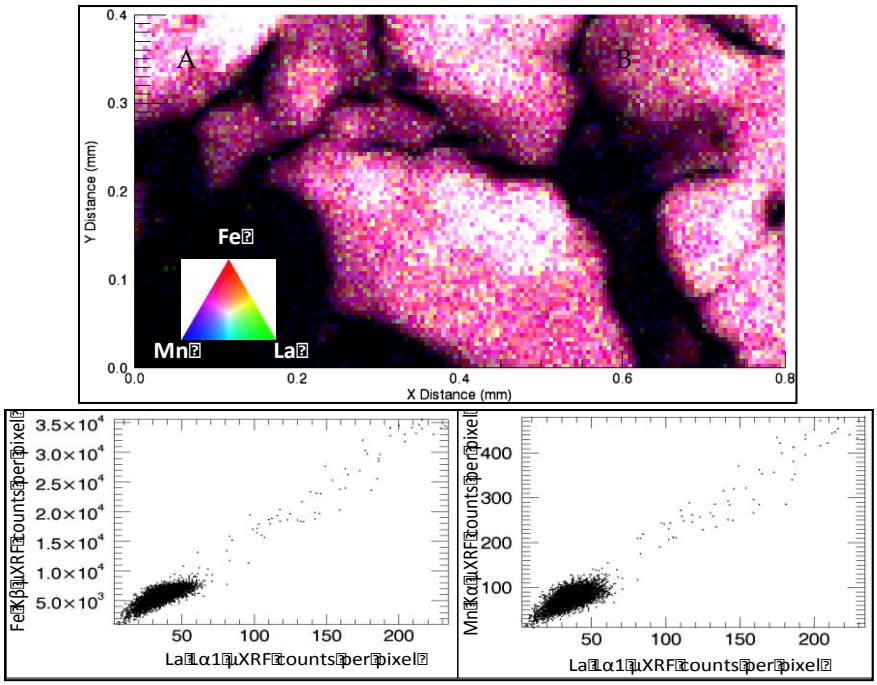

Figure 4 µXRF element map and associated element correlation plots for REEs on colloid sample SW1 – October 2011. Element counts are directly proportional to element concentrations (Jamieson and Gault, 2012).

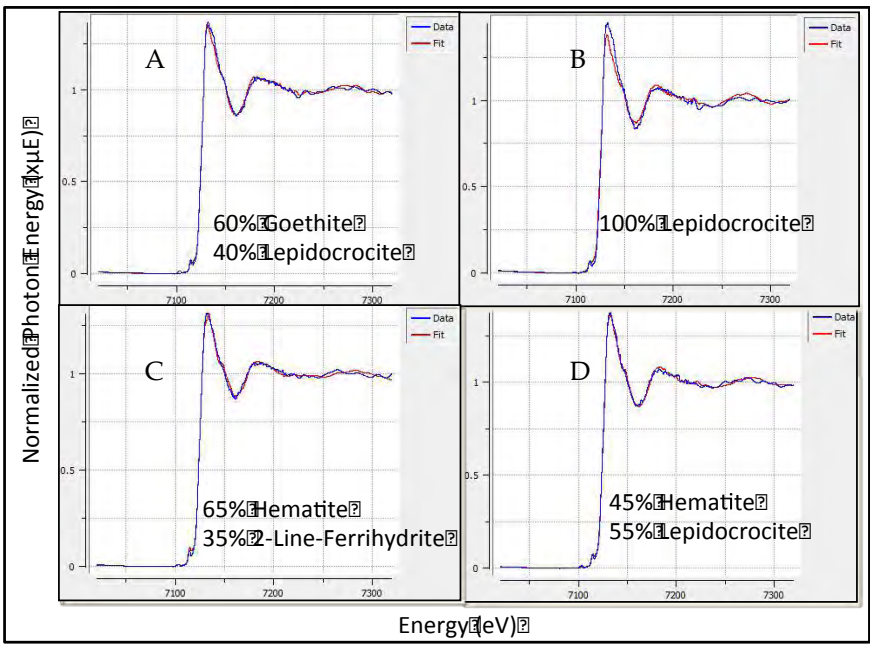

Figure 5 Fitted Fe μXANES collected from SW1 and SW2 colloid samples from October 2011. Background subtracted Fe μXANES collected on 2 targets from SW1 (A and B) and 2 targets on SW2 (C and D) were fitted using the standard reference μXANES patterns for 14 Fe minerals. The blue lines represent the collected, background subtracted scan for the sample and red lines represent the fit of the standard reference scans to the data.

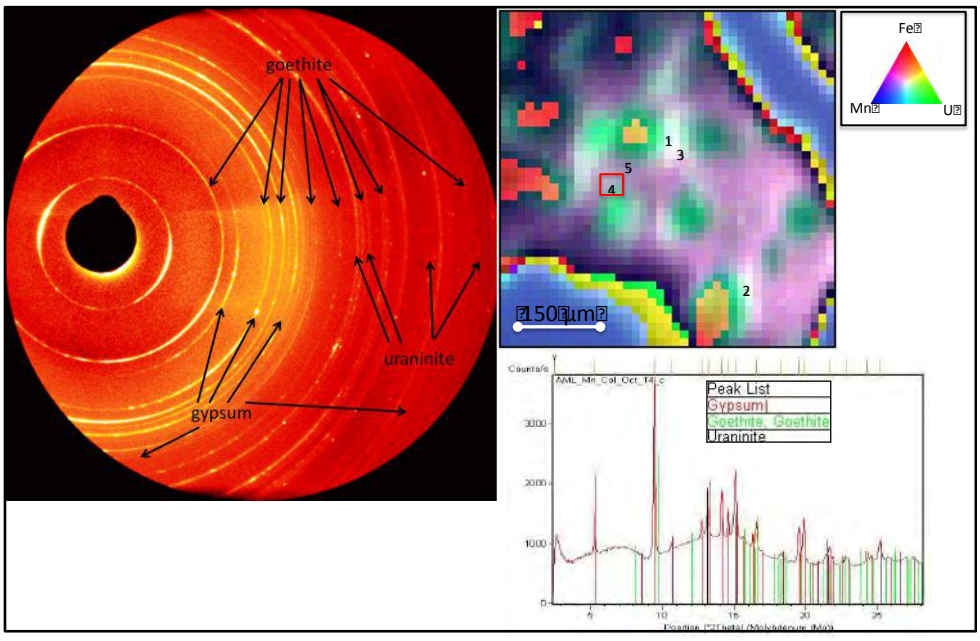

Figure 6 2D μXRD image showing Debye-Scherrer rings for goethite, gypsum and uraninite and corresponding target location on the tricolor μXRF map of the SW2 – October 2011 sample. Mixtures of red, blue and green imply a mixture of Fe, Mn and U.

XRF element mapping, in Figure 6, shows a good correlation between Mn and U only at low concentrations. At higher U concentrations, U shows poor correlations with both Fe and Mn,

suggesting that U is primarily hosted by nanoparticulate ore minerals, rather than secondary Fe- and Mn-oxyhydroxides.

Uraninite

Uraninite (UO_2) was identified in the SW2 colloid sample using μ-XRD (Figure 6). This is most likely a detrital phase, as UO_2 is a primary ore mineral in the Bicroft deposit and is not likely to precipitate from the relatively oxidized tailings effluent. Furthermore, other high-U targets from XRF mapping showed no discernable XRD pattern, but bright spotty images, which are associated with micro-analysis of nano-crystalline particles larger than the spot size of the synchrotron beam. Micro-XANES analyses of colloids with high U and low Fe and Mn concentrations showed that most U was present as U(IV), providing further evidence for detrital U grains in the colloid fraction. This observation is important, as detrital UO_2 transported downstream may oxidize to U(VI) over time, enhancing both the mobility and potential toxicity of this contaminant in the surrounding environment.

Characterization of U and REEs in sediments

Primary grains of UO_2 were identified in the grey, unoxidized section of the tailings core, in sediments downstream in the upper portion of the tributary stream, and in the Retention Pond sediments. The presence of these detrital, nanoparticle-size, grains downstream of the tailings impoundments is important, as they may be a source of further contamination if not maintained in the reduced state. From analysis of the colloids and fine tailings located immediately near the outlet of the tailings dam, it is clear that these UO_2 grains are mobilized from the tailings impoundments and released into the stream and wetland system through effluents.

Generally, most U was present as U(VI) in bulk stream sediments; however both U(IV) and U(VI) were present below the Retention Pond. Variation in the amount of U(IV) and U(VI) present depended on the local mechanism of attenuation. While goethite, maghemite, and lepidocrocite were the predominant Fe-oxyhydroxide minerals observed upstream of the Retention Pond, downstream of the Retention Pond a notable change in the predominant Fe-oxyhydroxide mineralization in stream sediments, to hematite, ferrihydrite and lepidocrocite, was observed. The presence of goethite and lepidocrocite above the Retention Pond is likely related to the relatively rapid precipitation of these phases from tailings pond effluent. Hematite however, is generally formed as a secondary mineral due to the internal rearrangement and dehydration of precipitated goethite, ferrihydrite and lepidocrocite. Uranium adsorbed to these Fe-oxyhydroxides may undergo reduction through dehydration or incorporation into the crystal structure by recrystallization, increasing the relative proportion of U(IV) in these sediments (Marshall *et al.* 2014).

CONCLUSION

The release of U and REEs from U mine wastes into surface waters is of concern for water quality, and the health of humans, organisms, and the surrounding environment. At the Bicroft Mine, an enhanced natural stream and wetland system has passively attenuated these elements of concern from tailings effluents for over 50 years, and sequestered these contaminants into local stream and wetland sediments. If the sediments and adsorbed species in this stream and wetland system

remain undisturbed, U and REEs sequestered in these sediments could be immobilized for many years. The results of this research have led to the following five main conclusions:

- The release of U, Ce, and La into the tributary stream and wetland system is associated with both oxidative and reductive dissolution of tailings within the impoundments, and subsequent release in mine tailings effluent;
- Colloids in the stream and wetland system are dominantly composed of Fe-oxyhydroxides;
- Detrital grains of UO_2 are present in the colloid fraction above the Retention Pond;
- REE-hosts in stream and wetland sediments are primarily composed of Fe- and Mn-oxyhydroxides, while U is present mainly in the dissolved phase;
- After 50 years, the stream and wetland at the Bicroft Mine continue to be an effective passively attenuating remediation system for effluent from low-grade U mine tailings.

ACKNOWLEDGEMENTS

This work was partially funded by Environmental Geoscience Program of the Earth Science Sector at Natural Resources Canada. The authors would like to thank Andrew Gault, Tony Lanzirotti (NSLS), and Robert Gordon (APS) for the many conversations regarding the preparation, use and collection of data from synchrotron facilities. This is contribution number 20140272 of the Earth Sciences Sector, Natural Resources Canada.

REFERENCES

Brookins, D.G. (1989). Chapter 8: Aqueous geochemistry of rare earth elements. In Geochemistry and Mineralogy of Rare Earth Elements. Eds. Lipin, B.R. and G.A. McKay. Reviews in Mineralogy. Mineralogical Society of America. 21:201-226.

Cantrell, K.J. and R.H. Byrne (1987). Temperature dependence of europium carbonate complexation. Journal of Solution Chemistry. 16:555-566.

Evans, A.M. (1962). Geology of the Bicroft Uranium Mine, ON. PhD Thesis – Queen's University.

Goldberg, E.D., Koide, M., Schmitt, R.A. and R.H. Smith (1963). Rare earth distributions in the marine environment. Journal of Geophysical Research. 68:4209-4217.

Groudev, S.N., Bratcova, S.G. and K. Komnitsas (1999). Treatment of waters polluted with radioactive elements and heavy metals by means of a laboratory passive system. Mineralogical Engineering. 12:261-270.

Guegen, C., Belin, C. and J. Dominik (2002). Organic colloid separation in contrasting aquatic environments with tangential flow filtration. Water Research. 36:1677-1684.

Jamieson, H.E., and A.G. Gault. 2012. Application of synchrotron microanalysis to studies of soils, sediments, dust and mine waste. In: Quantitative Mineralogy and Microanalysis of Sediments and Sedimentary Rocks, Mineralogical Association of Canada Short Course 42, ed. P. Sylvester, St. John's NL, May 2012, 35-53.

Kersting, A.B., Efurd, D.W., Finnegan, D.L., Rokop, D.J., Smith, D.K. and J.L. Thompson. (1999) Migration of plutonium in ground water at the Nevada Test Site. Nature. 397:56-59.

Klaine, S.J., Alvarez, P.J.J., Batlye, G.E., Fernandes, T.F., Hnady, R.D., Lyon, D.Y., Mahendra, S., McLaughlin, M.J. and J.R. Lead (2008). Nanomaterials in the Environment: behavior, fate, bioavailability, and effects. Environmental Toxicology and Chemistry. 27:9:1825-1851.

Kretzschmar, R. and T. Schäfer (2005). Metal Retention and Transport on Particles in the Environment. Elements. 1:197-203.

Laidlow, A.M. (2013) Characterization of uranium and rare earth element mobility and attenuation downstream of decommissioned tailings impoundments at the Bicroft Mine near Bancroft, Ontario. MSc Thesis, Queen's University, Kingston, Ontario, Canada (https://qspace.library.queensu.ca/handle/1974/8022).

Lentz, D. (1996). U, Mo, and REE mineralization in late-tectonic granitic pegmatites, southwestern Grenville Province, Canada. Ore Geology Reviews. 11:197-227.

Lottermoser, B.G. and P.M. Ashley (2005). Tailings dam seepage at the rehabilitated Mary Kathleen uranium mine, Australia. Journal of Geochemical Exploration. 85:119-137.

Marshall, T.A., Morris, K., Law, G.T.W., Livens, F.R., Mosselmans, J.F.W., Bots, P. and S. Shaw. 2014. Incorporation of Uranium into Hematite during Crystallization from Ferrihydrite. Environmental Science and Technology. 48:7:3724-3731.

Ministry of the Environment (MOE) (2003). Bancroft Area Mines (Madawaska, Bicroft and Dyno Mines) Assessment of Impacts on Water, Sediment and Biota from Historic Uranium Mining Activities. Ministry of the Environment, Environmental Sciences and Standards Division, Environmental Monitoring and Reporting Branch. 1-48.

Parsons, M.B., Friske, P.W.B., Laidlow, A.M., and H.E. Jamieson (2014) Controls on uranium, rare earth element, and radionuclide mobility at the decommissioned Bicroft Uranium Mine, Ontario. Geological Survey of Canada, Scientific Presentation 24, poster. doi:10.4095/293623.

Quinn, K. A., Byrne, R. H., & J. Schijf (2006a). Sorption of yttrium and rare earth elements by amorphous ferric hydroxide; influence of pH and ionic strength. Marine Chemistry. 99:128-150.

Schöner, A., Noubactep, C., Büchelc, G. and M. Sauter (2009). Geochemistry of natural wetlands in former uranium milling sites (eastern Germany) and implications for uranium retention. Chemie der Erde – Geochemistry. 69:91-107.

Veselic, M., Gantar, I., Karahodzic, M. and B. Galicic (2001). Towards passive treatment of uranium mine waters. In: Prokop, G. (Ed.), 1st. Image-Train Cluster-Meeting. Federal Environmental Agency Ltd., Austria (Wien), Karlsruhe, Germany. 116-128.

Wigginton, N.S., Haus, K.L. and M.F. Hochella Jr (2007). Aquatic environmental nanoparticles. Journal of Environmental Monitoring. 9:1306-1316.

Copper Toxicity and Organic Matter: Resiliency of Watersheds in the Duluth Complex, Minnesota, USA

Nadine Piatak, Robert Seal, Perry Jones and Laurel Woodruff
U.S. Geological Survey, USA

ABSTRACT

We estimated copper (Cu) toxicity in surface water with high dissolved organic matter (DOM) for unmined mineralized watersheds of the Duluth Complex using the Biotic Ligand Model (BLM), which evaluates the effect of DOM, cation competition for biologic binding sites, and metal speciation. A sediment-based BLM was used to estimate stream-sediment toxicity; this approach factors in the cumulative effects of multiple metals, incorporation of metals into less bioavailable sulfides, and complexation of metals with organic carbon.

For surface water, the formation of Cu-DOM complexes significantly reduces the amount of Cu available to aquatic organisms. The protective effects of cations, such as calcium (Ca) and magnesium (Mg), competing with Cu to complex with the biotic ligand is likely not as important as DOM in water with high DOM and low hardness. Standard hardness-based water quality criteria (WQC) are probably inadequate for describing Cu toxicity in such waters and a BLM approach may yield more accurate results. Nevertheless, assumptions about relative proportions of humic acid (HA) and fulvic acid (FA) in DOM significantly influence BLM results; the higher the HA fraction, the higher calculated resiliency of the water to Cu toxicity. Another important factor is seasonal variation in water chemistry, with greater resiliency to Cu toxicity during low flow compared to high flow.

Based on generally low total organic carbon and sulfur content, and equivalent metal ratios from total and weak partial extractions, much of the total metal concentration in clastic streambed-sediments may be in bioavailable forms, sorbed on clays or hydroxide phases. However, organic-rich fine-grained sediment in the numerous wetlands may sequester significant amount of metals, limiting their bioavailability. A high proportion of organic matter in waters and some sediments will play a key role in the resiliency of these watersheds to potential additional metal loads associated with future mining operations.

Keywords: baseline characterization, mineral deposits, water quality criteria, Biotic Ligand Model

INTRODUCTION

The characterization of baseline conditions in unmined mineralized watersheds of the Mesoproterozoic Duluth Complex, northeastern Minnesota (Figure 1), is essential to responsible extract minerals from a region with some of the greatest mineral development potential in the United States. Mining has the potential to release metals into watersheds that already contain ecologically-significant naturally-occurring concentrations of some elements such as Cu and nickel (Ni). The potential for metals to be toxic to aquatic organisms is influenced by the amount of organic carbon in the aquatic environment, the cumulative effects of multiple metals, cation competition for biologic binding sites, and speciation of metals. As a result, we estimated toxicity in mineralized watersheds using approaches that incorporate these water and sediment quality parameters.

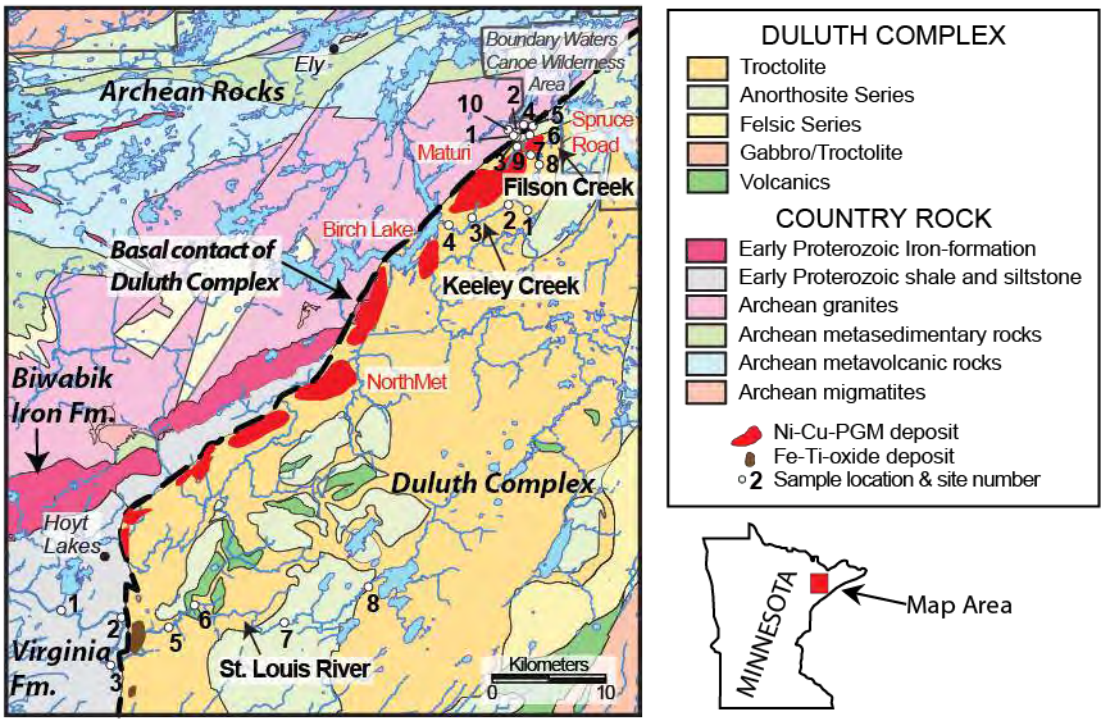

Figure 1 Bedrock geology, mineral deposits, and sample locations in northeastern Minnesota.

Surface-water and streambed-sediment samples shown in Figure 1 were collected from sites along three geologically distinct watersheds: 1. Filson Creek, where Cu-Ni-PGM (Platinum Group Metal) mineralization occurs at the bedrock surface along the basal Duluth Complex; 2. Keeley Creek, where Cu-Ni-PGM mineralization occurs only at great depth; and 3. the headwaters of the St. Louis River in the vicinity of iron (Fe) and titanium (Ti) oxide ultramafic intrusions, which occur in the subcrop beneath glacial cover. The headwaters of the St. Louis River are upstream of drainage from the taconite mining. Samples were collected in watersheds characterized by abundant wetlands, and some lakes and streams. Filson and Keeley creeks have smaller flows compared to the St. Louis River, which is a significantly larger river system. The watersheds are characterized by times of relatively low baseflow during the hot and dry late summer and early fall and again during winter

when creeks and rivers are ice-covered. Medium to high flow rates occur following storms, generally wet periods, and snowmelt, commonly in the spring and early summer.

METHODOLOGY

Surface-water and streambed-sediment samples were collected during September 2012 under baseflow conditions and surface waters were resampled during June 2013 (at medium-high flow), September 2013 (near baseflow), and April 2014 (near peak flow). In Figure 2, the daily mean discharge and instantaneous flow for the separate sampling events are shown for site 6 in the St. Louis River. Sampling locations included 10 sites in Filson Creek, 4 sites in Keeley Creek, and 7 sites in the St. Louis River (Figure 1); however, not every site was sampled during each sampling event.

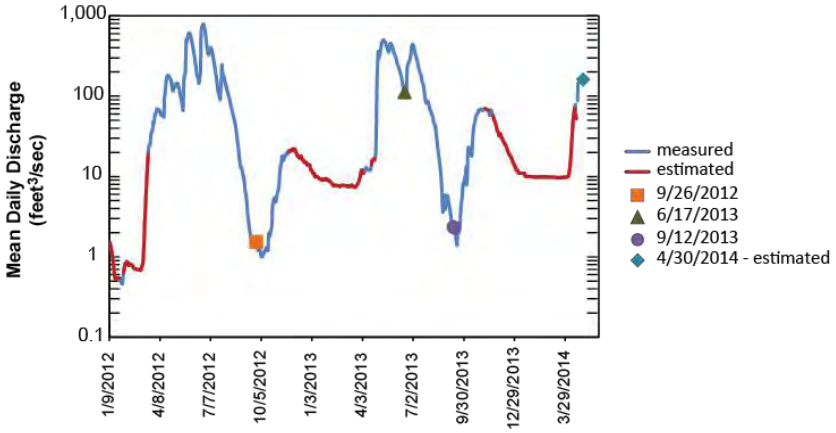

Figure 2 Daily mean discharge for St. Louis River, site 6, from http://waterdata.usgs.gov/nwis. Instantaneous discharge measured during sample collection shown as discreet symbols.

Surface-water samples were collected using United States Geological Survey (USGS) protocols (Wilde & Radtke, 1998; Wilde et al., 1999).Water quality parameters (e.g., pH, water temperature) were determined by discrete measurements at the time of water sample collection. Water samples included a less than 0.45 μm filtered (dissolved) sample and an unfiltered (total) sample. Major ions and trace elements in filtered and unfiltered surface waters acidified with ultrapure nitric acid were analyzed using inductively coupled plasma-atomic emission spectroscopy (ICP-AES) and inductively coupled plasma-mass spectrometry (ICP-MS) (Taggart, 2002). Major anions were analyzed on non-acidified filtered splits using ion chromatography (Taggart, 2002). Samples were analyzed for alkalinity on non-acidified filtered splits by titration; dissolved organic carbon (DOC) was measured by infrared spectrometry on filtered samples preserved with trace element grade hydrochloric acid (Taggart, 2002).

Composite streambed-sediment samples were collected according to USGS protocols (Shelton & Capel, 1994). Sediments were composites of approximately 30 surface subsamples collected in a grid pattern. The composite was homogenized and then sieved to a diameter of less than 2 mm. Samples were analyzed for total concentrations of major and trace elements using a combination of ICP-MS and ICP-AES following acid digestion using a mixture of HCl-HNO_3-$HClO_4$-HF. Total organic carbon is calculated as the difference between total carbon and carbonate carbon, which were determined using an elemental analyzer and coulometric titration, respectively. In order to

determine elements not tightly bound to silicates, partial extractions were conducted using HCl-H_2O_2 and a Diisobutyl Ketone (DIBK) solution; extracted metal concentrations were determined by ICP-AES. (For details regarding previously mentioned analytical methods for sediments see: http://minerals.cr.usgs.gov/projects/analytical_chem/references.html). Samples were also analyzed for acid volatile sulfide - simultaneously extracted metals (AVS-SEM) using a procedure modified after United States Environmental Protection Agency (USEPA, 1991). The AVS is operationally defined here as the sulfide fraction released by extraction with 1.2 N HCl at approximately 80º C; the metal fraction released during the AVS extraction is the SEM.

RESULTS AND DISCUSSION

Water and sediment chemistry

The geochemistry of the surface waters and stream sediments reflects underlying rock types, glacially transported unconsolidated materials, mineralization style within each watershed, and geochemical processes occurring in the streams. The water chemistry is also influenced by the ambient and flow conditions and therefore changes daily and seasonally. In general, the surface water is oxic, near neutral to slightly acidic (pH 5.0 to 7.6), has low total dissolved solids (38 to 110 mg/L), and is characterized by low hardness (10 to 53 mg/L $CaCO_3$), moderate carbonate species concentrations (4 to 44 mg/L $CaCO_3$ as bicarbonate), low sulfate (< 0.8 to 3.1 mg/L), and high DOC concentrations (18 to 47 mg/L) (Figure 3). The dominant dissolved trace elements are Fe (400 to 4,000 µg/L), Al (59 to 320 µg/L), Cu (< 0.8 to 9.6 µg/L), and Ni (0.6 to 7 µg/L).

For each specific sampling event, the average pH values are slightly lower and Cu and Ni concentrations are higher in water samples collected from the Filson Creek watershed, where the basal contact of the Duluth Complex is exposed. In contrast, the concentrations of major cations such as Ca and Mg, and, thus, hardness, as well as alkalinity are commonly highest in the St. Louis River for each sampling event compared to the other watersheds. Dissolved organic carbon is found in similar ranges of concentrations for all three watersheds during all sampling events, with a few exceptions; sulfate is generally low (Figure 3).

In addition to variation among watersheds, the chemistry of the streams changes with flow. Water samples collected during medium-high and peak flows (June 2013 and April 2014) are slightly more acidic, less alkaline, and generally more dilute with lower concentrations of some major and trace elements including Ca, Fe, Mg, and Na compared to water samples collected during low flow (Figure 3). Lower dissolved concentrations of elements are consistent with dilution after rainstorms or periods of snowmelt. However, despite generally more dilute conditions, the amount of dissolved elements (load) transported by the stream is greater under high flow conditions relative to low flow conditions as illustrated in Figure 4. In fact, the instantaneous loads for nearly all elements are greater during medium-high flow than under low flow and not correlated with element concentrations (Figures 3 and 4). During the drier and/or winter low flow conditions, major and trace elements and sulfate may accumulate in the wetland areas and in groundwater. These constituents may then be flushed from the reservoirs downstream during spring and summer high flow events. Similarly, DOC loads in the streams increase significantly during higher flow conditions, which also may be result of stream recharge through wetland areas that are organic-rich and oxygen-poor, as suggested by Berndt & Bavin (2012) for increased DOC concentrations following a major storm event in the St. Louis River watershed in August 2010.

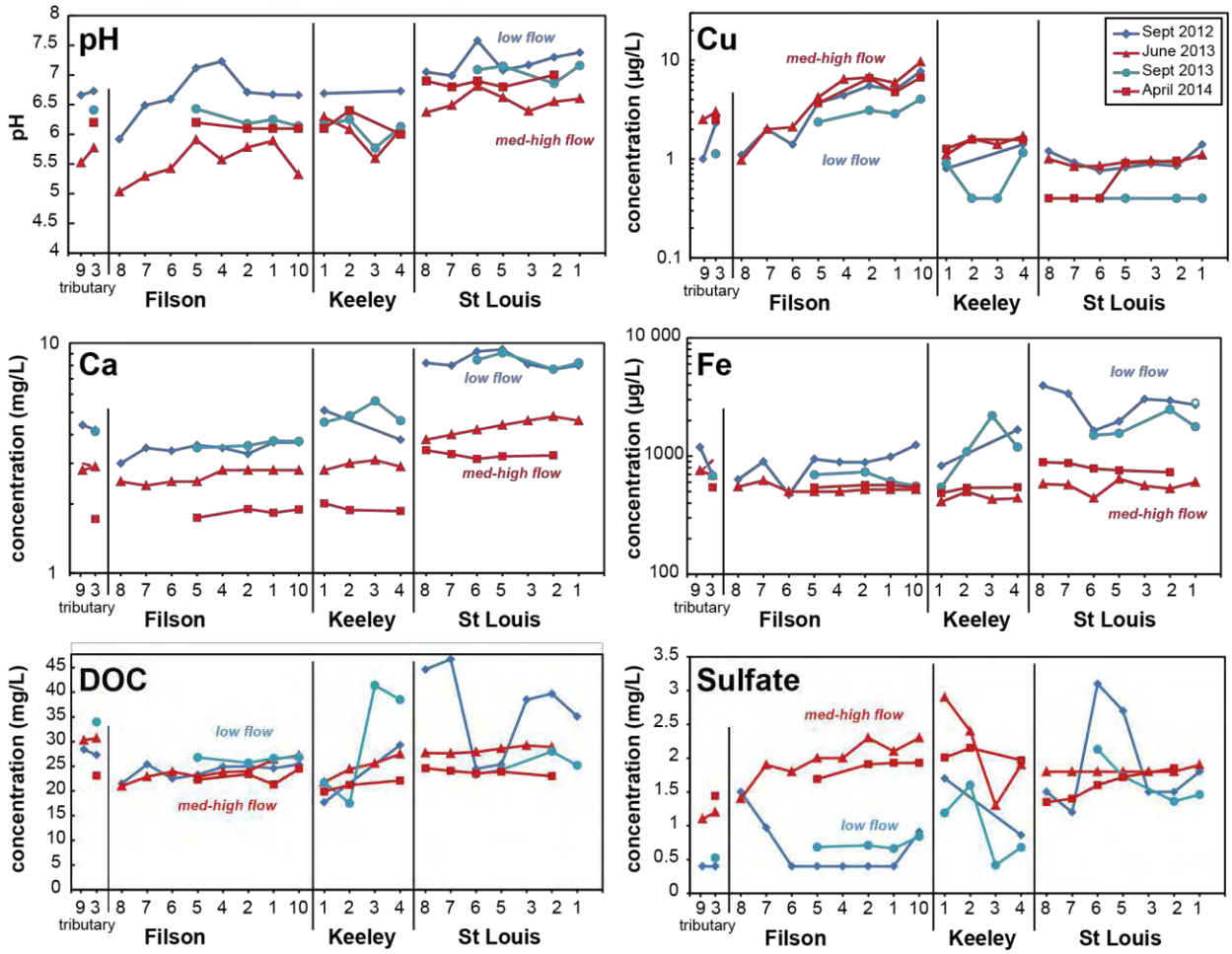

Figure 3 The pH and dissolved (< 45 µm) concentrations of Cu, Ca, Fe, DOC, and sulfate for each watershed plotted upstream to downstream (right to left for each watershed). Site numbers are given on the x-axis.

Stream sediments contain significant Al (7 to 11 weight percent, wt. %), Ca (1.5 to 6 wt. %), Fe (1 to 7 wt. %), and Na (2 to 4 wt. %). Sulfur is very low (< 0.05 wt. %). Organic carbon reaches 4.7 wt. % in one sample but is ≤ 1.5 wt. % in all the other samples. Trace metals are dominated by Cr (14 to 346 mg/kg), Cu (10 to 179 mg/kg), Ni (13 to 127 mg/kg), and Zn (23 to 95 mg/kg). On average, Cu and Ni are highest in Filson Creek stream sediments where Cu-Ni-PGM mineralization occurs at the surface (Figure 5). Samples collected from the St. Louis River watershed, where Fe-Ti oxide-bearing ultramafic rocks and a Paleoproterozoic shale/greywacke unit (Virginia Formation) occur, contain the highest average concentrations of many other trace elements including As, Cr, Fe, Pb, and Zn.

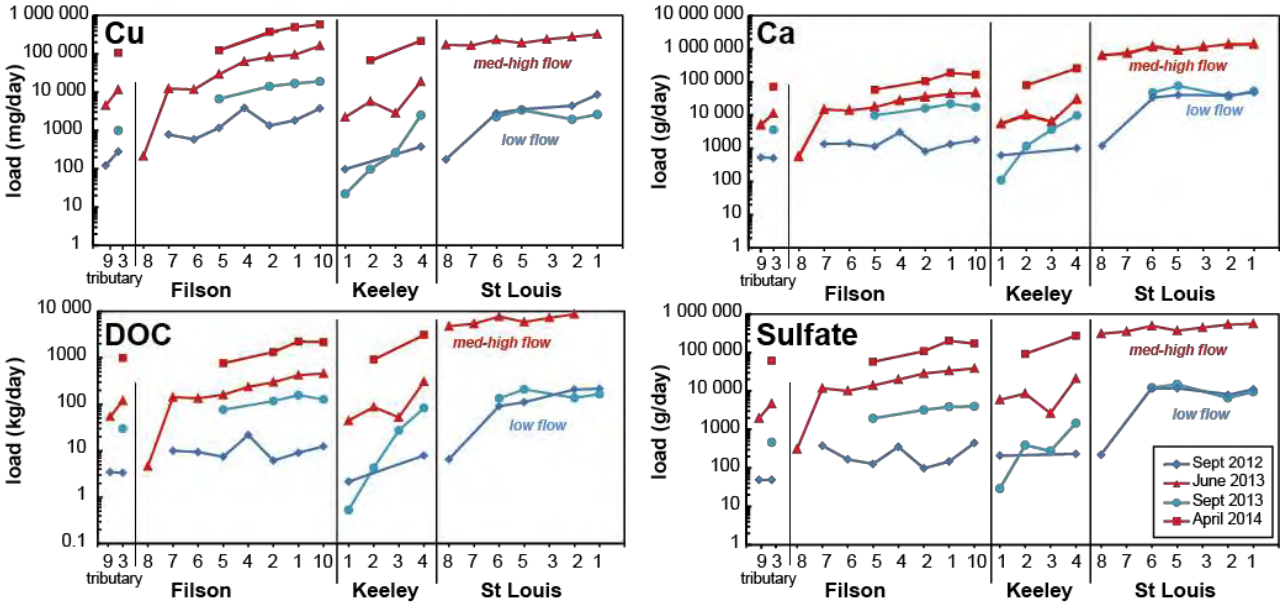

Figure 4 Instantaneous dissolved loads for Cu, Ca, DOC, and sulfate for each watershed plotted upstream to downstream. Flow data are not available for Keeley 1 or sites in the St. Louis River for April 2014.

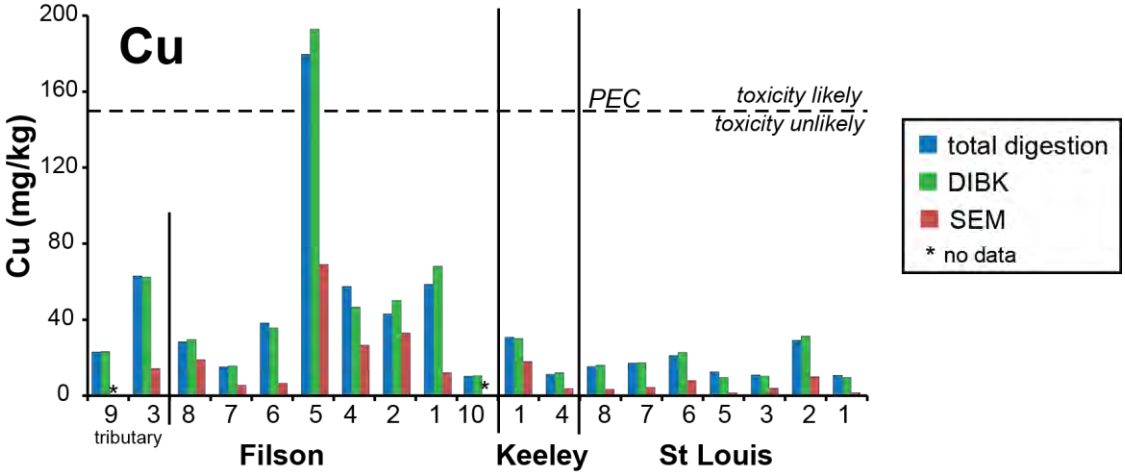

Figure 5 Concentrations of Cu in stream sediments for various digestion procedures for each watershed plotted upstream to downstream. Probable Effect Concentration (PEC) from MacDonald, Ingersoll, & Berger (2000).

Toxicity

In water, the toxicity of most metals is assessed on the basis of hardness-based criteria that adjust for the protective effects of Ca and Mg ions, which compete with metal ions for binding sites on organisms (USEPA, 2014). For sediment, consensus-based total-metal guidelines (i.e., Probable

Effect Concentration, PEC) are routinely used and rely on laboratory toxicity tests that document increased toxicity caused by increased metal concentrations (MacDonald, Ingersoll, & Berger, 2000). However, new guidelines that rely on the BLM utilize a more sophisticated approach incorporating a greater array of water and sediment quality parameters including the cumulative effects of multiple metals in sediment, metal speciation in water, and organic carbon complexes in both water and sediment (Di Toro et al., 2005; USEPA, 2007). The surface-water and sediment metal concentrations can be compared to aquatic guidelines using the hazard quotient (HQ), which is the ratio of the concentration of a metal in the sample to the guideline value. Values above 1 imply toxic conditions, whereas those below do not.

Copper is the main element of concern in these baseline-condition waters with regard to aquatic toxicity. Using hardness-based criteria, chronic toxicity HQs for Cu in water are greater than 1 for many sites during both medium to high and low flow conditions in the Filson Creek watershed and a few sites in Keeley Creek during medium-high flow (Figure 6A). However, as shown in Figure 6A, nearly all chronic toxicity HQs for Cu in water calculated based on the BLM model are less than 1 (assuming a high HA fraction, i.e., 60 %), suggesting a lack of toxicity in most samples. The radically different results from the hardness-based and BLM-based approaches suggest that the former approach routinely used by regulators may be inadequate to describe metal toxicity in these DOM-rich watersheds because it is based on a more limited set of parameters (i.e., only hardness).

In addition, the complexation of Cu with DOM likely significantly affects the bioaccessiblity of dissolved Cu in these watersheds, helping to mitigate its toxicity. However, the relative proportions of HA and FA in DOM greatly influence Cu complexation. The results from the BLM using various ratios of HA and FA at low and medium-high flow conditions for a site in Filson Creek are shown in Figure 6B; also, the range of HA (i.e., 10-60 %) that the BLM model is calibrated for is also shown. The concentration of Cu in the stream exceeds the chronic WQC for a medium-high flow sampling (June 2013) when WQC are calculated assuming a 10 % HA fraction. This is a conservative assumption for the percentage of HA that is recommended by HydroQual (2007) when HA and FA fractions are not known. If this reactive HA component makes up a higher proportion of the DOM, as is suspected for these waters (research currently ongoing), the WQC may increase above the Cu concentrations in the stream (Figure 6B). As illustrated by this example, it may therefore be important to quantify these acid fractions in order to accurately assess toxicity when using BLM, particularly for sites with HQ values close to 1. It is also apparent from Figure 6B that the Cu concentrations in the stream do not vary significantly with flow; however, other chemical changes in the stream result in significantly different WQC under different flow conditions.

The main elements of concern regarding benthic organism toxicity from streambed sediments include Cu as well as Ni and Cr. Partial digestions using a DIBK extraction suggest metals such as Cd, Cu, Pb, and Zn are likely partitioned into the more soluble and bioaccessible phases and not tightly bound to less reactive silicates (Figure 5). Although not analyzed in the DIKB extractions, only a small fraction of Ni and Cr was extracted during the AVS-SEM procedure suggesting that these elements, in addition to Cu, are not bound to less bioaccessible sulfides (Figure 5). Overall, both extractions suggest potentially toxic metals in sediments may be hosted in more bioaccessible forms such as sorbed onto clays and hydroxide phases that are available for benthic organism uptake.

Similar to the inconsistent predictions for water toxicity based on the BLM and hardness-based approaches, the sediment BLM approach suggests a different level of toxicity from sediments than would be predicted from consensus-based guidelines.

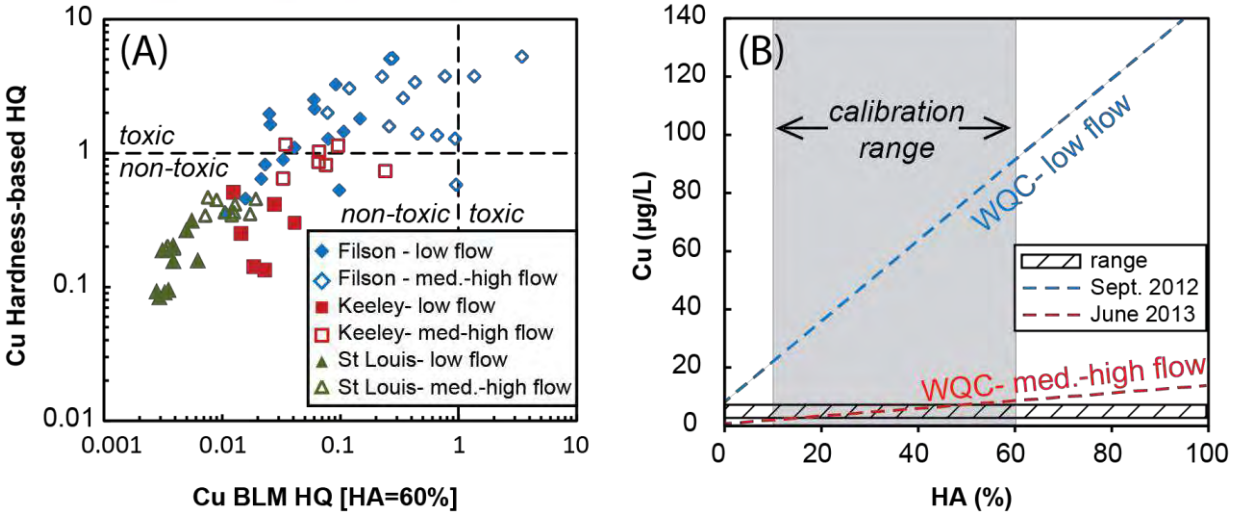

Figure 6 (A) Hardness-based and BLM-based HQs of chronic Cu toxicity. (B) Range in Cu concentrations and BLM- based chronic WQC for various proportions of HA for low and medium-high flows for Filson Creek site 2.

Several HQs for Ni and one HQ for Cu are greater than 1 when calculated using the consensus-based guidelines (i.e., PEC), which suggests toxic conditions (Figure 7A). In comparison, no toxicity (< 130 micromoles per gram of organic carbon, µmol/gOC) to uncertain toxicity (130 to 3,000 µmol/gOC) is predicted based on Equilibrium Partitioning Sediment Benchmarks (ESB) (USEPA, 2005) (Figure 7B). This approach includes: 1. determining extractable (a proxy for bioaccessible) metal concentrations (i.e., combined simultaneously extracted metals, ΣSEM = $SEM_{Cd}+SEM_{Cu}+SEM_{Ni}+SEM_{Pb}+SEM_{Zn}$); 2. adjusting them for potential incorporation into less bioaccessible sulfides (i.e., acid volatile sulfide, AVS); and 3. Adjusting for complexation with organic carbon (i.e., fraction of organic carbon, f_{oc}). The high organic carbon in some of the sediments could sequester significant amounts of trace elements; however, the low AVS suggest trace elements bound to sulfides are not significant components in these sediments.

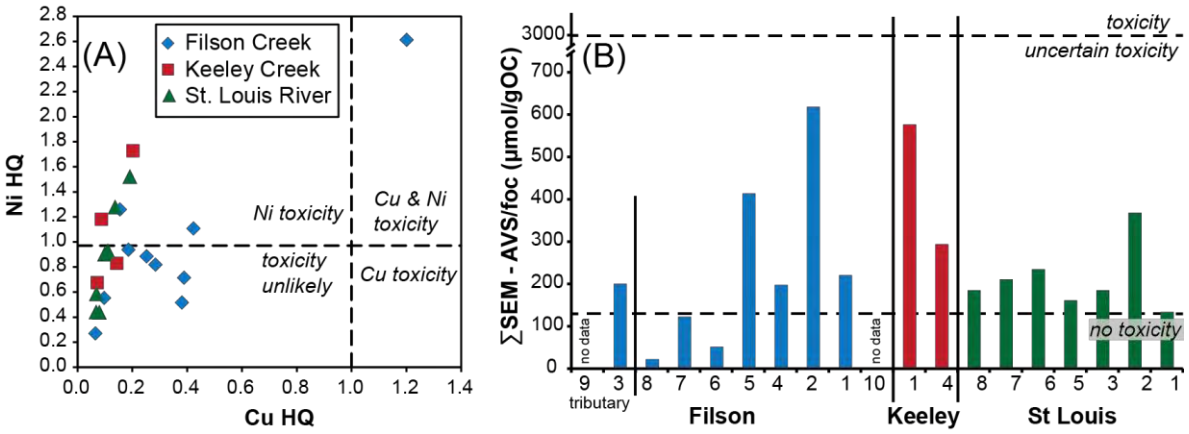

Figure 7 (A) Consensus-based HQ for Ni and Cu in sediment. (B) ESB for sediment samples by watershed and plotted upstream of downstream.

CONCLUSION

The chemistry of surface water and stream sediment in three watersheds from the Duluth Complex is variable due to different mineralization styles. The water chemistry also changes seasonally for most major and trace elements. However, the concentration of Cu, the main element of concern in these watersheds with regard to aquatic toxicity, and DOC only vary within a narrow range for each watershed among the various seasons and flow conditions sampled. The complexation of Cu with DOM significantly limits the bioaccessibility of dissolved Cu, and the generally consistent concentrations of DOM ensure the continued resiliency of water in Duluth watersheds to toxicity year round. As for the sediments, Cu and trace elements may occur in the more bioaccessible forms; however, organic carbon in some of the sediments may help to sequester significant amounts of trace elements. The high organic matter in waters and some sediments certainly plays a key role in protecting aquatic organisms from naturally-occurring concentrations of Cu and other elements in these mineralized watersheds. Nonetheless, the productivity and subsequent organic content of the stream waters and sediments could change if their chemistry is impacted by drainage from future mining (i.e., increase in metals and acidity). Changes in the amount of organic matter and its composition (i.e., changes in the fraction of humic and fulvic acids) could also influence the capacity of organic matter to bind metals and thus limit toxicity to aquatic organisms.

ACKNOWLEDGEMENTS

This research was supported by funding from the Mineral Resources Program and Midwest Region of the U.S. Geological Survey. The use of product names is for descriptive purposes only and does not imply endorsement by the U.S. government.

REFERENCES

Berndt, M., and Bavin, T. (2012) On the cycling of sulfur and mercury in the St. Louis River watershed, northeastern Minnesota: An Environmental and Natural Trust Fund Final Report, Minnesota Department of Natural Resources, 91 p., available at http://files.dnr.state.mn.us/lands_minerals/reclamation/BerndtandBavin2012b.pdf.

Di Toro, D.M., McGrath, J.M., Hansen, D.J., Berry, W.J., Paquin, P.R., Mathew, R., Wu, K.B., and Santore, R.C. (2005) Predicting sediment metal toxicity using a sediment biotic ligand model: Methodology and initial application, Environmental Toxicology and Chemistry, vol. 24, no. 10, pp. 2410-2427.

HydroQual, Inc. (2007) The Biotic Ligand Model Windows Interface, Version 2.2.3, User's Guide and Reference Manual, 2005, HydroQual, Inc., Mahwah, New Jersey.

MacDonald, D.D., Ingersoll, C.G., and Berger, T.A. (2000) Development and evaluation of consensus-based sediment quality guidelines for freshwater ecosystems, Archives of Environmental Contamination and Toxicology, vol. 39, no.1, pp. 20-31.

Shelton, L.R. and Capel, P.D. (1994) Guidelines for collecting and processing samples of stream bed sediment for analysis of trace elements and organic contaminants for the National Water-Quality Assessment Program, U.S. Geological Survey Open-File Report 94-0458, 20 p., available at http://pubs.er.usgs.gov/publication/ofr94458.

Taggart, J.E. (ed.), 2002, Analytical methods for chemical analysis of geologic and other materials, U.S. Geological Survey, U.S. Geological Open-File Report 02-223, variously paginated, available at http://pubs.usgs.gov/of/2002/ofr-02-0223/OFR-02-0223.pdf

U.S. Environmental Protection Agency (1991) Draft Analytical Method for Determination of Acid Volatile Sulfide in Sediment, U.S. Environmental Protection Agency EPA-821-R-91-100, 18 p.

U.S. Environmental Protection Agency (2005) Procedures for the derivation of equilibrium partitioning sediment benchmarks (ESBs) for the protection of benthic organisms: Metal mixtures (cadmium copper, lead nickel, silver, and zinc), U.S. Environmental Protection Agency 600-R-O2-011, variously paginated.

U.S. Environmental Protection Agency (2007) Aquatic life ambient freshwater quality criteria – Copper 2007 revision, U.S. Environmental Protection Agency EPA-822-F-07-001, 49 p.

U.S. Environmental Protection Agency (2014) National recommended water quality critera, accessed September 2014, at http://water.epa.gov/scitech/swguidance/standards/criteria/aqlife/index.cfm

Wilde, F.D., and Radtke, D.B., eds. (1998) Field measurements: U.S. Geological Survey Techniques of Water-Resources Investigations, book 9, chap. A6, variously paginated.

Wilde, F.D., Radtke, D.B., Gibs, J., and Iwatsubo, R.T., eds. (1999) Collection of water samples, U.S. Geological Survey Techniques of Water-Resources Investigations, book 9, chap. A4, 156 p.

Prediction of Acid Neutralizing Potential of Wetlands Affected By Gold Mining in a Semi-Arid Area

Julien Lusilao-Makiese, Ewa Cukrowska, Hlanganani Tutu, Luke Chimuka and Isabel Weiersbye
University of the Witwatersrand, South Africa

ABSTRACT

South Africa's mining activities play an important role in ensuring the country's position in the global market. Unfortunately, the country's mining history also has resulted in dramatic environmental consequences especially, in the case of acid rock drainage (ARD) production from gold mines of the Witwatersrand. The legacy of mining continues to affect water resources even long after mining operations have ceased.

The issue of ARD at both historic and active mines has led to the worldwide need to implement prediction methods and for the assessment of the acid generation potential during the exploratory phase of mine development.

In this study, static acid base accounting (ABA) tests were conducted on and around an active gold mine tailings dam to predict the risk of acid generation at the site. Sediment samples were collected from wetlands (natural and constructed) and tailings materials were obtained from a Tailings storage facility that has been built about a century ago. The Sobek method was used for the ABA test. Total metals and speciation (BCR extraction) analyses were also carried out on the collected samples.

Results of ABA tests showed variable Net Neutralization Potentials (NNPs) for surface samples (generally negative for tailings and positive for sediments), although the obtained NNPs fell within the range of uncertainty (i.e. -20 < NNP < 20), which demonstrated the need for kinetic tests. Natural wetland samples appeared to have a greater acid forming potential compared to the constructed ones. Moreover, the experiment also showed that acidic conditions would dominate after complete oxidation of the samples. Metals studies revealed not only high total metals values in the samples but also, for several metals, a strong correlation between fraction of "reducible" species (metals bound to sulfides or organic matters) and sulfur. Once exposed to oxygen, these non-soluble metals-sulfides can generate ARD and become available in acidic waters.

Keywords: Acid-Base Accounting, Net Neutralization Potential, Acid Mine Drainage

INTRODUCTION

Acid rock drainage (ARD) is produced by the oxidation of sulfide minerals, frequently pyrite (FeS_2). This is a natural chemical reaction that proceeds when minerals are exposed to air and water. ARD is found around the world as a result of both naturally occurring processes and activities associated with land disturbances, such as mining where acid-forming minerals are exposed at the surface of the earth. Mine tailings and waste rock have much greater surface area than in-place geologic material due to their smaller grain size and are, therefore, more prone to generating ARD. Metals that were once part of the host rock are solubilized and exacerbate the deleterious effects of low pH on terrestrial and aquatic receptors (Jennings *et al.*, 2008). Water contaminated by ARD often contains elevated concentrations of metals, which are toxic to aquatic organisms, leaving receiving streams devoid of most living creatures (Kimmel, 1983).

As elsewhere in the world, the activities of the mining sector in South Africa have resulted in serious environmental consequences, notably with respect to poor environmental and water management and, in the case of the gold mines of the Witwatersrand, production of ARD. Reappraisal of the risks attributable to ARD formation has become increasingly necessary in view of the looming crisis in the mining basins of the Witwatersrand region (Inter-ministerial committee, 2010). ARD and the mitigation thereof are critically important to South Africa. Mine waste particularly tailings, are a large contributing factor to ARD generation. Characterization of the acid generating properties of mine waste is fraught with uncertainty and deficiencies that create difficulties in evaluating and selecting suitable interventions for mitigating associated ARD risks in line with cleaner production and sustainable development principles (Kotelo, 2013).

Accurate prediction of acidic drainage from proposed mines is recognized as a critical requirement of mine permitting and long-term operation (Skousen and Ziemkiewicz, 1996). Mine drainage chemistry can be quantitatively predicted by investigating the geochemistry of rocks to be disturbed by mining (Pope *et al.*, 2010).

Prediction of acid generating potential from geologic formation, referred to as acid-base accounting (ABA), is essentially the ability to identify and quantify both acid-forming and neutralizing minerals in the geologic materials to be unearthed during mining operations (Skousen *et al.*, 2002; Smart *et al.*, 2002). A standardized EPA protocol known as the Sobek method (Sobek *et al.*, 1978) was developed to characterize mine soil and overburden. Although, this method is still used mainly due to its simplicity and low cost analytical procedures (USEPA, 1994), various modifications of the original procedure have been developed that "correct" some of the observed drawbacks from the original method (Chotpantarat, 2011).

In this study, the modified Sobek method (Skousen *et al.*, 1997) was adopted to predict the acid neutralizing potential of wetlands sediments and tailings materials collected from an active gold mine site in South Africa. This method involves the addition of hydrogen peroxide (H_2O_2), which oxidizes the ferrous iron in the dissolved siderite, yielding lower alkalinity predictions.

METHODOLOGY

Sampling

Forty-five sediments profile samples were collected at a gold mine site near Carletonville (North-West Province, South Africa). The samples were obtained from both natural (31 samples) and constructed wetlands (5 samples) near a tailings storage facility (TSF) which was built more than seven decades ago, and tailings materials (9 samples). The constructed wetlands (CWs) in the area are reed beds that are part of a succession from young trees colonizing water ponds and are less than five years old. Sediments in the CWs were "tailings like", especially at the surface, and were characterized by a low percentage carbon (between 0.2 and 1.3 %). Due to the wet conditions of the ponds on the day of sampling, only one CW profile (down to 50 cm depth) was collected from a relatively dryer pond. Natural wetlands (NWs) were characterized by a natural plants colonization and the sediment had a percentage carbon that varied between 0.3 to 2.1% with the highest values mostly measured at top layers. NW profiles were collected down to 100 cm depth whereas tailings materials were obtained from the TSF in horizontal profiles of 40 and 50 cm length. All profiles were later on divided, where possible, into layers of 10 cm each.

Analytical methods

Once in the laboratory, samples were homogenized and a representative aliquot of each sample was dried then pulverized with a pestle and mortar to approximately < 2 mm.

The samples were digested in a microwave assisted extraction system at 800 W for 30 min using a mixture of HCl, HNO_3, HF and H_3BO_3. The samples were then diluted with deionized water and stored in a fridge until analysis. A sequential extraction was performed according to the procedure recommended by the Standards, Measurements and Testing Programme of the European Union (SM& T, formerly BCR), for the determination of some elements of interest in the collected samples. The chosen extraction scheme is an operationally defined and standardized procedure (Tokalioglu *et al.*, 2003; Davidson *et al.*, 1999) in which the reagent used at each stage is intended to release metals associated with particular soil phases such as acid soluble, reducible, oxidizable, and residual. Reported results were related to the extraction step numbers as shown in Table 1. Thus, Fe1, Fe2, and Fe3 refer to the concentration of iron (Fe) in fraction 1, 2, and 3, respectively. Metal determination in the extracts was carried out by ICP-OES.

Table 1 The BCR three-stage sequential extraction scheme.

Extraction step	Reagents/ concentration/ pH	Solid phase
1	CH_3COOH (0.11 M) pH 2.85	Exchangeable, water & acid soluble (e.g. carbonates)
2	$NH_2OH.HCl$ (0.1 M) pH 2	Reducible (e.g. Fe/Mn oxides)
3	H_2O_2 (8.8 M) following by CH_3COONH_4 (1.0 M) pH 2	Oxidizable (e.g. organic substance and sulfides)

Total sulfur (S) used for ABA was determined using a LECO S632 analyzer, and Statistica software (Statistica® 7, USA) was used to check for correlation between the different studied parameters.

Static tests

Static ABA was performed on each pulverized sample. The following are the procedures used for the static ABA studies:

Initial pH

A sample mass of 5 g was weighed and added 50 ml of deionized water and was left for 24 hrs., after which the initial pH was measured (Usher *et al*, 2003).

Final pH

A volume of 80 ml of H_2O_2 (30% w/v) was added to a mass of 2 g of pulverized sample. The reaction was left to oxidize for 24 hrs, after which the final pH was measured (Usher *et al*, 2003).

The acid production potential

The acid production potential (AP) was determined from the total S content as follows:

AP (kg $CaCO_3$/t equivalent**)** = 31.25 x %S

Neutralization Potential (NP)

The peroxide siderite correction for Sobek method, as developed by Skousen *et al.* (1997), was used for determination of neutralization potential (NP). An initial fizz test was performed to select the volume and normality of HCl that was added to the sample prior titration. After the HCl addition, the sample was boiled until the reaction was complete. The resulting solution was back titrated to pH 7 with NaOH to determine the amount of acid consumed in the reaction between HCl and the sample. Blank titrations were also carried out to determine the blank constant critical for the calculation of the amount of acid consumed. NP was then calculated as follows:

NP (kg $CaCO_3$ equivalent / ton of material) = (ml of acid consumed) x (25.0) x (Normality of added HCl).

The net neutralizing potential (NNP) was determined by subtracting the AP from the NP and is a measure of the difference between the neutralizing and acid forming potentials.

RESULTS AND DISCUSSION

Elemental analysis

The results of selected elements concentrations in surface sediments and tailings materials are shown in Table 2. High metal concentrations relative to background levels were measured in the study samples with values sometimes reaching the percentage level, as was the case for aluminum (Al), Fe, and manganese (Mn), to mention a few. The measured concentrations are a clear indication of a pollution occurring at the site, probably from surrounding TSFs. Analysis of wetlands surface waters (Table 3) also revealed elevated concentrations in both CWs and NWs for elements such as Ca, Fe, Mg, Mn and S.

Table 2 Selected element concentrations (mg kg^{-1}) in surface sediments and tailings

Sample	Al	As	Co	Cu	Fe	Hg	Mn	Pb	S	Zn
NW1	15913	34	23	32	33301	0.3	5486	65	1070	67
NW2	12898	18	18	18	22877	0.5	5096	154	9102	35
NW3	14832	89	109	6309	28473	0.8	14191	112	1755	334
CW	13926	29	23	41	28571	0.1	284	22	1176	29
Tailings	53373	100	70	98	40103	0.9	662	84	3289	180
Background	7000	7	10	8	25246	0.1	234	80	220	24

Table 3 Mean values for field parameter and selected elements concentrations (mg kg^{-1}) in wetlands waters

Sample	pH	Eh (mV)	EC (mS cm^{-1})	Al	Ca	Co	Cu	Fe	Mg	Mn	Ni	S	Zn
CW	5.8	460	5.1	2.14	390	0.68	0.02	0.70	346	25.4	0.06	354	0.32
NW	6.4	246	4.1	0.09	125	0.24	0.02	12.5	207	27.9	0.05	490	0.48

Acidity in ARD is comprised of mineral acidity (Fe, Al, Mn, and other metals depending on the specific metal-sulfide minerals present) and hydrogen ion acidity (Skousen *et al.*, 2000). The extremely high concentrations of Fe (and S) could be due to the abundance of pyrite (FeS_2) in the overburden material. It was observed that Fe had a positive linear correlation with S (Figure 1). BCR sequential extraction procedure (SEP) also showed, in some cases, positive correlations between Fe3 (i.e. oxidizable) and S (Figure 1).

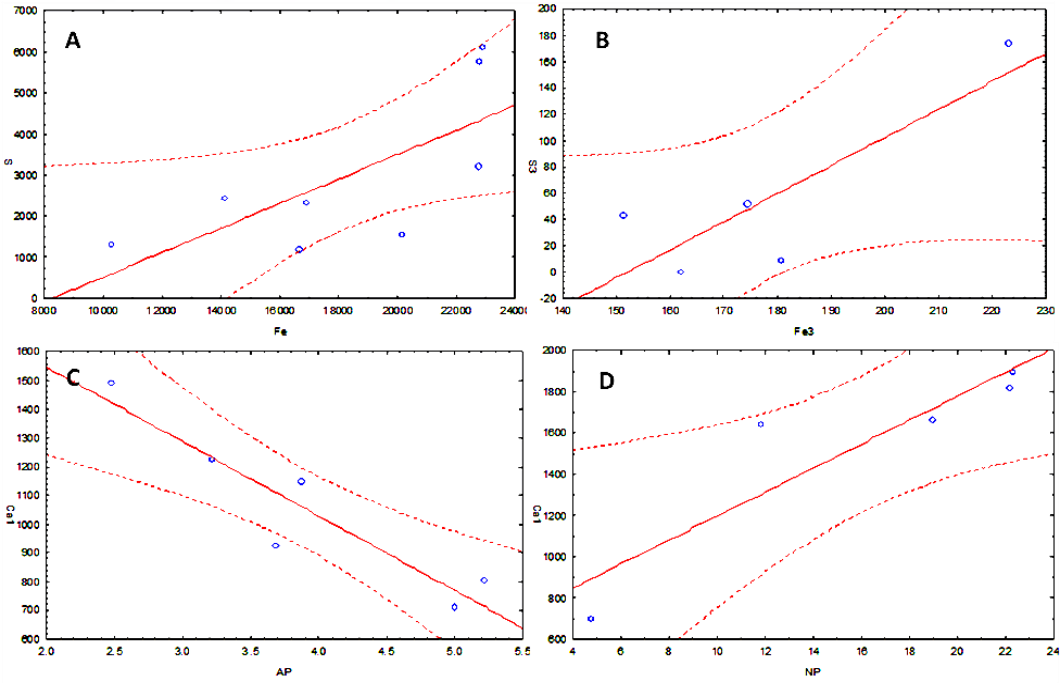

Figure 1 Correlation plots between total Fe and S (A), oxidizable Fe and S (B); Exchangeable Ca and AP (C), and Exchangeable Ca and NP (D), in natural wetlands sediments. Concentrations are in mg kg^{-1}.

The observed correlations could indicate the presence of pyrite in the overburden material, although other forms of Fe-S (e.g. pyrrhotite or $FeSO_4$) could also be present in the samples, as a good correlation was also found between total Fe and S. Good correlations were also observed between S and oxidisable cobalt (Co), copper (Cu), Mn and zinc (Zn) (Figure 2). It is known that these metals can complex with sulfides to form chalcopyrite ($CuFeS_2$), covellite (CuS), and sphalerite (ZnS). Pyrite commonly occurs with these other metal sulfides, and therefore ARD is likely to occur where Cu, Pb, and Zn are mined. The determination of the samples' mineralogy is, therefore, critical to reaching better conclusions about specific deposits.

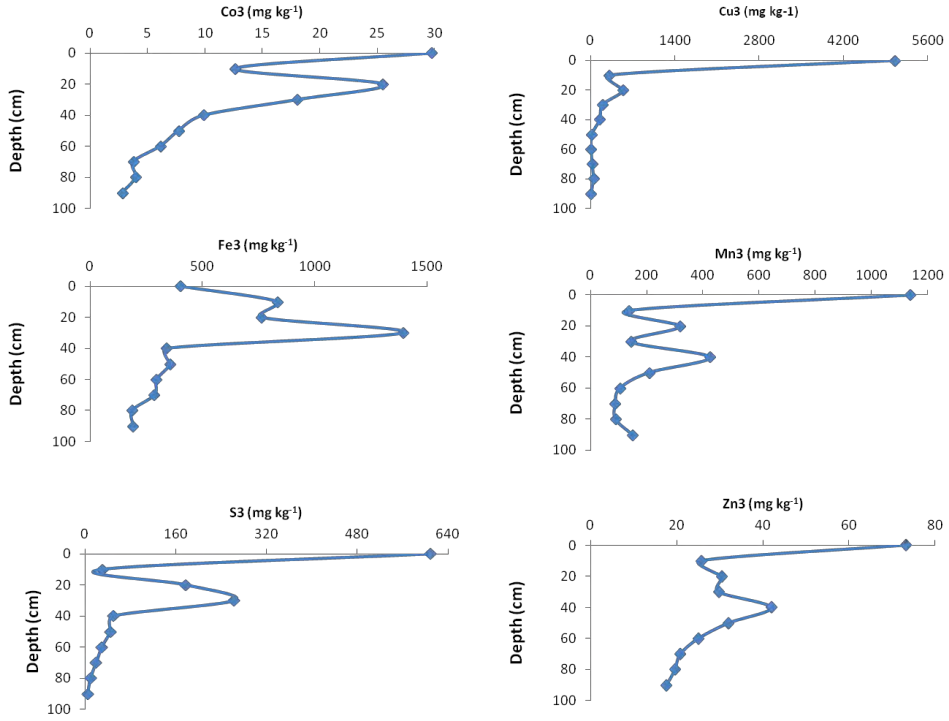

Figure 2 Trends of oxidizable forms of selected elements in a natural wetland sediment profile

Static tests

A plot of average pHs of the samples (Figure 3) shows that the initial average pH values ranged of 5.1 to 6.9.

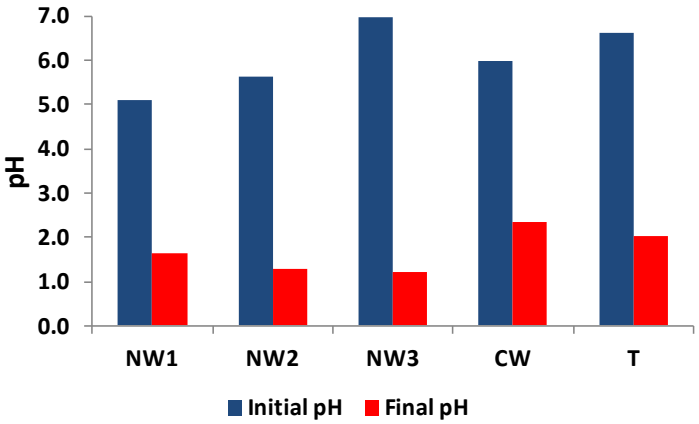

Figure 3 Average pH values of the samples before and after oxidization

The initial pH indicates the immediate acidic or basic characteristic of the sample and it could also indicate if acid generation has already been generated (Usher *et al.*, 2003). Note that, with the exception of NW3 which showed initial pH values close to neutrality, the majority of NW and CW samples had acidic pH, especially in bulk sediments were pH values as low as 3.8 were measured. This could be an indication that acid generation is already occurring at the site as a result of the oxidation of the above mentioned pyrite in the area. Acidic pH values were also measured in wetlands waters (Table 3). The final pH values suggest that after complete oxidation, the pH of each of the study samples would be less than 2.5

ABA tests revealed (Table 4) that the NNP (and NPR) values for the majority of the samples fell within the range of uncertainty (i.e. -1.3 ≥ NNP ≤ 9.1, or 0.9 ≥ NPR ≤ 2.8), except for the sample profile collected from one of the natural wetlands (i.e. NW1), which had an average NNP of 85.2 and falls within the non-acid forming range. This location exhibited higher NP values (up to about 190 Kg $CaCO_3$/t) at deeper layers (30 to 70 cm depth).

Table 4 ABA results of study samples

		AP (Kg $CaCO_3$/t)			NP (Kg $CaCO_3$/t)			NNP (Kg $CaCO_3$/t)		
Sample	n	Min	Mean	Max	Min	Mean	Max	Min	Mean	Max
NW1	11	3.3	6.2	9.5	4.7	91.5	187.6	-0.5	85.2	181.6
NW2	10	3.7	8.7	19.1	2.1	7.44	14.3	-13.9	-1.3	5.6
NW3	10	4.6	26.2	63.8	8.54	25.3	50.7	-51.8	-0.9	22.7
CW	5	1.3	5.0	7.7	-4.7	14.1	22.3	-6.0	9.1	16.9
Tailings	9	5.6	7.2	8.8	5.4	8.7	11.6	-0.2	1.5	2.8

These results may suggest an important source of acid-consuming constituents at this location. Since carbonates are known to be one of the main sources of alkalinity production (Sobek *et al.*, 2000), correlations have been plotted between the BCR SEP exchangeable fractions of selected elements and NP or AP, as that BCR fraction is known to contain carbonate-bound metals. Among all the study elements, a positive correlation was found between Ca1 (i.e. exchangeable Ca) and NP whereas a strongly negative correlation was observed for the same Ca fraction and AP (Figure 1), indicating that $CaCO_3$ could be the main acid-neutralizing agent in the study samples. Additionally, it has to be noted that the sample profile NW1 had the highest concentrations of exchangeable Ca.

With the exception of the above-mentioned sediment profile NW1, all the sediments also showed a strongly positive correlation (r^2 up to 0.899) between the pH after oxidization (final pH) and NNP. This implies that samples with the lower final pH (NW2 and NW3) might have been depleted of the total available carbonates leaving a lesser source of alkalinity to buffer the acid. Another reason may be that there were more acid-producing constituents than acid-consuming constituents in the sample as these two sample profiles had negative average NNP (i.e. Average AP > Average NP). Sample profile NW3 showed the lowest mean final pH, the lowest NNP, as well as the highest AP (Figure 2). The high AP values obtained in this profile may suggest an important presence of acid-producing constituents, such as metal sulfides. Furthermore, at the point where the lowest NNP was recorded, the concentration of total S was as high as 2% and NP was at one of its lowest recorded values in this profile (i.e. 12 kg $CaCO_3$/t). The more negative NNP could also imply,

therefore, that the sediment did not have enough $CaCO_3$ to neutralize the acidity in the soil hence there was a potential of ARD in the area.

It is important to recall that the method used in this study is based, in part, on calculation of potential acidity from total S measurements. However, potential acidity is known to be overestimated where organic S, sulfate S, and some sulfide compounds make up a substantial portion of the total S content (Schumann *et al.*, 2012). Thus, a method speciating S, such as the chromium reducible S (CRS) method, would be useful to refine the obtained results.

In general, NNP values were lower at depth in the sediments profiles (Figure 4). This could be attributed to anoxic conditions encountered at deeper layers in wetland sediments, which favor the reduction of sulfate, as well as \ formation of non-soluble metal-sulfides. Thus, in case of land disturbance (or water infiltration), there is a possibility for these sulfide-rich layers to become exposed to oxygen and undergo different reactions that lead to ARD generation and subsequent solubilization of toxic metals.

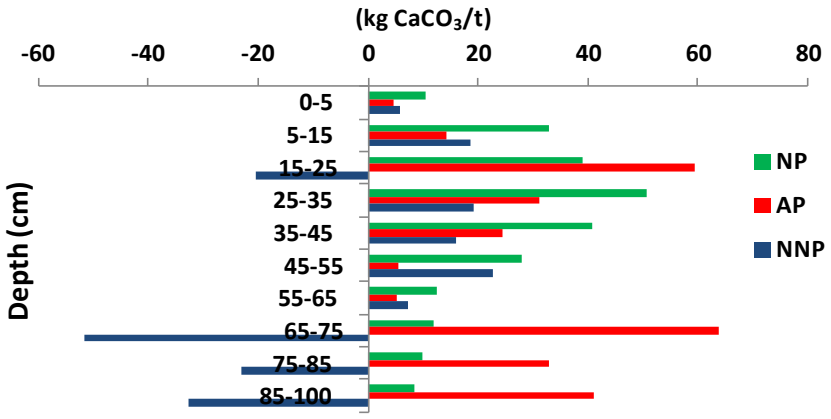

Figure 4 ABA results of the sediment profile NW3

CONCLUSION

Static ABA tests were performed in different samples collected from a gold mine site. Results showed that NNP (and NPR) values were mostly in the range of uncertain acid production, which suggests the need for kinetic tests, although pH tests revealed a risk of acid production if samples were exposed to more oxidizing conditions. Elemental analysis showed contamination already occurring at the site, and the pollution source is believed to be the presence of massive TSFs at the site. Generally, sample from the natural wetlands (and tailings) exhibited higher acid-forming potential than the constructed wetlands. BCR extraction helped to identify FeS_2 and $CaCO_3$ as the likely sources of acid- and alkalinity-production, respectively, in the samples. Mineralogical data would be necessary to verify the specific minerals contributing to ABA analysis and reported results.

ACKNOWLEDGEMENTS

The authors would like to thank NRF-THRIP (South Africa) and the Wits University Research Committee (URC, South Africa) for the financial support.

REFERENCES

Chotpantarat, S. (2011) A Review of Static Tests and Recent Studies, American Journal of Applied Sciences, vol. 8, 4, pp. 400-406.

Davidson, Ch., Ferreira, P.C.S. and Ure, A.M. (1999) Some sources of variability in application of the three-stage sequential extraction procedure recommended by BCR to industrially-contaminated soil, Fresenius J. Anal. Chem., 363, pp. 446–451.

Inter-ministerial committee (2010) Mine water management in the Witwatersrand Gold Fields with special emphasis on acid mine drainage, Report to the Inter-Ministerial Committee on Acid Mine Drainage, Department of Water Affairs, Pretoria.

Jennings, S.R., Neuman, D.R. and Blicker, P.S. (2008) Acid Mine Drainage and Effects on Fish Health and Ecology: A Review, Reclamation Research Group Publication, Bozeman, MT.

Kimmel, W. G. (1983) The impact of acid mine drainage on the stream ecosystem. Pennsylvania Coal: Resources, Technology, and Utilization, Pennsylvania Academic Science Publications, pp. 424-437.

Kotelo, L.O. (2013) Characterising the Acid Mine Drainage Potential of Fine Coal Wastes, MSc dissertation, UCT.

Pope, J. , Weber, P. , Mackenzie, A. , Newman, N. and Rait, R.(2010) Correlation of acid base accounting characteristics with the Geology of commonly mined coal measures, West Coast and Southland, New Zealand, New Zealand Journal of Geology and Geophysics, vol. 53, 2, pp. 153-166.

Schumann R., Stewart, W., Miller, S., Kawashima, N., Li, J. and Smart, R. (2012) Acid–base accounting assessment of mine wastes using the chromium reducible sulfur method, Science of the Total Environment, 424, pp. 289–296.

Skousen, J. G., and P.F. Ziemkiewicz (1996) Acid Mine Drainage Control and Treatment, Second Edition, Morgantown, W.V., West Virginia University and the National Mine Land Reclamation Center.

Skousen, J., Renton, J., Brown, H., Evans, P., Leavitt, B., Brady, K., Dohen, L. and Ziemkiewicz, P. (1997) Neutralization potential of overburden samples containing siderite, Journal of Environmental Quality, vol. 26, 3, pp. 673-681.

Skousen J, Sexstone, A and Ziemkiewicz, PF. (2000) Acid mine drainage treatment and control, in: Barnhisle, R, Daniels, W and Darmody, R (eds), Reclamation of Drastically Disturbed Lands, American Society of Agronomy, Madison, WI, pp.131—168.

Skousen, J., Simmons, J., McDonald, L.M. and Ziemkiewicz, P. (2002) Acid – Base Accounting to Predict Post-Mining Drainage Quality on Surface Mines, Journal of Environmental Quality, vol. 31, pp. 2034-2044.

Smart, R., Skinner, B., Levay, G., Gerson, A., Thomas, J., Sobleraj, H., Schumann, R., Welsner, C. and Weber, P. (2002) Prediction of Kinetic control of Acid Mine Drainage, AMIRA International, ARD Test Handbook Project, P387A.

Sobek, A., W. Schuller, J.R. Freeman, and R.M. Smith (1978) Field and Laboratory Methods Applicable to Overburdens and Minesoils, Cincinnati, OH, U.S. EPA, EPA-600/2-78-054: 203.

Sobek, A.A., J.G. Skousen, and S.E. Fisher, Jr. (2000) Chemical and physical properties of overburdens and minesoils, in: Reclamation of drastically disturbed lands, Agronomy Monogr, 41, ASA, Madison, WI, pp. 77–104.

Tokalioglu, S., Kartal, S. and Birol, G. (2003) Application Of A Three-Stage Sequential Extraction Procedure For The Determination Of Extractable Metal Contents In Highway Soils, Turk J Chem, 27, pp. 333–346.

U.S. EPA (1994) Acid Mine Drainage Prediction, Technical report, EPA 530-R-94-036.

Usher, B.H., Cruywagen, L.M., de Necker, E. and Hodgson, F.D.I. (2003) On-site and Laboratory Investigations of Spoil in Opencast Collieries and the Development of Acid-Base Accounting Procedures, Water Research Commission, WRC Report No. 1055/2/03, ISBN 1-77005-053-1, Vol.2.

Assessment of As and Hg in Mine Tailings and Indigenous Grass: A Case Study of Non-Functional New Union Gold Mine, South Africa

Tsedzuluso Mundalamo, Jabulani Gumbo, Confidence Muzerengi and Francis Dacosta
School of Environmental Sciences, University of Venda, South Africa

ABSTRACT

The present study was carried out to assess the uptake of toxic metals, arsenic (As) and mercury (Hg), by *Cynodon dactylon* grass species at New Union gold mine tailings, Limpopo Province, South Africa. The samples were collected from New Union Gold Mine tailings and from Ka-Madonsi Village (control), and concentrations of As and Hg in soil and plant material were determined by ICP-MS. The average dry weight concentrations of As and Hg in mine tailing dam A were 2.53 and 1.18 μg/g, respectively, and 2.24 and 0.91 μg/g, respectively, in mine tailings B. The average dry weight of As and Hg in the control soil samples were 0.30 and 0.05 μg/g, respectively. The *C. dactylon,* on average dry weight, absorbed 5.45 μg/g of As, and 1.72 μg/g of Hg from mine tailings A, and 4.29 μg/g of As; and 1.55 μg/g of Hg from mine tailings B. The control grass, on average dry weight, absorbed 0.53 μg/g and 0.01 μg/g of As and Hg, respectively. In most cases, significant differences were observed between bioaccumulation of Hg and As in plant tissue from mine sites and control sites. The study showed that the bioconcentration factor was less than 1 for the acidic mine tailings, with exception of the root and rhizome system which was greater than 1. This contrasted sharply with the control site where the pH was alkaline, and As and Hg levels were low. The pH values were significantly different ($p < 0.05$) between the soils originating from mine tailings and the control site. The electrical conductivity (EC) of soil at mine tailings A and B were 1847.35 and 1777.5 μS/cm, respectively. The EC for the control site was significantly different ($p < 0.05$) at 543.3 μS/cm. *C. dactylon* was found to be capable of bioaccumulation of As and Hg, effective at soil stabilization, and grew well under the acidic conditions. The control grass was healthy and thrived under the alkaline conditions.

Keywords: toxic heavy metals; *Cynodon dactylon*; re-vegetation; mine tailings

INTRODUCTION

Mining operations contribute wealth to an economy in a variety of ways, but mine wastes can negatively impact the environment. Abandoned mine tailings sites are a source of environmental problems throughout the world and the number of these sites is on the increase (Lodenius and Malm, 1998; Bell *et al*., 2001; Ogola *et al*., 2002; Naicker *et al*., 2003; Mendez *et al*., 2007; Schuwirth *et al*., 2007; Mulugisi *et al*., 2009). This study focuses on the abandoned mine tailings at New Union Gold Mine, Malamulele, Limpopo province, South Africa, an arid region with limited rainfall. During the processing of the gold ore at New Union Gold mine, the gold was recovered after addition of amalgam (mercury) (Janisch, 1986). The mine operated from 1935 to 1998 in Giyani greenstone belt under various mining companies such as New Union Mining, Northfields Gold Pty Ltd, New Union Gold, Noorde, Offspring and Barberton until the exhaustion of the underground gold ore (Potgieter and De Villiers, 1986; Du Plessis, 2011). According to Potgieter and De Villiers (1986) the gold ore was associated with sulfur-rich arsenopyrite in garnetiferous, biotite-rich bands. Thus, the mine processing wastes were probably rich in arsenic (As) and mercury (Hg), and were discarded to the mine tailings dams. These mine tailings dams are thinly covered by vegetation on slopes and on the surface such that water and wind erosion are likely to occur (Figure 1).

Figure 1 Thinly covered vegetation at New Union Gold Mine tailings showing water erosion

The study of Rösner and Schalkwyk (2000) in the mine tailings of Witwatersrand goldfields, South Africa showed that water erosion contributed to loading of heavy metals in nearby and deteriorated water quality in nearby rivers. The studies of Mulugisi *et al.* (2009) and Magonono *et al.* (2010) at New Union Gold Mine demonstrated the presence of heavy metals such as manganese, zinc, copper, lead, As, cadmium, and cobalt in the mine tailings. The study of Winde *et al.* (2004) showed that the contamination of the streams adjacent to the Witwatersrand goldfields mine tailings posed

a health risk for the people in the nearby informal settlements who drink the river water without appropriate treatment.

It is known that some plant and, more specifically grass, species are able to remove heavy metals from contaminated soil and water (Comino *et al*., 2008). Plant species that accumulate large amounts of heavy metals from soils are referred as hyper-accumulator species (Madejón *et al*., 2002; Li *et al*., 2007). The use of plants to remove heavy metals from contaminated soils is an environmentally friendly and cost-effective method, termed phytoremediation (Cunningham *et al*., 1995; McLaughlin *et al*., 2000; Mulugisi *et al*., 2009). At New Union Gold Mine tailings an indigenous grass, *Cynodon dactylon*, has been growing in different patches on the mine tailings. According to Soleimani *et al.* (2009), *C. dactylon* can hyper-accumulate nickel and lead and was one of the candidate methods for cleaning up heavy metal contamination of soil and sediments in Shadegan wetland, Iran. *C. dactylon* has an extensive roots system which is suitable for soil stabilization (Smith *et al*., 1998; Rizzi *et al*., 2004), and the studies of Smith *et al.* (1998) and Madejón *et al*. (2002) also showed that *C. dactylon* has a widespread creeping ability, which is useful for the stabilization of mine tailings. A similar, but separate study of Nelushi *et al.* (2013) of *C. dactylon* under field conditions at New Union Gold Mine showed that the grass was able to bioaccumulate significant amounts of chromium and uranium. The study on the bioaccumulation potential of As and Hg uptake by *C. dactylon* under field conditions are rather limited. The main aim of this study was to assess the uptake of As and Hg in different parts of *C. dactylon* plants (roots, rhizomes, stems, and leaves) from the New Union Gold Mine tailings under field conditions. A second objective was to determine pH and electric conductivity (EC) of the mine tailings, and how these contribute to availability of the toxic metals, As and Hg.

METHODOLOGY

Sample collection and preparation

The samples were collected from tailings dams at the New Union Gold Mine and control samples from Ka-Madonsi village, South Africa, on June 2010. The study area is well described in Mulugisi *et al*. (2009). The samples, C. *dactylon* and soils were obtained from the same spot from the mine tailings and the control site. The samples were collected at the following geographical coordinates: 23º01'05"S and 30º43'50"E; 23º00'59"S and 30º43'53"E; 23º01'06"S and 30º43'47"E; and 23º01'04"S and 30º43'45E"; for sample tailings A1, A2, B1 and B2, respectively. The samples were then sealed in sample bags and transported in coolers to the laboratory at the University of Venda for further analysis.

The grass samples were washed with distilled water, oven dried at 55 °C (Vacutec oven, Labcon, South Africa) to constant weight for a week and subsequently cut into plant sections (roots, rhizome, stems, or leaves). After drying soil samples for a week, the individual samples were ground with a Retsch RS 200 grinding mill (Retch, United Kingdom) to 80% fine or < 75µm, and were then weighed to 5.00g, using an AS 220/C/2 analytical balance (Radwag, United Kingdom). All grass and soil samples were acid-digested following the procedure of the APHA (2006), and were sent, in duplicate, to the ARC Institute of Soil, Water & Climate, Pretoria, South Africa for metal analysis.

Determination of pH and EC

The soil samples were weighed to 50 g, (BP 1200 balance) and mixed thoroughly with 50 ml of distilled water (Sampanpanish *et al.,* 2006) prior to conducting pH and EC measurements, for which a Crison Basic Model meter was used. The pH and EC measurements were determined in duplicate.

Determination of metals, arsenic and total mercury

The acid digested samples were analyzed, in duplicate, for As and Hg using cold vapour/hydride generation ICP-MS (Chen *et al*., 2008), using a Thermofischer ICP MS Model X Series II.

Data analysis

The concentrations of As and Hg were reported on a dry weight basis (d.w.). Statistical analyses were carried out using single factor ANOVA, with a significance level of $p < 0.05$. The bioconcentration factor (BCF) was calculated as per procedure of Al-Qahtani (2012). The BCF ratio, which was calculated as metal concentration in plant divided by metal concentration in soil, represents the ability of the plant to bioaccumulate the metal in question.

RESULTS AND DISCUSSION

The pH and EC of soil samples mine tailings and control sites

The research findings, presented in Table 1, indicate that the mine tailing dams were highly acidic and the control site was neutral.

Table 1 Average pH and EC of soil samples from at New Union Gold Mine tailings and the control site

Sample ID	pH	EC (µS/cm)
Mine tailing (A1)	3.55±0.04	1712.70±37.4
Mine tailing (A2)	3.49±0.01	1982.00±9.3
Mine tailing (B1)	3.62±0.01	1568.00±8.2
Mine tailing (B2)	3.66±0.05	1983.00±14.8
Control site	7.59±0.17	548.33±0.7

The pH results for replicate mine tailings samples were not significantly different ($p>0.05$) from each other, but were significantly different ($p<0.05$) from the control site. The acidity of the mine tailings was probably due to oxidation of pyrite and other sulfide minerals of geological origin (Potgieter and De Villiers, 1986; Mulugisi *et al.,* 2009; Magonono *et al.,* 2010). According to Al-Qahtani (2012) and Nelushi *et al.* (2013), soil pH, EC, organic content, and metal speciation may influence the plant-bioavailability of metals. The EC values of soil samples from mine tailings were higher than those from the control site (Table 1). The EC values of the mine tailings A and B were not significantly different ($p>0.05$, and their relatively high EC values probably result from oxidation of pyrite and sulfide minerals exposed to oxygen and water (James, 1997). Electrical conductivity of the soil is an indirect measure of the Total Dissolved Solid (TDS) present in the soil,

which has negative impacts on plant growth due to increased osmotic pressure of the soil solution, thereby inhibiting water and nutrient uptake by plants (James, 1997). Thus the acidic conditions are conducive to metal availability in the mine tailings soil coupled with easier metal uptake by the plants. Additionally, once the metals are in solution, they contribute to EC, as supported in this study. In contrast, the neutral conditions at the control site do not promote dissolution of metals, thus contributing to low electrical conductivity.

Concentrations of toxic metals in mine tailings and control sites

The research findings showed that As and Hg were significantly elevated in the New Union Gold Mine tailings in comparison with the control site (Figure 3). The range in concentrations of As and Hg in the mine tailings were 1.48 to 3.58 ug/g and 0.59 to 1.27 ug/g d.w., respectively. The levels of As and Hg in the mine tailings were higher than the control site, which may be attributed to the gold ore-amalgam processing and presence of sulfur-rich arsenopyrite in garnetiferous, biotite-rich bands.

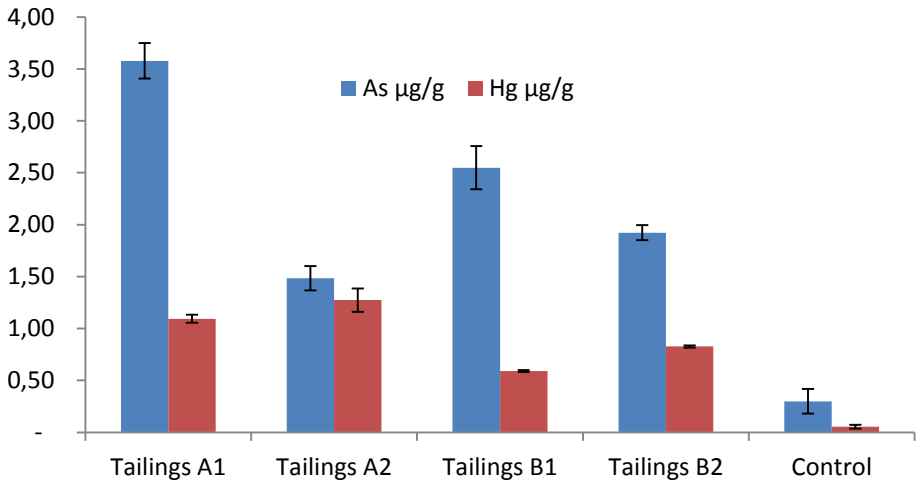

Figure 3 Average dry weight concentrations, based on duplicate analyses, of As and Hg in mine tailings at New Union Gold Mine and at the control site, whiskers reflect standard error

For both As and Hg, the mine tailings A and B were not significantly different ($p > 0.05$) from each other, but were significantly different from the control for Hg, ($p < 0.05$), with an insignificant difference for As ($p > 0.05$). This supports that the source of Hg likely originates from the New Union Gold Mine, where Hg was used to extract gold during operations (Janisch, 1896). Additionally, as previously described, the presence of As in the mine tailings is probably geological, coming from sulfur-rich arsenopyrite (Potgieter and De Villiers, 1986).

These findings are in agreement with numerous studies from a variety of mine sites, such as Amono-Neizer *et al*. (1996) which reported 12.92 µg/g and 0.93 µg/g of As and Hg, respectively, in soils around the gold mining town of Obuasi in Ghana. Furthermore, the As concentrations are similar to the study of Madojen *et al*. (2002) at the Aznallcollar mine spill (SW Spain), who found levels of of 9.59 µg/g in soils, and the study of Visoottiviseth *et al.* (2002), which reported As concentrations in soil of 14 µg/g. The research findings are also in agreement with the study of

Fernandez-Martizer (2009) which recorded Hg concentrations ranging from 0.59 µg/g to 1.59 µg/g in soils.

Toxic metal concentration in different parts of *Cynodon dactylon*

The concentrations of As and Hg were also determined in the different plant parts (roots, rhizome, stem and leaves) of *C. dactylon* harvested from the study sites (Figure 4). The *C. dactylon* growing on the mine tailings accumulated more As and Hg in the leaves and stems than the *C. dactylon* growing on the control site (Figures 4a and b), with a significant difference of $p < 0.05$. There were significant differences in the accumulation of As and Hg in plant parts from the various mine tailings sites. *C. dactylon* collected from the mine tailing sites was shown to accumulate higher levels of As and Hg in leaves than in stems. The metals under study, As and Hg, have no known biological function in plants (Comino *et al.*, 2009) and are reportedly toxic to plants including the *C. dactylon*; being detrimental to plant health and wellbeing. According to Comino *et al*. (2009), the As-uptake by plants was inhibited by the presence of antimony and phosphate, but was promoted by the presence of molybdate.

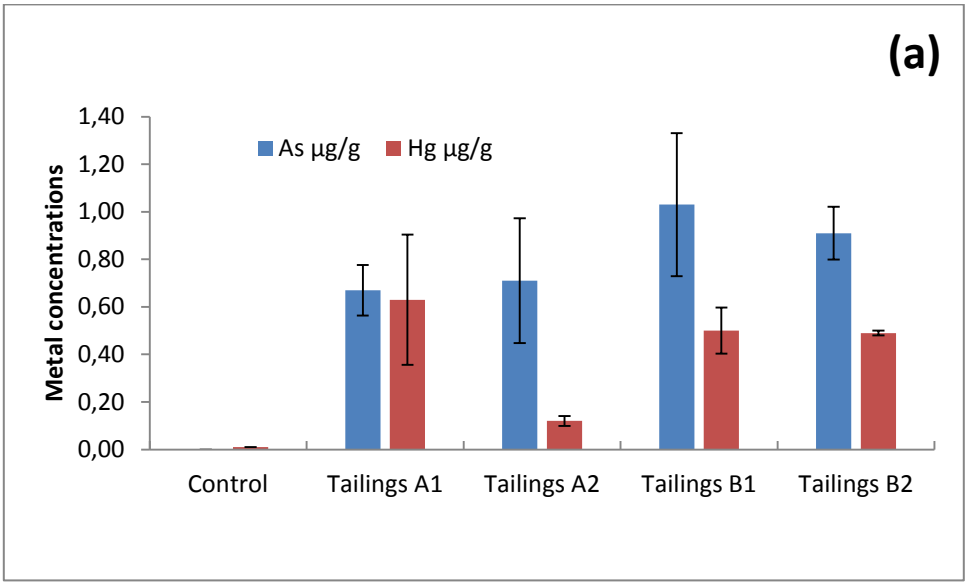

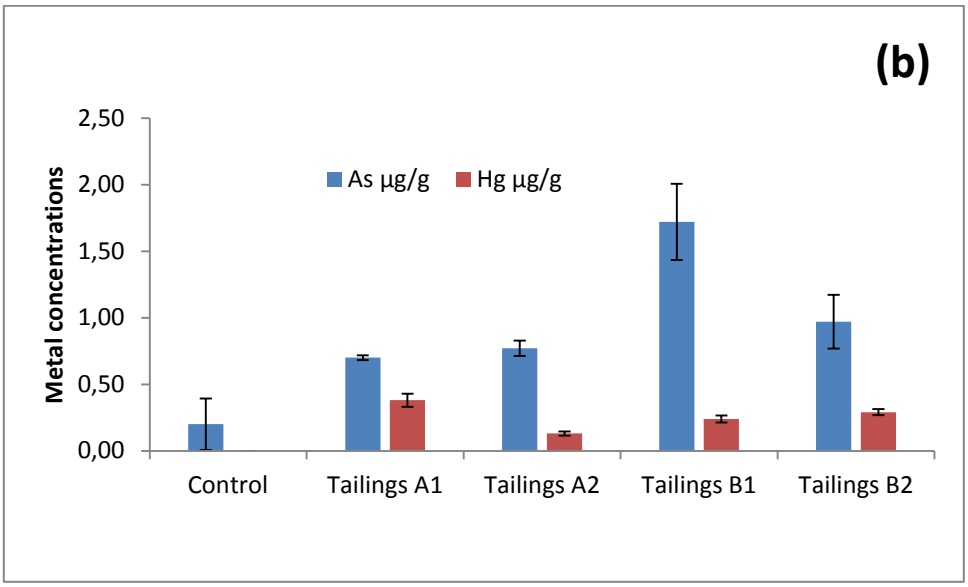
(b)
Metal concentrations
2,50
2,00
1,50
1,00
0,50
0,00
As µg/g
Hg µg/g
Control
Tailings A1
Tailings A2
Tailings B1
Tailings B2

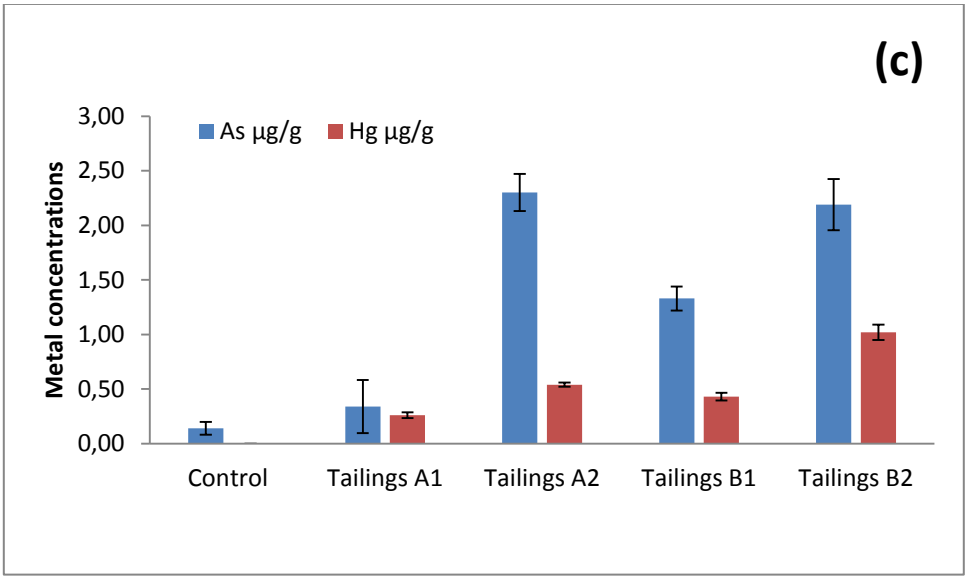
(c)
Metal concentrations
3,00
2,50
2,00
1,50
1,00
0,50
0,00
As µg/g
Hg µg/g
Control
Tailings A1
Tailings A2
Tailings B1
Tailings B2

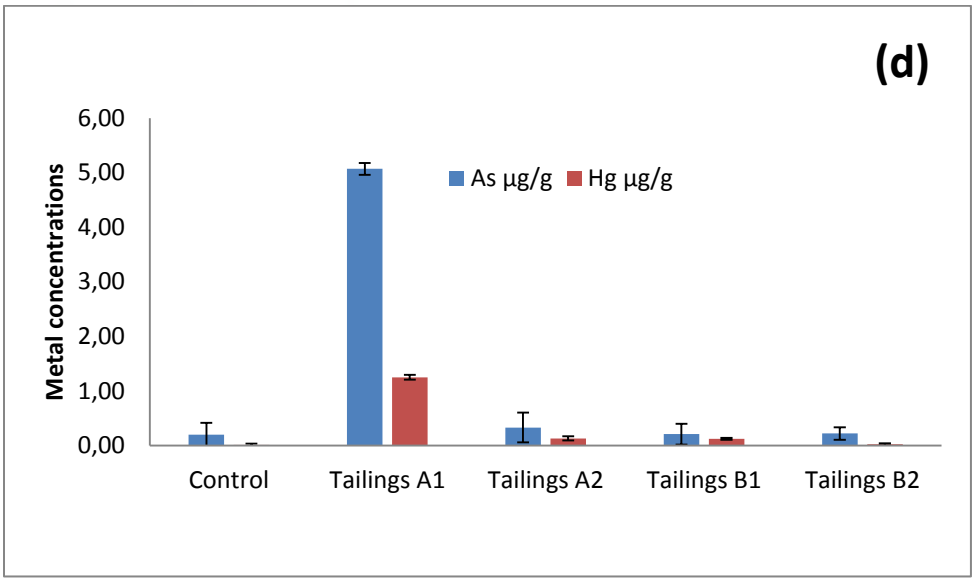

Figure 4 Average dry weight concentrations, based on duplicate analyses, of As and Hg in (a) leaves, (b) stems, (c) roots and (d) rhizomes of *C. dactylon* mine tailings at New Union Gold Mine and at the control site, whiskers reflect standard error

Similar to observations from the leaves and stems, *C. dactylon* growing on the mine tailings accumulated more As and Hg in the roots and rhizome than the *C. dactylon* that was growing on the control site (Figures 4c and d), with significant differences from the control ($p < 0.05$). This was expected since the roots grow deeper into mine tailings than the rhizome. Significant differences ($p<0.05$) in the accumulation of As and Hg were observed among the mine tailings sites. The *C. dactylon* was shown to bioaccumulate more As than Hg in roots than rhizome. This was expected since soil samples from mine tailings had higher concentrations of As than Hg (Figure 3), and thus the *C. dactylon* had access to more As than Hg. It is also possible that As and Hg compete with each other for uptake, as was shown by the study of Comino *et al*. (2009) in tomato plants. In the same study Comino *et al*. (2009) also showed that the uptake of Hg by tomato plant was inhibited by selenate, which has chemical similarities to certain forms of As. It may, therefore, be possible that As was inhibiting Hg uptake with a similar mechanism, thereby leading to higher As uptake by *C. dactylon*.

Generally, the most toxic metals such as As and Hg are highly bioavailable to grass under acidic conditions, conditions in which metals are more soluble (Okunola *et al.*, 2007). The research findings are in agreement with Smith *et al*. (1998), who reported that *C. dactylon* may tolerate pollution of trace elements (e.g. up to 30,000 µg/g of As in soil). The research findings are also in agreement with the study of Madejón *et al.* (2002), who reported that *C. dactylon* had a high bioconcentration of As (up to 75 µg/g) in a contaminated site in Spain.

Bioconcentration factors of *Cynodon dactylon*

The availability of metals for uptake by plants is determined by factors such as soil pH, EC, natural organic matter in soil; and metal speciation (Al-Qahtani, 2012). The bioconcentration factor (BCF) was calculated as metal concentration in plant divided by the metal concentration in soil, which

thus represented the ability of the plant to bioaccumulate the metal in question. Using this calculation, a BCF < 1 indicates lower bioavailability of a metal, while a BCF >1 indicates a higher bioavailable metal. The research findings showed that the BCF ratios were variable between the *C. dactylon* growing on mine tailings and that growing at the control site (Table 2). This BCF variability may be attributed to metal mobility and bioavailability as a result of acidic versus alkaline conditions. The study of Comino *et al*. (2009) showed that the uptake of As and Hg at the same time and space may interfere with each other, a finding that may support our results. Al-Qahtani (2012) stated that neutral to alkaline conditions restrained metal mobility and therefore the metal bioavailability in plant uptake and translocation into plant tissues. This is consistent with our study, where the alkaline conditions inhibited metal mobility and probably contributed to low BCF ratios for the control site. Our study showed that in the acidic mine tailings, the BCF was less than 1 with exception of the root and rhizome system which was greater than 1 for mine tailings such as A2 and B2 (Table 2). The location of accumulation of As in plant tissue was variable, but generally absorbed more in roots and the rhizome. Conversely, although the location of accumulation of Hg was also variable, it was generally absorbed more in leaves and the roots.

Table 2 Bioconcentration factors (BCF) of *C. dactylon* for As and Hg

	Tailings A1		**Tailings A2**		**Tailings B1**		**Tailings B2**		**Control**	
pH	3.55		3.49		3.62		3.66		7.59	
	As	**Hg**	**As**	**Hg**	**As**	**Hg**	**As**	**Hg**	**As**	**Hg**
Leaves	0.2	0.6	0.5	0.1	0.4	0.8	0.5	0.3	0.0	0.0
Stem	0.2	0.3	0.5	0.1	0.7	0.4	0.5	0.2	0.6	0.0
Rhizome	1.4	1.1	0.2	0.1	0.1	0.2	0.1	0.0	0.7	0.2
Roots	0.1	0.2	1.6	0.4	0.5	0.7	1.1	0.6	0.5	0.0

CONCLUSION

The ability of *C. dactylon* to uptake metals under acidic conditions and stabilize slopes as a result of creeping ability, makes it a suitable vegetation cover for the exposed mine tailings from a remedial perspective. However, this study showed that soil and *C. dactylon* samples at New Union Gold Mine tailings contain high levels of As and Hg in comparison to the control site. The acidic mine tailings likely solubilize the metals As and Hg, thus making these elements available for uptake by the C. *dactylon*. In contrast with control sample, the alkaline conditions were not conducive to metal solubility thus limiting uptake by *C. dactylon*. At the mine tailings sites in this study, the presence of As and Hg in the leaves and stem of this grass is worrisome, because grasses are frequently grazed upon by livestock and wild animals, which may lead to biomagnification in the food chain. The presence of animals at the mine tailings was shown by animal droppings. At the New Union Gold mine, there is presently no one to look after the property and the mine tailings are not fenced; the animals can thus freely graze on *C. dactylon* that was growing on the mine tailings.

ACKNOWLEDGEMENTS

The Chief of Madonsi village, community and Triangle cc for granting us access to the New Union Gold Mine. The University of Venda and International Council for Science (ICSU) and National Research Foundation (NRF) gave financial support for the study project (I431) and travel costs to attend and present at the 10th ICARD IMWA 2015 conference in Chile.

REFERENCES

APHA, (2006) *Standard Methods for the Examination of Water and Wastewater*, Washington, DC, USA.

Al-Qahtani KM (2012) Assessment of Heavy Metals Accumulation in Native Plant Species from Soils Contaminated in Riyadh City, Saudi Arabia. *Life Science Journal*, 9:384-392.

Amonoo-Neizer, E H, Nyamah, D, Bakiamoh, S B (1996) Mercury and arsenic pollution in soil and biological samples around the mining town of Obuasi, Ghana. *Water, Air, and Soil Pollution*, *91*(3-4), 363-373.

Bell, LC, Jones, CJ (1987) Rehabilitation of the base tailings case studies in mining rehabilitation 87 (Ed T.P Farrell),

Chen, CY, Pickhardt, PC, Xu, MQ, Folt, CL (2008) Mercury and Arsenic Bioaccumulation and Eutrophication in Baiyangdian Lake, China. Water Air Soil Pollut 190:115–127

Comino, E., Fiorucci, A., Menegatti, S., & Marocco, C (2009) Preliminary test of arsenic and mercury uptake by *Poa annua*. *Ecological Engineering*, *35*(3), 343-350.

Cunningham, SC, Berti, RW, Huang, JW (1995) *Bioremediation of Inorganics*. Battelle Press, Columbus, OH, 33-54.

Du Plessis, GA (2011) National Instrument 43-101 Technical Report for the Madonsi Project, Limpopo Province, South Africa. http://www.sahra.org.za/sites/default/files/additionaldocs/case%20id%202262-OCR_Part2.pdf (date accessed 15/02/2015)

James, AR (1997) The prediction of pollution loads from coarse sulphide-containing waste materials. Water Research

Janisch, PR (1986) Gold in South Africa. Commission Report No.559/1/97, Pretoria *J.S. Afr. Inst. Min. Metall*. 86(8):273-316

Li, MS, Luo, YP, Su, ZY (2007) Heavy metal concentrations in soils and plant accumulation in a restored manganese mineland in Guangxi, South China. Environmental pollution.147:168-175.

McLaughlin, MJ, Hamon, RE, McLaren, RG, Speir, TW, Rogers, SL (2000) Review: A bioavailability-based rationale for controlling metal and metalloid contamination of agricultural land in Australia and New Zealand. *Soil Research*, *38*(6), 1037-1086.

Madejón, P, Murillo, JM, Marañón, TF, Cabrera, López, R (2002) Bioaccumulation of As, Cd, Cu, Fe and Pb in wild grasses affected by the Aznalcóllar mine spill (SW Spain). The Science of Total Environment.290:105-120

Magonono, FA, Gumbo, JR, Chigayo, K, Dacosta, FA, Mojapelo, P (2011) Bioaccumulation of Toxic Metals by *Hyparrhenia* Grass Species: A Case Study of New Union Gold Mine Tailings and Makhado Town, Limpopo, South Africa. International Mine Water Conference

Mendez MO, Glenn EP, Maicer RM (2007) Phytostabilization Potential of Quaibush for mine tailings, Growth, Metal Accumulation and Microbial Community Changes, J Environ Qual,36: 245-253.

Mulugisi, G, Gumbo, JR, Dacosta, FA, Muzerengi, C (2009) The use of indigenous grass species as part of rehabilitation of mine tailings: A case study of New Union Gold Mine. Proceedings of the International Mine Water Conference. Pretoria, South Africa.

Naicker, K, Cukrowska, E, McCarthy, TS (2003) Acid mine drainage arising from gold mining activity in Johannesburg, South Africa and environs. Environmental Pollution. 122: 29-40.

Nelushi, K, Gumbo, JR, Dacosta, FA (2013) An investigation of the bioaccumulation of chromium and uranium metals by *Cynodon dactylon*: A case study of abandoned New Union Gold Mine Tailings, Limpopo, South Africa. African Journal of Biotechnology. 12:6517-6525.

Ogola, JS, Mutuilah, WV, Omulo, MA (2002) Impact of gold mining on the environment and human health: a case study in the Migori Gold Belt, Kenya, Environmental geochemistry and health, 24: 141- 158.

Okunola, OJ, Uzairua, Ndukwe, G (2007) Levels of trace metals in soil and vegetation along major and minor roads in metropolitan city of Kadun, Nigeria, African Journal of Biotechnology.6: 1703-1709.

Potgieter, GA, De Villiers, JPR (1986) Controls of mineralization at Sutherland Greenstone Belt. South African Journal of Geology. 1: 197- 203.

Rizzi, L, Petruzzelli, G, Poggio, G, Vigna, Guidi, G (2004) Soil Physical Changes and Plant Availability of Zn and Pb in a Treatability Test of Phytostabilization. Chemosphere. 57: 1039-1046.

Rösner, T, Schalkwyk, A (2000) The environmental impact of gold mine tailings footprints in the Johannesburg region, South Africa. Earth and Environmental Science.137 -148.

Sampanpanish P, Pongsapich W, Khaodhiar S, Khan E (2006) Chromium removal from soil by phytoremediation with weed plant species in Thailand. *Water Air Soil Poll. Focus*. 6: 191-206.

Schuwirth N, Voegelin A, Kretzschmar R, Hofmann T, (2007) Vertical distribution and speciation of trace metals in weathering flotation residues of a Zinc/Lead sulphide mine. J. Environ. Qual. 36:61-69. doi:10.2134/jeq2006.01148.

Smith, E, Naidu, R, Alston, AM (1998) Arsenic in the Soil Environment: a review. Adv. Agron. 64: 149-195.

Smith, LA, Means, JL, Chen, A, Alleman, B, Chapman, CC, Tixier, JS, Jr, Brauning, SE, Gavaskar, AR, Royer, MD (1995) *Remedial Options for Metals-Contaminated Sites*, Lewis Publishers, Boca Raton, FL.

Soleimani, M, Hajabbasi, MA, Afyuni, M, Charkhabi, AH, Shariatmadari, H (2009) Bioaccumulation of Nickel and Lead by Bermuda Grass (*Cynodon dactylon*) and Tall Fescue (*Festuca arundinacea*) from Two Contaminated Soils . Caspian Journal of Environmental sciences. 7(2):59-70.

Visoottiviseth, P, Francesconi, K, Sridokchan W (2002) The potential of Thai indigenous plant species for the phytoremediation of arsenic contaminated land. Environmental pollution. 118: 453-461.

Winde, F, Wade, P, Van der Walt, IJ (2004) Gold tailings as a source of water-borne uranium contamination of streams-the Koekemoerspruit (South Africa) as a case study-part III of III: fluctuations of stream chemistry and their impacts on uranium mobility. *Water SA*, *30*(2), 233-239.

Acid Rock Drainage in Antarctica: An Important Source for Trace Elements in the Southern Ocean

Bernhard Dold[1], Elena Gonzalez-Toril[2], Angeles Aguilera[2], Maria Eugenia Cisternas[1], Enrique Lopez-Pamo[3] and Ricardo Amils[2]

1. *Instituto de Geología Económica Aplicada (GEA), Universidad de Concepción, Chile*
2. *Centro de Astrobiologia (INTA-CSIC), Spain*
3. *Instituto Geológico y Minero de España (IGME), Spain*

ABSTRACT

Here we describe biogeochemical processes that lead to the generation of acid rock drainage (ARD) on the Antarctic landmass and show that ARD is an important source of trace elements for the Antarctic Ocean. During three expeditions, 2009 – 2011, we examined three sites on the South Shetland Islands in Antarctica. Two of them displayed intensive sulfide mineralization (up to 10 wt.% of pyrite) and generated acidic (pH 3.2 – 4.5), iron and trace element-rich drainage waters. The formation of ARD in the Antarctic was catalyzed by microorganisms found in acid mine drainage in cold climates, including *Acidithiobacillus ferrivorans* and "*Thiobacillus plumbophilus*".

At Cardozo Cove, lowest pH (3.2) with highest element concentrations were detected and infiltrated mainly as groundwater into the sea, and as superficial runoff (as Fe^{3+}), latter with the formation of schwertmannite in the sea ice (with up to 100 mg/L Fe (as Fe^{2+}), 95.2 mg/L Al, 19.7 mg/L Mn, 3.4 mg/L Zn, 1.46 mg/L Cu, 1.06 mg/L Ni and Rare Earth Elements (REE) up to 16.2 µg/L). At Marian Cove, the pH values were slightly higher and the element loads were generally lower than at Cardozo Cove (in the range of 10 – 25 %). In contrast, the liberation of trace elements from the non-mineralized control site (Punta Hannah) was in the range of 3 to 4 orders of magnitude less than from the two mineralized sites. Thus, our results show that ARD has to be seen important sources of trace elements to the sea. The increased iron and trace element input correlates with increased phytoplankton production close to the source. This might even be enhanced in the future by a global warming scenario, and could be a process counterbalancing global warming if the biomass is buried effectively in the sediments.

**There is no full article associated with this abstract.*

10th ICARD IMWA 2015 | 10th International Conference on Acid Rock Drainage & IMWA Annual Conference

In Situ Attenuation of Selenium in Coal Mine Flooded Pits

Alan Martin, Robert Goldblatt and Justin Stockwell
Lorax Environmental Services Ltd., Canada

ABSTRACT

Suboxia is a prerequisite for the bioremediation of selenium (Se), whereby Se is removed from solution as reduced species (*e.g.*, elemental Se). In this regard, flooded open pits offer suitable repositories for the bioremediation of Se given the tendency of these systems to develop suboxic conditions through either passive or active means. Specifically, the geometry of flooded pits and their water column density characteristics often make them conducive to permanent stratification (meromixis) and the development of bottom water suboxia. In order to assess the potential for Se bioremediation in a coal mine flooded pit in northern Canada, a combination of high resolution physical profiling (temperature, dissolved oxygen and conductivity) and water quality sampling was conducted. Vertical profiling revealed a stratified water column with respect to both temperature and salinity, with the pycnocline occurring at a depth of 5 m. Dissolved oxygen was absent below a depth of 20 m, suggesting that the water column stratification is permanent. Profiles of other redox-sensitive species (dissolved manganese and nitrate) further support the presence of bottom water anoxia below 20 m. The data for nitrate, for example, show evidence of denitrification immediately below the oxic-suboxic boundary. Dissolved Se shows evidence of attenuation in response to the vertical redox gradient in the water column, with surface values (12 to 20 µg/L) decreasing to <3 µg/L in the suboxic zone. Overall, the data reveal evidence of both denitrification and Se reduction, with Se being removed from solution presumably as either selenite (Se^{+4}) (via adsorption to settling particles) or as precipitation of elemental Se (Se^{0}) or selenide (Se^{2-}). The implications of the data with respect to mine water management and Se bioremediation are discussed.

Keywords: coal, mining, bioremediation, passive treatment

INTRODUCTION

For coal mine districts throughout North America, selenium (Se) is a water quality parameter of concern with respect to environmental compliance and the protection of aquatic resources. The common occurrence of elevated Se concentrations in coal source rocks (*e.g.*, wasterock, pit walls, tailings, coal reject, *etc.*), and leaching through natural weathering, can increase levels of Se in mining-influenced drainages to well over background levels. Due to potential environmental consequences aquatic taxa exposure to Se in mine-affected settings, considerable effort has been placed on the development and evaluation of active and passive treatment systems for Se removal (CH2MHILL, 2010, 2013). In particular, the potential for the passive removal of Se through various forms of bioremediation has received considerable attention due to the favourable cost implications and the ineffectiveness of traditional chemical precipitation methods for reducing Se to environmentally-acceptable limits (Frankenberger *et al.*, 2004).

Engineered passive and active treatment systems designed to remove Se from solution generally rely upon the development of suboxia. Under suboxic conditions, the potential for Se attenuation is enhanced by a suite of microbially-mediated processes that favour the reduction of selenate (Se^{+6}) and removal of dissolved Se from solution via adsorption and precipitation reactions. Such suboxic mechanisms include: 1) reduction of selenate (Se^{6+}) to selenite (Se^{4+}) followed by adsorption of selenite to particles; 2) precipitation of elemental Se (Se^{0}); 3) precipitation of Se as inorganic/organic selenides (Se^{2-}); and 4) co-precipitation of Se with reduced sulfur (Masscheleyn and Patrick, 1993). Suboxia is also required to reduce nitrate (through denitrification), the presence of which can inhibit Se reduction and hence its potential for attenuation (Oremland *et al.*, 1991).

Mine settings offer significant opportunities for the bioremediation of Se through the natural and/or engineered development of suboxia within mine facilities. Specifically, large-scale zones of suboxia may occur in pit lakes (Castro and Moore, 2000), within the pore spaces of saturated wasterock (Bianchin *et al.*, 2013), and in some cases, within unsaturated zones of large wasterock dumps (Kuo and Ritchie, 1999). Further, such suboxic zones have the potential to be incorporated into water management strategies designed to reduce Se loadings from mine operations.

In this paper, the potential utility of flooded open pits as bioremediation cells for Se is discussed through examination of water quality data from a mine in northern Canada. Mine pit lakes often differ from natural lakes in that they are typically deeper, more saline, and less susceptible to wind mixing (due to small fetch and topographic sheltering from pit walls). These features can lead to the development of permanent stratification (meromixis), resulting in the development of suboxic bottom waters. Specific objectives this study are as follows: 1) describe the physical and chemical limnological setting of the flooded pit; 2) delineate the biogeochemical processes governing the behaviour of Se and other mine-related parameters; and 3) discuss potential applications of flooded pits for Se bioremediation through passive and engineered methods.

ENVIRONMENTAL SETTING AND METHODOLOGY

The study site is situated at a closed coal mine in northern Canada at an elevation of ~1,500 m. The open pit was developed between ~1987 and ~1995 and partially backfilled with spoils from ~1995 to ~1998. Passive flooding of the pit began in 1998, reaching a static water level in 2002. The maximum water depth in the pit is 72 m, encompassing a total water volume of 2.35 million m^3. Due to the generally low total sulfur content (generally <1%) and high abundance of carbonate minerals in

host rocks, waste materials in the region are not acid generating. Environmental concerns relating to Se are typically associated with neutral to basic-pH leaching from subaerial (unsaturated) wasterock.

On July 31, 2013, the flooded pit was sampled through a combination of *in situ* profiling and water sample collection. *In situ* vertical profiling (20 cm vertical resolution) of conductivity, temperature, pH, dissolved oxygen (DO) and fluorescence was conducted over the deepest portion of the pit using a Sea-Bird Electronics™ conductivity-temperature-depth (CTD) profiler (SBE 19plus SEACAT Profiler, Bellevue, Washington). The CTD was configured with a WETLABS ECO Fluorometer™ to measure vertical variations in chlorophyll concentration in the water column (proxy for photosynthetic algal biomass). Water quality samples were collected at depths of 1, 2, 4, 6, 8, 10, 12, 15, 20, 30, 40, 50 and 60 m, and analyzed for physical parameters, anions, nutrients and total/dissolved trace elements. Trace element concentrations were determined via inductively-coupled plasma mass spectrometry (ICP-MS), while anions were analyzed via ion chromatography (Dionex).

RESULTS AND DISCUSSION

Water column physical structure

High resolution profiles of temperature and conductivity show the presence of a stratified water column in the flooded pit, with a pronounced thermocline observed between 3 and 6 m (Figure 1). The thermocline overlaps with a sharp gradient in salinity as revealed by the profile of specific conductivity. The combined effect of the temperature and salinity gradients result in a pronounced density gradient (pycnocline) that is spatially consistent with the temperature and conductivity gradients observed in the uppermost 6 m of the water column (Figure 1).

Salinity gradients in the flooded pit are dominantly governed by vertical variations in the concentrations of sulfate, calcium and alkalinity, all of which represent products of mine waste weathering (wasterock and pit walls) (Figure 2). Sulfate is liberated through the oxidation of reduced sulfur minerals (*e.g.* pyrite) while calcium and alkalinity represent the products of carbonate mineral dissolution which are abundant in the host Cretaceous sedimentary rocks. Sulfate concentrations in the water column (750 to 1,000 mg/L) are strongly elevated above background values, and illustrate the pronounced mine-related signature in pit waters. The range in sulfate concentration is comparable in magnitude to values observed in wasterock seepages in the region.

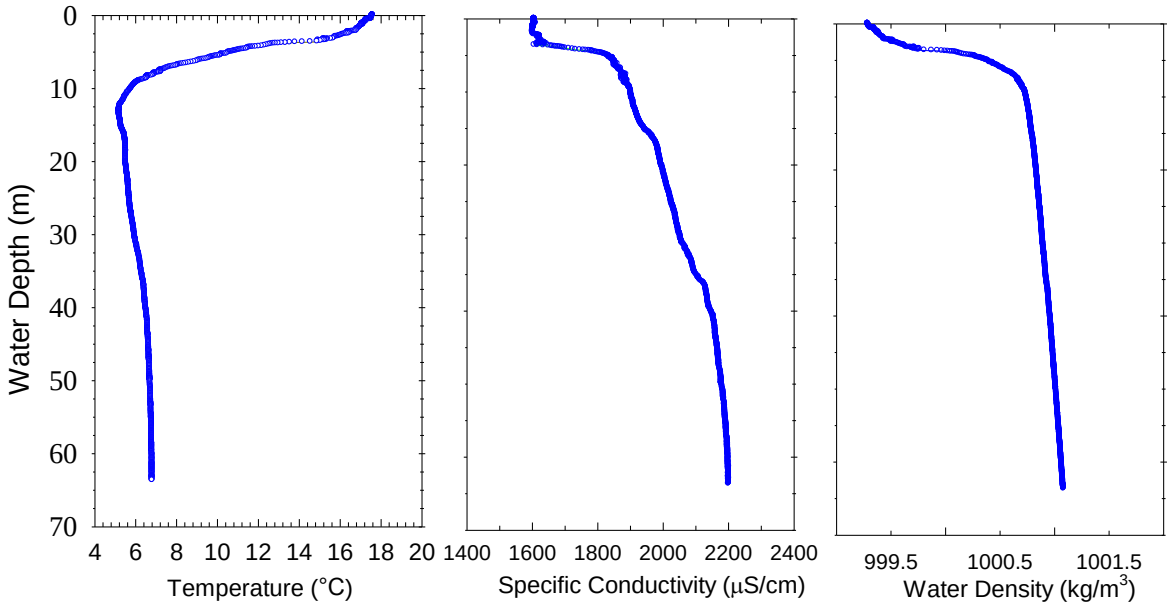

Figure 1 High vertical resolution (20 cm spacing) profiles of *in situ* temperature, specific conductivity and calculated water density in the flooded pit.

Redox conditions

Redox conditions have been shown to be the dominant variable governing Se speciation, precipitation/dissolution, sorption/desorption, methylation and volatilization in water and sediments (Masscheleyn and Patrick, 1993; Zhang and Moore, 1996). Accordingly, an understanding of redox conditions is essential to support interpretations of Se behavior. In natural systems, redox reactions are driven by the oxidation of organic matter, which can be defined by a series of microbially-mediated reactions (Table 1). In the presence of dissolved oxygen, aerobic bacteria will utilize O_2 as a terminal electron acceptor since this redox reaction affords the greatest energy yield. However, in systems where the rate of O_2 consumption exceeds the rate of re-supply, O_2 will become depleted and other secondary oxidants will be utilized by facultative anaerobic bacteria. These, in order of their free energy yield, are nitrate, manganese oxides, iron oxides, and sulfate (Table 1). In this sequence of redox reactions, selenate reduction occurs at a similar redox potential to that of nitrate.

Table 1 Oxidation/reduction reactions associated with the re-mineralization (oxidation) of organic matter. Parameters measured to elucidate redox conditions are highlighted in bold.

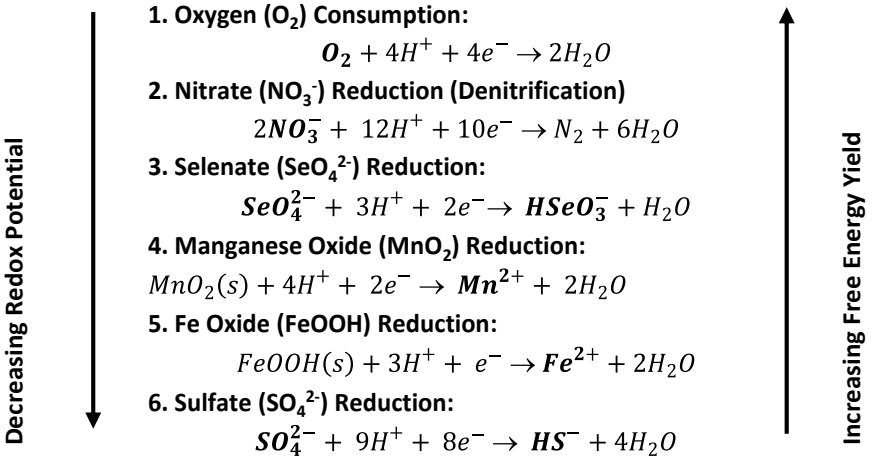

Water column redox conditions in the flooded pit were assessed through examination of various redox-sensitive indicators including dissolved oxygen (DO), nitrate, ammonia, dissolved Fe and dissolved Mn (Figure 2). Overall, the presence of lake stratification has a pronounced effect on water column redox conditions. DO levels show a progressive decline below the thermocline, from a maximum of 12 mg/L (at 5 m) to undetectable concentrations below a depth of 22 m. The absence of DO below 22 m provides strong evidence to indicate that the flooded pit is permanently stratified. If a mixing event had occurred in the previous months, some residual DO would be expected to persist in lake bottom waters.

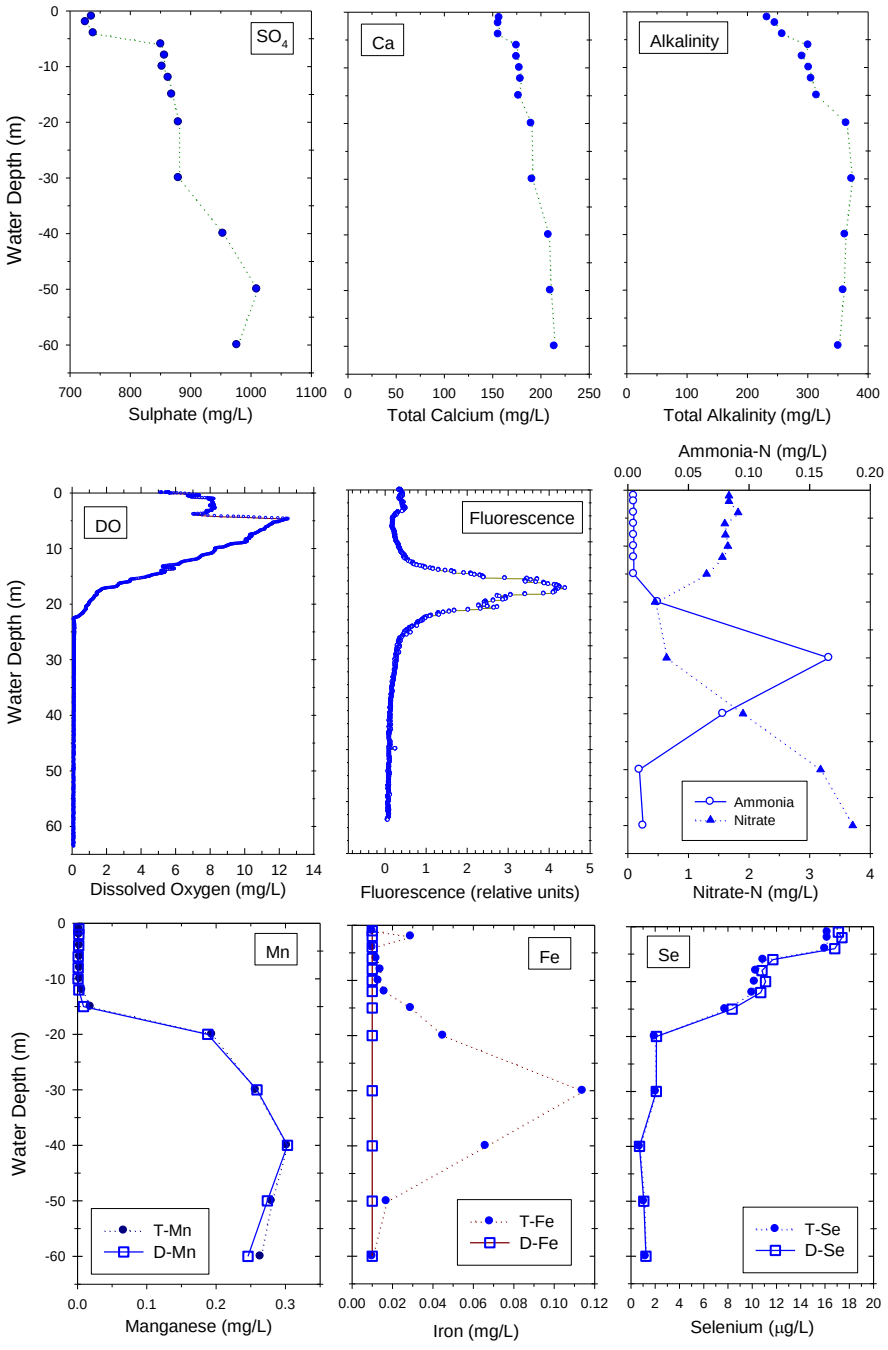

Figure 2 Vertical profiles of sulfate, total calcium, total alkalinity, dissolved oxygen, fluorscence, nitrate-N, ammonia-N, manganese, iron and selenium in the flooded pit. Data for fluorescence and dissolved oxgyen were collected via high vertical resolution *in situ* profiling.

Nitrate shows a pronounced mine-related signature in surface waters (1.6 mg/L), and reflects the input of residual nitrogen-based blasting residues. Below the oxic-suboxic boundary at 22 m, nitrate-N values decline to a minimum value of 0.5 mg/L at a depth of 20 m. The horizon of low

nitrate concentration is interpreted to result from denitrification (microbially-mediated nitrate reduction) in the suboxic zone below 20 m. Below the nitrate minimum, nitrate-N values progressively increase to a bottom water maximum of 3.7 mg/L, presumably reflecting the original mine-related signature established post-filling. Overall, the data suggest that the nitrate profile is in non-steady-state, whereby denitrification is progressively depleting the nitrate inventory in the suboxic zone below 20 m.

The occurrence of nitrate reduction near the oxic-suboxic boundary may in part be related to the peak in photosynthetic biomass (*e.g.*, algae) observed between 16 and 23 m, which will supply a source of organic detritus (and oxygen demand) to this portion of the water column. The magnitude of the fluorescence peak is indicative of oligotrophic conditions, which is common to pit lake environments. The influence of the autotrophic peak is also illustrated by the ammonia data, which show a concentration maximum in the upper portion of the suboxic zone (Figure 2). This ammonia peak is inferred to represent a product of organic matter remineralization. The presence of ammonia also provides additional evidence in support of suboxic conditions below water depths of 20 m, given the chemical instability of this species in the presence of DO.

Below the oxic-suboxic boundary at 22 m, dissolved Mn concentrations increase to a maximum of 0.3 mg/L. This is consistent with the reductive dissolution of Mn-oxides in the suboxic water column, which will liberate dissolved Mn^{2+} into solution. In contrast to Mn, dissolved Fe does not show any evidence of bottom water enrichment. Low levels of particulate Fe (as inferred from the total Fe profile) are evident; however, the data do not indicate the occurrence of Fe-oxide reductive dissolution. Collectively, the data for redox proxies are indicative of mildly suboxic conditions below 20 m, as inferred by the absence of DO, evidence of denitrification, presence of ammonia, and elevated levles of dissolved Mn. Indicators of more strongly reducing conditions, as would be revealed by Fe oxide reductive dissolution and/or sulfate reduction, are not observed.

Selenium

Profiles for dissolved and total Se are congruent, indicating that Se is present almost exclusively as dissolved species (Figure 2). Se shows evidence of attenuation in response to the vertical redox gradient in the water column, with surface values (12 to 20 μg/L) decreasing to <3 μg/L in the suboxic zone (Figure 2). The low Se values below the oxic-suboxic boundary, and the strong parallels between Se and DO, suggest that the behaviour and attenuation of Se is tied to vertical variations in redox conditions. Specifically, the data strongly suggest that the decrease in Se concentrations below 20 m reflects the removal of dissolved Se from solution as reduced Se phases, presumably as either selenite (Se^{+4}) (via adsorption to settling of particles) or as precipitation of elemental Se (Se^{0}) or selenide (Se^{2-}). The redox-controlled attenuation of Se is supported by the data for other redox proxies, which show evidence of both denitrification and Mn-oxide reductive dissolution. Specifically, the selenate/selenite redox couple occurs between nitrate reduction and Mn-oxide reduction (Table 1) Importantly, these data demonstrate that Se removal is achievable under mildly suboxic conditions in the presence of nitrate, which could be expected to hinder Se reduction.

The mechanism of Se attenuation described here is consistent with other forms of passive and engineered Se removal systems that rely on suboxic conditions, including passive wetland treatment (Martin *et al.*, 2011), passive removal in saturated wasterock (Bianchin *et al.*, 2013),

constructed permeable reactive barriers (Morrison *et al.*, 2001), and active biological treatment systems (CH2M HILL, 2010, 2013).

A conceptual model for Se bioremediation is shown in Figure 3. The required elements to support selenate reduction and removal from solution include: 1) a stratified water column, which allows the development of bottom water suboxia; and 2) a source of oxygen demand, which in this case is provided by *in situ* photosynthetic activity. The input of terrestrial organics via surface runoff likely also provides a source of organic carbon (and oxygen demand) to the system.

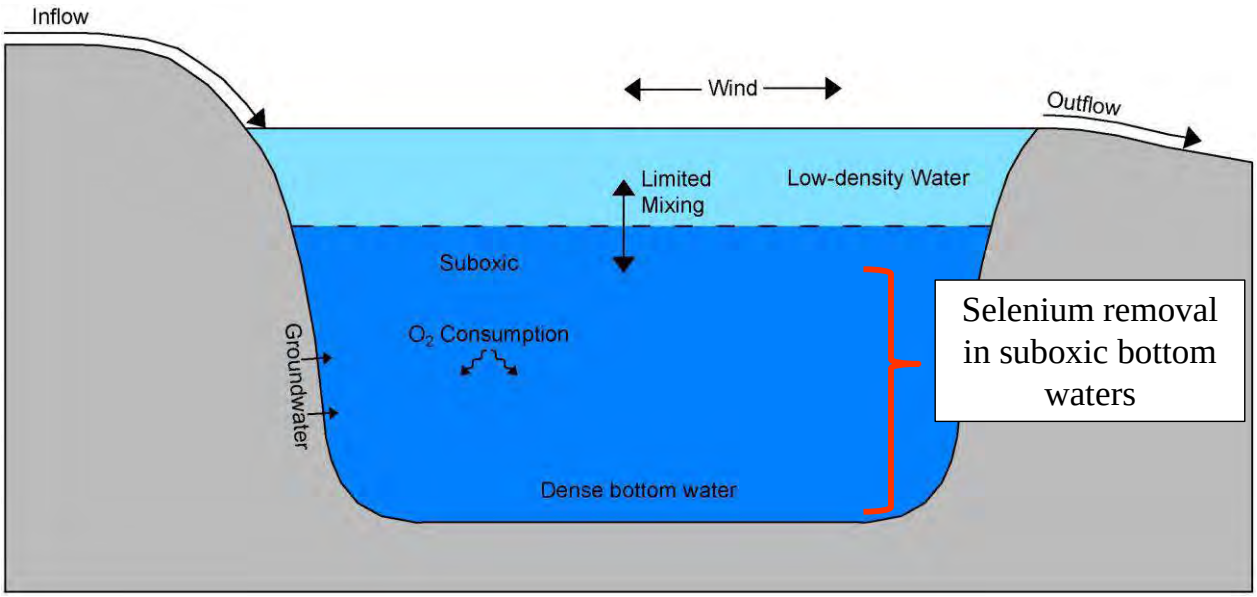

Figure 3. Conceptual model for selenium removal in a stratified flooded pit.

CONCLUSIONS AND IMPLICATIONS FOR MINE WATER MANAGEMENT

Overall, the data provided here illustrate the potential utility of flooded pits as *in situ* bioremediation cells for the removal of Se. The scale of Se removal can be illustrated by the volume of water in this system showing Se concentrations <5 µg/L, which equates to approximatly 1 million m^3 (below a depth of 20 m). There is also the potential to enhance rates of Se removal via the addition of organic amendments. Lake fertilization, for example, can provide an effective means to increase rates of *in situ* algal production and associated carbon generation (Dessouki *et al.*, 2005; Martin *et al.*, 2009). Such methods rely upon the well-established links between phosphorus limitation and algal growth (Schindler *et al.*, 1980). This form of amendment is very cost effective, given that only small additions of phosphorus can promote extensive carbon production. Alternatively, successful Se removal has been achieved via the direct addition of organic amendments to flooded pits (as liquid or solid forms) (Park *et al*., 2006).

Flooded pits that exhibit stratified and suboxic water columns also offer the potential to passively treat other site contact flows. This is illustrated in Figure 4 which shows a conceptual model depicting the injection of contact waters (*e.g.*, wasterock seepage) into the suboxic (bottom) zone of a flooded pit. Following mixing and Se attenuation in pit bottom waters, waters are then withdrawn from the pit for final discharge, which may require aerobic polishing prior to release to

receiving streams. The input of contact waters to the pit bottom will introduce DO, which has the potential to push the system to a less favourable redox regime (more oxic). In this regard, the addition of fertilizer and/or innoculum (*e.g.*, Se and nitrate reducing microbes) could be used to sustain suboxia and the desired redox state conducive to Se removal (also illustrated in Figure 4). This form of semi-passive treatment has been implemented at the Island Copper Mine, which uses a combination of ARD injection to bottom waters and surface water fertilization to promote more reducing conditions in the lower water column (Polling *et al.*, 2003).

With regards to mine water management, the data presented here also highlight the merits of maximizing saturated storage volumes in the design of mine waste facilities, which can passively, or through augmentation, form large-scale zones of suboxia. This requires consideration during mine planning (pit morphometry), potential use of in-pit berms to maximize in-pit water levels, mine waste management and water management.

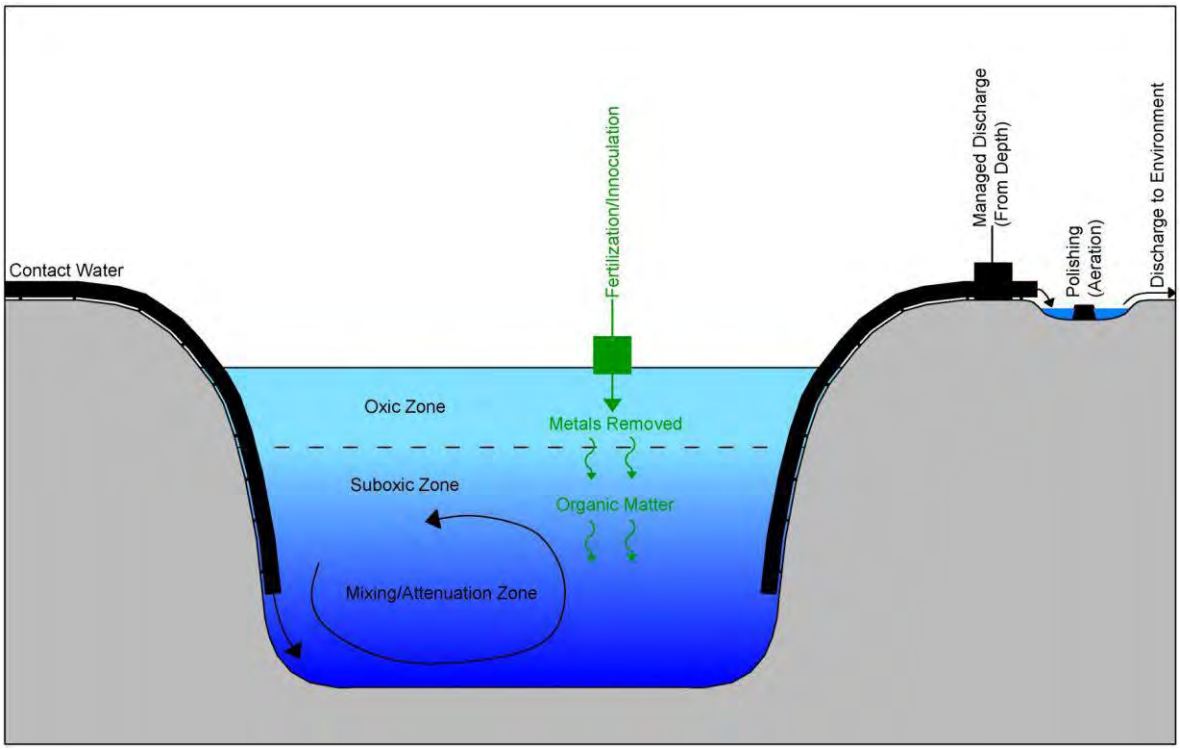

Figure 4. Conceptual model that desecribes a contact water injection system to pit bottom waters and associated removal in support of engineered Se removal system. Fertilization and polishing components

REFERENCES

Bianchin M., Martin A.J., Adams W.J. (2013) In-Situ Immobilization of Selenium within the Saturated Zones of Backfilled Pits at Coal-Mine Operations, Proceedings of 37th Annual British Columbia Mine Reclamation Symposium, September, 2013, Vancouver, BC.

Castro J.M., Moore J.N. (2000) Pit lakes: their characteristics and the potential for their remediation. Environ. Geol. 39:1254-1260.

CH2MHILL (2010) Review of Available Technologies for the Removal of Selenium from Water. Prepared for North American Metals Council. Prepared by CH2MHILL, June 2010.

CH2MHILL (2013) Review of Available Technologies for the Removal of Selenium from Water - Addendum. Prepared for North American Metals Council. Prepared by CH2MHILL, March 2013.

Dessouki T., Hudson J., Neal B., Bogard M. (2005) The effects of phosphorus additions on the sedimentation of contaminants in a uranium mine pit-lake. Wat. Res. 39:3055-3061.

Frankenberger W.T., Amrhein J.C., Fan T.W.M., Flaschi D., Glater J., Kartinen E., Kovac J.K., Lee E., Ohlendorf H.M., Owens L., Terry N., Toto A. (2004) Advanced treatment technologies in the remediation of seleniferous drainage waters and sediments. Irrig. Drainage Syst. 18:19-41.

Kuo E.Y., Ritchie A.I.M. (1999) The Impact of Convection on the Overall Oxidation Rate in Sulfidic Waste Rock Dumps. Conference Proceedings, Sudbury '99—Mining and the Environment, Paper AD2, vol. 1, pp. 9–18.

Martin A.J., Jones R., Buckwalter-Davis M. (2009) Passive and Semi-Passive Treatment Alternatives for the Bioremediation of Selenium from Mine Waters., Proceedings of 33rd Annual British Columbia Mine Reclamation Symposium, September 14-17, 2009, Cranbrook, BC.

Martin A.J., Simpson S., Fawcett S., Wiramanaden C.I.E., Pickering I.J., Belzile N., Chen Y.-W., London J., Wallschläger D. (2011) Biogeochemical mechanisms of selenium exchange between water and sediments in two contrasting lentic environments. Environ. Sci. Technol. 45:2605-2612.

Masscheleyn P.H., Patrick W.H. (1993) Biogeochemical processes affecting selenium cycling in wetlands. Environ. Tox. Chem. 12:2235-2243.

Morrison S., Metzler D. and Carpenter C. E. (2001). Uranium precipitation in a permeable reactive barrier by progressive irreversible dissolution of zerovalent iron. Environ. Sci Technol., 35, 385-390.

Oremland, R. S., Steinberg, N. A., Presser, T. S., & Miller, L. G. (1991). In situ bacterial selenate reduction in the agricultural drainage systems of western Nevada. Appl. Environ. Microbiol., 57(2), 615-617.

Park, B.T., Wangerud, K.W., Fundingsland, S.D., Adzic, M.E., and Lewis, N.N. (2006). In situ chemical and biological treatment leading to successful water discharge from Anchor Hill Pit Lake, Gilt Edge Superfund Site, South Dakota, U.S.A. Barnhisel, R.I. (Ed), 7th International Conference on Acid Rock Drainage, American Society of Mining and Reclamation, Lexington, KT, 1065-1069.

Poling G., Pelletier C., Muggli D., Wen M., Gerits J., Black K. (2003) Field Studies of Semi-Passive Biogeochemical Treatment of Acid Rock Drainage at the Island Copper Mine Pit Lake, 6th International Conference on Acid Rock Drainage, Cairns, Australia, July 2003. pp. 549-558.

Schindler D.E. (1980) The effect of fertilization with phosphorus and nitrogen versus phosphorus alone on eutrophication of experimental lakes. Limnol. Oceanogr. 25:1149-1152.

Zhang Y., Morre J.N. (1996) Selenium Fractionation and Speciation in a Wetland System. Environ. Sci. Technol. 30:2613-2619.

Biogeochemical Selenium Sequestration in Unsaturated Coal Reject Piles

Chris Kennedy[1], Stephen Day[1], Daniel Mackie[1] and Nicole Pesonen[2]

1. *SRK Consulting, Canada*
2. *Walter Energy Inc., Canada*

ABSTRACT

Predicting the source and fate of selenium (Se) from mine waste requires a multi-disciplinary understanding of the biogeochemical and hydrogeological processes that can occur, as differences in rock processing, waste storage configuration and resulting hydraulic properties can lead to orders of magnitude differences in the rate of Se release.

Non-acid generating coal reject piles stored on-site at the Willow Creek Mine, north-eastern British Columbia, Canada, were identified as a Se-leaching risk during environmental assessment studies. A condition of the mine permit included moving the piles to an alternative storage location to mitigate the risk of impacts to the nearby Pine River. Rates of Se leaching assumed for environmental studies were based on laboratory and small-scale site geochemical studies, performed under aerobic conditions that were ideal for Se release. However, to date, none of the available monitoring data have shown elevated Se concentrations in groundwater surrounding the piles.

To better understand why the coal reject piles did not appear to be leaching Se at predicted rates, a multi-disciplinary characterization study of the piles was performed that included borehole instrumentation of the piles to monitor gas composition and temperature, as well as collecting solid samples for microbial characterization coupled with geochemical and physical testing results from operational sampling.

Results from the study indicated the piles were sub-oxic and support a microbial community capable of reducing selenate, nitrate and ferric iron. Despite the piles being in an unsaturated state, the small particle size of the coal rejects and high residual moisture content has likely led to the observed sub-oxic conditions that provide a mechanism for Se sequestration within the piles resulting in low to non-detectable release rates to the surrounding environment. Findings from this study suggest there is currently no need to move the piles, and raises the question of whether re-handling would perturb established Se sequestration mechanisms.

Keywords: Selenium sequestration, biogeochemistry, coal rejects, field instrumentation

INTRODUCTION

The Willow Creek Mine (WCM) is located approximately 45 kilometres west of Chetwynd, British Columbia. Metallurgical grade coal seams are recovered by open pit methods and processed on site. The most recent operational phase for the mine was between 2010 and 2014, with operations placed on care-and-maintenance in the middle of 2014 due to low coal prices.

The economic coal seams are mined from the Lower Cretaceous Gething Formation. Surrounding the coal seams are sandstones, shales, siltstones, and mudstones, which are typical of the coal-bearing strata in the Rocky Mountains of western Canada Also typical of these rock types, and notably for the coal mines in eastern BC, is the enrichment of selenium (Se) when compared to typical global values for sandstones (Price 1997) On average Se concentrations range from 2-4 mg/kg Se, but have been reported as high as 15 mg/kg (Western Coal 2010; Kennedy et al, 2012).

Unsaturated coal reject (CR) piles stored on an alluvial fan (Figure 1) at the WCM were identified as a Se leaching risk during Mines Act Permit C-153 amendment (MAPA) studies to re-open the mine in 2010 (Western Coal 2010). A condition of the Mines Act Permit included moving the piles to an alternative storage location to mitigate the potential for impacts to the nearby Pine River. Rates of Se leaching assumed for environmental studies were based on laboratory and small-scale site geochemical studies, performed under aerobic conditions that were ideal for Se release. However, none of the available monitoring data before or the year after the MAPA studies were completed showed elevated Se concentrations in groundwater surrounding the piles. As a result, in 2011 a multi-disciplinary study was initiated by SRK Consulting (Canada) Inc and Walter Energy Inc. to assess the Se leaching potential from the CR piles currently stored near the plant site and better understand the implications of moving the piles to another location as currently stipulated in the Mines Act Permit.

Conceptual model and program design

A conceptual model was used as the basis for designing the study to determine if the pile is a long term risk for Se loading to the receiving environment. The model was divided into hydrogeology and biogeochemical components. A schematic of the overall conceptual model is provided in Figure 2.

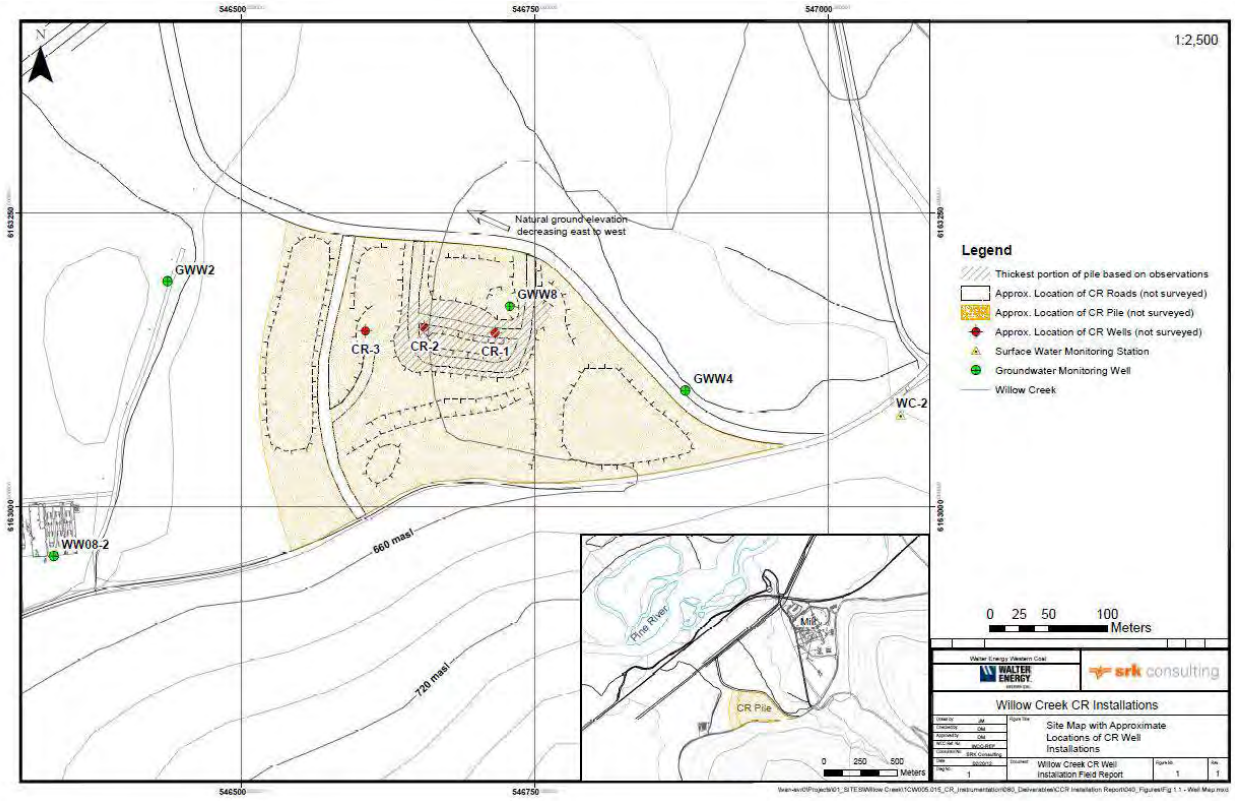

Figure 1 Location of coal reject pile on alluvial fan study site at Willow Creek Mine

Hydrogeology conceptual model

The groundwater flow system in the CR has two main components: (1) existing flow within the alluvial fan groundwater system and (2) seepage from the CR pile (Figure 2).

Groundwater is expected to move in the alluvial fan system from relatively high elevations near the apex of the fan, towards lower elevations and the Pine River. Recharge to the groundwater system comes from infiltration of direct precipitation, leakage from Willow Creek, and runoff from the mountains. Groundwater discharges to the Pine River. Seepage from the CR pile originates from precipitation infiltrating the pile and drain down of pore water within the pile when it was deposited. Precipitation on the CR pile either evaporates (or sublimates), runs off the pile, or infiltrates. The relatively fine-grained nature of the pile and presence of standing ponds indicate that infiltration is not likely to be excessive. Drain-down from within the pile itself is not likely significant.

Infiltration that does reach the base of the pile can infiltrate into the underlying substrate of the alluvial fan or run out along the ground surface and daylight as seeps at the toe of the pile. Water that does infiltrate into the alluvial fan percolates to the water table, then moves in the same direction as overall groundwater flow. There is the potential for silty interbeds to locally perch water, but all water will eventually reach the fan groundwater system.

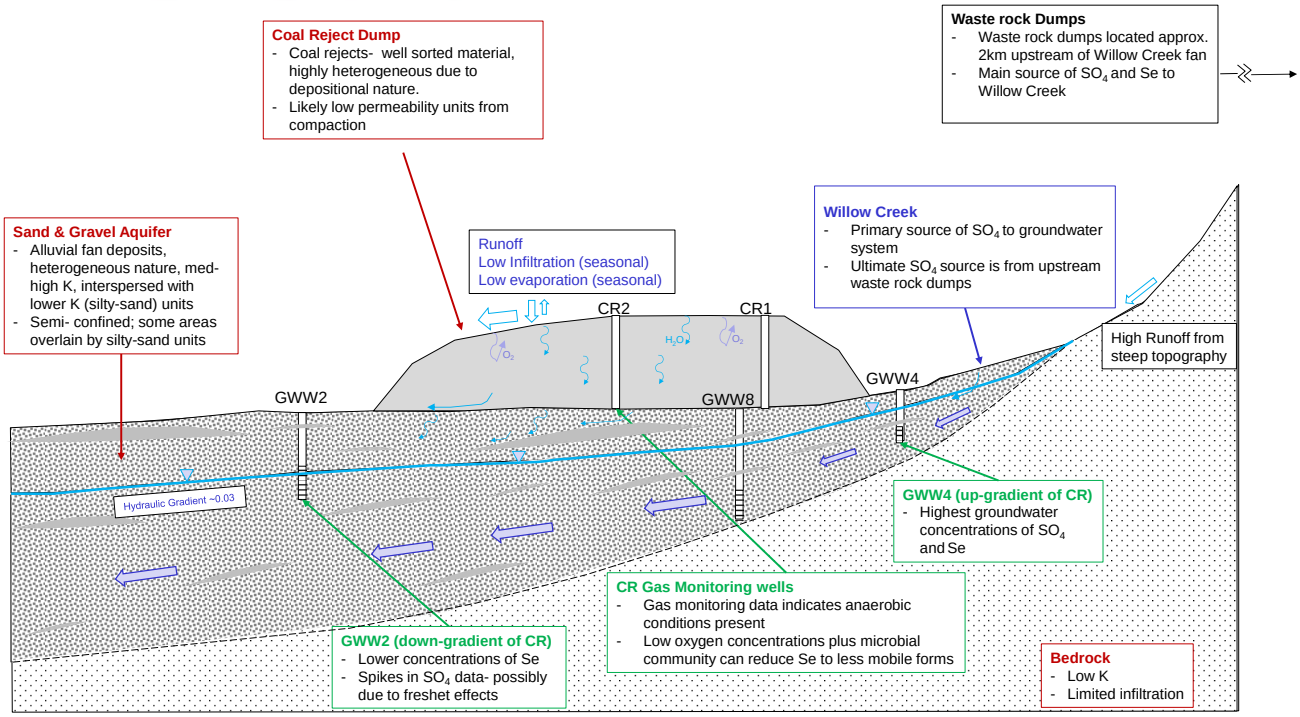

Figure 2 Conceptual model schematic for the WCM CR piles

Biogeochemical Conceptual Model

Selenium release from coal waste materials in British Columbia is generally understood to occur due to oxidative dissolution of pyrite, meaning that Se release is dependent on conditions favourable for the oxidation of sulfide minerals (Kennedy et al. 2012). Oxygen is the most likely oxidant and therefore if low level oxygen conditions are present in the CR piles, this should slow down the oxidation of sulfides and therefore Se release.

The following processes could be occurring in the CR pile:

- A thin layer on the exposed surfaces of the CR pile oxidizes producing soluble sulfate and Se, and dissolved organic carbon. Due to their concurrent release, Se and sulfate concentrations are expected to be correlated.
- Infiltrating precipitation dissolves Se, sulfate, and organic carbon.
- At depth, suboxic conditions develop and a microbial population that favours reduction becomes dominant, leading to conversion of Se to reduced states (selenite, potentially elemental Se and selenide).
- Sulfate may not undergo reduction unless anoxic conditions develop. As a result, the correlation between sulfate and Se diverge if Se is removed from solution.
- Selenium is sequestered in the pile by either selenite adsorption to reactive surfaces or by forming elemental Se and selenides (a solid phase precipitate).

Ultimately all of the above processes could result in leachate leaving the CR pile and travelling into groundwater with low Se, and relatively unchanged sulfate.

METHODOLOGY

In order to further understand the processes occurring in the CR piles, a multi-disciplinary characterization study of the piles was performed that included borehole instrumentation of the piles to monitor gas composition and temperature, as well as collecting solid samples for microbial characterization coupled with geochemical and physical testing results from operational sampling. The details of each component are provided below.

CR pile instrumentation and monitoring

Three monitoring boreholes were installed in 2012 using air rotary drilling into the CR piles. Each hole had thermistor strings installed and Solinst continuous multilevel tubing (CMT) with multi-level gas monitoring systems. Locations of these wells (CR-1, CR-2 and CR-3) are shown on Figure 1.

Monitoring of the gas wells included carbon dioxide and oxygen concentrations using an RKI Eagle multi-parameter gas sampling probe. Temperature was monitored by a multimeter capable of measuring the resistance in the thermistor strings.

Solids chemistry and reactivity assessment

Geochemical characterization of the CRs was based on previous studies from the MAPA study (Western Coal 2010) and supplemented by additional grab samples in 2010 and 2011 by WCM staff. The MAPA study included analysis of 44 operational samples from 2005 and 2006 and another 69 samples from operations after the mine re-started.

Analytical testing of all samples included acid-base accounting (Sobek et al. 1978) and element composition by aqua-regia digestion and ICP-MS. Neutralization potential (NP) is site specific at the WCM as defined in permit C-153 where NP for CR is calculated as Sobek NP (in kg $CaCaO_3$/t) multiplied by 0.8 plus 0.71. Acid potential (AP) for all rock types is calculated from sulfur concentrations determined by ICP-MS following aqua-regia digestion. Mineralogy of CR was characterized by semi-quantitative XRD and optical petrography descriptions.

Weathering kinetics were assessed using a humidity cell test (referred to as the "CCR H Cell" in the MAPA study), a 200 to 300 kg field barrel test and meteoric water mobility procedure (MWMP, NDEP 1990) tests on weathered samples collected in 2005 and 2006.

Microbial characterization

Grab samples were recovered aseptically from each borehole and shipped to the Microbial Geochemistry Laboratory at the University of Toronto, Ontario, for microbial analysis. A cultivation presence/absence approach was selected due to difficulties recovering DNA from the surface of the coal, which was found to be somewhat hydrophobic.

Media for anaerobic cultivation were prepared by mixing an artificial groundwater solution with solutions to support one of: nitrate; selenate; iron; or sulfate reduction. Lactate, acetate and pyruvate were used as the carbon sources. All solutions were sterilized (i.e. autoclaved) prior to inoculating with CR sediment. Sand and silt sized particles of CR were transferred into cultivation vials in an anaerobic chamber and stored at room temperature for 5 weeks. Successful cultivation

was indicated by biofilm accumulation on the vial walls for the nitrate and iron reducing media and by the presence of pink precipitates in the Se media.

Groundwater and surface water chemistry

In 2005, eight groundwater monitoring wells were installed in the Willow Creek Fan and the Pine River floodplain. The purpose of these wells was to assess groundwater quality and to develop a hydrogeological conceptual model for the fan in preparation for construction of the CR pile (Western Coal 2010). Five of the eight monitoring wells are located in the fan itself, although only GWW2, GWW4, and GWW8 are used in this study (Figure 1). Groundwater sampling data were available from late 2005 to 2013, with analyses including pH, sulfate, alkalinity, chloride, fluoride, nitrogen species, phosphorus species, dissolved organic carbon, and a 32 element scan by ICP MS for dissolved ions.

The spatial context of the fan monitoring locations (Figure 1) and context for interpreting water quality data are as follows:

- WC-2 represents upstream surface water that carries sulfate and Se from the up-land waste rock dumps at WCM.
- Groundwater generally follows topography, flowing from higher elevation portions of the fan towards the Pine River (i.e. GWW4 towards GWW2, passing GWW8), a distance of approximately 600 m horizontally from the toe of the CR pile.
- GWW4 is located upgradient of the CR pile and will not be impacted by the pile. The monitoring screen in GWW4 is within sandy gravel materials at a depth of 10 to 13 m below ground surface. The water table is about 7 m below ground surface at this location.
- GWW8 is screened below the CR pile footprint and has the potential to be impacted by the CR pile. The monitoring screen in GWW8 is within silty sand and gravel materials at a depth of 19 to 28 m below ground surface. The water table is about 9 m below ground surface at this location.
- GWW2 is located about 90 m down gradient of the CR piles and has the potential to be impacted by the CR piles. The monitoring screen in GWW2 is within sand and gravel materials at a depth of 10 to 16 m below ground surface. The water table is about 9 m below ground surface.

RESULTS AND DISCUSSION

Gas composition and temperature of the coal reject pile

Gas composition changes quickly over the first two metres below the surface with oxygen dropping below 4% and concentrations near detection at 8 metes below the surface. Carbon dioxide concentration shows an opposite trend in that it immediately increases below the surface to 3% and is relatively stable thereafter to the base of the pile.

Temperatures also appear to be higher inside the pile than regional ambient conditions during parts of the year, notably winter. Temperature monitoring of ambient conditions of the CR piles was not performed, although the average temperature during winter (November to March) in Chetwynd, British Columbia, ranges between -10°C and -5°C.

Geochemical characteristics

The CRs were characterized by relatively low sulfide sulfur (average of 0.16% interpreted from ICP aqua regia results) and levels of Se (average of 2.6 mg/kg) typical of coal waste material in eastern British Columbia. A statistical summary of the 69 grab samples that were analysed since the MAPA is provided in Table 1. When compared to the 2005 and 2006 operational samples (Western Coal 2010), sulfide sulfur and NP were somewhat lower in the grab samples. However, the overall difference between the acid-base account (NP divided by AP) of the two samples sets was small with averages for both around 3.0. Selenium concentrations were very similar between the two sample sets, with the average Se concentration in the 2005 and 2006 samples approximately 3 mg/kg.

The main sulfide mineral identified was pyrite, with possible pyrrhotite and trace levels of sphalerite and chalcopyrite also noted. X-ray diffraction determined that calcite, dolomite/ankerite and siderite were the main carbonates present.

The previous assessment of the CR piles by SRK (2007) and Western Coal (2010) indicated that the ARD potential was low. Grab sample results provided by WCM since the 2007 assessment support the original finding when an NP/AP criterion of 2 is used to delineate between PAG and non-PAG. While some of the samples have produced some acidity (as interpreted from a negative NP), water quality results from around the pile (Western Coal 2010) support that the piles overall are not a source of acidity despite being allowed to weather for several years.

Table 1 Summary of geochemical characteristics for operational coal reject samples

Statistic	Sulfide %S	AP kg $CaCO_3$/t	NP(Sobek) kg $CaCO_3$/t	NP/AP	Se mg/kg
Minimum	0.030	0.94	-3.3	-1.0	0.05
5th Percentile	0.040	1.3	3.4	0.64	0.94
25th Percentile	0.08	2.5	7.1	1.5	1.5
Mean	0.16	4.9	16	3.2	2.6
75th Percentile	0.21	6.6	18	5.0	3.2
95th Percentile	0.35	11	39	14	6.1
Maximum	0.61	19	108	43	8.9

Concentrations of Se and sulfide sulfur were compared in this study to confirm previous findings from other coal mines in British Columbia that Se was likely associated with sulfide (Kennedy et al. 2012). Selenium substitutes for sulfur and is often present as an accessory element in pyrite. The correlation coefficient for total sulfur (which will include any organic sulfur and sulfate sulfur) and Se was poor (r = 0.26, 99% confidence = 0.31), but improved when sulfide sulfur and Se were correlated (r = 0.45). Figure 3 compares of sulfide sulfur and Se in the CR samples.

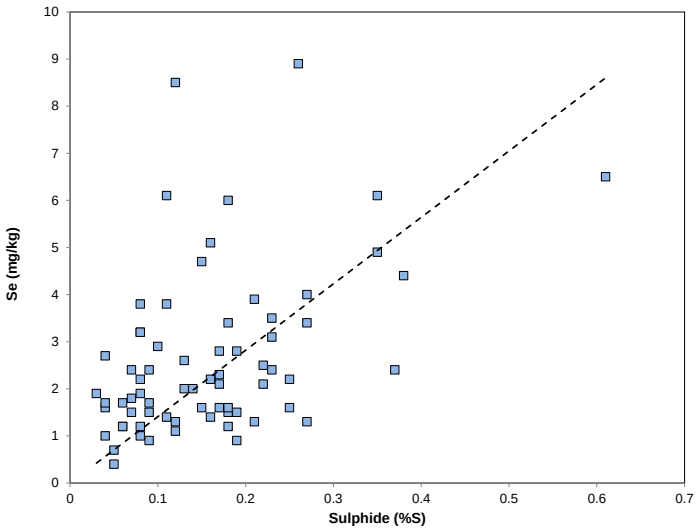

Figure 3 Comparison of Se and sulfide sulfur in WCM CR samples

Based on the results presented in Figure 3 and experience at other coal sites in British Columbia (e.g. Kennedy et al, 2012), Se leaching is expected to result from sulfide oxidation and generally at elevated levels compared to background levels (e.g., greater than 0.1 mg/L).

The field barrel test produced leachate pHs between 7.7 and 8.1, sulfate concentrations ranging from 283 to 2300 mg/L, and Se concentrations between 0.18 to 0.49 mg/L. Results from the MWMP tests confirmed these findings, as did the humidity cell tests, albeit at lower concentrations owing to the higher dilution in the humidity cell test (Western Coal 2010).

Microbial characterization

Results of microbial cultivation analysis demonstrated the viability of nitrate-, selenate- and iron-reducing communities of bacteria. Sulfate-reducing bacteria do not appear to be viable based on the cultivation tests.

The microbial communities identified are consistent with the low oxygen conditions present in at least portions of the CR piles. Bacteria respiring on selenate for electron transfer results in the formation of the more reduced forms of Se, such as selenite and elemental Se (Oremland 1994). These more reduced forms are readily removed from the soluble phase in groundwater by either adsorption or precipitation (selenite will adsorb, elemental Se will precipitate) (Neal & Sposito, 1989; Ralston, Unrine & Wallschläger, 2008). Nitrate and selenate are reduced at very similar oxidation potentials, while iron reduction requires more reducing conditions. Finding all three communities is a good indication that conditions are ideal to support suboxic to anoxic microbial communities and also that other requirements for survival are available, such as dissolved organic carbon and trace nutrients.

Based on the microbial characterization results, it is likely that a microbial community capable of converting selenate to more insoluble forms (e.g. selenite and elemental Se) will persist in the CR piles so long as suboxic conditions are maintained. It is likely a microbial communtiy is able to inhibit elevated concentrations of Se entering the receiving environment that was predicted by MAPA studies based on reactivity of the CRs under aerobic laboratory and field testing conditions.

Groundwater and surface water chemistry

Concentrations of sulfate and Se in groundwater and surface water are compared to infer the potential reactions occurring within the CR piles. This is because field and laboratory leach tests from previous studies indicated that pyrite in the CR oxidizes to release sulfate and if no other processes were occurring within the CR piles, a plume of sulfate and Se would be expected in the groundwater below and down gradient of the CR pile.

At the upstream surface water monitoring station WC-2 (Figure 4), sulfate concentrations are highest compared to all other monitoring stations, with seasonal spikes typically around 100 mg/L over the last four years. Sulfate concentrations in the groundwater wells typically decreases in a downstream direction. Monitoring well GWW2 shows moderate (~60 mg/L) seasonal spikes in sulfate concentrations, potentially indicating that this location is impacted more by surface water than GWW8 during certain times of the year. There are gaps in the record for GWW4, so it is not possible to confirm if seasonal spikes also occur at this location, but it is considered likely based on historic comparison of GWW4 and WC-2. Monitoring well GWW8 has shown a slow increase in sulfate concentration over time, roughly intermediate between GWW4 and GWW2 on an average annual basis.

Selenium concentrations were highest at WC 2 and GWW4 (Figure 4) at around 0.005 and 0.003 mg/L. Concentrations downstream the CR piles (i.e., GWW8) are near analytical detection limits (0.0005 mg/L) (Figure 5) and an order of magnitude lower than WC2 and GWW4 (i.e. than upstream of the pile). The step change in Se concentrations in 2010 is likely a function of changing detection limits in the analytical laboratory, although this has not been confirmed.

Sulfate and Se concentrations at WC-2 were well correlated ($r = 0.85$, 99% confidence = 0.2) whereas at GWW8 they were not ($r = -0.3$) (Figure 5). The divergence at GWW8 is likely evidence of conditions in the sub-surface supporting reduction of selenate to selenite and possible elemental Se. While redox was not measured in the wells, using the concentration of redox sensitive elements and compounds under alkaline conditions (pH of about 8), the redox level of the groundwater is estimated to be approximately 400 mV, which is near the redox potential required to reduce selenate to selenite (Ralston, Unrine & Wallschläger, 2008). This is interpreted from the concentrations of nitrate and nitrite at GWW8 (0.1 and 0.01 mg/L, respectively) and also from dissolved iron concentrations. Iron occasionally spikes in GWW8 (up to 0.11 mgFe/L), which could simply be a result of poor filtering (i.e. partiulcate iron oxide contamination), or indicate times when redox conditions are closer to 0 mV and favour the formation of elemental Se. Under alkaline pH conditions, iron is only soluble when it is present in the reduced form as ferrous iron.

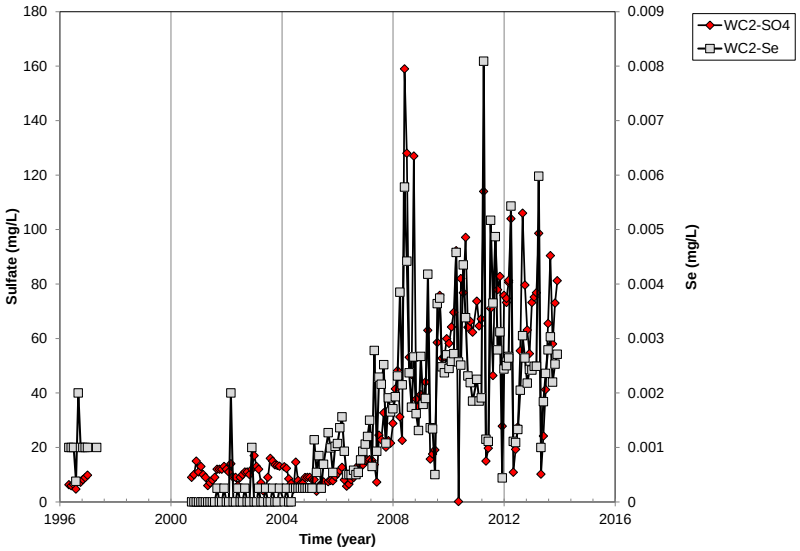

Figure 4 Sulfate and Se concentrations at surface water station WC2

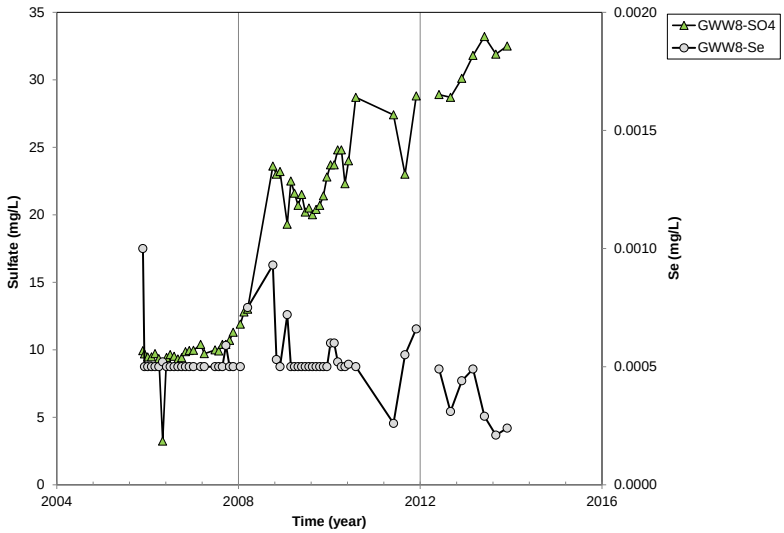

Figure 5 Sulfate and Se concentrations at groundwater monitoring station GWW8

CONCLUSION

A multi-disciplinary characterization approach was used to assess the Se leaching potential from the CR piles at the WCM. Based on the results of this study, the piles appear to be sub-oxic and support a microbial community capable of reducing selenate. Despite the piles being in an unsaturated state, the conditions within the CR piles provide a suitable environment for selenate reduction and therefore Se sequestration to occur resulting in low to non-detectable release rates to the surrounding environment. Findings from this study suggest there is currently no need to move the piles, and raises the question of whether re-handling would perturb established Se sequestration mechanisms.

ACKNOWLEDGEMENTS

SRK acknowledges Alex Brissard and Meghan Irvine of Walter Energy for their assistance for collection of operational samples and coordinating multiple information requests with various member of the WCM team for this study. SRK also acknowledges Veronika Shirokova of SRK (formerly of the University of Toronto) for her assistance with microbial characterization work.

REFERENCES

Kennedy, C, Day, S, MacGregor, D, Pumphrey, J (2012) Selenium Leaching from Coal Waste Rock in the Elk Valley, BC. Proceedings of the 9th International Conference on Acid Rock Drainage, May 20-26, 2012. Ottawa, Canada.

Neal, RH, Sposito, G (1989) Selenate adsorption on alluvial soils, Soil Science Society of America Journal, vol. 53, pp. 70-74.

Nevada Division of Environmental Protection. 1990. Meteoric Water Mobility Procedure, Bureau of Mining Regulation and Reclamation, Nevada Division of Environmental Protection, 9/19/90. 6 pages. http://ndep.nv.gov/bmrr/mobilty1.pdf.

Oremland, RS, Hollibaugh, JT, Maest, AS, Presser, TS, Miller, LG, Culberton, CW (1994) Isolation, Growth, and Metabolism of an Obligately Anaerobic Selenate-Respiring Bacterium, Strain SES-3. Applied and Environmental Microbiology, vol. 60, pp. 3011-3019.

Price, WA, (1997) Draft Manual of Guidelines and Recommended Methods for the Prediction of Metal Leaching and Acid Rock Drainage at Minesites in British Columbia. B.C. Ministry of Employment and Investment. 141 pp.

Ralston, NVC, Unrine, J, Wallschläger, D, (2008) Biogeochemistry and Analysis of Selenium and its Species. Prepared for: North American Metals Council. 61 pp.

Sobek, AA, Schuller, WA, Freeman, J R, and Smith R M, (1978) Field and laboratory methods applicable to overburden and minesoils. USEPA Report No. 600/2-78-054, 203 pp.

SRK (2007) Management of Coal Reject at Willow Creek Mine – Geochemical Investigations. Letter to Western Canadian Coal Corp. December 31, 2007.

Western Coal (2010) Willow Creek Mine – 3.8 Mt/a Environmental Assessment, Mine Permit, Effluent Permit, & Air Permit Amendments.

10th ICARD IMWA 2015 | 10th International Conference on Acid Rock Drainage & IMWA Annual Conference

Established and Emerging Passive and Hybrid Biological Sulfate Removal from Mining Effluents

Michael Bratty*[1], Tom Rutkowski[2], Eric Blumenstein[2] Kevin Conroy[2] and Andre Van Niekerk[3]

1. *Golder Associates, Peru*
2. *Golder Associates, USA*
3. *Golder Associates, South Africa*

ABSTRACT

Changing regulations and water scarcity combined with increased fiscal pressure in the mining industry have increased the calls for new, lower cost methods for sulfate removal from mining effluents. In the last decade, membrane-based processes have been implemented on a large scale for advanced sulfate removal and have achieved a level of commercial acceptance in the mining industry. But membrane systems are complex and costly. On the other hand, many applications of sulfate removal in mining do not require a high removal efficiency, so simpler systems that are less costly may be more appropriate. Passive treatment offers the potential for reduced cost on sites where sufficient land area is available to construct treatment cells. Passive treatment has been demonstrated at a large number of sites, but has well-known drawbacks that encourage innovation. This paper will describe a recent project in passive biological sulfate removal for a mining effluent, and reports on the emerging concept of hybrid biological treatment. Hybrid treatment is intended to reduce the land area needed for passive treatment and thereby to make passive systems applicable for larger flow rates.

Keywords: Passive Treatment; Advanced Sulfate Removal; Hybrid Treatment

INTRODUCTION

Increasing pressure on water resources, changing regulations, and increasing awareness of the impacts of mining on water quality have led to increasing need for sulfate removal from mining effluents. Lime treatment has traditionally been used to reduce metals and acidity, but is able to remove sulfate only to the limit of gypsum solubility. The term "advanced sulfate removal" has been adopted by many to refer to sulfate removal below the level of gypsum solubility. Depending on the jurisdiction, and on the assimilative capacity of the receiving environment, some operations may be required to achieve an "end of pipe" sulfate limit of 300-500 mg/L, while others may be under even more strict limits.

In the last decade, a number of operators have successfully demonstrated advanced sulfate removal using membrane processes, at large flow rates, to achieve sulfate levels in product water of 100 mg/L or below (Hutton 2009). Examples include the eMalahleni water treatment plant (started 2005) and the Optimum Coal mine water treatment plant (2009) in South Africa, a facility at Kennecott Mine for treatment of impacted groundwater (2006) and the Northern West Virginia Water Treatment Plant (2013) in the USA. The product water from the eMalahleni and Kennecott plants is sent directly to local municipalities to provide drinking water.

On the other hand, alternatives to these large scale "active treatment" processes are sought which are less costly for applications where strict discharge limits are not required, for example, in cases where only 30-50% removal is desired. The cost of treatment to moderate sulfate levels should be significantly lower than the cost to meet strict levels. One option is to bypass part of the flow, allowing for a smaller capacity membrane plant, so the mixture of treated water and bypass water meets the objectives. Another option is to select membrane types which are semi-permeable to the target ions, thereby increasing the sulfate level in the effluent, and hopefully, decreasing costs. All the active treatment options, however, require a fully-staffed mechanical treatment plant with appropriate skills and training and attention to process control, to prevent costly problems such as scaling.

"Passive treatment" can offer sulfate removal with a greatly reduced level of complexity, greatly reduced staffing levels and skills, and as a result, potentially offers cost savings. Passive treatment research and development has been carried out over a period of decades. A large number of facilities have been constructed, but a relatively small subset of these projects involves designs specifically targeting sulfate removal. Passive treatment for advanced sulfate removal has met with mixed success, however the limitations of the process are beginning to be well understood and companies can now evaluate the passive treatment option with greater confidence. In general, passive treatment requires a much larger land area than active treatment, and as a result the process has not been frequently applied to large flow rates.

"Hybrid treatment", also known as semi-passive treatment, is an emerging concept that combines aspects of active treatment and aspects of passive treatment. In hybrid treatment, a biological sulfate reduction process takes place in a lined earthen vessel containing inert media and bacteria,

fed with a soluble electron donor and nutrients. The use of a soluble electron donor reduces the size of the vessel, and improves control, compared to passive treatment. The result is a process having low complexity, relatively low cost, and less operator input, but without necessarily requiring a large land area. The hybrid process has been successfully demonstrated on a small scale for selenium removal, however early attempts in sulfate removal have encountered problems.

BIOLOGICAL SULFATE REMOVAL

Biological treatment removal utilizes an organic carbon source, or hydrogen, as an electron donor to and sulfate as a terminal electron acceptor, thereby achieving reduction to sulfide through cellular metabolism. In a broader context, a variety of organisms use a variety of terminal electron acceptors in cellular metabolism, depending on the environment. A conceptual model of electron transfer in cellular metabolism is provided in Figure 1.

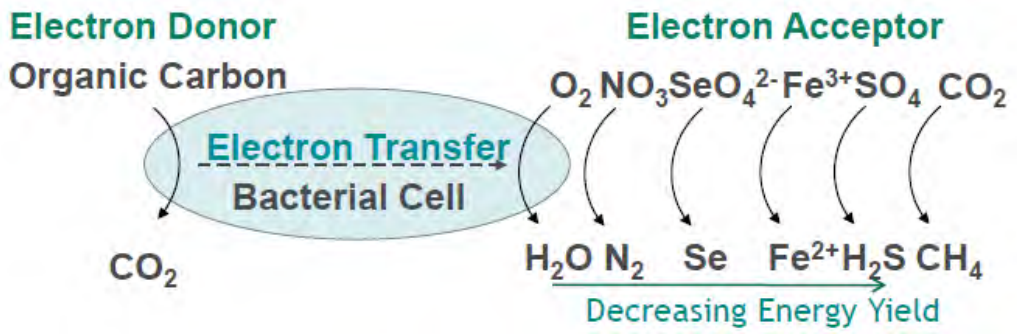

Figure 1 Electron donors and acceptors

There is a decreasing energy yield for successive electron acceptors illustrated by the figure, and, for example, oxygen and nitrate must be depleted prior to sulfate being reduced. The oxidation of organic carbon and the reduction of sulfate produces carbon dioxide (present at neutral pH as bicarbonate), water, and sulfide (present at neutral pH as a mixture of dissolved hydrogen sulfide and bisulfide).

A range of organic carbon sources have been employed for sulfate reduction, including but not limited to: methanol, ethanol, sugarcane waste, agricultural waste, sawmill waste, abattoir waste, sewage sludge, compost biosolids, cleared vegetation, and garden waste (Kumar 2011, Liamlean 2007). Selection of the lowest cost electron donor depends on the availability of materials close to the mine, and on the pre-processing costs that are required to deliver the material to the system.

Sulfide Sequestration

For biological treatment to be successful, it is essential that, once sulfate reduction is achieved, the resulting sulfide be removed from the system. The reasons are, firstly, sulfide is toxic and generally must be removed from effluents to low levels prior to release to natural water bodies. Secondly,

sulfide can off-gas from a treatment system as hydrogen sulfide, which is a health and safety or aesthetic concern and can add complexity to operation and maintenance. Thirdly, if not removed from the bioreactor effluent, sulfide can be oxidized back to sulfate through exposure to oxygen, in a process called reversion, which defeats the purpose of the process.

Some of the failures or difficulties of biological sulfate removal in the past have been associated with sulfide sequestration rather than sulfate reduction. Sulfide sequestration can be achieved in a variety of ways. In water sources that contain significant quantities of metals, the sulfide will act as a ligand and many base metals will precipitate. Alternatively, some of the sulfide may be removed using air-stripping, however this option produces a sulfide off-gas, and, practically, cannot achieve low levels of dissolved sulfide in the effluent. Air stripping may be combined with oxidation of sulfide to elemental sulfur, which is a solid and can be normally be separated from the liquids. The sulfur oxidation process can be biologically catalysed and is pH dependent. However, the process of oxidizing sulfide to sulfur can be difficult to control in passive systems, increasing the chance of reversion to sulfate, and creating polysulfides.

If the metals in the feed are not sufficient to sequester all of the sulfide, then a supplemental source of metals may be provided, and this usually consists of an abundant, low-cost iron carbonate, oxide or hydroxide material. Iron sulfate or chloride salts are not appropriate, since the resulting release of the sulfate or chloride ion to the effluent is counter to the overall objectives. Other base metal hydroxides can sequester sulfide, and their use depends on local availability. Also, the material should not contribute undesirable impurities, such as lead or arsenic, to the effluent. A reduced or partially reduced iron source is preferred, such as ferrous hydroxide, or magnetite to prevent redox reactions that contribute to reversion. Ferrous hydroxide sequesters sulfide as follows in equation 1.

1) $Fe(OH)_2 + H_2S = FeS(s) + 2H_2O$

In the case of an oxidized iron source, such as ferric hydroxide or ferrihyrite, the ferric ion will be preferentially be reduced to ferrous ion, resulting in the oxidation of sulfide and the production of elemental sulfur, as described in equation 2. Depending on the pH, some of the elemental sulfur will be soluble as polysulfide, as shown in equation 3. The polysulfide, if present, is undesirable since it is likely to report to the effluent and eventually revert to sulfate. Therefore, the success of sequestration processes using oxidized iron involves the control of the formation of polysulfide, and the separation of the elemental sulfur.

2) $2Fe^{3+} + S^{-2} = 2Fe^{2+} + S^{o}(s)$

3) $S^{2-} + n\ S^{o} = S^{o}_{n}S^{2-}$

If ferric hydroxide ($Fe(OH)_3$) is used as the iron source, then one third of the sulfide mass could follow this pathway, while two thirds would deport at FeS. Magnetite, ($Fe^{2+}Fe^{3+}{}_2O_4$) has been successfully used as a sequestering agent, and is discussed in the passive treatment case study below. Magnetite is an insoluble, black mineral that is widely available. It may be finely ground and added to the mixture of media as part of a sulfide sequestration system. The makeup of the media, the predicted longevity, and testing of such, are the subjects of recent and ongoing work (Blumenstein 2012, Van Niekerk 2015). A final stage of aeration is typically required to polish the

effluent to remove excess nutrients from the biological treatment system, and to oxidize a trace amount of residual sulfide downstream of the sulfide sequestration system. The final aeration also serves to increase the dissolved oxygen concentration of the effluent prior to discharge.

PASSIVE TREATMENT EXPERIENCE

Passive treatment systems commonly consist of biochemical reactors (BCRs), sulfide sequestration, and final polishing/aeration. A BCR is typically a gravity-flow bioreactor with a limestone-buffered organic treatment medium that is intended to require minimal operation and maintenance (Gusek, 2002). Passive BCRs consist of a series of geomembrane-lined cells or ponds filled with organic media, located outdoors. The organic media in the BCRs typically consists of woodchips and/or hay and limestone. A considerable amount of innovation has been seen in the development of the media for the BCR, to facilitate biological processes and to promote hydraulic conductivity. This organic matter provides a surface for the growth of microbial colonies and is gradually degraded to generate the organic carbon required for sulfate reduction. The typical construction of a BCR is shown in Figure 2.

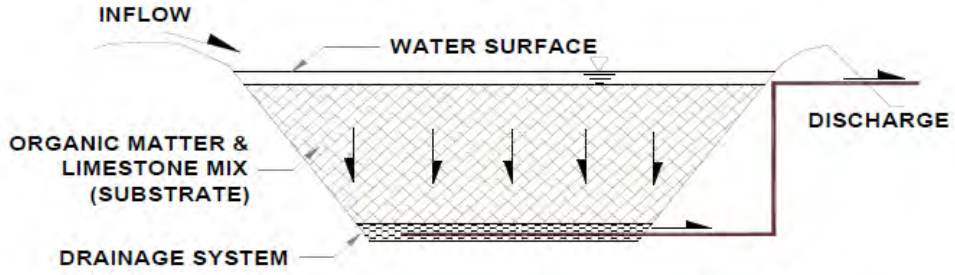

Figure 2 Profile of a BCR

A range of treatment mechanisms may be working in a BCR, depending on the particular feed conditions and the design as summarized below (Reisman 2009):

- biological reduction of sulfate to sulfide and subsequent precipitation of metal sulfides,
- alkalinity increase due to biological sulfate reduction and dissolution of limestone contained within the substrate,
- precipitation of metal hydroxides, and
- sorption of trace metals (e.g., Cd, Cu, Pb, Zn) to metal hydroxides and the organic medium.

The rate of degradation of organic material varies with media age and temperature and is likely the limiting factor in sulfate reduction in a BCR. Sulfide sequestration is achieved using an anaerobic sulfide polishing cell (SPC) that contains iron media. Effluent from the BCRs that contains high levels of sulfide flows through the SPC where sulfide is precipitated as an iron sulfide solid. Flow through a passive system is achieved through gravity flow and chemical addition is generally not required. Maintenance is performed at periodic intervals, for example, with SPCs media renovation every 3-5 years and BCRs media replacement every 10-20 years.

Advantages and disadvantages of passive biological sulfate removal

Passive treatment is well-researched and the benefits and limitations of the process are well understood:

- Passive treatment is not well suited to meeting strict effluent limits, due to a lack of process feedback signals and lack of process control mechanisms.
- Passive sulfate removal is founded on a biological process which is sensitive to low temperatures, and therefore may be sensitive to cold climates. However, as a mitigating measure, the BCR may be covered by an insulating layer of water, soils or even foam, to prevent freezing. Nevertheless, BCRs generally need to be sized for ambient feed water temperatures; lower temperatures require larger reactors.
- The breakdown of organic matter to produce volatile fatty acids (VFA) is believed to be the rate limiting step, and it is not directly linked to the subsequent consumption of VFAs for sulfate reduction. Under normal operation, most passive systems suffer from some degree of nutrient leakage. Nutrient leakage can result in failure to meet water quality objectives in terms of nitrogen, phosphorous or biological oxygen demand. An aerobic polishing cell, trickling filter, and/or lagoon may be installed downstream to help address the problem.
- Passive systems require large land areas, particularly for large flow rates. The availability of land near mining operations may be the limiting factor for passive systems.
- Passive systems benefit from a low degree of complexity. Often, little or no concrete, mechanical, electrical and structural work is required, drastically reducing capital costs compared to conventional active treatment systems, and simplifying maintenance operations.
- Passive systems cannot treat for chloride and generally do not result in a reduction in total dissolved solids (TDS) where chloride, magnesium, or other common anions are present.
- Passive systems benefit from low power consumption and are suitable for remote sites without access to line power. Depending on the site, water generally flows by gravity through the treatment system.
- Passive systems benefit from lower labour inputs, due to inherent differences including lower complexity, compared to active systems.
- Passive system can take advantage of low grade, lower cost carbon sources, which make the operating cost competitive compared to active biological sulfate removal systems.

Passive sulfate removal treatment case study

Golder Associates has been actively developing passive systems for various applications over the past 10 years both in the Americas and in Africa. In spite of a large number of published case studies involving passive treatment, there are few that have been designed specifically for sulfate removal. One such case is an operating coal mine located in a rainy and temperate part of Canada, shown in Figure 3. The feed sulfate level, typically 400-700 mg/L and the target for treatment is 300 mg/L, so the treatment effciency need not be high. This is considered an excellent application for passive treatment.

The feed is predominantly calcium sulfate, with a limited amount of metals available to sequester sulfide. The system contains a biochemical reactor (BCR) for sulfate reduction, an anaerobic sulfide

polishing cell (SPC), and aerobic lagoon and a settling pond. The SPC consists of a mixture of woodchips and a locally available magnetite. The pilot demonstration work commenced in 2009 (Blumenstein 2012) and a demonstration system at a quarter of the full scale (planned to be approximately 65 m3/hr) was constructed summer of 2012. The land area required from the demonstration scale was 0.8 ha. The feed and effluent sulfate data is shown in Figure 4, below. Data collection and compilation are ongoing.

The preliminary results from the case study are promising, and the system will continue to be adjusted through operations. The anaerobic sulfide polishing cell was commissioned in early 2013. The effluent from the SPC consistently is below 1 mg/L sulfide, and this residual is oxidized in the aerobic cells.

Figure 3 Passive BCR in Canada (2012)

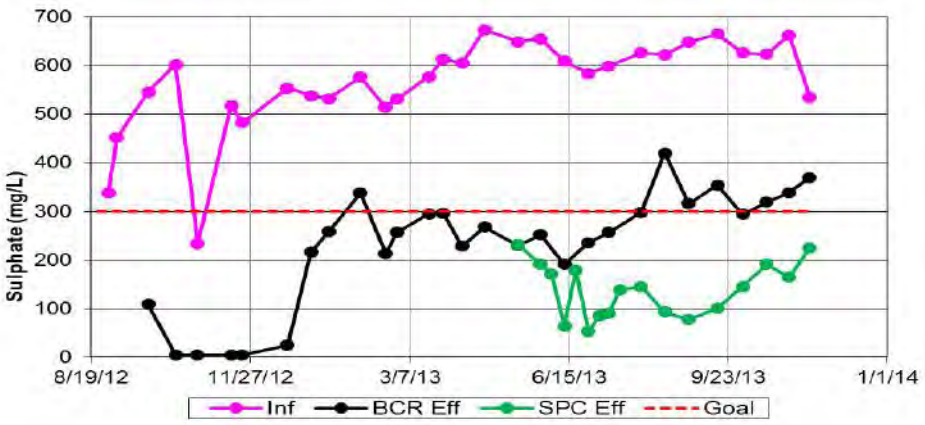

Figure 4 Preliminary Results from a Passive BCR in Canada

Notes: Inf – Influent to the BCR; BCR Eff – BCR Effluent; SPC Eff – SPC Effluent

HYBRID TREATMENT

The hybrid biological reactor concept has been developed to address some of the limitations of passive treatment systems, and to make passive treatment more applicable to large flow rates. Hybrid reactors operate on the principles of biological sulfate reduction, except the reactors are constructed using inert media in lined, covered, earthen basins, and are fed a soluble nutrient source by means of a metering pump. Although the biological sulfate reduction process can be engineered in an "active" mechanical treatment plant, but this process has all the disadvantages of cost and complexity of the membrane plants mentioned above. As a result, there are very few commercial examples of the active biological sulfate reduction process. Hybrid reactors, in contrast, are designed to contain few moving parts, draw very little electrical power, and to require a minimum of operator intervention. Hybrid systems are intended for cases where only partial sulfate reduction is required and where strict process control is not necessary, including cases with a relatively constant flow rate. The hybrid system takes advantage of the benefits of both active and passive systems, with lower costs than active systems and using less land area than conventional passive systems. While hybrid biological sulfate systems are in the early stage of development, they are anticipated to offer the following benefits:

- A variety of soluble electron donors can be utilized, including low cost or dilute options that are not recommended for conventional active treatment systems, such as compost leachate, silage or waste biological sludge.
- Hybrid systems eliminate most of the concrete, steel, mechanical equipment, electrical equipment, and much of the ancillary infrastructure, along with the engineering and construction costs associated therewith.
- Hybrids decouple sulfate reduction from the rate-limiting carbon metabolism of a BCR, reducing the size of the sulfate reducing bioreactor.
- Hybrids, like passive reactors, may be buried to protect from freezing in cold climates.
- Bioreactors may be constructed using a variety of on-site materials, such as coal beneficiation rejects, taconite wastes, or gravels.
- Hybrids are unique compared to passive systems in that they may be back-flushed, reducing problems with hydraulic conductivity, greatly extending their life span and allowing for higher loading. Early problems with passive treatment have commonly been associated with the mundane problem of flow distribution and distribution piping.
- Hybrids are intended to eliminate heating of water needed for typical active biological processes, by increasing the size of the bioreactor bed but at a reasonable cost.
- Hybrids require a small amount of electrical power, but unlike active biological or membrane systems, do not necessarily require access to line power.
- Hybrids, like passive systems, eliminate continuous operator attention and reduce labour costs compared to active systems.
- Hybrids improve control of nutrient leakage.
- The largest operating cost of a hybrid system is the electron donor. For a case study employing ethanol, the cost is estimated to be less than \$0.10 per m^3 of feed to reduce

sulfate from 600 mg/L to 300 mg/L, assuming the current market price for ethanol of $830/t. Lower cost alternatives, using waste products, are also possible.

Golder Associates has successfully applied the hybrid concept to selenium reducing bioreactors at a demonstration site. Biological selenium removal operates on similar principles as sulfate removal. The hybrid concept was applied at the Leviathan Mine, and this case study offers insight on early variations on the concept applied to base metal removal, at relatively low flows of 2-7 m3/hr (Mayer 2006, Tsukamoto 2002). A pilot scale hybrid system fed with ethanol and molasses was tested on scrubber blowdown in the Minnesota Iron Range (Eger, 2004). Like passive treatment, hybrid treatment requires a system to sequester sulfide, usually based on contact of the water with iron compounds (ideally ferrous oxides or hydroxides). An example process flow diagram is shown in Figure 5, below.

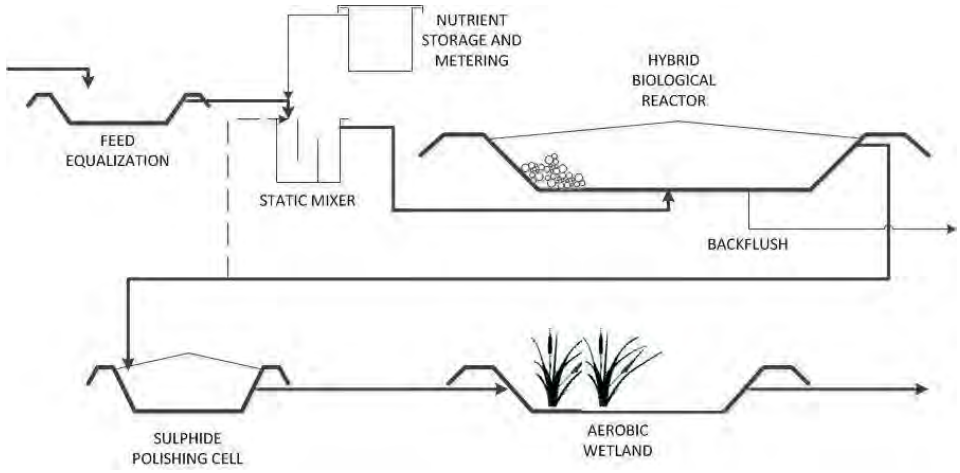

Figure 5 Example Hybrid System Process Flow Diagram

Sludge from the bioreactor back-flush is an organic material, mixed with feed suspended solids, and precipitated metal sulfides, depending on the application. The media in the sulfide polishing cell may be drawn from a range of locally available materials, ideally magnetite or other iron oxides. Depending on the specific feed water, part of the hybrid reactor overflow may be recycled to provide a ligand for specific influent metals. Lessons from the design of passive bioreactors inform the detailed design of hybrid reactors, such as: sizing, hydraulics, packing, flow distribution, and prevention of clogging and short-circuiting.

CONCLUSION

Active treatment, using membrane separations, has been demonstrated at a number of sites around the world, and has achieved commercial acceptance at large flow rates for advanced sulfate removal. Active treatment in general suffers from a high degree of complexity and as a result, a high cost. Furthermore, many operators require only partial removal of sulfate, for example, 50% removal, therefore less capital and operator intensive processes are more suitable.

Passive treatment has recently been successfully demonstrated for advanced sulfate removal. The process suffers from certain drawbacks, including the requirement for large land areas to treat large flow rates, and the risk of nutrient loss to the effluent. A key element of the most recent passive treatment case studies is the successful sequestration of sulfide using magnetite containing media, reducing the problems of sulfide gas release, or of reversion of sulfide to sulfate which in the past have hampered the success of certain passive biological sulfate removal case studies.

Hybrid biological treatment seeks to combine the best features of both active and passive treatment to offer cost savings for large scale sulfate removal projects without requiring a large land area. Hybrid treatment is an emerging concept, but is already commercially proven at least two sites for selenium reduction and has been demonstrated for base metal removal. Hybrid treatment seeks to decouple the processes that break down complex organic carbon sources from the sulfate reduction process. Such systems are designed to make use of readily available inert mine wastes as media to achieve a low unit cost for the bioreactor. Hybrid systems are unique compared to passive systems in that they may be back-flushed and thus offer longer reactor life spans.

REFERENCES

Blumenstein E, Gusek J,; The Development of a Demonstration Passive Treatment System for Removing Sulfate; 2012; National Meeting of the American Society of Mining and Reclamation, Tupelo, MS Sustainable Reclamation June 8 – 15, 2012. R.I. Barnhisel (Ed.) Published by ASMR, 3134 Montavesta Rd., Lexington, KY 40502

Eger P, Moe T, Engesser T; The Use of Sulfate Reducing Bacteria to Remove Sulfate from Iron Mining Tailings Water; Paper was presented at the 2004 National Meeting of the American Society of Mining and Reclamation and The 25th West Virginia Surface Mine Drainage Task Force, April 18-24,2004. Published by ASMR, 3134 Montavesta Rd., Lexington, KY 40502.

Gusek, J.J., 2002. Sulfate-Reducing Bioreactor Design and Operating Issues: Is This the Passive Treatment Technology for Your Mine Drainage? In: Proceedings of the National Association of Abandoned Mine Land Programs, Park City, Utah, September 15-18, 2002.

Hutton B, Kahan I, Thubendran N, Gunther, Operating and Maintenance Experience at the eMalahleni Water Reclamation Plant; 2009 Abstracts of the International Mine Water Conference 19th – 23rd October 2009 Pretoria, South Africa

Kumar R McCullough C Lund M Newport M; Sourcing Organic Materials for Pit Lake Bioremediation in Remote Mining Regions Mine Water Environ Technical Communication; Published online 08 Mar 2011

Liamleam W, Annachhatre A,; Electron donors for biological sulfate reduction; Biotechnology Advances 25 (2007) 452–463

Mayer, K, Bates, E, (2006) Compost-Free Sulfate-Reducing Bioreactors at Aspen Seep, http://www.epa.gov/aml/tech/leviathan.pdf

Reisman T, Rutkowski T, Smart P, Gusek J, Sieczkowski M,; Passive Treatment and Monitoring at the Standard Mine Superfund Site, Crested Butte, CO.; 2009 National Meeting of the American Society of Mining and Reclamation, Billings, MT, Revitalizing the Environment: Proven Solutions and Innovative

Approaches May 30 – June 5, 2009. R.I. Barnhisel (Ed.) Published by ASMR, 3134 Montavesta Rd., Lexington, KY 40502.

Tsukamoto TK, Miller GC (2002) Sustainable bioreactors for treatment of acid mine drainage at the Leviathan Mine. In: CD Proceedings of the conference on hard rock mining 2002, Denver, CO, USA, platform session 10, p 3

Van Niekerk, A; personal communication, February 2015

Mine water treatability studies for passive treatment of coal mine drainage

Alexander Sutton[1], Devin Sapsford[1] and Arabella Moorhouse[2]

1. *Cardiff University, United Kingdom*
2. *Coal Authority, United Kingdom*

ABSTRACT

The closure of coal mines in the United Kingdom, and the subsequent rebounding of the groundwater has caused widespread pollution of watercourses. This has largely been through the deposition of hydrous ferric oxides, commonly known as ochre. This research has been conducted to further the understanding of the treatability of mine waters with respect to the rates of ferrous iron oxidation and particulate ferric iron settling that occur. Iron oxidation and settling rates were measured in freshly emerged mine waters using a 2.5 m high, 45 L capacity settling column, with periodic sampling from three different depths over a 48 hour duration. Mine waters with initial iron concentrations of between 3 mg/L and 18 mg/L, from sites across South Wales (UK) and New Zealand were tested. The results indicated that the limiting step for treatment on waters above pH 6 and below 18 mg/L iron was settling, which has significant implications for design interventions intended to increase treatment efficiency. The results also demonstrate the complexity of the mine water in relation to the rate of iron removal and the need for a test to determine the iron removal rate for individual mine waters. Furthermore the effect of decreased temperature on mine water treatability, which is important for understanding seasonal effects and the impacts of heat extraction from mine waters with heat pumps, was also examined, with results showing a decrease in mine water treatability at temperatures between 17.6 ˚C and 1.6 ˚C.

Keywords: Oxidation, settling, passive, heat extraction

INTRODUCTION

Treatment of iron (Fe) bearing mine water using passive treatment systems has been occurring in the United Kingdom (UK) for two decades. A considerable amount of research has been conducted on the chemistry of the processes by numerous authors, which has been utilized in the design of passive treatment systems. These passive treatment systems in the UK are predominantly a combination of settling ponds and aerobic wetlands suitable for the circumneutral ferruginous mine waters issuing from former coal mines.

The design of past and current settling ponds has been based upon various criteria by different researchers. These include a 48 hour hydraulic retention time (NCB, 1982), anticipated Fe removal rate of 10 g/m²/d (Hedin, Nairn & Kleinmann, 1994) and 100 m² of pond area per L/s of mine water (PIRAMID, 2003). The calculation of the required area of wetlands is most often based upon one of two methods. The first was devised by Hedin, Nairn and Kleinmann (1994) and establishes a contaminant removal rate of 10 g/m²/d for a system that must meet regulatory standards or 20 g/m²/d for reasonable improvement (PIRAMID, 2003). Tarutis, Stark and Williams (1999) proposed that the removal rate of Fe in wetlands was by first order removal instead of zero order removal, which the previous criteria are based upon. These criteria produce sizably different scale treatment systems meaning that some are undersized, whilst others may be oversized (PIRAMID, 2003). Undersized schemes can lead to pollution incidents, whereas oversized schemes result in an unnecessary financial burden. A better understanding of the physicochemical processes influencing Fe removal for each site could reduce these uncertainties, taking into account the individual chemistry of the mine waters at each specific location.

The treatability of mine water with respect to the application of passive systems depends upon the rates of the processes governing Fe removal. Overall Fe removal in these systems requires (i) sufficient oxygen (O_2) transfer into the water to satisfy the O_2 demand of ferrous iron (Fe(II)) oxidation (ii) adequate residence time for Fe(II) oxidation and (iii) sufficient residence time to remove particulate ferric iron (Fe(III)) through filtration, accretion, or settling. The widely accepted rate law for oxidation of Fe(II) in pH >4 indicates a reaction that is influenced most significantly by the variation in pH (Stumm & Lee, 1961; Hove, Van Hille & Lewis, 2007; Millero, Sotolongo & Izaguirre, 1987). Studies on the rate of particulate Fe(III) settling are sparse and are usually combined with Fe(II) oxidation studies. One study on particulate Fe(III) settling rates using settling columns and laboratory simulated mine waters focused upon circumneutral and high pH waters in the range of 6-10 and found that there was no significant difference between settling rates of Fe at each pH tested (Hove, Van Hille & Lewis, 2007). Settling rates of particulate Fe(III) were found to demonstrate first-order behavior with respect to the concentration of particulate ferric iron, with settling rates varying for different mine waters (Sapsford, 2013). Hedin & Nairn (1990) suggested that "Fe removal rates are correlated with Fe concentration" for wetlands, but whether this is applicable to settling ponds is unknown.

Aeration of the mine water prior to flowing into the settling pond is seen as an essential step in the treatment of ferruginous mine water (PIRAMID, 2003). This is to ensure that the Fe(II) is oxidized to Fe(III) so that it may precipitate in the settling pond. For some mine waters aeration cascades benefit by stripping dissolved carbon dioxide, therefore raising the pH and increasing the Fe oxidation rate (Geroni & Sapsford, 2011; Stumm & Lee, 1961; Hove, Van Hille & Lewis, 2007; Millero, Sotolongo & Izaguirre, 1987).

Temperature affects the treatability of mine water and the kinetics of Fe(II) oxidation (e.g. Stumm & Lee, 1961; Millero, Sotolongo & Izaguirre, 1987). Temperature might reasonably be expected to affect settling behavior of particulate Fe(III), although literature is interestingly lacking on this subject. Heat extraction from mine water has been demonstrated to be feasible and economic (Banks et al, 2004), however little consideration has been given to the effects it may have upon the treatability of the mine water. In the UK mine water is typically at a temperature of 10-12 °C year-round (Banks et al, 2004). Decreasing this temperature by the typical 5 °C (Banks et al, 2004), would be expected to cause a subsequent decrease in the rate of oxidation of the Fe(II) and possibly impact settling rates.

This paper aims to (i) demonstrate a method for examining the treatability of different circumneutral ferruginous mine waters, which shows the rates of Fe(II) oxidation and settling of particulate Fe(III) under quiescent conditions for different mine waters, (ii) demonstrate the effect of aeration versus non-aeration and (iii) assess the effect of temperature reduction on mine water treatability.

METHODOLOGY

Iron removal tests were conducted for five mine waters from across South Wales and South Island in New Zealand. These studies were conducted using columns 2.5 m in height, (similar to a typical settling pond depth) and contained 45 L of mine water. Experiments were carried out on aerated and non-aerated mine water samples to determine the effects of aeration on the iron removal rates. Initial iron concentrations were between 3 mg/L and 17 mg/L. The experiments were run between 48 hours and 158 hours.

Iron Removal Rates

Mine Water Collection

A number of mine waters from coalfields in South Wales and New Zealand were used in the study, including active coal mine sites and passive treatment schemes. All of the samples from South Wales were collected prior to any aeration cascades. The sites were four passive treatment systems in South Wales (Glyncorrwg, Lindsay, Morlais, and Taff Merthyr) and one active mine in New Zealand, where the outfall from old mine workings pass over a waterfall prior to sampling. At each site 30 L containers were filled to the top to inhibit oxygenation in transit and transported back to the laboratory. Times varied from two hours to seven hours between sampling and commencement of the experiments.

Settling Column

The settling column was designed to replicate the processes occurring within a settling pond, although a difference in behavior might be expected where flow through the pond is not laminar. A relationship between the Fe concentration and column depth with time was determined by sampling every three hours from three sampling ports. An initial volume of 20 ml was extracted from each port and used to wash the beaker for each sample. A further 45 ml was extracted, from which 20 ml was used for total Fe analysis (i.e. particulate Fe(III) plus dissolved Fe(II)), 20 ml was filtered through a 0.2 μm syringe filter for total dissolved Fe and 5 ml was used for Fe(II) analysis. Prior to analysis 1 ml of 20% hydrochloric acid was added to the 20 ml samples.

Two settling columns were used for the water from each mine. In one column, the mine water was aerated by twice pouring the mine water between buckets held one meter above the other, in order to mimic the effects of an aeration cascade. In the second column, the non-aerated mine water was pumped directly from the 30 L container, through a pipe that passed down to the base of the column, thus minimizing the O_2 transfer into the mine water. The mine water was vigorously agitated in the sealed containers to re-suspend any sediment prior to being pumped into the columns. The columns were filled to within 0.05 m of the rim and remained undisturbed throughout the experiment.

Inorganic Elements Analysis

For the samples collected in South Wales total Fe was measured using a Perkin and Elmer Optima 2100DV inductively coupled plasma-optical emission spectrometer against certified standards. In New Zealand total Fe was determined using a portable Hach spectrophotometer with FerroVerr as the reagent. Iron concentrations above 3 mg/L were diluted using deionized water before analysis on the spectrophotometer. Ferrous iron from mine waters in Wales was determined spectrophotometrically using a Hitachi U1900 spectrophotometer at a wavelength of 510 nm. The reagent used was 1,10-phenathroline at Fe concentrations less than 15.0 mg/L. The mine water samples in New Zealand were measured using a portable Hach spectrophotometer with Hach Fe(II) reagent. Fe(II) concentrations above 3.0 mg/L were diluted using deionized water before analysis on the Hach spectrophotometer.

Data Logging

Throughout the duration of the experiment dissolved oxygen (DO), pH and temperature were measured using a HANNA 9828 multi-parameter probe. The probe was immersed in the mine water within the column at a height of 1.86 m. Calibration of the probe was undertaken before each experiment. Temperature, pH and DO were also measured in the field when the mine water was collected.

Heat Abstraction

Mine water collected from Taff Merthyr in South Wales was used for the heat abstraction experiments and was obtained in the same manner and analyzed using the same techniques as the column experiments above. The mine water was cooled during transport by storing in a cool box at reduced temperatures prior to refrigeration. The mine water in both columns was aerated prior to transfer into the column.

Settling Column

Two settling columns were used, one was kept at room temperature of 17.6°C and the second stored in a fridge at 1.6°C. The settling columns were 20 L square barrels, 0.55 m in height, 0.20 m in width and 0.20 m deep, filled to within 0.05 m of the rim. Samples were extracted from 0.1 m below the surface of the mine water. The experiment was repeated using different temperatures of 12.9°C for the room temperature and 4.3°C in the fridge.

RESULTS AND DISCUSSION

Iron Removal Rate & Aeration

The following can be inferred from the data presented below. Aeration of the mine water made little difference to the overall removal of iron for the mine water at Glyncorrwg (Figure 1), which was roughly linear with an iron removal rate of 0.07 mg/L/hr. This indicates that for this mine water particulate settling was likely to be the rate limiting step. At Lindsay (Figure 2) the data indicates that particulate settling was likely the rate limiting step for this mine water, with similar removal of total Fe after 48 hours between the aerated and the non-aerated columns. The impact of aeration on the Lindsay mine water is more evident and it is noteworthy that after 20—30 hours the majority of Fe was in particulate Fe form, which may have been easier to remove (by filtration) if the water was passing through an aerobic wetland at these times. Total Fe removal in Figure 2 did not follow a linear trend over the duration of the experiment at Lindsay. The mine water for Morlais was most clearly impacted by the aeration as seen in Figure 3, with the total Fe removal in the aerated column being approximately 58% lower in concentration than in the non-aerated column after 48 hours. This indicates that for this mine water, both the Fe(II) oxidation rate and particulate Fe(III) settling rate are important in the overall treatability of the mine water. Again the overall iron removal is approximately linear over the duration of the experiment and is circa 0.20 mg/L/hr.

The mine water Taff Merthyr indicates that for this mine water particulate Fe(III) settling is the rate limiting step and thus controls the overall removal of iron for this mine water (Figure 4). Iron oxidation rates are different between the aerated and non-aerated mine waters, but this has negligible impact on the overall Fe removal rate. The mine water at the active mine site in New Zealand (Figure 5) shows a case where there is no requirement for the oxidation of Fe(II) and that all the Fe is in the form of particulate Fe(III), thus Fe removal is solely governed by the rate of settling.

The Fe(II) and total Fe concentrations between the three sampling ports in the columns were found to be very similar in all cases, typically within 4.4% and 3.0% of each other for total Fe and Fe(II) respectively. Consequently the average value between the three sampling ports was used to create the following Fe concentration versus time graphs. This means that the settling rates of Fe(III) are irrespective of the depth, which has implications for design of settling lagoons.

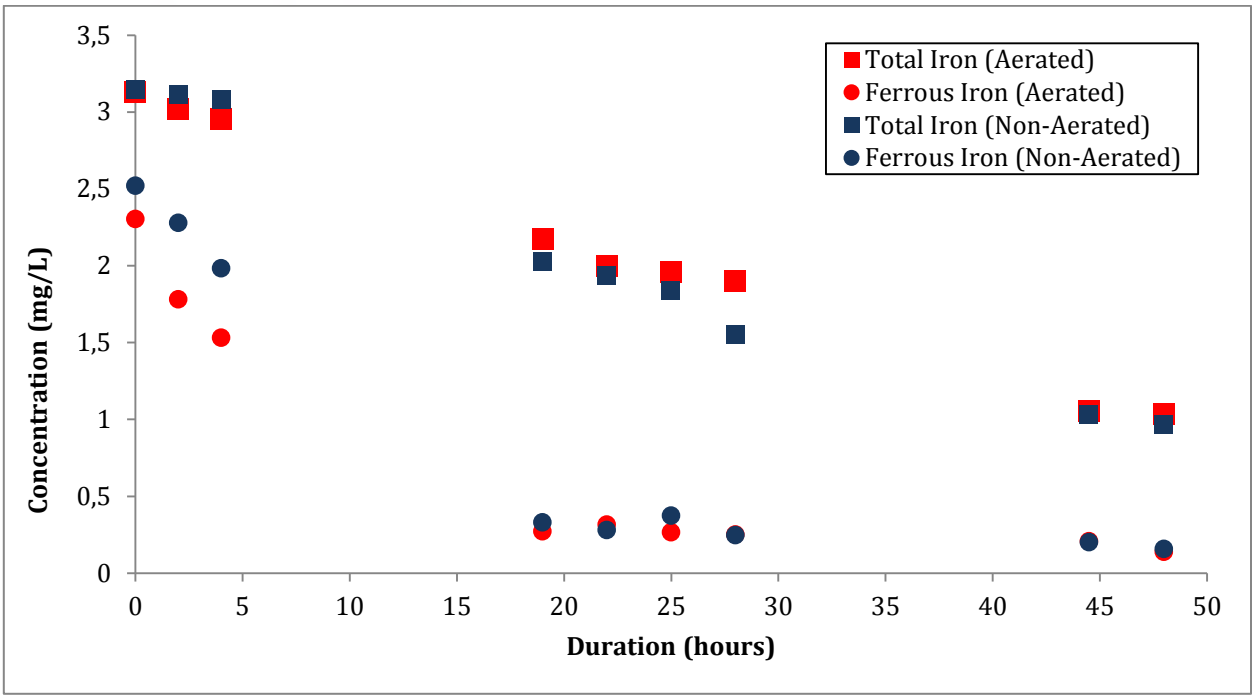

Figure 1 Change in Fe(II) and total Fe concentration with time in column at Glyncorrwg. Mean pH and initial DO during test = 6.52 and 4.99 mg/L respectively for aerated and 6.17 and 3.44 mg/L for non-aerated

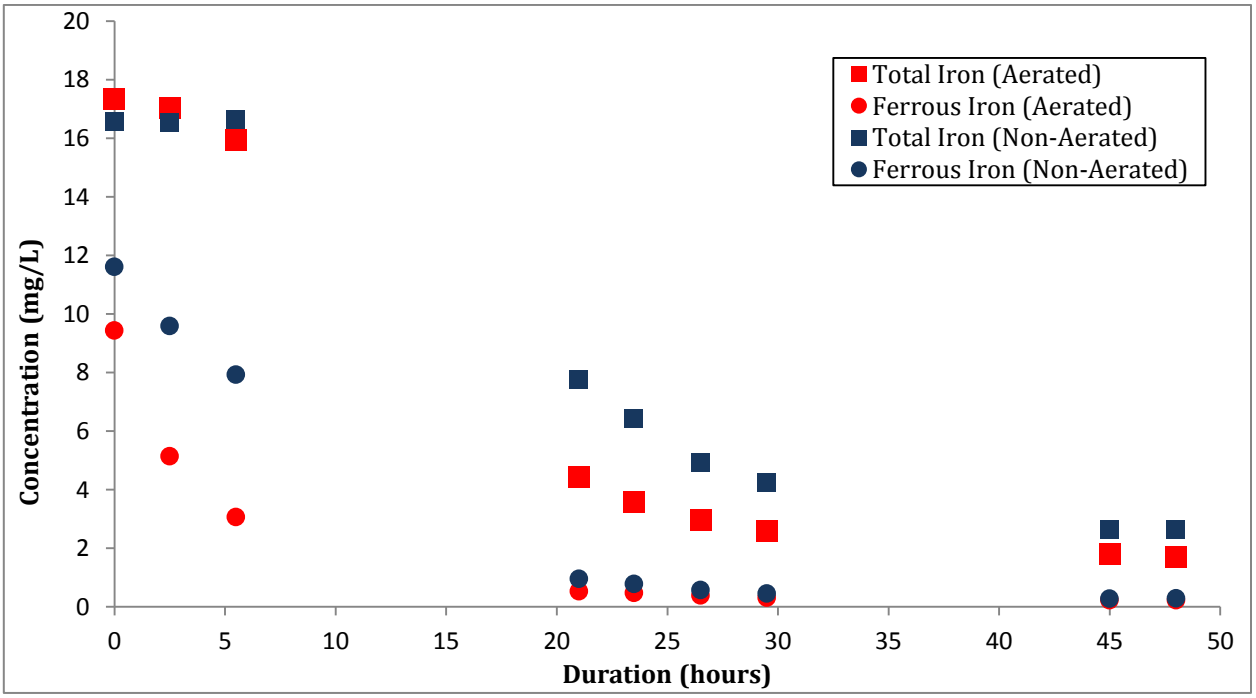

Figure 2 Change in Fe(II) and total Fe concentration with time in column at Lindsay. Mean pH and initial DO during test = 6.58 and 8.00 mg/L respectively for aerated and 6.59 and 2.67 mg/L for non-aerated

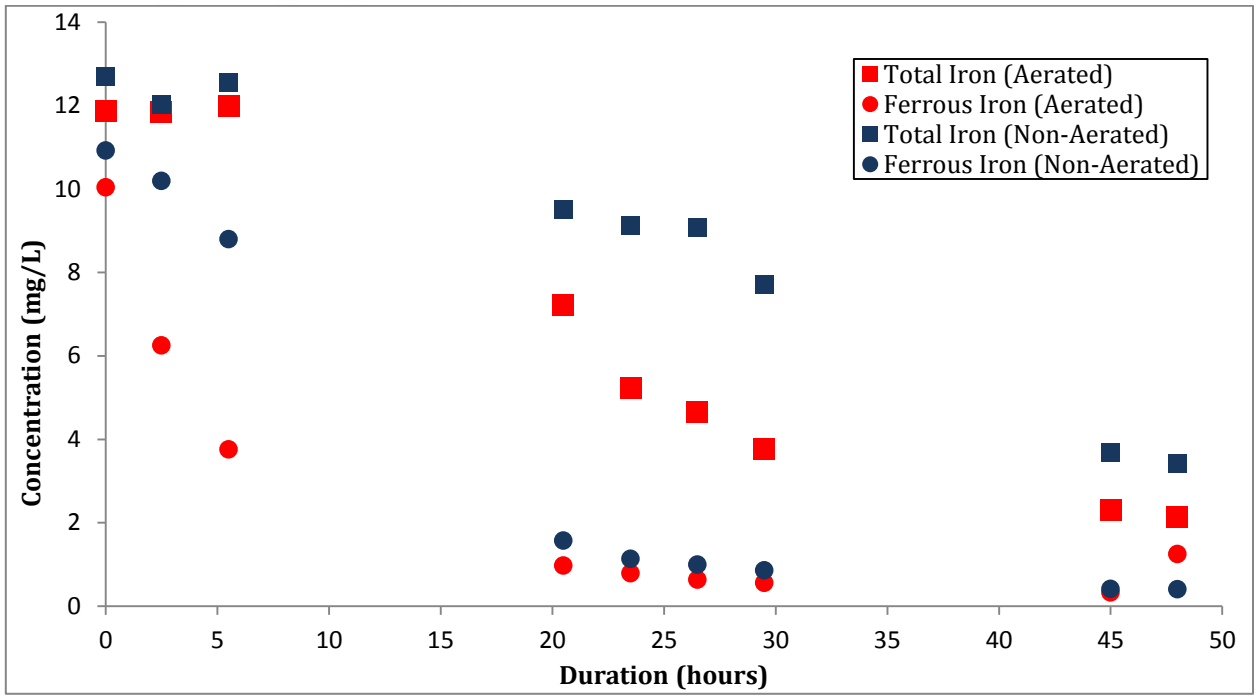

Figure 3 Change in Fe(II) and total Fe concentration with time in column at Morlais. Mean pH and initial DO during test = 6.06 and 5.01 mg/L respectively for aerated and 6.36 and 3.23 mg/L for non-aerated

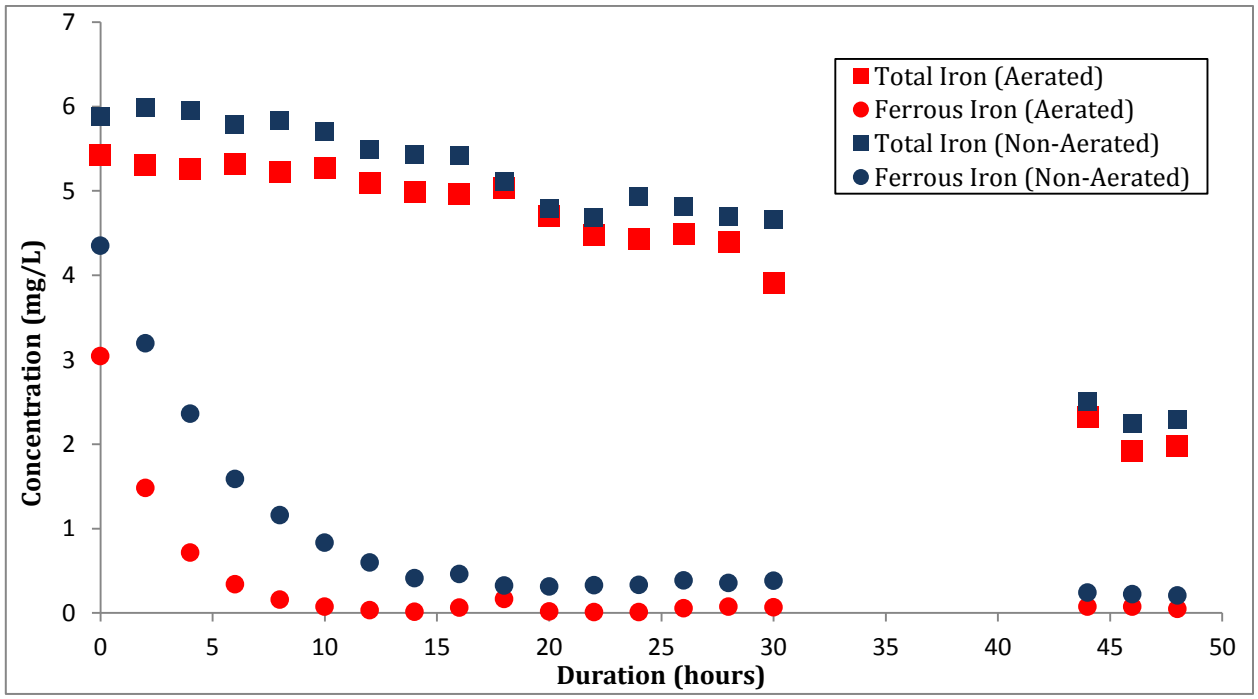

Figure 4 Change in Fe(II) and total Fe concentration with time in column at Taff Merthyr. Mean pH and initial DO during test = 7.09 and 8.52 mg/L respectively for aerated and 7.11 and 2.62 mg/L for non-aerated

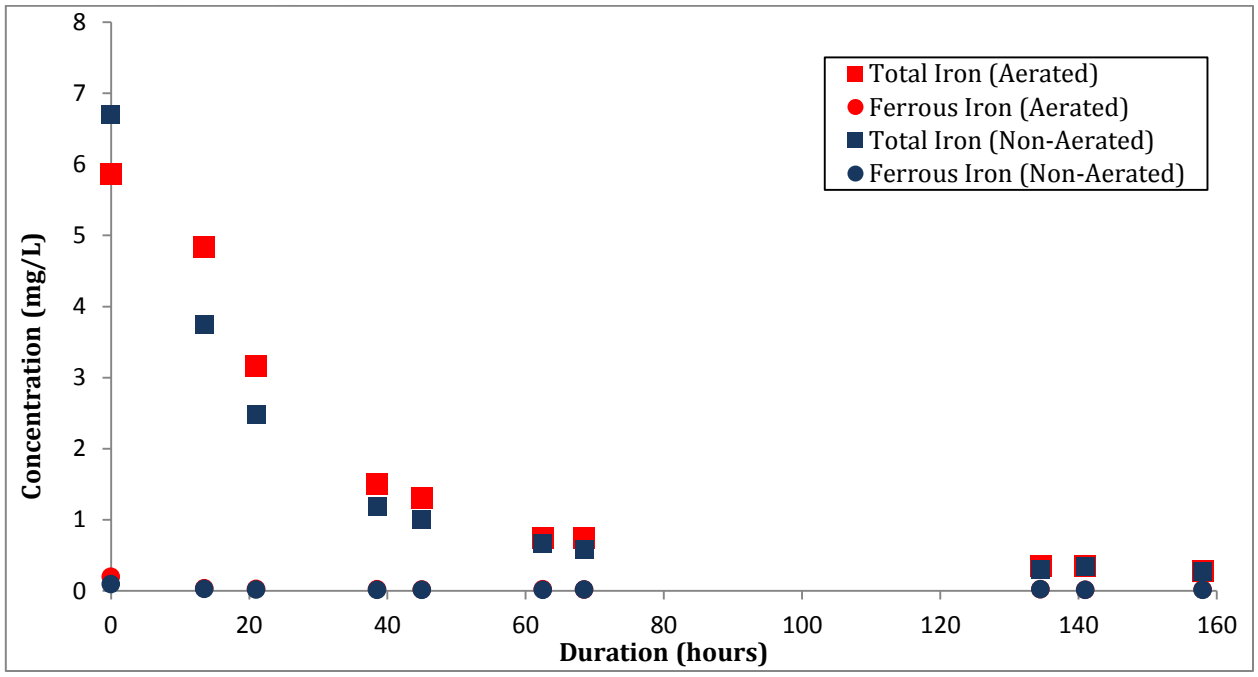

Figure 5 Change in Fe(II) and total Fe concentration with time in column at active mine site in New Zealand. Mean pH during test = 6.48 for aerated and 6.48 for non-aerated

Heat Abstraction

Experiment one was conducted at a mean water temperature of 1.6 °C for the refrigerated sample and 17.6 °C for the room temperature sample. Experiment two was conducted at 4.3 °C for the refrigerated sample and 12.9 °C for the room temperature sample. The Fe removal rates have a similar linear relationship between total Fe concentration and time to the previous column tests at Taff Merthyr.

Reduction in temperature in experiment one shows a decrease in the Fe removal rate between the room temperature sample and the refrigerated sample, with a difference in final Fe concentration of 0.8 mg/L after 48 hours. A similar decrease was seen in experiment two, with a difference in final total Fe concentration of 0.9 mg/L after 48 hours. Comparing the experiments shows that the Fe removal rates are variable and not solely dependent upon temperature, as the removal rate at 4.3 °C and 12.9 °C is higher than that recorded at 17.6 °C.

Table 1 Iron removal rates for mean temperatures of 1.6—17.6 °C, pH 6.4—6.8 and initial DO 6.0—6.2 mg/L, duration of 48 hours

Mean Temperature (°C)	Initial Fe(II) Concentration (mg/L)	Final Fe(II) Concentration (mg/L)	Initial Total Fe Concentration (mg/L)	Final Total Fe Concentration (mg/L)	Fe Removal Rate (mg/L/h)
1.6	2.32	0.12	5.13	2.24	0.03
17.6	2.49	0.27	4.85	1.39	0.07
4.3	3.22	0.13	5.13	2.09	0.07
12.9	3.30	0.13	5.20	1.24	0.08

CONCLUSION

In conclusion, the findings of this study were as follows:

(i) Particulate Fe(III) settling displays unusual settling behavior where the concentration is seen to decrease concurrently and equally at different heights within a column of quiescent mine water.

(ii) For mine waters of similar character (low Fe concentration, pH 6.0—7.5, DO 2.62—8.52 mg/L) the treatability of the mine waters is different and show instances where the relative rates of Fe(II) oxidation and particulate Fe(III) settling becomes more or less important. This information is very important for design, particularly where treatment efficiency is trying to be increased. The data presented thus demonstrate the importance of mine water treatability studies for each new mine water to be treated.

(iii) Decreasing the temperature of the mine water by between 8.6—16°C leads to a reduction in the treatability of the mine water.

ACKNOWLEDGEMENTS

The authors wish to thank the Coal Authority and the EPSRC for funding this research and CRL Energy Ltd for assisting with the research on the coal mine water in New Zealand.

REFERENCES

Banks D., Skarphagen H., Wiltshire R., and Jessop C (2004) *Heat Pumps as a Tool for Energy Recovery from Mining Wastes*, Energy, Waste and the Environment: a Geochemical Perspective, Vol.236, pp.499–513.

Geroni JN., Sapsford DJ (2011) *Kinetics of Iron (II) Oxidation Determined in the Field*, Applied Geochemistry, Vol.26, 1452–7.

Hedin RS., and Nairn RW (1990) *Sizing and Performance of Constructed Wetlands: Case Studies*, Mining and Reclamation Conference and Exhibition, West Virginia .

Hedin RS., Nairn RW., and Kleinmann RLP (1994) *Passive Treatment of Polluted Coal Mine Drainage*, Bureau of Mines Information Circular 9389, United States Department of Interior, pp.35.

Hove M., Van Hille RP., and Lewis AE (2007) *Iron Solids Formed from Oxidation Precipitation of Ferrous Sulfate Solutions*, AIChE Journal, Vol.53 (10), pp.2569–77.

Millero FJ., Sotolongo S., and Izaguirre M (1987) *The Oxidation Kinetics of Fe(II) in Seawater*, Geochimica et Cosmochimica, Acta, Vol.51 (4), pp.793–801.

National Coal Board (1982) *Technical Management of Water in the Coal Mining Industry*.

PIRAMID Consortium (2003) *Engineering Guidelines for the Passive Remediation of Acidic and/or Metalliferous Mine Drainage and Similar Waste Waters*, A Research Project of the European Commission 5th Framework Programme.

Sapsford DJ (2013) *New Perspectives on the Passive Treatment of Ferruginous Circumneutral Mine Waters in the UK*, Environmental Science and Pollution Research, Vol.20 (11), pp. 7827–36.

Stumm W., and Lee GF (1961) *Oxygenation of Ferrous Iron*, Industrial Engineering Chemistry, Vol.53, pp.143–6.

Tarutis WJ., Stark LR., and Williams FM (1999) *Sizing and Performance Estimation of Coal Mine Drainage Wetlands*, Ecological Engineering, Vol.12, pp.353-72.

10th ICARD IMWA 2015 | 10th International Conference on Acid Rock Drainage & IMWA Annual Conference

Case Study: 19 Years of Acid Rock Drainage Mitigation after a Bactericide Application

James Gusek[1] and Van Plocus[2]

1. *Sovereign Consulting Inc., USA*
2. *Diamond Engineering, USA*

ABSTRACT

The Fisher site is a backfilled and reclaimed (in 1984) surface coal mine in western Pennsylvania, USA. A post-closure toe seep at the site discharged acid rock drainage generated in pyritic rock zones that were identified using geophysical techniques. In 1995, sodium hydroxide and bactericide solutions were injected through cased boreholes into the pyritic zones in a two-step process: sodium hydroxide followed by bactericide. Prior to the event, the toe seepage had been treated with the addition of sodium hydroxide followed by a series of settling ponds and wetland zones. Post-injection, the seepage exhibited net-alkaline chemistry and the sodium hydroxide amendment was discontinued. Based on the prevailing wisdom at the time, the effects of the injection event were expected to be temporary. Almost two decades later, the beneficial effects of the two-step injection event persist and bond release for the site is pending. The seep chemistry has been monitored for over 25 years and the data suggest that the steady-state condition of net alkalinity in the seep water entering the ponds and wetland may be permanent. One current view is that the initial suppression of *Acidithiobacillus ferrooxidans* bacterial community with the sodium hydroxide and bactericide has been maintained by the seasonal infusion of bactericidal organic acids derived from the robust vegetative cover. The situation appears to be self-sustaining.

Keywords: sustainability, surfactant, coal, ARD, probiotics

INTRODUCTION

World-wide, reclaimed/re-vegetated mine sites (both coal and hard rock) continue to experience significant acid rock drainage (ARD) problems. The sites represent a perpetual treatment problem for the mine operator, contribute to environmental degradation of surface water and groundwater resources, and may prevent bond release. Conventional and passive treatment methods typically treat the symptoms of ARD, not its source. As evidenced by ARD being discharged from mines that were operated by the Romans over two thousand years ago, ARD can persist for millennia. Considering the billions of tonnes of acid-prone waste rock and tailings that are generated annually, a commitment to perpetual treatment is clearly not sustainable. ARD source control is clearly the "pathway to walkaway", but the mining industry seems to be reluctant to embrace unproven technologies. The recurring question is: "show us the data". Even when data are available, sampling protocols (if they are ever documented) can change over time, data gaps may occur for no reason, and even the sampling points can shift. This is the situation for this particular case history; the data set is not robust but the authors believe it is complete enough to be useful.

The iron-oxidizing bacteria, *Acidithiobacillus ferrooxidans (ATBFO)*, have proven to play a critical role in creating ARD and are strongly associated with the formation of acid rock drainage (Kleinmann, et.al. 1981; Schrenk et. al., 1998). Metals found in mine soils, including iron, manganese, aluminum, magnesium, lead, copper, zinc, cadmium, and selenium are solubilized, creating drainage that is toxic to the environment. Suppression of *ATBFO* has proven to significantly reduce the generation of ARD at mine sites (Rastogi 1996).

Bactericide usage history

Anionic surfactants are effective inhibitors of *ATBFO*, as they destroy the integrity of the cytoplasmic membrane of the bacteria thus allowing the acid that they create to enter the cells and destroy them. Their use was first promoted in the late 1970's and was successfully applied in the early 1980's (Kleinmann, 1979; Kleinmann and Erikson, 1983). However, skeptics in the mining community and mining regulators have argued (and rightfully so), that the inhibitory effects of anionic surfactants are temporary, as these highly soluble reagents can be rinsed from the treated mine wastes and *ATBFO* communities can rebound. To address this problem, commercial, slow release anionic surfactants such as ProMac™ were developed in the late 1980's.

More recently, researchers at the Wyoming Research Institute (Jin 2008) determined that a biofilm nurtured by waste milk or other dairy products, inoculated with a "probiotic" bacterial community, could out-compete *ATBFO* on the surfaces of pyrite grains and thus suppress ARD. Again, however, the question remains: what happens when the milk/dairy waste is consumed? Will the *ATBFO* community recover and dominate the situation?

Fortunately, anionic surfactants are not the only *ATBFO* inhibitors. Almost 35 years ago, Pichtel and Dick (1990) found that the following materials, some considered waste by modern society, can suppress ARD:

- Composted sewage sludge (biosolids),
- Composted paper mill sludge,
- Pyruvic acid (an organic acid), and
- A water-soluble extract from composted sewage sludge.

The ARD inhibitory effects of organic acids were cited by Sobek et al. (1990) as an important component in the long term (i.e., greater than three years) success of anionic surfactant usage. An excerpt from this paper follows.

> *Control of acid generation for prolonged periods greatly enhances reclamation efforts and can reduce reclamation costs by reducing the amount of topsoil needed to establish vegetation. Three natural processes resulting from strong vegetative cover for three years or more can break the acid production cycle. These processes are:*
>
> - *A healthy root system that competes for both oxygen and moisture with acid-producing bacteria;*
> - *Populations of beneficial heterotrophic soil bacteria and fungi that are re-established, resulting in the formation of organic acids that are inhibitory to T. ferrooxidans (Tuttle et al. 1977); and*
> - *The action of plant root respiration and heterotrophic bacteria increase CO_2 levels in the spoil, resulting in an unfavorable microenvironment for growth of T. ferrooxidans."*

Two reclaimed mine sites, one near Steubenville Ohio, USA and another near Clarksburg, West Virginia USA received slow release anionic surfactant treatments in 1984 and 1987, respectively (Rastogi, 1996). Increased vegetative growth was the primary goal of the surfactant applications; ARD suppression was a secondary benefit. The sites were investigated in 1994 and the benefits of the anionic surfactant persisted well beyond the normal longevity of the surfactant itself. However, the vegetative response in the treated portions of the sites was so strong that the ARD seepage was virtually eliminated. The somewhat less vegetated control plots still discharged ARD. Concurrent investigation results revealed that *ATBFO* populations in the treated soils were vastly outnumbered by beneficial heterotrophic bacteria by two to three orders of magnitude.

Despite the laboratory and overwhelming field evidence, the use of bactericides to suppress ARD was never a commercial success. It was not considered a permanent remedy. A decade of positive performance was apparently not enough.

SUBSURFACE INJECTION OF BACTERICIDE

As of the mid-1990's, anionic surfactants had only been applied to surface sources of ARD. That changed when Plocus and Rastogi (1997) demonstrated that subsurface application of anionic surfactants using injection techniques could successfully reduce ARD at the Fisher Site in Banks Township, Indiana County, Pennsylvania. This was accomplished by identifying the acid-generating zones using geophysical techniques and designing a multiple-stage borehole based injection program that targeted the ARD "hot spots".

Geophysical mapping with electromagnetic terrain conductivity meters and magnetometers were utilized to identify pyritic zones which were responsible for the high acid production on the Fisher Site. See Plocus and Rastogi (1997) for a more detailed discussion of the geophysical investigation.

The Fisher Site in Banks Township, Indiana County, western Pennsylvania USA represents a typical reclaimed mine site which continued to generate post-reclamation ARD. The Fisher Site layout is found in Figure 1.

A single coal seam (~2m thick) was mined in the early 1980's using surface mining techniques. Anecdotal information suggested that a high-ash coal containing pyritic shale partings had been buried in the pit during the coal removal process. Infiltrating precipitation and contact with

groundwater in these zones of concentrated pyritic material resulted in localized ARD production. A resultant ARD plume eventually surfaced as an acidic seep with levels of iron, manganese and pH exceeding effluent limits. Table 1 presents water quality data on the raw ARD seep on the Fisher Site and the associated limits for these parameters.

Site reclamation consisting of pit backfilling and re-vegetation; this effort was completed in 1984. The effluent from a small (0.25 ha) passive treatment system, constructed in 1985 to manage the raw seepage, did not meet Pennsylvania Department of Environmental Protection (PA DEP) standards. To remedy this situation, two treatment ponds were constructed after the passive treatment system; supplementary semi-active treatment with a sodium hydroxide solution comprised the long-term treatment plan for this reclaimed and re-vegetated surface mine. With the exception of the post-mine discharge which exceeded effluent limits, the Fisher Site had met all requirements established by the PA DEP for bituminous coal extraction and reclamation.

Table 1 Fisher Site ARD chemistry and regulatory limits

Parameter	Raw Seep Value	Pre-Injection Wetland Effluent	Regulatory Limits (Monthly avg.)	Regulatory Limits (Instant. Max.)
Iron (mg/L)	8 to 42	17.7	3.0	7.0
Manganese (mg/L)	6 to 12	12.4	2.0	5.0
pH (s.u.)	5 to 6	5.5	6.0 to 9.0	
Acidity (mg/L)	>alkalinity	Est. ~54	n/a	n/a

In 1993, the pollution liability of this site was transferred from the coal company to a third party. Because the site effluent met existing regulatory limits due the sodium hydroxide amendment as a fall-back position, this site was viewed an opportunity to evaluate ARD source control alternatives, in particular, the injection of anionic surfactants.

The prevailing theory (in 1993) was that the source of ARD on the Fisher Site was similar to other reclaimed sites: it was primarily located in the buried mine spoil. Unfortunately, conventional surface application of anionic surfactants is ineffective on re-vegetated sites as it cannot penetrate through subsoil, topsoil and vegetation. An alternative, more-invasive and focussed surfactant delivery method was needed and injection through multiple boreholes was a logical choice. Injecting surfactant into the entire mine spoil mass was not practical, however. As subsequently determined, neither was it necessary.

Plocus and Rastogi (1997) developed an innovative approach to (1) identify the source of ARD on the Fisher Site using geophysical mapping, (2) install subsurface injection wells, and (3) inject sodium hydroxide and an anionic surfactant into the toxic zones within the subsurface strata of the Fisher Site. Among the many uncertainties at the time was: if the procedure worked in suppressing ARD, how long would its effects last?

Site characterization and geophysical mapping

Identification of backfill zones with elevated pyrite concentration was critical in determining the target locations for installation of injection wells. Space limitation constraints preclude a detailed discussion of the relationship between these holes and those identified in Figure 1. A 3.2-ha portion

of the backfilled pit immediately up-gradient of the seep was mapped using data gathered with non-invasive geophysical techniques. Based on the results of geophysical mapping, three primary acid producing zones were suspected; the center of each zone received an exploratory boring and the cuttings were analysed for acid-base accounting parameters. This effort, coupled with geophysics data interpretation, yielded six target zones for surfactant injection. Three of the most significant target zones were selected for subsurface injection of the anionic surfactant.

Application of subsurface injection techniques

After the acid-producing areas were delineated, four deep wells were drilled in June 1995 into the acid aquifers for sodium hydroxide injection to neutralize the existing acid waters, and 25 shallower wells were selected to be drilled into the pyritic zones for injection of an anionic surfactant bactericide to prevent future acid generation. During drilling activities, mine spoil samples were collected at one-meter intervals for overburden analysis.

A series of twelve 11-mm diameter drill holes were placed at the source of the acid producing area. Grout packers were installed to permit pressure injection. Injection wells were cased with 50 mm diameter PVC pipe with 1.5-meter screens and sealed with bentonite and concrete. The screen helped in pressurized distribution of the sodium hydroxide and the anionic surfactant. The depth of the shallow injection wells was approximately three (3) meters while the depth of the 17 deep injection wells (28 wells total) and overburden wells averaged 16 meters. The location of injection wells, monitoring wells, artificial wetlands and treatment ponds are shown in the site map in Figure 1.

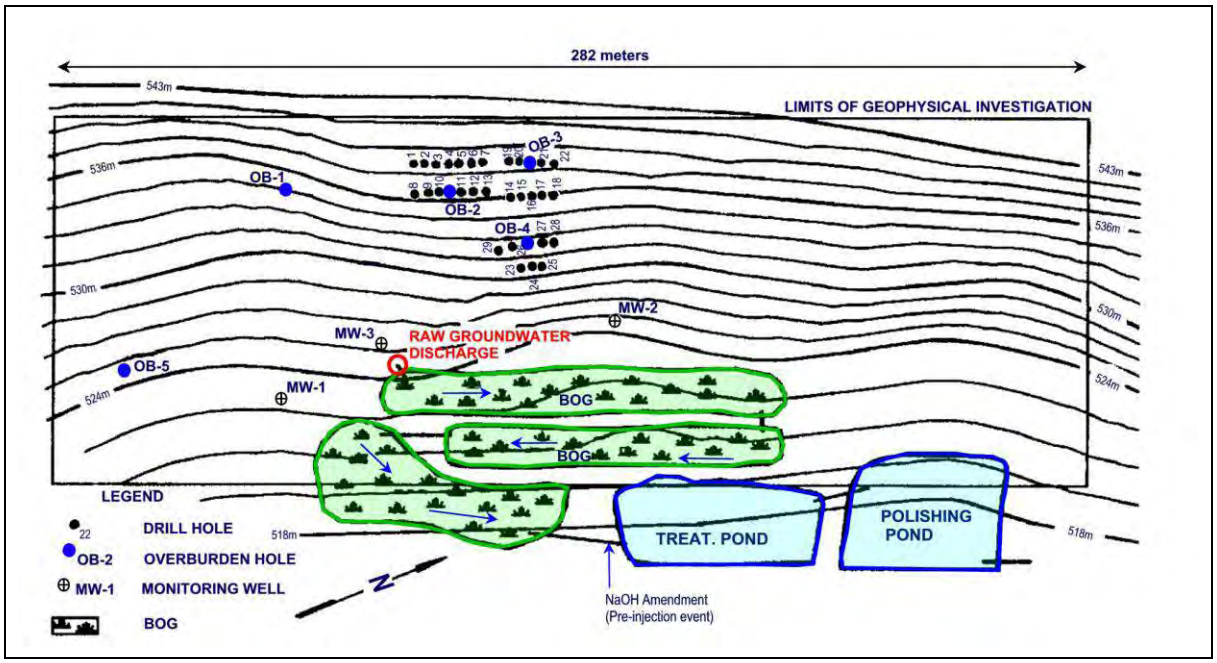

Figure 1 Injection site layout (After Plocus & Rastogi, 1997)

Injection of a 20% solution of sodium hydroxide began in mid-June, 1995 using pumps capable of pumping at pressures of 20.7MPa. Each injection well received about 1,140 liters of caustic solution.

This was followed by injection of about 570 liters of a 2% solution of the anionic surfactant bactericide. A total of six overburden wells were also injected with the anionic surfactant. In total, about 33,000 liters of 20% sodium hydroxide solution and 40,000 liters of 2% strength surfactant were injected over the span of 30 days. In 1995, the cost of these reagents was about $US8400.

The chemical amendment treatment system already in place at the Fisher Site was maintained for a one-month period after the initial injection. By that time, the quality of the raw seep prior to entering the passive treatment system had improved enough that the post-passive treatment chemical amendment addition was discontinued.

RESULTS

The raw groundwater discharge point (Figure 1) represents the acid seep discharge into the artificial wetland, or bog, which historically flowed at an average rate of 50 to 150 gpm. Figures 2 through 6 summarize results for alkalinity/acidity, pH, iron, manganese, and sulfate for this location, respectively. Rather than focus on instantaneous responses to drought or elevated flows, the discussion that follows will address long-term trends and offer plausible explanations in the context of the suppression of the acidophilic community.

Acidity, Alkalinity and pH:

Prior to subsurface injection, acidity typically exceeded alkalinity on the Fisher Site at the point of raw groundwater discharge. See Figure 2. After subsurface injection of sodium hydroxide and the anionic surfactant, alkalinity has exceeded acidity, and this condition was typically maintained even during and immediately after a prolonged drought. This is a condition necessary for bond release. The raw data is quite scattered due to the effects of drought and other unknown factors. Loading (flow times concentration) estimates are typically used to evaluate the overall effectiveness of a remedy. Figure 2 indicates a "tipping point" occurred about 13 years after the injection event when negative acidity results produced an even wider spread between acidity and alkalinity loading. The precise reasons for this apparently favourable situation are unclear and they may be an artefact of the analytical method. The pH results (Figure 3) for the same period do not reflect any dramatic improvement but about a year later, a pH improvement trend is evident and it continues to persist in 2014. On the average, pre-injection acidity loadings were about 7.1 kg/day; post-injection acidity loadings were about 1.0 kg/day and appear to be on a steady, stable (negative) trend.

The data in Figure 2 suggest that the positive effects of the injection event were quite pronounced in the three years following it. While the magnitude of the effects (the difference between acidity and alkalinity) appeared to abate, the conditions for bond release have been satisfied for the last 19 years.

Iron and Manganese:

Prior to subsurface injection activities, iron concentrations at the discharge seep ranged from 8 to 42 mg/L between 1984 and 1995 (Plocus & Rastogi, 1997). After the injection event in 1995, the seepage chemistry exhibited an overall decreasing trend in total iron and total manganese. On the average, iron loading decreased from 4.2 kg/day pre-injection to 2.4 kg/day post-injection. Manganese pre-injection and post-injection average loadings were 1.9 kg/day and 0.7 per day, respectively. Again,

post-1995 data is quite scattered but loading trends indicate a general and persistent decrease in iron and manganese mobilization from the treated area. See Figures 4 and 5. Note that the decrease in pH, iron and manganese occur a few years after the decrease in acidity loads. This suggests that iron and manganese levels did not account for the decreased acidity. Aluminum levels were not measured and this constituent may be the reason for the acidity data disconnection.

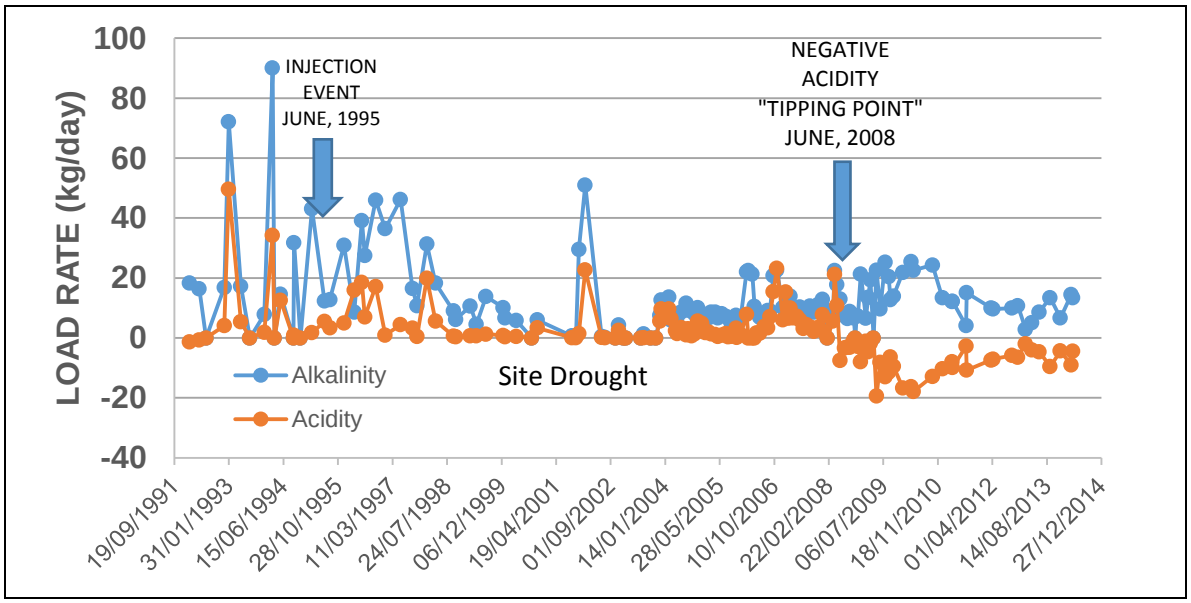

Figure 2 Seep acidity and alkalinity 1991 to 2014

Decreased sulfate levels:

As further evidence of the reduction of acid formation, sulfate concentration in the seep discharge decreased compared to pre-injection event levels. See Figure 6. This decrease, coupled with maintenance of an alkalinity level exceeding acidity levels indicates the quality is being maintained long after the immediate effects of alkaline injection and bactericide have worn off. The acidophilic community appears to be suppressed by mechanisms that are sustainable.

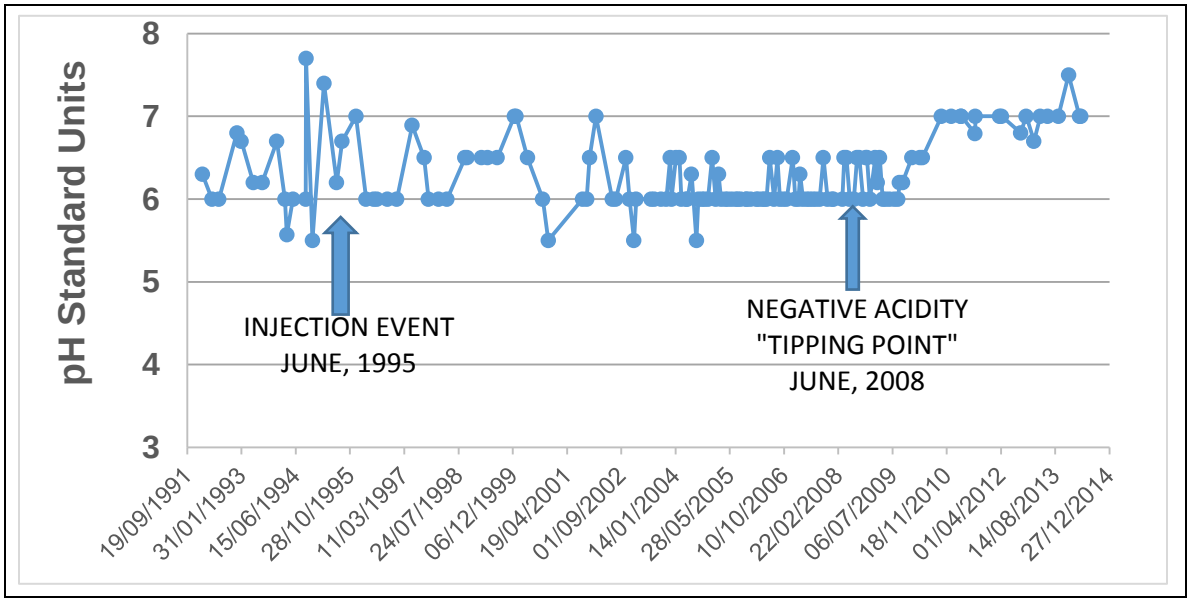

Figure 3 Seep pH 1991 to 2014

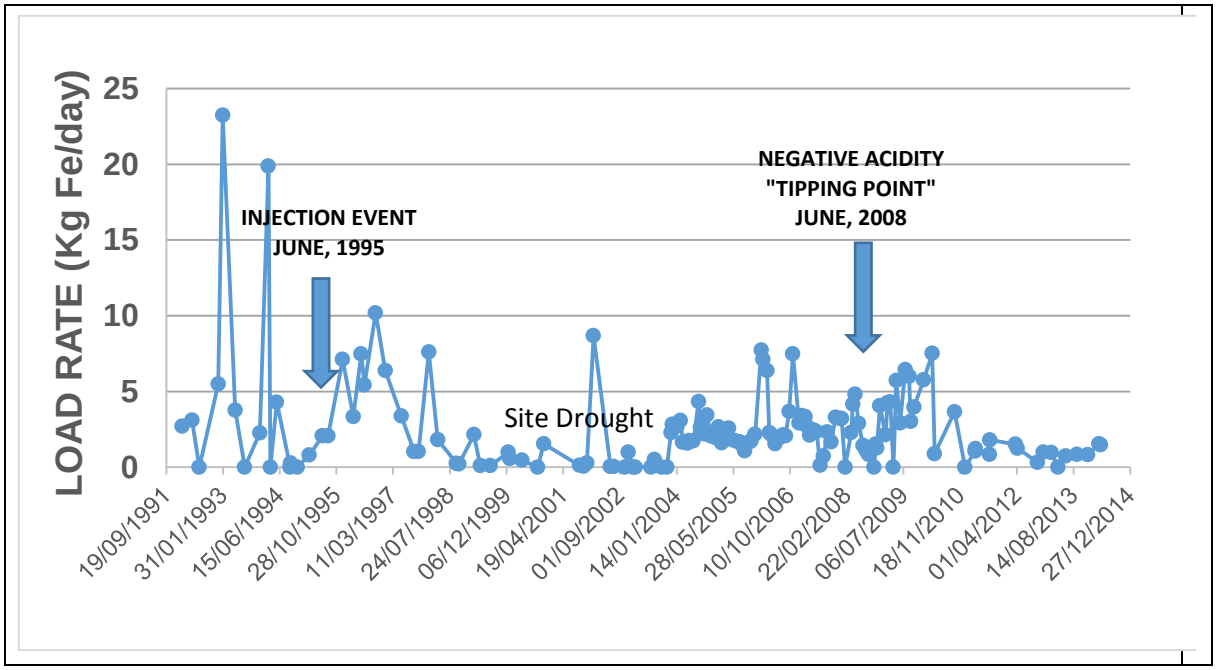

Figure 4 Seep iron loading 1991 to 2014

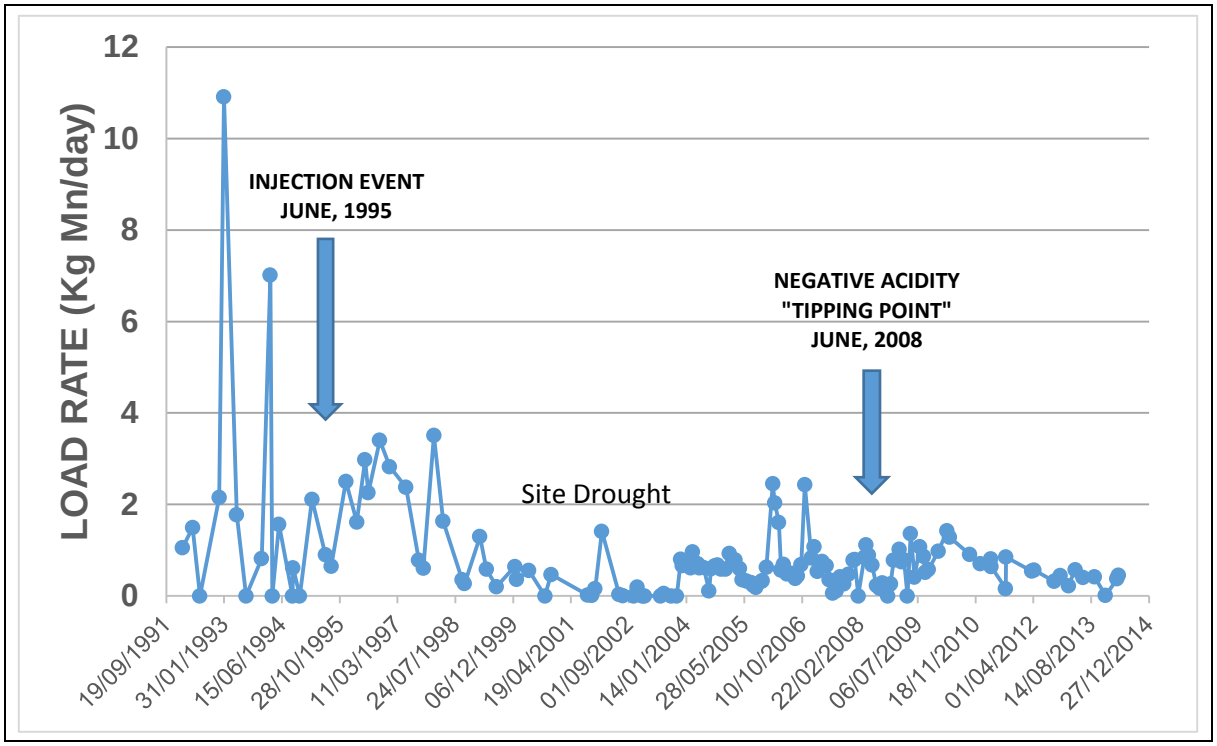

Figure 5 Seep manganese loading 1991 to 2014

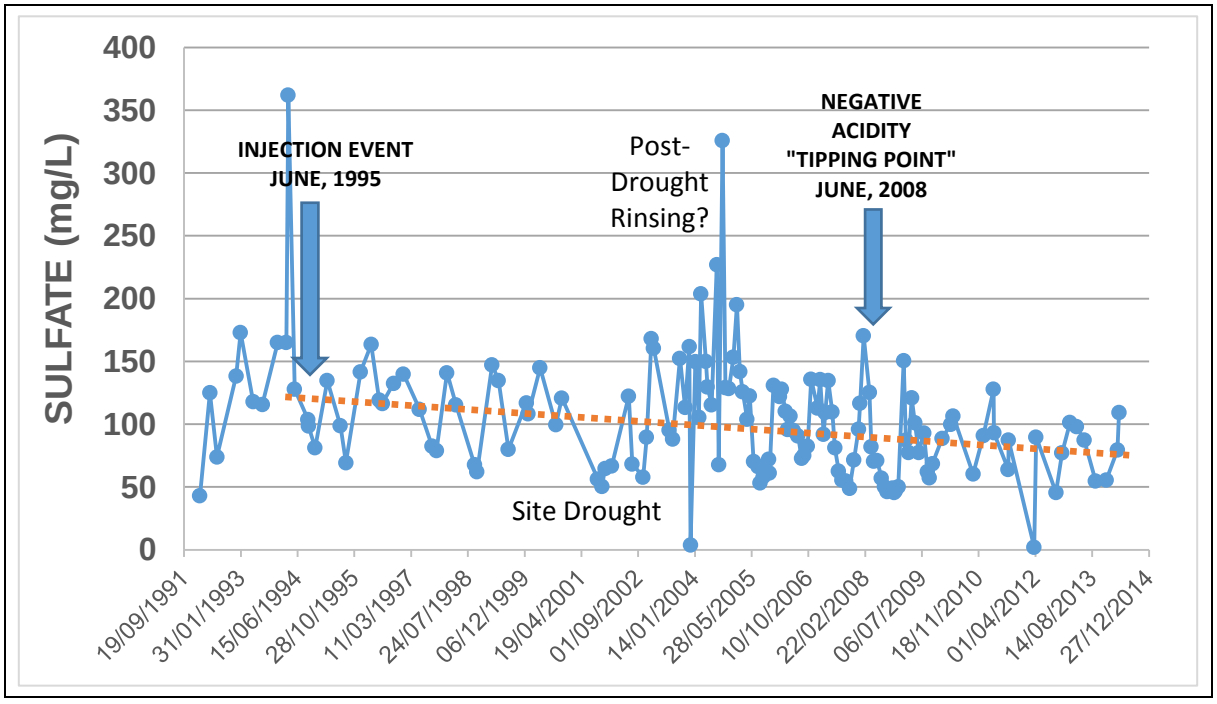

Figure 6 Seep sulfate concentration trend 1991 to 2014

DISCUSSION

Granted, the chemistry of Fisher Mine MIW was not as "aggressive" as ARD from more challenging mining sites that are too numerous to name. However, the data presented in figures 2 through 6 suggest that the positive effects of a single anti-bacterial application/injection event can persist for almost two decades. These observations are encouraging. The acidity/alkalinity "tipping point" is worthy of additional discussion. Unpublished laboratory data (Clark, 2013) suggests that the concentrations of sodium lauryl sulfate in the injected solution used at the Fisher Site would have certainly decimated the acidophilic community. However, it also probably decimated the isolated populations of beneficial heterotrophic bacteria as well, leaving the treated zone in an almost sterile condition. Kirby and Cravotta (2005) discussed hot acidity testing protocol and found that the presence of ferrous iron (Fe^{+2}) may result in negative acidity values; the oxidation with hydrogen peroxide could force ferrous iron to ferric, which reaction consumes hydrogen ions, raising the pH. Unfortunately, iron speciation, dissolved oxygen, or oxidation reduction potential (ORP) data for the Fisher seep is non-existent.

If the ratio of acidophilic to heterotrophic bacteria counts was about equal, one might expect ferric iron to predominate the seep discharge chemistry. However, if the heterotrophic populations finally grew to outnumber the acidophiles, one might expect to observe ferrous iron (and the associated negative acidity values) in the effluent samples. Whether this could occur in as short a time span as suggested in Figure 2 is uncertain and is worthy of additional study. However, it appears to be a persistent condition for the past six years. Future research work at the site (or elsewhere) might focus on better understanding this phenomenon. It is interesting that the sulfate levels decreased slowly, whereas acidity, pH and iron and manganese levels decreased abruptly in response to the injection event. Residual gypsum or sulfate salts from 11 years of unsuppressed pre-injection pyrite oxidation (which would be slow to rinse) may account for a portion of this lag in sulfate response. Other microbial-related mechanisms could have also contributed.

CONCLUSIONS

The Fisher Site subsurface injection project represented the first time that a combination of geophysical mapping and well injection of alkaline materials followed by efforts to inhibit bacterial production had been used to mitigate acid seeps from a reclaimed site. Almost two decades of data suggest that the beneficial effects of the method appear to be permanent and may improve even more in the future. Granted, the Fisher Site may not have presented an "extreme" biogeochemical challenge. However, one must start somewhere and this technology (coupled with a better understanding of the biogeochemistry of a given site) may offer a permanent remedy to ameliorate discharge problems leading to protection of groundwater resources, elimination of permanent surface treatment facilities, and ultimately the release of mine reclamation bonds on re-vegetated mine sites currently experiencing ARD problems.

REFERENCES

Clark, T. (2013) Pers. Comm.

Jin, S., Fallgren, P. H., Morris, J. M., and Cooper, J. S. (2008) Source Treatment of Acid Mine Drainage at a Backfilled Coal Mine Using Remote Sensing and Biogeochemistry. Water Air Soil Pollution 188:205–212.

Kirby, C. S. and C. A. Cravotta III. (2005) Net alkalinity and net acidity 2: Practical considerations, Applied Geochemistry 20 (2005) p1941–1964.

Kleinmann, R.L.P (1979) Biogeochemistry of acid mine drainage and a method to control acid formation. Ph.D. Thesis, Princeton University, Princeton, N.J. 104 pp.

Kleinmann, R.L.P. and Erickson, P.M. (1983) Control of acid drainage from coal refuse using anionic surfactants. Bureau of Mines RI 8847, 16 pp.

Pichtel, J.R. and Dick, W.A. (1991) Influence of Biological Inhibitors on the Oxidation of Pyritic Mine Spoil. Soil Biology and Biochemistry, Vol 23, No. 2, 1991, pp 109-116.

Plocus, V. G. and Rastogi, V. (1997) Geophysical Mapping and Subsurface Injection for Treatment of Post-Reclamation Acid Drainage. Paper presented at the 1997 National Meeting of the American Society for Surface Mining and Reclamation, Austin, Texas, May 10-15, 1997. pp 34-42.

Rastogi, V. (1996) "Water quality and reclamation management in mining using bactericides," Mining Engineering pp. 71-76 April 1996.

Schrenk, M.O., Edwards, K.J., Goodman R.M., Hamers, R.J., and Banfield, J.F. (1998) Distribution of thiobacillus ferrooxidans and leptospirillum ferooxidans: implications for generation of acid mine drainage. Science 279(5356): 1519-1522.

Sobek, A.A., Beneditti, D.A., and Rastogi, V. (1990) Successful reclamation using controlled release bactericides: Two case studies, Proceedings of the 1990 Mining and Reclamation Conference and Exhibition, Charleston, WV, Vol 1, pp. 33-41.

Tuttle, J.H., Dugan, P.R and Apel, W.A. (1977) Leakage of cellular material from Thiobacillus ferrooxidans in the presence of organic acids. Applied and Environmental Microbiology 33:459-469.

10th ICARD IMWA 2015 | 10th International Conference on Acid Rock Drainage & IMWA Annual Conference

Removal of Metals from Circum-Neutral Mine Water by Biologically-Induced Diurnal Ph Cycling

David Jones [1,2], Robert Jung[3] and Bernard Chapman[1,3]
1. Formerly: CSIRO Coal and Energy Technology, Australia
2. Currently: DR Jones Environmental Excellence, Australia
3. Currently: Insight Trading Pty Ltd, Australia

ABSTRACT

In surface freshwater streams the pH is typically controlled by the carbon dioxide, bicarbonate, carbonate buffer system. Photosynthesis during daylight hours leads to removal of carbon dioxide and/or bicarbonate from the water column with an associated increase in pH. Additionally, a locally strongly oxidizing environment can be created owing to production of high dissolved oxygen concentrations. These conditions can lead to enhanced removal of metals from the water column via precipitation of hydroxide and carbonate species, adsorption on sediments, or oxidation to insoluble forms.

This paper describes the findings from field and laboratory investigations of the removal of substantial amounts of manganese (Mn) and zinc (Zn) from a surface stream system, as a final polishing step for partially treated circumneutral metalliferous mine drainage produced from an underground lead/Zn mine. Diurnal pH modulation by the naturally occurring algal assemblage dominated by the filamentous cyanobacterium *Schizothrix calcicola* ,combined with formation of amorphous manganese dioxide coatings on the stream bed, were found to be the drivers of this process. Selective chemical extraction of the filamentous phototrophic biofilm material indicated that Zn was removed by surface adsorption or precipitation of carbonate phases and that Mn was largely removed by oxidation on the surface of the cyanobacterial filaments.

The findings from this work indicate the key role that photosynthetically driven pH cycles can play in metal removal in minewater treatment systems, and highlight the importance of maintaining shallow open water areas. The occurrence of diurnal cycles in metal concentrations downstream of mine water inputs emphasises the need to address this process in the design of water quality sampling programs being used to assess perfomance of these systems.

Keywords: mine drainage, diurnal pH cycles, metal removal, cyanobacteria, passive water treatment

INTRODUCTION

In aquatic systems dissolved metals can be removed from the water column by precipitation, adsorption to suspended sediment (followed by sedimentation), adsorption to the bed sediment, or by uptake by aquatic plants (Chapman, Jones & Jung, 1983). Precipitation, or co-precipitation of another metal present at lower concentration, followed by sedimentation can occur if the hydroxide or carbonate complexes become supersaturated. For trace metals (cations and oxyanions), pH is the key variable that controls the extent of adsorption and/or precipitation in oxic surface waters.

In most aquatic systems the pH is controlled by the carbonate buffer system. When photosynthesis occurs during daylight hours, carbon dioxide and/or bicarbonate is removed from the water column and the pH rises (Lucas & Smith, 1973). Additionally, a strongly oxidizing environment can be created locally as a result of the production of high dissolved oxygen concentrations. Variation in pH and oxygen concentrations due to photosynthetic activity can lead to fluctuations in the concentrations of contaminants in the water column as the solubility and/or state of adsorption-desorption equilibrium changes (Gammons, Nimick & Parker, 2014).

Over the past decade many observations have been made of diurnal cycles in concentrations of zinc (Zn) and manganese (Mn), in particular, in circum-neutral streams impacted by drainage from historic mines (Gammons, Nimick & Parker, 2014). The process is driven by the daily cycling of pH induced by the photosynthesis (light) and respiration (dark) of phototrophs attached to the stream bed. The importance of these processes in controlling metal removal, and their consequent relevance for obtaining meaningful measurements of metal concentrations downstream of mine water sources, has been the subject of a recent review (Gammons, Nimick & Parker, 2014). It is noted by these authors that although observed daily diurnal ranges of pH occasionally exceed one unit, in most locations they vary less than this.

There are few well-documented examples of the importance of diurnal pH cycling in driving metal removal in full scale mine water treatment systems. This study documents the findings from investigations of the passive water treatment system at the underground Hilton lead-zinc-silver mine located 20 km north of Mt Isa in central-northern Australia (Figure 1). Mt Isa Mines Ltd (the owners of the resource in the late 1980s) needed to dewater the underground ore-body in the lead up to developing production from the mine.

The concentration of Zn at site D3 (Figure 1) needed to meet the water quality discharge limit of 2 mg/L set by the Queensland state regulator. Coincidentally this target for removal of Zn also met the quality requirement for re-use of this water for mineral processing, an important consideration in this semi-arid environment. A 20 km pipeline transported water from the Hilton pump weir at D4 to the mineral processing plant at Mt Isa.

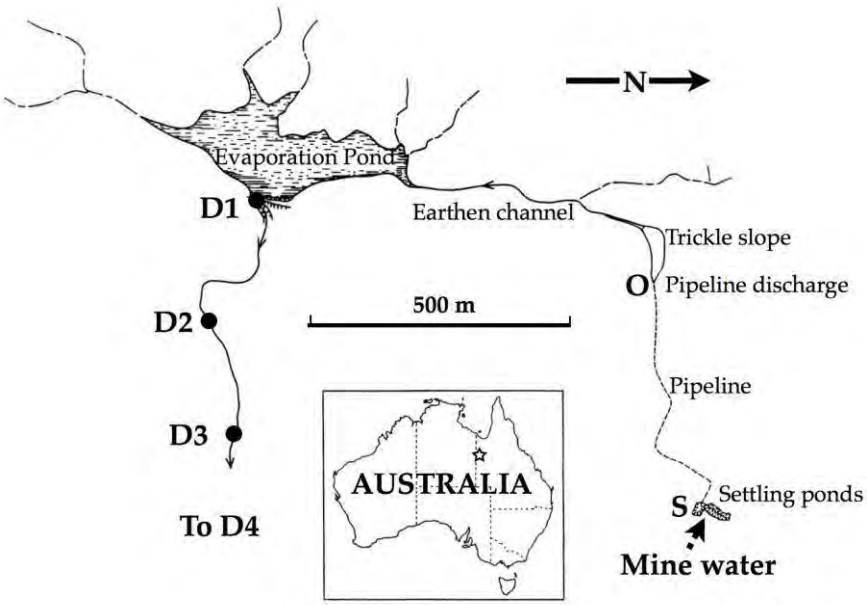

Figure 1 Location (star on map) of the Hilton mine and schematic of the mine water treatment system.

A passive treatment system was constructed to strip the metals from the mine water with the aim of meeting both process water and environmental discharge requirements for Zn. The present study was carried out to identify the specific removal processes involved to:

- facilitate optimization of contaminant removal, and
- to ascertain whether they could continue to operate satisfactorily into the future.

A detailed description of the complete treatment system for the pH circumneutral mine water has been published previously (Jones, Chapman & Jung, 1995). During the 18 month period of this study the total dewatering rate ranged between 2000-6000 m^3/day. There were no diluting inflows from other sources, such as rainfall or stream tributaries, to complicate interpretation of the results.

The focus of this paper is the downstream (from locations D1 to D4, Figure 1) section of the treatment system, wherein the residual dissolved Zn is further removed to acceptable levels. The stream between D1 and D4 was typically shallow (<0.3 m deep at the centre), with a maximum width of 2 m. It comprised sections of interconnected shallow pools punctuated by steeper riffle zones, as the watercourse descended by about 10 m over the reach. The gravel/cobble bed was covered by copious growths of green filaments (Figure 2).

METHODOLOGY

The field work described in this paper was conducted over three campaigns in October 1984, October 1985 and February 1986, with detailed chemical analysis work and laboratory experiments being conducted between the first two field visits and after the last one.

Figure 2 Mats of filamentous biofilm containing *S. calcicola* covering the stream bed

Water chemistry

Measurements of pH were made *in situ*. Water samples for total and dissolved (<0.1 μm) metals were collected in acid leached plastic bottles. All samples were preserved by the addition of nitric acid (to 0.1 %) within 1h of sample collection. The concentrations of major cations were determined by atomic absorption spectroscopy (AAS) or Inductively Coupled Plasma Atomic Emission Spectroscopy (ICPAES), and the concentrations of iron, Mn, and Zn measured by ICPAES. Sulfate was determined by ICPAES or ion chromatography and bicarbonate concentrations were measured in the field by titration with standardised hydrochloric acid.

Collection and analysis of microbial and sediment samples

Samples of the filamentous microbial material were collected from the bed of the stream at D1 and D3, and at several locations between, using plastic scoops. They were stored at 4 ℃ in plastic bottles for two days prior to being processed in the laboratory. Detritus such as leaves and twigs was removed by hand sorting. Filaments were washed by re-suspending them in 0.05 M NaCl solution. The sample was then consolidated by centrifugation. The supernatant was decanted and the washing and centrifugation step repeated.

Subsamples of the wet biofilm were separately extracted at room temperature with 0.1 M pH 4 acetic acid/sodium acetate buffer and 0.1 M hydroxylamine hydrochloride solution in the pH 4 acetate buffer to investigate the modes of binding of Zn and Mn in the algal filaments The extraction methods used were adapted from Tessier, Campbell & Bison, 1979.

Aliquots of supernatant solutions were withdrawn at 10, 20, 40 and 65 min to track the time course of increase in the extracted Zn and Mn concentrations. The concentrations extracted at 65 min were used to estimate the amounts of Zn and Mn associated with the phases targeted by the extract solutions, as the concentrations in solution approached an asymptote value at this time. Total extractable concentrations of Zn and Mn were obtained by digesting finely pulverised freeze-dried samples with a 1:1 mixture of concentrated HNO_3 and HCl acids. A similar digestion was used for the stream sediments. The concentrations of metals in the extract and digest solutions were determined by ICPAES. The oxidation state of Mn in the surface coatings on the stream sediments was determined using the iodometric method of Murray, Balistrieri & Paul, 1984.

Semi-quantitative powder X-ray diffraction (XRD) was used to identify crystalline mineral phases present in finely ground freeze-dried samples of the microbial material and the bed sediments.

Microbial strain identification

Samples of the microbial mat were collected from the stream bed between D1 and D3 were sent to the National Herbarium of New South Wales in Sydney for identification using optical microscopy. The dominant species was found to be a clumped ecoform of the widely occurring cyanobacterium (colloquially known as blue green algae) *Schizothrix calcicola*. It was noted by the phycologist at the Herbarium that this ecoform had a much higher amount of extracellular polymeric substances (EPS) associated with the filaments, than was usual for the species.

RESULTS AND DISCUSSION

Water chemistry

The concentrations of select major ions and of Mn and Zn between sites D1 and D4 in October 1984, are plotted in Figure 3. Only the data for 1984 are shown here as the behaviour of the solutes was found to be the same for the subsequent field campaigns.

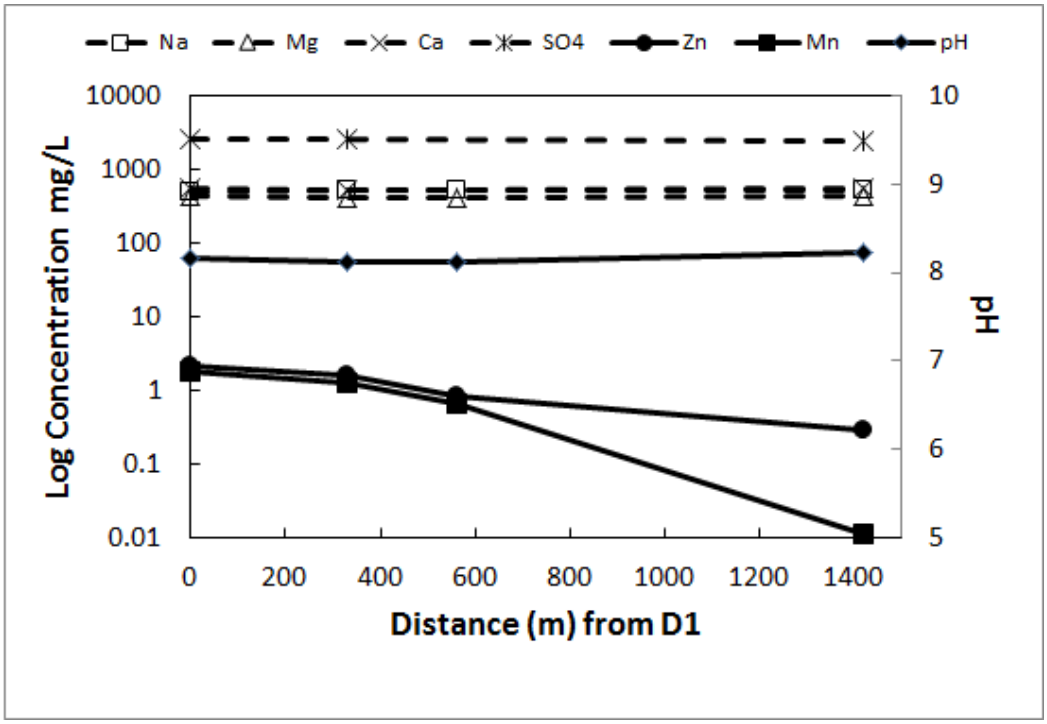

Figure 3 Concentrations of major ions, pH and Zn and Mn downstream of D1 (October 1984)

Only the dissolved concentrations are shown in Figure 3 as there were no substantial differences between the total and dissolved concentrations in this reach. The fact that the concentrations of the major cations did not change significantly between D1 and D4 indicates that there were no significant diluting inflows or losses of water by evaporation. In contrast to the major ions, the concentrations of soluble Zn and Mn decreased substantially (approximately 2.5 fold) between D1

(0 m) and D3 (560 m), with Mn concentrations being below detection limit (0.04 mg/L) at D4 (1420 m).

All of the water samples were collected in daylight hours within 30 min of one another. The possibility of artefacts being introduced due to sampling time, as discussed by Gammons, Nimick & Parker, 2014, was thus minimised.

Mineral Solubility

To determine which solid phases could potentially be removing Mn and Zn from solution, saturation indices (SI) were calculated using the MINEQL chemical equilibrium computer code (Westall, Zachary & Morel, 1976). The saturation index (SI) is defined as the logarithm of the ratio of the activity product of the component ions of the solid in solution to the solubility product for the solid. Values greater than zero indicate super-saturation and values less than zero, under-saturation. The SI calculations showed that calcium (Ca), Zn and Mn carbonates were marginally over saturated (SI values of 0.5, 1 and 1, respectively at D1) in the bulk flowing water downstream of D1, indicating that precipitation of these phases could be controlling the solubility of these metals. The SI for $MnCO_3$ declined below zero downstream of D3.

Investigation of the microbial material and stream sediments by XRD did not show the presence of Zn or Mn carbonate mineral phases, although low concentrations of Ca carbonate were detected. The non-detection of Zn and Mn carbonates does not mean that they were not present, as the limit of detection of XRD is typically around 1-2 wt % in a complex matrix (Chung F & Smith DK, 1999). Reference to Table 1 shows that the total concentrations of Zn and Mn in the microbial material, if all were present as carbonates, would be at or below the detection limit of this technique.

Mechanisms of metal removal– microbial mats

To investigate possible diurnal behaviour (an indicator of photosynthetic activity), the flowing water from mid-stream was sampled over a two-day period in October 1985 at D1 and at D3 (Figure 4). It is noted that the concentration of Zn at D1 at this time was approximately twice that in October 1984, whilst the concentration of Mn was about the same.

The concentrations of both Zn and Mn were considerably reduced (on average by factors of 2 and 4, respectively) along this reach of the stream. Moreover, there was a marked diurnal variation in concentrations which did not originate in the evaporation pond (the overflow of which corresponds to D1), but which occurred during the passage of the water between D1 and D3. Significantly in this reach of stream there was close contact between the water and extensive microbial filaments (primarily the commonly occurring cyanobacterium *Schizothrix calcicola*, hereafter abbreviated to *S. calcicola*) (Figure 2).

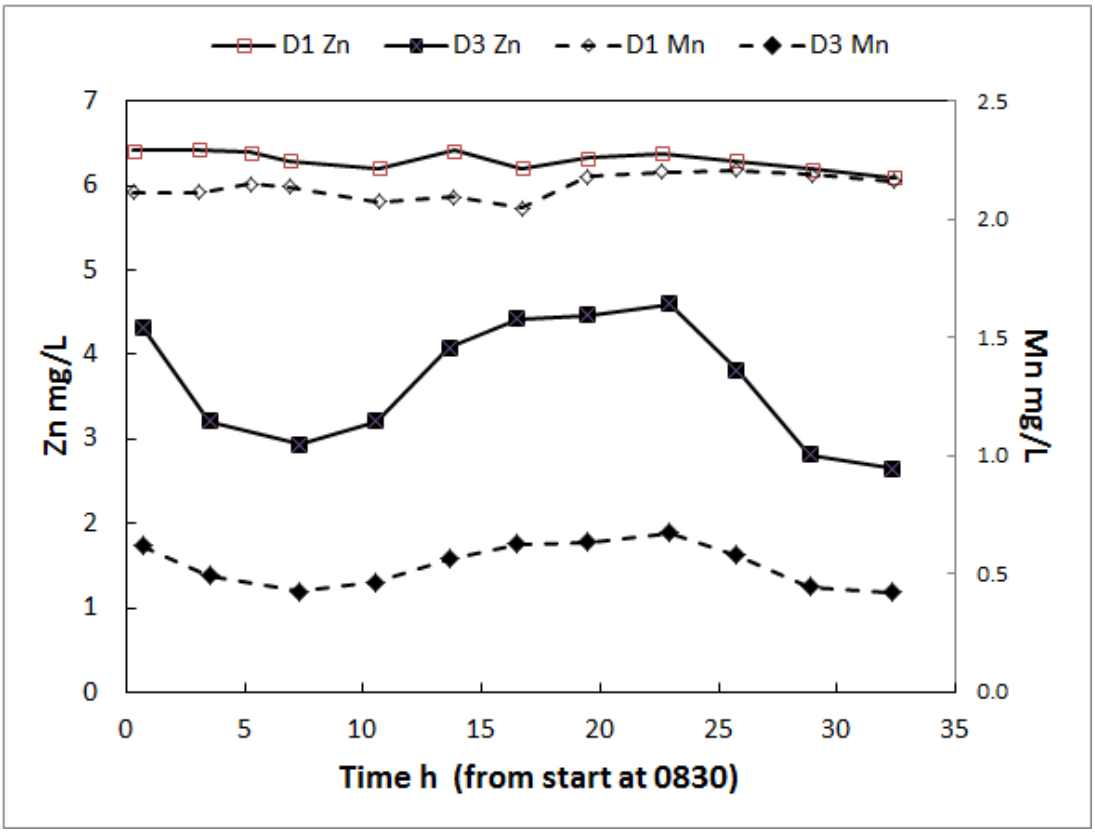

Figure 4 Concentrations of Zn and Mn at D1 and D3 over a two day period (October 1985)

A subsequent study was undertaken at D1 in February 1986 to test the hypothesis that the increase in pH associated with photosynthesis was a driver for metal removal. At this time the Zn concentrations were much lower than in October 1984 and 1985 because there was a lower proportion of the Zn-rich water derived from the orebody in the total volume of water being discharged.

The pH and concentrations of Zn close to a microbial mat were compared with that in mid-stream between sunrise and sunset (Figures 5 and 6). At sunrise, the pH values of both the stream water and the water close to the microbial mat were close to pH 7.9, with similar Zn concentrations (0.88 mg/L) at both locations. As the sun rose, the pH in the water close to the filaments rose steadily to a maximum value of 8.6-8.8, whereas the water in mid-stream remained close to 7.9. Coincidentally with the rise in pH near the *S. calcicola* filaments, the concentration of Zn in solution fell to 0.6 mg/L, whilst that in the bulk flowing water remained at its initial concentration. As the sun was setting, the pH near the *S. calcicola* filaments began to decline rapidly until, by nightfall, it had returned to its original early morning value. The pH increase measured in the field was consistent with *in vitro* laboratory measurements in a closed system that showed that the pH in vessels containing the *S. calcicola* varied by as much as 1.5 pH units over a simulated day/night cycle.

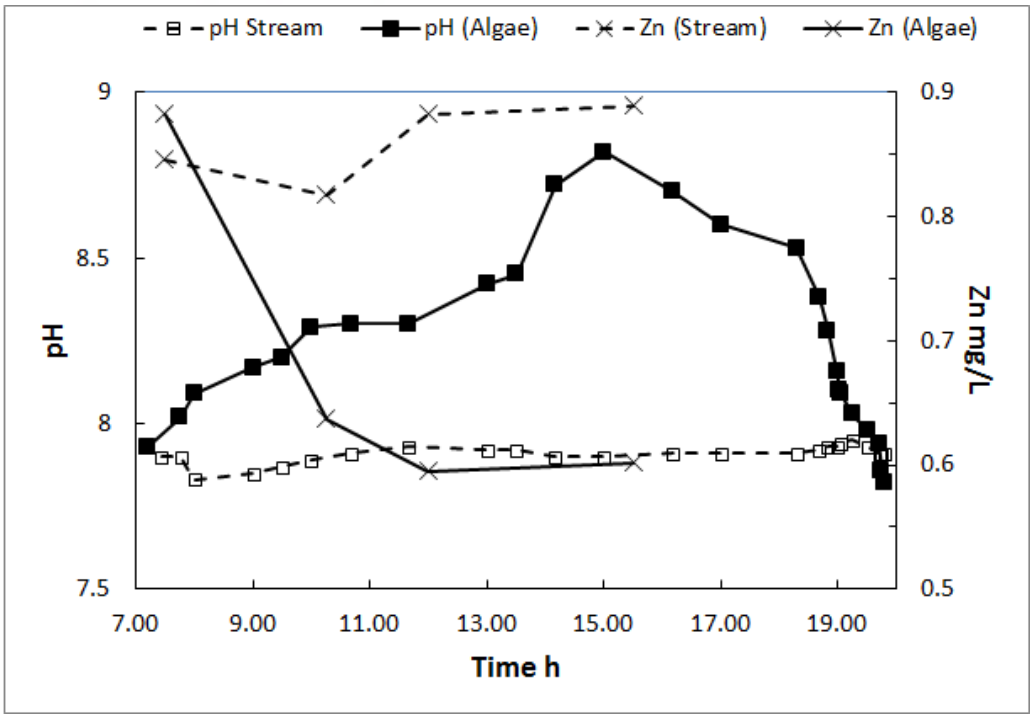

Figure 5 Comparison of pH and Zn concentrations in the middle of the stream and in a microbial mat at D1

Some properties of the microbial material collected at D1 are summarised in Table 1. The rapid rates of dissolution of the metals from intact *S. calcicola* filaments material by extraction reagents (pH 4 acetate buffer and 0.1 M hydroxylamine hydrochloride at pH 4) indicates that a high percentage of the total amounts of these metals are located on the surface of the *S. calcicola* filaments. In contrast to Zn, only 30 % of the Mn was extracted with the pH 4 buffer. However, the majority of the Mn was rapidly dissolved at pH 4 in the presence of a reducing agent (hydroxylamine) that is selective for Mn dioxide and Mn oxyhydroxides (Tessier, Campbell & Bison, 1979).

The extraction results are consistent with) metal removal by surface adsorption/complexation on and/or by enhancement of pH-dependent (precipitation, oxidation) removal processes on the surface of the cyanobacteria filaments. The EPS produced by the cyanobacteria may provide increased surface area for metal binding. The potential importance of EPS in binding and concentrating Zn on the surface of algal cells has been noted by others (Podda et al, 2000).

The increases in pH and oxygen concentrations produced as a result of photosynthesis may favour the precipitation of Zn and Mn carbonates and the oxidation of Mn(II) to produce insoluble Mn(III)/Mn(IV) oxides on the microbial filaments. Whilst concentrations of dissolved oxygen were not measured in the field, the occurrence of copious small bubbles on the surfaces of the microbial mats during daylight hours suggested the presence of elevated concentrations of oxygen in the vicinity of the filaments.

The role of photosynthesizing cyanobacterial or other types of phototrophic filaments in facilitating the precipitation of hydrozincite (a zinc hydroxy-carbonate phase) on their surfaces has been documented by Kwong et. al., 1994, and Podda et al, 2000. Support for these types of processes occurring downstream of D1 is provided by the findings from the selective extractions described above.

Table 1 Chemical extraction of Zn and Mn from D1 *S. calcicola* samples

Extract medium	Likely Phases	Zn	Mn
pH 4 acetate, 10 min	Adsorbed Zn and Mn, labile Zn and Mn carbonates (I)	62 %	23 %
pH 4 acetate, after 65 min	Adsorbed Zn and Mn, labile Zn and Mn carbonates(I)	77 %	30 %
pH 4 hydroxylamine, 10 min	(I) plus Mn oxyhydroxides and Mn oxides	65 %	84 %
pH 4 hydroxylamine, 65 min	(I) plus Mn oxyhydroxides and Mn oxides	90 %	98 %
Aqua regia digest (total)		17200 mg/kg dry weight	8330 mg/kg dry weight

The effectiveness of photosynthetically driven processes for metal removal will be a function of maximum day time temperature, day length and solar radiation intensity. The climate data (available from the Australian Bureau of Meteorology: www.bom.gov.au) for the Mt Isa region show that these parameters do not change substantially over the year at the Hilton mine. Consequently, it is not expected that there would be substantial variation in the effectiveness of biological removal processes through the year. This situation contrasts strongly with that existing in the temperate latitudes from which much of the published literature on diurnal cycling of metal removal has been produced.

Mechanisms of metal removal – inorganic sediments

Samples of the gravelly streambed sediment were collected 60 m downstream of D1. Gravelly soil was also collected from the banks of the stream at this location to provide a control for experiments to investigate the role that the bed material could play in removing dissolved Zn and Mn from the water. The only obvious physical difference between the two types of solids was that the gravel substrate from the channel bed was covered with a soft black coating. Samples of each (on-bank and in-stream) of these solids were agitated with aliquots of water from D1, and the decrease in metal concentrations monitored. Both sediment types removed similar amounts of Zn from solution (50 % after 20 h), but only the material collected from the stream bed removed Mn (97 % after 10 h for stream sediment, 0 % after 72 h for bank material).

Bacteria are known to catalyse the oxidation of soluble Mn(II) to insoluble Mn(IV) (Diem & Stumm, 1984). However, in this case the addition of the biocide sodium azide did not inhibit the removal of Mn by the stream sediment, indicating that the reaction must have been an abiotic process. X-ray diffraction, and chemical and redox speciation (Murray, Balistrieri & Paul, 1984) analysis of the black material coating the stream sediment particles showed it to be primarily amorphous manganese dioxide with considerable associated Zn (Mn/Zn=4). Pre-formed Mn(IV) oxides are known to catalyse the oxidation of initially adsorbed Mn(II) (Hem, 1978). The ability of Mn oxide

coatings on stream beds to remove Mn(II) from solution at pH values for which the abiotic rate of oxidation in solution would otherwise be very slow has been noted by others (Gordon & Burr, 1988) as has the ability of these types of coatings to absorb substantial amounts of Zn (Shope, Xie & Gammons, 2006).

Conclusions and significance of findings

Both abiotic (formation of Zn-rich manganese oxides on bed substrate) and biologically-mediated (adsorption and/or precipitation on *S. calcicola* filaments) processes have been shown to contribute to the reduction in Zn and Mn concentrations downstream of site D1 at the Hilton mine. The diurnal variations observed in the downstream concentrations of these metals occurring in concert with the daily cycling in pH adjacent to the *S. calcicola* filaments, imply that a significant proportion of the metals are removed as a result of the photosynthetically-induced pH oxygen concentration increases in the water close to the filamentous biomass in the stream channel.

Selective chemical extractions of the filamentous material indicated that Zn was removed by surface adsorption or precipitation of carbonate phases and that Mn was largely removed by oxidation. Uptake of Mn and Zn by manganese oxide coatings on the stream bed also contributed to the attenuation of these metals. Whilst it was not possible to definitively apportion the extent of Mn and Zn removal between the biotic and abiotic pathways, consideration of the physical context suggests that the phototrophic pathway may be the dominant one, as the *S. calcicola* filaments are in continuous intimate contact with the water column and the microbial mats provide a diffusion barrier to the Mn oxide coating on the underlying stream bed.

One of the primary objectives of water quality monitoring programs in surface water, whether it be a pristine or an impacted water body, is to obtain an accurate representation of the chemical status of the system. In the case of a mine-water treatment system, both regulatory compliance and metal removal efficiency typically need to be assessed. However, if diurnal variations in water quality are not adequately accounted for in the design of the monitoring program, then potentially flawed conclusions may be drawn. Indeed very different conclusions about system performance can be drawn depending on when in the day a system is sampled. This aspect has been well illustrated by a recent review (Gammons, Nimick & Parker, 2014). In the case of the Hilton Mine passive treatment system, substantive net removal of both Mn and Zn occurs throughout the diurnal cycle.

ACKNOWLEDGEMENTS

The permission of Mt Isa Mines Ltd (MIM) to publish the findings from this study and the assistance provided by MIM staff and CSIRO technical support staff for the conduct of this work is gratefully acknowledged by the authors. The National Herbarium of New South Wales in Sydney identified the cyanobacterium in the microbial-mat samples.

REFERENCES

Chapman, B, Jones, D & Jung, R (1983) Processes controlling metal ion attenuation in acid mine drainage streams. Geochimica Cosmochimica Acta, 47, 1957-1973.

Chung F & Smith DK (1999) Industrial Applications of X-Ray Diffraction, CRC Press, 1024p.Diem, D & Stumm, W (1984) Is dissolved Mn^{2+} being oxidised by O_2 in absence of Mn-bacteria or surface catalysts? Geochimica Cosmochimica Acta, 48, 1571-1573.

Gammons, C, Nimick, D & Parker S (2014) Diel cycling of trace elements in streams draining mineralize areas- a review, Applied Geochemistry, in press, http://dx.doi.org/10.1016/j.apgeochem.2014.05.008.

Gordon, J & Burr J (1988) Manganese treatment by two novel methods at abandoned coal strip mines in North Alabama. Proceedings of the 42nd Industrial Waste Conference, Purdue University, pp. 907-918.

Hem, J (1978) Redox processes at surfaces of manganese oxide and their effects on aqueous metal ions. Chemical Geology, 21, 199-218.

Jones, D, Chapman, B & Jung, R (1995) Passive treatment of mine water, in Proceedings of Sudbury '95 - Mining and the Environment, Hynes, T.P. and Blanchette, M.C. (eds), May 28 - June 1, 1995, Sudbury, Ontario, Canada, Vol. 2, pp. 755-763.

Kwong, Y.T.J, C. Roots, and W. Kettley(1994) Lithochemistry and aqueous metal transport in the Keno Hill mining district, central Yukon territory. In: Current Research 1994-E; Geological Survey of Canada, pp.7-15.

Lucas, WJ & Smith, FA (1973) The formation of alkaline and acid regions at the surface of *Chara corallina* cells, Journal of Experimental Botany, 24, 1-14.

Murray, J, Balistrieri, L & Paul, B (1984) The oxidation state of manganese in marine sediments and ferromanganese nodules. Geochimica Cosmochimica Acta, 48, 1237-1247.

Podda, F, Zuddas, P, Minacci, A, Pepi M & Baldi, F (2000) Heavy metal coprecipitation with hydrozincite [$Zn_5(CO_3)_2(OH)_6$] from mine waters caused by photosynthetic microorganisms, Applied and Environmental Microbiology, 66, 5092-5098.

Shope, C, Xie, Y & Gammons C (2006) The influence of hydrous Mn-Zn oxides on diel cycling of Zn in an alkakine stream draining abandoned mine lands, Applied Geochemistry, 21, 476-491.

Tessier, A, Campbell, P & Bisson M (1979) Sequential extraction procedure for the speciation of particulate trace metals, Analytical Chemistry, 51, 844-851.

Westall, J, Zachary, J & Morel, F (1976) Technical Note 18. Water Quality Laboratory, Dept. of Civil Engineering, MIT, Cambridge, Massachussets.

Biogeochemical Cycle of Mercury in Wetlands Ecosystem Affected by Gold Mining in a Semi-Arid Area

Ewa Cukrowska[1], Julien Lusilao-Makiese[1], Hlanganani Tutu[1], Luke Chimuka[1] and Isabel Weiersbye[2]

1. Molecular Sciences Institute, University of the Witwatersrand, South Africa,

2. School of Animal, Plants and Environmental Science, University of the Witwatersrand, South Africa

ABSTRACT

Wetlands are essential habitats in the environment since they fulfill a variety of ecological functions and support rich biodiversity. One major characteristic of wetlands is their ability to act as chemical sinks. There have been biogeochemical models developed for wetlands in Europe and North America but these systems differ from those found in South Africa, where most wetlands are river-fed and therefore undergo seasonal saturations, with periods of flooding in summer followed by drying during winter. High evapotranspiration rates also concentrate pollutants to very high levels. The nature, level and impact of mercury in the environment have not been extensively studied in South Africa, particularly in areas that have been significantly affected by gold mining activities.

Aims of this research were to determine the biogeochemical cycling of mercury in permanent and seasonal aquatic ecosystems (rivers, dams, natural and manmade wetlands) that have been heavily affected by mining activities (acid rock drainage) in semi-arid areas with extreme seasonal changes.

Research methodology included seasonal sampling, sequential extractions, determination of mercury speciation and modeling.

Results show that natural wetlands in South Africa have a greater capacity to trap mercury than manmade wetlands. Most leachable mercury exists in oxidizable form followed by unleachable residue. Organomercury species are produced in anaerobic deeper levels where organic carbon and reduced sulfur content is high. Evapotranspiration and surface precipitation during the dry season exhibited a strong seasonal relationship to acidity and redox conditions.

These research results are supported by a biogeochemical model may be used for identification and implementation of potential mercury remediation measures.

Keywords: mercury, wetlands, biogeochemical cycling, sequential extraction, bioavailability

INTRODUCTION

Changes in chemical and physical properties in the lithosphere can influence the release of heavy metals from mine tailings into the ecosystem and increase the likelihood of uptake by living organisms (Kim et al. 2001). These changes include acid rock drainage (ARD) (Durkin and Hermann 1994; Wildeman et al. 1991, Han et al., 2003).

Understanding the processes that influence the distribution, concentration, and bioavailability of potentially toxic metals, such as arsenic (As), cadmium (Cd), lead (Pb), mercury (Hg), and selenium (Se) is critical for successful management of chronically affected ecosystems. Such understanding can be used to identify and target pathways that have the greatest immediate and long-term impact on the environment. Such knowledge provides the scientific foundation for making decisions, developing strategy, and assessing remediation alternatives by governmental institutions as well as mining companies or local agencies charged with minimizing the environmental and health impacts of these toxic elements.

Gold mining has played a significant role in the socioeconomic life of South Africa (SA) for over one hundred years. Unfortunately, the wastes from this activity have been identified as a significant source of Hg and other heavy metals contamination of the environment. Heavy metals associated with mining are of particular interest for a number of reasons. They exhibit a tendency to accumulate in sediments and soils and persist as they are not biodegradable. Metals can be derived from the erosion of source rocks, or can accumulate following application of metal-enriched water as well as via deposition of atmospheric dust and fluvial reworking mined sediments (Getaneh W., 2006).

Acid rock drainage (ARD) is considered one of the mining industry's toughest challenges. Most water remediation techniques are time-consuming and costly, and ARD can continue in perpetuity, long after the mining activities cease. Constructed wetlands (CW) have been considered a possible solution to the long-term remediation of ARD. Wetlands successfully support improved water quality, providing a continuous, low-cost and effective solution to the ARD problem in some settings (Fennessy & Mitsch 1986; Kadlec 1985; Perry & Kleinman 1991; Snyder & Aharrah 1985). .

Wetlands functions that aid in the amelioration of ARD .include adsorption and ion exchange, bioaccumulation, biotic and abiotic oxidation, sedimentation, neutralization, reduction, and dissolution of carbonate minerals (Perry & Kleinmann 1991).

Processes within natural wetlands (NW) have been found to remediate contaminants found in ARD: imitation of these processes can work similarly in constructed wetlands. Wetlands have organic-rich substrates which capture/exchange dissolved metals (Wildeman et al. 1991). Wetland sediments are generally anaerobic below a thin oxidized surface layer and contain organic carbon needed for microbial growth (Gambrell & Patrick 1978). The anoxic zone of the sediments provide conditions which favor microbial and chemical reducing processes (Fenessy & Mitsch 1989). Soluble metals are converted to insoluble forms by the anoxic conditions of wetland sediments. Plants, microflora and bacteria also generate microenvironments that assist in oxidation and reduction processes (Wildeman et al. 1991; Mitsch & Gosselink 1986).

The toxicity of mercury depends strongly on the chemical form of the element (its speciation) but also on water environmental conditions like pH, redox potential, and the presence of dissolved and suspended carbon. Also dramatic differences may occur through time (high seasonality) and space. This is very important when establishing links between mercury emissions and levels in biota (Harris et al. 2005). The reactions and interactions may also vary with depth in wetland zones. For

example, the biogeochemical processes of complexation, adsorption, and precipitation may release or sequester certain metal species due to varying levels of biological activity (Baird and Cann 2012). Mercury behaves differently from other metals, forming volatile elemental mercury and even more volatile and toxic organomercury species under the anaerobic conditions which exist in deeper wetland sediments (Harris et al. 2005).

The nature, extent and impact of mercury in the environment have not been extensively studied in South Africa, particularly in areas that have been significantly affected by mining activities. To date, no analysis of seasonal changes in mercury bio-accessibility has been reported. This study addresses that gap, providing a detailed assessment and evaluation of the impact of mercury in Gauteng area of SA, very densely populated area with associated intensive water usage. The results would be useful in considering various remediation strategies.

Sequential extraction procedures (SEPs)

The toxicity, bioavailability and mobility of metals are related to their species (Quevauviller et al, 1994). However, the determination of chemical species is difficult and sometimes impossible. Therefore, the use of sequential extraction procedures for environmental studies provides an important tool for the determination of the different chemical forms or ways of binding between trace metals and sediment components (Rauret et al, 1999).

Sequential extraction procedures (SEPs) are employed to assess operationally defined metal fractions, which can be related to chemical speciation, as well as compound mobility, bioavailability or ecotoxicity. It is generally accepted that the ecological effects of metals (e.g., their transport, bioavailability, and ecotoxicology) are related to such mobile fractions rather than to the total metal concentration (Cordos et al, 2003).

Chemical fractionation schemes for partitioning trace metals in soils and sediments have been used extensively (Tessier, A., et al, 1979; Rauret G., et al, 1999; Han, F. X., et al, 2003; Ianni, C,et al, 2001; Navas, A., Lindhorfer, H. 2003; Hlavay, J., 2004. The European Community Bureau of Reference, the BCR method, standardizes SEPs (Ure et al. 1993) in order to: 1) minimize errors in the treatment and analysis of samples, 2) identify the most appropriate analytical procedure and 3) to supply reference materials for comparisons of the results. This standardized method appears to be more operationally effective than others previously proposed. (Sheppard and Stephenson, 1997).

METHODOLOGY

Sampling sites and sample pre-treatment

Samples were collected from a deposit of mine tailings (West Wits (WW)) in the Witwatersrand basin of South Africa (Figure 1). The sampling included natural and constructed wetlands, tailings and the soil next to the tailings. Redox potential, pH, temperature and conductivity were measured during sample collection. Samples were freeze dried and stored prior to analysis.

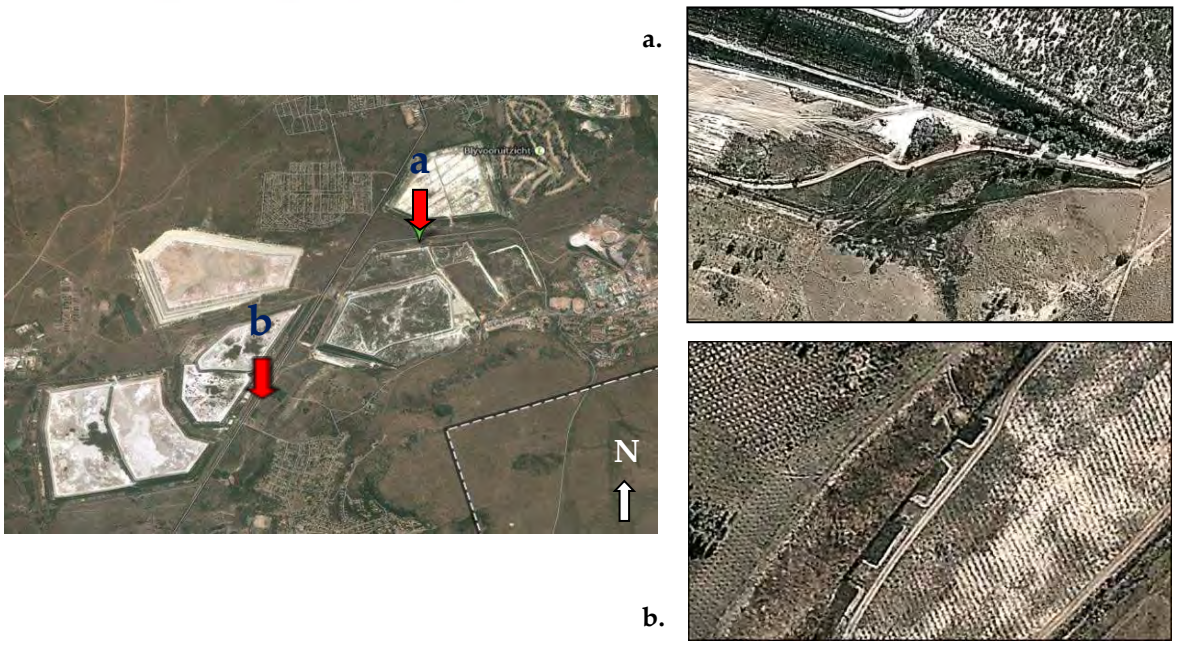

Figure 1 West Wits sampling site. a. natural wetlands (NW), b. constructed wetlands (CW)

Three stage BCR sequential extraction (BCR SE)

The BCR sequential extraction scheme with reagents and extracted fractions is shown on Figure 2.

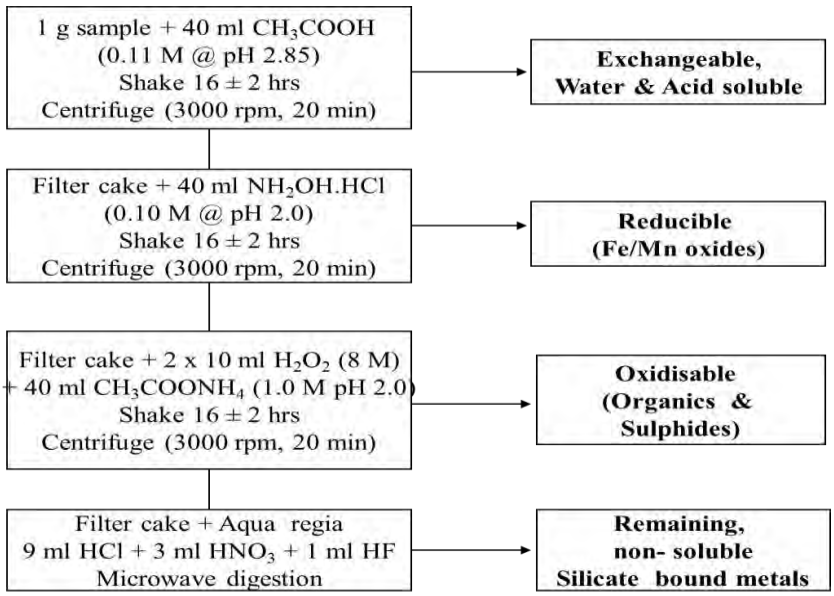

Figure 2 European Community Bureau of Reference (BCR) SE

Reagents and stock solutions

The following extraction solutions were prepared: (a) 0.11 M CH_3COOH solution adjusted to a pH of 2.0 by super pure grade HNO_3; (b) 0.10 M $NH_2OH.HCl$ solution adjusted to a pH of 2 with ultra-pure grade HNO_3; (c) 30 % H_2O_2 and 1.0 M CH_3COONH_4 adjusted to pH 2 with HNO_3 (d) ($HCl+HNO_3+HF$). Aqueous solutions of 3 % HCl (v/v) and 1.1 % $SnCl_2.2H_2O$ (in 3 % HCl v/v) were also prepared for the determination of Hg. Reagents used for Hg analysis were all certified heavy metals free (i.e. 99.999% pure).

Instrumentation

The determinations of metals in the extracts were performed by ICP – OES (Spectro, Germany) whereas Hg was analysed using an automated Hydride Generation Flow Injection Atomic Absorption Spectrometer (HG-FI-AAS, Perkin Elmer).

RESULTS AND DISCUSSION

The pH, Eh and organic carbon profiles recorded in wetlands sediments during the wet season are shown in Figure 3.

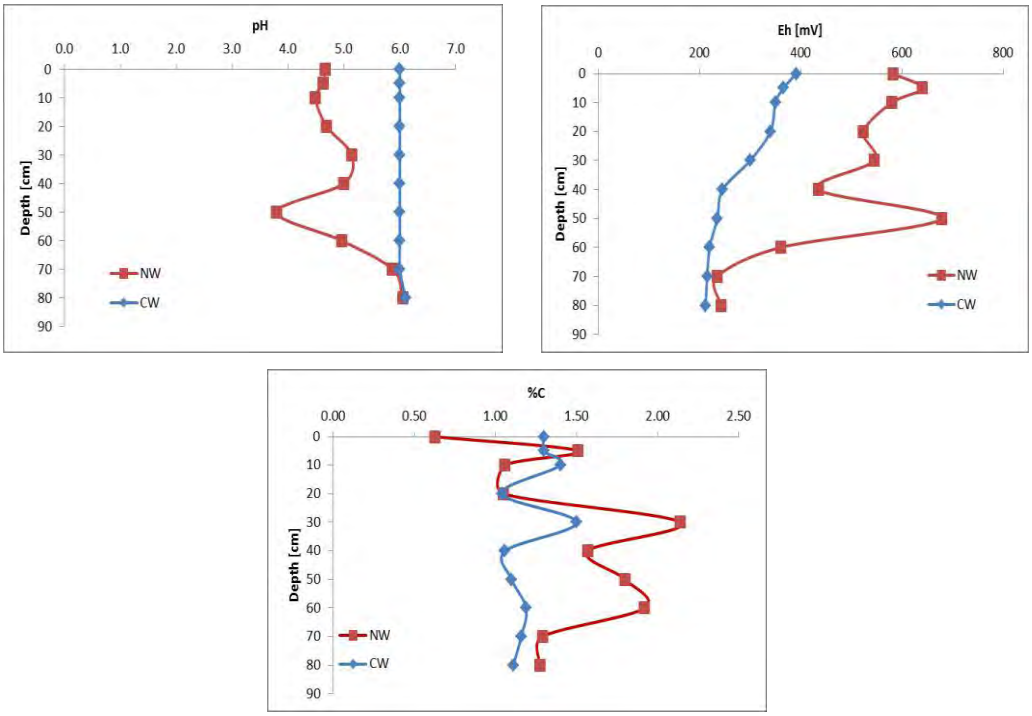

Figure 3 Sediment profiles of pH, Eh and carbon in NW and CW during wet season.

The CW profile was much more uniform to a depth of 70 cm, with a higher pH and lower redox potential and organic carbon content than the NW profile. , exhibiting almost the same levels in the lower-most sediments in both NW and CW. This might be attributed to the ageing process and to

the accumulation of organic matter. The CW is younger with sediments being removed operationally every few (3-4) years.

The total concentrations of Hg, iron (Fe) and sulfur (S), among others, were determined in wetlands, the tailings facility (TSF) and soil near the TSF (Table 1). The results of BCR sequential extraction for the same elements are presented in Figure 4.

Table 1 Total Hg, Fe and S in the wetlands and tailings

Sample ID	Depth (cm)	Hg ($\mu g\ Kg^{-1}$)	Fe ($mg\ Kg^{-1}$)	S ($mg\ Kg^{-1}$)
Soil near	0	1162	42459	1157
TSF	10	1196	34783	914
	20	987	38386	795
	30	1450	38460	692
	40	1171	38485	572
	50	1390	43693	544
	60	1198	41386	320
Tailings	0	1670	35205	1575
	10	1619	36551	1788
	20	1614	36712	1711
	30	1774	37598	1847
	40	1893	37258	1930
NW (WW)	0	312	33301	1070
	5	195	32247	1049
	10	207	27787	857
	20	803	34597	1298
	30	202	35042	1648
	40	294	31890	1321
	50	184	61115	2603
	60	207	26228	2112
	70	106	36164	1999
	80	237	47232	1421
CW (WW)	0	39	28571	1176
	20	111	41121	589
	40	234	39796	784
	60	315	61310	409
	80	194	51476	226

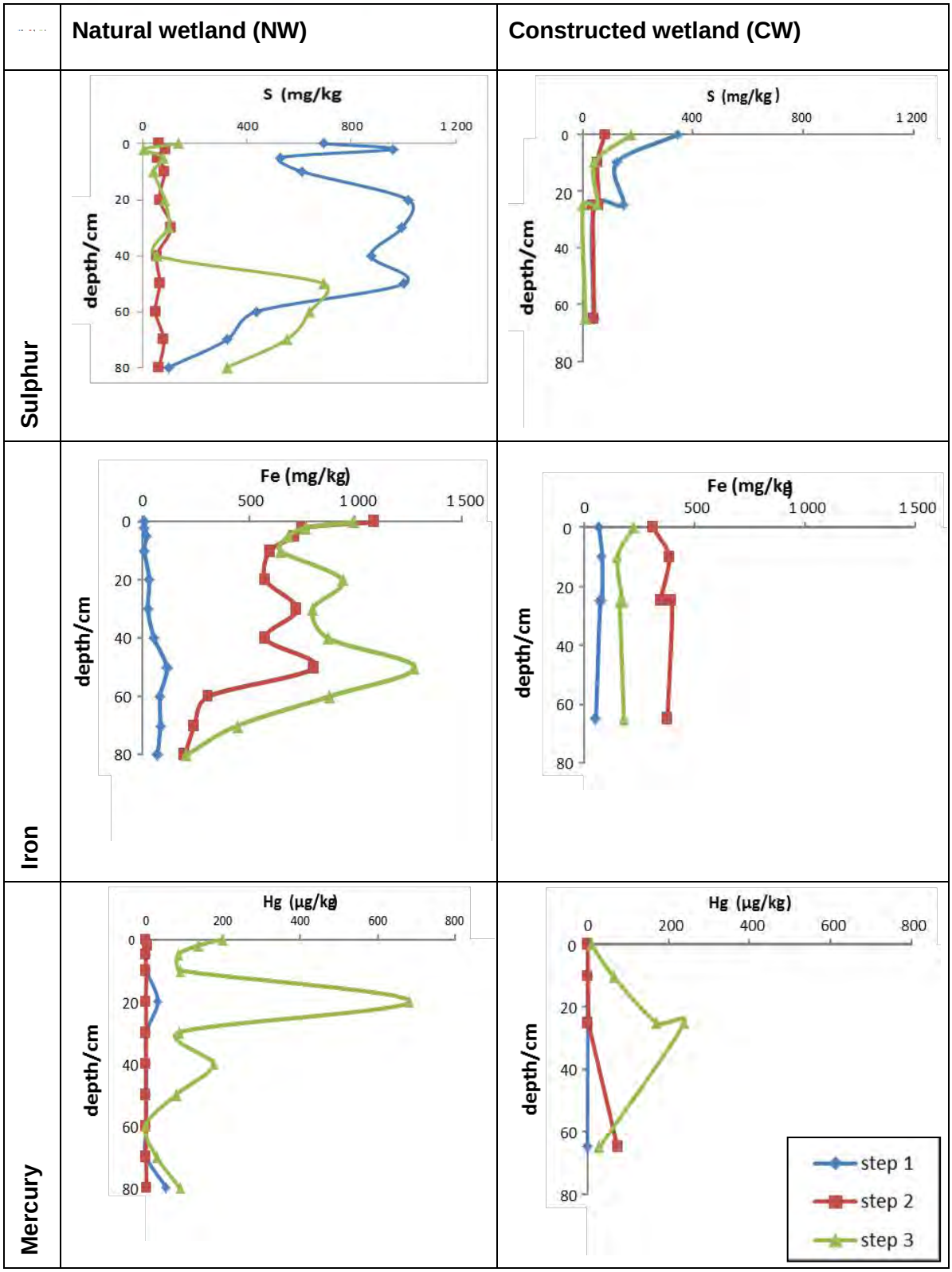

Figure 4 BCR sequential extraction (3 steps) for S, Fe and Hg in NW and CW sediments.

Mercury speciation in both wetlands shows the largest fraction leached in step 3 – oxidizable fraction; this situation is especially evident in the middle sediment levels. This is strongly correlated to sulphur and organic carbon for NWs. The relative quantities leached suggest the importance of ageing (maturity) in the case of CWs.

Seasonal distribution of mercury in wetlands

Distribution patterns for mercury were very similar in both wet and dry seasons. However, the total mercury (Hg^{TOT}) concentration in sediment was much higher in the latter (Figure 5). Also, in the dry season, pH was higher and redox potential was lower in water above the sediments. The equilibrium speciation modeling of Hg in wetlands waters was plotted on an Eh-pH diagram (Lewis and Plant, 2005) (Figure 6).

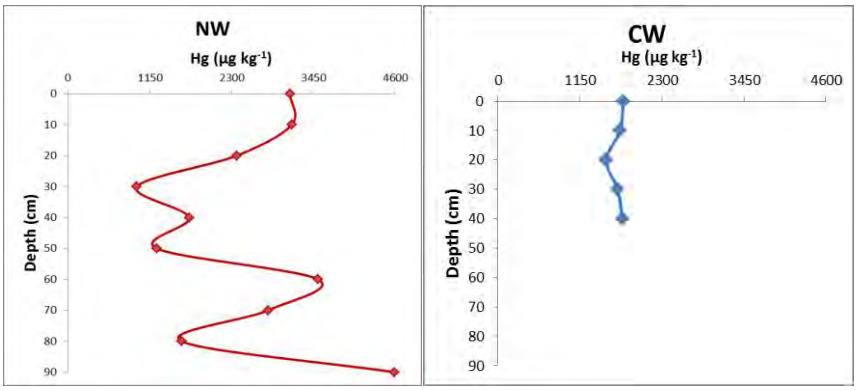

Figure 5 Comparison of Hg^{TOT} in constructed (CW) and natural (NW) wetland sediment in the dry season.

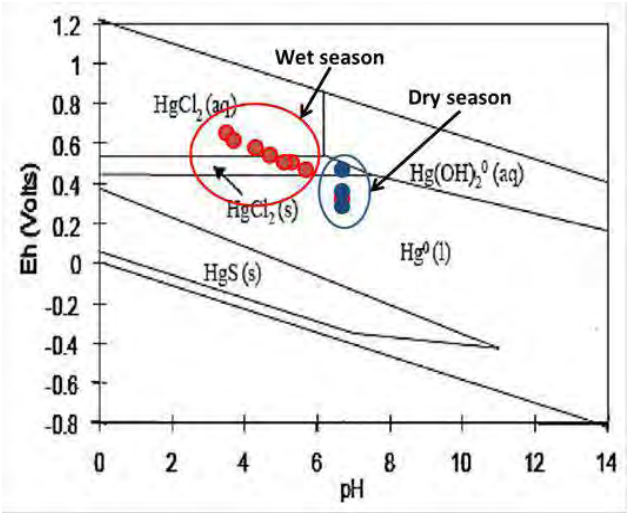

Figure 6 Eh-pH diagram showing seasonal mercury speciation in wetlands

The results showed that the predominant form of Hg in wet season waters is soluble $HgCl_2(aq)$ whereas the highly insoluble and volatile Hg^0 predominated in the dry season. This explains the elevated dissolved mercury concentration during the in wet season and its decrease in the corresponding sediment samples. This might be due to the acidification of the water during wet

season, which can occur when oxidation by products are flushed from mine tailings.. The lowering of the water pH during the rainy season is known to favour the solubilisation of heavy metals such as Hg, thus increasing Hg^{TOT}. There is, therefore a probable Hg remobilisation from the lower sediment horizons with the water's acidification during wet season and an eventual atmospheric release and/or re-precipitation during winter which explains its overall decrease in watersheds. The concentration of sulfate and chloride were also higher during the wet season, explaining the higher electrical conductivity values measured in these sampling time.

CONCLUSIONS

This study compares the performance of natural and manmade wetlands in trapping Hg as well the seasonal Hg distribution in both ecosystems. In general, natural wetlands performed better as "Hg sinks" compare to constructed ones. The lack of biodiversity in planting from the CWs and their younger ages could explain their lower effectiveness in Hg trapping. The constructed wetlands, therefore, require relatively more maturity and treatment prior to a meaningful assessment of their capacity retaining pollutants. Seasonal changes in Hg load in wetlands waters confirm that Hg is remobilized during the wet season and precipitates into sediment and/or evaporates into the atmosphere during the dry season. Selective extraction procedures revealed the predominance of in-soluble Hg compounds, especially at lower redox potential inorganic-rich sediments typical of wetlands. The fractionation of mercury in the BCR selective extraction depends strongly on the sample matrix as well as on the Hg concentration.

ACKNOWLEDGEMENTS

The authors would like to thank the following for their contribution and support during this study: Technology and Human Resources Programme (THRIP, SA) and AngloGold Ashanti Ltd (SA).

REFERENCES

Baird, C. and Cann, M. (2012). Environmental chemistry. W.H. Freeman, New York

Cordos E, Rautiu R, Roman C, Ponta M, Frentiu T, Sarkany A, Fodorpataki L, Macalik K, McCormick C, Weiss (2003). Characterization of the rivers system in the mining and industrial area of Baia Mare, Romania. The European Journal of Mineral Processing and Environmental Protection, 3 (3): 324-335.

Durkin, T.V. and J.G. Herrmann (1994). Focusing on the Problem of Mining Wastes: An Introduction to Acid Mine Drainage. IN Managing Environmental Problems at Inactive and Abandoned Mine Sites. US EPA Seminar Publication.

Fennessy, S. and W.J. Mitsch. (1989). Design and use of wetlands for renovation of drainage from coal mines. IN Ecological Engineering: an introduction to ecotechnology. W.J. Mitsch and S.E. Jorgensen (Ed.),. John Wiley & Sons, New York, NY, pp. 232-252

Gambrell, R.P. and W.H. Patrick Jr.. (1978) Chemical and microbiological properties of anaerobic soils and sediments. IN Plant Life in Anaerobic Environments. D.D. Hook and R.M.M. Crawford (Ed.). Ann Arbor, MI.

Getaneh W., Alemayehu T. (2006). Metal contamination of the environment by placer and primary gold mining in the Adola region of southern Ethiopia, Environ. Geol., 50(3), 339–352

Han, F. X., Banin, A., Kingery, W. L., Triplett, G. B., Zhou, L. X., Zheng, S. J., Ding, W. X. (2003) Advances in Environ. Research, vol. 8, pp. 113.

Harris, R., Krabbenhoft, D.P. Mason, R., Murray, M.W. Reash, R. , Saltman, T.ed. (2007). Ecosystem Responses to Mercury Contamination. CRC Press, Taylor & Fransis, New York.

Hlavay, J., Prohaska, T., Weisz, M., Wenzel, W., Stingeder, G.J., (2004) Determination of trace elements bound to soil and sediment fractions (IUPAC Technical Report). Pure Appl. Chem, , vol. 76, no. 2 pp. 415-442.

Ianni, C., Ruggieri, N., Rivaro, P. and Frache, R.: (2001) 'Evaluation and comparison of two selective extraction procedures for heavy metal speciation in sediments', Anal. Sci. 17, 1273–1278.

Kadlec, R.H. (1985). Aging phenomena in wastewater wetlands. IN Ecological Considerations in Wetlands Treatment of Municipal Waters. E.R. Kaynor, S. Pelczarski, and J. Benforado (Ed.). pp. 338-347. Van Nostrand Reinhold, NY.

Kim K.-K., Kim K.-W., Kim J.-Y., Kim I.S., Cheong Y.-W., Min J.-S., (2001) Characteristics of tailings from the closed metal mines as potential contamination source in South Korea, Environ. Geol., 41(3–4), 358–364

Lewis, R.A. and Plant, J.A. (2005) Mercury in the environment with reference to mining operations, Imperial College (ed), London.

Mitsch, W.J. and J.G. Gosselink. (1986). Wetlands. Van Nostrand Reinhold, NY.

Navas, A., Lindhorfer, H. 2003. Geochemical speciation of heavy metals in semiarid soils of the central Ebro Valley, Spain. Environ International 29 (1), 61-68.

Perry, A. and R.L.P. Kleinmann. (1991). The use of constructed wetlands in the treatment of acid mine drainage. Natural Resources Forum vol. 5, pp. 178-184.

Quevauviller, P., Rauret, G., Muntau, H., Ure, A. M., Rubio, R., Lopez-Sanchez, J. F., Fiedler, H. D., Griepink, B., (1994) Evaluation of a sequential extraction procedure for the extractable trace metal contents in sediments. Fresenius J. Anal. Chem., vol., 349, pp. 808-814.

Rauret, G López-Sánchez, J.-F. Sahuquillo, A. Barahona,E. Lachica,M. Ure,A.M. Davidson,C.M. Gomez,A. Lück,D. Bacon,J. Yli-Halla,M. Muntau H. and Quevauviller.,P. (2000) Application of a modified BCR sequential extraction (three-step) procedure for the determination of extractable trace metal contents in a sewage sludge amended soil reference material (CRM 483), complemented by a three-year stability study of acetic acid and EDTA extractable metal content J. Environ. Monit., vol. 2, pp. 228-233.

Sheppard, M.I., Stephenson, M., (1997). Critical Evaluation of Selective Extraction Methods for Soils and Sediments, Contaminated Soils. INRA (Les Colleagues, 85), Paris

Snyder, C,D. and E.C. Aharrah. (1985). The Typha community: a positive influence on mine drainage and mine restoration. IN Wetlands and Water Management on Mined Lands: Proc. of a Conf. 23-24 Oct. 1985 The Pennsylvania State University. pp. 187-188. University Park, PA.

Tessier,A.,Campbell,P.G.C., Bisson,M., (1979). Sequential extraction for the speciation of particulate trace metals. Anal. Chem. Vol. 51,pp. 844 – 851

Ure, A.M., Quevauviller, Ph., Muntau, H., Griepink, B., (1993). Speciation of heavy metal in soils and sediments. An account of the improvement and harmonisation of extraction techniques undertaken under the auspices of the BCR of the Commission of the European Communities. Int. J. Environ. Anal. Chem. Vol. 51, pp. 135 - 151.

Wildeman, T., J. Gusek, J. Dietz and S. Morea. (1991). Handbook for Constructed Wetlands Receiving Acid Mine Drainage. US EPA, Cincinnati.

Use of Genomic Methods to Characterize Microbial Community in Assessment of ARD Impacts and Mine Closure Activities

Melanie Blanchette[1], Mark Lund[1] and Lisa Kirk[2]

1. *Mine Water and Environment Research Centre (MiWER), Edith Cowan University, Australia*
2. *Center for Biofilm Engineering, Montana State University, USA*

ABSTRACT

Until recently, our understanding of the microbial ecology of mined materials and ARD-affected water has been hampered by the selective effects of culturing microbial taxa (Archaea, Bacteria and Fungi). Recent advances in genomic technologies – such as next generation high-throughput DNA sequencing – now allows rapid, low-cost, and comprehensive investigations into microbial community diversity and function. From an environmental management perspective, analysis of microbial communities from ARD-affected water can provide insight into the effectiveness of mine management programs by rapidly indicating environmental impacts as well as changes resulting from remedial action. However, incorporating microbes as part of routine environmental assessment requires dealing with (as yet) unknown issues such as the effect of scale, determination of physico-chemical drivers, taxonomy, the potential effect of sequencing platform/bioinformatics on identification, and information organization and communication.

Here, using a community ecology approach, we explore the utility of genomic analysis to the management and study of mine-affected waters through case studies in the USA and Australia: 1. acidic pit lakes in Collie, Western Australia, and 2. the hydraulically plugged Glengarry adit near Cooke City MT. These case studies highlight how microbes can be used for identifying and evaluating the impacts of ARD in post-mine pit lake and hydraulically plugged underground mine workings, and as potential tools for environmental management.

**There is no full article associated with this abstract.*

10th ICARD IMWA 2015 | 10th International Conference on Acid Rock Drainage & IMWA Annual Conference

Comparative Analyses of Metagenomes from Acid Rock Drainage

Ana Moya-Beltrán[1], Francisco Issotta[1], Harold Nuñez[1], Francisco Ossandón[1], David Holmes[1,3] and Raquel Quatrini[1,3*]

1. Microbial Ecophysiology Laboratory, Fundación Ciencia y Vida, Chile
2. Center for Bioinformatics and Genomic Biology, Fundación Ciencia y Vida, Chile
3. Facultad de Ciencias Biológicas, Universidad Andrés Bello, Chile

ABSTRACT

Acid rock drainage (ARD) is a worldwide environmental problem. ARD is generated by microbially mediated oxidative dissolution of sulfide minerals and is characterized by low pH and high concentrations of sulfate and metals, thus representing an extreme environment for microbial life. Current knowledge about the structure and functioning of these communities is limited mainly because most studies characterizing ARD environments have relied on culture-dependent techniques or molecular taxonomy studies based on 16S rRNA information. Cultivation-independent metagenomic approaches are generating new opportunities to investigate community structure and the metabolic potential and functional significance of ARD microbes by directly assessing genomic information from environmental samples.

In this work, a comparative analysis of six microbial metagenomes has been undertaken from ARD sites: 5-Way and UBA biofilms from Richmond (biofilm), Kristineberg mine (biofilm and planktonic samples); Carnoulès mine (arsenic-contamined effluents) and Los Rueldos mine (mercury contaminated effluents). Taxonomic analysis of 384 Mbp of sequence information demonstrates that *Acidithiobacillus-like*, *Leptospirillum-like* and some Archaea are the most abundant and widespread taxa. Community-wise comparative analyses also showed that different ARD microorganisms partition according to specific environmental and geochemical conditions (e.g pH, temperature, etc.) and that in general one type of microorganism is dominant in each condition (e.g *Acidithiobacillus ferrivorans* in the Kristineberg metagenome). On these bases, and using available sequenced reference genomes, read recruitment analyses have been undertaken and strain-level variations assessed on high coverage genomic regions.

Acknowledgements: Fondecyt 1130683, 1140048, Conicyt Scholarship 3130376, Basal PFB-16.

**There is no full article associated with this abstract.*

Targeted Metagenomic Analysis of Mynydd Parys Acid Rock Drainage Microbial Communities

Harold Nuñez[1], Juan Pablo Cardenas[1,2], Ana Moya[1], Francisco Issotta[1], Mónica Gonzalez[1], D. Barrie Johnson[4], Raquel Quatrini[1,2]

1. Microbial Ecophysiology Laboratory, Fundación Ciencia y Vida, Chile
2. Facultad de Ciencias Biologicas, Universidad Andres Bello, Chile
3. National center of genomics, proteomics and bioinformatics, Chile
4. School of Biological Sciences, University of Wales, United Kingdom

Acid rock drainage (ARD) is an environmental problem resulting from the oxidative dissolution of pyrite and other sulfide minerals. The high sulfate concentration, extreme acidity and toxicity of metal-rich solutions derived from ARDs impose unique selective pressures to the microorganisms thriving in these econiches. Analysis of ARD microbial communities have been primarily based on 16S rRNA gene library sequencing, DGGE and/or T-RFLP profiling, providing relevant insights into the structure and evolution of acidophilic microbial communities. Nonetheless, these approaches lack the depth and coverage of modern sequencing techniques, thus little information has been collected on the microdiversity and the distribution of strain variants of the dominant taxa.

Here we combined Illumina-based technology with classic 16S phylogenetic (V3-V4 regions) and Multi Locus Sequence Typing marker analysis, an approach referred to as Targeted Metagenomics, to assess the microdiversity within the genus *Acidithiobacillus* in Mynydd Parys copper mine acid rock drainage. Mynydd Parys (Parys Mountain) mine, located in north-west Wales and now abandoned, contains a large body of acidic (pH ~ 2.5) metal-rich water that has accumulated within the underground workings, raising serious environmental concerns. High sequencing depth and resolution achieved through this strategy enabled us to analyze the microbial diversity in great detail, uncovering whole-community structure and sharp differences in species composition and abundance between sampling sites. Based on an improved SNPs-discovery routine diversity within the *Acidithiobacillus* was further explored providing insight into the strain-level richness. Results obtained also revealed the presence within the Parys acid rock drainage of several sequence clusters of undefined taxonomic assignment, further contributing to the understanding of the biodiversity of this system.

Acknowledgements: Conicyt Scholarship 3130376; Fondecyt 1140048, Basal PFB-16.

**There is no full article associated with this abstract.*

10th ICARD IMWA 2015 | 10th International Conference on Acid Rock Drainage & IMWA Annual Conference

Bioaccessibility Testing of Sulfidic Rocks and Wastes

Eleanor van Veen[1], Anita Parbhakar-Fox[2] and Bernd Lottermoser[1, 2]

1. Environment and Sustainability Institute / Camborne School of Mines, University of Exeter, United Kingdom

2. School of Physical Sciences, University of Tasmania, Australia

ABSTRACT

Knowledge of the fraction of metal concentrations in mine wastes, which is accessible to plants, is integral to establishing effective and sustainable post-mining vegetation. Numerous tests have been designed to predict the bioaccessibility of metals in sediments and agricultural soils, however, it remains uncertain whether such tests can be applied to mine soils and in particular sulfidic rock and waste samples. This work aims to identify an appropriate test for the prediction of plant bioaccessibility of environmentally significant metals in sulfidic rocks and wastes.

Plant bioaccessibility extraction tests have evolved from extraction techniques used in the agricultural industry for almost half a century. Improvements in detection limits of analytical techniques to determine element concentrations in extractants (e.g. ICP-MS, ICP-AES) have allowed the use of less aggressive extraction reagents in more recent years. Sequential extraction procedures (e.g. Tessier and BCR sequential extraction procedures) can help determine the overall partitioning of total metals into different phases, however, they are expensive and time consuming. By contrast, single step extractions offer a snapshot of bioaccessibility and are operationally attractive being quicker. Simple salt solutions (e.g. $CaCl_2$, $NaNO_3$, NH_4NO_3) have gained favor in recent years over more aggressive complexing agents such as EDTA and DTPA. However, there are no universally accepted extraction solutions and the current snapshot may not be an indication of future metal bioaccessibility following weathering and oxidation of sulfidic waste rocks.

The results of a case study are presented, where the third step of the BCR sequential extraction procedure is applied to sulfidic rocks and wastes to predict the bioaccessibility of metals associated with sulfides in these materials. Based on literature review and case study analyses, this work is able to make recommendations for plant bioaccessibility testing of metals in sulfidic rocks and wastes.

**There is no full article associated with this abstract.*

10th ICARD IMWA 2015 | 10th International Conference on Acid Rock Drainage & IMWA Annual Conference

Removing Heavy Metals from Acid Mine Drainage Through the Biological Generation of High-Value Metal Nanoparticles

Giovanni Ulloa, Bernardo Collao and José Manuel Pérez
Laboratorio de Bionanotecnología y Microbiología/ CBIB/ Universidad Andres Bello, Chile

ABSTRACT

Acid drainage affects a significant proportion of mine waste and is one of the major environmental problems faced by the mining industry. Its causes, prediction, and treatment have become the focus of a number of research initiatives commissioned by governments, the mining industry, universities and environmental groups. Ferrous and sulfur-oxidizing bacteria catalyze the oxidation of sulfides, reducing the pH of the solution and increasing the concentration of heavy metals such as Cd, As, Te, Pb, Se, etc.

The objective of the present work was to analyze the ability of bacteria present in the bioleaching processes and acid mine drainage (AMD) to biosynthesize nanobiotechnological products, such as fluorescent nanoparticles (quantum dots, QDs) (patent application PCT/CL2014/000074). QDs are semiconductor nanoparticles with potential application in biotechnological and industrial settings, including solar cells, new generation TVs, and biomedicine because of their optoelectronic properties.

In general, the nanoparticle synthesis protocol described in this work involves sulfur-oxidizing microorganisms currently used in Chilean mining industry, in the presence of inorganic phosphate and metals, which allow the cellular incorporation and tolerance of heavy metals. The method of QD synthesis is related to the degradation of intracellular granules of polymeric phosphate, and the release of hydrogen sulfide in the presence of metals. Here we demonstrate that divalent cations are incorporated in the presence of inorganic phosphate by atomic absorption spectroscopy. Sulfur reacts with cellular molecules containing fluorescent nanoparticles to generate compounds of heavy metals and sulfur with the spectroscopic characteristics typical of biosynthesized nanoparticle QDs.

The QD market is forecast to grow globally to a value of $67 million. This market is expected to grow over the next five years at a compound annual growth rate of 59.3%, reaching $ 1185.4. In Chile, the generation of nanoparticles by the mining industry will allow the creation of a new, sustainable and revolutionary business area.

**There is no full article associated with this abstract.*

Trace Elements of Economic Value and Environmental Concern in Acidic Drainage, Biofilms and Mineral Precipitates

Lori Manoukian[1], Bryn Kimball[1], Danielle Fortin[2], Heather Jamieson[1]* and Claudio Andrade[3]

1. *Department of Geological Sciences and Geological Engineering, Queen's University, Canada*
2. *Department of Earth Sciences, University of Ottawa, Canada*
3. *Barrick Gold, Canada*

ABSTRACT

Remediation of closed mine sites that continue to produce acidic drainage from waste rock, underground workings or tailings may require a commitment of decades of water managment and treatment. The overall objective of our research is to explore the possibility of decreasing the financial burden and environmental impact of water treatment by recovering elements of significant market value or isolating elements that are particularly problematic. Processes that occur in mine waste such as the concentration of elements of interest by precipitation of efflorescent minerals and microbial sequestration and transformation of elements have been investigated.

We have sampled drainage waters, mineral precipitates and biofilms where present at El Indio, Lagunas Norte, and Pierina mines. These are epithermal high-sulfidation gold deposits that tend to produce acid drainage and have a distinctive suite of trace elements. Water samples were analysed for major and trace elements in aliquots that were unfiltered, filtered to 0.45 μm and ultrafiltered to 0.01μm. Mineral samples were characterized using SEM-MLA, XRD, EMPA and synchrotron-based microanalysis. Identification of the microbial population diversity in solid and liquid samples has been carried out with DNA extraction and amplification.

Secondary sulfate minerals from these deposits are known to sequester Cu, Zn, Cd, As and other trace elements. From previous work, microorganisms are known to control the mobility of redox-sensitive trace elements such as As and Te. The results of our research will provide a detailed geochemical and microbiological characterization of these mineral-water-biofilm systems associated with epithermal high-sulfidation gold deposits and provide the basis for innovative management approaches to ARD.

**There is no full article associated with this abstract.*

CHAPTER 2

APPLIED MINERALOGY AND GEOENVIRONMENTAL UNITS

Setting ARD Management Criteria for Mine Wastes with Low Sulfide and Negligible Carbonate Content

Stephen Day and Chris Kennedy
SRK Consulting, Canada

ABSTRACT

Evaluation of ARD potential for rock with low (less than <1% by weight) sulfide content using conventional acid-base accounting criteria (e.g. net neutralization potential and neutralization potential ratio) can result in invalid classifications because neutralization potentials do not adequately represent the ability of acid-consuming silicate minerals to neutralize weak acidity. Rocks containing low sulfide concentrations generate acid at low rates that do not necessarily require fast-reacting carbonates to buffer pH to near neutral levels. Instead, meteoric weathering of silicate minerals by carbonic acid can deliver sufficient dissolved bicarbonate to offset acid generated and buffer pHs well above 7. Because silicate minerals dominate the mineralogy of many common rock types, bulk neutralization potential is effectively infinite compared to acid generation potential, and the determination of ARD potential depends on the rate of silicate weathering relative to sulfide oxidation rate. Furthermore, the bulk sulfide oxidation rate is typically correlated to sulfide content allowing sulfide content thresholds to be used as management criteria.

This paper will present an example of the use of this conceptual model to develop waste rock management criteria for the NorthMet Project in the nearly carbonate-absent Duluth Complex of northern Minnesota, USA. The method involved measurement of silicate weathering rates for rocks containing negligible sulfide and development of a relationship between sulfide content and oxidation rates. Interpretation of the data obtained provided an explanation for the lack of net acid generation in decades-long kinetic-testwork performed by the Minnesota Department of Natural Resources on samples containing less than 0.2% sulfur as pyrrhotite and chalcopyrite. The findings were used to develop waste rock management criteria for the proposed mine using sulfur content.

Keywords: silicate weathering, silicate alkalinity, Duluth Complex, low sulfide

INTRODUCTION

Conceptual Geochemical Model – Contact Water pH Modification By Silicate Minerals

The tendency for mine wastes to yield contact waters containing unacceptable concentrations of regulated contaminants largely hinges on weathering pH because most of the the contaminants are metals and solubility is in part a function of pH typically represented by reactions such as:

$$Cu^{2+} + 2H_2O \leftrightarrow Cu(OH)_2 + 2H^+ \quad (1)$$

While higher pHs do not guarantee that concentrations will be below regulatory limits, the relationship between pH and metal concentrations indicates that concentrations will tend to be much higher at lower pHs. The trend is reversed when amphoteric behavior allows solubility to increase at higher pHs.

The weathering environment pH in mine wastes is commonly attributed to the balance between acid generating reactions represented by:

$$FeS_2 + {}^{15}\!/_4 O_2 + {}^{7}\!/_2 H_2O \rightarrow Fe(OH)_3 + 2SO_4^{2-} + 4H^+ \quad (2)$$

and the consumption of acid (H^+) by carbonate minerals:

$$4Ca(CO)_3 + 4H^+ \rightarrow 4Ca^{2+} + 4HCO_3^- \quad (3)$$

The balance between these reactions is usually evaluated by analytical methods which are proxies for the iron sulfide and carbonate minerals (for example, acid-base accounting, ABA, Sobek et al., 1978; Lawrence & Wang, 1991 and net acid generation, NAG, AMIRA International, 2002).

This conventional theory and the analytical approaches used to quantify acid generating and acid consuming mine waste components fall short of correctly incorporating the role of silicates in modifying contact water pH because silicate minerals react much less rapidly than carbonate minerals and weathering rates are a function of pH. For example, neutralization potential (NP) determined as part of ABA is commonly observed to yield more apparent acid-consuming capacity than can be accounted for by the carbonate content (for example, Day, 2009) and this difference is assigned to acid consumption by silicate minerals. The aggressive low pH of the test conditions in the NP procedure (and similarly in the NAG procedure) result in acid neutralization by reactions such as:

$$CaAl_2Si_2O_8 + 8HCl \rightarrow Ca^{2+} + 2Al^{3+} + 2SiO_2 + 8Cl^- + 4H_2O \quad (4)$$

Hydrolysis reactions for the resulting dissolved aluminum buffer pH in the range 4 to 5:

$$Al^{3+} + 3H_2O \rightarrow Al(OH)_3 + 3H^+ \quad (5)$$

Therefore, the low pH of the tests encourages silicate mineral dissolution, which buffers pHs through aluminum release (reaction (4)) at levels too low to usefully influence metal solubility relative to regulated limits. Furthermore, due to the slow weathering reaction kinetics of the consumption of acid by the above types of reactions and the method used to determine the amount of acid in the analytical procedures, the NP methods do not quantify the silicate mineral reservoir potentially available to neutralize acid.

The actual role of silicates in controlling contact water pH is represented by weathering reactions between carbon dioxide and silicate minerals, such as:

$$CaAl_2Si_2O_8 + 2H_2O + 2H_2CO_3^0 \rightarrow Ca^{2+} + 2Al(OH)_3 + 2SiO_2 + 2HCO_3^- \quad (6)$$

This reaction is comparable to reaction (4) but involves carbonic acid (i.e. dissolved CO_2) rather than sulfuric acid and yields dissolved bicarbonate which can in turn be involved in buffering contact water pH in the near neutral pH range through reversible reactions such as:

$$Ca^{2+} + HCO_3^- \rightarrow CaCO_3 + H^+ \quad (7)$$

The potential role of silicates in modifying contact water pH at higher pHs is therefore limited to the delivery of alkalinity due to slow weathering resulting in exchange of protons with alkali and alkali earth cations in silicates. These reaction rates are very slow relative to dissolution of carbonate minerals and are therefore probably unimportant in carbonate-rich systems. They become much more important in carbonate-deficient systems containing low sulfide concentrations where the rate of acid generation can be balanced by the slow generation of alkalinity by silicate weathering. Furthermore, the silicate mineral reservoir is far greater than the acid that could be generated by sulfide oxidation resulting in an effectively perpetual source of alkalinity even when passivation of silicate mineral surfaces by secondary silicates occurs. In this setting, the rate of acid generation by sulfide oxidation therefore becomes the controlling variable rather than the actual quantity of silicate minerals.

This paper describes quantification of silicate weathering for a nearly carbonate-absent geological environment and the resulting definition of sulfide sulfur management criteria for waste rock management.

Study Area – Duluth Complex

The Duluth Complex in northern Minnesota is a layered gabbroic complex intruded approximately 1 billion years ago. The base of the complex contains copper and nickel sulfides, and platinum group elements formed from sulfide melts. The dominant minerals in the Duluth Complex are olivine and plagioclase, and carbonates were not formed as part of the original magmatic processes. Deuteric processes resulted in localized formation of secondary carbonates but at very low concentrations which are commonly undetectable.

The State of Minnesota recognized the benefits of economic recovery of metals from the Duluth Complex and initiated studies to support resource development (State of Minnesota 1979). Interest in large-scale open pit and underground mining accelerated in the 2000s and several projects are in various stages of economic and regulatory assessment. This includes PolyMet Mining Inc.'s NorthMet Project, which is the subject of this paper.

Previous Studies

The Lands and Mineral Division of the Minnesota Department of Natural Resources (MDNR-LAM) continues to conduct several test programs designed to evaluate the long term weathering of Duluth Complex rocks (e.g. Lapakko & Antonson, 2006). These have included chemical and mineralogical characterization, conventional humidity cells (ASTM, 2001) and other custom-designed laboratory kinetic tests, and monitoring of drainage from small field test piles and full-

scale waste rock piles. The latter are stockpiles of Duluth Complex rocks resulting from stripping to access iron ore in the LTV Steel Mining Company's Dunka Pit.

The laboratory kinetic tests operated for over 18 years by MDNR-LAM (Lapakko & Antonson, 2006) have shown consistent leaching features including lack of pH depression in samples containing about 0.2% sulfur (Figure 1a), correlation of timing of pH depression and sulfur content (Figure 1b,c,d), recovery of pH following pH minimums (Figure 1b,c), and correlation of sulfide oxidation rates with sulfide content.

Program Design

The NorthMet Project would be an open pit mine with a proven and probable ore reserve of 275 million tonnes with a copper equivalent grade of 0.79% (Desautels & Zurowski, 2013). The sulfur block model for the deposit indicated that waste rock would contain sulfur concentrations ranging from 0.01% to greater than 1%. The majority of waste rock would contain less than 0.1%. A kinetic test program was designed in consultation with MDNR-LAM to develop waste management criteria. The detailed design evaluated the relationship between variables that could conceivably affect rock weathering behavior including sulfur content, rock type (variability between plagioclase- and olivine-rich troctolite end-members), sulfide mineralogy (iron versus copper and nickel sulfides as represented by samples of waste, low grade ore and ore), stratigraphic layer in the complex, and waste rock particle size. The influence of test protocol on outcomes was evaluated by parallel testing using conventional ASTM and MDNR-LAM-designed methods. The distribution of sulfur concentrations tested is shown in Figure 2. Several samples were selected containing 0.02% sulfur thereby indicating weathering chemistry for rock essentially containing no sulfide. Samples containing the highest sulfur concentrations in the test program were from the surrounding host rocks of the Duluth Complex rather than the intrusions themselves.

METHODOLOGY

Sample Acquisition and Preparation

Samples were selected from drill core using logged characteristics and analytical data in the exploration database. Two sections of each core interval were retained for mineralogical characterization and the balance was crushed to meet the specifications of the various test methods.

Mineralogy

Mineralogy was described using optical methods on polished thin sections. For each mineral, the crystal shape, grain size and texture were described. Electron microprobe was used to determine concentrations of major element oxides, arsenic, cobalt, copper, iron, nickel, titanium and zinc in grains of all major silicates, oxides and sulfides.

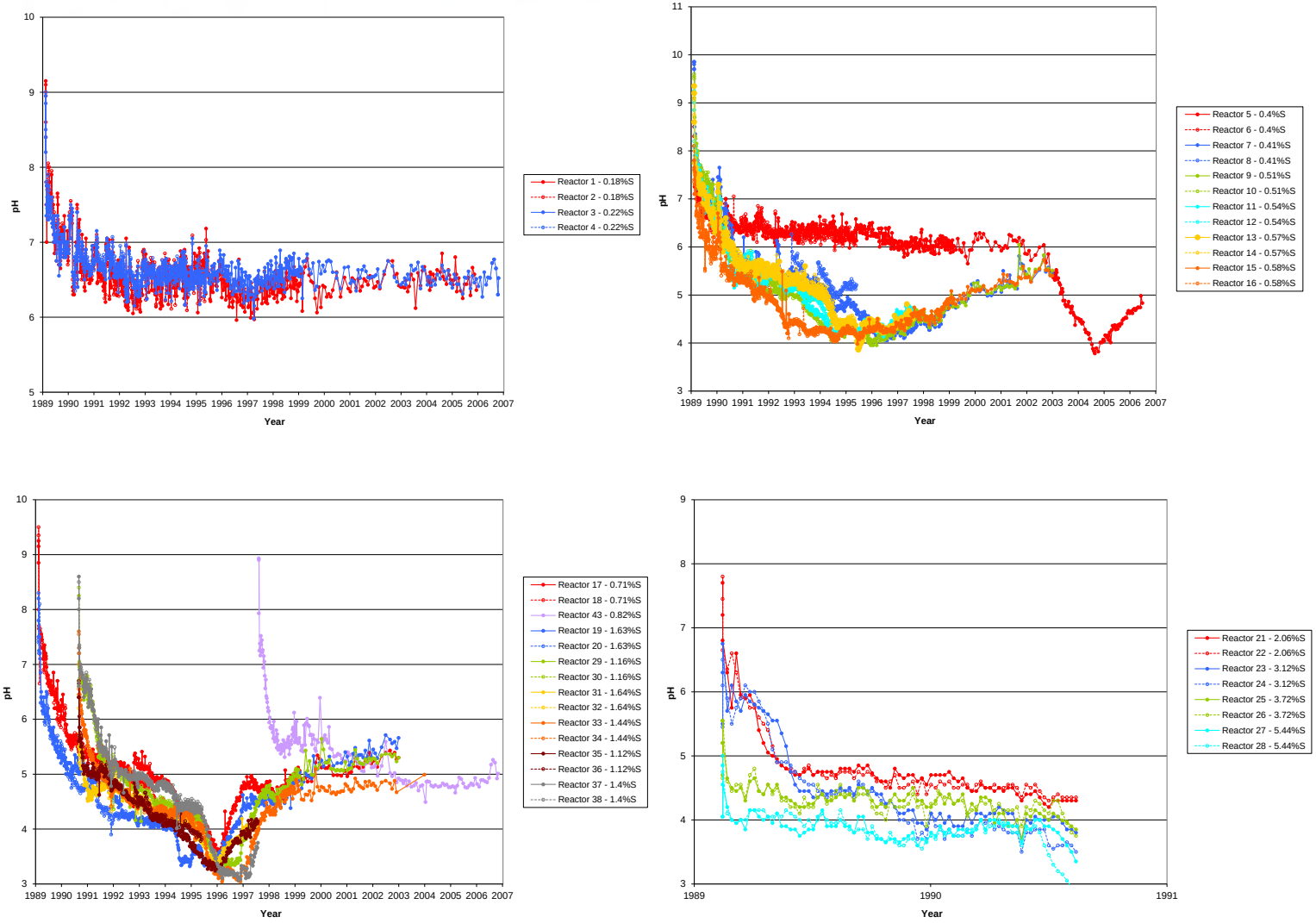

Figure 1 pH Trends for a selection of long term laboratory kinetic tests operated by MDNR-LAM

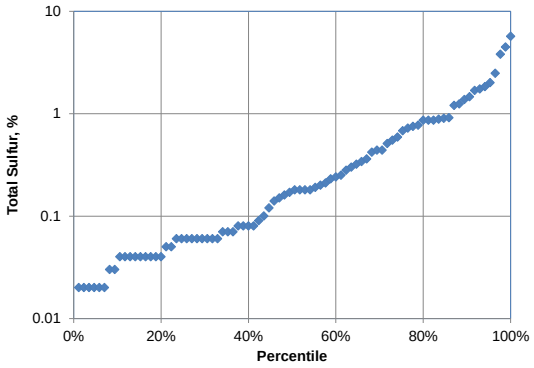

Figure 2 Distribution of sulfur concentrations in rock humidity cells for the NorthMet project. Each symbol is one test.

Humidity Cells

Humidity cells were performed using the ASTM (2001) methodology. The sample charge was 1 kg and the weekly leaching volume was 0.5 L. Leachate analysis included weekly pH, conductivity and ORP; sulfate, acidity, alkalinity, chloride and fluoride every two weeks, and an element scan every two weeks. For every fourth week, the element scan was performed using a low level ICP-MS method. ICP-OES was used for the intervening weeks. This approach recognized that the test work was expected to proceed for many years and therefore was selected to control costs. As the program proceeded, analytical frequency was further reduced. Some humidity cells have now been operating for over 10 years.

Quality Assurance and Quality Control

Routine quality assurance measures included analysis of 10% of solids and leachates in duplicate. In addition, 10% of all kinetic tests were operated in duplicate and blank kinetic tests.

RESULTS AND DISCUSSION

Mineralogical Characteristics

The dominant minerals in all Duluth Complex samples were plagioclase and olivine. Clinopyroxene and orthopyroxene were present in minor quantities with chlorite and serpentine as alteration products. Using microprobe data, plagioclase was determined to be of approximate labradorite composition being calcium enriched and the average composition of olivine was 57% forsterite (Mg_2SiO_4) and 43% fayalite (Fe_2SiO_4).

Dominant sulfide minerals determined from thin sections were pyrrhotite ($Fe_{1-x}S$) and chalcopyrite ($CuFeS_2$). Chalcopyrite was dominant when sulfur concentrations were very low (<0.05%) and in low grade and ore grade samples. Otherwise pyrrhotite dominated. The dominant nickel sulfide was pentlandite ($(Fe,Ni)_9S_8$) and cubanite ($CuFe_2S_3$) tended to be present in comparable amounts to pentlandite. Trace levels of various cobalt, copper, lead, nickel, iron and zinc sulfides and arsenides were identified. Calcite was very rarely identified.

Humidity Cell Results

Leachate Chemistry

Leachate pH trends for two groups of waste rock cells are shown in Figure 3. Samples containing less than or equal to 0.05% sulfur have consistently yielded pHs near 7 following initial decline in pH which lasted approximately 1 year. There has been a slight overall tendency for pH to increase over time in the long term testwork. Samples with more than 0.05% sulfur have also mostly yielded pHs between 6 and 7 with only three samples containing sulfur concentreations exceeding 0.4% showing lower pHs. Alkalinity concentrations have been consistently detected above 1 mg $CaCO_3$/L and tend to be less than 10 mg $CaCO_3$/L.

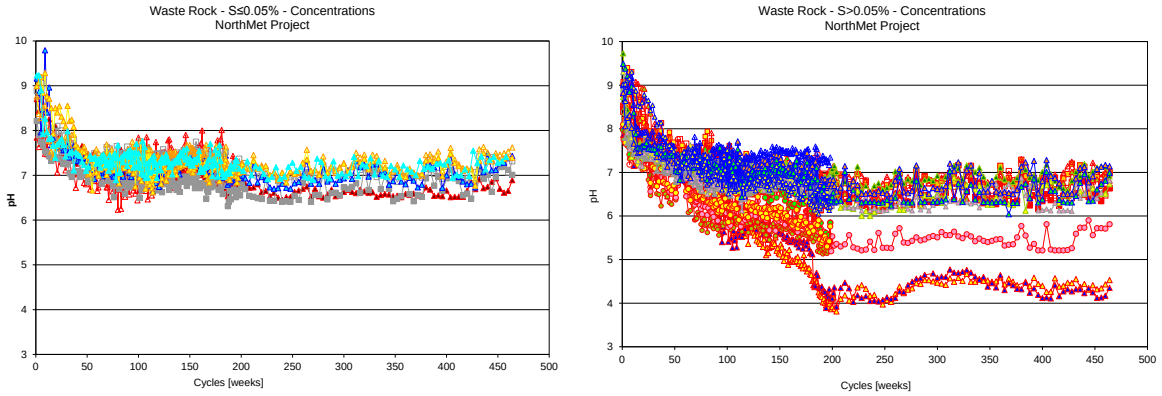

Figure 3 Selected humidity cell results for Duluth Complex samples from the NorthMet project grouped according to sulfide content

Interpretation of Sulfide Threshold for Acid Generation

Method

Long term test work on Duluth Complex samples performed by both MDNR-LAM and PolyMet Mining Inc. shows that samples with 0.4% and greater initial sulfur content generate acidic leachates under laboratory conditions. In this instance, acid generation is defined as a pH of 5.5 which is consistently below that of the deionized water used to leach the samples. MDNR-LAM's long term test work also shows that samples containing about 0.2% sulfide do not generate acid after 20 years of weathering. A sample containing 0.2% sulfur in the NorthMet program has shown pH near 5.5 (Figure 3) but detectable alkalinity (> 1 mg $CaCO_3$/L) is also released. These test data imply that a sulfur criterion for segregation of waste rock should be between 0.2% and 0.4%; however, a residual concern is that any of the MDNR-LAM or NorthMet Project tests with 0.2% sulfur could start to generate acid in the future. The NorthMet data were therefore interpreted to evaluate what the potential threshold of alkalinity release from weathering of silicates could be in order to offset acid generation from sulfide oxidation. The interpretation method used was as follows:

- Leachate from samples containing lowest sulfur concentrations were interpreted to determine if the chemistry was consistent with the silicate minerals that appear to be weathering, and were then used to establish alkalinity generation rates in the near absence of sulfide minerals.
- The correlation between oxidation rates and sulfur content was evaluated.
- Acid generation rates were compared to alkalinity generation rates to determine if a threshold sulfur concentration could be identified and used as a waste managemetn criterion.

Mineralogical Interpretation of Leachates

Selected typical leachates from six humidity cells containing 0.02% sulfur and carbonate content at or below the detection limit of 0.2% CO_2 were modeled using Geochemist's Workbench® to evaluate if leachate composition was consistent with the mineralogy of the samples. Three samples were described as troctolite and three as anorthosite. The latter contains a relatively greater proportion of plagioclase compared to olivine. The minerals assumed to be reacting were chalcopyrite ($CuFeS_2$, reacting amount calculated from sulfate concentrations), anorthite ($CaAl_2Si_2O_8$, reacting amount calculated from calcium), albite ($NaAlSi_3O_8$, reacting amount calculated from sodium), forsterite (Mg_2SiO_4, reacting amount calculated from magnesium) and fayalite (Fe_2SiO_4. reacting amount calculated from magnesium and the composition of olivine indicated by microprobe). The reaction was assumed to occur at 20°C (laboratory temperature) in the presence of fixed atmospheric oxygen (fugacity of 0.2) and carbon dioxide (fugacity of $10^{-3.4}$). Controlling secondary minerals were assumed to be amorphous ferric hydroxide ($Fe(OH)_3$), malachite ($Cu_2CO_3(OH)_2$), gibbsite ($Al(OH)_3$), kaolinite ($Al_2Si_2O_5(OH)_4$) and amorphous silica (SiO_2).

Measured and modelled leachate pHs were strongly correlated though the model over-predicted leachate pH in all six cases (Figure 4). Over-prediction was greater for the troctolite samples. Modelled alkalinity was very close to measured alkalinity for all six samples (Figure 4). Average modeled silicon concentrations were 1.9 mg/L compared to average measured concentrations of 1.2 mg/L. This modeling demonstrates that measured alkalinity generation can originate from meteoric weathering of the dominant silicate minerals confirming the conceptual model and indicating silicate weathering is a long term source of alkalinity. Stability of long term trends (approaching 10 years for this dataset and 20 years for the MDNR's dataset, Figure 1) has provided sufficient time for stripping of carbonate minerals even if present at the detection limit.

Based on this finding, longer term stable data from humidity cells were used to calculate an average alkalinity generation rate of 3.3 ± 0.4 mg $CaCO_3$/kg/week. The 5th to 95th percentile range for the rates was 2.1 to 5.3 mg$CaCO_3$/kg/week. For subsequent calculations and comparison to acid generation rates, 2.9 mg$CaCO_3$/kg/week as the lower confidence limit (at α=0.05) on the mean was selected to represent long-term base-level alkalinity generation by weathering of silicate minerals. Because the humidity cell tests were operated by leaching with 0.5 L of deionized water, the rate used corresponds to a concentration of about 5.8 mg$CaCO_3$/L

Relationships Between Sulfide Concentrations and Sulfate Release

Average sulfate release rates (calculated after an initial flush of sulfate from the humidity cells had completed at the start of the tests) were compared to sulfide concentrations (Figure 5). The correlation was very strong for sulfur concentrations below 0.1% but was weaker at higher sulfur concentrations where it appeared that some samples yielded distinctively lower sulfate release for a given sulfur content, whereas

others showed higher sulfate release at the same sulfur concentration. Correlations of sulfate release and sulfide content have also been reported by MDNR-LAM researchers (Lapakko and Antonson, 2006).

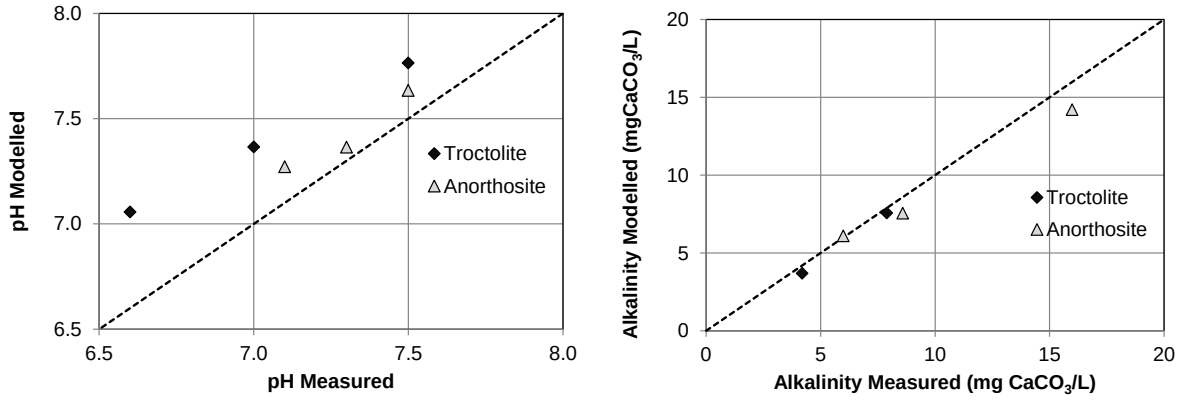

Figure 4. Comparison of measured and modeled humidity cell leachate pH and alkalinity for low sulfur samples. The dashed line indicates parity.

Grouping of samples according to Cu/S weight (mg/mg) ratios (i.e. reflecting the relative amounts of pyrrhotite and chalcopyrite) showed that samples with higher ratios (chalcopyrite enriched) yielded higher sulfate release rates whereas those with lower ratios (pyrrhotite enriched) yielded lower sulfate release. This finding applied across the range of sulfur concentrations including those with low sulfur content (Figure 5). Broadly, the ratio grouping correlates with the economic classification into low grade ore and waste. Three samples classified as lean ore but with lower ratios did not group with the waste rock samples but their sulfate release rates were unstable at the time of the interpretation and subsequently yielded low release rates.

The finding that chalcopyrite appears to oxidize faster than pyrrhotite was counter-intuitive because pyrrhotite is usually considered to be more reactive than chalcopyrite. It was expected that the difference in reactivity could be attributed to differences in mineralogical occurrence (e.g. grain size or crystallinity) but no satisfactory explanation was developed.

DEVELOPMENT OF SULFUR CRITERIA FOR ACID GENERATION POTENTIAL

The conclusion that sulfate release is correlated with sulfide content when Cu/S ratios are considered, was then used to propose sulfur criteria for acid generation potential because a direct link exists between sulfur content and the alkalinity required to offset acid generation. The data in Figure 5 were used to define the two regression equations shown:

$$\text{For Cu/S<0.3: Total S (\%)} = 0.40\ R_{SO_4}\ (\text{mg/kg/week}) - 0.70\ (n=15, r=0.98) \quad (8)$$

$$\text{For Cu/S>0.3: Total S (\%)} = 0.046\ R_{SO_4}\ (\text{mg/kg/week}) - 0.01\ (n=37, r=0.93) \quad (9)$$

The alkalinity generation rate (2.9 mg $CaCO_3$/kg/week) was used to calculate a balancing acid generation rate in sulfate equivalents of 2.9 mg SO_4/kg/week which was then used to calculate threshold sulfur

concentrations by the two regression equations. Due to the need to incorporate conservatism in the estimates for waste management, prediction envelopes were calculated for the regression equations based on a significance level of α=0.05.

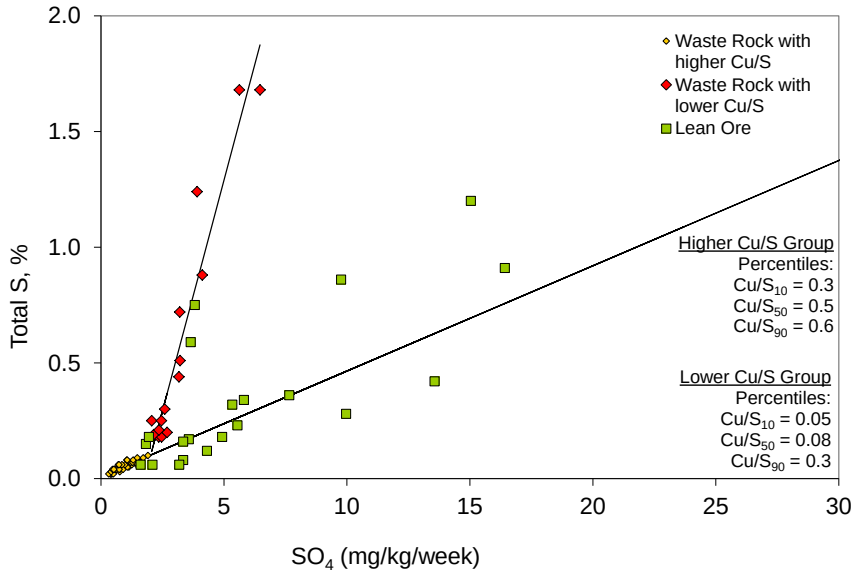

Figure 5 Relationships between average sulfate release and sulfur content

The resulting proposed sulfur criteria were 0.12% for higher Cu/S ratios and 0.31% for lower Cu/S ratios. Both criteria are consistent with the long term testwork performed by MDNR-LAM which showed acid generation occurred for samples with sulfur content greater than 0.4% and a smilar study by Campbell et al. (2012).

For the purpose of waste management, the project proceeded based on a single sulfur criterion of 0.12% due to the lack of an explanation for the difference in sulfide reactivity that resulted in the higher criterion of 0.31%.

CONCLUSIONS

Long term kinetic testwork performed on rocks from the Duluth Complex in northern Minnesota shows that alkalinity generated by weathering of silicate minerals provides a plausible explanation for the lack of acid generation in samples containing low sulfide concentrations. It is concluded that steady alkalinity generation offsets low levels of acid generation. Due to the overwhelming abundance of silicate minerals compared to acid generating sulfide minerals, waste segregation for acid geneation potential is appropriately based on sulfide content rather than coventional acid-base accounting methods. For the NorthMet Project, a site-specific sulfur criterion of 0.12% was adopted.

ACKNOWLEDGEMENTS

The authors gratefully acknowledge permission from PolyMet Mining Inc. to publish these results. Interpretation of the testwork results have benefitted from numerous discussions with individuals at MDNR-LAM (particularly Kim Lapakko, Paul Eger, Mike Berndt, Zach Wens and Mike Olsen), PolyMet (Jim Scott) and Barr Engineering (Tamara Diedrich).

NOMENCLATURE

ABA	Acid base accounting
MDNR-LAM	Minnesota Department of Natural Resources Lands and Minerals
NAG	Net acid generation
NP	Neutralization Potential

REFERENCES

AMIRA International (2002) ARD Test Handbook. Prediction & Kinetic Control of Acid Mine Drainage, Project P387A. May 2002.

ASTM (2001) Standard Test Method for Accelerated Weathering of Solid Materials Using a Modified Humidity Cell, D 5744 – 96 (Reapproved 2001).

Campbell, G, Haymont R, Amoah, N, (2012) A testing approach to assess the weathering behaviour of lithotypes characterized by a trace-sulphide/carbonate-deficient mineralogy: application to altered andesites/diorites at the Boddington Gold Mine, Western Australia. Proceedings of 9th International Conference on Acid Rock Drainage. Ottawa, Canada, May 20 to 26, 2012.

Day, S, (2009) Estimation of calcium and magnesium carbonate neutralization potential for refined acid-base accounting using electron microprobe and x-ray diffraction, Proceedings of 8th International Conference on Acid Rock Drainage. Skellefteå, Sweden, June 23 to 26, 2009.

Lapakko, KA,.Antonson, DA,(2006) Laboratory dissolution of Duluth Complex Rock from the Babbitt and Dunka Road Prospects, Status Report. MN Dept. Natural Resources, Division of Lands and Minerals, St. Paul, MN. October 2006. 35p.

Lawrence, RW, Wang (1996) Determination of neutralization potential for acid rock drainage prediction, MEND Project 1.16.3.

Pierre Desautels, P, Zurowski, G, (2013) Updated NI 43-101 Technical Report on the NorthMet Deposit Minnesota, USA, Prepared for PolyMet Mining Corp. January 14, 2013.

Sobek, AA, Schuller, WA, Freeman, JR, Smith, RM, (1978) Field and laboratory methods applicable to overburden and minesoils, USEPA Report No. 600/2-78-054, 203 pp.

State of Minnesota, (1979) The Minnesota Regional Copper-Nickel Study 1976-1979. Minnesota Environmental Quality Board. August 31, 1979.

A Desulfurization Flotation Approach for the Integrated Management of Sulfide Wastes and Acid Rock Drainage Risks

Jennifer Broadhurst and Susan Harrison
Minerals to Metals Initiative, Department of Chemical Engineering, University of Cape Town, South Africa

ABSTRACT

Wastes from the primary processing of hard-rock sulfide ores and coal have the potential to cause prolonged pollution of the local environment as a result of the long-term generation of acid rock drainage (ARD). Changes in legislation and global thinking have prompted a growing trend towards the development of approaches that remove the ARD pollution risks in perpetuity. In this regard, a two stage process has been developed at the University of Cape Town, which uses froth flotation to both recover valuable material and remove pyritic sulfur from fine mineral waste.

The technical feasibility of this process has been demonstrated at the laboratory scale for porphyry copper and fine coal wastes, with results indicating that it is possible to recover a useable product whilst generating a tailings waste stream with a negligible ARD risk. On the basis of this work, an order-of-magnitude financial model for a fictitious coal waste treatment plant has been developed and applied to demonstrate the economic viability for a selected case study. Furthermore, a life cycle assessment (LCA) study indicated that the pre-disposal removal of sulfide minerals from base metal tailings results in reduced eco-toxicity and human toxicity impacts. However, the LCA revealed that climate change and fossil fuel depletion impacts are increased due to additional energy consumption by the desulfurization process. This LCA study also highlighted the potential to reduce abiotic resource depletion through further processing and recycling of the separated tailings fractions.

The overarching objective of these studies, the key findings of which are presented in this paper, is to improve the environmental sustainability of coal and metal sulfide processing operations by both maximizing resource productivity and minimizing environmental burden.

Keywords: sulfide mine wastes, acid rock drainage, desulfurization flotation, economic feasibility, life cycle assessment

INTRODUCTION

The extraction and processing of coal and sulfide mineral deposits give rise to large volumes of solid and slurry wastes, which are conventionally disposed of in surface impoundments. These mine wastes frequently still contain residual sulfide minerals, particularly pyrite, which can result in the formation of acid rock drainage (ARD) upon exposure to air and moisture (Lottermoser, 2007). Acid rock drainage from sulfide mine waste deposits is typically characterized by low pH, high total dissolved solids and elevated levels of trace elements, and can cause prolonged degradation and pollution of local environments (see for example reports by Bell *et al*., 2001; Lottermoser, 2007; Rosner *et al*., 2001). Solid mine wastes also frequently represent a loss of valuable mineral resources due to incomplete separation during ore processing.

The long-term costs of on-going remedial action, coupled with increasing legislative and public pressure on mines to improve their environmental performance, has prompted a trend towards the development of preventative approaches that are aimed at minimizing or avoiding the generation of ARD (Johnson & Hallberg, 2005). Currently, such approaches focus mainly on avoiding exposure of sulfide minerals to oxygen and moisture, and involve techniques such as backfilling, blending and co-disposal, as well as the use of covers and seals (Johnson & Hallberg, 2005). However, these techniques do not completely remove the risk of ARD formation over the long-term, and in most cases their ability to provide a "walk-away" post-closure situation is yet to be proven. An alternative, and more sustainable, approach is to selectively remove the sulfide minerals from the waste prior to disposal, thereby effectively eliminating the risk of ARD formation in perpetuity (Cilliers, 2006; McCallum & Bruckard, 2009). Previous studies have shown froth flotation to be a technically feasible and cost-effective technique for removing sulfide minerals from a number of base metal and gold process tailings (Benzaazoua *et al*., 2000 & 2008; Benzaazoua & Kongolo, 2003, Bois *et al*., 2004 and Leppinen *et al*., 1997). The conventional desulfurization process produces two mineral waste fractions: a large volume sulfide-lean fraction which can be land disposed without posing an ARD risk, and a smaller volume sulfide-rich fraction which can be used as backfill (Benzaazoua & Kongolo, 2003) or processed further into useful by-products such as sulfuric acid.

Ideally, the pre-disposal treatment of sulfide mine tailings should be used in an integrated approach that not only removes risks of ARD pollution, but also provides opportunities for value recovery and re-allocation of unavoidable wastes as feedstock for other uses (Benzaazoua *et al*., 2008; Hesketh *et al*., 2010a). In this regard, studies at the University of Cape Town have demonstrated that desulfurization flotation of a porphyry-type copper sulfide tailings can be conducted in stages through manipulation of the reagent regime, producing an additional metal-rich stream that could be recycled to the conventional metal recovery plant (Hesketh *et al*., 2010a). The concept of using froth flotation to both recover value and remove ARD risks from mine waste has subsequently been extended to fine coal wastes in a two-stage process that recovers coal by means of oily collectors in stage 1, followed by desulfurization flotation to remove pyritic sulfur in stage 2 (Amaral Filho *et al*., 2011; Kazadi Mbamba *et al*., 2012). Selected case studies have also been conducted to explore the economic viability (Jera, 2013) and broader environmental implications (Broadhurst *et al*., 2014) of the proposed desulfurization flotation approaches.

This paper presents the key findings of these studies, with a view to demonstrating the techno-economic and environmental feasibility of using froth flotation to both recover valuable material and remove ARD risks from fine metal sulfide and coal processing wastes.

METHODOLOGY

Laboratory-scale flotation tests

All flotation tests were carried out in a 3-liter modified Leeds batch flotation cell at the natural pH of the slurry in tap water (pH 6-8), an impeller speed of 1200 rpm and an aeration rate of 5-6 L/min. Detailed experimental procedures are outlined by Hesketh *et al*. (2010a) for the porphyry copper case study and by Kazadi Mbamba *et al*. (2012) for the coal case studies. Acid generating potential was determined using standard acid-base accounting (ABA) and net acid generation (NAG) static tests (Stewart *et al*., 2006), as well as the batch biokinetic test developed at the University of Cape Town (Hesketh *et al*., 2010b)

Porphyry copper case study

In this case study, an oxidized low-grade porphyry copper ore, milled to 70 % passing 150 μm, was used as a proxy for a typical porphyry-type copper sulfide tailings. The ore had a sulfur and copper grade of 3.84 % and 0.16 %, respectively. Pyrite (7.03 %) and chalcopyrite (0.12 %) were the major sulfide minerals. Flotation was carried out in stages (maximum 4), using methyl isobutyl carbinol (MIBC) frother (30 g/ton) and a diothiophosphate collector from CYTEC mining chemicals, at a dosage rate of 9 kg/ton for each stage. The retention time for stage 1 was 8 minutes, and thereafter 5 minutes for each stage. Solids were analyzed for iron, copper and total sulfur.

Coal waste case studies

Two-stage laboratory-scale flotation tests were carried out on the following coal waste samples: fine thickener underflow slurry waste from an operating colliery in Middleburg, South Africa-filtered and milled to 75 % passing 150 μm; fine flotation tailings waste from an operating colliery in Criciúma, Brazil; coal discard, generated through the destoning of low-grade coal by means of an experimental X-ray sorter at a South African coal-fired power plant, and subsequently crushed and milled to 75 % passing 106 μm.

Dodecane (1.86 kg/t) or oleic acid (2.89 kg/t) were used as coal collectors in stage 1, together with isobutyl carbinol (0.11-0.28 kg/t) as a frother. Desulfurization flotation of the coal flotation tailings was subsequently carried out using potassium amyl xanthate (PAX) as a sulfide collector (2.33 kg/t), dextrin as a coal depressant (0.93 kg/t) and methyl isobutyl carbinol (MIBC) as a frother (0.11 kg/t). All flotation tests were carried out at a solids content of 6-7 %, and collection periods of 5 minute and 20 minutes for the coal and desulfurization flotation stages, respectively. Samples were analyzed for ash and total sulfur content.

Economic assessment: coal case study

A framework was developed for providing an order-of-magnitude cost estimate (± 30 % to ± 50 % accuracy) for a fictitious two-stage coal flotation desulfurization plant to treat nominal coal fines from a dump of an abandoned mine in the Witbank/Middleburg coal field (Jera, 2013). The plant flow sheet was based on the laboratory-scale test results obtained for the South African fine coal waste, as described in the previous section, and included milling, flotation, filtration, thickening and pumping as key operations. A plant throughput of 100 t/h with a capacity of 720,000 tons per annum was assumed, at a plant life and availability of 15 years and 82 % respectively. Capital costs were based on major equipment costs in combination with Lang costing factors. Operating costs

were based on "rule of thumb" industry estimates and flow sheet data. Revenue was generated from the sale of the coal product at a price of 349 South African rands (R) per ton. The net present value (NPV) and internal rate of return (IRR) were calculated at a discount rate of 14 %, using Microsoft Excel.

Life cycle assessment: base metal case study

Two scenarios for the treatment of a base metal sulfide tailings stream were developed to evaluate the environmental consequences of incorporating a desulfurization flotation unit into a conventional tailings management plant, which entails dewatering in a thickener and disposal of the thickener underflow to a tailings impoundment (base case scenario). Input-output data for the two tailings management options were derived from a combination of literature information, in-house knowledge and mass balance calculations. An empirical base metals case study by Benzaazoua & Kongolo (2003) formed the basis of this study (Table 1), producing two output streams: a non-acid generating sulfide-lean tailings comprising 72% of the feed; and a sulfide-rich concentrate which could be recycled to the primary extraction plant for additional metal and/or acid recovery.

Background data for electricity production were derived from the Eco-invent database (version 2.2), whilst data for the production of xanthate were obtained from a recent in-house study of the local production of liquid ethyl xanthate at Senmin® International in Sasolburg, South Africa (Kunene *et al*., 2013). Life cycle assessment modelling for each of the scenarios was conducted at a reference flow rate of 100 tons of dry tailings per day, using Simapro Software (version 7.3.3) and USEtox (eco-toxicity and human toxicity impacts) and ReCiPe (climate change, fossil fuel depletion, terrestrial acidification, urban land occupation and natural land transformation) impact assessment methodologies. The detailed methodology and case study assumptions are outlined in Broadhurst *et al*. (2014).

Table 1 Desulfurization flotation LCA case study data[1] (after Benzaazoua & Kongolo, 2003)

Component	Stream compositions (mass %)			Recovery to concentrate (% of feed)
	Feed tailings	Desulfurized tailings	Sulfide-rich concentrate	
Pyrite	17.4	2.18	56.53	91[2]
Sphalerite	0.19	0.02	0.62	90
Chalcopyrite	0.10	0.07	0.19	61
Calcite	2.70	3.38	0.96	10[3]
Other (gangue)	79.61	94.36	41.67	15[2]
Sulfide sulfur	9.38	1.17	30.49	91
Total solids	100	100	100	28

[1]Desulfurisation carried out at pH 6-11, using KAX (potassium propyl xanthate) as a collector and Sasfroth Sc 39 as a frother (Benzaazoua & Kongolo, 2003); [2]derived from mass balance calculations; [3]assumed on the basis of literature information (Broadhurst *et al*., 2007).

RESULTS AND DISCUSSION

Laboratory-scale flotation tests: porphyry copper case study

Flotation tests on the porphyry copper sulfide sample indicated that, whilst the recovery of both pyrite and chalcopyrite increased on increasing the dosage of collector from 9 g/t to 27 g/t, the effect was more significant in the case of pyrite. This differential effect of collector dosage created the opportunity to selectively recover copper in a multi-stage process using 9 kg/t collector in stage one and an additional 27 kg/t collector in subsequent stages. This approach resulted in three tailings fractions: a low volume value-rich fraction containing 58 % of the copper; a low volume sulfide-rich fraction containing > 85 % of the sulfur; and a large volume sulfide-lean fraction containing ~ 90 % of the total mass and < 6% of the total sulfur (Figure 2 and Table 2).

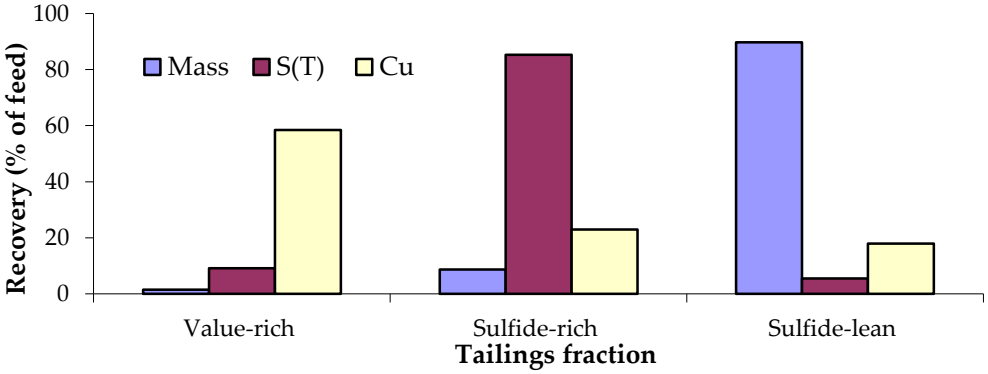

Figure 2 Recovery to tailings fractions in the multi-stage desulfurization of porphyry copper

Table 2 Flotation test results for the multi-stage desulfurization of porphyry copper

Stream	Content (mass %)		NAPP	ARD classification[1]
	Total sulfur	Copper	(kg/t H_2SO_4)	
Feed	3.8	0.16	97.4	Acid forming
Value-rich fraction	2.1	5.7	n/d	n/d
Sulfide-rich fraction	33.7	0.39	n/d	n/d
Sulfide-lean fraction	0.21	0.03	-19.2	Acid neutralizing

[1]In accordance with standard static and biokinetic test results (Hesketh *et al.*, 2010b)
Where: NAPP is net acid producing potential determined by the standard Acid Base Accounting (ABA) method, and n/d is not determined

Laboratory scale ARD prediction tests, using both acid base accounting (ABA) and net acid generating (NAG) protocols, indicated that the sulfide-lean tailings fraction, with a sulfur content of 0.2 %, can be classified as non-acid forming (Hesketh *et al.*, 2010a). Subsequent biokinetic tests confirmed that this sample was net-acid neutralizing, even under conditions of microbial activity (Hesketh *et al.*, 2010b).

Laboratory-scale flotation tests: coal waste case studies

Experimental results for the two-stage flotation process are presented in Table 3 and Figure 3.

Table 3 Flotation test results for the coal waste samples

	A: Tests usingdecane as a collector in stage 1							
	South African fine coal slurry[1]				Brazilian coal tailings			
	Feed	Coal product	Sulfide-rich	Sulfide-lean	Feed	Coal product	Sulfide-rich	Sulfide-lean
Yield (mass %)	100	20	13	67	100	35	43	22
Ash (mass %)	34.4	13.5	28.9	40.8	56.4	24.7	70.4	87.2
Sulfur (mass %)	1.1	0.5	2.7	0.4	5.1	1.6	1.8	0.5
NAPP (kg/t H_2SO_4)	3	n/d	65	-45	-7	n/d	27	-23
ARD classification[2]	PAF	n/d	AF	NAF	PAF	n/d	AF	NAF
	B: Tests using oleic acid as a collector in stage 1							
	South African coal discards				Brazilian coal tailing			
	Feed	Coal product	Sulfide-rich	Sulfide-lean	Feed	Coal product	Sulfide-rich	Sulfide-lean
Yield (mass %)	100	41	23	36	100	56	24	46
Ash (mass %)	56.4	32.1	53.8	82.4	56.4	42.2	85.3	88.8
Sulfur (mass %)	5.1	3.0	18.7	0.2	5.1	1.6	1.4	0.6
NAPP (kg/t H_2SO_4)	110	n/d	501	-70	-7	n/d	15	-67
ARD classification[1]	AF	n/d	AF	NAF	PAF	n/d	PAF	NAF

[1]After Kazadi Mbamba *et al.* (2012) [2]In accordance with standard static and biokinetic test results

Where: NAPP is net acid producing potential, PAF is potentially acid forming, AF is acid forming, UC is uncertain, NAF is non-acid forming, n/d is not determined.

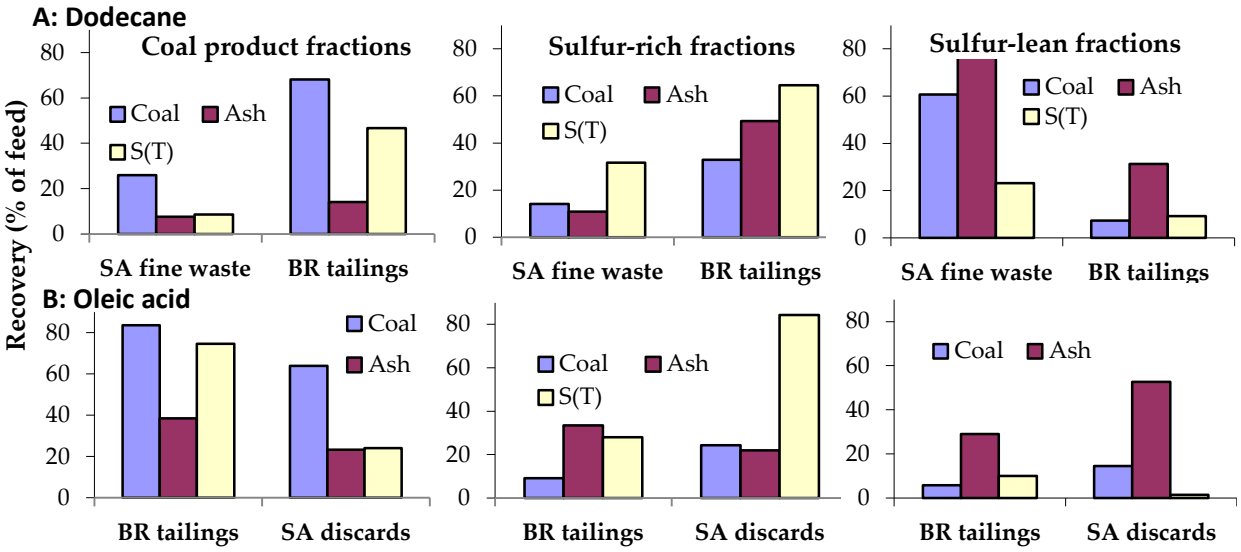

Figure 3 Deportment of key coal components to the flotation output streams, using dodecane (A) and oleic acid (B) as coal collectors (stage 1), and PAX as a sulfide collector (stage 2)

The results indicate that the relative deportment of key components (coal, ash and sulfur) to the flotation output streams varies quite significantly for different coal wastes. This variability can probably be attributed largely to differences in the mineralogical, petrographic and surface characteristics of the coal wastes (Kazadi Mbamba *et al*., 2012). The type of collector also appears to have a significant effect on coal yields in stage 1, with oleic acid resulting in higher recoveries of coal from the Brazilian coal tailings than dodecane. A similar trend has been observed for other coal wastes, and has been attributed to the stronger interaction between the hydrophobic component of the coal surface and the carbon-oxygen double bond of the oleic acid molecule (Kazadi Mbamba *et al*., 2013). Performance variability notwithstanding, in all case studies the two-stage flotation process resulted in a coal product with reduced ash and sulfur contents, and a final tailings fraction with reduced sulfide content and negligible ARD risk potentials.

Economic assessment: coal case study

The results of the order-of-magnitude economic assessment, for the specific coal waste case study described in the methodology section, are summarized in Table 4.

Table 4 Economic assessment results: fine coal waste case study

Item	Unit	Amount	Comment
Capital costs	R 000 000	198	Installed capital costs based on a combination of supplier estimates for major equipment and Lang factors
Operating costs	R 000 000 per annum	161	Based on a combination of flow sheet data and "rule-of-thumb" estimates from the industry and a contingency of 20%
Revenue	R 000 000 per annum	201	Based on a sales price of ZAR349/t
Project NPV	R 000 000	50	Calculated at a discount rate of 14% and based on earnings
Internal rate of return	%	19	before interest, taxes, depreciation and amortization

Although the financial model is based on one case study only, the results in Table 4 are indicative of the potential economic viability of the two-stage flotation process for the recovery of coal and removal of sulfur from coal wastes. Reagent costs were relatively high, contributing 54 % to total operating costs (Jera, 2013). The net present value (NPV) was found to be particularly sensitive to coal sales price, coal yield and reagents costs (Jera, 2013).

Life cycle assessment: base metal case study

The life cycle inventory (LCI) results for the conventional and desulfurization flotation treatment scenarios are compared in Figures 4A and B.

The desulfurization flotation process scenario consumes more carbon than the conventional tailings treatment scenario (base case), and results in higher emissions of carbon dioxide and sulfur dioxide, due largely to the higher consumption of fossil-fuel based electricity in the flotation circuit (Broadhurst *et al*., 2014). However it also results in a decrease in aqueous emissions, whilst simultaneously enhancing the potential to recover water and metal values from the tailings.

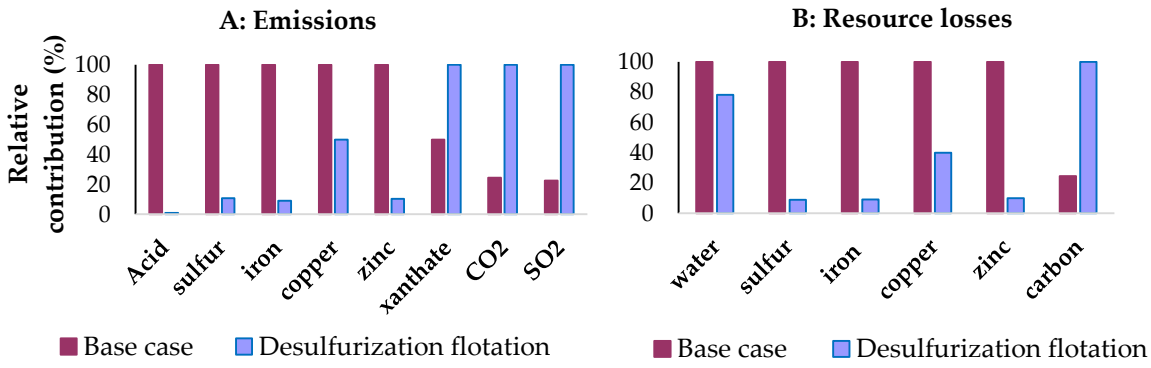

Figure 4 Relative environmental emissions (A) and resource losses (B) for the two tailings treatment scenarios (Broadhurst *et al*., 2014)

The results of the subsequent life cycle impact assessment (LCIA) modelling (Figure 5) indicate that the desulfurization flotation scenario results in higher climate change, fossil fuel depletion and terrestrial acidification impacts than the conventional treatment scenario, which can once again be attributed largely to the higher consumption of fossil-fuel based electricity in the flotation circuit (Broadhurst *et al*., 2014). Desulfurization flotation also results in a considerable reduction (more than 80 %) in both eco-toxicity and human toxicity impacts, due largely to a decrease in the amount of zinc that deports to the tailings and is thus available for subsequent release into the environment (Broadhurst *et al*., 2014). Incorporation of a desulfurization flotation unit into the conventional (base case) tailings treatment circuit also results in lower urban land occupation and natural land transformation impacts than the base case scenario, due to the smaller volumes of land-disposed tailings.

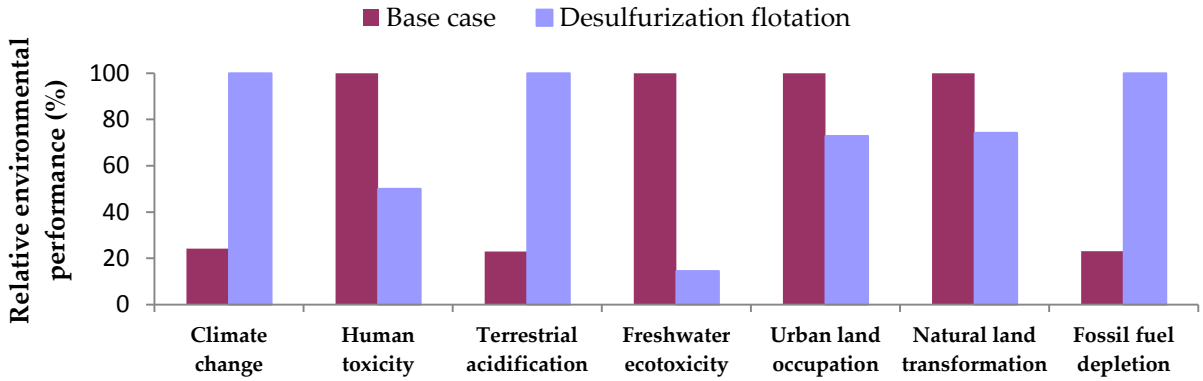

Figure 5 Relative environmental performance for the two tailings treatment scenarios

The study also highlighted the deficiencies of current LCIA tools, in terms of their ability to adequately assess the environmental impacts associated with solid mineral wastes and their management. This pertains, in particular, to aqueous acidification, salinization and trace metal impacts (Broadhurst *et al*., 2014).

CONCLUSION

The technical feasibility of using froth flotation in a two-stage process to both recover valuable material and remove sulfur from mine waste has been demonstrated at a laboratory-scale for the case of porphyry-copper and a range of different coal processing wastes. All case studies resulted in a sulfide-lean tailings stream, which is non-acid generating, thus effectively eliminating long-term ARD risks. Furthermore, a preliminary economic assessment showed the potential viability of the desulfurization flotation treatment process when combined with value recovery. A holistic environmental study using life cycle assessment tools highlighted the environmental benefits of the desulfurization flotation tailings management approach in terms of reduced aqueous emissions and waste burden as well as enhanced resource recovery. However, the flotation process also consumes additional electricity, which results in higher climate change, fossil fuel depletion and acidification impacts in cases where the production of electricity is coal-based.

Studies are in progress to identify and evaluate downstream management options for the sulfide-rich and sulfide-lean phases, with a view to further reducing waste burden and maximizing utilization of mineral resources. Further research and development is also currently underway to optimize the two-stage process in terms of key performance variables, particularly electricity, reagent consumption and waste characteristics, and to extend the techno-economic-environmental studies to a range of sulfidic mine wastes. These studies will form the basis for future publications.

ACKNOWLEDGEMENTS

The authors would like to acknowledge the contribution of the following post-graduate students: Alexander Hesketh, Christian Kazadi Mbamba, Juarez Amaral Filho, Melody Jera and Makhosazane “Chucky” Kunene. This work is based on research supported by the Water Research Commission of South Africa, Senmin® International and the Research Chairs Initiative of the South African Department of Science and Technology and National Research Foundation.

REFERENCES

Amaral Filho, J., Kazadi Mbamba, C., Franzidis, J-P, Broadhurst, J., Harrison, S.T.L and Schneider, I.A.H (2011). Froth flotation for desulphurization and coal recovery: A comparative study of South African and Brazilian colliery wastes, Flotation ’11, Cape Town, 14-17 November 2011.

Bell, F., Bullock, S., Hälbich, T. and Lindsay, P. (2001) Environmental impacts associated with an abandoned mine in the Witbank Coalfield, South Africa, International Journal of Coal Geology, vol. 45 (2-3), pp. 195-216.

Benzaazoua, M., Bussière, B., Kongolo, M., McLaughlin, J. and Marion, P. (2000) Environmental desulphurization of four Canadian mine tailings using froth flotation, International Journal of Mineral Processing, vol.60, pp. 57-74.

Benzaazoua, M. and Kongolo, M. (2003) Physico-chemical properties of tailing slurries during environmental desulphurization by froth flotation, International Journal of Mineral Processing, vol. 69, pp. 221-234.

Benzaazoua, M., Bussière, B., Demers, I., Aubertin, M., Fried, E. and Blier, A. (2008) *Integrated mine tailings management by combining environmental desulphurization and cemented paste backfill: Application to mine Doyon, Quebec, Canada,* Minerals Engineering, vol. 21, pp. 330-340.

Bois, D., Poirier, P., Benzaazoua, M. and Bussière, B. (2004) A feasibility study on the use of desulphurized tailings to control acid mine drainage, 36th Annual Meeting of the Canadian Mineral Processors, Ottawa, Canada.

Broadhurst, J.L., Petrie, J.G. and von Blottnitz, H. (2007) Understanding element distribution during primary metal production, Transactions of the Institute of Mining and Metallurgy: Section C-Mineral Processing and Extractive Metallurgy, vol. 116 (1), pp. 1-16.

Broadhurst, J.L., Kunene, M.C. and von Blottnitz, H. (2014) Life cycle assessment of the desulfurisation flotation process to prevent acid rock drainage: A base metal case study. Minerals Engineering, In press, available online 27 November 2014.

Cilliers, J. (2006) Active and passive gangue in mineral processing, disposal and economics, Proceedings of the XXIII International Minerals Processing Congress, 3-8 September, Istanbul, Turkey.

Hesketh, A., Broadhurst, J. and Harrison, S.T.L. (2010a) Mitigating the generation of acid mine drainage from copper sulfide tailings impoundments in perpetuity: A case study for an integrated management strategy, Minerals Engineering, vol. 23(3), pp. 225-229.

Hesketh, A.H., Broadhurst, J.L., Bryan, C.G., van Hille, R.P., Harrison, S.T.L (2010b) Biokinetic test for the characterisation of AMD generation potential of sulfide mineral wastes, Hydrometallurgy, vol. 104(3), pp. 459-464.

Jarvis, A.P. and Younger, P.L., 2000. Broadening the scope of mine water environemntal impact assessment: A UK perspective, Environmental Impact Assessment Review, vol. 2(2000), pp. 85-96.

Jera, M. (2013) An economic analysis of coal desulphurization by froth flotation to prevent acid rock drainage (ARD) and an economic review of capping covers and ARD treatment processes, Masters dissertation, University of Cape Town.

Johnson, D.B. and Hallberg, K.B. (2005) Acid mine drainage remediation options: a review, Science of the Total Environment, vol. 338, pp. 3-14.

Kazadi Mbamba, K., Harrison, S.T.L., Franzidis, J-P and Broadhurst, J. (2012) Mitigating acid rock drainage risk while recovering low-sulphur coal from ultrafine colliery wastes using froth flotation, Minerals Engineering, vol. 29, pp. 13–21.

Kazadi Mbamba, C., Franzidis, J-P., Harrison, S.T.L. and Broadhurst, J.L. (2013) Flotation of coal and sulphur from South African ultrafine colliery wastes, The Journal of the South African Institute of Mining and Metallurgy, vol. 133, pp. 399-405.

Kunene M., Broadhurst, J. and von Blottnitz H. (2013) Life cycle assessment of xanthate salts: a comparison of new and old production routes, 6th SETAC (Society for Environmental Toxicology and Chemistry) Africa conference, Lusaka, Zambia, 2-5 September 2013.

Leppinen, J.O., Salonsaari, P. and Palosaari, V. (1997) Flotation in acid mine drainage control: beneficiation of concentrate, Canadian Metallurgical Quarterly, vol. 36(4), pp. 225-230.

Lottermoser, B.G. (2007) Mine Waste Characterization, Treatment, Environmental Impacts, 2nd ed, Berlin: Springer

McCallum, D.A. and Bruckard, W.J. (2009) The development of a diagnostic protocol for the assessment and testing of sulphide tailings in relation to future sustainable tailings management, In: Wiertz, J. and Moran, C.J. (eds.), Proceedings of the First International Seminar on Environmental Issues in the Mining Industry (Enviromine), Santiago, Chile.

Rosner, T., Boer, R., Reyneke, R., Aucamp, P. and Vermaak, J. (2001) A preliminary assessment of pollution contained in the unsaturated zone beneath reclaimed gold-mine residue deposits, Water Research Commission Report No 797/1/01, Pretoria, South Africa.

Stewart, W.A., Miller, S.D. and Smart R. (2006) Advances in acid rock drainage (ARD) characterisation of mine wastes. In: 7th International Conference on Acid Rock Drainage, American Society of Mining and Reclamation, Lexington, KY, March 27-30 2006, pp. 2098-2119.

Pre-mining Characterization of Ore Deposits: What Information Do We Need to Increase Sustainability of the Mining Process?

Bernhard Dold
SUMIRCO (Sustainable Mining Research & Consultancy), Chile

ABSTRACT

The efficiency of the metallurgical process can be increased by the incorporation of mineralogical data during the process. Moreover, mineralogy plays a key role in the efficiency of biomining operations and is necessary to predict the formation of acid mine drainage. Decision making in mining operations is currently mainly based on element concentrations (e.g. ore grade, cut-off, acid base accounting) assuming mineral associations of these elements (often with or without sufficient mineralogical data). This can lead to inefficiency of the mining process and environmental problems. Standard prediction methods for acid mine drainage are not accurate enough and there are no methods available, for example, to predict the stability of mine waste under reducing conditions as would apply to submarine tailings disposal (STD), a tailings management strategy that is seeing a revival in the mining industry. To overcome these problems, advanced methodologies have to be applied to characterize new ore deposits before exploitation starts. This approach gives the opportunity to design optimized processes for efficient metal recovery of the different mineral assemblages in an ore deposit and at the same time to minimize the future environmental impact and costs for mine waste management. Additionally, the whole economic potential is evaluated including strategic elements such as rare earth elements (REE). The methodology should integrate high-resolution geochemistry by sequential extractions and quantitative mineralogy in combination with optimized kinetic testing (oxidizing or reducing conditions, depending on the final waste deposition environment). The resulting data set allows the identification of units with similar geochemical behaviors in the ore deposit and to predict the behavior of each economically or environmentally relevant element throughout the mining process and in the final deposition site.

Keywords: process efficiency, acid mine drainage, prediction, geometallurgy, biogeometallurgy

INTRODUCTION

Metal mining is the base industry for the technological development of human society. However, metal mining has not always been very efficient in processing and has had many environmental problems associated. Therefore, it is necessary to predict and improve the efficiency of the mining process from the beginning of an operation through to the final closure plan including waste management and environmental protection (Dold and Weibel, 2013). Together with a social license to mine, these are the basic goals needed to achieve a more sustainable mining process (Dold, 2008; Dold and Weibel, 2013). Most of the problems concerning efficiency of the mineral processing is based on the use of incorrect parameters for decision making during mine operation, and also for the prediction of environmental problems such as acid mine drainage (AMD). This work highlights the problems associated to today's mining process and suggests a methodology to predict the geochemical behavior along the flow-path of the mineral during the mining process (Figure 1).

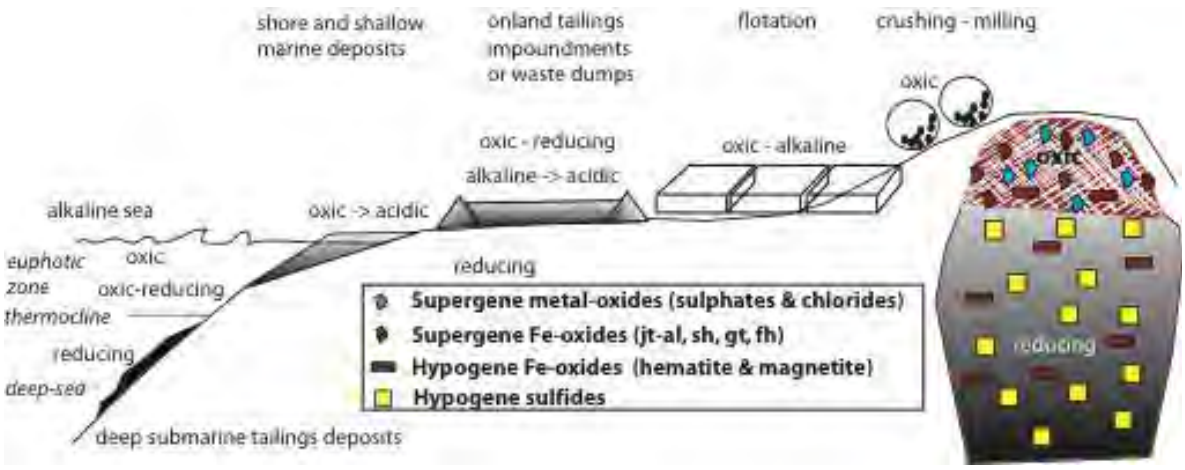

Figure 1 Overview of the flow path of the form the ore deposit with its different mineral associations through the mineral processing and the final mine waste deposition and the geochemical regimes in the different compartments of the process.

Currently, decision making is mostly based on element concentrations (e.g., cut-off grade, and acid-base account), but the metallurgical processes depend on the interactions between mineral surfaces and reagents, for example the flotation process and biomining operations (Dold, 2014b). For example, chalcopyrite is not acid leachable and it also is not efficiently oxidized by bacteria below 50°C, so that in most large scale bioleaching operations (dump leaching), chalcopyrite is not efficiently oxidized. However, this mineral responds well to flotation. In contrast, the presence of covellite and chalcocite in the mineral assemblage lowers the recovery of copper in the flotation, but these minerals are easily acid leachable (Dold, 2014b). Therefore it is crucial to know which minerals are sent to which processes in order to ensure the highest possible recovery rates. This goal is only possible if the mineralogical information is available.

The same is also true for acid mine drainage prediction, where currently very simple and mostly unsuitable tests are used to predict if a material will produce acid drainage and release certain elements into solution. Here, element concentrations such as from sulfur are also calculated as pyrite equivalent for the acid potential and a titration is used to calculate the neutralization potential. However, there are many other sulfide minerals that produce less acidity than pyrite and some even produce no acidity. On the other hand there are carbonates, such as siderite, that may even produce acidity due to hydrolysis of the iron ion. Iron hydroxides, such as ferrihydrite and goethite, and hydroxysulfates, such as jarosite and schwertmannite can acidify the system due to their dissolution chemistry (Alarcon et al., 2014). Thus, mineralogy is similarly key for the correct prediction of acid mine drainage (Dold, 2010).

Therefore, an advanced mineralogical and geochemical approach is suggested in order to predict accurately the behavior of the mineral assemblage throughout the mining process towards final deposition of the waste material.

METHODOLOGY

In order to predict accurately the geometallurgical, metallurgical, bioleaching, and environmental behavior, quantitative mineralogy is needed. This information allows for the possibility of predicting the behavior of the material in the communition process (e.g. crushing, milling and flotation); during hydrometallurgy in the bioleaching process, or for the accurate prediction of acid mine drainage formation (acid-base accounting). Today advanced technologies are available for automated mineralogical analysis such as QEMSCAN® or MLA. If thoroughly calibrated with the ore mineralogy, these techniques give an accurate quantification of the complete mineral assemblage, degree of liberation, as well as grain size distributions, all of which are important ito increase the efficiency of the extraction process. For example in case of the Andina Mine (CODELCO), the utilization of this information could increase the recovery by 2 % (Cruz et al., 2012).

However, this methodology does not give information on trace element associations to specific minerals or mineral groups. This information is crucial to predict if a certain contaminant may be liberated from its host mineral, or to develop a methodology for recovery of economically valuable trace elements such as rare earth elements (REE). Therefore, the mineralogical data are combined with high-resolution geochemical data from a seven-step sequential extraction procedure developed for the primary and secondary mineralogy present in typical porphyry copper deposits (Dold, 2003). These seven steps are as follows: step 1 liberates the water-soluble fraction (1.0 g sample into 50 mL deionized H_2O shake for 1 h at room temperature (RT)), step 2 liberates the exchangeable fraction (1 M NH_4-acetate, pH 4.5, shaken for 2 h, RT), step 3 addresses the Fe(III) oxyhydroxides fraction (0.2 M NH_4-oxalate, pH 3.0, shaken for 1 h in darkness, RT), step 4 dissolves the Fe(III) oxides fraction (0.2 M NH_4-oxalate, pH 3.0, heat in water bath 80 °C for 2 h), step 5 (35 % H_2O_2 heat in water bath for 1 h) dissolves organic matter and supergene Cu sulfides and partly primary sulfides, step 6 ($KClO_3$ and HCl, followed by 4 M HNO_3 boiling) dissolves more resistant primary sulfides, and step 7 (HCl, HF, $HClO_4$, HNO_3) dissolves the residual fraction (silicates). The leach solutions are then analyzed by inductively coupled plasma–atomic emission spectroscopy. In addition to the typical elements measured in the leachates, REE are analyzed in the different steps by inductively coupled plasma–mass spectroscopy (ICP-MS), in order to identify additional extractable byproduct commodities in the ore deposit and its mineralogical associations. The

sequential extraction data can additionally be used to perform a high-resolution acid-base account (ABA) (Dold 2010) and should be correlated with the mineralogical data for quality control, and in order to predict AMD formation and element liberation of any mined material. It is important to note that this extraction sequence must be adapted to the solubility of the specific minerals (primary and secondary) present in an ore deposit, as this may differ significantly among different ore deposit types.

RESULTS AND DISCUSSION

Exploitation efficiency

As described above, we extract minerals in the mining process, not elements, but the elements are associated with minerals. Therefore, we have to consider the mineralogy in order to develop efficient exploitation methods, to predict the stability of certain minerals during the extraction process, and in a long-term, for environmental protection.

Each mineral has a specific set of conditions where it remains stable. If we expose this mineral to other geochemical conditions, for example during the mining process (Figure 1), it will destabilize, resulting possibly in its oxidation, reduction, and/or dissolution. In these processes, associated trace elements from the mineral may be liberated and therefore possibly contaminate the process solution or the environment. Thus, if we know the exact mineralogy and the trace elements associated with those minerals prior to mining, we will be able to predict how these mineral will behave along the production flow-path, and we can even model this behavior with geochemical codes.

The evaluation process begins with the exploitation technique of the ore deposit. For example, it makes a difference if we exploit an open pit in the Atacama desert (e.g. Chuquicamata or Escondida) or if we exploit a porphyry deposit by block-caving in a more humid climate (e.g., El Teniente in Central Chile). In both cases, sulfide minerals are extracted. In the case of El Teniente, a slight pre-oxidation of the ore is observed (redox potential is slightly oxidizing and pH slightly acidic) due to the fracturing of the ore-body related to block caving and contact with rainwater percolating through the mineralization. These effects are evident in sequential extraction data for example through the association of Mo with secondary Fe(III)hydroxides (Dold and Weibel, 2013). In the crushing and milling process, water and reagents are added, so that the geochemical system then becomes more oxidizing before it is sent to an alkaline flotation process (Eh ~ 200-300 mV; pH ~ 9-11). Due to this geochemical change, secondary Fe(III) hydroxides are destabilized and may undergo reductive dissolution and adsorbed oxyanions such as molybdate or arsenate may be desorbed and enter into solution as a contaminant. This process can continue in an active tailings impoundment as the geochemical conditions maintain a reducing setting (Eh ~ 100-200 mV; pH ~ 8-10) at this stage (Smuda et al., 2014; Smuda et al., 2008). If operations then cease, the geochemical system of the tailings will change to oxidizing and acidic conditions may ensue due to sulfide oxidation (Dold, 2014a). Sulfides will be depleted in the oxidation zone and the iron will form secondary Fe(III)hydroxides, which serve as sorbents for oxyanions such as arsenate, molybdate, and sulfate at low pH condition (Dold and Fontboté, 2001). If we would now change again the geochemical system to reducing conditions by re-deposition of fresh tailings as in the case of Talabre/Chuquicamata (Smuda et al., 2014) or by an implementation of a cover system or flooding (Jenk et al., 2009), then the sorbent (Fe(III)hydroxides) will be destabilized and undergo reductive dissolution, liberating the adsorbed oxyanions into solution, possibly producing secondary

contamination (Jenk et al., 2009). A similar effect is observed when tailings containing Fe-oxides are deposited in the deep sea (Eh ~ -200 - +100 mV, pH 8) through submarine tailings disposal (Dold, 2014c). Thus, if we have exact knowledge before exploitation regarding which mineral contains which trace elements, we can predict their stability in the different geochemical systems during the exploitation process and thus increase exploitation efficiency and assess final and secure waste disposal scenarios.

Biomining

The relationship between ore and waste mineralogy and their fate has also been observed in the so called biomining operations, where in many giant mining operations, valuable metals can be recovered from the material that has an ore grade below cut-off but above the waste definition line (in case of porphyry copper systems usually between 0.1-0.2 and 0.3-0.6 wt.% Cu (Dold, 2014b)). The material of this grade is normally from the primary ore zone (without supergene enrichment with minerals such as covellite and chalcocite) and contains principally chalcopyrite as ore mineral. Chalcopyrite is not acid leachable and cannot be oxidized efficiently by the microbial community present at temperatures below 50°C. Thus the bioleaching process is very inefficient (10 - 20 % recovery). Recoveries can reach 40 % only if significant amounts of supergene Cu-sulfides are present, as in case of Escondida. However, this result is not due to efficient bioleaching, but to acid leaching of the supergene mineral assemblage. Thus, a thorough mineralogical characterization is also necessary in order to increase the efficiency of biomining. Here, the assessment of the presence of toxic trace elements in the ore minerals for the microbial community is also needed to predict efficiency of the bioleaching operation. These data can be obtained from sequential extractions.

Acid mine drainage (AMD) prediction and environmental assessment

As discussed above, standard AMD prediction, includes an acid-base accounting calculation based on sulfur concentrations, calculated as pyrite equivalent and neutralization potential, calculated based on a titration of the carbonate neutralization potential. All these calculations have many drawbacks and fundamental sources of error in the calculation (Dold, 2010). Therefore, if we rely on quantitative mineralogical data (such as optical microscopy, QEMSCAN or MLA), a more precise ABA can be estimated (Figure 2). A high resolution ABA can be performed even with sequential extraction data. If both methods are available, a thorough quality control is possible.

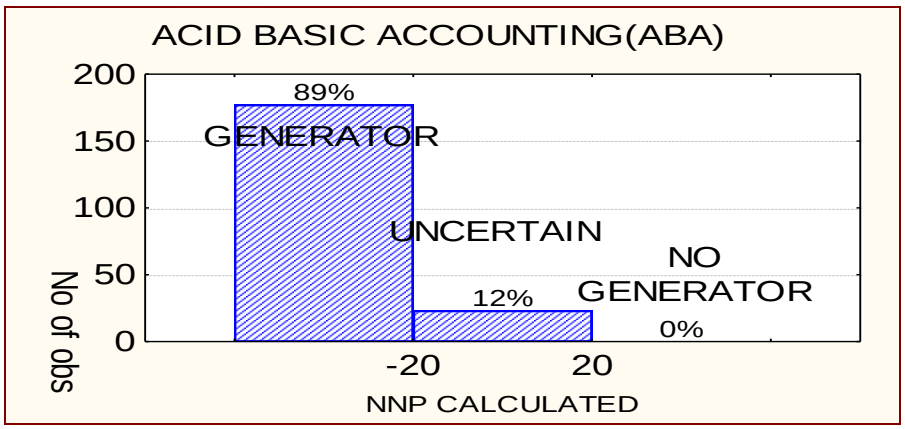

Figure 2 Example of the distribution of acid-base accounting data of a typical porphyry copper deposit calculated based on quantitative mineralogy, showing that 89 % of the samples are AMD generating and 12% range in uncertainty.

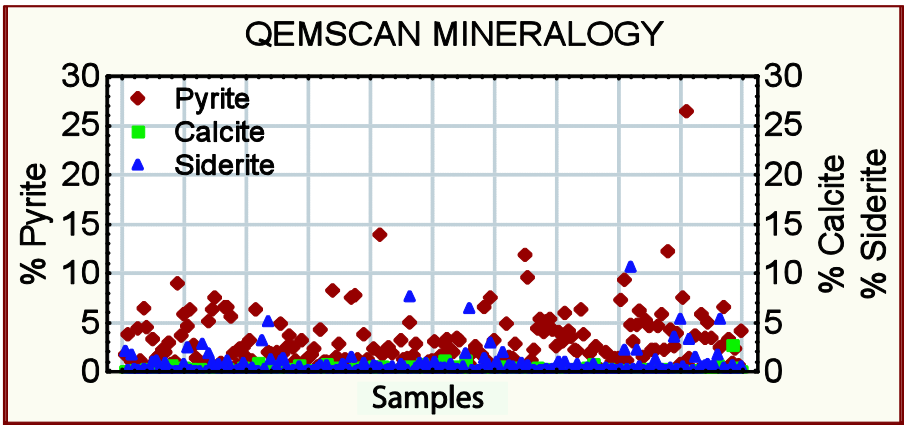

Figure 3 Quantitative mineralogy (QEMSCAN®) data for pyrite, calcite, and siderite of a typical porphyry copper deposit, showing the carbonate neutralization potential is mainly associated to siderite and not to calcite, so that standard ABA calculation would attribute higher neutralization potential, as the acid potential from the liberated iron from siderite (mobility of ferrous iron under reducing conditions or hydrolysis of ferric iron) is ignored.

For example, if unoxidized material from a porphyry copper deposit has 1.5 % pyrite (which has 1 % associated arsenic), 7 % siderite and 3 % anhydrite (Figure 3). A simple ABA would suggest that this material will not produce AMD. However, with the information given above based on quantitative mineralogy and sequential extractions, it can be predicted that this material in the active tailings impoundment will produce concentrations of approximately 1500 mg/L of SO_4 in solution due to equilibrium with gypsum (hydrated from anhydrite). Once operation has ceased, AMD will be produced, as siderite is not able to neutralize all the acidity produced by the pyrite oxidation. Siderite can be even a net acidity producer depending on the circumstances (Dold, 2010). Additionally, the AMD will carry significant amounts of arsenic.

CONCLUSION

The examples described above show that only if we rely on an accurate quantitative mineralogical characterization and chemical data on the trace elements with these minerals, can an accurate prediction of the behavior of the material in the different geochemical conditions during the extraction process, and during final deposition of the waste material be made. This approach is crucial to increase the efficiency of the extraction process, and to ensure environmentally sound waste management.

REFERENCES

Alarcon, R., Gaviria, J., and Dold, B., 2014, Liberation of adsorbed and co-precipitated arsenic from jarosite, schwertmannite, ferrihydrite, and goethite in seawater: Minerals, v. 4(2), p. 603-620.

Cruz, J., Bustos, C., Martínez, C., and Suazo, H., 2012, Daily mineralogical control of Andina Division Concentrator CODELCO CHILE, Geomet2012.

Dold, B., 2003, Speciation of the most soluble phases in a sequential extraction procedure adapted for geochemical studies of copper sulfide mine waste: Journal of Geochemical Exploration, v. 80, p. 55-68.

—, 2008, Sustainability in metal mining: from exploration, over processing to mine waste management: Reviews in Environmental Sciene and Biotechnology, v. 7, p. 275-285.

—, 2010, Basic concepts in environmental geochemistry of sulfide mine-waste management, in Kumar, S., ed., Waste Management, http://www.intechopen.com/books/show/title/waste-management, p. 173-198.

—, 2014a, Evolution of Acid Mine Drainage formation in sulphidic mine tailings: Minerals, v. 4(2), p. 621-641.

—, 2014b, Mineralogical and Geochemical Controls in Biomining and Bioremediation, in Parmar, N., and Singh, A., eds., Geomicrobiology and Biogeochemistry, Volume 39: Soil Biology, Springer Berlin Heidelberg, p. 119-135.

—, 2014c, Submarine Tailings Disposal – A Review: Minerals, p. 642-666.

Dold, B., and Fontboté, L., 2001, Element cycling and secondary mineralogy in porphyry copper tailings as a function of climate, primary mineralogy, and mineral processing: Journal of Geochemical Exploration, v. 74, p. 3-55.

Dold, B., and Weibel, L., 2013, Biogeometallurgical pre-mining characterization of ore deposits: An approach to increase sustainability in the mining process: Environmental Science and Pollution Research, v. 20, p. 7777-7786.

Jenk, U., Meyer, J., and Paul, M., 2009, Flooding of Wismut's uranium mines after closure - Key findings and unexpected effects, Securing the Future and 8th ICARD: Skelleftea, Schweden.

Smuda, J., Dold, B., Spangenberg, J.E., Friese, K., Kobek, M.R., Bustos, C.A., and Pfeifer, H.-R., 2014, Element cycling during the transition from alkaline to acidic environment in an active porphyry copper tailings impoundment, Chuquicamata, Chile: Journal of Geochemical Exploration.

Smuda, J., Dold, B., Spangenberg, J.E., and Pfeifer, H.R., 2008, Geochemistry of fresh alkaline porphyry copper tailings: Implications on sources and mobility of elements during transport and early stages of deposition: Chemical Geology, v. 256 p. 62-76

Mobility of Strategic Elements in Chilean Tailings in the Context of Secondary Mining Processes

Maria Ussath[1], Corinne Wendler[1], Nils Hoth[1], Ursula Kelm[2], Frank Haubrich[3], Michaela Hache[4], Gerhard Heide[1], Marlies Grimmer[1] and Carsten Drebenstedt[1]

1. *TU Bergakademie Freiberg, Faculty of Geosciences, Geoengineering and Mining, Germany*
2. *Institute of Applied Geology, Universidad de Concepción, Chile*
3. *Erz & Stein Gesellschaft für Lagerstätten- und Rohstoffberatung BR, Germany*
4. *GFI Grundwasserforschungsinstitut GmbH, Germany*

ABSTRACT

After a long time of dumping, tailings are characterized by hydrogeochemical reorganization processes that are reflected in weathering zones (mobilization) and accumulation zones (immobilization). These processes are connected to substantial secondary mineral formation. Accumulation zones are thereby often connected to iron phases and also have an increased content of trace elements. This knowledge is relevant for Chilean mining dumps because some of them are already affected by these long time processes.

Chilean mining companies are interested in information on the occurrence and extractability of secondary minerals and strategic elements (minor and trace elements of economic interest) from tailings. The German-Chilean project SecMinStratEl (Secondary Mining of Strategic Elements) aims to provide an understanding of the accumulation processes and will also evaluate opportunities for selective extraction. The project is actively supported by significant Chilean mining companies and universities.

Tailings considered in the study consist of granular material, which was ground during primary mining. Due to its potential content of elements of economic importance, the material is nowadays becoming an interesting resource for secondary mining. Exposed tailings suffer from weathering processes; mine waters, especially dump leachates, are enriched in some metals and trace elements which may also constitute a potential environmental hazard.

By means of specific characterization of accumulation horizons in dumps, a description of metal contents and their mobilization behavior is possible. Differentiation between the elemental contents of different layers is achieved with XRF analyses. Furthermore, a sequential extraction is performed in order to describe the partitioning of elements in mineral phases. Thus, the extractability of major, minor and trace elements can be estimated. With these findings, conclusions about extraction technologies for these elements and the environmental risk potential can be made.

Keywords: tailings, secondary mining, mine water

INTRODUCTION

Chile is the world's largest producer of copper ore. Extensive mining and processing over almost a century has left a large number of old mining legacies, which also have associated environmental issues (dust, acidic water, geotechnical instability). As metal production from processed ores was mostly directed towards copper, the tailings and heaps still contain significant amounts of other metals and minor and trace elements of economic interest. Furthermore, by today's standards old tailings are characterized by high copper contents due to earlier less efficient ore processing technology. The tailings are therefore an interesting target for secondary mining efforts.

The state-funded German-Chilean project "SecMinStratEl" (Secondary Mining of Strategic Elements) investigates minor and trace element content, distribution and extractability in Chilean tailings and the formation of secondary minerals. It aims to better understand reorganization processes due to the mobilization of the elements. Methods for the extraction of trace metals from relevant tailings will be evaluated on a conceptual level. In this context, the Institutes for Mining, Mineralogy and Mineral Processing Machines of TU Bergakademie Freiberg are cooperating with the Chilean universities Universidad de Concepción (UdeC) and Universidad de Atacama (UdA). As the project is still ongoing and deals with many different locations and tailings, only a small part of the whole investigation can be discussed here.

This article deals with one tailing of Chilean copper mining, which contains processed waste material from the copper production. The deposit has been exploited since the early 20th century, when the processing technology was much less efficient compared to today. The tailings consist of the processed material from the original ore body and its accompanying rock. Therefore, elemental contents of the mined deposits are of great interest. The tailing material originated from a porphyry copper-molybdenum deposit, which is characterized by copper sulfide minerals (bornite, digenite, chalcopyrite) and molybdenite. Furthermore, this deposit type is characterized by ore-bearing alteration zones accompanied by magnetite and rutile, as well as ilmenite and titanite (Buschmann 2014). Thus, it can be concluded, that the tailing material may contain concentrations of Au, Ag, Ti, Ga, Sn, W, Nb, In and other trace elements in addition to copper and molybdenum. Krause (2014) identified by means of XRD analysis quartz, micas (muscovite, phlogopite), chlorite, feldspars (andesine, albite, orthoclase), pyrite, and rutile to be typical minerals in the tailing material.

Due to the relatively long time of deposition of the tailings, they are affected by hydrogeochemical reorganization processes that are reflected in weathering zones (mobilization) and accumulation zones (immobilization). Accumulation zones are often related to secondary mineral formation of Fe phases with an increased content of trace elements. The intention of the study is a better understanding of the formation of these enrichment zones due to mobilization and immobilization reactions.

During an on-site sampling at the tailing in Chile, aqueous and solid samples were taken. At the surface of the tailing, the authors found efflorescent mineralization. It indicates a mobilization of metals with a subsequent accumulation at the surface due to the evaporation of pore water. Therefore, seepage waters from the tailings were sampled and analyzed to determine element contents. Solid samples were collected from different layers of the tailing at different sampling points, so that accumulation zones can be distinguished. The formation of different layers could be seen visually, however, for the geochemical description of the layer material, pXRF analyses and grain-size analyses were carried out. Another approach for the characterization of mobility inside

the tailings was sequential extraction on tailing material. Integrating these measurements, conclusions about the distribution of weathering, accumulation and enrichment zones can be made. Furthermore, ideas for the selective recovery and extraction of elements of economic interest can be developed.

METHODOLOGY

General Sample Characterization and Analyses

Solid samples were collected from freshly exposed profiles at a tailing, which was exposed approximately three years earlier. Back in Germany, the samples were homogenized and dewatered. After that, they were divided for different analysis methods, e.g. sequential extraction, X-ray fluorescence analysis and grain-size analysis (derived from German standard procedure DIN 66165 with 50 g of sample).

Water samples were taken from water outflows at the base of a tailing dam. On-site, environmental parameters (pH, pE, electrical conductivity) of the waters were measured. Water samples were bottled and acidified for the analyses of element concentrations in an external laboratory (ICP-MS, Actlabs Canada).

X-Ray Fluorescence Analyses

The X-ray fluorescence (XRF) spectrometer is an instrument used for non-destructive detection of major elements and selected trace elements during the investigation of rocks, ores and soils. A portable X-ray fluorescence (pXRF) analyzer allows operating on-site for immediate analysis. Field measurements, which were carried out by means of pXRF at exposed profiles, provide an overview about the elemental distribution (of major elements) in different horizons and help characterize tailing.

For this study, a pXRF Niton XL3t980 analyzer (equipped with an Ag-Anode 50 kV X-ray tube and Silicon-Drift-Detector 8 mm spot) was used. Raw data were visualized in spectra, where x-axes represent element-specific fluorescence energies (unit keV), and y-axes quantify counts of photons (unit cps) received by the detector. Analysis is possible for most of the elements with atomic numbers ranging from 12 (magnesium) to 92 (uranium), thus, for various trace metals a semi quantitative determination is possible. Results are comparable to wet-chemical analysis, though, pXRF has higher detection limits.

It should be noted that several factors have an effect on the measurement and the data output provided by the device: surface conditions (roughness), moisture content, matrix effects and calibration for the respective solid matrices (calibration used for quantification must be appropriate to the material of the sample analyzed). For major und trace elements device-specific, standard-based correction factors for normalized, homogenized and dried samples were developed, which were determined by measuring certified reference materials (publication prepared for CANAS 2015, Grimmer et al. (2015)). Values used in this article are corrected using these factors.

Sequential Extraction

Sequential extraction is an enhanced type of leaching of granular material, which distinguishes different bonding types of elements. The same material is treated with progressively stronger leaching solutions in order to determine extractable metal concentrations of each step. Seven pH-dependent extraction steps with water, followed by saline, complexing, reducing and oxidating reactants were carried out. By that, a correlation between extracted element contents and sequentially dissolved minerals, and therefore bonding types, is possible. An evaluation of the selective extraction method provides information about the extractability and thus mobility of different major and trace elements. The project partner GFI Dresden (Kassahun, Hache) developed a sequential extraction method, which is a variation from the method of Zeien (1995) and comparable to Dold & Fontboté (2001). In each step, eluates are analyzed for pH value, redox potential, electrical conductivity, TIC, Fe(II) and elemental concentrations (ICP-MS analysis). The steps of the sequential extraction used in this project are shown in Table 1.

Table 1 Overview of extraction steps of the altered sequential extraction method (modified from Zeien (1995) and Graupner et al. (2007))

Step	Extracted phase	Leaching solution	Conditions
It	Water soluble	Ultrapure water	
II	Exchangeable	Ammonium nitrate	pH 7
IIIa	Carbonates and specific bonds	Ammonium acetate	pH 6
IIIb	Reducible	Ammonium acetate Hydroxylamine hydrochloride	pH 6
IV	Organically bound (Oxidizable)	EDTA	pH 4.6
Va	Amorphous and poorly crystallized iron and aluminium hydroxides	Ammonium Oxalate Oxalic acid	pH 3.25
Vb	Crystalline iron and aluminium hydroxides	Ammonium Oxalate Oxalic acid Ascorbic acid	pH 3.25

RESULTS AND DISCUSSION

X-Ray Fluorescence Analyses – Field measurements

Eleven profiles (spatially relatively close to each other) were registered on the tailing. An exemplary result is the distribution of the copper concentration with depth in Profile 4 (left diagram of Figure 1). In this regard, the direct field measurement (blue) is compared to the measurement of samples in the laboratory (orange). Visually and granulometrically distinguishable horizons are labeled A to G. The result of the sieve analysis, i.e. the grain-size characterization, is shown in between the two diagrams of Figure 1. The abbreviation FSa stands for fine sand, MSa for medium sand, si for silty (si2 means < 15 wt% of silt, si4 > 30 wt% of silt). Enrichment zones of copper in the lower horizon areas are clearly revealed. Horizon E, which consists of medium grained silt, shows characteristics of an enrichment horizon based on these results. However, sequential extraction results are needed to verify this conclusion – as this can also be a production/process-related phenomenon. In general, copper contents of the profiles range from 0.15 to 0.3 %, but locally reach 0.5 % and more.

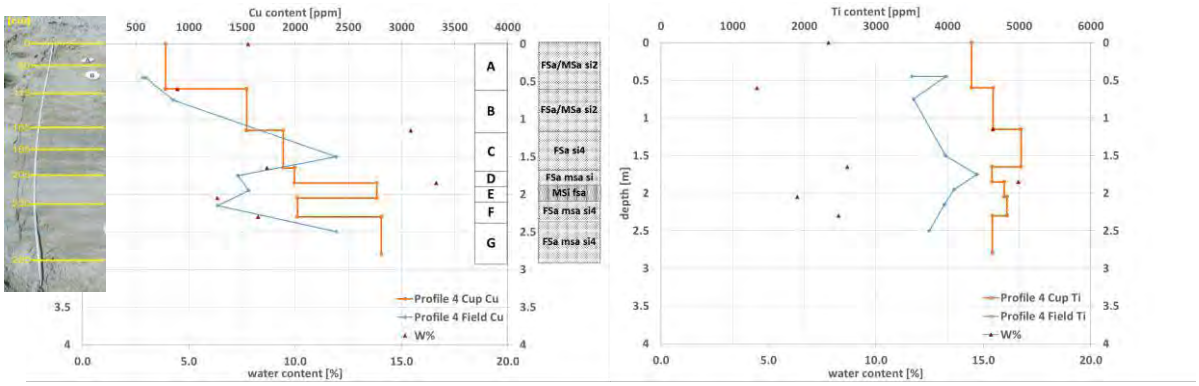

Figure 1 Copper and titanium distributions as function of the depth measured by means of pXRF; photo of profile at sampling site (left); grain size characterization of horizons (center)

These distribution diagrams were created for all profiles and major elements. In the right diagram of Figure 1, the distribution of titanium is shown. Titanium contents range within an order of magnitude of 0.5 %. This element shows less variation between the horizons than copper.

Unfortunately, results for rare earth elements analyses using complete chemical digestion are still pending at the beginning of 2015. Furthermore, deep boreholes (up to 60 m depth) were made into the tailing. They were characterized (e.g. color, granular structure) and sampled and provide an overview of the entire tailing body. From these, comparisons of oxidized and reduced deep zones and estimated element contents of the tailing can be conducted. These investigations are planned for 2015.

Grain-size analyses coupled with pXRF measurements

After sieve analyses, samples of the different fractions remain. These fractions were measured separately with the pXRF analyzer resulting in a distribution of elements depending on the fraction. For the lower horizons D to G of profile 4 the copper distribution is shown representatively in Figure 2.

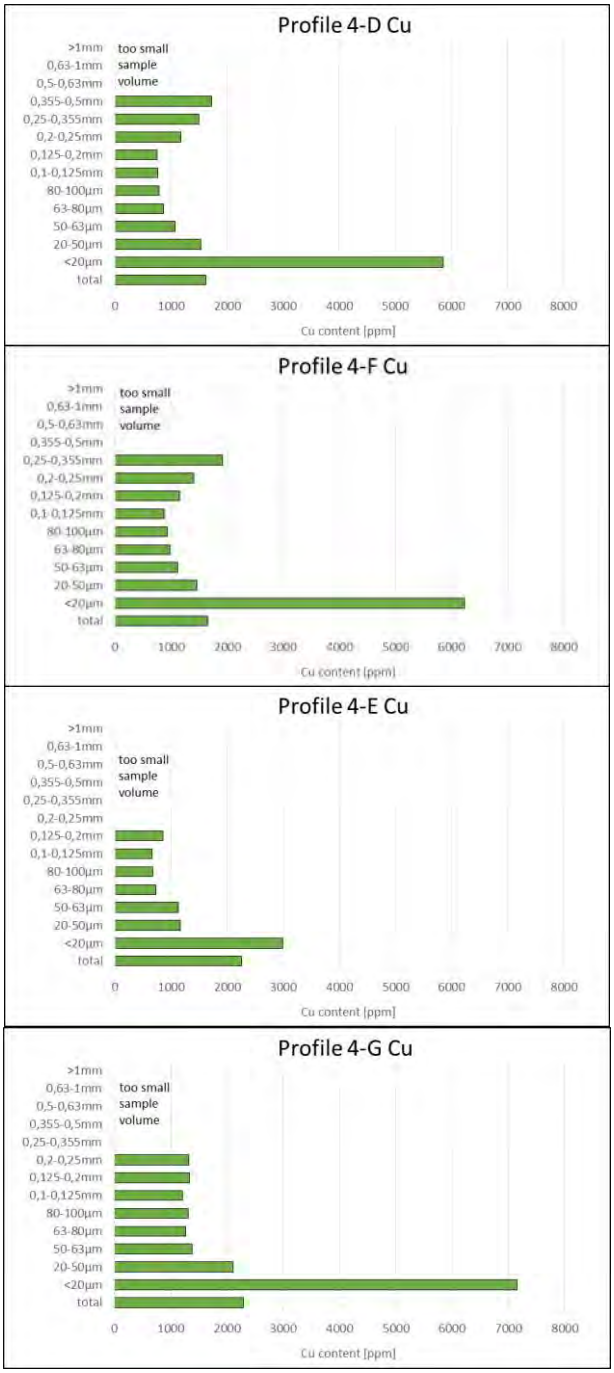

Figure 2 Grain-size dependence of copper content [ppm] measured by means of pXRF

It should be noted that the copper content in ppm refers to the respective particle size fraction whereas the masses of the fractions are not in the focus of this article. The knowledge of the fraction mass is used to estimate the fraction dependent copper contents or other elemental concentrations. In Figure 2 a higher copper content in the fractions 0.2 to 0.5 mm was identified. The highest concentrations are observed at grain sizes smaller than 50 μm.

In addition to copper, grain size dependencies were also examined for the following elements: Al, Ca, K, S, Si, Zn, V, Fe, Ti, As, Mo, and Mn. The results vary depending on the respective horizons, and show random enrichments of these elements in other fractions than <50 μm. Ongoing investigations will further elucidate these relationships.

Sequential Extraction

Evaluations of eluate analyses show varying characteristics of the extraction behavior of major and trace elements. A differentiation between a high and a low percentage of extracted element content has to be made. A low percentage means that after step Vb the bigger part of the element content still is bound to the remaining solid (especially sulfides, silicates). The pXRF measurements provide an estimation of the total element content in the original tailing material for the comparison with the extracted content. Another differentiation can be made between easily soluble/extractable elements, which are detected in the eluates from steps I, II and III and more strongly bound elements from the steps IV, Va and Vb.

Copper

Copper was the objective of primary mining processes. However, due to the evolution in ore processing technologies, the remaining copper content in the older tailings is nowadays of interest for secondary mining.

Figure 3a shows the results of the sequential extraction for copper. In comparison to total copper contents determined by XRF, copper is completely extracted by the leaching steps. Furthermore, except of layer A, which has experienced weathering processes, more than 75 % of copper is extracted from the tailing material within the leaching steps I, II, IIIa or IIIb. These results show the great mobility of copper in the sampled tailing.

(a)

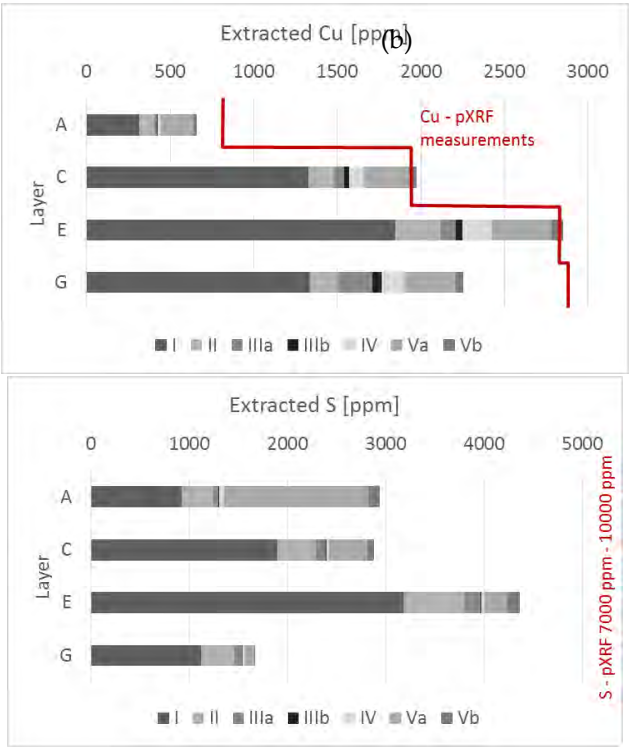

Figure 3 Extractable copper (a) and sulfur (b) during sequential extraction

More than half of the available copper can be recovered by a simple water extraction (step I). Solubility and thus removal of copper was also detectable as a loss of mass during wet sieving analyses. Copper complexes such as copper sulfate are very soluble and highly mobile. Thus, relocation to the depth (with seepage water) or due to evaporation and capillary action to the surface can lead to efflorescences. In this context, the formation of chalcanthite was observed in coarse tailing material with low moisture contents.

The remaining copper content is almost completely recoverable by means of ammonium oxalate as the extracting solution, i.e. during sequential extraction step Va (Table 1). This extractant dissolves amorphous and poorly crystallized iron and aluminum oxides.

Sulfur

Based on the assumption, that sulfur occurs mostly as (copper) sulfate inside the tailing, the sequential extraction of sulfur was examined. Figure 3b presents these results and furthermore shows the total sulfur amounts determined by pXRF (7000 – 10000 ppm). In contrast to copper, sulfur has not been extracted completely within the sequential leaching, as can be seen in comparison to the pXRF value. Extracted phases of sulfur are sulfates (step I), but also sulfur adhered to iron hydroxides (steps Va and Vb).

Arsenic

The behavior of arsenic shows the importance of considering the mobility of some elements. Arsenic levels up to 100 ppm are detected in tailing samples by pXRF. According to the findings from the sequential extraction, arsenic is barely dissolved until step Va (ammonium oxalate). This

means arsenic is difficult to mobilize, which is also confirmed by the analysis of tailing water outlets.

Other elements

In case of strategic elements, such as yttrium, cerium and vanadium, mobilization starts with extraction step IV (organically bound, oxidizable), which means they can be mobilized by EDTA. Molybdenum is partly dissolved during extraction steps IIIa, IIIb and IV, i.e. it is soluble with an acetic buffer. Therefore, these elements are more difficult to extract from the tailing compared to copper and they are less mobile.

Water Samples

Water samples were analyzed with ICP-MS in order to characterize mobile fractions, which were dissolved inside the tailing and transported with the seepage water. Due to dissolution processes within the tailing, specific elements are mobilized. It is assumed, that outflowing tailing waters mainly contain easily extractable elements. One example for that is arsenic, which is difficult to extract and in fact was not to be found in outflowing tailing waters.

Table 2 lists measured ranges of element concentrations of copper and selected light and heavy rare earth elements: cerium, dysprosium, gadolinium, lanthanum, neodymium, samarium and yttrium. Maximum copper concentrations of 888 mg/l are an indication for significant solubility and high mobility. In the second row, maximum concentrations measured in a pond at the base of the tailing are included. These values show the high potential capacity for element mobility within the tailing. Evaporation as a cause of enrichment has to be taken into account, as samples were taken during the summer. Nevertheless, the pond water accumulations show also a significant amount of rare earth elements, which originate from the tailing material.

Table 2 Overview of ICP-MS analysis results for copper and selected rare earth elements (contents in μg/l)

element	Cu	Ce	Dy	Gd	La	Nd	Sm	Y
Outflow waters - range	100000 - 350000	20 - 50	11 - 19	8 - 17	6 - 20	19 - 62	7 - 17	70 - 118
pond water	888000	275	75	53	90	183	48	510

CONCLUSION

During the first part of the investigation, eleven profiles at a tailing of a Chilean copper mine are characterized. Investigated tailing shows a formation of horizons, which are due to a variety of processes. The geochemical composition (e.g. copper content) of the horizons is initially influenced by the original ore body and by primary recovery processes or attributes such as coarseness, flotation fluids and their chemical properties, hydraulic dumping of the processed waste material, and exposure time among others. Apart from that, hydrogeochemical reorganization processes cause mobilization and immobilization of elements and also the formation of distinct horizons. It is possible to get a general idea of the horizontal zonation of the tailing and the approximate

elemental contents of the respective horizons by means of pXRF measurements. However, the tailing composition is not yet fully understood, especially in terms of mineralogy.

Understanding of hydrologic processes and especially the generation and location of accumulation zones inside the tailing is important. For instance, Dold & Fontboté (2001) described cases, "where evaporation exceeds precipitation, the water-flow direction may change to upwards migration via capillary forces. […] Supersaturation controls the precipitation of mainly water-soluble secondary sulfates (e.g. bonattite, chalcanthite) and leads to partly strong enrichment at the top of the tailings". Distributions of the fine granular materials are important, e.g. copper shows enrichments in the fine material (< 50 μm). Based on the sequential extraction results the following recommendations for secondary copper production from tailing sites can made: in the case of hydraulic mining, water is not only a transport medium, but also an extracting agent and should be completely collected, as already done with seepage waters of several copper tailings in Chile. Otherwise the majority of the copper content will be lost.

Future investigations will deal with the development of simplified extracting methods for leaching as a secondary mining solution. Furthermore, immobilization horizons will be characterized mineralogically in order to provide a basis for selective mining. For that, more detailed examination of the potential of minor and trace elements in the tailing samples will be conducted.

ACKNOWLEDGEMENTS

The project SecMinStratEl is funded by the German Federal Ministry of Education and Research (BMBF) as a part of the CLIENT-program "International Partnerships for Sustainable Technologies and Services for Climate Protection and the Environment" (grant no. (FKZ) 033R118A).

REFERENCES

Buschmann, B. (2014) *SecMinStratEl – Recherche zu ökonomisch relevanten Typen metallischer Lagerstätten Chiles*, Internal Report, Erz&Stein Gesellschaft für Lagerstätten- und Rohstoffberatung BR

Dold, B.; Fontboté, L. (2001) *Element cycling and secondary mineralogy in porphyry copper tailings as a function of climate, primary minerology, and mineral processing*, Journal of Geochemical Exploration 74, 3-55

Graupner, T.; Kassahun, A.; Rammlmair, D.; Meima, J.A.; Kock, D.; Furche, M.; Fiege, A.; Schippers, A.; Melcher, F. (2007) *Formation of sequences of cemented layers and hardpans within sulfide-bearing mine tailings (mine district Freiberg, Germany)*, Applied Geochemistry, vol. 22, p. 2486-2508

Grimmer, M., Haque, Z., Ussath, M. & Hoth, N. (2015) *Field portable X-Ray fluorescence analyzer (pXRF) – correction method for measurements in a silicon based matrix*, Proceedings Colloquium Analytische Atomspektroskopie – CANAS 2015

Krause, P. (2014) *Mineralogische Untersuchungen an Aufbereitungsrückständen, Chile*, Bachelor Thesis, Technical University Bergakademie Freiberg, Institute for Minerology

Zeien, H. (1995) *Chemische Extraktion zur Bestimmung der Bindungsformen von Schwermetallen in Böden*, Inaugural-Dissertation Rheinische Friedrich-Wilhelms-Universität Bonn, Institutee for Pedology, Bonner Abhandlungen, 17

10th ICARD IMWA 2015 | 10th International Conference on Acid Rock Drainage & IMWA Annual Conference

Tracking the Fate of Metals in Mining Waste Rock Using Metal Stable Isotopes

Elliott Skierszkan[1], Ulrich Mayer[1], Roger Beckie[1] and Dominique Weis[2]

1. Department of Earth, Ocean and Atmospheric Sciences, University of British Columbia, Canada
2. Pacific Centre for Isotopic and Geochemical Research (PCIGR), Department of Earth, Ocean and Atmospheric Sciences, University of British Columbia, Canada

ABSTRACT

The characterization of metal release and attenuation in mining waste rock drainage has traditionally relied upon an array of mineralogical and geochemical techniques. Recent advances in analytical instrumentation now allow robust measurements of minute variations in the isotopic composition of metals in environmental samples, which have become a powerful new tracer of their fate. Here we provide an overview of the application of these "non-traditional" stable isotopes to characterize metal release and attenuation in mining waste rock. First, we briefly review the theoretical framework of stable isotope geochemistry and its application to environmental studies. Second, we present results from an isotopic investigation of Mo and Zn at the Antamina mine, Peru. At Antamina, isotopic compositions of Mo and Zn have been determined in waste rock drainage waters and ore-mineral samples as a first step to determine whether isotope analyses can serve as a tool to track the geochemistry of these metals in waste rock dumps. The range in isotopic compositions measured thus far at Antamina spans 1.88‰ for $\delta^{98/95}$Mo and 0.65‰ for $\delta^{66/64}$Zn. This variability confirms that isotopic fractionation is occurring during metal release and/or attenuation reactions and indicates the potential for metal stable isotopes to track the mobility of metals in mining waste rock dumps. Linking this variability to distinct release and attenuation mechanisms (e.g. dissolution, adsorption and secondary mineral precipitation) will require further investigations to characterize the isotopic signatures of these mechanisms.

Keywords: Metal stable isotopes, drainage geochemistry, waste rock

INTRODUCTION

The complex hydrogeological and geochemical nature of waste rock dumps makes a detailed characterization of the fate of metals in this setting particularly challenging to achieve using conventional geochemical methods. An alternative and complimentary tool is stable isotope analysis of metals to track release and attenuation processes which would otherwise be difficult to identify. Subtle but measureable variations in isotopic compositions of metals occur as a result of isotopic fractionation during chemical reactions. By measuring these isotopic variations, metal release and attenuation processes can be unveiled. Over the last sixty years, the stable isotope approach has developed into a mature technique for tracking the fate of elements C, N, H, O and S, often called the "traditional" stable isotopes. Moreover, recent improvements in mass spectrometry permit the analysis of isotopic variations of other elements, including the transition metals, opening the door to their application in environmental studies.

This paper's objective is to introduce the use of metal stable isotope analysis to characterize processes in mining waste rock. Part 1 provides a brief review of isotopic fractionation and its applications and analytical considerations. Part 2 presents early results from a survey of metal stable isotope compositions measured in waste rock drainage, waste rock and ore minerals from the Antamina mine, Peru. These samples were analyzed in order to identify whether variations in isotopic compositions of Mo and Zn are present in Antamina waste rock materials, and consequently whether these can be useful to identify sources and attenuation mechanisms.

THEORY, APPLICATONS AND ANALYTICAL CONSIDERATIONS

Theory

Stable isotopes co-exist for many elements in the periodic table. The isotopes of a given element differ by the number of neutrons they contain, while the number of protons is constant. It is this slight difference in atomic masses and nuclear properties which causes differences in reactivity and result in isotopic fractionation. These isotopic variations are denoted as per mil (‰) deviations in the isotopic ratios of a sample relative to a standard using the delta (δ) notation, where superscripts *i* and *j* denote two isotopes of a given element *X*:

$$\delta^{i/j}X\ (‰) = 1000 \times \left(\frac{\left(\frac{^{i}X}{^{j}X}\right)_{sample}}{\left(\frac{^{i}X}{^{j}X}\right)_{standard}} - 1 \right)$$

Mass-*dependent* isotope fractionation occurs as a result of the differences in the strength of chemical bonds involving light and heavy isotopes for a given element: heavy isotopes form bonds which are thermodynamically stronger than those involving light isotopes, and thus are less reactive. Mass-dependent isotopic fractionation is further broken down into two categories, *equilibrium* isotope fractionation and *kinetic* isotope fractionation, an overview of which can be found in (Weiss et al., 2008). Some elements also display mass-*independent* fractionation (MIF) which can be a useful tracer of environmentally-relevant reactions. While not the focus of this work, MIF has been reviewed elsewhere (e.g. Buchachenko, 2013).

Recent Applications of Metal Stable Isotopes

A growing number of studies have successfully used stable isotope analyses to track sources of metal release and attenuation processes in the environment which are summarized in reviews such as (Weiss et al., 2008; Baskaran, 2012). Efforts to apply stable isotopes to track metals in mining environments have begun, including some noteworthy case studies: (Foucher et al., 2009) used mercury stable isotope analyses to identify the release of Hg from a Slovenian mine to riverine sediments and were able to quantify the contribution of the mine to sedimentary Hg downstream from the release site. Copper and Zn isotopes have been useful in identifying processes controlling metal mobility in acid mine drainage such as dilution, weathering and adsorption (Balistrieri et al., 2008; Kimball et al., 2009; Fernandez and Borrok, 2009; Aranda et al., 2012). Strong isotope fractionation during Cr and U removal from groundwater via reduction reactions makes analyses of their isotopic compositions very useful to identify and quantify attenuation of these elements (Heikoop et al., 2014, Baskaran, 2012, A. Shiel, 2013, pers. comm., Oct 16). Taken together, these studies demonstrate the use of stable isotopes to improve our understanding of metal mobility in a variety of environments including mine sites.

Analytical considerations

The stable isotope analysis of metals from environmental samples is not trivial. Analysis is typically done using either thermal ionization mass spectrometry (TIMS), or multi-collector inductively coupled-plasma mass spectrometry (MC-ICP-MS); the latter is becoming the instrument of choice because of the ICP's more efficient ionization ability. Accurate and precise metal isotope ratio measurements require careful sample handling. High-purity grade reagents are used in sample processing, in a metal-free clean laboratory. Samples must undergo chemical purification prior to analysis in order to extract the analyte element from the rest of the sample matrix. Finally, during mass spectrometry, a rigorous correction scheme is required because the MC-ICP-MS system fractionates isotopes during the measurement by as much as three orders of magnitude more than the fractionation present in natural samples. Fortunately, these analytical challenges have been overcome and stable isotope ratio protocols exist for most metals and metalloids of interest to the mining industry (e.g. Cr, Fe, Ni, Cu, Zn, Mo, Cd, Hg, U, Se, W, Ag). At present, analytical capabilities are mainly available within university and government research laboratories where instrumentation is available and knowledge of analytical protocols exists.

STABLE MO AND ZN ISOTOPIC FRACTIONATION AT THE ANTAMINA MINE, PERU

At the Antamina mine a multi-isotope study is currently under way in which the objective is to determine whether stable isotope analyses can be useful to track sources of metal release and processes of metal attenuation in waste rock dumps. The Antamina mine extracts Cu-Zn-(Ag-Mo) ores from one of the world's largest polymetallic skarn deposits, located high in the Peruvian Andes. The deposit formed in association with a quartz monzonite intrusion into carbonate terrain, producing a heterogeneous array of local lithologies which include skarns, hornfels, marbles and intrusives. Good understanding of Mo and Zn release and attenuation processes in waste rock dumps comprised of these materials is critical in order to predict long-term drainage water quality. However, this is a challenging objective to achieve by conventional geochemical and mineralogical approaches, and is further complicated by the geological heterogeneity of waste rock. Stable isotope

analyses could prove useful to gain insights into the fate of metals in waste rock dumps. As a first step, the variability in Mo and Zn isotopic compositions of drainage waters collected from field barrels and experimental waste rock dumps as well as select ore-grade rock samples must be determined to investigate this possibility.

At Antamina, the hypothesized Mo release mechanism to solution from mining waste rock is oxidative weathering of molybdenite (MoS_2). Upon release to solution as molybdate $(MoO_4^{2})^{-}$, Mo may be attenuated via adsorption onto (oxy)hydroxide minerals and clays or via precipitation as secondary minerals. Adsorption of molybdate onto various inorganic substrates peaks at a pH range of 3-5 (Goldberg et al., 1998), while it is minimal in alkaline and very acidic conditions. However, Conlan et al., (2012) and Hirsche (2012) showed that Mo solubility in neutral to alkaline conditions can be limited by precipitation of secondary minerals, including wulfenite ($PbMoO_4$) and powellite ($CaMoO_4$).

To date, no studies have examined Mo stable isotope compositions in mining waste. However, a growing body of literature is shedding light on the isotopic behavior of Mo. It has been shown that light isotopes of Mo are preferentially scavenged during adsorption onto Fe and Mn (oxy)hydroxides leaving a residual aqueous Mo pool which is isotopically heavier (Barling & Anbar, 2004; Siebert et al., 2006; Wasylenki et al., 2008; Goldberg et al., 2009; Wasylenki et al., 2011). Molybdenum isotopic fractionation during chemical weathering in various conditions show that Mo leached from rocks may have isotopic compositions which are similar to, or heavier than the parent material by up to 1 ‰ (Siebert et al., 2003; Liermann et al., 2011; Voegelin et al., 2012). The isotopic fractionation occurring during secondary mineral precipitation of Mo has not yet been studied.

Zinc in mining waste rock is released from the weathering of sphalerite (Hirsche, 2012; Matthies et al., 2014a). Possible attenuation mechanisms include adsorption onto (oxy)hydroxide minerals and carbonates and precipitation as secondary minerals (e.g. $ZnCO_3$, $Zn(OH)_2$) (Al et al., 2000; Hirsche, 2012). Zn adsorption shows a strong pH dependency, with minimal adsorption occurring in acidic conditions (<pH 5) and greater adsorption occurring for mildly acidic to alkaline pH values (Pokrovsky et al., 2005).

A small, but growing literature has begun investigating zinc isotopic variations in mining wastes (Balistrieri et al., 2008; Fernandez & Borrok, 2009; Aranda et al., 2012; Matthies et al., 2014a; Matthies et al., 2014b). Zinc adsorption onto Mn, Al and Fe oxides exhibits a small isotopic fractionation of <0.2 ‰ (Pokrovsky et al., 2005). Consistent with Mo, oxidative weathering of sphalerite-rich tailings leads to aqueous Zn which is isotopically heavier by ~0.1-0.2 ‰ (Matthies et al., 2014a). Complexation with carbonates yields residual aqueous solutions which are up to 1‰ lighter than the starting solution (Pichat et al., 2003; Fujii et al., 2011).

Methodology for Antamina Isotope Study

Antamina's geochemical investigation program includes a series of ~10m high experimental waste rock piles (each containing 30,000 tonnes of rock) and ~1m high field barrels (each containing 350kg of rock) which were installed in order to characterize drainage water quality for different waste rock types (Fig. 1). Water samples from these field barrels and experimental waste rock piles were collected in order to determine the range in isotopic compositions associated with different waste rock materials at Antamina. In addition, Mo and Zn ore minerals (molybdenite and sphalerite) from

various locations in the open pit were also sampled for isotope analysis because it is the chemical weathering of these minerals which is expected to be the dominant source of Mo and Zn in waste rock drainage waters.

Figure 1 Experimental field barrels, 1m high and containing ~350 kg of waste rock (left); and experimental waste rock dumps, 10m high and containing ~30,000 kg of waste rock (right) at Antamina.

Water samples were filtered in 0.22 μm filters and acidified prior to shipment to the laboratory for analysis. Molybdenites and sphalerites were hand-picked from ore-grade rock samples and dissolved in inverse *aqua regia*. Mo and Zn concentrations were determined using an ICP-MS (Agilent 7700x, Agilent, USA). Sample aliquots were then reconstituted in 7N HCl and processed through an anion-exchange purification scheme modified from Shiel et al. (2013) which isolates Mo and Zn from the sample matrix. In order to correct for instrumental and laboratory mass fractionation, a ^{97}Mo-^{100}Mo double-spike was equilibrated with samples prior to ion-exchange purification (Siebert et al., 2001). Zn instrumental mass fractionation was corrected using a combined standard-sample bracketing and external normalization procedure as in Shiel et al. (2013). Isotopic analyses were conducted using a Nu Plasma MC-ICP-MS (Nu Instruments Ltd., UK) hosted at the Pacific Centre for Isotopic and Geochemical Research (PCIGR), University of British Columbia, Vancouver, Canada. Isotopic compositions in this study were normalized using the NIST-SRM-3134 for Mo and using PCIGR-1 for Zn as delta-zero per mil standards. PCIGR-1 is ~0.11 ± 0.05 ‰ heavier than the commonly used JMC-Lyon Zn isotope standard. All reagents used in the laboratory were prepared using ultra-pure <18.2 MΩ H_2O and commercial environmental-grade acids were sub-boiled in PFA sills to reduce contaminants to trace levels. Laboratory work was carried out in metal-free Class 1000 clean laboratories at PCIGR.

Results and Discussion

Isotopic compositions of Mo and Zn measured in Antamina samples show variations of up to 1.88‰ for $\delta^{98/95}$Mo and 0.65‰ $\delta^{66/64}$Zn. These isotopic ranges are well in excess of the analytical precision of <0.10‰ and <0.12 ‰ for $\delta^{98/95}$Mo and $\delta^{66/64}$Zn, respectively, indicating that significant and resolvable isotopic fractionation is occurring during release and/or attenuation of Mo and Zn at Antamina.

Molybdenum isotopes

Isotopic compositions of molybdenites exhibit a range of 1.09‰ among various ore samples collected in the deposit (Fig. 2) The range in isotopic composition of molybdenites analyzed here bear some relationship with the lithological origin of its host rock: intrusive-hosted molybdenite spans –0.79 to -0.04 ‰ while skarn-hosted molybdenite is isotopically heavier (-0.46 to 0.37 ‰), though there is some overlap. The observed variability in $\delta^{98/95}$Mo in molybdenites at Antamina is consistent with studies of other molybdenite deposits worldwide, and is thought to be caused by a kinetic isotope fractionation associated with Mo reduction from Mo(VI) to Mo(IV) in hydrothermal fluids during molybdenite hydrothermal precipitation (Hannah et al., 2007; Greber et al., 2014).

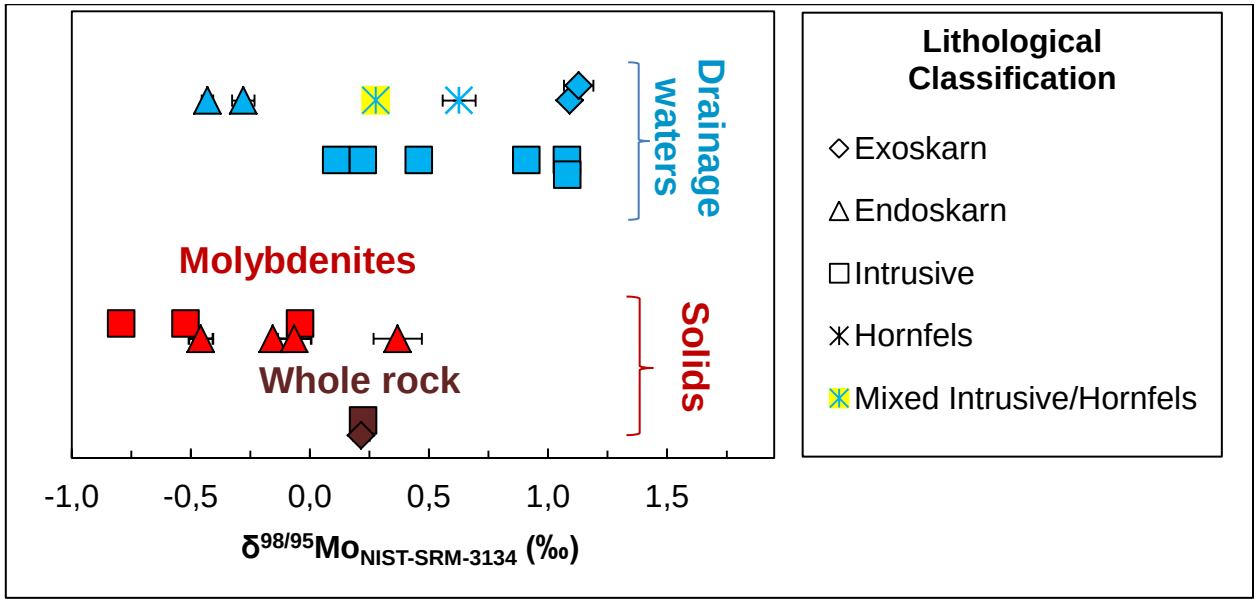

Figure 2 1-D representation of Mo isotopic composition of drainage waters (blue symbols), molybdenites (red symbols) and whole-rock (maroon symbols) by lithology (indicated by symbol shape) in Antamina waste rock material. Data are spread vertically for clarity. Error bars are ±2SD for a triplicate analysis on the MC-ICP-MS.

The range in $\delta^{98/95}$Mo in leachate water samples collected from field barrels and experimental waste rock piles is considerable, spanning 1.56 ‰. Leachate tends to be isotopically heavier than molybdenites, assumed to be the source of Mo. While at this point it is not possible to say specifically what causes this shift, it is possible to formulate hypotheses based on current knowledge of Mo isotope behavior. Heavier $\delta^{98/95}$Mo in drainage waters are consistent with previous studies, which have attributed this phenomenon to isotopic fractionation during oxidative weathering and adsorption onto (oxy)hydroxide minerals (Siebert et al., 2003; Barling and Anbar, 2004; Goldberg et al., 2009; Liermann et al., 2011; Voegelin et al., 2012). Sequential extractions and SEM analyses performed on Antamina waste rock dump material performed by Laurenzi (in prep.) show an association of Mo with oxidized mineralogical phases including Fe/Mn (oxy)hydroxides.

However, adsorption alone cannot fully explain Mo isotope compositions found in Antamina waters because the isotopically heaviest waters in this study included samples with pH ranges from 7.2-8.0, where Mo adsorption is expected to be minimal. Therefore another fractionating process can be invoked to explain this isotopic shift. Previous work shows that Mo attenuation via powellite

($CaMoO_4$) mineral precipitation is possible in these geochemical conditions (Conlan et al., 2012), although it is kinetically limited. While we cannot confirm which process is causing this isotopic shift at this point in time, a powellite precipitation hypothesis can be invoked as a possible explanation to explain this data: Ca- and Mo- bearing exoskarn is releasing Mo and Ca to solution, which then precipitate as $CaMoO_4$ albeit with a kinetic limitation. Kinetic isotope fractionation theory predicts that lighter Mo isotopes will be scavenged in this precipitation process, resulting in an isotopically heavy solution. Experimental testing of this hypothesis is an obvious next step. Finally, the endoskarn field barrel sampled in this campaign exhibited an opposite behavior to all other samples: water was isotopically lighter (-0.43 to -0.28 ‰) relative to molybdenite found in that field barrel (-0.16 ‰), suggesting another as of yet unknown process is causing isotopically light waters.

Zinc isotopes

In contrast with molybdenites, sphalerites at Antamina have a remarkably homogeneous Zn isotopic composition of 0.11 ± 0.01 ‰ (Fig. 3), which is consistent with a worldwide survey of Zn isotopic compositions in sphalerites by (Sonke et al., 2008). The range in Zn isotopic compositions measured in drainage water samples spans from -0.35 to 0.30 ‰, indicating that Zn isotopes are fractionated after release into solution from sphalerite oxidation. The isotopic composition of drainage waters is dependent upon the waste rock type: exoskarn and hornfels drainage is isotopically light, ranging from -0.35 to -0.02 ‰, while intrusive drainage is isotopically heavier, spanning from 0.03 to 0.30 ‰. One sample collected from an experimental waste rock pile (Pile 5-D) containing a mixture of hornfels and intrusive material had an intermediate isotopic composition of -0.01 ‰.

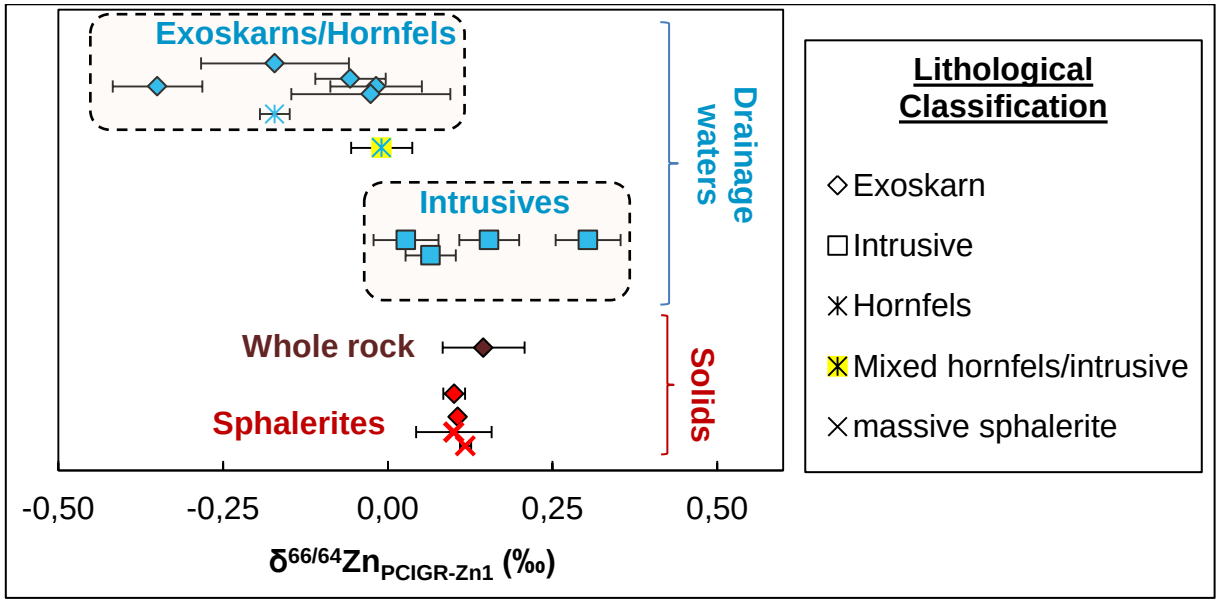

Figure 3 1-D representation of Zn isotopic composition of drainage waters (blue symbols), sphalerites (red symbols) and whole-rock (maroon symbols) in Antamina waste rock material by lithology (indicated by symbol shape). Data are spread along vertically axis for clarity. Error bars are ±2SD.

As is the case with Mo isotopes, at this point it is only possible to suggest hypotheses for the isotopic Zn variability measured at Antamina. Oxidative weathering, adsorption and precipitation of Zn-bearing carbonate minerals are all expected to cause some shifts in $\delta^{66/64}$Zn (Pichat et al., 2003; Fujii et al., 2011; Matthies et al., 2014a) and the variability measured here is likely an expression of one or several of these processes. The association of $\delta^{66/64}$Zn to waste rock lithology shows that Zn isotopes are a promising indicator for the provenance of Zn in waste rocks dumps which contain a mixture of different rock types. The intermediate isotopic composition of the hornfels/intrusive sample (Pile 5-D) could be an example of this application.

Laurenzi (in prep) has found evidence of Zn attenuation via adsorption onto Fe oxides and association with carbonate minerals in waste rock material collected from Antamina's waste rock dumps. Both of these attenuation mechanisms are possible in exoskarn waste rock material, because of its high carbonate content (2.8-31.3% by weight, (Peterson, 2014) and pH range (pH ~7-8) which is favorable for Zn adsorption (Pokrovsky et al., 2005). However, the shift towards isotopically light $\delta^{66/64}$Zn values in leachates from carbonate-rich waste exoskarn and hornfels materials are consistent with the precipitation of a Zn-carbonate mineral as an attenuating process (Pichat et al., 2003; Fujii et al., 2011).

SU MMARY AND CONCLUSION

Recent analytical improvements in MC-ICP-MS instrumentation allow the application of stable isotope analysis of heavy metals to track geochemical processes in mining waste rock and tailings. Mo and Zn isotope variations measured in Antamina waste rock materials are considerable and show that fractionation processes are occurring. Further experimental work will constrain the isotopic signature of environmentally relevant processes (e.g. adsorption, oxidative dissolution, secondary mineral precipitation) and improve our ability to use isotopes to diagnose the fate of these metals in full-scale waste rock dumps.

ACKNOWLEDGEMENTS

K. Gordon and Dr. M. Amini assisted in operating the MC-ICP-MS and developing analytical protocols. B. Harrison, M. Lorca-Ugalde, M. St-Arnault and L. Laurenzi assisted with sample collection along with Antamina field staff. B. Harrison, L. Laurenzi and M. St-Arnault and two anonymous reviewers provided invaluable comments to improve this manuscript. Funding was provided by NSERC and Compañía Minera Antamina.

REFERENCES

Al T. A., Martin C. J. and Blowes D. W. (2000) Carbonate-mineral / water interactions in sulfide-rich mine tailings. Geochim. Cosmochim. Acta 64, 3933–3948.

Aranda S., Borrok D. M., Wanty R. B. and Balistrieri L. S. (2012) Zinc isotope investigation of surface and pore waters in a mountain watershed impacted by acid rock drainage. Sci. Total Environ. 420, 202–13.

Balistrieri L. S., Borrok D. M., Wanty R. B. and Ridley W. I. (2008) Fractionation of Cu and Zn isotopes during adsorption onto amorphous Fe(III) oxyhydroxide: Experimental mixing of acid rock drainage and ambient river water. Geochim. Cosmochim. Acta 72, 311–328.

Barling J. and Anbar A. D. (2004) Molybdenum isotope fractionation during adsorption by manganese oxides. Earth Planet. Sci. Lett. 217, 315–329.

Buchachenko A. L. (2013) Mass-Independent Isotope Effects. J. Phys. Chem. 117, 2231–2238.

Baskaran, M. (Ed.) (2012) Handbook of Environmental Isotope Geochemistry. Springer Heidelberg Dordrecht London New York. 951 p.

Conlan M. J. W., Mayer K. U., Blaskovich R. and Beckie R. D. (2012) Solubility controls for molybdenum in neutral rock drainage. Geochemistry Explor. Environ. Anal. 12, 21–32.

Fernandez A. and Borrok D. M. (2009) Fractionation of Cu, Fe, and Zn isotopes during the oxidative weathering of sulfide-rich rocks. Chem. Geol. 264, 1–12.

Foucher D., Ogrinc N. and Hintelmann H. (2009) Tracing mercury contamination from the Idrija mining region (Slovenia) to the Gulf of Trieste using Hg isotope ratio measurements. Environ. Sci. Technol. 43, 33–9.

Fujii T., Moynier F., Pons M.-L. and Albarède F. (2011) The origin of Zn isotope fractionation in sulfides. Geochim. Cosmochim. Acta 75, 7632–7643.

Goldberg S., Lesch S. M. and Suarez D. L. (1998) Predicting Molybdenum Adsorption by Soils Using Soil Chemical Parameters in the Constant Capacitance Model. Soil Sci. Soc. Am. J. 66,1836–1842.

Goldberg T., Archer C., Vance D. and Poulton S. W. (2009) Mo isotope fractionation during adsorption to Fe (oxyhydr)oxides. Geochim. Cosmochim. Acta 73, 6502–6516.

Greber N. D., Pettke T. and Nägler T. F. (2014) Magmatic–hydrothermal molybdenum isotope fractionation and its relevance to the igneous crustal signature. Lithos 190-191, 104–110.

Hannah J. L., Stein H. J., Wieser M. E., de Laeter J. R. and Varner M. D. (2007) Molybdenum isotope variations in molybdenite: Vapor transport and Rayleigh fractionation of Mo. Geology 35, 703.

Heikoop J. M., Johnson T. M., Birdsell K. H., Longmire P., Hickmott D. D., Jacobs E. P., Broxton D. E., Katzman D., Vesselinov V. V., Ding M., Vaniman D. T., Reneau S. L., Goering T. J., Glessner J. and Basu A. (2014) Isotopic evidence for reduction of anthropogenic hexavalent chromium in Los Alamos National Laboratory groundwater. Chem. Geol. 373, 1–9.

Hirsche D. T. (2012) A field and humidity cell study of metal attenuation in neutral rock drainage from the Antamina mine, Peru. M.Sc. Thesis, University of British Columbia, 152 p.

Kimball B. E., Mathur R., Dohnalkova A. C., Wall A. J., Runkel R. L. and Brantley S. L. (2009) Copper isotope fractionation in acid mine drainage. Geochim. Cosmochim. Acta 73, 1247–1263.

Laurenzi, L., in prep. Metal attenuation studies in operational waste rock piles: A combined mineralogical and geochemical approach. ICARD conference, Santiago, Chile, April 20-25 2015.

Liermann L. J., Mathur R., Wasylenki L. E., Nuester J., Anbar a. D. and Brantley S. L. (2011) Extent and isotopic composition of Fe and Mo release from two Pennsylvania shales in the presence of organic ligands and bacteria. Chem. Geol. 281, 167–180.

Matthies R., Krahé L. and Blowes D. W. (2014a) Zinc stable isotope fractionation upon accelerated oxidative weathering of sulfidic mine waste. Sci. Total Environ. 487, 97–101.

Matthies R., Sinclair S.A and Blowes D. W. (2014b) The zinc stable isotope signature of waste rock drainage in the Canadian permafrost region. Appl. Geochemistry 48, 53–57.

Peterson H. E. (2014) Unsaturated hydrology, evaporation and geochemistry of neutral and acid rock drainage in the highly heterogeneous mine waste rock at the Antamina mine, Peru. PhD Thesis, University of British Columbia, 307 p.

Pichat S., Douchet C. and Albarède F. (2003) Zinc isotope variations in deep-sea carbonates from the eastern equatorial Pacific over the last 175 ka. Earth Planet. Sci. Lett. 210, 167–178.

Pokrovsky O. S., Viers J. and Freydier R. (2005) Zinc stable isotope fractionation during its adsorption on oxides and hydroxides. J. Colloid Interface Sci. 291, 192–200.

Shiel A. E., Weis D., Cossa D. and Orians K. J. (2013) Determining provenance of marine metal pollution in French bivalves using Cd, Zn and Pb isotopes. Geochim. Cosmochim. Acta 121, 155–167.

Siebert C., McManus J., Bice A., Poulson R. and Berelson W. M. (2006) Molybdenum isotope signatures in continental margin marine sediments. Earth Planet. Sci. Lett. 241, 723–733.

Siebert C., Nägler T. F., von Blanckenburg F. and Kramers J. D. (2003) Molybdenum isotope records as a potential new proxy for paleoceanography. Earth Planet. Sci. Lett. 211, 159–171.

Siebert C., Nägler T. F. and Kramers J. D. (2001) Determination of molybdenum isotope fractionation by double-spike multicollector inductively coupled plasma mass spectrometry. Geochemistry Geophys. Geosystems 2, 2000GS000124.

Sonke J., Sivry Y., Viers J., Freydier R., Dejonghe L., Andre L., Aggarwal J., Fontan F. and Dupre B. (2008) Historical variations in the isotopic composition of atmospheric zinc deposition from a zinc smelter. Chem. Geol. 252, 145–157.

Voegelin A. R., Nägler T. F., Pettke T., Neubert N., Steinmann M., Pourret O. and Villa I. M. (2012) The impact of igneous bedrock weathering on the Mo isotopic composition of stream waters: Natural samples and laboratory experiments. Geochim. Cosmochim. Acta 86, 150–165.

Wasylenki L. E., Rolfe B. A., Weeks C. L., Spiro T. G. and Anbar A. D. (2008) Experimental investigation of the effects of temperature and ionic strength on Mo isotope fractionation during adsorption to manganese oxides. Geochim. Cosmochim. Acta 72, 5997–6005.

Wasylenki L. E., Weeks C. L., Bargar J. R., Spiro T. G., Hein J. R. and Anbar a. D. (2011) The molecular mechanism of Mo isotope fractionation during adsorption to birnessite. Geochim. Cosmochim. Acta 75, 5019–5031.

Weiss D. J., Rehkämper M., Schoenberg R., Mclaughlin M., Kirby J., Campbell P. G. C., Arnold T., Chapman J., Peel K. and Gioia S. (2008) Application of nontraditional stable-isotope systems to the study of the sources and fate of metals in the environment. Environ. Sci. Technol. 42, 665–664.

Using Spatially Explicit Data and Modeling to Inform Ecological Risk Assessment at Mining Sites

Brad Parks[1], Sean Kosinski[2], Les Williams[2] and Andrew Nicholson[2]

1. *Integral Consulting, Chile*
2. *Integral Consulting, USA*

ABSTRACT

The ecological effects of mine development are typically assessed using very conservative assumptions inherent in screening level ecological risk assessments (SLERAs) vis-à-vis toxicity and exposure estimates. We recommend a simple efficient SLERA followed by a focused population-level risk assessment designed by risk assessors in consultation with mine planners and geochemists. We provide an example of an evaluation of potential risk using spatially explicit modeled data and empirical site data for multiple media including soil and expected future sediment and surface water conditions at a mining site. These data were used in conjunction with an expanded list of toxicity values and exposure pathway models to evaluate risks to ecological receptors at the site. Results indicate a handful of chemicals of potential concern based on exceedances of low-effect criteria for bats, barn swallow, and spotted sandpiper. In an effort to focus risk management, a third-tier risk assessment was conducted using an individual-based model (IBM) to evaluate uncertainties in the risk assessment approach and characterize population-level impacts for the bat *Myotis* spp. as an example species. This population modeling effort expands upon the exposure scenarios and anticipated future site habitats used to evaluate both baseline risks and potential mitigation of risks by overlaying material to reduce exposure to areas with higher levels of chemicals of interest. The results demonstrate the usefulness of population modeling tools in assessing future exposure scenarios to meet risk management objectives in the real-world currency of natural resources (i.e., population abundance) as opposed to the pass/fail hazard-quotient paradigm currently utilized in risk assessment. This study also illustrates the importance, even at a screening level, of a robust, spatially explicit site-specific data set in understanding future conditions and site management alternatives.

INTRODUCTION

Ecological risk assessment (ERA) is a process for evaluating the likelihood that adverse ecological effects may occur or are occurring as a result of exposure to one or more stressors. Typically, ecological risk assessments use toxicological, ecological, and geochemical information to evaluate risk of impacts to wildlife and habitats from human activities such as chemical spills, resource extraction, and land conversion. If ecological risks are unavoidable, the ERA process can help identify opportunities to minimize or mitigate these risks (USEPA, 1998). This process at the lowest-tier consists of utilizing maximum exposure concentrations to ecological receptors which not surprisingly results in overly conservative risk estimates. At the second-tier, ecological risk assessors can utilize detailed spatially explicit site date including analysis of the mine activities, mine geochemistry, habitat formation, habitat access, and contributions of the pit lake water quality, sediment quality, and wall rock concentrations in evaluating ecological risk. A third-tier assessment involves investigating population-level effects for those ecological species which exhibited risk based upon the spatially-informed assessment (i.e., second-tier). This evaluation utilizes population models or population viability analyses built upon the body of scientific literature describing life history characteristics for the receptor of interest. A subset of these models, individual-based models (IBMs) allow the risk assessor to incorporate ecosystem complexities such as physiological factors, intra- and inter-specific interactions, resource availability, habitat structure, and abiotic factors. Ultimately, the results from IBMs provide a refined assessment with a potential range of risk outcomes in ecosystem metrics that are potentially simpler to conceptualize than the hazard quotient construct. These metrics include population abundance, extinction or quasi-extinction risk, and population growth rates relative to a control condition (i.e., no stressor in the system).

As an example of this three-tiered ERA approach, we present the results of an ERA which was conducted to evaluate a proposed expansion of the Twin Creeks Mine in the arid Great Basin ecosystem of northern Nevada, USA. State and federal permitting requires an evaluation of ecological risk associated with mining activities. In the case of proposed pit mine expansion, several spatial and temporal issues complicate the ERA approach. The assessment must be conducted for an ecosystem (a pit lake) that does not yet exist, using predictions of what hydrologic, chemical, and biological conditions are likely to be present several decades into the future as the lake infills. The ERA needs to account for spatial heterogeneity of chemicals to evaluate chemicals that animals will be exposed to once the pit lake exists. The risk assessment also needs to incorporate site geochemistry, which influences the bioavailability of metals and other chemicals to which wildlife may be exposed (Flynn *et al.*, 2003; Suedel *et al.*, 2006). These issues call for spatially and temporally explicit approaches in order to accurately predict risk and, if risks of adverse effects are found, inform the approach to reduce or mitigate these risks. The uncertainty associated with the dynamic lake condition offers another benefit to the three-tiered assessment approach whereby incorporating temporal and spatial variability in exposure profiles into a probabilistic population modeling scenario to further inform risk management.

METHODS

A screening-level ecological risk assessment was conducted, consistent with regulatory guidance (USEPA, 1997; USEPA, 1999; USEPA, 2001), which uses maximum concentrations of chemicals in the proposed pit vicinity, assumes complete bioavailability, and compares chemical data to conservative toxicological criteria. The conservatism of this approach resulted in a long list of metals that may cause risk, with substantial uncertainty about the realism of these risks under future conditions.

To address these uncertainties, a spatially explicit ERA was then conducted as a second-tier assessment. This approach incorporated an expanded set of modeled and empirical data over multiple time scenarios to evaluate expected future sediment and surface water conditions, including:

- Spatially explicit data sets were used to evaluate what concentrations of metals might be expected at the pit wall surface to which the ecological community could be exposed (Figure 1). This effort included detailed characterization of the vertical extent of concentrations throughout the geologic section (Figure 2).
- Estimates of pit lake surface water elevation and water quality was modeled over the complete 200 years of lake infill by other workers (Itasca, 2010; Geomega, 2010).
- A conceptual site model was designed to look at how ecological communities of the lake might be expected to develop after pit closure and infill (Figure 3).

These data sets and conceptual models were used to inform a site-specific wildlife exposure model. The model creates estimates of exposure to local wildlife that might be expected to colonize or forage in the habitats that develop as the pit lake is created and habitat is formed (Figure 4). These estimates of exposure were evaluated relative to toxicological criteria for concentrations of metals that have been shown in the scientific literature to cause no or low levels of adverse effects to wildlife exposed to these metals.

Based on the risk outcomes from the second-tier ERA, a third-tier assessment was conducted to illustrate the usefulness of population models for an example receptor which exceeded the low-effect criteria. We developed an IBM which accounts for the reality that individual organisms are distributed in a non-uniform way and may respond differently to identical environmental conditions depending on sex, age, and health. Hexsim is a publically available modeling software developed for the purpose of analyzing individuals within an ecosystem over time by layering prey, habitat preferences, and movement patterns in a probabilistic manner (Heinrichs *et al.*, 2010). The model is individual-based, spatially-explicit through user-defined spatial data which capture landscape structure, habitat quality, and stressor distribution, and trait-based through user-definitions such as age, sex, and fitness (Figure 4). The model was run using annual time-steps over the first 50 years of pit lake infill. Incorporating best-case and worst-case behavioral traits for the receptor species allows us to evaluate uncertainty in the evaluation. The results of this analysis allow us to compare population-level endpoints (i.e., abundance, population growth rate) over varying modeled assumptions and assist in gauging the environmental reality of presumed risks following the second-tier.

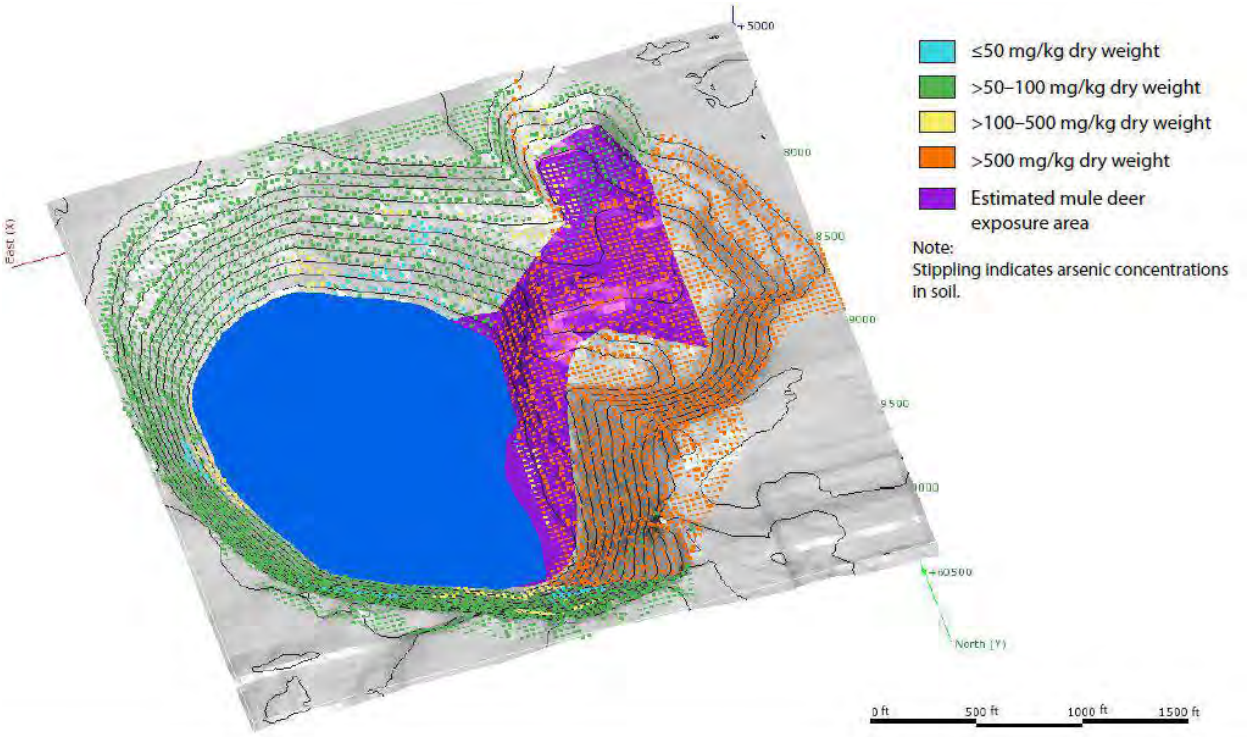

Figure 1 Predicted pit-lake geometry and arsenic distribution in the Vista Pit.

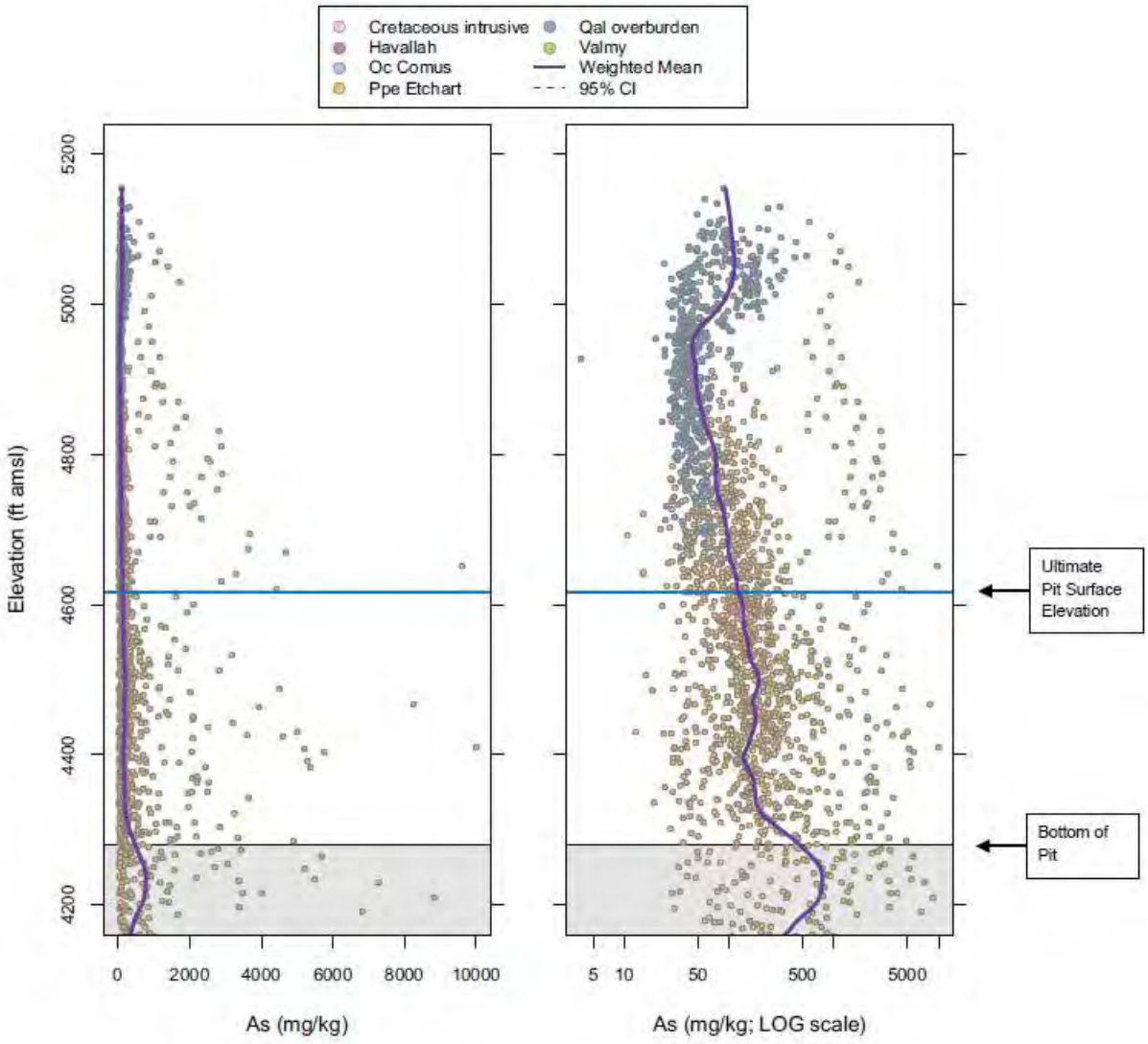

Figure 2 Arsenic concentrations as a function of depth in the proposed Vista Pit.

RESULTS AND DISCUSSION

Results of the wildlife exposure model included:

- No risks were predicted to modeled granivorous birds or ducks from exposure to chemicals at the site (Table 1).
- Low risks were predicted to ungulates, which could be redressed by considering pit wall mitigation. Exposures to antimony and arsenic were greater than the no-effect criteria for these metals if mule deer were conservatively assumed to spend all their time at the site. This risk could be eliminated if overburden (surficial materials removed prior to mining) is applied to the areas of the pit most likely to be frequented by grazing ungulates (Figure 2).
- A handful of metals were retained as chemicals of potential concern that exceeded low-effect criteria for one or more taxa of invertivorous mammals and birds (Table 1). However, there are important aspects of the model and the site conditions that are likely to reduce these risks:

- Predictions of risk were largely related to necessarily simplifying assumptions in the model of uptake factors from foods to consumers. When applied to bioaccumulation of metals, these factors often overestimate uptake, particularly at higher concentrations (Drexler *et al.*, 2003).
- The model assumes complete bioavailability of these metals; however, geochemical modeling indicates that at this site, several metals are likely to be in valence states or composite forms that reduce their bioavailability. For example, surface water pH greater than 5 is likely for this site, which would maintain aluminum in insoluble form, substantially limiting bioavailability of this chemical.

The availability of littoral habitat is likely to play a major role in shaping the ecological community of the site. Rapid infill rates over the first 20 years or so is likely to preclude the development of littoral habitat and will lead to the formation of a deep, mesotrophic pit lake. As lake infill slows, littoral habitat development will be regulated by the spatial proximity of shallow lake waters to horizontal pit wall benches that could allow for the development of a shallow vegetated photic zone. Low organic matter content in this arid ecosystem is likely to slow and limit shoreline soil capable of supporting substantial vegetation, further limiting habitat development.

CONCLUSIONS

The use of spatially and temporally explicit geochemical and ecological modeling to inform risk assessment has substantively improved our understanding of the ecological trajectory and potential for risk at the future Vista Pit lake. In an effort to further refine the risk characterization and weight-of-evidence for risk management alternatives, a third-tier assessment involving population model projections for receptor species of interest was conducted. Following closure and infill from groundwater, Vista Pit is likely to function as a deep, mesotrophic pit lake. The development of shallow littoral habitat capable of supporting wildlife will depend on the intersection of pit geometry and final surface level equilibrium, is likely to be prevented during initial rapid infill rates, and will be limited in the long term by low rates of organic matter accumulation in this arid ecosystem. Most chemicals that were evaluated were not found to be present at concentrations that suggest the potential for adverse effects on wildlife. Steps such as the use of overburden to cover pit wall surfaces that present a high likelihood of exposure may also be helpful in mitigating risk.

ACKNOWLEDGEMENTS

This work was funded and sponsored by Newmont Mining Corporation through subcontract to Enviroscientists, Inc.

REFERENCES

Drexler, J., N. Fisher, G. Henningsen, R. Lanno, J. McGeer, and K. Sappington. 2003. Issue paper on the bioavailability and bioaccumulation of metals. Submitted to: U.S. Environmental Protection Agency, Risk Assessment Forum, Washington D.C.

Flynn, H.C., A.A. Meharg, P.K. Bowyer, and G.I. Paton. 2003. Antimony bioavailability in mine soils. *Environmental Pollution*, Vol.124 No.1.

Geomega. 2010. Vista VII Pit Lake Chemogenesis. Final Draft. Prepared for Newmont Mining Corporation, Carlin, NV. September 9, 2010.

Heinrichs, J., D. Bender, D. Gummer, and N. Schumaker. 2010. Assessing critical habitat: evaluating the relative contribution of habitats to population persistence. *Biological Conservation*. 143: 2229-2237.

Itasca. 2010. Appendix D: Predictions of Vista Phase 7 lake infilling. 2010 Update of Twin Creeks numerical groundwater flow model and simulations for Vista Phase 7 Pit. Memorandum submitted to Newmont Mining Corporation. Lakewood, CO. Itasca Denver Inc. August 5, 2010.

Suedel, B., A. Nicholson, C. Day, and J. Spicer. 2006. The value of metals bioavailability and speciation information for ecological risk assessment in arid soils. *IEAM 4*(2):355-364.

USEPA. 1997. Ecological risk assessment guidance for Superfund: Process for designing and conducting ecological risk assessments. EPA 540-R-97-006. Interim final. U.S. Environmental Protection Agency, Office of Emergency and Remedial Response, Washington D.C.

USEPA. 1998. Guidelines for ecological risk assessment. EPA 630-R-95-002F. U.S. Environmental Protection Agency, Washington D.C.

USEPA. 1999. Screening Level Ecological Risk Assessment Protocol for Hazardous Waste Combustion Facilities Peer Review Draft. Appendix C: Media-to-receptor bioconcentration factors (BCFs).

USEPA. 2001. The role of screening-level risk assessments and refining contaminants of concern in baseline ecological risk assessments. ECO Update Intermittent Bulletin. EPA 540/F-01/014. U.S. Environmental Protection Agency, Washington D.C.

Table 1. Summary of toxicological criteria exceedances[a] using the wildlife ingestion model.

Receptor:	Chukar	Mule Deer	Myotis	Barn Swallow	Mallard	Spotted Sandpiper
Feeding guild:	Granivore	Browsing Ungulate	Aerial Invertivore	Aerial Invertivore	Omnivore	Shoreline Invertivore
Aluminum	—	—	X	X[b]	—	X
Antimony	—	X[b]	X[c]	No criteria	No criteria	No criteria
Arsenic	—	X[b]	X[b,c]	—	—	X[c]
Barium	—	—	—	—	—	—
Beryllium	—	—	—	No criteria	No criteria	No criteria
Cadmium	—	—	—	—	—	—
Chromium	—	—	X[b,c]	X[b,c]	—	X[b,c]
Copper	—	—	X[b,c]	X[b]	—	X [b]
Iron	—	—	—	—	—	—
Lead	—	—	—	X[b,c]	—	X [b]
Manganese	—	—	—	—	—	—
Mercury	—	—	—	X	—	X
Nickel	—	—	—	—	—	—
Selenium	—	—	X[b]	X[b]	—	X[b,c]
Silver	—	—	—	—	—	—
Zinc	—	—	—	—	—	—

Notes:

— = Criteria not exceeded.

X = Criterion exceeded

[a] Exposures at three time scenarios: 50 years of lake infill, 100, and 200 years were run and all results are summarized here.

[b] Criterion for lowest observed adverse effect is not exceeded, indicating risk is low

[c] For one or more time scenarios, concentration does not exceed criterion.

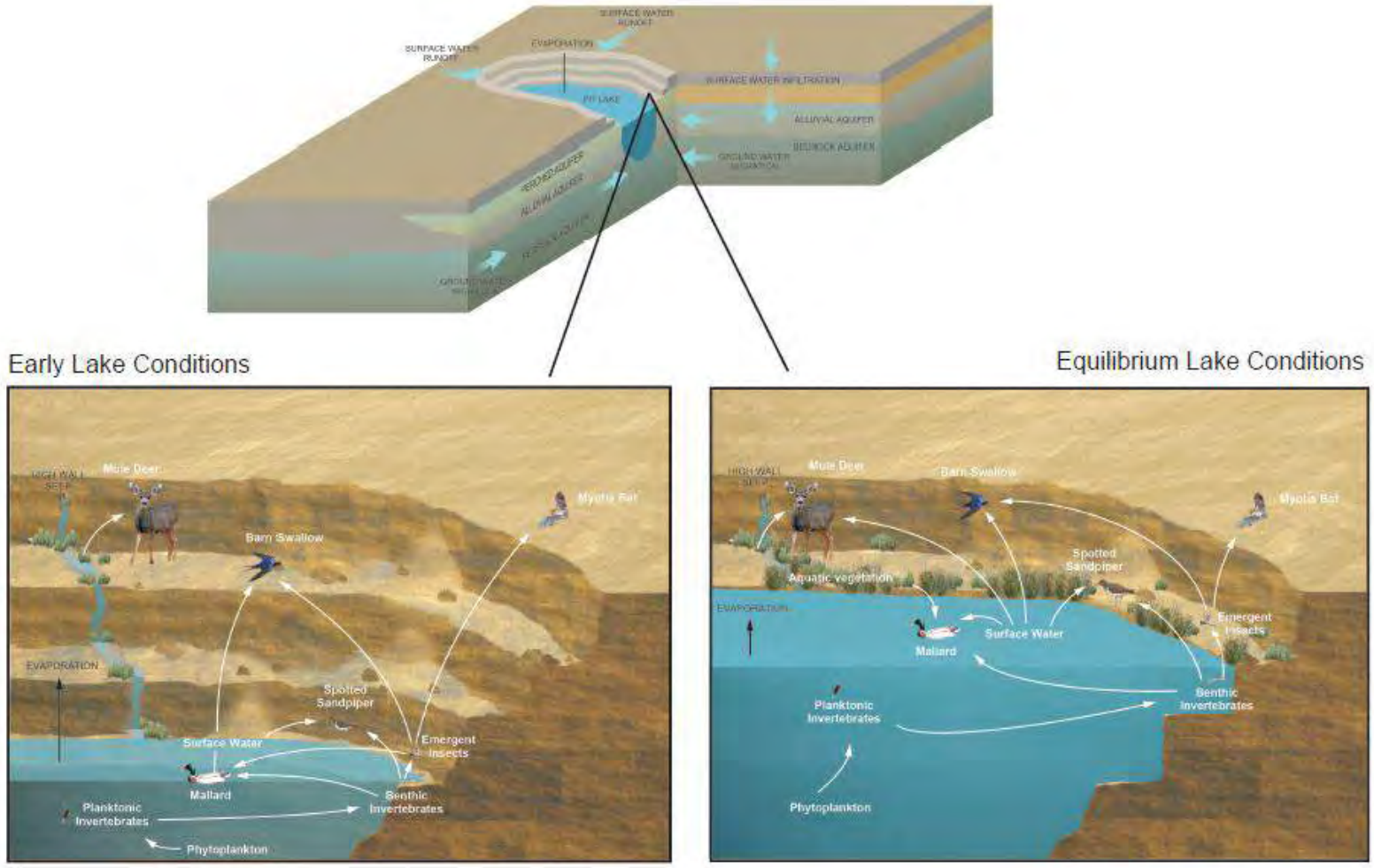

Figure 3 Ecological conceptual model of pit infilling and habitat development.

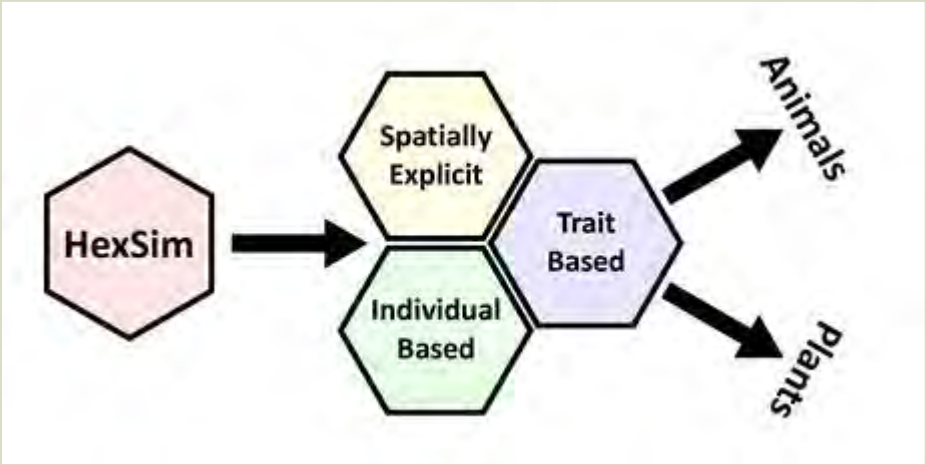

Figure 4 Simplified modeling diagram depicting HexSim individual-based model structure.

Effluent Chemistry of Closed Sulfide Mine Tailings: Influence of Ore Type

Päivi Kauppila and Marja Räisänen
Geological Survey of Finland

ABSTRACT

The seepage water quality of old sulfide mine tailings was studied from eleven closed sulfide metal mines in Finland to assess the influence of ore type on the drainage quality of tailings in the long-term. The studied sites represent a wide variety of ore types and commodities (e.g. Mo; Cu and Zn; Ni and Cu; Cu, W, As, Ag; Fe). Also the operation periods of the mines vary, from the 1750s to 1990s. Mining operations had ceased at the sites some 15–62 years ago (prior to sampling), but most of the facilities were left without any cover after mine closure. Only three of the tailings impoundments were covered with a thin layer of till or peat.

The seepage quality varied largely between the different mine sites. The pH of the seepages was between 2.8–7.3 and the total metal content (Zn + Cu + Cd + Pb + Co + Ni) between 0.004–207 mg/L. Overall, the high-acid, high-metal waters were related to Cu mine tailings, whereas the seepages from the other tailings deposits (i.e. from Ni, Fe, Mo, and Zn mines) were mostly near-neutral, low-metal containing waters. Unexpectedly, the most acidic seepage waters were found at the two sites where the tailings were covered with till after closure. One of the sites represented tailings from a Cu mine and the other from a Ni mine.

The results of the study show that there is a correlation between the tailings effluent quality and the ore type. However, other factors such as weathering period of the tailings also influence the seepage quality. These types of data contribute to the prediction of the long-term drainage quality of the new mining sites and in defining the requirements for their waste management and water treatment.

Keywords: Tailings, sulfide mining, seepage water, ore type, Finland

INTRODUCTION

Low-quality mine drainage from mine wastes is one of the major environmental issues that the mining operators struggle with. This is in particular at mines extracting base metals from sulfide-rich deposits, since the sulfide minerals oxidize once exposed to atmospheric oxygen and water. Depending on the balance between acid producing and neutralizing minerals in the waste, the drainage can be either low pH acid mine drainage ('AMD`) or non-acidic neutral mine drainage ('NMD') (Younger, 1995; Cravotta *et al.*, 1999; Pettit *et al.*, 1999; Heikkinen *et al.*, 2009). Regardless of the pH, these mining influenced waters can contain elevated to high concentrations of dissolved base and trace metals (*e.g.* Fe, Ca, Mg, Na, K, Cu, Ni, Zn) and sulfate originating from the weathering of sulfide, carbonate, oxide and silicate minerals in the waste (Pettit *et al.*, 1999; Plumlee *et al.*, 1999; Cravotta, 2008). Before opening a mine, quality of the future drainage should be estimated to assess the environmental impacts of the disposal of mine waste and to define the requirements for the waste management and water treatment techniques to prevent or minimize these impacts.

Prediction of the long-term quality of the waste effluents is a challenging task and is usually based on geochemical characterization of mine wastes using *e.g.* static and kinetic tests (White *et al.*, 1999; Sapsford *et al.*, 2008; INAP, 2009; Rousseau, 2012). Static tests provide one-time results and target to evaluate whether the waste is acid producing or not, whereas kinetic tests provide evaluation of the time dependent rates of chemical reactions in longer term. However, it has been recommended that the prediction should not be based on the tests alone, but they should be supplemented with water quality data from mine sites with similar types of geological deposits, because effluent chemistry shows ore type-specific features (Plumlee *et al.*, 1999; Lapakko, 2003; Seal & Hammarström, 2003).

In this study, preliminary results of the seepage water quality of tailings from eleven closed Finnish sulfide metal mine sites, representing six different genetic ore types, is presented to study the ore type-related effluent geochemical characteristics. At most of these sites the tailings have been uncovered since the mining operations ceased, and the tailings have had 15–62 years to weather. However, some of the tailings facilities were covered after closure with a layer of till or peat, so the influence of soil covers on the seepage water quality is also discussed. The focus of the study is in particular on the acidity and trace metal content of the seepages.

METHODOLOGY

Description of the studied sites

Seepage water samples were collected from tailings facilities of eleven closed sulfide metal mines in Finland (Figure 1), located in a temperate climate with an annual average precipitation of 600–700 mm. At all sites, the tailings were disposed above ground level into ponds constructed with earthen dams and utilizing natural depressions (*e.g.* small ponds/lakes or peatlands). The mines included Mätäsvaara Mo mine, Hammaslahti Cu-Zn mine, Laukunkangas Ni-Cu mine, Hällinmäki Cu-mine, Kotalahti Ni-Cu mine, Ylöjärvi Cu-W-As-Ag mine, Aijala Cu-Zn mine, Orijärvi Cu-Pb-Zn mine, Vihanti Zn-Cu-Pb-Ag mine, Rautuvaara Fe-Cu mine and Raajärvi Fe mine (Table 1). The ore deposit represented genetically 6 different ore types: volganogenic massive sulfide deposits, sedimentary exhalative type, porphyry copper deposits, magmatic nickel deposits, skarn and iron oxide ore types (Eilu *et al.*, 2012).

Figure 1 Locations of the studied mine sites (Contains data from the National Land Survey of Finland)

The mines operated variably from 1750s to 1990s (Puustinen, 2003, Eilu *et al.*, 2012), thus a variety of ore processing methods have been employed at the sites. Mining operations ceased at the sites some 15–62 years before the seepage water sampling (Table 1). Only three of the eleven tailings facilities (Hammaslahti, Laukunkangas, Vihanti) were covered after closure, so the tailings have been in most of the sites susceptible to oxidation. In Hammaslahti, the till cover was 35 cm thick in average (varying 10–60 cm) and it was partly covered with 10–15 cm layer of peat. Laukunkangas tailings area was covered with 50 cm till layer with 5 cm humus layer on top of it, whereas in Vihanti some 5 cm thick peat layer has been applied to revegetate the tailings facility. Covering of the sites has occurred only after some ten years after the mine closure and the end of the tailings disposal. Therefore, weathering of tailings has also initiated at these sites prior to covering.

Table 1 Commodity, ore type, operation period and amount of tailings of the studied mine sites

Mine site	Commodity	Ore deposit type[1]	Operation period[2]	Tailings (Mt)[3]
Aijala	Cu, Zn	VMS (bimodal, felsic dominated)	1949–58	2.0
Hammaslahti	Cu, Zn	Sedimentary exhalative	1972–86	5.3
Hällinmäki	Cu	VMS? (mafic)	1966–84	4.1
Kotalahti	Ni, Cu	Magmatic Ni sulfide	1959–87	9.4
Laukunkangas	Ni, Cu	Magmatic Ni-Cu-PGE	1985–94	6.6
Mätäsvaara	Mo	Porphyry (Cu, Au, Mo, W, Sn, Ag)	1903, 1910s, 1920–22, 1932–33, 1939–47	1.0
Orijärvi	Cu, Pb, Zn	VMS (bimodal, felsic dominated)	1758–1882, 1929–55	1.0
Raajärvi	Fe	Skarn (Zn-Pb-Ag, Cu, Au, Fe, W)	1964–75	2.2
Rautuvaara	Fe, Cu	Iron oxide-copper-gold	1962–88	8.0
Vihanti	Zn, Cu, Pb, Ag	VMS (bimodal, felsic dominated)	1954–92	1.4
Ylöjärvi	Cu, W, As, Ag	Close to Cu porphyry	1943–66	2.8

[1]Eilu *et al.*, 2012; [2]Puustinen, 2003; [3]Räisänen *et al.*, 2013; VMS = volcanogenic massive sulfide deposit

Sampling and analytical methods

Seepage water samples were collected from locations where water surfaces through the tailings dams. Samples were collected during early summer to midsummer (27th May to 3rd July). One seepage water sample was taken from each mine site. EC, pH, O_2, O%, and redox potential were measured in the field using a multi-parameter field meter (YSI 556 Multiprobe system), and alkalinity was determined with a Hach digital titrator with 0.1600 N or 1.600 N H_2SO_4 to an end point of 4.5. Unfiltered samples were collected for anion measurements and filtered (0.45 μm), HNO_3-acidified samples were collected for dissolved major cation and trace metal analyses. Major anions were determined with ion chromatography and major cations and trace metals with ICP-OES or ICP-MS. Duplicate samples and field blanks were taken for quality control. All the laboratory analyses were carried out at the FINAS-accredited testing laboratory of Labtium Ltd.

RESULTS AND DISCUSSION

Overall chemistry of the seepage waters and influence of the ore type

The seepage water quality varied largely between the different mine sites. The pH of the seepage waters varied between 2.8–7.3 and the total metal content (Zn, Cu, Cd, Pb, Co, Ni) between 0.004–207 mg/l (Figure 2). In general, the most abundant trace metals in the seepages were Zn, Ni, Co, and Cu and the seepages contained also high concentrations of SO_4, Ca, and Mg, which are typically released in the weathering of sulfide minerals and subsequent weathering of carbonate and silicate minerals (Figure 3).

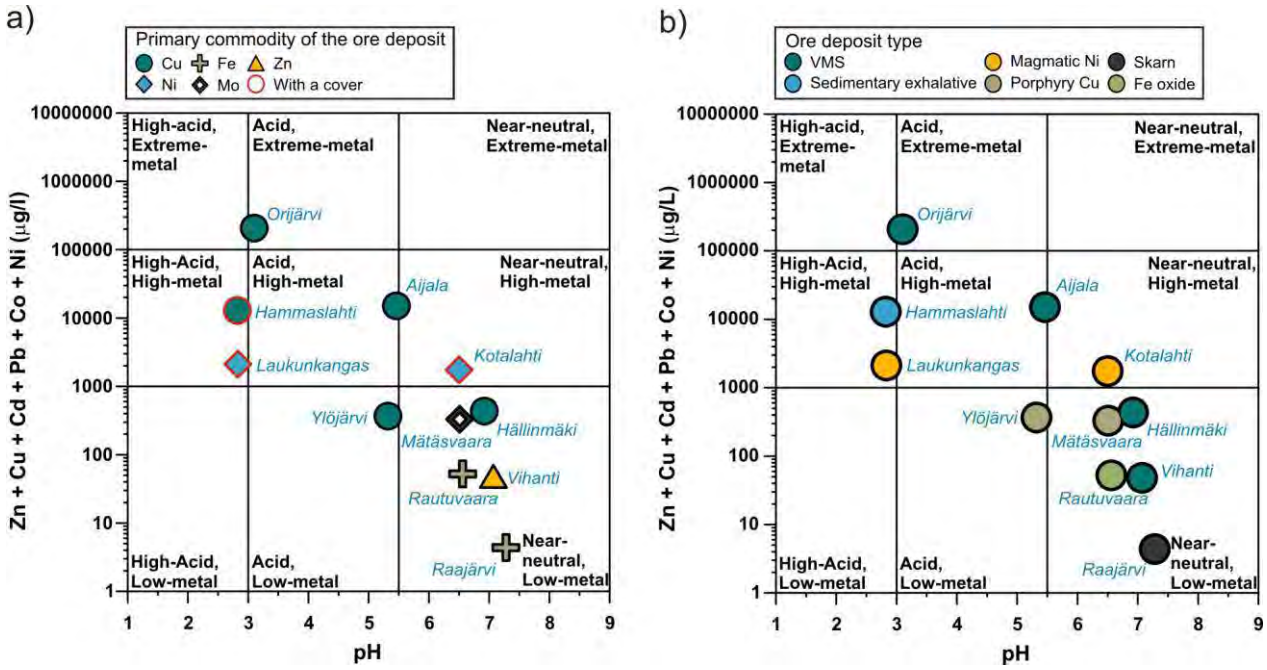

Figure 2 Ficklin diagrams (Plumlee *et al.*, 1999) of the tailings seepage waters showing the sum of dissolved heavy metals (Zn, Cu, Cd, Pb, Co, Ni) in µg/l plotted against pH value. Mine sites classified a) based on primary commodity of the ore deposit and b) based on genetic type of the ore deposit (VMS = volcanogenic massive sulfide deposit)

Based on the Ficklin diagram (Plumlee *et al.*, 1999), one third of the tailings seepages classified as high-acid/acid, high-metal waters, and half were near-neutral, low-metal drainages (Figure 2). Overall, the seepages at the sites where Cu ore had been extracted represented AMD type waters whereas the tailings effluents from most of the other types of deposits produced NMD (Figure 2). The most acidic seepage waters with highest metal contents were found at the sites where volcanogenic massive sulfide and sedimentary exhalative Cu ore types had been extracted, namely at Hammaslahti, Orijärvi and Aijala. These deposits contain typically high concentrations of sulfide minerals hosted by felsic rocks, having high acid production capacity and low neutralization capacity, and thus are prone to AMD. In contrast, the most neutral seepages with lowest metal contents were at the Raajärvi and Rautuvaara mine sites, which are iron oxide deposits containing only small amounts of sulfide minerals. However, the tailings produced in the extraction of magmatic Ni deposits (Laukunkangas and Kotalahti), porphyry deposits (Ylöjärvi and Mätäsvaara) and volcanogenic massive sulfide deposits (Vihanti, Hällinmäki, Aijala, Orijärvi) produced both AMD and NMD type seepage waters (Figure 2). These major ore type classes contain heterogeneous ore deposits, whose host rocks vary from ultramafic to felsic rocks, with varying buffering properties (Table 1). Host rocks of magmatic Ni deposits typically include ultramafic rocks with good buffering capacity, but in the Laukunkangas deposit the host rocks also contain black schists which are highly acid producing rocks (Grundström, 1985). Evidently, a more detailed classification of the ore type would likely better reveal the differences between the various ore deposits.

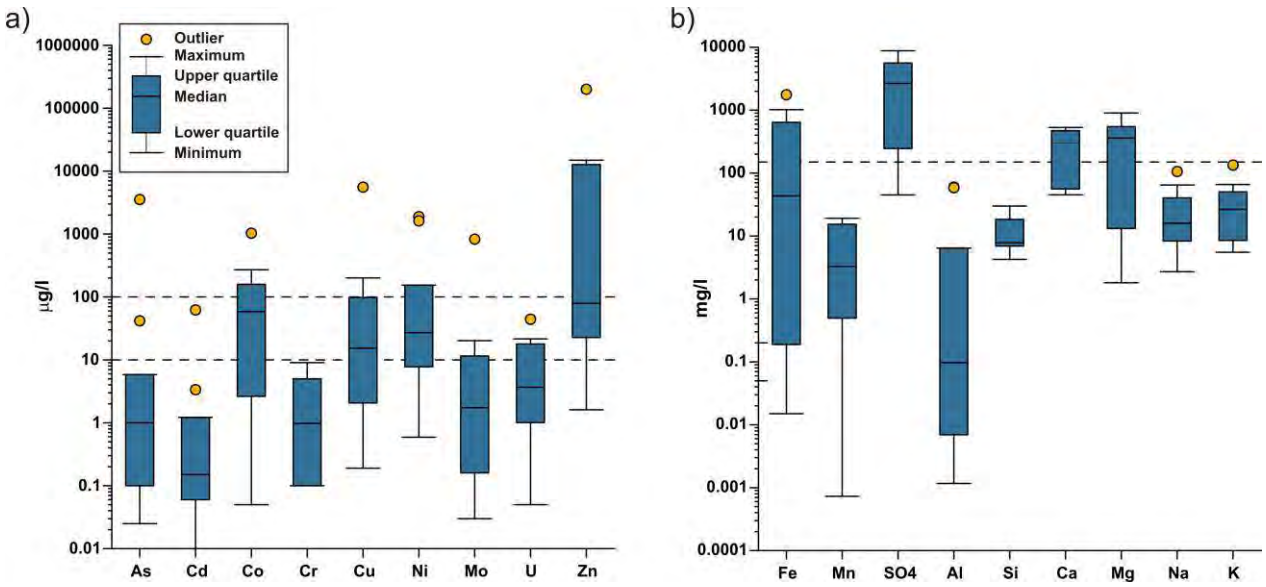

Figure 3 Box-Whisker plots for selected a) trace metal and b) major element and SO_4 contents of the tailings seepage waters

The loadings of trace metals in the seepages is a matter of the availability of the metals in the tailings (*i.e.* source of the metal) and the pH-Eh conditions controlling mineral weathering. Obviously, the tailings effluents of magmatic Ni deposits (Kotalahti and Laukunkangas) with abundant Ni sulfides in the tailings contained notably higher amounts of Ni than the other deposit types, whereas Cu concentrations were highest in the seepages of the Cu deposits (*e.g.* Orijärvi, Hällinmäki, Hammaslahti) rich in Cu sulfides (Figure 4). In addition, Zn was a typical trace metal in the seepages of the Cu deposit in which Zn occurred in exploitable amounts (Figure 4 and Table 1). However, occurrence of Zn in the seepages was also strongly linked to the pH conditions and thus in the weathering state of the tailings. For example, at the closed Vihanti Zn mine, the seepage water pH was > 7 and contained only minor amounts of Zn, even though there should be an abundant Zn source (sphalerite) in the tailings (Eilu *et al.*, 2012). The seepages of the Ylöjärvi porphyry deposit were distinct from the other seepages and had high As, U, and Co content originating from the weathering of arsenopyrite (As), uraninite (U) and presumably Co-bearing Fe-sulfides (Co). The seepages of the Fe deposits (Raajärvi and Rautuvaara) had in general very low contents of trace metals (Figure 4). The highest concentrations of Fe and SO_4 in the seepage waters occurred at the sites with the lowest pH and highest metal content, i.e. the sedimentary exhalative Cu deposit of Hammaslahti, Cu-rich VMS deposits of Orijärvi and Aijala, and the magmatic Ni deposit of Laukunkangas, indicating extensive sulfide oxidation in the tailings (Figures 2 and 4).

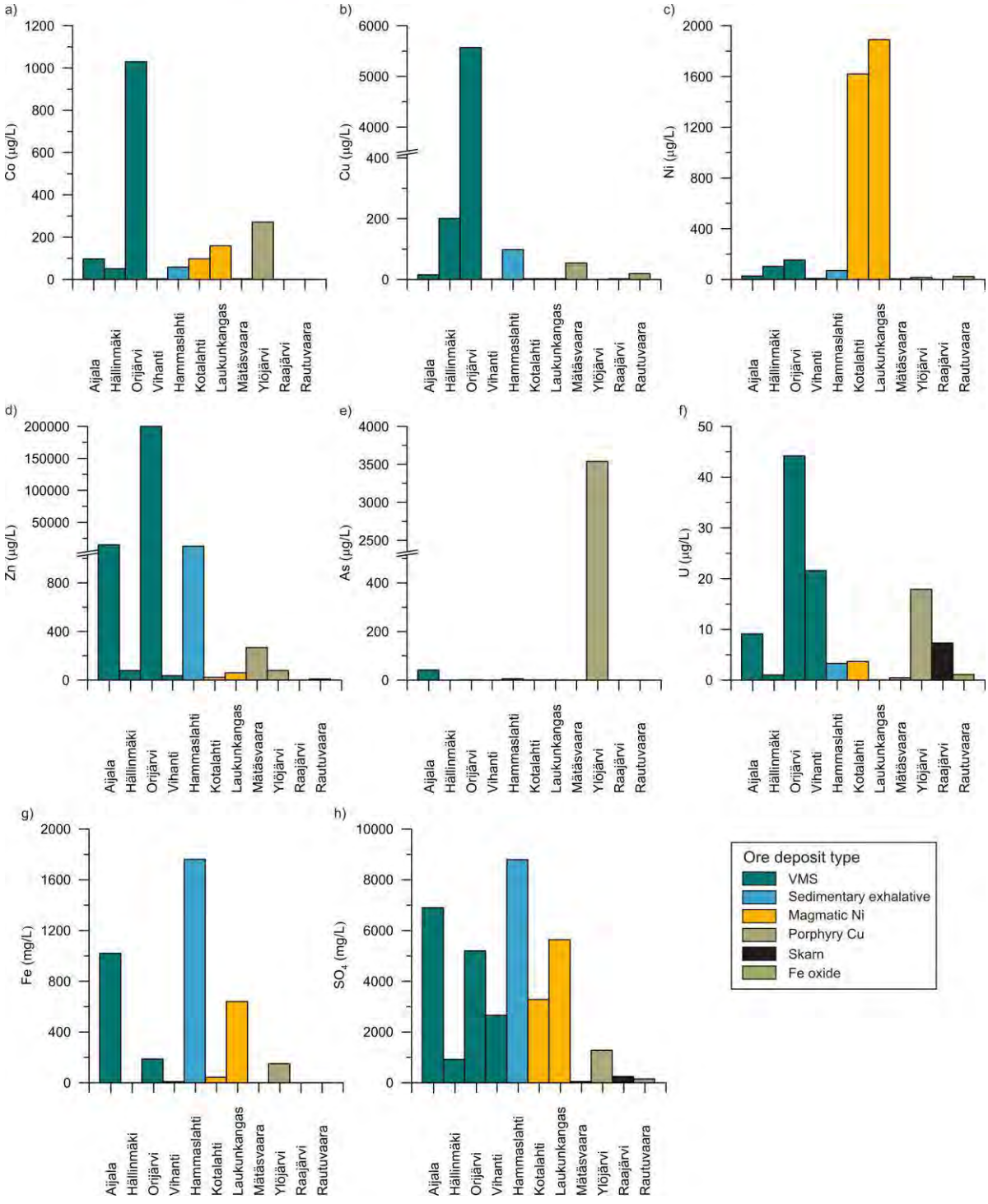

Figure 4 Concentrations of a) Co, b) Cu, c) Ni, d) Zn, e) As, f) U, g) Fe and h) SO_4 in the tailings seepage waters

The influence of the weathering period of the tailings on the drainage trace metal content was especially well seen in the seepage quality of the Orijärvi and Aijala sites. At these sites, the highest metal contents were measured and the time period after the cessation of tailings disposal was the

longest (> 40 years, Table 1). In particular, seepage waters of the Orijärvi tailings showed high concentrations of Cu, Co, Zn and U (Figure 4). High metal loadings at Orijärvi can also be related to the undeveloped processing methods of the ore leaving notable amounts of valuable metals in the tailings, since the mine operated in the early 20th century (Table 1).

Influence of the tailings covers

Covering of the tailings facility appeared to be a less important factor than the deposit type in controlling the seepage quality. Hammaslahti and Laukunkangas tailings facilities were covered in the 1990's and 2000's with less than a half a meter thick layer of till and Vihanti tailings with a 5 cm layer of peat. Despite this, the tailings facilities of the Hammaslahti and Laukunkangas generated seepages with some of the highest metal contents and lowest pH values (Figure 2). The applied cover structures were only thin soil covers that are not regarded as sufficient to prevent infiltration of rainwater into the tailings and to prevent the oxidation of sulfide minerals in the tailings (INAP 2009). Presumably the primary aim of the covers has been to prevent the dusting and to promote the spreading of vegetation. In addition, the covering of the tailings was made only after some years from the cessation of the tailings disposal. The delay in the covering of sulfide tailings contributes to the onset of sulfide oxidation and AMD production in tailings (*e.g.* Heikkinen 2009).

CONCLUSION

The tailings seepage water data collected from eleven closed mine sites in Finland, representing six different genetic ore types, showed that the ore type can be a starting point for the prediction of the future drainage quality of the tailings at new mine sites. Data indicated that especially tailings from processing of volcanogenic massive sulfide Cu deposits and sedimentary exhalative Cu deposits are susceptible to produce high-metal (*e.g.* Cu, Zn), high-acid drainage waters containing also high SO_4 and Fe concentrations. In addition, tailings effluents of certain types of magmatic Ni deposit may also be highly acidic with high metal (particularly Ni), SO_4 and Fe contents, whereas the Fe deposits seemed to be the least problematic concerning the tailings water quality. Tailings seepages from porphyry deposits may contain high levels of As, U and Co.

Covering of the tailings had little or no effect on the quality of the tailings seepage waters, because of the delay in the covering and too thin cover layers. The covers were made in the 1990's and in 2000's and apparently the primary aim was then to prevent dusting and promote the spreading of vegetation.

These types of data are valuable in defining the requirements for water treatment and tailings disposal at new mine sites. However, a larger data set and more detailed descriptions of the ore types are needed to better define the relationship between the seepage quality and the ore type. In a future study, the data set will be enhanced by collecting tailings seepage water data also from operating mine sites in Finland.

ACKNOWLEDGEMENTS

Authors are grateful to the Geological Survey of Finland for the funding of the sampling campaign and the analysis of the seepage waters.

REFERENCES

Cravotta, CA III (2008) Dissolved metals and associated constituents in abandoned coal-mine discharges, Pennsylvania, USA, Part 1: Constituents quantities and correlations, Applied Geochemistry 23:166–202.

Cravotta, CA III, Brady, KBC, Rose, AW, Douds, JB (1999) Frequency Distribution of the pH of Coal-Mine Drainage in Pennsylvania, In: Morganwalp, DW, Buxton, H (Eds) U.S. Geological Survey Toxic Substances Hydrology Program. Proceedings of the Technical Meeting, Charleston South Carolina, March 8-12, 1999, Volume 1 of 3, Contamination from Hard-Rock Mining, U.S. Geological Survey Water-Resources Investigation Report 99-4018A:313–324.

Eilu, P, Ahtola, T, Äikäs, O, Halkoaho, T, Heikura, P, Hulkki, H, Iljina, M, Juopperi, H, Karinen, T, Kärkkäinen, N, Konnunaho, J, Kontinen, A, Kontoniemi, O, Korkiakoski, E, Korsakova, M, Kuivasaari, T, Kyläkoski, M, Makkonen, H, Niiranen, T, Nikander, J, Nykänen, V, Perdahl, J-A, Pohjolainen, E, Räsänen, J, Sorjonen-Ward, P, Tiainen, M, Tontti, M, Torppa, A & Västi, K (2012) Metallogenic areas in Finland, Geological Survey of Finland, Special Paper 53, pp. 207–342, 90 figures and 43 tables.

Grundström, L (1985) The Laukunkangas nickel-copper deposit In: Papunen, H & Gorbunov, GI (Eds) Nickel-copper deposits of the Baltic Shield and Scandinavian Caledonides, Geological Survey of Finland, Bulletin 333, pp. 240–256.

Heikkinen, PM (2009) Active sulphide mine tailings impoundments as source of contaminated drainage: controlling factors, methods of characterization and geochemical constraints for mitigation, Geological Survey of Finland, Espoo, 38 p.

Heikkinen, PM, Räisänen, ML, Johnson, RH (2009) Geochemical characterization of seepage and drainage water quality from two sulphide mine tailings impoundments: Acid mine drainage vs. neutral mine drainage, Mine Water and the Environment 28:30–49.

INAP (2009) The GARDGuide. The Global Acid Rock Drainage Guide. The International Network for Acid Prevention (INAP), http://www.gardguide.com/.

Lapakko, KA (2003) Developments in humidity-cell tests and their applications, In: Jambor, JL, Blowes, DW, Ritchie, AIM (Eds) Environmental aspects of mine wastes, Mineralogical Association of Canada, Short Course Series, Vol. 31, pp.147–163.

Pettit, CM, Scharer, JM, Chambers, DB, Halbert, BE, Kirkaldy, JL, Bolduc, L (1999) Neutral mine drainage, In: Goldsack, DE, Belzile, N, Yearwood, P, Hall, GJ (Eds) Mining and the environment II, Conference proceedings, Sudbury '99, Volume 3, pp. 829–838.

Plumlee, GS, Smith, KS, Montour, MR, Ficklin, WH, Mosier, EL (1999) Geologic Controls on the Composition of Natural Waters and Mine Waters Draining Diverse Mineral-Deposit Types, In: Filipek, LH, Plumlee, GS (Eds) The Environmental Geochemistry of Mineral Deposits, Part B: Case Studies and Research Topics, Reviews in Economic Geology, Vol. 6B, pp. 373–432.

Puustinen, K (2003) Suomen kaivosteollisuus ja mineraalisten raaka-aineiden tuotanto vuosina 1530–2001, historiallinen katsaus erityisesti tuotantolukujen valossa, Geologian tutkimuskeskus, arkistoraportti, M 10.1/2003/3, 578 p, http://weppi.gtk.fi/aineistot/kaivosteollisuus/.

Rousseau, PDS (2012) A critical review of static geochemical test methods applied to mining wastes, including their applicability to field conditions, In: McCullough, CD, Lund, MA, Wyse, L (Eds) International Mine Water Association Symposium, Bunbury Australia 2012, ISBN 978-0-7298-0707-4, pp. 499–504.

Räisänen, ML, Tornivaara, A, Haavisto, T, Niskala, K, Silvola, M (2013) Suljettujen ja hylättyjen kaivosten kaivannaisjätealueiden kartoitus, Ympäristöministeriön raportteja 24, Summary: Inventory of closed and abandoned extractive waste facilities, Reports of the Ministry and the Environment 24/2013, 45 p. http://www.ym.fi/download/noname/%7BC66A2100-E323-4ADD-A630-5239E6F49A1E%7D/75982.

Sapsford, DJ, Bowell, RJ, Dey, M, Williams, KP (2008) Humidity cell tests for the prediction of acid rock drainage, Minerals Engineering 22:25–36.

Seal, RR, II, Hammaström, JM (2003) Geoenvironmental models of mineral deposits: Examples from massive sulfide and gold deposits, In: Jambor, JL, Blowes, DW, Ritchie, AIM (Eds) Environmental Aspects of mine wastes, Mineralogical Association of Canada, Short Course Series, vol. 31, pp. 11–50.

Younger, PL (1995) Hydrogeochemistry of minewaters flowing from abandoned coal workings in County Durham, Quarterly Journal of Engineering Geology 28:S101–S113.

Challenges in Prediction of Acid Rock Drainage Potential for Skarns – Use of Modified Testing

Felipe Vasquez[1], Jacob Waples[1] and Javier Condor[2]

1. *Golder Associates, USA*
2. *Compañía Minera Milpo S.A., Peru*

ABSTRACT

The Hilarion Mining Project, located in the Peruvian Andes, is anticipating the use of thickened tailings as disposal method for the projected QuenhuaRagra tailings storage facility. A comprehensive geochemical program of tailings samples was performed to characterize them in terms of acid mine drainage (AMD) and metal leaching potentials. Two samples representative of the Zn-Ag-Pb polymetallic skarn-type deposit were used.

Skarn deposits typically pose a challenge for traditional kinetic testing programs. High neutralization potential and high sulfur contents can lead to extended testing times, as the high content of each extends the depletion times. This makes it difficult to evaluate uncertain materials or potential lag times. In this case mineralogical results indicated the presence of high concentrations of neutralization minerals and high concentrations of acid generation minerals. Acid base accounting tests confirmed high neutralization potential, together with a high acidic potential.

Humidity cell tests (HCT) were performed to confirm static test results and to determine lag time for the onset of acidic conditions. After a first stage of testing (89 and 54 cycles), the results reported circum-neutral pH conditions and low release of sulfate and metal concentrations. This result combined with depletion calculations predicting acid generation, the static tests results, and uncertainties from the net acid generating test made the AMD potential classification a challenge.

To better understand the skarn tailings geochemistry, hydrogen peroxide was used as lixiviant for the HCTs in a second stage of the testing. After a decrease in pH, both samples returned to their previous pH values; however, sulfate and metal release did react to the change. After 21 and 18 HCT cycles with hydrogen peroxide, acidic conditions were not reached.

Accelerated kinetic test provided useful information for waste management. While acidic conditions are doubtful, oxidation of sulfides will produce release of metals and sulfate.

Keywords: skarns, extended lag time, hydrogen peroxide

INTRODUCTION

The geologic characteristics of mineral deposits exert important controls on the natural environmental signatures that could result from mining and mineral processing. A good understanding of the environmental geology of mineral deposits is therefore crucial to the development of effective mining-environmental prediction, mitigation, and remediation practices (Plumlee 1999).

Skarns are coarse-grained metamorphic rocks formed when magmatic-hydrothermal fluids are expelled from the magmas and react chemically with sedimentary rocks. The skarn alteration frequently introduces calc-silicate minerals replacing carbonate-bearing rocks. The skarn ores may include massive sulfide lenses and veins occurring within and/or replacing the sedimentary host rocks (Plumlee *et al.* 1999). This type of replacement increases the acid generation capacity by increasing the content of acid-generating sulfides in rocks and may decrease the acid-neutralizing capacity by removing carbonate minerals (Plumlee 1999). However, the original host rocks frequently still retain a high carbonate content. This results in geoenvironmental model signatures of circum-neutral pH values, and low metal concentrations with a few exceptions, including copper and zinc (Plumlee *et al.* 1999).

Evaluation of a material with high contents of sulfides and high carbonate content poses a challenge for the geochemical characterization programs and the determination of the acid generation potential because an extended kinetic testing time may be required to deplete one or the other, even in an accelerated test. The long lag times to acid generating conditions or to depletion of the neutralization potential are impractical compared to other aspects of mine planning and permitting and do not allow useful decisions to be made during the design process.

The Hilarion project in Peru is a Zn-Ag-Pb skarn-type deposit hosted in a contact zone of the calcareous sedimentary sequence of the Chulec-Pariatambo-Pariahuanca Formations (early Cretaceous) and an acidic intrusive stock (likely Tertiary). The calcareous sedimentary sequence ranges from predominantly claystone in the Pariatambo formation to limestones in the Chulec formation. The intrusive rocks present in the zone are a potential source of mineralization and are characterized as dioritic, feldspar porphyry, quartz monzonitic porphyry, and granodioritic types, affected by hydrothermal alteration mainly of the kaolinite and sericite into plagioclase and chloritic in amphiboles.

Compania Minera Milpo S.A.A. (Milpo) is currently developing the Hilarion project, which is located in the Peruvian Andes at an altitude varying between 4,500 and 5,200 meters above sea level, approximately 230 kilometers north of Lima and 80 kilometers southeast of the city of Huaraz. Milpo is considering the use of thickened tailings as a disposal method in the planned tailings storage facility (TSF).

As part of the permitting efforts, Milpo and Golder developed a geochemical characterization program to assess the acid generation and metal leaching potential of tailings samples representative of the polymetallic skarn-type deposit present at the Hilarion project following standard phased geochemical programs, including static and kinetic testing. However, given the

difficulties and extended time required to evaluate materials with high carbonate and high sulfide contents, the latter was modified through the addition of an oxidizing agent for further evaluation of the materials.

This case study provides an overview of the geochemical characterization program and its results, including the challenges presented by the nature of the material investigated and the modifications applied to a standard kinetic test to better understand the geochemical behavior of the Hilarion tailings samples.

METHODOLOGY

Tailing samples from pilot scale metallurgical work were tested as a part of the geochemical characterization program. The samples represented tailings from the ore material, following all metallurgical processes, that will be mined from the skarn deposit and that are expected to be deposited in a valley fill tailings storage facility (TSF). This study evaluated the expected environmental behavior of the tailings in the TSF, after metallurgical leaching processes. The study was designed to provide information for future waste management and water management strategies for the TSF, including water management strategies for runoff water and seepage, water management strategies for the tailings pond, water balance, and recirculation requirements, and whether and when treatment might be required.

Three tailings samples were evaluated. For sample 1 and sample 2, a complete geochemical testing program, including static and kinetic testing by humidity cells, was performed following standard guidance (*e.g.*, INAP 2009, MEND 2009). The geochemical testing program for these samples is summarized in Table 1. As part of confirmatory efforts during the static testing phase, an additional sample (sample 3), was sent to the lab to perform confirmatory analyses with respect to mineralogy and with respect to oxidation potential of the sulfides (i.e., the sequential net acid generation procedure).

The focus of this study was to better understand the geochemical behavior of the samples in the long term; as such, a second phase of kinetic testing was undertaken for samples 1 and 2. This second phase of testing was a modified kinetic test as described below. Given the interest in the long-term behavior, this paper focuses on the kinetic test results; however, the results of the static testing phase are also summarized to provide the context for the interpretation of the kinetic test results.

Table 1. Summary of complete geochemical testing program

Program	Analysis	Sample 1	Sample 2	Sample 3
Static	Elemental content by acid digestion	X		
	Acid base accounting	X	X	
	Net acid generation	X	X	
	Net acid generation test effluent analysis	X	X	
	Short term leaching procedure	X	X	
	Sequential net acid generation test			X
	X-ray diffraction with Rietveld refinement	X	X	X
	Acid base accounting after humidity cell test	X	X	
Kinetic	Humidity cell test	X	X	
	Modified humidity cell tests	X	X	

The humidity cell test (HCT) method (based on ASTM 2007) was used as the kinetic test in this project. The ASTM HCT, a cyclic kinetic test, was selected primarily given its common use and regulatory acceptability. For the modified kinetic testing, the original HCTs were continued into a second phase of testing with a modified procedure. In this phase, the lixiviant was changed from deionized water to hydrogen peroxide. The second phase of testing was initiated at cycles 89 and 54 for samples 1 and 2, respectively. After the lixiviant change, the modified HCTs were continued for additional 21 and 18 cycles (to 110 and 72 cycles, respectively).

Hydrogen peroxide is commonly used as a part of the net acid generation (NAG) test developed by AMIRA (AMIRA 2002) and is intended to accelerate oxidation of sulfides and challenge the neutralization potential present in the sample. The objective of using hydrogen peroxide in this case was to attempt to reach acidic conditions predicted by the static test results and depletion calculations.

After kinetic tests were terminated acid base accounting (ABA) testing was performed on the sample remaining in the humidity cells to confirm the depletion calculations based on the HCT results and to evaluate changes to the original acid generation potential classification following kinetic testing.

Laboratory testing, with the exception of the mineralogical analysis, was performed by a commercial laboratory in Lima, Peru. The laboratory has its own quality control, and quality

assurance program and experience performing ASTM HCT method. The mineralogical analysis was performed by the University of British Columbia, Vancouver, Canada.

RESULTS

Static tests results summary.

Mineralogical results for the three samples are presented in Table 2. The results of the XRD were consistent with the general understanding of the site geology, with a polymetallic skarn type mineralization of Zn-Ag-Pb. A high concentration of calcite was determined with a range between 8.1 and 10.4% by weight. Sulfide presence was highly dominated by pyrrhotite (15.8 to 18.0% by weight), followed by lower concentrations of pyrite and sphalerite.

Results of the static testing program indicated inconsistent results for sample 01. This sample is considered to have the potential for acid generation based on standard ABA calculations (both net neutralizing potential ratio (NPR) and net neutralization potential (NNP) calculations). While the neutralization potential (NP) of the sample was high (156 kg CaCO3/t, consistent with the 10 % by weight calcite content), this sample has a high acid potential (227.5 kg $CaCO_3$/t) consistent with an elevated sulfide content (20.3% by weight sulfides, including 17.7 % by weight pyrrhotite and 1.9% by weight pyrite). In contrast, the net acid generation (NAG) test did not confirm this classification for sample 1, reporting neutral pH values after the procedure. However, the NAG test is subject to complications for samples with high sulfide contents; insufficient hydrogen peroxide may have been added to oxidize all of the sulfides present.

Results of the static testing program indicated that sample 02 is considered to have an uncertain potential for acid generation based on the NPR result (i.e., 1.8), while the NAG result reported a circum-neutral pH value. This uncertain classification is again due to the high NP (207 kg CaCO3/t, consistent with the 10.4 % by weight calcite content), this sample has a high acid potential (115 kg CaCO3/t) consistent with an elevated sulfide content determined by mineralogical analysis (18.4% by weight sulfides, including 15.8 % by weight pyrrhotite and 1.6 % by weight pyrite).

Due to the inconsistency between the NAG test and the ABA results, a sequential NAG test (AMIRA 2002) was performed over a confirmatory sample (sample 3). A three step sequential NAG test was performed over the sample. The results after the three cycles reported a pH of 2.3 and elevated metal concentrations. This test confirmed that the one step NAG test performed over the original samples was inadequate to completely oxidize all the sulfide material present and confirmed the acid generating potential of the tailings samples.

Table 2. Tailings samples mineralogical test results (% by weight)

Minerals	Formula	RE-HI10-01	RE-HI10-02	RE-HI10-04
Quartz	SiO_2	5,8	6,5	6,0
Clinochlore	$(Mg,Fe^{2+})_5Al\ (Si_3Al)O_{10}(OH)_8$	3,4	4,4	3,1
Muscovite	$KAl_2AlSi_3O_{10}(OH)_2$	1,9	--	--
Biotite	$K(Mg,Fe)_3(AlSi_3O_{10})(OH)_2$	--	0,8	--
Actinolite	$Ca_2(Mg,Fe)_5Si_8O_{22}(OH)_2$	--	--	1,0
K-Feldspar	$KAlSi_3O_8$	18,5	20,5	14,8
Andradite	$Ca_3Fe_2^{3+}(SiO_4)_3$	--	--	4.1
Calcite	$CaCO_3$	10	10,4	8,1
Siderite	$FeCO_3$	0,7	0,4	0,3
Clinozoisite	$Ca_2Al_3(SiO_4)_3(OH)$	6,6	6,4	5,8
Diopside	$CaMgSi_2O_6$	12	14,2	11,7
Grossular	$Ca_3Al_2Si_3O_{12}$	20,9	17,7	22,5
Sphalerite	(Zn,Fe)S	0,7	1,0	1,6
Pyrrhotite	$Fe_{1-x}S$	17,7	15,8	18,0
Pyrite	FeS_2	1,9	1,6	3,1
Ilmenite	$FeTiO_3$	--	0,4	--
Total		100	100	100

Kinetic test results

The objectives of the kinetic test were to:

- Address the uncertainties provided by the initial static test results,
- Evaluate potential lag times to acidic conditions, and
- Evaluate the geochemical behavior of the tailings samples under acidic conditions.

The results of the HCTs would then be used in predictions of water quality and tailings behavior in the TSF during operation and after closure to assist with TSF design.

Tailings samples 1 and 2 had a first phase of the kinetic testing program in HCTs based on the standard ASTM method. However, following 89 and 54 cycles for sample 01 and 02, respectively, the HCTs had maintained neutral conditions, with pH values between 7.3 and 7.6. Metals concentrations were generally low with the exception of manganese, which is mobile at these pH values. The manganese concentrations by cycles 89 and 54 reported values between 0.28 and 1.5 mg/l.

A preliminary evaluation of the results was performed midway through the first phase of testing. Based on the ABA results, sequential NAG testing, and the high concentration of sulfide minerals, it was expected that the tests would result in acidic conditions, at least for sample 01 by this time of the HCT procedure. Additionally, forward-looking depletion calculations also indicated eventual acidic conditions. However the preliminary evaluation demonstrated that leachate from both samples reported circum-neutral pH values, a sulfate concentration around 100 mg/l, and low metal concentrations. These results indicate that not only were acidic conditions not attained, but also significant oxidation was not occurring.

At this point, it was decided to modify the HCT procedure expecting to accelerate the oxidative processes in one of the samples. Starting in cycle 54, the lixiviant for sample 02 was changed from deionized water to hydrogen peroxide, capable of accelerate the sulfides oxidation rates. Sample 02 was under this lixiviation scheme until cycle 72, when the test was terminated.

The sample 01 continued to be leached using the standard procedure for comparison until cycle 89. Based on the results reported up to that cycle, it was decided to also modify this cell and start using hydrogen peroxide as the lixiviant. The sample 01 HCT was tested until cycle 110 with hydrogen peroxide.

The results after 110 and 72 cycles (including 21 and 18 cycles using hydrogen peroxide) for samples 01 and 02, respectively, can be summarized as follow:

- Acidic conditions were not generated in any of the cells, even after the use of hydrogen peroxide as the lixiviant. The pH values for both samples ranged between 6.1 and 8.3 (Figure 1).
- After the first addition of hydrogen peroxide, pH value for sample 02 reported a decrease from 7.6 down to 6.6, but returning to pH values pre-hydrogen peroxide after 5 cycles.
- Sample 01 did not report significant changes in its leachate pH value after the change to hydrogen peroxide, keeping leachate pH values between 7.3 and 8.0 until the end of the test.
- While both samples were lixiviated using deionized water sulfate and metal concentrations remained low, reporting stable or decreasing trends.
- The addition of hydrogen peroxide in both cells resulted in a significant increase in sulfate concentrations. Both samples reported a one order of magnitude increase immediately after the first hydrogen peroxide cycle. The increase of sulfate concentration remained stable in cell 02 until terminated; while cell 01 reported a decrease in sulfate concentration after ten cycles using hydrogen peroxide, but still elevated compared to the concentrations reported when using deionized water (Figure 2).
- Metals concentration also reacted to the change in lixiviant. In both cells, similar parameters reacted to the addition of the strong oxidant. In most of the cases the increases in concentration

were above one order of magnitude. The parameters that reported increases in concentration for both samples included: barium, calcium, cadmium, cobalt, chromium, copper, magnesium, manganese, molybdenum, nickel, lead, selenium, silica, strontium, and zinc. For example, Figures 3 and 4 present the results for copper and zinc, respectively.

- After the initial peak in concentrations following the change to hydrogen peroxide, most of the parameters reported decreasing concentrations; however none of them returned to the concentrations exhibited before the change in lixiviant. Only magnesium remained stable or reporting increasing trends until the cells were terminated.

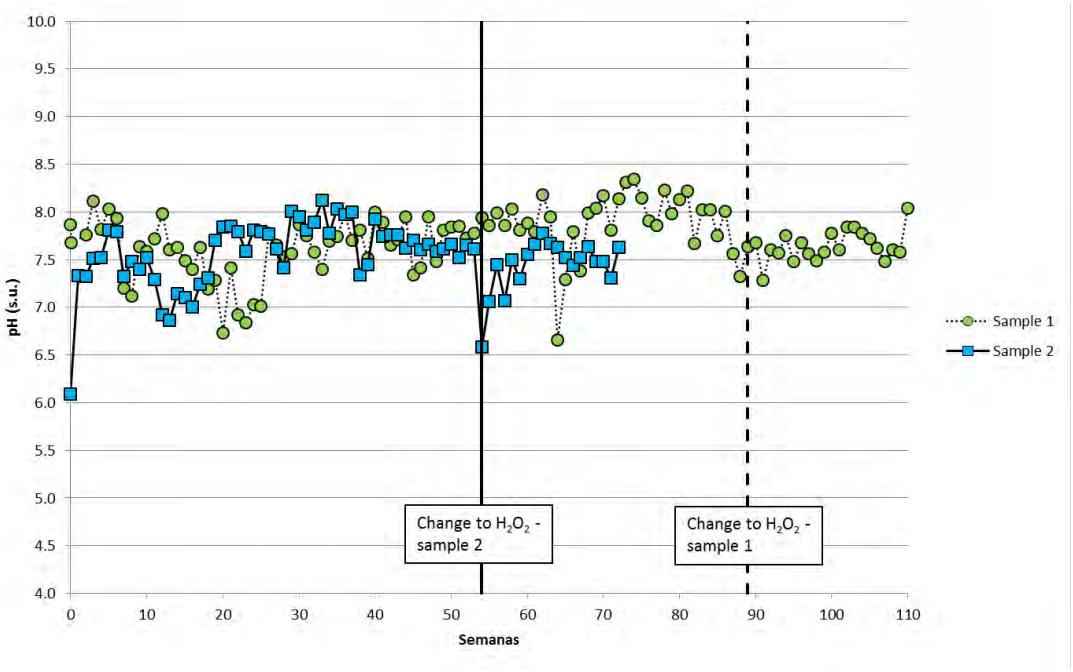

Figure 1. Kinetic test results – pH values

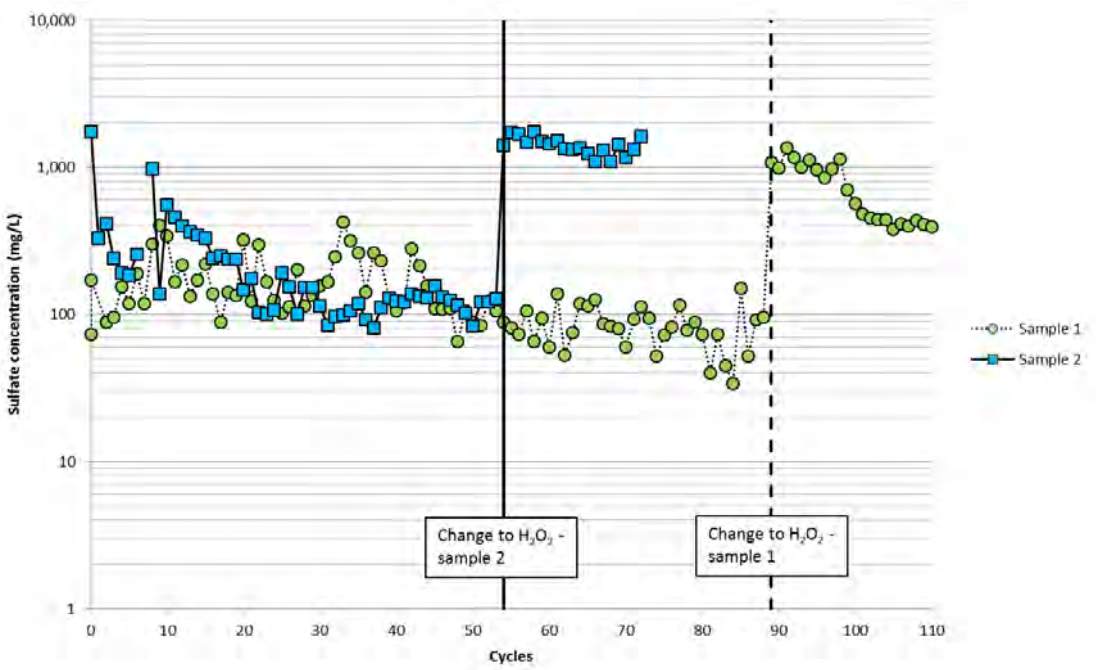

Figure 2. Kinetic test results – Sulfate concentrations

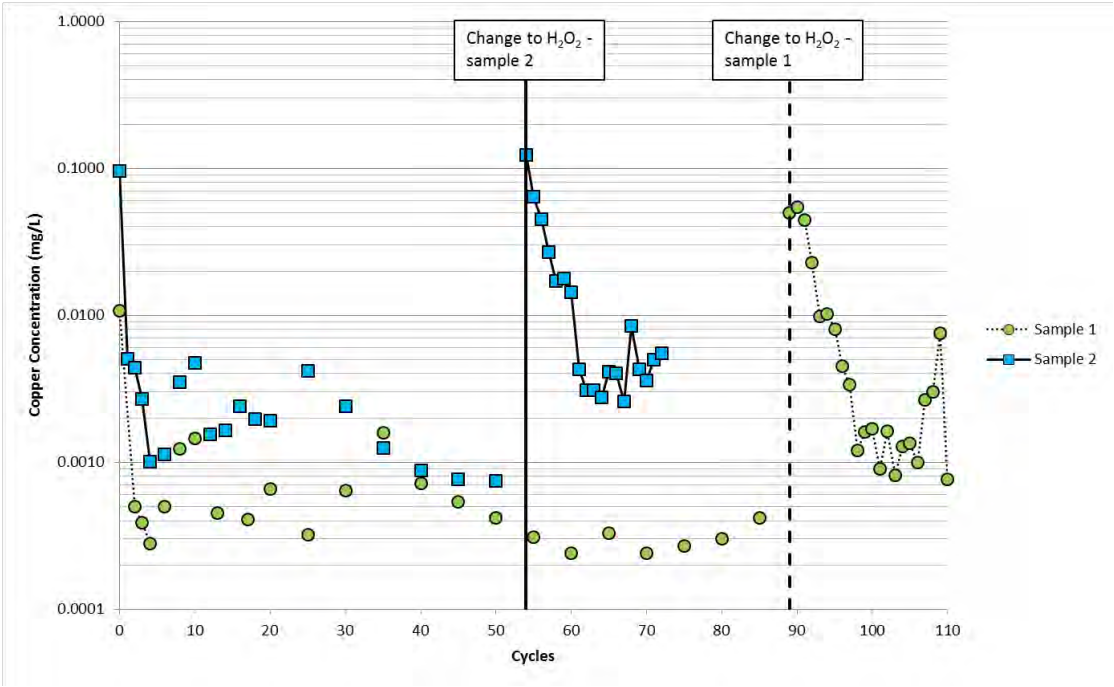

Figure 3. Kinetic test results – Copper concentrations

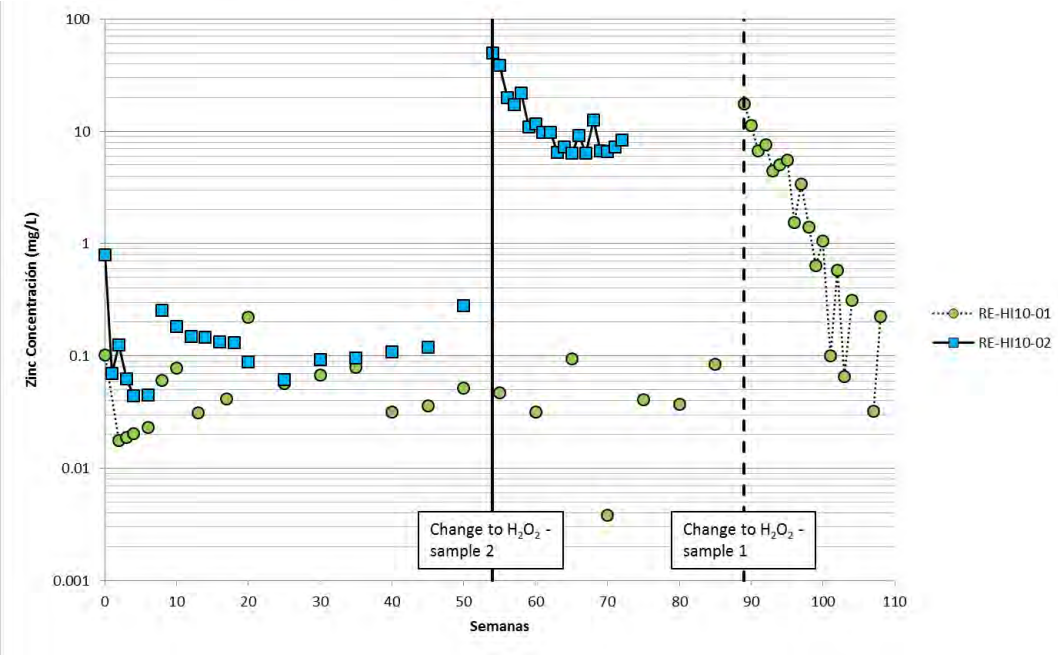

Figure 4. Kinetic test results – Zinc concentrations

DISCUSSIONS AND CONCLUSIONS

Skarn deposits pose a challenge for geochemical characterization programs. Excessive contents of carbonates and sulfides can lead to unreasonably long depletion times even in accelerated kinetic tests, resulting in uncertainty in the final acid generation behavior of waste materials.

Pilot plant tailings samples associated with the Hilarion project had high sulfide content (18.4 to 20.3 % by weight, primarily as pyrrhotite) and high carbonate content (10 to 10.4 % by weight calcite). Static ABA and sequential NAG testing resulted in predictions of potentially acid generating to uncertain. In this type of scenarios, humidity cell tests are performed to confirm the expected behavior in the future, after oxidizing conditions are applied to the samples. Humidity cell tests are used for a number of reasons, including confirmation the acid generation potential and the release rates of metals. Unfortunately, humidity cell test duration is not definitive and will depend on the results obtained, which at the same time are dependent in the type of materials studied.

Up to 88 and 54 cycles of kinetic testing by standard humidity cells did not resolve the potential uncertainty based on the ABA results. Additionally, depletion calculations indicated that exceptionally extended testing times (up to 15 years) would have been required to resolve this issue. While it was expected that the humidity cells would reach acidic conditions, the preliminary results of the kinetic test, under standard conditions, did not provide consistency with the static test results. The change of lixiviant from deionized water to hydrogen peroxide, a strong oxidant, was

performed to accelerate the oxidation of sulfide minerals present in the samples and to reach acidic conditions.

The second stage of modified humidity cell testing provided useful information for mine design, operational planning, and closure planning. The second stage of humidity cell testing involved the use of an oxidant (hydrogen peroxide, as in the NAG test) as a lixiviant of up to 21 cycles of testing. Even after 21 and 18 cycles of leaching with the oxidant for samples 1 and 2, respectively, acidic conditions were not achieved, contrary to predictions of potentially acid generation behavior based on the ABA testing and with concentration of sulfides of up to 20.3%. However, sulfide oxidation was achieved by using the oxidant as a leachate, as shown by increases in the sulfate and metals concentrations in the leachate. Oxidation, based on sulfate generation, was greatest immediately following addition of the oxidant, and remained elevated for up to 18 cycles. For sample 1, sulfide oxidation decreased 10 cycles after the initiation of the oxidant lixiviant; however, the oxidation rates from this point through the final 110 cycles of testing (again based on sulfate release) were still elevated (4 to 5 times higher) relative to initial test conditions, indicating oxidation was still occurring despite the decrease. Even under these scenarios, available NP was sufficient to prevent development of acidic conditions.

While oxidation was occurring in the second stage of kinetic testing, significant metals and sulfate release was also observed. Increases in metals and metalloids concentrations, including Ba, Cd, Co, Cr, Cu, Mn, Mo, Ni, Pb, Se, Sr, and Zn, were observed in the second stage of kinetic testing. It is expected these metals were released by sulfide oxidation and/or micro, localized acidic zones (even if the overall tests did not result in acidic conditions). Concentrations of Cd, Mn, Mo, SO_4, Se, and Zn, several of which are expected to be mobile even at low pH values, were elevated sufficiently to pose a risk to exceeding applicable regulatory standards based on water quality modeling for the TSF. As such, design for the TSF needed to consider potential water treatment if sulfide oxidation occurs. However, a lag time to sulfide oxidation is expected based on the first stage of kinetic testing and given that the climate and design of the TSF will keep the tailings saturated, at least through operations.

While the kinetic testing may not have definitively resolved discrepancies with respect to AMD and the static testing, the expected release of metals under neutral conditions once sulfide oxidation is initiated is significant for mine, operation, and closure planning. As such, use of this modified test to further accelerate weathering reactions provided useful information with respect to the overall expected tailings behavior.

REFERENCES

AMIRA. International Ltd. (2002)ARD Test Handbook – Prediction and kinetic control of acid mine drainage, environmental geochemistry international Pty. Ltd. and Ian Wark Institute, University of South Australia.

ASTM (2007). Standard test method for laboratory weathering of solid materials using a humidity cell, D 5744-07, The American Society of Testing and Materials ASTM International, West Conshohocken, Pennsylvania.

INAP (2009). Global Acid Rock Drainage Guide (GARD Guide),The International Network for Acid Prevention, http://www.gardguide.com.

MEND (2009). Prediction manual for drainage chemistry from sulphidic materials, MEND Report 1.20.1.

Plumlee, G.S. (1999). The environmental geology of mineral deposits, in ed. Filipek, L.H., and Plumlee, G.S. The Environmental Geochemistry of Mining Deposits: pp. 71–116.

Plumlee, G.S., Smith, K.S., Montour, M.R., Ficklin, W.H., and Mosier, E.L. (1999) Geologic controls on the composition of natural waters and mine waters draining diverse mineral-deposit types, in ed. Filipek, L.H., and Plumlee, G.S. The Environmental Geochemistry of Mining Deposits: pp. 373–432.

Smith, K.S., and Huyck, L.O. (1999). An overview of the abundance, relative mobility, bioavailability, and human toxicity of metals, in ed. Filipek, L.H., and Plumlee, G.S. The Environmental Geochemistry of Mining Deposits: pp. 29–70.

10th ICARD IMWA 2015 | 10th International Conference on Acid Rock Drainage & IMWA Annual Conference

Geochemical Characteristics of Oil Sand Tailings and Bitumen Upgrading By-Products, Alberta, Canada

Bronwen Forsyth[1], Stephen Day[1] and Oladipo Omotoso[2]

1. *SRK Consulting, Canada*
2. *Suncor Energy Inc, Canada*

ABSTRACT

Few studies have characterized the metal leaching and acid rock drainage (ML/ARD) potential of tailings from oil sand production, and associated by-products from bitumen upgrading. In order to address this gap, Suncor Energy Inc. undertook sampling to characterize their various tailings and by-products using ML/ARD characterization methodologies typically applied to coal and metal mine wastes. Tailings types characterized were mature fine tailings (MFT), dried mature fine tailings (DMFT), and froth treatment tailings (FTT). Bitumen upgrading by-products characterized were coke and coke ash. Methods used included conventional acid-base accounting, net acid generation testing, X-ray diffraction, and humidity-cell testing.

The characteristics of MFT, DMFT, and FTT reflected the mineralogy of the McMurray Formation, which includes pyrite, siderite, ankerite, and various clay minerals. In contrast, the characteristics of coke are carried over from the bitumen though pyrite is not destroyed because cokers operate under reducing conditions. Coke ash is mostly composed of amorphous aluminosilicate melts, and contains readily leachable concentrations of nickel and vanadium. The application of standard ML/ARD characterization methods to oil sands is complicated by the presence of residual bitumen, which makes tailings hydrophobic and rich in organic carbon.

Keywords: oil sands, metal leaching, acid rock drainage

INTRODUCTION

Tailings management remains one of the most difficult environmental challenges for the oil sands mining sector with over 77 square kilometers of oil sands tailings ponds in Alberta (Alberta Government, 2013). Government regulations introduced in 2009 (Directive 074) require operators to dewater the tailings ponds for reclamation purposes, and to reuse the water for production. In response, recent studies have focused on developing methods to reduce water within the ponds (COSIA, 2014a; Wang *et al.*, 2014). Few studies have characterized the metal leaching and acid rock drainage (ML/ARD) potential of tailings from oil sand production, and associated by-products from bitumen upgrading, or assessed the ML/ARD implications of dewatering the saturated tailings (Kuznetsov *et al.*, 2015). Furthermore, guidance on addressing ML/ARD potential is not available within best practice guidelines for oil sands tailings management (COSIA, 2012 and 2014b). In order to address this gap, Suncor undertook sampling to characterize the ML/ARD potential of their various tailings and bitumen upgrading by-products using existing methodologies typically applied to coal and metal mine wastes.

Suncor extracts bitumen from oil sands in the Lower Cretaceous McMurray Formation of northern Alberta, Canada, which are mainly deposits of fine-grained quartzitic bituminous sands and sandstones (Flach, 1984). Bitumen is extracted from crushed oil sand ore through a process of gravity separation and flotation. The process yields bitumen, bitumen froth, fluid tailings, and coarse sand tailings. The bitumen froth contains some fine minerals and oleophilic heavy minerals (including pyrite), and is mixed with naphtha to allow further separation of bitumen from residual water and minerals in centrifuges and inclined plate settlers. The residual water and minerals in the froth stream constitute the bulk of *froth treatment tailings* (FTT). FTT is a small percentage of the tailings produced during bitumen extraction and is handled separately from the rest of the tailings stream. Fluid tailings from the primary flotation circuit are further processed in secondary flotation circuits to remove residual bitumen. Fine tailings from the flotation circuits are combined with coarse sand tailings, and transported to a sand placement area where the sand fraction deposits along shallow slopes, and the fines are transferred to a pond where they settle to form *mature fine tailings* (MFT). After a few years, MFT settles to a solids content of approximately 30 to 40 wt%. MFT are later removed from the pond, mixed with polymer and placed in thin lifts in a dedicated disposal area where they are dewatered and dried to become *dried MFT* (DMFT).

Extracted bitumen is upgraded to lighter hydrocarbon products through a process of reductive coking at approximately 450 °C. The resulting *coke* is disposed in coke pits, or utilized for heat generation and reclamation purposes. Combusted coke results in *coke ash*, which is transported to storage ponds as slurry. The ash is composed of approximately 20 % bottom and mid-ash and 80 % fly ash.

This paper details the geochemical characterization of the oil sand tailings (MFT, DMFT, and FTT) and bitumen upgrading by-products (coke and coke ash), discusses the application of standard ML/ARD characterization methodologies, and highlights some of the methodological limitations for practitioners to consider when interpreting the results.

METHODOLOGY

Sample Collection

Suncor collected 57 MFT, 12 DMFT, five FTT, eight coke, and three coke ash samples for geochemical and mineralogical analysis. MFT samples were collected from three depths at various pond locations using a suction dredge. DMFT samples were collected as grab samples directly from dedicated disposal areas. Two FTT samples were collected from the tailings line prior to discharge, and three were collected as deposited samples from 3, 5, and 20 m below the pond water line in order to capture any compositional differences as a result of tailings deposition. Coke was collected monthly as grab samples across an eight-month period. Coke ash sampling consisted of a bottom ash, fly ash, and a combined coke ash grab sample collected from an ash storage pond.

Sample Preparation and Analysis

Samples were prepared and analyzed by Maxxam Analytics in Calgary, Alberta, and Vancouver, British Columbia. Coke and coke ash samples were air-dried prior to analysis. Each tailings sample was split into two subsamples, with one fraction air-dried to remove the bulk of the water and volatile hydrocarbons, and the second fraction taken as-received for Dean Stark extraction to determine the bitumen, mineral, and water contents (Dean and Stark, 1920). The method uses hot toluene to extract hydrocarbons.

The air-dried coke and coke ash, and toluene-treated tailings were analyzed for major elements by X-ray fluorescence (XRF) spectroscopy, minor elements by four-acid digestion and inductively coupled plasma mass spectrometry (ICP-MS), and particle size by dry and wet sieving methods.

Acid-base accounting (ABA) was undertaken on coke, coke ash, and air-dried tailings. This included total sulfur (Leco), sulfur speciation (ASTM D2492-02), total carbon (Leco), total organic carbon (TOC) (Leco analysis on residue of hydrochloric acid leach), total inorganic carbon (TIC) (by difference), paste pH and electrical conductivity, and neutralization potential (Sobek *et al.*, 1978) with siderite correction (Skousen 1997).

Net acid generation (NAG) testing (EGi 2006) was undertaken on air-dried and toluene-treated tailings. The toluene-treated tailings were hydrophobic. Therefore, when the NAG reagents were first added to the samples, they were dispersed in an ultrasonic bath until streaming birefringence was observed signifying complete dispersion.

Humidity-cell tests (Price 2009) were undertaken on coke, coke ash, and air-dried tailings for a minimum duration of 20 weeks, with leachates analyzed for pH, conductivity, sulfate, acidity, alkalinity, hardness, and trace elements by ICP-MS.

Mineralogy by X-ray diffraction (XRD), with quantification by Rietveld Refinement was undertaken by the University of British Columbia on the toluene-treated tailings. Selected FTT, coke, and coke ash samples were analyzed by Laue X-ray diffraction (μ-XRD) by the Canadian Light Source Inc. at the University of Saskatchewan.

Quality Assurance

No quality issues were identified in the final data on the basis of satisfactory certified reference material recoveries, laboratory duplicates, and ion balances for leachate analyses. Analytical and data interpretation issues encountered as a result of sample hydrophobicity and organic matter content are discussed within the results.

RESULTS

Mineralogy

In MFT, DMFT, and FTT, major minerals (those greater than 10 wt%) were quartz, kaolinite, and mica. Minor minerals (1 to 10 wt%) were microcline, clinochlore, and albite. Trace minerals (those less than 1 wt%) were pyrite, siderite, calcite, ankerite, various titanium oxides, zircon, and tourmaline.

Coke was composed of refractory organic matter with no crystalline phases detected by μ-XRD. Coke ash was mostly composed of an amorphous aluminosilicate melt (69 % for bottom ash, 91 % for fly ash, 93% for combined coke ash) with crystalline phases consisting of silica (quartz and cristobalite), aluminosilicate (mullite), feldspars (microcline, and plagioclase), and titanium and aluminum oxides (pseudobrookite and hercynite, respectively). Gypsum and magnesite were also identified in the combined coke ash sample.

Acid Potential

The presence of pyrite in MFT, DMFT, and FTT indicated that it is likely to be the principal source of acidity. Total sulfur by Leco analysis was not a good measure of pyrite content due to significant sulfur concentrations being associated with the insoluble fraction (mostly organic) (Figure 1a). Sulfide determined by the ASTM D2492 method correlated well with mineralogical sulfide by XRD for DMFT and most MFT samples (Figure 1b), although the correlation was poor for FTT and three MFT samples that contained FTT. These samples were likely to have contained amorphous phases that resulted in an over-estimation of mineral sulfide by XRD due to normalization of reported mineral abundances to 100 %.

FTT had the highest sulfide content, ranging from 0.29 to 0.58 % as S. Elevated sulfide concentrations in MFT samples were associated with the presence of small amounts of FTT. Coke contained no detectable sulfide. Sulfur was inferred to be present as refractory carbonaceous matter. Coke ash contained the highest sulfate concentrations, which were present as gypsum on the basis of μ-XRD results. In fly ash, sulfate was likely to be present as iron and aluminum sulfates on the basis of contact water chemistry. Elemental sulfur was not detected but is expected based on the conditions under which the ash is formed.

Acid potential in the tailings is conventionally associated with oxidation of pyrite, whereas coke has negligible acid potential, and coke ash has acid potential associated with soluble acid sulfates and possibly elemental sulfur.

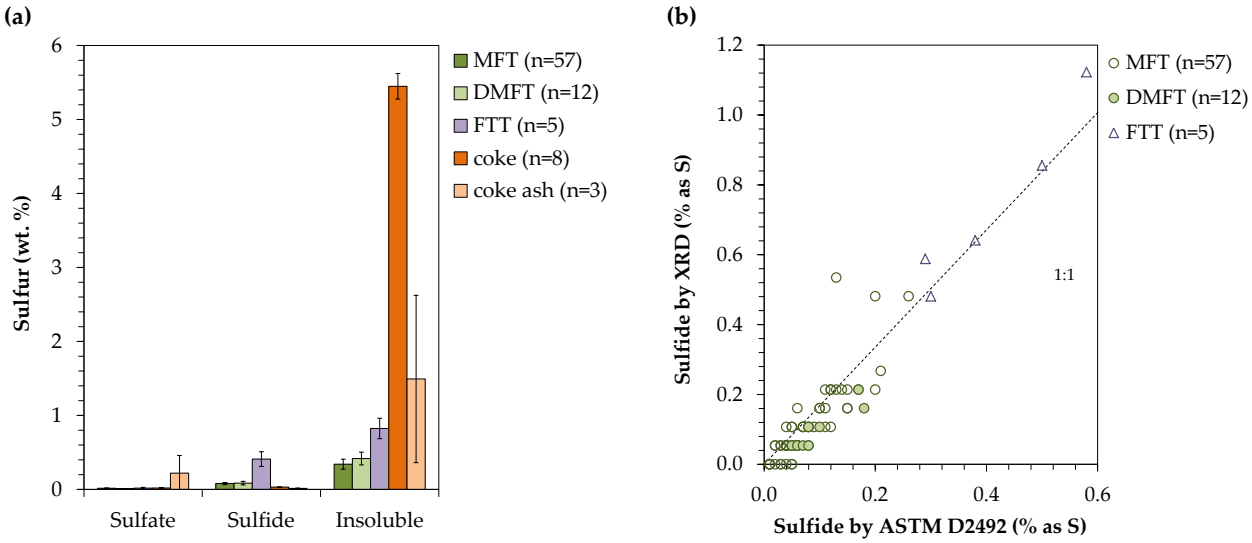

Figure 1 (a) Sulfur speciation (ASTM D2492) of oil sand tailings, coke, and coke ash presented as arithmetic average values with error bars indicating 95 % confidence intervals; and (b) comparison of sulfide concentrations in tailings as determined by ASTM D2492 and quantitative XRD

Acid Neutralization Potential

The form of neutralization potential in MFT, DMFT, and FTT was evaluated by comparing carbonate analyses, measured Sobek neutralization potentials (NPs), and carbonate neutralization potentials (CaNPs) calculated from quantitative XRD. Carbonate content was determined by difference between total carbon and residual carbon following hydrochloric acid leach. It was not correlated with carbonate content estimated from mineralogy (Figure 2a). This effect is likely attributable to the high organic carbon content and hydrophobic nature of the samples. The results of this procedure were not considered further.

XRD determinations of carbonate mineral content were used to calculate the neutralization potential associated with calcium and magnesium in calcite and ankerite (Day, 2009). Ankerite composition was assumed to be $CaFe(CO_3)_2$ for the purpose of the calculation. When compared to NP determined using the siderite-corrected method (Skousen, 1997), CaNP was correlated but generally lower (Figure 2b). Possible explanations are that the siderite-corrected NP included the influence of silicates, and that the peroxide treatment did not fully oxidize Fe^{2+} released by dissolution of siderite and ankerite. Carbonaceous matter in the samples may have competed for the hydrogen peroxide and also allowed redox to remain low. Due to these uncertainties, the mineralogical method was considered more reliable though it likely over-estimated bulk carbonate content as a result of amorphous phases in the samples.

Coke and coke ash samples had relatively low siderite-corrected NP (average 2.3 kg $CaCO_3$/t and -0.6 kg $CaCO_3$/t, respectively). Quantitative mineralogical data were not obtained. Due to the thermal process involved in converting coke to ash, carbonate minerals are not expected to be present except possibly as a result of carbonation by atmospheric CO_2 of calcium and magnesium oxides.

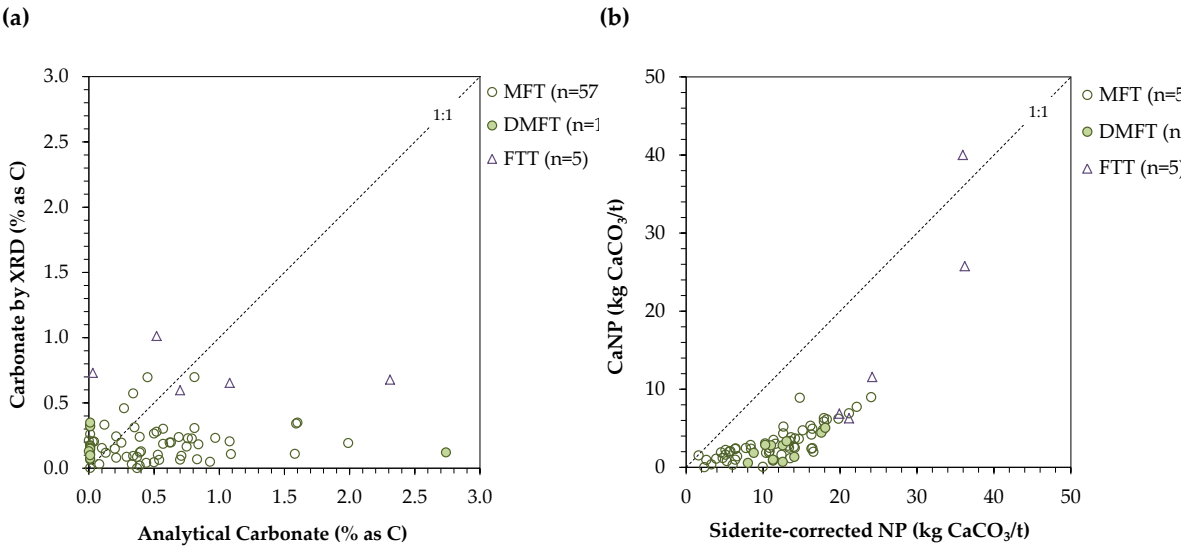

Figure 2 (a) Comparison of analytical carbonate determined as the difference between total carbon and total organic carbon, and carbonate by quantitative XRD; and (b) comparison of siderite-corrected NP and carbonate NP, whereby CaNP is calculated from calcium and magnesium-bearing carbonates

ARD Potential

ARD potential for tailings was assessed using CaNP/AP ratios. Potentially ARD-generating (PAG) tailings were defined by a CaNP/AP ratio of less than 1, whereas non-PAG tailings were defined by a CaNP/AP ratio greater than 2. CaNP/AP ratios between these limits were classified as uncertain. A value of 2 was considered to be appropriate because NP was based on Ca and Mg carbonate. Siderite-corrected NPs were not used due to their apparent tendency to over-estimate reactive carbonate NP as indicated by mineralogy. A second consideration for classification of ARD potential is that at very low sulfide content, the rate of acid generation is sufficiently slow that silicate minerals can play a role in consuming acid. For the purpose of this project, a sulfide concentration of 0.1% (acid potential 3.1 kg $CaCO_3$/t) was selected.

The majority of MFT and DMFT samples were classified as non-PAG on the basis of low sulfide content (Figure 3a). Three of the five FTT samples were classified as PAG, with variability in classification largely attributable to variable calcium and magnesium carbonate content.

In the absence of quantitative mineralogical data, ARD potential for coke and coke ash was assessed using siderite-corrected NP/AP ratios. A ratio of 3 was used to delineate uncertain and non-PAG classifications given the uncertainty in the source of NP. Coke was classified as non-PAG because it had low sulfide content (average 1.0 kg $CaCO_3$/t) and low NP (average 2.3 kg $CaCO_3$/t). Similarly, coke ash samples were low in sulfide content (average 0.4 kg $CaCO_3$/t) and NP (average -0.6 kg $CaCO_3$/t). The bottom ash and combined ash samples were non-PAG, whereas the fly ash sample was acidic (paste pH 2.8) due to the likely presence of elemental sulfur and acid sulfates.

NAG test results were compared to ARD potential classifications (Figure 3b). Samples classified as PAG by the NAG test (NAG pH < 4.5) were also classified as PAG by CaNP/AP. However, the majority of samples classified as PAG or uncertain by CaNP/AP had NAG pH greater than 4.5. The weak relationship between NAG pH and CaNP/AP may be a result of low sulfide content in the tailings, and the contribution of silicates to acid neutralization.

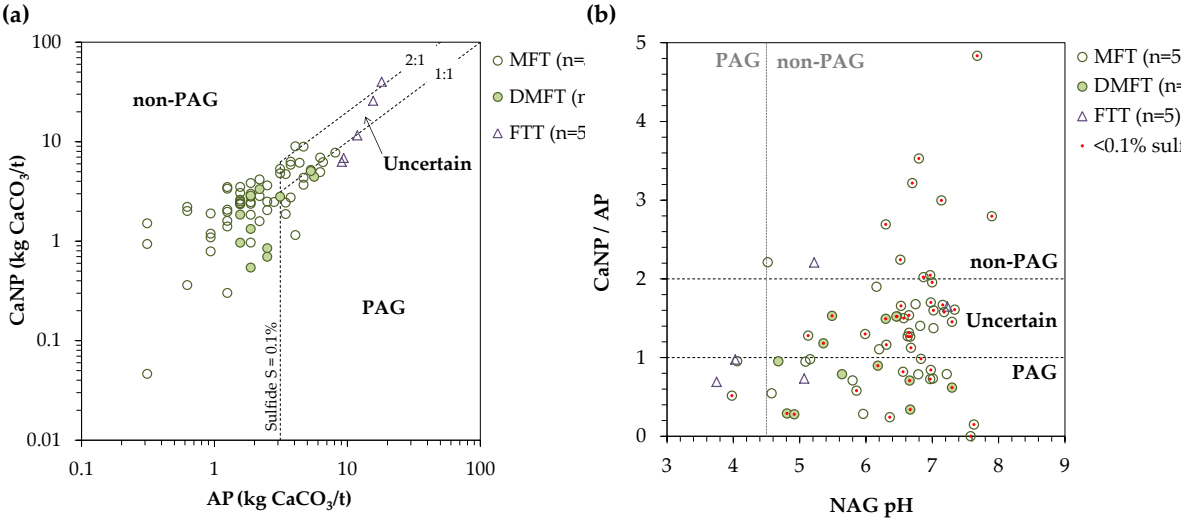

Figure 3 (a) ARD potential classifications for MFT, DMFT, and FTT; and (b) comparison of neutralization potential ratio (defined by CaNP and AP) and NAG pH

Pretreatment of the samples using the method of Dean and Stark (1920) removed bitumen prior to the NAG test. Samples pretreated to remove bitumen were characterized by greater NAG pH values than samples not subject to pretreatment (Figure 4). Sample pretreatment appears to have been effective in reducing bitumen contents and the subsequent formation of organic acids during the NAG test.

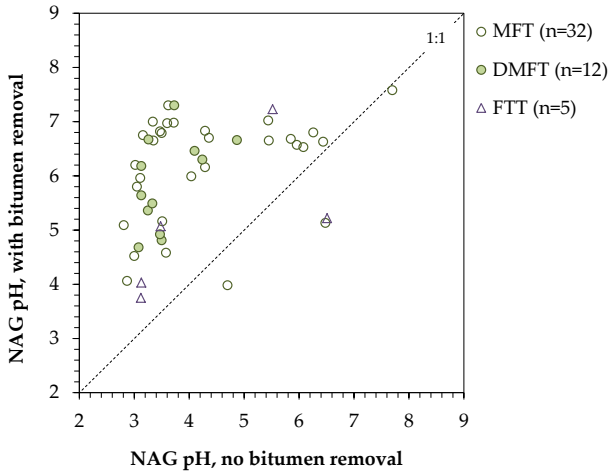

Figure 4 NAG pH before and after bitumen removal using the Dean and Stark (1920) method

Trace Element Leaching

Comparison with Global Average Values

Potential for trace element leaching was inferred by comparing concentrations in MFT, DMFT and FTT with global average values for sandstone and shale (Price 1997). The McMurray Formation is mainly sandstone but shale is locally present. As a result, tailings may have characteristics intermediate between that of sandstone and shale. Concentrations more than an order of magnitude higher than global average values were considered significant; however, potential for metal leaching needs to be considered in the context of the element-phase associations.

Relative to sandstones, cobalt, molybdenum, nickel, selenium, and uranium were enriched in MFT; cobalt and nickel were enriched in DMFT; and cobalt, molybdenum, nickel, selenium, and uranium were enriched in FTT (Table 1). These elements were not enriched relative to shale. Cobalt, molybdenum, and nickel in MFT and DMFT were correlated ($r \geq 0.78$) with insoluble sulfur and sulfide inferring an indistinguishable association with organic matter and pyrite, respectively. Cobalt ($r=0.84$) and nickel ($r=0.88$) in FTT were correlated with insoluble sulfur, whereas molybdenum ($r=0.91$) was correlated with sulfide. Uranium was correlated ($r \geq 0.96$) with titanium in all tailings implying an association with rutile, anatase, and ilmenite. These minerals are resistant to weathering and are not expected to leach uranium.

Comparison of trace concentrations in coke and coke ash with lithological average values did not yield meaningful indications of trace element leaching potential because the original minerals do not exist in these materials. The main feature of these products is the presence of percent level nickel and vanadium which occur in the organic structures of metalloporphyrins (Dechaine and Gray, 2010). Molybdenum concentrations were elevated due to the use of a Mo-based catalyst for coking.

Table 1 Element concentrations summarized as average ± 95% confidence interval

Material Type	Element Concentration (mg/kg)					
	Co	Mo	Ni	Se	U	V
MFT (n=57)	12±1.6	1.2±0.23	21±3.3	0.72±0.088	3.3±0.78	110±14
DMFT (n=12)	11±1.8	0.98±0.38	23±5.7	<0.5	3.3±1.2	99±27
FTT (n=5)	28±3.8	2.2±0.68	44±6.8	1.2±0.23	26±8	190±13
Coke (n=8)	7.2±0.49	47±2.5	370±15	n.d.	n.d.	930±41
Coke ash (n=3)	150±100	370±430	1900±600	0.63±0.26	18±13	>10000
Avg. sandstone (Price 1997)	0.3	0.2	2	0.05	0.45	20
Avg. shale (Price 1997)	19	2.6	68	0.6	3.7	130

Humidity Cells

Humidity cells are weathering tests, which provide some indication of how leaching potential correlates to concentrations in contact waters. None of the 12 tests on MFT, DMFT and FTT generated acid during the 20 weeks of testing. Tests on four PAG tailings were extended to 49 weeks, and did not generate acid. The lack of acidic conditions during the test reflects the neutralizing effects of carbonate minerals, thereby confirming their role in consuming sulfuric acid. The humidity cell tests, therefore, indicated leaching effects under neutral to slightly alkaline conditions (pH 6.3 to 8.6).

Initial humidity cell leachate chemistry was influenced by process water which is dominated by sodium, bicarbonate, and chloride. As the tests proceeded, leachate chemistry became increasingly influenced by weathering of the materials themselves including sulfate concentrations (correlated with sulfide content) and products of acid neutralization (calcium and magnesium). Increasing trends in manganese concentrations suggested that siderite was dissolving. Low leachable uranium concentrations were consistent with the expected association with chemically resistant oxides. Humidity cells on coke and coke ash generally showed leaching effects consistent with dissolution of soluble phases likely to occur in association with refractory organic matter in coke, and amorphous aluminosilicate melt in coke ash.

DISCUSSION

ML/ARD Potential of Oil Sands Processing Products

Test work performed for this study indicated that ARD potential of tailings (MFT, DMFT and FTT) is generally low because sulfide content is low relative to carbonate content. Calcite and ankerite contribute sufficient reactive neutralization potential as Ca and Mg carbonate to offset acid potential from sulfide. The exception to this general conclusion is that FTT, and DMFT and MFT containing mixed-in FTT may be classified as PAG due to the presence of pyrite. These conclusions are clearly linked to the host mineralogy of the McMurray Formation, and indicate that a site specific approach is needed to evaluate ARD potential.

Based on ABA characteristics and humidity cell test results, these oil sand tailings are expected to weather under basic conditions so that mobility of the trace constituents of pyrite (inferred to be cobalt, molybdenum, nickel, and selenium) will depend on how they speciate in waters. Cobalt and nickel are expected to have low mobility at neutral to alkaline pH, whereas the elements forming oxyanions may be more mobile. Dissolution of siderite during acid neutralization may release manganese into solution. Elements associated with carbonaceous matter (nickel and vanadium) and those associated with detrital oxides (uranium) are not expected to be mobile due to their relative stability of their hosts compared to pyrite.

Coke and coke ash contained relatively little sulfide. Coke is the most stable due to the occurrence of metals primarily hosted in refractory organic matter. Coke ash shows greater leachability due to the presence of soluble sulfate and oxide minerals.

Application of Standard ML/ARD Potential Characterization Methods

In addition to providing data on the ML/ARD potential of various oil sand tailings and bitumen upgrading by-products, this study also highlighted the challenges of applying standard methods developed for coal and metal mine wastes. One challenge was related to the hydrophobicity of the samples, which affected the application of water-based methods. For example, determining neutralization potential required the use of dispersants to break up the oil and sonification to allow the reagent to properly react with the sample. Hydrophobicity is due to the presence of bitumen in the samples, which is a source of organic carbon.

The high amounts of organic carbon relative to carbonate affected the determination of carbonate content. The use of hydrochloric acid to remove the carbonates was not effective on the basis of the poor correlation between the carbonate determinations and mineralogy. As a result, quantitative XRD may represent an alternative to the determination of carbonate mineralogy provided that measures are included to correct for the presence of amorphous matter, such as the addition of mineral standards in XRD samples.

Finally, humidity cells were used to evaluate weathering. The procedure appeared to be effective as results could be interpreted within the context of pore water leaching and mineralogical characteristics of the samples. Application of the results to site conditions requires careful consideration of sample hydrophobicity and scaling. The dominant presence of organic carbon and high moisture content of the tailings is likely to limit oxygen diffusion under field conditions.

CONCLUSIONS

The ML/ARD potential of the oil sand tailings sampled by this study and analyzed using standard ML/ARD characterization methods appears low and restricted to FTT. Metal leaching predominantly occurs under basic weathering conditions. Coke produced in the bitumen upgraders has low ARD potential but ash generated by burning coke contains soluble sulfates and oxides, some of which may be acidic. This study provides an important basis for the design of future oil sand ML/ARD characterization programs that should include careful consideration of analytical measures to address the presence of residual bitumen and associated hydrophobicity and organic carbon content.

ACKNOWLEDGEMENTS

The authors gratefully acknowledge permission from Suncor Energy Inc. to publish results of this study.

REFERENCES

Alberta Government (2013) Oil Sands Tailings. http://oilsands.alberta.ca/tailings.html (accessed October 13, 2014).

COSIA (2012) Technical Guide for Fluid Fine Tailings Management. Canada's Oil Sands Innovation Alliance (COSIA), August 30, http://www.cosia.ca/uploads/documents/id7/TechGuideFluidTailingsMgmt_Aug2012.pdf (accessed October 13, 2014).

COSIA (2014a) COSIA's Tailings Environmental Priority Area. http://www.cosia.ca/initiatives/tailings (accessed October 13, 2014).

COSIA (2014b) Guidelines for Performance Management of Oil Sands Fluid Fine Tailings Deposits to Meet Closure Commitments. Canada's Oil Sands Innovation Alliance (COSIA), February, http://www.cosia.ca/uploads/documents/id5/FFT%20Performance%20Management_Feb2014.pdf (accessed October 13, 2014).

Day, S.J. (2009) Estimation of calcium and magnesium carbonate neutralization potential for refined acid-base accounting using electron microprobe and X-ray diffraction. 8th International Conference on Acid Rock Drainage (ICARD), Skelleftea, Sweden, June 22-26.

Dean E.W. and Stark D.D. (1920) A Convenient Method for the Determination of Water in Petroleum and Other Organic Emulsions. Industrial and Engineering Chemistry. 12(5): 486-490.

Dechaine, G.P. and Gray, M.R. (2010) Chemistry and Association of Vanadium Compounds in Heavy Oil and Bitumen, and Implications for their Selective Removal. Energy and Fuels. 24: 2795-2808.

EGi (2006) Single Addition Net Acid Generation (NAG) Test Procedure. Environmental Geochemistry International Pty Ltd, Balmain, Australia.

Flach, P.D. (1984) Oil sands geology – Athabasca deposit north. Geological Survey Department, Alberta Research Council, Edmonton, Alberta.

Kuznetsov, P., Kuznetsova, A., Foght, J.M., Siddique, T. (2015) Oil sands thickened froth treatment tailings exhibit acid rock drainage potential during evaporative drying. Science of the Total Environment 505: 1-10.

Price, W.A. (1997) Draft Guidelines and Recommended Methods for the Prediction of Metal Leaching and Acid Rock Drainage at Minesites in British Columbia. Reclamation Section, Energy and Minerals Division, Ministry of Employment and Investment, British Columbia.

Price, W.A. (2009) Prediction Manual for Drainage Chemistry from Sulphidic Geologic Materials MEND Report 1.20.1. CANMET Mining and Mineral Sciences Laboratories, Smithers, British Columbia.

Skousen, J. (1997) Neutralization potential of overburden samples containing siderite. Journal of Environmental Quality. 26(3): 673-681.

Sobek, A.A., Schuller, W.A., Freeman, J.R., Smith, R.M. (1978) Field and Laboratory Methods Applicable to Overburdens and Minesoils. Report EPA-600/2-78-054, U.S. National Technical Information Report PB-280 495.

Wang, C., Harbottle, D., Liu, Q., Xu, Z. (2014) Current state of fine mineral tailings treatment: A critical review on theory and practice. Mineral Engineering 58: 113-131

10th ICARD IMWA 2015 | 10th International Conference on Acid Rock Drainage & IMWA Annual Conference

Pyrite Oxidation Rates from Laboratory Tests on Waste Rock

Kim Lapakko[1] and Edward Trujillo[2]

1. *Minnesota Department of Natural Resources, USA*
2. *University of Utah, USA*

ABSTRACT

Fourteen samples of pyrite-bearing waste rock were characterized (particle size distribution, chemistry, mineral content, degree of pyrite liberation, extent of precipitate coating on pyrite) and subjected to dissolution testing for 52 weeks. Approximately one-kilogram samples ($0.18 \leq d < 6.25$ mm) were placed into cells similar to that described in ASTM D5744-13. The modified testing procedure was divided into three phases. First, in the leach phase, the sample was soaked with 500 mL of deionized water for one hour, after which the leachate was collected in a flask for two hours then left exposed to ambient conditions for the rest of the day. Second, a drying phase started on the second day by pumping dry air (1 L/m) into the bottom of the cell for three days. Third, after drying, the humidity cell was kept unattended with the top lid on for the remaining three days. Leachate was analyzed for pH, sulfate, a number of other solutes, and bacterial growth. Pyrite was reported to be absent from four samples, at concentrations of 0.01 to 0.1 percent in three samples, and in the range of 0.7 to 4 percent in the remaining seven samples. Rates of pyrite oxidation were determined for all samples in which pyrite was detected, using sulfate release rates during weeks 37 to 52 and the calculated exposed pyrite surface area. For samples with pyrite contents of at least 0.7 percent, the oxidation rates determined were reasonably consistent with those predicted in the literature. For this same subset, oxidation rates for samples producing acidic drainage (~3.3-3.8) were one to twelve times those for samples producing circumneutral drainage (~7.0-7.5).

Keywords: pyrite oxidation rates, kinetics, humidity cell, laboratory weathering, mine rock drainage quality prediction

INTRODUCTION

Pyrite oxidation is a major concern related to waste rock excavated during mining operations. Pyrite and other iron-bearing sulfide minerals oxidize in the presence of oxygen and water and can produce acid, as well as iron oxyhydroxides and sulfate (reaction 1). Some or all of the acid produced can be neutralized by reaction with other minerals present in the rock. The acidity of drainage from an unmitigated waste rock facility is ultimately dependent on the balance of acid-producing and acid-neutralizing reactions. If the rate of acid production exceeds the rate of acid neutralization the drainage will be acidic. Quantification of pyrite oxidation rates and the attendant acid production benefits interpretation of kinetic test data, extrapolation of laboratory data to the field, and is required to model waste-rock drainage quality based on waste-rock composition.

$$FeS_{2(s)} + 3.75O_2 + 2.5H_2O \rightleftharpoons FeOOH_{(s)} + 2SO^{-2}_{4(aq)} + 4H^{+}_{(aq)} \quad (1)$$

Monomineralic dissolution studies have been conducted to determine rates of pyrite oxidation in oxygen saturated water (Williamson and Rimstidt, 1994) and in the presence of moist air (Jerz and Rimstidt, 2004). Using a method approximating that of Option B of ASTM D5744-13e (ASTM International 2013) for weathering a suite of greenstone rock samples, Lapakko and Antonson (2006) attributed sulfate release to oxidation of pyrite in the fine fraction in which water was retained. The pyrite oxidation rates determined were in good agreement with those presented by Williamson and Rimstidt (1994) for abiotic oxidation of pyrite by oxygen.

Jerz and Rimstidt (2004) conducted laboratory experiments at 25 °C, 96.7 % relative humidity, and oxygen partial pressures of 0.21, 0.61, and 1.00 atmosphere (atm). They derived the following expression for the rate of pyrite oxidation in moist air:

$$\frac{dFeS_2}{dt} = 10^{-6.6} P^{0.5} t^{-0.5} \quad (2)$$

where, $dFeS_2/dt$ is the rate of pyrite oxidation (mol m^{-2} s^{-1}), P is the partial pressure of oxygen (atm) and t is time in seconds. They reported that the reaction rate decreased over time due to formation of a precipitate layer on the mineral surface that inhibited oxygen transport.

The present humidity-cell studies were conducted using a one-day period for rinsing and draining of the cell followed by a three-day period during which dry air was introduced to the cell. After the drying cycle samples were retained undisturbed in the cells. The conditions for pyrite oxidation were consequently much dryer than those used by Lapakko and Antonson (2006), and may simulate conditions near the boundary of waste rock piles in an arid environment. The following

sections investigate pyrite oxidation rates for 10 waste-rock samples under these conditions and compare them to rates published for monomineralic pyrite oxidation studies.

METHODS

Materials

Fourteen rock samples for humidity-cell testing were collected from waste-rock piles (7 samples), outcrops (6 samples) and scars (1 sample) at the Questa molybdenum mine in northern New Mexico (Chevron, 2005). Samples from the waste-rock piles were collected from trenches (McLemore et al., 2005), homogenized and sieved to obtain the size fraction finer than 6.35 mm (McLemore et al., 2008). Rock samples were staged crushed with 1.27- and 0.635-cm jaw crushers to obtain the -0.635 cm size fraction (McLemore et al., 2008). Due to concerns regarding flow transmission during humidity-cell testing, all samples were dry-sieved to remove the fraction finer than 0.18 mm prior to testing. Dry sieving employing 12 Tyler screens was used to determine particle size distributions of the bulk sample, the sample submitted for humidity-cell testing, and the samples following termination of the humidity-cell tests.

The resultant samples were subjected to chemical, mineralogic, and petrographic analysis (McLemore et al., 2008; 2009). Mineral Services (2008) provided descriptions of hand samples, microscopic analysis of thin sections, Rietveld x-ray diffraction analyses, and analyses by scanning electron microscopy (SEM) with energy-dispersive x-ray spectrometry (EDS). Pyrite contents used in the present paper were selected based on consideration of chemical analyses and mineralogic analyses by both New Mexico Tech and Mineral Services. Pyrite grain-size distributions (McSwiggen, 2008a) and the extent of pyrite coating were also determined (McSwiggen, 2008b).

Humidity Cell Tests

Humidity-cell testing was performed at room temperature using a modified version of ASTM D5744-13e (ASTM International, 2013) for one year. Approximately one kilogram of sample was charged to each cell. The modified testing procedure was divided into three phases, i.e., (1) leach phase, (2) drying phase and (3) stand-alone phase over a seven-day cycle. During the first day (the leach phase), 500 mL of deionized water (or synthetic water) was delivered to the cell from the separatory funnel and the sample was allowed to soak for one hour. The leachate was then collected in a flask for two hours, after which the humidity cell was left undisturbed. Leachate was analyzed (1) directly for temperature, pH, and Eh; (2) after filtration (0.45 μm) for sulfate, fluoride, and ferrous iron; and (3) after filtration and acidification (ultrapure nitric acid) for cations. The drying phase started on the second day by pumping air dried to a dew point of -40 °C (Balston model 76-10 membrane air dryer) at 1.0 liter/minute from the bottom of the cell for three days. After drying, the humidity cell was left alone for the remaining three days. Dry air flow rates, temperatures, pressure drops and humidity were measured for each cell periodically. Cell masses before and after the leach and after the dry-air portion of each weekly cycle were determined.

Samples used for the GHN-KMD-0088 cells were inoculated and analyzed for bacteria growth at weeks 5, 26, 38, 50, and 52. All leachate samples were analyzed in duplicate using MPN tests at 24 °C (Richins et al. 2008). The microbial humidity-cell inoculum was produced from rock samples from the mine that were provided for characterization and inoculum production. The inocula were produced using characterized media for enhanced growth of each general population group. The inocula were a unique composite of separately produced populations of (1) general heterotrophic species, (2) general sulfate-reducing species, (3) general *Acidithiobacillus* and *Leprotspirillum* species, (4) general acidophilic species, and (5) general *Archaea* species. The inocula contained concentrations of the five generalized population groups that mirrored the relative concentrations in the original sample.

Calculations

Pyrite grain size and liberation were determined in two steps (McSwiggen 2008a). First, the average pyrite grain size was determined for particles with diameters ranging from roughly 1 to 3 mm. The image analysis program NIH ImageJ was used to interpret backscatter electron signals collected using a JEOL 8600 Electron Probe Microanalyzer. The image analysis program identified sulfide mineral grains and determined the longest length, perimeter, and area of each grain. The "circular diameter" (diameter assuming a circular particle = 4 x particle area/particle perimeter) of each particle and total grain area present were calculated. The resultant data were sorted from smallest to largest particle area, and the percent cumulative areas for the sorted grains were calculated. The median grain diameter was defined as the circular diameter for which the percent cumulative area was 50. The probability of a sulfide grain being exposed was then calculated using the following equation:

$$P = 100 - 100[(R_1 - R_2)^2/R_1^2] \quad (3)$$

P = probability of sulfide grain being exposed,

R_1 = radius of host rock grains,

R_2 = median radius of all pyrite

Rates of pyrite oxidation were determined by dividing molar rates of sulfate release by twice the liberated pyrite surface area. Sulfate release rates were determined for periods from 6 to 9 and 37 to 52 weeks. The rate for a specific period was calculated by averaging the weekly sulfate release rates observed during the period.

The exposed pyrite surface area of a sample was determined by summing the exposed pyrite surface area in each particle size fraction, which was calculated as follows:

$$A_{py,i} = \left(\frac{\%FeS_2}{100}\right)\left(\frac{6}{\rho\, d_{gm,i}}\right)\left(\frac{M_i\, L_i\, (SR)}{100}\right) \quad (4)$$

where

$A_{py,i}$ = pyrite area in particle size fraction i, m^2,

$\%FeS_2$ = percent pyrite of sample, assumed to be constant among size fractions,

ρ = pyrite density = 5.02×10^6 g m^{-3},

$d_{gm,i}$ = geometric mean diameter of particle size fraction i, m,

M_i = mass of rock in particle size fraction i, g,

L_i = percent pyrite exposure in particle size fraction i, and

SR = surface roughness factor for pyrite estimated as 4.9, the mean of five literature values presented by Lapakko and Antonson (2006).

RESULTS

Rock Characterization

The rocks examined were collected from rock piles and outcrops at the Questa mine site and reflected characteristics of the andesitic lava and rhyolitic ignimbrite rocks at the site (Dunbar, Heizler & Sweeney, 2008). Mineralogical analyses indicated that pyrite was absent from four of the samples and this paper will focus on the remaining ten samples. Six of these samples were from rock piles and four were collected from outcrops. Six of the samples were classified as andesite and four as rhyolite, with respective QSP alteration ranges of 0 to 90 percent and 0 to 70 percent (McLemore et al. 2008).

Particle size distributions for the humidity cell samples revealed that one to five percent of the sample mass was generally finer than 0.18 mm. Samples had been dry-sieved with the intent of removing this fraction but this method was not entirely effective. In particular sample BCS-VWL-0004 had about seven percent reporting as finer than 0.18 mm. Particle size distributions for five of the samples appeared to provide a central tendency for these data. The respective ranges for percent finer than 1.7 mm and 0.5 mm for these samples were 36 to 47 percent and 14 to 17 percent. Two samples were coarser and three finer than these samples.

Major whole rock components (and typical ranges) were SiO_2 (60-70 wt. %), Al_2O_3 (13-14 wt. %), total FeO and K_2O (both 3-5 wt. %). Respective sulfide and sulfate content ranges for the samples were 0.03-2.49 wt. % and 0.04 to 0.55 wt. % (Table 1). Although carbon contents of eight of the ten samples did not exceed 0.07 percent, one value was reported as 1.58 wt. % for a sample in which wood fragments were detected (BCS-VWL-0004; Table 1). Quartz was typically the dominant mineral present (19-51 wt. %), and other major minerals were potassium feldspar (5-27 wt. %), illite-sericite (9-33 wt. %), and plagioclase (<1 – 30 wt. %) (McLemore et al. 2008).

Pyrite was the dominant sulfide mineral present, with jarosite and gypsum observed in some samples (Table 1). New Mexico Tech estimated jarosite and gypsum contents based on the sulfate content determined by chemical analysis, but the presence of these minerals was verified by petrographic examinations in six and two samples, respectively. Similarly, calcite contents were estimated assuming all carbon was present as calcite but its presence was verified in only three samples (Table 2).

Pyrite contents ranged from 0.01 to 4 wt. % (Table 1). Based on examination of 89 to 1033 pyrite grains per sample, median pyrite diameters ranged from 12 to 1100 μm (Table 1). It should be noted that the median values were selected as the 50th percentile of cumulative area, and they do not reflect the large number of very fine pyrite grains in the samples. The percentage of pyrite particles finer than 10 μm ranged from roughly 60 to 90 percent. However, with one exception, the fraction of the total pyrite surface area contributed by this fine fraction did not exceed 7.2 percent. Based on the particle size distribution, the pyrite content, and the median pyrite grain size, liberated pyrite surface areas in the samples typically ranged from about 0.02 to 0.2 m^2 (Table 1). Coatings of 6 to 7 μm thickness were reported on three of the samples. The primary chemical constituents of the coatings were FeO (74-80 wt. %), SiO_2 (9-16 wt. %), CaO (3-5 wt. %), and SO_3 (0-14 wt. %).

Table 1 Paste pH and chemistry, mineral content, and pyrite characteristics related to oxidation.

ID	GHN-JRM 0009	ROC-NWD 0002	SPR-JWM 0002	PIT-VTM 0600	GHN-KMD 0096	PIT-RDL 0007	GHN-JRM 0001	GHN-JRM 0002	BCS-VWL 0004	GHN-KMD 0088
PASTE PH[1]										
	3.97	4.4	6.26	7.16	2.56	2.29	2.14	2.15	4.29	2.63
WHOLE ROCK CHEMISTRY, WEIGHT PERCENT										
S	1.31	2.49	1.79	0.92	0.06	0.81	1.80	0.00	0.03	0.69
SO_4	0.51	0.11	0.54	0.04	0.37	0.22	0.55	0.33	0.42	0.23
C	0.07	0.03	0.06	0.25	0.02	0.04	0.06	0.04	1.58	0.05
SULFUR-BEARING AND CARBONATE MINERAL CONTENT, WEIGHT PERCENT										
jarosite	1.7	0.01	NR	NR	1.4	1	2	0.01	2	NR
jarosite observed[2]	Yes	No	No	No	Yes	Yes	Yes	Yes	Yes	No
gypsum	0.8	0.5	2	0.2	0.5	0.02	0.8	1.5	0.4	1
gypsum observed[2]	No	No	No	No	No	No	Yes	No	Yes	No
calcite	0.5	0.1	0.5	2	0.2	0.2	0.4	0.3	0.2	0.3
calcite observed[2]	Yes	No	Yes	Yes	No	No	No	No	No	No
PYRITE CHARACTERIZATION										
pyrite, wt. %	2	4	0.7[3]	2	0.1	1	3	0.01	0.1	1
coating, μm	0	0	7	6	0	0	0	7	0[4]	0
med. d^5, μm	850	1100	100	250	12	45	154	190[6]	46	35
grains	662	393	1033	559	89	593	518	654	98	647

examined[7]										
A_T(py)[8], m^2	0.25	0.29	0.41	0.52	0.49	1.27	0.98	0.0032	0.13	1.66
A_L(py)[9], m^2	0.20	0.20	0.053	0.20	0.018	0.11	0.38	0.0011	0.021	0.14

[1] McLemore et al. 2008

[2] Observed by New Mexico Tech or Mineral Services

[3] Reported as 3 wt. % by New Mexico Tech. Alternative value selected is in closer agreement with pyrite

content based on post-leach sulfide content (0.5 wt. %), initial normative CIPW value reported by New

Mexico Tech (0.8 %), and Mineral Services Rietveld analysis (0.7 wt. %).

[4] McSwiggen found no pyrite grains in the 60 mesh fraction of the sample but reported coating remnants.

[5] Median sulfide grain diameter.

[6] Number of grains reported is inconsistent with low pyrite content.

[7] Pyrite grains examined to determine median diameter.

[8] Total pyrite surface area.

[9] Liberated pyrite surface area.

Humidity Cell Tests

As mentioned earlier, humidity cell testing was conducted at room temperature using compressed air, dried to zero humidity. This resulted in some cells being completely dried during the dry-air cycle. However, this did not happen consistently. Sometimes the residual water saturation would go to zero while for other weeks it would remain high. This can probably be attributed to preferential gas flow paths developing over time in the cells or a decrease in the air flow rate caused by uneven pressure distribution. Thus it is difficult to say how much moisture was present over the seven-day period for pyrite oxidation for each cell over time.

Initial pH values from five of the samples were in the range of 2.3-2.9, three ranged from 3.1-4, and the remaining two were 6.5 and 6.8. These values reasonably reflected those determined by McLemore et al. (2008) for paste pH (Figure 1). The pH reflected three trends: a neutral/basic group (pH 6.5-8.0), composed of SPR-JWM-002 and PIT-VTM-0600, a pH 5-6 group (BCS-VML-004), and an acidic group (pH 2.5-4.5) (Figure 2). The reproducibility of duplicated samples, SPR-JWM-002, GHN-KMD-0088 and GHN-JRM-0001 is demonstrated in Figure 2. Most cations and anions showed relatively high concentrations in the first few weeks of the humidity cell test, which is attributed to the initial pore water quality, the reaction of very small fines and soluble salts. Total iron concentrations generally corresponded with pH, with the lowest pH cells having the highest

iron concentrations and cells producing neutral or basic pH yielding iron concentrations at or below detection limits.

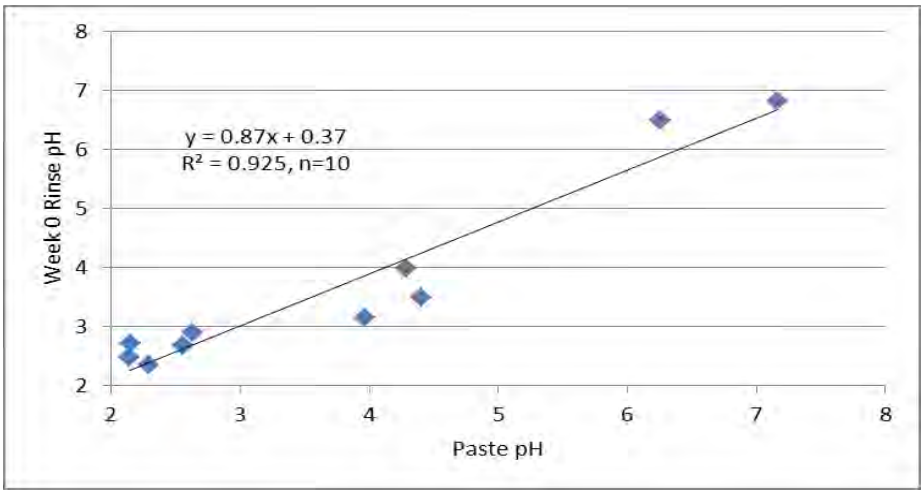

Figure 1 Effluent pH at week 0 correlated closely with paste pH.

Sulfate concentrations decreased rapidly in the initial stages of the experiment, reflecting removal of residual oxidation products generated during sample storage and preparation, as well as oxidation of highly reactive particles. In particular, such reaction could include oxidation of fine particles with high specific surface areas. Sulfate release ultimately plateaued toward the end of the period of record for most samples (Figure 2). Drainage quality for most samples was fairly stable after week 37, although release from some continued to oscillate within a constant range or decline slowly.

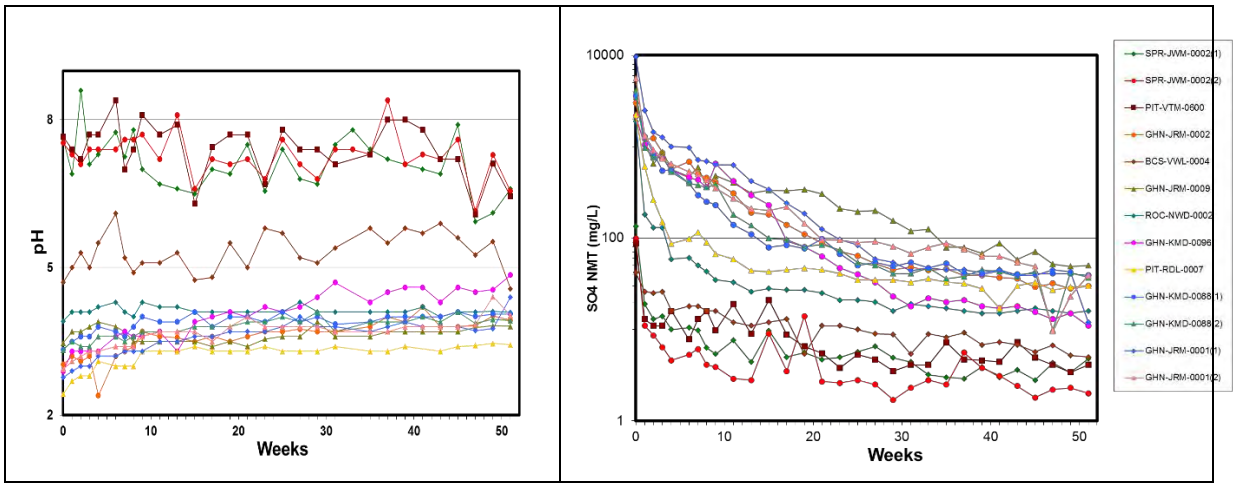

Figure 2 pH and sulfate concentration over time for all 10 samples. SPR-JWM-0002, GHN-KMD-0088 and GHN-JRM-0001 were run in duplicate.

Average sulfate release rates for weeks six through nine were calculated as an indicator of the rate of sulfate release after the initial rapid release, and the interval from week 37 to 52 was selected to represent a period of "fairly stable" sulfate release (Table 2). Ratios of the latter rate to that observed during weeks 6-9 was calculated to describe the degree to which sulfate release rates declined over the period of record. The ratios fell into two general ranges: 0.04-0.1 and 0.3-0.5 (Table 2). The lower range was associated with samples collected from trenches at the Goat Hill North rock pile. These samples were finer-grained materials that had been subjected to oxidation in the field for 30 to 35 years (McLemore et al., 2009). The remaining samples were generated from crushing larger rocks. The finer-grained Goat Hill North samples likely contained more labile sulfate generated from weathering in the field than the rock samples. The relatively rapid release of this sulfate resulted in a larger decline in sulfate release rates for the weathered samples. The trench samples also generally produced large changes in pH over this period, suggesting that the sulfate source was an acidic mineral rather than, for example, gypsum. Solid-phase analyses do not provide convincing corroboration for this suggestion (Table 1). Samples generating neutral or basic pH tended to produce low sulfate concentrations, whereas more acidic leachates generally had elevated sulfate concentrations. However, GHN-JRM-0009 consistently produced much higher sulfate concentration than the PIT-RDL-0007 despite a consistently higher pH.

Bacteriological results showed that sulfate-reducing bacteria and heterotrophic bacteria grew over time in all cells, even the ones not inoculated, however the *Acidithiobacillus* and *Leptospirillum sp*. were only detected in low numbers in a few of the cells (Richins et al. 2008). This may be due to lack of nutrients or the loss of microbes by pure water washes. Thus, it appears that *Acidithiobacillus* did not play a significant role in these humidity cells and pyrite was primarily oxidized abiotically by oxygen.

Pyrite oxidation rates were calculated for all ten samples based on the average weekly rates of sulfate release between weeks 37 and 52 and the calculated liberated pyrite surface area. Rates determined for two of the three samples in which pyrite content was reported as 0.1 percent or less were considerably higher than those for the remaining samples. The pyrite content of the latter seven samples ranged from 0.7 to 4 wt. %, and the following discussion focuses on the pyrite oxidation rates determined for these samples.

Table 2 Humidity cell data summary. Shaded values of dpy/dt indicate py ≤ 0.1 wt %.

Sample ID	GHN-JRM 0009	ROC-NWD 0002	SPR-JWM 0002	PIT-VTM 0600	GHN-KMD 0096	PIT-RDL 0007	GHN-JRM 0001	GHN-JRM 0002	BCS-VWL 0004	GHN-KMD 0088
pH_o[1]	3.15	3.49	6.49	6.81	2.67	2.35	2.47	2.71	3.99	2.89

pH_i[2]	3.11	3.52	6.88	6.95	3.12	2.80	2.96	3.19	4.26	3.25
pH_f[3]	3.45	3.68	6.75	7.36	3.93	3.16	3.54	3.72	4.60	3.70
pH_f - pH_i	0.34	0.16	-0.13	0.41	0.81	0.36	0.58	0.53	0.34	0.45
$dSO4/dt_0$[4]	258	124	8.13	5.25	148	153	460	155	2.63	269
$dSO4/dt_i$[5]	36.2	3.10	0.50	0.896	28.0	6.39	32.4	31.8	1.23	25.0
$dSO4/dt_f$[6]	3.65	1.17	0.253	0.324	1.03	1.93	2.74	2.08	0.434	2.80
$rate_f/rate_i$[7]	0.10	0.38	0.51	0.36	0.037	0.30	0.085	0.065	0.35	0.11
dpy/dt[8]	9.3	2.9	2.4	0.80	29	8.8	3.6	950	10	9.8

[1] Initial rinse pH, arithmetic mean used for duplicate cells.

[2] Arithmetic mean pH, weeks 6-9.

[3] Arithmetic mean pH, weeks 37-52.

[4] Sulfate release rate, week 0, mol s^{-1} x 10^{-10}; assumes one week reaction time.

[5] Average sulfate release rate, weeks 6-9, mol s^{-1} x 10^{-10}.

[6] Average sulfate release rate, weeks 37-52, mol s^{-1} x 10^{-10}.

[7] Ratio of average sulfate release rate for weeks 37-52 to that for weeks 6-9.

[8] Average pyrite oxidation rate, weeks 37-52, mol m^{-2} s^{-1} x 10^{-10}.

The resultant oxidation rates ranged from 0.8 x 10^{-10} to 9.8 x 10^{-10} mol m^{-2} s^{-1}, with all but one value exceeding 2 x 10^{-10} mol m^{-2} s^{-1} (Table 2). The calculated rates exhibited a mild dependence on pH although this dependence must be viewed with caution. The data fall into two clusters at roughly pH 3.5 and 7.3 (Figure 3). The intent of this analysis was to aid in description of the data and not to deduce a mechanistic interpretation. It should further be noted that the two points near pH 7.3 were both generated by samples in which pyrite coatings of 6-7 μm were detected. These coating likely contributed to the lower oxidation rates observed for these samples.

The pyrite oxidation rates observed were lower than those reported for oxidation of pyrite present in greenstone samples (Lapakko and Antonson 2006) (Figure 3). Using the two linear regressions as descriptors, the Questa oxidation rates are about 30 to 60 percent of those for the greenstone samples. One factor contributing to this discrepancy is the difference in reaction conditions between the two experiments. In the greenstone experiments, no air was introduced to the humidity cells, and typically 130 to 150 mL of water was retained in the cells throughout the weekly cycle. Pyrite

oxidation in this experiment was described as occurring in the fine fraction of rock particles that were in contact with oxygen saturated water. This was consistent with the agreement of observed rates with those reported by Williamson and Rimstidt (1994).

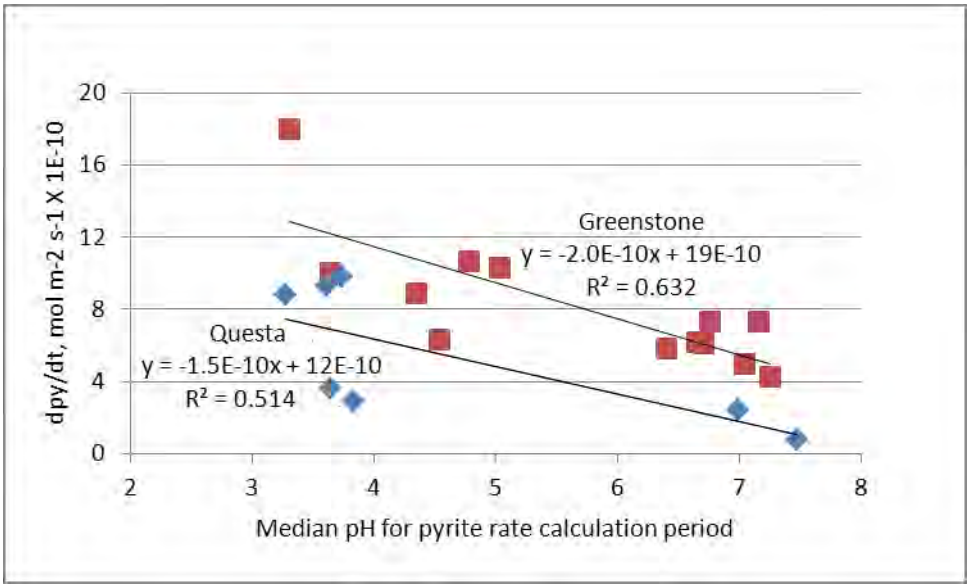

Figure 3 Pyrite oxidation rates for the Questa samples were lower than those reported for greenstone samples (Lapakko and Antonson 2006). The drier oxidation conditions of Questa samples during the weekly cycle likely contributed to the lower rates.

In contrast, the cells in the present study were subjected to three days of dry air following the day during which samples drained. During this day, oxidation likely occurred in the presence of oxygen saturated water. During the next three days water evaporated from the cell, sometimes to total dryness. Thus, during this period, oxidation could occur with pyrite grains in contact with oxygen saturated water, water saturated air as observed by Jerz and Rimstidt (2004), or with air of variable water saturation. Because it is not possible to confidently describe the precise reaction conditions, oxidation rates for several possible conditions were calculated to compare theoretical rates (i.e. Williamson and Rimstidt 1994 and Jerz and Rimstidt 2004) with those observed. The overall range of rates calculated for various time periods for abiotic oxidation by oxygen in water and oxidation in humid air was 0.3 x 10^{-10} to 7.2 x 10^{-10} mol m^{-2} s^{-1}. The observed range for the samples in this study was 0.8 x 10^{-10} to 9.8 x 10^{-10} mol m^{-2} s^{-1}, within or slightly above the theoretical range.

SUMMARY

Rates of pyrite oxidation were determined for seven waste rock samples subjected to humidity cell testing for one year based on observed rates of sulfate release and liberated pyrite surface area.

Liberated pyrite surface area was determined using pyrite content and size distributions of pyrite grains and the rock subjected to testing. The equation used for this determination yielded rates that were consistent with those reported in the literature for samples with pyrite contents between 0.7 and 4 percent. For two samples with pyrite contents near 0.1 percent, the calculated rates were one and three times those for the samples of higher pyrite content. The oxidation rate for a sample with a reported pyrite content of 0.01 percent was almost three orders of magnitude above the range for higher pyrite contents. This suggests that the method yields reasonable results for sample with pyrite contents above 0.1 percent, but for samples with lower pyrite content the method has limitations. For samples of low pyrite content the method may underestimate the liberated pyrite surface area surface area due to low pyrite concentrations or the occurrence of pyrite as very fine grains on rock surfaces. Alternatively, a highly reactive sulfide or sulfate mineral may have been present at low concentrations in these samples.

ACKNOWLEDGEMENTS

Chevron Mining provided funding for the humidity cell testing. Kelly Donahue of Brown and Caldwell provided initial review of sample collection methods and general petrology. Mike Moncur of Alberta Innovates – Technology Futures and Bob Seal of the United States Geological Survey provided constructive review of the draft submitted.

REFERENCES

ASTM International (2013) D5744-13e, Standard test method for laboratory weathering of solid materials using a humidity cell. In Annual book of ASTM Standards, 11.04. American Society for Testing and Materials International, West Conschohocken, PA. 23 p. (http://www.astm.org/Standards/D5744.htm?A).

Chevron (2005) Standard operating procedure no. 5: Sampling outcrops, rock piles, and drill core (solid), rev. 5v8, 2/07/05: unpublished report to Chevron. 19 p.

Dunbar, N., Heizler, L. and Sweeney, D. (2008) DRA-4. Mineralogical characterization of Questa rock-pile samples by petrographic and electron microprobe analysis: unpublished report to Molycorp, Inc., DRA-4. 19 p.

Jerz, J.K. & Rimstidt, D.J. (2004) Pyrite oxidation in moist air. Geochchim. Cosmochim. Acta 68. p. 701-714.

Lapakko, K.A. and Antonson, D.A. (2006) Pyrite oxidation rates from humidity cell testing of greenstone rock. In Proc. 2006, 7th ICARD, March 26-30, 2006, St. Louis MO. Published by ASMR, 3134 Montavesta Rd., Lexington, KY 40502. p. 1007-1025.

McLemore, V.T., Heizler, L., Dunbar, N., Phillips, E., Donahue, K., Sweeney, D., Dickens, A. and Ennin, F. (2008) Petrographic Analysis of Humidity Cell Samples: unpublished report to Chevron, Task B1.5.2. 29 p. plus appendices.

McLemore, V.T., Walsh, P., Donahue, K., Gutierrez, L., Tachie-Menson, S., Shannon, H.R. and Wilson, G.W. (2005) Preliminary status report on Molycorp Goathill North trenches, Questa, New Mexico, 2005 National Meeting, of the American Society of Mining and Reclamation. American Society of Mining and Reclamation, Breckenridge p. 507-532.

McLemore, V.T., Heizler, L., Donahue, K. and Dunbar, N. (2009) Characterization of weathering of mine rock piles: Example from the Quest mine, New Mexico, USA. In Proc. Securing the Future and 8th ICARD, June 23-26, 2009, Skellefteå, Sweden, CD-ROM. 10 p.

McSwiggen, P. (2008a) Sulfide mineral liberation. Technical memo by Peter McSwiggen, McSwiggen & Associates, P.A. Micro Analytical Services, St. Anthony, MN. 29 July 2008. 11p.

McSwiggen, P. (2008b) Part B3-Sulfide mineral coatings in unleached samples. Technical memo by Peter McSwiggen, McSwiggen & Associates, P.A. Micro Analytical Services, St. Anthony, MN. 28 August 2008. 3 p.

Mineral Services (2008) Petrographic and mineralogical characterization of 14 samples from the rock piles of the Questa molybdenum mine (New Mexico, USA). Report prepared for Mark J. Logsdon, Geochimica Inc. by Mineral Services Canada Inc., North Vancouver, B.C. 16 April 2008. 80 p.

Richins, B., Eschler, J., Kennedy, J. and Adams, D.J. (2008) Questa Mine Site: Humidity Cell Microbial Evaluation. University of Utah.

Williamson, M.A. and Rimstidt, J.D. (1994) The kinetics and electrochemical rate-determining step of aqueous pyrite oxidation. Geochim. Cosmochim. Acta, 58. p. 5443-5454.

Iron Sulfides Ain't Iron Sulfides. A Comparison of Acidity Generated During Oxidation of Pyrite and Pyrrhotite in Waste Rock and Tailing Materials

Russell Schumann[1], Alan Robertson[2], Andrea Gerson[3], Rong Fan[3], Nobuyuki Kawashima[3], Jun Li[3] and Roger Smart[3]

1. Levay & Co Environmental Services, University of South Australia
2. RGS Environmental Pty Ltd, Australia
3. Minerals and Materials Science and Technology, Mawson Institute, University of South Australia

ABSTRACT

It is generally recognized that acid and metalliferous drainage (AMD) occurs as a result of oxidative dissolution of iron-containing sulfide minerals, while oxidation of sulfides containing low or no iron such as sphalerite or galena do not generally result in highly acidic drainage, but may lead to elevated concentrations of sulfate and metals., e.g. Zn, Pb. Therefore common understanding suggests that the amount of iron sulfide present in an ore deposit or mine waste plays a crucial role in determining the characteristics of the mine drainage. It is generally less appreciated that the oxidative behavior of different iron sulfide minerals varies appreciably, and the characteristics of mine drainage depends markedly on the particular iron sulfide minerals present.

In order to quantify differences in the oxidative behavior of pyrite and pyrrhotite-containing wastes, both simulated sulfidic mine wastes and actual mine tailings were leached under kinetic leach column test conditions. Synthetic mine wastes containing 5 wt% pyrite or pyrrhotite, together with 5 wt.% chlorite, 10 wt.% amazonite and 80 wt.% quartz, produced 71 % and 6 % respectively of the expected acidity based on acid base accounting during 120 weeks of leaching. Nickel mine tailings containing nearly 30 % pyrrhotite also produced much lower than expected acidity (<1 %) after 107 weeks of leaching.

Sulfur speciation analysis of both solids and the drainage demonstrate that, for both the simulated pyrrhotite mine waste and the nickel mine tailings, around 85 % of the oxidized sulfur converted to elemental sulfur, a reaction path which does not generate acidity. In contrast, for the simulated pyrite mine waste, only 2 % of the oxidized sulfur converted to elemental sulfur, with the majority oxidising through to sulfate. While elemental sulfur can further oxidize to sulfate with concomitant acid production, this reaction is very slow in the absence of oxidative bacterial catalysis. Analysis of the oxidized zone of the nickel mine tailings storage facility also demonstrated the predominant oxidation product to be elemental sulfur, suggesting that even in field conditions, pyrrhotite oxidation will likely produce significantly less acidity than is predicted by standard AMD assessment methods.

Keywords: pyrite, pyrrhotite, acid potential, elemental sulfur

INTRODUCTION

In the assessment of the acid generating potential of a mine waste material, the initial screening method usually includes acid base accounting (ABA) and, in some cases, the net acid generation (NAG) test (INAP, 2009). In its most basic form, ABA includes calculation of the acid potential (AP) of a waste usually by determining the sulfide content of the material. The use of sulfide content without further distinction between the various sulfide minerals is based on the abundance of iron sulfides, particulalry pyrite, in mine wastes. AP is then calculated from the sulfide sulfur content based on the stoichiometry of the reaction of pyrite with oxygen and water to produce one mole of sulfuric acid per mole of sulfur. It is generally regarded that other iron sulfides such as pyrrhotite, marcasite and arsenopyrite will also react simiarly to produce acid, while some sulfides such as sphalerite and galena, which can undergo oxidative dissolution to release metal ions and sulfate without iron oxyhydroxide precipitation, may not produce much if any acidity (INAP, 2009, MEND, 2009, DTIR, 2007).

Under the conditions of the accelerated oxidation NAG test (hydrogen peroxide), results from testing of various individual sulfide minerals suggest that all iron sulfides react in a similar way to pyrite, producing one mole of sulfuric acid per mole of sulfur (Stewart et al., 2003, Jennings et al., 2000). Therefore in the use of these simple screening methods for assessment of acid potential, there is generally no consideration given to different potential reaction pathways for oxidative dissolution of the various iron sulfides and the possible effects of these reaction pathways on drainage chemistry. However, a number of studies have identified that, unlike the oxidative dissolution of pyrite where sulfate is invariably the major final product of sulfide oxidation, during oxidation of pyrrhotite signficant quanities of elemental sulfur have been identified (Cruz et al., 2005, Belzile et al., 2004, Mikhlin et al., 2002, Kalinkin et al., 2000, Nicholson & Scharer, 1994). In addition to laboratory studies, investigations into weathering of pyrrhotite in site tailings storages have shown that elemental sulfur is present as a result of pyrrhotite oxidation (McGregor et al., 1998, Janzen et al., 1997).

Table 1 shows some potential overall reaction pathways for the dissolution of pyrite and pyrrhotite, ranging from oxidative dissolution to produce iron oxyhydroxide and sulfate (2 moles H^+ produced per mole S) to non-oxidative dissolution to hydrogen sulfide (2 moles H^+ consumed per mole S). It is clear from these equations, that the pathway(s) along which iron sulfide dissolution occurs will influence the amount of acidity produced (or consumed) with direct conseqence on drainage quality. It is also apparent that if oxidation of pyrrhotite proceeds only as far as elemental sulfur, then no proton acidity will be produced. If this reaction pathway becomes the dominant path for oxidative dissolution, then AP and NAG measurements will likely greatly over estimate the amount of acidity that can be expected from pyrrhotite containing waste matereials.

In order to determine and quantify the different reaction pathways of various sulfide minerals during oxidation, we have investigated the behavior of simulated mine wastes containing various sulfides including pyrite and pyrrhotite using kinetic leach column tests (AMIRA 2002). At the same time, as part of investigations into the geochemistry of tailings in the tailings storage facility (TSF) at the Savannah Nickel Mine (SNM) in the Kimberly region of Western Australia (Robertson et al. 2015), we have studied the oxidative behaviour of pyrrhotite-containing tailings both in laboratory leach columns and *in situ* in the SNM TSF. This paper details the results of these investigations, including quantification of the relative amounts of various reaction products and the subsequent acidity produced.

Table 1 Different reaction pathways for oxidative and non-oxidative dissolution of pyrite and pyrrhotite and the corresponding number of protons released per S

Product	Sulfide	Reaction	H^+ Released/S	H^+ Stored/S
Goethite & sulfate	Pyrite	$FeS_2 + 3.75O_2 + 2.5H_2O \Rightarrow FeOOH + 2SO_4^{2-} + 4H^+$	2 (100%)	0 (0%)
	Pyrrhotite	$Fe_{(1-x)}S + 0.75(3-x)O_2 + 0.5(3-x)H_2O \Rightarrow (1-x)FeOOH + SO_4^{2-} + 2H^+$	2 (100%)	0 (0%)
Goethite & jarosite	Pyrite	$FeS_2 + 3.75O_2 + 2.5H_2O + 1/3K^+ \Rightarrow 1/3KFe_3(SO_4)_2(OH)_6 + 4/3SO_4^{2-} + 3H^+$	1.5 (75%)	0.5 (25%)
	Pyrrhotite	$Fe_{(1-x)}S + 0.75(3-x)O_2 + 0.5(3-x)H_2O + 1/3(1-x)K^+ \Rightarrow 1/3(1-x)KFe_3(SO_4)_2(OH)_6 + 1/3(1+2x)SO_4^{2-} + (1+x)H^+$	1+x (55% for $Fe_{0.9}S$)	1-x (45% for $Fe_{0.9}S$)
Goethite & elemental sulfur	Pyrite	$FeS_2 + 0.75O_2 + 0.5H_2O \Rightarrow FeOOH + 2S$	0 (0%)	2 (100%)
	Pyrrhotite	$Fe_{(1-x)}S + 0.75(1-x)O_2 + 0.5(1-x)H_2O \Rightarrow (1-x)FeOOH + S$	0 (0%)	2 (100%)
Sulfide	Pyrrhotite	$Fe_{(1-x)}S + 2H^+ \Rightarrow (1-3x)Fe^{2+} + 2xFe^{3+} + H_2S$	-2 (-100%)	4 (200%)

METHODOLOGY

Kinetic leach column tests using simulated sulfidic mine wastes

To compare the oxidative behaviour of pyrite and pyrrhotite under conditions that might be comparable to the oxidative zone of a waste rock storage facility, simulated sulfidic mine wastes containing either pyrite or pyrrhotite were subjected to leaching for a period of 120 weeks. In addition to 5 wt.% sulfide, the simulated sulfidic wastes also contained 5 wt.% chlorite, 10 wt.% amazonite and 80 wt.% quartz. Leaching was conducted using the standard kinetic leach column method (AMIRA 2002).

All of the individual mineral samples used for producing the simulated sulfidic mine wastes were characterized by bulk assay and quantitative XRD analysis. The results show that pyrite and quartz were essentially pure minerals (>98%). The pyrrhotite sample contained 65 wt.% pyrrhotite, 10 wt.% pentlandite and 8 wt.% chalcopyrite. Scanning electron microscopy (SEM) analysis using energy dispersive x-ray spectroscopy (EDS) suggested an average iron content of 46.5 atomic % in the pyrrhotite, which is close to that for the iron deficient monoclinic pyrrhotite Fe_7S_8. Analysis results for the chlorite sample indicate it contained around 75% chlinoclore, with 15% quartz and 10% albite. The amazonite was an 80:20 mixture of microcline and albite.

Kinetic leach column tests using pyrrhotite tailings from SNM

Quantitative XRD analysis of the fresh tailings from SNM indicated a pyrrhotite content of 29.1%, which, if it is assumed that the sulfide content is 11.4% (Total S 11.5% - sulfate S 0.1%), is very close to the 29.3% pyrrhotite calculated from the sulfide S content assuming a formula of $Fe_{0.90}S$ for the pyrrhotite determined by EDS analysis. SEM-EDS analysis identified essentially pyrrhotite as the only sulfide, with very minor amounts of mackinawite ($(Fe, Ni)_{(1+x)}S$). No pyrite was found. XRD analysis using a high intensity, high resolution synchrotron source indicated the pyrrhotite in the fresh tailings was around 90% hexagonal, consistent with an average iron content of 47.4 atomic % ($Fe_{0.90}S$).

XRD analysis identified both anthophyllite and ferroan enstatite as magnesium bearing silicates in the tailings. SEM analysis confirmed the presence of magnesium iron silicate phases, which are likely to contribute significantly to the neutralising potential (NP) of the tailings. Inorganic carbon analysis indicated there are no carbonates in the fresh tailings (inorganic C <0.02%).

Fresh tailings collected from the SNM concentrator were placed into columns 150 mm diameter by 600 mm height. The columns were constructed in four segments, each segment containing liquid and solids sampling points. The tailings were placed into the columns as slurries in process water as received. Approximately 15 kg of tailings (dry weight) were packed into each column. After allowing the bed to consolidate, water was allowed to drain from the columns. The consolidated tailings bed had a porosity of close to 0.40, similar to that estimated for the tailings in the SNM TSF.

KLC tests were run with tailings at 50 and 75 % average saturation. However, after allowing Column 1 (target 50 % saturation) to drain under gravity for four months the average degree of saturation of the tailings bed had not dropped below 75 %, presumably due to the high suction pressure of this material. Following the first flush, Column 1 was allowed to drain until no further water was collected. Vacuum was then applied to the column until sufficient water was removed to give an average degree of saturation of 50%. After about six months of operation, it was found that small volumes of water were required to be added to Column 2 to maintain 75% average saturation.

Flushing of the tailings was achieved by adding 3 L of deionized water to the columns and allowing the flush water to remain in the column for 24 h prior to draining. Water was collected in clean plastic-lined foil bags so that air was excluded during collection. pH and oxidation-reduction potential (ORP) measurements were made at each of the liquid sampling points (top, middle and bottom segments) for each column immediately prior to collection of the flush water. Flushes were conducted at weeks 16, 26, 39, 52, 65, 78, 91 and 107. Solids were sampled from each segment following flushes at weeks 26, 52, 78 and 107. Approximately 10 g of wet solids were removed from each sampling point by inserting a hollow tube through the entire width of the column. The samples were weighed and then dried under vacuum at 50°C prior to analysis.

Characterization of sulfur species in tailings from SNM

Core samples from TSF1 at SNM were collected using a drilling rig fitted with an auger bit in which the core was collected in 40 mm diameter tubes, each of 700 mm length. Using this method, the cores had very limited exposure to air during sampling and no drilling water was used so pore water was not diluted during sampling. Samples from the drill holes were bagged immediately in air tight plastic bags and transported to the metallurgical laboratory on site as collected.

Measurements including pore water pH, Eh and dissolved oxygen (DO) were made in a glove bag under an argon atmosphere. Remaining pore water was filtered and appropriately preserved and then transported to our laboratories in Adelaide. The remaining core samples were frozen and transported to Adelaide without thawing. Samples were stored frozen until they were analysed when they were thawed and a portion dried under vacuum at 50°C.

Analysis of column leachates and solids, and tailings storage facility pore waters and solids

Samples of simulated sulfidic mine waste, fresh tailings and TSF core samples from SNM were characterized using standard static test procedures (NP, total S, chromium reducible sulfur (S_{CR}), NAG) in addition to mineralogical analysis by quantitative XRD and SEM-EDS analyses. Sulfur speciation analysis was conducted on both fresh tailings and on samples of weathered tailings from

the kinetic leach column tests and on core samples collected from the SNM TSF. Sulfur speciation analysis was also conducted on solids removed from the kinetic leach column tests conducted on simulated sulfidic mine wastes after 120 weeks of leaching.

NP and NAG analyses were conducted according to the methods described in the AMIRA ARD Test Handbook (AMIRA 2002). S_{CR} analysis was conducted using the method of Sullivan et al. (2004). Sulfur speciation analyses were carried out using the methods of Li et al. (2007) and Stewart et al. (2009). Because of the high concentration of pyrrhotite in the SNM tailings samples, it is likely that pyrolysis of the tailings does not result in complete removal of the pyrrhotite (Li et al., 2007). Therefore a portion of the pyrrhotite would report as HCl extractable sulfur which also includes insoluble sulfates such as jarosite. Consequently HCl extractions were not conducted and estimates of jarosite content were not made. Determination of elemental sulfur was achieved by extraction of the solids with acetone followed by analysis of the extract by liquid chromatography (McGuire and Hamers, 2000).

RESULTS AND DISCUSSION

Kinetic leach column tests using simulated sulfidic mine wastes

During KLC testing of the simulated sulfidic mine wastes containing pyrite and pyrrhotite, coloration of the pyrrhotite waste suggested significant oxidation had taken place, but acidity measured in leachates was surprisingly low in comparison to the expected acidity based on either ABA or NAG tests (Table 2). In an attempt to understand the lower than expected leachate acidity, sulfur mass balance was undertaken to determine reaction pathways of sulfide oxidative dissolution. Sulfur mass balance included sulfur species contained in leachates, sulfur in acetone extracts of solids (elemental sulfur) and sulfur species in 1M KCl extracts of the solids (soluble sulfates, e.g. gypsum, melanterite, etc.).

Based on sulfur mass balance undertaken at 120 weeks of leaching, less than 20 % of pyrite and more than 70 % of pyrrhotite had undergone oxidation, consistent with the visual evidence that suggested substantial oxidation of the simulated pyrrhotite waste and in line with previous studies, which suggest pyrrhotite oxidation rates one to two orders of magnitude higher than for pyrite (Belzile et al., 2004). Correction of expected acidities based on the amount sulfide oxidized, gave much closer agreement with measured acidity for the simulated pyrite waste, but the measured acidity was still significantly lower than that expected from oxidation of the simulated pyrrhotite waste if oxidation was assumed to proceed to goethite and sulfate (Table 2). However, the sulfur mass balance indicated that the dominant (85 %) sulfur oxidation product in the case of the simulated pyrrhotite waste was not sulfate but elemental sulfur (Table 2), a reaction which will not produce acidity (Table 1). Further correction of the expected acidity to take into account oxidative dissolution to elemental sulfur, shows much closer agreement with the measured acidity for the simulated pyrrhotite waste.

Further analysis of leachate solutions and 1M KCl extracts of the solids were undertaken to determine the processes that may lie behind the difference in measured and expected acidity, even after reaction to elemental sulfur is taken into account. The results of these analyses are shown in Figure 1. The figure shows the titrated acidity (released acidity) together with stored acidity measured by titration of the KCl extract. It also shows released and stored alkalinity, which were calculated from concentrations of Ca, Mg and Na in leachates and KCl extracts respectively,

assuming the presence of these ions results from neutralising reactions. When stored and released acidities and alkalinities are combined, their sum is in good agreement with the expected acidities (Fig. 1). The results demonstrate that for the pyrite waste, the majority of acidity is released, with minor stored acidity and limited neutralization provided by chlorite in the simulated waste. In the case of the simulated pyrrhotite waste, the proportion of expected acidity which was released under KLC conditions was much less, with more stored acidity and some neutralising by chlorite (Jambor et al., 2007).

Table 2 Comparison of expected and measured acidity in leachates after 120 weeks of KLC testing conducted on simulated sulfidic wastes containing either pyrite or pyrrhotite

Sulfide	AP (kg $CaCO_3$/t)	NAG (kg $CaCO_3$/t)	Titrated leachate acidity (kg $CaCO_3$/t)	Total sulfide oxidized (%)	Expected acidity (kg $CaCO_3$/t)	Relative amount oxidized to S^o (%)	Expected acidity S^o excluded (kg $CaCO_3$/t)
Pyrite	84	65	10	17	14	2.0	14
Pyrrhotite	50	32	2.0	73	37	85	5.6

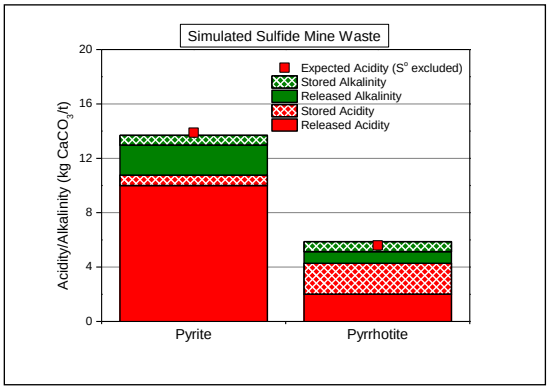

Figure 1 Acidity and alkalinity measured in leachates (released) and in KCl extracts of solids (stored) after 120 weeks of KLC testing conducted on simulated sulfidic mine wastes containing either pyrite or pyrrhotite

Kinetic leach column tests using pyrrhotite tailings from SNM

Similar to observations made during KLC tests of simulated pyrrhotite waste, visual inspection of the SNM tailings during column leach testing suggested extensive oxidation, but acidities measured in leachates remained low (Table 3) and in the case of the tailings leached at an average saturation of 75 %, almost non-existent (Table 4). With a pyrrhotite content of around 30%, these tailings were predicted to be strongly acid producing. Sulfur mass balance analysis indicated around 40% of the pyrrhotite had undergone oxidation during two years of leaching at 50 % average saturation and around 10% was oxidized during two years of leaching at 75 % average saturation (Tables 3 and 4), suggesting both columns should have produced substantial acidity if oxidation had proceeded to sulfate (Table 1). However, as for the simulated pyrrhotite waste, sulfur analysis demonstrated that the major pathway for pyrrhotite oxidation during leaching of the SNM tailings was via oxidation

to elemental sulfur, with around 90 % of oxidized sulfur in the tailings leached at 50 % saturation and around 80 % of oxidized sulfur in the tailings leached at 75 % saturation, reacting to produce elemental sulfur and no acidity (Tables 3 and 4). When this non-acid producing reaction pathway is taken into account, expected and measured acidities are much closer, although there was still significantly less measured acidity than expected, especially for the column leached at 75 % saturation.

Table 3 Comparison of expected and measured acidity in leachates during 107 weeks of leaching of SNM tailings with and average saturation of 50%

Leaching time (weeks)	AP (kg $CaCO_3$/t)	NAG (kg $CaCO_3$/t)	Titrated leachate acidity (kg $CaCO_3$/t)	Total sulfide oxidized (%)	Expected acidity (kg $CaCO_3$/t)	Relative amount oxidized to S^o (%)	Expected acidity S^o excluded (kg $CaCO_3$/t)
26	356	213	0.03	7.6	27	91	2.5
52			5.2	25	87	88	11
78			7.4	44	155	90	16
107			9.3	39	139	88	17

Table 4 Comparison of expected and measured acidity in leachates during 107 weeks of leaching of SNM tailings with and average saturation of 75%

Leaching time (weeks)	AP (kg $CaCO_3$/t)	NAG (kg $CaCO_3$/t)	Titrated leachate acidity (kg $CaCO_3$/t)	Total sulfide oxidized (%)	Expected acidity (kg $CaCO_3$/t)	Relative amount oxidized to S^o (%)	Expected acidity S^o excluded (kg $CaCO_3$/t)
26	356	213	0	2.0	7.1	80	1.4
52			0.02	7.9	28	79	5.9
78			0.03	10	36	79	7.7
107			0.05	9.5	34	73	9.2

The results of a similar analysis of stored and released acidity and alkalinity in leached SNM tailings to that conducted for the simulated sulfidic wastes are shown in Figure 2. Again, when stored and released alkalinity (neutralized acidity) are summed together with stored and released acidity, there is good agreement with the expected acidity based on the total amount of sulfide oxidized and the percentage of reaction leading to elemental sulfur. In some cases, the expected acidity is not entirely accounted for by the measured neutralization and stored and released acidity. These small differences are likely due to stored acidity in jarosite which was not quantified, but was detected during XRD analysis of the leached tailings.

Figure 2 shows that acidity released during oxidation of pyrrhotite in the SNM tailings comprized only a very small fraction of the total acidity generated and that the majority of the acidity has been neutralized, although at 50% saturation, there is also a significant fraction of stored acidity. Analysis of leachates and KCl extracts indicate that most of this neutralization comes from

magnesium bearing minerals, possibly enstatite. The results suggest that if the tailings can be maintained at near or above 75% saturation, then pyrrhotite oxidation is likely to be sufficiently slowed to allow the small amount of acidity generated from oxidation through to sulfate (Table 1), to be neutralized by reactive silicates present in the tailings. Under these conditions, released acidity is likely to be less than 1% of that predicted by ABA or NAG tests.

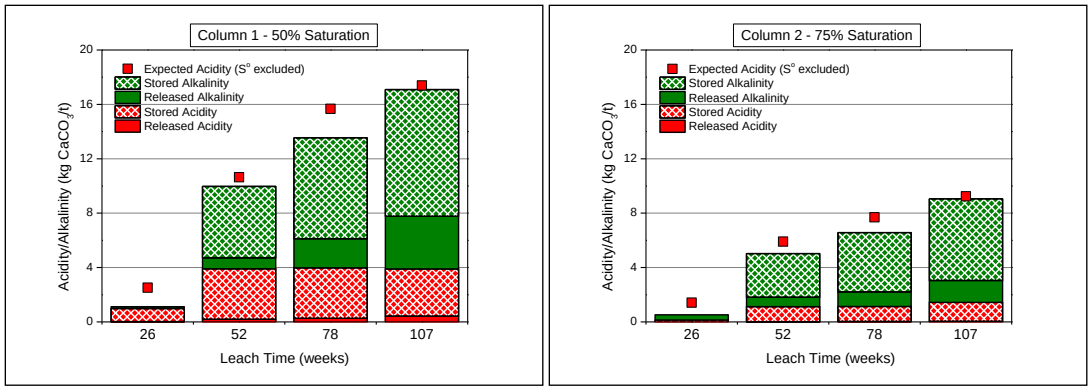

Figure 2 Acidity and alkalinity measured in leachates (released) and in KCl extracts of solids (stored), during 107 weeks of leaching of SNM tailings at an average saturation of 50% (left) and an average saturation of 75% (right)

Characterization of sulfur species in tailings from SNM

As a part of the study of geochemical reactions which occur during weathering of the SNM tailings, core samples were taken from several locations at the TSF. Core samples were taken through the full depth of the tailings deposited in the TSF and represented tailings deposited over about a five year period. Surface tailings, which had formed a hardpan, represented material deposited during the previous 1.5–2.5 years. Sulfur speciation analysis was undertaken on the core samples. The results of these analyses are show in Figure 3.

For each core sample taken, in the oxidized hardpan layer, elemental sulfur was the dominant sulfur species present with only minor sulfide (pyrrhotite) remaining. It was not possible to determine with any accuracy the relative proportion of oxidation of pyrrhotite to elemental sulfur vs oxidation to sulfate, as the amount of sulfate produced could not be determined since it is not quantitatively retained within the hardpan. Nevertheless, an estimate of the relative amounts of oxidation to elemental sulfur and sulfate could be made based on the results of sulfur speciation. For example, if in the Geochem 4 hardpan sample it is assumed that the original sulfide sulfur content is similar to the sulfide sulfur content of the tailings immediately below the hardpan, then sulfide sulfur decreased from 9.2 to 1.0 %. At the same time the elemental sulfur content increased from 0.1 to 7.1 %. This equates to an 86 % conversion of sulfide sulfur to elemental sulfur, suggesting that oxidation to elemental sulfur is the dominant reaction pathway for oxidation of pyrrhotite in the TSF hardpan.

These results suggest that under the conditions prevailing in the TSF, further oxidation of elemental sulfur is very slow in comparison to pyrrhotite oxidation, and that therefore the acidity generated by pyrrhotite oxidation will be substantially less than that predicted from ABA and NAG tests. This

was confirmed by results of tailings pore water analysis and ground water monitoring around the TSF, which showed elevated concentrations of sulfate, Ca and Mg, but neutral pH and no acidity, results consistent with the laboratory-based leaching tests conducted on SNM tailings.

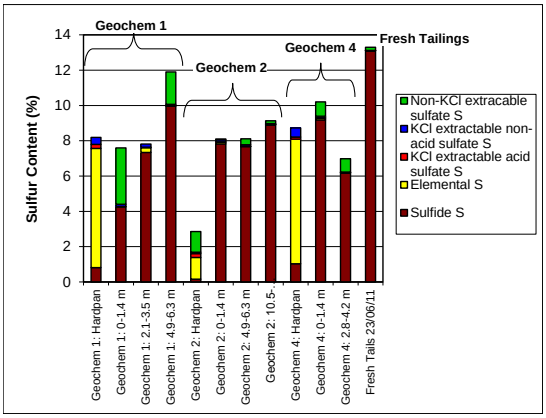

Figure 3 Results of sulfur speciation analysis of core samples taken from the SNM TSF

CONCLUSIONS

Oxidation of iron sulfides is recognized as being the cause of AMD, but generally no distinction is made between different iron sulfides in prediction of acid potential. Despite the fact that it has long been recognized that oxidation of pyrrhotite produces elemental sulfur as well as sulfate, with the former reaction generating no net acidity, there appears to have been no previous studies which have quantified the contribution of reaction to elemental sulfur to the overall oxidation of pyrrhotite. In this study, oxidation of simulated sulfide mine wastes containing pyrite or pyrrhotite under kinetic leach column tests conditions, demonstrated that oxidation of pyrite was dominated by the reaction to produce sulfuric acid (98 %), while pyrrhotite oxidation primarily (85 %) produced elemental sulfur and consequently significantly less acidity (~5 %) than would be expected based on AP calculations or NAG testing.

Similar results were obtained during column leaching of mine tailings containing around 30% pyrrhotite. About 90 % of oxidized sulfur in the tailings leached at 50 % saturation and around 80 % of oxidized sulfur in the tailings leached at 75 % saturation, reacted to produce elemental sulfur and no acidity. Consequently measured acidities were around 6 % of the predicted acidity in the tailings leached at 50 % saturation and less than 0.2 % of the predicted acidity in the tailings leached at 75 % saturation. The very low acidity from the tailings leached at 75% saturation was not only due to oxidation principally occurring via production of elemental sulfur, but also because the majority of acidity produced by the alternative oxidation pathway to sulfuric acid was neutralized by magnesium silicates also present in the tailings.

While further oxidation of elemental sulfur to produce sulfate and acid may occur, especially in the presence of bacterial catalysis, analysis of the oxidized zone of the tailings in the mine TSF suggests that, similar to laboratory column leach tests, *in situ* oxidation of pyrrhotite led to elemental sulfur as the main product. The results from the TSF suggest that further oxidation of elemental sulfur with natural bacterial populations is relatively slow in conditions at SNM. These results indicate that tailings and mine waste rocks where the major iron sulfide is pyrrhotite, are likely to produce

signficantly less acid than those containing pyrite. The results of this study further suggest that if pyrrhotite oxidation can be sufficiently slowed, for example by maintaining adequate levels of saturation in tailings, then silicates present in many mine wastes may be reactive enough to neutralize most, if not all, of the acidity produced. In short, complete assessment of the acid potential of a mine waste material will include not only the amounts, but also the identities of any iron sulfides present.

ACKNOWLEDGEMENTS

Funding from a Linkage Grant from the Australian Research Council and sponsors of the AMIRA P933A project (BHP Billiton Iron Ore, Savage River Rehabilitation Project, Hidden Valley Services PNG, Rio Tinto, Teck Metals) in supporting the investigations of simulated sulfidic mine wastes is gratefully acknowledged. The authors also acknowledge the assistance and funding by Panoramic Resources Limited for the work conducted on pyrrhotite tailings.

REFERENCES

AMIRA/EGi (2002) ARD Test Handbook (Smart R, Skinner W, Levay G, Gerson A, Thomas J, Sobieraj H, Schumann R, Weizener C, Weber P, Miller S, Stewart W), *AMIRA International*, http://www.amira.com.au/web/documents/downloads/P387AProtocolBooklet.pdf .

Belzile, N., Chen, Y-W., Cai, M-F., Li, Y. (2004) 'A review on pyrrhotite oxidation' *J. Geochem. Explor*., vol 84, pp. 65–76.

Cruz, R., González, I., Monroy, M. (2005) "Electrochemical characterization of pyrrhotite reactivity under simulated weathering conditions' *App. Geochem*., vol 20, pp. 109–121.

DTIR (2007). *Leading practice sustainable development program for the mining industry. Managing acid and metalliferous drainage*, Department of Industry, Tourism and Resources, Canberra, ACT, Australia.

INAP (2009). *Global Acid Rock Drainage Guide (GARD Guide)*, Document prepared by Golder Associates on behalf of the International Network on Acid Prevention (INAP) http://www.gardguide.com.

Jambor, J.L., Dutrizac, J.E., Raudsepp, M. (2007) 'Measured and computed neutralization potentials from static test of diverse rock types' *Environ. Geol*., vol 52, pp. 1019–1031.

Janzen, M.P., Nicholson, R.V., Scharer, J.M. (1997) 'The role of enhanced particle surface area, crystal structure and trace metal content on pyrrhotite oxidation rates in tailings' *Proceedings 4th International Conference on Acid Rock Drainage*, May 31-June 6, Vancouver, BC, Canada.

Jennings, S.R., Dollhopf, D.J., Inskeep, W.P. (2000) 'Acid production from sulfide minerals using hydrogen peroxide weathering' *App. Geochem*., vol 15, pp. 247–255.

Kalinkin, A.M., Forsling, W., Makarov, D.V., Makarov, V.N. (2000) 'Surface oxidation of synthetic pyrrhotite during wetting-drying treatment' *Environ. Eng. Sci*., vol 17, pp. 329–335.

Li, J., Smart, R.StC., Schumann, R.C., Gerson, A.R., Levay, G. (2007) 'A simplified method for estimation of jarosite and acid-forming sulfates in acid mine wastes' *Sci Total Environ*., vol 373, pp. 391–403.

McGregor, R.G., Blowes, D.W., Jambor, J.L., Robertson, W.D. (1998) 'Mobilization and attenuation of heavy metals within a nickel mine tailings impoundment near Sudbury, Ontario, Canada' *Environmental Geology*, vol 36, pp. 305–319.

McGuire, M.M., Hamers, R.J. (2000) 'Extraction and quantitative analysis of elemental sulfur from sulfide mineral surfaces by high-performance liquid chromatography' *Environ. Sci. Technol*., vol 34, pp. 4651–4655.

MEND, 2009. *Prediction Manual for Drainage Chemistry from Sulphidic Geologic Material*, MEND Report 1.20.1, Natural Resources Canada, www.mend-nedem.org.

Mikhlin, Y.L., Kuklinskiy, A.V., Pavlenko, N.I., Varnek, V.A., Asanov, I.P., Okotrub, A.V., Selyutin, G.E., Solovyev, L.A. (2002) 'Spectroscopic and XRD studies of the air degradation of acid-reacted pyrrhotites' *Geochim. Cosmochim. Acta*, vol 66, pp. 4057–4067.

Nicholson R.V., Scharer J.M. (1994) 'Laboratory studies of pyrrhotite oxidation kinetics' In *Environmental Geochemistry of Sulfide Oxidation*, ACS Synposium Series 550, CA Alpers and DW Blowes (Co-Eds.), American Chemical Society Washington DC.

Robertson, A.M., Kawashima, N., Smart, R.St.C., Schumann, R.C. (2015) 'Management of pyrrhotite tailings at Savannah Nickel Mine – a decade of experience and learning' *Proceedings 10th International Conference on Acid Rock Drainage*, April 21–24, Santiago, Chile, Gecamin, Santiago, Chile, pp.

Stewart, W., Schumann, R., Miller., S, Smart, R. (2009) 'Development of prediction methods for ARD assessment of coal process wastes' *Proceedings 8th International Conference Acid Rock Drainage*, June 22-26, Skelleftea, Sweden, http://www.proceedings-stfandicard-2009.com/

Stewart, W., Miller., S, Smart, R , Gerson, A., Thomas, J., Skinner, W., Levay, G., Schumann, R. (2003) 'Evaluation of the net acid generation (NAG) test for assessing the acid generating capacity of sulfide minerals' *Proceedings 6th International Conference on Acid Rock Drainage*, July 14-17, Cairns, QLD, Australia, Australasian Institute of Mining and Metallurgy, pp. 617–625.

Sullivan, L.A., Bush, R.T., McConchie, D., Lancaster, G., Clark, M., Lin, C., Saenger, P. (2004) *Chromium reducible sulfur (SCR)-method code 22B*. In: Ahern, C.R., Sullivan, L.A., McElnea, A.E. (eds). Laboratory method guidelines 2004 - acid sulfate soils. Queensland acid sulfate soil technical manual; Department of Natural Resources, Mines and Energy, Indooroopilly, Queensland, Australia.

Prediction of Acid Rock Drainage (ARD) from Calculated Mineralogy

Ron Berry[1], Julie Hunt[2], Anita Parbhakar-Fox[2] and Bernd Lottermoser[2,3]

1. CODES-UTAS, Australia
2. CRC ORE-UTAS, Australia
3. Camborne - School of Mines, United Kingdom

ABSTRACT

The acid-forming potential of ore and waste can be calculated based on a detailed knowledge of mineralogy, especially sulphide and carbonate contents. However, most mineralogical techniques (e.g., semi-quantitative X-ray diffraction (qXRD), scanning electron microscopy/energy dispersive spectroscopy (SEM/EDS) point counting) are too expensive for routine application. Mineralogy can be calculated from assay data using linear programming (simplex method) which is a mature method with application to real world quantities that cannot be negative. In order to apply this method, a table of mineral compositions is required for all the significant minerals in the study area. Unlike least squares methods, the mineral list can exceed the number of elements included in the assay data. Several carbonate compositions with a range of neutralising potential can be included. To use the linear programming method, a calibration must be established based on known compositions. This calibration can be based on qXRD or SEM/EDS point counting methods.

Not all types of assay data are sufficient for calculating mineralogy reliably. The best assay data comes from X-ray fluorescence analysis of major elements, including "loss on ignition" (LOI). Adding measured C content to this analysis provides a robust data set for calculating sulphide and carbonate contents of rocks. The mineralogy can be calculated without measured C, if LOI and SiO_2 are included in the analysis. However, typical mine databases contain multi-element assays based on a four-acid digestion method. In this case SiO_2 is not analysed and there is no "LOI" or total C. With typical four acid digestion data it is not possible to estimate the original carbonate content even when the mineralogy is simple. In rocks with complex mineralogy, mixed carbonates and/or multiple sulphides, qXRD and full chemical analyses are required to calculated acid rock drainage potential from mineralogy.

Keywords: calculated mineralogy, linear programming, ARD, carbonate

INTRODUCTION

In mining operations, the rock mineralogy is a key parameter controlling the acid generation/neutralisation potential (Paktunc, 1999). An efficient measurement of mineral abundance in waste samples is the key to understanding large scale acid rock drainage (ARD) potential. This can be done via calculated mineralogy and there are a number of methods that can be used to determine modal mineralogy from chemical assay. Two of these methods with potential application in the minerals industry are discussed here. These methods have been applied to two data sets, one with a simple mineralogy and a second data set from rocks with multiple sulphide and carbonate minerals.

METHODOLOGY

There has been a long history of calculating mineralogy from assay data. An early version was Bryan et al. (1969) which was improved on by Le Maitre (1981) and a more recent version was published by Paktunc (1998, 2001). All of these programs are based on simple least squares models and thus suffer from two serious limitations: 1) The nature of least squares models requires the number of minerals to be less than the number of elements in the analyses, and 2) the methods used do not enforce non-negativity constraints, so often the calculated mineralogy is impossible. The standard method for calculating a least squares model with non-negative constraints was published by Lawson and Hanson (1995). However, this method can now be readily carried out using the non-linear minimization routine included in the "Solver" tool within EXCEL®; an easily accessible version of this was presented by Herrmann and Berry (2002).

There is an additional problem with simple least squares minimisation methods, in that these methods assume that the errors on all input data are the same in absolute terms. For example, the absolute errors on SiO_2 and CO_2 values are considered to be the same. In practice, the relative errors are similar so that high abundance elements such as SiO_2 are over fitted and low abundance elements such as S and CO_2 are under fitted. A better result is obtained if the fit errors are weighted by the measurement errors (Press et al., 1986). This is especially important when merging data with very different errors such as quantitative Xray diffraction (qXRD) and assay data. Berry et al. (2011) addressed these problems and suggested two solutions suitable for calculation of mineralogy applicable to mine wastes: weighted least squares and Linear Programming.

There are many choices involved in selecting the most suitable assay data set for a mining environment. We have carried out a full major element analysis (including Ba and Cu) by X-ray fluorescence (XRF) with associated measurement of "loss on ignition" (LOI). H_2O+ and CO_2 were measured using a Flash Elemental Analyser. No organic C was observed so all C is assumed to be in carbonate. Quantitative XRD results were obtained using SiroQuant™ ver3.0 using the Rietveld method which is a standardless, full pattern approach to semi-quantitative phase analysis.

In most cases mine assays do not included any estimate of the volatile components. In addition it is now common for multi-element data to be four-acid digestions where SiO_2 is not analysed. To show how the absence of these components in the analyses affects the accuracy of the calculation, the mineralogy was calculated from several different subsets of this data.

All results reported here are based on 50 samples. For the linear programming, a separate group of 50 samples was used as a training set. No samples from the training set were included in the test data. The mineralogy of the training set was estimated using the weighted least squares method and all available analytical data.

Weighted least squares to combine assay and qXRD results

The assay data alone do not include enough constraints to calculate complex mineralogy. One way to overcome this problem is by measuring the mineralogy by qXRD. The qXRD results provide many additional constraints that can be used in calculated mineralogy and the calculation can include all major minerals. In the examples reported here, we calculated the abundance of 26 distinct mineral compositions with 34 constraints. Berry et al. (2011) applied this technique using the "NNLS" (non-negative least squares) subroutine of Lawson and Hanson (1995). Here we have used the non-linear "Solver" routine in EXCEL®. All calculated mineral abundances were limited in the Solver routine to be ≥0 (non-negative constraint) and ≤100% (as required by closure constraints on modal abundance).

For the assay results the measurement error was estimated as 3% relative plus 0.05% absolute. The errors for the qXRD results are based on repetitions of samples, error estimates reported in the literature and consideration of the fit errors achieved. For qXRD results the errors were set at 6% relative plus 0.5% absolute. At this weighting the problem can be stated as finding a modal mineralogy consistent with the chemical analysis which is as close as possible to the qXRD results. All samples in this study could be adequately explained (chi-squared probability of valid fit greater than 25%) based on these error estimates.

Linear programming and the Simplex Method

The second method of calculating the modal mineralogy from chemical analyses suggested by Berry et al. (2011) was linear programming using the Simplex method (Press et al., 1986). For the results reported here, the calculations were carried out using the linear routine in "Solver" with EXCEL®. This method requires a training set to calibrate the objective functions required. It can calculate mineral modes from an extended mineral list and additional linear constraints can be added as required. In this method, as in the weighted least square method, calculated mineral abundances were limited to ≥0 and ≤100%. For some minerals additional upper limits to abundance were enforced. A list of 45 distinct mineral compositions was included in the calculation.

Experimental Data

Experiment A: Simple assemblage

An evaluation program has been run on samples from a Cu porphyry deposit with a relatively simple mineralogy where carbonate is dominated by calcite and the significant sulfides are pyrite and chalcopyrite. Extensive mineral liberation analyzer (MLA) measurements failed to detect dolomite, ankerite or siderite above detection levels.

For these samples the mineralogy was calculated by:

a) weighted least squares using qXRD, major elements, total C and H_2O+
b) linear programming using major elements, total C and H_2O+
c) linear programming using major elements and LOI
d) linear programming using major elements except SiO_2

For experiment A the weighted least squares results were used to calculate the preferred "best" values for acid generating potential (AP) and neutralising potential (NP).

Experiment B: Complex assemblage

In the second experiment, the deposit type was IOCG (iron oxide-copper-gold) and the mineralogy relevant to ARD is more complex. Calcite, siderite, dolomite and ankerite were detected at significant and highly variable levels. Sulphides include significant chalcocite, bornite and chalcopyrite as well as pyrite which was at relatively low levels (i.e., typically less than 1%). In many ways this represents a worst case scenario for calculating ARD potential from assay data. The only significant sulphate was barite so problems with estimating other sulphates were not tested. Because of the mineralogical complexity, the mineralogy of all samples was measured using a SEM/EDS point count method (20,000 points) on grain mounts (Fandrich et al., 2007).

For these samples the mineralogy was estimated by:

a) SEM/EDS point counting
b) weighted least squares using qXRD, major elements and LOI
c) linear programming using major elements and LOI
d) linear programming using major elements except SiO_2

The linear programming estimates of the carbonate minerals, in experiment B, were calculated as end-member compositions for calcite, dolomite and siderite. Since the preferred estimate of acid neutralising capacity from intermediate carbonates is a linear sum of the cations (Paktunc, 1999), no attempt was made to estimate the actual proportion of ankerite in these analyses. For experiment B the SEM/EDS point count data were used to calculate the preferred "best" values for AP and NP.

Since the application of interest here is prediction of ARD, the results will be discussed in terms of AP and NP. No pyrrhotite was detected in these samples so AP is primarily due to pyrite. Thus the AP was calculated simply, as suggested by Paktunc (1999):

$$AP = 16.33 * X_{pyrite} \quad \text{in kg sulfuric acid equivalent per tonne}$$

The NP was calculated using the factors listed in Table 1.

Table 1 Estimates of NP from the literature (Skousen et al., 1997, Jambor et al., 2003, 2006, 2007, Hammarstrom et al., 2003). Siderite NP is for end-member siderite based on non-oxidisable cations as recommended by Paktunc (1999). All sulphides, tourmaline, fluorite, titanite and barite are assumed to have an NP of 0.

mineral	NP (calcite eq Kgms/t)	mineral	NP (calcite eq Kgms/t)
amphibole	3	K feldspar	1
ankerite	970	magnetite	2
apatite	8	muscovite	1
biotite	4	plagioclase	1
calcite	1000	pyroxene	5
chlorite	6	quartz	0
dolomite	1086	rhodochrosite	870
epidote	1	rutile	0
hematite	2	siderite	0
kaolinite	0		

RESULTS AND DISCUSSION

Experiment A: Simple assemblage

The abundance of calcite totally controls the NP results in experiment A. In this environment any method that considers the CO_2 content will produce an accurate assessment of the NP (Fig. 1). Where there is only a general indication of the volatile content, in this case a measure of LOI, the carbonate content can still be inferred but in these experiments the estimate is about 20% (relative) too high (Fig. 2). Using only the commonly available limited assay data, with no SiO_2 or LOI, the estimate is poor (Fig. 3) but still perhaps of some value as a general indication of which rock packages have acid neutralising potential.

The AP for the samples in experiment A is totally controlled by pyrite and with this simple mineralogy S analyses (with correction for barite and chalcopyrite) provide an excellent estimate of the pyrite content. Thus all the analytical methods tested give the same AP (Figs. 4, 5, 6). In this case even the simple four-acid analytical data commonly available in mine databases provides an excellent indication of AP.

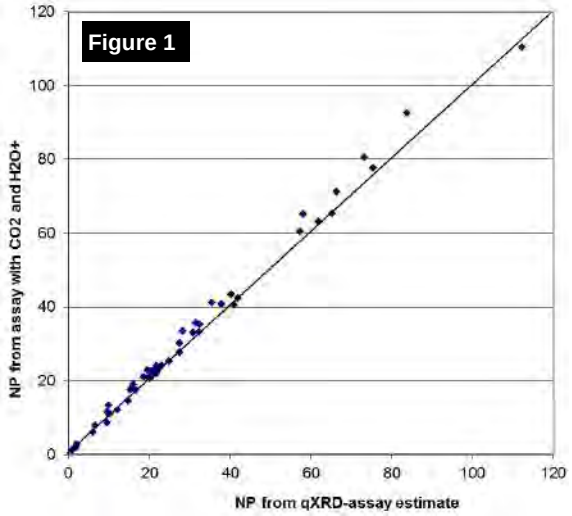

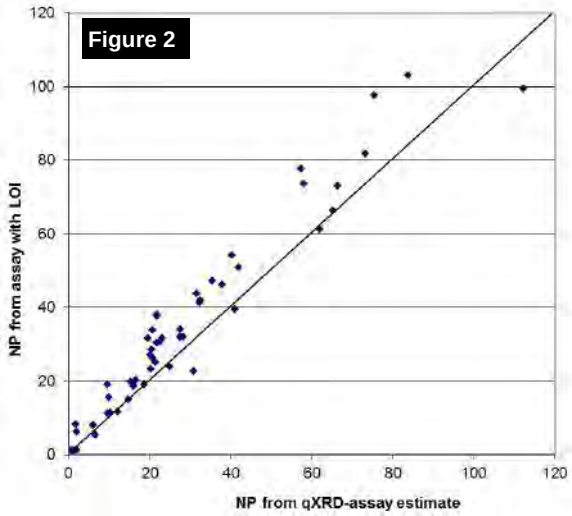

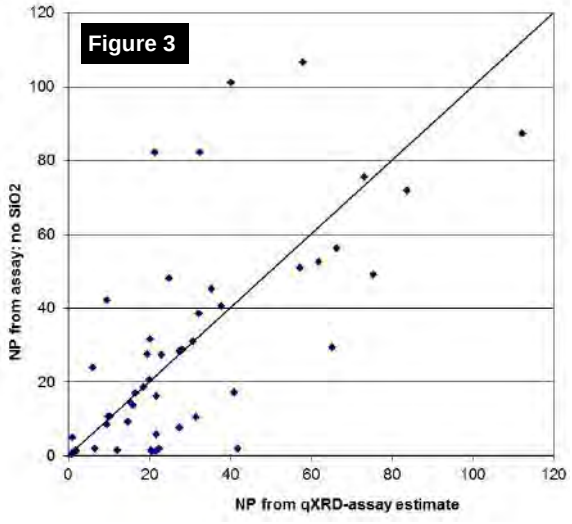

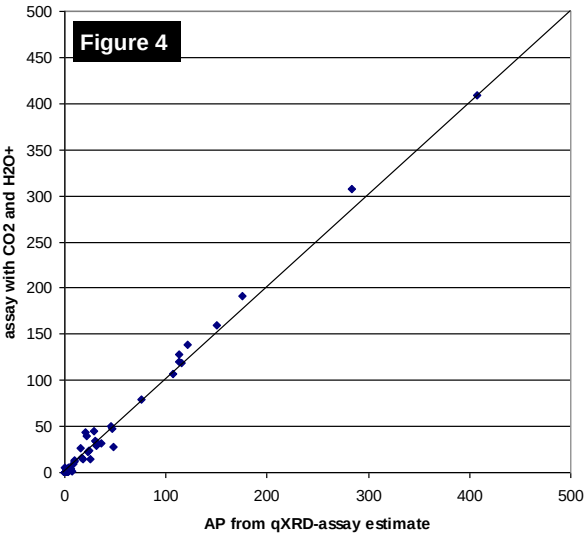

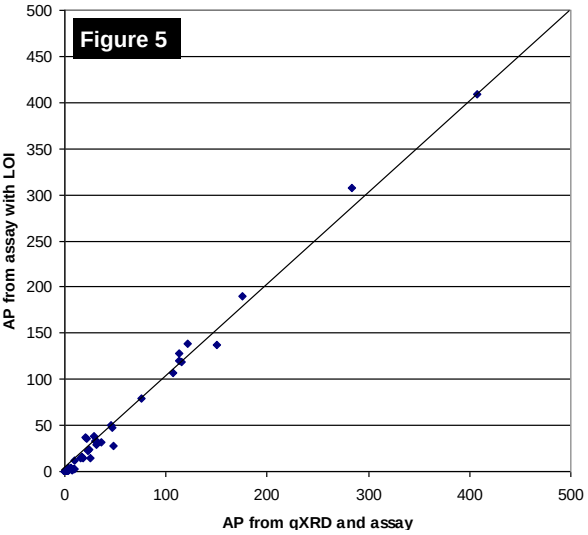

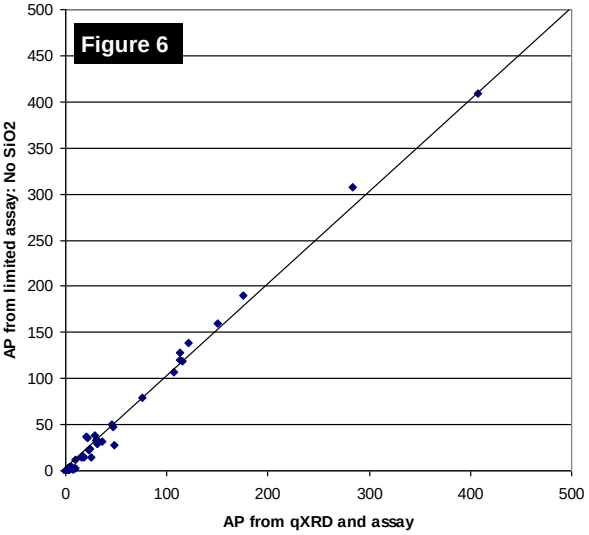

Figures 1 to 3. NP ($CaCO_3$ eq kg/t). X-axis = NP determined from combined qXRD and assay by weighted least squares method. **1)** Y-axis = predicted NP from linear programming with CO_2 and H_2O vs. Root mean squared

(RMS) difference of linear programming estimated from weighted least squared estimate 3.0; **2)** Y-axis = predicted NP from linear programming with LOI. RMS difference 9.3; **3)** Y-axis = predicted NP ($CaCO_3$ eq kg/t) from linear programming using limited assay data and no SiO_2. RMS difference 21.6;

Figures 4 to 6. AP (kg H_2SO_4/t)**.** X-axis = AP determined from preferred weighted least squared estimate. **4)** Y-axis = predicted AP from linear programming with CO_2 and H_2O. RMS difference 8.4; **5)** Y-axis = predicted AP from linear programming with LOI. RMS difference 7.6; **6**) Y-axis = predicted AP from linear programming using limited assay data and no SiO_2. RMS difference 7.5.

Experiment B: Complex assemblage

There are three different estimates of calculated mineralogy for the complex case. Using weighted least squares to combine qXRD and full major element assays by XRF gives an un-biased but not very accurate measure of NP. This can be seen by comparing the result with the more reliable SEM/EDS point counting method (Fig. 7). Using only analyses with LOI it is very difficult to balance the hydrous and carbonate minerals. In this example (Fig. 8), the NP was over-estimated by ~20 $CaCO_3$ eq kg/t at relatively low carbonate contents. With typical limited assay data (Fig. 9) the overestimate of the NP value was closer to ~30 $CaCO_3$ eq kg/t. These values suggest that, for the complex case in these experiments, the combined qXRD-assay method is required to adequately estimate NP. It is possible that a full assay (i.e. XRF + LOI) with CO_2 analysis would be sufficient but that was not tested on these rocks.

The qXRD analysis was strongly affected by the high X-ray fluorescence background in these high Fe rocks despite the use of a Co X-ray tube. The XRD laboratory noted that there was interference from an intense hematite XRD peak onto one of the main peaks of pyrite and they predicted that many of the low pyrite contents reported were too high. The combined qXRD-assay results inherit this bias to high pyrite estimates (Fig. 10). The comparison with the AP values determined from mineralogy based on SEM/EDS point counting suggests the pyrite content is overestimated by about 0.5%. This bias is seen as AP values that are about 10 kg H_2SO_4/t too high (Fig. 11) using the qXRD-assay estimates of mineralogy.

Using the assay data with LOI alone the AP values are generally too low (Fig. 12). With S allocated to four sulphides it is difficult to correctly predict the mixture on a routine basis. Most samples are close to the correct value but there are two outliers where the AP estimate is 20 kg H_2SO_4/t too low. The estimate based on a limited assay (Fig. 13) gives a similar result. While these methods are less robust than the qXRD-assay method they are not affected by the qXRD interference and have smaller average errors in AP value.

Figures 7 to 9 (below). NP ($CaCO_3$ eq kg/t). X-axis = NP determined from mineralogy based on SEM/EDS point counting. 7) Y-axis = predicted NP from weighted least squares integration of qXRD and assay data. RMS difference 10.6; 8) Y-axis = predicted NP from linear programming with LOI. RMS difference 20.9; 9) Y-axis = predicted NP from linear programming using limited assay data and no SiO_2. RMS difference 24.8.

Figures 11 to 13 (below). AP (kg H_2SO_4/t). X-axis = AP determined from mineralogy based on SEM/EDS point counting. 11) Y-axis = predicted AP weighted least squares integration of qXRD and assay data. RMS difference 5.4; 12) Y-axis = predicted AP from linear programming with assay data and LOI. RMS difference 5.3; 13) Y-axis = predicted AP from linear programming limited assay data and no SiO_2. RMS difference 4.1.

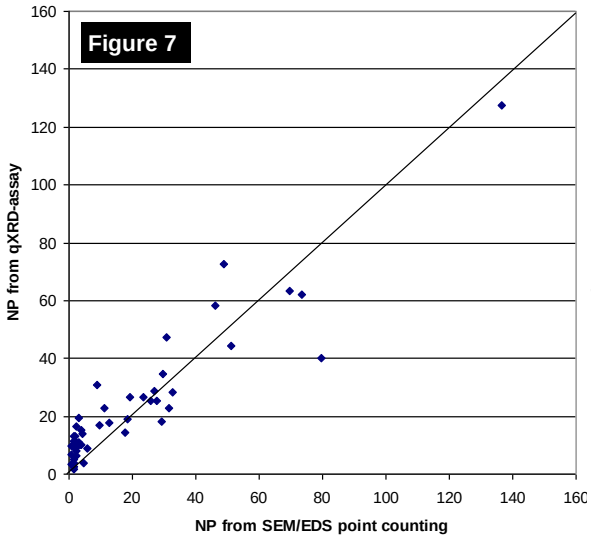
Figure 7
NP from qXRD-assay
NP from SEM/EDS point counting
0
20
40
60
80
100
120
140
160

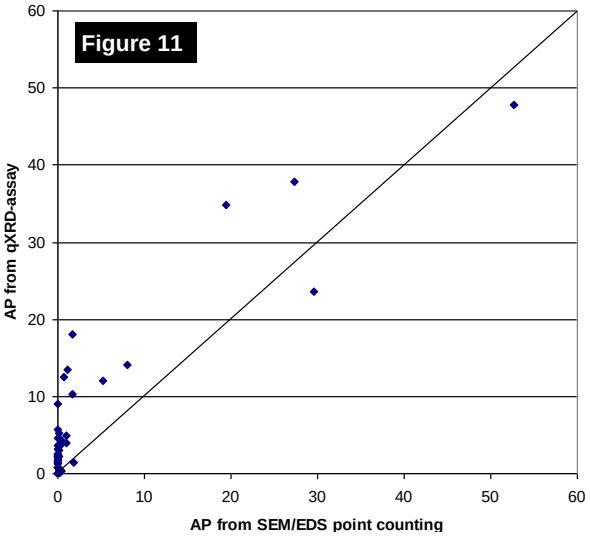
Figure 11
AP from qXRD-assay
AP from SEM/EDS point counting
0
10
20
30
40
50
60

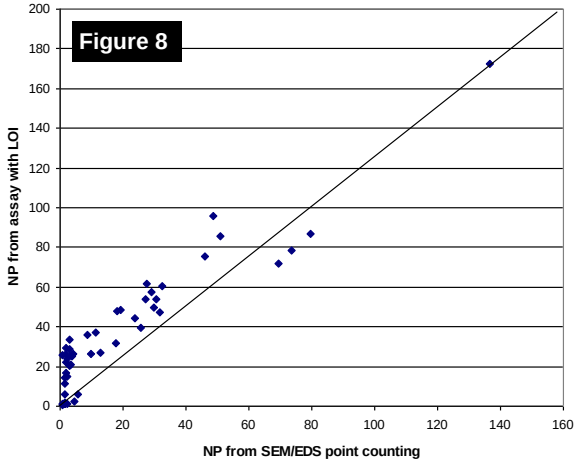
Figure 8
NP from assay with LOI
NP from SEM/EDS point counting
0
20
40
60
80
100
120
140
160
180
200

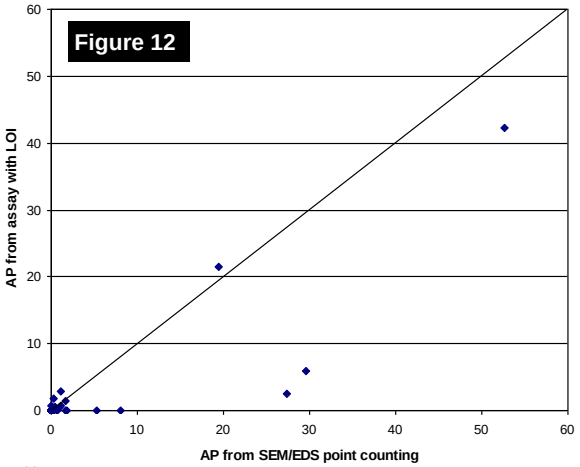
Figure 12
AP from assay with LOI
AP from SEM/EDS point counting
0
10
20
30
40
50
60

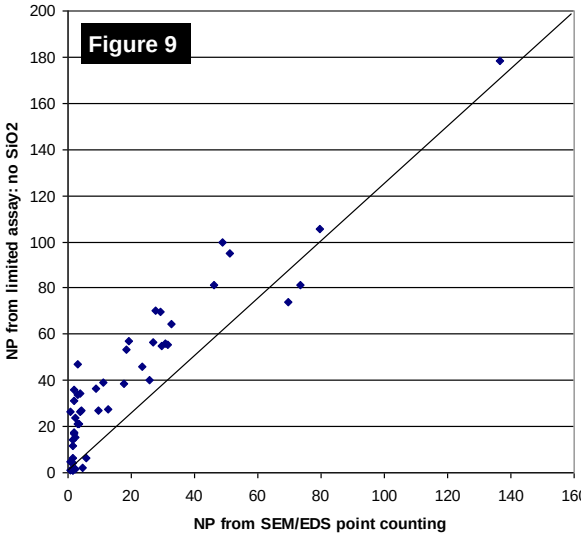
Figure 9
NP from limited assay: no SiO2
NP from SEM/EDS point counting
0
20
40
60
80
100
120
140
160
180
200

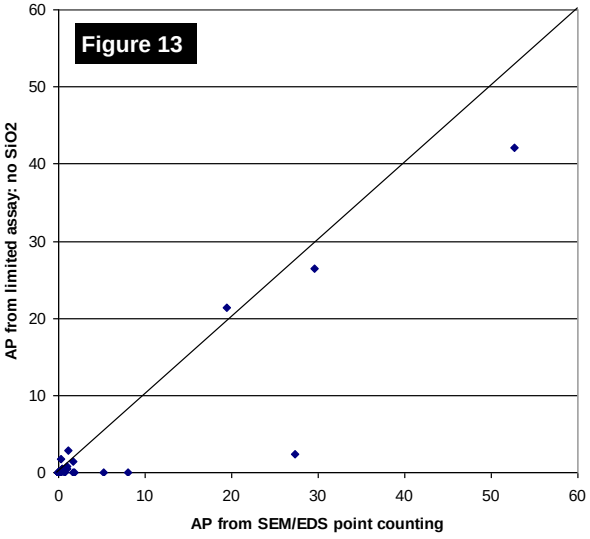
Figure 13
AP from limited assay: no SiO2
AP from SEM/EDS point counting
0
10
20
30
40
50
60

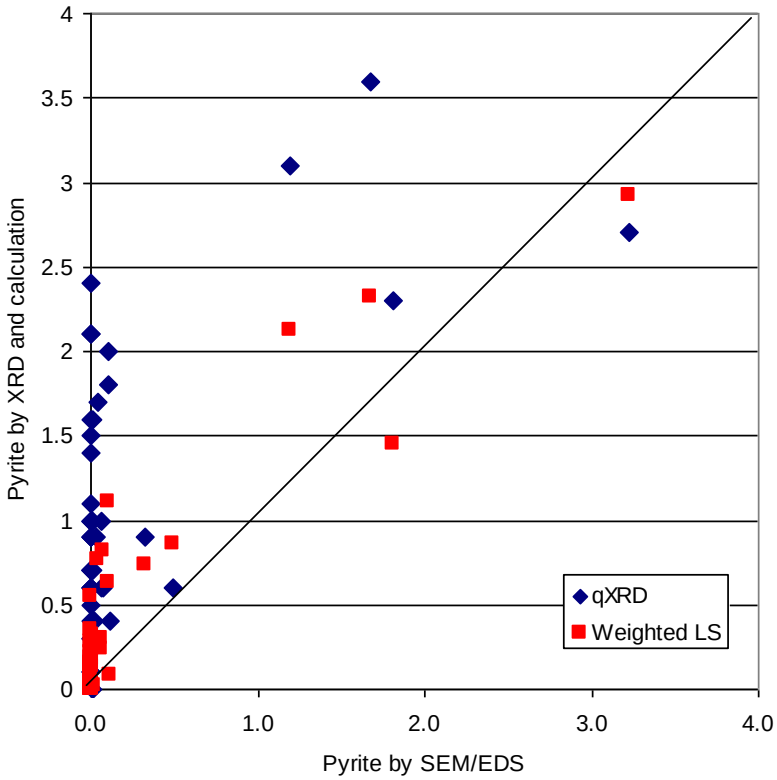

Figure 10. Comparison of pyrite estimates from qXRD alone (blue diamonds) and after merging qXRD with assay data using a weighted least squares method (red squares), with the more accurate estimate using SEM/EDS point counting.

CONCLUSION

Mineral grade calculated from assay data has potential to provide a low cost prediction of ARD potential, albeit, provided care is taken in the calibration and in selection of suitable assay characteristics. Quantitative (q)XRD is a robust method for identifying the major minerals in a sample. However the precision is poor and especially so at abundances less than 5%. Combining assay data with qXRD results leads to a substantially improved estimate of the mineralogy. Where there is an adequate training set of samples with "known" mineralogy, it is possible to estimate the mineralogy from assay data alone using linear programming.

In waste rocks with simple mineralogy it is possible to predict the ARD potential of rocks based on major element analyses where at least LOI is measured. However if the only available analysis are from four-acid assay data (no Si, no LOI) the NP cannot be accurately predicted and therefore the net acid production potential cannot be quantified.

Where the mineralogy is complex, with multiple S-bearing phases and/or mixed carbonates, ARD potential can be predicted from samples which have both qXRD and assay data. If only major element analyses with LOI are available the calculation of AP and NP are inaccurate and with only four-acid data no realistic estimate of ARD potential is possible.

ACKNOWLEDGEMENTS

Some of the C and H_2O+ analyses used in this paper were carried out at the Central Science Laboratory, University of Tasmania. The qXRD results were provided by Stafford Mcknight, University of Ballarat. Support for the data collection in this report was provided by AMIRA P843.

REFERENCES

Berry, RF, Hunt, JH and McKnight, SW (2011) Estimating mineralogy in bulk samples. In Dominy SC (ed) First AusIMM International Geometallurgy Conference (GeoMet) 2011, pp. 153-156.

Bryan, WB, Finger, LW and Chayes, F (1969) Estimating proportions in petrographic mixing equations by least squares approximation. Science, vol. 163, pp. 926-7.

Fandrich, R, Gu, Y, Burrows, D and Moeller, K (2007) Modern SEM-based mineral liberation analysis. International Journal of Mineral Processing, vol. 84, pp. 310-320

Hammarstrom, JM, Piatek, NM, Seal, RR, Briggs, PH, Meier, AL, Muzik, TL (2003). Geochemical characteristics of TP3 mine wastes at the Elizabeth copper mine superfund site, Orange County, Vermont. United States Geological Survey Open-File Report 03-431, pp. 83.

Herrmann, W and Berry, RF (2002) MINSQ - A least squares spreadsheet method for calculating mineral proportions from whole rock major element analyses. Geochemistry: Exploration, Environment, Analysis, vol. 2, pp. 361-368.

Jambor, JL (2003) Mine-waste mineralogy and mineralogical perspectives of acid-base accounting. In: Jambor, JL, Blowes, DW and Ritchie, AIM (Eds.), Environmental Aspects of Mine Wastes. Mineralogical Association of Canada, Short Course Series, 31, pp. 117-145.

Jambor, JL, Dutrizac, JE, Raudsepp M (2006) Comparison of measured and mineralogically predicted values of the Sobek Neutralization Potential for intrusive rocks. In: Barnhisel, RI (Ed.), Proceedings of the 7th International Conference on Acid Rock Drainage (ICARD), pp. 820-832.

Jambor, JL, Dutrizac, JE, Raudsepp, M (2007) Measured and computed neutralization potentials from static tests of diverse rock types. Environmental Geology, vol. 52, pp. 1019-1031.

Lawson, CL, and Hanson, RJ (1995) *Solving least squares problems.* SIAM classics in Applied Mathematics, Philadelphia, 337 pp.

Le Maitre, RW (1981) GENMIX – A generalised petrological mixing model program. Computers and Geosciences, *vol.* 7, pp. 229–247.

Paktunc, AD (1999) Mineralogical constraints on the determination of neutralising potential and prediction of acid mine drainage. Environmental Geology, vol. 39, pp. 103-112.

Paktunc, AD (2001) MODAN a computer program for estimating mineral quantities based on bulk composition: Windows version. Computers and Geosciences, vol. 21, pp. 883-886.

Press, WH, Flannery, BP, Teukolsky, SA and Vettering, WT (1986) *Numerical Recipes: The Art of Scientific Computing.* Cambridge University Press: Cambridge, 818 pp.

Skousen, J, Renton, J, Brown, H, Evans, P, Leavitt, B, Brady, K, Cohen, L, Ziemkiewicz, P (1997) Neutralization potential of over burden samples containing siderite. Journal of Environmental Quality, vol. 26, pp. 673-681.

Characterization of Weathering Products and Controls on Metal Mobility at a Cu-Ni-PGE Deposit

Paul Fix[1], Tamara Diedrich[2], Chris Kennedy[3] and Stephen Day[3]

1. Department of Earth and Environmental Sciences, University of Minnesota, USA
2. Barr Engineering Company, USA
3. SRK Consulting (Canada) Inc., Canada

ABSTRACT

Secondary minerals and other weathering products (for example, secondary sulfates, carbonates, oxides, and amorphous coatings) can serve as an important control on the concentration of trace metals in mine-impacted water. This becomes particularly true for mine features like waste rock stockpiles with engineered covers that are designed to minimize water flux, thereby increasing the likelihood that constituents released during mineral weathering are going to be retained within the feature. Standard methods designed to characterize constituent release rates (i.e., humidity cell tests) do not provide information on secondary mineral controls under mine site conditions due to the high water:rock ratio employed in these tests. Other types of tests that use less water may provide empirical evidence for weathering product-related controls, but, because they lack information on control mechanism or weathering product identities, it can be a challenge to extend the results to mine site conditions. Here, we report on the results of an ongoing study into controls exerted by weathering products on trace metal mobility from a magmatic sulfide Cu-Ni-PGE deposit within the Duluth Complex, located in Minnesota, USA. Key aspects of this study include: (1) utilization of weathered samples collected from outcrops on site as proxies for potential future oxidized waste rock; and (2) application of complementary analytical techniques, from both commercial and university labs, selected to achieve the chemical sensitivity and high-spatial resolution necessary to characterize secondary minerals in weathered rocks (including, but not limited to, X-ray diffraction, electron-microprobe analysis, and chemical analysis following sequential extraction). Results of this work are being used to refine the conceptual model for the mobility of trace metals that would be released during weathering of potential future waste rock.

Keywords: secondary minerals, metal attenuation, scanning electron microscope, X-ray diffraction, mineral characterization

INTRODUCTION

The Duluth Complex, Minnesota, USA, is a large composite mafic intrusion emplaced during a failed mid-continental rifting event that occurred in the region approximately 1.1 billion years ago and has been identified as one of the world's largest Cu-Ni-PGE resources (Miller et al., 2002). Multiple magmatic sulfide Cu-Ni-PGE deposits in the Duluth Complex are currently the subjects of ongoing mineral exploration, mine planning, and environmental review. While there is likely to be variability in the chemistry of mine-impacted waters from different potential future mines in the Duluth Complex, similarities in mineralogy, geology, and regional characteristics throughout the complex suggest that the following aspects of a site geochemical model may be typical for Duluth Complex deposits:

- The region has a wet, continental climate with abundant valuable water resources. Any potential future mine would likely be required to utilize engineered systems that minimize contact water as part of the mine water and waste rock management plans, for example, utilization of advanced stockpile cover systems, where appropriate.

- Oxidation of sulfide minerals is a potential source of acidity, sulfate, iron, and other metals (Lappako & Antonson, 2012; Lappako, Olson, & Antonson, 2013; Lappako, 1993). Within Duluth Complex magmatic deposits, sulfur content, as well as the sulfide mineralogy, show wide variability (Ripley & Alawi, 1986). The typical sulfide mineral assemblage includes pyrrhotite ($Fe_{(1-x)}S$), chalcopyrite ($CuFeS_2$), cubanite ($CuFe_2S_3$), and pentlandite ($(Fe,Ni)_9S_8$). Sulfide minerals may contain trace metals in addition to those indicated by the mineral formula. Whereas a larger suite of metals may be environmentally relevant for Duluth Complex rocks, this study is focused on Cu, Ni, Co, and Zn.

- Carbonate minerals are generally absent or at low concentrations in Duluth Complex rocks; instead, neutralization potential is supplied by dissolution of silicate minerals (Lappako et al., 2013). The silicate mineralogy for Duluth Complex rocks is dominated by anorthite-rich plagioclase feldspar, olivine, and pyroxene (Miller et. al 2002), of which, anorthite-rich plagioclase and olivine may provide significant neutralization potential. For rocks of sufficiently low sulfide content, this neutralization mechanism may be adequate to maintain circum-neutral conditions (Day & Kennedy, in press; Miller et al., 2010).

Ultimately, metal concentrations in mine-impacted water will reflect combined effect of constituent release from sulfide minerals, as well as, attenuation during weathering from mechanisms such as precipitation of secondary phases, sorption onto solid phase surfaces, and co-precipitation. In this context, the term "secondary phases" refers to minerals and other solid phases that form as a result of rock weathering after being exposed at the surface. Evidence for metal attenuation by ferric (oxy)hydroxides and related iron-rich secondary phases has been widely reported in the literature (for example, Carbone et al., 2012; Alpers et. al. 1994; Jambor & Dutrizac, 1998). With respect to Duluth Complex rocks, metal attenuation has been inferred for field leach piles with acidic pH (Kelsey et al., 1996). However, the role of attenuation by secondary phases would likely be more

significant for systems with low-sulfide waste rock where drainage maintains circum-neutral pH (Smith et al., 2013), because many of these attenuation mechanisms are pH dependent. Whereas extensive characterization has been performed on constituent release rates from Duluth Complex rock (Lappako, Olson & Antonson, 2013), relatively little work has characterized the relevant attenuation mechanisms, in particular, under circum-neutral conditions.

The following work aims to characterize weathering products and related attenuation mechanisms that could be active in mine-impacted drainage at a potential future Duluth Complex mine. Characterizing weathering products can be challenging due to the poor crystallinity and micro- to nanometer-scale size of features (e.g. thin surface coatings). To overcome some of these limitations, an assortment of high-resolution techniques, including scanning electron microscopy (SEM) methods, x-ray diffraction (XRD), and chemical sequential extraction were used, employing resources at both university and commercial labs.

METHODOLOGY

Low-sulfur waste rock piles of Duluth Complex rock are not available; therefore, weathered rock from exposures (both natural outcrops and historical railroad cuts) of Duluth Complex were collected and used as analogues for waste rock that may be produced by a potential future project. This approach has some limitations, for example, differences in time scales between natural weathering and mining, difference in surfaces, and poorly constrained drainage chemistry. Opportunistic sampling was conducted at six locations to capture the variety of visual alteration. Samples included both rock with visible weathered rinds as well as, white crusts (Figure 1). Of the six sampling locations, one captured rock from a meta-sedimentary rock that underlies the Duluth Complex. This paper focus on the Duluth Complex samples from the remaining five sampling locations. At each location, a grab sample (small clasts typically less than 1-2 inches, about 1 kg) and separate hand samples (about 1 kg) were collected.

Figure 1 Left image shows example of a field sampling location where Duluth Complex rock was exposed during construction of a railroad. Right image shows "white crust" observed at the site.

Secondary Mineral Characterization Techniques

Rietveld X-Ray Diffraction

Rietveld X-ray diffraction (XRD) was performed at the University of British Columbia. Grab samples were ground (< 10 μm) under ethanol in a vibratory McCrone Micronizing Mill for 7 minutes. Step-scan X-ray powder-diffraction data were collected over a range 3-80° 2θ with CoKα radiation on a Bruker D8 Advance Bragg-Brentano diffractometer equipped with an Fe monochromator foil, 0.6 mm (0.3°) divergence slit, incident- and diffracted-beam Soller slits and a LynxEye-XE detector. The long fine-focus Co X-ray tube was operated at 35 kV and 40 mA, using a take-off angle of 6°. The detection limit for this method is about 0.5 percent.

Qualitative powder X-Ray Diffraction

To supplement Rietveld XRD on whole rock samples, coatings on hand samples were isolated for additional analysis by XRD. Samples were viewed under a binocular microscope to identify visually distinct weathered areas. Alteration coatings were then scraped with a stainless steel pick onto a plastic weigh boat. While viewing the granular scrapings under a binocular microscope, material that appeared as primary mineral grains (i.e. unweathered materials) was removed. Samples were ground with an agate mortar and pestle and mounted on zero-background plates. Using a Phillips XPert MPD diffractometer at the University of Minnesota-Duluth with CuKα radiation source, each sample was scanned between 5° and 65° 2θ at a scan rate of 0.05 deg./min. X-rays were refined with a graphite monochromator, 1° divergence slit, incident and diffracted Stoller slits, a 10 mm mask and collected with a point scintillator detector. The X-ray tube was operated at 40 kV and 40 mA. The long collection time gave sufficient counts to match patterns from the database for some secondary phases. Diffraction data were processed with X-Pert HighScore software and compared to mineral patterns in the International Centre for Diffraction Data (ICDD) database.

Scanning Electron Microscopy

The morphology and semi-quantitative coating chemistry were characterized using a SEM. Preparation included crushing (< 1 mm), mounting in epoxy, polishing, and carbon coating (15 nm). A JEOL JSM-6590LV scanning electron microscope, combined with an INCA X-ACT energy dispersive spectroscopy system (EDS) and complementary software, was operated at the University of Minnesota-Duluth. Operating conditions were optimized independently for imaging in backscattered mode and EDS mode; moderate accelerating voltage (15 kV) produced optimal results. EDS calibration was performed on metallic Cu and is considered semi-quantitative. Additional work was performed on a JEOL 8600 Electron Microprobe operated in EDS mode by McSwiggen & Associates, a commercial lab in St. Anthony, Minnesota. The procedure was standardless, and therefore semi-quantitative.

Chemical Sequential Extraction

A sequential extraction procedure was chosen based on a hypothesis that metals of interest could be divided into six solid phases or groupings. Groupings coincide with relative environmental stability mineral classes. One gram of pulverized material was used as the starting mass for each sample. The chemical extraction was analyzed by ICP-OES.

Table 1 Abbreviated sequential extraction procedure.

Extraction Step	Extraction Target Phase	Associated Mineral Groups	Method Reference
1	Water soluble	• Sulfate salts	Dold 2003
2	Weakly acid soluble (pH 5)	• Carbonates • Adsorption to primary and secondary Fe oxides, kaolinite and montmorillonite. • Apatite	Tessier et al. 1979
3	Weakly reducible	• Al-hydroxides • Poorly crystalline Fe-oxide/ (oxy)hydroxides	Chao and Zhou 1983
4	Strongly reducible	• Goethite • Primary Fe-oxides • Ilmenite	Chao and Zhou 1983
5	Oxidizable	• Sulfides • Pyrrhotite • Chalcopyrite	Chao and Sanzolone 1977 in Leinz et al. 2000
6	Residual	• Various silicates	

RESULTS AND DISCUSSION

X-Ray Diffraction

XRD with Reitveld analysis on powdered bulk rock samples confirmed a primary mineral assemblage consistent with typical Duluth Complex lithologies. Samples were largely composed of the primary minerals: plagioclase feldspar, olivine, pyroxene, and ilmenite. For most samples, sulfide minerals were likely below the detection limit (about 0.5 %), although chalcopyrite was detected in one sample. Results from bulk XRD did not yield secondary iron-oxide mineral identifications. This may be due to low mineral abundance and/or iron-rich coatings that were amorphous or poorly crystalline. There were isolated occurrences of the efflorescent sulfate salts alunogen and epsomite, as well as, the silicate weathering products, kaolinite and montmorillonite. Several phyllosilicate minerals (biotite, actinolite, clinochlore) were identified that may have resulted from late-stage processes associated with the igneous intrusion, such as deuteric alteration of primary silicates.

The powder XRD on the hand sample coatings provided evidence for additional weathering products. Diffraction of iron-rich material generally did not produce diffraction patterns that

allowed phase identification, suggesting the rind material structure is very poorly crystalline to amorphous. However, in one case, poorly crystalline goethite was identified and appeared to be a product of sulfide- mineral replacement (Figure 2). The presence of goethite (FeOOH) may indicate crystalline transformation of iron oxide-rich coatings (Guo & Barnard, 2013 and references therein) or *in situ* formation due to the lower pH micro-domain proximal to the primary sulfide grain undergoing alteration as suggested by Jambor, 2003. An additional efflorescent sulfate salt was identified in one sample as rozenite ($Fe(SO_4)\bullet 4(H_2O)$) (Figure 3).

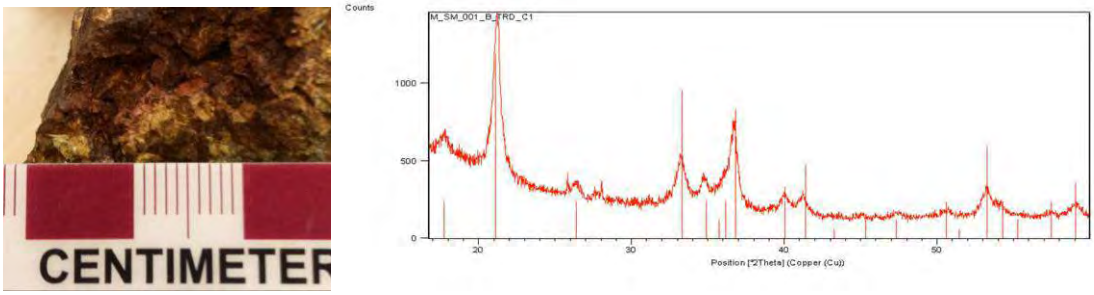

Figure 2 Hand sample showing rust-colored sulfide-replacement texture (left). XRD pattern of pictured material with the matched pattern (vertical lines) from ICDD database for goethite (ID card 000080097) (right).

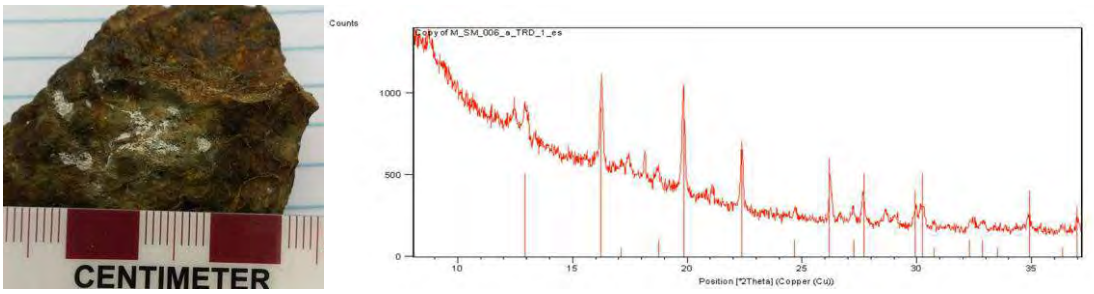

Figure 3 Hand sample showing visible weathering (left). Diffraction pattern of the white precipitate from this sample along with the pattern (vertical lines) from ICDD database for rozenite (ID card 000160699) (right).

Electron Microscope Analysis

Secondary mineral occurrences observed using back-scattered electron (BSE) images include: along fractures/ grain boundaries; as sulfide replacement; and on the exposed surfaces of mineralized rock. Chemical composition data gathered with energy dispersive spectroscopy (SEM-EDS) performed at University of Minnesota Duluth indicate the coatings commonly contain iron and silica as major components and variable amounts of aluminum, sulfur, and metals (e.g. copper) as minor elements (Table 2). BSE images and associated chemical composition suggests variations in solution chemistry (cyclic chemical compositions) during deposition of these features.

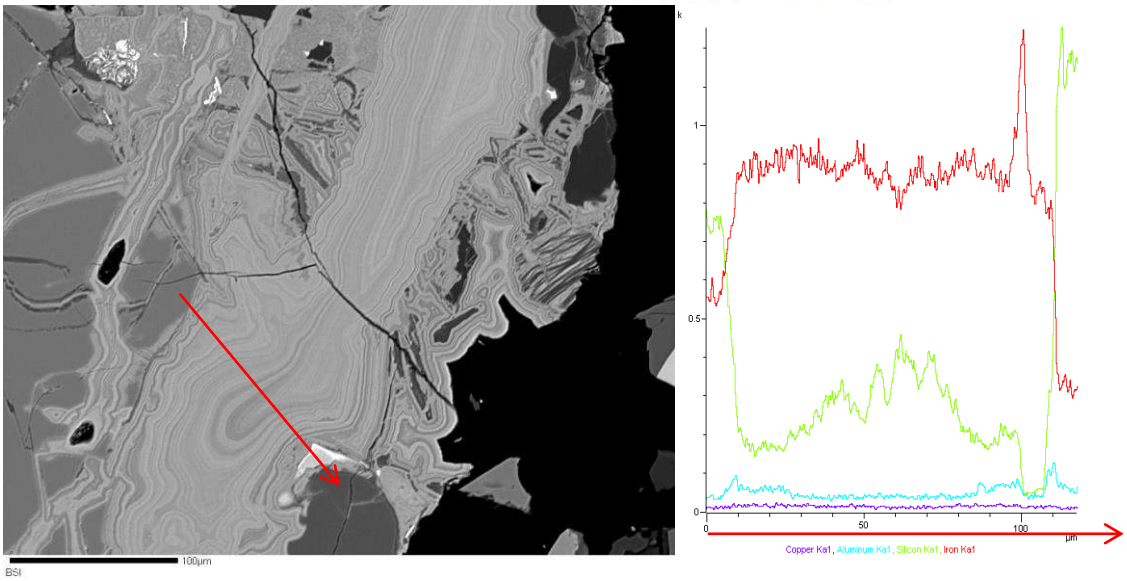

Figure 3 BSE image and location of cross-section line scan of an iron-rich coating (left). Relative chemical abundance plot Fe (red) and Si (green) Al (blue) and Cu (purple) showing variation across iron rich rind (right).

Table 2 Typical range of composition for iron rich coatings, oxygen not reported.

Element	Range of values* observed (weight percent)
Fe	45-66
Si	4-10
Al	1-2
S	0-5
Cu	0-3

* Semi-quantitative values.

Additional energy dispersive spectroscopy (EDS) analyses, performed by McSwiggen & Associates, indicated that the iron oxide-rich layers can contain up to 6 wt% CuO. These compositions were determined using a standardless technique, and therefore were semi-quantitative. Consistent with the analyses performed at the University of Minnesota Duluth, the amount of copper contained within the iron oxide-rich layers is highly variable. For some samples, the copper content was below the detection limit of the instrument under the operating conditions described (approximately 0.1 wt.%). On-going investigations are working to resolve certainty related to Cu speciation, association, and the upper limit of trace metal concentration.

The SEM analysis indicates that the width of individual layers within the layered iron oxide-rich features ranges from approximately < 1-3 µm. Spatial resolution for the EDS analysis is on the order

of 1 μm at 15 kV. Therefore, individual EDS analyses are likely sampling multiple layers, especially when layers are not oriented parallel to the electron beam. Our analyses likely represent a composite composition of several rind layers. If this is the case, it can be expected that true variability in the chemical composition of individual layers is greater than what is suggested by EDS data. Furthermore, these techniques cannot assess the form of the Cu, for example sorbed species on Fe oxide and/or fine-grained Cu secondary minerals.

Sequential Extraction

Results from sequential extraction confirm SEM observations of trace metals associated with iron oxide-rich layers. Iron oxides are expected to report within the reducible fractions. Results from sequential extraction indicate that these fractions can contain significant copper, nickel (Table 3). Similar trends for Co and Zn were also observed. For each of these elements, up to approximately half of the total amount of that element was associated with the reducible fractions.

Table 3 Sequential extraction results for **c**opper and nickel.

Extraction (mg/kg)	**Water soluble**		**Weakly acid soluble**		**Reducible***		**Oxidizable**		**Residual**	
	Cu	Ni	Cu	Ni	Cu	Ni	Cu	Ni	Cu	Ni
SM1	2.2	0.3	346.5	5.0	1030.0	158.7	727.9	151.5	40.1	29.6
SM2	1.1	1.0	137.1	5.6	740.3	191.7	1302.8	135.5	18.8	31.2
SM4a**	327.0	198.2	916.2	94.2	909.5	178.7	2314.1	175.8	8.4	24.9
SM4b	22.8	28.3	201.6	47.6	832.9	220.0	5331.2	376.7	8.5	27.0
SM5	5.7	11.1	64.0	21.6	770.4	179.1	5430.9	529.1	6.3	25.5

* Both reducible extractions (step 3 and 4) summed

** SM4a contained white crusts (see Figure 1, right)

CONCLUSION

Collectively, the mineral characterization techniques employed provide evidence for attenuation of constituents released during weathering of Duluth Complex rock by means of: (1) silicate mineral alteration to clays (kaolinite, montmorillonite); (2) precipitation of sulfate salts (epsomite, alunogen, rozenite); and (3) formation of iron-oxide rich layers which also contain variable amounts of trace metals, silicon, and aluminum. Assuming that the iron-oxide layers behave similarly to hydrous ferric oxide, the degree to which iron oxide layers will attenuate copper, nickel, zinc, and cobalt from mine-impacted water will be a function of drainage pH, total iron content, trace metal content, and reactive surface area (Dzombak & Morel, 1990). Micro-scale heterogeneity may indicate the presence of micro-geochemical environments and/or temporal fluctuations in water chemistry.

ACKNOWLEDGEMENTS

We would like to thank Andrew Thrift of Teck American Inc. for supporting this work. We also thank Dr. Jim Miller for facilitating industry support for this work through the Precambrian Research Center (PRC). Dr. Bryan Bandli at UMD provided excellent guidance for both XRD and SEM analyses. Bronwen Forsyth (SRK) designed the sequential extraction procedure and related data processing/interpretation. University of British Columbia (QXRD), Vancouver Petrographics (thin sections), and McSwiggen and Associates (microprobe) provided essential data and products. We would also like to thank two anonymous reviewers for comments that resulted in a number of improvements to this manuscript.

NOMENCLATURE

BSE	Back-scatter electron
EDS	Energy dispersive spectrometer
ICDD	International Center for Diffraction Data
ICP-OES	Inductively coupled plasma- optical emission spectrometry
SEM	Scanning electron microscope

REFERENCES

Alper, C., Blowes, D., Nordstrom, D &Jambor, J., (1994) *Secondary minerals and acid mine-water chemistry, In: Jambor, J., Alpers, C., & Blowes, D. (Eds) The environmental geochemistry of sulfide mine-wastes.* Mineralogical Association of Canada. Short Course Series 22, pp. 245-270.

Carbone, C., Marescotti, P., Lucchetti, G., Martinelli, A., Basso, R., & Cauzid, J. (2012) *Migration of selected elements of environmental concern from unaltered pyrite-rich mineralizations to Fe-rich alteration crusts,* Journal of Geochemical Exploration, vol. 114, pp. 109–117.

Chao, T. T. & Zhou, L. (1983) *Extraction techniques for selective dissolution of amorphous iron oxides from soils and sediments*, Soil Science Society of America Journal, vol. 47, pp. 225-232.

Day, S. & Kennedy, C. (2015) *Setting ARD management criteria for mine wastes with low sulfide content*, 10th ICARD (this volume).

Dold, B. (2003) *Speciation of the most soluble phases in a sequential extraction procedure adapted for geochemical studies of copper sulfide mine waste,* Journal of Geochemical Exploration, vol. 80, pp.55-68.

Dzombak, D., & Morel, F. (1990) *Surface complexation modeling*, New York: Wiley, (p. 393).

Guo, H., & Barnard, A. S. (2013) *Naturally occurring iron oxide nanoparticles: morphology, surface chemistry and environmental stability*, Journal of Materials Chemistry A, vol. 1 pp. 27-42.

Jambor, J. L., & Dutrizac, J. E. (1998) *Occurrence and constitution of natural and synthetic ferrihydrite, a widespread iron oxyhydroxide*. Chemical Reviews, vol. 98, pp. 2549–2586.

Jambor, J.L., (2003) *Mine-waste mineralogy and minerological perspectives of acid-base accounting, In: Jambor, J., Blowes, D., Ritchie, A. (Eds) Environmental Aspects of Mine Wastes*, Mineralogical Association of Canada, Short Course Series 31, pp. 117-145.

Kelsey, P., Klusman, R., & Lapakko, K. (1996) *Equlibrium Modeling of Trace Metal Transport from Duluth Complex Rockpile*, In: 13th Annual Meeting of the American Society for Surface Mining and Reclamation p. 671–680.

Lapakko, K. (1993) *Rock Field Dissolution of Test Piles of Duluth Complex*, Minnesota Department of Natural Resources: Report to US Bureau of Mines, p. 148.

Lapakko, K., & Antonson, D. A. (2012) *Duluth Complex Rock Dissolution and Mitigation Techniques : A summary of 35 years of DNR research*, Minnesota Department of Natural Resources, (p. 56).

Lapakko, K., Olson, M., & Antonson, D. (2013) *Dissolution of Duluth Complex Rock from the Babbitt and Dunka Road Prospects: Eight-year laboratory experiment*, Minnnesota Department of Natural Resources, (p. 99).

Miller, J.D., Jr., Green, J.C., Severson, M.J., Chandler, V.W., Hauck, S.A., Peterson, D.M., & Wahl, T.E. (2002) *Geology and mineral potential of the Duluth Complex and related rocks of northeastern Minnesota*. Minnesota Geological Survey Report of Investigations (p. 207).

Miller, S.D, Warwick, S.S., Rusdinar, Y., Schummann, R.E., Ciccarelli, J.M., Li, J & Smart, R. (2010) *Methods for estimation of long-term non-carbonate neutralisation of acid rock drainage.* Science of the Total Environment, vol. 408, pp. 2129-2135.

Ripley, E., & Alawi, J. (1986) S*ulfide mineralogy and chemical evolution of the Babbitt Cu-Ni deposit, Duluth Complex, Minnesota,* Canadian Mineralogist, vol. 24, pp. 347–368.

Smith, L. J. D., Bailey, B. L., Blowes, D. W., Jambor, J. L., Smith, L., & Sego, D. C. (2013) *The Diavik waste rock project: Initial geochemical response from a low sulfide waste rock pile,* Applied Geochemistry vol. 36 pp. 210-221.

Tessier, A., Campbell, P. G. C. & Bisson, M. (1979) *Sequential extraction procedure for the speciation of particulate trace metals*, Analytical Chemistry, vol. 51, pp. 844-851.

Mineralogically-Based Determinations of Neutralization and Acid Potential Using Automated Mineralogy

Martha Buckwalter-Davis[1,2], Colin Lussier-Purdy[1,3] and Heather Jamieson[1]

1. *Department of Geological Sciences and Geological Engineering, Queen's University, Canada*
2. *Now at Golder Associates, Ireland*
3. *Now at Arktis Solutions Incorporated, Canada*

ABSTRACT

The determination of the neutralization potential (NP) and acid potential (AP) of environmentally reactive material is a crucial step in the characterization and prediction of acid rock drainage (ARD) and metal leaching (ML) in mine waste for environmental planning. The calculations performed from laboratory tests (static testing) make assumptions regarding acidification and neutralization potential without mineralogical information. The role of mineralogy in ML/ARD is significant and mineralogical characterization can be used to check assumptions or enhance the prediction of water quality.

Mineral Liberation Analyzer (MLA), a scanning electron microscopy-based software program, can provide highly detailed information regarding the abundance, variability, chemistry, and physical characteristics of various acid producing and acid neutralizing minerals. Mineralogical information was determined for several mining projects in Canada using MLA and AP and NP were calculated from modal mineralogy. These results were compared to the results of static testing. Automated mineral analysis is suitable for mining projects with unusual circumstances, such as cases where detailed characterization of acid-neutralizing and acid-generating phases is called for or where concentrations of key mineral phases are below detection limits of other mineralogical characterization techniques such as XRD. Notably, the energy dispersive X-ray spectroscopy associated with MLA is ideal for the identification and quantification of iron and manganese bearing carbonates such as siderite and ankerite, which are measured as carbonates in static tests of NP but can contribute acidity from iron and manganese when dissolved. In addition, there are many other factors that control ML/ARD that can be analysed using automated mineral analysis, including mineral associations, exposure of minerals, and grain size.

Keywords: automated mineralogy; acid base accounting

INTRODUCTION

Automated quantitative mineralogy is a powerful tool that allows us to answer questions regarding mineralogical controls on the behavior of mining-related waste in the environment. Mineral Liberation Analyzer (MLA), an SEM-based mineralogical software program, and its sister software QEMSCAN have traditionally been used by the metallurgical industry for characterizing ore and mill feed. Tailings, waste rock, polished rock thin sections, mining impacted soils, and other sediments can be analyzed using MLA to determine the relative abundance of minerals in mine waste to better understand the processes that formed them and their fate. MLA has been applied to whole rock thin sections of waste rock to develop a mineralogical ARD index by Parbhakar-Fox et al. (2011), to assess the levels of base metals in mining-impacted estuarine sediments in Cornwall by Pirrie et al. (2003), and to identify mineralogical products important to weathering processes from waste rock at the Antamina Mine in Chile (Blaskovich, 2013).

In our research program, we have applied SEM-MLA to the following mine waste problems: (1) determination of acid potential and neutralization potential of mine tailings, with results that compare favorably with static testing, (2) comparison of the modal mineralogy of mine-impacted stream sediments based on SEM-MLA, bulk-XRD, and X-ray absorption spectroscopy, (3) prediction the fate of Hg, As, Cd and other elements in tailings from a complex, oxidized orebody (4) calculation of the relative proportions of anthropogenic and natural As-bearing grains in lake sediments and (5) explanation of variations in Pb bioaccessibility in tailings samples. This paper focuses on the first application.

Laboratory static tests for AP and NP are not mineralogically based and do not take into account the variability in chemical content of various acid-producing and acid-neutralizing minerals. Mineralogy plays a significant role in the neutralization of ARD and mineralogical characterization is recommended as part of every drainage chemistry prediction program to check assumptions made by laboratory tests (Price, 2009). The most important acid neutralizing minerals are in the carbonate group, which react readily and freely. Some silicate minerals such as olivine and wollastonite provide neutralization (Jambor et al., 2002) but with very slow reaction rates. It is expected that the onset of ARD precedes the reaction rates of neutralizing silicates (Jambor et al., 2002) and most researchers recommend the use of neutralization potential derived from carbonates such as calcite and dolomite, excluding iron and manganese carbonates (Jambor, 2000; Price, 2009).

The presence of iron and manganese carbonates such as siderite [$FeCO_3$], rhodochrosite ([nCO_3] and ferroan dolomite [$Ca(Fe,Mg)(CO_3)_2$, Fe>Mg] complicates neutralization potential, because the alkalinity produced by the dissolution of the carbonates is offset by the acidity contributed by iron and manganese oxidation and hydrolysis (Frostad, Price & Bent, 2003; Price, 2009). At present, the industry standard is static laboratory tests to determine sulfur species and neutralization potential, and kinetic laboratory tests where material is leached over a period of time to analyze reaction rates and metal loads. These tests utilize crushed samples and do not take mineralogical factors explicitly into account.

Automated mineralogy provides a way to look at the mineralogical and physical factors that control metal leaching and acid rock drainage. For these studies, modal mineralogy was obtained from MLA, an automated, quantitative SEM-EDS based mineralogical software program. MLA works on particle thin sections and determines modal mineralogy while collecting sample images and allowing for the analysis of sample texture and particle size. These results were expressed in

terms of AP and NP, and then compared with conventional laboratory determinations of these parameters. This approach was applied to tailings from three unique sites: a massive sulfide ore that does not produce acid drainage, a syenite-hosted rare earth element (REE) deposit with very low sulfide content, and a massive sulfide ore that is known to produce ARD.

Investigated Sites

New Calumet

The former New Calumet Mine is located on Ile du Grand Calumet in Quebec, Canada, approximately 90 km northwest of Ottawa, Ontario. The New Calumet deposit consists of massive sulfide lenses and disseminated sulfides associated with cordierite-anthophyllite-bearing gneisses that have been metamorphosed from hydrothermally altered rocks (Corriveau et al. 2007). The ore consists mainly of sphalerite and galena with smaller amounts of pyrrhotite, silver, gold, chalcopyrite, and tetrahedrite. Gangue minerals are quartz, calcite, amphibole, pyroxene, biotite, orthoclase, plagioclase (anorthite and albite), titanite, goethite, and spinel (Williams, 1992).

From 1943 to 1968, 3.8 million tonnes of Pb-Zn ore grading 5.8% Zn, 1.6% Pb, 65 g/tonne Ag, and 0.4 g/tonne Au were extracted using flotation processing (Bishop, 1987). Approximately 2.5 million tonnes of tailings remain exposed on site in multiple locations: the Gobi Desert (GD), Mount Sinai (MS), and the Beaver Pond (BV). To date, remediation has been limited to re-vegetation in some areas.

The pH of drainage from the three New Calumet tailings deposits remains neutral to alkaline based on testing from the 1960s to present day (Doonkervort, 2007; Praharaj & Fortin, 2008; Dongas, 2013). However, Jaggard (2012) noted the occurrence of anglesite [$PbSO_4$], a mineral stable under acidic conditions, in the fine (<20 μm) fraction. This suggests the presence of an acidic environment, even if only on a small scale or in certain environments within the tailings.

Nechalacho

The unmined Nechalacho rare earth element deposit is situated at Thor Lake, approximately 100 km east of Yellowknife, Northwest Territories, Canada. The deposit is hosted within a hydrothermally altered layered nepheline-sodalite syenite in the peralkaline Blatchford Lake complex. The main REE ore minerals are zircon, fergusonite, allanite, monazite, bastnäsite, and synchysite/parisite. Gangue minerals are largely K-feldspar, albite, biotite, quartz, and magnetite (Sheard et al., 2012). Sulfides are uncommon in the deposit, representing < 0.01 % of the mineralogy (Purdy, 2014), most commonly occurring as pyrite, although sphalerite, galena, molybdenite, and chalcopyrite have also been reported in trace quantities (Pinckston & Smith, 1995; Purdy, 2014; Sheard et al., 2012). Carbonate minerals are also not abundant in the deposit, typically comprising about one to two percent of the rock, and include ankerite, siderite-magnesite, calcite, dolomite, bastnäsite, and synchysite/parisite (Purdy, 2014). It remains unclear how much neutralization potential is contributed by bastnäsite and synchysite/parisite.

Geco

Geco is a former Cu-Zn-Ag-Au massive sulfide producer located near Manitouwadge, roughly 250 km east of Thunder Bay, Ontario. The deposit is situated within the Manitouwadge greenstone belt,

locally hosted in quartz-feldspar-biotite ± hornblende gneisses and quartz-sillimanite ± muscovite schists (Petersen, 1986). The ore mineralogy comprises chiefly of pyrite, pyrrhotite, sphalerite, and chalcopyrite, with minor galena, and marcasite. Gangue minerals are largely quartz, plagioclase, K-feldspar, muscovite and amphibole (Jamieson, Shaw & Clark, 1995), although other minerals have been documented in the deposit (Petersen, 1986). Carbonate minerals occur only in trace amounts and acid drainage from tailings has been documented (Jamieson, Shaw & Clark, 1995).

METHODS

Tailings samples from New Calumet Mine were prepared as thin sections for MLA by Vancouver Petrographics in Langley, BC, Canada. Samples were impregnated with set epoxy, mounted to glass slides, and ground to 30-50 μm thickness. Thin sections are doubly-polished and liftable, and mounted onto glass using Krazy Glue™. Water and heat were not used during preparation of thin sections, to avoid any chemical alteration of the samples. Kerosene was used when fluids were necessary.

Tailings from the Nechalacho deposit and Geco Mine were prepared at Queen's University, Kingston, Ontario, Canada. The Geco samples were sieved into three size fractions (< 125 μm, 63-125 μm, and < 63 μm), and the Nechalacho samples were left unsieved due to their fine grind size (80 % passing at 38 μm). All samples were mixed 2:1 with graphite to decrease particle density and particle agglomeration before being mixed with epoxy in a plastic vial lightly coated with petroleum jelly. The mixture was stirred thoroughly to ensure the entire sample was suspended in the epoxy and then placed in an ultrasonic bath for 10 minutes to reduce particle agglomeration. Samples from the Geco Mine were left as epoxy mounts and polished, whereas the samples from the Nechalacho deposit were cut vertically and mounted as thin sections before being polished. Water was used in the sample preparation of both the Nechalacho and Geco samples as dissolution of secondary phases was not identified as a concern.

Samples were carbon coated and analyzed under high vacuum at Queen's University on a Quanta 650 FEG-E-SEM with FEI's MLA software.

MLA Methods

MLA requires optimization of several project specific parameters, such as operating voltage, magnification, spot size, brightness and contrast. FEI recommends calibrating brightness and contrast on the brightest (highest atomic number) mineralogical phase in the sample to achieve the best range of gray scale coloring in back scatter electron view for particle distinguishing.

An important part of using Mineral Liberation Analyzer is the creation of an accurate and complete Mineral Reference Library that is used to classify the minerals in a sample or sample suite (Fandrich et al., 2007). The Mineral Reference Library is made up of mineral names or chemical composition groupings with associated EDS spectra. Each EDS spectra collected in an MLA run is compared to the Mineral Reference Library and assigned a classification (mineral name or chemical composition grouping) based on the EDS spectra it matches most closely. An accurate mineral reference library is critical, as multiple mineral types contribute to acid generation and acid neutralization.

Static Testing – Acid Base Accounting

All of the samples collected from New Calumet and Geco, and one mixed sample of mixed tailings from Nechalacho were subjected to static tests at a commercial laboratory. The analyses included paste pH, total inorganic carbon, sulfur speciation, determination of AP and NP, method modified after Sobek and CO_3-NP(Price, 2009).

RESULTS AND DISCUSSION

Determination of Neutralization Potential

Table 1 compares the NP calculated by SEM-MLA based on the modal amounts of carbonate minerals with the NP measured using chemical tests (total inorganic carbon or CO_3-NP, and the modified Sobek test). Calculating the neutralization potential of material from modal mineralogy via MLA allows for the consideration of Fe and Mn carbonates (Frostad, Price & Brent, 2003; Paktunc, 1999). For the Calumet samples, the ferroan dolomite grains contain an average iron mole % of 3.9%, and for the Nechalacho samples, the ankerite grains contain an average iron mole % of 16.24% (Buckwalter-Davis, 2013; Purdy, 2014). The total NP was calculated according to Frostad, Price & Bent (2003) from two components. $CaCO_3$-NP takes into account the modal mineralogy of calcite and dolomite and subtracts the contribution from iron (Equation 1) and $FeCO_3$-NP takes into account ferroan dolomite/ankerite and siderite and removes the contribution from iron (Equation 2).

$$\mathrm{CaCO_3 - NP}\left(\frac{\mathrm{kg\ CaCO_3}}{\mathrm{t}}\right) = \left\{\mathrm{calcite\ wt\ \% + dolomite\ wt\ \% + \left(ferroan\ dolomite\ wt.\ \% \times \left(1 - \left(\frac{Fe\ mole\%}{100}\right)\right)\right)}\right\} \times 10 \quad (1)$$

$$\mathbf{FeCO_3 - NP}\left(\frac{\mathbf{kg\ CaCO_3}}{\mathbf{t}}\right) = \frac{\left(\mathbf{(ferroan\ dolomite\ wt.\ \% \times Fe\ mole\%) + siderite\ wt.\ \%}\right)}{\mathbf{115.86^{*} \times 100.09^{\#} \times 10}} \quad (2)$$

*115.86 = molecular weight of $FeCO_3$

#100.09 = molecular weight of $CaCO_3$

The NP values calculated from MLA are broadly similar to those measured by CO_3-NP (static test) for all three mine sites. The CO_3-NP value, based on total inorganic carbonate, is generally considered to be a more relevant static test than the modified Sobek, which can overestimate NP by including non-carbonate neutralizing minerals that are unlikely to actually react in the field (Price, 2009). Studies to measure the neutralization potential of common rock-forming minerals and common rock types and compare it to NP calculated from modal mineralogy have been done by Jambor et al. (2002); Jambor, Dutrizac & Raudsepp (2006); and Jambor, Dutrizac & Raudsepp (2007). Non-carbonate minerals (with estimated NPs) that may contribute to NP in a minor way in a modified Sobek test include plagioclase, chlorite, enstatite, anthophyllite, muscovite, and orthoclase (Jambor et al., 2002; 2006). The Nechalacho ore minerals bastnäsite and synchysite-parisite are fluorocarbonates with possible neutralization potential; however they were not included in the calculation as their contribution to NP remains uncertain.

Table 1 Neutralization Potential calculated from MLA vs. determined by static testing

Sample	$CaCO_3$-NP (MLA)	$FeCO_3$-NP (MLA)	Total NP (MLA)	CO_3-NP (static test)	Modified Sobek NP (static test)
	(kg $CaCO_3$/t)	(kg $CaCO_3$/t)	(kg $CaCO_3$/t)	(kg $CaCO_3$/t)	(kg $CaCO_3$/t)
New Calumet					
GD-VEG1	83	1.7	85	93.33	104.0
GD-VEG2	77	1.3	78	75.00	85.0
GD-non VEG	71	0.7	71	69.17	77.5
BV-VEG	65	1.7	67	66.67	74.6
BV-non VEG	45	1.3	47	44.17	54.7
MS-non VEG	10	1.7	12	8.33	14.4
Nechalacho					
UZLG	6.8	2.9	10	13.4	22.4
UZAG	10	3.4	14	13.4	22.4
BZMP	15	3.0	18	13.4	22.4
BZAG	11	2.2	14	13.4	22.4
Geco					
Main Tailings Beach	0.05	0.02	0.07	0.1	4.7
Glory Hole	0.45	0.00	0.45	0.1	0.4
Red Pond	0.46	0.10	0.56	0.1	4.3
E3 Dam	0.19	0.02	0.21	0.2	1.9

Acid Potential

Acid potential can be calculated from modal mineralogy by calculating the sulfur content of acid-generating minerals. Static testing uses a determination of the amount of sulfur in the sample to calculate acid potential. The total sulfur results from static testing compare well to the total sulfur assay determined by MLA (Table 2). Sulfide sulfur from static testing was calculated by subtracting the sulfate sulfur content from the total sulfur measurement. This is a recommended indirect method for estimating sulfide sulfur where organic sulfur is not present (Price, 2009).

Table 2 Comparison of measured total sulfur between MLA and static testing

Sample	MLA %S (total)	Static Testing %S (total)
New Calumet		
GD-VEG1	0.44	0.43
GD-VEG2	2.66	2.28
GD-non VEG	2.40	2.32
BV-VEG1	3.89	2.92

BV-non VEG	3.11	2.25
MS-non VEG	2.04	2.46
Nechalacho		
UZLG	0.003	0.039
UZAG	0.010	0.014
BZMP	0.001	0.008
BZAG	0.005	0.006
Geco		
Main Tailings Beach	4.32	7.04
Glory Hole	1.44	1.17
Red Pond	12.64	9.84
E3 Dam	15.21	15.1

AP from modal mineralogy was calculated in two ways: with pyrite and pyrrhotite and arsenopyrite only (Py+Po+As) and with all the sulfides that have the potential to oxidize (sulf). Table 3 shows that MLA-calculated AP is generally similar to AP determined by laboratory-measured %S.

Table 3 Comparison of measured and calculated acid potential (AP)

	%S(S_2) (py+po+as) MLA	%S(S_2) (sulf) MLA	%S(S_2) %S(total)-%S(SO_4) Static	AP (py+po+as) MLA	AP (sulf) MLA	AP Static
New Calumet						
GD-VEG1	0.32	0.45	0.40	9.85	14.11	12.50
GD-VEG2	2.07	2.74	2.23	64.75	85.72	69.69
GD-non VEG	1.57	2.37	2.04	48.93	74.08	63.75
BV-VEG1	2.85	4.01	2.87	89.13	125.2	89.69
BV-non VEG	2.24	3.20	2.21	69.97	99.87	69.06
MS-non VEG	1.59	2.06	1.95	49.78	64.46	60.94
Nechalacho						
UZLG	0.005	0.005	< 0.01	0.17	0.17	0.31
UZAG	0.010	0.010	< 0.01	0.33	0.33	0.31
BZMP	0.001	0.001	< 0.01	0.02	0.02	0.31
BZAG	0.005	0.005	< 0.01	0.17	0.17	0.31
Geco						
Main Tailings Beach	4.29	4.35	6.79	134	136	212
Glory Hole	0.36	0.36	1.15	11.3	11.3	35.9
Red Pond	12.40	12.65	8.04	388	395	251
E3 Dam	14.78	15.11	13.6	462	472	425

Neutralization Potential Ratio

Acid base accounting involves taking the results of static testing, including paste pH, sulfur species, and neutralization determination, to make estimations as to the potential for metal leaching and acid rock drainage. The neutralization potential ratio (NPR) evaluates NP/AP. For this analysis, two NPR calculations are compared in Table 4. NPR (static testing) is calculated from AP(static testing) and the NP calculated from modal mineralogy, and NPR(MLA) is calculated from the AP and NP calculated from modal mineralogy. Samples are considered potentially net acid generating (PAG) if the NPR < 1, non-PAG if NPR > 2 and uncertain if NP/AP is between 1 and 2 (Price, 2009). Three of the samples from New Calumet are potentially acid-generating based on these criteria, one non-acid-generating, and two uncertain. Subsequent MLA analysis on five additional samples from Mt. Sinai (MS) confirmed NPRs near zero for all samples (Dongas 2013). The Nechalacho tailings all have high NPR and are thus non-PAG, whereas the Geco tailings have very low NPR and are classified as PAG.

Table 4 Neutralization Potential Ratios calculated from values obtained by MLA and static testing

Sample	NPR (MLA NP/ MLA AP)	NPR (MLA NP/ static AP)	NPR (static CaNP /static AP)
New Calumet			
GD-VEG1	8.63	6.8	7.47
GD-VEG2	1.2	1.12	1.08
GD-non VEG	1.45	1.11	1.08
BV-VEG	0.75	0.75	0.74
BV-nonVEG	0.67	0.68	0.64
MS-non VEG	0.24	0.2	0.14
Nechalacho			
UZLG	58	31	33.3
UZAG	41	44	33.3
BZMP	1103	59	33.3
BZAG	81	44	33.3
Geco			
Main Tailings Beach	0.001	0.000	0.02
Glory Hole	0.039	0.012	0.01
Red Pond	0.001	0.002	0.02
E3 Dam	0.000	0.000	0.00

CONCLUSIONS

Our results have shown that the NP and AP calculated from SEM-MLA results compare well with the results of static tests for three different mine sites, and the calculated NPR places the samples in the same category with respect to potential acid generation as the static testing.

NP and AP calculated from modal mineralogy provide several advantages over laboratory tests, notably the explicit consideration of Fe and Mn carbonates, and the identification and quantification of important acid-generating or acid neutralizing minerals that may be found in smaller amounts and with greater chemical accuracy than could be detected by other quantitative techniques such as XRD.

Particle size and liberation were not analyzed here, as they are not comparable between thin section analysis using MLA and static testing. MLA works on intact samples and preserves sample texture and particle size. Static testing utilizes subsamples crushed to <74 micrometers or <120 micrometers (depending on laboratory) and the crushing and grinding creates new particles and surfaces (Price, 2009). However, preliminary assessment of the degree of liberation of sulfide minerals in the New Calumet samples suggest that after 50 years of exposure, most of the remaining sulfide grains are very small (<50 micrometers) and locked within silicate grains, and likely unavailable to contribute to AP even in samples crushed for static testing. This would explain the persistently pH-neutral drainage at this site despite the NPR value between 0 and 1 for most samples.

REFERENCES

Bishop, C. (1987). Report on the New Calumet Mine Gold Property; Grand Calumet Township, Southwestern Quebec.

Blaskovich, R.J. (2013) Characterizing waste rock using automated quantitative electron microscopy. MSc. Thesis, University of British Columbia. Available at: https://circle.ubc.ca/handle/2429/44496.

Buckwalter-Davis, M. (2013) Automated Mineral Analysis of Mine Waste. MSc. Thesis, Queen's University. Available at: http://qspace.library.queensu.ca/handle/1974/8200

Corriveau, L., Perreault, S., and Davidson, A. (2007) Prospective metallogenic settings of the Grenville Province, *in* Goodfellow, W.D., ed., Mineral Deposits of Canada: A Synthesis of Major Deposit-Types, District Metallogeny, the Evolution of Geological Provinces, and Exploration Methods: Geological Association of Canada, Mineral Deposits Division, Special Publication No. 5, pp. 819-847.

Dongas, J. (2013) Detailed mineralogical analysis to determine the differences of depletion rates between sulfides and carbonates in mine tailings of Mount Sinai from the New Calumet Mine, QC. B.Sc. Thesis, Queen's University, Kingston, Ontario. Available at: ftp://ftp.mrn.gouv.qc.ca/Public/Gestim/Dossiers_New_calumet/Dongas_Thesis_2013-1.pdf

Doonkervort, L. (2007) A Mineralogical and Geochemical Study of the Mine Tailings from the New Calumet Mine, Ile du Grand Calumet, Quebec. B.Sc. Thesis, Queen's University, Kingston, Ontario.

Fandrich, R., Y. Gu, D. Burrows, and K. Moeller. (2007) "Modern SEM-based Mineral Liberation Analysis." *International Journal of Mineral Processing* 84 (1-4): 310–320.

Frostad, S.R., Price, W.A. & Bent, H. (2003) Operational NP determination–accounting for iron manganese carbonates and developing a site-specific fizz rating. In Proceedings of Sudbury '95, Mining and the Environment III, Sudbury, Ontario, pp.231–237.

Jaggard, H.N. (2012) Mineralogical characterization of tailings and respirable dust from Pb-rich mine waste and its potential effects on human bioaccessibility from the New Calumet Mine, Quebec. M.Sc. Thesis. Queen's University, Kingston, ON.

Jambor, J.L. (2000) The relationship of mineralogy to acid-and neutralization-potential values in ARD. Environmental mineralogy: Microbial interactions, anthropogenic influences, contaminated land and waste management, pp.141–159.

Jambor, J., Dutrizac, J. E., Groat, J. & Raudsepp, M. (2002) Static tests of neutralization potentials of silicate and aluminosilicate minerals. Environmental Geology, 43(1-2), pp.1–17.

Jambor, J. L., Dutrizac, J. E. & Raudsepp, M. (2007) Measured and computed neutralization potentials from static tests of diverse rock types. Environmental Geology, 52(6), pp.1173–1185.

Jambor, John L., Dutrizac, John E. & Raudsepp, M. (2006) Comparison of measured and mineralogically predicted values of the Sobek neutralization potential for intrusive rocks. In Proceedings of the 7th international conference on acid rock drainage. ASMR, Lexington. pp. 820–832.

Jamieson, H.E., Shaw, S.C. & Clark, A.H. (1995) Mineralogical factors controlling metal release from tailings at Geco, Manitouwadge, Ontario. In Proceedings of Sudbury '95, Mining and the Environment, Sudbury, Ontario, pp.405-413.

Paktunc, A.D. (1999) Mineralogical constraints on the determination of neutralization potential and prediction of acid mine drainage. Environmental Geology 39(2), pp. 103-112.

Parbhakar-Fox, A., Edraki, M., Walters, S. & Bradshaw, D., (2011) Development of a textural index for the prediction of acid rock drainage, Minerals Engineering: An International Journal Devoted to Innovation and Developments in Mineral Processing and Extractive Metallurgy, 24, (12) pp. 1277-1287.

Peterson, E.U. (1986) Tin in Volcanogenic Massive Sulfide Deposits: An Example from the Geco Mine, Manitouwadge District, Ontario, Canada. Economic Geology 81, pp. 323—342.

Pinckston, D.R. & Smith, D.G.W. (1995) Mineralogy of the Lake Zone, Thor Lake rare-metals deposit, N.W.T., Canada. Canadian Journal of Earth Science, 32, pp.516-532.

Pirrie, D., Power, M.R., Rollinson, G., Camm, G.S., Hughes, S.H., Butcher, A.R. & Hughes, P. (2003) The spatial distribution and source of arsenic, copper, tin and zinc within the surface sediments of the Fal Estuary, Cornwall, UK. Sedimentology, 50(3), pp.579–595.

Purdy, C. (2014) The geochemical and mineralogical controls on the environmental mobility of rare earth elements from tailings, Nechalacho deposit, Northwest Territories. M.Sc. Thesis. Queen's University, Kingston, ON.

Praharaj, T. & Fortin, D. (2008) Seasonal variations of microbial sulfate and iron reduction in alkaline Pb–Zn mine tailings (Ontario, Canada). Applied Geochemistry, 23(12), pp.3728–3740.

Price, W.A. (2009) Prediction manual for drainage chemistry from sulphidic geologic materials. Mine Environment Neutral Drainage Report 1.20.1.

Sheard, E.R., Williams-Jones, A.E., Heiligmann, M., Pederson, C. & Trueman, D.L. (2012) Controls on the concentration of zirconium, niobium, and the rare earth elements in the Thor Lake rare metal deposit, Northwest Territories, Canada. Economic Geology, 107, pp.81-104.

Williams, P.J. (1992) Metamorphosed boninitic basalts, arc tholeiites, and cryptic volcanic stratigraphy from the Elzevir Terrane of the Grenville Province, Calumet mine, Quebec. *Canadian Journal of Earth Sciences*, 29(1), pp.26–34.

10th ICARD IMWA 2015 | 10th International Conference on Acid Rock Drainage & IMWA Annual Conference

The Effect of Aluminium Source and Sludge Recycling on the Properties of Ettringite Formed During Water Treatment

Devin Sapsford[1], Sandra Tufvesson[1], Richard Coulton[2], Tom Penny[2] and Keith Williams[2]

1. *Cardiff School of Engineering, Cardiff University, United Kingdom*
2. *Siltbuster Process Solutions Ltd, United Kingdom*

ABSTRACT

A range of techniques are available for the removal of sulfate ions from mine waters and industrial effluents. A number of processes involve the removal of sulfate as ettringite, a calcium aluminium sulfate ($Ca_6Al_2(SO_4)_3(OH)_{12}{\cdot}26H_2O$) at elevated pH (11.5 – 13). Various process configurations have been proposed using lime and a source of aluminium to react with the sulfate in the process feed. This paper presents a study of the effect of the source of aluminium (when mixed with lime and synthetic sodium sulfate rich effluent) on the physicochemical properties of the resultant ettringite sludge and on the propensity of the precipitate, when recirculated, to form high density sludge (HDS). The study demonstrates that sodium aluminate ($NaAlO_2$), aluminium chloride ($AlCl_3$), aluminium nitrate ($Al(NO_3)_3$) and polyaluminium chloride (PAC) all form ettringite and remove sulfate, with $AlCl_3$ being the most successful during 'single-pass' treatment. Furthermore, synthetic $Al(OH)_3$ was demonstrated to be unreactive and the study also confirms the results of earlier literature that crystalline gibbsite does not form etttringite. The continuous trial with $NaAlO_2$ suggests that recirculation of sludge does improve the reaction kinetics of ettringite precipitation with lower residual sulfate concentrations being reached in similar residence time in the reaction tank when influent water is contacted with recirculated sludge. Different aluminium sources play a key role in determining the resultant sludge volume with $NaAlO_2$ forming a voluminous sludge and $AlCl_3$-derived etttringite forming a denser single-pass sludge. Both reagents show only a slight tendency to form HDS upon recirculation. Microscopy images show differences in the precipitate morphology between Al sources and recycled precipitates. These results highlight the importance of understanding how reagent choice influences the properties of the resultant sludge properties, with the commensurate implications for process design, when applying the ettringite precipitation process for the removal of sulfate from effluents.

Keywords: Sulfate removal; high density sludge (HDS); sodium aluminate

INTRODUCTION

Elevated concentrations of the sulfate ion ($SO_4^{2-}{}_{(aq)}$) occur in water bodies impacted by acid mine drainage (AMD). The sulfate results from oxidation of the sulfur moeity of pyrite,. Elevated sulfate concentrations are also common in other industrial effluents from smelting operations, pulp and paper mills, textile mills and tanneries (Galiana-Aleixandre et al. 2005; GBC 2000). Sulfate in itself is not toxic to humans. The taste threshold depends on the form in which the sulfate is present, but generally lies between 250 mg/L and 1000 mg/L. No health related issues have been reported or fully proven to be the result of any sulfate concentration and in terms of water quality standards no target have been set by WHO although their recommendation lies at 250 mg/L due to taste (WHO 2011). At concentrations greater than about 500 mg/L sulfate becomes a concern if the water contacts concrete infrastructure because it can cause deterioration of concrete, this can restrict disposal of sulfate-rich effluent to sewers.

The treatment of sulfate has for a long time been of secondary importance in water treatment due to the relatively low toxicity of sulfate compared to other contaminants. However, in the recent years environmental regulators have become more concerned with high sulfate concentrations in effluents especially when it is a key contributor to high total dissolved solids which are becoming a target of more stringent regulation. According to the International Network for Acid Prevention (INAP) it is therefore likely more demanding regulations will appear in the future (Lorax 2003). A number of treatment approaches for treating sulfate rich water have been variously reviewed in the literature (e.g. Bowell, 2004; Lorax, 2003). Some methods, in particularly those used for AMD, are developed to also clean water from metals and reduce the acidity. The existing methods can be broken down into four types (Lorax 2003) (i) Chemical treatment with mineral precipitation (ii) Membranes (iii) Ion exchange and (iv) Biological treatment. Note that ultimately membrane processes result in a concentrated sulfate brine which will require precipitation or crystallisation to produce a solid for final disposal. Biological processes generally rely on conversion by reduction to H_2S and either removed as metal sulphide or zero valent sulphur. Chemical treatments involve precipitation of the insoluble/sparingly soluble sulfate salts including gypsum, ettringite, barium sulfate (e.g. Bosman et al. 1990).), and jarosite. The Lorax(2003) report highlights ettringite precipitation processes as being particularly promising.The reaction occurs at elevated pH and involves reaction of dissolved sulfate with a source of aluminium (Al) and calcium (Ca) such that ettringite ($Ca_6Al_2(SO_4)_3(OH)_{12}\bullet 26H_2O$) precipitates. This paper concerns the ettringite precipitates that form during water treatmentfor the removal of sulfate.

Properties of ettingite precipitates

Ettringite can refer to both the mineral and the ettringite crystal structure (Tishmack and Burns 2004; Damons and Petersen 2002). The distinguishable features of the ettringite crystal structure are parallel columns comprising Ca^{2+}, Al^{3+} and OH^- structured units of $[Ca_6Al_2(OH)_{12}\cdot 24H_2O]^{6+}$. Between the columns channels are formed where water is present as well as sulfate ions which balance out the structural charge (Johnson, 2004; Damons and Petersen 2002). The mineral can exchange some of its ions without adverse structural change (Damons and Petersen 2002). The actual water content of ettringite can change (24-32 moles per mole of ettringite) and a change in water content does

have an impact on the XRD peaks. (Tishmack and Burns 2004). Most research on ettringite is in conjunction with concrete where it is a common constituent phase. Much literature is focused on secondary ettringite formation which can be problematic due to growth and expansion of the mineral which causes cracking. A comprehensive study by Cody et al. (2004) investigated how the nucleation and growth of the ettringite crystals were affected by different chemicals. The findings from the study showed that different precipitate morphologies were found and were dependent on the type and amount of additives.

Although there are some publications covering the effectiveness of different reagents in removing sulfate by ettringite precipitation (e.g. Janneck et al, 2012), there is an absence of studies looking at the influence on the resultant sludge. This study came about after inital continuous trials of an ettringite precipitation process (detailed below) resulted in excessive volumes of precipitate, as compared to other mine water sludges that the authors are familiar with. This paper thus aimed to examine (i) the influence of aluminium source on the properties of the resultant sludge and (ii) to examine whether recirculation of the sludge leads to a densification of the final sludge. Sludge recirculation is well established in the High Density Sludge (HDS) process used commonly for the removal of metals from AMD (add reference). Recirculation of the sludge results in denser HDS (in terms of m/v) than single-pass sludge with better settling rates, dewaterability and reduced resistance to filtration which equates to better process economics (Coulton et al 2004). Among the published ettringite based sulfate removal processes, those of Outotec and Veolia incorporate sludge recirculation. Note that sludge recirculation is included in the SAVMIN process but only after regeneration of the sludge to active $Al(OH)_3$ so this process is not comparable with that presented here.

METHODOLOGY

Initial Continuous Trial of Sodium Aluminate

The initial experiment began with a continuous pilot plant trial using sodium aluminate ($NaAlO_2$), based upon early trials showing that $NaAlO_2$ was a suitable source of soluble aluminium for ettringite precipitation. The pilot plant was supplied by G.U.N.T. Gerätebau GmbH. A photograph of the plant in use with $NaAlO_2$ and lime and a close-up of the ettringite precipitates can be seen in Figures 1 and 2. The plant consists essentially of a raw water tank, a reactor tank followed by a flocculation/coagulation train with up-and-over weirs, followed by a lamella clarifier. Reagents are dosed from reagent containers with feed pumps. Manual setting of the lime flow to the reactor tank was performed with regular pH measurements with a portable instrument. A sludge recirculation pump was installed and for most of the work up to two lime slurry feed pumps were installed. All chemical analyses were performed using the portable Hach Spectrophotometer following standard procedures (add reference).

The plant was configured to add lime and $NaAlO_2$ concurrently into the cylindrical precipitation vessel, where recirculated sludge was also added. Raw water feed rate was fixed initially at 10 litres per hour, giving a nominal residence time in the vessel of 1 hour excluding the influence of the thickened sludge re-circulation. Lime was added as a 5% m/v suspension to maintain the pH at the required value in the precipitation tank (pH > 11.5) and $NaAlO_2$ was dosed as a solution at 5 % m/v based on the stoichiometric amount of Al required. Anionic flocculant (NA 120 L) was dosed as an aqueous solution at a concentration of 0.005 % m/v to give a dosage between 1.3 and 2.6 mg/l of

dry polymer. Recirculation of sludge was achieved with the peristaltic pump (yellow in colour on Figure 1).

Figure 1. Photograph of plant in operation showing the ettringite precipitate in the clarifier and the external sludge recirculation pump in the foreground

Figure 2. Close-up of the clarifier with subdued lighting showing ettringite precipitates and clear overflow

Batch testing of different aluminium sources

The batch experiments treated a sodium sulfate solution by addition of stoichiometric quantities of aluminium (in various forms) and a 10 % stoichiometric excess of lime. The solution was kept at SO_4 = 1500 mg/L to avoid precipitation of gypsum. The chemicals used were 2.22 % m/v Na_2SO_4 solution, 5% m/v $Ca(OH)_2$ slurry, and the aluminium sources trialed were as follows: 25 % $AlCl_3.6H_2O$, $NaAlO_2$, polyaluminium chloride (10% m/v), 22 % (m/v) $Al(NO_3)_3{\cdot}9H_2O$, aluminium hydroxide powder and synthesised aluminium hydroxide. The synthesised aluminium hydroxide was produced by neutralising 250 ml of a 2 % m/v $AlCl_3$ solution with NaOH. This resulted in a gel which was filtered, rinsed and dried.

Batch tests were carried out as follows: 100 ml of the Na_2SO_4 feed solution was added to a beaker placed on a magnetic stirrer. Reactions were started by introduction of 4 ml of the $Ca(OH)_2$ slurry. This was followed by aluminium addition (in which ever form). Immediately afterwards an additional 1.1 ml of the $Ca(OH)_2$ was added to the beaker. The suspension was allowed to stir for a total of 15 minutes. The suspension was then placed in a settling cylinder and the sludge allowed to settle for 15 minutes and then sludge volume recorded. This was the end point for 'single pass' experiments. For all non-final cycle (i.e. where the sludge was to be recycled) experiments, at the end of settling the supernatant was carefully decanted off and the sludge returned to the reaction beaker. 100 ml of Na_2SO_4 feed solution was added to the sludge in the reaction beaker and the next cycle begun. The experiments were thereafter repeated according to this procedure for between 1

and 12 cycles for $AlCl_3$ and 6 cycles for $NaAlO_2$. To obtain images of the precipitate morphology 0.5 ml of suspension was removed during the 14th minute of the final cycle for recycled sludge experiments. The sample was spread across a petri dish and immediately oven-dried at 35°C prior to imaging under an optical microscope. At the end of all experiments solids were recovered by filtration, oven-dried at 35°C (for 24 hours) and weighed.

RESULTS AND DISCUSSION

Continuous pilot plant trial with sodium aluminate

Operation in this mode proved to be extremely challenging and in hindsight it would have been prudent to perform bench-scale batch tests (as was done for the remainder of the study) to determine whether sludge recirculation lead to densification of the ettringite sludge. It soon became impractical to return the thickened sludge to the precipitation tank using the peristaltic pump alone. For that reason it became necessary to employ a laborious method of filtering the sludge in a large Buchner funnel arrangement and return solids as a much thicker paste than was possible using the plant thickener. Nevertheless it was possible to keep running for about three weeks, treating about 800 litres of raw water containing up to 2350 mg/l of sulfate.

Figure 3 depicts the reduction in sulfate concentrations achieved throughout the pilot plant operation with $NaAlO_2$ as the source of Al and shows that a substantial improvement in removal efficiency took place as plant operation proceeded. In order to explain this trend it is necessary to consider the variations in other parameters that took place. Of particular note are the changes in aluminium dosages and rise in solids concentration in the reactor as time progressed. The pH in the precipitation reactor was slowly increased over time but was always above the target value of about 11.5 for ettringite precipitation. The improved sulfate removal cannot be attributed directly to the increase in aluminate dosage that occurred at Day 8. $NaAlO_2$ dose was increased from 0.17 l/h to 0.34 l/h after day 8 and then reduced to 0.25 l/h for days 15–25. It is more valid to examine the influence of stoichiometric amounts of Al present in the reactor. Up to Day 8 the removal of sulfate ion was approximately 10,000 mg/h. The Al addition rate was 2.8 g/h, thus representing an approximate stoichiometric excess of 50 %. Between Days 8 and 15 the removal of sulfate ion increased to about 20,000 mg/h whilst the excess of Al stayed at about 50 %. After Day 15 it was possible to add Al at approximately stoichiometric amounts and achieve removals of sulfate of up to 22,000 mg/h. It is concluded that the improved performance in terms of increase in the sulfate removal kinetics (implied by lower sulfate concentrations for the residence time) is the result of adding recycled solids to the precipitation vessel. It is interesting to note that very little improvement in sulfate removal efficiency occurred after the solids concentration exceed about 2 % m/v (i.e. 20 g/l).

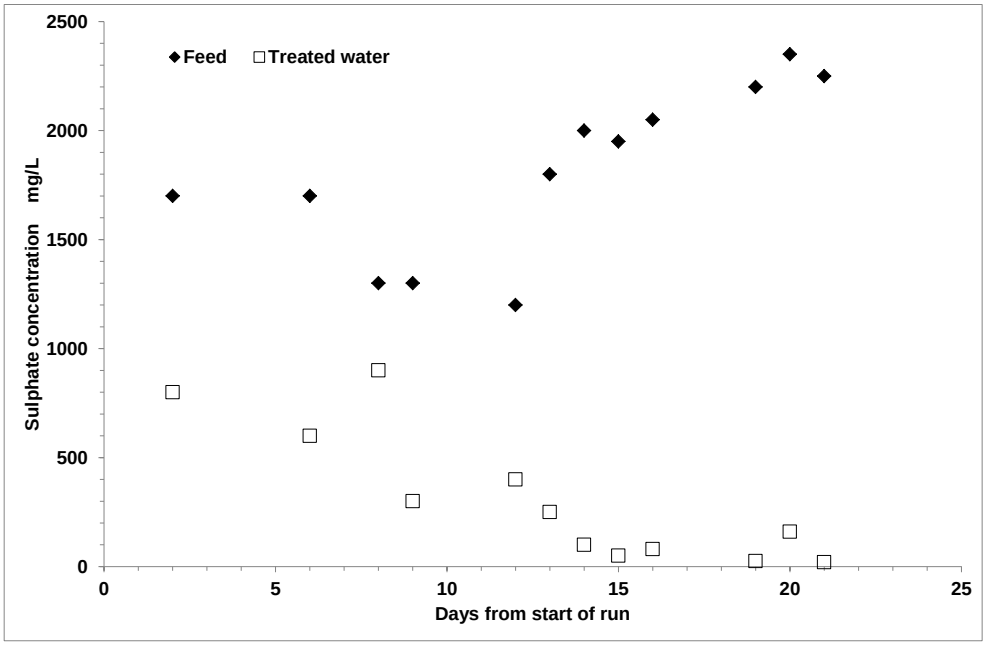

Fig 3. Variation in sulfate concentrations during pilot plant operation. pH > 11.5, Al dose variable (see text).

Batch trials with different aluminium reagents

In all cases where an obvious reaction occurred, the resultant precipitated solid was determined to be ettringite through XRD analyses. Furthermore ICP-OES on digested precipitates demonstrated the Ca, S, Al ratio expected for ettringite.

Initial Sludge Volumes

Table 1 shows the results of the single-pass ettringite precipitation experiments with various reagents providing the source of aluminium. Several important observations are as follows: In agreement with literature $Al(OH)_3$ powder is found to be largely unreactive, synthetic $Al(OH)_3$ was also found to be unreactive. $AlCl_3$ forms the least voluminous single pass sludge, and removes sulfate to the lowest residual level. The use of $NaAlO_2$ results in the most voluminous sludge (80 ml per 100 ml of influent treated) and relatively poor sulphate removal.

Propensity for sludge to densify during recycling

Figure 4 shows the effect of recycling the ettringite sludge on the resultant sludge volume where $NaAlO_2$ or $AlCl_3$ has been used as the Al source for ettringite precipitation. The 'predicted' sludge volumes are based on projections of sludge volume accumulating at the same volume that the single-pass sludge precipitated, and assuming incompressibility of the sludges. It can be seen that the initial trend of relatively high precipitant volume is observed to continue over 6 cycles for the

$NaAlO_2$ based sludge (in fact, the experiment had to be abandoned after 6 cycles due to impracticality of recycling the sludge). However, there is some evidence of sludge densification due to recycling of the sludge compared to projections based on single pass sludge volumes. Similarly, it can be again seen that $AlCl_3$ forms a much lower volume precipitate and that recycling of this precipitate leads to a slight densification over the volume of sludge expected from projection of the single-pass sludge volumes. However, beyond 9 cycles no further benefit is observed. These data indicate that sludge recycling confers some small benefits in terms of sludge densification as well as improved reaction kinetics.

Table 1 Mean residual sulfate and settled sludge volumes for different aluminium sources when precipitating ettringite from solutions with initial sulfate concentration = 1467 mg/L

Reagent	Number of experimental repeats	Mean Residual sulfate concentration (mg/L± stdv)	Settled sludge volume* (mL per 100ml of influent)
$NaAlO_2$	3	525 (± 19.2)	80 (± 17)
$AlCl_3$	4	365 (±193)	16 (± 2)
$Al(NO_3)_3{\cdot}9H_2O$	2	383	28
PAC	3	639 (±263)	22 (±2)
$Al(OH)_3$powder	1	1269	94
$Al(OH)_3$ synthetic	1	1464	95

*In 15 mins of settling time

Morphological characteristic of ettringite sludge

The optical microscopy reveals that the morphology of the ettringite precipitates varies for different Al source and also by recycling of the sludge. Figure 5 (a) and (b) show the $NaAlO_2$ single-pass and 6x recycled sludge. It can be seen that both the single pass sludge and the recycled sludge do not show the classical needle-like morphology of ettringite, but rather that small spherical particles dominate, this is particularly clear for the recycled sludge. Interestingly Cody et al. (2004) observed that large amounts of Na (added as NaCl) leads to the formation of spheres of ettringite precipitate rather than needles. Figure 5 (c) and (d) shows the $AlCl_3$ single-pass and 12x recycled sludge. The single-pass sludge demonstrates amorphous masses of crystals whereas the 12x recycled sludge shows that this early morphoogy has changed to a prounounced needle-like morphology (with needles of up to 100 μm) more typical of pure ettringite. It is clear that during recycling the precipitates have changed its morphology, whether this is due to ageing or through crystal growth is not known.

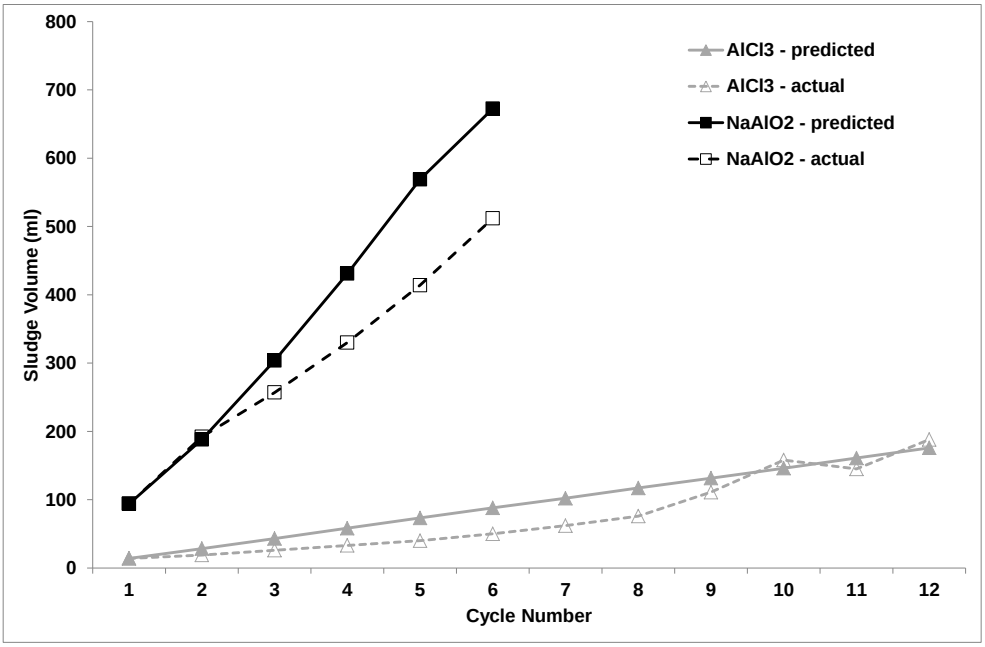

Fig 4. Effect of sludge recycling on volume of ettringite precipitation. Predicted volumes are based on projection of the single-pass sludge volume (corrected for measured sulfate removal)

Cody et al. (2004) describe how (i) nucleation of ettringite may becompletely inhibited and another less stable mineral suchas calcium aluminate monosulfate forms, (ii) how nucleation gel/colloid can form or nucleation (iii) or crystal growth can be inhibited and can affect growth in numerous ways depending on which crystal planes are poisoned by foreign ions. This study along with Cody et al. (2004) indicates that ettringite precipitates seem to be sensistive to the aqueous environment from which they form and that this can have profound effects on the nature of the sludge formed.

CONCLUSIONS

The following conclusions are drawn from this study:

- Sodium aluminate produced a voluminous ettringite sludge during both continous operation and batch testing relative to aluminium chloride
- Using aluminium chloride as the aluminium source leads to the lowest residual sulfate levels in single-pass operation.
- Recirculation of the sodium aluminate based sludges yielded improvements in sulfate removal, which in the context of the continuous operation equates to better removal process kinetics

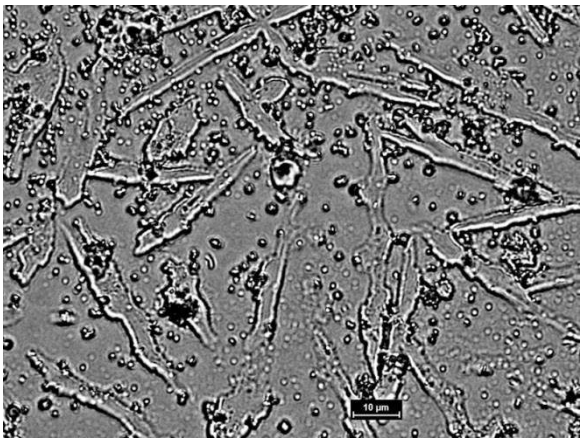

(a) $NaAlO_2$ single-pass sludge, 100 x magnification

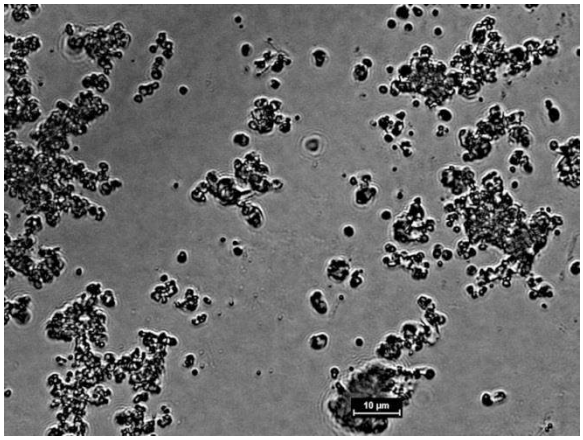

(b) $NaAlO_2$ 6 x recycled sludge, 100 x magnification

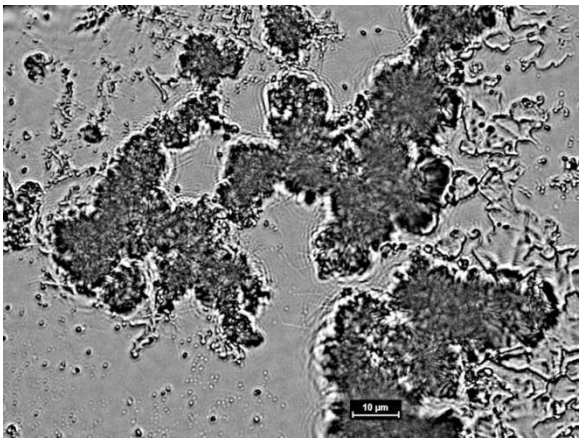

(c) $AlCl_3$ single-pass sludge, 100 x magnification

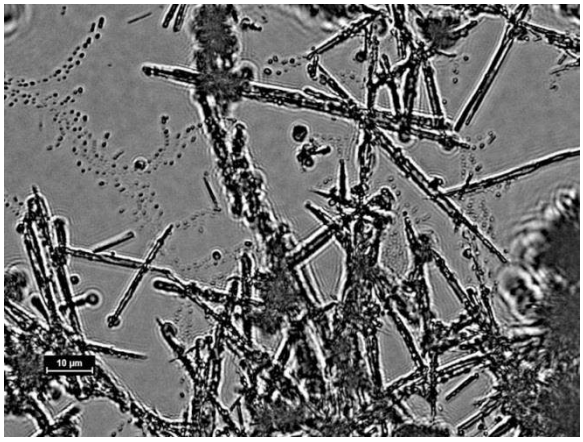

(d) $AlCl_3$ 12 x recycled sludge, 100 x magnification

Fig 5. Optical mineralogy of air dried ettringite sludge.

- Recirculation of the sodium aluminate and aluminium chloride based sludges showed that the sludges have the propensity to slightly densify on recycling
- Morphological differences were observed between precipitates formed from different reagents and when recycled
- The choice of Al-bearing reagent will influence the morphology of the precipipate formed during the ettringite precipitation process, crucially these microscopic morphological changes correlate with macroscopic sludge characteristics.

REFERENCES

Bosman, D.J. Clayton, J.A. Maree, J.P. Adlem, C.J.L. (1990). Removal of Sulphate from Mine Water using Barium Sulphide. International Journal of Mine Water. 9(1-4), pp. 149-163

Bowell, R. J. (2004) "A review of sulfate removal options for mine waters." Proceedings of IMWA (2004): 75-88.

Cody, A.M., Lee, H., Cody, R.D., Spry, P.G. (2004). The effects of chemical environment on the nucleation, growth, and stability of ettringite [Ca3Al(OH)6]2(SO4)3.26H2O. Cement and Concrete Research 34(5), pp. 869-881

Coulton, R. H., Bullen, C. J., Williams, C. R., & Williams, K. P.(2004). The formation of high density sludge from mine waters with low iron concentrations. Proceedings of IMWA (2004), 25-30.

Damons, R.E. and Petersen, F.W. (2002). An Aspen Model for the Treatment of Acid Mine Water. European Journal of Mineral Processing and Environmental Protection. 2(2), pp. 69-81

Galiana-Alexiandre, M.V. Iborra-Clar, A. Bes-Pia, B. Mendoza-Roca, J.A. Cuartas-Uribe, B. Iborra-Clar, M.I. (2005). Nanofiltration for sulphate removal and water reuse of the pickling and tanning processes in a tannery. Desalination. 179(1-3), pp. 307-313

GBC. (2000). Water Quality: Ambient Water Quality Guidelines for Sulphate – Overview Report [Online]. Available at: http://www.env.gov.bc.ca/wat/wq/BCguidelines/sulphate/sulphate.html#top. Accessed: 22 Sep. 2014

Janneck, E., Cook, M., Kunze, C., Sommer, K., & Dinu, L. (2012). Ettringite Precipitation vs. Nano-Filtration for Efficient Sulphate Removal from Mine Water. IMWA conference

Johnson, C.A. (2004). Cement stabilization of heavy-metal containing wastes. In: Gieré, R. and Stille, P. (eds). Energy Waste and the Enivironment: a Geochemical Perspective. London: The Geological Society Special publication 236, pp. 596-606

Lorax. (2003). Treatment of Sulphate in Mine Effluent. International Network for Acid Prevention

Tishmack, J.K. and Burns, P.E. (2004). Chemistry and Mineralogy of Coal. In: Gieré, R. and Stille, P. (eds). Energy Waste and the Enivironment: a Geochemical Perspective. London: The Geological Society Special publication 236, pp. 223-246

World Health Organization. (2011). Guidelines for Drinking-water Quality. 4th ed. WHO publications

Management of Pyrrhotite Tailings at Savannah Nickel Mine: A decade of Experience and Learning

Alan Robertson[1], Nobuyuki Kawashima[2], Roger Smart[2] and Russell Schumann[3]

1. *RGS Environmental Pty Ltd, Australia*
2. *Minerals and Materials Science and Technology, Mawson Institute, University of South Australia*
3. *Levay and Co. Environmental Services, Ian Wark Research Institute, University of South Australia*

ABSTRACT

Savannah Nickel Mine is an underground mine located in the Kimberley region of Western Australia and is owned and operated by Panoramic Resources Limited (Panoramic). The open cut mine commenced in 2005 and rapidly progressed to an underground operation. Tailings generated from processing ore are stored at an above-ground valley fill Tailings Storage Facility (TSF). The initial mine approval was based upon a number of studies, which incorporated preliminary geochemical data, and included a requirement to tranfer the tailings from the TSF to the open cut void at the end of mine life. Recent exploration success has demonstrated that the open cut void has insufficient storage capacity to store the volume of tailings predicted to be generated over the life of mine.

Over the past decade, a substantial body of geochemical and mineralogical information has demonstrated that the geochemical behaviour of the tailings in the TSF is much more benign than initially predicted. Despite containing almost 30% pyrrhotite, the tailings generate only a fraction of the acidity predicted by classical static geochemical test techniques, and the rate of acidity generation is more than compensated by the inherent non-carbonate acid neutralizing capacity available from specific silicate minerals within the tailings matrix. These studies have shown that leaving the tailings in situ at mine closure and using a cover system will produce a sustainable environmental outcome, and the mine operator has recently received regulatory approval to increase the storage capacity of the TSF and implement this closure strategy.

The mine operator now has a very good understanding of the geochemistry of the tailings, although geochemical, mineralogical and a broad range of other related studies are continuing, moving towards mine closure.

Keywords: Tailings, Pyrrhotite, Geochemistry, Mineralogy, Mine Closure

INTRODUCTION

In order for mining companies to obtain approval and finance for mining and mineral processing projects, a broad range of technical studies need to be completed, including the geochemical and mineralogical assessment of mine waste materials. These studies should commence during exploration and ultimately continue throughout the various phases of the life of the operation through to closure. Successful completion of these studies can lead to the development and implementation of appropriate environmental management strategies, which can significantly reduce the risk of the development of Acid Rock Drainage (ARD) and Metal Leaching (ML).

Acquisition of timely geochemical and mineralogical information on the characteristics of waste materials can be used to develop innovative design solutions, limit the potential for environmental impacts, and promote sustainable closure (Miller, 2014). During the mine planning and regulatory approvals stage, there may be a limited amount of information available on the long-term geochemical behaviour of waste materials. This can lead to the development of impractical mine waste management solutions and prescriptive approval conditions, which may not result in the best environmental outcome. Some flexibility should remain during the mine operational phase to improve mine waste management strategies, based on additional knowledge and experience gained during the mine life.

Geochemical and Mineralogical Studies

Whilst technical guidelines for the geochemical and mineralogical assessment of mine and mineral process waste materials have been developed in Australia (DITR, 2007) and internationally (INAP, 2009), it is important to consider the individual characteristics of sites and waste material types when selecting the best test methods to use. Classical geochemical characterisation techniques can sometimes produce inconclusive and unexpected results. In such cases, further study using more specialised geochemical and mineralogical tests can be warranted, particularly where some uncertainty remains over the long-term geochemical behaviour of waste materials.

The information acquired from geochemical and mineralogical tests on mine waste materials can assist with predicting the level of environmental risk and potential impacts. However, due to scale-up and other factors such as the heterogeneity of the mine waste materials and the redox conditions experienced by mine waste materials in the field, simplistic direct comparison of leachate chemistry with existing water quality guidelines should be treated with caution. Where uncertainty exists, modelling is often used to assess the complex behaviour of mine waste materials and potential impacts from mine waste storage facilities (Mayer *et al*., 2003).

Focus of Paper

This paper presents a case study from Savannah Nickel Mine located in the Kimberley region of Western Australia, which illustrates the benefits of ongoing geochemical and mineralogical characterisation and assessment studies on mine tailings materials throughout mine life and in planning for closure. These studies form an integral part of broader operational and closure planning studies completed for the site Tailings Storage Facility (TSF), such as geotechnical

stability, cover design, geomorphology, solute transport modelling, ecotoxicology and ecological assessment of downstream aquatic fauna.

Classical geochemical classification techniques completed at the mine planning stage of the project produced results that were not replicated in the field and led to regulatory conditions of consent, which not produce the most effective long-term environmental outcome at the site. Geochemical, mineralogical and other related studies completed over the past ten years show that leaving the tailings *in situ* at mine closure and using a store and release cover system will produce a more sustainable environmental outcome. Whilst some researchers have had some success with reactive alkaline cover systems, the use of such a cover system is not required st this site (Quispe *et al*., 2013) The mine operator has now received regulatory approval to increase the capacity of the TSF and implement this closure strategy.

CASE STUDY

Project Background

Savannah Nickel Mine is owned by Panoramic Resources Limited (Panoramic) and is located in a semi-arid to sub-tropical part of Australia with an average annual rainfall of approximately 557 mm (ranges from 280 to 1,310 mm) and an average annual evaporation of approximately 3,200 mm. Most rainfall occurs in the hot summer months between December and March.

Commencing in 2005 as an open pit operation, the mine is now an underground operation, and tailings are currently disposed of as a cement-based backfill underground or stored at an above-ground valley fill TSF. The original mine approval required the mine operator to remove the tailings from the TSF back into the underground workings and open pit at the end of mine life. Approximately six million tonnes of tailings had been placed at the TSF by the end of 2014.

Additional mineral resources were identified at the project resulting in an extension of the mine life and a requirement for additional capacity to accommodate additional tailings generated from mineral processing. In 2007, Panoramic began assessing options for the long-term management of tailings at the operation to match revised life of mine ore reserve estimates. The preferred option was to increase the capacity of the TSF in a series of embankment raises and leave the tailings *in situ* at mine closure before covering with a suitable cover system. The high evaporation to rainfall rate at the site (over 5:1) essentially precludes the use of a permanent water cover system for the tailings.

Geochemical information presented in the original approvals documentation (Notice of Intent) in 2002 predicted that the tailings would be Potentially Acid Forming (PAF) and could pose a significant long-term risk to the environment from potential seepage of ARD and ML. However in 2008, an independent peer review found that removing tailings from the TSF and returning them to the open pit was unlikely to produce the best environmental outcome at closure. A broad range of technical studies were recommended to assess the tailings at the TSF and the merits of vairous mine closure options. These studies included geochemistry, mineralogy, surface water and groundwater hydrology, cover design, geomorphology, solute transport modelling, ecotoxicology and ecological assessment of downstream aquatic fauna. A network of surface and groundwater monitoring infrastructure was already in place at the site.

The additional technical studies outlined above were commissioned in 2008 and completed in 2013, and included consultation with relevant stakeholders, including State Government agencies. Site

visits and risk workshops were held to communicate the ongoing findings of the technical studies and demonstrate a transparent process for seeking approval for the preferred operational and post-closure tailings storage option. In 2013, Panoramic received approval from the WA State Government to increase the capacity of the existing TSF and implement the preferred long-term tailings storage option at closure. Panoramic has continued to fund long-term geochemical and mineralogical studies on tailings, and some of the latest findings are included in this paper.

RESULTS AND DISCUSSION

Tailings Characteristics

Geochemical studies completed on a simulated tailings sample in 2002 concluded that pyrite was present as the main sulfide species and classified the tailings as PAF. Subsequent geochemical and mineralogical studies completed over the past ten years have found that 'actual' tailings generated at the project and deposited in the TSF contain pyrrhotite rather than pyrite and react in a very different way to that originally assumed in 2002. Whilst the 'actual' tailings are still classified as PAF using static geochemical classification methods, the bulk tailings continue to generate very little acidity, and contain sufficient neutralising capacity to produce circumneutral pH leachate with excess alkalinity and low metal concentrations (Robertson *et al*, 2012). At the TSF surface, the tailings form a trafficable hardpan surface about 3 cm thick and the oxidation front has not progressed below the hardpan layer. Below the surface hardpan, the tailings remain relatively fresh/unoxidised and do not generate acid conditions after a storage period of up to ten years (Robertson *et al.*, 2012) as evidenced by:

- The visual appearance of the tailings at the TSF,
- *In situ* geochemical and mineralogical data for tailings in and below the hardpan surface;
- The findings of a "tailings-at-depth" geochemical assessment down to 20m;
- Water quality seepage data at the downstream Water Storage Facility;
- Groundwater monitoring data downstream of the TSF; and
- Geochemical and mineralogical studies completed over the past ten years.

Water quality monitoring downstream of the TSF indicates that seepage water is typically pH-neutral, with excess alkalinity and elevated conductivity, mostly attributable to dissolved sulfate, calcium and magnesium, whereas the concentration of dissolved iron is low. The elevated sulfate is attributable to a number of factors including the oxidation of near-surface tailings stored in the TSF (*i.e*. hardpan formation) and recycling of sulfate rich water from dewatering of the water storage facility seepage and underground workings at the mine.

Geochemical and mineralogical studies of *in situ* bulk tailings at the TSF demonstrate that below the hardpan surface, bulk tailings remain pH neutral (due to the neutralizing capacity of magnesium silicates) are slightly brackish, and containing low concentrations of trace metals suggesting limited oxygen diffusion into the bulk tailing material (possibly through a combination of surface hardpan formation, elevated tailings saturation levels, and maintenance of reducing/anoxic conditions at depth in the TSF). The results of ongoing kinetic leach column (KLC) studies on tailings over the past seven year mirror these findings. A key finding is that under anoxic conditions, the tailings pore water contains very low concentrations of soluble reduced iron and sulfate sulfur species

indicating limited potential for any latent acidity in TSF seepage. However, this does not entirely explain the geochemical behaviour of the *in situ* bulk tailing materials at the TSF. A significant amount of elemental sulfur was also found to be present in both the bulk tailings at depth and the oxidised hardpan, which suggests that alternative pyrrhotite reaction mechanisms are occurring in the bulk tailings.

Tailings Hardpan

The relatively benign geochemical nature of the tailings solids at the TSF is unusual as this material can contain up to 30 wt. % pyrrhotite. A review of the available literature over the past 15 years suggests that pyrrhotite is less well studied that pyrite, but is commonly associated with nickel sulfide deposits (Schippers *et al.*, 2007, Heikkinen and Räisänen, 2008; Robertson *et al.*, 2012).

The rate of pyrrhotite oxidation slows when a hardpan layer is present on tailings under both dry and saturated cover conditions (Gilbert *et al*., 2003). McGregor and Blowes (2002) suggested that a TSF hardpan layer could act as a hydraulic and diffusive barrier against the migration of rainfall infiltration and oxygen. The authors presented a case study for uncovered pyrrhotite tailings at a TSF in Canada (Fault Lake), and highlighted that the hardpan layer had grown to 20 cm and the oxidation front had migrated only an additional 18 cm after 25 years of exposure to atmospheric conditions. Further numerical simulations of the Fault Lake tailings concluded that, over a time period of 1,000 years, only the top three metres of tailings would become oxidised (Romano *et al.*, 2006), which aligns with earlier tailing modelling work which indicated that the overall rate of oxidation of the near surface tailings was eventually controlled by the diffusion of oxygen into the tailings mass rather than by the reaction kinetics in the tailing (Elberling *et al.*, 1994). No information on water quality was presented in either of these references. These references illustrate the characteristics of a tailings surface hardpan and clarify the expected rate of progression of the oxidation front into the bulk tailings material over time.

At Savannah Nickel Mine TSF, the tailings form a surface hardpan, which also appears to limit oxygen diffusion or at least maintain a high level of saturation in the bulk tailings and generally retains the bulk tailings in a mostly reducing/anoxic environment. This has been confirmed by recent work completed on the tailings (Schumann *et al*, 2015), which indicates a slow and comparable rate of progression of the hardpan layer and oxidation front into the tailings (1cm per year if tailings are maintained above 75 % saturation). Another attribute of the tailings is that they contain significant amounts of potentially acid-neutralising gangue silicate minerals (*e.g*. enstatite), which can provide both short- and long-term neutralisation of acid generated through pyrrhotite oxidation (Ciccarelli *et al*, 2008).

Soil-atmosphere modelling results associated with the proposed final cover design for the TSF prepared by O'Kane Consultants demonstrate that a saturation level of 75 % in the tailings below the cover material is likely at depths of 5m or greater below the tailing-cover interface (Panoramic, 2012). At shallower depths in the tailings profile, a reduced level of saturation is expected, although at a depth of 1 m, a saturation level in the range 62 to 68% is still likely. This modelling takes no account of the surface hardpan maintaining higher levels of saturation in the bulk tailings. Hence the predicted level of saturation, together with the surface hardpan, will serve to significantly slow the pyrrhotite oxidation rate at the TSF to a rate that is likely to be matched by the silicate dissolution rate within the bulk tailings.

Reaction Pathways

In order to explain the relatively benign nature of the project tailings, the reaction mechanisms of pyrrhotite should be considered. The dissolution behaviour of pyrrhotite is less studied than that of pyrite; however a number of studies from both laboratory and field investigations have been published (*e.g.* Nicholson and Scharer, 1994; Thomas *et al*., 1998, 2000; and Belize *et al*., 2004). Pyrrhotite can follow a number of reaction pathways that can be acid forming or non-acid forming (Thomas *et al*., 2001). The non-acid forming reaction pathway involves the generation of goethite and elemental sulfur. Another potential pathway for pyrrhotite oxidation is where iron is converted to goethite and in this situation sulfur is fully oxidised to produce sulfuric acid. The two main reaction pathways which are considered to potentially operate within the tailings are provided below.

Reaction Pathway 1

$$Fe_{(1-x)}S + 3(1-x)/4O_2 + (1-x)/2H_2O \rightarrow (1-x)FeOOH + S^0 \quad [1]$$

Pyrrhotite + Oxygen + Water → Goethite + Elemental Sulfur

Reaction Pathway 2

$$Fe_{(1-x}S + 3(3-x)/4O_2 + (3-x)/2H_2O \rightarrow (1-x)FeOOH + H_2SO_4 \quad [2]$$

Pyrrhotite + Oxygen + Water → Goethite + Sulfuric Acid

Both acid forming and non-acid forming reactions could be occurring in the tailings at the TSF. However, the KLC test results, "tailings at depth" assessment, and seepage and groundwater quality observations downstream of the TSF suggest that, although pyrrhotite may be acid generating to some extent in the hardpan tailing material, it is generally non-acid forming or acid neutral in the bulk tailing material. The presence of elemental sulfur in the bulk tailings hardpan and at depth, and the lack of oxygen below the tailing hardpan surface (dissolved oxygen was measured in the tailing porewater during a drilling and sampling program at the TSF) suggests that a non-acid forming pathway is likely to be favoured. It is noted that no reduced sulfur species (such as sulfite) were found in the bulk tailings pore water at depth and iron concentrations were very low suggesting that the potential for latent acidity to occur in seepage from the TSF is low.

Any acid generated according to an acid generating reaction pathway in the tailings is likely to be neutralised by alkalinity from residual lime from the tailings and/or from mineral dissolution reactions. Recent mineralogical assessment work has established that the tailings contain enstatite, a magnesium silicate with a dissolution rate comparable to the measured oxidation rate of pyrrhotite in near saturated tailings and which provides a source of alkalinity at a rate comparable to the acid generation rate from pyrrhotite oxidation. This results in pH neutral drainage with excess alkalinity and low levels of dissolved metals as well as elevated salinity from sulfate, calcium and magnesium. These results are consistent with observations reported in the literature regarding other pyrrhotite-bearing tailings wastes (Schumann *et al.*, 2015).

KLC Tests

Long-term KLC tests have been operated for bulk (25 kg) tailings samples from the project over the past seven years to investigate the likely quality of seepage from tailings stored at the TSF. When operated under anoxic, saturated conditions the leachate chemistry closely resembles that of groundwater monitoring data for seepage from the TSF (*i.e.* pH neutral, excess alkalinity and low concentrations of trace metals). The KLC data has been used in other study components (*e.g.* post-closure TSF seepage modelling and potential groundwater impacts), to facilitate prediction of the likely quality of any long-term TSF seepage and potential for environmental impact.

More recently, three KLC tests have been established to determine the oxidative dissolution behaviour of pyrrhotite in the tailings as a function of water content and in the absence of additional alkalinity inputs **(Figure 1**). The three KLC tests have been operated with average levels of saturation of 50 **%**, 75 **%** and 100 % to investigate what geochemical processes are likely to occur in the tailings stored in the TSF in the post-operational period, during which saturation levels and alkalinity inputs may be less than those which currently occur during operations.

The tailings used in the more recent KLC tests were fully characterised prior to commencement of the tests. The pyrrhotite content of the tailings is around 29 wt. %, and no pyrite was found. The tailings contain no carbonate minerals, but contain magnesium silicates such as enstatite and anthophyllite, which are likely to provide some neutralising capacity. After eighteen months "weathering" of the tailings under KLC test conditions, the following conclusions can be drawn:

For fully saturated conditions –

- Leachates from the column are pH neutral with no acidity;
- Leachates are composed essentially of calcium and sulfate with most metals being non-detectable;
- There is little evidence of pyrrhotite oxidation (approximately 6 % estimated oxidation);
- The main geochemical process occurring in the tailings under fully saturated conditions is dissolution of gypsum which is present in the tailings as a precipitated phase when the tailings are deposited in the TSF.

At 75 % saturation –

- Leachate pH dropped to around pH 4.5 after eighteen months with low levels of acidity;
- Leachates are composed essentially of calcium, magnesium and sulfate with low levels of metals;
- Around 15 % of the pyrrhotite in the tailings has undergone oxidative dissolution;
- The main geochemical processes occurring in the tailings at approximately 75 % saturation are oxidative dissolution of pyrrhotite to produce goethite and elemental sulfur as the major reaction (64 %) and goethite and sulfate as the minor reaction pathway (36 %). Less than 2 % of the oxidised sulfur is leached from the column as soluble sulfate; the majority of sulfate remaining within the tailings as partially soluble sulfates (e.g. gypsum, epsomite, melanterite) or less soluble salts such as jarosite or schwertmannite. Dissolution of magnesium silicates (enstatite and anthopyllite) is also occurring.

Figure 1 KLC test setup.

At 50 % saturation –

- Leachate pH dropped to around pH 4 after eighteen months with acidity around 10 times higher than that in leachate from the tailings weathered at 75% saturation;
- Leachates are composed essentially of magnesium, iron, calcium and sulfate with the concentrations of other metals being low;
- Around 57 % of the pyrrhotite in the tailings has undergone oxidative dissolution over the 18 months of leaching;
- The main geochemical process occurring in the tailings at approximately 50 % saturation are essentially the same as those occurring at 75 % saturation, except that the rates are increased in the tailings with lower water content.

These results confirm that even under unsaturated conditions, the dominant reaction pathway for pyrrhotite oxidative dissolution in tailings produces elemental sulfur which, in the absence of further oxidation, is a non-acid producing reaction (Robertson *et al*, 2012). Of the pyrrhotite, which is fully oxidised to sulfate, the majority appears to precipitate as poorly soluble sulfate salts which contain stored acidity. This stored acidity in compounds such as jarosite is likely to redissolve at a sufficiently slow rate such that dissolution of magnesium silicates in the tailings will match that of acid production eliminating or greatly reducing acidity.

The low amount of acidity generated during weathering of the tailings can clearly be seen from the data shown in **Table 1**. Even under conditions of 50% saturation where nearly 60% of the pyrrhotite in the tailings has oxidised, the acidity measured in leachate is only 0.2% of the expected acidity based on ABA analysis. Therefore it is likely that even if fully saturated conditions cannot be maintained post operation, oxidation of pyrrhotite will result in a significantly reduced acidity load than is predicted by classical static geochemical tests.

Table 1 Measured versus expected acidity during eighteen months of tailings KLC testing

Saturation (%)	Amount pyrrhotite oxidised (%)	Expected acidity[A] (kg H_2SO_4/t)	Measured acidity (kg H_2SO_4/t)	Measured acidity as a percentage of expected acidity
50	57	145	0.34	0.23
75	16	41	0.039	0.10
100	6	15	0.035	0.23

A. Expected acidity calculated by multiplying the measured net acid producing potential (NAPP) (255 kg H_2SO_4/t) by the percentage of pyrrhotite oxidised.

The results of these KLC tests also demonstrate that there is an inverse correlation between the moisture content of the tailings and the rate of pyrrhotite oxidation, indicative of oxygen diffusion as the rate controlling process. These results suggest that at saturation levels likely to occur in the TSF following closure, the oxidation rate of pyrrhotite is likely to be sufficiently slow to be matched by the dissolution rate of magnesium silicates in these tailings resulting in pH neutral or low acidity leachate. Further testing is continuing to verify whether this situation is maintained.

CONCLUSIONS

A case study has been used to illustrate the complexity of the geochemical and mineralogical processes associated with tailings material at a nickel mining operation in Australia. Whilst detailed and targeted geochemical studies in the early stages of mine feasibility and planning can provide important information of the characteristics of mine waste materials, this paper illustrates that ongoing study and flexibility are required throughout the life of mine to ensure that the most appropriate operational and closure options are developed and implemented for tailings storage.

The results of this case study indicate that there is now a very good understanding of the geochemistry and mineralogy of tailings material at the mining operation based on a number of studies by recognised experts and peer reviews, where field evidence at the TSF matches predicted geochemical behaviour over time. The downward movement of the surface hardpan and oxidation

front into the bulk tailings at the TSF is very slow and predicted to remain so even without a cover system in place. The final cover design for the TSF predicts a high level of saturation in the bulk tailings below the cover material, but does not take into account the positive effects of the surface hardpan on maintaining the elevated tailings saturation level. Mineralogical and kinetic geochemical studies show that the rate of pyrrhotite oxidation and acid generation in the tailings is likely to be matched by the magnesium silicate dissolution rate. At the TSF, this results in pH neutral drainage with excess alkalinity and low levels of dissolved metals as well as elevated salinity from sulfate, calcium and magnesium. Further testing is continuing to confirm that this situation is maintained in the longer term.

ACKNOWLEDGEMENTS

The project was primarily undertaken by RGS Environmental Pty Ltd and Levay & Co. Environmental Services at the University of South Australia. The authors acknowledge the assistance and funding of the project by Panoramic Resources Limited over the past eight years.

REFERENCES

AMIRA (2002) *ARD Test Handbook – AMIRA Project P387A: Prediction & Kinetic Control of Acid Mine Drainage*. Environmental Geochemistry International and Ian Wark Research Institute.

Belize, N., Chen, Y.W., Cai, M.F. and Li, Y. (2004) *A review of pyrrhotite oxidation*, Journal of Geochemical Exploration 84, pp65-76.

Ciccarelli, J.M., Li, J., Smart, R., Schumann, R. and Miller, S. (2008) *Estimation of acid neutralising silicate minerals using kinetic dissolution cell method*. In Proceedings of the Sixth International Workshop on Acid and Metalliferous Drainage (Eds Bell, L.C. *et al.*), pp 377-381, Burnie, Tasmania, 15-18 April, 2008, Australian Centre for Minerals Extension and Research (ACMER), Sustainable Minerals Institute, University of Queensland, QLD Australia.

DTIR (2007) *Leading practice sustainable development program for the mining industry. Managing acid and metalliferous drainage*, Department of Industry, Tourism and Resources, Canberra, ACT, Australia.

Elberling, B., Nicholson, R.V. and Scharer, J.M. (1994) *A combined kinetic and diffusion model for pyrite oxidation in tailings: a change in controls with time,* Journal of Hydrology, V157, pp47-60, November.

Gilbert, S.E., Cooke, D.R., and Hollings, P. (2003) *The effects of hardpan layers on the water chemistry from leaching of pyrrhotite-rich tailing materials*, Environmental Geology, 44, 687-697.

Heikkinen, P.M. and Räisänen, M.L. (2008) *Mineralogical and geochemical alteration of Hitura sulphide mine tailing with emphasis on nickel mobility and retention*, Journal of Geochemical Exploration 97, 1-20.

INAP (2009) *Global Acid Rock Drainage Guide (GARD Guide)*. Document prepared by Golder Associates on behalf of the International Network on Acid Prevention (INAP). June (http://www.inap.com.au/).

Mayer, K.L.I., Blowes, D.W. and Frind, E.O . (2003) *Advances in reactive-transport modelling of contaminant release and attenuation from mine-waste deposits*. (Eds Jambor, J.L. *et al.*) Environmental Aspects of Mine Wastes, Mineralogical Association of Canada Short Course Series, Vol 31, ISBN 0-921294-31-X, pp. 283-302.

McGuire, M.M. and Hamers, R.S. (2000) *Extraction and quantitative analysis of elemental sulphur from sulphide mineral surfaces by high-performance liquid chromatography*, Environmental Science Technology, 34, pp4651 – 4655.

McGregor, R.G. and Blowes, D.W. (2002) *The physical, chemical and mineralogical properties of three cemented layers within sulfide-bearing mine tailings*, Journal of Geochemical Exploration 76, pp195–207.

Miller, S. (2014) *Leading practice solutions for Acid Rock Drainage prevention and control: A key to achieving a sustainable future for minerals resource development*, In Proceedings of the Eighth Australian Workshop on Acid and Metalliferous Drainage, Adelaide, South Australia. 29 April – 2 May (Eds. Miller, H. and Preuss, L.) pp 51-66 (JKTech Pty Ltd: Brisbane).

Nicholson, R.V. and Scharer, J.M . (1994) *Laboratory studies of pyrrhotite oxidation kinetics*, In Environmental Geochemistry of Sulfide Oxidation, ACS Synposium Series 550 (Eds. Alpers, C.A. and Blowes, D.W., American Chemical Society Washington DC.

Quispe, D. Pérez-López, R. Acero, P. Ayora, C. Nieto, J.M. and Tucoulou, R. (2013) *Formation of a hardpan in the co-disposal of fly ash and sulfide mine tailings and its influence on the generation of acid mine drainage.* Chemical Geology 355: 45-55.

Panoramic (2012) *Savannah Project Stage 2 Tailings Storage Facility Amendment.* Report prepared by Panoramic Resources Limited for the Western Australian Department of Mines and Petroleum, June.

Robertson, A.M., Kawashima, N., Smart, R.St.C. and Schumann, R.C. (2012) *Ongoing evaluation of tailings geochemistry: An integral component of mine closure planning,* In Proceedings of the 9th International Conference on Acid Rock Drainage (ICARD). Ottawa, Canada. 20-26 May 2012. (Eds. Price *et al.*). Paper 0260.

Romano, C.G., Mayer, K.U. and Blowes, D.W. (2006) *Reactive Transport Modelling of AMD Release and Attenuation at the Fault Lake Tailings Area, Falconbridge, Ontario*, Proceedings of the 7th International Conference on Acid Rock Drainage (ICARD), March 26-30, 2006, St Louis MO. Published by the American Society of Mining and Reclamation (ASMR), 3134 Montavesta Road, Lexington, KY 40502.

Schippers, A., Kock, D., Schwarz, M., Bottcher, M.E., Vogel, H. and Hagger, M. (2007) *Geomicrobial and geochemical investigation of a pyrrhotite-containing mine waste tailing dam near Selebi-Phikwe in Botswana*, J. Geochem. Exploration, 92, pp151 – 158.

Schumann, R.C., Robertson, A.M., Gerson, A.R., Fan, R., Nobuyuki, K., Li, J. and Smart, R.St.C. (2015) *Iron sulfides ain't iron sulfides. A comparison of acidity generated during oxidation of pyrite and pyrrhotite in waste rock and tailing materials,* Paper No. 201 accepted for the 10th International Conference on Acid Rock Drainage (ICARD). Santiago, Chile 21-24 April.

Thomas, J.E., Skinner, W.M. and Smart, R.St.C. (1998) *The Role of Sulfur Species in the Inhibition of Pyrrhotite Dissolution in Acid Conditions*, Geochim. Cosmochim. Acta, 62(9), pp1555-1565.

Thomas, J.E., Smart, R.St.C. and Skinner, W.M. (2000) *Kinetic Factors for Oxidative and Non-Oxidative Dissolution of Iron Sulfides*, Minerals Engineering, 13, pp1149-1159.

Thomas, J.E., Skinner, W.M. and Smart, R.St.C. (2001) *A mechanism to explain sudden changes in rates and products for pyrrhotite dissolution in acid solution'.* Geochimica et Cosmochimica Acta, Vol 65(1), pp1-12.

10th ICARD IMWA 2015 | 10th International Conference on Acid Rock Drainage & IMWA Annual Conference

Waste Rock Modelling to Improve ARD Prediction and Project Economics: A Case Study

Emily Luscz and Terre Lane
Global Resource Engineering, USA

ABSTRACT

Treatment of mine water impacted by acid rock drainage (ARD) can be a significant cost item for mining projects. Accurate predictions of potentially acid generating (PAG) waste and associated metals are important for estimating project economics, for detailed mine planning, and for developing waste rock management plans to protect downstream water quality. In this study, the methods used to predict ARD are described for an open pit mining project in southern Peru with waste rock containing significant sulfide mineralization. In conjunction with a geochemical testing program, two approaches were used to characterize potentially acid generating waste for the project. The first approach predicted PAG waste based on rock type, and utilized a conservative management strategy to handle all mineralized rock types as PAG, regardless of the variability within each rock type. The second approach used additional waste rock samples and geostatistical evaluation to construct an ARD block model that included an estimate of acid generating potential and contained metals. This allowed for scheduling of waste rock to minimize special handling of PAG materials with an associated reduction in handling cost. The results showed that while the first approach relied on less data, the second approach resulted in cost savings for the project. In addition, relying on rock type alone resulted in some potentially non-acid generating waste being classified as PAG. This case study illustrates the value of geospatial modeling of acid-generation potential to support project planning. The improved economics for the project compensated for the additional cost of the second approach.

Keywords: Acid rock drainage prediction, mine waste geochemistry, block modeling

INTRODUCTION

The Corani project is a proposed silver-lead-zinc project owned by Bear Creek Mining Company (BCMC) and is located in a high-altitude region of southern Peru. Initial feasibility work completed in 2010/2011 projected that the open pit would produce 256 million tonnes of waste rock over an 18-year mine life with waste rock being placed in several dump locations and as pit-backfill. A significant portion of the waste rock will contain sulfide mineralization, and as a result, mitigation of potential acid rock drainage from the waste facilities is a concern for the project. Additionally, naturally-occurring ARD, from weathering of exposed sulfide-bearing formations, and ARD, from historic mining, impact the project area.

Accurate prediction of geochemical risk is important for any project facing potential ARD risk and has implications for project economics, permitting, mine planning and environmental management. Guidelines for testing procedures and the approach to geochemical characterization are given in the Global Acid Rock Drainage (GARD) Guide (INAP, 2009) and several ASTM standards (i.e. ASTM E1915-11 (2011) and ASTM D5744-07e1, (2007)), but the amount of data collected and how this data is integrated into the mine plan and economic model varies between projects and depends on the stage of the project, the type and level of geochemical risk and the regulations and permitting requirements for the project.

In order to better understand the ARD potential of the proposed project and to develop a program for managing ARD at the project, a preliminary geochemical characterization was completed as part of the feasibility work (Dorey & Breckenridge, 2013). This program included static tests, LECO Furnace total sulfur and total carbon assays, and on-site kinetic cell tests. This was combined with geologic and metallurgical characterization of lithologies and material types. The conclusions from this work included the following:

- The geochemistry of the project will be dominated by certain mineralization types; in particular, mineralized lithic tuff with fine black sulphides (FBS) and mineralized tuff with pyrite and marcasite (PM).
- Whole rock analysis indicated that several metals of environmental and processing concern exist at high levels; synthetic precipitation leaching procedure testing suggested that many of these metals are readily leachable.
- The kinetic tests showed that many waste types were acid generating though the behaviour among certain mineralization types was mixed.

Following this work, additional samples were collected for geochemical testing. In total, static testing was completed on over 400 samples with an additional 200 samples analyzed by LECO Furnace.

Two different approaches were used to assess the geochemical risk of the project. The first approach (*Method 1*) predicted potentially acid generating (PAG) waste based on rock type and utilized a conservative management strategy to handle all mineralized rock types as PAG, regardless of the variability within each rock type. Given the availability of additional samples and optimization work being completed for the project, the second approach (*Method 2*) used an ARD block model that included an estimate of acid generating potential and contained metals. The methods used to calculate the amount of PAG material for the project are described below.

METHODOLOGY

Method 1

The initial geochemical testing program revealed that much of the mineralized material could be considered PAG. Consequently, a conservative approach was used to estimate the amount of PAG material generated by the project. It was assumed that all mineralized tuff material would have acid-generating potential and would be managed using encapsulation. Based on this assumption, all blocks classified as mineralized tuff in the resource model were also classified as PAG. This allows a straight-forward approach to predicting total PAG waste, but does not allow the variability of acid-generation potential to be considered.

The annual PAG and NAG quantities were reported from the mine plan in order to stage the design of the waste storage facilities. The design included selective management of PAG waste, including encapsulation within inert waste and engineered cover zones. The calculations confirmed that enough non-acid generating (NAG) material would be available to line and cover the waste rock storage facilities, and in addition, to provide enough NAG material for construction of the tailings dam and for road construction.

Method 2

Following the collection of the additional geochemical samples, an ARD block model was developed to refine the PAG volume estimate as well as to allow the PAG production schedule to be estimated in conjunction with detailed mine planning. The ability to schedule PAG waste strategically as part of the planning process can allow waste handling and placement scenarios to be optimized. Waste with the highest PAG potential is ideally placed in the central portion of the encapsulation zones where oxygen permeation and precipitation infiltration are less important. In addition it may be possible to mine high ARD potential zones during the dry season and low ARD potential zones during the wet season, minimizing ARD risk from active placement areas. Method 2 also results in a reduction in the predicted total quantity of PAG material that must be managed, and increases the quantity of NAG material available for use as a construction material.

TECHBASE was used for data compilation and analysis of the geochemical data. TECHBASE is a database management program that includes capabilities for statistical analysis, spatial modelling and generating advanced graphics. The geochemical data, drillhole collars and survey data were loaded into the database along with the project block model.

Since samples varied in length, samples were composited into intervals with a minimum length of 1 and a maximum length of 8 meters. Once the geochemical samples were composited, composited intervals were assigned a lithology and geometallurgical type from the block model. This was accomplished by using nearest neighbour to assign lithology values from the block model to composite intervals in TECHBASE. Since there is 100% overlap between the block model and the geochemical samples, a maximum of 1 data point was used to estimate each point.

In order to estimate geochemical parameters from the geochemical samples to each block in the model, data was subset by lithology (mineralized tuff or non-mineralized tuff) and variograms were created for each parameter. Strong trends were not evident in the directional variograms so models were only fit to global variograms. In addition, the variograms revealed that for most parameters, spatial trends were only evident to about 75-150 meters.

Based on the variogram models, each parameter was estimated for each block in the block model using kriging. The result is an estimate of geochemical properties for each block in the resource model.

RESULTS

The Corani waste rock exhibits highly inconsistent geochemical behaviour. As indicated above, the initial geochemical test work showed a large degree of variability in acid generating potential, composition, and leachability of contained metals. These conclusions were confirmed by the additional static testing following the initial test work. Table 1 reports the summary statistics for net neutralizing potential (NNP) and metals of concern for both the entire sample database and for each mineralization type.

Table 1 Summary statistics for the sample database for all mineralized samples and by mineralization type (362 samples).

Group	NNP				Arsenic (ppm)				Cadmium (ppm)				Mercury (ppm)			
	Avg	SD	Min	Max	Avg	SD	Min	Max	Avg	SD	Min	Max	Avg	SD	Min	Max
All-362*	-66	99	-469	-4	286	554	13	5560	15	47	0.02	569	1.07	1.84	0.01	18.80
FBS-116	-33	50	-288	-5	206	478	15	3910	22	64	0.02	569	0.67	1.22	0.01	7.70
FEO3-37	-63	90	-397	-7	312	927	15	5560	5	13	0.15	79	1.52	3.30	0.01	18.80
FEO4-81	-158	142	-469	-4	281	489	13	3150	12	46	0.02	412	1.83	1.85	0.05	6.50
MNO-6	-226	75	-284	-86	644	312	293	1155	28	24	3.86	68	3.07	1.35	1.23	4.76
PM-106	-25	20	-101	-11	378	541	18	4280	15	39	0.17	277	0.69	1.51	0.01	10.60
QSB-16	-48	90	-376	-13	98	119	24	491	2	2	0.05	7	0.81	1.05	0.07	4.43

Table 2 Summary statistics for the sample database for all non-mineralized samples (64 samples).

Group	NNP				Arsenic (ppm)				Cadmium (ppm)				Mercury (ppm)			
	Avg	SD	Min	Max	Avg	SD	Min	Max	Avg	SD	Min	Max	Avg	SD	Min	Max
Non-Min	-9	16	-93	-3	36	24	10	188	0	1	0.02	4	0.04	0.08	0.01	0.42

The table indicates that most of the mineralization types have average NNPs that exceed the generally accepted criteria for determining likely acid generating waste (an NNP less than -20). However, the range shows that some samples, even in the most likely acid generating mineralization types have NNPs in the uncertain range (NNP between -20 and 20). MnO was the only waste type to show consistent potentially acid generating behaviour based on ABA results. The whole rock analysis results also show a high degree of variability as indicated by the results presented for arsenic, mercury, and cadmium.

Based on the *Method 1* approach, the open pit will produce an estimated 129 million tonnes of PAG material. Using the *Method 2* approach, it is estimated that only 81 million tonnes of PAG material will be produced. *Method 2* also provides an estimate of contained metals for each block.

Figure 1 shows boxplots of selected metals for the sample database and for the block model using *Method 2*. The close symmetry between the boxplots from the sample database and the block model suggest that the estimation processes did not introduce significant bias.

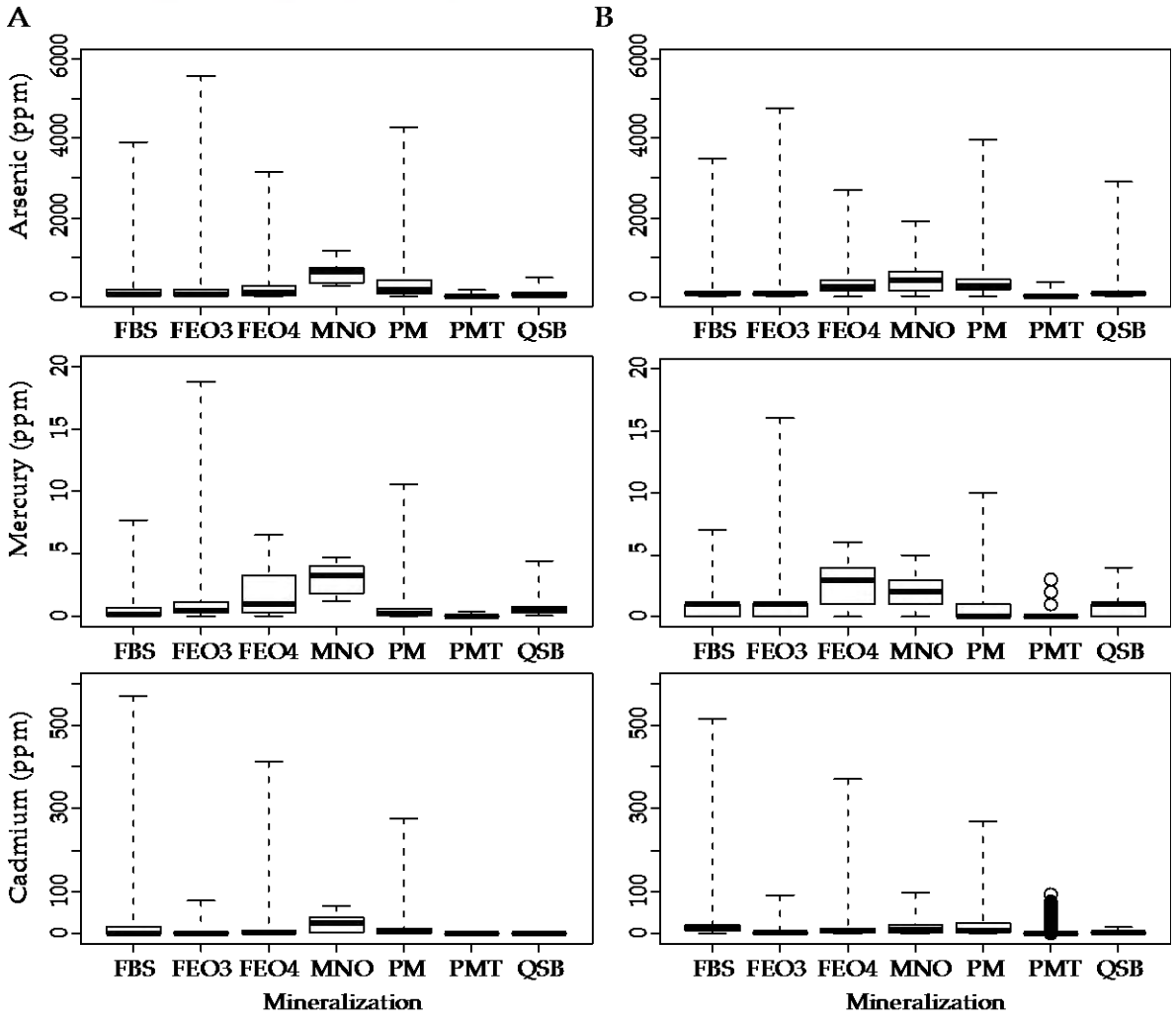

Figure 1 Box plots of selected metals by mineralization type for (A) the sample database and (B) the block model

Figure 2 is a typical cross-section through the Corani pit showing predicted net neutralizing potential using both methods. The mineralization of the section is also shown.

A significant portion of material previously classified as PAG using *Method 1* is classified as NAG using *Method 2*. In addition to an improvement in the outlook for the amount of PAG material requiring special handling, *Method 2* provides a spatially detailed description of PAG behaviour and contained metals. For instance, there are two areas in the cross-section with clearly elevated acid generating potential (centred near x=315900 and x=316800).

DISCUSSION

As the results indicate, depending on the selected method, the estimated volume and strength of PAG material can vary significantly. Each approach has a unique set of benefits and detractors

which must be considered when selecting the appropriate approach to ARD prediction. The pros and cons of each approach are outlined in Table 2.

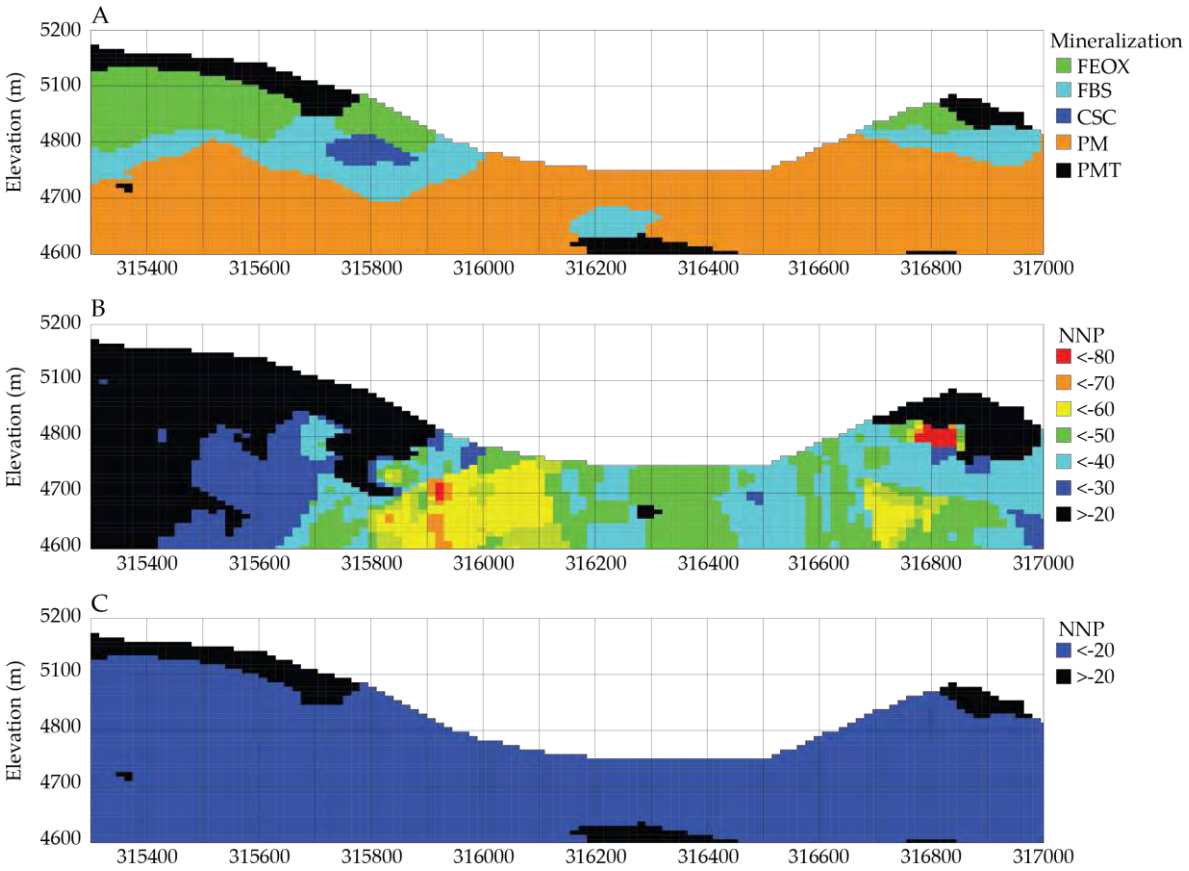

Figure 2 Typical cross-sections through the block model showing (A) mineralization (B) net neutralizing potential predicted using Method 1 and (B) net neutralizing potential predicted using Method 2. Mineralization types include iron oxide (FEOX), fine black sulfide (FBS), coarse sulfide and celadonite (CSC), pyrite marcasite (PM), and post mineral tuff (PMT-non-mineralized material).

Method 1 provides a less detailed prediction of PAG material characteristics. However, this approach relies on less data and is conservative in terms of cost and long-term treatment requirements. This method is appropriate during early stages of project development or for projects where testing of the waste rock indicates consistent acid-generating behaviour.

Method 2 introduces spatial detail to ARD prediction which can be used to refine several aspects of the mine plan. Most significantly, there are several opportunities to use this information to refine the economics of the project. Since the Corani project includes a waste encapsulation and pit backfill plan for managing PAG material, the refinement in PAG volume estimates allows for optimization in where mineralized material will be placed. For instance, if mineralized material is determined to be NAG, it may be placed in the least costly location rather than being transported to the pit or the dump where waste encapsulation is occurring. In addition, estimates of contained metals can be used to refine the estimate of smelter penalties. It appears that some mineralization types contain lower amounts of some metals than others and therefore, it would be appropriate to

assume that these may incur lower smelter penalties. *Method 2* is best applied in cases where acid generating potential is spatially variable or there is a need to refine the waste handling plan to improve project economics or to optimize waste handling procedures.

Table 2 Pros and Cons of two approaches for ARD prediction.

Method	Pro	Con
1	• Requires fewer samples • Straight-forward • Conservative	• Less detailed description of ARD hazard • May produce an overly conservative cost for treatment and processing • Cannot be used to optimize waste handling practices
2	• Includes spatial detail in ARD estimate • Can be used to optimize mine plan, processing and waste handling • Addition of detail may improve project economics	• Uncertainty is introduced from the block model • Requires more samples

The most conservative management practice for handling waste rock at a project is to classify all mineralized waste rock as potentially acid generating for purposes of basic engineering. The estimates generated using *Method 2* can then be used to refine the waste handling procedures and improve environmental conditions in detailed design and operations. Using the ARD block model, additional precautions can be taken for the waste that appears to be the most strongly acid generating. For instance, it can be placed during the dry season or more strongly encapsulated. Similarly, the same approach can be used for waste rock with large contents of arsenic or other elements of concern. This has the potential to lessen the impacts to surface water and/or reduce long-term treatment requirements.

CONCLUSIONS

Both methods considered here have strengths and weaknesses. The first method relies on a smaller sample database, is conservative, straight-forward to apply and is based on the conservative management practice of considering all mineralized material to be acid-generating. The second method requires more data but has the potential to improve project economics and optimize waste handling. The selection of the appropriate method depends on the stage of the project, the ARD risk associated with the project and the project management philosophy along with several other factors. A detailed ARD model is not only useful for environmental management, but also can be a tool in mine and process scheduling. As with all components of the mine plan, the ARD management approach should be re-evaluated and evolve along with the project. A management strategy selected during scoping is not necessarily appropriate for feasibility or final planning.

ACKNOWLEDGEMENTS

The authors would like to thank Bear Creek Mining Company for support in publishing this work and Mike Norred at Techbase International for providing software support during the preparation of this paper.

REFERENCES

ASTM D5744-07e1. (2007). Standard Test Method for Laboratory Weathering of Solid Materials Using a Humidity Cell. American Socitey of Testing and Materials.

ASTM E1915-09. (2009). Standard Test Method for Analysis of Metal Bearing Ores and Related Materials for Carbon, Sulfur, and Acid-Base Characteristics. American Society for Testing and Materials.

Dorey, R. and Breckenridge, L. (2013) Mine Waste Geochemistry Assessment, Corani Project, Puno, Peru. In A. Brown, L. Figuero, & C. Wolkersdorfer (Ed.), *Annual International Mine Water Association Conference – Reliable Mine Water Technology*, vol. 1, pp. 331-337.

The International Network for Acid Prevention (INAP). (2009) Global Acid Rock Drainage Guide (GARD Guide).http://www.gardguide.com/

Meliadine Gold Project: Investigation of the Buffering Capacity of Waste Rock

Valérie Bertrand[1], Jennifer Cole[1] and Stéphane Robert[2]

1. *Golder Associates, Canada*
2. *Agnico-Eagle Mines, Canada*

ABSTRACT

The Meliadine Gold project is located near Rankin Inlet in Nunavut, Canada. The Project currently comprises six deposits along a 20 km section of the Meliadine Trend. Gold occurs in low-sulfide gold-quartz veins in a prominent fault zone, hosted in an oxide iron formation and mafic volcanic flows, a Package that is similar in all deposits. Although waste rock from each deposit has low sulfur and low acid rock drainage (ARD), the acid-buffering capacity varies between deposits. Those situated west and central to the trend possess excess calcite and dolomite-ankerite buffering capacity, while deposits located to the east are slightly more silicified and possess a greater proportion of iron-bearing carbonate minerals. Various testing methods were used to define the acid-buffering capacity of waste rock from these east-side deposits, including mineralogy, static test methods, mathematical accounting methods based on mineralogy and measured carbonate content, as well as kinetic weathering test methods. Net acid generation (NAG) and kinetic test results show the presence of active and sustained buffering capacity from carbonate minerals, which corroborate the results of modified Sobek buffer capacity tests. Conversely, mineralogy and carbonate content frequently inferred the absence of buffering carbonate minerals; this could be due to the low resolution of X-Ray Diffraction (XRD), and to the possible heterogeneity of the sample which is exacerbated at trace mineral content. The compendium of results was, therefore, used to assess the ARD potential of waste rock from these deposits. Waste rock management strategies will include mixing of rock types where the proportion of uncertain or potentially acid generating (PAG) rock is small, additional tests during operation and strategic placement of potentially acid generating waste rock, and cover where the proportion is higher. These management plans are designed to overcome uncertainty on acid generation potential where it exists and avoid acidification of PAG waste rock in the long-term.

Keywords: buffering capacity, neutralization potential, mineralogy, metal carbonates.

INTRODUCTION

Agnico-Eagle Mines Ltd. (AEM) is currently studying the feasibility of constructing and operating a gold mine known as the Meliadine gold project located approximately 25 km north of Rankin Inlet in Nunavut, Canada. The Meliadine property comprises several gold deposits in a low sulfur mineralization system. Some of the lithologies from two of these deposits, Discovery and F Zone, have very low carbonate content but static and kinetic tests show sustained buffering. Multiple geochemical analyses and calculations were conducted to better define the long-term acid rock drainage (ARD) potential of these low sulfur and low carbonate rocks.

This article describes the analyses completed on waste rock from the Discovery and F Zone deposits and compares results of the different tests and concludes with recommendations for greater clarity on the determination of effective buffering capacity in low sulfur and low carbonate rocks.

GEOLOGY OF THE MELIADINE DEPOSITS

The gold deposits of the Meliadine property are hosted in volcanic flows and sediments of the Archean-age Rankin Inlet Greenstone Belt (Pincock Allan & Holt, 2008). Gold deposits occur along the east-west-trending splay off the regional Pyke Fault and on structures parallel to it. Gold is mostly present in quartz-vein stock works, laminated veins, and in weakly sulphidized iron formation, which is folded and sheared. The Meliadine ore deposits are low-sulfide, gold-quartz vein deposits as per the geo-environmental classifications provided in Plumlee et al. (1999).

The geology of each deposit is similar. Waste rock includes iron formation, which is both volcanic-hosted and sediment-hosted. It comprises greywackes, siltstones and argillites with magnetite and chert layers. Schistose and carbonate-altered mafic volcanic rocks make up most of the footwall waste rock. The hanging wall rock comprises fine-grained turbiditic meta-sediments that include greywacke, sericite-altered siltstones, graphitic argillites and gabbro dykes (AEM, 2011; AEM 2014).

PROPOSED MINE DEVELOPMENT

The six deposits to be mined includee: Wolf, Tiriganiaq, Pump, Wesmeg, F Zone and the Discovery. Waste rock from the first 4 deposits will be mixed in two large rock storage facilities. Waste rock in these mixed piles has ample excess buffer capacity; there is no concern for acidification from these stockpiles. Conversely, waste rock from F Zone and Discovery deposits will be stored in individual waste rock storage facilities adjacent to their respective open pits. Some samples of waste rock from F Zone and Discovery deposits have an uncertain acidification potential, hence the importance of defining the reactivity of the available buffering capacity of all waste rock from these deposits in order to design appropriate stockpile management plans.

ANALYTICAL METHODS

Mineralogy

Mineralogical analyses were carried out by XRD at the University of British Columbia, Earth and Ocean Sciences Department. Samples consisted of a 2 mg split of a fraction of the pulverized portion (reground to <10 μm) of the waste rock sample. The X-Ray diffractograms were analyzed using the International Centre for Diffraction Database PDF-4 using Search-Match software by Siemens (Bruker). X-Ray powder-diffraction data were refined with Rietveld program Topas 3 (Bruker AXS). This method allows evaluating quantitatively the crystalline mineral phases with a detection limit of approximately one weight percent (1 wt%). Mineral quantities represent the relative amounts of crystalline phases normalized to 100%. Non-quantitative identification to <1% was made by UBC, however, the precision of the instrument decreases substantially below one wt% (errors margins up to 100%; M. Raudsepp, 2014, pers. comm., 27 March). Concentrations less than 1% are imprecise.

Laboratory measurement of buffering capacity

The following methods of accounting for buffering capacity were completed:

1996 Modified NP Procedure (bulk NP), (MEND, 2009) – This method quantifies the total buffering capacity of a sample, including contributions from slower reacting or less reactive aluminosilicate minerals. The buffering capacity is calculated from the amount of base consumed to neutralize acid remaining from the sample acid-digested at room temperature. Bulk NP is expressed as kg $CaCO_3$/tonne.

Carbonate mineral NP (CaNP), (Price, 1997) – This method quantifies the buffering capacity from the carbonate content of a sample assuming that all the carbonate is present as calcite. CaNP is calculated from the carbonate (CO_3) content as follows: CaNP (kg $CaCO_3$/tonne) = CO_3 (wt%) *(100.09*10)/60.01. Where siderite and other divalent metal carbonates are present, the CaNP can be overestimated since these minerals release less neutralization per mole of carbonate ions than calcite or dolomite.

Mineralogical Carbonate NP (CaNP-min), (Paktunc, 1999) – This represents the buffering capacity provided by the carbonate minerals that are identified by XRD. In this study, they include calcite, ankerite and siderite. The effective carbonate NP is calculated following methods outlined in Paktunc (1999) where the amount of buffer available from each mineral is proportioned to the available carbonate ions per its idealized mineral formulae as follows: Calcite and dolomite 100%; ankerite 70%; siderite 0%. This method utilizes the weight percent (wt%) XRD results, thus it was applied only to samples subjected to mineralogical analysis. The CaNP-min value is expressed as kg $CaCO_3$/tonne.

Adjusted Carbonate Mineral NP (CaNP-adj) – This represents the NP from carbonate minerals (CaNP) based on the chemical content of inorganic carbon (TIC) rather than the weight percent of XRD carbonate minerals, but adjusts the buffering capacity according to the carbonate minerals present in the sample defined by XRD analysis. The adjustment is also based on the proportion of available carbonate ions from each mineral identified (Paktunc, 1999). Thus, if XRD identified that 50% of the carbonate minerals present in the sample were calcite and 50% siderite, CaNP-adj was

set at half of the CaNP value defined from TIC analysis. If a sample had no mineralogical data, it was assumed to have the average carbonated mineral content tabulated for the sample's lithology. The CaNP-adj value is expressed as kg $CaCO_3$/tonne.

Laboratory measurement of acid potential (AP)

There are no documented occurrences of primary sulfate minerals in the Meliadine deposit (Pincock Allan & Holt, 2008; AEM, 2011; AEM 2014). Where chemical analysis identified sulfate, it was attributed to weathering of the sample after extraction. Thus, AP was calculated from the total sulfur (S) content, based on the theory that all the sulfur in the sample occurs as available di-sulfide minerals (AP (kg $CaCO_3$/tonne) = 31.25 x S (%)). The total sulfur content of the sample was determined by LECO furnace with a S-analyzer following ASTM E 1915. A subsample was pre-treated with cold hydrochloric acid (HCl) to remove sulfate and the resulting material was analyzed for total sulfur. The difference between the two total sulfur values was assumed to be sulfate sulfur.

Evaluation of ARD potential

The determination of the ARD potential of waste rock was evaluated by acid-base accounting (ABA) using net potential ratio (NPR) of NP to AP, whereby NPR = NP/AP. The NPR was evaluated for the various forms of NP, as follows:

- NPR = bulk NP/AP
- CaNPR = CaNP/AP
- CaNPR-min = CaNP-min/AP
- CaNPR-adj = CaNP-adj/AP

Leaching test pH and sulfate content

The distilled water shake flask extraction (SFE) (ASTM D3987-06) and the paste pH (Price, 1997) were carried out on all samples. An increase in the pH of the leaching solution (initial pH was approximately 5.5) indicated the presence of readily available buffering capacity.

The single addition net acid generation (NAG) test (AMIRA, 2002) was completed on a subset of samples from each lithology. The subset of samples selected for NAG tests was different than the subset selected for mineralogical analysis.

Kinetic weathering tests were carried out following the humidity cell test (HCT) procedure (ASTM D 5744-96) on the same subset of samples subjected to mineralogical testing. Kinetic tests were run for a period of 20 to 40 weeks. Leachates were analyzed by inductively coupled plasma - mass spectrometry. These tests were used to investigate the kinetics of mineral reaction.

RESULTS AND DISCUSSION

Mineralogy

Pyrite (FeS_2) is the most common sulfide mineral found in the waste rock away from ore zones, with lesser arsenopyrite (FeAsS), trace pyrrhotite ($Fe_{1-x}S$) and rare chalcopyrite (CuFeS). F Zone and Discovery waste rock have low quantity of calcite and a greater proportion of metal-bearing

carbonate minerals such as siderite and ferroan dolomite (ankerite). The iron content of the ankerite was not defined during this study. Aluminosilicate minerals including biotite, muscovite, plagioclase feldspars and clinochlore which are documented to possess buffering capacity (Jambor et al. 2002; Jambor, Dutrizac and Raudsepp, 2007; Matson, 2009), occur in large quantities in Discovery and F Zone samples (TABLE 1).

Table 1 Minerals identified by XRD with Reitveld refinement

Mineral Group/Name	Ideal Mineral Formula	Discovery Deposit Greywacke/ Siltstone				Discovery Deposit Iron Formation			F Zone Deposit Iron Formation		
		1	2	3	4	5	6	7	8	9	10
Calcite	$CaCO_3$	-	-	0.30	-	0.45	1.0	1.9	-	-	-
Ankerite	$Ca(Fe,Mg,Mn)(CO_3)_2$	-	-	-	-	-	-	-	3.7	3.6	5.8
Siderite	$FeCO_3$	-	-	-	-	-	-	-	0.59	2.7	6.5
Dolomite	$CaMg(CO_3)_2$	-	-	-	-	-	-	-	-	-	-
Pyrite	FeS_2	-	-	-	-	0.85	-	-	-	0.43	-
Pyrrhotite	$Fe_{1-x}S$	-	-	-	-	-	1.7	-	8.7	3.6	7.0
Arsenopyrite	FeAsS	-	-	-	-	-	-	-	-	0.63	-
Quartz	SiO_2	32	31	30	31	42	42	34	69	75	72
Plagioclase	$(Na,Ca)AlSi_3O_8$	30	35	39	37	5.9	11	8.0	-	-	-
Biotite	$K(Mg,Fe)_3(Al,Fe)Si_3O_{10}(OH,F)_2$	6.1	7.5	8.4	6.4	3.0	5.6	7.1	-	-	-
Muscovite	$KAl_2(AlSi_3)O_{10}(OH)_2$	20	16	7.5	18	-	-	-	-	-	-
Clinochlore	$(Mg,Fe^{2+})_5Al(Si,Al)_4O_{10}(OH)_8$	11	9.9	9.2	7.5	1.2	5.4	5.4	4.7	1.4	2.0
Magnetite	Fe_3O_4	-	-	-	-	38	10	22	3.1	3.6	0.37
Actinolite	$Ca_2(Mg,Fe)_5Si_8O_{22}(OH)_2$	-	-	3.9	-	8.8	8.6	8.2	-	-	-
Cumming-tonite	$Mg_7Si_8O_{22}(OH)_2$	-	-	-	-	-	14	12	10	9.0	6.6

- not detected; values <1 wt% are approximate

ABA results for samples subjected to mineralogical analysis are summarized in TABLE 2 along with the average for samples from each lithology.

Table 2 Summary of ABA results and lithological average values

Mineral Group/Name	Discovery Deposit Greywacke/Siltstone					Iron Formation				F Zone Deposit Iron Formation			
	1	2	3	4	avg. (n=54)	5	6	7	avg. (n=33)	8	9	10	avg. (n=7)
paste pH	9.3	9.7	9.6	9.6	9.7	9.1	8.8	9.0	9.0	8.4	8.6	8.5	8.5
SFE pH	7.9	8.6	8.2	8.0	8.4	7.7	7.7	7.9	8.0	8.0	8.0	7.0	8.0
Net Acid Generation (NAG) pH	3.3	4.5	7.1	na	6.7	na	na	na	9.0	na	na	na	na
Bulk NP	7.4	7.3	12	8.1	14	15	22	44	29	31	34	53	72
CaNP	1.5	3.1	6.5	1.2	6.0	2.0	12	26	19	16	34	27	56

CaNP-adj	1.5	3.1	6.5	1.2	1.7	2.0	12	26	19	9.6	14	8.8	25
CaNP-min	0.0	0.0	3.1	0.0	0.8	4.6	10	20	12	26	26	41	31
Total Sulfur (wt%)	0.25	0.12	0.15	0.15	0.13	0.66	0.78	0.37	0.45	2.6	1.3	3.2	1.9
AP	7.7	3.9	4.5	4.6	4.1	21	24	12	14	81	42	100	59
bulkNPR	1.0	1.9	2.6	1.8	4.7	0.7	0.9	3.8	2.7	0.4	0.8	0.5	15
CaNPR	0.2	0.8	1.4	0.3	2.8	0.1	0.5	2.3	2.0	0.2	0.8	0.3	13
CaNPR-adj	0.2	0.8	1.4	0.3	0.7	0.1	0.5	2.3	2.0	0.1	0.3	0.09	5.7
CaNPR-min	0.0	0.0	0.7	0.0	0.2	0.2	0.4	1.7	0.7	0.3	0.6	0.4	0.4

na: not analyzed; avg: average

Evaluation of buffering capacity

Bulk NP values are consistent, and often substantially higher than CaNP indicating that a large portion of the buffering capacity accounted for in bulk NP is from non-carbonate minerals. The reactivity of this buffering capacity cannot be verified in the long-term, thus, these measurements were not retained to assess ARD potential.

Because of the documented presence of iron carbonates the use of CaNP was not retained either. CaNP is an imprecise evaluation of buffering capacity for the Meliadine project because it negates the NP-lowering effect of metal carbonate minerals and the buffering capacity of reactive silicate minerals.

Mineralogy-based CaNP (CaNP-min) tended to be the most conservative assessment of buffering capacity. However, this method was not considered appropriate for ARD assessment because of the following factors: the uncertainty of the quantitative estimate from XRD data due to the low resolution of the instrument for trace mineral content; the evidence of available buffering capacity (from paste pH, NAG pH, and kinetic testing) in samples where little to no carbonate minerals were identified by XRD; and the substantial discrepancy between carbonate content measured by chemical analysis and weight percent carbonate content from XRD results.

Adjustment of CaNP using mineralogical data (CaNP-adj) accounts for both the trace content of carbonate defined by chemical analysis and the presence of iron carbonate minerals identified in the samples. Although this method still negates buffering capacity from aluminosilicate minerals, it is considered to be appropriately conservative for NP determination.

Supporting Information

The highly alkaline paste pH values of most samples and the neutral to alkaline SFE pH values demonstrate the presence of immediately available buffering capacity in all samples, including those where no carbonate minerals were identified by XRD. This suggests that either some effective calcite or low iron dolomite was present at concentrations that are below the XRD detection limit, and/or other effective aluminosilicate minerals are available to buffer the solution pH.

Most end-pH values of the NAG tests were also above 4.5 with little acidity released, suggesting that most samples tested (which targeted low AP and low NP samples) have enough buffering capacity to avoid ARD (except for samples 1 and 2 in TABLE 2). Corresponding mineralogical data was available for three samples of Discovery greywacke/siltstone. These show that the non-potentially acid generating (NPAG) sample (sample 3) has a low, but detectable, calcite content (0.3wt %), a low sulfur content (0.15 wt%), a bulk NPR of 2.6 and a CaNPR-adj above 1. Conversely,

samples 1 and 2 yielded acidic NAG pH values suggesting they have a potential to generate acid in the long-term. They had no detectable carbonate mineral content and lower bulk NP and CaNP-adj values than sample 3 and similar to higher sulfur contents. Samples 1 and 2 have bulk NPR values above 1 but CaNPR, CaNPR-min and CaNPR-adj values of less than 1. The relationship between CaNPR-adj, AP and mineralogy may form a trend that needs to be verified with a larger database of NAG pH values and mineralogical data.

Kinetic testing on Discovery and F Zone samples also showed active and sustained buffering capacity for the duration of testing including for samples with no XRD-detectable carbonate minerals (FIGURES 2 and 3). The very low sulfate values suggest very slow mineral reaction rates in the short to medium term. Given the dry arctic conditions at site and corresponding low leaching rate, the 40 week test duration is estimated to cover a period at site which is longer than the planned mined life (13 years).

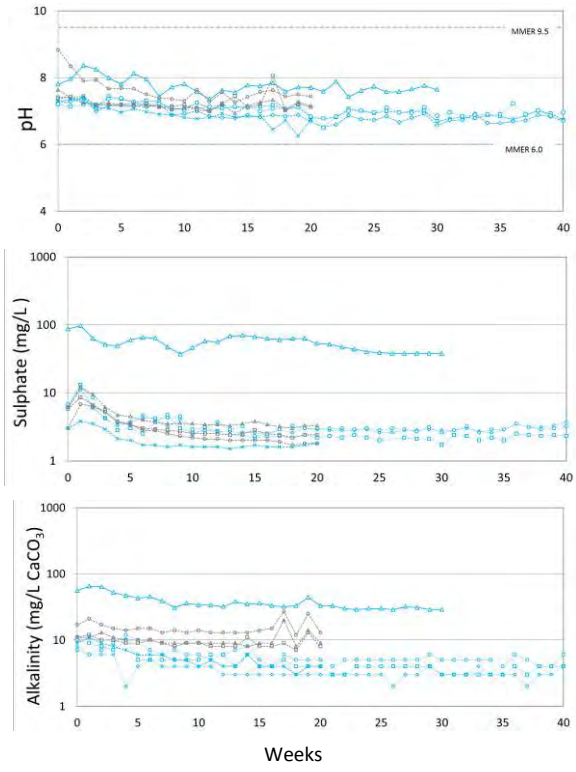

Figure 2 Kinetic test results for Discovery greywacke/siltstone samples (blue) and iron formation samples (grey)

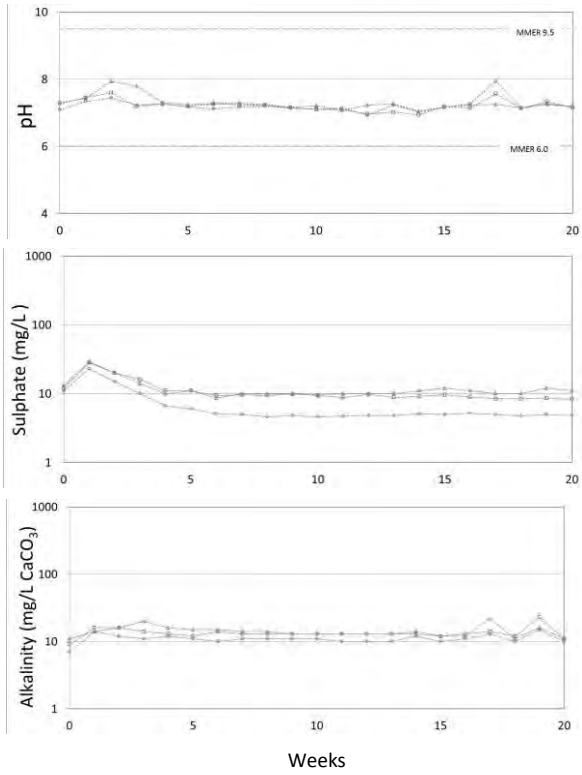

Figure 3 Kinetic test results for F Zone iron formation samples

CONCLUSION

The available neutralization capacity observed for many low carbonate samples based on paste pH, kinetic testing, NAG pH (for other samples not presented here) and carbonate content was often not reflected in XRD analysis. Similarly, the presence of sulfur identified by chemical analysis did not always correspond to identifiable sulfide mineral phases in XRD, including for samples having a total sulfur content of up to 0.55 wt%. This incongruence suggests that XRD-Rietveld does not possess a sufficiently elevated resolution to identify potentially important minerals in ARD reactions in low S, low carbonate rocks. This could be due to many factors, which include: the small subsample size subjected to XRD and the heterogeneity of the sample, the imprecision in identifying minerals that occur in trace quantities, the presence of mineral solid solutions such as the dolomite-ankerite series and that mineral phases with similar diffractogram patterns are difficult to distinguish. These factors are accentuated when the targeted element or mineral is present in trace quantities.

This imprecision decreases the relevance of relying solely on mineralogy-based evaluations of NP and NPR. Notwithstanding this, mineralogical data should be used to guide evaluations of buffer capacity, in conjuction with chemical analysis of carbonate content. Indeed, imprecise mineral identification or quantification, the presence of mineral solid-solutions (such as dolomite-ankerite) and the presence of reactive aluminosilicate minerals can lead to errors in the evaluation of the potential to generate acidic drainage.

Buffer capacity evaluation methods that are based on mineralogy require a greater mineralogical database for the project studied, and more powerful and precise mineral identification techniques such as Qemscan or Scanning Electron Microscope (SEM) with energy dispersive X-Ray (EDX) or a mineral liberation analyzer (MLA). The MLA was shown to successfully identify trace quantities of minerals down to 0.01wt% ranges (Barazzuol et al, 2012). Mineralogical analysis should be done in conjunction with chemical analyses including chemical scan, carbonate content, NAG pH with NAG solution analysis to verify that all the sulfur in the sample has been oxidized.

Results from the compendium of analytical techniques used suggest that Discovery waste rock is not likely to generate ARD in the short to medium term under the arctic (very dry and cold) site conditions. However, the development of acidic conditions in the long-term is uncertain. The uncertainty stems from the lack of precision in identifying the type and availability of buffering minerals present in trace amounts. This is also the case for F Zone iron formation rock, however this lithology constitutes a minor proportion (8%) of the total quantity of waste rock to be stored in F Zone WRST, the balance of which is NPAG and has excess carbonate-mineral buffering capacity.

Waste rock management control strategies will include mixing of rock types where the proportion of uncertain or potentially acid generating rock is small, such as in the F Zone waste rock stockpile, and for Discovery PAG rock, will include strategic placement the PAG waste rock in the stockpile and placement of a thermal cover having little to no PAG rock. These methods are planned to overcome uncertainty where it exists and avoid acidification of the Discovery and F Zone PAG waste rock in the long-term.

ACKNOWLEDGEMENTS

This study is presented thanks to Agnico-Eagle Mines Technical Services Division. The authors thank the staff of Agnico-Eagle Mines Inc. for their assistance in the studies described in this paper.

REFERENCES

Agnico-Eagle Mines Ltd. (AEM) (2014) Final Environmental Impact Statement (FEIS) Support document SD 6-3 Geochemistry Baseline Report, May 2014.

Agnico-Eagle Mines Ltd. (AEM) (2011) Project Description, Meliadine Gold Project, April 2011.

AMIRA International Ltd. (AMIRA) (2002). ARD Test Handbook – Project P387A Prediction and Kinetic Control of Acid Mine Drainage. May, 2002.

American Society for Testing and Materials (ASTM) (2006) ASTM D3987-06, Standard Test Method for Shake Extraction of Solid Waste with Water. ASTM Technical Committee D34-01-04 on Waste Leaching Techniques.

American Society for Testing and Materials (ASTM) (1996) ASTM D 5744-96, Standard Test Method for Accelerated Weathering of Solid Materials Using a Modified Humidity Cell, ASTM Committee D-34 Waste Management, Subcommittee D34.02 Physical and Chemical Characterization.

Barazzuol, L., K. Sexsmith, C. Bucknam and D. Lopez (2012) *Application of an Advanced Mineralogical Technique: Sulfide Mineral Availability and Humidity Cell Interpretations based on MLA Analysis*, Proc. of the 9th International Conference on Acid Rock Drainage, May 20-26, 2012, Ottawa, Canada.

Jambor, J.L., J.E. Dutrizac and M. Raudsepp. (2007) *Measured and Computed Neutralization Potentials from Static Tests of Diverse Rock Types*, Environmental Geology. No. 52, pp. 1019-1031.

Jambor, J.L., J.E. Dutrizac, L.A. Groat and M. Raudsepp. (2002) *Static Tests of Neutralization Potentials of Silicate and Aluminosilicate Minerals*, Environmental Geology, No.43, pp. 1-17.Snowden (2008), Comaplex Minerals Corp. Tiriganiaq Gold Deposit, Nunavut – Resource Update (NI 43-101 report), Amended April 2008.

Matson, B. (2009) *Assessing the Availability and Source of Non-Carbonate Neutralization Potential by Pre-treatment of Kinetic Test Samples*, Proceedings of the Securing the Future and Eighth International Conference on Acid Rock Drainage, June 23-26, 2009, Skelleftea, Sweden.

MEND (2009) *Prediction Manual for Drainage Chemistry from Sulphidic Geologic Materials*, MEND Report 1.20.1. Mining Environment Neutral Drainage Program, Natural Resources Canada, December 2009.

Paktunc, A.D. (1999) *Mineralogical constraints on the determination of neutralization potential and prediction of acid mine drainage*, Environmental Geology, vol. 39 (2), pp. 103-112.

Pincock, Allen and Holt (2008) Technical Report for the Meliadine East Project (NI 43-101 report), prepared for Meliadine Resources Ltd. on Behalf of the Meliadine East Joint Venture, April 18, 2008.

Plumlee. G.S., K.S., Smith, M.R., Montour, W.H. Ficklin, and E.L. Mosier (1999) *Geologic Controls on the Composition of Natural Waters and Mine Waters Draining Diverse Mineral-Deposit Types*, The Environmental Geochemistry of Mineral Deposits, Part B: Case Studies and Research Topics, Reviews in Economic Geology, vol. 6B, Society of Economic Geologists, Inc.

Price, W.A. (1997) *Draft Guidelines and Recommended Methods for the Prediction of Metal Leaching and Acid Rock Drainage at Mine sites in British Columbia*, Ministry of Energy and Mines, p. 159.

Walker, S.R., J. Millard, J. Andrina and S. Sibbick (2012) *Predicting ML/ARD from Low Sulfide and Low Neutralization Potential Waste Rock; Baffinland Iron Mines Mary River Project, Nunavut, Canada*, Proc. of the 9th International Conference on Acid Rock Drainage, May 20-26, 2012, Ottawa, Canada.

10th ICARD IMWA 2015 | 10th International Conference on Acid Rock Drainage & IMWA Annual Conference

Effect of Geological Models on ML/ARD Characterization Program Design at the KSM Project

Mark Nelson[1], Mike Lechner[2], Kelsey Norlund[1], Clem Pelletier[1] and Brent Murphy[3]

1. *ERM Rescan, Canada*
2. *Resource Modellin Inc., USA*
3. *Seabridge Gold, Canada*

ABSTRACT

The effect of different geological classification systems on a ML/ARD characterization program is investigated for the KSM Au-Cu porphyry project in northwest BC, Canada. Geological models enable predictive modeling of the ML/ARD potential of material during excavation and long term storage of waste rock by allowing the representation of a large mass of material by a relatively small mass of sampled material. A robust sampling plan typically attempts to collect samples in proportion to the mass of material to be excavated. Geological models developed during advanced exploration are often used during the geochemical characterization program; however, biases towards ore at the expense of waste rock and future pit walls frequently exist. Perceived uncertainty introduced through "lumping" or "splitting" of datasets can be carried into ML/ARD prediction and water quality models and regulatory approvals. Therefore, the choice of geological model is essential as a geochemistry baseline program advances to determine quantities of potentially acid generating (PAG) and not-PAG waste rock for waste rock and water management planning and to address stakeholder and government concerns.

Three geological models of the KSM project were assessed: Lithology, Alteration, and a hybrid Mine Model. Using the proportion of samples classified as PAG in each model unit, the material to be excavated was classified as PAG or not-PAG.

These results were then compared to an ABA block based on each of the three geological models. Differences in the proportions of PAG material were identified and the underlying cause of the differences is presented.

Keywords: ML/ARD; KSM; Model

INTRODUCTION

The KSM (Kerr-Sulphurets-Mitchell) Project is located in northwestern British Columbia, Canada (Figure 1). Gold and copper mineralization is hosted in a cluster of porphyry related, deformed, and dismembered deposits. The deposits are spread over an area of roughly two by ten kilometers and contain a 2.16 billion tonne resource with an average grade of 0.55 g/t Au, 0.21 % Cu, 2.74 g/t Ag, and 44.7 ppm Mo.

Figure 1 Location of the KSM Project

The work presented here focuses on the material that will be exposed during development of the Kerr open pit. The structural dismemberment of the deposit hinders the use of a pure alteration or lithology model, therefore a hybrid model has been used during the exploration program. This hybrid model (Mine Model) uses predominantly lithological terms above the major thrust faults, where protolith is more easily recognized, and alteration below the thrust faults where pervasive alteration has obliterated primary minerals and structures.

METHODOLOGY

To characterize the acid rock drainage (ARD) potential of the KSM Project each sample was analyzed to obtain its acid generating potential (AP) and acid neutralizing potential (NP). Standard acid-base accounting (ABA) methods (Sobek et al., 1978) were used to determine the sulfide sulfur content and the Sobek neutralization potential.

The neutralization potential ratio (NPR) is the NP:AP ratio. In this paper a generic NPR value of 2.0 was used as a cut-off for the designation of potentially acid generating (PAG; NPR < 2.0) or not-PAG.

PROJECT GEOLOGY

The setting provided in this report is a summary of previously completed descriptions of the regional geology (Ditson, Wells, and Bridge 1995; Fowler and Wells 1995; Kirkham and Margolis 1995; Lechner 2008). A detailed description of the local lithologies, alteration, mineralization, and structures can be found in the 2011 Pre-Feasibility Study Update (Wardrop 2011), this information was summarized in *2012 KSM (Kerr-Sulphurets-Mitchell) Prefeasibility Study* (Tetra Tech 2012).

The Sulphurets District is located along the eastern side of the Coast Mountains, approximately 25 km east of the Coast Plutonic Complex, a north-northwesterly trending belt of Cretaceous to Early Tertiary intrusions and high grade metamorphic rocks. The area lies near the western edge of the middle Jurassic to Cretaceous age Bowser Basin within the Stikine Terrane, also known as Stikinia, which was possibly accreted to the North American continental margin in the Middle Jurassic Period. Stikinia is interpreted as Triassic and Jurassic volcanic arcs resting on Palaeozoic basement (not present at site) and overlain by Jurassic basinal sedimentary rocks.

The upper Triassic Stuhini Group has two major subdivisions. A lower, dominantly sedimentary sequence consisting of turbidites and sandstones. Overlain by an upper dominantly volcanic sequence of volcanic pillowed flows and volcaniclastic breccias.

The Lower Jurassic Hazelton Group is inferred to represent a volcano-sedimentary island arc and back arc complex. The sedimentary sequence consists of a coarse basal sedimentary sequence overlain by a lower volcanic/volcaniclastic sequence, an upper felsic volcanic-pyroclastic unit (Mount Dilworth Formation), and an uppermost marine sedimentary sequence containing subaqueous mafic volcanic flows. The upper contact of the Hazelton Group is gradational with the Bowser Lake Group.

The Hazelton sedimentary sequence is intruded by a suite of porphyritic, Early Jurassic (189 to 195 million years) rocks including alkali feldspar granite, quartz monzonite, syenite, and granodiorite collectively referred to as the Mitchell Intrusions or Texas Creek Plutonic Suite. Below the Sulphurets and Mitchell thrust faults (STF and MTF), pre- and intra-mineral intrusions have historically been exploration targets. A conceptual summary of the evolution if the Project is presented in Figure 2.

There are two main structures at the project (Figure 3) – the Mitchell Thrust Fault (MTF) and the Sulphurets Thrust Fault (STF). The STF can be identified as the primary structure at the Kerr Deposit. The footwall of each deposit is usually more altered and more sheared than the hangingwall. In most instances this alteration and shearing has obliterated primary textures making identification of the protolith difficult. Where evident the protolith is classified as either volcaniclastic or sedimentary belonging to the Stuhini Group. The host rocks have been intruded by multi-phases of the Mitchell Intrusions.

The project fits within a broad porphyry alteration model. Weak hornfelsed alteration assemblages are evidence of contact metamorphism during the emplacement of the Mitchell Intrusions. There is a broad and pervasive propylitic halo characterized by chlorite alteration with variable secondary carbonate. More proximal to the intrusions and along hydrothermal conduits phyllic (QSP; quartz-sericite-pyrite) and intermediate argillic (IARG; clay minerals) alteration dominates, generally destroys primary mineral assemblages and structures. The more intense QSP and IARG alterations are the primary targets for gold and copper exploration. Potassic alteration has been noted but is volumetrically minor in waste rock. The pyrite halo is most intense within the QSP and IARG alterations and pyrite contents can reach 20 %.

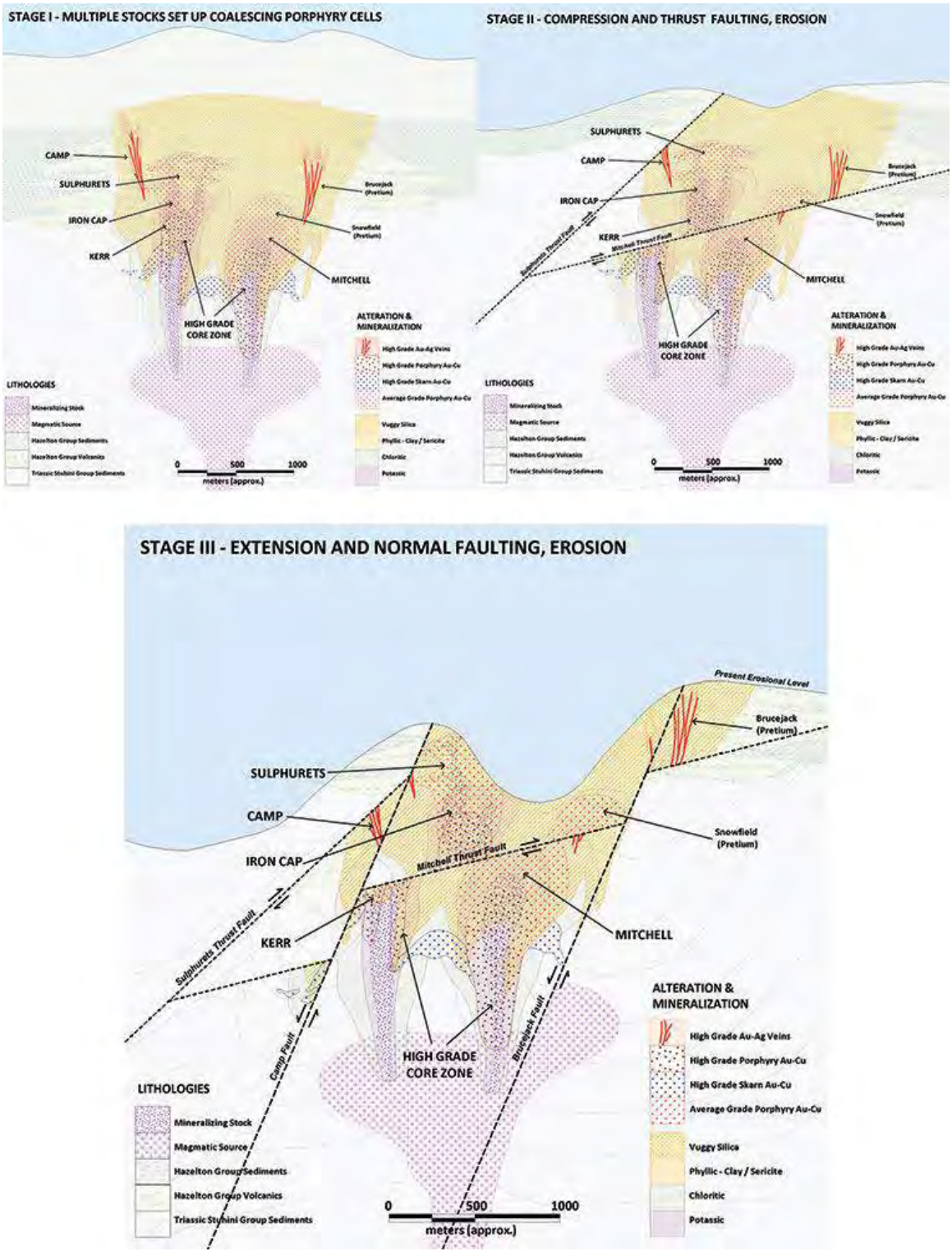

Figure 2 Conceptual geological evolution of the KSM deposits

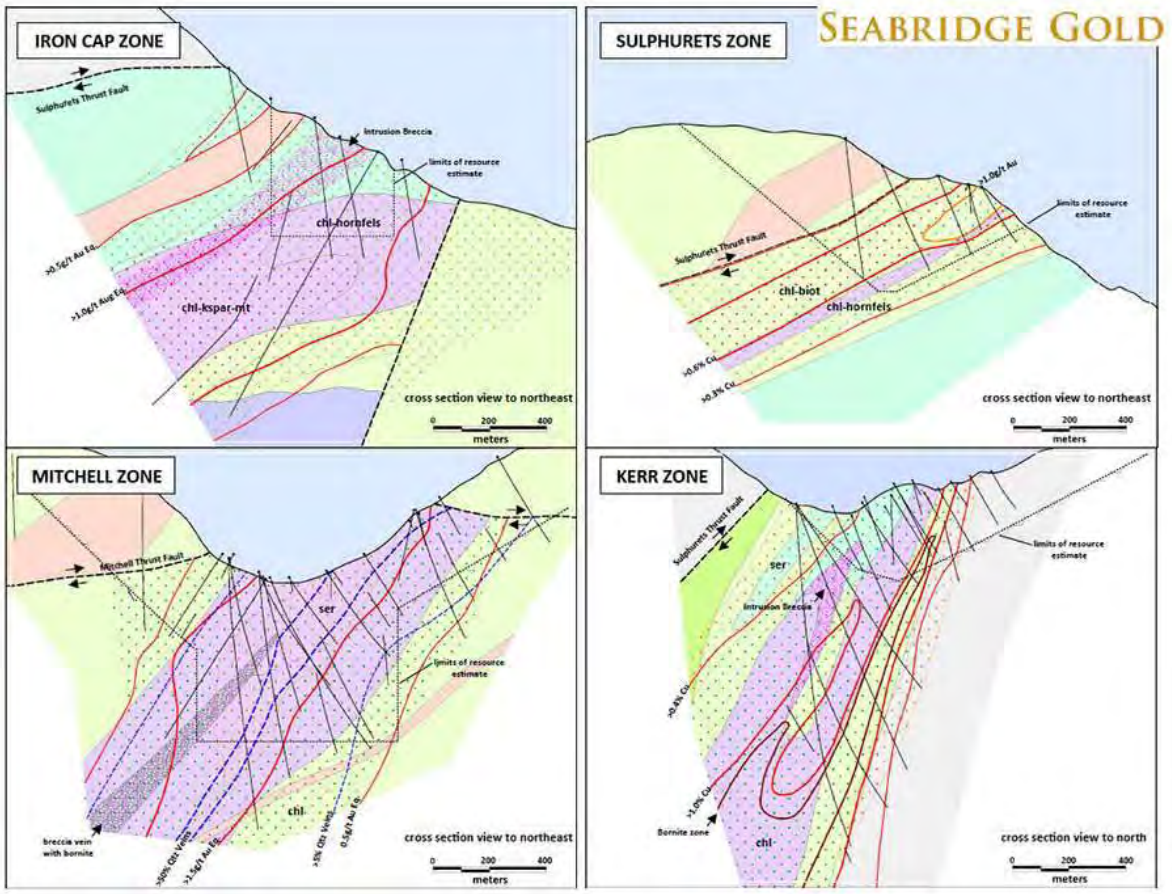

Figure 3 Schematic cross sections through KSM Project deposits

BLOCK MODEL

ABA block models were constructed for the KSM project in 2010, 2011, and 2012. Those models were updated in 2014 with additional static ABA sample data and refined geological models. The ABA block models were constructed with data collected from relatively wide-spaced drill holes from materials thought to be representative of "ore" and "waste". The resolution of individual model blocks is 25 m x 25 m x 15 m, which should allow for large excavators to segregate materials on a pit-bench scale. A general outline of the method used to generate the ABA block model is given below:

The ABA models are based on samples collected from existing drill hole assay pulps. Basic descriptive statistics were tabulated for AP and NP based on block model rock types, alteration types, degree of mineralization, and stratigraphic position relative to major thrust faults.

The models were constructed using three distinct methods outlined below and simplified in Figure 4:

- direct assignment of ABA values to blocks "pierced" by ABA samples;
- two-pass inverse distance estimation methods; and

- assignment of ABA values based on average values calculated by rock/alteration/mineralization type.

Individual model blocks pierced by an ABA sample were assigned NP and AP values from the sample and flagged as being estimated and off limits for subsequent estimation methods.

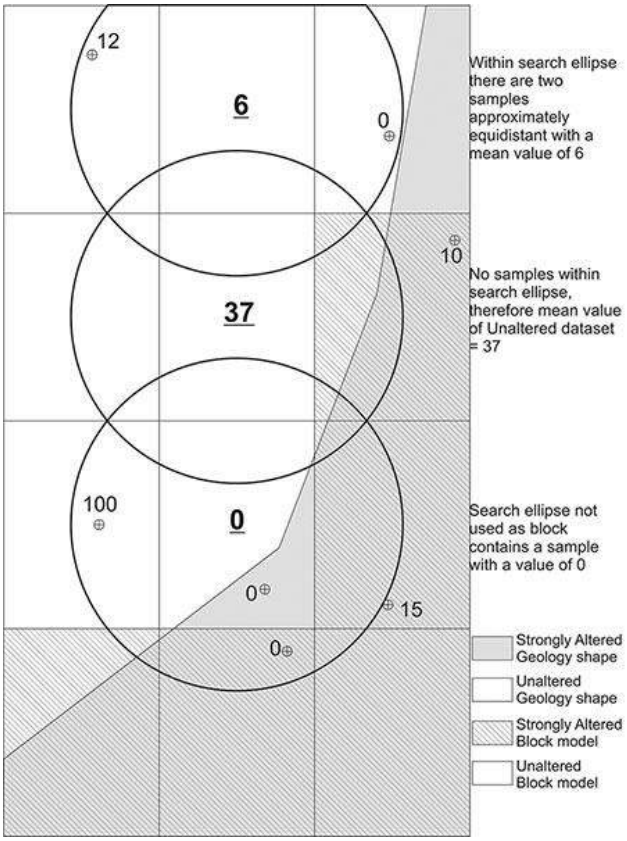

Figure 4 Conceptual diagram showing three methods for assigning a value to a block

After direct ABA assignment was completed, a two-pass inverse distance estimation method was implemented. The first pass used a 100 m x 100 m x 60 m search ellipse to locate eligible ABA samples. A minimum of one sample was required with a maximum of 8 samples used to interpolate NP and AP values. Blocks estimated by this method were flagged as being estimated and not subjected to subsequent estimates. The second estimation pass used a 200 m x 200 m x 120 m search ellipse with the same sample selection used for the first pass. Strict block/sample matching was used in both inverse distance estimation passes. This means that blocks of a certain rock type could only be estimated by samples with the same rock type. Unique search ellipse orientations were used for the Kerr, Sulphurets, and Mitchell zones. A minimum of 1 sample was required, with a maximum of 8 samples allowed with no more than 2 samples from each drill hole. An inverse distance weighting power of 2 was selected.

For blocks beyond 200 m of ABA sample data, class average values were assigned to blocks based on rock, alteration, or mineralization codes. The average values for NP and AP for these static samples are influenced by mineralization intensity. Typically, as gold and/or copper grades increase NP values decrease and AP values increase. Commingling mineralized and unmineralized

ABA samples has provided a certain degree of conservatism because most of the mineralized material will be processed and not sent to a waste rock disposal area. After the estimate and assignment of block ABA values was completed, the NPR was calculated.

RESULTS AND DISCUSSION

Lithology Model

The primary difference between the two approaches is the large difference in predicted PAG material from the heavily altered and uncategorized material below the STF (Table 1). The result is that the two approaches have an approximately 28 % difference in the total mass of predicted PAG material.

Table 1 Lithology model comparison

	From Block Model		From ABA Samples		
Lithology Model Code	PAG	not-PAG	PAG	not-PAG	Tonnage of waste (Mt)
Kerr					
Overburden	100 %	0 %	26 %	74 %	20.3
Stuhini Group	0 %	100 %	0 %	100 %	70.4
HW Intrusive Rock	97 %	3 %	64 %	36 %	51.1
Premier Dike	100 %	0 %	100 %	0 %	9.3
Hornblende Dike	100 %	0 %	N.S.	N.S.	0.1
HW Mixed	98 %	2 %	82 %	18 %	32.9
FW Mixed	100 %	0 %	82 %	18 %	11.0
HW Uncategorized	**100 %**	**0 %**	**91 %**	**9 %**	**200.5**
FW Uncategorized	**99 %**	**1 %**	**50 %**	**50 %**	**240.6**
Unclassified	100 %	0 %	N.S.	N.S.	25.6
Kerr Total Mass	585.7	76.1	401.9	234.2	661.8

N.S. = no sample collected

Major units are represented by bold font

Alteration Model

The two Alteration Model approaches predict a 24 % difference in the mass of PAG material (Table 1). The two major units have much higher predicted masses of PAG material through the block model approach compared to the ABA samples.

Table 2 Alteration model comparison

Alteration Model Code	From Block Model PAG	From Block Model not-PAG	From ABA Samples PAG	From ABA Samples not-PAG	Tonnage of waste (Mt)
Kerr					
CL-PR	100 %	0 %	93 %	7 %	18.5
QSP	**99 %**	**1 %**	**86 %**	**14 %**	**208.2**
Weak CL-QSP	100 %	0 %	86 %	14 %	110.4
Premier Dike	100 %	0 %	86 %	14 %	13.3
Hornblende Dike	100 %	0 %	N.S.	N.S.	0.3
Uncategorized/unaltered	**79 %**	**21 %**	**43 %.**	**57 %**	**311.0**
Kerr Total Mass	596.0	65.7	436.9	224.5	661.7

N.S. = no sample collected

Major units are represented by bold font

Mine Model

In the Mine Model the difference between the block model and the ABA samples can be large for major units (Table 3). Using just the ABA samples the volume of PAG material would be underestimated by approximately 129 Mt at Kerr, approximately 21 % of the mass of waste rock produced.

Table 3 Mine model comparison

Mine Model Code	From Block Model PAG	From Block Model not-PAG	From ABA Samples PAG	From ABA Samples not-PAG	Tonnage of waste (Mt)
Overburden	100 %	0 %	100 %	0 %	20.3
Premier Dike	100 %	0 %	100 %	0 %	1.3
Chlorite-propylitic alteration	100 %	0 %	93 %	7 %	15.5
QSP alteration	**99 %**	**1 %**	**85 %**	**15 %**	**175.2**
Weak chlorite-QSP alteration	100 %	0 %	91 %	9 %	91.1
Stuhini Volcanics	0 %	100 %	0 %	100 %	63.0
HW Intrusive Rock	95 %	5 %	60 %	40 %	0.0
FW Weak QSP alteration	99 %	1 %	88 %	12 %	33.3
FW Propylitic Hornfels alteration	99 %	1 %	42 %	58 %	51.4
HW Propylitic Hornfels alteration	**100 %**	**0 %**	**64 %**	**36 %**	**175.0**
Kerr Total Mass	560.8	65.3	431.3	194.8	626.1

Major units are represented by bold font

DISCUSSION

The differences between the proportions calculated from the ABA samples and the proportions calculated from the Block Models are a function of block model edge effects and the influence high AP values. Blocks near the periphery of the Kerr open pit have AP and NP values assigned by either inverse distance estimation or average value of model unit. Both methods favor higher AP assignment, as both methods are influenced by the drilling and sampling focused in the mineralized and highly altered footwall. The average value assignment method is not responsible for as many assigned values as inverse distance estimation.

Figure 5 uses fictional data to illustrate the difference in calculated proportions of PAG material based on using the ratio of ABA samples (left grid) or using inverse distance estimation (right grid). In the example five samples are identified with varying NP and AP values and placed in a two dimensional grid to simulate a block model. When just the ABA sample data are used (left grid) the example predicts 60 % of the material to be not-PAG (shaded grey); based on three of five samples having a NPR more than 2.0. This result indicates that the bulk of the material in the block is not-PAG. Note that using the ratio of PAG to not-PAG samples from an ABA database does not take into account the spatial layout of samples.

Using the same example data in the same grid inverse distance estimations were used to calculate AP values for each block (Figure 5, right grid). The single high AP value in the center dominates an inverse distance estimation resulting in very few blocks being classified as not-PAG. The end result is less than 10 % not-PAG (shaded grey) by inverse distance estimation, compared with 60 % not-PAG by ABA sample. This result indicates that the bulk of the block is PAG and may require segregation or special handling.

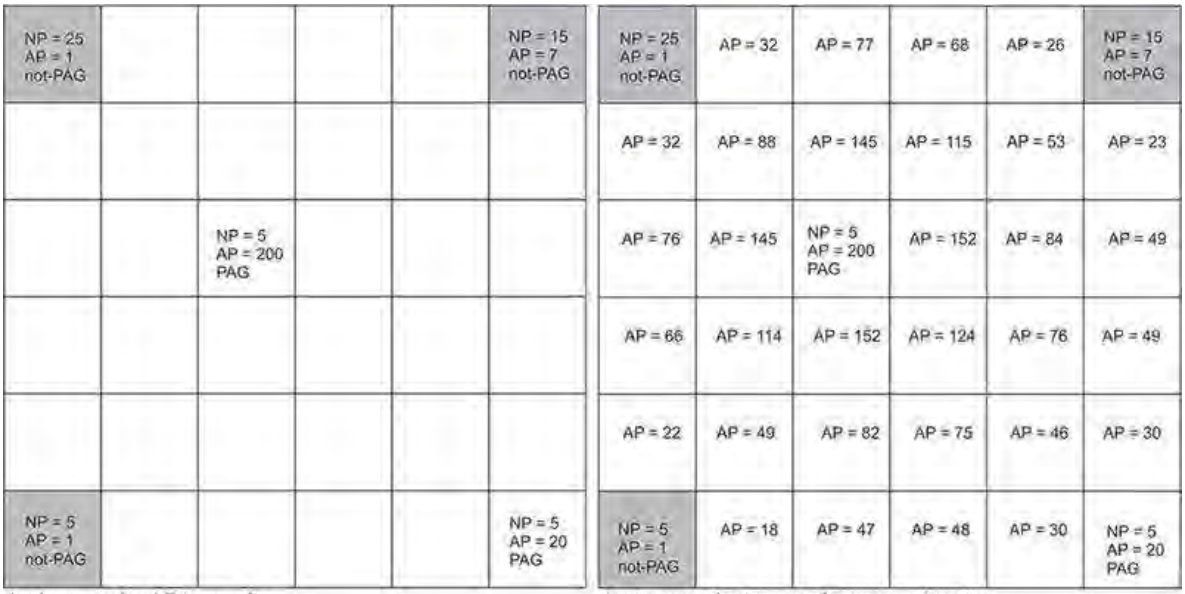

Figure 5 Conceptual diagram showing proportion of material estimated to be PAG by two differing methods

CONCLUSION

Differences were noted when comparing the proportion of PAG material predicted for the three Kerr block models to the proportions of samples classified as PAG. In the Lithology, Alteration, and Mine Models the block model predicted a higher proportion of PAG material than the ABA sample data. The primary reason for the difference is the overwhelming effect a single high AP value can have on surrounding blocks if NP and AP are usually moderate to low.

The results presented illuminate the need to consider Block Models and ABA datasets when predicting the proportions of PAG material. Additionally, the masses predicted by the deposit Block Models were quite similar irrespective of the geological model used to generate the Block Model. This result indicates that at the Kerr Deposit the Block Models are a robust and conservative approach to ARD prediction.

REFERENCES

Ditson, G.M., R.C. Wells, and D.J. Bridge (1995) Kerr: The geology and evolution of a deformed porphyry copper-gold deposit, northwestern British Columbia, in *Porphyry Deposits of Northwestern Codillera of North America*. Canadian Inistitute of Mining, Metallurgy and Petroleum, Special Volume 46, pp. 509-523.

Fowler, R.V. and R.C. Wells, (1995) The Sulphurets Gold Zone, northwestern British Columbia, in *Porphyry Deposits of Northwestern Codillera of North America*. Canadian Inistitute of Mining, Metallurgy and Petroleum, Special Volume 46, pp. 484-498.

Kirkham, R.V. and J. Margolis (1995) Overview of the Sulphurets area, northwestern British Columbia, in *Porphyry Deposits of Northwestern Codillera of North America*. Canadian Inistitute of Mining, Metallurgy and Petroleum, Special Volume 46, pp. 473-483.

Lechner, M. (2008) Updated Mitchell Creek Technical Report Northern British Columbia, Tuscon, AZ, prepared for Seabridge Gold Inc.

Sobek, A.A., W.A. Schuller, J.R. Freeman and R.M. Smith (1978) *Field and laboratory methods applicable to overburden and minesoils*, EPA 600/2-78-054, 203pp.

Tetra Tech (2012) 2012 KSM (Kerr-Sulphurets-Mitchell) Prefeasibility Study, Vancouver, BC, prepared for Seabridge Gold Inc.

Wardrop (2011) Kerr-Sulphurets-Mitchell (KSM) Prefeasibility Study Update 2011, Vancouver, BC, Prepared for Seabridge Gold Inc.

10th ICARD IMWA 2015 | 10th International Conference on Acid Rock Drainage & IMWA Annual Conference

A Metal Attenuation Study on Waste Rock Collected from the East Dump, Antamina Mine, Peru: A Combined Mineralogical and Geochemical Approach

Laura Laurenzi, K. Ulrich Mayer and Roger Beckie

Department of Earth, Ocean and Atmospheric Sciences, University of British Columbia, Canada

ABSTRACT

In this study we evaluate the influence of secondary minerals on metal attenuation using a suite of geochemical and mineralogical tests on three samples collected from different depths in the East Dump, Antamina Mine in Peru. The bulk elemental content and mineralogy are determined using trace metal analysis by inductively coupled plasma mass spectrometry (ICP-MS) after digestion and X-Ray Diffraction (XRD), respectively. A sequential extraction procedure (SEP) is used to identify the phases associated with the metals. Optical mineralogy and scanning electron/back-scatter electron microscopy (SEM/BSE) are used to identify secondary mineral phases, elements associated with the secondary minerals and the mode of occurrence of the secondary minerals.

Precipitation of weak-acid soluble phases and sorption/co-precipitation with amorphous reducible phases are the predominant attenuation mechanisms for the metals studied (i.e., arsenic, copper, lead, molybdenum and zinc). Copper, lead, and zinc are associated with weak-acid soluble phases and reducible phases. Arsenic and molybdenum are associated with reducible phases. Iron oxides are the predominant reducible phases forming coatings around sulfides and silicate minerals, or discrete mineral grains. Metal carbonates/sulfates (with variable Cu and Zn content) and zinc silicates are the predominant weak-acid soluble phases forming coatings on calcium carbonates and silicate grains, or as discrete mineral grains. This combined mineralogical and geochemical approach elucidates the nature of secondary minerals and associated metal attenuation processes.

Keywords: Metal Attenuation, Waste rock, Geochemistry, Mineralogy

INTRODUCTION

Mine waste rock often contains sulfide minerals that oxidize when exposed to oxygen and water. Without sufficient carbonate mineral buffering capacity in the waste rock, acidic conditions can develop leading to acid rock drainage (ARD); however, if the waste rock contains sufficient carbonate minerals to buffer the acidity generated by the oxidation of sulfides, neutral conditions can persist resulting in neutral rock drainage (NRD). Dissolved metal concentrations differ in ARD and NRD because metal mobility is highly dependent on pH. In ARD, Al, Fe, Cu, Pb, Zn, Cd, Mn, Co, and Ni are generally mobile (Al et al., 2000), while in NRD metals which are either weakly hydrolyzing such as Zn, Ni or oxyanion forming such as Mo, As, Se, and Cr are generally mobile (Price, 2009). This is because in NRD, cationic trace metals can be sequestered in secondary mineral phases and sorbed onto metal (oxy)hydroxides and clay minerals (Smith, 1999; Al et al., 2000). Oxyanions are more mobile in NRD because sorption onto iron oxides increases as pH drops below neutral. Thus, secondary minerals are an important control on the quality of water emanating from waste materials (van der Sloot and van Zomeren 2012; Al et al., 2000). Understanding the mechanisms that attenuate metals from waste rock is essential for reliable predictions of water quality (Mayer et al., 2003; Al et al., 2000). The objective of this study is to identify the secondary minerals and processes that attenuate metals by examining samples collected from the full scale operating waste dump, the East Dump at the Antamina Mine, Peru. Results from this study can be compared to the results of laboratory and smaller scale tests also conducted on waste rock material from this site.

METHODOLOGY

Project Site and Sample Collection

The Antamina deposit is a copper-zinc-molybdenum skarn formed by the intrusion quartz monzonite into limestone (Lipten & Smith, 2004; Love et al., 2004; Redwood, 1999). Waste is subdivided into classes based on the criteria summarized in Table 1. The East Dump, the focus of this study, receives all classes of waste rock and is therefore geochemically heterogeneous.

Table 1 Antamina Waste Rock Classification System

Class	Description	Zn	As	Sulfide
A	(Exo,Endo)skarn, intrusive, hornfels, Marbles Limestone	>1500 ppm	>400 ppm	> 3%
B	Hornfels, marble, limestone	700-1500 ppm	N/A	<2-3%
C	Hornfels, marble, limestone	<700 ppm	<400 ppm	<2-3%

The waste rock samples used for this study were collected from two boreholes at site BH-1 drilled using a reverse circulation drill rig. At the time of drilling, the deepest material in East Dump had been in place for over ten years, while the shallowest material for more than 5 years. Composite samples of waste rock material (at 1.5 m intervals) were collected and sieved using a 2 mm (#10) mesh. Sixteen samples were initially characterized for bulk elemental content, X-ray Diffraction (XRD) and sequential extraction procedure (SEP) testing, the results of which were used to focus scanning electron/back-scatter electron microscopy (SEM/BSE) tests on three samples. The results of the geochemical and mineralogical testing on the three samples are discussed here.

Testing Framework

The bulk elemental content of the samples was determined using ICP-MS analysis after a 4-acid digestion by SGS in Vancouver, Canada. XRD was used to identify crystalline minerals. XRD data were collected using a Bruker D8 Focus Diffractometer with a scanning step of 0.029° 2θ and counting time of 100.1 s/ over a range of 3-80° 2θ. While XRD is useful for crystalline mineral phases, XRD cannot identify minerals below ~1% abundance or those that are amorphous or nano-crystalline. Accordingly, the sequential extraction procedure (SEP) proposed by Hall et al. (1996) (Table 2) was used to identify the predominant secondary phases and attenuation mechanisms for As, Cu, Mo, Pb, and Zn.

Three samples that showed elevated metal concentrations in the SEP were investigated in more detail. Thin sections of these three samples were prepared and examined using transmitted/reflected light microscopy where individual mineral grains were targeted for SEM/BSE imaging and Electron Dispersion Spectra (EDS) analysis. For the SEM/BSE analysis, the thin sections were coated with evaporated carbon and examined on a Philips XL30 SEM equipped with Bruker Quantax 200 Microanalysis system and light element XFLASH 4010 Silicon Drift detector. Semi-quantitative analysis of the EDS yielded weight percent (wt.%) of elements associated with the secondary minerals.

Table 2 Sequential extraction procedure used on samples (Hall et al., 1996)

Step	Phases	Method(1)
1	Water Soluble	50 mL deionized water shake for 1h at room temperature
2	Weakly sorbed /Exchangeable(2)	40 mL 1M $MgCl_2$ shake for 1 hour at room temperature
3	Weak-acid soluble	20 mL 1M CH_3COONa (sodium acetate) at pH 5 shake for 6h centrifuge for 10min Repeat Step
4	Amorphous reducible phases	20 mL 0.25M NH_2OH*HCl (hydroxylamine hydrochloride) in 0.25 HCl place in 60^{0}C water bath for 2h every 30min vortex contents Repeat Step but heat for only 30 min
5	Crystalline reducible phases	30 mL of 1 M NH_2OH*HCl (hydroxylamine hydrochloride) in 25% CH_3COOH (acetic acid) place in 90^{0}C water bath for 3h, vortex every 20 min Repeat Step but heat for only 1.5 hours
6	Residual Phases	4 - Acid Digest(3)

NOTES:

(1) Steps 3 – 5 are repeated using the same liquid solid ratio (LSR). Leachates are analyzed separately and the concentrations are summed.

(2) Weakly sorbed/exchangeable step taken from (Tessier et al., 1979)

(3) Residual fraction was determined by 4-acid digest at SGS, Burnaby (BC, Canada)

Results

From the lithologic logs produced at the time of drilling (not shown), samples BH-1s (1.5 – 3.0) and BH-1d (90.0 – 91.5) are composed predominantly of marble and marble diopside lithologies. Both samples contain some skarn while BH-1d (90.0 – 91.5) also contains some igneous intrusive rock. BH-1d (19.5 – 21.0) is predominantly igneous intrusive, with some marble.

The bulk elemental content of As, Cu, Mo, Pb, and Zn are presented in Table 3. Among the three samples, BH-1s (1.5 – 3.0) has the highest content of Mo and Pb and BH-1d (19.5 – 20.0) and BH-1d (90.0 – 91.5) have the higher Cu and Zn. Total arsenic is highest in BH-1d (90.0 – 91.5).

Table 3 Total metal concentrations for select elements

	Units	BH-1s (1.5 - 3.0)	BH-1d (19.5 - 21.0)	BH-1d (90.0 - 91.5)
As	ppm	104	49	118
Cu	ppm	1340	5740	5530
Mo	ppm	468	104	73.3
Pb	ppm	2080	195	593
Zn	ppm	674	4900	>10000

Generally, the primary mineralogy of the samples is consistent with the primary lithology of the samples, which includes quartz, orthoclase, albite, biotite, actinolite and calcite in all samples. Diopside, garnets, and vesuvianite were additionally found in marble diopside and skarn bearing samples, BH-1s (1.5 – 3.0) and BH-1d (90.0 – 91.5). Table 4 summarizes the sulfide and secondary mineralogy of the samples determined from XRD. The secondary minerals noted in the XRD are chlorite, gypsum, smithsonite, otavite, wulfenite, and hemimorphite. In addition there was a strong amorphous background in the diffraction patterns, indicative of amorphous minerals such as iron oxides and aluminum hydroxides. Although hemimorphite is a secondary mineral that could form in the dump due to the weathering of Zn bearing sulfides, it is also part of the supergene mineralization of the Antamina deposit (Personal communication 2013, L. Plascencia). Wulfenite found in the XRD of samples from site BH-1 (not shown here) confirms previous work using batch and field experiments that indicate that Mo precipitation is likely in the form of wulfenite (Hirsche et al. 2012; Conlan 2009).

Table 4 Mineralogy as determined by XRD

Mineral	Chemical Formula	BH-1s (1.5 - 3.0)	BH-1d (19.5 - 21.0)	BH-1d (90.0 - 91.5)
	Sulfides			
Pyrite	FeS_2	x	x	x
Molybdenite	MoS_2	x		
Chalcopyrite	$CuFeS_2$		x	x
	Secondary minerals			
Chlorite	$(Mg,Fe)_3(Si,Al)_4O_{10}(OH)_2 \cdot (Mg,Fe)_3(OH)_6$	x	x	x
Gypsum	$CaSO_4$	x	x	x
Smithsonite	$ZnCO_3$		x	x
Otavite	$CdCO_3$			x
Hemimorphite	$Zn_4Si_2O_7(OH)_2 \cdot H_2O$			x
Amorphous Background	n/a	x	x	x

Sequential Extraction Procedure

Figure 1 presents the SEP results for As, Cu, Mo, Pb and Zn. Only Ca and S were found in the water soluble leach step (step 1) and indicate that gypsum is the only water-soluble phase. Table 5 presents the range in concentrations extracted (in μm) for the SEP steps 2 – 5 and the % extracted for each step when compared to the total amount extracted from the SEPs. From Table 5, weak-acid soluble phases and amorphous reducible phases are considered attenuation mechanisms for Cu, Pb, and Zn and reducible phases are considered to have some attenuating control on As and Mo.

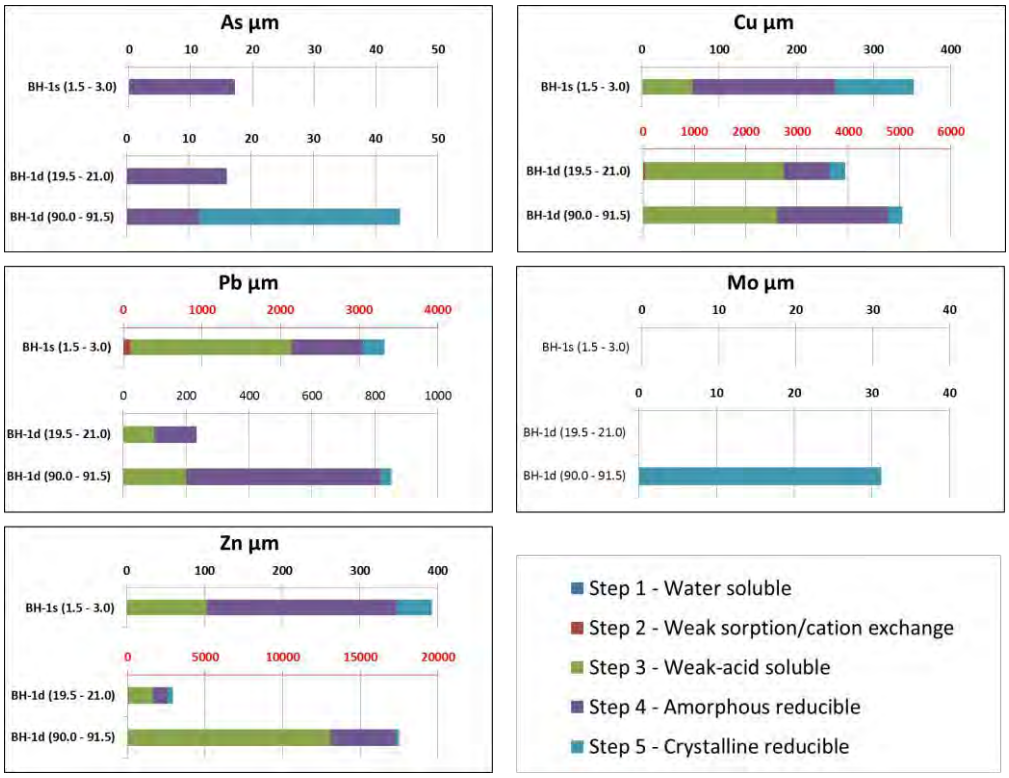

Figure 1 Sequential extraction results for select elements in µg as leached from a 1g sample. Each sub-figure has the same scale unless otherwise indicated using red text

Table 5 SEP results in ppm and % for steps 2 - 5

	As	Cu	Mo	Pb	Zn
step 2 - Weak sorption/cation exchange					
µm extracted	-	DL – 34.6	-	DL – 90.0	DL – 44.7
% extracted(1)	-	0 - 0.65	-	0 – 2.66	0 - 0.96
step 3 - Weak-acid soluble					
µm extracted	-	65.4 – 2707.5	-	99.8 – 2048.4	103.4 – 13081.1
% extracted(1)	-	6 – 51.0	-	23.1 – 60.4	13.7 – 72.2
step 4 - Amorphous reducible					
µm extracted	0.4 - 0.6	185.2 – 2156.9	-	133.8 – 906.3	243.9 – 4125.9
% extracted(1)	12.0 – 49.3	16.9 – 37.8	-	26.7 – 70.8	20.1- 32.2
step 5 - Crystalline reducible					
µm extracted	DL – 32.3	101.1 – 298.9	DL – 31.2	DL – 280.0	45.4 – 365.5
% extracted(1)	0.0 – 33.3	4.8 – 9.2	0.0 – 62.6	0.0 – 8.3	1.6 – 7.7

Notes:

(1) % extracted compared to the total extracted from all steps of the SEP

(2) DL – indicates that concentrations were below detection limit and mass extracted was not calculated

Optical Microscopy and SEM/BSE imaging

Weak-acid Soluble Phases

Figure 2 to Figure 4 present transmitted light microscopy and SEM/BSE images for mineral grains suspected of contributing to Cu and Zn found in the weak-acid soluble leach step. Carbon is included in the semi-quantitative analyses in these figures because it is suspected that these secondary minerals are either carbonates or sulfates or some carbonate/sulfate mix and that the carbon coating used in the method preparation would not contribute significantly to the results. Figure 2 shows two distinct mineral coatings a dark black Zn/Cu carbonate, and a blue/green Cu/Zn carbonate/sulfate coating a silicate/carbonate mineral grain. Figure 3 shows a Cu/Zn carbonate mineral associated with hemimorphite. Figure 4 shows a discrete Zn/Cu carbonate mineral grain. A weak-acid soluble secondary mineral with Pb association was not found although SEP leachate results indicate that this is a potential attenuation mechanism for Pb. These results indicate that more than one Cu/Zn weak-acid soluble phase is forming. In addition, hemimorphite ($Zn_4Si_2O_7(OH)_2 \cdot H_2O$) dissolved in the weak-acid used for this step (Laurenzi, unpublished).

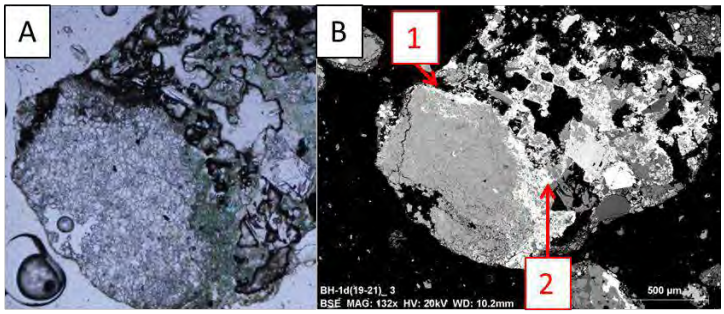

Figure 2 A) Plane-polarized transmitted light photograph of silicate/calcite mineral with black and blue/green secondary mineral coating. B) SEM/BSE image of same mineral: 1) black mineral semi-quantitative analysis; 9 wt.% Cu, 28 wt.% Zn, 22 wt.% O, 8 wt.% C, 0.2 wt.% S.; 2) blue/green mineral semi-quantitative analysis; 46 wt.% Cu, 1.5 wt.% Zn, 15 wt.% O, 5 wt.% C, 6 wt.% S

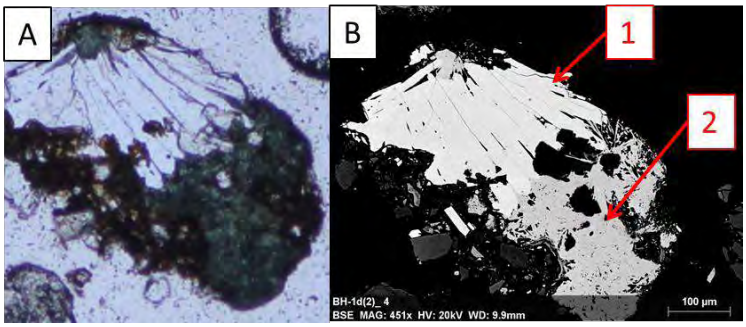

Figure 3 A) Plane-polarized transmitted light photograph of zinc silicate mineral (hemimorphite) with blue/green secondary mineral coating. B) SEM/BSE image of mineral: 1) Hemimorphite semi-quantitative analysis; 50 wt.% Zn, 16 wt.% O, 9 wt.% Si, 2 wt.% C. 2) blue/green mineral semi-quantitative analysis; 42 wt.% Cu, 13 wt.% Zn, 23 wt.% O, 9 wt.% C

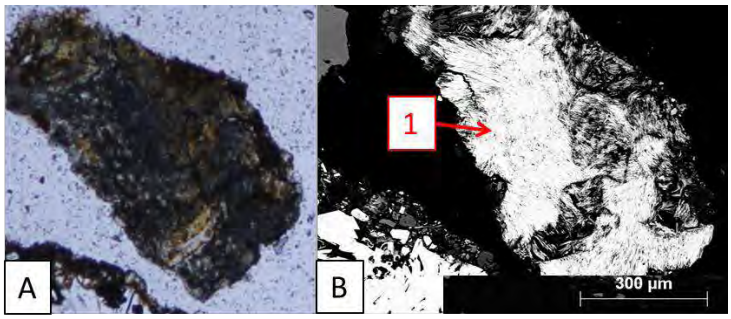

Figure 4 A) Plane-polarized transmitted light photograph of mineral. B) SEM/BSE image of same mineral: 1) mineral semi-quantitative analysis; 18 wt.% Cu, 32 wt.% Zn, 18 wt.% O, 10 wt.% C

Amorphous Reducible Phases

The predominant reducible phases are iron oxides. Figure 5 to Figure 6 present transmitted light and SEM/BSE images for iron oxides found in the samples. The iron oxides form as coatings around sulfide minerals, silicate minerals and as discrete mineral grains (not shown here). Iron oxides were found in all samples and contained variable concentrations of Cu (0.0 wt.% - 2.0 wt.%), Pb (0.0 wt.% - 4 wt.%), and (1wt.% - 7wt.%) Zn. The iron oxide in Figure 6 was determined to have 0.1 wt.% Mo.

Although As associations were not identified using SEM/BSE, the results of the SEP indicate that the As and Mo concentration may be below the detection limits of the SEM/BSE instrument. Sorption and co-precipitation onto these reducible phases is assumed to be one of the attenuation mechanisms for these metals.

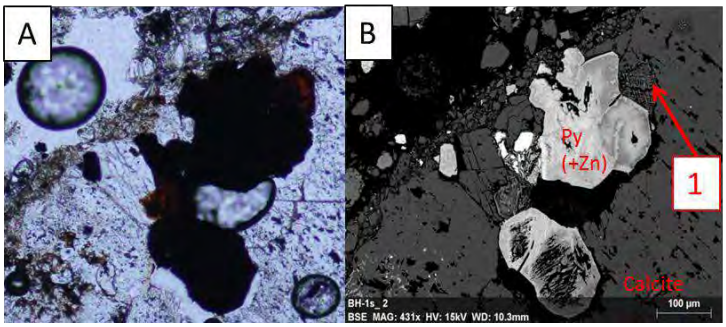

Figure 5 A) Plane-polarized transmitted light photograph of pyrite mineral with iron oxide coatings. B) SEM/BSE image of same mineral. Semi-quantitative analysis of iron oxide 1) 28 wt.% Fe, 21 wt.% O, 1 wt.% Zn, 4 wt.% Pb

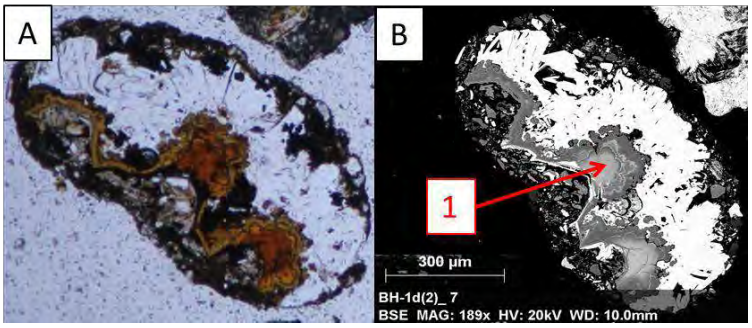

Figure 6 A) Plane-polarized transmitted light photograph of iron oxide coating hemimorphite (white mineral). B) SEM/BSE image of same mineral. Semi-quantitative analysis of iron oxide 1) 41 wt.% Fe, 26 wt.% O, 8 wt.% Zn, 2 wt. % Cu, 2 wt. % Pb, 0.01 wt. % Mo

DISCUSSION

The geochemical and mineralogical testing framework shows that weak-acid soluble and amorphous reducible phases are the predominant attenuation processes for Cu, Pb, and Zn. The main weak-acid soluble phases are copper and zinc bearing; however, their composition determined by SEM/BSE is not indicative of a single mineral phase. This supports field - experimental pile scale conclusions, that identified a blue (mostly amorphous copper sulfate) precipitate containing some malachite in a pile composed of Class A intrusive material (Peterson 2014). More work is required to determine the mineralogy of these weak-acid soluble phases. Hemimorphite, potentially a secondary mineral that formed in the East Dump, should also be considered a weak-acid soluble phase in which Zn is attenuated. The main reducible phases are iron oxides and can contain as much as 2.0 wt.% Cu, 4 wt.% Pb and 7 wt.% Zn. The variability in metals associated with the iron oxides is considered to be due to differences in the total metal content in the waste rock, flow patterns within the pile and the release rate of these metals from the waste rock. Low concentrations of As and Mo are associated with reducible phases dissolved in the SEP leachates. For As these associations were not identified in the SEM/BSE investigation possibly due to low content. While for Mo, sorption onto iron oxides, as determined from the SEP and SEM/BSE investigations, and precipitation of wulfenite, identified by XRD, are the likely attenuation processes. Based upon the results of the SEP, a lead-bearing weak-acid soluble phase was expected but was not identified in the mineralogical and SEM/BSE investigations. More work is required to identify the attenuating mechanism for lead. The metal/mineral associations seen in this study are considered to be the results of pore waters high in Zn and Cu and SO_4 and CO_3, from which Cu-Zn bearing minerals are precipitating. Due the presence of calcite in the samples the pH of the water is suspected to be near neutral, thus limiting the sorption of As and Mo.

CONCLUSION

This work focused on 3 samples collected from depth in an operational waste rock pile. This study highlights the benefit of detailed mineralogical and geochemical investigations to constrain metal attenuation phases and processes. It is important to examine samples collected from the field to support inferences made from laboratory tests.

Results from the SEP, microscopy and SEM/BSE investigations indicate that precipitation of weak-acid soluble phases and sorption onto amorphous reducible phases are the predominant attenuation mechanism for Cu, Pb and Zn. Cu and Zn are associated together with variable concentrations in weak-acid soluble phases. SEP tests show that Pb is being attenuated in a weak-acid soluble phase; however, this phase was not identified in the mineralogy or SEM/BSE work. SEP tests indicate that As is associated with reducible phases. SEP leachates and XRD tests indicate that Mo attenuation is via sorption onto iron oxides and precipitation of wulfenite, respectively.

ACKNOWLEDGEMENTS

Funding for this Project was provided in-part by Compañia Minera Antamina. Many thanks to Bevin Harrison from Antamina for her time and effort in reviewing this submission; as well as, Celedonio Aranda, Edsael Sanchez and Bartolome Vargas for excellent technical and field support at Antamina. Special thanks to my supervisors Roger Beckie and K. Ulrich Mayer and my cohorts Elliot Skierszkan, Maria Eliana Lorca Ugalde, Melanie St. Arnault, and Daniele Pedretti for their assistance in collecting samples, support and thoughtful reviews.

References

Al, T. A., C. J. Martin, and D. W. Blowes. 2000. "Carbonate-Mineral/water Interactions in Sulfide-Rich Mine Tailings." *Geochimica Et Cosmochimica Acta* 64 (December): 3933–48.

Conlan, Michael Joseph William. 2009. "Attenuation Mechanisms for Molybdenum in Neutral Rock Drainage". University of British Columbia.

Hall, G.E.M., J.E. Vaive, R. Beer, and M. Hoashi. 1996. "Selective Leaches Revisited, with Emphasis on the Amorphous Fe Oxyhydroxide Phase Extraction." *Journal of Geochemical Exploration* 56: 59 –78.

Hirsche, Dustin Trevor, R. D. Beckie, Michael J. W. Conlan, Sharon Blackmore, J. L. Smith, B. Klein, K. Ulrich Mayer, C. A. Aranda, Luis A. Rojas Bardón, and Raúl Jamanca Castañeda. 2012. "Stacked Field Cells as a Means for Studying Metal Attenuation by Waste Rock Mixing at the Antamina Mine in Peru." In *Proceedings Ninth International Conference on Acid Rock Drainage*, 9. Ottawa, Canada.

Mayer, K. Ulrich, D. W. Blowes, and E.O. Frind. 2003. "Advances in Reactive-Transport Modelling of Contaminant Release and Attenuation from Mine-Waste Deposits." In *Environmental Aspects of Mine Wastes*. Vol. 31. Mineralogical Association of Canada Short Course Series (eds. Jambor, J.L.,Blowes, D.W., Ritchie, A.I.M.

Peterson, H. E. 2014. "Unsaturated Hydrology, Evaporation, and Geochemistry of Neutral and Acid Rock Drainage in Highly Heterogeneous Mine Waste Rock at the Antamina Mine, Peru."

Price, William A. 2009. "Prediction Manual for Drainage Chemistry from Sulphidic Geologic Materals."

Smith, K.S. 1999. "Metal Sorption on Mineral Surfaces: An Overview with Examples Relating to Mineral Deposits." In *The Environmental Geochemistry of Mineral Deposits*, edited by G.S. Plumlee and M.J. Logsdon. Society of Economic Geologists.

Van der Sloot, Hans Albert, and Andre van Zomeren. 2012. "Characterisation Leaching Tests and Associated Geochemical Speciation Modelling to Assess Long Term Release Behaviour from Extractive Wastes." *Mine Water and the Environment* 31 (2): 92–103. doi:10.1007/s10230-012-0182-8.

Management of Spontaneous Combustion for Metalliferous Mines

Matt Landers and Brent Usher
Klohn Crippen Berger, Australia

ABSTRACT

Spontaneous combustion of mine waste is usually associated with coal mines. It occurs to a lesser extent with ore deposits that contain pyrite (FeS_2) or pyrrhotite ($Fe_{1-x}S$) and carbonaceous materials. Limited research has been conducted into the prediction of spontaneous combustion and currently no single method exists for all mine sites. Prediction requires classification of the material based on geochemical properties that can be coded into a block model. The potential spontaneous combustion materials are managed accordingly to minimize atmospheric oxidation and contact with water.

Spontaneous combustion results in the production of heat (> 270 ºC near the surface and up to 1,200 ºC deep in a Waste Rock Dump; WRD), which has implications for; *inter alia*, blasting while in the pit or underground and the release of hazardous gasses such as sulfur dioxide (SO_2).

Spontaneous combustion often evolves and material can be classed according to stages of development, including: potential, current and extinct. The "potential" class includes material that has the geochemical properties that, under field conditions could lead to spontaneous combustion, but has not yet started reacting. "Current" spontaneous combustion materials have already begun to combust and therefore prevention is no longer an option; rather the material requires remediation and containment. Zones of "extinct" spontaneous combustion materials are usually associated with precipitated minerals that may contain elevated metal concentrations that need to be managed. Several metalliferous mines in Australia have issues with spontaneous combustion occurring within the pit and on WRDs. These mines have implemented a number of control techniques that can be incorporated into WRD design and mine planning to minimize the effects of spontaneous combustion and ultimately prevent it from occurring. This paper describes some of the control measures that are being implemented for one Australian metalliferous mine.

Keywords: Spontaneous Combustion, Metalliferous Mine, Pyrite oxidation

INTRODUCTION

Spontaneous combustion of mine waste is usually associated with coal mines. It occurs to a lesser extent with ore deposits that contain sufficient pyrite (FeS_2) and carbonaceous materials. Several metalliferous mines in Australia have issues with spontaneous combustion occurring within the pit and on the waste rock dump.

Limited research has been conducted into the prediction of spontaneous combustion and currently no single method exists for all mine sites. This paper outlines the factors of importance in spontaneous combustion and the onsite experience with this phenomenon at a metalliferous mine; the site is to remain anonymous and will be referred to as "Site X".

Spontaneous Combustion Process

Spontaneous combustion (also referred to in this paper as "smokers") is a phenomenon usually associated with ore deposits that contain pyrite (but may also include the sulfide minerals, *inter alia*, pyrrhotite, galena, sphalerite, arsenopyrite, chalcopyrite and molybdenite) and carbonaceous materials. The oxidation of pyrite is exothermic and can lead to a significant increase in heat.

Spontaneous combustion is usually associated with finely grained disseminated pyrite (framboidal pyrite) which is a major constituent at some metalliferous mines. The mining process contributes to exposing the pyrite and decreasing the particle size of the rock mined. This results in an increase in the surface area and reactivity of the rock. The spontaneous combustion process begins with the exposure of the material to atmospheric oxidation or contact with oxygenated water (usually rainwater).

The oxidation of pyrite and other sulfides results in a gradual increase in temperature immediately surrounding the point of oxidation. This point is insulated by surrounding rocks, preventing the release of heat, which results in further increases in temperature. Over time, the temperatures become high enough to ignite any carbon and/or organic matter that may be present, releasing gas (e.g. CO_2, SO_2, etc.) and steam. As the heat increases the rate of pyrite reaction increases. The process has been determined to be a three-stage process: stage A (ambient to 100°C), stage B (> 100°C) and stage C (> 350°C) (Rosenblum and Spira 1995; Rosenblum et al. 2001). Once the reacted material cools down, complex minerals precipitate (e.g. sulfates, halides and native sulfur); usually containing a concoction of trace elements.

Spontaneous combustion may also result from galvanic interaction. The presence of an electrolyte and two sulfides (e.g. galena and sphalerite) with different rest potential may form a galvanic cell (Kwong et al., 2003), with the sulfide with the higher rest potential forming the cathode and the lower forming the anode. Spontaneous combustion results from galvanic sulfide interaction with a rest potential difference (ΔV) greater than 0.2 V, whereas mixtures with $\Delta V < 0.1$ V do not combust (Payant et al., 2011).

Spontaneous combustion is time dependent, and early detection of the potential sources of the problem may allow for the issues to be managed appropriately, preventing the problem from developing into full – scale combustion. If combustion has already begun, management of the materials is more problematic, as excavation and movement of materials will allow further atmospheric oxidation, allowing the conditions to be optimized for sulfide oxidation, potentially increasing the rate of pyrite oxidation.

Spontaneous Combustion Prediction and Detection

Prediction of spontaneous combustion requires classification of the material based on its inherent properties. The characteristics of a material that can be used to identify the potential for material to spontaneously combust include (*inter alia*): the geochemical constituents of the materials and chemical analysis of drill core samples/waste piles (e.g. sulfur content (particularly pyrite); combustible carbon content; moisture content; environment oxygen content; oxygen avidity; presence of other volatile materials; and, temperature). Another method of prediction/ detection includes modeling the rate of heat generated versus the rate of heat dissipated (Carnes and Saghafi, 1998).

Early detection of spontaneously combustible materials allows for the associated materials to be managed appropriately, which may prevent the material from developing further into a smoker. The main detection characteristics include (*inter alia*) temperature increases, gas odor and observation of vapor/gases. Heat haze and "steam" plumes may be observed as well as efflorescence caused by the oxidation of pyrite and sublimation of sulfur. Infrared monitoring instruments or thermal probes inserted into the WRD may be used for early detection of spontaneous combustion. Spontaneous combustion has a distinctive smell; the most common and prevalent of the gases produced is SO_2, which is odorless at low concentration, however, may have a pungent rotten egg smell at high concentrations.

The intensity and the rate at which a "smoker" develops are dependent on a combination of factors; some of these factors include: composition (the presence and availability of sulfide [pyrite and other sulfides,], carbon and oxygen); friability, particle size and surface area (which can be related to mining method, such as blasting); moisture content; climatic conditions (temperature, relative humidity, barometric pressure and oxygen concentration); and, stockpile compaction, height and method of stockpiling (e.g. end – dumping versus paddock dumping).

METHODOLOGY AND SITE PROPERTIES

A spontaneous combustion management plan was developed for Site X, a metalliferous mine in Australia. The management plan was based on the factors that promote the evolution of spontaneous combustion, and has been separated into classes according to stages of development, namely: potential, current and extinct. The management options were developed based on site observations including monitoring of temperature. The Site's historical geochemical database was reviewed to develop geochemical trends; however, the outcomes from this review are not discussed in this paper. Several of the more practical methods for managing (remediating) spontaneous combustion were tested at the Site.

All of the lithological domains at Site X contain sulfide minerals (pyrite, sphalerite and galena) with some units being characterized by elevated pyrite, ranging from 10 to 27 wt %. For lithologies containing galena and sphalerite, their median abundances were low, ranging from 1 to 2 wt %. All lithologies contain carbonates (dolomite, calcite and ankerite) with dolomite being the dominant acid neutralizing mineral in all lithological units. Other non-sulfide/carbonate minerals include: quartz, mica, K-feldspar (microcline) and moderate to trace quantities of kaolinite, chlorite, montmorillonite, vermiculite, plagioclase (albite) and gypsum.

Several of the waste lithological units contained elevated sulfide concentrations with average values including: X Shale (~8.6 wt % S), Y Shale (~7.2 wt % S) and Z Shale (~5 wt % S). The sulfide is

mainly associated with framboidal pyrite (Figure 1). The overburden waste also contains significant organic carbon (> 0.5 wt %).

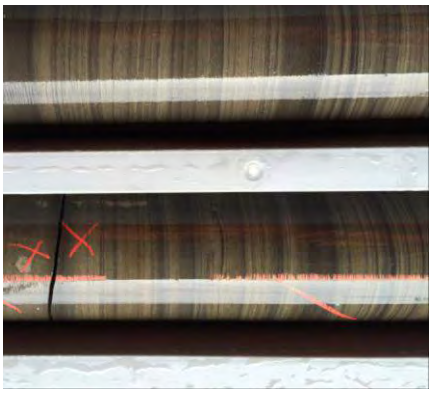

Figure 1 Interbedded framboidal pyrite and dolomite.

RESULTS AND DISCUSSION

Spontaneous Combustion Prevention, Control and Remediation

There are a number of control techniques that can be incorporated into the WRD design and mine planning to minimize the effects of spontaneous combustion and ultimately prevent it from occurring; however, there is no single control that has been proven to be completely reliable or successful. Effective control of spontaneous combustion is usually achieved by using a combination of techniques, and these techniques are dependent on individual mining situations.

Some of these controls include measures to reduce or eliminate oxygen. This may be achieved with: sealing agents; compaction of the surface material (dozing over, truck haulage routes or compaction); buffer blasting; covering the area of concern with inert material (e.g. non-acid forming [NAF] material, clay); application of a final cover layer with good water retention properties (e.g. fly ash-water slurry); and, subaqueous deposition. Control measures that have been proposed or used at several Australian sites to reduce the temperature and lower the reaction rate include: water cannons; firefighting foam; injection of water; water spraying; nitrogen injection; and, carbon dioxide injection. Other control measures to eliminate the process may include: excavation of hot or burning material; controlling the morphology of high sulfide material cells (layering etc.); the use of low-angle slopes to minimize the effects of wind (i.e. reduce "chimney effect"); the use of artificial wind barriers; submersion in water (e.g. backfill in pit and flooding); and, spreading the affected material into thin piles to allow to cool. The effectiveness of a cover is generally dependent on composition, particle size and bulk density; water content of the cover; air filled void space; heat transfer capacity; oxygen transfer; and cover thickness.

Geochemical Management: Spontaneous Combustion

The management options for spontaneous combustion can be separated according to the different stages of development of smokers, these stages include: potential smokers, current smokers and extinct smokers. The "potential smokers" class includes material that has the geochemical characteristics of a smoker, but is not currently combusting or is not currently associated with elevated temperatures (> 60 °C). Current smokers have already begun to combust and therefore prevention is no longer an option; rather the material requires remediation and containment.

Extinct smokers are materials that were active smokers but became extinct due to depletion of sulfide, oxygen or combustible carbon. These materials may result in precipitation of soluble minerals which contain trace elements that need to be managed.

Potential Smokers

Potential smokers can be detected through the block model (populated by drilling sample analysis) and/or field investigations (handheld XRF of drill mounds) prior to blasting and excavation. The most critical step in preventing spontaneous combustion from developing is to limit contact or reduce contact time with oxygen and water. Therefore, if material has the characteristics that may result in spontaneous combustion it is handled preferentially with appropriate management controls. This can prevent the material from developing spontaneous combustion and reduce the need for remediation. Potentially reactive materials are be mined shortly after blasting and managed appropriately.

Management of potential smokers - Option P1:

One of the preferred options to consider for future operations is subaqueous disposal of reactive waste. The disposal method typically involves the storage of reactive waste in a series of pits below the water table (Figure 2); the material is stored below the water table where oxygen is inhibited. The process reduces the risk of natural or manmade incidents associated with flooded impoundments or complex engineered covers. In addition to groundwater saturation, a thick (3 to 4 m) pervious cover (which may include oxygen consuming materials such as organics), is placed over the reactive waste. The reactive waste is placed such that it will remain saturated under the water table to beyond a 1 in 50-year dry condition. During the periods when the reactive waste is not saturated (for example if water tables and infiltration decrease in a prolonged drought) the system will rely on the oxygen consuming cover. Similarly, excess water from dewatering may be pumped over the reactive PAF such that the material is not exposed over dry periods. Additional benefits of this option include the reduced foot print compared to conventional disposal facilities as well as reducing volumes of encapsulation materials required elsewhere on site for waste mitigation.

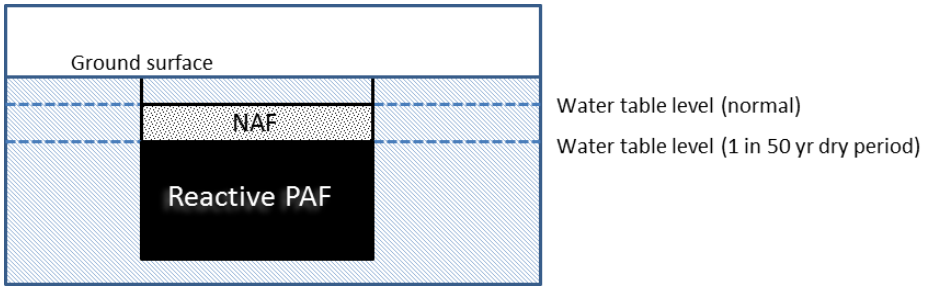

Figure 2 Subaqueous disposal of reactive PAF below groundwater level.

Management of potential smokers – Option P2:

A second option to consider for future operations is co-disposal, which involves the disposal of both tailings and waste rock simultaneously within a storage compartment (e.g. compacted clay lined dam) (e.g. Figure). The waste rock at the Site is commonly coarse, meaning there are large void spaces when placed on the WRD. The tailings waste is very fine and may be deposited within

the void spaces of the waste rock. Co-disposal also has a number of other benefits, including: provides a storage option for both waste streams (waste rock and tailings); the tailings act as a barrier to atmospheric oxidation of the PAF, therefore reduced ARD generation; low permeability of the WRD means reduced seepage; structural integrity; smaller footprint (excludes the tailings facility); and, potentially less post closure maintenance.

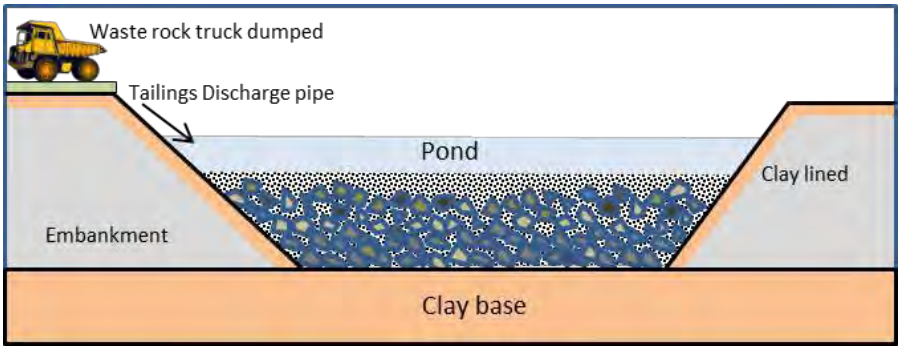

Figure 3 Co-disposal of tailings and waste rock (including reactive PAF).

Current Smokers (Remediation)

Current smokers are materials that are currently combusting (i.e. when excavated, stockpiled or during transportation; Figure 4) and are characterized as having temperature > 60 °C and/or produce gases. Remediation of current smokers also includes small quantities of material that may begin to react within the pit. There are also instances at Site X where materials used as windrows have been constructed with reactive PAF and begun to combust. These materials are all treated as current smokers.

Figure 4 Current and extinct smokers at Site X.

Remediation - Option R1

Remediation (Option R1) is only applicable for material that is combusting directly below the surface (e.g. ~ 50 cm; Figure 4). This option should not be considered for areas affected by deep "hotspots" as the material will continue to combust when encapsulated and could potentially develop into a much larger problem. Encapsulating a deep "hotspot" may cause the buildup of heat

and gases which may ultimately lead to an eruption – like event at the surface. A good understanding of the depth of the hot-spot is gathered at the monitoring stage or at least prior to any remedial work being conducted.

Generally, the smokers at Site X are associated with very steep sections of the WRD; the steeper slopes are also more difficult to compact and may be conducive to the "chimney" effect. The main step in this remediation is to reduce the WRD slopes; the chimney effect is significantly reduced and the hotspot may be less exposed to atmospheric oxidation.

If the smoking material can be spread loosely, it may be able to cool. Once cooling has occurred (this may take several weeks depending on the carbon and pyrite content of the affected area) and the slopes have been reduced, the affected area (which should show evidence of being dormant/extinct with low temperatures and no evidence of gases) is covered with NAF or clay and compacted (Figure 5). Given the intensity of the smoker and the likely minerals/metals which make up the efflorescence, a clay layer is also applied and compacted to prevent the mobilization and transportation of metals and further oxidation of any unreacted pyrite/ combustible carbon.

This management option has been tested at Site X and the observations and ongoing monitoring have indicated the materials have stopped combusting and become extinct.

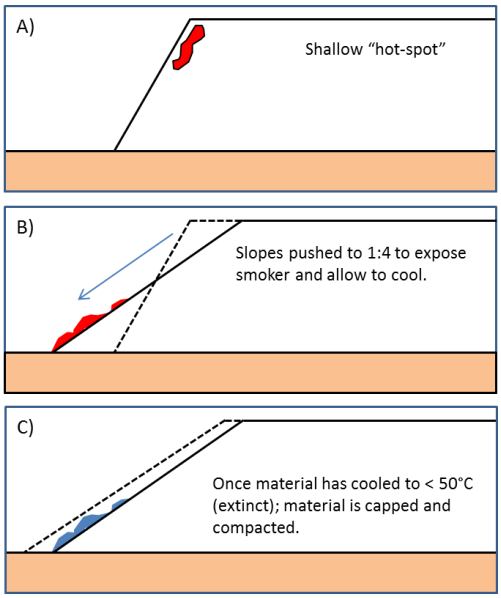

Figure 5 Spontaneous combustion remediation option 1 (R1) for shallow affected materials.

Remediation - Option R2

Remediation option R2 is used if the hot – spot proceeds deep into the WRD or for material that begins to react in the pit. Deep hotspots are usually associated with the precipitation of native sulfur, and the presence of hydrogen sulfide (H_2S) gas and cracks in the surface (presumably to release excess pressure). H_2S is generally only formed when there is not enough oxygen available for complete oxidation; often deep within a waste facility. The $H_2S_{(g)}$ is oxidized to native sulfur once exposed to atmospheric oxidation, and the presence of native sulfur often indicates that the formation of H_2S forming deep within the WRD where there is likely to be limited O_2.

The affected areas are excavated from the WRD and transported to a specially designed facility at identified and managed disposal locations. All material that is excavated and has a temperature > 60 °C is spread thinly and allowed to cool. The material is ideally truck dumped into loose ~ 2-m piles (via paddock dumping) within a specially designed facility (e.g. compacted clay layer) (Figure A). Previous investigations have shown that 2-m piles are below the critical mass for spontaneous combustion to occur (Waters and O'Kane, 2003); this assumption will also be investigated for materials at Site X. The 2-m piles are be monitored until the material is below 60°C and become extinct. This monitoring includes daily observations and the inclusion of several temperature probes in the piles to assess whether there are any temperature spikes. Once the material is shown to be extinct (i.e. monitoring indicates there are no temperature rises and there is no visible smoke), it can be spread evenly as a 2-m lift and then covered with inert material and compacted (Figure B). The excavation of the affected material causes rapid combustion once disturbed (i.e. the rate of pyrite oxidation is enhanced due to the availability of oxygen) producing excessive gas and vapor.

The spontaneous combustion storage facility should not be located in a place that receives runoff from other facilities, or above or adjacent to major streams. Similarly, the site should not be located near clean material (NAF and clay) stockpiles. The number of spontaneous combustion management sites is minimized, including the size of the footprint.

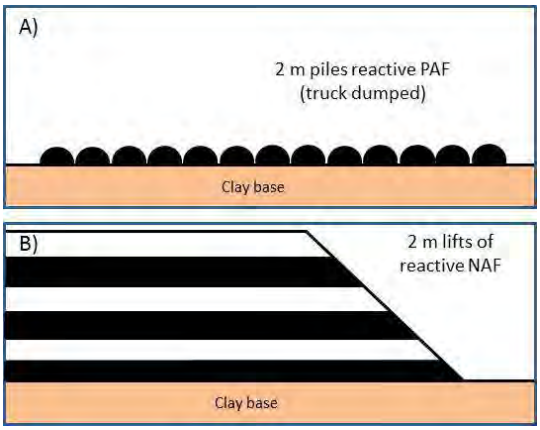

Figure 6 Spontaneous combustion Emplacement Facility.

Remediation - Option R3

Remediation option R3 is based on management and remediation strategies undertaken by another mine with similar geology, waste material and climate, which has also had issues with spontaneous combustion from reactive shale. A number of options were tested at this analogue site, with the most successful being the addition of a mixture of quicklime (CaO) and water to the affected area; this is now part of routine operations. The addition of the mixed quicklime/water slurry were able to achieve a reduction in temperature from 300 to 60 °C within 30 minutes of application for a 20-m cut/0.5-m lift.

Although the application of the quicklime/water mixture is proving to eliminate the issue, it is an expensive solution. The cost of quicklime delivered to site is ~A$600 ton (> A$2,000 for a single mixture).

Remediation - Option R4

The location of some smokers is such that this material is difficult or impossible to excavate and remove in a safe manner (e.g. smokers on the pit walls). There are limited remediation methods to deal with the issue in these cases. There are a few gel sealants which can be sprayed onto the affected area, although these are effective, they can generally be expensive. Miron (1995) and Chakravorty and Kolada (1988) investigated a number of gel sealants for the mitigation of spontaneous combustion for coal mines. These may be effective but were not considered applicable due to cost or scale at this Site.

Extinct Smokers

Extinct smokers should be closely monitored to make sure they are actually extinct. Residual heat (> 60 °C) is indicative that the material may still be combusting under the surface. The dormant/extinct smokers are associated with mineral precipitates (ash/efflorescence; Figure 4) which are likely to carry a large quantity of soluble solids and metal loads. The metals that are present as readily soluble salts are susceptible to leaching particularly after the first rains which may dissolve and transport these materials to sensitive receptors. For this reason the ash/efflorescence is excavated and encapsulated.

CONCLUSIONS

The management options for spontaneous combustion were separated according to the stages of development of spontaneous combustion (potential smokers; current smokers; and, extinct smokers). As spontaneous combustion develops from a potential smoker to a current smoker, the management options must change from prevention and confinement to remediation and confinement, respectively. The various options are summarized in Table for each stage of spontaneous combustion development. Some of the management options have tested this for current spontaneous combustion. The outcomes of these trials are summarized in Table 2.

Table 2 Remediation, management and monitoring options summary.

Developmen t Stafe	Management/ Remediation Option	Description	Trial Outcome
Potential Spontaneous combustion	P1 – Subaqueous Disposal	Disposal of reactive PAF material (and other reactive material) below groundwater table.	Not tested to date
	P2 – Co-disposal	Co-disposal of reactive PAF material with tailings within a facility.	Not tested to date
Current Spontaneous combustion	R1 – Decline slopes	Reduce the spontaneous combustion affected WRD slopes to 1:4, allow affected material to cool and then encapsulate. Closely monitor.	The trial was successful at eliminating spontaneous combustion with temperatures reduced to < 60 °C and reduction of gas emissions.

	R2 – Layer – cake	Material > 60°C is be spread thinly as a < 2 m^3 pile and allowed to cool. Once cooled the material is spread as a 2 m lift and covered with NAF. Closely monitor.	The trial was successful at eliminating spontaneous combustion with temperatures reduced to < 60 °C and reduction of gas emissions.
	R3 – Quicklime/ water	Application of quicklime/water mixture to spontaneous combustion affected areas.	The trial was not successful and enhanced pyrite oxidation resulting in the production of gases.
	R4 – Gel application	Application of gel to spontaneous combustion affected areas.	Not tested to date
Extinct Spontaneous combustion	Extinct material	Close monitoring.	
	Extinct Ash (soluble minerals)	Ash is excavated and encapsulated within a PAF cell.	

All of the management and remediation options need to be monitored closely to assure spontaneous combustion is not developing and contaminants are not being released to the environment. Monitoring may include: Oxygen levels; temperature; gas (O_2, SO_2 and H_2S associated with spontaneous combustion); surface water, seepage water and groundwater qualities and volumes; and, physical stability.

REFERENCES

Carnes, J and Saghafi, A (1998) Predicting spontaneous combustion in spoil piles from open cut coal mines, in Aziz, N (ed), Coal 1998: Coal Operators' Conference, University of Wollongong & the Australasian Institute of Mining and Metallurgy, 1998, pp. 617-625.

Chakravorty, R and Kolada, R (1988) Prevention and Control of Spontaneous Combustion in Coal Mines, Mining Engineering, pp. 952 – 956.

Kwong, Y, Swerhone, G, and Lawrence, J (2003) Galvanic sulphide oxidation as metal-leaching and its environmental implications. Geochemistry: Exploration, Environment, Analysis, vol. 3. pp. 337–343.

Miron, Y (1995) Gel Sealants for the Mitigation of Spontaneous Combustion Heating's in Coal Mines, Unite States Bureau of Mines, RI 9585.

Payant, R, Rosenblum, F, Nesset, J and Finch, J, (2011). Galvanic interaction and particle size effects in self-heating of sulphide mixtures. Proceedings of the 43rd Annual Canadian Mineral Processors Conference.

Rosenblum, F and Nesset, J (2001) Evaluation and control of self-heating in sulphide concentrates. CIM bulletin. Vol. 94, pp. 92.

Waters, P and O'Kane, M (2003) Mining and Storage of Reactive Shale at BHP Billiton's Mt Whaleback Mine. 6th ICARD, Cairns, Qld, 2003.

Evolution of a Waste Rock Dump Management Plan for a Metalliferous Mine

Matt Landers and Brent Usher
Klohn Crippen Berger, Australia

ABSTRACT

As part of sound mine waste management, a thorough understanding of the geochemical properties of waste materials is needed. Waste rock is a significant factor to consider in the environmental management of metalliferous mines and a detailed waste rock dump (WRD) management plan is required. These plans may evolve over the life of a metalliferous mine as new data and a better understanding of the geochemical nature of waste rock types become available. A case study in Australia is discussed where the plan had to undergo significant modifications as a result of a geochemical characterisation program that yielded a much improved understanding of key waste types and material volumes. Inaccurate geochemical classification of waste rock resulted in significant variance between the estimated volumes of non-acid forming (NAF) and potentially acid forming (PAF) materials quantified by the site's 'block model', and the true volumes disposed on the WRD or determined by pit technicians. The initial classification of PAF and NAF was quite broad and did consider different types of material which could lead to salinity, neutral mine drainage (NMD; metalliferous NAF) or which could identify acid consuming (AC) material. As a result, initial WRD design was geared to effectively mitigate sulphide oxidation and subsequent generation of acidity, metals and salinity. These discrepancies had large implications for mine planning and led to the adoption of new strategies and a revised WRD design to minimise the impacts of acid and neutral mine drainage (AMD and NMD). This case study discusses the evolution of the WRD design as the geochemical understanding has improved and measures that have been implemented by the mine to minimise reactivity and water quality impacts.

**There is no full article associated with this abstract.*

10th ICARD IMWA2015 | 10th International Conference on Acid Rock Drainage & IMWA Annual Conference

Deportment of Sulfide and Neutralization Potential by Particle Size Distribution in Limited Buffering Mine Wastes

David Tait[1], Andrew Barnes[1], Claudio Andrade[2], Matt Dey[1], Rob Bowell[1] and Carl Williams[1]

1. *SRK Consulting, United Kingdom*
2. *Barrick Gold, Canada*

The evaluation of Acid Potential (AP) and Neutralization Potential (NP) through industry standard static testing methods is a first step in mine waste characterisation programs and the assessment of Acid Rock Drainage (ARD). The common Acid Base Accounting (ABA) classifications often report results as 'uncertain' or 'low AP' for low sulfide-low carbonate materials.

Bulk sample analyses have limitations in applications to overall large field scale waste rock dumps. Reaction rates are dependent on grain-size and surface area, among other factors, with the potential for segregation of sulfide or carbonate minerals to the different size fractions to alter the effective ARD potential relative to the bulk measurements.

This study evaluated the deportment of sulfide sulfur, carbonate NP and bulk NP by grain-size in low NP waste rock samples. The aim was to evaluate potential bias introduced by the standard bulk analysis procedures, particularly due to the pulverisation of the bulk samples.

Samples were sieved to three size fractions: sub 1 mm, 1-5 mm and 5-12 mm. The sieved fractions were split into two portions: the first portion was analysed by the Modified Sobek procedure on the 'as sieved' material without grinding/grain-size reduction to provide a measure of the 'available NP' for each fraction (i.e., the quantity of NP available under field conditions). The second portion was subject to grinding and subsequent analysis by the conventional Modified Sobek method as well as sulfur and carbon content by LECO analysis.

Evaluation of the NP results showed that 'available NP' of the sieved non-pulverised materials was approximately an order of magnitude lower than bulk NP values, and agree with other similar studies conducted by the authors. Overall, the tests indicate that bulk NP data for low carbonate materials could present a considerable over-estimation of NP, and should be applied with care to ARD studies.

**There is no full article associated with this abstract.*

CHAPTER 3

PREDICTION OF DRAINAGE FLOW

The Calculation of Actual Evaporation from an Unsaturated Soil Surface

Murray Fredlund[1], Dat Tran[2] and Delwyn Fredlund[3]
1. SoilVision Systems Ltd., Canada
2. Thurber Engineering Ltd., Canada
3. Golder Associates, Canada

ABSTRACT

The calculation of Actual Evaporation, AE, is required when calculating the net moisture flux across the ground surface. The Wilson-Penman (1990) equation appears to provide reasonable estimations of actual evaporation, AE, from saturated clayey soils but tend to over-estimate actual evaporation from coarse-grained soils. Two distinct approaches have emerged in recent years for the calculation of actual evaporation from unsaturated coarse-grained surfaces. Both approaches are based on the concept that evaporation tends to "shut-off" as the natural water content approaches residual water content conditions. The first approach to calculating AE from unsaturated soils has involved the adjustment of calculated total suction at the soil surface. The second approach determines an "evaporation-rate reduction point" from the drying soil-water characteristic curve and then calculates a vapor pressure reduction factor when calculating AE. Both approaches constitute an attempt to take "surface resistance" to evaporation into consideration. The paper compares the theoretical context for both approaches (i.e., total suction adjustment and vapor pressure adjustment), for the calculation of actual evaporation.

Keywords: Actual evaporation, potential evaporation, total suction, surface resistance, vapor pressure.

INTRODUCTION

The primary components associated with the determination of water balance (or net infiltration, *I*) at ground surface are shown in Eq. [1].

Infiltration (*I*) = Precipitation (*P*) – Actual Evaporation (*AE*) – Transpiration (*T*) – Runoff (*R*) [1]

Evaporation models can first be classified on the basis of whether Potential Evaporation, *PE*, or Actual Evaporation, *AE*, is calculated (See Figure 1). Most methods used in geotechnical engineering practice are based on energy balance and aerodynamic considerations. It has become apparent that "surface resistance" plays an important role in the computation of actual evaporation, *AE*. Several evaporation models that have been used in geotechnical engineering practice until the late 1990s did not take the "surface resistance" of the soil into consideration. Examples of these models are shown in Figure 2.

The calculation of actual evaporation has proven to be one of the most complex analyses associated with unsaturated soil mechanics. Models that have been proposed and used in geotechnical engineering for calculation of evaporative flux can be divided into two broad categories; namely, those that take "surface resistance" into consideration and those that "do not take surface resistance" into consideration (See Figure 3). "Surface resistance" has proven to be a significant factor in calculating "actual evaporation".

Figure 3 shows that the Wilson (1990) and Wilson et al., (1997) models for actual evaporation have been incorporated into numerical modeling codes in two different ways; namely, where consideration is given to "surface resistance" (e.g., SVFlux 2009), and where consideration has not been given to "surface resistance" (e.g., SoilCover, 1994 and Vadose/W, 2008). The word "*modified*" has been added to the description identifiers for each method where "surface resistance" has been taken into consideration.

The effect of "surface resistance" turns out to be of particular significant when considering evaporation from dry, coarse soils in arid regions. Wilson (1990) noted that the Wilson-Penman (1990) method would over-predict actual evaporation from soil surfaces in dry regions. It now appears that the primary reason for the over-prediction of actual evaporation was the omission of the "surface resistance" term. Wilson (1990) also pointed out that osmotic suction effects were not taken into consideration in the Wilson-Penman method. This paper does not address the issues related to osmotic suction but focuses on clarifying the formulations that attempt to address "surface resistance".

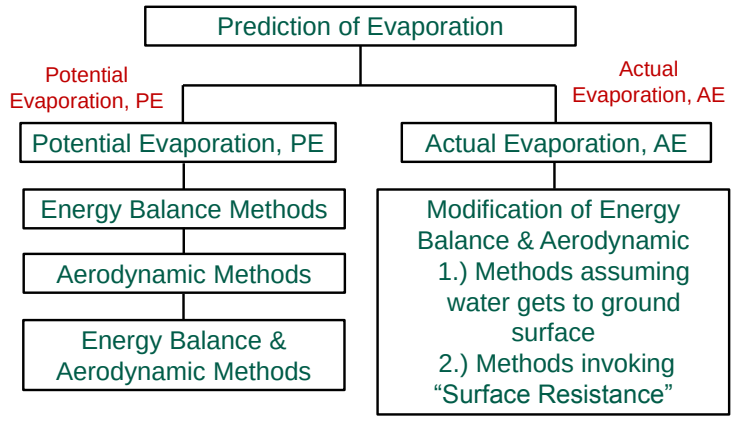

Figure 1 Evaporation models classified in terms of whether potential evaporation, PE, or actual evaporation, AE, is being calculated.

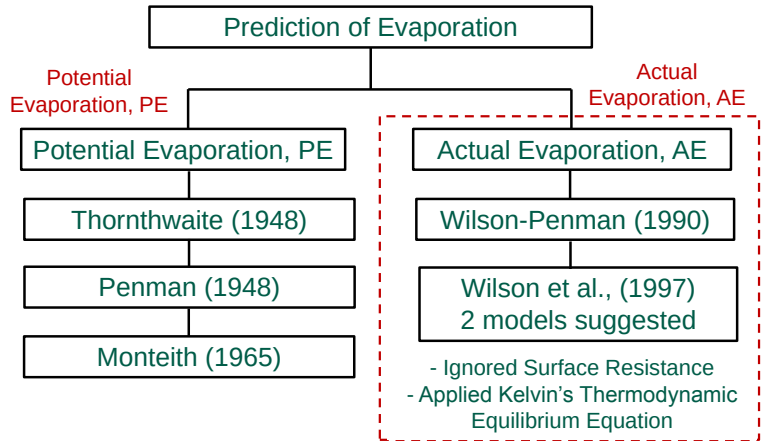

Figure 2 Evaporation models that did not take "surface resistance" of the soil into consideration.

Fredlund et al., (2012) suggested that an adjustment should be made to the total suction calculated at the soil surface to account for non-equilibrium conditions. The adjusted total suction was incorporated into the computer code of SVFlux (2009). The proposed procedure was verified using datasets found in the research literature. Actual evaporation models were solved using both "coupled" and "uncoupled" methodologies. The revised procedures to calculate actual evaporation were referred to as: i.) the *modified* Wilson-Penman (1990) method, ii.) the *modified* "Limiting Function" method (Wilson et al., 1997), and iii.) the *modified* "Experimental Function" method (Wilson et al., 1997).

Tran (2013) re-visited the Penman-Monteith (1965) formulation that incorporated the concept of a "canopy cover" (i.e., a type of "surface resistance") from vegetated surfaces and found that the formulation could also be applied to evaporation from unsaturated soil surfaces. In this case an empirical methodology was used to adjust the calculated vapor pressure at the soil surface. The calculated actual evaporations from the revised Penman-Monteith methodology were compared to measurements of evaporation made on several sand column tests. Consequently, there were now two methodologies available for the calculation of "actual evaporation" from unsaturated soil surfaces.

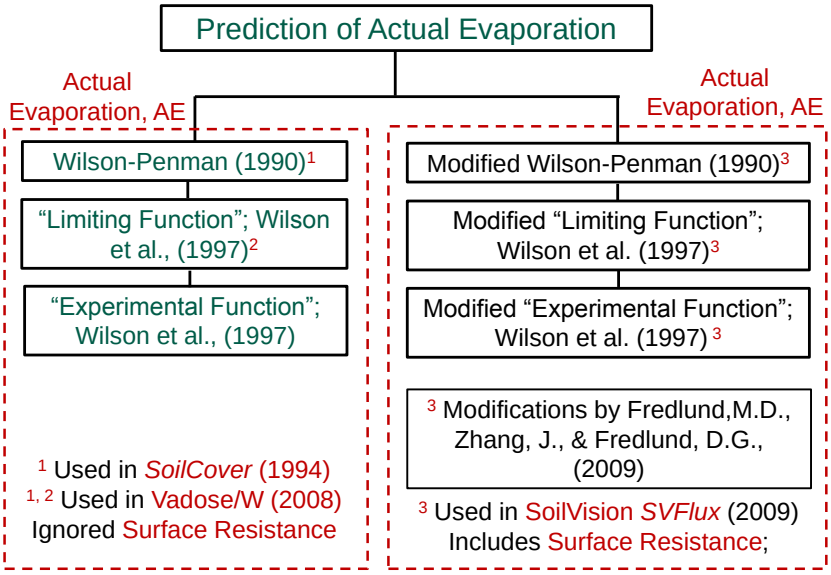

Figure 3 Broad classification of models based on modifications of the original Penman (1948) equation

The objective of this paper is to provide a summary (and clarification) of the various methods that have been proposed within geotechnical engineering for the calculation of actual evaporation, *AE*. The scope of this paper is limited to a presentation of the theories involved and reference is made to the datasets from laboratory column test measurements that have been used to verify the theoretical formulations.

Evaporation Models Based on Thermodynamic Equilibrium at the Evaporating Surface

Figure 4 identifies some of the variations of the Penman (1948) method that have been proposed for the calculation of actual evaporation. These models did not initially take "surface resistance" into consideration but were later *modified* by Fredlund et al., (2012) to account for "surface resistance".

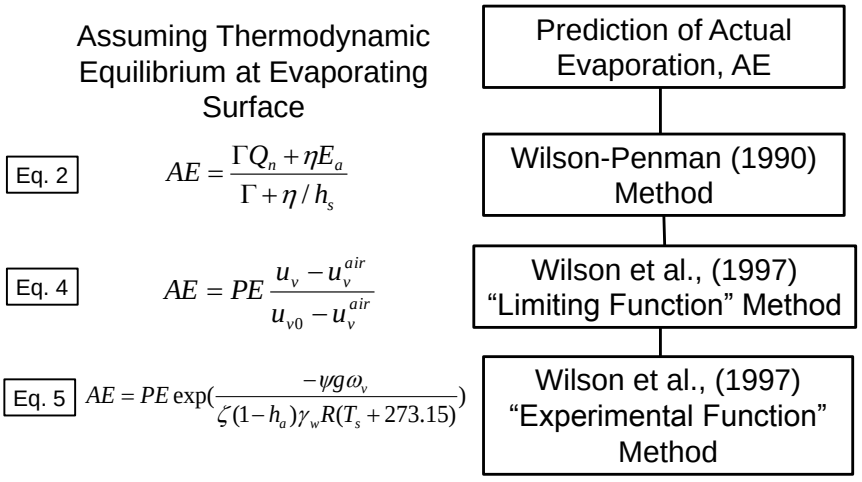

Figure 4. Actual evaporation equations based on thermodynamic equilibrium at the soil surface.

The Wilson (1990) and the Wilson et al., (1997) methods for calculating actual evaporation are assumed to be driven by a vapor pressure gradient that satisfy thermal equilibrium at the ground surface. The water in the soil at ground surface can be negative (i.e., corresponding to an equivalent

total suction). Soil suction (i.e., total suction) at ground surface was assumed to reduce the vapor pressure and thereby reduce evaporation from ground surface. The Wilson (1990) and the Wilson et al., (1997) equations appears to provide reasonable calculations of actual evaporation when the clay soils at ground surface remain near saturation but appear to over-estimate actual evaporation from unsaturated, coarse-grained soils.

The 1948 Penman equation was based on the vapor pressure gradient between the water surface and the overlying air as the primary driving mechanisms that influenced the vapor pressure gradient; namely, net radiation and wind speed (i.e., mixing of air) at the ground surface. The properties of the soil did not come into the analysis and it was assumed that water was available for evaporation at ground surface.

Wilson-Penman (1990) Model

Wilson (1990) made one modification to the Penman (1948) equation which then became known as the Wilson-Penman (1990) equation as shown in Figure 4:

$$AE = \frac{\Gamma Q_n + \eta E_a}{\Gamma + \eta / h_s} \qquad [2]$$

where: AE = actual evaporation rate from a soil surface in mm/day; Γ = slope of saturation vapor pressure versus temperature curve, $kPa/^oC$, Q_n = net radiation at the water (or saturated ground) surface, mm/day, η = psychrometric constant, $kPa/^oC$, $E_a = 2.625(1 + 0.146W_w)(u_{vo}^{air} - u_v^{air})$, mm/day, W_w = wind speed at 2 m, km/hr, h_s = relative humidity at the soil surface (i.e., $h_s = u_v^{soil}/u_{vo}^{soil}$, where u_{vo}^{soil} = saturated vapor pressure in the soil at ground surface, kPa). The inclusion of the relative humidity term in the denominator took into consideration the affinity (or holding power) of the soil for water at ground surface. While net radiation (and wind) attempted to remove water vapor away from the soil surface, the soil attempted to retain water. The Wilson-Penman (1990) model appeared to provide reasonable results in situations where the soil at ground surface remained essentially saturated and the permeability of the near ground surface soil was such that water could be transmitted to the soil surface.

Actual evaporation was calculated in an uncoupled manner when using the Wilson-Penman (1990) method. The assumption was made that the ground surface thermal flux was zero. The soil surface temperature was computed using the following empirical relationship.

$$T_{soil} = T_a + \frac{1000\left(R_n - R_g\right) - L_v AE}{C_f \eta f\left(u\right) L_v} \qquad [3]$$

where: T_{soil} = soil temperature at soil surface, ^oC, T_a = air temperature, ^oC, C_f = conversion factor, (i.e., 1 kPa = 0.00750 mHg), η = psychrometric constant, 0.06733 $kPa/^oC$, $f(u)$ = function depending speed, $f(u)$ = 0.35 (1.0 + 0.146 W_w), W_w = wind speed, km/hr, R_n = net radiation, $J/m^2/day$, R_g = ground surface thermal flux, $J/m^2/day$, and L_v = volumetric latent heat of vaporization, J/m^3.

Wilson-Fredlund-Barbour (1997) "Limiting Function" Model

Wilson et al., (1997) suggested that actual evaporation could be written as a "Limiting Function" between actual evaporation and potential evaporation (See Figure 4). This model assumed that the temperature at the soil surface was the same as the air temperature. Therefore, the vapor pressure (and relative humidity) at the ground surface was the same as the relative humidity in the air above the ground surface.

$$AE = PE\,\frac{u_v - u_v^{air}}{u_{v0} - u_v^{air}} \qquad [4]$$

where: u_v = actual vapour pressure at the soil surface, kPa; u_{v0} = saturated vapour pressure at the soil surface temperature, kPa; u_v^{air} = vapour pressure in the air above the soil surface, kPa. Calculations using the Wilson-Fredlund-Barbour (1997) "Limiting Function" model were essentially the same as those from the Wilson-Penman (1990) model. Once again, the model over-predicted actual evaporation for dry, coarse-grained soils in arid regions.

Wilson-Fredlund-Barbour-Penman (1997) "Experimental Function" Model

A series of drying tests were undertaken in the laboratory on thin layers of sand, silt and clay soils (i.e., about 1 mm thick). It was observed that all three soils with different grain sizes gave similar ratios between actual and potential evaporation as shown in Figure 5.

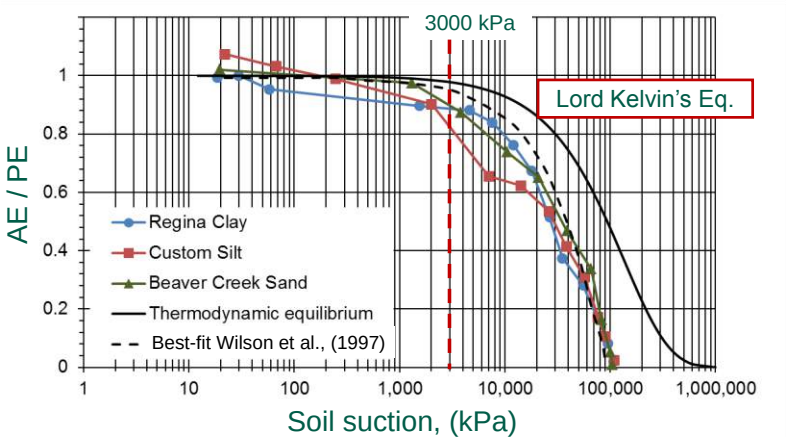

Figure 5 Ratio of actual evaporation to potential evaporation for thin soil layers (Wilson, 1990).

Also shown on Figure 5 is Lord Kelvin's equation. The laboratory data has a similar shape to the Lord Kelvin equation; however, it is translated to the left by approximately 70% of a log cycle. The dashed line in Figure 5 is the result of incorporating an empirical factor of 0.7 into Lord Kelvin's equation.

$$AE / PE = \exp\left(\frac{-\psi g \omega_v}{\zeta(1-h_a)\gamma_w R(T_s + 273.15)}\right) \qquad [5]$$

where: ζ = a dimensional empirical parameter with a suggested value of 0.7; h_a = relative humidity of overlying air; ψ = total suction (i.e., matric suction plus osmotic suction), kPa; ω_v = molecular

weight of water, 0.018 kg/mol; γ_w = unit weight of water, 9.807 kN/m^3; g = gravity acceleration, m/s^2; R = universal gas constant, 8.314 J/(mol.K); and T_s = soil surface temperature, ^{o}C. Equation [5] was based on, and is applicable for evaporation from thin soil layers. The air and soil temperatures were assumed to be the same.

Limitations of Evaporation Models Based on Thermodynamic Equilibrium at the Evaporating Surface

Numerous attempts have been made to apply Lord Kelvin thermodynamic equilibrium equation at the ground surface (McCumber and Pielke, 1981; Camillo et al., 1983; Wilson, 1990). However, attempts to apply thermodynamic equilibrium at ground surface failed to take into consideration the resistance to water movement at the soil-atmosphere interface. Researchers began to realize that Lord Kelvin equation was invalid close to the soil surface (Wetzel and Chang, 1987 Kondo et al., 1990 and Lee and Pielke, 1992).

Figure 6 compares relative evaporation, RE, and relative humidity to soil suction for a sand column test performed by Wilson (1990). The results show that RE dropped to approximately 40% at a suction of 20 kPa while the relative humidity began to reduce at soil suctions in excess of 3000 kPa. The results suggest that another physical mechanism is involved in evaporation near-ground-surface for drying of sand.

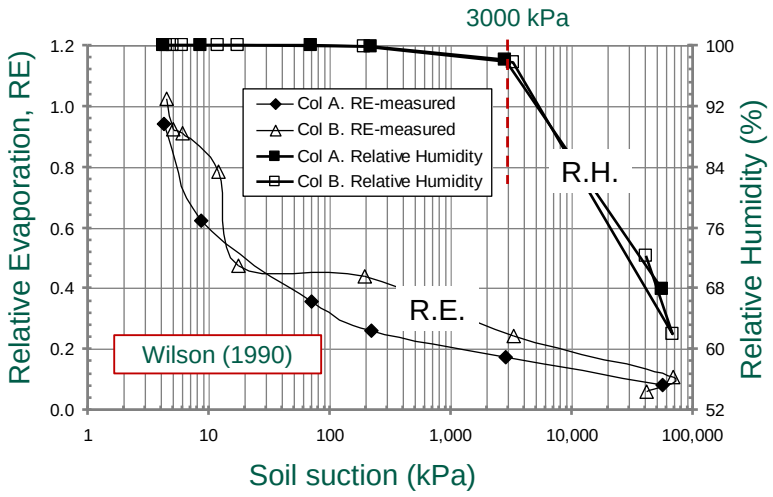

Figure 6 Measured relative evaporation, RE, and relative humidity, RH, from a sand column tested by Wilson (1990).

Similar results from a column evaporation test on sand have been presented by Bruch (1993) and Yanful and Choo (1997). The observed deficiencies in applying the thermodynamic equilibrium equation have led to the development of two types of models that attempt to take "surface resistance" into consideration.

Actual Evaporation Models that take Surface Resistance into Consideration

There are two main classes of models that provide a more reliable calculation of the relative humidity (or vapor pressure) at the soil surface. Both classes of models have been proposed to more accurately calculate actual evaporation from unsaturated and dry soil surfaces. For the first class of models, the relative humidity at ground surface is calculated through use of a modified thermodynamic relationship as suggested by numerous researchers (Alvenas and Jansson, 1997;

Bittelli et al., 2008; Fredlund et al., 2011; and recently Dunmola, 2012). A complete model has been formulated by Fredlund et al., (2012) and is referred to as the "total suction adjustment" approach. The corresponding model has been implemented in SVFux (2009) software from *SoilVision Systems.* The total suction at the soil surface depends on residual suction conditions defined by the drying soil-water characteristic curve, SWCC. The model is referred to as the Fredlund-Zhang-Fredlund method. Details of the method have been published in the SVFlux (2009) User's Manual and by Fredlund et al., (2012).

The second class of models utilizes an empirical method of modifying the relative humidity at the soil surface humidity based on the findings of several researchers (Kondo et al., 1990; Lee and Pielke, 1992; Tran, 2013). The formulation of the model is based on the original Penman-Monteith (1965) equation that incorporates the "canopy concept" associated with evaporation from vegetated surfaces. Tran (2013) formulated a model utilizing the concept of "surface resistance". The model is based on evaporation-rate reduction observed when drying soils near residual water content conditions. The procedure is referred to as the "vapor pressure adjustment" procedures.

The relationship between the "total suction adjustment" procedure and the "vapor pressure adjustment" procedure is illustrated in Figure 7. The evaporation of moisture near ground surface has been shown to be quite complex. As a result it is not possible to simply apply the thermodynamic equilibrium equation at the soil surface without applying an adjustment to either total suction or relative humidity.

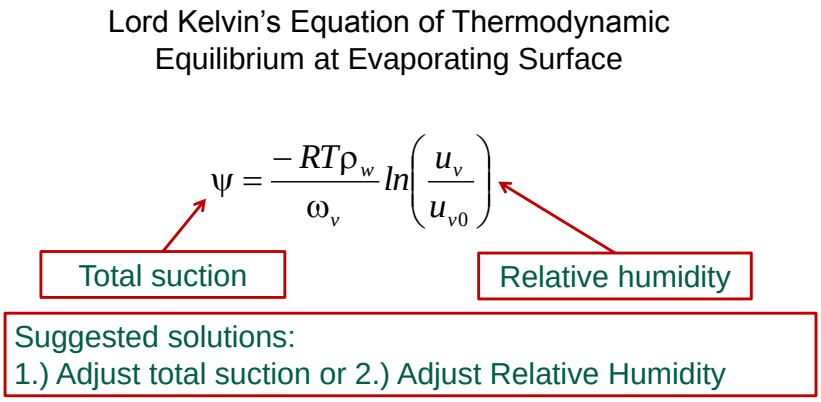

Figure 7 Relationship between adjustments applied to either total suction or relative humidity to accommodate "surface resistance".

There are two distinctly different classes of actual evaporation models that take the concept of "surface resistance" into consideration (See Figure 8). While the formulation of the two models is different, both models appear to capture the importance of significantly reduced evaporation rates from dry, coarse-grained soils. Column evaporation datasets have been used to show that both models provide reasonable predictions of actual evaporation under dry conditions (Fredlund et al, 2012; Tran, 2013).

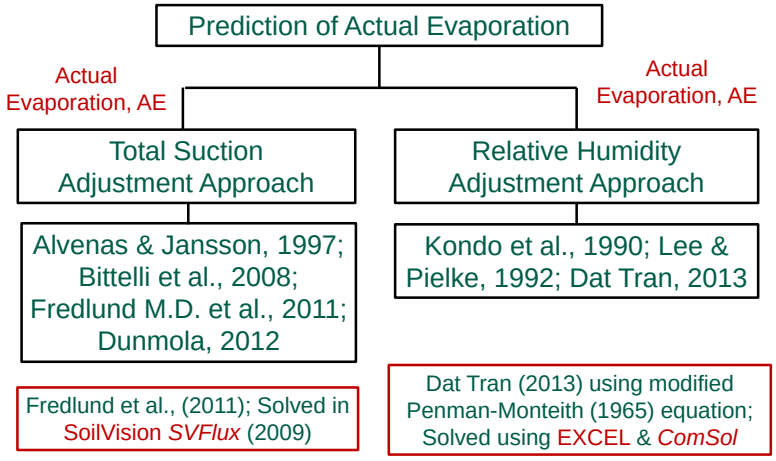

Figure 8 Classification of models taking the concept of "surface resistance" into consideration.

Definition of "Surface Resistance"

"Surface resistance" can be defined as the resistance to water vapor diffusion from near the soil surface (Aluwihare and Watanabe, 2003). The original usage of the term was in connection with evaporation from leaves and vegetated ground surfaces (i.e., the canopy effect) (Monteith, 1965). "Surface resistance" was illustrated by Aluwihare and Watanabe, (2003) and is reproduced in Figure 9.

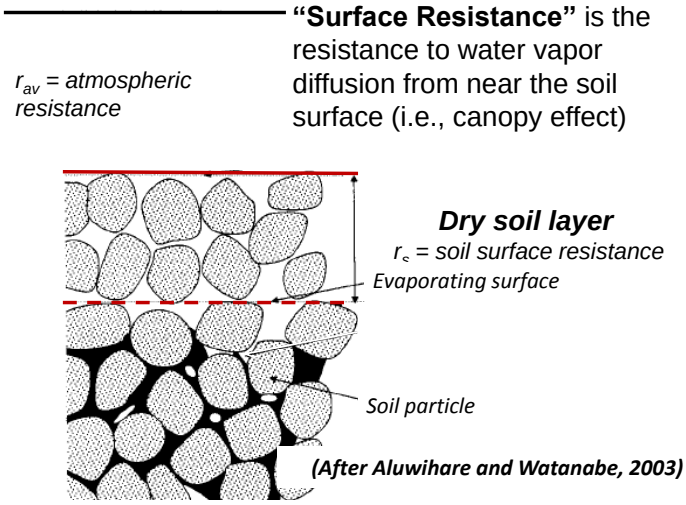

Figure 9 Illustration of "surface resistance" components (after Aluwihare and Watanabe, 2003).

Several researchers have attempted to quantify "surface resistance" and have written its magnitude in terms of the inverse of hydraulic conductivity (Fen Shu, 1982; Carmillo & Gurney, 1986; and van de Griend & Owe, 1994). Evaporation from a soil surface is based on molecular diffusion through a thin layer at the soil surface and turbulent diffusion in the air.

Fredlund-Zhang-Fredlund (2009) Formulation Using the "Total Suction Adjustment" Approach

Several researchers have attempted to adjust the total suction at the surface of a drying soil in order to more accurately simulate actual evaporation (Alvenas & Jansson, 1997; Bittelli et al., 2008; Fredlund, M.D. et al., 2011; Dunmola, 2012). The formulations take the form of a further modification to the Penman (1948) equation and makes use of an adjustment to total suction. The

formulation is called the "total suction adjustment" approach. Details of this approach were proposed by Fredlund, M.D. et al., (2011) and were also implemented into the SVFlux (2009) computer model (Fredlund et al., 2012). The equation for relative humidity can be used to describe the ratio between *AE*/*PE*; however, it is necessary to apply an adjustment factor, δ, to the total suction values as shown in equation [6]:

$$h_s = \exp\left(\frac{10^{\delta}\psi g \omega_v}{\gamma_w R(273.15+T_{soil})}\right) \quad [6]$$

where: δ = a dimensionless total suction adjustment factor generally varied from 0 to 3.

The Total Suction Adjustment Factor

The empirical total suction adjustment factor, (written in terms of negative pore-water pressures, u_{wa}), is shown in equation [7].

$$u_{wa} = u_{wo}10^{\delta} \quad [7]$$

where: u_{wa} = adjusted negative pore-water pressure, u_{wo} = original pore-water pressure from water phase partial differential equation, and δ = empirical adjustment factor. The adjustment of the negative pore-water pressure must be made when using the Wilson (1990) and Wilson et al., (1997) formulations for actual evaporation. An adjustment factor of 1.8 closely simulated the evaporation rate from columns of sand tested by Wilson (1990). The adjustment factor varies for different soils with the largest values being applicable for coarse-grained soils. The adjustment of the total suction applies for coupled and uncoupled solutions. The adjustment factor should remain equal to zero when evaporation is being computed from a saturated clay soil. The adjustment in the total suction attempts to simulate "surface resistance" near ground surface.

Figure 10 illustrate the rationale behind the calculation for the δ adjustment factor. The residual suction from the drying SWCC, is used as the reference point for calculating the δ adjustment factor. The empirical adjustment factor, in essence, translates the SWCC over to the 3000 kPa point on Lord Kelvin's curve. Typical values of the δ adjustment factor for various residual suction values are illustrated in Figure 11. The maximum δ adjustment factor for coarse sand soils is 3.48 while no adjustment is required for clayey soils with a high air-entry value.

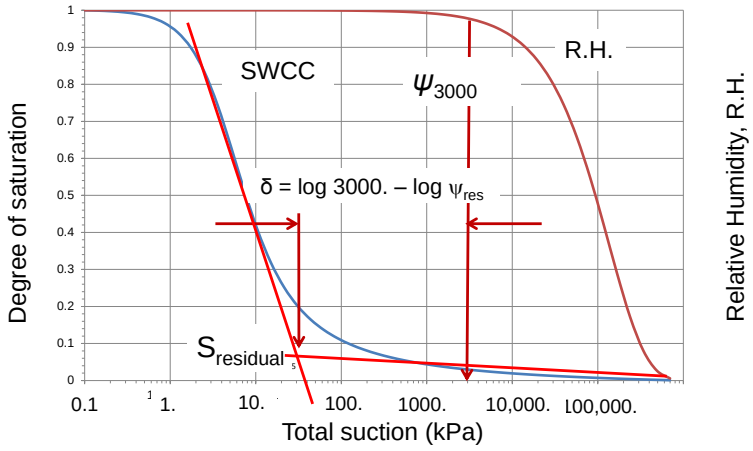

Figure 10 Illustration of the construction procedure to obtain the δ adjustment factor.

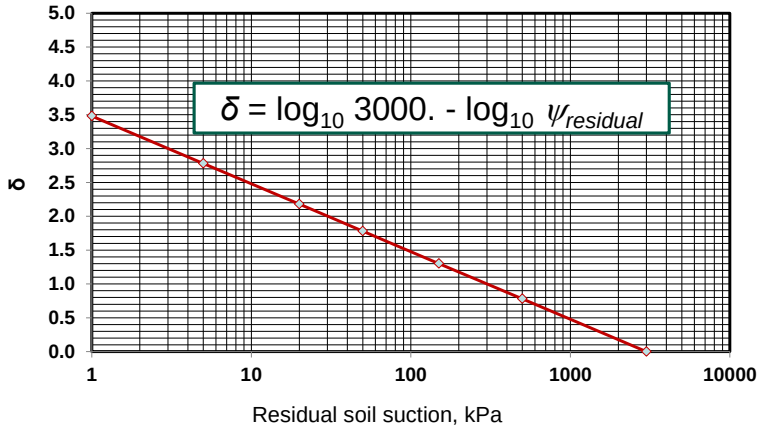

Figure 11 The δ adjustment factors for various residual suction values.

Fredlund-Zhang-Fredlund (2009) Model Calculations of Actual Evaporation from Sand Columns

Measurements by Wilson (1990) of evaporation from a sand soil column can be compared with numerical model calculations using the Fredlund-Zhang-Fredlund (2009) model in the SVFlux and SVHeat software (*SoilVision,* 2009). Both "coupled" and "uncoupled" solutions provided a reasonable simulation of actual evaporation from a sand soil. The numerical simulation results used a δ value of 1.8 and were published in Fredlund et al., (2011) and Tran et al., (2014). Space does not permit repeating the results of the simulation in this paper.

Tran (2013) Evaporation-Rate Reduction Model utilizing the Penman-Monteith (1965) equation

Several researchers have suggested the use of an empirical and indirect parameterization of the surface humidity (Kondo et al., 1990; Lee and Pielke, 1992; Tran, 2013). The complete formulation of the model is based on the Penman-Monteith (1965) model with "surface resistance".

Evaporation-Rate Reduction Point

A reduction in actual evaporation rate has been observed from the data collected on a series of soil columns tests in the research literature. The evaporation-rate starts to reduce from potential evaporation-rate when the suction is somewhere between the air-entry value and residual suction.

$$\psi_R = \begin{cases} \psi_{aev} & if \;\; a=0 \\ \psi_{res} & if \;\; a=1 \\ \psi_{res}^{a} \times \psi_{aev}^{1-a} & if \;\; 0<a<1 \end{cases} \quad \textbf{[8]}$$

where: ψ_R = suction at evaporation-rate reduction point, kPa; ψ_{aev} = air-entry value based on the SWCC, kPa; ψ_{res} = residual suction from the SWCC, kPa; a = an empirical factor which varies between 0 and 1. Published results show that the best-fit value of "a" for sand and silt are 0.60 and 0.75, respectively.

Proposed Methods for Predicting Relative Humidity

Predicting the relative humidity at the soil surface is required in the evaporation model. Lee and Pielke (1992) used the soil moisture availability term, β, to designate the evaporation-rate reduction point, θ_R.

$$\beta = \begin{cases} \frac{1}{4}\left[1-\cos\left(\frac{\theta}{\theta_R}\pi\right)\right]^2 & \theta < \theta_R \\ 1 & \theta \geq \theta_R \end{cases} \quad [9]$$

where: β = coefficient representing the surface moisture availability; θ_R = volumetric water content at evaporation-rate reduction point; θ = soil volumetric water content of the top soil layer.

The actual water vapour pressure can be computed from the soil moisture availability factor.

$$u_v = \beta \times u_v^{sat} + (1-\beta) \times u_v^{air} \quad [10]$$

where: u_v = actual vapor pressure at the soil surface, kPa; u_v^{sat} = saturated vapor pressure at the soil surface, kPa; u_v^{air} = actual air pressure immediately above the soil surface, kPa.

Calculation of Soil Surface Resistance

Several researchers introduced equations to estimate "surface resistance" including Fen Shu (1982), Camillo and Gurney (1986) and van de Griend and Owe (1994). Soil surface resistance varies from zero at the wet soil surface to several thousand at the dry soil surface. The van de Griend and Owe's (1994) equation for soil surface resistance is shown and is written as follows:

$$r_s = 10 \times e^{0.3563(\theta_{\min} - \theta_{top})} \quad [11]$$

where: r_s = soil surface resistance at top 0 – 1 cm, s/m; q_{top} = volumetric water content of the top 1 cm layer, (%); q_{min} = an empirical minimum above which the soil is able to deliver vapor at a potential rate, (%). The original model sets q_{min} = 15% as a fixed value for all soils.

Tran's (2013) Modified Penman-Monteith (1965) Equation

The Penman-Monteith's equation, (i.e., combination of energy balance and mass balance) was used to derive a soil-atmospheric equation that considers the effect of "surface resistance" on actual evaporation.

$$AE = \frac{\Gamma Q + \eta \dfrac{f'(u)}{f(u)} E_a}{\Gamma + \eta A \dfrac{f'(u)}{f(u)}} \qquad [12]$$

where: AE = transpiration rate from a soil, mm/day; E'_a = aerodynamic evaporative term, $E'_a = f(u)(u_{ao} - u_a)$, mm/day/Pa; Q_n = heat budget, mm/day; u_{ao} = saturation vapor pressure of the mean air temperature, kPa; u_a = vapor pressure of the air above the surface, kPa; $f(u)$ and $f'(u)$= the transmission functions for mass and heat, respectively. Further details related to the transmission functions, $f(u)$ and $f'(u)$, can be found in Tran (2013).

Ability of the Tran (2013) Model to Simulate Actual Evaporation from Sand Soils

Soil column drying tests for the Beaver Creek sand (Wilson, 1990) and Processed Silt (Bruch, 1993), were re-analyzed using the Tran (2013) model. The actual evaporation rate obtained using the numerical model (i.e., using ComSol Metaphysics software and Excel); along with measured water contents and temperatures at the soil surface showed close agreement was observed between all the laboratory results and the computed results. Comparisons between the numerical model results and laboratory test results can be found in Tran (2013) and Tran et al., (2014).

The proposed soil-atmosphere flux equation describing evaporation from a soil surface takes into consideration net radiation, wind speed, relative humidity of the air and soil surface, and "soil surface resistance". The evaporation rate is shown to decrease during the drying process mainly as a result of an increase in soil surface resistance.

Concluding Remarks on Modeling Actual Evaporation

Two approaches were examined that attempted to incorporate "surface resistance" into the formulation of the models. One approach was referred to as the "total suction adjustment" approach and the other was referred to as the "relative humidity adjustment" approach. The application of the modified actual evaporation models have been compared to measured evaporation rates from several sand column tests. The comparative simulations showed that both the total suction adjustment approach and the relative humidity adjustment approach produced greatly improve the simulation of actual evaporation.

References

Aluwihare, S., and Watanabe, K. 2003. Measurement of evaporation on bare soil and estimating surface resistance. Journal of Environmental Engineering, Vol. 129, No. 12, pp. 1157–1168

Alvenas, G., and Jansson, P.E. 1997. Model for evaporation, moisture and temperature of bare soil: calibration and sensitivity analysis, Agricultural and Forest Meteorology, Elsevier Science, 88:47-56.

Bittelli, M., Ventura, F., Campbell., G., Snyder, R., Gallegati., F. and Pisa, P. 2008. Coupling of heat, water vapor and liquid water fluxes to compute evaporation in bare soils. Journal of Hydrology, Vol. 362, pp. 191–205.

Bruch, P.G. 1993. A laboratory study of evaporative fluxes in homogeneous and layered soils. Master of Science Thesis, University of Saskatchewan, Saskatoon, SK., Canada.

Camillo, P.J., and Gurney, R.J. 1986. A resistance parameter for bare-soil evaporation models. Soil Science, Vol. 141, No. 2, pp. 191-205.

Camillo, P.J., Gurney, R.J., and Schmugge, T.J. 1983. A soil and atmospheric boundary layer model for evapotranspiration and soil moisture studies. Water Resources Research, Vol. 19, No. 2, pp. 371-380.

Dunmola, A.S. 2012. Predicting evaporative fluxes in saline soil and surface-deposited thickened mine tailings. Ph.D. Thesis, Department of Civil and Environmental Engineering, Carleton University, Ottawa, Ontario, Canada.

Fen Shu, S. 2012. Moisture and heat transport in a soil layer forced by atmospheric conditions. Master of Science thesis, University of Connecticut, USA.

Fredlund, D.G., Rahardjo, H., and Fredlund, M.D. 2012. Unsaturated Soil Mechanics in Engineering Practice, John Wiley & Sons, New York, N.Y.

Fredlund, M.D., Zhang, J.M., Tran, D.T.Q., and Fredlund, D.G. 2011. Coupling heat and moisture and moisture flow for the computation of actual evaporation. Paper No. 1058, Proceedings of the Canadian Geotechnical Conference and Pan-American Conference, Toronto, ON, Canada, October 2-6.

Kondo, J., and Saigusa, N. 1992. A model and experimental study of evaporation from bare-soil surfaces, Journal of Applied Meteorology, American Meteorological Society, Vol. 31, pp. 304-312.

Kondo, J., Saigusa, N., and Sato, T. 1990. A parameterization of evaporation from soil surfaces. Journal of Applied Meteorology, American Meteorological Society, Vol. 29, pp. 385-389.

Lee, T.J., and Pielke, R. 1992. Estimating the soil surface specific humidity, Notes and Correspondence, Journal of Applied Meteorology, American Meteorological Society, Vol. 31, pp. 480-484.

McCumber, M.C., and Pielke, R.A. 1081. Simulation of the effects of surface fluxes of heat and moisture in a mesoscale numerical model. Part I: Soil layer. Journal of Geophysical Research, Vol. 86, pp. 9929-9938.

Monteith, J.L. 1965. Evaporation and the environment. In the movement of water in living organisms. XIX Symposium Society for Experimental Biology, Swansea, Cambridge, University Press, Vol. 19, pp. 205–234.

Penman, H.L. 1948. Natural evaporation from open water, bare soil and grass, Proceedings of the Royal Society of London, Series A193: pp. 120-145.

SoilCover (1994). User's Manual, Version 1.0, Department of Civil Engineering, University of Saskatchewan, Saskatoon, SK., Canada.

SVFux (2009). User's Manual for SVFlux, SoilVision Systems, Saskatoon, Sask., Canada

Thornthwaite, C.W. 1948. An approach toward a rationale classification of climate. Geographical Review, Vol. 48, pp. 55-94.

Tran, D.T.Q., 2013. Re-visitation of actual evaporation theories. Ph.D. Thesis, Department of Civil and Environmental Engineering, University of Alberta, Edmonton, Alberta, Canada.

Tran, D,T.Q., Chan, D.H., and Fredlund, D.G. 2014. Re-assessment of soil suction at the evaporation-rate reduction point for saturated-unsaturated soil surfaces. Proceedings of the 2014 Geo-Congress Conference, Sustainability, Energy, and the Environment, Atlanta, GA, Feb. 23 – 26.

van de Griend, A.A., and Owe, M. 1994. Bare soil surface resistance to evaporation by vapor diffusion under semiarid conditions. Water Resources Research, Vol. 30, No. 2, pp. 181–188.

Wetzel, P.J., and Chang, J. 1987. Concerning the relationship between evapotranspiration and soil moisture. Journal of Applied Meteorology and Climatology, Vol. 26, pp. 18-27.

Wilson, G.W. 1990. Soil evaporative fluxes for geotechnical engineering problems, Ph.D. dissertation, University of Saskatchewan, Saskatoon, SK., Canada.

Wilson, G.W., Fredlund, D.G. and Barbour, S.L. 1997. The effect of soil suction on evaporative fluxes from soil surfaces. Canadian Geotechnical Journal, 34(4): pp. 145-155.

Yanful, E.K., and Choo, L.P. 1997. Measurement of evaporative fluxes from candidate cover soils. Canadian Geotechnical Journal, Vol. 34, pp. 447-459.

Near-Surface Water Balances of Waste Rock Dumps

Mike O'Kane[1], Tyler Birkham[1], Amy Goodbrand[1*], S. Lee Barbour[2], Sean Carey[3], Justin Straker[4], Trevor Baker[4] and Rob Klein[5]

1. *O'Kane Consultants, Canada [1]*formerly*
2. *University of Saskatchewan, Canada*
3. *McMaster University, Canada*
4. *Integral Ecology, Canada*
5. *Teck Resources, Canada*

ABSTRACT

The near-surface water balance of mine impacted landscapes is a key control on re-vegetation performance, and on the hydrologic and water quality impact at the watershed scale. As part of Teck Resources Limited's applied research and development program focused on managing water quality in mine-affected watersheds, 12 sites in western Canada (southeastern British Columbia and western Alberta) representing a range of waste rock dump reclamation surface management options (i.e. soil cover, surficial mounding) were instrumented in 2012 to measure meteorological and soil water response and to quantify the near-surface water balances with a focal objective to improve estimates of ranges of net percolation into waste rock dumps under a range of scenarios.

Subsurface water and meteorological conditions varied substantially, as expected for the range of elevation, slope aspects, vegetation, soil covers, geographic location and surface preparation of the selected sites. Patterns in water balance trends emerged in the first year of analysis with net percolation (NP) into underlying waste rock typically decreasing for increased vegetation and soil cover, as well as for decreases in rainfall or snowmelt. Increased vegetation cover resulted in a greater volume of water removed from near-surface through evapotranspiration. The lowest NP (as % of water input) was estimated for a mature, reclaimed conifer forest site and a dense agronomic grass/alfalfa covered site. Net percolation estimated for a soil covered waste rock slope was approximately 15% (of water inputs) less than an adjacent bare waste rock slope. Decreased NP was partly attributed to greater water storage in the finer-textured soil cover. Net percolation through the soil cover is expected to further decrease with time as vegetation establishes relative to the bare waste rock slope. Net percolation for a mounded, bare waste rock slope was less than estimated for an adjacent smooth slope. Net percolation below a trough was similar to the smooth slope, but decreased at the crest and mounded mid-slope positions due to thinner snowpack (less snowmelt) from wind scouring. Additional monitoring and analysis of site-specific water balances will help define the shift in the relative proportions of water entering the deposits as vegetation matures.

INTRODUCTION

Mining activities undertaken by Teck Resources Limited (Teck) to access the metallurgical coal resource in the Elk Valley of southeastern British Columbia and in northwestern Alberta result in waste rock dumps with material susceptible to long term weathering and erosion processes. The waste rock is known to increase concentrations of some constituents of interest (CIs) in downstream surface water and groundwater systems. Post-depositional weathering of the waste rock is accelerated by oxygen ingress and weathering products can be transported with infiltrating water. These two processes are both controlled by the degree of saturation of the unsaturated waste rock.

The amount of water that infiltrates into waste rock landforms is a function of the near-surface water balance. This surface water balance is a key control on vegetation establishment and its long term performance and will affect the hydrology, hydrogeology and geochemistry of affected watersheds. For example, selenium (Se) concentrations in mine-affected rivers are reported to have increased over the last three decades (Lussier, Veiga & Baldwin, 2003; Chapman, Berdusco & Jones, 2007) and the understanding of Se release and transport from waste rock dumps is still developing. Research has indicated that Se is more readily transported in the soluble form of selenate suggesting a strong link to water movement (Chapman, Berdusco & Jones, 2007).

Controls on the movement of water through and out of waste rock dumps include the volume, rate, and flow path of net percolation (NP) waters. The term 'net percolation' is defined as water that migrates into and downward in the material profile to depths not influenced by atmospheric processes (i.e. evapotranspiration). This water may eventually be released from waste rock to adjacent groundwater or surface water. Important aspects of NP include:

- Volume: NP volumes are a primary control on water volumes reporting as basal and toe seepage from waste rock dumps and have important implications for mine-affected watershed water balances and water management strategies. NP volumes may be an important control on solute loadings in basal and toe seepage;
- Rate: The flow velocity of NP through mine wastes, as well as the height of the waste deposit, will control the residence time of pore-water in the waste rock profile. Residence time may be an important consideration on the dissolution of CIs; and
- Flow Path: Water may move via preferential pathways (i.e. macro-pore flow) or via matrix flow, which is more distributed. Preferential flow through waste rock will decrease the surface area contacted by NP and residence time of NP in waste rock dumps, which are opposite to the trends for matrix dominated flow. Preferential flow paths will increase the time required to flush CIs from a waste rock dump compared to matrix dominated flow as NP following preferential flow paths bypasses and does not flush oxidation products from all of the waste rock.

As part of Teck's applied research and development program focused on managing water quality in mine-affected watersheds, 12 sites representing different waste rock dump reclamation surface management options were instrumented in 2012 to measure meteorological and soil water dynamics. Data from these sites was used to quantify the near-surface water balances with a focal objective to improve estimates of ranges of NP into waste rock dumps for a variety of conditions.

METHODOLOGY

The study sites are located at four coal mining operations in the Elk Valley, BC and one in northwestern Alberta: Line Creek (LC); Greenhills (GH); Elkview (EV); Fording River (FR); and Cardinal River (CR; Figure 1). The climate at all of the study sites is humid continental. Climate normals data (1981-2010, Environment Canada, Sparwood station at 1140 m asl) indicate the Elk Valley mines are located in a region with mean annual precipitation of 613 mm (411 mm as rainfall, 202 mm as snow). Mean annual precipitation from climate normals data (1981 – 2010, Environment Canada, Jasper East Gate at 1003 m asl) for the Cardinal River area is 599 mm (448 as rainfall, 151 mm as snow). The study sites monitoring instruments were commissioned in the summer and fall of 2012 and have been collecting data since. This paper reports on data for each site over one hydrologic year starting October 1st, 2012 through September 30th, 2013. A large rainfall event in the Elk Valley from June 18th – 21st, 2013 largely influenced the amount of precipitation observed in the first year of monitoring as this event resulted in 81% more rain in June than the monthly climate normal for that month.

General Site Descriptions

The study sites were chosen to investigate the effect of elevation, surface soil placement, re-vegetation types, site orientation (slope/aspect) and microtopography on the near-surface water balance (Table 1). The study site locations include two instrumented sites at Greenhills Operation North Thompson mine area that are part of a paired cover trial with a uniform sloped soil cover (GH_NTC) and bare waste rock (GH_NTW) slope. A soil cover was also placed on the Turn Creek dump (FR_TCR) at Fording River Operation. Three sites (LC_BHE, LC_RHE and LC_RME) were installed on benched plateaus of the West Line Creek dump at the Line Creek Operation at different elevations and with varying degrees of vegetation cover. A reclaimed mature forest site (FR_CSP) at the Fording River Operation provided an optimal scenario to understand the effect of mature tree re-vegetation on near-surface water retention and net percolation. Data collected on a south-facing, vegetated slope of the Bodie Dump (EV_BRD) at the Elkview Operation allow quantification of the effect of a thick grass-legume vegetation cover and slope aspect. Similarly, instruments installed at the Cardinal River Operation north-facing (CR_B5D) and south-facing (CR_B4D) slopes were used to observe differences due to aspect and soil placement. The sloped surface in the Greenhills Rosebowl mine area (GH_RMS) and Cardinal River Cheviot area (CR_CMS) have been prepared using a mounding technique creating crests, mid-slopes and troughs, which help evaluate the effect of mounding on re-vegetation success and overall NP rates.

Performance Monitoring Instrumentation

All sites were instrumented with both soil profile monitoring (suction, temperature and water content) and meteorological stations with the exception of CR_B4D, which was installed with only a net radiation sensor. Components of a soil monitoring station included one primary *in situ* water content monitoring station consisting of eight thermal conductivity (pore-water suction) and eight time-domain reflectometry (TDR, water content) sensors, and four secondary *in situ* water content monitoring stations, each consisting of four TDR sensors. Meteorological stations measured rainfall (CS700 Tipping Bucket Rain Gauge), air temperature and relative humidity (HC2-S3 Probe), wind speed/direction (R.M. Young Model 05103AP-10 Wind Monitor), net radiation (Net Radiation Kipp & Zonen model NR-LITE2 Net Radiometer), and snow depth (Sonic Ranger 50A). Eddy covariance stations were installed at LC_RHE, LC_BHE, FR_CSP, and GH_NTW, and included a gas analyzer

(either LICOR Li-7200 closed-path for forest and grasses, or a Li-7700 open-path CO_2/H_2O analyzers for bare waste rock), an ultrasonic anemometer (Windmaster, Gill Instruments), an air temperature and relative humidity sensor (HMP45 sensor, Vaisala), and a net radiometer (CNR4, Kipp & Zonen). Nine Gee lysimeters were installed under the trough, crest, and slope areas of the GH_RMS study to directly measure net percolation rates. Lastly, 24 sap flow sensors were installed in 12 trees at FR_CSP to measure sap flow velocity and estimate water uptake rates by each tree.

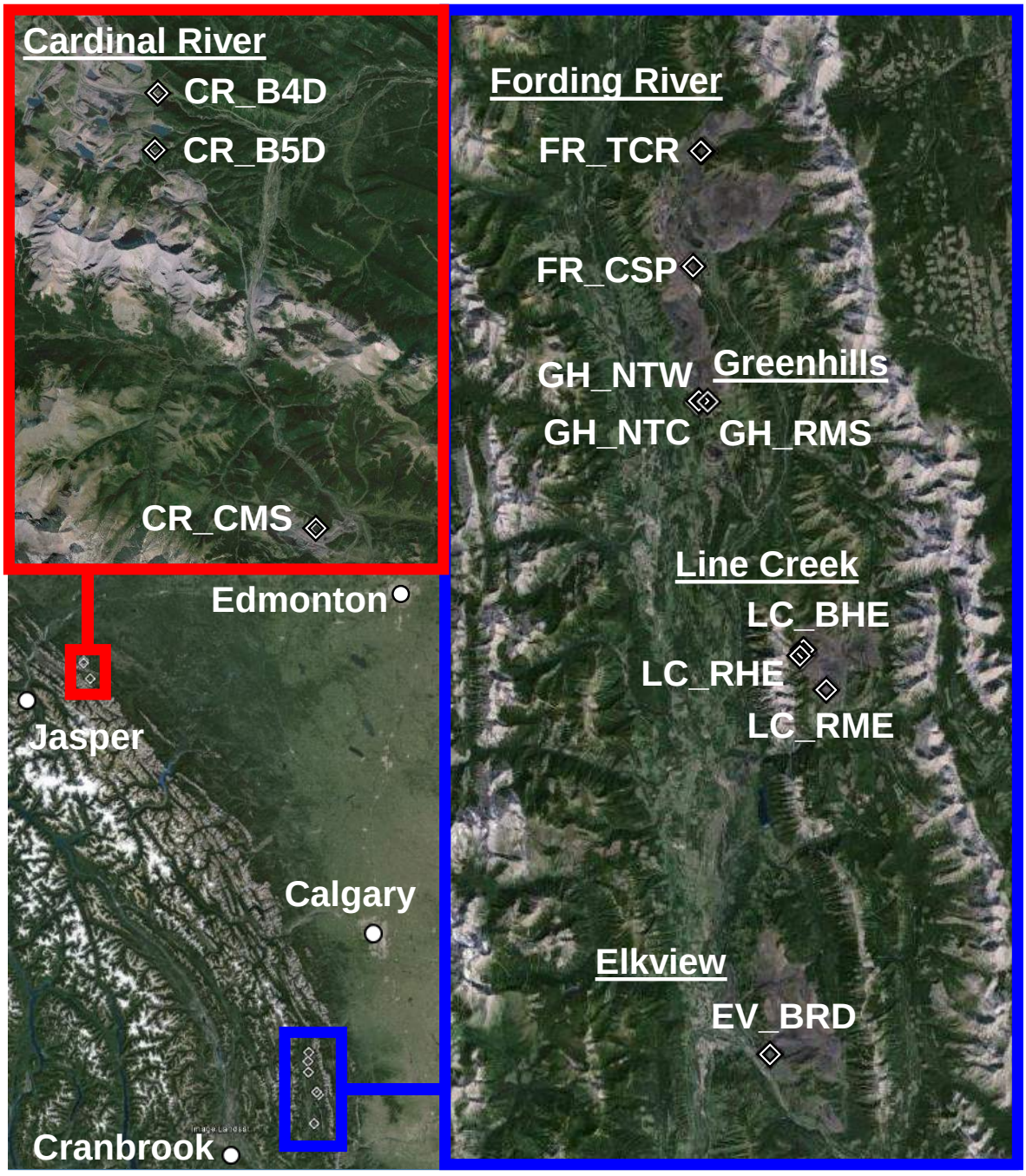

Figure 1 Aerial map showing locations of study sites.

Table 1 Summary of characteristics at study sites located in southeast BC and northwest AB

Site	Easting	Northing	Mine Area	Elevation (m asl)	Cover Soil	Surface	Slope (°)	Aspect	Topographic Shading	Vegetation
GH_NTW	5550564	651834.7	N Thompson Ck	1800	No	Smooth	26	W	No	Planted Seedlings
GH_NTC	5550651	651875	N Thompson Ck	1800	2-Lift Surface Soil	Smooth	26	W	No	Planted Seedlings/ Natural Regeneration
GH_RMS	5550429	652172.1	Rosebowl	1920	No	Mounds	26	SW	No	Planted Seedlings
LC_BHE	5535363	658257.9	West Line Ck	2150	No	Smooth/ Harrow	-	Level	No	Planted Seedlings
LC_RHE	5535020	658138.9	West Line Ck	2075	No	Smooth/ Harrow	-	Level	No	Agronomic Grasses/ Legumes
LC_RME	5533016	659655.7	West Line Ck	1790	No	Smooth/ Harrow	-	Level	No	Agronomic Grasses/ Legumes
FR_CSP	5559029	348453.1	C Spoil	1690	No	Smooth	26	E	No	~25 Year Old Regenerating Conifer Forest
FR_TCR	652279	5566138	Turn Creek	1800	Salvaged Soil/ Overburden	Smooth/ Harrow	-	Level	Yes	Planted Seedlings
EV_BRD	5510559	343964.9	Bodie Rock Drain	1470	No	Smooth	26	SW	No	Agronomic Grasses/ Legumes
CR_B5D	5879971	475328.5	Luscar B5	1630	Regolith	Smooth	26	NE	No	Agronomic Grasses/ Legumes
CR_B4D	5878010	474278.7	Luscar B4	1690	No	Smooth	26	S	Partial Winter	Agronomic Grasses/ Legumes
CR_CMS	5864953	479802.9	Cheviot 1930	1930	Salvaged Soil (Till)	Mounds	26	S	No	Planted Seedlings/ Natural Regeneration

*Substrate for all sites was waste rock.

Water Balance Analysis

Water balances were developed for each site over one hydrologic year starting October 1st, 2012 through September 30th, 2013. For these snow-dominated sites, water input was defined as the sum of rainfall minus rainfall interception, plus snowmelt (hereafter referred to as effective precipitation, P_{eff}). The following components of the water balance were measured or estimated to calculate daily changes in storage (ΔS) in the top ~1 m of material at the primary station profiles:

$$\Delta S = R + M - AE(T) - RO - NP \quad (1)$$

where: R is rainfall, M is snowmelt, $AE(T)$ is actual evaporation or evapotranspiration where appropriate, RO is surface runoff, and NP is net percolation (all units are mm d^{-1}). Runoff at all sites was assumed to be zero as a result of the high hydraulic conductivity of the waste rock and cover soils.

Precipitation

Rainfall (volume and intensity) was measured with a tipping bucket rain gauge (TBRG, Campbell Scientific 700). Precipitation was verified by comparing multiple TBRG records at sites with similar elevation, the precipitation record from the Sparwood, BC climate station (1140 masl, Environment Canada) and other total precipitation gauges operated by McMaster University and Teck. Precipitation was assumed to be rain if the mean daily air temperature was greater than 2°C.

Daily average snow depth was measured continuously using an automated Sonic Ranger 50A (SR50) sensor. Snow surveys completed at the end of March 2013 provided snow depth and density data to calculate a transect-average snow-water equivalent (SWE) across each site. A continuous record of snowpack SWE was estimated with snow density equations (Bartlett, MacKay & Verseghy, 2006).

Melt

Point-based daily snow ablation amounts for each site were estimated using the energy balance equation and daily averages of meteorological data using the approach reported by Dingman (2002) and Burles & Boon (2011). The energy fluxes from ground heat flux and rain were assumed to be zero. Sensible heat was calculated as a function of measured wind speed and air temperature. Sublimation and evaporation were accounted for by the latent heat term which was a function of the vapour pressure gradient between the air and snow surface. The melt period was initialized with peak SWE and run to complete snowpack removal. The SR50 snow depth record in combination with field observations (including time-lapse photos) were used to determine the timing of snowpack disappearance.

Evapotranspiration

Potential evaporation was estimated using the Penman (1948) or Penman-Monteith combination method (Monteith, 1965) for sites with well-established vegetation. Canopy conductance (C_{can}) was estimated using leaf area index data collected in 2013 (Integral Ecology, 2013). A relationship

between evapotranspiration (E(T)) and soil water deficits was used to relate potential evapotranspiration (PE(T)) to actual E(T) via the following equations:

$$AE(T) = PE(T) \cdot Available\ Water\ Ratio \quad (2a)$$

$$Available\ Water\ Ratio = (VWC - WP)/(FC - WP) \quad (2b)$$

where: VWC is the volumetric water content of the surficial soil profile (average of top 15 to 30 cm depending on vegetation and expected depth range accessible to evapotranspiration), WP is the wilting point and FC is the field capacity. WP and FC are defined as the volumetric water contents at 1500 and 10 kPa of suction, respectively. The available water ratio approached 1 at FC and declined as the availability of water decreased to the WP for plants (available water ratio = 0). Eddy covariance estimates of AE(T) were found to positively correlate with measured leaf area index (LAI) (Integral Ecology, 2013); therefore, AE(T) estimates calculated using Eq. 3a and 3b were constrained using the developed LAI-AE(T) relationship for conditions ranging from bare to vegetated ground.

Interception

Rainfall intercepted was assumed to be evaporated daily and estimated using a modified version of the forest rainfall interception model in Rutter and Morton (1977). Daily maximum rainfall interception was set equal to the canopy storage capacity for conifers (1 mm; Schmidt & Gluns, 1991). Intercepted snowfall in the trees at Fording River C-spoil was not considered during the first year of analysis due to the complexity in quantifying this process and scope of the study.

Storage

Changes in water storage (ΔS) through the soil profile were calculated using the volumetric water content (CS616 Time Domain Reflectometry Sensors) measured at the primary monitoring station. The volume of water was weighted for sensor depth and summed over the entire profile.

Net Percolation

It was assumed that NP occurred when there was a downward vertical hydraulic gradient as calculated from the soil suction values between 75 and 100 cm depth and if there was a net loss in storage within the bottom half of the instrumented profile. For this case, NP was assumed to be equal to the net loss in storage from the bottom half of the profile, as it was assumed AE(T) fluxes would not affect water storage at that depth. This assumption was supported by matric suction depth profiles (not presented) which exhibited the greatest changes with time and occurrence of upward gradients in the upper 50 cm.

If the water storage capacity of the bottom soil profile exceeded the field capacity (FC; 10 kPa of suction) during snowmelt infiltration or rainfall events, then NP was estimated via the water balance in Eq. 1. This NP estimation method was used during snowmelt infiltration and rainfall events as there was often a surplus of water during melt and rainfall events if the gradient / storage method for calculating NP described above was used. It was assumed that seepage rates could be near steady-state during melt and rainfall events and that NP could be occurring even if there was not a measured decrease in storage.

Analytical Model Calibration

Water retention curves (WRC) were developed using the water content and suction monitoring data. These were then used to estimate values of FC and WP. Water retention curves, however, are difficult to develop for heterogeneous, coarse-textured materials. Estimates of AE(T) were most sensitive to FC and WP parameters; therefore, sensitivity of water balance estimates were assessed by varying the FC and WP values ± 2 to 10%. Measured water content and the match of measured and calculated water storage was used to inform FC and WP estimates and constrain AE(T) values. Assuming no runoff, water input that was not removed by AE(T) was then assumed to eventually report to NP.

RESULTS AND DISCUSSION

The soil water contents and meteorological conditions were variable, which was expected given the range of elevation, slope aspects, vegetation, soil covers, geographic location and surface preparation of the selected sites. Meteorological conditions at the various sites were similar but with key differences that can be attributed to elevation, geographic location, and slope aspect. Precipitation increased with increasing elevation. LC_BHE, the highest elevation site (2,150 m asl) had the greatest measured total annual precipitation (1,210 mm). For sites in the 1,500 to 1,800 m asl elevation range, total annual precipitation ranged from approximately 800 to 950 mm. Sites located at the Cardinal River Operation were greatly influenced by the dry, warm winds blowing down the eastern slopes of the Rocky mountains. Data records indicate snowpack disappearance occurred earlier on the south-facing CR_B4D slope compared to north-facing B5D likely due to higher solar energy input received on the south-facing slope. Earlier snowmelt and snowpack disappearance was also observed on other south-facing slopes including EV_BRD and CR_CMS.

Patterns in water balance trends emerged in the first year of analysis with NP into underlying waste rock typically decreasing for increased vegetation and soil cover, as well as for decreases in rainfall or snowmelt. The highest NP occurred at LC_BHE due to greater P_{eff}, low AE(T), and less water holding capacity in the coarse waste rock compared to other monitored sites (Table 2). Increased vegetation cover resulted in a greater volume of water removed from the near-surface through AE(T), that would have otherwise resulted in NP. For example, the lowest NP (as % P_{eff}) calculated was for the mature, reclaimed conifer forest site (FR_CSP) and the dense agronomic grass/alfalfa covered site (EV_BRD). Lower NP at EV_BRD compared to FR_CSP was attributed to a higher water holding capacity in the material underlying the thick grass cover combined with lower P_{eff} on a south-facing slope. As the individual site cover systems evolve, vegetation communities mature, and water balance trends become more apparent the mechanisms having the largest impact on controlling net percolation through waste rock dumps and achieving re-vegetation objectives can be identified, quantified and evaluated as potential watershed management tools.

Net percolation estimated for a soil covered, waste rock slope (GH_NTC) was approximately 15% (of P_{eff}) less than an adjacent bare waste rock slope (GH_NTW). Research has shown that cover systems have the potential to limit infiltrating water (i.e. NP) through a waste rock dump (MEND, 2012). Water storage in the shallow subsurface was greater in the finer-texture soil cover at GH_NTC compared to GH_NTW (Figure 2). NP through the soil cover is expected to further decrease in future years as vegetation establishes, thus more available soil water will be removed through AE(T) (Integral Ecology, 2012).

The water balances for the covered sites at FR_TCR and GH_NTC, and the mature forest site at FR_CSP, were analyzed over a shorter period than other sites as data was not available until later in the fall. NP estimates (as a % of P_{eff}) are likely slightly over-estimated for these sites as heavy rainfall in early October prior to the first day of the water balance estimations were not included in the P_{eff} values but may have been contributing to NP during the analysis period.

The weighted net percolation for a mounded, bare waste rock slope (GH_RMS), considering the overall effect of troughs and crests, was lower than that calculated for an adjacent smooth slope (GH_NTW) (Table 2). Net percolation estimates at the GH_RMS were corroborated by direct measurement of NP by lysimeters. Net percolation in a trough at GH_RMS was similar to the smooth slope at GH_NTW, but decreased at the crest and mounded mid-slope positions due to thinner snowpack (less snowmelt) from wind redistribution. Increased water availability in the troughs, as well as wind and sun shading, are expected to increase vegetation productivity over time in the troughs relative to the crests which will increase AE(T) and further decrease NP at GH_RMS.

CONCLUSION

Patterns in near-surface water balances have begun to emerge in the first year of monitoring of a range of waste rock dump reclamation surface management options. Net percolation as estimated from data collected from field moisture and climate instruments decreased with increasing vegetation cover and the addition of a surficial soil cover. Overall NP at a mounded waste rock site was estimated to be less than for an adjacent smooth waste rock slope. The effect of mounding on NP should be considered on a site-specific basis, however, as differences in precipitation, depth of troughs, slope aspect and prevailing wind direction will influence the results.

Table 2 Cumulative annual water balance fluxes for all 12 study sites. All fluxes are presented in millimeters. Net percolation values are presented as a percentage of effective water inputs (rainfall plus snowmelt).

Site	Elev m asl	Description	Rain	Melt	Effective Precipitation (P_{eff})	Actual E(T)	Net Percolation (NP)	Meas ΔS	Calc ΔS	NP as % of P_{eff}	Sensitivity of NP (as % of P_{eff})
LC_BHE	2150	Bare, plateau	530	640	1170	**150**	970	60	50	**83%**	**79 – 85%**
LC_RHE	2075	Grass/legume, plateau	530	590	1120	**280**	780	65	65	**70%**	**68 – 71%**
LC_RME	1790	Grass/legume, plateau	630	270	900	**170**	640	90	85	**71%**	**68 – 73%**
GH_NTW	1800	Seedlings, bare, slope	510	430	940	**150**	750	30	35	**80%**	**77 – 83%**
GH_NTC[1]	1800	Seedlings, soil cover, slope	480	340	820	**180**	550	80	90	**67%**	**65 – 71%**
GH_RMS **Trough**	1920	Seedlings, bare, mounded, slope	510	470	980	**150**	810[4]	10	15	**83%**	**79 – 85%**
GH_RMS **Crest**	1920	Seedlings, bare, mounded, slope	510	130	640	**150**	450[5]	55	45	**70%**	**63 – 77%**
FR_CSP[2]	1690	Trees, bare, slope	620	350	970	**380**[6]	560	40	35	**58%**	**55 – 61%**
FR_TCR[3]	1800	Seedlings, soil cover, plateau	600	250	850	**150**	730	-30	-30	**86%**	**82 – 89%**
EV_BRD	1470	Grass/legume, slope	690	190	880	**320**	460	100	100	**52%**	**49 – 55%**
CR_B5D	1630	Grass/legume, slope	460	420	880	**330**	590	-45	-40	**67%**	**64 – 70%**
CR_B4D	1690	Grass, legume, slope	460	400	860	**250**	650	-45	-40	**76%**	**72 – 79%**
CR_CMS	1930	Seedlings, cover, mounded, slope	450	300	750	**200**	570	-20	-20	**76%**	**72 – 79%**

[*] Runoff assumed to be zero for all sites.

[1] Water balance period starting 18 Oct 2012

[2] Water balance period starting 15 Oct 2012

[3] Water balance period starting 25 Oct 2012

[4] Drainage measured using Gee lysimeters was 780 mm

[5] Drainage measured using Gee lysimeters was 65 mm

[6] Rainfall canopy interception was estimated to be 70 mm of AE(T)

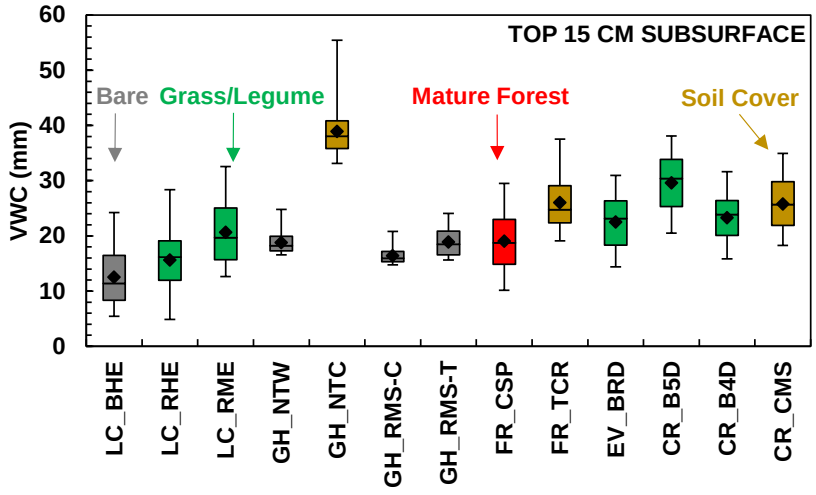

Figure 2 Box and whisker plot showing inter-site variability in mean daily VWC for the top 15 cm of material during the non-frozen period (May 1st to September 30th, 2013). Whiskers indicate the maximum and minimum values, the box represents the 25th and 75th percentiles, while the median values are represented by the mid-range lines. Mean values are presented as black diamonds to indicate the skew in the distribution of the data set.

REFERENCES

Bartlett, P.A., MacKay, M.D., and Verseghy, D.L. (2006) Modified snow algorithms in the Canadian Land Surface Scheme: Model runs and sensitivity analysis at three Boreal forest stands, *Atmos. Ocean*, vol 43, pp. 207–222.

Burles, K. and Boon, S. (2011) Snowmelt energy balance in a burned forest plot, Crowsnest Pass, Alberta, Canada. *Hydrological Processes*, vol. 25, pp. 3012–3029.

Chapman, P.M., Berdusco, R.J., and Jones, R. (2007) Update on the status of selenium investigations in the Elk River Valley, B.C.

Dingman, S.L. (2002) Physical Hydrology, 2nd Edn. Prentice-Hall Inc: Upper Saddle River, New Jersey; 600 pp.

Integral Ecology Group Ltd (2013) Teck Resources Limited Applied Research and Development Program: 2013 reclamation assessment – Draft.

Integral Ecology Group Ltd (2012) Teck Resources Limited Applied Research and Development Program: Evapotranspiration and vegetation contributions to soil water balances on reclaimed sites – an interpretive review. Project No. TCLWRD-11.

Lussier, C., Veiga, V., & Baldwin, S. (2003) The geochemistry of selenium associated with coal waste in the Elk River Valley, Canada. Environmental Geology, vol. 44, issue 8, pp. 905–913.

MEND 1.61.5c. (2012) Cold Regions Cover System Design Technical Guidance Document. Canadian Mine Environment Neutral Drainage Program.

Monteith, J.L. (1965) Evaporation and environment. In New York, NY: Cambridge University Press, *Proceedings of the 19th Symposium of the Society for Experimental Biology*, pp. 205–233.

Penman, H. L. (1948) Natural evaporation from open water, bare soil and grass. *Proceedings of the Royal Society of London. Series A. Mathematical and Physical Sciences*, vol. 193, pp. 120–145.

Schmidt, R. A., and Gluns, D. R. (1991) Snowfall interception on branches of three conifer species. *Canadian Journal of Forestry Research*, vol. 21, pp. 1262–1269.

Water Balance Modeling of Preferential Flow in Waste Rock Materials

Jason Keller[1], Michael Milczarek[1] and Guosheng Zhan[2]

1. *GeoSystems Analysis, Inc, USA*
2. *Barrick Gold Corporation, USA*

ABSTRACT

For waste rock with a high percentage of gravel particles the spatial distribution of the gravel particles can create macropores and discontinuity in the pore-size distribution. Consequently, many studies have shown that preferential flow may dominate unsaturated flow conditions in waste rock in some cases and that two or more functions may be needed to describe the unsaturated flow in waste rock materials. Most unsaturated flow models use the Richards' equation to predict unsaturated flow behavior in soil matrix, and cannot simulate preferential flow through macropores. Alternatively, MACRO 5.1, a dual-permeability model, uses a kinematic wave equation to describe water flow in macropores, while the Richards' equation is used for water flow in micropores (soil matrix).

In order to simulate the potential for preferential flow, MACRO 5.1 was used to predict unsaturated flow behavior in a planned waste rock facility at a proposed mine in northwestern Pakistan. The site is extremely dry with a ratio of annual potential evaporation (3900 mm) to precipitation (32 mm) of 120. For this kind of climate region, if a model only involves matrix flow mechanism and neglects preferential flow, it would project unrealistic no deep percolation. The influence of waste rock dump geometry (area and thickness) on predicted percolation volumes exiting the base of the dump were also evaluated to predict wetting front arrival times and percolation rates.

The modeling results demonstrate that the large evaporative demand results in minimal deep percolation and a long delay from the time of waste rock dump placement to the beginning of outflow from the dump. For the higher dump, outflow from the dump is predicted to begin 204 years after dump placement and reach a maximum outflow rate 612 years after placement. Outflow from the lower dump is predicted to begin 82 years after dump placement and attain its maximum outflow rate 490 years after placement.

Keywords: Unsaturated flow, waste rock, macropore, dual-permeability model, kinematic wave equation

INTRODUCTION

For waste rock with a high percentage of gravel particles the spatial distribution of the gravel particles can create macropores and discontinuity in the pore-size distribution (Milczarek et al., 2006; Al-Yahyai et al., 2006; Poulsen, 2002). Therefore, the moisture retention characteristic relationship between water content and soil water pressure potential and relationship between unsaturated hydraulic conductivity and water content (K(θ)) or soil water potential (K(ψ)) may require two or more functions to describe the unsaturated hydraulic properties for the entire pore-size distribution.

Most unsaturated flow models use the Richards' equation to predict unsaturated flow behavior, such as HYDRUS (Simunek et al., 1998), UNSAT-H (Fayer, 2000), SWIM (Verburg et al., 1996), and VADOSE/W (GEO-SLOPE International Limited, 2002). However, for gravelly materials the existence of macropores can lead to macropore flow (preferential flow), which cannot be simulated by the Richards' equation. For arid climates that experience periodic high intensity precipitation events, neglecting preferential flow may result in large under predictions of deep percolation. For porous media containing macropores, Larsbo et al. (2005) proposed a dual-permeability model (MACRO 5.1), where a kinematic wave equation (Germann, 1985) is employed to describe the water flow in macro-pores, while the Richards' equation is used for the water flow in micropores (soil matrix).

In order to account for macropore flow in a proposed waste rock facility in arid northwestern Pakistan, the one-dimensional dual-permeability model MACRO 5.1 was used to predict unsaturated flow behavior in the unvegetated waste material. The simulations predicted wetting front arrival and deep percolation rates under conditions which account for evaporation and surface run-off. The influence of waste rock dump geometry (area and thickness) on predicted percolation volumes exiting the base of the dump were evaluated using the MACRO 5.1 model predicted wetting front arrival times and percolation rates.

METHODOLOGY

Model

MACRO 5.1 is a dual-permeability model, separating the total porosity into two separate flow components, micropores and macropores. Each flow domain is characterized by a degree of saturation, conductivity, and water flow rate. The two domain model describing water flow requires modifications to the traditional van Genuchten (1980) moisture retention curve (MRC) function. The modified van Genuchten MRC function of the soil matrix (micropores) is described by (Larsbo et al., 2005):

$$S = \frac{\theta_{mi} - \theta_r}{\theta_s^* - \theta_r} = (1 + |\alpha_{vg}\psi|^{n_{vg}})^{-m_{vg}} \qquad (1)$$

where S is the effective soil water saturation. This equation assumes a fictitious saturated water content (θ_s*), which is defined in place of the saturated water content (θ_s), where $\theta_s^* \leq \theta_s$. θ_{mi} is the micropore water content and the remaining parameters are the same as that in the standard van

Genuchten equation; θ_r is the residual water content and α_{vg}, n_{vg}, and m_{vg} are fitting parameters related to pore-size distribution of the material (where m_{vg} is set equal to 1 - 1/n_{vg}).

The modified van Genuchten-Mualem equation utilized in MACRO 5.1 is in the form (Larsbo et al., 2005):

$$K_{mi} = K_b \left(\frac{S}{S_{(\theta b)}}\right)^l \left\{ \frac{1-(1-S^{1/m_{vg}})^{m_{vg}}}{1-(1-S_{(\theta_b)}{}^{1/m_{vg}})^{m_{vg}}} \right\}^2, \ \theta \le \theta_b \qquad (2)$$

where K_{mi} is the unsaturated hydraulic conductivity in the soil matrix, l is the tortuosity factor (assumed to be equal to 0.5 (Mualem, 1976)), $S_{(\theta b)}$ is the effective water saturation at the break point between macro- and microporosity (θ_b), and K_b is the hydraulic conductivity at θ_b (K_b = saturated hydraulic conductivity for soil matrix). The other parameters are the same as in equation 1.

Larsbo et al. (2005) define the hydraulic conductivity function for the macropores (K_{ma}) as a simple power law of the macropore degree of saturation (S_{ma}):

$$K_{ma} = K_{s(ma)} S_{ma}{}^{n^*} = (K_s - K_b) S_{ma}{}^{n^*}, \ \theta > \theta_b \qquad (3)$$

where $K_{s(ma)}$ is the saturated hydraulic conductivity of the macropores, n^* is a "kinematic" exponent reflecting macropore size distribution and tortuosity, and K_s is the total saturated hydraulic conductivity.

Model Domain

The total depth of the domain was 8 m, conservatively below the "zero flux plane", which is an imaginary plane above which water can move upward due to evaporation but below which water moves downward only. Node spacing near the surface was made smaller (e.g. 0.3 cm) to facilitate an accurate solution under conditions of large and rapid changes of soil water pressure potential in response to evaporation and precipitation. Node spacing at other depths were set to be progressively larger (e.g. 0.4 to 4 cm) to reduce model run time.

Hydraulic Properties

Average waste rock material hydraulic parameters were developed from a database of waste rock material saturated hydraulic conductivity and moisture retention data compiled by GeoSystems Analysis, Inc (GSA). The materials were chosen to represent coarse, high permeability material in order to provide a conservative estimate of percolation. Geometric mean K_s and van Genuchten (1980) hydraulic properties used for the simulation are provided in Table 1.

The soil water pressure potential at which macropores and the soil matrix partition (ψ_b) varies in the literature. Schaap (2005) suggested $0 > \psi_b \ge -4$ cm, while Jarvis (2007) reported the range $-6 \ge \psi_b \ge -10$ cm based on his literature review. At matric potentials above the partition point (less negative), K(θ) can increase by up to several orders of magnitude (e.g., Poulsen et al., 2002). To error on the side of greater macropore flow, a conservative ψ_b of -10 cm was assigned.

The hydraulic parameters needed to describe micro- and macropore flows as defined in equations 1 through 3 are presented in Table 1. K_b (soil matrix saturated hydraulic conductivity) applied in equation 2 and the kinematic exponent (n*) listed in equation 3 were established from previous work in which equations 1 through 3 were fit to moisture retention and unsaturated hydraulic

conductivity measurements made on two waste rock samples (Keller et al., 2009). Based on the similarity of the fine earth fraction (<4.75 mm) for the Keller et al. (2009) sample and the database samples, K_b was assigned as the estimated unsaturated hydraulic conductivity of the Keller et al. (2009) sample at -10 cm (1.06×10^{-4} cm/sec) and n* was set equal to 2.4, the average of the Keller et al. (2009) measured values of 2.0 and 2.8. The modified van Genuchten soil water retention function and hydraulic conductivity function used in the simulations are presented on Figure 1.

Table 1 Waste rock material van Genuchten parameters

K_s (cm/sec)	α (cm^{-1})	n (-)	θ_r (cm^3/cm^3)	θ_s (cm^3/cm^3)	Ψ_b (-cm)	θ_b (cm^3/cm^3)	K_b (cm/sec)	n* (-)
4.50×10^{-2}	0.131	1.911	0.048	0.315	10	0.215	1.06×10^{-4}	2.4

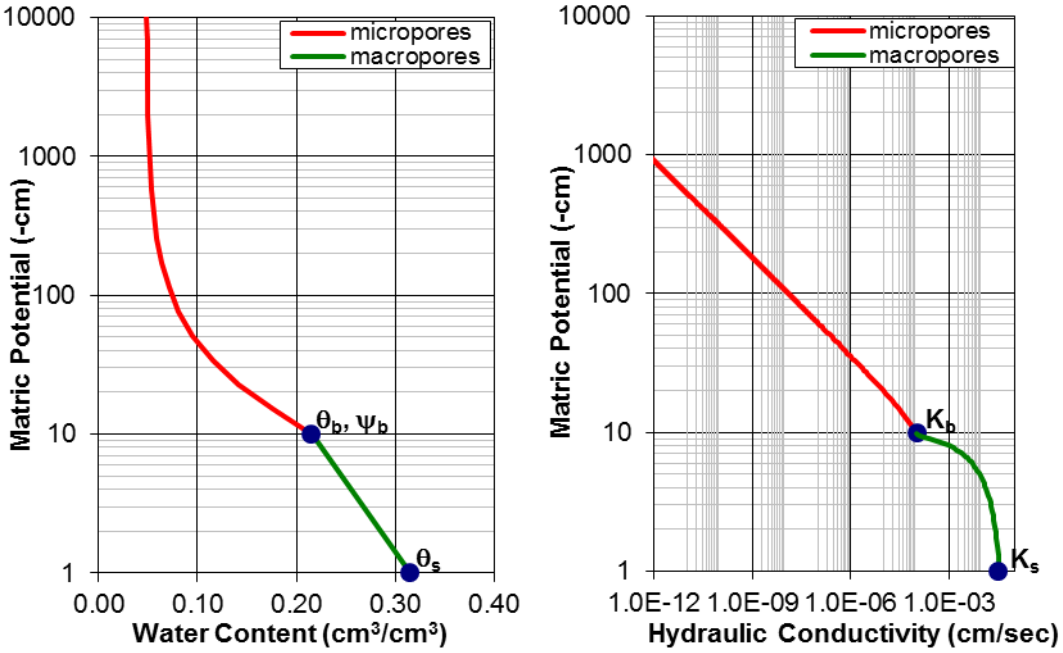

Figure 1 van Genuchten soil water retention function (left) and hydraulic conductivity function (right)

Climate Data

Synthetic daily 100-year precipitation data for the project site developed from historical climate records was used as the precipitation data input for the simulation. For the synthetic 100-year dataset, the maximum daily rainfall was 72 mm and the maximum annual rainfall was 192 mm. Hourly rainfall data was generated from daily rainfall data by assigning rainfall durations from one to twenty-four hours for each day and dividing the daily rainfall amount by the assigned rainfall duration. Rainfall durations were assigned using a random generator with the assumption of an even distribution of rainfall durations. Hourly rainfall intensities ranged from a high of 15 mm to less than 1 mm, with the majority of hourly rainfall intensities being less than 1 mm. This range of rainfall intensities is similar to measured rainfall intensities, which ranged from 29.3 mm/hr to 0.9

mm/hr for rainfall durations of 1 to 24 hours and reoccurrence intervals of 5 to 1000 years. The calculated hourly rainfall for each day was applied beginning at the first hour of the day and applied at each subsequent hour until the daily rainfall amount was satisfied.

Average daily temperature (maximum and minimum) and potential evapotranspiration (PET) required as model input were derived from a 3.25 year temperature and PET data record collected at the project site weather station. The applied sinusoidal annual temperature and PET relationships are shown on Figure 2.

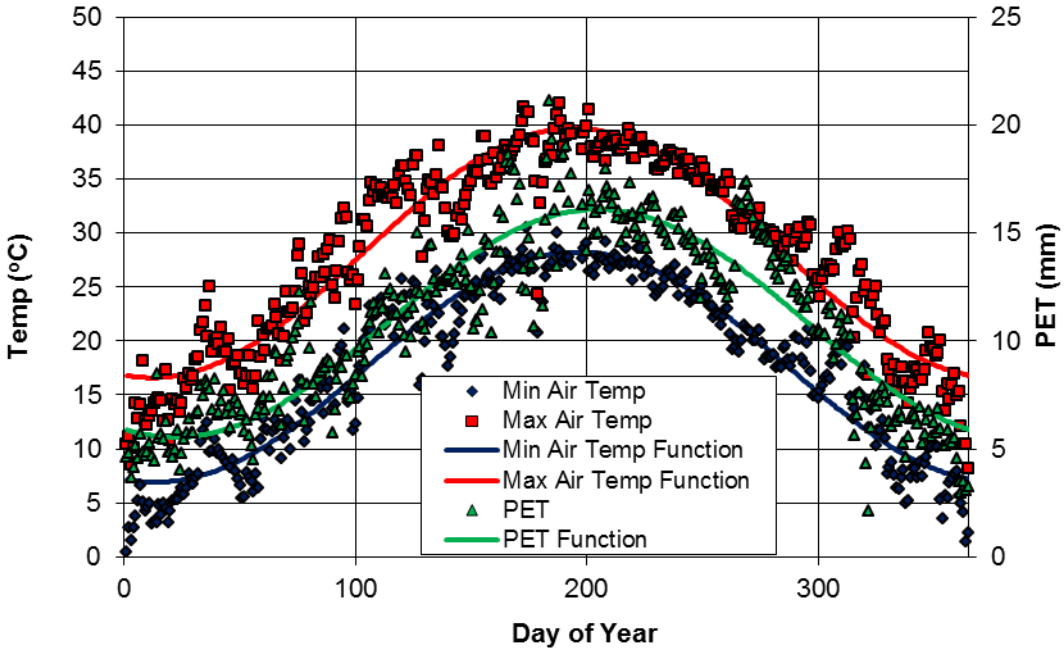

Figure 2 Measured average minimum and maximum air temperature and PET and sinusoidal functions applied in the model

Runoff Estimate

MACRO 5.1 does not model runoff but instead assumes all precipitation either evaporates or infiltrates into the soil micro- and macropores. Not considering runoff could potentially lead to a significant over prediction of deep percolation. As an alternative, the SCS runoff curve number method (USDA, 1986) was used to estimate runoff. The SCS runoff curve number method provides an estimate of runoff depth (*RO*) using the empirical relationship:

$$RO = \frac{(P - 0.2S)^2}{P + 0.8S} \qquad (5)$$

where *P* is rainfall and *S* is equal to 1000/*CN* – 10. *CN* is the curve number whose major factors are hydrologic soil group, cover type, and surface treatment. *CN* values obtained from USDA (1986) for newly graded, nonvegetated areas ranged from 77 for soils with high infiltration rates (hydrologic soil group A) to 91 for soils with low infiltration rates (hydrological soil group C). A CN value of 77 was assigned considering that the waste rock material will be relatively coarse. Estimated daily runoff was subtracted from the precipitation for that day and this modified precipitation amount (or net precipitation) was used as the daily precipitation input for the model.

Boundary and Initial Conditions

The upper boundary was set to allow evaporation while receiving hourly precipitation input. The lower boundary was set to allow free drainage (unit gradient flow). Given the arid conditions at the project site, it was assumed that the waste rock will be laid down at a very dry moisture content equivalent to a pressure head of -40,000 cm (approximating the permanent wilting point for desert plants), which is equivalent to a water content of 0.049 cm^3/cm^3. This initial water content was uniformly applied over the model domain.

Waste Rock Dump Geometry and Estimated Waste Rock Dump Outflow

The design of both dumps consists of three lifts. In order to estimate infiltration into, and outflow from the entire waste rock dump, each dump was mimicked by three columns. Each column represented the cumulative height (L) of the dump bench and the surface area (A) of the bench, as depicted on Figure 3. Column (i.e. bench) height and surface area and total dump waste rock volume are provided in Table 2. The column representation of the waste rock piles was relatively accurate, though slightly overestimated the design volume by 4 to 5 percent.

Table 2 Column (bench) height, surface area, and total dump waste rock volume

Dump	Column	Height (m)	Area (m^2)	Waste Rock Volume (m^3)
	1	60	2,085,224	
Higher	2	120	1,833,968	2,609,465,039
	3	180	12,579,308	
	1	24	1,075,843	
Lower	2	84	1,048,152	390,921,729
	3	144	1,924,005	

The model predicted average deep percolation rate and average water content increase at 8 m below ground surface (bgs) was then used to calculate the cumulative percolation volumes that exit the bottom of the dump. The percolation volume (Q) exiting the dump as a function of time was calculated and summed using:

$$Q(t) = \sum_{i=1}^{n+1} Q_i(t) = \sum_{i=1}^{n+1} \cdot q_i(t) \cdot A_i \qquad (6)$$

where t is time, q is the model predicted deep percolation rate at the bottom of column i, and A is the area of the dump with a thickness equal to column i.

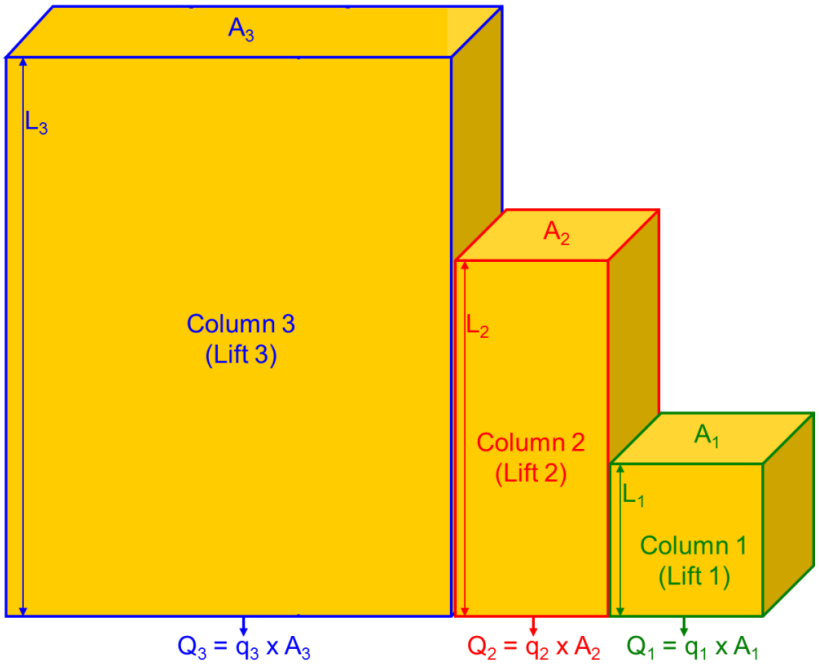

Figure 3 Hypothetical dump geometry consisting of three column heights

RESULTS AND DISCUSSION

Simulation of Waste Rock 100-Year Water Balance

The 100-year model predicted deep percolation, defined as the predicted percolation at 8 m bgs, and water content at 8 m bgs are presented on Figure 4. The simulated water balance is presented in Table 3. The large evaporative demand of the arid climate results in evaporation of the majority of precipitation (70%). Twenty percent of precipitation is predicted to become deep percolation with the remaining 10% of precipitation mass going to runoff or storage.

Arrival of the leading edge of the wetting front at 8 m bgs occurs at approximately 20 years as depicted by a sharp increase in water content (Figure 4). There is an approximate 4 year lag time before first arrival of the wetting front and the beginning of deep percolation, during which time the water content increases until reaching the water holding capacity of the waste rock material. After deep percolation begins, moisture content and percolation rate display moderate perturbations in response to arrival of water pulses stemming from larger precipitation years. From the onset of deep percolation to simulation year 100 the average deep percolation rate is 8.5 mm/yr (2.7×10^{-8} cm/s). The average water content during this same time period is 0.078 cm^3/cm^3, representing a 0.029 cm^3/cm^3 increase from initial water content conditions.

Table 3 Model predicted 100-year water mass balance at 8 m bgs

Total Precip (mm)	Total Runoff		Storage		Total Evaporation		Total Percolation	
	mm	% Precip	mm	% Precip	mm	% Precip	mm	% Precip
3191	117	4%	186	6%	2218	70%	654	20%

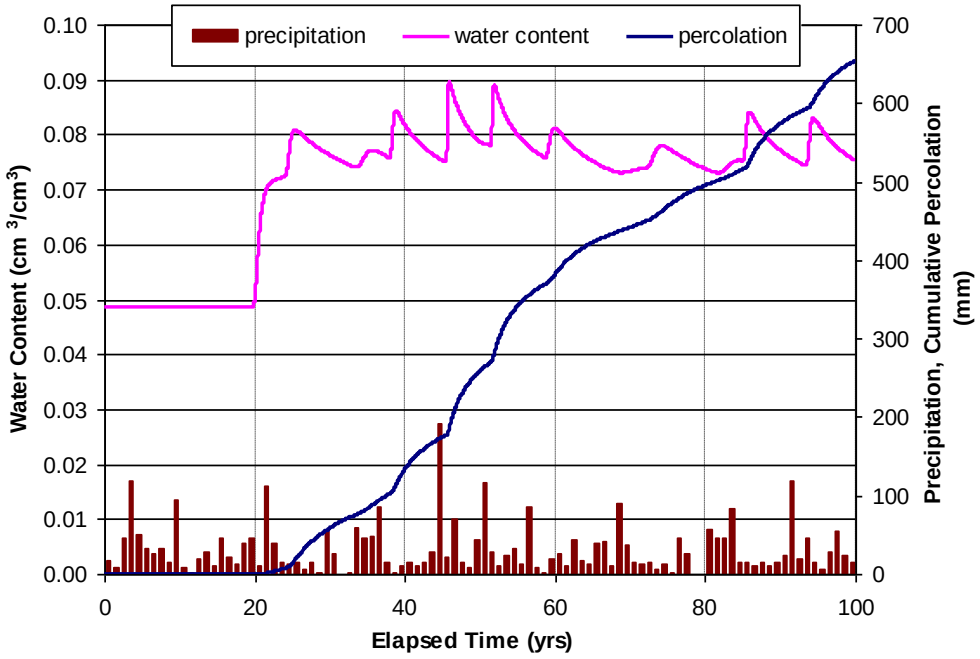

Figure 4 Precipitation and model predicted water content and percolation at 8 m bgs

Predicted Long-Term Outflow Volumes for the Waste Rock Dumps

Long-term percolation volumes from the base of the higher dump and lower dump waste rock columns were estimated from the model predicted average deep percolation and associated change in water content at 8 m bgs. Using a 60 m waste rock column as an example, to increase the waste rock water content by 0.029 cm^3/cm^3, such that deep percolation can occur, is equivalent to adding 1.74 m of water to the 60 m column. Based on an estimated average deep percolation rate of 8.5 mm/yr, the addition of 1.74 m of deep percolation would take 204 years, at the end of which the average percolation rate at 60 m bgs will be 8.5 mm/yr. This calculation was performed for each column and cumulative dump outflow calculated using the profile surface area and Equation 6. Like the model simulations, the calculation of long-term dump outflow assumes one-dimensional flow under homogeneous material conditions. The calculation also assumes that the 100-year synthetic climate record used in the simulation continues for subsequent centuries.

Figure 5 presents estimated cumulative dump outflow over a 750 year period, and dump outflow rates for the higher dump and lower dump. For the higher dump, outflow from the lowest 60 m lift at the average percolation rate is predicted to begin 204 years after placement of waste rock with outflow from the 120 m column 408 years after dump placement. Maximum drainage from the higher dump is predicted to begin 612 years after placement of the waste rock, at which time the dump outflow attains a predicted flow rate of 4.5 l/sec (71 gal/min). Outflow from the lower dump is predicted to begin 82 years after placement of waste rock from the lowest lift with a doubling of flow 286 years after dump placement in response to deep percolation from second lift. Maximum drainage from the lower dump is predicted to occur 490 years after dump placement, with the outflow rate reaching 1.1 l/sec (17 gal/min).

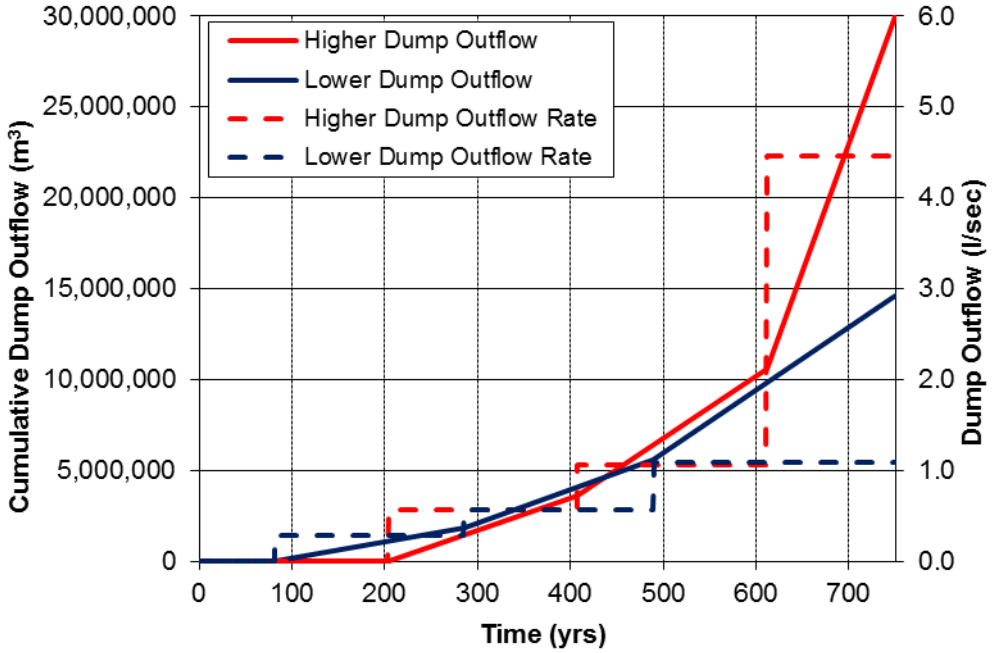

Figure 5 Predicted cumulative outflow and outflow rate.

CONCLUSION

The modeling results demonstrate that the large evaporative demand results in minimal deep percolation and a long delay from the time of waste rock dump placement to the beginning of outflow from the dump. An increase in water content from initial conditions (0.049 cm^3/cm^3) to 0.078 cm^3/cm^3 is predicted to occur before dump outflow begins. For the higher dump, outflow from the dump is predicted to begin 204 years after dump placement and reach a maximum outflow rate of 4.5 l/sec (71 gal/min) 612 years after placement. Outflow from the lower dump is predicted to begin 82 years after dump placement and attain its maximum outflow rate of 1.1 l/sec (17 gal/min) 490 years after placement.

The dump outflow predictions are conservative due to the hydraulic property assignment assuming homogeneous coarse, high permeability material. Finer grained waste rock material will reduce deep percolation due to greater moisture retention and evaporation and also increase total moisture retention. Furthermore, textural contrasts within waste rock can dominate flow processes by promoting lateral spreading, thereby increasing the time for deep percolation to occur at depth.

Other factors contributing to the predictions being conservative are:

- The analysis assigned a conservative value for the soil water pressure potential at which macropores and the soil matrix partition, resulting in greater macropore flow and less evaporation.
- Airflow within waste rock dumps can act to redistribute water and increase evaporative losses which would also decrease deep percolation.

REFERENCES

Al-Yahyai, R., B. Scheffer, F. S. Davies, and R. Munoz-Carpena, 2006, Characterization of soil-water retention of a very gravelly loam soil varied with determination method, Soil Sci., 171 (2): 85-93.

Fayer, M. J., 2000. UNSAT-H Version 3.0:Unsaturated soil water and heat flow model: Theory, User Manual, and Examples. PNNL-13249, Pacific Northwest National Laboratory, Richland, WA.

GEO-SLOPE International Limited, 2002, Vadose/W user's manual. GEO-SLOPE International Limited, Calgary, Alberta, Canada.

Germann, P. F., 1985, Kinematic water approach to infiltration and drainage into and from soil macropores. Trans. ASAE 28:745-749.

Jarvis, N. J., 2007, A review of non-equilibrium water flow and solute transport in soil macropores: principles, controlling factors and consequences for water quality, European Journal of Soil Science, 58, 523-546.

Keller, J. M. Milczarek, S. Peng, T. Yao, and D. van Zyl, 2009, Characterization and Modeling of Macro-pore Flow in Heap Leach and Waste Rock Material. 8th ICARD, June 23–26, 2009, Skellefteå, Sweden.

Larsbo, M., S. Roulier, F. Stenemo, R. Kasteel, and N. Jarvis, 2005, An improved dual-permeability model of water flow and solute transport in the vadose zone, Vadose Zone Journal 4: 398-406.

Milczarek, M. A., D. van Zyl, S. Peng and R. C. Rice, 2006, Saturated and Unsaturated Hydraulic Properties Characterization at Mine Facilities: Are We Doing it Right? 7th ICARD, March 26–30, 2006, St. Louis MO. Published by ASMR, 3134 Montavesta Rd., Lexington, KY 40502.

Mualem, Y., 1976, A new model for predicting the hydraulic conductivity of unsaturated porous media. Water Resour. Res. 12:513522.

Peng, S., M. Milczarek, A. Graham, T. Yao, and J. Keller, 2009, Hydraulic Property Characterization and Unsaturated Flow Modeling for Two Gravelly Soils, submitted to Vadose Zone Journal.

Poulsen, T. G., P. Moldrup, B. V. Iverson, and O. H. Jacobsen, 2002, Three-region Campbell model for unsaturated hydraulic conductivity in undisturbed soils, Soil Sci. Soc. Am. J., 66,744-752.

Schaap, M.G. and M.Th. van Genuchten, 2006. A Modified Mualem-van Genuchten formulation for improved description of the hydraulic conductivity near saturation. Vadose Zone Journal, 5(1): 27-34.

Simunek, J., M. Sejna, M. Th. van Genuchten. The Hydrus-1D Software Package for Simulating the One Dimensional Movement of Water, Heat, and Multiple Solutes in Variably-Saturated Media. U.S.Salinity Laboratory,1998.

SoilCover, 2000. Soil Cover User's Manual, Unsaturated Soils Group, Department of Civil Engineering, University of Saskatchewan, Saskatoon, Saskatchewan, Canada.

United States Department of Agriculture, 1986, Urban hydrology for small watersheds, Technical Release 55, Natural Resources Conservation Service.

van Genuchten, M. Th., 1980. A closed form equation for predicting the hydraulic conductivity of unsaturated soils. Soil Sci Soc Am J, 44:892-898.

Verburg, K., P. J. Ross, and K. L. Bristow, 1996. SWIM v.2.1 User Manual. Divisional Report No130, CSIRO, Division of Soils, Australia, 77 pp.

Prediction of Seepage from a Platinum-Group Metals Tailings Storage Facility

Koovila Naicker and Keretia Lupankwa
Golder Associates, South Africa

ABSTRACT

The Platreef mineralized belt is located in the Northern Limb of the Bushveld Igneous Complex (BIC) in South Africa's Limpopo Province and hosts the highest concentration of Platinum Group Elements (PGE) and gold in Africa. The BIC comprises of the mafic-ultramafic Rustenburg Layered Suite (RLS) that is separable into five distinct compartments one of which is the Northern or Potgietersrus limb (length of 110km and a width of 15 km). The Critical Zone of the RLS is dominated by pyroxenite, anorthosite, norite and olivine- rich rocks and is characterized by regular layering of chromite and PGE-mineralization. The Platreef is correlated to the Upper Critical Zone with chromitites and PGE rich zones being direct correlates of the Upper Group 2 and Merensky Reefs. Sulphide minerals: Pyrrhotite [Fe_7S_8], pentlandite [$(Ni,Fe)_9S_8$], chalcopyrite [$CuFeS_2$], millerite [NiS], troilite [FeS], pyrite [FeS_2] and cubanite [$CuFe_2S_3$] occur in the BIC.

Geochemical characterisation conducted on the Upper Critical Zone lithologies involved static and kinetic testwork (by use of humidity cells) for ore, wall rock, waste rock and tailings material. The geochemical characterisation data was use to assess groundwater impacts from the proposed Tailings Storage Facility (TSF) from the Project.

Selected ore, hanging wall and footwall units or 28% of samples representing the underground mine unit classified as likely (sulphide sulphur >0.3% and Net Potential Ratio <1) acid generation potential. The Platreef Rougher tailings material was found to be non-acid generating due to low sulphide-sulphur content (0.015%). Humidity cell tests (HCT) results indicated low metal loading rates for tailings and rock samples after two weeks. Seepage mass load ranges were modeled as a function of tailings material properties, Goldsim water balance and HCT results and used as source-term input in the solute-transport model to assess impacts to the groundwater regime.

Keywords: Bushveld Igneous Complex, platinum tailings, humidity cell, source-term; groundwater

INTRODUCTION

A geochemistry prefeasibility study was conducted to assess the risk of Acid Rock Drainage (ARD) and Metal Leaching (ML) associated with a PGE project, as part of the Environmental and Social Impact Assessment. The proposed Tailings Storage Facility (TSF) presents unique specific water quality risks during operational and post closure phases of the TSF, partly associated with the ARD/ML potential of the tailings material. The geochemistry study aimed to quantify these risks based on the Goldsim TSF water balance, static and kinetic (humidity cell test - HCT) results from laboratory generated tailings material. The source-term developed for the proposed TSF was used as inputs in the Feflow solute transport model.

BACKGROUND

The Project includes a recently discovered underground deposit of thick PGE-nickel-copper-gold mineralization, in the Northern Limb of the Bushveld Igneous Complex (BIC). The PGE deposit will be extracted using conventional underground mining methods over a period of 30 years. Tailings material and residue (from the water treatment plant) will be produced at a rate of 3.81 million (dry) tpa.

Geology

Archaean rocks belonging to the western end of the Pietersburg Greenstone Belt and associated granitoid gneisses constitute the oldest rocks (3.6 -2.5 Ga) in the area surrounding the Project and include:

- Goudplaats- Hout River Gneiss Suite: banded migmatitic gneiss with leucocratic to dark-grey granites and pegmatites;
- Turfloop Granite: Fine to medium grained, grey and pink granodioritic /monzogranitic;
- Lunsklip Granite: Medium to coarse grained or porphyritic pink to grey syenogranite; and
- Uitloop Granite: Medium grained to porphyritic reddish alkali granite.

The Transvaal sequence overlies the Archaean basement greenstones and granitoids to the east. The BIC intrudes the Transvaal Supergroup and is the world's largest mafic layered intrusion (Cawthorn and Boerst , 2006). The BIC is subdivided into three suites namely, the mafic-ultramafic Rustenburg Layered Suite (RLS), the Lebowa Granite Suite and the Rashoop Granophyre Suite (Figure 1). According to (Cawthorn and Boerst, 2006), the RLS typically consists of the following zones from bottom to top:

- The Marginal Zone: Comprised of generally finer grained rocks and contains abundant xenoliths of country rocks. The main rock type is norite. This unit is not always present.
- Lower Zone: Dominated by pyroxenite and harzburgite. Completely absent in some areas.
- Critical Zone: Dominated by pyroxenite, anorthosite, norite and olivine- rich rocks. It is characterized by regular rhythmic layering of cumulus chromite and PGE mineralization.
- Main Zone: Consists of norite and gabbronorite, minor mottled anorthosite and pyroxenite.

- Upper Zone: consists of magnetite gabbronorite, olivine-magnetite gabbronorite and olivine-apatite diorite. It is characterized by vanadium mineralization.

The RLS is separable into five distinct compartments known as the Western Limb, the far- Western Limb, the Eastern Limb, the Northern or Potgietersrus limb and the Southern Limb. The northern limb is a slightly sinous, north-west striking sequence of igneous rocks (dip 40º to 45º W) with a length of 110km and a width of 15 km (Kinnard, 2004).

The RLS hosts major deposits of PGEs, chromite ($FeCr_2O_4$), vanadium (V) and nickel (Ni), with minor copper (Cu), gold (Au) and silver (Ag) mineralization. The PGEs (mainly platinum [Pt] and palladium [Pd]) are hosted in three major mineralized horizons, namely: Upper Group 2 (UG2) chromitite and Merensky reef in the Critical Zone of the western and eastern limbs; and the Platreef of the northern limb (Cawthorn and Boerst 1999).

Six separate mineralized zones occur throughout the Upper Critical Zone of the Project. Cyclic units T1M and T2 are the best developed and show good continuity. The other mineralized zones contain erratic mineralization and disrupted continuity. Much thicker than the normal Merensky Reef, the Turfspruit T1M and T2 ore zones are much less affected by contamination from sedimentary xenoliths than most of the other units in the footwall. The Pseudo and UG2 Reefs found stratigraphically below the TCU usually are less continuous, being disrupted by sedimentary xenoliths and associated contamination/alteration. Sulphide minerals that occur in the BIC include, Pyrrhotite [Fe_7S_8], pentlandite [$(Ni,Fe)_9S_8$], chalcopyrite [$CuFeS_2$], millerite [NiS], troilite [FeS], pyrite [FeS_2] and cubanite [$CuFe_2S_3$] Schouwstra and Kinloch, 2000.

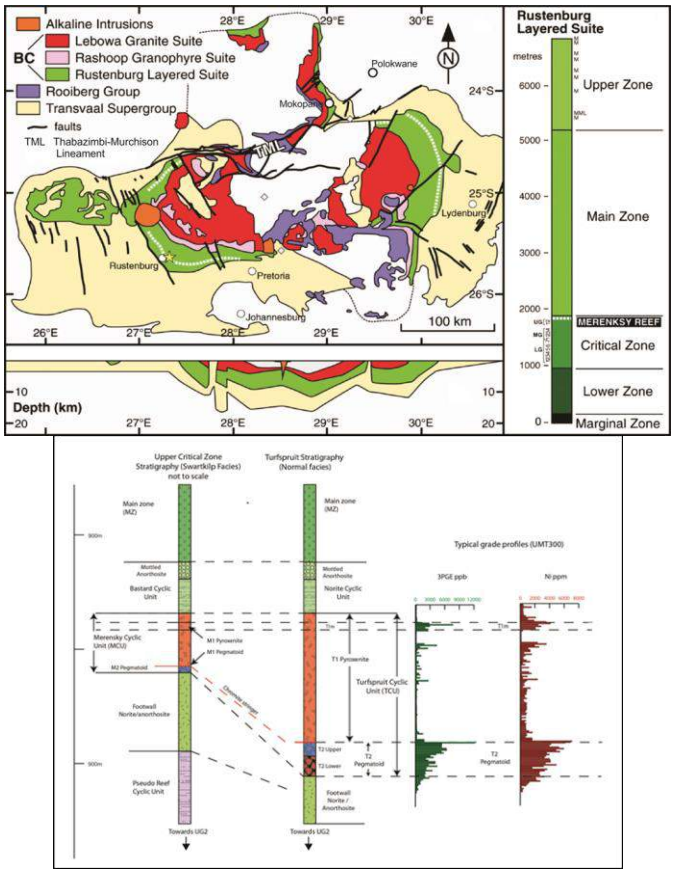

Figure 1 a) Simplified geological map of the BIC showing RLS b) Revised stratigraphy for the Project area

The stratigraphic sequence in the Project area have been revised following a recent discovery of a cyclic magmatic (Figure 1b) sequence consists of apparently uncontaminated pyroxenite, harzburgite, and dunite in the upper part of the Platreef (Grobler et al., 2012). This sequence has been termed Turfspruit Cyclic Unit (TCU) and correlated to the Upper Critical Zone of the Western and Eastern Limbs. Mineralization in the TCU shows generally good continuity and is confined to pegmatoidal orthopyroxenite and harzburgite.

In the project area, sulphides occur typically as disseminated grains, varying in size from a 5 μm to 2 cm blebs. The blebs occur mainly in serpentinized peridotite and calc-silicate rocks. The base metal sulphides also occur in places as intergrowth with secondary silicates (alteration assemblages dominated by talc, tremolite and serpentine) and in secondary hydrothermal veins traversing primary or secondary silicates.

Climate

The project area is situated in the Central Bushveld bioregion in the South Africa, with an altitude of approximately 1100 m above mean sea level. The project area lies within a water scarce region. The available information indicates only 10.5 years of combined rainfall data from weather stations in the area. The area falls in a summer rainfall climate region with the peak rainfall period from November to February when the area receives ~70% of the annual average rainfall (Figure 1). The annual minimum and maximum temperatures are 13.0 ^{0}C and 26.3 ^{0}C (average temperature is 19.7 ^{0}C). The area falls in evaporation zone 1C (Midgely et al, 1990). The mean annual S-pan evaporation is 1 700 - 2 000 mm/a.

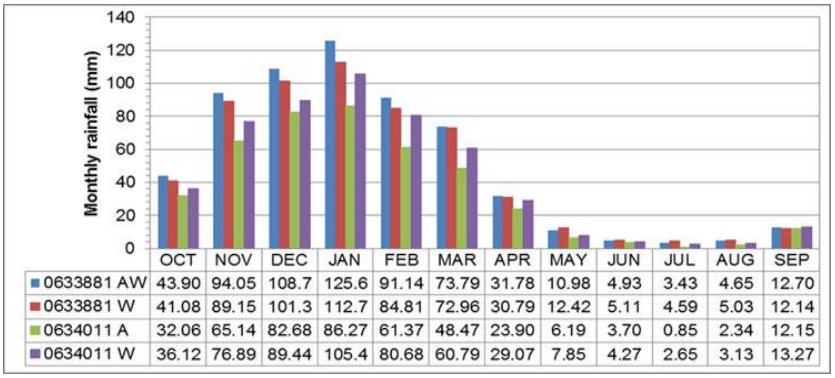

	OCT	NOV	DEC	JAN	FEB	MAR	APR	MAY	JUN	JUL	AUG	SEP
0633881 AW	43.90	94.05	108.7	125.6	91.14	73.79	31.78	10.98	4.93	3.43	4.65	12.70
0633881 W	41.08	89.15	101.3	112.7	84.81	72.96	30.79	12.42	5.11	4.59	5.03	12.14
0634011 A	32.06	65.14	82.68	86.27	61.37	48.47	23.90	6.19	3.70	0.85	2.34	12.15
0634011 W	36.12	76.89	89.44	105.4	80.68	60.79	29.07	7.85	4.27	2.65	3.13	13.27

Figure 2 Average monthly rainfall for rainfall stations in study area

Water Balance

A water balance model for the proposed TSF was constructed in Goldsim on a daily time step. Gauge number 0633881 (MAP=572 mm) was used. Runoff factors were informed by average runoff for the quaternary catchment (Middleton et al., 2009). Design criteria for the TSF, used in the water balance modeling are summarized in Table 1. The simulated water balance results are provided in Figure 3 and that water balance is a deficit water balance.

Table 1 Design criteria for proposed TSF

Parameter	Design Specifications
Total storage capacity	135 000 000 tonnes (over 36.5 years)
Deposition rate	3 800 000 dry tonnes/annum
Footprint area	250 ha (Basin area 203 hectare)
Slurry density	50% solids by mass
Tailings SG	3.13
Deposition method	Spigot
Decant method	Barge

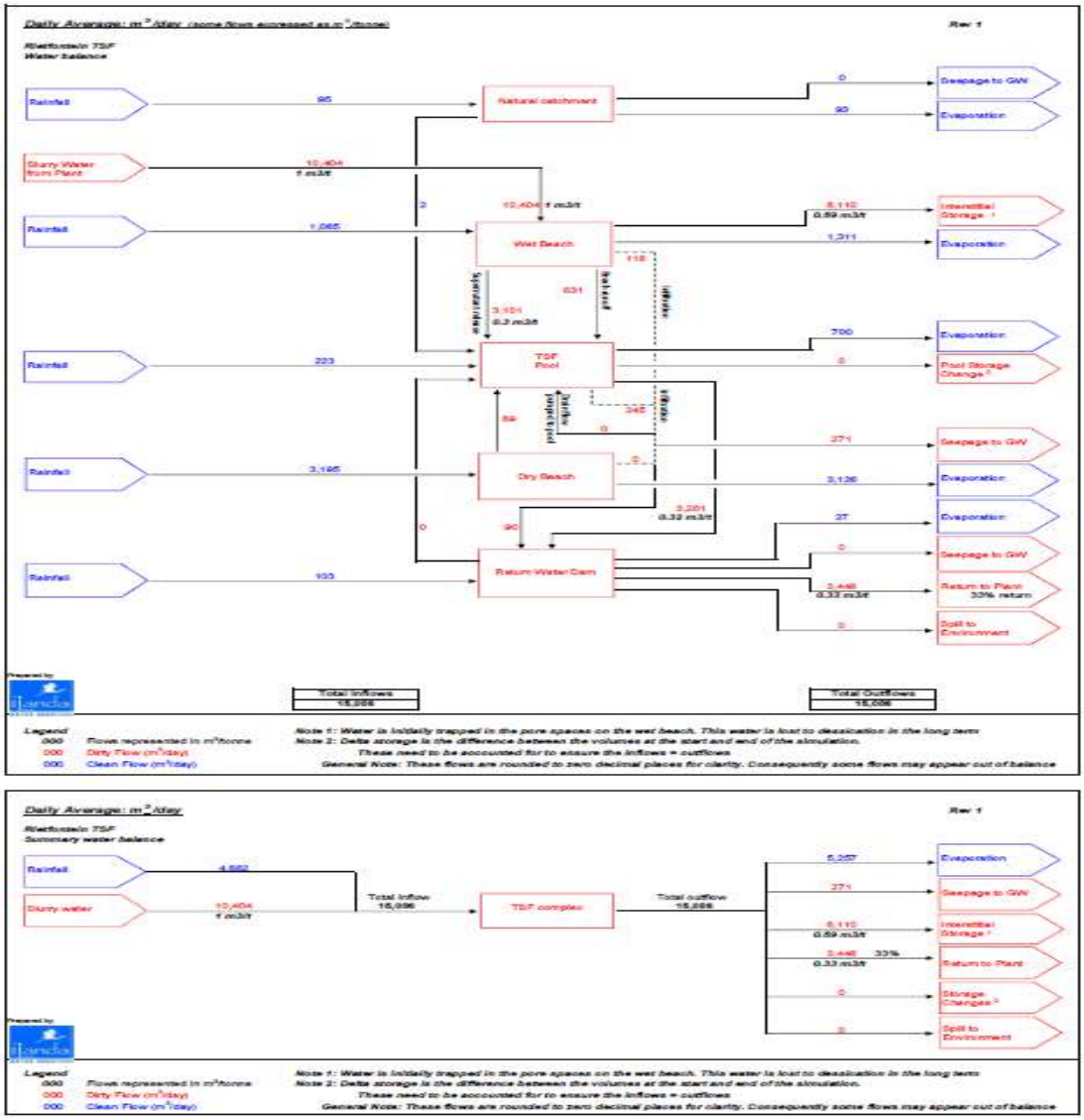

Figure 3 TSF water balance diagram

TAILINGS MATERIAL CHARACTERISATION

Rougher tailings material was received from a scoping study batch test done on a composite sample representing the current LOM blend: 15%T1; 42.5%T2U and 42.5%T2L. The Rougher tailings sample comprised 90-95% of the final tailings material. Metallurgical lock cycle test results for the final tailings indicated; particle size distribution of 80% passing 75µm and total S (0.25%), Cu (0.06%) and Ni (0.14%) concentration. The assay results for the Rougher tailings (open circuit) sample decreased by half for S, Cu and Ni. The assumption that the Rougher tailings sample tested is representative of the final tailings that will be produced is unknown and represented a limitation of the geochemical prefeasibility assessment.

Static Results

Acid base Accounting

Acid Base Accounting (ABA) results for the Rougher tailings sample is provided in Table 2. The circum-neutral paste pH (6.8) indicates the short-term pH of pore fluid in the sample and correlates with the low sulphide-sulphur (0.015%) concentration recorded.

Table 2 ABA results for Rougher Tailings

Parameter	Unit	Value
Paste pH	-	6.8
Total C	%C	0.16
Total S	%S	0.10
Sulphide-S	%S	0.015
Sulphate-S	%S	0.020
Neutralization Potential (NP)	kg $CaCO_3$eqv/t kg	5.99
Sulphide Acid Potential (SAP)	kg $CaCO_3$eqv/t kg	1.56
Sulphide Neutralizing Potential Ratio (SNPR)	ratio	3.84

X-Ray diffraction

Table 3 summarizes the mineralogical composition of the Rougher tailings. Silicate minerals dominate the tailings mineralogy and is consistent with the Platreef geology which is mainly mafic-ultramafic rocks, consisting of > 90% mafic minerals (enstatite, diopside, augite, actinolite, lizardite, biotite, chlorite) and anorthosite, which is felsic. Pyrite and/or pyrrhotite were not detected due to the limit of detection (<0.5%)

Table 3 Mineralogical composition (wt%) results of Rougher tailings material

Weathering Rate[1]	Mineral Name	Formula	Rougher Tailings (%)
Fast Weathering	Biotite	$KMg_{2.5}Fe^{2+}_{0.5}AlSi_3O_{10}(OH)_{1.75}F_{0.25}$	12
	Chlorite	(Mg,Fe2+)5Al(Si3Al)O10(OH)8	6.7
	Diopside	$CaMgSi_2O_6$	6.2
Intermediate Weathering	Enstatite	$Mg_2Si_2O_6$	45
	Actinolite	Ca2(Mg,Fe2+)5(Si8O22)(OH)2	5.3
Slow weathering	Lizardite	$Mg_3(Si_2O_5)(OH)_4$	3.6
	Talc	$H_2Mg_3(SiO_3)_4$	13
	Plagioclase	Na,Ca)(Si,Al)$_4O_8$	7.8
Resistant	Quartz	SiO_2	0.93

[1] *after SRK, 1989; Sverdrup, 1990; SRK, 1998*

Whole rock analysis

The extent of element enrichment in Rougher tailings was assessed with the aid of the geochemical abundance index (GAI), which compares the measured concentration of a particular element with the estimated median crustal abundance (INAP, 2010). Elements with a GAI value ≥ 3 (12 to 24 times the median crustal abundance) included Cr, Pt, Mo and Te and are of potential contaminants of concern (PCOC) in the tailings material.

Supernatant Analysis

The supernatant (process) water of the Rougher Tailings sample was separated from the tailings solid for analysis. The supernatant was found to have alkaline pH (8.52) and TDS of 202 mg/l. Chemical constituents contributing to the dissolved salt load included Cl, Alkalinity, NO_3, SO_4, Ca, Mg, Na, K and Si. Trace metals that are likely PCOC are B, Ba and Mo (concentrations > 0.1 mg/l). The dissolved Mo concentration (0.25 mg/l) observed for the tailings supernatant was in the same order as the distilled water leach (0.13 mg/l) and acid leach Mo (0.66 mg/l) concentration.

Kinetic Results by humidity cell method

The ASTM D 5744-96 method (Standard test method for accelerated weathering of solid material using a modified humidity cell) covers the procedure that accelerates the natural weathering rate of geologic materials. For the initial (week 0) flush 750 ml of distilled water was used according to MEND (2009) HCT method. The HCT (week 0) TDS was recorded as 423 mg/l (Figure 4a) and decreases in first two weeks due to the flushing of historically oxidized ARD and weathering products. Loading rates of major and trace metals followed the same trend and thereafter varied slightly with small changes in pH, due to solubility changes. An increase in the week 12 Ni loading (Figure 4b) can be expected as Ni is released as pentlandite is oxidized/weathered.

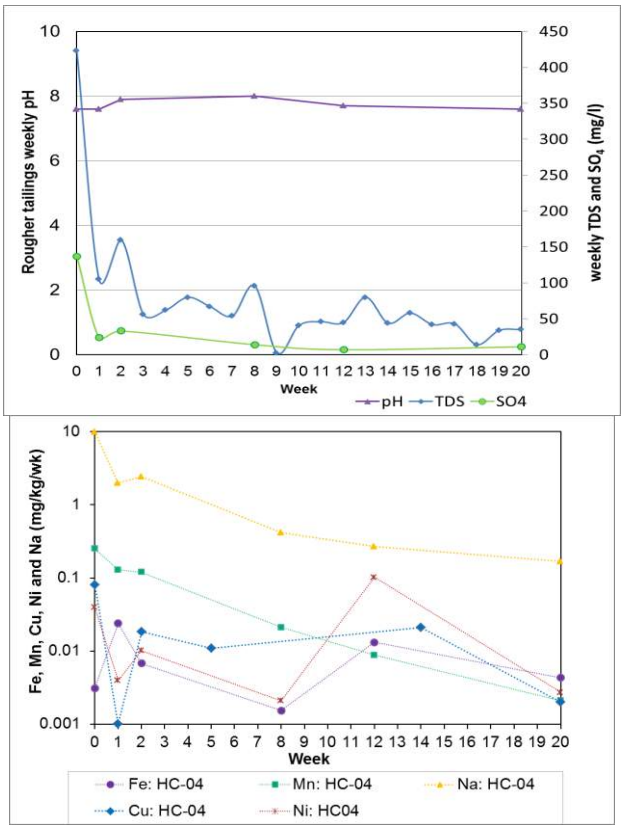

Figure 4 Rougher tailings HCT results: a) Variation of pH, TDS and SO_4 b) Weekly loadings Fe, Mn, Cu, Ni and Na

TSF SOURCE-TERM DEVELOPMENT

The TSF source-term model consisted of two key components: a flow module and a geochemical module supported by the TSF water balance and humidity cell results.

Flow Module

The water balance simulations of the average seepage to ground water (271 m^3/day, Figure 3) provided guidance on the average vertical seepage emanating from the base of the proposed TSF. Staged development curves (tonnes/area)) for the proposed TSF was sourced from the TSF capacity design analysis. The pool and wet beach seepage volumes (low, likely and high case) were modeled dynamically; using the surface area at the time of calculation.

The modeled seepage volume from the TSF base and entering groundwater is provided in Figure 5a-b. The predicted seepage volumes under post-closure are significantly lower than during operational phase. Seepage from the TSF at post-closure is driven by rainfall infiltration (unsaturated flow processes) and evaporation. The following assumptions were made for the flow module:

- Dry conditions are expected for the dry beach and TSF wall resulting in runoff (only and no seepage flow contribution from these areas. The assumption is based on the water balance model that assumed that no deposition occurs on the dry beach;
- The saturated conditions at the pool section are associated with the permanent head of water at the pool and moist conditions associated with the wet beach. In practice, the wet beach moves as the deposition location changes resulting in higher infiltration losses and a gradual increase in return water followed by a sudden reduction;
- The pool (and wet beach) area varies from 2-5% (average case 2.4%) of the total area, after evaporation effects. Seepage from pool and wet beach was calculated by applying the Darcian equation with K= $1e^{-7}$ m/s (based on laboratory measurements on final tailings – fine fraction);
- The calibrated groundwater flow model provided the average recharge of 1% or $1.24e^{-05}$ m/d based on average low aquifer transmissivities ~$1.0x10^{-3}$ m^2/d in the Turfloop Granite underlying the TSF site The contact zone between diabase dykes and the host Turfloop Granite rocks at the TSF site, are clayey and non-water bearing thus assumed not to be a conduit;
- It is assumed that approximately 95% of the vertical seepage is captured by the under drainage seepage collection system. and downstream cut--off drains.; and
- The recedence of the phreatic surface was assumed to be 10 years. For closure to post-closure phases, infiltration rates of 0.5-1.5% MAP (without cover) were assumed for the dry TSF.

Geochemical Module

Kinetic testing (HCT method) is not a direct indication of on-site drainage chemistry but simulates accelerated metal-mine waste material weathering rates. The difference between actual field conditions and HCT can differ by at least an order of magnitude. Liquid to solid ratios were used for field scaling evaporation in the project area is high.

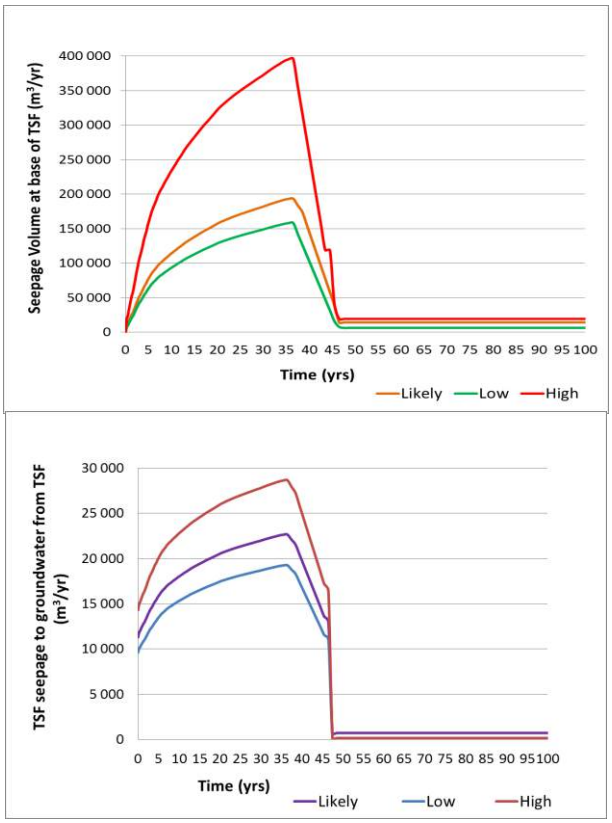

Figure 5 Modeled seepage flow volumes a) from the base of proposed TSF b) entering groundwater

Equilibrium-speciation modeling assessed mineral solubility controls on the weekly HCT seepage under oxidizing conditions (pe 2-5) and gas equilibration). Ferrihydrite - $Fe(OH)_3$ and Gibbsite - $Al(OH)_3$) were found to control dissolved Fe and Al concentrations in the seepage. The following assumptions were made for the geochemical model and source-term development:

- Operational input seepage qualities were assumed to remain constant over time i.e. the measured supernatant TDS of 202 mg/l was used without considering evaporation and recirculation effects;
- Post-closure field capacity of 15-22% (average 20%) was assumed for scaling HCT data. The HCT utilized 500 ml deionized rinse water weekly (except week 0) for 1000 g Rougher tailings sample (1:2 liquid: solid ratio). Based in assumed field capacity the average weekly TDS concentration (77 mg/l, Figure 4a) was scaled up by factor 2.3, 2.5 and 3.3 for the low, likely and high case seepage TDS concentration;
- Salt depletion rate (~7%) was estimated from the week 0 (high case) TDS and 77 mg/l; and
- The TSF seepage quality interaction with the underlying weathered zone does not change the seepage quality that is reporting to the groundwater.

Seepage concentration and TSF source-term mass loading ranges to ground water is shown in Figure 6a-b. The sharp increase in the modeled post-closure high case TDS concentration (256 mg/l)

is based on the 15% m/m moisture content; and to a lesser extent from ARD products generated from trace sulphide minerals (0.015%) as phreatic surface recedes and the TSF dries out.

CONCLUSION

A source-term has been developed for platinum TSF by integrating; PFS engineering design, Goldsim model simulation results, and geochemical characterisation results. The source-term TDS concentration time series was input into the solute transport groundwater model to quantify impacts. Several assumptions were made during the geochemical assessment and source-term development; including limited representativeness of the final tailings, and need to be addressed in the feasibility assessment.

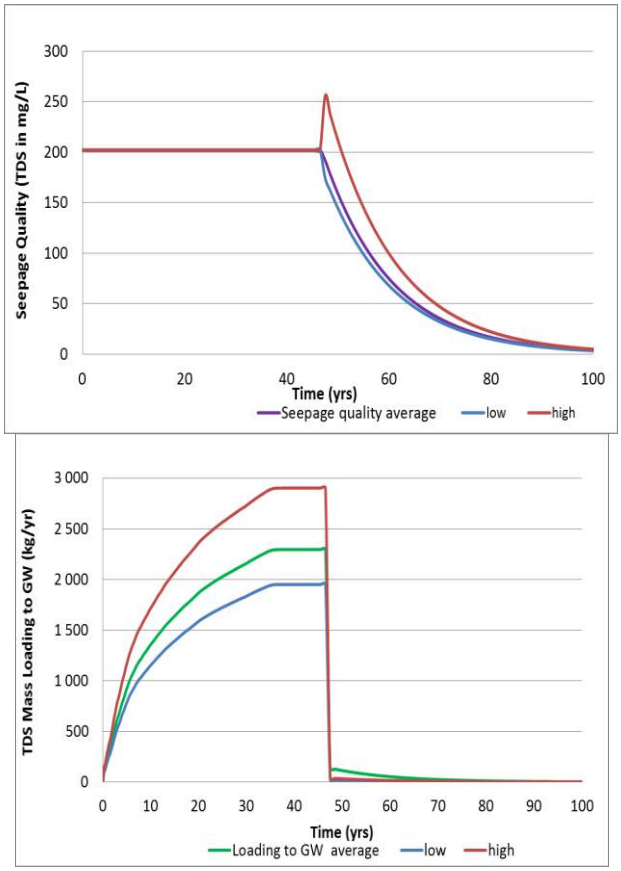

Figure 6 Proposed TSF source-term seepage a) TDS concentration and b) TDS mass loading ranges

REFERENCES

Cawthorn and Boerst, R.G., 1999. The Discovery of the Platiniferous Merensky Reef in 1924. SAJG, v. 102 (3), 178 – 183.

Cawthorn, R.G. and Boerst K., 2006. Origin of the Pegmatitic Pyroxenite in the Merensky Unit, Bushveld Complex, South Africa. Journal of Petrology, 47, 1509-1530.

INAP, 2010. International Network for Acid Prevention- Global Acid Rock Drainage (GARD) Guide. V 0.8. www.gardguide.com.

Kinnaird, J.A., 2004. An overview of the Platreef. Abstract Volume, Geoscience Africa, University of the Witwatersrand, July 2004 345-346.

Kinnaird, J.A. and McDonald, I., 2005. An introduction to the mineralization of the northern limb of the Bushveld Complex: Transactions of the Institution of Mining and Metallurgy, v. 114, B194-B198 .

Grobler, D.F., Nielsen, S.A., and Broughton, D. 2012. Upper Critical Zone (Merensky Reef-UG2) correlates within the Platreef on the Turfspruit 241KR, Northern Limb, Bushveld Complex: 5th Platreef Workshop. Mokopane, 9th – 11th November, 2012Schouwstra and Kinloch, 2000; Rose et al, 2011; van der Merwe et al, 2012).

Schouwstra R. P. and Kinloch E. D., 2000. A short Geological review of the Bushveld Complex. Platinum Metals Rev. No. 44, vol 1, 33-39.

SRK, 1989, Draft ARD Technical Guide, volume 1. British Columbia AMDTask Force (1985-90).

Sverdrup, H.U., 1990, The kinetics of base cation release due to chemical weathering: Lund University Press, Lund, 246.

Middleton, B.J. and Bailey, A.K., Water Resources of South Africa, 2005 study (WR2005), 2009. WRC Report No TT 382/08.

Midgley, D.C., Pitman, W.V., Middleton, B.J. Surface Water Resources of South Africa,1990. WRC Report No 298/2.1/94, Volume 1.

Resistivity Tomography with Hydraulic and Geotechnical Data to Conceptualize Weathered Hydrogeology

Paul Hubbard and Anthony Rex
SRK Consulting, United Kingdom

ABSTRACT

In low permeability metamorphic rock increased fracturing associated with weathering and fault zones can exert a significant control on shallow groundwater flow and solute transport. Formulating a detailed understanding of these structural and lithological controls is therefore critical for the development of a hydrogeological conceptual model for the weathered zone. Electrical resistivity tomography (ERT) is a shallow geophysical technique that can significantly aid fracture zone characterization; however the data needs to be integrated with other site investigation data for detailed interpretation.

In this study a hydrogeological conceptual model for seepage from a tailings facility in West Africa was developed through the integration of ERT with geotechnical and hydrogeological test data. This paper presents the results of geophysical, geological and hydrogeological investigation and interpretation to create a hydrogeological conceptual model for fracture flow in the shallow weathered zone. Fracture logging and vertical hydraulic data were found to be essential for fully interpreting the ERT data and the depth of the relatively permeable weathered zone. The depth of the fractured weathered zone at the site was found to be highly variable, which was considered to be a result of the anisotropy of the host rock. This variability in the depth of the weathered zone, combined with a complex fault zone geometry, led to a conceptual model with shallow 'weathered channels' and zones of fracturing influencing groundwater flow and solute transport.

In an area of sparse drill data the development of such a refined hydrogeological conceptual model would have not have been possible without the ERT interpretation. Thus, the ERT technique proved to be an effective method to characterise shallow weathered hydrogeology, but only when integrated with relevant geotechnical and hydrogeological field data. The benefits of this analysis have continued through to the follow-on saturated zone solute transport modelling and helped to inform the groundwater monitoring plan.

Keywords: hydrogeological conceptual model, resistivity tomography

INTRODUCTION

A combined hydrogeological, geophysical and geotechnical investigation was undertaken as part of an assessment of seepage impacts from a tailings facility. The main objectives of the project were to develop a groundwater model for predicting the potential for solute transport and to inform on-going monitoring and mitigation measures. To achieve these aims a hydrogeological conceptual model was needed that characterized the potential increase in flow in the shallow fractured zone, which was initially presumed to be located between 30m to 80m depth. This paper focuses on how Electrical Resistivity Tomography (ERT) combined with geotechnical and hydrogeological test data were used to characterise the depth and flow within the weathered zone as well as indicating potential flow boundaries from sub-vertical fault structures, thus improving our understanding of shallow groundwater flow at this site.

Hydraulic measurements in shallow, weathered horizons in metamorphic basement terrain can often provide highly variable results. Often this variability can be due simply to weathering profile heterogeneity or the presence of previously unidentified fault features. Improved conceptualisation of the weathered fractured zone can aid weathered layer definition and the general understanding of shallow flow at a site, which in turn informs hydraulic test interpretation, numerical model design etc.

The use of ERT as a rapid, cost effective tool in weathered hydrogeology is well documented (Krishnamurthy, Chandra, & Kumar, 2008; Singal, 2010; Elster, Holman, Parker, & Rudge, 2014). ERT sections can allow for a more detailed understanding of subsurface variations. However, the changes observed in the resistance can be the result of a number of factors such as lithology, structure or fluids, as well as interference effects, hence the sections must be interpreted with relevant ground data.

This paper describes how geotechnical logging of weathering, fractures and lithology, supported by hydraulic test data, can be used with ERT data to interpret the weathering profile. ERT sections were used to interpolate the base of the fractured weathered zone and the occurrence of faults. This data was used to significantly improve the hydrogeological conceptual model at a mine site scale.

BACKGROUND

The site

The site is situated in Saharan Africa in Archean rocks of the West African Craton basement. The regional geology comprises volcanic and volcanosedimentary rocks metamorphosed to greenschist to lower amphibolite facies. In the study area the main lithologies are steeply eastward dipping meta-basalts to the east and meta-volcanosedimentary/volcaniclastic sandstones and grits to the west. The lithological units strike north to south, with a similar north to south orientated, steeply east dipping foliation.

The dominant structural trend is also north to south in accordance with the main shear zone to the west, which hosts the mineralisation. Splay faults are typically observed near lithological contacts and later stage east to west orientated faults off-set lithological units. The area is cross cut by thin, north northeast to south southwest and west to east trending non-foliated mafic dikes.

The topography is peneplainal; very flat with the exception of the tailings facility. The area is void of surface water, with rare sharp torrential rainfall events leading to overland flow along dry river beds (Wadis) and localised flooding due to the clays in the upper soil.

The hydraulic gradient across the site is generally quite flat and only increases noticeably near the open pits. Seepage from the base of the tailings facility at the site has led to a slight rise in groundwater levels in the vicinity of the facility.

Packer tests had previously been conducted around the pit area as part of an earlier feasibility study. A low hydraulic conductivity was reported for the fresh basement of $1x10^{-9}$m/s to $1x10^{-11}$m/s. The hydraulic conductivity range for the shallow rocks was much more variable with values between $1x10^{-5}$m/s to $1x10^{-10}$m/s given for packer tests shallower than 80m depth. Based on the packer data no consistent depth range was apparent for the fractured weathered layer.

Groundwater in the area is generally very saline, with fresher water limited to the shallow alluvium found beneath the courses of larger wadi features at distance from the site. The tailings seepage water is also very saline and has no appreciable difference in salinity to the local groundwater (both have a total dissolved solid content in the range of approximately ~30g/l to 60g/l).

The weathered hard rock aquifer model

The typical model for hard rock weathered aquifers in crystalline systems has been described in various studies as a composite layered groundwater system, with layer permeability largely driven by the weathered condition of the rock (Wyns, Baltassat, & Lachassange, 2004; Lachassagne, 2008; Dewandel, 2006). Subvertical tectonic zones or brittle cooling zones from dikes can then create localised deeper zones of increased permeability within the fissured and basement layers. The principle layers of the composite weathered aquifer are described as:

Saprolite: a high porosity, low permeability, clay rich, oxidised layer often up to tens of metres in thickness, which can act as a major storage reservoir for the aquifer. The saprolite can be divided into two sub-units comprising an upper regolith and a lower more structured 'laminated layer'. If fractures are well preserved the base of the laminated layer may also exhibit increased tranmissivity (Dewandel, 2006);

Fissured layer: a layer of increased, open, sub-horizontal joints formed through weathering and decompression resulting in zones of high transmissivity. Typically, denser jointing is present in the upper part of the fissured (fractured) layer with a frequency of joints decreasing downwards as the layer transitions into fresh basement. In isotropic rocks such as granites, joints tend form parallel to topographic surface, whereas in highly foliated metamorphic rocks, such as the project site, joints will also develop along foliation planes;

Fresh basement: characterized by a low number of open fractures with negligible permeability except in tectonic or dike zones, and low storage.

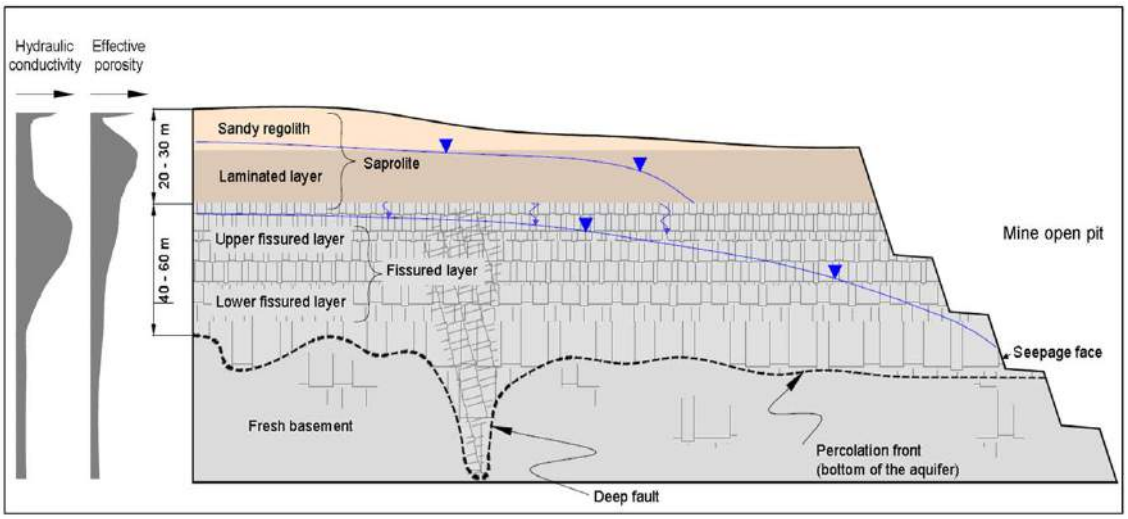

Figure 1 Idealised conceptual model of single phase weathered profile layers cross cut with a vertical fault zone, with dewatering under active mining conditions. Based on work by Wyns, Baltassat, & Lachassange, 2004; Dewandel, 2006; Elster, Holman, Parker, & Rudge, 2014 and SRK

The conceptual model for a weathered crystalline system for a single phase of weathering, with dewatering occurring through mining is shown in Figure 1. A multi-phase weathering model is described by Dewandel (2006) as leading to more variability in the weathered base and a reduced fractured layer thickness. Whilst this weathered hard rock model was generated based on crystalline/granite research, and has since been applied in weathered metamorphic systems e.g. (Courtois, Lachassagne, Wyns, & Blanchin, 2010), it is clear that foliation in metamorphic rocks may lead to more inclined joints.

FIELD METHODS

The hydrogeological characterisation of the study site was developed from existing data derived from nearby open pit studies, such as drill logs, packer test results, and water level measurements combined with additional field methods undertaken for this study. These included diamond core and down-the-hole hammer (DTHH) drilling with geotechnical and lithological logs; ERT geophysics; and airlift, rising head and constant rate pumping tests.

The main methods applied in this paper are discussed below:

Electrical resistivity tomography (ERT)

The electrical response of the earth is essentially influenced by porosity, saturation, fluid type, clay content and metal (sulfide) content. Therefore ERT (or electrical imaging) methods can be effective for weathering depth surveys as they can give a strong response to the high porosity and clay content in the saprolite. Additionally, in the case of the project site, the salinity of groundwater would be expected reduce the resistivity further in highly saturated zones.

ERT measurements are taken along an array of electrodes with the active electrode spacing increasing on each traverse to gain a greater penetration depth. ERT was selected for this investigation due to the need for additional, cost effective ground data, its ability to pick up sharp

lateral variations needed to identify fault systems, and the fact that the field work can be conducted rapidly with relatively low cost.

Relevant limitations of the ERT method include: suppression, which is the difficulty to clearly resolve thin bodies of a slightly higher resistivity below thicker low resistivity surface layers such as saprolite; non-uniqueness, which, for this study, could occur from saline seepage zones or clay rich saprolite zones both showing similar resistivities; and accurate resolution of smaller anomalies at greater depths, which for this study may affect the resolution of deeper faults.

The ERT sections were taken on the ground around the tailings facility and to the north and south of the tailings facility, perpendicular to structural trends. The lines were placed to avoid known structures with potential interference effects such as power lines, metallic fencing or pipes and active roads. Parallel sections were taken in some areas to aid structural interpretation. A dipole to dipole array of 96 electrodes was used with an electrode spacing of 10m to provide a maximum investigation depth of approximately 100m.

Geotechnical logging

Diamond-core drill holes were carried out directly along the ERT sections primarily to verify lithology and weathering against resistivity. Core was logged for lithology, weathering description, foliation, joints and fractures. Fracture parameters included dip, fill, aperture and roughness.

Hydraulic tests

Instability in the weathered zone required that core holes were immediately converted to piezometers without the opportunity to carry out spinner tests (impeller flow logging) as originally planned. Hydraulic tests were carried out in a later DTHH drilling programme designed to identify suitable well locations. The majority of these rotary boreholes were located using favourable geophysics results, whilst others were based on client preference and historic water quality data. Hydraulic measurements comprised drill-stem airlift (or blow yield), constant rate airlift tests and rising head tests; and in wells with sufficient flows, constant rate pumping tests.

RESULTS AND ANALYSIS

Interpretation of weathered layers

Core holes in the investigation area showed that the foliation of the rock mass was steeply dipping at between 60° and 70°. The dip of open joint planes in the weathered zone included both sub-horizontal and sub-vertical joint sets in both units due to the high angle foliation. A stronger foliation and therefore more foliation jointing was found in the volcaniclastics.

The relationship between resistivity measurements and weathering zone was principally determined through comparison with weathering logs and open joint count for both the saprolite and the fractured layer. The correlation between the base of the saprolite layer and resistivity data was generally clearer for both lithologies. In contrast, the transitional base of the fractured layer was less clear, particularly in the volcaniclastics. This is partly due to the variability in foliation within the unit. The correlation of the fractured base level to resistivity data was improved by comparison to hydraulic data, as discussed below.

Figure 2 shows an example of the lithological, weathering and joint count logs for a core hole in basalt superimposed on resistivity data. At this location the saprolite was logged to a depth equivalent to ~11Ω.m (ohm-meter), whereas open joints were recorded in the resistivity range of ~11to 30Ω.m.

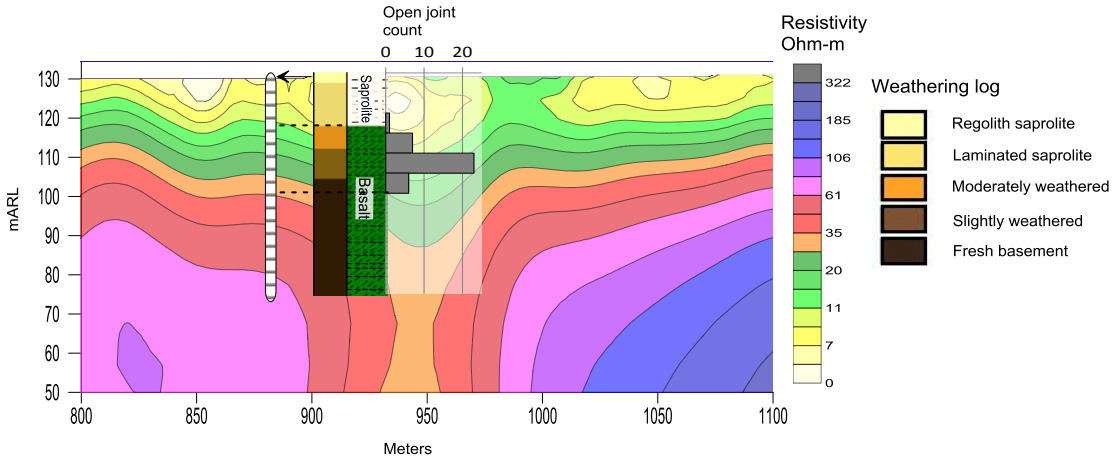

Figure 2 An example of the comparison between ERT results and the weathering log, lithology log and open joint count for an along-section vertical core hole in the basalt.

The initial interpretation of the weathered layers was compared with vertical airlift flows during drilling to identify permeable fractures and to refine the depth of the weathered fractured zone. The interpolated static piezometric groundwater level was used to identify locations where the base of the fractured zone was likely to be below saturated pressure. An example of this comparison is shown in Figure 3. Although airlift yields during drilling have limited accuracy, they can provide useful quantitative data for interpreting inflow zones. For example, in well GW02 the rapid drop-off in airlift yield to zero following water strike, indicates a shallow perched lens of limited capacity. Subsequent water quality analysis showed that this was undiluted leakage from the tailings facility (See Figure 3). Airlift yield measurements showed a good relationship between inflows and areas of interpreted fractured weathered rock below the piezometric level (e.g. wells GW01, GW03, GW04 and GW11 in Figure 3). Conversely, little or no groundwater yield was recorded for some well locations that were selected purely based on site preferences without the use of the geophysical data. These wells were typically located in areas where fresh rock had been interpreted above piezometric level (e.g. wells GW12a and GW02).

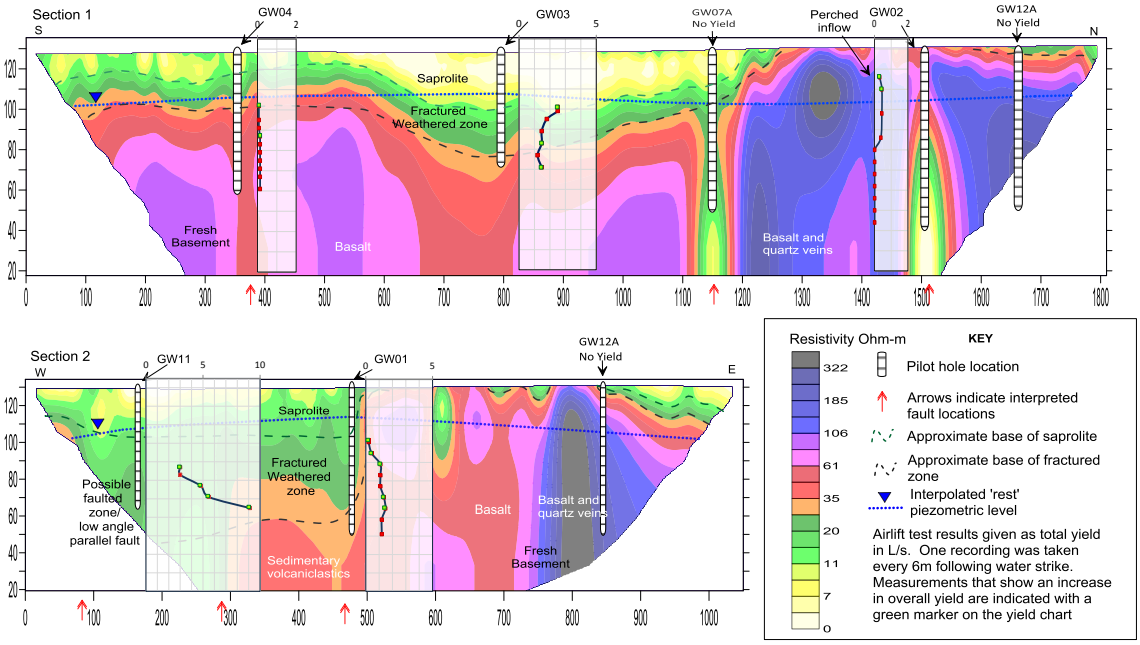

Figure 3 ERT sections with interpreted base of weathered saprolite and the fractured zone overlain by pilot hole locations, graphs of recorded airlift yields (L/sec) for yielding wells and interpolated piezometric level of the groundwater. Section 1 is a north to south section in basalt. Section 2 is a west to east section in sedimentary volcaniclastics and basalt. Both sections suggest that the weathered fractured zone is only present below the piezometric level in parts of the site.

A very deep, low resistivity zone in the ERT originally thought to be anomalous (as shown between 200m and 300m in Section 2, Figure 3) was partly verified through comparison of yield data. Well GW11 passed through a thick saprolite layer before striking water at ~44mbgl and showed water gains until the hole was stopped due to the collapsing nature of the shattered zone intercepted below ~70maRL. It should be noted that the resistivity results may show some depth inaccuracy in this area due to the thick layer of very low resistivity material at the surface.

A number of results can be drawn from the comparison of hydraulic and geotechnical data with ERT sections:

- Consistent with the classic crystalline weathered model significant increases in pilot hole yield were found in the saturated upper fractured zone (e.g. as seen in pilot holes GW11, GW03 and GW01 in Figure 3). Subsequent pumping test analysis confirmed well inflows were likely to originate from only a few principal fractures in most wells and these depths matched well with the inflow depths observed from airlift tests during drilling. In the lower part of the fractured zone there was generally no noticeable additional yield and the fresh basement generally exhibited no noticeable additional yield;
- The depth and thickness of weathering is variable across the site with the base of the fractured zone showing considerable variation. Visually this compares better to the 'multiphase weathered model' presented by Dewandel et al (2006). However, this is likely to be due to the increased variability in metamorphic rocks, particularly in folitation strength;

- Due to this weathered depth variability the base of the fractured zone is only below the piezometric level in certain parts of the site including beneath and around the tailings facility where groundwater levels were locally mounded due to seepage;
- Owing to the salinity of the water fault structures were visible on ERT sections as near vertical, thin, low resistivity zones (See Section 1, Figure 3). Based on core data and fault mapping in the pits it is expected that the majority of fault structures are permeable. These structures were not intercepted in any of the test wells (despite attempts e.g. GW02, GW07a). However, in some cases subsequent pumping test analysis has indicated permeable boundary structures consistent with the locations of these fault structures.

Table 1 Approximate resistivity ranges attributed to geological formations

Weathering Layer	**Approximate Resistivity (Ω.m)**	
	Meta-Basalt	**Meta-volcaniclastics**
Saprolite	0-10	0-25
Fractured layer	~10-45	~26-100
Fresh rock	>45	>100

Table 1 summarises the resistivity measurements for the different weathered zones deduced from comparing the ERT data to fracture logging, weathering logging and hydrogeological data. The resistivities are lower than would typically be expected for these lithologies due to the salinity of the groundwater and the high clay content of the weathered rock.

Saturated fractured layer and fault mapping

The results of the ERT surveys indicate that only parts of the upper fractured layer are below groundwater level. 'Channels' of higher permeability are formed where this layer is below groundwater level. As the majority of groundwater and solute flow would occur along these zones of higher permeability, as well as along the faults, mapping the channels and faults was an important part of the conceptual model development.

Resistivity sections were compiled into Leapfrog™ 3D geological modelling software for cross comparison (Figure 4). The interpreted base of the weathered fractured layer was interpolated between the resistivity sections with drill data used where larger gaps were present between sections. The area below the tailings facility, together with other zones of limited data, represents areas of considerable uncertainty in terms weathering depth, fault location and water.

For the interpolation of vertical structures dikes were separated from faults by overlaying aerial magnetic survey data and comparing with the ERT sections (the mafic dikes are clearly defined in the magnetic results). The fault structures were then interpolated with a confidence rating of 1 to 5 applied to the interpolations. The interpolated north to south trending faults (Figure 4) are consistent with structural mapping and some show good correlation with surface fault mapping.

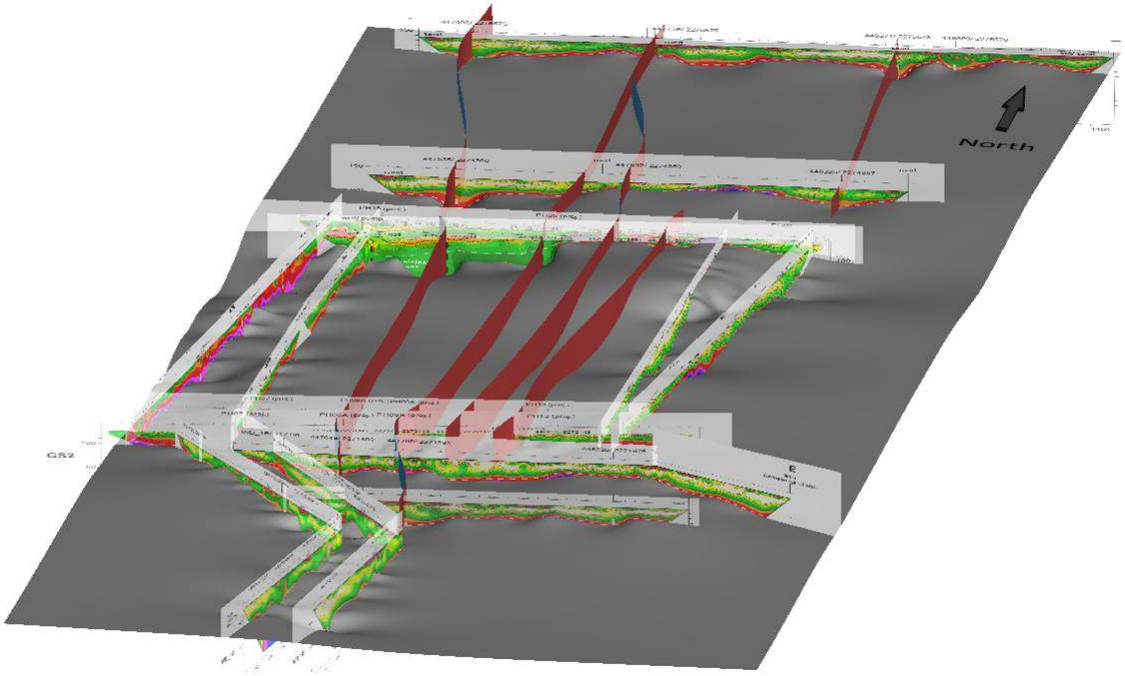

Figure 4 Compilation of ERT sections with the interpolation of the base of fractured layer (grey) and major north to south trending fault interpolations (burgundy and blue).

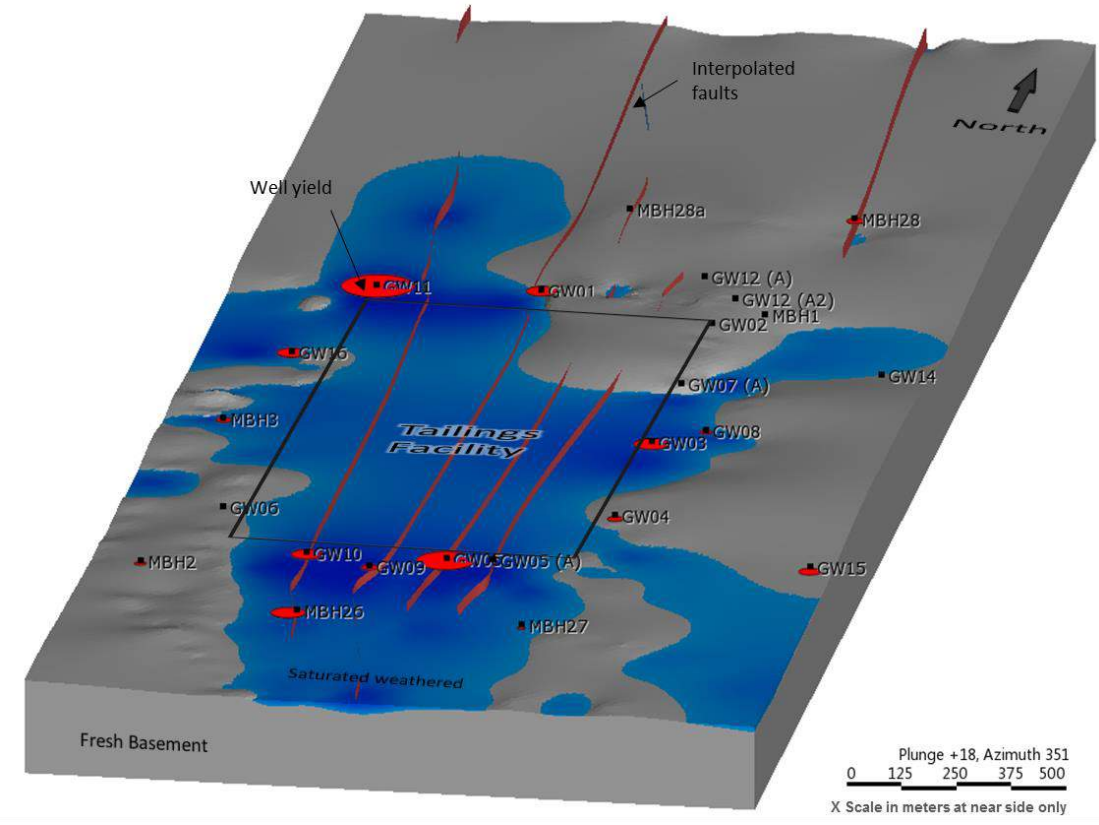

Figure 5 Interpolated base of the fractured weathered layer with a colour flood showing areas below the piezometric surface. Darker blue shading indicates an increased thickness of saturated weathered layer. Black

dots mark DTHH boreholes where water yield was measured. The relative yields from the boreholes are indicate by the size of red circles

Overlaying the groundwater level with the interpolated base of the fractured weathered layer shows a roughly north northwest to south southeast orientated channel that represents the 'saturated fractured weathered layer' material beneath the site and the tailings facility (blue area Figure 5). A deepening of the weathered layer is also seen to the east of the tailings facility (as evident in Section 1 Figure 3). Total yields from airlift tests indicate a good correlation between high borehole yield and the boreholes' positions relative to the weathered channels. Conversely there is a good correlation with zones of elevated fresh basement and boreholes which were drilled with no yield recorded (e.g. in the area North of GW07[A] in Figure 5) with only some minor exceptions (e.g. MBH02, GW04 and GW15).

Furthermore, the channel area mapped around the tailings facility was found to be consistent with groundwater quality samples containing tailings solute, indicating that solute migration was likely to be preferentially occurring along these weathered channels. Long-duration pumping at some of the wells has since established drawdown relationships between wells to the north and south of the tailings facility, which may be a result of hydrogeological connection within the weathered channels or the north – south oriented faults.

CONCLUSIONS

An ERT survey supported with lithological, geotechnical and hydrological data was used to characterise the shallow weathered zone and fault locations for a hydrogeological conceptual model in weathered metamorphic rock as part of a tailings seepage study. In the comparative analysis the open joint locations generally correlated well to inflow zones, which in-turn could be broadly correlated to a range of resistivities. However, the depth of the fractured layer itself was not apparent from the resistivity results alone. Therefore, the combination of both geotechnical and vertical hydrogeological data was found to be indispensible when interpreting the ERT measurements, leading to improved confidence in the overall interpretation of the system.

Despite some limitations to the method, the ERT measurements helped to show that weathered zone thickness at the site is considerably variable. The variable weathering depth differs to the classic single phase weathered model, which is considered to be a result of increased anisotropic structure of metamorphic rocks (particularly foliation). The weathered fractured zone is only present below the piezometric surface in certain parts of the site, with mapping of the fractured layer revealing a channel system where the fractured zone is saturated. This compares well with elevated hydraulic test results and water quality data showing that tailings water is migrating along these higher permeability channels. A number of faults were also determined from mapping of the ERT data, with locations that are supported by existing structural data. Some of these faults have since been evidenced hydraulically by pumping test analysis.

ERT integrated with geotechnical and hydrological data proved to be an invaluable tool in the refinement of the conceptual model for this hydrogeological study. It has led to important changes in our understanding of shallow flow and potential flow barriers, and, in turn, the potential for solute transport. The conceptual model has assisted with the siting of subsequent groundwater monitoring wells, the development of a numerical flow and solute model as well as the interpretation of hydraulic and water quality test data at the site.

Acknowledgments

The authors would like to thank the client for the use of their data in this paper, Terratec for the resistivity field work, and the SRK structural geologists and geotechnical engineers involved in the project for their input.

REFERENCES

Courtois, N., Lachassagne, P., Wyns, R., & Blanchin, R. (2010). Large scale mapping of the hard rock aquifer properties applied to Burkina Faso. *Groundwater, 48*(2), pp. 269-283.

Dewandel, P. L. (2006). A generalized 3-D geological and hydrogeological conceptual model of granite aquifers controlled by single or multiphase weathering. *Journal of Hydrology*.

Elster, D., Holman, I., Parker, A., & Rudge, L. (2014). An investigation of the basement complex aquifer system in Lofa county, Liberia, for the purpose of siting boreholes. *Quarterly Journal of Engineering Geology and Hydrogeology*(v.47; p159-167).

Krishnamurthy, N., Chandra, S., & Kumar, D. (2008). Geophysical Characterization of Hard Rock Aquifers. *Groundwater Dynamis in Hard Rock Aquifers*.

Lachassagne, P. (2008). From a new hydrogeological conceptual model for hard rock aquifers to enhanced practical applications. In S. A. al, *Groundwater Dynamics in Hard Rock Aquifers.* Springer.

Singal, G. (2010). *Applied Hydrogeology of Fractured Rocks, 2nd edition.* Springer.

Wyns, R., Baltassat, J., & Lachassange, P. (2004). Application of proton magnetic resonance sounding to groundwater reserve mapping in weathered basement rocks (Brittany, France). *Bulletin of the Geological Society of France, 175*, 21-34.

Alberta Oil Sands Cover System Field Trial: Development, Construction, and Results Two Years In

Larisa Barber, David Christensen, and Lindsay Tallon
O'Kane Consultants, Canada

ABSTRACT

Syncrude Canada Ltd. (SCL) has developed a field scale cover system trial at the Aurora North mine operations in Fort McMurray, Alberta, Canada. O'Kane Consultants Inc. (OKC) is part of the multi-discipline team that includes university researchers and industrial partners. The overall objective of the trial is to determine appropriate soil cover system designs and capping depth(s) for reclamation using available surface soil materials, while understanding and addressing the risk and uncertainty associated with the presence of oil sand (naturally occurring hydrocarbons) in the overburden and soil reclamation materials. The field scale cover system trial consisted of 36 one hectare cells, made up of 12 treatment options constructed in triplicate. The research cells were instrumented and planted with three native boreal forest tree species in varying densities.

OKC's primary research objective of the field trial was to investigate internal overburden disposal area dynamics, and develop an understanding for the key mechanisms and processes that influence the performance of various soil cover system prescriptions. Instrumentation was installed to monitor water balance parameters and groundwater, and to collect pore-water. Of the cells examined, the treatments with peat as a surface material had the lowest net percolation, due to higher water storage capacity. Groundwater levels revealed small, dynamic hydraulic gradients across the trial, and groundwater chemistry was generally typical of mine affected groundwater elsewhere at the Aurora North mine. Results from the study will serve to identify optimal cover system configurations and will be used by SCL to guide future reclamation operations.

Keywords: cover system, net percolation, overburden

INTRODUCTION

Syncrude Canada Ltd. (Syncrude) has developed a field-scale soil capping study at their Aurora North mine operations in Fort McMurray, Alberta, Canada. The overall research objective of the Aurora soil capping study (ASCS) is to determine appropriate soil cover system designs and capping depth(s) for reclamation using readily available surface materials, while understanding the risks and uncertainties associated with overburden and soil reclamation materials containing naturally occurring oil sand (petroleum hydrocarbons).

Syncrude has undertaken the study to examine alternatives for rehabilitation of their overburden areas. Rehabilitation practices must optimize the available reclamation materials to provide the foundation for re-emergence of sustainable, productive ecosystems. It is the research team's expectation that a wide range of land capability will be required within reclaimed areas and, as a result, reclamation treatments might change from one area to the next within the final landform. Consequently, the differences in performance between different surface materials, the thickness of the surface material, and the influence of the underlying subsoil materials need to be defined.

Indicators of cover system performance include net percolation and health of vegetation. OKC's contribution to the multi-disciplinary study is to examine the hydrological performance of the treatment alternatives. As soil moisture dynamics and vegetation health are interrelated, indirect indicators of vegetation performance such as plant available water and soil temperature are also considered. Further conclusions on vegetation health are within the scope of other researchers on site and are supported by data collected by OKC.

BACKGROUND

Oil sands mining is an open-pit mine operation. It involves removal of surficial geologic materials within the mine footprint that are suitable for use later in reclamation. This primarily includes discrete salvage of upland surface topsoil and subsoil materials and peat materials from lowland bogs and fens. Following reclamation soil salvage, overburden is removed to the oil sand ore body. The overburden is transported to a designated disposal area (generally above-grade or out of pit) where it is landform graded to defined elevation and grade specifications and capped with previously salvaged soil reclamation materials.

The appropriate soil reclamation capping design and depth is dependent on the underlying overburden quality and risk. For Syncrude's Aurora North mine, there are a number of risks and uncertainties associated with their overburden reclamation. Due to the geologic processes that took place at the end of the last glaciation, naturally occurring sand material which contains petroleum hydrocarbons have been mixed in the overburden and the soil reclamation materials in the region. Naturally occurring hydrocarbons are present in the entire matrix of the overburden, while they are present as discrete bands or chunks of varying size and proportion within the soil matrix. The removal, disruption, and spreading of these materials in a new setting poses a risk to the closure landscape, and the appropriate soil cover design and thickness is also uncertain.

A second issue Syncrude faces with overburden reclamation at the Aurora North mine is the large abundance of sandy (coarse textured) mineral reclamation materials. Although Syncrude has over 30 years of reclamation experience in the region, the Aurora North mine coarse textured surficial geological materials differs from previous mining locations. The appropriate use of available soil

reclamation materials to re-establish similar vegetation that was present prior to the disturbance has not been determined.

The ASCS has been constructed to address the risks and uncertainties with overburden reclamation at the Aurora North mine. The objective is evaluate the risks present and provide an appropriate soil cover system design and depth that will mitigate these risks. It is a large-scale, replicated multi-disciplinary study that spans key disciplines such as soil physics, soil chemistry, geochemistry, hydrology, plant growth and soil microbiology.

METHODOLOGY

Twelve treatment options (Figure 1) were constructed in triplicate to facilitate scientifically rigorous comparisons, resulting in a total of 36 cells (Figure 2). Surface layer materials include peat (a material of high organic content, salvaged from bogs), LFH (forest floor material), and Centre pit Bm (sandy subsoil material). Instrumentation for measurement of groundwater and various parameters of the water balance was installed in the cells (Figure 2). The research cells were planted with three native tree species in varying densities.

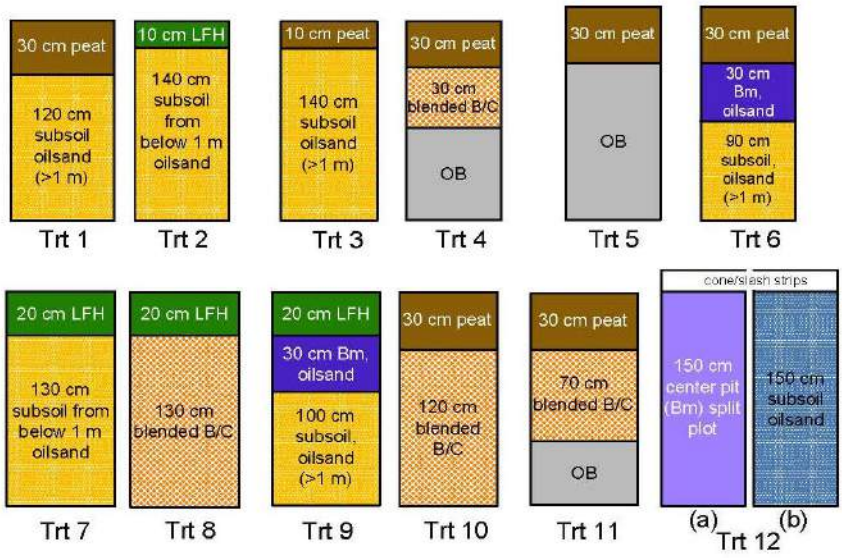

Figure ¡Error! No hay texto con el estilo especificado en el documento. Twelve treatment options applied at the ASCS. B/C = B and C soil horizons, Bm = slight colour and structural changes from the parent material (Soil Classification Working Group, 1998).

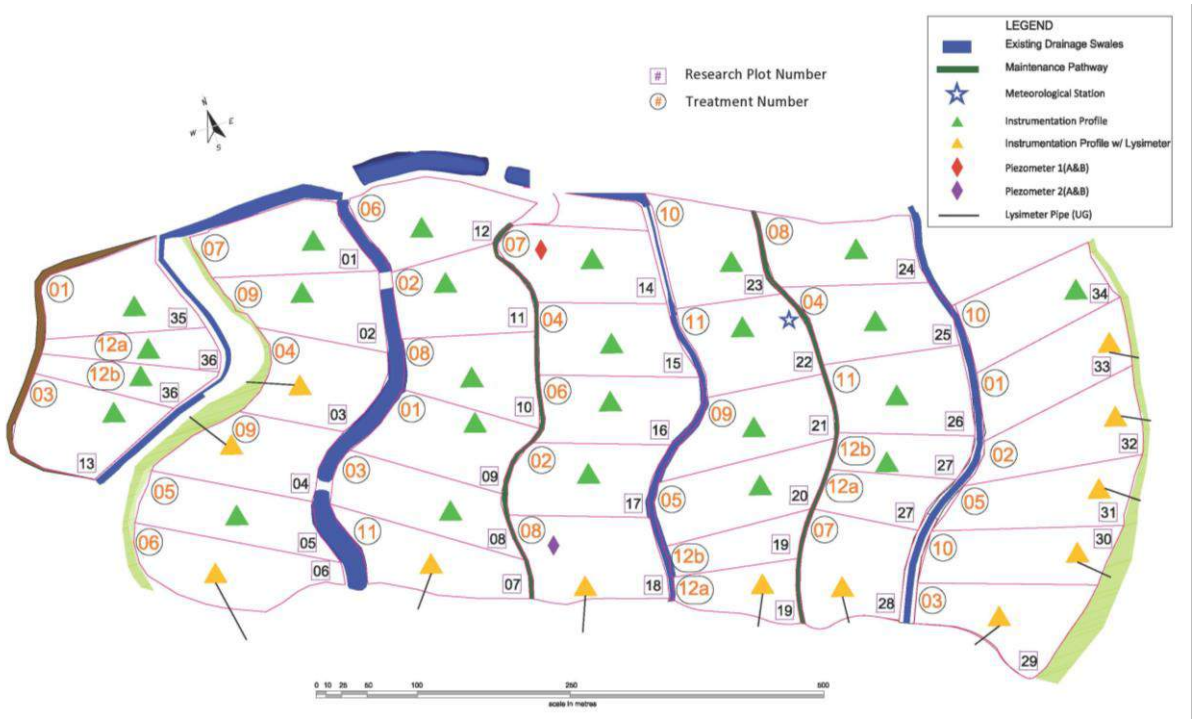

Figure 2 Study layout and instrumentation installed at the ASCS.

Water balance method

Analytical water balances were performed for cells on the perimeter of the ASCS to quantify the volume of water percolating through the cover systems in the 2012 - 2013 water year (November 1, 2012 to October 31, 2013). Water balances use calculated, estimated and field measured components as inputs to solve the water balance equation [1] on a daily basis during frost-free periods. In this way, the water dynamics of the various cover system treatments, and the hydrology of the system as a whole, can be characterized.

$$PPT = RO/S + AET + NP + dS \quad [1]$$

PPT = precipitation (rainfall plus snow water equivalent (SWE)),

RO/S = runoff and sublimation,

AET = actual evapotranspiration,

NP = net percolation, and

dS = change in moisture storage.

A meteorological station was erected at the ASCS on Cell#22 to measure site-specific climatic parameters (Figure 2). The station included instrumentation to monitor air temperature, relative humidity, net radiation, wind speed and direction, rainfall, snow depth, and air pressure.

Potential evapotranspiration (PE) was estimated using the modified Penman-Monteith method (Vanderborght et. al, 2010) and site meteorological data collected by the meteorological station. AET was calculated based on climate data and rates of PE, while AET/PE ratios were based upon

soil saturation levels, and field capacity and wilting point values, and adjusted to match the calculated storage to the measured storage in the water balance.

Vadose zone water dynamics in the cover systems and overburden at the ASCS were monitored by Campbell Scientific (CS) model 616-L volumetric water content sensors and CS229-L matric suction sensors. Data from these sensors was used to determine measured change in storage for the water balance. Pairs of soil water sensors were installed by hand in all layers of cover materials and in overburden, with focus on material interfaces.

CS229-L matric suction sensors also recorded soil temperatures. Soil temperature data was used to determine the frost-free period, and assist with the interpretation of water content data. In addition, the season when vegetation on the test cells is active is heavily influenced by soil temperatures.

Net percolation through the cover system treatments was monitored by large-scale lysimeters (Figure 2). The large-scale lysimeters were installed in the upper overburden profile of 12 of the perimeter test cells. Smaller scale Gee drain gauges were installed to assist in the characterization of water flow dynamics. Water balance net percolation was estimated using lysimeter and Gee gauge data, and the change in water storage at the base of the cover system.

Runoff is not directly measured at the site. Runoff and sublimation from the snowpack were estimated from the water balance.

Groundwater monitoring instrumentation

Four standpipe piezometers were installed at the ASCS (Figure 2) to measure groundwater levels and facilitate groundwater sampling, using Barber Dual Rotary and Coring Rigs. SP-1A and SP-2A are deep standpipes, while SP-1B and SP-2B are shallow standpipes. Groundwater levels were manually recorded in August and September of 2013, and samples taken using an inertial pump.

RESULTS AND DISCUSSION

Two cells with the surface treatment types of 20 cm LFH (top 15 cm of soil which consists of litter layer plus a portion of the immediately underlying mineral material) (Cell#18) and 30 cm peat (surface peat salvaged from bogs and fens) (Cell#30) were selected for presentation of results, but trends for research cells with large scale lysimeters and located on the perimeter of the study area are also discussed.

Temperature

Cells with peat as a surface material had dampened freezing penetration, in that they did not freeze as deep or as quickly as cells with LFH as a surface material. Freezing penetration occurred to approximately 90 cm for Cell #30 (Figure 3), versus approximately 200 cm for Cell #18 (Figure 4). In addition, freezing was more gradual for Cell#30 than for Cell#18 which showed an immediate spike of freezing to approximately 50 cm depth.

The number of days that soil temperatures at 10 cm depth exceeded 5°C was determined for the four major surface treatment types (Figure 5). The criteria of 5°C at 10 cm depth was used as an approximate indicator for when vegetation becomes active (Novak, 2005). The cells with 20 cm LFH at the surface had a greater number of days with active vegetation than cells with 30 cm of surface peat. Peat is an excellent insulator and more easily transmits energy from the material surface to the atmosphere relative to the sandy textured LFH. If soil-water is present to meet vegetation demand, increased soil temperature (more active vegetation days) in the boreal forest will likely translate into increased tree growth.

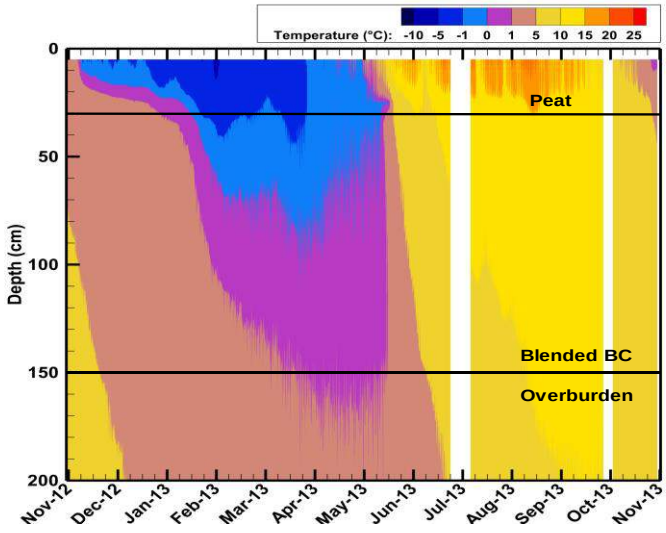

Figure 3 *In situ* soil temperature contours measured at Cell#30 (30 cm peat cover treatment) during the 2012-2013 water year.

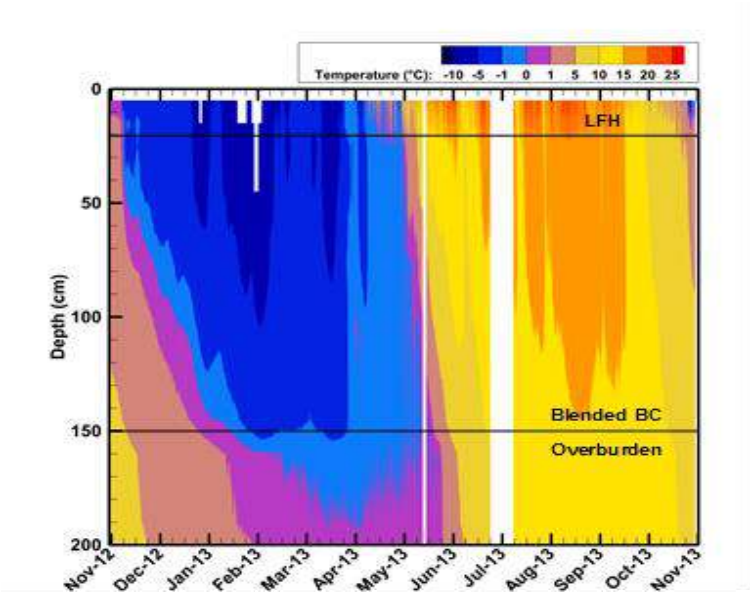

Figure 4 *In situ* soil temperature contours measured at Cell#18 (20 cm LFH cover treatment) during the 2012-2013 water year.

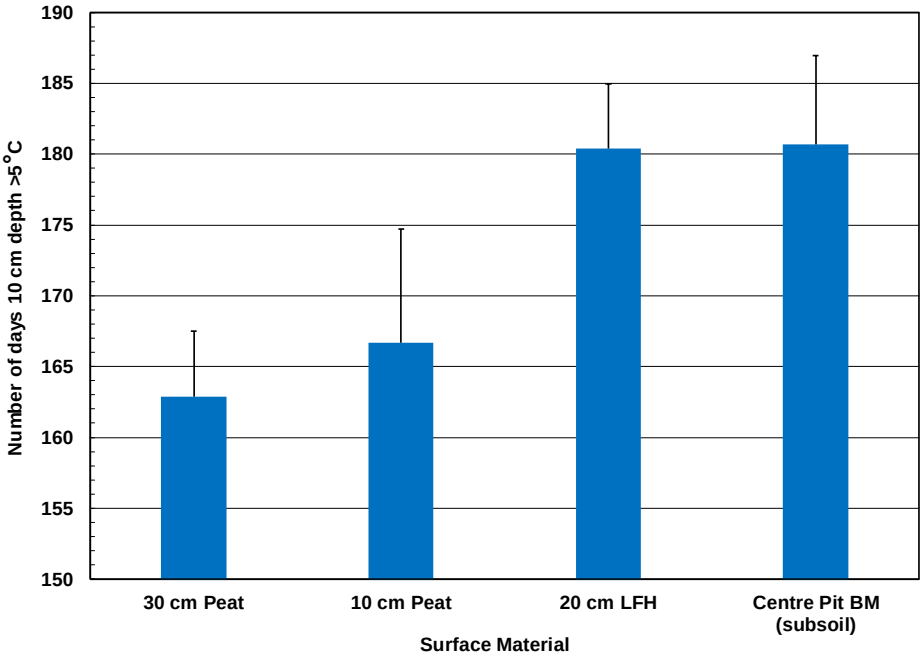

Figure 5 Number of days soil temperature at 10 cm depth was greater than 5°C for surface materials during the 2012 - 2013 water year.

Water balances

Water balances were completed for all research cells with large scale lysimeters and located on the perimeter of the study area. Calculated and measured storages matched well for Cell #30 (Figure 6) and Cell#18 (Figure 7) for the 2012 – 2013 water year, and for all water balances. Runoff and sublimation were higher for Cell#30, as well as for the majority of cells with peat as a surface material. AET rates were similar for Cell#18 and Cell#30, and ranged between 61% and 76% for all water balances constructed. AET rates did not have a discernible pattern based on material type. Rainfall for the year was above average, with two major rainfall events resulting in the majority of net percolation through the cover systems.

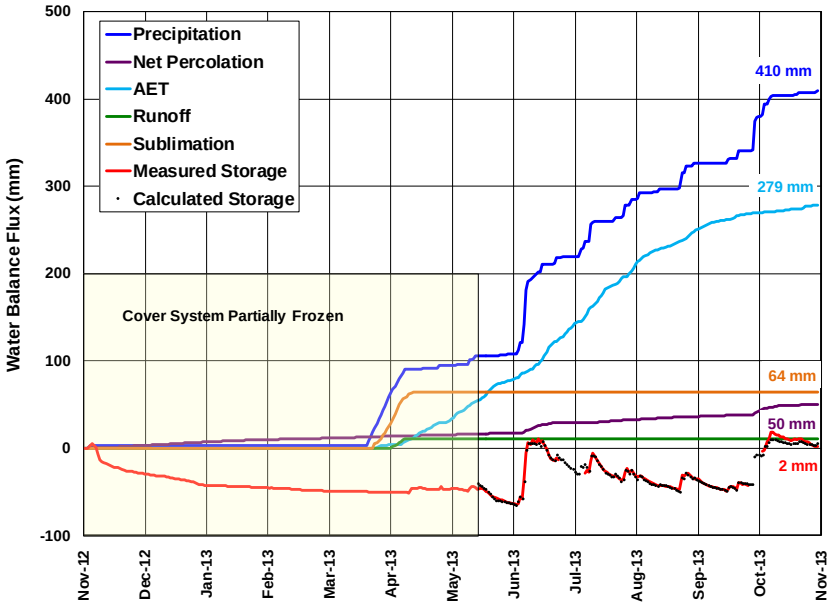

Figure 6 Cumulative water balance fluxes for the Cell#30 (30 cm peat cover treatment) for the 2012 - 2013 water year.

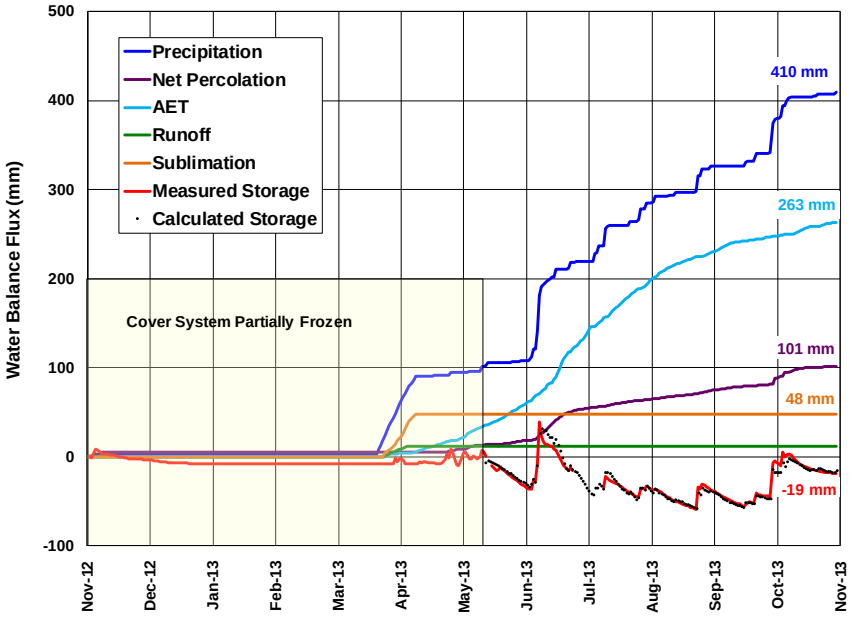

Figure 7 Cumulative water balance fluxes for the Cell#18 (20 cm LFH cover treatment) for the 2012 - 2013 water year.

Net percolation is an indicator of storage water potential of the cover system treatments,which can have implications on soil-water availability for vegetation growth and groundwater recharge rates. The net percolation rate for Cell#30 for the 2012 – 2013 water year, at 12% of annual precipitation was lower than the rate for Cell#18, at 25%. Following this trend, on average, cells with 30 cm of peat as a surface material had lower net percolation rates, at 14%, than cells with LFH as a surface material, at 23% (Figure 8). This is attributed to the higher storage capacity of peat, which improves the water store and release mechanism of the cover systems. In addition, it is possible that textural discontinuity between peat and subsurface materials inhibits drainage from peat to subsurface materials.

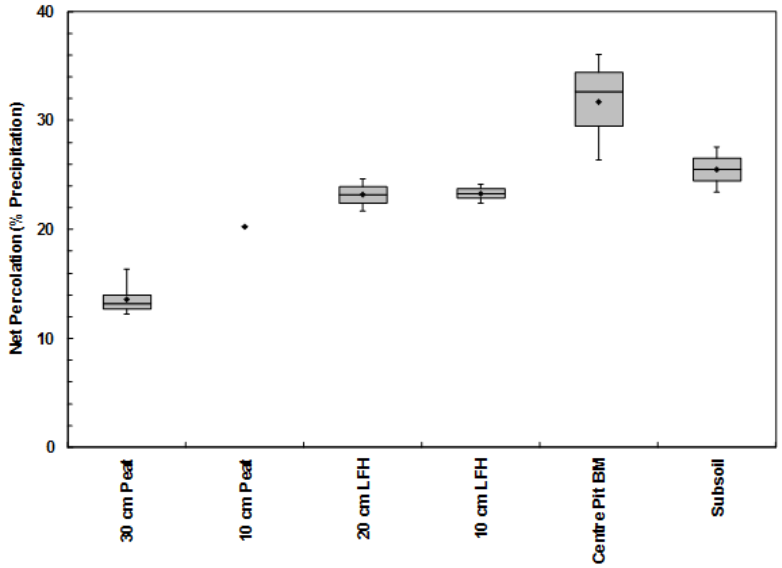

Figure 8 Net percolation box and whisker plot for all surface treatment options.

Groundwater levels and chemistry

Deep and shallow water tables were identified by manual water level measurements at SP-1A and SP-2A, and SP1-B and SP-2B, respectively. The average hydraulic gradient between SP-1A and SP-2A (the deep seated piezometers) in the 2012 - 2013 water year was -0.0098 m/m, translating into a north to south flow. The average hydraulic gradient between SP-1B and SP- 2B (the shallow seated piezometers) for the 2012 - 2013 water year was 0.0027 m/m, which translates to a south to north water flow.

Select results from chemical analyses of groundwater samples taken in standpipes (Table 1) were typical of mine-affected groundwater sampled elsewhere at the Aurora North mine.

Table 1 Select results of groundwater chemistry analyses.

Parameter	SP-2B	SP-1B	SP-1A
pH	7.35	7.89	7.88
EC (uS/cm)	2,760	3,860	2,680
TDS (mg/L)	2,340	3,060	2,240
Organic C (mg/L)	83.6	92.7	21.7
Dissolved Ca (mg/L)	429	205	436
Dissolved Mg (mg/L)	96.1	62.3	93.4
Dissolved Na (mg/L)	276	824	225
Dissolved S04 (mg/L)	955	1,360	1,060
Dissolved V (mg/L)	<0.0002	0.0024	0.0036
Dissolved As (mg/L)	<0.0004	0.001	0.0022
Dissolved Chloride (mg/L)	74.7	241	204

CONCLUSION

The influence of cover system treatments on soil temperature and water content were measured at an oil sands reclamation research study referred to as the Aurora soil capping study. Net percolation rates for the 2012 - 2013 monitoring year for treatments with 30 cm of peat at the surface were 14% of annual precipitation, which was lower than treatments with LFH (23% of annual precipitation) at the surface. The greater soil-water content of the treatments with peat at the surface is attributed to peat having a higher water storage capacity. In addition, textural discontinuity between peat and underlying sandy subsurface materials potentially inhibits drainage. Peat as a surface material also had an influence on soil temperature. Due to its ability to insulate the soil from the atmosphere, the number of active growing days was significantly lower in the peat cover treatments relative to the LFH cover treatment. Although peat may improve vegetation production in terms of water storage, it has the potential to reduce a soils effective growing season. These relative advantages and disadvantages over a range of wet-dry conditions and whether they persist as the site soil and vegetation mature may shape the preferred reclamation soil cover design strategy.

The first full year of monitoring the dynamics of the overburden disposal area at the ASCS have shown the interactions of the vegetation, cover materials, and climate are complex and further study is required to determine the preferred cover system treatment(s) for closure of the area. Data collected so far was sufficient to provide a comparison of cover system performance and identify key trends that will affect long-term performance such as net percolation, and the length of the vegetation growing season.

REFERENCES

Vanderborgh, J., Graf, A., Steenpass, C., Scharnagl, B., Prolingheuer, N., Herbst, M., Franssen, H.H., and Vereecken, H. (2010) *Within Field Variability of Bare Soil Evaporation Derived from Eddy Covariance Measurements Special Section: Patterns*, Vadose Zone Journal, vol. 9, pp. 943–954.

Novak, M.D. (2005) *Soil temperature,* Hatfield, J.L. and J.M. Baker (eds). Micrometeorology in agricultural systems. ASA-CSSA-SSSA.

Soil Classification Working Group (1998) The Canadian System of Soil Classification. Agric. And Agri-Food Can. Publ. 1646 (Revised).

Rheology and Hydrogeological Behavior of Thickened Tailings Disposal using Field Experimental Cell

Abdelkabir Maqsoud, Mamert Mbonimpa and Bruno Bussière
Université du Québec en Abitibi-Témiscamingue, Canada

ABSTRACT

Due to the current global context of the mining industry, many open pit mine projects are being developed. In the cases where the dimensions of the open pits are very important (order of km), the mining industry faces many challenges, particularly the management of mine tailings produced during mineral extractions. For that, different surface disposal technologies can be used such as dry, paste and thickened tailings disposals. These methods allow reducing the deposition area covered by the tailings and limit the environmental footprint. The rheological behavior of the tailings influences their flow distance, which in turn can affect the segregation behavior. The hydrogeological behavior of these types of deposition is mainly related to soil-atmosphere exchange.

To evaluate the geotechnical properties of thickened tailings and their hydrogeological behavior during their deposition, an experimental cell was constructed with three instrumented monitoring stations. The tailings thickness was included between 28 and 40 cm. These monitoring stations allowed to measure changes in volumetric water contents, suctions and pore pressures. Also, before tailings deposition in cell, grain-size distribution and % solids were analyzed. The % solids, rheological yield stress used as the initial design criterion correspond to 68 % and 16 Pa, respectively. During deposition, tailings samplings were performed and these samples were used to evaluate the grain size distribution and rheological properties.

The grain size distributions are typical for hard rock and did not present any segregation during tailings deposition. Rheology properties analysis show that the yield stress values obtained with the Bingham and Herschel-Bulkley models are very close to 8 Pa. The Sicko and Cross models provide similar values for the dynamic viscosity η_∞ (= 0.46 Pa.s) at high shear stress or rate ranges. Volumetric water content (VWC) measurements performed show that after tailings deposition and during drainage, the VWC are higher in the bottom and in middle than in the top tailings layer. These values remain higher in the bottom, whereas in the middle and top layer there is a rapid decrease indicating that the tailings materials drain relatively well. Finally pore pressure measurements showed that the pressure dissipation takes about 10 days to reach the initial state. These results allow concluding that these materials can be used as thickened tailings and allow to manage properly the wastes tailings and to limit the environment impact.

Keywords: Mine tailings, Experimental cell, Rheological properties, Hydrogeological

INTRODUCTION

The extraction of mineral resources plays an important role in the Canadian economy. However, ore extraction generates large amount of wastes. In Canada, about 650 Mt of solid wastes are generated each year by mining operations (*in* Winfield et al. 2002). These wastes include overburden, fine-grained mill tailings produced by the ore processing plant and waste rock extracted to reach the orebody.

Due to the current global context of the mining industry, many open pit mine projects are being developed. In the cases where the dimensions of the open pits are very important (order of km), the mining industry faces many challenges, particularly the management of mine tailings generated during mineral extractions (Oxenford & Lord 2006; Fourie 2009). Over the last few years, new and modified approaches have been proposed to increase the geotechnical and geochemical stability of mine tailings to better insure environmental protection (Bussière 2007). For the surface disposal, different technologies can be used such as 1) thickened (Robinsky 1999, Oxenford and lord 2006), 2) slurry, 3) paste (Hassani and Archibald, 1998; Benzaazoua et al. 2004), and 4) dry tailings disposals (Devies and Rice 2001, Kemp 2005). These technologies allow reducing the deposition area covered by the tailings and limit the environmental footprint.

The thickened paste technology offers significant economic incentives and environmental benefits (Meggys and Jefferies, 2012) because particle segregation cannot occurs during process, the paste material exhibits much greater stability than conventional tailings; there is no need for a pond on top of the deposit; which itself forms a gently sloping surface promoting runoff of rain water; and the overall costs are lower than for conventional slurry technologies

To evaluate the hydrogeological behavior of thickened tailings during and after deposition, an experimental cell was constructed and instrumented using monitoring stations. The main objectives of this paper are to evaluate in first the possible segregation of tailings during deposition and their rheological properties and in second the drainage behavior of the thickened tailings after deposition.

This article starts by field experimental cell description and its instrumentation followed by material characterization and rheological properties. Then hydrogeological behavior using volumetric water content and water pressure are presented. Finally this paper ends by a conclusion

FIELD EXPERIMENTAL CELL AND MATERIALS CHARACTERISATION

Experimental cell and monitoring stations

The field experimental cell was constructed using three dykes in the north, east and west side (see Fig. 1). Then three monitoring stations were installed in the thickened tailings flow direction, station 1 being closest to the discharge point. Each station is equipped with 1) 5TM sensors for volumetric water content and temperature measurements; 2) MPS sensors for the suction measurement (see Figure 1). Volumetric water content and suction sensors are connected to data logger for continuous measurements (see Maqsoud et al. 2007). The location of different sensors from the bottom, corresponding to the initial surface before deposition of tailings cell, is shown in Table 1 where one can observe that the average spacing between sensors is about 10 cm.

At each monitoring station, a well point was installed prior to the tailing depositions and it is equipped with a mini-Diver logger for continuous measurement of water pressure (see Figure 1).

Table 1 Sensor locations from the bottom surface installed at different monitoring stations

	Bottom sensors	Middle sensors	Top sensors
Station 1	10 cm	20 cm	35 cm
Station 2	7 cm	21 cm	32 cm
Station 3	9 cm	18 cm	28 cm

Figure 1 Experimental cell: a) Location of the different monitoring stations; b) details of instrumentation

After installation of monitoring stations, solid percent were verified using different methods then tailings deposition occurred in the experimental cell. Two layers were deposited in the experimental cell and during deposition 5 tailings samples were collected for each layer (see Fig. 2 for sampling locations).

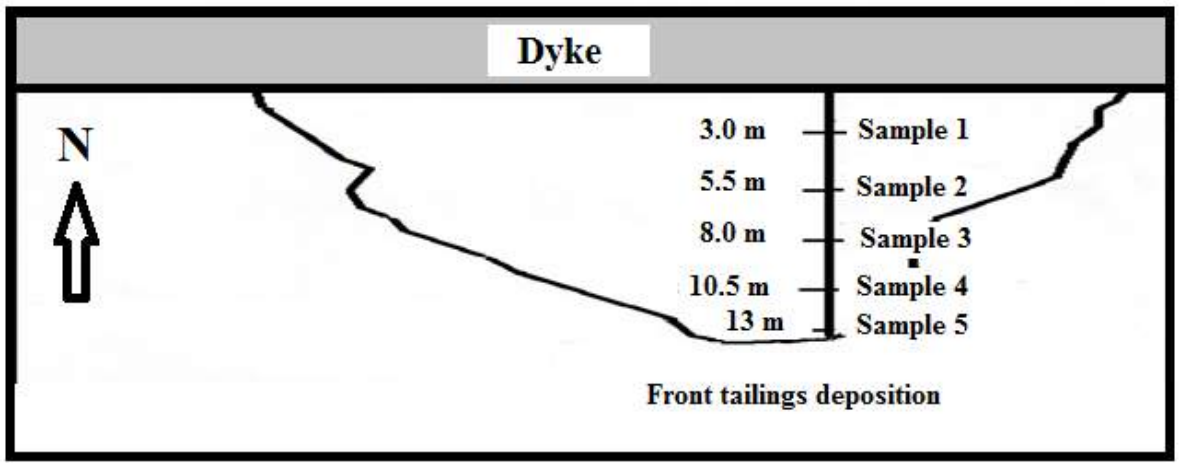

Figure 2 Samples location during tailings depositions

Grain size distribution and rheological properties

The grain-size distribution of the tailings was measured with a particle size analyzer based on laser diffraction. The apparatus used is a Mastersizer Standard Type S from Malvern Instrument (Merkus

2008; ASTM D 6913-04, 2009). The grain size measured with this equipment is included between 0.01 and 1000 μm.

The rheological properties of tailings were studied using an AR 2000 apparatus from TA Instruments. The tests were performed following the protocol:

- Preparation of a small pastefill batch (50 ml) at a given solid content;
- Pastefill mixing for 2 minutes;
- Rheological testing on a specimen of 28 mL at times t = 10 min (t =0 corresponds to the beginning of pastefill mixing);
- Each tests series was triplicated to ensure reproducibility of the results.

The rheological tests were performed at 20°C using a 14 -diameter by 42 mm-high vane geometry. The gap between the rotating vane and the wall of the stationary cylinder was 1 mm. This geometry gap must be at least 10 times higher than the largest grain size of the tested mixture. The following shear protocol was used:

- Conditioning step: a pre-shear stage of 30 s at a shear rate of 800 s^{-1} is performed;
- Flow procedures: the specimen was sheared from 800 to 0 s^{-1} using a continuous shear ramp test, stepped flow step and a steady state flow step.

The down flow and viscosity curves obtained were fitted using 4 models available in *TA instruments* data analysis software to obtain some rheological parameters such as the yield stress, etc.:

- Bingham and Herschel-Buckley models for flow curves;
- Cross and Cisko models for viscosity curves.

The Herschell–Bulkley and Bingham models are described with equations (1) and (2), respectively.

$$\tau = \tau_{0HB} + K_{HB}\dot{\gamma}^{n_{HB}} \quad [1]$$

$$\tau = \tau_{0B} + \eta_B\dot{\gamma} \quad [2]$$

The Sisko and Cross equations are defined with equations (3) and (4), respectively.

$$\eta = \eta_\infty + K_S\dot{\gamma}^{n_S-1} \quad [3]$$

$$\eta = \eta_\infty + \frac{(\eta_0-\eta_\infty)}{1+K_C\dot{\gamma}^{n_C}} \quad [4]$$

In equations (1) to (4),τ is the shear stress, $(\dot{\gamma})$ is the shear rate, and η is the dynamic viscosity. ($=\tau/\dot{\gamma}$). In eq. (1), τ_{oHB}, K_{HB} and n_{HB} represent the Herschell–Bulkley yield stress, viscosity (or consistency) and flow rate index, respectively. The following behavior applies: $n_{HB} < 1$ for shear-thinning, $n_{HB} > 1$ for shear-thickening and $n_{HB} = 1$ for Binghamn behavior (see eq. 2). In eq.(2), τ_{oB}, η_B correspond the Bingham yield stress and viscosity. In eqs. (3) and (4), η_0 and η_∞ are dynamic zero-rate ($\dot{\gamma} = 0$) and infinity-rate ($\dot{\gamma} \to \infty$) viscosities, respectively. K_s and K_c are consistency parameters and n_s and n_c are viscosity rate indexes. The performance of the different models can be compared using the standard error (SE) defined with equation (5). SE is deemed acceptable when it is less than 20 ‰ (TA Instrument manual).

$$SE = \left[\frac{\left(\frac{\sum(x_m - x_c)^2}{(N-2)}\right)^{1/2}}{\text{Range}} \times 1000\right] \quad [5]$$

where Range = difference between the maximum and minimum value measured, N is the number of points, x_m and x_c represent measured and calculated (with the fitting model) values, respectively.

MAIN RESULTS

In this paragraph, one can find results of the grain-size characterization, rheological properties and hydrogeological behavior of tailings during and after deposition.

Grain size distribution

The grain size distributions of different sampled materials are presented in figure 3 where one can observe that grain size range included between 2 and 74 µm (corresponding to silt fraction) corresponds to percent included between 65 and 69. The other percent corresponds to sand fraction. These different curves were used for determination of the geotechnical parameters D_{10}, D_{60} *and coefficient of uniformity* ($Cu = D_{60} / D_{10}$). These values are presented in Table 2, where one can observe that D_{10} is included between 6.47 and 7.16 (mean = 6.84) µm; D_{60} is included between 53.47 and 61.94 (mean = 59.84) µm and Cu, is included between 7.97 and 9.13 (mean = 8.75). These values are typical for hard rock tailings (see Aubertin et al. 2002).

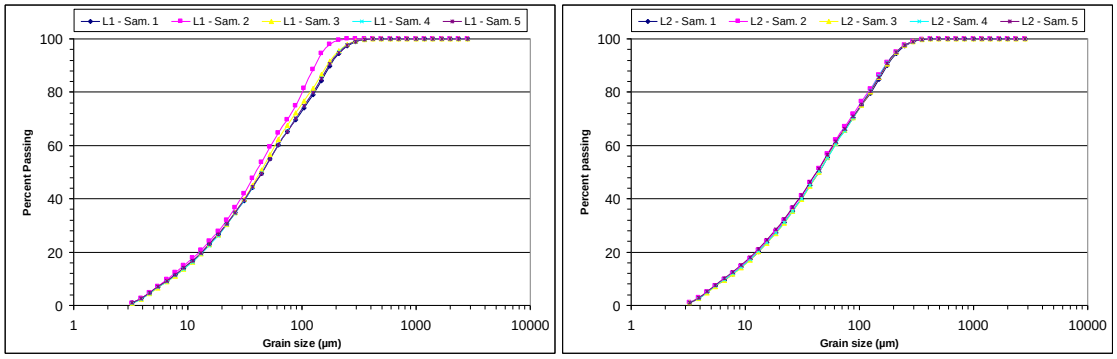

Figure 3 Grain-size distribution of tailings sampled during deposition (L1: layer 1, L2: layer 2, Sam: sample)

Tableau 2 Geotechnical parameters of tailings (Sam: sample)

	Layer 1					Layer 2				
	Sam 1	**Sam 2**	**Sam 3**	**Sam4**	**Sam 5**	**Sam 1**	**Sam 2**	**Sam 3**	**Sam 4**	**Sam 5**
D_{10} (µm)	6.96	6.71	7.16	7.11	6.93	6.77	6.66	6.93	6.74	6.47
D_{60} (µm)	61.8	53.47	58.23	61.55	61.93	60.81	58.28	61.94	61.33	59.06
Cu	8.89	7.97	8.13	8.66	8.94	8.99	8.76	8.94	910	9.13

Rheological properties

Figures 4 shows typical flow and viscosity curves obtained from the tests made following the three flow procedures. These figures show that all obtained results using different procedures are very

close. These triplicated results were merged using built-in rheological data analysis software to obtain one representative flow curve and viscosity curve. The merged flow and viscosity curves were fitted with the rheological models described above by applying the best fitting option available in the software (See Figure 5).

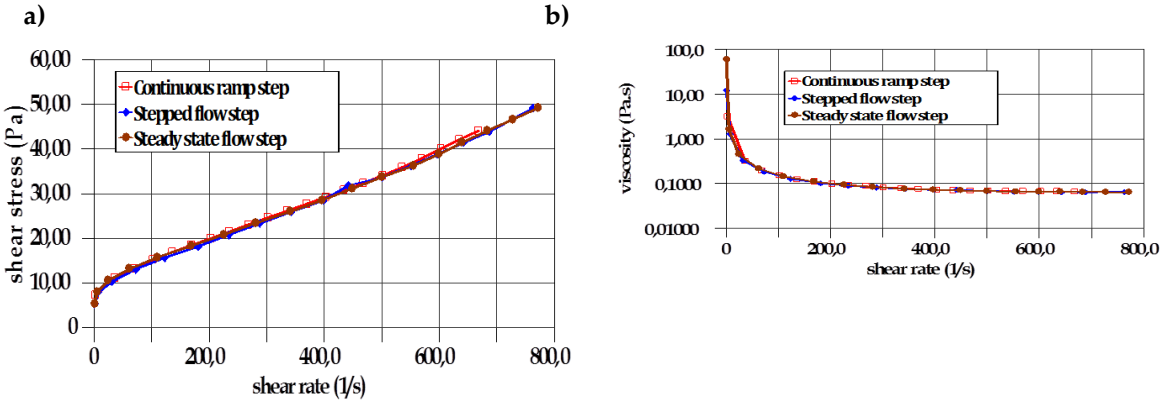

Figure 4 Flow (a) and viscosity (b) curves obtained for different flow procedures

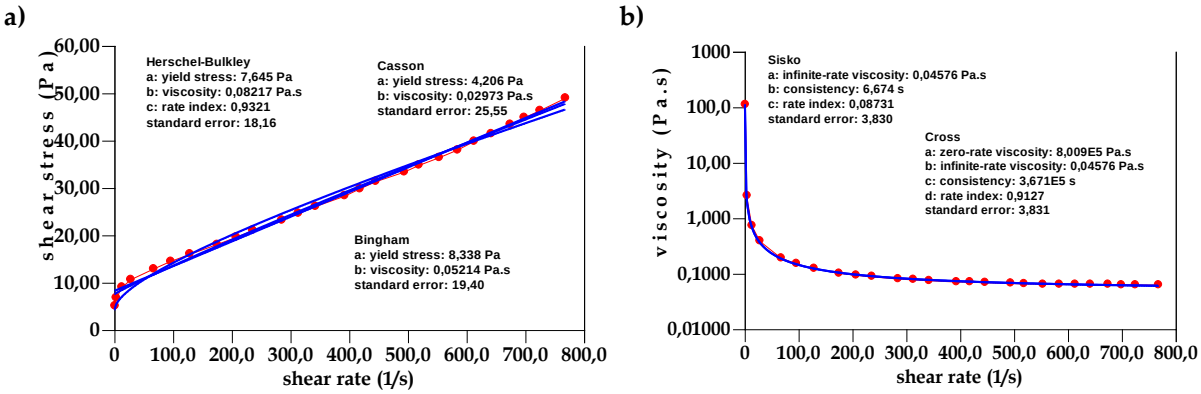

Figure 5 Merged flow (a) and viscosity (b) curves fitted with differents models

Table 3 summarizes the model parameters obtained. The yield stress values obtained with the Bingham and Herschel-Bulkley models are very close about 8 Pa.

Table 3 Rheological parameters obtained by fitting the merged flow and viscosity curves with different rheological models

Parameters	Models			
	Bingham	Herschel-Buckley	Cross	Sisko
Yield stress τ_{0B} or τ_{0HB} (Pa)	8.3	7.6	/	/
Viscosity η_B (Pa.s)	0.052	/	/	/
Consistency K_{HB} (Pa.s)	/	0.082		6.7
Rate index		0.93	0.91	0.87
Zero-rate viscosity η_0 (Pa.s)	/	/	$8x10^5$	
Infinite-rate viscosity η_∞ (Pa.s)	/	/	0.046	0.046
Consistency K_c	/	/	3.7×10^5	/
Standard error SE (‰)	19.4	18.2	3.8	3.8

The Sicko and Cross models provide similar values for the dynamic viscosity η_∞ (= 0.46 Pa.s) at high shear stress or rate ranges.

Hydrogeological behavior of tailings

Volumetric water content measurement

Volumetric water content (VWC) measurements performed at stations 1, 2 and 3 (see Fig. 1 for location) are presented in Figures 6 a, b and c. Due to the experimental cell configuration (tilt from north to south) and the limited volume of deposited tailings, sensors placed at the top (see table 1 for location) were not completely covered at stations 2 and 3. For these raisons, measurements results from these sensors are not presented.

Figures 6a, b and c show that VWC at saturation is about 0.44. Also, one can observe that after tailings deposition and during drainage, the VWC are higher in the bottom and in middle than in the top tailings layer. These values remain higher in the bottom, whereas in the middle and top layer there is a rapid decrease indicating that the tailings materials drain relatively well.

It is important to recall that after tailings deposition, different fluctuations were observed in the VWC. Some of these changes are related to precipitations, such as those that took place during November 23, that induce an increase in the volumetric water content. Other fluctuations are induced by temperatures decrease (below the freezing point) causing the water freezing and therefore reducing the amount of liquid water that can be measured by the equipment (figure 6d). This effect is illustrated by the lower VWC (close to residual volumetric water content) observed at the top of the layer at stations 1 (figure 6d)

Suction measurements

Suction measurements were performed in the top and bottom at the station 1 and 3. However, for the station 2, suction measurements were performed in the bottom and middle of the layer. Due to the limited volume of tailings deposition, sensor installed in the top of station 3 was not completely covered by tailings; consequently measurements results at this level will not be presented.

Suctions measurements results (not shown here due to space limitations) indicate that there is a good agreement between volumetric water contents and suctions measurements at different tailings layers: when volumetric water contents increase, there is a drop in the suction values while when volumetric water contents fall, suction value increase. Also, in the bottom layer suction remain constant at about 10 kPa, and this until November 24. After November 24, the measured suctions value show different fluctuations (exception for station 1). It is important to recall that the observed fluctuations and particularly the suction increases are related to freeze effect. Also, in the top and in middle the tailings layer, the measured suctions show many variations that are related to drying effect during water distribution and to wetting effect of tailings by precipitations.

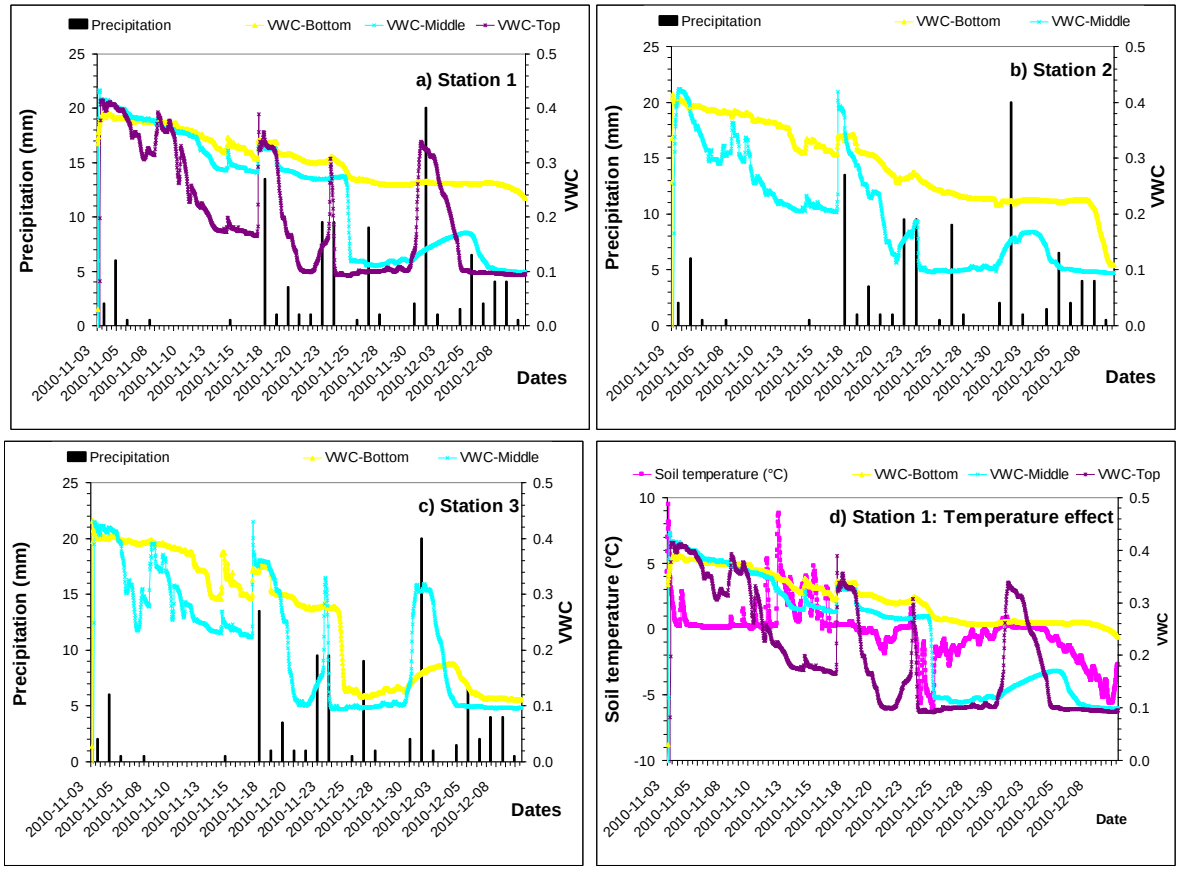

Figure 6 Volumetric water content measurements: a) station 1, b) station 2, c) station 3 and d) temperature effect

Well point pressure

Water pressures measured in the three well points are presented in Figure 7. Thus, in the three well points, one can observe in first an increase in water pressure during tailings depositions (2 and 3 November). Then there is a drop in the water pressure to reach the initial level after about 10 days (see Figure 7). Then one can observe that water pressure increases, especially during the 14, 17 and 23 November; these increases in water pressure are related to the precipitation that occurred in the region. As final remark, it is important to note that the water pressure decreases from the well point P1 (near the deposition area) to the well point P3 (at the bottom of the cell). The tailings thickness being greater near P1, it is fitting that the pore pressure is greater than that P2 and P3.

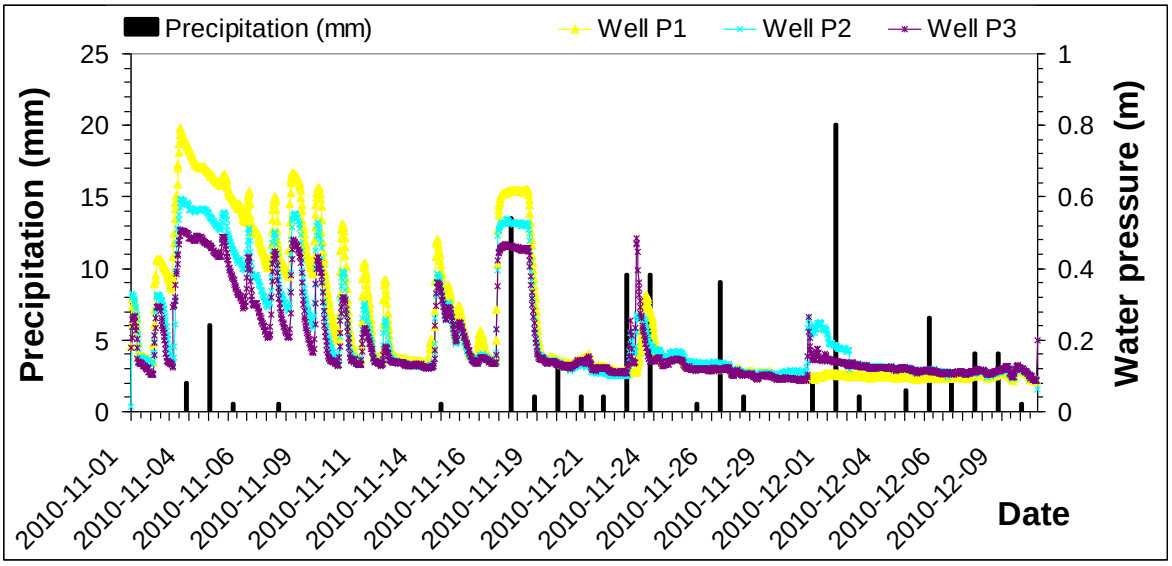

Figure 7 Water pressures measured in the three well points: P1, P2 et P3

CONCLUSION

An experimental field cell was constructed to evaluate the drainage behavior of the thickened tailings during and after deposition. Three monitoring stations were installed for volumetric water content, suction and water pressure measurements. During deposition, 10 thickened tailings samples were collected for analysis of grain size distributions and rheological properties.

Analysis results show that the grain size distributions are typical for hard rock where silt fraction corresponds to percent included between 65 and 69. Also, grain size analyzes show that there is no particle segregation during thickened tailings deposition. Rheology properties analyses show that the yield stress values, obtained with the Bingham and Herschel-Bulkley models, are very close about 8 Pa. The Sicko and Cross models provide similar values for the dynamic viscosity η_∞ (= 0.46 Pa.s) at high shear stress or rate ranges. Measurements show that after tailings deposition and during drainage, the VWC decrease from the bottom to the top layer. These VWC values remain higher at the bottom, whereas in the middle and top layer there is a rapid decrease indicating that the tailings materials drain relatively well. After tailings deposition, different fluctuations were observed in the VWC. Some of these changes are related to precipitations but others are related to freezing effect. Finally pore pressure measurements showed that the pressure dissipation takes about 10 days to reach the initial state. These results allow concluding that these materials can be used as thickened tailings and all to manage properly the wastes tailings and limit the environment impact.

REFERENCES

ASTM D 6913-04, (2009) 'Standard Test Methods for Particle-Size Distribution (Gradation) of Soils Using Sieve Analysis'.

Aubertin, M., Bussière, B. and Bernier, L. (2002). 'Environnement et gestion des rejets miniers.' Manuel sur cédérom, Presses internationales Polytechnique.

Benzaazoua, M., Pérez, P., Belem, T., and Fall, M. 2004. 'A laboratory study of the behaviour of surface paste disposal' *In* Proceedings of the 8th International Symposium on Mining with Backfill, The Nonferrous Metals Society of China, Beijing, September 2004. pp. 180–192.

Bussière, B. 2007 'Colloquium 2004: Hydrogeotechnical properties of hard rock tailings from metal mines and emerging geoenvironmental disposal approaches' Revue canadienne de géotechnique, 2007, 44(9): 1019-1052.

Devies and Rice 2001, Davies, M.P., and Rice, S. 2001. 'An alternative to conventional tailings management – "dry stack" filtered tailings' *In* Proceedings of the 8th International Conference on Tailings and Mine Waste '01, Fort Collins, Colo., 15–18 January 2001. A.A. Balkema, Rotterdam, the Netherlands. pp. 411–420.

Fourie, A. (2009). 'Preventing catastrophic failures and mitigating environmental impacts of tailings storage facilities' *Procedia Earth and Planetary Science*, *1*(1), 1067-1071.

Hassani, F.P., and Archibald, J. 1998. 'Mine backfill' Canadian Institute of Mining, Metallurgy, and Petroleum [CD-ROM], Montréal, Que.

Kemp, D. 2005. 'Designing a sustainable tailings impoundment for permafrost – the Raglan experience' [CD-ROM]. *In* Symposium 2005 on Mining and the Environment, Rouyn-Noranda, Que, 15–18 May 2005. Canadian Institute of Mining, Metallurgy, and Petroleum.

Maqsoud, A., Bussière, B., Mbonimpa, M., Aubertin, M., Wilson, W.G. (2007) 'Instrumentation and monitoring of covers used to control Acid Mine drainage' Proceeding of the Mining Industry Conference, CIM, Montréal CD-rom.

Meggyes, T. and Jefferis, S. (2012) 'Mine Paste Backfill–The Behaviour of Thickened Tailings and Pipeline Design' ASCE, GeoCongress 2012: pp. 4116-4125. doi: 10.1061/9780784412121.423

Merkus, H. (2008); 'NEW Particle Size Measurements: Fundamentals, Practice, Quality' Springer-Verlag New York Inc, ISBN-13, 9781402090158.

Oxenford, J., & Lord, E. R. (2006, April). 'Canadian experience in the application of paste and thickened tailings for surface disposal' In *Proceedings of the 9th International Seminar on Paste and Thickened Tailings, Paste* (pp. 93-105).

Robinsky, E.I. 1999. 'Thickened tailings disposal in the mining industry' E.I. Robinsky Associates, Toronto, Ont.

Winfield, M., Coumans, C., Kuyek, J. N., Meloche, F., Taylor, A. (2002). 'Looking beneath the surface: An assessment of the value of public support for the metal mining industry in canada' Institut Penbina and Mine alerte repport, ISBN 0-921719-84-1.

Experimental Analysis on Soil-Water Characteristic Curve of CH_3COO^- Contaminated Clay

Liwen Cao, Tianyu Xu, Yong Wang and Pan Huo
School of Resource and Earth Science, China University of Mining and Technology

ABSTRACT

Based on the soil-water characteristic curve (SWCC) of CH_3COO^- contaminated clay determined by test, SWCC parameters and equations, as well as SWCC factors and its application of forecasting on permeability and shear strength of the CH_3COO^- contaminated clay are confirmed.

Comparative study on CH_3COO^- contaminated clay and non-contaminating clay are carried out, and the fitting parameters are gotten. It is found that Van Genuchten model and Fredlund-Xing model are suitable for CH_3COO^- contaminated clay. Then, such factors as concentration, initial moisture content and initial dry density influence on the soil-water characteristic curve of the CH_3COO^- contaminated clay are explored. Specially, the SWCC of CH_3COO^- contaminated clay is used to predict the permeability coefficient and shear strength of the CH_3COO^- contaminated clay in this article. The researches show as follows: with the increase of concentration of CH_3COO^-, value of air-entry suction and residual water content are reducing gradually; meanwhile, saturation moisture content is increasing, and the SWCC curve slope is rising, which indicate that water-holding capacity is declining with CH_3COO^- concentration increase. When the initial water content is equal to plastic limit, such parameters as saturation moisture content, value of air-entry suction and residual water content reach to maximum, at the same time, the soil-water characteristic curve becomes flat, which represents the maximum water-holding capacity. With the increase of initial dry density, the value of air-entry suction and residual water content are increasing, and saturation moisture content is declining. Additionally, with increasing matric suction, the permeability coefficient of the CH_3COO^- contaminated clay declines and the shear strength increases, but the changing rate becomes slower and slower.

Keywords: CH_3COO^- contaminated clay; Soil-water characteristic curve; Fitting; Engineering geological properties prediction

INTRODUCTION

The soil contaminated by leachate is a common type of contaminated soil in the nature. CH_3COO^-, a common composition in the organic acid, influences the physical-mechanical properties of soil greatly. For example, the compression coefficient and deformation value of the foundation soil increasing obviously due to contamination will induce the buildings to crack. The determination of Soil-water characteristic curve is a premise of the study on physical-mechanical properties of soils. Thus, it is important to research contaminated soil and its soil-water characteristic curve (SWCC).

The researches on contaminated unsaturated soils are performed widely at home and abroad. A migration model on heavy metal in unsaturated soil was established (Chen W *et al*., 2010). The component and physical property of clay before and after the contamination of hydrochloric acid and sodium hydrate were analyzed (Zhang X.L. 2007). Bo researched the physical-mechanical properties and structure as well as corrosion mechanism of hydrochloric acid contaminated red clay (Bo T.Z. 2012), and Cao researched the influence of concentration of sulphuric acid and corrosion time on the physical-mechanical properties of clay (Cao H.R. 2012). Additionally, some researchers focused on salt contaminated soils, for example, physical-mechanical properties of clay change with the concentration of salt solution (Niu X.L. 2009). In the aspects of soil-water characteristic curve of unsaturated soil, the relationship between void ratio and soil-water characteristic curve of unsaturated soil, as well as the prediction of soil-water characteristic curve through any initial void ratio was involved (Chen G.F. *et al*., 2008.Cai G.Q. *et al*.,2010).

However, the leachate contaminated clay, especially CH_3COO^- contaminated clay, is scarcely touched upon. Based on theory of the unsaturated soil mechanics, the author investigates the soil-water characteristic curve of CH_3COO^- contaminated clay, and its influence factors, and then the parameters and equations of CH_3COO^- contaminated clay are confirmed.

THE SOIL-WATER CHARACTERISTIC CURVE OF CH_3COO^- CONTAMINATED CLAY

The SWCC feature of CH_3COO^- contaminated clay

The CH_3COO^- contaminated clay sample was prepared through soaking in 10% of acetic acid solution. According to the test data, soil-water characteristic curve of CH_3COO^- contaminated clay is obtained.

As is illustrated in Figure 1, the SWCC of CH_3COO^- contaminated clay shows the same tendency with that of uncontaminated clay. With increasing matric suction, the water content is declining, specially, the water loss rate declines obviously in high matric suction stage. Furthermore, the SWCC of uncontaminated clay can be divided into three sections named as boundary effect region, transition region and residual region by two inflection points G_1 and G_2. Similarly, the SWCC of CH_3COO^- contaminated clay can be divided into two sections named as transition region and residual region by one inflection point G_2 without boundary effect region. The same feature is

presented in CH_3COO^- contaminated clay and non-contaminated clay in the transition region and residual region.

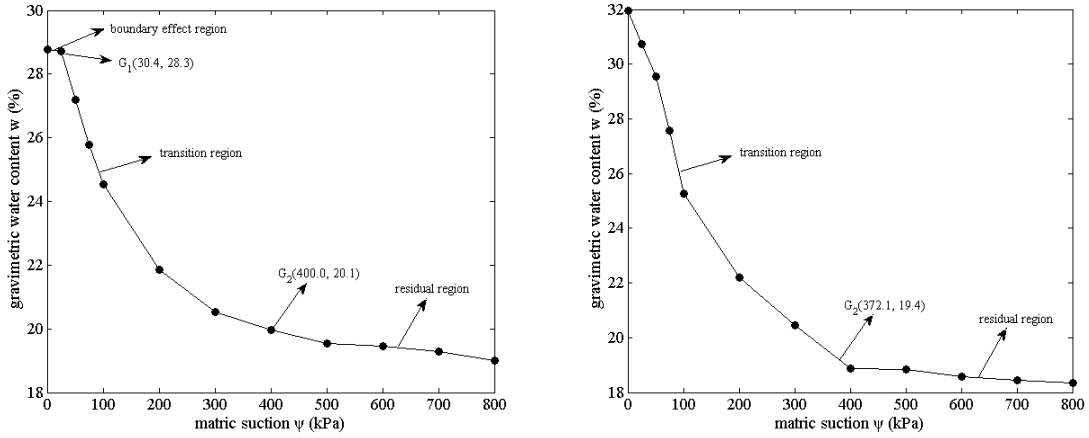

(a) SWCC of uncontaminated clay (b) SWCC of 10% of CH_3COO^- contaminated clay

Figure 1 SWCC of uncontaminated and 10% of CH3COO- contaminated clay

Meanwhile, the saturation moisture content of CH_3COO^- contaminated clay is greater than that of uncontaminated clay; however, the residual moisture content shows a contrary trend. Additionally, the gradient of soil-water characteristic curve of CH_3COO^- contaminated clay is larger than that of uncontaminated clay, which indicates the moisture holding capacity of the clay declines due to CH_3COO^- contamination.

The SWCC model of CH_3COO^- contaminated clay

Among the soil-water characteristic curve models, Van Genuchten model and Fredlund-Xing model are frequently used with characteristic of considering more factors and higher representative (Guo *et al.*, 2013).

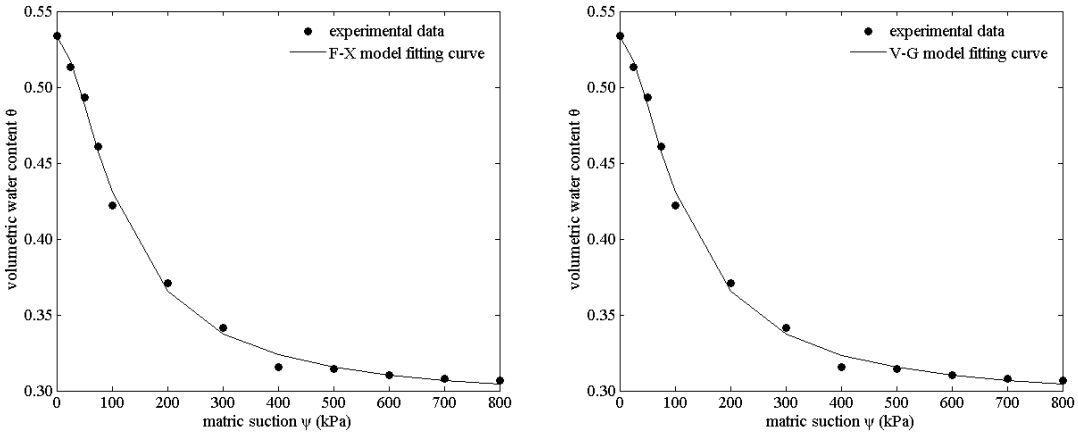

(a) V-G model fitting (b) F-X model fitting

Figure 2 The fitting curves of 10% CH_3COO^- contaminated clay

In this paper, the scatter diagram on soil-water characteristic curve of CH_3COO^- contaminated clay is drawn from experimental data, then, Van Genuchten model (V-G model) and Fredlund-Xing model (F-X model) are used for fitting, as showed in Figure 2.

The soil-water characteristic curve model equations are demonstrated as follows:

$$\theta_w = 0.279 + \frac{0.255}{\left[1+\left(0.23\varphi\right)^{1.72}\right]^{0.88}} \quad (1)$$

$$\theta_w = 0.281 + \frac{0.253}{\left\{\ln\left[e+\left(0.13\varphi\right)\right]^{1.66}\right\}^{1.97}} \quad (2)$$

THE EFFECT FACTORS ON SWCC OF CH_3COO^- CONTAMINATED CLAY

The effect of acetic acid concentration on SWCC of CH3COO- contaminated clay

The CH_3COO^- contaminated clay samples with four concentrations: 1%, 4%, 7% and 10% of acetic acid were prepared. The SWCCs of the clay samples are tested as shown in Figure 3 with the corresponding relation between volumetric water content and matric suction displayed in Table 1.

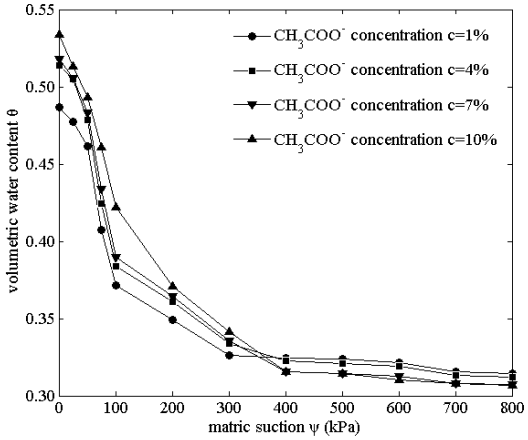

Figure 3 The SWCC of contaminated clay with different acetic acid concentrations

With increasing acetic acid concentration, the saturation moisture content of CH_3COO^- contaminated clay is rising. In the stage of lower matric suction (0-350kPa), the corresponding moisture content is increasing gradually with the acetic acid concentration rising as to the same matric suction, on the other hand, the SWCCs in the stage of higher matric suction (>350kPa) show a contrary trend.

Suffered from acetic acid pollution, the clay mineral compositions change significantly. For instance, mental salts are dissolved. High valence ions such as Al, Si and Fe, as well as Na, Mg, K, Ca and other elements content reduce significantly. With the increase of acetic acid concentration,

the dissolution increases obviously, while the adsorption capacity of soil particles to water and water holding capacity gradually decreases. Meanwhile, with the increase of acetic acid concentration, the clay porosity and pore size increase, thus inducing the decrease of value of air entry, water holding capacity and residual water content.

Table 1 The volumetric water content and matric suction of contaminated clay with different concentrations

matric suction （kPa）	contaminated clay with 1% acetic acid	contaminated clay with 4% acetic acid	contaminated clay with 7% acetic acid	contaminated clay with 10% acetic acid
0	0.4865	0.5141	0.5182	0.5337
25	0.4775	0.5050	0.5053	0.5135
50	0.4614	0.4783	0.4830	0.4932
75	0.4072	0.4245	0.4338	0.4607
100	0.3716	0.3837	0.3900	0.4218
200	0.3492	0.3607	0.3644	0.3710
300	0.3261	0.3340	0.3355	0.3414
400	0.3246	0.3224	0.3153	0.3154
500	0.3236	0.3211	0.3145	0.3145
600	0.3214	0.3191	0.3128	0.3105
700	0.3154	0.3135	0.3077	0.3078
800	0.3146	0.3123	0.3075	0.3065

The effect of initial water content on SWCC of CH_3COO^- contaminated clay

The CH_3COO^- contaminated clay samples with three initial water contents: 15%, 21% and 27% were prepared. The SWCCs of the clay samples are tested as shown in Figure 4 with the corresponding relation between volumetric water content and matric suction displayed in Table 2.

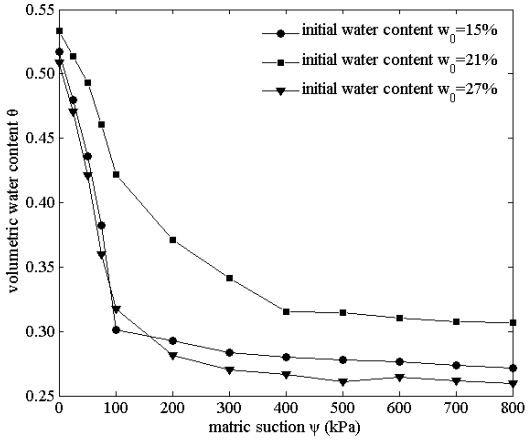

Figure 4 The SWCC of contaminated clay with different initial water contents

Table 2 The matric suction and volumetric water content under different initial water content of CH_3COO^- contaminated clay

matric suction kPa	w_0=15%	w_0=21%	w_0=27%
0	0.5172	0.5337	0.5086
25	0.4796	0.5135	0.4703
50	0.4357	0.4932	0.4215
75	0.3825	0.4607	0.3597
100	0.3013	0.4218	0.3173
200	0.2928	0.3710	0.2812
300	0.2837	0.3414	0.2701
400	0.2801	0.3154	0.2668
500	0.2778	0.3145	0.2610
600	0.2765	0.3105	0.2648
700	0.2733	0.3078	0.2617
800	0.2714	0.3065	0.2598

When the initial water content is equal to plastic limit 21%, such parameters as saturation moisture content, value of air-entry suction and residual water content reach the maxima, at the same time, the soil-water characteristic curve becomes flat, which represents the maximum water-holding capacity.

The initial water content has important effect on clay pore structure. When initial water content is small, the clay possesses lower value of air entry and the water holding capacity. When the water content increases to plastic limit, the clay possesses optimal pore arrangement, inducing the water holding capacity, saturated moisture content and residual water content reached the maxima. When the water content increases continually, the adsorption ability of clay particles decrease, causing the water holding capacity, saturated moisture content and residual water content declines as well.

The effect of initial dry density on SWCC of CH_3COO^- contaminated clay

CH_3COO^- contaminated clay samples with three initial dry densities: 1.64g/cm^3, 1.72g/cm^3 and 1.78g/cm^3 were prepared. The SWCCs of the clay samples are tested as shown in Figure 5 with the corresponding relation between volumetric water content and matric suction displayed in Table 3.

With the increase of the initial dry density, the CH_3COO^- contaminated remolded clay has the smaller saturation moisture content, but the bigger value of air-entry suction and residual water content. The curve slope increasing represents the water holding capacity rising.

The influence of initial dry density on SWCC of CH_3COO^- contaminated clay is realized by changing clay pore structure. With increasing initial dry density, the clay pore space decline gradually, thus decreasing the water storage space and saturated water content of the clay. With the increase of dry density and the decrease of pore space, the specific surface area of clay particles

increases, enhancing the adsorption to water, water holding capacity, air entry value and residual water content greatly under the same matric suction.

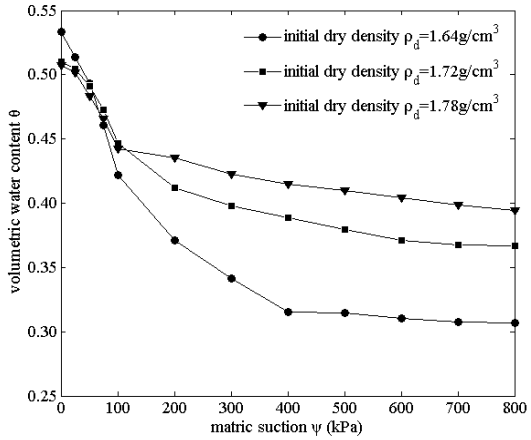

Figure 5 The SWCC of CH_3COO^- contaminated clay with different initial dry densities

Table 3 Matric suction and volumetric water content under different initial dry density

matric suction kPa	ρ_d=1.64g/cm^3	ρ_d=1.72g/cm^3	ρ_d=1.78g/cm^3
0	0.5337	0.5102	0.5075
25	0.5135	0.5043	0.5018
50	0.4932	0.4911	0.4832
75	0.4607	0.4725	0.4653
100	0.4218	0.4468	0.4424
200	0.371	0.4117	0.4356
300	0.3414	0.3981	0.4223
400	0.3154	0.3885	0.4148
500	0.3145	0.3793	0.4096
600	0.3105	0.3713	0.4045
700	0.3078	0.3674	0.3989
800	0.3065	0.3668	0.3944

Additionally, with the matric suction increasing, the permeability coefficient of the CH_3COO^- contaminated clay declines and the shear strength increases, but the changing rate becomes slower and slower.

FORECASTING ON PERMEABILITY COEFFICIENT AND SHEAR STRENGTH OF THE CH_3COO^- CONTAMINATED CLAY

In this paper, SWCC was used to predict the permeability coefficient and shear strength of the CH_3COO^- contaminated clay. Jackson equation and Vanapalli equation are used to predict the

permeability coefficient and shear strength of the CH_3COO^- contaminated clay as to the same permeability coefficient and shear strength of the CH_3COO^- contaminated clay sample. The relevant forecasting equations show as follows:

$$k = 6.38\times10^{-13}\times\left(2.76\times10^{15}\right)^{\theta} \tag{3}$$

$$k = e^{-8.8-0.04\varphi+6.16\times10^{-5}\psi^2} \tag{4}$$

$$\tau = 4.3\times10^{5} - 3.3\times10^{-5}e^{25\theta} - 4.3\times10^{5}e^{7.69\times10^{-6}\theta} \tag{5}$$

$$\tau = 5.4\times10^{5} - 19e^{-0.02\psi} - 5.4\times10^{5}e^{1.43\times10^{-6}\theta} \tag{6}$$

The above equations can be used to forecast the permeability coefficient and shear strength of the CH_3COO^- contaminated clay.

CONCLUSIONS

Based on the experiment of the CH_3COO^- contaminated clay, the soil-water characteristic curve (SWCC) of CH_3COO^- contaminated clay and their SWCC parameters as well as equations are obtained, meanwhile, SWCC factors and its application of forecasting on permeability and shear strength of the CH_3COO^- contaminated clay are confirmed.

(1) It is found that Van Genuchten model and Fredlund & Xing model are suitable for CH_3COO^- contaminated clay.

(2) Such factors as concentration, initial moisture content and initial dry density influence on the soil-water characteristic curve of the CH_3COO^- contaminated clay are explored, meanwhile, their influence mechanism are touched upon.

With the increase of concentration of CH_3COO^-, value of air-entry suction and residual water content are reducing gradually; meanwhile, saturation moisture content is increasing, and the SWCC curve slope is rising, which indicate that water-holding capacity is declining with CH_3COO^- concentration increase. When the initial water content is equal to plastic limit, such parameters as saturation moisture content, value of air-entry suction and residual water content reach the maxima, at the same time, the soil-water characteristic curve becomes flat, which represents the maximum water-holding capacity. With the increase of initial dry density, the value of air-entry suction and residual water content are increasing, and saturation moisture content is declining. The shape of the water content curve is more sensitive to the initial dry density value than the concentration of acetic acid.

(3) The SWCC of CH_3COO^- contaminated clay is used to predict the permeability coefficient and shear strength of the CH_3COO^- contaminated clay, and the related forecasting equation are obtained.

ACKNOWLEDGEMENTS

This research is jointly supported by the National Natural Science Foundation of China No. 41372326, No.41072236 and project funded by the Fundamental Research Funds for the Central Universities (2014ZDPY27) and the Priority Academic Program Development of Jiangsu Higher Education Institutions.

NOMENCLATURE

k	permeability coefficient
w	gravimetric water content
θ	volumetric water content
ρ_d	initial dry density
τ	shear strength

REFERENCES

Wei Chen, Zeshi Gao,Yilin Yang &Aiguo Zhang.(2010). The theory analysis for the transport of heavy metal pollutant in unsaturated soil [J]. Journal of Anhui University: Natural Science Edition, 34(5): 98-103.

Xiaolu Zhang.(2007). Experimental research on soil contaminated by acid and alkali [D]. NanJing: HoHai University.

Tongzhen Bo.(2012). Acid pollution of laterite macro and micro characteristics and corrosion mechanism research [D]. KunMing: Kunming University of Science and Technology.

Hairong Cao.(2012). Research on physical-mechanical property of soil contaminated by acid in laboratory [J]. Journal of Hunan University of Science &Technology: Natural Science Edition, 34(5): 98-103.

Xiaoling Niu.(2009). Experimental study on soil contaminated by salt environment [D]. TaiYuan : Taiyuan University of Technology.

Gaofeng Chen, Yujun Cui, Yingfa Lu,&Xianqi Luo.(2008). Study of soil-water characteristical curve and its influential factors [J]. Rock and Soil Mechanics, 29(9):2481-2486.

Guoqing Cai, Yan Liu, Xuedong Zhang,&Chenggang Zhao.(2010). Research on influence of soil density on soil-water characteristic curve [J]. Rock and Soil Mechanics, 31(5): 1463-1468.

Lina Guo, Bin Hu, Youjian Song,&Guochao Zhang.(2013). Contrast study on forecast of shear strength of unsaturated soil using soil water characteristic curve [J]. Journal of Engineering Geology, 21(6): 849-856.

Simulation of Contaminant Transportation in Saturated Transparent Rock Fractures

Wanghua Sui and Hao Qu
School of Resources and Geosciences, China University of Mining and Technology

ABSTRACT

This paper presents an experimental investigation of flow of contaminated water in saturated rock fractures by using a transparent fractured rock replica for visualizing contaminant transport. The transparent fractured rock model is composed of transparent silica blocks and matched refractive index pore fluids. A dyed fluid is used for simulating contaminants. The experimental setup consists of a Plexiglas container, a contamination injection system and three CCD cameras. The transport images during testing are captured by the three cameras in orthogonal directions. Digital image processing is applied to analyze the greyscale to detect the edge of the transportation front and to calculate penetration length and area at different times. A roughly circular plume is found when the fractures filled with transparent silica grains. The results indicate a square relationship between the penetration length and the cubic root of injection time, and a square relationship between the propagation area and the injection time in the fractures. The results also verified the possibility for simulation of contaminant transport in a fractured rock mass by using a transparent rock replica.

Keywords: Contaminant transport; rock fracture; digital image correlation; transparent rock replica; transparent soil

INTRODUCTION

In recent years, transparent models have been successfully applied to investigate contaminant transport in porous media (Mannheimer and Oswald 1993; Iskander et al. 2003; Liu et al. 2005; Lo et al. 2008; Fernandez et al. 2011; Liu et al. 2013). However, the transparent model has not been used to study contaminant transport in fractured rock mass. The difficulty of the visualization inside a rock mass limits the understanding of contaminant transport during water drainage due to mining. This paper presents a preliminary extension of the transparent soil modelling techniques to simulate contaminant transport in rock fractures. A transparent rock replica is constructed to document contaminant propagation in saturated fractures filled with fused silica grains.

EXPERIMENTAL SET UP AND PROCEDURE

Experimental setup and transparent model preparation

The experimental setup consists of a transparent fractured rock replica, an injection system, an optical detecting system and data collectors. All of the experimental devices were built on a vibration isolation optical platform.

Transparent fractured rock model

Silica blocks that were 2 cm (length) × 2 cm (width) × 2 cm (depth) in size were used to replicate fractured rock in this experimental investigation. The apertures between silica blocks were considered as rock fractures. A regular fracture network could be built when the silica blocks were placed in order. The fractures in the blocks were filled with fused silica grains with a particle size between 0.1 to 1 mm. The refractive index (RI) of the fused silica was 1.4585. The related physical properties of the fused silica can be found in Liu et al. (2013) and were generally similar to those of Chinese standard sand. Calcium bromide solution was applied as pore fluid, which can be made the same RI as the fused silica and can be completely mixed with the fused silica. $CaBr_2$ which is white powder or crystals with a purity of more than 96% was used to prepare the calcium bromide solution. A series of trial and error tests shows that the RI of calcium bromide solution reached 1.4585 at a concentration of approximately 65% thus the best transparency achieved. An ink-dyed calcium bromide solution was used to simulate the contaminant. When the contaminant propagates among the fractures, the position of the contaminant front in every fracture could be easily observed and recorded since the fractured rock replica is transparent.

The injection system and the optical detecting system

Fig. 1 shows an overall schematic of experiment set up. A similar drip injection method was used by Hayashi, et al. (2006). The injection pressure was about 1500 mm high which approximates a pressure of 15 kPa. An injection needle with an inner diameter of 1.2 mm was inserted into the model at a depth of 25 mm below the sample surface. The injection system was connected with transparent pneumatic tubes. A point contaminant source was then simulated by the injection at the end of the needle.

The optical system was a modified particle image velocimetry (PIV) system. Three black and white Charge Coupled Device (CCD) cameras were connected to a computer for image capturing and collecting. The CCD cameras had a resolution of 1024 × 768 pixels and a maximum frame rate of 30

frames per second (fps). The CCD cameras were controlled by a computer through the MV Capture 2.0 program.

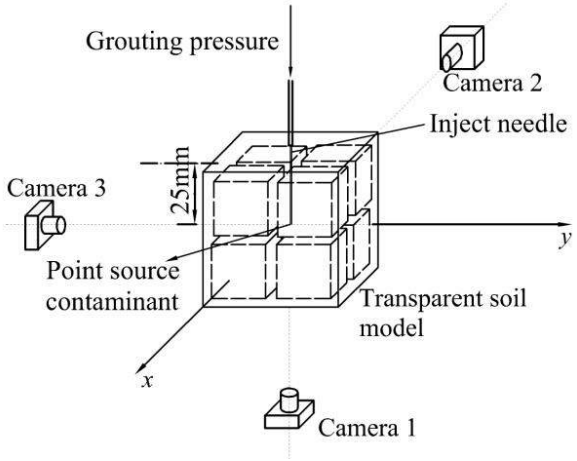

Figure 1 Schematic of experimental set up

Transparent model preparation

The transparent model was constructed in a transparent Plexiglas mold with an inner size of 5 cm (length) × 5 cm (width) × 5 cm (depth). Four silica blocks were evenly and symmetrically packed in blocks of 2 × 2 to form a layer of the rock replica. The fractures with an aperture of about 3 mm were filled with fused silica grains and pore fluid. The model was then de-aerated by using a vacuum pump to achieve the best transparency. Fig. 2 shows the transparent replica and its transparent effect.

Test procedure

A background image was taken before the injection. Once the injection pipe was turned on, a series of images were then captured during the injection at a frame rate of 30 fps until the test stopped after 22 s of contaminant injection.

RESULTS AND ANALYSIS

Propagation characteristics of contaminant front

Fig. 3 shows some images captured by Camera 2 at different times during the experiment, in which the contaminant transport process lasted for about 22 s and approximately 2000 images were captured. The contaminant propagates almost symmetrically. The contaminant first penetrates in a nearly circular shape inside the fractures; see Figs. 3(a) to 3(e). However, the contaminant did not propagate in an entirely circular shape; see Figs. 3(f) to 3(j). The contaminant front appeared inside the fractures where the penetration was faster. With a longer time, the propagation boundary became more irregular. The pore structure of the fused silica sands themselves caused the plume-shaped edges of the propagation front.

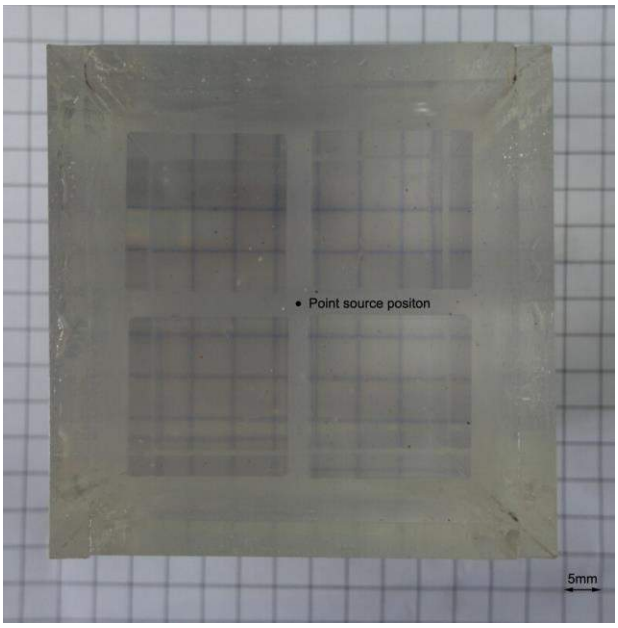

Figure 2 Transparent silica rock replica

Contaminant penetration length and propagation area

The images captured in the test were analyzed by digital image process software. The propagation front was traced to acquire perimeter. The propagation area was calculated according to the traced data. Table 1 lists the image scale coefficients calculated in accordance with the pixel value and real size of the silica blocks.

Table1 Scale coefficients of images in accordance with size of silica block

Location	Pixel value	Real size (cm)	Length scale coefficient (cm^{-1})	Area scale coefficient (cm^{-2})
Camera1, underneath the model	256	2	128	16384
Camera 2, behind the model	233	2	116.5	13572
Camera 3, on the left of the model	233	2	116.5	13572

Fig.4 shows the maximum penetration length of the contaminant in the images. The equations are as follows

$$L_N = -2.31t^{2/3} + 18.01t^{1/3} - 13.16 \quad (1)$$

$$L_B = -1.18t^{2/3} + 11.52t^{1/3} - 7.96 \quad (2)$$

$$L_L = -1.23t^{2/3} + 12.76t^{1/3} - 8.71 \quad (3)$$

Where L_N = contaminant penetration diameter taken from underneath the model, mm; L_B = contaminant penetration diameter taken behind the model, mm; L_L = contaminant penetration

diameter taken on the left side of the model, mm; and t = injection time, s. The start times of contaminant propagation in three locations were 0.412 s, 0.456 s and 0.535 s, respectively.

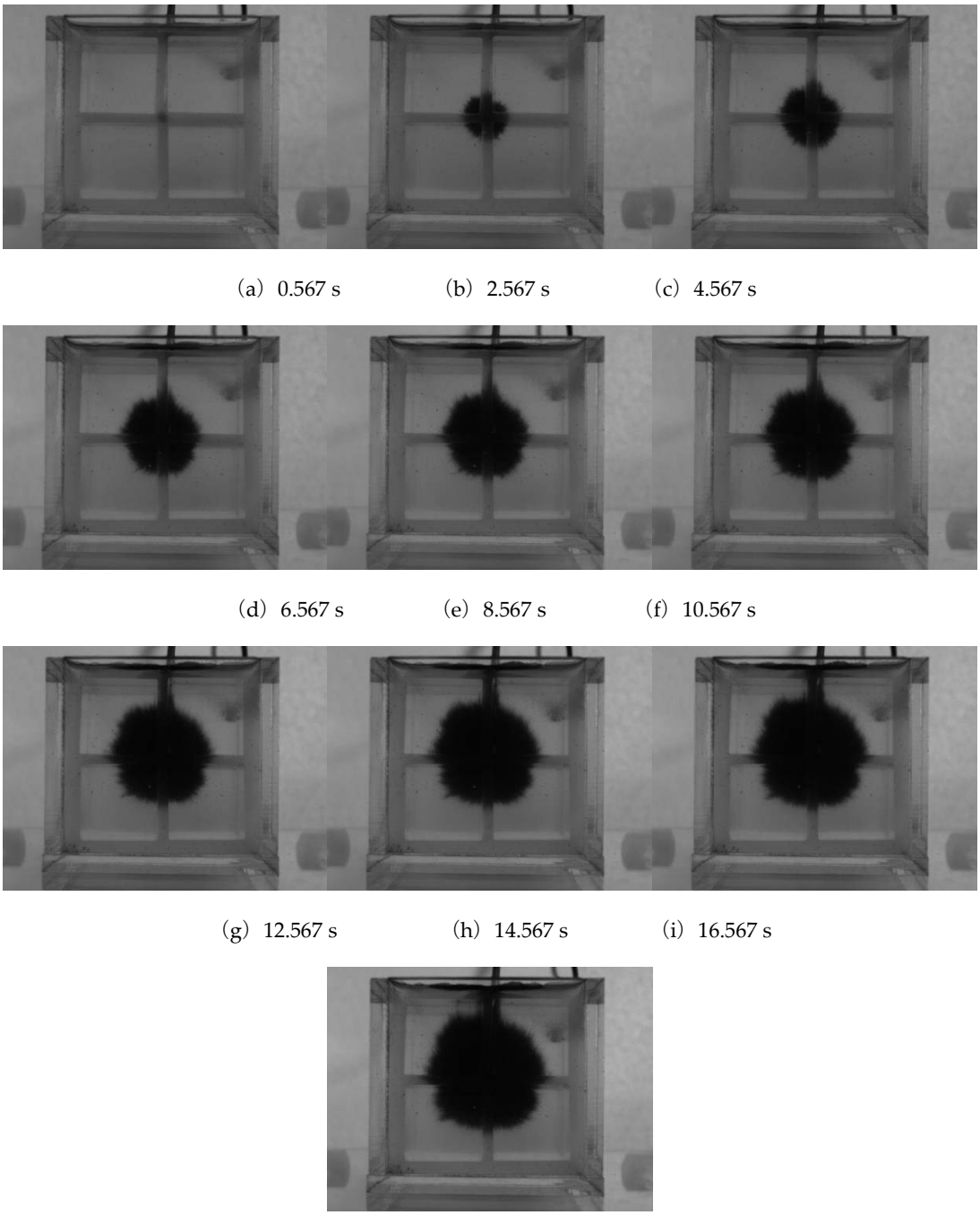

(a) 0.567 s (b) 2.567 s (c) 4.567 s

(d) 6.567 s (e) 8.567 s (f) 10.567 s

(g) 12.567 s (h) 14.567 s (i) 16.567 s

(j) 18.567 s

Figure 3 Contaminant propagation images captured by Camera 2 at different times

The border of the propagation for every image was approximately traced, and the propagation area was calculated. Fig. 5 shows the variation in the contaminant propagation area with time. The equations are as follows

$$A_N = -0.020t^2 + 0.892t - 0.758 \quad (4)$$

$$A_B = -0.006t^2 + 0.532t - 0.120 \quad (5)$$

$$A_L = -0.005t^2 + 0.550t - 0.199 \quad (6)$$

Where A_N = contaminant propagation area taken from underneath the model, cm²; A_B = contaminant propagation area taken behind the model, cm²; A_L = contaminant propagation area taken on the left side of the model, cm²; and t = injection time, s. The start times are 0.332 s, 0.455 s and 0.590 s, respectively.

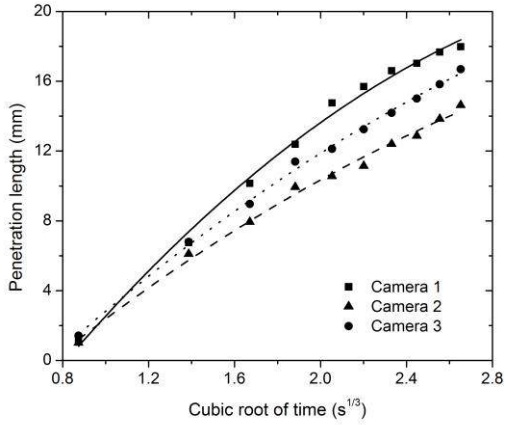

Figure 4 maximum penetration lengths with time

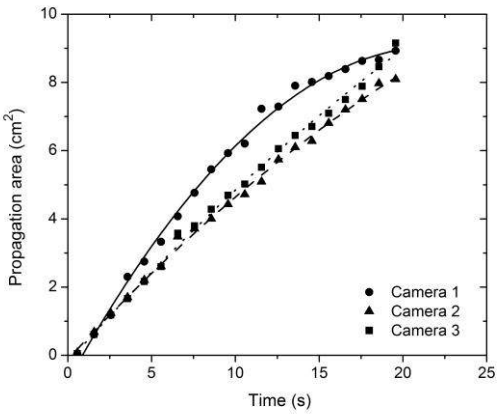

Figure 5 Contaminant propagation areas with time

CONCLUSIONS

This paper has presented an experimental investigation in which contaminant transportation phenomena were observed in a saturated transparent fracture replica filled with sand grains by using three CCD cameras. A series of images during contaminant transport have been captured and analyzed to identify the plume boundary, penetration length, and propagation area.

The results indicate that there is a square relationship between the maximum penetration length and the cubic root of injection time, and also a square relationship between the contaminant transport area and injection time when the pressure head is constant.

This paper is a very preliminary attempt to investigate the possibility of real-time observation of contaminant transport in a rock fracture replica. There are still many factors that need to be taken into consideration in further studies for more real and complicated geological conditions, such as different fracture shapes, dip angles, groundwater pressures. Furthermore, physical and chemical interactions should also be considered in future investigation.

ACKNOWLEDGEMENTS

The authors would like to acknowledge the financial support of the Natural Science Foundation of China under Grant No. 41472268, the 973 Program under Grant No. 2013CB227903 and PAPD.

REFERENCES

Fernandez, R., Iskander, M. and Tabe, K., (2011) 3D contaminant flow imaging in transparent granular porous media, Geotechnique Letters, Vol.1, pp. 71–78.

Hayashi, S., Chai, X. J., Matsunaga, K., and Toki, A. (2006) Drip injection of chemical grouts: a new apparatus, Geotechnical Testing Journal., Vol. 29, pp. 108–116.

Lo, H-C., Tabe, K., Iskander, M., and Sung, H. (2008) Modelling of Multi-Phase Flow and Surfactant Flushing Using Transparent Aquabeads, Geo Congress, pp. 846–853.

Iskander, M., Liu, J., and Sadek, S., (2003) Modelling 3D flow & soil structure interaction using optical tomography. National Science Foundation Final Report Project No. CMS 9733064.

Liu, J., Gao, Y., and Sui, W. (2013) Visualization of Grout Permeation inside Transparent Soil, IACGE 2013, pp. 188–194.

Liu, J, Iskander, M, Tabe, K. and Kostarelos, K (2005) Flow Visualization Using Transparent Synthetic Soils. Proceedings 16 ICSMGE, Vol. 4, pp 2411–2414.

Mannheimer, R.J. and Oswald, C.J. (1993) Development of transparent porous media with permeabilities and porosities comparable to soils aquifers and petroleum reservoirs. Ground Water, Vol.31, pp 781–788.

Reactive Transport Model of the Carbonate-Evaporite Elk Point Group Underlying the Athabasca Oil Sands

Matt Neuner and Skya Fawcett
Golder Associates, Canada

ABSTRACT

A reactive transport model was constructed to investigative how the carbonate-evaporite aquifer system within the Devonian Elk Point Group in northeast Alberta has evolved over geologic time and to evaluate connectivity in the present system. The mineable area of the Athabasca Oil Sands overlies the Elk Point Group where regional dissolution of halite and anhydrite has eroded the Prairie Evaporite Formation from a thickness of approximately 260 m to as thin as 20 m. Groundwater chemistry changes along the flowpath towards the Athabasca River, reflecting the evaporite distribution. Water types change from bicarbonate- to sulphate- to chloride-types, and salinities increase exponentially toward saturation with respect to halite. The model was constructed as a 1-D domain in PHREEQC to simulate the regional dissolution of the evaporites, using hydraulic testing results, isotopic data, and the measured hydrochemistry to constrain the transport parameters. The dual porosity function in PHREEQC was needed to calibrate the model to the measured chloride distribution over the 90 km-long model domain, indicating the role of mass transfer from poorly-connected regions of the aquifer system. The simulated duration of the regional dissolution was on the order of 50,000 to 500,000 years, suggesting that the phases of dissolution postulated from geologic evidence from the pre-Cretaceous to the Holocene (Stoakes et al. 2014a) may have consisted of relatively shorter pulses of dissolution. Two types of accelerated anhydrite dissolution and dedolomitization are identified for the current conditions: anhydrite/gypsum removal by low-TDS, bicarbonate-dominated waters and increased anhydrite/gypsum solubility with higher salinity. Both of these processes appear to be occurring within approximately 20 km east of the Athabasca River. Reactive transport modelling of the regional system may help to identify local areas of karst development and vertical connection to open-pit mines in the overlying McMurray Formation.

Keywords: Reactive transport carbonate evaporite karst

INTRODUCTION

The mineable Athabasca Oil Sands Area (AOSA; Figure 1) is underlain by a carbonate-evaporite aquifer system with hydraulic heads >50 m above the planned base of the open-pit mines. A karst-type inflow of saline water to one of the mines in 2010 demonstrated the high degree of vertical connectivity to this aquifer system where hydraulic windows exist (Wozniewicz et al. 2014). Characterization of the Devonian strata and specifically the aquifer system within the Elk Point Group in the region has increased significantly since the 2010 karst inflow event.

This study presents a reactive transport model that provides an investigative tool to aid in attempts to identify regions with highly-transmissive karst and potential vertical connectivity between the Elk Point Group and overlying McMurray Formation. The model was also used to explore the evolution of the Elk Point aquifer system over geologic time and to postulate a mechanism for the present-day hydrochemical distribution. Data from previously published studies were used to calibrate the model, as the geochemical interpretation from recent field programs at several operating mines is ongoing. Dedolomitization is assessed at a regional scale, as it has been recognized as a key process resulting in enhanced permeability laterally within the Elk Point aquifer system and potentially also enhancing vertical connectivity (Wozniewicz et al. 2014).

BACKGROUND

Geologic Setting

The mineable AOSA is near the northeast edge of the Western Canadian Sedimentary Basin (Figure 1), where the Phanerozoic strata form a wedge over the Canadian Shield with maximum thickness of approximately 700 m. Devonian strata consisting primarily of marine carbonates regionally dip to the southwest (Figure 2) due to subsidence associated with formation of the Rocky Mountains. Cretaceous sediments including the McMurray Formation, which hosts the oil sands deposit, overlie a 200 million year gap in the geologic record referred to as the Pre-Cretaceous unconformity.

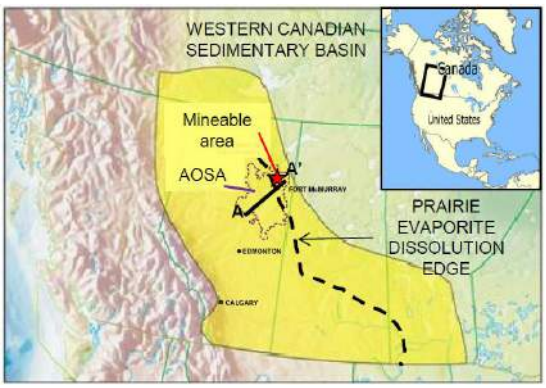

Figure 1 The mineable Athabasca Oil Sands Area

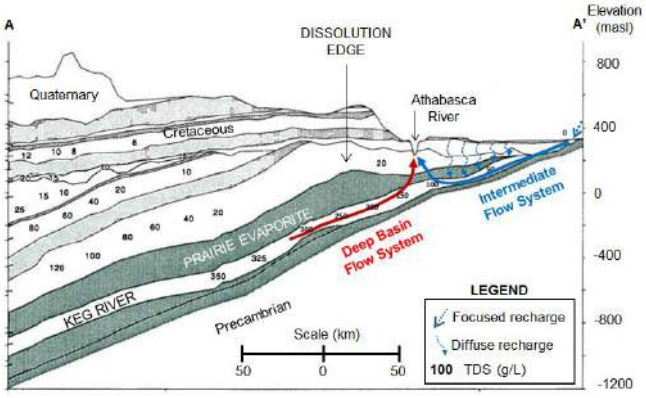

Figure 2 Cross section through Northeast Alberta

The Devonian Elk Point Group includes porous reef buildups of the Keg River Formation and an evaporative sequence in the Prairie Evaporite Formation, which on-laps the reefs. The Prairie Evaporite Formation was deposited as brining-upward sequences of dololaminites, anhydrite, and halite (Stoakes et

al. 2014b). These two formations are overlain by approximately 60 m of primarily marine carbonates and shales, which are referred to here as the Upper Devonian.

Infiltrating meteoric waters to the eastern edge of the basin have dissolved the Prairie Evaporite Formation from an initial thickness of approximately 260 m west of the dissolution edge (Figure 1) to as thin as 20 m near the basin edge. This dissolution resulted in extensive collapse of the overlying strata and enhanced permeability within the Prairie Evaporite Formation.

Physical Hydrogeology

Dololaminites in the lower Prairie Evaporite Formation form a highly transmissive (10^{-3} to 10^{0} m^2/s) aquifer where they have been more extensively dedolomitized, as evident in regional responses to the 2010 inflow event (Wozniewicz et al. 2014). This event provided direct evidence of karst in the Devonian strata and of good connection in places between the Elk Point and the overlying McMurray Formation, neither of which had previously been unequivocally accepted (e.g., Alsands 1981). Reefs in the Keg River Formation form aquifers capable of sustained wastewater injection (1,733,000 m^3 over ten years; Husky 2011). Most multi-day hydraulic tests in the region have been conducted over both of these formations and have yielded transmissivities on the order of 10^{-5} m^2/s. The Prairie Evaporite Formation on-laps to the sides of reefs suggesting some degree of connection; hence, the two aquifers are collectively referred to as the Elk Point aquifer system.

The Elk Point aquifer system is highly heterogeneous, and flow paths at the sub-lease scale are thought to follow complex fracture networks with a wide range of connectivity. At the regional scale, the subcrop of the Elk Point Group beneath Quaternary sediments near the provincial border (Figure 3) provides focused recharge to the aquifer system. Groundwater flows from the subcrop generally westward toward the discharge zone at the Athabasca River, and the system also receives more diffuse vertical recharge through the overlying units (Figure 2).

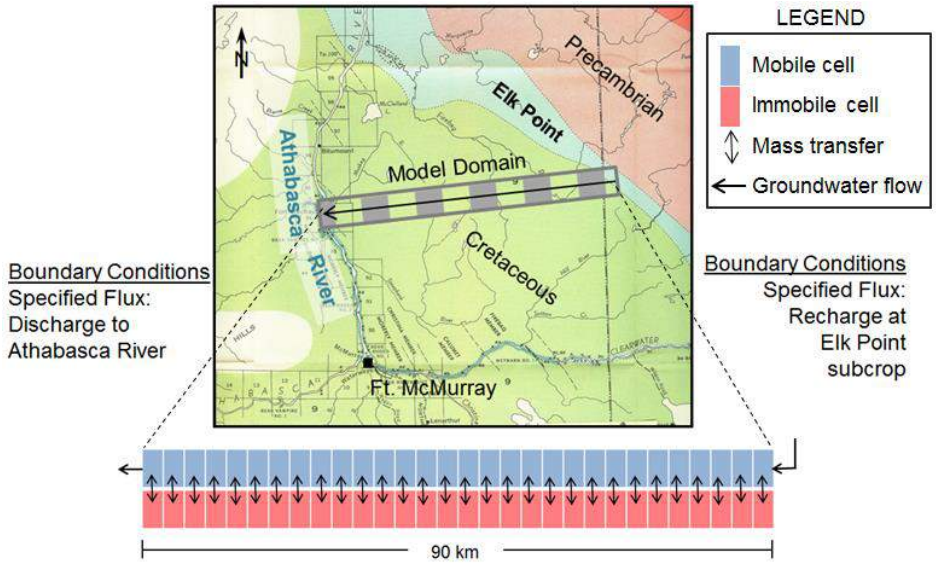

Figure 3 Geologic map: units subcropping beneath Quaternary sediments (Norris 1963), adapted with regional flow directions in the Elk Point and the 1-D domain for the reactive transport model.

GEOCHEMISTRY OF THE ELK POINT AQUIFER SYSTEM

The regional distribution of evaporite minerals in the Prairie Evaporite Formation (Figure 4) provides a primary control on the hydrochemistry within the Elk Point aquifer system. Generally in the region, halite is still present and dissolving between the dissolution edge and the Athabasca River. Within approximately 20 km to 30 km east of the Athabasca River halite has been removed and anhydrite is dissolving, while in the eastern part of the region both halite and anhydrite have been removed leaving an extensively collapsed region with dolomite the primary mineral (Figure 4; Schneider and Grobe 2013).

A preliminary model was constructed in PHREEQC (v. 3.06; Parkhust and Appelo 2013) to begin investigating the relationship between dissolution of the Prairie Evaporite over geologic time and the present day hydrochemistry. A batch model domain of one litre was filled with an approximate composition of Prairie Evaporite Formation prior to dissolution, based on publically-available geologic logs: 40% dolomite ($CaMg(CO_3)_2$), 20% halite (NaCl), 20% anhydrite ($CaSO_4$), 20% calcite ($CaCO_3$), and 10% porosity. The model domain was then successively flushed with pure water equilibrated with atmospheric CO_2 (pCO_2 10^{-2} atmospheres [atm]) and allowed to equilibrate to these minerals and CO_2 at 10°C at each step. The results of this preliminary modelling exercise are shown in Figure 5.

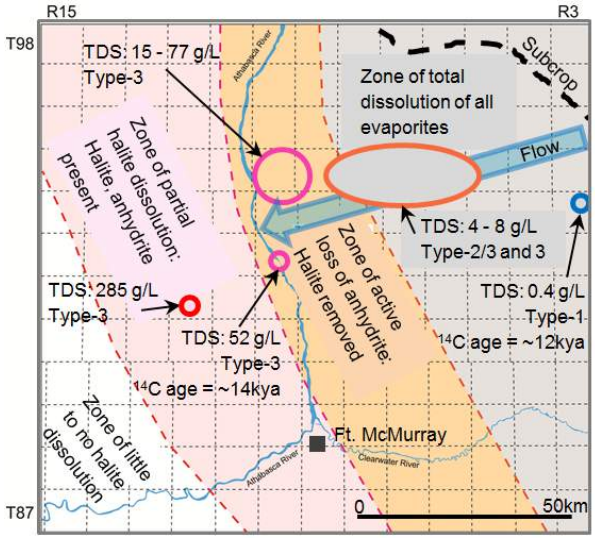

Figure 4 Prairie Evaporite dissolution map (adapted from Schneider and Grobe 2013); samples from Elk Point wells and saline a saline spring (1 to 9 wells per oval).

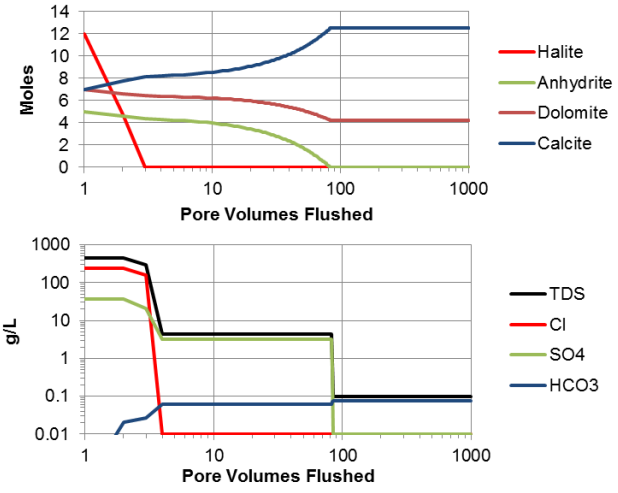

Figure 5 Results from a preliminary modelling exercise: successive flushing with fresh waters of a one litre domain representing the Prairie Evaporite Formation.

Three distinct zones were simulated with the preliminary model, similar to the regional dissolution map (Figure 4). The simulation illustrates that halite in the Elk Point Group was dissolved after only a few pore volumes had been flushed by infiltrating fresh recharge waters, such that regions with halite remaining and salinity of >300 g/L TDS can be assumed to have had little contact with fresh waters. An intermediate region was simulated having anhydrite remaining but halite removed and waters dominated by sulphate and salinity of approximately 5 g/L TDS (Figure 5). Where on the order of one hundred pore volumes or more had been flushed in the preliminary model, the anhydrite was removed leaving only dolomite, calcite, and bicarbonate-dominated waters with salinity on the order of 0.1 g/L.

Water types and salinities in samples collected from the Elk Point aquifer system in the region are shown on Figure 4 (Alsands 1981, ARC 1975, Cenovus 2011, Golder 2002, Gue 2012, and Husky 2011). Water type classifications developed here are listed in Table 1. The samples exhibit an evolution along the east to west flowpath that reflects the mineralogy and is generally similar to the results from the preliminary modelling exercise. Near the focused recharge zone at the Elk Point subcrop, a sample had salinity of 0.4 g/L TDS and was dominated by bicarbonate. Approximately 45 km to 60 km downgradient of the subcrop, salinities range from 6 g/L to 8 g/L TDS with dominant anions of sulphate and chloride. Within 15 km of the Athabasca River, salinities in the Elk Point increase to 77 g/L TDS with chloride the dominant anion (Figure 4). West of the river a chloride-dominated sample with salinity of 285 g/L TDS has been collected, and similar samples have been collected from wells farther to the west.

Table 1 Water types in the Elk Point aquifer system, northeast Alberta

Water Type	Dominant Anion	Origin of Water	Salinity	Residence (m=million; k=thousand)	Occurrence
Type 1	Bicarbonate	Meteoric	< 2 g/L	< 10k yrs	Near subcrop
Type 2	Sulphate	Meteoric	3 to 5 g/L	< 10k yrs	~20 to ~50 km east of Athabasca R.
Type 3	Chloride	Meteoric	5 to 300 g/L	5k to 40k yrs	East of dissolution edge
		Connate	> 250 g/L	> 1m yrs (?)	West of dissolution edge
Intermediates	HCO_3, SO_4, Cl	Meteoric	1 to 10 g/L	< 40k yrs	East of Athabasca R.

The main geochemical processes, based on the mineralogy, hydrochemistry, and preliminary modelling, are: halite (NaCl) dissolution, anhydrite ($CaSO_4$) dissolution, dolomite ($CaMg(CO_3)_2$) dissolution, and calcite ($CaCO_3$) dissolution/precipitation. Ion exchange in the Elk Point in the region is thought to be less significant than the main mineral interactions listed above, but is significant enough to characterize the samples east of the dissolution edge as having meteoric origin, using the Index of Bases Exchange (IBE) formulation of Collins (1975). Samples west of the dissolution edge have IBE greater than the diagnostic cut-off for connate water defined by Collins (1975) of 0.129, indicating deep basin water with residence time of millions of years or more.

Isotopic signatures further characterize origins of waters in the Elk Point. Deep basin waters sampled in the Edmonton area have $\delta^{18}O$ and $\delta^{2}H$ signatures of warm recharge and a high degree of water-rock interaction (Simpson 1999). Samples from Elk Point wells and saline springs east of the dissolution edge in the region have meteoric $\delta^{18}O$ and $\delta^{2}H$ signatures of cold water recharge, with $\delta^{18}O$ values ranging from -19.2‰ to -24.6‰ (Cenovus 2011, Gue 2012, Wallick and Dabrowski 1982). These values and ^{14}C groundwater age estimates of approximately 10,000 to 30,000 years indicate that Elk Point waters east of the dissolution edge represent a mixture of meltwater from the Laurentide ice sheet, which melted in the region approximately 10,000 years ago and has a $\delta^{18}O$ signature of -25‰ to -28‰, and warmer water similar to present-day recharge (-17.7‰ to -19‰) (Grasby and Chen 2005; Gue 2012).

Karst development in the region is caused by halite dissolution, anhydrite/gypsum dissolution, and dedolomitization. These processes accelerate carbonate dissolution, which is otherwise controlled by pH of the water and specifically carbonic acid sourced from atmospheric CO_2. Dedolomitization causes a large increase in the dolomite dissolution rate (e.g., Palmer 2007; Escoria et al. 2013) due to dissolution of both dolomite and anhydrite. It causes a process referred to as the common-ion effect, with ideal stoichiometry (Appelo and Postma 2005):

$1.8CaSO_4 + 0.8CaMg(CO_3)_2 \rightarrow 1.6CaCO_3 + Ca^{2+} + 0.8Mg^{2+} + 1.8SO_4^{2-}$.

Anhydrite and dolomite dissolution both produce calcium ions, driving precipitation of calcite.

1-D REACTIVE TRANSPORT MODEL

A 1-D reactive transport model was constructed in PHREEQC to attempt to simulate salinities above 5 g/L TDS where halite has been completely or almost completely removed, and to provide an investigative tool to potentially identify areas with higher dissolution rates. The model domain represents a 90 km flow path from the Elk Point subcrop to the Athabasca River, using 30 mobile and 30 immobile cells (Figure 3).

The initial conditions represent the Elk Point prior to dissolution, based on publically-available logs from the region: 40% halite, 40% dolomite, 10% anhydrite, and 10% calcite; 6% porosity; and 1 mol/L dissolved organic carbon (oil and bitumen). Boundary conditions are specified flux into the east end of the domain yielding a groundwater velocity of 10 m/yr through the model domain, and an equivalent discharge rate at the west end. Recharge was simulated as pure water equilibrated to atmospheric CO_2 with pCO_2 of 10^{-2} atm. No transverse flow boundaries are necessitated by the 1-D model geometry: an important limitation, which assumes zero vertical recharge through the overlying Cretaceous sediments and Upper Devonian into the Elk Point aquifer system. This limitation is discussed further below.

A high degree of simulated heterogeneity was required to approximately match the hydrochemistry in samples along the flow path. Dispersion was simulated using a dispersivity of 1000 m for the regional flowpath. The dual-porosity function in PHREEQC was also required: the domain was divided into 30 cells through which the simulated groundwater flows laterally, referred to as mobile cells, and 30 adjacent cells referred to as immobile cells (Figure 3). Rate-limited mass transfer between immobile and mobile cells is allowed, simulating a store-and-release function in the poorly-connected regions of the domain similar to the concept of Harvey and Gorelick (2000). The mobile and immobile cells initially have very high salinity due to equilibration with halite; as the mobile cells are flushed with meteoric recharge, Na and Cl in particular diffuse from the immobile cells into the mobile cells.

The simulated flow velocity of 10 m/yr was chosen based on corrected radiocarbon ages (Figure 4; Cenovus 2011, Gue 2012) and 1-D Darcy flux using hydraulic conductivity from multiple-day hydraulic tests (Alsands 1981, Golder 2002, Husky 2011), average hydraulic gradient of 0.002, and porosity of 10%. Both approaches yielded flow velocity estimates ranging from 1 to 10 m/yr. Flow velocities may have been lower at early stages of the dissolution of the Prairie Evaporite Formation. During the later glacially-driven stages of dissolution, flow velocities could have been an order of magnitude higher or more due to an increased pressure gradient imposed by the receding glacier.

Reactive transport is simulated in PHREEQC by solving equilibrium equations and shifting reaction products from each cell to the next cell along the flowpath, as calculated according to the flow velocity. At each time step in the model (representing approximately 300 yr), the water in each cell (3,000 m length) equilibrates with aqueous and mineral phases using the ThermoChimie database in PHREEQC, which utilizes the specific ion interaction theory (SIT) approach. The SIT approach estimates ion activities based on ionic strength and is hence suitable for solutions with high salinity; the Pitzer approach was not used due to its limited database in PHREEQC. Flow and transport of the reaction products are then simulated by input of the recharge to the eastern-most mobile cell and shifting the water in each mobile cell to the next mobile cell, followed by dispersion, rate-limited mass transfer from the immobile cells, and re-equilibration.

MODEL RESULTS

Dissolution Fronts and Simulation of Present Conditions

A halite dissolution front was simulated advancing from east to west over geologic time, followed by an anhydrite dissolution front (Figure 6). Dissolution fronts were delayed in the immobile model cells, which represent poorly-connected regions in or adjacent to the Elk Point aquifer system.

Figure 7 shows the simulated distribution of salinity and major ions along the flowpath for the present conditions, compared to concentrations in samples (Alsands 1981, ARC 1975, Cenovus 2011, Golder 2002, Gue 2012, and Husky 2011). Present conditions were simulated by 50,000 years of active freshwater recharge. At that time in the simulation, halite was completely removed from the mobile cells and partially remained in immobile cells within 10 km of the Athabasca River. The dissolution front for anhydrite, modelled as gypsum, is simulated to have advanced approximately 15 km (Figure 6), with anhydrite still present in the rest of the model domain.

The modelled concentrations of major ions and TDS in the Elk Point aquifer system (solid lines in Figure 7) approximately match the majority of the concentrations from samples, where available along the regional flowpath. The modelled distribution of water types generally matches those measured in samples: Type-1 in the east, Type-2/3 in the central part of the region, and Type-3 in the western part of the flowpath near the Athabasca River.

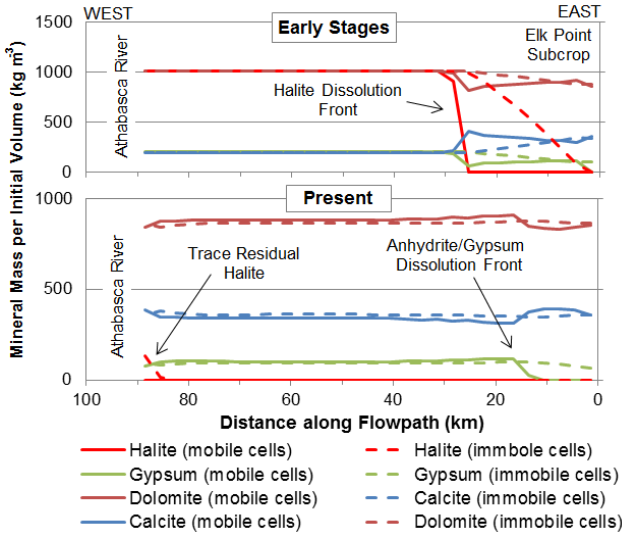

Figure 6 Model results: mineral mass and dissolution fronts along the flowpath, at early stages in the evolution and for the simulated present conditions.

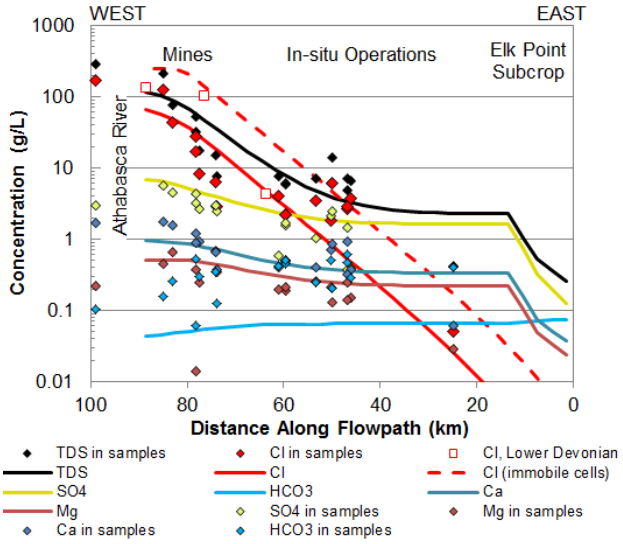

Figure 7 Model results for present conditions, as the 50,000 year simulation: major ions modelled (lines) and in Elk Point (◇) and Lower Devonian (□) samples.

Halite dissolution resulted in removal of more than half of the mass in the model. This large loss in volume was accommodated by regional collapse (not modelled). Anhydrite dissolution and dedolomitization resulted in increases in porosity of <1% to approximately 5%, based on the reactive transport model results.

Areas with Higher Degree of Connectivity

Rates of dissolution of halite, anhydrite, and dolomite were examined with the reactive transport model. Simulated rates of dissolution were highest as the halite dissolution front moved through the region: on

the order of 1,000 g m^{-3} yr^{-1} for halite and in excess of 100 g m^{-3} yr^{-1} for anhydrite and dolomite. As the evolution of flow velocities over geologic time is unknown, modelled dissolution rates are presented for comparison only. The flow rate in the model assumes the halite dissolution products are advanced forward. In the actual system, the halite forms an aquiclude that was being dissolved entirely at the eastern edge and would likely have forced the dissolution products upward, possibly along collapse features at the dissolution front, further enhancing these vertical connections.

Dissolution rates for anhydrite and dolomite at the anhydrite dissolution front (Figure 6) were on the order of 10 g m^{-3} yr^{-1}. Dissolution rates were lower over much of the model domain, except within 20 km of the Athabasca River where they ranged from 0.5 g m^{-3} yr^{-1} to 10 g m^{-3} yr^{-1}. Simulated dissolution rates indicate two types of enhanced anhydrite/gypsum dissolution and dedolomitization: input of Type-1 water (~15 km on Figure 6) and where gypsum solubility is higher due to increased salinity (elevated SO_4 at ~70 to 90 km on Figure 7).

A minority of samples in the area of the mines have Cl concentrations an order of magnitude lower than the regional trend simulated with the model (Figure 6). These low Cl concentrations, which correspond with lower SO_4 and higher HCO_3, indicate greater vertical recharge in those areas. Input of vertical recharge in the eastern area of the mines could provide a driver for circulation of freshwater to development of karst. Mine operators should carry out geochemical modelling at the scale of the lease to further investigate higher dissolution rates.

Model Sensitivity

Model sensitivity was investigated for these parameters:

- Groundwater velocity;
- Mass transfer rate;
- Initial mineral composition; and
- Initial and boundary pH.

Simulations were run with flow velocity one order of magnitude lower and higher than the base case of 10 m/yr by varying the number of shifts as an analogue to flow rate. The higher velocity (100 m/yr), possible during glacial melt, corresponded with a reasonable match to the major ions in samples at a duration of 3,000 years, with dissolution fronts travelling an order of magnitude faster, and dissolution rates approximately 30% faster. Isotopic values and geologic evidence, however, necessitate a longer duration such that a high velocity could have occurred only for a relatively short time. With the lower velocity (1 m/yr), the match to major ions in samples was poor except when a reduced mass transfer rate was used. Dissolution fronts moved an order of magnitude slower, but peak dissolution rates were approximately the same as for the base case. While this slower velocity may have prevailed at earlier phases of the geologic evolution, an average velocity at this rate would necessitate a high proportion of vertical recharge to result in detection of modern carbon. Such a case may result in decreasing groundwater ages along the flowpath, which is not measured in samples.

The distribution of sodium and chloride, in particular, were sensitive to the mass transfer rate. A change of less than half an order of magnitude from the base case $5x10^{-13}$ mol s^{-1} yielded poor matches. The model results were not sensitive to the initial halite, dolomite, or calcite amounts (within +/- 50% of base case), but the timing of the anhydrite/gypsum dissolution front was sensitive to the initial anhydrite amount. Although carbonate reactions can be highly sensitive to pH, changing the recharge boundary pH or the initial conditions from pH 7 to either 6 or 8 yielded essentially no change in the results. The model also

was not sensitive to the initial pCO2 value, and was not equilibrated with CO_2 (although the preliminary model was).

The simulated duration of active groundwater flow through the Elk Point and movement of dissolution fronts are sensitive to the selection of present-day groundwater velocity, and hence represents a lower estimate on the duration and an upper bound on dissolution front velocity, each with uncertainty of approximately an order of magnitude. Dissolution rates at the regional scale were less sensitive to the flow velocity. The model was not sensitive to whether halite was remaining in the poorly-connected model cells or completely removed: elevated chloride can be explained by either diffusion or active interaction with residual halite.

CONCLUSIONS

Karst inflow from the carbonate-evaporite Elk Point aquifer system to the overlying mines of the Athabasca Oil Sands Area is a major geohazard for the operators in the region. The following conclusions from investigative geochemical modelling with a 1-D reactive transport model are highlighted:

- The hydrochemistry within the Elk Point is directly related to mineral dissolution.
- Poorly-connected regions provide an important store-and-release function affecting the regional distribution of salinity in the Elk Point.
- Removal of anhydrite by Type-1 (TDS <1 g/L, HCO_3-dominated) water is associated with accelerated dedolomitization occurring in the eastern part of the region and possibly in areas of increased vertical recharge.
- Anhydrite dissolution and dedolomitization are also accelerated within approximately 20 km of the Athabasca River where salinity is greater than approximately 10 g/L, yielding increased anhydrite and gypsum solubility.
- The modelled dissolution rates suggest that dissolution of the Prairie Evaporite appears to have occurred as shorter periods of active dissolution (total duration 50,000 to 500,000 years) within phases of karst development in the Jurassic, Cretaceous, Tertiary, and Quaternary (Stoakes et al. 2014a).

The modelling approach used in this regional study has several limitations: the 1-D domain assumes zero or constant vertical recharge such that focused vertical recharge was only identified by mismatch to the model; mineral dissolution rates may not be applicable to shorter time scales, as kinetics were not included; an aggregate flow system was simulated rather than realistic geometries of flowpaths; and geologic information at the lease-scale to sub-lease scale were not included. This modelling approach is used as an investigative tool to improve the understanding of the evolution of the aquifer system and to aid in identification of areas of higher connectivity, rather than comprehensively modelling the system.

ACKNOWLEDGEMENTS

This work was initiated with direction from Hugh Abercrombie. Comments from Valerie Bertrand and an anonymous reviewer are greatly appreciated.

NOMENCLATURE

Cl = chloride HCO_3 = bicarbonate SO_4 = sulphate TDS = total dissolved solids

$\delta^{18}O$ = isotopic ratio for oxygen-18 to oxygen-16 $\delta^{2}H$ = isotopic ratio for hydrogen-2 to hydrogen-1

REFERENCES

Alsands Energy Ltd. (Alsands). 1981. *Hydrogeology Part 2, Groundwater Hydrology, Alsands Project—In support of Development and Reclamation Plan*. Dated May 1981.

Appelo, C.A.J., and D. Postma. 2005. *Geochemistry, groundwater and pollution, 2nd edition.* CRC Press, New York. 649 p.

Alberta Research Council (ARC). 1975. *Groundwater Observation Well Network: Athabasca Oil Sands Area*. Information Series 69. 1272 p. including updates to 1977.

Cenovus Energy (Cenovus). 2011. *Telephone Lake Project – Volume 2: Environmental Impact Assessment*. Submitted to the Alberta Energy Resources and Conservation Board.

Collins , G. 1975. *Geochemistry of Oil Field Waters*. Elsevier. 495 pp.

Escoria, L-.C., E. Gomez-Rivas, L. Daniele, and M. Corbella. 2013. *Dedolomitization and reservoir quality: insights from reactive transport modelling.* Geofluids VII: Paris 2012. 11 p.

Golder Associates Ltd. (Golder). 2002. *Firebag In-Situ Oil Sands Project: Deep Well Disposal Program and Monitoring Plan.* Consultant report submitted to Alberta Energy and Utilities Board and Alberta Environment. 723 p.

Grasby, S.E., and Z. Chen. 2005. *Subglacial recharge into the Western Canada Sedimentary Basin – Impact of Pleistocene glaciation on basin hydrodynamics.* GSA Bulletin, 117(3/4): 500-514.

Gue, A. 2012. *The Geochemistry of Saline Springs in the Athabasca Oil Sands Region and their Impact on the Clearwater and Athabasca Rivers*. M.Sc. Thesis. Calgary, AB: University of Calgary.

Harvey, C., and S.M. Gorelick. 2000. *Rate-limited mass transfer or macrodispersion: Which dominates plume evolution at the Macrodispersion (MADE) site?* Water Resources Research, 36(3):637-650.

Husky Energy Ltd. (Husky). 2011. *Addendum Application for Project Amendment Submitted under Application No. 1673591 for ERCB Scheme Approval No. 10419*. Calgary: ERCB.

Norris, A.W. 1963. *Devonian stratigraphy of northeastern Alberta and northwestern Saskatchewan.* Geological Survey of Canada, Memoir 313, 168 p.

Palmer, A.N. 2007. *Variation in Rates of Karst Processes*. Proceedings of Time in Karst Symposium, Postojna, Slovenia, March 14 to 18, 2007: 15-24.

Parkhurst, D.L., and Appelo, C.A.J. 2013. *Description of input and examples for PHREEQC version 3—A computer program for speciation, batch-reaction, one-dimensional transport, and inverse geochemical calculations: U.S. Geological Survey Techniques and Methods*, book 6, chap. A43, 497 p.

Schneider, C.L., and M. Grobe. 2013. *Regional Cross-Sections of Devonian Stratigraphy in Northeastern Alberta (NTS74D, E)*. Alberta Energy Regulator, AER/AGS Open File Report 2013-05, 25 p.

Simpson, G.P. 1999. *Sulfate Reduction and Fluid Chemistry of the Devonian Leduc and Nisku Formations in South-central Alberta.* Ph.D thesis, University of Calgary. Alberta, Canada. 265 p.

Stoakes, F.A., M. Verhoef, and R. Mahood. 2014a. *Multiphase solution removal of the Prairie Evaporite Formation in northease Alberta (Implications for the oil sands mining community)*. GeoConvention 2014. Calgary, Canada.

Stoakes, F.A., M. Verhoef, and R. Mahood. 2014b. *Evolution of a regional interconnected diagenetic aquifer in the Lower Prairie Evaporite of northeast Alberta.* GeoConvention 2014. Calgary, Canada.

Wallick, E.I., and T.L. Dabrowski. 1982. *Isotope hydrochemistry of the Alsands project area, Athabasca Oil Sands, northeast Alberta.* Proc. 2nd National Hydrogeologic Conference, Winnipeg, Feb. 2-4. 50-58.

Wozniewicz, J.S., F.A. Stoakes, M. Davies, M. Verhoef, R. Mahood. 2014. *Update of Devonian Hydrostratigraphy in the Athabasca Mineable Oil Sands Area, NE Alberta*. GeoConvention 2014. Calgary.

10th ICARD IMWA 2015 | 10th International Conference on Acid Rock Drainage & IMWA Annual Conference

Using Instrumentation Data to Develop Detailed Conceptual Models for Waste Rock Geohydrology

Steven Pearce[1] and Bonnie Dobchuk[2]

1. *O'Kane Consultants, Australia*
2. *O'Kane Consultants, Canada*

ABSTRACT

The installation of instruments within waste rock dumps (WRD) enables the conceptual understanding of unsaturated zone hydrology using recorded data. Instrumentation has been used for many years as part of the assessment and monitoring of cover systems on WRDs. Conversely, the installation of instrumentation at greater depths within WRDs is less common (with the exception of tailings dams). The general understanding of unsaturated zone hydrogeology and geochemistry deeper in WRDs is typically based on academic theory and conjecture, rather than being derived from measured field data.

O'Kane Consultants Pty. Ltd. has completed the installation of over 150 instruments in WRD landforms in the Pilbara, WA. The instruments were installed to depths of 100 m as part of a long term monitoring and assessment program.

Data from the instrumentation installed to date has been used to develop some fundamental concepts for a detailed conceptual model for the geohydrology of WRDs within a semi-arid environment. The concept of advective drying for example has been determined as a significant factor in the process of wetting up of the waste rock. The analysis of matric potential and temperature sensor data indicates that significant moisture cycling through the waste rock dumps occurs as a result of advection forced drying. A key consequence of advective drying is to increase theoretical timeframes for "wetting up" of waste rock to occur as the overall water balance for the waste rock dump is significantly impacted by this process that is not commonly included as part of traditional water balance calculations. The process also results in transfer of oxygen and moisture through waste dumps in the vapour phase that stimulates oxidation reactions in material buried deep within the waste dump that would be considered as being "oxygen and moisture limited" based on theoretical understanding of waste dump geohydrology.

**There is no full article associated with this abstract.*

CHAPTER 4

PREDICTION OF DRAINAGE CHEMISTRY

The ADTI/SME Prediction Volume: Techniques for Predicting Metal Mining Influenced Water: The Consensus Process and What's New

R. David Williams[1], Lisa Kirk[2], Linda Figueroa[3] and Sharon Diehl[4]
1. U. S. Department of Interior, Bureau of Land Management, USA
2. Enviromin, USA
3. Colorado School of Mines, USA
4. U. S. Geological Survey (retired), USA

ABSTRACT

Techniques for Predicting Metal Mining Influenced Water, which addresses the prediction and management of mine-affected water, is Volume 5 in the series of collaborative publications between the Acid Drainage Technology Initiative (ADTI), and the Society for Mining, Metallurgy and Exploration (SME),. Other volumes in the ADTI/SME series have included: Volume 1, *Basics of Metal Mining Influenced Water*, Volume 2, *Mitigation of Metal Mining Influenced Water*, Volume 3, *Mine Pit Lakes, Characteristics, Predictive Modeling, and Sustainability*, and Volume 4, *Sampling and Monitoring for the Mine Life Cycle.* A final volume addressing methods for modeling future water quality is in preparation.

Acidic and metal-enriched mine-affected water is a worldwide environmental problem resulting from weathering of mine-tailings and waste-rock. Management of mined materials is necessary to control impacts on surface and groundwater. The Prediction Volume summarizes the status of acid drainage and metal leaching prediction methods within the context of current best management practice. The volume repeatedly stresses the importance of a detailed understanding of geology including lithology, mineralogy and alteration history to interpret both static and kinetic acid drainage test results. The volume also proposes flexibility for kinetic test duration through the development of a site-specific objective-based framework that can be developed and modified to address project specific objectives.

INTRODUCTION

ADTI and the partnership with SME (after Hornberger, et al., 2000)

In 2014, the Acid Drainage Technology Initiative (ADTI)/Society of Mining, Metallurgy and Exploration (SME) published their prediction volume*: Techniques for Predicting Metal Mining Influenced Water (Prediction)*, one of several guidance documents being prepared by ADTI. The ADTI was initiated in 1995 by federal agencies, the National Mining Association, and the Interstate Mining Compact Commission to identify, evaluate and develop cost-effective and practical acid drainage management technologies. A founding team of regulatory, academic, and industry scientific experts envisioned that a consensus could be developed on reliable, standard static and kinetic test methods and other aspects of mine drainage prediction in the Appalachian Coal Basin. The name ADTI was also selected to emphasize the organization's central focus on technology development and transfer, rather than regulatory or policy issues. Early meetings of the Working Groups demonstrated the great value of coal-mining and metal-mining representatives working together on common objectives to address acid drainage problems confronting both sectors of the mining industry. Although initial efforts at developing various ADTI guidance went well, significant differences between coal mining and metal mining suggested the need for a Metal Mining Sector of ADTI (ADTI-MMS) to more effectively represent the interests of the metal-mining industry and the agencies involved in regulating and remediating metal mine sites. A more detailed historical review of the foundation of ADTI is provided by Hornberger et al., 2000.

The ADTI mission is to use the consensus process to refine prediction methods and management technology for the prevention, treatment and abatement of AMD/ARD pollution in an effective and economical manner. ADTI members believe that it is more productive to solve differences of opinion through the application of good science and consensus process rather than litigation.

Five technical focus areas were identified: (1) Sampling/Monitoring, (2) Prediction, (3) Mitigation, (4) Pit Lakes, and (5) Modeling. In 2007 the ADTI-MMS entered into an agreement with the Society for Mining, Metallurgy and Exploration (SME) to publish the workbooks noted above. The first of these workbooks was published in 2008: *Basics of Metal Mining Influenced Water*. Subsequent volumes include: *Mitigation of Metal Mining Influenced Water* (2009), *Mine Pit Lakes Characteristics, Predictive Modeling and Sustainability* (2009), and in most recently, in 2014, the volume described here, *Techniques for Predicting Metal Mine Influenced Water* and another, *Sampling and Monitoring for the Mine Life Cycle*. The last of the five volumes, on the subject of modeling, is anticipated in 2015.

Prediction Volume

Work on the ADTI prediction volume, began shortly after SME and ADTI agreed to coordinate on the series of workbooks in 2007. As with all the workbooks, volunteer collaboration within the consensus process has proceeded somewhat slowly. Initial drafts of the volume prepared with input from multiple authors were circulated in 2010. Following extensive reviews and edits, a final version was delivered to SME in the fall of 2013 for more detailed editing by SME. The volume was released in March of 2014.

Much of the volume's topics will look familiar to anyone working with rock characterization and acid drainage prediction:

- Chapter 1: Introduction
- Chapter 2: Acid Rock Drainage, Sulfide Mineral Geochemistry Affecting Drainage
- Chapter 3: Prediction: Background
- Chapter 4: Overview of Predictive Methods (Tools)
- Chapter 5: Evaluation
- Chapter 6: Application and Conclusion
- Appendices of Test Methods

Chapter 2, taken largely from Lapakko et al. (2004), focuses on mineral dissolution reactions that influence mine-waste drainage quality. The reactions presented result in acid generation, acid neutralization, and trace metal release. Within the chapter, soluble and insoluble ferrous and ferric solid phases of interest in mine and process waste characterization are identified.

Chapter 3 focuses on geology, lithology, and alteration, and includes a discussion of geoenvironmental models which can provide an initial assessment of potential water quality impacts based on characteristics of a mineral deposit. The chapter also includes a discussion of analytical techniques used to identify sample mineralogy, a critical need for interpreting both static and kinetic tests as noted below.

Chapter 4 includes a more detailed discussion than the GARD Guide (INAP, 2011) of the various static tests, short term and field leach tests, and kinetic tests, including field test methods that are, or have been used to, characterize materials. The strengths and limitations of the tests are discussed here and some examples of their use are also in Chapter 5, Evaluation.

Prediction of the acid-generating material at mine sites is now recognized as a crucial element of mine feasibility, permitting, and environmental review. Predictive technology has advanced considerably in recent years but still requires a detailed understanding of the entire range of complexities in the various units at a mine site needing evaluation. The ADTI/SME Prediction volume attempts to present a thorough discussion of the variety of predictive tests that might be considered for evaluating material that has the potential to be acid-generating:

- Will the material to be mined produce acid?
- Will the properties of the material change as mining proceeds?
- Are there units to be mined that can be used to neutralize or isolate acidic units?
- Will any acid produced impact ground- or surface water(s)?
- What series of test protocols accurately characterizes the material?
- Of these tests, which can be used to operationally segregate material that might need special handling or storage?
- Can any of the tests be interpreted to supplement geochemical modeling?
- Can any of the tests be used to develop field-scale tests that may help to confirm the laboratory tests?
- Can field-scale tests be interpreted to confirm geochemical predictions and modeling?

Together this iterative process should lead to a waste characterization system that enables a mine to accurately characterize and manage material at operational scales and timeframes. This system must incorporate all the information from all the testing and it must be both continuous and flexible enough to allow for the recognition and management of changed conditions.

The volume highlights the importance of a detailed understanding of sample mineralogy. The mineralogy of rock mined from ore deposits may host many generations of minerals, with many associated elements. Mineral composition and surface area, habit, encapsulation, and solubility direct influence reactivity, and therefore control sulfide oxidation and metal/metalloid release potential. A detailed evaluation of the minerals and their composition thus may be required, not only for the purpose of ARD potential and waste characterization but also for efficient recovery of the desired economic products. The choice of methods used for mineral and/or element analysis will depend on the questions that need to be answered. For example, is it more important to know the bulk concentration of an element of interest, or the mineralogical residence of that element? A number of analytical methods used for these purposes, such as XRD and SEM-EDX, are reviewed and discussed in the volume. Regardless of the technology or evaluation method selected, it is critical to remember that an understanding of the mineralogy is essential to understanding and interpreting any of the various predictive tests, not the other way around.

Evaluation

Where the ADTI/SME prediction volume differs from the GARD guide (INAP, 2011) and other guidance documents describing ARD testing methods is the discussion of evaluation provided in Chapter 5. Because these materials require: (1) subjective judgement in deciding when HC tests should be terminated, (2) may be used to answer multiple questions, and (3) are complex to interpret, the ADTI-MMS Steering Committee requested that the editors of the prediction volume examine this issue and include a discussion of humidity cell duration and provide a recommended framework that might aid in clarifying HC test objectives and termination criteria.

Although many have attempted to standardize the methods used to evaluate and predict the geochemistry of mined materials, the application of the individual analytical methods within testing programs continues to vary between jurisdictions and mine localities. One reflection of this is the varied duration of humidity cell (HC) tests during mine permitting baseline studies, which was raised as an issue during the preparation of this volume. Early work on HC method development indicated the potential need for extended run times (Lapakko, 1988, 1990; White and Jeffers, 1994), yet the initial ASTM standard developed in 1996 mentioned a minimum run time of 20 weeks (ASTM, 1996). Though other sections of the ASTM clarified that this was meant to be a minimum, this 20-week duration nevertheless became the "standard" run time. This led, inevitably, to arguments over humidity cell tests not being run long enough to accurately represent the potential for material to produce problematic drainage in a real world setting. It also, of course, led to the over-testing of some types of materials. Examples include samples with obvious potential to produce acidity in the short term being run longer than necessary to make an accurate determination of the material's need for special handling. Another, and particularly interesting example of this are inert materials, which have both low sulphide and low neutralization potential, which may appear to have uncertain potential for acid generation when they have little if any potential to produce acidity at all.

This framework/guidance is complicated by the fact that HC tests are often asked to answer two separate questions, neither of which the test is specifically designed to do:

1) How will the material perform in a real world setting and
2) What short term tests can be linked to the HC test results and then be used to accurately characterize the material so it can be managed and handled in a real time setting at a minesite?

Results generated during HC tests are not known in advance, so it is not possible to establish a specific test duration prior to test initiation. This makes it all the more important to develop rational objectives and criteria for test duration.

An understanding of the detailed objectives and rational criteria for test duration is necessary and should include a discussion of which samples are being collected and why samples are tested and evaluated: Why do we run these tests and what is it we're trying to accomplish? A mining company may use HC tests for internal environmental management programs or tests may be run as part of a larger, public permitting program. Tests may be run to identify material for selective handling, and terminated as soon as their character relative to that selective handling strategy (e.g., impoundment or encapsulation) has been identified (i.e., acid material in an HC test terminated at 10 weeks). Tests may also be run to predict the long term water quality of a material and therefore merit longer testing duration to evaluate metal release potential. The intended use, applicable regulatory guidelines, and relevant management scenarios identify the key stakeholders who define the objectives and criteria.

The objectives and rationale developed envision the involvement of knowledgeable stakeholders to develop site specific criteria for the following different possible objectives:

- Confirmation of Static Testing Results

    a) For strongly acidic or basic samples
    b) For neutral/inert or slightly basic samples

- Evaluation of Reactivity and Leachate Quality for Segregating Mine Waste

    a) For neutral/inert samples
    b) For inert/non-reacive

Each of the above possible objectives can involve criteria, which includes pH trends, sulfate release rates, Ca/Mg:S ratios, or ANP/AGP ratios among other possibilities. These criteria must be developed on a site/project-specific basis based on the site-specific lithology, mineralogy, trace-metal characteristics, and potential environmental risks.

- Evaluation of Quantity of Neutralization Potential (NP) Available to React with Produced Acid

In the event detailed information on the actual availability and timing of neutralization is critical to developing a comprehensive waste management plan, the following factors must be considered

    a) Duration will be based on when NP of carbonate or other neutralizing minerals has been consumed. Tests based on this objective can be expected to have extended durations, potentially years rather than weeks.
    b) Mine-waste constituents that are mobilized during weathering need to be identified and characterized.

- Prediction of leachate quality (metals/metalloids)

Given the potential duration of HC tests, the importance of early test initiation cannot be overstated. Other considerations include: (1) ongoing field pilot study tests, which can be used to

supplement HC results and support detailed geochemical modeling; (2) geoenvironmental comparisons with closely related deposits; and (3) the possible need for duplicate cells for lithologies with complex mineralogy or conflicted static test results as an alternative to restarting humidity cells with disputed termination decisions.

Once the objectives and criteria for HC tests have been satisfied, this information can then, hopefully be used to develop a sequence of testing that can be used at an operational scale to effectively segregate and manage material at the mine site to meet environmental requirements.

CONCLUSION

The volume describes an iterative process characterizing and classifying mined material. One of five guidance documents developed through a unique consensus process within the ADTI, this volume addresses some key elements of management practice which include the perspective of regulators, corporations, and other stakeholders. While any waste characterization program should be based on clear set of sampling and testing objectives, criteria for terminating kinetic tests which are appropriate to the goals of the overall program (e.g., selective handling vs. use of material for construction, for example). In developing criteria for test duration, a thorough understanding of the following is needed:

- The petrology, mineralogy, alteration, and sequential mineralization history of material.
- The actual procedures used in the static and kinetic tests of the material

This detailed understanding will allow correct evaluation of results from both the static and kinetic tests performed on samples. Characterization of large tonnages of mining and processing waste requires complex and geostatistically sound sampling and characterization programs throughout the mine life to assure that relevant environmental standards can be met both throughout the mine life and beyond as the mine is closed and reclaimed.

The ADTI/SME Prediction volume also presents some ideas on a possible framework that might be used by stakeholders to develop rational objectives and criteria for the duration of HC tests that will contribute to reducing uncertainty and level of risk associated with mineral development.

Collectively this information will help assure that mines identify and manage materials that might adversely affect the environment if not handled appropriately.

ADTI-MMS continues to work towards its goals through coordination with the International Network for Acid Prevention (INAP) and its partners in the Global Alliance; South Africa's WRC (Water Research Commission), MEND (Mine Environment Neutral Drainage) in Canada, PADRE (Partnership for Acid Drainage Remediation in Europe) in the European Union, SANAP (South American Network for Acid Prevention) in South America, SMIKT (Sustainable Minerals Institute, Knowledge Transfer) in Australia, INAD (The Indonesian Network for Acid Drainage), and the CNAMD, The Chinese Network for Acid Mine Drainage in China.

REFERENCES

ASTM D 5744-96 and subsequent revisions. (2000). *Standard Test Method for Accelerated Weathering of Solid Materials Using a Modified Humidity Cell,*. West Conshohocken, PA ASTM International. pp. 257–269.

Brady, K. B. C., Smith, M. W., and Schueck , J. (1998). *Coal mine drainage prediction and pollution prevention in Pennsylvania*, Department of Environmental Protection, Pennsylvania.

Caruccio, Frank T., and R.R. Parizek. (1967). An Evaluation of Factors Influencing Acid Mine Drainage Production from Various Strata of the Allegheny Group and the Ground Water

Interactions in Selected Areas of Western Pennsylvania. *Special Research, Report SR-*

65, Department of Geology and Geophysics, College of Earth and Mineral Science, the Pennsylvania State University, University Park, Pa.

Hornberger R. J., Lapakko K. A., Krueger, G. E., Bucknam C. H., Ziemkiewicz, P. F., Dirk J.A. vanZyl, D. J. A., and Posey, H. H. 2000 The Acid Drainage Technology Initiative, *Proceedings from the Fifth International Conference on Acid Rock Drainage. Littleton, CO: Society for Mining Metallurgy and Exploration*. 2000.

INAP (International Network for Acid Prevention). 2011. *Global Acid Rock Drainage Guide* (GARD Guide), http://www.gardguide.com/. Accessed October 2, 2014.

Lapakko, K.A. 1988. Prediction of acid mine drainage from Duluth Complex mining wastes in northeastern Minnesota, In *Mine Drainage and Surface Mine Reclamation*. Vol. 1, Mine Water and Mine Waste. Proceedings of the 1988 Mine Drainage and Surface Mine Reclamation Conference. Bureau of Mines IC 9183. pp. 180–190.

Lapakko, K.A. 1990. Regulatory mine waste characterization: A parallel to economic resource evaluation, In *Proceedings of the Western Regional Symposium on Mining and Mineral Processing Wastes.* Edited by F. Doyle. Littleton, CO: SME. pp. 31–39.

Lapakko, K.A., and Antonson, D.A. 1994. Oxidation of sulfide minerals present in Duluth Complex rock: A laboratory study., In *Environmental Geochemistry of Sulfide Oxidation*. ACS Symposium Series 550. Washington, DC: American Chemical Society. pp. 593–607.

Lapakko, K.A., Engstrom, J.N., and Antonson, D.A. 2004. Long term dissolution testing of mine waste, Report on Contract No. DACW45-02-P-0205 to US Army Corps of Engineers by the Minnesota Department of Natural Resources.

White III, W. W., and Jeffers, T. H. 1994. Chemical predictive modeling of acid mine drainage from metallic sulfide-bearing waste rock., Chapter 37 in *Environmental Geochemistry of Sulfide Oxidation.* ACS Symposium Series 550. 1994.

A Risk Assessment of ARD Prediction and Control

Shannon Shaw[1] and Andrew Robertson[2]

1. *pHase Geochemistry Inc., Canada*
2. *Robertson GeoConsultants Inc., Canada*

ABSTRACT

Risk assessments are routinely conducted for many of the specialized aspects or features of a mine site or design, but rarely completed as a focussed evaluation of acid rock drainage and metal leaching, or ARD/ML risk. ARD/ML and water quality impacts however are often one of the most significant risks associated with mining projects in terms of long term environmental impacts, public and regulatory image and closure costs.

Risk assessments are often done via the Failure Modes and Effects Analysis (FMEA) methodology in which potential failure modes are identified, the anticipated effects of those failures are documented and the likelihood of occurrence and consequences of occurrence are rated. Failure modes as they relate to ARD/ML can arise from errors and uncertainties in predictions, as well as errors and uncertainties associated with control measures. The FMEA can be used as a tool to better mitigate and manage these errors and uncertainties.

This paper uses the FMEA approach to classify and share an understanding of relative risks for mines with respect to ARD/ML. By way of case studies and examples, a listing of failure modes that should be considered in ARD/ML prediction programs and management and control plans is provided, as are factors that contribute to each failure mode.

INTRODUCTION

A common risk management tool used by engineers in the mining industry is the failure modes and effects analysis (or FMEA). This analysis tool is meant to identify potential events that could cause a consequence that is unacceptable. In this way, unacceptable risks can be identified and mitigated or managed with the objective of reducing those risks to acceptable levels.

Acid rock drainage and metal leaching (ARD/ML) has been identified and is generally thought of as one of the larger risks associated with mining in sulphide rich deposits, with those risks including not only risks to the receiving environment (water quality, aquatic species, agriculture, livestock and wildlife as well as humans) but also risks to the financial health of mining proponents and their shareholders, tax payers and other stakeholders.

The potential occurrence of ARD/ML is therefore often included as a failure mode in a more encompassing risk assessment at any one project or site with the consequence ultimately being an impact to receiving water quality. When ARD/ML occurs, the view is often that there was a fundamental error in one, or more of the following; (1) the identification and characterization of the potential for ARD/ML, (2) the prediction of water quality effects and/or effectiveness of control measures, or (3) the performance of management of waste for the control of ARD/ML. Significant work goes into each of these aspects at considerable cost to a proponent and considerable implication to the overall risk profile for a project. In the authors' experience there are components of each of these aspects (characterization, prediction and management) that can affect the ultimate risk of a project related to ARD/ML. These components can be framed within the context of an FMEA for the purpose of ARD/ML characterization, prediction and management with the objective of better quantifying the overall ARD/ML risk and then applying applicable mitigation measures to lower risk of a project. In other words, what are the failure modes and consequences of ARD/ML evaluation and management programs themselves? What risk do these represent for the project, so that mitigation measures can be applied to reduce risk? This paper attempts to identify and describe those failure modes that are most common and/or have the highest consequences.

METHODOLOGY

The risk assessment approach used in this study was that of a Failure Modes and Effects Analysis (or FMEA), which consists of the quantification of the likelihood and consequence of a failure or event (Robertson, 2012).

A failure mode can be naturally initiated (e.g. 1:500 year flood event) or initiated by a failure of an engineered system (e.g. leakage from a contaminated water storage pond), or by an operational error (e.g. accidental release of contaminant to the receiving environment).

The assessment of the effects or consequences of these failure modes is site specific though in large part based on precedence, experience at other mines (case histories) and professional judgement by experienced personnel. A suggested basis or metric by which the likelihoods and consequences can be quantified is provided, each based on metrics defined in 5-point scales as detailed in Tables 1 and 2 below.

Table 1 provides the likelihoods of an event occurring ranging from not likely to expected. The not likely category is defined here as having a <0.1% chance of occurrence (or one in a thousand) while the expected case has been defined as a >50% chance of occurrence (or a one in two probability of

occurring). The period of consideration may the annual likelihood or the likelihood over the life of the project. Likelihood increases for the period under consideration. The authors have a preference for working with the likelihood of the period of operation of the mine, or in the case of post closure risk, a period of 100 years.

Table 1 Scale used to define the likelihood of a risk.

Likelihood Class	Likelihood of Occurrence of event within the period of consideration
Not Likely (NL)	<0.1% chance of occurrence
Low (L)	0.1 to 1% chance of occurrence
Moderate (M)	1 to 10% chance of occurrence
High (H)	10 to 50% chance of occurrence
Expected (E)	>50% chance of occurrence

Consequences in Table 2 have been categorized or grouped in a manner used commonly for FMEAs in the mining industry; specifically as geochemical impacts (often compared to water quality guidelines or biological metrics), regulatory effects (compliance), social license, health and safety and costs. The example scalars used here to assess the consequences, or the severity of effects should an event occur range from negligible to extreme. A negligible consequence would be one that had no measurable geochemical impacts on the receiving environment, that did not exceed regulated limits, that did not result in social attention or a health and safety concern, and for which repair or mitigate costs less than $10,000. An extreme consequence on the other hand would be an event that resulted in a geochemical impact that was considered very large and irreversible, that resulted in exceedances of regulatory obligations at a level that might shut down an operation or impose severe restrictions on an operation, that resulted in social outcry and the loss of social trust, that may result in fatalities and cost $10 million dollars or more to clean-up or mitigate. This scale can be modified to suit the sensitivities of each mine or project and the site and project specific conditions.

Risk is the product of likelihood and consequence:

Likelihood x Consequence = Risk

The risk rank can be quantified as either a number (the product of the likelihood rank and the consequence rank) or as a colour.

The matrix provided in Figure 1 below illustrates this as a color-coded (or ranked) system with warmer colors representing higher risks (with higher likelihoods and consequences) and colder colors representing lower risks (with lower likelihoods and consequences). A numerical quantification is also provided with the risk value for each failure mode being the multiplication of the likelihood rank times the consequence rank.

A separate risk matrix can be generated for each risk consequence: Geochemical Impacts; Regulatory Effects; Social Licence; Health and Safety; and Costs. This paper addresses geochemical failure modes, likelihood, consequences and risk.

FAILURE MODES

Geochemical failure modes identified in this paper have been organized here into those that are related to (1) prediction of geochemical behaviour, (2) prediction of effectiveness of control measures and (3) performance of control measures. In addition, the dimension of time (or kinetics)

as related to each possible failure mode is discussed. This temporal aspect can relate to prediction of geochemical behaviour (e.g. the rate of neutralization depletion), the prediction of the effectiveness of control measures (e.g. the predicted infiltration rate through covers) and the performance of control measures (e.g. the effect of climatic effects such as a 1 in 1000 year flood on control measure performance).

Table 2 Example of a scale used to define the severity of effects (consequences).

Consequences	Geochemical Impacts	Regulatory Effects	Social License	Health and Safety	Costs
Negligible (N)	No measurable impact	Meet regulatory obligations or expectations	No stakeholder (e.g. locals, NGO) attention	No concern	<$0.01 million
Low (L)	Minor impact on WQ (less than order of magnitude change)	Seldom or marginally exceed regulations. Some loss of regulatory tolerance, increasing reporting	Infrequent local, international and NGO attention addressed by normal public relations and communications	First aid required; or small risk of serious injury	$0.01 to $0.1 million
Moderate (M)	Moderate, temporary, reversible impact on WQ	Occasionally (less than one per year) or moderately fail regulatory obligations or expectations - fined or censured	Occasional local, international and NGO attention requiring minor procedure changes and additional public relations and communications	Lost time or injury likely: or some potential for serious injuries	$0.1 to $1 million
High (H)	Significant, irreversible impact on WQ or large, reversible	Regularly (more than once per year) or severely fail regulatory obligations - large increasing fines and loss of regulatory trust	Local, international activism resulting in political and financial impacts on company 'license to do business' and in major procedure or practice changes	Severe injury or disability likely: or some potential for fatality	$1 to $10 million
Extreme (E)	Catastrophic impact on WQ (irreversible and large)	Unable to meet regulatory obligations or expectations; shut down or severe restriction of operations	Local, international outcry & protests, results in large stock devaluation: severe restrictions of 'licence to practice'; large compensatory payments etc.	Fatality or multiple fatalities expected	>$10 million

		LIKELIHOOD				
		NOT LIKELY [1]	LOW [2]	MODERATE [3]	HIGH [4]	EXPECTED [5]
CONSEQUENCE	EXTREME [5]	5	10	15	20	25
	HIGH [4]	4	8	12	16	20
	MODERATE [3]	3	6	9	12	15
	LOW [2]	2	4	6	8	10
	NEGLIGIBLE [1]	1	2	3	4	5

Figure 1 Risk Matrix Illustrating the Combination of Likelihood and Consequence

Prediction of Geochemical Behaviour

Potential/common failure modes related to prediction programs aimed at characterizing the geochemical behaviour of a material have been identified below.

Failure Mode 1.1: Errors related to geological variability. Geotechnical engineers who use the FMEA tool extensively in the mining industry are used to working with variability in parameters such as shear strength and permeability where variability in values can be substantial but where there is a predictable range for a given rock type. Geochemical variability for a given rock type can result from a number of components that could include variations in the quantity of key minerals, variations in textures and particle sizes, variability in the liberation of key minerals and how each is exposed during blasting etc. Without substantive testing and quantification, geochemical variability for a given rock type therefore is difficult to predict and project specific.

Failure Mode 1.2: Errors related to representativeness of samples. Generally sampling for geochemical characterization is done, at least initially, on the basis of guidelines that suggest a

number of samples be collected for a specific tonnage of waste for each key rock type. Prior to mining, this is further limited by the availability of drill core available to sample. This drill core is generally representative of rock within or close to ore zones and not necessarily encompassing of all likely waste. Uncertainties therefore arise from the frequency and spatial distribution of samples selected. During operations or on closure this uncertainty is often reduced by the fact that sampling can be much more targeted to the material of interest and/or can be done at a higher frequency, with better temporal and spatial certainty.

Failure Mode 1.3: Errors related to representativeness of models. Modelling tools are used extensively in the industry. Often models are used to extrapolate data from the samples collected and characterized spatially in order to forecast the geochemical behaviour of waste rock before it is mined. These models have great value for waste planning particularly on projects where there is waste handling of material with one geochemical characteristic that differs from others. Uncertainties in the models however exist. These uncertainties may be greater for some deposits than for others, for examples extrapolation of a sulphur value from one sample across many meters of rock in a model for a deposit where sulphides are present as veins may have a much higher degree of uncertainty than if the sulphides were evenly disseminated throughout the rock mass.

Failure modes related to the development or utilization of models exist as do failure modes related to the use of the output. Practitioners need to understand the limits of models when making decisions on the basis of those models. Misguided use or over-reliance on model outputs can therefore also lead to failure modes.

Failure Mode 1.4: Errors related to definition of operational waste management. Many projects have waste handling procedures that are intended to segregate one type of rock from another. These programs are often developed to support project licensing prior to obtaining an understanding of how rock will blast, how sulphides and carbonates will partition in blasted rock, how well operations will be able to forecast and identify zones of differing geochemical behaviour, how diligent and dedicated operations will be to segregating rock etc. Predictions of how effective waste handling will be are often optimistic and not practical or conservative and may be unrealistic in estimating effectiveness.

Failure Mode 1.5: Errors in quantification of oxidation rates. Uncertainties that related to the tools and test methods standardly used to quantify oxidation rates (e.g. humidity cell tests, intrinsic oxygen consumption tests etc.) can also lead to failure modes. Because these tests are long in duration they are expensive. Sample selection therefore becomes a critical component of these programs. Inadequate sample representation can therefore lead to failure modes. Additionally, because there are standard methods for this quantification, programs tend to use the standard methods as a default. Adaptation of the methods to better suit site specific needs is rarely done and the duration of testing is often dictated by guidelines (e.g. 20 weeks, 40 weeks) rather than being dictated by each individual sample behaviour.

Failure Mode 1.6: Errors in the extrapolation of lab-based kinetic data to field conditions. Lab-based kinetic tests are typically used to quantify the rate of sulphide oxidation, depletion rates of buffering minerals and release rates of elements of interest. Test conditions seldom represent field conditions and numerical modeling is often inadequate to reliably extrapolate test conditions to field conditions. Data is used to calculate the lag time or delay to the onset of ARD conditions, when they are predicted to occur, as well as using release rates to predict water quality associated with waste facilities. Uncertainties and errors in the way in which lab rates are used in these

calculations and predictions represent another failure mode with potentially significant consequences.

Failure Mode 1.7: Deficiencies in the industry-wide knowledge base. Much of the characterization and predictive work relies in large part on case studies, analogs and the successes and failures experienced at other sites. Our ability to better predict water quality impacts and to better manage or sort waste on the basis of geochemical criteria therefore would have less uncertainties if operations and practitioners were able to, or required to, re-visit predictions and evaluate if there are differences in predictions and observed conditions what may have contributed to those differences. It is recognized that this is only really partially achievable, particularly at locations where there is a lag phase and sometimes decades between the period of time when predictions are made and conditions represented by those predictions occur. Comparing apples to apples therefore becomes a particular challenge when relying on case studies and analogs. However 'calibration' against precedence of other projects or historical behaviour on a given projects are important methods for improving prediction accuracy and risk mitigation.

Prediction of Effectiveness of Control Measures

Control measures most typically evaluated and utilized at mine sites in order to limit the effects of ARD/ML include measures aimed at (1) limiting sulphide oxidation (source control), (2) limiting migration of contaminants generated by sulphide oxidation (migration control), and/or (3) limiting the release of contaminants, if generated, into the receiving environment (collection and treatment). There are a number of potential failure modes related to the prediction of how these control measures may perform that should be considered.

Failure Mode 2.1: Effectiveness of source controls. This failure mode would include potential errors in waste management aimed at controlling ARD/ML which, depending on the waste management at any particular site, could include: ineffective prediction of, or design of, segregation and sorting programs for waste rock; ineffective prediction of or design of blending or layering strategies for waste rock; inaccurate prediction of performance of amendments to lower reaction rates or increase lag times, inaccurate prediction of measures to reduce oxygen ingress, and potentially errors related to the design of sub-aqueous disposal of wastes.

Failure modes could occur where there is inability to, or inadequate planning for, the potential partitioning of the neutralization potential (NP) and acid potential (AP) into different particle size fractions when rock is blasted versus how it is accounted for in samples available prior to mining (i.e. pulverized drill core). This could influence design of segregation and/or blending strategies.

Others could include insufficient planning of amendment application or dosage with the result that reaction rates and/or lag times are faster than anticipated.

Control of ARD/ML by sub-aqueous disposal could also have potential failure modes associated with it. For example, the inability to keep waste submerged resulting from errors in water balance predictions or resulting from severe climatic changes.

Failure Mode 2.2: Effectiveness of migration control measures. In the scenario where ARD/ML generation controls are not considered achievable or are cost prohibitive, control measures aimed at limiting migration are sought and are most often focussed on the design of covers aimed at reducing infiltration into a waste storage facility. Failure modes could occur in the design of appropriate covers for instance if test plots are too shallow or too narrow influencing the parameters which are used to design the most effective covers. Failure modes could also occur by

errors related to assumptions or inaccuracies of modelling relied upon to design covers. Even if designed properly, failure modes can occur during construction and/or as a result of long term changes in cover properties (biotic intrusion, desiccation and settlement cracking etc.).

Failure Mode 2.3: Errors related to collection and treatment measures. If neither oxidation control nor migration control are achievable, the ability to collect and treat impacted waters becomes critical. Failure modes that could occur in the prediction and design stage of collection and treatment control measures might relate again to errors in water balance or site water quality models, inadequate baseline assessments of hydrological or hydrogeological conditions etc. with the potential result that there is either too much water or much less than engineered for and/or that the treatment technology does not treat effectively or for all the parameters of concern.

Performance of Control Measures

Beyond the potential errors involved in characterization of ARD/ML and errors that could occur during the prediction or assessment of control measures for ARD/ML there are failure modes related to the performance of control measures put in place. This could in part be related to a failure to implement a design as planned or a failure to plan and design for implementation challenges.

Failure Mode 3.1: Errors related to operational waste management and deposition. Many projects have waste handling procedures that are intended to segregate one type of rock from another. Operational errors can occur whereby a zone on a pit bench is marked as a non-potentially acid generating zone or domain where in fact it is potentially acid generating and that block gets moved to the wrong disposal area. This could result from blasthole sampling at an inadequate frequency for accurate waste block designation or as a result of operator error where a truck operator who is supposed to take rock to one dump takes it instead to another. Rock management could also be prone to failure modes resulting from other operational constraints (e.g. a road washes out) resulting in all rock going to one area for a period of time. The simple process by which rock is placed can also create variability in a dump. For end-dump waste piles, segregation by rock size can occur down slope, this may result in partitioning of one rock type, perhaps intended to add carbonate buffering to the mix being deposited in one zone and another rock type, perhaps a harder rock that blasts in larger particle sizes, segregating down slope in another zone.

Failure of blending and layering management could result from partitioning of the neutralization potential (NP) and acid potential (AP) into different particle size fractions post blasting whereby neutralization is not effective and the standardized NP/AP ratios are either overly conservative or not protective. Failures could also occur if neutralizing minerals get blinded by secondary mineral precipitation on particle surfaces.

Control of ARD/ML by sub-aqueous disposal could also have potential failure modes associated with it: for example resulting from severe climatic changes; containment structure breaches etc.

Failure Mode 3.2: Migration control failures. Failures in covers due to root action, frost action, erosion and/or deterioration of liners all fall within this failure mode. Often the consequences of these failures occur slowly and gradually over time.

Failure Mode 3.3: Collection and treatment control failures. Failure modes that would occur within the context of collection and treatment systems could include ice and sediment blockages in diversion ditches, landslides blocking water management structures, flood events. Failure modes could also include temporal changes in water quality resulting in changing treatment requirements

and/or changing water quality standards and regulations resulting in changing treatment requirements.

EFFECTS

In the case of the failure modes above, be they related to prediction errors, error in the prediction of control measures or the effectiveness of those measures, the effects can be described as (1) that monitoring detects the failure mode and remediation is taken or (2) monitoring does not detect the failure mode and an impact, perhaps temporarily, to the receiving environment occurs. The likelihood and consequences of geochemical related risks are therefore intimately dependent on the monitoring programs and highlight the importance of appropriate monitoring and response plans. Where monitoring is not adequate and failure modes occur, it may be that emergency response and clean-up plans need to be initiated.

Effects are also tied intimately to the receiving environment in which a project is located, the assimilative capacity, cumulative effects etc. The risk of cover failure in an area of high rainfall may have a much greater effect than if the same failure were to occur over similar waste in a dry environment.

Risks are also cascading. For example, if source control fails – for example if PAG and non-PAG rock segregation or blending is not effectively executed, then migration controls become the primary reliance measure. If migration controls fail, then collection and treatment systems become more important. Collection and treatment controls may have greater assurance where the likelihoods of an event are diminished, however costs are increased.

EVALUATION

This FMEA approach can be illustrated by way of example. For instance, consider a porphyry style open pit project whereby sulphides are both disseminated and structurally controlled and where carbonate content is generally low and present in veinlets. In this example, pre-mining characterization work identified a variable range of both PAG and non-PAG rock that was not strongly lithological-dependent and an operational segregation and sorting plan was developed based on a sulphide value criterion. Waste management in this example is done on the basis of blasthole sampling, on-site testing for sulphur and flagging of dig blocks on the pit face on the basis of those results. Waste planning includes PAG rock disposal in one location and non-PAG rock identified as construction rock and or disposal in a separate facility. The closure plan assumed and allocated closure costs for a cover placement on the PAG rock pile to minimize infiltration and predictions indicated there would be no need for collection and treatment to protect the downstream environment.

Potential failure modes for the characterization program, the prediction of control measures and the performance of the plan are provided in Table 3.

Precedence for this type of deposit would suggest that one possible failure mode is that not all PAG rock is identified or segregated correctly because the original sulphide criteria was not sufficiently protective or due to variability on a scale not adequately represented by sampling etc.. This could result in the PAG rock getting placed in a non-PAG rock pile or used as construction rock. The effects could be very different depending on whether or not monitoring was sufficient to detect and mitigate for this failure mode. Monitoring for this type of failure mode could include a verification

program initiated during construction and early operations aimed to identify whether or not that the criterion be adjusted and/or water quality monitoring detects increased concentrations of indicator parameters.

In the example provided, there were a few failure modes identified related to extrapolation of kinetic data. The first example illustrates a potential error related to oxidation rate expectations. If in a case where control of ARD/ML from a PAG pile is reliant on a cover for infiltration control, the lag phase needs to be sufficient to prevent significant ARD/ML generation until such time as a cover can be placed. Kinetic tests are also relied on for prediction of water chemistry of contact water from non-PAG sources. If the tests or predictions based on those tests are not conservative enough, one effect could be that water chemistry associated with a non-PAG pile is still not of discharge quality and would also potentially require cover placement and/or seepage collection. A robust seepage quality monitoring program becomes a key factor at early identification of these potential failure modes and allowance for early mitigation by additional cover placement in the control plan would reduce risk.

SUMMARY

The FMEA methodology, which has found great utilization in the mining industry particularly in the regard to stability of geotechnical structures (dams, slopes, waste dumps), can also be a valuable tool for risk assessment of ARD/ML control programs and waste planning. In this paper a number of potential failure modes have been identified with greater discussion, by way of example, provided for a subset of these. The importance of consistent, robust and targeted monitoring is illustrated as a key risk mitigation and management tool.

REFERENCES

Robertson, A. MacG. (2012). FMEA Risk Analysis: Failure Modes and Effects Analysis. Presentation at Gestao de Riscos e Seguranca de Barragens de Rejeitos, Seminario 2012. http://www.infomine.com/library/publications/docs/Robertson2012b.pdf, accessed May, 2014.

Table 3 Example output of FMEA for ARD/ML Prediction and Prevention Program.

FAILURE MODE	EFFECTS	LIKELIHOOD	CONSEQUENCES					Highest Risk Rating
			Geochemical Impacts	Regulatory Effects	Social License	Health and Safety	Costs ($M)	
Characterization Program								
Error related to geological variability	Sulphur criterion not adequate for PAG sorting, PAG rock to non-PAG pile	3	3	4	3	1	2	
Errors related to representativeness of samples	Blasthole sampling not spaced adequately to define PAG blocks, PAG rock to non-PAG pile	2	3	4	3	1	2	
Errors related to representativeness of models	Modeling of vein hosted sulphides and carbonates difficult and PAG waste volumes underpredicted	3	2	2	1	1	4	
Errors related to definition of operational waste management	Operational errors lead to occasional PAG rock placement in the non-PAG pile	3	2	2	2	1	1	
Errors in quantification of oxidation rates	PAG pile produces acidity before cover placement, seepage collection required	3	3	4	2	1	5	
Errors in the extrapolation of lab-based kinetic data to field conditions	Water chemistry different then expected and requires collection	3	3	4	2	1	5	
Deficiencies in the industry-wide knowledge base	Analogs or precedents not available to support predictions	1	3	4	2	1	1	

Table 3 Example output of FMEA for ARD/ML Prediction and Prevention Program (continued).

FAILURE MODE	EFFECTS	LIKELIHOOD	CONSEQUENCES					Highest Risk Rating
			Geochemical Impacts	Regulatory Effects	Social License	Health and Safety	Costs ($M)	
Prediction of Control Measures								
Effectiveness of source controls	Predictions for non-PAG pile to have good seepage chemistry not accurate	2	4	4	3	1	4	
Effectiveness of migration control measures	Predictions of infiltration through PAG pile not accurate, potentially higher seepage rates	4	3	2	1	1	4	
Errors related to collection and treatment measures	Not predicted to be required but as a result of other failures is needed	3	3	4	4	2	5	
Performance of Control Measures								
Errors related to operational waste management and deposition	Non-PAG pile contaminated by PAG rock, seepage not of discharge quality	2	4	4	4	2	4	
Migration control failures	Cover failure due to root action etc., seepage higher than expected requires collection	2	4	4	4	2	4	
Collection and treatment control failures	Collection and treatment not adequate to protect downstream environment	1	5	5	5	3	5	

10th ICARD IMWA2015 | 10th International Conference on Acid Rock Drainage & IMWA Annual Conference

Acid Mine and Metalliferous Drainage (AMD); Sample Selection an Intricate Task

Edgardo Alarcón León, Carel van der Westhuizen and Lucy (Xin) Du
Pendragon Environmental Solutions, Australia

ABSTRACT

Although acid rock drainage (ARD) exists in nature, acid mine and metalliferous drainage (AMD) as a consequence of mining remains one of the most difficult environmental problems to deal with. AMD has the potential to persist long after closure, requiring extensive and expensive on-going remediation and monitoring of local and surrounding downstream environments.

AMD characterization requires in-depth investigations to understand the key processes involved in the oxidation of sulfides and the subsequent release and transport of solutes. Approaches and solutions to mine-waste characterization and management during resource exploitation require accuracy but is site specific. Regulators, miners and scientists have different views on the numbers and types of sample specimens; these differences should be recognised and considered as they play an important role in the overall decision making process. Over time, many different approaches and methodologies to ascertain the number of samples have been developed. These range from a dominant geo-statistical approach, such as the theory of sampling (ToS), to methods inclusive of a combination of statistical, mineralogical, geochemical, environmental and economic analyses.

Despite which approach is followed, sample types and numbers are often subject to unwarranted critique. Regulation may further complicate matters, particularly where decision makers are risk averse. An innovative approach that centres around a risk-based approach and combines geological, mineralogical, geochemical and hydrogeological characteristics of the mine site into a conceptual model, from which the AMD investigator is able to define the type and number of samples and relative amount of material, appears the most appropriate approach to extricate this fundamental problem in investigating and assessing AMD. This global yet site specific approach, will assist during the various stages of mining and will provide assurance that subsequent rehabilitation and closure are achieved with little difficulty and expense.

Keywords: AMD, characterization, sample, selection, number.

INTRODUCTION

Although acid rock drainage (ARD) exists widely in nature, acid mine/metalliferous drainage (AMD) is a significant environmental concern for the mining industry and one that may persist long after closure, often requiring extensive and expensive remediation.

ARD/AMD is caused by the exposure of sulfide minerals to oxygen and water which produces acidity and triggers the dissolution of metals and metalloids, which are harmful to site and neighbouring downstream environments (Alarcón and Anstiss 2002). Owing to the complex physical, chemical and biological processes occurring during the weathering of sulfides, the production of AMD can be severe, or may not occur if the media remains in a reducing condition. This uncertainty adds further complexity to the assessment of a mining project and thus, the characterization of mine wastes becomes fundamental to develop cost effective management approaches including preventive and containment measures.

Regulators, miners and scientists have differing views on the types, number and origins of samples that would fully characterize mine waste. These differences within the various stages of mine development create a complicated paradigm and impact adequate mine-waste identification and management. Responses to these complexities include numerous research investigations and publications that incorporate an all-inclusive approach of statistical, mineralogical, geochemical, environmental and economic analyses. However, these approaches have not fully addressed the intricacies of defining *adequate sampling quality and population*, which remains a paradigm.

With reference to AMD, there are several questions that need to be answered over the life of a mining project, these including but are not limited to:

- Should samples be profiled for AMD characteristics during the exploration stages?
- What constitutes a sample for AMD assessment?
- How many, which kind and what sizes of samples are sufficient to hydrogeochemically characterize the proposed new mine?
- How are we dealing with heterogeneity and how might lithological samples express this complexity?
- How much analysis is required and what parameters need to be investigated?
- How may laboratory analyses be extrapolated to real mine conditions?

SAMPLING PARADIGM

It is accepted that samples for AMD investigations should be *site-specific and depend on the phase of the project, but must be sufficient to adequately represent the variability/heterogeneity within each geological unit and waste type* (DITR 2007). Certain key parameters including the extent of mineral variability, mineralogical alterations and sulfide types/concentrations are often omitted from AMD assessments. These parameters are required to reveal baseline conditions of the overburden/waste rock and ore (high and low grades), and assess the risks that a mining project imposes on the environment.

Whilst numerous sample selection methodologies are used worldwide, the general theory of sampling (ToS, Francis Pitard, 1989) takes into account both technical and statistical aspects of sampling. ToS was developed by the French academic Pierry Gy and addresses all facets of sampling. The main contribution attributed to this theory is the proposition of a mathematical definition of heterogeneity (Rossi *et al*, 2010).

In nature, this concept is paramount as we need to know the lithology, mineralogy, alterations and the variability of the physical, mechanical, hydraulic and chemical properties of the rocks. Alternate sampling strategies range from purely statistical to fixed-frequency approaches. The British Columbia AMD Task Force (1989) proposed that samples be collected in a fixed-frequency approach, based on the mass/volume of waste, and recommends a minimum number of samples expressed as:

$$N = 0.0026M^{0.5}$$

where N is the number of required samples and M is the mass of the geologic unit in tons (M should be > 6×10^3 tons). Based on this approach, a minimum number of 25 samples are required per 1 million tons geologic unit, or one sample for every 40,000 tons (Figure 1). However, as the waste volume increases beyond 1.5E+8 tons, the number of samples decreases. Gene Farmer of the U.S. Forest Service suggested collecting 50 samples for each 1 million tons of waste (USDA Forest Service, 1992). The specifics of Gene Farmers' approach indicate that for each 1 million tons of waste rock, eight to twelve samples of each significant rock type (as a minimum) should be collected (Schafer 1993). Brady and Hornberger (1989) proposed a minimum number of samples per coal seam based solely on acreage, calculated as [acres/(100acres)]+2. A similar approach was suggested by Freeman *et al* (1987), which allowed the areal extent of a coal mine to be used as the basis for determining the number of samples.

In general, fixed-frequency sampling methods imply that each individual sample used to test and classify larger volumes of waste, would allow lithological stratification mixing and sample chemistry blend. Consequences of this approach may be far reaching as information about sample variability could be lost, imposing a degree of liability (British Columbia AMD Task Force, 1990). In addition, sample lithotype mixture may not necessarily be applicable in highly heterogeneous conditions such as at base metal mines (SENES, 1994).

Although the scheme is not specific for AMD, a prominent code on statistical sampling theory and practice has been developed by the Joint Ore Reserve Committee for the mining industry (JORC 2012). Reporting standards on sampling methods, measurements of sampling error and correctness and Public Report transparency regarding exploration results (JORC 2012), are included in this code. The proposed method of sample selection is similar to those used to evaluate recoverable mineral resources (assay samples), which employ estimation variance (ANOVA and variant method) to determine the optimum threshold of parameters (such as total sulfur), as a function of sample density and characterization (Modis and Komnitsas 2007; Kentwell *et al* 2012; Servida *et al* 2013). If the parameter of interest is either well above or below the threshold of interest, the total unit or volume of a rock type can be classified as either potential acid forming (PAF) or non-acid forming (NAF) and managed accordingly. However, the spatial distribution of the element within a rock category may not necessarily be homogeneous across the entire volume of each rock type; this may raise questions pertaining to heterogeneity, sampling intensity and sample density.

CHARACTERIZATION AND ASSESSMENT METHOD

The methodologies used in several AMD studies (Table 1) are inclusive of a global ARD and AMD knowledge base, and experiences gained in different climatic and geological-hydrogeological settings. However, the methodology the authors practice differs slightly as it incorporates the development of a mine hydrogeochemical conceptual model as a first step in the assessment of AMD (Table 2). The conceptual model is developed to account for the potential of overburden, waste rock, and the ore body

(all grades) to possess either acid or base characteristics. Studies incorporated for this assessment include geological, hydrogeochemical, hydrological and hydrogeological data gathered during exploration activities. These parameters are assessed on merits of their natural occurrences and interactions and are subsequently risk assessed with regard to potential short- to long-term social, economic and environmental impacts.

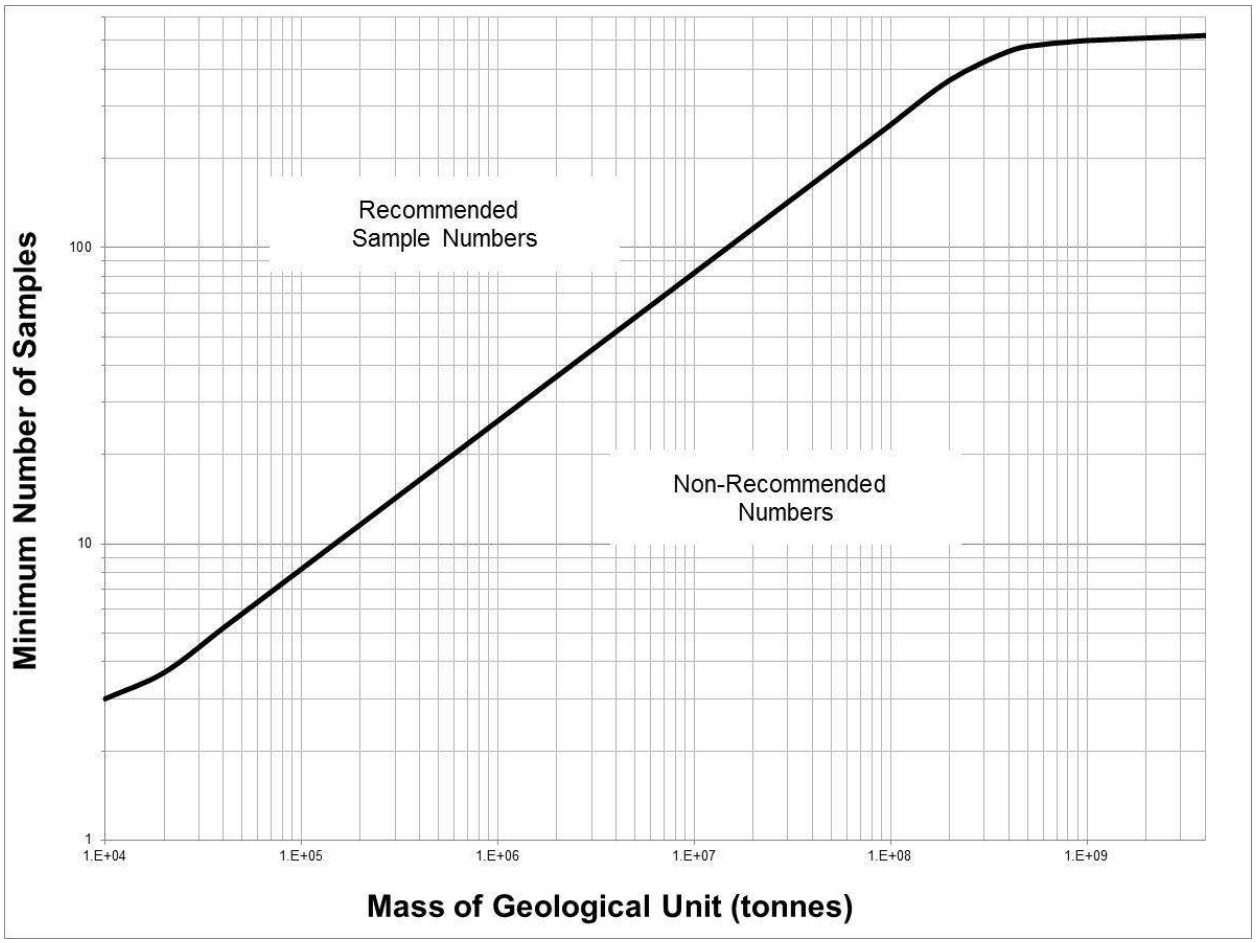

Figure 1 Recommended Minimum Number of Samples as a function of Mass of Each Geologic Unit

The conceptual model becomes a key interpretive AMD framework which provides a basis for the prediction of chemical processes that may develop during operations and post-mining. The derived framework is then tested by limited sampling and analysis which incorporates additional geochemical testing in the form of acid base accounting (ABA) and kinetic testing if required. Although the question of up scaling remains, field kinetic testing is recommended as it fosters the resemblance of actual climatic conditions and can be adapted to investigate new findings arising during the subsequent stages of mining.

Table 1 Selected AMD Investigations

Project Name	Project Location	Client	Characteristic
Area C Iron Project	NT, Australia	Sherwin Iron Pty Ltd.	EIS component
Beatons Creek	Western Australia	Novo Resources Corp.	EIS Component
Frances Creek	NT, Australia	Territory Iron Pty Ltd.	Rehabilitation
Goldsworthy Mine	Western Australia	BHP Billiton	Remediation and Closure
Kapulo Copper Project	Congo	Mawson West Ltd.	EIS component
Old Pirate Mine	NT, Australia	ABM Resources NL	MMP Component
Railway Project, Yandi	Western Australia	United Mineral Corporation	EIS component
RedbankMine Site	NT, Australia	Redbank Cooper Ltd.	EIS component
Western Desert Iron Ore Project	NT, Australia	Western Desert Resources Ltd.	EIS component
Westgold Project	NT, Australia	Westgold Resources Ltd.	EIS component

An example of conclusions reached during the conceptual model stage at one of the projects (Table 1) is presented below.

- Deposit C, due to its mineralogical characteristics and low sulfide concentrations, has a low likelihood of producing acid mine and metalliferous drainage.
- Low sulfur concentrations (<0.25%S) in more than 99% of the samples (Table 2) indicate that potential acid forming (PAF) materials occur sporadically, are highly localised and are confined to about nine locations (RC bores). Four locations (RC bores) contain samples located beneath the direct shipping ore (DSO) body.
- Most PAF materials (84% of samples) occur outside the perimeters of the proposed open pit and/or are beneath the base thereof.
- The ground water level is likely to remain below the base of the open pit. Localised perched waters in shallow highly weathered and/or fracture systems are not a cause for concern.
- Deep ground water may be impacted by infiltrating rain from the open pit (partially backfilled with a large void remaining after closure) migrating through the underlying undisturbed PAF bodies. However, PAF bodies are small and isolated and evaporation exceeds rainfall by several orders of magnitude, which limit the quantity of water that may infiltrate through the base of the open pit. Rain falling into the open pit may also be diverted away from areas where PAF bodies are known to exist.

This preliminary assessment indicated no need for a rigorous AMD evaluation but to comply with regulatory requirements, further assessments were undertaken. Using the fixed-frequency sampling approach a minimum of 404 samples across the different sandstone (Sst), siltstone (Slt), shale (Shl), ferruginous sandstone (Fst) and other layers would have been required. However, a total-S global statistical approach indicated that at a 95% confidence level, a maximum of 50 samples would yield a low global 1.41% margin of error (Table 3).

Table 2 Mine Geochemical Conceptual Models

Project Name	Exploration Geochemistry, Mineralogy and Geology								Interactions	Conceptual Model						AMD Potential
	XRF (No samples; %)				XRD		Petrography	SEM		Perceived Risks:						
	No Samples	<0.25%	0.25% - 0.3%	>0.3%	No Samples	Sulfides				Issue / Cause	Insignificant	Minor	Moderate	Major	Catastrophic	
Redbank Cooper Project	140	*50*	*6*	*44*	40	Yes			Surface / Ground water	Acidic seepages from waste rock dumps (WRD), tailing storage facilities (TSF) and pits.				X		Likely
Sherwin Iron Ore Project	2541	*99*	*0.3*	*0.7*	21	Yes	6		Surface / Ground water	Acidic seepages from waste rock dumps (WRD), tailing storage facilities (TSF) and pits.		X				Unlikely
Old Pirate, ABM Resources	1743	*99.8*		*0.2*		Yes			Surface / Ground water	Acidic seepages from waste rock dumps (WRD), tailing storage facilities (TSF) and pits.	X					Unlikely
Western Desert Iron Ore Project	5286	*72*	*7*	*21*	50	Yes		46	Surface / Ground water	Acidic seepages from waste rock dumps (WRD), tailing storage facilities (TSF) and pits.			X			Likely
Westgold Project	500	*99.5*		*0.5*	150	Yes		15	Surface / Ground water	Acidic seepages from waste rock dumps (WRD), tailing storage facilities (TSF) and pits.	X					Unlikely
Frances Creek	1747	*83*	*1*	*16*		Yes			Surface / Ground water	Acidic seepages from waste rock dumps (WRD), tailing storage facilities (TSF) and pits.				X		Likely

Table 3 Number of Samples Required and Analytically Assessed for AMD Investigations

Project Name	Required number of samples by fixed-frequency analysis (refer Figure 1)	Confidence level 95% with pre-established margin error (±20%)		Number of samples selected for analytical assessment		
		Sample No.	Margin Error (%)	ABA Test	NAG Test	Leaching Test
Redbank Cooper Project	354	40	7.5	42	42	23
Kapulo Cooper Project*	142	50	2.2	50	50	20
Sherwin Iron Ore Project	404	50	1.41	54	54	27
Western Desert Iron Ore Project	1491	250	2.7	204	204	204
Westgold Project	115	30	1.2	17	17	17

*Iron and cooper concentrations used for the statistical assessment.

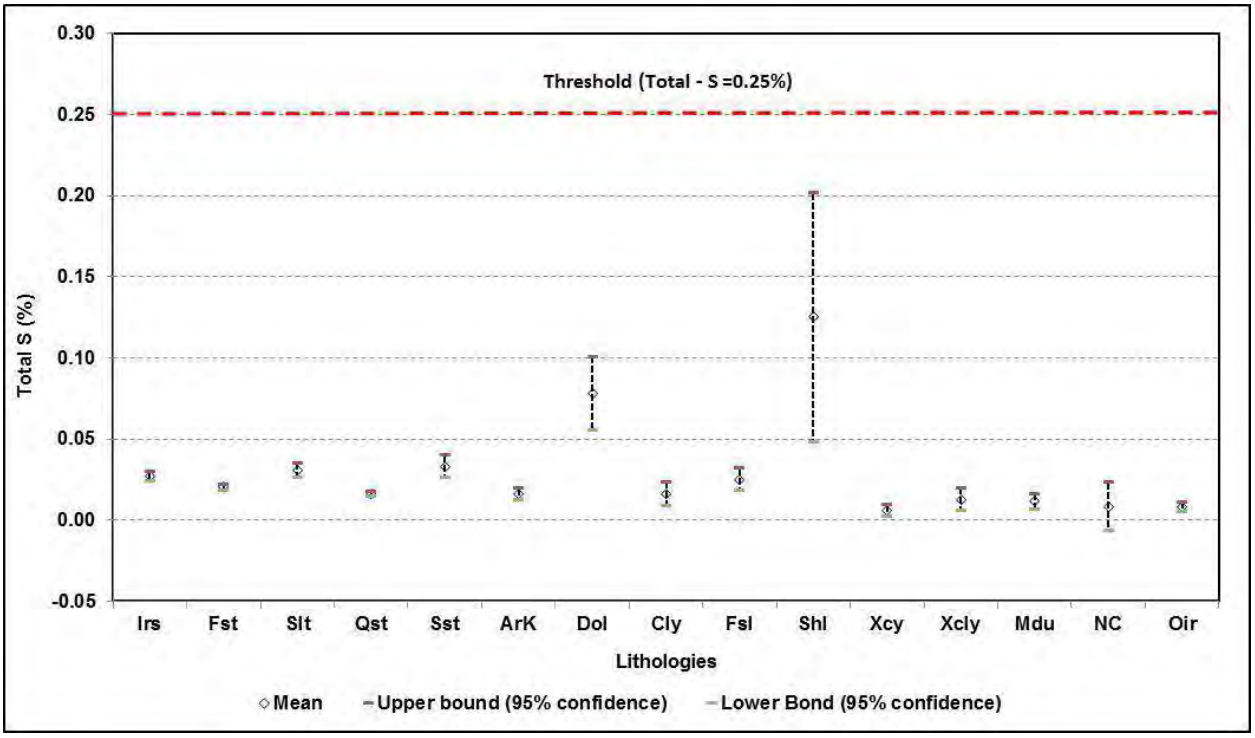

Figure 2 95% Confidence Intervals for Waste Lithologies at Deposit C

A further statistical assessment of the sample population in relation to global lithological distribution based also on total-S concentration (Figure 2) indicated that the threshold sulfur value of 0.25% is well above of the highest mean of 0.13% of the shale (Shl). The 95% confidence level of this highest mean ranges from 0.05% to 0.20% and all rocks may be classified as non-acid forming (NAF) materials.

In summary, the development of the conceptual model assisted with defining the degree of rigour with which the exploration data needed to be assessed, as a first step of sample number definition and

quantification. The statistical assessment, to comply with regulatory requirements, allowed verification of the optimum number of samples (Table 3) submitted for analytical assessment. The highest confidence levels tolerated indicated that the sample population selected would produce high confidence levels and contain the true sample population value which, provided confidence to verify the assumptions made during the development of the geochemical conceptual model.

The conceptual model approach with clearly defined objectives abridged the premise that *samples must be selected to characterize both the type and volume of rock materials and also to account for the variability of materials that will be exposed during the life of the mine* (DITR 2007; DMP 2009). In addition, it assisted with determining the extent of the mine AMD management plan (including sampling methodologies and monitoring requirements) and a site specific standard operation procedure (SoP) for the daily management of PAF/NAF waste materials.

AMD ASSESSMENT APPROACH

Sample qualification and quantification are generally regulated by various authorities and approval agencies, and supplemented by a series of guidelines which despite postulating sample location, quantity and type, are seldom specific in regard to analytical assessment methodology. The use of these guidelines in distinguishing an approach to sampling should not be regarded as a stringent *step-by-step,* but instead be considered in conjunction with a risk-based approach, incorporating interpretation of the wider interactions of site conditions with current ARD and AMD scientific knowledge, and adjusted accordingly. Guidelines, rather than being prescriptive, should aid stakeholders to factor internal and external influences of and for the project. This in essence should set a framework that integrates the processes for identifying and managing risks, strategies and planning for the management of potential acid forming materials.

Included in the development of the hydrogeochemical conceptual model are the environmental risk assessment of AMD and an overall evaluation of social, economic and environmental impacts of the project. The analysis of these parameters primarily assists with defining the potential extent of impacts and perceived value of onsite and offsite environments. These are also considered to ascertain the degree of rigour required by further sampling and help in setting adequate analysis to characterize sources, pathways and receptors. For example, if the mine is located within a sensitive environment with likely downstream impacts by AMD formation, the sample number and sampling frequency are likely to increase as a consequence of the risks coupled with a stricter more detailed assessment by the regulator. However, if the site has no significant potential for AMD and is located in a remote locality with little or no predicted downstream environmental impacts, the AMD assessment may be concluded after finalising the conceptual model, with limited confirmatory sampling and analysis.

In summary, if the analysis of key parameters incorporates a quantifiable risk of the local and regional site conditions, the wider geological and geochemical analysis, qualification and quantification of wastes and a hydrogeochemical assessment, a site specific investigation should provide a good base to evaluate AMD and their implications for mining development (Figure 3).

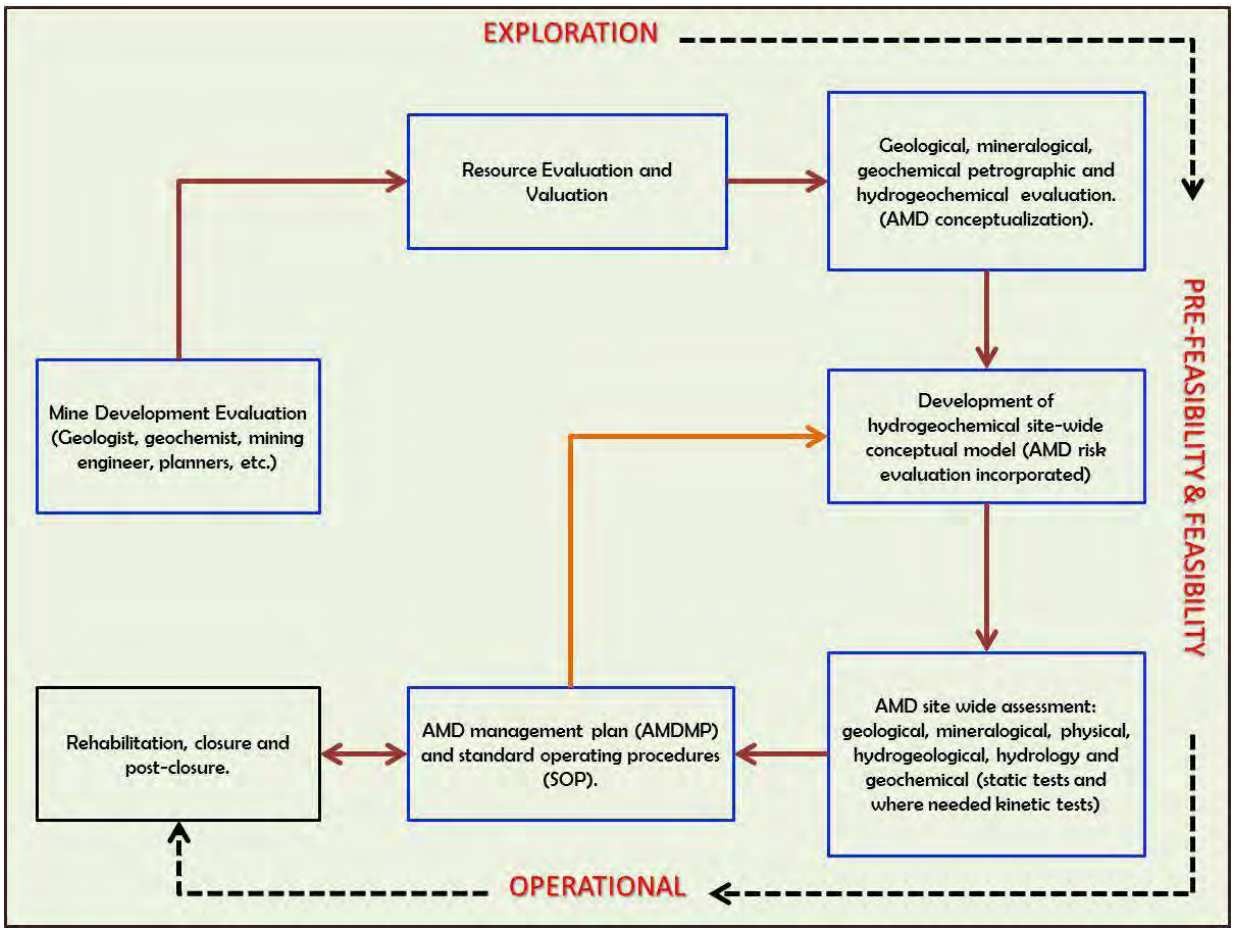

Figure 3 Flow Diagram to be adopted at the Exploration Stage

However, this approach needs to be incorporated at the exploration stage and continued through to the pre-feasibility, feasibility and operation phases. A good opportunity to further AMD studies is also presented by the grade control drilling program during feasibility studies and subsequent mining. This drilling program is developed to better understand grade distribution and variability of recoverable resources. Thus the development of a site wide hydrogeochemical conceptual model during the early stages of the exploration program should be used as a forum to:

- Analyse the potential for AMD formation.
- Assess the environmental sensitivity of the site and potential risks than this may pose.
- Assess the potential short- to long-term social, economic and environmental consequences.
- Define sample quality and number.
- Define methodologies to be used for AMD investigations and assessments.

REFERENCES

Alarcón León, E., Anstiss, R.G. (2002) Selected trace elements in Stockton, New Zealand Waters. New Zealand Journal of Marine and Freshwater Research 36. pp 81 -87.

Brady, K.B.C.. Hornberger, R.J. (1989). A manual for premining prediction of coal mine drainage quality. Common wealth of Pennsylvania Department of Environment and Resources, Bureau of Mining and Reclamation.

British Columbia Acid Mine Drainage Task Force (1991). 1990/1991 annual report. What happens if?—some remarks on useful geostatistical concepts in the design of sampling patterns. Proceedings of the symposium on sampling practices in the minerals industry, Australasian Institute of Mining and Metallurgy, pp 1– 15.

DMP (2009). Environmental notes on mining: Acid Mine Drainage. Government of Western Australia, Department of Mines and Petroleum.

DITR (2007). Managing acid and metalliferous drainage. Australian Government, Department of Industry Tourism and Resources. Leading Practice Sustainable Development Program for the mining Industry. 108 pp.

Freeman, J.R., Sturm, J.W., and Smith, R.M. (1987). Acid-base accounting in United States coal mine spoils and prep plant refuse. Proceedings of Acid Mine Drainage Seminar/Workshop. Environment Canada Halifax, Nova Scotia, Canada, 263-286.

Joint Ore Reserves Committee (2012). The JORC Code (2012 Edition). AusIMM the Minerals Institute. 44 pp.

Kentwell, D., Garvie, A., and Chapman, J. (2012). Adequacy of Sampling and Volume Estimation for Pre-mining Evaluation of Potentially Acid Forming Waste: Statistical and Geostatistical Methods. Proceedings of Life-of-Mine Conference, 10-12 July 2012, Brisbane, Australia (The Australasian Institute of Mining and Metallurgy: Melbourne).

Modis, K., and Komnitsas, K. (2007). Optimum Sampling Density for the Prediction of Acid Mine Drainage in an Underground Sulphide Mine. Mine Water Environment, 26: 237-242.

Rossi, L, Rumley, L, Ort, C., Minkkinen, P., Barry, DA., Chevre, N.; (2010). Sampling-helper: A web-based tool to assess the reliability of sampling strategies in sewers and receiving waters. Novatech 2010. Pp. 1-10.

Schafer, W.M.; (1993). Design of Geochemical Sampling Programs, presented at Mine Operation and Closure Short Course, Helena, Montana, USA, April 27-29.

SENES Consultants Limited, (1994). Review of Waste Rock Sampling Techniques, MEND Project 4.5.1-1.

Servida, D., Comero, S., Dal Santo, M., de Capitani, L., Grieco, G., Marescotti, P., Porro, S.,Lázár Forray, F., Gál, A., Szakács, A. (2013). Waste rock dump investigation at Rosia Montanaˇ gold mine (Romania): a geostatistical approach. Environmental Earth Science. 70: 13-31.

USDA Forest Service (1992). A Conceptual Waste Rock Sampling Program for Mines Operating in Metallic Sulfide Ores with a Potential for Acid Rock Drainage (G Farmer, Department of Agriculture, Forest Service, Ogden, Utah, USA).

Opportunistic AMD Sampling from Multi-Discipline Drilling Programs for Large Mining Companies

Joshua I Pearce[1] and Juan Gutierrez[2]

1. *O'Kane Consultants, Australia*
2 *Golder Associates, Australia*

ABSTRACT

The application of drilling surveys to assess economic viability, ground stability and hydrogeological conditions are typically completed prior to commencement of mining. It is generally accepted that in many instances insufficient geological samples are collected from these drilling programs specifically for geochemical analysis to effectively characterise the acid and metalliferous drainage (AMD) potential of the deposit. To minimise risk associated with incomplete characterisation of AMD potential, a continuing AMD sampling and analysis program can be developed and implemented to ensure adequate sample collection occurs.

The focus of this paper is to outline a case study of the development of such a sampling program for a large mining company that incorporates all of their Western Australian iron ore operations. The program utilises multi-discipline drilling programs at all stages of mine development to minimise AMD risk.

The continuing sampling and analysis program is initiated at the long term drilling schedule planning stage by selecting relevant upcoming programs. Potential drilling programs include exploration, geotechnical, hydrogeological and grade-control drilling. Engagement with project teams responsible for the individual drilling programs to express interest in drill core is initiated early with upfront cross-discipline drilling planning meetings. Once approval has been given to select splits of drill core, a sampling plan is developed and provided to the responsible project teams along with a detailed and easy to follow sample collection and dispatch procedure.

The implementation of the program over the previous ten months has successfully seen the selection and collection of geological samples from more than 35 drilling programs across 25 deposits spanning six mining operations within Western Australia. In addition to increasing the size of their regional environmental geochemical database, this has resulted in significant cost-savings by incorporating AMD sampling into existing drilling programs. Designing the program to have minimal impact on existing procedures and the positive adoption of site personnel to reducing AMD risk has contributed strongly to the success of the program.

Keywords: AMD sampling and analysis, large scale sampling, multi-discipline drilling

INTRODUCTION

Geological samples, in some form or another, are collected from the first to last drill hole for any given mining project. Drilling programs to assess economic viability, ground stability and hydrogeological conditions are typically completed prior to commencement of mining and all present opportunities for the collection of geological material. However, sufficient environmental geochemical samples to adequately characterise a site for its potential to generate acid and metalliferous drainage (AMD) are not commonly collected. This deficiency in waste rock geochemical knowledge can be due to a number of reasons:

- Exploration programs do not generally actively target waste units which are typically the key materials of interest for AMD predictions, rather they focus on ore bodies.
- Minimum sampling requirements for AMD assessments set by regulatory bodies are often vague and/or poorly interpreted by those developing sampling programs.
- AMD sampling programs are often considered to be complete and are ceased once approval to mine has been granted.
- The true monetary value of AMD risk is often poorly understood and/or insufficiently weighted against exploration/production targets.

AMD sampling programs can also have the propensity to be set at a level that is too intensive in the early stages of mine development. Intensive analysis of geological materials for AMD assessments prior to developing a sound geological understanding of the deposit can lead to disproportionate analysis of waste units. This can in many cases result in unnecessary expenditure by mining companies on environmental geochemical data not providing the value of its capital outlay.

These potential causes for insufficient sample collection or conversely early phase over-intensive analysis for AMD assessments, can be addressed by implementing an iterative sampling program throughout the life of the mining operation (Kentwell et al. 2012). Leveraging off the multiple drilling programs routinely completed as part of resource assessment can mean costly standalone drilling programs specifically for AMD assessments may be avoided.

Successfully taking advantage of drilling programs designed for purposes other than AMD sampling requires close interaction with the multiple stakeholders specific to each drilling program. Carefully designed and easy to follow procedures are critical to ensure consistency and sample integrity is achieved in sample selection and collection stages.

As part of geochemical risk management activities, an ongoing AMD sampling and analysis program was developed for the Western Australian iron operations of a large iron-ore mining company by the authors in collaboration with the mining company. The program developed utilises multi-discipline drilling programs at all stages of mine development to minimise AMD risk. This paper presents the various stages that comprise the developed ongoing sampling program including the incorporation of a data management and tracking procedure to ensure sample and data integrity is maintained.

METHODOLOGY

The mining company's ongoing sampling and analysis program comprises multiple stages with input required from various groups within the company. To ensure that sample and data integrity could be maintained over such a large program, a data tracking and management procedure was incorporated into the ongoing sampling and analysis program. The stages of the developed program are presented in Figure 1 and are:

- Identification and initiating involvement with key drilling programs and program stake holders.
- Development of a consistent sample selection procedure.
- Development of consistent sample collection procedure.
- Data tracking and management.
- AMD Data interpretation.

Adoption by Key Stakeholders

The first step to designing an ongoing sampling and analysis program that is to be successfully adopted by multiple operations and disciplines is understanding the drivers of each of the key stakeholders. That is, when taking advantage of planned drilling programs for opportunistic AMD sampling, the program must be designed to work around the key stakeholder's objectives.

For individual AMD sampling plans created within the ongoing sampling and analysis program, requesting site personnel or those responsible for the planning of the drilling programs to significantly alter an established process was deliberately avoided. The objective being to minimise the burden (perceived or actual) of the AMD sampling, particularly for site staff.

Some key factors that the effective adoption and implementation of the program (by multiple stakeholders) depended on, included:

- Frequent and open communications with site personnel and drilling program coordinators.
- Understanding the various sampling/logging/dispatch procedures employed across the site(s), e.g. geotechnical versus hydrogeological versus exploration versus grade control.
- Understanding the limitations of each drilling technique employed and therefore the limitations for AMD sampling.
- Designing the sampling and analysis plans to be cohesive with planned drilling programs.
- Avoiding requests for unnecessary collection of samples.

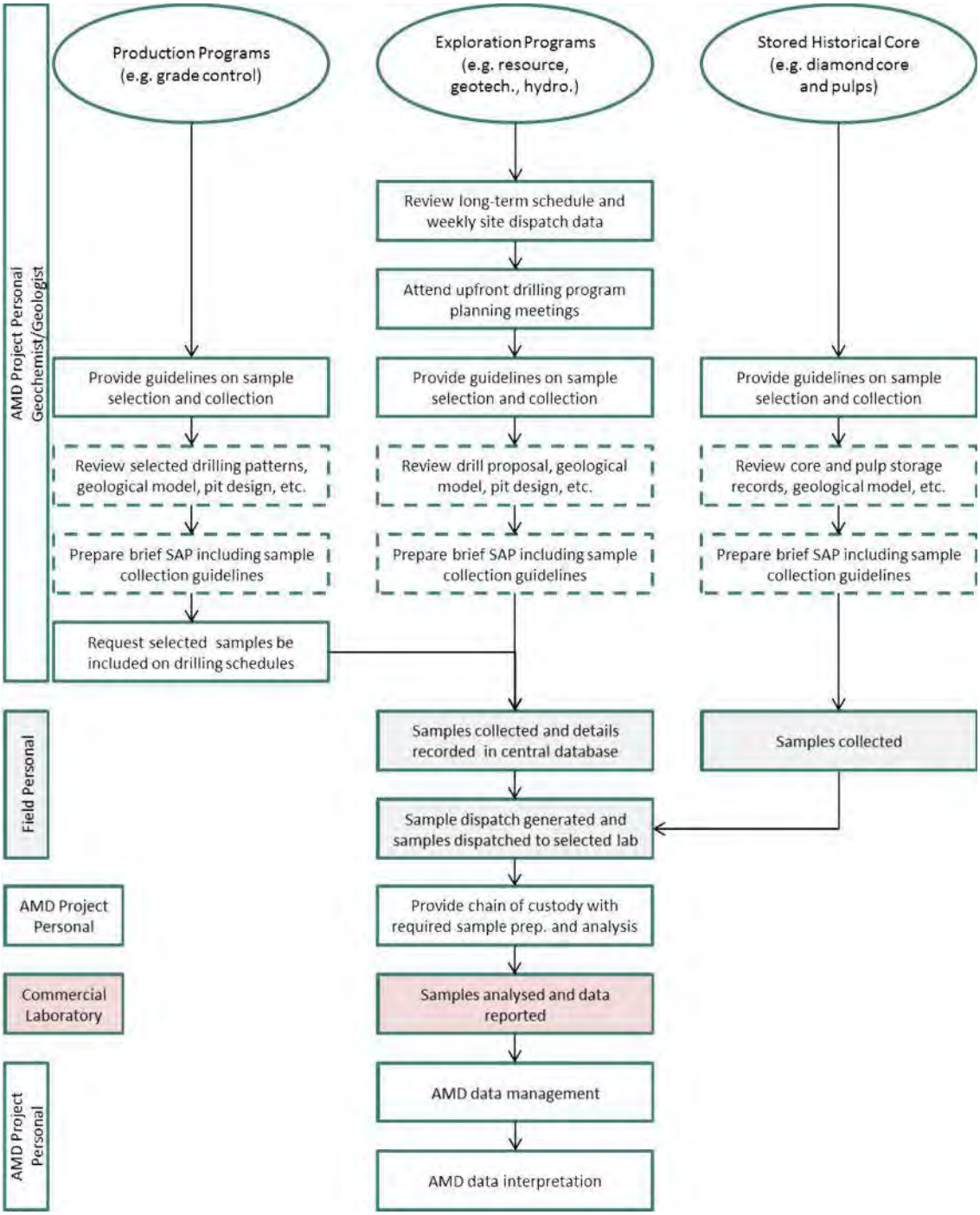

Figure 1 Ongoing sampling and analysis program flowchart

Identification and Initiating Involvement with Key Drilling Programs

The ongoing sampling and analysis program is initiated at the long term drilling schedule planning stage by selecting relevant upcoming programs. Potential drilling programs include exploration, geotechnical, hydrogeological and grade-control drilling. Engagement with project teams responsible for the individual drilling programs to express interest in drill core was initiated early with upfront cross-discipline drilling planning meetings.

For large mining companies with several standalone mining operations, careful consideration must be given to which drilling program is selected to avoid unnecessary expenditure. Unnecessary expenditure are not limited to direct laboratory costs but also the time taken by employees to select and collect samples.

Some key questions asked when deciding whether to pursue a planned drilling program included:

- Does the planned drilling program target a deposit of significant interest to the company?
- Will the drilling program intersect key lithological units with respect to AMD generation?
- Will the drilling program intersect lithological units for which little data is currently available?
- Is there sufficient knowledge of the orebody and potential pit shell to avoid unnecessary sampling, i.e. is it worthwhile waiting for an infill drilling program planned at a later date?
- Is the drilling method conducive to the collection of meaningful AMD samples?

Development of a Consistent Sample Selection Procedure

Once approval had been granted by project teams responsible for the individual drilling programs to select splits of drill core, a sampling plan was developed. A sample selection procedure was developed to promote consistency across the various operations. The procedure included the selection of samples from upcoming drilling programs and the selection of stored core/pulps.

The sample selection procedure was designed to be used for each phase of sampling with each preceding phase informing the current planned phase and is therefore iterative in nature. Several informed decisions are required throughout the procedure which are primarily based on the sampling program objectives, the size of the drilling program, the type of drilling method and existing geochemical information.

The sample selection procedure was comprised of the steps presented in Figure 2.

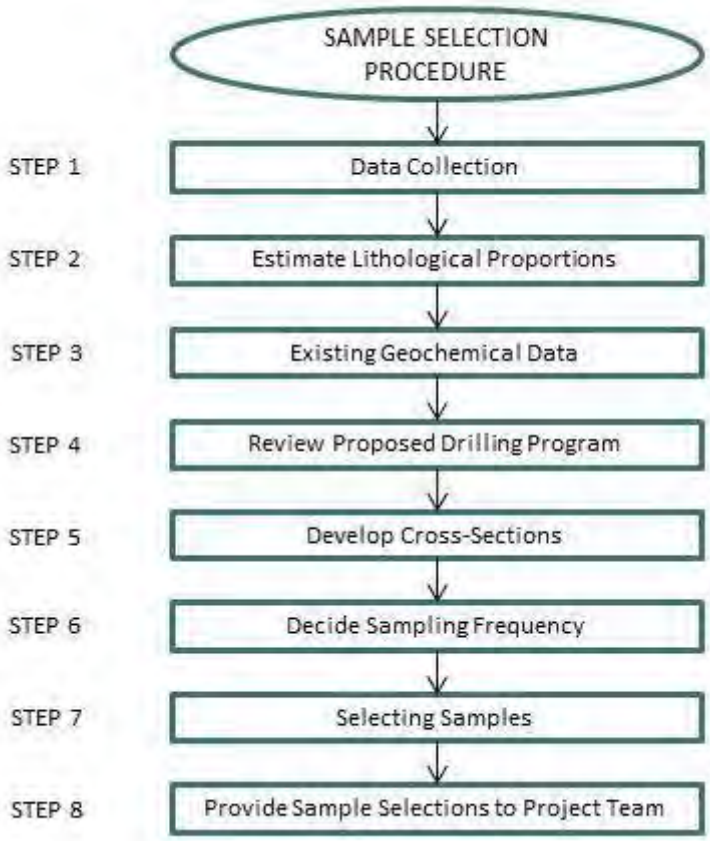

Figure 2 Sample selection procedure flowchart

Initially, the most up to date drilling proposal and geological resource model from the central database was collected (Step 1). Then, using geological modelling software, the percentages of each waste lithology to be mined within the proposed pit shell was estimated as well as lithologies remaining in the pit wall (Step 2).

To ensure informed sample selections incorporated all applicable data collected prior, relevant geochemical data for the deposit including the current assay database was reviewed (Step 3). If sulfur data was available within the assay database, the sulfur distribution within the geological model was assessed to identify any regions of high sulfur concentrations. The average sulfur concentrations per lithology was also estimated.

Following the review of all relevant data, the proposed drilling program was studied within the resource model to assess what lithologies may be intersected (Step 4). The potentially intersected lithologies were cross-checked with:

- Any lithologies previously identified as important with respect to AMD processes such as sulfide/carbonate bearing units or enrichment in elements of concern.
- Results of the existing geochemical data review (Step 3).

To assist site personal with sample selection and to also aid the later stages of data interpretation, geological modelling software was used to create cross sections (Step 5). Cross-sections included, at a minimum, proposed drill holes, historical drill holes (if appropriate), geological information (lithological domains, ore zone(s), weathered zones), proposed pit shell(s) and pre-mining water tables.

For drilling programs covering the entire deposit, cross-sections were spaced at relatively equal distances spanning the deposit in order to achieve a good spatial representation. For smaller targeted drilling programs (geotechnical, etc), all drill holes were presented on the cross-sections.

Several factors need to be considered when deciding the sampling frequency for Step 6. For large, deposit encompassing drilling programs, sufficient numbers of samples should be taken to accurately characterise the variability and central tendency (e.g. average, median, and 10th and 90th percentiles) of the different waste materials, project components and geological units (DoITR, 2007 and Price, 2009). For smaller targeted drilling programs (e.g. geotechnical) the sample frequency was largely reduced and was not necessarily focussed on spatial representativeness.

Figure 3 presents some of the factors to be considered when deciding on the sampling frequency for an individual drilling program.

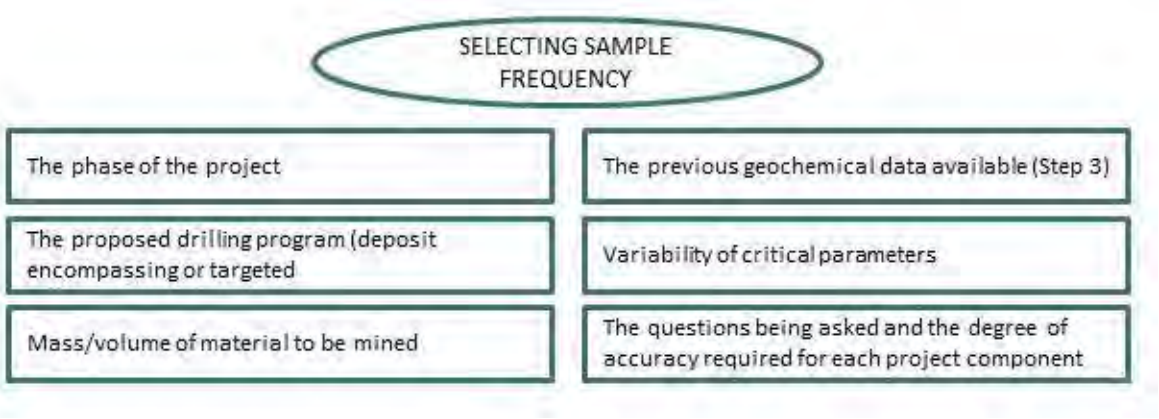

Figure 3: Selecting sample frequency

Providing good spatial, geological and geochemical representation in the sample population is important as AMD may be produced by only a portion of the geological materials (Price, 2009). For large deposit encompassing programs, the aim was to select sample proportions equivalent to the waste material to be mined as determined in Step 2.

Sampling locations (Step 7) were largely based on:

- The required accuracy and precision of the sampling program.
- Knowledge of the deposit.
- Areas of notable physical, mineralogical, geochemical and degrees of weathering differences.
- Findings from Step 3 and Step 4.

The proportions of specific lithologies may increase if lithologies to be intersected have been identified in previous geochemical assessments as units of interest. In addition, lithologies may have been targeted for extra sampling if specific drainage prediction questions were being investigated.

Once all samples were selected, selections were tabulated and their corresponding details were provided in a format easily followed by field personal (Step 8).

Development of a Consistent Sample Collection Procedure

To maintain sample and data integrity, particularly within a large company with multiple disciplines responsible for sample collection and dispatch, a consistent and easy to follow sample collection procedure is essential and as such was developed.

Sample recording, bagging, labelling and dispatch instructions were clearly provided in the sample collection procedure. The recording and entering of sample details into the central database represents the commencement of the phase that follows the ongoing sampling and analysis program (data tracking and management procedure).

Clear sample collection instructions for each drilling technique were needed to ensure sample integrity was maintained. Three separate sub-procedures were therefore developed for the three main drilling techniques employed at the various operations:

- Diamond Core – exploration, geotechnical, metallurgical and hydrogeological.
- Reverse Circulation – exploration, geotechnical, metallurgical and hydrogeological.
- Blast hole – grade control.

Diamond Core (Exploration, Geotechnical, Metallurgical and Hydrogeological)

Sampling of diamond core for AMD testing was undertaken in various ways because of the multiple programs employing this drilling method. Quarter core splits were generally collected and were largely obtained following a coarse crushing stage. Greater proportions than quarter were generally only permitted when core was not to be assayed.

Timing was critical for the requesting of diamond core intervals because generally all core was processed; if the request was delayed samples may have not been available. Therefore, when core arrived at the processing facilities, borehole logs had to be reviewed within the geological model as a priority prior to submitting a sample request form.

Reverse Circulation (Exploration, Geotechnical, Metallurgical and Hydrogeological)

Drilling programs employing reverse circulation drilling collected requested samples as a split sample directly from the cone or rotary cone splitter. For exploration drillholes, one composite sample was collected per rod (3 m interval).

Unlike diamond core selections which were selected after reviewing borehole logs, sample selections from reverse circulation drilling were made prior to drilling. Therefore, targeted lithologies were often missed as field staff collected requested intervals irrespective of the material intersected. This was counteracted by over-selection during the sample selection phase as the cost to collect and dispose of additional unwanted samples was considered to outweigh falling short on collection of key lithologies.

Blast hole (Grade Control)

Although the quality of samples collected from blastholes for environmental geochemistry purposes were considered lower than samples collected from diamond and reverse circulation drilling, there is still benefit in utilising this source for AMD characterisation. .

Taking the limitations into consideration, only one sample was collected for any given blasthole and specifically from the middle 3 m interval. This was to minimise contamination from the upper bench blasting pattern and bias introduced from collecting material from the lower portion of the drillhole.

Data Tracking and Management

The data tracking and management procedure begins when sample collection details are recorded and entered into the central database (Figure 4). Samples are then dispatched under a standardised dispatch system.

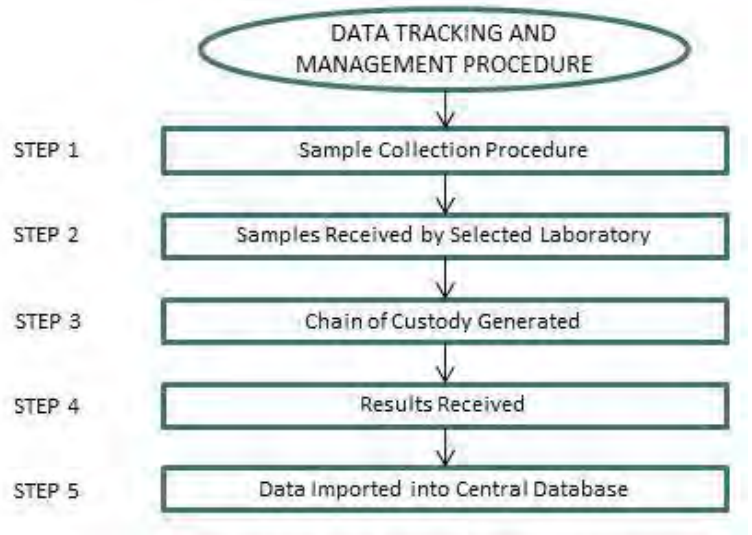

Figure 4: Data tracking and management procedure flowchart

Once samples arrived at the laboratory, received samples were assessed and analysis requests (chain of custodies) were prepared. This also provided an opportunity to review assay data if available for specific intervals to reduce unnecessary analysis. It also provided an additional control step to identify primary samples sent to the environmental laboratory that should have been directed to the metallurgical laboratory.

To streamline the importation of laboratory data into the central database, a database compatible format was developed. This file was provided to internal database specialists.

Data Interpretation

Once all data is located within the central database, it needs to be readily available for inclusion in AMD assessments for specific operations. To streamline the collation of required data for AMD assessments, an "AMD Export" file (readable as a csv) was developed that included all critical

available information for AMD assessments. The export includes a range of parameters for each data point, such as:

- Project and orebody.
- Borehole name, drilling method, borehole coordinates and coordinates grid name.
- Unique internal sample number and unique laboratory sample number.
- Sample depth.
- Lithology, waste/ore, degree of weathering, above or below water table.
- Laboratory results (environmental and assay where available).

RESULTS AND CONCLUSIONS

The implementation of the program over its first ten months successfully saw the selection and collection of geological samples from more than 35 drilling programs across 25 deposits spanning six mining operations within Western Australia. In addition to increasing the size of the regional environmental geochemical database, this has resulted in significant cost-savings by incorporating AMD sampling into existing drilling programs.

Designing the program to have minimal impact on existing procedures and the positive inclusion and "buy in" of site personnel to reducing AMD risk has contributed strongly to the success of the program. As a result of the careful consideration for implementation, it was noted that as the program developed teams in other disciplines were willing to allow redesigning of planned drilling programs for AMD specific drillholes. This was considered a positive sign of internal acceptance and approval of the program.

Some key learnings from the implementation of the program included:

- Understanding the limitations of the drilling methods and the already established sample collection procedures was required to ensure sensible sample requests were made.
- Understanding the limitations of the selection/collection procedures was paramount to (a) understanding the limitations of the data collected, and (b) appreciate that not all targeted units may be collected and to prepare inbuilt contingencies within the sampling plans.
- When selecting samples from geological block models, it is important to recognise the limitations in resolution/accuracy and select samples accordingly. That is, the successful collection of a targeted lithology is more likely if a wider interval range is provided to field personal (15-21m opposed to 15-18m).
- Different field staff may interpret requested sample intervals differently; one composite sample (3 m) collected within the requested 10 m interval opposed to the entire interval being collected (three samples). For this reason, the analysis request step was not included at the dispatch stage which allowed the prevention of unnecessary analysis.

Potential areas for further program development include:

- Incorporate other parameters where available into the sample selection procedure that may also be recorded within resource block models, (calcium, magnesium, selenium, etc).

- Where possible, request field staff to differentiate between sub-units when selecting and collecting samples. For example, sub-units can have significantly different acid forming potentials and reaction rates leading to different management options.

ACKNOWLEDGEMENTS

We would like to acknowledge the mining company and their staff for their assistance in developing and establishing the program. We would also like to acknowledge the advice provided by both the mining company and Golder Associates Pty Ltd staff.

REFERENCES

DoITR (2007) Leading Practice Sustainable Development Program for the Mining Industry - Mine Rehabilitation. Canberra, Australia, Commonwealth of Australia.

Kentwell, D, Garvie A, Chapman J (2012) Adequacy of Sampling and Volume Estimation for Pre-mining Evaluation of Potentially Acid Forming Waste: Statistical and Geostatistical Methods. Proceedings of Life-of-Mine Conference, 10–12 July 2012, Brisbane, Australia (The Australasian Institute of Mining and Metallurgy: Melbourne).

Price, W (2009) Prediction Manual for Drainage Chemistry from Sulphidic Geologic Materials. Smithers, British Columbia, Mine Environment Neutral Drainage (MEND) Program.

Difficulties of Interpretation of NAG Test Results on Net Neutralizing Mine Wastes: Initial Observations of Elevated pH Conditions and Theory of CO_2 Disequilibrium

Jessica Charles, Andrew Barnes, Julien Declercq, Ruth Warrender, Christopher Brough, and Robert Bowell
SRK Consulting, United Kingdom

ABSTRACT

Hydrogen peroxide leach tests (NAG tests) are increasing in use by the mining industry for determining acid rock drainage characteristics of mine wastes. The test uses an excess of hydrogen peroxide (H_2O_2) to rapidly oxidise sulfide minerals in a sample, thus releasing acidity related to sulfide oxidation. The acidity released is neutralized by available (carbonate) neutralizing potential, theoretically resulting in a measure of Net Acid Generation (NAG) based on material reactivity. In addition, chemical analysis of the NAG leachates can be undertaken to provide an indication of solutes that may be mobilised during sulfide weathering.

NAG tests are complimentary tests to standard Acid Base Accounting (ABA), allowing clarification of ABA characteristics and better characterization of samples that show uncertain characteristics based on ABA testwork. However, experience has shown that the use of the NAG test method on samples with elevated carbonate content can result in excessively basic pH conditions which may be misleading and result in uncertainty in interpretation.

To understand the uncertainty mentioned above, tests were completed to measure and evaluate the pH change throughout the NAG test method. The results indicate that much of the pH change can be attributed to carbon dioxide (CO_2) disequilibrium during the heating stage of a NAG test. The study is supported by diagnostic mineralogical and geochemical investigation. In addition, the influence of CO_2 on NAG test pH conditions is demonstrated through numerical interpretation using the USGS thermodynamic equilibrium code PHREEQC.

Keywords: ARDML, NAG, PHREEQC, carbon dioxide, hydrogen peroxide

INTRODUCTION

Environmental concerns coupled with the strengthening of environmental legislation, has necessitated the development a range of testwork methods for the prediction of Acid Rock Drainage and Metal Leaching (ARDML) from mine wastes. One of the most accepted and widespread methods is the Acid Base Accounting (ABA) test, which is used to determine the balance between acid generation potential (AP) and acid neutralization potential (NP) of a material based on sulfide and carbonate content, respectively. Recently, the complimentary NAG) test method has seen increasing use within the industry. This test allows for the rapid determination of ARD characteristics of tailings and waste rock samples through the use of hydrogen peroxide (H_2O_2). The typical NAG test procedure is based upon H_2O_2 oxidation testing that has been developed over the past 40 years by: Smith *et al*. (1974), Sobek *et al*. (1978), O'Shay & Hossner, (1984), Finkelman & Giffin (1986), O'Shay *et al*., (1990), Miller *et al*. (1997), and most recently by Stewart *et al*. (2003); Stewart (2005) and Stewart *et al*. (2006).

Solutions generated during the NAG test can additionally be analysed to provide an indication of metal and metalloid (e.g. zinc, copper, lead, cadmium, arsenic) mobility during weathering and oxidation of the waste. Furthermore, there are possible advantages to using NAG tests and derivations of the NAG test (such as kinetic NAG) as a substitute for kinetic tests (Miller *et al*., 1997; Stewart *et al*., 2006; Sapsford *et al*., 2010) and for preliminary prediction of seepage water quality from mining waste facilities (Barnes et al., 2013; Barnes et al., 2015).

Although NAG tests allow for improved understanding of ARDML characteristics and classification of samples that show uncertain acid generating characteristics from ABA testing, it is not without its limitations. These limitations have been highlighted in studies undertaken on the NAG testing of coal spoils by Stewart, (2005) and Stewart *et al*., (2006). In addition, other authors have highlighted the sensitivity of the oxidising agent H_2O_2 to: base metal cations and dissolved carbonates (Lee *et al*., 2000 and references therein); and to elevated reaction temperatures (Yazici & Deveci, 2010).

Further to the above limitations with respect to the instability of H_2O_2, it has also been observed by the authors that the use of the NAG test method on samples with elevated transition metal carbonate content (such as ankerite) can produce excessively basic NAG pH conditions which may be misleading and result in uncertainty in interpretation. This paper intends to shed light on the mechanisms that induce the generation of excessively basic solution. It is hypothesised that the elevated pH conditions can be attributed to carbon dioxide (CO_2) disequilibrium during the heating stage of a NAG test.

METHODOLOGY

Ten waste rock samples were collected from a gold mine site in the UK. Local geology at the site consists of clastic marine sediments, minor volcanic units, sandstone and auriferous quartz-carbonate veins. The major gold-bearing formation comprises mixed semi-pelites, quartz semi-pelites, and psammites. The project area contains mesothermal gold mineralization, with gold disseminated in quartz-sulfide veins.

Acid base accounting testwork

ABA testing was undertaken in accordance with the method described in EN15875 (CEN, 2011). The method assesses the speciated carbon and sulfur content of the samples to determine the balance of acid generating sulfides (AP) and acid neutralizing carbonate minerals (NP). ABA testing does not make allowances for mineralogy and assumes all sulfide is present as pyrite and all carbonates are present as calcite. AP is calculated from the sulfide sulfur content of the samples whilst the NP is based on a modified Sobek procedure in which acid addition is determined from the Total Inorganic Carbon (TIC) content of the sample. The determination of a samples AP and NP in kg $CaCO_3$ equivalents per tonne allows for the calculation of net neutralizing potential (NNP) and neutralization potential ratio (NPR) which describe the samples potential for acid generation:

$$Net\ Neutralizing\ Potential\ (NNP)(kg\ CaCO_3) = NP - AP$$

$$Neutralization\ Potential\ Ratio\ (NPR) = {}^{NP}/_{AP}$$

An assessment of paste pH was also undertaken to determine the immediate sample pH without oxidation of the sample.

Mineralogical analysis

A mineralogical investigation was undertaken on the samples to assist in interpretation of the NAG test results. This consisted of optical and scanning electron microscopic (SEM) analysis and spectroscopic analysis using SEM electron dispersive X-Ray (EDX) analysis of grab samples from the drill core sample intervals. The investigation focussed on quartz, carbonate, and sulfides within mineralized veins.

Net acid generation testwork

The static NAG test differs from the ABA test in that it provides a direct empirical estimate of the overall sample reactivity, including any acid generated by semi-soluble sulfate minerals (e.g. alunite), as well as other potentially acid-generating sulfur-bearing minerals. As such, the NAG test provides a better estimate of potential for field acid generation than the more widely-used ABA methods. ABA defines acid potential based solely on sulfide sulfur, or total sulfur content, and assumes pyrite to be the dominant sulfide mineral present.

NAG testing was carried out in accordance with the method described in the AMIRA guidelines (2002) as follows: 250 mL of 15% H_2O_2 was added to 2.5g of pulverised sample. The H_2O_2 was allowed to react with the sample overnight, and the following day the NAG solution was gently heated, using a hot plate to near boiling for a minimum of 2 hours; deionised water was added as required to maintain an approximately constant volume of solution. The NAG solution is heated to remove excess H_2O_2 and also facilitate the release of inherent neutralizing capacity (carbonate buffering). The solution was then allowed to cool to room temperature, and at this point the NAG pH was measured and recorded. The test also reports the NAG value, measured in equivalent kilograms of sulfuric acid (H_2SO_4) per tonne.

The above method was adapted for the test samples in order to track the pH change through the latter portion of the test. pH was measured at the following times to determine the evolution of solution pH:

- *Step 1*: Prior to solution heating following completion of NAG test procedure (20 °C)
- *Step 2*: Following 2 hour heating step (at approximately 100 °C) after the solution is allowed to cool to room temperature (20 °C) - and then made up with deionised water - typical NAG pH
- *Step 3*: After solution allowed to equilibrate with atmosphere for 24 hours
- *Step 4*: After solution allowed to equilibrate with atmosphere at room temperature for 1 week.

The leachate generated during the NAG test was analysed for major ions, dissolved metals and metalloids using inductively coupled plasma mass spectrometry (ICP-MS). The aggressive oxidising conditions of the H_2O_2 used in the NAG test, effectively oxidises all physically exposed or chemically available sulfide minerals. Analysis of the NAG solution provides an indication of the potential for high level metal(loid) release that would occur during exposure of the mine-waste material to oxygen.

Thermodynamic equilibrium modeling

Thermodynamic equilibrium calculations were carried out to validate and numerically recreate the observations of the NAG testwork and demonstrate the influence of CO_2 on NAG pH. Thermodynamic calculations were carried out using the geochemical modelling code PHREEQC, version 3.1.2.8538 (Parkhurst & Appelo, 1999) together with the MINTEQ v8 database. This database is largely consistent with the MINTEQ v4 provided with PHREEQC, including updated thermodynamic data for arsenic and manganese. The NAG solutions defined in TABLE 1 were run initially in PHREEQC without any carbonate equilibrium phases, then the same simulations were run with CO_2 at atmospheric pressure (CO_2 partial pressure of 0.0003 bar). Forty PHREEQC simulations (four per initial starting solution; TABLE 1) were carried out in order to replicate the NAG experiment as described below:

- *Simulation 1*: Initial solution – at room temperature (20 °C)
- *Simulation 2*: Boiling initial solution (100 °C) - degassing of CO_2 in solution to atmospheric equilibrium
- *Simulation 3*: Cooling of solution back to room temperature (20 °C) – system at disequilibrium with respect to CO_2 and carbonate minerals with CO_2 in solution much lower than equilibrium CO_2 concentration
- *Simulation 4*: System allowed to reach equilibrium with respect to CO_2 (20 °C)

The input solution chemistries outlined in TABLE 1 were experimentally derived from the NAG test. Bicarbonate alkalinity was not measured directly and was determined via major ion charge balance.

Table 1 PHREEQC initial input solutions derived from NAG leachate analysis

Sample ID	1	2	3	4	5	6	7	8	9	10
Temp (°C)	20	20	20	20	20	20	20	20	20	20
units	mg/L	mg/L	mg/L	mg/L	mg/L	mg/L	mg/L	mg/L	mg/L	mg/L
NAG pH (pre boiling)	7.03	7.38	7.21	7.42	7.22	7.35	7.22	7.00	7.37	7.12
HCO_3-	49.5	57.9	56.2	50.9	48.4	52.3	50.1	29.9	39.2	21.0
SO_4	1	1.2	6	3.8	1.6	1	11	1	1	1
Ca	18	19	22	19	18	17	22	12	15	8.6
K	1.9	4.8	2.7	3	2.1	4.6	3.5	1.4	2	2.5
Mg	0.5	0.5	0.5	0.5	0.5	0.5	0.5	0.5	0.5	0.5
Na	0.5	1.1	0.5	0.5	0.5	1.6	1	0.5	0.5	0.5
As	0.06	0.0055	0.028	0.14	0.011	0.024	0.076	0.018	0.125	0.017
Cu	0.0012	0.0023	0.0026	0.0017	0.0036	0.001	0.0068	0.0011	0.012	0.0038
Fe	0.056	0.048	0.059	0.105	0.062	0.032	0.054	0.063	0.056	0.035
Mn	0.35	0.16	0.21	0.225	0.245	0.04	0.195	0.455	0.215	0.13
Ni	0.0047	0.005	0.012	0.024	0.0078	0.0038	0.011	0.0057	0.071	0.0085
Zn	0.001	0.001	0.001	0.0025	0.001	0.001	0.0011	0.001	0.099	0.001

RESULTS

ABA testwork

ABA testwork results for the ten samples are summarised in TABLE 2. Based on the results all samples are classified as Non Acid Forming (NAF). Paste pH of the samples ranged from 8.12 to 8.96 with an average of 8.47. The total sulfur concentrations range from 0.01 wt% to 0.16 wt%. The samples are classified as NAF based on their NNP and NPR values which were calculated from the NP and AP values. Nine of the 10 samples have a greater NP than AP and are therefore classified as net neutralizing mine waste. An NNP result of <-20 and an NPR result of <1 is indicative of a potentially acid forming (PAF) sample, whereas an NNP of >20 and an NPR of >3 is representative of a NAF sample. All samples except for sample 10 report an NPR of >3.

Table 2 Sample summary

Sample ID	Total S (%)	Sulfide S (%)	Paste pH	TIC (%)	AP (kg $CaCO_3$ eq/t)	NP (kg $CaCO_3$ eq/t)	NPR	NNP (kg $CaCO_3$ eq/t)	ARD Classification
1	0.01	0.01	8.52	0.09	0.31	1.463	4.68	1.15	NAF
2	0.06	0.06	8.96	0.24	1.88	20.30	10.83	18.43	NAF
3	0.05	0.05	8.55	0.21	1.56	12.79	8.18	11.23	NAF
4	0.16	0.16	8.22	0.23	5.00	17.29	3.46	12.29	NAF
5	0.07	0.07	8.31	0.11	2.19	22.25	10.17	20.06	NAF
6	0.03	0.03	8.32	0.36	0.94	19.03	20.29	18.09	NAF
7	0.15	0.15	8.14	0.19	4.69	17.13	3.65	12.44	NAF
8	0.01	0.01	8.67	0.06	0.31	5.46	17.48	5.15	NAF
9	0.07	0.07	8.12	0.16	2.19	19.24	8.79	17.05	NAF
10	0.03	0.03	8.86	0.21	0.94	0.00	0.00	-0.94	Uncertain

PAF – Potentially Acid Forming; NAF – Non-Acid Forming; TIC – Total Inorganic Carbon

Mineralogical assessment

Optical microscope and SEM investigation confirmed the main sulfide mineral present within the deposit as pyrite (FeS_2), which was present in two main textural associations. First, pyrite was frequently present in trace (<1%) proportions within the main quartz-mica-schist (QMS) fabric; usually fine-grained and aligned along the foliation direction. Second, coarse to medium-grained euhderal to subhedral pyrite within cross-cutting veins. This pyrite was closely associated with quartz and ankerite (the main carbonate mineral observed). In addition to pyrite there was subordinate chalcopyrite ($FeCuS_2$), aikinite ($CuPbBiS_3$), enargite (Cu_3AsS_4), lautite (CuAsS), and galena (PbS). Mg-poor ankerite was the primary carbonate present in the samples, with an approximate stoichiometry of $0.5Ca0.2Mg0.3(Fe,Mn)CO_3$.

NAG testwork

The NAG pHs recorded during the various stages of the NAG tests are reported in TABLE 3 and FIGURE 1. In general, a NAG pH less than 4.5 and a NAG value greater than 5 kg H_2SO_4 equivalents per tonne are indicative of a PAF material. All NAG pH values recorded in the various stages of the testwork are neutral to alkaline (7.0 to 10.67). The table shows that following the NAG test but prior to the pre-heating stage, the measured pH for all solutions is in the range of 7.0 to 7.5 with little deviation. Comparison of the pre-boiling NAG pH with measured paste pH shows that pre-boiling NAG pH is consistently in the region of 1 to 1.5 pH units lower than paste pH.

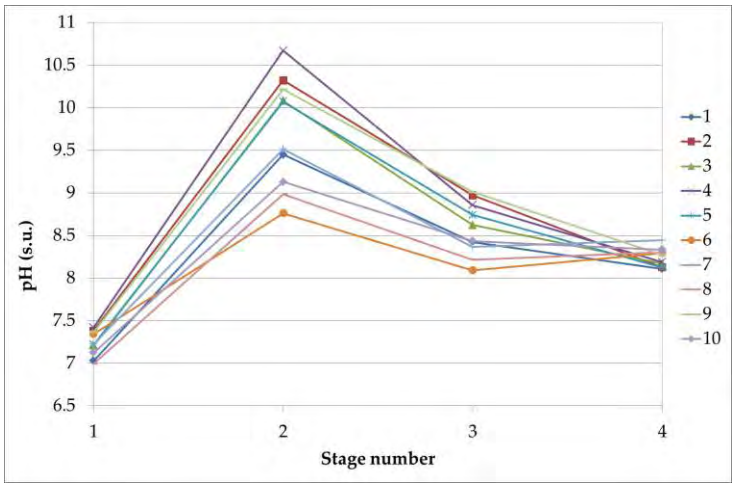

Figure 1 pH variability in NAG experiments

Following the initial pH measurement the NAG solution was heated as per the protocol for a period of approximately 2 hours. Following the heating step, the solution was allowed to cool back to room temperature and was then filled to 250mL with deionised water. Solution pH was then measured a second time (stage 2). The results show that the NAG pH of the solutions greatly increases following the boiling of the solution, suggesting that the solutions are out of equilibration with CO_2 when samples are allowed a standard cooling time. The average pH of the ten solutions increased from 7.23 at stage 1 to 9.72 at stage 2. The average pH dropped from 9.72 at stage 2 to 8.57 at stage 3 following 24 hours of further oxidation and equilibration. After a week, the pH of seven of the ten samples showed further decline, with the average pH decreasing from 8.57 at stage 3 to 8.24 at stage 4.

PHREEQC output results

The PHREEQC output results are in TABLE 3 and are compared with the results of the laboratory testwork in FIGURE 2. The results of thermodynamic equilibrium modelling using PHREEQC exhibit the same pH variability as seen in the laboratory based NAG testwork. The solutions were reacted at a temperature of 100°C; this resulted in the degassing of CO_2 to equilibrium with the atmosphere. The subsequent cooling of the solution back to room temperature results in the system being at disequilibrium with respect to atmospheric CO_2. Average pH increased from 7.23 in the input solution to 9.93 following the boiling and subsequent cooling of the solutions. Comparison between the laboratory data and the thermodynamic equilibrium simulation show good agreement with respect to average pH characteristics with average values in both the disequilibrium case and fully equilibrated cases showing agreement within 0.5 pH units.

Table 3 Comparison between NAG test pH and simulated pH

	Pre heating pH		**NAG pH (2 hours)**		**NAG pH (24 hours)**		**NAG pH (168 hours)**	
Sample ID	**Test - Stage 1**	**Sim 1**	**Test - Stage 2**	**Sim 3**	**Test - Stage 3**	**Sim**	**Test - Stage 4**	**Sim 4**
1	7.03	7.03	9.45	9.95	8.42		8.11	8.17
2	7.38	7.38	10.32	9.98	8.97		8.13	8.23
3	7.21	7.21	10.08	9.96	8.62		8.17	8.22
4	7.42	7.42	10.67	9.95	8.86		8.19	8.18
5	7.22	7.22	10.07	9.95	8.74		8.13	8.16
6	7.35	7.35	8.76	9.97	8.09		8.3	8.19
7	7.22	7.22	9.52	9.94	8.37		8.44	8.17
8	7	7	8.99	9.87	8.22		8.3	7.95
9	7.37	7.37	10.21	9.92	9.01		8.27	8.07
10	7.12	7.12	9.13	9.8	8.44		8.33	7.8
Average	**7.23**	**7.23**	**9.72**	**9.93**	**8.57**	**-**	**8.24**	**8.11**

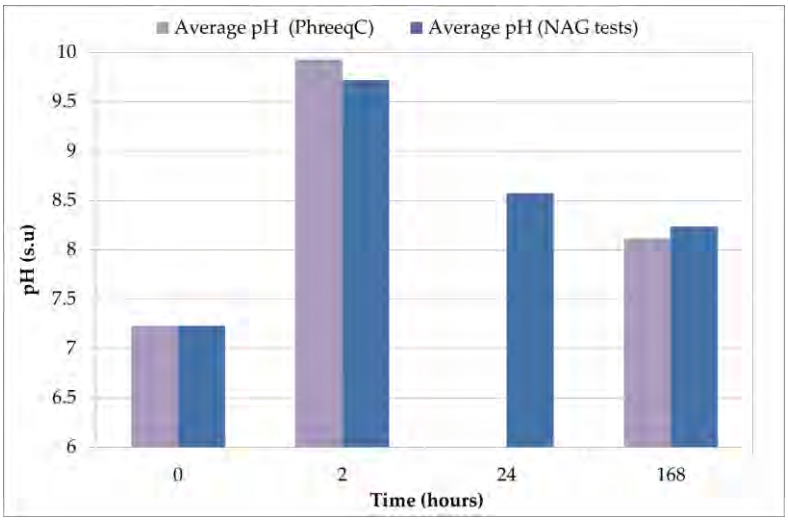

Figure 2 Average of PHREEQC results for all solutions compared to NAG test results

DISCUSSION

The generally accepted NAG test method outlined in Stewart *et al*. (2006) instructs that the NAG solution is boiled to facilitate the breakdown of residual H_2O_2 and also the dissolution of carbonate neutralization potential (NP) buffering. The results of this work have shown that the boiling step in the NAG test methodology can lead to the over estimation of basic pH conditions when the NAG solutions are allowed the standard cooling time. It is postulated that this is the result of the solutions being out of equilibration with respect to CO_2 gas and carbonate minerals. Therefore, the use of such data may lead to a misleading prediction of solution composition, if NAG solution analysis for dissolved metals is to be undertaken.

In order to understand what is occurring in the NAG solution as a result of boiling, it is necessary to understand the carbonate buffer system in detail. Unlike a number of other naturally occurring buffer systems, such as borate, the carbonate buffer system has a gaseous component, and therefore the pH behaviour of the buffer is dependent on interaction between the solution phase and the gaseous phases (Stumm & Morgan, 1996). Furthermore, the nature of the NAG test, in which acidity rapidly dissolves carbonate minerals, means conditions are suitable for gas phase disequilibrium to occur in accordance with the following stoichiometry:

$$\textit{(Sulfide Oxidation by } H_2O_2 \textit{ – Chirita (2007))}\ FeS_2 + 7.5H_2O_2 \rightarrow Fe^{3+} + 2SO_4^{2-} + H^+ + 7H_2O$$

$$\textit{(Neutralization reaction)}\ 2H^+ + CaCO_{3(s)} \leftrightarrow 2HCO_3^+ + Ca^{2+}$$

$$\textit{(Gas Phase Equilibration)}\ HCO_3^+ \leftrightarrow CO_{2(g)} + OH^-$$

Owing to the sensitivity of gas solubility to solution temperature (in accordance with Henry's Law), any changes in solution temperature may have a marked effect on solution pH. Furthermore, the relatively shallow concentration gradients involved in $CO_{2(g)}$ equilibrium with a solution phase due largely to the relatively low atmospheric concentration, means the rates of CO_2 gas transfer between gaseous and solution phases (as described by Fick's law) is slow, requiring hours or days to attain.

The use of the typical NAG test method involving a heating step on NAF samples with elevated carbonate content can therefore produce excessively basic NAG pH as an artefact of test conditions. The basicity of the NAG solution pH reported in this study immediately following cooling after the boiling step may lead to the following potential issues:

- Increased mobility of certain elements, especially the oxyanions potentially including arsenic, selenium antimony, and chromium
- Decreased mobility of certain elements, especially metals whose minimum hydroxide solubility is above pH 9 such as zinc, nickel and cadmium.
- Potential misinterpretation of pH conditions from mine-waste rock drainage leading to incorrect classification of acid generation characteristics.

CONCLUSION

NAG testing has emerged as a useful tool in the assessment of ARDML at mine sites. However, the results of this study and previous work undertaken utilising NAG tests have identified that there is still much to understand about the nature of these tests, and the chemical mechanisms that control the stability and behaviour of the H_2O_2 solution. This study has focused on methodological variations in NAG test pH conditions, resulting from carbonate disequilibrium, resulting from the

particular prescribed methodology. The results suggest that the pH variations seen in the test may be attributed to CO_2 disequilibrium during the heating stage of the NAG test. Therefore NAG pH according to the standard test methodology (for certain net alkaline solutions) cannot be fully relied on as an indication of mine water pH, due largely to the gas phase disequilibrium created.

In order to address this, it is recommended that the pH of a NAG solution be recorded pre- and post-boiling in order to identify the discrepancy in pH disequilibrium. In addition, if the intention is to analyse the NAG solution to give an indication of the potential for mobilization of problematic elements, it is advised that the solution is collected prior to solution heating stage to avoid under- and/or over-reporting metal mobility.

ACKNOWLEDGEMENTS

The Authors would like to thank Cardiff University School of Engineering for use of their facilities.

REFERENCES

AMIRA (2002) ARD Test Handbook. Project P387A Prediction & Kinetic Control of Acid Mine Drainage. Authored by Ian Wark Research Institute & Environmental Geochemistry International Pty Ltd on behalf of AMIRA International Ltd. May 2002.

Barnes, A., Sapsford, D.J., Bowell, R.J., Dey, M. (2013). An assessment of Rapid-Turnaround Tests for ARD Prediction. Presentation given at the 23rd World Mining Congress. August 11th 2013, Montreal, Canada.

Barnes, A., Bowell, R.J., Warrender, R., Sapsford, D.J., Sexsmith, K., Charles, J.C., Declercq, J., Santonastaso, M. and Dey, B.M. (2015) Comparison between long-term Humidity Cell testing and static Net Acid Generation (NAG) tests: Potential for NAG use in preliminary mine site water quality predictions. In: *Proceedings of the 10th International Conference on Acid Rock drainage* (Santiago, Chile, 21-24 April 2015). *ppTBC*

CEN (2009) EN15875 - Characterisation of waste – Static test for the determination of Acid Potential and neutralisation potential of sulfidic waste. European Centre for Standardisation (CEN). October 2011.

Chirita, P. (2007) Kinetic Study of Hydrogen Peroxide Decomposition in Presence of Pyrite. *Chem. Biochem. Eng. Q.* 21 (3) pp. 257–264

Finkelman, R.B. and Giffin, D.E. (1986) Hydrogen Peroxide Oxidation: An Improved Method for Rapidly Assessing Acid-Generating Potential of Sediments and Sedimentary Rocks. Reclamation and Reveg. Res. 5.

Lee, H.H.B., Park, A-H., Oloman, C. (2000) Stability of hydrogen peroxide in sodium carbonate solutions. *TAPPI Journal* 83(8).

Miller, S., Robertson, A., and Donohue, T. (1997) Advances in Acid Drainage Prediction Using the Net Acid Generation (NAG) Test. p. 535-549. In: *Proceedings of the 4th International Conference on Acid Rock Drainage* (Vancouver, May 31-June 6, 1997), vol II.

O'Shay, T.A., Hossner, L.R. (1984) The determination of potential acidity of overburden sediments. In Proceedings of surface mine reclamation workshop. (San Antonio, TX, October 9-10). pp. 13-14.

O'Shay, T.A., Hossner, L.R., Dixon, J.B. (1990) A modified hydrogen peroxide oxidation method for determination of potential acidity in pyritic overburden. *Journal of Environmental Quality* 19. pp. 778-782.

Parkhurst, D.L. and Appelo, C.A.J. (1999) User's guide to PHREEQC (version 2)--A computer program for speciation, batch-reaction, one-dimensional transport, and inverse geochemical calculations: U.S. Geological Survey Water-Resources Investigations Report 99-4259, p. 312.

Sapsford, D. Bowell, R., Dey, M., Williams, C. and Williams, K. (2008) A Comparison of Kinetic NAG tests with Static and Humidity Cell Tests for the Prediction of ARD. In: *Proceedings of 10th International Mine Water Association Congress* (Karlovy Vary, Czech Republic, 2-5 June 2008).

Sobek, A.A., Schuller, W.A, Freemen, J.R. and Smith R.M. (1978) Field and Laboratory Methods Applicable to Overburdens and Minesoils. Report EPA-600/2-78-054, US National Technical information Report.

Stumm, W. and Morgan, J.J. (1996). *Aquatic Chemistry: Chemical Equilibria and Rates in Natural Waters*. 3rd Edition. John Wiley & Sons. Inc. 1022 pages.

Stewart, W., Miller, S., Smart R. Gerson, A., Thomas, J.E., Skinner, W., Levay, G., and Schumann, R. (2003) Evaluation of the Net Acid Generation (NAG) Test for Assessing the Acid Generating Capacity of Sulphide Minerals. pp. 617-625. *Proceedings of the Sixth International Conference on Acid Rock drainage* (Cairns, 12-18th July 2003).

Stewart, W.A. (2005) Development of Acid Rock Drainage Prediction Methodologies for Coal Mine Wastes. Thesis Submitted In Fulfilment of the Requirements for the Degree of Doctor of Philosophy in Applied Science (Minerals and Materials). Ian Wark Research Institute, University of South Australia. February 2005.

Stewart, W.A., Miller, S.D., Smart, R. (2006) Advances in Acid Rock Drainage (ARD) Characterisation of Mine Wastes. Paper Presented at the 7th International Conference on Acid Rock Drainage (ICARD), March 26-30, 2006

Yazici, E.Y., Deveci, H. (2010) Factors Affecting Decomposition of Hydrogen Peroxide. In: *Proceedings of the XIIth International Mineral Processing Symposium.* 6th–8th Octoberm 2010, Cappadocia-Nevsehir, Turkey. pp.609-616.

10th ICARD IMWA 2015 | 10th International Conference on Acid Rock Drainage & IMWA Annual Conference

Applicability of a New and More Efficient Approach to the ABCC Test

Carla Calderón Rosas, Natalia Farfán and Carolina Soto
Fundación Chile

ABSTRACT

Acid Rock drainage (ARD) from mining waste such as tailings, waste rock, leach piles, etc, is currently one of the most important environmental concerns of mining activities. In order to address this problem, different prediction tests exist that allow the characterization of mine wastes and the assessment if these have the potential to generate acid drainage in the future.

One of the existing prediction tests is the ABCC (Acid Buffering Characteristic Curve) test, which allows one to determine the percentage of the neutralization potential (NP) of a sample that effectively reacts to neutralize acid at different pH values (MEND Report 1.20.1 (2009); Warwick A. et al. 2006). This test involves a slow titration with hydrochloric acid (HCl), and the continuous recording of pH values. The shape of the resulting curve indicates the capacity of the sample to neutralize acids.

The procedure of the ABCC test consists of adding water to a sample in a proportion of 2% (w/v), and then titrate every 15 minutes with HCl (under continuous agitation), until the mixture reaches a pH value of 2.8.

This test yields a good estimation of the neutralization capacity of a sample; however, one of its main disadvantages is the long analysis time per sample. Therefore, the objective of this study is the search of an appropriate development time of the test, which would result in fewer analysis times per sample and thus a cost reduction.

The results show that reducing the time of acid addition resulted in curves with no significant statistical variations when compared to the ones obtained with the original protocol. In consequence, it can be established that it is possible to conduct the ABCC test in a significantly shorter time while still obtaining meaningful results.

Keywords: Test ABCC, NP, Acid drainage, static test, massive mine waste

INTRODUCTION

Acid Rock Drainage (ARD) is a phenomenon which is produced through the exposure of sulphide minerals (such as pyrite) to atmospheric oxygen and water. As a product of mining activities, this phenomenon can be accelerated due to the increased exposure of these minerals to the environment, as is the case with massive mine wastes, such as tailings, waste rock and leach piles, among others. Consequently, ARD is one of the most important environmental problems of mining activities today.

To address this problem, a series of procedures were developed that allow for the characterization of the materials which compose mining wastes, in order to assess whether or not these will potentially generate acid drainage in the future. Among the most common methods are static prediction tests, i.e., those which include only one measurement in time. These tests are conducted on a laboratory scale, and include the most well known and performed tests the ABA (Acid Base Accounting) test and the NAG (Net Acid Generation) test.

On the other hand, there are other static prediction tests that are not as common, but similarly produce important information that permits the characterization of these minerals. One of these tests is the ABCC test, which has the objective to determine which percentage of the NP of a sample effectively reacts to neutralize the pH at different pH levels (MEND Report 1.20.1 (2009); Warwick A. *et al.* 2006).

The ABCC test involves a slow titration of a mixture of 100 mL DI water and 2 g sample with HCl, until a pH of 2.8 is reached, which is monitored continuously. Approximately every 15 minutes small volumes of HCl are added, and the pH value is recorded once it is stable. The volume and concentration of the added acid varies according to the range of NP values of the sample. High acid volumes and concentrations are used on samples with high NP values, and vice versa. Finally, the added quantity of HCl is converted into kg CaCO3/tonnes, the latter which is then plotted (x-axis) against measured pH (y-axis) (MEND Report 1.20.1 (2009); Warwick A. *et al.* 2006).

Although this test gives a good estimation of the neutralization capacity of a sample, it has the main disadvantage that the analysis per sample is time consuming. Therefore, the objective of this study is to find an appropriate execution time, which can secure reliable results while reducing associated costs.

METHODOLOGY

The study compromised the application of the original ABCC test as well as a modified protocol, in which the time interval of HCl addition was varied (15, 5 and 3 minutes) by using tailings samples which correspond to samples from the copper flotation process. Afterwards, results were compared to determine whether or not significant differences could be observed. This comparison used statistical tools for each of the analyses conducted. Additionally the NP was determined to characterize the sample and to estimate the capacity of neutralizing acid, which is necessary in

order to define the conditions of the ABCC test. The methodology of the conduction of the study is described below.

Preparation and ID of the sample

The preparation of the sample consisted of: (1) drying the sample (not exceeding 40°C), and (2) the mechanical preparation of the sample, to obtain a sample of a grain size of 75 μm (for the conduction of ABCC test and determination of NP).

"ABCC-X" corresponds to the sample ID, where "-X" changes according to the analysis or test (Table 1).

Table 1 ID of the sample according to the analysis or test.

ID of the sample	Analysis or Test
ABCC-NP	NP determination
ABCC-(15)	ABCC test every 15 minutes
ABCC-(5)	ABCC test every 5 minutes
ABCC-(3)	ABCC test every 3 minutes

Mineralogical characterization

The mineralogical characterization of the sample was conducted by X- Ray Diffraction using TOPAS software. As observed in Table 2, the XRD analysis showed a sample characterized by the presence of quartz and aluminosilicates, and no presence of neither pyrite nor sulphide ore was detected.

Tabla 2 XRD characterization of the tailing sample tested

Mineral	Chemical Formula	Percentage (%)
SiO_2	Quartz	23.3
$Si_{2.83}\ Al_{1.17}\ Na_{0.84}\ Ca_{0.16}\ O_8$	Oligoclase An16	22.0
$Si_{2.72}\ Al_{1.28}\ Na_{0.75}\ Ca_{0.25}\ O_8$	Oligoclase An25	10.7
$Si_{1.5}\ Al_{0.5}\ Na_{0.07}\ K_{0.93}\ O_8$	Sanidine Na0.07	13.7
$Si_{1.5}\ Al_{0.5}\ Na_{0.1}\ K_{0.9}\ O_8$	Sanidine Na0.1	11.9
$K_{0.9}FeAl_{0.5}Si_{1.5}\ O_5(OH)$	Muscovite 2M1	11.0
$K_{1.4}Al_{2.3}Si_{1.7}O_8(OH)_2$	Muscovite 1M	3.1
$H_8\ Al_{1.75}\ Fe_{0.25}\ Mg_5\ O_{18}\ Si_3$	Chlorite IIb	0.6
$Al_2\ H_8\ Mg_5\ O_{18}\ Si_3$	Clinochlore 2M	1.9
$Al_2\ Si_2\ O_5\ (OH)_4$	Dickite (BAILEY)	1.8
$Na_3Mn_5Si_8O_{24}$	Ungarettiite	0.0
FeS_2	Pyrite	0.0

Determination of Neutralization Potential (NP)

The determination of the neutralization potential of the sample was conducted using the Bulk Acid Neutralization method according to Modified Acid Base Accounting (1989). The procedure starts with the "fizz rating" test, which consists of adding 3-4 drops of a 25% HCl solution to a sample mass of 0.5 g, placed in a glass flask or a piece of aluminum foil, in order to observe any "fizz" and its magnitude, which is classified as "none, slight, moderate, or strong fizz". Afterwards, approximately 2 g of the sample are placed into a 250 mL Erlenmeyer flask, to which HCl is added. The volume and normality (N) of the acid depend on the "fizz rating" (Table 3). In this study, 20 mL of 0.1N HCl were used.

Table 3 Volume and Normality of HCl for NP determination, based in the Fizz Rating (After MEND Project 1.16.1b (2008).

Fizz Rating	Volume (mL)	Normality
None	20	0,1
Slight	40	0,1
Moderate	40	0,5
Strong	80	0,5

The HCl-sample mixture was left to react for 24 hours, placing the Erlenmeyer flask on a shaking apparatus. Finally, the sample is titrated with 0.1N NaOH (corresponding to the normality of HCl used), until a pH of 8.3 was reached. With the data obtained from the titration, the NP was determined in units of kg $CaCO_3$per tons of material, through the following equation:

$$NP = \frac{50a\left[x-\left(\frac{b}{a}\right)y\right]}{c} \quad (1)$$

Where:

NP: neutralization potential in kg $CaCO_3$/tonnes; a= normality of HCl; c= sample weight in grams; x= volume of HCl added in mL; y= volume of NaOH added to reach pH 8.3 in mL; b= normality of NaOH

Test ABCC (Acid Buffering Characteristic Curve)

The ABCC test is an analysis that allows the determination of the percentage that effectively reacts with and neutralizes acid (at different pH values) as it is directly related to the determination of NP described above. For this study, the ABCC test was conducted according to the protocol, as well as with modifications conducted by Fundación Chile.

ABCC TEST (Original Protocol) (MEND Report 1.20.1 (2009); Warwick A. et al. 2006)

This test consists of weighing approximately 2 g of sample into a 250 mL Erlenmeyer flask, and adding 100 mL of DI water. Afterwards, the mixture is slowly titrated until a pH of 2.8 is reached, the latter which is continuously monitored. This is carried out by adding 0.1 mL of 0.1 M (molar) HCl every 15 minutes, recording the pH value during this time. The volume and concentration of HCl used in the ABCC test depend on the NP value of the sample (Table 4).

Table 4 Suggested incremental additions and concentration of HCl (After MEND Report 1.20.1 (2009).

NP of sample (kg CaCO3 /tonnes of material)	Concentration of HCl (Molar)	Increments of HCl (mL)
10	0,1	0,1
20	0,1	0,2
50	0,1	0,5
100	0,5	0,2
200	0,5	0,4
500	0,5	1,0
1000	0,5	2,0

Finally, the quantity of HCL added in this test is converted into values of kg $CaCO_3$/tonnes of material (Equation 2), which are plotted against the pH (Y axis) measured every 15 minutes, obtaining the buffering curve.

$$\text{kg CaCO3} = \frac{[(\text{volume HCl (mL)addedx molar concentrationx100})/2]}{\text{sample weight (g)}} \quad (2)$$

ABCC TEST (FCh Protocol)

The procedure of the ABCC test developed by Fundación Chile is similar to the one described above. The difference is that the time interval of acid addition to the sample was modified, with the objective to reduce the time to conduct the test. In this procedure, the same sample and water quantities were used, as well as the concentration and volume of added HCl, as in the original protocol, while adding HCl and recording the pH value every 3 or 5 minutes. As in the original ABCC protocol, results in kg CaCO3/tonnes of material (x-axis) were plotted against the measured pH values (y-axis) to obtain the buffering curve.

Effective neutralization percentage (%RN)

Because the ABCC test allows determining what percentage of the NP actually reacts with and neutralizes acid, this percentage was determined for each of the three curves in this study; afterwards, the obtained results were compared with each other.To determine the percentage of neutralization (%RN) that effectively reacts, it is considered that neutralization reactions only occur until a pH value of 4.0, and the total neutralization capacity of a sample is determined through the Bulk Acid Neutralization Method. In consequence, the amount of NP that reacts is determined from the ABCC curve, with the value of kg CaCO3/tons of material that corresponds to a pH of 4 (Equation 3):

$$\%RN = \frac{(kgCaCO3/tonnesapH\ 4)}{(kgCaCO3/tonsofbulkacidneutralization)} x100 \quad (3)$$

Statistic Analysis

Statistical analysis was applied in order to assess if obtained results are acceptable. To achieve this goal, each ABCC test was conducted in triplicate, and the NP determination in duplicate.

To compare the results obtained from curves ABCC-(5) and ABCC-(3) with the reference curve ABCC-(15), t-student tests were performed for each point (average) of the curves, to determine if significant statistical differences exist. The t-test consists of determining the t value of student calculated from analytical experience, and compare this value with the so-called critical value, which is obtained from the t-student table for a given percentage of reliability. If no significant differences exist between 2 groups, the calculated "t" has to be smaller than the "t" value from the table (ISP (2010)). For all of the statistical measures, a 95% confidence interval was used.

RESULTS AND DISCUSSION

Determination of Neutralization Potential (NP)

The results of the determination of the NP of the samples present an average NP of 3.257 ±0.085 kg $CaCO_3$/tonnes (Table 5). As this is a positive value, it can be concluded that the sample does not have a high neutralization capacity.

Table 5 Results from the determination of NP.

ID sample	Fizz Test	NP (kg $CaCO_3$/tonnes)	Average NP (kg $CaCO_3$/tonnes)
ABCC-NP (A)	None	3,316	**3,257 ± 0,085**
ABCC-NP (B)	None	3,197	

ABCCTest (Acid Buffering Characteristic Curve)

The results presented below correspond to the analysis of one sample of tailings material, through the ABCC test, conducted in two forms, the original protocol and the modified one (FCh). To obtain reliable results, the sample was analyzed in triplicate for each of the protocols, so that results presented correspond to average values. The first results correspond to the curves obtained from adding HCl at three different time intervals. This volume of HCl was chosen, as all of the tests conducted, especially the original protocol, reached a pH of 3 with this volume. The results of the original protocol were used as a reference of comparison for the results of the modified test.

Comparing the results from the modified tests to the results of the original protocol, it can be seen that no significant differences exist for each of the points of the curve, neither in pH nor kg CaCO3/tonnes values.

Moreover, it can be observed that pH values of the ABCC-(15) curve are slightly greater than for the other two curves, with exception of the first points of the curves (before acid addition). It can be seen that the kg CaCO3/ton values are practically the same in all three curves (see Figure 1).

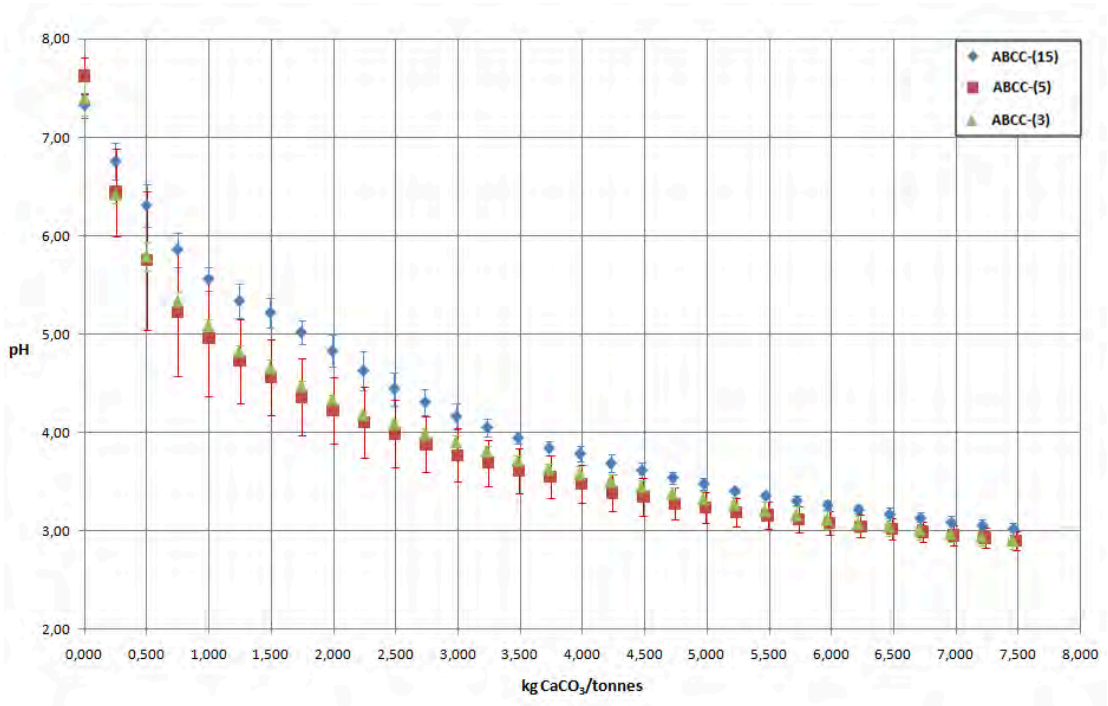

Figure 1 Acid Buffering Characteristics Curves of ABCC-(15) of reference, ABCC-(5) and ABCC-(3) protocols

It can be seen in Figure 1 that the three obtained curves show a similar behavior, and the major difference occurs in the first part of the curve. If the standard deviation is considered, the curves could be even more similar.

Another parameter to compare is the behavior of pH values concerning the amount of HCl added, as shown in Figures 2 and 3. It can be observed that pH values show greater differences among the different tests.

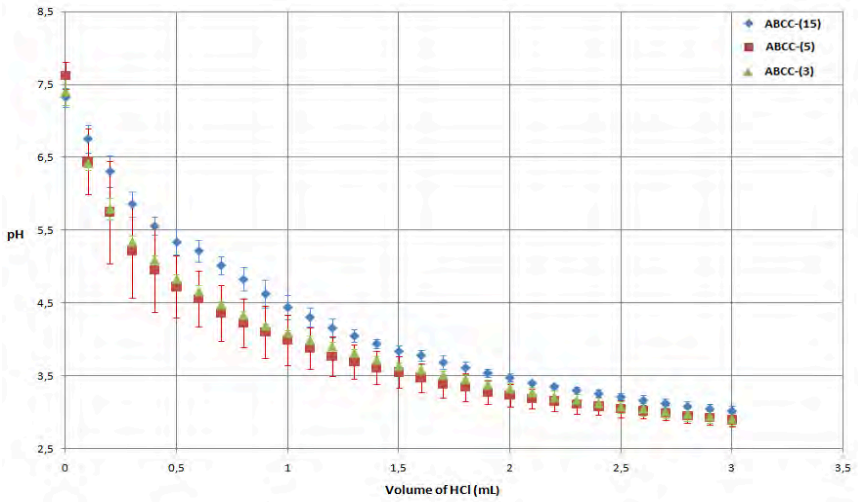

Figure 2 pH vs HCl added for reference ABCC-(15), ABCC-(5) and ABCC-(3) protocols

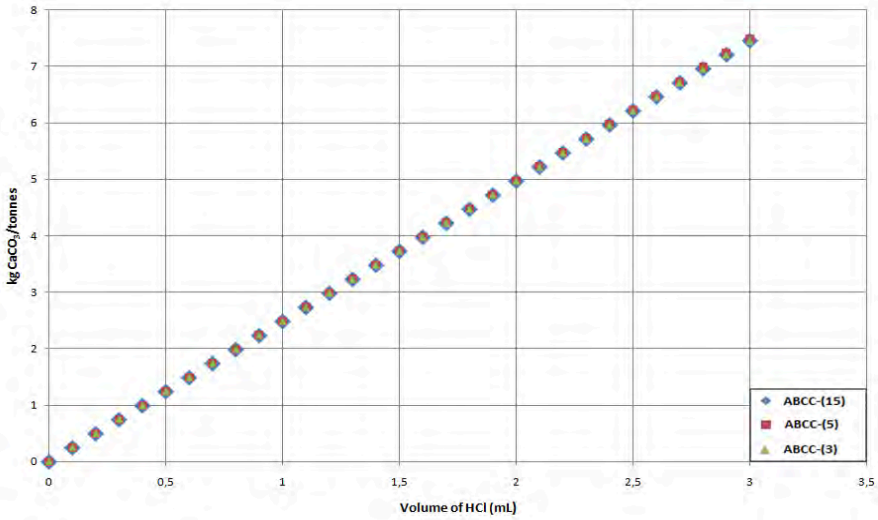

Figure 3 kg $CaCO_3$/tonnes vs HCl added for reference ABCC-(15), ABCC-(5) and ABCC-(3) protocols

All the values obtained and presented in each of the curves can be considered acceptable, as they show standard low deviation values and variation coefficients (%CV), the latter which are < 10% for all points, except 3 pH values in the ABCC-(5) curve (namely, 5.75±0.65; 5.22±0.65 and 4.96±0.59).

To analyze the differences between values of curves ABCC-(5) and ABCC-(3) related to the reference ABCC-(15), it can be concluded that these are quite low, as the first two curves show percent recovery (%R) between 80% and 110%, low systematic bias values, and complies with the rule that all tcal are smaller than tcrit for the t-student test. Thus, all values are acceptable and no significant differences exist between the reference curve and curves ABCC-(5) and ABCC-(3).

Effective percentage of neutralization (%EN)

This value was determined using the NP value obtained through the Bulk Acid Neutralization Method and of each of the ABCC curves. As in the reference curve (ABCC-(15)), a pH of 4 (4.05) was reached with a volume of 1.3 mL of HCl added, this value was used to determine the kg $CaCO_3$/tonnes values of the ABCC-(5) and ABCC-(3) curves for the determination of the %RN of both curves. The results are presented in Table 6 and 7.

Table 6 Neutralization Potential (NP) through the Bulk method and the capacity neutralization observed in ABCC curves at pH 4.

NP Bulk method (kg CaCO3/tonnes)	NP ABCC-(15) at pH 4(kg CaCO3/tonnes)	NP ABCC-(5) at pH 4(kg CaCO3/tonnes)	NP ABCC-(3) at pH 4(kg CaCO3/tonnes)
3,257	3,232	3,242	3,230

Table 7 Percentage of real neutralization (%RN) calculated of the 3 ABCC curves.

%RN ABCC-(15)	%RN ABCC-(5)	%RN ABCC-(3)
99,22	99,53	99,17

The results indicate that the three calculated %EN values from the ABCC curves are closely related. It can be observed that between curves ABCC-(15) and ABCC-(5), there is a difference of 0.0313 units in %EN; between ABCC-(15) and ABCC-(3), this difference is 0.049. It can be concluded that the difference between the three obtained %RN values is small, and is smaller between ABCC-(15) and ABCC-(3).

CONCLUSION

From the obtained results, it can be concluded that it is feasible to reduce the conduction time of the ABCC test in the manner proposed in this study, as the results indicate that no significant statistical differences exist in the data (curves) when comparing results from the original ABCC test and the test ABCC test modified by Fundación Chile. As shown in this study, the ABCC test with smaller time intervals for the addition of HCl, reliable data are obtained, which are very similar to those obtained by adding acid every 15 minutes.

Thus it was determined that the ABCC test can be conducted in a significantly shorter time, which permits developing studies and projects with reduced response times and costs, while working with reliable data.

Concerning the parameters assessed in the ABCC test, it can be concluded that the pH is the parameter that varies most, i.e. is the most sensitive, and could present an error, as it depends on the conditions under which the test is conducted, as it is an experimental parameter. Changes in kg

CaCO3/ton are minor, as this parameter is determined through a mathematical equation, which always should show a minor error.

It is important to note that all ABCC tests were conducted until a pH of 2.8 was reached as shown in protocols; however, only data until a pH of 3 were used as it was considered appropriate to work until this pH was reached. The results below a pH of 3 showed a very small variation by adding acid. The system is stable below a pH of 3, not producing any significant changes in pH values.

The protocols of the conducted ABCC tests in this study should use standard curves to compare results of a sample; as this was not possible in this study, the ABCC-(15) curve was used as a reference for all comparisons instead.

Finally, to mention that the ABCC tests conducted in this study were based on the description of two standard protocols: (1) MEND ("Prediction Manual for Drainage Chemistry from Sulphidic Geologic Materials (2009) and (2) Warwick A. et. al. (2006). Both protocols indicate that between each addition of acid solution 15 minutes must be waited and no additional information is provided about the reason of this determined time.

ACKNOWLEDGEMENTS

The authors would like to thank the geochemical team of the Environmental Risk Management Group, Department of Sustainability of Fundación Chile, for allowing the conduction of this study, which helps the constant development of tools and analyses for the characterization and prediction of acid rock drainage.

NOMENCLATURE

NP Neutralization Potential

ABCC Acid Buffering Characteristic Curve

%RN Real Percentage of Neutralization

kg $CaCO_3$/tonnes kilograms of calcium carbonate per tonnes of material

REFERENCES

Prediction Manual for drainage Chemistry from Sulphidic Geologic Materials (2009). MEND Report 1.20.1. Chapter 15, pp. 15-7 – 15-8.

Warwick A. Stewart, Stuart D. Miller and Roger Smart (2006). Advances in Acid Rock Drainage (ARD) Characterisation of mine Wastes. In: 7th Conference on Acid Rock Drainage (ICARD), St. Louis MO, March 26-30. R.I. Barnhisel (ed) Published by the American Society of Minning and Reclamation (ASMR). 3134 Montavesta Road, Lexington. KY 40502. Pp. 2101-2102.

ARD Test Handbook Project AMIRA P387A Prediction & Kinetic Control of Acid Mine Drainage (2002).Prepared by: Ian Wark Research Institute and Environmental Geochemistry International Pty Ltd. May.Pp. G-1 and G-2.

Acid Rock Drainage Prediction Manual (2008). MEND Project 1.16.1b. Chapter 6, pp. 34-37.

Validación de métodos y determinación de la incertidumbre de la medición "Aspectos generales sobre la validación de métodos" (2010). Instituto de Salud Pública de Chile (ISP). Pp.8, 10, 11, 12, 13, 14, 37, 40.

A Detailed ABA Study of the Coal-Bearing Formations in the Waterberg Coalfield, Limpopo Province, South Africa

Lorie Marie Deysel and Danie Vermeulen
Institute for Groundwater Studies, University of the Free State, South Africa

ABSTRACT

Coal constitutes 77% of the primary energy needs in the country, with the Waterberg Coalfield estimated to host about 40% of the remaining South African coal resources. The Karoo coals were deposited in a reduced environment that have the potential to produce sulphides within the sediments they are hosted. The sulphur content within the coal can range from 0.1 wt.% to as high as 10 wt.%. Mining generates a disturbance in the natural groundwater levels and affects the surrounding water chemistry when sulphate is produced as a result of pyrite oxidation.

Acid base accounting (ABA) was used to determine the balance between the acid producing potential (AP) and acid neutralizing potential (NP). From the analysis the Net Neutralising Potential (NNP) classified samples as either acid or non-acid producing. ARD does not only result in the generation of acid but is accompanied by decreased pH and increased values of specific conductance, dissolved metals and sulphate.

The ABA results showed that interburden and coal samples have higher risks of producing acid upon oxidation than overburden samples. Higher concentrations of neutralising minerals are present in overburden samples. ABA indicated that the material 60m below ground surface had a higher acid producing potential than the material above. The analysis from kinetic tests showed the long-term behaviour of different samples, with the electrical conductivity (EC) and pH changing over time. Samples with lower pH continued to produce more sulphate, while calcium continued to increase until it was depleted from the samples. Inductively coupled plasma analysis determined the release of the heavy metals which can be detrimental to the environment, such as As, Co, Ni and Pb.

The water demand will increase as mining continues in the area, with inter-catchment transfers identified to overcome local water scarcity issues. ARD poses a big threat to both groundwater and surface water resources.

Keywords: New coal mine, ABA, lithology classified

INTRODUCTION

The Waterberg coalfield (Figure 1) has been noted as the continental powerhouse of coal fuelled electricity production (Waterberg Municipality, 2013). The shortage of water is a problem as new mining communities are emerging. The impacts of acid mine drainage has been under investigation for years, in both operating and closed mines around the world.

Different methods are available for the prevention, management, treatment and prediction of ARD but no method can guarantee the remediation of ARD impact. No impacts have been noticed so far in the Grootegeluk mine, but according to the ABA done in the area (Vermeulen *et al.*, 2011) some of the lithology shows a very high acid potential.

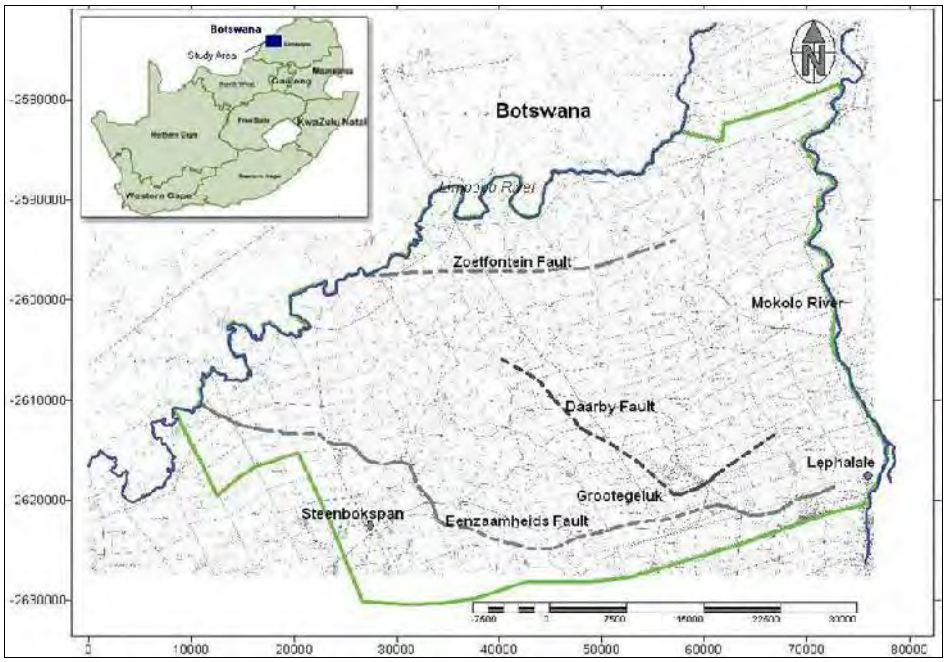

Figure 1 Location of study area. Insert: Map of South Africa indicating the position of the coalfield

Acid base accounting is used as a prediction tool to determine the acid potential of the lithological units. The 11 coal-bearing zones in the Waterberg coalfield are mined in benches and handled according to their intended use. There are two main coal-bearing formations in the Waterberg coalfield (Jeffrey, 2005); these coal zones extend from the Volksrust formation into the Vryheid formation. Vermeulen *et al.* (2011) described three main categories of coal thickness (identified by Bester, 2009), based on the weathered phase of the geology in the area. Figure 3 shows the three categories, green for full succession of coal, yellow for Middle Ecca and pink where area has been weathered in parts.

METHODOLOGY

Samples from different exploratian companies were collected from the study área in Figure 1. The investigation was conducted on various zones of borehole stratigraphy and on discards from the only active mine's beneficiation plant. The sampled material consisted of overburden, the mined interburden and discard after the coal material was liberated, as well as fly ash sampled form the Matimba Power Station.

Acid-Base Accounting was designed to evaluate the acid producing capability of coal mine wastes, and it is now used in a broader field to evaluate both the coal and the metal mine wastes (Lapakko *et al.*, 1999). The detection limits and outlines of static ABA criteria is shown in Table 1. The criteria is used during the analyses of the overburden and interburden. The balance between the acid producing potential (AP) and the neutralising potential (NP) is measured. The acid potential is calculated from the determination of the sulphur content and also represents the sulphur contained in the acid generating sulphide minerals within the sample. NP is determined by subjecting the mine waste samples to some form of acid digestion and represents the amount of acid-neutralising carbonate minerals present in the sample. Net Neutralising Potential (NNP) is the difference between NP and AP. NNP measurements classify rock or coal samples as potentially acid or non-acid producing. A greater NP than AP produces a positive NNP; on the contrary, if NP is less than AP, the resulting NNP will be negative.

Table 1 Detection limits and outlines of the Static ABA analyses

	Static ABA
Analyses / Used for	Used to determine the acid generating potential.
Data format	Expressed as calcium carbonate equivalents and compared to compute net acid-producing or neutralising potential.
Standards used	According to Usher et al. (2002), "material exhibiting a net acid production potential of 5 tons/ 1000 tons of overburden material or more as calcium carbonate equivalent, is classed as toxic or potentially toxic".
Sample preparation	Crushed by Retsch KG 5657 Haan BB100, milled by Giebtechnik Labor-Scheibenschwingmmuhle.

Oxidation products are analysed by using peroxide where only the reactive species (Usher, 2003) will oxidise. The reaction will produce acid and provides an indication of the heavy metal content. The final water quality is also provided as a result of the oxidation reaction.

Metal release

Metal and trace element content were analysed using the inductively coupled plasma optical emission spectroscopy (ICP-OES). This was used to analyse the release of the elements Ag, Al, As, Ba, Be, Ca, Cd, Cr, Co, Cu, Fe, K, Li, Mg, Mn, Mo, Na, Na, Ni, Sb, Se, Sn, Sr, Pb, V, Zn and SO_4. As the oxidation process takes place, metals are mobilized and some become soluble. In the case of the iron species it converts from Fe^{3+} to Fe^{2+} at a pH of 3.1 (Hodgson *et al.*, 1999). If the sample has not yet oxidized in the field the initial pH of a sample will have a higher concentration of sodium carbonate. Calcium/magnesium carbonate exists at a pH of 6 and decreases as the pH decreases during acidification.

Kinetic test

Table 2 lists the kinetic cells used in the study and the ABA results of the same samples. A total of 13 samples used in the analysis were taken from Grootegeluk, Sasol and Sekoko cored boreholes. The criteria that were used to select the samples are the ones that gave inconclusive ABA results, and samples which had extremely high or low NNP from the ABA analysis.

Table 2 Kinetic cell samples as selected from the ABA results

Kinetic cell	Initial pH	Final pH	AP (Open)	AP (Closed)	NNP (Open)	NNP (Closed)
S8	7.86	1.98	32.35	64.71	7.25	14.51
S14	7.11	1.88	20.47	40.94	-11.28	-21.74
S15	6.77	1.72	11	22	-10.12	-21.12
S16	6.80	1.81	1.19	2.38	-0.07	-1.26
S34	6.8	1.8	2.09	4.18	2.64	4.73
SEK 1	6.94	2.08	0.82	1.63	-4.18	-4.99
SEK 3	6.17	2.97	0.58	1.16	-1.60	-2.18
S38	8.53	7.88	1.67	3.34	49.16	50.83
G10	8.14	6.73	0.04	0.08	3.34	3.38
G12	8.62	8.6	0.14	0.27	310.8	310.9
G18	7.71	4.82	0.50	1.00	-5.18	-5.68
SEK 2	7.18	4.07	0.20	0.41	3.16	3.37
SEK 4	6.95	6.54	21.01	42.01	18.29	39.29

Comparison of Leco (%S) with H_2O_2 (%S)

The total sulphur content of the samples was determined by the Leco method. Total S will overestimate the acid potential if a significant amount of sulphate S, organic S or other non-pyritic forms occur in the sample. The same samples were selected and analysed by both the Leco and H_2O_2 method. The relationship of the different methods of analyses for %S is illustrated in Figure 2.

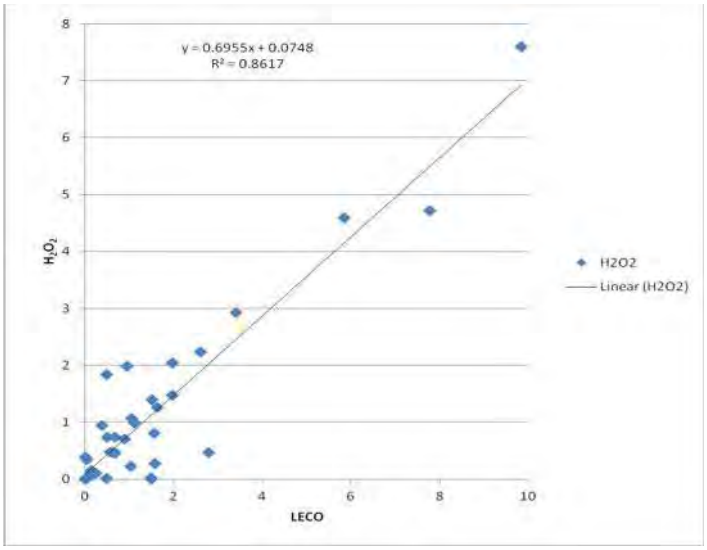

Figure 2 Comparison between the %S of the LECO method and the %S H_2O_2 method. The linear correlation between the two methods establishes that both methods %S can be used to determine the acid potentials of samples.

The Leco method has higher sulphur values than those obtained for the H_2O_2 method; however, the values for the H_2O_2 method compared well to the values of the Leco analyser. Due to this similarity, the H_2O_2 methods sulphur values can be used to determine the total sulphur present in the samples.

RESULTS AND DISCUSSION

Acid Base Accounting

The ABA and kinetic tests highlighted the lithological units that are prone to become acidic or poses a neutralising potential. The geological units with a NP above the coal units included calcrete and sandstone. These units typically consist of quartz, kaolinite, muscovite, calcite, dolomite, rutile and feldspar. The minerals identified within the mudstone and shale units included quartz, kaolinite, muscovite, pyrite, hematite, marcasite and calcite. A summary of the geological logs, the minerals within the units as well as their AP and NP, are illustrated in Figure 3.

Mineralogy

The samples with a NP mainly contained the minerals calcite and ankerite/dolomite. This is due to the carbonate content within the mineral chemistry. Pyrite is the dominant mineral in the acidifying samples. The mineral chemistry of pyrite contains iron and sulphide elements, which under favourable conditions, contribute to the production of acidic waters.

There is a difference in the mineral distribution of the three successions over the various lithologies. The different minerals found in the mudstones are shown in Table 3.

Table 3 The mineral distribution found in mudstones in the different successions.

Minerals	Full succession	Partly weathered	Middle Ecca
Quartz	■	■	■
Kaolinite	■	■	■
Siderite	■		
Calcite	■	■	
Muscovite	■	■	■
Rutile	■	■	■
Pyrite	■	■	
Marcasite	■		
Hematite	■		
Apatite		■	
Pyrrothite		■	
Feldspar			■

The mudstones have both neutralising and acid generating potential, which are associated with their mineral chemistry. The mineral chemistry for the sandstones from the three successions appears to be relatively similar with minor exceptions for hematite, ilmenite and feldspar (Table 4).

Table 4 The mineral distribution found in sandstones in the different successions.

Minerals	Full succession	Partly weathered	Middle Ecca
Quartz	■	■	■
Kaolinite	■	■	■
Siderite	■	■	■
Muscovite	■	■	■
Rutile	■	■	■
Pyrite	■	■	■
Hematite		■	
Ilmenite			■
Feldspar			■

On average, the samples with an acidifying potential and those with a base potential, contain similar concentrations of SiO_2. The major difference is found between the CaO and MgO of the samples, with a base potential to be 50% less in the samples which acidify.

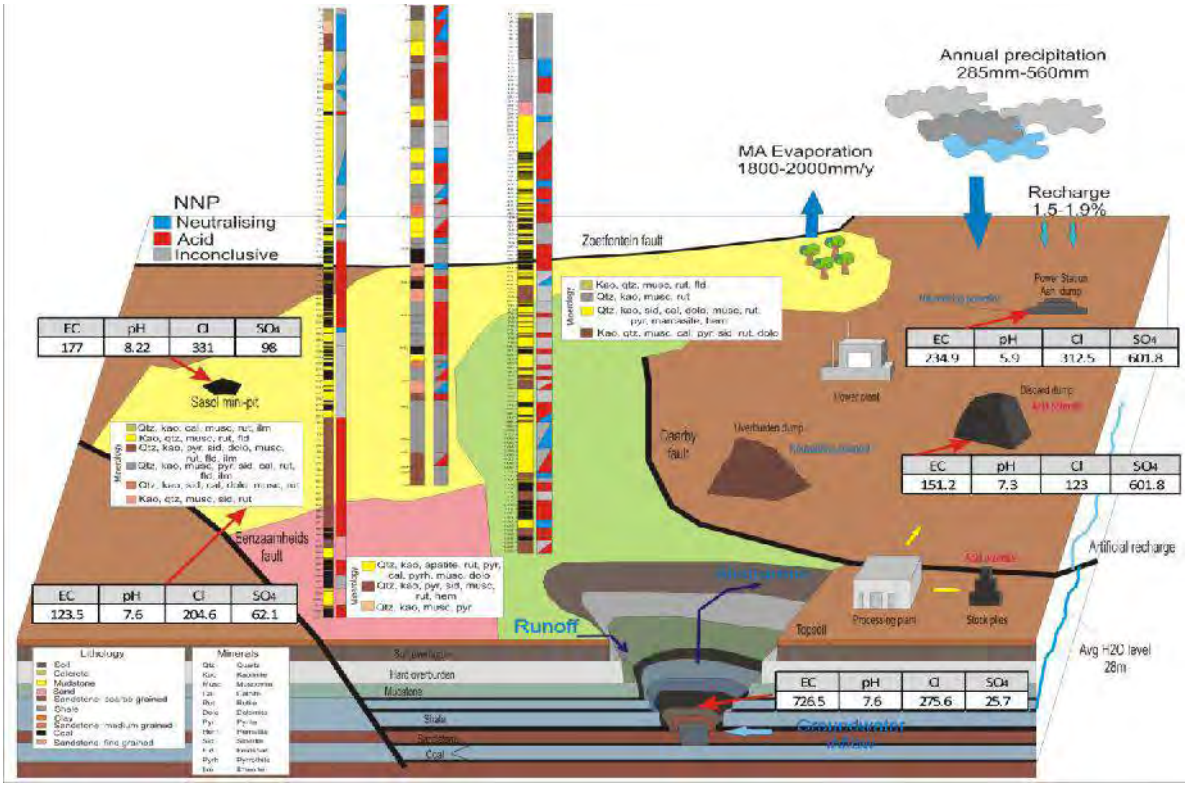

Figure 3 Summary of the acid and neutralising potential of the various contributing factors over the extent of the study area (Macdonald, 2014).

Metal release

Elements such as sodium, potassium and nickel (Figure 4) are present in quantities below their solubility limits. This is denoted by a decrease in concentration with a drop in the pH (Hodgson *et al.*, 1999). Calcium/ magnesium carbonate exist as a form of a buffer which will cause the pH to increase, and will again decrease when the buffering species are depleted.

Iron and sulphate (Figure 5) exhibit an associated rise indicating that pyrite is the most common sulphide mineral present. Calcium and magnesium concentrations increase until they are depleted from the rock and coal through reaction with the acid. Sodium ranges from low to intermediate levels, and the higher sodium levels often coincide with high pH-levels, suggesting the presence of sodium carbonate species.

Figure 4 shows that the sulphate values will increase as the pH decreases in the case of Sasol samples; Exxaro samples show very low concentrations of sulphate even when the pH drops. This might be because of the dominance of the carbonaceous material that is found in the Exxaro samples.

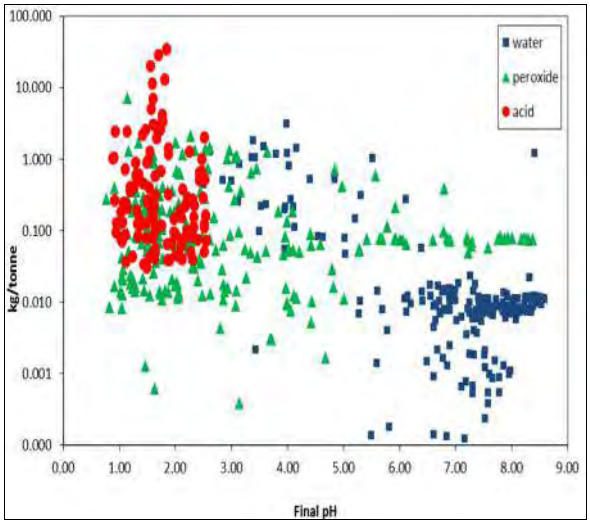

Figure 4 Nickel versus pH

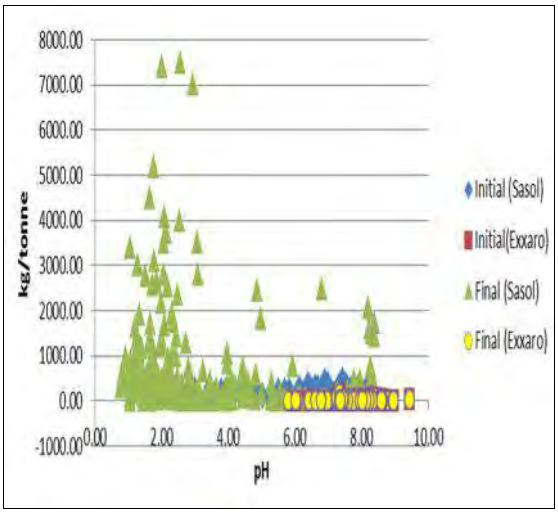

Figure 5 Sulphate versus pH

Kinetic test results

The thirteen samples are from different areas. Eight of the samples provided a closed NNP (-20 to 20 kg/tonne $CaCO_3$) which indicates inconclusive results and the other five had a higher closed NNP which classifies the samples as having the potential to turn acidic or basic. The Sasol samples (S6 to S38) were collected from the interburden and overburden (shale/mudstone) and interburden (sandstone). The Grootegeluk samples (G10 to G18) were taken from the partly weathered overburden which consists of carbonaceous mudstone and the Sekoko samples (SEK1 to SEK4) were taken from the Middle Ecca interburden. Figure 6 shows the pH of the 13 samples that were analysed. Throughout the leaching test the pH values of the samples remained high; an exception being S14 and S15 which showed a drop in pH over 20 weeks and which remained acidic.

Figure 7 shows the release of sulphate from the interburden samples; the analysis shows that the production rate for all the samples was lower at the beginning of the analysis. The highest recorded sulphate concentration at the end of week 20 is in S14 and S15, with an approximate production rate between 250 mg/kg/wk and 50 mg/kg/wk. The majority of the samples showed an increase in

the first three weeks, then decreased again thereafter due to the removal of already oxidised products. The increase in sulphate coincided with the decrease in pH. The samples which gave inconclusive closed NNP all produced rates that were below 150 mg/kg/wk in the first three weeks, and the production rate continued to decrease, which is indicative of the oxidised products that continued to be removed.

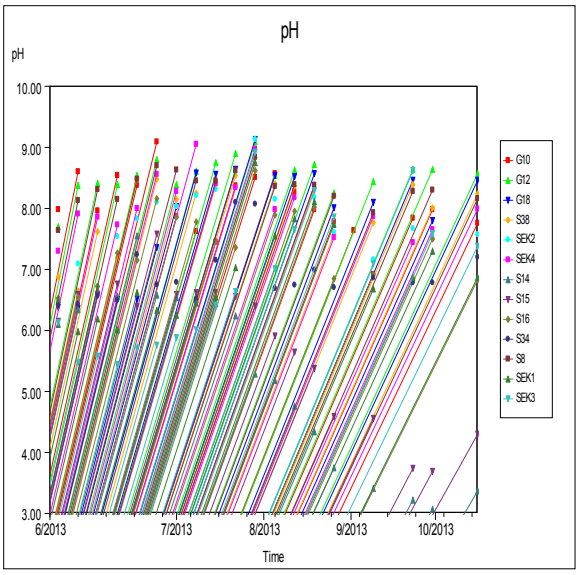

Figure 6 pH *values for Kinetic tests*

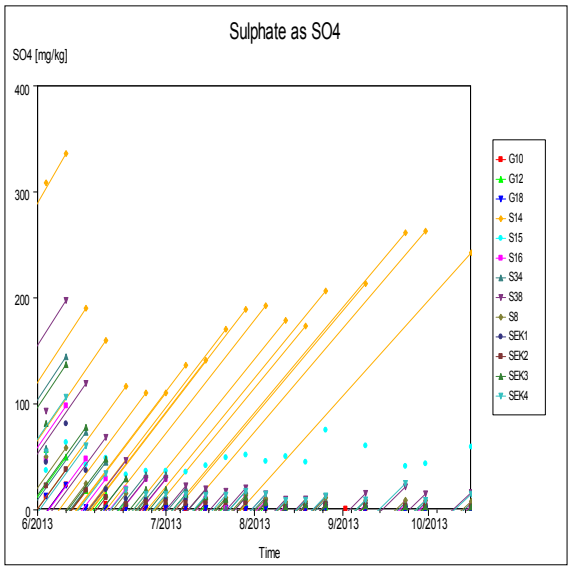

Figure 7 Sulphate *realease for interburden and overburden*

CONCLUSION

The ABA results showed that the coal seam has the highest AP, whilst overburden and shale have a NP. Leaching of heavy metals is evident when the pH decreases. This provides an idea of the post mining environment. Sample analyses was done on the interburden, overburden as well as the coal samples. The results indicated that over 35% to 50% of the samples in the different lithologies (interburden, overburden) have an excess AP. This classifies the samples as having a higher risk for acid generation. About 30% to 40% of the samples have a NP. The remainder of the samples have a medium risk for acid generation.

The ABA results determined that the interburden and discards used as backfill material has a potential to generate acid. This includes the composite samples with various densities from the processing plant. Overburden material has a NP. The ABA illustrated that the shale and mudstone samples have both acid and neutralising potentials and the majority of sandstone samples beneath 60 m have a distinct AP.

The composite material can be used as backfill material within the pit. It only becomes a risk upon exposure to oxygen and water. The Waterberg area has a relatively low annual rainfall, high evaporation and deep groundwater levels, thus the risk to produce acid from infiltrating water is limited. The risk of exposure to oxygen leads to the spontaneous combustion of discard material.

Kinetic test analysis were carried out on the overburden and interburden samples. The pH results showed variations throughout the analysis with all the samples having pH values above 5.5 for the first nine weeks of analysis. The majority of the samples exhibit a high pH throughout the course of

the analysis; a difference is only seen in two samples from the interburden which showed a drop below pH 4. According to ABA results the seven weathered interburden samples from the Middle Ecca have a higher risk of generating acid with the highest at pH of 2.97. An increase in sulphate production is directly related to an increase in EC. Six samples in the kinetic test results were classified as medium to lower risk of acid generation according to results with the lowest pH of 4.07. From the kinetic results, the samples also showed a final pH >7. After week 14 the sulphate production was below 50 mg/kg and the calcium production below 5 mg/kg, The EC values also remained low at constant values.

The pH variations of sandstone and mudstone within the overburden and interburden allowed the materials to be combined at an optimal ratio to ensure a neutral pH within the pit. The initial pH results before testing indicated no oxidation before ABA analysis were done. The interburden material with pH below 4 had correspondingly high sulphate loads (20000-350000 mg/kg). The overburden materials had a lower sulphate load between 5000-35000 mg/kg. The analyses indicated that the interburden material is more likely to generate acid.

The mining industry is always seeking new, cost-effective methods of improving operational efficiency within the mining infrastructure. There have been considerable improvements made to the various aspects of backfilling systems, including the availability and supply of fill materials, different types of backfill systems, backfill preparation procedures for transportation and placement, and the use of alternative cementing agents used in underground mining.

The preferred handling method for the waste generated at the coal mines is the *high and dry* method. Waste is placed layered in between non-reactive material (acidic potential and spontaneous combustion). At the bottom of the mined pit non-reactive interburden is placed in compartments and sealed on the sides and along the top of the backfilled heap. The individual heaps should not exceed 22° and not stacked higher than 17 m. The interburden must be the initial layer, stacked above the natural groundwater level. The stacking will not be affected as on-going mining operations will result in lowering the groundwater levels. The high and dry method places the acid prone material above the natural groundwater level, ensuring minimal to no contamination to groundwater bodies. The individual heaps are stacked to the specified heights and angles and then continue towards the mining advance. Overburden is used as sealing material, due to the shale and clay's low propensity of spontaneously combust or generate acid.

One suggestion to the handling would be to interlayer ash from Matimba Power Station close by. The ash is available, and the research showed it has a high neutralizing potential in ratios of 2:1 and 5:1, and it would help to reduce the volume of the final mine void. Ash reduces the iron and sulphate from acidic waters and continues to increase the pH by precipitating the problematic elements from the solution. It is however, a great challenge to transport ash in the study area due to the limited amount of water and the availability of ash material. The fine particles should be kept wet during transport. Cost of transport can be reduced when the same conveyor system that is already in place, is used to take ash back to the mine.

ACKNOWLEDGEMENTS

This report was written as part of the WRC report submitted in March 2014. We appreciate the advice and assistance during progress meetings from the reference group, organized by the WRC. We also thank the WRC for the funding and the support provided by them.

NOMENCLATURE

ABA	Acid base accounting
NP	Neutral potential
AP	Acid potential
Ovb	Overburden

REFERENCES

Bester, M (2009) "Groundwater resource assessment of the Waterberg Coal reserves." Unpublished M.Sc Thesis, University of the Free State, Bloemfontein, South Africa

Hodgson, F, Grobbelaar, R, Cruywagen, L-M and de Necker, E (1999) Acid-base accounting and long term mine water chemistry at Douglas Colliery. Institute for Groundwater studies, University of the Free State, Bloemfontein, South Africa

Jeffery L (2005) Challenges associated with the further development of the Waterberg coalfield. *The journal of the South African Institute of Mining and Metallurgy*, 105 (6) 453-458

Lapakko, KA, Cox, RL and White, WW (1999) The Environmental Geology of Mineral Deposits. In: G.S. Plumlee and M.J. Logsdon (Eds.), Static test methods commonly used to predict Acid-mine drainage: Practical guidelines for use and interpretation., Part A: Processes, Techniques and Health Issues, Reviews in Economic Geology Vol. 6A, Society of Economic Geologists, Inc., 325-338

Macdonald, N (2014) The Management of spoils in the Waterberg coalfield, Unpublished M.Sc Thesis, Institute for Groundwater studies, University of the Free State, Bloemfontein, South Africa

Usher BH, Cruywagen LM, De Necker E and Hodgson, FDI (2003) *On-site and Laboratory Investigations of Spoil in Opencast Collieries and the development of Acid-Base Accounting Procedures*. WRC Report no 1055/1/03, Pretoria, South Africa

Vermeulen, PD, Bester, M, Cruywagen, LM and van Tonder, GJ (2011) "Scoping level assessment of how water quality and quantity will be affected by mining method and mining of the shallow Waterberg coal reserves west of the Darby fault." WRC Report no 1830/1/10, Pretoria, South Africa

Waterberg Municipality (2013) Mining. http://www.waterberg.gov.za/index.php?page=mining (accessed 15 February, 2013)

Estimation of Immediate Acid and Neutralization Rates within ARD Waste Rock Storage Facilities

Jun Li[1], Andrea Gerson[1], Nobuyuki Kawashima[1], Rong Fan[1], Roger Smart[1] and Russell Schumann[2]

1. Minerals and Materials Science and Technology, Mawson Institute, University of South Australia

2. Levay & Co Environmental Services, University of South Australia

ABSTRACT

The weathering rate of primary silicate minerals in a waste rock storage facility determines dump drainage pH and associated behaviour of contaminants in the later stages of the acid rock drainage (ARD) profile due to their long-term acid neutralization capacity. This long-term non-carbonate neutralization rate (ANRnc) value can be used, for more economical ARD management, to estimate the cover thickness and saturation required to control the acid generation rate (AGR) within the waste storage facility, so that the two parameters (ANRnc and AGR) are matched, potentially providing an initial design target for emplacement and cover design. We previously established two methods to determine the ANRnc in a waste sample: i) silicate mineralogy using the available pH-dependent dissolution rate database from the literature; and ii) long-term column leach solution assays with the ANRnc calculated from cation release. The ANRnc values estimated using the two methods for a given waste show good agreement and reproducibility at pH < 4.

As part of the AMIRA International funded project "Alternative Treatment Options for Long-term ARD Control" (P933A), four case studies were carried out to estimate immediate AGR and ANRnc within weathered ARD waste rock storage facilities using mine site water monitoring data in combination with the waste mineralogical tests. These estimates may represent a useful tool to monitor, plan and ultimately help reduce the effects of ARD at mine sites; i.e. to determine what strategies may be necessary to attempt to reduce the AGR to equal the ANRnc.

This paper focuses on the results from our investigations of AGR and ANRnc within a number of mining waste dumps. Estimates of the evolution of dump profiles were determined with a view towards matching the values of the AGR and ANRnc within the wastes.

Keywords: long-term non-carbonate neutralization rate, acid generation rate, waste rock storage facility, site mineralogy, water quality monitoring

INTRODUCTION

The weathering rate of primary silicate minerals in a waste rock storage facility determines dump drainage pH and the associated behavior of contaminants in the later stages of the acid rock drainage (ARD) profile due to their long-term acid neutralization capacity. Given the abundance of these silicates in most mine wastes, the widespread occurrence of ARD shows that in many circumstances, silicates in the absence of carbonates do not provide neutralizing capacity at a sufficiently fast rate to neutralize acidity resulting from sulfide oxidation (Gerson et al., 2014a, Gerson et al., 2014b). The acid generation rate (AGR) from sulfide oxidation is therefore required to be reduced and the long-term non-carbonate neutralization rate (ANRnc) from dissolution of silicates needs to be measured so that the two parameters can be matched for long-term ARD management. These measurements can potentially provide an initial design target for emplacement and estimation of the cover thickness and saturation required to control the AGR within the waste storage facility. This paper will explain these estimates, their current limitations and their application to real ARD wastes.

We previously established two methods to determine the ANRnc in a waste sample: i) from silicate mineralogy using the available pH-dependent dissolution rate database from the literature (Palandri and Khraka, 2004); and ii) from long-term column leach solution assays with the ANRnc calculated from cation release. The ANRnc values estimated using the two methods for a given waste have shown good agreement and reproducibility at pH values < 4 (Miller et al., 2010). However, it has been noticed that at greater pH, ANRnc values calculated from mineralogy generally exceeded those calculated from leach column testing (Gerson et al., 2014a, Gerson et al., 2014b) possibly due to removal of some cations by precipitation in the leach columns. In a similar approach, Morin and Hutt (2011) compared ANRnc values derived from mineralogy with those obtained from short-term humidity cell tests. They found that the rates calculated from mineralogy were similar to, or substantially less than, the measured values. Most recently, we carried out four case studies to estimate immediate AGR and ANRnc within four weathered ARD waste rock storage facilities.

Site A

Site A is a zinc and lead mine located in Alaska. The site is sufficiently cold to support permafrost. Mean annual rainfall at the mine site is 467 mm with a mean measured ground temperature of -2 °C. The waste dump contains approximately 36 million tonnes (Mt) of potentially acid forming (PAF) waste rock. Acid rock drainage (ARD) from the stockpile is towards a tailings impoundment and is treated to meet specific water quality standards prior to discharge.

Site B

The Bingham Canyon porphyry Cu deposit is located in the Oquirrh Mountains immediately west of Salt Lake City, Utah. Large scale open pit Cu mining began at the Kennecott Utah Copper Bingham Canyon (KUCBC) mine in 1906 and mining is currently planned to continue for more than a decade. Waste rock placement on the eastern margin of the Oquirrh Mountains (Eastside dumps) began in 1953 and is still on-going (Borden 2003; Borden et al., 2006). The total mass of waste rock classified as PAF materials within the Eastside dumps was estimated to be approximately 2.2 billion tonnes up to 2004. Copper concentrations within the placed waste rock have averaged less than

0.1% (Borden, 2003). From 1941, Cu was recovered from the waste rock dumps by active heap leach operations, in addition to beneficiation and smelting operations (Borden et al., 2006), until all leach water applications were terminated in September 2000. Since infiltration into the dumps occurred only from natural rainfall after leaching was terminated, drain down of acidic water (at a flow rate of 45 L/s in 2004) has been collected, treated and used in the process water circuit (Borden et al., 2006).

Site C

The Savage River iron ore mine is located in north-west Tasmania, Australia. To date, mining operations have generated in excess of 50 million m^3 of ore and 300 million m^3 of waste rock since about 1975. Current mining plans allow for the potential of a further 100 million m^3 of waste rock over the next 15 years (Gerson et al., 2014a). However, ARD, emanating from legacy (sulfide-containing) waste-rock dumps at the mine site, which flows into both Main Creek and the Savage River, is impacting the river and its tributaries. The historic B-dump was identified as a significant source of ARD at the site and D-type PAF waste is responsible for the major part of the AMD issues in B-dump. From early 1970 to 1996, about 13 Mt of D-type PAF waste rock was placed into B-dump, from which approximately 40% of the total Cu load emanated, and which flows down the river through Main Creek (Li et al., 2011, Li et al., 2012). To reduce impact to the river, combined water shedding and alkaline (A-type chlorite-calcite schist) covers were constructed over the dump in 2006 for long-term ARD control. It has been reported that the average rainfall infiltration was reduced to 9% by the water shedding cover (Hutchison et al., 2009). The alkaline side cover allows rainwater infiltrating the cover to take up alkalinity from the A-type material, and this alkalinity can then react with, and neutralize, existing acid drainage (Hutchison et al., 2009). It was found that alkalinity from the side cover has been migrating down into the D-type PAF waste below, forming passivating layers on pyrite grains, but it may be some time before the remaining PAF waste in the dump is fully passivated (Li et al., 2011).

Site D

The Mount Whaleback mine is an iron ore mine located in the Pilbara region of Western Australia, six kilometers west of Newman. The mine is majority-owned (85%) and operated by BHP Billiton, and is one of seven iron ore mines the company operates in the Pilbara. Approximately 10 wt% of the total remaining waste rock at the BHPBIO Mount Whaleback Mine has been identified as PAF materials that contain sulfide minerals > 1 wt%; e.g. altered black shale from the Mount McRae shale contains 4 wt% pyrite, 50 wt% chlorite, 27 wt% muscovite, 2 wt% dolomite, 1 wt% hematite and 16 wt% quartz (Webb et al., 2006). The earliest acidic drainage found at the Mt Whaleback site was from seepage at the toe of the W39 Terrace Dump in 1995 (Huys, 2010). There are about 40 Mt of waste rock placed in the dump covering a surface area of 0.51 km^2. Based on the average annual rainfall of 314 mm in the Mt Whaleback area (Newman Aero weather station), the average seepage rate was estimated to be 5.08 L/s (assuming full rainfall infiltration). To manage this ARD, an ARD Dam (clay compacted floor) that is below and adjacent to the dump (capacity = 850 ML; surface area = 0.32 km^2) was constructed in 1995 to collect the seepage and some surface run-off waters from the mine site.

The aim of this study was to scale up our AGR and ANRnc estimation methodology to these four real waste rock storage facilities using existing mine site water monitoring data in combination with the waste mineralogical tests. This paper describes the results from our investigations of AGR and

ANRnc within the four ARD waste rock storage facilities, as well as combining the AGR and ANRnc to produce estimates of the evolution of the dump profiles towards matching these values within the wastes.

METHODOLOGY

Waste rock sample preparation

Site A and Site B waste rock samples were provided by their respective companies. Site C-dump waste rock sample (D-type, potentially acid forming) was collected through an excavation of the eastern alkaline side cover of the dump in 2010 (Li et al., 2011). A Site D waste rock sample of Mt McRae black shale was collected from WB 0505-403 at the mine site and column leached for 2.5 years. The leached residue solid is expected to have similar mineral composition to that in the W39 Terrace Dump. All the rock samples (particle size < 4 mm) were initially dried in an oven at 50 °C overnight with argon purging, ground, and dry sieved through a 75 μm screen. For X-ray diffraction (XRD) analyses, all the samples were micronized to -2 μm to reduce particle orientation effects on XRD data collection and corundum (α-Al_2O_3, 15 wt%) was added to each sample as an internal standard to quantify the amorphous content in the sample. Corundum (0.3 g) was added to 1.7 g of pulverised material (-75 μm) and then micronized with 10 mL of ethanol using a McCrone Micronizing Mill for 10 minutes. Each suspension obtained was dried in an oven at 50 °C and stored in a sealed tube prior to XRD analysis.

Silicate mineralogy

The simplest method of estimating ANRnc is to calculate the parameter from the known silicate mineralogy of the waste, determined at the time that the pH and AGR are measured using the available pH-dependent dissolution rate database from the literature. The mineralogy of waste samples was determined by XRD and mineral dissolution rate data used in the study is from Palandri and Kharaka (Palandri and Kharaka, 2004) and Lowson and coworkers (Lowson et al., 2007, Lowson et al., 2005) for chlorite. The methodology of the ANRnc calculation steps is described in detail in Miller et al. (2010).

XRD analyses of solid samples were conducted at the Bragg Crystallography Facility, School of Chemistry and Physics, the University of Adelaide. The data collection was performed on a Bruker D4 Endeavor diffractometer with Co Kα radiation (1.7902 Å) at 30 kV and 20 mA. Diffraction patterns were collected with $\theta/2\theta$ geometry from 5 to 80 °2θ at 0.02 °2θ increments with a rotating sample stage to ameliorate preferred orientation effects. Phase identification was carried out using the DiffracPlus EVA software (Bruker) with the ICDD-PDF2 database (International Center for Diffraction Data, 2000). Bruker-AXS TOPAS V4.2 software was then used to quantify each phase. Crystal structure information for all the minerals was obtained from the Bruker Structure Database.

Estimations from water quality monitoring data

An alternative method of estimating ANRnc can be formulated using solution assay data from long-term standard kinetic column leach tests of -4 mm crushed waste rocks and tailings (Smart et al., 2002) with the ANRnc calculated from cation release (Na, K, Ca, Mg and Al) (Miller et al., 2010). The ANRnc (mg H_2SO_4/kg/week) formulation was first developed by (Paktunc, 1999) and extended by (Miller et al., 2010) as expressed as Equation 1.

$$ANR_{nc}(mgH_2SO_4Kg^{-1}week^{-1}) = \frac{R_f \times 49}{m \times 1000} \times \left[\left(\frac{Na}{M_{w(Na)}} + \frac{K}{M_{w(K)}}\right) + \left(\frac{Mg}{M_{w(Mg)}} + \frac{Ca}{M_{w(Ca)}}\right) \times 2 + \left(\frac{Al}{M_{w(Al)}} \times 3\right)\right] \quad (1)$$

where, R_f is the measured drainage flow rate (L/week), m is the mass of a waste rock sample in the column (t), Na, K, Mg, Ca and Al are dissolved metal concentrations in the drainage (mg/L), M_w is the molecular weight and the factor 49 converts mmol H^+ ions to mg H_2SO_4.

In this study, Equation 1 was used to calculate immediate ANRnc within a waste rock storage facility using water quality monitoring data from each mine site.

RESULTS AND DISCUSSION

Site A

The waste rock collected in 2008 in the stockpile contains 13.9 wt% pyrite with 3.6 wt% sphalerite as sulphide minerals, 5.5 wt% barite and 0.1 wt% gunningite (sulfate minerals), 60.3 wt% quartz, 10.7 wt% biotite with 2.5 wt% albite, 2.2 wt% muscovite and 1.2 wt% sanidine, and is classified as PAF by the acid-base account (ABA) and net acid generation (NAG) testing. However, our recent XRD analyses on waste rock collected in 2010 in the stockpile but at a different area revealed a different mineral composition of 3.3 wt% pyrite, 3.0 wt% sphalerite, 2.5 wt% galena, 70.3 wt% barite and 20.9 wt% quartz within the waste rock. This suggests that the mineral composition of the waste rock varies significantly across the whole stockpile. Since the recent waste rock sample does not contain any silicates other than quartz the silicate mineralogy of the sample collected in 2008 was used for estimation of mineralogical ANRnc and the ANRnc value of 141 mg H_2SO_4/kg/week was obtained for the waste as shown in Table 1 the predominant contribution coming from biotite at the dump pH 2.7.

Water monitoring data for the samples collected from Site A in 2002 were averaged and are listed along with other measured parameters in Table 2 for the ANRnc and AGR (based on dissolved sulfate concentration) estimations. The average pH of these samples was low at 2.5. Solution assay data for a typical sample with pH 2.7 (collected in 2008 at the stockpile) was also used for the estimations (Table 2). Table 2 shows relatively high Mg and Al concentrations in the seep waters and the concentrations increased with weathering (six years), consistent with the dissolution of biotite identified in the waste rock mineralogy (Table 1). A relatively high Ca concentration and low K concentration are most likely due to dissolution of gypsum and formation of jarosite in the stockpile although these two secondary mineral phases were not identified by XRD, probably due to their relatively low content and ultrafine jarosite deposition.

The ANRnc value from leached cations was 0.8 mg H_2SO_4/kg/week. The AGR of 2.2 mg H_2SO_4/kg/week estimated from sulfate concentrations was about three times greater than the ANRnc in the stockpile in 2008 (Table 3). It is worth noting that the AGR within the stockpile decreased by a factor of five from 10.7 mg H_2SO_4/kg/week in 2002 to 2.2 mg H_2SO_4/kg/week in 2008 and the AGR/ANRnc ratio for the stockpile decreased from 14 to 3 during the six years of weathering (Table 3). These differences represent the evolution of the Site A waste rock oxidation with time; they suggest the stockpile is over the peak and on the downward path in its AGR/ANRnc ratio vs time profile. In 2008, it was clearly further down the path than in 2002.

Table 1 Calculated ANRnc (mg H_2SO_4/kg/week) from silicate mineralogy of different waste rock materials.

Site A				**Site C**			
Mineral	Mass fraction	Mineral ANR* at pH 2.7	ANRnc at pH 2.7	Mineral	Mass fraction	Mineral ANR* at pH 3.4	ANRnc at pH 3.4
Quartz (SiO_2)	0.603	-	-	Quartz (SiO_2)	0.41	-	-
Biotite ($KMg_{1.5}Fe_{1.5}AlSi_3O_{10}(OH)_2$)	0.107	1147	123	Clinochlore# ($Mg_{3.6}Fe_{1.4}Al_2Si_3O_{10}(OH)_8$)	0.12	1612	193
Albite ($NaAlSi_3O_8$)	0.025	479	12	Albite ($NaAlSi_3O_8$)	0.14	472	66
Muscovite ($KAl_3Si_3O_{10}(OH)_2$)	0.022	42	1	Muscovite ($KAl_3Si_3O_{10}(OH)_2$)	0.22	21	5
Sanadine ($KAlSi_3O_8$)	0.012	461	6				
Total			**141**	**Total**			**264**
Site B				**Site D**			
Mineral	Mass fraction	Mineral ANR* at pH 2.9	ANRnc at pH 2.9	Mineral	Mass fraction	Mineral ANR* at pH 4.2	ANRnc at pH 4.2
Quartz (SiO_2)	0.52	-	-	Quartz (SiO_2)		-	-
Clinochlore# ($Mg_{3.6}Fe_{1.4}Al_2Si_3O_{10}(OH)_8$)	0.15	2549	382	Clinochlore# ($Mg_{3.6}Fe_{1.4}Al_2Si_3O_{10}(OH)_8$)	0.25	285	71
Muscovite ($KAl_3Si_3O_{10}(OH)_2$)	0.10	35	4	Muscovite ($KAl_3Si_3O_{10}(OH)_2$)	0.45	1.1	0.5
Orthoclase ($KAlSi_3O_8$)	0.13	366	48				
Total			**434**	**Total**			**72**

*kinetic dissolution rate data from Palandri and Khraka (2004).
#Clinochlore dissolution rate data from Lowson et al.. (2005; 2007).

The 2008 ANRnc (2.2 mg H_2SO_4/kg/week) estimated from seep assays is about two orders of magnitude slower than that (141 mg H_2SO_4/kg/week) calculated from the mineralogy of the waste rock collected at the same time. The mineralogy estimate assumes a 38-75 μm size fraction with average surface area of 1 m^2/g whereas the standard column leach used sieved -4 mm material. It was reported that waste rock in a storage facility commonly contains 10 - 30 wt% of -4 mm materials (Kempton, 2012) . Given the particle surface area differences, the difference between ANRnc values estimated using the waste stockpile seep assays and mineralogy/laboratory column leach assays are not surprising. This suggests that a scale factor of the order of 0.01 should be applied to the mineralogical estimate here and in the other case studies below. A closer estimate of the effective surface area in the -4 mm samples is currently being defined.

Table 2 Selected cation concentrations from water monitoring data of waste storage facility at different mine sites for AGR and ANRnc estimation.

Parameters	Site A		Site B	Site C	Site D
	Year 2002	Year 2008			
Flow rate (L/week)	2,831,198	2,831,198	27,216,000	4,294,080	1,632,960
Waste mass (t)	17,800,000	33,000,000	22,000,000	3,941,212*	40,091,000
pH	2.5	2.7	2.9	3.4	4.2
Acidity (mg $CaCO_3$/L)	-	18,000	30,000	300	67
Na (mg/L)	3	21	40	19	182
K (mg/L)	3	1	0	5	26
Ca (mg/L)	235	540	500	226	446
Mg (mg/L)	445	1,100	10,000	400	693
Al (mg/L)	435	610	3,000	55	44
SO_4 (mg/L)	65,980	25,000	60,000	2,496	4,124

*The type D waste rocks in side cover area.

Table 3 Calculated ANRnc (mg H_2SO_4/kg/week) using water monitoring data from different waste storage facilities at the mine sites.

	pH	ANRnc	AGR	AGR/ANRnc	ANRc mineralogy
Site A (2002)	2.5	0.8	10.7	14.2	-
Site A (2008)	2.7	0.8	2.2	2.8	141
Site B (2004)	2.9	71.7	75.8	1.1	434
Site C (2009)	3.4	2.7	2.8	1.0	264
Site D (2008-2009)	4.2	0.5	0.6	1.0	72

Site B

The Site B waste rock contains 5 wt% pyrite (sulfide), 3 wt% alunite, 2 wt% jarosite and 1 wt% gypsum (sulfate minerals), 52 wt% quartz, 15 wt% clinochlore, 13 wt% orthoclase, 2.2 wt% muscovite and 10 wt% muscovite (silicate minerals) and are classified as PAF materials. Based on the silicate mineralogy, an ANRnc value of 434 mg H_2SO_4/kg/week, predominantly contributed from clinochlore, at the effluent pH of 2.9, was calculated (Table 1).

The typical water quality data reported by Borden et al. (Borden et al., 2006) for the seeps from the dump toe in 2004 show the seep waters were highly acidic (pH 2.9) with high Mg, Al and sulfate concentrations (Table 2). In addition to Al, Fe (250 mg/L), Mn (350 mg/L), Cu (140-600 mg/L) and Zn (170 mg/L) were also significant metals in the water (Borden et al., 2006) that contributed to a high titratable acidity (30 g $CaCO_3$/L). The high Mg and Al concentration is consistent with the predominant dissolution of clinochlore at pH 2.9 (Table 1). The ANRnc (72 mg H_2SO_4/kg/week) and AGR (76 mg H_2SO_4/kg/week) within the dumps were calculated. It was found that the ratio of AGR/ANRnc was close to 1 (Table 3). However, in this case the AGR may be underestimated due to formation of gypsum, jarosite and alunite, as identified by XRD. It is well known that the use of effluent sulfate concentration can lead to an underestimation of the AGR arising from pyrite

oxidation as formation of S containing secondary sulfate minerals may occur. In practice, this can be corrected using oxygen consumption measurements (e.g. using a sulfide oxidation cell). Table 3 shows that the ANRnc (72 mg H_2SO_4/kg/week) estimated from seep assays is about one order of magnitude slower than that (434 mg H_2SO_4/kg/week) calculated from the rock mineralogy.

Site C

The use of waste dump drainage assays and mineralogy methods to estimate ANR and AGR in the wastes may provide a possible measure for B-dump cover performance in ARD control at the Savage River Mine site. The D type PAF waste rock collected from the eastern side cover of the dump in 2010 was quantified to contain 2 wt% pyrite, 12 wt% clinochlore, 14 wt% albite, 22 wt% muscovite, 41 wt% quartz and 9 wt% amorphous. The mineralogical ANRnc was calculated to be 264 mg H_2SO_4/kg/week at pH 3.4 and the clinochlore chlorite in the rock contributed most of the ANRnc (Table 1).

B-dump water monitoring data extracted from Koehnken (2010) were used to calculate ANR and AGR (Table 2). Since the B-dump seep between the two Main Creek water monitoring points (Main Creek at Pilot Plant and Main Creek at Dolomite Dam) was predominantly from the side cover area under which there are 30 wt% of total D-type PAF rocks in the B-dump, the D-type waste rock mass of about 3.9 Mt was used for the rates calculation (Table 2). The relatively high Ca and Mg concentrations associated with a low Al concentration in the pH 3.4 seep water suggest some alkalinity from the side cover by the partial dissolution of calcite and dolomite, in addition to the dissolution of clinochlore in the D-type PAF waste rock. The sulfate concentration was low (Table 2), consistent with the partial passivation of pyrite surfaces observed in the cover - D type waste interface which has resulted in a reduced sulfide oxidation rate within the dump (Li et al., 2012, Li et al., 2011). The ANR (2.7 mg H_2SO_4/kg/week) and AGR (2.8 mg H_2SO_4/kg/week) with in the dump were calculated and the ratio of AGR/ANR was close to unity as expected (Table 3). Again, the ANR is about two orders of magnitude slower than the mineralogical ANRnc of 264 mg H_2SO_4/kg/week at pH 3.4.

Site D

Our recent XRD analysis has identified the mineralogy of the BHPBIO weathered waste rock as containing 25 wt% clinochlore, 45 wt% muscovite, 26 wt% quartz and 4 wt% amorphous. The mineralogical ANRnc was calculated as being 72 mg H_2SO_4/kg/week at pH 4.2 and the clinochlore in the rock contributed all of ANRnc with a very minor contribution from muscovite (Table 1).

Water monitoring data for five water samples was extracted from a water quality dataset collected at the ARD Dam from March 2008 to August 2009 and averaged for the ANRnc and AGR calculation (Table 2). A dilution factor of 1.6 was used for the calculation according to the Dam surface area and the annual rainfall. Table 1 shows that the average water pH was relatively high at 4.2 with a very low titratable acidity. Since carbonate alkalinity in the water was less than 1 mg $CaCO_3$/L (not shown), high Mg with corresponding Al and Si concentrations in the solution is consistent with dissolution of clinochlore ($Mg_{3.6}Fe_{1.4}Al_2Si_3O_{10}(OH)_8$) being the major neutralization mechanism within the dump. The high Ca concentration may have resulted from dissolution of other reactive silicate minerals in amorphous form, e.g. anorthite as a secondary product from gypsum during weathering in the dump. Values of ANRnc (0.6 mg H_2SO_4/kg/week) and AGR (0.6 mg H_2SO_4/kg/week) were estimated from the water monitoring data with an AGR/ANRnc ratio of 1.0 (Tables 2 and 3). The ratio of AGR/ANRnc of unity indicates that the AGR was fairly close to the

ANRnc provided by silicate minerals within the W39 Terrace Dump in 2008-2009 and that any further reduction in the acid generation rate will result in less acidic drainage from the dump with a subsequently increased water pH in the ARD Dam. Similar to other dumps, the ANRnc is about two orders of magnitude slower than the mineralogical ANRnc of 72 mg H_2SO_4/kg/week at pH 4.2.

Combination of AGR and ANRnc as a function of pH

We previously investigated the influence of the ratio of AGR to ANRnc on the pH of leachate from a number of long-term column leach tests and results are shown in Figure 1. When the AGR/ANRnc ratio approaches 1 the effluent pH starts to increase, but can still be as low as 3 when the AGR and ANRnc are matched (Miller et al., 2010). We have now extended this to include AGR/ANRnc and pH data from this study, which is also shown in Figure 1. The figure shows that the calculated AGR/ANRnc data estimated from each of the ARD waste storage facilities fall within the values measured for long-term column leach tests, suggesting that the estimates made for the facilities are quite reasonable.

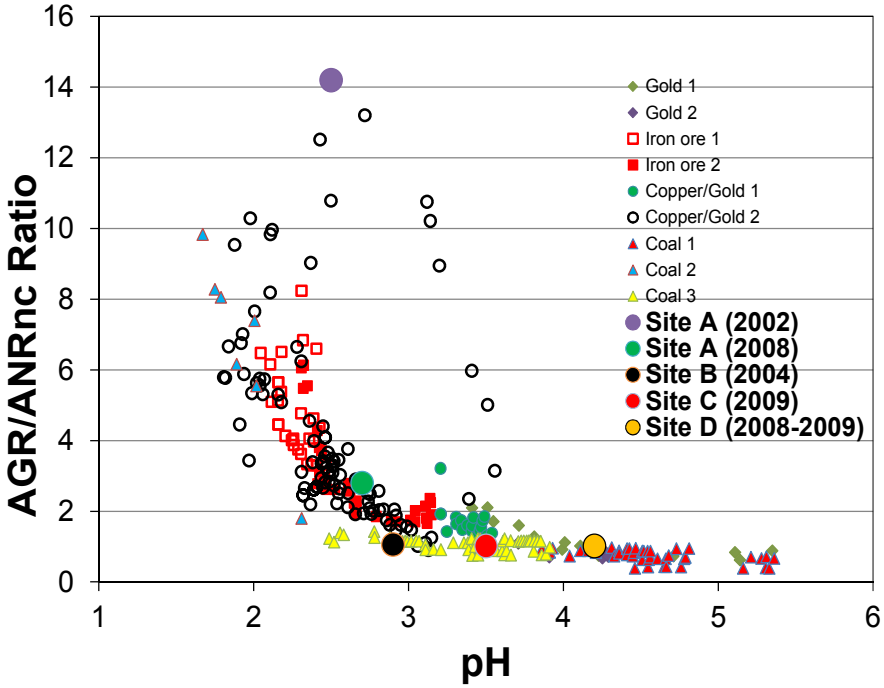

Figure 1 A comparison of ratios of AGR/ANRnc vs pH for different ARD waste rock storage facilities and columns

The evolution of ARD within the Site A stockpile can be seen in the data shown in Figure 1. In 2002, the AGR/ANRnc ratio estimated from water assays was around 14, but this had dropped to approximately 3 by 2008, indicating that AGR may well be matched by ANRnc in the future. The AGR/ANRnc was about unity for the other three dumps and these too appear to approaching the matching rate. However, for the Site B dumps, the low pH (2.9) and high acidity conditions suggest that these first-level estimates involve possible overestimation of the ANRnc and underestimation of the AGR. There is still 5 wt% active pyrite along with alunite (3 wt%) and jarosite (2 wt%) in the dumps requiring long-term management.

CONCLUSION

An initial estimation of the immediate AGR and ANRnc within a weathered ARD waste rock storage facility can be achieved using mine site water monitoring data in combination with waste mineralogical tests. Given the possible effects of climate, preferential flow paths and variation of waste rock mineralogy by weathering etc. on the pore water chemistry in a storage facility, the ANRnc estimated by the water monitoring data may sometimes involve large uncertainties. As an alternative, the dump ANRnc can also be simply determined from the mineralogy, at time scales significantly shorter than traditional kinetic methods but this requires refinement of the effective surface area in the estimate. Uncertainties in AGR estimates from sulfate release alone can be reduced by comparison with oxygen consumption measurements. These estimates may then represent a useful tool to monitor, plan and ultimately help reduce the effects of ARD at mine sites; i.e. to determine what strategies may be necessary to attempt to reduce the AGR to match the ANRnc in the long term evolution of the dump.

ACKNOWLEDGEMENTS

A Linkage Grant from the Australian Research Council, the assistance of Gray Bailey (Project Coordinator) and sponsors of the AMIRA P933A project (BHP Billiton Iron Ore, Savage River Rehabilitation Project, Hidden Valley Services PNG, Rio Tinto, Teck Metals) and permission to publish the results from SRRP, BHPB Iron Ore, Hidden Valley Services, Rio Tinto and Teck Ltd is gratefully acknowledged.

REFERENCES

BORDEN, R. K. 2003. Environmental geochemistry of the Bingham Canyon porphyry copper deposit, Utah. *Environmental Geochemistry,* 43**,** 752-758.

BORDEN, R. K., PEACEY, V. & VINTON, B. 2006. Groundwater response to the end of forty years of copper heap leach operations, Bingham Canyn, Utah. *In proceeding of the 7th International Conference on Acid Rock Drainage (ICARD), March, St. Louis MO.,* March 26-23**,** 214-232.

GERSON, A. R., LI, J., SMART, R. S. C., SAINT, C. P., SHORT, M. D. & SCHUMANN, R. C. 2014a. Responsible Management of Acid Mine Wastes: Geochemical and Microbiological Resources. *In:* JARVIE-EGGART, M. & MUGA, H. E. (eds.) *Responsible Mining: Sustainable Practices in the Mining Industry.* SME Publications, Littleton, Colorado (USA).

GERSON, A. R., SMART, R., LI, J., KAWASHIMA, N., FAN, R., ZENG, S., SCHUMANN, R., LEVAY, G., DIELEMANS, P., MC LATCHIE, P., HUYS, B., HUGHES, A., KENT, S. & HUTCHISON, B. Mineralogy Of Mine Site Neutralising Materials: A Missing Link In AMD Control Planning. *In:* L.C. BELL, B. M. D. B., C. REID AND R.W. MCLEAN, ed. Eighth Australian Workshop on Acid and Metalliferous Drainage, 2014b. JKTech Pty Ltd, Indooroopilly, Qld, Australia.

HUTCHISON, B., BRETT, D., KENT, S. & FERGUSON, T. 2009. Acid rock drainage management and remediation through innovative waste rock management techniques and mine planning at Savage River. *In proceeding of the 8th ICARD, June 23-26 2009, Skelleftea, Sweden***,** 1-10.

HUYS, B. 2010. Acid Rock Drainage - ARD, Presentation Slides. *BHPB Environment, June 2010***,** 1-24.

KEMPTON, H. 2012. A review of scale factors for estimating waste rock weathering from laboratory tests. *In Proc. 9th Int. Conf. Acid Rock Drainage (9 ICARD), 21–25 May, 2012 Ottawa, Canada.* www.mend-nedem.org.

KOEHNKEN, L. 2010. Summary of mass-balance investigation in Main Creek, December 2009. *Report to the SRRP, V1, February 2010*, 1-11.

LI, J., KAWASHIMA, N., KAPLUN, K., SCHUMANN, R., SMART, R. S. C., HUGHES, A., HUTCHISON, B. & KENT, S. 2012. Investigation of alkaline cover performance for abatement of ARD from waste rock dumps at Savage River Mine. *In Proceedings of the 9th International Conference on Acid Rock Drainage, May 20–26, 2012, Ottawa, Canada. Edited by W.A. Price, C. Hogan, and G. Tremblay. Kanata, ON: Golder Associates.* www.mend-nedem.org.

LI, J., KAWASHIMA, N., SCHUMANN, R., HUGHES, A., HUTCHISON, B., KENT, S., KAPLUN, K., CICCARELLI, J. M. & SMART, R. S. C. 2011. Assessment of alkaline cover performance for abatement of ARD from waste rock dumps at Savage River Mine *In Proceedings of the 7th Australian Workshop on Acid and Metalliferous Drainage, Emerging Trends in Acid and Metalliferous Drainage Management. Indooroopilly, Qld, Australia: JKTech.* , 241–253.

LOWSON, R. T., BROWN, P. L., COMARMOND, M. C. J. & RATJARATNAM, G. 2007. The kinetics of chlorite dissolution. *Geochimica et Cosmochimica Acta,* 71, 1431-1447.

LOWSON, R. T., COMARMOND, M. C. J., RATJARATNAM, G. & BROWN, P. L. 2005. The kinetics of the dissolution of chlorite as a function of pH at 25ºC. *Geochimica et Cosmochimica Acta,* 69, 1687-1699.

MILLER, S. D., STEWART, W. S., RUSDINAR, Y., SCHUMANN, R. E., CICCARELLI, J. M., LI, J. & SMART, R. S. C. 2010. Methods for estimatin of long-term non-carbonate neutralisation of acid rock drainage. *Science of the Total Environment,* 408, 2129-2135.

MORIN, K. A. & HUTT, N. M. 2011. A Case Study of Important Aluminosilicate Neutralization. *Internet Case Study 25.* www.MDAG.com.

PAKTUNC, A. D. 1999. Characterization of mine wastes for prediction of acid mine drainage. *In:* AZCUE, J. M. (ed.) *Environmental Impacts of Mining Activities.* Berlin: Springer-Verlag.

PALANDRI, J. L. & KHARAKA, Y. K. 2004. A compilation of rate parameters of water-mineral interaction kinetic for application to geochemical modeling. *Open-file rep. 2004-1068, U.S. Geological Survey, Menlo Park, California*.

SMART, R., SKINNER, B., LEVAY, G., GERSON, A., THOMAS, J. E., SOBIERAJ, H., SCHUMANN, R., WEISENER, C. G. & WEBER, P. A. 2002. ARD Test Handbook. *AMIRA International Limited, University of South Australia* http://www.amira.com.au/web/documents/downloads/P387AProtocolBooklet.pdf 14-15.

WEBB, A. D., DICKENS, G. R. & OLIVER, N. H. S. 2006. Carbonate alteration of the Upper Mount McRae Shale at Mount Whaleback, Western Australia - implications for iron ore genesis. *Applied Earth Science (Trans. Inst. Min. Metall. B)* 115, 161-166.

10th ICARD IMWA 2015 | 10th International Conference on Acid Rock Drainage & IMWA Annual Conference

Acid Mine Drainage Risk Assessment Utilizing Drill-Hole Data and Geological Modelling Tools

Claire Linklater, Alison Hendry and John Chapman
SRK Consulting, Australia

ABSTRACT

For an Australian iron ore operation in the Pilbara region of Western Australia, an acid and metalliferous drainage (AMD) study has considered available drill-hole data (chemical assays and geological logging information) combined with mine planning information to conduct a high level assessment of the potential for AMD from mined waste storage facilities and within the pit void.

Geological modelling tools (Vulcan, Leapfrog) were used to generate 3D visualisations of the distribution of sulfur (a key parameter indicative of AMD risk) within the mined volume. The final sulfur model was aligned with the existing block model to aid future mine planning. Small volumes representing sulfur-bearing 'hot-spots' were identified and pit void maps were generated to determine the location of these hot spots on exposed pit walls. Similarly, volumetric quantities of sulfur-bearing material that would report to waste rock dumps and ore stockpiles were estimated.

Outcomes from the assessment were used to focus ongoing geochemical characterisation activities, and can be used as a basis for scoping calculations to predict the possible quality of drainage waters from mined waste storage facilities and pit walls. This paper describes the overall assessment approach and summarises outcomes from the AMD risk assessment.

Keywords: acid mine drainage, sulfur distribution, geological modelling

INTRODUCTION

There are numerous iron ore mines within the Pilbara, Western Australia. In many, mineralized ore is located within the Dales Gorge Member of the Brockman Iron Formation which is part of the Early Proterozoic Hamersley Group. The Brockman Iron Formation is stratigraphically underlain by the Mount McRae Shale, which is known to contain sulfidic mineralization. Due to the possible exposure of sulfidic materials during mining it is necessary to assess the potential for acidic and/or metalliferous drainage (AMD) at the site from mined materials placed above ground and also exposed on walls within the pit void (Figure 1).

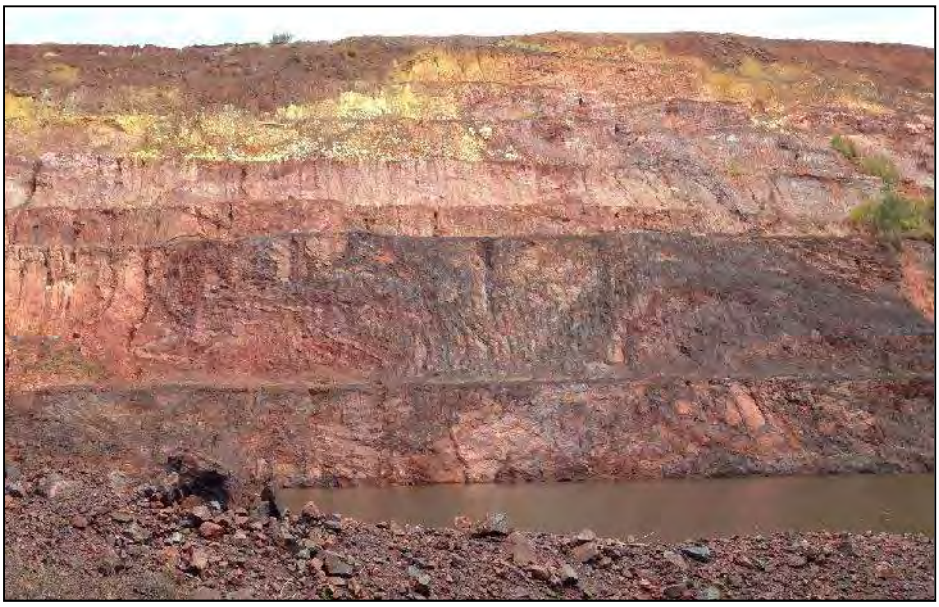

Figure 1 Photograph of exposed Mount McRae Shale (dark colored rock) on pit walls

This paper describes how sulfur data (a key parameter indicative of AMD risk) have been used to develop an approach to assess the risk of AMD. Geological modelling tools were utilized to build an understanding of the spatial distribution of sulfur within the mined void, helping to inform assessment of risk. Outcomes have been used to focus ongoing geochemical characterization activities, as a basis for scoping calculations to predict the possible quality of drainage waters, and as a foundation for closure planning.

APPROACH

The propensity for mined materials to generate acid is a balance between the abundance of acid forming minerals (i.e. sulfides) and acid neutralizing minerals (e.g. carbonates). In the current work, the geochemical characteristics of mined lithologies were assessed principally on the basis of geochemical data within the drill-hole database. These data comprised XRF results for the following parameters: Al_2O_3, CaO, Fe, K_2O, MgO, MnO, P, S, SiO_2, TiO_2.

Sulfur (S), was used to infer maximum acid potential (AP) based on the assumption that all sulfur present is in the form of reactive sulfide. This is a conservative approach, as some proportion of the sulfur may be present as sulfate in the form of gypsum or other non-acid forming minerals. CaO and MgO were assessed as possible surrogates for carbonate-based neutralization potential (NP)

but were found to over-estimate NP when compared to available acid-base accounting data – probably due the presence of Ca- and Mg-bearing silicates in the materials.

Because CaO and MgO were found to be unreliable surrogates for NP, the most conservative approach was to assume no NP and to classify materials on the basis of a sulfur cut-off threshold. Additionally, materials are flagged as 'pyritic' in the drill-hole database if they had been logged as un-oxidized Mount McRae Shale (i.e. Mount McRae Shale sourced from below the oxidation zone). This approach provided two broad categories of classification namely pyritic waste and non-pyritic waste; the non-pyritic waste is assumed non-acid forming (NAF) whereas the pyritic waste is categorized as potentially acid forming (PAF) only if the sulfur content is above 0.2%. Material with sulfur content below the sulfur threshold was considered to represent a low risk of acid generation.

To develop an understanding of the waste distribution and material classification, a statistical analysis was carried out to establish the occurrence of sulfur within each lithological unit using all data within the mining void. To account for materials that would be removed from site (i.e. ore), data were differentiated as ore or waste. Figure 2 illustrates sulfur statistics for waste, with the pyritic waste classification shown separately. The figure shows that the median values of sulfur content for the waste classification were low and fell below the 0.2% sulfur cutoff. The corresponding range (as indicated by the whiskers) of the assays also fell below the cutoff for the majority of the lithological units. The range of assays for some of the lithologies however exceeded the sulfur cutoff. In the absence of significant NP this may indicate a risk of acid generation.

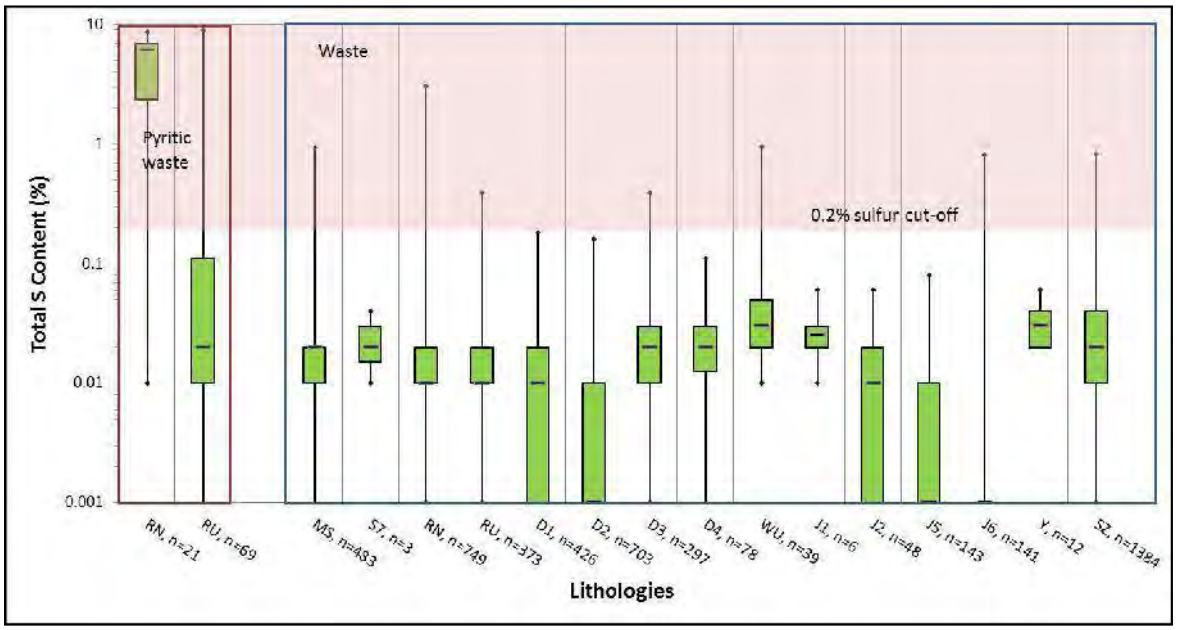

Figure 2 Box and whisker plots showing sulfur statistics in waste materials, by lithology

Note: The box and whisker plots show the minimum and maximum sulfur values (short horizontal dashes), median sulfur values (bold black dashes), and data falling within the 25th and 75th percentiles (green boxes). The number of samples, n, from each lithological unit is shown along the x-axis.

RU, RN – Mt McRae Shale (Upper and Nodular Zone, respectively); MS – Mt Sylvia, undifferentiated; S7 - Mt Sylvia (Bruno's Band); SZ – Surface Scree

Brockman Iron Formation: D1-4 – Units within the Dales Gorge Member; WU – Upper Whaleback Shale; J1-6 – Units within the Joffre Member; Y – Yandicoogina Shale.

Consistent with its classification, material categorized as pyritic waste contained a higher median sulfur grade, most notably for the Mount McRae Shale from within the Nodular Zone (RN); the majority of data for pyritic RN was above the 0.2% sulfur cut-off threshold. The Upper Zone of the Mount McRae Shale (RU) whilst classified as pyritic waste, showed a median sulfur content below the cutoff, but exhibited a large range in sulfur content.

On the assumption of a 0.2 % sulfur cutoff, the statistical analysis shows that the waste classification system would capture PAF materials within the pyritic waste category; however this is not necessarily the case for the waste category as illustrated by the range of assays exceeding the cutoff value for the remaining lithologies.

Therefore, the above analysis showed that to assess the overall potential risks of AMD, the range of sulfur values contained within each lithology is likely to influence the outcomes. Furthermore in the absence of NP data, a further level of conservatism in the form of a lower sulfur cut-off of 0.1 % was included in the subsequent evaluation.

Leapfrog® 3D modelling software[1] was used to process the drill-hole database to visualize the occurrence of the high sulfur zones within the mining void and that exposed on the final pit shell areas of reactive zones. To enable this, in addition to sulfur, the information imported into Leapfrog for 3D modelling purposes included:

- Geological wireframes;
- Pre-mining and proposed final (as mined pit shells) topographies; and,
- Pre-mining water table contours.

The resulting models were used to generate estimates of:

- Volumes of sulfur-bearing material that would report to waste rock dumps and ore stockpiles; and,
- Estimates of the pit wall exposure as a function of lithology and sulfur content.

Using these outcomes it was possible to build an understanding of the spatial distribution of sulfur-bearing materials.

The drill-hole assay data coordinates were then aligned with the block "mid-points" of the current mining models using Vulcan™ (3D modelling and mine planning) software[2], and blocks were classified according to the client's waste classification definitions, including a PAF waste category if > 0.2 % sulfur, to inform future mine planning and closure options at the site.

[1] Leapfrog® Mining 3D modelling software was used for this study, which utilises a "toolbox" approach to 3D geological modelling, allowing processing, viewing and interpretation of drill-hole data. Leapfrog® is 3D geological modelling software which is designed to be used in the mining, exploration, environmental and geothermal energy industries. Leapfrog® is the registered trademark of ARANZ Geo Limited.

[2] Vulcan™ is 3D modelling and mine planning software, allowing users to validate and transform raw mining data into dynamic 3D models, mine designs and operating plans. Vulcan™ is trademark registered to Maptek™.

RESULTS

Geochemical Characteristics of Mined Lithologies

Based on the sulfur statistics (see Figure 2), the majority of the lithologies to be mined would be considered to pose a low risk of acid generation. However, the sulfur ranges for many lithologies extend to maxima that lie above the sulfur cut-off thresholds, indicating that there may be quantities of material from several of the lithological units that could pose a risk of AMD.

Potential for Acid and Metalliferous Drainage - Pit Walls

Figure 3 is a Leapfrog image of the final pit shell showing the lithological composition of the exposed pit walls. One approach to assess the potential for AMD from the pit walls is to examine the sulfur statistics for the lithologies in question. Based on the statistical evaluation, the proportion of data with sulfur values above the cut-off threshold can be quantified and used a guide to the proportion of PAF material present. However, this approach takes no account of potential spatial variability in the distribution of sulfur within the lithological units.

Figure 4 shows another Leapfrog image of the final pit shell, this time showing the distribution of sulfur on the pit wall based on the sulfur model developed from the available drill-hole data.

The degree of correlation between lithological exposure and sulfur content is not entirely clear cut, which may reflect the fact that the density of data available to support the geological model is greater than that available to support the sulfur model. However, comparison of Figures 3 and 4 shows that higher sulfur values are often coincident with exposure of the Mount McRae Shale and the immediately overlying Colonial Chert Unit (D1). Most of these exposures are located at or near the base of the pit. Sulfur 'hot-spots' are shown to also extend up to the pit crest, many of which are coincident with exposure of surface scree.

Using the Leapfrog model, it was possible to quantify the composition of the exposed pit wall according to sulfur content, by elevation (Table 1). Note that having taken account of spatial variability the total percentage of PAF exposed on the pit wall is greater than was estimated on the basis of bulk sulfur statistics. Pit wall rock with total sulfur content greater than 0.1% is now 6%, rather than 3%, and wall rock with sulfur content greater than 0.2% is 5% rather than 0.3%.

Having developed a model of the spatial distribution of sulfur on the pit wall, a more robust risk assessment for the potential for AMD can be achieved. For example, the location of higher sulfur materials relative to post-closure water levels can be accounted for in the long term risk assessment; only materials remaining above the long term water table would be expected to continue to represent a potential source of AMD post-closure.

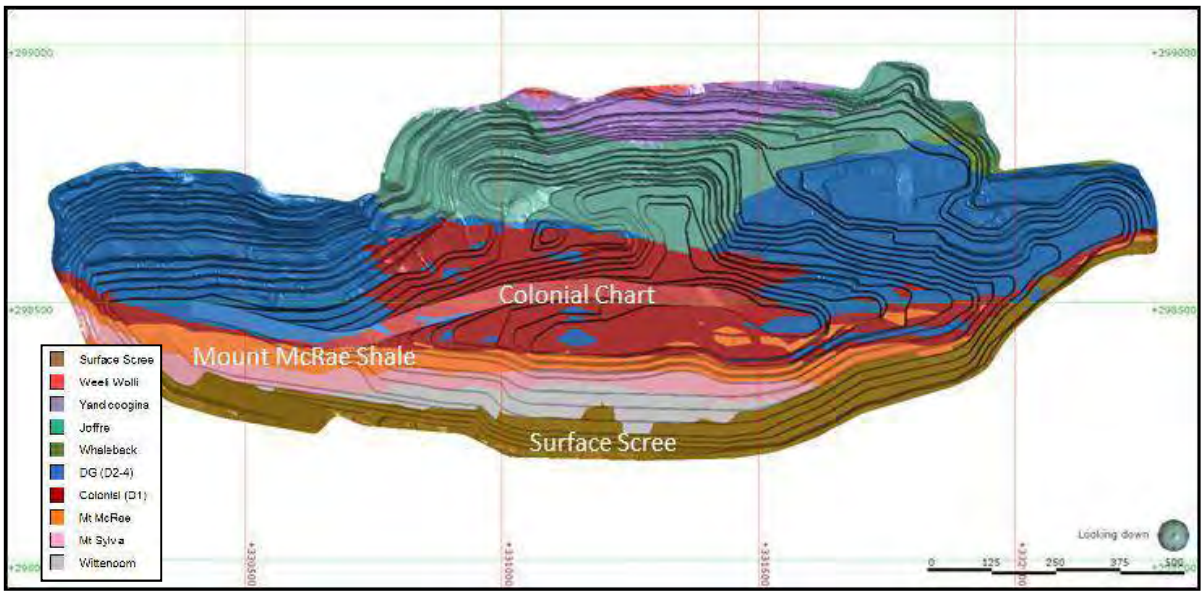

Figure 3 Leapfrog image of the pit shell, and showing lithological composition of the pit walls

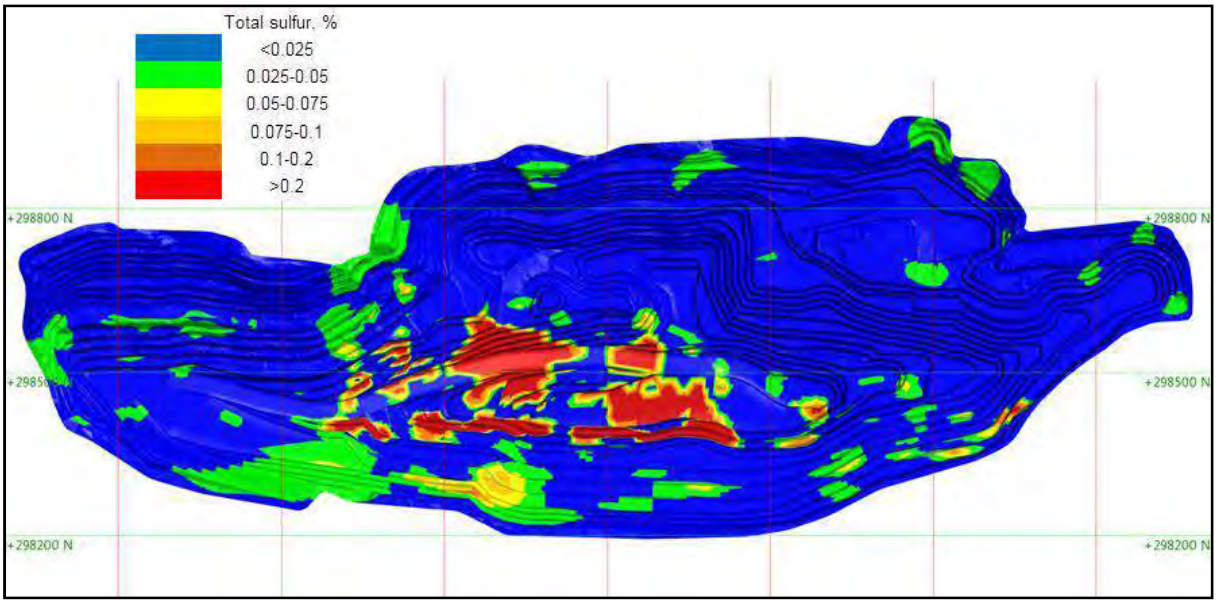

Figure 4 Leapfrog image of the pit shell showing the distribution of sulfur on the pit walls

Table 1 Estimate of the Areas of Exposed Sulfur-Bearing Rock, By Sulfur Category

Elevation Range (m)	Total Surface Area (m²)	Surface Area (m²), by Sulfur Category			
		<0.1%	0.1-0.2%	0.2-1%	>1%
382-390	13,000	13,000	-	-	-
390-400	54,000	35,000	5,000	13,000	1,000
400-410	52,000	35,000	3,000	7,000	6,000
410-420	43,000	34,000	2,000	2,000	5,000
420-430	53,000	40,000	2,000	4,000	8,000
430-440	48,000	40,000	1,000	2,000	5,000
440-450	60,000	52,000	2,000	3,000	3,000
450-460	83,000	77,000	2,000	2,000	1,000
460-470	86,000	82,000	1,000	4,000	-
470-480	88,000	85,000	1,000	2,000	-
480-490	146,000	145,000	1,000	-	-
490-500	144,000	143,000	1,000	-	-
500-505	34,000	34,000	-	-	-
505-510	76,000	76,000	-	-	-
510-515	49,000	49,000	-	-	-
515-520	81,000	81,000	-	-	-
520-530	73,000	73,000	-	-	-
530-540	80,000	80,000	-	-	-
540-550	55,000	55,000	-	-	-
550-560	46,000	46,000	-	-	-
560-570	31,000	31,000	-	-	-
570-580	14,000	14,000	-	-	-
580-590	13,000	13,000	-	-	-
590-600	12,000	12,000	-	-	-
600-610	11,000	11,000	-	-	-
610-620	6,000	6,000	-	-	-
620-630	4,000	4,000	-	-	-
630-640	-	-	-	-	-
Totals	1,458,000	1,368,000	21,000	39,000	30,000
Percentage of Total Surface Area		**94%**	**1%**	**3%**	**2%**
Estimates based on evaluation of bulk sulfur statistics		**97%**	**3%**		
		99.7%		**0.3%**	

Note: Highlighting has been used to indicate material with total sulfur content above sulfur cut-off thresholds (i.e. PAF). Note that an elevation range from 382 (pit base) to 640 mRL has been considered in the analysis. The images presented in Figure 3 and 4 have been clipped at approximately 505 mRL (the level of the lowest point along the pit crest)

In the current assessment, the potential for AMD in pit wall runoff is considered low due to the relatively low proportion of higher sulfur material exposed. With respect to the small proportion of higher sulfur material identified:

- Material located on or near the pit floor is hosted by Mount McRae Shale and Colonial Chert. These lithologies are known to host sulfide mineralization, and could represent sources of AMD. Because these materials would be expected to be submerged following water table rebound, they would not represent long-term sources of AMD, post-closure. Short-term leaching of pre-existing soluble oxidation products is possible.

- Material located near the pit crest is hosted by surface scree. Though some sulfur in this lithology is expected to be non-sulfidic (e.g. gypsum), geochemical characterization studies have confirmed the presence of sulfidic sulfur in a small subset of samples. Data from ongoing detailed geochemical characterization activities suggest that sufficient neutralization potential is present to classify the materials generally as NAF. These materials may however represent a potential source of neutral mine drainage (NMD).

Potential for AMD - Waste Storage Areas

The lithological composition of waste to be mined is shown in Figure 5, based on Leapfrog modelling of the lithological volumes within the pit shell. Estimates of the overall proportion of PAF material present in the waste is shown in Table 2. The estimates combine the volume of each lithology with the bulk sulfur characteristics of the materials.

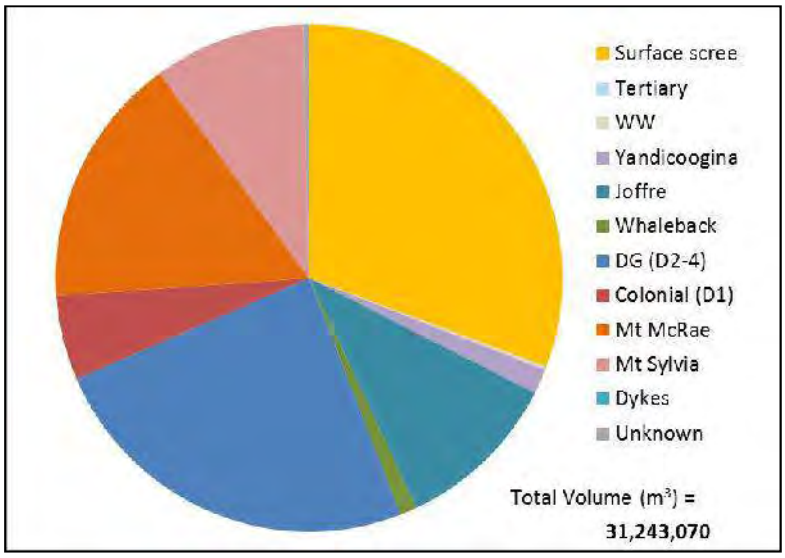

Figure 5 Pie-chart showing the lithological composition of waste to be mined from the pit

Table 2 Estimated proportions of PAF material in waste

Lithological Unit	% of waste volume	0.1% sulfur cut-off		0.2% sulfur cut-off	
		Proportion of PAF material in unit[1]	% of PAF material	Proportion of PAF material in unit[1]	% of PAF material
SZ	31%	10%	3%	5%	1.5%
WW	0.2%	[2]			
HJ	0.002%	[2]			
HE	0.05%	[2]			
Y	2%	0%	-	0%	-
J6	5%	1%	0.05%	1%	0.05%
J5	3%	1%	0.03%	0%	0%
J2	2%	1%	0.02%	0%	0%
J1	0.2%	5%	0.01%	0%	0%
WU	1%	10%	0.1%	5%	0.05%
D4	5%	5%	0.3%	0%	0%
D3	7%	5%	0.4%	1%	0.07%
D2	12%	1%	0.1%	1%	0.1%
D1	5%	3%	0.2%	1%	0.05%
RU	6%	5%/25%[3]	0.4%[4]	1%/5%[3]	0.1%[4]
RN	10%	5%/98%[3]	0.8%[4]	1%/95%[3]	0.4%[4]
S7	0.03%	0%	-	0%	-
S	10%	5%	0.5%	1%	0.1%
UN	0.4%	[2]			
Totals	**100%**		**5.9%**		**2.5%**

Notes:

[1] Proportion of PAF-classed material estimated on the basis of the percentile of the dataset that lies above the sulfur cut-off (0.1% or 0.2%).

[2] No data available for this volumetrically insignificant unit.

[3] General/un-oxidised 'pyritic' waste categories – as recorded in drill-hole logs

[4] Accounting for contributions from both general and pyritic waste categories

SZ – Surface Scree; Z – Tertiary Detritals; HJ – Weeli Wolli Iron Formation; HE – Weeli Wolli Dolerite; K – Dykes/Sills

Brockman Iron Formation: D1-4 – Units within the Dales Gorge Member; WU – Upper Whaleback Shale; J1-6 – Units within the Joffre Member; Y – Yandicoogina Shale

RU, RN – Mt McRae Shale (Upper and Nodular Zone, respectively); S – Mt Sylvia, undifferentiated; S7 - Mt Sylvia (Bruno's Band);

Potential for AMD – Stockpiled Ore

As was the case with waste, the volumetric proportion of PAF material in ore grade materials was estimated to be low. Combined with short residence times within stockpiles, the ore materials were considered to represent a low to negligible risk of AMD.

AMD RISK AND WATER QUALITY

As described in the previous section, the approach developed allowed the identification and quantification of potential AMD sources for waste storage areas, ore stockpiles, and exposed pit walls. Based a semi-qualitative assessment the AMD risks associated with the potential sources were considered low. However, a more robust assessment would include the estimation of water quality and solute loadings that would result from each of these sources, and then determining the potential impacts on the downstream environmental receptors. The approach presented herein provides fundamental inputs that are required to complete such an assessment, comprising properties, quantities and exposures for materials that have a potential to generate AMD. The assessment would however also require kinetic test data (to provide reaction rates and solute release rates) water flow rates (i.e. infiltration, runoff) and flowpath analysis to understand impacts on the receptors.

The outcomes risk assessment can also be used to infer possible closure management strategies at the site which may include backfilling of the pit void. If the pits were backfilled to above the long-term regional groundwater table, groundwater flow would be re-established and flow would likely pass through the backfill. Upon inundation, oxygen would be excluded from the backfill to very low levels and oxidation of any residual sulfides present would essentially cease. Readily soluble solutes contained in the backfill placed below the final water table (i.e. generated prior to inundation) would be released to the groundwater following inundation. The total potential for solute release would depend on the degree of oxidation (i.e. the duration of exposure) of sulfide minerals prior to inundation. Solute generation would be expected to continue in reactive materials (backfill and wall rocks) that remain above the water table.

Should the pits remain as open voids post closure (or be backfilled to below the long-term groundwater elevation), they could act as indefinite sinks for groundwater and would capture some seepage and runoff from waste storage areas that fall within the draw-downs that would occur around the voids. Under this scenario, although the pit lakes would be anticipated to salinize over time due to evapo-concentration, impacts on the key environmental receptors would be unlikely.

CONCLUSIONS

Sulfur has been used as an indicator of the potential for AP, and therefore AMD risk (a conservative approach since surrogates for NP in the geological database were found to be unreliable). Using geological modelling tools, drill-hole data were utilized to develop models of sulfur distribution within the mine volumes to provide estimates of quantities of materials, and wall rock exposure on the final void, that may pose a risk of AMD. This information is required to semi-quantitatively infer the potential risk of AMD. Taking into account spatial variability in the distribution was found to be an important foundation for the assessment of AMD risk. With respect to the pit walls, if spatial variability was not accounted for, the potential for AMD could be under-estimated.

ACKNOWLEDGEMENTS

Fabio Vergara and Ben Jupp provided geological modelling support and prepared the Leapfrog images. Jemini Bhargava assisted with the alignment of drill-hole assay data to the current mining model. The paper has also benefited from comments made by an anonymous reviewer.

Weathering and Oxidation Rates in Black Shales – A Comparison of Laboratory Methods

Claire Linklater[1], Alex Watson[1], John Chapman[1], Rosalind Green[2] and Steven Lee[2]

1. *SRK Consulting, Australia*
2. *Rio Tinto Iron Ore, Australia*

ABSTRACT

Kinetic testing has been conducted on six samples of sulfidic Mount McRae Shale from the Pilbara, West Australia. The total sulfur content of the samples ranged from 0.2 to 8.9%. Whilst the sulfide mineralization was predominantly pyrite, the bulk mineralogy of the samples was dominated by silicates and iron oxides. Acid neutralizing capacity was low and sample classification ranged from Uncertain (UC) for the low sulfide samples, to potentially acid forming (PAF) for the higher sulfide samples.

Various small scale test methods have been developed within the industry to assess the rate of oxidation and solute release from mine waste materials. Whilst humidity cell tests (HCTs) were developed in North America as part of the MEND program, an alternate but similar free draining method was developed in Australia, referred to as the AMIRA free-draining method. These methods are conducted at a similar scale, but differ primarily in the frequency of irrigation, and the temperature at which testing is undertaken. The methods were compared to assess the implications on leach rates and water quality predictions.

Under acidic conditions, both test methods generated similar trends, and produced approximately equivalent results. One sample contained neutralizing capacity and the two methods yielded different pH profiles; the HCT remained circum neutral, whilst the AMIRA test developed acidic conditions. A possible cause of the discrepancy is comparatively high consumption of neutralization capacity in the saline AMIRA leachate environment. Further work is required to develop a more robust understanding of neutralization processes, and their effectiveness, as a function of leachate salinity.

The test results for acidic conditions would yield similar outcomes when used as the basis for water quality predictions at a larger scale, however, this was not the case for the sample containing reactive ANC.

Keywords: Sulfide oxidation, kinetic testing

INTRODUCTION

The stratigraphic sequence in the Pilbara, Western Australia, includes shale and lignite lithologies, both of which are known to host sulfide mineralization (Green and Borden, 2011). Extensive geochemical characterization programs have been conducted to build an understanding of the geochemical behavior of these materials.

Laboratory-scale testing methods are employed to give insights into sulfide oxidation rates, acid/neutralization potential of the material and solutes released. The results are the foundation for predictive modelling of future mine-affected water quality and are used to guide mine waste management decisions (Green and Borden, 2011; MEND, 2009; INAP, 2009).

In the current study, two kinetic test methods were evaluated in parallel: i) AMIRA free-draining columns and ii) humidity cell tests (HCTs). In addition, the work was performed to compare the results from the two methods in order to evaluate the test method constraints, functionality and reliability or accuracy.

METHODS AND MATERIALS

Two kinetic test methods were employed:

- **AMIRA Free-Draining Column Method** (AMIRA, 2002). The method involves placing 2 kg dry weight of crushed rock (< 10 mm) on a mesh in a free-draining container and subjecting it to periodic leaching with a known volume of de-ionized water (400 mL/kg). The sample is flushed once every four weeks. In the weeks between flush events, the sample is moistened by the addition of a small volume (100 mL/kg) of de-ionized water. Heat lamps are applied at regular intervals to ensure the sample dries out between solution applications and to ensure that the temperature remains in the range 30 to 35 °C.
- **Humidity Cell Test Method** (MEND, 2009). Humidity cell tests (HCT) involve loading approximately 1 kg dry weight of crushed rock (< 10 mm) into a humidity cell. In the initial week (Week 0) the sample is wetted and flushed. This is followed by a weekly cycle, involving continuously pumping dry air for three days, and humid air for a subsequent three days, through the sample. The sample is then flushed with 500 mL of de-ionized water on the seventh day. Tests are operated at ambient laboratory temperature, approximately 23 °C.

In both methods, after each leach cycle, the leachate draining from the sample is collected and analyzed.

Six rock samples sourced from Mount McRae Shale were selected to represent a range of sulfur contents and various classifications, as shown in Table 1. Four samples were subjected to both kinetic testing methods. Since insufficient sample mass was available for the remaining two samples to conduct both methods, one was tested as an AMIRA column and the other as a HCT.

In later stages of AMIRA testing for samples ETD297 and EUG180, insufficient leachate was generated to meet analytical requirements – possibly because physical properties of the samples were changing over time (e.g. reduction in porosity, permeability, leading to an increase in moisture retention). Consequently from approximately Week 40 onwards these samples were flushed at a higher rinse volume (500 mL/kg).

All testing and analyses were undertaken at the SGS Laboratories in Perth.

Table 1 Acid-Base Accounting Results and Sample Classification

Parameter	Units	Sample ID					
		EPP357	ETD297	EUG180	EZL155	ESI115	EUE765
Sulfur speciation and potential acid generation potential							
Total S	%	0.16	0.55	1.4	1.8	5.1	8.9
CRS	%	n.m.	n.m.	0.9	n.m.	3.4	6.3
HCl soluble SO_4 - S	%	0.08	0.05	0.3	1.3[4]	0.3	0.9
Pyrite-S[1]	%	n.d.	0.4	1.0	1.7	4.0	8.8
Jarosite-S[1]	%	n.d.	n.d.	0.1	n.d.	0.3	0.4
MPA	**kg H_2SO_4/t**	4.9	16.8	42.8	55.1	156.1	272.3
AP	**kg H_2SO_4/t**	2.4	15.2	32.7	15.3	146.3	244.2
Carbon speciation and acid neutralization capacity							
TOC	%	n.m.	0.96	1.4	3.4	0.53	2.1
TIC	%	n.m.	0.13	0.08	0.24	0.65	0.14
Siderite-C[1]	%	n.d.	n.d.	n.d.	n.d.	0.6	n.d.
ANC	**kg H_2SO_4/t**	<1	8.2	4.7	9.6	4.4	<1
CarbNP[2]	**kg H_2SO_4/t**	-	10.6	6.5	19.6	53.1	11.4
Net acid generation (NAG) test results							
NAG pH	**pH Unit**	4.7	7.1	3.1	2.5	2.2	2
NAG (pH 4.5)	**kg H_2SO_4/t**	0.5	0.5	4.9	33	33	210
NAG (pH 7.0)	**kg H_2SO_4/t**	1.5	<0.5	10	44	59	230
Acid Base Accounting and Sample Classification							
NAPP[3]	**kg H_2SO_4/t**	3.9	8.6	38.1	45.5	151.7	271.3
NPR[3]	**-**	0.2	0.5	0.1	0.2	0.1	0.1
Classification	**AMIRA**	UC(NAF)	UC(NAF)	PAF-LC	PAF	PAF	PAF

n.d.=not detected; n.m.=not measured

S – Sulfur; SO_4 – Sulfate; CRS=Chromium reducible sulfur; ANC – Acid Neutralizing Capacity; NAG – Net Acid Generation; MPA – Maximum Potential Acidity; AP – Acid potential; TIC=Total Inorganic Carbon; TOC=Total Organic Carbon; CarbNP – Carbonate Neutralizing Potential; NAPP – Net Acid Producing Potential; NPR – Net Potential Ratio; NAF – Non Acid Forming; UC – Uncertain; PAF – Potentially Acid Forming; LC – Low Capacity.

Notes:

[1] Calculated from XRD results.

[2] CarbNP was calculated from the total inorganic carbon content of the sample.

[3] NAPP and NPR calculated using the ANC and MPA.

[4] Anomalous (high) as it is inconsistent with other results for this sample, e.g. the pyrite content as determined by XRD, and the NAG test results.

RESULTS

Figure 1 and 2 show leachate pH and calculated sulfate release rates for each test, as a function of time. As applicable results from both AMIRA columns and humidity cell tests are shown on the same plot for ease of comparison.

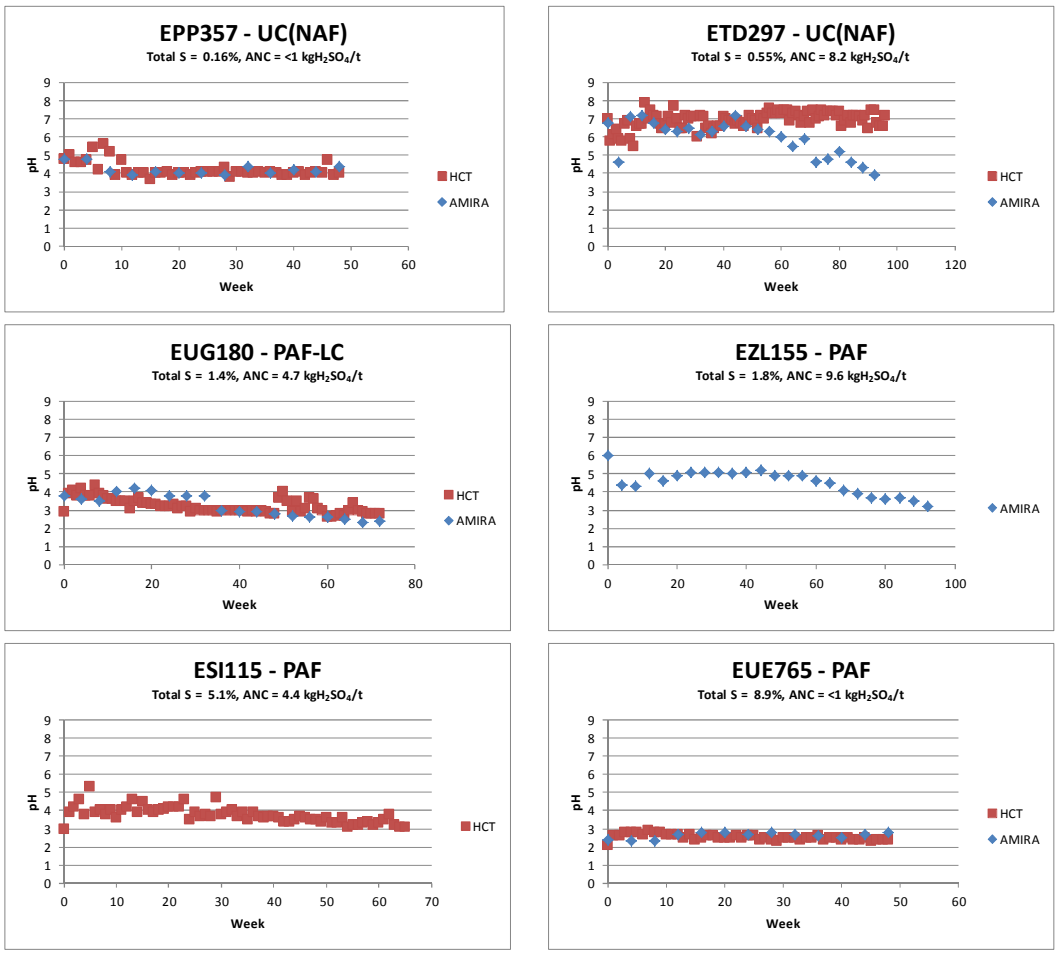

Figure 1 Leachate pH as a Function of Time
[The plots are arranged in order of sulfur content, reading from left to right]

Although a range of sample classifications was represented - UC(NAF), PAF-LC and PAF (see Table 1 footnote) - most of the tests progressed to acidic conditions (stable long-term average leachate pH values ranging from 2 to 4). The exception was the HCT test for sample ETD297 which remained circum neutral throughout (92 weeks). Though circum neutral at first, the AMIRA test for this sample progressed to acidic conditions at around Week 48 (not long after the increasing the rinsing volume from 400 mL/kg to 500 mL/kg).

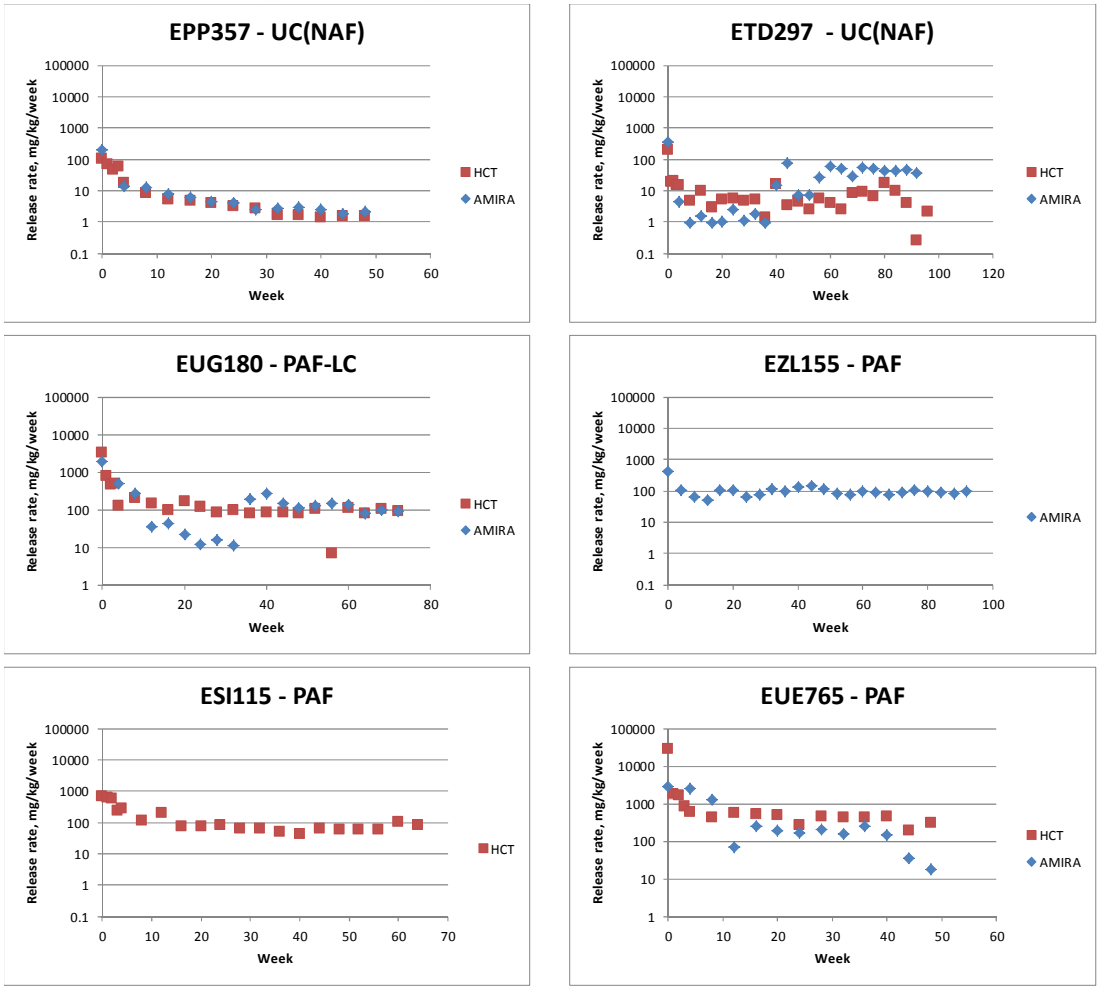

Figure 2 Calculated Sulfate Release Rate as a Function of Time.
[The plots are arranged in order of sulfur content, reading from left to right]

Sulfate release was highest in the early cycles of testing, and decreased in subsequent cycles, for the majority of tests, irrespective of test method. This reflects leaching of pre-existing readily soluble sulfate from the samples. The sulfate concentrations tended to stabilize at an approximately constant value in later stages for many of the tests, allowing calculation long-term average sulfate release rates. Exceptions were:

- AMIRA tests for samples ETD297 and EUG180 which showed a significant increase in release rate (by an order of magnitude or more) coincident with the increase in rinse volume
- AMIRA test containing sample EUE765 which showed a progressive decrease in release from Week 40 onwards.

Table 3 tabulates average release rates calculated for selected parameters.

Table 3 Average Release Rates Calculated for Selected Parameters

Sample	Lithology	Test duration, weeks	Week Trends Stabilised	Leachate pH	Average release rates, mg/kg/week[1]										
					SO_4	Ca	Fe	K	Mg	Si	Co	Cu	Ni	Se	Zn
AMIRA Columns															
Approx. detection limit[2]					*0.07*	*0.01*	*0.0003*	*0.007*	*0.007*	*0.001*	*0.00007*	*0.00007*	*0.00007*	*0.0002*	*0.00007*
EPP357	LGG	48	32	4.2	2	0.3	0.0003	0.08	0.3	0.5	0.0002	0.00007	0.0008	0.0002	0.0008
ETD297	SHL	96	40[3]	4.5	41	9.0	0.035	0.6	2.8	0.9	0.007	0.0011	0.012	0.001	0.013
EUG180	SHC	72	40[3]	2.6	119	3.3	4.8	0.06	3.7	1.0	0.2	0.1	0.8	0.006	3.0
EZL155	SHL	96	20	3.8	95	3.1	0.182	2.5	1.2	0.4	0.10	0.057	0.2	0.002	0.9
EUE765	SHC	48	16[4]	2.7	195	0.9	71	0.03	4.7	0.1	0.03	0.05	0.08	0.0009	0.05
Humidity Cell Tests															
Approx. detection limit[2]					*0.4*	*0.08*	*0.002*	*0.04*	*0.04*	*0.008*	*0.0004*	*0.0004*	*0.0004*	*0.0008*	*0.0004*
EPP357	LGG	48	32	4.0	2	0.08	0.002	0.1	0.08	0.6	0.0004	0.0004	0.0008	0.0008	0.002
ETD297	SHL	120	12	6.9	6	2.9	0.02	0.5	0.8	1.0	0.0004	0.0004	0.0004	0.0008	0.003
EUG180	SHC	72	32	2.9	83	0.5	3.2	1.0	1.7	4.3	0.1	0.1	0.5	0.006	1.9
ESI115	SHC	72	20	3.4	70	2.8	8.1	0.3	4.3	0.8	0.03	0.0006	0.07	0.0014	0.2
EUE765	SHC	48	16	2.5	394	0.1	152	0.2	5.3	4.3	0.03	0.07	0.1	0.007	0.07

Grey values are close to the approximate detection limits

Notes:

[1] Calculated from later column leachates, after most chemical parameters start showing stable trends (the week when stable conditions were attained is shown).

[2] Some calculated release rates are based on detection limit values and are therefore overestimates. The detection limit given in the table is approximate because, for the same analytical detection limit, the calculated release rate varies according to the volume of leachate collected and the mass of solid in the column.

[3] Average rates are based on data collected after the rinse volume had been increased.

[4] For this test, trends showed a sharp decline after 36 weeks, possibly due to armouring of reactive surface (see main text for discussion). The average release rates have been calculated using the data obtained between Week 16 (trends stabilised) and Week 36 (immediately prior to the declining trend).

DISCUSSION

Sulfide Oxidation, Acid Generation and Neutralization

Sulfate release rates from kinetic columns can be used to infer sulfide oxidation rates, assuming that no other geochemical processes increase or decrease sulfate concentrations in the leachates. PHREEQC modeling indicated that gypsum solubility may have controlled sulfate release in some of the early leaching cycles. At later stages, other sulfur-bearing minerals, e.g. hydroxysulfates such as jarosite, may have influenced leachate chemistry. However, the influence of these minerals on sulfate concentrations would have been limited by the low concentrations of other mineral constituents such as Al, K or Fe.

Figure 3 plots the average sulfate release rates against the sulfide sulfur content of the sample. The results from AMIRA columns and HCTs show the same general trend toward higher sulfate release rates as the sulfide sulfur content increases.

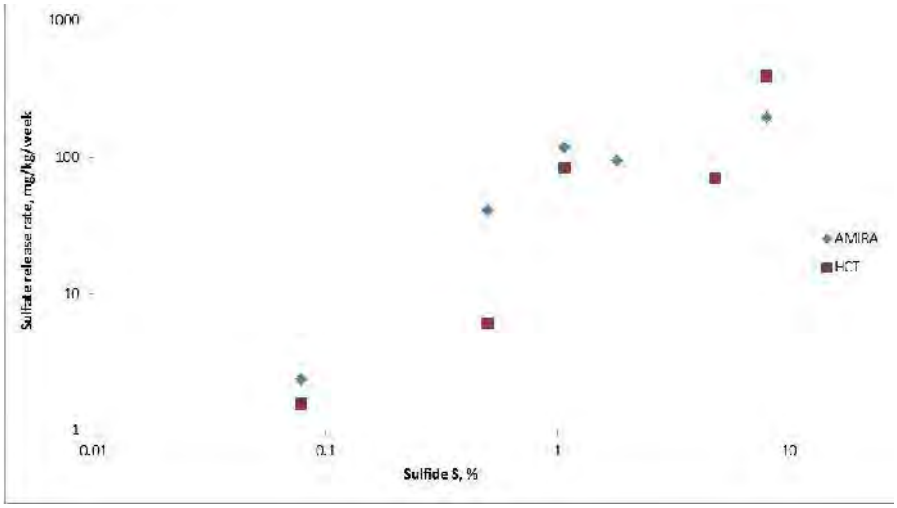

Figure 3 Sulfate Release Rate as a Function of Sulfide Content

Whilst sulfide content is interpreted as the primary variable controlling oxidation rates in the test materials, leachate pH clearly plays a role, explaining the higher sulfate release calculated in the AMIRA column (acidic) for sample ETD297 (about 0.5 % S) when compared to the equivalent HCT (circum neutral). The higher oxidation rate for the AMIRA test can be explained by:

- Catalysis by acidophilic bacteria is expected to be more effective under acidic conditions;
- An increased influence from ferric iron (Fe^{3+}) as an oxidant at acidic pH;
- Armoring of reactive surfaces is more likely under the circum neutral conditions of the HCT, and may have slowed reaction rates in this test.

Sample ETD297 was the only material that showed any evidence of effective neutralization during testing. In the early stages of both methods, circum neutral pH and $(Ca+Mg)/SO_4$ molar ratios in the leachates were interpreted as evidence of carbonate-based neutralization.

In the AMIRA test the leachate remained circum neutral until Week 40, when the pH started to decrease (Figure 1). The change in pH coincided with an increase in rinse volume. The increased rinse volume is

believed to have resulted in more effective flushing of accumulated products. The observed pH response suggests that either: (i) available neutralization capacity in the AMIRA method depleted at the same time as the operational conditions changed, or, (ii) the change in operating conditions somehow influenced the effectiveness of pH buffering in the material. The latter explanation is considered more likely, and could also explain why the results for the AMIRA test on sample EUG180 indicated a pH decrease coincident with a change in operating conditions (from pH 3 to pH 2; Figure 1).

Leachate pH is a complex balance of multiple influences, e.g. minerals that contribute acidity, and, minerals and aqueous complexes that can provide pH buffering. These complex equilibria are likely to be affected by changes in the leachate solute load (salinity). It appears that for the AMIRA test on sample ETD297 pH buffering was no longer effective following the increase in solute load. From that point onward in the test, increased oxidation rates (in response to the more acidic conditions) would have compounded the effect.

When compared to the AMIRA test leachates, solute concentrations in the HCT leachates were more dilute (due to more frequent rinsing with a higher volume of water). Perhaps for this reason, pH buffering remained effective for longer – explaining the continued neutralization observed in the HCT test for sample ETD297.

It is noteworthy that for all the samples the average Ca (and Mg) release is higher for the AMIRA tests than for the equivalent HCT tests, possibly indicating that the Ca/Mg mineral source is more reactive and/or soluble under the more saline condition of the AMIRA tests. In general terms, as most tests were acidic, this would indicate that pH neutralization is generally not effective (possibly indicative of a sideritic carbonate mineral source – siderite identified in ESI115, Table 1).

Elemental Release

Major elements, Al, Fe and Mn, and minor elements, As, Cd, Co, Cu, Ni, Sr, and Zn, release rates in general were in reasonable agreement between the two methods (Table 3 shows data for some of these elements); some deviations noted for sample ETD297 were related to the circum neutral pH observed for the leachates from the HCT method. Key controls on release were interpreted to be:

- Oxidizing sulfides – positive correlation with sulfate release suggested that some elements (e.g. Fe, Cu, As, Se) could be present in the matrix of the dissolving sulfide, whilst others (e.g. Al, Mg) could be sourced from minerals (e.g. carbonates, silicates) reacting in response to the acidic conditions produced by sulfide oxidation.
- Mn-bearing mineral – Cd, Co, Ni and Zn all showed strong correlation with Mn release. The identity of the mineral is unknown, possibilities are: manganese hydroxide, or Mn-bearing siderite or iron oxide. Release of Cd, Co, Ni and Zn (under acidic conditions) was also correlated to the bulk elemental content of the sample. As Mn itself did not correlate with bulk content it is inferred that only one of multiple Mn-bearing mineral sources in the material is reactive under the conditions of the tests.
- Mineral solubility – Fe and Al concentrations in some leachates were consistent with control by the solubility of iron and aluminium hydroxides and hydroxysulfates. Other possible solubility controls identified were amorphous silica (Si) and barite (Ba).

Comparison of Results from the Two Methods

Both methods were developed to measure sulfide oxidation and consequent solute release. The expectation is that all the soluble reaction products will be flushed entirely from the column during each irrigation event. The resulting leachate chemistries should therefore give a measure of the rate at which those reaction products are generated, provided the solutes are mobilized from the sample. Incomplete flushing of the oxidation products subject to solubility constraints would lead to underestimation of actual oxidation rates and solute release rates.

Table 3 Ratio of Calculated Average Long-Term Release Rates from HCTs: AMIRA Columns

Sample	Total S, %	Average long-term leachate pH		Rate HCT: Rate AMIRA[1]										
		AMIRA	HCT	SO_4	Cl	F	Al	Ca	Fe	K	Mg	Mn	Na	Si
EPP357	0.16	4.2	4.0	0.7	1.4	1.8	1.5	0.3	5.9	1.3	0.3	0.5	2.6	1.1
ETD297	0.55	4.7	6.9	0.1	1.5	4.5	0.4	0.3	0.7	0.8	0.3	0.0	0.4	1.2
EUG180	1.4	2.6	2.9	0.7	4.3	13.7	0.6	0.1	0.7	17.6	0.5	0.7	1.1	4.4
EUE765	8.9	2.7	2.5	2.0	5.3	19.5	1.0	0.2	2.1	7.2	1.1	0.5	5.4	47.6
				As	**B**	**Ba**	**Bi**	**Cd**	**Co**	**Cr**	**Cu**	**Hg**	**Mo**	**Ni**
EPP357	0.16	4.2	4.0	5.9	0.9	2.3	5.9	5.9	2.0	5.9	5.9	5.9	5.9	1.0
ETD297	0.55	4.7	6.9	5.1	2.4	0.7	4.5	0.4	0.1	6.0	0.5	6.0	10.8	0.0
EUG180	1.4	2.6	2.9	1.5	2.3	11.5	6.1	0.6	0.6	0.9	0.9	4.7	4.7	0.7
EUE765	8.9	2.7	2.5	1.6	9.7	68.5	5.5	1.6	0.9	1.4	1.5	5.3	5.3	1.6
				Pb	**Sb**	**Se**	**Sn**	**Sr**	**Th**	**Ti**	**Tl**	**U**	**V**	**Zn**
EPP357	0.16	4.2	4.0	5.9	4.7	4.9	5.9	0.2	5.9	5.9	5.9	5.9	5.9	2.8
ETD297	0.55	4.7	6.9	6.0	6.7	0.8	6.0	0.3	4.5	6.2	6.0	5.8	6.0	0.3
EUG180	1.4	2.6	2.9	4.7	5.3	1.2	4.7	1.6	0.6	4.7	4.7	0.9	1.1	0.7
EUE765	8.9	2.7	2.5	5.3	5.5	8.5	5.3	12.2	2.6	5.3	5.3	2.7	1.7	1.3

Notes:

[1] Grey shading indicates ratios for parameters leaching close to or below analytical detection limits in both test methods. For an equivalent analytical detection limit, where the detection limit is adopted for the calculation, the calculated release rate for an HCT will be five times that for an AMIRA column (due to the weekly versus 4-weekly rinse frequency, and accounting for the different rinse volumes involved)

Elements not unduly affected by proximity to detection limits in general indicated the following:

- Reasonable agreement was observed between the two methods with HCT:AMIRA ratios often between 0.5 and 2 (i.e. rates were within a factor of two) for many elements.
- For sample ETD297, ratios were often less than 0.5, suggesting a significantly greater release rate from the AMIRA test. Note that the AMIRA test was acidic, whilst the HCT was circum neutral.
- Ca (and Mg, except for sample EUE765) release was consistently greater from the AMIRA columns, by a factor of between 3 and 10 (i.e. giving ratios between 0.1 and 0.3). This may be indicative of a temperature response. However, systematic temperature effects are not evident for other elements, and therefore an alternative explanation such as the influence of salinity is considered more likely.

- K and Si release rates from the two methods were in reasonable agreement for the lower sulfide content materials, but were greater in the HCT for higher sulfide materials. For the higher sulfide materials, the behavior may reflect a combination of incomplete rinsing of products from the AMIRA test, and/or the influence of solubility constraints.

CONCLUSIONS

Relative Merits of the Two Methods

The AMIRA and HCT methods showed the same broad trends, and equivalent release rates were observed. It should be noted however that most of the materials tested contained little or no effective neutralizing capacity, and leachates were mostly acidic.

The sample that contained available neutralization capacity, ETD297, yielded different pH profiles for the two methods; the HCT remained circum neutral over a testing period of 92 weeks, whilst the AMIRA test yielded acidic conditions after 40 weeks. The differing pH trends were interpreted as evidence that, for the higher solute and acidity concentrations expected during an AMIRA rinse event, (carbonate) neutralization is consumed or dissolved at a comparatively higher rate, and is more easily 'overwhelmed' (or armoured be secondary minerals), than is the case for more dilute leachates and higher frequency of flushing that occur for the HCT method. This interpretation may explain the differing pH profiles obtained for the ETD297 sample, and also the observation that Ca and Mg release is consistently greater for the AMIRA methods than for the HCT method. This difference in test outcomes has important implications with respect to utilization of the results for water quality predictions.

In terms of operational performance, the following is noted:

- Release profiles calculated from the AMIRA method tended to show a greater degree of variability than for the equivalent HCT method – interpreted as an increased sensitivity to the efficiency of leaching during individual rinse events.
- Leaching of pre-existing soluble salts (where present) was completed in a shorter time frame in the HCT – due to the more frequent rinsing regime.
- Limits of detection were encountered more often for the HCT method. For slow reacting samples, the AMIRA method facilitated collection of quantitative release rates for a wider range of elements when compared to the HCT methodology.

Implications for Data Utilization in Water Quality Prediction

Generally, trends in kinetic test datasets are used to examine relationships between sample properties (e.g. sulfur content) and oxidation rates, and to build confidence in conceptual models of processes controlling solute release. The current dataset showed that for acidic operating conditions, both test methods generated similar trends, and produced approximately equivalent datasets for use as a basis for estimating potential seepage quality from acid generating materials.

Leachate pH is a key influence on many geochemical processes, and an important aim of kinetic testing is to gain insight to the effectiveness and availability of neutralization capacity present, and facilitate estimation of times to the onset of acidic conditions. The different trends shown by sample ETD297 have important implications; the AMIRA method and the HCT gave different test outcomes, and led to differing conclusions with respect to the timescale, or even the likelihood, that acid conditions would develop in waters contacting this material type. The main cause of the discrepancy is interpreted to be a

comparatively high consumption of neutralization capacity in the more saline AMIRA leachate environment.

The climate in the Pilbara is arid, characterised by hot summers with periodic heavy rain and mild winters with occasional rain. In a full scale waste rock facility, time periods between 'rinse' events may be long, and the volumes of water involved low. Thus, contact waters would be expected to be saline. It is possible therefore that the outcomes from the AMIRA method could be more representative of neutralization behavior in a larger scale facility.

The current study included only one sample that allowed insight to the effectiveness of neutralization processes in the tests. Also, the internal variability for each of the test methods (i.e. effects of subsample variability, method variability, flushing efficiency etc.) has not been established for either method. Further work, on sample types known to contain effective neutralization capacity, would be necessary to develop a more robust understanding of neutralization processes, and their effectiveness, as a function of leachate salinity.

ACKNOWLEDGEMENTS

The HCTs and AMIRA columns were operated by SGS Laboratories, Perth, Australia. This paper has benefited from comments made by an anonymous reviewer.

REFERENCES

AMIRA AMIRA International Limited (2002), ARD Test Handbook: Project P387A Prediction and Kinetic Control of Acid Mine Drainage, May 2002.

Green, R. and Borden, R.K. (2011) Geochemical risk assessment process for Rio Tinto's Pilbara iron ore mines, Integrated Waste Management – Volume I (Ed. Sunil Kumar), 365-390. ISBN 978-953-307-469-6.

International Network for Acid Prevention (INAP) (2009) Global Acid Rock Drainage Guide (GARD Guide) - http://www.gardguide.com/.

MEND (2009), Prediction Manual for Drainage Chemistry from Sulphidic Geologic Materials. Report 1.20.1, December 2009

10th ICARD IMWA 2015 | 10th International Conference on Acid Rock Drainage & IMWA Annual Conference

Lessons Learned in the Interpretation of Mine Waste Static Testing Results

Cheryl Ross and Rens Verburg
Golder Associates, USA

ABSTRACT

A mine waste geochemical characterization program is a fundamental component of the Environmental and Social Impact Assessment (ESIA) for a proposed mine. Typically, the primary objective of the geochemical characterization program is to characterize the acid rock drainage and metal leaching (ARD/ML) potential of mine materials (e.g., development rock, tailing and ore). Often, the laboratory testing program begins with static testing followed by kinetic testing, if deemed appropriate. Static testing is conducted to describe the bulk chemical characteristics of a material and evaluate the potential of a material to leach metals or generate acid. If static testing indicates an ARD/ML potential, kinetic testing is typically conducted to verify whether the various ARD/ML potentials identified will indeed be realized over time, to determine reaction rates, and to assess lag times to acid generation. Static and kinetic testing results often form the basis for the prediction of water qualities during operations and at closure.

This paper discusses the interpretation of results for industry standard static testing procedures. Laboratory testing examples are presented to demonstrate how static test results can be affected by the selection of a particular analytical method or the execution of the selected method. The examples presented include: (1) the potential for contamination from laboratory reagents to affect Net Acid Generation (NAG) test leachate concentrations; (2) the potential for filter selection to bias Synthetic Precipitation Leaching Procedure (SPLP) leachate pH values; and, (3) differences in sulfur and carbon determinations using different analytical methods.

This paper demonstrates the importance of a comprehensive understanding of the laboratory methods and the inclusion of data validation procedures in the development of a robust static testing data set for use in prediction of ARD/ML potential and water quality prediction.

Keywords: static, laboratory, NAG, SPLP, ABA, data validation

INTRODUCTION

A mine waste geochemical characterization program is a fundamental component of the Environmental and Social Impact Assessment (ESIA) for a proposed mine. Typically, the primary objective of the geochemical characterization program is to characterize the acid rock drainage and metal leaching (ARD/ML) potential of mine materials (e.g., development rock, tailing and ore). Often, the laboratory testing program begins with static testing followed by kinetic testing, if deemed appropriate. Static testing is conducted to describe the bulk chemical characteristics of a material and evaluate the potential of a material to leach metals or generate acid. If static testing indicates an ARD/ML potential, kinetic testing is typically conducted to verify whether the various ARD/ML potentials identified will indeed be realized over time, to determine reaction rates, and to assess lag times to acid generation. Static and kinetic testing results often form the basis for the prediction of water qualities resulting from the interaction between mine waste materials and the ambient environment during operations and at closure.

Leach testing is conducted to characterize the metal leaching potential of a mine material. The results of leach tests are sensitive to the methodology used (e.g., solid to solution ratio, nature of the lixiviant, grain size reduction). Therefore, although leach tests provide an estimation of which metals are most likely to leach from a particular material, leachate metal concentrations will exhibit variability related to the specific test methodology used and may not be representative of field-scale conditions. Two examples of how leach test method implementation can affect test results are presented in this paper.

Acid base accounting (ABA) is the industry standard method used to provide an initial assessment of ARD potential of a mine material. The acid generation potential (AP) of a material is derived from a sulfur determination. The most environmentally conservative approach to calculate AP is to make the assumption that all sulfur in a sample is potentially reactive and therefore capable of generating acid; however, this ignores the fact that not all sulfur will contribute acidity. Total sulfur is often determined using a combustion method (e.g., Leco furnace) but acid digestion methods may also be used. Results from these methods are compared in this paper to show differences in calculated AP. The neutralization potential (NP) of a material is often estimated based on carbon analysis. Differences in carbon analysis results by method are also presented.

STATIC TEST RESULTS AND POTENTIAL PITFALLS

Net Acid Generation Leachate

The Net Acid Generation (NAG) test is an acid-base accounting test developed initially in Australia but now widely applied internationally. The NAG procedure uses a strong oxidant (hydrogen peroxide) to rapidly oxidize sulfide minerals in a crushed rock sample (AMIRA 2002). The NP of the sample then can be directly challenged by the acidity generated by rapidly oxidizing sulfides. If the sample has sufficient available NP, the alkalinity of the whole rock will not be entirely depleted, and the system is expected to have the capacity to remain circum-neutral. If there is inadequate available NP, then the pH of the test solution will fall below 4.5 and there will be net acidity rather than net alkalinity. In this case, a sample shows potential for acid generation.

The steps in the single-addition analytical procedure from AMIRA (2002) are summarized below:

- **Step 1:** Place 2.5 grams of a pulverized rock sample to a conical beaker.
- **Step 2:** Add 250 millilitres (mL) of 15% hydrogen peroxide (H_2O_2)
- **Step 3:** Cover the beaker with a watchglass and place in a fume head. Allow the sample to react until boiling or effervescence ceases.
- **Step 4**: Once the reaction is complete, place the beaker on a hot plate and heat until effervescence stops or a minimum of 2 hours.
- **Step 5:** Allow the sample to cool to room temperature. Add deionized water to increase the volume to 250 mL.
- **Step 5:** Measure the pH of the solution.
- **Step 6:** Titrate with sodium hydroxide (NaOH) to a final pH of 7.0.

Increasingly, comprehensive chemical analysis of NAG test leachate is conducted following Step 5 (i.e. prior to back titration). These results may then be used in mine water quality predictions as an indication of worst case or terminal water quality.

For quality assurance/quality control (QA/QC) purposes, it is critical that a blank sample be analysed in association with any NAG leachate analysis. The reagent grade hydrogen peroxide typically used by laboratories contains a number of impurities, including metals. Phosphorus is also present due to the use of phosphoric acid as a stabilizer. Other chemicals used for stabilization may also impart impurities (e.g., colloidal stannates, organophosphonates and colloidal silicates). The pH of hydrogen peroxide is variable due to the presence of stabilizing agents. Acids and bases used in pH adjustment of the hydrogen peroxide are another possible source of impurities. The NAG test method stipulates a target hydrogen peroxide pH between 4.5 and 6.0.

As an example, the specifications for a 30% reagent grade hydrogen peroxide, American Chemical Society (ACS) certified, are shown in Table 1 (Fisher Scientific 2014). An example analysis of a NAG blank for a test conducted with reagent grade hydrogen peroxide is shown in Table 2.

Table 1 Example of 30% reagent grade hydrogen peroxide specifications

Parameter	Maximum Permissible Concentration (mg/L)
Iron (Fe)	0.5
Nitrate (NO_3)	2
Sulfate (SO_4)	5
Copper (Cu)	0.1
Nickel (Ni)	0.1
Ammonium (NH_4)	5.
Chloride (Cl)	3
Heavy Metals (as Pb)	1
Phosphate (PO_4)	2

Table 2 NAG Blank Analysis Results

Param.	Conc.	Param.	Conc.	Param.	Conc.	Param.	Conc.
pH	5.24	Ag	0.00006	Cu	0.00358	Se	<0.00004
Alkalinity	1,600	Al	0.459	F	<0.06	Si	0.15
Cl	4.9	As	0.0005	Fe	0.206	Sn	10.7
SO_4	5.0	B	0.0128	Hg	<0.00001	Sr	0.0285
P	45.9	Ba	0.00493	Li	0.000327	Ti	0.00237
Ca	5.44	Be	0.000011	Mn	0.0061	Tl	0.000025
Mg	1.43	Bi	<0.000007	Mo	0.00885	U	0.00018
Na	44.2	Cd	0.000425	Ni	0.0388	V	0.00001
K	0.579	Co	0.000878	Pb	0.00094	Zn	0.018
		Cr	0.0536	Sb	0.006	Zr	<0.002

Param = parameter
Conc. = concentration in mg/L for all parameters with the exception of pH

The NAG blank results indicate the presence of a number of metals at concentrations above their respective analytical reporting limits. For some metals/metalloids (e.g., antimony), the reported concentrations are of the same order of magnitude as the water quality standards against which leach test results are often compared (e.g., United States Environmental Protection Agency [USEPA] drinking water maximum contaminant level [MCL] [USEPA 2009]). Phosphorus was measured at a concentration of almost 50 mg/L. The hydrogen peroxide therefore is a likely source of metals and phosphorus. The concentrations of phosphorus and chloride measured in the blank are higher than their respective maximum permissible concentration in the reagent grade hydrogen peroxide. The results for other parameters (e.g., alkalinity and tin) demonstrate the importance of a blank in the interpretation of NAG leachate results.

To reduce the potential for the hydrogen peroxide to be a source of contamination, it is recommended that ultra-pure hydrogen peroxide be used in NAG testing when leachate analysis is performed. This change will result in a significant increase in the cost of laboratory analysis. The cost of reagent ACS grade hydrogen peroxide currently is approximately 15 US$ per litre compared to 500 US$ per litre for ultra-pure hydrogen peroxide. Regardless of the type of hydrogen peroxide used, it is recommended that a blank analysis always be performed in association with NAG leachate analyses.

Synthetic Precipitation Leaching Procedure

The USEPA Synthetic Precipitation Leaching Procedure (SPLP) simulates the short-term interaction between meteoric water and a material (USEPA 1994). This test is frequently used in the mining industry to characterize the metal leaching potential of mine materials.

The SPLP test is conducted at a 20:1 solution to solid ratio. The lixiviant is prepared by the addition of a 60/40 weight percent mixture of sulfuric and nitric acids to reagent water to an end point pH of either 4.2 or 5.0, intended to be comparable to the pH of rainwater. The method calls for use of a pH 4.2 or 5.0 lixiviant for sites located east and west of the Mississippi River, respectively. Sample

preparation may include particle size reduction (<9.5 cm). Following 18 hours of reaction time, the leachate is filtered through a 0.6 to 0.8 μm glass fiber filter prior to chemical analysis.

Review of SPLP test results from multiple commercial laboratories has shown that an increase in leachate pH is sometimes observed following filtration. Example SPLP pH results for five waste rock samples tested using a pH 5.0 lixiviant are shown in Figure 1. These tests were conducted at a 4:1 solution to solid ratio instead of the standard 20:1 ratio. Leachate pH values were measured in the SPLP extraction vessel at the conclusion of testing (blue bars) and after filtration (green bars). The blank sample showed an increase in pH from 5.0, prior to filtration, to 6.2 after filtration. Significant increases (i.e. 10 to 20%) in pH were also observed for two of the five waste rock samples. The samples that demonstrated an increase in pH reported an initial value close to that of the lixiviant. As shown in Figure 2, these samples reported the lowest alkalinity and acidity concentrations and are therefore described as poorly buffered solutions. Poorly buffered solutions are the most susceptible to changes in pH following addition of an acid or base.

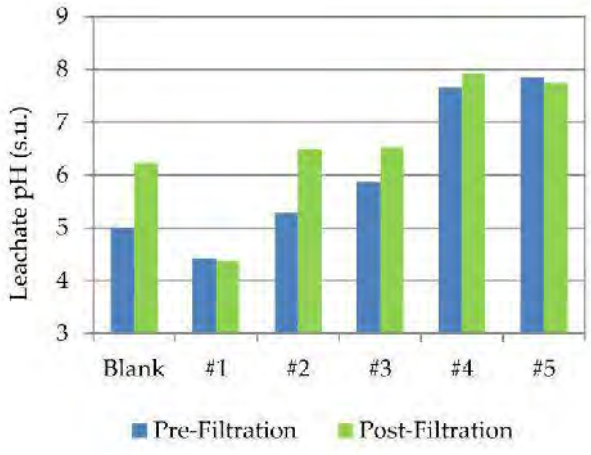

Figure 1 SPLP leachate pH results

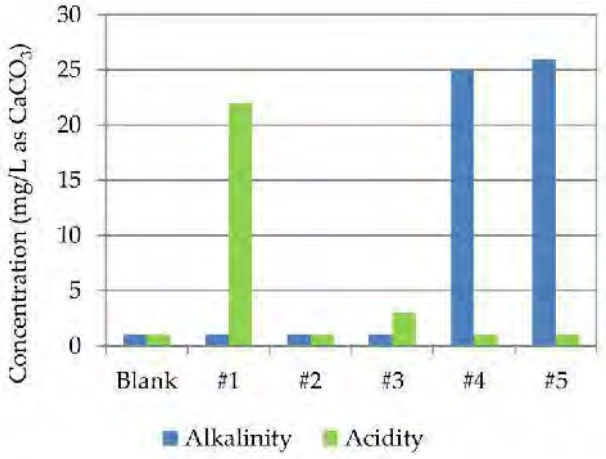

Figure 2 SPLP leachate alkalinity and acidity

Based on the results of additional laboratory testing, it was determined that improper filter preparation was the cause of the observed increase in pH. The potential for changes in the partial pressure of carbon dioxide in sample leachates was considered and discounted as the primary cause of the increase in pH.

The SPLP method stipulates that when evaluating the mobility of metals, filters shall be acid-washed and rinsed prior to use (USEPA 1994). Because the mobility of many metals is pH dependent, often decreasing as pH increases, a change in leachate pH has the potential to affect leachate metal concentrations. Therefore, use of a filter that does not impart a change in leachate pH is fundamental to the accurate determination of metal leaching.

Method specifications for SPLP filters include (USEPA 1994):

- Filters shall be made of borosilicate glass fiber, shall contain no binder materials, and shall have an effective pore size of 0.6 to 0.8 μm.
- Pre-filters must not be used.
- When evaluating the mobility of metals, filters shall be acid-washed prior to use by rinsing with 1 normal (N) nitric acid followed by three consecutive rinses with reagent water (a minimum of 1-liter per rinse is recommended).

To evaluate the potential for filters to affect leachate pH, it is recommended that a method blank be performed in association with all SPLP tests. Although not stipulated in the SPLP method, it is further recommended that leachate pH be measured before and after the filtration step.

Total Sulfur Analysis

Accurate determination of total sulfur is an essential component of many mine waste management programs. Two common methods for total sulfur determination are combustion (i.e. Leco furnace) and strong acid digestion. Total sulfur determinations using these methods for samples from a magmatic sulfide deposit are compared in Figures 3 and 4 (both figures present the same data on a linear and logarithmic scale, respectively). Each analytical method is described below:

- **Sulfur by Combustion (ASTM 2009) –** Sulfur content is determined by the combustion of a dry and pulverized sample in an oxygen atmosphere. Sulfur in the sample is converted to sulfur dioxide gas. The amount of sulfur dioxide gas evolved is measured by infrared adsorption.
- **Sulfur by Acid Digestion (Rudolph 1979)** - Characterization of the elemental (including sulfur) composition of a sample is a two-step process that includes an acid digestion to release elements into the solution phase followed by analysis of the elements in the resulting digestion. The 4-acid digest used in this study was a mixture of hydrochloric (HCl), hydrofluoric (HF), nitric (HNO_3) and perchloric ($HClO_4$) acids. The digestion was analysed by inductively coupled plasma (ICP).

In Figures 3 and 4, sample results with relative percent difference (RPD) values between the two results less than 35% are identified. An RPD less than 35% represents acceptable precision for solid phase duplicate analysis (USEPA 2010). These figures show that, at sulfur values greater than approximately 0.15 wt.%, the two analyses yield similar results. Below this concentration threshold, total sulfur values determined by the 4-acid digestion method were consistently higher than values reported by Leco furnace. As shown in Figure 3, at low sulfur values, the combustion method returns values that range from 0.005 to 0.1 wt.%; however, the 4-acid digestion method yields results for these same samples that are consistently higher (i.e. generally in the range of 0.1 to 0.2 wt.%). The reporting limits (RL) for total sulfur by combustion and 4-acid digestion are the same (0.005 wt.%) according to the method descriptions. At total sulfur values greater than 1 wt.%, although the two methods yielded similar results (i.e. RPD <35%), total sulfur by combustion consistently yielded higher values than the 4-acid digest method. This trend is likely attributable to loss of sulfur by volatilization with the 4-acid digest method. Based on the assumption that the Leco furnace results are more accurate, acid potential estimated from total sulfur determined by 4-acid digest would result in a biased high estimate of acid potential at low total sulfur concentrations and a biased low estimate of acid potential at high total sulfur concentrations. Use of mineralogical results is recommended to verify that sulfur determinations provide accurate estimates of AP.

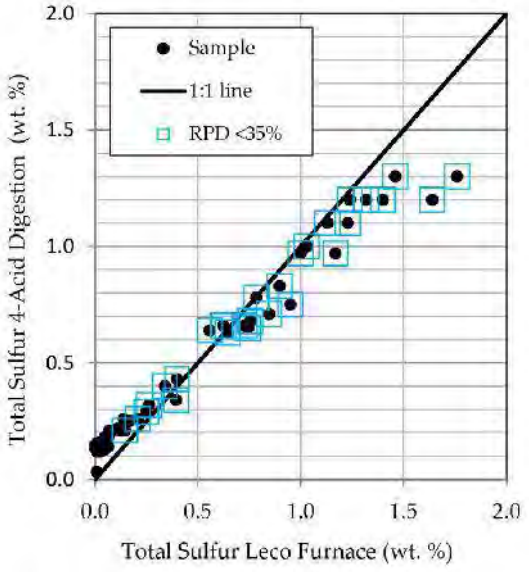

Figure 3 Total sulfur by Leco versus 4-acid digestion (linear scale)

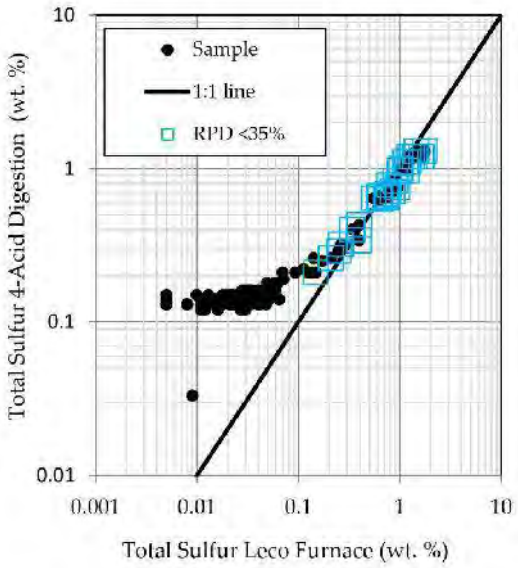

Figure 4 Total sulfur by Leco versus 4-acid digestion (logarithmic scale)

Carbon Analysis

The American Society for Testing Materials method (ASTM E1915-09) for total inorganic carbon (TIC) analysis provides two options: acid leach or pyrolysis (ASTM 2009). For both methods, total carbon (TC) is determined by the combustion of a dry and pulverized sample in an oxygen atmosphere. Carbon in the sample is converted to carbon dioxide gas. The amount of carbon dioxide gas evolved is measured by infrared adsorption. For the acid leach option, TIC analysis is conducted following the method described for TC; however, the sample is treated with hydrochloric acid (HCl) prior to analysis to remove the inorganic carbon fraction. TIC is then determined by difference (i.e. TC minus residual carbon following an acid leach). The pyrolysis method does not include a pre-treatment step. Instead, the sample is combusted at 550 °C to promote volatilization of organic carbon. The residual carbon (residue) is reported as TIC. Because siderite [$FeCO_3$] may decompose below 550 °C, the pyrolysis method may underestimate the TIC content of a sample when siderite is present (ASTM 2009).

TIC analysis results for 20 gold mine tailing samples are shown in Figure 5. For these samples, TIC values determined by HCl leach consistently yielded higher concentrations than TIC determined by pyrolysis. As shown in Figure 6, TIC by HCl leach was essentially equal to TC. TIC determined by pyrolysis indicated the presence of an organic carbon fraction (i.e. organic carbon equal to the difference between TC and TIC).

Mineralogical analysis by X-ray diffraction (XRD) indicated that the dominant carbonate mineral in all tailing samples was calcite [$CaCO_3$], with concentrations ranging from 1.2 to 5.8 wt.%. Siderite was identified in six samples at concentrations of <1 wt.%. TIC values determined by the acid leach and pyrolysis methods are compared to TIC calculated from mineralogy in Figure 7. Compared to the mineralogy results, TIC by acid leach generally overestimates TIC and TIC by pyrolysis often underestimates TIC. The presence of siderite does not appear to affect this trend.

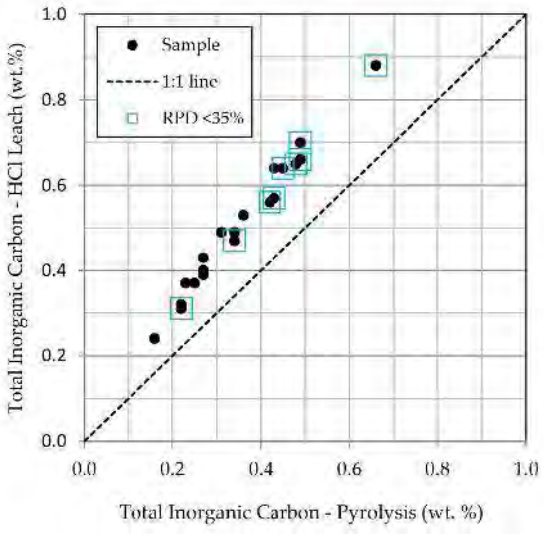

Figure 5 Total inorganic carbon by two methods

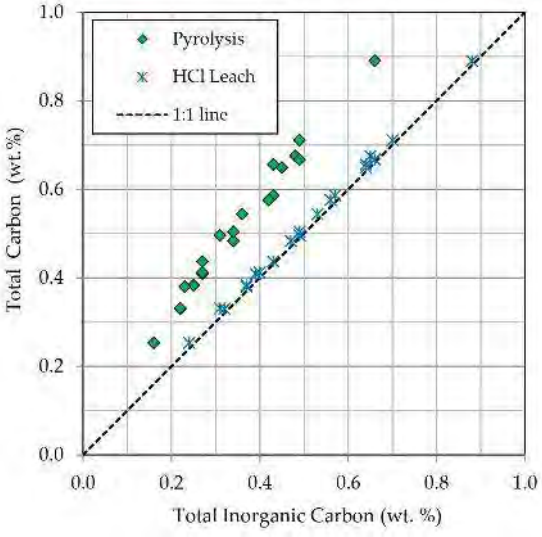

Figure 6 Total inorganic carbon versus total carbon

The average AP of the 20 tailing samples calculated from sulfide sulfur was 61 kg $CaCO_3$/t, whereas the average NP determined from calcite was 31 kg $CaCO_3$/t. The average difference in NP determined from TIC by the two methods was 13 kg $CaCO_3$/t, roughly one third of total NP. For a few samples, the difference in calculated NP is significant as the difference resulted in a change in the ARD classification of the sample as determined by neutralization potential ratio (NPR). Therefore, for these samples, even a small difference in estimated NP based on TIC is considered significant. Use of mineralogical results is recommended to verify that TIC determinations provide accurate estimates of NP.

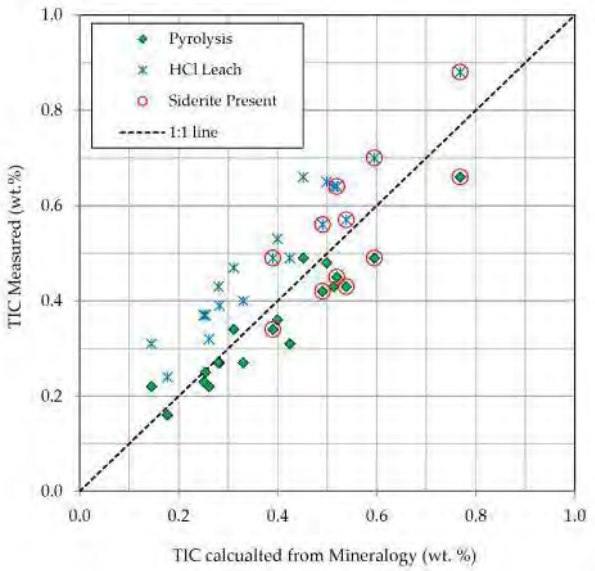

Figure 7 Comparison of total inorganic carbon by three methods

SUMMARY AND CONCLUSION

The examples presented in this paper demonstrate the importance of a comprehensive understanding of the laboratory methods and the inclusion of data validation procedures in the development of a robust static testing data set for use in water quality predictions. Development of QA/QC procedures is required to evaluate the accuracy and precision of the analytical results prior to use in predictions.

As demonstrated by the NAG and SPLP examples, inclusion of a method blank is recommended for QA purposes. Method blank results should be used to evaluate laboratory contamination and confirm the target lixiviant pH. Although not specified in the SPLP method, measurement of leachate pH before and after filtration is recommended. When NAG leachate analysis is conducted, use of ultra-pure hydrogen peroxide is recommended.

Acid base accounting is the industry standard method to provide a preliminary indication of a material's ARD potential. As demonstrated by the examples presented in this paper, the analytical method selected for sulfur and carbon determinations may affect the results, and therefore the estimates of AP and NP. For the total sulfur determination example presented in this paper, total sulfur determined by Leco furnace is considered more accurate than total sulfur determined by 4-acid digest. For both sulfur and carbon determinations, use of mineralogical analysis results is recommended to verify that total sulfur and TIC determinations provide accurate estimates of AP and NP, respectively.

REFERENCES

AMIRA International Ltd. (AMIRA) (2002) *ARD Test Handbook – Project P387A Prediction and Kinetic Control of Acid Rock Drainage (Appendix C)*, May, pp. D1– D5.

American Society of Testing Materials (ASTM). 2009. Standard Test Methods for Analysis of Metal Bearing Ores and Related Materials by Combustion Infrared Adsorption Spectometry. E 1915-09.

Fisher Scientific (2014) Hydrogen Peroxide, 30% (Certified ACS), Fisher Chemical Specifications, http://www.fishersci.com/.

Rudolf, B. (Ed.) (1979) A Handbook of Decomposition Methods in Analytical Chemistry, Halsted Press, Div. Wiley & Sons, New York.

United States Environmental Protection Agency (USEPA) (1994) *Method 1312 – Synthetic Precipitation Leaching Procedure (Revision 0)*, September.

USEPA (2009) National Primary Drinking Water Regulations, EPA 816-F-09-004, May.

USEPA (2010) USEPA Contract Laboratory Program National Functional Guidelines for Inorganic Superfund Data Review – Final, EPA 540-R-10-011, January.

Kinetic Tests to Evaluate the Relative Oxidation Rates of Various Sulfides and Sulfosalts

Aurélie Chopard[1], Mostafa Benzaazoua[1], Benoît Plante[1], Hassan Bouzahzah[1] and Philippe Marion

1. *Research Institute on Mines and Environment (RIME), Université du Québec en Abitibi-Témiscamingue, Canada*
2. *Géoressources, École Nationale Supérieure de Géologie (ENSG), Université de Lorraine, France*

ABSTRACT

Mine wastes produced from sulfide-bearing ores exploitation and processing are often characterized by acid mine drainage (AMD) generation, which leads to high dissolved metal concentrations in addition to acidity. When the acidic drainage is neutralized (generally through neutralization by carbonates), the phenomenon is called contaminated neutral drainage (CND). The quality of these drainages can be predicted by static tests, which can quickly assess the acid-generating potential (AP) and the neutralization potential (NP) by chemical and/or mineralogical calculations. With the Paktunc static test, the mineralogical composition of the sample is used to calculate both AP and NP. For AP calculation, equal oxidation rates are assumed for all sulfides. Since the sulfide minerals oxidize at different rates, the objective of the present paper is to compare the oxidation rates of various sulfides and sulfosalts often encountered in mine wastes in order to take them into account in AP prediction. Thus, seventeen pure sulfide minerals and sulfosalts (pyrite, pyrrhotite, bornite, chalcocite, chalcopyrite, covellite, galena, sphalerite, arsenopyrite, stibnite, gersdorffite and fahlore) were characterized physically, chemically and mineralogically, and submitted to kinetic tests (modified weathering cells) in order to compare their oxidation rates, acidity generation, and metal leaching potentials (As, Cu, Fe, Ni, Sb or Zn). The oxidation rates vary from 2 to 15 times between the sulfide minerals studied. Moreover, the metal concentrations in leachates from the sulfosalts are 30 to 40 times higher than those of the sulfide minerals.

This study fills a knowledge gap in the oxidation rates of common sulfides and sulfosalts, which enable a more precise prediction of AMD and CND generation, mainly through the integration of a kinetic parameter in the modified Paktunc AP calculation.

INTRODUCTION

Solid mine wastes resulting from extraction and ore treatment are often stored at the surface in waste rock piles and tailings impoundments. Mine wastes from sulfide-bearing ores contain different sulfide minerals which, upon exposure to atmospheric conditions, may generate acidic effluents in the absence of neutralizing minerals. The phenomenon, well-known as Acid Mine Drainage (AMD), is a complex process of chemical, physical and biological reactions. The prediction of water quality is of significant importance for the mining industry, due to increasingly restrictive regulations and higher social awareness.

AMD is very well documented in the literature (Brodie, Broughton & Robertson, 1991; Alpers & Nordstrom, 1999; Aubertin, Bussière & Bernier, 2002; Blowes et al., 2014). A reliable prediction of the quality of mine drainage at the earliest stage of the mining projects is beneficial. Different water quality prediction tools such as static and kinetic testing were developed in the past 30 years (Sobek et al., 1978; Adam et al., 1997; Lawrence & Scheske, 1997; Paktunc, 1999; Blowes et al., 2014). Prediction static procedures often examine the balance between the acid generating potential (AP) and neutralization potential (NP) of samples and are called acid–base accounting (ABA) tests (Ferguson & Morin, 1991). There are distinct classes of static tests: chemical methods and mineralogical methods. Chemical methods require testing in a chemistry lab, while mineralogical methods are mainly based on the mineralogical composition of the mine wastes. The AP and NP are calculated as the sum of the individual contributions of each acidifying and neutralizing mineral, based on their proportions in the sample and their relative reactivity (only for NP). The NP procedure has been largely investigated in the literature (e.g. Lapakko, 1994; Lawrence & Wang, 1997; Li, 1997; Paktunc, 1999). On the other hand, the AP is still often simply calculated on the basis of the bulk sulfide concentration in the sample, considering all sulfides are present as pyrite and based on the stoichiometry of pyrite oxidation (EQUATION 1). Thus, this simple AP calculation is biased because the possible different acid generation (on a molar basis) of other sulfides is not taken into account. To overcome this issue, (Paktunc, 1999) proposed an AP calculation based on the theoretical oxidation rates of the different sulfides (EQUATION 2).

$$AP = 31.25 \times \%Ssulfide \quad (kg\ CaCO_3/t) \quad (1)$$

$$AP = \sum_{s=1}^{m}\left(\frac{n_s \times 98 \times X_s \times 10}{w_s}\right) \quad (kg\ H_2SO_4/t) \quad (2)$$

- AP: acidification potential;
- ns: number of moles of H2SO4 formed by the oxidation of one mole of sulfide mineral s;
- 98: molecular weight of H2SO4 (g.mol–1);
- 10: conversion factor for recasting in kg.t–1;
- Xs: amount of sulfide mineral s in wt%;
- ws: molecular weight of sulfide mineral s (g.mol–1);
- m: number of sulfide minerals in the sample.

This equation improves the AP calculation but does not take into consideration the relative acidity production rates of the different sulfides; the latter was evaluated by several other authors (Nicholson, 1994; Rimstidt, Chermak & Gagen, 1994; Jambor & Blowes, 1998; Plumlee, Logsdon & Filipek, 1999). Moreover, based on the Paktunc equation, Bouzahzah, Benzaazoua & Bussière (2013) proposed another modified equation taking account the relative rates of acidity production of each sulfide by using a relative reactivity factor. This factor is determined by the average of the total

acidity produced by each sulfide calculated relatively to the acidity production of pyrite. However, only five common sulfides have been studied (arsenopyrite, chalcopyrite, galena, pyrite and sphalerite). Thus, based on their work, seventeen sulfide minerals were submitted to kinetic testing. The main objective of this study is to compare the acidity production rate of various sulfide minerals and sulfosalts often encountered in mine wastes, including pyrite (FeS_2), As and Ni-bearing pyrite, and pyrrhotite ($Fe_{(1-x)}S$, $0<x<0,17$) (hereinafter referred to as iron-sulfides); bornite (Cu_5FeS_4), chalcocite (Cu_2S), chalcopyrite ($CuFeS_2$), covellite (CuS), galena (PbS), sphalerite ((Zn,Fe)S), and sphalerite-Fe (hereinafter referred to as base-metals sulfides); arsenopyrite (FeAsS), fahlore (tetrahedrite-tennantite solid solution) $(Cu,Fe,Ag,Zn)_{12}(Sb,As)_4S_{13}$), gersdorffite (NiAsS), and stibnite (Sb_2S_3) (hereinafter referred to as As/Sb-bearing sulfides). To do this, a series of standard sample were prepared by mixing pure sulfide minerals with quartz (considered as inert). The reactivity of each compound within standard samples is evaluated by laboratory kinetic tests in modified weathering cells (small-scale humidity cell tests; see Cruz et al., 2001 and Benzaazoua et al., 2004 for details).

METHODOLOGY

Materials

A total of 17 sulfides and sulfosalts were selected based on their presences in typical polymetallic sulfides-rich deposits. These sulfides were acquired as pure mineral samples from a specialized minerals supplier. Five of these seventeen sulfides (arsenopyrite, chalcopyrite, galena, pyrite and sphalerite) were previously studied at the RIME (Bouzahzah, Benzaazoua & Bussière, 2013; Bouzahzah et al., 2008). The other samples were hand sorted to remove macroscopic impurities under a binocular lens before grinding to reach typical tailings grain size distribution (Bussière, 2007) according to their own grindability. Representative samples of the pure mineral powders were submitted to a full characterization and then used into the kinetic test.

Polished sections of the powders were examined and showed that some materials contain minor sulfide and/or gangue contaminants. Pure quartz was mixed with the pure sulfides and sulfosalts (95 wt% quartz and 5 wt% pure minerals) for kinetic testing.

Solid material characterization

The physical, chemical and mineralogical properties were determined for all studied materials (pure and mixtures). The grain size distributions were measured with a Microtrac S3500 laser grain size analyzer. The D_{10}, D_{50} and D_{90} values taken from the grain size distributions are presented below. The grain size distributions of the studied pure minerals are typical of tailings with D_{10} values ranging approximately from 1 to 20 µm and 80 to 95 % passing 130 µm. The total sulfur content S_t, including S from sulfide and sulfate minerals, was analyzed by an ELTRA induction furnace coupled with an infrared analyzer. The bulk chemical composition was analyzed by ICP-AES (Perkin Elmer Optima 3100-RL) following a multi-acid digestion ($HNO_3/Br_2/HF/HCl$). TABLE 1 summarizes the physical and chemical properties of the pure minerals.

Table 1 Physical and chemical properties of the pure studied minerals as solid samples

Mineral	D_{10} (µm)	D_{50} (µm)	D_{90} (µm)	St (%)	Fe (%)	Cu (%)	Zn (%)	Pb (%)	As (ppm)	Ni (ppm)	Sb (ppm)	Other traces (<2000ppm)
Iron-sulfides												
Pyrite 1	8.7	49.0	129.2	50.1	46.46	0.04	0.01					
Pyrite 2	5.8	29.8	75.9	45.62	45.29	0.14	2.48	0.65	1110	458	<4	Bi, Cd, Co, Mn
Pyrite 3	6.2	35.9	98.3	34.89	32.75	1.72	0.1	0.15	3280	498	<4	Bi, Cd, Co, Mn
Pyrrhotite 1	4.6	21.1	74.3	36.63	64.29	0.24	0.11	0.04	1050	71	<4	Bi, Co, Mn
Pyrrhotite 2	11.7	54.5	128.8	37.67	58.2	0.22	0.03	0	917	47410	981	Bi, Co, Mn
Base-metals sulfides												
Bornite	19.9	75.9	163.7	24.13	11.44	61.56	0.18	0.02	148	9	699	Bi, Co, Mn
Chalcocite	17.1	66.1	151.3	20.34	0.04	78.57	0.23	0.02	<30	10	90	Co, Mn
Chalcopyrite 1	6.2	33.3	94.8	32.5	34.49	21.1	1.55	0.01	752	69	<4	Bi, Co, Mn, Se
Chalcopyrite 2	10.5	44	161.0	32.77	29.74	30.2	0.02	0.02				
Covellite	14.4	72.2	161.7	32.39	0.02	64.18	0.21	0.01	<30	12	6	Se
Galena	6.1	41.3	115.1	12.64	<0.001	0	<0.0055	87.36	<30	6	527	
Sphalerite	4.6	43.2	160	32.19	6.9	0.01	63.1	0.02				Cd, Mn
Sphalerite-Fe	10.4	57.9	142.1	32.94	11.6	0.1	60.43	0.01	177	16	<4	Co, Mn (0.5%)
As/Sb-bearing sulfides												
Arsenopyrite	3.6	18	102.9	18.83	32.35	0.01	0	0.07	434000	94	399	Bi, Mn
Gersdorffite	4.2	18.2	49.2	11.56	0.8		0.12		385000	235500	14900	Mn, Co (3.5%), Se
Fahlore	4.5	21.9	68.7	24.81	4.71	40.63	2.03	0.01	105000	240	62000	Bi, Co, Mn
Stibnite	4.5	30.5	84.6	28.74	<0.001	0.02	<0.0055	<5	<30	<5	712000	Co, Se

Polished sections were observed by optical microscopy to identify the gangue minerals or/and other minor sulfides. The composition of gersdorffite and fahlore was first evaluated using a JEOL J7600F Field Emission Scanning Electron Microscope (FE-SEM) coupled with an Oxford EDS (Energy Dispersive X-ray Spectrometry) spectrometer. Then, the more precise composition of these two samples and trace elements in pyrite 2 and 3, pyrrhotite 1 and 2, and in sphalerite-Fe (choosed along the assay of the sample and/or the oxidation behavior) was determined by analyzing 10 particles from each section using a Castaing Cameca SX100 Electron Probe MicroAnalyser (EPMA) coupled with a WDS (Wavelength-dispersive X-ray Spectometry) spectrometer for the microanalysis. All quantitative EPMA were done in wavelength-dispersive mode with an

accelerating voltage of 20 kV and a constant beam current of 20 nA. The counting time on each peak was 10 s with the exception of Mn (40 s), Ag (40 s) and trace elements (Cd, Co:40 s). The results are shown in TABLE 2. Gersdorffite is a solid solution (Fanlo et al., 2004; Ahmed, Arai & Ikenne, 2009) which contains more As and less S and Ni than the gersdorffite approved by the IMA, and which also contains Co. Fahlore is a solid solution between the tetrahedrite and tennantite poles.

Table 2 Microanalysis by EPMA of the pure studied minerals as solid samples

Element (w%)	S	Fe	Cu	Zn	As	Ag	Sb	Ni	Cd	Mn	Co
DDL (ppm)	672	1067	1046	1222	664	959	1805	546	440	461	329
Fahlore	**27.73**	**3.58**	**42.68**	**3.31**	**14.97**	**0.12**	**8.23**				
Gersdorffite	**11.8**	**0.63**			**56.65**			**27.24**			**5.21**
Pyrite 2 (As)	**53.27**	**47.12**			**0.1**						
Pyrite 3 (Ni)	**52.47**	**46.24**						**0.24**			**0.13**
Pyrrhotite 1 (SEM)	**40.38**	**60.83**									
Pyrrhotite 2	**39.19**	**57.44**						**1.18**			
Sphalerite-Fe											
50% of type 1	**33.57**	**7.29**		**58.98**					**0.08**		
50% of type 2	**33.65**	**8.71**		**56.54**					**0.16**	**1.18**	

Modified kinetic testing

The samples were submitted to kinetic testing in modified weathering cells. These weathering cells (Cruz et al., 2001) are small-scale humidity cells which render similar results for the rates of reactions (Cruz et al., 2001). These tests could be considered as reproducible (Demers et al., 2011). Moreover, weathering cells can be used as an alternative to humidity cells when working on small sample quantities (< 100 g). This method is also known to be more aggressive than humidity cells (Villeneuve, 2004). The procedure consists of a 100 mm Büchner funnel with a 0.45 µm glass-fiber filter holding a 67 g sample. The sample is leached twice a week (3 days between flushes) with 50 mL deionized water. The cells were placed in a controlled-weather box to maintain the samples under optimal saturation conditions and avoid extreme drying (Bouzahzah, Benzaazoua & Bussière, 2013). Leachates from the weathering cells were analyzed for pH, conductivity, acidity, sulfur and elemental concentrations. The element concentrations in the leachates are analyzed by ICP-AES on an aliquot acidified to 2% HNO_3 for preservation. The weathering cells were run for 55 to 70 cycles (stopped upon reaching steady-state).

RESULTS AND DISCUSSION

pH

FIGURE 1 shows the comparison of the pH leachate of all studied minerals. The pyrrhotite 1 provided neutral pH at the beginning of the test which is related to the neutralization by calcite (6.8%). After its complete dissolution, the pH became acidic and then reached the pH value of the pyrrhotite 2. Almost all of the iron sulfide minerals showed more acidic pH at the beginning, certainly due to the dissolution of secondary products at the surface of the samples. The sphalerite

and sphalerite-Fe display very similar pH around 6. The covellite pH fluctuated between 5 and 6. The arsenopyrite generated the most acidic leachates of all samples. The gersdorffite produces acidic leachates at the test start and increases to more neutral pH along the test.

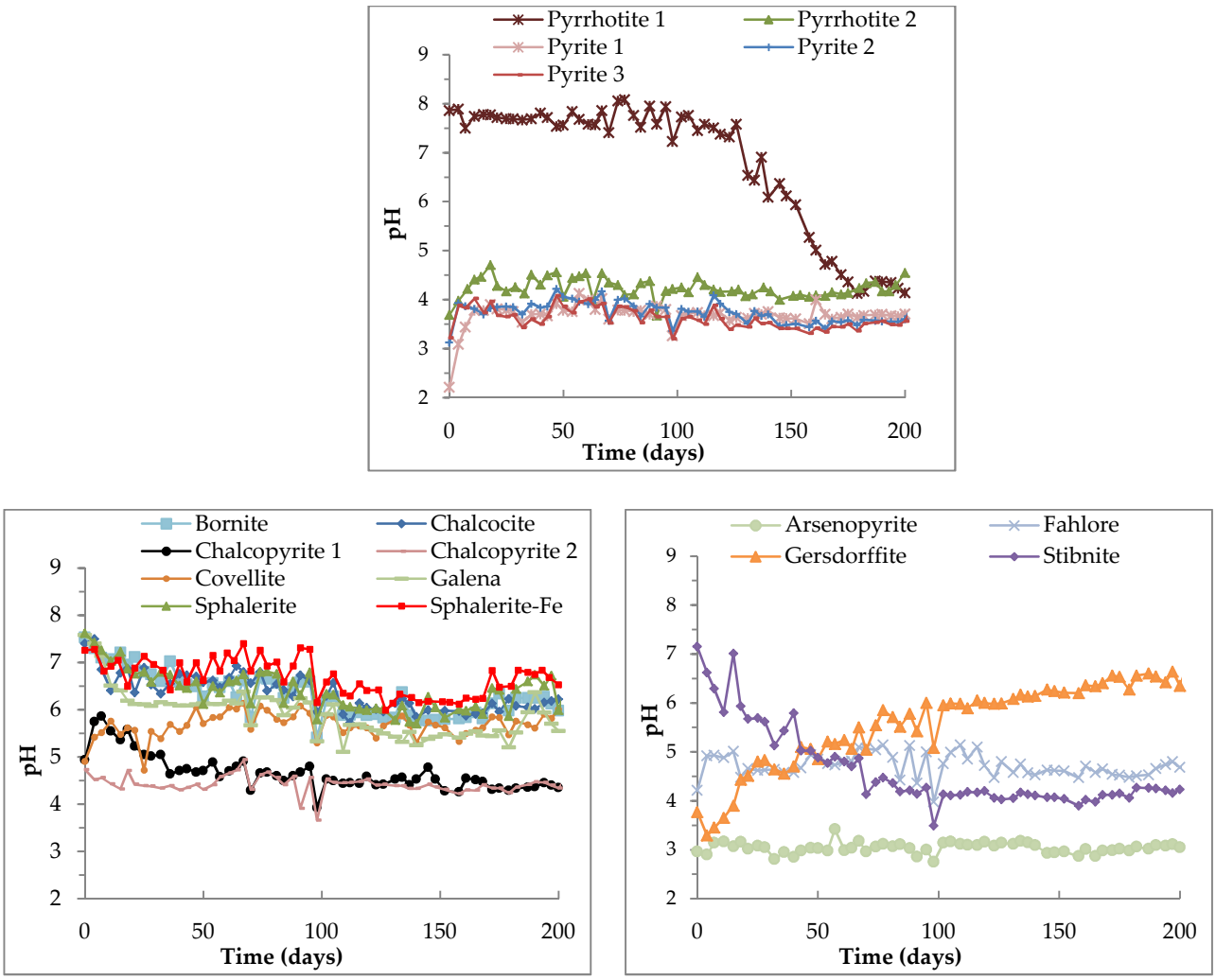

Figure 1 pH results of the leachates of the weathering cells for all minerals studied

Reactivity rates

As no other S-bearing oxidation products are suspected to form under the acidic and highly oxidative conditions of the kinetic tests, it is assumed that the entire S was present as sulfate in solution (pH > 2 and Eh > 0.4 V during all experiments) and ended up in the leachates. Therefore, this study uses the rate of sulfate production as the direct indicator of the acid generation rate and of the sulfide oxidation rate. The cumulative dissolved element loads are normalized regarding the initial sample mass for expressing the rates. The Specific Surface Area (SSA) of the studied minerals will be determined in a further study to take into account the influence of particle sizes in the oxidation rates.

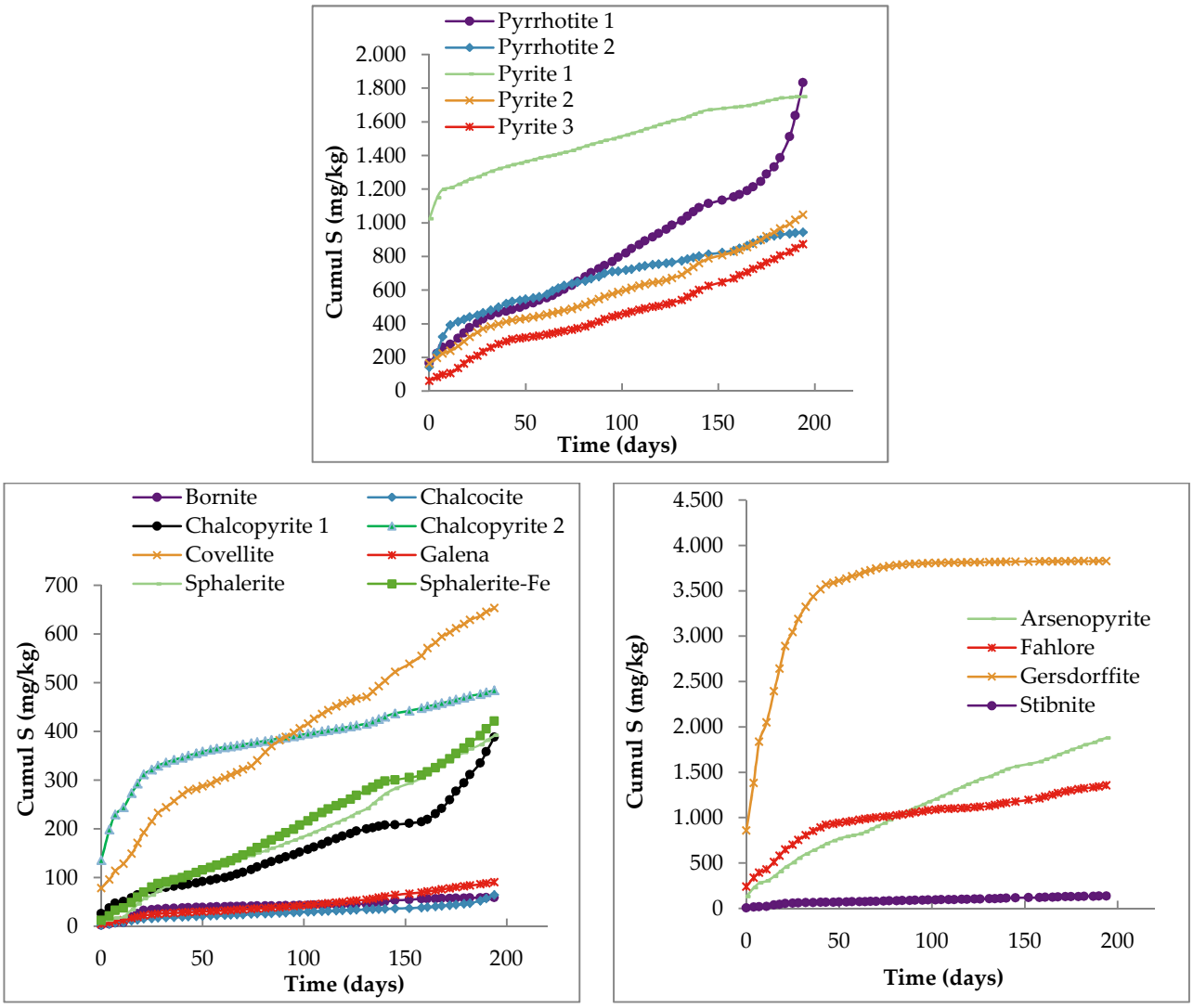

Figure 2 Cumulative normalized charges of S for the studied sulfides. Black arrows show points of inflexion for three specific minerals curves

FIGURE 2 shows the S release rate of the studied sulfides. The inflexion point of pyrrhotite 1 is due to the complete depletion of the carbonates content in the sample. The inflexion points of the sphalerites and chalcopyrites need further investigations and are not currently explained. We can note that the Mn content of the sphalerite-Fe may influence its rate of oxidation. This will be verified in a further study. TABLE 3 shows the oxidation rates of the studied sulfides, obtained by calculating the slope of the linear regression within the stabilized portion of these cumulative normalized loadings over time (mg of S/kg/day). These rates allowed the classification of iron-sulfides based on their reactivity as follows: pyrrhotite 1 > pyrite 2 > pyrite 3 > pyrrhotite 2 > pyrite 1. We have to mentionnthat the pyrrhotite 2 sample is not pure and contains 10 % of pentlandite. Moreover, this pyrrhotite contains trace Ni, certainly in its crystal network (about 1%, see TABLE 2), which may influence its reactivity (Dold, 2010). For this mineral, the Ni concentration in the leachates is higher (from 2 to 16 mg/L). The high concentration of Ni in pyrrhotite's leachates is

probably both due to the presence of pentlandite and trace Ni in the pyrrhotite grains. At the end of the test, the outline of almost all pyrrhotite grains is altered. For the base-metals sulfides, the classification is as follow: sphalerite-Fe > covellite > sphalerite > chalcopyrite 1 > chalcopyrite 2 > galena > chalcocite > bornite. Chalcopyrite 1 is more reactive than chalcopyrite 2 because it contains 26.5% of pyrrhotite. The sphalerite-Fe is more reactive than the sphalerite because of the presence of trace Mn (see TABLE 2) and its higher Fe-content. The As/Sb-bearing sulfides can be classified as: gersdorffite >>> arsenopyrite > fahlore > stibnite. We have to keep in mind that the gersdorffite is very reactive at the beginning of the test. Actually, the stabilized portion for gersdorffite either shows a depletion of the mineral of 70% (calculated by depletion of S) or could be due to a passivation of the reactive surfaces. Another duplicate test is currently ongoing.

Table 3 Experimental oxidation rates for the studied sulfides

Oxidation rates (mg of S/kg/d)					
Iron-sulfides		*Base-metals sulfides*		*As/Sb-bearing sulfides*	
Pyrrhotite 1	8.2	**Bornite**	0.23	**Arsenopyrite**	6.9
Pyrrhotite 2	2.6	**Chalcocite**	0.28	**Gersdorffite**	93.6
Pyrite 1	2.4	**Chalcopyrite 1**	2.0	**Fahlore**	3.2
Pyrite 2	4.8	**Chalcopyrite 2**	1.0	**Stibnite**	0.49
Pyrite 3	4.6	**Covellite**	2.7		
		Galena	0.53		
		Sphalerite	2.3		
		Sphalerite-Fe	3.2		

CONCLUSIONS AND FURTHER WORK

In order to complete the lack of knowledge about the oxidation rates of certain sulfide and sulfosalt minerals often encountered in mine wastes, the oxidation rates of seventeen of them were assessed by a modified weathering cell test. Based on the obtained results, these minerals can be classified in terms of oxidation based on their S release rates from the highest to the lowest: gersdorffite > pyrrhotite > arsenopyrite > pyrite > fahlore > covellite > sphalerite-Fe ≥ chalcopyrite > sphalerite > galena > stibnite > chalcocite > bornite. The results highlight the importance of trace element composition in the stability of individual sulfides (Dold, 2010). Pyrrhotite 2, which contains around 1.2% Ni, is less reactive than the pure pyrrhotite 1. Gersdorffite shows a different behavior which can be interpreted as a high initial oxidation rate and a high initial release of As. On the other hand, this study demonstrates that minerals could be very problematic for the environment, even if present at low concentrations in a sample. In fact, gersdorffite (As), arsenopyrite (As), stibnite (Sb) and fahlore (As, Sb) are very reactive minerals and release metal and metalloids. Further work will consist in the evaluation of their influence in real mine waste samples. Moreover, other metals or metalloids, like Cd, Co, Mo, Mn, Ni or Zn have been found in the leachates at concentrations over the existing regulation. More work will be done to improve the prediction of CND.

REFERENCES

Adam, K., Kourtis, A., Gazea, B. & Kontopoulos, A. (1997). "Evaluation of static tests used to predict the potential for acid drainage generation at sulphide mine sites." Transactions of the Institution of Mining and Metallurgy-Section A-Mining Industry **106**: A1.

Ahmed, A. H., Arai, S. & Ikenne, M. (2009). "Mineralogy and Paragenesis of the Co-Ni Arsenide Ores of Bou Azzer, Anti-Atlas, Morocco." Economic Geology **104**(2): 249-266.

Alpers, C. & Nordstrom, D. (1999). "Geochemical modeling of water-rock interactions in mining environments." The environmental geochemistry of mineral deposits. Part A: processes, techniques, and health issues **6**: 289-323.

Aubertin, M., Bussière, B. & Bernier, L. (2002). Environnement et gestion des résidus miniers. P. I. d. Polytechnique. Corporation de l'École Polytechnique de Montréal, Montréal. **Manuel sur cédérom**.

Benzaazoua, M., Bussière, B., Dagenais, A.-M. & Archambault, M. (2004). "Kinetic tests comparison and interpretation for prediction of the Joutel tailings acid generation potential." Environmental Geology **46**(8): 1086-1101.

Blowes, D. W., Ptacek, C. J., Jambor, J. L., Weisener, C. G., Paktunc, D., Gould, W. D. & Johnson, D. B. (2014). 11.5 - The Geochemistry of Acid Mine Drainage. Treatise on Geochemistry (Second Edition). H. D. Holland &K. K. Turekian. Oxford, Elsevier**:** 131-190.

Bouzahzah, H., Benzaazoua, M. & Bussière, B. 2013. «Acid-generating potential calculation using mineralogical static test : modification of the Paktunc equation». In *World Mining Congress (WMC 2013)* (Montréal, Québec, Canada., Août 11-14, 2013.

Bouzahzah, H., Califice, A., Benzaazoua, M., Mermillod-Blondin, R. & Pirard, E. 2008. «Modal analysis of mineral blends using optical image analysis versus X ray diffraction». In *Proceedings of International Congress for Applied Mineralogy ICAM08* (AusIMM.

Brodie, M., Broughton, L. & Robertson, A. 1991. «A conceptual rock classification system for waste management and a laboratory method for ARD prediction from rock piles». In *Proc. Second International Conference on the Abatement of Acidic Drainage* (Montreal, Quebec), p. 119-135. Quebec Mining Association, Ottawa.

Bussière, B., (2007). Colloquium 2004: Hydrogeotechnical properties of hard rock tailings from metal mines and emerging geoenvironmental disposal approaches. Canadian Geotechnical journal 44, 1019-1052.

Cruz, R., Bertrand, V., Monroy, M. & González, I. (2001). "Effect of sulfide impurities on the reactivity of pyrite and pyritic concentrates: a multi-tool approach." Applied Geochemistry **16**(7–8): 803-819.

Demers, I., Bussière, B., Aachib, M. & Aubertin, M. (2011). "Repeatability evaluation of instrumented column tests in cover efficiency evaluation for the prevention of acid mine drainage." Water, Air, & Soil Pollution **219**(1-4): 113-128.

Dold, B. (2010). "Basic concepts in environmental geochemistry of sulfidic mine-waste management." Waste management: 173-198.

Fanlo, I., Subías, I., Gervilla, F., Paniagua, A. & García, B. (2004). "The composition of Co–Ni–Fe sulfarsenides, diarsenides and triarsenides from the San Juan de Plan deposit, Central Pyrenees, Spain." The Canadian Mineralogist **42**(4): 1221-1240.

Ferguson, K. & Morin, K. 1991. «The prediction of acid rock drainage - Lessons from the database». In *Second international conference on the abatement of acidic drainage. Conference proceedings* (Montreal, Quebec), p. 83-106. Quebec Mining Association, Ottawa.

Jambor, J. & Blowes, D. (1998). "Theory and applications of mineralogy in environmental studies of sulfide-bearing mine wastes." Modern Approaches to Ore and Environmental Mineralogy: Ottawa, Canadá, Mineralogical Association of Canada, Short Course Series **27**: 367-401.

Lapakko, K. A. 1994. «Evaluation of neutralization potential determinations for metal mine waste and a proposed alternative». In *Proceeding: of the international land reclamation and mine drainage conference and 3rd ICARD* (Pittsburgh), p. 129-137.

Lawrence, R. W. & Scheske, M. (1997). "A method to calculate the neutralization potential of mining wastes." Environmental Geology **32**(2): 100-106.

Lawrence, R. W. & Wang, Y. 1997. «Determination of neutralization potential in the prediction of acid rock drainage». In *Proc. 4th International Conference on Acid Rock Drainage, Vancouver, BC*, p. 449-464.

Li, M. 1997. «Neutralization potential versus observed mineral dissolution in humidity cell tests for Louvicourt tailings». In *Proceedings of the Fourth International Conference on Acid Rock Drainage*, p. 149-164.

Nicholson, R. (1994). "Iron-sulfide oxidation mechanisms: laboratory studies." Environmental Geochemistry of Sulphide Mine-Wastes **22**: 163-183.

Paktunc, A. D. (1999). "Mineralogical constraints on the determination of neutralization potential and prediction of acid mine drainage." Environmental Geology **39**(2): 103-112.

Plumlee, G. S., Logsdon, M. J. & Filipek, L. H. (1999). The environmental geochemistry of mineral deposits, Pacific Section Society of economic.

Rimstidt, J. D., Chermak, J. A. & Gagen, P. M. 1994. «Rates of reaction of galena, sphalerite, chalcopyrite, and arsenopyrite with Fe (III) in acidic solutions». In *ACS symposium series*, p. 2-13. Washington, DC: American Chemical Society,[1974]-.

Sobek, A. A., Schuller, W., Freeman, J. & Smith, R. (1978). "Field and Laboratory Methods Applicable to Overburdens and Minesoils." US Environmental Protection Agency, Cincinnati, Ohia **45268**: 47-50.

Villeneuve, M. (2004). Évaluation du comportement géochimique à long terme de rejets miniers à faible potentiel de génération d'acide à l'aide d'essais cinétiques. Maîtrise, Université de Montréal - Ecole Polytechnique Montréal.

10th ICARD IMWA 2015 | 10th International Conference on Acid Rock Drainage & IMWA Annual Conference

A Kinetic Approach to Assessing the Risk of Groundwater Acidification from Sulfidic Soils

Karen Mackenzie[1], Hannah Dannatt[1], Andrew Barker[1], Chris Wendt[2] and Christian Wallis[1]

1. *Golder Associates, Australia*
2. *Theiss Degremont Services Joint Venture; Watersure, Australia*

ABSTRACT

To assess potential impacts to groundwater from the disturbance of acid sulfate soils at a large construction project in coastal Victoria, Australia, an extensive program of fieldwork was undertaken to provide geological, meteorological and hydrogeological inputs into a site conceptual model to assess source, pathway and receptor linkages at the site. Soils were geochemically and geotechnically characterised from both background and disturbed areas, and free draining kinetic columns were constructed using local rainwater as the leachant.

The results of a ten month kinetic leach program were used to assess the potential long term risk posed to the receiving environment from insitu and stockpiled soils and assist in the development of groundwater management measures and improved water management at the constructed facility.

Keywords: Kinetic leach trial, acid sulfate soils

INTRODUCTION

The site is located in an area comprising gentle undulating terrace sand covered plains and alluvial floodplains and swamps (Rosengren and Boyd, 2008) of the early to mid Holocene, affected by both periods of drought (during 2007-2009) and flooding (during the winter of 2013). The groundwater level within the overburden groundwater aquifer at the site was reported to seasonally fluctuate by up to 1.5 m. Soils comprising acid sulfate soils (ASS) are present above and below the groundwater level, across the site, with soils with the highest potential to generate acidity present within the low lying swampy areas.

During the development of the site, ASS had been excavated and placed in stockpiles to represent artificial dunes, while in other areas, insitu ASS was dewatered due to construction activities. Concerns were raised about long term risks presented by ASS oxidation. In response, an extensive program of work was undertaken to evaluate the potential impact of ASS at the site on the surrounding environment.

To assess the risk associated with the release of acid from the disturbed soils a probabilistic statistical assessment of the sulfidic soils sampled at the site was conducted (Barker and Wallis, 2014). A GoldSim model was constructed to undertake a preliminary assessment of fate and transport of non-attenuated solute (i.e. acidic leachate) migrating off-site. In particular, the time it could take for a non-attenuated solute to migrate towards key environmental receptors was conservatively estimated. Two potential receptors; the Powlett River, situated approximately 1100 m east/northeast from the site and a tributary of the Powlett River, situated approximately 500 m from the site were identified.

The results demonstrated that there was a 50% probability that (a non-attenuated) leachate could reach the Powlett River in 12 years and the tributary in 4 years. There was a 5% probability that the leachate would reach the River in less than 2 years. Given the potential for impacts to the surrounding environment, an intensive investigation was undertaken to better understand the acid loads and timing of acidification.

Characterisation of the site conditions comprising assessment for the presence of ASS (using Suspension Peroxide Oxidation Combined Acidity & Sulfur (SPOCAS) analysis) combined with kinetic geochemical characterisation methods was undertaken. Groundwater quality at the site was monitored at a high frequency, through a network of groundwater wells within the overburden material, with a view to capturing local variations to groundwater quality from the construction activities that were ongoing (Dannatt and Wallis, 2014).

The kinetic methods employed were those typically used for mine-related acid drainage projects, this was one of the few construction projects known in Australia where kinetic techniques have been employed in any assessment. The free draining leach column method was modified from the standard methodology (with respect to leachate volumes and frequency of leach events) to reflect the site conditions encountered and the material properties (adapted from McElnea and Ahern (2000)).

The specific objectives of this geochemical leach assessment were to quantify the acid load released from each of the insitu and exsitu areas and provide an indication of the length of time that active management practices would be required.

METHODOLOGY

Sample Collection

Sample locations were selected based on the ASS test results obtained from previous soil investigations. The purpose was to obtain a range of different soil types with varying acidity regimes which would represent typical insitu and exsitu soil conditions. Approximately 4 kg of soil sample was collected from each location using a Geoprobe® drill rig with a push tube system. The soil samples were logged using the Unified Soil Classification System.

Sample Analysis

Samples were submitted to a National Analytical Testing Authority (NATA) accredited laboratory for static geochemical analytical work. A sub-sample of approximately 500 g was sent to Golder geotechnical laboratory for geomechanical testing. Soil samples were analysed for the parameters listed in Table 1.

Table 1 Soil and groundwater analysis methods and parameters

	Standard Parameters	Limit of Reporting
Soil		
Geomechanical	Atterberg Limits	1% and (0.5% for Linear Shrinkage)
pH/Electrical Conductivity	pH (1:5)	0.1 pH units
	EC (1:5)	1 µS/cm
Static Acid Base Account	SPOCAS Suite	pH unit, 2 mole H+/T, 0.02%S
Multi-Elements in Solids	Total Metals (Al, As, Ba, Be, Cd Cr, Co, Cu, Fe, Pb, Mn, Ni, V, Zn)	1-50 mg/kg
	Hg	0.1 mg/kg
	Sulfate	50 mg/kg
	Chloride (Cl-)	10 mg/kg
	Soluble Major Cations (Ca, Mg, Na, K)	10 mg/kg
Multi- Elements in water	Leachable Metals (Al, As, Ba, Be, Cd Cr, Co, Cu, Fe, Pb, Mn, Ni, V, Zn, Hg)	0.0001-0.01 mg/L
Soil Parameters	Cation Exchange Capacity (CEC), Organic Matter, Moisture Content,	0.1 meq/100 g, 0.5%, 1%
X-Ray Fluorescence (XRF)	Fused disc XRF	SiO2 – 0.05%, Cr2O3, MnO, P2O5 – 0.005%:
		Others: 0.01%

X-Ray Defraction (XRD)	XRD and Siroquant Analysis	Generally 0.1%
Leachate		
Acidity	Acidity	1 mg/L
Dissolved Major Anions and Cations	Cl, SO_4, Alkalinity and Ca, Mg, K and Na	1 mg/L
Dissolved Metals	As, Ba, Be, Cd, Co, Cr, Cu, Mn, Ni, Pb, V, Zn, Fe, Al and Hg	Al – 0.01 mg/L, Cd-0.0001 mg/L, Zn–0.005 mg/L, V/Fe–0.05 mg/L Others:0.001 mg/L

Kinetic Leach Column Testing

Two procedures for kinetic testing of solid mine waste materials; the Free Draining Leach Test, described in Appendix E of the AMIRA International ARD Test Handbook (2002) developed in Australia and the ASTM Designation: D 5744 – 96 (Reapproved 2001) accelerated weathering test method developed in the USA. Modifications to the above methods have been made based on available refereed literature describing ASS studies that have utilised column experiments. Further modifications, described below, were made during the running of the leach experiments.

Rainfall collected at the site was used as the leachant. The volume of rainwater used per leach event was initially based on the Bureau of Meteorology's monthly climate statistics for the Wonthaggi Weather Station obtained during the period 1981 to 2010. The aim was to leach the columns with the same amount of water as that which falls on the site in a 20 year period. Based on an average monthly rainfall of 79.2 mm (and taking into account total annual actual evapotranspiration), the volume of rainwater required to be leached through the columns over a 10 month period (to simulate a 20 year period), was 3.4 litres per week (total of 136 L).

Approximately 2.5 kg of 'as received' soil (i.e. no drying or grinding), was placed in each column (C01-C09) except for columns C05 and duplicate column C06 where approximately 1.8 kg of soil was used in the column. The sample weight was corrected to 'dry weight' using the soil moisture content test results.

Four columns comprised soil samples collected from the stockpiled soil (C01, C03, C04, C05) and two columns comprised soil samples collected from the insitu, expected dewatered zone, (C07 and C09). Three duplicate columns (C02 duplicate of C01, C06 duplicate of C05 and C08 duplicate of C07) were also included in the program.

A total of 20 leach events were undertaken for all columns except C05 and C06, where the experiments were terminated early due to the dispersive nature of the material (only 14 and 12 leach events were completed respectively). Samples of leachate are then collected and analysed (presented in Table 1).

During the first one to two leaching events, it was attempted to leach 3.4 Litres through the soil samples, however, due to low the permeability of the soil the method required modification; the frequency of leach events and the volume of leachant had to be reduced. The frequency of leaching

events was reduced from weekly to approximately every 2 weeks and the volume of leachant was reduced to approximately 1.7 litres per sampling event. In addition, following the first leach event, a vacuum pump was employed to assist in the collection of samples as insufficient sample was leaching by free drainage.

For four of the columns (C02, C03, C05 and C06), the volume of leachant had to be further reduced due to the highly dispersive nature of the fines. These challenges provide useful information regarding the soil behaviour and aided the development of the site conceptual hydrogeological model. The total volume of leachant added to each column over the leach events was between 20.1 and 37.4 Litres. This volume is equivalent to that which would be received at the site over a 3 to 5.5 year period.

RESULTS AND DISCUSSION

Pre leached Static

Soils sampled for this study comprised medium plasticity soft silty clay overlying low to medium dense silty sand . The organic matter content ranged from less than 0.5 %, in C09, to 2.1 %, in C07.

The pH (1:5 soil:water) of the exsitu samples range from 5.4 to 6.9 pH units. The pH of the insitu samples ranged from 4.9 to 5.5 pH units with samples from C07 returning the lowest pH values of 4.9 and 5.1 pH units. The EC values of the exsitu samples ranged from 325 to 718 µS/cm and are higher than the EC of the two insitu samples which are 147 µS/cm and 207 µS/cm. The titratable actual acidity (TAA) test results of the exsitu samples ranged from 6 to 13 moles H+/t and were generally lower than the TAA results for the insitu samples which range from 5 to 59 moles H+/t. Insitu soil samples from C07 exhibited the highest TAA test results compared to other samples.

The potential sulfidic acidity (S_{POS}) test results of the exsitu samples ranged from <10 to 47 moles H+/t although the majority of the samples had S_{POS} test results between 12 and 24 moles H+/t. Only one sample (from C04) returned a S_{POS} value of 47 moles H+/t. The SPOS test results of the exsitu samples are generally lower that the S_{POS} test results of the insitu samples which ranged from <10 to 178 moles H+/t. Test results from insitu soil samples from C09 were considerably higher than test results from other soil samples.

Nine of the 12 samples returned S_{POS} values above the laboratory limit of reporting. None of the exsitu or insitu samples contained any retained acidity. None of the exsitu or insitu samples contained acid neutralising capacity (ANC), as measured by acid reacted magnesium or acid reacted calcium. The 'net acidity' values of the exsitu samples ranged from <10 to 54 moles H+/t and were generally, lower than the 'net acidity' value of the insitu samples which ranged from 24 to 183 moles H+/t.

Post-Leach Testing

The concentration of metals within the leachate, over the course of the project is presented in Figure 1.The pH (1:5 soil:water) of all post-leach samples remained comparable to the pre-leach test results except for samples from C01, which returned a higher pH, and samples from C04, C05 and its duplicate C06, and C09 which returned a lower pH. The sample in C01 was the only sample that was leached of all its actual acidity and it is likely that the pH of the post-leach soil was influenced by the pH of rainfall more so that the samples in the other columns. Columns C04 and C09

generated the most amount of acidity via oxidation of sulfides whilst C05 and C06 could not be leached for the full extent of the monitoring program and may have retained some acidity.

Based on the S_{POS} test results of the leached soil, the entire measureable pyrite content of the soil placed within the columns had oxidised during the 10 month leaching program except at C01 and C09 where S_{POS} results of 18 moles H^+/t were recorded post the leach program. At C01, the post-leach S_{POS} result exceeded the pre-leach S_{POS} result (by 4 H^+ mole/tonne) which was likely due to the sample heterogeneity. As C09, the post-leach S_{POS} results was significantly less than the pre-leach S_{POS} result (i.e. reduced by 150 moles H^+/t) however, some potential acidity remained.

The TAA test results are above the laboratory limit of reporting for all samples except C01. This is inferred to indicate that all leached soils, apart from that at C01, contain some actual acidity which has the potential to be leached in the future; moderate levels of TAA (~30 moles H+/t) were recorded in columns C04, C07 and C08 whilst low levels (<15 moles H+/t) were recorded in the remaining columns.

Leachate Quality

In general, leachate from C04 (exsitu soil) and C09 (insitu soil) contained the highest concentrations of metals (Figure 1). At C09, the concentrations of metals in the leachate rose until leach event 4 to 5 after which the dissolved metal concentrations in the leachate began to decline. This trend is consistent with the trends in decreasing pH and increasing sulfate (Figure 2). A second increase in dissolved Al, As, Fe and Zn concentrations was observed in the leachate from C09, following leach event 10. This trend is consistent with a second rise in sulfate concentration and drop in pH post leach event 10 (Figure 2 (iii)).

The trend in dissolved metal concentrations (i.e. decrease following initial leach events) was similar for all metals except Cu where the concentration generally increased during the testing period. Based on this trend, the dissolved Cu test results suggest that Cu in the soil in column C09 is more strongly attenuated than other metals tested and the rate of Cu release increases when the pH drops to below approximately 2.6 pH units. Low levels of dissolved Al and Fe were detected in the leachate which was expected given the static test results for these metals.

Dissolved Al is likely present due to the dissolution of aluminosilicate clay minerals following the drop in pH whilst the dissolved Fe is likely present due to the dissociation of pyrite within the samples.

Leachate results were compared to groundwater quality at the site. Groundwater quality was found to be relatively stable when teh whole site was considered. Localised variability was recorded, but these impacts could be correlated to the construction activities in close proximity to the monitoring point, thus impact from the acidic run off were not identified . Nevertheless, as a precautionary measure, run off from the stockpiles at the site is collected in a network of drains and treated.

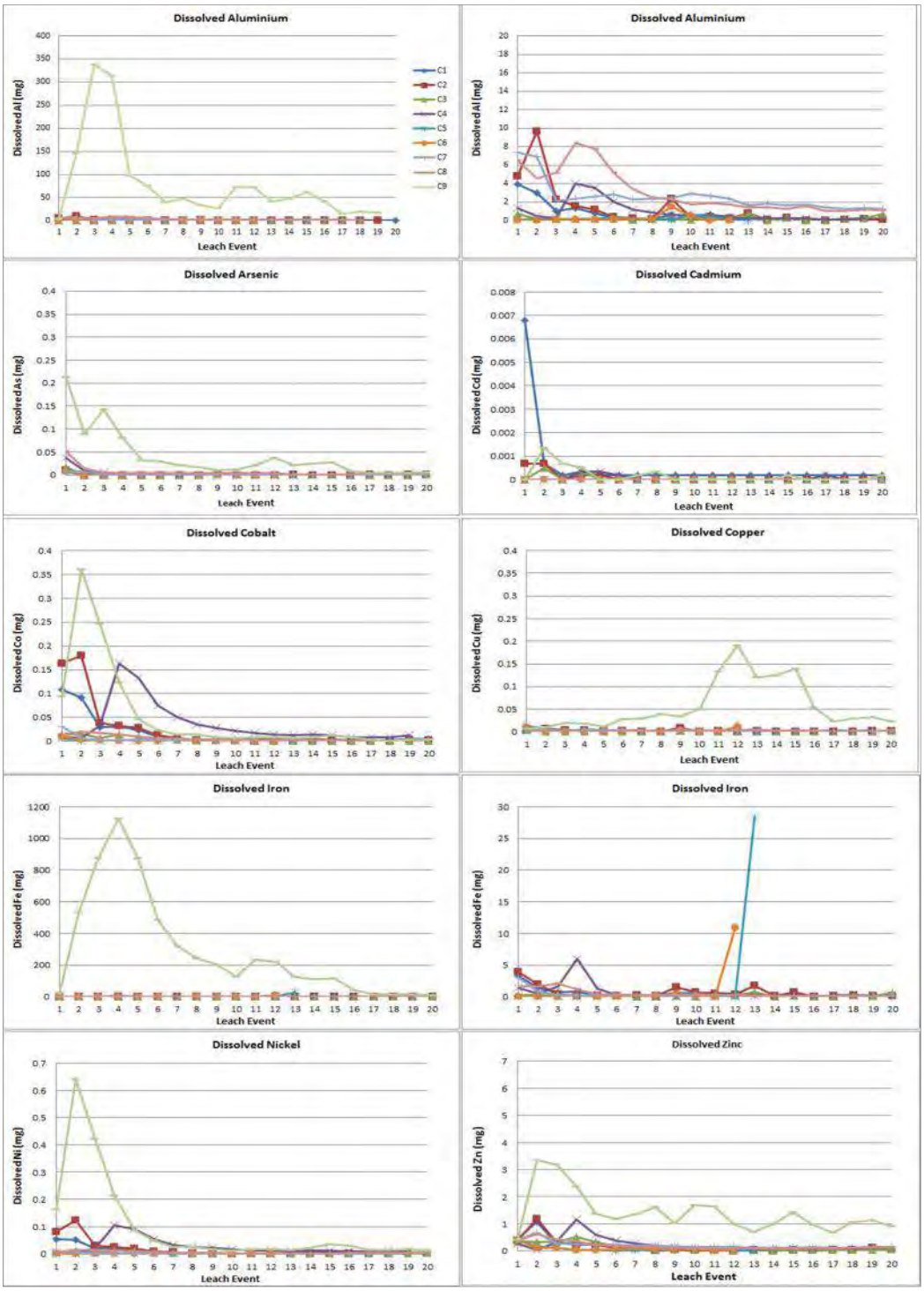

Figure 1 Comparison of dissolved metal concentrations in leachate.

XRF/XRD Analysis

Based on the results of the XRF analysis, the leached samples predominantly comprised silica (SiO_2) with lesser amounts of Aluminium Oxide (Al_2O_3; up to 9.55%), Iron Oxide (Fe_2O_3; up to 2.42%) and Potassium Oxide (K_2O; up to 1.46%).

Secondary iron minerals, such as jarosite and schwertmannite which commonly precipitate from iron-sulfate rich waters, were not identifiable within samples via XRD. This may be because they are only a minor component of the sample matrix (i.e. newly formed minerals). Alternatively they lack sufficient crystallinity to be detected. Freshly precipitated secondary minerals are likely to be highly amorphous and lack a regular crystalline structure.

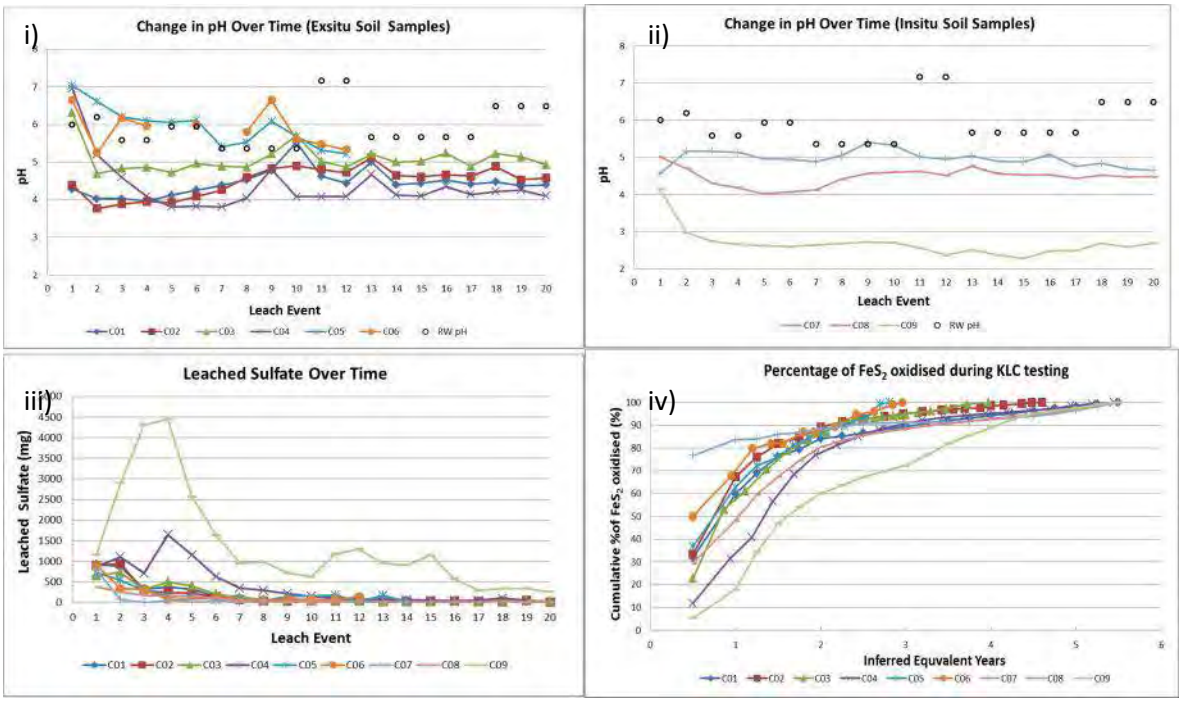

Figure 2 Change in pH over the leaching period for exsitu (i) and insitu (ii) samples. Rainwater pH (RW pH) also shown, iii) Sulfate export from the columns, iv) rate of sulfate generation / pyrite oxidation, assumes 100% of sulfate was leached during experiment.

Pyrite Oxidation Rates

Preliminary pyrite oxidation rates were calculated using the static and kinetic leach testing results. The assumptions used during this assessment are summarised as follows: (i) the samples are representative of the material in the constructed dunes; (ii) total pyrite content is calculated from the sum of sulfate in the leachate; (iii) the role of Fe(III) in the pyrite oxidation is limited given the low Fe concentration in waters at the site; (iv) by leach event 20, all of the pyrite has oxidised.

The cumulative percentage of FeS_2 oxidised over the course of the experiment was calculated through measurement of the sulfate generation over time and assuming oxygen as the primary oxidant. The rate of pyrite oxidation was plotted against the inferred equivalent field time (based on volume of leachant), as shown in Figure 2 (iii) and (iv).

It was noted that the oxidation rate decreased at approximately the 2.5 year mark, thus the assessment of acid loads to the environment two rates were used: within the first 2.5 years of oxidation, and following 2.5 years of oxidation. The oxidation rates for soil collected from the site are summarised as follows; oxidation rate within 2.5 years of disturbance, was estimated to range between 2 x 10-7 to 1.3 x 10-6 % pyrite oxidised per second. Oxidation rate following 2.5 years of disturbance, was estimated to range between 1 x 10-7 to 3.6 x 10-7 % pyrite/ sec. These rates are within the range reported in the literature (1 x10-7 to 2 x 10-4 % pyrite/ sec, (Hipsey and Salmon, 2008).

CONCLUSION

Based on the pyrite oxidation rates estimated during these works, the risks to groundwater from the oxidation of pyrite (within insitu and exsitu ASS) was most significant during the first and second year of soil disturbance and dewatering (2009 and 2010). However, based on groundwater monitoring (Dannatt and Wallis, 2014), the acid load released to groundwater during this time may not have caused acidic conditions to form; the construction period being as long as the acid generation period. Thus, the significant amount of high alkalinity construction materials (i.e. concrete) used at the site to potentially buffered the groundwater pH.

As the acid formation from the insitu and exsitu ASS is likely to reduce with time, as the rate of oxidation of pyrite stabilises and the potential acid load is significantly depleted, the long term risks to groundwater (i.e. following 2013) are likely to be limited. As a response to this, groundwater monitoring frequency has been reduced to quarterly events.

ACKNOWLEDGEMENTS

We would like to thank Dr Silvana Santomartino for her contribution to the project. Her expertise in the laboratory analysis of acid sulphate soils and data processing was most useful in the early phase of the project. We also wish to thank Dr Angus McElnea for his mentorship of Silvana.

REFERENCES

ASTM D5744-96, Standard Test Method for Accelerated Weathering of Solid Materials Using a Modified Humidity Cell, ASTM International, West Conshohocken, PA, 2001, www.astm.org

ANZECC (2000). Australian Water Quality Guidelines for Fresh and Marine Waters, Australian and New Zealand Environment and Conservation Council, Australia.

Ball and Nordstrom (1991). Ball, J.W., and Nordstrom, D.K., 1991, User's manual for WATEQ4F, with revised thermodynamic data base and test cases for calculating speciation of major, trace, and redox elements in natural waters: U.S. Geological Survey Open-File Report 91-183, 189 p. (Revised and reprinted August 1992.)

Barker, A, and Wallis, C (2014) An application of probabilistic modelling of total acid loads to improve ASS risk characterisation and communication. In: "Proceedings of the 4th National Conference on Acid Sulfate Soils". 20th-21st May 2014, Perth, Australia.

Dannatt. H, and Wallis, C. (2014) Application of high frequency groundwater monitoring to distinguish potential ASS impacts from the dynamic nature of background conditions. In: "Proceedings of the 4th National Conference on Acid Sulfate Soils". 20th-21st May 2014, Perth, Australia.

Golder Associates Pty Ltd 2013, Geochemical Assessment of Exsitu and Insitu Acid Sulfate Soil, unpublished report, Australia.

Hipsey, M.R., Salmon, S.U. (2008) Numerical Assessment of Acid-Sulfate Soil Impact on the River Murray Lower, Centre for Water Research, Western Australia.

Ian Wark Research Institute and Environmental Geochemistry International (2002) AMIRA P387A Project ARD Test Handbook, AMIRA International Limited, Australia.

McElnea AE, Ahern CR (2000) Effectiveness of Lime and Cement Kiln Dust as Acid Sulfate Soil Ameliorants – Leaching Column Experiments. In 'Acid Sulfate Soils: Environmental Issues, Acid Sulfate Soils Laboratory Methods Guidelines, Version 2.1, A1 – 11, Assessment and Management, Technical Papers'. (Eds CR Ahern, KM Hey, KM Watling, VJ Eldershaw) pp. 30/1–30/12 (Queensland Department of Natural Resources: Brisbane).

National Environmental Protection Council (NEPC) (1999). National Environment Protection (Assessment of Site Contamination) Measure (NEPM). Guideline on Investigation Levels for Soil and Groundwater, Groundwater Investigation Levels.

Rosengren. N, and Boyd. C (2008) Existing site conditions, Impacts and Risk Assessment, Geology, Geomorphology and Acid Sulfate Soils, Rosengren. N, and Boyd. C, Bendigo, Victoria.

Comparison of Actual and Calculated Lag Times in Humidity Cell Tests

Kelly Sexsmith[1], Dylan MacGregor[1] and Andrew Barnes[2]

1. *SRK Consulting, Canada*
2. *SRK Consulting, United Kingdom*

ABSTRACT

It is common practice to run humidity cell tests on potentially acid generating rock or tailings samples to determine the amount of time it will take for acidic conditions to develop—often called "lag time". Defining lag time is important for understanding when management plans need to be in place for preventing or mitigating acid rock drainage. The lag time is a function of the amount of neutralization potential (NP) present in the rocks and rate of sulphide oxidation and therefore NP depletion. Although direct observations of lag times are possible, it is relatively rare for acidic conditions to develop over the course of a laboratory test. Therefore, lag times are more often calculated.

This paper explores the relationships between actual measured lag times versus calculated lag times for two groups of samples: 1) where acidic conditions developed following a distinct lag time, and 2) where acidic conditions should have developed, but did not develop despite an extended period of testing. The results show that actual lag times tend to be shorter than calculated lag times, demonstrating the importance of using conservative assumptions in the calculations of lag time as well as running some tests for an extended period of time to obtain site specific information on lag times. In addition the paper reiterates the importance of quantifying available NP rather than simply adopting measured NP results available from commonly measured NP procedures.

Keywords: Lag Time, Humidity Cell Test, Prediction, Management

INTRODUCTION

Generation of acid rock drainage (ARD) is a time dependent process in which oxidation of sulphide minerals results in the release of sulphate and acidity. Weathering of silicate minerals and/or dissolution of carbonate minerals may produce sufficient alkalinity to buffer the pH. In addition, reactions between sulphide oxidation products and carbonate and/or silicate minerals may further buffer the pH. In potentially acid generating mine wastes, the relative rates of acid production and acid consumption will determine: 1) whether acidic conditions will develop rapidly – due to insufficient rates of neutralization; or 2) whether there will be a delay in the onset of acidic conditions - due to a finite or limited amount of neutralization potential (NP). Along with rates of acid production, the amount and the availability of the NP will determine how long buffering reactions will persist.

Where present, the delay in the onset of acidic conditions is typically referred to as the "lag time". Lag times are important for understanding when management plans need to be in place to prevent or mitigate the effects of ARD. For example, where lag times are sufficient to ensure neutral pH conditions can be maintained for a period of time, it may be possible to backfill, place covers, or freeze the material to prevent ARD from developing. Similarly, it may be possible to delay the construction of a treatment plant, and thereby defer some of the start-up costs for period of time.

The lag time is a function of the amount and availability of NP present in the rocks and rate of sulphide oxidation and therefore NP depletion occurring as these rocks are exposed to air and water. Although direct observations of lag times are possible, it is relatively rare for acidic conditions to develop over the course of a laboratory test – even in samples that are potentially acid generating. More often, acidic conditions develop very early in the lab test due to insufficient rates of neutralization, or they don't develop at all due to slow rates of NP depletion. Therefore, lag times are more often calculated using data from humidity cell tests. Although the calculations are based on reasonably straightforward inputs, they are subject to a number of uncertainties, including the accuracy of measuring the NP and the rates of sulphide oxidation and NP release, the availability and reactivity of the NP, and other factors such as deposition of secondary minerals on mineral surfaces which may reduce the availability of the NP or result in reduced reaction rates. Estimates of lag times are also typically adjusted to reflect field conditions such as differences in temperature which can reduce reaction rates and further delay the onset of acidic conditions.

To better understand the magnitude of uncertainty in estimating lag times in the laboratory setting, we compiled data from a number of long term humidity cell tests and explored the relationship between actual versus calculated lag times in two groups of samples: 1) where acidic conditions developed following a distinct lag time, and 2) where calculations indicated that acidic conditions should have developed, but didn't develop despite an extended period of testing.

METHODOLOGY

SRK has compiled an inventory of results from over 229 humidity cell tests representing 33 sites internationally. Of these, 42 tests from 15 of these sites were identified as possible candidates for this study either because acidic conditions developed after distinct lag time to onset of acidic conditions, or acidic conditions had not developed, but the predicted lag times were reasonably close to or less than the test duration, indicating that acidic conditions could have developed. Key static and kinetic test results for each of these samples were compiled, and the calculations of NP

depletion were checked to ensure that consistent calculation methods were applied. On further review, 12 of the non-acidic tests were eliminated because the calculated lag times exceeded the test duration (i.e. there was no reason to expect that acidic conditions should have developed). The final dataset was comprised of 30 tests from 14 sites, with test durations ranging from 80 to 520 weeks. Thirteen of these tests are still operating.

Due to the large number of programs and the time frame over which these tests were completed – dating back almost 20 years, there were some minor variations in the static and kinetic testing methods. Most of the ABA tests included analysis of total inorganic carbon (TIC), and either Modified Sobek NP (MEND 1991), Sobek NP (Sobek et al., 1978), or with the European Standard EN15875 (CEN, 2011) procedure which itself is based on the Modified Sobek NP procedure. All of the humidity cell tests were completed using either flood or trickle leach variations of the MEND or ASTM method for humidity cell tests (ASTM 2001, MEND 1991). Lastly, the mineralogy was characterized using petrographic analysis and/or Reitveld XRD for most of the samples.

The actual lag time was defined as the point in time where the pH dropped below a value of pH 5, as shown in Figure 1. This pH was selected to ensure that acidic conditions were due to sulphide oxidation, rather than equilibrium with atmospheric carbon dioxide.

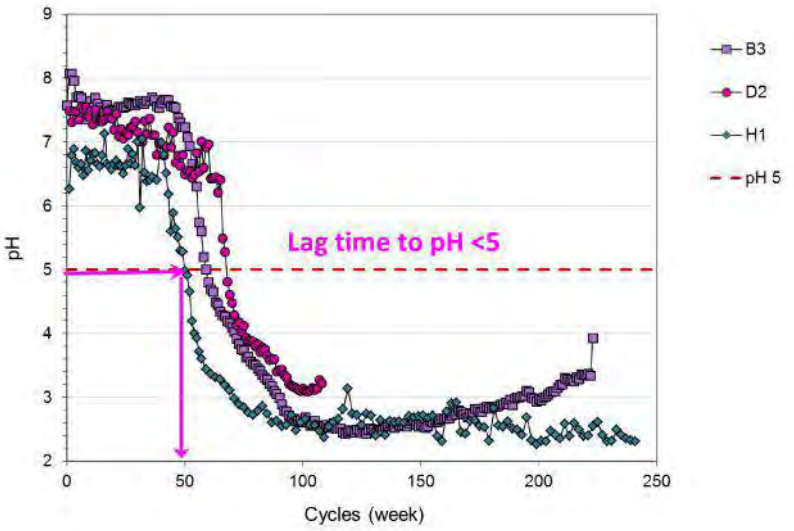

Figure 1 Definition of "actual lag times" used in this study

Calculated lag times were determined using the following two methods:

$$Time\ to\ NP\ depletion\ = \frac{NP*}{(Ca+Mg)\ release\ rate} \qquad \text{(equation 1)}$$

or,

$$Time\ to\ NP\ depletion\ = \frac{NP*}{SO_4\ release\ rate} \qquad \text{(equation 2)}$$

Where: NP* is the available NP in units of kg $CaCO_3$ eq/t (described below)

(Ca+Mg) and SO_4 release rates are the steady state non-acidic release rate from the humidity cell test in units of kg $CaCO_3$ eq/t/year.

For most of the samples examined in this study, these two calculation methods gave similar depletion times because the molar ratios of SO4/(Ca+Mg) in the humidity cell leachate were close to unity.

The available NP (NP*) was estimated based the TIC or NP titration method (Sobek, Modified Sobek or EN15875) that was considered to be most appropriate for the sample or project site, and further adjustments to account for limitations on the availability and/or reactivity of the NP. The following types of adjustments were made to account for these limitations:

- Site specific "unavailable" NP was estimated based on the TIC or NP found in samples with acidic paste pH values, and was subtracted from the TIC or NP.
- TIC was multiplied by a factor that represented the Ca+Mg content of the carbonates (Day 2009).
- TIC or NP was divided by a factor representing the relative availability of NP/AP (NP/AP_{crit}) established through kinetic testing. (NP/AP_{crit}) is typically a value between 1 and 1.5.
- For sites where there was no specific information as to whether TIC or NP was more appropriate for a site, or where site specific correction factors could not be established, the lesser of the TIC or NP value was selected and this was divided by an NP/AP_{crit} factor of 1.5.

For one site (Site N), NP was measured using both the normal EN15875 method in finely pulverized material, and an alternative method on samples with a particle size distribution equivalent to that used in the humidity cell test – without size reduction, making it possible to determine the amount of NP that was physically available in the humidity cell test. The results ranged from 0.34 to 0.66 (average of 0.53), indicating that roughly half of the NP was physically available. However, for consistency with the other data sets which did not have this type of data, these results were not explicitly considered in determining of NP* for these tests.

The (Ca+Mg) and SO_4 release rates were based on the steady state release rates established for the period of the test prior to the onset of acidic conditions. This is an important point because these rates often increase in response to decreasing pH conditions, and since the point of the calculation is to determine the time to onset, rates must reflect the period prior to onset of acidic conditions. Additionally, it was important to establish that these rates were not governed by dissolution of primary gypsum or anhydrite in the samples or by gypsum precipitation – which can occur in samples with very high oxidation rates and large amounts of calcite.

The comparisons of actual and calculated lag times inherently consider the combined effects of the variables that are included in these calculations – notably NP* and the (Ca+Mg) or SO_4 release rates. To explore secondary relationships, regression analysis was used to establish the relationship between actual and calculated values, and the residuals were plotted against other variables, including the rate of acidification (i.e. pH unit/week), the difference between NP* and TIC, (Ca+Mg)/SO4 release rates, sulphur content and sulphate production rates. A more qualitative approach was used to assess potential influences of mineralogy on the results.

RESULTS AND DISCUSSION

Sample Characteristics

Table 1 presents key results from the static and kinetic tests, and the actual and calculated lag times for each of the samples.

The ABA results (Table 1 and Figure 2) indicate that the majority of these samples had very low TIC and NP and high AP, with TIC/AP and NP/AP ratios consistently well below 1, indicating that they were all samples with a strong potential for ARD. As indicated previously, these samples represent a relatively small portion of the total number of samples in the kinetic test inventory, which suggests that delayed onset to acidic conditions is relatively rare and almost always occurs in material with very low NP and relatively high sulphide contents.

The pH profiles from the humidity cell tests (Figure 3) show a range of patterns. In some tests (Figure 3a), there is a distinct period when pH conditions are maintained at constant levels in the range of pH 6.5 to 8, and then a rapid drop in pH. In some (Figure 3b, 3c), there is a distinct period with constant pH, but then a more gradual drop in pH that is sometimes accompanied by large oscillations in pH over an extended period of time. In others (Figure 3d), the pH starts to drop early on in the test, but decreases very gradually, resulting in effective delays of more than 20 weeks before dropping below a pH of 5. Arguably samples from this last group does not show a distinct lag to onset of ARD, but were retained for use in the study to see if they would provide further insights in the determination of lag time.

Calculated versus Actual Lag Times

Comparisons of calculated versus actual lag times are shown in Figure 4. The results indicated that a small number of tests (5/30) had calculated lag times that were shorter than actual lag times. However, in most tests, calculated lag times were longer than actual values, and there was a reasonable relationship between these values (r = 0.62 and 0.67 for the two calculation methods respectively). A small number of tests were also treated as outliers because they had calculated lag times that were much longer than actual values. Further discussion of the outlier results is provided in the following section.

Although we expected to find a number of tests where the acidic conditions should have developed but didn't develop over the course of the test, only one test met this criterion (plotted on Figure 4 using test duration in lieu of actual lag time). This also supports the conclusion that acidic conditions tend to develop more rapidly than expected based on standard calculation methods used to assess lag times.

Linear regressions on these relationships indicate that, on average, predictions of lag time would be improved if the calculated lag times are multiplied by a factor of 0.73 (based on the calculation shown in equation 2). In other words, predicted lag times should be calculated as follows:

$$predicted\ lag\ time\ = 0.74 \times \frac{NP*}{SO_4\ release\ rate} \qquad \text{(equation 3)}$$

Interestingly, this factor is reasonably close to the "physical availability" that was measured in samples from Site N, suggesting that more rapid onset of acidic conditions could be, in part, a function of reduced NP availability in coarser particles in these samples.

Table 1 Sample Characteristics, Actual and Calculated Lag times

Test	Duration	S(T)	S(SO4)	AP	TIC	NP	NP*	NP*/AP	Release rates		Calculated Lag		Actual Lag time		Rate of	Mineralogy
									Ca+Mg	SO4	eqn 1	eqn 2	to pH<6	to pH<5	pH change	
	weeks	%	%	kg CaCO3/t					kg CaCO3 eq/yr		years		years		su/wk	
A1	295	0.71	0.01	22	0.83	10	0.83	0.04	0.38	0.33	2.2	2.5	3.3	4.5	0.01	no carbonate, Ca+Mg silicates
A2	295	1.86	0.01	58	1.7	9.2	1.7	0.03	0.67	0.61	2.5	2.7	1.4	2.1	0.04	calcite > analytical TIC, Ca+Mg silicate
A3	266	2.21	0.02	68	12	18	12	0.17	1.3	1.4	(8.7)	(8.3)	1.1	1.3	0.09	calcite, Ca+Mg silicates
B1	442	0.73	0.01	23	7.5	7.0	5.4	0.24	0.8	0.31	6.4	(17.4)	4.1	4.7	0.02	Ankerite/ankerite dolomite
B2	223	0.93	0.02	29	4.2	4.0	3.1	0.11	1.4	1.4	2.1	2.2	1.0	1.1	0.25	Ankerite/ankerite dolomite
B3	223	0.98	0.02	31	5.0	3.0	2.3	0.08	1.7	1.6	1.4	1.4	1.1	1.2	0.25	Ankerite/ankerite dolomite
B4	223	1.1	0.02	34.4	52	5	3.8	0.11	2.3	1.3	1.7	3.0	>4.3	>4.3	na	
C1	154	3.27	0.06	100	5.8	10	4.9	0.05	1.7	2.2	2.8	2.2	1.2	1.7	0.04	tr calcite, 40% quartz, 40% illite.
D1	98	0.57	0.01	18	0.80	3	0.53	0.03	0.43	0.52	1.2	1.0	0.7	0.8	0.14	no carbonate
D2	108	0.27	0.02	6	1.7	3.5	1.1	0.19	0.42	0.33	2.7	3.4	1.3	1.3	0.18	tr carbonate
D3	81	0.38	0.01	11	0.80	1.2	0.53	0.05	0.18	0.28	3.0	1.9	0.5	0.7	0.10	no carbonate
D4	104	0.59	0.01	16	0.83	8.5	0.56	0.03	0.27	0.37	2.1	1.5	0.6	1.0	0.06	tr carbonate
E1	313	36	0.72	1087	72	62	41	0.04	32	32	1.3	1.3	1.4	1.8	0.06	calcite
F1	173	2.91	0.34	80.3	20	11	7.1	0.09	2.0	2.0	3.5	3.4	2.3	2.8	0.05	no data
F2	118	1.15	0.11	35.9	39	19	6.2	0.17	1.8	1.8	3.5	3.5	1.9	2.3	0.05	no data
G1	296	9.1	0.04	283	11	15	7.6	0.03	0.36	0.44	(21.0)	(17.2)	1.2	1.5	0.05	no carbonate by XRD
G2	296	6.7	0.1	198	6.8	6.5	4.3	0.02	2.4	2.8	1.8	1.6	0.0	0.9	0.03	calcite
G3	296	6.4	0.1	189	6.8	6.2	4.1	0.02	4.3	4.8	1.0	0.9	0.0	0.3	0.11	no carbonate
H1	241	6.04	0.1	186	8.0	1.0	4.7	0.03	4.3	4.3	1.1	1.1	0.8	1.0	0.20	calcite and dolomite, but low mod NP
H2	369	2.48	0.05	76	58	5.2	3.1	0.04	1.2	1.3	2.6	2.4	2.1	3.0	0.02	high siderite
I1	96	1.6	0.01	50	4.1	6.8	2.8	0.05	2.0	2.2	1.4	1.3	0.5	0.6	0.15	no data
J1	520	4.4	0.01	136	11	6.0	7.3	0.05	1.7	1.8	4.2	4.1	2.7	4.0	0.02	pale brown carbonate (poss ankerite)
J2	520	2.4	0.01	73	48	57	32	0.43	3.8	4.4	8.3	7.2	3.4	5.2	0.01	calcite vienlets
K1	201	13.2		243.5	na	7.3	4.9	0.02	na	0.96	na	5.1	1.4	2.1	0.01	no carbonate
L1	113	1.16	0.01	36	2.0	6.4	1.4	0.04	1.0	0.90	1.4	1.5	1.1	1.7	0.04	calcite with minor ankerite and
M1	79	1.06	0.04	30	25	23	20	0.65	5.2	7.0	3.8	2.8	0.6	0.7	0.25	no data
N1	169	3.25	0.27	93	8.3	11	5.6	0.06	2.0	1.8	2.7	3.0	1.9	2.9	0.03	calcite
N2	169	2.92	0.11	88	57	36	24	0.27	1.5	1.5	(16.3)	(15.9)	1.9	2.5	0.02	-
N3	169	0.76	0.05	22	3.3	4.8	2.2	0.10	0.5	0.4	4.8	5.5	1.9	2.8	0.03	-
N4	169	3.07	0.29	87	3.3	3.8	2.2	0.03	0.9	1.0	2.5	2.2	1.5	2.1	0.03	-

Notes: Blue text indicates less than detection limits. Red text indicates outliers.

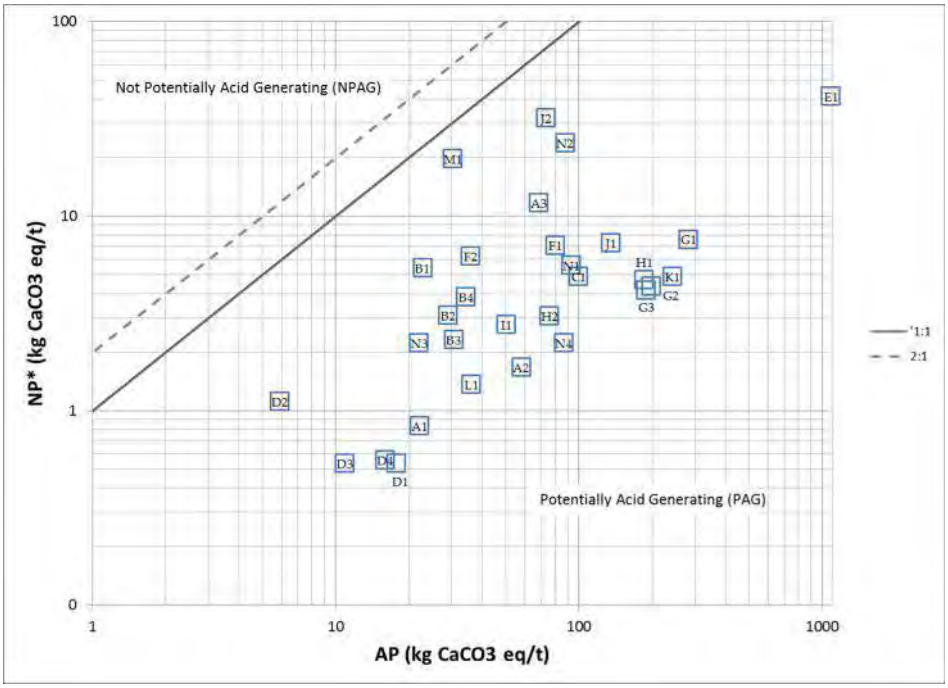

Figure 2 NP versus AP results for this dataset. Labels indicate the site and test number

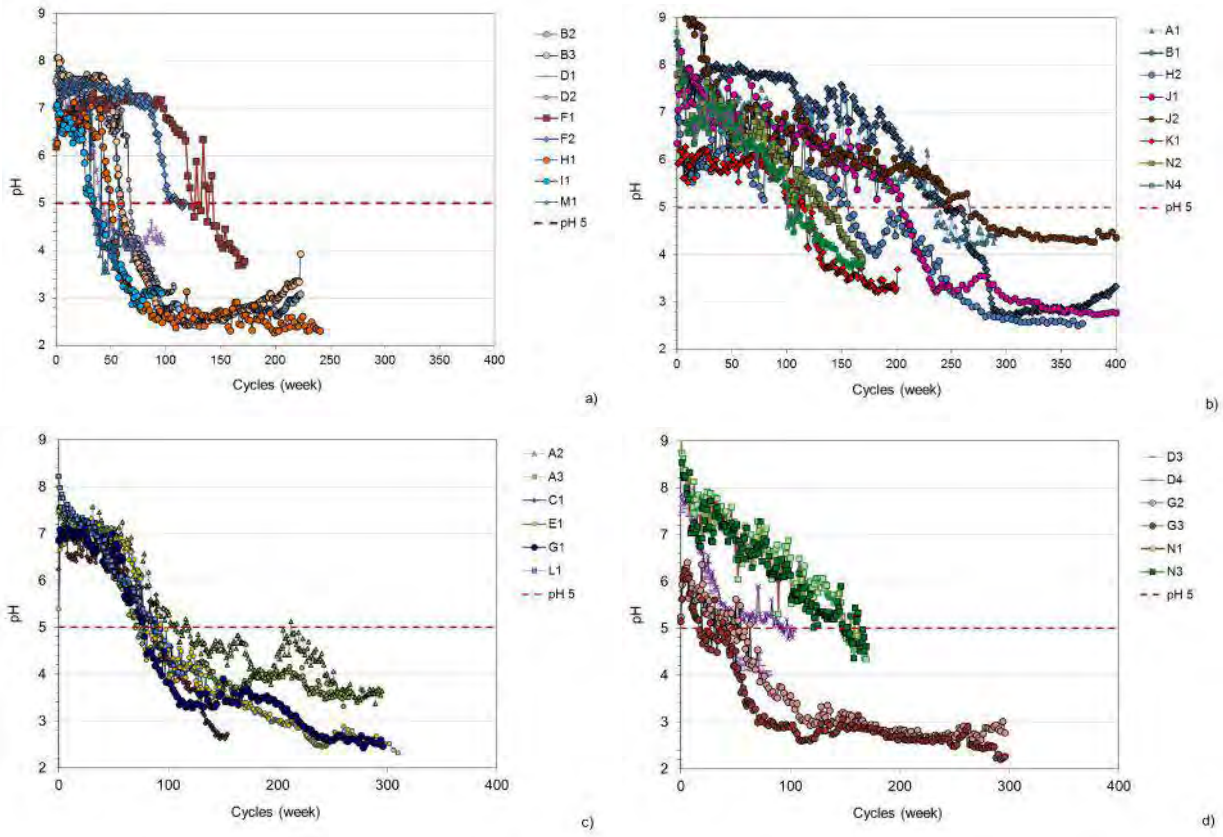

Figure 3 pH profiles from humidity cell tests.

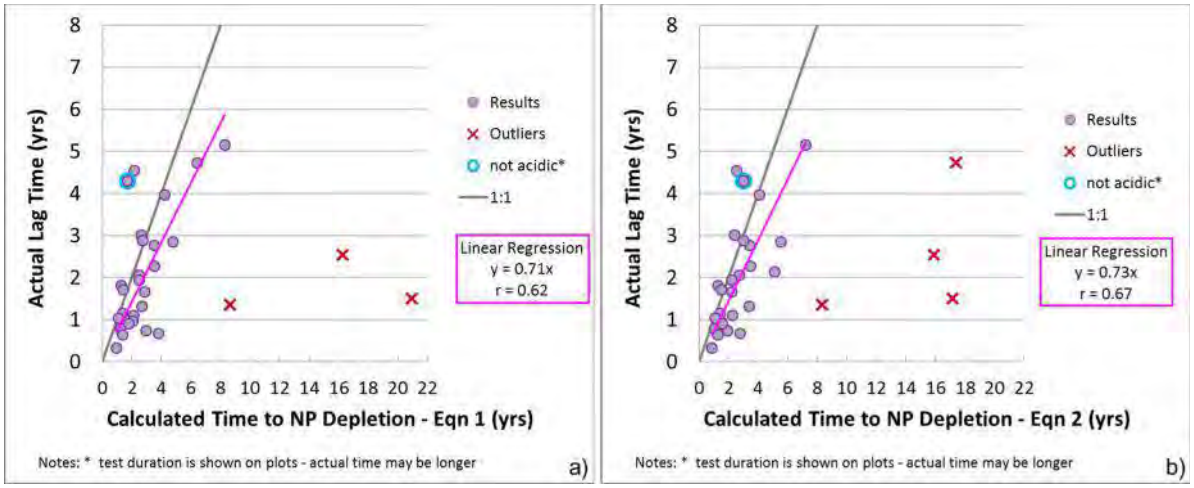

Figure 4 Comparison of actual versus calculated lag times a) using NP release rates (equation 1), b) using SO4 release rates (equation 2).

To assess the potential effects of other variables, the difference between actual and predicted lag times (equation 3) was calculated, and these residuals were plotted against other variables, including the rate of acidification, the difference between NP and TIC, (Ca+Mg)/SO4 release rates, sulphur content and sulphate production rates. The results are summarized as follows:

- The rate of pH change showed the strongest secondary relationship explaining 25% of the remaining variance (r^2 = 0.25) (Figure 5a). Samples that exhibited more gradual (slow) acidification tended to show longer than expected lag times, while samples that exhibited faster acidification tended to show shorter than expected lag times. This may be explained in part by the choice of pH used to define lag time in this study. If a higher pH threshold had been selected, actual lag times would be much shorter in the samples with slow pH changes, and essentially unchanged for the samples with more rapid pH changes.
- Samples with large differences between NP and TIC also tended to show longer than expected lag times (Figure 5b). However, this is based on only two samples with large differences between NP and TIC, and may not be statistically significant. In these samples, the TIC may have been contributing some buffering capacity not accounted for by the NP titration, or the discrepancy could indicate that the NP was underestimated.
- There was essentially no relationship between the residuals and ratios of (Ca+Mg)/SO4, total sulphur content or sulphate production rates.

A more qualitative approach was used to evaluate potential relationships with mineralogy, specifically the presence of calcium magnesium carbonates, iron carbonates, and calcium magnesium silicate minerals. Samples with relatively low carbonate, but with favorable silicate minerals tended to have longer than expected lag times, and samples with iron carbonates tended to have longer than expected lag times. However there were several exceptions and no clear patterns were evident. We also note that samples with shorter than expected lag times had NP measurements that were inconsistent with mineralogy or TIC, suggesting that the differences could have been due to analytical variability. Given that this dataset tended to have such low NP, it is not surprising that variability in lab measurement could be an important factor.

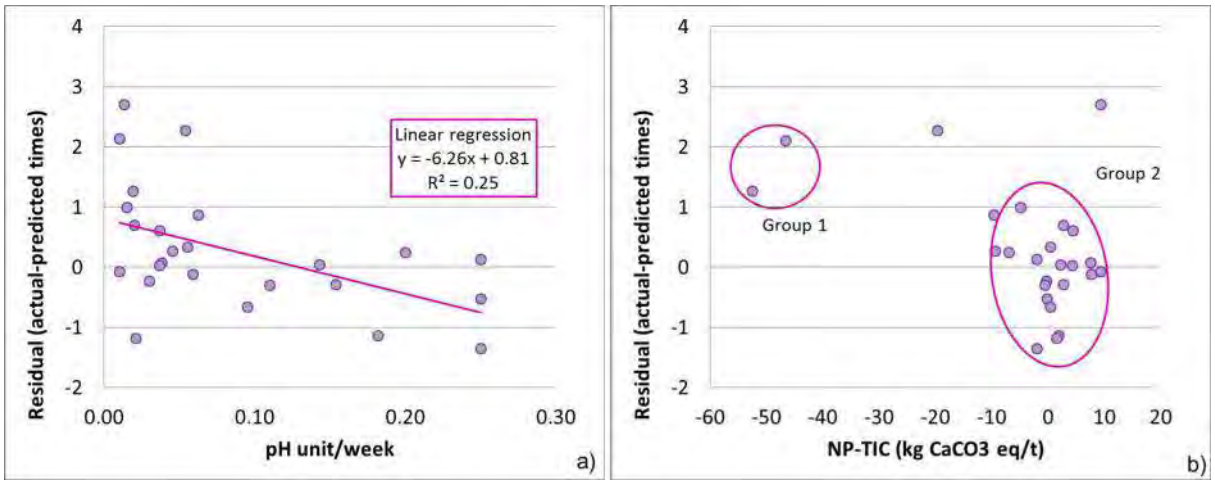

Figure 5 Relationships between residuals and a) rate of pH change and b) NP minus TIC

Outliers

Both calculation methods resulted in a small number of samples with calculated lag times that were substantially longer than the lag times actually observed in those tests. The calculated lag times based on equation 1 produced three outliers, while the calculated lag times based on equation 2 produced four outliers. The outliers were all from different sites. The outliers were closely examined to determine whether there were any unique features that could explain the large discrepancies between calculated and actual lag times, however, none were identified. Although it is believed that these differences could be due to inaccuracies in the quantification of available NP, they do suggest that calculations of lag time can lead to erroneous results. This finding emphasizes the importance of considering a range of samples in the determination of lag time, conducting quantitative mineralogy to provide independent verification of chemical determinations and having thorough QA measures in place to validate analytical results through duplicates and re-checks.

CONCLUSIONS

Data were compiled from a number of long term humidity cell tests to explore the relationship between actual versus calculated lag times. These number of tests in which lag time can be measured is rare and represents a relatively small portion of the total number of tests that were reviewed (30 out of 229 tests). The vast majority of samples that showed a distinct lag time prior to onset of acidic conditions had very low NP and relatively high sulphide concentrations. Key findings of this study are as follows:

- Calculated lag times were typically longer than actual lag times, but were significantly correlated ($r = 0.67$).
- Estimates of lag time can be improved by selecting the most appropriate NP (usually the lesser of TIC or NP), and by applying correction factors to account for availability/reactivity. These may be further improved by considering limitations on the physical availability.

- Tests with the longer than expected lag times showed a relatively gradual change in pH.
- The results emphasize the value of running some tests for an extended period of time either to determine actual lag times or to demonstrate that there is a prolonged period of neutral pH conditions in cases where the lag times are expected to last for an impractically long time.

It is emphasized that these conclusions may not be appropriate for samples with higher NP and/or lower sulphide content. However, there is insufficient data on lag times for those types of samples due to the long times required to measure onset of acidic conditions. Estimation of lag times in the field present further challenges and should be verified through appropriate monitoring programs.

ACKNOWLEDGEMENTS

Data used in this study was from a number of geochemical characterization programs that were completed by SRK in support of mining or mine development projects. We would like to acknowledge and thank the many companies that funded these programs and allowed us to use the data. Additionally, we are grateful for the support provided by our colleagues at SRK that helped to prepare the sample inventory and identify candidate tests for this work.

NOMENCLATURE

AP	acid potential
ARD	acid rock drainage
NP	neutralization potential
NP*	available neutralization potential
TIC	total inorganic carbon (a measure of carbonate content)

REFERENCES

ASTM, 2001 (and subsequent revisions). Standard Test for Accelerated Weathering of Solid Materials Using a Modified Humidity Cell. Designation: D 5744-96 (Reapproved 2001).

Day, S. 2009. Estimation of Calcium and Magnesium Carbonate Neutralization Potential for Refined Acid-Base Accounting Using Electron Microprobe and X-Ray Diffraction. Proceedings of 8th International Conference on Acid Rock Drainage. Skellefteå, Sweden, June 23 to 26, 2009.

MEND, 1991. Acid Rock Drainage Prediction Manual. MEND Project 1.16-1b. Report prepared by Coastech Research for CANMET. (see http://www.nrcan.gc.ca/mms/canmet-mtb/mmsllmsm/mend/mendpubs-e.htm for publication information).

CEN, 2011. EN15875 - Characterization of waste – Static test for the determination of Acid Potential and neutralization potential of sulfidic waste. European Centre for Standardization (CEN). October 2011.

Sobek A A, Schuller W A, Freeman J R, and Smith R M., 1978, Field and laboratory methods applicable to overburden and minesoils. USEPA Report No. 600/2-78-054, 203 pp.

Evaluation of Humidity Cell Test Precision from an Ongoing Geochemical Characterization Program

Stephanie Theriault[1], Tamara Diedrich[1] and Stephen Day[2]

1. *Barr Engineering Company, USA*
2. *SRK Consulting, Canada*

ABSTRACT

Data from humidity cell tests (HCTs) are often used during mine development to design appropriate rock management plans and engineered systems, and can provide critical source terms in the predictive modelling of mine-impacted water quality. Information on reproducibility and repeatability of HCTs, in general, can be useful in providing a basis of reference during both the design of the HCT programs, and in the review of the quality of data used for making decisions, or forming inputs to the predictive models. Lapakko and White (2013) conducted repeatability and reproducibility analyses of duplicate HCTs on several rock types, including gabbro from the Duluth Complex with sulfur content ranging from 0.56% to 1.39%. An ongoing geochemical characterization program for a project in development to mine Duluth Complex rock presents an opportunity to augment this previous study with additional data from HCTs. As part of a characterization program, seven duplicate humidity cell tests (representing 14 individual tests) were conducted on Duluth Complex rock with total sulfur content from 0.04% to 3.79%, following the ASTM standard method D 5744-96 (Reapproved 2001) (ASTM, 2001). Results from this study indicate that for duplicate HCTs, maximum difference from the mean for pH varies between 0.05 and 0.18 units, while average difference from the mean for constituent release rates for sulfate, calcium, and magnesium were mostly within 15%. Variability in release rates for copper and nickel were greater, with average difference from the mean ranging from approximately 15-29%.

Keywords: Humidity cell tests (HCT), repeatability, precision, Duluth Complex

INTRODUCTION

Data from humidity cell tests (HCTs) are routinely used to estimate the rates by which constituents will be released during subaerial weathering of waste rock. These estimates may then be used as inputs to predictive geochemical models that serve as the technical bases for making decisions related to environmental assessment, mine design, and financing for mining projects. The U.S. Environmental Protection Agency Guidance for Quality Assurance Project Plans (USEPA, 2012), a guidance on quality assurance for environmental data, including data produced from models, recommends that a systematic planning process is used to establish criteria for the "Data Quality Indicators" (DQIs) that are consistent with the overall "Data Quality Objectives" (DQOs) for the project. DQIs for environmental data include properties such as precision, bias, representativeness, completeness, and sensitivity. Following from the above, characterizing the precision of HCTs may be a key component in evaluating whether geochemical model outcomes meet the DQOs for the overall project. In addition, knowledge of the precision of HCTs is required to assess representativeness and accuracy of the dataset. For the purpose of this paper, precision is defined as "an evaluation of agreement among replicate measurements of the same property under similar conditions; also referred to as random error or measured variability" (USEPA, 2012) whereas accuracy is defined as "a measure of the closeness of an individual measurement to a known or reference value" (USEPA, 2012) and is measured through both precision and bias. There is currently a limited amount of published data on repeatability and reproducibility of HCTs, factors that are used to quantify the overall precision. The current study aims to augment this existing body of information by opportunistic evaluation of the HCTs conducted for the quality assurance/quality control component of the ongoing geochemical chemical characterization program for a potential future mining project located in Duluth, north-eastern Minnesota.

Lapakko and White (2013) conducted repeatability and reproducibility analyses of duplicate HCTs on several rock types, including Duluth Complex gabbro (sulfur content ranging from 0.56% to 1.39%). The results of this study were used as a basis for the precision parameters in the present ASTM standard (method D 5744-96). Consistent with ASTM protocols (ASTM, 2011), repeatability refers to precision under conditions where the same test is performed by the same operator in the same lab within short periods of time, whereas reproducibility reflects precision when the test is performed by different operators at different labs. The majority of the repeatability HCTs analyzed by Lapakko and White (2013) were conducted over 59 weeks with a few extending up to 265 weeks. Comparisons were based on pH and release rates for sulfate, calcium, and magnesium. The maximum difference of the mean was used to compare drainage pH values whereas the percent difference from the mean was used for sulfate, calcium, and magnesium rate comparisons. The equations for both values are listed below:

(1) Maximum Difference of the Mean pH = maximum value for $|pH - pH_{ave}|$ where $pH_{ave} = -\log[(10^{-pH_1} + 10^{-pH_2})/2]$

(2) Percent Difference from the Mean = $100 * |rate - rate_{ave}|/rate_{ave}$

The percent difference from the mean was calculated for each individual rinse cycle and the mean and standard deviation of the percent difference was reported.

ASTM method D5744-96 includes two protocol options (Options A and B). Option A involves weekly cycles of three days of dry air followed by three days of water-saturated air pumped through the sample, with a water leach on the last day. Alternatively, Option B has six days of

controlled and constant temperature and humidity and oxygen is supplied via diffusion (and possibly advection), not pumping, followed by a water leach occurring on the last day (ASTM, 2011). Lapakko and White (2013) evaluated both of these options. For Option A, both leaching alternatives were evaluated (drip and flood) for repeatability and reproducibility analyses whereas for Option B the drip and flood leach alternatives were only evaluated for the repeatability analysis (Lapakko and White, 2013).

Lapakko and White (2013) found that for the Option A drip alternative gabbro samples, repeatability of each laboratory was satisfactory. Two-thirds of the duplicate samples had a pH within 0.10 units of the mean. Similarly, sulfate, calcium, and magnesium rates were within 10% of the mean for over three-quarters of the samples. Deviations from the mean increased the longer the HCT was conducted. Reproducibility of the drip alternative for Option A were similar to that of the repeatability analysis during the first 125 weeks and as the length of testing increased, the percent difference from the mean increased as well. The increases were ultimately attributed to elevated temperature of the reaction environment resulting in an increase in sulfate release and lower drainage pH. Seasonal temperature changes resulted in differences in sulfate rates, most notably with increased rates in the summer months; increased oxidation rates also resulted in a lower pH. Similar trends were observed in the Option A flood alternative samples, as well as slightly lower pH values. One gabbro sample was run using each Option B method (drip and flood); initial results were similar between the leach alternatives and did not deviate with increasing time, presumably resultant to the stable temperature reaction environment (Lapakko and White, 2013).

The HCTs evaluated for the present study also contain rock from the Duluth Complex which enabled a direct comparison to Lapakko and White (2013). However, an expanded range in sulfur content was considered (duplicate HCT's use samples with sulfur content of 0.04-3.79%).

METHODOLOGY

An ongoing geochemical characterization program for a project in development to mine Duluth Complex rock presents an opportunity to augment this previous study with additional data from humidity cell tests on similar rock. This program was designed in cooperation with the Minnesota Department of Natural Resources Lands and Minerals Division and included seven duplicate HCTs (fourteen total) conducted on samples with a sulfur content ranging from 0.04% to 3.79% (Table 1) for 198 weeks. All humidity cells were analyzed by a single laboratory, allowing for the evaluation of the repeatability of the data only. Lithological designations for the Duluth Complex rocks are based on modal percentages of plagioclase, olivine, and pyroxene minerals present, using the classification scheme created by Phinney (1972). Humidity cell tests used in this study were conducted in accordance with ASTM standard method D 5744-96, Option A, flood leach. Sulfur content was determined using a LECO furnace. Aqueous metal concentrations were analyzed using ICP-MS and ICP-OES (alternating) bi-weekly. The ICP-OES was conducted to evaluate trends in major elements and provided trace metal concentrations, but at higher detection limits than the ICP-MS. pH was collected weekly. Results were recorded as mg/L and all non-detect data were recorded at the detection limit. For the purpose of this paper, only calcium, copper, magnesium, nickel, sulfate, and pH were evaluated.

Table 1 Duplicate HCT details

Sulfur Content	Lithology
0.04%	Anorthositic
0.04%	Troctolitic
0.06%	Ultramafic
0.09%	Anorthositic
0.25%	Troctolitic
1.68%	Troctolitic
3.79%	Virginia/Graywacke

Repeatability of the HCT samples is evaluated in a manner consistent with Lapakko and White (2013), as follows:

- pH: the difference from the mean (negative logarithm of the average hydrogen ion concentration) is determined by calculating an average pH between the duplicate HCTs (or group of non-duplicate, similar sulfur HCTs) for each weekly test cycle and the difference between the pH of individual HCT and the average. The maximum and average difference from the mean were determined and reported for each duplicate and similar sulfur content, non-duplicate groups.
- Release rates: the percent difference from the mean is determined by first converting concentration of ions to a release rate (µmol/kg/wk). Then, an average release rate is calculated for each test cycle and the difference between individual HCT analyses and the cycle average is calculated. The average of these differences for each test cycle is expressed as a percentage of the mean release rate for each cycle ("the percent difference from the mean"). The average percent difference from the mean is reported here for each duplicate set and similar sulfur content, non-duplicate groups.

The method of calculation conducted by Lapakko and White (2013) assumes a normal distribution. Additional analyses were conducted on sulfate and pH to determine to actual distribution as well as the upper confidence limit (UCL) of the mean concentration based on that distribution. The statistical software program ProUCL 5.1.00 was used to determine the data distribution and UCL mean concentrations (Singh et al., 2013). The non-detect values are easily identifiable in ProUCL and are input at the detection limit.

RESULTS AND DISCUSSION

Results of the repeatability analysis of the duplicate HCTs are shown in Table 2. For sulfate, calcium, and magnesium, the average percent difference from the mean for release rates was less than 15%, except for the duplicate samples run on ultramafic material. For pH, the maximum difference from the mean was found to be between 0.05 and 0.18. These results are slightly higher, yet consistent, with findings reported in Lapakko and White (2013) Duplicate HCTs with less than 0.10% S are closer to the findings of Lapakko and White (2013) than those with more than 0.25% S, except in the case of ultramafic samples. Figures 1-3 portray the time sequence of release rates for duplicate HCTs for sulfate, calcium (trends for magnesium release rates are similar to calcium) and

pH. For individual pairs of duplicate HCTs, there are no obvious trends in the difference from the mean, either in terms of test duration (i.e., the difference from the mean did not consistently increase or decrease as the HCT progressed) or relationship to the analytical detection limit (analyses closer to the detection limit did not show consistently greater differences than those far away).

Table 2 Repeatability of duplicate HCTs: maximum difference from the mean (pH) and average percent difference from the mean (SO_4, Ca, Mg release rates)

HCT IDs	Sulfur Content	Lithology	pH	SO4	Ca	Mg
37, 41	0.04%	Anorthositic	0.12	7.9%	11.2%	10.0%
51, 57	0.04%	Troctolitic	0.05	8.7%	8.9%	9.6%
61, 72	0.06%	Ultramafic	0.18	17.1%	35.0%	34.1%
1, 9	0.09%	Anorthositic	0.17	7.5%	8.7%	8.3%
38, 48	0.25%	Troctolitic	0.08	13.4%	12.6%	8.4%
10, 20	1.68%	Troctolitic	0.12	12.1%	8.9%	9.2%
58, 63	3.79%	Graywacke	0.12	12.8%	12.3%	14.0%

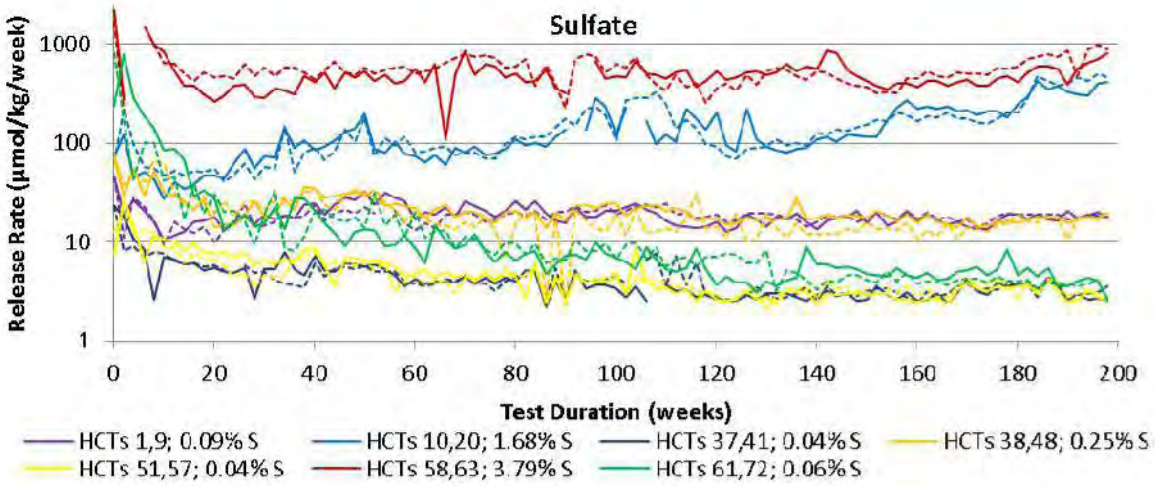

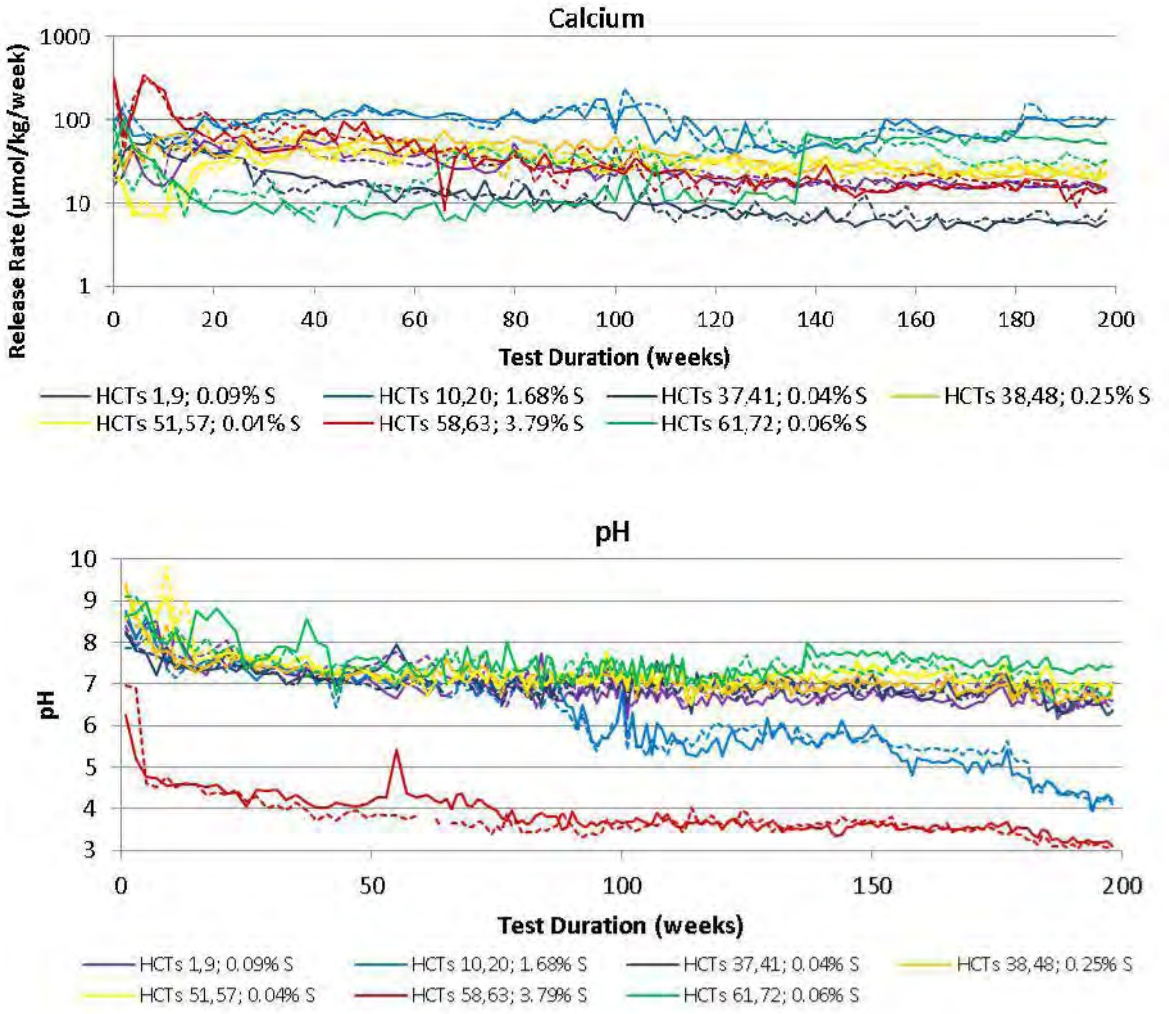

Figures 1-3 Sulfate and calcium release rates and pH for duplicate HCTs (shown by solid and dashed lines of the same color) throughout the 198 weeks of testing

Two different analytical methods, ICP-OES and ICP-MS, were used to measure constituent concentrations in HCT rinseate. The ICP-OES analyses, with detection limits up to two order of magnitude greater than the ICP-MS, were often dominated by analyses less than the detection limit for copper and nickel; therefore, only the ICP-MS data were used in the evaluation of copper and nickel repeatability. Repeatability of copper and nickel release rates using ICP-MS data are shown below in Table 3. The average percent difference from the means for all duplicate pairs are approximately 15% or greater for both copper and nickel release rates. For the duplicate HCTs, there does not appear to be a direct relationship between percent difference from the mean and closeness to the analytical detection limit. While repeatability was weaker for these trace metals than the major ions, trends in metal release was the same for duplicate pairs and distinctive differences between tests were maintained.

Table 3 Duplicate HCT repeatability analysis results: average percent difference from the mean for copper and nickel release rates

HCT IDs	Sulphur Content	Lithology	Cu	Ni
37, 41	0.04%	Anorthositic	22.2%	14.7%
51, 57	0.04%	Troctolitic	22.6%	16.3%
61, 72	0.06%	Ultramafic	26.2%	25.1%
1, 9	0.09%	Anorthositic	18.2%	18.2%
38, 48	0.25%	Troctolitic	21.2%	18.7%
10, 20	1.68%	Troctolitic	17.5%	21.5%
58, 63	3.79%	Virginia/Graywacke	29.4%	16.8%

The distribution of sulfate release rates and pH values for the duplicate humidity cells were conducted on results after the first 52 weeks of study using ProUCL. Significant variability occurred within the first 52 weeks and may not be indicative of long-term conditions encountered. Additionally, as previously mentioned, the Lapakko and White (2013) study based their analysis on the data being normally distributed, however, further analysis indicated that only 36% and 57% of the humidity cells sulfate release rates and pH values, respectively, were characterized as being normally distributed. The 95% UCL of the mean for each humidity cell was determined based on distribution criteria outlined in Singh et al. (2013).

Table 4 Repeatability of duplicate HCTs based on statistically determined distribution: maximum difference from the mean (pH) and average percent difference from the mean (SO_4 release rates)

HCT IDs	Sulfur Content	Lithology	pH		Sulfate	
			95% UCL	Max. Diff.	95% UCL	Ave. Percent Diff.
37	0.04%	Anorthositic	6.9	0.06	3.9	5.7%
41			7.0		3.5	
51	0.04%	Troctolitic	7.2	0.01	3.8	0.7%
57			7.2		3.8	
61	0.06%	Ultramafic	7.3	0.07	7.5	6.3%
72			7.5		6.6	
1	0.09%	Anorthositic	7.0	0.13	19.0	0.8%
9			6.7		19.3	
38	0.25%	Troctolitic	7.0	0.01	19.4	10.1%
48			7.0		15.8	
10	1.68%	Troctolitic	5.9	0.01	200.8	4.1%
20			5.8		217.8	
58	3.79%	Graywacke	3.6	0.07	582.9	4.8%
63			3.7		529.8	

The recalculated maximum difference from the mean pH value was approximately one-half of those assuming normal distribution for all the samples. Similarly, the recalculated average percent difference from the mean sulfate release rates were 2 to 10% lower than those previously determined. Therefore, it is possible that with more rigorous statistical analyses, with particular attention on the distribution of the data as well as long-term stability of the dataset, the repeatability of the HCT improves.

CONCLUSION

Humidity cell test data is key input for predictive modelling of the quality of mine-impacted water. Understanding the repeatability of that data is necessary for accessing the quality of data being used for these models. Results from this study indicate that for duplicate HCTs, pH varies between 0.05 and 0.18 units from the mean, while constituent release rates for sulfate, calcium, and magnesium were within 15% of the mean, except for the ultramafic duplicate samples. This is consistent, although slightly higher, than precision parameters published in the ASTM method. Duplicate HCTs with less than 0.10% S are more consistent with the findings of Lapakko and White (2013) than those with more than 0.25% S, except in the case of ultramafic samples. The average difference from the mean for copper and nickel was greater than that of the major ions. Trends were not observed between either test duration or closeness to the detection limit and precision. Statistical analyses of the distribution of pH and sulfate release rates for data collected after the first 52 weeks of testing resulted in lower differences from the mean and therefore increased apparent repeatability of the humidity cell testing.

ACKNOWLEDGEMENTS

The authors gratefully acknowledge permission from the mining company to publish these results. Interpretation of the test work results have benefitted from numerous discussions with individuals at both MDNR-LAM and the company. The authors would also like to acknowledge the contribution of two anonymous reviewers whose comments resulted in a much improved manuscript.

NOMENCLATURE

HCT humidity cell test

REFERENCES

ASTM Standard D5744-96 (2001). Standard Test Method for Accelerated Weathering of Solid Materials Using a Modified Humidity Cell. ASTM International, West Conshohocken, PA, 2001.DOI: 10.1520/D5744-96, www.astm.org.

Lapakko, K.A. and White, W.W. (2013). Interlaboratory Study to Establish Precision Statement for ASTM D5744-2013, Test Method for Laboratory Weathering of Solid Materials Using a Humidity Cell. Research Report: D34-1019. Committee D34 on Waste Management, Subcommittee D34.01.04 on Waste-Leaching Techniques, ASTM International.

Phinney, W.C. (1972) Duluth Complex, history and nomenclature, *in* Sims, P.K. and Morey, G.B., eds., Geology of Minnesota: A centennial volume: Minnesota Geologic Survey, p. 333-334.

Singh, A. and Singh, A.K. (2013). ProUCL Version 5.0.00 Technical Guide, Prepared for the US EPA. EPA/600/R-07-041. September 2013.

SRK Consulting (2007). RS53/RS42 – Waste Rock Characteristics/Waste Water Quality Modeling - Waste Rock and Lean Ore – NorthMet Project - DRAFT. [RS53/RS42 Draft-01]. SRK Project 1UP005.001. July 2007.

USEPA (2001). Data Quality Objectives Decision Error Feasibility Trials Software (DEFT)-USER'S GUIDE, EPA 240-B-01-007. September, 2001.

USEPA (2012). U.S. Environmental Protection Agency Guidance for Quality Assurance Project Plans, CIO 2106-G-05 QAPP. Final Draft, 17 January, 2012.

Evaluation of Lag Times for Tailings in Extreme Arid Climates by Long-Term and Delayed-Rinse Kinetic Tests

Jacob Waples[1], Troy Jones[2], Guillermo Aguierre[3] and Christian Wisskirchen[4]

1. *Golder Associates, USA*
2. *Teck Resources, Canada*
3. *Teck Resources, Chile*
4. *Golder Associates, Chile*

ABSTRACT

For operations and closure planning, understanding lag times to the potential development of acidic conditions is critical for management of a tailing storage facility (TSF). While this is important for many mines, for the site presented herein (and similar projects) the climatic and hydraulic conditions expected for TSFs in the extreme arid climate of the Atacama Desert present specific challenges for prediction of lag times to acidic conditions and subsequent metals leaching.

Long term humidity cell testing (up to 151 total cycles) was undertaken for several fractions of pilot plant tailings for a copper porphyry deposit. Modified humidity cell tests were also utilized with weekly cycles of humid and dry air and rinses every 20 cycles. The delayed rinse cells were used to provide insight for conditions where wetting of tailings will occur very infrequently following deposition.

Tailings evaluated had total sulfur contents near 1.0% and low neutralization potential. While predicted to be acid generating by static testing, extended lag times were observed. Long term humidity cell testing indicated a lag time of 40 cycles to significant acid generation and a slow process of acidification (reaching stable final pH values near 2.5 took almost 115 cycles). Metals leaching, as expected, increased with acidic conditions. The delayed rinse cells indicated longer lag times to acidification and reduced loading rates for key metals.

Evaluation of the potential development and timing of onset of acidic conditions in the TSF considered the results of the long-term and delayed-rinse testing, pre- and post-testing mineralogy, as well as the hydraulic conditions expected in the TSF under the extreme climate conditions. These include: high evaporation rates, salt migration, and hardpan formation. This paper describes the test work, results, and how the results were used to guide design efforts for both operations and closure planning.

Keywords: Closure planning, arid climate, humidity cell lag time, prediction

INTRODUCTION

While mine wastes may be predicted to be potentially acid generating (PAG), the lag time to the generation of acidic conditions in the field has important implications for mine and closure planning. The lag time may dictate how the material may be handled, stored, or treated prior to acidification. Understanding lag times, and the factors that affect them, is critical in order to effectively design, operate, and prepare for closure of a mine. There are a number of factors that may affect a lag time, including geochemical factors (such as sulfide content, sulfide mineral availability and morphology, secondary mineral coating, available neutralization potential) and physical factors (such as exposure time, grain size and surface area, and moisture content).

Understanding the timing to the onset of acidic conditions is important for facility design, operation, and closure because once acidic conditions are initiated they can persist over the long term. Acidic conditions may require a spectrum of water management practices, water treatment needs, or mitigation strategies, all of which may also evolve with time from operations to closure. For tailings storage facilities (TSFs), these measures may include: seepage capture systems, water treatment facilities, water management for run-on and runoff, amendments, and closure covers. Implementation of these strategies is generally more costly and difficult to perform without preparation or in a retroactive fashion; therefore, it is important to understand these needs as early as possible in the design of a TSF (INAP 2009).

For tailings, the overall dynamics for acid generation are generally well understood. Highest oxidation generally occurs shortly after tailings deposition ends (Blowes et al. 2003). Oxidation rates are generally the highest at the initiation of oxidation and the majority of acid generation occurs during the early stages of acid generation (e.g., MEND 1997). Oxidation occurs at the surface of the TSF and an oxidation front typically progresses downward from the TSF surface. This process results in a profile that includes an upper oxidized zone where sulfides have oxidized, an oxidation zone, where oxidation is occurring, and an un-oxidized layer underneath (e.g., Blowes et al. 2003). The location of an actual acidic front within this profile is dependent on the infiltration rates and the balance of acid generation versus neutralization potential. The acidic front will either remain within the upper zones of the profile or be carried downward by infiltration and, if it overwhelms the neutralization potential below, acidic seepage can result.

The depth and development of the oxidation profile and acidic front is dependent on a range of factors, such as the tailings' acid-base characteristics, saturation state, oxygen diffusion, and age of the facility. Saturation state of the tailings is considered a key parameter for tailings facilities, as higher saturation will restrict oxygen entry, limit oxidation, and subsequently control the development and location of acidic conditions.

In the Atacama Desert, the saturation state of the tailings is an important parameter for consideration of the generation of acidic conditions. The Atacama Desert is one of the driest places in the world with annual average precipitation under 15 millimeters (mm) for an average year and on the order of 100 millimeters per year for a 100 year return period. Coupled with this, evaporation is high, with an annual average evaporation near 2500 mm per year. In addition, precipitation is infrequent with many successive years registering zero precipitation. When precipitation does occur it is typically concentrated in one larger event. The extreme arid climate will affect geochemical and hydraulic factors of the oxidation profile and warrant consideration in the design, management, and closure planning for TSFs in arid climates.

As a part of permitting and design of a TSF in the Atacama Desert for development of a copper porphyry deposit, a kinetic testing program was undertaken for several fractions of pilot plant tailings. The kinetic testing program included long-term (up to 151 cycles) humidity cells and modified humidity cells with extended time between rinse cycles. The objective of the modified humidity cells was to evaluate the lag time under dry conditions with infrequent wetting and rinsing, as found at the climate of the site. The testing program was designed to meet both permitting requirements and informational needs to provide inputs to engineering design, operations planning, and closure planning activities.

METHODOLOGY

Three tailings samples were included in the kinetic testing program, including whole tailings, underflow tailings, and overflow tailings. The whole tailings sample represents materials from a process plant mill that will then be cycloned to produce the overflow (two stages, combined for this sample) and underflow materials. The underflow sample represents the sands that will be used to build the dam for the TSF. A combination of whole tailings and overflow tailings are planned to be placed in the TSF. All tailings samples were produced by a metallurgical pilot plant.

A standard and complete static testing program (e.g., INAP 2009, MEND 2009) was performed on all tailings samples, including acid base accounting (ABA), mineralogy by x-ray diffraction (XRD) with Rietveld refinement, elemental content, grain-size distribution, net acid generation testing (NAG), and short term leach testing. Pertinent ABA and mineralogy results are provided in Tables 1 and 2, respectively. All tailings have moderate amounts of sulfur (0.78 to 1.1 wt. %) and are estimated to be potentially acid generating (PAG) from the results of both ABA and NAG testing (using criteria presented in INAP (2009) and MEND (2009)). These results are confirmed by the mineralogical testing that indicates moderate pyrite content (between 1.3 and 2.0 %) and limited minerals with neutralization potential.

Kinetic testing was performed utilizing two types of humidity cells. The first was based on the standard humidity cell test (ASTM D5744-07), utilizing standard cycles of humid air and dry air during a week, followed by a week-end leach. However, these humidity cells were run for extended periods, including 60, 130, and 151 cycles for the overflow, underflow, and whole tailings samples, respectively.

The second test was a modified humidity cell, referred to herein as a delayed humidity cell. In this test, the standard procedure was modified so that that leach cycle was performed every 20 cycles rather than weekly. The weekly dry and wet air cycles were still performed. Delayed humidity cells were performed for two samples, the whole tailings and the underflow tailings. Delayed humidity cells were run for 80 cycles and were leached 4 times during the testing period.

At the termination of the humidity cell tests, splits from the humidity cells were tested for post-testing ABA and mineralogy (Tables 1 and 2, respectively). Post-testing ABA results indicate a depletion of sulfides and neutralization potential during kinetic testing. Post-testing mineralogical results indicate depletion of sulfides and the presence of reaction products such as jarosite and gibbsite, as expected. This is also consistent with post-testing ABA results as well. An increase in carbonates (calcite and ankerite) was detected in the post-testing XRD analysis, inconsistent with both the expected depletion and the ABA results; this result is considered likely due to heterogeneous materials.

Table 1 ABA results

Parameter	Units	Whole		Overflow		Underflow	
		Pre	Post(1)	Pre	Post(1)	Pre	Post(1)
Paste pH	s. u.	8.2	3.7	8.0	5.1	8.3	6.1
Total S	wt.%	1.04	0.44	0.86	0.77	0.78	0.73
Sulfide-S	wt.%	0.99	0.27	0.77	0.65	0.69	0.60
TIC	% CO_2	0.02	<0.01	0.03	<0.01	0.01	<0.01
NAG pH	s. u.	2.7	--	2.9	--	2.9	--
NP	kg $CaCO_3$/ton	4.8	<0.1	4.9	1.3	3.4	2.0
CO3-NP	kg $CaCO_3$/ton	0.50	<0.8	0.70	<0.8	0.20	<0.8
NNP	kg $CaCO_3$/ton	-26.1	-7.94	-19.2	-19.0	-18.2	-16.8
NPR	--	0.16	0.06	0.20	0.06	0.16	0.11

(1) Post-testing results shown for standard humidity cell sample.
(2) NNP and NPR based on standard NP and AP calculated from sulfide sulfur.

Table 2 XRD results

Mineral	Ideal Formula	Weight Percent					
		Whole		Overflow		Underflow	
		Pre	Post(1)	Pre	Post(1)	Pre	Post(1)
Quartz	SiO_2	34.6	31.5	32.9	28.6	41.4	36.4
Chlorite/Clinochlore	$(Mg,Fe^{2+})_5Al(Si_3Al)O_{10}(OH)_8$	2.5	7.1	2.5	6.9	1.5	4.4
Muscovite	$KAl_2AlSi_3O_{10}(OH)_2$	16.0	15.7	18.2	17.7	11.6	13.2
Biotite/Phlogopite	$K(Mg,Fe)_3(AlSi_3O_{10})(OH)_2$	4.4	4.9	4.4	5.9	3.2	5.2
K-Feldspar	$KAlSi_3O_8$	17.8	16.4	17.6	14.8	18.5	15.7
Plagioclase/Albite	$NaAlSi_3O_8 – CaAl_2Si_2O_8$	20.8	20.2	21.6	19.6	21.0	19.5
Pyrite	FeS_2	2.0	0.3	1.6	1.1	1.3	0.7
Chalcopyrite	$CuFeS_2$	0.5	--	--	--	--	--
Magnetite	Fe_3O_4	0.3	--	--	--	0.2 (2)	--
Halite	NaCl	0.5(3)	0.2(3)	--	--	--	--
Rutile	TiO_2	0.7	--	0.6	--	0.5	--
Calcite	$CaCO_3$	--	0.6	0.8	1.8	0.8	0.7
Ankerite	$CaFe(CO_3)_2$	--	0.8	--	0.8	--	1.0
Jarosite	$KFe_3(SO_4)_2(OH)_6$	--	1.8	--	1.9	--	2.1
Gibbsite	$Al(OH)_3$	--	0.4	--	0.8	--	0.6
Total	--	100.1	99.9	100.2	99.9	99.8	99.5

(1) Post-testing results shown for standard humidity cell sample.
(2) Mineral quantity at methods detection limit, mineral not confirmed.
(3) Halite is an artifact of the pilot plant test solutions and is not associated with tailings mineralogy.

RESULTS OF THE KINETIC TESTING PROGRAM

Results for the leachate pH values with time for all kinetic test types are shown in Figure 1a. Concentrations of sulfate are shown on Figure 1b and concentrations of copper are shown on Figure 1c. The humidity cell leachates initially have near neutral pH values for all tests and a typical first flush of elevated sulfate concentrations and metals is observed. Following the first flush, an extended lag time to acidic conditions is observed for all tailings samples under the test conditions, during which pH values remain above 7 and sulfate concentrations steadily decrease.

Following the lag period, sulfide oxidation and subsequent acid generation occurs. For the whole tailings sample in the standard humidity cell, increasing sulfate concentrations (indicating sulfide oxidation) and increasing calcium concentrations (indicating dissolution of calcite) are observed starting at cycle 35. The pH begins a steady decline following this in cycle 40. The pH continues to drop with subsequent cycles to cycle 116 when the pH stabilizes near a value of 2.5, which is maintained for the final 35 cycles of testing (151 cycles total). During the final acidic phase, calcium concentrations decrease (likely indicating depletion of carbonate) and a decrease in sulfate concentrations to between 300 and 450 mg/L occurs. Concentrations for metals are elevated, including: aluminum, barium, beryllium, cadmium, chromium, cobalt, copper, iron, lead, lithium, manganese, nickel, thallium, uranium, and zinc.

The lag time under testing conditions was greater for the cyclone fractions. The underflow fraction sample had the greatest lag time to initiation of sulfide oxidation and to initiation of acidic conditions (starting at approximately 83 cycles with a drop in leachate pH below 7 and an increase in sulfate concentrations). Additionally, the final stable pH for the underflow humidity cell test was higher, at a value near 5. For the overflow sample, sulfate concentrations followed a similar trend as the whole tailings sample, with increasing concentrations beginning near cycle 40 and an initiation of a decrease in pH beginning in cycle 58. Given similar behavior to the whole tailings, this test was terminated at this time.

For the delayed humidity cells, the lag time was not exhausted during the testing period. The pH values for the entire duration of testing were greater than 7. Additionally, a change in sulfate and overall metals mass loading was not generally observed in the leachate over time. Leachate sulfate and metals concentrations were generally elevated in the delayed humidity cell test relative to that of the standard test because removal of mass load from the cells only occurred every 20 cycles. Calculation of mass flux from the standard humidity cell compared to that of the delayed humidity cell at cycles 20, 40, 60, and 80 are presented for sulfate, copper, arsenic, and antimony on Figures 2a through 2d (results shown for whole tailings samples only).

DISCUSSION

The majority of the geochemical characterization data indicate that the tailings (whole and cycloned fractions) have potential to be acid generating under appropriate conditions, such as assuming the presence of sufficient moisture following desaturation of the tailings. With the onset of acid generation, pore water quality would be expected to have low pH values between 2.5 and 3 with elevated concentrations of sulfate and metals. For a copper porphyry deposit with sulfide tailings this is not an unexpected result. From a planning perspective for design, operations, and closure, the most pertinent results are those from the kinetic testing with respect to the lag time. A significant lag time is expected based on the results of the standard humidity cell test. The lag time was observed to vary between the different tailings fractions, with the shortest lag time for

initiation of acidic conditions observed for the whole tailings (40 cycles) and longest for the underflow (80 cycles). For this site, translation of laboratory lag times to the field is significant. One equivalent cycle under field conditions could take many years to occur as there can be successive years without precipitation or without precipitation sufficient to wet more than the surface of the tailings due to the high evaporation rate.

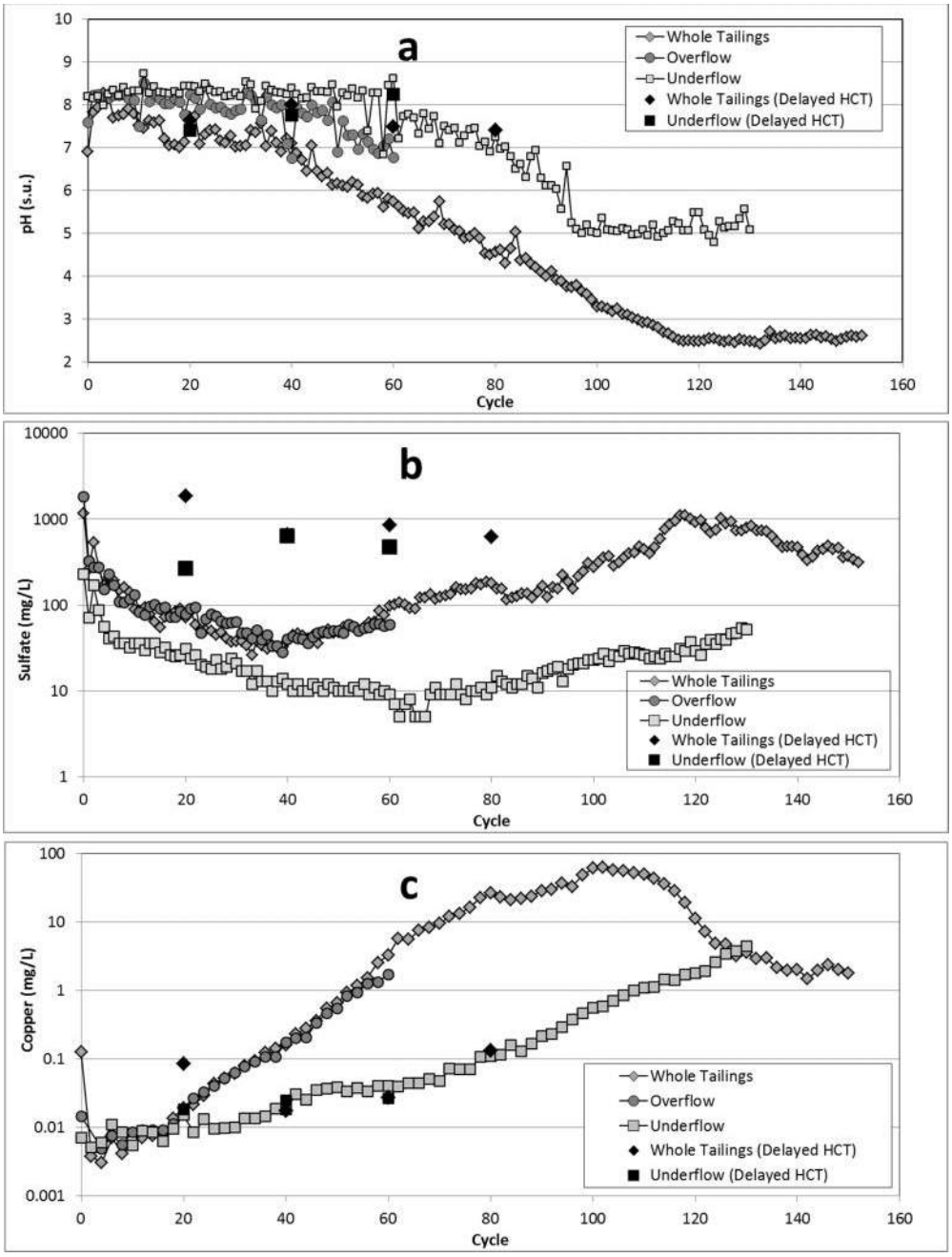

Figure 1 Leachate a) pH, b) sulphate and c) copper concentrations with time

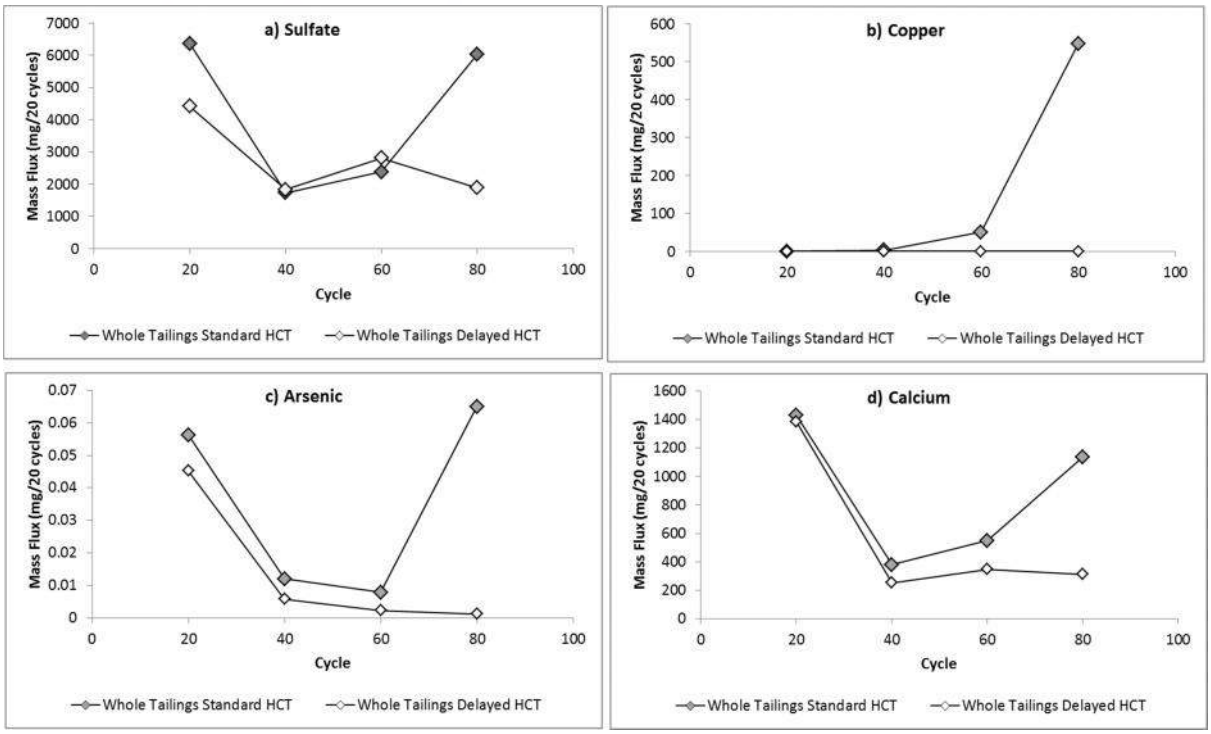

Figure 2 Mass flux from standard and delayed humidity cells over 20 cycles for: a) sulfate, b) copper, c) arsenic, and d) calcium

The results of the delayed humidity cells confirm the lag time and indicate that the lag time may be extended further with less frequent wetting as expected in drier conditions. The pH of the delayed humidity cells remained constant through testing (80 cycles) and no increase in sulfate or metals concentrations is observed. This indicates that initiation of sufficient oxidation to affected leachate water quality is postponed in the absence of weekly rinsing cycles.

Trends of mass flux from the standard humidity cells compared to that of the delayed humidity cells provide greater insight into the oxidation behavior. Mass flux for sulfate (Figure 2a) and most metals (similar to that of copper and arsenic, as shown on Figures 2b and 2c) are similar for the standard and delayed humidity cells for the first 40 cycles, indicating similar rates of oxidation and metals release up to this time. Following the initiation of sulfide oxidation just before 40 cycles in the standard humidity cells, a slight increase in cumulative loading is observed for the standard humidity cells, resulting in higher loading rates compared to the delayed humidity cells at 60 cycles. At 80 cycles, the pH values of the standard humidity cells have dropped below 5, sulfate and metals mass flux increases dramatically. In comparison, mass flux of metals and sulfate from the delayed humidity cells remains relatively constant between cycles 40 and 80.

The mass flux trends indicate that whole tailings in both the standard and delayed humidity cells had similar oxidation and metals release during the initial phases of the test (i.e., the first 40 cycles). Because the mass flux changes for the standard cells, but not the delayed humidity cells, this implies that the initiation of significant oxidation is delayed by less-frequent wetting and it is not a mechanism of neutralization that delays acid generation. Calcium mass flux (Figure 2d), which

would provide an indication of calcite dissolution, is also similar between the standard and delayed humidity cells until significant oxidation and acidic conditions are apparent in the standard cell.

The delay in the initiation of oxidation could be due to factors such as an initial surface coating of sulfide surfaces with secondary minerals that may form during initial processing (e.g., Jambor 1994; Thomas et al. 1998) or throughout the testing, sulfide mineral availability, initially available neutralizing minerals, or buffering capacity of initial process solutions. The limited flushing in the delayed humidity cell test may not sufficiently remove oxidation products from the pyrite surface, thereby further limiting initiation of significant oxidation (e.g., Blowes and Ptacek 1994, Jerz and Rimsdit 2004, Huminicki and Rimstidt 2009).

A second pertinent result from a TSF design and planning standpoint is that following initiation of sulfide oxidation and depletion of the neutralization potential, the development of fully acidic conditions was gradual under the test conditions. While terminal pH values were near 2.5 with elevated metals concentrations, it took greater than 75 cycles to reach these conditions after sulfide oxidation initiated between cycles 35 and 40 (based on the increasing sulfate concentrations at this time). Peak sulfide oxidation rates (based on sulfate release) are reached in cycle 116, as a pH of 2.5 is reached, and then sulfide oxidation rates decrease through the conclusion of the test at 151 cycles. The greatest sulfide oxidation rates are expected for tailings at the beginning of acidic conditions (e.g., MEND 1997). In this case, a similar result is observed, but only after fully acidic conditions were attained (i.e., at the start of consistent pH values near 2.5). While the neutralization potential of the tailings was expected to be limited based on initial ABA and XRD analyses, sufficient available neutralization potential from the tailings (and possibly process solutions) was available to slow the acidification process.

Implications for Design

The results of the geochemical testing program, while initially developed for permitting using standard characterization tests, were incorporated into the design and planning for the facility, considering both operations and closure. The design and planning process also considered the extreme arid climate, combined with its implications on the hydraulics of the TSF, in light of the geochemical characterization results. Additional hydraulic considerations included the high evaporation rates, salt migration, and hardpan formation which may also affect saturation state. All of these factors warrant consideration in the design, management, and closure planning for TSFs in the Atacama Desert, as well as site in other arid climates.

Operations

Given the extended lag time for the tailings and the saturation state of freshly deposited tailings, acidic conditions will not develop in the TSF during operations. Tailings will be deposited wet, in lifts by spigots. The upper portion of a lift will undergo drying; however, it will be re-wetted to a limited extent as it is subsequently covered by a fresh layer of tailings. However, due to the arid climate, limited rewetting is expected, with infiltration modeling indicated that infiltration and rewetting will be interrupted after 5 to 8 days by evaporation processes. The results of the delayed humidity cells indicate that the limited wetting and drying will further extend the already significant lag time to the initiation of significant oxidation (a minimum of 40 cycles based on the standard humidity cells) and development of full acidic conditions (a minimum of 116 cycles in the standard humidity cells). Furthermore, one cycle in the laboratory scaled to an equivalent wetting

and drying cycle in the field following cessation of deposition may represent many years at the site location due to the climate conditions.

The long lag time and slow development of fully acidic conditions with peak oxidation rates has other implications for TSF management. Given acidification either may not occur at all due to the climate or it will take a very long time to develop acidic conditions, monitoring of any seepage from the tailings facility will provide a long lead time to develop and implement mitigation measures.

From an oxidation potential perspective, underflow sands in the dam can be a concern due to their grain size and position in the dam that allows for drainage and lower moisture contents. Cycloning tailings can also result in concentration of sulfides in the underflow sands. However, in this case, the latter was not observed with similar sulfide contents in the whole and underflow tailings as measured by both ABA and XRD. Additionally, the grain-size distribution for underflow sands is generally larger, resulting in a lower specific reactive surface area. The lower specific surface area and similar sulfide content resulted in less reactive underflow tailings in this case. The underflow sands exhibited a longer lag time and the terminal pH values were relatively high (values near 5) with corresponding lower concentrations of sulfate and metals. As such, significant acid generation from the underflow sands is also not expected during operations.

Given these observations, the TSF design was focused on water conservation as water quality is not expected to be a concern. These factors, combined with the expected geochemistry of the tailings, indicate a very low risk of water quality impacts during operations.

Closure

Following closure, the upper tailings will be unsaturated, allowing oxidation and acidification. However, the significance of acidification will be limited due to several factors. The most important is that following cessation of operations and deposition of tailings, the climate conditions will not provide sufficient water to mobilize seepage through the facility. Secondly, as described, a delay to acidification is expected and the dry climate will limit wet and dry cycles and mobilization of acidity. The delayed humidity cells demonstrate that persistent dry conditions and lack of flushing will increase the lag time. A lack of mobilization of constituents from the oxidized zone may also limit oxidation as secondary products may blind off reactive surfaces. Finally, while a significant unsaturated zone at the surface of the TSF is expected due to the climate, formation of a hardpan is also expected by natural and secondary salts (e.g., Coggans et al. 1999) that may limit oxidation diffusion. Natural hardpans are currently present at the site due to the climate, providing an analog for expected future conditions, and hardpan formation was observed in geotechnical laboratory studies for the tailings. Given the above considerations, limited or no water management requirements are expected following closure of the TSF to be protective of the environment.

ACKNOWLEDGEMENTS

The authors thank Derek Amores for his contributions. Jacob Waples and Christian Wisskirchen acknowledge being compensated for the original laboratory work and analysis for Teck Resources.

NOMENCLATURE

ABA	acid-base accounting
ASTM	American Society for Testing and Materials
CO3-NP	carbonate neutralization potential
HCT	humidity cell test
NAG	net acid generation test
NNP	net neutralization potential
NP	neutralization potential
NPR	neutralization potential ratio
PAG	potentially acid generating
TIC	total inorganic carbon
TSF	tailings storage facility
XRD	x-ray diffraction

REFERENCES

Blowes D.W. and C.J. Ptacek (1994) Acid-Neutralization Mechanisms in Inactive Mine Tailings. In The Environmental Geochemistry of Sulfide Mine-Wastes, Short Course Handbook, D.W. Blowes and J.L. Jambor, editors. Mineralogical Association of Canada, Vol. 22.

Blowes D.W., C.J. Ptacek, and J. Jurjovec (2003). Mill Tailings: Hydrogeology and Geochemistry. In Environmental Aspects of Mine Wastes, J.L. Jambor, D.W. Blowes and A.I.M. Ritchie, Mineralogical Association of Canada, Short Course Series Volume 31.

Coggans, C.J., D.W. Blowes, W.D. Robertson, and J.L. Jambor (1999) The Hydrogeochemistry of a Nickel-Mine Tailings Impoundment. In The Environmental Geochemistry of Mineral Deposits, Part B: Case Studies and Research Topics. L.H. Filipek and G.D. Plumlee, editors. Reviews in Economic Geology Volume 6B, Society of Economic Geologists, Inc.

Huminicki, D. M, and J.D. Rimstidt. Iron Hydroxide Coating of Pyrite for Acid Mine Drainage Control. Applied Geochemistry, 24, pp. 1626-1634.

INAP (2009) Global Acid Rock Drainage Guide (GARD Guide), The International Network for Acid Prevention, http://www.gardguide.com.

Jambor J.L. (1994) Tailings Mineralogy. In The Environmental Geochemistry of Sulfide Mine-Wastes, Short Course Handbook, D.W. Blowes and J.L. Jambor, editors. Mineralogical Association of Canada, Vol. 22.

Jerz, J.K. and J. D. Rimstidt (2004) Pyrite Oxidation in Moist Air. Geochimica et Cosmochimica Acta, Vol. 68, No. 4, pp. 701-714.

MEND (1997) A Survey of In Situ Oxygen Consumption Rates on Sulfide Tailings: Investigations on Exposed and Covered Tailings. MEND Project 4.6.5ac

MEND (2009) Prediction manual for drainage chemistry from sulphidic materials, MEND Report 1.20.1.

Thomas, J.E, C.F. Jones, W.M. Skinner, and R.S. Smart (1998) The Role of Surface Sulfur Species in the Inhibition of Pyrrhotite Dissolution in Acidic Conditions. Geochimica et Cosmochimica Acta, Vol 62, No. 9. Pp. 1555-1565.

10th ICARD IMWA 2015 | 10th International Conference on Acid Rock Drainage & IMWA Annual Conference

Pyrite Oxidation in Well-Constrained Humidity Cell Tests

Mark Williamson
Geochemical Solutions, USA

ABSTRACT

Owing to its significance in the formation of acid mine drainage, the rate of pyrite oxidation has received persistent attention for many years. The vast majority of experimental rate measurements have been made under saturated (liquid) conditions (no gas phase), and a few are available for the reaction in vapor-only (humid oxygenated air) conditions. However, in field settings, either naturally occurring or associated with mineral extraction activity, liquid+vapor conditions with moist air and water present are perhaps the most common.

As part of environmental permitting programs, the mineral industry has come to rely on empirical measurements of pyrite (and other sulfide mineral) reaction rates using the Humidity Cell Test (HCT). This laboratory test exposes crushed mine rock samples to liquid+vapor water in the presence of atmospheric oxygen, provided in excess. The HCT is a standardized test method that has been evaluated for reproducibility, but limited effort has been made to assess rates, specifically pyrite, relative to existing geochemical literature.

In the present work, a series of well-constrained HCT experiments have been and are being conducted using simple mineral assemblages, with known mineral grain sizes/reactive surface area. Tests have been conducted using pyrite + quartz and pyrite + quartz + calcite. Additional testing has been conducted using two separate pyrite grain sizes. Though difficult to constrain, the proportion of liquid to vapor water in the system has also been investigated by altering the established procedure to increase the vapor relative to liquid phase (vapor-enhanced).

Results to date indicate that the rate of pyrite oxidation slows with time. Initial rates are significantly faster than in liquid-only experiments (Williamson and Rimstidt, 1994), and diminish with time. Results were consistent with trends observed in vapor-only laboratory experiments. Terminal, near steady-state rates of pyrite oxidation approached the same value for all test conditions, and were consistent with well-stirred liquid-only initial rates. Thus, hypothetical retention of reaction products that might explain the both the reduction in rate and the similarity among tests seems improbably. Terminal rates showed no relationship to rate of water supply (flushing). Rates scaled directly with pyrite reactive surface area, but sulfate production (concentration) did not scale directly with grainsize.

Keywords: pyrite oxidation, HCT, kinetics

INTRODUCTION

Owing to its significance in the formation of acid mine drainage, the rate of pyrite oxidation has received persistent attention for many years. Understanding has grown from a characterization of oxygen, temperature, sulfide mineralogy and bacterial action as reaction drivers of pyrite oxidation (Caruccio, 1968) through development of quantitative rate expressions that identify the significance of reactive surface area of pyrite. Currently, rate expressions for pyrite oxidation have been developed for water-saturated conditions (Williamson and Rimstidt, 1994) and water vapor-only conditions (Williamson, 2013). However, in field settings, either naturally occurring or associated with mineral extraction activity, liquid+vapor water conditions are the most common.

As part of environmental permitting and mine waste management programs, the mineral industry has come to rely on empirical measurements of pyrite (and other sulfide mineral) reaction rates using the Humidity Cell Test (HCT). This laboratory test exposes prepared mine rock samples to liquid+vapor water in the presence of atmospheric oxygen, both provided in excess. Initially, the HCT was thought to be an accelerated weathering test, as it was thought that the procedure removed reaction products from the test cell that would otherwise impede reaction progress (Sobek, et al, 1978). The HCT is a standardized test method (ASTM, 2012) that has been evaluated for reproducibility, but limited effort has been made to assess reaction rates relative to existing geochemical literature.

Only a few studies have tried to quantify the rate of pyrite oxidation in a two-phase water system (liquid+vapor). Of these, only a limited number of studies have been conducted for which the reactive surface area of pyrite is known or estimated. Lappakko and Antonson (2006) report rates of pyrite oxidation present in Duluth Complex rock matrices determined in an HCT; Watzlaff and Hammack (1990) made measurements in a vertical column with continual air flow and a weekly leach; and Leon, et al (2004) present results of batch-style tests with limited amounts of liquid water present in an otherwise humid environment without forced airflow. Data from other two-phase studies are reported in the literature, but reactive surface area and/or grainsize is either unknown or beyond estimation.

The worldwide database of two-phase (presence of moist air plus liquid water) results is overwhelmingly for mine rock using the HCT. These materials often represent complex mineralogy and virtually never report reactive surface area for pyrite, although the test procedure itself does restrict the grain size of the material with which the cell is charged. Thus, it is impossible to reliably compare and contrast pyrite oxidation rates with fundamental geochemical understanding, or compare other tests on various mine rock samples. The purpose of the present study is to employ a simplifying approach to begin to study simple systems that will eventually lead to the defensible interpretation of specific reactions in humidity cell tests and support reliable predictive modeling.

METHODOLOGY

In the present work, a series of well-constrained HCT experiments have been conducted using simple mineral assemblages, with known mineral grain sizes/reactive surface area. Tests have been conducted using test cell charges comprised of pyrite (py) + quartz (qtz) and pyrite + quartz + calcite (cal). Testing has been conducted using two separate pyrite grain sizes. Though difficult to constrain or quantify, the effect proportion of liquid to vapor water in the system as well as rinsing has also been investigated by altering the established HCT procedure (ASTM, 2012) to increase the

vapor relative to liquid phase (vapor-enhanced).

Approach

In contrast to the inherently more complex situation when testing poly-mineralic materials (i.e. mine rock, tailings), with a restricted but wide range in grainsize (with unknown reactive surface area), and fixed rate of water supply, the present work has taken a decidedly reductionist approach. The study has utilized a simple mineralogic composition (pyrite, calcite and quartz) with restricted grainsize, known reactive surface area. Two distinct values of reactive surface area for pyrite were examined and the rate of water supply was varied by a factor of about two. Table 1 summarizes the four tests currently being conducted, and provides a statement of test objective for each. All tests were run at 22 ± 1.5 C.

Table 1 Summary of experimental conditions.

Test Cell ID	Cell Charge (gm)			Flushing Frequency	Test Objective
	Pyrite	*Calcite*	*Quartz***		
HCT-1	100*	0	900	Weekly	Measure of pyrite oxidation rate at standard conditions
HCT-2	40*	200	760	Weekly	Contrasted with HCT-1, measure of pyrite oxidation rate in carbonate buffered solution, at conventional 3:1 ratio of neutralization to acid potential
HCT-3	100**	0	900	Weekly	Contrasted with HCT-1, assessment of pyrite oxidation rate at different grain size/surface area
HCT-4	100*	0	900	Bi-Weekly	Contrasted with HCT-1, assessment of pyrite oxidation rate at lower flushing frequency/rate
HCT-5	0	0	1000	Weekly	Blank

* Grain size = 0.4 mm (0.297 mm < sample < 0.5 mm) = 70 m^2/gm (Foust et al., 1980)

** Grain size = 2.4 mm (2 mm < sample < 2.83 mm) = 19 m^2/gm

*** Grain size = 0.85 mm (0.85 mm < 93.6% < 1 mm sieve)

Materials

The pure pyrite (FeS_2) used in this study was sourced in Peru, and is the same material used by Williamson and Rimstidt (1994) and Jerz and Rimstidt (2004). The sieved pyrite was washed with alcohol to remove fine-grained material as much as possible. Pure calcite ($CaCO_3$) was obtained from Ward's Scientific (optically clear; variety Iceland Spar) and was sieved to collect the 0.5 mm fraction as described above for pyrite. Silica sand (SiO_2) was purchased commercially, sourced in Wedron, Illinois, with a reported assay of 99.7% SiO_2 and less than 0.01% calcite. Mineral mixtures were loaded carefully into the test cells to avoid any gravity separation effects.

RESULTS AND DISCUSSION

Analytical Results

Analytical results for test cells' leachate over time are presented in Figures 1 to 4. Figure 1 illustrates the mass of water retained by each cell following the leach cycle. Of particular note are the results for HCT-4, which was only rinsed bi-weekly, showing the cell essentially drying out between leaching. Other cells display a loss of entrained water, but clearly maintain the presence of liquid water (not dried out) and moist vapor during the experiment.

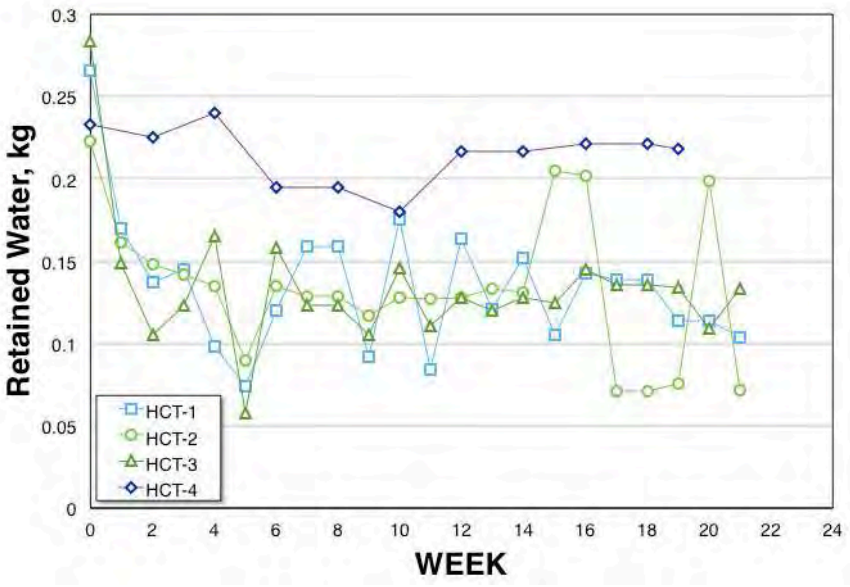

Figure 1 Cell water retention over time

Figure 2 is a graph of pH over time, and shows an expected decrease for two of three py+qtz cells. HCT-1 and HCT-4 (same pyrite grainsize, HCT-4 flushed bi-weekly) begin an immediate, but not instantaneous drop, reaching a value of 4 after 24 weeks. Oddly, HCT-3 (larger pyrite grainsize) remained generally steady for about 18 weeks, and then became more erratic, and trending toward lower values. As expected, the test containing calcite remained near neutral, but significantly below a value of about 8.2 that would be expected for qtz+cc without pyrite. The blank cell maintained a pH ranging from 5.7 to 6.3 throughout.

Figure 3 present results for sulfate, which shows an immediate and significant decrease over the first four weeks. All tests are generally steady after six weeks. Iron (Figure 4) shows an increase in tests where pH decreases. Sulfate and iron analyses for the blank cell produced were determined to be zero throughout.

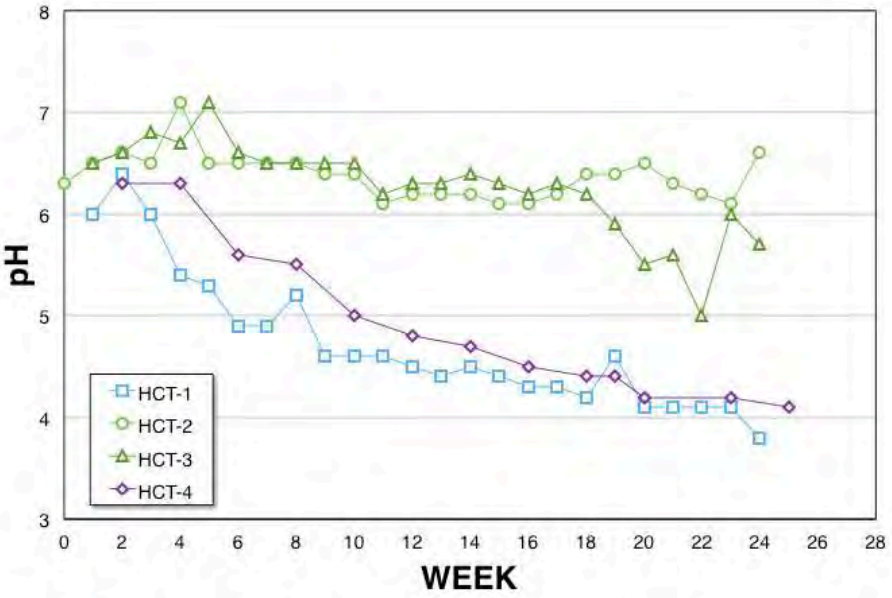

Figure 2 Leachate pH variation over time

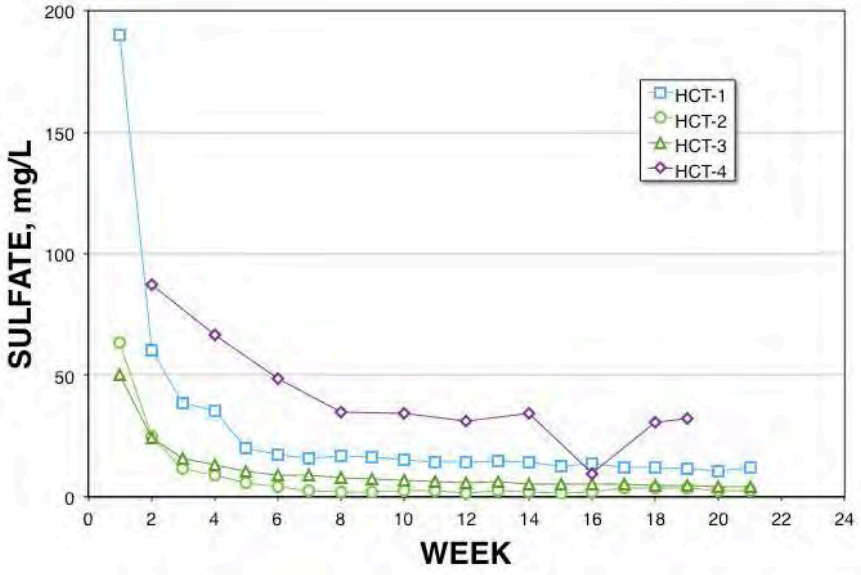

Figure 3 Leachate sulfate concentrations over time

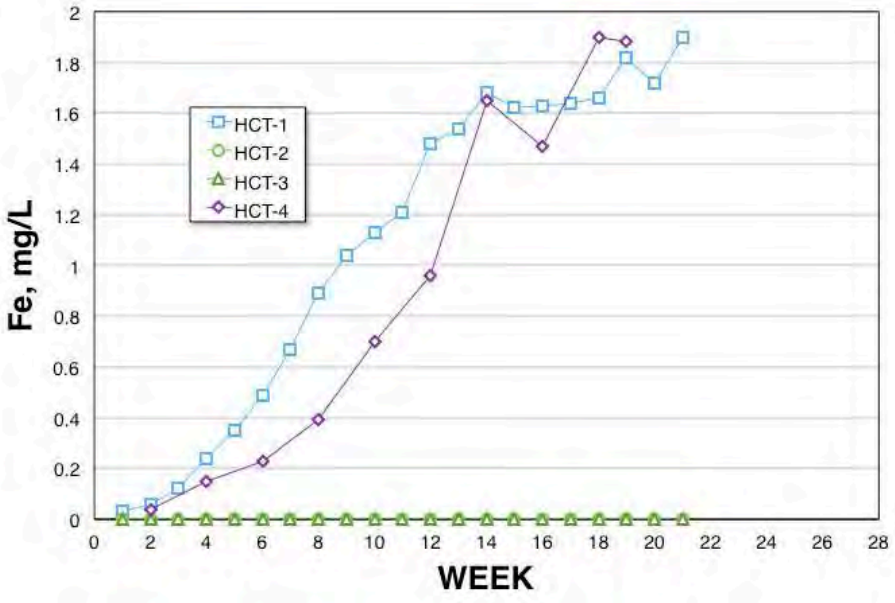

Figure 4 Leachate iron concentrations over time

Discussion

As expected, in py+qtz experiments, acidity is immediately produced by pyrite oxidation and the pH of leachate solutions begins to drop. However, despite the basic absence of acid neutralizing minerals (calcite), the pH decreases more gradually than might be expected. One py+qtz experiment, with larger grainsize pyrite, maintained near-neutral pH for about 18 weeks before it displayed a (slight) trend toward acidic conditions.

Consistent with common convention of reporting the results of HCT work, Figure 5 is a graph of the cumulative sulfate production in each test cell. In this case the sulfate production has been normalized to the mass of pyrite in the cell and not the total mass in the cell (1 kg). If the end-point of each test is used to calculate the overall rate of pyrite oxidation, the bi-weekly rinse test (HCT-4) produces less sulfate than the base case (HCT-1) and, therefore, might be interpreted to represent a slower rate of reaction. Similarly, the larger grainsize pyrite test (HCT-3) would also appear slower than the base case. However, a more appropriate basis upon which to compare rates of reaction, both between tests and with established literature is that of moles of pyrite destroyed, per meter squared, per second (mol py/m^2/s; Williamson and Rimstidt, 1994, Lappakko and Antonson, 2006), and can be calculated for each point (week) during the test.

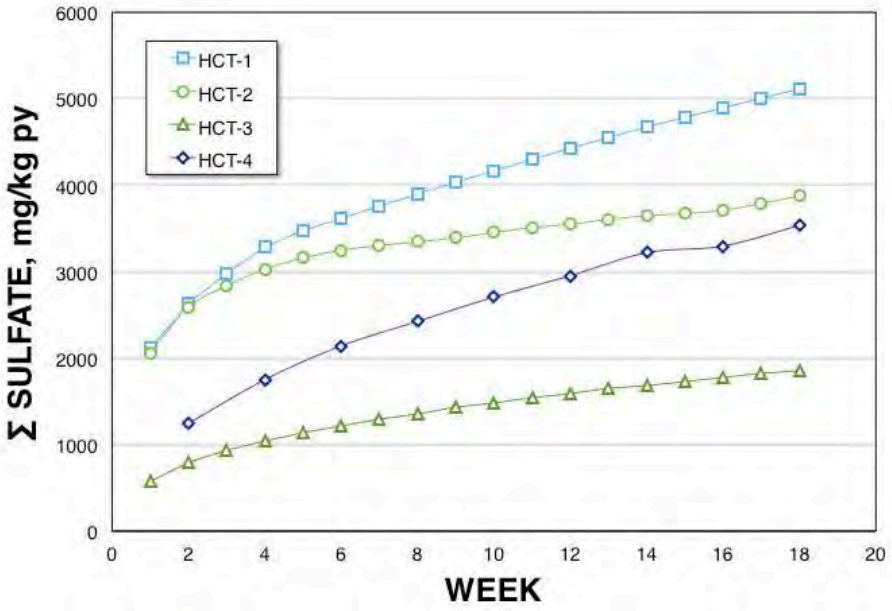

Figure 5 Cumulative sulfate production over time

When data are recast to mol py/m²/s, calculated for each period of measurement (either one week or two), the rates of pyrite oxidation show very consistent trends. Figure 6 illustrates the pyrite oxidation rates on this basis. Owing to the simple mineralogical composition and texture of the experiments, the data plot in a remarkably smooth fashion. All but one experiment (HCT-4) shows a relatively rapid initial rate that rapidly diminishes with time. All experiments converge to essentially the same fundamental rate. Thus, the presence of calcite and bi-weekly flushing ultimately appear to have little effect on the rate of pyrite oxidation. The agreement between cells with different grainsizes, confirms that the fundamental link between rate and reactive surface area applies under HCT conditions.

The observed rapid decrease in the rate of reaction (Figure 6) is consistent with literature for the oxidation of pyrite in vapor-only conditions. Over the course of many individual experiments, Jerz and Rimstidt (2004) observed the same basic trend. Figure 7 illustrates some typical data from one of their experiments. Like the rates in the current study, the initial rate is relatively fast, and rapidly diminishes to near steady rates with time. Jerz and Rimstidt (2004) attributed this observation to the build up of an adsorbed water layer that restricted oxygen transfer to the mineral surface via diffusion. Their estimates of the amount of pyrite destroyed did not lead to a conclusion of iron precipitate armoring of the pyrite grains. Such an effect may not apply to the current results, as the HCT provides for weekly rinsing However, a similar passivation may occur in HCT work as a result of armouring by weathering products (retention of iron) or a change in electrochemical properties of the pyrite itself (Williamson and Rimstidt, 1994). Although currently unavailable, on-going microscopic analyses intend to address these possibilities.

In the present experiments, each retained iron. This is shown clearly in Figure 4 for HCT-2 and HCT-3. Although the remaining two cells discharged iron, it was less than the stoichiometric amount expected from consideration of sulfate release. Thus, armoring by iron precipitates might be anticipated. However, in comparison with literature reports for pyrite oxidation in well-stirred,

liquid-only experiments, such armoring seems unlikely as reaction products are rapidly swept form the mineral surface.

Figure 8 illustrates the rate of reaction in the present test cells as a function of the pH, for each week. As described above, the rate drops rapidly and, in some cases, the pH decreases. The figure also shows the rate of reaction according to rate laws for liquid-only experiments (solid line; Williamson and Rimstidt, 1994) and for vapor-only rate laws for 100% relative humidity (Williamson, 2013). As shown, the present rates, over time, approach the rates for well-stirred liquid-only rates, (line for Williamson and Rimstidt, 1994 in Figure 8) where accumulation of iron precipitates is limited, to non-existent. Thus, the slowing of rates in the present test cells, despite retention of iron, does not appear to be explained by the accumulation of iron precipitates.

Lappakko and Antonson (2006) present a comparison of surface area corrected pyrite oxidation rates in their HCT cells with the rate laws of Williamson and Rimstidt (1994) and likewise conclude that there is close agreement, although the comparison is less favorable than the present cells. This difference is likely to be related to the great, but expected, difficulty in estimating reactive surface area for their clearly more complex test cell charges (rock).

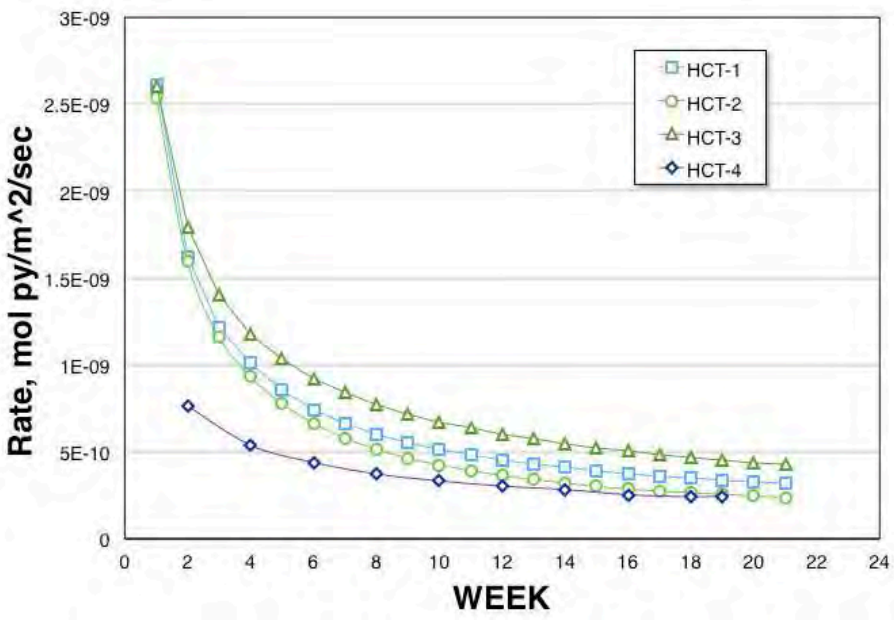

Figure 6 Rate of pyrite oxidation over time

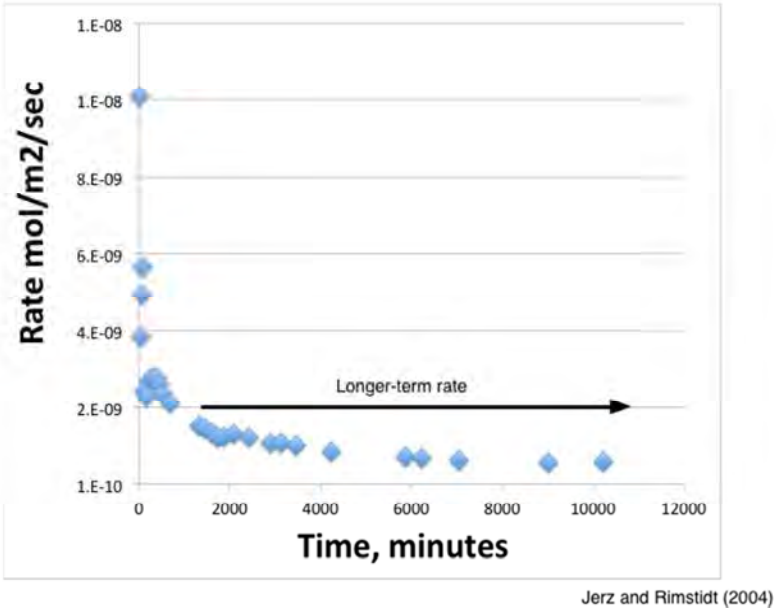

Figure 7 Rate of pyrite oxidation over time in vapour-only experiments

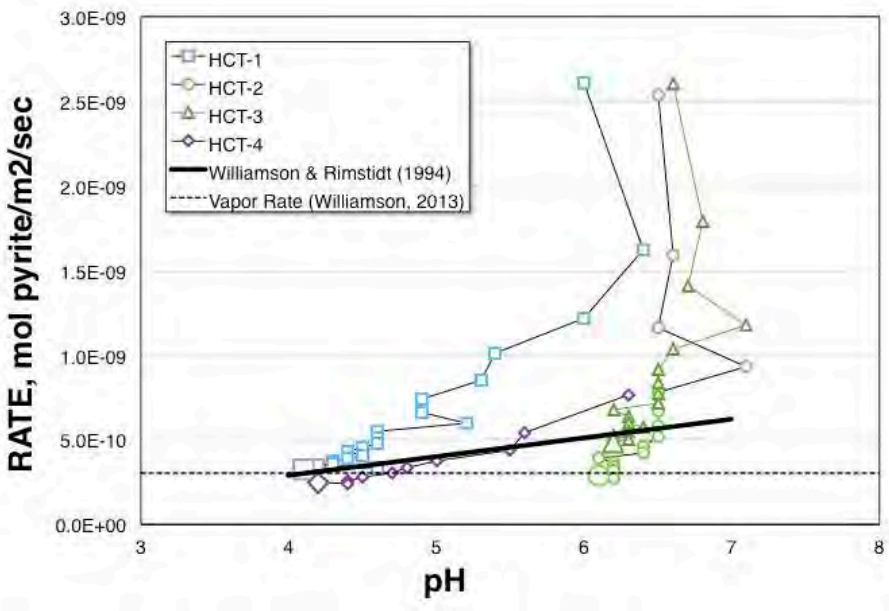

Figure 8 Rate of pyrite oxidation over time

CONCLUSION

The rate of pyrite oxidation in HCT liquid+vapor conditions, with routine flushing, is in close agreement with literature rates of reaction in liquid-only conditions and for vapor-only 100%

relative humidity. Although there is some thought that HCTs might retard the rate of reaction due to the retention of reaction products, it did not appear to be appreciable in the present test cells. There was only very limited difference in observed rate when pH was buffered by the presence of calcite, or for cells with pyrite of different reactive surface area, or indeed the rate of flushing.

ACKNOWLEDGEMENTS

The author acknowledges and appreciates the support and assistance of ACZ Laboratories of Steamboat Springs, Colorado, USA for providing a discount on costs and for their patience and willingness to prepare materials and run tests per experimental design.

REFERENCES

ASTM (2012) Standard Test Method for Laboratory Weathering of Solid Materials Using a Humidity Cell. *American Society for Testing and Materials.* Method D5744 – 12.

Caruccio 1968 An evaluation of factors affecting acid mine drainage production and ground water interactions in selected areas of western Pennsylvania. In *Proceedings of the Second Symposium on Coal Mine Drainage Research.* Bituminous Coal Research Inc. Monroeville, Pennsylvania.

Hammack, R. W. and G. R. Watzlaf (1990). The effect of oxygen on pyrite oxidation. Proceedings of the 1990 Mining and Reclamation Conference and Exhibition.

Jerz, J. and J. D. Rimstidt (2004). Pyrite oxidation in moist air. *Geochimica et Cosmochimica Acta*, **68**: 701-714.

Lapakko, K. and D. A. Antonson (2006). Pyrite oxidation rates from humidity cell testing of greenstone rock. *Seventh International Conference on Acid Rock Drainage*, St. Louis, Missouri, USA, American Society of Mining and Reclamation.

León, E. A., et al. (2004). Weathering of sulphide minerals at circum-neutral-pH in semi-arid/arid environments: influence of water content. *SuperSoil 2004: 3rd Australian New Zealand Soils Conference*, University of Sydney, Australia.

Sobek, A. A., et al. (1978). Field and Laboratory Methods Applicable to Overburdens and Minesoils. Cincinnati, *U.S. Environmental Protection Agency*. EPA-600/2-78-054

Williamson, M.A. (2013) Pyrite oxidation in two phase liquid+vapor conditions. *Geological Society of America Annual Meeting Programs with Abstracts.*

Williamson, M.A. and J.D. Rimstidt, J.D. (1994) The kinetics and electrochemical rate-determining step of pyrite oxidation. *Geochim. Cosmochim. Acta.* **58**: 5443-5454.

Comparison between Long-Term Humidity Cell Testing and Static Net Acid Generation (NAG) Tests: Potential for NAG Use in Preliminary Mine Site Water Quality Predictions

Andrew Barnes[1], Robert Bowell[1], Ruth Warrender[1], Devin Sapsford[2], Kelly Sexsmith[3], Jessica Charles[1], Julien Declercq[1], Marco Santonastaso[2] and Brian Dey[1]

1. *SRK Consulting, United Kingdom*
2. *Cardiff University School of Engineering, United Kingdom*
3. *SRK Consulting, Canada*

ABSTRACT

Kinetic testing is one of the key tools for predicting the long-term weathering of mine waste materials and their potential environmental impacts. The standard methodology commonly undertaken for kinetic testing of mine waste is the ASTM D 5744 humidity cell test procedure. However, this test requires a significant time period to generate representative data, with typical test duration in excess of 40 weeks. In some cases, it may even require years before suitable information is obtained. This long lead time can have significant impact on mine development schedules especially if the data is required by environmental regulators for the permit application procedures. Due to the time constraints of mine development programs, it is highly desirable to identify complimentary test methods that are able to deliver the required data for water quality predictions in a shorter period of time. One of the more promising methods is the use of hydrogen peroxide (H_2O_2) leach test (a common variant being the Net Acid Generation or NAG tests). The resulting NAG leach solutions can potentially be scaled to field conditions to allow for a preliminary prediction of mine waste seepage water quality. This paper compares results from NAG testing and long term humidity cell testing, including correlations between the two data sets to show whether NAG leaching is an appropriate method for preliminary rapid assessment of mine site drainage water quality.

Keywords: NAG test; Humidity Cell; Seepage prediction

INTRODUCTION

Exposure of sulfide minerals during mining results in gradual oxidation of these minerals and the associated release of solutes and acidity to the environment. This is commonly referred to as acid rock drainage (ARD) and metal(loid) leaching (ML) or ARDML. ARDML can result in significant detrimental ecological impacts which makes the prediction of water quality from mine sites one of the most critical aspects of the evaluation of mine design for permitting and/or closure applications. Prediction of ARDML and associated water quality impacts have become mandatory for studies in many mining jurisdictions and/or where international bank financing is required.

One of the primary objectives of an ARDML study is to determine if contaminants will be released and to predict the rate at which they will be released from each mining waste type. In order to do this, it is necessary to undertake a series of characterization tests. These tests can generally be classified into two types (MEND, 2009):

- Static tests – rapid testing procedures that deliver information on the finite materials characteristics, for instance, if the material is potentially acid generating, if it is enriched in certain elements of concern, what the immediate mobility of such elements are, and the potential for long term release of certain elements if the samples are fully oxidized.
- Kinetic tests –laboratory or field column tests that are used to determine the rate at which acidity is generated and solutes are released. Kinetic tests require a longer time period than static testing, and are usually run for 40 weeks or more.

Kinetic testing methods vary based on the particular scenario that is being examined and the required test outcome. The most commonly used kinetic test is the ASTM D 5744 Humidity Cell Test (HCT) (ASTM, 2013). This is an optimized weathering test in which a sulfidic material is exposed to alternating dry and humid air cycles followed by weekly flushing with deionized water at a high liquid to solid ratio. The test is intended to ensure that appreciable oxidation and solute release is achieved and is not designed to directly simulate field conditions.

The long lead time between the initiation of the tests and the time at which the test matures i.e. when the data obtained from the test is suitable for use in long term water quality predictions, can be many months (eg. Sexsmith et al, 2015). This is especially applicable with materials which are slow reacting and demonstrate a significant lag time to the onset of persistent acidic leaching conditions at which solute mobility and release from the cell is at its highest and most representative of long term weathering.

In many cases, the significant maturation time of kinetic testing does not fit in with the mine development schedule where timely water quality predictions are essential in order to ensure that the most suitable and cost effective mitigation measures are designed into the project at the earliest possible opportunity. In order to avoid such situations, it would be beneficial to develop a complementary methodology that can be used to undertake preliminary predictions of water quality far in advance of that provided by kinetic tests.

One of the most promising methods to address these needs is the use of solute release data obtained from Net Acid Generation (NAG) test. NAG tests are commonly used as a complimentary method to Acid Base Accounting (ABA) for the confirmation of a materials acid generating potential. In a standard NAG test, a 2.5g portion of pulverized sample is leached in 250mL of 15% hydrogen peroxide (H_2O_2) solution. The NAG test intends to fully oxidize the sulfide minerals contained within the sample, generating acidity, releasing sulfide-associated elements into solution and reacting with fast-reacting acid buffering carbonate minerals. As well as providing information on

acid generating characteristics, multi-element analysis of the generated NAG solution can reveal significant information on potential release of metals, metalloids and salts from the sample after complete sulfide weathering.

The NAG procedure has been sequentially developed by a number of researchers over the past 40 years; Smith et al. (1974), Sobek et al. (1978), O'Shay et al, (1990), Stewart et al (2006) and references therein; but so far, the use of NAG test data in the preliminary prediction of water quality for mine sites has not been addressed. The most likely reason for this is that analysis of NAG solution chemistry is not widely practiced and a reliable empirical database comparing standard kinetic (HCT) release rates and mass release from standard NAG test data is not readily available.

The purpose of this paper is to make comparison between multi-element assay of the NAG solution and the HCT results from the perspective of using NAG data to make a preliminary prediction of water quality suitable for use in mining development studies as a complementary methodology to (rather than a substitution for) standard kinetic testing methods.

The potential benefits of using such static tests for early water quality predictions would be to allow for better costing of engineering designs early on in a feasibility study program to mitigate the potential impact of ARDML to the environment without inclusion of excessively cautious designs approaches.

Prediction of water quality through scaling of kinetic data

Although it can be argued that the use of HCT data for the prediction of mine site water quality is less than ideal (i.e. Sunkavalli, 2014), it is not the intention of this paper to examine this. Therefore in this study, kinetic testing refers to standard ASTM D-5744 HCT and the resulting solute release rates. However, the author acknowledges that elemental release rates can be obtained from a large variety of kinetic tests, some of which are arguably superior to HCT more closely simulating field conditions in terms of fluid flow, temperature or liquid to solid ratio.

In order to convert laboratory derived solute release rate (R*lab)* into field water quality predictions, it is necessary to upscale R*lab*, to take into account such factors as oxygen availability, particle size distribution, and field temperature variation to give a primary field release rate (R*field*). Once R*field* has been calculated, it is then possible to estimate a concentration in pore water by taking into account the difference between laboratory and field liquid to solid ratio. The solute concentrations calculated using this method then need to be equilibrated using a thermodynamic equilibrium code (such as PHREEQC, Parkhurst and Appelo, 2013) to take into account such things as mineral saturation and adsorption to mineral surfaces. The resulting solutions 'source term' concentration can then be incorporated into site wide water quality predictions and / or assessed against relevant water quality guidelines, and used to develop suitable mitigation controls in the design and cost estimates prior to mine development.

Alternative methods of water quality prediction may also be undertaken such as deriving water quality from primary mineral weathering rates (effectively from first principals i.e. Linklater et al (2005) and references therein). However, these methods are complex and require data that is usually difficult to obtain during a mine development study. In addition, the first principal method of modeling commonly does not take into account all of the contaminants released from a deposit which would be included if scaling of kinetic test data is included. It is also possible to make a preliminary prediction of water quality from empirical relationships and analogue sites. This is often a very useful first approach (MEND, 2009) but again, does not take into account intricacies and variations that can be obtained through the scaling of leaching test data.

Potential for substitution of kinetic "rates" with static test release data

It is plausible that R*lab* obtained from kinetic testing can be substituted for an alternative rate derived from static testing methods. However, static tests generate only a mass release (usually referred to in mg/kg) and thus a release rate has to be assigned - for example, by assuming that all of the sulfide-S content of a sample is released as sulfate equally over a given time period. Furthermore, in the case of water leaching tests such as EN12457 or MWMP tests, the mass released often represents only the dissolution of soluble salts that are rinsed from the sample surface and do not take into account the release of solutes due to the oxidative dissolution of sulfides, and associated acidity driven dissolution.

The NAG test has the benefit of being able to determine (i) the solute release attributed to sulfide oxidation though the reaction of hydrogen peroxide (H_2O_2), and (ii) the solubility of the solutes at the pH of the final NAG solution. Therefore this method shows the most promise for use in rapid prediction of long-term weathering water quality. However, due to the very rapid reaction of H_2O_2 with the sulfide minerals within a mine waste sample, complete oxidation is commonly achieved within a matter of hours. Although attempts have been made to measure NAG release rates (Kinetic NAG), the exothermic breakdown of H_2O_2 during the test often results in very high temperatures which make measurement of a sulfide oxidation rate difficult.

Any rate used to substitution for R*lab* (HCT) must be derived in some way from the total mass release. The NAG tests simply gives a bulk release of sulfide-associated elements, an average for the entire humidity cell release if it were to be run to sulfide exhaustion. Additionally, NAG tests suffer many additional complications. For instance, incomplete oxidation of sulfides is often observed in samples due to the decomposition of H_2O_2 during the test. This is promoted by increasing pH and by the presence of catalytic metal ion, such as Mn, Fe and Cu or, in alkaline solution, by the presence of the carbonate ion (Liochev and Fridovich, 2004 and references there in) and in some cases simply by the method employed for the analysis (Charles et al, 2015). Despite these drawbacks, NAG tests may represent one of the most favorable static tests for rapid determination of water quality impacts.

Comparison of NAG data with HCT data

Eight samples of moderate to high sulfur waste rock materials were subjected to long term (greater than 160 weeks) ongoing HCT testing, details of the ARD characteristics of the samples are given in **TABLE 1.** The deposit utilized for the testing is a magnetite resource within an Iron Oxide Copper Gold (IOCG) style of mineralization. The deposit is characterized by a moderately elevated coarse grained sulfide (pyrite / pyrrhotite / chalcopyrite) content hosted in quartz veins within amphibolites, diorites and schists lithologies. Total sulfur (almost all present as sulfide sulfur) is in the range of 0.1 to 5 wt.%. In addition to sulfides, the deposit also has a relatively uniform but low magnitude carbonate mineral assemblage with inorganic carbon consistently between 0.05 - 0.5 wt.% and averaging 0.08 wt.%. All the static testing undertaken on the samples demonstrated them to be acid generating and all NAG tests produced pH conditions below pH 4.5.

Comparisons are made of data between times at which the HCTs were at circum-neutral pH and them later at acidic pH. It is important to note that within ARD systems, as pH decreases to < 4, dissolved Fe(III) becomes increasingly soluble and more important than O_2 as the (direct) sulfide oxidant. Laboratory data indicate that sulfide oxidation rates are circa one order of magnitude higher under acidic conditions than rates under neutral (O_2 dominated) pH conditions (cf.

McKibben and Barnes (1986); Olson (1991) and Rimstidt et al (1994). Observation made by the authors from previous kinetic testing have shown that, the ratio between sulfide oxidation rates at neutral pH and peak (maximum) sulfide oxidation rates under acidic condition may reach the factor of 10 and in some cases exceed this. However, this was generally only observed for a short duration (<10 weeks) and was not representative of average sulfide oxidation rates under acidic conditions. When the long term neutral and long term acidic sulfate release rates were compared, the ratio between neutral and acidic rates decreased significantly with a median ratio value of 4.87 and ranges between 1.8 and 8 (see inset graph in **FIGURE 1)**

Table 1 Summary of geochemical characteristics of waste material used in humidity cell testing

Sample No.	Material Type	Acid Base Accounting							NAG pH	Ave. week 151 – 160 HCT pH
		TIC	Total Sulfur	AP	NP from TIC	NP from Titr.	NNP Titr.	NPR Titr.		
		%	%	kg CaCO3 eq/t						
1	Skarn	0.10	3.25	93.31	8.33	11.00	-82.31	0.118	2.7	4.75
2	Schist	0.68	2.92	87.81	56.64	35.50	-52.31	0.404	2.8	4.27
3	Amphibolite	0.07	1.98	58.75	5.83	7.25	-51.50	0.123	3.3	5.97
4	Amphibolite	0.04	3.07	86.75	3.33	3.75	-83.00	0.043	2.8	*3.81*
5	Amphibolite	0.04	0.76	22.02	3.33	4.75	-17.27	0.216	3.7	4.92
6	Diorite	0.10	2.18	61.25	8.33	5.50	-55.75	0.090	3.2	5.60
7	Diorite	0.05	1.74	52.18	4.17	4.00	-48.18	0.077	3.3	6.35
8	Diorite	0.04	0.53	14.51	3.33	4.50	-10.01	0.310	4.2	6.80

NP	Neutralizing Potential	AP	Acid Generating Potential
NNP	Net Neutralizing Potential (NP-AP)	TIC	Total Inorganic Carbon
NPR	Neutralizing Potential Ratio (NP/AP)		

The main plot in **FIGURE 1** compares the rate of sulfate release at different periods within the HCT to the total sulfate mass release from the corresponding NAG tests. The red points represent early stage weathering (weeks 21 to 40) during which time pH of all HCT leach solutions was above pH 7 whilst ensuring that the early stage flushing of soluble sulfate salts had occurred. The second period is between weeks 151 and 160 which is the most recent data available and represents the cells at their lowest recorded pH and highest sulfate release (blue points). In both cases, a reasonable correlation can be drawn between the NAG release and HCT release rates with R^2 of 0.72 for weeks 21 to 40 and 0.93 for weeks 151 to 160, for linear best fit and zero intercepts. The slope of the correlation for weeks 21 to 40 is 0.0012 (1/776), whilst this is roughly double for weeks 151 to 160 at 0.0025 (1/391). This demonstrates the following:

1) That the rate of release in the HCT is proportional to the NAG sulfate release and likewise the total sulfur content of the samples. This is logical for samples such as these where sulfides (and their exposed surface area) are distributed uniformly through the sample.
2) That this proportionality between HCT S release rate and NAG S release is maintained at later stages of the HCT when pH is lower, albeit with higher HCT sulfate release rates.

3) That as with other literature, sulfide oxidation rates within the HCT increase as pH conditions become more acidic. In the example given here, the sulfate release rate has doubled between neutral and mildly acidic pH conditions of the test.

The upper orange line in **FIGURE 1** represents a 4.87 increase in the neutral oxidation rate as discussed above. Applying a factor of 4.87 to the week 21 to 40 rate slope of 1/776 gives a predicted sulfate release rate (under acidic conditions) / NAG sulfate release slope equal to 0.00635 (1/157.5) x the total NAG S. Or restated for clarity, after 157.5 weeks, the total sulfur content of the sample would be released at a fixed rate to exhaustion.

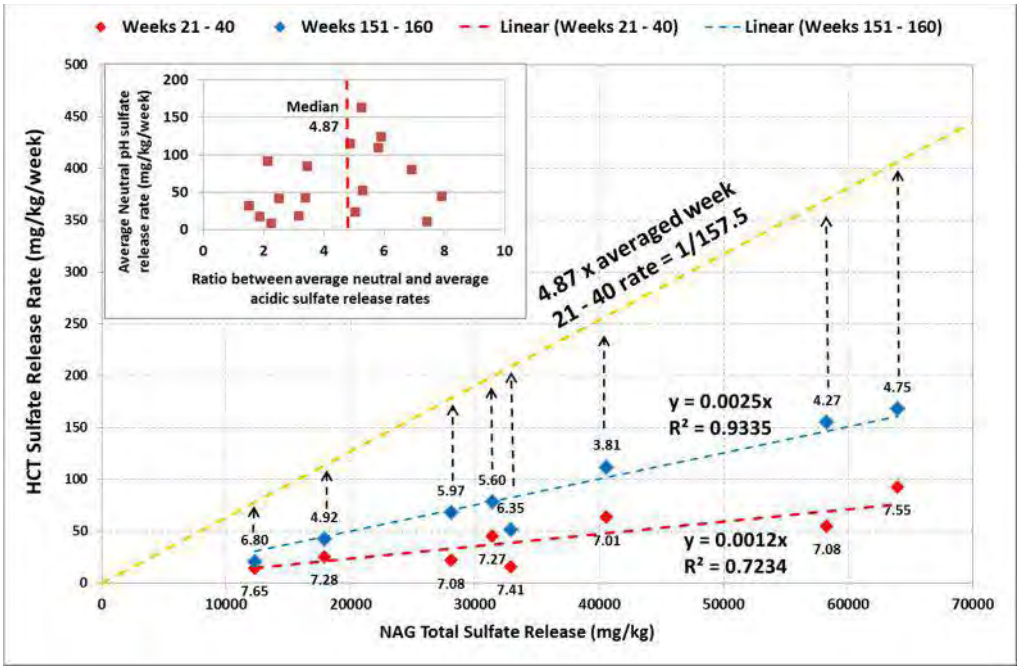

Figure 1 Variation between NAG release (mg/kg) and HCT sulfate release rate (mg/kg/week) for weeks 21 to 40 and weeks 151 to 160 HCT data respectively. Data point labels correspond to the average HCT pH for the period. The orange dashed line corresponds to 4.87 times multiplication of the weeks 21 to 40 slope rate resulting in a slope of 1/157.5. The inset graph shows the range of ratios between sulfate release rates under neutral and acidic conditions from previous HCT data.

Logically, for sulfide-bound metals, the rate at which sulfide is oxidizes and sulfate is released should correspond to the rate at which other sulfide-associated elements are released – except where solubility limits constraint this. The plots in **FIGURE 2** compare HCT release rates for Cu, Co, Ni and Zn with the corresponding calculated metals release rates using NAG test data divided by a factor of 157.5 (i.e. assuming that under acidic conditions within the HCT, that the total NAG metals are released linearly over 157.5 week period). Also shown is the line of unity between HCT and calculated NAG release rates. Measured HCT release rates are shown for both the average week 21 to 40 data and the 141 to 150 data.

It is clear that measured releases are significantly higher in the 141 to 150 period compared with the 21 to 40 period. In fact, during the early weeks of testing, both Cu and Co concentrations were consistently below the analytical detection limit (ADL) within the tests which accounts for the flat trend observed. Ni and Zn were both above ADL during the week 21 to 40 period with Ni showing a good linear correlation with calculated NAG Ni release rates.

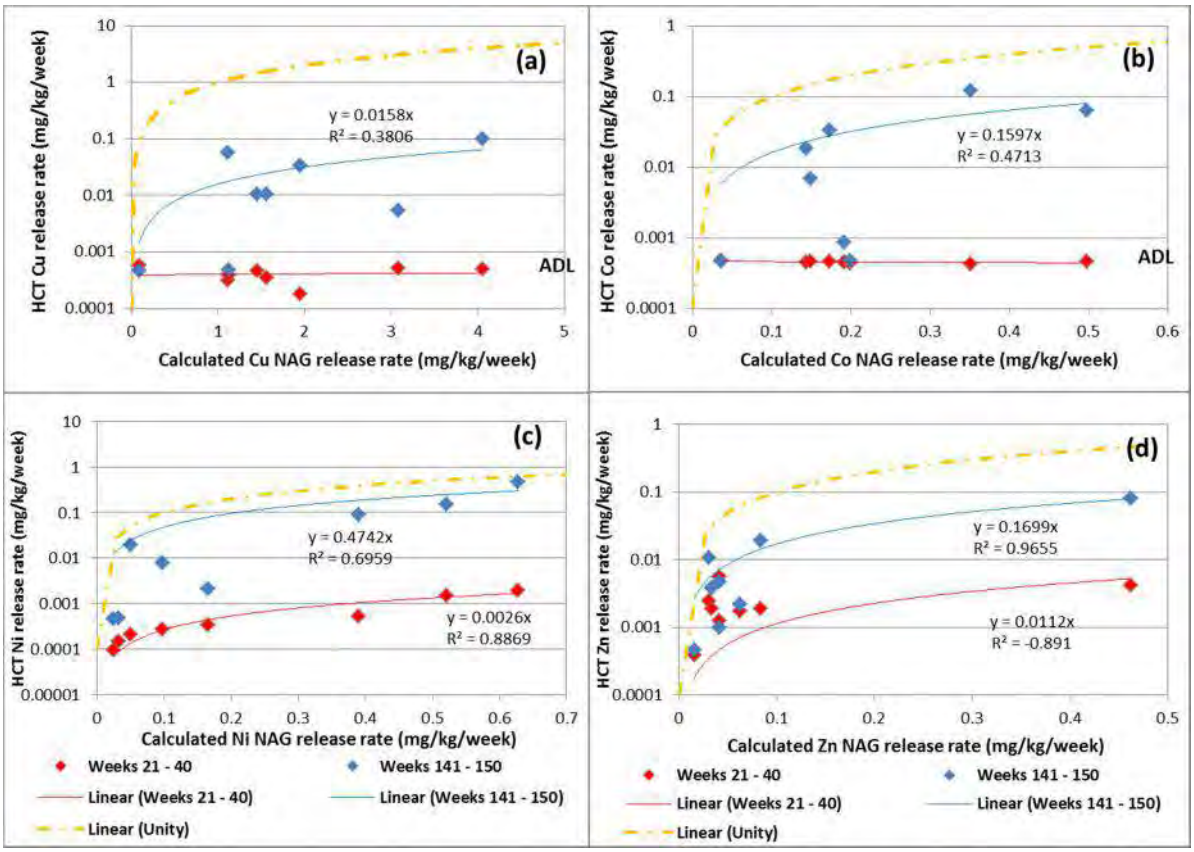

Figure 2 Comparison between measured HCT metals release rate (mg/kg/week) and calculated NAG release rate using the factor of 157.5 correction (as mg/kg/week equivalent) for a) Cu b) Co c) Ni and d) Zn. Comparison is made for HCT weeks 21 to 40 data and HCT weeks 141 to 150 data. The orange dashed shows 1:1 ratio between measured HCT release rates and calculated NAG release rates.

Metals release rates from the HCT increase significantly for Co, Cu, Ni and Zn, in most samples, between early stage and late stage leaching. However, it can be demonstrated that this increase in metals release is largely a result of the increasingly acidic pH as opposed to purely an increase in the rate of sulfide oxidation and primary release. For example, where the rate of sulfate release between early stage and late stage HCT weathering increases by a factor of about 2, in most cases, metals release increases by about 2 orders of magnitude for Co, Cu and Ni, and 1 order of magnitude for Zn. Therefore, the increasing sulfide oxidation rate cannot directly account for the increasing metals release. In order to further clarify this, a plot comparing metals release rate from the early stage and late stage HCT for Co, Cu, Ni and Zn against pH was produced (see **FIGURE 3**). This shows the clear log linear correlation between metals release rate and pH, behavior typical for transition metals cations due to retention through adsorption to iron oxides (Dzombak and Morel, 1999). The strong pH control of transition metal cations makes decoupling of the two processes of (i) primary release from sulfide minerals and (ii) actual release from the HCT column extremely difficult from HCT that have not reached acidic pH (pH << 4) due to the high proportion of metals being retained within the column. Due to the HCT metals release rate being compounded by sulfide oxidation rate and metals retention, it is difficult to use immature HCT release data to predict future release rates under acidic conditions without allowing the tests to run until such time as acidic pH conditions are reached. Because of the low final NAG pH, the calculated NAG metals

release rates are not anticipated to be significantly moderated by sorption (in this example) and therefore, use of the calculated NAG release rate allows a better indication of long term release rates than could be achieved through scaling of premature HCT test data alone. This is where NAG test data can prove highly beneficial, to demonstrate this, the calculated NAG metals release rate plotted against the NAG test solution pH has also been included in **FIGURE 3**.

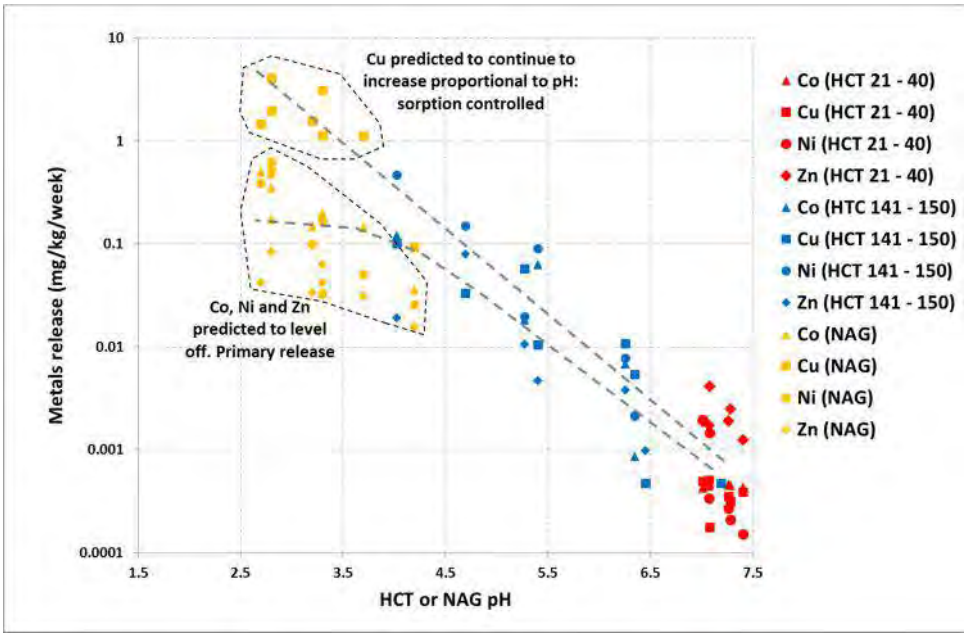

Figure 3 HCT metals release rates (mg/kg/week) verses pH for weeks 141 to 150 data. Also shown are predicted metals releases corresponding to NAG release rate (mg/kg) divided by a factor of 157.5.

The difference between measured and actual metals release rate are most apparent with the behavior of Cu. This is due to its high affinity for adsorption to iron oxides and the low adsorption edge relative to Co, Ni and Zn (Dzombak and Morel, 1999). The lower pH adsorption edge of Cu means that even at week 141 – 150, where most cells are generating mildly acidic pH solutions, a significant proportion of the Cu released through sulfide oxidation is likely to be retained within the cell through adsorption to iron oxides. It is only when the pH within the HCT drops significantly below 4 (assuming that this will occur) that the Cu release are predicted to increase to levels reflect by the proportion relationship with the NAG test data. Once the pH within the HCT solutions have declined below the adsorption edge of a particular metal, then the concentration of the metal within the solution should correlate with the sulfate release rate as the metal will no longer be retained within the cell. This can only be fully clarified by continuing the HCT tests until stable acidic pH are reached.

CONCLUSION

- For the particular samples and deposit type described in this paper, a good correlation was identified between HCT sulfate release rates and NAG test total sulfate release. This reflects the total available sulfur content within the sample which for these samples is correlated to the exposed sulfide mineral surface area.

- For samples that are expected to become acidic, the sulfide oxidation rate (in line with observations and literature) is expected to increase. It is possible that the initial sulfate release rate can be extrapolated to the final acidic pH release rate.
- The scaling of release rates under neutral condition to those under acidic conditions although logical for sulfate release, may not be applied to metals release so readily due to retention of metals by adsorption within the column. NAG test data shows promise for supplementing HCT prediction data by giving an indication of the maximum sulfide-associated metals release that can be expected under acidic conditions.

REFERENCES

ASTM (2013) Standard Test method for Laboratory Weathering of Solid Materials Using a Humidity Cell. ASTM D 5744-13e1.

Charles, J.C., Barnes, A., Declerq, J., Warrender, R., Brough, C., Bowell, R.J. (2015). Difficulties of interpretation of NAG test results on net neutralizing mine wastes: initial observations of elevated pH conditions and theory of CO2 disequilibrium. In: Proceedings of the 10th International Conference on Acid Rock Drainage and IMWA Annual Conference. April 21 – 24, 2015. Santiago, Chile. ppTBC

Dzombak, D. and Morel, F. (1990). Surface Complexation Modeling: Hydrous Ferric Oxide. J. Wiley, New York.

Linklater, C.M., Sinclair, D.J., Brown, P.L. (2005). Coupled chemistry and transport modeling of sulphidic waste rock dumps at the Aitik mine site, Sweden. Applied Geochemistry 20. 275-293.

Liochev, S.I., Fridovich, I. (2004) Carbon dioxide mediates Mn(II)-Catalyzed decomposition of hydrogen peroxide and peroxidation reactions. PNAS 101(34). 12485-12490.

McKibben, M.A., Barnes, H.L. (1986). Oxidation of Pyrite in Low Temperature Acidic Solutions: Rate Laws and Surface Textures. Geochimica Et Cosmochimica Acta 50(1). 509-520

MEND. (2009). Prediction Manual for Drainage Chemistry from Sulphidic Geological Materials. MEND Report 1.20.1. Report prepared by Price, W.A. December 2009. pp579.

Olson, G.J. (1991). Rate of pyrite bioleaching by *Thibacillus ferrooxidans* – results of an interlaboratory comparison. Applied Environmental Microbiology 57. 642-644.

O'Shay, T.A., Hossner, L.R., Dixon, J.B. (1990) A modified hydrogen peroxide oxidation method for determination of potential acidity in pyritic overburden. Journal of Environmental Quality 19. 778-782.

Parkhurst, D.L. Appelo, C.A.J. 2013. Description of Input and Examples for PHREEQC Version 3--A Computer Program for Speciation, Batch-Reaction, One-Dimensional Transport, and Inverse Geochemical Calculations

Rimstidt, J.D., Chermak, J.A., Gagen, P.M. (1994). Rates of reaction of galena, sphalerite, chalcopyrite and arsenipyrite. In *Environmental geochemistry of sulfide oxidation*. (eds. C.N. Alpers and D.W. Blowes), American Chemical Society, Washington, DC, vol. 550, pp. 2-13.

Sapsford, D. Bowell, R., Dey, M., and Williams, K. A (2009) Humidity cell tests for the prediction of acid rock drainage. Minerals Engineering 22(1). 25-36.

Sexsmith, K., MacGregor, D., Barnes, A. (2015) Comparison of actual and calculated lag times in humidity cell tests. In: Proceedings of the 10th International Conference on Acid Rock Drainage and IMWA Annual Conference. April 21 – 24, 2015. Santiago, Chile. ppTBC

Sobek, A.A., Schuller, W.A, Freemen, J.R. and Smith R.M. (1978). Field and Laboratory Methods Applicable to Overburdens and Minesoils. Report EPA-600/2-78-054, US National Technical information Report. PB-280495.Stumm, W. and Warner, J.J. (1996). Aquatic Chemistry: Chemical Equilibria and Rates in Natural Waters. 3rd Edition. Environment Science and Technology.

Stewart, W.A., Miller, S.D., Smart, R. (2006). Advances in Acid Rock Drainage (ARD) Characterisation of Mine Wastes. Paper Presented at the 7th International Conference on Acd Rock Drainage (ICARD), March 26-30, 2006, St Louis MO. R.I. Barnhisel (ed.) Published by the American Society of Mining and Reclamation (ASMR), 3134 Montavesta Road, Lexington, KY 40502. Pp 2098 – 2119

Sunkavakki, S.P. (2014). Gap between Humidity Cell Testing Data and Geochemical Modelling of Acid Rock Draiange. Hydrology Current Research 5(1).

Coupled Modeling of Iron Loads from Lignite Mining Dump Groundwater to the Pleiße River

Heike Büttcher[1], Holger Mansel[1] and Lutz Weber[2]

1. *Ingenieurbüro für Grundwasser GmbH, Germany*
2. *Lausitzer und Mitteldeutsche Bergbau-Verwaltungsgesellschaft, Germany*

ABSTRACT

The lignite mining dump of Witznitz in Central Germany is characterized by iron concentrations in groundwater up to 4 g/L. Rising groundwater levels after the mine was closed in 1993 have resulted in the discharge of consistently high iron loads to the adjacent Pleiße river.

The quantity of groundwater discharge to the stream is described by a 3D groundwater flow model using the program PcGeofim. In order to predict the groundwater hydrogeochemistry, a batch model using the PHREEQC geochemical modeling package was firstly set up to reproduce the genesis of dump groundwater by considering the processes of iron disulfide weathering, solution of calcite and silicates as well as the formation of new minerals such as gypsum and siderite. The model was calibrated using a set of 350 groundwater analyses from 50 wells in the dump and investigations on the solid phase of the dump material. As a result, the mean iron disulfide degree of weathering was determined to be 18% of the total dump iron disulfide.

Based on this, both models were coupled using a Python script by implementing the hydrogeochemical batch model including mineral phases into each cell of the groundwater flow model. Thereby, the spatial variability of the degree of iron disulfide weathering was taken into account by Monte Carlo simulations. As a result, groundwater solute concentrations were predicted to decline in conjunction with the groundwater recharge and solution of the secondary mineral pool takes place, whereas the velocity of the process is determined by the rate of groundwater recharge as well as groundwater flow. Implementing the Pleiße river as a boundary condition in the model makes it possible to predict the quality and quantity of groundwater discharge into the river.

Keywords: reactive solute transport modeling; iron loads; dump aquifer; PcGeofim

INTRODUCTION

The surface water quality of the Pleiße river in the lignite mining area south of Leipzig, Germany, shows total iron concentrations of up to 6 mg/L during periods of low water. Besides the visual impact, the high iron concentration results in iron clogging of the river bottom as well as negative effects on the aquatic ecosystem. By this, the achievement of a good ecological potential in accordance to the European Water Framework Directive is hindered.

Iron originates from the lignite mining dumps alongside the river, whose groundwater exfiltrates into the river. Due to iron disulfide oxidation of tertiary sediments, the dumps are often rich in bivalent dissolved iron. During the transition from the anoxic groundwater to the aerated environment of the river, oxidation to trivalent iron takes place as well as further formation of iron(3)-hydroxides or -hydroxysulfates, respectively. The process is accompanied by the formation of acidity.

One major source of iron in the Pleiße river is the dump of the former surface mine Witznitz, which was operated between 1946 and 1993. Dump material mainly consists of quaternary flood sediments and tills as well as tertiary marine overburden and the adjacent sediments of the removed coal seams. After the devastation of the original river bed, the Pleiße river was relocated directly across the dump during the 1960s. Following the termination of operations, uplift of the groundwater table, which was formerly lowered by mining activities, began. This is connected with a direct discharge of dump groundwater into the river.

Recent mean total iron concentrations measured in dump groundwater are 1050 mg/L, whereas the mean pH is slightly acidic at 5.3. The ionic balance is decisively influenced by the concentrations of both calcium (480 mg/L) and sulfate (3700 mg/L). The spatial variability of iron concentrations is great, ranging from 26 to 4510 mg/L. This is due to a varying geochemical composition of the source material of the dump as well as a differing intensity of oxygen contact and iron disulfide weathering taking place during fore field drainage and dump formation as well as on active mining slopes and exposed dump surfaces.

In order to predict future dump-originated solute inputs to the Pleiße river, a reactive solute transport model was developed for the Witznitz dump, which allows a spatially differentiated calculation of groundwater discharge to the river both in quantity and quality.

METHODOLOGY

Reactive solute transport modeling was realized by coupling the groundwater flow and solute transport model PcGeofim (Blankenburg et al., 2013) with the hydrogeochemical simulator model PHREEQC (Parkhurst & Appelo, 1999). By coupling the two models, it is possible to take into account reactions within the liquid phase, interactions between liquid and solid phase, such as iron disulfide weathering, as well as gas exchange processes in combination with transport modeling.

Model coupling was taken out by a programming script using the language Python. For each time step in the model, groundwater flow and solute transport was calculated, taking into account 11 different migrating solutes. Using the solute concentrations resulting from this calculation, hydrogeochemical batch calculations were carried out between liquid, solid and gas phases for each cell. Thereby, the pH, which is a non-conservative parameter, is recalculated in every batch calculation based on the charge balance. The resulting solute concentrations are then used for the

groundwater flow and solute transport calculation of the next time step. Solid phase contents and cation exchange allocation are saved using internal storage.

Groundwater flow model

The 3D groundwater flow model of the Witznitz dump is part of a large-scale model which comprises the whole lignite mining area south of Leipzig. The surrounding consists of mining dumps as well as active mining areas with a still massive lowering of the groundwater table. PcGeofim calculations are based on the method of finite volumes.

The model grid of the Witznitz dump is 62.5 x 62.5 m. In vertical direction the dump is divided into six aquifer layers and coupled onto the adjacent natural aquifers. The hydraulic conductivity of the dump aquifer was calculated from the silt and clay content using an empirical relationship according to Kaubisch (1986). Kf-values of the upper dump are in the order of 10^{-6} m/s, whereas the lower dump is characterized by values in the order of 10^{-8} m/s. Groundwater flow therefore takes place primarily in the upper part of the dump aquifer. Surface waters such as the Pleiße river as well as mining lakes are implemented as boundary conditions. Groundwater recharge is derived from the catchment model ArcEGMO (Becker et al., 2002) and amounts to an average of 80 mm/yr considering the whole dump body.

The groundwater flow model was calibrated using measured hydraulic heads from 65 piezometers within the dump body. The standard deviation between measured and calculated hydraulic heads was 1.3 m.

Hydrogeochemical batch model of dump genesis

The batch model represents the genesis path of dump hydrogeochemistry originating from the initial unweathered substrates during dump formation to the recent monitored conditions. Similar modeling approaches were used *e.g.* by Wisotzky & Obermann (2001) for the Rhineland lignite mining area.

The primary minerals of the model are iron disulfide FeS_2, calcite $CaCO_3$, clay minerals (for the sake of simplicity represented by kaolinite $Al_2Si_2O_5(OH)_4$) as well as primary silicates such as feldspars or micas (fig. 1). The mineral contents were derived from the measured contents in the original geological layers that now form the dump body, taking into account the portions of the single layers in the dump structure.

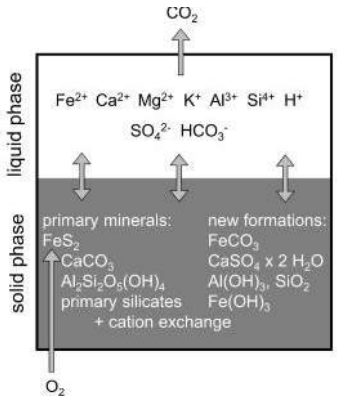

Figure 1 Hydrogeochemical process model

This results in an overall initial iron disulfide content of 2.1 mass-% and calcite content of 0.5 mass-% for the purpose of the model. Kaolinite is simplistically assumed to be abundant, whereas the weathering of primary silicates is coupled to the turnover of iron disulfide and fitted during calibration.

A stepwise addition of oxygen leads to an oxidation of iron disulfide and a release of iron, sulfate und acidity. Buffering is primarily provided by calcite and after depletion at lower pH values by clay mineral solution. Dissolution of primary silicates is a kinetically slow process which takes place in parallel with the processes mentioned before. As a result, the ionic strength of the liquid phase increases. On one hand, CO_2 originating from calcite weathering degasses in part; on the other hand, new mineral phases start to form. Siderite ($FeCO_3$) is a transient mineral formation of the released iron, which, however, gets resolved at lower pH values. A further new mineral formation is represented by gypsum ($CaSO_4x2H_2O$). Solution of silicates and clay minerals leads to the formation of aluminum hydroxide as well as silicon dioxide. Beyond that, precipitation of a mineral phase of trivalent iron is implemented in the model, as weathering of iron disulfides takes place mainly during unsaturated oxic conditions. At pH values > 3, iron hydroxides, oxyhydrates, or hydroxisulfates are formed. Exhibiting higher degrees of crystallization, part of these are irreversibly fixed within the dump substrate and are therefore stable against reductive dissolution during the uplift of the groundwater table. In the model this irreversible reaction was considered by an additional iron sink, which is coupled to the degree of iron disulfide weathering. Finally, the model takes into account the cation exchange of calcium, manganese, potassium, iron, and aluminum with an overall exchange capacity of 2.1 $cmol_c/kg$, which reflects the measured mean conditions in soil samples obtained from the dump body.

The model was calibrated using 350 chemical analyses from 50 monitoring wells and piezometers within the dump body as well as 87 soil samples, which were mainly analyzed for sulfur and carbon species as well as main cations and the cation exchange capacity. Based on the measurements, the process model was adjusted by varying solubility products of mineral phases, the portion of irreversibly bound trivalent iron minerals as well as the maximum partial pressure of CO_2. The computational realization was done by means of the simulator PHREEQC using the database wateq4f.dat.

Solute transport model of dump discharge

Model coupling of the groundwater flow and solute transport model with the hydrogeochemical batch model was realized alongside nine representative 2D vertical-plane cuts crossing the dump in groundwater flow direction to the Pleiße river. In principal, 3D modeling would also be possible. The advantage of the 2D cuts, however, is a clarity, which facilitates an understanding of the ongoing processes.

Discretization of the cuts was 50 m in the horizontal and 5 m in the vertical direction. Parameterization of hydraulic conductivity as well as hydraulic boundary conditions and groundwater recharge was taken from the 3D groundwater flow model of the Witznitz dump.

The hydrogeochemical batch model was implemented into every model cell using a Python script for model coupling. It considers primary iron disulfide oxidation taking place by fore field drainage and trapped oxygen during dump construction as well as on active mining slopes previous to the fill-up of the dump with groundwater. Spatial variability of the degree of iron disulfide oxidation as a percentage of the initial iron disulfide content was taken into consideration by Monte Carlo

simulations using a random generator based on a normal statistical distribution to calculate the turnover for every model cell.

Secondary iron disulfide oxidation takes place via the dump surface after the termination of the dump formation. It is accounted for by an additional oxygen input and corresponding iron disulfide turnover, which decreases successively with the age of the dump as growing vegetation reduces the oxygen input by soil respiration and iron disulfide minerals get less accessible to weathering due to passivation. In cases of oxic conditions close to the dump surface as a result of iron disulfide depletion, the formation of schwertmannite is allowed to take place according to the formula $Fe_{16}O_{16}(OH)_{9.2}(SO_4)_{3.4}x36H_2O$ (Bigham et al., 1996) in addition to the processes defined in the hydrogeochemical batch model.

The model was calibrated by using the same analytical data as for the calibration of the hydrogeochemical batch model, but also considering spatial patterns in total iron concentrations, particularly, variation with depth. Fitting parameters were given by the degree of primary iron disulfide oxidation including its standard deviation for Monte Carlo simulations to reproduce the measured variation of iron concentrations as well as by the quantity of secondary iron disulfide oxidation via the dump surface. The calculation was carried out beginning from the termination of dump formation, which is between 1951 and 1970 for the single cuts, for a time interval of 450 years.

RESULTS AND DISCUSSION

Grundwater flow regime

Groundwater dynamics within the Witznitz dump are essentially determined by surrounding surface waters (fig. 2). Due to comparably low hydraulic conductivities a groundwater cap is formed within the northern part of the dump at a level of +140 m above sea level (a.s.l.).

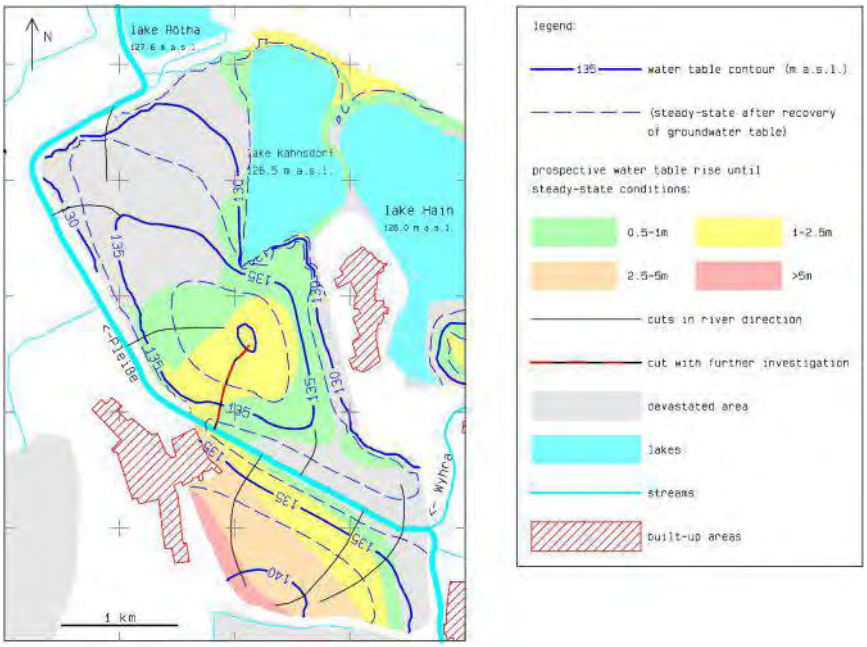

Figure 2 Steady-state water table contours, prospective rise and cuts in river direction for the transport model

Groundwater flow from the dump takes place to the Pleiße river, as well as to the mining lakes Kahnsdorf and Hain. The dump body south of the river is characterized by a groundwater flow to the river from southeastern direction at steady-state conditions after the completion of the groundwater table uplift.

In the northern part of the dump the groundwater table uplift is nearly complete. Future rises are below 2.5 m (fig. 2). By contrast, in the southern part of the dump there is a future rise of up to 6 m expected, which is caused by a further groundwater uplift in the dump surroundings. By means of the large-scale model, this could be considered in the groundwater flow calculation of the Witznitz dump.

The modeled groundwater inflow from the Witznitz dump to the Pleiße river amounts to 0.78 m^3/min for steady-state conditions.

Hydrogeochemistry of dump genesis

The model of dump genesis was realized by a stepwise increase of the degree of iron disulfide weathering releasing iron, sulfate, and acidity to the groundwater. Subsequently, several accompanying reactions take place, which are shown in the upper left plot of fig. 3 in relation to the sulfate concentration, which serves as an indicator of the degree of iron disulfide weathering.

The first buffering process is given by the solution of calcite and lasts up to sulfate concentrations of approximately 1800 mg/L.

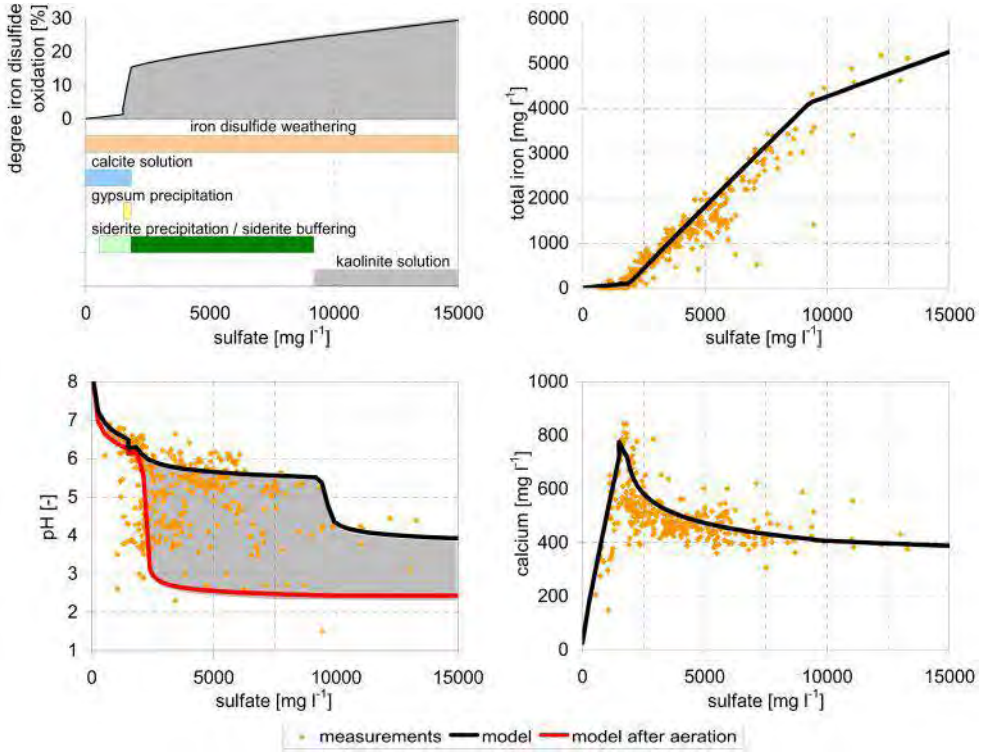

Figure 3 Mineral transformations during iron disulfide weathering and development of iron and calcium concentrations as well as pH as a function of the master variable sulfate; measurements and batch model

As a result of the rising calcium and sulfate concentrations in the solution, precipitation of gypsum starts at sulfate concentrations of about 1500 mg/L. It stops in parallel with the calcite solution as calcium is needed for the formation of gypsum. Siderite precipitation starts at sulfate concentrations of approximately 500 mg/L and similarly terminates with the end of calcite solution as carbonate for siderite formation is no longer available. At sulfate concentrations higher than 1800 mg/L resolution of siderite takes place connected with the release of hydrogen carbonate, which serves as a buffering mechanism up to sulfate concentrations of about 9200 mg/L. Afterwards solution of clay minerals represented by kaolinite begins.

Concentrations of total iron increase with rising sulfate concentrations (fig. 3, upper right plot). At sulfate concentrations of up to 1800 mg/L iron concentrations are low, which is due to siderite fixing. At higher sulfate concentrations, there is a clear rise in iron concentrations, as iron is firstly released by iron disulfide weathering and secondly by the resolution of siderite minerals. The slope of the curve decreases at sulfate concentrations above 9500 mg/L because of a depletion of siderite. The model results fit well with the measured data.

The pH decreases with an increasing degree of iron disulfide weathering (fig. 3, lower left plot, black line). During calcite buffering, the pH is above 6.3, within the siderite buffering interval it amounts to 5-6, whereas buffering by clay minerals (represented by kaolinite) results in a pH of about 4. Principally, iron appears in bivalent form in the dump groundwater. Trivalent iron occurs in traces only, as firstly the groundwater is anoxic due to prevalent iron disulfides and secondly trivalent iron is precipitated at pH values greater than 3. Nonetheless, partial aeration took place during groundwater sampling. Because of the low hydraulic conductivity of the dump material, part of the samples had to be taken from the standing water in the pipe after dry pumping on three consecutive days. This led to an iron oxidation and precipitation of hydroxides or hydroxysulfates respectively, which is connected with a release of acidity and a decrease of the pH. Measurements are mostly in between the black (no aeration) and the red line (full aeration) in the plot, indicating a partial aeration during the sample procedure.

Calcium firstly shows an increase (fig. 3, lower right plot), which is due to calcite dissolution. Concentrations decrease again with the beginning of gypsum precipitation to a level of 400 to 600 mg/L. Measurements fit well with the model.

The considered solubility product pK_{sp} of the mineral phase calcite is -8.48, which is in line with the value of the wateq4f.dat database. With respect to gypsum, pK_{sp} was selected as -4.53, which represents a very slight supersaturation of +0.05 for precipitation to occur compared to the considered database. Based on the measurements, pK_{sp} of siderite was determined to be -9.25, which implies a supersaturation of +1.2. This is in line with the findings of Lenk & Wisotzky (2007). This is possibly due to surface effects during the process of precipitation or the formation of mixed iron(2)-calcium-carbonates. Matching measured liquid and solid contents resulted in the assumption that one third of the iron released during iron disulfide weathering gets irreversibly bound by the formation of trivalent iron oxyhydrates. The maximum allowed partial pressure of CO_2 is 30%.

Resulting from the batch model, the great variability of measured groundwater quality data can be described by the variation of the degree of iron disulfide oxidation, which is a consequence of the varying exposure of the dump material connected with a differing contact to oxygen. The overall mean degree of iron disulfide weathering determined from the mean sulfate concentration of the dump groundwater, which is 3660 mg/L, amounts to 18%.

Future development of dump groundwater quality and solute discharge

The coupled groundwater flow and reactive solute transport model was realized for nine vertical-plane cuts in groundwater flow direction to the Pleiße river (fig. 2). In the following, one cut representing the groundwater flow from northern direction to the Pleiße river in the region of the river crossing the dump is investigated in detail (red-black dashed cut in fig. 2).

By implementing the hydrogeochemical batch model into every model cell, the model simulates the discharge of the solutes originating from iron disulfide oxidation with the groundwater flow. Considering a homogenous distribution of the iron disulfide oxidation rate, iron concentrations in the cut for the year 2010 are between 2000 and 4000 mg/L in the upper part and between 1000 and 2000 mg/L in the lower part of the dump (fig. 5). Concentrations are reproduced in the model by considering the iron disulfide turnover during the dump formation and shortly thereafter. Low hydraulic conductivities and slow groundwater flow lead to the preservation of high iron concentrations in the dump body for long time intervals. The vertical concentration gradient is due to the oxygen input via the dump surface leading to a secondary iron disulfide oxidation next to the primary one within the whole dump body. For the year 2100, the model predicts a clear reduction of iron concentrations in the upper aquifer because of diluting effects by groundwater recharge and the solute discharge to the river. This effect continues into the future. Correspondingly, modeled concentrations for the year 2300 are below 250 mg/L in the upper aquifer. In contrast, solute discharge from the lower aquifer is small, as the hydraulic conductivity is comparably low in this part of the dump.

Results considering a random distribution of the iron disulfide oxidation rate using Monte Carlo simulations show the same trend, though iron concentrations in the cut are additionally influenced by scattering.

Solute fluxes from the dump into the direction of the Pleiße river were calculated as weighted means per length of the respective river section combining the results of all nine cuts. From this, iron loads of approximately 1000 kg/d are calculated for a time interval of the next 100 years (fig. 4). Afterwards fluxes decline to 190 kg/d in 2400. Derived sulfate loads are in the order of 3500 kg/d during the next 100 years and decline to 2000 kg/d until 2400. Compared to iron the decrease of fluxes with time is less significant, as there is a great pool of gypsum bound in the dump, whose resolution takes place during a very long time interval. Monte Carlo simulations show similar solute fluxes compared to the homogenous distribution of iron disulfide oxidation, which indicates that spatial variability is averaged in the dump discharge.

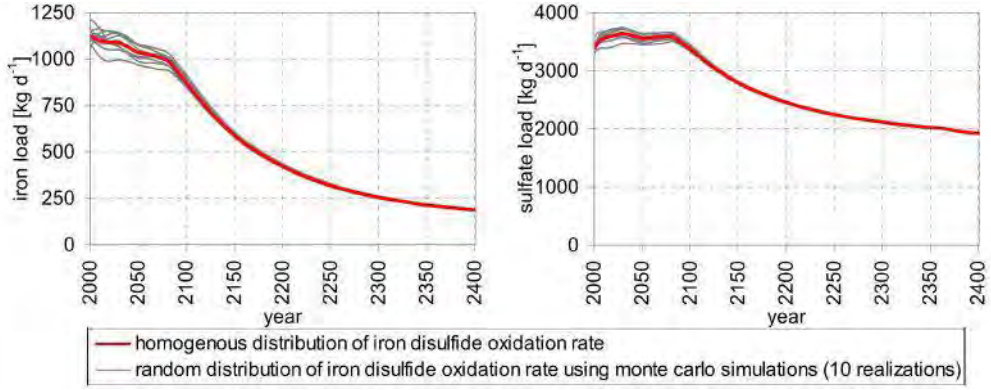

Figure 4 Modeled fluxes of iron and sulfate from the dump in direction of the Pleiße river

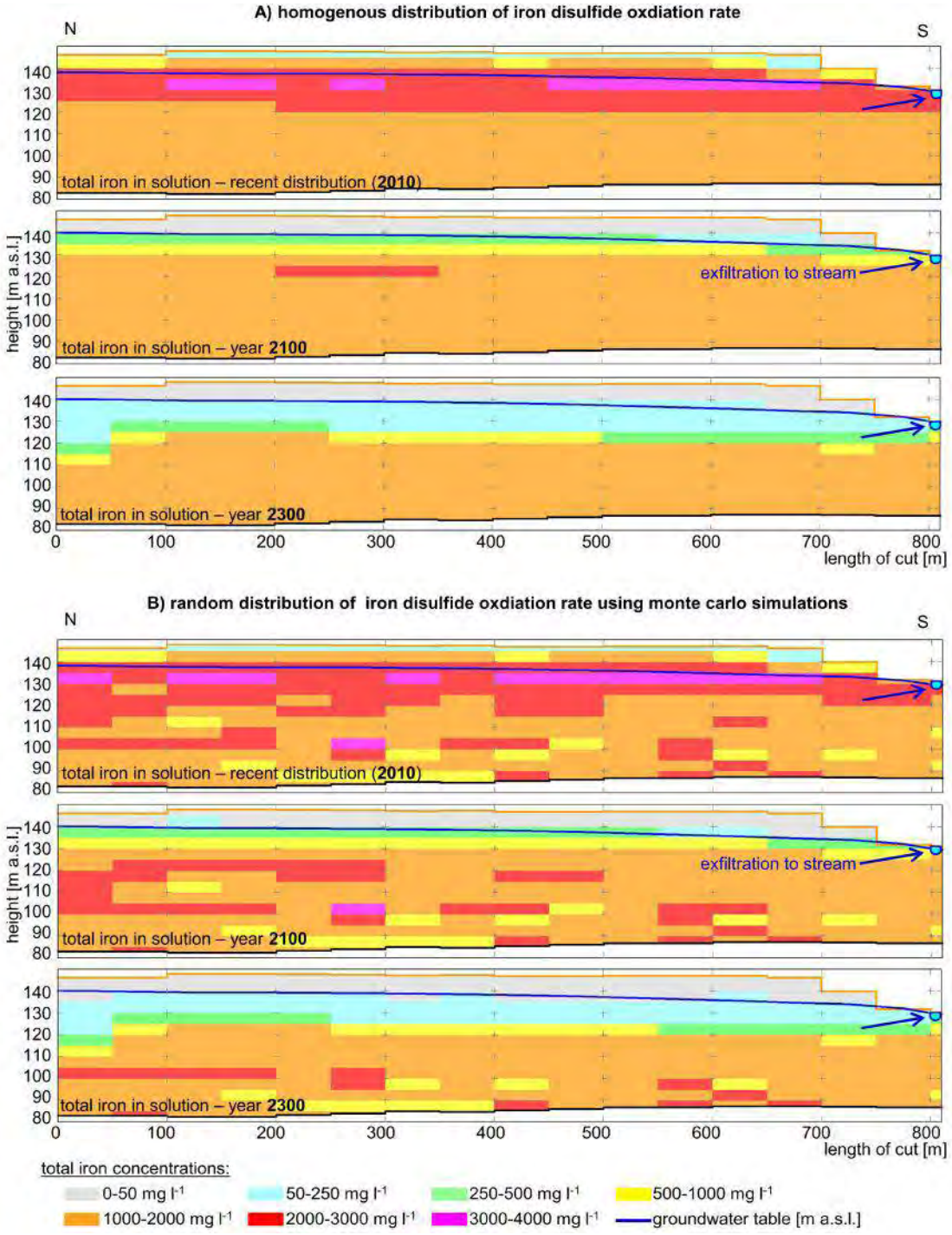

Figure 5 Modeled concentrations of total iron in den liquid phase along the red-black dashed cut (cf. Fig 2), time slices 2010, 2100 and 2300

CONCLUSION

The presented study is based on a large data pool of groundwater analyses and investigations on the solid phase of the dump material. This allows a detailed examination of the ongoing processes and the derivation of a process-oriented model. It was therefore possible to determine the relevance of single mineral phases during the genesis of the dump groundwater and to derive the solubility products of the participating mineral phases. This enables extrapolation to other areas with a less comprehensive pool of data.

The wide scattering of measured iron and sulfate concentrations is most likely due to the varying degree of iron disulfide oxidation. During solute transport modeling this was taken into consideration by a Monte Carlo simulation.

The newly developed model coupling allows a precise prediction of the future development of dump hydrogeochemistry and the expected solute fluxes into the Pleiße river, indicating that the process of solute discharge from lignite mining dumps exhibiting low hydraulic conductivities takes place on very long time intervals.

ACKNOWLEDGEMENTS

The study was funded by the Lusatia and Central German Mining Administration Company (LMBV), which also provided the immense data pool for investigation.

REFERENCES

Becker, A., Klöcking, B., Lahmer, W. & Pfützner, B. (2002) *The Hydrological Modeling System ArcEGMO*, in: Singh, V.P. & Frevert, D.K. (eds.), Mathematical Models of Large Watershed Hydrology, Water Resources Publications, Littleton / Colorado, pp 321–384.

Bigham, J.M., Schwertmann, U., Traina, S.J., Winland, R.L. & Wolf, M. (1996) *Schwertmannite and the chemical modeling of iron in acid sulfate waters*, Geochimica et Cosmochimica Acta, vol. 60, no. 12, pp. 2111–2121.

Blankenburg, R., Mansel, H., Sames, D. & Brückner, F. (2013) *Consideration of Open Cast Mining Progress and more using the Finite Volume Model PCGEOFIM*, in: Maxwell, R., Hill, M., Zheng, C. & Tonkin, M. (eds.), MODFLOW and More 2013 – Conference Proceedings, pp. 283–286.

Kaubisch, M. (1986) *Zur indirekten Ermittlung hydrogeologischer Kennwerte von Kippenkomplexen, dargestellt am Beispiel des Braunkohlenbergbaus*, doctoral thesis, Technical University of Freiberg, 129 pp.

Lenk, S. & Wisotzky, F. (2007) *Chemische Beschaffenheit und modellierte Genese von Grundwässern in Braunkohlenabraumkippen des Tagebaus Inden*, Grundwasser, vol. 12, pp. 301–313.

Parkhurst, D.L. & Appelo, C.A.J. (1999) *User's guide to PHREEQC (Version 2) – a computer program for speciation, batch-reaction, one-dimensional transport, and inverse geochemical calculations*, Water Resources Investigations Report 99-4259, Denver, Colorado, 312 pp.

Wisotzky, F. & Obermann, P. (2001) *Acid mine groundwater in lignite oberburden dumps and its prevention – the Rhineland lignite mining area (Germany)*, Ecological Engineering, vol. 17, pp. 115–123

Simulating the Performance of a Dry Stack Tailings Design for Water Control Permitting

Amy Hudson[1], April Hussey[1], **Andrew Harley**[1] and **Timothy M. Dyhr**[2]
1. Tetra Tech, USA
2. Nevada Copper Corp., USA

ABSTRACT

Dewatering tailings to below saturation prior to placement in a permanent storage facility, referred to as "dry stacking", offers significant advantages over conventional slurried tailings storage, especially in arid environments. These include significantly reduced water requirements, a much smaller environmental footprint, and reduced long-term water management costs. Even with these clear benefits, dewatered tailings have not previously been permitted in the state of Nevada. In order to demonstrate to the regulators that the proposed tailings design is feasible and to lay out a clear path for evaluating the performance of the facility design, a series of models and presentations were developed.

The modeling results provided clear evidence that the facility design and phased stacking plan would produce unsaturated tailings, limiting the potential flow of water into the subsurface and impacts to groundwater. A sensitivity analysis of the modeling was conducted to evaluate the parameters used and the possible facility performance under less than ideal conditions. The sensitivity modeling suggested that flux into the foundation layer is most affected by the water content of the placed tailings. Geochemical modeling was also conducted, incorporating results from the Meteoric Water Mobility Procedure results of site specific tailings samples. The geochemical modeling predicted that the geochemistry of the interstitial fluids in the tailings would be of generally good quality and below state standards.

The facility's Water Pollution Control Permit was issued in August 2013, conditionally approving the placement of dewatered, unsaturated tailings in the facility. The project has agreed to construct and monitor a field test cell over a minimum of a one-year period. Additional project work is currently underway to monitor water contents in the initial operating cells of the tailings storage facility. Both of these seek to validate the modeling results and demonstrate the efficacy of the tailings storage facility design.

Keywords: Modeling, dewatered tailings, geochemistry, permitting

INTRODUCTION

Dewatered tailings, also known as dry stack tailings (DST), are better suited for the arid southwest than traditional slurried tailings disposal due to the reduced water requirements, environmental footprint, long-term water management, and seepage. Additionally, concurrent reclamation can be completed on DST facilities because of the increased trafficability of the material compared to slurried tailings. Despite these clear benefits, as a DST facility had not previously been constructed or permitted in the state of Nevada, additional steps were necessary to permit such a facility with the Nevada Department of Environmental Protection (NDEP).

Prior to developing the predictive models to support the permitting of the DST facility, a presentation was provided for the regulators to help educate them on the operational design and function. This approach had previously been proven successful for permitting a DST facility in Arizona. The initial presentation was conducted in late 2011, and included the general concepts of dry stacking (including the water content of unsaturated "dry" tailings, the conveyance process, stacking plans, stability of DST, seepage mechanisms, and trafficability) and a path forward for additional site-specific field investigations, laboratory analyses, and modeling that could be used to verify the proposed design concept.

A second presentation was held in early 2012. The time between the presentations allowed the regulatory officials to digest the original information and develop specific follow-up questions about the project. The second presentation focused on the specific design proposed for the project and results of the predictive modeling. This second meeting also focused on presentation of a proposed alternative lining concept. For this project, an alternate liner system consisting of 0.45 meters (m) (18 inches [in]) of compacted tailings with a maximum permeability of $4x10^{-4}$ centimeters per second (cm/s) was proposed. These presentations and the predictive modeling laid the groundwork for open communication, which allowed for approval of the water pollution control permit application. The remainder of this paper focuses on the predictive modeling that was used to support these presentations and ultimately the permit application.

CONCEPTUAL MODEL

The predictive modeling was developed to supplement the engineering design report for the DST facility. Figure 1 shows the conceptual model of a DST facility. The conceptual model for a DST facility is similar to other mining facilities. The conceptual model shown in Figure 1 illustrates the system water balance components which consist of precipitation, evaporation, runoff, infiltration, and seepage. The tailings material will also contain some solution when it is placed in the facility (interstitial water), adding to the initial water balance of the facility. The gravimetric water content of the tailings at placement is expected to range from 15% to 17%, equivalent to a volumetric water content of 26%.

MODELING TECHNIQUE AND INPUTS

VADOSE/W (GEO-SLOPE, 2007a), a two-dimensional variably saturated flow model that is part of the Geo-Studio suite of programs, was used to simulate the flow of water through the tailings mass in the DST facility. To determine the quality of the water that could potentially seep from the base

of the facility into the foundation soils, fate and transport modeling was completed using a combination of particle tracking and geochemical modeling.

The objectives of the infiltration and seepage analyses were to assess:

- The performance of the proposed closure cover configuration;
- The rate of infiltration into the tailings mass;
- The rate of seepage to the drains; and
- The rate of seepage from the DST to the foundation soils.

The objective of the fate and transport analysis was to:

- Predict the geochemical quality of the seepage from the base of the DST facility;
- Evaluate the potential for seepage into the foundation soils; and
- Evaluate the potential for any seepage to impact the regional groundwater system.

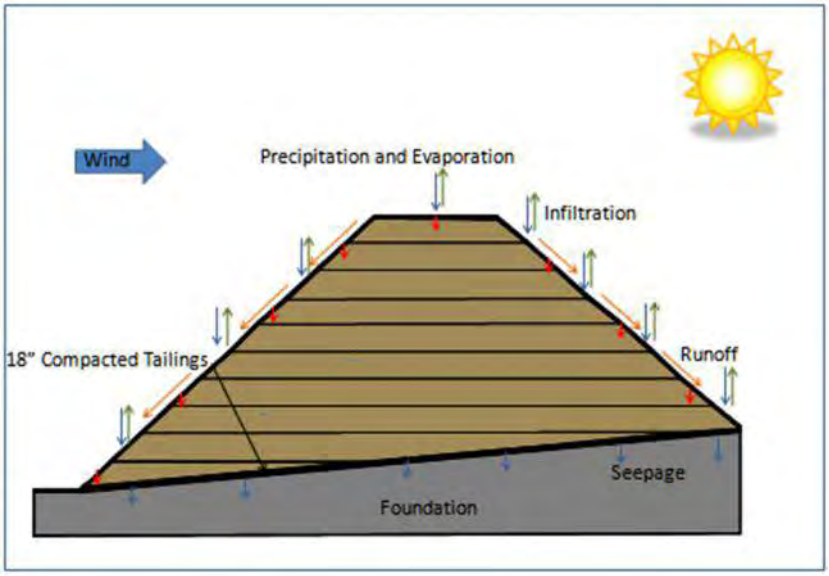

Figure 1 Conceptual Flow Model DST Facility

Climate

The Project is located in low barren hills above a dry alluvial valley. The climate is arid with hot summers and relatively mild winters, allowing nearby mining operations to work year round. Vegetation in the immediate project area is sparse low brush with local grasses suitable for limited cattle grazing. The alluvial Mason Valley to the west, hydrogeologically separate and different from the project area, contains numerous agricultural fields, primarily alfalfa, onions, vegetables, and pasture lands. These fields are watered by irrigation canals from the nearby Walker River and groundwater wells.

Daily climate data were used for the analyses. Actual daily precipitation and minimum and maximum temperatures were obtained from a meteorological station in Yerington, Nevada (WRCC Station 269229). The relative humidity and wind speed were obtained from Fallon Naval Air Station, Nevada (TuTiempo Station 724885[KNFL]). A data set spanning from 1914 through 2010 was assembled. The average annual precipitation is 12.2 cm (4.81 in) and the median precipitation is

11.7 cm (4.61 in) for the years included in the data set. A year matching the median precipitation, 1970, was chosen for use in the modeling to represent the typical conditions. The 75th percentile precipitation for the data set is 14.8 cm (5.83 in), occurring in 1918. This year was modeled to represent above average precipitation conditions. The daily measured precipitation for 1970 (median precipitation) and 1918 (above average precipitation) was applied over the models in 24-hour time periods distributed according to a sinusoidal function that peaks at noon (normal distribution).

Material Properties

Table 1 summarizes the material parameters used in the VADOSE/W (GEO-SLOPE, 2007a) models for the DST facility. The material properties used in the VADOSE/W (GEO-SLOPE, 2007a) models were based on the design properties of the facility, laboratory and field testing of actual Project materials, and literature values where no site specific data was available.

Table 1 Material Properties

Material Type	Porosity	Dry Density# (g/cm^3)	Saturated Hydraulic Conductivity (cm/s)	Initial Volumetric Water Content# (%)	Thermal Properties
Soil Cover	0.40*	1.92	5.0×10^{-4}*	10	silt
Capillary Break	0.34*	1.92	7.2×10^{-3}*	10	sand
Tailings	0.39^	1.60	3.1×10^{-3}^	26	sand
Compacted Tailings Layer	0.42^	1.92	1.8×10^{-5}^	26	silt
Foundation Soil	0.29^	1.92	8.7×10^{-4}^	6 - 8	sand

* Literature values

\# Assumed values

^ Laboratory testing of site specific material

Facility Design

The configuration of the DST facility includes a 0.45 m (18 in) thick layer of compacted tailings placed directly on the foundation soils. The compacted layer of tailings will act as the liner unit to limit the flux of water into the underlying foundation soils. Over the compacted tailings layer, a network of gravel drains will be placed that will be used to collect and convey the solution draindown from the tailings into lined ditches and ponds. The gravel drains will be piped such that the draindown solution will be removed from the drainage network to an adjacent lined pond, where it will be managed. The DST will be placed over the compacted tailings and drainage network in 9 m (30 foot [ft]) lifts using mobile conveyors. Equipment traffic will be limited on the tailings surface as to avoid development of compacted zones, to minimize the changes to the material properties after stacking, and to limit the development of preferential flow paths. The stacking plan has been designed such that after the placement of each lift of tailings material, the tailings mass will be allowed to drain for an average duration of one year prior to the placement of the next lift. This will maximize the amount of solution that will be able to freely drain from the facility, and minimize the amount of solution remaining in the tailings material when future lifts are placed. The cover designs that were evaluated included both a single-layer and two-layer system incorporating a capillary break.

INFILTRATION AND SEEPAGE MODELING

The DST facility was modeled at three points in time (after placement of the first lift, mid-operations, and fully stacked facility). In order to assess the quantity of infiltration that is expected under ambient conditions and above average precipitation conditions, as well as the performance of the cover system, the model simulated typical climate conditions, a worst case runoff conditions, and a multi-day storm (worst case infiltration conditions)

RESULTS AND DISCUSSION

The first model simulated the placement of the first lift of the DST in the facility. The drainage of the first lift of the tailings material was considered to be the most likely to influence the water content of the foundation soils, thus the highest potential to impact the regional groundwater system. Additionally, the first lift model precipitation events have the shortest flow path to the foundation layer.

The volumetric water content of the tailings decreases steadily after placement, as illustrated in Figure 2. Figure 2 presents the simulated change in water content at individual points along a vertical profile through the central portion of the first lift of the DST facility. The locations near the surface of the lift decrease most rapidly because water is being removed by both downward flux and evaporation. The deeper portions of the lift have a slower decline in water content because this area is not subject to evaporation and this area is receiving water from the upper portions of the lift. The one point starting with a lower water content of approximately 17% by volume is representative of the compacted tailings layer at the base of the facility. It should be noted that based on the results of the sensitivity analysis, regardless of the starting volumetric water content, over the one year period after placement of the first lift, the tailings drain to a water content that is just above the residual water content of the material.

The second scenario simulated the flux through the DST facility after five lifts of tailings have been placed (approximately the mid-point of the mine life). The volumetric water content of the mid-operations scenario model one year after placement is presented in Figure 3. The flux into the drainage network at the base of the facility decreases with time and as additional lifts are stacked on top, because the water content of the tailings in the lower layers of the dry stack is smaller than the water content in the newly placed tailings material. The water in the newly placed tailings material has fewer connected pathways to travel through to the lower layers because the underlying layers have a lower water content causing the pore spaces to be physically disconnected from each other. At the beginning of the placement of the fifth lift, the water begins to migrate downward. However, there is sufficient storage capacity within the underlying tailings material that the water “spreads out” through the facility ensuring low water contents throughout the entire facility.

The final DST facility modeling scenario was the completely constructed facility. When the last lift of the DST facility is placed, the water within the tailings moves downward through the facility as observed from the mid-operations model. As with the mid-operations model, because the lower lifts have partially drained, there is sufficient storage capacity within the tailings material to dissipate the water content throughout the facility, resulting in only small zones of slightly increased water content.

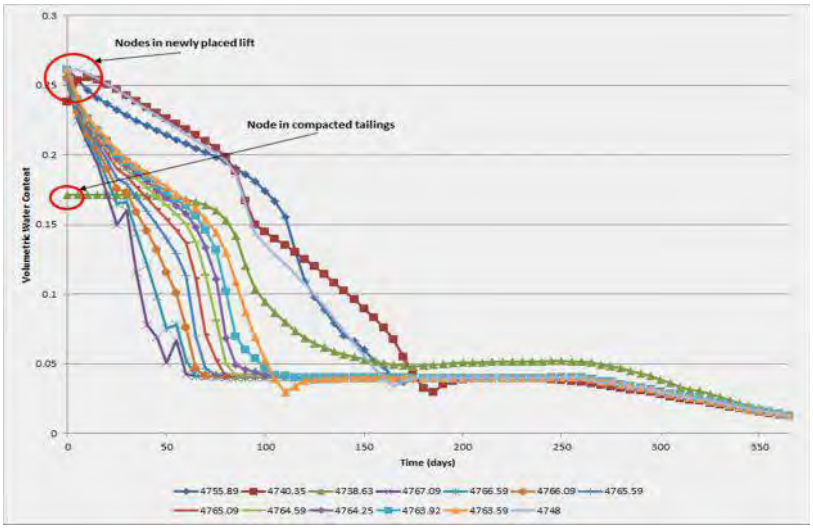

Figure 2 Volumetric Water Content with Depth – First Lift Model

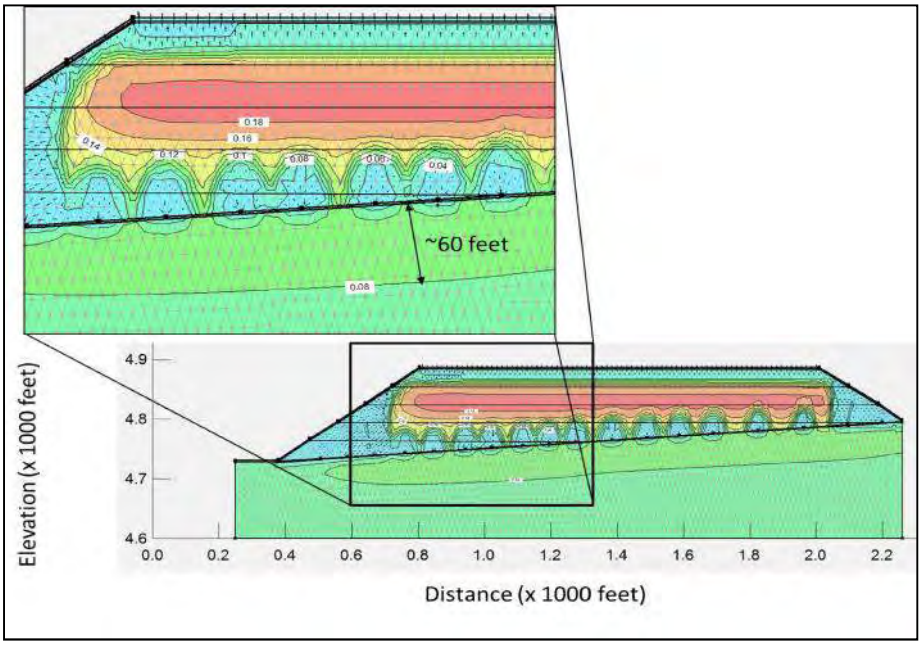

Figure 3 Volumetric Water Content DST Facility - Lift Five Model One Year After Tailings Placement

The net negative water balance of the site limits the amount of precipitation that infiltrates into the DST material. On average, only 29 days each year have measureable precipitation with approximately 18 cm (7 in) of snow. Based on the modeling, infiltration into the facility will be minimal under median and above average precipitation conditions. Figure 4 presents the daily flux of water into or out of the DST facility for the four climate scenarios modeled. The results suggest that only isolated storm events may result in infiltration into the upper surface of the tailings, and because of the high evaporation, this water is then later lost as it is drawn back out of the facility.

This behavior is typical of a store and release design, such as the evaluated cover systems. Annual evaporative water loss through the cover is calculated to be greater than annual precipitation for the Project. The placement of the cover improves the performance of the facility surface by reducing the flow of water, both into and out of the facility, by approximately 25%. These models only considered a one year period after placement of complete cover.

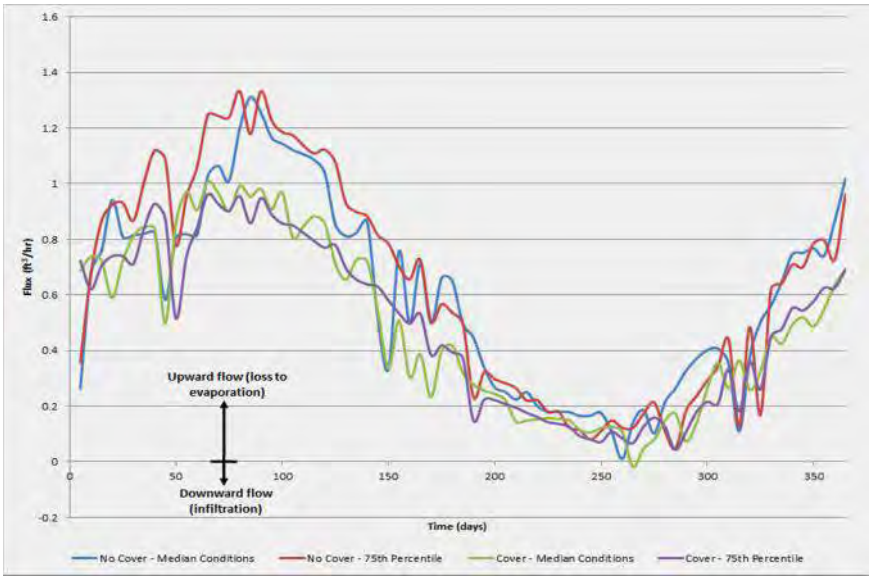

Figure 4 DST Water Flux at Tailings Surface – Completely Constructed Facility

FATE AND TRANSPORT MODELING

The flow modeling determined the quantity of water infiltrating into and seeping through the tailings in the DST facility, including the time of contact. To determine the quality of water that could potentially move downward from the base of the facility and seep into the foundation soil and possibly impact the underlying groundwater system, fate and transport modeling was completed.

Conceptual Fate and Transport Model

The fate and transport models were built from the same geometry and material properties as the infiltration and seepage models. As determined from the infiltration and seepage modeling, the general flow path through the DST is in the vertical direction. Therefore, the fate and transport modeling focused on the potential transport paths, both upward and downward within the DST.

Fate and transport modeling was completed in two separate steps. The first step involved particle tracking to determine the path of the water flow, including which materials the flow would come in contact with and the time required to reach the subsurface. The next step was a simple geochemical mixing model representing the water quality due to contact with the materials in the facility. The results of these two modeling steps were an estimation of where potential seepage would occur, including the water quality of the potential seepage. The following sections provide more detail of these two modeling steps.

Particle Tracking

Particle tracking modeling was performed using the program CTRAN/W (GEO-SLOPE, 2007b), another component of the GeoStudio software suite. The particle-tracking portion of the modeling estimated the flow paths of the water entering, traveling through, and exiting the DST facility. The particle tracking modeling also determined how long the water was in contact with each of the materials, and if seepage would be expected to travel into the foundation materials. The particle tracking model was run for a period of 10 years to allow sufficient time to determine water velocities, should it be determined that water is seeping into the foundation soil. This would allow for the calculation of travel times through the subsurface and the time required for water to reach the top of the regional groundwater system.

Geochemical Modeling

Geochemical modeling was conducted using the computer code PHREEQC (Parkhurst and Appelo, 1999), a reaction path chemical equilibrium model supplied by the U.S. Geological Survey (USGS). In addition to a computer code, geochemical modeling requires a database of thermodynamic and kinetic parameters associated with the chemical reactions. For this Project, the WATEQ4F database (Ball and Nordstrom, 1991) was chosen. However, this database did not include all of the metals of concern to the Project, so additional metals were added to the file. The information added was obtained from the PHREEQ database published with the computer code (Parkhurst and Appelo, 1999). The combination of the two databases provided the broad range of metals needed to predict water quality.

Model Construction

The particle tracking model used the same geometry and material properties as the infiltration and seepage model. The water content and flow conditions resulting from the flow modeling were also used as the starting conditions of the particle tracking models. The particles were placed near the top of the tailings surface, and throughout the facility. The model was run using a forward tracking solver, which calculates the path of the water flux within the facility and associated velocities.

The input solutions representing the leachable constituents in the geochemical modeling were based on the Meteoric Water Mobility Procedure data for three site specific tailings samples: Northwest Open Pit, Northwest Underground, and East/E2. All three samples are representative of tailings material to be placed within the DST facility. Solution concentration data from all three samples were mixed in equal proportions as the starting solution for fate and transport modeling. Each of the starting solutions was equilibrated with atmospheric concentrations of oxygen and carbon dioxide, which was also used to determine the relative pe (redox potential expressed as –log of electron activity). Starting solutions were also equilibrated with mineral phases commonly found within the DST to allow for precipitation or dissolution of minerals from solution.

Model Results

Based on the seepage and infiltration modeling, the water in the DST facility is expected to move downward through the tailings until drainage of the pore water is compete or the pore spaces become sufficiently disconnected to prevent further drainage. Therefore, fate and transport

modeling was completed to determine if water draining to the compacted base of the facility would be captured by the drainage network, or if the water would seep through the compacted base, enter the foundation soils, and potentially be transported into the groundwater system.

The model showed that there is minimal downward movement of water within the DST after the initial drainage of the interstitial water, as would be expected because the system is not saturated. Modeling that focused on the first lift of the DST facility showed that the particles primarily moved laterally towards the drains. None of the particles were shown to travel from the facility into the underlying foundation soils. This suggests that the slightly increased water content in the foundation soils observed in the seepage modeling is an equilibration condition instead of actual water movement. The results of the particle tracking of the full facility also show minimal movement of the particles. The greatest movement is only in the zone of highest water content, which does drain downward. Once those zones draindown, the remaining particles moved very little. The particles placed near the outer surface of the facility show the strong influence evaporation has on this facility. The particles in this area are moving upward toward the surface of the facility. The lower water contents and drying in the outer areas of the facility supports this movement.

Even though the flow and the particle tracking models suggests that no water will be transported to the regional groundwater system, the quality of the seepage from the facility was estimated using a geochemical mixing model to demonstrate it would meet regulatory standards. The results of the mixing model suggest that any potential seepage from the DST facility would still be of generally good quality and below NDEP Profile 1 Reference Values.

CONCLUSION

Based on the results of the infiltration and seepage modeling, the DST facility is not expected to impact the regional groundwater system. Under median and above average climate conditions, the water balance of the facility is negative, where draindown of entrained water into the network of drains and subsequent ponds and evaporation are the largest components of the system. Under these conditions potential seepage is limited to the entrained solution in the tailings material, and not precipitation. The flow of entrained solution into the foundation soils and increase in water content of the foundation soils is anticipated to be minimal throughout operations and into closure. The stacking plan includes periods of draining prior to the placement of subsequent tailings lifts, which maximizes the amount of solution that is allowed to drain into the drainage networks.

The compacted tailings layer placed under the main tailings mass is sufficiently impermeable to limit the seepage of water into the foundation soils, and to help move the drained solution to the drainage network. Regardless of the permeability of the compacted tailings layer, even with minor seepage into the foundation soils, there would only be a two percent increase in the volumetric water content. The depth of influence based on the modeling is less than 24 m (80 ft) below the base of the facility, indicating no anticipated impact to regional groundwater system, approximately 90 m (300 ft) below the facility. Based on particle tracking, there is no movement of water from the DST to the zone of influence suggesting equilibration of the system rather than transport.

NDEP reviewed the modeling and through discussions with the mining company, approved the facility's Water Pollution Control Permit in August 2013 including the DST facility. A field test cell was agreed upon to demonstrate over a minimum of a one-year period that the DST concept and the alternate lining approach would be fully protective of the environment, particularly the

underlying groundwater system. Initial tailings deposition cells will be constructed with an HDPE liner while the test cell is constructed and data analyzed. Additional project work is currently underway to develop, design, construct, instrument, and develop success criteria for the test cell to demonstrate its protectiveness of the environment.

REFERENCES

Ball, J.W. and Nordstrom, D.K., (1991). WATEQ4F – User's Manual with Revised Thermodynamic Database and Test Cases for Calculating Speciation of Major, Trace, and Redox Elements in Natural Water. USGS Open-File Report 90-129, 185 p.

GEO-SLOPE International, Ltd. (GEO-SLOPE), (2007a). Vadose Zone Modeling with VADOSE/W 2007: An Engineering Methodology. GEO-SLOPE International Ltd.: Calgary, Alberta, Canada.

GEO-SLOPE, (2007b). Contaminant Modeling with CTRAN/W 2007: An Engineering Methodology. GEO-SLOPE International Ltd.: Calgary, Alberta, Canada.

Parkhurst, David L. and Appelo, C.A.J., (1999) User's Guide to PHREEQC (Version 2) – A Computer Program for Speciation, Batch-Reaction, One-Dimensional Transport, and Inverse Geochemical Calculations. USGS WRIR 99-4259.

Tetra Tech, 2010a. NI 43-101 Preliminary Economic Assessment Update. Pumpkin Hollow Copper Project. Prepared for Nevada Copper Corporation. January 13, 2010.

Western Regional Climate Center (2011). Yerington, Nevada (269229) Period of Record Daily Precipitation. http://www.wrcc.dri.edu. Accessed May 1, 2011.

Using PhreePlot to Calibrate Mining Related Geochemical Models: A User's Perspective

John Mahoney
Mahoney Geochemical Consulting, USA

ABSTRACT

With the release of the program PhreePlot, geochemists obtained a method to better understand and quantify geochemical processes. PhreePlot's ability to optimize a wide range of parameters in PHREEQC based models provides a simple and direct method to better calibrate geochemical models. In its fitting routines, PhreePlot calculates the weighted residual sum of squares [W(RSS)] between the measured (observed) and modeled data. The optimization routine minimizes this value by changing user defined variables in the attached PHREEQC model. The combination of several fitting options, plus flexibilities inherent in PHREEQC, allows for a range of approaches in quantitative geochemical data evaluation. The simplest applications permit straightforward fitting of experimental or field measurements for solubility product calculations. The fitting of surface complexation reactions over a large range of experimental conditions is another straightforward application. Many parameters in PHREEQC such as surface site densities, and rate constants are suitable for fitting and can be used to match measured data with modeled results. The quantitative understanding from these rigorous fits can produce stronger insights about the geochemical processes and potentially simplify regulatory reviews.

Keywords: PHREEQC, PhreePlot, Model optimization, Arsenic, Surface complexation

INTRODUCTION

The program PhreePlot (Kinniburgh and Cooper 2011) uses PHREEQC (Parkhurst and Appelo 2013) to prepare a wide variety of figures including species distribution plots, Eh-pH diagrams, and other types of activity - activity plots. To construct these figures, PhreePlot cycles through a range of user defined conditions such as pH, oxygen fugacities or pe, and component concentrations. Numerous options are available to make these figures and even animations can be prepared using the Hunt and Track method (Kinniburgh and Cooper 2004) to define the Eh-pH conditions, and a separate looping option to set a range of concentrations (see PhreePlot Website). Because it uses a large thermodynamic database the figures are more accurate than the simpler plots described in many textbooks and references.

The ability to change a "tagged" parameter(s) provides a means to optimize selected parameters through the fitting routine. There are several fitting options in PhreePlot, and it is this capability that is described below. In the current PhreePlot user's guide there are a limited number of fitting examples. The following describes a range of applications and efforts to learn how to prepare optimized geochemical models.

A comment about program installation is appropriate. Although installation of PhreePlot and its two supporting programs GPL Ghostscript and GSview appears daunting, it is straightforward. The key issue I have run into is to make sure that the path to the pdf maker is correctly listed in the pp.set file.

COMPARISON OF PhreePlot TO UCODE_2005

Before PhreePlot was released in 2011 one optimization method that was commonly employed was to couple a batch version of PHREEQC with UCODE_2005 (Poeter et al. 2005). Mahoney et al. (2009) used such an approach to fit four uranyl surface complexation constants onto the hydrous ferric oxide (HFO) surface. It was decided that these data sets and models would provide a reasonably straightforward test of PhreePlot capabilities. Both UCODE and PhreePlot use a similar method to "tag" the adjustable parameters and to tabulate observations. Consequently, the original batch PHREEQC input files and observation data files required little updating to accommodate the PhreePlot requirements. The same order of fitting the constants as described in Mahoney et al. (2009) was used. The K_1^{int} and K_2^{int} values were first fit using carbonate free experimental data, and then K_3^{int} was fit and finally the K_4^{int} value was fit. PhreePlot calculated the essentially same log K^{int} values (Table 1) reported in Mahoney et al. (2009).

Table 1 Comparison of batch PHREEQC/UCODE_2005 values of surface complexation constants to values estimated using PhreePlot, the NEA database for uranyl complexes was used in all calculations.

Uranyl Surface Complexation Species	Fitted K^{int}	Reaction	Method	Optimized Log K	Standard Deviation	No. of Observations/Data Sets
Strong Site Uranyl	K_1^{int}	Hfo_sOH + UO_2^{+2} = Hfo_sOUO_2^{+} + H^+	PHREEQC/ UCODE_2005	3.792	±7.97E-01	38/2 Strong and weak site complexes fit simultaneously
			PhreePlot	3.7897	±8.3788E-01	
Weak Site Uranyl	K_2^{int}	Hfo_wOH + UO_2^{+2} = Hfo_wOUO_2^{+} + H^+	PHREEQC/ UCODE_2005	2.507	±3.33E-01	
			PhreePlot	2.508	±3.4097E-01	
Uranyl Monocarbonate	K_3^{int}	Hfo_wOH +UO_2^{+2} + CO_3^{-2} = Hfo_w$OUO_2CO_3^{-}$ + H^+	PHREEQC/ UCODE_2005	9.150	±1.25E-01	81/10
			PhreePlot	9.1474	±1.2389E-01	
Uranyl Dicarbonate	K_4^{int}	Hfo_wOH + UO_2^{+2} + $2CO_3^{-2}$ = Hfo_w$OUO_2(CO_3)_2^{-3}$ + H^+	PHREEQC/ UCODE_2005	15.28	±1.16E-01	217/12
			PhreePlot	15.2753	Not reported	

SCORODITE AND YUKONITE SOLUBILITY DATA

PhreePlot was used as part of an effort to calculate the solubility product constant (K_{sp}) and formula for yukonite, a calcium ferric arsenate, which may control arsenic concentrations under some conditions, has had various formulas reported in the literature. The first step was to determine if PhreePlot could provide a log K_{sp} value and a reasonable stoichiometry for a known phase. Scorodite ($FeAsO_4 \cdot 2H_2O$) was selected for several reasons. Its formula is well defined and I had worked with the data set presented in Langmuir et al. (2006), and like yukonite it is also a ferric arsenate. In the 2006 paper, we used a trial and error method with a simple sum of the squared residuals to confirm the fits. As an exercise, a data set was used to verify the previously reported solubility product (log K_{sp}) for crystalline scorodite. The data set contained 34 points. In the model, the log K_{sp} was adjusted to optimize the fit by minimizing the difference between the "observed" target saturation indices (SIs), which were set to zero, and having PhreePlot fit the SIs by adjusting the log K_{sp} value. These calculations can easily be conducted using just PHREEQC and averaging the saturation indices, but to accomplish further fittings using PhreePlot this step was required. PhreePlot uses tags, which are identified by less than and greater than symbols < > within the PHREEQC part of the file. For the initial setup only the <log_k1> value changed.

```
Scorodite_fitted        405

        FeAsO4:2H2O = Fe+3 + AsO4-3 + 2H2O

        log_k               <log_k1>
```

For crystalline scorodite, Langmuir et al. (2006) reported a log K_{sp} value of -25.83±0.07. For the PhreePlot calculations, the observation file defined the SIs for all samples at 0.00. This is different from calculations typically run using PhreePlot, where the measured data set shows the variance. In these calculations, the observed values (the SIs) were set to zero so there is no variance, but the experimental data do contain the variance, so the weighted residual sum of squares [W(RSS)] is still calculated. PhreePlot calculated log K_{sp} of -25.78±0.0724 for crystalline scorodite. For the 34 data points, an average log K_{sp} calculated with PHREEQC was -25.774 (Figure 1a).

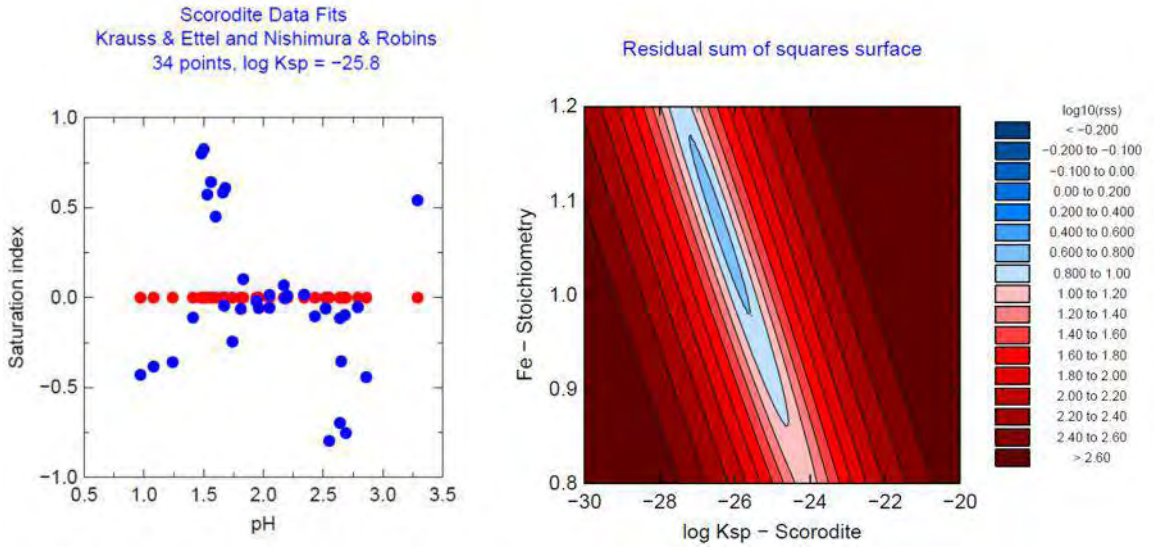

Figures 1a,b PhreePlot prepared figure showing saturation indices as a function of pH. The "observed" values (red dots) are all set to zero. The blue dots represent the model calculated saturation indices after the program has adjusted the log K_{sp}. Figure (b) RHS, shows a contour plot showing the relationship between log K_{sp} and stoichiometric value for Fe

The next calculation was an effort to simultaneously calculate the log K_{sp} for scorodite and the stoichiometric coefficient for Fe^{+3}. This effort was a precursor to the yukonite calculations. To accomplish the second part of the fit the dissolution equation was redefined and the -no_check option was included:

Fe<stoic1>AsO4:2H2O = <stoic>Fe+3 + AsO4-3 + 2H2O

The relationship between <stoic1> and <stoic> was defined by the following numericTag:

numericTags <stoic1> = 1.00*<stoic>

The final estimates were close to the previous estimate with values of:

log_k1 = -26.40 ± 0.34799, stoic = 1.0739 ± 0.040576

For such a large dataset a fit closer to 1.0 for the Fe stoichiometry was expected; the fit is somewhat disappointing. The contour plot is a feature in PhreePlot that helps refine optimization search strategies. Figure 1b shows the RSS as a function of log K_{sp} and Fe stoichiometry. A blue lens (valley) shows the strong relationship between the two variables, and without other data it would be difficult to further refine the result.

The subsequent yukonite modeling required the simultaneous fitting of up to four parameters (calcium, iron, arsenic and the solubility product constant). Data were provided by Dr. George Demopoulos and his students from McGill University.

The general formula for yukonite is $Ca_xFe_y(AsC_4)_z(OH)_A$, where A balances the charge according to:

$$A = 2.0\,X + 3.0 \times Y - 3.0 \times Z$$

Due to convergence issues with the hydroxide term, most models were run using the Bound Optimization BY Quadratic Approximation (BOBYQA) method rather than the simpler Non-Linear Least Squares (NLLS). The BOBYQA method uses fitting parameter ranges. In one series of calculations, calcium was fixed at 2.0 and in the BOBYQA method the ferric and arsenate stoichiometries were allowed to vary within a small range. Both methods produced similar conclusions with a possible log K_{sp} near -111, and a formula of $Ca_2Fe_3(AsO_4)_{3.03}(OH)_{3.92}$ (Figure 2a), or - $Ca_2Fe_3(AsO_4)_3(OH)_4$. Waters of hydration were not estimated. The room temperature results remain suspect; X-ray diffraction did not confirm yukonite in most of these samples. Furthermore, activities of the Fe^{+3} component show a large variation, which influences the calculations. A simulation using data from 75°C and confirmed to contain Yukonite produced a log K_{sp} of -119 and a formula of $Ca_2Fe_3(AsO_4)_2(OH)_7$. The fit appears to be poorer than the room temperature fit. The discrepancy between the formulas and log K_{sp}'s and the visually poor fits for the data at 75°C (Figure 2b) raise questions about all the optimization results.

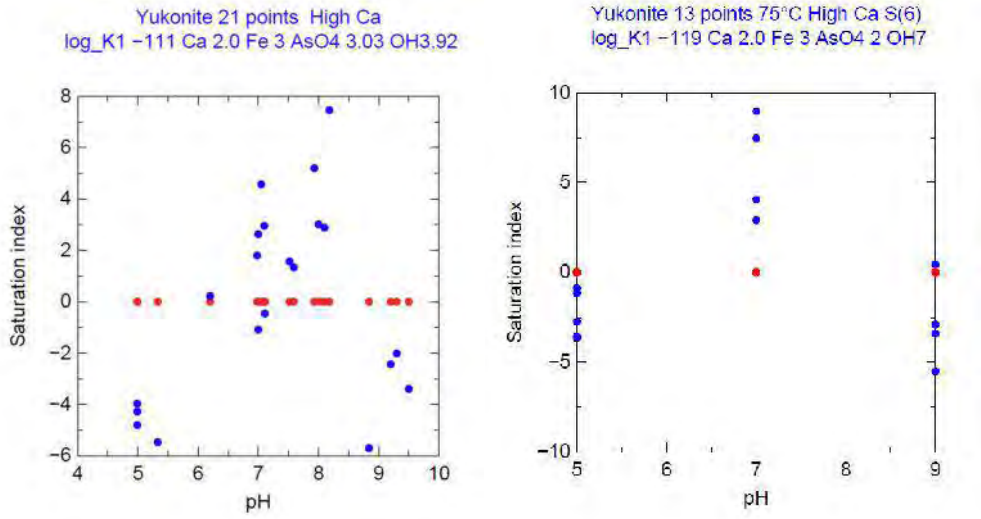

Figure 2a, 2b Example PhreePlot calculations to estimate Yukonite solubility. Figure 2a (left) shows the saturation indices for the 21 samples (blue dots) at room temperature after fitting, compared to "observed" values which were set to zero (red dots). Figure 2b (right) was for 13 samples run at 75°C.

Detailed contour plots based upon 52 data points were used to better define the relationship between the Fe and AsO_4 stoichiometric proportions. PhreePlot sweeps through a defined range of reaction coefficient values, and using the activities of the components in the solutions and the assigned stoichiometries the program calculates a log K_{sp} value. Using the measured concentrations, PhreePlot then calculates a W(RSS) and prepares contour plots of the $\log_{10}$(rss) values. Numerous data sets were evaluated. Figures 3a and 3b show some of these results. Unlike the deep narrow valley shown for scorodite (Figure 1b) the yukonite figures indicate that there are large "flat" zones where the iron stoichiometric values, in particular, show a large degree of uncertainty. For the $Ca_2Fe_y(AsO4)_z(OH)_a$ calculations for the oval that represents the minimum RSS (darkest blue), the

range for Fe is more than 2.0 units long, and even the As ranges from 1.65 to 2.65. To get a sense of how the Ion Activity Product (IAP) changes with changing stoichiometries, calculations were prepared using 1200 mg/L arsenic as arsenate, 1000 mg/L Ca, 2500 mg/L sulfate, the pH was fixed at 7.5 and ferrihydrite was present. These IAP values do not represent saturated conditions. "Yukonites" show a large spread in their log *IAP* values, for the upper point with Fe at 2.6 and AsO_4 at 2.4 (Figure 3a) the log *IAP* is -96.10. The smallest Fe value within the oval was Fe at 0.55 and AsO_4 at 1.65, and the log *IAP* value was -29.70. For the $Ca_3Fe_y(AsO4)_z(OH)_a$ formulas (Figure 3b) the upper and lower *IAP* values were -126.16 and -44.61. These ranges are too great to develop unique formulas and log K_{sp} values.

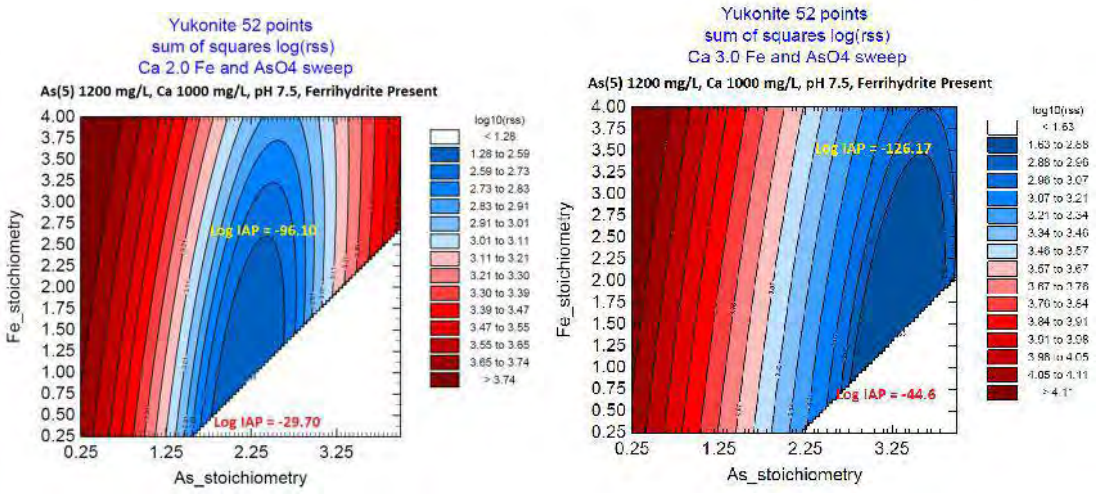

Figure 3a, 3b PhreePlot calculations used to evaluate stoichiometry factors for Fe and As for Yukonite. Figure 3a (left) used a Ca value of 2 and Figure 3b (right) used a Ca value of 3. White regions failed to converge in PHREEQC

Based upon the simpler scorodite calculation the approach appears to work, but it is highly sensitive to the quality of the data, and for yukonite the final parameter fit remains inconclusive at this time. It may be that ferric activities change as these samples age, further complicating the fitting calculations. This type of approach may be best for an iterative evaluation of laboratory data.

CALCULATION OF SURFACE SITE CONCENTRATIONS

The ability to vary any parameter in a PHREEQC model, provided one has sufficient data, means that better geochemical models can be developed, tested and refined using PhreePlot. In preparing a surface water discharge model for a uranium mill Mahoney and Frey (2014) used PhreePlot in several ways to produce a more rigorous model. One example is shown below.

The surface discharge model performed a series of mixing calculations for each year's discharge. The model is mainly a mixing model that uses site specific water balances to mix the various waters including surface waters and precipitation (rain and snow) at the discharge point. Additional surface water and precipitation dilute the composition in the two downstream lakes. The model was setup to allow for a wide range of options including evaporation, mineral precipitation and surface complexation. When appropriate, reactions in the receiving water bodies are included. Each model year was simulated independently. There was no year to year carry over in the models.

In the surface water discharge model, source waters are mixed at a discharge point (reservoir) and the waters flow through two additional bodies of water. By volume the two most important waters are from pit dewatering operations followed by the treated effluent from the mill. Chemical loads come from the treated mill water (Mill Discharge in Figure 4). For many major ions, simple mixing and dilution processes explain their concentrations in the downstream locations. However, arsenic concentrations are too low in the reservoir to be explained solely by mixing and dilution, so there must be an alternative geochemical process. Initial source term concentrations are too low for mineral solubility controls, so surface complexation becomes a means for arsenic attenuation. There is sufficient dissolved iron, particularly from the pit dewatering wells, that ferrihydrite appears to form and settle at the mixing/discharge point. Therefore, as part of the arsenic evaluation a surface complexation sub-model was included in the overall setup. Previous experience with arsenic surface complexation in pit lake models indicated that arsenic concentrations are unrealistically low when the standard site density parameter of 0.2 moles of weak HFO sites per mole of ferrihdyrite precipitated is used. Therefore, it was decided to prepare a model that tracked the amount of HFO that formed as the waters were mixed at the discharge point, and then fit the surface site density to obtain the best fit for the arsenic in the three lakes. Twelve data points, each representing annual averages for the various source terms and the concentrations in the three lakes for a total of 36 points were used. Surface complexation constants reported in Gustafsson and Bhattacharya (2007) for arsenic were used instead of the values in Dzombak and Morel (1990), speciation reactions defined in Langmuir et al. (2006) and Marini and Accornero (2010) were included. Based upon other observations, it was decided to estimate two different site concentration values. The first one was for the first six years, followed by another estimate for the final six years. The calculations adjusted the <sitedens> value. For years 1 through 6 the PHREEQC input follows:

```
SURFACE 1012000
 Hfo_wOH Ferrihydrite    equilibrium_phase <sitedens>    53400
 Hfo_sOH Ferrihydrite    equilibrium_phase <Strong>
```

The lines of input shown above tell PHREEQC to define the weak site surface concentration Hfo_wOH based upon the moles of ferrihydrite present as an equilibrium_phase times the value of sitedens. The surface area is assumed to be 600 m^2/g or 53400 m^2/mole of Ferrihydrite present as the equilibrium_phase. The strong site concentration Hfo_sOH is defined in a similar manner, but the strong site value is related to the weak site concentration through the following numericTag, <Strong>="<sitedens>/40". A similar setup was used for years 7 through 12, but the terms were <sitedens2> and <Strong2>. As ferrihydrite only forms in the first lake it is also the only location where surface complexation takes place. The lowering of concentrations in lakes 2 and 3 is caused by dilution from surface waters and rainfall/snowfall.
The PhreePlot estimated site density values were:

sitedens = 9.0497E-02 ± 1.7243E-02

sitedens2 = 1.2961E-01 ± 1.4404E-02

The site density values for the Hfo_wOH sites are about half of the value originally defined in Dzombak and Morel (1990), they defined a value of 0.2 sites per mole of HFO precipitated for weak sites. The fitted model uses smaller values and is considered to be more conservative (i.e., protective of the environment). Figure 4 compares different model setups for arsenic. The figure

shows a mixing/dilution only scenario (purple circles) which clearly overestimates estimates arsenic concentrations. The red lines are the optimized arsenic modeled concentrations based upon the fitted site densities. Surface complexation also appears to influence uranium concentrations, but a problem was noted, the site density values when fitted to the arsenic data produced models that underestimate uranium surface complexation and overestimate uranium concentrations in the lakes. The differences between the arsenic and uranyl fits suggest a disconnect in the surface complexation databases. It was decided to retain these lower site density values because higher surface site concentrations would lower dissolved arsenic concentrations producing a less conservative model. Also, the values tend to predict somewhat high uranium concentrations, which are considered to produce a more conservative model.

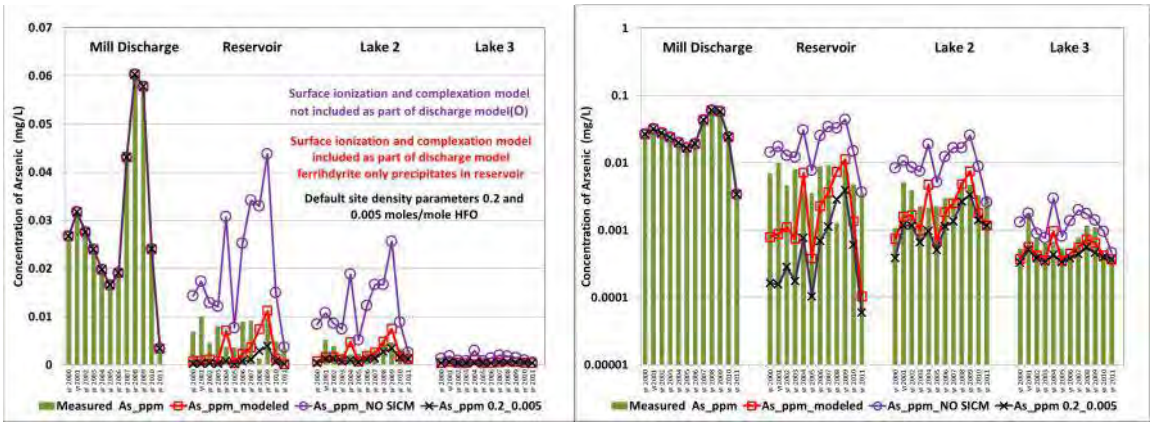

Figure 4a, 4b Surface water discharge model for arsenic, linear (a) and log concentrations (b). The figures shows observed values as green lines, the open circles did not include surface complexation reactions, red squares represent PhreePlot fitted model with surface complexation reactions on precipitated HFO. Black X's used the default site densities defined in Dzombak and Morel (1990)

ESTIMATION OF RATE LAW CONSTANTS

The following example shows how laboratory leach tests can be used to optimize a parameter in a geochemical model. Rate constants for kinetic models can also be fit using PhreePlot. Leach amenability studies (also called bottle roll tests) were used to determine rate constants for uraninite (UO_2) dissolution for a proposed in-situ uranium recovery operation in the Powder River Basin (Wyoming). The rates and rate law were subsequently included in a PHAST (Parkhurst et al. 2012) model to understand the nature of the leaching process in a three dimensional reactive transport system. The tests are used to demonstrate that the uranium mineralization is capable of being leached using conventional in-situ leach (ISL) methodologies. The leaching solution consisted of sodium bicarbonate (1 g/L $NaHCO_3$) as the carbonate complexation agent. Hydrogen peroxide at 0.5 g/L H_2O_2 (equivalent to 235 mg/L of dissolved oxygen) was used as the uranium-oxidizing agent. These tests were conducted at ambient pressure.

The bottle roll tests used 300 grams of solid and 1500 ml of leachate, the subsequent PHREEQC models maintained these proportions and used 200 grams of solid for 1 L of solution. The bottles were rolled for 16 hours (5.76e4 seconds), with eight hours available to collect samples and set up the next cycle, each sample under went six cycles. Ten tests were run and the ten samples covered a range of concentrations.

A kinetic model was developed to obtain a rate constant (k) for the dissolution of uraninite. A modified version of the rate law developed by Posey-Dowty et al. (1987) was used. The original rate law was:

$$dU/dt = k\left({}^{SA}/_{V}\right)(O_2)^{0.5}((U_s - [U])/U_s)$$

Where: k is the rate constant at 4.9(±2.2)e-5 (mole)(1)(m)$^{-1}$(atm)$^{-1/2}$(min^{-1}) reported by Posey-Dowty et al., (1987). Converting to seconds the value is 8.166 e-7(mole)(1)(m)$^{-1}$(atm)$^{-1/2}$(sec^{-1}), and

- SA is surface area in m^2,
- V is volume of water in liters,
- O_2 is the partial pressure of oxygen in solution in atmospheres,
- U_s is the uranium concentration at saturation, and [U] is the concentration of uranium at that point in time (units are moles) in the model.

The original paper was vague in defining the *(Us-[U])/Us)* term. They did not define the mineral that was to attain saturation or provide a limiting value for U_s, so the rate law was changed to:

$$dU/dt = k\,(SA/V)(O_2)^{0.5}((1\text{-}SR(\text{“}Schoepite\text{”}))^{*}(m/m0)^{power}$$

SR is the saturation ratio (IAP/K_{eq}), and the term *((1-SR(“Schoepite”)* slows the overall dissolution rate as the solution approaches saturation with schoepite. This type of limiting term is commonly used in many PHREEQC rate laws. At equilibrium, the SR = 1.0 and the dissolution process halts. For these models, uraninite was originally considered as the limiting mineral, but leaching conditions were so far from saturation with uraninite, that the SR term is exceedingly small, and would not have any impact as dissolution proceeded. The m0 value represents the moles of uraninite at time 0.0, and m represents the number of moles as the dissolution process proceeds. The *(m0/m)* term provides a means to adjust the rate as the uraninite particles get smaller and the surface area decreases. For theoretical reasons, the term is usually raised to the 0.67 power, but better fits were noted in the models where the power was 1.0.

The preferred RATES keyword for uraninite dissolution written in BASIC is:

```
RATES; Uraninite; -start
10 if(si("Uraninite")>=0) then goto 50
15 if (m <= 0) then goto 50
20 rate=<Rate_constant>*parm(1)*((10^SI("O2(g)"))^0.5)*(1-
SR("Schoepite"))*((m/m0))
30 moles = rate * time
40 if (moles > m) then moles = m
50 save moles
-end
```

The model also required a surface area (SA/V) value and uraninite concentrations, i.e., the m0 terms for each sample. Laboratory data provided the uraninite concentrations and QEMSCAM data indicated that the average diameter of the uraninite particles was 20 microns. The particles were assumed to be spherical, the areas were calculated. These surface areas are the parm(1) term in each model.

The 2012 models were prepared using PHREEQC and the rate constant was estimated using a trial and error method. The fit was based upon the Test 8 results, which had the largest concentration of uranium. Each bottle roll test was modeled using a one cell six shift TRANSPORT model. Essentially, the “beaker” (or cell in PHREEQC syntax) contained 0.2 kilograms of solid sample and

contacted 1 liter of fresh leaching solution six times. The time for each contact was assumed to be 16 hours or 5.76e4 seconds. For the trial and error approach this provided the needed concentrations as a function of time. The rate constant was used to prepare models of the other nine tests and the observations were compared to the modeled values. The trial and error fits were acceptable. To get the sequence of data in the SELECTED_OUTPUT file for the PhreePlot calculations, rather than use six shifts, an initial non-transport step was used, followed by five shifts in the TRANSPORT step, and the PRINT keyword turned writing to the SELECTED_OUTPUT file off and on, as needed (D. Parkhurst, personal communication).

The earlier trial and error method produced a rate constant of 2.8e-7(mole)(1)$(m)^{-1}(atm)^{-1/2}(sec^{-1})$, the value was subsequently used in a PhreePlot calculation to estimate the W(RSS) and for the sixty data points, the W(RSS) was 1.5754e04. Two different models were run using PhreePlot. The first model used the $(m/m0)^{0.67}$ function (Figure 5) and the second model used a 1.0 power. A smaller W(RSS) was produced for the $(m/m0)^{1.0}$ model. This is probably because the uraninite particles are not all 20 micron spheres. The best fit value is 2.433e-7 ±1.011e-8 (mole)(1)$(m)^{-1}(atm)^{-1/2}(sec^{-1})$. This value is close to the trial and error value estimates in 2012. Both rate constants are less than the value reported by Posey-Dowty et al. (1987). But differences are relatively small and could be related to differences in sample storage and handling, particle size estimates and subsequent estimation of surface areas, or differences between the two ore deposits.

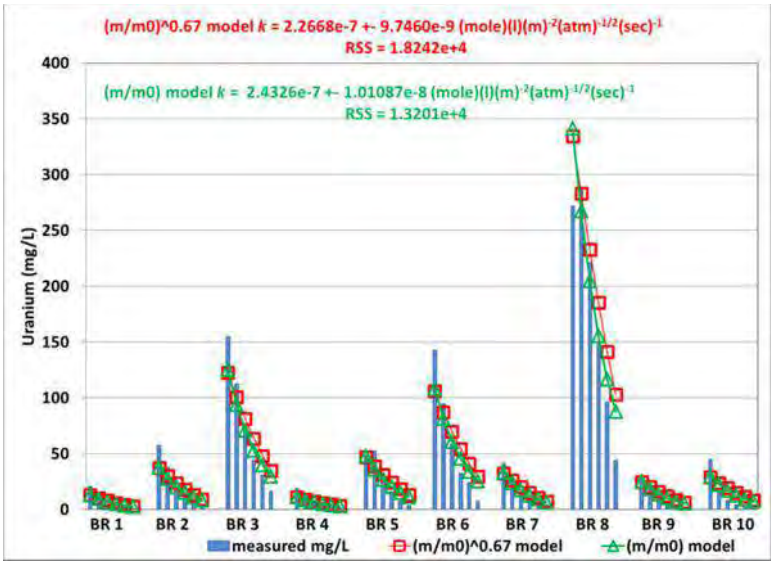

Figure 5 Bottle roll test data (blue lines) and PhreePlot Model fits. Red squares used an $(m0/m)^{0.67}$ term, green triangles used an $(m0/m)^{1.0}$ term

CONCLUSIONS

Nearly any parameter in a PHREEQC model can be fit using PhreePlot to better match observational data and produce a better model. Potential future applications might include: adjusting mixing parameters in a pit lake model to match early recovery time concentration data in the nascent lake to further refine the water balance, or for a 1 dimensional transport model, the length of time for shifts in a series of cells can be fit to calibrate transport velocities by matching the concentrations observed over time in a down gradient well with the modelled estimates. Such

calibrations even with limited early data produce better long term predictive models. The surface water discharge model described previously demonstrates this process. An improved understanding of the role of different processes also provides further insights about the whole discharge operation, which further strengthens the "what if" scenarios that are typically considered in predictive models.

This paper has shown just a few applications of the fitting capabilities in PhreePlot. It is hoped that other users will continue to apply PhreePlot to their specific studies.

REFERENCES

Dzombak, D.A. and Morel, F.M.M., 1990. Surface complexation modelling: hydrous ferric oxide. Wiley-Interscience, New York, 393 p.

Gustafsson, J.P., and Bhattacharya, P. , 2007. Geochemical modeling of arsenic adsorption to oxide surfaces. (Chapter 6). *in* Arsenic in Soil and Groundwater Environment, P. Bhattacharya, A. B. Mukherjee, J. Bundschuh, R. Zevenhoven, R. H. Loeppert (Editors) Trace Metals and other Contaminants in the Environment, Volume 9, pp. 159–206 Elsevier B.V.

Kinniburgh, D. G., and Cooper, D. M., 2004. Predominance and mineral stability diagrams revisited. Environ. Sci. Technol.. v. 38, No.13, pp. 3641-3648.

Kinniburgh, D. G., and Cooper, D. M., 2011. PhreePlot – Creating graphical output with PHREEQC. Available at http://www.phreeplot.org/, original date June 2011, last updated December 17, 2014, 606 p.

Langmuir, D., Mahoney, J., and Rowson, J., 2006. Solubility products of amorphous ferric arsenate and crystalline scorodite ($FeAsO_4{\cdot}2H_2O$) and their application to arsenic behavior in buried mine tailings: Geochimica et Cosmochimica Acta., vol. 70, pp. 2942-2956.

Mahoney, J.J., Cadle, S.A., and Jakubowski, R.T., 2009. Uranyl adsorption onto hydrous ferric oxide – a re-evaluation for the diffuse layer model database. Environ. Sci. and Technol., v. 43, no. 24, pp. 9260-9266. DOI 10.1021/es901586w.

Mahoney, J.J., and Frey, R.A., 2014. Calibration of a PHREEQC Based Geochemical Model to Predict Surface Water Discharge Compositions from an Operating Uranium Mill in the Athabasca Basin. Presented at URAM 2014, Material for the Nuclear Fuel Cycle: Exploration, Mining, Production, Supply and Demand, Economics and Environmental Issues. IAEA. Vienna, Austria. (in press).

Marini, L., and Accornero, M., 2010. Erratum to: Prediction of the thermodynamic properties of metal–arsenate and metal–arsenite aqueous complexes to high temperatures and pressures and some geological consequences. Environ. Earth Sci. Vol. 59, pp. 1601-1606.

Parkhurst, D.L., and Appelo, C.A.J., 2013. Description of input and examples for PHREEQC version 3 — A computer program for speciation, batch-reaction, one-dimensional transport, and inverse geochemical calculations: U.S. Geological Survey Techniques and Methods, book 6, chap. A43, 497 p., available only at http://pubs.usgs.gov/tm/06/a43.

Parkhurst, D.L., Kipp, K.L., and Charlton, S.R., 2010. PHAST Version 2 —A program for simulating groundwater flow, solute transport, and multicomponent geochemical reactions: U.S. Geological Survey Techniques and Methods 6–A35, 235 p.

Poeter, E. P., Hill, M. C., Banta, E. R., Mehl, S., Christensen, S., 2005. UCODE_2005 and Six Other Computer Codes for Universal Sensitivity Analysis, Calibration and Uncertainty Evaluation; Techniques and Methods 6-A11; USGS: Reston, VA.

Posey-Dowty, J.,Axtmann, E., Crerar, D., Borcsik, M., Ronk, A., and Woods, W. 1987. Dissolution rate of uraninite and uranium roll-front ores. Economic Geology, Vol. 82, pp. 1493 -1506.

Hydrogeochemistry Tailing Model to Evaluate Future Water Quality – Mina Vazante MG, Brazil

Flávio Vasconcelos[1], Caroline Zanetti[2], Debora Almeida[3] and Adelson de Souza[3]

1. *Hidrogeo Assessoria Ambiental Ltda., Brazil*
2. *Amplo Engenharia e Gestão de Projetos Ltda, Brazil*
3. *Votorantim Metais, Brazil*

ABSTRACT

Aroeira dam received for the last 10 years, zinc silicate tailing material (willemite $Zn_2(SiO_4)$ from the mill plant (USICON) of Vazante Mine. Votorantim Metals is nowadays developing a Feasibility Project of Zinc-Ambrosia oxidized sulphide zinc deposit, located in the nearby municipality of Paracatu / MG. This new ore deposit is subdivided into two parts (North and South Cava), and the North Cava has 800,000 tons of oxidized sulphide zinc ore. The financial feasibility of the ore exploitation of this new deposit requires the disposal of the new tailings into Aroeira dam. Work recently carried out by Votorantim Metals technicians using acetic acid leaching test in several samples of tailings had values for lead and cadmium relatively high. However, test results from the same samples using water leaching test (using distilled water) had values of the same parameters (Pb and Cd) below the detection limit of the analytical methods for most of the samples. Considering the above issues presented here in terms of the solid waste metal leaching, Ambrosia tailing characteristics should be considered in the final tailing disposal. In addition, the actual tailings are low in sulfide and have large neutralizing capacities, so decreasing in pH conditions are not expected. The work presented here aims to demonstrate through a hydrogeochemical model, using geochemical waste material characterization data and the software PHREEQC the environmental impact of disposal of Ambrosia mining waste into Aroeira tailings dam. The study developed here required the water sampling and tailing geochemical characterization according to MABA, NAG, water leaching test, and SPLP and the use of these results together with the dam physical characterization for the development of a future water quality model for this reservoir. Results obtained from this work allow someone to state that the disposal of Ambrosia tailings will not impact the local water resources.

Keywords: Water quality prediction, Hydrogeochemical modeling.

INTRODUCTION

Aroeira dam received for the last 10 years, zinc silicate tailing material (willemite $Zn_2(SiO_4)$ from the mill plant (USICON) of Vazante Mine. Votorantim Metals is nowadays developing a Feasibility Project of Zinc-Ambrosia oxidized sulphide zinc ore deposit, located in the nearby municipality of Paracatu / MG. This new ore deposit is subdivided into two parts (North and South Cava), and the North Cava has 800,000 tons of oxidized sulphide zinc ore. The disposal of the new tailings into Aroeira dam is fundamentally important for the financial viability of this new project. Considering the above issue presented here in terms of the solid waste management, Ambrosia tailing characteristics should be considered in the final tailing disposal. So, Aroeira tailing dam will receive new solid waste coming from Ambrosia ore deposit and also coming from other zinc mine (Extremo Norte mine). The first one is an oxidized sulphide lead and zinc ore deposit and the last one is a zinc silicate ore deposit hosted in a geological carbonate formation. The aim of this work is to demonstrate, using a PHREEQC model, that the current tailing dam can receive this new tailing material (Ambrosia deposit and Extremo Norte mine) without significant changes in the water quality of the current conditions of this reservoir.

METHODOLOGY

The water sampling of the tailing pond was carried out on July/2014 by the technicians of HidroGeo & Amplo consulting companies with the help and support of an employee from Votorantim Metals who was the boat operator for the water sampling collection. The water sampling was based on the Brazilian technical standards ABNT NBR 9897 - Planning sampling of liquid effluents and receiving bodies and ABNT NBR 9898 - Conservation and sampling techniques of liquid effluents and receiving water. This technical norm presents the fundamental aspects that should be followed during any water sampling campaign. All the technical aspects related to water sampling were strictly executed by field technicians.
The methods of analysis of water samples were those recommended by the Standard Methods for the Examination of Water and Wastewater, in its 21st edition of 2005. Some methodologies of the Environmental Protection Agency (EPA) were also adopted regarding the collection and analysis of industrial effluents and receiving waters.

Water and tailing sampling

Eight water samples were collected at four points inside the Aroeira tailing dam at two depths as shown in Table 1 below. To collect these samples field technicians used the Van Dorn bottle. Table 1 presents the identification and characteristics of the sampling points, and the depth of the collection. Tailing samples of the future waste material that will be discharged into the Aroeira reservoir were obtained from metallurgical plant, provided by Votorantim Metals for geochemical characterization.

Tailing samples from the Aroeira reservoir were collected at the same time that water samples were collected (Table 1).

Table 1 List of water and tailing sampling points at Aroeira reservoir

Point	ID	Date	Hour	Location: coordinate UTM SAD 69 Zone 23		Sample Depth (m)
1	ARO 01	07/02/2014	12:31	307906	8012222,	0.5
	ARO 02		13:30	307906	8012222	2.0
2	ARO 03	07/02/2014	14:27	307597	8012347	0.5
	ARO 04		15:00	307597	8012347	2.5
3	ARO 05	07/02/2014	15:27	307689	8012245	0.5
	ARO 06		15:50	307689	8012245	6.5
4	ARO 07	07/02/2014	16:30	307746	8012169	0.5
	ARO 08		16:50	307746	8012169	8.5

The parameters temperature, pH, dissolved oxygen (DO), electrical conductivity (EC) and redox potential (Eh) were measured in situ with a multiparameter equipment Hanna HI9828. The equipment was calibrated daily as part of the protocol (QA / QC) for data collection in the field.

The samples were filtered and preserved in the field with membrane of 0.45 μm to determine the dissolved metals (Figure 1).

Figure 1 Photo of the water sampling and filtering procedure in the Aroeira tailing dam.

Tailing Geochemical characterization (Mill plant, Vazante tailing, Extremo Norte tailing, Ambrosia tailing)

Geochemical characterization for acid generation (static tests) and metal leaching potential were performed in all tailing samples. For acid generation it was used modified acid base account (MABA) and net acid generation (NAG) and for metal leaching it was used synthetic precipitation leaching procedure (SPLP) and a Brazilian version of TCLP test that uses diluted strong acids and acetic acid at pH 5 (ABNT NBR 10,005) and another Brazilian test that uses water leaching procedure for characterization of solid waste (ABNT NBR 10,006). All these metal leaching tests were used to better understand the potential metal leaching capacity of sample at normal and extreme condition of water pH. Results and comments are presented in the next section.

Underneath there is a schematic profile representing the sampling points along the main axis of the tailing dam (Figure 2).

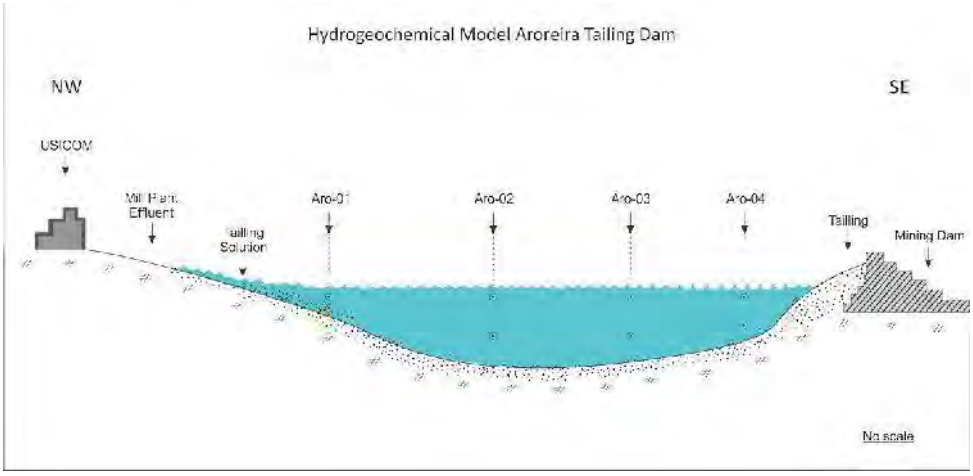

Figure 2 Schematic representation of the sampling points of water and tailings from Aroeira dam.

Conceptual Site Model (CSM)

To be able to develop a hydrogeochemical model using PHREEQC it is necessary to develop a conceptual site model (CSM) based on the tailing's water balance and solutions chemical composition. Five solutions were considered in this model and they are the following: Solution 1- Underground mine effluent; Solution 2- Mill plant effluent; Solution 3- Rainfall precipitation; Solution 4- Tailing water; and Solution 5- Tailing spillway. These solutions are represented in the following CSM figure (Figure 3). Groundwater contribution was not relevant for this case; therefore, it was not considered in the CSM presented here.

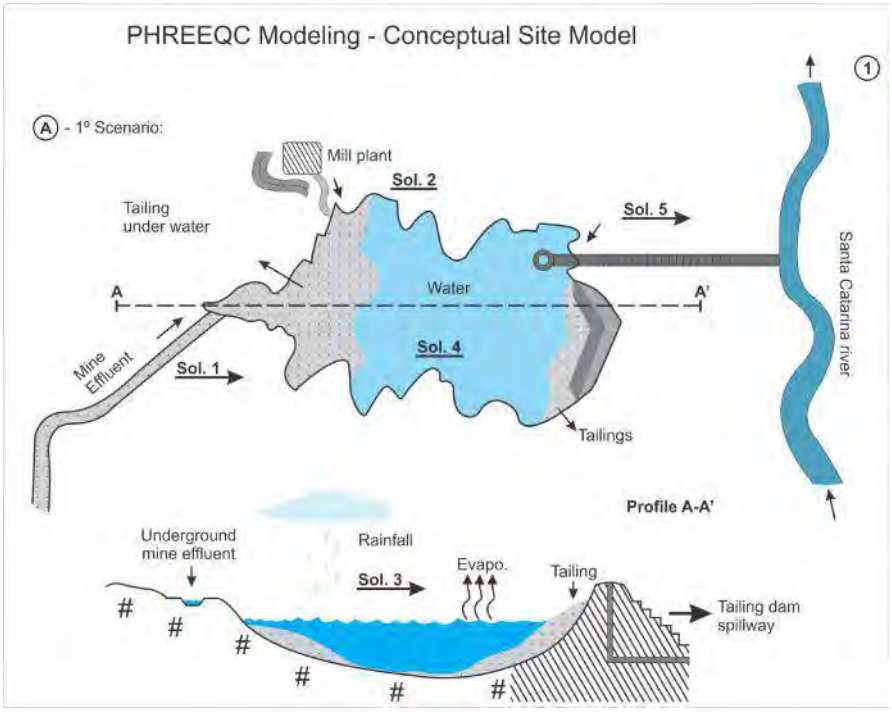

Figure 3 Conceptual site model (CSM) representing a map and a profile of the site, and no scale.

PHREEQC input data

The PHREEQC used in this paper took MINTEQ database to run the model and the input data is basically the water quality of each solution that compound the system to be modelled and the percent volume of each solution, then three scenarios were simulated. The first one was the current tailing scenario where the underground mine effluent mix with the mill plant effluent to make the tailing water composition. The other two scenarios are derivatives of the first one, where just the second solution (solution 2), coming from the mill plant effluent would change considering the new type of ore material that will be processed there.

Hydrogeochemistry model calibration

To be able to calibrate the model the following approach was used. Based on the CSM tailing water chemical composition (solution 4) is derived from the mix of solution 1 (underground mine effluent) and solution 2 (mill plant effluent). Therefore, in this work, solution 4 was used to calibrate the mix of solution 1 and 2. Once, the results obtained from the model come out very similar to the results obtained from solution 4 the model was considered calibrated and it was run for the other two scenarios where solution 2 would change in function of the new ore material or mix of ore that would be processed in the mill plant. So, the only solution that will change from scenario 1 to 2 and 3 is solution 2 (Table 2).

Table 2 Hydrogeochemical calibration of PHREEQC using current scenario of the tailing dam

Solutions	*Solution ID*
Solution 1	Underground Mine Effluent (sampling point ARO 09)
Solution 2*	Current mill plant tailing; Ambrosia; Mix of tailings (Ambrosia, Vazante and Extremo Norte)
Solution 3	Annual precipitation water quality
Solution 4	Tailing dam water quality (Average of sampling points)
Solution 5	Spillway of the dam (sampling point ARO 10)

* Solution 2 will change in function of the 3 scenarios.

RESULTS AND DISCUSSION

Geochemical characterization of the tailing samples

The potential to generate acidity conducted from static tests can be interpreted by various types of graphical forms. In this study, it was chosen one type of interpretation often used for this purpose (INAP, 2009; MEND, 2009) (Figure 4).

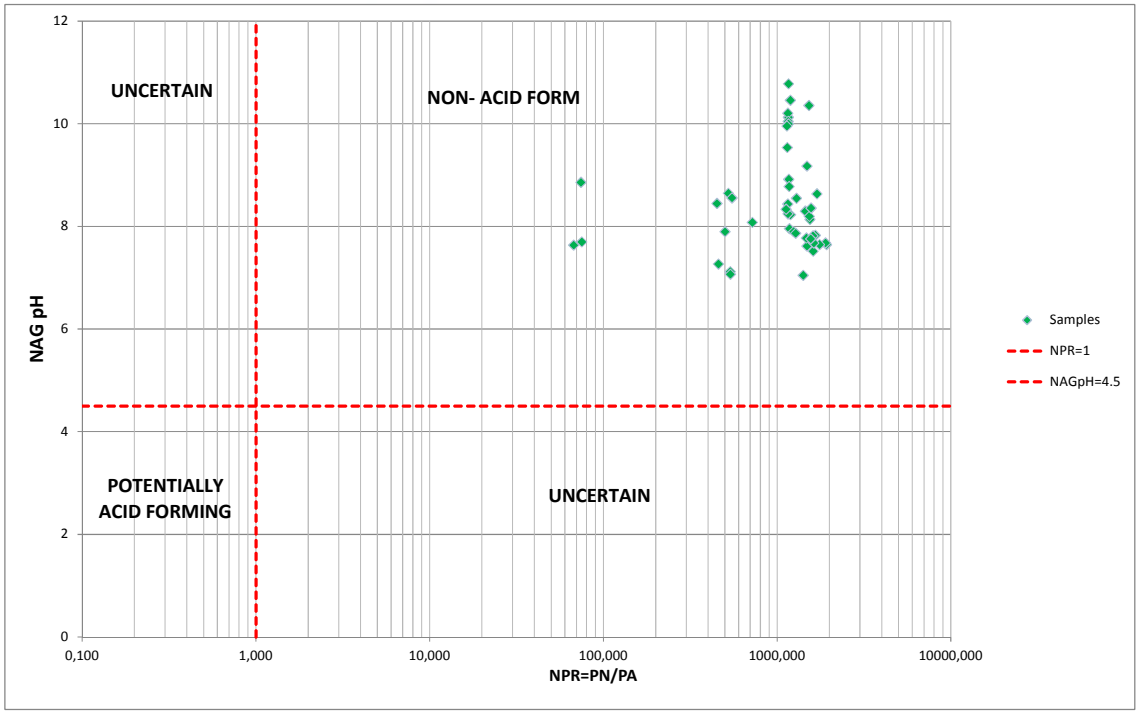

Figure 4

From the results obtained in the MABA and NAG tests presented above it can be concluded that it is very low and unlikely that these tailing samples already displaced or that will be disposed into the Aroeira reservoir will generate acidity. These results are consistent with the mineralogical composition of the rocks that generated Vazante tailing samples that are metamorphosed carbonate sediments, as marls and dolomites, intercalated with phyllites. The geological formation of this zinc deposit is a classical karst environment. In addition, underground water flow in the underground mine is super critic with a water flow rate of 10,315 m^3/hr.

Results of metal leaching test according to the North American standard SPLP, using diluted strong acid at pH 5, (US EPA 1312) presented very similar numbers and the only parameter that showed the greatest potential for leaching was just lead (values varied from 3.74 mg/L to 10.43 mg/L). For modeling purpose neither SPLP test nor the Brazilian acetic acid leaching test results (ABNT NBR 10,005) were used because they do not accurately represent tailing physical chemical conditions. Water leaching results from a mix of tailings at the following proportion 10% (Ambrosia Mine); 40% (Extreme North); 50% (Vazante Mine), used for modeling purposes, is presented in the underneath table (Table 3).

Table 3 Water leaching test in mixed tailings.

Element	*Unit*	*T_1*	*T_2*	*T_3*	*T_4*	*T_5*
Al	mg Al/L	<0.005	<0.005	0.046	0.,027	0.036
As	mg As/L	<0.01	<0.01	<0.01	<0.01	<0.01
Ba	mg Ba/L	0.243	0.228	0.264	0.241	0.273
Cd	mg Cd/L	<0.001	<0.001	<0.001	<0.001	<0.001
Pb	mg Pb/L	<0.01	<0.01	0.03	0.02	<0.01
CN	mg CN-/L	<0.01	<0.01	<0.01	<0.01	<0.01
Cl	mg Cl-/L	<2.0	<2.0	<2.0	<2.0	<2.0
Cu	mg Cu/L	<0.003	<0.003	0.006	<0.003	<0.003
Cr	mg Cr/L	<0.01	<0.01	<0.01	<0.01	<0.01
Fe	mg Fe/L	<0.05	<0.05	<0.05	<0.05	<0.05
Mn	mg Mn/L	<0.03	<0.03	<0.03	<0.03	<0.03
NO_3	mg N_NO_3/L	<0.05	<0.05	<0.05	<0.05	<0.05
pH solution (ratio 2:1)	-	9.04	9.08	9.17	9.1	9.18
Ag	mg Ag/L	<0.003	<0.003	<0.003	<0.003	<0.003
Se	mg Se/L	<0.01	<0.01	<0.01	<0.01	<0.01
Na	mg Na/L	8.08	8.23	7.54	7.67	7.57
SO_4	mg SO4/L	24.1	23.7	27.1	27.8	23.7
Zn	mg Zn/L	0.006	<0.005	0.013	0.011	0.006

The only trace metal with significant water leaching values was lead (Pb = 0.03 and 0.02 mg/L). However, this order of magnitude of values obtained for lead (i.e., decimals ppm) is not considered high because of the dilution factor that should be also counted for in this analysis.
Water quality of each solution is presented in the table underneath (Table 4). The water percent volume is presented right after (Table 5). It is noticeable that the solution 1 coming from the underground mine effluent is the biggest percent volume and probably will play major role in the final tailing water composition (solution 4) considering its volume.

Table 4 Water quality input data for PHREEQC model for Aroeira tailing dam at different scenarios.

Element	*Solution 1 (mg/L)*	*Solution 2 (mg/L)*		
		Scenario 1 Current tailing	**Scenario 2 Ambrosia tailing**	**Scenario 3 Mixture of tailings**
Alkalinity	191	200	200	200
Al	0.033	0.005	0.0025	0.005
Cd	0.0005	0.0005	0.0005	0.0005
Ca	33.7	15.6	11.64	11.26
Cu	0.0015	0.0015	0.0015	0.0015
Fe	0.025	0.050	0.025	0.025
Mg	20.8	6.71	9.4	6.75

Mn	0.015	0.03	0.024	0.0225
N(5)	0.57	0.11	0.025	0.025
pH	7.0	9.1	8.2	9.23
K	0.87	1.3	3.6	1.17
pe	4.57	4.0	4.0	4.0
Pb	0.005	0.005	0.005	0.005
Zn	0.04	0.0106	0.1649	0.019

Considering that there is no gain or loss of water from or to the groundwater in the tailing dam area, the tailing reservoir (Solution 4) is made out of approximately 92% of water coming from the underground mine effluent and 8% of water coming from the mill plant (Table 5). The percent of water coming from rainfall precipitation is not significant therefore it was neglected in this study in particularly.

Table 5 Percent volume of each type of solution used in the hydrogeochemical model.

Solutions	*Volume (m^3/year)*	*Solution ID*	*Percent Volume (%)*
Solution 1	90,436,000.00	Underground mine	91.87
Solution 2	168,340.87	Mill plant	8.10
Solution 3	70,927.57	Rainfall	0.03
Solution 4	2,080,297.39	Tailing water	-
Solution 5	85,759,000.00	Spillway	-

PHREEQC output data

The current tailing pond is basically composed of water from the underground mine (sol. 1 = 91.87%) and solution waste from the beneficiation plant (USICON) (sol. 2 = 8,10%). The mixture of these two solutions must generate another solution very similar in composition to the water dam (sol. 4). The PHREEQC output data for the three modeled scenarios are shown at Tables 5, 6 and 7 below. Scenario 1 is considered in this exercise the calibration operation. It is remarkable that pH from the underground mine effluent raised com 7.3 to 8.4 after being displaced in the tailing dam (sol. 4). This fact means that solution alkalinity coming from the inlet increases in more than 10 times. PHREEQC model was able to consistently represent the field data. For most of the other parameters the different in concentration were not higher than 35%, so this represents a fair agreement between field data and model results , only trace metal such as: Fe, Mn, Zn and Cu that had very low concentration presented relative difference higher than 35% (Table 6).

Table 6 PHREEQC Output data for scenario 1 (model calibration)

Elements	*MIX of Sol. 1 and Sol. 2 (mg/L)*	*Water tailing Sol. 4 (mg/L)*	*Relative difference (%)*
Al	0.033	0.0211	36.6
Ca	33.37	28.79	13.7
Cd	0.0005	0.0005	0.0
Cl	1.00	1.00	0.0
Cu	0.002	0.003	50
Fe	0.025	0.050	100
K	0.861	1.436	20.6
Mg	20.60	20.25	24.6
Mn	0.015	0.030	6,2
Ni	0.005	0.010	100
Pb	0.005	0.005	0.0
Zn	0.040	0.023	42.5
pH	7.3	8.40	1.8

Once we got the model calibrated in relation to the tailing water (solution 4), the next step was to run the same model framework in terms of solution volume but now solution 2 would change accordantly to the water leaching from the tailing material generated by the mill plant. Result obtained demonstrates that the addition of tailing from Ambrosia ore deposit to the reservoir will not change significantly water quality of Aroeira tailing dam (Table 6). Sensitivity analysis was done further on to demonstrate that even when someone double the metal leaching results obtained from the geochemical test, simulating a more conservative scenario, final modeling results in the tailing dam still similar to the one obtained here (results not presented). Aluminum and zinc concentration was lower in the current tailing solution and it is probably due to some sorption of this metal with ferryhydrite or another form of iron oxyhydroxides.

For the other scenarios the same procedure as the previous one was used. The system framework was kept the same, except the water composition of solution 2. Now this solution was obtained from a mix of tailing water leaching composition (Table 6). Again the difference between the mix of solution 1 and 2 was close to the standard solution 4 that we use to evaluate the model results. In this particular case sodium and sulfur different was even higher than before and this must be related to field tailing water composition tailing characterization procedure. The mix of sample definitely was not processed with sodium sulphide and sodium carbonate.

Table 6 PHREEQC output data for scenarios 2 and 3

Elementos	*MIX Sol. 1 e Sol. 2 (mg/L) Scenario 2*	*MIX Sol. 1 e Sol. 2 (mg/L) Scenario 3*	*Água Barragem (Sol. 4) Reference (mg/L)*
Al	0.061	0.0611	0.021
Ca	27.39	27.315	28.79
Cd	0.001	0.001	0.001
Cl	2.0	2.0	1.0
Cu	0.003	0.003	0.003
Fe	0.002	0.002	0.050
K	2.177	1.788	1.436
Mg	17.65	17.21	20.25
Mn	0.032	0.032	0.030
Ni	0.010	0.010	0.010
Pb	0.010	0.010	0.005
Zn	0.076	0.076	0.023
pH	8.25	8.25	8.40

CONCLUSION

All tailings evaluated (current mill plant tailing; Ambrosia tailing; Mix of tailings, Vazante and Extremo Norten tailings) did not show potential to generate acid drainage and have low potential for metal water leaching. They also have very similar geochemical behavior comparing to the waste currently disposed at the bottom of the Aroeira tailing dam. The hydrogeochemical modeling performed in this study using a computational tool PHREEQC, was used to demonstrate this behavior and it reflected the boundary conditions presented above. The solution 1 from the underground mine, due to its large volume (92% of the total water volume), will dominate the water quality of the Aroeira tailing dam and other tailings solutions from the processing plant, solution 2, (i.e., mix of Ambrosia and mix waste) will not be able to change the current quality of the reservoir. Therefore, water quality in the Aroeira dam will not turn into acid and no significant metal solubility from tailing displaced in the dam to the water will occur. So, it is possible to conclude that this new disposal of tailings will not cause any harm to the local environment.

ACKNOWLEDGEMENT

Authors of the paper would like to make some acknowledgement to Votorantim Metais S.A. that allow the group to develop and publish this work. We also would like to acknowledge the ICARD technical committee for the selection of this paper for publication and presentation.

REFERENCES

ASSOCIAÇÃO BRASILEIRA DE NORMAS TÉCNICAS (ABNT) – NBR 10005, Procedure for obtaining leachate extract from solid waste. Rio de Janeiro/RJ. 2004.

ASSOCIAÇÃO BRASILEIRA DE NORMAS TÉCNICAS (ABNT) – NBR 10006, Procedure for obtaining leachate extract from solid waste. Rio de Janeiro/RJ. 2004.

MEND, Prediction Manual for Drainage Chemistry from Sulphidic Geologic Materials. MEND Report 1.20.1. December 2009.

THE INTERNATIONAL NETWORK FOR ACID PREVENTION (INAP).Global Acid Rock Dranaige Guide (GARD). International Network for Acid Prevention. Skellefteå, Sweden. 2009 Acessado em 10/09/2012: www.gardguide.com.

UNITED STATES ENVIRONMENTAL PROTECTION AGENCY (US EPA 1312), Synthetic Precipitation Leaching Procedure. September ,1994. Washington.30 pp

Reaction Modeling of Drainage Quality in the Duluth Complex, Northern Minnesota, USA

Robert Seal[1], Kim Lapakko[2], Nadine Piatak[1] and Laurel Woodruff[1]

1. *U.S. Geological Survey*
2. *Minnesota Department of Natural Resources (retired), USA*

ABSTRACT

Reaction modeling can be a valuable tool in predicting the long-term behavior of waste material if representative rate constants can be derived from long-term leaching tests or other approaches. Reaction modeling using the REACT program of the Geochemist's Workbench was conducted to evaluate long-term drainage quality affected by disseminated Cu-Ni-(Co-)-PGM sulfide mineralization in the basal zone of the Duluth Complex where significant resources have been identified. Disseminated sulfide minerals, mostly pyrrhotite and Cu-Fe sulfides, are hosted by clinopyroxene-bearing troctolites. Carbonate minerals are scarce to non-existent. Long-term simulations of up to 20 years of weathering of tailings used two different sets of rate constants: one based on published laboratory single-mineral dissolution experiments, and one based on leaching experiments using bulk material from the Duluth Complex conducted by the Minnesota Department of Natural Resources (MNDNR). The simulations included only plagioclase, olivine, clinopyroxene, pyrrhotite, and water as starting phases. Dissolved oxygen concentrations were assumed to be in equilibrium with atmospheric oxygen. The simulations based on the published single-mineral rate constants predicted that pyrrhotite would be effectively exhausted in less than two years and pH would rise accordingly. In contrast, only 20 percent of the pyrrhotite was depleted after two years using the MNDNR rate constants. Predicted pyrrhotite depletion by the simulation based on the MNDNR rate constant matched well with published results of laboratory tests on tailings. Modeling long-term weathering of mine wastes also can provide important insights into secondary reactions that may influence the permeability of tailings and thereby affect weathering behavior. Both models predicted the precipitation of a variety of secondary phases including goethite, gibbsite, and clay (nontronite).

Keywords: acid mine drainage, mineral dissolution, mine tailings, water quality prediction, REACT

INTRODUCTION

Predicting long-term weathering behavior of mine waste, though a formidable challenge, holds great importance for the mining industry. Traditional static tests, such as acid-base accounting, provide information about maximum potential acidity, but offer no insight about how that acidity may evolve over time. Results from static tests have great value as screening tools, which form the basis for more costly and labor-intensive studies, such as kinetic tests. Kinetic tests, such as humidity-cell experiments, provide empirical information about the time-dependent weathering of mine waste, but are generally limited by the experimental duration. The longest duration leaching experiments are probably those conducted by the Minnesota Department of Natural Resources (MNDNR), which have been ongoing for more than 24 years, on waste rock from the Duluth Complex, northern Minnesota (Kellogg et al., 2014). The MNDNR also has weathering test results from ongoing 10-year experiments on tailings derived from pilot metallurgical tests on Duluth Complex low-sulfide ores hosted by troctolitic rocks (Lapakko, Olson & Antonson, 2013a). For permitting purposes, time scales of these lengths are challenging as is scaling laboratory tests up to a mine scale. Barrel tests and instrumented tests on waste-rock and tailings piles are being used once mine development has begun to help address this challenge (Smith et al., 2013; Lindsay et al., 2009).

Uncertainty about the long-term behavior of mine waste clouds the decision-making process for many mine-permit applications. Extrapolating laboratory results significantly into the future has significant uncertainty, particularly for experiments in which the acid-generating potential has not been exhausted. This report explores the possibility of using geochemical reaction modeling to predict the long-term weathering behavior of mill tailings from low-sulfide Duluth Complex Cu-Ni-(Co)-PGM ores (Fig. 1). Acid-generating potential is the initial focus of this ongoing study. Major and trace element behavior will be a future emphasis.

The Duluth Complex of northern Minnesota has high potential for future mining of large tonnage, low grade Cu-Ni-(Co)-PGM resources (Ripley, 2014). Collectively, estimated reserves exceed 4.4 billion tons with approximately 0.66 percent Cu, 0.2 percent Ni, and total PGMs ranging between 0.3 and 0.6 mg/kg (Pd > Pt) (Listerud and Meineke (1977). The ores are found in troctolites and gabbros in the lower 100 to 300 m of the Partridge River and South Kawishiwi intrusions (Fig. 1) (Ripley, 2014). The host rocks comprise plagioclase, clinopyroxene, and olivine, with minor amounts of orthopyroxene, biotite, potassium feldspar, and ilmenite; the rocks are essentially devoid of carbonate minerals (Lapakko, Olson & Antonson, 2013a; Ripley, 2014). The principal sulfide minerals are pyrrhotite, chalcopyrite, cubanite, and pentlandite.

METHODOLOGY

Conceptual framework

The goal of this study is to explore the feasibility of using geochemical reaction computer software to model the long-term weathering behavior of tailings generated from the disseminated, low-sulfide ores at the base of the Duluth Complex for time periods spanning decades. The 10-year weathering test results for pilot-test tailings from the Duluth Complex low-sulfide ores are used as a basis to validate various simulation parameters (Lapakko et al., 2013a). The disseminated sulfide ores at the base of the complex are characterized by a low sulfide content (generally < 1 wt. % S)

and virtually no carbonate minerals (Lapakko and Antonson, 2012; Lapakko, Olson & Antonson, 2013a; Ripley, 2014). Thus, the acid-neutralizing potential of the mine waste is supplied by silicate minerals such as plagioclase, olivine, and pyroxene.

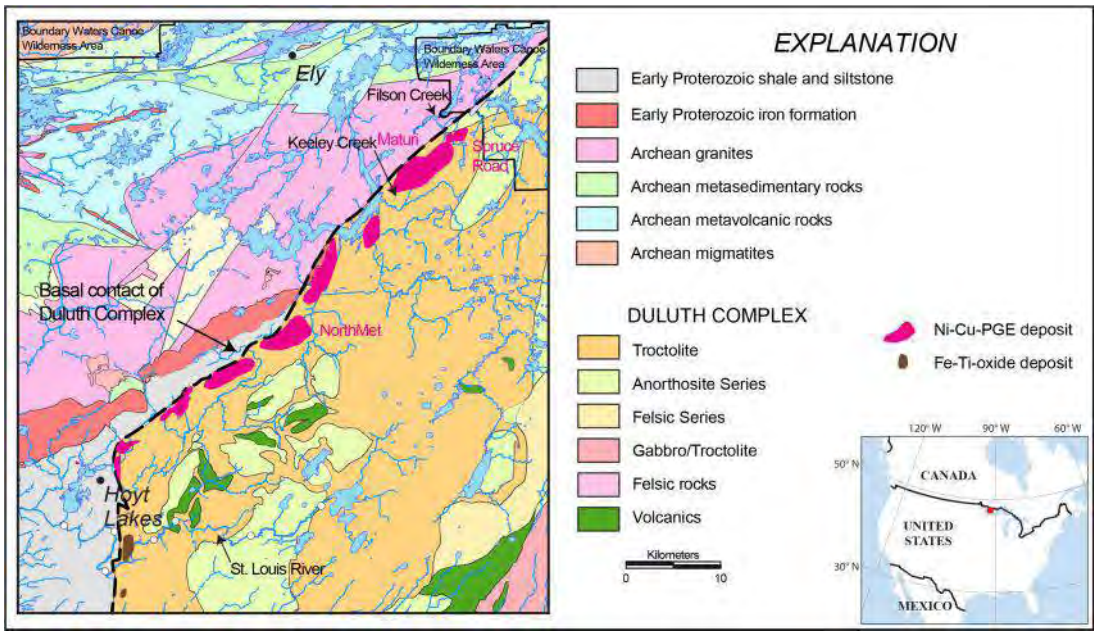

Figure 1 Geologic map of the Duluth Complex and older rocks in the vicinity of the disseminated Cu-Ni-(Co)-PGM deposits.

Software

The software package used in this study is the suite of programs included in the Geochemist's Workbench, primarily the program REACT (Bethke, 2008; Bethke and Yeakel, 2014). REACT simulates the reaction of a specified mass of solid with 1 kg of solution. Equilibrium modeling titrates increments of the solid into the solution, following a specified number of steps, allowing reaction progress to be followed. Kinetic modeling, using user-defined rate constants for solids, reacts a specified amount of solids with 1 kg of solution for a specified amount of time.

Thermodynamic and Kinetic Data

This study used the Lawrence Livermore National Laboratory (LLNL) thermodynamic database supplied with the Geochemist's Workbench for these simulations, because it contained data applicable to the silicate, sulfide, and sulfate phases included in the study. Two sets of kinetic data were used. The first set is the compilation of published single-mineral rate constants from Palandri & Kharaka (2004). The second set, from Kellogg et al. (2014), is based on normative-style calculations from weathering tests on waste rock from the Duluth Complex.

The initial system

The model system used in this study is based on the 10-year laboratory weathering tests by Lapakko, Olson & Antonson (2013a) performed in small reactors on mill tailings derived from metallurgical testing. The sample comprised plagioclase (An_{57}; 57 %), clinopyroxene (X_{Mg} 0.77; 11 %), olivine (X_{Mg} 0.55; 9.8 %), quartz (9.8 %, assumed to be contamination of the sample from the country rock), and biotite (X_{Mg} 0.65; 5.7 %) with trace amounts of ilmenite, potassium feldspar, and orthopyroxene. The sample contained 0.2 wt. % sulfur, assumed for the purposes of modeling to be present as pyrrhotite, which is known to be the most common sulfide mineral in the Duluth Complex (Ripley, 2014). Lapakko, Olson & Antonson (2013a) were only able to identify chalcopyrite in their mineralogical characterization of their tailings sample, but they assumed the presence of both pyrrhotite and pentlandite.

For this exercise, the mineralogy of the starting model system was simplified to consist of plagioclase, clinopyroxene, olivine, and pyrrhotite. To account for solid-solution effects, the two end members of binary solid-solution series were included in proportion to the average composition for these minerals as described by Lapakko, Olson & Antonson (2013a). Thus, the simulations included plagioclase as both albite and anorthite, clinopyroxene as diopside and hedenbergite, and olivine as forsterite and fayalite. Pyrrhotite was assumed to be stoichiometric troilite (FeS). The masses of these phases, normalized to 100 percent, are presented in Table 1.

Table 1 Mineralogical composition of model system and dissolution rate constants.

Mineral	Component	Abundance	Surface Area	Rate Constant (k)	Rate Constant (k)
Units		mass %	$cm^2\ g^{-1}$	mol $cm^{-2}\ sec^{-1}$	mol $cm^{-2}\ sec^{-1}$
Source		Lapakko, Olson & Antonson (2013a)	Estimated This Study	Palandri & Kharaka (2004)	Kellogg et al. (2014)
Plagioclase	Albite	31.1	330.0	2.75E-17	6.2E-17
	Anorthite	41.2	330.0	1.6E-15	6.2E-17
Clinopyroxene	Diopside	10.7	330.0	1.1E-16	8.8E-16
	Hedenbergite	3.2	330.0	1.1E-16	8.8E-16
Olivine	Forsterite	7.1	330.0	1.0E-14	1.4E-16
	Fayalite	5.7	330.0	2.0E-15	1.4E-16
Pyrrhotite	Pyrrhotite	1.0	330.0	2.0E-12	2.2E-14

The grain size and surface area of reacting phases were estimated on the basis of the particle-size distribution data of Lapakko, Olson & Antonson (2013a). All minerals were assumed to have the same particle size (Table 1).

A dilute surface-water solution was chosen from Filson Creek, upstream of the mineralized basal zone of the Duluth Complex (Piatak et al., 2015; Table 2). At an active mine, waters percolating through tailings piles will likely be a combination of process water and local precipitation. The solution was assumed to be saturated with respect to atmospheric oxygen and buffered by the atmosphere.

Table 2 Starting solution composition for modeling simulations

Parameter	Units	Concentration
pH	S.U.	6.7
Na	mg L^{-1}	1.3
K	mg L^{-1}	0.2
Ca	mg L^{-1}	3.7
Mg	mg L^{-1}	2.8
Al	mg L^{-1}	0.1
Fe	mg L^{-1}	0.1
SiO_2	mg L^{-1}	1.0
SO_4^{2-}	mg L^{-1}	1.6
HCO_3^-	mg L^{-1} as $CaCO_3$	12.2
Cl	mg L^{-1}	1.0

Modeling Approach

This modeling exercise attempts to reproduce the laboratory weathering results of Lapakko, Olson & Antonson (2013a), focusing on acid generation and neutralization, and sulfur geochemistry. The tailings examined by Lapakko, Olson & Antonson (2013a) had an acid-generating potential (AP) of 6.2 kg $CaCO_3$/t and an acid-neutralizing potential (NP) of 19 kg $CaCO_3$/t, which results in a neutralizing potential ratio (NPR) of 3.1, and a classification of "not potentially acidic drainage generating". Their study was designed to investigate mineral dissolution rates under air saturated conditions rather than to simulate field conditions. Additional information that is useful for validation purposes can be found in Lapakko, Olson & Antonson (2013b), Lapakko et al. (2013), and Wenz et al. (2013). For the weathering tests on tailings (Lapakko, Olson & Antonson, 2013a), pH dropped from a starting value of approximately 7.5 to a minimum value of approximately 6.4 over the course of the 10-year experiment. The pH drop was most rapid in the first year of the experiments, and showed generally gradual decreases for the remainder of the experiments. Sulfate was released at the greatest rates in the first two years of the experiment and then leveled off. At the end of 10 years, the amount of remaining sulfur in the solids was between 45 and 49 percent of the starting concentration (0.2 wt. %). In contrast, Kellogg et al. (2014) conducted similar tests on waste rock (75 g; particle size 50 – 150 μm diameter) of varying starting sulfide sulfur contents ranging from 0.18 to 1.64 wt. %. In these experiments, pH started at near-neutral values (7 – 8), but reached minimum values of approximately 3 in the most sulfur-rich samples. The pH profiles were more complex with the high sulfur samples exhibiting increased pH values after reaching their minima. Sulfate release was similarly complex, with significant release early and a decrease over time, followed by maxima that correlated with pH minima in the high sulfur samples. In these experiments, the amount of sulfur remaining in the solids ranged between 0 and 55 percent of the starting concentration.

Using the starting conditions described above, the interaction of the solution with tailings was simulated by allowing fixed amounts of solids to react with 1 kg of solution for either 10 or 20 years. Under these scenarios, the sensitivity of the simulations was evaluated by using the different sets of rate constants described above, by varying the water/rock ratio, changing the starting concentration of sulfide-sulfur, and by changing the pyrrhotite dissolution rate constant relative to silicate rate constants. The pH of the model simulations is the primary screening tool to assess the success of the modeling at this stage, followed by the sulfur geochemistry.

RESULTS AND DISCUSSION

Rate Constants

Two sets of rate constants for the dissolution of silicate minerals and pyrrhotite were used in this study (Table 1): (1) Those based on single-mineral laboratory experiments compiled from the literature (Palandri & Kharaka, 2004); and (2) Those based on weathering tests on waste rock from the Duluth Complex (Kellogg et al., 2014). The variation of pH over the course of a 10-year simulation shows distinct differences between the two sets of rate constants (Fig. 2a). The simulations based on the MNDNR (Kellogg et al., 2013) values show a steady decrease from the starting value (6.7) to a value of 6.3 at 10 years, which is similar to pH evolution observed in the weathering tests of Lapakko, Olson & Antonson (2013a). In contrast, the rate constants based on single-mineral laboratory experiments have a distinctly different pattern. This simulation has a more rapid drop in pH, reaching a mínimum of approximately 5.8 between Years 1 and 2, followed by an increase in pH to approximately 8.4 in Year 9. Therefore, the rate constants based on single-mineral experiments predict the exhaustion of acid-generating potential from pyrrhotite and acid-neutralization by silicates that are significantly faster than the empirical observations in the tailings weathering tests (Lapakko, Olson & Antonson, 2013a). However, the rate constants based on the weathering tests on Duluth Complex waste rocks provide a better description of the pH evolution in the tailings weathering tests. Kellogg et al. (2014) summarized their pyrrhotite dissolution rate constants in terms of minimum, maximum, and average values. A comparison of these values, and that of Palandri & Kharaka (2004) relative to the MNDNR silicate rate constants shows that the MNDNR maximum value best describes the tailings weathering test (Fig. 2b). The MNDNR silicate rates were used for the remainder of the simulations. Because of the limited pH range shown by the experiments of Lapakko, Olson & Antonson (2013a), the silicate dissolution rates were assumed to be constant.

Water/Rock Ratio

The water/rock ratio of the experiment has a profound effect on the resulting pH of the simulation. Weathering tests using 1 kg of solid, which is leached with 0.5 kg of water on a weekly basis, would be exposed to a water/rock ratio of 26/1 per year or 260/1 over the course of 10 years. Simulations were made using water/rock ratios of 1/1, 10/1, 100/1, 260/1, and 1000/1 (Fig. 3). Based on these results, the water-dominated simulations appear to describe the tailings weathering experiments better than that the rock-dominated simulations. The water/rock ratio corresponding to 10 years of weathering tests (260/1) results is a lower pH than observed, which suggests that: (1) the effective reactive (i.e., exposed) mass of pyrrhotite may be significantly less than the total present; (2) the pyrrhotite dissolution rate constant used is too fast; (3) that the silicate dissolution rate constants are too slow; or (4) a combination of these factors.

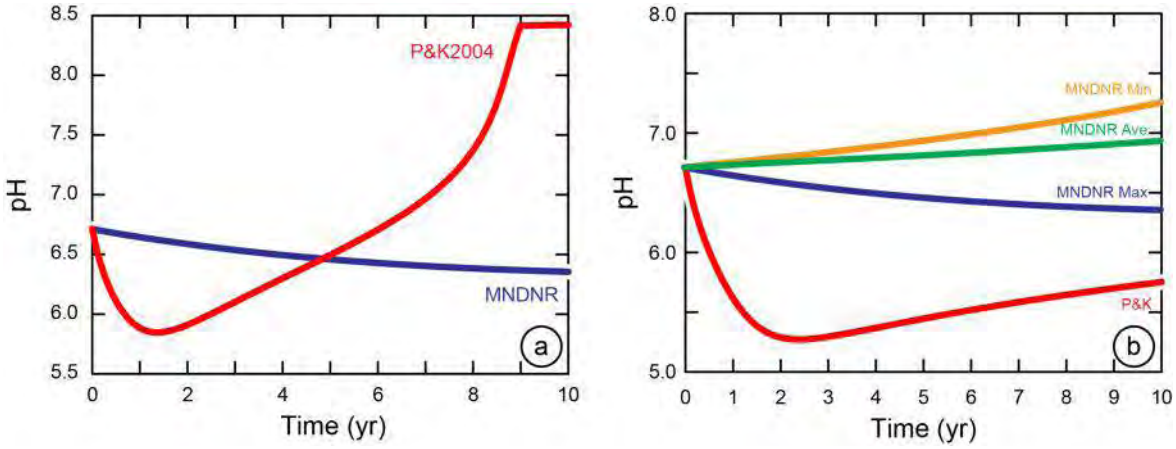

Figure 2 Comparison of rate constants for the dissolution of minerals in tailings. a. Comparison of single-mineral constants (P&K2004, Palandri & Kharaka, 2004) and empirical constants (MNDNR, Kellogg et al., 2014); b. Comparison of pyrrhotite dissolution constants from Kellogg et al. (2014) for their maximum (MNDNR Max) average (MNDNR Ave) and minimum (MNDNR Min) observed rates and from Palandri & Kharaka (2004; P&K).

Effect of Sulfide Content

The sulfide content of mine waste determines its acid-generating potential. To assess the sensitivity of the model simulations to sulfide content, simulations were run at various sulfide contents that span the range that has been observed in the ores in the basal zone of the Duluth Complex: 0.2, 0.5, 1.0, and 2.0 wt. % S (Kellogg et al., 2014; Lapakko, Olson & Antonson, 2013a, b; Fig. 4a). The simulations show the influence of sulfide content on pH. The simulations with the highest sulfide content produced the lowest pH values, reaching a low of 3 in the simulation with 2 wt. % S. These relationships of sulfide content to pH variations are similar to those observed by Kellogg et al. (2014) for weathering tests on waste rock from the Duluth Complex. They divided their samples into three groups on the basis of sulfide content and origin of sample material. Their Group I (0.18 – 0.22 wt. % S) produced pH values above 6, Group II (0.4 – 0.58 wt. % S) reached a low of approximately pH 3.5, and Group III (0.71 – 1.64 wt. % S) reached a low of pH 3.

The effectiveness of this modeling approach can also be evaluated by comparing the predicted depletion of sulfide-sulfur in the tailings with observed depletion in the weathering tests (Lapakko, Olson & Antonson, 2013a). Figure 4b shows both the measured depletion of pyrrhotite (red dots) and the predicted depletion of pyrrhotite (blue line) with time. The measured depletion reflects a greater initial loss of pyrrhotite in the first year, perhaps due to oxidation of very fine sulfide grains, but the rate slows in subsequent years compared to the predicted loss of pyrrhotite. However, the general agreement between the observed and predicted depletion of pyrrhotite indicates that the model provides a reasonable description of pyrrhotite weathering.

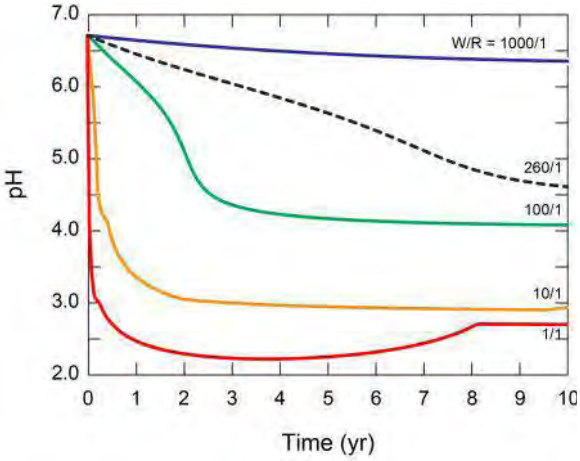

Figure 3 The effect of water rock ratio on the pH variation of 10-year model simulations.

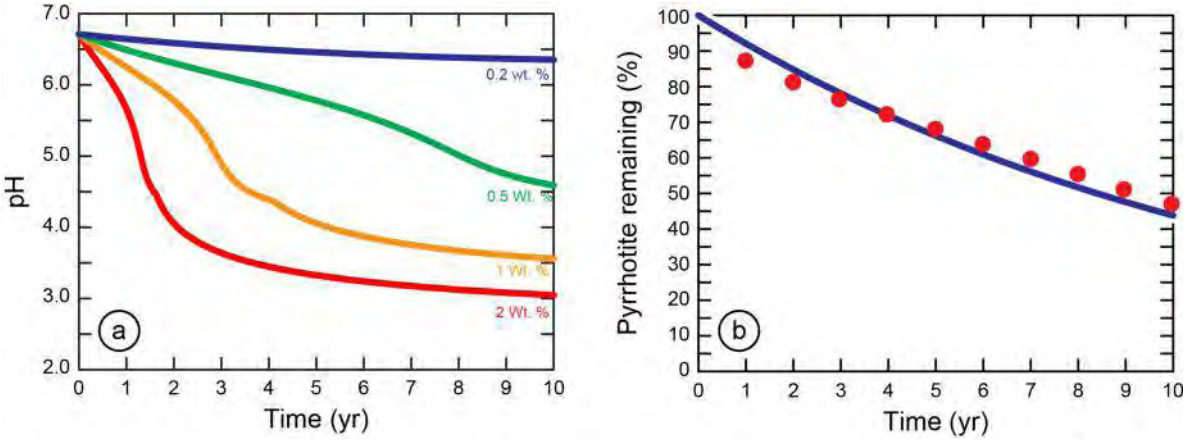

Figure 4 Influence of sulfur geochemistry. a. The effects of different total sulfide contents on pH. b. Comparison of predicted (blue line) with observed depletion of sulfide-sulfur (red dots).

Long-Term Implications

The effectiveness of REACT to describe the general aspects of tailings weathering for the low-sulfide ores of the Duluth Complex suggests that useful insights can be gained from reaction modeling. The pH reaches a minimum around Year 13 (Fig. 5a), indicating that the amount of pyrrhotite has been exhausted to the point where the rate of acid neutralization exceeds the rate of acid generation. The pyrrhotite content at the end of year 20 is predicted to be 20 percent of the starting concentration.

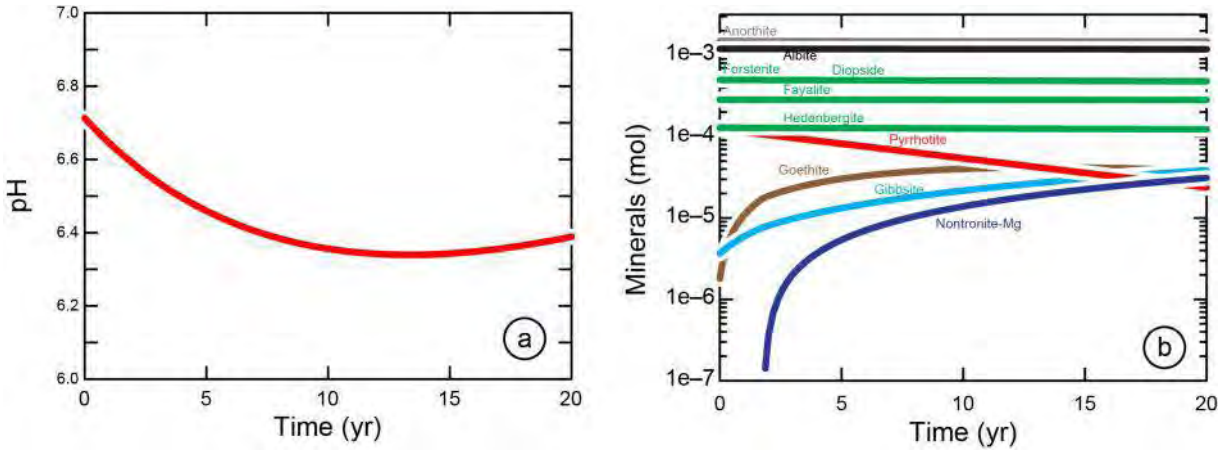

Figure 5 Twenty-year simulation of the weathering of low-sulfide tailings from the Duluth Complex. a. Variation of pH with time. b. Variation of primary and secondary minerals

The simulation indicates that pyrrhotite dissolution occurs at a much greater rate than plagioclase, olivine, and clinopyroxene dissolution (Fig. 5b). The simulation predicts the secondary phases, including aluminum and ferric hydroxides, and clay (nontronite), should form (Fig. 5b). In a tailings pile, these secondary phases could decrease permeability and limit weathering rates. The sulfate salts gypsum and epsomite are predicted to be significantly undersaturated throughout at the simulation at high water/rock ratios. However, at low water/rock ratios, gypsum becomes saturated. Thus, gypsum may be an important secondary phase that could limit the infiltration of water in the vadose zone of tailings storage facilities.

CONCLUSION

In concert with established methods, computer-based reaction modeling represents another promising tool to assess the long-term behavior of tailings. One of the greatest limitations for applying this approach is the lack of appropriate rate constants for mineral dissolution. Rate constants derived from single-mineral laboratory experiments appear to be unrealistically fast to describe weathering tests. Rate constants based on weathering tests are more realistic, but their derivation is more problematic because multiple minerals are dissolving simultaneously in these experiments. Long-term simulations can identify potential secondary phases that can influence the permeability of tailings and affect their weathering behavior, and thus permit a more insightful interpretation of other types of mine-waste weathering data.

ACKNOWLEDGEMENTS

This research was supported by funding from the Mineral Resources Program and Midwest Region of the U.S. Geological Survey. The use of product names is for descriptive purposes only and does not imply endorsement by the U.S. government. Additional funding was provided by the Minnesota Department of Natural Resources.

REFERENCES

Bethke, C.M. (2008) *Geochemical and Biogeochemical Modeling*, Cambridge University Press, Cambridge, UK, 2nd Edition, 543 p.

Bethke, C.M., and Yeakel, S. (2014) *Reaction Modeling Guide, The Geochemist's Workbench, Release 10.0*. Aqueous Solutions LLC, Champaign, Illinois, 98 p.

Kellogg, C., Lapakko, K., Olson, M., Jenzen, E., and Antonson, D. (2014) Laboratory dissolution of blast hole samples of Duluth Complex rock from the South Kawishiwi Intrusion: Twenty-four year laboratory experiment, Minnesota Department of Natural Resources Report, 314 p. Accessed 16 Sept. 2014 at http://files.dnr.state.mn.us/lands_minerals/reclamation/mndnr_blast_hole_expt_2014.pdf

Lapakko, K.A., and Antonson, D.A. (2012) Duluth complex rock dissolution and mitigation techniques: A summary of 35 years of DNR research 51 p. Accessed 16 Sept. 2014 at http://files.dnr.state.mn.us/lands_minerals/reclamation/mndnr_research_summary_2012.pdf

Lapakko, K.A., Olson, M.C., and Antonson, D.A. (2013a) Duluth Complex tailings dissolution: Ten-year laboratory experiment, Minnesota Department of Natural Resources Report, 54 p. Accessed 16 Sept. 2014 at http://files.dnr.state.mn.us/lands_minerals/reclamation/mndnr_dc_tailings_2013.pdf

Lapakko, K.A., Olson, M.C., and Antonson, D.A. (2013b) Dissolution of Duluth Complex Rock from the Babbitt and Dunka Road Prospects: Eight-year laboratory experiment, Minnesota Department of Natural Resources Report, 88 p. Accessed 16 Sept. 2014 at http://files.dnr.state.mn.us/lands_minerals/reclamation/mndnr_dc_wasterock_2013.pdf

Lapakko, K., Leopold, L., Mehleis, E., Theriault, S., Jagunich, A., and Antonson, D.,(2013) Subaqueous Disposal of Sulfidic Waste Rock: Seven-year laboratory column experiment, Minnesota Department of Natural Resources Report, 62 p. Accessed 16 Sept. 2014 at http://files.dnr.state.mn.us/lands_minerals/reclamation/mndnr_subaqueous_columns_2013.pdf

Lindsay, M. B., Condon, P. D., Jambor, J. L., Lear, K. G., Blowes, D. W., and Ptacek, C. J. (2009) Mineralogical, geochemical, and microbial investigation of a sulfide-rich tailings deposit characterized by neutral drainage. Applied Geochemistry, v. 24, p. 2212-2221.

Listerud, W.H., and Meineke, D.G. (1977) Mineral resources of a portion of the Duluth Complex and adjacent rocks in St. Louis and Lake counties, northeastern Minnesota. Minnesota Department of Natural Resources, Division of Minerals, Report 93, 74 p.

Palandri, J.L., and Kharaka, Y.K. (2004) A compilation of rate parameters of water-mineral interaction kinetics for application to geochemical modeling. U.S. Geological Survey Open-File Report 2004-1068, 64 p.

Piatak, N.M., Seal, R.R., II, Jones, P.M., and Woodruff, L.G. (2015) Copper toxicity and organic matter: Resiliency of watersheds in the Duluth Complex, Minnesota, USA. Proceedings, ICARD-IMWA2015, 10 p.

Ripley, E.M. (2014) Ni-Cu-PGE Mineralization in the Partridge River, South Kawishiwi, and Eagle Intrusions: A Review of Contrasting Styles of Sulfide-Rich Occurrences in the Midcontinent Rift System. Economic Geology, v. 109, p. 309-324.

Smith, L. J., Moncur, M. C., Neuner, M., Gupton, M., Blowes, D. W., Smith, L., and Sego, D. C. (2013) The Diavik Waste Rock Project: Design, construction, and instrumentation of field-scale experimental waste-rock piles. Applied Geochemistry, v. 6, p. 187-199.

Wenz, Z., Lapakko, K., and Antonson, D. (2013) Rock composition, leachate quality and solute release as a function of particle size for three waste rock types: An 18-year laboratory experiment, Minnesota Department of Natural Resources Report, 117 p. Accessed 16 Sept. 2014 at http://files.dnr.state.mn.us/lands_minerals/reclamation/the_particle_size_experiment_report_2013.pdf

10th ICARD IMWA 2015 | 10th International Conference on Acid Rock Drainage & IMWA Annual Conference

Modelling Humidity Cell Experimental Data by Making Use of the PHREEQC Code

Nicolaus Van Zweel, Rainier Dennis and Ingrid Dennis
Centre for Water Sciences and Management, North West University, South Africa

ABSTRACT

Most of South Africa' energy is generated by coal fired power stations. South Africa has rich coal deposits concentrated in the north-east of the country and as the demands for electricity are growing so are the associated mining activates, a large number of which are shallow opencast mines. The mining method results in post-closure back filled pits and above ground disposal facilities. Leachate emanating from these disposal sites is saline and in most cases highly acidic. Currently the standard testing procedure to quantify expected leachate qualities include Acid Base Accounting (ABA) with static and kinetic leaching.

The aim of this study is to model standard humidity cell leach tests performed in these studies using the PHREEQC code. This model can then be scaled up to field conditions to model 1D reactive mass transport. It is commonly accepted that the rate of pyrite oxidation in backfilled pits and waste storage facilities is governed by the rate of oxygen ingress and that no pyrite oxidation takes place in the saturated zone. This is not the case for humidity cells, as sufficient oxygen is available for reaction. Pyrite reaction rates in humidity cells are expected to be governed by a combination of available reaction surface and ash layer resistance. This is modelled in PHREEQC (Parkhurst & Appelo, 1999) using the KINETIC block. Leachate composition is then modelled in the column, making use of the TRANSPORT block. The experimental data is fitted by means of the reactive surface and ash layer diffusion coefficient.

This model can then be used to estimate long term water qualities beyond the twenty week norm. The model can then be scaled up to field conditions by compensating for the oxygen ingress component.

Keywords: ABA, Humidity Cell, Leach Test, Shrinking Core Model, PHREEQC Modelling

INTRODUCTION

Most of South Africa's energy is generated by coal fired power stations. South Africa has rich coal deposits concentrated in the north-east of the country and as the demands for electricity are growing so are the associated mining activates, a large number of which are shallow opencast mines. The mining method results in post-closure back filled pits and above ground disposal facilities comprising of mined out rock and discard from the beneficiation process respectively. Leachate emanating from these disposal sites may range from acidic to alkaline, with commonly observed elevated levels of sulfate, iron, manganese and aluminium (Usher et al., 2002). In order to implement a successful mitigation strategy, sources of pollution must be identified and there must be a good understanding of the related source term governing the pollution. According to Nordstrom (2000) several points must be considered when looking at geochemical modelling. Firstly when referring to a model, it is not necessarily implied that the model is a computer code or a mathematical approach. It can consist of a well constrained logical proposition with the goal to improve or refine a conceptual model of the problem. A geochemical model can provide invaluable insight in this this regard and can assist in the interpretation of field data (Linklater et al., 2005). In order to develop such a model Usher et al. (2002) suggested the Acid-Base: Accounting, Technique and Evaluation (ABATE) strategy to develop a model of the geochemical problem at hand.

Field data/Experimental data

Acid Base Accounting (ABA) is generally used as a first order classification procedure in acid rock drainage (ARD) prediction methodologies (Usher et al., 2002) and results provide information about the potential of a sample to generate ARD (Price, 1997). Net Acid Generating (NAG) tests are also performed to aid in improving the interpretation of the ABA results (Miller et al., 1997). Usher et al., (2002) recommends a kinetic leach test methodology adapted from the D5744-96 Standard Test Method (ASTM, 2001). The minimum suggested duration of this leach test is twenty weeks and this is in some cases insufficient for sulphate production to stabilize. Static methods do not address the transient behaviour of ARD formation; humidity leach test supplements statics test in this regard and can assist in obtaining rates of reaction and a generalized indication of the potential mineral leaching behaviour of rock samples (Price, 1997). In the ABATE strategy mineralogy is required before the kinetic leach test is performed. In most cases mineralogy in the form of XRF is performed with the kinetic leach test.

Numerical geochemical modelling

Numerical geochemical modelling is the last step in the ABATE strategy. The need for numerical modelling will depend on the objectives of the study. Kinetic modelling of a spoils heap becomes complex as the concentrations of chemical components in the effluent is a function of both space and time. In turn the concentrations depend on the sulfide mineral oxidation rate, water infiltration rate and chemical oxidation rates (Pantelis et al., 2001). Several mathematical models that describe the leaching process in spoils heaps, has been developed over the last couple of years (Davis & Ritchie, 1986; Molson et al., 2005; Linklater et al., 2005; Pantelis et al., 2001).

Sulfide mineral oxidation

The dominant sulfide mineral in mine waste is pyrite (FeS_2). The oxidation of pyrite is a multi-step complex reaction consisting of both the oxidation of disulphide (S_2^{2-}) and of ferrous iron (Fe^{2+}) (Appelo & Postma, 2005). The following balanced reaction is generally accepted to represent the overall oxidation of pyrite at atmospheric conditions (Appelo & Postma, 2005; Lefebvre et al., 2001):

$$FeS_2 + \frac{15}{4}O_2 + \frac{7}{2}H_2O \rightarrow Fe(OH)_3 + 2SO_4^{2-} + 4H^+ \quad (1)$$

Oxidation of pyrite by oxygen has been shown to be slow and does not account for the rapid decrease in pH commonly observed from field conditions. This may be explained by the influence of pyrite oxidation by ferric iron (Fe^{3+}) (Lefebvre et al., 2001) and bacterial catalization of the reaction (Andre, 2009). Kinetics reported by Williams and Rimstidt, and also referenced by Appelo & Postma (2005) for the oxidation rate of pyrite by O_2 is as follows:

$$r = 10^{-8.19} m_{O_2}^{0.5} m_{H^+}^{-0.11} \quad (2)$$

where r is the rate with the units (mol/m²/s) and m_x denotes the molar concentration of x. It can be seen that the rate has a square root dependency on the concentration of O_2. This results in a significant effect on the rate if the oxygen concentration is low and a small effect at high oxygen concentrations. This effect is explained by Appelo & Postma (2005) by referring to the work conducted by Nicolson et al., (1988) as the pyrite surface becomes saturated with oxygen. A general rate law describing the dissolution/precipitation of minerals can be written as follows (Appelo & Postma, 2005):

$$r = k\frac{A_0}{V}\left(\frac{m}{m_0}\right)^n g(C) \quad (3)$$

where r is the overall reaction rate with the units (mol/L/s) and k is the specific rate with the units (mol/m²/s). The initial area and solution volume is denoted by A_0 and V respectively. The factor $(\frac{m}{m_0})^n$ accounts for the change in surface area where m_0 is the initial moles of the solid and m is the moles at a given time. The function $g(C)$ accounts for the effect of the solution composition on the rate e.g. the pH of the solution or the distance from equilibrium.

Sulphate mineral oxidation in tailing facilities

In the well-known work of Davis & Ritchie (1986) and also later Molson et al. (2005) the shrinking core model is used to describe the reaction kinetics of pyrite oxidation in a waste dump. In this approach it is assumed that the rate of oxygen diffusion to the reaction area is the rate limiting step. This is also discussed as an important factor in the oxidation of pyrite soils (Appelo & Postma, 2005). It is noted that oxygen transport is only important in the unsaturated zone. In the saturated

zone the approximate amount of oxygen available for pyrite oxidation is 0.33 mM O_2, suggesting that the unsaturated zone is the most reactive and the greatest source of sulfide oxidation.

Davis & Ritchie (1986) further assumes that the rate of unreacted core shrinkage is much slower than the oxygen diffusion rate within the particle (Levenspiel, 1962). It is assumed that the reaction at the surface of the particle is instantaneous and that ash layer diffusion is the rate determining step.

In the model developed by Davis & Ritchie (1986), it is assumed that diffusion is the only means of oxygen transport. Fick's second law with a consumption term is used to describe the diffusion process mathematically:

$$\frac{\partial U_A}{\partial t} = D_1 \frac{\partial^2 U_A}{\partial z^2} - q(z,t) \tag{4}$$

The model describes a two-stage diffusion process to the reaction sites. The first stage consists of oxygen diffusion through the air filled pores. D_1 is the diffusion coefficient for this stage. The consumption term $q(z,t)$ in Equation 4 represents the change in volume due to the oxidation of pyrite, and can be expressed as follows (Molson et al., 2005):

$$q(z,t) = D_2 \frac{3(1-\theta)}{R^2}\left(\frac{r_c}{R-r_c}\right)\frac{[O_2]_a}{H} \tag{5}$$

where D_2 is the diffusion coefficient, R is the particle radius, r_c is the unreacted core radius, θ is the porosity, $[O_2]_a$ the concentration of oxygen dissolving into the water film surrounding the particle and H is Henry's constant for a given temperature. The diffusion coefficient D_2 represents the forming ash layer that is shielding the shrinking particle. The schematic representation of an oxidizing particle is shown in Figure 1.

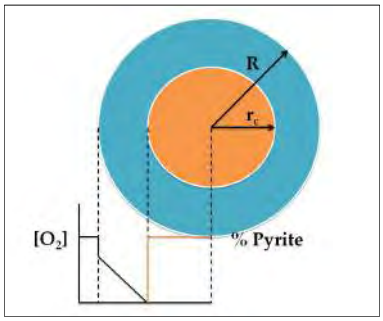

Figure 1 Schematic representation of an oxidizing particle (Davis, 1983)

From Equation 5 and Figure 1 it is clear that the change in oxygen due to pyrite oxidation can be related to the change in unreacted core radius (r_c):

$$\frac{dr_c}{dt} = \frac{D_2(1-\theta)}{\epsilon \rho_s} \frac{R}{r_c(R-r_c)} \frac{[O_2]_a}{H} \tag{6}$$

where ϵ represents the ratio of oxygen to sulphur consumed on the basis of reaction stoichiometry (Equation 1). The density ρ_s is calculated from the bulk density and the weight fraction of pyrite present.

METHODOLOGY

Actual humidity cell leach test (HCT) data were modelled using the PHREEQC code. Only the main principles are discussed here. PHREEQC has the ability to model dynamic processes using such as reaction kinetics, 1D reactive transport using the RATES block and TRANSPORT block respectively.

HCT approximated as a continues stirred tank reactor

The HCT is approximated as a continuous stirred tank reactor (CSTR) as shown in Figure 2. This may be an over simplification of the system as it do not account for preferential flow paths in the HCT It is assumed that the leachate has come into contact with all the particles before exiting the cell or reactor.

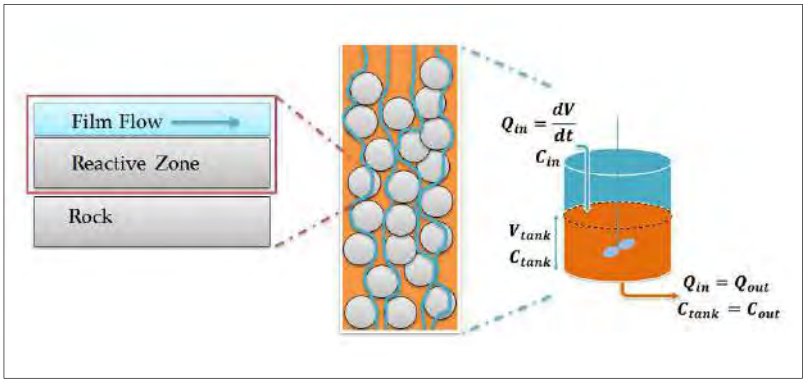

Figure 2 Schematic representation of the CSTR approximation (Andre, 2009)

The CSTR can be described by the following equation:

$$\tau = \frac{V_{tank}}{dV/_{dt}} \tag{7}$$

where τ is the residence time and V represents the volume of the tank. In work conducted by Tiruta-Barna (2008), a CSTR is modelled by solving the differential equation in the RATES block of PHREEQC. The reactor can also be modelled by making use of the TRANSPORT block in

PHREEQC. In the TRANSPORT block stagnant cells can be defined to interact with 'active' transport cells using the MIX block. Reaction kinetics and solution composition can then be defined for individual cells.

Input parameters

The mineral composition of the sample was calculated from the XRD data of the sample (Table 1). The reaction kinetics of pyrite oxidation was defined substituting Equation 2 in Equation 3 and compensating for the influence of the saturation state, rendering the following rate expression:

$$r = \left(\frac{A_0}{V}\right)\left(\frac{m}{m_0}\right)^n \left(10^{-6.07} m_{O_2}^{0.5} m_{H^+}^{-0.11}\right)(1 - SR(Pyrite)) \quad (8)$$

The unit of the rate expression is (mol/L/s) and *SR (Pyrite)* represents the saturation state. The exponent n is a function of the particle geometry and for cubical dissolving particles a value of n = 2/3 can be assumed (Appelo & Postma, 2005).

It was assumed that oxygen is present in excess. This was defined in the EQUILIBRIUM block of PHREEQC. The PHREEQC TRANSPORT block was used to describe the flow characteristics of the system approximated as a CSTR.

Table 1 XRD data of sample used in the humidity cell leach test

Mineral	Weight %
Anatase	3.43
Dolomite	1.83
Kaolinite	51.69
Muscovite	5.45
Pyrite	6.98
Quartz	30.28
Siderite	0.33

Shrinking core model

The shrinking core model can also be applied in PHREEQC by making use of the RATES block. The rate of pyrite oxidation (mole/litre bulk/s) is defined as follows (Mayer, 1999):

$$r = -10^3 S_i \frac{D_2}{3.5} \frac{R}{(R - r_c) r_c} [O_2]_a \quad (9)$$

where S_i is the reaction surface at time t_i and is defined as:

$$S_i = 10^{-3} \frac{3\varphi_i}{r_c} \quad (10)$$

where φ_i is the volume fraction of minerals defined in units (m^3 mineral/m^3 bulk). The concentration of oxygen dissolved in the liquid film can be calculated using Henry's law. Usually the Henry's law constants are reported at a reference temperature of 25°C and 1 atm. The following two equations can be used for temperature (Koretsky, 2003):

$$\left(\frac{\partial lnH_i}{\partial P}\right) = \frac{H_i^{\infty} - h_i^{v}}{R} \tag{11}$$

where R is the gas constant, H_i^{∞} is the partial molar enthalpy and h_i^{v} is the pure species enthalpy. A similar equation describes the correction for pressure, but it is beyond the scope of this study due to the fact that the pressure will always be at 1 atm. Assuming the mole fraction of oxygen in ambient conditions is $y_{O_2} = 0.21$, the partial pressure of O_2 is then formulated as follows:

$$P_{O_2} = (0.21)P \tag{12}$$

where P is the atmospheric pressure. The concentration of oxygen in solution is the calculated using the Henry's coefficient for oxygen in water ($H_{O2} = 44252.9$ Bar @ 25°C and 1 atm):

$$x_{O_2} = \frac{y_{O_2}P}{H_{O_2}} = \frac{0.21(bar)}{44253.9(bar)} = 4.75 \times 10^{-6} \tag{13}$$

The concentration of oxygen, $[O_2]$ in molality, is expressed as:

$$[O_2] = \frac{n_{O_2}}{V} \tag{14}$$

Where V is 1 litre of water and n_{O_2} is the molar amount of dissolved oxygen. The concentration of dissolved oxygen is then calculated as:

$$[O_2] = x_{O_2}\frac{n_{O_2}}{V} = 2.63 \times 10^{-4} M \tag{15}$$

By defining the partial pressure of oxygen as $\log(P_{O_2}) = -0.67$ in the EQUILIBRIUM_PHASES block and defining a set oxygen concentration in the liquid film surrounding the particles, the above described kinetics were used to model the oxidation of pyrite. The PHREEQC result together with the validation from the equivalent mathematical model in MATLAB is presented in Figure 3.

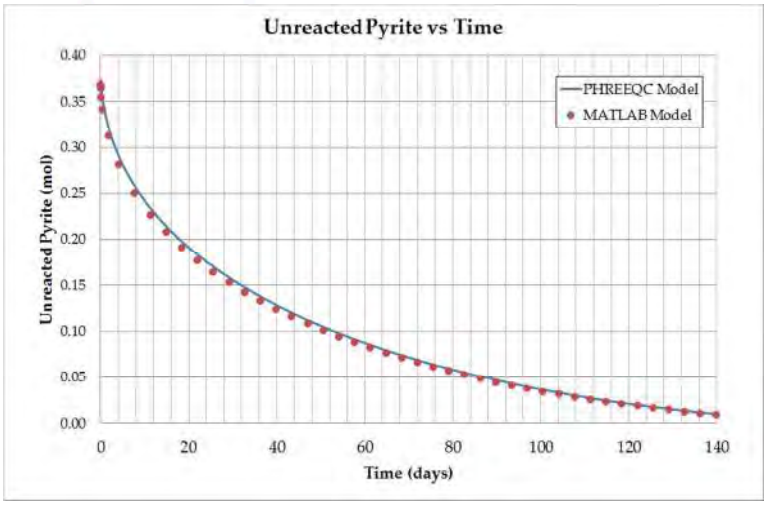

Figure 3 Model results of PHREEQC shrinking core model validated with MATLAB

PHREEQC does not have functionality for gas transport to describe the change in pore gas phase composition over time (Equation 4). This makes the use of this rate expression problematic as the gas phase composition will have to be changed for every time step outside the PHREEQC environment.

Analytical Approximate Solution

Due to the complexity of implementing Equation 4 in PHREEQC it is suggested to use the Analytical Approximate Solution (AAS) proposed by Davis & Ritchie (1986). By using this approach the rate of sulphate production already accounts for the rate limiting effect of oxygen diffusion.

In order to use the AAS model to describe a HTC, it must be assumed that oxygen is in fact rate limiting for sufficiently small particles (tailing samples) with a high moisture content. This assumption can be tested by making use of Fick's second law, and assuming an infinite homogeneous slab. The oxygen concentration profile can be described by the following equation:

$$U_a(x,t) = U_{a0}\left[1 - erf\left(\frac{x}{2\sqrt{D_1 t}}\right)\right] \tag{16}$$

where U_{a0} is the surface concentration of oxygen. The value of D_1 can be calculated from the following equation:

$$D_1 = 3.98 \times 10^{-9}\left[\frac{\theta_A - 0.05}{0.95}\right]T^{1.5} \tag{17}$$

where θ_A is the effective porosity and T is the temperature (K). From Equation 16 and Equation 17 it is clear that the oxygen concentration decreases linearly for a standard leach cell and that the percentage of saturation will only influence the oxygen profile at high levels of water saturation.

RESULTS AND DISCUSSION

The data obtained from an HCT was modelled using both the AAS model (Davis & Richie, 1986) and the Surface Kinetic (SK) model as shown in Figure 4. The SK model shows a better fit for the leach data. Although gypsum was not detected in the mineralogy, it is apparent from the leachate analysis that gypsum might be present as a minor component material and may not necessarily be picked up by the XRD analysis. In both models, gypsum was defined to dissolve kinetically to account for initial high sulfate leach values. The AAS method shows a moderately good fit to the data. It can clearly be seen that the shrinking core model does not describe the kinetic behavior of the oxidation of pyrite accurately under the conditions observed in the HCT. In the AAS model it is assumed that ash layer diffusion is the rate controlling step; this may be an over simplification of the system. The shrinking core model can be expressed to account for both ash layer controlled and chemical reaction controlled rates (Levenspiel, 1962). Although this approach may yield a better fit, it introduces more variables to the model and either the diffusion coefficient D_2 or the rate constant of the chemical reaction rate must be determined experimentally to define the system in such a manner so that a reasonable model can be constructed.

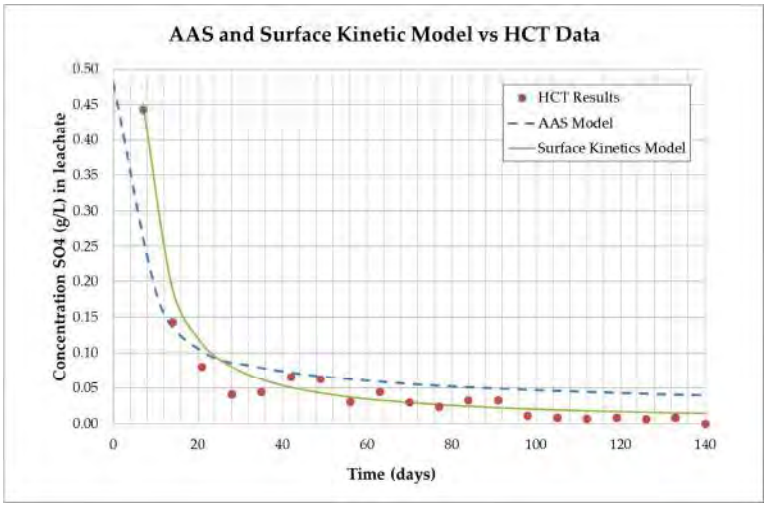

Figure 4 Comparison of AAS Model and SK Model fitted to HCT data

CONCLUSION

Both the AAS model and the SK model showed a reasonable fit to the HCT data. The SK model does however describe the data better. It was found that assuming the ash layer diffusion as the only rate controlling factor is a gross over simplification of the system. This results in compensating for the influence of chemical reaction controls to obtain a more accurate model. The standard HCT setup will not provide this data and further experimental data will be required to obtain either the kinetic rate constant for the chemical reaction controlled step or the diffusion coefficient.

REFERENCES

Andre, B.J. (2009) Generation of acid mine drainage: reactive transport models incorporating geochemical and microbial kinetics, PhD thesis: University Of Colorado At Boulder Appelo, C.A.J. & Postma, D. (2005) Geochemistry, groundwater and pollution, Boca Raton: CRC Press, 2nd ed.

ASTM (2001) Standard test method for accelerated weathering of solid materials using a modified Humidity Cell, D 5744-96ASTM (2007) Standard test method for laboratory weathering of solidmaterials using a humidity cell, D5744-07, pp. 1–19.

Davis, G.B. (1983) Mathematical modelling of rate-limiting mechanisms of pyritic oxidation in overburden dumps, PhD thesis: The University of WollongongDavis, G.B. & Ritchie, A.I.M. (1986) A model of oxidation in pyritic mine waste: part 1 equations and approximate solution, Applied Mathematical. Modelling, vol. 10, pp. 314–322.

Koretsky, M.D. (2003) Engineering and Chemical Thermodynamics, USA: John Wiley & Sons.

Lefebvre, R., Hoclley, D., Smolensky, J. & Gélinas, P. (2001) Multiple transfer processes in waste rock piles producing acid mine drainage 1: Conceptual model and system characterization, Journal of Contaminant Hydrology, pp. 137–164.

Levenspiel, O. (1962) Chemical Reaction Engineering, New York: Wiley, 3rd ed.

Linklater, C.M., Sinclair, D.J. & Brown, P.L. (2005) Coupled chemistry and transport modelling of sulphidic waste rock dumps at the Aitik mine site, Sweden, Applied Geochemistry, vol 20, 275–293.

Mayer, K.U. (1999) Numerical Model for the Multicomponent Reactive Transport in Variable Saturated Porous Media, PhD thesis: The University of Waterloo.

Miller, S., Robertson, A. & Donahue, T. (1997) Advances in acid drainage prediction using the net acid generation (NAG) 4th international conference on acid rock drainage.

Molson, J.W., Fala, O., Aubertin, M. & Bussière, B. (2005) Numerical simulations of pyrite oxidation and acid mine drainage in unsaturated waste rock piles, Journal of Contaminant Hydrology, vol 78, pp. 343–371.

Nordstrom, D.K. (2000) Advances in the hydrogeochemistry and microbiology of acid mine waters, International Geology Review, vol 42, pp. 499–515.

Pantelis, G., Ritchie, A.I.M. & Stepanyants, Y.A. (2002) A conceptual model for the description of oxidation and transport processes in sulphidic waste rock dumps, Applied Mathematical Modelling, vol 26, pp. 751–770.

Parkhurst, D.L. & Appelo, C.A.J. (1999) User's guide to PHREEQC (version 2)— a computer program for speciation, batch-reaction, one-dimensional transport, and inverse geochemical calculations, Report 99-4259, pp. 312.

Price, W.A. (1997) Guidelines and recommended methods for the prediction of metal leaching and acid rock drainage at minesites in british columbia (DRAFT). British Columbia Ministry of Employment and Investment, Energy and Minerals Division, Smithers: BC, pp.143.

Tiruta-Barna, L. (2008) Using PHREEQC for modelling and simulation of dynamic leaching tests and scenarios. Journal of Hazardous Materials, vol 157, pp. 525–533.

Usher, B.H., Cruywagen, L-M., De Necker, E. & Hodgson, F.D.I. (2002) On-site and laboratory investigations of spoil in opencast collieries and the development of acid-base accounting procedures, Water Research Commission.

10th ICARD IMWA 2015 | 10th International Conference on Acid Rock Drainage & IMWA Annual Conference

Diavik Waste Rock Project: Reactive Transport Simulation of Sulfide Weathering

David Wilson[1], Richard Amos[2], David Blowes[1], Jeff Langman[1], David Sego and Leslie Smith

1. *Department of Earth and Environmental Sciences, University of Waterloo, Canada*
2. *Department of Earth Sciences, Carleton University, Canada*
3. *Department of Civil and Environmental Engineering, University of Alberta, Canada*
4. *Department of Earth, Ocean and Atmospheric Sciences, University of British Columbia, Canada*

ABSTRACT

The Diavik Waste Rock Project consists of laboratory scale and field scale experiments with one of its primary goals being the development of scale-up techniques for the prediction of impacts from mine wastes on groundwater and surface water. As part of the Diavik project, humidity cell experiments have been conducted to assess the long term geochemical evolution of the low sulfide content waste rock. Reactive transport modelling has been used to assess the significant geochemical processes controlling oxidation of sulfide minerals and subsequent sulfate and metals release from the humidity cell experiments. The geochemical evolution of effluent from waste rock with sulfide content of 0.16 wt. % (primarily pyrrhotite) in a subset of the humidity cells was simulated with the reactive transport model MIN3P under the conceptual model of constant water flow and that sulfide oxidation is controlled by the availability of ferric iron. Elevated metal concentrations in the humidity cell effluent were released through sulfide oxidation, which is controlled by diffusion of ferric iron to the unreacted particle surface and aerobic oxidation of the released ferrous iron. Elevated sulfate concentrations in solution are influenced by the production of intermediary sulfur compounds (represented in the model by S^0). Comparison of humidity cell experiments containing rock of varying sulfide content and temperature indicate available surface area and temperature also play important roles in rates of sulfide oxidation and subsequent sulfate production. The simulations also indicate that secondary mineral formation affects solute release. The humidity cell simulations are intended to provide a baseline for future reactive transport simulations of the larger scale field experiments at the Diavik site.

Keywords: sulfide oxidation, shrinking core model, reactive transport

INTRODUCTION

An important component of the planning of a mining project is the prediction of waste-rock effluent quality. The potential for mine waste rock to generate acid and elevated solute concentrations in effluent and the associated long term effects to the surrounding environment are often characterized using laboratory scale humidity cell experiments (Lapakko, 2003; Ardau, Blowes & Ptacek, 2009; Sapsford et al., 2009). The subsequent prediction process commonly involves the extrapolation of contaminant leaching rates derived from humidity cell experiments using empirical scale factors. The resulting scaled leaching rates are used to assess the potential for poor quality effluent from full scale waste-rock piles (commonly referred to as scale-up). Scale factors often include parameters understood to influence effluent quality such as pH, grain size, moisture content, temperature, oxygen availability and mineral surface area and volume (Kempton, 2012). The empirical scale factor method is often rendered incapable of accurate effluent quality prediction since site specific heterogeneities that arise during scale-up such as variability in flow mechanisms and geochemical reaction mechanisms are difficult to model given the simplified parameters. Reactive transport modelling has the potential to address some of the complexities associated with scale-up by providing a detailed, mechanistic, and quantitative approach to assessing effluent quality that encompasses the capability to take site specific processes into consideration.

The reactive transport model MIN3P (Mayer, Frind & Blowes, 2002) is used to simulate the weathering of waste rock to allow assessment of the primary geochemical processes involved. This article presents a conceptual model of pyrrhotite weathering in low S waste rock using the results of humidity cell effluent quality sampling and the resulting estimated weathering rate, and mineralogical and hydraulic properties from the humidity cell experiments and field scale experiments. The simulations are intended to provide a comprehensive geochemical conceptual model that will later be included in modelling of larger scale field experiments.

HUMIDITY CELL METHODOLOGY

As part of the Diavik Waste Rock Project (DWRP), 36 humidity cell experiments were conducted at the University of Waterloo over a period of approximately six years using representative run of mine waste rock collected at Diavik Diamond Mine (Diavik). The experiments were designed to assess the primary geochemical mechanisms controlling effluent quality from waste rock piles at the mine site. The primary sulfide mineral present in the waste rock is pyrrhotite wherein minor substitution of Ni and Cu for Fe has occurred in the following approximate ratio: [$Fe_{0.852}Ni_{0.004}Co_{0.001}S$] (Jambor, 1997). Given the relatively low sulfide content of the waste rock, the humidity cell experiments were used to assess the potential for acid generation as well as increased concentrations of solutes such as sulfate [SO_4], Fe, Ni, Cu, and Zn.

The Diavik waste rock used in the humidity cell experiments was collected in 2004 and 2005 and includes approximately 75 % granite (primarily quartz [SiO_2], k-feldspar [$KAlSi_3O_8$], and albite [$NaAlSi_3O_8$]), 14 % pegmatitic granite, 10 % biotite schist, and 1 % diabase (Blowes & Logsdon, 1998; Langman et al., 2014). The biotite schist is composed primarily of albite (35–55 %), quartz (20–50 %), and biotite [$KMg_2FeAlSi_3O_{10}(OH)_2$] (10–25 %) and contains a mean sulfide content of 0.24 wt. % S (Langman et al., 2014). Static testing was conducted on each of the humidity cell samples to determine S and C content (Langman et al., 2014). Other sulfide minerals present in the waste rock include minor amounts of chalcopyrite [$CuFeS_2$], sphalerite [ZnS], and pentlandite [$(Ni,Fe)_9S_8$]. The

waste rock is sorted into three types according to sulfur content (Type I < 0.04 wt. %, Type II 0.04 to 0.08 wt. %, and Type III > 0.08 wt. % S) (Smith et al., 2013).

Each humidity cell contained 1 kg of Type I, Type II, or Type III waste rock, through which deionized water was flushed at a rate of 500 mL·wk^{-1}. Once per week water was added to the cells and held for approximately one hour then allowed to drain from the cells. Draining of the cells typically lasted four to six hours and was followed by periods of dry air flow (three days at < 10 % relative humidity) and humid air flow (three days at > 95 % relative humidity) lasting the remainder of the week (Langman et al., 2014). The experiments followed the American Society for Testing and Materials (ASTM) method for humidity cell testing (ASTM, 1996) with increased flooding in the early stages according to the ASTM method modification described by Lapakko and White (2000). Duplicate sets of humidity cell experiments were conducted at two control temperatures (one set at approximately 22 °C and one set at approximately 5 °C).

CONCEPTUAL MODEL

The conceptual model presented here was based on the Type III (sulfide content of 0.16 wt. %), room temperature humidity cell experiments conducted as part of the DWRP and described by Langman et al., 2014. Because of the abundance of oxygen and moisture in the system, sulfide oxidation has been posited to be the significant geochemical process contributing to elevated concentrations of sulfate, Ni, and Co in the humidity cell effluent. Water flow through the model domain is described as continuous infiltration at a rate of 500 mL·wk^{-1}. Although the addition of water to the cells was conducted as flooding events (i.e. 500 mL over the period of a few hours), continuous infiltration was assumed to be a reasonable approximation because weekly flooding and limited evaporation during the dry air influx period did not likely result in significant moisture content reduction.

The oxidation of pyrrhotite was represented by a series of three primary reactions designed to simulate the reaction pathways for sulfide mineral oxidation outlined by Schippers & Sand (1999) and Rohwerder et al. (2003). Following the reaction mechanism for sulfide oxidation, ferric iron was considered as the dominant sulfide oxidizer according to the following overall reaction (Nicholson & Scharer, 1998; Janzen, Nicholson & Scharer, 2000; Belzile et al., 2004):

$$Fe_{(1-x)}S + (8-2x)Fe^{3+} + 4H_2O \rightarrow (9-3x)Fe^{2+} + SO_4^{2-} + 8H^+ \quad (1)$$

The reaction mechanism presented by Schippers & Sand (1999) and Rohwerder et al. (2003) includes the polysulfide pathway wherein several partially oxidized S species (primarily S^0 in the absence of sulfur oxidizing bacteria) can be produced as the reaction sequence progresses towards the fully oxidized product SO_4. The polysulfide pathway is appropriate for the oxidation of monosulfides such as pyrrhotite (Schippers & Sand, 1999; Rohwerder et al., 2003). Elemental S was selected as a proxy for the intermediary components in the MIN3P simulations. Introducing S^0 as an intermediary component results in the following reaction sequence (Nicholson & Scharer, 1998) where equation 2 represents an oxidation process and equation 3 represents an oxidation and dissolution process:

$$Fe_{(1-x)}S + (2-2x)Fe^{3+} \rightarrow (3-3x)Fe^{2+} + S^0 \quad (2)$$

$$S^0 + 1.5O_{2(aq)} + H_2O \rightarrow SO_4^{2-} + 2H^+ \quad (3)$$

Equations 2 and 3 were ultimately driven in the simulations by the oxidation of Fe^{2+}, facilitating the replenishment of Fe^{3+} represented by the following reaction (Singer & Stumm, 1970; Schippers & Sand, 1999; Rohwerder et al., 2003):

$$Fe^{2+} + 0.25O_{2(aq)} + H^{+} \leftrightarrow Fe^{3+} + 0.5H_2O \quad (4)$$

The rate of sulfide oxidation (equation 2) was simulated using the shrinking core model (Levenspiel, 1972; Wunderly et al., 1996; Mayer, Frind & Blowes, 2002) and was represented in the model using the following rate expression (after Mayer, Frind & Blowes, 2002):

$$R_{Po\ ox} = -10^3 S_{Fe_{0.852}Ni_{0.004}Co_{0.001}} \left[\frac{r^p}{(r^p - r^r)r^r}\right] D_{Fe^{3+}} \left[\frac{Fe^{3+}}{1.714}\right] \quad (5)$$

where $R_{Po\ ox}$ represents the rate of pyrrhotite oxidation using the shrinking core model [mol·L^{-1}·d^{-1}] and $S_{Fe_{0.852}Ni_{0.004}Co_{0.001}}$, r^p, r^r, and $D_{Fe^{3+}}$represent the reactive surface area [m^2 mineral·dm^{-3} porous medium], average particle radius [m], unreacted particle radius [m], and effective diffusion coefficient [m^2·s^{-1}] of Fe^{3+} to the unreacted surface, respectively.

In addition to chemical oxidation processes, microbial populations play an important role in the oxidation of sulfide minerals (Nordstrom & Southam, 1997; Blowes et al., 2003). Most probable number bacteria count data from the DWRP humidity cell experiments (Langman et al., 2014) indicates that neutrophilic sulfur oxidizing bacteria (nSOB) were the dominant microbiological catalyst in the system. As a result, biotic oxidation was represented in the rate expressions associated with equations 3 and 4 by simulating the increase in reaction rate with increasing substrate (in this case Fe^{2+} and S^0) concentration to represent the increase in microbial activity.

The rate of ferric iron production (equation 4) was simulated using the rate expression (after Singer & Stumm, 1970; Mayer, Frind & Blowes, 2002; Roden, 2008):

$$R_{Fe^{2+}-Fe^{3+}} = -S\left[k^1_{Fe^{2+}-Fe^{3+}}[Fe^{2+}][O_{2(aq)}] + k^2_{Fe^{2+}-Fe^{3+}}[Fe^{2+}][O_{2(aq)}][OH^-]^2\right]$$
$$-k^3_{Fe^{2+}-Fe^{3+}}\left[\frac{[Fe^{2+}]}{K_s+[Fe^{2+}]}\right] \quad (6)$$

The first two terms in equation 6 represent the chemical oxidation of Fe^{2+} by aqueous oxygen where $R_{Fe^{2+}-Fe^{3+}}$ represents the rate of Fe^{2+} oxidation [mol·L^{-1}·d^{-1}] and S, $k^1_{Fe^{2+}-Fe^{3+}}$, and $k^2_{Fe^{2+}-Fe^{3+}}$ represent a scaling factor [-], the reaction rate constant for pH < ~ 3.5 [L·mol^{-1}·d^{-1}] (Singer & Stumm, 1970), the reaction rate constant for pH > ~ 4.5 [mol·L^{-1}·d^{-1}] (Singer & Stumm, 1970), respectively. The third term in equation 6 represents the biotic oxidation of Fe^{2+} by microbes where $k^3_{Fe^{2+}-Fe^{3+}}$ and K_s represent the reaction rate constant [mol·L^{-1}·d^{-1}] and half-saturating constant [mol·L^{-1}], respectively.

Sulfate concentrations in humidity cell effluent were simulated by the bioitic oxidation of S^0 to SO_4 according to the reaction stoichiometry in equation 3. The rate of S^0 oxidation is dependent on the presence of both oxygen and the S^0 however, due to the abundance of oxygen in the system only S^0 is represented in the following rate expression (after Roden, 2008):

$$R_{S^0-SO_4} = -k_{S^0-SO_4}\left[\frac{[S^0]}{K_s+[S^0]}\right] \quad (7)$$

where $R_{S^0-SO_4}$represents the rate of biotic S^0 oxidation by [mol·L^{-1}·d^{-1}] and $k_{S^0-SO_4}$and K_s represent

the reaction rate constant [mol·L^{-1}·d^{-1}] and half-saturating constant [mol·L^{-1}] respectively.

Minor constituent sulfide minerals chalcopyrite, sphalerite, and pentlandite, were also included in the simulations undergoing oxidation by Fe^{3+} according to the shrinking core model (equation 5, Table 1). Additional primary minerals were simulated to dissolve as surface controlled reactions (Table 1) according to pH dependent (calcite, biotite, muscovite, and albite) or transition state rate expression (k-feldspar and quartz).

Secondary minerals (primarily iron-bearing oxides and hydroxysulfates) are expected to precipitate in association with the oxidation of sulfide minerals (Blowes et al., 2003; Jambor, 2003). Several secondary minerals were added to the system based on saturation index analysis conducted using Type III, room temperature humidity cell effluent chemistry data in conjunction with the geochemical speciation software PHREEQC (Parkhurst & Appelo, 1999). The saturation index analysis indicated that minerals ferrihydrite [$Fe(OH)_3$], jarosite [$KFe_3(SO_4)_2(OH)_6$], and gibbsite [$Al(OH)_3$] were supersaturated in the humidity cell effluent at various points of the experiments. These minerals were allowed to precipitate or dissolve during the simulations according to equilibrium controlled rate expressions. Amorphous silica [$SiO_{2(am)}$] was also allowed to precipitate according to an equilibrium controlled rate expression to prevent excess Si build up.

Table 1 Reaction stoichiometry used in sulfide weathering simulations

Mineral	Primary Minerals	log K
(1) pyrrhotite	$Fe_{0.852}Ni_{0.004}Co_{0.001}S + 1.714Fe^{3+} \rightarrow 2.566Fe^{2+} + 0.004Ni^{2+} + 0.001Co^{2+} + S^0$	--
(2) sphalerite	$ZnS + 2Fe^{3+} \rightarrow 2Fe^{2+} + Zn^{2+} + S^0$	--
(3) chalcopyrite	$FeCuS_2 + 4Fe^{3+} \rightarrow 5Fe^{2+} + Cu^{2+} + 2S^0$	--
(4) pentlandite	$Fe_{4.5}Ni_{3.6}Co_{0.9}S_8 + 18Fe^{3+} \rightarrow 22.5Fe^{2+} + 3.6Ni^{2+} + 0.9Co^{2+} + 8S^0$	--
(5) calcite	$CaCO_3 \rightarrow Ca^{2+} + CO_3^{2-}$	-8.48
(6) biotite	$KMg_2Fe(AlSi_3O_{10})(OH)_2 + 10H^+ \rightarrow K^+ + 2Mg^{2+} + Fe^{2+} + Al^{3+} + 3H_4SiO_4$	--
(7) muscovite	$KAl_2(AlSi_3O_{10})(OH)_2 + 10H^+ \rightarrow K^+ + 3Al^{3+} + 3H_4SiO_4$	--
(8) k-feldspar	$KAlSiO_8 + 4H_2O + 4H^+ \rightarrow K^+ + Al^{3+} + 3H_4SiO_4$	0.08
(9) albite	$NaAlSi_3O_8 + 4H_2O + 4H^+ \rightarrow Na^+ + Al^{3+} + 3H_4SiO_4$	--
(10) quartz	$SiO_2 + 2H_2O \rightarrow H_4SiO_4$	-3.98
	Secondary Minerals	
(11) ferrihydrite	$Fe(OH)_{3(am)} + 3H^+ \leftrightarrow Fe^{3+} + 3H_2O$	4.89
(12) jarosite	$KFe_3(SO_4)_2(OH)_6 + 6H^+ \leftrightarrow K^+ + 3Fe^{3+} + 2SO_4^{2-} + 6H_2O$	-9.21
(13) silica (am)	$SiO_{2(am,gl)} + 2H_2O \leftrightarrow H_4SiO_4$	-3.02
(14) gibbsite	$Al(OH)_{3(am)} + 3H^+ \leftrightarrow Al^{3+} + 3H_2O$	8.11

Table 2 Stoichiometry used in intra-aqueous reactions

Primary Components	Intra-aqueous Reactions	log K
(1) Fe(II)/Fe(III)	$Fe^{2+} + 0.25O_{2(aq)} + H^+ \leftrightarrow Fe^{3+} + 0.5H_2O$	--
(2) SO_4^{2-}/HS-	$HS^- + 2O_{2(aq)} \leftrightarrow SO_4^{2-} + H^+$	-138.38
(3) S^0- SO_4^{2-}	$S^0 + 1.5O_{2(aq)} + H_2O \rightarrow SO_4^{2-} + 2H^+$	--

MODEL PARAMETERS

The humidity cell experiments were conducted in cylinders with diameter of approximately 0.1 m resulting in an average height of waste rock of 0.1 m. Flow through the humidity cells was simulated as a 1-D column with the vertical domain set at 0.1 m, discretized into 100 1 mm control volumes. The simulations were run for a 2240 d period corresponding approximately to the data set available as of September 2014. Because atmospheric air (humidity adjusted) was used for the air flow portions of the experiment and the infiltrating deionized water was not isolated from atmospheric conditions, the cells were assumed to be in equilibrium with atmospheric oxygen and carbon dioxide at all times. The temperature of the simulations was set at 22 °C to be consistent with the conditions of the experiments. Flow parameters (Table 3) including porosity, hydraulic conductivity, and soil hydraulic function parameters were based on the work of Neuner et al., 2013 or by analysis of humidity cell data; dispersivity along the 0.1 m flow path was ignored. Mineral weight percent (Table 4) for pyrrhotite, calcite, biotite, muscovite, k-feldspar, albite, and quartz were calculated based on the general waste rock content documented by Jambor (1997), with values for chalcopyrite and sphalerite estimated from the molar ratios of Cu^{+2} and Zn^{+2} to Ni^{+2} in humidity cell effluent. The resulting estimates for the weight percent of chalcopyrite and sphalerite were consistent with values estimated by Bailey (2013). The weight percent for pentlandite was calibrated as part of the simulations. The initial volume fractions of secondary minerals expected to precipitate were set to an arbitrary low value (i.e. 1 x 10^{-10}).

Table 3 Physical parameters used in simulations

Parameter		Value
hydraulic conductivity ($m \cdot s^{-1}$)		2.5 x 10^{-4}
van Genuchten soil hydraulic parameters	α (m^{-1})	8.8
	n	1.7
flow rate ($m \cdot s^{-1}$)		1.0 x 10^{-9}
Porosity		0.26

Table 4 Composition of waste rock

Mineral	wt. %
pyrrhotite	0.17[1]
chalcopyrite	0.01[1]
sphalerite	0.01[1]
pentlandite	0.01[1]
calcite	0.07[1]
biotite	7.0[2]
muscovite	2.3[2]
k-feldspar	38.0[2]
albite	20.3[2]
quartz	30.4[2]

[1]Based on results of static testing with adjustment during calibration phase of model.

[2]Based on results of Jambor 1997

Dissolution and precipitation reactions involving primary minerals were kinetically controlled and irreversible (with the exception of calcite, which was simulated as a reversible reaction). Secondary mineral precipitation and dissolution reactions were kinetically controlled and reversible.

RESULTS AND DISCUSSION

To evaluate the conceptual model and assess the resulting simulations, the output of the MIN3P simulations were optimized for best fit to measured effluent concentrations of selected solute parameters from the Type III, room temperature humidity cells. All hydraulic parameters were fixed during the optimization process. Initial elevated concentrations of SO_4 and cations were not considered since they were likely a result of the initial blasting process (Bailey et al., 2013). Subsequent to the initial flush of blasting residuals, measured solute concentrations increased from relatively low concentrations to peak concentrations over a period of ten to approximately 24 weeks depending on the parameter (SO_4 concentrations peaked at approximately ten weeks whereas Ni^{2+} and Co^{2+} concentrations peaked at approximately 24 weeks).

To assess the general applicability of the simulations to other humidity cells and field scale experiments, the simulated rate of sulfide oxidation was compared to the rate of sulfide oxidation for the Type III waste rock calculated using the concentrations of SO_4 in the Type III, room temperature humidity cell effluent by Langman et al. (2014) (Figure 1). The good fit over most of the simulated period indicates that the model captures the general rate of oxidation suggesting a reasonable approximation of the overall sulfide oxidation process at the laboratory scale.

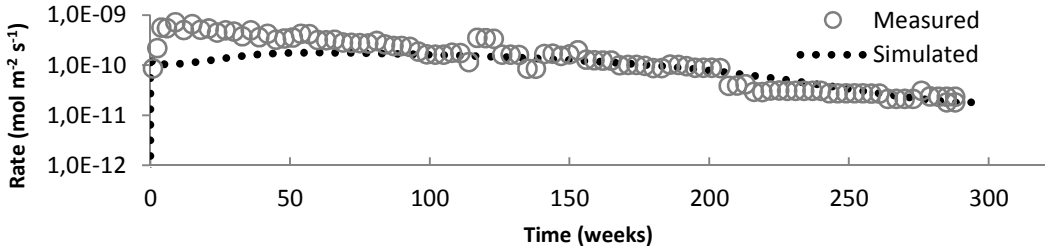

Figure 1 Rate of sulfide oxidation [mol·m^{-2}·s^{-1}] versus time [weeks] as estimated from measured SO_4 concentrations in humidity cell effluent compared to MIN3P sulfide oxidation simulation results

To assess specific processes, the measured effluent concentrations of SO_4,Ni^{2+}, and Co^{2+} from the Type III humidity cells are compared to the simulation results (Figure 2). The effective rate constants for non-sulfide minerals were used to calibrate the simulations to allow best fit to the measured effluent chemistry data. For sulfide minerals, the reactive surface area was used to calibrate the simulations.

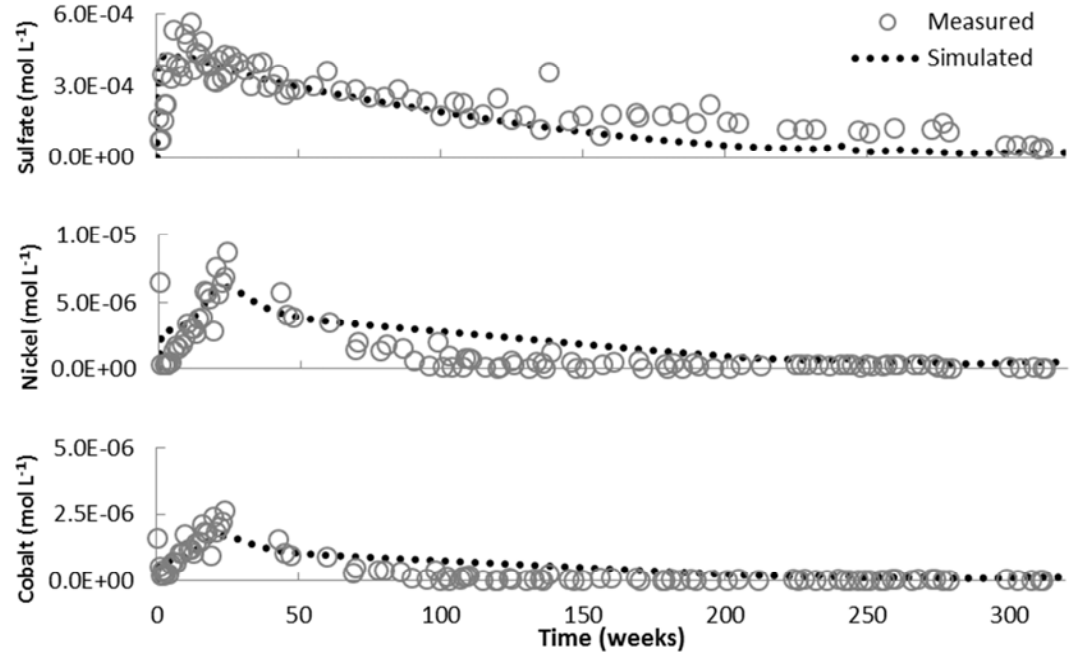

Figure 2 Concentrations of sulfide oxidation products SO_4, Ni^{2+}, and Co^{2+} [mol·L^{-1}] versus time [weeks] measured in humidity cell effluent compared to aqueous concentrations exiting the simulation domain

Simulated sulfate concentrations show a good fit to the measured data throughout the modelled period indicating an initial increase to peak concentrations at approximately ten weeks followed by a monotonic decrease. These trends are simulated through changes in the rates of microbially mediated oxidation reactions and available reactive surface area, as described by the shrinking core model.

Simulated Ni^{2+} and Co^{2+} concentrations followed a pattern generally similar to SO_4, with peak concentrations occurring slightly later than the sulfate concentration peak (Ni^{2+} and Co^{2+} concentrations peaked at about 24 weeks). The later peak concentrations of cations are attributed to slower oxidation rates for pentlandite when compared to the oxidation rate of pyrrhotite.

CONCLUSIONS

The general agreement between the simulated solute concentrations and the measured humidity cell concentrations indicates a reasonable conceptual geochemical model has been put forward for the oxidation of sulfides contained in Diavik waste rock. The major components controlling oxidation of the sulfide minerals were identified by the modelling study to be the biotic influence on the rate of S^0 oxidation and the available reactive surface area of sulfide minerals. Further work is required to identify the major controls on iron concentrations and biotite dissolution rates, which will facilitate use of the geochemical conceptual model for the field scale experiments that are part of the DWRP.

ACKNOWLEDGEMENTS

Funding for this research was provided by a Collaborative Research and Development Grant from the Natural Sciences and Engineering Research Council of Canada (NSERC) awarded to D.W. Blowes, Principal Investigator; Diavik Diamond Mines, Inc.; the International Network for Acid Prevention; and the Mine Environment Neutral Drainage Program.

NOMENCLATURE

$\boldsymbol{R_{Po\ ox}}$	rate of pyrrhotite oxidation
$S_{Fe_{0.852}Ni_{0.004}Co_{0.001}}$	reactive surface area
r^p	average particle radius
r^r	unreacted particle radius
$D_{Fe^{3+}}$	effective diffusion coefficient of Fe^{+3} to the unreacted surface
$\boldsymbol{R_{Fe^{2+}-Fe^{3+}}}$	rate of Fe^{+2} oxidation
$k^1_{Fe^{2+}-Fe^{3+}}$	reaction rate constant for pH < ~ 3.5
$k^2_{Fe^{2+}-Fe^{3+}}$	reaction rate constant for pH > ~ 4.5
S	scaling factor
$k^3_{Fe^{2+}-Fe^{3+}}$	reaction rate constant
K_S	half saturating constant
$\boldsymbol{R_{S^0-SO_4}}$	rate of S^0 oxidation
$\boldsymbol{k}_{S^0-SO_4}$	reaction rate constant

REFERENCES

American Society for Testing and Materials. *Test Method for Laboratory Weathering of Solid Materials Using a Humidity Cell*; ASTM International, 1996; p. 19.

Ardau, C., Blowes, D.W., Ptacek, C.J., 2009. Comparison of laboratory testing protocols to field observations of the weathering of sulfide-bearing mine tailings. J. Geochem. Explor. 100, 182-191.

Bailey, B.L., Smith, L.J.D., Blowes, D.W., Ptacek C.J., Smith, L., Sego, D.C., 2013. The Diavik Waste Rock Project: Persistence of contaminants from blasting agents in waste rock effluent. App. Geochem., Vol. 36, pp 256-270.

Bailey, B.L., 2013. Geochemical and microbiological characterization of effluent and pore water from low-sulfide content waste rock. Ph.D. thesis, University of Waterloo, 399 p.

Belzile, N., Chen, Y.W., Cai, M.F., Li, Y., 2004. A review on pyrrhotite oxidation. J. Geochem. Explor. 84, 65–76.

Blowes, D.W., Logsdon, M.J., 1998. Diavik geochemistry baseline report. Prepared by Sala Groundwater, Inc. and Geochimica, Inc. for Diavik Diamond Mines and submitted to Canadian Environmental Assessment Agency, 121 p.

Blowes, D.W., Ptacek, C.J., Jambor, J.L., Weisener, C.G., 2003. The geochemistry of acid mine drainage. In: Lollar, B.S. (Ed.), Environmental Geochemistry, 9, Treatise on Geochemistry, Elsevier-Pergamon, pp. 149–204.

Jambor, J.L., 1997. Mineralogy of the Diavik Lac de Gras kimberlites and host rocks. Prepared by Leslie Investment, Ltd. for Diavik Diamond Mines and submitted to the Canadian Environmental Assessment Agency, 1997, 187 p.

Jambor, J.L., 2003. Mine-waste mineralogy and mineralogical perspectives of acid-base accounting. In: Jambor, J.L., Blowes, D.W., Ritchie, A.I.M. (Eds.), Environmental Aspects of Mine Wastes: Mineralogical Association of Canada Short Course Series. Economic Geology Publishing Company, pp. 117-145.

Janzen, M.P., Nicholson, R.V., Scharer, J.M., 2000. Pyrrhotite reaction kinetics: reaction rates for oxidation by oxygen, ferric iron, and for nonoxidative dissolution, Geo. Cos. Acta 64(9), 1511–1522.

Kempton, H., 2012, A review of scale factors for estimating waste rock weathering from laboratory tests: International Conference on Acid Rock Drainage (ICARD) Ottawa, 9th, Canada, 20–24 May 2012, Proceedings.

Lapakko, K.A., 2003. Developments in humidity-cell tests and their application. In: Jambor, J.L., Blowes, D.W., Ritchie, A.I.M. (Eds.), Environmental Aspects of Mine Wastes: Mineralogical Association of Canada Short Course Series. Economic Geology Publishing Company, pp. 147-164.

Lapakko, K.A., White, W.W., 2000. Modification of the ASTM 5744-96 kinetic test. In *Proceedings of Fifth International Conference on Acid Rock Drainage*; Society for Mining, Metallurgy, and Exploration: Littleton, Colorado, 2000; pp. 631–639.

Langman, J.B., Moore, M.L., Ptacek, C.J., Smith, L., Sego, D., Blowes, D.W., 2014. Diavik Waste Rock Project: evolution of mineral weathering, element release, and acid generation and neutralization during a 5-year humidity cell experiment. Minerals 4(2), 257–278.

Levenspiel, O., 1972. Chemical Reaction Engineering, 2nd ed., John Wiley & Sons, New York, 361–371.

Mayer, K.U., Frind, E.O., Blowes, D.W., 2002. Multicomponent reactive transport modeling in variably saturated porous media using a generalized formulation for kinetically controlled reactions. Water Resour. Res. 38(9), 13-1–21.

Neuner, M., Smith, L., Blowes, D.W., Sego, D.C., Smith, L.J.D., Fretz, N., Gupton, M., 2013. The Diavik Waste Rock Project: water flow though waste rock in a permafrost terrain. Appl. Geochem. 36, 222–233.

Nicholson, R.V., Scharer, J.M., 1998. Laboratory Studies of Pyrrhotite Oxidation, MEND Project 1.21.2.

Nordstrom, D.K., Southam, G., 1997. Geomicrobiology of sulfide mineral oxidation. Rev. Mineral. Geochem. 35, 361–390.

Parkhurst, D.L., Appelo, C.A.J., 1999. *PHREEQCi (version 2)* – A computer program for speciation, batch reaction, one dimensional transport, and inverse geochemical calculations: U.S. Geological Survey Water-Resources Investigations.

Roden, E.E., 2008. Microbiological Control on Geochemical Kinetics 1: Fundamentals and Case Study on Microbial Fe(III) Oxide Reduction. In: Brantley, S.L., Kubicki, J.D., White, A.F. (Eds.), Kinetics of Water-Rock Interaction. Springer Science+Business Media, pp. 335-415.

Rohwerder, T., Gehrke, T., Kinzler, K., Sand, W., 2003. Bioleaching review part A: Progress in bioleaching: fundamentals and mechanisms of bacterial metal sulfide oxidation. Appl. Microbiol. Biotechnol. (2003) 63: 239-248.

Sapsford, D.J., Bowell, R.J., Dey, M., Williams, K.P., 2009. Humidity cell tests for the prediction of acid rock drainage. Minerals Engineering, Vol. 22, pp. 25-36.

Schippers, A., Sand, W., 1999. Bacterial leaching of metal sulfides proceeds by two indirect mechanisms via thiosulfate or via polysulfides and sulfur. Appl. Environ. Microbiol. 65(1), 319–321.

Singer P.C., Stumm, W., 1970. Acidic Mine Drainage : The Rate-Determining Step. Science, New Series, Vol. 167, No. 3921 (Feb. 20, 1970), pp. 1121-1123.

Smith, L.J.D., Bailey, B.L., Blowes, D.W., Jambor, J.L., Smith, L., Sego, D.C., 2013. The Diavik Waste Rock Project: initial geochemical response from a low sulfide waste rock pile. Appl. Geochem. 36, 210–221.

Wunderly, M.D., Blowes, D.W., Frind, E.O., Ptacek, C.J., 1996. Sulfide mineral oxidation and subsequent reactive transport of oxidation products in mine tailings impoundments: A numerical model. Water Resour. Res. 32, 3173–3187.

Assessing the Robustness of Antamina's Site Wide Water Balance/Water Quality Model over 5 Years of Implementation

James Tuff[1], Bevin Harrison[2], Sergio Yi Choy[2], Roald Strand[1] and Brent Usher[1]

1. *Klohn Crippen Berger, Australia*
2. *Compañía Minera Antamina, Peru*

ABSTRACT

Predicting water chemistry resulting from mining activities is arguably one of the most important aspects of environmental management at mines. The water quality within waste storage facilities presents an especially important consideration in mine planning and the ability to accurately simulate the chemical evolution within such facilities is a major goal for environmental planning.

To illustrate the concepts in development of a predictive model, a water quality model for the tailings storage facility (TSF) at the Antamina mine in Peru is presented. The model is based on fundamental mineralogical and thermodynamic controls and monitoring data from the mine's regular monitoring and field research programs.

The model has developed as a collaborative effort between KCB and Antamina. The geochemical controls and water balance mechanisms simulate the interaction in the TSF and these are continually calibrated against observed data. This iterative process has resulted in the construction of a robust model that can predict, with confidence, water quality originating from the facility for the life of mine and after closure.

Here we outline the main control mechanisms built into the model and compare these to the observations of the tailings storage facility at Antamina. By introducing 'stresses', such as erroneous water flows or large inputs of sulfate, we can demonstrate that the model is robust and able to handle a variety of alternative scenarios. We also use established geochemical modelling software, such as PHREEQC and GWB, to cross-check predicted mineral and geochemical controls and compare the equilibria predicted in these models to those that have been constructed in the Antamina water quality model. The results show that that model's mechanisms and simulation algorithms are robust and versatile and may be utilised successfully at this mine site but also in a variety of mining waste rock dumps, tailings storage facilities and water catchments.

Keywords: GoldSim, modeling, geochemistry

INTRODUCTION

The Antamina mine is a polymetalic skarn deposit situated in the Peruvian Andes, approximately 270 km northeast of Lima. The mine produces copper, zinc and molybdenum concentrates. Waste material generated by the mining process is deposited in two waste rock dumps (WRD) and a tailings storage facility (TSF).

Due to the distinct wet and dry season climate (Harrison *et al.*, 2012), Compañía Minera Antamina (Antamina) manages water using infrastructure such as: diversion channels; passive treatment wetlands; capture and pump-back and operational controls such as flocculation and neutralization. Antamina conducts regular monitoring of water quality and flows across the mine site and compliments this information with a comprehensive geochemical testing program. The program includes static testing (acid-base accounting, whole rock analysis, mineralogy and leachate testing) and kinetic testing through laboratory and field testing methods (*e.g.* field cells and instrumented waste rock piles).

KCB uses the geochemical testing data, site water quality and flows to understand site interactions, construct feasible conceptual models for each of the major mine site components, calibrate and test the operation of the model. This collaborative effort has resulted in a mine site-wide integrated water balance and water quality model (IWBWQM).

The IWBWQM has been built using the GoldSim Pro software developed initially in partnership with Golder Associates and the United States Department of Energy for water balance purposes. The Antamina IWBWQM is a coupled water balance and water quality model built to simulate a variety of different scenarios including: predicting water levels, flows, seepage, pumping needs, and water quality as a solution of up to 42 water quality parameters at a variety of locations throughout the system. GoldSim was considered an appropriate choice for Antamina due to its capacity for complex modelling in terms of handling of data arrays, measurement unit continuity, error checking and user interface. GoldSim simulation software is capable of deterministic and probabilistic modelling as well as providing sensitivity analyses. Specific to this project, multiple realizations of the water balance can be achieved and the sensitivity of different input parameters or processes can be determined. The GoldSim model construction means the model is flexible enough to make impact assessments even given a broad range of potential future water management scenarios.

The Antamina IWBWQM encompasses the entire project area. Here, we focus on the construction and development of the modelled TSF facility. In this paper we demonstrate the fundamental concepts that form the underlying infrastructure of the TSF model, the integration of this framework with data provided by Antamina and comparisons between the predicted evolution of the TSF with historical data. Finally, we demonstrate that the principles in the TSF model construction can be applied to other components of the mine site and that the Antamina mine provides the ideal setting to test this.

METHODOLOGY

The conceptual design and construction of the IWBWQM have been detailed by Strand *et al.* (2010). This study focuses on the design, construction and subsequent testing of the TSF.

The TSF is the most interconnected facility to simulate in the model, with contributions from over 20 inflows and 10 outflows, geometric calculations and area balances. TSF inputs and outputs are based on processes and controls operating at Antamina. The transport of reaction products is taken into account primarily from the dissolved flows and tailings reactivity. Geochemical systems are simulated in both the pond and the tailings pore space as separate systems, with mass transfers between the pond and the tailings as a function of flows and diffusion. Use was made of PHREEQC (Parkhurst and Appelo, 1999) and Geochemist's Workbench (Bethke, 2008) in both the pond and pore space. Mine infrastructure plans, waste schedules and static geochemical test results are used to define the mass of reactants available. Field kinetic cells are used to define the expected reaction sequence and kinetic loading rates under oxidizing (beach surface) and reducing (beach pores and base pores) conditions. The site's water quality monitoring record is used to define the expected behaviour, provide reasons for observations and deviations from expected flows or concentrations. The approach is summarised schematically in Figure 1.

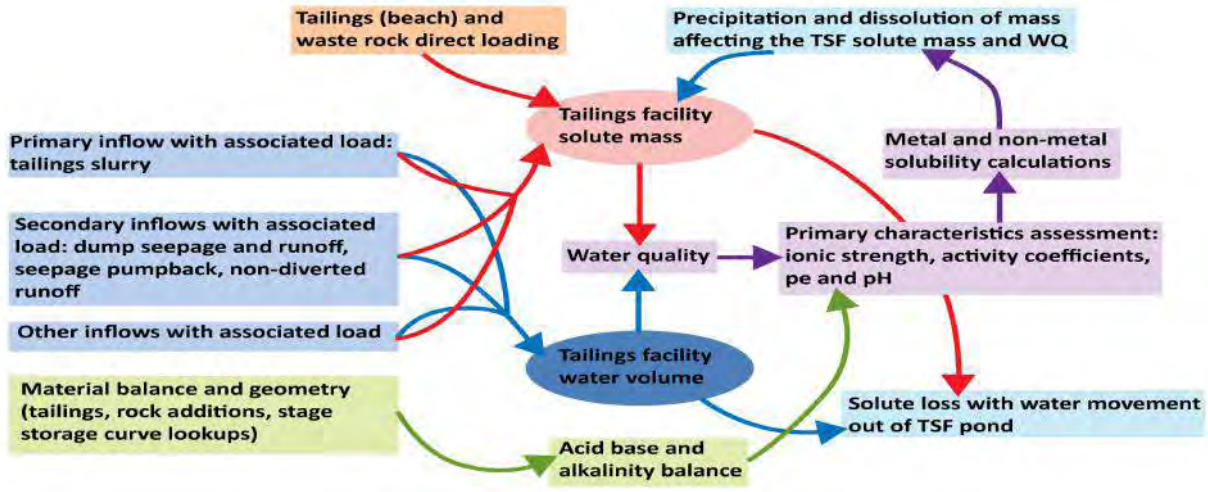

Figure 1 TSF model conceptual components

The TSF pond is the central reservoir and is affected by all of the water inflows and outflows of this section of the model. The most significant inflow to the system is the tailings slurry, which regulates the chemistry in the TSF pond by constant addition of dissolved load and high pH water. Secondary inflows from the waste dumps are the greatest contributors of dissolved metals. These flows include direct precipitation, runoff and contact flows from the waste rock dump or water inflows from non-contact sources. Direct loading from the tailings beach and waste rock also provides a significant contribution. Solute loss is controlled through the precipitation of minerals within the pond, or loss associated with water movement out of the TSF via dam seepage to the seepage pumpback system.

Time and mass dependent loading rates are calculated by multiplying the effluent concentrations by the effluent volume and dividing by the sample mass and the sample interval to produce a mg/kg/week value, Equation 1.

$$Loading\ Rate = \frac{[X]v}{\frac{m}{t}} \quad (1)$$

where X is the concentration in the effluent, v is the effluent volume, m is the mass of the source term used (rock mass) and t is the time interval between measurements.

Subaqueous deposition is associated with considerably slower kinetic rates than aerated deposition. Reaction rates are derived from the kinetic geochemical testing program. The kinetic rates are obtained from the humidity cell data and subsequent field cells operated by Antamina; there are cells currently in operation which continue to provide data for model population.

The model uses a mass balance approach combined with an acid-base accounting and alkalinity balance system and subsequent pH modelling to assess the net load of acid or alkalinity entering the TSF pond via loading at each time step. The TSF load, (the result of water concentration and flow) entering the TSF is a function of all sources considered. Therefore, because those sources vary rapidly, it is assumed that incoming acidic loads only neutralise according to the total concentration of alkalinity present in aqueous solution; thereafter neutralisation is due to the tailings material itself.

The total mass of dissolved solute present in the pond is simulated. All dissolved solute is added to this "reservoir", and all precipitation or physical removal via outflow is removed directly from this element. Dissolved loads that are associated with inflows and dissolution of secondary precipitates also contribute. The solute mass is a primary input for the tailings pond free water quality.

Since the TSF is a mixing pond of several different water flows, preliminary acid base accounting is undertaken through a series of algorithms prior to depleting neutralizing potential (NP) in the TSF. If a water flow is assumed to be acid, then the acidity from that inflow is allowed to deplete the dissolved alkalinity load reporting to the TSF. The net addition of alkalinity and acidity to the pond is the difference between the various alkalinity and acidity contributors. Excess acidity is simulated to then consume the available NP in the tailings, which is present as calcite and small amounts of dolomite in the tailings solids. This differs from other facilities, which consider pyrite oxidation (based on conservative estimates) as the primary driver for the source term systems with acidity generation through sulfide oxidation and subsequent neutralization of acidity by carbonate minerals. From this point, however, acidity as a driver is handled much the same as in source term facilities. Excess acidity consumes minerals contributing to neutralization potential of the tailings.

The TSF pond is modelled using the established carbonate-bicarbonate-CO_2 equilibrium detailed in Strand *et al.* (2010). In the model, the 'central pillar' is considered to be the alkalinity within the TSF pond, which can be estimated as the molar concentration of bicarbonate (HCO_3^-). A certain amount of alkalinity is present in the pond; this is based on measurements provided by Antamina. When the model is operated, any acidity added to the pond (e.g., from the mill) consumes alkalinity. This in turn shifts the equilibrium so that the net effect is to dissolve calcite ($CaCO_3$) to produce more bicarbonate (Strand *et al.*, 2010). The shift in equilibrium results in the dissolution of CO_2, which is assumed to be in equilibrium with the atmosphere (Strand *et al.*, 2010). The model thus combines calcite dissolution/precipitation and CO_2 dissolution/degassing to buffer acidity additions to the TSF pond, provided solid calcite remains in the system (atmospheric CO_2 is considered to be constantly replenished). Alkalinity is also added to the pond from the various additions (e.g., from the mill slurry), which are simulated in the model based on data provided by Antamina.

Calcite provides the major buffering mechanism in the TSF, but bicarbonate is stable within a pH range of ~ 6 – 9. At lower pH levels, other mineral buffering systems are more appropriate and

these have been built into the model. Minerals and secondary precipitates that neutralize acid and buffer pH, using similar principles to the calcite system, have been assigned the pH ranges in the model as follows, after Blowes & Ptacek (1994):

1. Calcite and /or dolomite (6.3 pH – 9 pH)
2. Siderite (4.8 pH – 6.3 pH)
3. Alumosilicates and gibbsite (pH 4.0 – 4.5)
4. Iron Oxides Ferrihydrite and/or Goethite (2.5 pH – 3.5 pH)
5. Jarosite (1.8 pH – 2.0 pH)

Geochemical processes controlling water quality at Antamina

TSF concentrations are governed by kinetic reaction rates, equilibrium controls on saturation and associated water volumes. The major mineral assemblages are dominated by calcium containing carbonates (Strand *et al.*, 2010). Water quality variation appears to be most strongly affected by the oxidation of sulfide minerals, which drives the increase in salinity, sulfate and the acidity. Neutralization of the acidity may occur through the water's natural alkalinity, but occurs principally through the dissolution of Ca-containing carbonates. Sulfide oxidation and concurrent buffering increases salinity and releases the associated metal in the sulfide (*e.g.*, Fe, Cu, Zn or Pb). The resultant increased sulfate and calcium culminates in gypsum ($CaSO_4$) precipitation (Fig. 2). The continued presence of carbonates maintains neutral to alkaline conditions, which limits mobilization of many of the metals, apart from neutral drainage species, such as As and Mo.

Using the sulfate generation rate allows an estimation of the amount of acidity and the amount of carbonate needed to buffer this acidity (i.e. depletion of calcite/dolomite as a result of sulfide oxidation). The site observations confirm that the concentrations of the majority of metals are a function of the pH conditions, overall salinity and mineral solubility constraints. From these observations the required geochemical mechanisms including pH determination, acid generation and neutralization, salinity calculation and solubility constraints have been built into the model (Strand *et al.*, 2010).

TSF solution chemistry was analyzed using PHREEQC to assess the precipitate phases most likely to govern solution chemistry and GWB to observe the potential speciation and the relationships between solubility, concentration and pH. Since the purpose of the IWBWQM is to simulate dynamic conditions, algorithms are used to assess how far the system is from the equilibrium condition. This is achieved by calculating the solubility product, K_{sp}, for a particular mineral at supersaturation and undersaturation. Equations 2 and 3 are examples, for gypsum, of the basis of the quantification of these non-equilibrium conditions:

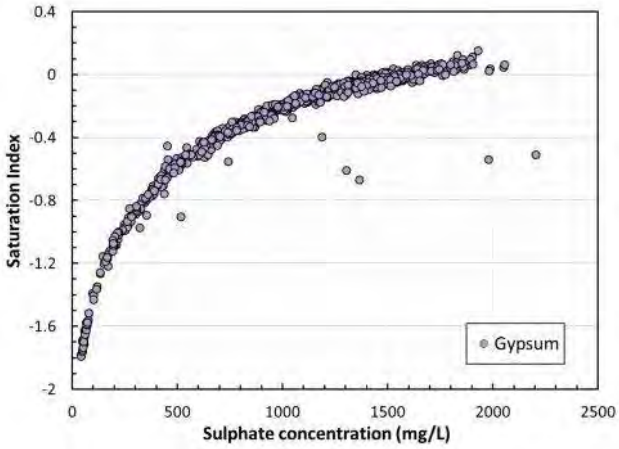

Figure 2 Saturation state of gypsum with increasing sulfate concentrations at the Antamina east waste rock dump

Undersaturated: $([Ca^{2+}] + \delta[Ca^{2+}]) \cdot ([SO_4^{2-}] + \delta[SO_4^{2-}]) = K_{sp(gypsum)}$ (2)

and

Supersaturated: $([Ca^{2+}] - \delta[Ca^{2+}]) \cdot ([SO_4^{2-}] - \delta[SO_4^{2-}]) = K_{sp(gypsum)}$ (3)

These calculate the change in the molar concentration (δ) that is required to bring the solution back to equilibrium. A series of these relationships is included in the model to move sensitive parameters in and out of solution as the pH and other variables change; those used in the TSF are shown in Table 1.

Table 1 Primary mineral controls used in the TSF section of the IWBWQM

Mineral	Formula	Mineral	Formula	Mineral	Formula	Mineral	Formula
Calcite	$CaCO_3$	Gypsum	$CaSO_4$		Cr_2O_3	Otavite	$CdCO_3$
Dolomite	$CaMg(CO_3)_2$	Anglesite	$PbSO_4$	Malachite	$Cu_2CO_3(OH)_2$		$Pb(OH)_2$
Siderite	$FeCO_3$	Brucite	$MgCO_3$	Manganite	MnO(OH)	Rhodochrosite	$MnCO_3$
Gibbsite	$Al(OH)_3$	Cerrusite	$PbCO_3$	Molybdate	Ca/Cu/Pb /$ZnMoO_4$	Smithsonite	$ZnCO_3$
Goethite	FeO(OH)						

Antamina site monitoring data and field kinetic testing suggests that sorption has an important control on metal concentrations at the TSF. This is taken into account in the model by calculating sorption of metal species to Fe-precipitates. The model assumes that the total iron in the TSF is the amount produced by pyrite oxidation; the dissolved iron is governed by solubility calculations. The iron precipitated at each time-step results from the total iron minus the dissolved iron. At a given pH and provided enough precipitated iron is present, the proportion of As, Mo and Se adsorbed to the precipitate is based on PHREEQC determined adsorption ratios. Although metals are typically

desorbed from other minerals present as pH decreases, this is not always the case. Figure 3 shows how the fraction of MoO_4^{2-} sorbed to a surface decreases as pH increases. In contrast, other Mo species, such as H_2MoO_4, remain sorbed at high pH.

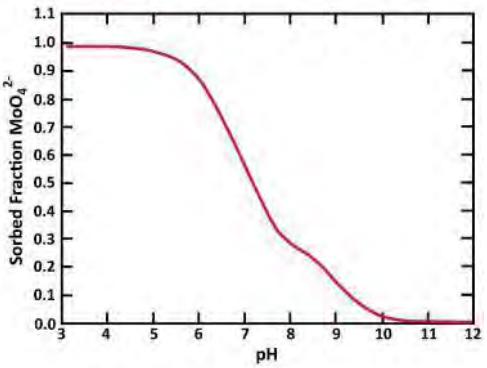

Figure 3 Sorption of MoO_4^{2-} with pH

Once the mass loss and gain and its effect on the TSF pond water dissolved solute has been determined in each time step, the dissolved solute mass for each parameter controlled by minerals/pH is assumed to be 'near' equilibrium in the pond. The concentration of solutes in the pond water is assumed to be the water quality in the pond for that time step. Any outflows from the system (barge pumped, seepage through the tailings-water interface, or other) are assigned this water quality.

RESULTS AND DISCUSSION

TSF IWBWQM model output was compared to TSF monitoring data provided by Antamina. Figure 4 shows the simulated output normalized to the site monitored data and expressed as a percentage above and below the monitored concentrations (set at 1). Simulated sulfate and chloride concentrations are within 20 % of the monitored values for the majority of the five year simulation period: this error is comparable to the analytical error associated with the monitoring data.

Figure 5 shows simulated pH levels normalized to those monitored at the TSF and expressed as percentages above and below the real values. For the majority of the simulated period, pH values are within 20 % of the real values (often within 10 %). This is comparable to analytical error. Figure 5 also shows the simulated TSF pond water volume normalized to water balance data provided by Antamina. The TSF IWBWQM produces a close calibration with the real water balance and is within 10 % of monitored values for the majority of the simulated period. In addition, Figure 5 shows the effect of deliberately 'stressing' the water balance; in this case adding an erroneous water flow of 50 L/s to the TSF pond. In this scenario the model rapidly loses the close calibration to the real data, indicating that the TSF IWBWQM is performing in close agreement to the observed water balance.

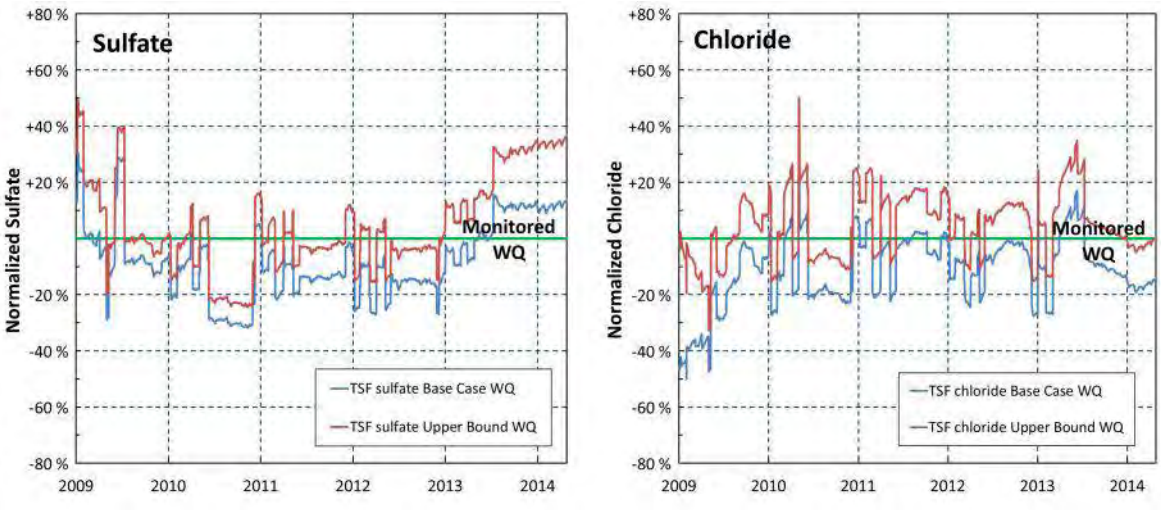

Figure 4 Simulated sulfate and chloride concentrations normalized to monitored concentrations at the TSF

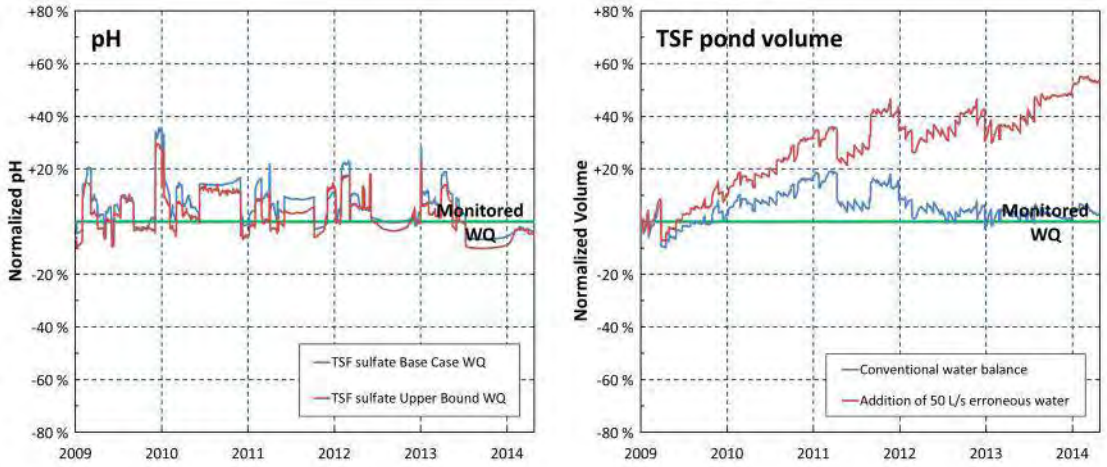

Figure 5 Simulated pH normalized to monitored pH values (LHS) and simulated TSF pond volume normalized to monitored values (RHS)

PHREEQC saturation assessment and the effect of increased sulfate to the TSF

Saturation indices of the IWBWQM mineral controls (Table 1) were calculated using PHREEQC, based on monitored TSF water qualities under the conditions of the mine site. Using PHREEQC in conjunction with the model is an iterative process and allows for continual adjustment of the controls as more data become available. Figure 6 shows that there is generally a good agreement between the TSF IWBWQM expected minerals (which, for equilibrium should be zero) and the saturation indices calculated in PHREEQC.

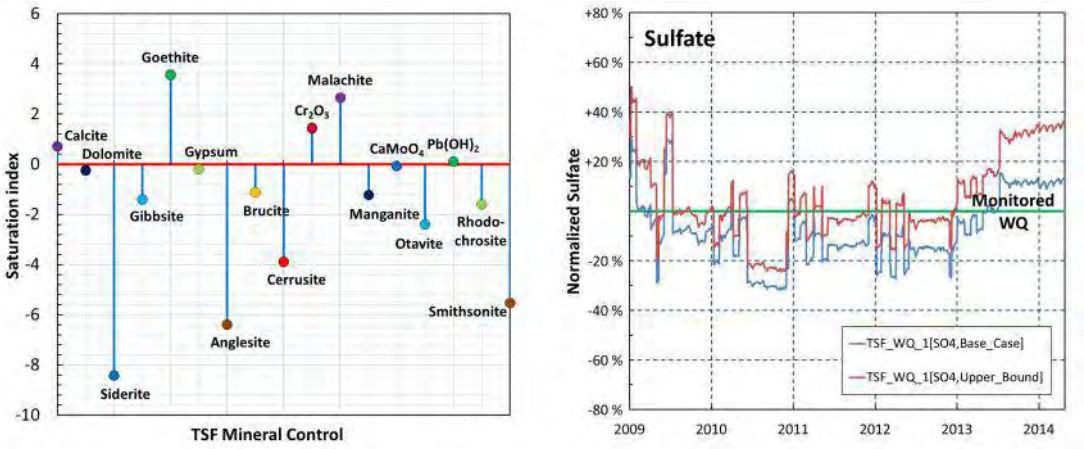

Figure 6 PHREEQC saturation indices using the water quality monitored in the TSF by Antamina (LHS) and normalized TSF sulfate concentrations after a 6-fold sulfate increase at 100 L/s (RHS)

The IWBWQM was tested for its robustness to changes in conditions by simulating an increased sulfate addition to the TSF. Figure 6 shows that, in spite of the increased sulfate input (here this is simulated as a 6-fold sulfate increase at 100 L/s), the TSF sulfate concentrations remain within 20 % of the monitored values (*cf.* Fig. 4) and suggests that the mineral control mechanisms built into the model can adjust to this influx; the IWBWQM moderates the impact of the additional sulphate by allowing oversaturated minerals to precipitate.

The Antamina site is ideal for applying the IWBWQM principles to other mine site facilities. Figure 7 compares the simulated normalized concentrations at the East Waste Rock Dump (EWRD). Although simulated sulfate is consistently lower than shown in the monitoring data, the values are, nonetheless, within 20 % for the majority of the simulation.

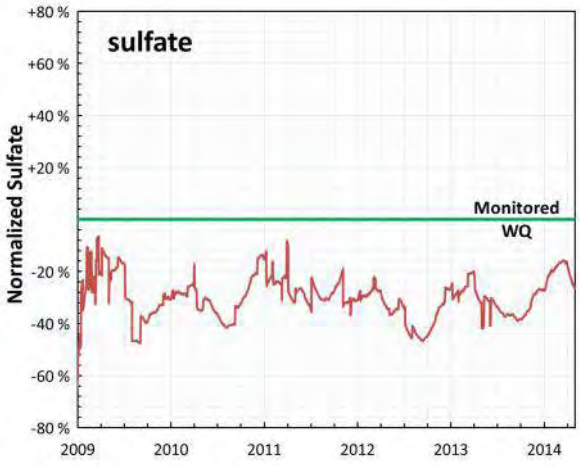

Figure 7 Simulated sulfate concentrations normalized to monitored concentrations at the EWRD, Antamina

CONCLUSIONS

This report outlines the infrastructure of the TSF IWBWQM and testing that has recently been conducted to check the mechanisms and controls within the model. The model is based primarily on site observations and fundamental geochemical principles: monitored water qualities are used provide the provisional model calibration and the water balance and water quality components of the model are continually updated as more information becomes available. Testing of the TSF IWBWQM has shown that the simulated water quality is within 20 % of that monitored at the mine site. The simulated TSF is closely calibrated with water balance data provided by Antamina.

Comparison with hydrogeochemical modelling programs, such as PHREEQC, shows that the TSF IWBWQM is operating as predicted by these programs. Nevertheless, the mechanisms built into the model are continually revised (with the aid of programs such as PHREEQC) to optimise the performance of the model. It is expected that this process will continue.

This paper has focused on the TSF facility at Antamina, but the mine site provides an ideal setting to test the application of the model to other facilities. Here we show examples applied to the East Waste Rock Dump.

ACKNOWLEDGEMENTS

Thanks are extended to all of the field technicians and staff for their hard work in data collection. Without their diligence, this model would not have the inputs and trends to support its calibration. We would like to acknowledge the collaborative efforts of UBC and the many consultants who have provided supporting studies to aid modelling of the various systems.

REFERENCES

Bethke, C M (2008) *Geochemical and Biogeochemical Reaction Modelling*, Cambridge University Press, pp. 547.

Blowes, D W and Ptacek, C J (1994) Acid-neutralization mechanisms in inactive mine tailings. In: Blowes, D W and Jambor, J L (eds). *The environmental geochemistry of sulfide mine-wastes*, 22, Short Course handbook: Waterloo, mineralogical association of Canada pp. 271-292.

Harrison, B, Aranda, C, Sanchez, M and Vizconde, J (2012) Waste Rock Management at the Antamina Mine Overall Strategy and Data Application in the Face of Continued Expansion. In: *Proceedings of the 9th International Conference on Acid Rock Drainage (ICARD)*, May 20-26, 2012, Ottawa, Ontario, Canada.

Strand, R, Usher, B, Strachotta, C and Jackson, J (2010) Integrated water balance and water quality modelling for mine closure planning at Antamina. In *Proceedings of the 5th International Conference on Mine Closure*, Nov 23-26, 2010, Viña del Mar, Chile.

Parkhurst, D L and Appelo, C A J (1999) User's guide to PHREEQC (Version 2): a computer program for speciation, batch-reaction, one-dimensional transport, and inverse geochemical calculations. U.S. Geological Survey: Earth Science Information Center, Open-File Reports Section [distributor], *Water-Resources Investigations Report* 99-4259, xiv, 312 pp.

Leachability of Suspended Particles in Mine Water and Risk of Water Contamination

Elvis Fosso-Kankeu[1], Frans Waanders[1], Antoine Mulaba-Bafubiandi[2] and Sibusio Sidu[3]

1. *School of Chemical and Minerals Engineering, North West University, South Africa*
2. *Minerals Processing and Technology Research Center, University of Johannesburg, South Africa*
3. *Gold One International Limited, South Africa*

ABSTRACT

Water released from underground mine fissures is either pumped at the surface or accumulates in ponds underground. Fine particles of ore suspended in such solutions are susceptible to weathering under environmental conditions or through the effect of indigenous autotrophic microorganisms living in the ore. The leachability of the suspended solids determines the risk of water contamination underground and at the surface as well as the need of a pretreatment process. In this work environmental conditions are partly considered, as aggressive methods are also used for leaching. Water samples collected underground and at the surface of a mine, were filtered and the suspended particles were separated from the solution through filtration and analyzed by SEM-EDS, XRD and XRF. The solid was leached under simulated environmental conditions or ultrasonic acid digestion at various temperatures. The metal mobility test was carried out according to the German standard Norm DIN 19730. The XRD analysis revealed the presence of iron sulfide (pyrite) in underground samples and iron oxides (maghemite and mackinawite) and zeolite in samples collected at the surface, while the SEM-EDS and XRF results showed the presence of trace elements such as chrome, titanium, calcium, zinc, nickel, manganese, lead, copper, cobalt and magnesium. The amount of mobilized metals detected by ICP analysis indicates that the metal could be released from the suspended solids, however, further investigations are required to determine the extent and rate of metal leaching under environmental conditions.

The natural weathering of the suspended solids is possible and this could therefore contribute in the degradation of water quality by decreasing the pH and increasing metal concentration; this implies that pretreatment of mine water is required to mitigate the risk of contamination of water sources.

Keywords: Mine water, suspended particles, metal mobility, leachability, underground and surface waters

INTRODUCTION

Mining of ore as well as recovery of metals and other resources from the ores using mineral processing and hydrometallurgical processes generally results in the accumulation of suspended particle matters (SPM) also referred to as fluid fine mineral tailings. These particles often contain sulfide minerals which, if not properly stored can be oxidized, resulting in the formation of acid mine drainage (AMD), usually containing high concentrations of dissolved potentially toxic elements (PTE) and sulfate (SO_4^{2-}). According to several authors (Bird et al., 2008; Fuge et al., 1991; Allan, 1988; Helgen and Davis, 2000; Miller et al., 2007), the release of contaminant metals into the fluvial environment within mining-affected river catchments generally results from (1) acid mine drainage, (2) the release of waste slurries containing solute and particulate-associated metals, (3) dumping of mining and milling waste that is subsequently leached or dispersed downstream. Interaction of ground water and surface water with the suspended particle matters will result in the mobility of the trace elements from the solid phase after a time often determined by environmental conditions. Depending on the hydrogeochemical environment, the dissolution of SPM may give elevated concentrations of the trace elements and create potential contamination of associated ground water and surface water systems. The oxidation of sulfide minerals such as pyrite, chalcopyrite, arsenopyrite and pyrrhotite, will eventually result in the dispersion overtime of large amount of toxic metals into the ecosystem impacting the freshwater resources. From such sources, metal can easily move along the food chain causing genotoxicity among living organisms (Patra et al., 2004).

This study focuses on the investigation of the leachability of suspended particles in water from underground mine fissure and tailing ponds.

METHODOLOGY

Sampling

Water was collected from underground mine fissures and from tailings ponds at the surface. Suspended particles were collected from water samples by filtration through filter paper (Whatman 150 mm, Cat No 1440 150). The recovered suspended solid was dried at 50°C in the oven until constant weight.

Characterization of suspended particles

The suspended solid samples were ground in a mortar and for the determination of the mineralogical phase, they were subjected to X-ray diffraction (XRD) analysis using the Philips model X'Pert pro MPD, at a power of 1.6 kW used at 40 kV; Programmable divergence and anti-scatter slits; primary Soller slits: 0.04 Rad; 2θ range: 4-79.98; step size: 0.017°. The proportion of elements in the suspended solids was determined by X-ray fluorescence (XRF) using the MagiX PRO & SuperQ Version 4 (Panalytical, Netherland); a rhodium(Rh) anode was used in the X-ray tube and operated at 50 kV and current 125 mA; at power level of 4 kW.

Scanning Electrom Microscopy (SEM)

A FEI Quanta 200 ESEM Scanning Electron Microscope, integrated with an Oxford Inca 400 energy dispersive x-ray spectrometer was used for the analysis of the suspended particles.

Leaching experiments

The suspended solid samples were submitted to batch leaching with three different approaches aiming to test the mobility and rate of release of elements from the three suspended solid samples. The aggressive test using aqua regia aimed to approximate total metals not associated with silicate. In all experiments, about 0.1 g of samples was leached with 10 ml of lixiviant.

Leaching with synthetic acid rain

The Eastern Transvaal Highveld is the area in South Africa where large metal working industries and coal burning power stations are located; in this particular area acid rain can occur at an average pH of 4.2. To simulate the natural lixiviant, synthetic acid rain (SAR) was prepared by diluting the mixture of H_2SO_4 and HNO_3 to a pH of 4.2; this solution (SAR) was used in batch leaching at room temperature. Leaching was performed with simultaneous shaking on horizontal at a speed of 150 rpm and six shaking periods: 1, 2, 3, 4, 7 and 24 hours; a long term leaching test was performed without shaking over a period of nine weeks (simulation of environmental conditions).

Metal mobility test

The mobility of the elements was measured on the basis of the procedure described in the German Norm DIN 19730 (Deutsche-Norm DIN, 19730, 1997). The suspended solids were leached in deionized water without subsequent change of pH for 2 h at constant shaking speed of 20 rpm and at room temperature (~20°C).

Ultrasound assisted acid digestion method

To maximize the extraction of elements from the suspended solids, the leaching was performed using aquaregia; the mixtures in 250 ml flasks were immersed into the ultrasonic water bath and subjected to ultrasonic energy of 35 KHZ for 20 min. The three temperatures of the ultrasonic water bath considered were 30, 50 and 70°C.

ICP analysis

After the leaching process, the sample from each of the above test was collected into a 50 ml centrifuge tube, then centrifuged at 4000 rpm for 20 min and the supernatant carefully recovered without disturbing the pellet. The metal content of the supernatant was analyzed using the ICP-OES (ICP Expert II, Agilent Technologies 720 ICP-OES).

Leachability of elements

The leachability of an element was calculated by considering the approximate total metal (expressed in leached amount) and the percentage leached value for the element.

The leached amount was calculated using the following equation:

$$Ca = CL \times VL/S \quad (1)$$

Where Ca is the leached amount of an element in mg/g; CL is the concentration of an element in the leachate in mg/L; VL is the volume of the leachate in L, S is the mass of the suspended solid in g.

The percentage leached was calculated using the following equation.

$$Cp = Ca/Csp \times 100 \quad (2)$$

Cp is the percentage leached in %; Csp is the total concentration of an element in the suspended solid, estimated by XRF analysis.

RESULTS AND DISCUSSION

The susceptibility of suspended solids from mine ponds to release metals in the environment is investigated in this study with consideration of natural or environmental conditions impacting on the leachability of metals. **Minerals and elements in the suspended particles**

The chemical characteristic of the suspended particles may determine the rate of reaction with the lixiviant. The mineralogical composition as determined by the XRD showed (Table 1) higher content of pyrite (FeS_2) in underground suspended particles (SP). It is assumed that the lower content of pyrite in surface SP is associated with longer exposure to weathering and dissolution of pyrite, hence the presence of iron oxides such as maghemite and mackinawite. The zeolite was identified only in surface samples (B and C), while quartz (SiO2) was abundant in all the SPs.

Table 1 Mineralogical composition (XRD) of the suspended solids samples

Sample A		Sample B		Sample C	
Phase name	**Wt %**	**Phase name**	**Wt %**	**Phase name**	**Wt %**
Pyrite	12.74	Silicon Oxide	17.67	Calcium silicate	19.31
Potassium Iron Oxide	33.55	Clinoptilolite	27.46	Zeolite	12.59
Silicon Oxide	26.59	Mackinawite	24.42	Silicon Oxide	16.86
Magnetite	27.11	Maghemite	30.45	iron(III) oxide	24.45
				Iron Sulfide	26.79

Based on the consideration of Price et al. (1997), the above table shows that there will be negligeable clay or carbonate minerals neutralisation potential.

The SEM-EDS analysis (Figure 1) shows the abundance of elements such as Fe, Si, Ti, Cr, Al, K, Mg and S in all the samples which can be correlated to the presence of pyrite and aluminosilicates as revealed by the XRD results; the element composition was confirmed by XRF results in Table 2.

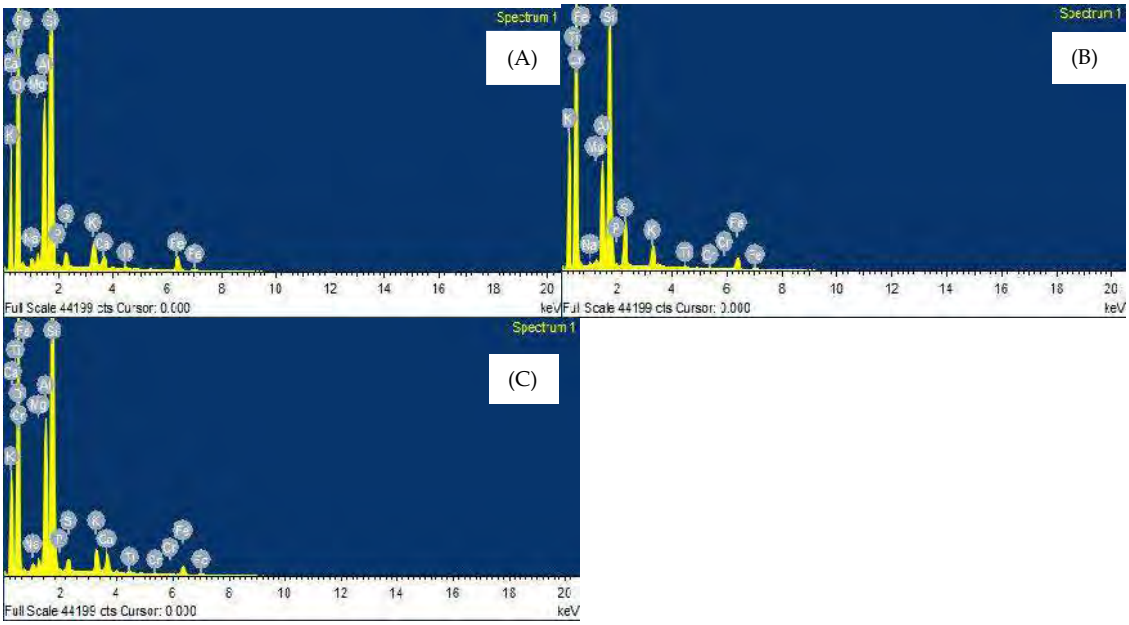

Figure 1 SEM-EDS analysis of suspended particles

Table 2 Chemical composition of suspended particles

Elements	Mass %		
	A	B	C
Na_2O	0.24	0.82	0.94
MgO	0.37	1.65	1.73
Al_2O_3	10.70	18.65	20.11
SiO_2	67.50	63.56	61.40
P_2O_5	0.07	0.06	0.06
SO_3	9.05	2.78	2.88
K_2O	3.09	2.83	3.37
CaO	0.07	4.04	2.55
TiO_2	0.50	0.65	0.64
Cr_2O_3	0.24	0.17	0.19
MnO	0.02	0.07	0.06
Fe_2O_3	7.82	4.28	5.69
Co_2O_3	nd	0.01	0.01
NiO	0.03	0.03	0.03
CuO	0.01	0.01	0.02
ZnO	0.01	0.05	0.09
As_2O_3	0.12	0.03	0.04
Rb_2O	0.01	0.01	0.01
SrO	0.01	0.02	0.02
ZrO_2	0.05	0.04	0.03
BaO	nd	0.06	0.07
PbO	0.06	0.02	0.03
U_3O_8	0.03	0.01	nd

The Fe enrichment of the SPs is associated with Fe-rich sulfides and Fe oxides as observed with XRD analysis (Table 1) and also reported in the mine residues such as tailings (Hochella et al., 1999; CourtinNomade et al., 2003).

Mobility of elements under environmental conditions

The percentages of Al, Fe, Mn, Ni, Sr, Zn and Cr leached from the samples (A, B and C) are plotted in Figures 2a and b which correspond to metal release by long term leaching (simulation of environmental conditions) and mobility test, respectively. It is observed that the metals are easily leached from the SPA which has acidic tendency as revealed by the decrease of pH after nine weeks contributing to dissolution of the mineral. Furthermore the presence of zeolite in surface samples (B and C) reduces the mobility of metals due to its cation exchange and molecular sieving properties; it is reported (Jiwan et al., 2013) that zeolite if often used to reduce the leachability of metals in compost. The long term leaching was carried out without stirring in synthetic acid rain (SAR) which are similar to environmental conditions. The mobility test is carried out at the same pH as the original solution of the SP and could therefore reflect the dissolution likely to occur in mine water at the site; it is observed that (Figure 2B) under such condition all the metals were mobilized from the SPA and only Mn, Sr and Zn from SPB and SPC; overall Fe, Ni, Sr and Zn were found to be the elements with higher leachability.

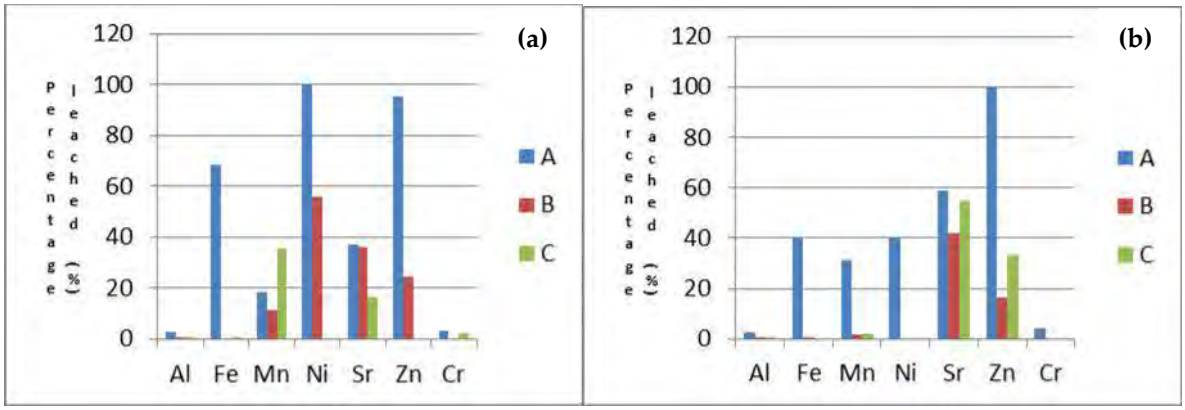

Figure 2 Percentage leached of metals from suspended particles following (a) long term leaching and (b) mobility test

To better understand the leachability of the element the correlation of their mobility and their concentrations in the SPs was evaluated; as shown in Table 2, the values of the coefficient of determination (R^2) were relatively low, implying very little correlation, therefore the mobility of the element is not strictly related to its concentration in the SP, similar results have been reported by Jankowski et al. (2006). Except for Fe and Zn, there was no obvious correlation between mobility of element and the long term leaching; trace elements may exist in different oxidation states in mineral matters and therefore respond differently to leaching (Wadge et al., 1987; Jackson and Miller, 1998).

Table 2 Correlation between mobility of elements, total concentration of elements and long term leaching

Elements	Mobility vs Total concentration	Mobility vs long term leaching
Al	-0.9792	0.9304
Fe	0.834	0.9998
Mn	0.9326	-0.4852
Ni	-0.8992	0.944
Sr	0.6583	-0.9435
Zn	0.74	0.99
Cr	0.9346	0.7551

This also implies in our study that the dissolution of the metal is mostly dependent on the chemical reactions given the distinctiveness with regard to the mineralogical composition of the samples.

Leachability of elements from suspended particles

Environmental monitoring often requires the determination of metal content of suspended particles, but most importantly the susceptibility of release by dissolution. Figures 3a, b and c below show the percentage of Al, Fe Mn, Ni, Sr, Zn and Cr released through ultrasonic digestion of SPs. The predominant factor during such leaching approach is the temperature which increased the reactivity between the lixiviant and the SP, but also important in this case, a very aggressive lixiviant namely aqua regia was used to ensure the maximum extraction of the metal from the SPs. This test is basically conducted to detect elements which can be a drainage chemistry concern but is not a direct measure of their threat to the environment (Price et al., 1997). It is observed that irrespective of the temperature, approximately all the metals were extracted from the SPs. The impact of temperature is however noticeable as for metals such Al, Sr and Cr there is significant increase of percentage of metal leached with increase of temperature.

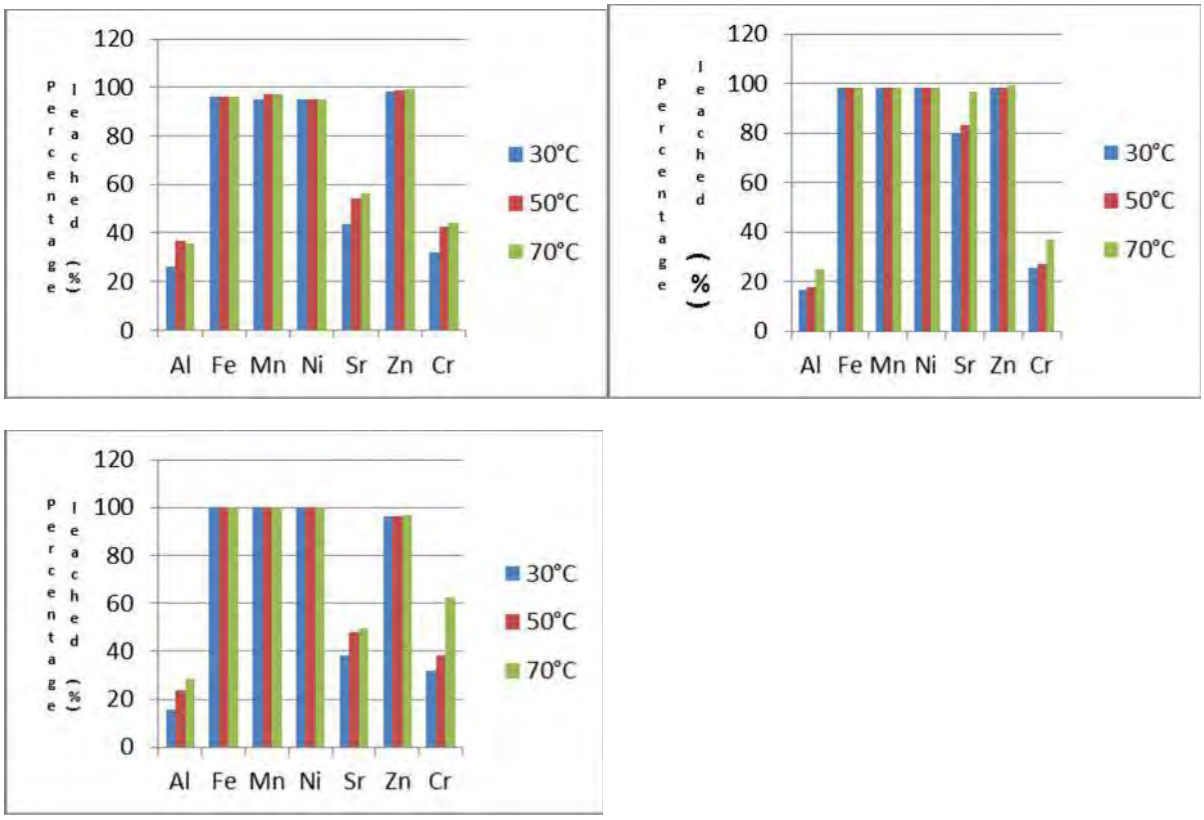

Figure 3 Percentage leached metals from ultrasonic assisted acid digestion of suspended particles

Maximum recovery close to 100% was achieved in most cases for Fe, Mn, Ni and Zn; Kazi et al. (2000) have also reported similar percentage recovery using ultrasonic acid assisted digestion for the recovery of Cd, Cr, Ni and Pb. This result indicates that weathering of the suspended particles over a relative long period of time will likely result in the release of most of the metals into the environment resulting in the pollution of water sources.

CONCLUSION

The suspended particles studied contained several metals in relatively high amounts with regard to environmental impact. The suspended particles collected underground were more likely to release the metals, the SP mineralogical propertyy is therefore and important parameter determining the mobility of the metals. The methods of metal extraction considered indicate that these metals will be released at various rates in the water system after short or long period of time. However, environmental conditions being only partly considered, the data could not be used for exact prediction of actual leachability at the mine site.

ACKNOWLEDGEMENTS

The authors are grateful to the contribution of Ms N Baloyi and Mr E Malenga from the Laboratory of Extraction Metallurgy at the University of Johannesburg; Mr G Van Rensburg from the Laboratory of Mineral Processing in the School of Chemical and Minerals Engineering – North-West University.

REFERENCES

Allan RJ. 1988. Mining activities as sources of metals and metalloids to the hydrosphere. In: Strigel G. (Ed.), Metals and Metalloids in the Hydrosphere: Impact Through Mining and Industry, and Prevention Technology. UNESCO, Paris, pp. 45 – 67.

Bird G, Brewer PA, Macklin MG, Balteanu D, Serban M, Driga B, Zaharia S. 2008. River system recovery following the Novat-Rosu tailings dam failure, Maramures County, Romania. Applied Geochemistry. 23: 3498 – 3518.

Courtin-Nomade A, Bril H, Neel C, Lenain J-F. 2003. Arsenic in iron cements developed within of a former metalliferous mine-Enguiales, Aveyron, France. Appl. Geochem. 18: 395 – 408.

Fuge R, Laidlaw IMS, Perkins WT, Rogers KP. 1991. The influence of acidic mine and spoil drainage on water quality in the mid-wales area. Environ. Geochem. Health. 13: 70 – 75.

Helgen SO, Davis A. 2000. Quantifying metal contributions from multiple sources to the Clark Fork River, Montana, USA. J. Environ. Forensics. 1: 55 – 62.

Hochella MFJr, Moore JN, Golla U, Putrus A. 1999. A TEM study of samples from acid mine drainage systems: metal-mineral association with implications for transport. Geochim. Cosmochim. Acta. 19/20: 3395 – 3406.

Jackson BP, Miller WP. 1998. Arsenic and selenium speciation in coal fly ash extracts by ion chromatography-inductively coupled plasma mass spectrometry. J. Anal. Atom. Spectrom. 13: 1107-1112.

Jankowski J, Ward CR, French D, Groves S. 2006. Mobility of trace elements from selected Australian fly ashes and its potential impact on aquatic ecosystems. Fuel. 85: 243 – 256.

Kazi TG, Jamali MK, Arain MB, Afridi HI. 2000. Evaluation of an ultrasonic acid digestion procedure for total heavy metals determination in environmental and biological samples. Journal of Hazardous Materials. 161: 1391-1398.

Patra M, Bhowmik N, Bandopadheyay B, Sharma A. 2004. Comparison of mercury, lead and arsenic with respect to genotoxic effects on plant systems and the development of genetic tolerance. Environ. Experimental. Bot. 52: 199 – 223.

Price WA, Morin K, Hutt N. 1997. Guidelines for the prediction of acid rock drainage and metal leaching for mines leaching in British Columbia: Part II. Recommended procedures for static and kinetic testing. Fourth International Conference on Acid Rock Drainage. Vancouver, B.C. Canada. May 31 – June 6, 1997.

Wadge A, Hutton M. 1987. The leachability and chemical speciation of selected trace elements in fly ash from coal combustion and refuse incineration. Environ. Pollution. 48: 85-99.

Release of Explosives Originated Nitrogen from the Waste Rocks of a Dimension Stone Quarry

Teemu Karlsson and Tommi Kauppila
Department of Land Use and Environment, Geological Survey of Finland

ABSTRACT

Emissions of nitrogen compounds, including $NH4^+$, $NO3^-$ and $NO2^-$, from mining areas can have detrimental effects on the environment through either eutrophication or direct toxicity. Besides environmental effects, contamination by nitrogen originated from explosives may be problematic, depending on definitions and classifications of inert waste. In certain jurisdictions, nitrogen contamination of otherwise mineralogically and chemically inert waste rocks of good technical quality may hinder utilization of these product streams. This is an important economic and environmental issue, especially at dimension stone quarries.

To study the amount of nitrogen contamination in waste rocks produced by these types of quarrying operations, two 1 m^3 lysimeters were installed at a selected quarry. The test units were filled with fresh waste rock immediately after the excavation of a block of dimension stone. The rainwater flowing through the test units was collected in separated plastic tanks and sampled regularly over a one year period.

The results indicate that the "first flush" of recharge water occurs rapidly, only after a few weeks, after which the nitrogen drainage settles to near natural rainwater levels. Calculations on the amount of nitrogen leached out of the test units and the remaining nitrogen detected on the rocks after the monitoring period suggest that a little more than half of the explosive residuals had remained within the waste rock material. The total amount of nitrogen derived from explosives in the waste rock material at a dimension stone quarry seems to be in the order of 0.1 mg/kg, which is well below the amounts commonly detected in waste rocks produced by larger scale mines and thus indicate that the environmental risks associated with these type of waste rocks are relatively low.

Keywords: Explosives, nitrogen, waste rock, dimension stone

INTRODUCTION

The presence of nitrogen compounds in mining areas can have detrimental effects on the environment through eutrophication or direct toxicity (Forsyth et al. 1995). Use of explosives is one of the main sources of nitrogen emissions in the mining industry (Morin & Hutt 2009). Besides environmental effects, contamination by nitrogen compounds derived from explosives may be problematic due to varying definitions and classifications of inert waste. Nitrogen contamination of otherwise mineralogically and chemically inert waste rocks of good technical quality may hinder the utilization of these product streams, which is an important economic and environmental issue at several quarries and mines.

To study the rate of dissipation and amount of nitrogen contamination on waste rock surfaces and to investigate the reactivity of the materials, a long term field study was conducted at a selected quarry.

METHODOLOGY

The study area was a dimension stone quarry located in Varpaisjärvi in the Lapinlahti municipality in the region of Northern Savonia (Figure 1).
The main stone extracted at the selected quarry is black diabase, with an average density of 3 080 kg/ m^3. The total amount of extraction is approximately 28 500 m^3/year, of which around 24 000 m^3 i.e. 73 920 tons is waste rock. The use of explosives, mainly nitroglycol and diatomite containing K-pipecharges by Forcit Oy, is roughly 5 700 kg/year, the specific charge (powder factor) being around 0.065 kg / t. The average nitrogen concentration of K-pipecharge is 4.2 % (Forcit Oy 2013). The water resistance of K-pipecharges is reasonable, but the unexploded agent dissolves gradually into water. The waste rocks consist mainly of the same diabase material as the final products.

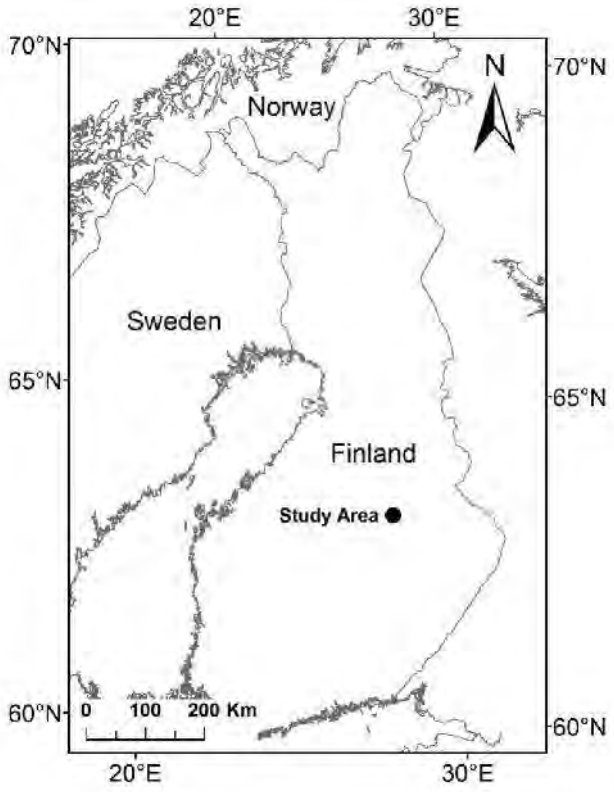

Figure 1 The test site (a dimension stone quarry) is located in Varpaisjärvi in the Northern Savonia region of Finland

To evaluate the temporal changes in the quality of water emanating from waste rock produced by the quarry, two lysimeters were installed at the quarry site, and filled with waste rock material collected immediately after the excavation of a large diabase block. The rock material in both lysimeters was identical and the purpose of setting up two units was to examine the repeatability of the test. Unit 1 contained approximately 1 970 kg of rocks with 38 % porosity, and Unit 2 contained approximately 1 790 kg of rocks with 44 % porosity. The test units are shown in Figure 2.

The rain water flowing through the lysimeters was collected in separate 70-liter plastic tanks and analysed frequently, 9 times in total, between the 10th of October 2012 and the 16th of October 2013, excluding the winter months when the test units were frozen. The sampling interval was 2 weeks during the first month and once a month during the rest of the monitoring period.

The monitored parameters included nitrogen species ($NO2^-$, $NO3^-$, $NH4^+$ and total-N), Cl^-, pH, Ec and temperature. Chloride (Cl^-) is present in rock dust and in the blasting residuals (as sodium chloride) and is considered as a good indicator of the first flush of water through the test units (Bailey et al. 2013).

At the end of the observation period, the test units were filled (washed) with tap water and sampled three times (Unit 2 only once) to remove the remaining nitrogen of explosive origin and to determine the porosity and approximate weight of the rocks inside the test units. The chemical composition of the tap water used for washing was analyzed as well.

Figure 2 The aging test units 1 (front) and 2 (behind). The rain water flowing through the units was collected in the green plastic tanks below. Photo: Lauri Solismaa / GTK

Field measurements and sampling

The untreated samples were collected into HDPE sample bottles that had been triple-rinsed with sample water. The sample bottles were sent to the laboratory in a cool box during the sampling day. The samples arrived at the laboratory next morning and were analysed as soon as possible, to minimize the alteration of the samples, especially the sensitive $NO2^-$.

The pH, temperature, electric conductivity, nitrite and ammonium were measured in the field. The pH was measured by the Mettler Toledo SevenGo pH-meter. The electrical conductivity and temperature were measured with the WTW-electric conductivity meter Cond 340i. The nitrite and ammonium concentrations were analyzed with a portable Hach Lange DR2800 spectrophotometer using Lange cuvette tests LCK342 (0.6-6 mg/l NO2-N) and LCK 304 (0.015-2 mg/l NH4-N). The amount of rain water accumulated in the tanks was measured and the tanks were emptied after every sampling occasion.

Besides field measurements, the nitrogen species were also analysed in a laboratory to estimate the accuracy of the spectrophotometric measurements and to investigate the effects of transportation of the water samples to the laboratory. The results seemed to be similar with both methods although the portable spectrophotometer gave lower concentrations when the weather was colder.

Laboratory measurements

The laboratory measurements included total nitrogen, nitrite, nitrate and chloride in an accredited laboratory (Labtium Oy). The $NO2^-$ was measured by spectrophotometry. The anions $NO3^-$ and Cl^- were measured using ion chromatography (IC) according to the standard SFS-EN-ISO 10304-1. $NH4^+$ was measured by the Aquakem analysator (salicylate-spectrophotometric method). Total nitrogen was measured by the peroxosulphate oxidation and Aquakem analysator (hydrazine reduction and spectrophotometric sulphanilamide method).

RESULTS AND DISCUSSION

The monitored concentrations and values followed similar trends in both test units, but the concentrations were somewhat lower in Test Unit 2. At first the electric conductivity and concentrations, e.g. of total-N and Cl^- were relatively high, but declined rapidly to the average local rain water values after the "first flush" (Figure 3). Cl^- declined more sharply and remained low for the remainder of the study. The nitrogen concentrations were more erratic, but the absence of Cl^- suggests that most of the nitrogen was delivered from rain water / atmosphere.

The most abundant nitrogen species was NO3-N, around 60 % of the total first flush N concentration. The NH4-N concentrations were relatively high during the first flush, around 40 % of the total N. Later, the proportion of the NO3-N increased to 67 – 94 % and the proportion of NH4-N decreased to 1 – 9 %. The field measurement values of $NH4^+$ and $NO2^-$ were mainly higher than those measured in laboratory, which may indicate the instability of these nitrogen species during transport.

The total-N concentrations in rainwater have been measured by the Finnish Environment Institute (SYKE) at the nearest weather station at Maaninka (about 40 km south west from Varpaisjärvi) during 2004 – 2012. The rainwater samples collected at the test units at Varpaisjärvi had similar total-N concentrations to Maaninka, around 0.6 mg/L. During two observation periods (30th of April 2013 and 20th of August 2013) the rainwater tanks were full and probably overflowed.

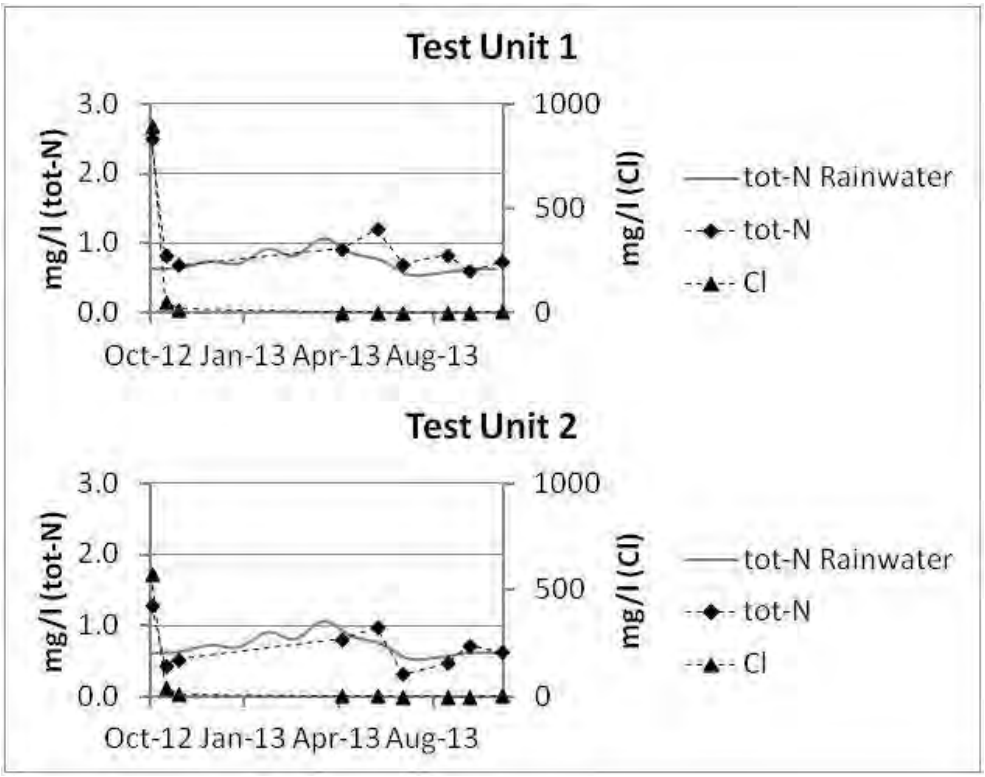

Figure 3 Total-Nitrogen and Chloride concentrations in the recharge waters of the Test Unit 2 and total-N of rainwater in Maaninka (monthly averages during the years 2004-2012) measured by the Finnish Environment Institute

The amount of water required to fill the Unit 1 was 380 litres and 440 litres for the Unit 2 (i.e. the porosities were 38 % and 44 %). The rock masses of the units were calculated by the volume and density of the diabase (in Unit 1 approximately 1 970 kg and in the Unit 2 approximately 1 790 kg).

The amounts of total nitrogen released from the test units were calculated by multiplying the amounts of water (litres) by the nitrogen concentrations (Table 1). The nitrogen concentrations of the first flush were determined by subtracting the background value (0.6 mg/L in October) from the measured concentrations. The first flush includes the first samplings in October 2012 when the concentrations were higher than the background values of rainwater (Unit 1 10th October 2012 and 25th October 2012, Unit 2 only 10th October 2012).

The amount of nitrogen originating from explosives was detected in Test Unit 1 was 138.8 mg i.e. 0.07 mg/kg Waste Rock and 32.5 mg i.e. 0.02 mg/kg Waste Rock in Test Unit 2. About half of the total nitrogen seemed to be left in the test units after one year of ageing. Presumably some traces of explosive nitrogen were also released after the first flush, but the nitrogen concentrations were so close to the average rain water values that assessment of exact numbers is difficult. Some small residual amounts probably also remained in the stone material after washing. Considering the uncertainty factors, the amount of nitrogen derived from explosives in the type of rock material used in this study is around 0.1 mg/kg or 0.1 g/t. Multiplying this by the annual average amount of waste rocks (24 000 m^3 i.e. 73 920 t) remaining at the test site results in blasting-related nitrogen load of around 7.4 kg/year from the waste rock pile.

Table 1 The amounts of total nitrogen released from the test units during first flush and washing. *NH4-N + NO2-N concentrations.

Sample	tot-N (mg/L)	Water (L)	Released N (mg)
Test Unit 1			
10.10.2012	1.9	28	53.2
25.10.2012	0.2	48	9.6
1st wash	0.1	380	38
2nd wash	0.1	380	38
3rd wash	0.0	380	0
Total N			**138.8**
Test Unit 2			
10.10.2012	0.7	27.5	19.3
1st wash	0.03*	440	13.2
Total N			**32.5**

Lysimeters used in this study were relatively small scale compared with the size fractions of normal waste rock material, which introduces a bias to the test setup. In addition, the residuals of explosives are heterogeneously distributed in a waste rock material as demonstrated by the differences between the test units. The rock material in the test units presented a ”worst case”; real waste rock contains also larger boulders, so it has less surface area / kg (= less explosives-N / kg)

than the finer material in the test units. This indicates that in practice, the amount of leaching from the waste rock material should be less.

Waste rocks produced by the natural stone industry seem to contain less explosives originated nitrogen than waste rocks produced by larger mining activities. For example waste rock at the Diavik diamond mine in Canada contains tot-N around 4.6 mg/kg (Bailey et al. 2013) and ore and waste rocks at the Kemi chromium mine around 20 mg/kg (Mattila et al. 2007).

The leaching tests conducted in this study apply to the K-pipecharge explosives used at the test quarry, which contain relatively low amounts of nitrogen, about 4.2 %. Different types of explosives exist for different purposes and their nitrogen contents and solubilities may vary. In general, the nitrogen content of different rock blasting explosives varies between 20 – 30 % of total weight (Chloth 2011).

CONCLUSIONS

Based on the observation period of more than a year the "first flush" of nitrogen occurs rapidly, during the first few weeks (or first rain events), after which the nitrogen drainage settles to natural rainwater levels. Based on the current results, the first flush removes approximately half of the total nitrogen, mainly in NO3-N and NH4-N forms.

Calculations on the nitrogen leached out of the test units during the observation period and the remaining nitrogen detected on the rocks after the test period indicate that some residuals of explosives remain within the test material. The remaining nitrogen is leached out fairly slowly, promoting loss to the atmosphere.

The two seemingly identical units had different nitrogen concentrations, which suggest that the undetonated explosives are heterogeneously distributed in a waste rock pile.

The total amount of nitrogen derived from explosives in the waste rock material of a dimension stone quarry seems to be on the scale of 0.1 mg/kg, which is well below the amount detected in waste rock produced by larger scale mines. The main reason for the difference is probably the moderate use of low nitrogen containing explosives in natural stone quarrying.

As the nitrogen contamination of dimension stone quarrying waste rock is relatively low to begin with and enhanced by the rapid flushing by rainwater, the residues of explosives should not be considered to prevent the utilization of otherwise mineralogically inert waste rocks of good technical quality.

ACKNOWLEDGEMENTS

This study was conducted as a part of the Finnish Green Mining project MINIMAN, which concentrated on the behaviour of nitrogen compounds in mining environments, and developing technologies for management of nitrogen discharges. The research project was realized during the years 2012-2014 as a cooperative project between the Geological Survey of Finland (GTK), Technical Research Centre of Finland (VTT) and Tampere University of Technology (TTY) together with several industrial and international partners.

REFERENCES

Bailey, B., Smith, L.J.D., Blowes, D., Ptacek, C. Smith, L., Sego, D. 2013. The Diavik Waste Rock Project: Persistence of contaminants from blasting agents in waste rock effluent. Applied Geochemistry 36 (2013) pp. 256-270.

Chlot, S 2011. Nitrogen effluents from mine sites in northern Sweden: nitrogen transformations and limiting nutrient in receiving waters. Licentiate thesis, Luleå tekniska universitet, Luleå. Licentiate thesis / Luleå University of Technology

Forcit Oy 2013. K-pipecharge / KK-pipecharge Product information version 02.04.2013.

Forsyth, B., Cameron, A. and Miller, S. 1995. Explosives and water quality. Sudbury '95, Mining and the environment, Sudbury Canada. pp. 795-803.

Mattila, K., Zaitsev, G., Langwald, J. 2007. Biological removal of nutrients from mine waters. Final report. Finland. Finnish Forest Research Institute

Morin, K. and Hutt, N. 2009. Mine-Water Leaching of Nitrogen Species from Explosive Residues. Proceedings of GeoHalifax 2009, the 62nd Canadian Geotechnical Conference and 10th Joint CGS/IAH-CNC Groundwater Conference, Halifax, Nova Scotia, Canada, September 20-24, pp. 1549-1553.

Predicting Water Quality for a High Altitude Mine Waste Facility in Peru

C. James Warren[1], Dawn Kaback[2] Gokhan Inci[2] and Daniel Neff[3]
1. AMEC Foster Wheeler Environment & Infrastructure, Canada
2. AMEC Foster Wheeler Environment & Infrastructure, USA
3. M3 Engineering and Technology Corporation, USA

ABSTRACT

AMEC Environment & Infrastructure (AMEC) was retained by M3 Engineering and Technology Corporation (M3) to provide an assessment of the acid rock drainage and metals leaching potential (ARD/ML) of waste rock and ore to be produced at an open pit copper mine located at high elevation (3,000 – 4,500 masl) in Peru. The mine is expected to produce about 573 Mt of ore for milling, 173 Mt of low-grade ore for heap leach, and about 1,360 Mt of waste rock over 25 years of operation. The current plan is to construct an on-site waste storage facility (WSF) by co-blending milled tailings with waste rock in an alpine valley. The WSF, which will also partially cover the heap leach residue pad located at the top of the valley, will contain underdrains directed to a single pond at the toe. Geochemical testing included analyses of 1000 samples from five major lithologies representing waste rock and ore for acid base accounting and content of total metals. Selected samples of waste rock, simulated tailings, and heap leach residue were submitted for mineralogical, humidity cell, and other geochemical testing. Geochemical results were modeled by considering the configuration of the WSF to predict water quality of the leachate at the toe. Leachate pH is expected to be mildly alkaline due to alkalinity generated primarily by the tailings. Although the heap leach residue is expected to contribute some acidity, alkalinity from the tailings will minimize the contribution. The results indicate that arsenic, chromium, mercury, and zinc may be of possible concern, requiring treatment prior to discharge.

Keywords: Tailings, Alpine, Waste Rock, Humidity Cells, ABA

INTRODUCTION

AMEC Environment & Infrastructure, a division of AMEC Americas Limited (AMEC), was retained by M3 Engineering and Technology Corporation to assess the acid rock drainage and metals leaching potential (ARD/ML) of waste rock and ore to be placed in a high elevation (3,000 – 4,500 masl) waste storage facility (WSF) in Peru. The WSF is designed to contain milled tailings from high-grade ore (573 Mt) co-blended with waste rock (1,360 Mt). The co-blended material is expected to partially cover a spent heap leach residue pad (total 173 Mt) when mining operations cease after 21 years. The WSF including the heap leach residue pad (total 2,106 Mt) will be located in an existing alpine valley with constructed underdrains directing leachate to a pond at the toe.

A geochemical testing program was conducted to enable prediction of potential water quality from the WSF to support mine planning activities. The objective of the program was to develop an integrated geochemical-hydrological loading model to predict water quality at the toe of the WSF using data derived from static and humidity cell testing of waste rock, simulated mill tailings, and heap leach residue as well as local meteorological data.

METHODOLOGY

Sample Selection

A total of 1000 samples were selected for static geochemical testing from available drill core from 205 diamond drill holes totaling 92,760 m spaced about 50 to 75 m apart. Preliminary estimates based on the block model for the mine identified six major rock types (lithologies) as listed in Table 1 with estimated proportions and number of samples selected for testing.

Table 1 Estimated Proportions of Major Identified Lithologies (Rock Types) and Sample Numbers

Lithology	Percentage of Waste Rock	WSF Weighted Proportion	Number of Waste Rock Samples	Number of High-grade Ore Samples	Number of Low-grade Ore Samples
Siltstone	18.2%	12.9%	178	13	4
Quartzite	32.1%	22.7%	494	49	24
Quartz Monzonite (fine-grained)	15.2%	10.7%	16	25	2
Quartz Monzonite (coarse-grained)	19.3%	13.6%	36	20	6
Feldspar-Megacrystic Quartz Monzonite (coarse-grained)	15.3%	10.8%	71	41	13
Monzodiorite	0.4%	Included	5	2	1
TOTAL	100.0%	100.0%	800	150	50

ABA Testing and Assay Database

The 1000 core samples were collected for acid base accounting (ABA) analyses to provide preliminary estimates for the potential acid generating (PAG), or non-PAG nature of the rock. Samples were analyzed for total sulfur, sulfate-sulfur, and pyritic-sulfur (sulfide-sulfur). Organic-sulfur was reported as the difference between total sulfur and the combination of the sulfate-sulfur

and pyritic sulfur. The Acid Generating Potential (AGP) was calculated based on sulfide analyses, whereas the. Acid Neutralization Potential (ANP) was determined following the State of Nevada Modified Sobek Procedure (2010). The potential for acid generation was assessed based on Neutralization Potential Ratio (NPR = ANP/AGP).

A metallurgical assay database for the 92,760 m of drill core, containing analyses for a total of 30,858 drill core samples, including concentrations of copper (Cu), molybdenum (Mo), iron (Fe), bismuth (Bi), antimony (Sb), arsenic (As), mercury (Hg), lead (Pb), and zinc (Zn), was reviewed to assess metal leaching (ML) potential prior to kinetic humidity cell testing.

In addition, composite samples representing simulated tailings and heap leach residue obtained from bench/pilot-scale metallurgical testing were submitted for the same ABA analyses used for waste rock and ore samples. The simulated tailings sample was derived from a blend of high-grade ore core samples and the simulated heap leach sample was derived from blended low-grade ore.

Humidity Cell Testing

Based upon results of static testing, kinetic testing (humidity cells) was initiated for nine of the waste rock samples and for single samples of simulated tailings and simulated heap leach residue obtained from bench/pilot-scale metallurgical tests. The nine samples of waste rock were selected to represent each major rock type (lithology), with two samples per lithology; one of either PAG rock (NPR<1) or uncertain (1<NPR<2) categories along with a non-PAG (NPR>2) sample from the same lithology. In addition, consideration was given to samples enriched in total contents of metals [copper (Cu), silver (Ag), molybdenum (Mo), bismuth (Bi), antimony (Sb), and arsenic (As)] based on assay analyses.

Humidity cell testing was conducted based on ASTM D5744-07 and EPA Method 1627. Testing for three of the nine waste rock samples was terminated after 20 weeks, because release rates of key parameters had stabilized. Humidity cell testing for the remaining six waste rock samples was continued for a total of 32 weeks. Humidity cell testing for the simulated tailings and heap leach samples was terminated after 20 weeks. Leachate samples were collected weekly for analysis of:

- pH, specific conductivity, total dissolved solids (TDS), alkalinity, and acidity;
- Concentrations of sulfate, chloride, fluoride, bicarbonate, and nitrate+nitrite nitrogen;
- Concentrations of calcium, magnesium, potassium, and sodium by inductively coupled plasma optical emission spectroscopy (ICP-OES); and,
- Concentrations of dissolved aluminum, antimony, arsenic, barium, beryllium, cadmium, chromium, copper, iron lead, manganese, mercury, nickel, phosphorous, selenium, silver, thallium, and zinc by inductively coupled plasma mass spectroscopy (ICP-MS).

Carbonate Analyses

The 11 humidity cell samples (nine waste rock, one simulated tailings and one simulated heap leach residue) were analyzed using a LECO C/S analyzer for (1) total carbon content and (2) carbon content of a subsample digested with hydrochloric acid to predict acid-insoluble carbon. The content of carbonate carbon (acid soluble carbon) was determined by difference and used to calculate carbonate NP. Although only a very limited number of samples were analyzed, the values were extrapolated to the remainder of the 800 sample waste rock database using linear regression to estimate carbonate NP for the entire waste rock database.

Other Analyses

The nine humidity cell waste rock samples were also submitted for X-ray diffraction using Rietveld refinement (RXRD) to provide a semi-quantitative estimate of mineral content. These waste rock samples and the two samples of metallurgical residues representing simulated tailings and heap leach residue were analyzed using the single addition net acid generation (NAG) test. On completion of humidity cell testing, the nine waste rock samples were submitted for particle size (grain size) analysis. Particle size data for composite bench/pilot-scale test samples were determined during metallurgical testing. Grain size analysis is typically used to estimate specific surface area of material in the humidity cells.

RESULTS AND DISCUSSION

Acid Base Accounting (ABA)

Methods for assessment of waste rock and ore as PAG or non-PAG vary depending on jurisdiction. As an initial PAG/non-PAG screening criterion for waste rock, MEND (2009) recommends NPR values greater than 2 to identify non-potentially acid generating (non-PAG) rocks; NPR values between 1 and 2 as having an uncertain acid-generating potential, requiring further testing for accurate assessment; and NPR values less than 1 as rock considered to be potentially acid generating (PAG). All samples with NPR values less than 2 are considered PAG until additional testing has been conducted. These criteria may also be applied to tailings; however, some jurisdictions recognize a lower NPR threshold for differentiating PAG and non-PAG tailings; however this requires site-specific studies. For this study, the MEND screening criteria (MEND, 2009) described earlier were applied to the ore/tailings as well as to the waste rock. It should be noted that the individual ore samples submitted for static testing were not subjected to metallurgical processing prior to analyses. The ABA characteristics and metal content of tailings derived from the ore could differ greatly from these analyses depending on the milling and heap leach processes. Average values for NPR, calculated from the ABA data (ANP/AGP) for the various lithologies where AGP is based on pyritic sulfur are summarized in Table 2.

Table 2 Proportion of 1000 Sample Database Based on NPR and Carbonate NPR (CNPR)

Lithology	Number of Samples	Sobek-NP		Avg.	Carbonate NP		Avg.
		NPR<2	NPR>2	NPR[1]	NPR<2	NPR>2	CNPR[1]
Low-grade Ore	50	48%	52%	1.8	72%	28%	0.6
High-grade Ore	150	48%	52%	1.4	79%	21%	0.4
Siltstone	178	14%	86%	2.8	22%	78%	1.1
Quartzite	494	20%	80%	1.6	56%	44%	0.2
Quartz Monzonite (fine-grained)	16	6%	94%	6.6	38%	63%	1.1
Quartz Monzonite (coarse-grained)	36	6%	94%	6.2	6%	94%	4.3
Feldspar-Megacrystic Quartz Monzonite	71	11%	89%	5.1	42%	58%	1.4
Monzodiorite	5	40%	60%	0.9	nd	nd	nd

Note: 1. Average for samples within a lithology or grade category
nd = not determined

Individually, the Siltstone, Quartz Monzonite (fine-grained), Quartz Monzonite (coarse-grained) and Feldspar Megacrystic Quartz Monzonite (coarse-grained) lithologies are non-PAG; collectively representing 67% of the waste rock. The Monzodiorite (<1% of the waste rock) was classified as PAG with an average NPR of 0.9, and the Quartzite (32% of the waste rock) was classified as uncertain with respect to ARD potential with an average NPR of 1.7. High-grade ore (feed stock for the mill) and low-grade ore (for use in the heap leach facility) had average NPR values of 1.4 and 1.8, respectively, indicating that the samples have uncertain ARD potential (1<NPR<2) with respect to the initial screening criteria. Overall, 52% of the ore samples were classified as non-PAG (NPR>2); 33% PAG (NPR<1) and 15% uncertain (1<NPR<2). Average values for Carbonate Neutralization Potential (CNPR) in Table 2 are discussed in the sections below.

Carbonate Carbon and NAG pH

The content of carbonate carbon for the nine waste rock humidity cell samples was used to calculate carbonate neutralization potential (CNP as $CaCO_3$ equivalent) for all samples in the database via linear regression. To calculate CNP, it is assumed that all neutralization potential (NP) is due to carbonate. For the waste rock and ore samples, CNP values represented between 15% and 70% of the Modified Sobek NP with an average of 26%. The values for carbonate content and the resulting carbonate NPR values (CNPR) show high variability with respect to acid generation potential and that the Quartz Monzonite (coarse-grained), Quartzite, and Feldspar-Megacrystalic Quartz Monzonite (coarse-grained) are either PAG (CNPR<1) or uncertain (1<CNPR<2) with respect to acid generation potential. Although the variability within each lithology (represented by only 2 samples each) was high, the CNPR values agreed with the NAG pH results. Comparison of NPR and CNPR values, NAG pH, and corresponding ARD classifications for the nine individual humidity cell samples is summarized in Table 3. Tailings and heap leach residue CNPR values and classification are compared to NAG pH classification in the same table. These values were used to calculate the average CNPR values for each lithology listed in Table 2.

Refinement of ABA Classification

Although the degree of variability for the CNP is higher than the Modified Sobek NP due to the limited number of samples, the amount of NP supplied by carbonate alone (CNP) provides a more conservative estimate of effective NP in the long term compared to modified Sobek NP values. Neutralization potential (NP) based on carbonate content (CNP) was used instead of Sobek NP as the primary means to assess ARD potential in these materials. Values for average CNPR, calculated as CNP/AGP, where AGP is based on pyritic sulfur, for the individual humidity cell samples with different lithologies is provided in Table 2 along with the average Sobek NPR values. Based upon the Sobek NP and the sulfide AP measurements, the waste rock had a weighted average NPR (based upon estimated percentages of the various lithologies in the waste facility; Table 1) of 3.9, indicating that overall the WSF is non-PAG. Based on the carbonate-carbon data, the weighted average of CNPR calculated for the waste rock overall based on the proportions of each lithology (Table 1) was 1.7, indicating that the waste rock, overall, has uncertain ARD potential. Based upon the CNPR data (Table 2), the quartzite waste rock was PAG with an average value of 0.2. The Siltstone, Quartz Monzonite (fine-grained), and Feldspar-Megacrystic Quartz Monzonite (coarse-grained) had CNPR values between 1 and 2, indicating uncertain ARD potential and the Quartz

Monzonite (coarse-grained) had an average CNPR of 4.3, indicating non-PAG material. Both the high-grade and low-grade ore had CNPR values less than 1, indicating that these materials are PAG. Note that these estimates for ARD potential for the site should be viewed as having a very high degree of variability, as the data were extrapolated to all 1000 samples using the original static data based on the carbonate analyses for the nine waste rock humidity cell samples, one tailings (cf. high-grade ore) sample, and one heap leach (cf. low- grade ore) sample.

The NAG test uses pH of 4.5 as a cutoff to differentiate between PAG and non-PAG rock. Based on this assessment, five of the nine waste rock samples were predicted to be PAG, including both samples of quartzite, and four samples were predicted to be non-PAG (Table 3). The simulated tailings sample had a NAG pH of 9.2, indicating it was non-PAG and the master composite sample (heap leach residue/low-grade ore) had a NAG pH of 3.4, indicating that it was PAG (Table 3).

Table 3 ABA and NAG pH Results for Individual Samples from Humidity Cells

Sample ID/Lithology	NPR ANP/AGP	ARD Class	CNPR CNP/AGP	ARD Class	NAG pH	ARD Class
015/Siltstone	10	Non-PAG	8.1	Non-PAG	6.0	Non-PAG
198/Siltstone	1.3	Uncertain	0.0	PAG	3.3	PAG
050/Quartzite	5.7	Non-PAG	0.9	PAG	3.5	PAG
101/Quartzite	1.4	Uncertain	0.2	PAG	3.1	PAG
247/Quartz Monzonite (fine-grained)	0.4	PAG	0.0	PAG	4.1	PAG
247b/Quartz Monzonite (fine-grained)	17	Non-PAG	5.4	Non-PAG	5.4	Non-PAG
017/Quartz Monzonite (coarse-grained)	1.4	Uncertain	1.0	Uncertain	5.2	Non-PAG
142/Feldspar-Megacrystic Quartz Monzonite	8.0	Non-PAG	1.5	Uncertain	9.9	Non-PAG
164/Feldspar-Megacrystic Quartz Monzonite	0.6	PAG	0.2	PAG	3.3	PAG
MT / Simulated Mill Tailings	nd	nd	1.6	Uncertain	9.2	Non-PAG
MC / Simulated Heap Leach Residue	nd	nd	0.9	PAG	3.4	PAG

Mineralogical Analyses

Results for mineralogical content of the nine samples, as determined by RXRD are as follows:

- The quartzite lithology was predominantly quartz (>95%) with some muscovite and metallic iron with one sample contained measurable quantities (0.5%) of pyrite.
- The siltstone samples contained quartz and muscovite (about 87%) with minor kaolinite and rutile. One sample also contained K-feldspar, andalusite, and detectable pyrite (0.4%).
- The quartz monzonite samples (fine-grained and coarse-grained) had similar mineralogy, containing quartz, feldspars, muscovite and kaolinite. The coarse-grained sample and one of

the fine-grained samples contained 2-3% jarosite, suggesting that the materials may have an acid generating source mineral in addition to sulfides (e.g., pyrite).

- The two Feldspar-Megacrystic Quartz Monzonite samples were very similar mineralogically, containing quartz, feldspars, muscovite, chlorite, pyrite, calcite, and siderite. Siderite ($FeCO_3$) is slow reacting compared to calcite, and estimates for carbonate NP were corrected in these two samples based on the mineralogical analyses.

Waste Rock Humidity Cells

After 20 weeks of waste rock humidity cell testing, leachate concentrations in three of the nine samples was terminated because release rates of key parameters had stabilized. The remaining six waste rock humidity cell samples were continued through 32 weeks. Based on humidity cell testing, preliminary estimates for exhaustion of sulfide-S (primary acid generation source) and carbonate NP (neutralization source) for waste rock samples in the nine humidity cells are summarized in Table 4. It should be noted that estimates for the humidity cells are based on best available data for the humidity cells, which may or may not have stabilized. Estimated rates of sulfate loss from the columns ranged from 0.25 to 26 mg/kg/week. Rates of alkalinity loss were similar for all columns at about 2.5 mg/kg/week with the exception of the Feldspar-Megacrystic Quartz Monzonite samples, which were 8.7 and 6.9 mg/kg/week. Using these values, predicted times required to exhaust sulfide and alkalinity in the humidity cells did not agree well with the original Sobek NPR values calculated from the static ABA testing. This indicates a high amount of variability within each lithology, particularly those samples containing low concentrations of sulfide and carbonate alkalinity. Note that these time estimates are for crushed samples under ideal laboratory conditions, whereas rates in the field are typically slower due to lower specific surface area values associated with larger rock fragments, ambient soil temperatures, and less contact with reactive surfaces as water flows among the larger rock fragments.

Table 4 Estimates of Years for Exhaustion of Sulfide and Carbonate in the Humidity Cells

Sample ID/ Lithology	CNPR CNP/AGP	Years to Exhaust Sulfide	Years to Exhaust Carbonate	Year to Acidification
015/Siltstone	8.1	23	19	19
198/Siltstone	0.0	14	0	Immediate
050/Quartzite	0.9	<1	38	Never
101/Quartzite	0.2	53	6	6
247/Quartz Monzonite (fine-grained)	0.0	4	6	Never
247b/Quartz Monzonite (fine-grained)	5.4	26	26	Never
017/Quartz Monzonite (coarse-grained)	1.0	157	5	5
142/Feldspar-Megacrystic Quartz Monzonite	1.5	<1	0	Never
164/Feldspar-Megacrystic Quartz Monzonite	0.2	11	13	Never

Tailings and Heap Leach Residue Humidity Cells

Humidity cell testing and analyses for the two metallurgical residue samples were completed through 20 weeks. Results indicated that the pH of the leachate from the Master Composite heap leach residue sample was 5.3 and the filtered tailings was 7.8. These data are assumed to represent long-term water quality for these materials, although they may or may not have stabilized during the 20-week testing. Based on the humidity cell leachate results, concentrations of metals released from the tailings are not anticipated to contribute high amounts of metals to the WSF leachate; however, it should be noted that the humidity cell data do not represent stabilized conditions; it is likely that metal leaching may not have been initiated due to the limited timeframe for leaching.

PROPOSED WASTE STORAGE FACILITY

Based on the mine plan, mill tailings derived from high-grade ore (about 573 Mt) are to be mixed with waste rock (about 1,360 Mt) for permanent storage in the on-site WSF. The WSF will also partially cover the heap leach facility (HLF; about 173 Mt), which will have been treated (surface irrigation) with about 2% H_2SO_4 for metal extraction. After mining operations cease (after 21 years) the entire WSF including the HLF not covered by co-mingled waste rock and tailings will be capped with a 2.5 m thick layer of tailings compacted to a dry bulk density of about 1.6 tonnes/m^3 and the compacted tailings will be covered with a 1 m thick layer of "inert" waste rock composed of roughly equal portions of Quartz Monzonite fine-grained; Quartz Monzonite coarse-grained and Feldspar-Megacrystic Quartz Monzonite coarse-grained lithologies. The waste rock layer will be covered with 0.5 m of growth media (soil) to support re-vegetation.

Water quality predictions for the leachate and ARD potential of the blended storage facility was based on the following assumptions:

- Release rates of acidity/alkalinity and metals from the co-mingled WSF at constant rates based on steady state data obtained from the humidity cells and on the proportion of materials during construction and after completion of mining;
- Instantaneous placement of the 2.5 m thick compacted tailings cover and 1 m of waste rock after 21 years of mining reducing the volume of infiltrating water. The volume and quality of water released at toe decrease and the results of the model presented herein represent worst case conditions;
- Ideal (perfect) mixing of rock types within the waste rock dump according to proportion of their lithologies (Table 1);
- Mill tailings are allocated to fill all pore space within the waste rock;
- The final configuration of the WSF covers an area of about 6,702,780 m^2 (6.7 km^2) receiving average annual precipitation of 963.8 mm, of which about 95% is received during the months of October to April. Evaporation from the surface of the WSF is assumed to be about 50% of precipitation. Losses from surface runoff and to groundwater are negligible.
- The HLF is assumed to be 100% PAG as it is leached with 2% H_2SO_4
- The proportion of PAG and non-PAG materials in the WSF are based on carbonate NP and a cut-off CNPR value of 2;
- Rates of releases for metals are based on the humidity cell data scaled up to field conditions.
- The waste rock is assumed to have an effective specific surface area of 13 m^2/tonne based on a total surface area of 20 m^2/tonne and 65% contact with water;

- Tailings and the heap leach residue are assumed to have specific surface areas the same as the respective humidity cell materials and will react to provide similar water quality.
- For the purposes of calculations, the internal temperature of the WSF is assumed to be constant at 15°C.

WATER QUALITY PREDICTIONS

Based on available data and assumptions, estimates for water quality of the WSF leachate are provided in Table 5. Leachate from waste rock will likely have a pH of approximately 4.6, calculated as weighted proportions of leachate contacting waste rock, tailings, and heap leach residue, at equal rates of flow through all materials, with equal contact. In reality, the majority of water flowing through the WSF is likely to be in contact with the larger pores of the waste rock with lesser contributions from the tailings and heap leach residue; however, estimates for water flow and proportions contacting each of the materials require a more detailed hydrological and hydrogeological assessment.

Table 5 Estimated Water Quality for WSF Leachate

Parameter	Units	Leachate	MPL[1] Liquid Effluent	NEQSW[2] Category 1
pH	su	4.6	6-9	6.5-8.5
Sulfate	mg/L	469		250
Calcium	mg/L	54		
Magnesium	mg/L	8		
Potassium	mg/L	21		
Sodium	mg/L	15		
Aluminum	mg/L	4.0		0.2
Antimony	mg/L	0.030		0.006
Arsenic	mg/L	0.242	0.1	0.01
Barium	mg/L	1.383		0.7
Beryllium	mg/L	0.006		0.004
Cadmium	mg/L	0.006		0.003
Chromium	mg/L	0.093	0.1	0.05
Copper	mg/L	12	0.5	2
Iron	mg/L	53	2	0.3
Lead	mg/L	0.045	0.20	0.01
Manganese	mg/L	0.400		0.1
Mercury	mg/L	0.001	0.002	0.001
Nickel	mg/L	0.116		0.02
Phosphorus	mg/L	0.278		0.1
Selenium	mg/L	0.050		0.01
Silver	mg/L	0.014		
Thallium	mg/L	0.003		
Zinc	mg/L	0.119	1.5	3

Notes: 1.Maximum Permissible Limits to unload liquid Effluents by Metallurgical Mining Activities.
2. National Environmental Quality Standards for Water Category 1: Potable Water

It is anticipated that water will flow through the much finer textured mill tailings at a much slower rate and consequently the volume of flow contributed from the tailings is expected to be less compared to flow and loadings from the waste rock; however, an estimate of the magnitude and proportions are beyond the current scope of this work.

The key parameters of concern appear to be pH, arsenic, copper, and iron. Some of the iron released from the WSF may precipitate from the leachate as it becomes more oxygenated by contact with the atmosphere. This may also reduce the concentrations of copper and arsenic due to co-precipitation or adsorption; however, concentrations may or may not be reduced to levels acceptable to Peruvian regulations, and thus may require active water treatment.

CONCLUSIONS

Based on static and humidity cell testing and the water quality model described herein, predictions indicate that leachate from the WSF is anticipated to contain elevated concentrations of iron, arsenic, and copper as well as acidic pH values less than the acceptable minimum required by Peruvian authorities for discharge to the environment. Water treatment measures may be required to reduce concentrations of metals as well as increase pH prior to discharge to the environment. Additional information on flow conditions, a detailed hydrological and hydrogeological assessment and water quality of downstream waters are required for further assessment.

REFERENCES

AMEC, 2012. Exploration Core Sample Selection for Geochemical Characterization of Waste Rock and Ore. AMEC File 742015150000, Technical Memorandum October 30, 2012.

ASTM D 5744 – 07, "Standard Test Method for Laboratory Weathering of Solid Materials Using a Humidity Cell". ASTM International, West Conshohocken, PA, www.astm.org.

EPA Method 1627, "Method 1627: Kinetic Test Method for the Prediction of Mine Drainage Quality". U.S. Environmental Protection Agency, 1200 Pennsylvania Avenue, NW, Washington, DC 20460, EPA Document Number - September 2008.

British Columbia Ministry of Energy and Mines, (BCMEM) 1998. Policy of Metal Leaching and Acid Rock Drainage at Minesites in British Columbia.

International Finance Corporation, World Bank Group, (IFC-WBG) 2007. Environmental, Heath, and Safety Guidelines, Mining. World Bank Group December 10, 2007.

MEND, 2009. Prediction Manual for Drainage Chemistry from Sulphidic Geologic Materials, MEND Report 1.20.1, (2009).

State of Nevada Modified Sobek Procedure, 2010. http://ndep.nv.gov/bmrr/file/sobek.pdf, Revision 1.0, 5/2010 – Addition of siderite correction method, NDEP, 2010.

Impacts of Artisanal Small-Scale Gold Mining on Water Quality of a Tropical River (Surow River, Ghana)

Karunia Macdonald, Mark Lund and Melanie Blanchette
Mine Water and Environment Research Centre, Edith Cowan University, Australia

ABSTRACT

Rivers in Ghana provide environmental and economic services such as fishery and farming, and are also the main sources of clean drinking water. Artisanal small-scale gold mining (ASGM), a significant industry in Ghana, typically occurs near streams and rivers in order to obtain a source of water for processing and waste discharge. ASGM is subsistence mining carried out by individuals or small collectives using rudimentary technologies for both extraction and processing of ore. Using small quantities of mercury for gold extraction, ASGM also releases high quantities of sediment, (along with metals and other contaminants) into local water bodies, posing environmental and downstream human health risks. In Ahafo, Ghana, we undertook a detailed assessment of the effect of ASGM on the water quality of the Surow River over one year (January 2013 to April 2014). Physico-chemical properties of the water at 11 sites along the river (above and below ASGM sites) were measured monthly. Our research indicates that the impacts of ASGM extend beyond Hg contamination, with the main effects of ASGM on river systems being changes in water conductivity, sediment loads, and metals, as well as alteration of river morphology. Dewatering water was responsible for significant increases in conductivity. We did not detect mercury above drinking water standards, with the exception being at the headwaters, presumably from natural sources. In general, we found that sites with associated ASGM activities had water qualities that did not meet Ghanaian national standards for drinking water, with manganese at particularly high concentrations. We also saw temporal variability in water quality parameters, likely due to the combination of fluctuating ASGM activities and the natural seasonal hydrology of tropical river systems.

Keywords: ASGM, sedimentation, mine dewatering, river ecosystems

INTRODUCTION

Rivers in Ghana provide not only environmental and economic services such as fishery and farming, but are also the main source of clean drinking water. Rural communities, particularly in areas where access to clean water is limited, often use untreated river water for domestic purposes including drinking. Where water is treated before consumption, declines in water quality within the rivers from pollutants and sediment loads from agriculture, industry, mining and forestry increase treatment costs (Fianko et al. 2010; Gyau-Boakye and Biney 2002). Coupled with declines in water quality, increasing demand (Gyau-Boakye and Biney 2002), and declining rainfall (Gyau-Boakye and Tumbulto 2000; Owusu and Waylen 2009), rivers in Ghana are under pressure.

Artisanal small-scale gold mining (ASGM) is a globally-significant industry, providing rural employment directly to at least 15 million people and indirectly to over 100 million in more than 70 countries (WHO 2013). Many ASGM operations occur near streams and rivers for easy access to alluvial ores, but also to supply water used in processing and as a receiving environment for mine waters. Although ASGM contributes to rural economies, it often results in degraded environmental, safety and social conditions due to the rudimentary mining and processing techniques used (Hilson 2002; Telmer and Veiga 2009). ASGM traditionally relied upon secondary and tertiary materials easily found near to the surface or river banks. However, due to depletion of alluvial resources and increased technical and financial capacities, contemporary operators are increasingly mining primary ore found underground, by manually digging vertical shafts or tunnels up to 30 to 35 m deep. These shafts and tunnels often require dewatering, with large volumes of untreated dewatering water often pumped out of these underground operations into nearby rivers and streams. Metal released from processing, dewatering or acid rock drainage can further degrade river water quality. Particularly concerning in ASGM is the widespread use of mercury amalgamation techniques in processing, although cyanide processing is increasingly being used in reprocessing of tailings (de Andrade Lima et al. 2008; Velásquez-López et al. 2011). Mercury processing emits toxic vapours, with predicted global mercury emission by ASGM to be 727 tonnes: 35% of the total world anthropogenic emission of mercury (UNEP 2013). The toxicity of mercury derived from ASGM operations to people and, to a lesser extent, the environment, has been well studied (Bose-O'Reilly et al. 2010; Castilhos et al. 2006; Donkor et al. 2006). However, the impact of AGSM operations on the broader water quality of these river and streams has been largely overlooked.

Previously, we identified a range of potential environmental impacts of ASGM on rivers, such as changes in hydrology and water quality (particularly increased turbidity), as a result of land clearing, erosion, mining and processing (Macdonald et al. 2014). Hydrological changes in rivers can alter available hydrological habitat for aquatic biota (Blanchette and Pearson 2013), and increased turbidity may lead to smothering of aquatic plants, habitats, and biota. Clearing of riparian vegetation, unregulated sewage from mining camps and rubbish disposal can impact on the rivers nutrient concentrations and habitats. In Ghana, these environmental impacts are temporally variable, with ASGM demands for water during dry seasons and excess water in wet seasons altering the flow of the river/stream (pers. obs.). Further, degradation of the river water quality and ecology can have flow-on impacts to cultural values associated with the river, as well as fishing and suitability for drinking.

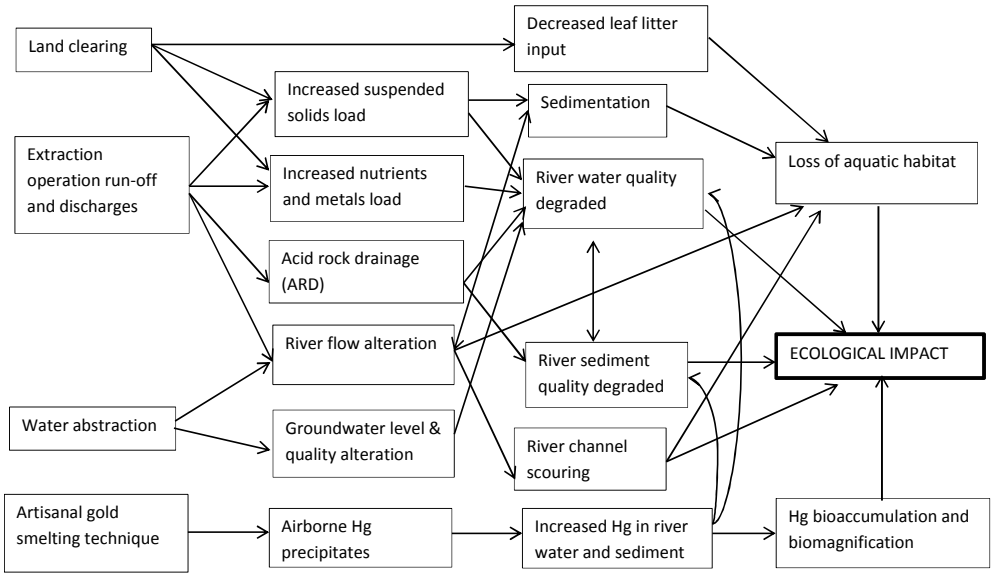

Figure 1 The impacts of artisanal small-scale gold mining (ASGM) on riverine systems (from Macdonald et al., 2014)

The impact of ASGM on tropical rivers has been investigated in Ghana, the Philippines, and Brazil, but the focus of these studies has been on elevated mercury concentrations and mercury cycling as a result of rudimentary processing techniques (Appleton et al. 2006; Bastos et al. 2007; Brabo et al. 2003). These studies were conducted on large river systems such as the Amazon in Brazil (Santos et al. 2000; Telmer et al. 2006) or the Pra (Donkor et al. 2005)and Ankobra Rivers in Ghana (Akabzaa et al. 2009) which have extensive and long-established ASGM operations with chronic mercury inputs. However, the scale and age of these systems prevents identification of other possible impacts besides mercury contamination. In contrast, ASGM activities in smaller rivers are easier to trace due to acutely concentrated nature of measurable impacts (see Webster et al. 1992). Therefore, this study is different from previously published research because of the focus on a smaller river, with the intention of more clearly defining the suite of impacts from ASGM operations.

The aim of this study was to identify the possible impacts of ASGM operations on water quality in the Surow River, a small tributary of the Tano River in Brong Ahafo, Ghana.

METHODOLOGY

Study site background

The Surow River catchment is located in the upper Tano River Basin in the Brong Ahafo region, Ghana, approximately 300 km northwest of the capital city of Accra (Figure 2). Major land uses in the Surow catchment are ASGM and agriculture among tracts of natural forest. Farming activities in the area include cash crop (cocoa), ranching and subsistence farming (vegetables and tubers). The Tano River (400 km long and 15,000 km^2 of catchment) is a major source of potable and domestic water for south west Ghana, and the Surow River is approximately 16 km long with a 3,500 ha. catchment. Located in a wet tropical region, the major rains occur during April to June (average

precipitation 294 mm/month) with minor rains from September to November (average precipitation 234 mm/month) and the driest months are from December to February (average precipitation 16 mm/month and evaporation 105 mm/month) (unpublished meteorological report NGGL, 2013). Therefore, rivers in the Tano Basin exhibit classical wet-dry hydrological patterns, driven by rainfall.

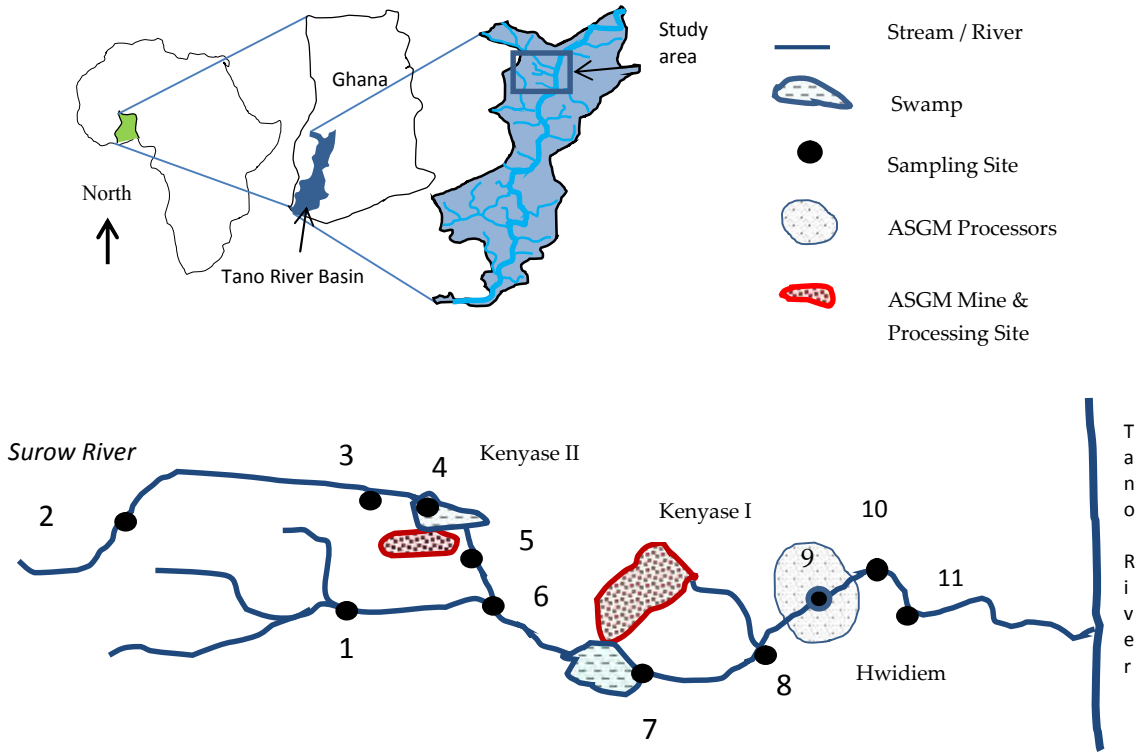

Figure 2 Location of sampling sites (1-11) along the Surow River, Ghana (not to scale)

ASGM has been practiced in many parts of Ghana for hundreds of years (Donkor, et al. 2005). However, operations are relatively new (9 years) to the Surow River catchment. ASGM in this area was started in 2005, following the commencement of a large multi-national gold mining project that discovered gold in the region. During the study period (February 2013 to April 2014), ASGM communities operated along the river at Kenyase I, Kenyase II and Hwidiem townships (Figure 2). At Kenyase I and II, small operators extracted secondary or tertiary alluvial ores easily found in the river banks, while larger operators extracted primary ore mined underground. Ores from these two sites are processed on site as well as sold to other processors mainly scattered near to the river at Hwidiem township. Loose gravel, sands and milled ores are processed via mechanical crushing, elutriation and, in most cases, mercury amalgamation followed by gold smelting and refining (see Macdonald et al. 2014).

Ghanaian legal provisions on mining exclude foreigners and foreign investments in ASGM operations. The sector, nevertheless, received foreign investments at least until March/April 2013 when the Ghanaian government deported as many as 4000 foreigners involved in the industry. As a result, many ASGM operators across the country (including those in Kenyase I and II) ceased most of their operations in May 2013, mostly due to lack of financial support previously provided by

foreign investors. Although underground mining activity was substantially reduced, dewatering of existing mine pits continued, especially during the wetter months. Smaller mining operators and processors, comprised of local citizens, continued to operate after the deportation.

Sampling program

Eleven sites on the Surow River were sampled monthly for 14 months from February 2013 to April 2014, typically within a 12 h period. Sites were chosen based on access, safety, and representativeness of catchment land use (Table 1). In addition, direct sampling of dewatering water at the Kenyase I ASGM site (sample site 8) was conducted once in April 2014.

Table 1 Hydrology and land use of sites (numbered upstream to downstream) on the Surow River, Ghana (February 2013-April 2014)

Sample site	Dominant site hydrology	Major land use
1	Riffle/run	Minimal use
2	Riffle/run	Minimal use
3	Pool/slow run	Minimal use, rural dwelling
4	Swamp	Mining, processing waste
5	Riffle/run	Minimal use
6	Run	Minimal use
7	Swamp	Mining, processing waste
8	Rifle/Run	Dewatering water
9	Riffle/Run	Processing
10	Riffle/Run	Cattle, cocoa farming
11	Pool/slow run	Rural dwelling

On each sampling occasion, and at each site, water depth and velocity (Marsh-McBirney Flowmeter, USA) were measured. Physico-chemical parameters of pH, oxygen reduction potential, dissolved oxygen (DO), temperature, electrical conductivity (EC), and turbidity were measured *in situ* using a Quanta Multimeter (Hach, USA). Water samples were collected 0.1 m below water surface and immediately divided into unfiltered and filtered (through 0.5 μm GF/C; Pall Ltd Metrigard) aliquots. All samples were stored at <4°C prior to analysis.

Aluminum, As, Cd, Cu, Cr, Mn, Pb, Zn in filtered water was analyzed using inductively coupled plasma mass spectrometry (ICP-MS) following USEPA Method 200.8; Fe and Mg were analyzed using ICP (USEPA Method 200.7), and Hg was quantified using cold vapour atomic absorption (CVAA; USEPA Method 245.1,detection limit of 0.0002 mg/L). Dissolved organic carbon was analyzed following USEPA Method 5310B. On unfiltered samples, total Kjeldahl nitrogen (TKN)

was analyzed via block digester method (USEPA M351.2); and total phosphorus was analysed with an auto ascorbic acid method (USEPA M365.1). The above samples were airfreighted to ACZ Laboratory in Colorado, USA.

Analysis of ammonia/ammonium (NH_3-N), nitrate/nitrite (NOx-N) and sulfate (SO_4) on filtered water were performed at the Newmont Ghana Ltd. environmental laboratory at Ahafo using a Hach DR 2800 spectrophotometer following APHA (2005) methods 4500B&C, USEPA Method 375.4; and USEPA Method 365.2 respectively.

Data Analysis

Water quality data was ordinated using principal components analysis (PCA) to illustrate patterns in the data, then compared among sites using permutational ANOVA (PERMANOVA). Data were prepared for ordination and analysis by selecting parameters where more than half of the samples were above detection; values below detection were replaced with half the detection limit, missing data were replaced by the average of any other data for that time and treatment, and auto-correlated parameters were reduced to a single representative parameter. Data were also normalized in Primer v6 prior to ordination and analysis. Significance testing of the multivariate data among sites was undertaken on PERMANOVA, using a two-way, unreplicated design with time (fixed) and site (random) as factors, followed by pairwise comparisons between sites. All analyses were performed on Primer v6 (Primer-E; Clarke and Gorley 2006).

RESULTS AND DISCUSSION

Water quality varied among sites (pseudo-F 2.36, $P<0.01$) and over time (pseudo-F 3.92, $P<0.01$), reflecting stochastic events, seasonal trends, and anthropogenic impacts. A PCA of water quality data, separated by month, illustrates the effect of seasonal trends on the data is presented in Figure 3 (note different axis scales). On most occasions, water quality at the headwater sites (1, 2, 3), and minimal land use sites (5, 6) were closely associated with each other, with the exception of site 6 in September and October 2013. Water quality at sites 1, 2 and 6 were not significantly different to each other, but were different to 5 (Table 2). Water from sites 1, 2 and 3 (headwaters) had low EC (0.11-0.35 mS cm^{-1}), turbidity levels generally below the Ghanaian EPA standard of 75 NTU (except on one occasion at site 2, and six occasions for site 3 where turbidity peaked at 247 NTU), and pH levels between 6.03 to 7.81. Water quality at the headwater sites reflects catchment mineralization (NGGL 2005), with silicate and carbonate mineral weathering, precipitation, and agricultural activities the most significant processes influencing the water quality in the area (Banoeng-Yakubo et al. 2009; Yidana 2009).

In March 2013, Hg concentrations at sites 1 and 3 exceeded the Ghanaian drinking water standards of 0.002 mg L^{-1}, reaching 0.003 mg L^{-1} – at no other time or site were standards exceeded. Mean (±SE) Fe concentrations declined downstream from 1.07±0.35 at site 1, to 0.25±0.10 by site 9. The Ghanaian drinking water standard for Fe is 0.3 mg L^{-1} and the EPA standard is 1 mg L^{-1}; essentially, exceedances occurred at headwater sites. Manganese exceeded the Ghanaian drinking water standards (0.05 mg L^{-1}) in 93 out of 130 samples, and the EPA standard (0.1 mg L^{-1}) in 67 samples across all sites and times (Figure 4). Although there were exceedances of both standards at sites 1 and 2, at site 3 every sample exceeded the drinking water standard. Sites 4, 5 and 6 (further downstream) had progressively fewer exceedances of the drinking water standard for Mn.

Therefore, Hg, Fe, and Mn concentrations in the Surow River do not appear to be directly related to ASGM operations, instead reflecting local geologies.

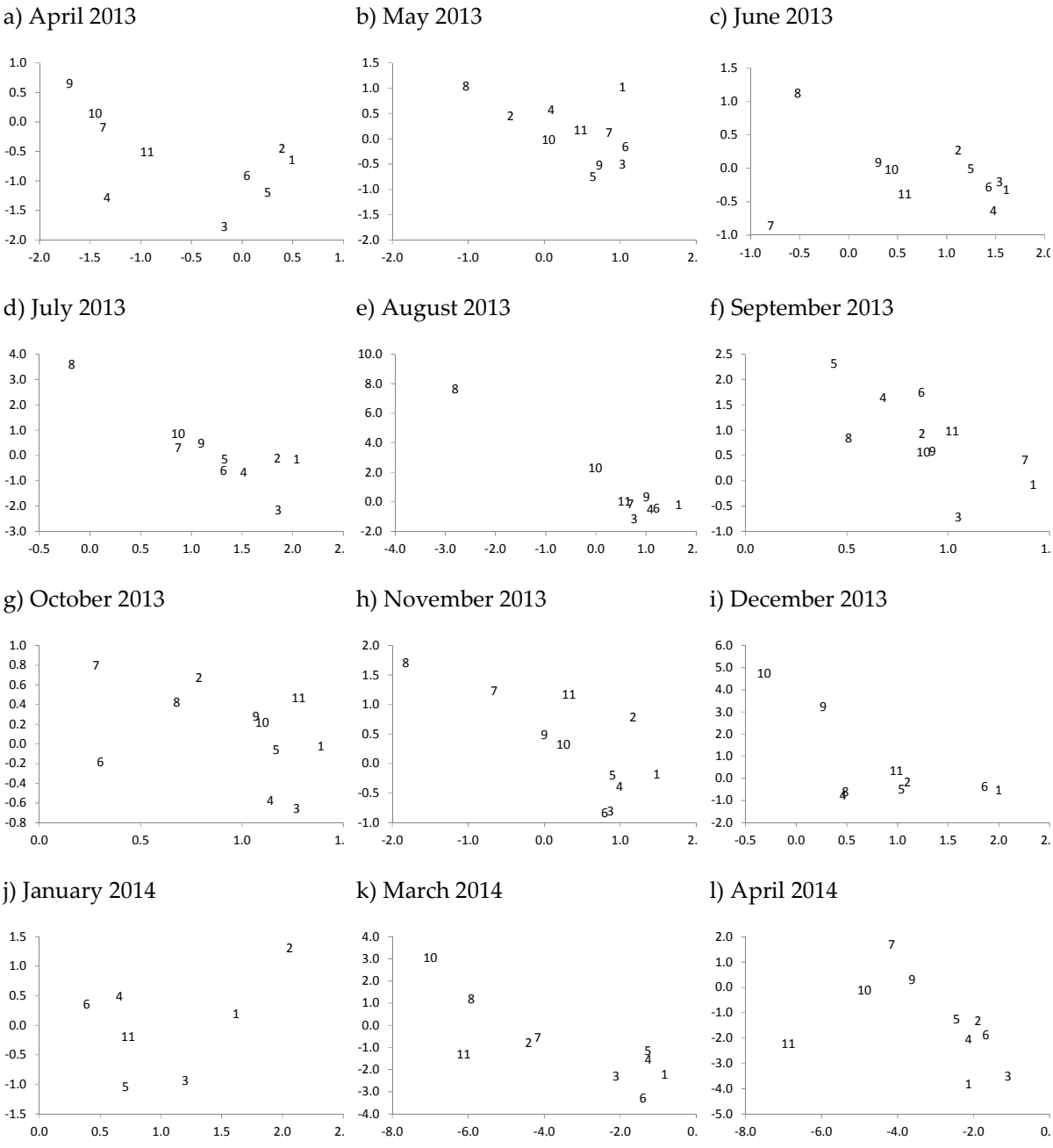

Figure 3 PCA of water quality data per sampling month (a-l) showing each site. Each graph is a subset of a single PCA on all available data. Note different axis scales

Sites 5 and 6 were similar to 1, 2, and 3 on most occasions (Figure 3), even during the period of highest ASGM activity (prior to May 2013) at site 4. At sites 5 and 6, EC ranged between 0.14—0.31

mS cm^{-1}, turbidity was 30—247 NTU and pH was 6.57—7.69, with metal concentrations similar to that of the upstream sites, except for Mn concentrations, which were among the highest of all sites at site 5 ranging between 0.03—3.11 mg L^{-1} (mean 0.8±0.3 mg L^{-1}). The similarity of sites above and below site 4, a site of intense ASGM activity, suggests that the impacts of ASGM, as measured, are highly localized.

Site 4 was separated from headwater sites (1-3) in April 2013 at the height of AGSM operations. Pairwise comparisons between all sites (across all times) show no significant differences between the two main ASGM sites 4 and 7, with 5 similar to 7 but not to 4. The start of the wet season in September 2013 altered the relationship among all sites. Although ASGM activity partially returned to site 4 in April 2014, the impact on overall water quality was not pronounced (as indicated by a lack of separation from other sites; Figure 3), possibly due to the heavy rainfall and high flows at this time. Magnitude and timing of flows appeared to have a variable impact on how different site 4 was from the rest of the data set.

At site 4, accumulation of sediment from processing at Kenyase II turned the defined river channel into a broad swamp. The site had a wider range of water temperatures (23.4-31.6 ^{o}C) than other sites - possibly due to its lack of canopy cover. The site had EC similar to the headwater sites (0.11—0.24 mS cm^{-1}) despite its proximity to an ASGM site, although underground mining activities were not significant during the study period (i.e., highly conductive groundwater was not being discharged into the river) Surface mining and ore processing were the main activities, resulting in high turbidity (peak >2000 NTU; mean 277±141 NTU) and sedimentation at site 4 (Figure 4). The number of exceedances of the Ghanaian EPA standard for turbidity was the same as site 3, although values were lower at site 3. Although the impact of ASGM operations on increasing turbidity are clearly visible before April 2013, after this time turbidity was also being generated at site 3. Higher flows during the wet seasons are naturally high in turbidity, with the sedimentation generated at site 3 washed downstream to site 4, and then carried further downstream to site 7. With the exception of Mn, dissolved metal concentrations were also similar at up- and downstream sites (5 and 6). Mean Mn concentrations at site 4 (0.51±0.24 mg L^{-1}) were higher than at site 3 (0.21±0.03 mg L^{-1}), indicating that ASGM activity was a source of the metal. Further, the only times that Mn concentrations were higher at site 4 than at site 3 was during periods of mining activity (April 2013, 2014, and December 2013). Mn is a hematological toxicant in fish, mammals and human (Crossgrove and Zheng 2004). Over discharge of manganese into aquatic ecosystems may affect the survival of natural fish population (Agrawal and Srivastava 1980).

In addition to site 4, sites 7 and 8 were highly impacted by ASGM activities, and tended to separate from other sites, particularly in June, July August, and November 2013 (Figure 3). Site 7 was highly turbid (up to 2000 NTU), particularly in comparison to headwater sites (Figure 4). At site 7, EC ranged from 0.20-0.95 mS cm^{-1}, pH ranged between 6.7—8.2, and occasionally had very high concentrations (and consequently mean concentrations) of NOx-N, TKN, Ca, and P compared to site 6 (site 6 being directly upstream of site 7, and unimpacted by mining). At site 7, metals were similar in concentration to site 6, with the exception of Mg which between December 2013 and April 2014 has concentrations at least an order of magnitude higher than site 6. There was a marginal increase in Mg seen at site 4 during April 2013.

a) Manganese b) Turbidity

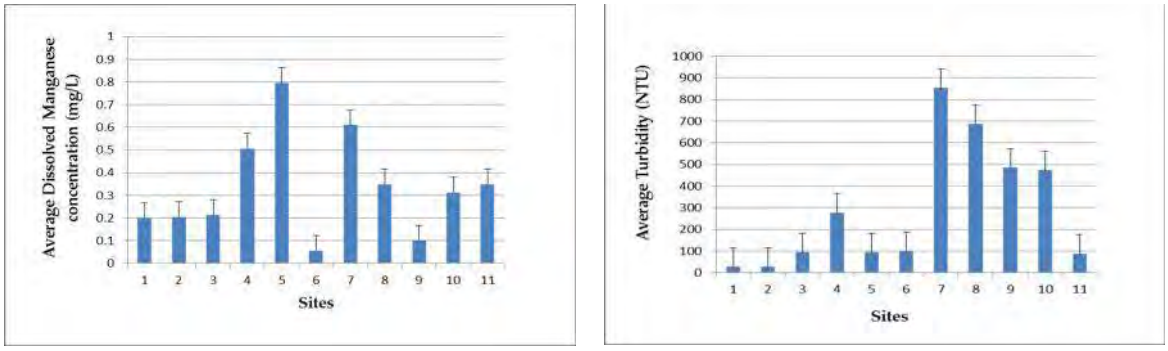

Figure 4 Mean (+SE) of a) manganese and b) turbidity at sites in the Surow River between February 2013 and April 2014. Sites are ordered upstream (1) to downstream (11)

The occasional spikes seen in nutrient concentrations at site 7 might be related to surrounding farming activities (cocoa plantation and cattle). Alternatively, in a forested stream, following a disturbance such as deforestation in the catchment, vegetative nutrient uptake is reduced while mineralization of organic matter is accelerated, which can result in elevated concentrations of NOx-N, Ca, Mg, K and Na (Webster et al. 1992). Site 7 is a swamp resulting from the deposition of sediment that came with the run-off from the exposed land, elutriation boxes, unregulated tailing, and waste material disposal at Kenyase I site. The size of ASGM operations at Kenyase I (site 7, 8) was larger than Kenyase II (4) this was also reflected in the relative size of the two swamps and mean turbidity values (Figure 4). River sediment is a sink of many pollutants and a medium for bio-geological processes including methylation of mercury; the quality of river water and habitats can strongly be influenced by quality of sediment (Chon et al. 2012; Kehrig et al. 2003).

Table 2 Significance of pairwise comparisons between sites from PERMANOVA (ns = P>0.05, t<1.3; s= P<0.05, t>1.3). See Table 1 for site details

	2	3	4	5	6	7	8	9	10	11
1	ns	s	s	s	ns	s	s	s	s	s
2	-	s	s	s	ns	s	s	s	ns	ns
3	-	-	s	s	s	s	s	s	s	s
4	-	-	-	s	s	ns	s	s	s	ns
5	-	-	-	-	s	ns	s	s	s	ns
6	-	-	-	-	-	s	s	s	s	ns
7	-	-	-	-	-	-	s	s	ns	ns
8	-	-	-	-	-	-	-	s	ns	s
9	-	-	-	-	-	-	-	-	s	ns
10	-	-	-	-	-	-	-	-	-	ns

Site 8 was significantly different to all other sites except 10 (Table 2), and was characterized by high EC (0.58±0.08 mS cm^{-1}; peak 1.02 mS cm^{-1} in April 2013) for the duration of the study, particularly during the height of ASGM operations (February-April 2013). Five out of 13 times EC exceeded the

Ghanaian drinking water standard (0.5 mS cm^{-1}) but not the EPA standard of 1.5 mS cm^{-1}. Site 8 received dewatering water from the underground mines at Kenyase I via a drain. Dewatering water at the Kenyase I mine was sampled directly in April 2014 and had an EC of 1.3 mS cm^{-1}, suggesting this as the most likely source of the high EC at site 8. Calcium, Mg and Zn concentrations were generally similar to site 7; and higher than sites 1 to 6, particularly during the dry seasons (although the reason for this pattern was unclear). Site 8 had a pH between 6.7—8.5 (the highest recorded pH at any site during the study); turbidity was high between 19—2000 NTU, with the low turbidities occurring during the wet season when discharge of a large amount of dewatering water occurred.

Sulfate concentrations were substantially higher at site 8 than at all other sites (108.3±46.4 mg L^{-1} compared to <13 mg L^{-1} at sites 1—6), except for in December 2013 when sulfate at site 7 was 281 mg L^{-1}. Sulfate concentrations exceeded the drinking water standard of 250 mg L^{-1} on four occasions. Dewatering water appears to be source of the sulfate obtained from the mineralization of the ores in the area, which mostly contain sulfide composites (NGGL 2005) typical of the Sefwi belt of the Birimian host rocks, the main source of gold and diamonds that extends across Ghana (Akabzaa, et al. 2009). Similarities between sites 7 and 8 were not observed in May, July and August 2013, where site 7 had water quality similar to the headwater sites, possibly reflecting the downturn in ASGM activity at this time.

Site 9 is surrounded by ASGM processors, but no mining activities, and water quality at site 9 was significantly different from all other sites except site 11 (Table 2). Although the high turbidity recorded at sites 7 and 8 also occurred at site 9, values at site 9 were generally lower (Figure 4). The high EC at site 8 did not persist at site 9, and concentration of most metals at site 9 were lower than at sites 7 and 8 –below the Ghanaian drinking water standard with exceptions of Fe (2 occasions) and Mn (8 occasions). Broadly, water quality at sites 9, 10 and 11 tended to be similar (Figure 3, Table 2), with the exception of after December 2013 where 11 separated from 9 and 10 (although water quality overall at site 11 was not significantly different to sites 9 and 10; Table 2). Although overall water quality at sites 9, 10 and 11 tended to be significantly different to upstream sites (Table 2), this distinction was not reflected in the PCA ordinations for May, June, October and November 2013, possibly due to increased hydrological connectivity during the times of highest rainfall.

Water quality at site 11 was only significantly different to sites 1, 3 (headwaters) and 8 (ASGM dewatering), likely because as the most downstream site, site 11 represents the cumulative impacts of land use within the catchment.

CONCLUSIONS

Previously, we identified a range of possible environmental impacts of ASGM on riverine systems. In the Surow River, Ghana, ASGM activities increased sedimentation, altered river morphology, and elevated Mn concentrations. As evidenced by high pH across all sites and times, we did not observe acid mine drainage, although the mineralogy of the area made it unlikely because it contains low levels of pyrite. Mercury was only detected in headwater sites, presumably from natural rock sources. Dewatering water discharges were found to substantially increase EC in the river, although, as with most observed parameters, impacts were local. During the wet seasons, we observed that higher flows in the river tended to reduce the differences between sites. Overall, water quality in the river at many sites did not meet the standards set for the environment by the Ghanaian EPA and for drinking water. Future work will investigate the effect of ASGM activities on river ecology.

ACKNOWLEDGEMENTS

The authors wish to acknowledge support and assistance received from various institutions and individuals, including but not limited to: (1) Mr Anthony Loh and Ms Rita Lebene-Tibu of Newmont Ghana Gold Limited (NGGL) at Ahafo for their assistance in airfreighting the samples to be analysed at ACZ in the USA, (2) the NGGL Environment Laboratory staff at Ahafo, (3) Mr. Mumin Zakaria and Mr. Yakubu Ibrahim of Hwidiem, Ghana, (4) Nana Osuodumgya Berima Apiedwaa, Chief of Hwidiem Town (5) Dr Clint McCullough of Golder Associates (Perth) for his contributions to project design, and (6) Kenyasi I Galamsey (ASGM) Committee, Brong Ahafo, Ghana.

REFERENCES

Agrawal, S. J., Srivastava, A. K. (1980). Haematological responses in a fresh water fish to experimental manganese poisoning. *Toxicology, 17*(1), 97-100.

Akabzaa, T., Jamieson, H., Jorgenson, N., Nyame, K. (2009). The Combined Impact of Mine Drainage in the Ankobra River Basin, SW Ghana. *Mine Water and the Environment, 28*(1), 50-64. doi: 10.1007/s10230-008-0057-1

Appleton, J. D., Weeks, J. M., Calvez, J. P., Beinhoff, C. (2006). Impacts of mercury contaminated mining waste on soil quality, crops, bivalves, and fish in the Naboc River area, Mindanao, Philippines. *Sci Total Environ, 354*(2-3), 198-211.

Banoeng-Yakubo, B., Yidana, S., Anku, Y., Akabzaa, T., Asiedu, D. (2009). Water quality characterization in some Birimian aquifers of the Birim Basin, Ghana. *KSCE Journal of Civil Engineering, 13*(3), 179-187. doi: 10.1007/s12205-009-0179-4

Bastos, W., de Almeida, R., Dórea, J., Barbosa, A. (2007). Annual flooding and fish-mercury bioaccumulation in the environmentally impacted Rio Madeira (Amazon). *Ecotoxicology, 16*(3), 341-346.

Blanchette, M., Pearson, R. (2013). Dynamics of habitats and macroinvertebrate assemblages in rivers of the Australian dry tropics. *Freshwater Biology, 58*(4), 742-757.

Bose-O'Reilly, S., Drasch, G., Beinhoff, C., Rodrigues-Filho, S., Roider, G., Lettmeier, B., et al. (2010). Health assessment of artisanal gold miners in Indonesia. *Sci Total Environ, 408*(4), 713-725.

Brabo, E. S., Angélica, R. S., Silva, A. P., Faial, K. R. F., Mascarenhas, A. F. S., Santos, E. C. O., et al. (2003). Assessment of Mercury Levels in Soils, Waters, Bottom Sediments and Fishes of Acre State in Brazilian Amazon. *Water, Air, & Soil Pollution, 147*(1), 61-77.

Castilhos, Z. C., Rodrigues-Filho, S., Rodrigues, A. P. C., Villas-Bôas, R. C., Siegel, S., Veiga, M. M., et al. (2006). Mercury contamination in fish from gold mining areas in Indonesia and human health risk assessment. *Science of The Total Environment, 368*(1), 320-325.

Chon, H. S., Ohandja, D. G., Voulvoulis, N. (2012). The role of sediments as a source of metals in river catchments. *Chemosphere*.

Crossgrove, J., Zheng, W. (2004). Manganese toxicity upon overexposure. *NMR in Biomedicine, 17*(8), 544-553.

de Andrade Lima, L. R., Bernardez, L. A., Barbosa, L. A. (2008). Characterization and treatment of artisanal gold mine tailings. *J Hazard Mater, 150*(3), 747-753.

Donkor, A. K., Bonzongo, J.-C. J., Nartey, V. K., Adotey, D. K. (2005). Heavy Metals in Sediments of the Gold Mining Impacted Pra River Basin, Ghana, West Africa. *Soil and Sediment Contamination: An International Journal, 14*(6), 479 - 503.

Donkor, A. K., Bonzongo, J. C., Nartey, V. K., Adotey, D. K. (2006). Mercury in different environmental compartments of the Pra River Basin, Ghana. *Sci Total Environ, 368*(1), 164-176.

Fianko, J., Lowor, S., Donkor, A., Yeboah, P. (2010). Nutrient chemistry of the Densu River in Ghana. *The Environmentalist, 30*(2), 145-152.

Gyau-Boakye, P., Biney, C. A. (2002). Management of freshwater bodies in Ghana. *Water international, 27*(4), 476-484.

Gyau-Boakye, P., Tumbulto, J. W. (2000). The Volta Lake and Declining Rainfall and Streamflows in the Volta River Basin. *Environment, Development and Sustainability, 2*(1), 1-11. doi: 10.1023/a:1010020328225

Hilson, G. (2002). The environmental impact of small-scale gold mining in Ghana: identifying problems and possible solutions. *Geographical Journal, 168*(1), 57-72.

Kehrig, H., Pinto, F., Moreira, I., Malm, O. (2003). Heavy metals and methylmercury in a tropical coastal estuary and a mangrove in Brazil. *Organic Geochemistry, 34*(5), 661-669.

Macdonald, K. F., Lund, M., Blanchette, M., McCullough, C. (2014). *Regulation of Artisanal Small Scale Gold Mining (ASGM) in Ghana and Indonesia as Currently Implemented Fails to Adequately Protect Aquatic Ecosystems.* Paper presented at the 12th International Mine Water Association, China.

NGGL. (2005). Environmental and social impact assessment. Ahafo South Project. Accra, Ghana: Newmont Ghana Gold Limited.

Owusu, K., Waylen, P. (2009). Trends in spatio-temporal variability in annual rainfall in Ghana 1999 - 2000. *Weather, 64*(5), 6.

Santos, E. C., Jesus, I. M., Brabo, E. S., Loureiro, E. C., Mascarenhas, A. F., Weirich, J., et al. (2000). Mercury exposures in riverside Amazon communities in Para, Brazil. *Environ Res, 84*(2), 100-107.

Telmer, K., Costa, M., Simões Angélica, R., Araujo, E. S., Maurice, Y. (2006). The source and fate of sediment and mercury in the Tapajós River, Pará, Brazilian Amazon: Ground- and space-based evidence. *Journal of Environmental Management, 81*(2), 101-113.

Telmer, K. H., Veiga, M. M. (2009). World emissions of mercury from artisanal and small scale gold mining. In R. Mason & N. Pirrone (Eds.), *Mercury Fate and Transport in the Global Atmosphere* (pp. 131-172): Springer US.

UNEP. (2013). Global Mercury Assessment 2013. Sources, emissions, releases and environmental transports (I. a. E. Divison of Technology, Trans.) *Global Mercury Assessment 2013* (pp. 44). Geneva: United Nations Environmental Programme.

Velásquez-López, P. C., Veiga, M. M., Klein, B., Shandro, J. A., Hall, K. (2011). Cyanidation of mercury-rich tailings in artisanal and small-scale gold mining: identifying strategies to manage environmental risks in Southern Ecuador. *Journal of Cleaner Production, 19*(9-10), 1125-1133.

Webster, J., Golladay, S., Benfield, E., Meyer, J., Swank, W., Wallace, J. (1992). Catchment disturbance and stream response: an overview of stream research at Coweeta Hydrologic Laboratory. *River conservation and management, 15*, 232-253.

WHO. (2013). *Preventing disease through healthy environments. Mercury exposure and health impacts among individuals in the Artisanal Small-Scale Gold Mining (ASGM) Community.* Geneva.

Yidana, S. (2009). The hydrochemical framework of surface water basins in southern Ghana. *Environmental Geology, 57*(4), 789-796.

10th ICARD IMWA 2015 | 10th International Conference on Acid Rock Drainage & IMWA Annual Conference

National Assessment of Sediment-Related Diffuse Mining Pollution in England and Wales

William Mayes[1], Áron Anton[1], Carl Thomas[1], Hugh Potter[2], Sian Rudall[3], Jaime Amezaga[4], Catherine Gandy[4] and Adam Jarvis[4]

1. *Centre for Environmental and Marine Sciences, University of Hull, United Kingdom*
2. *Environment Agency, United Kingdom*
3. *Schlumberger Water Services, Chile*
4. *School of Civil Engineering and Geosciences, Newcastle University, United Kingdom*

ABSTRACT

In catchments affected by diffuse mining-related pollution, the effectiveness of future remediation efforts at point discharges (e.g. mine drainage adits) may be severely limited as diffuse sources persist in elevating instream contaminant concentrations. This paper aims to systematically map potential diffuse mining pollution sources across catchments in England and Wales through (1) undertaking a risk-based classification of all waste rock mining features mapped between 1840 and the present (e.g. waste rock, tailings and processing plants), and (2) screening national datasets of fluvial metal(loid) concentrations in mine-affected catchments. A total of 2402 waste rock features (total surface area: 91 km^2) are identified in mining catchments, which in 11 priority catchments accounts to >10% of the catchment area. Many of these waste rock features are located in steep, upland catchments where risk for ongoing contaminated sediment delivery to watercourses is highlighted by topographic analyses (e.g. distance from stream features, slope and drainage areas) for each feature. There also appears to be a considerable inventory of within-stream potential diffuse pollution sources. In 69% of mine-affected catchments with available fluvial sediment concentration data, lead (Pb) exceeds the Probable Effects Level (PEL), above which potential negative effects on sediment dwelling organisms would be anticipated. The data highlight the ubiquity of diffuse-mining related pollution, and data presented for one catchment in north east England illustrate the importance of diffuse source mining pollution to overall metal export from such river systems. Such information will be of use for managers in catchment scale source apportionment studies and remedial planning for point discharges.

Keywords: diffuse pollution; metal mine; zinc; lead; geographic information system

INTRODUCTION

The persistent environmental legacy of abandoned metal mine discharges on the aquatic environment has long been recognised (e.g. Lewin et al. 1977). There has been a considerable associated growth in research in recent decades to try and address these legacy pollution issues, through the development of passive treatment systems requiring modest maintenance and running costs (e.g. Gandy and Jarvis, 2012). In catchments affected by metal mine pollution, the long term effectiveness of remedial action at point discharges (i.e. discrete discharges from mine adits or drainage levels) needs to be considered in the light of the broader controls on water quality within the wider catchment. Environmental regulators have increasingly focussed management on the catchment scale as a result of legislative drivers (e.g. the Water Framework Directive in Europe) that recognise that investment in remedial action must lead to demonstrable improvements in water quality and ecology at a catchment scale. As such, an awareness of the transient influence of different polluting sources on water quality at downstream regulatory compliance points is required. In catchments affected by abandoned metal mining, there are often multiple point discharges contributing to any instream water quality failure in addition to a range of diffuse metal inputs, the significance of which (and subsequent mobility of metals) will vary under differing hydrological conditions.

Where studies on the nature and extent of diffuse mining pollution have been undertaken, diffuse inputs into river systems have been found to be ubiquitous (e.g. Mighanetara et al., 2009; Byrne et al., 2013; Jones et al., 2013). These diffuse pollution mechanisms range from direct diffuse input of contaminated groundwater into surface waters to runoff from waste rock heaps, through to the remobilisation of weakly associated sediment-bound metals from instream sediments into the water column (for example during a fall in stream pH that may occur after heavy rainfall in peatland-rich upland catchments). The latter mechanism has been highlighted as important by several workers (e.g. Banks et al., 2010, Gozzard et al., 2011) as a significant portion of metals are typically found in sediment fractions that are either readily exchangeable or remobilised with change in pH or redox (Environment Agency, 2006). Studies have shown that these diffuse inputs are also visible from scales ranging from individual reaches (10s of metres) around mine sites (e.g. Gozzard et al. 2011) through to river basin scale (100s of km^2: e.g. Mayes et al., 2013). Indeed, in catchments with large inventories of metal-contaminated sediments in floodplain deposits, modelling studies have suggested it may take centuries for sediment metal concentrations to return to pre-mining levels (e.g. Dennis et al. 2009).

In the UK, national metal mine water management strategies have been focussed on catchment-scale management, with exercises to identify water bodies impacted by metal mining pollution (both point and diffuse) and subsequently prioritise them for potential remedial action (Jarvis and Mayes, 2012; Mayes et al. 2009). These large scale exercises have also provided detailed inventories for metal flux arising from point metal mine discharges (e.g. Mayes et al., 2010). However, no systematic assessment of potential diffuse metal mine pollution sources has yet to be established. Diffuse pollution issues were cited as a common occurrence at 187 of 256 mine sites in national surveys of environment managers (Jarvis and Mayes, 2012), however no specific detail on the nature and extent of these issues were provided.

This paper provides an overview of national scale GIS-based analysis to systematically identify potential diffuse metal mining pollution sources across England and Wales. By using a range of spatial resources (e.g. topographic maps, national geochemical atlases) we: (1) identify the extent of potential diffuse sources in priority mine-impacted catchments (e.g. extent of waste rock; establish

sediment metal concentrations), and (2) undertake a risk-based assessment of individual waste rock features based on physical attributes. These resources will be useful to river basin managers to help inform operational catchment-scale management, for example in terms of identifying potential locations for monitoring diffuse pollution inputs (e.g. upstream and downstream of waste rock) in catchment scale remedial planning investigations. A case study of the River South Tyne catchment, in north east England, concludes the paper. It highlights the importance of effective monitoring of both aqueous and particulate metals to quantify diffuse pollution, and also illustrates the challenges involved in managing such diffuse sources.

METHODOLOGY

Catchment descriptors

All spatial analyses were undertaken in Arc GIS v.10, with statistical analyses undertaken in Minitab v.15. Sediment metal concentration data were normally distributed after log transformation (Kolmogorov Smirnov $P>0.05$) so parametric methods are used. Spatial analyses focussed on the 264 water bodies in England and Wales deemed to be impacted or probably impacted by abandoned metal mine pollution (see Mayes et al., 2009 for detailed description of impact categories), which account for around 6% of all streams and rivers. In these priority water bodies, a range of physical and chemical environmental characteristics were derived to assist in the interrogation of catchment-scale water quality studies (e.g. Gozzard et al., 2011). The characteristics generated are detailed in Table 1 and utilise a range of datasets such as national topographic layers, Landmark waste rock data (from national Ordnance Survey mapping – see below) and GBASE stream sediment data. The latter is a geochemical atlas collated by the British Geological Survey (BGS) of individual sediment analyses at roughly 1km^2 grid square resolution nationally (Lister and Johnson 2005).

Waste rock heap mapping

Waste rock heaps are mapped digitally in the UK by the Ordnance Survey under the Historic Landmark dataset and provide a potential basis for systematic mapping of waste rock (e.g. waste rock, tailings) associated with abandoned metal mines. The Landmark data consists of shapefiles (polygons of areas) marked as waste rock or potential mining wastes digitised from historic OS maps (from 1st Edition c. 1840 to present). The datasets contain many features that may not be related to metal mining, so the first process was a manual check as to the likelihood of individual mapped features being related to historic metal mining (and not for example, due to aggregate extraction). This was done through combining the shapefiles from different mapping dates then:

- Screening for only those features that fell within a 1000m radius of a mineral vein (buffer analysis).
- Clipping the Landmark dataset to only the priority catchments identified by Mayes et al. (2009).
- Manually comparing remaining features against aerial photography (ESRI World Imagery) to assess whether features could be readily discounted as not being related to metal mining - for example, if aerial photography showed the feature to be a limestone quarry in a mineralised district. Features clearly related to other non-metal mining extractive activities were filtered from subsequent analyses.

These screening procedures reduced the number of features from an initial 85,478 features to 2,402.

Table 1 Water body descriptors of relevance to diffuse pollution risk.

Catchment descriptor	**Source / processing**
Average elevation (m)	National digital terrain model – zonal statistics to derive catchment average
Average slope (°)	National digital terrain model, processed for slope – zonal statistics to derive catchment average
Waste rock area (km²)	Based on processed Landmark data (see below) – zonal statistics to derive catchment total
Waste rock as percentage of catchment area	Based on above and water body catchment area
Average sediment Cd concentration (mg/kg)	GBASE data filtered for stream sediments only; spatial join to derive average (and count) based on number of GBASE sample points in each water body
Average sediment Cu concentration (mg/kg)	As above
Average sediment Pb concentration (mg/kg)	As above
Average sediment Zn concentration (mg/kg)	As above

Waste rock risk assessment

The identified potential metal mine waste rock heap polygons were subject to a range of analyses to assess the potential risk for delivering contaminated sediments into adjacent river systems, which may become remobilised in the water column. Waste rock features were then assigned a relative risk score based on a series of criteria. The boundaries for these criteria were set to give a roughly even distribution of features in each class. The Calculate Geometry Tool was used to determine the area of individual features (Table 2). Each polygon was then given a risk score based on proximity to the nearest watercourse (taken from the 1:50000 river network shapefile). Buffer distances and Risk Scores were obtained as per Turner *et al*. (2011) and are shown in Table 2.

Topographic Wetness Index (TWI) is a tool widely used in assessing slope stability in many geotechnical settings (e.g. railway embankments and cliffs). TWI is a function of local slope and the drainage area feeding an individual point on the slope (as a surrogate of potential soil moisture). We followed the method of Miller *et al.* (2012) to derive the TWI for all waste rock heaps based on 10m Digital Terrain Models (DTM) for the UK. TWI is given by the following:

$$TWI = \ln (\alpha / \tan \beta)$$

where α is the local upslope contributing are draining through a specific point and β is the local slope. The 10m DTM was used to create a Slope raster using the Slope Tool (Spatial Analyst), in degrees. Subsequently, a Flow Direction Raster was created, with the Flow Direction Tool (Spatial Analyst). The Flow Accumulation tool was then applied to determine the number of cells draining to every point of the 10m DTM (see Mayes et al. 2008).

Table 2 Risk Scores for each of the waste rock / landscape criteria

Risk Score	Area (m^2)	Distance to river (risk category)	TWI score
6	>100000	Direct contact : <2m (extreme risk)	<11
5	20001-100000	2 – 50m (very high)	11-12.5
4	10001-20000	50 – 100m (high)	12.5-13.5
3	5001-10000	100 – 250m (moderate)	13.5-14.5
2	2001-5000	250 – 500m (moderate-low)	14.5-15.5
1	301-2000	>500m (low)	>15.5

Average slope was calculated for each waste rock feature (using the Zonal Statistics Tool), while the maximum drainage area in km^2 was also calculated for each feature. TWI Risk Categories were then computed according to Table 2. It is worth noting that given the form of the TWI equation, a lower value equates to greater risk (i.e. increased slope or drainage area at a point).

After these steps, an overall Risk Score was derived for each polygon using the following equation:

> Risk Score (values between 3 – 18) = Area Risk Score (1-6) + Distance to stream Risk Score (1-6) + TWI Risk Score (1-6)

RESULTS AND DISCUSSION

Catchment descriptors

Of the catchment descriptors generated, those that are most revealing in terms of national generalisation on the extent of diffuse mining pollution sources are (a) catchment average sediment metal concentrations, and (b) the areal extent of waste rock in mine-affected catchments. The GBASE coverage covers 202 of the 264 Impacted / Probably Impacted catchments, however, a cursory examination of the available GBASE data highlights several patterns. Firstly, where data are available, the catchment average metal concentrations are usually derived from multiple instream samples (average of 11 samples per catchment; range from 1-169), which gives a reasonable level of resolution on which to consider sediment metal concentrations. Figure 1 shows the relationship between Pb and Zn (left panel) and Cd and Cu (right panel), which provide an indication of mining provenance and highlight the potential additive effects on biota of multiple metals in fluvial sediments. The relationships between the four metals are all positive and significant (r: 0.42-0.63; $P<0.05$ for all permutations). Similar patterns are seen in analysis of mine discharges themselves (e.g. Jones et al. 2013) and represent the nature of mineralisation in many of the UK orefields. The chief Pb ore (galena: PbS) is often found with sphalerite (ZnS) in many orefields (e.g. Dunham, 1985; 1990), while Cd is commonly found in sphalerite as an impurity (Dunham, 1990). Cu enrichment is less common across the orefields of England and Wales (hence

the weaker correlations), but peak concentrations found in the orefields of the Lake District and Cornwall and Devon are typically found in combination with other Zn and Pb minerals. Superimposed on Figure 1 are the respective Threshold Effects Levels (TEL – green line) and Predicted Effects Levels (PEL – red line) for fluvial sediment contamination (Buchman, 2008). These values, derived by Environment Canada (PLA, 2014), offer an initial screening tool to assess the likelihood of negative effects of metal concentrations on sediment-dwelling organisms in river systems. A value below the TEL would not be expected to impact on aquatic biota, whereas a value in excess of the PEL would be expected to result in negative impacts on sediment-dwelling organisms. The distribution of the catchment average sediment concentrations show that for Zn, Pb and Cd that the majority of catchments exceed TEL values (between 85 and 94% of catchments), with a significant portion of catchments above PEL values (between 17 (Cd) and 69% (Pb)). Elevated Cu concentrations are rarely an issue in most priority catchments with only 35% above TEL and 3% above PEL values. Comparisons with such preliminary screening tools should be undertaken with caution, however the data highlight that sediment metal concentrations (notably for Zn and Pb) are elevated at levels of potential concern for aquatic ecosystem health in most priority catchments. Screening for sediment metal concentrations in non-priority catchments shows TEL exceedance in less than 5% of cases (data not shown). While such a coarse-scale analysis cannot provide detail on the provenance of the metals, the body of evidence from smaller scale studies consistently highlight the importance of mining activity in elevating sediment metal concentrations above pre-mining levels (Environment Agency 2006). This would suggest that secondary diffuse metal pollution sources in fluvial sediments are widespread.

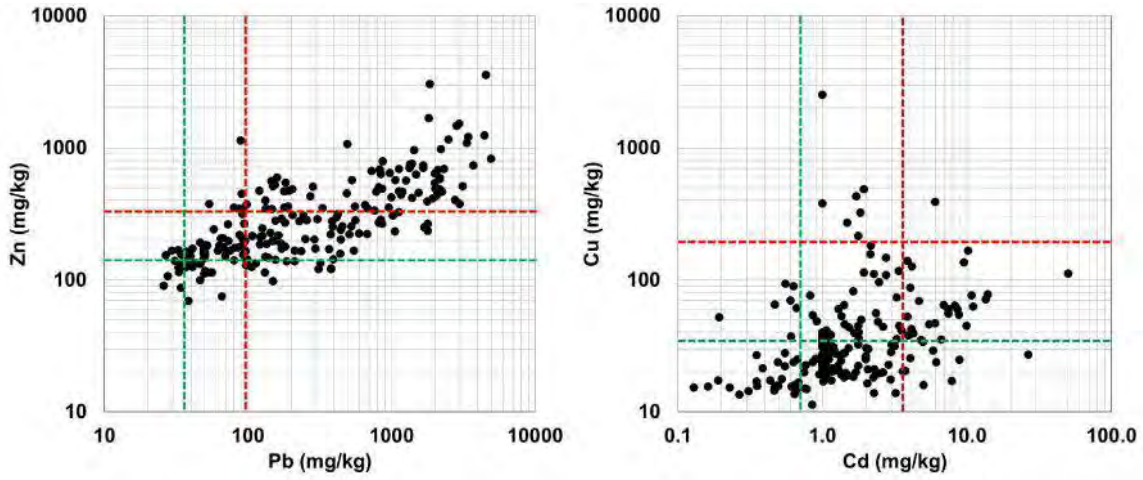

Figure 1 The relationship between Zn and Pb (left panel) and Cu and Cd (right panel). Green lines show respective Threshold Effects Levels (TEL), red lines show Predicted Effects Levels (PEL). Data from GBASE: Licence No.2012/069GB British Geological Survey © NERC

The waste rock cover data offer another good insight into key diffuse pollution sources. In the priority catchments the average areal extent of waste rock was 0.06 km^2. The maximum recorded extent of waste rock was up to 6.4km^2 in the upper Wharfe catchment in the Yorkshire Pennines. When the areal extent of waste rock is compared with catchment area, the average percentage cover of waste rock is 0.8%, with maximum values in four catchments where waste rock exceeded 25% of the entire catchment area (Hicks Mill Stream, Upper and Lower River Carnon in Cornwall and the

mid-reaches of the Lathkill in Derbyshire). Generally, those with the highest waste rock cover are dominated by catchments from the Pennines and South West of England. Whether this is a feature of more systematic mapping in some regions is uncertain (possibly those where mining was more recent and therefore better represented in spatial data, such as the extensive reworking of waste rock in Pennine catchments for fluorspar and barytes in the 1960s/70s: Dunham 1990) and warrants further investigation of the Landmark datasets.

Waste rock heap risk maps

The waste rock heap overall risk score effectively provide a relative risk assessment of metal delivery to the fluvial environment based on the parameters detailed above (slope, flow accumulation, proximity to stream, waste rock area). Figure 2 shows a screengrab of the layer in the Upper Tyne catchment. The waste rock areas with the higher risk scores are generally closer to, or overlap rivers on steep slopes, while those with the lower scores are typically on low gradient summit plateaux near catchment boundaries. This relative risk assessment provides a coarse-scale screening tool to focus more detailed remedial planning investigations. We envisage this layer to be used alongside point mine discharge data to (a) determine the most suitable positions for potential instream sample stations (e.g. upstream and downstream of major waste rock heaps) in catchment scale synoptic surveys (e.g. Gozzard et al. 2011), and (b) assist in interpreting catchment loading data, for example suggesting on which reaches diffuse input from riparian waste rock would be anticipated. During such catchment scale investigations field validation of the relative risk assessment (e.g. visual inspection for evidence of contaminated sediment delivery to surface waters) would provide the scope for future refinement of the spatial analyses.

Case study: the River South Tyne catchment

The River South Tyne, in north east England, has a catchment area of approximately 800 km^2. It drains a large section of the North Pennine orefield, which was heavily mined for several centuries, primarily for lead and zinc. The widespread abandoned mines in the area most severely impact the Rivers Nent, and East and West Allen (Figure 2). In addition to numerous point sources of mining pollution (there are 5 major discharges to the River Nent alone), diffuse pollution (both aqueous and particulate) adds a significant additional burden to the overall flux of metals to the River South Tyne (Gozzard et al. 2011; Rudall, 2012). The main metal of concern is zinc.

Figure 2 (yellow inset) shows the waste rock heap risk map for the River Nent, a major tributary of the River South Tyne. In particular, Figure 2 shows that there are extensive tracts of waste rock in the vicinity of the headwaters of the Nent, which are assigned a risk score of 12-13 according to the methodology described above. Sneddon et al (2008) estimated that 615 000 tonnes of waste rock material were dumped along the River Nent during the period of mining, containing 0.4 wt% Pb and 3.5 wt% Zn.

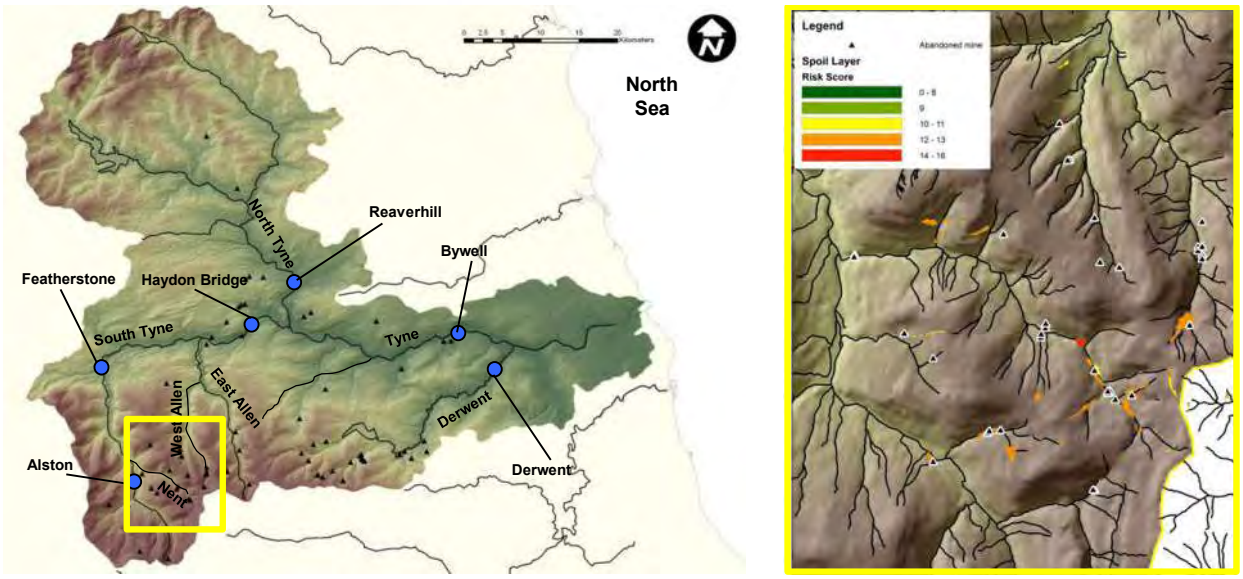

Figure 2 Screenshot of waste rock layer (with risk categories) and river network in the Upper Tyne catchment (yellow inset) and the broader Tyne catchment

The contribution of point sources of pollution to the overall flux of Zn in the River Nent is relatively constant. For example, an investigation during 1997 and 1998 suggested that the combined flux of Zn from the 5 point source discharges did not exceed 40 kg/d (in both particulate and aqueous fractions: Nuttall, 1999). More recent monitoring of Zn flux shows that this remains the case to this day. However, Zn flux monitoring in the River Nent, below the areas of waste rock, and also at two locations on the River South Tyne, downstream of the River Nent, shows that riverine fluxes of zinc are far in excess of that which can be accounted for by the point source discharges. Figure 3 shows zinc flux as a function of river flow-rate on the River Nent, and also on the River South Tyne at Featherstone and at Haydon Bridge, during 2010 and 2011. It is clear that there is a sharp increase in flux as flow increases on the River Nent, which is a result of waste rock heap runoff and remobilisation of secondary metal contamination associated with metal-rich instream sediments. The flux of Zn in the River South Tyne at Featherstone is attributable almost entirely to the metal pollution from the River Nent. Further downstream, at Haydon Bridge (Figure 2) Zn flux is greater than that at Featherstone during highest flows (up to a maximum of instantaneous flux of 1 678 kg Zn/d), and this is due to the contribution of zinc from the Rivers East and West Allen. Point source mining pollution is often the focus of remedial efforts, but observations such as those for the River South Tyne have major implications for the benefits of such remediation. Specifically, point source treatment may not result in downstream water and sediment quality objectives being met, particularly at higher river flows when diffuse source pollution is significant.

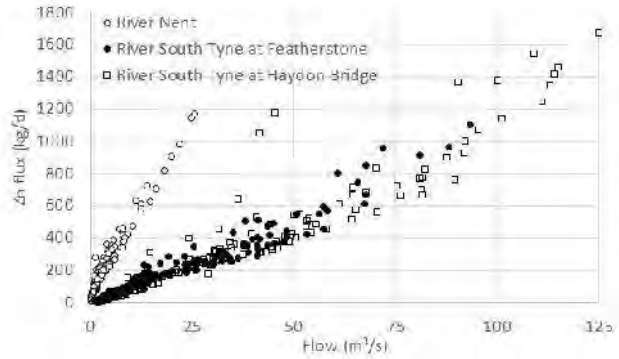

Figure 3 Zn flux in the River Nent and River South Tyne under varying hydrological conditions, illustrating the substantial contribution of diffuse sources of mining pollution

CONCLUSION

Diffuse sources of metal pollutants are ubiquitous in catchments in which extensive former metal mining has occurred. This includes both waste rock heaps, which total 91 km^2 in area and contaminated instream sediments. The analysis of fluvial sediment metal concentrations across the orefields of England and Wales shows in most catchments deemed priorities for remedial action, concentrations are often in excess of prescribed screening thresholds. The positive correlations between Zn, Cd, Pb and Cu highlights that contaminated sediments in mine-affected catchments typically contain a cocktail of numerous metals in high concentrations giving rise to the prospect of synergistic impacts on aquatic biota. The GIS screening exercises undertaken here provide environmental managers with datasets that can assist in catchment scale remedial planning. In the UK, this typically consists of catchment scale synoptic sampling of contaminant loads to identify the contribution of individual point and diffuse discharges to instream contamination. A case study of the River South Tyne illustrates how mapping waste rock coverage can highlight the potential importance of diffuse pollution, and guide the design of monitoring programmes to quantify the relative contributions of point and diffuse source pollution.

ACKNOWLEDGEMENTS

This work was funded by the UK Government Department for Environment, Food and Rural Affairs under Project WT0969. We are grateful to the project steering committee (Dr Abby Moorhouse, Dr Ian Watson, Victor Aguilera) for comments on the methodological approach. BGS GBASE data are used under licence 2010/069GCB. The views expressed in the paper of those of the authors and not necessarily those of the funding agency.

REFERENCES

Banks, V.J. & Palumbo-Roe, B. (2010) Synoptic monitoring as an approach to discriminating between point and diffuse source contributions to zinc loads in mining impacted catchments. Journal of Environmental Monitoring, 12:1684-1698

Byrne, P., Reid, I., Wood, P. (2012) Stormflow hydrochemistry of a river draining an abandoned metal mine: the Afon Twymyn, central Wales. Environmental Monitoring and Assessment. 45: 211-222.

Dennis I.A., Coulthard T.J., Brewer P., Macklin M.G. (2009) The role of floodplains in attenuating contaminated sediment fluxes in formerly mined drainage basins. Earth Surface Processes and Landforms. 34:453–66

Dunham, K.C. (1990) *Geology of the Northern Pennine orefield, volume I, Tyne to Stainmore. Economic Memoir of the British Geological Survey, 2nd edition* HMSO, London, 299 pp.

Environment Agency. (2008) *Assessment of metal mining-contaminated river sediments in England and Wales.* Environment Agency Science Report SC030136/SR4. Bristol, UK.

Gozzard E., Mayes W.M., Potter H.A.B. & Jarvis A.P. (2011) Seasonal and spatial variation of diffuse (non-point) source zinc pollution in a historically metal mined river catchment. Environmental Pollution. 159: 3113-3122.

Jarvis AP & Mayes WM (2012) *Prioritisation of abandoned non-coal mine impacts on the environment. XII. Future management of abandoned non-coal mine water discharges*. Report for Defra and Environment Agency SC030136/R14. 61pp.

Jones A., Rogerson M., Greenway G., Potter HAB. and Mayes WM. (2013) Mine water geochemistry and metal flux in a major historic Pb-Zn-F orefield, the Yorkshire Pennines, UK. Environmental Science & Pollution Research, 20: 7570-7581.

Lewin, J., Davies, B.E. & Wolfenden, P.J. (1977) Interactions between channel change and historic mining sediments. In: Gregory, K.J. (editor) *River channel changes.* John Wiley and Sons, Chichester, pp. 353-367.

Lister, T.R.; Johnson, C.C.. 2005 *G-BASE data conditioning procedures for stream sediment and soil chemical analyses.* British Geological Survey, 85pp. (IR/05/150)

Mayes, W.M., Johnston, D., Potter, H.A.B. & Jarvis, A.P. (2009a). A national strategy for identification, prioritisation and management of pollution from abandoned non-coal mine sites in England and Wales. I. Methodology development and initial results. Science of the Total Environment. 407: 5435-5447.

Mayes, W.M. Potter, H.A.B. & Jarvis, A.P. (2010). Inventory of contaminant flux arising from historic metal mining in England and Wales. Science of the Total Environment. 408: 3576-3583.

Mighanetara K, Braungardt C.B., Rieuwerts J.S., Azizi F. (2009). Contaminant fluxes from point and diffuse sources from abandoned mines in the River Tamar catchment, UK. Journal of Geochemical Exploration,100:116–24.

Miller, P.E., Mills, J.P., Barr, S.L., Birkinshaw, S.J., Hardy, A.J., Parkin, G. and Hall, S.J. (2012) A remote sensing approach for landslide hazard assessment on engineered slopes. *IEEE Transactions on Geoscience and Remote Sensing*. DOI: 10.1109/TGRS.2011.2165547

Nuttall, C.A. (1999) Aquatic zinc pollution from abandoned mines: Assessment and passive treatment in the Nent valley, Cumbria, UK. Unpublished PhD thesis, Newcastle University, UK.

PLA (2014) http://www.pla.co.uk/Environment/Canadian-Sediment-Quality-Guidelines-for-the-Protection-of-Aquatic-Life [last accessed 23.09.2014]

Rudall, S.E (2012) Metal pollution dynamics under varying hydrological conditions in a mining-impacted river catchment. Unpublished PhD thesis, Newcastle University, UK.

Sneddon, I., Orueetxebarria, M., Hodson, M., Schofield, P. and Valsami-Jones, E. (2008) Filed trial using bone meal amendments to remediate mine waste derived soil contaminated with zinc, lead and cadmium. Applied Geochemistry. 23(8): 2414-2424.

Turner, A.J.M., Braungardt, C., & Potter, H. (2011). Risk-based prioritisation of closed mine waste facilities using GIS. In R.T. Rüde, A. Freund, & Ch. Wolkersdorfer: Managing the challenges (p. 667-671), Aachen, Germany.

Comparison of Laboratory and Field-Scale Predictions of Processed Kimberlite Effluent in the Arctic

Michael Moncur[1], Lianna Smith[2] and Dogan Paktunc[3]

1. *Alberta Innovates – Technology Futures, Canada*
2. *Rio Tinto, Diavik Diamond Mines, Yellowknife, NT, Canada*
3. *CANMET Mining and Mineral Sciences Laboratory, Natural Resources Canada*

ABSTRACT

When assessing mine closure options, predicting mine waste effluent water quality is a particular challenge. Conventional static and kinetic tests on small sample volumes are typically used to assess if the mine wastes will be acid generating. However, using these small scale tests to assess if or when field-scale waste piles will release poor quality effluent requires recognizing scale-up issues between laboratory and field conditions. At the Diavik Diamond Mine, up to 42 million tonnes of fine processed kimberlite (FPK) will be deposited onsite for permanent storage. To evaluate the effectiveness of using lab scale experiments to predict mineral weathering and the evolution of porewater geochemistry from the FPK storage impoundment, testing was done to quantify the relationship between laboratory humidity cells and large field-scale tanks. Three fractions of FPK were used for the humidity cell experiments including fine, medium and coarse grained fractions of slurry-deposited FPK. Humidity cells representing the three grain sizes were run for 80 weeks in duplicate at 4°C and 20°C, following the ASTM method. Concurrently, three 5700 L high-density polyethylene tanks were filled with the same fractions of FPK material as the humidity cells. The three tanks were constructed to represent unsaturated conditions. Each tank was instrumented in detail to measure pore water geochemistry, gas-phase concentrations and oxygen diffusion, matrix pressure and flow, evolution of temperature, as well as to resolve mass and flow balances. Results from this study will be used for closure plans at Diavik and potentially other Diamond mines in the Canadian North.

Keywords: Sulfide oxidation, neutralization, processed kimberlite, humidity cells, scale-up

INTRODUCTION

Processed kimberlite (PK) is discharged by slurry to permanent tailings impoundments at diamond mines in Canada's arctic. The Diavik Diamond Mine (Diavik) is an operating mine with two completed open pits and an underground mine. Up to 42 million tonnes of slurry-deposited fine processed kimberlite is expected to be permanently retained on-site in the Processed Kimberlite Containment (PKC) facility. Slurry-deposited PK is defined by Diavik as the < 1 mm fraction of the PK stream and is referred to as fine PK (FPK). Diavik is located 300 km northeast of Yellowknife, NT, Canada (Figure 1) in the remote barren lands of the Canadian arctic. The area is dry and cold with a mean annual temperature, rainfall, snowfall and lake evaporation of -12°C, 164 mm, 187 mm and 271 mm, respectively.

Laboratory humidity cell experiments and *in situ* 5700 L tank experiments were initiated in 2012 to complement an on-going *in situ* PKC experiment at the Diavik Diamond Mine (Moncur and Smith, 2012) to understand better the complexities of using small-scale laboratory experiments for long-term predictions of seepage quality.

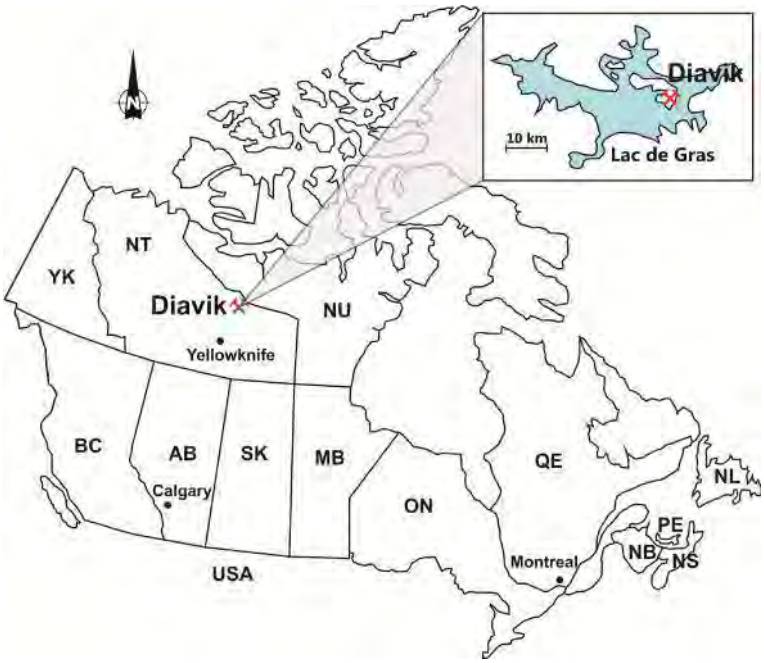

Figure 1 Location of Diavik Diamond Mines in NT, Canada.

METHODOLOGY

Processed kimberlite used for this study was deposited by slurry in 2011 on the East Beach of the PKC. Using a track hoe, FPK was excavated and transported by dump truck on August 2, 2012 to the experiment site. The coarse fraction of FPK (CT) was collected near the toe of the containment dam; the fine fraction of FPK (FT) was collected approximately 200 m from the dam, adjacent to the standing pond water; and the medium FPK fraction (MT) was collected mid-way between the pond

and the containment dam. During FPK excavation every attempt was made to remove the overlying unsaturated FPK to prevent the collection of previously weathered material. Material collected for the tanks was excavated from within the saturated and frost zones of the impoundment.

Tank design and construction

Instrumentation was selected to measure pore water geochemistry, gas-phase concentrations and oxygen diffusion, matrix pressure and flow, evolution of temperature, as well as to resolve mass and flow balances, developed after Smith et al. (2013).

Each tank was constructed from a 2 m in height by 2 m diameter 5700 L HDPE tank. The top of each tank was cut off at a 1.8 m and a 44.5 mm drainage hole was drilled in the wall of the tanks near the bottom for drainage. Water discharging from the bottom of each tank was channeled through a 37.5 mm schedule 40 PVC pipe into a sealed sample cell (Figure 2). Overflow from the sample cell discharged into a data-logging tipping bucket rain gauge so that a continuous record of flow could be maintained to provide bulk chemistry and volume of flow from each tank.

Figure 2 Photos showing (A) completed PK tanks, from left to right FT, MT, CT (B) tank bottom drain pipe discharging into the sample cell and tipping bucket (C) instrumentation on tank tops.

Soil water solution samplers (SWSS) were installed in each tank to provide point measurements of pore water solute concentrations by extracting pore water using applied suction from an area of influence around the probe tip. SWSS were installed at depths of 0.25, 0.5, 1.0, 1.5 and 1.7 m.

Decagon Devices ECH$_2$O-TE probes were installed in each tank at depths of 0.25, 0.5, 0.75, 1.0 and 1.5 m to provide discrete measurements of electrical conductivity (EC), volumetric water content and temperature. Measurements of volumetric water content through space and time can be used to monitor the wetting front propagation through each tank in which discontinuous zones of ice may form, and may indicate the locations and/or transient nature of any preferential flow paths. Continuous monitoring of EC at various depths will provide an understanding of the evolution of pore water during weathering, precipitation and freeze/thaw events. All ECH$_2$O probes were connected to a Decagon Devices EM50 data logger that continually records measurements every 4 hours.

A thermistor string consisting of 10 thermistors was installed at 0.0, 0.25, 0.5, 0.75, 1.0, 1.25, 1.5 and 1.75 m depths through each tank to allow the determination of spatial and temporal variations in permafrost formation, as well as the quantification of thermal contributions from exothermic sulfide oxidation reactions. Nine of the thermistors were attached to a 37.5 mm PVC stand pipe for support, with the bottom thermistor placed on the tank bottom. The PVC stand pipe was filled with FPK to prevent the conduction of air temperatures down the pipe annulus. Thermistor strings were connected to Lakewood Systems UltraLogger data loggers for continuous measurements.

Gas sampling lines consist of 0.63 mm I.D. low density polyethylene tubing installed at 0.1, 0.2, 0.3, 0.4, 0.5, 0.7, 0.9, 1.1, 1.3, 1.5 and 1.7 m depths within each tank. Internal gas compositions in each tank will be used to understand O_2 gas transport mechanisms, O_2 consumption rates from the oxidation of sulfide minerals, and CO_2 production or consumption rates from the dissolution or precipitation of carbonate minerals. Measured O_2 consumption rates can be used to determine sulfide mineral oxidation rates assuming sulfide oxidation is the only process consuming O_2 (Linklater, Sinclair and Brown, 2005).

Soil moisture 2725ARL Jet FI11 tensiometers were installed in the unsaturated zone of the tanks to measure pressure potential (matrix potential) in the FPK at depths of 0.25, 0.5, 1.0, 1.5 and 1.7 m. Pressure potential measurements will be used to calculate the gradient pressure in order to determine the rate of water movement through the unsaturated zone in the tanks.

Each tank was filled with the assigned FPK fraction in lifts of 0.3 to 0.4 m. Filling the tanks in lifts was necessary to accurately place the instruments and insure material was applied uniformly and compacted. Tanks were filled with FPK to a height of 1.7 m above the tank bottom. During filling of the tanks, a 20 L composite sample from each tank was collected for humidity tests and analyses of mineralogy, grain size, total sulfur and carbon, whole rock analyses, acid-base accounting and neutralization potential. All tanks were filled and instrumented on August 3, 2012 and remain exposed to ambient conditions year-round.

Sampling

Water sampling was initiated on August 28, 2012. Porewater was collected into SWSS by applying a vacuum of approximately 70 kPa two days prior to sampling. Water samples were collected from SWSS and drain sample cells using 60 mL polyethylene (PE) syringes. Measurements of pH, Eh and electrical conductivity (EC) were made on unfiltered samples in the field. The resulting water samples were passed through 0.45 μm filters and split into three aliquots. One aliquot of water was acidified with 12 *N* trace-metal grade HNO_3 to a pH of <1 for cation analysis, and another aliquot was left unacidified to use for anion analysis. The remaining water was used for alkalinity and NH_3 analyses. Water samples collected for anion and cation analyses were immediately refrigerated until analyses. Determination of major cations and trace elements was performed by inductively coupled plasma–optical emission spectroscopy (ICP–OES) and inductively coupled plasma-mass spectrometry (ICP–MS), respectively. Ion chromatography was used to measure inorganic anion concentrations. Concentrations of O_2 and CO_2 gas were measured from gas lines using a Grafton Model 902 O_2/CO_2 analyzer. Air temperature and precipitation data from site was provided by Diavik.

Humidity Cells

Two samples of each the fine-, medium- and coarse fractions of FPK were split from the tank material for an 80 week kinetic testing program. Kinetic testing followed the ASTM (1996) 5744-07

protocol, with the exception that samples were not crushed. Original size fractions were maintained in order to observe any geochemical variation caused by differences in grain size distributions. One set of fine, medium and coarse humidity cells was operated at room temperature (~22°C) and one set was operated at 4°C. The cells were subjected to a weekly cycle of a 3-day dry period (0% relative humidity), 3-day wet period (>95% relative humidity), and a 1-day flood leach with 500 mL of DI water. Effluent from each humidity cell was analyzed weekly for pH, ORP, acidity, alkalinity and SO_4. Dissolved metals, Cl and F were analyzed weekly from week 1-20, bi-weekly from week 20-40, and every six weeks from week 40-80.

RESULTS AND DISCUSSION

Mineralogy

The kimberlite pipes at Diavik are intrusions within supracrustal rocks and late Archean granitoids of the Slave structural province (Moss, Russell, and Andrews, 2008). The pipes are composed of bedded volcaniclastic kimberlite, consisting of both kimberlite and mudstone xenoliths. Processed kimberlite used for this study was composed of olivine, calcite, quartz, garnet, lizardite, biotite, albite, saponite, and both framboidal and massive pyrite. Pyrite grains are mostly encapsulated in fragments of serpentine and aluminosilicate clays. The acid generating potential (AP) and neutralizing potential (NP) of the FPK were calculated following the Modified ABA test described by MEND (1991). The AP values are similar among the three grain size fractions, 5.3 - 7.8 kg $CaCO_3$ eq/t, however not all of the AP would be available due to the occurrence of some pyrite as locked particles in other mineral fragments. The NP of the samples are similar, 165 - 218 kg $CaCO_3$ eq/t, and far exceed the acid generating potentials (Table 1). Olivine and calcite were the primary neutralizing minerals.

Sieve analyses using sieves +20, -20+35, -35+60, -60+100, -100+120, -120+200, -200+270 and -270 show the differences in grain size between the FPK in the three tanks and humidity cells (Table 1). The FPK from the FT and MT samples were similar with FT having slightly finer FPK, whereas the FPK from CT was coarser with a lower uniformity coefficient (Table 1).

Table 1 Grain size distribution, sulfur content, neutralization potential (NP), acid-generating potential (AP) and net neturalizing potential (NNP) for the tank and humidity cell experiments.

Tank	d10	d60	Uniformity Coefficient	Sulfur (%)	NP (kg $CaCO_3$ eq/t)	AP (kg $CaCO_3$ eq/t)	NNP (kg $CaCO_3$ eq/t)
FT	0.07	0.39	5.8	0.23	218.4	5.3	213
MT	0.08	0.44	5.3	0.34	203.1	7.8	195
CT	0.18	0.82	4.6	0.26	165.3	6.6	159

Processed kimberlite tanks

The pH from the tank drains were circumnetural to alkaline and showed little variation between tanks during the active period of June 1, 2013 to August 31, 2013 (Figure 3). The Eh and alkalinity trends were similar to that of pH, with all tanks exhibiting oxidized conditions and alkalinity typically >40 mg L^{-1} (as $CaCO_3$) (Figure 3), consistent with calculated NNP. Concentrations of SO_4 remained relatively constant for each tank but with the FT tank drain having much lower concentrations (Figure 3). The CT tank had slightly higher concentrations than the MT tank (Figure 3). The EC trends for the tanks mirror the SO_4 concentration trends with the highest concentration of dissolved SO_4 observed from the CT tank and the lowest from the FT tank (Figure 3).

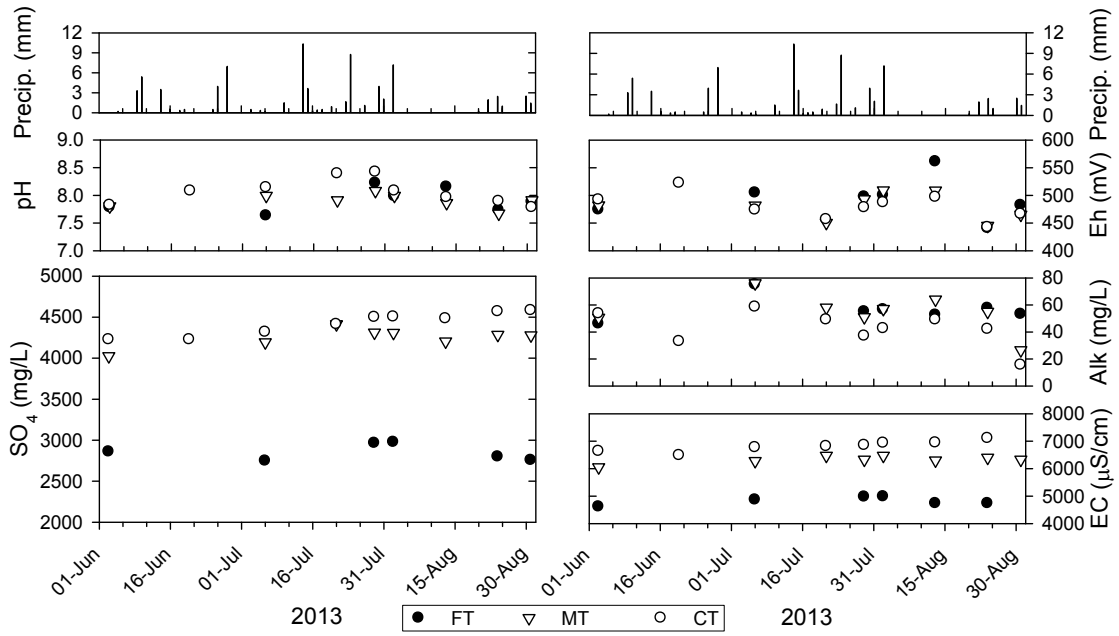

Figure3 Temporal variation of precipitation, pH, SO_4, Eh, alkalinity and EC from the PK tanks between June 1, 2013 and August 31, 2013.

The pH in the SWSS from all three tanks remained circumneutral to alkaline at all depths and was slightly higher in the MT and CT tanks for 2013 than for 2012 (Figure 4), possibly as accumulated reaction products began to flush through the tanks. Similarly, alkalinity concentrations in all tanks at all depths remained similar for both 2012 and 2013 (Figure 4), consistent with calculated NP values and alkalinity concentrations measured in porewater from the unsaturated zone at the PK facility (Moncur and Smith, 2012). Dissolved sulfate concentration in PK slurry water from the end-of-pipe ranged from 59 to 380 mg/L. Porewater concentrations of dissolved sulfate in the tanks approached 5000 mg L^{-1} and remained relatively constant between 2012 and 2013 sampling events (Figure 4). These elevated dissolved sulfate concentrations suggest that sulfide oxidation is likely occurring throughout the tanks (Lindsay et al., 2015). Depletions in O_2 in the FT and MT tanks were observed for 2012, but O_2 concentrations remained near atmospheric levels in 2013 and for both years in the CT tank (Figure 4). Volumetric water content (VWC) was typically higher in 2012 than in 2013 but varied with depth. The similar peaks and trends between sample years suggest the changes in VMC are not an artefact of sample timing dates (i.e. sampling during a particularly dry or wet time) and may suggest compositional differences by depths that affect wetting front propagation.

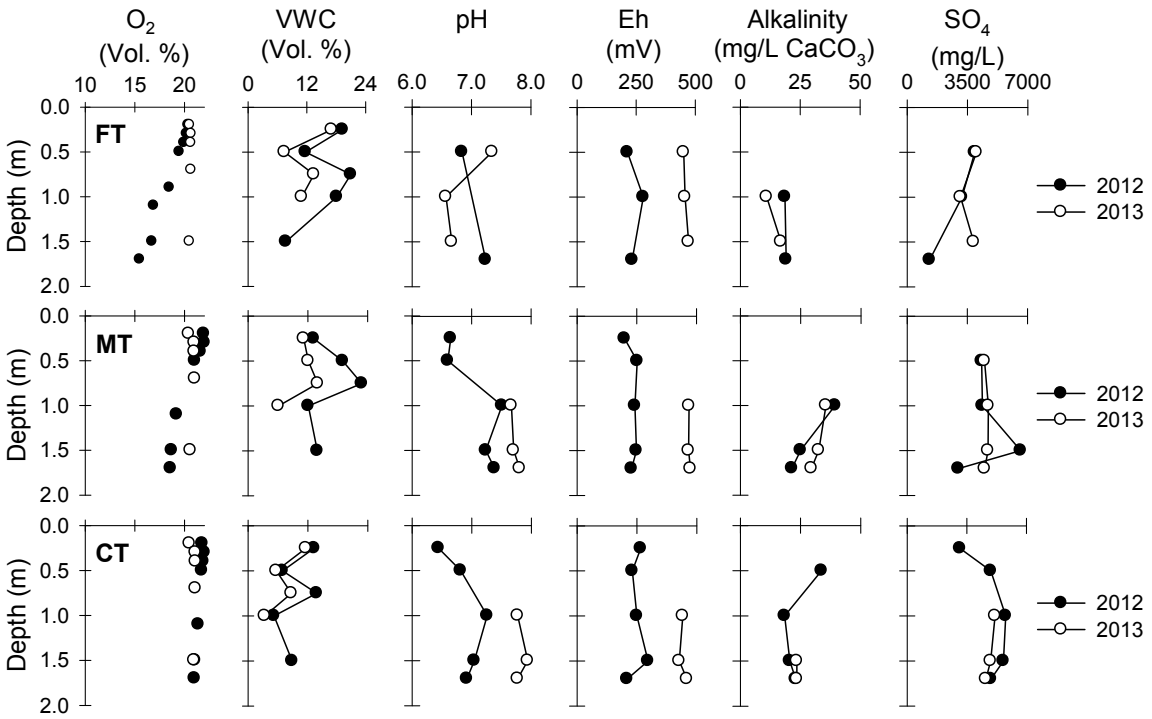

Figure 4 Depth profiles of oxygen gas, volumetric water content (VWC) and selected porewater chemistry from the PK tanks measured in 2012 and 2013.

Humidity cells

The pH in all humidity cell charges remained circumneutral to alkaline for the duration of the experiment with pH values ranging from 7.1 to 8.4 (Figure 5). The cells in the cold room consistently exhibited higher pH compared to the corresponding cell at room temperature. The room temperature cell with CT material exhibited lower pH and erratic fluctuations compared to the other five cells, possibly as a result of preferential flow paths reducing contact and reaction time with the cell material. However, alkalinity measurements from the same cell did not exhibit the same erratic behavior. Alkalinity remained >60 mg/L (as $CaCO_3$), for the duration of the experiment (Figure 5). Conditions within all cells remained oxidized with ORP ranging from 300 to 450 mV, consistent with the tank data.

Sulfate release rates were slightly higher for room temperature cells than for cells operated at 4°C, and in descending order, FT, MT and CT cells (Figure 5). Data from the first three weeks represent flushing of accumulated reaction products. Release rates from week 4 – 24 declined rapidly, and then declined at a more moderate rate from week 24 – 55. Sulfate release rates become more stable after week 55 until the end of the experiment at week 80 (Figure 5). Mass calculations suggest 77-85% of total sulfur and 73-81% of sulfides remain in the test charges after the 80 week experiment; however the decreasing rates suggest available sulfide surfaces are becoming limited by a reduction of available free grains, sulfide armoring or other limiting processes within the test cells.

Preliminary pH and alkalinity tank data are typically consistent with both the humidity cell experiments and the static tests which indicate that there is an excess of neutralization potential

over acid-generating potential. On-going monitoring of the tanks will determine if SO_4 release rates in the tanks follow the observed humidity cell trends of rapidly declining release rates despite >70% of measured sulfides remaining in the samples. Though not directly comparable, the difference between tanks in drain SO_4 concentration trends from humidity cell release rate trends suggest additional processes are occurring *in situ*. These processes need to be identified and evaluated for any scaling calculations.

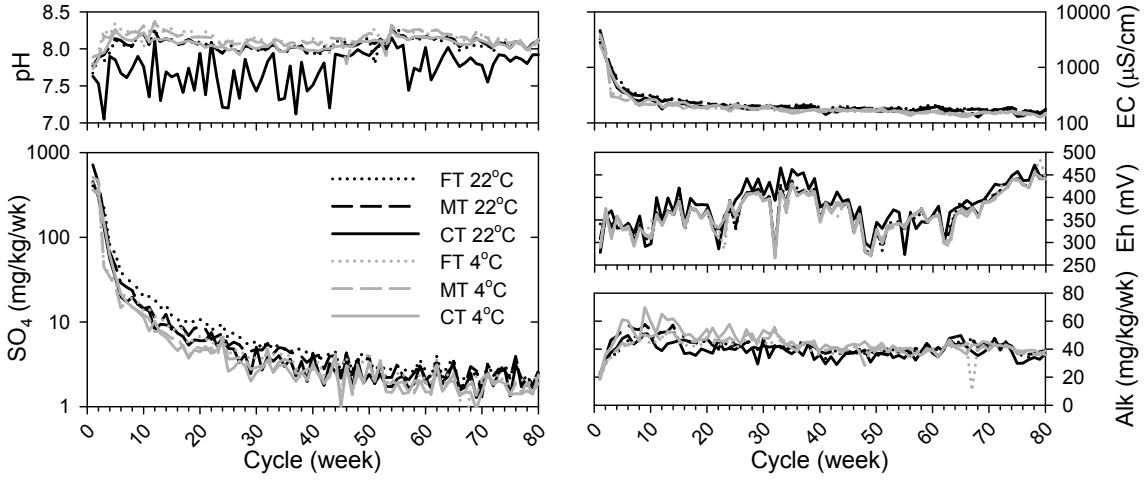

Figure 5 Temporal variation of pH, SO_4, EC, Eh and alkalinity of leachate from the FT, MT and CT humidity cells at 22°C and 4°C.

CONCLUSION

Comparing humidity cell reaction rates to the *in situ* tank experiment results are preliminary because the low amount of precipitation and infiltration and short thaw season limits the release of reaction products from the tanks and products are expected to take more than one thaw year to flush from the tanks. On-going monitoring of the tank experiments will permit the calculation of an *in situ* sulfate release rate(s) that accounts for local climatic factors that affect sulfide oxidation. Tank release rates can then be compared to humidity cell release rates to determine the applicability of using the small-scale tests to predict long-term seepage quality from the PKC facility. Diavik will use the results from the tank and humidity cell experiments to predict and refine long-term seepage quality from the PKC facility.

ACKNOWLEDGEMENTS

We would like to thank David Blowes, Kevin Tattrie, Jeff Bain, Sean Sinclair, Kent Richardson, David Wilson, Gord Macdonald, Emily Taylor, and the Diavik Environment team for their advice and technical assistance. This project was funded by Rio Tinto-DDMI. We thank an anonymous reviewer for their constructive evaluation of this manuscript. The use of trade names is for descriptive purposes only.

NOMENCLATURE

PK	Processed kimberlite
PKC	Processed kimberlite containment facility
FPK	Fine processed kimberlite
FT	Tank with fine FPK fraction
MT	Tank with medium FPK fraction
CT	Tank with coarse FPK fraction
SWSS	Soil water suction sampler
EC	Electrical conductivity

REFERENCES

ASTM (American Society for Testing and Materials) (1996) Test method for laboratory weathering of solid materials using a humidity cell, ASTM International, West Conshohocken, PA, USA.

Lindsay, M.B.J., Moncur, M.C., Bain, J.G., Jambor, J.L., Ptacek, C.J., Blowes, D.W. (2015) Geochemical and mineralogical aspects of sulfide mine tailings, Applied Geochemistry

doi:http://dx.doi.org/10.1016/j.apgeochem.2015.01.009

Linklater, C.M., Sinclair, D.J., Brown, P.L. (2005) Coupled chemistry and transport modelling of sulphidic waste rock dumps at the Aitik mine site, Sweden, Applied Geochemistry, vol. 20, pp. 275–293.

MEND. (1991). Acid rock drainage prediction manual. MEND Project 1.16.1b, report by Coastech Research. MEND, Natural Resources Canada, Ottawa, Ontario.

Moncur, M.C., Smith, L.J.D. (2012) Processed kimberlite porewater geochemistry from Diavik Diamond Mines, Inc., In: W.A. Price (Ed.), 9th International Conference on Acid Rock Drainage, Ottawa, ON, May 20-26, 12p.

Moss, S., Russell, J.K. and Andrews, G.D.M. (2008) Progressive infilling of a kimberlite pipe at Diavik, Northwest Territories, Canada: Insights from volcanic facies architecture, textures, and granulometry, Journal of Volcanology and Geothermal Research, vol. 174, pp. 103-116.

Smith, L.J.D., Moncur, M.C., Neuner, M., Gupton, M., Blowes, D.W., Smith, L., Sego, D.C. (2012) The Diavik waste rock project: design, construction and instrumentation of field-scale experimental waste rock piles, Applied Geochemistry, vol. 36, pp 187-199.

The Evolution of Tailings Seepage Chemistry at One of Australia's Largest and Longest Operating Mines

Bronwen Forsyth[1], Mansour Edraki[2] and Thomas Baumgartl[2]

1. *SRK Consulting, Australia*
2. *Centre for Mined Land Rehabilitation, Sustainable Minerals Institute, The University of Queensland, Australia*

ABSTRACT

The Mount Isa mines have been active for more than 90 years and have played a significant role in the economy of Queensland. Process tailings from both copper and lead-zinc production streams are deposited in a large valley fill tailings storage facility which currently has an approximate surface area of 14 km^2. The site is a world class sedimentary deposit with climatic conditions typified by prolonged dry seasons with relatively short, high intensity wet seasons. This paper discusses the mineralogical and geochemical characterization of the tailings, and the assessment of the potential for metal leaching, to aid mine closure planning.

Historical tailings at Mount Isa are generally non-acid forming based on conventional acid base accounting, mineralogical examination, and kinetic testing. However, modern tailings are characterized by higher sulfide and associated trace element content, and lower carbonate mineral content than historical tailings. Changes in tailings composition are likely attributable to changes in ore and mineral processing methods, and time since tailings deposition. Strategies are currently being developed for the placement of a suitable cover system to reduce surface water – tailings interaction following decommissioning of the TSF. This study demonstrates the benefit of integrating detailed geochemical characterization into closure and rehabilitation planning.

Keywords: Mount Isa Mine, tailings, seepage

INTRODUCTION

Mount Isa is located in North-West Queensland, Australia, approximately 360 km south from the Gulf of Carpentaria and 960 km west of the Coral Sea (20° 43' S, 139° 29' E) (Figure 1). Mineralization in the Mount Isa region was first discovered in 1923 and subsequently a large number of mining leases were established with ore extracted through numerous shallow open pit operations. In 1924, Mount Isa Mines was incorporated, consolidating a number of the major leases and initiating the development of an underground mining operation. Today, ore is sourced from both underground and open pit mines. Copper ore is mined and processed separately from lead and zinc ore. The ore is concentrated by grinding and flotation, followed by smelting. Typically 30% of the combined copper and lead-zinc tailings stream is utilized as hydraulic fill in underground mine operations and the remaining portion is sent to a tailings storage facility (TSF).

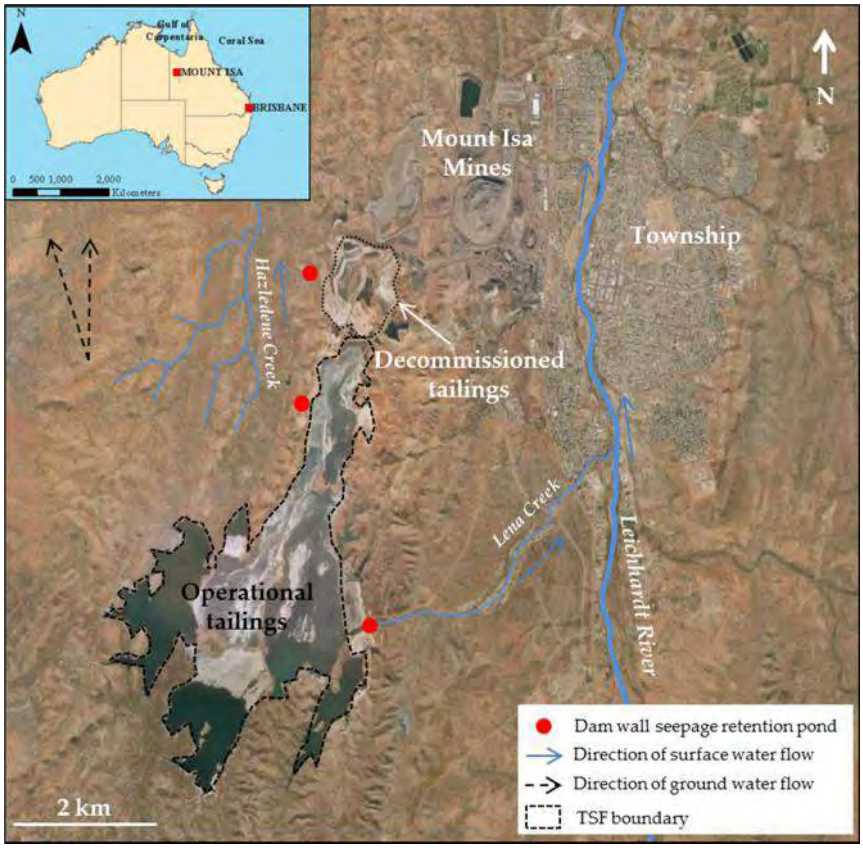

Figure 1 Site locality

The TSF is approximately 14 km² in surface area. The area is contained by three visible dam walls, with a further two dam walls buried under a waste rock dump to the north. Toe seepage emanates from the base of the dam walls at rates of less than 1 to 5 L/s and is captured in retention ponds prior to being pumped back to the TSF. It is characterized by neutral pH (7.3 to 8.2) and elevated sulfate (3100 to 8400 mg/L SO_4), with concentrations of arsenic, boron, cadmium, cobalt, copper, lead, manganese, and zinc slightly elevated in comparison to Australian National Water Quality Guidelines for 95% aquatic ecosystem protection (ANZECC, 2000) and regional surface and ground waters.

The TSF is composed of decommissioned cells to the north, and operational cells to the south (Figure 1). Decommissioned cells were operational from the early 1950s to the mid-1960s. Tailings within the decommissioned cells (hereon referred to as 'decommissioned tailings') have been exposed to approximately 40 years of weathering and exposure. Since decommissioning of the northern cells, tailings have been actively deposited within the operational cells ('operational tailings'). Tailings deposition is cycled through the different operational cells so that the operational tailings sampled by this study had been exposed for less than two years.

This paper discusses the mineralogical and geochemical characterization of the tailings, and the potential release of metals and acidity due to long-term mineralogical weathering.

Climate and Geology

The climate of Mount Isa is semi-arid and subtropical, characterized by average annual pan evaporation (3100 mm) exceeding average annual rainfall (430 mm), and warm to hot temperatures (19 to 32 °C mean monthly minimum and maximum) (BoM, 2012). On average, 75% of annual rainfall occurs between the months of December and March ('wet season') with the intervening months of April to November typified as the 'dry season'.

The Mount Isa Mines' ore deposits are located within the Mount Isa Inlier; an area of more than 50,000 km^2 of Early and Middle Proterozoic rocks host to economically significant quantities of lead-zinc, copper, uranium, cobalt, and gold (Blake *et al.*, 1990). Mount Isa shares some geological similarities to other well-known shale-hosted massive sulfide deposits, such as the Red Dog and Lik deposits in Alaska (Kelley *et al.*, 1995; Kelley and Taylor, 1997), and McArthur River and Broken Hill deposits in Australia (Huston *et al.*, 2006).

A distinct feature of Mount Isa is the occurrence of spatially separate lead-zinc and copper ore bodies. Both occur within the Urquhart Shale, a unit of metamorphosed pyritic and dolomitic shale approximately 1000 m thick at the mine. The main economic sulfides within lead-zinc ore are galena (PbS) and sphalerite (ZnS) with minor amounts of silver occurring in close association with galena. Copper ore principally occurs as chalcopyrite ($CuFeS_2$). The main gangue sulfide is pyrite (FeS_2). The main carbonates are dolomite ($CaMg(CO_3)_2$) and calcite ($CaCO_3$), with ankerite ($Ca(Fe,Mg)(CO_3)_2$) and siderite ($FeCO_3$) also present. Other gangue minerals include quartz, chlorite, K-feldspar, muscovite, biotite, albite, rutile, and carbonaceous material (Heinrich *et al.*, 1995; Chapman, 2004).

METHODOLOGY

Sample Collection

Decommissioned and operational tailings were sampled to less than 1 m depth with the assistance of an excavator, and to depth using a truck-mounted drill rig equipped with a push-in piston sampler. Drill cores were sub-sampled at 1 m intervals from 0 to 3 m below the tailings surface, and at 3 m intervals to bedrock (typically 27.5 m below surface). A total of 20 samples from four locations within decommissioned tailings, and 30 samples from 10 locations within operational tailings were collected.

The selection of sample sites at Mount Isa was ultimately constrained by accessibility. The unconsolidated nature of operational tailings restricted sampling to areas accessible by internal roads that run the length of the TSF. Analytical data were interpreted with supporting information

from secondary sources including aerial photography, ore geology and mineral processing publications, concentrator records, annual Xstrata sustainability reports, and personal communication with long-term mine staff.

Mineralogy

The mineral composition of tailings samples was determined using X-ray diffraction, optical microscopy, Scanning Electron Microscopy coupled with Energy Dispersive Spectroscopy (SEM-EDS), and Mineral Liberation Analysis (MLA). All analyses were undertaken at the University of Queensland.

Static Testing

Tailings were analyzed for acid base accounting (ABA) (AMIRA International, 2002) and elemental composition by four-acid digestion and ICP-MS analysis. Maximum Potential Acidity (MPA) was calculated using sulfide sulfur corrected for non-acid generating forms of sulfide, specifically sphalerite and galena using zinc and lead concentrations, respectively. Acid Neutralization Capacity (ANC) was measured using the Sobek method modified to oxidize and hydrolyze dissolved ferrous iron during the titration step (AMIRA International, 2002). Analyses were undertaken at the University of Queensland and a commercial laboratory (ALS) in Brisbane, Australia. Quality checking and assurance consisted of duplicate, certified reference material, and method blank inclusion in each sample batch.

Column Leaching

Three decommissioned and three operational tailings column samples were extracted from in-situ, near-surface (0 to 1 m depth) deposited tailings. The samples were collected intact with minimal disturbance to stratigraphy by inserting the column tubing housed within a soil corer directly into the tailings profile. The columns were 125 mm in length and 70 mm in internal diameter. The tailings were leached with deionized water supplied under constant head pressure using a Mariotte-type design. A flow rate of 2 to 5 mL/hr was targeted as this allowed the accumulation of leachate sufficient in volume to be collected at least once every two days. The columns were subject to four phases (Figure 2):

a) Saturated leach 1. Deionized water was slowly introduced from the column base over the course of one to two weeks to exclude air from pore spaces while minimizing loss of pore structure from increasing pressure, and then leached under saturated conditions until electrical conductivity showed little variation between collected samples (typically two to three months).
b) Suction and aeration. Drying was induced within the columns by applying suction (-15 to -60 kPa). The concept was to empty pores of water and increase oxygen ingress. Compressed air was fed directly into the tailings via an inlet on the side of each column for a period of one week. This was to encourage oxidation reactions and to hasten the mineral weathering process.
c) Saturated leaching 2. Deionized water was re-introduced in order to mobilize any soluble constituents released as a result of the suction and aeration step.
d) End of leach characterization. A non-reactive tracer test (KCl) was conducted to estimate solute transport parameters. Chloride break-through curve data were modelled using a non-equilibrium dual porosity, Mobile-Immobile Model within Hydrus-1D (Version 4.14) (Simunek *et al.* 2008). Further method detail is provided by Forsyth *et al.* (2013).

Collected leachate was analyzed for pH, electrical conductivity, oxidation-reduction potential, sulfate, chloride, major cations by ICP-AES, and trace elements by ICP-MS. Element release rates (mg/kg/day) were calculated for leach phases 1, 2a, and 2b as shown in Figure 2.

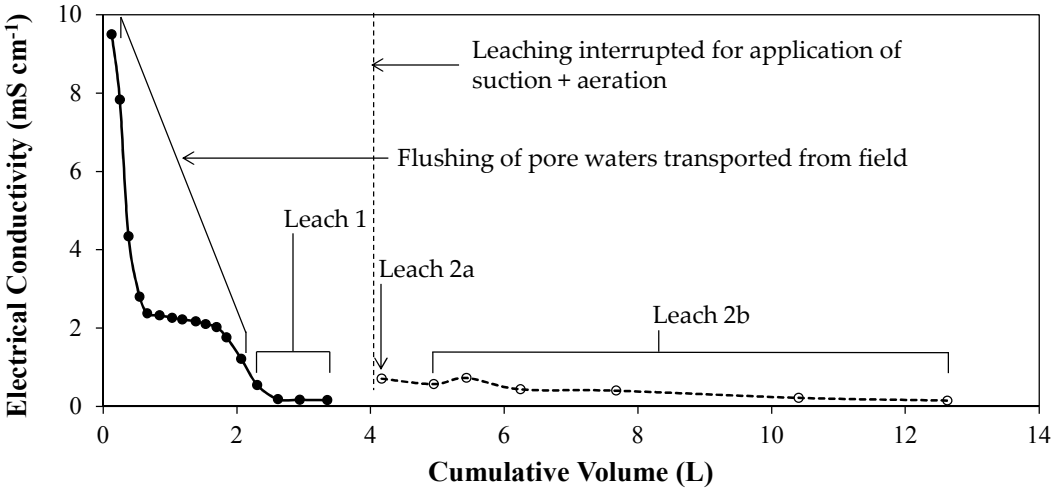

Figure 2 Column leach phases

RESULTS AND DISCUSSION

Tailings Characterization

Mineralogy

Bulk mineralogy was similar between decommissioned and operational tailings. The main minerals were quartz, K-feldspar, chlorite, muscovite, dolomite, calcite, and pyrite. Quantitative XRD showed that operational tailings contained more pyrite (12 to 15 wt. %) and less dolomite (6 to 16 wt. %) than decommissioned tailings (1 to 2 wt. % and 11 to 18 wt. %, respectively). Pyrrhotite, chalcopyrite, galena, sphalerite, ankerite, and siderite were observed in low abundance (less than 2 wt. %) in both tailings types.

Secondary minerals within decommissioned tailings included goethite and gypsum in sub-surface samples, and gypsum, hexahydrite, jarosite, melanterite/rozenite, chalcanthite, and poitevinite in surface samples. SEM-EDS analysis on decommissioned tailings indicated the presence of poorly crystalline iron (oxy)hydroxides, iron oxyhydroxysulfates, and a calcium-iron-silica gel of variable chemical composition. Secondary mineralization in operational tailings was restricted to gypsum.

Acid Base Accounting

ABA classifications were defined using ANC/MPA ratios (Figure 3), with samples forming four groups reflective of their origin within the TSF:

a) Group 1: decommissioned tailings, 0 to 1 m depth below surface. Samples within this group were depleted in ANC (geometric mean 110 kg H_2SO_4/t) and MPA (20 kg H_2SO_4/t) as a result of over 40 years of mineral weathering and exposure.

b) Group 2: decommissioned tailings, 1 to 27.5 m depth below surface. Samples within this group contained high ANC (320 kg H_2SO_4/t) and low MPA (120 kg H_2SO_4/t), and were classified as non-acid forming (NAF) or uncertain.
c) Group 3: operational tailings, 0 to 12 m depth below surface. Samples within this group typically contained less ANC (160 kg H_2SO_4/t) and more MPA (200 kg H_2SO_4/t) than operational tailings below 12 m depth, and were classified as potentially acid forming (PAF) or uncertain.
d) Group 4: operational tailings, 12 to 27.5 m depth below surface. Samples within this group were characterized by ANC (240 kg H_2SO_4/t) intermediate to that of group 2 and 3, and low MPA (120 kg H_2SO_4/t), and were classified as uncertain.

No samples were acidic. Paste pH ranged from 6.0 to 8.0, with group 3 samples at the lower end of the range (pH 6.0 to 7.4).

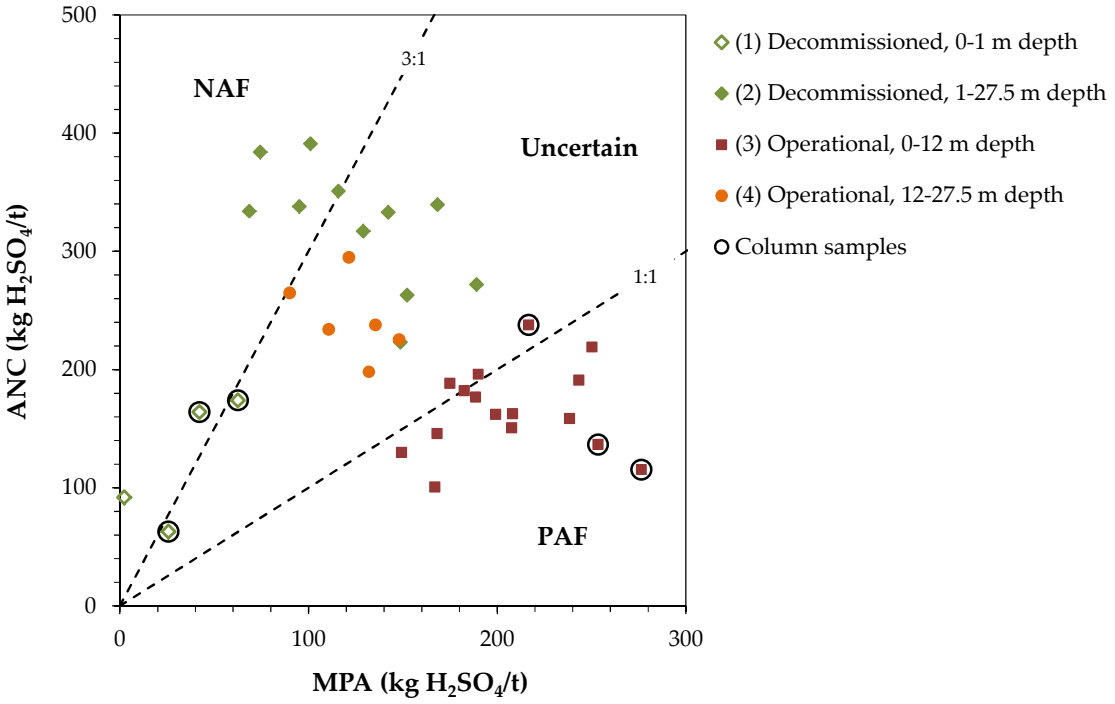

Figure 3 Acid base account plot for decommissioned and operational tailings

Trace Element Analysis

A comparison of decommissioned and operational tailings using a two-sample t-test indicated that operational tailings from 0 to 12 m depth contained significantly ($p \leq 0.01$) greater concentrations of trace elements commonly associated with mineral sulfides, including arsenic, copper, lead, molybdenum, nickel, and zinc (Table 1). Slightly elevated concentrations of some metals were observed in near-surface decommissioned tailings, including copper, molybdenum, nickel, and zinc (Table 1). These metals are likely to occur in association with efflorescent sulfate salts.

Table 1 Element concentrations by four-acid digestion summarized as the geometric mean with minimum and maximum values in parentheses

Tailings Group	As	Cu	Pb	Mo	Ni	Zn
	mg/kg	mg/kg	mg/kg	mg/kg	mg/kg	mg/kg
Decommissioned 0-1 m depth (n = 7)	480 (200, 790)	1900 (1000, 4600)	4200 (3200, 5700)	4 (2, 100)	22 (15, 32)	5500 (4400, 6800)
Decommissioned 1-27.5 m depth (n = 11)	330 (210, 460)	960 (790, 2000)	2800 (1800, 6100)	1 (1, 2)	11 (8, 14)	3700 (2200, 5900)
Operational 0-12 m depth (n = 21)	810 (610, 1400)	2200 (1300, 6100)	5400 (2400, 8500)	26 (3, 220)	26 (19, 35)	8600 (3400,20000)
Operational 12-27.5 m depth (n = 6)	540 (440, 800)	1200 (690, 1500)	4000 (2600, 6600)	2 (2, 3)	16 (12, 22)	4800 (4300, 7100)

Note: All values are reported to two significant figures.

Changes in Mine Operation Influencing Tailings Composition

In comparison to historical tailings, the modern tailings stream at Mount Isa, represented by operational tailings from 0 to 12 m depth, is characterized by higher sulfide and associated trace element content, and less carbonate. Information from secondary sources suggests changes in tailings composition are likely attributable to changes in ore source and processing.

Decommissioned tailings were primarily derived from the processing of shallow copper ore bodies (200, 400, 500 and 600 mRL) which are predominantly dolomitic in composition (Wilde *et al.*, 2006), and lead-zinc ore from the Mount Isa underground mine. In contrast, operational tailings were derived from the processing of deeper, more siliceous copper ore bodies (1100, 1900, 3000 and 3500 mRL), and lead-zinc ore from George Fisher underground and Handlebar Hill and Black Star open pit mines.

The introduction of ore preconcentration and ultra-fine grinding technologies such as the IsaMill allowed the processing of lower grade ores (Gao *et al.*, 2002), which contain more pyrite, and resulted in a finer, higher sulfide tailings stream.

Mineral Reaction Rates

Column Leaching

Leachate pH remained near-neutral throughout the experiment with little difference between the ranges of decommissioned (pH 7.5 to 8.3) and operational tailings (pH 7.3 to 8.4). Major ions were dominated by calcium and sulfate, with leachate from two of the three decommissioned tailings remaining supersaturated with respect to gypsum throughout the experiment.

The columns were characterized by long pore water residence times (15 to 53 hours) and high water retention with 84 to 98% of pores remaining water-filled after the application of -60 kPa pressure. However, this small change in water content in operational tailings was sufficient to increase sulfate, and calcium and magnesium release rates (indicative of sulfide mineral oxidation and acid neutralization, respectively), and release rates for certain trace elements, including manganese, cobalt, and zinc (for example, operational tailings column 2, Table 2). The increase in element release rates from operational tailings was accompanied by a 0.4 to 0.7 unit decrease in leachate pH.

Saturated hydraulic conductivity (Ks) under constant head increased during the experiment (Table 2). In two columns, this was attributed to the formation of fine vertical cracks observed after the application of suction. In other columns, it was attributed to the slow dissolution of soluble phases (particularly gypsum) resulting in more pores contributing to water flow.

Sulfate, calcium, and magnesium release rates were used to calculate rates of acid generation and neutralization, whereby:

$$\text{Sulfide oxidation rate (kg } H_2SO_4\text{/t/day)} = SO_4 \text{ production rate (kg/t/day)} \times \frac{98.08}{96.06} \quad \textbf{(1)}$$

$$\text{ANC consumption rate (kg } H_2SO_4\text{/t/day)} = \text{sulfide oxidation rate (kg } H_2SO_4\text{/t/day)} \times \frac{[Ca\ (mol)+Mg(mol)]}{SO_4(mol)} \quad \textbf{(2)}$$

Leachate solutions saturated and/or supersaturated with respect to gypsum were excluded from the calculations.

A comparison of the calculated rates (Table 3) indicated that ANC would likely be consumed before the acid-generating sulfides in operational tailings 1 and 2 under all test conditions, which supports a PAF classification. Conversely, ANC was unlikely to be consumed before the acid-generating sulfides in decommissioned tailings, which supports a NAF classification. Operational tailings 3 were classified as uncertain using static ABA. Kinetic testing suggests this sample has the potential to become acid generating if conditions were to remain unsaturated and highly oxidizing.

CONCLUSIONS

Modern tailings at Mount Isa are characterized by higher sulfide and associated trace element content, and lower carbonate mineral content than historical tailings. Changes in tailings composition are likely attributable to changes in ore and mineral processing methods, and time since tailings deposition.

Strategies are currently being developed for placement of a suitable cover system to reduce surface water – tailings interaction following decommissioning of the TSF. It is anticipated that covering the surface tailings would potentially limit the accumulation of efflorescent sulfate salts on the tailings surface, which if allowed to accumulate, would be subject to dissolution and transportation during wet season rain events. Infiltrated water that passes through the oxidation zone is expected to be readily neutralized by ANC in the tailings below. Modification of the final tailings layer prior to deposition to remove or pacify pyrite could also potentially be considered as an alternative to a suitable cover system.

Table 2 Element release rates from operational tailings column 2

Leach Phase[a]	Water Content	pH	SO_4	Ca	Mg	Mn	Co	Zn
	cm^3/cm^3		mg/kg/day	mg/kg/day	mg/kg/day	mg/kg/day	mg/kg/day	mg/kg/day
1	53 (100%)	8.1	18	10	0.33	0.0074	0.00006	0.0093
2a	49 (92%)	7.7	450	160	40	1.1	0.059	2.0
2b	53 (100%)	7.9	77	31	5.8	0.14	0.006	0.14

Note: (a) Refer to Figure 2.

Table 3 Sulfide oxidation and ANC consumption rates measured from column leaching

Column	Leach	Mean K_s	Acid Generation			Neutralization			Class.
	Phase[a]		MPA	Sulfide Oxidation Rate	Depletion Time in Lab	ANC	ANC Consumption Rate	Depletion Time in Lab	
		cm/day	kg H_2SO_4/t	kg H_2SO_4/t/day	years	kg H_2SO_4/t	kg H_2SO_4/t/day	years	
Decommissioned 1	1	1.2	71	0.17	1.1	174	0.10	4.9	NAF
	2a	3.5	71	0.54	0.4	174	0.34	1.4	NAF
	2b	0.9	71	0.13	1.5	174	0.09	5.4	NAF
Operational 1	1	0.3	293	n.a.[b]	n.a.[b]	115	n.a.[b]	n.a.[b]	n.a.[b]
	2a	0.4	293	0.32	2.5	115	0.26	1.2	PAF
	2b	12	293	0.10	7.9	115	0.09	3.4	PAF
Operational 2	1	0.2	276	0.03	25	137	0.03	13	PAF
	2a	62	276	0.46	1.6	137	0.45	0.8	PAF
	2b	120	276	0.09	8.7	137	0.09	4.2	PAF
Operational 3	1	1.6	231	0.07	9.4	238	0.04	15	NAF
	2a	83	231	0.23	2.8	238	0.55	1.2	PAF
	2b	120	231	0.20	3.2	238	0.15	4.3	NAF

Notes: (a) Refer to Figure 2. (b) Rate indeterminate due to gypsum saturation.

ACKNOWLEDGEMENTS

This research was undertaken by the Centre for Mined Land Rehabilitation and funded by Glencore's Mount Isa Mines. Dr Laurent Lassabatere of Université de Lyon, France, is thanked for his role in the modelling of column solute transport parameters. John Chapman of SRK Consulting Australia and Jason Jones of Glencore are thanked for their thoughts and suggestions regarding this paper.

REFERENCES

AMIRA International (2002) ARD Test Handbook. AMIRA P387A Project: Prediction and Kinetic Control of Acid Mine Drainage. Melbourne, Australia, Ian Wark Research Institute and Environmental Geochemistry International.

ANZECC (2000) Australian and New Zealand Guidelines for Fresh and Marine Water Quality. Australian and New Zealand Environment and Conservation Council and Agriculture and Resource Management Council of Australia and New Zealand.

Berkman, D. (1996) *Making the Mount Isa Mine, 1923-1933*. The Australasian Institute of Mining and Metallurgy, Carlton, Victoria.

Blake, D. H. (1987) Geology of the Mount Isa Inlier and environs, Queensland and Northern Territory. *Bureau of Mineral Resources, Geology and Geophysics Bulletin*, 225, 1-83.

BoM (2012) Climate Statistics for Australian Locations: 029126 Mount Isa Mine Dataset IDCJCM0036_029126. Australian Government Bureau of Meteorology.

Chapman, L. H. (2004) Geology and Mineralization Styles of the George Fisher Zn-Pb-Ag Deposit, Mount Isa, Australia. *Economic Geology*, 99, 233-255.

Forsyth, B., Lassabatere, L., Edraki, M., and Baumgartl, T. 2013, 'Contaminant Release from Sulfidic Mine Tailings: Column Experiments and Geochemical Modeling'. *3rd International Seminar on Environmental Issues in Mining (Enviromine)*, Centre for Mined Land Rehabilitation and Gecamin, Santiago, Chile, 4-6 December.

Gao, M., Young, M. F. & Allum, P. (2002) IsaMill Fine Grinding Technology and its Industrial Applications at Mount Isa Mines. *Canadian Institute of Mining, Metallurgy and Petroleum 104th Annual General Meeting*, Vancouver, British Columbia, 28 April - 1 May.

Heinrich, C. A., Bain, J. H. C., Mernagh, T. P., Wyborn, L., Andrew, A. S. & Waring, C. L. (1995) Fluid and Mass Transfer during Metabasalt Alteration and Copper Mineralization at Mount Isa, Australia. *Economic Geology*, 90, 705-730.

Huston, D. L., Stevens, B., Southgate, P. N., Muhling, P. & Wyborn, L. (2006) Australian Zn-Pb-Ag Ore-Forming Systems: A Review and Analysis. *Economic Geology*, 101, 1117-1157.

Kelley, K.D., Seal, R.R., Schmidt, J.M., Hoover, D.B. & Klein, D.P. (1995) Sedimentary Exhalative Zn-Pb-Ag Deposits. In: du Bray, E.A. (Ed.) Preliminary Compiliation of Descriptive Geoenvironmental Mineral Deposit Models, U.S. Geological Survey Open-File Report 95-831, Denver, Colorado, 225-233.

Kelley, K. D. & Taylor, C. D. (1997) Environmental geochemistry of shale-hosted Ag-Pb-Zn massive sulfide deposits in northwest Alaska: natural background concentrations of metals in water from mineralized areas. *Applied Geochemistry*, 12, 397-409.

Simunek, J. & Van Genuchten, M. T. (2008) Modeling Nonequilibrium Flow and Transport Processes Using HYDRUS. *Vadose Zone Journal*, 7, 782-797.

Wilde, A. R., Jones, D. R., Gessner, K., Ailleres, L., Gregory, M. J. & Duncan, R. J. (2006) A Geochemical Process Model for the Mount Isa Copper Orebodies. *Economic Geology*, 101, 1547-1567.

10th ICARD IMWA 2015 | 10th International Conference on Acid Rock Drainage & IMWA Annual Conference

Investigation of Pore Gas Oxygen and Internal Temperature in a Waste Rock Dump, Antamina Mine, Peru

Maria Eliana Lorca, Ulrich Mayer and Roger Beckie
Department of Earth, Ocean and Atmospheric Sciences, University of British Columbia, Canada

ABSTRACT

Sulfide mineral oxidation in waste rock dumps tends to increase internal temperatures and may lead to oxygen depletion. The objective of this study is to address how waste rock heterogeneity affects dump-internal gas and temperature distributions. Waste rock dumps built by end dumping are characterized by a high degree of grain size segregation, where coarse rock fragments rest at the bottom, and smaller particles remain near the surface. Due to truck traffic, the fine-grained material located near the surface is compacted. In addition, chemical heterogeneity, in particular sulfide content, also affects internal reactivity and oxygen demand. A drilling program was initiated at Antamina to investigate pore gas and temperature distribution within one of the operating dumps. The investigated dump is 400 m tall and the material is geochemically highly heterogeneous, containing waste rock composed of skarn, hornfels, marbles and intrusives. Two sites where drilled: At Site 1 a shallow borehole was completed, and at Site 3 a shallow and a deep borehole were completed. The sulfur content of the drilled material showed a high degree of chemical heterogeneity with depth; the average sulfur content is 2.5%, but some of the intervals present sulfur content higher than 10%. A thermistor string and oxygen probes were inserted in the boreholes for monitoring of in-situ sulfide mineral oxidation. Areas of increased reactivity (elevated temperature and low pore gas oxygen) correspond to intervals of waste rock with high sulfur content. Regarding the overall reactivity, Site 1 is warmer than Site 3 and shows a higher degree of oxygen depletion. The nature of temperature and oxygen profiles in the deep borehole (Site 3) indicates the presence of reactive hotspots and complex pore gas and pore water migration patterns. These results highlight the role that physical and chemical heterogeneities have on waste rock reactivity.

Keywords: Waste Rock; Oxidation; Heterogeneity, Heat Generation

INTRODUCTION

In this study we investigate the effect of waste rock heterogeneity on dump-internal oxygen concentration and temperature distributions. Sulfide mineral oxidation in waste rock dumps increases internal temperatures, due to the exothermic nature of the sulfide mineral oxidation, and reduces oxygen concentration in the pore gas with respect to atmospheric levels.

Waste rock dumps built by end dumping are characterized by a high degree of grain size segregation, where coarse rock fragments rest at the bottom, and smaller particles remain near the surface (Smith and Beckie 2003; Amos et al. 2014). Due to truck traffic, the fine grained material located near the surface is compacted. (Lefebvre et al. 2001; Amos et al. 2014; Wels, Lefebvre, and Robertson 2003). Laboratory reactivity studies have shown that pyrite oxidation is higher with decreasing particle size (Stromberg and Banwart 1999; Hollings et al. 2001).

In addition, chemical heterogeneity, in particular sulfide content of the dump also affects internal reactivity and oxygen demand. Everything else being equal, zones of the dump where the sulfide minerals are abundant will present increased reactivity, elevated temperature and lower oxygen concentration.

The ingress of fresh air from the atmosphere brings oxygen to supply the reaction. This air can be drawn into the dump by advection/convection due to pressure and/or temperature gradients, but diffusion will also supply oxygen in presence of concentration gradients. Wels et al. (2003) provide an overview of gas flow in waste rock dumps. The main processes are depicted in Figure 1.

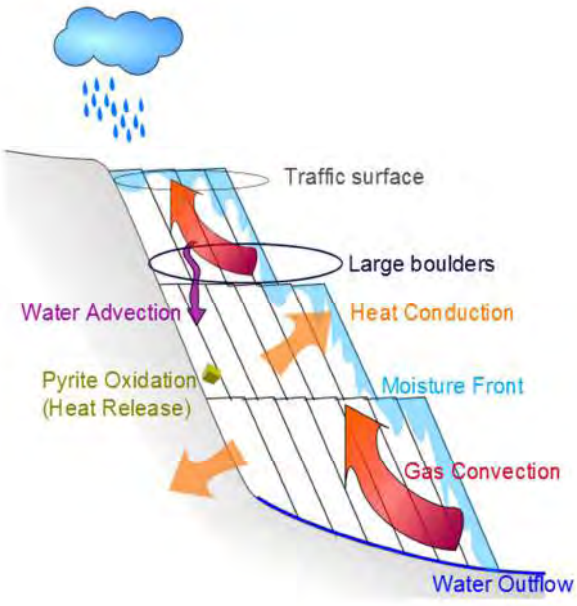

Figure 1 Conceptual model of the processes affecting oxygen transport within waste rock dumps.

Boreholes provide an opportunity to monitor the interior of waste dumps. Borehole construction is difficult and expensive, often limiting installation possibilities. In the past, some waste rock dumps and coal spoils have been successfully drilled, instrumented and monitored (Harries and Ritchie 1981; Lefebvre et al. 2001; Milczarek et al. 2009).

The traditional model of waste rock dump weathering considers that the oxidation processes occur in the exterior of the piles, whereas the interior stays oxygen deprived (Ritchie 2003). Numerical models show that bulk convection can occur in some dumps, where sulfide oxidation rates are high and permeability and diffusion are enhanced, allowing the ingress of oxygen deep into the dump.

METHODS

Site Description

The Antamina mine is located approximately 270 km northeast of Lima, Peru in the department of Ancash. It is located in the high Andes, at an elevation ranging between 4200 and 4700 m.a.s.l. There are two marked wet and dry seasons, the annual precipitation ranges between 1200 and 1500 mm, and the average annual temperature ranges between 5.4 and 8.5°C (Harrison et al. 2012).

Antamina is a polymetallic skarn deposit. It produces copper, zinc, and molybdenum concentrates, and silver and lead concentrates as by-products. The intrusion that produced the mineralization is hosted in sedimentary carbonate sequences (Love, Clark, and Glover 2004). There are five major lithologies in the mine: intrusive, skarn, hornfels, marble and limestone.

Drilling and Instrumentation

A drilling program was initiated at Antamina in conjunction with UBC to investigate pore gas and temperature distribution within one of the operational waste dumps. The investigated dump is 400 m tall and the material is geochemically highly heterogeneous, containing waste rock composed of skarn, hornfels, marbles and intrusives. A photograph of the dump with the location of the boreholes is shown in Figure 2. Two sites where drilled: At Site 1 a shallow borehole was completed, and at Site 3 a shallow and a deep borehole were completed 10 m apart from each other. The two sites are 1 km apart.

The boreholes were drilled with a percussion hammer (Casagrande C3 drill rig). The samples were retrieved by reverse air circulation using a cyclone, and there was neither use of drilling lubricants nor water. Casing was advanced using approximately 2 m lengths of welded steel casing. The percussion hammer breaks the rocks into smaller pieces therefore the particle size distribution of the samples is not representative of the deposit.

Solid phase analysis and ABA testing was done at ALS Peru. In this paper we present data on sulfur content. Analysis of secondary minerals for selected intervals of boreholes from site 1 is presented by Laurenzi el al. (2015).

After the borehole drilling was completed the instrumentation was installed in the borehole by attaching it to a central pipe (steel for the deep borehole and PVC for the shallow ones). A Geokon thermistor string and KE-50 Figaro oxygen probes were inserted in the borehole for monitoring of in-situ sulfide mineral oxidation.

Figure 2 Drilling sites. Arrows point to the monitoring borehole sites

To complete the installation, the borehole was backfilled with either silica sand/gravel, waste rock or bentonite using a tremie pipe. Each interval of the casing was retrieved one meter at a time during backfilling. Bentonite intervals were wetted with water to ensure proper sealing. The sensors were surrounded with material selected to optimize data collection, in the case of the oxygen readings, the probes were surrounded with quartz pea gravel.

Limitations

The construction of the boreholes was more difficult than initially anticipated. The height of the Antamina dump, the drilling method and the wide range in material size posed challenges for the successful completion of the installation. In particular, a deep borehole was considered to be included on site 1, but because of the difficulties this borehole was not completed at the time. The site 3 deep borehole has 2 sections of trapped casing underground (25 – 45 m and 100 – 120 m). These sections could not be brought back to the surface because the welds broke at the moment of casing retrieval.

RESULTS AND DISCUSSIONS

The sulfur content of the drilled material showed a high degree of heterogeneity with depth; the average sulfur content was 2.5%, but some of the intervals presented sulfur content up to 20%. The distribution of high sulfur content intervals is random, linked to the original lithology of the deposit. At Antamina, the abundance of carbonate rocks leads to acid-base-accounting (ABA) results that are mostly indicative of neutral drainage conditions, with a few exceptions in the high sulfur intervals.

The deep and shallow boreholes on site 3 (BH3d and BH3s respectively) show moderate oxygen depletion (i.e., about 10%-15% O_2) whereas the shallow borehole from site 1 (BH1s) shows steadily declining oxygen concentrations with depth to almost complete depletion at 20m depth (Figure **4**).

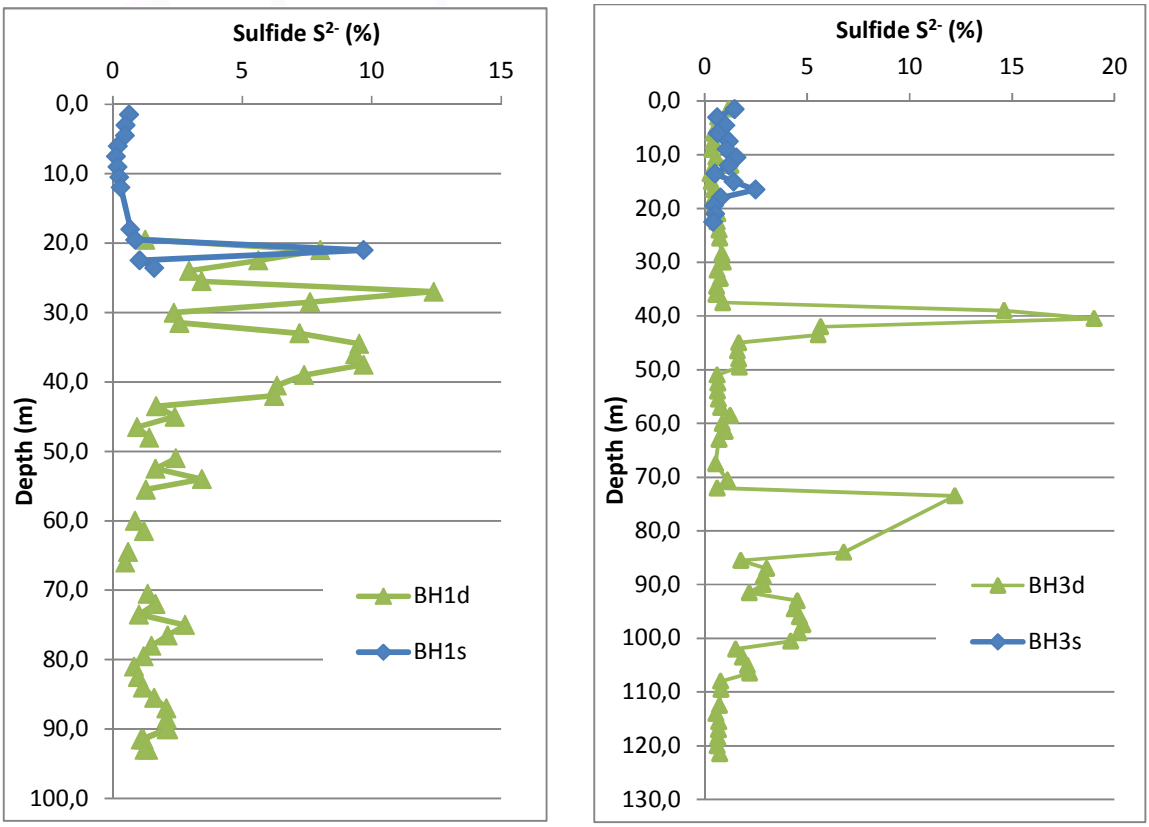

Figure 3 Sulfur content of the solid phase samples

Site 1 is warmer than Site 3, shows a higher degree of oxygen depletion and presents several intervals with higher than average sulfur content which could explain the increased reactivity. Nevertheless, higher overall sulfur content is observed in specific intervals at Site 3, .

The deep hole at Site 3 shows an increase in temperature at 40 m depth and then a decrease at 65 m. The same pattern is repeated at the bottom of the borehole. The lower temperature zones are correlated with the base of the lifts on which the dump was constructed. These zones are presumed to be a result of the lower reactivity of the boulders that rest at the base of each lift.

Waste rock dumps built by end dumping are segregated with coarse material resting the bottom, producing high permeability areas for oxygen ingress, similar to what Wels et al. describe as the "chimney effect". In the case of the borehole BH3d it is observed that O_2 content is higher in the location where coarse fragments are located (60-70 m), but rapidly decreases again in the new lift, where it is expected that fine material is present, but also there is an increase in sulfur content at 75 m.b.g.s.

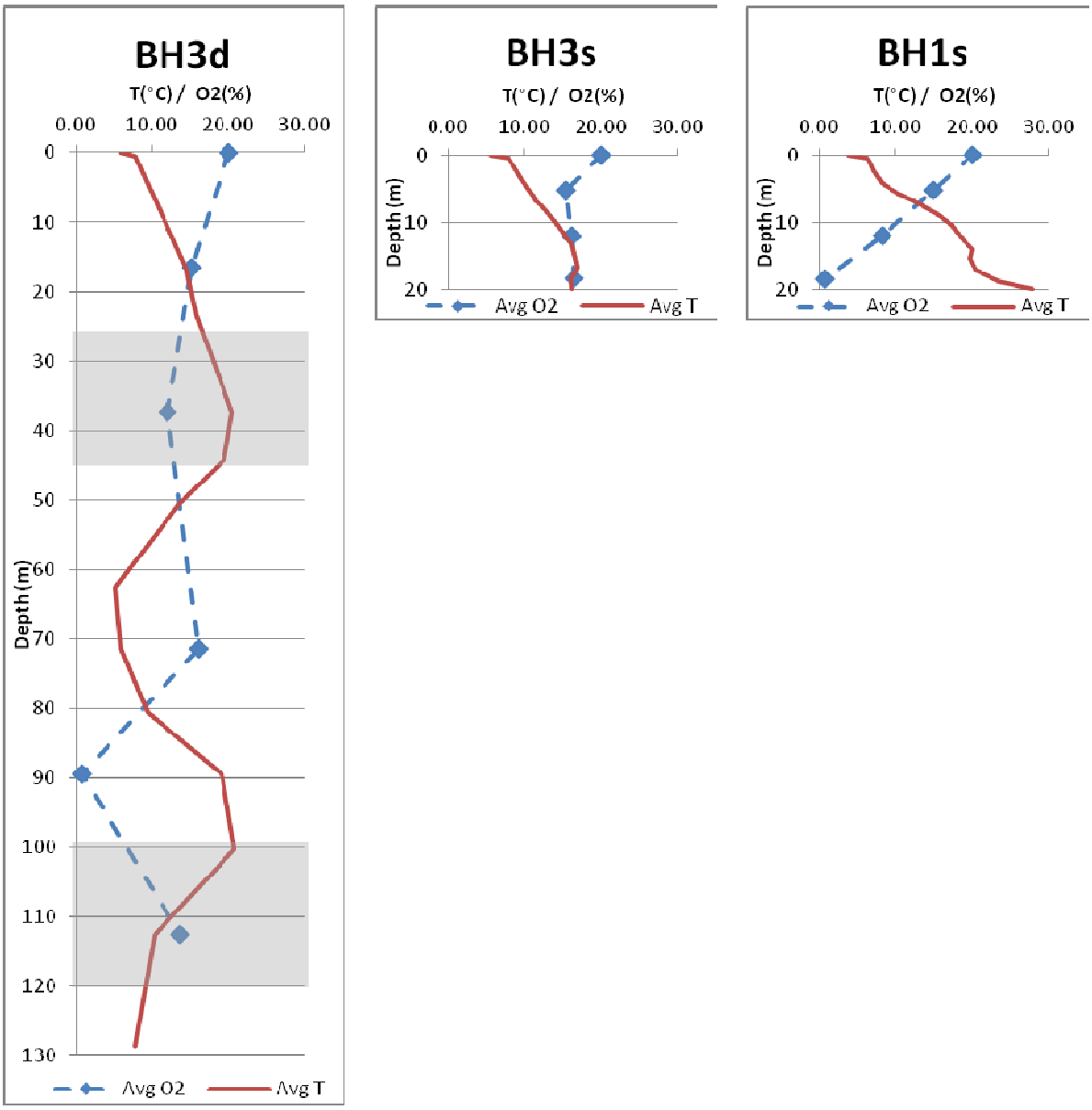

Figure 4 Average O_2 and T profiles for the boreholes. The shaded areas for BH3d represent the trapped casing

When oxygen is supplied by 1D-diffusion only, the oxygen concentration at depth can be solved analytically (Ritchie and Miskelly, 2000):

$$u(x) = \frac{\cosh(\varepsilon(x-1))}{\cosh \varepsilon} \tag{1}$$

$$\varepsilon = \sqrt{\frac{h^2 S_o}{D C_o}} \tag{2}$$

$$X_l = \sqrt{\frac{2 D C_o}{S_o}} \tag{3}$$

where u is the oxygen concentration as a function of $x = z/h$, z is the depth, h is the height of the pile, S_o is the intrinsic oxidation rate, D is the effective diffusion coefficient, C_o is the oxygen concentration at the surface and X_l is the diffusion length. The oxygen concentrations expected using these equations are shown in Figure 5.

The oxygen concentration profiles differ from an expected diffusion profile, and this could be explained because of either heterogeneity leading to complex diffusion patterns in three dimensions or gas migration processes other than diffusion, namely convection/advection. The isolated zones of high temperatures and low oxygen in the deep borehole (Site 3) indicates the presence of reactive hotspots and complex pore gas migration patterns that are not consistent with 1D-diffusion as explained by Ritchie and Miskelly (2000).

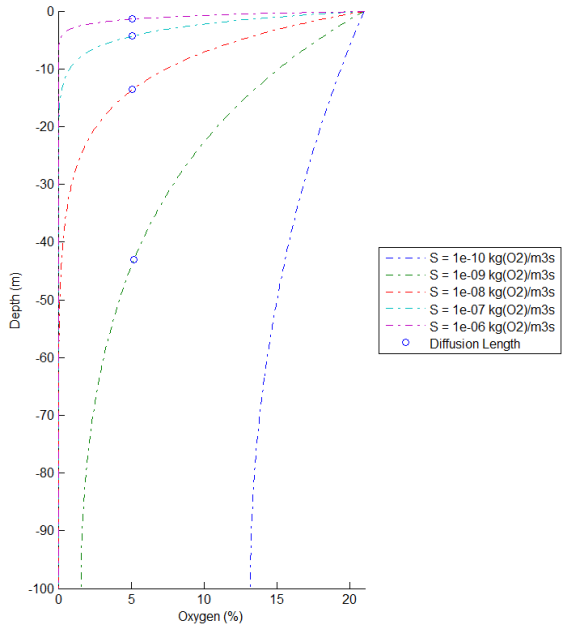

Figure 5 Expected oxygen concentration profiles for varying range of intrinsic oxidation (S) in a hypothetical 100 m tall dump considering homogeneous oxidation rate and 1D-diffusion as the only oxygen supplying mechanism

A previous study in an 10 m high experimental waste rock pile at Antamina showed decreased oxygen concentration down to 7% (Singurindy et al. 2012). The temperature increase at the experimental pile scale was up to 13.3 °C. It was observed at the experimental pile scale that the zones of greatest oxygen depletion were well correlated with the traffic surface, whereas at the operating dump scale zones in the interior of the dump show the highest degree of oxygen depletion. The experimental pile material is comprised of sulfur up to 4.6% which is lower than the high sulfur intervals of the dump.

Based on these results, the chemical and physical heterogeneity play important roles in the oxygen demand and distribution within waste rock dumps. Other factors, such as moisture content will affect fluid transport; increasing moisture content limits the ingress of fresh air into the dump by decreasing the air permeability and diffusivity.

CONCLUSIONS

We measured oxygen concentration and internal temperature within an operational waste rock dump. There is evidence of sulfide mineral oxidation at the two investigated locations. Areas of increased reactivity (elevated temperature and low pore gas oxygen) corresponded to intervals of waste rock with high sulfur content. Oxygen content and temperature were highly variable within the investigated dump, inconsistent with a 1D-diffusion – dominated system. The nature of temperature and oxygen profiles indicates the presence of reactive hotspots and complex pore gas and pore water migration patterns. It is often conceived that gas distribution in waste dumps is relatively smooth. This might be the case in relatively homogeneous dumps, however we show that in the presence of geochemical and physical heterogeneity this conventional view is not applicable. Because of the variability of waste rock, we recommend site-specific investigations.

ACKNOWLEDGMENTS

We thank Laura Laurenzi and Mehrnoush Javadi from UBC. The design of the boreholes and instrumentation was developed in conjunction with GeoSystems SA. We appreciate the support provided by Bevin Harrison, Celedonio Aranda, Edsael Sanchez, Bartolome Vargas, and Haydee Aguirre from Antamina. The funding for this project was provided by Compañia Minera Antamina.

REFERENCES

Amos, Richard T., David W. Blowes, Brenda L. Bailey, David C. Sego, Leslie Smith, and A. Ian M. Ritchie. 2014. "Waste-Rock Hydrogeology and Geochemistry." *Applied Geochemistry* In press. doi:10.1016/j.apgeochem.2014.06.020.

Harries, Jr, and Aim Ritchie. 1981. "The Use of Temperature Profiles to Estimate the Pyritic Oxidation Rate." *Water Air and Soil Pollution* 15 (4): 405–23. doi:10.1007/BF00279423.

Harrison, Bevin, Celedonio Aranda, Michael Edsael Sanchez, and Janeth Vizconde. 2012. "Waste Rock Management at the Antamina Mine: Overall Strategy and Data Application in the Face of Continued Expansion." In *Proceedings of the 9h International Conference on Acid Rock Drainage*. Ottawa, Canada.

Hollings, P., M. J. Hendry, R. V. Nicholson, and R. A. Kirkland. 2001. "Quantification of Oxygen Consumption and Sulphate Release Rates for Waste Rock Piles Using Kinetic Cells: Cluff Lake Uranium Mine,

Northern Saskatchewan, Canada." *Applied Geochemistry* 16 (9–10): 1215–30. doi:10.1016/S0883-2927(01)00005-1.

Laurenzi, Laura, K. Ulrich Mayer, and Roger Beckie. 2015. "Metal Attenuation Studies in Operational Waste Rock Piles: A Combined Mineralogical and Geochemical Approach." In *Proceedings of the 10th International Conference on Acid Rock Drainage (ICARD)*. Santiago, Chile.

Lefebvre, R., D. Hockley, J. Smolensky, and P. Gelinas. 2001. "Multiphase Transfer Processes in Waste Rock Piles Producing Acid Mine Drainage 1: Conceptual Model and System Characterization." *Journal of Contaminant Hydrology* 52 (1-4): 137–64. doi:10.1016/S0169-7722(01)00156-5.

Love, D. A., A. H. Clark, and J. K. Glover. 2004. "The Lithologic, Stratigraphic, and Structural Setting of the Giant Antamina Copper-Zinc Skarn Deposit, Ancash, Peru." *Economic Geology And The Bulletin Of The Society Of Economic Geologists* 99 (5): 887–916.

Milczarek, Michael, Dale Hammermeister, Margaret Buchanan, Bryce Vorwaller, and Teresa Conner. 2009. "In Situ Monitoring of a Closed Waste Rock Facility." In *Proceedings of the 8th International Conference in Acid Rock Drainage (ICARD)*. Skellefteå, Sweden.

Ritchie, A. I. M. 2003. "Oxidation and Gas Transport in Piles of Sulfidic Material." In *The Environmental Aspects of Mine Wastes*, edited by J. L. Jambor, David W. Blowes, and A.I.M. Ritchie, 73–94. Short Course Series 31. Ottawa: Mineralogical Association of Canada.

Ritchie, Ian, and P. Miskelly. 2000. "Geometric and Physico-Chemical Properties Determining Sulfide Oxidation Rates in Waste Rock Dumps." In *Proceedings of the Fifth International Conference on Acid Rock Drainage*. Littleton, Colorado.

Singurindy, Olga, María E. Lorca Ugalde, H. Peterson, Trevor Hirsche, M. Javadi, S. Blackmore, C. A. Aranda, K. U. Mayer, R. Beckie, and Leslie Smith. 2012. "Spatial and Temporal Variations of O2 and CO2 Pore Gas Concentrations in an Experimental Waste Rock Pile at the Antamina Mine, Peru." In *Proceedings of the 9th International Conference on Acid Rock Drainage*. Ottawa, Canada.

Smith, Leslie, and R. D. Beckie. 2003. "Hydrologic and Geochemical Transport Processes in Mine Waste Rock." In *Environmental Aspects of Mine Wastes*, edited by J. L. Jambor, D. W. Blowes, and A. I. M. Ritchie, 31:51–72. Short Course Series. Ottawa: Mineralogical Association of Canada.

Stromberg, B., and S. Banwart. 1999. "Weathering Kinetics of Waste Rock from the Aitik Copper Mine, Sweden: Scale Dependent Rate Factors and pH Controls in Large Column Experiments." *Journal Of Contaminant Hydrology* 39 (1-2): 59–89.

Wels, Christoph, René Lefebvre, and A. Robertson. 2003. "An Overview of Prediction and Control of Air Flow in Acid Generating Waste Rock Dumps." In *Proceedings of the 6th International Conference on Acid Rock Drainage*. Cairns, Queensland, Australia.

10th ICARD IMWA 2015 | 10th International Conference on Acid Rock Drainage & IMWA Annual Conference

Comparison of Pre-Mining Geochemical Predictions to Operating Conditions for New Afton Tailings

Emily O'Hara and Scott Davidson
New Afton Mine, Canada

ABSTRACT

New Afton is a block cave mine that sustains processing of an average of 14000 tonnes per day of ore. The mine produces an average of 80,000 ounces of gold and 750,000 pounds of copper annually over a 12 year mine life. New Afton is located near Kamloops, BC which is hosted by a grassland ecosystem classified as semi-arid, with annual average precipitation of 305mm and evaporation of 608mm.

Prediction of acid rock drainage (ARD) and metal leaching (ML) for tailings supernatant and leachate is typically carried out early in the permitting process when access to tailings samples is often limited to those generated from metallurgical testing programs which often do not reflect the range of geological conditions that are present in an ore body or surrounding waste rock. Early prediction of potential effects, is essential to ensure mitigation programs can be effectively developed and implemented. New Afton has a variety of practices available to understand and control potential effects of ARD or ML. With 2 years of operating conditions, comparisons are now being carried out to reflect on the predicted versus actual conditions. This paper examines the comparison of pre-mining geochemical predictions with actual observed conditions while also commenting on some of the challenges in linking the two.

The New Afton ore body is classified as having low acid generating potential, with a high neutralizing capacity. The predicted Net Neutralizing Potential (NNP) for tailings samples is between 177 and 263 tCaCO3/1000t, with paste pH between 8 and 8.6. Predicted tailings supernatant ranged between 7.85 and 9.28 and actual supernatant at the Tailings Storage Facility (TSF) has ranged between 7.83 and 9.79, over the last 2 years of operation. Additional tailings samples have been taken based on "actual" conditions, and humidity cell tests (HCTs) are in progress to determine the variability between the pilot plant samples. The two original humidity cells generated from metallurgical testing have been running for 6 years with no evidence of acidic conditions and pH results between 7.81 and 8.33. However, humidity cells, and tailings supernatant indicate that low level metal leaching may occur under neutral or high pH conditions.

Keywords: Tailings, Permitting, ARD, ML

INTRODUCTION

New Afton is located approximately 10km west of Kamloops in British Columbia, on the historic Afton Mine site. Kamloops is approximately 350km North East of Vancouver. The site is within the Interior Plateau region of British Columbia that lies in the rain shadow of the Coastal Mountains (Rescan, 2007). Precipitation in this area is very low, on average receiving 305mm per year with annual evaporation rate of 608mm (Environment Canada, 2014). The New Afton site is zero discharge, with all runoff being contained onsite. New Afton uses the "block cave" mining method.

The New Afton ore body is an alkalic porphyry copper-gold deposit comprised predominately of hypogene mineralization, with lesser amounts of supergene mineralization and intermediate mesogene mineralogy located in upper elevations of the deposit. The hypogene type ore has constituted over 85% of the mill feed to date, as the block cave mining sequence extracts ore from the lower levels of the current mining lift. The proportion of mesogene ore and supergene ores has gradually increased, as ore from higher levels in the block cave are extracted.

Pyrite is the main sulphide gangue mineral with the concentration of up to 0.5% in hypogene ore. Mesogene samples include higher proportion of carbonates (13% compared to 2-3% for the other ore types). A pyrite "halo" surrounds the ore zone, with sulphur values ranging between 0.02% and 8.1% (Rescan, 2006). Arsenic mineralization in the ore is found to be primarily tennantite with some tetrahedrite, and only trace amounts of arsenopyrite.

New Afton does not suffer from significant ARD/ML issues due to three main factors; low precipitation, low acid generating capacity and high neutralizing capacity. The block cave mining method does not generate significant waste rock, and all waste rock bought to surface is disposed of in the old Afton Pit. As waste rock generation is low, and disposal is fully controlled, the primary geochemical focus is acid rock draining and metal leaching (ARD/ML) potential of the tailings. While ARD potential for the tailings is very low, some metal leaching has been seen to occur at neutral or higher pH.

Tailings Dam Design

The New Afton tailings storage facility (TSF) is made up of five dams. Two dams were constructed at final elevation, and three were constructed as started dams to be raised throughout the mine life. The three construction dams use the centerline method of dam construction. New Afton also has the ability to use Pothook Pit for tailings deposition. Seepage ponds are located at the base of each of these dams, with pumping capacity to return water to the tailings impoundment.

The relevance to TSF design to geochemistry is the use of tailings sands as construction material. Raw tailings are processed using cyclones to produce a not acid generating (NAG) construction sand. Should the tailings be considered potentially acid generating (PAG), this method of construction would be less appropriate.

TESTING PROGRAM

Tailings geochemical prediction often has significant limitations primarily due to the availability of representative tailings samples. During the early stages of permitting and economic assessment, tailings samples are generated as part of metallurgical, laboratory based, pilot plant testing programs to determine which mill flow sheet will provide the best results. These tests are designed

based on expected geological conditions and availability of core samples and may be designed and conducted in a fashion that does not reflect the proposed process. It is the remains from this test work that is then available for predictive testing.

Tailings Geochemistry Tests

Static Tests

Three samples based on ore type were selected for static acid base accounting (ABA) testing during the permitting process. The three samples were based on the three ore types, mesogene, hypogene and supergene with the results being demonstrated in Table 1.

Table 1 Historic Laboratory and Pilot Plant Tailings Samples

	Static Tests Only			Static and HCTs	
	JUN 20-06 LCT Hypogene Tails	**JUN 21-06 LCT M2 Mesogene Tails**	**JUN 22-06 LCT MS1 Mesogene/Supergene Tails**	**Tails Rougher 2092P6**	**Tails Final 2092P6**
Paste pH	8.3	8.2	8.3	8.6	8.5
%S (Total)	0.15	0.18	0.12	0.52	0.42
%S (Sulphide)	0.13 (Calc)	0.14 (Calc)	0.11 (Calc)	0.33	0.27
%S (Sulphate) Carbonate Leach	0.01	<0.01	0.02	0.02	0.05
%S (Sulphate) HCL Leachable	0.02	0.04	0.01	0.02	0.01
Measured NP (kg $CaCO_3$/t)	57	269	193	267	276
SNNP (kg $CaCO_3$/t)	53	264	190	252	264
SNPR	15.2	53.8	61.8	17.6	22.3
As ppm	5.6	37.2	64.7	1090	772
Cu ppm	1055	1650	2210	7890	6380
Se ppm	1	1	1	4	4

As per ore quality at New Afton, the tailings samples have been shown to be heavily neutralizing with the potential for acid generation being very low. Most of the Bulk NP is likely associated with the carbonate-based minerals, based on CaNP levels (Rescan, 2007).

Follow-up Static Tests

The mine permit for New Afton does not contain any geochemical monitoring program requirements for tailings. Since operation of the TSF began only 5 static samples have been taken in order to provide more representative data for the composite tailings. The grab sample program will continue throughout the life of mine to ensure continued understanding of tailings conditions. Samples will be selected based on mill feed characteristics. The ore feed is a blend of the 3 primary

types so the collection of blended samples will provide a better understanding of actual conditions than analyses run on pure ore materials.

Table 2 Actual Tailings Samples 2014

	Static Tests Only		Static and HCTs		
	JUN 25-14 Whole Tailings	**JUN 25-14 Tailings Cyclone Underflow**	**Q2 2014 Overflow Tailings (SCOF)**	**Q2 2014 Underflow Tailings (STUF)**	**Q2 2014 Final Tailings (FTML)**
Paste pH	8.1	8.3	7.8	8.7	8.5
%S (Total)	0.9	0.74	0.73	0.35	0.55
%S (Sulphide)	0.82	0.71	0.69	0.31	0.52
%S (Sulphate) Carbonate Leach	0.08	0.03	0.04	0.04	0.03
%S (Sulphate) HCL Leachable	0.07	0.01	0.03	0.03	0.04
Measured NP (kg $CaCO_3$/t)	112	101	170	144	162
SNNP (kg $CaCO_3$/t)	88.6	79.1	149.4	135.3	147.0
SNPR	4.8	4.6	8.2	16.5	10.8
As ppm	36.5	38.5	25.3	35.8	32.5
Cu ppm	1730	1740	901	1980	1400
Se ppm	1.41	1.46	1.33	1.01	1.15

The ore type is predominately hypogene, however concentrations of each ore type will vary throughout the mine life. Table 3 shows the mill feed by ore type for April to August 2014 to illustrate the current level of variability. BCKGR is partially mineralized ore, and is treated as hypogene for processing requirements.

Table 3 Ore Composite by Type April – August 2014

	Tons	**Supergene**	**Hypogene**	**Mesogene**	**BCKGR**
April 2014	366,941	2.2%	75.9%	8.9%	13.0%
May 2014	392,151	2.5%	74.2%	8.1%	15.3%
June 2014	380,528	2.2%	73.9%	8.1%	15.9%
July 2014	400,030	1.8%	76.5%	8.8%	12.9%
August 2014	413,887	1.4%	75.4%	9.1%	14.1%

Figure 1 shows the expected mill feed as a function of ore type over the life of mine. It can be seen that the relative portion of mesogene and supergene ore increases later in the mine life.

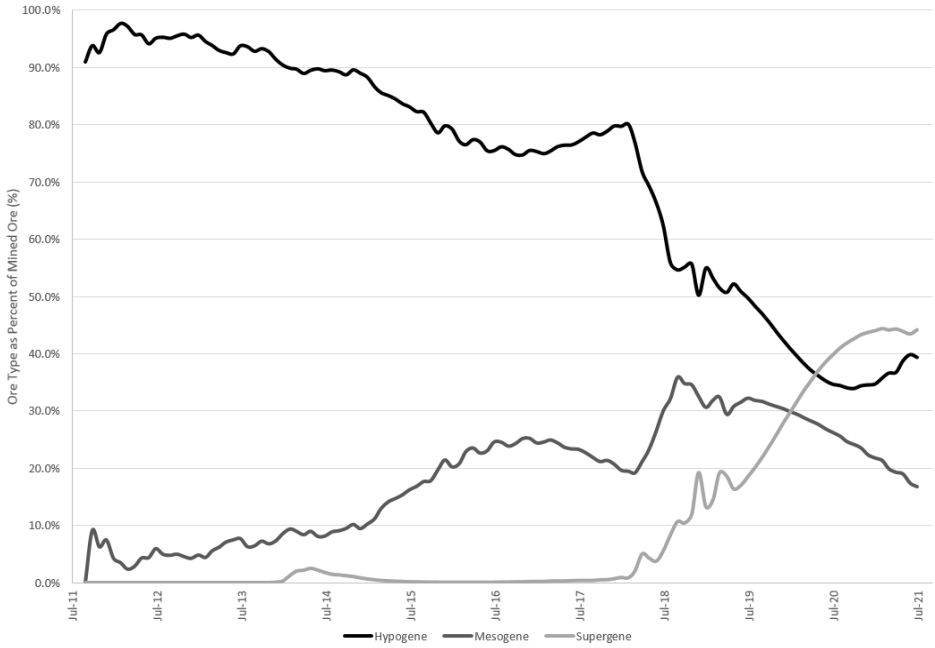

Figure 1 Mill Feed by Ore Type over Life of Mine

Initial Kinetic Tests

New Afton started two humidity cell tests (HCTs) on the 29th May 2008. Initial characterization results are shown above for the two HCTs in Table 1. The two samples were generated during two stages of a pilot plant, rougher and final tails (Rescan, 2012a) and these tests have been running for 329 weeks. The samples for the HCT tests were generated from mesogene ore material. Hypogene ore was also selected for pilot plant testing, however it is believed that there was not enough sufficient tailings produced from this ore type to allow for kinetic testing. Table 4 demonstrates the mineralogy of the tailings samples. No arsenic or antimony bearing mineral phases were identified in these mesogene tailings samples by Rietveld X-Ray Diffraction (XRD), however tennantite and tetrahedrite are considered the main contributing arsenic compound in mesogene ore (Rescan, 2012b).

Table 4 Rietveld X-Ray Diffraction Mineralogy for Tailings Humidity Cell Tests

Mineral	Ideal Formula	2092P6 Final Tls Sands	2092P6 Ro Tls Sands
Dolomite (wt.%)	$CaMg(CO_3)_2$	32.6	32.6
Muscovite, total (wt.%)	$KAl2AlSi_3O_{10}(OH)_2$	21.4	22.3
Plagioclase (wt.%)	$NaAlSi_3O_8$-$CaAl_2Si_2O_8$	18.3	17.2
Quartz (wt.%)	SiO_2	16.9	16.3
K-feldspar (wt.%)	$KAlSi_3O_8$	6.1	6.5
Kaolinite (wt.%)	$Al_2Si_2O_5(OH)_4$	3.4	3.6
Calcite (wt.%)	$CaCO_3$	1	1
Anatase (wt.%)	TiO_2	0.5	0.5

A secondary issue with the samples taken for initial HCT tests is that the feed sample was not representative of witnessed feed grade since operation, even considering mesogene ore feed. The feed grade in the pilot plant test was approximately 2% copper, which is around double what has been seen on average. The tails grade was also disproportionately high, as the pilot plant was targeting a specific concentrate grade not attempting to optimize recovery. This has resulted in elemental content of tailings being higher than average feed grade. For example, the As values for the tails used in the HCTs was 1090 ppm and 772ppm, whereas for 2014 the As values in Final Mill tailings (FTML) ranged between 7.4ppm and 58.5ppm. These are not seen as an error in sample collection, but a challenge when dealing with limited sample availability.

Due to low sulphur content and high neutralization potential, these HCTs were not expected to become acid generating. Metal leaching rates were not predicted for these samples. Figures 2, 3 and 4 demonstrate pH, arsenic and copper results seen for the two original tailings HCTS. While other metal concentrations have been decreasing, arsenic values have been increasing since week 258. It is believed that this increase could be the result of cleaning of fines that had accumulated under the screen which were then placed back on top of the solid sample. A spike in arsenic was also seen at a similar time in some waste rock cells following similar cell maintenance.

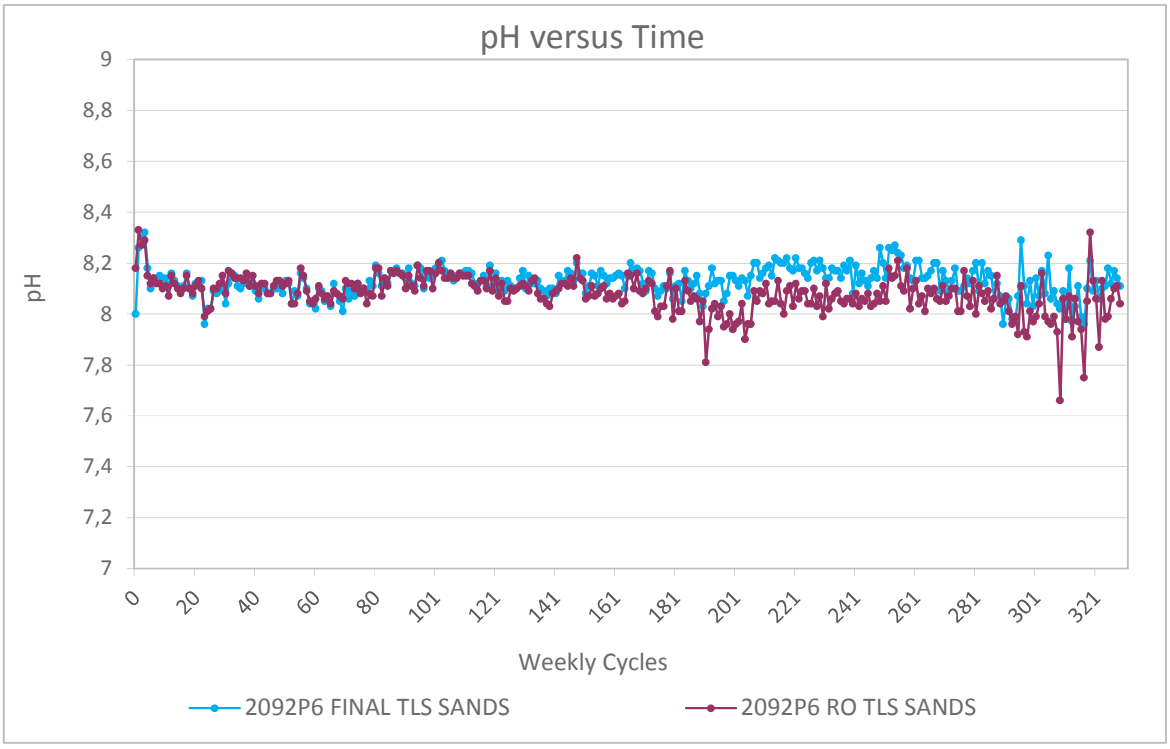

Figure 2 Pre-Operations HCTs pH vs Time

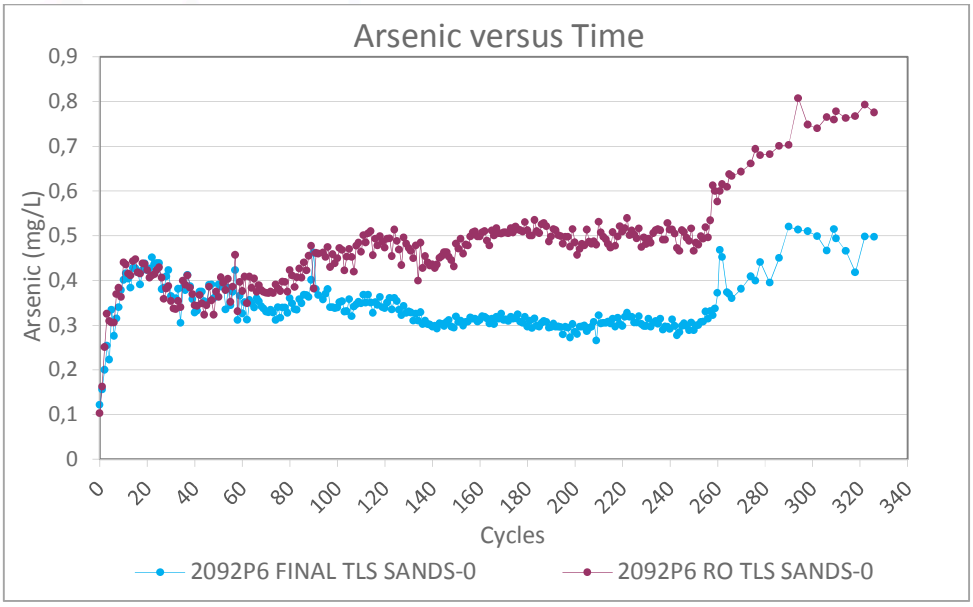

Figure 3 Pre-Operations HCTs Arsenic vs Time

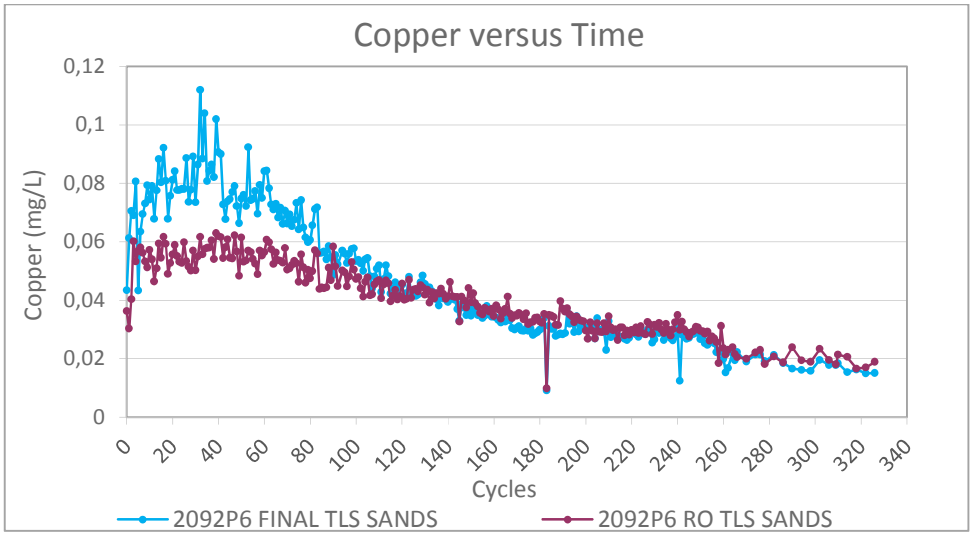

Figure 4 Pre-Operations HCTs Copper vs Time

Secondary Kinetic Tests

In the second quarter of 2014, a weighted composite of tailings was collected for Final Tailings (FTML), Secondary Tailings Underflow (STUF) and Secondary Tailings Overflow (SCOF). FTML is the total tailings that is sent from the mill to the TSF, STUF is the tailings sands that are used for dam construction, and SCOF is the fine slimes that are sent to the center of the TSF. This composite was collected over a 4 month period, in order to obtain required weights of samples for humidity cell testing.

There is currently not sufficient data to estimate time to ARD onset with the new humidity cells, as high loadings of sulphate is being exhibited due to initial flushing. The secondary humidity cells are intended to be continued throughout the life of mine. Additional HCT testing will be initiated later in the mine life when there is a higher portion of mesogene and supergene ore in the mill feed as these will reflect the final tailings produced during the mine.

Tailings Water Quality Tests

TSF water quality is of significant interest to regulators, and local communities of interest. While the water contained in the TSF is reused within the milling process, and the water is understood to be contaminated, monthly monitoring is carried out to ensure a good understanding of this water quality.

Laboratory Supernatant Analysis

Both fresh and 7-day aged supernatant analysis was carried out for the lock cycle test bulk tailings samples for hypogene tails, mesogene tails and a mesogene/supergene blended tails. A sample of these results are shown in Table 5.

Table 5 Lab Tested Tailings Supernatant Results and Actual New Afton TSF Supernatant

		Laboratory Test						Actual
		LCT H2 Hyp Tails Sol'n		**LCT M2 Mes Tails Sol'n**		**LCT MS1 Mes/Sup Tails Sol'n**		**SW17 - TSF**
	Units	**Fresh**	**7-Day Aged**	**Fresh**	**7-Day Aged**	**Fresh**	**7-Day Aged**	**Average 2012-2014**
TSS	mg/L	700	412	140	124	3240	32	38
pH	pH	8.93	8.34	8.85	7.85	9.28	8.87	8.58
Acidity	Mg/L as $CaCO_3$	<2	<2	<2	<2	<2	<2	2.5
Alkalinity	Mg/L as $CaCO_3$	152	138	170	170	261	204	92
Conductivity	uS/cm	548	554	692	663	647	665	7700
SO_4	mg/L	69	86	97	110	78	99	4448
As – Total	mg/L	0.0085	0.0072	0.0561	0.0488	0.328	0.142	0.023
Cu – Total	mg/L	3.17	1.1	0.185	0.0958	6.33	0.412	0.03
Mo - Total	mg/L	0.0141	0.017	0.0205	0.0242	0.00482	0.0128	0.1585
Pb - Total	mg/L	0.0121	0.0104	0.00112	0.0012	0.0572	0.0068	0.0013
Se – Total	mg/L	<0.003	<0.003	0.006	0.005	<0.003	0.003	0.0416
As – Dissolved	mg/L	0.0079	0.008	0.04	0.0474	0.134	0.123	0.021
Cu – Dissolved	mg/L	0.718	0.592	0.0034	0.0054	0.178	0.0037	0.004
Mo - Dissolved	mg/L	0.0184	0.0202	0.0211	0.0231	0.01416	0.017	0.1549
Pb - Dissolved	mg/L	0.00832	0.0082	0.0001	0.0001	0.0043	0.0003	<0.0005
Se – Dissolved	mg/L	<0.0003	<0.0003	0.006	0.006	0.006	0.005	0.044

Monthly Water Quality Samples

New Afton monitors tailings supernatant monthly as per permit requirements. Table 5 shows monthly averages when compared against the laboratory supernatant tests. pH at the TSF has ranged between 7.83 and 10.4. Higher pH results are likely associated with lime that is added to the mill process, rather than neutralization that is occurring. The major difference between the laboratory and field tests has been conductivity and sulphate. Figure 5 and Figure 6 demonstrate the pH, conductivity, sulphate and alkalinity results seen at the New Afton TSF since operation commenced.

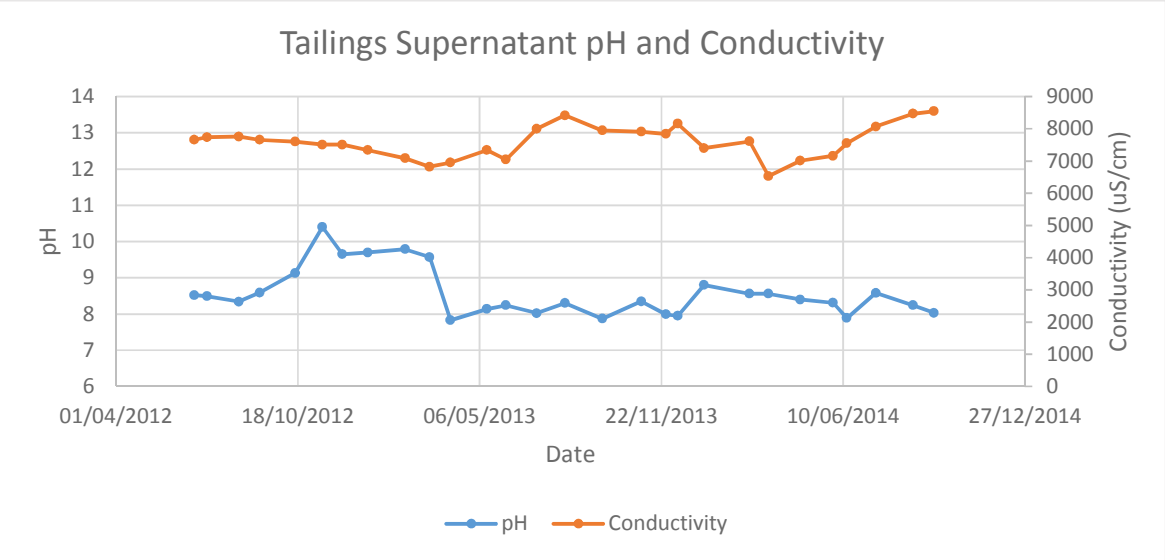

Figure 5 Actual Tailings Supernatant pH and Conductivity

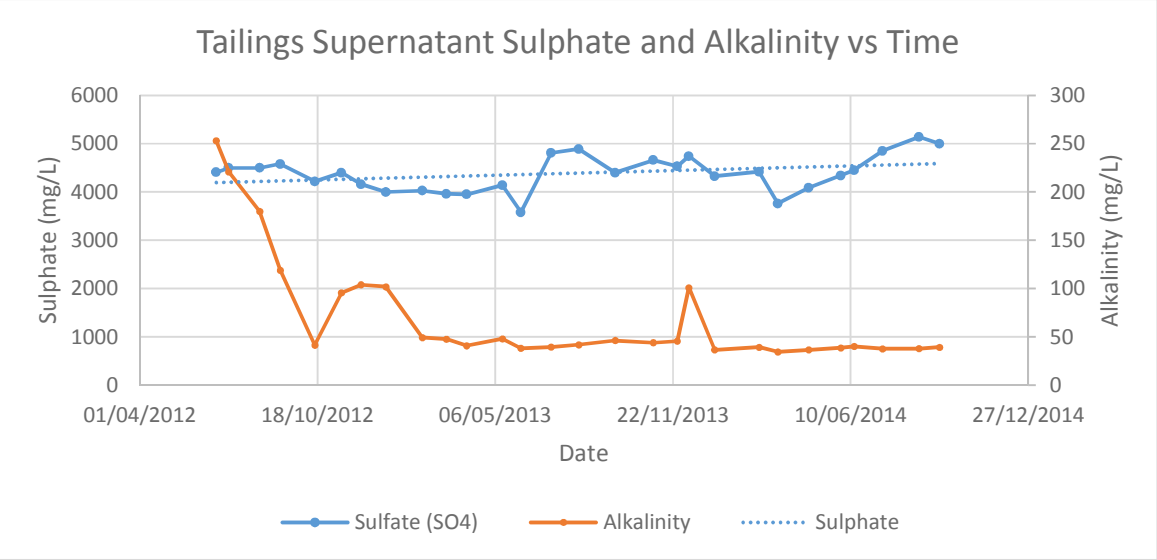

Figure 6 Actual Tailings Supernatant Sulphate vs Time

RESULTS AND DISCUSSION

Overall, kinetic, static and supernatant test results indicate that New Afton should not expect tailings to become acid generating, or have significant issues with ML. Both lab and mill produced tailings demonstrated low acid potential and high neutralizing potential, which was expected based on ore properties. The pre-operation humidity cells are an outlier in comparison to other test results with respect to elemental content.

Operational characterization programs have been developed in order to ensure that there is adequate characterization of the tailings that are being produced over the life of mine. The development of these operational characterization programs is important given with the need to validate or refute the representative nature of the pre-mining characterization samples.

Humidity Cell Results

Humidity cells to date indicate neutral pH and generally low metal loadings. BC Fresh Water Aquatic Life (BCFWAL) concentration guidelines have seen exceedances for antimony, arsenic, copper and selenium. Metal loadings have generally been decreasing throughout testing, however arsenic has seen increasing concentrations since week 250. The samples used in these HCTs, as provided by the pilot plant do not represent actual conditions, with As values in the Final Tails pilot plant sample being greater than 10 times the maximum seen during 2014 operations when the mill feed was primary hypogene ore.

It is expected that these samples were used for HCTs, as no other testing would provide sufficient sample weight to run HCTs. However, there was no documented discussion during permitting or reporting regarding the appropriateness of these samples, so it cannot be determined if these anomalies were picked up prior to initiating the tests.

It is expected that the metal leaching that is occurring under neutral pH is associated with these high metal concentrations and has not been identified as a risk to operation or closure of the New Afton TSF. As results are received for the operating tailings HCTs, it is expected that metal loadings will be lower than those seen in the pre-operations test results.

Tailings Supernatant

It is expected that differences in tailings supernatant results can be explained by the addition of lime in the milling process, processing of the historic Teck Ore Stockpile, and the circulating loads due to the reuse of process water. Lime addition was not included in pre-testing, as it was not expected to be required. This lime addition would contribute to the increased conductivity seen in the supernatant water. The added lime also results in the suppression of pyrite during the flotation circuit resulting in more pyrite reporting to the tailings waste stream. Weathering of the pyrite in the cyclone sands used to construct the impoundment will result in some increases in sulphate concentrations. Early in operation, New Afton processed approximately 129,000 tons of historic ore from the Afton Mine which was operated by Teck and closed around 1995. This ore was significantly weathered and oxidized, which could explain the increase in sulphate loading from the start of the TSF operation. No leachate tests were completed on this ore however. New Afton expects that concentrations will increase throughout life of mine, as metals and nutrients are circulated throughout the process.

It is difficult to make significant comparisons of aging tests versus actual supernatant due to variances in operating conditions, and the recycling of process water. No discussion around scale-up or estimations were completed for the permitting report.

ARD and ML Management

New Afton has the ability to manage ARD through draw control and blending, should a high pyrite or high arsenic zone be identified. To date, this practice has not been necessary and draw control has been based primarily on ore grade requirements and maintaining cave operations. Waste rock was generated primarily through the development of the access declines to construct the underground mine although some waste rock is generated from the base of columns within the block cave. All waste rock produced from the underground mine is disposed of in the historic Afton open pit.

If waste rock is to be used onsite for construction, it must first be tested and meet the requirements of New Afton's M229 permit as NAP waste rock. These conditions include a paste pH of greater than six or NPR greater than two. The open pit is the final location for all PAG waste rock, however, standard practice since operations began has been that all waste rock is disposed of within the historic open pit.

CONCLUSION

Prediction of ARD and ML is an essential part of the permitting process to ensure that environmental effects are planned for and managed correctly however, geochemical characterization programs are often based on small samples that are available at the time of testing. These samples may not always reflect the actual operating conditions, and in the case of New Afton HCTs the samples chosen are statically significantly different to witnessed operating conditions. Scaling up tailings samples is particularly difficult, due to the limited availability of samples produced during the laboratory metallurgical testing process. These challenges do not indicate that these tests should not be completed, but that ongoing checks and verification of the results is important. Lessons learned from the permitting aspect of New Afton, is that documentation for reasons behind sample selection is essential and verification of appropriateness of sample should be carried out. A review of As levels was completed in 2012, however no reasoning for why As levels were significantly higher in the samples was provided. It was recommended that additional tailings HCTs be set up based on actual tailings samples to provide a comparison.

In New Afton's case, it is expected that metal leaching will demonstrate lower concentrations than those predicted through the initial humidity cells. While pre-operation research is valuable, it is important for companies to continue to improve and increase their knowledge of ARD and ML based on actual operating conditions in order to confirm or refute the initial predictions. This ensures that adequate resources are available as needed to control ARD/ML after the mine has closed.

While New Afton does not expect to see any detrimental effects from changes in predictions, there has been significant benefit in repeating ARD/ML tests based on mill produced tailings. This allows New Afton to have greater confidence when communicating to regulators and communities of interest that potential effects are well understood and managed.

ACKNOWLEDGEMENTS

The authors appreciate the work that Rescan Environmental (ERM) completed as part of the permitting process and in setting up the HCTs. There was also ongoing reporting associated with these HCTs which has provided significant information to the New Afton site.

It is appreciated that New Gold Inc has allowed the time to prepare this paper and provide significant management review.

REFERENCES

Rescan Environmental Services Ltd. (Rescan) (2012a) *New Afton Humidity Cells Report 2012,* Prepared for New Gold Inc. by Rescan Environmental Services Ltd., pp. 3-15.

Rescan Environmental Services Ltd. (Rescan) (2012b) *Assessment of Elevated Arsenic in Tailings Humidity Cell Leachate,* Prepared for New Gold Inc. by Rescan Environmental Services Ltd., pp. 1-10.

10th ICARD IMWA2015 | 10th International Conference on Acid Rock Drainage & IMWA Annual Conference

Effective Field-Based Testing Tools for Rapid ARD Prediction

Anita Parbhakar-Fox[1], John Aalders[1] and Bernd Lottermoser [1, 2]

[1] *School of Physical Sciences, University of Tasmania, Australia*

[2] *Environment and Sustainability Institute / Camborne School of Mines, University of Exeter, United Kingdom*

ABSTRACT

Accurate prediction of acid rock drainage (ARD) during early life-of-mine stages is critical for the development of effective waste management strategies. However, tests and methodologies used by industry focus on the extensive use of geochemical tests i.e., those associated with acid base accounting. Due to the high costs and turn-around time of such tests, only a limited number of samples are selected for predictive testwork. Consequently, detailed ARD characteristics of a deposit cannot be understood, resulting in the development of inadequate waste management plans and rehabilitation strategies. Instead, industry requires effective tools and protocols which allow for a greater number of samples to be evaluated, and are simple enough to perform in a field-laboratory, thus keeping costs to a minimum and turn-around time short. To satisfy such requirements, simple field-based pH tests should be utilised. In addition, methods to improve mineralogical characterisation in drill core materials should be employed including an ARD focused logging code, chemical staining and the use of portable instruments (i.e., portable XRF, Equotip). Finally, methods for evaluating geometallurgical data for ARD prediction should be used, and have real potential to add-value to existing datasets.

These new tools and protocols were developed and tested using drill core and waste rock materials obtained from several Australian mines with differing geology, mineralogy and mineralisation style. Our research shows that by adopting these improved tests and methods, the industry will be able to: i) perform effective predictive ARD testwork; ii) achieve detailed deposit-wide characterisation, iii) develop the best possible waste management plan; and iv) evaluate only the most suitable rehabilitation options.

Keywords: management, geochemical, prediction, waste rock, test

INTRODUCTION

Oxidative dissolution of sulphidic minerals present in mine waste materials (e.g., waste rock, tailings) has the potential to release acidic leachate (acid rock drainage, ARD), sulphate and potentially deleterious elements e.g., As, Ag, Cd, Cr, Cu, Hg, Ni, Pb, Sb, U and Zn. Therefore, in order for mining operations to adequately control and manage ARD during the entire life-of-mine, a comprehensive approach to ARD prediction must be adopted, benefits of which will be minimisation of environmental impacts, and reduction of financial liabilities associated with closure. Such an approach requires: i) analysis of an adequate number of samples, and ii) a short turnaround time frame in which to collect pertinent ARD data to allow for basic waste classification. The current industry approach to ARD prediction relies upon using geochemical tests (e.g., static, kinetic). However, limitations of static testing have long-since been established (i.e., the use of sulphide-sulphur vs. total sulphur in calculation of maximum potential acidity (MPA), variations in reaction times and chemicals in acid neutralising capacity (ANC) experiments). Furthermore, kinetic tests run for a minimum of 30 weeks i.e., data returned too slowly to guide development of an adequate waste management strategy. Most significantly, neither static nor kinetic testwork are suitable to perform on regulator recommended number of samples for ARD testwork during early life-of-mine stages (e.g., several hundred; Australian Government, 2007) due to the costs involved. For example, a basic net acid producing potential (NAPP) and net acid generating (NAG) package costs A$50 (Australian Laboratory Services, 2014) and can take at least 5 days (on sample receipt) for data to be reported. Performing such screening tests on best practice number of samples (e.g. 500 samples) would cost at least A$25,000, excluding sample preparation and handling costs. Additional mineralogical testwork would likely be required (average cost per sample: A$50-150), and any further geochemical testing (i.e., sulphide-sulphur determination, pH testing, advanced NAG tests) would result in significant financial expenditures.

Ideally, industry needs to have a field-appropriate ARD prediction toolbox that allows useful data to be collected more time-efficiently and cost-effectively. If such tests can be readily performed at mine sites, then samples for more detailed ARD testwork (i.e., using the established methods) can be better chosen. Considering this, we have evaluated several test methods (both geochemical and mineralogical) for rapid field-based ARD prediction. These included: i) chemical staining to identify neutralising potential, ii) field-based pH testing, iii) field portable instruments and iv) ARD focused logging. All results were validated against established methods e.g., X-ray diffractometry (XRD), X-ray fluorescence (XRF), and static tests (total-sulphur, multi-addition NAG and Sobek methods). These methods were tested using drill core and waste materials collected from several Australian mine sites, including two operational volcanogenic massive sulphide deposits located in Western Tasmania, and one abandoned lode gold deposit located in Queensland. Examples from these studies are presented in this paper.

METHODOLOGY

Both drill core and waste rock samples were collected from three sites (1, 2 and 3) between 2007 and 2013. Site 1 is an operational polymetallic volcanic-hosted massive sulphide deposit located on the western coast of Tasmania. Site 2 is an abandoned lode-Au mine operations in Queensland where the dominant waste rock lithologies comprise hydrothermally altered rhyolite/ rhyolite tuffs which host sulphide bearing quartz lodes. Site 3 is a deposit part of the large Cambrian hybrid volcanogenic-magmatic Cu-Au-Ag system at Mount Lyell, Western Tasmania.

Sample preparation

Each sample from site 1 and 2 was sawn in two to allow for photography and logging of a fresh surface. One portion was subjected to crushing and milling to <63 μm for geochemical and mineralogical testwork. The other portion was kept intact for mineralogical and chemical analyses using stains and field-appropriate equipment. Drill core from site 3 were first subjected to chemical staining and geometallurgical testwork, followed by the selection of representative samples every 1 m for validation geochemical and mineralogical analyses. These samples were also crushed and milled to <63 μm.

Chemical staining

Chemical staining techniques are under-utilised in the mining industry despite being simple and inexpensive tools to distinguish mineralogy and texture in a range of sample types (i.e., drill core, grain mount and thin section). Various carbonate staining techniques exist as published by Freidman (1959), Warne (1962) and Reid (1969). The methods presented in Freidman (1959) were used in this study as these are the most commonly used (Hitzman, 1999). The advantage of using chemical stains on drill core is that carbonate materials (particularly effective neutralisers such as calcite and dolomite) can be confidently identified, thus allowing for improved estimations of their modal abundance during logging or initial ARD assessments.

All drill core samples (n= 51- site 1; 70 m - site 3) were subjected to staining. Prior to staining, drill core materials were etched with dilute hydrochloric acid (HCl) for 2 to 3 minutes, and subsequently washed with water. Samples were then left to dry for approximately 30 minutes. Site 1 samples were placed directly in a plastic container containing the stain and left to soak for approximately 15 minutes in a dual stain comprising the organic dye Alizarin red-S (ARS) and potassium ferricyanide (PF) dissolved in HCl. For site 3, samples were stained directly with the same stain using a paintbrush. The ARS produces a pink to red stain on any carbonate that will react with dilute acid. The more reactive carbonates such as calcite and aragonite stain red, but the less reactive such as dolomite and siderite, remain unstained (Friedman, 1959; Hitzman, 1999). Whilst pure dolomite does not stain, if iron is substituted into the dolomite lattice, it becomes more reactive thus; ferroan dolomite and ankerite stain with ARS (Hitzman, 1999). The PF stain is more effective at identifying ferrous carbonates, as it reacts with ferrous iron causing a precipitate of Turnbull's blue to form (Dickinson, 1966). Siderite does not react with this stain. Therefore where zones of high acid neutralising capacity (ANC) are reported, but no staining colour is observed, the effective ANC can be considered low as siderite is not an effective carbonate neutraliser. After staining, samples were imaged to allow for comparison against unstained images.

Environmental logging

Textural analysis is largely absent from predictive acid rock drainage (ARD) assessments despite the direct control of texture on acid formation as discussed in Parbhakar-Fox et al. (2011). Motivated by this, these authors developed the 'ARD Index' (or ARDI) which allows for simple textural evaluations to be performed. The generated ARDI values are recommended for use in conjunction with sulphur assay or paste pH data to domain ARD forming potential. The ARDI proposed by Parbhakar-Fox et al. (2011) required assessments to be performed on both a mesoscale and microscale. However, a modified ARDI has since been developed for site 1 to allow for the performance of simpler, more time efficient assessments. An assessment was performed on all

samples, over an 8.5 cm x 5.5 cm size area, with the area most dominated by sulphide chosen for assessment, as the most conservative ARDI value was sought.

Field pH testing

Paste pH testing represents the most efficient manner by which to assess a sample's immediate acid forming characteristics. Considering this, it was performed on all samples at the University of Tasmania (UTas, School of Physical Sciences, CRC ORE laboratory), with the ASTM D4972-01(2007) method used on drill core materials (i.e., site 1 and 3) following recommendations given in Noble et al. (2012). For weathered materials from site 2, the AMIRA P387A Handbook method (Smart et al., 2002) was used. The pH value of each tested sample was measured in triplicate, with the standard deviation calculated as <0.5.

A method to accelerate the paste pH test by using a hot electrolyte solution to encourage faster reaction kinetics was trialed. Select pulverised (< 63 μm) materials from sites 1 and 3 (n=20) were paste pH tested using three different electrolyte solutions: i) tap-water; ii) deionised water (DI); and iii) 0.01M $CaCl_2$. Certified reference materials KZK-1 and NBM-1 (purchased from CANMET; Natural Resources, Ottawa) were also tested. These solutions were heated to 100°C and poured onto 10 g of sample weighed out in 50 ml glass beakers, with a 1:2 solid: solution ratio used. Once poured, beakers were stirred for 30 seconds and allowed to cool to room temperature. Measurements of pH and EC were taken after 1 hour in triplicate, with standard deviation calculated as <0.01.

Field instrumentation

Short-wave infrared

The application of short-wave infrared (SWIR) spectroscopy in determining pale, fine-grained alteration minerals has been demonstrated in ore-deposit characterisation studies (e.g., Thompson et al., 1999; White et al., 2010). Mineral identification is based on absorption spectra collected from clean, dry, flat, rock surfaces (Gifkins et al., 2005). SWIR therefore has potential to improve mineral identification of altered drill core samples for ARD characterisation. Two instruments were selected for testing in this research on samples from site 2; a portable infrared mineral analyser (PIMA; manufactured by Integrated Spectronics, Australia) and a TerraSpec spectroradiometer (manufactured by analytical spectral device (ASD) Inc.). Materials from site 3 were tested using the TerraSpec only, however in this study, both intact pieces and homogenised powders from each 1 m interval were analysed to assess which is a more appropriate sample type.

Portable XRF

Accurately measuring chemistry and comparing these data to ARD parameters (e.g., paste pH, total-sulphur) allows for a first-pass indication of potential leachate quality issues which may arise towards the life-of-mine end (i.e., mine closure). This in turn allows the development of appropriate waste management plans. Field-portable XRF (pXRF) instruments have in recent years been used in mine site characterisation studies for determining element concentrations (e.g., Haffert and Craw, 2010; Higueras et al., 2012). Most recently, Parbhakar-Fox et al. (2014) discussed its application in mesotextural classification at abandoned mine-sites. In this study, a hand-held Olympus-InnovX instrument was used (UTas, School of Earth Sciences) on intact drill core (three

areas selected) and homogenised powders at site 1, and powders taken at 1 m intervals at site 3, with reference standards NIST 2781, GXR3-538 and GXR4-2843 used throughout the analyses. A benchtop Innov-X X50 XRF instrument was used to analyse waste materials collected from site 2. Both homogenised powders and intact portions (three areas analysed) were tested in this particular study. The instrument was routinely calibrated by the material supplied by the manufacturer during the analyses (i.e., after ever 10th measurement).

Equotip

Measuring the susceptibility of a lithology to weathering is required to understand how rapidly acid forming minerals will become exposed in a waste rock pile. Therefore, the application of Equotip (a non-destructive, core-based measurement technique) which measures hardness was explored. The Leeb (Ls) hardness value (0 to 1000) is automatically calculated, and is the quotient of the rebound velocity over the impelled velocity multiplied by 1000 (Keeney, 2008). The impact body rebounds faster from harder test samples than it does from softer ones, resulting in a greater value. Approximately 3000 Equotip measurements were collected on site 3 material only, using an Equotip 3 (Proceq) instrument, across the whole 70 m interval. Average values were calculated for each 1 m interval based on measurements taken at 2.5 cm intervals. These values were used alongside total-sulphur values for comparison with NAG pH vs. paste pH data. This has the potential to allow for a low-cost first-pass understanding of lag-time to ARD on a deposit-scale.

Geochemical and mineralogical validation testing

Rapid and accurate measurement of total sulphur (wt.%) for comparison against Equotip and calculation of maximum potential acidity (MPA) was performed on samples from sites 1 and 3 using an Eltra C-S 2000 instrument at UTas (School of Physical Sciences). For site 2 samples, total sulphur was measured using a Thermo Finnigan 1112 Series Flash Elemental Analyser instrument (Central Science Laboratory (CSL), UTas). Appropriate standard materials were analysed on both instruments during all analyses. In addition, the total element chemistry of samples from site 2 was measured for comparison against pXRF data using a Philips PW1480 X-ray Spectrometer (UTas, School of Physical Sciences). Acid neutralising capacity (ANC) was measured by the Sobek method at ALS Brisbane for samples from all three sites. The multi-addition net acid generation (mNAG) test was performed on materials from all sites at UTas (School of Physical Sciences) following the AMIRA P387A method (Smart et al., 2002).

Mineralogical determination of material from sites 1 and 3 was performed using a benchtop Bruker D2 Phaser X-ray diffractometer at UTas (School of Physical Sciences). Mineralogical analyses for samples from site 2 were performed at the University of Ballarat, Australia, using a traditional Siemens D501 diffractometer.

RESULTS AND DISCUSSION

Domaining neutralising potential: staining

The dominant carbonate textures observed in drill core material from site 3 comprised of clasts (in limestone conglomerates) and veins. The Alizarin red S-potassium ferricyanide (ARS-PF) stain appropriately reacted with calcitic material in both textural forms; with the pink stain appropriately uptaken, with corresponding XRD data confirming this as calcite. Comparison of samples analysed

by the stain painted directly on, and those soaked directly in the stain, confirmed that stains were better uptaken by the latter method (Figure 1).

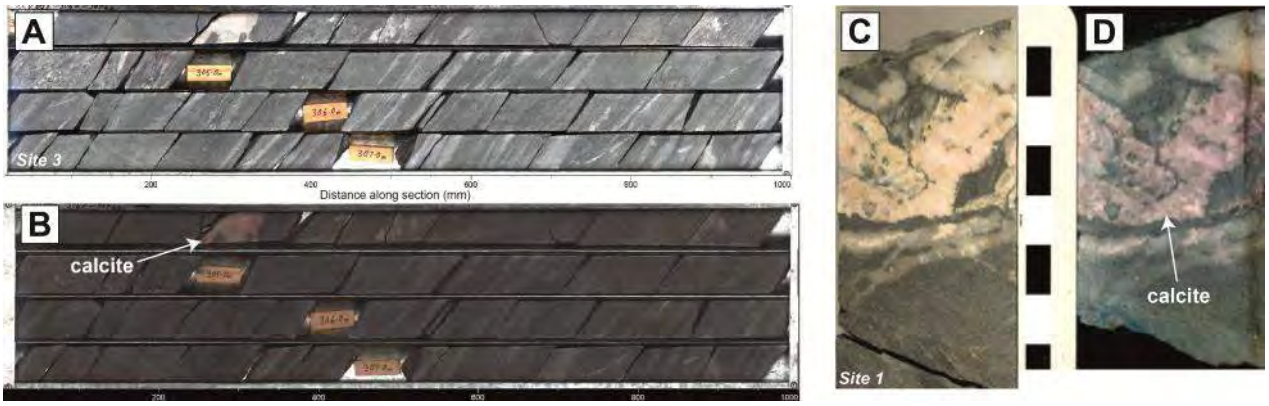

Figure 1 Photograph images of drill core from site 3 (massive sulphide deposit, western Tasmania, Australia); A) unstained and B) after several coatings of stain were painted directly on; C) unstained drill core sample from site 1 (operational polymetallic mine, western Tasmania, Australia); C) stained drill core sample from site 1 after soaking in stain bath for 30 minutes. The pink colour seen in both examples indicates the presence of calcite thus identifying effective acid neutralising capacity

Domaining neutralising potential: SWIR

Whilst major rock forming minerals can be easily recognised in hand-specimen based on their different rock properties (i.e., hardness, lustre, habit), hydrothermally altered minerals are much harder to identify. Typically, they can appear as pale and fine-grained, and with such a grain size, potential for participating in neutralising reactions (cf. Plumlee, 1999) is much greater. As stated, homogenised powder samples from site 2 were used in a study to compare two commonly used SWIR instruments, namely the PIMA and TerraSpec. Muscovite was confirmed by XRD as the dominant alteration mineral in these hydrothermally altered rhyolite samples. Two examples of typical PIMA and TerraSpec results are shown in Figure 2. Spectra collected by TerraSpec (Figure 2b and d) were better defined (i.e., less noise), and show better agreement with the reference spectra. Results from PIMA showed greater deviation from the reference spectra for sample 1 (Figure 2a), and were aspectral from sample 2 (Figure 2b). Based on these results, the TerraSpec is given preference for use. Furthermore, the TerraSpec is not restricted to analysis of pale-coloured minerals like PIMA and can detect a greater range of minerals including iron-oxyhydroxides.

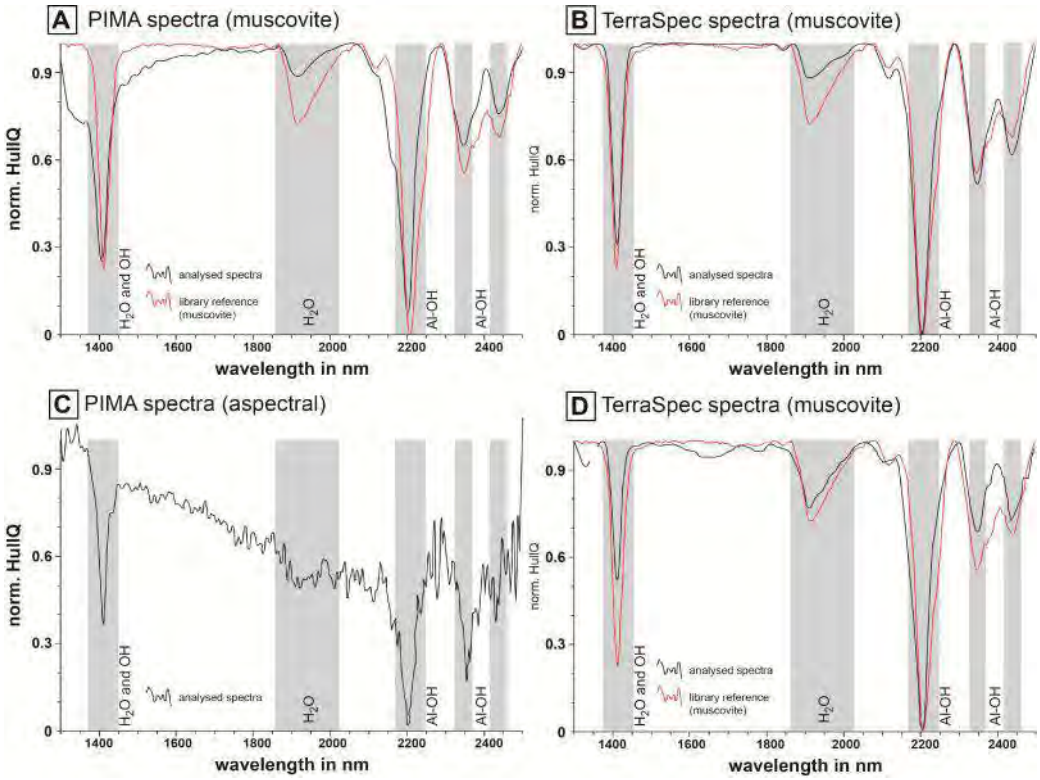

Figure 2 Example of alteration mineral identification in Site 2 (abandoned lode-Au mine, Queensland) waste rock materials; A) Sample A analysed on a PIMA with muscovite identified; B) Sample A analysed on a TerraSpec with muscovite confidently identified; C) Sample B analysed on a PIMA with an aspectral result; and D) Sample B analysed on a TerraSpec with muscovite confidently identified

In order to identify the best sample type for TerraSpec analysis, both powdered and intact drill core materials from site 1 were tested. For powdered samples, noisy spectra were collected, which were classified as aspectral, therefore, preference is given to using intact drill core. However, in validation testwork, the TerraSpec was less accurate than XRD. Whilst the TerraSpec was able to confidently identify the presence of calcite, muscovite and chlorite in 52% of the samples, it occasionally misidentified minerals such as tourmaline and epidote, which were neither logged, nor detected by XRD. Furthermore, whilst the TerraSpec instrument correct detected the presence of carbonate minerals in 52% (i.e., identified as calcite) of these samples, the exact carbonate mineral type was only correctly identified in 10% of samples when compared to XRD. This is likely explained by having performed these analyses on intact drill core (i.e., non-homogenised, randomly selected areas for analysis); therefore there is a high likelihood of conflicts when compared to XRD data. Based on these results, it is evident that applications of TerraSpec for ANC domaining are limited.

Assessing acid forming characteristics

Paste pH measurements are shown in Figure 3 with data compared against NAG pH and total sulphur measurements as recommended in Parbhakar-Fox et al. (2011). A spread of data was seen for all sites. Site 1 samples were mostly classified as potentially acid forming to non-acid forming;

site 2 samples showed a range of classifications with both extremely acid forming and non-acid forming materials identified; and site 3 samples were potentially acid forming to acid forming.

Accelerated paste pH data (DI water, tap water and ASTM D4921-01) were compared against standard ASTM D4921-01 results for drill core materials from site 1 (Figure 4a) and site 3 (Figure 4b). In general, for site 1 the accelerated ASTM D4921-01 returned the lowest pH values by up to 2.3 units. Results from both accelerated water electrolyte experiments were in close approximation (R^2= 0.995). However, when values were compared against standard ASTM D4921-01 method data, they were neither consistently higher, nor lower (pH unit difference range of +1.2 to -2.2). A similar trend was seen for site 3, with the accelerated ASTM D4921-01 test returning the lowest pH values for the accelerated tests. When these were compared against the standard ASTM D4921-01 method, an inconsistent trend was once against observed with a pH unit different range of +1 to -2.25. These results confirm that the accelerated test is encouraging reaction kinetics to proceed quicker as all accelerated values differ to the standard ASTM method. In order to understand the changes occurring during these tests, the supernatant chemistry will be assessed and a detailed XRD study of the residual powder will be undertaken. In addition, a re-evaluation of field-NAG tests is to be undertaken. The aim of this will be to produce a simple pH testing methodology (which can be performed at mine sites), the results from which can be used in more informative paste pH vs. NAG pH classifications.

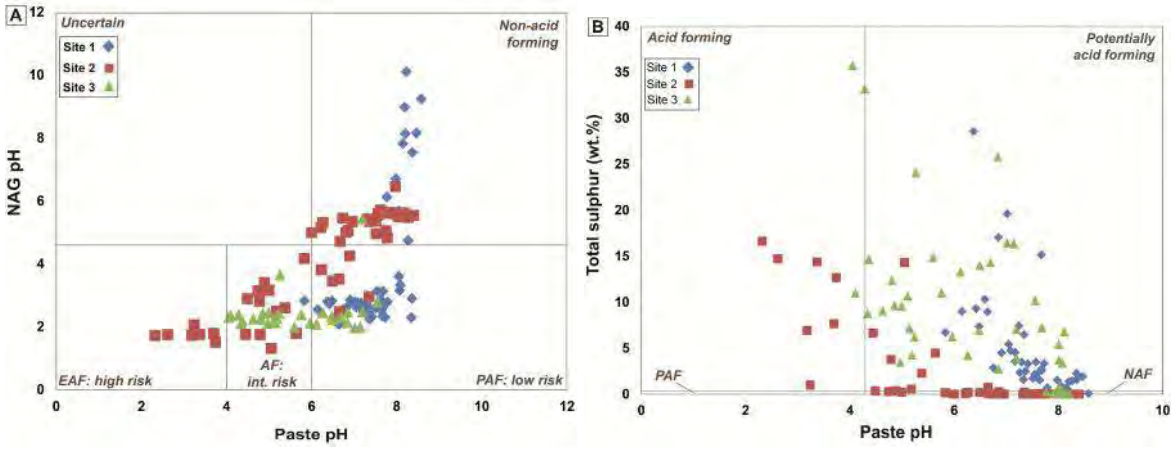

Figure 3 Paste pH measurements performed on drill core and waste materials from sites 1, 2 and 3; A) NAG pH compared against paste pH (after Weber et al., 2006); B) Total sulphur compared against paste pH (after Parbhakar-Fox et al., 2011). Abbreviations: AF, acid forming; EAF, extremely acid forming; PAF, potentially acid forming; NAF, non-acid forming)

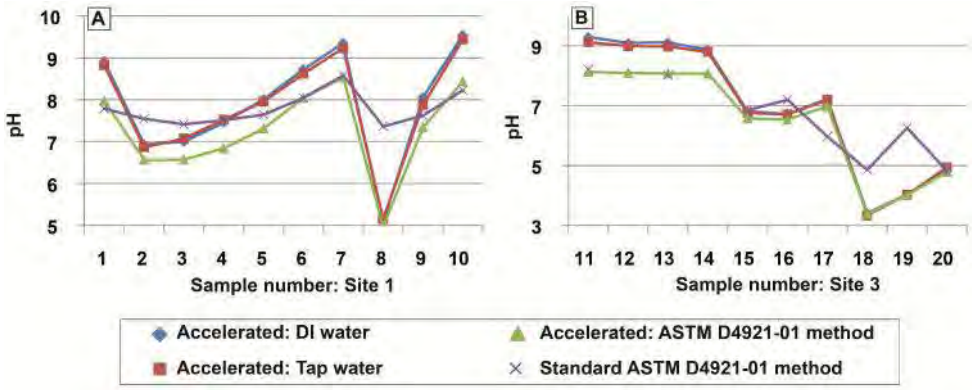

Figure 4 Paste pH test results for 10 samples from site 1 (operational polymetallic mine, western Tasmania, Australia; 1 to 10) and site 3 (massive sulphide deposit, western Tasmania, Australia; 11 to 21). Data from four experiments (3 accelerated, and one standard) are shown

Determination of bulk chemistry

Measurements of sulphur are essential for the calculation of MPA. However, the turnaround time for assay data may be significant (i.e., >48 hours). Alternatively, sulphur can be measured using a portable XRF or a benchtop element analyser. To test the accuracy of the various sulphur measurement techniques, materials from site 2 were subjected to measurements using an: i) element analyser; ii) traditional XRF; and iii) pXRF with results shown in Figure 5. Data from the element analyser and XRF were in close approximation (R^2= 0.9979), however, data from the pXRF was in less agreement when compared with both methods (R^2= 0.886 against EA; R^2= 0.8197 against XRF). Based on these results, the use of pXRF to directly calculate MPA should be avoided. Instead, this can be accurately determined using an element analyser (e.g., Eltra CS 2000 instrument), whereby reliable sulphur data can be collected efficiently. Instead, data from a pXRF instrument could be used to aid the identification of samples requiring such testwork, i.e., those with relatively high sulphur (i.e., above the specified total-sulphur cut-off).

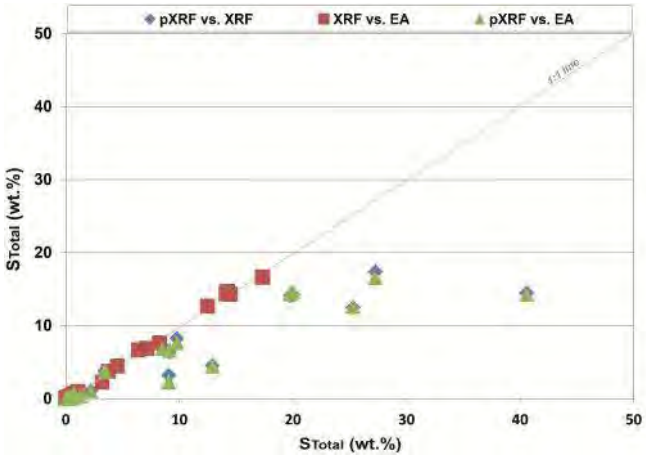

Figure 5 Total sulphur measurements made by three different analytical instruments (portable XRF, pXRF; XRF and an element analyser, EA) on samples from site 2 (abandoned lode Au-operations, Queensland, Australia)

The bulk chemistry was measured by XRF and pXRF for samples from site 2. Results for six elements commonly of environmental concern which were measured above detection limit are shown in Figure 6. Both techniques returned results in very close agreement (range of $R^2 = 0.9413$ for Sb, to $R^2 = 0.998$ for Pb). This indicates that element data collected from pXRF is relatively accurate, and therefore can be confidently used in classification schemes such as Ficklin plots (Plumlee, 1999). A similar conclusion as to the accuracy of pXRF instruments for waste classification purposes at the MacArthur River Mine, Australia was made by Landers et al. (2014).

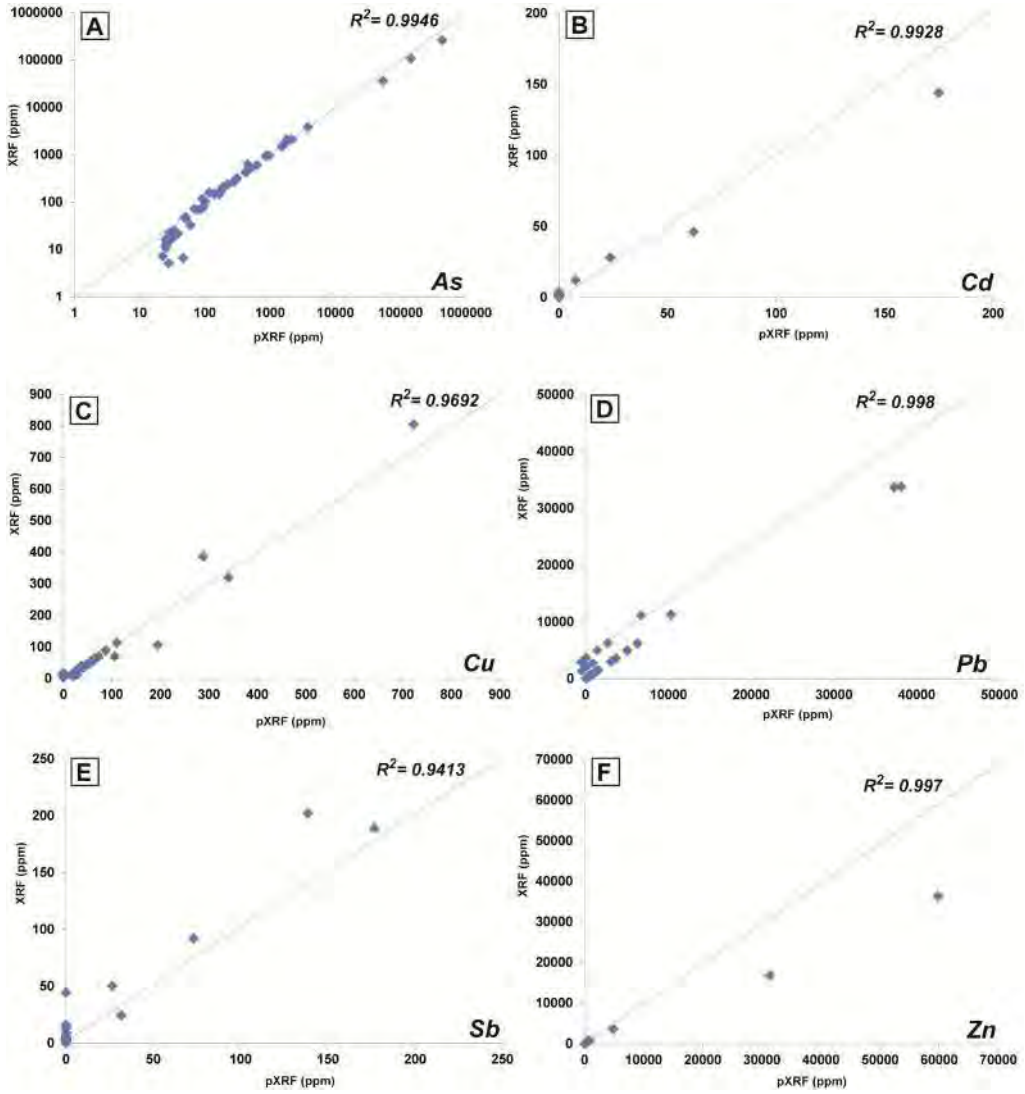

Figure 6 Concentrations (ppm) of selected elements: As (A); Cd (B); Cu (C); Pb (D); Sb (E); and Zn (F) measured in waste rock materials from site 2 (abandoned lode-Au, Queensland, Australia) by portable XRF (pXRF) and XRF techniques.

The type of sample to use in pXRF tests was evaluated using material from site 1. Both were homogenous powders and intact drill core were examined with results for the sum of metals (as considered in Ficklin plots) is shown in Figure 7. In general, there is positive correlation between both datasets (R^2= 0.81), with powdered samples generally returning higher values. From an efficiency perspective, collection of data on intact drill core is preferred; however, subjective (bias) sampling is introduced through identifying a particular interval for analysis. Furthermore, over a given interval (i.e., 1 m or 5 m), if one final value is to be utilised, how many analysis should be performed, and should an average value calculated and used? If analysis on drill core is to be pursued, a standard operating procedure must be enforced. To reduce such sampling issues, pXRF should be performed on powdered materials (again, it would be advantageous to use the same powdered materials as in total-sulphur and paste pH testing). In doing so, appropriate certified reference materials (CRMs) used here and described in Hall et al. (2014) and Piercey and Devine (2014) should also be analysed. Additionally, samples should be systematically selected for validation (using routine whole-rock analysis techniques) and if necessary, specific correction factors developed.

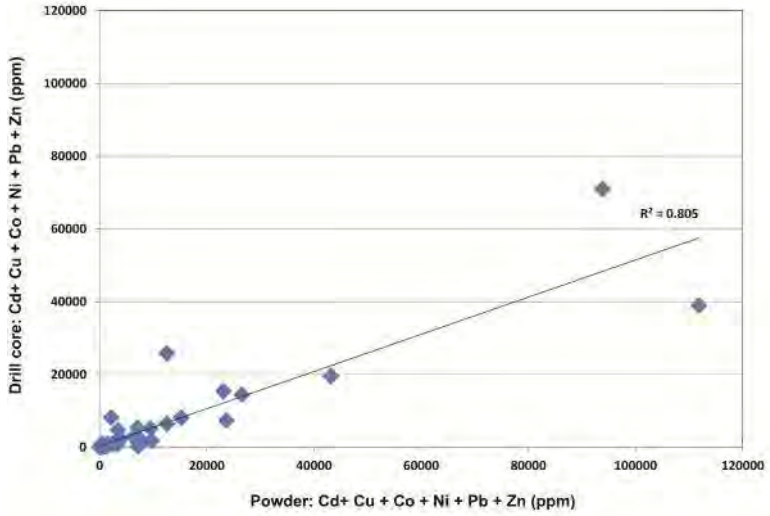

Figure 7 Total metal concentrations (Cd, Cu, Co, Ni, Pb, Zn in ppm) measured by portable XRF (pXRF) in drill core and homogenised powdered sample material collected from site 1 (operational polymetallic mine, western Tasmania, Australia, n= 51)

Using hardness for waste classification

Mineral hardness data was measured by Equotip for all drill core material collected from site 1 (304 m to 375 m). Whilst the objective was to domain ARD risk for the sulphidic schist material (345 m to 375 m), the Equotip data also allowed for ANC assessment for the carbonate-breccia material (304 m to 344 m). Comparisons of Equotip data against total sulphur and paste pH values are shown in Figure 8. If a mineral hardness value was <648 Ls, it was classified as soft in accordance with Keeney (2008). The schist material was classified as 'PAF-rapid ARD likely' by the criteria: paste pH <5.5, total-sulphur >0.3 wt. %, and < 648 Ls. Such a classification indicates that the material is susceptible to weathering as it is friable, which was observed in the field and during handling. Therefore, there is a greater likelihood of acid generation at a rapid rate, as sulphides in this material (i.e., pyrite and chalcopyrite) will be quickly liberated. These findings are in agreement

with the NAG pH vs. paste pH classification (Figure 3a). Materials were classified as having ANC by the criteria: paste pH ≥8, total-sulphur values < 0.3 wt. % and <648 Ls (e.g., 309 m to 315 m; Figure 8d).These were taken to represent the most effective neutralisers. This study indicates the potential assistance of Equotip data when performing field-based ARD studies. It is noteworthy that in the absence of paste pH data, mineral hardness and total sulphur data would have been sufficient to conservatively classify the behaviour of these materials.

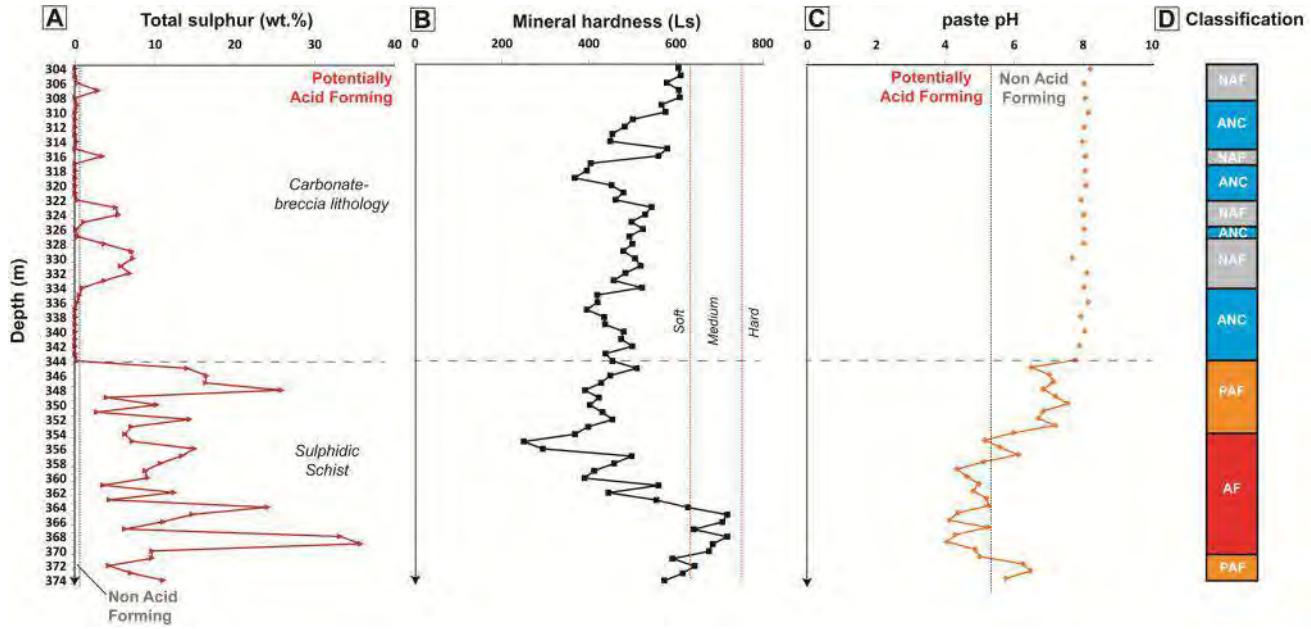

Figure 8 Downhole geochemical and geometallurgical data from site 3 (massive sulphide deposit, western Tasmania, Australia) drill core material (304 m to 375 m, change of lithology indicated by the horizontal dashed line at 345 m; A) Total sulphur values (wt. %; n=70) with 0.3 wt. % used as the classification cut-off criterion (Parbhakar-Fox et al., 2011); B) Mineral hardness values as measured by Equotip and reported in Leeb (Ls), with criteria for defining hard, medium and soft samples shown (Keeney, 2008); C) Paste pH values (n=55) with pH 5.5 used as the classification cut-off criterion; D) ARD classifications based on total sulphur, mineral hardness and paste pH values. Abbreviations: AF, acid forming, high risk with rapid ARD formation, ANC, acid neutralising capacity, highly effective; NAF, non-acid forming; PAF, potentially acid forming, medium risk with lag-time to ARD formation.

Geoenvironmental logging

A validation study of the acid rock drainage index (ARDI) was performed on drill core materials from site 1, whereby ARDI values collected in mesotextural scale drill core material only were compared against geochemical data (Figure 9). The ARDI was able to correctly identify samples with acid forming capacity (PAF, AF and EAF) when compared against total sulphur (Figure 9a), NAPP values (Figure 9b) and NAG pH (Figure 9c). The ARDI was more conservative in its classification of samples with neutralising capacity with several identified as NAF by the ARDI, but were identified as having an ANC by Sobek testing (Figure 9d). In this instance, the ARDI was

considered more accurate, as it evaluated the content of sulphides in proximity to, and the mineral associations of carbonate minerals. This study demonstrates the application of the ARDI, consequently, more mine sites should adopt such an ARD focused logging code in order to populate their mine database with this environmental attribute. Additionally, this method can be performed at mining operations in various stages of the life-of mine; for example: during exploration on hand specimen samples, during mine operations to check the correct placement of waste materials, and post-closure at historic or abandoned sites.

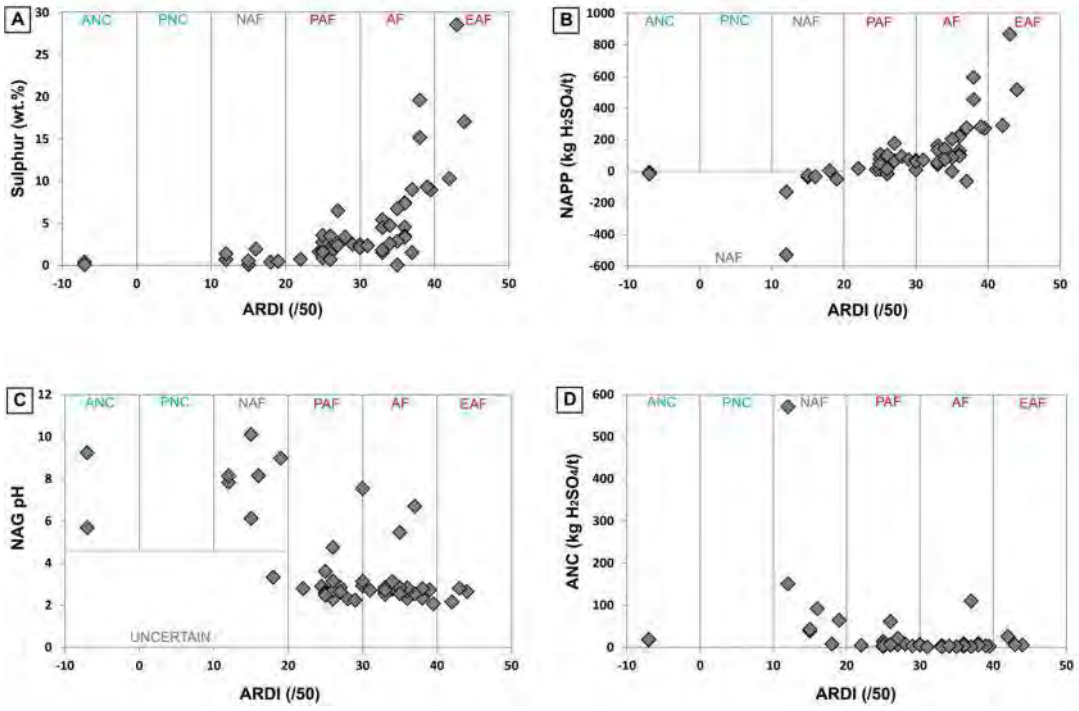

Figure 9 Comparison of acid rock drainage index (ARDI) scores given to site 1 (operational polymetallic mine, western Tasmania, Australia) drill core materials (n=51) against: A. Total sulphur (wt. %); B.net acid producing potential values (NAPP; kg H_2SO_4/t); C. net acid generation (NAG) pH; and D. acid neutralising capacity (ANC; kg H_2SO_4/t).

CONCLUSION

To effectively select the most appropriate samples for detailed geochemical and mineralogical test work, which allows for ARD prediction and waste classification during early life-of-mine operations, a pre-screening testing stage is required as described in Parbhakar-Fox et al. (2011). Such a stage must allow for a deposit-appropriate number of samples to be evaluated in order to build a database of ARD information allowing for the construction of a deposit-wide ARD model. Such a pre-screening stage must utilise efficient and cost-effective field-based tools. This permits site-based staff to characterise their own materials, thus reducing turnaround time for obtaining ARD relevant data, and improving the quality of decision making with regards to waste management (e.g., scheduling, handling and placement). A range of both existing and newly developed tools were examined in this study using materials collected from three Australian mine sites.

Our study indicates that chemical staining is an appropriate technique by which to identify the presence of carbonates if traditional mineral identification methods fail (e.g., if it is very fine grained and present in the rock matrix). Whilst the best stain responses are returned from soaking drill core directly in chemical stains, it may not be practical to perform in a field laboratory. Therefore, painting stains directly onto core gives sufficient results. Carbonate staining responses should be used to assist with environmental logging using a modified ARDI (i.e., mesoscale analysis evaluation only). The use of automated hyperspectral loggers (e.g., HyLogger) as used for geometallurgical testwork should be considered, as was demonstrated in Parbhakar-Fox and Lottermoser (2014). Short-wave infrared data collected by a TerraSpec instrument can be used to confirm the presence of carbonate but will only provide an indication of the exact carbonate mineral. Such analysis should only be performed on intact drill core materials and not on homogenised powders. In order to classify the geochemical behaviour of the materials, paste pH tests should be performed and used against portable XRF data (collected from homogenised powders) on Ficklin plots. However, paste pH testing must be standardised industry-wide, and methods in which to turn this simple method into a predictive test must be developed. The accelerated paste pH test represents one option; however, alternatives exist such as using a field NAG pH test. In addition, sulphur data should be collected on a bench-top instrument (if no assay data exist), and used with mineral hardness values (as collected by Equotip) and paste pH to domain lag-time to ARD.

The benefit of utilising these field-based techniques is that it enables a database of ARD data to be collected and held on site thus allowing for in-house expertise to be built up. Ultimately, this will lead to an improved quality of waste management strategies, and better forecasting of appropriate of rehabilitation options. Additionally, as demonstrated by using materials from site 2 (abandoned lode-Au operations, Queensland, Australia) these simple field-techniques can be used at mines in the final life-of-mine stage i.e., post-closure.

ACKNOWLEDGEMENTS

The authors would like to acknowledge the support of CRC ORE, established and supported by the Australian Government's Cooperative Research Centres Programme. The two western Tasmanian mines (sites 1 and 3) are thanked for access to drill core materials. Additionally, the Queensland Department of Natural Resources and Mines are thanked for granting access to the abandoned lode-Au mine operations (site 2). Peter Harding and Dr. David Green of Minerals Resources Tasmania (MRT) are thanked for allowing drill core testing on materials from site 3 to be performed at MRT. Finally from the University of Tasmania, Dr. Nathan Fox, Craig Winter and Angela Escolme are acknowledged for analytical assistance.

REFERENCES

American Society for Testing and Materials ASTM D4972-01 (2007) Standard test method for pH of soils, ASTM D4972-01(2007). ASTM International, West Conshohocken.

Australian Government Department of Industry, Tourism and Resources (2007) Managing acid and metalliferous drainage, Leading Practice Sustainable Development Program for the Mining Industry, Canberra, 96p.

Australian Laboratory Services (2014) Service Catalogue, pp. 42-43.

Bowell, RJ, Rees, SB, and Parshley, JV (2000) Geochemical predictions of metal leaching and acid generation: geologic controls and baseline assessment. *Geology and Ore Deposits: The great Basin and Beyond Proceedings 2*, pp.799-823.

Dickinson, JAD (1966) Carbonate identification and genesis as revealed by staining, *Journal of Sedimentary Petrology*, vol.36, pp.491-505.

Freidman, GM (1959) Identification of carbonate minerals by staining methods, *Journal of Sedimentary Petrology*, vol.29, pp.87-97.

Gifkins, C, Herrman, W, and Large, R (2005) Altered Volcanic Rocks: a guide to description and interpretation, University of Tasmania, 275 pp.

Haffert, L, Craw, D, and Pope, J (2010) Climatic and compositional controls on secondary arsenic mineral formation in high-arsenic mine wastes, South Island, New Zealand, *New Zealand Journal of Geology and Geophysics*, vol.53, pp.91-101.

Hall, GEM, Bonham-Carter, GF, and Buchar, A (2014) Evaluation of portable X-ray fluorescence (pXRF) in exploration and mining: Phase 1, control reference materials. *Geochemistry: Exploration, Environment, Analysis,* 10.1144/geochem2013-241.

Higueras, P, Oyarzun, R, Iraizoz, JM, Lorenzo, S, Esbri, JM, and Martinez-Coronado, A (2012) Low-cost geochemical surveys for environmental studies in developing countries: Testing a field portable XRF instrument under quasi-realistic conditions. *Journal of Geochemical Exploration*, vol.113, pp.3-12.

Hitzman, MW (1999) Routine staining of drill core to determine carbonate mineralogy and distinguish carbonate alteration textures. *Mineralium Deposita*, vol.34, p.794-798.

Jambor, JL, Dutrizac, JE, Groat, L, and Raudsepp, M (2002) Static tests of neutralization potentials of silicate and aluminosilicate minerals. *Environmental Geology*, vol.43, pp. 1-17.

Keeney, L (2008) Equotip hardness testing: Aqqaluk (including a guide on how to use Equotip). *AMIRA P843 Technical Report 2*, (ed: J Hunt), pp.17.1-17.20.

Kruse, F.A (1994) Identification and mapping of minerals in drill core using hyperspectral image analysis of infrared reflectance spectra. http://www.spectralcameras.com/fi les/Applications/Kruse_Core94.pdf

Landers, M, Usher, B, Faulkner, D, Marianelli, P, and Masterman, K (2014) Field and desktop waste rock classification guide for a metalliferous mine in the northern territory, Australia. *Proceedings of the Eighth Australian Workshop on Acid and Metalliferous Drainage* (Eds H Miller and L Preuss) pp.159-172.

Noble, TL, Lottermoser, BG, and Parbhakar-Fox, A (2012) Evaluating pH tests for mine water prediction, in *3rd International Congress on Water Management in the Mining Industry*, (eds: F Valenzuela, J Wiertz) pp. 504-512.

Parbhakar-Fox, A, and Lottermoser, B (2014) Domaining acid rock drainage risks using geometallurgical data. In *Proceedings of the Eighth Australian Workshop on Acid and Metalliferous* (Eds H Miller and L Preuss) pp. 483-494.

Parbhakar-Fox, A, Edraki, M, Hardie, K, Kadletz, O, and Hall, T (2014) Identification of acid rock drainage sources through mesotextural classification at abandoned mines of Croydon, Australia: Implications for the rehabilitation of waste rock repositories, *Journal of Geochemical Exploration*, vol. 137 pp. 11-28.

Parbhakar-Fox, AK, Edraki, M, Walters, S ,and Bradshaw, D (2011) Development of a textural index for the prediction of acid rock drainage, *Minerals Engineering*, vol. 24, pp.1277-1287.

Piercey, SJ and Devine, MC (2014) Analysis of powdered reference materials and known samples with a benchtop, field portable X-Ray fluorescence (pXRF) spectrometer: evalution of performance and potential applications for exploration lithogeochemistry. *Geochemistry: Exploration, Environment, Analysis*. 10.1144/geochem2013-199

Plumlee, GS (1999) The environmental geology of mineral deposits, in *The Environmental Geochemistry of Mineral Deposits Part A: Processes, Techniques and Health Issues*, (eds: GS Plumlee, MJ Lodgson), Reviews in Economic Geology, Vol. 6B pp.71-116.

Reid, WP (1969) Mineral staining tests, *Colorado School of Mines: Mineral Industry Bulletin*, vol.12, pp.1-20.

Smart, R, Skinner, WM, Levay, G, Gerson, AR, Thomas, JE, Sobieraj, H, Schumann, R, Weisener, CG, Weber, PA, Miller, SD and Stewart, W.A (2002) ARD test handbook: Project P387A, A prediction and kinetic control of acid mine drainage, Melbourne, Australia: AMIRA, International Ltd, Ian Wark Research Institute.

Thompson, AJB, Hauff , PL, and Robitaille, AJ (1999) Alteration mapping in exploration: application of short-wave infrared (SWIR) spectroscopy, *Society of Economic Geology Newsletter*, vol .39, 13 p.

Warne, S (1962) A quick field or laboratory staining scheme for the differentiation of the major carbonate minerals, Journal of Sedimentary Petrology, vol.32, pp.29-38.

Weber, PA, Hughes, JB, Conner, LB, Lindsay, P, and Smart, R (2006) Short-term acid rock drainage characteristics determined by paste pH and kinetic NAG testing: Cypress prospect, New Zealand, Paper presented at the 7th International Conference on Acid Rock Drainage (ICARD).

White, A, Robb, VM, Robb, LJ, and Waters, DJ (2010) Portable infrared spectroscopy as a tool for the exploration of gold deposits in tropical terrains: A case study at the Damang deposit, Ghana, *Society of Economic Geologists Special Publication 15*.

10th ICARD IMWA 2015 | April 20 - 25. Santiago, Chile
icard@gecamin.com +56 2 2652 1577

The Effects of Preferential and Matrix Flow and Water Residence Time on Seasonal Fluctuations in Mine Waste Rock Effluent Water Quality

Holly Esther Peterson[1], K. Ulrich Mayer[2] and Roger Beckie[2]

1. *Department of Geology, Guilford College, USA*
2. *Department of Earth, Ocean and Atmospheric Sciences, University of British Columbia, Canada*

ABSTRACT

Unsaturated flow regimes in mine waste rock control the volume, timing and quality of dump effluent water. The objectives of this research are to determine the role of particle size distribution on water residence times and to assess how unsaturated flow regimes affect water quality in a two-season (wet/dry) climate. Effluent flow and water quality data are presented for three 36 m x 36 m x 10 m experimental waste rock piles composed of distinct waste rock types at the Antamina Mine in Peru. In boulder- and cobble-dominated carbonate waste rock (Pile 1), matrix flow velocities are 3-12 cm/day and preferential flow velocities are up to 20 m/day. Most dissolved solute concentrations are lowest during the wet season in Pile 1 effluent due to shorter residence times, activation of preferential flow paths, and dilution at the base of the pile. In gravel- and sand-dominated intrusive waste rock (Pile 2), matrix flow velocities are 2-3 cm/day and evidence of fast preferential flow is limited. Pile 2 effluent solute concentrations are highest during the wet season, partly due to solute accumulation in the finer-grained matrix material during dry season and displacement during the wet season. In gravel- and sand-dominated skarn waste rock that contains a significant proportion of boulders in the outer slope (Pile 3), matrix flow velocities are <2-4 cm/day and there is strong evidence of fast preferential flow (up to 2.5 m/day). Most dissolved solute concentrations are lowest during the wet season in Pile 3 due to activation of preferential flow paths and dilution at the base of the pile. Results highlight the effect of particle size on flow distribution and water residence times, which in turn affect seasonal solute concentrations. The results are relevant for predicting seasonal fluctuations in drainage quantity and composition in a variety of waste rock materials.

Keywords: Unsaturated flow; Aqueous geochemistry; Solute accumulation; Dilution; Antamina

INTRODUCTION

The factors controlling mine waste rock effluent water quality are numerous and complex. Simplified, they include waste rock elemental and mineralogical composition, particle size, hydrological properties, microbiology, and meteorology, many of which are strongly linked. Many of the geochemical processes of acid mine drainage in waste rock and tailings, such as sulfide oxidation and acid neutralization, have become relatively well understood through numerous, comprehensive geochemical studies (e.g., Blowes et al., 2003; Moncur et al., 2005), and the amount of research conducted concerning waste rock hydrology is also increasing (e.g., Smith et al., 1995; Eriksson et al., 1997; Smith and Beckie, 2003; Nichol et al., 2005; Neuner et al., 2013). As our understanding of the geochemical and hydrological processes controlling waste rock water quality increases, so does the need to provide the links between the two disciplines, both at the mechanistic level (e.g., Sracek et al, 2004; Stockwell et al., 2006; Wagner et al., 2006; Bay et al., 2014) and through reactive transport modelling (e.g., Lefebvre et al., 2001; Linklater et al., 2005; Molson et al., 2005; Fala et al., 2013). As the research body concerning interactions between hydrology, material type, reaction rates, and metal release and attenuation grows, reactive transport models will become more accurate and uncertainty associated with water quality predictions will be reduced.

The primary purpose of this study is to experimentally investigate quantitative links between waste rock hydrology and geochemistry. Specifically, the study focusses on variability of solute concentrations due to high water residence times and solute accumulation, solute flushing during periods of high precipitation and increased matrix velocities, and dilution of higher-concentration water by lower-concentration water travelling through preferential flow paths. While the study focusses on a limited number of processes, it is recognized that other processes simultaneously affect seasonal fluctuations in water quality, such as variable sulfide oxidation rates, changes in pH, and secondary mineral precipitation and dissolution, and those processes are discussed separately (Nordstrom 2011; Peterson, 2014).

The conclusions of this study are based on observations of seasonal solute concentration fluctuations in the effluent water of three experimental waste rock piles composed of physically and mineralogically distinct materials. The experimental piles are located at the Antamina Mine in Peru and are exposed to almost identical meteorological conditions, isolating the effect of material type – and specifically that of particle size -- on unsaturated flow regimes and effluent water quality.

PROJECT DESCRIPTION

The open-pit Cu-Zn-Mo Antamina Mine in Ancash, Peru consists of a skarn deposit formed during an upper Miocene quartz-monzonite porphyry intrusion (Love et al., 2004). The mine is expected to produce 2.2 billion tonnes of waste rock by proposed mine closure in 2029 (Harrison et al., 2012). Antamina's multi-scale waste rock research program focuses on the characterization, linkage, and scaling of flow, evaporation, and biological and geochemical processes in waste rock. This study focuses specifically on the hydrology and geochemistry of three of the project's five 36 m x 36 m x 10 m experimental waste-rock piles (Figures 1 and 2), which are located at the mine and are exposed to the distinct wet (September-April; approximately 1100 mm to 1300 mm of rain annually) and dry (May-September; approximately 100 mm to 200 mm of rain annually) seasons of the high Peruvian Andes (elevation ~ 4500 m).

The experimental piles were constructed with run-of mine waste rock using the end-dump/push-dump technique, mimicking the construction of the full-scale dumps. Waste rock was placed/dumped on the piles in four phases: a protective layer at the base of the pile and three end-dumped 'tipping phases' building progressively outward. The piles are each composed of a single rock type (i.e., carbonate, intrusive, or skarn), but rocks from each phase originate from different locations in the open pit. Pile 1 consists of marble/hornfels rock with estimated high neutralization potential and low acid production potential. Pile 2 consists of intrusive rocks with estimated low neutralization potential and moderate acid production potential. Pile 3 consists of skarn rocks that have estimated moderate neutralization potential and moderate acid production potential.

Figure 1 Photo of the five experimental waste rock piles

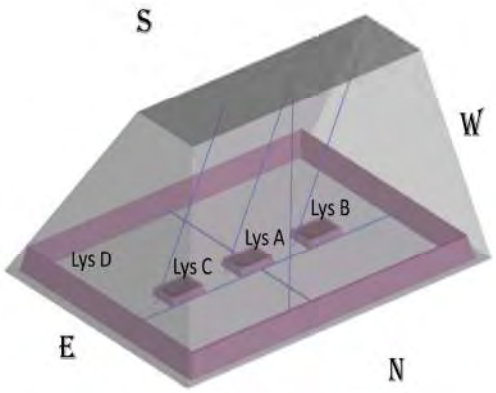

Figure 2. Schematic of the experimental piles, including three internal Sub-Lysimeters A, B, and C (4 m x 4 m) and outer Lysimeter D (36 m x 36 m).

FLOW AND TRANSPORT CHARACTERIZATION

Matrix flow and preferential flow are two hydrological components that directly affect solute concentrations by way of water residence time and dilution. In this study, matrix flow is defined as capillary flow through the granular matrix that adheres to the Richards (1931) equation and has pore water velocities on the order of millimeters to centimeters per day. The term preferential flow has different definitions in different disciplines, and for this study is considered to be 'the observation of water or solute movement faster than expected by an experimental observer or the concentration of flow into spatially localized areas' (Nichol et al., 2005). 'Fast' preferential flow is considered for this study to be water velocities on the order of meters per day.

A few tests were performed to evaluate hydrological and geochemical factors controlling seasonal concentration fluctuations, including particle size distributions (PSD), observations of effluent flow rates and patterns, a tracer study, and analysis of aqueous geochemistry. The details of these tests are described below.

Particle size distribution (PSD) analyses were performed for samples from each of the tipping phases and protective layers for all three experimental piles. Analyses were conducted by Golder Associates during the construction process according to method ASTM D 5519, and are described in Aranda (2009).

Recharge volumes and flow rates were measured continuously using acrylic tipping bucket flow meters. There is no runoff leaving the piles, so all precipitation that falls on the piles evaporates, is stored within the pile, or infiltrates to the collection lysimeters at the bases of the piles (internal Lysimeters A, B, and C = 4 m x 4 m; outer Lysimeter D = 36 m x 36 m; Figure 2) Most of the results presented here are from the D lysimeters, which account for ~97% of the lysimeter area and which collect ~97% of recharge.

The conservative tracer bromide was applied as individual, artificial rain events on the crowns (but not the slopes) of each of the three experimental waste-rock piles in January 2010 according to the methods in Blackmore et al. (2012) and Peterson (2014). The tracers were applied at rates of 6.0-8.5 mm/hr and corresponded to approximately to 7 to 8-year, 5-year, and 6 to 7-year rain events for Piles 1, 2, and 3, respectively. Reported preferential and matrix flow velocities were calculated using peak concentration arrival times as opposed to mean tracer mass arrival times because not all of the applied tracer mass had been recovered by the end of the study period. Sharp spikes in lysimeter bromide concentrations shortly after tracer application represent faster preferential flow, and more gradual increases and decreases in bromide concentrations represent slower matrix flow.

Effluent water was analysed on a weekly to monthly basis for anions, cations, dissolved and total metals, and alkalinity by external laboratories (2007-2009: Envirolab S.A, Lima Peru; 2010-2013: SGS Del Per, S.A.C.).

RESULTS AND DISCUSSION

Particle size distributions

From the PSD analysis we observed that Pile 1 is composed of coarser-grained, boulder- and cobble-dominated marble and hornfels waste rock (Figure 3). Pile 2 is finer-grained, sand- and gravel-dominated intrusive waste rock that is relatively homogeneous with a narrow range of PSD curves among material sub-types. Pile 3 skarn waste rock is similarly finer-grained as Pile 2 and is also sand-and gravel-dominated, but is more heterogeneous with a broader range of PSDs among tipping phases, including a significant amount of large (>1m) boulders in the outer tipping phase of the pile.

The discussions that follow highlight the effect of the boulder size fractions in Piles 1 and 3 on the development of preferential flow paths through waste rock in those piles, and the effect of the relatively finer-grained, homogeneous nature of the Pile 2 waste rock on solute accumulation within slower matrix flow paths in that pile.

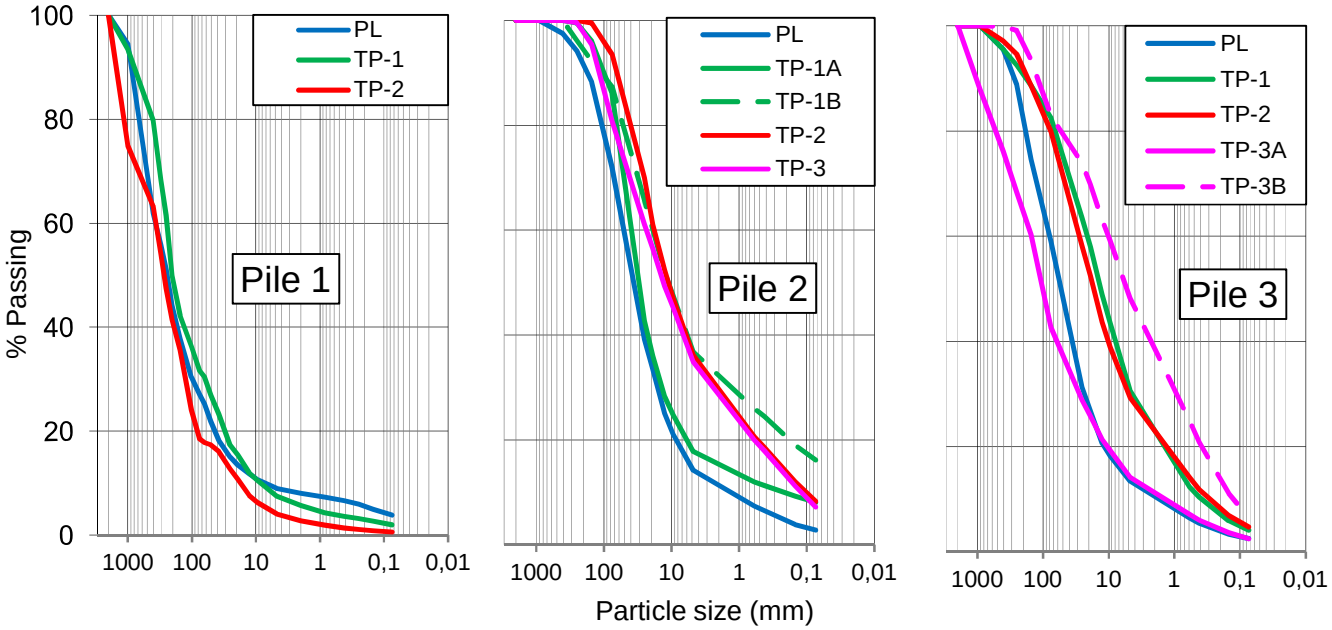

Figure 3 Waste rock particle size distributions for the protective layer (PL) and each tipping phase (TP)

Tracer study and effluent flow

All three piles are matrix-flow dominated, as shown by tracer mass release that is consistent with matrix flow conditions for the corresponding pile material (Peterson, 2014). Matrix flow velocities (v_m) as calculated with bromide breakthrough curves from the coarser-grained Pile 1 are much higher with a broader range (v_m range 3-12 cm/day; Figure 4). Matrix velocities are low in the relatively homogeneous, finer-grained Pile 2 (v_m range 2-3 cm/day), and velocities are spatially uniform throughout that pile as evidenced by relatively smooth, delayed bromide breakthrough curves (Figure 5) and closely matching lysimeter hydrographs for all four Pile 2 lysimeters). Compared to Pile 2, matrix flow velocities are similar in value but broader-ranged in the similarly finer-grained but comparatively heterogeneous Pile 3 (v_m range <2-4 cm/day). Velocities of wetting fronts are approximately five to ten times higher in the wet season than in the dry season for all three materials, as evidenced by internal moisture content probes (Peterson, 2014).

Spikes in waste rock drainage flow rates are often observed following large precipitation events in Piles 1 and 3, as evidenced by outflow hydrographs (Figure 5). The spikes – for example those observed at the beginning of the peak of the wet season in January 2010 for the slope-dominated C and D lysimeters of the carbonate (Pile 1) and skarn (Pile 3) waste rock – may indicate fast preferential flow in those materials, especially underneath the slopes.

Rapid effluent response in response to rain events does not always indicate the presence of preferential flow (Nichol et al., 2005), but bromide breakthrough curves from the tracer study confirm that there is indeed a greater proportion of faster preferential flow in Piles 1 and 3 than in Pile 2 (Figure 4). Specifically,

spikes in bromide concentrations soon after tracer application correspond to preferential flow velocities up to 20 m/day (Pile 1) and up to 2.5 m/day (Pile 3). It is hypothesized that preferential flow in Pile 3 primarily occurs as fast flow over the surfaces of boulders present in the outermost tipping phase of that otherwise finer-grained waste rock pile.

When assessing these flow patterns in light of the waste rock PSDs for each pile, it is reasonable to conclude that the boulder (Piles 1 and 3) and cobble (Pile 1) size fractions most strongly influence the development of preferential flow paths in those piles, likely as fast flow over the surfaces of the larger clasts. Dominant sand and gravel size fractions result in relatively low, narrow ranges in matrix flow velocities in Piles 2 and 3. This is especially the case for the more homogeneous Pile 2, which additionally has relatively spatially uniform matrix flow velocities. The PSDs and flow patterns, in turn, play important roles in solute accumulation in finer-grained waste rock, and solute displacement and dilution during periods of high precipitation, as discussed below.

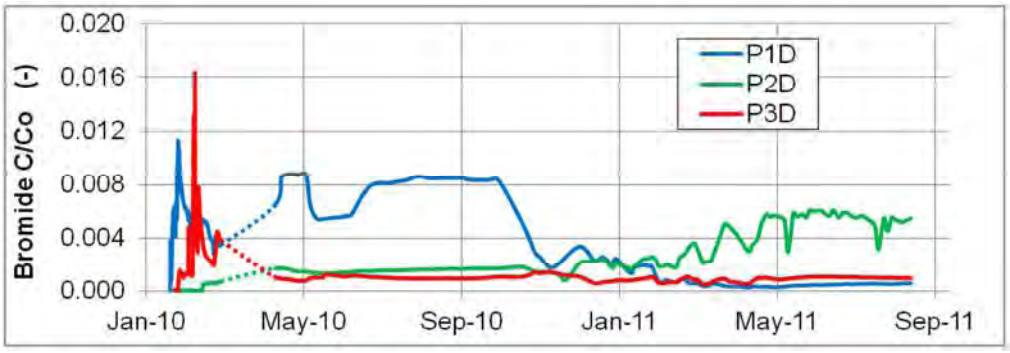

Figure 4 Bromide tracer breakthrough curves from Piles 1, 2, and 3 Lysimeter D

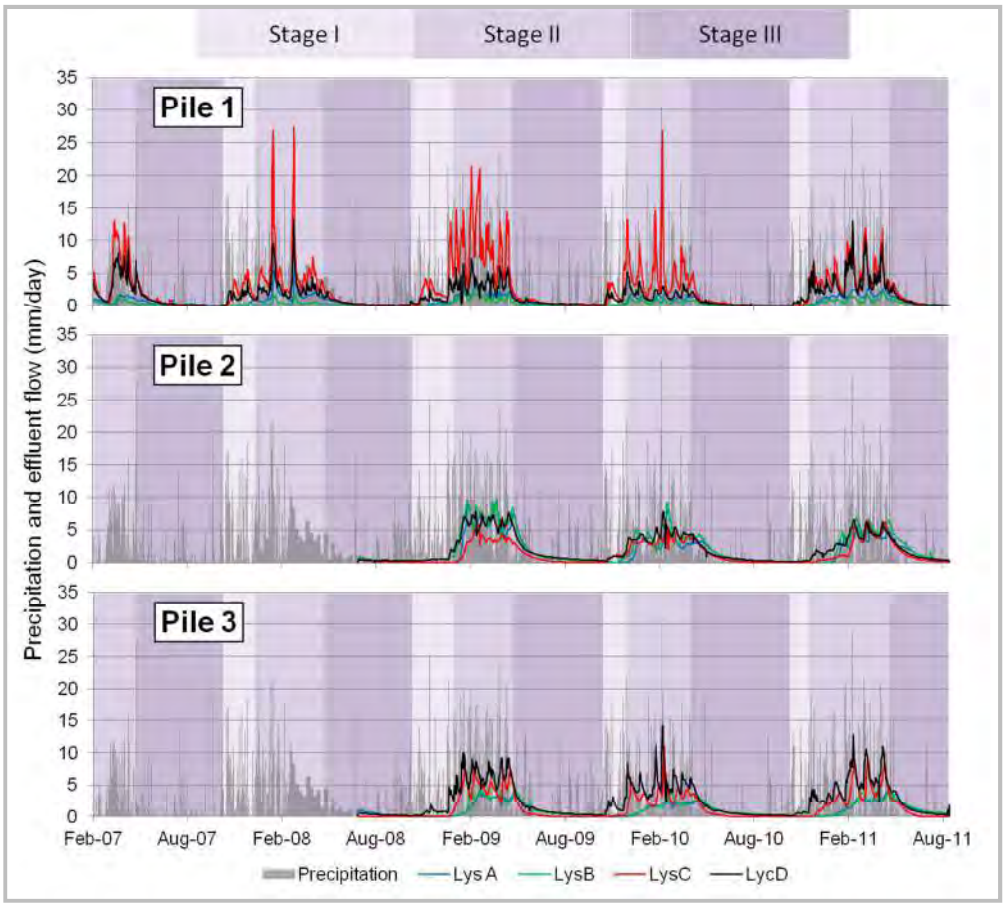

Figure 5 Precipitation and area-normalized effluent flow from Lysimeters A, B, C, and D during Stage I (beginning of the wet season), Stage II (peak of the wet season), and Stage III (draindown and dry season)

Water Quality

Dissolved solute concentrations in experimental waste rock pile drainage fluctuate significantly between the wet and dry seasons for most solutes in all three piles. Peak concentration patterns (i.e., the seasons during which solute concentrations are highest) depend on the solute and waste rock material type. There are several hydrological and geochemical controls on seasonal solute concentration fluctuations (e.g., changes in pH, secondary precipitation and dissolution, changes in internal moisture content), including solute accumulation during periods of low precipitation, displacement during periods of high precipitation, and dilution at the base of a waste rock pile, as discussed below.

An illustrative example is the behaviour of dissolved Zn concentrations, which fluctuate significantly between the wet and dry seasons for all three piles (Figure 6). Specifically, concentrations are highest for Pile 2 during the wet season (e.g., October 2008-April 2009), which can be associated with the flushing out of solutes that accumulate during the dry season when velocities are lower and residence times are longer. The pattern is the opposite for Zn concentrations in Piles 1 and 3, however, where concentrations are

highest during the dry season and decrease during the wet season, which can be associated lower residence times and dilution of higher-concentration water at the base of the pile.

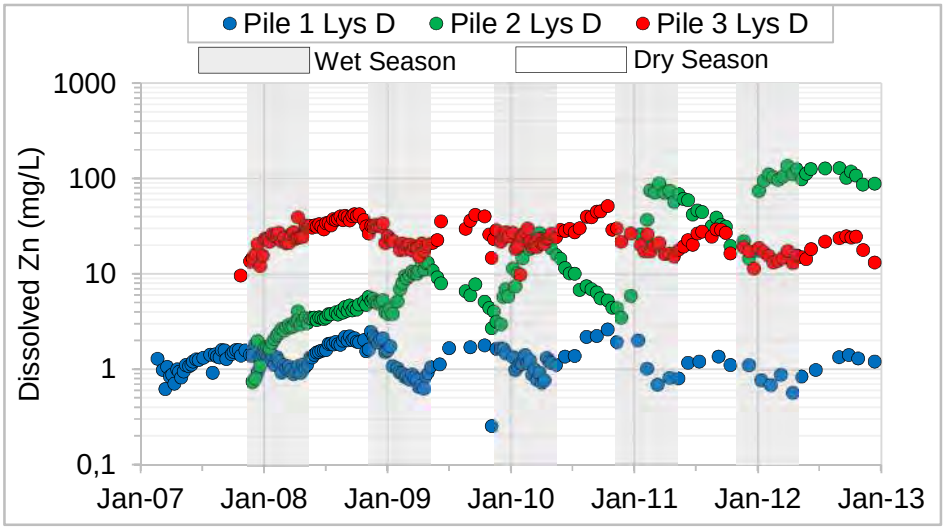

Figure 6 Dissolved zinc concentrations for Piles 1, 2, and 3

Linking particle size distributions, flow patterns, and seasonal fluctuations in solute concentrations

The coarser-grained nature of boulder- and cobble-dominated Pile 1 causes fast flow and low residence times during the wet season, which in turn contribute to solute dilution of the base of the pile and lower effluent concentrations. The more homogeneous, finer-grained nature and lack of boulders in sand- and gravel- dominated Pile 2 leads to higher, spatially even matrix velocities without the activation of fast preferential flow paths in the wet season, resulting in the flushing out of high-concentration water that accumulates during the dry season, without strong dilution at the base of the pile. Similar flow and solute flushing patterns (and hence, higher concentrations during the wet season) should also be expected from the finer-grained, sand- and gravel-dominated Pile 3 skarn, but instead the opposite is true. Solute concentrations tend to decrease in the wet season, indicating dilution from low-residence time preferential flow water, most likely resulting from fast flow over the surfaces of boulders in the outer tipping phase.

CONCLUSIONS

In finer-grained, sand- and gravel- dominated waste rock materials that have spatially uniform unsaturated matrix flow velocities with little preferential flow, higher solute concentrations can be expected during wet seasons as they are flushed from the pile after periods of low precipitation. Solute concentrations from similarly finer-grained materials that do have a significant component of preferential flow, however, can be expected to decrease during high precipitation months as a result of dilution at the base of the pile by high-velocity fresh water travelling through fast flow paths with shorter residence times. Solute concentrations in effluent from coarser-grained, boulder- and cobble- dominated waste rock

can also be expected to decrease during periods of high precipitation as a result of dilution from water traveling through faster flow paths with lower residence times.

Physical flow mechanisms effects on drainage water quality are often not considered over the recognized controls imposed by the biogeochemistry of the waste. While factors such as pH, the precipitation and dissolution of secondary minerals, and changes in seasonal sulfide oxidation rates due to temperature variations are significant and widely recognized controls on drainage chemistry, it is also important to consider physical hydrological controls when assessing or prediction waste rock effluent water quality in light of site, climate, and waste rock characteristics. As our knowledge of the links between waste rock unsaturated hydrology and geochemistry increases, the uncertainty in water quality predictions will decrease.

ACKNOWLODGEMENTS

Funding for this project was provided mine by Teck-ART, Compañia Minera Antamina S.A., and the National Sciences and Engineering Research Council of Canada (NSERC). Special thanks to Daniele Pedretti for his scientific and editorial contributions.

REFERENCES

Aranda, C. (2009). Assessment of waste rock weathering characteristics at the Antamina mine based on field cells experiment. M.Sc., University of British Columbia.

Bay, D., Corazao Gallegos, J. C., Smith, L., Mayer, K. U., & Beckie, R. (2014, submitted). Hydrological and hydrogeochemical characteristics of neutral drainage from a waste-rock test pile. Submitted to Mine Water and the Environment.

Blackmore, S., Speidel, B., Critchley, A., Beckie, R., Mayer, K. U., & Smith, L. (2012). The influence of spatial heterogeneity and material characteristics on fluid flow patterns through two unsaturated, mixed waste-rock piles. Proceedings of the 9th International Conference on Acid Rock Drainage (ICARD), Ottawa, ON, Canada.

Blowes, D., Ptacek, C., Jambor, J., & Weisener, C. (2003). The geochemistry of acid mine drainage. Treatise on Geochemistry, 9, 149-204.

Corazao Gallegos, J. C. (2007). The design, construction, instrumentation, and initial response of a field-scale waste rock test pile. M.A.Sc., The University of British Columbia.

Eriksson, N., Gupta, A., & Destouni, G. (1997). Comparative analysis of laboratory and field tracer tests for investigating preferential flow and transport in mining waste rock. Journal of Hydrology, 194(1), 143-163.

Fala, O., Molson, J., Aubertin, M., & Bussière, B. (2005). Numerical modelling of flow and capillary barrier effects in unsaturated waste-rock piles. Mine Water and the Environment, 24(4), 172-185.

Harrison, B., Aranda, C., Sanchez, M., & Vizconde, J. (2012). Waste rock management at the Antamina Mine: Overall management and data application in the face of continued expansion. *Proceedings of the 9th International Conference on Acid Rock Drainage (ICARD),* Ottawa, ON, Canada.

Lefebvre, R., Hockley, D., Smolensky, J., & Gélinas, P. (2001). Multiphase transfer processes in waste-rock piles producing acid mine drainage: 1. Conceptual model and system characterization. Journal of Contaminant Hydrology, 52(1–4), 137-164.

Linklater, C. M., Sinclair, D. J., & Brown, P. L. (2005). Coupled chemistry and transport modelling of sulphidic waste rock dumps at the Aitik Mine site, Sweden. Applied Geochemistry, 20(2), 275-293.

Molson, J., Fala, O., Aubertin, M., & Bussière, B. (2005). Numerical simulations of pyrite oxidation and acid mine drainage in unsaturated waste-rock piles. Journal of Contaminant Hydrology, 78(4), 343-371.

Love, D. A., Clark, A. H., & Glover, J. K. (2004). The lithologic, stratigraphic, and structural setting of the giant Antamina copper-zinc skarn deposit, Ancash, Peru. Economic Geology, 99(5), 887-916.

Moncur, M. C., Ptacek, C. J., Blowes, D. W., & Jambor, J. L. (2005). Release, transport and attenuation of metals from an old tailings impoundment. Applied Geochemistry, 20(3), 639-659.

Neuner, M., Smith, L., Blowes, D. W., Sego, D. C., Smith, L. J. D., Fretz, N., et al. (2013). The diavik waste rock project: Water flow through mine waste rock in a permafrost terrain. Applied Geochemistry, 36(0), 222-233.

Nichol, C., Smith, L., & Beckie, R. (2005). Field-scale experiments of unsaturated flow and solute transport in a heterogeneous porous medium. Water Resources Research, 41(5), W05018.

Nordstrom, D. K. (2011). Hydrogeochemical processes governing the origin, transport and fate of major and trace elements from mine wastes and mineralized rock to surface waters. Applied Geochemistry, 26(11), 1777-1791.

Peterson, H.E. (2014). Unsaturated hydrology, evaporation, and geochemistry of neutral and acid rock drainage in highly heterogeneous mine waste rock at the Antamina Mine, Peru. Ph.D., The University of British Columbia.

Smith, L., & Beckie, R. (2003). Hydrologic and geochemical transport processes in mine waste rock. In J. L. Jambor, D. W. Blowes & A. I. M. Ritchie (Eds.), Environmental aspects of mine wastes, short course series. Mineralogical Association of Canada.

Smith, L., Lopez, D., Beckie, R., Morin, K., Dawson, R., & Price, W. (1995). Hydrogeology of waste rock dumps. British Columbia Ministry of Energy, Mines and Petroleum Resources and CANMET.

Sracek, O., Choquette, M., Gélinas, P., Lefebvre, R., & Nicholson, R. V. (2004). Geochemical characterization of acid mine drainage from a waste-rock pile, Mine Doyon, Québec, Canada. Journal of Contaminant Hydrology, 69(1-2).

Stockwell, J., Smith, L., Jambor, J. L., & Beckie, R. (2006). The relationship between fluid flow and mineral weathering in heterogeneous unsaturated porous media: A physical and geochemical characterization of a waste-rock pile. Applied Geochemistry, 21(8), 1347-1361.

Wagner, K., Smith, L., & Beckie, R. (2006). Hydrogeochemical characterization of effluent from mine waste rock, Cluff Lake, Saskatchewan. Proceedings of the 7th International Conference on Acid Rock Drainage (ICARD), St. Louis MO.

Final Outcome of Sulfate Transport Modelling and a Prediction of Ground and Surface Water Quality in Aquifers Influenced by Lignite Mining in Germany

Anne Walther[1], Nils Hoth[1], Heike Büttcher[2], Anne Weber[3], Marion Geißler[4], Michael Struzina[5] and Beate Lucke[6]

1. *TU Bergakademie Freiberg, Institute of Mining and Special Civil Engineering, Germany*
2. *Ingenieurbüro für Grundwasser, Germany*
3. *Grundwasserforschungsinsitut, Germany*
4. *GEOmontan GmbH Freiberg, Germany*
5. *Mitteldeutsche Braunkohlengesellschaft mbH, Germany*
6. *Lausitzer und Mitteldeutsche Bergbau-Verwaltungsgesellschaft mbH, Germany*

ABSTRACT

Lignite mining in central Germany has played an important role for more than 100 years. Former and present mining activities, as well as remediation processes, affect the aquifers. The investigation area, south of the city Leipzig, occupies 205 km². For this area, the environmental objectives of the European Union (EU)'s Water Framework Directive are currently not achieved. A prediction of ground and surface water qualities has been established focussing on pyritic sulfuroxidation and the generation of sulfate .

To predict the sulfate migration out of overburden dumps into unaffected aquifers, as well as the influence on surface waters, several steps were necessary. The first step involved characterization of the un-disturbed overburden material to predict the geochemical behaviour of the dumps. Therefore, a geological model, generated from several thousand drillings, was formed. Furthermore the concentrations of sulfur and carbonate, within the different geological layers, were examined in the geochemical model. The average dump compositions were based on a blending of the geochemical parameters with the thickness of the different geological layers.

The prediction of dump water quality was carried out using PhreeqC (Parkhust & Apello, 1999) modelling. Predicted amounts of weathering products were used to calculate the equilibrium between groundwater, secondary minerals (gypsum, siderite) and CO_2 concentration of the gas phase by consideration of redox reactions, mineral dissolution, precipitation and cationic exchange. The flow and one component transport modelling for the investigation area was carried out by the existing large scale model (HGMS) of the company IBGW Leipzig and was based on the flow and transport code PCGEOFIM®. Selected "Hotspot zones" were subsequently modelled using a reactive hydro-geochemical transport model, based on the program code PHT3D.

The results describe an expansion of dump water plumes into unaffected aquifers within the stratigraphic sequence from the upper to the lower layers.

Keywords: lignite mining, groundwater quality, pyrite oxidation, hydro-geochemical modelling, prediction

INTRODUCTION

The Central German Mining District has been influenced by lignite mining for more than 100 years. Due to former and present mining activities, aquifers in this area are significantly affected and the environmental objectives of the EU's Water Framework Directive are currently not achieved for the area south of Leipzig. This region is a main part of the Central German Mining District, which occupies a working area of 205 km^2. The University of Freiberg has been commissioned by operators of remediation (LMBV) and active mining (MIBRAG) to predict the future mass fluxes of sulfate in the groundwater bodies and the impact on surface waters. Overburden of tertiary and quaternary age contains distinct proportions of pyrite. During the mining process, the aeration of reduced sulfur compounds in overburden material causes high concentrations of sulfate, iron and trace metals in pore water, which can subsequently be mobilised.

After the mining process has been completed, groundwater levels rise, natural flow systems are re-established and Acid and Metalliferous Drainage (AMD) may occur. In order to predict the potential impact of overburden dump pore waters on unaffected aquifers a geological model, which includes the regular sequences of geological layers, was generated. Concentrations of total sulfur, sulfide-sulfur and carbonate were balanced from existing drilling data in the geochemical model. Simultaneously, the actual groundwater compositions in the investigation area were recorded, to assess the groundwater quality for the mining districts. Migration processes in groundwater were simulated using the existing large scale model (HGMS) of IBGW Leipzig, based on the transport code PCGEOFIM® and sulfate distribution in 2100 main pollution plumes out of overburden dump bodies were assessed. Furthermore, the trend of sulfate concentration was presented on several virtual water gauges. To estimate the overburden dump water impact on surface water bodies, the sulfate mass flow in selected rivers and lakes was calculated. Selected "Hotspot zones" were modelled subsequently, by means of a reactive hydro-geochemical transport model, based on the program code PHT3D.

METHODOLOGY

Determination of the dump groundwater chemistry

Initial concentrations of the main dissolved constituents in overburden dump pore water are a key input into transport modelling and the prediction of future groundwater pollution. Predictions are based on the geological structure of the investigation area (geological model) and the chemical behaviour of the groundwater observed in the field (geochemical model).

Geological model

To verify the distribution of geological layers in the investigation area, petrographic data were collected. Afterwards, several thousand drillings were used to generate a geological model, which describes the deposits and sequences of the overburden layers. Different vertical layers of silt, clay, sand or gravel were detected. According to their chemical properties, these layers are combined to stratigraphic units. Table 1 shows the stratigraphic units with high acidity potential or buffering potential.

Table 1 chart of geological layers in the investigation area

Unit-nr.	Stratigraphy		Lithology	Acidity potential	Buffering effect
1	Quaternary	Quaternary, cohesionless	gravel, sand	0	0
2		Quaternary, cohesive	alluvial clay glacial till banded clay	0	++++
3		Late pleistocene	rubble	0	0
4	Tertiary (Paleogene)	"Thierbach" layers, cohesionless	gravel, sand	(+)	0
5		"Thierbach" layers, cohesive	silt	(+)	0
6		Aquifers 2.2, 2.4	sand	+	0 – (+)
7		Aquifer 2.5	shell sand, shell silt	+	(+) - +
8		Aquifers 2.6, 2.7	silty sand, glauconite silt	+++	0
9		Aquifer 3	fine and coarse sand	+++	+
10		Aquifer 4	Sand, silty sand	++	0
11		Aquifer 5	sand	+	0
12+13+14		Cohesive intermediate material	clay, silt	(+) - +	0

Occurrence of the characteristic:	
0	not
(+)	very low
+	low
++	high
+++/ ++++	very high

Geochemical model and balancing

In order to characterize overburden materials related to their chemical and physical properties, results of geochemical investigations of about 200 drilling locations were used. During the investigation, parameters such as total sulfur content, sulfate-sulfur content, total carbon content (Ct), carbonate content ($CaCO_3$) and exchange capacity (CEC) were determined for sediments in each geological layer. The analyzed parameters were then integrated using a laminar interpolation, to determine the geochemical potentials of several areas. A weighting of geochemical parameters, according to their thickness inside the geological layer, was found to be necessary (Hoth et al., 2000). The interpolation is based on a kriging method, realized with the modeling and visualization software SURFER®. Fig. 1 illustrates the results of interpolation for Unit 4. Total-sulfur contents in sediments of this unit are shown in Fig. 1(a). In summary, 58 drillings with 160 soil samples located into aquifer 2.6 or 2.7 were analyzed. The red parts of this map illustrate very high total sulfur contents up to 3 wt%. The calculated buffering potential in materials of this unit is shown in Fig.1(b). Beside some northern parts, Unit 4 is nearly free of carbonate. This causes a very high potential for acidification.

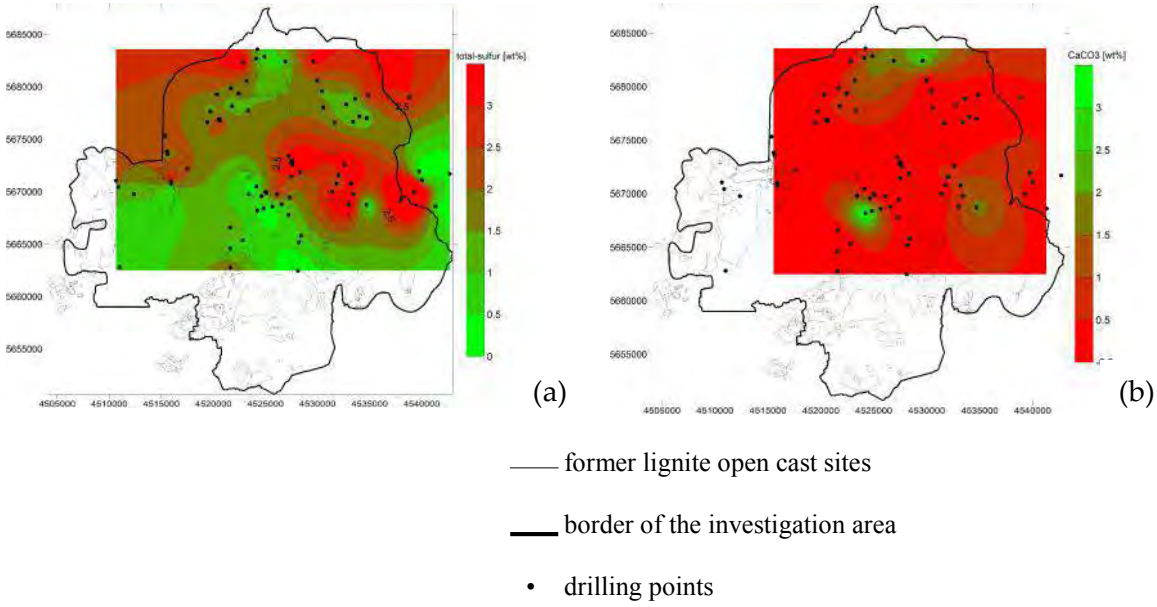

Figure 1 Predicted total-sulfur (a) and $CaCO_3$ (b) contents (wt%) in unit 4

Predicted dump pore water quality

Determination of average dump compositions is based on a "blending" of geochemical parameters with the thickness of the stratigraphic units. The investigation area is rasterized with a spacing of 125 x 125 meter. Geochemical parameters, derived from analyses, are converted into predicted parameters for overburden dumps (Hoth et al., 2000).

The prediction of overburden dump pore water quality is carried out using the hydro-geochemical equilibrium model PHREEQC (Parkhust & Appelo, 1999) and the important initial amounts of minerals including pyrite, calcite, dolomite, siderite and gypsum are used. The potential of precipitation of ($Fe(OH)_3$ and kaolinite) is respected as modelling minerals. Furthermore, the CO_2 content of the pore waters and in the gas phase is also considered and is related to the equilibrium of carbonic minerals. To calculate the equilibrium of groundwaters, an initial CO_2 concentration in the gas phase was defined. Also, the equilibrium between water solution and predicted CEC was included in the model, based on standard exchange coefficients of the PHREEQC database.

Analysis of current groundwater conditions

Characterization of the groundwater conditions of the whole investigation area is based on an intensive data analysis for generating a fundamental database. Data total of 1300 groundwater observation wells were used. To describe the actual sulfate pollution of groundwater, a series of measurements from 2009 to 2014 were considered and medians determined.

The saturation state of the groundwaters, related to relevant mineral phases (gypsum, calcite, siderite) was also determined using PHREEQC. At sulfate concentrations around 1600 mg/l a reduction of calcium is observed, because of precipitation of gypsum.

Saturation indexes of calcite and siderite depend mainly on pH values. Groundwater samples of dumps with pH values according to buffer range of calcite and siderite are often characterized as saturated groundwaters.

Overburden dump aquifers show the highest sulfate concentrations (on average 1650 mg/l) in the investigation area. The reason for elevated sulfate concentrations, greater than 3000 mg/l, appears to be the combination of overburden material behavior (high content of pyrite) and very low carbonate contents (no buffering) together with low clay contents (allowing oxidizing conditions via air access). Furthermore, slopes and edges of active mining and overburden dumps have high sulfate concentrations, due to exposure to oxygen in air. In some parts of the investigation area, groundwater of unaffected aquifers also shows high sulfate concentrations related to aeration during the artificial lowering of the groundwater level. The interaction with outflowing of dump pore waters also plays an important role. For modelling sulfate transport in groundwater, initial concentrations of sulfate were defined for every stratigraphic unit.

Mass flow and one-component transport modelling

Groundwater flow model

Results of overburden characterization and groundwater analysis were combined into an existing large scale model for mass flow modelling (called HGMS) (IBGW Leipzig). The program code PCGEOFIM® was used to calculate groundwater flow and migration processes. The model was based on the expected geological structure. Natural geological layers, overburden dumps and parameters of active mining were included in HGMS (see IBGW GmbH, 2010). The geological series of layers included all aquifers of the investigation area and zones between aquifers were regarded as aquitards. The model was adjusted for hydraulic parameters such as flooding concepts or lake-water levels using water levels from 11.000 observation wells within the calculations.

Concept and parameterization of sulfate transport

The rise of groundwater level influences the solute migration process of overburden dumps. For the simulation of the migration process, including advection, dispersion and relevant chemical reactions, PCGEOFIM® was used. Intended operations in active open cast mines were also considered alongside the mass flow inside unsaturated dump material. The sulfate concentration in groundwater was impacted by chemical reactions. Accordingly, a concept for consideration of minerals in solid matter was developed. The formation of gypsum, during the genesis of dumps and the rise of groundwater level, was found to be important. Therefore, the additional storage of gypsum was described with isotherms, including the thermodynamic equilibrium between formation and dissolving. In summary, nine classes of isotherms were defined (Figure 2).

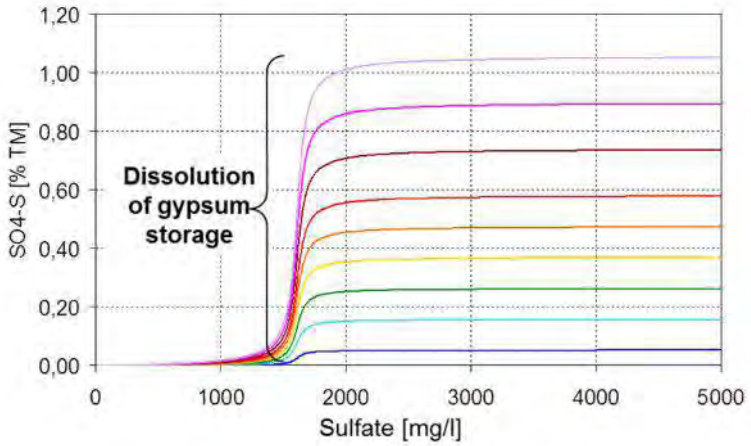

Figure 2 Dissolution of gypsum, considered as isotherms

The consideration of mass flux by using HGMS was possible in lateral and vertical direction. The first step was to investigate zones likely to have considerable plumes in future. Thereafter, current groundwater conditions were included and the mass flow out of overburden dumps was considered and future groundwater compositions simulated up to the year 2100.

Reactive transport model

A reactive transport model was used to investigate the three-dimensional reactive processes of mass flow, for two small scale parts of the whole investigation area. Using this approach, a model which describes sulfate formation and sulfate release, according to other substances in aqueous solution or in solid phases, was generated. The large scale model HGMS, including hydraulic parameters and storages of substances, was used as a background for reactive transport modelling. Calculations of reactive transport and the regional distribution of sulfate were based on the computer code PHT3D, it combines geochemical modeling (PHREEQC) with three-dimensional groundwater flow.

RESULTS AND DISCUSSION

Predicted dump compositions and hazard potentials

After the blending of geological structures and geochemical conditions, predicted dump compositions were derived. Figure 3 presents the predicted total-sulfur (a) and carbonate (b) contents for two selected overburden dumps. Red coloured areas in figures (a) and (b), depict high total-sulfur contents and very low carbonate contents and are described as hazard areas, because of high acidity potential and low buffering effect.

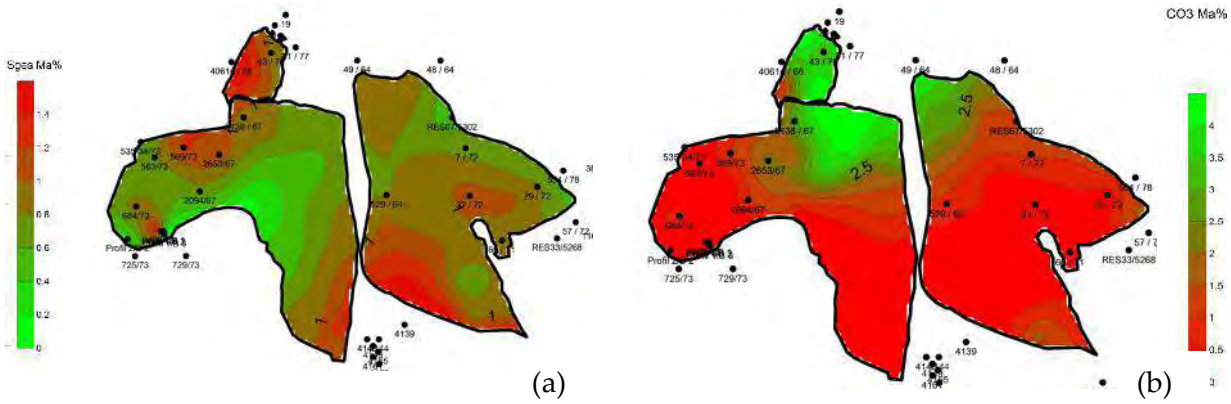

Figure 3 Predicted dump pore water composition (a) total-sulfur and (b)carbonate content in two overburden dumps

Predicted overburden dump pore water qualities

The predicted sulfate concentrations for one part of the investigation area are presented in Figure 4, along with monitoring measurements from the observation wells (coloured points). In the northern dump (called dump Witznitz), very high sulfate concentrations (up to 6000 mg/l) were calculated. Overall, not every measuring point could be reproduced by hydro-geochemical modelling. In these overburden dumps (especially Witznitz) the displacement of overburden because of the mining technology was not considered in the modelling, therefore the red area could be shifted. Furthermore, the measurements represents the part of the filter (around 2 m) and therefore weathering zones were not considered. In summary, the main groundwater condition could be simulated by the model.

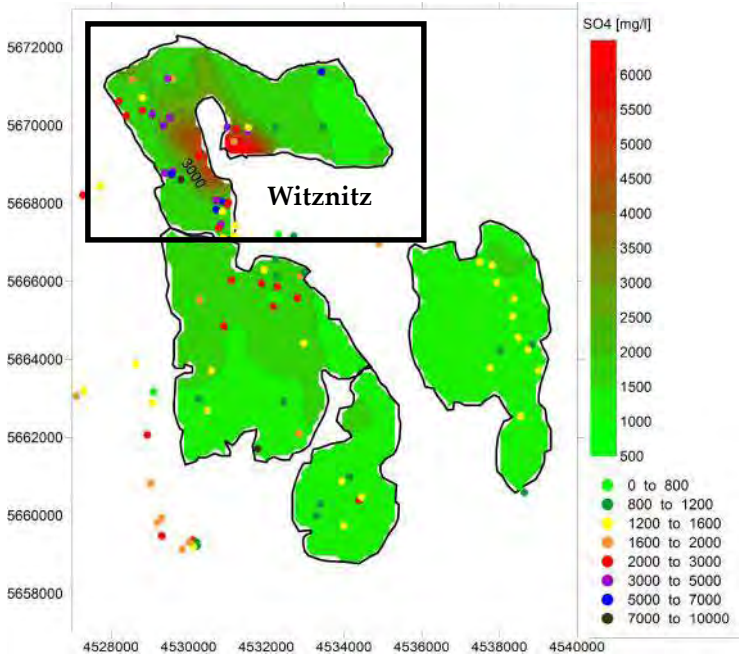

Figure 4 Predicted sulfate concentrations compared with measurements in observation wells

Results of sulfate transport modelling

Figures 5 and 6 present the sulfate concentrations in the outflow of the overburden dumps for selected stratigraphic units in the year 2100. Yellow, orange and red coloured areas suggest groundwater pollution because of dump pore water migration. In unaffected areas the sulfate concentration is around 300 mg/l. According to hydro-dynamical circumstances, stationary conditions are expected in the year 2100.

Overall, the pollution plumes with sulfate concentrations higher than 600 mg/l widen out within the stratigraphy. Local plumes around the dump boarders appeared in the upper layers, because of dilution effects (groundwater recharge) and groundwater seepage into watercourses.

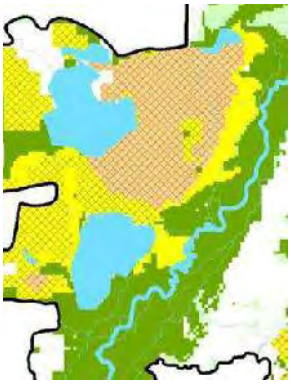

Figure 5 sulfate concentrations in 2100 after transport modelling, aquifers 1.1-1.7

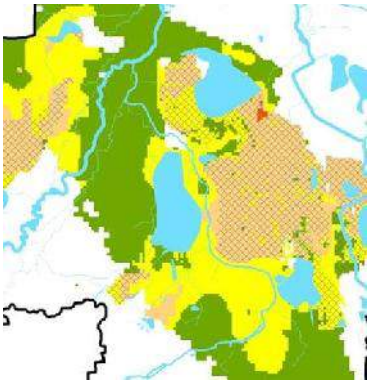

Figure 6 sulfate concentrations in 2100 after transport modelling, aquifer 4

The development of the sulfate mass flow from groundwater to lakes is shown in Figure 7, and is illustrated for one selected lake (Kahnsdorfer See) in the investigation area. This relic lake is next to Witznitz, one of the overburden dumps with the highest sulfate concentrations in pore water. According to Figure 7, the sulfate mass flow into the lake will be reduced from 4210 m^3/d in 2013 to 762 m^3/d in 2100, by nearly constant groundwater influxes.

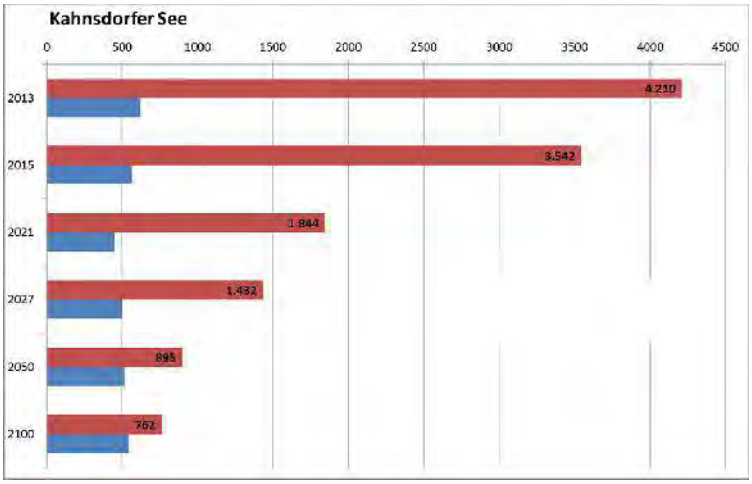

Figure 7 sulfate balance till 2100 for one lake in investigation area

CONCLUSION

Calculated geochemical parameters from overburden dump sediments, especially sulfate, carbonate and total carbon, have been used to describe conditions for every stratigraphic unit and depict hazard potentials. In these zones, high sulfate concentrations, as a result of pyrite oxidation, were generated. Sulfate migration into groundwater and flow to unaffected areas has resulted in AMD effects, as buffering geological materials are generally not available. The main AMD problems were related to two stratigraphic units - unit 8 (aquifers 2.6, 2.7) and unit 6 (aquifers 2.2, 2.4), with high sulfur and low carbonate contents, combined with the high permeability. The results were integrated into a sulfate transport model and the current groundwater conditions determined by analysing numerous data of observations wells and dump gauges. The highest sulfate concentrations, of more than 6000 mg/L, were detected in dump aquifers. An average sulfate concentration of 1650 mg/L was shown for dump pore waters. For stratigraphic units 6 and 8, high sulfate concentrations in unaffected aquifers were also detected. The evaluation of saturation states in aquifers, and respective gypsum, calcite and siderite contents indicate that pore water in overburden dumps and the zones discussed are predominantly saturated or oversaturated. Based on the current groundwater conditions and calculated geochemical potentials of the overburden dumps, initial parameters were defined and implemented in the sulfate transport model. The first results of sulfate transport modelling indicate mainly local pollution plumes in areas adjacent to the overburden dumps.

In summary, the investigations show, that the downstream area of the polluted aquifers will be impacted by the inflow of dump groundwater for several decades. Whilst there are identified pollution plumes; areas between these plumes will not be affected.

REFERENCES

Hoth N., Wagner S., Häfner F. (2000) Predictive modelling of dump water impact on the surroundings of the lignite dump site Jänschwalde (Eastern Germany). Journal of Geochemical Exploration 73, 113-121

IBGW GmbH (2010) Auswirkungen des Grundwasserwiederanstiegs und der daraus folgenden Exfiltration eisenbelasteter Grundwässer aus den Kippen des ehemaligen Tagebaus Witznitz in die Fließgewässer Pleiße und Wyhra. Teilbericht 4: Aufbau eines reaktiven Stofftransportmodells für den Kippenkörper Kahnsdorf und Prognose der zukünftigen Stoffeinträge aus dem Kippenkörper in die Pleiße. Leipzig.

Parkhust D.L., Appelo, C.A.J. (1995) User´s Guide to PHREEQC. U.S. Geological Survey, Water Resources Investigations Report, Denver-Colorado

10th ICARD IMWA 2015 | 10th International Conference on Acid Rock Drainage & IMWA Annual Conference

Distinctive Estimation of Stored Acidity Forms in Acid Mine Wastes

Andrea Gerson[1], Jun Li[1], Rong Fan[1], Nobuyuki Kawashima[1], Roger Smart[1] and Russell Schumann[2]

1. *Minerals and Materials Science and Technology, Mawson Institute, University of South Australia*
2. *Levay & Co Environmental Services, University of South Australia*

ABSTRACT

It is well known that weathering and sulfide mineral oxidation in sulfide-containing waste rock dumps and tailings dams can result in release of acidity and potentially biotoxic metal species as acid mine drainage. In addition to the acid generated by the dissolution of the sulfide minerals, 'stored' acidity can also be released with changing pH by hydrolysis and dissolution of several non-sulfide oxidation products formed during weathering particularly in the unsaturated zones of the mine wastes. The matching of acid and neutralization release rates in kinetically controlled processes is, in principle, the only sustainable option for long-term mine closure but, to date, there is little predictive capacity regarding secondary mineral behavior in tailings. Due to this, secondary mineralization is rarely effectively analyzed and usually not considered in site environmental risk assessments or by regulatory authorities.

Secondary mineralization is generally ultra-fine grained with high surface area and mobility. Secondary minerals formed within mining wastes can act as a both a sink and source of latent acidity and biotoxic metal species *e.g*. As, Se, Cu, Zn, Pb, Ni and several other metals of direct environmental impact. Acid sulfate salts including iron sulfates (e.g. melanterite), jarosites, and schwertmannite can be formed in the unsaturated oxidation zone of these wastes together with ferrihydrite and goethite. These secondary mineral products have widely different acid release rates at different pH and strongly affect drainage water acidity dynamics. Some of the crystalline secondary products (*e.g*. Na, K-jarosites, goethite) dissolve very slowly and can mitigate release rates of toxic species to acceptable concentrations in effluent from tailings. Others, *e.g.* H-jarosite, schwertmannite and amorphous mineralloids, form initially with similar uptake of biotoxic metals but subsequently recrystallize to more stable minerals. Whether they release or transfer these metals during recrystallization is not known but is clearly important in acid and metalliferous drainage control. A four -step extraction procedure to quantify jarosite and schwertmannite separately with various soluble sulfate salts has been validated with synthetic and real sulfide waste materials with XRD and SEM verification. Correction to acid potential and estimation of acid and some toxic metal release rates can be based on this method.

**There is no full article associated with this abstract.*

10th ICARD IMWA2015 | 10th International Conference on Acid Rock Drainage & IMWA Annual Conference

Humidity Cell Test with Pyrite Concentrate from Tailings Flotation

Refugio González[1], Antonio Barrera[2], Liliana Lizárraga[1] and Carmen Durán[2]

1. *Universidad Autónoma del Estado de Hidalgo, Mexico*
2. *Universidad Nacional Autónoma de México*

ABSTRACT

A humidity cell test was performed with tailings from a massive sulfide mine, located in the State of Mexico, Mexico. These wastes have a high acid generation potential and null net neutralization potential. The aim of this work was to compare the leachate characteristics from the tailings and the sulfide concentrate obtained by tailings flotation, in order to show how trace neutralizing minerals affect pH evolution. The samples were analyzed by XRD: pyrite, sphalerite, quartz, clinochlore, calcite and muscovite were identified in the tailings, whereas dolomite, sphalerite with cobalt, hydroxisilicate of potassium, magnesium and aluminum and moscovite with vanadium and barium were identified in the flotation gangue and only pyrite was detected in the sulfide concentrate. The tailings and pyrite concentrate were submitted to a modified humidity cell test from ASTM D 5744-96 method, by circulating 3 $Lmin^{-1}$ of air on the surface and dropping 50 mL of water during the wet period. The cycle duration was 14 days with a one-day wet period, the test was performed for 4 cycles. The starting leachates pH were 4.60 and 4.63 and electrical conductivity (EC) were 3673 and 235.5 μScm^{-1} respectively, for the tailings and the concentrate. The lowest leachate pH for the pyrite concentrate was 4.15, and 4.48 in the original sample. EC increased 5 times in the concentrate (1246 μScm^{-1}) and decreased to 2785 μScm^{-1} in the tailings. These results suggest that traces of neutralizing minerals can partially buffer the acidity generated in the first oxidation stages and flotation can improve tailings characterization.

**There is no full article associated with this abstract.*

10th ICARD IMWA 2015 | 10th International Conference on Acid Rock Drainage & IMWA Annual Conference

Mine Water Quality Prediction over the Long Term: A 15-Year Column Test for a Flooded Uranium Mine

Ulf Jenk, Jürgen Meyer, Marcus Frenzel and Michael Paul
Wismut GmbH Chemnitz, Engineering and Radiation Protection Division, Germany

ABSTRACT

Within the Wismut Remediation Project the Uranium mine at Schlema-Alberoda, where about 80,000 tonnes of uranium had been mined conventionally between 1946 and 1990, have been flooded since 1991. The mine water is contaminated with uranium, radium, iron, manganese, and arsenic and has to be treated for discharge into the Mulde River over the long term.

In order to understand the basic hydrogeochemical processes and to predict the future trend of mine water composition, column tests have been set to work in 1999 on a pilot scale (volume 1 m^3, filled with mine typical ores and materials). Two scenarios are being simulated with 9 columns over a time period of about 15 years: a) saturated conditions with oxygen limitation (simulating flooded mine areas) and b) unsaturated conditions (simulating surface near mine areas which are flooded temporarily)

The most important finding is that most of the concentration trends have been developed stable not before 2 to 4 years, and a number of parameters are still in movement. In general, under unsaturated conditions weathering processes and pollutant mobilization (As, U, Ra) keeps on whereas in the saturated columns reductive immobilisation, particularly of uranium, is ongoing. First geomicrobiological investigations show sulphate reducing bacteria in the saturated columns. The results confirm the long term nature of pollutant behaviour in flooded mines. Short term experiments are not able to describe these time depending processes in an adequate way.

**There is no full article associated with this abstract.*

10th ICARD IMWA 2015 | 10th International Conference on Acid Rock Drainage & IMWA Annual Conference

Leachability of Metals from Gold Tailings: A Modeling and Experimental Approach

Bronwyn Camden-Smith[1], Raymond Johnson[2] and Hlanganani Tutu[1]

1. *Molecular Sciences Institute, School of Chemistry, University of the Witwatersrand, South Africa*
2. *SM Stoller Corporation, USA*

ABSTRACT

Mine leachates emanating from gold tailings in the Witwatersrand Basin, South Africa, usually contain elevated concentrations of metals and sulphates that tend to impact negatively on water and soil quality in the vicinity. This study aimed at assessing the leachability of metals from oxidised by rainwater. Leaching of tailings was conducted experimentally using artificial rainwater and simulated using the PHREEQC geochemical modelling code to further understand the dominant processes. The formation of evaporite secondary minerals was also simulated to understand processes leading to their formation from tailings leachates and surface water.

The results indicated that the predominant metals in tailings were aluminium, copper, cobalt, iron, lead, manganese, nickel, uranium and zinc. These were found to be held in secondary mineral phases, mainly sulphates that constituted the readily soluble fraction. Results from modelling showed that the secondary minerals were chemically similar to leachates from oxidised tailings while leachates from oxidised tailings and unoxidised tailings would likely mix to form the immediate groundwater. The secondary minerals consisted of simple sulphate salts and complex multi-element sulphates that formed along a flow path between tailings and receiving surface water systems. Dissolution of these salts would likely cause episodic pollutant input to receiving water.

**There is no full article associated with this abstract.*

To the technical staff of consulting companies that worked at the EIS, who provided complementary information and handled our requests for clarification (alphabetically ordered): Carlos Aguilera M. (Process Engineer. Fluor); Michael K. Herrel (Geochemist. Golder Associates); Alfredo Híjar (Environmental Consultant); Rafael S. Dávila (Principal, General Manager. Golder Associates); Simon Mansell (Senior Project Manager, Schlumberger Water Services); Mayra Medina (Consulting. Metis Gaia Consultores); Nathan Nadramija (General Manager. Metis Gaia Consultores); Xavier G. Panozo M. (Project Manager. Knight Piésold Consulting); Roberto Parra (Environmental Consultant); Abelardo de la Torre Villanueva (Asesores Técnicos Asociados, S.A.); Javier Torrealva (Lider Grupo Hidrotecnia. Golder Associates); and Mario Villavisencio (General Manager. Knight Piésold Consulting).

Finally, to all those who answered to our call for meetings both in Cajamarca and Lima, to incorporate their invaluable information to the expert report (alphabetically ordered): Narda Alarcón Rojas (UPAGU); Hugo Arévalo Escaró (PROESMIN); Nicole Bernex (Pontificia Universidad Católica del Perú); Luis Céspedes Ortiz (General Manager. Chamber of Commerce and Production of Cajamarca); Antenor Floríndez Díaz (ONG CUENCAS); Cristian H. Gálvez Ruiz (Director. Chamber of Commerce and Production of Cajamarca); Héctor Garay Montáñez (Universidad Particular Antonio Guillermo Urrelo (UPAGU); Ever Glicerio Hernández Cervera (Regional Governor Cajamarca Region); José J. Huamán Mantilla (PSI SIERRA – MINAG); José Carmelo Martínez Lázaro (Bishop of Cajamarca); Mirco H. Miranda Sotil (Advisor to the High Direction of High Water Authority); Rosa Olivera González (AGRORURAL – MINAG); Telmo Ramón Rojas Alcalde (ONG CUENCAS); Hugo Loli Salomón (Director of Committees. Chamber of Commerce and Production of Cajamarca); Francisca Torres Hernández (Josemar Consultores EIRL).

OFFER

Those interested in obtaining further information, not for commercial use, may ask for the complete expert report (in Spanish) and a power point presentation (rfrubio@gmail.com).

REFERENCES

Fernández Rubio, R. (1991). Tratamiento biológico de aguas en pantanales. Tecno Ambiente 1: 37-44. Madrid.

Fernández Rubio, R.; López García, L.; Martins Carvalho, J. (2012). Dictamen pericial internacional. Componente hídrico del estudio de impacto ambiental del proyecto minero Conga (Cajamarca - Perú). Elaborado para la Presidencia del Consejo de Ministros de Perú. 261 pp. Lima.

Fernández Rubio, R.; Lorca Fernández, D. & Novo Negrillo, J. (2014). Mitos y realidades de las cabeceras de cuencas andinas peruanas. El Ingeniero de Minas. Col. Ing. del Perú. 20-26. Lima.

Knight Piésold Consulting. (2010a) Proyecto Conga. Estudio de Impacto Ambiental. Informe Final. Realizado para Minera Yanacocha S.R.L. 20.467 pp. Lima.

Knight Piésold Consulting. (2010b). Levantamiento de Observaciones. Ministerio de Energía y Minas. 6.919 pp. Lima.

MINAM. (2006). ECA para el agua, con alrededor de 80 parámetros agrupados por uso en cuatro categorías. Art. 81º y 82º del Reglamento de la LGA. Aprobado por D.S. Nº 002- 2008. Lima.

10th ICARD IMWA 2015 | 10th International Conference on Acid Rock Drainage & IMWA Annual Conference

Development of Technical Criteria for the Chemical Stability in Mining Facilities

María Carolina Soto[1], Raquel Charte[1], Angela Oblasser[1], Lilian Valdebenito[2] and Jorge Campos[2]

1. Fundación Chile

2. SERNAGEOMIN, Chile

ABSTRACT

In 2011, a new Mine Closure and Mining Facilities Law was promulgated in Chile, requiring that all mining companies submit a Closure Plan of all their facilities for approval by the National Geological and Mining Survey (SERNAGEOMIN) prior to implementation of the exploitation.

Prior to the introduction of this law, regulations regarding mine closure considered only the physical stability of mining facilities. The new law and its regulations include a new requirement related to ensure chemical stability of the mine waste; however, it does not give details or technical criteria on how this should be assessed and guaranteed. This new requirement constitutes a major challenge towards more sustainable mining operations, which involves the integrated management of massive mine waste and mine facilities during the life cycle of a mining project.

Since mid 2013, Fundación Chile and SERNAGEOMIN are working on a project that considers the development of a methodology and technical criteria to evaluate and ensure chemical stability at mining facilities in order to guide the actions necessary during the lifetime and closure of a mining project. One of the results of this project is the development of a technical guide, that is expected to be published in December of 2014, that will gather information from national and international documents and guides related to chemical stability, mining-influenced water, acid and neutral mine drainage, mobility of contaminants and risk assessment, among others, and will be applied to the geological, mining and climatic conditions in Chile. Also, the project includes validation of the methodology and technical criteria in public-private workshops, in which all related stakeholders, participate. This work is co-funded by the Government Production Development Corporation (CORFO).

**There is no full article associated with this abstract.*

CHAPTER 5

MINE WATER DRAINAGE COLLECTION AND TREATMENT – PHYSICAL CHEMICAL ACTIVE TREATMENT

Commercial Case Studies of Life Cycle Cost Reduction of ARD Treatment with Sulfide Precipitation

David Kratochvil[1], Songlin Ye[1], and Oscar Lopez[2]

1. *BioteQ Environmental Technologies, Canada*
2. *BioteQ Water Chile SpA, Chile*

ABSTRACT

Sulphide-based precipitation of divalent metals has been shown to greatly reduce life cycle costs and waste generation for the treatment of acid rock drainage (ARD) at mine sites. BioteQ's ChemSulphide® process has been applied in multiple countries and continents and has proven to be a more cost effective solution than HDS or LDS lime plants on their own. Two case studies are presented in which the ChemSulphide® process has been applied to reduce the life cycle cost of water treatment at sites facing active ARD treatment in perpetuity. The case study examines the lessons learned and causes of plant downtime at the Wellington Oro water treatment plant. The plant, which has been operating for over five years, has continually been able to meet strict discharge requirements for cadmium and zinc while entirely eliminating the production of waste sludge, however mechanical and secondary process issues had reduced plant availability. Lessons learned and mitigation methods that are currently being implemented are presented and discussed. The second case study looks at the ChemSulphide® plant installed upstream of a HDS lime neutralization plant treating ARD at the Yinshan Mine in China. The plant selectively recovers copper as a commercial grade concentrate with the net revenues largely offsetting treatment costs to achieve both economic and environmental benefits. The net present value of the savings generated by the ChemSulphide® plants at Wellington Oro and Yinshan are also analysed and discussed.

Keywords: acid rock drainage, metal recovery, life cycle costs, sulphide precipitation, environmental compliance

INTRODUCTION

Preventing acid rock drainage (ARD) has become a key component of mine development planning and operations. Unfortunately, there are many legacy sites and/or active mines where despite the adoption of best management practices, the generation of ARD cannot be avoided, leading to the need for active treatment in perpetuity. The life cycle cost of active treatment over several decades can be very high and the amount of solid waste generated in the treatment process and the composition of this waste may not only significantly contribute towards the overall life cycle costs (LCC) but also impart long-term liabilities.

This paper presents two commercial case studies of active ARD treatment using BioteQ's ChemSulphide® process at sites with prolonged time horizons of water treatment. One is at an abandoned mine where the ChemSulphide® plant has been in operation since 2009 and where BioteQ recently performed a plant review as part of the customer follow-up process. The other is at an operating mine currently undergoing expansion and where a new ARD treatment system that combines HDS lime neutralization with ChemSulphide® was commissioned in 2014. The long-term benefits of the ChemSulphide® process including the reduction in LCC, process robustness to meet stringent discharge limits, and the reduction or elimination of waste sludge are discussed.

Traditionally, ARD has been treated with lime neutralization in a typical flow sheet shown below in Figure 1. In this process, lime is added to the metal laden water to neutralize the dissolved metals.

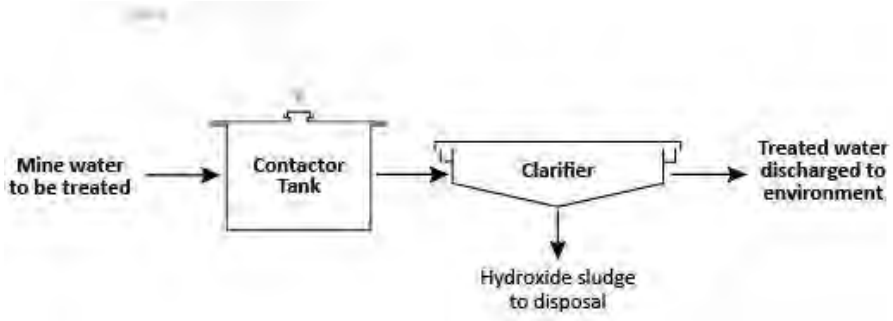

Figure 1 Traditional ARD Treatment Flow Diagram

As shown above, all metals in the ARD are precipitated in a voluminous hydroxide sludge that will bring significant disposal costs and associated liabilities. Adding to the complexity of sludge management is that storage and disposal is controlled by site-specific licenses or permits in some jurisdictions.

Sulphide precipitation technology, depending on the ARD composition, can recover all the metals as salable metal sulphide products and completely eliminate the sludge generation and disposal, or partially recover the valuable metals to reduce the overall sludge management cost.

CASE STUDY: WELLINGTON ORO MINE

The Wellington Oro (WO) treatment plant is located approximately five kilometres east of the Town of Breckenridge, Colorado. A former United States Environmental Protection Agency (EPA) superfund site, the WO mine was seeping ARD with zinc and cadmium from its historic underground workings to waterways and a downstream fishery (US EPA, 2014). An international call for proposals resulted in ChemSulphide® being selected as the best available technology to meet site-specific effluent discharge regulations and minimize the quantity of solid waste generated and stored on-site. Since it is impossible to prevent water ingress into the mine, ARD treatment will be required for many decades and possibly in perpetuity at the site. The flow diagram of the ChemSulphide® treatment process designed by BioteQ and installed at WO is shown in Figure 2.

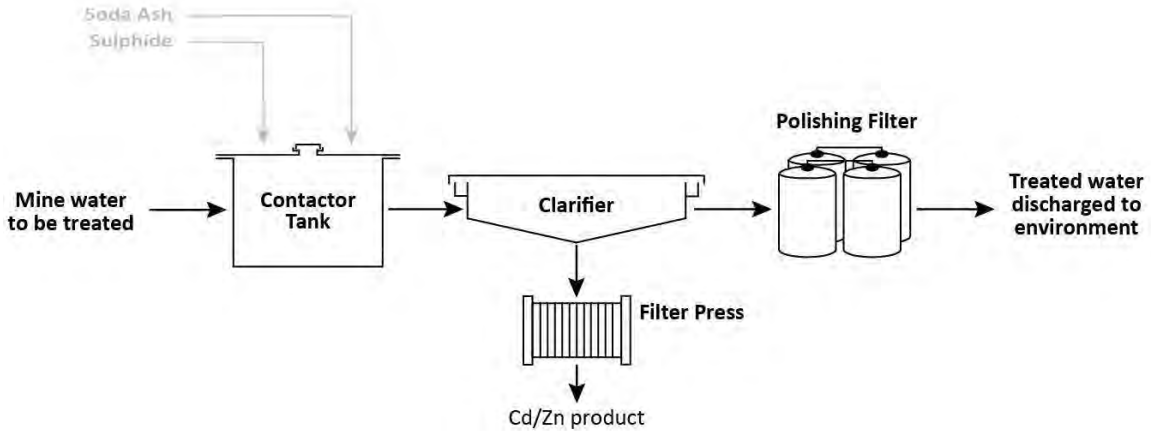

Figure 2 WO ChemSulphide® Process Flow Diagram

The ARD treatment at the site works by selectively precipitating the dissolved Cd/Zn in the mine water as metal sulphide solids using chemical sulphide as the primary reagent. The water is then separated from the Cd/Zn solid and sent to polishing filters before being discharged to the environment. The Cd/Zn solids are filtered to remove excess water, producing a high-grade metal product suitable for refining.

The plant was constructed and commissioned in 2008. Within approximately three months following the plant start-up, the treatment plant was meeting all project objectives summarized in Table 1.

Table 1 Wellington Oro Treatment Objectives and Results

Parameter	Feed	Objective	Result
Zn	132 mg/L	< 225 ppb	< 67 ppb
Cd	122 ppb	< 4 ppb	< 0.5 ppb
pH	6.15	6.5 to 9.0	7.5 to 8.5
Waste sludge generation	-	Zero waste	Zero waste
Hydraulic flow	-	9 to 27 m^3/hr	16 m^3/hr

Following the successful commissioning of the plant and training of local operators, the Town of Breckenridge took over responsibility for plant operations. In Q1 2014, the city made the decision to take advantage of the available follow-up services and invited BioteQ to perform an on-site review and optimization of the plant, five years after start-up.

BioteQ's review revealed that while the ChemSulphide® plant has continuously met regulatory discharge limits and successfully eliminated waste sludge, which were the primary benefits of the process, the overall plant availability was impacted due to several issues as summarized in Table 2.

Table 2 Wellington Oro Plant Availability Impacts

Operational Issue	Impact on Operability
Frequent soda ash pump seal failure	Increased downtime, higher maintenance costs
Hard scale deposit build-up in polishing filters	Higher operating cost to include media filter replacement every 6 months
Significant % of time spent in recycle	Reduced plant availability

Further review of the plant operating data and discussions with plant operators revealed that over the course of the past five years, plant operating conditions changed substantially from the original design. The key parameters that have changed are noted in Table 3.

Table 3 Wellington Oro Plant Changes in Operating Conditions

Parameter	Unit	Design	Actual Results
Feed flow	m^3/hr	9 to 34	< 9 m^3/hr
Feed alkalinity	mg/L as $CaCO_3$	0	120 to 150
Metal acidity	mg/L as H_2SO_4	410	150 to 175

The changes in the operating conditions needed to be taken account during the on-site review and plant optimization to determine the extent to which they contributed to the operational issues identified in Table 2 and the recommendations to address the plant availability impacts.

Elucidating Pump Seal Failure

The soda ash pumps installed at WO are centrifugal pumps with a single mechanical seal. Originally, the seal flush plan was based on using the pump discharge (6% soda ash solution) as the source of gland water. This was recognized by the operators as the main cause of seal failure due to the build-up of soda ash crystals in the seal. The new flush plan involved using local groundwater as the gland water source. By switching the flush plan to groundwater, the frequency of seal failure was reduced but not enough to have a positive impact on the overall plant availability.

BioteQ's review of the groundwater quality data revealed the water contained very high levels of calcium hardness (~ 1,200 mg/L). Although this type of water may be suitable as gland water for many pumping applications, its use as gland water for pumping concentrated soda ash solution at WO is problematic. The reaction between calcium hardness and sodium carbonate results in the precipitation of calcium carbonate inside the pump seal which is the most likely cause of pre-mature seal failures.

Therefore, BioteQ provided the city with two options to remedy the current situation including: 1) install a small house size water softener for reducing calcium hardness upstream of pump glands, and 2) replace soda ash with caustic soda as the alkali used for pH adjustment in the ChemSulphide® process.

Elucidating the Formation of Hard Scale Deposit in Polishing Filters

Samples of the scale that built up in the multimedia filters were analyzed and revealed that the solids contained calcium and iron carbonate. As part of the on-site review, BioteQ reviewed the current plant feed water quality data and completed acid titrations of the feed water to confirm the alkalinity present in the mine drainage. Water quality data showed the feed to contain approximately 400 mg/L Ca with the titration results indicating a feed pH of 6.3 and alkalinity of approximately 130 mg/L. This data points to the fact that the plant feed is saturated with respect to $CaCO_3$.

Based on the original design criteria it was expected the feed would contain zero alkalinity and high metal acidity which would result in the generation of free acid and a drop in solution pH in the metal precipitation stage via reaction (1). Therefore, the original design included the addition of soda ash into the metal sulphide precipitation contactor in order to buffer the pH in the reactor.

$$Zn^{2+} + NaHS = ZnS + Na^{+} + H^{+} \quad (1)$$

Due to the fact the feed already contains 130 mg/L alkalinity and metal acidity is only 175 mg/L, the addition of soda ash to the treatment process results in a significant increase in the alkalinity of the treated water. This was confirmed by an acid titration performed on the reactor discharge solution indicating that the alkalinity increased by 260 mg/L to 390 mg/L as $CaCO_3$.

The increase in alkalinity produces solution supersaturation and significantly increases the scaling potential of the treated water where both $FeCO_3$ and $CaCO_3$ can precipitate out of solution. Scale formation in the multimedia filters can be explained by the filter media having a high solid surface to liquid volume ratio inside the filter housing. This acts as seed for relieving at least a portion of the solution supersaturation.

It is also likely that the gradual build-up of scale inside the filters was exacerbated by a less than optimal back-flush regime where it is imperative that the best possible conditions are created to

remove solids trapped inside the filters. The current back-flush conditions are far from optimal due to the following:

- The plant flow rate is below the minimum back-flush flow required (multimedia filters use filter discharge to back-flush); and
- Limited volume of water in the backwash feed tank.

Based on this process analysis, BioteQ recommended the following three remedies: 1) automate the filter backwash based on the level in the filter feed and backwash collation tanks to ensure adequate backwash volume and time is allocated to cleaning the filters; 2) move the soda ash addition downstream of the polishing filters; and/or 3) replace soda ash with caustic as the alkali of choice to control the pH in the process and for discharge. While moving the soda ash addition is a more versatile solution that is applicable over a wide range of feed water quality, it may still result in scaling in the effluent piping. The replacement of soda ash with caustic completely eliminates carbonate formation and scaling but is applicable only when the plant feed contains sufficient alkalinity to buffer the pH in the metal sulphide precipitation stage.

Elucidating the Cause of Poor Plant Availability Due to Recycle

The ChemSulphide® process is designed for continuous operation; as such, any time there is a plant upset that causes the process to shut down, there will be a certain amount of operating time before on spec water can be produced again. Typically, the longer the process is shut down, the longer it takes to get the process back up to steady state.

The current plant configuration does not allow for an automatic recycle of off spec water back to the mine if a minor upset occurs. If an off-spec issue occurs, the plant automatically shuts down and requires operator intervention to start back up. As the plant was designed for operation with limited supervision, there are times when the process will be idle for 10-12 hours depending on operator availability. This can turn a small process upset, which with a recycle loop would result in a minor upset, into the plant being shut down for an extended period and then taking 3-5 days for the process to restart.

In order to keep the process running following an upset, BioteQ recommends that automated valves and a recycle line should be added to the discharge line to ensure the plant can continue to circulate water when producing off-spec water. This should reduce the 3-5 day timeframe for plant restart to a matter of hours. The existing manual valves can be modified to accept a pneumatic or electric actuator and, along with a few modifications to the PLC program, the plant will be able to recycle automatically.

Plant Review Summary

The review of the ChemSulphide® plant operation five years after plant start-up revealed the following:

- The ChemSulphide® process is robust and has been successful in meeting project objectives that include compliance with stringent discharge limits and the elimination of waste sludge;
- To ensure high plant availability and low maintenance costs, it is important to use only soft water as gland water for centrifugal pumps used for conveying soda ash solutions for pH control;
- Where mine drainage may contain significant alkalinity, the plant design should allow for the use of caustic in addition to soda ash to avoid the risk of scaling in polishing filters; and
- When sizing the filter feed and backwash tanks, it is important to consider not only the maximum design flow but also the minimum design flow.

Positive Impact of Metal Recovery on Life Cycle Costs

On average, the WO ChemSulphide® plant treats and discharges over 45,000 m^3 of water annually while recovering over 99% of the zinc and cadmium in the ARD. The recovered metals equate to roughly 23,000 lbs of Zn/Cd which are formed into a filter cake concentrate and shipped to a smelter. By recovering these metals, the WO treatment plant avoids the production of HDS lime sludge which would necessitate the construction of dedicated sludge ponds and/or significant costs of ultimate sludge disposal in a final resting place such as an industrial waste landfill.

CASE STUDY: YINSHAN MINE

In Q2 2014, BioteQ along with its joint venture partner Jiangxi Copper Corporation (JCC), completed the construction and commissioning of a new water treatment plant at JCC's Yinshan mine. The treatment plant combines conventional high density sludge (HDS) lime neutralization with the ChemSulphide® process to treat ARD and recover copper. The plant is the second such plant built by the partners. The first was constructed at the nearby Dexing Mine in 2007 and has been operating continuously and successfully since start-up.

At Yinshan, there are two main sources of ARD including surface run-off collected from the open pit and toes of the waste rock dumps, and water collected and pumped from underground mine workings. The initial objective for the site was ARD treatment to meet regulatory requirements with a properly designed HDS plant. However, during the project definition stage, it became evident that the copper and zinc concentrations in the ARD have sufficient economic value to warrant potential metal recovery. A subsequent engineering feasibility study confirmed this and the decision was made to expand treatment to include the ChemSulphide® process to recover copper with a further allowance made for a possible future expansion to include zinc recovery. The flow sheet of the ARD treatment system installed at Yinshan is schematically depicted in Figure 3.

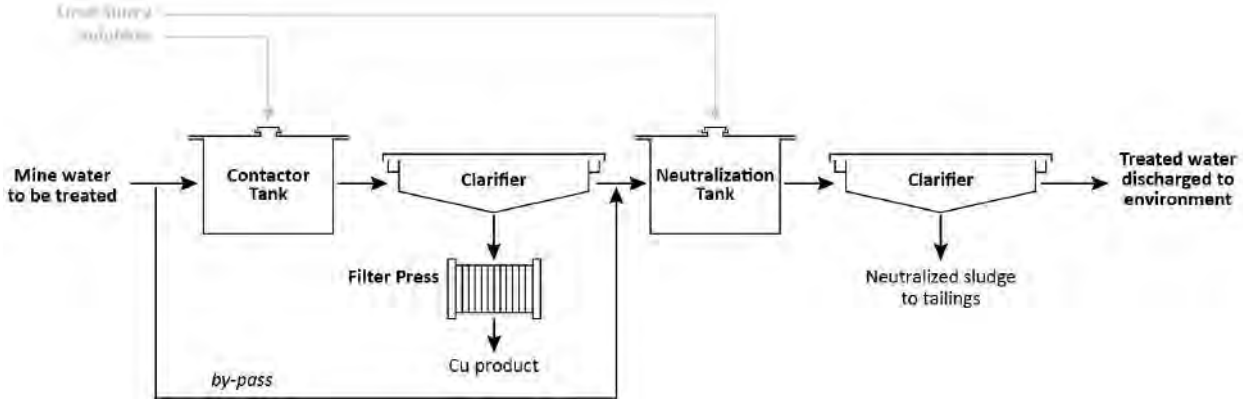

Figure 3 Yinshan ChemSulphide® Process Flow Diagram

As can be seen from Figure 3, a portion of the mine water is designed to by-pass the copper recovery stage. This is due to the fact that not all sources of mine impacted water at Yinshan contain sufficient amounts of copper to warrant recovery and the need to reduce the capital cost of the overall treatment. A chemical sulphide reagent is used to precipitate the dissolved copper in the ARD into a copper sulphide slurry. The slurry is dewatered to produce a high-grade copper concentrate that is sold to a local smelter.

Although the ChemSulphide® circuit of the overall treatment currently recovers only copper, the operating conditions of the plant also removes arsenic and cadmium from the ARD to ultra-low levels which is deported to the copper concentrate hence preventing them from being discharged to the environment. A downstream HDS lime plant is currently used to remove zinc (before the Zn recovery is put into place) along with aluminum and iron, prior to final discharge. The plant effluent is discharged into a local river that is part of the watershed of the largest fresh water lake in China – the Poyang Lake. The HDS lime sludge with reduced metal content is disposed of in the tailings pond.

Due to permitting and construction delays of the ARD collection and storage facilities, the plant has yet to reach and operate at the maximum design capacity for an extended period of time. Average copper concentrations in the plant feed are also lower than designed for the same reasons. The plant has been fully tested during the May to July 2014 storm season peak flow days and has met all design expectations. Table 4 summarizes the key design objectives against the actual averages since the start of operation.

Table 4 Yinshan Treatment Objectives and Results

Parameter	Feed	Objective	Result
Cu	80 mg/L	1 mg/L	< 1 mg/L
Cu concentrate grade	-	35%	31-33%
Cu recovery	-	90%	90%
pH	2.6	2.2	2.2
Hydraulic flow – Cu recovery	-	700 m^3/hr	400 m^3/hr
Hydraulic flow – HDS	-	1,000 m^3/hr	600 m^3/hr

BioteQ continues to provide technical support for ongoing plant operations.

Positive Impact of Metal Recovery on Life Cycle Costs

Using the actual capital cost of the fully installed plant and the operating cost figures from the first three months of operation, the projected LCC of ARD treatment with a 20 year net present cost (NPC) was estimated for three treatment scenarios: HDS alone, HDS with the current copper recovery, and the future possible scenario of HDS with copper and zinc recovery.

The LCC were calculated using a 5% discount rate with no adjustment for future cost escalation for inflation, and assumes a fixed copper price of $3.30/lb and zinc price of $1.13/lb over the life of the project. It should be noted that base metals in China trade at a price premium of approximately 10 to 15% over the London Metal Exchange prices.

The calculated LCC are also based on zero sludge disposal costs. This is true for the Yinshan mine operation where HDS lime sludge is pumped to an existing tailings facility nearby. However, in many cases of active ARD treatment, this option for sludge disposal is not available and the sludge handling and disposal costs can be quite significant.

From this perspective, the LCC presented in Table 5 represent the worst case scenario for the positive impact of metal recovery by the ChemSulphide® process on the overall economics of ARD treatment. For illustration of the additional potential benefit of the ChemSulphide® process for other sites, the sludge reduction associated with metal recovery are also provided.

Table 5 Yinshan Plant Life Cycle Cost Comparison (US$)

	HDS	HDS + Cu	HDS + Cu/Zn
CAPEX			
ChemSulphide®	-	$ 3,400,000	$ 3,900,000
HDS Lime	$ 5,300,000*	$ 4,300,000	$ 4,300,000
OPEX			
ChemSulphide®	-	$ 1,100,000	$ 2,117,000
HDS Lime	$ 875,000	$ 827,000	$ 807,000
Value of Metal Recovery			
Cu	-	$ 1,768,000	$ 1,768,000
Zn	-	-	$ 1,224,000
Net OPEX (incl Metal Value)	($ 875,000)	($ 159,000)	$ 68,000
LCC (20 yr NPC @ 5%)	$ 16,200,000	$ 9,681,000	$ 7,353,000
Cost per m^3 ARD treated	$ 1.17	$ 0.70	$ 0.53
Sludge Reduction (tons/year)	0	1,440	5,160
Sludge Reduction (m^3/year)	0	1,030	3,690

*** Construction of a HDS plant alone would cost $1 M more due to cost efficiencies from shared infrastructure and mechanical/electrical installation when a HDS plant is built in conjunction with a ChemSulphide plant.**

As indicated by the LCC comparisons, copper recovery can offset the HDS treatment cost and reduce the long-term liability associated with treating ARD by more than $ 6 M. On an initial capital cost of $7.7 M for the HDS + Cu recovery option, the LCC is $9.7 M to treat ARD for 20 years.

When zinc is also recovered in combination with copper recovery, the liability of treating ARD can be turned into a profit centre. The capital cost for HDS + Cu/Zn is $ 8.2 M. The LCC is $ 7.4 M. Over a 20 year treatment period, the project will have generated a profit of $ 800,000.

CONCLUSION

ChemSulphide® is a robust and efficient process technology for the treatment of mine impacted waters to meet regulatory compliance while contributing positively to the LCC of the project. The technology has been applied at multiple sites with different site conditions and requirements.

At Wellington Oro, the ChemSulphide® plant has operated for five years, successfully meeting stringent discharge requirements and generating no waste for disposal. By eliminating waste and its associated liabilities, operational costs are reduced. And as operating conditions change over time from the initial design, the process can be modified to maximize plant operability.

The newly installed Yinshan plant illustrates how a metal recovery component when treating ARD can reduce project LCC. Depending on the value of metals in the ARD, the flow rate and metal prices, the revenues generated can range from offsetting treatment costs to becoming a profit centre.

The two cases presented in this paper can be applicable to many mine sites that have similar ARD issues. Sulphide precipitation, due to its high process efficiency and metal selectivity, can also be combined with other mine water treatment applications such as ion exchange and membranes to address complex ARD issues, or meet ultra-low effluent discharge limits.

Mine water treatment is a necessity but can be costly. The two cases in this paper demonstrates that options now exist to treat ARD to comply with environmental regulations and reduce LCC, thereby improving overall project economics.

REFERENCES

USEPA (2014) *French Gulch*, September 16, 2014, http://www2.epa.gov/region8/french-gulch

10th ICARD IMWA 2015 | 10th International Conference on Acid Rock Drainage & IMWA Annual Conference

The Feasibility of Treatment of Acid Mine Drainage with Seawater

Devin Sapsford, Lawrence de Leeuw, James Phillips and Peter Brabham
Cardiff University, United Kingdom

ABSTRACT

This paper presents results from an experimental study on the interaction of acid mine drainage from the abandoned Parys Mountain mine site (UK) and seawater with a focus on its potential use as a reagent in mine water treatment. Parys Mountain is a former copper mine, the acid mine drainage discharge measured during the study was pH 2.1 – 2.4 with elevated iron concentrations (up to 490 mg/L) and a range of other elevated metal concentrations including copper (34 mg/L), zinc (11 mg/L), lead (109 μg/L) aluminium (57 mg/L), and cadmium (135 μg/L). Currently the discharge (circa 10 L/s) flows via the Afon Goch for approximately 2 km to discharge to the Irish Sea. Remediation options have been considered for the site and include active and hybrid active-passive treatments with active treatment being favoured given the challenging AMD chemistry. Because active treatment is costly, alternative remediation strategies would be favourable. Considering that seawater has alkalinity due to the presence principally of dissolved carbonates and borates, this study looks at the feasibility of using seawater as a reagent to treat the mine drainage. Field titrations were performed using seawater to titrate the acidic mine drainage whilst pH was monitored and samples withdrawn for analyses of dissolved species. It was determined that mixing of mine water with seawater in ratio 1:1 was found to give the following removals (quoted as load removal with residual metal concentration in parentheses): Cd 77% (16 μg/L); Zn 77% (1.3 mg/L); Cu 74% (4.5 mg/L); Al 68% (9.2 mg/L) and Fe 36% (58 mg/L), thought to be due to precipitation of K-jarosite. The load removal is reasonably good at simple mixing ratio of 1:1 but the residual concentrations are relatively high. Clearly if stringent concentration-based discharge consents were imposed then mixing (1:1) with seawater would not satisfy these consents (mixing at higher ratios might), however, if the aim is to reduce metals loading to the coastal water for as low a cost as possible, then seawater mixing and removal of precipitated metals may be a promising avenue to explore further.

Keywords: Neutralization; metals removal; remediation

INTRODUCTION

Acid mine drainage is a widespread problem for mining operations around the world, both for active sites and former mine sites. One such legacy site is Parys Mountain, Anglesey, UK where AMD currently pollutes local water courses and the near-shore environment. This study focusses on AMD from the Dyffryn Adda adit discharge which enters the Afon Goch Amlwch watercourse, which then flows through the town of Amlwch and into the Irish Sea. Parys Mountain is an Ordovician/Silurian volcanogenic massive sulphide ore deposit (Barrett et al. 2001). The "mountain" lies approximately three kilometres from the north Anglesey coast in North Wales, and reaches a peak height of < 150 m above ordnance datum. The ore bodies' occurrences comprise both massive and banded polymetallic sulphide lenses, hosting copper, zinc, lead, silver, and gold. Despite the range of metals in the ore, the mountain has been predominantly mined for copper. Archaeological evidence suggests that mining activity has been present on the site for approximately 4000 years, and around the time of the industrial revolution, circa 1750, it was Britain's and one of the World's primary sources of copper. A range of treatment technologies for the principal Parys Mountain discharge have been reviewed including active treatment using standard chemical precipitation of metals and long sea outfall without treatment. The regulatory framework to achieve compliance is detailed by the requirements of the European Water Framework Directive. The CAPEX and OPEX associated with conventional lime treatment and uncertainty about the success of passive treatment drives the research and development of novel approaches to treating problematic discharges without excessive cost.

Aims

The key aims of the present study were to (i) examine the interaction of mine water with seawater (ii) to determine whether this presents a viable potential treatment method for removing dissolved metals. There is a paucity of studies that examine the interaction of mine water with seawater, exceptions include Braungardt et al. (2003) and Achterberg et al. (2003) who studied AMD / seawater interactions in estuary systems. There is also no mention of seawater as a reagent in water treatment with the exception of the study by Muraviev et al. (1997) which examined the use of seawater as a reagent to regenerate ion exchange resins used in mine water treatment.

Figure 1 Parys Mountain mine site, Anglesy, UK

METHODOLOGY

Field experiments were undertaken to determine the ratio of sea water to mine water required to raise the pH to 7 and determine any concurrent removal of dissolved metals. Mine water neutralization experiments were carried out using water directly from the Dyffryn Adda Adit. Each ratio of mine water to seawater mixing (1:1 to 1:90) was conducted as a separate experiment rather than sequentially adding seawater. pH, DO, Redox potential (presented corrected to v. SHE) were measured in the field using a Hanna HI 9828 Multiparameter probe throughout the process and water samples for dissolved metals analyses were taken at the different stages. Acidity/Alkalinity and anion determination ion (using IC) were carried out in the laboratory. In a second round and third round of neutralization experiments, air was bubbled through each mine water/seawater mixture (using a 12V air compressor) for 10 minutes. In addition to aeration, in the 3rd round of neutralization experiments the seawater was reacted with limestone chippings (4 – 10 mm) for 24 hours prior to the mixing experiments. All water samples for metals analyses were filtered (0.45 μm) and acidified with 1ml of 10% nitric acid, diluted x 10 and analysed by ICP-MS.

RESULTS AND DISCUSSION

Mine water neutralization

The water quality parameters of the Parys Mountain mine water were as follows on the two sampling occasions: pH 2.37, Eh 419 mV, pH 2.10, Eh 402 mV and acidity 1786 mg/L. Corresponding data for the seawater used was as follows, pH 8.14, Eh 300 mV. The seawater used in the aeration experiment was pH 7.50, Eh 290mV and a third batch of seawater attained a pH of 8.26 and Eh of 215 mV on 24 hour contact with limestone chips. Fig 2 shows the results of mixing 1 part mine water with increasing amounts of seawater. It can be seen that neutralization to pH 7 requires 90 parts seawater to 1 part Parys Mountain mine water when simply mixed. If the mixture is aerated for 10 minutes after the seawater addition a reduction can be seen in the volume of seawater required to bring the pH to 7 (MW:SW of 1:40). This is probably due to stripping of dissolved CO_2 from the mixture as it is formed during the reaction of HCO_3^- in the seawater with H^+ in the mine water. The increase in alkalinity (116 to 182 mg/L as $CaCO_3$) imparted to the seawater by soaking it in limestone for 24 hours explains the reduction in the volume of this pretreated seawater required to reach pH 7 (MW:SW of 1:25). The mine water flow at Parys Mountain is cicra 10 L/s. An upper estimate of a viable seawater mixing ratio for use in treatment is 1:10 (MW:SW) which would result in a combined flow of 110L/s (comparable to some of the larger coal mine drainage treatment flows in the UK). It can be seen that at 1:10 ratio that the pH values are 4.9, 5.33 and 5.79 respectively.

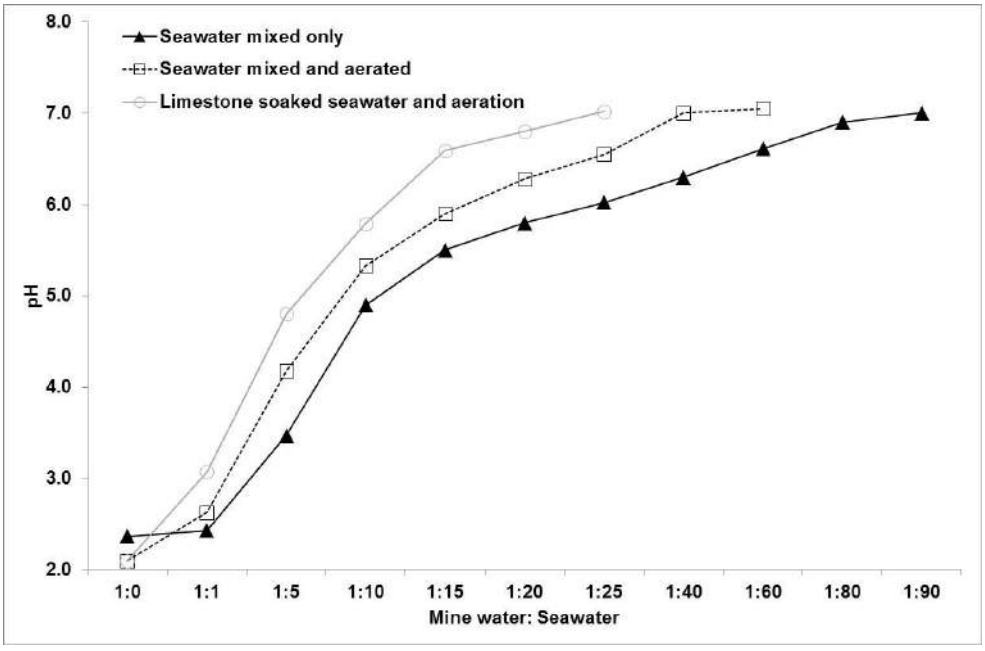

Figure 2 pH of mine water and seawater mixtures

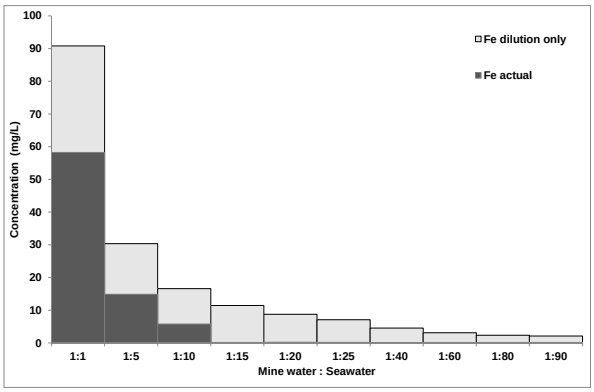

(a) Fe

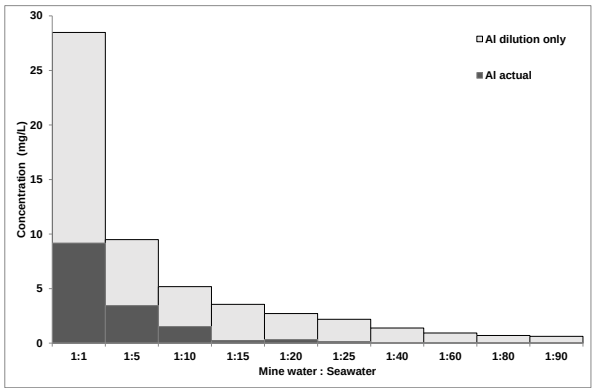

(b) Al

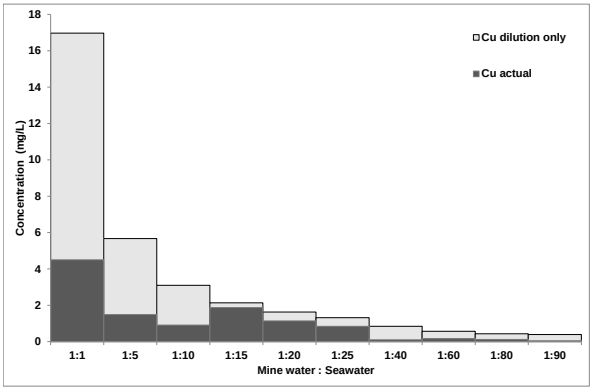

(c) Cu

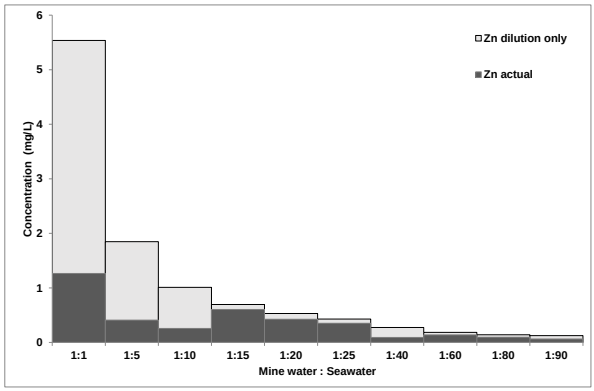

(d) Zn

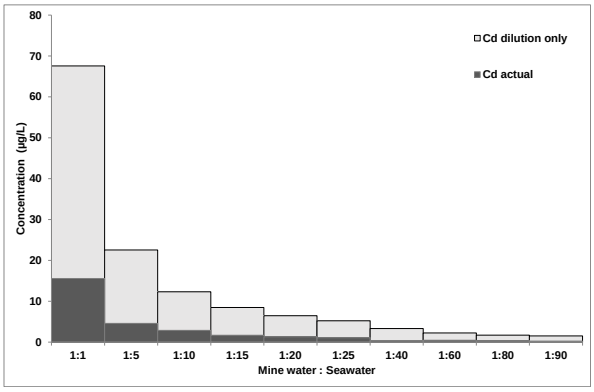

(e) Cd

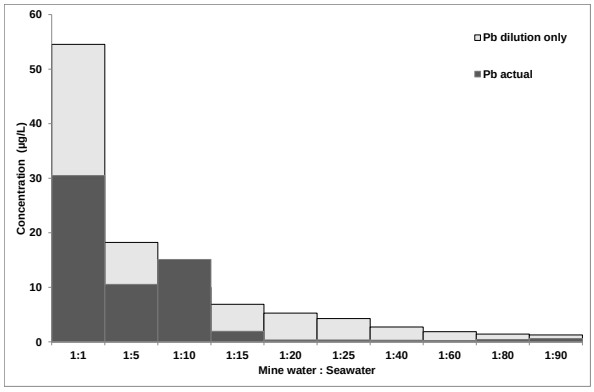

(f) Pb

Figure 3 Residual dissolved metals after mixing with seawater at different ratios. Shown are concentrations predicted from dilution of mine water and actual measured concentrations.

Metals removal

Mixing of the mine water with equal parts seawater led to an instantaneous colour change from colourless to orange indicative of precipitation of iron, with higher proportions of seawater the orange colour was less detectable due to the high volume of seawater. As the pH increased, metals began to precipitate out and form a layer on the bottom of the mixing container. The resultant settled sludge can be seen in Fig 4 at the base of the reaction vessel. Fig 3 shows the concentrations of residual dissolved Fe, Al, Cu, Zn, Pb and Cd in solution after mixing with various amounts of seawater. Since when creating mine water and seawater mixtures the high concentrations of metals in the mine water are diluted, each graph also shows the decrease in concentration expected by dilution alone. It can be seen that in all cases (except for Pb at a ratio of 1:10) at all dilution ratios, the residual dissolved metals concentrations are considerably lower than by simple dilution indicating that metals have been removed from solution during mixing with seawater. For Fe (Fig 5) it can be seen that 36% of the dissolved Fe is removed by simple mixing 1:1 with seawater, this indicates (also suggested by the observed colour change) that an Fe(III)-bearing precipitate formed, which also buffered the pH (only a small change in pH observed (see Fig 2). 92 – 99% of Fe is removed at ratio of 1:15 and above. 68 % of the Al is removed by mixing 1:1 with seawater, with 88 – 99 % of the Al removed above 1:15 (where the pH < 5.5) as expected from the solubility of Al. The removal of Fe and Al at1:1 ratio whilst the pH is low suggests the precipitation of an Fe-Al mineral, possibly jarosite-alunite. PHREEQC modelling with the mine and seawater compositions demonstrates that precipitation of K-jarosite can account for the observed decrease in Fe concentration.

Figure 4 Precipitate formed from mixture of mine water with seawater can clearly be seen at the bottom of the reaction vessel.

74% of Cu (Fig 4 (c) and Fig 5) was removed from solution by mixing 1:1 with seawater. Of note is the variable Cu removal; a high removal at 1:1 through to 1:10, very low removal of 12% at 1:15 though to a maximum Cu removal observed for MW:SW ratio of 1:40. This behaviour is also observed with Zn, with 77% being removed at 1:1, and the highest removal between mixing values of 1:1 and 1:10, whilst lows of 13% removal occurred at 1:15, and removals did not recovering above this ratio. This behaviour is indicative of complex adsorption behaviour, whilst there is an abundance of Fe/Al precipitates to sorb to, it is likely that at the pH reached 5 and above that

competitive sorption by the swamping excess of ions in the seawater outcompete Cu and Zn for sorption sites on these precipitates. Achterberg et al (2003) found that AMD source metals remain in the dissolved phase in an estuary (albeit at much lower concentrations). 77% of the dissolved Cd is removed by mixing 1:1 with seawater and removal thereafter remains reasonably constant with a high of 88% removal at ratio of 1:40. Why Cd behaviour is different to Zn and Cu is unknown but note the difference in magnitude of the starting concentrations. The removal of Cu, Zn and Cd at low pH at low mixing ratios may be due to the suspected jarosite-alunite precipitation. Cu, Zn, and Cd are known to be able to substitute into the jarosite-alunite structure.

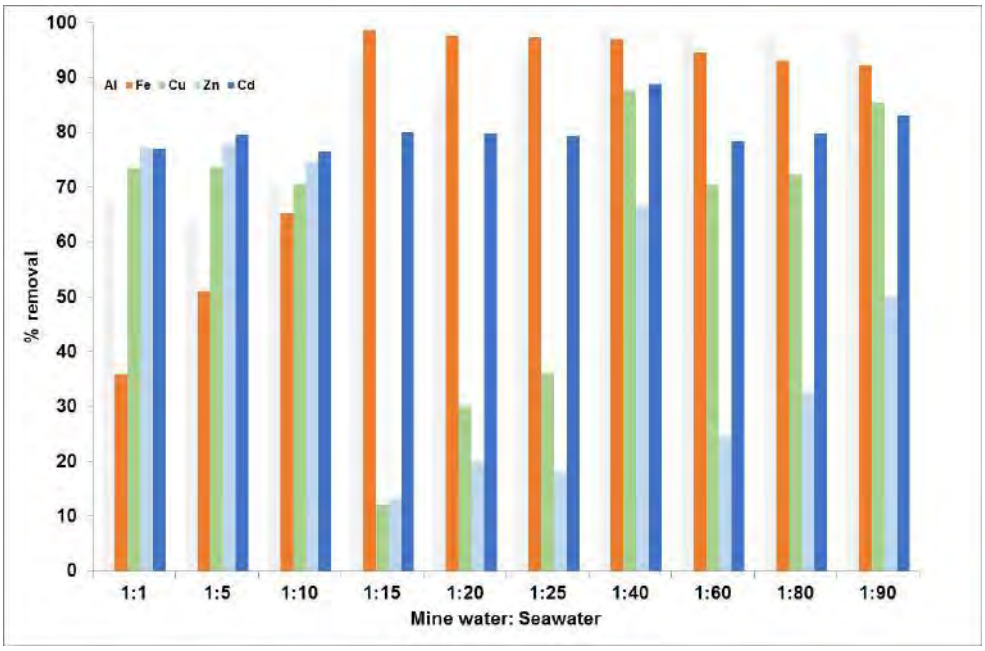

Figure 5 % removal of metals from solution upon mixing with different ratio of seawater

CONCLUSION

Mixing seawater with Parys Mountain AMD at ratios between 1:1 to 1:90 results in the removal of dissolved metals Fe, Al, Cu, Pb, Zn and Cd from solution. Cu and Zn showed decreased removal at certain ratios thought to be due to competitive sorption between Cu and Zn and seawater cations such as Mg^{2+}. This may have significant implications for the fate and transport modelling for AMD releases to sea. Neutralization of the AMD occurs as the mixing ratio is increased. Incorporating aeration, and contacting the seawater with limestone chips decreases the amount of seawater required to raise the pH of the mine water/seawater mixtures. Mixing of mine water with seawater in ratio 1:1 was found to give the following quoted as load removal with residual metal concentration in parentheses: Cd 77% (16 µg/L); Zn 77% (1.3 mg/L); Cu 74% (4.5 mg/L); Al 68% (9.2 mg/L) and Fe 36% (58 mg/L). Clearly the load removal is reasonably good at simple mixing ratio of 1:1 but the residual concentrations are relatively high.

Feasibity of use for AMD treatment at Parys Mountain

Treatment of Parys Mountain mine water (or other similar discharges close to the sea) is likely to comprise mine water capture, treatment and final discharge to the sea. The feasibility of using seawater as a reagent in mine water treatment would depend upon the regulatory framework for the discharge. Clearly if stringent concentration-based discharge consents were imposed then mixing (1:1) with seawater will not satisfy these consents (mixing at higher ratios might), however if the aim is to reduce metals loading to the coastal water for as low a cost as possible then seawater mixing and removal of precipitated metals may be a promising avenue to explore further. It should be noted that the mixing with seawater removes metals from solution, for full treatment a suitable liquid/solid separation would be required in the treatment train. For example settling ponds, VFRs (Sapsford et al., these Proceedings; Sapsford et al., 2007) or reedbeds. Thus a full system would comprise a pump and piping for seawater abstraction, a mixing chamber for seawater (perhaps contacted with limestone in a limestone drain to boost alkalinity) and mine water followed by the selected settling/filtration system. If pumping of seawater was not an option, there might be scope for a tidally driven mixing system which would further reduce costs.

ACKNOWLEDGEMENTS

The authors wish to thank Natural Resources Wales for the financial support and supporting data for this study.

REFERENCES

Achterberg, E. P., Herzl, V., Braungardt, C. B., & Millward, G. E. (2003). Metal behaviour in an estuary polluted by acid mine drainage: the role of particulate matter. Environmental Pollution, 121(2), 283-292.

Barrett, T. J., MacLean, W. H. and Tennant, S. C. 2001. 'Volcanic sequence and alteration at the Parys Mountain volcanic-hosted massive sulphide deposit, Wales, United Kingdom: applications of immobile element lithogeochemistry', Economic Geology, 96, 1279-1305

Braungardt, C. B., Achterberg, E. P., Elbaz-Poulichet, F., & Morley, N. H. (2003). Metal geochemistry in a mine-polluted estuarine system in Spain. Applied Geochemistry, 18(11), 1757-1771.

Muraviev, D., Noguerol, J., & Valiente, M. (1997). Seawater as auxiliary reagent in dual-temperature ion-exchange processing of acidic mine waters.Environmental science & technology, 31(2), 379-383.

Sapsford, D., Barnes, A., Dey, M., Williams, K., Jarvis, A., & Younger, P. (2007). Low footprint passive mine water treatment: field demonstration and application. Mine Water and the Environment, 26(4), 243-250.

Acid Drainage Treatment Using Phyllite Rock in an Underground Mine

José Santos, Alejandrina Castro, Angélica Cervantes, Ángeles Neri, Juan Goslinga and Guadalupe Isidro
Universidad Nacional Autónoma de México

ABSTRACT

Tizapa mine is located in the State of Mexico, Mexico, the ore deposit is volcanogenic and its mineralization consists of Fe, Zn, Pb, Cu and As sulfides and Ag sulfosalts. Pyrite is the most abundant sulfide mineral and is found in massive and disseminated form. The host rock is schist and graphitic phyllite, their composition is mainly quartz, plagioclase, chlorite and muscovite; but the phyllite also has abundant calcite as filling fissures. Presence of water in the underground mine generates acid mine drainage (AMD) in old working areas. Water source was evaluated by testing soil infiltration, permeability and fracturing of the rock. AMD pH varies from 2.4 to 3.4; it has high conductivity and soluble concentrations of Fe, Al, Cu, Cd, Mn, Zn and sulfates. The flow varies from 0.7 L/s to 1.7 L/s and the presence of water is mainly associated to an upper aquifer. AMD drains down a ramp and it is directed to an active treatment plant inside the mine. Treatment involves raising the pH using sodium carbonate to a 5.5 value. Phyllite associated with calcite allows proposing a passive treatment system alternative to control the AMD. The objective of this work is to develop a passive system using phyllite rock to neutralize the AMD within the mine to replace the current active treatment plant. Stirring batch tests were conducted to raise the pH to values between 6.2 and 6.6. Removal of 100% (Fe, Al, and Cu), 19-40% (Cd), 0-32% (Mn) and 4-36% (Zn) was achieved. Currently, the research is focused on the design of an open canal system with phyllite to install it in different parts of the mine and force the AD to flow through it.

Keywords: Acid mine drainage, passive treatment, phyllite rock, underground mine

INTRODUCTION

Acid mine drainage (AMD) is a natural phenomenon that occurs in mining working areas or waste deposits where sulphide minerals have been exposed to environmental conditions of weathering (Lottermoser, 2007). There has been much research on the development of treatment methods for the control of AMD, mainly into so-called passive treatments (López et al., 2002; Johnson et al., 2005). Some of the main passive treatment methods have been applied to AMD such as limestone canal systems (Alcolea et al., 2012) or permeable reactive barriers (Macías et al., 2012). These applications have been made to treat acid drainage generated in waste deposits, or acid drainage which comes from mining works and receives treatment outside of the mine. However, little research has been done on controlling acid drainage inside mines which are still in operation and where this may have further effects on the aquifers. The poor quality water in abandoned mining areas is partly associated with the generation of acid drainage from mining works (Younger et al., 2002; Wolkersdorfer, 2008). Tizapa mine is located in the State of Mexico, Mexico (Figure 1). The ore is a volcano-sedimentary deposit of massive Zn-Pb-Cu with Ag and Au values sulphide mineral (Coremi, 1996; Alfonso et al., 2011). Mineralization consists mainly of pyrite, sphalerite, chalcopyrite, arsenopyrite, pyrrhotite and freibergita. In old working areas located nearest to the surface, AMD is being generated by the presence of water, coming primarily from shallow aquifers and surface infiltration from rainwater. Inside the mine AMD is drained by canals leading to a treatment plant where it is then neutralized by a solution of sodium carbonate. The neutralized water is used for mineral processing.

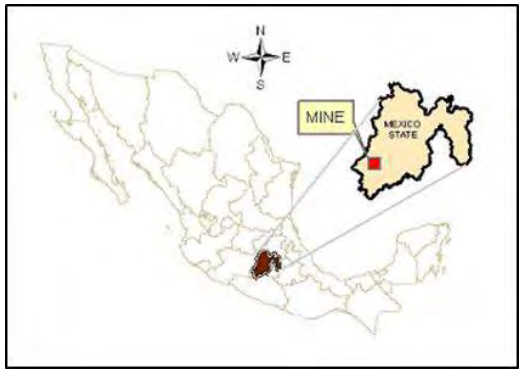

Figure 1 Mine location

Stratigraphy of the area consists of metamorphic rocks from the Triassic-Jurassic: phyllites and gneisses; above these, it is a set of metavolcanic rocks consisting of phyllites and schists of chlorite and sericite. Over the metamorphic rocks, lies a group of Cretaceous rocks: limestone and clastic rocks. Finally Quaternaries conglomerates and basalts cover the volcano-sedimentary sequence (Alfonso et al., 2011). The host rock associated to the ore deposit is chlorite and sericite schist at the base and graphitic phyllite at the top (Figure 2). Phyllite rock has abundant content of calcite mineral ($CaCO_3$), which allows considering its usefulness in a treatment system to neutralize the AMD. Also, near the mine there is a small outcrop of limestone which can be used for treatment too.

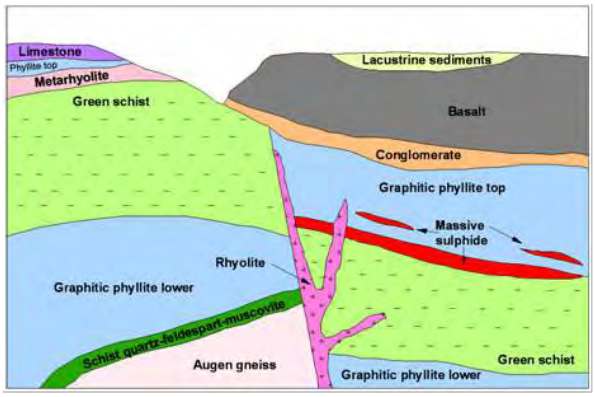

Figure 2 Mine stratigraphy and rocks associated to ore deposit

The aim of this work is to develop a passive treatment system using the phyllite rock, which could be installed inside the mine to control the AMD. Currently, work is carried out at laboratory level and conditions inside the mine are under study for the system installation.

METHODOLOGY

Identification and measurement of the AMD

Walks through the mine were performed to identify the AMD generating sites. The pH at each of these AMD generating sites was measured and located on the mine maps. The AMD flow rate was estimated by using the volumetric gauging method at each of the generating sites. The measurements were made three times, each one at different seasons of the year; the first one in May (end of low water season), the second one in July (in the middle of rainy season) and the third one in September (end of rainy season).

Water source

To determine from where the mine water is coming, analysis of the available information on rainfall (registered by a mine's weather station) and aquifers located in the area (information generated by the Water National Commission of Mexico) were conducted. Three infiltration tests were performed on the soil at the mine's surface, and the watershed runoff rate where the mine is located was determined. Furthermore, permeability tests were conducted on samples of three different rock types recovered by drilling cores: phyllite, shale and tuff. Finally, an analysis of the rock's fracturing, in places where acidic water is generated, was made.

AMD and rock characterization

Four mine's AMD samples were taken and analyzed to obtain the pH, electrical conductivity, and the concentration of major ions and trace elements. Trace elements were determined by Optical Emission Spectrometry with Inductively Coupled Plasma (ICP-EOS) on a Perkin Elmer instrument; and major ions by ion chromatography using an 883 Basic IC plus Metrohm chromatograph.

Three phyllite rock samples were taken inside the mine and a limestone sample was taken from an outcrop located outside the mine. The mineralogical composition of the rocks was determined by optical microscopy (parallel light and polarized light) and X-ray diffraction on a Shimadzu Lab X XRD-6000 equipment. The metal concentration was obtained by XRF on a Siemens SRS 3000 instrument. An analysis by scanning electron microscopy coupled with x-ray spectrometry by dispersive energy (SEM-EDS) was carried out.

Batch tests in flasks

Preliminary laboratory tests were made in batches; phyllite rock with acid drainage was stirred in 250 mL flasks at 200 rpm. During the first stage, the parameters evaluated were, the rock's grain size (2, 2.36 and 3.35 mm), the stirring time (18, 24 and 36 hours) and rock/AMD ratio (1/5, 1/10 to 1/20). With these tests, the schist's ability to neutralize acidity was determined. In the second stage, batch testing continued to determine the minimum time required to achieve a neutral pH; for this stage only rocks with a grain size of 3.35 mm was used, but the rock/AMD ratios remained (1/5, 1/10 and 1/20). The stirring was stopped every five minutes to measure the pH; tests were stopped when a pH value between 5 and 6 was achieved. The solutions obtained after neutralization were analyzed by ICP-EOS.

In a third stage, two step stirring tests were conducted. In the first step the AMD was stirred with phyllite rock until a pH value of 5 was reached, and in the second step the resulting solution was stirred with limestone to raise the pH above 7. The final solutions obtained were analyzed to determine the concentration of trace elements and major ions. Residual sediments obtained in both steps were analyzed by scanning electron microscopy coupled with x-ray spectrometry by dispersive energy (SEM-EDS) on a Hitachi Tabletop TM-1000

Filled cells testing

Currently, tests are carried out using an acrylic cell filled with the phyllite rock, through which the AMD flow passes. The cell can hold 3.5 L and 5 kg of rock with a size between 4.75 and 12.5 mm (Figure 3). The aim of these tests is to evaluate the retention time needed to raise the pH; therefore, the flow rate passing through the cell varies (2.5 to 12.5 ml/s).

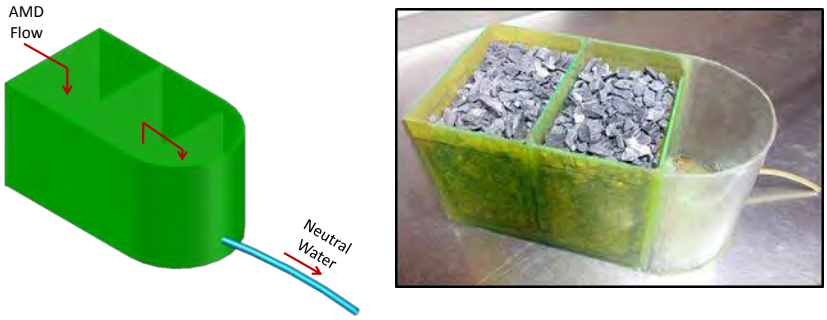

Figure 3 Testing in rock filled cell (currently in development)

The results are positive so far; however, are not reported in this paper because they are not yet considered conclusive. After these tests, the next step will be to upscale the system in order to perform a pilot test inside the mine.

RESULTS AND DISCUSSION

AMD generation

Eleven sites where AMD is generated were located within the mine, all of these connected to old mining works located between levels 1226 and 1040 m.a.s.l., and corresponding to the mine zone nearest to the surface. Measured pH varies from 2.4 to 4.6. All AMD runoff is driven by canals to the principal ramp where it is lead to the treatment plant.

The measured flow of AMD in May was 0.73 L/s, in July was 0.95 L/s, and in September was 1.74 L/s. Neutral water runoff was also found inside the mine and flows obtained were 2.05 L/s in May, 2.27 L/s in July and 1.8 L/s in September.

Water source

Infiltration tests on soils show that infiltration rates are slow to moderate (0.078 to 2.07 cm/h). Furthermore, measured permeability in the rock samples is very low; the average value is between 4.8 E-10 cm/s and 5.09 E-06 cm/s.

In order to determine rainwater infiltration volume in the study area, the average rainfall data recorded at the mine's meteorological station was used, and for the runoff coefficient the Mexican regulations methodology (SEMARNAT, 2002) was used. Furthermore, the subwatershed area was measured in the zone where AMD is generated. It was determined that the water runoff coefficient is 0.184 and, considering that subwatershed area is 0.151 km^2, it was estimated that rainwater infiltration volume is 0.031 Mm^3/year.

The maximum value of water running inside the mine, measured in September 3.54 L/s (AMD plus neutral water), was considered as a constant throughout the year, giving an estimation of 0.112 Mm^3 of water running inside the mine pear year. Comparing this value with the calculated stormwater infiltration value of 0.031 Mm^3/year, the rainwater represents only 27.7% of the total water in the mine.

In Zacazonapan town (4 km away from the mine) it is reported that the Temascaltepec aquifer is 1 to 2 meters deep and has a 1368 m.a.s.l. elevation (Conagua, 2008). This aquifer provides water to the stream "El Ahogado" which runs next to the mine at an elevation of 1226 m.a.s.l., and so, it is interpreted that the aquifer water flows over the old mining works which generate AMD.

Structural analysis of the rock where AMD is generated shows a high degree of natural fracturing at 1052, 1100 and 1200 m.a.s.l. elevations in two preferred directions: NW-SE and NE-SW.

From the information presented above it has been concluded that rainwater contribution to the water running through the mine is minimal, due the low permeability of soil and rock. From the information available about the aquifer, it is estimated that it runs close to surface level and above the mining works. Due the high fracturing level, water from the aquifer and rainwater flow through the fractures to the mining works thus generating AMD.

AMD and rock characterization

The pH values and electrical conductivity are shown in Table 1. The pH values obtained confirm the acidity of water and the high electrical conductivity is largely due the ions in solution and salts dissolved in water.

Table 1 Trace elements concentration in AMD

Sample	pH	EC (mS)	Al	Cd	Cu	Fe	Mn	Si	Zn
			mg/L						
DA 6	2.44	11.31	41	6	12	563	41	35	483
DA 6 - A	2.53	8.02	36	5	12	527	37	32	471
Pileta	2.9	4.72	9	2	2	178	26	17	363
DA 8	3.38	1.87	<LD	0.2	<LD	0.3	4	8	77

LD (mg/L): Al (0.08), Cu (0.12)

Significant concentrations of Al, Cd, Cu, Fe, Mn, Si and Zn were found (Table 1). Other elements, As, Cr, Mo, Sb, Se, Ti, Tl and V, were analyzed and are in concentrations below the detection limit.

Major concentrations of ions (Table 2) are high for Na, K, Ca and Mg cations due to the dissolution of silicate minerals present in the rocks which began to dissolve after the carbonates were consumed. A high concentration of sulphates indicates the chemical oxidation process of sulphides and is directly related to water soluble iron. Presence of chlorides is related to chlorite content in the schist rock.

Table 2 Major ion concentrations in AMD

Sample	Na^+	K^+	Ca^{2+}	Mg^{2+}	Cl^-	SO_4^{2-}
	ppm					
DA 6	228	21	438	1,759	92	18,732
DA 6 - A	197	4	369	1,674	82	16,555
Pileta	354	19	310	1,601	176	10,118
DA 8	114	14	252	380	35	2,896

Petrographic analysis showed that there is abundant calcite in the phyllite rock (Figure 4); however, the presence of plagioclase mineral is also interesting, since it is reported in literature that this could be used to neutralize AMD (Romero et al., 2007).

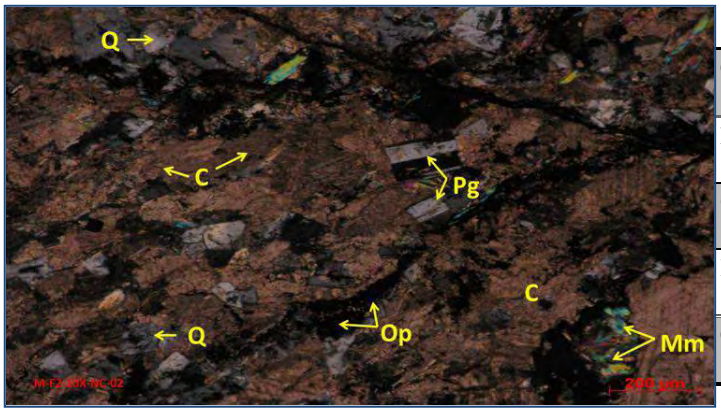

Op	Opaque minerals
Mm	Muscovite mica
C	Calcite
Pg	Plagioclase
Q	Quartz

Figure 4 Photomicrograph of phyllite rock 10 X magnification

XRD confirms that phyllite has high calcite content and abundant presence of plagioclase and micas. The mineralogy suggests that phyllite has potential to neutralize AMD. Limestone was also analyzed and dominance of calcite and quartz was observed; to a lesser extent, intermediate plagioclase and phyllosilicates (chlorite and mica) are also present.

Batch tests in flasks

In the first stage of the tests, pH values of 5.35 (3.35 mm, 18 hours, 1/20) to 7.36 (2 mm, 36 hours, 1/5) were achieved. The neutralization process is enhanced with smaller particle sizes, lower rock/AMD ratio, and increased stirring time. Figure 5 shows only the pH increase using 3.35 mm particle size; as larger particle sizes will be needed when moving forward in the research.

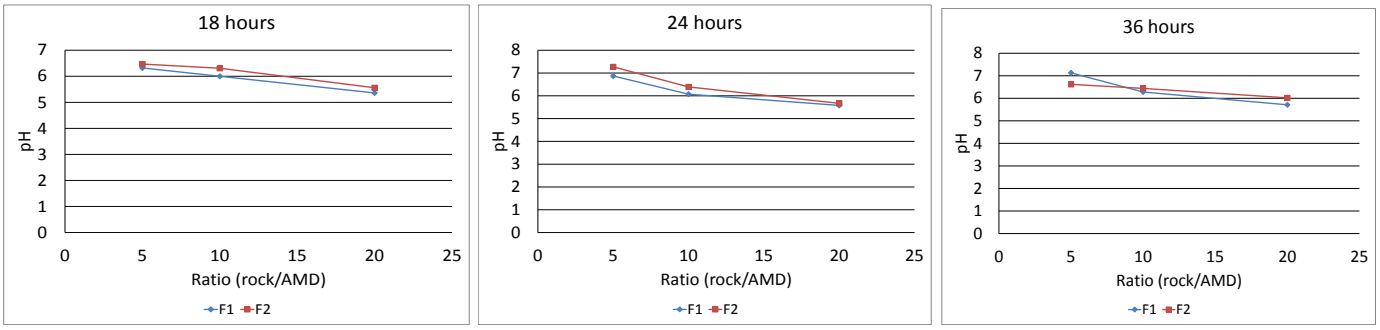

Figure 5 pH values reached in stirring tests with particle size of 3.35 mm

In the second stage of tests, the highest stirring time was necessary for the 1/20 ratio test, as 180 minutes were needed to reach a maximum pH value of 4.7. With the 1/5 ratio test, a minimum stirring time of 30 minutes was enough to reach a pH value of 5.55 (Figure 6).

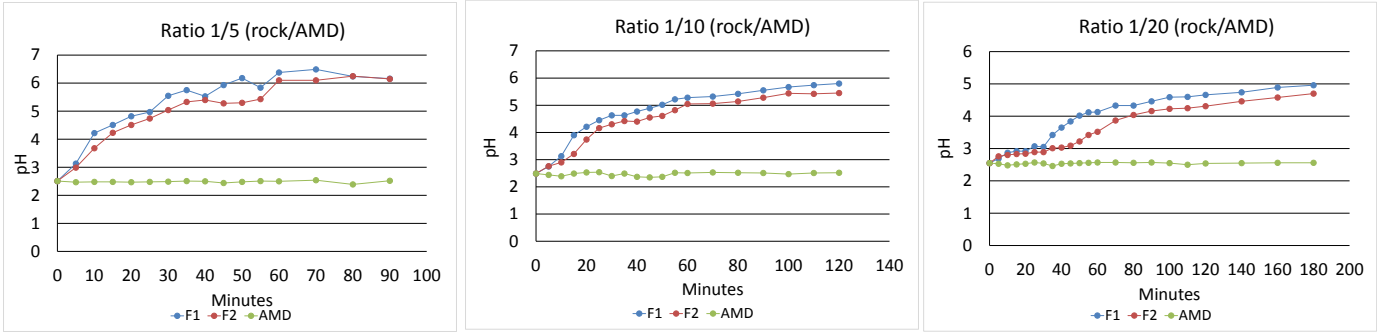

Figure 6 Minimum stirring times to achieve neutral pH values

Table 3 shows trace element concentrations in the solutions after neutralization; samples B-20, B-10 and B-5 correspond to acid drainage without treatment. A direct relationship between pH reached and rock/ AMD ratio is observed. The highest pH value was obtained with a 1/5 ratio. It is noted that with a 1/10 ratio, total removal of Fe, Al and Cu is achieved at a pH value of 4.97 (F1-10). Cd and Zn concentration decreases from pH values above 6.55 (F2-5), achieving at this value an 18% removal for Cd and 20% for Zn. In contrast, Mn remains practically at the same level, because this element requires pH values above 8 to precipitate (Luan, et al., 2012; Silva, et al., 2012.). Si removal is also high, between 65 to 76% with a 1/5 ratio.

Table 3 Trace element concentrations in neutralized solutions (second stage)

Sample	pH	EC (mS)	Al	Cd	Cu	Fe	Mn	Si	Zn
			mg/L						
B - 20	2.53	8.21	21	2	2	128	2	23	294
F1 - 20	4.39	7.62	1	2	1	<LD	3	20	295
F2 - 20	3.88	7.49	4	2	1	1	3	23	300
B - 10	2.49	8.02	19	2	2	116	2	21	293
F1 - 10	4.97	7.34	<LD	2	<LD	<LD	2	12	269
F2 - 10	4.73	7.38	<LD	3	0.1	2	4	22	319
B - 5	2.62	7.6	20	2	2	112	2	22	309
F1 - 5	6.57	6.96	<LD	2	<LD	<LD	3	5	217
F2 - 5	6.55	6.81	<LD	2	<LD	<LD	3	8	247

LD (mg/L): Al (0.08), Cu (0.12), Fe (0.01)

In the third stage, stirring was done in two steps, the first with phyllite rock and the second with limestone. Sample B corresponds to untreated AMD. Table 4 shows that pH values between 5.0 and 6.67 were reached with phyllite rock in the first step, and between 7.33 and 7.64 were reached in the second step with limestone rock. In the first step, 100% of Al, Cu and Fe was removed; and between 9 and 41% of Cd, 45 and 74% of Si, 2 and 12% of Zn and 0 and 32% of Mn, were removed. In the second step, almost 100 % removal of Cd was achieved, as well as a removal from 82 to 92% of Si, 95 to 99% of Zn and 89 to 97% of Mn.

Table 4 Trace elements concentration in neutralized solutions of 1st and 2nd steps (third stage)

Sample	pH		Al		Cd		Cu		Fe		Mn		Si		Zn	
			mg/L													
	1a	2a	1a	2a	1a	2a	1a	2a	1a	2a	1a	2a	1a	2a	1a	2a
B	2.74	2.82	19	18	2	2	2	2	112	102	23	22	24	23	320	309
F1	6.64	7.26	<LD	<LD	1.3	0.1	<LD	<LD	<LD	<LD	16	2	6	2	205	14
F2	5.00	7.33	<LD	<LD	<LD	<LD	<LD	<LD	<LD	<LD	20	1	10	2	259	1
F2-d	6.67	7.64	<LD	<LD	2	<LD	<LD	<LD	<LD	<LD	26	2	13	3	311	2

LD (mg/L): Al (0.08), Cd 80.02), Cu (0.12), Fe (0.01), Mn (0.007), Si (0.008) y Zn (0.007)

Concentration of Al, Fe, Zn and Mn in the phyllite rock, determined by XRF, were of 7.28%, 2.95%, 0.02% and 0.05%, respectively; in the after neutralization phyllite sediment photomicrographs (Figure 7 – A), it is observed an increase in the concentration of Fe (40.5%) and Zn (2.7%). The limestone rock has in its composition 3.69% of Al, 2.09% of Fe, 0.01% of Zn and 0.14% of Mn; the after neutralization limestone sediment photomicrographs (Figure 7 – B), also show an increase on Fe (2.5%), Zn (16.8%) and Mn (1.1%) concentrations. These results indicate that Fe, Zn and Mn are been retained in the rock's sediments after the neutralization of AMD.

At this stage it was determined that it is appropriate to use phyllite rock to increase pH to values between 5 and 6, and precipitate Al, Cu and Fe; then use limestone to raise pH above 7 and remove the largest portion of Cd, Mn and Zn.

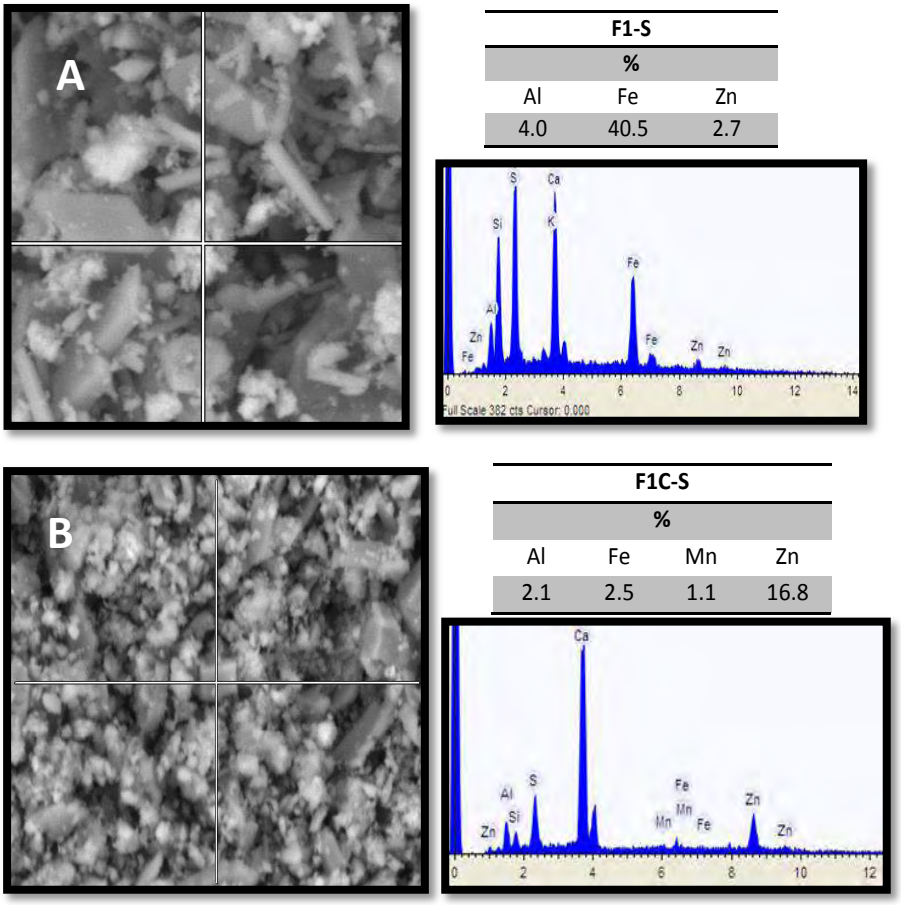

Figure 7 Photomicrographs obtained by SEM-EDS of phyllite (A) and limestone (B) sediments after neutralization.

CONCLUSIONS

The AMD inside the mine is generated in the old mining works, close to the surface level, due to the contact of exposed sulphide minerals with the water of a shallow aquifer and the rainwater flowing through fractured rock. It is possible to lead AMD through canals to the principal works of the mine for a subsequent treatment. The phyllite rock associated with the ore deposit is useful in neutralizing the AMD due to its high content of calcite. Laboratory tests results show that it is possible to achieve pH values between 6 and 7 with phyllite rock. The phyllite allows removal of 100% of Al, Fe and Cu at pH values between 5 and 6. Using limestone, available on an outcrop near the mine, it is possible to raise pH above 7 achieving removal of 100% of Cd, 95% of Zn and 89% of Mn. It is advisable to continue the tests with rock packed cells and then design a system that can be scaled to install it inside the mine.

ACKNOWLEDGEMENTS

This research is conducted with the assistance of the Support Program to Projects of Research and Innovation (PAPIIT IN 114113) from the National Autonomous University of Mexico (UNAM). We thank "Minera Tizapa, SA de CV" for the facilities provided to carry out this work.

REFERENCES

Alcolea A., Vázquez M., Caparrós A., Ibarra I., García C., Linares R., Rodríguez R. (2012). Heavy metal removal of intermittent acid mine drainage with an open limestone channel. Minerals Engineering. 26. 86-98.

Alfonso P., Torró L., Canet C., Parcerisa D., García-Vallés M., Mata-Perelló J., Mesa C., González-Partida E. (2011). Mineralorgía del yacimiento VMS de Zn-Cu-Pb-Ag-Au de Tizapa, México. Macla. 15. 27-28.

Conagua. (2008). Determinación de la disponibilidad de agua en el acuífero 1509 Temascaltepec, Estado de México. Comisión Nacional del Agua. México, D.F.

Coremi. (1996). Monografía geológico-minera del Estado de México. Consejo de Recursos Minerales. Secretaría de Comercio y Fomento Industrial. México. 148 p.

Johnson DB, Hallberg KB. (2005). Acid mine drainage remediation options: a review. Sci Total Environ 338:3–14.

López P. E., Aduvire O. y Barettino D. (2002). Tratamientos pasivos de drenajes ácidos de mina: estado actual y perspectivas de futuro. Boletín Geológico y Minero, 113 (1): 3-21.

Lottermoser B. (2007). Mine Wastes. Characterization, Treatment and Environmental Impacts. Second ed. Springer, USA.

Luan, F., Santelli, C. M., Hansel, C. M. & Burgos, W. D. (2012). Defining manganese (II) removal processes in passive coal mine drainage treatment systems through laboratory incubation experiments. Applied Geochemistry, Volumen 27, pp. 1567-1578.

Macías F., Caraballo A. M., Nieto J. M., Rötting S. T., Ayora C. (2012). Natural pretreatment and passive remediation of highly polluted acid mine drainage. Journal of Environmental Management. 104. 93-100

Romero, F., Armienta, M. & Gonzalez-Hernandez, G. (2007). Solid-phase control on the mobility of potentially toxic elements in an abandoned lead/zinc mine tailings impoundment, Taxco, Mexico. Applied Geochemistry, Issue 22, pp. 109-127.

Semarnat. (2002). NORMA Oficial Mexicana NOM-011-CNA-2000, conservación del recurso agua - Que establece las especificaciones y el método para determinar la disponibilidad media anual de las aguas nacionales. Secretaría de Medio Ambiente y Recursos Naturales. Diario Oficial de la Federación, 17 de abril de 2002.

Silva, A. M., Cunha, E. C., Silva, F. D. & Leao, V. A. (2012). Treatment of high-manganese mine water with limestone and sodium carbonate. Journal of Cleaner Production, 29(30), pp. 11-19.

Younger P.L., Banwart S.A., Hedin R.S. (2002). Mine water hidrology, pollution remediation. Kluwer Academic Publishers. Great Britain. 442 pp.

Wolkersdorfer Ch. (2008). Water management at abandoned flooded underground mines. Springer. Germany. 464 pp.

10th ICARD IMWA 2015 | 10th International Conference on Acid Rock Drainage & IMWA Annual Conference

Evaluation of Nanofiltration and Reverse Osmosis in the Treatment of Gold Acid Mine Drainage

Alice Aguiar, Laura Andrade, Wadson Pires and Miriam Amaral
Department of Sanitary and Environmental Engineering, Universidade Federal de Minas Gerais, Brazil

ABSTRACT

With the rising restrictive discharge standards, the reuse of effluents such as acid mine drainage (AMD) has become a viable option both environmental and economically. Membrane separation processes especially nanofiltration (NF) and reverse osmosis (RO) produces a permeate with high quality, which can usually be reused in the process. Therefore, the purpose of this study was to compare nanofiltration and reverse osmosis treating an acid mine drainage effluent from Minas Gerais, Brazil. Initially, a pretreatment study was conducted to compare the performance of the NF when operating with raw effluent and two pre-filtered effluents: one with qualitative filter and another using microfiltration. The performance was evaluated in terms of fouling and effluent quality (ions concentration, total solids and conductivity). The results showed that the type of pretreatment does not considerably affect membrane fouling, and effluent average flow was between 73 and 86% of the flow with water. The retention efficiency of major contaminants was very high: greater than 79% for solids, 98% for conductivity and 99% for sulphate. Moreover the pretreatment improved effluent quality in all aspects analyzed. Secondly, a comparative study of three membranes of NF and two membranes of RO was conducted. The membranes of NF analyzed were NF90, NF270 and MPS-34. The membranes of RO analyzed were TFC-HR and BW30. All five membranes showed high pollutants retention (sulphate >99% and conductivity >84%). The pollutants retention efficiencies of nanofiltration membrane (NF 270) were comparable to the retention efficiencies of the RO membranes; yet it was associated with the highest permeate flux (10 and 88 L/h.m² for RO and NF membrane respectively).

Keywords: Gold acid mine drainage; Nanofiltration; Reverse osmosis

INTRODUCTION

Gold is a substance of extreme important as monetary reserve and much of what was produced throughout history is now stored on national central banks or National Treasury of many countries. Its importance is also associated with the production of jewelry and its use in the electronic industry as well as its demand for dental and medical purposes (GFMS, 2014). Nevertheless, despite the clear economic benefits, exploitation and processing of gold are associated with various environmental impacts. Acid mine drainage (AMD) is one of the main environmental impacts related to gold mining, due to the difficulty of AMD control once initiated, the high volumes involved and associated treatment costs, and its perpetuity.

Mining effluents are usually treated by neutralization, precipitation and sedimentation (Langsch et al., 2012), although other technologies such as anaerobic bioreactors (Wildeman et al., 2006), sorption (Acheampong & Lens, 2014), coagulation and flocculation (Oncel et al., 2013), and crystallization (Fernández-Torres et al., 2012) may also be used. However, these methods may be insufficient to adjust the effluent properties to meet the discharge and/or reuse standards, require high consumption of chemical products, and may generate large sludge volumes (Wang et al., 2007).

Membrane separation processes (MSP) are promising technologies for treating acid mine drainage (AMD). According to Habert et al. (2006), MSP are technologies that use a selective barrier (membrane) that under a driving force can promote the separation of the components of a solution or suspension. Membrane separation process has significantly developed over the past few years, since it has unique characteristics compared to conventional separation processes. Some example of MSP characteristics are that they do not need phase transition to perform components separation (as in distillation), thus contributing to energy savings; do not require the addition of chemicals (as in liquid-liquid extraction); have high selectivity; can be easily scaled since they are modular; do not require extensive workforce, etc.

Among the MSP, nanofiltration (NF) and reverse osmosis (RO) stand out. These process are effective technologies to remove salts and metals from aqueous medium (Al-Rashdi et al., 2013) presenting high potential to treat mining effluents for reuse.

NF process is an intermediate process between RO and ultrafiltration (UF) that may retain dissolved molecules with molecular weight ranging between 200 and 1.000 g/mol and multivalent ions (Yu et al., 2010). Many works have shown that NF is an efficient system for secondary or tertiary treatment of effluents intended to supply water for industrial, agricultural and/or indirect reuse as drinkable water (Acero et al., 2010). The use of NF has been increasing due to advantages such as the ease of operation, reliability, low power consumption and high efficiency (Fu & Wang, 2011).

RO systems use membranes that are permeable to water, but substantially impermeable to salts, and therefore are suited to separate ions, dissolved metals and organic molecules of low molar mass (Baker, 2004). One of the main applications of RO membranes is seawater desalination, which accounts for more than 20% of all desalinated water supplied around the world (Fu & Wang, 2011). Moreover, RO membranes have become a promising technology for industrial effluents reclamation (Qi et al., 2011; Kurt et al., 2012).

Sierra et al., 2013 studied nanofiltration process for treating an acid mine drainage from an abandoned mercury mine. It was able to remove up to 99% of aluminum, iron and arsenic content,

and 97% of sulfate content. Chan & Dudeney, 2008 evaluated the treatment of wastewater from gold ore bioleaching treated by neutralization, precipitation and sedimentation followed by a post-treatment with GE Osmonics TFM-100 RO membrane. It was found that more than 90% of the arsenic that had not been removed by the first treatment was retained by the membrane. Another study evaluated NF and RO membrane performance to treat two synthetic acid mine drainage, including one with higher metal content (Al-Zoubi et al., 2010). It was found that NF membrane was more suited for such use as it handled higher permeate flux at lower power consumption, although its rejections were smaller than in RO membrane treatment.

Despite the successful cases using different membranes for treating mining plant effluents, there remains the need for further examination of the most appropriate system types, that is, NF or RO, membrane selection and operating conditions such as type of pre-treatment for each specific application. Such assessment would be targeted to find ways to increase retention efficiencies, decrease membrane fouling formation, reduce costs, and optimize the whole system.

Therefore, the aim of this study was to evaluate the use of MSP in the treatment of gold AMD. Initially, a study of pretreatment requirement was conducted. It compared the performance of the NF when operating with raw effluent, an effluent pre-filtered with qualitative paper filter (Fmaia - 8μm) and an effluent pre-filtered using microfiltration. After defining the appropriate pretreatment, the operation of two RO and three NF membranes was compared and the best membranes for the system studied were selected.

METHODOLOGY

Acid mine drainage

Acid mine drainage was collected in a gold mining company in the state of Minas Gerais, Brazil which has two underground gold mines and an industrial processing plant. AMD was collected in the underground mine, on the fourth level below ground. AMD characteristics vary throughout the year; the main characteristics of the AMD used in this study are presented on Table 1.

Table 1 AMD main characteristics

AMD	pH	Conductivity (μS/cm²)	Total solids (mg/L)	Sulfate (mg/L)	Chloride (mg/L)	Calcium (mg/L)	Magnesium (mg/L)
First collection	3.35	2,841	2,409	985	4.5	323	97
Second collection	2.74	2,744	2,926	1,406	1.6	282	125

Unit description

For the nanofiltration and reverse osmosis filtration tests a bench scale unit was used. The system is comprised of: one supply tank (ST); one pump; one valve for pressure adjustment; one rotameter; one manometer; one thermometer and one stainless steel membrane cell. Figure 1 shows a schematic of this unit.

The stainless steel membrane cell has 9.8 cm in diameter, providing a filtration area of 75 cm². The membranes tested were properly cut before being placed in the cell. A feed spacer was placed over the membrane to promote flow distribution. Permeate flow was measured by collecting the volume

of permeate in a measuring cylinder over 60 seconds for nanofiltration tests and 180 seconds for reverse osmosis tests. Permeate was collected for analysis and retentate was returned to the supply tank.

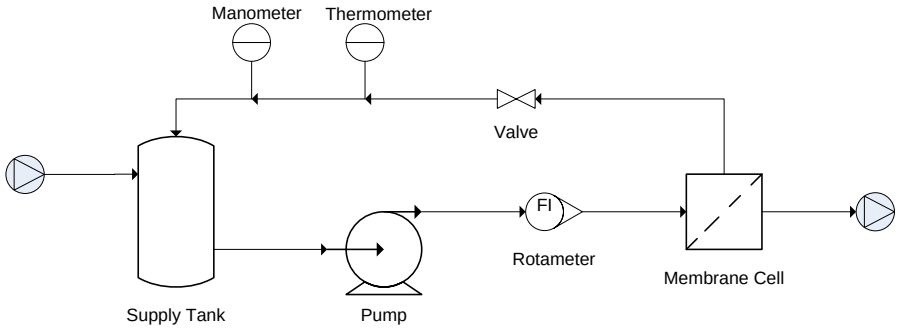

Figure 1 Schematic of NF and RO unit

Pretreatment study

Initially, a pretreatment study was conducted to compare the performance of the nanofiltration when operating with raw effluent and two pre-filtered effluents: one with qualitative filter paper (Fmaia - 8μm) and another using microfiltration. Microfiltration (MF) was performed using a submerged membrane module provided by Pam Membranas Seletivas Ltda., with filtration area of 0.04 m^2, average pore diameter of 0.4 μm and polyetherimide-based polymer. MF occurred at a pressure of 0.7 bar up to a recovery rate of 60%.

The nanofiltration tests were carried out with AMD from the first collection and used the NF90 membrane provided by the supplier Dow Filmtec. Initially, the membrane was washed in ultrasound bath first with citric acid solution at pH 2.5 followed by 0.1% NaOH solution for 20 minutes each. Water permeability at 25°C (K) was obtained by monitoring the normalized value of the stabilized permeate flux of clean water at pressures of 10.0; 8.0; 6.0 and 4.0 bar. Normalization to 25°C was accomplished by means of a correction factor calculated by the ratio of the water viscosity at 25°C and the water viscosity at the temperature of permeation:

$$K = \frac{J \cdot \mu(T)}{\Delta P \cdot \mu(25^{\circ}C)} \quad (1)$$

Where J is the permeate flux in $m^3/h.m^2$, μ is the permeate viscosity (water) in $N.s/m^2$ and ΔP is the system pressure in Pa. With the normalized water permeability, the intrinsic membrane resistance to filtration (R_m) was calculated:

$$R_m = \frac{1}{K \cdot \mu(25^{\circ}C)} \quad (2)$$

The nanofiltration of the acid mine drainage was carried out for two hours at fixed pressure of 10 bar, feed flow rate of 2.4 LPM and temperatures ranging between 25 and 35°C. Permeate flux and temperature were measured each 15 minutes. Final accumulated permeate was collected for analysis. Retentate was returned to the supply tank. The fouling resistance to filtration (R_f) was determined with the values of permeate flux and temperature obtained at the end of the experiment, as demonstrated by the equation:

$$R_f = \frac{\Delta P - \Delta \pi}{\mu(T) \cdot J} - R_m \quad (3)$$

Where (ΔP- Δπ) is the effective pressure of the system in Pa and Δπ is the osmotic pressure difference between the retentate and the permeate in Pa. The Δπ was calculated using the software ROSA 9.1 (The Dow Chemical Company, USA). The initial concentration of the main ions in solution inserted in the software were: 2,000 mg/L of sulfate, 10 mg/L of chloride, 150 mg/L of magnesium and 593 mg/L of calcium. These ions concentrations were typical values obtained for the AMD.

Feed and permeates were analyzed for conductivity (Hanna conductivity meter HI 9835), total solids and ions concentrations (Metrohm 850 Professional IC, Herisau, Switzerland, equipped with column type Metrosep C4-100/4.0 and Metrosep A Supp 5-150/4.0), in accordance with the Standard Methods for the Examination of Water and Wastewater (APPA 2005).

Evaluation of different NF and RO membranes

A comparative study of three nanofiltration (NF) membranes and two reverse osmosis (RO) membranes on the treatment of AMD was conducted. The NF membranes analyzed were NF90, NF270 and MPS-34. The RO membranes analyzed were TFC-HR and BW30. Table 2 shows the main characteristics of these membranes as provided by the suppliers, unless otherwise specified.

Table 2 Membranes characteristics as provided by the suppliers

Characteristic	TFC-HR	BW30	MPS34	NF90	NF270
Supplier	Koch Membranes	Dow Filmtec	Koch Membranes	Dow Filmtec	Dow Filmtec
Membrane Material	Composite Polyamide	Composite Polyamide	Composite	Composite Polyamide	Composite Polyamide
NaCl Retention	99.55% [a]	99.5% [b]	35% [c]	85-95% [b]	n.a.
$MgSO_4$ Retention	n.a.	n.a.	n.a.	>97% [d]	97% [d]
Molecular weight cutoff (Da)	100 [e]	n.a.	200 [f]	100 [g]	200-300 [f]

n.a. Not available

[a] Feed solution containing 2,000 mg/L of NaCl, filtration at 15.5 bar, 25°C, and recovery rate of 15%.

[b] Feed solution containing 2,000 mg/L of NaCl, filtration at 4.8 bar, 25°C, and recovery rate of 15%.

[c] Feed solution containing 50,000 mg/L of NaCl.

[d] Feed solution containing 2,000 mg/L of $MgSO_4$, filtration at 4.8 bar, 25°C, and recovery rate of 15%.

[e] Reference: (Xu et al., 2005)

[f] Reference: (Wang & Tang, 2011)

[g] Reference: (Zulaikha et al., 2014)

Membrane evaluation procedure was similar to the pretreatment study procedure. First the AMD was filtered using the MF submerged membrane module provided by Pam Membranas Seletivas

Ltda., at a pressure of 0.7 bar and up to a recovery rate of 60%. All five membranes were then washed in ultrasound bath first with citric acid solution at pH 2.5 followed by 0.1% NaOH solution for 20 minutes each.

AMD nanofiltration was carried out up to a recovery rate of 10% (defined as permeate volume by initial effluent volume) at 10 bar pressure, 2.4 LPM feed flow rate and temperatures ranging between 25 and 35°C. Permeate flux, temperature and permeate accumulated volume were measured from time to time and final accumulated permeate was collected for analysis. Retentate was returned to the supply tank.

Feed and permeates were analyzed for conductivity (Hanna conductivity meter HI 9835), total solids and ions concentrations (Metrohm 850 Professional IC, Herisau, Switzerland, equipped with column type Metrosep C4-100/4.0 and Metrosep A Supp 5-150/4.0), in accordance with the Standard Methods for the Examination of Water and Wastewater (APPA 2005).

RESULTS AND DISCUSSION

Pretreatment study

The initial osmotic pressure of the acid mine drainage calculated using the software ROSA 9.1 (The Dow Chemical Company, USA) was 0.75 bar.

The NF90 membrane water permeability (K), membrane resistance to filtration (R_m) and fouling resistance (R_f) obtained according to Equation 1, 2 and 3 respectively are presented on Table 3. The variations on water permeability are usual and often occur due to minute variations on membrane characteristics or the effectiveness of the membrane cleaning.

Table 3 Water permeability, membrane resistance, fouling resistance and average ratio of effluent flux by clean water flux of the NF90 for each of the pretreatment studied

	Water permeability ($m^3/s.m^2.Pa$)	Membrane resistance (m^{-1})	Final fouling resistance (m^{-1})	Effluent flux by water flux (%)
Raw effluent	9.6×10^{-12}	$1.2 \times 10^{+14}$	$3.6 \times 10^{+13}$	86.3
Qualitative filter	1.7×10^{-11}	$6.6 \times 10^{+13}$	$3.9 \times 10^{+13}$	73.6
Microfiltration	1.1×10^{-11}	$1.1 \times 10^{+14}$	$4.3 \times 10^{+13}$	78.5

To minimize the influences that variations on water permeability could have on the comparison of the effluent permeate fluxes, it is usual to express the ratio of the effluent flux by the water flux. The average ratios obtained are shown on Table 3. The average permeate flux of the microfiltered effluent was 26.4 $L/h.m^2$. Sierra et al., 2013 obtained with the NF2540 membrane a permeate flux of approximately 45 $L/h.m^2$ for mercury AMD at an effective pressure of 10 bar and feed flow rate of 1,000 LPM. Besides the difference in the applied membrane characteristics, the increase in feed flow rate increases the shearing forces and decreases membrane fouling which could explain the difference in permeate flux.

Moreover the small variations on fouling resistance indicate that the AMD do not cause severe fouling during nanofiltration. This is corroborated by the low initial concentrations of fouling components such as suspended solids and organic matter in the feed solution. One might think

then that it is best to use directly the raw effluent. However, it is important to consider that the presence of small quantities of fouling components (such as suspended solids and organic matter) can directly increase the frequency of cleaning and maintenance and therefore reduce membrane lifespan. Moreover, an industrial effluent such as AMD varies greatly throughout the year, which could cause an increase in fouling components and consequently damage the system.

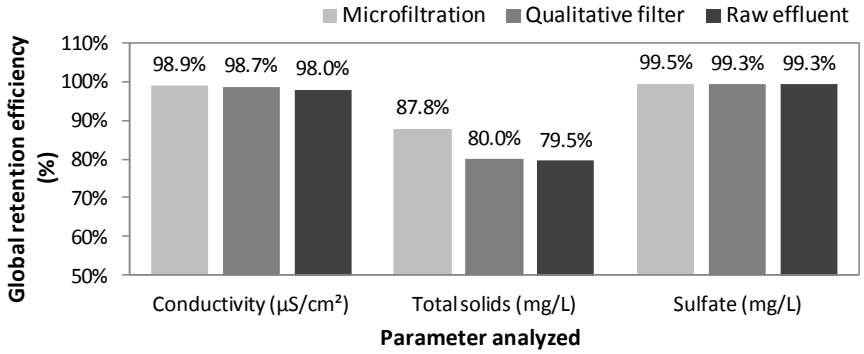

Figure 2 shows the global retention efficiencies of the main pollutants on the accumulated NF permeate for each pretreatment studied. These efficiencies comprised both the pretreatment efficiency as well as the NF efficiency and were called global retention efficiencies. All retention efficiencies obtained were very high, nevertheless it is observed that the stronger the pretreatment used, the better the final permeate quality. For instance, the total solids concentration on permeate with raw effluent was 495 mg/L, while the concentration with microfiltration was 293 mg/L, 41% smaller. The retention efficiencies for the microfiltered effluent were 98.9% for conductivity, 87.8% for total solids and 99.5% for sulfate.

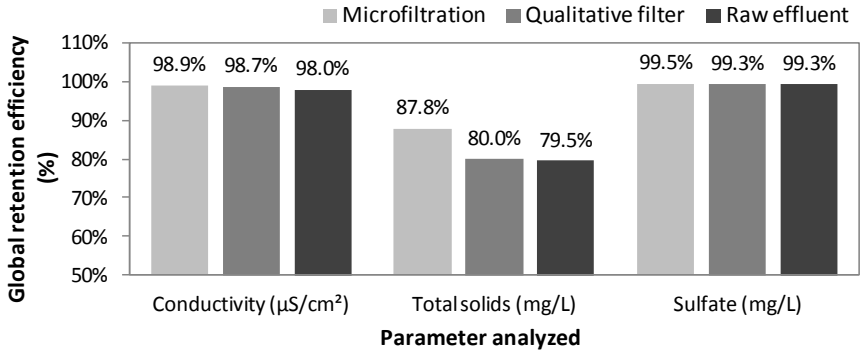

Figure 2 Pollutants retention efficiency for the three pretreatments studied

As the main objective of this treatment system is to obtain a permeate with quality appropriate for reuse as process water, the retention of sulfate and calcium must be optimized as these ions can precipitate in pipes and equipments, damaging systems. The increase in retention efficiency of sulfate corroborates that the use of microfiltration before the nanofiltration is ideal for the treatment system.

Evaluation of different NF and RO membranes

The normalized permeate fluxes for each of the five membranes as a function of effluent recovery rate is presented on Figure 3. The RO membranes (THF-HC and BW30) showed the lowest permeate flux during the filtration (the average permeate fluxes were 10.2 and 10.0 L/h.m² for THF-HC and BW30 respectively). These results are compatible with the structure of these membranes. RO membranes have a more closed polymeric structure, which increases membrane resistance and decreases permeate flux (Tu Nghiem et al., 2011). Among the NF membranes, the NF270 showed the highest permeate flux with average permeate flux of 88.6 L/h.m².

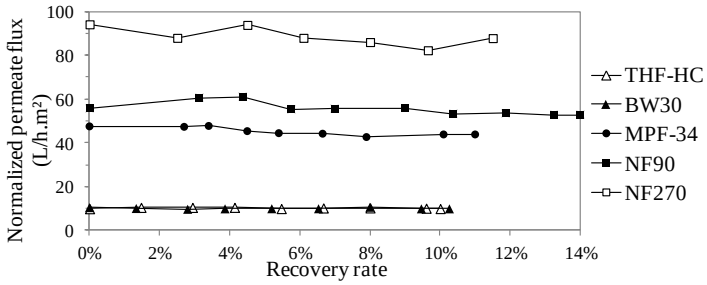

Figure 3 Normalized permeate fluxes of the five membranes as a function of effluent recovery rate

Table 4 shows the main pollutants final concentration of the accumulated permeates obtained for the five membranes tested. The final concentration of the permeate of the THF-HC membrane were the lowest for all parameters analyzed. This RO membrane is typically used on effluent treatment and water reuse due to its high efficiency (Fujioka et al., 2012). The BW30 membrane however showed higher permeate final concentration than the NF membranes studied. On the other hand pollutants concentrations of the NF membranes were only slightly higher than those of the THF-HC membrane. Permeate total solids may include other ions present in the AMD, especially monovalent ions which have smaller retention efficiencies.

Table 4 Pollutants final concentration on the permeate for the five membranes studied

	THF-HC	BW30	MPS-34	NF90	NF270
Conductivity (µS/cm²)	78	517	442	170	379
Total solids (mg/L)	38	849	295	146	207
Sulfate (mg/L)	2.2	9.7	4.1	4.5	2.6
Calcium (mg/L)	< 2.5	< 2.5	10.3	3.1	8.8

In the selection of the best membrane for a given application it should be considered the membrane area required since the cost of the NF or RO system directly depends on it. Given the low fluxes obtained for the THF-HC and BW30 membranes, its use on the treatment of gold AMD proved to be cost-prohibitive. Moreover, the pollutants retentions of the three NF membranes were similar to those of the THF-HC membrane, besides allowing for a much higher permeate flux. As a result, the NF membranes were selected over the RO membranes for this application, and among the NF membranes the NF270 was chosen as the membrane with the highest potential.

CONCLUSION

The pretreatment study showed that AMD filtration did not considerably affect initial membrane fouling resistance, indicating that the AMD initially does not cause severe fouling during nanofiltration. The average ratio of permeate flux by water flux were 86.3%, 73.6% and 78.5% for the raw effluent, the effluent filtered with qualitative filter and the microfiltered effluent respectively. On the other hand, the pretreatment of the AMD improved permeate quality in all aspects analyzed. The retention efficiencies of the microfiltered effluent were 87.8% for total solids, 98.9% for conductivity and 99.5% for sulfate.

Additionally, the five membranes studied showed high pollutants retention and the RO membrane THF-HC showed the highest pollutants retention among then. However, the NF membranes had a pollutant retention similar to the THF-HC retention associated with higher permeate fluxes. The NF270 membrane showed the highest permeate flux (88 L/h.m^2) and was chosen as the most indicated for this application.

ACKNOWLEDGEMENTS

The authors would like to thank the Coordination of Improvement of Higher Education Personnel (CAPES) and National Council for Scientific and Technological Development (CNPq) for the postgraduate scholarships provided.

NOMENCLATURE

K	water permeability at 25°C (m^3/h.m^2.Pa)
J	permeate flux (m^3/h.m^2)
μ	permeate viscosity (water) (N.s/m^2)
ΔP	system pressure (Pa)
$\Delta\pi$	osmotic pressure (Pa)
R	resistance to filtration (m^{-1})

REFERENCES

Acero, J. L., Benitez, F. J., Leal, A. I., Real, F. J., & Teva, F. (2010) Membrane filtration technologies applied to municipal secondary effluents for potential reuse. *Journal of hazardous materials*, v. 177, pp. 390-398.

Acheampong, M. A., & Lens, P. N. (2014) Treatment of gold mining effluent in pilot fixed bed sorption system. *Hydrometallurgy*, v. 141, pp. 1-7.

Al-Rashdi, B. A. M., Johnson, D. J., & Hilal, N. (2013) Removal of heavy metal ions by nanofiltration. *Desalination*, v. 315, pp. 2-17.

Al-Zoubi, H., Rieger, A., Steinberger, P., Pelz, W., Haseneder, R., & Härtel, G. (2010) Optimization study for treatment of acid mine drainage using membrane technology. *Separation Science and Technology*, v. 45, pp. 2004-2016.

APPA, A. (2005). WEF (2005) Standard methods for the examination of water and wastewater, *American Public Health Association*, Washington DC.

Baker, R. W. (2004) *Membrane technology and applications*. England: John Wiley and Sons.

Chan, B. K. C., & Dudeney, A. W. L. (2008) Reverse osmosis removal of arsenic residues from bioleaching of refractory gold concentrates. *Minerals Engineering*, v. 21, pp. 272-278.

Fernández-Torres, M. J. ; et al. (2012) A comparative life cycle assessment of eutectic freeze crystallisation and evaporative crystallisation for the treatment of saline wastewater. *Desalination*, v. 306, pp. 17-23.

Fu, F., & Wang, Q. (2011) Removal of heavy metal ions from wastewaters: a review. *Journal of Environmental Management*, v. 92, pp. 407-418.

Fujioka, T.; et al. (2012) Effects of feed solution characteristics on the rejection of N-nitrosamines by reverse osmosis membranes. *Journal of Membrane Science*, v. 409, pp. 66-74.

GFMS. *GFMS Gold Survey*. Thomson Reuters. London (UK). 2014

Habert, A.C.; Borges, C.P.; Nobrega, R. (2006) Escola Piloto em Engenharia Química: Processos de separação com membranas. Programa de Engenharia Química, COPPE/UFRJ, Rio de Janeiro, RJ, Brasil.

Kurt, E., Koseoglu-Imer, D. Y., Dizge, N., Chellam, S., & Koyuncu, I. (2012) Pilot-scale evaluation of nanofiltration and reverse osmosis for process reuse of segregated textile dyewash wastewater. *Desalination*, v. 302, pp. 24-32.

Langsch, J. E.; et al. (2012) New Technology for Arsenic Removal from Mining Effluents. *Journal of Materials Research and Technology*, v. 1, pp. 178-181.

Oncel, M. S., Muhcu, A., Demirbas, E., & Kobya, M. (2013) A comparative study of chemical precipitation and electrocoagulation for treatment of coal acid drainage wastewater. *Journal of Environmental Chemical Engineering*, v. 1, pp. 989-995.

Qi, L., Wang, X., & Xu, Q. (2011) Coupling of biological methods with membrane filtration using ozone as pre-treatment for water reuse. *Desalination*, v. 270, pp. 264-268.

ROSA 9.1 System Design Software, The Dow Chemical Company, USA. Available at http://www.dowwaterandprocess.com/en/resources/rosa_system_design_software. Accessed on: 01/07/2014.

Sierra, C., Saiz, J. R. Á., & Gallego, J. L. R. (2013) Nanofiltration of Acid Mine Drainage in an Abandoned Mercury Mining Area. *Water, Air, & Soil Pollution*, v. 224, pp. 1-12.

Tu, K. L., Nghiem, L. D., & Chivas, A. R. (2011) Coupling effects of feed solution pH and ionic strength on the rejection of boron by NF/RO membranes. *Chemical Engineering Journal*, v. 168, pp. 700-706.

Wang, Y. N., & Tang, C. Y. (2011) Protein fouling of nanofiltration, reverse osmosis, and ultrafiltration membranes—the role of hydrodynamic conditions, solution chemistry, and membrane properties. *Journal of Membrane Science*, v. 376, pp. 275-282.

Wang, Z., Liu, G., Fan, Z., Yang, X., Wang, J., & Wang, S. (2007) Experimental study on treatment of electroplating wastewater by nanofiltration. *Journal of Membrane Science*, v. 305, pp. 185-195.

Wildeman, T., A. Pinto, et al. (2006) Passive treatment of a cyanide and arsenic laden process water at the RPM Gold Mine, Minas Gerais, Brazil. *Proceedings, 7th International Conference on Acid Rock Drainage*, 26Á30 March.

Xu, P., J. E. Drewes, et al. (2005) Rejection of emerging organic micropollutants in nanofiltration-reverse osmosis membrane applications. *Water Environment Research*, pp. 40-48.

Yu, S., M. Liu, et al. (2010) Impacts of membrane properties on reactive dye removal from dye/salt mixtures by asymmetric cellulose acetate and composite polyamide nanofiltration membranes. *Journal of Membrane Science*, v. 350, pp. 83-91.

Zulaikha, S., W. Lau, et al. (2014) Treatment of restaurant wastewater using ultrafiltration and nanofiltration membranes. *Journal of Water Process Engineering*.

Sorption/Oxidation of Manganese in Aqueous System

Fernanda Camargo, Henrique de Leucas and Ana Cláudia Ladeira
Center for the Development of Nuclear Technology, Brazil

ABSTRACT

Manganese is considered one of the main contaminants of effluents from the mineral industry in Brazil. In some regions, mainly the ones with generation of acid mine drainage; the manganese concentrations in the acid effluent reach values up to 150 mg/L. However, the Brazilian Standard Limit for effluent discharging is 1.0 mg/L and the pH must be at 5 to 9. This study aims to evaluate the reduction of high levels of manganese contained in synthetic solutions simulating an acid effluent (about 150 mg/L) to the level required by the legislation. The manganese removal experiments were carried out by the adsorption of soluble Mn (II) in the presence of a solid substrate; manganese dioxide (MnO_2), which is a residue from the zinc electro winning process. The pH of the experiments was around 7, adjusted with NaOH or lime at room temperature (25 °C). The addition of NaClO and $KMnO_4$, during the experiments, was employed with the purpose of continuous activation of the surface sites of the substrate MnO_2. Batch experiments showed no difference between the levels NaClO added. The greatest Mn uptake was around 80 % and occurred when the initial pH solution was adjusted with lime. For the column experiments filled with solid MnO_2 and the residence time of 3.3 h, the manganese levels remained as low as 1 mg/L up to bed volume (BV) number 60. During the experiment, the pH of the out coming effluent decreased from 9.9 to 7.1. The maximum loading capacity of the solid was 18.6 mg/g. Attempts to regenerate the bed with $KMnO_4$ and NaOCl proved to be not possibly to achieve the total loading capacity of the fresh substrate. The loading capacity after regeneration was 11.6 mg/g and 6.3 mg/g, respectively.

Keywords: Manganese, manganese dioxide, acid mine drainage

INTRODUCTION

Acid mine drainage (AMD) is one of the most serious environmental problems faced by the mining industry in Brazil. The sulphide minerals such as pyrite when exposed to water and oxygen are oxidized producing sulfuric acid. The acidic water promotes the dissolution of metals of the soils which represent an important source of contamination to watercourses (Johnson & Halberg, 2006). In Brazil, Mn (II) has been found in concentrations up to 150 mg/L in acid drainage, as a consequence of high levels of this metal in the soils, while in the other countries the levels are up to 10 mg/L (Aguiar, Duarte & Ladeira, 2013). The standard limit for effluent discharge, according to Resolution CONAMA 430/2011, is 1.0 mg/L. Generally, liming procedure is used to remove dissolved Mn but in the case of high Mn concentration the pH must be above 10, to complete precipitate the metal. This stability of the Mn (II) in a wide range of pH increases the cost of the process and, moreover, the final pH of the effluent does not comply with the legislation which requires a pH at 5.0 to 9.0 for discharge (Aguiar, Duarte & Ladeira, 2013). Many studies have considered the removal of soluble manganese, although in these works the initial Mn levels are much lower than in the present investigation. Removal techniques include physical and chemical treatments such as addition of oxidants (chlorine, potassium permanganate, chlorine dioxide, ozone) to oxidize the Mn (II) to Mn (IV) and precipitating it (Islam et al., 2010), , ion exchange resins (Tafarel & Rubio, 2010), adsorption methods using zeolites, limestone (Silva et al., 2010), (Aziz & Smith, 1996), (Thornton, 1995), pyrolusite and oxides manganese (MnO_x). It is important to stress that MnO_x can be considered as a catalyst for the oxidation of manganese and it can be used either as a solid adsorbent or it can be formed onto the surface of a filter medium when the Mn (II) is oxidized by oxidants, such as permanganate ($KMnO_4$) and chlorine (Cl_2), or even by natural process. The soluble Mn (II) can be sorbed on the MnO_x coated filter media followed by surface oxidation. This removal process has been named as "natural greensand effects". Knocke et al. (1991) studied the kinetics of oxidation of manganese with potassium permanganate and chlorine dioxide and observed that the amount of Mn (II) removed from the system was slightly higher than that predicted by stoichiometry, due the presence of MnO_x. Hue, Cam & Nam (2008) developed a method for removing manganese from ground water using natural MnO_2. The experiments showed that using 10 g of ore, around 99.9 % of the manganese was removed from groundwater. According Knocke & Hargette (2001) the sorption capacity is proportional to the number of available sorption sites and also to the existing form of MnO_x, i.e., highly oxidized MnO_x, has greater removal efficiency. Moroever, they showed at pH 5-7, removal capacity of Mn (II) by MnO_x decreased by 80 % as compared to at pH 8. The present study aims to evaluate the reduction of high levels of Mn (II), around 150 mg/L, to the level required by legislation (1 mg/L) by simulating an acid effluent. Experiments were performed in the presence of a manganese dioxide (MnO_2), a residue from the zinc electrowinning process and two different oxidants were used in order to reactivate the MnO_2 sorption sites.

METHODOLOGY

Liquid samples

Laboratory solutions were prepared by diluting 0.461 g $MnSO_4.H_2O$ (Vectec Brazil) in 1.0 L of deionized water and the pH was adjusted by adding sodium hydroxide (NaOH) or lime. The Mn (II) concentration was determined by atomic absorption spectrophotometry – AAS (VARIAN, model AA240FS).

Solid samples

The MnO_2 was a residue from the zinc electro winning process. The specific surface area was 38.35 m^2/g, determined by Brunauer Emmett Teller (BET) method multiple point technique (Quantachrome Corp., NOVA-2200). MnO_2 content in the residue was around 64 %, determined by Energy Dispersive X-ray - EDX (SHIMADZU model EXD -720). In order to prepare the sample to the column experiments, 5 % of cement was mixed to the residue to obtain pellets with particle size between 1.19 and 1.68 mm.

Batch experiments

Experiments were conducted in glass beakers containing 200 mL of about 150 mg/L of Mn (II) solution, in the presence of 2.000 g MnO_2, under stirring and at room temperature (25 ºC ± 0.5). The pH was adjusted by adding sodium hydroxide or sulphuric acid during the first two hours. Sodium hypochlorite (NaOCl) was added at 12 min of reaction in order reactivate the MnO_x sorption sites. The amount NaOCl used corresponded to 5 %, 15 % and 25 % of the stoichiometry amount. Samples were collected at pre-established time and filtered in 0.45 μm membranes. Sulphuric acid and sodium bissulfite 5% (w/v) was added to the filtrate to avoid late precipitation of Mn.

Column experiments

Column experiments were carried out in a glass column with a 1.9 cm inner diameter and 35 cm of length. The glass columns were packed with a volume of 40.0 mL of MnO_2 pellets and fed with laboratory solution of Mn(II), at pH 7.0, adjusted with lime. After neutralization, the solution was filtered to remove some MnO_x that could have precipitated. The operation was performed at room temperature by downstream flow rate at 0.2 mL/min (residence time of 200 minutes), using a peristaltic pump Master Flex L/S model 7519—20. Liquid samples from the column outflow were collected periodically, by means of Spectra/Chrome Fraction Collector (model CF-1), acidified and analyzed to determine Mn by AAS. In order to reactivate the bed of MnO_2, each fixed bed was washed with oxidizing agent: $KMnO_4$ (4 % w/v) and NaOCl which chlorine content was 96.0 mg/L. After that, the fixed beds were washed with deionized water and then they were fed with a new laboratory solution of Mn(II), under the same experimental conditions.

RESULTS AND DISCUSSION

Influence of NaOCl on Mn removal

According to Knocke & Hargette (2001) the uptake of soluble manganese by sorption onto MnO_x coated filter media and its subsequent reactivation using free chlorine is an effective technique for

continuous removal of Mn (II). In the presence of chlorine, the sorption sites on the oxides surfaces can be regenerate increasing the removal of soluble Mn (II). When no oxidant is added, the uptake of Mn (II) occurs until all available adsorption sites are filled. According to Islam et al. (2010), chlorine is able to regenerate the adsorption sites of the oxide by the oxidation of the Mn (II) to Mn (IV), or Mn (III) to Mn (IV), both previously adsorbed on the oxide surface. Figure 1 shows the concentrations of Mn(II) in solution using MnO_2 and the addition NaOCl. The influence of sodium hypochlorite was assessed by adding different stoichiometric doses of NaOCl after 12 min of reaction with MnO_2 (time corresponding to a local raise in Mn concentration) in an attempt to make the removal more effective. For all the experiments, the curves present similar profile. Manganese removal without the addition of NaOCl was 29.0 mg/L, after two hours. It is observed that for the first eight minutes the kinetic is rapid and manganese concentration drops to values around 60 to 80 mg/L. After 8 minutes, the concentration increases slightly with a maximum at 12 minutes and then falls again until the ending of the experiment. It seems that low doses of NaOCl (0.05 and 0.15) have no effect on the oxidation process; the final concentration is slightly higher in the latter experiments if compared to the one without oxidant. However, there was an improvement on manganese uptake when the dose of NaOCl was equal to 0.25 and the pH initial solution was adjusted with lime, about 80 % manganese was removed. The authors understand that the chlorine in solution in fact oxidizes the soluble Mn(II) favoring the precipitation and that it is not able to regenerate the sites of the solid sorbent.

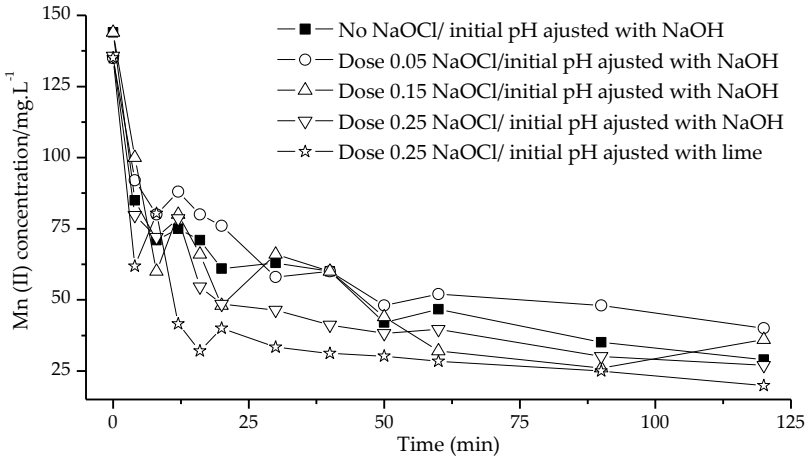

Figure 1 Manganese removal from solution at pH 7.0, T=25 °C , using different doses of NaOCl, 2.000 g of MnO_2, 200 mL of fresh solution

Although the experiment with lime proves to be the most effective in all its extension, the concentration of Mn remained in solution, i.e., 20 mg/L, was above the standard limit for discharging (1 mg/L) leading to a conclusion that the addition of the NaOCl was not effective. One possibility is that the doses of chlorine used were not sufficient to regenerate the adsorption sites of MnO_2, another possibility can be that the oxidation of the adsorbed Mn (II) by chlorine is slow and the reaction time was insufficient for the attainment of the desired value and comply with the legislation. Despite the sodium hypochlorite being not effective, others authors show that it is able to activate and regenerate the sites of MnO_2, making them available for the subsequent adsorption. Another oxidant commonly used for this purpose is $KMnO_4$. The ability of regeneration of this

reagent is reported in studies of Mn removal in fixed beds consisting MnO_2 and in the present study it was evaluated by means of column experiments described below.

Column experiments and regeneration.

Column experiments were carried out in fixed beds of MnO_2 pellets, at pH 7.0. Figure 2 shows the profiles where the Mn (II) concentration in the outflow was plotted versus cumulative bed volume (BV). The solid squares represent the column with fresh MnO_2 that was loaded up to the BV 190. The breakthrough point of the curve, chosen according to the standard limit of 1.0 mg/L, was attained at BV 52. From this point the manganese concentration gradually increased and reaches the feed value of 135 mg/L. This means that the saturation of the column was achieved for the inflow is equal to the outflow.

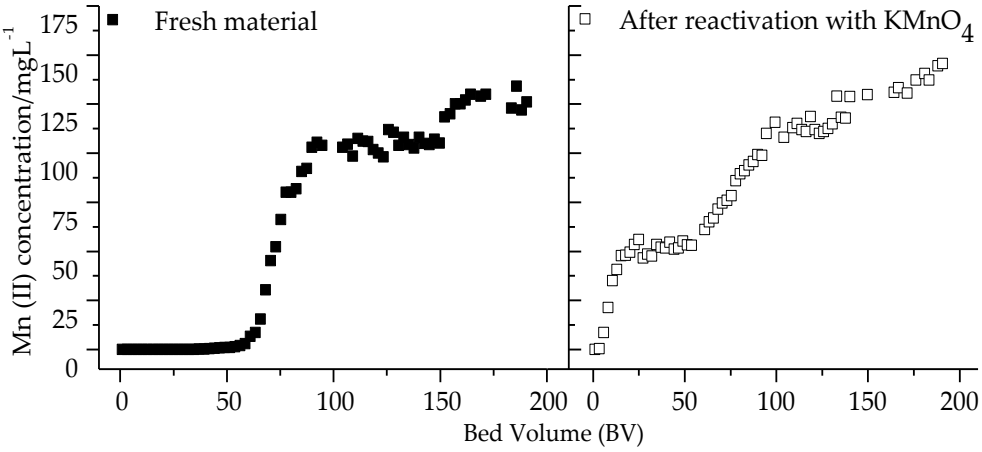

Figure 2 Sorption profiles for Mn removal with 40 mL of MnO_2, $[Mn]_{initial}$ = 140 mg/L, $pH_{initial}$ = 7.0 adjusted with lime; T = 25 °C; flow rate = 0.2 mL/min, reactivation with 4% w/v $KMnO_4$ solution.

The loading capacity of the first column from Figure 2, calculated by integrating the area above each curve, is 13.6 mg/g of MnO_2. The value was lower than the loading capacity obtained by Aguiar, Duarte & Ladeira (2013) 17.9 mg/g of MnO_2 whose initial concentration was 95 mg/L. The pH of the outflow solutions from Figure 2 was 8 in the first initials BVs and then increased slowly and reached the value of 9.5 up to BV 23. The pH enhancement was caused by the alkalinity of the cement; a component used to prepare the MnO_2 pellets. After BV 23, the pH of the outflow dropped and reached 7.1 at the end of the experiment. This pH decrease may indicate the oxidation of the Mn (II) because the oxide formation reactions produced H^+ ions in solution according to the reaction:

$$Mn^{2+} + 1/2O_2 + H_2O \rightleftharpoons MnO_2 + 2H^+ \quad (1)$$

The loading capacity calculated by Hue, Cam & Nam (2008) to manganese removal in underground water using as sorbent a manganese dioxide ore is 12.7 mg/g. This value is close the loading capacity shown previously (13.6 mg/g). Subsequently, it was washed with a solution of 4 %(w/v) $KMnO_4$ and then the experiment was run again under the same conditions of first loading. The

second curve from Figure 2 (open circle) shows the loading of Mn after regeneration of the fixed bed. It is observed that the bed was reactivated, however, the loading capacity (11.6 mg/g) is 15 % lower than the one determined for the fresh material. Despite the fixed bed had been reactivated, the breakthroug point was reached quickly at 4 BV, therefore the standard limit established by legislation (1.0 mg/L) was exceeded at the initial of the loading. The profile of manganese uptake after regenerations was not favorable.

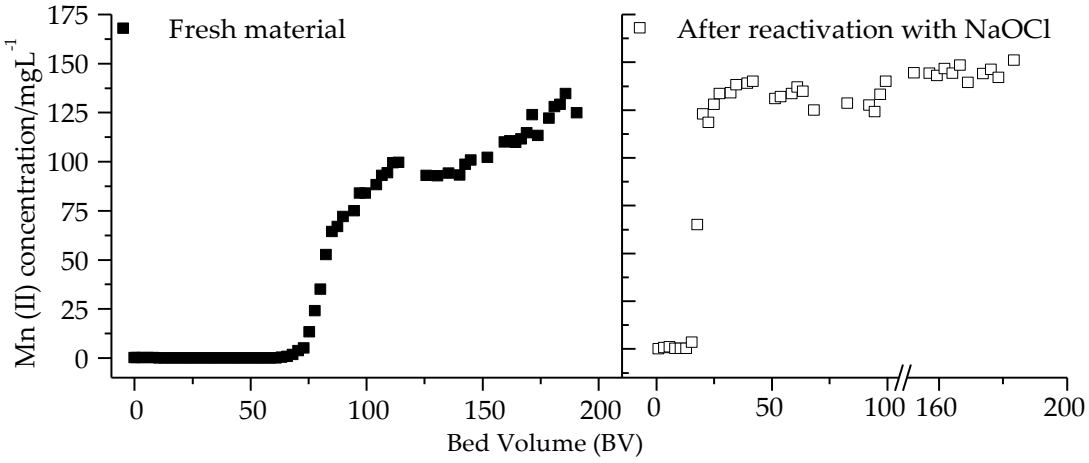

Figure 3 Mn removal with MnO_2, $[Mn]_{initial}$ = 150 mg/L, $pH_{initial}$ = 7.0 adjusted with lime; BV of 40 mL, T = 25 °C; flow rate = 0.2 mL/min, reactivated with NaOCl solution and flow rate 1.3 mL/min

Figure 3 shows the profiles for column filled with MnO_2 where the Mn (II) concentration in the outflow was plotted versus cumulative BV. It shows the loading experiment with fresh material and after regeneration with NaOCl. The experimental conditions were kept the same as in the experiment using $KMnO_4$. The breakthrough point was reached at BV 66, and the loading capacity of the fresh material was 18.4 mg/g of MnO_2; as previously determined. This value is close to the loading capacity obtained by Aguiar, Duarte & Ladeira (2013) 17.9 mg/g. After the reactivation with NaOCl (open circles), the loading capacity was 6.3 mg/g and the standard limit was reached at BV 12. Compared to Figure 2, the loading capacity of the column reactivated with NaOCl is lower than the one reactivated with $KMnO_4$, once the saturation point of the column is achieved at BV 98 in which the manganese concentration in the outflow is 140 mg/L. Despite the reactivation with $KMnO_4$ being more efficient, the discharging limit for both experiments was attained extremely quickly which makes the regeneration unfeasible. Data obtained through XPS spectroscopy (not shown) suggested that the soluble Mn(II) is converted into Mn(IV) during the removal process and the MnO_2 is perhaps the most likely form to be present on the surface of the Mn oxide.

CONCLUSION

The removal of Mn (II) at pH 7.0 in laboratory solutions was possible using MnO_2, allowing lower costs, since it is not necessary to raise the pH to 10 to attain the level of Mn (II) required by Brazilian legislation to discharge the effluent. The maximum loading capacity achieved was 18.4 mg/g of

MnO_2. Despite the reactivation with $KMnO_4$ being more efficient than the one with NaOCl, the loading capacities were respectively 11.6 mg/g and 6.3 mg/g which is considered not viable.

ACKNOWLEDGEMENTS

The authors would like to thank CNPq, FAPEMIG (Fundação de Amparo a Pesquisa de Minas Gerais) and Vale S.A. for the financial support.

REFERENCES

Aguiar, A. O., Duarte, R. A., Ladeira, A. C. Q., (2013) *The application of MnO_2 in the removal of manganese from acid mine*, Water Air Soil Pollution, vol. 224, pp. 1690-1697.

Aziz, H. A., Smith, P. G., (1996) *Removal of manganese from water using crushed dolomite filtration technique, Water* Research, vol. 30, n. 2, pp. 489-492.

Hargette, A. C., Knocke, W. R., (2001) *Assessment of fate of manganese in oxide-coated filtration systems*, J. Environmental Engineering, vol. 127, pp. 1132-1138.

Hue, N. T., Cam, B. D., Nam, L. T. H., (2008) *Removal of arsenic and manganese in underground water by manganese dioxide and diatomite mineral ores,* In: WEPA INTERNATIONAL FORUM, 6., Putrajaya, Mexico Retrieved May 23, 2014, from: http://www.wepa-db.net/pdf/0810forum/paper23.pdf.

Islam, A. A., Goodwill, J. E., Bouchard, R., Tobiason, J. E., Knocke, W. R., (2010) *Characterization of filter media MnOx(s) surfaces and Mn removal capability*, Journal of American Water Works Association, vol. 102, n. 9, pp. 71-83.

Johnson, D. B., Hallberg, K. B., (2005) *Acid mine remediation options: a review*, Science of the Total Environment, vol. 338, pp. 3–14.

Knocke, W. R., Benschoten, J. E. V., Kearney, M. J., Soborsky, M. J., Reckhow, D. A., (1991) *Kinetics of manganese and iron oxidation by potassium permanganate and chlorine dioxide,* J. American Water Works Association, vol. 83, n. 6, pp. 80-87.

Silva, A. M., Cruz, F. L. S., Lima, R. M. F., Teixeira, M. C., Leão, V. A., (2010) *Manganese and limestone interactions during mine water treatment*, Journal of Hazardous Materials, vol. 181, pp.514-520.

Taffarel, S. R.; Rubio, J., (2010) *Removal of Mn^{2+} from aqueous solution by manganese oxide coated zeolite*, Minerals Engineering, vol. 23, pp. 1131–1138.

Thornton, F. C., (1995) *Manganese removal from water using limestone-filled tanks*, Ecological Engineering, vol. 4, pp. 11-18.

10th ICARD IMWA 2015 | 10th International Conference on Acid Rock Drainage & IMWA Annual Conference

Effect of Feed Ph in the Nanofiltration of Gold Acid Mine Drainage

Alice Aguiar, Laura Andrade, Wadson Pires and Miriam Amaral
Department of Sanitary and Environmental Engineering, Universidade Federal de Minas Gerais, Brazil

ABSTRACT

Acid mine drainage (AMD) is knowingly one of the greatest problems caused by mining activities, not only for the associated environmental impacts, but also due to the large volumes produced and the related costs, the difficulty of its control once started, and its perpetuity. Due to the large volume associated with AMD, membrane separation processes especially nanofiltration (NF) are of great interest. Typically, NF produces a permeate with high quality, which can then be reused in the process. The present work aims to study the effect of different feed pH in the treatment with NF of a gold acid mine drainage effluent. The membranes studied were NF90, NF270 and MPS-34, which were chosen in a previous work for its high potential for AMD treatment. The results showed that the MPS-34 and NF90 membranes operating at natural AMD pH (3.2) obtained higher permeate fluxes than in other conditions. However, the conductivity retention efficiency of the MPS-34 membrane was very low, below 45% for all conditions. The NF270 membrane presented the highest permeate fluxes. Moreover, the retention of conductivity and sulfate were higher with the NF270 membrane than with the NF90 membrane. The fouling resistance of the NF270 at pH 5.5 was slightly smaller than at pH 4.2, indicating that this might be the most adequate condition for the treatment of gold AMD.

Keywords: Gold acid mine drainage; Nanofiltration; Feed pH

INTRODUCTION

Gold mining and gold ore processing are activities of great economic importance. Gold has been used in various applications, ranging from the manufacture of jewelry to the protective covering of satellites and medicinal use due to its distinguished physicochemical properties, such as high corrosion resistance, high electrical conductivity and high infrared radiation reflectance (Kwon et al., 2011; Savage, 2013).

On the other hand, gold mining and processing leads to many environmental impacts. They may vary from natural habitat destruction and consequent loss of biodiversity to the inappropriate disposal of large amounts of waste on the environment (Getaneh & Alemayehu, 2006). Soil, water and plants in areas near gold mining regions can become contaminated by many heavy metals, such as copper, manganese, aluminum, iron, zinc, nickel, chromium, lead, cobalt, etc (Abdul-Wahab & Marikar, 2012). This contamination is most pronounced when the mined rock contains significant amounts of pyrite and other sulfide minerals. These minerals can be oxidized leading to acid generation and consequent increase of heavy metals leaching (Abdul-Wahab & Marikar, 2012).

Metal sulfides oxidation is responsible for the formation of acid mine drainage (AMD), recognized as one of the greatest environmental impacts of mining (Hilsona & Murck, 2001; Akcil & Koldas, 2006). Several authors mention that AMD results from a complex series of chemical reactions involving direct and indirect mechanisms and microbial action (Costello, 2003; Akcil & Koldas, 2006). AMD environmental impacts include acidification of surface and groundwater, soil acidification, biodiversity loss, solubilization of harmful elements such as heavy metals (which could reach human food chain through bioaccumulation and biomagnification), generation of precipitates in water bodies harming benthic flora, etc (Borma & Soares, 2002; Campaner & Silva, 2009).

Therefore, the application of AMD control measures is essential for preservation of environmental quality. AMD traditional treatment consists of adding lime to neutralize the free acidity, oxidize metals and precipitate them as hydroxides (Costello, 2003; Akcil & Koldas, 2006). These technologies may be sufficient to adjust water characteristics to discharge standards; however they are unlikely to generate water with reuse quality, as salts concentrations in the treated effluent are still high.

Membrane separation processes (MSP) are technologies of great potential for mining effluent treatment, especially if the generation of reuse water is also the aim (Al-Zoubi et al., 2010; Sierra et al., 2013; He et al., 2014). Among the MSP, nanofiltration (NF) importance must be highlighted. Nanofiltration is considered an energy efficient and environment-friendly process. NF offers higher fluxes than reverse osmosis and significantly better retentions than ultrafiltration for small molecules such as sugars, amino acids, peptides and even ions (Luo & Wan, 2013).

Solutes separation by NF membranes occurs by several mechanisms including steric hindrance, Donnan and Dielectric effects (Nguyen et al., 2009). Therefore pore size and surface charge of the membrane pores influence salts and molecules retention. As the commercially available NF membranes are usually hydrophilic and prone to be hydrated and ionized in aqueous solution, the conformation and ionization of the membrane's polymer chains will change under different surrounding conditions, especially at different pH and ionic strength. Due to the nanoscale pore dimensions (~1 nm) and electrically charged materials of the NF membranes, even a minor change in pore size or charge pattern would have a clear impact on membrane permeability and molecules

retention (Luo & Wan, 2013). Hence, literature findings reveal that membrane separation performance can be highly dependent on solution pH, which in turn can significantly affect the operational conditions selection for a given type of effluent (Capar et al., 2006).

The effect of pH on NF performance is quite complicated as membrane properties and solutes diversity largely varies with pH, and these variations are dependent on membrane material and solute type. Although the behavior of NF membranes in both, single or multi-element solutions of a known composition has already been extensively studied and modeled (Szoke et al., 2003; Teixeira et al., 2005; Nguyen et al., 2009; Dalwani et al., 2011; Luo & Wan, 2013), the operational performance of these processes to treat actual effluents cannot easily be predicted.

Some authors have evaluated the NF of real effluent or water at different pHs (Qin et al., 2003; Capar et al., 2006; Wang et al., 2007), however retention mechanisms and fouling resistance were not thoroughly discussed. As a result, understanding and then manipulating the effect of feed pH on NF can improve effluent treatment, by enhancing separation performance and reducing membrane fouling.

The aim of this study was to evaluate the treatment of a gold acid mine drainage by nanofiltration. Three different commercial NF membranes were tested at feed pH ranging from 3.2 (natural pH) to 6.0.

METHODOLOGY

Acid mine drainage

Acid mine drainage was collected from a gold mining company in the state of Minas Gerais, Brazil which has two underground gold mines and an industrial processing plant. AMD was collected in one of the underground mines, on the fourth level below ground. The AMD characteristics vary over the year, in this study the effluent was characterized by a high conductivity (4,510 μS/cm²) and sulfate concentration (2,625 mg/L), and initial pH of 3.2.

Unit description

A bench scale unit was used during the nanofiltration tests. The system is comprised of: one supply tank (ST); one pump; one valve for pressure adjustment; one rotameter; one manometer; one thermometer and one stainless steel membrane cell. Figure 1 shows a schematic of this unit.

The stainless steel membrane cell has 9.8 cm in diameter, providing a filtration area of 75 cm². The membranes tested were properly cut before being placed in the cell. A feed spacer was placed over the membrane to promote flow distribution. Permeate flow was measured by collecting the volume of permeate in a measuring cylinder over 60 seconds for nanofiltration tests and 180 seconds for reverse osmosis tests. Permeate was collected for analysis and retentate was returned to the supply tank.

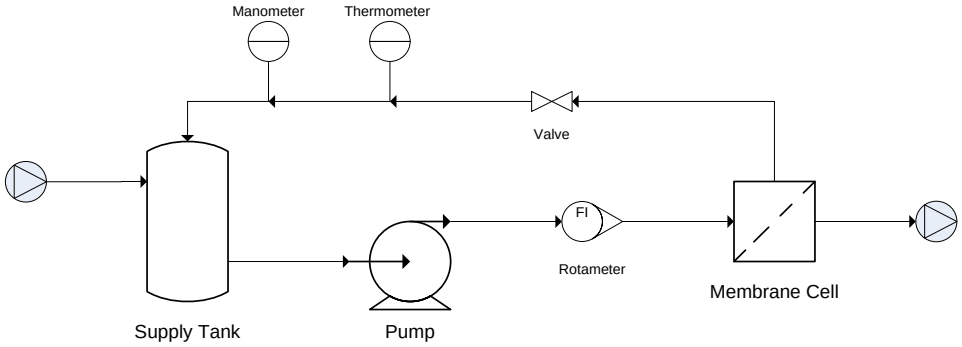

Figure 1 Schematic of NF unit

Evaluation of different feed pH values

A comparative study of three nanofiltration (NF) membranes on the treatment of AMD at feed pH ranging from 3.2 (natural pH) to 6.0 was conducted. The membranes of NF analyzed were NF90, NF270 and MPS-34. Table 1 shows the main characteristics of these membranes as provided by the suppliers, unless otherwise specified.

Process water cannot have acidic pH to prevent possible wear and corrosion of equipment and piping. Thus, for the reuse of the treated effluent, its pH must be adjusted to approximately 7.0 (Asano et al., 2007). Such adjustment can be performed before or after the membrane treatment system. Therefore, the membranes were tested at different pH values, namely 3.2, 4.2, 5.0, 5.5, and 6.0. Tests with pH above 6.0 were not performed as higher pH values did not enabled better process performance, as will be shown later. A solution 5.0 N of NaOH was used for pH adjustment.

Table 1 Membranes characteristics as provided by the suppliers

Characteristic	**MPS-34**	**NF90**	**NF270**
Supplier	Koch Membranes	Dow Filmtec	Dow Filmtec
Membrane Material	Composite	Composite Polyamide	Composite Polyamide
NaCl Retention	35% [a]	85-95% [b]	n.a.
$MgSO_4$ Retention	n.a.	>97% [c]	97% [c]
Molecular weight cutoff (Da)	200 [d]	100 [e]	200-300 [d]

n.a. Not available

[a] Feed solution containing 50,000 mg/L of NaCl.

[b] Feed solution containing 2,000 mg/L of NaCl, filtration at 4.8 bar, 25°C, and recovery rate of 15%.

[c] Feed solution containing 2,000 mg/L of $MgSO_4$, filtration at 4.8 bar, 25°C, and recovery rate of 15%.

[d] Reference: (Wang & Tang, 2011)

[e] Reference: (Zulaikha et al., 2014)

After pH adjustment, six liters of the AMD was ultrafiltered using a commercial submerged membrane (ZeeWeed) with a filtration area of 0.047 m², PVDF-based polymer and average pore diameter of 0.04 micrometers. UF occurred at a pressure of 0.7 bar up to 4 liters of permeate recovery.

The NF membranes were initially washed in ultrasound bath first with citric acid solution at pH 2.5 followed by 0.1% NaOH solution for 20 minutes each. Water permeability was obtained by monitoring the normalized value of the stabilized permeate flux of clean water at pressures of 10.0; 8.0; 6.0 and 4.0 bar. Normalization to 25°C was accomplished by means of a correction factor calculated by the ratio of water viscosity at 25°C and water viscosity at the temperature of permeation:

$$K = \frac{J}{\Delta P} * \frac{\mu(T)}{\mu(25^{\circ}C)} \quad (1)$$

With the calculated value of water permeability, intrinsic membrane resistance to filtration (R_m) was calculated:

$$R_m = \frac{1}{K * \mu(25^{\circ}C)} \quad (2)$$

Nanofiltration was carried out using four liters of pretreated acid mine drainage, during four hours at fixed pressure of 10 bar, feed flow rate of 2.4 LPM and temperatures ranging between 25 and 35°C. Permeate flux, temperature and accumulated permeate volume were measured each 15 minutes. Final permeate was collected for analysis. Retentate was returned to the supply tank. The fouling resistance to filtration (R_f) was determined with the values of permeate flux and temperature obtained at the end of the experiment, as demonstrated by the equation:

$$R_f = \frac{\Delta P - \Delta \pi}{\mu(T) * J} - R_m \quad (3)$$

Effluent osmotic pressure (π) for different recovery rates were calculated using the software ROSA 9.1 (The Dow Chemical Company, USA) up to a recovery rate of 65%. The recovery rate is defined as the ratio of the accumulated volume of permeates to the initial volume of effluent. Table 2 shows a summary of the main ions in solution and its respective concentration. These ions concentrations were typical values obtained for the AMD.

Table 2 Main ions in gold's acid mine drainage and its concentrations

Ions	Concentration (mg/L)
Sulfate (SO_4^{-2})	2,000
Chloride (Cl^-)	10.0
Magnesium (Mg^{+2})	150
Calcium (Ca^{+2})	593

Feed and permeates were analyzed for conductivity (Hanna conductivity meter HI 9835), total solids and ions concentrations (Metrohm 850 Professional IC, Herisau, Switzerland, equipped with

column type Metrosep C4-100/4.0 and Metrosep A Supp 5-150/4.0), in accordance with the Standard Methods for the Examination of Water and Wastewater (APHA 2005).

RESULTS AND DISCUSSION

Effluent osmotic pressure

A simulation of the acid mine drainage osmotic pressure calculated using the software ROSA 9.1 (The Dow Chemical Company, USA) for a recovery rate up to 65% is presented on Table 3.

Table 3 Osmotic pressure of gold's acid mine drainage

Recovery Rate	Osmotic pressure of retentate (bar)	Recovery Rate	Osmotic pressure of retentate (bar)
0%	0.75	35%	1.07
5%	0.78	40%	1.15
10%	0.82	45%	1.24
15%	0.86	50%	1.34
20%	0.90	55%	1.46
25%	0.95	60%	1.62
30%	1.01	65%	1.81

As expected, the osmotic pressure of the retentate increases with the increase in the recovery rate, as the concentration of ions in solution increase. The driving force of the nanofiltration is the effective pressure, defined as the operation pressure minus the osmotic pressure. Therefore, an increase in the recovery rate increases the osmotic pressure decreasing the filtration driving force and consequently decreasing the permeate flux.

However, it is important to point out that this software does not provide a full description of the system as it does not have all ions in solution. Hence, small variations in the effluent osmotic pressure are expected.

Membrane separation

To minimize the influences that variations on initial membrane water permeability could have on the comparison of the effluent permeate fluxes, it is usual to express the ratio of permeate flux to water flux. Figure 2 shows the ratio of permeate flux to water flux as a function permeation time and feed pH for membranes NF90 (Figure 2a), MPS-34 (Figure 2b) and NF270 (Figure 2c).

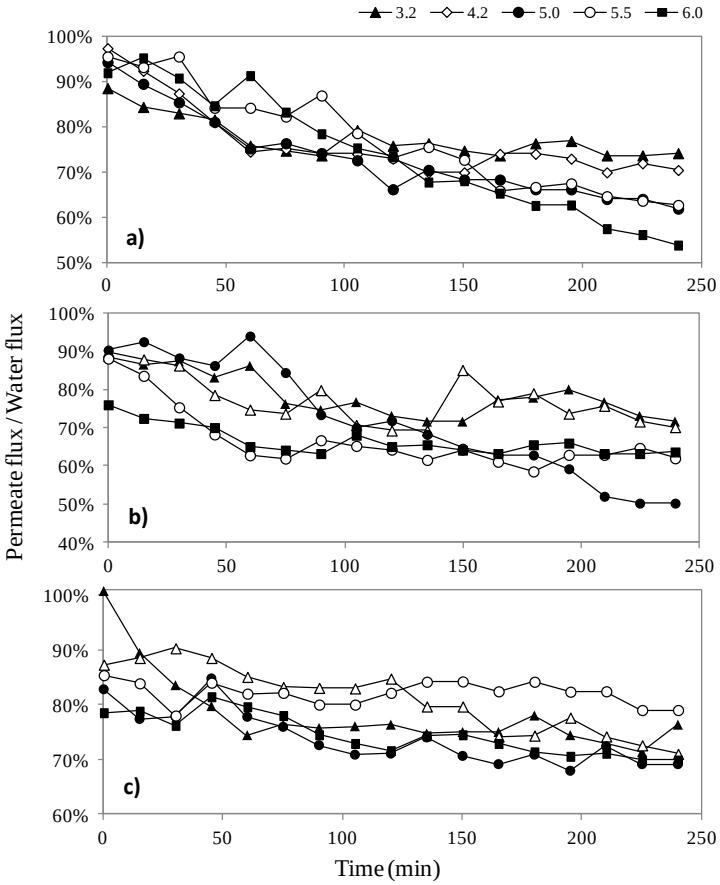

Figure 2 Ratio of permeate flux to water flux as a function permeation time and feed pH for membranes a) NF90, b) MPS-34 and c) NF270

The NF90 membrane operated best at natural pH (3.2). At this pH the average permeate flux obtained was 52.0 L/h.m^2 and the average ratio of permeate flux to water flux was 77.4%. However, as can be seen from Figure 2a, there is a considerable decrease in permeate flux at the beginning of the filtration. At the end of the filtration (recovery rate near 40%) the permeate flux was 49.5 L/h.m^2. At higher pH (6.0) the initial ratio of permeate flux to water flux was very high (91.9%) but it decreased rapidly and at a recovery rate of 40% its value had fallen to 67.9%.

The MPS-34 membrane obtained permeate fluxes similar to the NF90 membrane; and the best feed pH was also 3.2. At this pH the average permeate flux obtained was 51.9 L/h.m^2 and the average ratio of permeate flux to water flux was 78.3%. Even so, its retention efficiencies were very low, as will be shown later.

Finally, the NF270 membrane presented the highest ratio of permeate flux to water flux of all three membranes. This result is expected as the NF270 membrane has higher water permeability and larger pores than the other membranes (Wang & Tang, 2011; Nghiem & Hawkes, 2007). The NF270 membrane operated better at pH 4.2 and 5.5, as can be seen from Figure 2c the ratio of permeate flux to water flux for these two pH's are consistently higher than the rest. At pH 4.2 the average permeate flux obtained was 68.5 L/h.m^2, the average ratio of permeate flux to water flux was 81.0% and near the end of the filtration (recovery rate of 40%) the permeate flux was 62.7 L/h.m^2. At pH 5.5 the average permeate flux obtained was 64.2 L/h.m^2, the average ratio of permeate flux to water

flux was 82.1% and near the end of the filtration (recovery rate of 40%) the permeate flux was 64.4 L/h.m^2.

Table 4 shows the water permeability, membrane resistance and fouling resistance for the NF270 membrane at feed pH of 4.2 and 5.5 obtained from Equations 1, 2 and 3 respectively. For these two conditions, the values obtained for the water permeability and membrane resistance were very close, which means that the initial conditions of the system were similar. The lower fouling resistance with pH 5.5 indicates that this operational condition might be the most adequate in the treatment of the gold AMD.

Table 4 Water permeability, membrane resistance and fouling resistance of the NF270 at feed pH of 4.2 and 5.5

pH	K (m^3/s.m^2.Pa)	R_m (m^{-1})	R_f (m^{-1})
4.2	2.56×10^{-11}	$4.40 \times 10^{+13}$	$1.35 \times 10^{+13}$
5.5	2.53×10^{-11}	$4.44 \times 10^{+13}$	$1.20 \times 10^{+13}$

The conductivity retention efficiencies obtained for the MPS-34 with all the pH studied were very low (e.g. below 45%). The small permeate fluxes and low retention efficiencies indicate that this membrane is not the most appropriate for this specific application. Table 5 shows the main permeate characteristics for the NF90 membrane at pH 3.2 and NF270 membrane at pH 4.2 and 5.5.

Table 5 Permeate conductivity, sulfate and calcium concentrations for the NF90 membrane at pH 3.2 and NF270 membrane at pH 4.2 and 5.5

Membrane	pH	Conductivity (µS/cm^2)	Sulfate (mg/L)	Calcium (mg/L)
NF90	3.2	770	549	< 2.5
NF270	4.2	370	258	< 2.5
NF270	5.5	405	257	< 2.5

It is noted that the retention of conductivity and sulfate were better with the NF270 membrane than with the NF90 membrane. For the NF270 membrane at pH 5.5, the retention efficiencies of conductivity and sulfate were 91.0 and 90.2%, respectively. Calcium retention was high for all three conditions and final concentration was below the method's lowest detection limit.

CONCLUSION

Average permeate flux for the NF90 and the MPS-34 membranes operating at AMD natural pH (3.2) were very similar, equal 52.0 and 51.9 L/h.m^2 respectively. However, the permeate flux decrease in the NF90 membrane was considerably higher than the permeate flux decrease in the other membranes. The NF270 membrane showed the highest overall permeate flux and best fluxes were obtained at pH 4.2 and 5.5. At these pHs the average permeate flux were 68.5 and 62.7 L/h.m^2 respectively for pH 4.2 and 5.5 but permeate flux decline was smaller at pH 5.5 than at pH 4.2. Moreover, fouling resistance was lower at pH 5.5 than at pH 4.2. The retention efficiencies of conductivity and sulfate for the NF270 membrane at pH 5.5 were 91.0 and 90.2%, respectively.

ACKNOWLEDGEMENTS

The authors would like to thank the Coordination of Improvement of Higher Education Personnel (CAPES) and National Council for Scientific and Technological Development (CNPq) for the postgraduate scholarships provided.

NOMENCLATURE

K	water permeability at 25°C ($m^3/h.m^2.Pa$)
μ	permeate viscosity ($N.s/m^2$)
J	permeate flux ($m^3/h.m^2$)
ΔP	system pressure (Pa)
R_m	intrinsic membrane resistance to filtration (m^{-1})
R_f	fouling resistance to filtration (m^{-1})
$\Delta P - \Delta \pi$	effective pressure (Pa)

REFERENCES

Abdul-Wahab, S.A., Marikar, F.A. (2012) The environmental impact of gold mines: pollution by heavy metals. *Central European Journal of Engineering*, v. 2, pp. 304-313.

Akcil, A., Koldas, S. (2006) Acid Mine Drainage (AMD): causes, treatment and case studies. *Journal of Cleaner Production*, v. 14, pp. 1139-1145.

Al-Zoubi, H., Rieger, A., Steinberger, P., Pelz, W., Haseneder, R., & Härtel, G. (2010) Optimization study for treatment of acid mine drainage using membrane technology. *Separation Science and Technology*, v. 45, pp. 2004-2016.

APHA, A. (2005) Standard methods for the examination of water and wastewater, American Public Health Association, Washington, DC.

Burton, F., Leverenz, H., Tsuchihashi, R., Tchobanoglous, G. (2007). Water reuse: issues, technologies, and applications.

Soares, P. S. M., Borma, L. D. S. (2002) Drenagem ácida e gestão de resíduos sólidos de mineração. *Extração de Ouro-Princípios, Tecnologia e Meio Ambiente*. Rio de Janeiro, RJ, pp. 253-276.

Campaner, V.P., Silva, W.L. (2009) Processos físico-químicos em drenagem ácida de mina em mineração de carvão no sul do Brasil. *Química Nova*, v. 32, pp. 146-152.

Capar, G., Yilmaz, L., & Yetis, U. (2006) Reclamation of acid dye bath wastewater: effect of pH on nanofiltration performance. *Journal of membrane science*, v. 281, pp. 560-569.

Costello, C. (2003) Acid mine drainage: innovative treatment technologies. *US Environmental Protection Agency*.

Dalwani, M., Benes, N. E., Bargeman, G., Stamatialis, D., & Wessling, M. (2011) Effect of pH on the performance of polyamide/polyacrylonitrile based thin film composite membranes. *Journal of Membrane Science*, v. 372, pp. 228-238.

Getaneh, W., T. Alemayehu (2006) Metal contamination of the environment by placer and primary gold mining in the Adola region of southern Ethiopia. *Environmental Geology*, v. 50, pp. 339-352.

He, C., Wang, X., Liu, W., Barbot, E., Vidic, R.D (2014) Microfiltration in recycling of Marcellus Shale flowback water: Solids removal and potential fouling of polymeric microfiltration membranes. *Journal of Membrane Science*, v. 462, pp. 88-95.

Hilsona, G., Murck, B. (2001) Progress toward pollution prevention and waste minimization in the North American gold mining industry. *Journal of Cleaner Production*, v. 9, pp. 405-415.

Kwon, Y., Lai, S. C., Rodriguez, P., Koper, M. T. (2011) Electrocatalytic oxidation of alcohols on gold in alkaline media: base or gold catalysis?. *Journal of the American Chemical Society*, v. 133, pp. 6914-6917.

Luo, J., Wan Y. (2013) Effects of pH and salt on nanofiltration—a critical review. *Journal of Membrane Science*, v. 438, pp. 18-28.

Nghiem, L.D., Hawkes, S. (2007) Effects of membrane fouling on the nanofiltration of pharmaceutically active compounds (PhACs): Mechanisms and role of membrane pore size. *Separation and Purification Technology*, v. 57, pp. 176–184.

Nguyen, C. M., Bang, S., Cho, J., Kim, K. W. (2009) Performance and mechanism of arsenic removal from water by a nanofiltration membrane. *Desalination*, v. 245, pp. 82-94.

Qin, J. J., Oo, M. H., Wai, M. N., Wong, F. S. (2003) Effect of feed pH on an integrated membrane process for the reclamation of a combined rinse water from electroless nickel plating. *Journal of membrane science*, v. 217, n. 1, pp. 261-268.

ROSA 9.1 System Design Software, The Dow Chemical Company, USA. Available at http://www.dowwaterandprocess.com/en/resources/rosa_system_design_software. Accessed on: 01/07/2014.

Szoke, S., Patzay, G., Weiser, L. (2003) Characteristics of thin-film nanofiltration membranes at various pH-values. *Desalination*, v. 151, pp. 123–129.

Savage, N. (2013) Mine, all mine! Nature. *Nature*, v. 495(S3).

Sierra, C., J. R. Á. Saiz, et al. (2013) Nanofiltration of Acid Mine Drainage in an Abandoned Mercury Mining Area. *Water, Air, & Soil Pollution*, v. 224, pp. 1-12.

Teixeira, M.R., Rosa, M.J., Nyström, M. (2005) The role of membrane charge on nanofiltration performance. *Journal of Membrane Science*, v. 265, n. 1, pp. 160-166.

Wang, Y.-N. and C. Y. Tang (2011) Protein fouling of nanofiltration, reverse osmosis, and ultrafiltration membranes—the role of hydrodynamic conditions, solution chemistry, and membrane properties. *Journal of Membrane Science*, v. 376, pp. 275-282.

Wang, Z., G. Liu, et al. (2007) Experimental study on treatment of electroplating wastewater by nanofiltration. *Journal of Membrane Science*, v. 305, pp. 185-195.

Zulaikha, S., W. Lau, et al. (2014) Treatment of restaurant wastewater using ultrafiltration and nanofiltration membranes. *Journal of Water Process Engineering*.

Fulfilment of EPA Discharge Requirements for ARD Using Co-Precipitation Iron Process at Neutral PH

David Pascual[1] and Michael McPhee[2]

1. *Ecopreneur Chile*
2. *Unipure Corp, USA*

ABSTRACT

The dissolution of soluble metal compounds from ore and waste rock and the presence of contaminants in industrial and mining process water are a major concern for water treatment standards.

An improvement of alkaline precipitation methods to remove metals was the focus of this study. This system was based on iron co-precipitation technology, taking advantage of the beneficial characteristics of iron, such as natural coagulation, natural adsorption of heavy metals, good clarification and increased dewatering properties of solids.

Based on this iron co-precipitation technology, two different configurations were evaluated at Leviathan Mine Superfund Site (California, USA) for treatment of ARD containing the following metal concentrations (μg/L): Aluminium (107,800), Arsenic (3,240), Copper (2,150), Iron (456,430), Nickel (2,560), Cadmium (26,100), Chromium (341,000), Lead (6,200), Selenium (16,600), Zinc (538,000).

The objectives of the technology evaluation were to determine the removal efficiencies for target metals, verify reduction under discharge standards, document operating parameters, assess critical operating conditions, evaluate operational efficiency of solid separation and dewatering systems.

The treatment system was shown to be extremely effective in neutralizing acidity and reducing the concentrations of the target metals to below EPA discharge standards.

The mechanisms of this technology, combined with the characteristics of iron and operation at neutral pH, showed beneficial results that include less amount of base requirement, no requirement of final pH adjustment to fulfil discharge limits, better clarification with less settling area, and better solids dewatering.

Keywords: metal, precipitation, ARD, iron, neutral

INTRODUCTION

Conventional Alkaline precipitation

Alkaline Precipitation is an extensively used technology for removal of heavy metals. It is based on the occurrence of the following reaction:

$$M^{+2}{}_{(aq)} + 2(OH^-) \leftrightarrow M(OH)_{2\,(S)} \quad (1)$$

In this equation, the M^{2+} represents any divalent heavy metal. As it is indicated, the metal ion combines with hydroxide ion to form the insoluble metal hydroxide solid. This reaction is pH dependent; as more base is added, the reaction is driven further to the right to precipitate more of the metal complex. Conversely, as the pH is decreased, the thermodynamic equilibrium moves to the left, causing more of the metals to resolubilize. This reaction is fully reversible and results in a solubility curve (blue curve) similar to that shown in Figure 1.

The limitations of alkaline precipitation technologies result from secondary reactions which occur as more hydroxide is added. One common reaction is the combination of the metal hydroxide precipitate with additional hydroxide ion:

$$M(OH)_{2\ (s)} + OH^- \leftrightarrow M(OH)_3^-{}_{(aq)} \quad (2)$$

The metal hydroxide precipitate combines with additional hydroxide to form a soluble metal complex. Thus as the pH increases, the reaction proceeds to the right and the metal becomes more soluble. The solubility curve of this reaction (purple curve) approximately mirrors the curve of the first reaction as shown in Figure 1.

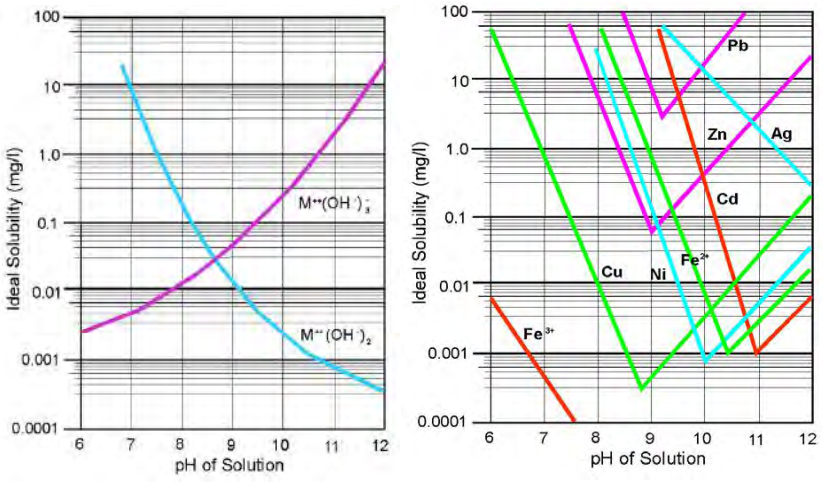

Figure 1 Solubility of metal hydroxides

By overlaying these two curves as shown in Figure 1, and then combining the effects of all the reactions which take place, the familiar V-shaped solubility curve for metal hydroxides is obtained as shown in Figure 1. The lowest point of this curve identifies the absolute lowest concentration of a particular metal which can be achieved, under ideal conditions, by alkaline precipitation technology. To obtain this concentration, pH must be maintained within a specified range to reduce the metal resolubilisation. In a wastewater stream with multiple metals, this problem becomes more challenging due to solubility dependence of metals on pH. Any operating pH is chosen to be optimal in reducing the solubility of dissolved species (Figure 1).

Iron co-precipitation process technology

Iron co-precipitation technology is based on the beneficial characteristics of iron: natural coagulation, adsorption of heavy metals onto iron solids, good clarification and increased dewatering properties solids formed.

Ferrous iron (Fe^{2+}), existing or added to water, tends to form a soluble chain-like structure in solution due to the weak ionic attractions between molecules. This close association between the heavy metals species and the iron species provides the mechanism by which the iron can be targeted to most efficiently remove the heavy metals (McPhee, n.d.).

After the soluble association is formed, base is added to control the pH and form a suspension of metal hydroxides; then, air is added to oxidize Fe (II) to Fe (III) and form crystals containing ferric ions as ferromagnetic oxides, such as Fe_3O_4, and/or oxyhydrates (or oxiyhydroxides) FeOOH, and further containing the metal ions originally in solution. Many kinds of heavy metals in the solution are substituted in the metal sites of the ferric crystal lattice to form various kinds of ferrites or of FeOOH crystal lattice. Other kinds of heavy metals are firmly adsorbed by the ferrites thus formed (Sugano, Tsuji, Kanamori, 1976).

These metals are "occluded" in the iron solids and are effectively enveloped in iron as shown in Figure 2. The occluded metals are insulated from the solution by the iron, and so are not allowed to resolubilize as solubility curves in Figure 1 would indicate. This phenomenon makes it possible to remove heavy metals from water to concentrations well below their thermodynamic solubility limits. The precipitates, ferric iron solids, can then be separated from the treated water by chemical coagulation, flocculation, and clarification processes (McPhee, n.d.).

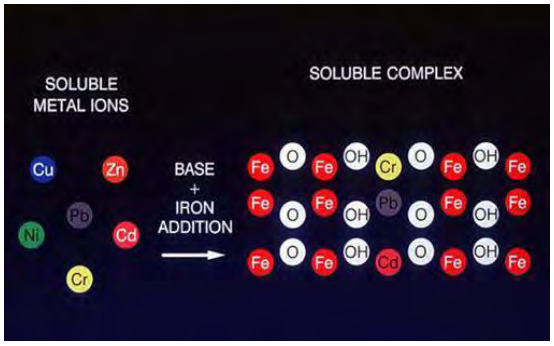

Figure 2 Soluble iron complex formation in iron co-precipitation process

Other metals which may not be removed by occlusion are adsorbed; ferric iron solids tend to adsorb heavy metals to their surface and acts as a catalyst for the oxidation of Fe(II) to Fe(III).

Process description

A treatment system based on iron co-precipitation technology was designed to treat ARD from holding ponds from an inactive underground copper mine and an open pit sulphur mines in the State of California (Siskind, 2002).

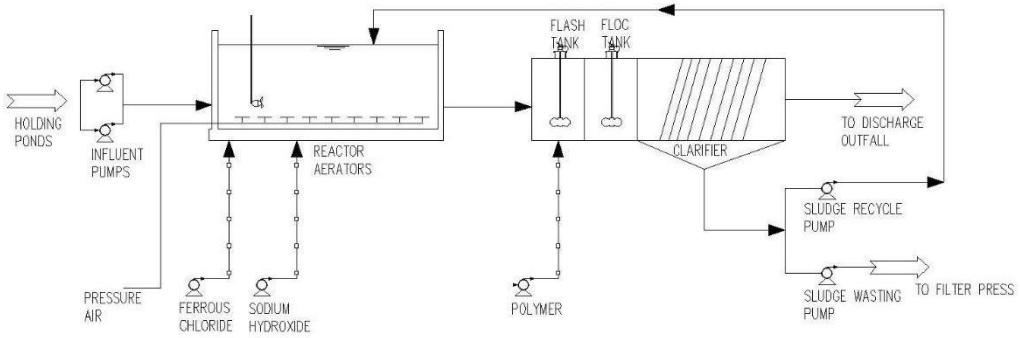

Figure 3 Co-precipitation metals treatment process flow diagram. One-stage system

The system was operated in two different modes, one-stage and two-stage. Operated as a one-stage system, the active treatment system was evaluated for its ability to treat a combined, moderate ARD flow without regard to the type of metal or concentration. Operated as a two-stage system, the active lime treatment system was evaluated for its ability to treat a high ARD flow where concentrations of arsenic were relatively high.

The treatment system for both modes involves reaction of lime with ARD (usually at a pH of 2 to 3), to raise the solution pH to 7.9 to 8.2. In one-stage mode, pH is rise to 7.8 to 8.2 in one stage. In two-stage mode the overall chemical reaction is the same as for the one-stage mode; however, metals precipitation is conducted in two steps. In stage I, the active treatment system is held at a pH of 2.8 to3.0 creating a small quantity of precipitate. In stage II, the pH is raised to 7.9 to 8.2 and the remaining metals are precipitated, creating a much larger quantity of solid waste.

The equipment for each stage consists of an aerated reaction tank (30 minutes retention time), flash and flocculation mixing tanks, plate clarifiers (settling rate of 1 m^3/m^2 h), filter press (only for first step of two-stages configuration) and a settling pond as shown in Figure 3 and Figure 4. Treatment chemicals used were lime and anionic polyacrylamide as polymer; no ferrous chloride or sulphate addition was needed due to a high concentration of iron in the ARD flow.

Ferric iron solids are present in the process as a result of the oxidation of ferrous iron, and as a result of recycle from the clarification step as shown in Figure 3 and Figure 4. The solids, due to a very high shear environment in the reaction vessel, are highly fractured resulting in a very high surface area and many active adsorption sites. The heavy metals in solution adsorb to the surface of these solids in the reactor. As ferrous iron enters the reactor with the contaminated stream, the iron

preferentially precipitates, due to the autocatalytic effect, on the solids which have already formed. This layering of iron precipitate on top of adsorbed heavy metals produces results similar to those achieved by the first mechanism; the heavy metals are effectively removed from solution and are isolated from the solution so that they cannot freely follow their solubility curves as the pH varies. This reaction mechanism also results in extremely dense solids since the precipitation is occurring directly on the surface of other solids (McPhee, nd).

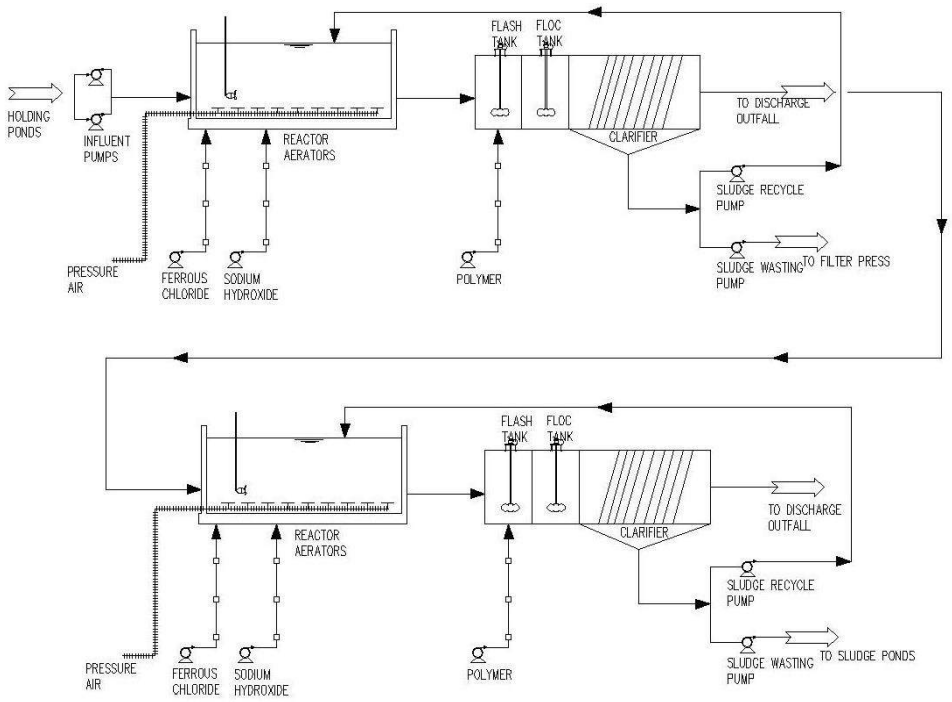

Figure 4 Co-precipitation metals treatment process flow diagram. Two-stage system

The principal objectives of the technology evaluations carried out by EPA (Bates, 2006) were: ability to neutralize acidity, determine removal efficiencies of ten metals (Al, As, Cu, Fe, Ni, Cd, Cr, Pb, Se and Zn) , determine the concentrations of the primary and secondary metals in effluent are below EPA-mandated discharge standards, document operating parameters, optimize system performance, monitor chemical composition of ARD as it passes through the treatment system, operational performance of solids separation systems, document solids transfer, dewatering, and disposal operations.

RESULTS AND DISCUSSION

The study was carried out over a two-year period. A total volume of 83,600 m^3 of ARD was treated with both systems, 93% of this volume with the two-stage system, 7% with the one-stage configuration. Three tables summarizing the outcomes are provided in Table 1 – 3.

Table 1 and 2 show the results of influent, effluent concentrations and removal efficiencies for the considered metals. This included one-stage and two-stage operations. Table 3 shows the amounts of waste generated during the evaluation and its composition.

Table 1 Active lime treatment system removal efficiencies: two-stage operation in 2002 and 2003

Target metal	Avg. influent conc. (µg/L)	Std. Dev.	Avg. effluent conc. (µg/L)	Std. Dev.	Exceeds discharge standards (Y/N)	Avg. removal efficiency (%)	Range of removal efficiencies (%)
Aluminium	381,000	48,792	1,118	782.00	N	99.70	99.20 to 99.90
Arsenic	2,239	866.00	8.60	1.90	N	99.60	99.20 to 99.80
Copper	2.383	276.00	8.00	2.50	N	99.70	99.40 to 99.80
Iron	461,615	100,251	44.90	66.20	N	100.00	99.90 to 100.00
Nickel	7,024	834.00	34.20	15.40	N	99.50	99.20 to 99.90
Cadmium	54.40	6.10	0.70	0.28	N	98.70	99.20 to 99.90
Chromium	877.00	173.00	5.70	12.20	N	99.30	93.80 to 99.90
Lead	7.60	3.60	2.00	1.10	N	78.30	69.20 to 86.70
Selenium	4.30	3.90	3.80	1.50	N	Not Calculated	Not Calculated
Zinc	1,469	176.00	19.30	8.90	N	98.70	97.40 to 99.40

In one-stage operation, the resulting solid waste stream exhibited hazardous waste characteristics due to high arsenic and nickel concentrations, and must be disposed of in an off-site treatment, storage and disposal (TDS) facility. In step I of two-stage operation, a small quantity of precipitate containing high arsenic concentrations is produced, which when dewatered, exhibits hazardous waste characteristics and requires off-site disposal in a TDS facility. In step II, a much larger quantity of solid waste is generated; however, arsenic concentrations are low enough that the step II solid waste is not classified as a hazardous waste and can be disposed of on site

Table 2 Active lime treatment system removal efficiencies: one-stage operation in 2003

Target metal	Avg. influent conc. (µg/L)	Std. Dev.	Avg. effluent conc. (µ/L)	Std. Dev.	Exceeds discharge standards (Y/N)	Avg. removal efficiency (%)	Range of removal efficiencies (%)
Aluminium	107,800	6,734	633.00	284.00	N	99.50	99.00 to 99.80
Arsenic	3,236	252.00	6.30	3.50	N	99.80	99.70 to 99.90
Copper	2,152	46.40	3.10	1.50	N	99.40	99.00 to 99.70
Iron	456,429	49,430	176.00	130.00	N	100.00	99.90 to 100.00
Nickel	2,560	128.00	46.80	34.70	N	97.90	95.70 to 99.30
Cadmium	26.10	14.10	0.20	0.03	N	99.10	98.40 to 99.70
Chromium	341.00	129.00	3.00	3.80	N	99.00	95.60 to 99.80
Lead	6.20	3.60	1.60	1.30	N	74.60	48.30 to 89.80
Selenium	16.60	13.60	2.10	0.43	N	93.10	91.00 to 94.40
Zinc	538.00	28.90	5.60	3.60	N	98.80	97.70 to 99.60

Table 3 Determination of hazardous waste characteristics of solid waste streams at Leviathan mine

Mode of Operation	Operational year	Solid waste stream evaluated	Total solid waste generated (DryTons)	TCLP	Waste handling requirement
Biphasic	2002	Phase I Filter cake	22.70	Pass	Off-site TSD facility
Biphasic	2002	Phase II Pit clarifier Sludge	118.00	Pass	On-site disposal
Biphasic	2003	Phase I Filter cake	21.10	Pass	Off-site TSD facility
Biphasic	2003	Phase II Pit clarifier Sludge	93.60	Pass	On-site disposal
Monophasic	2002	Filter cake	20.40	Pass	Off-site TSD facility

CONCLUSION

Both treatment systems were shown to be extremely effective at reducing metal concentrations of the ten target metals in the ARD flows to below EPA-mandated discharge standards. In general, removal efficiencies for the ten target metals exceeded ninety percent at a maximum pH value of 8.2.

In addition, the active two-stages treatment system was shown to be very effective at separating arsenic from ARD prior to precipitation of other metals, subsequently reducing the total volume of hazardous solid waste produced. Solids generated in stage II of two-stage configuration pass the EPA Toxicity Characteristic Leaching Procedure TCLP 1311, and the solids were allowed to be

disposed of in a municipal landfill or on-site, with a reduction in the cost of disposal from about 500 US$ per metric ton to as less as 20 US$ per metric ton.

In Table 4, a process and cost comparison is shown between the iron co-precipitation technology and High Density Sludge (HDS) technology, a common technology applied to treat ARD.

Table 4 Process comparison. Iron co-precipitation vs. HDS

Technology	Reactor TSS(mg/L)	Reactor HRT(min)	Process pH	Minimum Process No. steps
Iron Co-precipitation	500-3,000	20-30	6-8.2	1
HDS	10,000-25,000	30-60	6-11	2

Regarding capital cost comparison between Iron co-precipitation and HDS, for a regular metal-removal system for ARD, an HDS system will need 2 series-reactors and an sludge conditioning step where the lime or base is added to a sludge conditioning reactor prior to being returned to the primary reactor; on the other hand, an iron-co-precipitation system can be implemented in only 1 reactor step. Regarding expenditure costs, in a HDS system is needed to maintain a higher pH than in iron co-precipitation, with an increase in base consumption. It is important to remark the importance of running pilot test to ensure treatment characteristics in order to develop a complete installation.

REFERENCES

Bates, E. (2006) *Active and semi-passive lime treatment of acid mine drainage,* National risk management research laboratory, Cincinnati. United States Environmental protection agency, May 2006

McPhee, M. (n.d.) *Metals removal technology*, viewed 8 February 2013, <http://http://www.unipure.com/metals-removal-technology>

Siskind, D. (2002) 'Two-stage system tackles acid mine drainage', *Industrial Water World,* PennWell Corporation, vol 03.05

SGS Société Générale de Surveillance SA (2008), "Acid Rock Drainage", SGS MINERALS SERVICES – T3 SGS 855, viewed 6 February 2010, http://www.sgs.com/~/media/Global/Documents/Flyers%20and%20Leaflets/SGS-MIN-WA106-Acid-Rock-Drainage-EN-11.pdf

Sugano, I., Tsuji, T., Kanamori, M. (1976) *Method of extracting heavy metals from industrial wastewater,* Nippon Electric Company Limited, Japan. Patent #: 3,931,007.

Solving Mine Water Problems with Peat-Based Sorption Media

Paul Eger[1], Peggy Jones[2] and Doug Green[2]
1. *Global Minerals Engineering, USA*
2. *American Peat Technology, USA*

ABSTRACT

Mine water often contains trace metals that must be removed prior to discharge. Conventional technologies exist but generally are labor intensive and expensive. Peat-based sorption material can be a less expensive alternative and is easily deployed in either "semi-active" or passive treatment designs. The media is a hardened uniform granular material produced from reed sedge peat. It has a hydraulic conductivity of around 1 cm/sec, metal removal capacities ranging from 1 - 15% dry weight and been used successfully to remove suspended and dissolved metals from the Soudan iron mine in Minnesota and base metal mines in North America.

In November 2012, a pilot test was initiated at the Soudan mine. Since startup, over 62.4 million liters (> 32,000 bed volumes) have been treated with an average removal of around 75% for suspended copper and 60% for dissolved copper. Backwash is required at about 4000 bed volumes, but with a combination of air sparging and high flow backwash, the suspended material is effectively removed from the bed. The APTsorb media produced equivalent removal to the existing system but reduced the size and complexity of the system and reduced operating costs by 50%.

In October 2013, a pilot test began at a base metal mine in North America. The pilot was designed to model both a "semi-active" (pressurized tank) and passive (biocell) treatment system approach. Lead removal in both pilot systems was generally greater than 99%. Excessive solids in the mine discharge contaminated the pressurized tank and affected treatment at 6400 bed volumes. This reduced dissolved metal removal efficiency in the media from 99% to about 85% and caused the discharge to exceed the permit limit of 11.5 ug/l lead. The biocell was not affected and it continued to meet discharge limits up to 20000 bed volumes.

Keywords: Copper, lead, zinc, cadmium, ion exchange, passive treatment, adsorption,

INTRODUCTION

Mine water often contains trace metals above regulatory limits. For many situations, lime treatment is the preferred treatment since it is effective with most mine waters. However, it is expensive, generally requires a large infrastructure and has substantial ongoing operation and maintenance costs. Commercial ion exchange resins can provide an alternative treatment approach but the media is expensive and typically cannot effectively handle water containing suspended solids.

Peat is a natural material and has long been known for its ability to remove metals from water. As a result, metal concentrations in peat have been used as a geochemical prospecting tool and peat has been tested for its ability to treat wastewater (Lapakko & Eger, 1988, Salmi, 1959, Brown et al., 2000). Up to 10% copper was measured in peat from the Tantramar Swamp in New Brunswick and copper concentrations up to 8.9 % have been reported in samples used to treat wastewater (McDonald, 1976; Premi, 1970).

Peat, although relatively inexpensive, tends to be non-uniform and somewhat difficult to handle. Although loose, fibrous peat can have hydraulic conductivities on the order of 10^{-1} cm/sec, more decomposed and compacted peat can have conductivities of 10^{-3} to 10^{-4} cm/sec. These lower conductivities reduce the overall flow rate and increase the potential for channelization.

American Peat Technology (APT) has developed a granulation and low temperature hardening process to convert loose peat into an engineered sorption media (Figures 1, 2). The granules maintain their structure when wet and can be sized to any specification, which makes them readily adaptable to a variety of treatment systems. The standard media is 0.6 to 2 mm and has an estimated hydraulic conductivity around 1 cm/sec. Metal removal capacities measured in laboratory equilibrium tests have ranged from 1 to 15% dry weight metal.

Figure 1 Peat granules

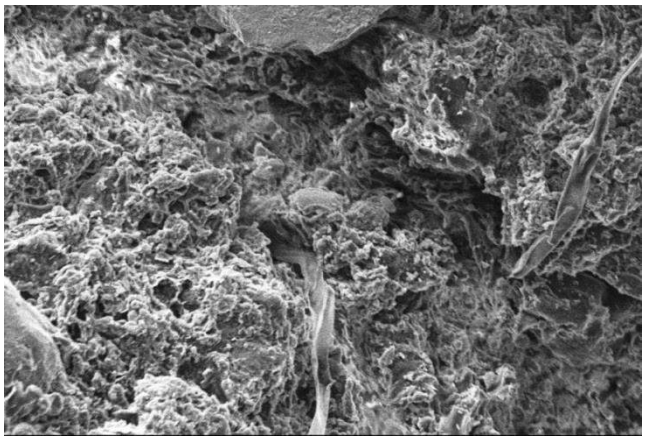

Figure 2 Sorption media surface at 1500X

APPROACH

Pilot tests were conducted at several sites to evaluate the ability of peat-based sorption media) to remove trace metals from mine drainage.

Soudan Mine; Suspended and Dissolved Copper

The Soudan Mine is an abandoned underground iron mine located in northeastern Minnesota. Mine water is discharged at an average flow rate of 227 L/min. The pH of the discharge is generally around 7 but contains low levels of copper and cobalt. Metals concentrations range from 30-50 ug/l copper and 10-15 ug/l cobalt, which exceed the permit limits of 17 and 4 respectively. About 75% of the copper is suspended but all the cobalt is dissolved. Water is currently treated with a commercial ion exchange system that employs prefiltration with bags, cartridge filters and activated carbon (Figure 3).

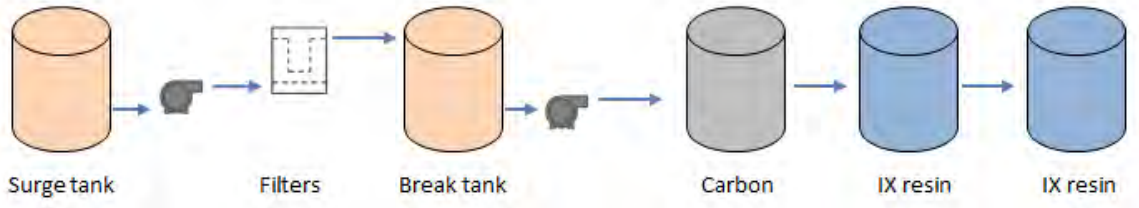

Figure 3 Existing water treatment, Soudan Underground mine

At the Soudan Mine, a pilot test was conducted to evaluate the ability of the peat-based sorption media to remove both suspended and dissolved metals from the overall mine discharge. About 1900total liters of media were installed in a 3785 liter treatment tank that was designed to be periodically backwashed (Figure 4).Typical flow rate was 189 L/min, but flow rates varied over the course of the pilot from 114 to 378 L/min.

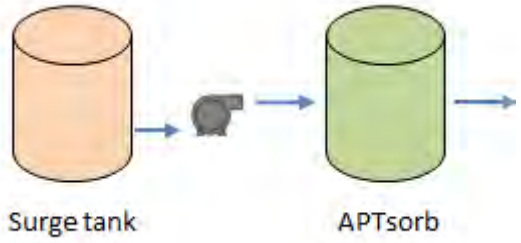

Figure 4 Pilot test, Soudan Underground Mine

Water quality samples were taken roughly on a weekly basis and analyzed by APT using a Perkin Elmer PinAAcle 900 graphite furnace. Periodic quality control samples were run by Pace Laboratories.

RESULTS

During the initial testing, samples were collected from before and after the media tank as well as after each component in the existing system. During this time, total copper in the mine discharge generally varied from 20 to 40 ug/l and dissolved ranged from 5 to 10 ug/l. A total of about 17 million liters was treated by the peat based sorption media system during the comparative test.

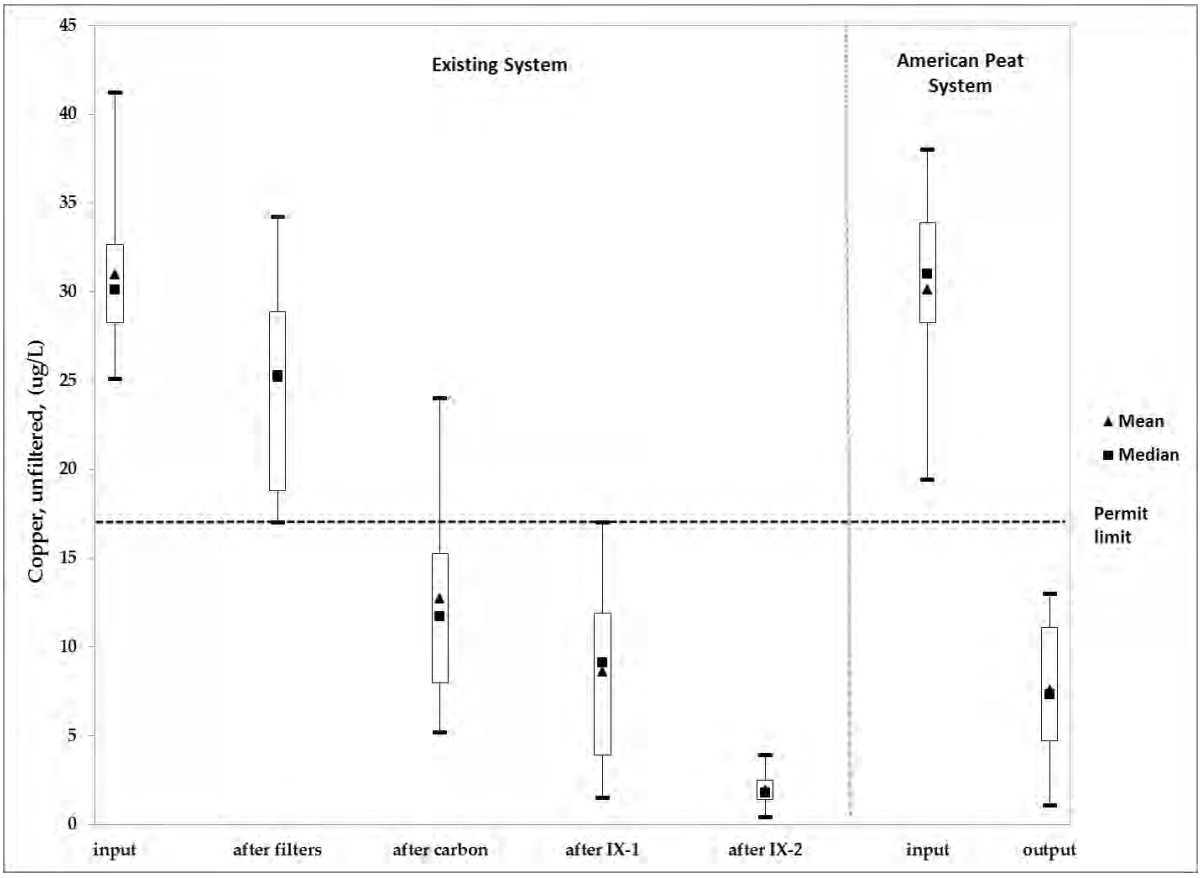

Figure 5 Comparison of existing system and APTsorb, November 2012 – April 2013

In the existing system, total copper concentrations decreased after each component, and were less than 5 ug/l after the last ion exchange tank. (Figure 5). After the peat media tank, total copper ranged from 4 to 13 ug/l and was always less than the permit limit of 17 ug/l.

Starting in May 2013, there were problems with an in-mine treatment system that pre-treated a small but concentrated flow, and the copper concentrations in the overall mine discharge began to

increase. It reached a maximum of 364 ug/l in July. The problems with the in-mine system were corrected by October, and concentrations returned to the typical range of 30 – 50 ug/l (Figure 6).

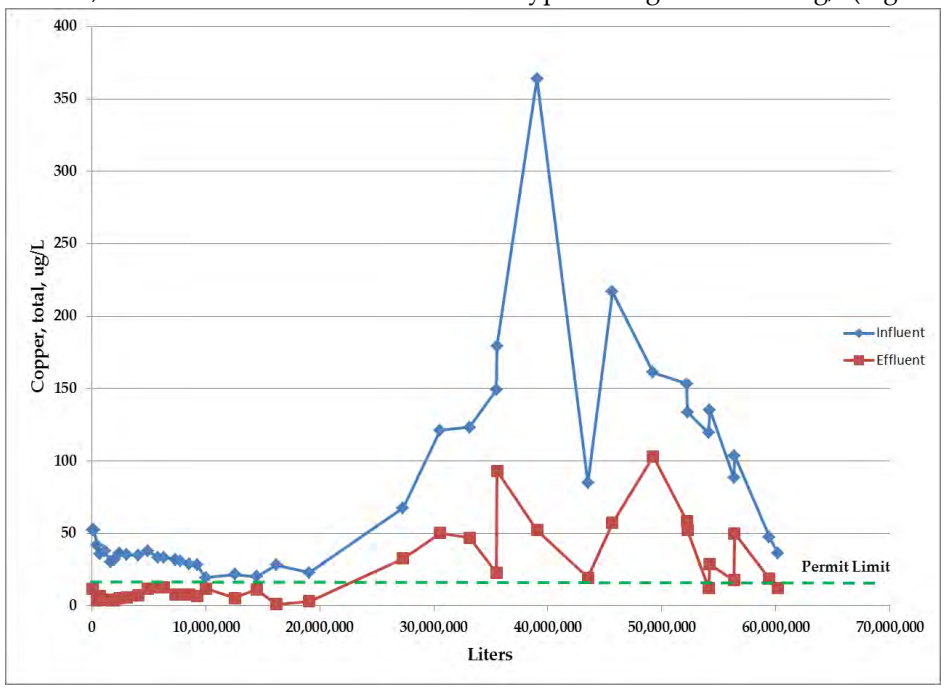

Figure 6 Total copper removal at the Soudan Mine, November 2012-2013

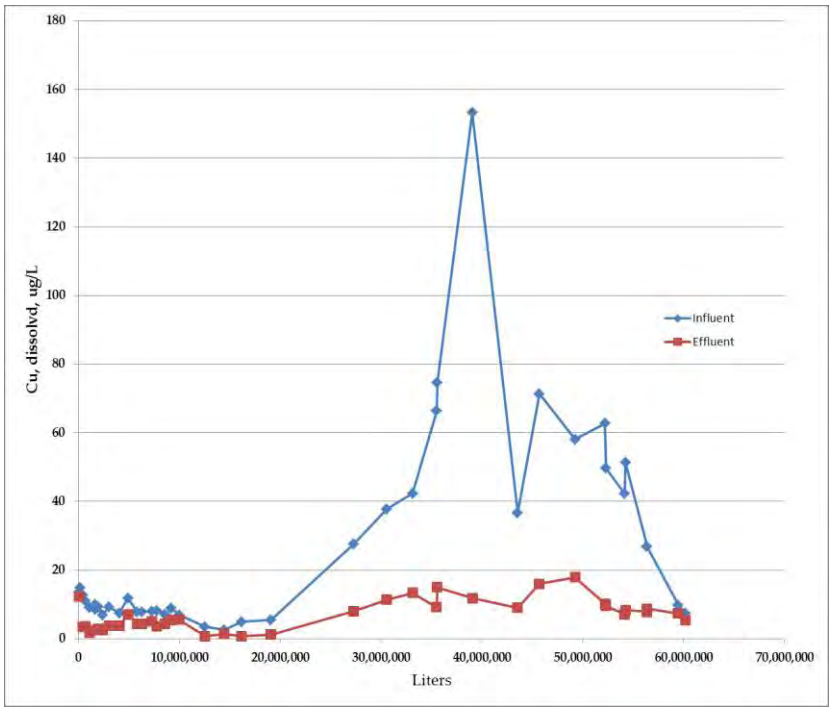

Figure 7 Dissolved copper removal at the Soudan Mine, November 2012-2013

When concentrations in the mine water increased, the peat media continued to remove both total and dissolved copper, but concentrations exceeded the permit limit of 17 ug/l. (Figures 6, 7). When

the influent copper concentrations decreased in the fall, the effluent concentrations also decreased and the discharge met the permit limit. Dissolved copper was removed continuously throughout the study despite an order of magnitude variation in input concentration. Treatment continued until November 2013 when the system had to be shut down and moved to a new treatment location. During the treatment period, about 62.4 million liters of water had been treated.

Base Metal Mine; Lead, zinc, cadmium

The second site is an active underground base metal mine in North America. The suspended solids in the mine water vary substantially but average around 30 mg/l. The water is circumneutral with average total metal concentrations of 2100 ug/l lead, 115 ug/l zinc and 0.8 ug/l cadmium; average dissolved concentrations were 150 ug/l lead, 70 ug/l zinc and 0.2 ug/l cadmium. Typical discharge is around 18,900 L/min. Water is currently discharged to a clarification basin.

Two pilots were constructed; one using a pressurized tank similar to the Soudan mine and the second a gravity flow system to simulate a passive treatment approach (biocell). Since the media has a high hydraulic conductivity, hydraulic loading rates of 40.8 L/min/m^2 are possible with minimal head pressure. The pressurized flow tank typically treated 189 L/min, but flow rates up to 378 L/min were tested. The biocells were operated at loading rates of 10.2, 20.4 and 40.8 L/min/m^2 (2.3 to 9.5 L/min). Since the discharge was directly from an active underground mine a sand filter was installed prior to both pilots to avoid excessive solids loading.

Pressurized tank

Treatment began in October of 2013. Lead concentrations in the input water were typically around 1000 ug/l, but spiked as high as 40,000 µg/l in December (Figure 8). The sand filter essentially removed all the suspended lead, although it plugged quickly during the high solids discharge. The peat media removed about 99% of the remaining lead with effluent concentrations well below the current permit limit of 11.5 ug/l (Figure 8).

Although the sand filter removed most of the suspended material, an excessive solids load plugged the sand filter within 30 minutes and solids were pushed into the media tank. In an effort to remove these solids, the peat media was backwashed.

The backwash did not effectively remove the solids but instead distributed them throughout the bed and contaminated the media. After the backwash, Lead concentrations immediately jumped to around 20 ug/l.

Biocell

Only the results from the biocell with the highest loading are presented. Treatment was similar in all biocells; those with lower flows just treated less volume.

The biocell removed about 99% of the lead for the first 10 weeks of the study (Figure 9). Concentrations increased gradually and reached the permit limit at about 30 weeks. Although suspended solids did enter the biocell, they were retained in the upper layer of the media.

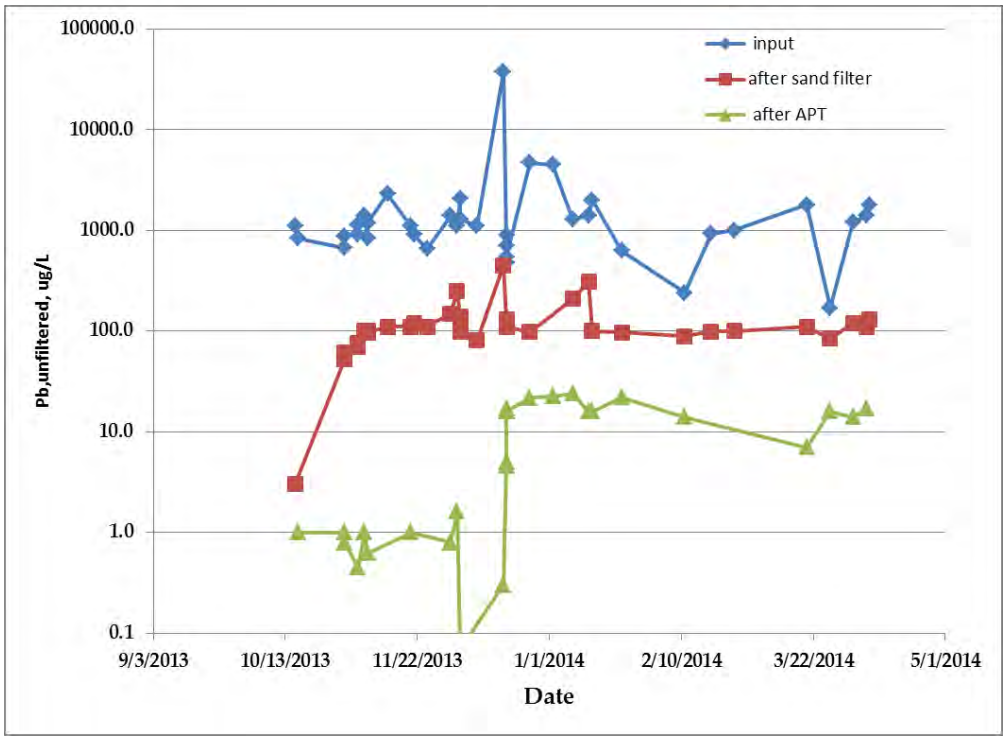

Figure 8 Lead removal, pressurized tank, October 2013-February 2014

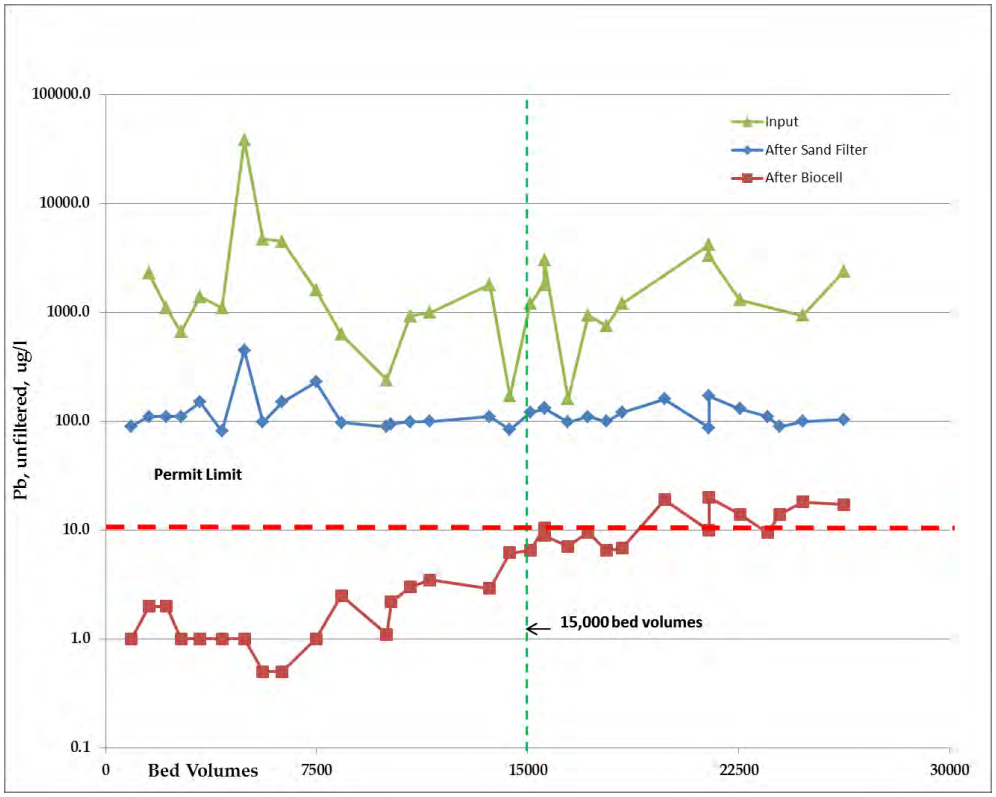

Figure 9 Lead removal, biocell October 2013 – August 2014

This caused a slight increase in head but the flow rate remained constant. No backwash was conducted on the biocell and the system continued to treat water until the test was terminated in August 2014. At the end of the experiment, Lead removal was still greater than 80%.

DISCUSSION

Lifetime

Treatment lifetime is often measured by the number of bed volumes treated. One bed volume is equal to the volume of the media; which in the pressurized tank is about 1890 liters. At the Soudan Mine, over 32,000 bed volumes have been treated, while the biocell at the base metal mine treated over 26,000 bed volumes (Figure 10). In both cases, the media was still removing substantial amounts of metal when the pilot ended.

At the base metal mine, the media treated 15,000 bed volumes before effluent concentrations approached the permit limit. The first sample that actually exceeded the permit limit of 11.5 ug/l was at 20,000 bed volumes. The standard procedure in media treatment is to employ a two-tank (lead/lag) design. The first tank would treat the first 15,000 bed volumes then a second or lag tank would be added to polish the effluent from the first tank to reduce the concentration below the permit limit. This extends the life of the media in the first tank. Although lead exceeded the permit limit in the biocell, the overall lead removal was still over 80% and the rate of increase in the lead concentration in the effluent was gradual, which suggests that breakthrough would be manageable and allow for methodical replacement of media.

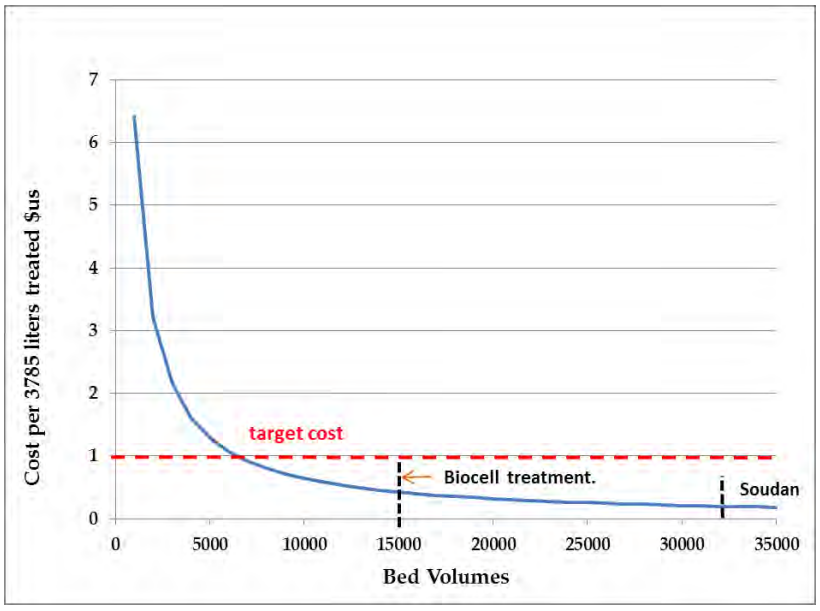

Figure 10 Treatment cost

Costs

As the number of bed volumes treated increases, the treatment cost (cost per liter treated) decreases (Figure 10). For copper treatment at Soudan the operating cost is on the order of 0.25 US$ per 3785 liters. For lead, the treatment cost using a single bed of media would be 0.43 US$ per 3785 liters.

At the Soudan Mine, a single tank of peat based sorption media provided equivalent (or better) copper treatment than the first four components of the existing system. Reducing the complexity of the system also reduced the overall cost associated with treatment. The estimated annual operating cost for the existing system was around 163,000 US$; this could be reduced to around 70,000 US$ by replacing the first part of the system with a tank of peat media.

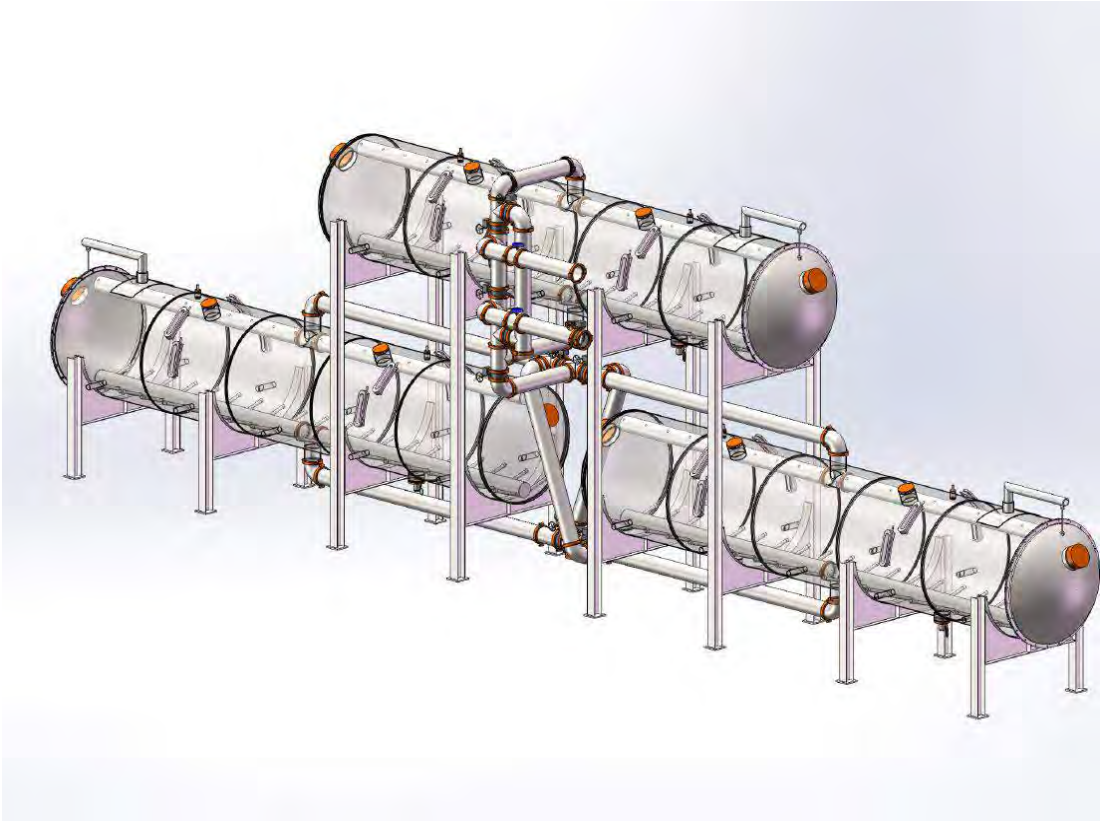

Figure 11 Three -tank module

At the base metal mine, a conceptual treatment approach was developed using a three tank modular system, containing a sand filter, and two tanks of media in a lead/lag configuration (Figure 11). Each module would be capable of treating up to 4540 L/min. The projected capital cost for the system was less than half that of a chemical treatment plant and the projected operating cost of 0.43 US$ per 3785 liters was significantly less than the company's target cost of 1 US$ per 3785 liters.

CONCLUSIONS

A variety of metal removal mechanisms occur in peat and include adsorption, ion exchange, complexation and chelation (Brown et al., 2000). This variety of mechanisms makes peat a very effective natural treatment media with the ability to cost-effectively remove a wide range of trace metals.

Peat resources are plentiful in Minnesota and the northern portion of the state still retains over 90% of its presettlement wetlands. Peat used to produce the media is harvested from an area that was drained in the early 1900's when there was a major effort to develop agriculture in northern Minnesota. The use of peat as a water remediation media is an example of using a resource in a sustainable, thoughtful way to maximize its best use potential.

Technically and politically, peat is described as a slowly-renewable resource and given the large area of wetlands in northern Minnesota overall accumulation exceeds the small extractive use. Peat accumulation rates are very slow but American Peat Technology is currently investigating methods to increase the rate of accumulation as part of its reclamation program.

REFERENCES

Brown, P. A., Gill, S. A. and Allen, S. J. 2000. Metal removal from wastewater using peat. Water Research Volume 34, Issue 16, Pages 3907-3916

Lapakko, K., Eger, P., 1988 Trace metal removal from stockpile drainage by peat. Proc. Mine Drainage and Surface Mine Reclamation Conference (USM Information Circular 9183), pp. 291-300

MacDonald, R. J., Hage, K. E., Dutrizoc, J. E. 1976. Copper recovery from copper-bearing peat moss. Miner. Res. Program, Miner. Science Lab. Report No. MRP/MSC 76-275

Salmi, M. 1959. On peat chemical prospecting in Finland. International Geological Congress Sym. De Exploration Geoguimica, Tomo 2, pp. 243-254

Conceptual Project on Eliminating Acid Mine Drainage (AMD) by Directed Pumping

Craig Sheridan[1], Ricky Bonner[1], Lenke Bruyns[1], Jo Burgess[2], Deanne Drake[1], Jon Paul Janet[1], Kevin Harding[1], Karl Rumbold[1], Nabeela Saber[1]

1. *Industrial and Mining Water Research Unit, University of the Witwatersrand, South Africa*
2. *Water Research Commission, South Africa*

ABSTRACT

Acid mine drainage (AMD) poses a serious threat to water quality in the Witwatersrand region (South Africa), owing to extensive mine voids that have been abandoned, and subsequently flooded. In response to the severity of the situation, the South African government has undertaken construction of facilities to lower the water level to a safe depth (e.g. where no AMD decants into the surrounding surface- or groundwater) through pumping and treatment. It is proposed that the infrastructure that is currently being installed could better manage the problem by pumping from a greater depth than originally intended. It is hypothesised that the anoxic conditions at greater depth (ca. 2 km) will preclude the generation of AMD and hence reduce the need for treatment, while maintaining the desired water level below ground. The increased energy required for pumping from 2 km was calculated relative to the intended depth (just below the environmentally critical level). The expected energy increase was ≈10%, suggesting that it is feasible to use the existing/planned pumping infrastructure at greater depth. The effects of pH, temperature and initial availability of oxygen in reaction water on the formation rate of AMD from Witwatersrand coal waste rock have been quantified.

No statistically significant effects of initial oxygen availability, pH, or incubation temperature on the production of SO_4^{2-} from coal mine waste rock were observed. In particular, decreased availability of O_2 in incubation water did not inhibit production of SO_4^{2-}. However, dissolved oxygen (DO) in many of the low DO treatment replicates increased, even though the incubation vessels were sealed, suggesting contamination.

The potential effects of pumping from depth on the aquifer were also investigated. In both cases, where oxygenated or low DO water was added to the surface and pumped from the bottom of an experimental column, the result was improved water quality with time (pH, EC, Fe, and SO_4^{2-}). However there is still considerable uncertainty as to whether this is a result of dilution without any formation of AMD or a result of dilution and no generation due to insufficient sulphide present to cause an ongoing reaction.

Keywords: Acid Mine Drainage (AMD), Acid Rock Drainage (ARD), Remediation, Pumping, Johannesburg.

INTRODUCTION

Extensive gold mining activity around the Witwatersrand Basin (South Africa) has resulted in the formation of acid mine drainage (AMD). It is estimated that the potential AMD decant is in excess of 200 Ml/day, and contains high levels of sulphate and dissolved metals (McCarthy, 2011; Council for Geoscience *et al*., 2010). The South African government has awarded tenders to various industrial partners to mitigate the problem by pumping the water table down to just below the Environmentally Critical Level (ECL) by pumping from the ECL, and treating the resulting effluent using the High Density Sludge Process (HDSP) (Odendaal, 2013). This process is energy intensive, as it requires transport of large quantities of lime to the treatment site, pumping between tanks and treatment ponds, and disposal of the treatment residues. Pumping and treatment can only, however, be a temporary solution to the problem, as fresh AMD will continue to be generated in the mine voids for an indefinite length of time and will continue to require treatment.

In this work it was hypothesised that if water were to be pumped from a lower level, whilst holding the same ECL, acid might not be generated (following removal of the initial acid present in the void) as opposed to pumping from the ECL, where acid would continuously be generated by freshly aerated water. This hypothesis is based on the premise that at depth, oxygen is very limited in water. This effect can be observed in marine environments, where corrosion (due to oxidation) occurs in the surf zone, as well as in deep lakes, where the deep levels in the lake are anaerobic. This project sought to simulate anaerobic, subsurface conditions with a view to testing this hypothesis.

LITERATURE

Background

Acid mine drainage is generated in mine voids, primarily where pyrite-containing minerals are exposed to oxygenated water. The result is acidic water that is rich in sulphates and dissolved metals; in South Africa this frequently includes uranium (Cukrowska *et al*., 2008). Acid mine drainage poses a particular danger to the local environment of the Witwatersrand owing to the high number of abandoned mines and characteristics of the water table in this semi-arid region (Durand, 2012). Decant of AMD is a serious threat to the safety of communities and the environment of the Witwatersrand (Council for Geoscience *et al*., 2010).

The immediate geological region of the Witwatersrand is named the Witwatersrand Supergroup, and consists of sedimentary rock approximately 7500 m thick (Durand, 2012). The Witwatersrand groundwater table is mainly supplied by karst aquifers located in the adjacent Transvaal Supergroup. Water flows from these dolomite-rich aquifers into the Witwatersrand Supergroup, and many of the gold mines in the area are located below the water level of karst aquifers. Hence, millions of litres of water were pumped out daily during peak mining activity periods. Mining activity depressed the water table by as much as 3 km (Durand, 2012). Following cessation of mining activities and associated pumping, groundwater has ingressed into pyrite-rich mine voids left behind, and is currently discharging into rivers in the provinces of Gauteng and the North West.

Mine voids in the Witwatersrand region are classified into the western basin, central basin and eastern basin. The western basin alone has an estimated void volume of at least 45 Gl. Durand (2012) reports that decant of approximately 36 Ml of AMD per day was released from this basin into

the Tweelopiesspruit river in Krugersdorp in 2010, although pumping undertaken at Rand Uranium has since reduced the decant considerably (Odendaal, 2013).

The severity of the AMD decant varies substantially with location. The water quality in the Witwatersrand Basin is seen to be most affected nearest mining operations, with some samples having pH < 2 and sulphate concentrations exceeding 7 000 mg/l in the worst cases (Cukrowska *et al*., 2008). High concentrations of iron (up to 1 010 mg/l), as well as other metals including copper, nickel, cobalt and uranium were also reported.

In some cases, there are sufficient concentrations of uranium and other radioactive elements in mine decant and water bodies to pose serious risk to human health. For example, samples from some lakes near mining operations have been found to contain 14.8 mg/l of uranium, more than 1000× the safe limit for irrigation water of 10 μg/l (Durand, 2012).

Mechanisms of AMD Generation

The mechanisms of AMD generation are extensively reported in literature. The principal process involved occurs when pyrite-containing rocks (FeS_2) are contacted by oxygenated water, where the overall reaction (Equation 1) occurs (Hallberg and Johnson, 2005):

$$FeS_2 + 15O_2 + 14H_2O \rightarrow 4Fe(OH)_3 + 18SO_4^{2-} + 16H^+ \quad (1)$$

The above reaction occurs in multiple stages, and the primary oxidant is ferric iron instead of molecular oxygen – the attack of the ferric iron on the pyrite mineral occurs first, then the resulting ferrous iron is converted back to ferric iron by re-oxidation using oxygen dissolved in the mine water. Oxygenated water is therefore, essential for continuation of the cycle that produces acidity (Hallberg and Johnson, 2005). While this is a naturally occurring reaction, it is accelerated when large surface areas are exposed in mine voids and water and oxygen gain access to the minerals. While the reaction can occur in the absence of bacterial activity, micro-organisms such as *Acidithiobacillus ferrooxidans* can substantially increase the rate of generation (Akcil and Koldas, 2006). As a result of the low pH, metals leach out of the solid state further contaminating the water. In the Witwatersrand, the primary metals of concern are manganese, aluminium, iron, nickel, zinc, cobalt, copper, lead, radium, thorium, and uranium (Durand, 2012).

Current Management Strategies

Three priority areas have been defined in the Witwatersrand (Council for Geoscience *et al*., 2010):

- Prevent uncontrolled decant. This is to be accomplished by pumping water out of the voids to keep the water table below the ECL.
- Limit the ingress of water into the mineshafts. This is to be accomplished by sealing as many large openings as possible.
- Treat the water removed from the voids before being released to the environment. This could be through neutralisation with lime, passive remediation in limestone beds, bioremediation using aerobic wetlands, bioreactors and more (Hallberg and Johnson, 2005). In situ and passive methods are currently regarded as unfeasible for the Witwatersrand Basin due to the size and complexity of the voids as well the large decant rates expected. The expected cost of active treatment of the discharge is ZAR11 /m^3 (Council for Geoscience *et al*., 2010); approximately USD1.1 /m^3.

In response to the AMD problem, these strategies are currently being implemented. The state-owned Trans-Caledon Tunnel Authority (TCTA) awarded a R319 million contract to Group Five Engineering in December 2012 (Odendaal, 2013) to construct pumping stations and HDSP treatment facilities for the central basin. In the western basin, upgrades are being carried out on the existing pumping and treatment facilities at Rand Uranium in order to expand capacity. Due to cost constraints, construction of pumping systems in the eastern basin has been postponed (Odendaal, 2013).

Increasing Pumping Depth

Previous work has shown that by increasing the pumping depth (Figure 1), the energy requirements do not increase as much as might be expected, *e.g.* depending on the initial conditions, doubling the pumping flowrate may only result in a 10% increase in the energy requirement (Figure 2) (Janet et al. 201x). In this paper, we present results of experiments conducted to determine if it is in fact possible to prevent the formation of AMD by using this strategy.

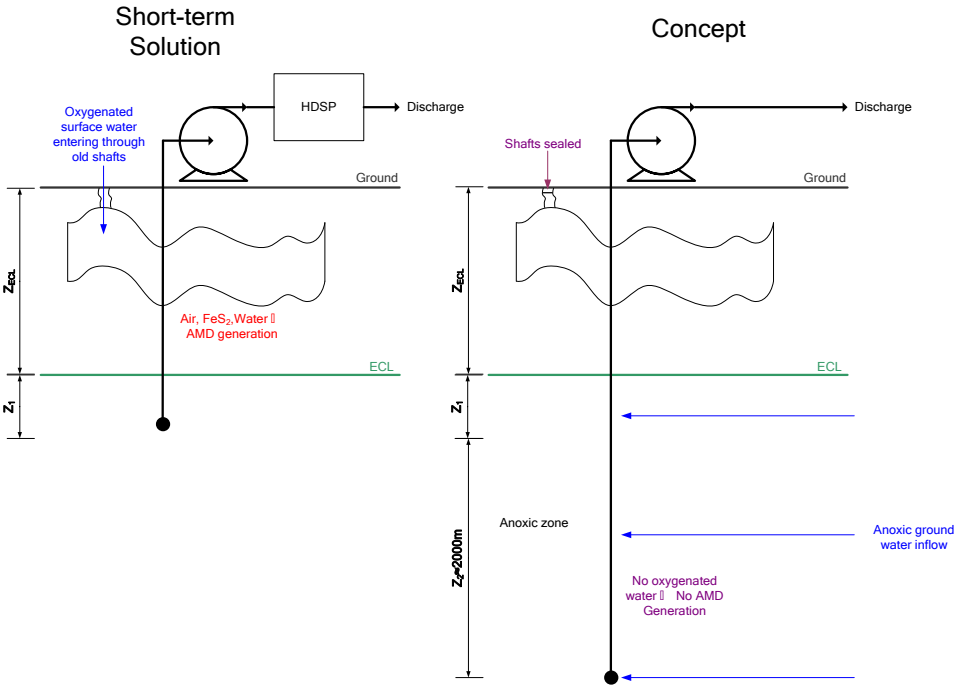

Figure 1 Schematic comparison of current short term intervention plan (left) and the proposed concept of pumping from depth (right) From Janet *et al.*, 201x

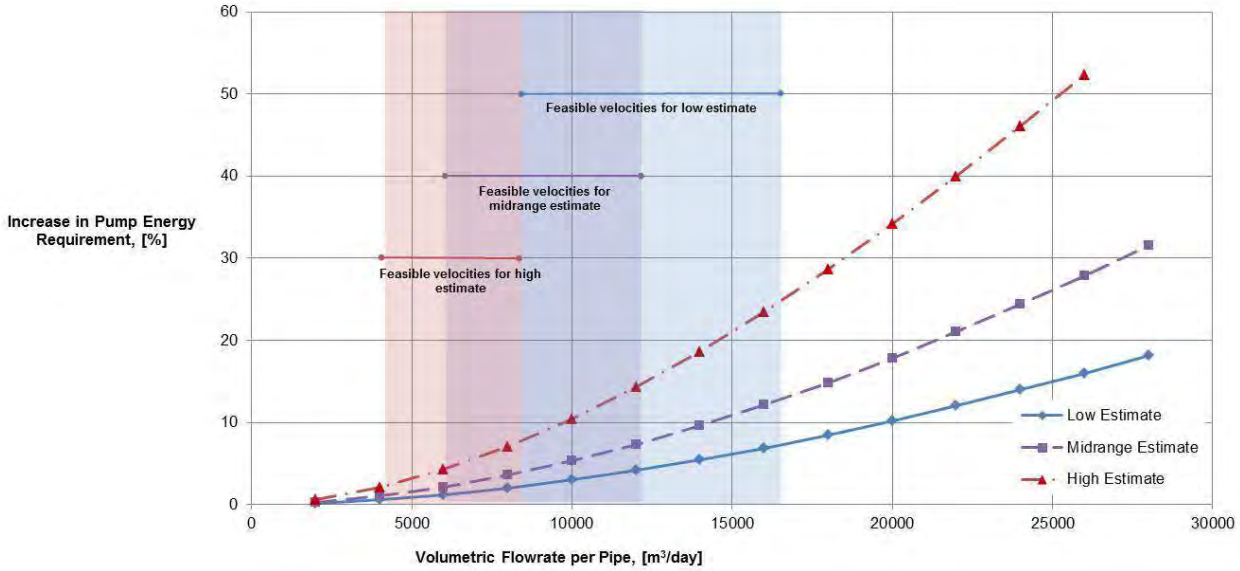

Figure 2 Comparison of percentage increase in pumping energy when increasing pumping depth for three scenarios (low, mid and high estimates) (Janet *et al*., 201x)

METHODOLOGY

Three PVC column reactors (6 m × 30 cm) were set up with pyrite-rich waste rock representative of an AMD-generating ore body (Figure 3), kindly provided by Optimum Coal. Each reactor had a solid casing installed in the centre, in which a peristaltic pump suction line could be inserted. The reactors had a cap at the surface to prevent air entering the system. Deoxygenated water was prepared by continuously bubbling nitrogen through a feed tank. Double head Watson and Marlow peristaltic pumps drew water from the base of each column whilst pumping deoxygenated water into the top of the column at the same flow rate of 31 ml/hour (equal to the net rainfall in the Witwatersrand). This equated to a 9 week hydraulic residence time.

The three columns were set up as follows:

- Column 1: Potable water added to surface, effluent (mimicking groundwater) removed from the base and DO, pH and SO_4^{2-} measured. This investigated what would happen if the only source of water was percolation from the ground surface, mimicking the generation of AMD at the surface. The experiment was also designed to demonstrate potential remediation of AMD as the recharge passed through the aquifer.
- Column 2: De-oxygenated water added to the surface, effluent (groundwater) removed from the lowest level and DO, pH and SO_4^{2-} measured. This experiment was designed to indicate whether AMD formed under anaerobic conditions.
- Column 3: De-oxygenated water added to different depths along the side of the central casing, effluent (groundwater) removed from the lowest level and DO, pH and SO_4^{2-} measured. The column was initially filled with previously boiled water and purged with nitrogen prior to and during filling to minimise DO. This experiment sought to reproduce ingress of DO-poor water at different depths, as would be expected in an aquifer.

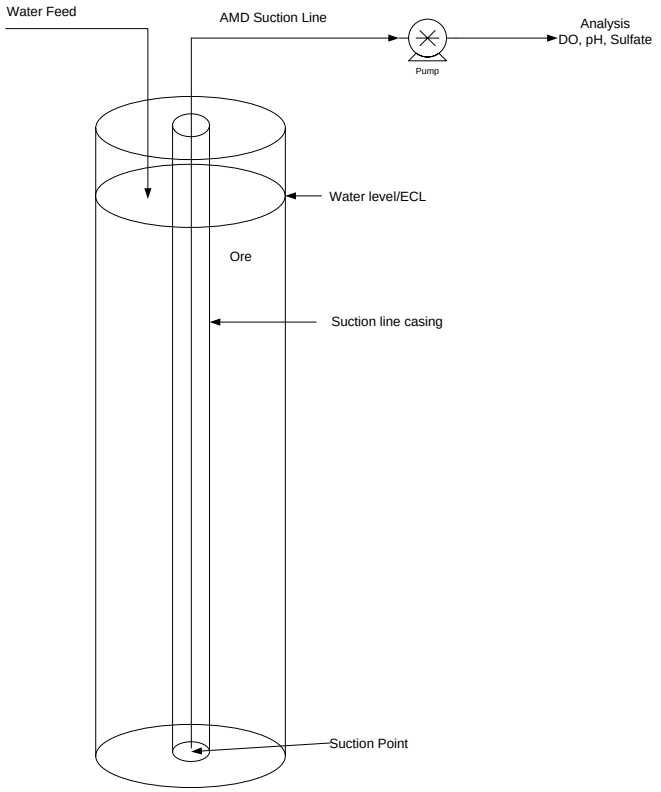

Figure 3 Column reactor, showing feed ingress at the top and effluent removal via a casing in the centre of the column

Upon completion of the initial experiments, Columns 1 and 3 were purged with air whilst still full of water for a period of 30 min in an attempt to generate additional acid such that it could be assured that the results seen were not as a result of the rate of dilution being greater than the rate of acid generation.

Sample DO, EC and pH values were measured using a handheld Consort C5010 multiprobe, which was calibrated prior to each use. Iron and sulphate were measured using a Merck Pharo 300 spectroquant, using test kit 1.14671.0002 for iron and test kit 1.14791.0001 for sulphate. Samples were prepared and analysed according to the manufacturer's directions. Measurements inside the columns (temperature and pH) were taken using a Hydrolab MS5 EC-pH probe.

RESULTS AND DISCUSSION

Comparison of Column 1 (oxygenated feed) with Column 3 (de-oxygenated water feed)

The change in pH of the columns' effluent is shown in Figure 4. Acid was rapidly generated in both columns and the pH gradually rose thereafter. The low DO column (Column 3) had a slightly higher pH than Column 1 after 5 weeks.

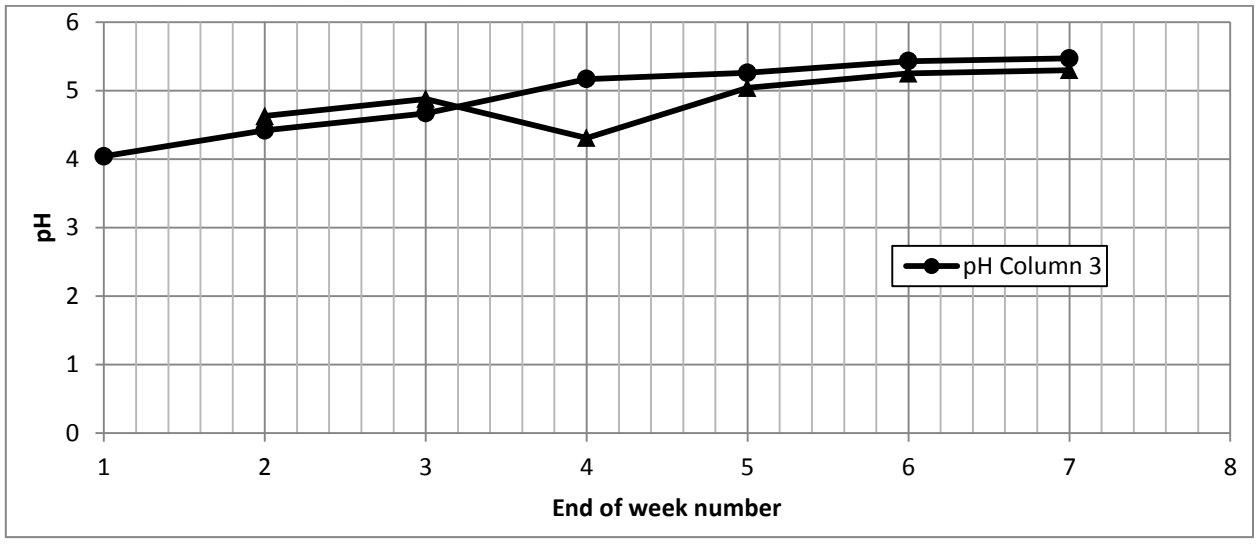

Figure 4 The pH in both columns over time

The DO concentrations in columns 1 and 3 are presented in Figure 5. The values were erratic, although there seemed to be a decrease in DO with time, suggesting that available oxygen was utilised as the reactions proceeded. However, the DO probe was adversely affected by low pH and high sulphate values; these data are not reliable.

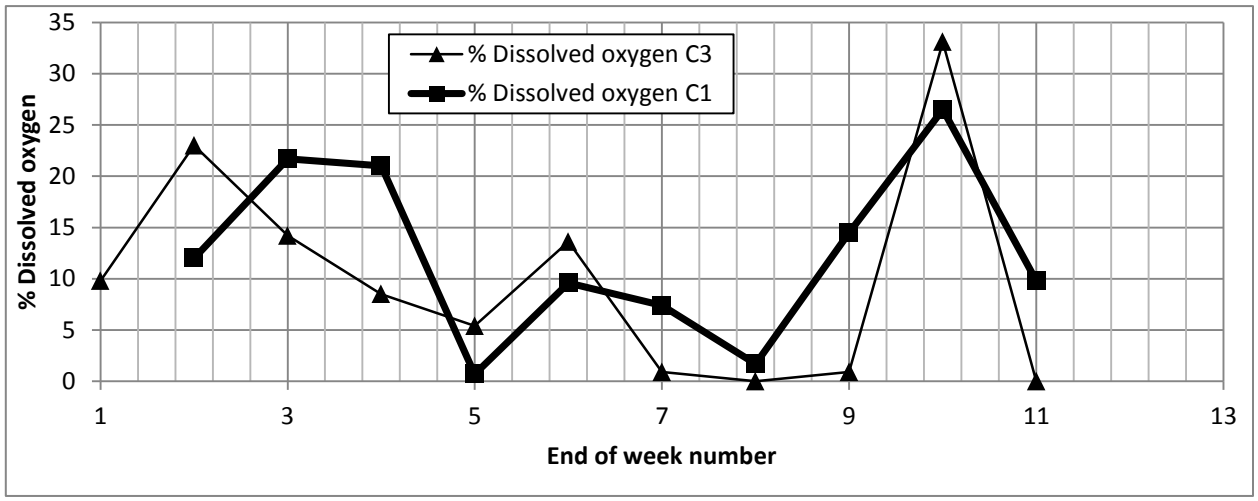

Figure 5 Dissolved oxygen in Columns 1 and 3, showing erratic nature of the data.

Both sulphate and iron concentrations in Column 1 rose rapidly and then decreased (Figure 6). The sulphate values fluctuated substantially throughout the experiment. It is believed that this is a result of the type of analysis used. It is understood that the BaCl test would give significantly more accurate results, and this is recommended for future work. The iron was shown to decrease.

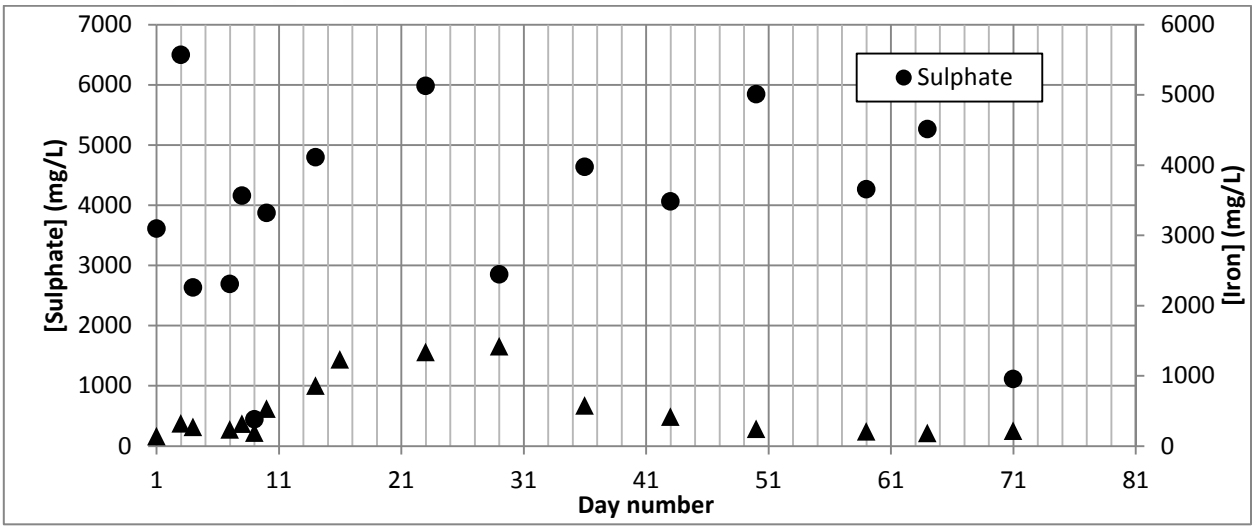

Figure 6 Variation of sulphate and iron in Column 1

The change in sulphate and iron in Column 3 is shown in Figure 7. Similarly to Column 1, concentrations rose rapidly within the first day and subsequently decreased. The two columns reached similar initial values and both showed a decreasing trend with time. The variation of the sulphate concentrations is once again observed.

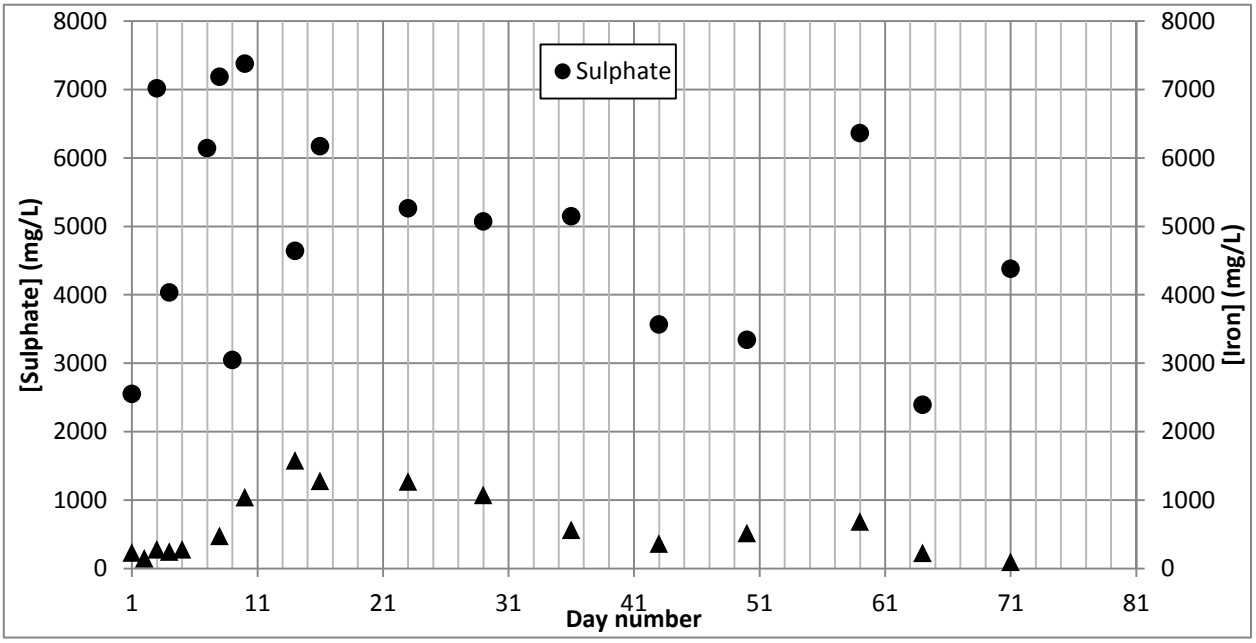

Figure 7 Variation of sulphate and iron in Column 3

Figure 8 illustrates the results when we inserted a Hydrolab MS5 autoprobe onto Columns 1 and 3. The Hydrolab MS5 auto probe, able to measure and record pH, EC and temperature was initially placed in Column 3 from 28 March 2014 to 16 April 2014 and then transferred to Column 1 from 16 April to 23 April. Whilst the probe did not record the beginning of the experiment in Column 1, the data recorded clearly showed an increase in pH, and a decrease in EC (Figure 8), and in Figure 9 the

data are presented for Column 3. The rise in pH is particularly evident in the low DO experiment where the pH increased by 1.5 and EC decreased by approximately 25% .

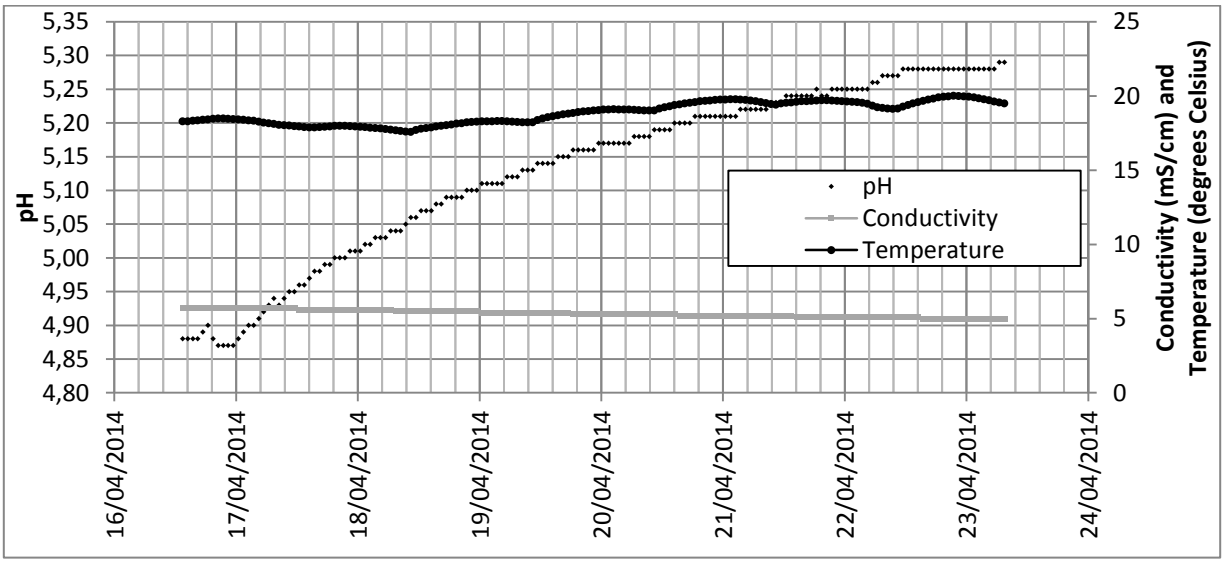

Figure 8 Temperature, pH, and EC profiles within Column 1

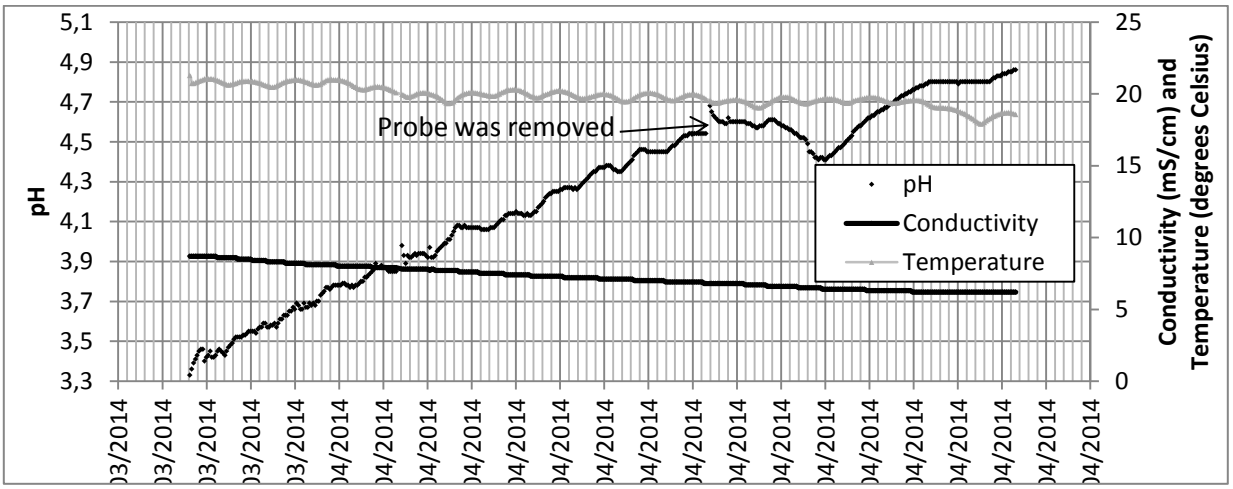

Figure 9 Temperature, pH, and EC profiles within Column 3.

The long-term measurements obtained from use of the Hydrolab probe indicated that by pumping from the bottom of the column, water quality improved and that improvement occurred regardless of the oxygen content of the feed.

CONCLUSION

It has been shown that the energy to pump water from 2 km below surface is not substantially different from removing water from just below the ECL. It has further been demonstrated that acid is rapidly generated by waste rock. With time, all water quality parameters improved significantly by pumping water from the base of the columns where AMD was unable to form. It was not

possible to conclude whether this improvement in quality was a result of dilution due to depletion of the mineral or if AMD was no longer being generated due to the establishment of anaerobic conditions. Future work to assess this will proceed.

ACKNOWLEDGEMENTS

The financial support of the Water Research Commission, South Africa, as well as the University Research Council (URC) of the University of the Witwatersrand, Johannesburg is gratefully acknowledged.

REFERENCES

Akcil, A, Koldas, K (2006) Acid mine drainage (AMD): Causes, treatment and case studies, *J Clean Prod* 14: 1139–1145.

Council for Geoscience, Department of Water Affairs, Department of Mineral Resources, Council for Scientific and Industrial Research, Mintek, Water Research Commission (2010) *Mine Water Management in the Witwatersrand Gold Fields with Special Emphasis on Acid Mine Drainage*, The Council for Geoscience.

Cukrowska, E, McCarthy, TS, Tutu, H. (2008) The chemical characteristics of acid mine drainage with particular reference to sources, distribution and remediation: The Witwatersrand Basin, South Africa as a case study, *Appl Geochem*, 23, 3666-84.

Durand, JF. (2012) The impact of gold mining on the Witwatersrand on the rivers and karst system. *J Afr Earth Sci*, 68, 24-43.

Hallberg, KB, Johnson, DB (2005) Acid mine drainage remediation options: a review, *Sci Total Environ*, 338, 3-14.

Janet, JP, Sheridan, CM, Drake, DC, Rumbold, K, Harding, KG (201x) Increasing Pumping Depth as a Solution in the Long-Term Management of Acid Mine Drainage, *WaterSA*, xx, xx-xx (submitted for peer review).

McCarthy, TS (2011) The impact of acid mine drainage in South Africa, *SA J Sci*, 5/6, 107.

Odendaal, N (2013) *Group Five starts work on TCTA AMD contract* [Online] Mining Weekly Available at: http://www.engineeringnews.co.za/article/group-five-starts-work-on-tcta-amd-contract-a-02-22 [Accessed 3 June 2013].

Diffusive Exchange System with Internal Precipitation for Acid Mine Drainage Treatment

Gustavo Chaparro, Norma Perez and Alex Schwarz
Centre of Water Resources for Agriculture and Mining (CRHIAM), Universidad de Concepción, Chile

ABSTRACT

Copper extraction is the principal mining activity in Chile. Acid mine drainages (AMDs) and mining effluents are characterized by high concentrations of copper, which can be recovered. Existing biochemical reactors utilize homogeneous substrates as percolation media to immobilize metals. However, microbial communities are exposed to the acid drainages within these systems and their toxicity often limits reactor reactivity.

Diffusive exchange systems on the other hand avoid direct contact of microorganisms with the AMD, significantly expanding the treatment range of biochemical reactors to include higher metal concentrations and lower pHs. A key innovation of this research is the use of vertical tubular screens to convey the AMD through the substrate while simultaneously allowing transverse diffusion of dissolved species and acting as reactors for precipitate formation and settling. This design minimizes clogging and facilitates the recovery of valuable metal. Furthermore, biochemical reactors with passive systems can be built taller and much smaller footprints can be achieved.

This work studied the performance of a 2-m long vertical diffusive exchange column with internal precipitation, allowing the simultaneous removal and recovery of copper from a synthetic AMD. Detailed insight was gained into reactions and transport processes within the tubular screen by the use of several sampling points along the column.

During the first two months the reactor was fed with increasing concentrations of sulfate and no metals, to determine its sulfate reduction potential. Then the reactor was fed with the AMD for one month; during this test effluent metals, sulfate, sulfide, acidity, alkalinity, pH, conductivity and ORP were monitored periodically. The sampling points allowed pH, ORP and metal concentrations to be measured throughout the reactor. High sulfate reduction rates of 0.2-0.6 moles/m^3-day were obtained. Also, during the first month of operation with influent metals, constant removal rates were achieved and precipitates were harvested.

Keywords: biochemical reactor; acid mine drainage; diffusion; copper; sulfate.

INTRODUCTION

Acid mine drainages (AMDs) are an environmental problem which has serious effects on the quality of both surface and ground water. These include acidification and increased concentrations of toxic metals and sulfate.

AMDs are produced by the oxidation of mineral sulfides, resulting in the dissolution of heavy metals and sulfate (Scheoran *et al*, 2010). The reaction involving the oxidation of pyrite is known and can be represented by the following equation (EPA, 1994):

$$FeS_2(s) + 14Fe^{3+} + 8H_2O \rightarrow 15Fe^{2+} + 2SO_4^{2-} + 16H^+. \quad (1)$$

AMD and mining operation effluents generated by the copper extraction industry contain high concentrations of copper which may in some cases be recovered. The complete oxidation of chalcopyrite can be written as (Dold, 2010):

$$CuFeS_2 + 4O_2 \rightarrow Cu^{2+} + Fe^{2+} + 2SO_4^{2-}. \quad (2)$$

Sulfate-reducing bioreactors or biochemical reactors (BCR) have proved to be an effective way of treating AMD (ITRC, 2012). The effectiveness of BCRs relies mainly on the activities of sulfate-reducing bacteria, which produce sulfide and bicarbonate inside the reactor. This leads to the formation of sulfides of metals such as copper, zinc and iron, which precipitate and can then be removed.

$$H_2S + M^{2+} \rightarrow MS\downarrow + 2H^+. \quad (3)$$

However, existing BCRs use a homogeneous bed as a percolation medium for immobilizing the metals in the system. This exposes the microbial communities to AMD, limiting the reactivity of the BCR.

Sulfidic diffusive exchange systems (SDES) avoid direct contact between the AMD and the microbial communities by separating the percolation medium into alternate layers or zones of high and low hydraulic conductivity (Schwarz & Rittmann, 2010). The idea of using this configuration is to separate the advecting contaminated water from the reactive material; in this way the microbial communities in a BCR are not exposed directly to the toxic metals in an AMD. This will enable the range of substrates treated in BCRs to be extended to high metal concentrations and lower pH values (Schwarz & Rittmann, 2007a).

The solutes are exchanged between the layers or zones of a SDES by diffusive processes, so solute exchange occurs because of the concentration gradient between the layers. In order for solute transport to be controlled by the diffusive processes, there should be a difference of at least two orders of magnitude between the hydraulic conductivity values of the reactive and conductive layers.

Using a SDES configuration for the substrate in a BCR allows certain disadvantages suffered by homogenous substrate BCRs to be overcome, such as: loss of organic matter reactivity due to metal crusting and precipitation; problems with blockages and preferential hydraulic flows; limitation of microbial activity due to toxic concentrations of metals; and limits on the height of the BCR because of diminished hydraulic conductivity (Schwarz & Rittmann, 2007b).

In view of the above, it would be of interest to find out whether a new prototype BCR with SDES would enable the equipment to be used to treat an AMD with a high copper concentration, which is impossible with a homogeneous bed BCR. This research developed a prototype BCR with SDES which may allow copper and other metals to be removed from an AMD by simultaneous

precipitation and sedimentation. We also evaluated whether the concentration of influent sulfate is a limiting factor for the functioning of a BCR with SDES, and determined the sulfate reduction rate.

METHODOLOGY

Design of a BCR with SDES

The proposed BCR with SDES uses vertical diffusive exchange columns as conductive zones, surrounded by the organic substrate (reactive zone). With this configuration it is expected that the majority of the metals will be removed by precipitation and accumulate at the bottom of the column.

The idea of using vertical columns as the AMD conductive zone is to promote precipitate formation and establish the exact area where the metals removed by the BCR would accumulate. The object of this is to project a BCR with SDES which would enable metals to be recovered from an AMD. Figure 1 shows the differences between a homogenous bed BCR and the proposed BCR with SDES.

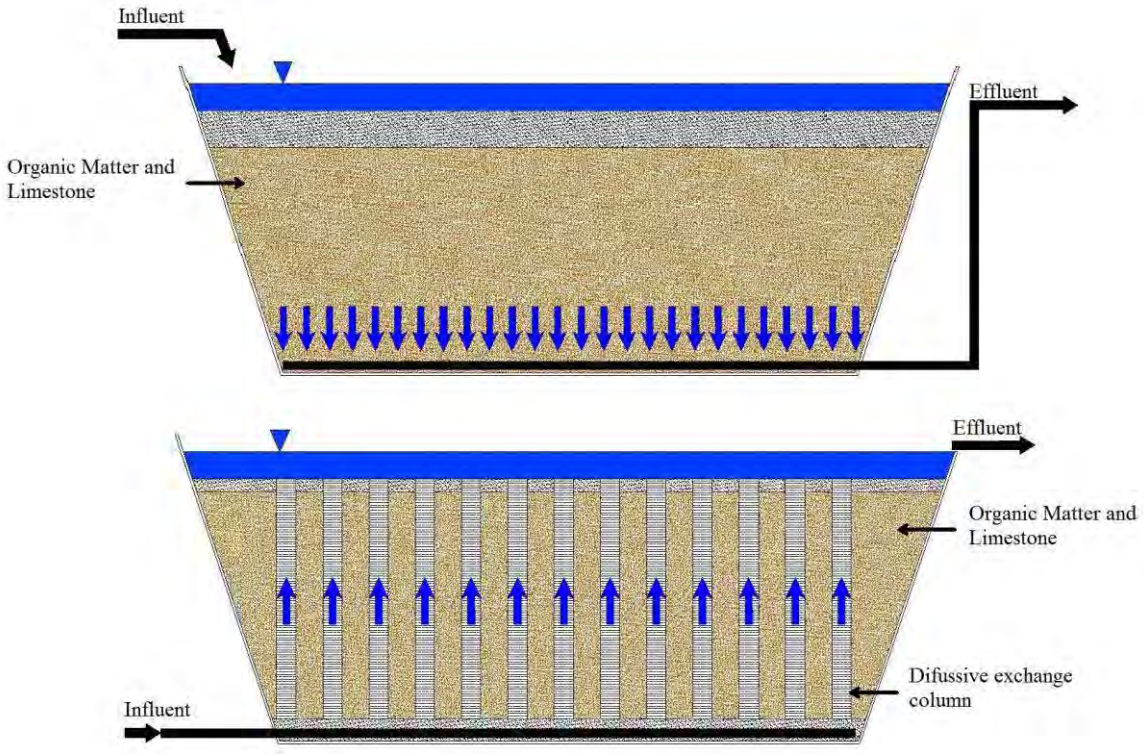

Figure 1 Diagram of a homogenous bed BCR (above) and a BCR with SDES (below). In the SDES reactor, the reactive mixture is crossed by screened tubes for the transport of fluid through the reactive bed. The screens retain the reactive mixture while allowing the lateral exchange of solutes between the advecing fluid and the bed pore space. Precipitates are expected to accumulate at the bottom of the screened tubes.

In the proposed BCR with SDES we decided to use an ascending flow to help sedimentation of the metal sulfide precipitates. The laboratory-scale BCR with SDES represents one of the several

reaction columns that may be found in a full-scale BCR with SDES. Figure 2 is a diagram of the laboratory-scale BCR with SDES constructed for the experiment.

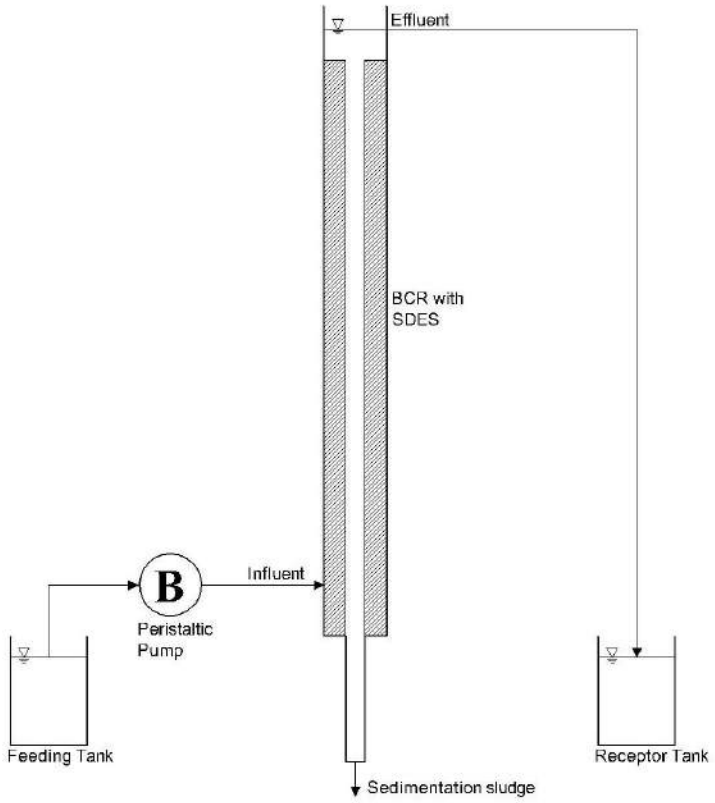

Figure 2 Diagram of the up-flow column reactor that simulates the processes that occur within a column of a BCR with SDES and its associated bed material. The reactor is made up of two concentric columns of which the interior one is screened. The reactive material is located in the inter-column space. The influent is feed into the inner column at the reactor bottom. Formed precipitates can be captured by sedimentation within the bottom extension of the screened tube.

ITRC (2012) recommends a maximum height of 1.8 m for the BCR, to avoid problems of reduced hydraulic conductivity in the lower layers of the substrate as a result of the excessive weight above. This problem does not apply to BCRs with SDES, but for practical reasons it was decided to make the laboratory-scale reactor 1.95 m high. The internal screened column is made of stainless steel, 6 cm in diameter and with aperture 0.75 mm. The outer column is made of PVC tubing, 19.3 cm in diameter. As a result, the volume occupied by the conductive central column in the reactor is 9.7%. A PVC tube 60 cm long, of the same diameter as the screened column, was placed below the column to collect the precipitates.

In order to study the reactor processes, five sampling points were fitted along the screen; these points were set at 6, 50, 100, 150 and 195 cm from the start of the reactive layer.

Organic matter

An important assumption in the choice and design of the substrate for the reactive layer was that microbial activity is sufficient to raise the pH of the AMD, because sulfate-reducing reactions produce bicarbonate and thus generate alkalinity (Scheoran, 2010). For this reason the reactive layer does not contain limestone or any other material to add alkalinity. Table 1 shows the materials used and their percentage by weight.

Table 1 Materials used in the reactive layer (% weight)

Function	Material	Percentage
Long term electron donor	Pure cellulose	50%
Short-medium electron donor	Manure	18.8%
	Leaf compost	31.2%

15 kg of organic matter were needed to fill the reactive layer in the reactor. The mixture was inoculated with 19 L of anaerobic digester content from the local sewage treatment plant. In addition, 15 L of distilled water were added to facilitate mixing and to saturate the organic matter. Figure 3 shows the organic matter used before and after mixing.

Figure 3 Organic matter utilized in the reactive mixture, before (left) and after (right) mixing

Finer organic matter can be used in BCR with SDES, since the substrate does not have to be kept permeable. The organic matter used in these reactors therefore has a larger contact area, with greater bio-availability to the microorganisms.

Experimental Tests

Four continuous experimental tests were carried out. In the first three, only the sulfate concentration in the influent was increased, while in the fourth metals were added. The purpose of

this was to study first whether sulfate is a limiting factor in the operation of a BCR with SDES. Table 2 shows the characteristics of the influent in the experimental tests.

The influent metal concentrations in the fourth test were: 568 mg Cu/L, 137 mg Zn/L, 35 mg Al/L and 0,8 mg Fe/L. These correspond to representative conditions of AMDs generated by large-scale copper mining in central Chile.

To characterize reactor functioning, samples were taken once per week from the effluent, the interior (bed pore water at a depth of 30 cm) and the five points along the screened column (numbered in the direction of flow). The sulfate and sulfide concentrations, the pH and the ORP were measured in the effluent, sampling point 5 (SP 5) and the interior. At SP 1 to SP 4, the sulfide concentration, the pH and the ORP were measured.

Table 2 Experimental tests

	Duration (weeks)	pH	Sulfate (mg/L)	Flow (L/day)
Test 1	6	5-5.5	2,218	2
Test 2	4	5-5.5	4,437	2
Test 3	4	5-5.5	6,655	2
Test 4	4	4-4.5	3,300	3

For three weeks before starting tests, 18 L of a solution with initial concentrations of 2,218 mg/L sulfate and 0.9 ml/L of lactate were recirculated through the reactor. The reactor was then fed for one week with a solution with the same initial concentrations as above, but without recirculation, at a flow of 2 L/day. This month of acclimatization is important in reactors of this type, to enable the bacteria to adapt and the communities to grow sufficiently to spread throughout the substrate.

RESULTS AND DISCUSSION

Variations in Sulfide, ORP and pH

Based on the interior screened column volume, the hydraulic residence time in the first three tests is 2.76 days, and in the fourth, 1.84 days. Table 3 shows the most important results of each test.

The results for SP 2 to SP 5 show the increase in sulfide concentrations as the contact time of the solution inside the reactor increases. All the sampling points reacted to the increased sulfate in the influent. SP 2 to SP 5, and the interior, present an increase in the average sulfide concentration as the influent sulfate increases.

At SP 2 to SP 5, when the sulfate concentration was doubled, the sulfide concentration increased on average by 51%. At these points, when the sulfate concentration was tripled, the sulfide concentration increased on average by 97%. It may therefore be concluded that the sulfide production in the reactor is limited to the influent sulfate. When the concentration of sulfate in the influent is increased, the sulfide inside the reactor also increases, in a proportion of two to one (percentage ratio).

The ORP measurements obtained during the tests at the five sampling points inside the reactor present similar behavior and appear to oscillate around the same average ORP regardless of the

sulfate concentrations in the influent. The ORP at SP 1 to SP 5 during these three tests was -108 mV on average, indicating that the reactor provides optimum conditions for anaerobic sulfate-reducing reactions, and that these conditions do not vary significantly along the reactor.

In the design it was assumed that the sulfate-reducing microbial reactions were sufficient to raise the pH of the influent. However, the average pH of the effluent during the three tests was 5.36, an average increase of only 0.06 over the pH of the influent.

Table 3 Variations in sulfide, ORP and pH during the tests with influent sulfate only (Tests 1-3)

		Sulfide average concentration (mg/L)	Sulfide maximum concentration (mg/L)	ORP (mV)	pH
	Effluent	2.4	5.5	-14.1	
	Interior	6.7	15.1	5	
	SP 1	16.9	23.0	-120.9	
Test 1	SP 2	15.2	21.1	-112.2	
	SP 3	14.5	21.5	-112.7	
	SP 4	14.8	22.8	-113.4	
	SP 5	14.7	21.1	-115.6	
	Effluent	9.5	12.5	-86.1	5.4
	Interior	8.8	14.8	22.3	5.1
	SP 1	11.2	21.5	-93.0	5.1
Test 2	SP 2	20	28.6	-94.3	5
	SP 3	24.7	30.7	-104.3	4.9
	SP 4	22.7	24.3	-106.5	5
	SP 5	21.9	23.2	-115.3	5
	Effluent	5	11.2	-71.5	5.4
	Interior	18.9	26.1	-22.7	5
	SP 1	9.2	20.7	-98.0	5.1
Test 3	SP 2	21.8	35.6	-109.5	4.9
	SP 3	32.8	33.9	-114.6	4.8
	SP 4	30.4	35.2	-113.0	4.9
	SP 5	31.2	43.6	-112.1	5.1

Variations in the Sulfate

Figure 4 shows the sulfate concentrations obtained during the three tests in the effluent, SP 5 and inside the reactor.

In the first test it was observed that the reactor reached a state of equilibrium immediately. This was because during bacterial acclimatization the reactor was fed with the same concentrations used in

Test 1. It had therefore already reached equilibrium for the concentration used in Test 1. In Tests 2 and 3, equilibrium was reached after 15 days' operation. The interior (organic matter) never reaches equilibrium because transport in this layer is diffusive, so the test times are too short for concentrations to equalize throughout the bed material within the reactor. However it is observed that the sulfate concentration in the interior increases, and that it is dependent on the concentration in the influent.

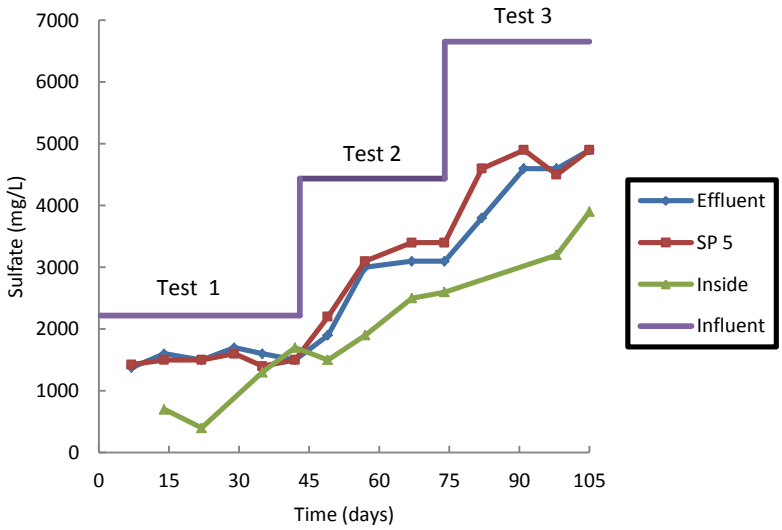

Figure 4 Variation of sulfate concentrations during the treatments with influent sulfate only (Tests 1-3). SP 5 is at the bed surface within the screened interior tube and the "inside" point is within the bed material at a depth of 30 cm.

For a homogeneous BCR, the volumetric sulfate-reduction rates are between 0.1 and 0.3 moles/m^3 of substrate/day (Gusek, 2002; ITRC, 2012; Wildeman & Schmiermund, 2004). The BCR with SDES constructed for this experiment presented average volumetric sulfate-reduction rates of 0.25, 0.5 and 0.72 moles/m^3 reactor/day for Tests 1, 2 and 3 respectively, based on total reactor volume (bed volume plus screened volume) (see Figure 5). Therefore the volumetric sulfate-reduction rate for a BCR with SDES depends on the influent sulfate concentration, and is directly proportional. In other words, if the influent sulfate concentration is doubled, the volumetric sulfate reduction rate will increase in roughly the same proportion.

The average sulfate removal percentages were 30.3, 30.9 and 29.4% in Tests 1, 2 and 3 respectively (see Figure 6). Thus the removal percentage did not vary significantly when the influent sulfate concentration was increased, remaining fairly constant at around 30%.

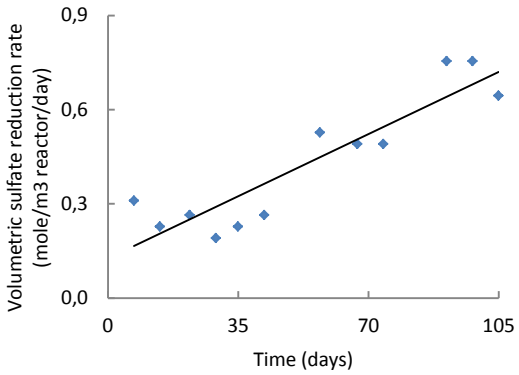

Figure 5 Volumetric sulfate reduction rates during treatment with influent sulfate only (Tests 1-3)

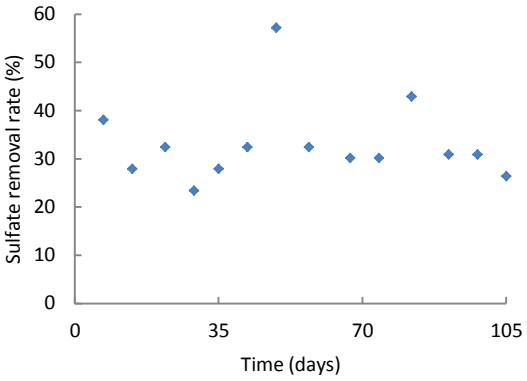

Figure 6 Sulfate removal rates during treatment with influent sulfate only (Tests 1-3)

Metal removal

In the fourth test the column was exposed to high concentrations of metals, particularly Cu and Zn, representative of AMD in central Chile. The flow was also increased by 50% to 3 L/day, to keep the reactor overloaded with metals. Under these conditions, the metal removals were 57% for Cu, 37% for Zn, and 50% for Al (Fig. 7). The overall volumetric metal removal rate was 300 mmol/m^3 reactor/day (Fig. 8). This experiment is continuing, to see whether the reactor can maintain these removal rates over time. Blackish precipitates were found in the bottom effluent, which may be mostly Covelite.

Based on sulfate reduction and metal removal rates one can compute the metal removal to sulfate removal yield, which is about two thirds or 67%. That is in average sulfate reduction would be only 67% effective in contributing to metal removal as sulfides.

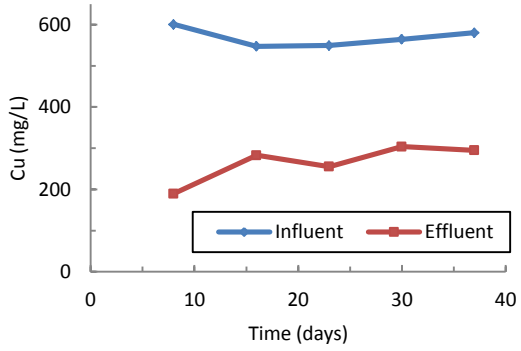

Figure 7 Influent and effluent copper concentrations during treatment with synthetic AMD (Test 4)

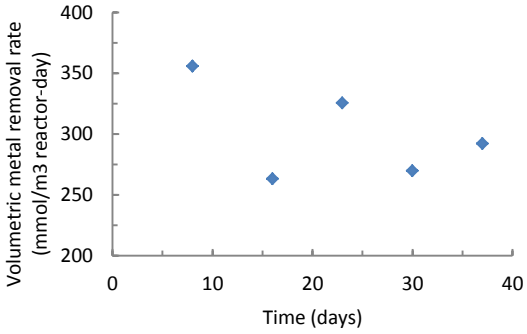

Figure 8 Overall volumetric metal removal rates during treatment with synthetic AMD (Test 4)

CONCLUSIONS

The BCR with SDES constructed at laboratory scale presented sulfate reduction rates of up to 0.75 moles/m^3 of reactor/day. This value is 2.5 times higher than the average sulfate reduction rate found in homogeneous BCRs, showing that the use of SDES in regard to substrate, can improve BCR functioning significantly.

The BCR with SDES reacted to increases in the influent sulfate concentration. The volumetric sulfate reduction rate increased proportionally with the sulfate concentration. On the other hand the sulfide inside the reactor increased by 50% on average when the sulfate concentration was increased by 100%. Thus the sulfate concentration in an AMD is a limiting factor in the operation of a BCR with SDES.

The BCR with SDES cannot raise the pH of the influent. Thus to neutralize the pH of an AMD it may be necessary to add limestone or some other alkaline material to the mixture.

During the first month of feeding with metals, the reactor removed a significant percentage of copper and zinc; however it remains to be seen whether this removal can be maintained over time. A precipitate was recovered from the bottom of the reactor, the purity of which is to be determined for copper recovery purposes.

Hence BCR with SDES hold promise for the treatment of AMD. Biological processes and chemical reactions are separated within theses systems. This zonation allows independent optimization of key processes. The biological system can be optimized for resistance and reactivity, while de chemical system can be optimized for metal precipitation and recovery.

REFERENCES

Dold, B. (2010) *Basic Concepts in Environmental Geochemistry of Sulfidic Mine-Waste Management,* Waste Management, pp. 173–198.

EPA (1994) *Technical Document. Acid Mine Drainage Prediction*, U.S. Environmental Protection Agency. Washington, D.C.

Gusek, J.J. (2002) *Sulfate reducing bioreactor design and operating issues: Is this the passive treatment technology for your mine drainage?* National Association of Abandoned Mine Land Programs and Reclamation. Park City. UE.

ITRC (2012) *Biochemical Reactor for Mining-Influenced Water,* Interstate Technology & Regulatory Council, Biochemical Reactor for Mining-Influenced Waste Team. Washington, DC.

Schwarz, A.O., and B.R. Rittmann (2007) *A biogeochemical framework for metal detoxification in sulfidic systems,* Biodegradation, vol. 18, pp. 675–692.

Schwarz, A.O., and B.R. Rittmann (2007) *Analytical-modeling analysis of how pore-water gradients of toxic metals confer community resistance*, Advances in Water Resources, vol. 30, pp. 1562–1570.

Schwarz, A.O., and B.R. Rittmann (2010) *The diffusion-active permeable reactive barrier,* Journal of Contaminant Hydrology, vol. 112, pp. 155-162.

Scheoran, A.S., V. Sheoran, and R.P. Choudhary (2010) *Bioremedation of acid-rock drainage by sulphate-reducing prokaryotes: A review,* Minerals Engineering, vol. 23, pp. 1073-1100.

Wildeman, T.R, and R. Schmiermund (2004) *Mining influenced waters: Their chemistry and methods of treatment,* National Meeting of the American Society and Reclamation. Lexington. UE. April.

10th ICARD IMWA 2015 | 10th International Conference on Acid Rock Drainage & IMWA Annual Conference

Designing a Mine Water Treatment Facility to Remove Sulfate

H. C. Liang, Joseph Tamburini and Frank Johns
Tetra Tech, USA

ABSTRACT

Due to the effects of weathering and oxidation of sulfide–containing ores, acid rock or acid mine drainage (ARD or AMD) from mining activities can generate sulfate–contaminated waters. Although sulfate has long been considered relatively harmless to human health and to the environment compared to other contaminants common in ARD or AMD, regulations for sulfate in mine water discharge have become more common, necessitating more advanced sulfate–removal processes at many mining operations. Where they apply, sulfate discharge standards in the United States typically range between 250 and 1,000 mg/L, with proposals in certain areas to apply sulfate discharge standards as low as 10 mg/L. The presentation highlights the design of a full–scale mine water treatment facility to remove sulfate in AMD–impacted waters at a mine in North America with a design flowrate of approximately 5 million gallons per day (MGD), where the average sulfate concentration is approximately 2,000 mg/L and would need to be treated to below 600 mg/L sulfate for discharge. The evaluation of chemical precipitation for sulfate removal such as gypsum and ettringite formation as well as the use of membrane filtration and the decision processes used to arrive at the final design are discussed.

Keywords: Sulfate, ettringite, gypsum, mine water

INTRODUCTION

Sulfate (SO_4^{2-}) is often produced in acid mine drainage (AMD) as a result of exposing pyritic rocks to air due to mining activities, which leads to a cascade of reactions forming both acidity and sulfate that can be summarized by Equation 1:

$$2FeS_2(s) + 7O_2(g) + 2H_2O(l) \rightarrow 2Fe^{2+}(aq) + 4SO_4^{2-}(aq) + 4H^+(aq) \quad (1)$$

Although acid mine drainage (AMD) is a major environmental concern (Liang & Thomson, 2010), and many AMD–impacted waters contain high levels of sulfate, most mine water treatment facilities have not been designed to remove the sulfate anion. Instead, when sulfate removal does occur at mine water treatment facilities, it usually occurs as an unintended consequence of using lime to raise the pH of the solution, which provides a source of calcium ions (Ca^{2+}) to precipitate and remove some of the dissolved sulfate ions as gypsum ($CaSO_4{\cdot}2H_2O$). One of the reasons why sulfate has been mostly ignored in mine water treatment is that it is traditionally considered a benign, non–toxic inorganic contaminant. For example, the U.S. Environmental Protection Agency (U.S. EPA) has not established an enforceable primary drinking water standard for sulfate and only has a non–enforceable secondary drinking water standard of 250 mg/L for sulfate. Because of the perception that sulfate is relatively harmless, mine water treatment has typically focused more on pH adjustment and the removal of more acutely toxic inorganic contaminants such as copper, cadmium, arsenic, antimony, selenium, and other inorganic contaminants that often occur as a result of AMD instead of on sulfate removal. Recently, however, research has shown that sulfate–reducing bacteria (SRB) can generate highly toxic and bioavailable methylmercury in the environment by methylating inorganic Hg^{2+} and converting inorganic mercuric compounds into methylmercury (Jeremiason et al, 2006). In addition, research has also shown that high sulfate levels in wetlands can induce the liberation of precipitated, bound phosphates in the sediment and lead indirectly to the eutrophication of wetland systems (Lamers, Tomassen & Roelofs 1998). Because of these issues, and because sulfate typically accounts for much of the total dissolved solids (TDS) in mining–impacted waters that need to be treated to acceptably low TDS levels to reduce the impact of mining waters on the salinity of the receiving waters, sulfate removal has become much more important in mining water treatment in recent years.

METHODOLOGY

The major criteria used to select the sulfate–removal treatment process were, in order of importance: 1) Capability to remove sulfate consistently to < 600 mg/L; 2) Treatment costs, which included examining the amounts of wastes generated by the treatment process; 3) Ease–of–operations. Any treatment process that in–and–of–itself cannot practically be expected to remove sulfate to < 600 mg/L on a consistent basis was not examined further.

As the stability diagram of sulfur in water shows (Figure 1), the sulfate anion is the predominant sulfur species under most conditions encountered in surface waters. Because of the high design

flowrate (~5 MGD) and fluctuating water quantities and qualities for the mine water treatment facility, it was determined that it would not be practical to pursue biological sulfate reduction. Therefore, assessment of the treatment options focused on chemical precipitation or membrane filtration to remove the sulfate.

Assessment of treatment options

Chemical precipitation to remove sulfate

Adding hydrated lime to neutralize acidic mine waters and for chemical precipitation of gypsum to remove sulfate is one of the more common practices encountered in mine water treatment. The hydrated lime ($Ca(OH)_2$) is added to supply Ca^{2+} ions for removing sulfate as gypsum, as represented by Equation 2:

$$Ca(OH)_2(s) + SO_4^{2-}(aq) + 2H_2O(l) \longrightarrow CaSO_4{\cdot}2H_2O(s) + 2OH^-(aq) \quad (2)$$

Because gypsum is slightly soluble in water ($K_{sp} = 3.14 \times 10^{-5}$), both theoretical calculations and field results show approximately 1,500 mg/L or higher of calcium would remain dissolved in solution after gypsum precipitation treatment. Therefore, gypsum precipitation by itself would not be sufficient to meet the 600 mg/L sulfate discharge limit at this mine.

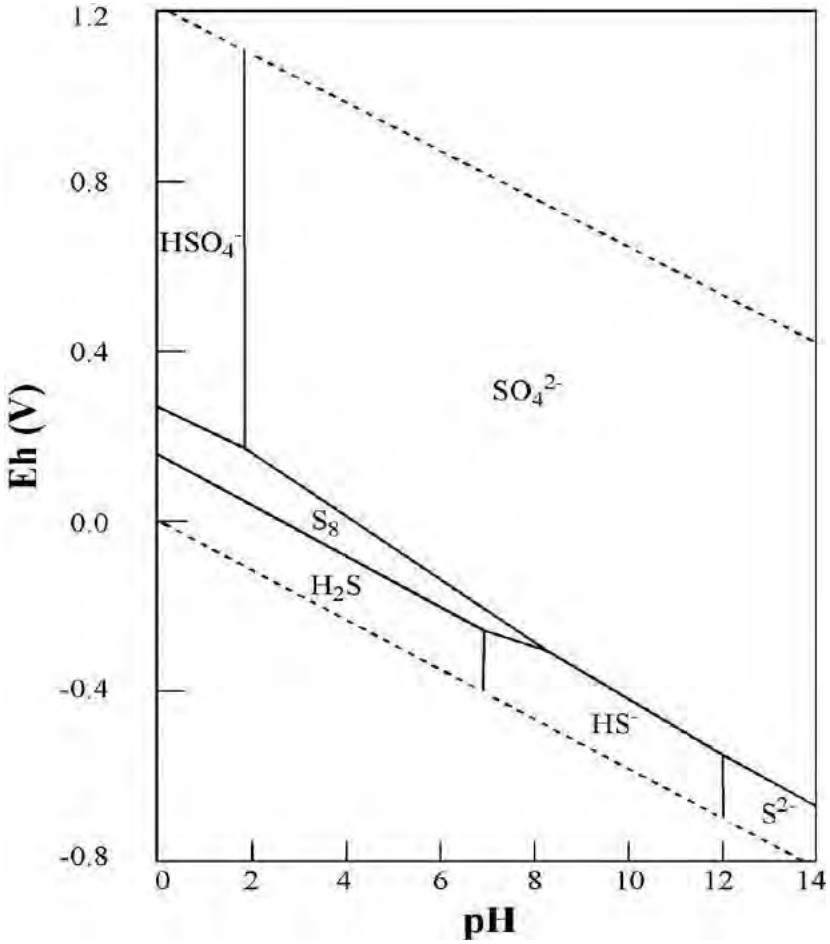

Figure 1 Stability diagram of sulfur showing the predominance of the sulfate anion in water. The dashed lines are the stability limits of water (Pourbaix, 1966)

Another chemical precipitation process, the formation of the insoluble mineral ettringite ($3CaO{\cdot}3CaSO_4{\cdot}Al_2O_3{\cdot}31H_2O$), was also explored (GARD Guide, 2014). Because ettringite is much more insoluble in water (K_{sp} = 2.8 x 10^{-45}) compared to gypsum, removal of sulfate by precipitating ettringite could consistently reduce the sulfate levels to below 600 mg/L (Equation 3):

$$6Ca^{2+}(aq) + 3SO_4^{2-}(aq) + 2Al(OH)_3(s) + 37H_2O(l) \rightarrow$$

$$3CaO{\cdot}3CaSO_4{\cdot}Al_2O_3{\cdot}31H_2O(s) + 6H_3O^{+}(aq) \quad (3)$$

One of the ettringite precipitation treatment processes that has been developed for sulfate removal is called the CESR process (Reinsel, 1999). In the CESR process, lime is first added to raise the pH and also to precipitate gypsum if the sulfate concentration is high enough and also to supply a calcium source to form the mineral ettringite. More lime and an aluminum reagent are then added in the next step, which results in the formation of the highly insoluble ettringite and the removal of most of the sulfate from solution (Figure 2).

Although bench scale testing showed that the CESR process can consistently remove sulfate down to < 200 mg/L, well below the 600 mg/L sulfate target (Reinsel, 1999), it was determined that CESR or similar ettringite–forming processes would not be suitable for several reasons. For example, careful examination of the stoichiometry of the ettringite formation reaction (Equation 3) shows that an exorbitant amount of sludge would be generated by the process, where more than four times the mass of sludge would be generated for every mass unit of sulfate removed. This compares to a mass ratio of less than two to one for the amount of gypsum sludge generated per mass unit of sulfate removed by the gypsum precipitation process (Equation 2).

Another reason for not considering further the CESR or related ettringite–formation processes for the full–scale mine water treatment plant to remove sulfate was because of the slow kinetics of the reaction to form ettringite using calcium aluminate as the reagent. Bench scale testing showed that it required long reaction times, up to 5 hours for completion (Liang et al., 2012). At a design flowrate of 5 MGD, a residence time of 5 hours would require more than one million gallons of capacity, which would be impractical for the full–scale water treatment system.

It should be pointed out that an ettringite–formation process using sodium aluminate as the aluminum source and hydrated lime as the calcium source to form ettringite has been developed and is reported to have much faster kinetics of ettringite formation (Outotec, 2014). Because of the large amounts of sludge generated by ettringite processes, the undesirable side effect of increasing sodium concentration in the treated water from using sodium aluminate, and the fact that the treated water sulfate concentration required at this site is not low enough to require ettringite formation, however, the ettringite process using sodium aluminate reagent was not considered either.

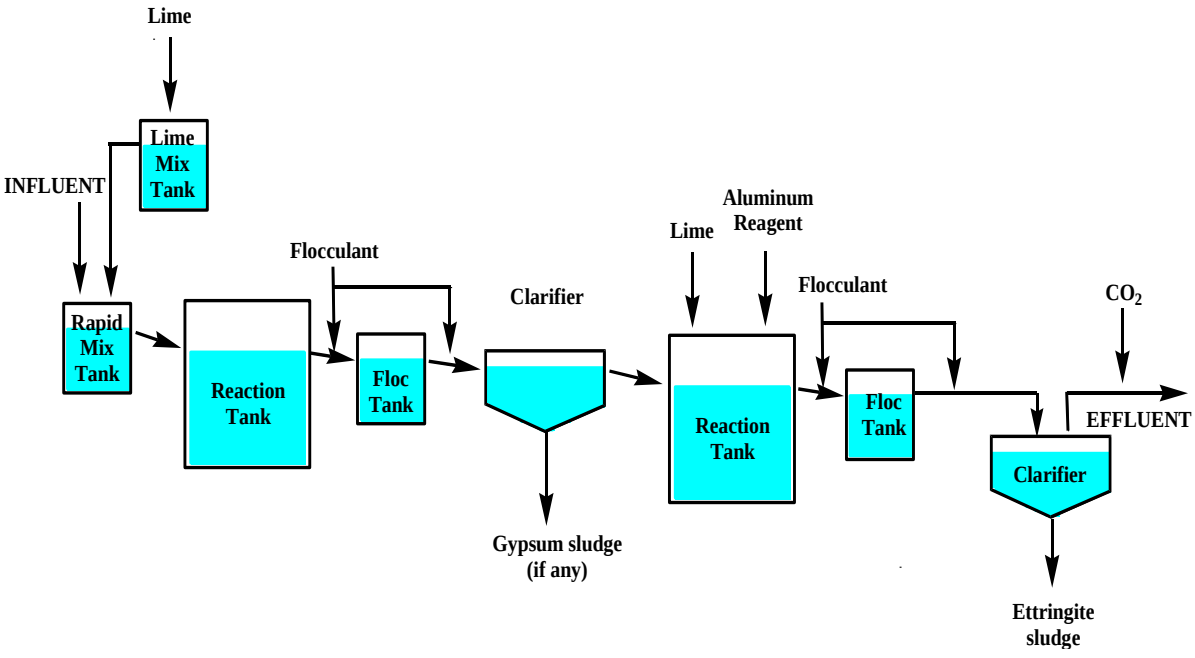

Figure 2 Schematic of CESR sulfate removal process

Membrane process for removing sulfate

Nanofiltration (NF) is also a potential option for sulfate removal for mine water treatment. NF can reject > 99% sulfate and would be able to consistently generate treated water with < 50 mg/L sulfate, much lower than the required 600 mg/L sulfate discharge target. Because of potential scaling issues on the NF membranes, especially for waters with high sulfate concentrations, pre–treatment for NF would need to be carefully considered. Another potential issue with using NF is that it would generate a lot of waste brine that would be expensive to manage. For example, at a 5 MGD flowrate and 70% recovery of the NF treatment process, 1.5 MGD of NF concentrate/brine waste would need to be managed and disposed (Figure 3).

Considering the issues of brine management and the fact that treating the water to < 50 mg/L sulfate would be an overkill at this mine site, it was determined that NF treatment in and of itself was not a viable option.

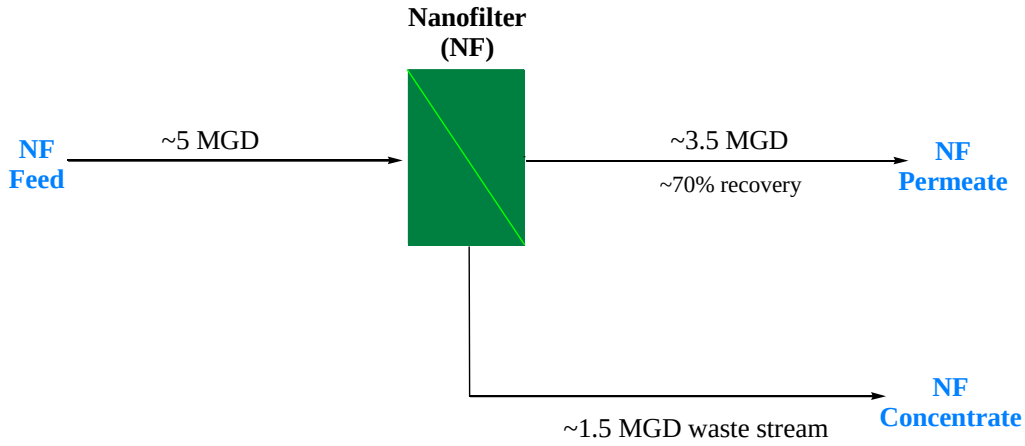

Figure 3 Schematic of NF treatment process showing need to manage large NF waste stream

RESULTS AND DISCUSSION

Hybrid membrane chemical precipitation sulfate removal process

Based on the issues with gypsum or ettringite precipitation and with NF membrane treatment discussed in the previous sections, preliminary evaluation of sulfate removal options for the mine water concluded that none of the options by themselves would be practical at the site.

Using the geochemical modeling software Phreeqc (USGS, 2014) to conduct chemical modeling suggested that a hybrid treatment process combining NF treatment with gypsum precipitation may be viable and meet the major criteria of consistently treating the water to < 600 mg/L sulfate and not generating as much waste sludge as the ettringite precipitation process. The concept was to use the NF to concentrate the stream so that more sulfate can be removed by gypsum precipitation in the NF concentrate stream compared to the more dilute full stream flow. And then the chemically treated NF concentrate stream can then be re–blended with the NF permeate stream so that no NF brine/concentrate stream will need to be managed or disposed separately; the re–blended stream will consistently meet the < 600 mg/L sulfate discharge limit due to the higher sulfate–removal

capacity of gypsum precipitation of the brine stream compared to gypsum precipitation of the full flow stream because of the higher concentration of sulfate in the NF brine stream. There would also be a recycle stream for the gypsum removal clarifier overflow that can be adjusted to fine–tune the blended discharge water quality.

The main components of the hybrid sulfate removal process are: 1) Pre–treatment using hydrated lime to decrease sulfate concentration to the gypsum saturation point. The pre–treatment process also precipitates and removes metals and silica to protect the nanofilter downstream in the process and increase the NF recovery; 2) Filtration upstream of the NF; 3) Nanofiltration process, which serves to concentrate the stream; 4) Hydrated lime treatment of NF concentrate stream to further remove sulfate as gypsum; 5) Re–blending of the chemically–treated NF concentrate stream with the NF permeate stream. The hybrid sulfate removal process is summarized and depicted in Figure 4.

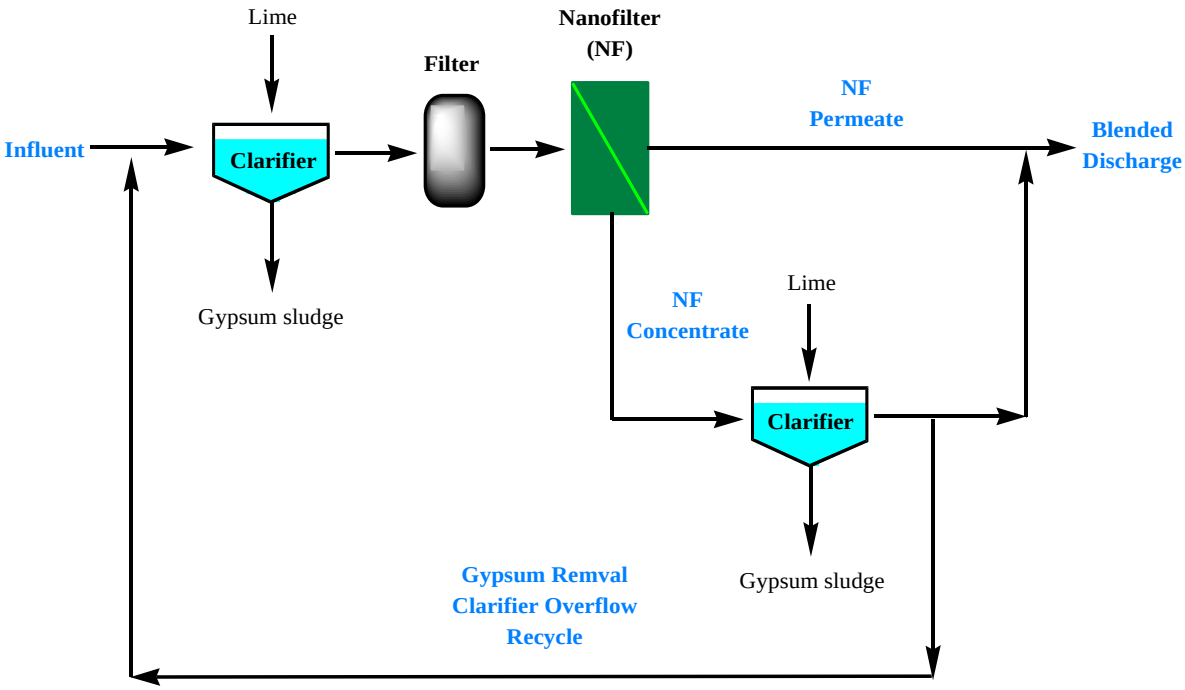

Figure 4 Schematic of hybrid gypsum precipitation and NF treatment processes

Pilot testing data

The hybrid treatment process depicted in Figure 4 and described above has been examined in a pilot test. The pilot testing was run for seven months at an average overall flowrate of approximately 20 gallons per minute (gpm), and the average NF recovery was approximately 70% with the use of a polyacrylate scale inhibitor and after iron, aluminum, and manganese were removed in the hydrated lime pre–treatment process. Data on the removal of these potentially scaling components in the lime pre–treatment process are shown in Table 1. It is of interest to note that aluminum was removed to low concentrations even at the pH of approximately 10. Data from major components of the pilot test are summarized in Table 2, which show data of the mass balance of sulfate removal across the hybrid treatment processes as determined from the pilot testing.

Table 1 Data from lime pre–treatment process to remove metals and increase NF recovery

	Al (Total, mg/L)	Fe (Total, mg/L)	Mn (Total, mg/L)
Raw Water	18	2.5	19
Lime Pre–Treated Water	0.15	0.02	0.01

Table 2 Data from pilot testing of hybrid gypsum precipitation and NF treatment processes (average values reported using two significant figures)

	pH	Sulfate (mg/L)	Total Dissolved Solids (TDS) (mg/L)
Raw Water	6.3	1,900	2,600
Lime Pre–Treated Water	10	1,400	2,200
NF Permeate	10	2.3	42
NF Concentrate	10	4,600	7,100
Lime–Treated NF Concentrate	11	1,800	2,400
Blended Discharge	7.5*	540	750
Treatment Goals	6.5–9	600	1,000

**After pH adjustment using CO_2*

As can be seen from the data presented in Table 2, the pilot study confirmed that it would be possible to use a hybrid treatment process to achieve the goal of treating sulfate down to 600 mg/L or less. Final design of the full-scale mine water treatment facility has been completed, and the mine water treatment plant is currently being constructed.

CONCLUSION

A full–scale mine water treatment facility has been designed and is currently under construction for treating up to approximately 5 MGD of water to remove sulfate to < 600 mg/L on a consistent basis. Assessment of chemical precipitation options showed that gypsum precipitation alone would not meet the 600 mg/L sulfate discharge target. So gypsum precipitation by itself was ruled out as a viable option. Although treating the water using ettringite precipitation would generate water that would meet the 600 mg/L sulfate discharge standard, it would also generate large amounts of waste sludge that would be difficult and expensive to manage. Additionally, bench scale testing showed that ettringite precipitation using calcium aluminate reagents were exceedingly slow and would require unrealistically large reaction tanks at a flowrate of 5 MGD, while using sodium aluminate, which is a potentially viable from a kinetics standpoint, would add too much sodium to the water as well as still generate exorbitant amounts of sludge. Therefore, chemical precipitation by itself, either using gypsum or ettringite precipitation, was ruled out as a practical option at the mine site. Evaluation of NF treatment also showed that while it would generate treated water that could easily meet the 600 mg/L sulfate discharge limit, the high flows of NF brine waste would be expensive to manage. Based on further evaluation of treatment options, a hybrid treatment process combining NF treatment and gypsum precipitation was developed first based on chemical modeling and then confirmed by pilot testing. The pilot testing confirmed that 600 mg/L sulfate in the treated water is achievable on a consistent basis.

REFERENCES

GARD Guide, Chapter 7, http://www.gardguide.com/index.php?title=Chapter_7, accessed October, 2014.

Jeremiason, J. D.; Engstrom, D. R.; Swain, E. B.; Nater, E. A.; Johnson, B. M.; Almendinger, J. E.; Monson, B. A.; Kolka, R. K. (2006) Sulfate addition increases methylmercury production in an experimental wetland. *Environ. Sci. Technol.* **40**: 3800–3806.

Lamers, L. P. M.; Tomassen, H. B. M.; Roelofs, J. G. M. (1998) Sulfate–induced eutrophication and phytotoxicity in freshwater wetlands. *Environ. Sci. Technol.* **32**: 199–205

Liang, H. C.; Thomson, B. M. (2010) Minerals and mine drainage. *Water Env. Res.* **82**: 1485–1533.

Liang, H. C.; Zinchenko, D.; Billin, S.; Barta, J.; Jones, R.; Willis, W. B.; Tamburini, S. (2012) Membrane vs. chemical treatment to remove mine water contaminants – Determining which process works best for mine water treatment needs. Proceedings of the SME Conference, Seattle, Washington, 600–603.

Outotec, http://www.eurominexpo.com/wp/wp–content/uploads/2014/06/12–thursday–13.30–outotec.pdf, accessed December, 2014.

Reinsel, M. A. (1999) A new process for sulfate removal from industrial waters. Proceedings of the Annual National Meeting – American Society for Surface Mining and Reclamation 16.

Pourbaix, M. 1966. *Atlas of electrochemical equilibria in aqueous solutions*, Pergamon Press, Oxford, New York.

USGS, http://wwwbrr.cr.usgs.gov/projects/GWC_coupled/phreeqc/, accessed April, 2014.

The High Density Sludge (HDS) Process and Sulphate Control

Bernard Aubé and Douglas Lee
Amec Foster Wheeler Environment and Infrastructure,Canada

ABSTRACT

The high-density sludge (HDS) process has been the standard in the mining industry for treating metal-containing acid rock drainage (ARD), providing low metal levels in the final effluent, and reducing waste sludge volumes compared to other lime based processes. It has been applied for 40 years at mine sites all over the world to meet discharge limits for metals and pH. Recently, various jurisdictions have introduced low discharge limits for sulphate concentrations that are difficult to meet with conventional treatment systems. Also, when treated water is recycled, high sulphate concentrations can cause some undesired downstream impacts. To assist in reducing effluent sulphate concentrations, the recent trend shows that HDS plants have been constructed with considerably higher retentions times in the neutralisation reactors. The reason for this increase in retention time is due primarily to the slow gypsum-precipitation reactions that are the key to minimising sulphate concentrations. These reactions and their effects are explained in detail in this paper. Also discussed are the potential synergies between the HDS process and other processes that treat sulphate more directly. This includes the combination with membrane filtration (reverse osmosis or nanofiltration), with ettringite precipitation, with ion exchange, and even barium precipitation.

Keywords: acid mine drainage sulfate lime treatment

INTRODUCTION

Although many different biological and chemical technologies exist for treatment of acid rock drainage (ARD – or acid mine drainage, AMD), lime neutralisation remains by far the most widely applied treatment method. This is largely due to the high efficiency in removal of dissolved heavy metals combined with the fact that lime costs are low in comparison to alternatives. Lime treatment essentially consists in bringing the pH of the raw water to a point where the metals of concern are insoluble. These metals therefore precipitate to form minuscule particles. A separation of these precipitates is then required to produce a clear effluent which meets regional discharge criteria. The solid/liquid separation forms a sludge which, for a high-density sludge (HDS) process, can contain 10 to 30% solids by weight. This sludge can be further processed to increase the solid content and must be disposed of in an environmentally acceptable manner.

The HDS process has met requirements in the past as the focus for discharge limits has been on toxic metals and acidity. In recent years, there are more and more jurisdictions also including sulphate as a regulated parameter, including Chile and Peru. The specifically applied limits depend on the jurisdiction and often also on the receiver. The limits vary from approximately 2,000 mg/L (as sulphate, SO_4^{2-}) in the high end to as low as 10 mg/L in the receiver.

Lime treatment processes alone cannot meet the low effluent sulphate limits and even the higher limits in some cases. But there are modifications that can be brought to the HDS process which help minimise the final sulphate concentration either as a stand-alone treatment or in conjunction with other sulphate treatment systems. In this paper, the lime treatment of ARD is summarised and the associated minimisation of sulphate concentration is also explained.

THE BASIC CHEMISTRY OF LIME TREATMENT

The principle of lime neutralisation of ARD lies in the insolubility of heavy metals in alkaline conditions. By controlling pH to a typical setpoint of 9.5, metals such as iron (Fe), zinc (Zn), and copper (Cu) are precipitated (see Figure 1). Other metals such as nickel (Ni) and cadmium (Cd) require a higher pH, in the range of 10.5 to 11 to effectively precipitate the hydroxides. The precipitates can be formed individually as minuscule particles smaller than a single micron (1 μm). In a high-density sludge process, the precipitates are formed onto existing particles recycled within the process. This creates larger and denser particles that settle and compress better than the precipitates created with direct lime addition. This essentially defines the greatest difference between the HDS process and other lime treatment processes: the method of precipitating and separating the solids and the sludge that is formed.

It is important to note that the precipitation reactions and resulting precipitates are shown and discussed as per theory. In reality, almost all of the precipitates are amorphous mixtures of many metals, hydroxides, sulphates, and other ions present in solution, with several of the ions adsorbed and not truly precipitated in the presented form. The only actual crystals often identified in fresh sludge are calcite and gypsum. Aged sludges can contain other crystalline forms (Zinck, 2005).

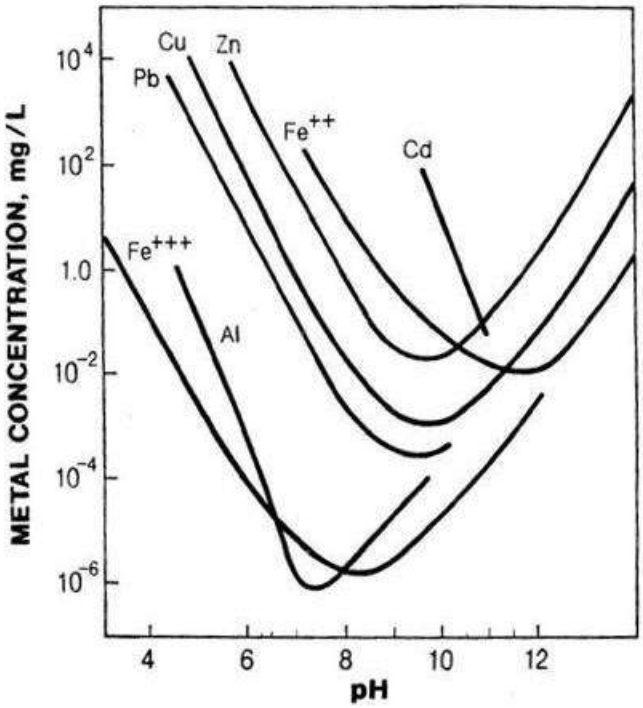

Figure 1 Metal Hydrolysis (from Aubé and Zinck, 2003)

Lime dissolution is the first step of the neutralisation process. For large treatment systems, quicklime is used. This lime must first be hydrated (slaked) and is normally fed to the process as a slurry. When fed to the process, the hydrated lime then dissolves to increase pH. The two following equations illustrate these reactions:

$$CaO + H_2O \Rightarrow Ca(OH)_2$$

$$Ca(OH)_2 \Rightarrow Ca^{2+} + 2OH^-$$

The increased pH then provides hydroxide ions which combine with the dissolved metals to produce precipitates. The following equations show the precipitation reactions with different metals:

$$Al^{3+} + 3OH^- \Rightarrow Al(OH)_3$$

$$Co^{2+} + 2OH^- \Rightarrow Co(OH)_2$$

$$Cu^{2+} + 2OH^- \Rightarrow Cu(OH)_2$$

$$Fe^{2+} + 2OH^- \Rightarrow Fe(OH)_2$$

$$Fe^{3+} + 3OH^- \Rightarrow Fe(OH)_3$$

$$Ni^{2+} + 2OH^- \Rightarrow Ni(OH)_2$$

$$Pb^{2+} + 2OH^- \Rightarrow Pb(OH)_2$$

$$Zn^{2+} + 2OH^- \Rightarrow Zn(OH)_2$$

The resulting water quality contains very low heavy metal concentrations due to this hydroxide precipitation. Proportional to the precipitation of these metals is the solubilisation of calcium from the lime. Effectively, for the dissolved ionic balance, Ca replaces the heavy metals in solution. This leads to the precipitation of gypsum as per the following equation:

$$Ca^{2+} + SO_4^{2-} \Rightarrow CaSO_4 \cdot 2H_2O$$

What differentiates gypsum from the metal hydroxides is that the metals precipitate very rapidly while gypsum precipitates slowly. Most lime treatment plant effluents are super-saturated for gypsum upon discharge. The reasons for this and the effects that are caused by this slow precipitation are discussed in greater detail in the following sections.

THE SULPHATE PROBLEM STATEMENT

In most sulphide mines, some precious metal mines, and some coal mines, the waste rock and tailings contain iron and other metal sulphides which oxidise to form AMD containing sulphuric acid and dissolved metals. This AMD problem is well documented in numerous other publications. Historically, AMD was either treated to remove toxicity and released to the environment or treated for recycle to the process (concentrator) with high sulphate concentrations.

Sulphate control has become a greater concern in recent years because it has been added as a regulated parameter in many jurisdictions. Sulphate concentrations can also present problems when the treated water is recycled. The gypsum formation discussed above also results in significant scaling issues, both within treatment plants and downstream. Within a conventional lime treatment plant there can be significant scaling on all surfaces, particularly in reactors where the lime is added when there is no sludge recirculation. Even with sludge recirculation, it is the clarifier overflow weir, effluent piping, flume, turbidimeters, and pH probes that sustain the greatest amount of scaling.

For some sites where the treated water is recycled as process water, the scaling caused by gypsum formation can be a critical cost issue. In one European underground mine, the recycled water used in the mine for cooling the drills (jumbos) via oil-water intercoolers results in significant scaling of these items and high maintenance costs. A gypsum-saturated solution also cannot be used as gland water for pumps due to the significant maintenance requirements. Scaling in process water piping and valves can also create issues with control and even safety concerns.

There are two main reasons for the scaling issues: 1) the gypsum precipitation reaction is slow and 2) gypsum is a crystal that preferentially forms on existing gypsum crystals.

While hydroxide reactions that cause the precipitation of metals are almost instantaneous, gypsum formation can take days to reach equilibrium. The comparatively slow precipitation is primarily a function of kinetics but can also be related to the solubility product constant (Ksp). The heavy metal hydroxide precipitates listed above have solubility constants in the order of 10^{-15} to 10^{-30}. Gypsum has a solubility product constant of 2.4×10^{-5} which is at least 10 orders of magnitude higher than that of the hydroxides. Kinetics can also be linked to size of the ions involved in the formation of the solid. In the case of the metal precipitates, all are related to the hydroxide ion, which is extremely mobile in an aqueous solution. For gypsum, the calcium mobility can be compared to that of the heavy metals, while the sulphate molecule, which is a much larger molecule than that of the hydroxide, is considerably less mobile.

Another important aspect of gypsum precipitation is that it occurs considerably more readily on existing gypsum crystals than by nucleation. Metal hydroxide particles readily nucleate in a solution that contains no solids, given the right pH conditions. Gypsum does not tend to nucleate but rather to form on a solid surface, preferably on existing gypsum. In clear water, without the presence of gypsum particles or other solids in suspension, the only existing surfaces are from the equipment and walls. An initial coating of gypsum forms on equipment surfaces, then these surfaces act as a seeding location for continued precipitation. This distinctiveness for gypsum explains why scaling on equipment surfaces occurs more readily in clear water, following solid-liquid separation.

THE HDS PROCESS

The high density sludge (HDS) process is the standard in the AMD treatment industry today (**Figure 2**). Instead of contacting lime directly to the AMD, this process first contacts recycled sludge with the lime slurry for neutralisation. To do this, the sludge from the clarifier bottom is pumped to a "Lime/Sludge Mix Tank" where sufficient lime to neutralise the AMD to the desired pH setpoint is also fed. This forces contact between the solids and promotes coagulation of lime particles onto the recycled precipitates. This mixture then overflows to the Lime Reactor (LR) where pH is controlled and the precipitation reactions are completed. Aeration is often added to this reactor to oxidise ferrous iron to ferric and form the more stable ferric hydroxide.

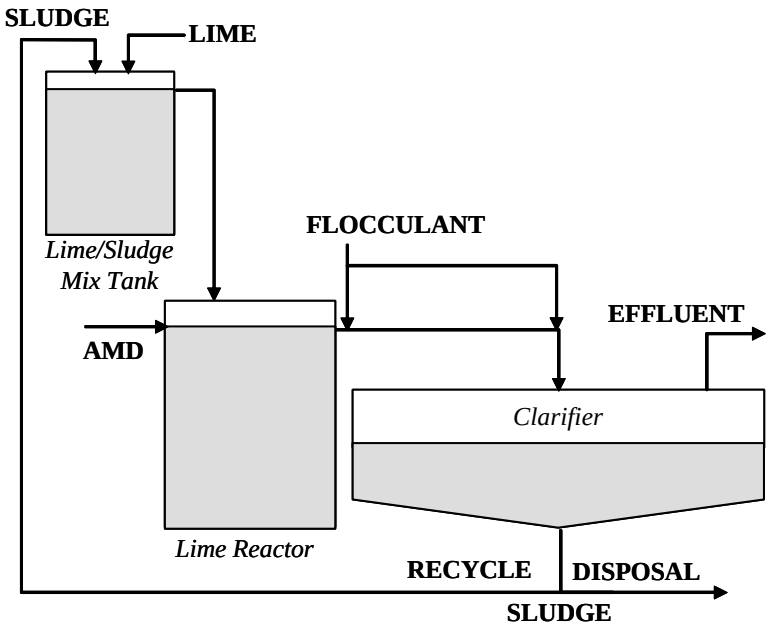

Figure 2 Simplified Representation of HDS Process

The slurry is then contacted to a flocculant solution either via a Flocculation Tank or by providing turbulence in the conduit leading from the Lime Reactor to the clarifier. A trough with baffles may be sufficient to ensure proper contact with the small particles. The flocculant serves to agglomerate

all precipitates and promote efficient settling in the clarifier. The clarifier overflow can either be discharged or recycled as process water as-is or polished prior to the next step. A simplified representation of the HDS process is shown in Figure 2.

The key to this process lies in the mixing of lime and sludge prior to neutralisation. The fact that the calcium hydroxide and recycled particles are combined causes the precipitation reactions to occur mostly on the surface of existing particles, thereby increasing their size and density. The precipitates from this process are therefore different from those where this lime/sludge mixture does not occur.

The HDS process presents significant advantages in operating costs over conventional lime addition, due the increased sludge density, decreased lime consumption, improved metal removal, and better solid/liquid separation (Aubé and Zinck, 1999). The higher sludge density means less waste is produced but also that more water is treated and released (or recycled).

Sulphate in the HDS Process

As discussed previously, a critical part of the HDS process is the Lime/Sludge Mix Tank, where recycled sludge is contacted with a concentrated lime slurry. The lime addition rate here is controlled by the desired setpoint in the Lime Reactor. Typically, the pH in this reactor is higher than 11 and can be as high as 12.5. As this high pH is due to lime dissolution, the calcium concentrations are very high. This promotes gypsum precipitation in this location and provides a high concentration of gypsum needles for the Lime Reactor. This is shown in Figure 3 in a scanning electron micrograph (SEM) of a freeze-dried slurry collected from an industrial Lime/Sludge Mix Tank. The needles in Figure 3 are gypsum crystals.

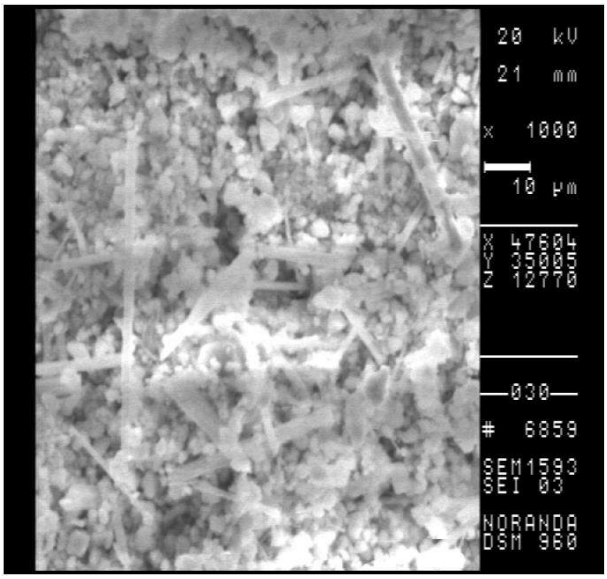

Figure 3 SEM Photograph of a Lime/Sludge Mixture

Modifications to the HDS Process for Improved Sulphate Removal

The major modification incorporated into the HDS process for improved sulphate control is to increase retention time in the reactors. This can be done by using multiple reactors in series. Table 1

shows a summary of HDS treatment plants built late in the past century (sites A to D), in comparison with more recent plants (sites 1 to 3) that were designed with a focus on sulphate concentrations. It is clear that the trend applied by process engineers in recent years is to add more reactors and greater retention time. In case of scaling issues, the reactors are often designed to be by-passed. This is true of the Geco plant (Site 1), for example, where either of the first two reactors can be by-passed. The other two examples can have any of the neutralisation reactors by-passed.

Table 1 Example HDS Plant Reactor Retention Times

Site	Start-up (year)	Treatment Flowrate (L/min)	Number of Reactors	Total Design Retention Time (minutes)
A	1984	3 000	2	40
B	1993	60 000	1	40
C	1993	10 000	1	40
D	1997	20 000	1	45
1	2005	15 500	3	150
2	2011	5 833	2	120
3	2014	30 000	3	120

A high sludge recycle rate also increases the concentration of gypsum crystals in the neutralising reactors to help promote additional gypsum precipitation. But the recycle rate can be limited by the efficiency of flocculant contact and solid/liquid separation; too high a recycle will lead to a high solid content in the slurry and can make flocculation difficult.

By applying these principles of increased retention time in the reactors where a continuous contact with existing gypsum crystals is provided by high sludge recycle, the resulting sulphate concentrations are lower as the slurry reaches the clarifier. There are limitations in the removal of sulphate in an HDS plant related not only to the kinetics of gypsum precipitation but also to the chemistry of the raw water. The gypsum precipitation occurs in large part due to Ca replacing heavy metals as the cation associated to sulphate. Some cations do not precipitate in HDS treatment, particularly alkali metals such as sodium (Na) and potassium (K). Magnesium may also remain in solution if the pH control point is less than 10. Sulphate concentrations will be higher in HDS-treated effluent if the AMD contains significant concentrations of these light metals. The final sulphate concentration therefore varies from site to site despite applying the same process, as the raw water chemistry varies significantly.

Some scaling is still likely to occur in HDS treatment plants, particularly in the effluent systems and reactor aeration systems. The more recent designs allow for maintenance to remove scaling where it may become problematic. Launders and flow-measuring devices are open or with removable covers for access to remove accumulated scaling. For the aeration systems in the reactors, the ability to by-pass a reactor can allow for maintenance while continuing treatment. Large man-doors are included in the design of the reactors for rapid access. Clarifiers can be equipped with larger access to facilitate using a small tractor (such as a Bobcat) to remove the accumulated scale. At mine sites

with high sulphate concentrations, it may be necessary to shut down on an annual basis for a week or two specifically for this clarifier cleaning.

Combination of HDS with Other Treatment Methods

In order to meet some effluent regulations for sulphate, HDS treatment cannot be applied alone. In these cases, other technologies can be used to treat for sulphate specifically. Four of these potential sulphate treatment technologies are discussed below, including membrane separation, ion exchange, ettringite precipitation, and barium precipitation.

The limitations inherent in the sulphate treatment technologies discussed below are the main reasons for their reduced applicability seen at the full scale. The following sections describe the opportunities to optimise these sulphate technologies through combination with the HDS process.

Membranes

The leading method of control for sulphate in the mining industry at this time is by membrane separation. These reverse osmosis (RO) or nano-filtration (NF) systems can produce a permeate capable of meeting any sulphate limit. The greatest disadvantage of this process is the formation of a concentrate (or brine) stream that often represents more than 30% of the initial raw water volume. The HDS process can be used to treat this high-sulphate concentrate to greatly reduce the final waste volume. Treatment of the brine with HDS can provide the required bleed of sulphate in the form of gypsum in the waste sludge, while the clarifier overflow can either be returned for re-treatment in the RO or mixed with the RO permeate depending on the target sulphate level in the final effluent.

The greatest challenge with membrane treatment for sulphate in the mining industry is the formation of gypsum in the membranes themselves, due to the super-concentration of the brine as it advances across the membrane. This gypsum precipitate is commonly due to the fact that the ARD contains sulfuric acid that has been neutralised with lime, thereby feeding a gypsum super-saturated solution to the membrane from the start. This scaling issue significantly reduces the service life of the membranes. Gypsum scaling can be reduced by decreasing recovery rates, backwashing, increasing tangential flow, and/or adding an anti-scalant. Each of these options increases treatment costs due to decreased discharge fractions (more recycled brine), increased pressures (higher energy costs), and/or high reagent costs.

Recent advances in membrane materials have resulted in NF membranes that can tolerate very low pH. In some applications, with a low pH stream containing high levels of metals and sulphate, it is possible to treat this stream with NF membranes with only particle filtration as a pre-treatment. At this low pH, prior to lime addition, the solubility level of gypsum is higher and the available calcium is lower, resulting in a decreased scaling potential in the NF membranes. This results in considerably higher recovery rates, with concentrate streams of less than 25% of the raw ARD feed. This can significantly reduce costs as the membranes last longer and the use of anti-scalants is reduced or even eliminated.

The NF permeate can then be combined with the balance of the AMD for further treatment in an HDS plant, but now the issues with gypsum scaling are reduced. The NF concentrate can be treated in an HDS process to further reduce the waste stream. If RO is required as a final treatment, the NF and RO concentrate streams can be combined and treated in the same HDS plant.

Essentially, membrane treatment alone would result in a significant waste stream and still require pH adjustment. To reduce waste, to present an outlet for sulphate (as gypsum), and increase overall water recovery in an economic manner, HDS is best used in conjunction with membrane treatment.

Ion Exchange

Another process offered by suppliers for sulphate treatment is ion exchange . In this process, two stages are applied with very specific ion exchange resins. One example of this process is the GYP-SIX process (Robertson and Rohrs, 1995). The cationic resin is specific for calcium and the anionic is specific for sulphate. The regeneration is performed with sulphuric acid on the cationic side and lime-saturated solution on the anionic side. The process produces gypsum as a by-product (or most likely as a waste). The proposed IX processes do not treat all contaminants to make the water compliant for discharge or recycle to a concentrator. One option is the application of the HDS process upstream of the IX process, and by minimising the concentrations of sulphate, it will be possible to reduce the overall costs of water treatment.

Ettringite

There are many suppliers presently proposing the ettringite process for sulphate control. This process has been proven to bring sulphate concentrations low but has the disadvantage of high costs due to the need for an aluminium (Al) reagent and the production of large volumes of low-density sludge. This is shown in the formula below.

$$6Ca^{2+} + 3SO_4^{2-} + 2Al(OH)_3 + 32\ H_2O \Rightarrow Ca_6Al_2(SO_4)_3(OH)_{12}{\cdot}26H_2O + 6H^+$$

In some cases, such as the CESR process (INAP, 2003), there is a metal precipitation step prior to ettringite formation. If the HDS process with an extended retention time in the neutralisation reactors were to be applied in this initial metal precipitation step, the initial sulphate concentrations for the ettringite step will be reduced. This would serve to decrease the consumption of the expensive Al reagent in the ettringite step. This will also significantly reduce the volume of sludge produced as the HDS process can form a sludge containing more than 20% solids with a significant sulphate (gypsum) content. The ettringite sludge is viscous and can contain less than 2% solids.

Barium Precipitation

Another well-known process for treatment of sulphate is precipitation using barium (Ba). It may be possible to integrate Ba into existing HDS treatment systems thereby reducing unnecessary and expensive capital investments. New systems could also incorporate Ba after lime addition. As a specific process for sulphate precipitation, Ba is not currently used in the full scale. This is due to high cost of the raw reagent, as Ba is not readily available in the quantities that would be required.

At a high pH, the addition of barium carbonate can be used to decrease sulphate concentrations via the following reaction:

$$Ca^{2+} + SO_4^{2-} + BaCO_3(s) \rightarrow BaSO_4(s) + CaCO_3(s)$$

It is also possible to use barium hydroxide directly, where the main process reaction would be the following:

$$Ba(OH)_2 + Me^{n+} + SO4 \rightarrow Me(OH)_n + BaSO_4(s)$$

Me represents the metal components of the effluent stream, typically iron, zinc, nickel, copper, cadmium, or cobalt. Barium chloride can also be used for sulphate precipitation but this process

will put into solution as much chloride as there is sulphate removed, thus exchanging one problem with another.

Prior treatment with the HDS process can help reduce the sulphate concentration and thus the operating costs of the sulphate treatment process as it decreases the consumption of barium.

CONCLUSION

Recent trends to improve the sulphate treatment in HDS plants involve longer retention time in neutralisation reactors as a primary modification. The process requires an optimised control of solids recirculation to provide sufficient gypsum seeding from sludge without negatively impacting the solid/liquid separation. The ability to access the equipment and by-pass reactors is also important for maintenance when treating high-sulphate waters.

The HDS process can be successfully combined with membrane filtration either before or after to control the effluent quality as required and minimise liquid waste from the concentrate. The HDS process is also uniquely suited to work with ettringite, barium, or ion exchange processes to reduce total treatment costs and waste management.

REFERENCES

Aubé B. and J.M. Zinck, 1999. "Comparison of AMD Treatment Processes and their Impact on Sludge Characteristics". Proceedings for Sudbury '99, Mining and the Environment II.

INAP, 2003. "Treatment of Sulphate in Mine Effluents". Online document available at http://www.inap.com.au/research/ (November 2014).

Janneck, E., M. Cook, C. Kunze, K. Sommer, and L. Dinu, 2012. Ettringite Precipitation vs. Nanofiltration for Efficient Sulphate Removal from Mine Water". Proceedings for IMWA 2012, pp. 206 I-206 R.

Robertson, A. and R.G. Rohrs 1995. Sulphate removal of acid mine drainage water after lime treatment. In: Proceedings of Sudbury '95: Mining and the Environment. 28 May to 1 June, Sudbury, Ontario.

Zinck, J.M., 2005. "Review of Disposal, Reprocessing and Reuse Options for Acidic Drainage Treatment Sludge". MEND report 3.42.3.

An Innovative Process to Reduce Sulfate in Membrane Concentrate Enhances Mine Water Recovery

Kashi Banerjee, Christopher Howell Charles Blumenschein and Herve Buisson
Veolia Water Technologies, USA

ABSTRACT

A treatment process was developed to reduce sulfate from nanofiltration (NF) concentrate to less than 100 mg/l. The treatment system is comprised of a two-stage chemical precipitation process. The impacts of sludge recirculation ratio, pH and chemical dosages were investigated. Calcium sulfate crystal growth kinetics was determined. Bench and two pilot-scale studies were conducted to evaluate the performance of the system. The studies also evaluated the performance of an NF system for removing sulfate from copper mine tailing pond water. Using the ion chromatography (IC) method, the concentration of sulfate in water was analyzed. Membrane performance was evaluated at various flux rates, water recovery rates and trans-membrane pressures. The process recovers more than 95% aluminum from the precipitated sludge for reuse. Based on the two pilot study results, a preliminary concept was developed. The innovative process increased overall water recovery significantly.

Keywords:

Sulfate; membrane concentrate; precipitation; calcium sulfoaluminate; water reuse

INTRODUCTION

The high solubility and stability of sulfate ions in aqueous solutions make processes for removal of this anion from water to low levels extremely complex. The application of nanofiltration (NF) for sulfate reduction is becoming popular with the promulgation of new regulations and increased interest in water reuse. However, handling of the NF concentrate with high sulfate is problematic. State-of-the-art sulfate treatment technology includes chemical precipitation, biological degradation, adsorption and/or ion-exchange, and membrane (nanofiltration and reverse osmosis) processes. Each of the processes is discussed in detail by Silva et al. (2010). Under favorable reaction conditions (water with low ionic strength), the desaturation process generates effluent containing about 1,800 mg/l of sulfate (as SO4). The major drawback of the biological reduction of sulfate is the generation of sulfide gas, a long residence time, and the metabolic waste products, which are difficult to handle. Evaporation/crystallization is an energy-intensive process. Ion exchange produces regenerants containing extremely high concentrations of sulfate, which are also difficult to handle. Therefore, a sulfate removal technology that can reduce the sulfate concentration in the treated effluent of the desaturation process down to a low level (say <100 mg/L) is needed.

The primary objectives of this project were to determine and validate an appropriate membrane (NF) process to reduce the sulfate concentration in the water as well as to establish an innovative sulfate treatment technology for the membrane reject. The treated effluent then could be blended with the NF permeate to achieve a higher water recovery for reuse.

METHODOLOGY

Initially, a treatability study was conducted to validate the proposed sulfate treatment system and to generate data that were used as baseline information for the on-site pilot-scale experiment.

Wastewater Sampling and Characterization

Samples were collected from the tailings pond of a copper mine site. The analytical results of the "as-received" sample are presented in Table 1. All metals were analyzed using the Inductively Coupled Plasma – Mass Spectroscopy (ICP-MS) method, and sulfate was analyzed using the Ion Chromatography (IC) method.

Table 1 Characteristics of Untreated Pond Water

Parameters	Concentrations
pH, S.U.	7.4
Total Alkalinity , mg/l $CaCO_3$	28
TDS, mg/l	3070
Turbidity, NTU	1.41
TOC, mg/l	2.4
Chlorides, mg/l	66.8
Sulfate, mg/l	1,830

Calcium, mg/l	692
Iron, mg/l	0.01
Magnesium, mg/l	21.1
Manganese, mg/l	0.17
Molybdenum, mg/l	0.25
Potassium, mg/l	124
Sodium, mg/l	104

Laboratory-Scale Study

Using the actual pond water sample from the mine site, a laboratory study was conducted, including molybdenum removal, SDI reduction followed by NF for sulfate reduction, and treatment of the NF concentrate.

Molybdenum Removal and SDI Reduction

To ensure a molybdenum concentration below 0.05 mg/l, iron (as Fe^{3+}) was added under slightly acidic condition (pH between 6.0 and 6.5), and SDI was reduced to <3 by adding a polymeric flocculent.

Sulfate Removal with NF

After pretreatment, the pH of the NF feed water was adjusted to about 7.5. The membrane was operated at a 60% water recovery rate. An antiscalant was used to protect the membrane from scaling. Samples were collected from the permeate and the reject line, and the trans-membrane pressure (TMP) was noted. The treated samples were analyzed for sulfate, calcium, conductivity, total dissolved solids (TDS), and other pertinent cations and anions. The detailed laboratory study procedures are presented elsewhere (Banerjee et al., 2012).

NF Reject Treatment

Sulfate present in the NF reject at a high concentration was removed as a precipitate of calcium sulfate by the desaturation process. The study was conducted in a continuous system for two weeks using Veolia Water's proprietary Turbomix® reactor (a draft-tube, high-speed reactor). A detailed description of the Turbomix reactor is provided elsewhere (Banerjee et al., 2010). The reactor was equipped with a sludge recirculation system. NF reject was pumped into the reactor where calcium ion was added. Lime or a combination of lime and calcium chloride was used as the source of calcium ions. The precipitation reaction was performed in the presence of a seed material. After precipitation, solids were separated from the liquid in a clarifier. A portion of the sludge was recycled back to the reactor, and the other portion was dewatered. Samples of the clarified effluent were filtered through 0.45-μ paper and analyzed for calcium and sulfate.

The effluent from the above process was further treated with aluminum-based salt to precipitate sulfate as a highly insoluble calcium sulfoaluminate mineral. A high-speed Turbomix® reactor was also used in this case. At a specified sludge recirculation ratio, a sulfate removal kinetic study was conducted. Calcium sulfoaluminate mineral was separated from the clear water, and aluminum ion was regenerated from the sludge, after pH adjustment, and recycled back to the process.

Pilot-Scale Study

Based on the laboratory study results, a 1.3 l/s (4.5 m^3/hour) pilot unit was designed and constructed. Pilot studies were conducted for about two months. The general process flow diagram of pilot study is included in Figure 1. The pretreatment included iron coagulation, gravity separation, and a Multimedia Filter (MMF). The NF system was comprised of three 200-mm-diameter elements (two DOW 90 – 400 elements and one DOW 270 – 400 element). The unit was run at three different flux rates ranging between 22 and 30 lmh, and was operated continuously (24 hours/7 days a week) at 350 percent $CaSO_4$ saturation. Using lime and calcium chloride in the presence of a seed material, sulfate from the NF reject was desaturated in the first-stage high-speed Turbomix® reactor. Under the same process condition, about 80% of the samples were collected and analyzed three times to check the reproducibility of the results. Using a HACH kit, sulfate was analyzed at the site, and Ion chromatography method was used to determine sulfate concentration in the laboratory. Using water from a coal mine site, the 2nd set of pilot study was conducted. A similar sampling, analytical, and replication procedures were followed as described above.

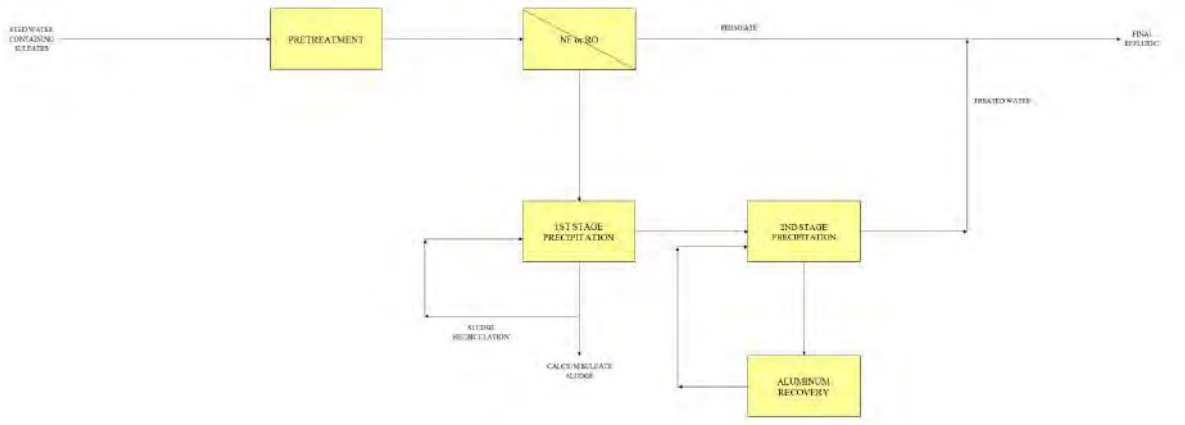

Figure 1 Pilot Flow Diagram

RESULTS AND DISCUSSION

Laboratory-Scale Study

The average calcium and sulfate concentrations in the NF feed water were 640 (as Ca^{2+}) and 1,600 mg/l (as SO_4^{2-}), respectively. More than 98% of the sulfate was rejected at the 60% water recovery rate. The average concentration of sulfate in the permeate was about 25 mg/l. Increasing the membrane flux rate did not affect the permeate quality significantly. The concentration of calcium in the NF reject at the 60% water recovery rate varied between 1535 and 1550 mg/l, and that of sulfate ranged between 3,500 and 4,100 mg/l. Results of the laboratory-scale membrane performance are shown elsewhere (Banerjee et al., 2012).

The results of calcium sulfate desaturation kinetics in the presence of seed material with sludge recirculation are shown in Table 2. As the table illustrates, sulfate in the treated water was reduced from 4,000 (average concentration) to 1,300 mg/l, which is less than the theoretical solubility limit of

1,800 mg/l as dissolved sulfate. The results also reveal that without the sludge recirculation, sulfate was reduced to about 2,000 mg/L. The seed material was added only once (during the process start-up). Detailed laboratory study results are presented elsewhere (Banerjee et al., 2012).

Table 2 Sulfate Removal after Calcium Sulfate Precipitation/Adsorption using Lime and Calcium Chloride, or Lime only, with Seed Material in a Sludge Recirculation System

Sludge Recirculation Ratio	20:1	15:1	10:1	15:1*	0*
pH	9.3	9.3	9.2	12.0*	12.0*
Dissolved Sulfate, mg/L	1,350	1,100	1,200	1,100*	2,000*

*This experiment was conducted only with lime.

The data show that sludge recirculation and seeding have a significant impact on the calcium sulfate desaturation process. The seed material used in this process has a highly reactive surface, which increases the reaction driving force and the available free energy of the system. It is anticipated that besides chemical precipitation, sulfate ions present in the NF reject are adsorbed onto the reactive surface of the seed material as well as onto the freshly precipitated calcium sulfate solids. Additionally, increased crystal growth of the precipitated solids takes place in the presence of the seed material.

Pilot-Scale Study

The sulfate concentration in the raw water ranged between 1,800 and 2,900 mg/l (average 2,300 mg/l). During the study, the sulfate concentration in the raw water increased by about 30%. The calcium concentration in the raw water did not change significantly, and the average turbidity in the water was about 25 NTU. After pretreatment, iron, manganese, molybdenum, and SDI were reduced to <0.3mg/l, <0.05mg/l, <0.05mg/l, and <3, respectively. Since the raw water contained a higher sulfate concentration, initially the NF was run at 50% water recovery to avoid scaling; after that, it was operated for two weeks at a 60% water recovery rate with an increased antiscalant dosage.

Sulfate and calcium rejection data are presented in Figures 2 and 3. As Figure 2 shows, about 98.5% of the sulfate was rejected, and sulfate in the NF permeate ranged between 25 and 55 mg/l. The average sulfate concentration in the permeate was 35 mg/l. The percent rejection of calcium ranged between 90 and 99% (see Figure 3). Calcium in the NF permeate ranged between 10 and 60 mg/l. Sulfate rejection showed a very stable line in the high 90's (Figure 1) in comparison to calcium rejection (Figure 2). Since the membrane surface is negatively charged, the membrane primarily rejects sulfate, and because of ion pairing, the sulfate holds back the positively charged calcium and magnesium ions from passing through the membrane.

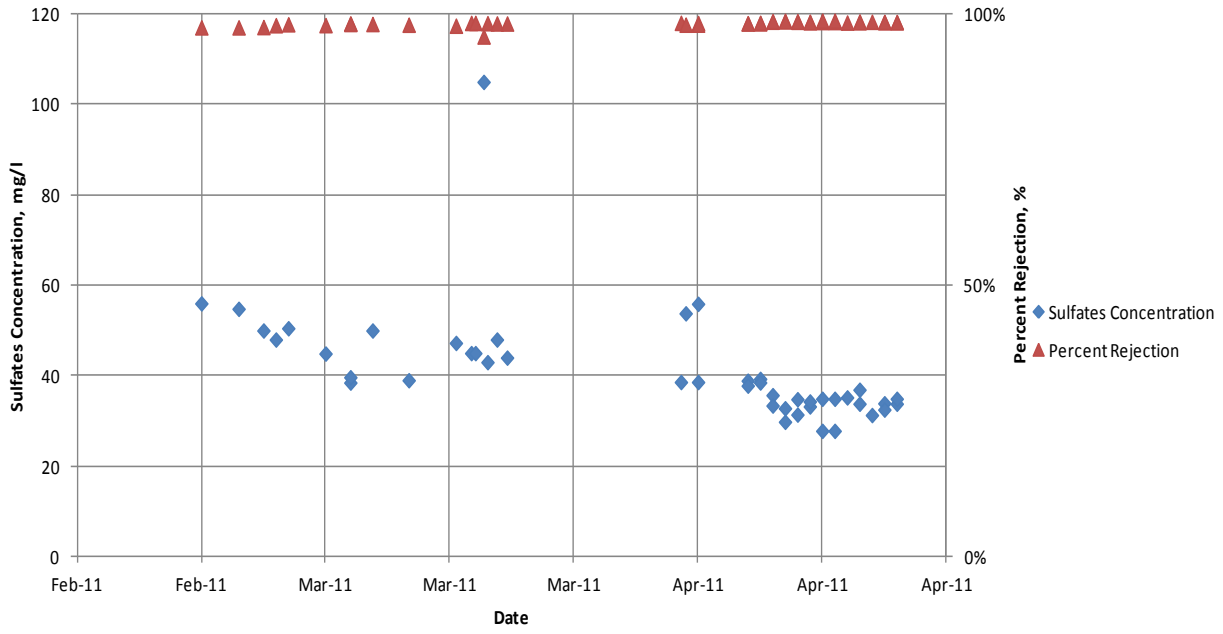

Figure 2 NF Permeate – Sulfate Concentrations and Percent Rejection

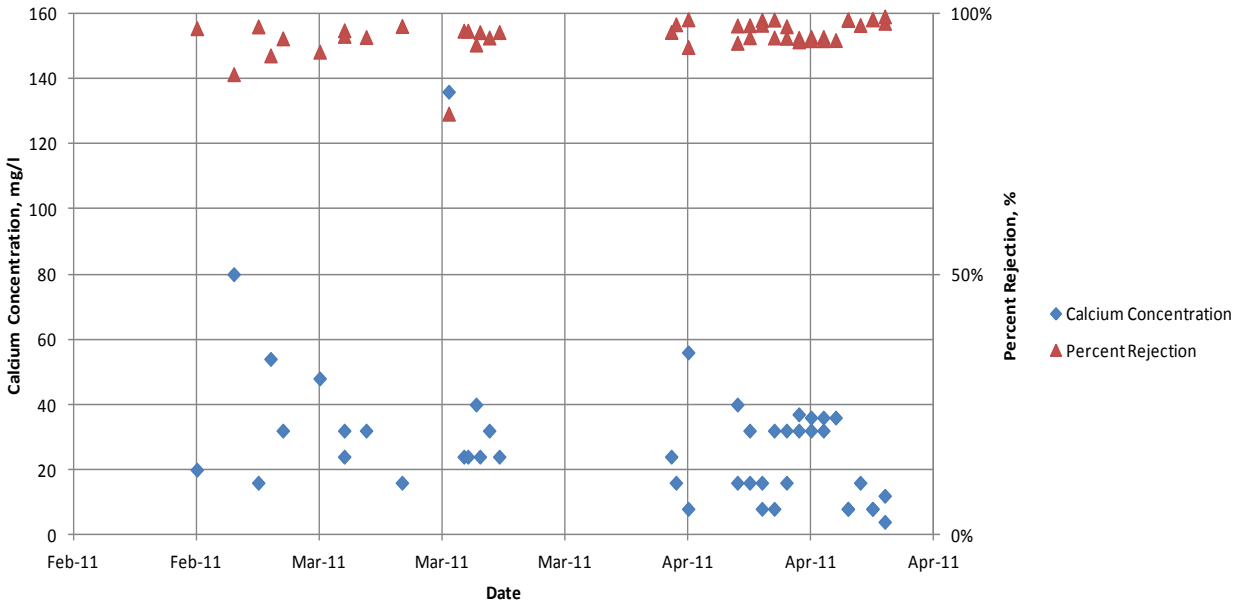

Figure 3 NF Permeate – Calcium Concentrations and Percent Rejection

The sulfate concentration in the NF reject ranged between 2,500 and 4,000 mg/l, and calcium in the reject varied between 800 and 1,800 mg/l. TMP across the membrane never exceeded 0.7 bar because of the low SDI values in the feed water and periodic flushing of the membrane with NF permeate. The membranes were flushed once every twelve hours.

Sulfate treatment results for NF concentrate by the desaturation process are presented in Figure 4. In this process, sulfate was removed through gypsum ($CaSO_4 \cdot 2H_2O$) precipitation using a combination of lime and calcium chloride under a controlled pH at a specified sludge recirculation ratio within 30 minutes of reaction in the presence of seed material, which was added one time during the study. During the desaturation process, utilizing a Turbomix™ reactor and MULTIFLO™ technology, sulfate was reduced to less than 1,500 mg/l.

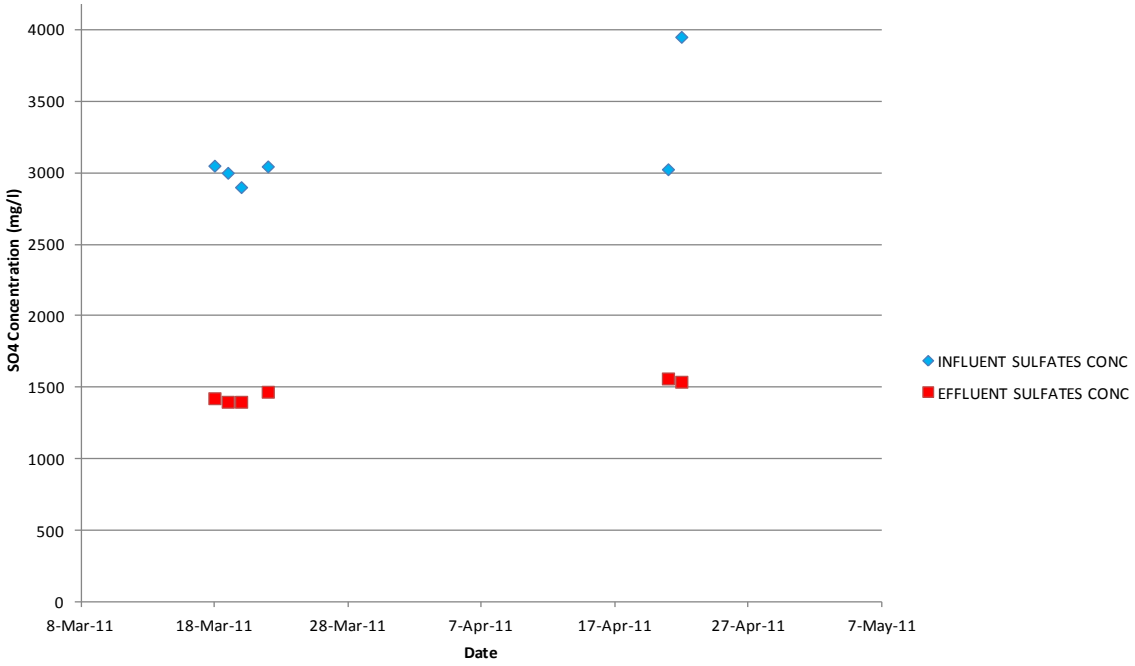

Figure 4 CaSO4 Desaturation with Sludge Recirculation and with Seed Material

Further Reduction of Sulfate by Calcium Sulfate Complexation

Dissolved sulfate from the desaturated calcium sulfate effluent was further reduced by forming an insoluble complex known as calcium sulfoaluminate mineral. The associated chemical dosages and sludge recirculation ratios were determined from the preliminary laboratory study results. Sulfate reduction kinetics results for the most efficient recirculation ratio are shown in Figure 5.

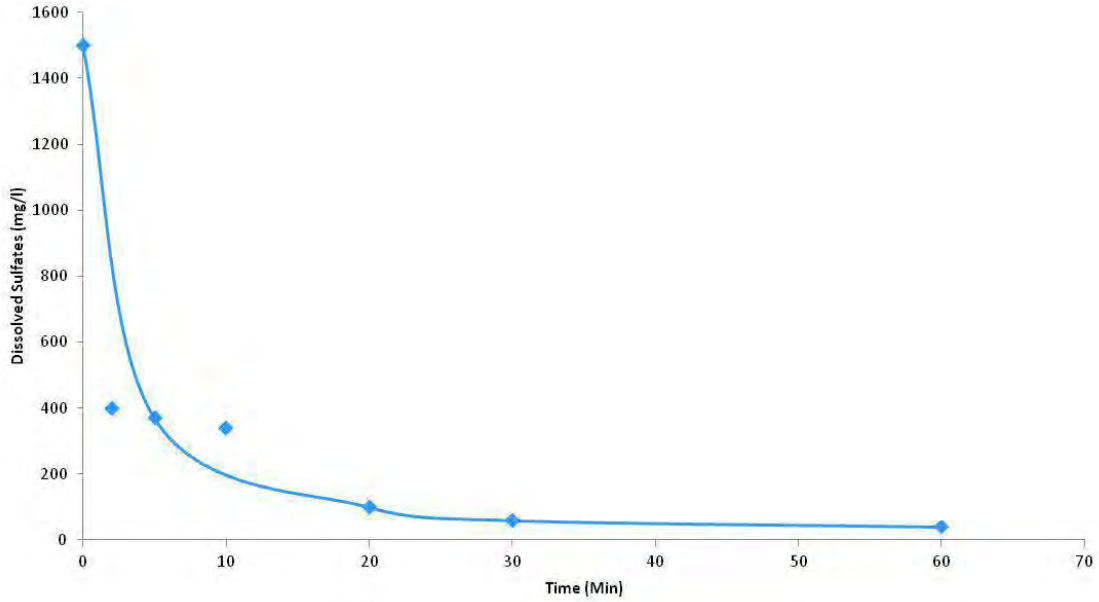

Figure 5 Sulfate Precipitations Kinetics as Calcium Sulfoaluminate Mineral

As the figure illustrates, increasing the reaction time decreased the sulfate concentration, and the reaction was completed within 20 minutes. During that period, dissolved sulfate was reduced to <100 mg/l.

As indicated earlier, using the water from a coal mine site, the 2nd set of pilot study was conducted. The primary objective was to recover aluminum from calcium sulfoaluminate (Ettringite) sludge, and reuse that in the process. The study was conducted for a period of 16 weeks. Freshly prepared tri hydroxide of aluminum (Gibbsite) was used for the first two weeks of the study to precipitate sulfate as the Ettringite mineral. Once the system reached to the steady state condition, regenerated tri hydroxide of aluminum was used for Ettringite precipitation.

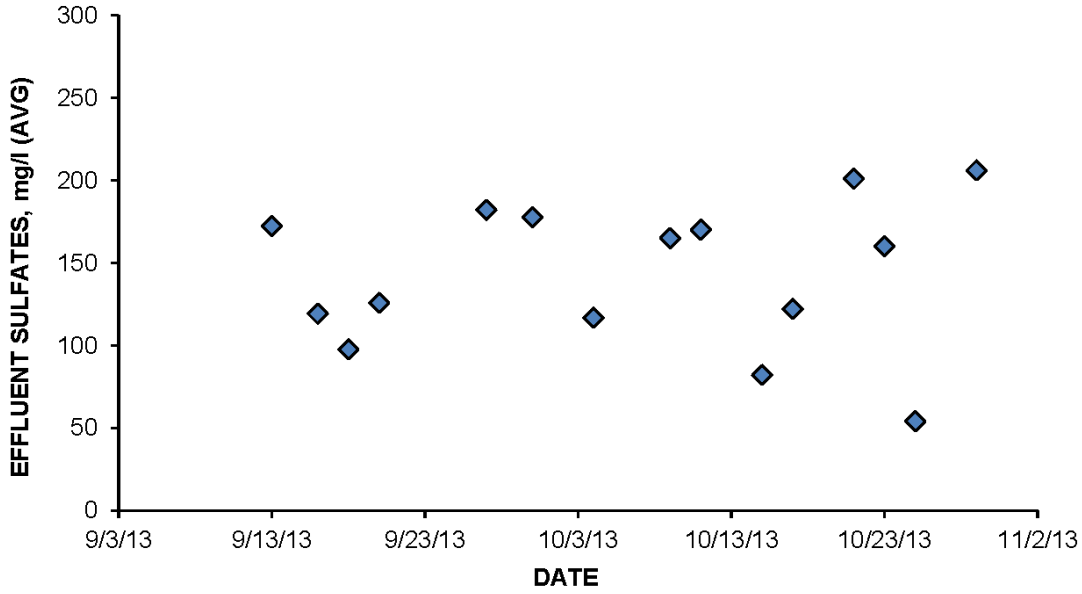

Figure 6 Effluent Sulfate with Regenerated Gibbsite

As indicated in Figure 6, after solid/liquid separation, sulfate was reduced to <100 mg/L The particle size distribution results (not shown in the paper; will be included in the presentation) revealed that the average particle diameter of the Ettringite solids is 20μ, and more than 1% of the particles have the diameter less than 1μ. Consequently, carry-over of the fine colloids of Ettringite has contributed to elevate the sulfate results. It is anticipated that with adequate sludge recirculation, the solids carry-over problem would be under control. Dissolved aluminum in the treated effluent ranged between 0.1 and 0.35 mg/L (see Figure 7).

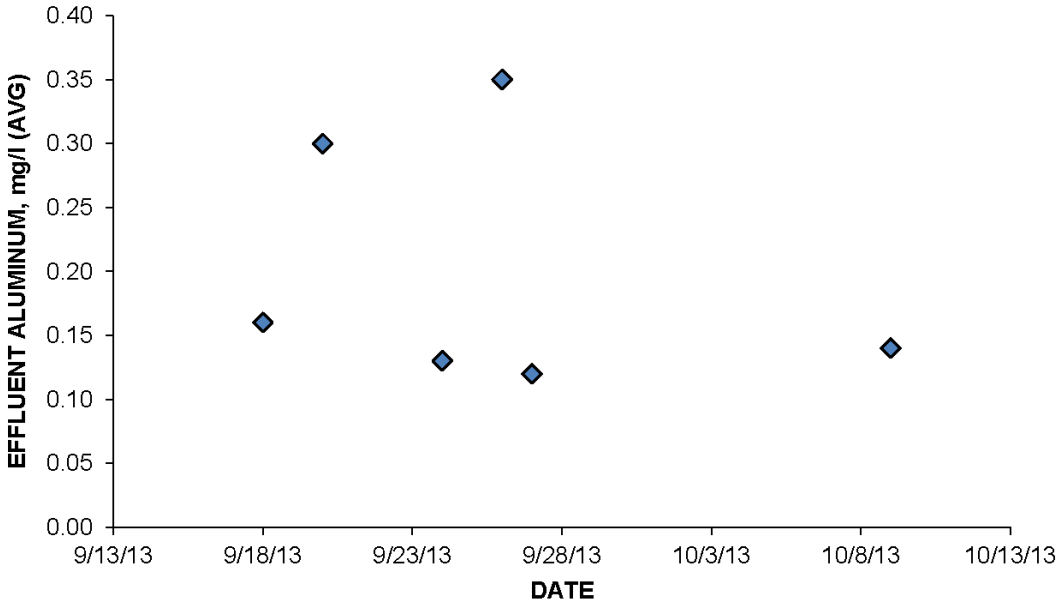

Figure 7 Aluminum in the Treated Effluent

Aluminum from the calcium sulfoaluminate precipitate was recovered by dissolving this mineral in acid. After solid/liquid separation, more than 95% of the aluminum-based salt was recovered and reused to precipitate calcium sulfoaluminate for sulfate reduction.

Based on the pilot-scale results, a flow and mass balance calculation was performed, and a conceptual process was proposed (see Figure 8). The process includes pretreatment for iron, manganese, molybdenum, total suspended solids (TSS), and other pertinent contaminants followed by NF for sulfate removal and sulfate reduction from NF reject by a two-stage chemical precipitation process. The flow and mass balance calculation for this specific site revealed that after blending the treated NF reject with the permeate, the overall water recovery increased from 60 to 90%.

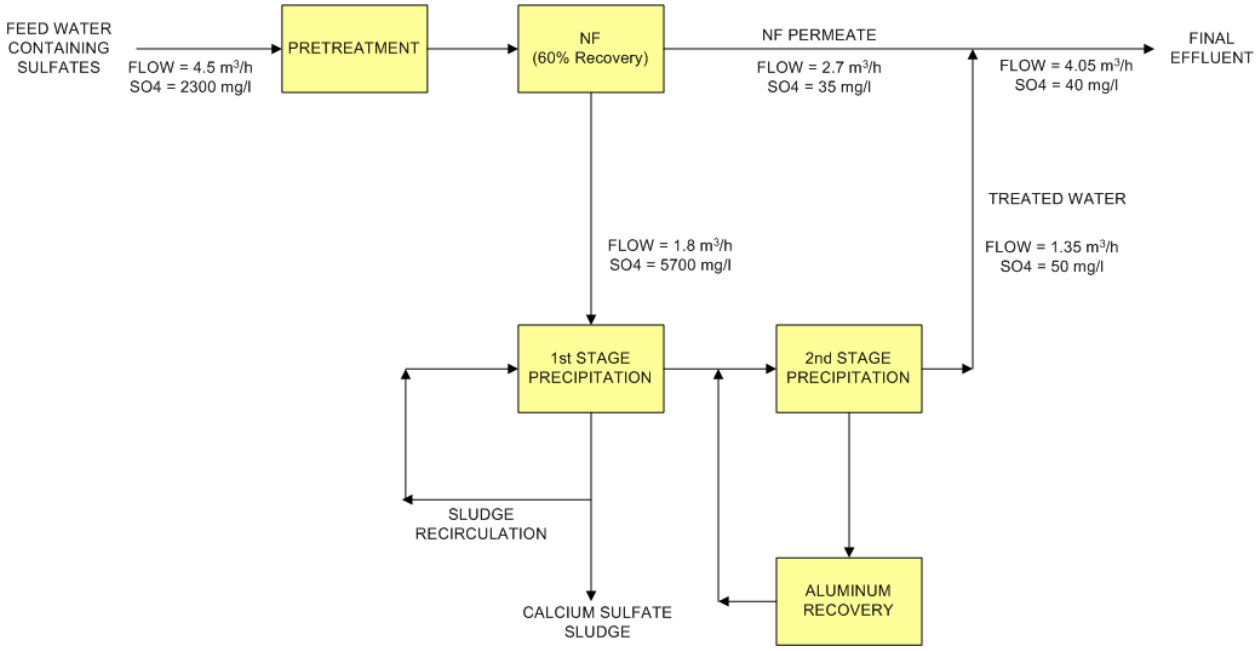

Figure 8 Process Flow Diagram

CONCLUSION

Sulfate from the NF reject can be reduced to less than 1,500 mg/l by a chemical precipitation and/or adsorption process in the presence of a seed material with sludge recirculation. Calcium sulfate crystal growth can be accomplished in a continuous system with a specified reaction time and sludge recirculation ratio. The sulfate concentration can be further reduced to less than 100 mg/l by a calcium sulfoaluminate precipitation process. The crystal growth and precipitation reaction kinetics of this process are fast and can be accomplished within 20 minutes of reaction. More than 95% of the aluminum was recovered and reused. This innovative concept increased overall water recovery significantly.

ACKNOWLEDGEMENTS

The authors gratefully acknowledge Sri Muddasani, Hillary Kronebusch, Carla Robinson, and Deb Livada for their contribution to the work for this paper.

REFERENCES

Silva, R.; Cadorin, L.; and Rubio, J. (2010) Sulfate ions removal from an aqueous solution: I. Co-precipitation with hydrolyzed aluminum-bearing salts. Mineral Eng. 23, 1220 – 1226.

Banerjee, K.; Muddasani, S.; Blumenschein, C. D.; Buisson, H. and Zick, R. (2012) An Innovative process for sulfate treatment of membrane concentrates from mining operations, Proc. IWA 9th Leading Edge Technology Conference, Brisbane, Australia, June 2012

Banerjee, K.; Blumenschein. C.D.; and Buisson, H. (2010) Comparison of Carbonate Crystal Growth in a Conventional Reactor versus a Proprietary Enhanced Reactor. Proc. IWA International Water Week, Singapore, 2010.

10th ICARD IMWA 2015 | 10th International Conference on Acid Rock Drainage & IMWA Annual Conference

Development of an Adsorbent Comprising Schwertmannite and its Utilization in Mine Water Treatment

Eberhard Janneck[1], Diana Burghardt[2], Elisabeth Simon[2], Stefan Peiffer[3], Michael Paul[4] and Tomas Koch[5]

1. *G.E.O.S. Ingenieurgesellschaft mbH, Germany*
2. *Institute for Groundwater Management, TU Dresden, Germany*
3. *University of Bayreuth, Germany*
4. *Wismut GmbH, Germany*
5. *Vattenfall Europe Mining AG, Germany*

ABSTRACT

Two different kinds of agglomerated and filter stable adsorbents were developed based on bio-technologically synthesized schwertmannite (SHM) from iron and sulfate containing lignite mine water. The adsorbents were obtained by compaction and by mixing SHM with an organic polymer without impairing its adsorption capacity regarding arsenic, respectively.

At first, both types of SHM adsorbents were tested in comparison to the commercially available iron hydroxide adsorbent (Ferrosorp®Plus, HeGoBiotec GmbH) in two batch test series with (1) tap water stocked with 20 mg/L As(V) and As(III), respectively and (2) drainage water from an abandoned uranium mine of the ore mountains (Eastern Germany) which contained about 1 mg As/L. Both types of SHM adsorbents showed higher maximum As(III) and As(V) adsorption capacities (28.0 to 31.1 mg/g adsorbent) than Ferrosorp®Plus (22.7 and 18.0 mg/g adsorbent, respectively).

Thereafter, two column test series were performed directly at the abandoned uranium mine site with the drainage water and a filter bed residence time of 11 to 34 minutes. Due to its slow adsorption kinetic, the effluent limit value of 0.1 mg As/L was exceeded significantly earlier in the Ferrosorp®Plus column than in the columns filled with SHM-adsorbents. The compacted product SHM-sorpP showed a better long time effect due to its 40% higher bulk density.

In dumping experiments with the As loaded SHM adsorbents and alternating rain water (pH 5) and continuous groundwater elution (pH 7), only 0.13 – 0.6% and 0.03% of the adsorbed As were desorbed within 285 days, respectively. Currently, further pilot scale trials are being prepared for testing the SHM agglomerates with various kinds of mine and industrial wastewaters.

*Corresponding author: G.E.O.S. Ingenieurgesellschaft mbH, Schwarze Kiefern 2, 09599 Freiberg, Germany, Phone: +49 3731 369129, Email: e.janneck@geosfreiberg.de

INTRODUCTION

The Vattenfall Europe Mining AG and the G.E.O.S. company are operating in close collaboration a pilot plant for microbial-mediated ferrous iron oxidation in the open pit lignite mine near Nochten (Lusatia, Germany) where schwertmannite (SHM) is synthesized as a byproduct of a worldwide unique water treatment process (Janneck et al, 2010 ; DE 102 21 756 B4). The pilot plant (Figure 1) is operated with iron and sulfate rich mine water from the Nochten pit. In the framework of a recently finished research project founded by the German Ministry of Education and Research (Peiffer et.al., 2012), two methods for the production of an agglomerated adsorbent based on SHM were developed for utilization of water stable agglomerates in passive treatment systems for Arsenic-contaminated mine waters.

MATERIALS AND METHODS

Adsorbents

The SHM-based adsorbents were fabricated a) by compaction (called SHM-sorpP thereafter) and b) by mixing SHM with an organic polymer (called SHM-sorpX thereafter), respectively. The latter was produced by using filter-moist SHM (approximately 48 wt-% water content), a binder amount of 8 wt% (in order to obtain a stable product), a drying step of 6 hours at 85°C and a curing step of 1 hour at 120°C thereafter. The binder-free adsorbent was produced by high-pressure compaction in a briquette press with controllable pressure gradient at the Höcker Polytechnik GmbH, Hilter, Germany (Figure 2). For this purpose, the SHM was dried at 60°C in order to obtain a water content of 10 to 20 wt-%. The moisture of the raw material SHM has an important influence on the briquette quality. SHM does not adhere and will still remain as a dusty powder if the water content is too low, even at sufficient pressure conditions. If the water content is too high, the substance exhibits thixotropic behavior. Details of the briquette fabrication are given in EU patent application EP 2664376A1.

The new SHM-based adsorbents (Figure 3) for the treatment of arsenic contaminated mine water should be compared to that of a commercially available iron-hydroxide adsorbent like Ferrosorp®Pus (HeGo Biotec GmbH). Table 1 summarizes the characteristic parameters of all three adsorbents.

Figure 1 1-2.5 m^3/h pilot plant in Tzschelln (left), where schwertmannite is generated as a byproduct of microbial catalysed lignite mine water treatment on special carrier elements (right)

Figure 2 Höcker BrikStar press (left) was used for production of cylindrical briquettes with 5 cm in diameter (right)

Figure 3 SHM-based adsorbents, obtained by mixing with an organic polymer (left) and high pressure compaction, crushing and sieving (right). Grain size: 1-2 mm in both pictures

Table 1 Selected parameters of the SHM-sorpX, SHM-sorpP and Ferrosorp®Plus

Adsorbent		**SHM-SorpX**	**SHM-SorpP**	**Ferrosorp®Plus**
Grain size	[mm]	1-2	1-2	0.63 -2
Grain density ρ_s	[g/cm^3]	2.43	3.06	3.02
Bulk density ρ_d	[g/cm^3]	0.6	1.0	0.60
Filter bed porosity	[%]	75	69	80
Specific surface area (SSA)	[m^2/g]	143.9	64.7	320.8
Micropore surf. area	[m^2/g]	8.7	25	276.6
Micropore volume	[cm^3/g]	0.0031	0.0044	0.0983
Intraparticle porosity*	[%]	0.75	1.29	29.7

*intraparticle porosity = grain density * micropore volume

Table 2 Selected parameters of the As(III) or As(V) enriched tap water used in batch tests and the drainage water of an abandoned uranium mine (Ore Mountains, Germany) used in pilot scale column tests

parameter	pH [-]	TIC	SO_4	Ca	Mg	Fe	Si	As
					[mg/L]			
Tap water	8.15	18.2	31.0	40.2	3.4	<0.1	1.9	(+10/ +20)
Drainage water	7.05	63.1	0.49	49.7	11.8	<0.1	10.0	0.85-1.8

Water

Two kinds of water were used in the study. For the investigation of the principal As adsorption behavior (adsorption capacities and kinetics), batch test series with As-enriched tap water were performed. The suitability of the new SHM adsorbents for practical water mine treatment was studied in two field site column test series at an abandoned uranium mining site (Ore Mountains, Eastern Germany) using drainage water. Table 2 summarizes the parameters of these waters.

Test methods

Batch tests In order to investigate the principal As adsorption behavior (adsorption capacities and kinetics) of the new SHM adsorbents, samples of SHM-SorpX and SHM-SorpP were prewashed to remove residual, superficially-adhered sulfate. The As uptake behavior was investigated in 250 mL glass bottles with screw caps at an initial As(III) and As(V) concentration of 10 and 20 mg/L tap water (quality mentioned in the pre-selection test section) as $Na_2HAsO_4*7H_2O$ p.a. and $NaAsO_2$ p.a., and an adsorbent mass of 0.5 g/L for an overall time of 24 days. Prior to the beginning of the experiments, the solution pH was adjusted to a value of 7.4 +/- 0.1 with diluted HCl. The bottles were gently shaken on a horizontal shaker at T= 22 ± 2°C. During the experiments, no pH buffering was done in order to simulate conditions of water treatment plants. Sampling of pH and As concentration was performed after 1, 3, 6, 11 hours and 1, 2, 4, 6, 10, 14 and 24 days. In order to compare the As(III) and As(V) adsorption capacities of both SHM-adsorbents with the iron hydroxide adsorbent Ferrosorp®Plus, parallel tests with 10 and 20 mg/L As(III) or As(V) and dose of 0,5 g/L of these adsorbents were performed and sampled after 1 hour and 14 days. As(III) experiments were carried out under nitrogen atmosphere in a glove box and the tap water used for the As(III) stock solution was degassed under vacuum.

Field site column tests Thanks to the support of WISMUT GmbH, two column test series could be performed directly at an abandoned uranium mining site. From these tests, the suitability of the new SHM adsorbents for passive mine water treatment systems could be investigated. Table 3 contains important data including trial periods, column dimensions and filter bed residence times. In the 1st column series, the column plant was placed directly at the outlet of the abandoned uranium mine (shaft G1), where the drainage contained about two-thirds arsenite (As(III)). Thereafter, the drainage flows through an aeration cascade and two sedimentation ponds and is decontaminated in a passive water treatment system subsequently (operated by the WISMUT GmbH). The residence time of the drainage water between the mine outlet and this treatment system is approximately 7 days, along the way As(III) is completely oxidized to As(V). Based on the results of the previous batch tests, where the SHM adsorbents offered better adsorption properties

for As(V), the column plant was placed directly at the inlet of the passive water treatment system (shaft G4B) for the 2nd column test series. Figure 4 shows the column set-up.

Table 3 Test parameters of the field site column test series

Test series	Location	Trial period	Dimension of the columns	C(As, influent)	Filter bed residence time
1	shaft G1	2012, sept.-dec. & 2013, may –sept.	D = 4 cm, L = 20 cm V_{column} = 251 cm^3	**ca. 1.8 mg/L:** 65% As(III), 28% As(V)	28 - 34 min
2	shaft G4B	2013, oct.- dec.	D = 3 cm, L = 14.5 cm V_{column}= 102 cm^3	**ca. 0.85 mg/L:** 100% As(V)	11 – 16 min

Sampling of each column influent and effluent were done three times a week, and ferrous iron and pH were estimated by a test kit. Arsenic was analysed by AAS (Perkin Elmer) after membrane filtration (0.2 µm Cellulose Acetate) and conservation by 1% HNO_3(c). The development of As-Species from shaft G1 to shaft G4B was investigated during a field campaign according to the method of (Le et al., 2000).

Figure 4 Field site column test design with a prefilter (sand column) and an admission pressure pump (left), the column test plant with effluent containers (middle) and the Plexiglas columns filled with adsorbents (right)

Dumping tests Dumping tests were performed to verify the long-term binding stability of SHM-sorpX and SHM-sorpP for arsenic. Therefore, the As-loaded SHM-adsorbents from the batch tests were tested under two "worst case" scenarios. (1) A rainwater elution scenario should represent a dumping site with an insufficient surface cover and (2) a groundwater elution scenario should simulate a dumping site without basic sealing. For the rainwater scenario, the SHM adsorbents were wetted by synthetic rainwater (pH 5, Ca: 0.6 mg/L, K, Na, NH_4, Mg: 0.3 mg/L, NO_3, SO_4: 2 mg/L, Cl: 0.5 mg/L) for 24 hours every 2 to 4 weeks. A non-contaminated mine water from Ehrenfriedersdorf (Ore Mountains, Eastern Germany) with pH 7.9, EC 445 µS/cm, SO_4: 102 mg/L, HCO_3^-: 47.3 mg/L, Si: 6,5 mg/L, Fe: < 0.1 mg/L and Mn: <0.1 mg/L was used for the groundwater

elution scenario respectively. In all tests, the water to adsorbent ratio was 1:10. The change of the equilibrium water phase and the subsequent As analysis (sample preparation and analytical method as mentioned above) were done every 2-4 weeks (in a total of 15 cycles) for an overall test time of 9.5 month (285 days).

RESULTS

Batch tests

Figure 5 shows the adsorption kinetic of As(III) and As(V) for both SHM-sorpX and SHM-sorpP. The amount of adsorbed As (q_t in mg/g adsorbent) was plotted against the square-root of the shaking time t (in days$^{0.5}$) in order to visualize different adsorption kinetic behaviours. According to (Weber & Morris, 1963), theses q_t-$t^{0.5}$-plots (with $q_t = k*t^{0.5}$ and the slope/equilibrium rate constant k) show multi-linearity, if not only an external diffusion of the adsorbate (As(III) or As(V)) to the surface of the adsorbents, but also intraparticle diffusion controls the adsorption behaviour. The main part of As adsorption was controlled by external diffusion of As to the adsorbent surfaces and appears within the first two days of the experiments, Intra-particle diffusion of superficially adsorbed As into the meso- or micropores of the SHM adsorbents could be evidenced in minor parts by a second, significantly lower slope of each q_t-$t^{0.5}$ plot. SHM-sorpX shows a faster 'short-time' adsorption behavior for As(III) and As(V) (steeper slopes of the first parts of the q_t-$t^{0.5}$-plots), whereas SHM-sorpP takes over thereafter (during the 'long-time' adsorption, steeper slopes of the second parts of the q_t-$t^{0.5}$-plots), especially in the experiments with As(V). During the contact with water in the batch test, SHM-sorpP seems to form higher intraparticle porosity than SHM-sorpX, which could be very advantageous for a longtime use in filter bed systems. This can be attributed to the curing of the SHM-sorpX product by the binder addition.

Table 4 contains the As(III) and As(V) adsorption capacities for SHM-sorpX, SHM-sorpP and Ferrosorp®Plus after 1 hour and 14 days, respectively. Whereas the As(III) adsorption to both SHM adsorbents was slightly lower than that of Ferrosorp®Plus after 1 hour, SHM-sorpP and SHM-sorpX had adsorbed more As(III) than the iron hydroxide adsorbent after 14 days. In contrast to this, the As(V) adsorption to SHM-sorpP and SHM-sorpX was always significantly higher than that of the iron hydroxide adsorbent, even after 1 hour. This could be referred to a more positive surface charge of the SHM because of a proton release during its hydrolysis.

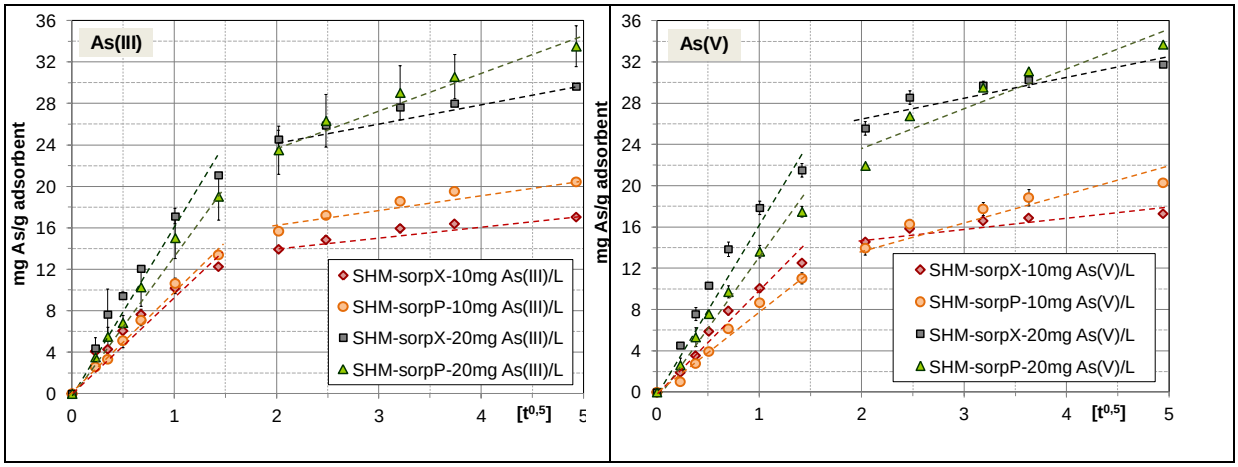

Figure 5 As adsorption kinetics of SHM-adsorbents, 0.5 g ads./L, pH_{start}: 7.4±0.1, no pH buffering during the tests

Field site column tests

In both test series, a significantly better performance could be demonstrated for the newly developed SHM adsorbents compared to Ferrosorp®Plus (Figure 6). Thereby, the higher bulk density of SHM-sorpP proved to be a major advantage. This allows 40% higher amounts of adsorbent in the filter beds and so their lifetimes can be increased greatly. In addition, it seems that the 'open' (in contrast to product SHM-sorpX not glued) surface structure allows a slight kinetic sorption (intraparticle diffusion), whereby initially superficial adsorbed arsenic is carried deeper into the granule structure and the surface adsorption area can receive new arsenic. The second series of experiments has been shown that the new SHM-adsorbents due to their, already in the laboratory tests (Tab.1) proven, better As (V) – adsorption kinetics have another big advantage compared to the adsorbent Ferrosorp®Plus. This enables much shorter residence times in the filter bed and the water flow rate could be increased significantly. Due to the beginning of the frost period, the test series 2 was completed by December 2013.

Table 4 As(III)- and As(V)- capacities estimated in batch tests with 0.5 g adsorbent/L and 20 mg As/L, pH_{Start}= 7,4±0,1 after 1 hour and 14 days (rather maximal adsorption capacities)

Adsorbent	after 1 hour		after 14 days	
	mg As(III)/g ($pH_{equilibrium}$)	mg As(V)/g ($pH_{equilibrium}$)	mg AsIII)/g ($pH_{equilibrium}$)	mg As(V)/g ($pH_{equilibrium}$)
SHM-sorpX	**4.4**±1.0 (pH 6.8)	**4.5**±0.7 (pH 6.9)	**28.0**±0.7 (pH 6.8)	**30.3**±0.2 (pH 6.8)
SHM-sorpP	**3.5**±0.4 (pH 7.0)	**2.6**±0.01 (pH 7.0)	**30.6**±2,1 (pH 6.6)	**31.1**±0.7 (pH 6.9)
Ferrosorp®Plus	**4.8**±0.1 (pH 7.6)	**1.6**±0.3 (pH 7.3)	**22.7**±0.4 (pH 8.2)	**18.0**±0.2 (pH 7.9)

Table 5 and 6 contain a summary of the characteristic parameters and the filter-bed volumes which could be exchanged up to the exceedance of the effluent limit concentration of 0.1 mg As/L. Because of the higher residence time in the 1st test series, the calculated, integral As loading of the adsorbents were in the same range. However, it should be considered, that the filter bed system with SHM-sorpP contained a 40% higher adsorbent mass. In the 2nd test series, the As loading of Ferrosorp®Plus was remarkably lower, and demonstrated its worse adsorption kinetic again.

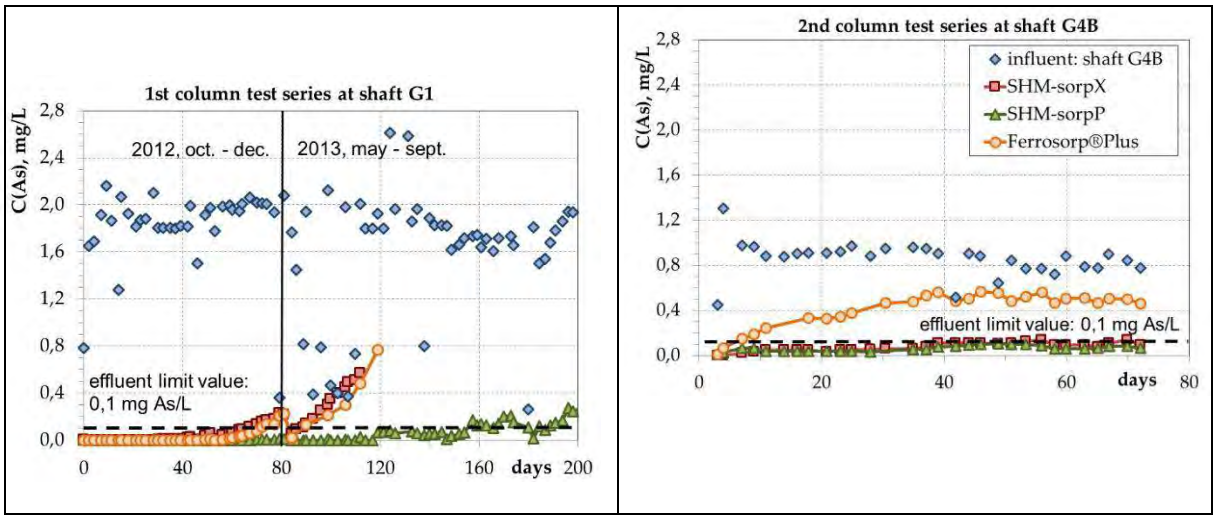

Figure 6 Development of As-concentrations in the column effluents of the 1st (left) and 2nd test series

Table 5 Summary of the 1st column test series at shaft G1

Adsorbent (mass)	**Filter bed residence time**	**Filter bed volumes treated $C(As)_{effl}$ >0.1 mg/L**	**Total through put / test time at $C(As)_{effl}$ >0.1 mg/L**	**Calculated As adsorp. capacity at $C(As)_{effl}$ >0.1 mg/L**
Ferrosorp®Plus (153 g)	34 min	2,784	501 L/ 72 d	6.1 mg As/g Ads.
SHM-sorpX (177 g)	32 min	3,633	654 L/ 90 d	6.1 mg As/g Ads.
SHM-sorpP (304 g)	28 min	6,389	1214 L/ 157 d	6.9 mg As/g Ads.

Table 6 Summary of the 2nd column test series at shaft G4B

Adsorbent (mass)	**Filter bed residence time**	**Filter bed volumes treated $C(As)_{effl}$ >0.1 mg/L**	**Total through put / test time at $C(As)_{effl}$ >0.1 mg/L**	**Calculated As adsorp. capacity at $C(As)_{effl}$ >0.1 mg/L**
Ferrosorp®Plus (73 g)	15.6 min	549	44 L/ 7 d	0.5 mg As/g Ads.
SHM-sorpX (66 g)	13.2 min	4,418	353 L/ 39 d	4.7 mg As/g Ads.
SHM-sorpP (118 g)	11.4 min	5,966	418 L/ 49 d	2.9 mg As/g Ads.

After the end of both column test series, the As-loaded SHM adsorbents were also analyzed by aqua regia digestion for their arsenic content in the inlet and outlet areas of the columns (Table 7). The results show, that the As adsorption capacities of the SHM adsorbents have not been fully exhausted compared to the values reached in the batch tests. If a series connection of two columns

will be used, As adsorption capacity up to 20 mg As/g should be achievable in the entire first column.

Table 7 As content of the SHM adsorbents after the end of the column tests

Column	SHM-sorpP		SHM-sorpX	
	inlet area	outlet area	inlet area	outlet area
Series 1	20.3 mg As /g	5.1 mg As/g	16.4 mg As/g	4.2 mg As/g
Series 2	8.4 mg As/g	1.7 mg As/g	13.4 mg As/g	2.8 mg As/g

Dumping tests

Sequential elution tests with groundwater and synthetic rainwater were performed with As loaded SHM adsorbents from the As(III) adsorption kinetic tests. Between 0.13% and 0.6% of the adsorbed As were desorbed by a total of 15 cycles of alternating wetting with rainwater and subsequent drying (Table 8). Leaching of As by continuous elution with groundwater for 285 days was not significant (0.03 % of the initial value). After one elution cycle, the concentration limit of 2.5 mg/L of dumping class DKIII (German DepVerwV, 2005) was not exceeded in any case of dumping. This assessment demonstrates that dumping of As-contaminated SHM adsorbents would be tolerable according to German dumping classes even under worst case conditions like a dumping site without an intact surface or bottom sealing and no additional treatment of the SHM adsorbents for immobilisation purpose is necessary.

Table 8 Desorption of As from SHM-adsorbents

Adsorbent	SHM-sorpX	SHM-sorpP	SHM-sorpX	SHM-sorpP
C(As, adsorbed)	32.8 mg/g	31.5 mg/g	32.8 mg/g	31.5 mg/g
Elution procedure	**Alternating rainwater elution (pH 5)**		**Continuous groundwater elution (pH 7)**	
Total As eluated (15 cycles)	0.13 %	0.60%	0.03 %	0.03%
C(As, eluated, 1st cycle)	1.41 mg/L	1.87 mg/L	1.57 mg/L	0.72 mg/L

CONCLUSION

Schwertmannite, biotechnologically synthesized in a pilot plant for lignite mine water treatment, was used for the production of two filter stable adsorbents (grain size 1-2mm) in order to use them in passive treatment systems for As contaminated mine waters. The adsorbents were obtained by compaction and by mixing SHM with an organic polymer, respectively.

In batch tests series with both SHM-adsorbents and a commercially-available iron hydroxide adsorbent (Ferrosorp®Plus, HeGo Biotec GmbH) as well as tap water enriched with 20 mg/L As(III) or As(V), 28.0 to 31.1 mg As/g SHM-adsorbents and 22.7 to 18.0 mg As/g Ferrosorp®Plus were estimated after 24 days equilibrium time, respectively. Thereafter, two column test series were performed directly at an abandoned uranium mining site with drainage water. Because of its worse adsorption kinetic, the effluent limit value of 0.1 mg As/L was exceeded in the Ferrosorp®Plus column significantly earlier than in the columns filled with SHM-adsorbents. Thereby, the

compacted product SHM-sorpP showed a better long time effect due to its 40% higher bulk density. In dumping tests with As loaded SHM adsorbents and alternating rain water (pH 5) and continuous groundwater elution (pH 7) elution, only 0.13 – 0.6% and 0.03% of the adsorbed As were desorbed into 285 days, respectively.

REFERENCES

DepVerwV (2005): Verordnung über die Verwertung von Abfällen auf Deponien über Tag und zur Änderung der Gewerbeabfallverordnung. 25.Juli 2005

DE 10221756 B4: Verfahren zur Reinigung/ Behandlung von sauren, eisen- und sulfathaltigen Wässern. Patentschrift Bundesrepublik Deutschland, Veröffentlichungstag 26.04.07

EP 2664376A1 An adsorbent comprising schwertmannite, a method of preparing the adsorbent and the use of the adsorbent for purifying water or gas; 14.05.2012

Janneck, E., Arnold, I., Koch, TH., Meyer, J., Burghardt, D., Ehinger, S. (2010): Microbial synthesis of schwertmannite from lignite mine water and its utilization for removal of arsenic from mine waters and for production of iron pigments. Proceedings IMWA Conference, Sydney, NS, Canada

Le, X.,Ch, Yalcin, S., Ma, M. (2000): Speciation of Submicrogram per Liter levels of Arsenic in Water: On-Site Species Separation Integrated with Sample Collection. Environmental Science and Technology, vol. 34, no. 11, p. 2342 – 2347.

Peiffer, S. Burghardt, D., Simon, E., Rostan, M., Janneck, E., Fischer, H., Patzig, A., Lambrecht, J., Schlömann, M., Wiaceck, C., Kipry, J., Mosler, S. (2012): Fertigstellung von Verfahren zur biotechnologischen Schwertmannit-Synthese und zur passiven Wasseraufbereitung durch Herstellung eines Schwertmannit-Agglomerates. BMBF-Abschlussbericht, FKZ 03G0821, TIB Hannover.

Weber, W.J., Morris, J.C. (1963): Kinetics of adsorption on carbon from solution. Journal of Sanitary Engineering Division. American Society of Civil Engineers 89, p. 31-59.

Investigation and Strategy on Iron Removal from Water Courses in Mining Induced Areas

Friedrich Carl Benthaus[1], Wilfried Uhlmann[2], and Oliver Totsche[1]

1. *LMBV, Germany*
2. *IWB, Germany*

ABSTRACT

The ground water table has been lowered for lignite mining purposes at Lausitz area between Cottbus and Dresden (Germany) for a long period of time. Pyrite contained in unconsolidated rocks as well as overburden oxidized intensively at up to 30 or 50 m depth. High quantities of soluble ferrous iron as well as insoluble ferric iron were generated.

While mining on large scale closed in this area, the ground water table rose in recent years. Water courses again are predominated by groundwater inflow. The iron input into the river Spree and into adjunct water creeks can be observed as a cloudy, reddish brown substance.

Large scale investigations have been carried out in order to detect the most important sources of iron contamination along the river Spree. Measuring the flow at different seasons and measuring pH, alkalinity, iron and sulfate along the river course at one day gives a perfect impression of the river status.

A high concentrated groundwater inflow in rivers had been detected not only in connection with dump areas. Increased ferrous iron concentrations have been detected for example at highly permeable aquifers and the outflow of former bog areas.

In order to remove iron from the Spree river water, various treatment units were designed and implemented. The concept for removing the iron followed the principles of simplicity in process, low cost design and minimal chemical additions. Former water treatment plants are reused as sedimentation ponds. Wetlands are constructed for settling of ferric oxyhydroxide solids. Even microbial treatment of groundwater is in test scale with encouraging results.

INTRODUCTION

Lignite mining makes an important contribution to the supply of electrical energy in Germany. In Lusatian district, the area between Dresden and Cottbus, nearly 65 million tonnes of lignite were extracted in 2013, about a third of Germany total production

The lignite seams are embedded in horizontal strata of soft rock sand and silt of Tertiary and Pleistocene age. In order to extract this coal from depths of 30 to 50 metres, the water in the overlying strata has to be lowered by draining. In the past a depression cone of approximately 2,100 square kilometres occurred (Fig.1), extending well over the borders of the opencast mining area.

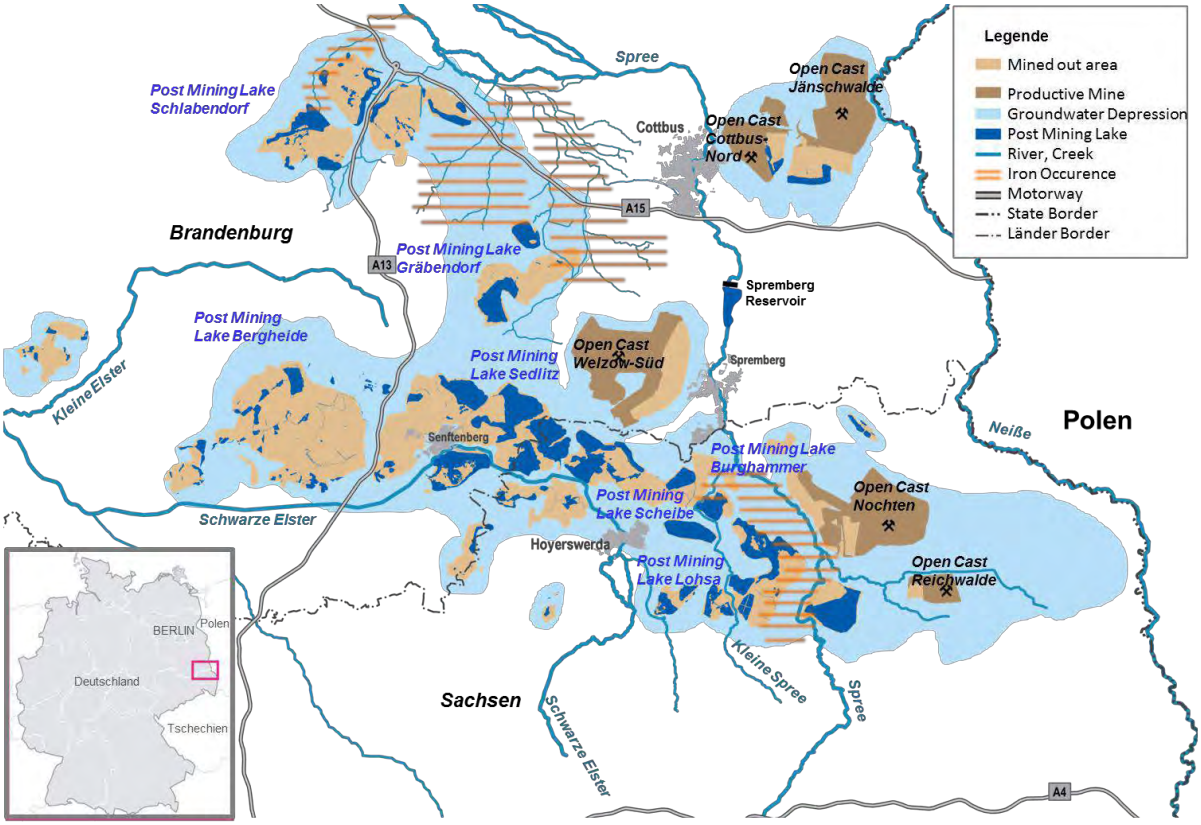

Figure 1 The Lusatian lignite mining district in Germany

Since 1990 a total of 32 lignite mines have had to be closed down. Either deposits have been depleted or the economic and competitive conditions have changed dramatically. The German mining legislation requires that all mines to be rehabilitated. The rehabilitation Lausitzer und Mitteldeutsche Bergbauverwaltungs GmbH (LMBV) has taken charge of. It comprises the removal of all installations, stabilisation of slopes, flooding the opencast mining areas and the restoring the natural water resources.

PROBLEMS OCCURRING WHILE GROUND WATER RISE

Pyrite layers accompanying the seams had previously been under the exclusion of air. While lowering ground water, the oxidation of the drained strata in the depression cone has resulted in soluble iron and sulphate compounds. As the groundwater level rises, these substances are now carried into the water courses.

While sulphate remains in solution in these waters, iron oxidises further, forming iron precipitate. Heavy loads of the resultant iron ochre represent a serious burden for the water course ecosystems affected (see Fig. 2). As a consequence, for example, water plants lack light because of suspended solids. Mussels are smothered by the fine silt and the turbidity deprives fishes of their spawning grounds through the accumulation of mud.

Figure 2 Iron burden in the "Kleine Spree" river (Photo: Theiss)

Investigations by IBW (2010b) and IWB (2013) have shown that there are various sources for the accumulation of iron ochre in water courses (Fig.3). Lignite mining in Lusatia has resulted in large disturbance of the catchment. Besides this, agricultural improvements such as surface draining (1) or turf cutting (6) or even bog iron ore extraction in the last century causes an "initial load" (Fig.3).

The aeration of aquifers following the groundwater depression, takes place even far outside the immediate opencast mining area (2). Oxidation in these aquifers is relatively weak compared with that in material that was relocated in inner dumps (3) or in outer dumps (4) during mining operations. The inner dumps will be submerged again once the water table has been restored. This will result in the cessation of the oxidation process, at least in the long run. The outer dumps will slowly become completely oxidised, and these substances will be carried into the groundwater as well as surface water bodies by precipitation. Groundwater outflows from acid post-mining lakes (5) partly are loaded with iron. In Lusatia the numerous moorlands are a very significant source of

iron (6) because large quantities of iron sulphide minerals have formed as they developed. As the ground water rises the oxidised iron compounds are washed out.

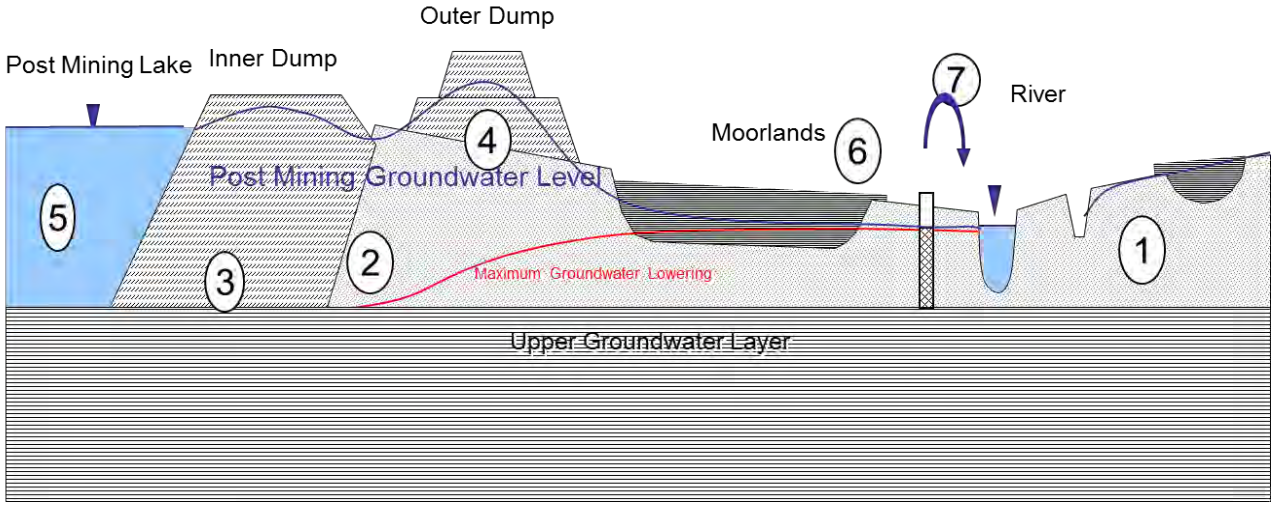

Figure 3 Sources of iron contamination in watercourses in Lusatian district (IWB 2013)

The following article deals with problems on aerated aquifers (2), inner dumps (3), and outer dumps (4).

IRON LOADS AND HOT SPOT AREAS

Initially an elevated concentration of iron was identified from 2003 onwards in a River Spree tributary, called "Kleine Spree" that is fed with ground water inflow. In the "Kleine Spree" river the concentration of iron rose continuously till 2010 up to approximately 10 mg/L while mean low water level in summer time. After a period of heavy precipitation in 2010 and 2011, high concentrations of iron could be seen and measured along some 20 kilometres of the River Spree.

This iron originates from the Pleistocene aquifer in the depression cone of the former Lohsa and Burghammer lignite opencast mines (Fig.4). The ground water level in the Pleistocene aquifer had been lowered by as much as 50 metres, and as a result the sediments had been aerated for many decades. There are no aquitards in the upper level of the aquifer. The clastic Pleistocene sediments show between 0.01 % and, at most, 0.05 % of pyrite by mass, while they do not contain any carbonate minerals whatsoever.

The pyrite weathered significantly because of the good permeability of the coarse, dewatered aquifer. Because of this, groundwater locally contains up to 400 mg/L of iron and 1,400 mg/L of sulphate. Groundwater that is so severely contaminated had previously only been encountered in well-aerated lignite opencast mine dumps. Following the raising of the ground water level, this groundwater now flows into watercourses (Fig. 4).

The historic level of iron in Lusatian water courses is approximately 1 mg/L. The iron comprises of differing proportions of dissolved iron(II), iron(II, III) humic acids and iron(III) hydroxide in suspension. The light adsorption is so strong that even relatively low concentrations of iron(III) hydroxide result in high degrees of turbidity. Above concentrations of about 2 mg/L, the iron(III)

hydroxide can be seen colouring bodies of water and water courses ochre and making them turbid (Fig. 2).

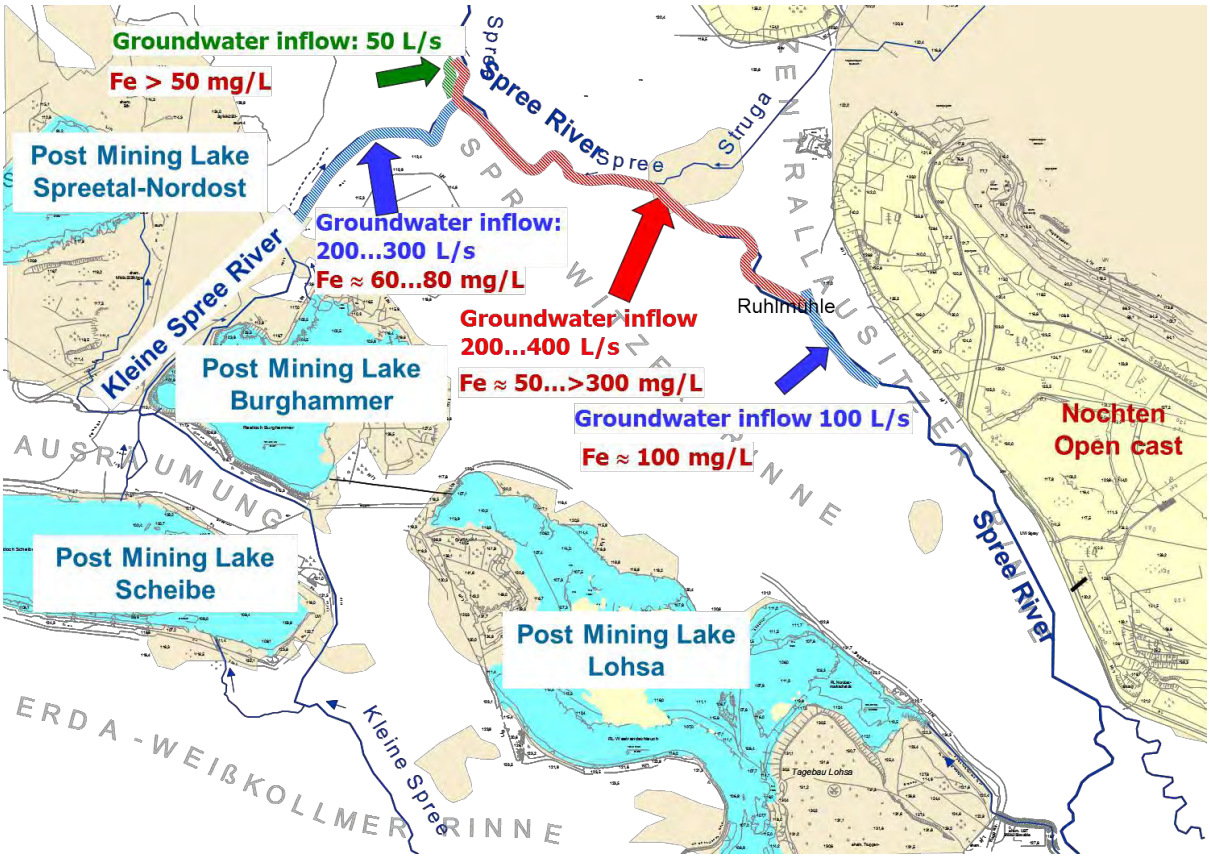

Figure 4 Iron loaded groundwater inflow into the River Spree and the River Kleine Spree

Because of the high quantity of groundwater inflow (1,0 m³/s) along the River "Kleine Spree", the concentration of iron has risen up to 20 and 30 mg/L. The iron is transferred from the groundwater as iron(II). The oxidation of iron(II) in the watercourses is dependant on temperature and pH value. The hydrolysis of iron(III) lowers the pH value so that conditions for iron oxidation in the watercourses deteriorate further. As a result, particularly in winter time when through flows are higher, the dissolved iron(II) is transported over considerable distances. At present iron(II) at a pH value ranging from 5 to 6 is being found in the River Kleine Spree because of the pH-limited oxidation.

Currently between 4 and 8 mg/L of total iron are measured in the River Spree (14 m³/s). The majority of the iron occurs as iron(III) hydroxide. During the winter months as much as 50% of the iron is found as dissolved iron(II).

The iron oxide sludge is deposited along the banks and stagnant water zones of the affected watercourses. It is re-suspended during high water periods and carried further by the flow. Consequently the total concentration of iron in the River Spree can reach 10 to 20 mg/L. Iron can currently be identified along Spree River as far as the Spremberg reservoir (fig. 5). This reservoir contains more than 20 million cubic metres. At average flow rates into the River Spree the retention period varies from 2 to 4 weeks. At present the Spremberg reservoir is providing reliable protection to downstream stretches of the River Spree. This includes the Spreewald biosphere reserve and tourism destination.

Figure 5 Iron load carried into the Spremberg reservoir (photo Rauhut)

Currently investigations are being carried out to determine whether the Spremberg Reservoir will retain its protective capacity. The reservoir had been erected for water management purposes, as increasing the flows during low water episodes and for flood control while high water. The high iron load of the River Spree is harmful to its ecology. European and German water legislation do not permit the deterioration of a body of water or of a water course. It requires to localise the sources of contamination precisely so that targeted preventive measures can be planned and implemented.

MONITORING

The localisation and quantification of inflow presents a challenge to hydrogeological monitoring. The diffuse iron-loaded inflows can be measured directly at very few sites. Depending on the local and hydrological conditions there are various methods that are suitable for measuring diffuse material discharges:

- hydrochemical groundwater exploration
- flow monitorings in the entire watercourses on particular days

Hydro chemical groundwater surveys in the immediate neighbourhood of the river allow the inflow area to be delimited. This requires a close-meshed network of groundwater wells. The Pleistocene aquifer is geohydraulically and hydro chemically very heterogeneous. In the entire River Kleine Spree, monitoring of flows and water quality on particular days are promising. When a section of the watercourse is closely covered with flow monitoring and sampling points, the volume and material inflows can be spatially defined with a high level of resolution. Errors had been minimised by multiple repetitions of targeted monitoring. To determine the loads of dissolved substances the monitoring was made on a particular day at low outflow rates and under stable hydraulic and geohydraulically conditions. To determine the hydraulic conditions, the water levels in the watercourses and the groundwater level near the river are measured with load cells and

continuously logged. With knowledge of the process dynamics along the river, the results of monitoring can be interpreted reliably. The sensitivity of the monitoring can be assessed using associated geohydraulic modelling.

A diffuse ground water inflow of between 200 and 300 L/s was identified along a stretch of the river "Kleine Spree" approximately 4 kilometres long (fig. 4). The emerging groundwater had a mean iron concentration of between 70 and 80 mg/L. An iron concentration ranging from 3 to 450 mg/L was measured at about 20 monitoring points in the groundwater surrounding the river "Kleine Spree". The median for iron concentration in the groundwater is between 50 and 60 mg/L.

In the Spree with comparatively high flow rates, the water quality has been successfully monitored at short intervals. The hydro chemical results have been associated with flow rates at continuously monitored wells. This allows a reliable determination of iron loads over a longer monitoring period. Drawing up an overall balance involves a number of specific problems. At low rates of flow, there is a relatively high proportion of diffuse inflows from ground water. Some of the iron remains in the riverbed as iron sludge. That iron is not registered by discrete monitoring. Usually the sedimented iron sludge is remobilised during a high water event. On the other hand, during such event the diffuse inflow of groundwater is pushed back. Consequently during high waters, in spite of the short flow times, mainly iron(III) hydroxide and hardly any dissolved iron(II) are found. In the Spremberg Reservoir three monitoring campaigns were set up: upstream of the auxiliary dam, downstream of it, and downstream of the main dam (Fig. 6).

As the flows at these positions are known, it was possible to assess the transformation and the retention of iron in the reservoir (5 to 20 million m^3). Using the results from the monitoring point above the Spremberg Rervoir the seasonal and hydrological influences on iron transport can be identified

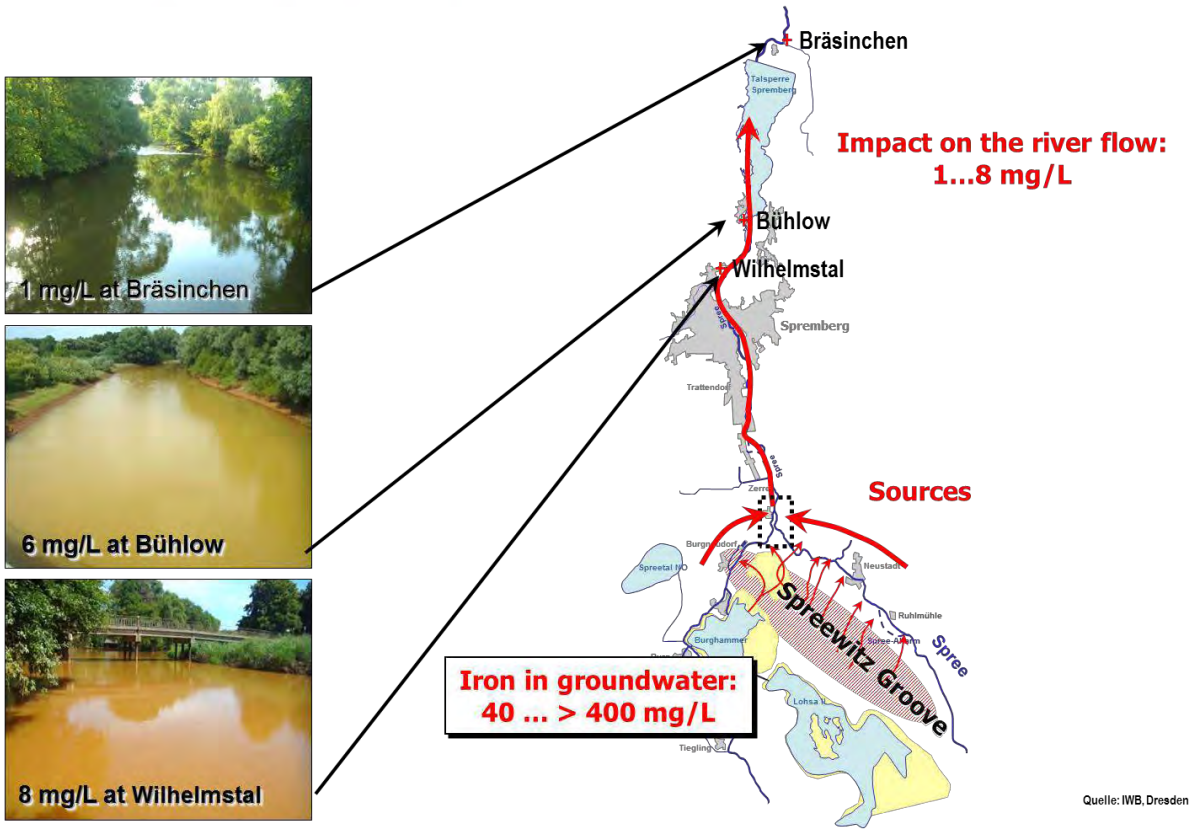

Figure 6 Iron sources and impact along the river Spree

In the "Kleine Spree" river, the volumetric flows of the diffuse groundwater inflow into the River Spree cannot be measured directly. Taking the regional water balance into account, and applying the values of a geohydraulic groundwater and runoff model, the volume of flow is estimated to be between 300 and 700 L/s (Fig. 4). The concentration of iron can be captured here at a few selected locations where groundwater monitoring wells have been installed.

A few local surface tributaries to the River Spree can be reliably measured. An oxbow parallel to the River Spree drains groundwater over a stretch of about one kilometer. The groundwater inflow into the oxbow is most stable during low and medium water periods. At an inflow between 100 and 130 L/s; here the iron concentration is about 150 mg/L. Another 600-metre long ditch for lowering local groundwater draws off about 20 L/s of groundwater containing over 350 mg/L of iron.

Planning preventive measures it is important to know the diffuse groundwater peak inflows into watercourses. This issue has both a hydraulic and a hydrochemical aspect. The maximal groundwater inflow into watercourses is expected when the groundwater rise will be completed in some years. Groundwater hydrographs show that the increase in groundwater levels has progressed far, but is not yet complete in all parts of the area under investigation.

In most places where groundwater is monitored the iron concentration has been stable for a long time. In some monitoring wells near the river the concentration of iron increases as the groundwater level rises. Reverse trends of a diminishing concentration of iron have not yet been observed. Consequently it can be assumed that the iron load in watercourses will continue to increase for some years.

At present, about 600 to 1,200 L/s of iron-loaded groundwater flows into the river "Kleine Spree". Only about 150 L/s of which stems from newly-formed aquifers in the catchment area. The remainder is produced by permeation losses from the Lohsa and Burghammer post-mining lakes. The volume of iron-loaded groundwater in the Spreewitz groove is estimated to be between 600 and 800 million m^3. The balance also shows that flows of iron-loaded groundwater into the watercourses must be expected to continue at least for the next 15 to 40 years.

REMEDIATION APPROACHES

To reduce the iron loading in the River Spree different approaches are followed:

- water treatment in or near the river
- water retention, drainage, and treatment

A water treatment plant and a natural wetland area in or near the river are being examined as potential solutions. Such treatment plant on the River Spree would have to be dimensioned for a volume flow of 12 m^3/s at initial inflow values of between 4 and 8 mg/L of iron. An appropriately dimensioned technical plant of this size and for these inputs would be very expensive to build and operate. A natural retention wetland on the other hand would require an area of between 30 and 60 hectares for treatment by sedimentation. Such areas at the end are not available in the intensively used landscape of the River Spree.

Nevertheless the technical effort is considerable. The technology includes four stages: extraction, raising the ground water, transfer it to a treatment plant, cleaning the iron-loaded groundwater, and finally treating the iron sludge.

Cleaning the iron-loaded groundwater is ideally carried out in a water treatment facility using alkaline and polymer flocculants. As an alternative to a treatment plant, the iron-rich groundwater can be pumped (no. 6) into the deep, anoxic area of a nearby post-mining lake. Because the surrounding post-mining lakes are acidified and therefore require long-term chemical treatment anyway, the sludge treatment can be dealt with in the process.

A remediation of the entire Pleistocene aquifer contaminated with iron is out of question because of its enormous costs. Quite apart from the fact, there is no state-of-the-art groundwater treatment technology for dealing with the iron load mentioned. It is acknowledged that there are possibilities for developing subsurface water treatment using heterotrophic sulphate reduction (no. 1). The significantly greater expense characteristic of this process is partly made up for by the absence of drainage, water treatment, and iron sludge treatment. Large-scale field trials in this context are being undertaken at present.

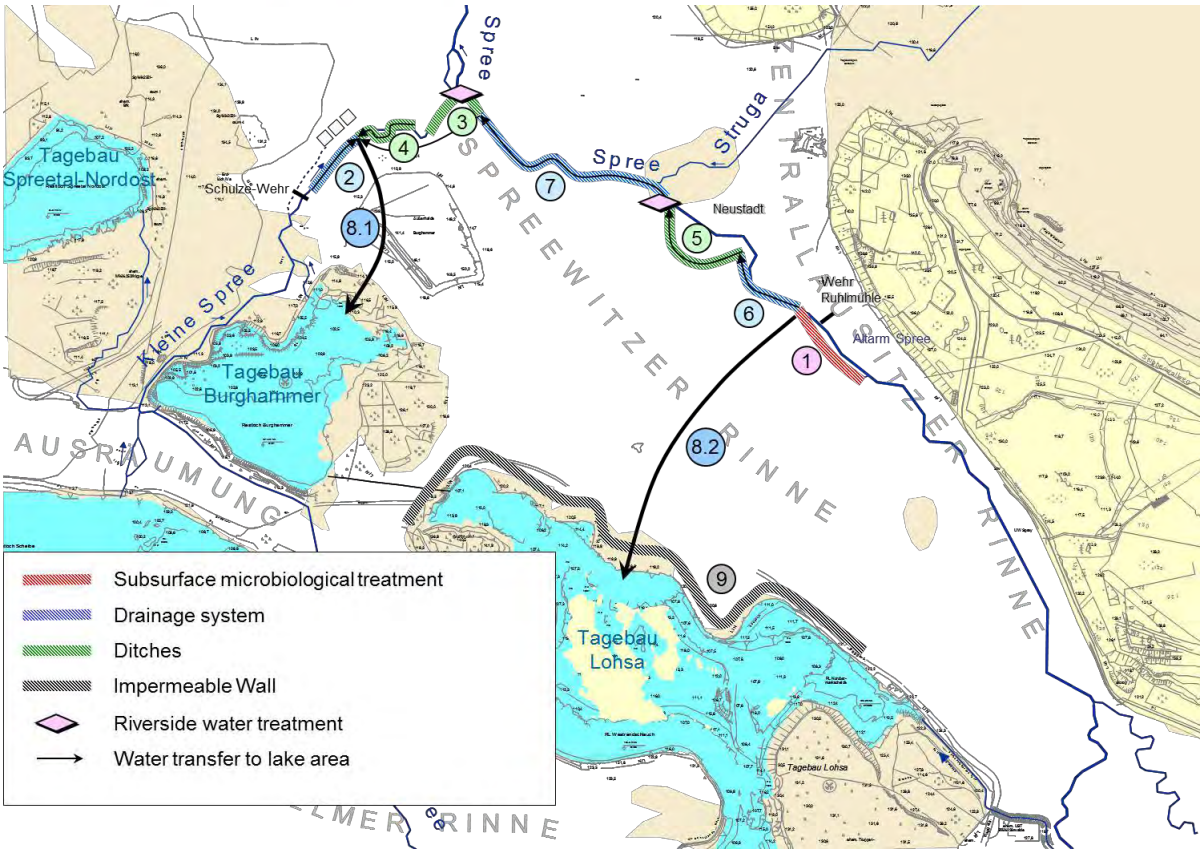

Figure 7 Measures to reduce iron discharge into the River Spree

As an hydraulic alternative the installation of a barrier wall on the northern border of the Lohsa post-mining lake (no. 9) is being examined. The intention would be to achieve a substantial reduction of the groundwater outflow, and thus of the iron loads being carried to the River Spree. A barrier solution could reduce measures near the river in the medium term.

SUMMARY

The Tertiary and Pleistocene strata in the Lusatian soil contain Pyrite which oxidised following the groundwater lowering in previous decades. This has resulted in the formation of groundwater that contains up to 400 mg/L of iron in places. This groundwater is now diffusely flowing into the watercourses of Spree river. A specific exploration scheme has been implemented to determine the loads along the river flow. Hydrochemical surveying of the groundwater at numerous monitoring well near to the river permits local differences in load levels to be determined. Varying loads were identified by repeating monitorings in summer and winter on specific days.

Depending on the varying loads along the course of the river flow a barrier concept had been developed to reduce the diffuse inflow. A substantial reduction of these discharges can be achieved economically over the medium term.

REFERENCES

(IWB 2010a) Uhlmann, W.; S. Theiss; W. Nestler, and Chr. Franke: Untersuchungen der hydrochemischen und ökologischen Auswirkungen der Exfiltration von eisenhaltigem, saurem Grundwasser in die Kleine Spree und in die Spree, Teil 1 Erkundung, Teil 2 Maßnahmen Institut für Wasser und Boden Dr. Uhlmann, Dresden, published in 2010: www.lmbv.de

(IWB 2010b) Uhlmann, W.; D. Seiler; K. Zimmermann; S. Theiss, Chr. Engelmann, und P. Lommatzsch: Studie zu den Auswirkungen des Grundwasseranstiegs auf die Beschaffenheit der Oberflächengewässer in den Sanierungsgebieten Seese/ Schlabendorf und Greifenhain/Gräbendorf, Institut für Wasser und Boden Dr. Uhlmann, Dresden,

(IWB 2012) Uhlmann, W.; S. Theiss; W. Nestler; K. Zimmermann, and Th. Claus: Weiterführende Untersuchungen zu den hydrochemischen und ökologischen Auswirkungen der Exfiltration von eisenhaltigem, saurem Grundwasser in die Kleine Spree und in die Spree, Präzisierung der Ursachen und Quellstärken für die hohe Eisenbelastung des Grundwassers, Institut für Wasser und Boden Dr. Uhlmann, Dresden, published in 2012: www.lmbv.de

(IWB 2013) Uhlmann, W.; S. Theiss; W. Nestler, and Th. Claus: Studie zu den Auswirkungen des Grundwasserwiederanstiegs auf die Beschaffenheit der Oberflächengewässer in den Sanierungsgebieten Seese/ Schlabendorf und Greifenhain/Gräbendorf, Vertiefung der Untersuchungen zur Präzisierung der Modellgrundlagen und der Bemessungsansätze für Wasserbehandlungsanlagen, Institut für Wasser und Boden Dr. Uhlmann, Dresden, published in 2013: www.lmbv.de

Evidences of Effective Treatment of Alkaline Mine Drainage with $BaCO_3$

Alba Gomez-Arias[1], Julio Castillo[1], Megan Welman-Purchase[2], Jan Posthumus[1] and Esta van Heerden[1]

1. *Department of Microbial, Biochemical and Food Biotechnology, University of the Free State, South Africa*
2. *Department of Geology, University of the Free State, South Africa*

ABSTRACT

An experimental lab scale reactor that treats alkaline mine drainage has been developed based on hydrogeochemical characteristics of most of the South African coal mines leachates, which generally have high concentrations of sulfates, TDS (total dissolve solid), salinity and heavy metals (mainly Fe^{3+} and Al^{3+}).

The experiment development was based on the DAS system (disperse alkaline substrate). In this case, barium carbonate ($BaCO_3$) was used as alkaline reactive, fixed to a non-toxic inert matrix (wood chips). The experiment was carried out with 3 different proportions of wood:$BaCO_3$ (w/w); 1:2, 1:3 and 1:4 with a residence time of 24 hours. SO_4^{2-} and Ca^{2+} contained in AMD precipitate as $BaSO_4$ and $CaCO_3$, respectively, according to (1) thermodynamic modelling by PHREEQC, (2) geochemical and (3) mineralogical characterization. The pH increased up to 9-10, which allowed the removal of divalent metals. Reactors were maintained for 6 months and the results that were acquired from all of them demonstrated their reactivity, without saturation or clogging in any of the columns, towards the total removal of nitrates (100%), 93% of sulfates, 50% hardness (Ca^{2+}, Mg^{2+} and Na^{2+}), as well as 68-93% of metal removal (Fe^{3+}, Al^{3+}, Cu^{2+}, Zn^{2+} and Mn^{2+}, in moderate concentrations). Therefore, parameters such as salinity, TDS and conductivity decreased throughout the experiment. Water volume treated was approx. 764 L during 26 weeks in the lab scale reactors and the physicochemical parameters of the water after treatment are within the allowable limits for drinking water, according to SANS 241 class 1 for Drinking Water (South African national standard, 2006; 2011).

INTRODUCTION

Coal mine drainage

South Africa has 95% of Africa's known coal reserves and the 9th biggest recoverable coal reserves (61 000 Mt) in the world where 27 400 Mt were proven coal reserves in 2012 (Energy Information Administration, 2014).

These coal deposits have about 4% of pyrite (Snyman & Botha, 1993; van Dyk, 2006) which is the cause for the coal mine drainage to contain sulphur. However the typical acidity produced by the oxidation of pyrite (equations 1 and 2) and by the subsequent oxidation and precipitation of Fe (equation 3 to 5) is neutralized by the CO_3^{-2} released from the calcite ($CaCO_3$) and dolomite ($CaMg(CO_3)_2$) that is contained in South African's coal; about 6.7% and 10.1% respectively (van Dyk, 2006). Therefore, coal mines in South Africa can generate acid, neutral or alkaline mine drainage (AMD) (Kirby, Dennis & Kahler, 2009). When pyrite and other sulfide minerals associated with coal deposits are exposed to water and oxygen, several chemical and biochemical reactions take place. These reactions can be seen in the Singer & Stumm (1970).

Oxidation of pyrite can be produced by oxygen (eq. 1) or ferric iron (eq. 2) in the presence of water. Further oxidation of Fe^{2+} to Fe^{3+} occurs when sufficient oxygen is dissolved in the water or when water is exposed to atmospheric oxygen (eq. 3). This reaction is also accelerated by the presence of oxidizing bacteria such as *Acidithiobacillus ferrooxidans*. Ferric iron can either precipitate as $Fe(OH)_3$, (eq. 4) or it can react directly with pyrite to produce more ferrous iron and acidity as shown by eq. 5. The presence of alkaline compounds such as calcite and dolomite decreases the acidity of the AMD by consuming protons (H^+) and releasing bicarbonate anion (HCO_3^-) as shows the eq. 6 and 7 (Pokrovsky, Golubev & Schott, 2005).

$$FeS_2 + 3.5\ O_2 + H_2O \rightarrow Fe^{2+} + 2SO_4^{2-} + 2H^+ \quad (1)$$

$$FeS_2 + 14Fe^{3+} + 8H_2O \rightarrow 15Fe^{2+} + 2SO_4^{2-} + 16H^+ \quad (2)$$

$$Fe^{2+} + 0.25\ O_2 + H^+ \xrightarrow{Acidithiobacillus\ ferrooxidans} Fe^{3+} + 0.5H_2O \quad (3)$$

$$Fe^{3+} + 3H_2O \leftrightarrow Fe(OH)_{3(S)} + 3H^+ \quad (4)$$

$$14Fe^{3+} + FeS_2 + 8H_2O \rightarrow 2SO_4^{2-} + 15Fe^{2+} + 16H^+ \quad (5)$$

$$CaCO_3 + H^+ \rightarrow Ca + HCO_3^- \quad (6)$$

$$CaMg(CO_3)_2 + 2H^+ \rightarrow Ca + Mg + 2(HCO_3^-) \quad (7)$$

Therefore the alkalinity of the coal mine drainage depends, among others, on the ratio between acidic and alkaline minerals of each specific coal deposit and surroundings.

Case study

The case study was done on the alkaline drainage generated by a coal mine situated at (25°42'23.2"S, 29°59'32.7"E), that is mining the coal from the north eastern coalfield of the Karoo basin, located in Mpumalanga province. The AMD generated is collected in the evaporation dam located SW within the facility area (25°42'20.4"S 29°59'28.4"E). This AMD has a pH of 7.45 and, in contrast, the electrical conductivity (EC), salinity (Sal) and total dissolved solids (TDS) are fairly high (2090 µS/cm, 980 mg/L and 100mg/L, respectively). The AMD has high concentrations of sulfates and nitrates (1 253 mg/L and 3 032 mg/L respectively) as well as dissolved Ca and Mg (262.41 mg/L and 132.60 mg/L respectively).

State of the art AMD treatments

Many passive and semi-passive treatments have been developed over the past three decades to remediate AMD, such as aerobic and anaerobic wetlands, Anoxic Limestone Drains (ALD), limestone sands, beds, ponds and open channels, diversion wells, reducing and alkalinity producing systems (RAPS), ReRAPS, water-powered devices, windmills, sodium carbonate briquettes, sodium hydroxide, hydrated lime and quick lime (e.g. Watzlaf et al., 2004). Recently, a new system has been developed with the aim to solve the clogging problem caused by the Al^{3+} and Fe^{3+} precipitation that has been documented in many of these systems (Robbins et al., 1996; Cravotta and Trahan, 1999; Watzlaf et al., 2000; 2002; Rees et al., 2001; Ziemkiewicz et al., 2003; Rose et al., 2004). This new system called Dispersed Alkaline Substrate (DAS) consists of an inert matrix of wood chips, which provide high permeability and reduce clogging problems, mixed with a fine-grained alkaline material such as limestone sand (Rotting et al., 2008).

The reactor system that the authors have developed on a laboratory scale is based on a modified DAS system. The modification includes the substitution of limestone ($CaCO_3$) with barium carbonate ($BaCO_3$) powder. This system, called B-DAS, has been designed with the aim to improve the removal of sulfates by precipitating it as $BaSO_4$ as well as improving the salinity (see reactions below). The aim is extended to find a system that is able to remediate not only acid mine drainage but neutral and alkaline mine drainages as well. $BaCO_3$ easily dissolves at a pH above 4 which makes it ideal to treat these drainages. The AMD used in this study has a pH of 7.45 which undergoes the dissolution process as follow; $BaCO_3$ is dissolved (eq. 8). Dissolved sulfates can precipitate as barium sulfates (eq. 9). The pH is increased to 10 by consuming protons and releasing hydroxide anion (eq. 8) and bicarbonate anion (eq. 10). The high pH and the presence of bicarbonate anions promote metal precipitation as carbonates (e.g. Ca and Mg):

$$BaCO_3 + H_2O \rightarrow Ba + HCO_3^- + OH^- \quad (8)$$

$$BaCO_3 + H_2SO_4 \rightarrow BaSO_4 + H_2CO_3^- \quad (9)$$

$$BaCO_3 + H^+ \rightarrow Ba + HCO_3^- \quad (10)$$

$$Me + HCO_3^- \rightarrow MeCO_3 + H^+ \quad (11)$$

METHODOLOGY

Column experiment

Three down-flow columns were constructed from PVC pipes (10 cm inner diameter, height 50 cm) and equipped with four additional lateral sampling ports. Each port had a small perforated pipe in the column matrix to promote homogeneous samplings and allow homogeneous flow within the columns by increasing the area of sampling while, avoiding, as far as possible, preferential flow.

Each column contained a layer of quartz gravel (particle size about 5-8 mm) at the bottom (2.5 cm). This layer was covered with a 40 cm reactive material layer, which consisted of $BaCO_3$ and wood shaving mixture. Each column had different ratios of wood: $BaCO_3$ (w/w); these were columns (A) 1:2 (260g:520g) , (B) 1:3 (240g:720g) and (C) 1:4 (220g:960g).

During the six months of the experiment the down-flow reactors, with supernatant open to the atmosphere, were fed with the AMD, as input water from the top using a peristaltic pump and flowed down gravitationally. The outflow was collected in a container that also functioned as an aeration and sedimentation tank. The flow rate was 1.09 mL / min with a residence time of 24 hours for each B-DAS columns. The porosity of the systems was 70% (volumetrically calculated).

Sampling

During the first week of the columns running, samples were taken daily from the outlet of each column (A, B and C) and after that sampling was done weekly for the next six. Another set of samples were taken monthly from the four sampling ports of each column, to evaluate the spatial evolution of each column during the experiment.

Finally, the columns were drained and column C was cut with an angle grinder to have access to the precipitates formed on the wood shavings (see left of figure 4). Three samples of precipitates were collected at the top, middle and bottom of the column for further analysis .

Analytical techniques

Water analysis

Source water was collected from the evaporation dam in 25L carboys, transported to the laboratory and stored at 4°C. pH, EC, Sal, TDS, redox potential (ORP) and temperature (T) was measured on site. These physicochemical parameters were also analysed from the columns weekly and monthly. The measures were done with the ExStix®II multi-probe and ExStix®II ORP probe. ORP measures were corrected to the Eh standard hydrogen electrode (SHE). Samples were analysed by ICP at the Institute for Groundwater Studies at UFS, filtered and acidified to pH < 2 with HNO_3 2% (v/v), to compare influent and effluent chemistry of the columns. Sulfate (SO_4^{2-}), Fe^{2+} and Fe^{Total} concentrations were analysed by a HACH spectrophotometer (model DR/900 colorimeter) according to the colorimetric methods described in the HACH Procedures Manual (Method Sulfate 608, Method Ferrous iron 255 and FerroVer 265, respectively).

Geochemical modeling

The precipitation of newly formed solid phases by the $BaCO_3$ was confirmed by using a thermodynamic model (PHREEQC) as well as by characterizing the final solid products. These saturated mineral phases in the system were estimated, assuming that the initial solution in contact with an alkaline material (in our case $BaCO_3$) reaches equilibrium with that material. The PHREEQC-2 geochemical speciation model (Parkhurst & Appelo, 2005) in conjunction with the MINTEQ thermodynamic database (Allison et al., 1991) was used to determine the aqueous speciation of solutions and saturation indices (SI) of solid phases that could control the concentration of dissolved species in the simulation SI=log(IAP/KS) where IAP is the ion activity product and KS is the solubility constant. Zero, negative or positive SI values indicate that the solutions are saturated, undersaturated and supersaturated respectively, with regards to a solid phase.

Mineralogical characterization

The Panalytical Empyrean x-ray diffractometer (XRD) was used under the following conditions: slit fixed at 10mm, Cu / Kα monochromatic radiation, 40mA and 45 kV. Samples were run at a speed of 2°θ /min (5-70°) to analyse the precipitates formed. Interpretation of data was done by the Highscore program. Samples were milled previously to a particle size less than 10 micron. Due to the small quantity of sample, a zero-background wafer sample holder was used.

The scanning electron microscope Jeol GSM 6610 equipped with energy dispersive system (SEM-EDS) was used for the analysis, along with Astimex 53 Minerals Mount MINM25-53 standards. The accelerating voltage of the beam during analysis was 20.0 kV with a spot size of 50 and working distance of 10 mm. Sample preparation for this method involves a strip of double-sided carbon tape attached to a glass section. The samples were coated with a thin layer of carbon (± 15-100nm) to prevent charging.

RESULTS AND DISCUSSION

Water analysis

Temporal evolution

Figure 1 indicates that the data of the three columns are similar; the pH increased from 7.5 to 9.8 and the rest of the parameters (TDS, Sal, Cond, Eh, sulfates and iron) decreased from the first sampling performed after 24 hours. Fe^{2+} and Fe^{Total} concentrations were always below detection limit (BDL). The sulfate concentration decreased from 1400 mg/L to BDL after one week. However Sal, TDS and Cond reached the lowest values after four months (from 980 mg/L, 1000 mg/L and 2090 µS/cm to 283 mg/L, 209 mg/L and 576 µS/cm, respectively). The Eh decreased from 296 to 150 mV within the first 24 hours and continued to decrease for two month to -21 mV, thereafter stabilized at about -35 ± 15 mV.

The ICP analysis (Table 1) shows that the concentration of the Ba in the water increased in the first sampling, this is probably because the $BaCO_3$ powder that is not attached to the wood shavings is released into the water, however the Ba concentration decreased and stabilized around 0.7 mg/L thereafter. Most of the compounds started to decrease within 24 hours such as Ca, Mg, Cl, NO_3, SO_4

and Zn; from 262.4, 132.6, 9.2, 3032, 1253, 0.007 mg/L to 36.8, 97.8, 4.1, 1766, 147 and 0.003 mg/L, respectively (calculated as the average of the three columns). The rest of the compounds, such as Na, K, Al, Fe and Mn clearly started to be removed from the second sampling (5th week) from 4.9, 5.9, 0.044, 0.057 and 0.03 mg/L to 3.1, 5.3, 0.03, 0.008 and 0.002 mg/L, respectively (calculated as the average of the three columns). At the end of the experiment all the compounds were within the limits allowable for drinking water according to SANS 241 (South African national standard 2006; 2011), except for the Mg that exceed the limit by 15mg/L. The final removal of each compound is shown in Table 2. The similar evolution of the three columns, allowed for the spatial evolution analysis to be performed in column B and the geochemical characterization of the precipitates in column C.

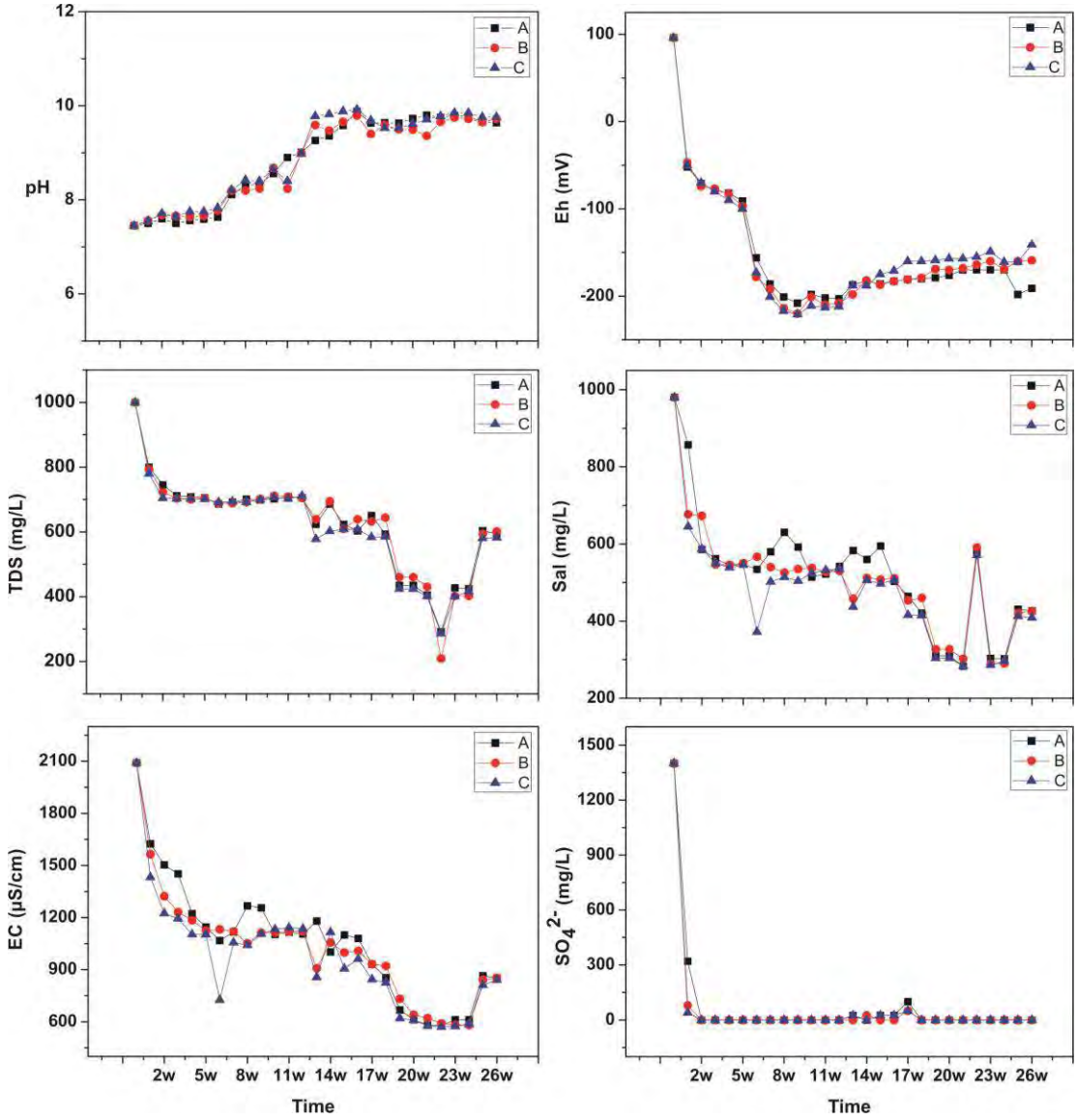

Figure 1 physicochemical parameters (pH, sulfates, Sal, TDS, Cond and Eh) of the water samples collected from the outlet of the three columns (A, B and C) over time

Table 1 ICP water analysis of the main chemical compounds at the inlet and outlet of the columns A, B and C (As, Cu, Cd, Ni, Pb and Cr were always below detection limit (BDL))

	NO_3	Ca	SO_4	Mn	Na	Fe	Al	Zn	Mg	K	Cl	Ba
INLET	**3032**	**262.4**	**1253**	**0.03**	**4.9**	**0.057**	**0.044**	**0.007**	**132.6**	**5.9**	**9.2**	**0.11**
Day 1												
Sept A	1784	45.6	233.3	0.065	6.9	0.071	0.044	0.004	89.7	23.6	4.3	92.79
Sept B	1843	27.1	133.5	0.034	5.2	0.009	0.027	0.003	112.9	32.7	4.1	76.37
Sept C	1670	37.8	74.4	0.042	7.2	0.027	0.041	0.003	90.9	12.8	4	77.07
Month 2												
Oct A	1685	11.2	240	0.002	2.9	0.008	0.029	0.006	132.3	4.6	5.9	0.95
Oct B	1701	9.7	218.2	0.002	3.2	0.011	0.029	0.004	137.8	5.2	5.6	1.36
Oct C	1715	10.6	253.1	0.003	3.1	0.004	0.031	0.004	133.2	6.1	5.4	1.45
Month 4												
Dec A	2.8	5.3	116	0.002	1.4	0.024	0.006	0.002	118.2	6.7	9.6	0.67
Dec B	1	5.3	71.9	0.001	1.8	BDL	0.002	0.004	141.8	3.7	6.3	0.80
Dec C	1.1	4.8	68.6	0.001	1.2	BDL	0.005	0.003	118	4	6.4	0.73
Month 6												
Feb A	0.3	4.7	78.8	0.002	BDL	0.006	0.008	0.002	111.1	4.8	6.6	0.75
Feb B	0.3	5	88.6	0.001	1.2	0.006	0.007	0.003	120	4.9	7.5	0.73
Feb C	0.3	5	96.6	0.003	BDL	0.055	0.009	0.003	113.2	11.8	14.8	0.74

Table 2 percentage removal of the main compounds in the three columns at the end of the experiment

Removal %	NO_3	Ca	SO_4	Mn	Na	Fe	Al	Zn	Mg
Column A	99.99	98.2	93.7	94.2	100.0	89.3	82.0	73.1	16.2
Column B	99.99	98.1	92.9	95.6	74.3	89.4	84.6	65.9	9.5
Column C	99.99	98.1	92.3	89.0	100.0	92.2	78.8	65.8	14.6
AVERAGE	99.99	98.1	93.0	92.9	91.4	90.3	81.8	68.3	13.4

Spatial evolution

Two sets of samples from the four sampling ports, named from top to bottom: one, two, three and four, were collected from column B and analysed. The residence time of the AMD in the column was 24 h, therefore the contact time with the reactive material of the samples from each port was approximately 6, 12, 18 and 24 h, respectively. The results (Figure 2) show that the removal of every compound analysed occurred mainly at port one. The composition of the water at port two, three and four had no significant differences. Therefore, the fast dissolution of the $BaCO_3$ in contact with the AMD is displayed. This is also demonstrated by the analysis of precipitates.

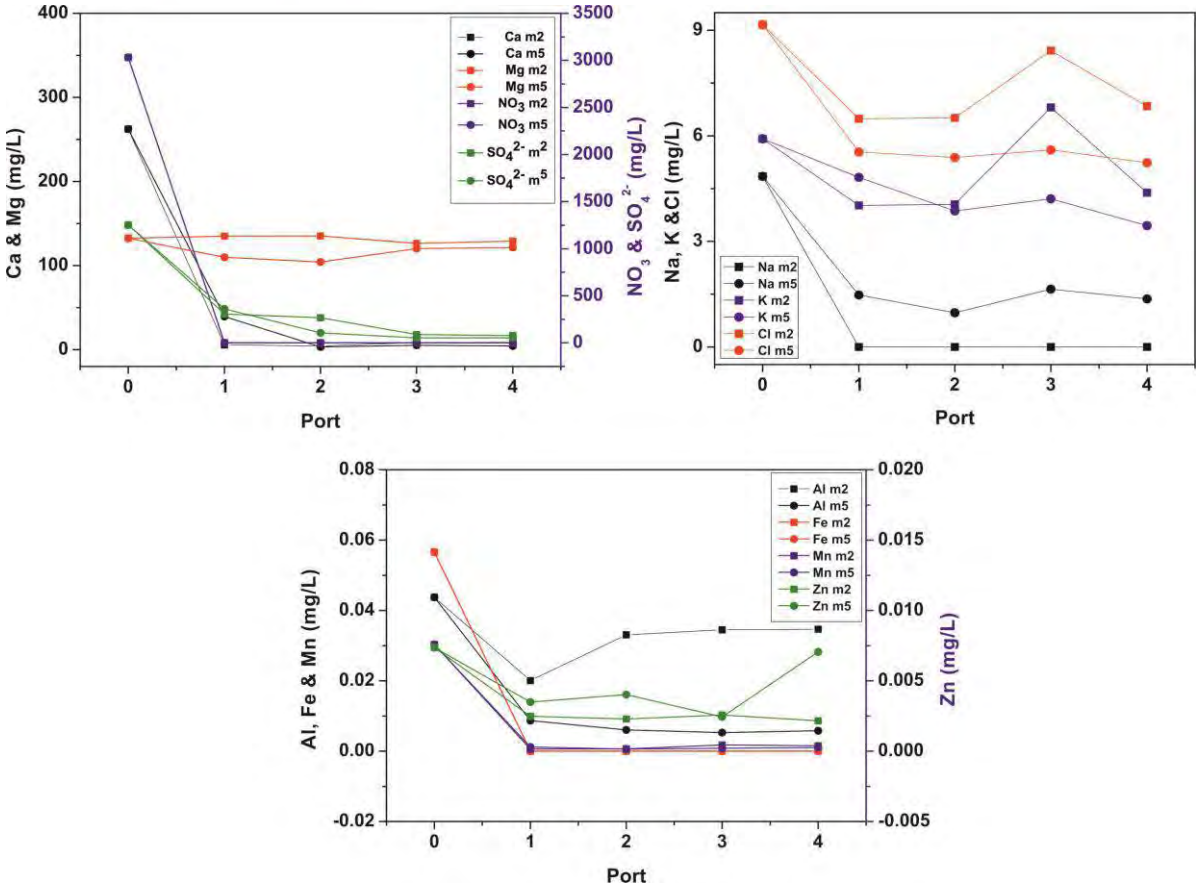

Figure 2 Spatial evolution of the main chemical compounds of the water throughout column C, from top (inlet) to bottom (port 4)

Geochemical modelling

The simulation was based on the physicochemical characteristics of the AMD used as the solution in this experiment. Witherite was assumed as equilibrium phase 0, since total dissolution was expected. The predicted precipitates were barite ($BaSO_4$; SI~3.49), calcite ($CaCO_3$; SI~1.25), dolomite ($CaMg(CO_3)_2$; SI~2.50), $Fe(OH)_{3(a)}$ (SI~1.75), hausmannite (Mn_3O_4: SI~15.34) and pyrolusite (MnO_2; SI~9.85). However, due the low concentration of Fe and Mn, those precipitates could be masked in the XRD analysis.

Mineralogical characterization

According to the SEM-EDS analysis of the bottom sample, the composition of most of the crystals were mainly Ba (79 - 95%), O (4 - 21%) and some of them also had trace amounts of sulfur (0.5 - 4%) in the form of clear needles smaller than 5µm. The XRD analyses determined that those crystals were 95.1% witherite ($BaCO_3$) and 4.9% barite ($BaSO_4$) (red diffractogram in Figure 4). In the middle

sample the concentration of witherite was lower (24.4%); the precipitation of barite increased (56.4%); the precipitation of Ca detected in SEM analysis (Figure 3c & d) was confirmed by the XRD analysis where calcite and aragonite where detected (6.4 and 12.8% respectively). However, the precipitation of Mg and K detected by SEM were masked in the XRD analysis, mainly due to the high concentration of barite (green diffractogram in Figure 4). In the top sample the concentration of witherite (Figure 3b) and barite were slightly lower (23.4 and 46.7%, respectively), but calcite and aragonite concentrations were higher (7.6 and 22.3%, respectively) (Figure 3a). In this section of the column precipitates with Al, Fe, Mg, Na, Si, Cl and K were also found (Figure 3b).

According to the analyses, the AMD dissolves the $BaCO_3$ in the top of the column and releases Ba^{2+} and HCO_3^-, both precipitate mainly as $BaSO_4$ and $CaCO_3$. Thereafter, the AMD was already remediated and did not continue to react with the $BaCO_3$ in the column. This is confirmed by the neoformed minerals found at the top and the middle, whereas the bottom sample still had reactive $BaCO_3$ and no neoformed mineral phase was found. Furthermore, in the picture of Figure 4 it can be observed that the bottom of the column is still white due the $BaCO_3$ that remained on it.

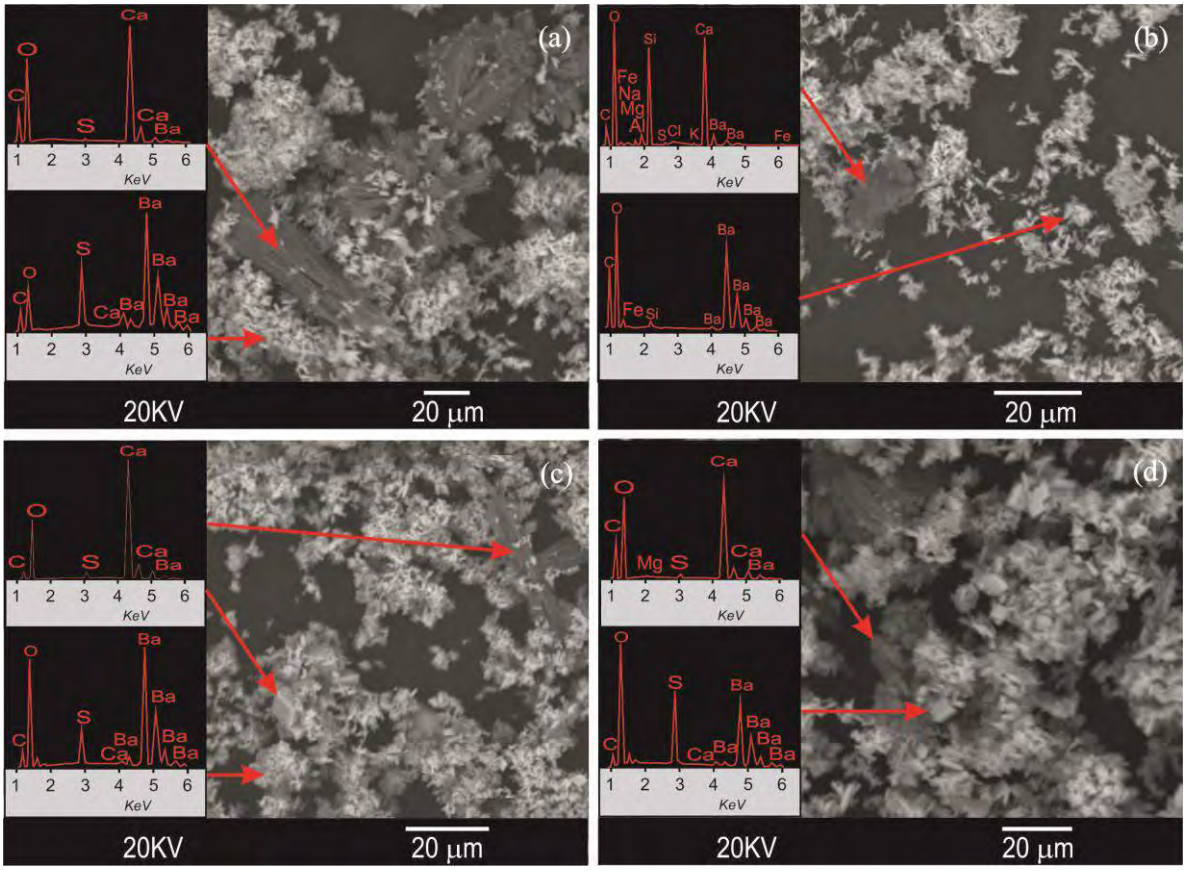

Figure 3 SEM images of (a) top sample: fibrous aggregates of $CaCO_3$, acicular $BaSO_4$, (b) amorphous precipitation and $BaCO_3$;(c) middle sample: fibrous and rhombohedral crystals of $CaCO_3$ and acicular $BaSO_4$ (d) globular $CaCO_3$ and orthorhombic $BaSO_4$.

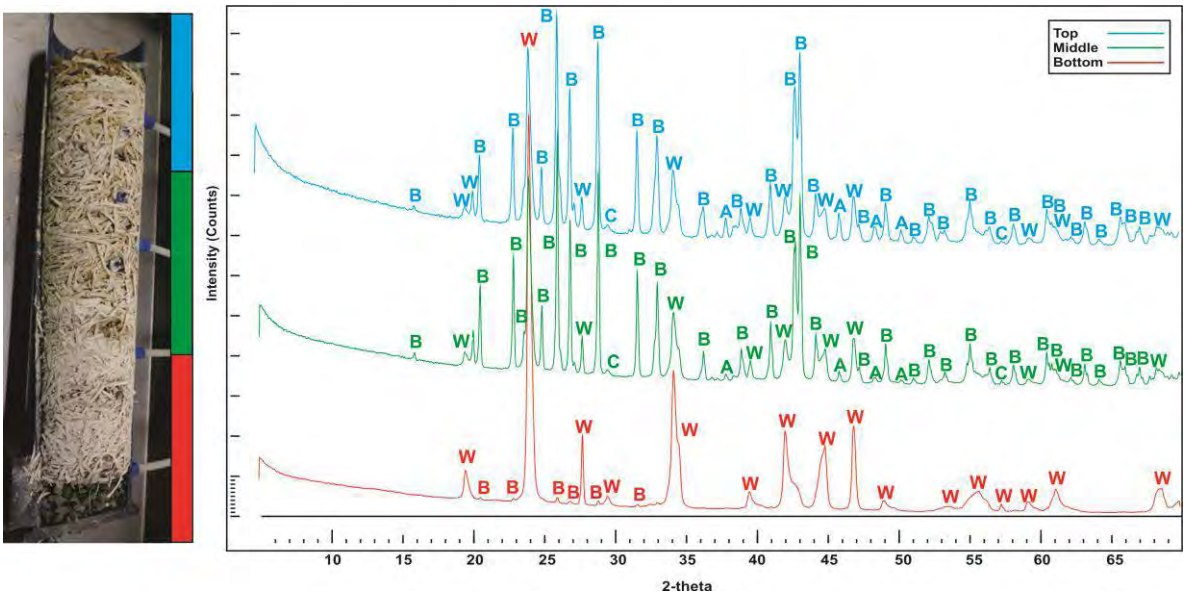

Figure 4 XRD difractograms of the three samples: bottom (red), middle (green) and top (blue) of column c (left picture). W: witherite, B: barite, C: calcite and A: aragonite

CONCLUSIONS

764 L of alkaline coal mine drainage from the site was treated by the B-DAS (Barium carbonate - disperse alkaline substrate) system in lab scale reactors. The aim to remove the high cations and anions concentration as well as the Sal and TDS from this drainage was achieved. According to the water analysis and the mineralogical characterization, the B-DAS system has demonstrated the capacity to remove 93% of sulfates through the precipitation of barite ($BaSO_4$); 98% of Ca by precipitation of calcite and aragonite ($CaCO_3$); remove Mn, Na, Fe, Al, Zn, Mg (93, 91, 90, 82, 68 and 13%, respectively). K and Si were also found in the neoformed precipitates. NO_3 was also removed (99.9%) from the AMD, but the absence of N in the precipitates and the extremely reductive condition in the reactor (Eh about -35 mV) could have promoted the denitrification process. The EC, Sal and TDS decreased about 50 – 70%.

According to the XRD analysis, after 6 months, column C had about 22 % of the $BaCO_3$ at the top and 95 % at the bottom of the column. Therefore, the reactive capacity of the $BaCO_3$ could be extended. Neoformed crystals were found in the top and middle samples, but not in the bottom sample, indicating that the dissolution of the $BaCO_3$ and the consequent precipitations took place in less than six hours (estimated residence time of the water in the top section of the column), demonstrating the effective treatment and the capacity of this system.

ACKNOWLEDGEMENTS

The authors gratefully acknowledge funding from the Technology Innovation Agency (TIA, South Africa). We thank Exxaro for site and sample access to the mining company's facilities, as well as the University of the Free State, in particular the Institute for Groundwater Studies and Department of Geology for the assistance in sample analysis.

REFERENCES

Allison, J.D., Brown, D.S. & Novo-Gradac, K.J. (1991) *MINTEQA2/PRODEFA2, A geochemical assessment model for environmental systems. Version 3.0 User's Manual,* Environmental Research Laboratory, Office of Research and Development, US Environmental Protection Agency, EPA/600/3-911021, Athens, Georgia.

Cravotta, C.A. & Trahan, M.K. (1999) *Limestone drains to increase pH and remove dissolved metals from acidic mine drainage,* Applied Geochemistry, vol. 14, pp. 581–606.

De Kortye, G.J. (2010) *Coal preparation research in South Africa,* International Coal Preparation, pp. 859–863.

Energy Information Administration (2014)*Countries: South Africa,* National Energy Information Center, Washington, DC, viewed 8 September 2014, <http://www.eia.gov/countries/cab.cfm?fips=sf>.

Kirby, C.S., Dennis, A. & Kahler, A. (2009) *Aeration to degas CO2, increase pH, and increase iron oxidation ratesfor efficient treatment of net alkaline mine drainage,* Applied Geochemistry, vol. 24, pp. 1175–1184.

Knyaston, H. (1906) *The geology of the Komati Poort Coal-field,* Transvaal Mines Department, Geological Survey, Memoir, pp. 2–55.

McQeen, K.G., Caldwell, J.R. & Millsteed, P.W. (1988) *Primary and secondary minerals at the Paddy's River Mine, Australian capital territory,* Australian mineralogist, vol. 3, pp. 83–100.

Parkhurst, D.L., Appelo, C.A.J. (2005) *PHREEQC-2 version 2.12: A hydrochemical transport model,* viewed September 2008. http://wwwbrr.cr.usgs.

Pokrovsky, O.S., Golubev, S.V., Schott, J. (2005) *Dissolution kinetics of calcite, dolomite and magnesite at 25 °C and 0 to 50 atm pCO2,* Chemical Geology, Vol. 217, pp. 239–255.

Robbins, E.I., Nord, G.L., Savela, C.E., Eddy, J.I., Livi, K.J.T., Gullett, C.D., Nordstrom, D.K., Chou, I.-M. & Briggs, K.M. (1996) *Microbial and mineralogical analysis of aluminum-rich precipitates that occlude porosity in a failed anoxic limestone drain, Monongalia County, West Virginia,* In: 13th Annual International Pittsburgh Coal Conference, Pittsburgh, pp. 761–767.

Rotting, T.S., Caraballo, M.A., Serrano, J.A., Ayora, C. & Carrera J. (2008) *Field application of calcite Dispersed Alkaline Substrate (calcite-DAS) for passive treatment of acid mine drainage with high Al and metal concentrations,* Applied Geochemistry, vol. 23, pp. 1660–1674.

Singer, P.C., Stumm, W. (1970) *Acidic mine drainage: the rate determining step,* Science, vol. 167, no. 3921 pp. 1121–1123.

South African bureau of standards 241: 2006 (2006). *Drinking water standard South Africa national* standards, SANS 241, Pretoria.

South African bureau of standards 241: 2011 (2011). *Drinking water standard South Africa national* standards, SANS 241, Pretoria.

Snyman, C.P. & Botha, W.J. (1993) *Coal in South Africa*, Journal of African earth science, vol. 16, No 1/2, pp. 171–180.

Van Dyk, J.C. (2006) *Understanding the influence of acidic components (Si, Al, and Ti) on ash flow temperature of South African coal sources,* Minerals Engineering, vol. 19, pp. 280–286.

Watzlaf, G.R., Schroeder, K.T., Kleinmann, R.L.P., Kairies & C.L. (2000) *Long term performance of anoxic limestone drains for the treatment of coal mine drainage,* Mine Water Environ, vol. 19, pp. 98–110.

Watzlaf, G.R., Kairies, C.L., Schroeder, K.T., Danehy, T. & Beam, R. (2002) *Quantitative results from the flushing of four reducing and alkalinity-producing systems,* Paper presented at the West Virginia Surface Mine Drainage Task Force Symposium; April 16-17.

Watzlaf, G.R., Schroeder, K.T., Kleinmann, R.L.P., Kairies, C.L. & Nairn, R.W. (2004) *The Passive Treatment of Coal Mine Drainage, DOE/NETL, 2004/1202*, US Department of Energy, Pittsburgh.

Low-Cost Carbon-Based Materials for Selective Removal of As(III) from Waste Waters

Yiannis Deligiannakis, Yiannis Georgiou, Eleftherios Mouzourakis and Ioannis Konstantinou
Lab of Physical Chemistry of Materials & Environment, Dept. of Environmental & Natural Resources Management, University of Patras, Greece

ABSTRACT

A low-cost carbon-based material from pyrolytic carbon from recycled tyres (PCrt) has been developed for selective removal of lead or arsenite from waste waters. The PCrt material has been characterized with X-Ray Fluorescence, XRD, And FTIR spectroscopies. Arsenite and Pb uptake was studied at the ppb level by Cathodic and Anodic Stripping Voltammetry (CSV). Adsorption isotherms, kinetic and pH-edge data show that PCrt can bind arsenite at a wide pH range from 4 to 9. More specifically, PCrt after mild treatment with HNO_3 and calcination at 500°C can adsorb 8.8 mg of As (III) and 27,7 mg Pb(II) per gram of material. PCrt can selectively uptake arsenite vs. lead when the two metals are present simultaneously in the aqueous solution. Importantly, when Pb is first adsorbed by PCrt, this forms PbS sites that act as additional arsenite binding sites. This is a unique example where one toxic metal, Pb(II), acts synergistically for adsorption of another toxic, As(III) on the appropriate matrix.

Keywords: low-cost, pyrolytic carbon, selective, Pb(II), As(III), metal uptake

INTRODUCTION

Disposal of waste tyres has become a serious source of environmental pollution [1]. More of 330 million waste tyres are discarded each year [2]. Tyre rubbers consist mainly of synthetic and natural rubber, tyre rubber additives i.e. like carbon black, sulphur and zinc oxide [1, 3]. A feasible solution for an environmentally friendly treatment of waste tyres would be to recycle them to valuable products that can be used in various applications.

Pyrolysis is an established process, which involves thermal decomposition of waste tyres at high temperatures (450-900 ^{o}C) under oxygen-free atmosphere, transforming them into useful products [3-4]. Tyre rubber pyrolysis results in the production of an oil- and a gas- fraction, plus the carbonized solid residue, the Pyrolytic Char from recycled tyres (PCrt) [3]. Pyrolytic oil and gas can be used as a source of chemical feedstock or a fuel with high calorific value for in-process, on-site or off-side applications [5]. PCrt may be used as carbon black filler for the tyre and printing-ink industries or as a precursor to manufacture low-cost adsorbent materials because of its high carbon content [4].

Arsenic may present in two main redox states Arsenites (As $^{3+}$) and Arsenate (As $^{5+}$) in natural waters, changes in solubility and mobility therefore occur as a function of redox potential and pH conditions in the environment and also are common in natural waters.[6] The World Health Organization (WHO) provisional guideline of 10 ppb (0.01 mg L^{-1}) have be adopted as the drinking water standard also U.S. Environmental Protection Agency (U.S EPA) required public drinking water to 10 ppb (0.01 mg L^{-1}). Arsenic is mobilized by natural weathering reactions, biological activity, geochemical reactions, volcanic emissions and other anthropogenic activities. Most environmental arsenic problems are the result of mobilization under natural conditions. However, mining activities, combustion of fossil fuels, use of arsenic pesticides, herbicides, and crop desiccants and use of arsenic additives to livestock feed create additional impacts.[7]. Pb (II) dominates in acid while $PbOH^{+}$ predominates in most environment pHs. The drinking water guideline recommended by WHO is 0.05 mg L^{-1}. The maximum allowable lead in drinking water has been set at a concentration of 15 ppb by U.S. EPA. Lead is widely used in processing industries such as electroplating, paint and dyes, explosive manufacturing, and lead batteries and in lakes and streams by acid. Also leads emitted into the atmosphere by combustion of fossil fuels and the smelting of sulfide ores.[8]. Also historic mining and industrial have produced numerous sites containing high concentration levels of As, Pb, Zn and Cd. Remediation of the contaminated sites is necessary because unthreaded effluent may have an adverse impact for the protection of the environment and public health.[9]. In the present study, priority heavy metal Pb (II) and metalloid As (III) were used as representative adsorbates which were removed from aqueous solutions by PCrt. Batch experiments were conducted to investigated kinetics and isotherms characteristic of arsenite and lead adsorption onto Pc. Finally we test the competitive adsorption of arsenite and lead onto PCrt.

METHODOLOGY

Preparation of tyre rubber pyrolytic char: The char was derived from the pyrolysis of used rubber tyres at 450^{o}C in oxygen-free atmosphere under vacuum for 4 hours. For the purification of as-received pyrolytic tyre char 2 gr of as received pyrolytic char suspended onto 2M HNO_3 for 2 hr . At the end of 2 hr suspension the material was collect and washed with deionized water for 6 times

to final pH =7 and solid was finally dried at room temperature. After room temperature drying, solid was calcinated at 500 °C under inert condition (N_2) for 1 hr.

Chemicals: Sodium meta-arsenite $NaAsO_2$ was obtained from Sigma-Aldrich, while HCl, NaOH and KNO_3. $Cu(NO_3)\cdot 3H_2O$, $Pb(NO_3)_2$ and HNO_3 were obtain from Merck. 2-(N-Morpholino) ethanesulfonic acid hydrate, 4-Morpholineethanesulfonic acid MES hydrate & 4-(2-Hydroxyethyl) piperazine-1-ethanesulfonic acid, N-(2-Hydroxyethyl) piperazine-N-(2-ethanesulfonic acid) HEPES used for pH buffering were obtained from Sigma-Aldrich. Ultrapure water was produced by a Milli-Q Academic system, Millipore. All solutions were prepared with analytical grade chemicals and ultrapure Milli-Q water with a conductivity of 18.2 μS cm^{-1}

Characterization of pyrolytic chars: The X-Ray powder Diffraction (XRD) patterns for the as received PCrt, char purified and $char_{500}$, were recorded by a Brüker Advance D8 instrument using Cu K_a radiation (λ = 1.5418 Å) in the 2θ range from 10° to 80°with a 2θ resolution of 0.02°. N_2 adsorption–desorption isotherms were obtained at 77 K using a Tristar Micrometrics Instruments and the specific surface area (S_{BET}) of the $Char_{500}$ was calculated using the Brünauer–Emmett–Teller (BET) method based on the adsorption data. The carbon, hydrogen, nitrogen and oxygen (CHNO) contents of the tyre - derived chars were determined using an elemental analyzer Perkin Elmer (2400 Series II) at 1.100 °C. Oxygen content was determined by mass difference. The ash content was determined by calcination of 1g of chars in a muffle furnace (800 °C, 4 h).

Analytical determination of As (III) and Pb (II): The concentration of metals in the aqueous solution was determined by Cathodic Stripping Voltammetry (CSV) using a Trace Master5-MD150 polarograph by Radiometer Analytica. An Ag/AgCl electrode with a double liquid junction was used as the reference electrode whilst a Pt electrode. Importantly, samples were not purged with N_2 gas in order to avoid loss of As(III) [10]. During the stripping step the solution was stirred at 525 rpm. For the measurements we used aliquots of 8.3 mL adjusted at pH 0.5 by HCl [11]. Then 8 ppm Cu^{2+} was added and the pH was readjusted if necessary to pH 0.5. In the following, As (III) was determined by square-wave CSV (SW-CSV) with accumulation potential E = -400 mV and accumulation time 60 s. As (III) was quantified by its signal at $E_{1/2}$ = -670 mV. The concentrations of Lead in the aqueous phase were determined by Anodic Stripping Voltammetry (ASV) .[12]

As (III) and Pb (II) sorption experiments: As (III) and Pb (II) uptake from aqueous solutions were studied in batch experiments. Adsorption kinetics of arsenite and lead onto PCrt, were screened for contact times ranging between 0 and 240 min at pH 7, $NaAsO_2$ = 3 mg L^{-1}, PCrt = 0.1 g L^{-1} and $Pb(NO)_3$=3 mg L^{-1} , PCrt= 0.1 g L^{-1} . In each experiment the supernatant was collected by centrifugation and then analyzed for arsenite and lead. Adsorption isotherms were recorded at pH 7 in the presence of $NaAsO_2$ and $Pb(NO)_3$ at concentrations between 10 to 50 mg gr^{-1} and 10 to 60 mg gr^{-1} respectively for 0.1 g L^{-1} of PCrt suspended in 50 mL buffer solution in polypropylene tubes.

Comparative adsorption were recorded at pH 7 in presence $NaAsO_2$ = 3 mg L^{-1} $Pb(NO)_3$=3 mg L^{-1} , PCrt = 0.1 g L^{-1} in 50 mL buffer for 120 min equilibrium time. Control experiments (without PCrt) showed no loss of initial As (III). The initial pH values of buffers were adjusted using small volumes of 2.5 M HCl or 2.5 M NaOH to the desired value. After metals addition, the suspension was allowed to equilibrate for 120 min at room temperature (25 °C ± 0.2) for arsenite and lead respectively while agitated in a magnetic stirrer. After completion of the equilibration, the suspension was centrifuged at 5000 rpm for 10 min the As (III) concentration of the supernatant solution was analyzed by Cathodic Stripping Voltammetry (CSV) and the Pb (II) concentration of

the supernatant solution was analyzed by Square Wave Anodic Stripping Voltammetry (SW-ASV) as described above.

RESULTS AND DISCUSSION

Characterization of the materials: The X-Ray Diffraction patterns of as receive PCrt, acid- treated PCrt, PCrt calcinated at 500 °C after acid- treatment, are presented in Figure 1. The XRD patterns show a typical peak of graphitic carbon 25° [13](Fig. 1). The peaks at 27°, 47° and 57° are characteristic of zinc sulfide (ZnS) [14]. On the other hand, the peak at 43° relates to iron carbides (Fe_3C).[14-15]

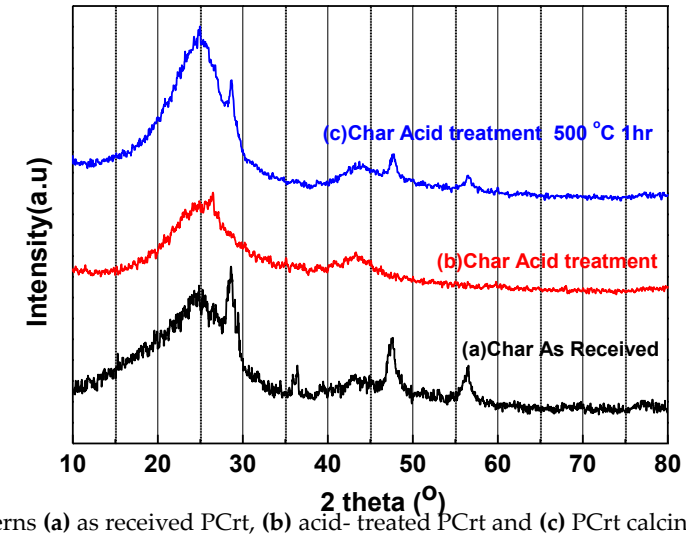

Figure 1 XRDs patterns **(a)** as received PCrt, **(b)** acid- treated PCrt and **(c)** PCrt calcinated at 500 °C after acid- treatment.

The IR spectra of the materials are shown in Fig. 2. The absorption peaks at 3400, 2380, 1600 cm^{-1} can be assigned to the =C-H, C-H and C=C stretching modes and shown in all materials [16]. The band at 1060 cm^{-1} is due to S=O stretching and appears in all materials [16]. The weak peak at 500 cm^{-1} indicates the existence S-S bonds and appears to as received char and char calcinated at 500 °C for 1 hour [16]. The band at 722 cm^{-1} is due to ZnS and shows up only at char calcinated at 500 °C for 1 hour[17]

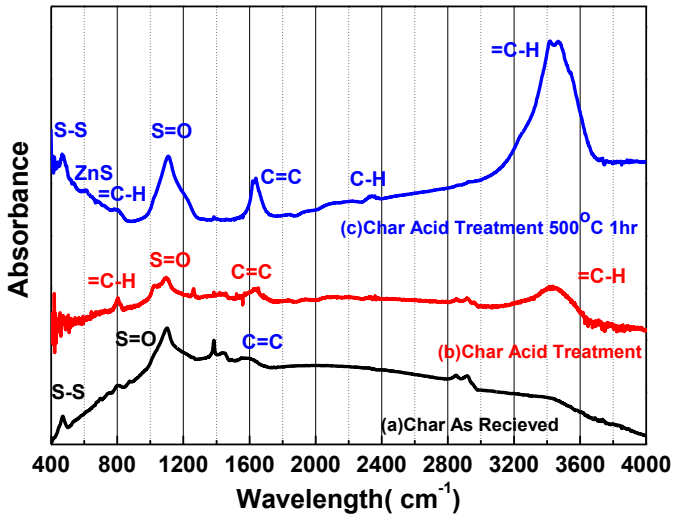

Figure 2 FTIR patterns **(a)** as received PCrt, **(b)** acid- treated PCrt and **(c)** PCrt calcinated at 500 °C after acid- treatment.

Arsenite and Lead adsorption: Adsorption kinetic data of arsenite onto PCrt in contact times ranging between 0 and 240 min (4 h). Arsenite uptake is accomplished after 120 min (data not shown). The maximum As (III) uptake capacity for the PCrt was evaluated at room temperature by fitting the experimental data with the Langmuir adsorption isotherm

$$q_e = \frac{q_m * K * C_e}{1 + K * C_e} \qquad \text{(Eq.1)}$$

Where q_e is the surface concentration or the surface density in mg g^{-1}. C_e has units of either mol L^{-1} or mg L^{-1}. The maximum q_m adsorption derived from the fit, listed in Table 1 is found 8,8 mg gr^{-1} of As(III) per gram at pH=7 (Fig. 3a).

Adsorption kinetic data of lead onto PCrt in contact times ranging between 0 and 240 min (4 h). Lead uptake is accomplished in the first 120 min (data not shown). The maximum Pb(II) uptake capacity for the PCrt was evaluated at room temperature by fitting the experimental data (see Table 1) with the Langmuir adsorption isotherm with equation 1 as describe above and was found 27.7 mg gr^{-1} of Pb(II) per gram at pH=7 (Fig. 3b)

Table 1 Langmuir Isotherm Constants at pH 7.0

Materials	Adsorbed	q_m (mg gr^{-1})	K_l	R^2
PCrt _acid_500^{0}C	As(III)	8,8	0,084	0,991
PCrt _acid_500^{0}C	Pb(II)	27,7	0,087	0,979
[[PCrt _acid_500^{0}C]- Pb(II)]	As(III)	31	0,69	0,989

For comparison, adsorption experiments with as received char and wash and char calcinated at 500 °C without acid-treatment show 1.8 mg gr^{-1} of arsenite at pH 7. This demonstrates that acid-treatment before the calcination step is essential for optimizing the PCrt surface for metal uptake.

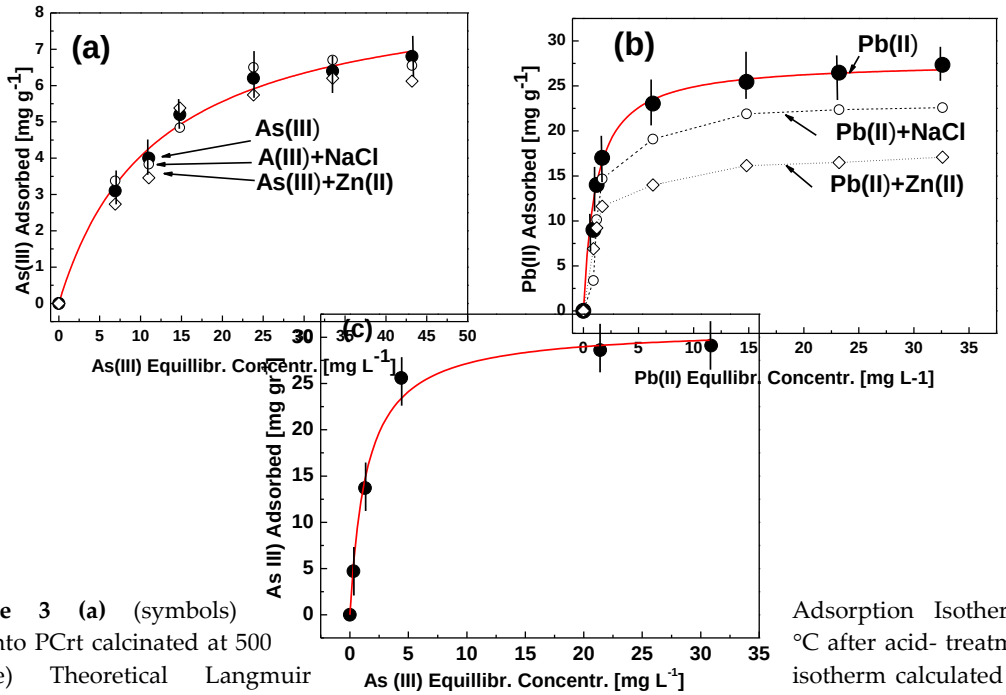

Figure 3 (a) (symbols) Adsorption Isotherm of As (III) onto PCrt calcinated at 500 °C after acid- treatment. (red line) Theoretical Langmuir isotherm calculated using the parameters listed in Table 1. Open symbls: As(III) uptake isotherms in the presence of 100mM NaCl, or 3mg/L Zn(II). **(b)** (symbols) Adsorption Isotherm of Pb (II) onto PCrt calcinated at 500 °C after acid- treatment. Open symbls: Pb(II) uptake isotherms in the presence of 100mM NaCl, or 3mg/L Zn(II) (red line) Theoretical Langmuir isotherm calculated using the parameters listed in Table 1, **(c)** (symbols) Adsorption Isotherm of As (III) onto [[PCrt _acid_500^{0}C]-Pb(II)]. (red line) Theoretical Langmuir isotherm calculated using the parameters listed in Table 1.

Selectivity of As(III) Uptake:

(a) Pb(II) enhances As(III) Uptake: Comparative adsorption Pb (II) and As (III) onto PCrt reveal an interesting phenomenon. When simultaneously present in the initial solution, 3 mg L^{-1} $NaAsO_2$ and 3 mg L^{-1} $Pb(NO)_3$ with 0.1 g L^{-1} PCrt, the adsorption of arsenite is strongly increased to 22.5 mg gr^{-1} and adsorption of lead show decrease to 16.9 mg gr^{-1}. This indicates that Pb (II) results in an –at first glance unexpected- enhancement of As (III) uptake. To further prove this we have performed an adsorption experiment where [i] first 27,7 mg gr^{-1} Pb (II) was allowed to be adsorbed on PCrt

_acid_500^{0}C for 2 hours, [ii] then As(III) adsorption was studied on the so-formed [[PCrt _acid_500^{0}C]- Pb(II)] material. The data reveal a significant boost of the As (III) uptake to 31 mg gr^{-1} after 30 min equilibrium time (Fig. 3c).This clearly demonstrates a novel phenomenon that can be explained if we consider the formation of PbS sites i.e. from adsorbed Pb (II) ions on S-sites that exist in the PCrt structure. In crystalline form, PbS has strong affinity for As (III) Bostick et al. [18] and Piquette et al. [19] that show arsenites adsorption onto PbS (galena). In the present case we consider that PbS sites are formed during lead adsorption, and these act as additional As (III) adsorption sites.

(b) Effect of electrolyte ions Na^+, Cl^-: Common electrolyte ions i.e. such as Na^+ and Cl^- have different effect on As(III) vs. Pb(II) uptake (compare open circles in Fig 3(a) vs. 3(b)). In the case of As(III) electrolyte ions at 100mM concentration have practically no effect, while Pb(II) uptake is inhbited by ~15%. This phenomenon can be explained as follows: at any pH<9 As(III) is in its neutral form H_3AsO_3 [6, 18] thus it is adsorbed preferentially on neutral sites of the adsorbing materials [6, 12,13b 18]. In contrast, Pb(II) cations are preferentially uptaken by anionic surface sites [12, 13b]. Thus electrolyte ions –which act via electrostatic forces in the electrostatic double layer at the interface- have no effect on the <H_3AsO_2-[neutral surface sites]> interaction whilst they do affect the <Pd(2+)-[surface anionic sites]> interaction.

(c) Effect of Zn(II): analogously, the presence of 3mg/L Zn(II) ions has negligible effect on As(III) uptake, see Figure 3a, while they severely compete for Pb(II) binding i.e. since both Pb(II) and Zn(II) cations compete for binding at the same anionic surface sites of PCrt.

Thus the present data reveal a selective As(III) uptake by the PCrt metarial that is not impaired by other common cations or anions.

Comparison with analogous As(III) sorbents: Low-cost Granular Activated Carbon, (GAC) and Fe-loaded GAC were reported to achieve an uptake of 0.4 mg As/g (GAC) and 3 mg/gr (GAC)-Fe respectively [20]. Other methods such as co-precipitation e.g. with Al or Fe hydroxides require significantly longer timescales i.e. days [6], *vs.* a max time of 120 minutes in the present systems. Moreover, the so formed precipitates have to be deposited on a low-cost substrate such as sand, Al_2O_3 or a carbon matrix [6, 21] in order to be usable in leaching-free column applications. For example Fe-hydroxide coated Al_2O_3 was shown to achieve As(III) uptake 7.6mg/g [6]. Our present approach suggests that PCrt-Pb outperforms these materials. When compared with more expensive materials prepared in our lab [12, 13d] the low-cost PCrt can be considered as a promising material on a performance/ cost basis.

Acknowledgements

This work is financially supported by the "SYNERGASIA" Program 11SYN_5_682 (O.P.Competitiveness & Entrepreneurship (EPAN II), ROP Macedonia- Thrace, ROP Crete and Aegean Islands, ROP Thessaly- Mainland Greece- Epirus, ROP Attica.

ΕΥΡΩΠΑΪΚΗ ΕΝΩΣΗ
ΑΝΤΑΓΩΝΙΣΤΙΚΟΤΗΤΑ ΕΠΙΧΕΙΡΗΜΑΤΙΚΟΤΗΤΑ ΕΠΑΝ II
η περιφέρεια στο επίκεντρο της ανάπτυξης
ΕΣΠΑ 2007-2013 πρόγραμμα για την ανάπτυξη
Υπουργείο Παιδείας και Θρησκευμάτων, Πολιτισμού και
Ε. Π. Ανταγωνιστικότητα και Επιχειρηματικότητα (ΕΠΑΝ ΙΙ), ΠΕΠ Μακεδονίας –

References

[1] E. L. K. Mui, W. H. Cheung, M. Valix, G. McKay, *Journal of Hazardous Materials* **2010**, *177*, 1001-1005.

[2] A. M. Cunliffe, P. T. Williams, *Energy and Fuels* **1999**, *13*, 166-175.

[3] G. S. Miguel, G. D. Fowler, C. J. Sollars, *Industrial and Engineering Chemistry Research* **1998**, *37*, 2430-2435.

[4] H. Teng, M. A. Serio, M. A. Wójtowicz, R. Bassilakis, P. R. Solomon, *Industrial and Engineering Chemistry Research* **1995**, *34*, 3102-3111.

[5] C. Roy, B. Labrecque, B. De Caumia, *Resources, Conservation and Recycling* **1990**, *4*, 203-213.

[6] D. Mohan, C. U. Pittman Jr, *Journal of Hazardous Materials* **2007**, *142*, 1-53.

[7] E. Amster, A. Tiwary, M. B. Schenker, *Environmental health perspectives* **2007**, 606-608.

[8] (a) P. Mushak, J. Michael Davis, A. F. Crocetti, L. D. Grant, *Environmental Research* **1989**, *50*, 11-36; (b) G. Flora, D. Gupta, A. Tiwari, *Interdisciplinary toxicology* **2012**, *5*, 47-58.

[9] (a)J. G. Dean, F. L. Bosqui, K. H. Lanouette, *Environmental Science & Technology* **1972**, *6*, 518-522; (b)A. S. Sheoran, V. Sheoran, *Minerals Engineering* **2006**, *19*, 105-116; (c)M. A. Acheampong, R. J. W. Meulepas, P. N. L. Lens, *Journal of Chemical Technology & Biotechnology* **2010**, *85*, 590-613.

[10] C. M. Barra, M. M. C. dos Santos, *Electroanalysis* **2001**, *13*, 1098-1104.

[11] V. Pallier, B. Serpaud, G. Feuillade-Cathalifaud, J.-C. Bollinger, *International Journal of Environmental Analytical Chemistry* **2011**, *91*, 1-16.

[12] M. Baikousi, C. Daikopoulos, Y. Georgiou, A. Bourlinos, R. Zbořil, Y. Deligiannakis, M. A. Karakassides, *The Journal of Physical Chemistry C* **2013**, *117*, 16961-16971.

[13] (a) E. S. Steigerwalt, G. A. Deluga, D. E. Cliffel, C. M. Lukehart, *The Journal of Physical Chemistry B* **2001**, *105*, 8097-8101; (b) C. Daikopoulos, Y. Georgiou, A. B. Bourlinos, M. Baikousi, M. A. Karakassides, R. Zboril, T. A. Steriotis, Y. Deligiannakis, *Chemical Engineering Journal* **2014**, *256*, 347-355; (c)A. Thomas, A. Fischer, F. Goettmann, M. Antonietti, J.-O. Muller, R. Schlogl, J. M. Carlsson, *Journal of Materials Chemistry* **2008**, *18*, 4893-4908.

[14] H. Darmstadt, C. Roy, S. Kaliaguine, *Carbon* **1995**, *33*, 1449-1455.

[15] W. Wu, Z. Zhu, Z. Liu, Y. Xie, J. Zhang, T. Hu, *Carbon* **2003**, *41*, 317-321.

[16] B. H. Stuart, *Infrared Spectroscopy: Fundamentals and Applications*, Wiley, **2004**.

[17] P. Griffiths, J. A. D. Haseth, *Fourier Transform Infrared Spectrometry*, Wiley, **2007**.

[18] B. C. Bostick, S. Fendorf, B. A. Manning, *Geochimica et Cosmochimica Acta* **2003**, *67*, 895-907.

[19] A. Piquette, C. Cannon, A. W. Apblett, *Nanotechnology* **2012**, *23*, 294014.

[20] Z. Gu, J. Fang, B. Deng, *Environ. Sci. Technol.*, **2005**, *39(10)*, 3833–3843.

[21] R. Singh, S. Singh, P. Parihar, V.P.Singh, S. M. Prasad *Ecotoxicology and Environemental Safety* 2015, 112, 247-270.

Functionalized Pyrolytic Carbon from Recycled Tyres: A Hybrid Material for Selective Removal of Pb, Cd from Waste Waters

Alexandra Mavrogiorgou and Maria Louloudi
Laboratory of Inorganic Chemistry, University of Ioannina, Greece

ABSTRACT

Carbon-based materials from recycled tyres (**PCox)** have been functionalized by covalently grafting organisilanised functionalities (**Si-L)** bearing ligating groups **L** [where **L**=4-imidazoledithiocarboxylic acid or 4-imidazolcarboxaldehyde]. These ligands **L** bear with high affinity for heavy metals. Here Pb^{2+}, Cd^{2+} uptake was studied by Adsorption isotherms and pH-edge data using Anodic Stripping Voltammetry (ASV). The maximum metal-uptake capacity of **L@PCox** material is 32.3 mg of Cd^{2+} per gram of **L@PCox** when L=4-Imid-ald (47.4 mg/gr when **L**=4-Imid-dithio) at pH 7.0. For Pb^{2+}, the max uptake is 17.1mg/g (for L=4-Imid-ald) and 34.2mg/g when **L**=4-Imid-dithio at pH 7. In the presence of competitive Zn^{2+} or Cu^{2+} ions, the **L@PCox** matrerials show a strong selectively for the Pb^{2+} or Cd^{2+} ions. This is attributed to the selectivity of the ligands **L** to the bigger lead or cadmium ions. When compared with the no functionalized pyrolytic carbon, the functionalised materials **L@PCox** show > 400% improvement for Cd and Pd uptake.

Keywords: pyrolytic carbon, fuctionalisation, Cd, Pb, metal uptake

INTRODUCTION

Pyrolytic char is one of the main products obtained after the pyrolysis process for disposing of waste tyres. It has contiguous structure with carbon black and this confers on it the general properties of carbonaceous materials such as thermal stability, high corrosion resistance in acid/base and low cost [1]. Concerning different technologies applied to the removal of heavy metal ions from aqueous bodies, metal adsorption onto solid supports such as activated carbon, zeolites, clays and metal oxides has been used so far [2]. However, the efficiency and selectivity of these solid supports are quite low, and improved metal absorbents have been prepared by coupling chelating ligands to support matrixes. The organic functionalities typically serve to form complexes with heavy metal ions, and the solid support allows easy removal from the liquid waste e.g. by filtration for example [3]. Various functionalized adsorbents with heavy metal complexing ligands have been reported [4,5] based mainly on polymers [6,7], clays [8,9], silica gel [3,10] and mesoporous silica [11,12].
Here, we report the functionalization of carbon-based materials from recycled tyres (**PC=Pyrolytic arbon)** *via* covalently grafting of organisilane-functionalities (**Si-L)** which bear ligating groups (**L)** with high affinity for heavy metals such as Pb^{2+}, Cd^{2+}. The so-prepared **L@PCox** hybrids contained functional groups **L**=4-imidazoledithiocarboxylic acid and 4-Imidazolcarboxaldehyde that are known to have specific ligation affinity for the heavy metals tested. Heavy-meta uptake was studied in aqueous solutions at pH 4-9 i.e. pertinent for industrial or surface waste waters.

METHODOLOGY

Oxidation of pyrolytic carbon. 5 gr of pyrolytic carbon (**PC**) were refluxed with 90 ml 65% v/v HNO_3 for 6h. The oxidized pyrolytic carbon (**PCox**) obtained was separated by filtration, washed exhaustively with distilled water until pH~7 and dried under reduced pressure at 40 °C for 12 h. DRIFTS-IR (cm^{-1}, selected peaks): 2919, 2855: ν(C-H); 1701: ν(C=O); 1542: ν(C=C); 1162: ν(C-O). Thermal analysis: the derivative thermogram of **PCox** shows a broad peak in the range of 130-420 °C assigned to the decomposition of –COOH surface groups with a 10.0 % weight loss and an intense peak at 600 °C assigned to the combustion of carbon support. The –COOH groups formed are *ca.* 2.2 mmol g^{-1} determined by thermogravimetric and elemental analysis. The **PCox** had an average surface area of *ca.* 687 m^2 g^{-1}.

Synthesis of Organosilane-ligands. *(a) Synthesis of organo-silanes* ***4-Imid-dithio-OS*** *and* ***4-Imid-ald-OS****.* 1.5 mmol of 4-imidazoledithiocarboxylic acid or 4-imidazolcarboxaldehyde and 1.0 mmol of (3-glycidyloxypropyl)-trimethoxysilane or (3-aminopropyl)-trimethoxysilane respectively were stirred for 24 h in 10 ml of MeOH under N_2 at 60°C in order to generate **L1-OS** and **L2-OS** silane-precursors. *(b) Formation of modified carbon materials.* The **L1@PCox** and **L2@PCox** materials were prepared through co-condensation of **4-Imid-dithio-OS** or **4-Imid-ald-OS** precursors with the –OH functional groups of oxidised carbon **PCox**. Accordingly, 0.5 g oxidised carbon **PCox** and 5 ml EtOH were added to the precursor **L1-OS** or **L2-OS** solution, and the resulting slurry was stirred at 60 °C for 24 h. The obtained solids, **4-Imid-dithio@PCox** and **4-Imid-ald@PCox,** were washed several times with MeOH and EtOH and dried under vacuum at 60 °C for 12 h.

4-Imid-dithio@PCox: DRIFTS-IR (cm^{-1}, selected peaks): 2918, 2853: ν(C-H); 1702: ν(C=O); 1652: ν(C=N); 1561: ν(N-H); 1542: ν(C=C); 1159: ν(C-S); 901: ν(C-O-Si). Thermal analysis provides a weight

loss of 14.1 % assigned to the decomposition of the surface –COOH groups and the anchored organic ligand. This material showed an average surface area of *ca.* 45 m^2 g^{-1}.

4-Imid-ald@PCox: DRIFTS-IR (cm^{-1}, selected peaks): 2923, 2855: ν(C-H); 1702: ν(C=O); 1597: ν(C=N); 1542: ν(C=C); 1107: ν(C-O); 799: ν(C-O-Si). Thermal analysis shows a weight loss of 15.1 % corresponds to the decomposition of the surface –COOH groups and the anchored organic ligand. This material had an average surface area of *ca.* 75 m^2 g^{-1}.

Analytical determination of Cd^{2+} and Pb2+: Determination of metal concentrations in aqueous phase was carried out by Anodic Stripping Voltammetry using a Trace Master5-MD150 polarograph by Radiometer Analytica as described earlier [3]. The measuring cells were borosilicate glass cell from Radiometer. The working electrode was a hanging mercury drop electrode (HMDE), with an Hg drop with 0.4mm diameter generated by a 70μm capillary. The reference electrode was an Ag/AgCl electrode with a double liquid junction. The counter electrode was a Pt electrode. Initially, before the stripping step N_2 gas (99.999% purity) was passed from the measuring solutions to remove any trace O_2. During this step the solution was under continuous stirring at 525rpm. During the stripping step the solution was not stirred. Square Wave (SW) measurements were performed in the anodic direction i.e. Square Wave Anodic Stripping Voltammetry (SW-ASV), to quantify metal ions. Typically under our experimental conditions, 1.05 10^{-6}M $Pb(NO_3)_2$ in 0.01M KNO_3 resulted in a current of Ip=0.851μA, Ep=-340mV at pH 6.5 and 1.05 10^{-6}M $Cd(NO_3)_2$ in 0.01M KNO_3 resulted in a current of Ip=0.820μA, Ep=-460mV at pH 6.5. Adsorption kinetics of cadmium and lead onto L@PCox , were performed for contact times ranging between 0 and 120 min at pH 7, L@PCox = 0.1 g L^{-1} and $Cd(NO)_3$ or $Pb(NO)_3$=3 mg L^{-1}. In each experiment the supernatant was collected by centrifugation and then analyzed for cadmium and lead. Adsorption isotherms were recorded at pH 7 in the presence of $Cd(NO_3)_2$ and $Pb(NO_3)_2$ at concentrations between 10- 50 mg g^{-1} , and 10- 60 mg g^{-1} respectively for 0.1 g L^{-1} of L@PCox suspended in 50 mL buffer solution in polypropylene tubes. The initial pH values of buffers were adjusted using small volumes of 2.5 M HNO_3 or 2.5 M NaOH to the desired value. After metals addition, the suspension was allowed to equilibrate for 120 min at room temperature (25 °C ± 0.2) for cadmium and lead, while agitated in a magnetic stirrer. After completion of the equilibration, the suspension was centrifuged at 5000 rpm for 10 min. The Cd^{2+} or Pb^{2+} concentration of the supernatant solution was analyzed by Square Wave Anodic Stripping Voltammetry (SW-ASV) as described above. In the competition experiments, $Cu(NO_3)_2$ or $Zn(NO_3)_2$ where added in the same reaction mixture together with lead or cadmium and determined using SW-ASV.

RESULTS AND DISCUSSION

Synthesis of the adsorbents

The methodology applied here for anchoring of chelating ligands onto pyrolytic carbon uses silylation reaction of silane-precursors, depicted in Figure 1. The key concept of the present method is, first, a reaction of bifunctional, commercially available, alkoxy-silanes with 4-imidazoledithiocarboxylic acid or 4-imidazolcarboxaldehyde producing **4-Imid-dithio-OS** and **4-**

Imid-ald-OS precursors which has the alkoxy-moiety intact, and, second, silylation reaction of the so obtained silane-precursors with the surfacial –OH groups of the oxidized pyrolytic carbon.

Overall, the present synthetic procedure involves: (i) oxidation of the pyrolytic carbon **PC** with concentrated HNO_3; (ii) derivatization of the 4-imidazoledithiocarboxylic acid or 4-imidazolcarboxaldehyde to form silane-compounds; and (iii) anchoring of the silane-precursors to the oxidised pyrolytic carbon **PCox**. Derivatization occurs *via* reaction of 4-imidazoledithiocarboxylic acid and 4-Imidazolcarboxaldehyde with (3-glycidyloxypropyl)- or (3-aminopropyl)-trimethoxysilane to generate **4-Imid-dithio-OS** and **4-Imid-ald-OS** silane-precursors respectively. The propyl-trimethoxysilane moieties of **4-Imid-dithio-OS** and **4-Imid-ald-OS** allows their covalent attachment on the oxidized pyrolytic carbon **PCox** surface via hydrolysis and co-condensation with the –OH functionalities of the **PCox** leading to the formation of **4-Imid-dithio@PCox** and **4-Imid-ald@PCox** hybrid materials respectively.

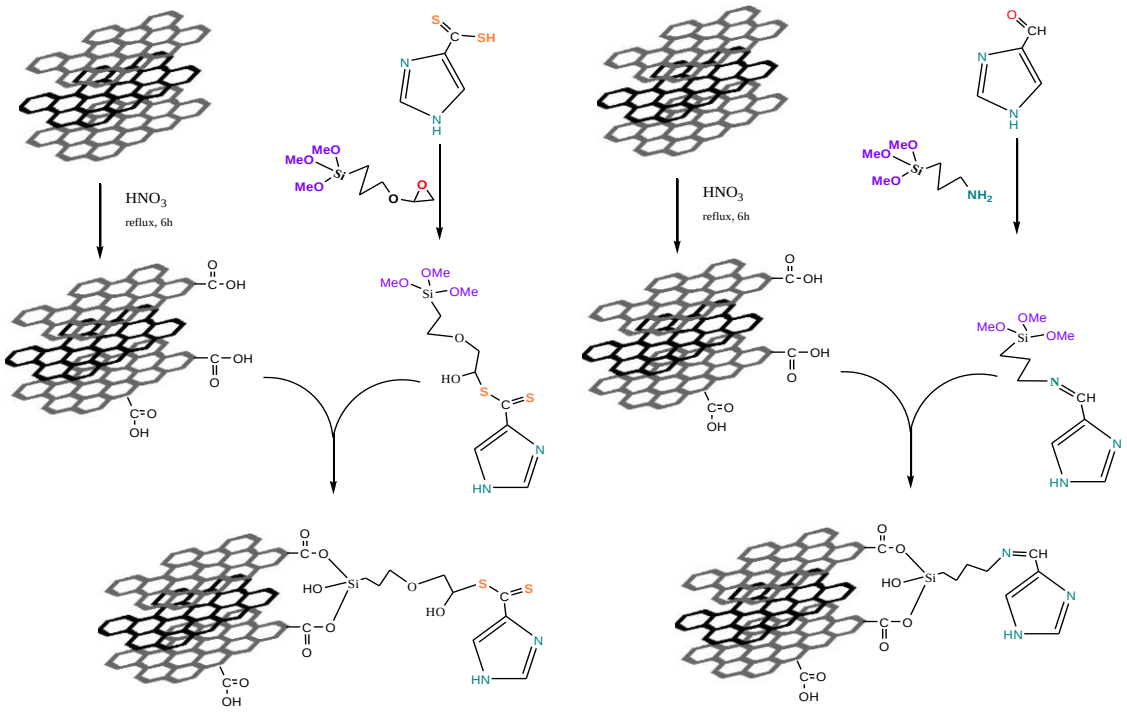

4-Imid-dithio@PCox **4-Imid-ald@PCox**

Figure 1 Grafting of 4-imidazoledithiocarboxylic acid and 4-Imidazolcarboxaldehyde on the surface of **PCox**

The DRIFTS-IR spectra of the **4-Imid-dithio@PCox** and **4-Imid-ald@PCox** show several bands corresponding to various structural units of the solid support as well as from the chelating ligands 4-imidazoledithiocarboxylic acid or 4-imidazolcarboxaldehyde. More specifically, the modified materials display the characteristic $-CH_2$ stretching bands in the region 2950–2850 cm^{-1} and $-CH_2-$ aliphatic deformation vibrations in the region 1500–1300 cm^{-1}, as weak intensity bands. The bands at 1702 cm^{-1} are attributed to ν(C=O) stretching vibrations. The C=N and C=C stretching vibrations of **4-Imid-dithio@PCox** were observed at 1652 and 1542 cm^{-1}, respectively. The same vibrations were also observed at 1597 and 1542 cm^{-1} attributed to imidazole ring in the **4-Imid-ald@PCox** material.
The derivative thermograms for **4-Imid-dithio@PCox** and **4-Imid-ald@PCox** show 14.1 and 15.1% weight loss respectively, in the range 130-400 °C, which corresponds to a loss of anchored organic moieties and surface oxidised functionalities. Taking into account that the parent **PCox** material bears 10.0 % [w:w] –COOH surface groups which are decomposed in the same temperature region, the additional weight loss of 4.1 and 5.1% is assigned to the decomposition of the anchored organic ligand 4-imidazoledithiocarboxylic acid and 4-imidazolcarboxaldehyde respectively**.** The loading of 4-imidazoledithiocarboxylic acid and 4-imidazolcarboxaldehyde is *ca.* 0.3 and 0.5 mmol g^{-1} respectively.

Heavy Metal Uptake

Pb^{2+} uptake: Figure 2 presents the uptake of Pb^{2+} ions by 4-imid-ald@PCox (2A) or 4-imid-dithio@PCox (2B). The functionalised materials have significantly i.e. at least fourfold, improved Pd-uptake compared to the untreated pyrolytic carbon material (PC). Then pH-egde profiles in Figure 2 indicate that 4-imid-ald@PCox binds Pb via the imidazole group which deprotonates at alkaline pH. In contrast or 4-imid-dithio@PCox can bind metal cations at all the pH values tested. This is attributed to Sulfur atoms that have strong affinity for Cd and Pb. The S atoms act synergistically with the imidazole, thus achieving a higher Pd-uptake than imidazole alone.

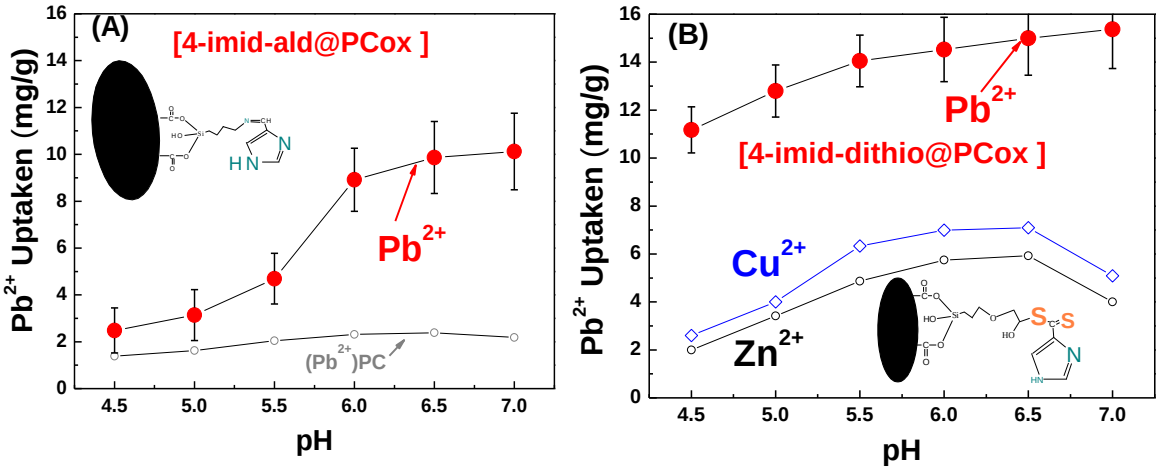

Figure 2 (A) Adsorption pH-edge for Pb^{2+} onto or 4-imid-ald@PCox (•) or untreated Pyrolytic Carbon (PC) (◦). (B) onto 4-imid-dithio@PCox (♦). In 2B, the pH-edge adsorprion of Cu^{2+} (◊) or Zn^{2+} (◦) ions is shown.

Cd^{2+} uptake: Figure 3 presents the uptake of Cd^{2+} ions by 4-imid-ald@PCox (A) or 4-imid-dithio@PCox (B). As in the case of Pb, the functionalised materials have significantly better Cd-uptake ability, than the untreated pyrolytic carbon material (PC). The beneficial role of the S-atoms in or 4-imid-dithio@PCox is also seen in Figure 3B e.g. *vs.* imidazole alone, in 4-imid-ald@PCox Figure 3B.

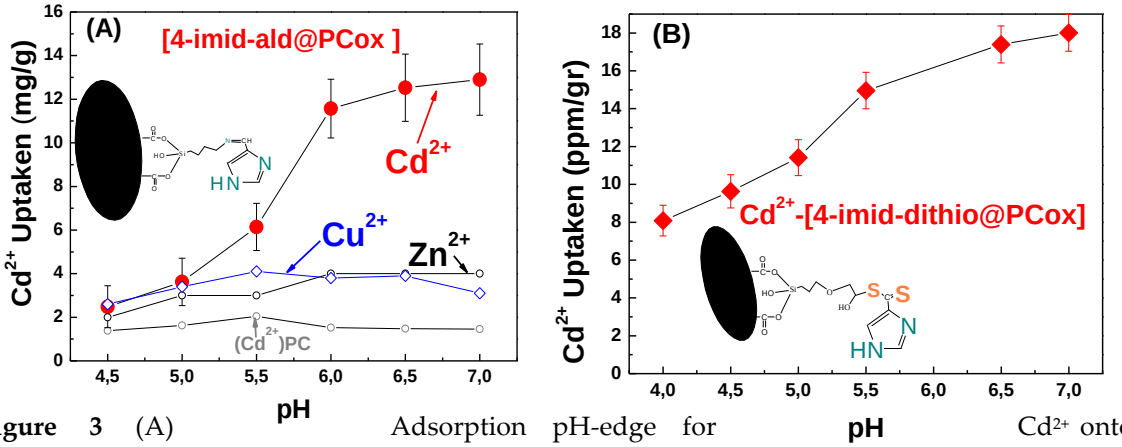

Figure 3 (A) Adsorption pH-edge for Cd^{2+} onto 4-imid-ald@PCox (•) or untreated Pyrolytic Carbon (PC) (◦). (B) onto 4-imid-dithio@PCox (♦).(♦). In 3A, the pH-edge adsorprion of Cu^{2+} (◊) or Zn^{2+} (◦) ions is shown.

As in the case of Pb-uptake, at pH 7, both materials show improved sorption capacities. This indicates the involvement of pH dependent surface groups in the mechanism of cadmium uptake. The origin of this phenomenon can be understood based on the Surface Complexation Model developed in our previous work [3] for analogous ligands grafted on SiO_2 [3]. According to this, the binding of Cd^{2+} and Pb^{2+} ions is determined by [i] their binding affinities towards the S-atoms and the imidazole in 4-imid-dithio while the imidazole is the only functional group in 4-imid-ald. On the other hand the high affinity of Pb for the S-atoms in 4-imid-dithio@PCox render this material stronger adsorbent for Pb-ions at all pH values. On the other hand imidazole has higher affinity for Cd binding than for Pb, thus the Cd-uptake by 4-imid-ald@PCox is higher for Cd than for Pb.

Competitive Metal Uptake: The data in Figure 2B, show that 4-imid-dithio@PCox has an almost 100% higher Pb-uptake affinity than for Cu^{2+}, and ~130% higher affinity for Pb^{2+} vs. Zn^{2+}. This is due to the high binding affinity of the imidazole/S unit for Pb^{2+} ions. Similarly, 4-imid-ald@PCox shows a significantly higher binding affinity for Cd^{2+} ions than for the Cu^{2+} or Zn^{2+} ions. In Table 1 we summarise the maximum metal uptake capacity for Cd^{2+} or Pb^{2+} when present simultaneously with Cu^{2+} of Zn^{2+} ions.

All experiments were performed at a neutral pH 7 for an initial metal concentration 50mg per gram of material. The binary-metal data, in Table 1 clearly exemplify the effect seen in the pH-edge data of Figures 2B and 3A. 4-imid-dithio@PCox shows a 4:1 to 2:1 selectivity for Cb over Cu or Zn respectively. 4-imid-dithio@PCox shows a 4:1 and 3:1 for Cd^{2+} over Cu and Zn respectively. The higher affinity for the bigger (Cd^{2+}, Pb^{2+}) ions is attributed to a chelation effect originating from the 4-imid-ald/dithio ligands on the oxidized pyrolytic carbon matrix.

Table 1 Maximum Metal Uptake Capacity of the functionalized PCox materials at pH 7.0

	Metal **sinlge-sorbates** (mg of metal uptaken per gr of material)		Metal **Binary-sorbates** (mg of metal uptaken per gr of material)			
Material	Cd^{2+}	Pb^{2+}	Cd^{2+}(Cu^{2+})	Cd^{2+} (Zn^{2+})	Pb^{2+}(Cu^{2+})	Pb^{2+} (Zn^{2+})
4-imid-dithio@PCox	32.3	30.1	29.4(5.8)	11.2(6.9)	23.0(4.6)	25.7(13.9)
4-imid-ald@PCox	47.4	27.2	36.2(9.4)	33.2(11.4)	26.1(8.7)	30.2(12.6)

Comparison with analogous metal-sorbents: the present pyrolytic carbon-based materials can be compared with other chars e.g. such as pyrolyitc wood [13], biochar or activated carbon that have been used for Cd and Pd uptake [14-16]. The present materials achieve 30-40 mg of Pb uptaken per gram for an initial metal concentration 50mg/gr i.e. >70% metal uptake. Chars derived from several pyrolytic woods [13] achieved <5mg Pb per gram at initial Pb >100mg [see review in 13]. Activated carbon from *Phaseulus* a. huls tested from Pb, Zn, Cu, Cd as in the present case at pH 7 achieved metal uptakes of 6-16mg/gr [16]. No completion/selectivity data were reported. In [14] binary metal sorbates (Cd-Cu) were evaluated by activated carbon (Aldrich Darco-120)., at very low initial concentrations (0.6mg/gr). Cd uptake was severely outcompeted by Cu which was >95%uptaken vs. <50% of the Cd [14]. Thus, the present functionalized PCox materials constitute an example of high performance/high selectivity materials for Cd, Pd uptake.

CONCLUSION

Covalent rafting of appropriate organic ligands on PCox may result in significant enhancement of metal uptake by the adsorbent, compared to untreated Pyrolytic Carbon. Noticeably, the immobilised multifunctional ligands such as 4-imid-dithio and 4-imid-ald, have exhibited high Cd and Pb uptake-capacity at acidic as well as at neutral pH values. The high binding affinities of the Pb and Cd ions for the S-atoms of 4-imid-dithio and the idazole ring respectively result in different pH-edge profiles for the two metals. The data show that the presence or absence of protonable groups on the ligand determines the pH-edge profile in combination with the hydrolysis profile of

the metal ion under study. Thus both the nature of the ligand as well as its surface concentration are of equal importance for the sorbing capacity of the material.

ACKNOWLEDGEMENTS

This research has been co-financed by the European Union (European Regional Development Fund – ERDF) and Greek national funds (EPAN-II), PEP–Sterea Ellada–Epirus-Thessaly within Action SYNERGASIA-2011.

Ε. Π. Ανταγωνιστικότητα και Επιχειρηματικότητα (ΕΠΑΝ ΙΙ), ΠΕΠ Μακεδονίας – Θράκης, ΠΕΠ

REFERENCES

1. J.L. Allen, J.L. Gatz, P.C. Eklund, *Carbon*, 37, (1999), 1487-1489.
2. S. Babel, T.A. Kurniawan, J. Hazard. Mater. 97 (2003) 219–243.
3. G. Grigoropoulou, P. Stathi, M. A. Karakassides, M. Louloudi, Y. Deligiannakis, *Colloids Surf. A: Physicochem. Eng. Aspects* 320 (2008) 25–35
4. T.P. Rao, R. Kala, S. Daniel, *Anal. Chim. Acta* 578 (2006) 105–116.
5. V. Camel, Spectrochim. Acta Part B 58 (2003) 1177–1233.
6. R.R.Navarro, K. Sumi, M. Matsumura, *Water Res.* 33 (1999) 2037–2044.
7. Y.H. Park, J.M. Lim, C.R. Park, *J. Appl. Polym. Sci*. 63 (1997) 773–778.
8. I.L. Lagadic, M. Mitchell, B. Payne, *Environ. Sci. Technol.* 35 (2001) 984–990.
9. L. Mercier, T.J. Pinnavaia, *Micropor. Mesopor. Mater*. 20 (1998) 101–106.
10. M. Zougagh, J.M. Cano Pav´on, A. Garcia de Torres, *Anal. Bioanal. Chem*. 381 (2005) 1103–1113.
11. A. Sayari, S. Hamoudi, Y. Yang, *Chem. Mater*. 17 (2005) 212–216.
12. L. Mercier, T.J. Pinnavaia, *Environ. Sci. Technol*. 32 (1998) 2749–2754.
13. D. Mohan, C.U. Pittman Jr., M. Bricka, F.Smith, J. Mohammad , P. H. Steele, M. F. Alexandre-Franco, B.Yancey, V. Gomez-Serrano, H. Gong *Journal of Colloid and Interface Science* 310 (2007) 57–73.
14. A. Seco, P. MArtzal, C. Gabaldon *J. Chem. Technol. Biotechnol*. 68 (1997) 23-30.
15. S. Badel, T. A. Kurniawan *J. Hazardous Materials B97 (*2003) 219-243.
16. I.Ali *Separation & Purification Reviews* 39 (2010) 95-171.

10th ICARD IMWA 2015 | 10th International Conference on Acid Rock Drainage & IMWA Annual Conference

Outotec Ettringite Process for Sulfate Removal from Mining and Metallurgical Waters

Laura Nevatalo[1], Tuomas van der Meer[1], Mika Martikainen[1] and Cristian Montes[2]

1. *Outotec Industrial Water Treatment, Finland*
2. *Outotec Chile*

The treatment of wastewaters from mining and metallurgical processes is becoming challenging due to tightening environmental regulation for water quality that is allowed for discharge to environment. Sulfate in form of sulfuric acid is one of the key components of acid mine drainage and acid rock drainage. Traditional lime neutralization neutralizes the acid and precipitates the metals, but sulfate will remain in the solution in gypsum saturation concentration. Removal of sulfate from these streams to meet the required concentration limits has been proven to be challenging due to high solubility of sulfate salts. Few technically feasible water treatment processes exist in the market that can be applied to decrease sulfate concentration below gypsum saturation level: biological sulfate reduction, membrane separation, ion exchange, evaporation and chemical precipitation. Some of these technologies are effective for treating wastewater, but there is typically a highly concentrated sulfate fraction left requiring still further treatment. Selecting the correct sulfate removal technology requires deep understanding of water chemistry and the effects of technology selection to overall water treatment plant capex and opex, and including also the necessary pre- and post treatment steps and solid waste management required around the core technology. Outotec has developed a sulfate removal solution: Outotec Ettringite process for treatment of gypsum saturated waters and waters with high Na_2SO_4 concentration, where sulfate removed to solid form as ettringite ($3CaO_3CaSO_4Al_2O_3*31H_2O$). Process equipment are reactors for ettringite precipitation, clarifier and filter for separation of ettringite solids and reactor for final neutralization with CO_2-gas followed by polishing $CaCO_3$ solids separation step. Typically the wastewaters to be treated contain 1-10 g/l sulfate and after ettringite process the sulfate concentration is 200 mg/l or even lower, this residual sulfate concentration can be controlled flexibly. Besides the sulfate concentration, the wastewater characteristics have an effect on the overall opex.

**There is no full article associated with this abstract.*

10th ICARD IMWA 2015 | 10th International Conference on Acid Rock Drainage & IMWA Annual Conference

Performance of Organic and Inorganic Polymers for the Removal of Suspended Solids from Mine Water

Elvis Fosso-Kankeu[1], Frans Waanders[1], I.O. Ntwampe[1] and Hermant Mittal[2]

1. *School of Chemical and Minerals Engineering, North West University, South Africa*
2. *DST/CSIR National Centre for Nanostructured Materials, Council for Scientific and Industrial Research, South Africa*

ABSTRACT

This study investigates the performance of synthesized organic and inorganic polymers in the flocculation of fine particles of suspended solids from mine water of different electrochemical properties.

Factors considered for the evaluation of the performance of coagulants included, coagulant type, pH conditions, turbidity removal efficiency, pH correction and sedimentation rate of the flocs.

It was observed that the monomeric inorganic coagulants had a relatively poor performance compared to the polymers. The organic polymer (GK-cl-P(AAm-co-AA)/Fe_3O_4 nanocomposite) was much effective in acidic solutions, while the monomeric inorganic polymer performed better under alkaline conditions; the response of the inorganic polymer af-PFCl to pH changes was inconsistent. The coagulants used were unable to correct acidic pH of the solutions. In general the coagulants could achieve a turbidity removal in the range of 67 to 99.5%, but GK-cl-P(AAm-co-AA)/Fe_3O_4 nanocomposite showed the greatest reactivity by achieving the fastest floc formation rate and shortest optimum sedimentation time of 5 mins.

Developed polymers have shown better flocculation potential and provide the advantage to reduce the formation of byproducts, improving the quality of mine effluents prior to discharge in the environment.

**There is no full article associated with this abstract.*

CHAPTER 6

MINE WATER DRAINAGE COLLECTION AND TREATMENT – BIOLOGICAL ACTIVE TREATMENT

Sulfidogenic Diffusive Exchange System for the Treatment of Acid Mine Drainage

Alex Schwarz and Norma Pérez
Center for Water Resources in Agriculture and Mining (CRHIAM), Universidad de Concepción, Chile

ABSTRACT

Sulfate-reducing bioreactors are good treatment options for acid mine drainage (AMD). In this technology, AMD flows through a bed containing reactive material, where sulfate, metals and acidity are removed by the metabolic activity of sulfate-reducing communities. The substrates should be affordable and provide organic matter that promotes the growth of microorganisms. We hypothesize that increasing organic substrate availability by utilizing finely ground organic material will increase sulfate reduction kinetics, although new reactor designs such as diffusive exchange systems (DES) will be needed to accommodate these finer substrates while keeping AMD throughput.

In this research, utilizing a fine organic substrate in a sulfidogenic DES bench scale reactor, we treated acidic AMD (pH down to 2.5) for a period of 14 months. Although the reactor was operated in a metal and acidity overloaded mode for the whole period, it achieved stable operation, reducing sulfate, removing metals and adding alkalinity. To our knowledge, this is the first time a biochemical reactor is operated passively, without external alkalinity source, at such low pH and high metal load. This stable operation indicates that a bioprotection mechanism based on chemical gradients protected the microbial community within the reactive layers of low permeability. In addition, the system did not show any permeability reduction. The metals precipitated along the interfaces between the reactive and conductive layers, where sulfide and metal gradients met, consistent with chemical-gradient-based bioprotection. Hence, the sulfidogenic DES holds promise for the passive treatment of highly acidic and toxic AMD. Higher reaction rates are possible within these reactors, and microbial consortia are protected from toxicity while no permeability reduction is observed.

Keywords: biochemical reactor, bioprotection, diffusive exchange, passive treatment, AMD.

INTRODUCTION

The mining waste rock and tailings represent a potential hazard for the environment, especially when the residues contain sulfide minerals that can be a source of acid mine drainage (AMD). The exposure of the metal sulfides to oxygen and water, accompanied by microbial activity, leads to the formation of drainage rich in sulfate, acidity and heavy metals (Dold, 2010). The AMD problem involves both active and abandoned mines dedicated to the extraction of metals or coal (Blowes et al., 2003).

In mines located in areas with intermittent precipitations, such as in Northern and Central Chile, and steep slopes where no flooding occurs, water, oxygen and sulfides strongly interact increasing the potential for AMD formation; additionally, the high evaporation rate causes the accumulation of sulfate salts that generate stronger AMD (Nordstrom, 2011). The potential AMD sources in Chile are significant: in 2002, 3,000,000 ton/day of waste rock were generated, and 650,000 ton/day of tailings (Ministerio de Minería & Consejo de Minería, 2002). On the other hand, Chile has a legacy of contamination of water resources due to past mining operations, which has to be addressed (Instituto de Ingenieros de Chile, 2011; Banco Mundial, 2011). Leaking tailing dams, acid mine drainage and small scale mining result in contamination of water resources that are often used for irrigation downstream. In Northern and Central Chile, many rivers present concentrations of metals and sulfate that exceed irrigation water quality standards. Since the 1980s, levels of arsenic, copper and sulfate have increased (Banco Mundial, 2011). These problems demand long-term passive solutions that are low cost and make use of local resources.

Several physicochemical and biological techniques have been developed to treat AMD. In conventional active treatment, acidity and metals are removed by continuous addition of alkaline substances (such as NaOH, $Ca(OH)_2$, CaO, Na_2CO_3 and NH_3), which can be expensive, specially when needed in high quantities; also, costs of operation and maintenance of active systems are high (Watzlaf et al., 2004). During the last decades, research has focused on the development of passive treatment systems for AMD, because passive systems have shown high metal removal at low pH values (pH 3-6), sludges that are chemically stable, low operational and maintenance costs, reduced chemical consumption and minimal consumption of energy. The passive treatment systems use addition of limestone to generate alkalinity and precipitate metals as oxides and/or use biological processes in which sulfate reduction takes place through which alkalinity is generated and metals precipitate as sulfides.

In biological treatment systems such as anaerobic wetlands, remediation of dissolved metals is mainly caused by sulfate reduction, which simultaneously removes sulfate, metals and acidity. Metals are also precipitated as a result of some abiotic reactions that result from the reducing ambient that is generated (Kosolapov et al., 2004) such as precipitation of metal oxides or carbonates driven by a pH increase (Gadd, 2000). The precipitation of metals by sulfate reduction occurs when the produced H_2S reacts with the metals to produce insoluble precipitates (Zagury et al., 2006). For sulfate reduction to be successful a pH range of 5 to 8 is required; outside this range, reduction diminishes and the capacity of metal removal is reduced. At low pH (< 5), sulfate reduction is normally inhibited and the solubility of metal sulfides increases (Neculita et al., 2007). However, sulfate-reducing bacteria (SRB) surviving at pH of 2.5 have been found, although with only slight alkalinity generation (Tsukamoto et al., 2004). Also, a reduced anaerobic medium is required for sulfate reduction with redox potential (Eh) of less than -100 mV (Rabus et al., 2006). The substrate usually used to drive sulfate reduction is principally made of organic residues such

as animal feces, compost and agricultural residues (Neculita et al., 2008). Adequate proportions of different organic sources are required for long-term operation of the biological treatment system (Sheoran et al., 2010). The efficacy of these systems will be affected by pH variations, metal concentrations, and concentrations of sulfide produced in-situ, which may be also toxic.

The development of biological treatment systems must be focused on the adequate proportions of different organic sources, avoiding AMD toxicity to microorganisms, and studying the key bacterial populations involved in treatment. Research results suggest that a good organic energy source for sulfate reducing communities must contain several carbon sources (Waybrand et al., 1998; Zagury et al., 2006). Substrates with cellulose have been confirmed to be more efficient than lignocellulosic substrates (Waybrand et al., 1998). An optimum mixture must contain equal proportions of cellulosic and non-cellulosic organic residues (Neculita et al., 2008). The non-cellulosic organic residues (compost and manure) accelerate the activity of sulfate reducers at the start of the system (Wildeman (2006), cited by McCauley et al., 2009). The cellulose delivers the long-term organic matter and must be hydrolyzed and fermented by a microbial consortium that provides the simple carbon sources to SRB.

Our research addresses protection from toxicity. We take advantage of chemical gradient-based bioprotection, a mechanism by which some bacteria in a community induce pore-water metal gradients (Schwarz & Rittmann 2007a; 2007b). Bioprotecting gradients can occur over a broad range of scales: μm - mm in biofilms, mm - cm in freshwater and marine sediments, and cm - m in groundwater aquifers. An excellent example of this community-based bioprotection mechanism involves SRB, which produce sulfide that can coordinate toxic free metals to form solids. Results of previous analytical and numerical modeling (Schwarz & Rittmann, 2007a; 2007b) provide evidence that gradient resistance ought to work much better in diffusion-dominated systems, compared to advection-dominated systems. This insight led us to develop the diffusive exchange system (DES) approach to be used in permeable reactive barriers or constructed wetlands. In DES reactors, layers of low conductivity (low-K) containing reactive organic materials are intercalated between layers of high conductivity (high-K) that transport the AMD across the reactor. Because diffusion dominates transport in the reactive layers, microbial communities can take advantage there of the chemical-gradient mechanism for protection from toxicants. Specifically, we experimented with a porous layered system where the reactive sulfate reducing layers with low hydraulic conductivity were intercalated between sand layers with higher hydraulic conductivity. The sulfide produced in the reactive layers diffused to the sand layers where the metals precipitated. This system avoided the direct contact between microorganisms and the flowing AMD.

METHODOLOGY

The DES reactor, with horizontal gravitational flow, had dimensions of 120 cm x 60 cm x 10 cm (L x H x W) (Fig. 1). It was filled with horizontal layers of 10 cm thickness of reactive material and sand (3 each). The flow was controlled by means of a peristaltic pump feeding the upgradient well (Masterflex, 0.02–100 rpm). Both upgradient and downgradient, a 10 cm zone was included to facilitate distribution of influent flow over the reactor height and retain the reactive material, respectively. The reactor had a glass wall on one side, to allow observation of materials, and positions where precipitates deposited.

The geometric design of the reactor fulfilled the analytical criteria of Schwarz & Rittmann (2007a) for chemical-based bioprotection. In this case, the criteria were used to define the minimum thickness of reactive layers and maximum flow velocity.

The reactive material was a mixture of *Pinus radiata* bark compost, digested sludge from a local wastewater treatment plant, sand, and calcium sulfate to promote initial sulfate reduction. To inoculate the mixture, it was wetted with anaerobic digester content of the same wastewater treatment plant.

The reactor was fed with local spring water modified to obtain a pH of 2.5–3.5 and concentrations of 450 mg/L Fe (II), 100 mg/L Zn, 20 mg/L Mn, 5 mg/L Cu and 3,100 mg/L SO_4^{2-}. During 14 months, the flow was controlled at 1.5 ml/min. Concentrations of SO_4^{2-} (Method 4500E (APHA, 2005)), H_2S-HS^- (Method 4500-S2-D (APHA, 2005)), Zn^{2+} (Method 3500-Zn-B (APHA, 2005)), Fe (Method 3500-Fe (APHA, 2005)), Cu (Method 3500-Cu (APHA, 2005)), Ni (Method PAN (HACH)), pH, and Eh, were determined in the influent and effluent weekly. Influent pH was initially 3.5, but then changed to 2.5 to chemically stabilize the reactor feed, since at pH of 3.5, precipitates were observed in the feed tank, probably due to Fe oxidation and precipitation.

During the last 5 months, the effluent was also fed to a 10-L bucket (the "settler"), to test the effect of oxidizing conditions on treatment performance and effluent quality.

Finally, after 3 months, the possibility of rejuvenating spent organic layers was tested. A solution of 20 g/L of microcrystalline cellulose (MCC) (Sigmacell, 20 μm) was injected into reactive layers at 5–cm intervals (27 g of MCC in total).

Figure 1 Experimental system

RESULTS AND DISCUSSION

Although the reactor was operated under metal and acidity overload for the entire period of 14 months, it consistently reduced sulfate and metal concentrations, and added alkalinity. This is the first time a biochemical reactor has been operated passively, without an external source of alkalinity, such as calcite, at very low pH and high metal load.

This stable operation is indicative of a bioprotection mechanism based on chemical gradients protecting the microbial community within the reactive layers of low permeability (Schwarz & Rittmann, 2007a; 2007b; 2010). Additionally, the system did not show any permeability reduction. Metals precipitated along the interfaces between the conductive and reactive layers, where sulfide and metal gradients meet, consistent with the bioprotection mechanism based on chemical gradients.

Fig. 2 shows measured concentrations of chemical parameters at the inlet and outlet of the reactor for the 14-months operation period. For the last 5 months, values at the outflow of the settler are also shown. Influent concentrations were measured at the feeding well, located immediately

upgradient of the porous materials. Similarly, effluent concentrations were measured at the downgradient well. These wells were separated from the porous materials by a fine mesh. In the entry well, pH and metal concentrations already differed from nominal values in the feeding tank. This difference was significant during the first 3 months due to iron oxidation and precipitation in the feeding tank and well. Hence metal concentrations are shown from month 4 on. Chemical instability of Fe was finally avoided by reducing the pH in the feed to 2.5. Even then, feeding well values fluctuated around nominal values probably because feeding well composition is already affected by biochemical reactions in the reactor.

The sulfide peak occurred after the MCC injection. This peak was coincident with a decrease in effluent sulfate. Although, the stimulating effect lasted less than 2 months, higher MCC concentrations could be used to make it last longer.

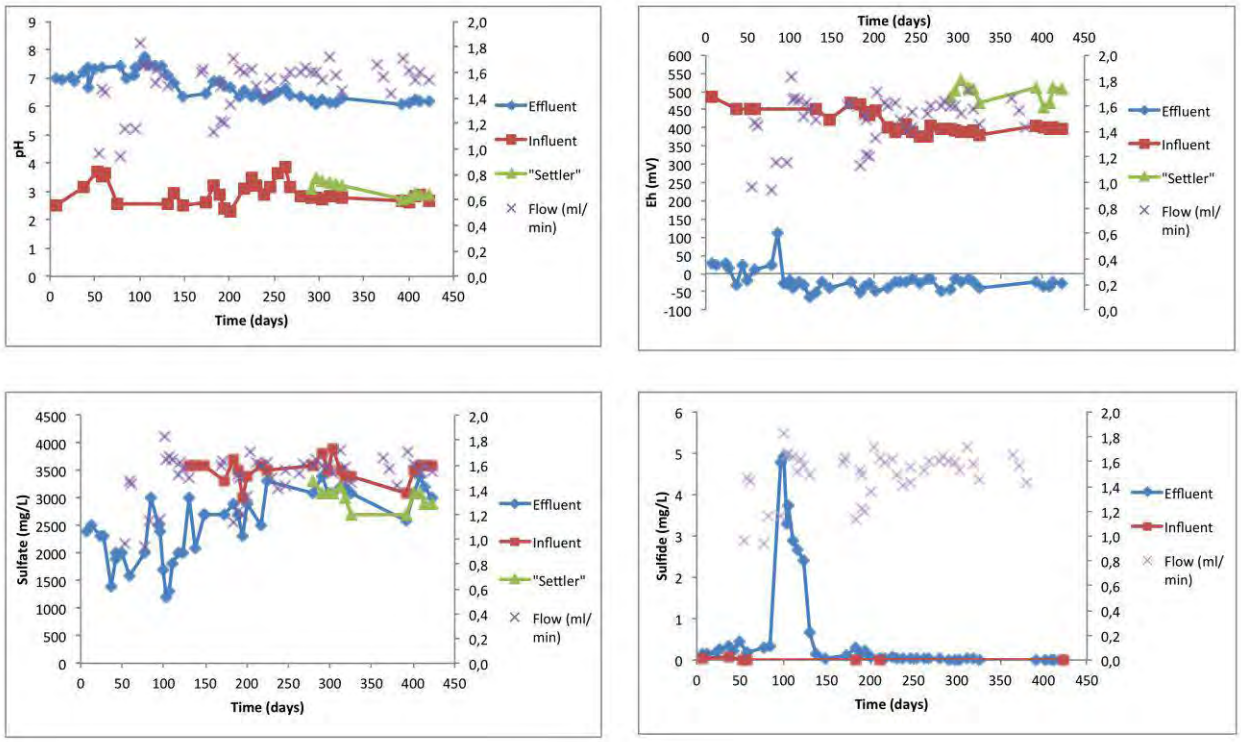

Figure 2 Measured values of pH, Eh, and concentrations of sulfate and sulfide

The effluent pH was near neutral all the time, and hence the reactor neutralized proton acidity, generating an adequate environment for the microbial community. On the other hand, the acidity coming from Fe (II) was only partially neutralized. Under oxidizing conditions in the settler, Fe (II) oxidation and Fe (III) precipitation occurred, and the pH dropped to influent values at which Fe (II) oxidation slowed down significantly. As the Fe graph shows (Fig. 3), the reactor itself removed little Fe, but a significant fraction was removed in the settler as hydroxides, thanks to the alkalinity added by the reactor, that also neutralized part of Fe acidity. Additionally, the reactor showed negative redox potentials, allowing successful establishment of sulfate reducing communities.

Zn removal (Fig. 3) occurred within the reactor, probably as sulfides, as evidenced by white precipitates along interfaces between reactive and conductive layers. Also, sulfide solubility

products are lower for zinc than for iron, hence sulfide generated in the reactive layers, reacted preferentially with zinc. Similarly, nickel was only removed in the reactor.

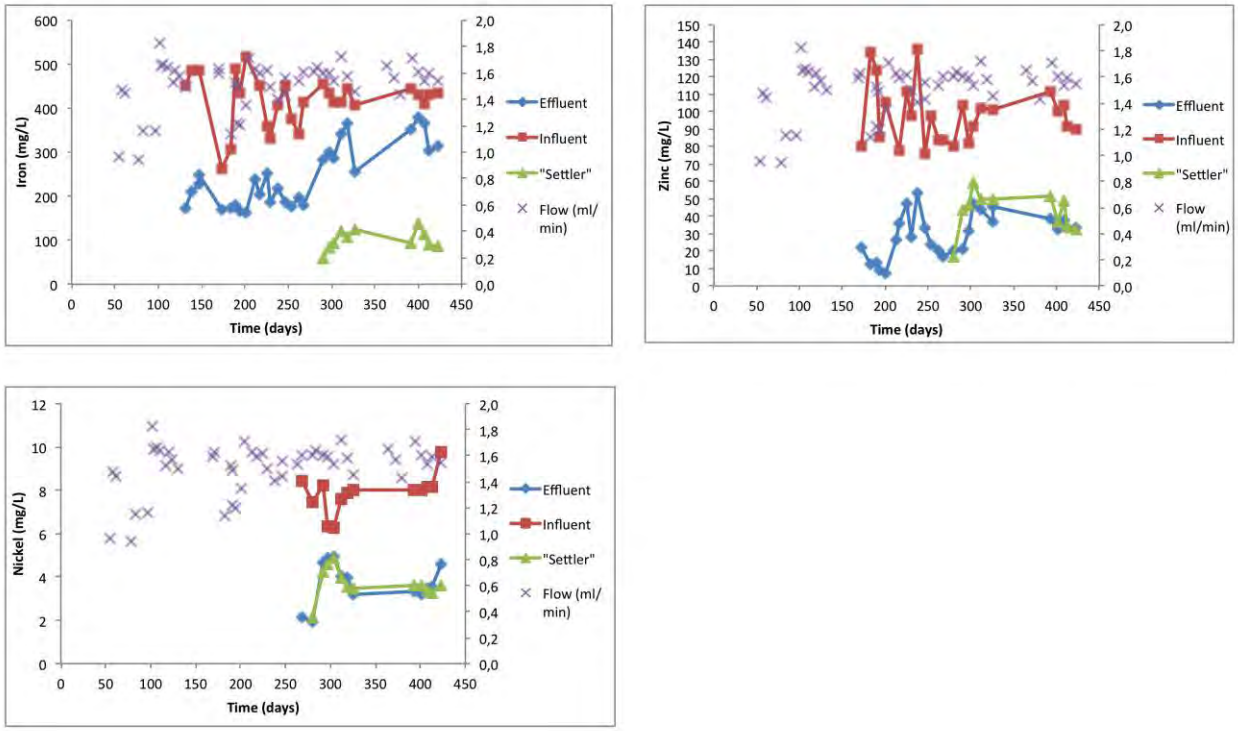

Figure 3 Measured concentrations of metals Fe, Zn, and Ni

Figure 4 shows white precipitates along the boundaries between layers, consistent with gradient-based resistance.

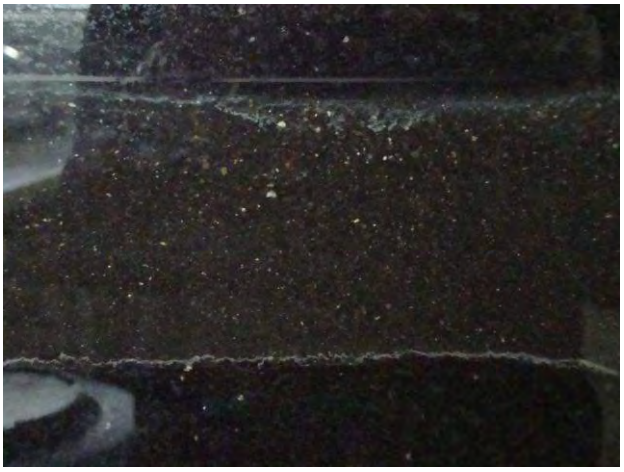

Figure 4 Location of precipitates along layer boundaries. The darker is the organic layer

CONCLUSIONS

DES reactors hold promise for passive treatment of highly acidic and toxic AMD, like the one generated by the copper mining industry in Chile. Within these reactors higher reaction rates are feasible, microbial consortia are protected from toxicity, and no permeability reduction due to precipitate formation is observed.

The key characteristic of DES systems is that reactive zones are separated from the zones of advective transport of contaminated water. An advantage of this zonation is that reactive and conductive zones can be optimized independently. The advection zone can be optimized to maintain an adequate hydraulic conductivity in the long term by using highly permeable materials. Similarly, higher sulfate–reducing rates in reactive zones of DES systems by using finely ground organic materials are possible.

ACKNOWLEDGEMENTS

Funding for this project was made possible through grant CONICYT/FONDAP/15130015.

REFERENCES

APHA (2005) *Standard methods for the examination of water and wastewater*, 20th edn, American Public Health Association, Washington, D.C.

Banco Mundial (2011) *Diagnóstico de la gestión de los recursos hídricos en Chile*, B. M., Santiago.

Blowes, D.W., Ptacek, C.J., Jambor, J.L. & Weisener, C.G. (2003) 'The geochemistry of acid mine drainage', in *Treatise on Geochemistry*, Elsevier, vol. 9, pp. 149–204.

Dold, B. (2010) 'Basic concepts in environmental geochemistry of sulfide mine-waste management', in *Waste Management*, INTECH, pp. 173–198.

Gadd, M. (2000) 'Bioremedial potential of microbial mechanisms of metal mobilization and immobilization', *Current Opinion in Biotechnology*, vol. 11, pp. 271–279.

Instituto de Ingenieros de Chile (2011) *Temas prioritarios para una política nacional de recursos hídricos,* I. I. CH., Santiago.

Kosolapov, D., Kuschk, P., Vainshtein, M., Vatsourina, A., Wiebner, A., Kastner, M. & Muller, R. (2004) 'Microbial processes of heavy metal removal from carbon-deficient effluents in constructed wetlands', *Eng. Life Sci.*, vol. 4, pp. 403–411.

McCauley, C.A., O'Sullivan, A.D., Milke, M.W., Weber, P.A. & Trumm, D.A. (2009) 'Sulfate and metal removal in bioreactors treating acid mine drainage dominated with iron and aluminum', *Water Research*, vol. 43, pp. 961–970.

Ministerio de Minería & Consejo Minero (2002) *Guía metodológica sobre el drenaje ácido en la industria minera*, M. M & C. M., Santiago.

Neculita, C., Zagury, G. & Bussiere, B. (2007) 'Passive treatment of acid mine drainage using sulfate-reducing bacteria: critical review and research needs', *Journal of Environmental Quality*, vol. 36, pp. 1–16.

Neculita, C.M. & Zagury, G.J. (2008) 'Biological treatment of highly contaminated acid mine drainage in batch reactors: long-term treatment and reactive mixture characterization', *Journal of Hazardous Materials*, vol. 157, pp. 358–366.

Nordstrom, D.K. (2011) 'Hydrogeochemical processes governing the origin, transport and fate of major and trace elements from mine wastes and mineralized rock to surface waters', *Applied Geochemistry*, vol. 26, pp. 1777–1791.

Rabus, R., Hansen, T. & Widdel, F. (2006) 'Dissimilatory sulfate– and sulfur–reducing prokaryotes', in *The Prokaryotes*, vol. 2., pp. 659 –768.

Schwarz, A.O. & Rittman, B.E. (2007a) 'Analytical–modeling analysis of how pore–water gradients of toxic metals confer community resistance', *Advances in Water Resources*, vol. 30, pp. 1562–1570.

Schwarz, A.O. & Rittmann, B.E. (2007b) 'Modeling bio–protection and the gradient–resistance mechanism', *Biodegradation*, vol. 18, pp. 693–701.

Schwarz, A.O. & Rittmann, B.E. (2010) 'The diffusion–active permeable reactive barrier', *Journal of Contaminant Hydrology*, vol. 112, pp. 155–162.

Sheoran, A.S., Sheoran, V. & Choudhary, R.P. (2010) 'Bioremediation of acid–rock drainage by sulfate–reducing prokaryotes: a review', *Minerals Engineering*, vol. 23, pp. 1073-1100.

Tsukamoto, T.K., Killion, H.A. & Miller, G.C. (2004) 'Column experiments for microbial treatment of acid mine drainage: low-temperature, low-pH and matrix investigations', *Water Research*, vol. 38, pp. 1405–1418.

Watzlaf, G.R., Schroeder, K.T., Kleinmann, R.L.P., Kairies, C.L. & Nairn, R.W. (2004) *The passive treatment of coal mine drainage*, DOE/NETL–2004–1202.

Waybrant, K., Blowes, D. & Ptacek, C. (1998) 'Selection of reactive mixtures for use in permeable reactive walls for treatment of mine drainage', *Environmental Science and Technology*, vol. 32, pp. 1972–1979.

Zagury, G., Kulnieks, V. & Neculita, C. (2006) 'Characterization and reactivity assessment of organic substrates for sulfate–reducing bacteria in acid mine drainage treatment', *Chemosphere*, vol. 64, pp. 944–954.

Mitigating Acid Rock Drainage with Land-Applied Biochemical Reactor Effluent

James Gusek
Sovereign Consulting Inc., USA

ABSTRACT

Perpetual treatment of acid rock drainage (ARD) is unsustainable; ARD suppression at its source is the logical strategy to avoid or lessen ARD impacts. Innovative mitigation concepts have been advanced in recent years; the concept of land-applying biochemical reactor (BCR) effluent to suppress ARD is another promising strategic tool. The concept's elegance lies with the merging of two well-developed mine remediation/processing technologies: BCRs and heap or dump leaching of metal ores. In the proposed innovative approach, organic-rich effluent from a BCR would be land-applied to acid-producing mine waste (e.g., tailings, waste rock, and coal refuse) with solution application methods typically used in heap leach pads. BCR effluent is typically anoxic and contains biochemical oxygen demand, excess alkalinity, dissolved sulfide ion, and dissolved manganese. The process would capitalize on these characteristics to coat mine waste with films of biosolids and/or manganese oxide that would suppress biological and abiotic pyrite oxidation. To the author's knowledge, this technology has not been implemented in a formal way but anecdotal information suggests that a properly-engineered application could yield significant long term environmental benefits.

Keywords: ARD, bactericide, sustainability, heap leaching

INTRODUCTION

A Medical Analogue

If one can embrace the medical analogue, much of the mining industry currently suffers from a massive bacterial infection. When pyrite-bearing or sulfide-bearing rock formations, tailings, or mine wastes are infected by *Acidithiobacillus ferrooxidans*, the likelihood of forming acid rock drainage (ARD) is almost guaranteed. The "pharmacy" of antibiotics available is extensive, ranging from solid alkaline amendments like limestone to liquid "medicines" such as sodium lauryl sulfate and sodium thiocyanate. Many of these materials may be in short supply (locally), or carry inconvenient side-effects. The danger of re-infection is a concern that also needs to be addressed. A "probiotic", naturally-sustainable regimen that introduces a microbial consortium that outcompetes the acidophiles may be the key to why some previous antibiotic applications continue to work for decades. See Gusek and Rastogi, 2015.

Unfortunately, the "geo-medical" teams of geochemists, microbiologists, engineers, and mine managers lack the tools to surgically apply these active ingredients where they are needed most with a minimum of waste. The implementation of up-to-date best management practices has not healed the patient; the equivalent of an intravenous drip of a very inexpensive generic medicine followed by a pro-biotic protocol is clearly needed.

An "Intravenous Drip" for ARD Suppression

The answer to this problem may lie with the merging of two well-developed mine remediation/ processing technologies: biochemical reactors (BCRs) and heap or dump leaching of metal ores. In the proposed innovative technology, organic-rich effluent from a BCR would be land-applied to acid-producing mine waste (e.g., tailings, waste rock, and coal refuse) using solution application methods typically used in precious metal heap leach pads.

BCR effluent is typically anoxic and contains biochemical oxygen demand, excess alkalinity, dissolved sulfide ion and manganese. If all these antibiotic and probiotic characteristics can be preserved and the BCR effluent solution can be dispersed over a large area of mine waste (which could be either revegetated or barren), the downward percolating solution should coat the mine waste with a film of probiotic bacteria-supporting biosolids that would suppress biological and abiotic pyrite oxidation. While to the author's knowledge this has never been implemented, it is believed that heap leach solution application techniques could accomplish this inexpensively. The mine waste ARD source would behave similar to a trickling filter in a waste water treatment plant. ARD might be suppressed for decades, perhaps longer, before a "booster shot" of BCR effluent might be required.

ARD REFRESHER

The formation of ARD is a natural process. In the presence of air, water, and acidophilic bacteria, sulfide minerals such as pyrite oxidize and produce sulfuric acid; concurrently, iron and other metals are released into the water. The problem can be associated with both coal and hard rock operations where previously buried sulfide minerals are exposed to oxygen and water. The descriptions of the bio-geochemical reactions responsible for ARD are found in many technical

papers and will not be repeated here. However, it may be reasonable to revisit the general conditions required for ARD to form.

ARD Tetrahedron

Considered simply, the elementary ingredients required for the formation of ARD are analogous to the components needed for the burning of combustible materials. To start a fire, one must have air, heat, and a fuel source. To generate ARD, one needs air, water, a pyrite source, and the bacteria to speed reactions that would otherwise occur slowly: consider an "ARD Tetrahedron" concept (see Figure 1), with each requirement positioned at a vertex. If any of the primary ingredients are missing, isolated, or chemically neutralized, fire/ARD will not form. Pyrite will oxidize in the absence of acidophilic bacteria; however, these bacteria are reported to accelerate the kinetics of pyrite oxidation by an order of magnitude (Baldi, et al. 1992).

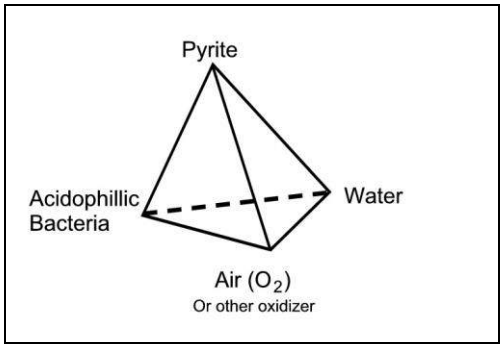

Figure 1 ARD Tetrahedron (Gusek, 1994)

Baseline Testing

The tendency of a given rock or material to produce ARD is predicted by a number of standard tests, including acid-base accounting, humidity cells, and column leach testing. Based on this author's experience, the microbial component of ARD production in these tests is rarely assessed. Even more rarely, probiotic measures such as the application of waste milk to create heterotrophic biofilms that outcompete acidophiles (Jin et al. 2008) have only recently been considered as viable technologies.

However, the concept of introducing competing bacteria is not new. Sobek, Benedetti, and Rastogi (1990) suggested that a probiotic process would complement the application of a slow-release acidophilic bactericide, sodium lauryl sulfate:

> "Inhibiting or destroying thiobacilli can significantly slow the rate of acid production. Anionic surfactants, organic acids and food preservatives (Onysko et al. 1984) act as bactericides and kill these bacteria; however; bactericides degrade over time and are lost because of leaching and runoff. To overcome the inherent short duration effectiveness of spray applications, controlled release systems to provide the bactericide slowly over a long time period were developed (Sobek et al. 1985).
>
> Control of acid generation for prolonged periods greatly enhances reclamation efforts and can reduce reclamation costs by reducing the amount of topsoil needed to establish vegetation. Three natural processes resulting from strong

vegetative cover for three years or more can break the acid production cycle. These processes are:

1) A healthy root system that competes for both oxygen and moisture with acid-producing bacteria;

2) Populations of beneficial heterotrophic soil bacteria and fungi that are re-established, resulting in the formation of organic acids that are inhibitory to *T. ferrooxidans* (Tuttle et al. 1977); and

3) The action of plant root respiration and heterotrophic bacteria increase CO_2 levels in the spoil, resulting in an unfavorable microenvironment for growth of *T. ferrooxidans.*"

Sobek, Benedetti, and Rastogi viewed antibacterial application as a method to reduce the volume of topsoil to revegetate potentially acid generating or PAG waste. They believed that at least three years of acidophilic bacterial suppression was sufficient to accomplish this goal.

The 21st century ARD-focused community of geochemists may be aware of how acidophilic bacteria promote ARD but they may not understand its kinetic importance. An informal survey suggests that inclusion of acidophilic inoculum, bactericides, and nutrients to support competing bacteria in humidity cell and column leach tests is rarely attempted because the effects of bactericides have always been considered temporary. As Sobek, Benedetti, and Rastogi (1990) suggest, that might be true but the limitation might be overcome by substitution of heterotrophic bacteria and fungi into the ARD generation zone coupled with a slow-release bactericide.

BIOCHEMICAL REACTOR TECHNOLOGY REFRESHER

Sulfate reduction in biochemical reactors (BCRs) has been shown to effectively treat ARD containing dissolved heavy metals, including aluminum, in a variety of situations. The chemical reactions are facilitated by the bacteria *Desulfovibrio* in BCRs as shown schematically in Figure 2 and the photo in Figure 3. However, a consortium of bacteria contribute to this effort as discussed in Seyler et al. (2003).

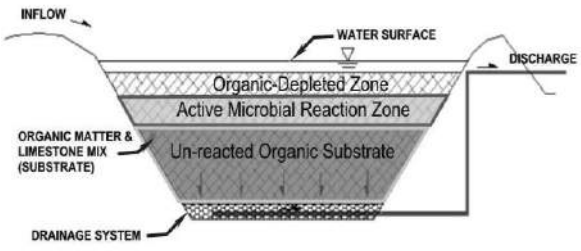

Figure 2 Down-flow Biochemical Reactor Schematic

Figure 3 A Typical Biochemical Reactor

The key conditions for sulfate reducing bacteria (SRB) health are a pH of 5.0 (maintained by the SRB itself through the bicarbonate reaction and/or the presence of limestone sand), the presence of a source of sulfate (typically from the ARD), and organic matter (from the substrate). BCRs have

been successful at substantially reducing metal concentrations, nitrate concentrations, and favorably adjusting pH of metal and coal mine drainages.

As discussed in Blumenstein & Gusek (2010), typical BCR effluent contains biochemical oxygen (BOD)/dissolved total organic carbon (TOC), and sulfide in varying concentrations. Ironically, when compared to the context of this paper, these are referred to as "nuisance" parameters that need to be addressed in order to allow the discharge of a BCR effluent to a natural receiving stream that might be impacted by BOD and the depressed dissolved oxygen characteristics of raw BCR effluent.

Fortunately, the BOC/TOC cited above are also probiotic nutrients that can support a microbial community that can occupy and quickly displace the niche occupied by the acidophiles.

It is noteworthy that BCRs do not remove manganese. Thus, any dissolved manganese present in the BCR present is available to create encapsulating and metal adsorption-capable films of MnO_2 ("desert varnish") under certain aerobic conditions.

HEAP LEACH TECHNOLOGY REFRESHER

Heap leaching technology was described by Agricola in the 16th century as a method for recovering alum for tanning of animal hides (Kappes, 2002). In America, a similar technology was used in Vermont in the early-1800's at the Elizabeth Mine for recovery of Copperas, or hydrated ferrous sulfate, that was used for curing and setting colors in hides and pelts, dye and ink manufacturing, and for treating timber (Hammarstrom et al. in Slack, 2001). Modern gold and silver heap leaching practices matured in the western USA in the early 1970s and are now used world-wide.

The recovery of metals from ore heaps or marginal mine waste dumps involves the application of a "barren" leach solution (typically sodium cyanide in the case of precious metals and sulfuric acid in the case of copper) to dissolve the metals to yield a pregnant or "preg" solution that is recovered by gravity and processed for the metal(s) of interest. After the metals are recovered from the preg solution, the resulting barren solution is recycled back to the heap to leach more metals. Several holding and process ponds are involved as shown in Figure 4.

Kappes (2002) provides an overview of the heap leaching process; design aspects related to the application of BCR effluent to mine wastes follow.

Solution distribution piping that is typically installed on top of the heap or dump is a leaching design feature of special interest with regard to ARD suppression. There are four mainstream methods for applying barren solution (Kappes, 2002):

- Drip emitters,
- Wobbler sprinklers,
- Reciprocating sprinklers, and
- High rate evaporative sprinklers.

To preserve the anoxic and geochemically reducing characteristics exhibited by BCR effluent, reciprocating and evaporative sprinklers would logically be avoided. The oxidation of BCR effluent as it traveled from the sprinkler head to the PAG rock surface or tailings surface would result in a deposit of biosolids and noxious odor.

Drip emitters or wobbler sprinklers would allow the well-buffered, soluble TOC containing solution to infiltrate into and percolate through the mine waste where ARD-suppressing biofilms should form along preferential pathways. This approach would be especially attractive in situations where the mine waste repository surface had already been revegetated. BCR effluent

would percolate through the plant growth medium and some buffering and organic matter addition would certainly bolster the productivity of the vegetative community.

A typical leach pad solution distribution system is comprised of a series of header pipes and sub-header pipes connected to a series of lateral pipes or hoses into which the drip emitters or wobbler sprinklers are installed. Whether or not the distribution piping is removed prior to a leach pad's or waste repository's receiving a fresh lift of ore-grade material will vary depending on site-specific economics. It may be more cost effective to abandon a piping network in place rather than expending the time and labor effort to dismantle, move, and reinstall it elsewhere on the site.

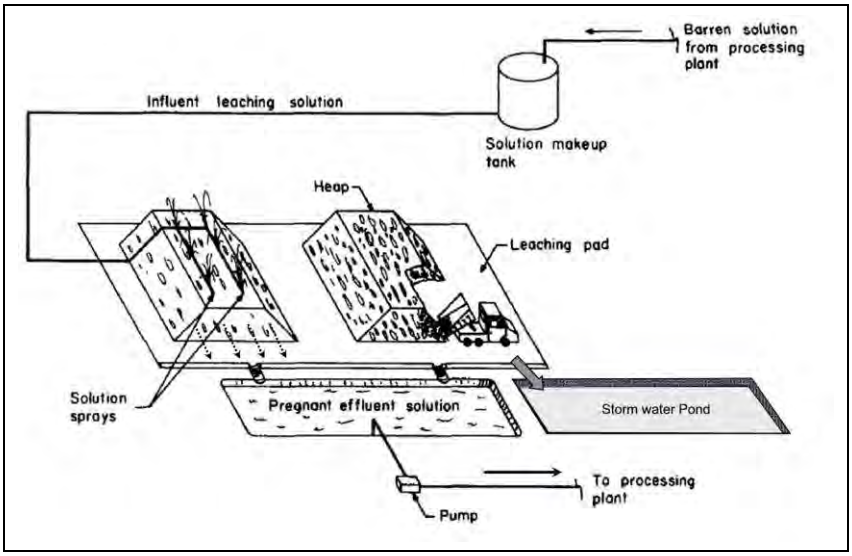

Figure 4 Heap Leach Pad Schematic (After Chamberlain & Pojar, 1984)

As subsequently discussed, it is unlikely that a BCR effluent solution distribution system would be abandoned in place due to the relatively temporary (compared to a "resource recovery" operation) deployment over an ARD-producing zone in the mine waste repository (which might include pit walls). Rather, the solution distribution system would be designed to be modular and easily transferred in a sequential fashion to where it would be needed next at the site.

If a heap leach pad contains PAG rock, it is probably only a matter of time before ARD becomes an issue. Cellan, et al. (1997) described the construction of a "Biopass" system at the closed Santa Fe gold mine in Mineral County, Nevada. The installation included retrofitting a geomembrane-lined solution pond into a BCR. The effluent from the BCR flowed by gravity through a buried pipeline to a leach field. The proposed ARD-suppressing process would differ from the Cellan et al. concept by recycling the effluent from the retrofitted pond(s) back to the source of the ARD. Of course, this will alter the water balance of the leach facility and a "circulating load" of mining influenced water would need to be managed. A new water balance estimate would be design necessity if BCR effluent is applied to the PAG waste in this fashion.

Faulkner (2015) described a "nuisance" condition where elevated BOD-containing BCR effluent from a newly commissioned unit was land-applied to a waste rock dump that exhibited elevated selenium concentrations. The selenium concentrations in the dump seepage co-incidentally decreased in response to the BCR effluent application. It is too early to say if the decreased selenium levels will persist after the land application activity was suspended.

VACCINATION VS MEDICATION?

Continuing with the medical analogy, vaccination to suppress ARD should ideally occur shortly after pyritic waste is either excavated or placed. Thus, vaccination would occur before the acidophilic bacterial community has a chance to mature. The medical sage advice of Benjamin Franklin, "an ounce of prevention is worth a pound of cure", is especially appropriate but it might be updated for a mine site application to read: "a tonne of ARD prevention is worth a hectare of passive treatment".

The advantages of pursuing this preventive protocol include:

- Closer control of ARD-suppressing solution application (focused only on PAG waste zones identified by geophysics, mining records, field testing, or other methods),
- Lower cost because the levels of stored acidity in the PAG waste (if it is fresh) should be low,
- Better management of ARD issues throughout the mine life instead of waiting until closure and attempting to gain control of a "Stage 4" geo-bacterial condition, and
- Lower costs of active treatment during operations.

The application of geo-medicines to suppress ARD on legacy sites that have been "cooking" for years offers a special challenge. This is the analogous "medication" scenario. As the surfactant-based bactericides such as sodium lauryl sulfate are organic compounds, they are susceptible to degradation when exposed to acidic conditions on the acidified mineral surfaces. In this author's opinion, any bactericide should be applied in a solution that is well-buffered and contains enough alkalinity to protect the bactericide's molecular integrity from the stored acidity in the mine waste. This suggests that medicating a "thoroughly-infected" mine waste material will be more expensive than the implementing vaccinating protocol described above for the same material.

The preference to engineer a "silver bullet" process to suppress ARD with bactericides and probiotic nutrients in a single "cocktail" application is a strong one. It will save costs and time. However, unpublished data suggests that some acidophilic bactericides are also toxic to probiotic bacterial communities. This finding suggests that a sequential application strategy may have a better chance of success in producing the desired outcome: decimation of the acidophilic community and its replacement with a self-sustaining heterotrophic community perpetually supported by organic acids from the healthy vegetation on the surface of the site.

Expected ARD Suppression Mechanisms

The percolating BCR effluent should contain at least five characteristics known to suppress ARD:

1. Dissolved organic carbon (measured as BOD or TOC),
2. Bicarbonate alkalinity,
3. Reducing oxidation reduction potential (ORP) of – 100 mv or less,
4. Low dissolved oxygen [DO] (<1 mg/L),
5. Dissolved sulfide ion, and
6. Dissolved manganese.

The alkalinity and low DO in the BCR effluent should decimate the acidophilic community. The sulfide ion and reducing ORP conditions should facilitate precipitating any dissolved ferrous iron

the solution encounters as a monosulfide (FeS). The BOD present in the solution should be oxidized and form a coating of biosolids on the mine waste particle surfaces. This biofilm layer should support a microbial community that outcompetes the acidophilic community and thereby suppress ARD formation. Based on the slow degradation of organic matter in municipal landfills, the beneficial effects of these combined mechanisms could persist for decades.

The benefits of manganese dioxide MnO_2 deposition would occur deeper in the rock/waste "column" under oxidizing conditions. The MnO_2 would tend to coat exposed rock surfaces along the preferential flow pathways. This reaction would only occur at circum-neutral pH such as that provided by well-buffered BCR effluent.

The proposed ARD suppression method is more appropriate to surface mining situations such as:

- Heap leach facilities,
- Tailing storage facilities,
- Waste rock repositories,
- Coal refuse disposal sites (fine and coarse refuse), and
- Pit walls.

Space limitations prohibit more detailed discussions on how BCR effluent application with heap leach pad drip emitters might be implemented in the above situations. However, it must be stressed that the long-term success of the proposed technology depends on the ultimate establishment of a robust vegetated cover to create a perpetual "probiotic" almost walkaway ARD remedy. Again, this "marriage" of BCR and heap leaching technologies is conceptual; to the author's knowledge, it has never been implemented.

MEDICATION CASE STUDIES

The application of BCR effluent to suppress ARD is a promising concept. Anecdotal information suggests that there may be sites in the USA where it is being evaluated. Consequently, only two case studies in the literature appear to be available to suggest that the concept could work with an appropriate level of design effort.

Antibiotic Case Study in Pennsylvania, USA

Plocus and Rastogi (1997) sequentially injected solutions of caustic soda (NaOH) and sodium lauryl sulfate at the Fisher Coal Mine in Pennsylvania USA in 1995. The PAG rock zone in a backfilled coal pit had been identified using geophysical techniques. The site was fully revegetated at the time of the two-step caustic/bactericide application through a network of shallow and deep injection boreholes that mimicked the pattern typically found in a heap leach pad. The effects of the injection process were dramatic. See Gusek and Plocus (2015). Chemistry of a toe seep at the site improved enough within 30 days that chemical treatment of the ARD was no longer required. In 2014, almost two decades later, this is still the case. The seepage chemistry is suitable enough to be polished in an aerobic passive treatment system. Bond release for the site is pending.

Probiotic Case Study in Tennessee, USA

An injection/treatment process similar to the one described by Plocus and Rastogi was implemented at the Sequatchie Valley coal mine in Tennessee. In this case, waste milk and a bacterial inoculum (biosolids) were injected into mine waste that had been reclaimed and revegetated. The project, completed by the Western Research Institute (Jin, et al., 2008 and ITRC, 2014) was undertaken to establish a bio-film of bacteria on the pyritic waste that would out-compete *Acidithiobacillus ferrooxidans* and thereby prevent ARD. While details are lacking, the technology was implemented in a 4 ha area exhibiting a seepage of about 0.12 m^3/min. (30 gpm).

Ground water upstream of the test plot exhibits typical ARD characteristics, depressed pH (5.5 to 6.0 standard units); the seepage downstream of the test plot exhibits a pH of 6.8 to 8 about four years after the initial injection event (ITRC, 2014). Plans are underway to evaluate this technology in a more con-trolled manner at the Sequatchie site.

It is interesting to note that this probiotic application did not include a specific bactericide as implemented by Plocus and Rastogi. This might be due to how the casein protein in milk behaves when it contacts an acidic environment: by curdling into a globular mass. One could theorize that this property imparts a "heat-seeking missile" effect to the patented process of using dairy products to suppress ARD. The milk proteins should selectively coat rock surfaces that are acidic. Regardless, conventional wisdom suggests that BCR effluent (with its high dissolved organic matter content) would be more similar to milk than to the two ARD-mitigating solutions that Plocus and Rastogi used sequentially at the Fisher site. Similar to milk's behavior, when BCR effluent encounters oxidizing conditions on a rock surface, a film of organic biosolids should be selectively deposited.

PRELIMINARY "MEDICATION" COST MODEL

Ultimately, the cost of implementing this ARD mitigation alternative would need to be compared to the costs of perpetual treatment. As a starting point, a drip irrigation cost estimating spreadsheet available from the University of Delaware Agricultural Extension (U. of D., 2014) was used to develop the cost of installing a drip irrigation system on a hypothetical 8.1 ha ARD "medication" situation site. The irrigation system was sized with a drip row spacing of about 1 meter to apply about 152.4 cm of BCR solution for over the span of a year.

This would amount to about 33.8 m^3 per day or 12344 m^3 per annum. The capital cost of the installation was about US$14500. The annual operating cost was estimated to be about US$19000, most of which was labor. Factoring in the useful life of the various capital components yielded an annual fixed cost of US$7200 to yield a total annual cost of about US$26000.

Gusek and Schneider (2010) cited a projected BCR unit treatment cost of US$0.31 per m^3 of effluent spread over the assumed 20-year BCR lifespan. This would amount to about US$4000 per year. Combining the drip sprinkler and BCR cost yielded an annual cost of about US$30000 per year or about US$3700 per ha or US$1500 per acre. Of course, the actual volume of BCR effluent required, its application rate, and duration may need to be adjusted for site-specific conditions which would be based on small scale field tests.

CONCLUSIONS

The re-purposing of BCR effluent to suppress ARD formation is a scientifically sound concept. It has never been implemented but if it works as expected, ubiquitous ARD suppressing materials such as wood chips, spoiled hay, straw, and animal manure could be locally procured to reduce costs and provide sustainable supplies that would be naturally grown, not manufactured. Carbon sequestration may be a small side benefit of the process. The upside potential of this innovative merging of two common mining technologies could provide a paradigm shift in mine remediation strategy that has incalculable benefits to society world-wide. This emerging technology could be another step on the "pathway to walkaway" with regard to mine closure.

REFERENCES

Baldi, F., Clark, T., Pollack, S.S. and Olson, G.J. (1992) Leaching of pyrites of various reactivities by Thiobacillus ferrooxidans. Appl. Envir. Microbiol. 58: 1853-1856.

Blumenstein, E. P. and Gusek, J.J. (2010) Nuisance Parameters in Passive Water Treatment Systems - A Specific Case Study. 2010 Annual Meeting of the American Society for Mining and Reclamation (ASMR), June. Pittsburgh, PA.

Cellan, R., Cox, A., Uhle, R., Jenevein, D., Miller, S., and Mudder, T. (1997) The Biopass System Phase II: Full Scale Design and Construction of an In Situ Anaerobic Biochemical System, presented at the Ann. Mtg. of the Am. Society of Surface Mining & Reclamation (ASSMR), Austin, TX. May 10-15, 1997.

Chamberlain, P. G. and Pojar, M. G. (1984) *Gold and Silver Leaching Practices in the United States*. US Bureau of Mines Information Circular (IC) 8968, U.S. Government Printing Office, Washington, D.C.

Faulkner, B. (2015) Pers. Comm.

Gusek, J.J., (1994) "Avoiding and Remediating Acid Rock Drainage" presented at Latin American Mining Opportunities, Randol at Vancouver '94, Oct. 30-Nov. 2, 1994.

Gusek, J.J. and Schneider, R. (2010) Passive Management of Mining Influenced Water at the Haile Gold Mine, SC. 2010 Annual Meeting of ASMR, June. Pittsburgh, PA.

Gusek, J.J and Plocus, V. (2015) Case study: 19 years of acid rock drainage mitigation after a bactericide application; paper accepted for oral presentation at the 10th International Conference on Acid Rock Drainage and IMWA Annual Conference, April 21~24, 2015 Santiago, Chile.

Hammarstrom, J. M., Seal II, R.R., Slack, J. F., Kierstead, M.A., and Hathaway, E. M. (2001) "Field Trip Days 1 and 2, Road Log for the Elizabeth and Ely Mines and Vicinity" (in) *Guidebook Series Volume 35, Part II. Environmental Geochemistry of Mining History of Massive Sulfide Deposits in the Vermont Copper Belt*. J.F. Slack, ed. Society of Economic Geologists and USGS, October, 2001.

Interstate Technology Regulatory Council (ITRC) website (2014) Sequatchie Valley Coal Mine project accessed June 10, 2014 (http://www.itrcweb.org/miningwaste-guidance/cs31_sequatchie.htm)

Jin, S., Fallgren, P. H., Morris, J. M., and Cooper, J. S. (2008) Source Treatment of Acid Mine Drainage at a Backfilled Coal Mine Using Remote Sensing and Biogeochemistry. Water Air Soil Poll. 188:205–212.

Kappes, D. (2002) Precious Metal Heap Leach Design and Practice. Mineral Processing Plant Design, Practice, and Control, Volume 1, Published 2002 by SME. Downloaded from www.kcareno.com May, 15 2014.

Plocus, V. G. and Rastogi, V. (1997) Geophysical Mapping and Subsurface Injection for Treatment of Post-Reclamation Acid Drainage. Paper presented at the 1997 National Meeting of ASSMR Austin, Texas, May 10-15, 1997. pp 34-42.

Seyler, J., Figueroa, L., Ahmann, D., Wildeman T.R., and Robustelli, M. (2003) "Effect Of Solid Phase Organic Substrate Characteristics on Sulfate Reducer Activity and Metal Removal in Passive Mine Drainage Treatment Systems" in Proceedings of National Meeting of the ASMR, Billings MT, June 3-6, 2003. Published by ASMR, 3134 Montavesta Rd., Lexington, KY 40502.

Sobek, A. A., Benedetti, D.A., and Rastogi, V. (1990) Successful Reclamation Using Controlled Release Bactericides: Two Case Studies. Paper presented at the 1990 Mining and Reclamation Conference and Exhibition, Charleston, West Virginia, April 23-26, 1990.

Tuttle, J.H., Dugan, P.R and Apel, W.A. (1977) Leakage of cellular material from Thiobacillus ferrooxidans in the presence of organic acids. Applied and Environmental Microbiology 33:459-469.

University of Delaware Agricultural Extension Website (2014) http://extension.udel.edu/ accessed June 10, 2014.

The Utilization of Cellulosic Biomass in treating AMD and the Subsequent Generation of Fermentable Sugars

Edzai Magowo, Karl Rumbold and Craig Sheridan
Industrial and Mining Water Research Unit, University of the Witwatersrand, South Africa

ABSTRACT

The drainage from closed and abandoned mines is often acidic with elevated heavy metal concentrations. The interaction between acid mine drainage (AMD) and the environment has a significant impact. Whilst temporary remediation can lessen this impact, complete amelioration is only possible using active and/or passive treatment. Active technologies are often costly and can produce a secondary waste stream which may require additional treatment. In this project we explored a passive option combining different technologies. We recognise AMD as a resource of sulphuric acid which we used as a pre-treatment on cellulosic feedstock. Following this, we enzymatically digested the partially hydrolysed cellulose to produce fermentable sugars (which could be used to produce bioethanol). Concurrently, the pH of the AMD increased from 2.11 to 5.46 and 62% of the iron was removed from solution. Previous research has shown that sulfate is also remediated (primarily through dissimilatory sulfate reduction [DSR]). In this research we were successfully able to combine two separate, yet established technologies and were able to remediate AMD with a cellulosic feedstock through DSR and Fe precipitation, whilst being able to use the cellulose residue as a feedstock for bioethanol production.

Keywords: Cellulose, AMD, Fermentation Feedstock

INTRODUCTION

Acid mine drainage (AMD) refers to the outflow of acidic water from (usually abandoned) metal and coal mines. It is characterized by low pH and high concentrations of sulfate and heavy metals (Acid mine Drainage (AMD) South Africa, 2011). It is considered the most important mining industry related pollution problem (Rob and Robson, 1995; Johnson and Hallberg, 2005; Kuyacak *et al*, 2011). AMD occurs when sulfide ores are exposed to the atmosphere, which can be magnified through mining and milling activities, where oxidation reactions are initiated (Jennings *et al*., 2008; Zipper *et al*., 2011; McCathy, 2011; Johnson and Hallberg, 2005). Upon exposure to oxygen and water, pyritic minerals oxidise to form acidic, iron and sulfate rich drainage. The oxidation of the pyritic minerals is the primary mechanism by which acid is released into AMD (Ackil and Kodas, 2006, Neculita *et al*., 2007, Sangita *et al*., 2010). The reactions involved in the formation of AMD are a multistep process involving oxygen-independent and oxygen dependant reactions. A general equation for the process is (Equation 1):

$$FeS_2(s) + 14Fe^{3+}(aq) + 8H_2O = 15Fe^{2+}(aq) + 2SO_4^{2-} + 16H^+(aq) \quad (1)$$

The net effect of these reactions is to release H^+, which lowers pH and maintains the solubility of ferric ions (Blodau 2006).

AMD treatment can be achieved through active, semi-passive or passive methods (Greben *et al*., 2009). A broad range of passive and active treatment approaches are available for dealing with AMD. Neutralisation (pH control) is the AMD treatment mechanism for both passive and active systems. By increasing pH to create alkaline conditions, the solubility of most metals is significantly decreased by precipitation (Taylor *et al*., 2005).

In previous work, biomass has been successfully used to treat AMD. The results indicated that grasses hold promise for remediating AMD, as a maximum of 99% iron removal, 80% sulfate removal, and a final pH of 8.5 was achieved from initial conditions of 2000mg/l iron, 6000mg/l sulfate, and a pH of 3. (Sheridan *et al*., 2013).

In this study, it is hypothesised that the lignin fraction of grasses and other cellulosic feedstocks contain numerous reactive groups which bind to and remove metals from AMD. Simultaneously the sulfuric acid in the AMD hydrolyses hemicellulose and exposes the cellular structure of cellulose whereby it can be subjected to a subsequent enzymatic hydrolysis step. In this study, we assess the potential use of the acidity present in AMD to (at least) partially hydrolyse cellulose. This would result in partially remediated AMD as well as a fermentable feedstock which could be utilised to produce, for example, bioethanol.

Materials

Two different cellulosic feedstocks were tested in this study: sugarcane bagasse and switch grass. Sugarcane bagasse was originally obtained from Illovo Sugar Company based in Kwazulu Natal. The switch grass, *Panicum virgitum* (an indigenous perennial grass) was obtained milled from the laboratory of the School of Chemical and Metallurgical Engineering. The second batch of switch grass was collected from the African Leadership Academy garden. It was obtained already dry. The

enzyme (cellulase) was supplied by Yakult Pharmaceutical Ind. Co., Ltd from Tokyo, Japan. The enzyme was obtained in powdered form. The product name of the enzyme is Cellulase "Onozuka" FA. The enzyme was composed of cellulase 12% and lactose 88%.

METHODOLOGY

The AMD feed was exposed to different cellulosic feedstocks for a period of 14 weeks. The resulting materialwas subsequently enzymatically digested with cellulase. The pH of the AMD exposed to the biomass was measured using a bench top pH meter. The iron concentration was analysed using the Merck test kit number 114761 and the Merck spectroquant Pharo 300 according to the manufacture's manual. Reducing sugars were measured using a 1200 series Agilent HPLC. Scanning electron microscopy was done using an FEI Quanta 400 E-SEM.

RESULTS

Dissolved iron and pH changes

Figure 1 and Figure 2 show the increase in pH and the decrease in the dissolved iron concentration during treatment of AMD using different lignocellulosic biomass over the 14 week experimental period.

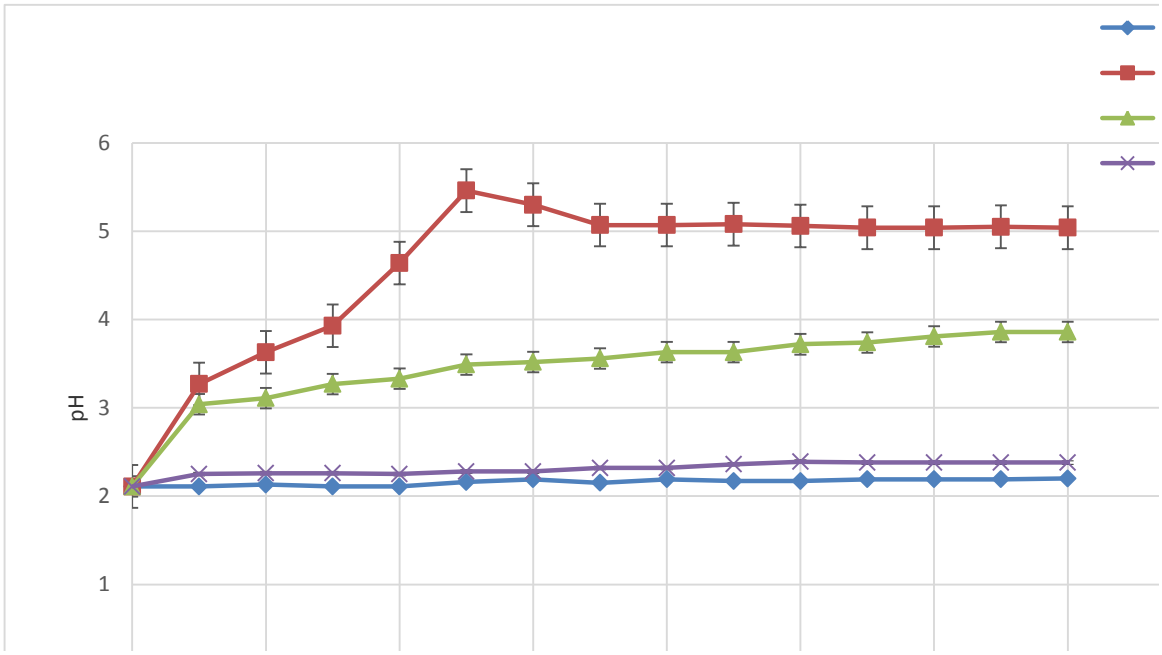

Figure 1 Changes in pH as effected through different types of lignocellulosic biomass

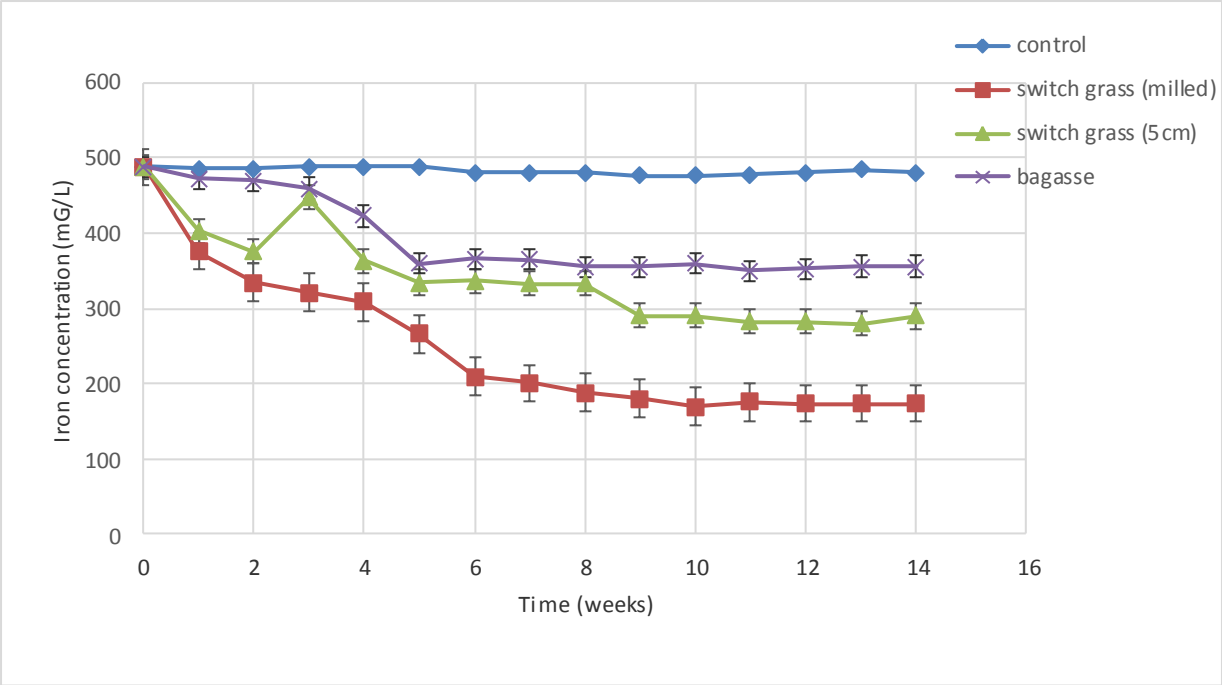

Figure 2 Changes in Iron concentration as effected by different types of lignocellulosic biomass

The data presented in Figures 1 and 2 indicate that the three sources of cellulosic biomass were able to effect some remediation of AMD. In all three cases dissolved iron concentration was reduced and pH was increased. The milled switch grass (≤2mm) was the most effective in the remediation of AMD. The milled switch grass was able to remove 65.2% of dissolved iron and increase the pH from 2.11 to 5.30. The maximum pH was obtained in a relatively shorter period of time (5 weeks). The switch grass (5cm) was able to remove 42% of dissolved iron and increased the pH from 2.11 to 3.86. Sugarcane bagasse had the least remedial effect on AMD. Sugarcane bagasse removed 28% of iron from AMD and increased the pH from 2.11 to 2.36; this was achieved in 14 weeks. The pH and the iron concentration of the control which contained only AMD did not change much during the experimental period, indicating that the biomass (switch grass and bagasse) caused the increase in alkalinity and the decrease in dissolved iron concentration. Similar results were obtained by Ramla (2012). In Ramla's investigation, two indigenous grass species, *Hyparrheia hirta* and *Setaria spacenta*. Maximum pH values of 8.48 and 99% percentage removal of iron from the AMD solution was reported in that study.

These values are comparable with the ones reported in literature for the biosorption and precipitation of metals on switch grass and other biomasses. According to literature the main mechanisms of metal ion removal in bioreactors are precipitation in the form of sulfides, hydroxides and carbonates and sorption mechanisms such as adsorption (Neculita *et al.*, 2007). The greatest effect on remediating the AMD was observed for the milled switchgrass. The decrease in dissolved iron in solution can be explained by the presence of a large number of active sites on the milled switch grass due to the increased surface area caused by milling. Functional groups capable

of metal sorption in biomass include phenolic, hydroxyl and carboxylic groups. Milling exposes these functional groups to the dissolved ions. These functional groups in the biomass are protonated at higher pH and presumably available for binding dissolved metals (Neculita *et al*., 2007). This explains the fact that the increase in pH is accompanied by a marked decrease in dissolved iron concentration (Figure 5.1).Increases in pH of acidic water effectively removes some metals due to the precipitation of metals in the form of hydroxides (Goatham, 2013).

Microbial activity also plays a role in the remediation of the AMD. Microbial activity was observed in the two switch grass series with the milled switch grass seeming to support more growth. IT is most probable that this microbial population is comprised of sulfate reducing bacteria (SRB). As explained by Ramla (2012), the increase in pH can be directly related to SRB population growth. The substrate may have been providing nutrients to sulfate reducing bacteria which contributed to the growth of the microbial population. The SRB activity reduces sulfate to sulfide and produces hydrogen carbonate (Equation 2). The hydrogen carbonate partially neutralises the AMD, while the hydrogen sulfide reacts with dissolved metals in the AMD, resulting in the precipitation of metals as metal sulfides (Equation 3) (Taylor *et al*, 2005).

$SO_4^{2-} + 2CH_2O + 2H^+ \rightarrow H_2S + 2H_2CO_3$ (Equation 2)

$H_2S + M^{2+} \rightarrow MS + 2H^+$ (Equation 3)

Where CH_2O are the sugars and M^{2+} represents metal ion.

The release of glucose during the treatment of AMD using milled switch grass (≤2mm)

The release of glucose was observed only in the milled switch grass, suggesting that milling was a significant factor in the generation of glucose. Milling reduces cellulose crystallinity and disrupts the lignin-carbohydrate complexes. This aids the acid treatment process and the subsequent enzyme hydrolysis (Mais *et al*., 2002: Carmen *et al*., 2013). The change in concentration of glucose is shown in Figure 3. Glucose started to appear in the third week of treatment where a rapid increase was observed. The maximum amount of glucose obtained was 8.4mg/ml in the seventh week. Thereafter the concentration decreased to 4.9mg/ml after 14 weeks. The decrease in glucose concentration may be explained by the consumption of glucose by sulfate reducing bacteria (SRB). The generation of glucose and other reducing sugars during AMD treatment is attributed to acid catalysis, where the sulfuric acid in the AMD catalyses the breakdown of cellulose and hemicellulose to release glucose, xylose and other degradation products. Hemicellulose, comprised mainly of mannan and xylan, accounts for up to a third of the total carbohydrate in many lignocellulosic materials (Pingali *et al*., 2010). In a study by Roman (2004), much higher levels of reducing sugars (306g/l) were produced. In that study, production was also followed by consumption. The consumption was accompanied by an increase in pH from 5.8 to 7. The increase in pH was found to be related to sulfate reduction and the production of alkalinity within the bioreactor.

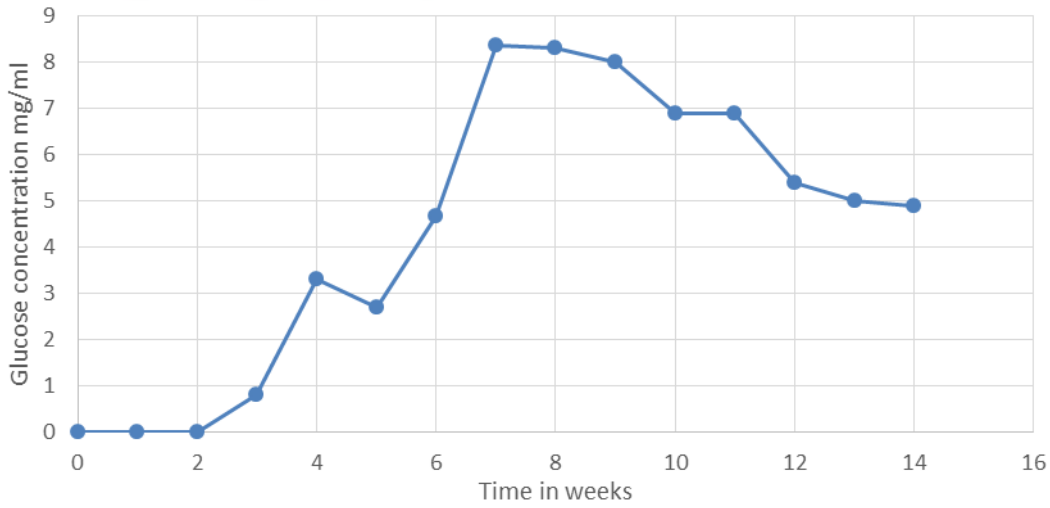

Figure 3 The release of glucose during treatment of AMD using milled switch grass

Scanning Electron Microscope (SEM) analysis of switch grass treated by water and AMD before and after enzymatic hydrolysis.

SEM was used to study the morphological features and surface characteristics of the switch grass treated by water and AMD before and after enzyme hydrolysis (Figure 4).

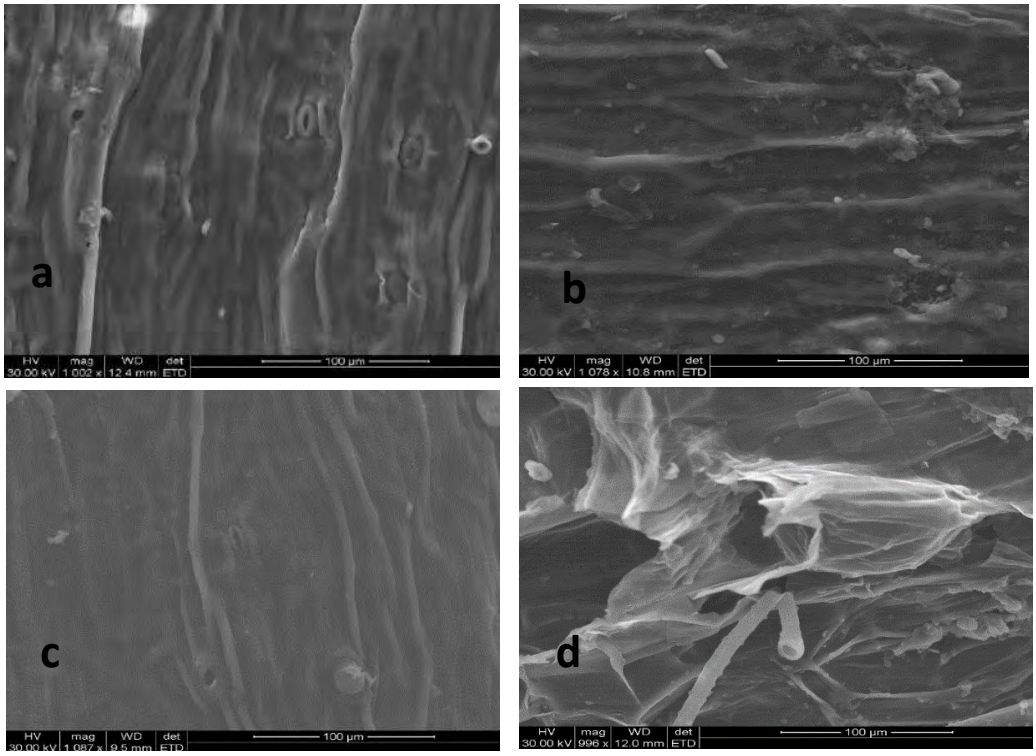

Figure 4 Scanning electron microscope images of switch grass (a) water treated, (b) AMD treated, (c) water treated followed by enzyme treatment and (d) AMD treated followed by enzyme treatment.

The SEM images reveal that pre-treatment induced significant morphological changes in the switch grass. Water treated switch grass exhibited rigid and highly ordered fibrils (Figure 4a). The fibres of the AMD treated switch grass appear to be distorted with some holes evident on the surface (Figure 4b). This renders the switch grass more accessible to cellulase, resulting in higher enzymatic hydrolysis rates and cellulose digestibility (Moxley *et al.*, 2008: Remli *et al*., 2013). The molecular structure of the water pre-treated and enzyme treated switch grass remained intact, showing no digestion occurred during the hydrolysis of the water treated switch grass (Figure 4c). The molecular structure of the switch grass which was pre-treated by AMD followed by enzyme digestion was completely destroyed (Figure 4d). The improved/altered morphological properties caused by AMD pre-treatment of switch grass appeared to be the primary source for the enhancement of enzymatic hydrolysis (Goshadrou *et al*., 2011). These micrographs are in agreement with the HPLC results shown in Table 1, which show high digestibility of AMD treated switch grass and no or very little digestibility in the water treated switch grass.

Enzymatic hydrolysis of AMD treated and untreated switch grass

Table 1 shows the concentrations of xylose and glucose after the enzymatic hydrolysis of the water treated and AMD treated switch grass as analysed using HPLC.

Table 1 Enzymatic hydrolysis of water treated and AMD treated switch grass.

	Water treated		AMD treated	
Enzyme %	Xylose mg/ml	Glucose mg/ml	Xylose mg/ml	Glucose mg/ml
0	0	0	0	0
0,5	0	0	1,9	0
2,5	0	0	3,3	3,8
5	0	0	0	4,8
10	1,4	0	3,4	3,7

The water treated sample was our control for this experiment. It is noted from Table 1 that the glucose yield for the water treated switch grass was zero for all the enzyme concentrations. The xylose yield was zero except for the 10% enzyme concentration which had xylose concentration of 1.4 mg/ml. The SEM images (Figure 4) showed that the water treated switch grass displayed no obvious signs of mechanical disruption of the general surface morphology. This rigid and compact structure of untreated lignocellulosic biomass hinders the effectivity of cellulase and prevents it from digesting the grass. The enzymatic digestion of the AMD treated switch grass show the concentrations of glucose and xylose in mg/ml. The maximum sugar concentration achieved with the milled switch grass were 4.8 mg/ml glucose at 5% enzyme concentration and 3,4 mg/ml xylose at 10% enzyme concentration. The enzyme concentration had a significant effect on the amounts of glucose and xylose obtained: there is a general increase of the glucose and xylose concentration with the increase in enzyme concentration. Small quantities of enzymes were ineffective in digesting the treated switch grass. The AMD treatment of the switch grass was therefore able to significantly improve the accessibility of the cell walls to enzymatic digestion, leading to greater sugar yields compared with the water treated switch grass.

DISCUSSION AND CONCLUSION

Switch grass has been shown in this study to have the capacity to effectively remove iron and acidity from AMD. The results indicate that milled switch grass (2mm) was more effective in remediating AMD than sugar cane bagasse or the large particle size switch grass (<5cm). The potential of switch grass, sugarcane bagasse and other lignocellulosic material to remove metals by adsorption is expected since such materials contain functional groups such as phenolic, hydroxyl, carboxyl and carboxylic (Harman *et al*., 2007). This theory is supported by Minawar and Riwandi (2010) who attributed the decrease in dissolved iron in the first two weeks of AMD treatment to iron retention by the organic matter rather than iron precipitation. In our study the milled switch grass which had a higher surface area was able to retain more iron resulting in lower dissolved iron concentration. Zagury *et al*., 2006 (cited in Munawar and Riwandi, 2010) explained that metal

removal tends to occur sooner than to sulfate reduction, through adsorption of metals to organic matter. Once reducing conditions are established metal precipitation rather than adsorption becomes the predominant mechanism of removal. Munawar and Riwandi (2010) reported the decrease of sulfate concentration in the third week of their study, using chicken manure mixed with AMD. This was attributed to sulfate reduction to metal sulfides such as iron sulfide. In our study microbial activity seemed to dominate in the third week of AMD treatment supporting Munawar and Riwandis' findings that sulfate reduction occurs at a later stage of AMD treatment. SRB activity produces hydrogen carbonate which increases the alkalinity of the AMD.

The milled switch grass was able to increase the pH of the AMD from 2.11 to 5.30 and to remove dissolved iron from the AMD by 65.2% by the fifth week. Both the pH and the dissolved iron content started to stabilise thereafter. To further increase the alkalinity and to reduce the dissolved iron concentration, periodic substrate loading may be considered in future for the long term remediation of AMD (Ramla 2012).

Santos *et al*., (2004) worked with different biomass concentrations and showed that an increase of the biomass (grape stalks) concentration up to 30g/L leads to a 20% reduction of the total content of dissolved iron in the AMD. In a similar study Greben *et al*., (2008) used cut grass serving as a carbon and energy source for continuous sulfate removal and obtained between 80 and 90% removal efficiency by adding cut grass loadings every two weeks. The increase in grass loadings provides new surface area for adsorption of metal ions, further reducing their concentration.

In our study the residue switch grass obtained from the AMD treatment process was prepared for a further enzymatic hydrolysis step. The preparation included washing to remove metal ions adsorbed to the surface. SEM was used to study the effects of the AMD on the switch grass. The results showed that AMD induced morphological changes in the switch grass (Figure 4). These changes are due to the hydrolysis of hemicellulose and to a lesser extent cellulose by the sulfuric acid in the AMD. The hemicellulose fraction is converted to its monomeric sugars which include pentose and glucose. This treatment is analogous to the pre-treatment of lignocellulosic biomass using acid. In literature dilute acid pre-treatments of lignocellulosic material are done at higher temperatures and pressure and are able to recover relatively higher amounts of fermentable sugars from the hemicellulose fraction of lignocellulose. Barrier et al., (1985) reported the conversion and recovery of sugars from the hemicellulose fraction treated with dilute acid to be more than 90% efficient. Dilute sulphuric acid in the range 0.5-1.5% and temperatures above 160 has been found the most favoured for industrial applications. Under these conditions high sugar yields from hemicellulose are obtained (Hisham and Mageed, 2008). In our study the conditions are mild (room temperature and pressure) and hence we expected reduced rates.

Glucose was detected during the treatment of AMD in the course of this study (Figure 3). A maximum glucose concentration of 8.4 g/ml was obtained in the seventh week of the study. After AMD treatment it is necessary to recover some of the sugars from the AMD/sugar liquor. The sugars in solution in the AMD are highly contaminated with metal ions and would need purification if they are to be recovered and to be used for further bioprocessing. It is difficult to recover the hemicellulose fraction of sugars from the AMD/sugar solution. The AMD/sugar liquor can be fermented to produce ethanol which can be recovered by distillation, or alternatively the AMD/sugar liquor could be used as a carbon and energy source for SRB in subsequent treatments. The remaining cellulose residue, instead of being discarded, could be further processed by

additional enzymatic hydrolysis as the cellulose residue contains the bulk of the glucose. Cellulase enzymes were used in our study to recover some of the sugars in the lignocellulose, with maximum values of glucose and xylose at 4.8 mg/ml and 3.4 mg/ml respectively. The xylose produced in the processing may also be fermented or used to produce other value added products. One possible use of the unconverted xylose is to produce fodder yeast (single cell protein) for animal feed (Barrier *et al*., 1985). This study has evaluated the potential of AMD treated switch grass in the production of fermentable sugars. From this study it can be concluded that:

a) Lignocellulosic material has the capacity to treat AMD,
b) The AMD treated switch grass has the potential to produce fermentable quantities of glucose upon enzymatic hydrolysis,
c) AMD is not only remediated but assists in a bioprocess to prepare second generation feedstock for industrial biotechnology.

The research is, however, at a very early stage of development. Substantial additional work is required to optimise the production of fermentable sugars as well as understanding the rates of AMD treatment. There is also still much work needed into developing a process which could be used commercially. This is the subject of ongoing research.

REFERENCES

ACID MINE DRAINAGE (AMD), SOUTH AFRICA, 2011.

ACKIL, A. AND KOLDAS, S. 2006, Acid Mine Drainage (AMD): causes, treatment and case studies. Journal of Cleaner Production, 14(12-13), pp1139-1145. BARRIER, J.W., MOORE, M.R., FARINA G.E., BRODER, J.D., FORSYTHE, M.L., 1985. Experimental production of ethanol from cellulosic material at low temperature acid hydrolysis. Biomass congresses, 1985. pp 587-600.

BLODAU, C., 2006. A review of acidity generation and consumption in acid coal mine lakes and their watershed. Science of the Total Environment, 369(1-3), 307-332.

CANAM, T., TOWN, J., IROBA, K., TABIL, L., DUMONCEAUX, T., 2013. Pretreatment of lignocellulosic biomass using microorganisms: Approaches, Advantages, and Limitations. http://dx.doi.org.10.5772/55088. Pp 181-189

GOATHAM, V., 2013. Treatment methods of acid mine drainage and a case study on selective recovery of metals. 13MI60R09. Mining engineering 2013. pp1-31.

GOSHADROU, A., KARIMI, K., TAHERDAZEH, M.S., 2011. Improvement of sweet sorghum bagasse hydrolysis by alkali and acidic pretreatments. World renewable energy congress, 2011. Linkoping, Sweden.

GREBEN, H.A., BALOYI, J., SIGAM VENTER, N.S., 2008. Bioremediation of sulphate rich effluents using grass cuttings and rumen fluid microorganisms. Journal of Geochemical exploration.doi:10.1016/j.gexpo.2008.01.004.

GREBEN, H., SIGAMA, J., BURKE, L AND VENTER, SN, 2009. Cellulose fermentation products as an energy source for biological sulphate reduction of acid mine drainage type waste water. Report to the Water Research Commission. Pp5-7.

HARMAN, G., PATRICK, R., SPITTLER, T., 2007. Removal of heavy metals from polluted waters using lignocellulosic agriculture waste products. Industrial Biotechnol. Winter, pp366-374.

HISHAM, F.M, MEGEED, M.E., 2008. Lignocellulosic biomass conversion technologies to biofuels, potentials in Egypt. A report submitted to UNIDO-Cairo-Egypt IMC. Pp6-20

JENNINGS, S.R., NEUMAN, D.R. AND BLICKER, P.S., 2008. "Acid Mine Drainage and Effects on fish health and ecology: A Review". Reclamation Research Group Publication, Bozeman, MT. pp1-29

JOHNSON, D.B AND HALLBERG, K.B., 2005. Acid mine drainage remediation options: review. Science of the Total Environment. 338, pp3-14.

KUYACAK, N., 2011. Mine water treatment: Application and Policy. Pp360-390.

MAISE, U., ESTEGHHLALIAN A., SADDLER, J., MANSFIELD, S., 2002. Enhancing enzymatic hydrolysis of cellulosic material using simultaneous ball milling. Applied Biochemistry and Biotechnology. 98 pp815-839.

MCCARTHY, T.S., 2011. The impact of acid mine drainage in South Africa. South African Journal of Science. 107(5/6) pp7, 712.

MOXLEY, A., ZHU, Z., ZHANG P.Y-H., 2008. Efficient sugar release by by the cellulose solvent based lignocellulose fractionation technology and enzymatic cellulase hydrolysis. J. Agric. Foodchem. 56 pp7885-7890.

MUNAWAR, A AND RIWANDI, 2010. Chemical characteristics of organic wastes and their potential use for acid mine drainage. Journal Nature Indonesia. 12(2) pp167-172.

NECULITA, M.C., ZAGURY, G.J., BUSSIRE, B., 2007. Effectiveness of sulfate reducing passive bioreactors for treating highly contaminated acid mine drainage: 11. Metal removal mechanisms and potential mobility. Applied Geochemistry. 23, pp3545-3560.

RAMLA, B., 2012. Potential utilisation of indigenous grass for acid mine drainage remediation. Master's thesis, University of the Witwatersrand. pp1-22.

REMLI, N.A.R., SHA, M.D., ABD-AZIA S., 2013.Effects of chemical and thermal pretreatments on enzymatic saccharification of rice straw for sugar production. Bioresources. 9(1) pp510-522.

ROB, G.A AND ROBSON, J.D.F., 1995. Acid drainage from mines. Geographical Journal, 107(5/6), pp38-39.

ROMAN, 2004. The degradation of lignocellulose in a biologically-generated sulphidic environment. Pp1-133.

SAHARAN, M.R., GUPTA, K.K., JAMAL, A., SHEORAN, A.S., 1995. Management of acidic effluents from tailings dams in metalliferous mines. Mine Water and the Environment. 14(annual issue, paper 7), pp85-94.

SANGITA, G., PRASAD, U., PRASAD, B., 2010. Studies on the environmental impact of acid mine drainage generation and its treatment: an appraisal. Indian J. Environmental Protection. 30(11) pp953-967.

SANTOS S., MACHADO, R., CORREIRA, N.J.M., CARVALHO, J.R., 2004. Treatment of Acid Mine Waters. 17 pp225-232.

SHERIDAN, C., HARDING, K., KOLLER. E. AND DE PRETO, 2013. A. A comparison of charcoal and slag based constructed wetlands for acid mine remediation. Water SA. 39(3) pp369-372.

TAYLOR, G., 2005. Biofuels and the biorefinery concept. Energy policy. 36(12) pp4406-4409.

ZAGURY, G.J., NECULTA, C., BUSSIERE, B, 2006. Passive treatment of acid mine drainage in bioreactors: short review, application, and research needs. Ottawa Geo2007, 14439-14446.

ZHANG, Y.P., DING, S.U., MIELENZ, J.R., CUI, J-B., ELANDER, T.R., LASER, M., HIMMEL, M.E., MCMILLAN J.R., LYND L.R., 2007. Fractionating recalcitrant lignocellulose at modest conditios. Biotechnology and Bioengineering, 97 pp214-222.

ZIPPER, C., SKOUSEN, J., JAGE. C., 2011. Passive treatment of Acid Mine Drainage. Virginia Cooperative Extension. Publication 460-133. Pp1-14.

Biomass Retention and Recycling to Enhance Sulfate Reduction Kinetics

Robert van Hille, Tynan Marais and Susan Harrison
Centre for Bioprocess Engineering Research, University of Cape Town, South Africa

ABSTRACT

Biological sulfate reduction represents a more sustainable option for the removal of sulfate from acid rock drainage, particularly if the resulting sulfide is used for metal precipitation or is partially oxidized to sulfur. Sulfate reducing bacteria are relatively slow growing and attach poorly to most solid substrates, so washout is a concern at low hydraulic residence times. This paper describes two strategies to achieve high cell concentrations in sulfate reducing reactors and reports on the resulting improvements in sulfate reduction efficiency.

A linear flow channel reactor was fitted with carbon microfibers, which provided a large surface area for attachment, without significantly reducing effective reactor volume. The surface properties of the carbon fibers enhance biomass attachment and colonization of the fibers occurred within two weeks. The hydrodynamic regime within the reactor ensured even substrate distribution without physical agitation. The second reactor system involved coupling a cross-flow microfiltration unit, fitted with a ceramic membrane, to a conventional continuous stirred tank reactor. The retentate, containing the biomass, was recycled back to the CSTR.

The reactors were fed a synthetic solution containing 1 g/L sulfate, with lactate as the carbon source and electron donor, at a COD to sulfate ratio of 0.7. The hydraulic residence time was reduced from 4 days to 0.5 days, with steady state data collected at each residence time. Maximum volumetric sulfate reduction rates of 47.5 and 65 mg/L.h were achieved in the channel reactor and membrane coupled reactor system respectively. These represent improvements of 20% and 50% over a conventional CSTR, where washout of part of the community occurred at HRTs below 1 day.

Keywords: Sulfate reduction, biomass retention, membrane separation, biomass attachment

INTRODUCTION

The contamination of surface and groundwater by acid mine drainage (AMD) and acid rock drainage (ARD) and the consequences for the environment, agriculture and human health are serious concerns in the regions of South Africa impacted by mining activities. Acid drainage is generated via the oxidation of sulfide minerals, typically pyrite, when exposed to oxygen and water. The process is usually catalyzed by iron and sulfur oxidizing microorganisms. In South Africa, mine water can be divided into two broad categories. The first, AMD, originates from the rebound of groundwater through abandoned mine workings, once dewatering has ceased and is characterized by large volumes of heavily impacted water. The volume and composition of the AMD precludes the application of biological treatment options in most cases. The second type, referred to as acid rock drainage (ARD) in this paper, originates from diffuse sources, such as waste rock dumps, tailings impoundments, coal discard heaps and unworked pits. These sites are more numerous, are likely to affect a greater area and can persist for decades. Acid rock drainage, from diffuse sources as well as end-of-pipe sources, is more amenable to biological treatment.

A variety of technologies have been developed for the treatment of AMD and ARD. The established methods are based on oxidation, neutralization, precipitation and sedimentation. The oxidation converts iron and aluminum to their less soluble oxidized form, which makes subsequent precipitation more efficient. The most appropriate treatment is dependent upon the volume of the effluent, concentration type of contaminants and the pH of the water (Gazea et al., 1996). Acid drainage treatment technologies can be divided into two broad categories, active and passive treatment systems.

Active treatment typically involves the installation of agitated reactors or similar units, which require constant energy input. Furthermore, the addition of alkaline chemicals and reagents to treat the acidic effluent can become costly, given that the drainage may persist for several decades, or longer, at decommissioned mine sites (Gazea *et al*., 1996). Many of the active treatment technologies depend on the addition of lime or limestone, which are non-renewable resources. Lime addition to sulfate rich effluents typically results in substantial gypsum precipitation, which needs to be managed. The long-term sustainability of many active treatment technologies is therefore questionable, both from an economic and environmental perspective. There is a diverse range of active treatment technologies, such as chemical precipitation, ion-exchange, membrane technology and biological sulfate reduction.

Passive systems depend on processes that are kinetically slower than those involved in active systems and thus require longer hydraulic retention times (HRTs) and larger areas to achieve similar results (Hedin *et al*., 1994). Passive treatment options include anoxic limestone drains, permeable reactive barriers, natural and constructed wetlands and engineered biological treatment systems.

Biological treatment has the potential to be more cost effective and sustainable than the physical and chemical processes mentioned above. The biological treatment of ARD is centered on the activity of sulfate-reducing bacteria (SRB), which are able to reduce sulfate to sulfide, coupled to the oxidation of an electron donor, typically an organic carbon molecule. Sulfate reduction may be assimilatory, where the sulfide is incorporated in sulfur-containing amino acids, or dissimilatory, where the sulfide is released to the external medium. The latter process forms the basis of ARD remediation processes. A generalized reaction for dissimilatory sulfate reduction is shown below (Zagury et al., 2007; Oyekola et al., 2009).

$$2CH_2O + SO_4^{2-} \rightarrow 2HCO_3^- + H_2S \quad (1)$$

The sulfate is reduced to sulfide, coupled to the simultaneous generation of alkalinity, predominantly as bicarbonate (HCO_3^-). From an ARD treatment perspective the alkalinity acts to neutralize the acidity while the sulfide is available for the precipitation of metals as metal sulfides (Johnson and Hallberg, 2005).

A number of commercial processes, based on biological sulfate reduction, have been developed, but their widespread application has been constrained by three factors. These are the cost of the electron donor, the relatively slow growth of sulfate reducers and the associated kinetic constraints and the management of the sulfide product. The research presented in this paper addresses the second constraint by investigating novel reactor configurations aimed at biomass retention and recycling. The first and third constraints have been addresses by previous and ongoing research within CeBER (van Hille and Mooruth, 2013; Harrison et al., 2014) and by others (Janssen et al., 1995; Molwantwa and Rose, 2013).

METHODOLOGY

Sulfate reducing bacteria (SRB) culture

The SRB mixed microbial community was obtained from the Department of Microbiology, Biochemistry and Biotechnology at Rhodes University, originally from the anaerobic compartment of a facultative pond at the Grahamstown sewage treatment works, and has been maintained at UCT since 1999. The stock culture has been maintained on modified Postgate B medium consisting of: 0.5 g/L KH_2PO_4, 1 g/L NH_4Cl, 2 g/L $MgSO_4.7H_2O$, 1 g/L Na_2SO_4, 1 g/L yeast extract, 6 mL/L 60% sodium lactate solution (Sigma), 0.3 g/L sodium citrate. The same solution was used to feed all experimental reactors. Unless otherwise stated, all regents were analytical grade, sourced from Merck.

Reactor units

Continuously stirred biological sulfate reduction reactor

Continuous experiments were performed in glass reactors with a working volume of 1 L. The reactor height was 200 mm, with a liquid volume height of 118 mm, and diameter 104 mm.

Agitation was provided by an overhead stirrer powering a four-bladed marine impeller (58 mm diameter) at 300 rpm. The reactor was fitted with four vertical baffles (10 mm width) to prevent vortex formation. Temperature was controlled at 30°C by pumping heated water through the external jacket or placing the reactors in a temperature-controlled water bath. Feed solution was continuously pumped into the reactor using a variable speed peristaltic pump.

Sulfate reduction reactor with microfiltration unit

The reactor configuration for the cross-flow microfiltration consisted of the standard 1 L glass reactor coupled to a microfiltration unit. The contents of the reactor were pumped through the membrane unit (ceramic membrane with a 0.2 μm pore size) at a rate of 1.7 L/min, meaning the entire volume passed through the membrane every 35 seconds. As a result, the reactor could be considered well mixed and additional agitation by the impeller was not required. This was confirmed through mixing studies.

Linear flow channel reactor (LFCR) with carbon microfibers

The channel reactor provided a flow-through reactor with medium stratification in place of homogeneity. It was constructed from Perspex (11 mm thickness). The front wall of the reactor was fitted with three sets of sample ports, located 60 mm, 120 mm and 180 mm from the inlet. At each distance, there were three ports, 25 mm, 55 mm and 90 mm from the base of the reactor. Each port was fitted with a GC septum and samples were withdrawn with a hypodermic needle. The reactor was fitted with three feed ports (25 mm, 60 mm and 95 mm from the base) in the left wall and three effluent ports (15 mm, 50 mm and 85 mm from the base) in the right wall. When the top outlet port was utilized the liquid height in the reactor was 85 mm, giving a working volume of 2.125 L. The reactor was fitted with a lid and an airtight silicon seal. A port fitted 10 mm below the lid in the left and right hand walls allowed the headspace to be flushed. A strip (38 mm wide) of carbon microfibers (AMT Composites, Cape Town) was attached to the bottom of the lid so that the fibers were submerged in the liquid. The strip had a bundle of microfibers (180 mm long) attached at 7 mm intervals on each side. The reactor was operated continuously by pumping feed in from the uppermost feed port and collecting effluent from the uppermost effluent port.

Analytical methods

All pH testing was done on a Cyberscan 2500 micro pH meter. The meter was calibrated daily using standard (pH of 4.0 and 7.0) buffer solutions. Aqueous sulfide was quantified using the colorimetric DMPD method (APHA, 2005). Aqueous sulfate concentrations were measured by HPLC using a Waters Breeze 2.0 system equipped with a Waters IC-Pak A HR (Anion High Resolution) column and a conductivity detector. The system was run isocratically using a sodium borate-gluconate mobile phase at a flow rate of 1 mL/min. Sample injection volumes of 100 μL were used. To quantify the ion concentrations standard solutions (20, 40, 60, 80 and 100 mg/L) were prepared using sodium sulfate (Na_2SO_4) salt. A full volatile fatty acids (VFAs) analysis was conducted to quantify the concentration of lactic, acetic, propionic, iso-butyric, butyric, iso-valeric and valeric acids. The concentration of each VFA was determined using HPLC on a Waters Breeze

2 HPLC system equipped with a Bio-Rad Organics Acids ROA column and a UV (210 nm wavelength) detector. The system was run isocratically using a mobile phase of 0.01 mol/L H_2SO_4 at a flow rate of 0.6 mL/min. Sample injection volumes of 100 μL were used. To quantify the VFA concentrations, standard solutions (100, 200, 300, 400 and 500 mg/L for each acid) were prepared.

Experimental programme

Baseline

Baseline data were generated in a standard CSTR operated at 30°C, using the modified Postgate B medium as the feed source. The reactor was started at a HRT of four days and sampled at least once per HRT. Once steady state had been established and monitored for at least three HRTs, the feed rate was increased, reducing the HRT to three days. The process was repeated a number of times, collecting data at each HRT (**Table 1**).

The reactors were sampled by removing 10 mL of solution and immediately using 20 μL to perform a sulfide assay. The pH and redox potential were measured using the remaining sample. A subsample (2 mL) was transferred to a 2 mL Eppendorf tube, to which 40 μL of zinc chloride solution was added. The tubes were mixed on a vortex mixer, then centrifuged at 14000 × *g* for seven minutes. The supernatant was used to prepare samples for analysis of anions and VFAs by HPLC.

Table 1 Summary of operating conditions for baseline CSTR, membrane unit and channel reactor. HRTs refers to the total number of hydraulic residence times under each set of conditions

	Baseline CSTR and membrane reactor			Channel reactor		
Desired HRT (days)	Mean flow rate (mL/min)	Mean HRT (days)	HRTs	Mean flow rate (mL/min)	Mean HRT (days)	HRTs
4	0.170	4.10	11.96	0.361	4.09	2.47
3	0.219	3.17	7.61	0.465	3.18	5.64
2.5				0.594	2.49	4.37
2	0.339	2.05	19.24	0.713	2.07	5.29
1.5	0.466	1.49	9.49	0.950	1.55	6.79
1	0.661	1.05	17.69	1.412	1.05	7.68
0.75	0.900	0.77	10.29	1.869	0.79	13.33
0.5	1.347	0.52	7.90	2.535	0.58	18.07
1.3				1.135	1.30	4.03

Membrane unit

The purpose of coupling the microfiltration unit to the continuous reactor was to separate biomass from suspension and recycle it back to the reactor, while discharging a cell-free permeate. This was chosen to build up a very high cell density. It was hypothesized that the high cell density would

support efficient sulfate reduction at HRTs below one day, owing to the de-coupling of the mean cell retention time (MCRT) and HRT.

The reactor coupled to the membrane filtration unit was set up and operated similarly to the reactor used to collect the baseline data. The feed rates, overall hydraulic retention times and number of hydraulic retention times under each set of conditions was identical to the control reactor (**Table 1**). Once steady state had been achieved at a four day HRT the pump was turned on and reactor contents were pumped through the membrane. Permeate was pumped from the membrane unit at the same rate as feed was pumped into the reactor to maintain a fixed operating volume across the system. Under normal operating conditions no effluent was collected from the overflow port of the reactor. However, if the membrane became fouled, reducing the transmembrane flux, or the permeate pipe became blocked, the volume in the reactor would accumulate and discharge through the overflow port. When this occurred, the membrane needed to be de-fouled.

The reactor was sampled as described for the control reactor, while permeate was sampled by collecting the outflow for 5-10 minutes. Reactor and permeate samples were analyzed for pH, redox potential, anions and VFAs.

Linear flow channel reactor

The channel reactor was initially operated at a 5.5 day HRT (0.27 mL/min) to allow for colonization of the microfibers. This was achieved successfully over a period of 20 days. From day 20, the feed rate was increased to achieve a HRT of 4 days. Samples (2 mL) were removed daily from the middle (FM) and lower (FB) sample ports in the first and third (BM and BB) rows. The pH and sulfide concentration were measured immediately, after which the remainder of the sample was treated with 40 µL of zinc chloride (100 g/L) and centrifuged at 14000 × g for seven minutes to remove sulfide as zinc sulfide. The supernatant was filtered through a 0.22 µm nylon membrane filter and retained for HPLC analysis (VFAs and anions). Effluent from the reactor was collected in a sealed bottle over varying time intervals and the volume quantified to confirm the HRT. A portion of the collected effluent was treated for HPLC analysis, while the rest was used to measure pH and redox potential. The operating conditions of the channel reactor are summarized in **Table 1**.

RESULTS AND DISCUSSION

The data presented in this section represent a summary of steady state data at the different retention times across the three reactors. Steady state was assumed when the change in key parameters, particularly residual sulfate concentration, was less than 10% for three successive HRTs following a change in system conditions.

Baseline date

The steady state profiles for sulfate consumption and measured sulfide are shown in Figure 1. The theoretical sulfide concentration, based on the molar concentration of sulfate reduced, is also

shown. The sulfate reduction is relatively consistent across the range of HRTs from four days down to one day, with between 870 and 920 mg/L of the 1000 mg/L feed being consumed. Based on molar stoichiometry, the theoretical sulfide concentration was just below 300 mg/L. However, the actual measured sulfide concentration was significantly lower, suggesting either a loss of sulfide to the surroundings or further reaction of the sulfide.

The reactor unit was sealed and any offgas passed through a sodium hydroxide sulfide scrubber, where gaseous hydrogen sulfide (H_2S) would be converted to aqueous bisulfide (HS^-). Analysis of the bisulfide concentration indicated no significant loss of H_2S from the reactor. This is consistent with the steady state pH (7.4 ± 0.15). Under these conditions the majority of the aqueous sulfide would exist as the HS^-. The result suggests partial oxidation or precipitation of a portion of the sulfide, although no metal sulfide precipitate could be observed. An experiment to quantify the abiotic sulfide oxidation under similar solution chemistry conditions (data not shown) indicated that only a small portion of the missing sulfide could be accounted for by abiotic oxidation. Visual observation of the reactor showed an elemental sulfur deposit at the air/water interface. This deposition was clearly visible when the reactors were taken down, suggesting biologically mediated partial oxidation to sulfur.

There was a significant decrease in the amount of sulfate reduced at a HRT of 12 hours (dilution rate of 0.083/h), with the conversion efficiency falling to around 50%. Despite the reduction in the sulfate conversion, the conversion of lactate remained at 99%. Based on the amount of sulfate reduced, the expected residual lactate concentration at this HRT should have been over 1000 mg/L. However, a residual concentration of below 30 mg/L was detected. This indicates that the sulfate conversion was not limited by lactate concentration.

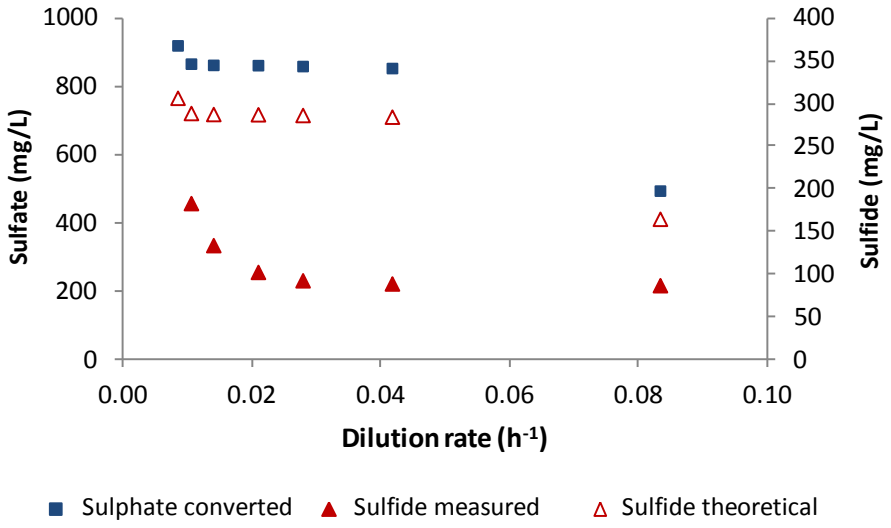

Figure 1 Sulfate conversion and measured and theoretical sulfide concentrations as a function of dilution rate. HRT plotted as dilution rate (1/HRT)

This observation also suggests that while sulfate reducers oxidized lactate at a rate near their μ_{max} another group of microorganisms characterized by higher μ_{max} and K_s values for lactate utilization were able to proliferate due to increased lactate loading at the high volumetric loading rate. Consequently, there was no accumulation of lactate. The decline in sulfate conversion was most likely a consequence of wash out of a portion of the sulfate reducing community when the reactor was operated at a dilution rate greater than their μ_{max}. These data are similar to those obtained by Moosa et al. (2002, 2005), Oyekola et al. (2009; 2010; 2012) and Baksaran and Nemati (2006). The study showed that the decrease in sulfate reduction efficiency coincided with a decrease in acetate formation and increase in propionate formation (Oyekola et al., 2009). Propionate production is an indication of lactate fermentation (Heimann et al., 2005). In addition Oyekola et al. (2012) performed a qualitative assessment of microbial community structure, which confirmed that the diversity of sulfate reducers decreased with increasing dilution rate.

Membrane unit

The redox potential in the reactor decreased from an initial value of around -350 mV to a steady state between -390 and -400 mV during the first 30 days of operation, as the sulfate reduction efficiency increased prior to attaining steady state at a four day HRT (day 30). During the same time the pH increased from around pH 7 to pH 7.4-7.5.

The redox potential of the permeate was typically similar to that of the bulk reactor fluid, except during periods where permeate flow decreased due to fouling or blockage of the tube draining the membrane unit. Under these circumstances oxidation of the permeate was near complete, resulting in a less negative redox potential. The pH of the permeate from the microfiltration membrane was consistently higher than the pH measured in the reactor, typically by 0.5 pH units.

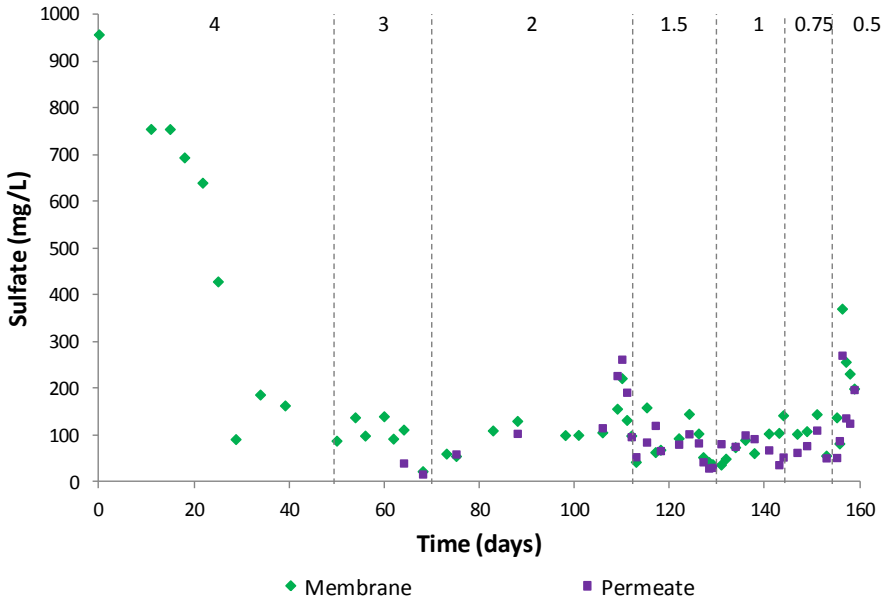

Figure 2 Residual sulfate data from the continuous reactor with microfiltration unit. Changes in HRT are shown by the dashed lines with the nominal mean HRT indicated. 'Membrane' refers to the sample from the bulk reactor fluid

The residual sulfate data (Figure 2) gave an indication of the efficiency of the system across the range of HRTs. The system took around 30 days to reach steady state at the initial four day HRT. The residual sulfate at steady state was approximately 140 mg/L, representing a removal efficiency of over 85%. This was consistent with the baseline data under similar operating conditions. The residual sulfate was relatively unchanged down to a HRT of 0.75 days and increased slightly at 0.5 days. The sulfate concentration measured in the permeate was similar or slightly lower in most cases, indicating that while partial oxidation of sulfide to sulfur occurred in the drainage tube, complete oxidation to sulfate did not.

The low residual sulfate, even at a HRT of 0.5 days, was indicative of very efficient performance. The recycling of the majority of the biomass, particularly under conditions where slower growing species would be washed out, resulted in a very high biomass concentration that could sustain efficient sulfate reduction at a high volumetric loading rate. The average VSRR measured across the 0.5 day HRT was 64.18 mg/L.h, over 50% higher than that achieved during the baseline study.

The sulfide concentration in the bulk fluid was similar to that in the baseline CSTR, while the permeate was consistently lower, fluctuating around 100 mg/L when the system was operating efficiently. The lower sulfide concentration, coupled with the increased pH suggested the partial oxidation of some of the sulfide to elemental sulfur. The silicone tubing used to drain the permeate is permeable to oxygen. Under oxygen limiting conditions the partial oxidation of sulfide is favored, according to the reaction below (Kuhn *et al*, 1983)

$$2HS^- + O_2 \rightarrow \tfrac{1}{4}S_8 + 2OH^- \quad (2)$$

The generation of hydroxide ions accounts for the increase in pH. As the pH increased, a portion of the remaining sulfide could be converted to polysulfides. The permeate was typically pale yellow color, consistent with the presence of some polysulfide. Sulfur production in the outlet pipes resulted in relatively frequent blockages, resulting in effluent draining from the reactor overflow port, rather than exiting as permeate. The problem was more pronounced at the shorter HRTs. At the 1.5 day HRT 76% of the total effluent was made up of permeate and 24% as overflow from the reactor. The proportion exiting as permeate fell to 67%, 69% and 44% at the 1 day, 0.75 day and 0.5 day HRTs respectively.

The sample from the reactor clearly contained suspended biomass, which became more apparent as the experiment progressed. The appearance of attached biofilm on the reactor walls and the presence of elemental sulfur in the bulk fluid prevented accurate quantification by either dry mass or optical density. The permeate sample was consistently cell free, indicating that the cells were recycled back to the reactor with the retentate. The absence of cells in the permeate was confirmed by light microscopy.

Linear flow channel reactor

The system experienced some perturbations during the initial operation and steady state, with respect to sulfate reduction, was achieved day 40 and on day 45 the HRT was reduced to 4 days. The sulfide data (Figure 3) show that a relatively high sulfide concentration was maintained in the reactor, even at a 0.5 day HRT.

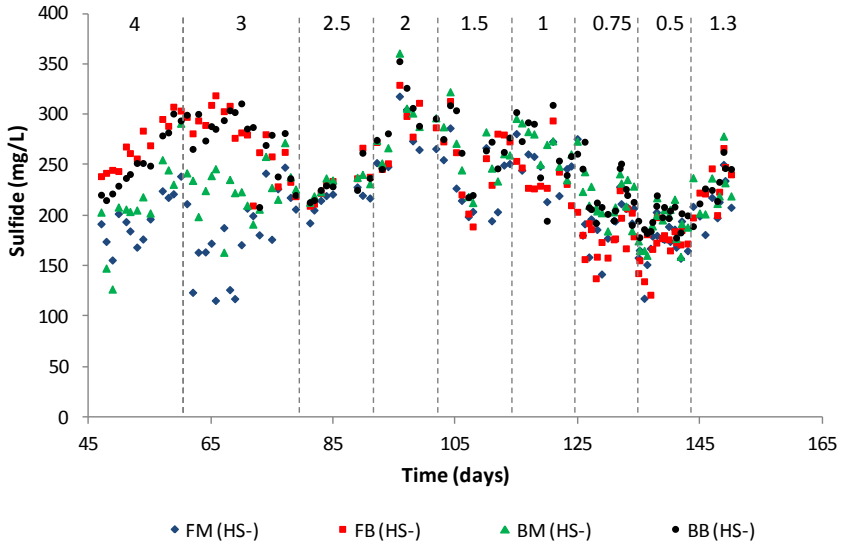

Figure 3 Aqueous sulfide concentration as a factor of HRT, measured at four points in the reactor. Changes in HRT are represented by dashed lines and mean HRT is indicated

At the longer HRT there was some inhomgeneity in the reactor, a function of the hydrodynamics within the reactor, with higher concentrations in the lower half of the reactor. While the sulfide levels did decrease to an extent as the HRT decreased, a relatively steady state was observed at each HRT and the decreased performance with decreasing HRT, below the critical maximum specific growth rate of the cells, observed in the CSTR, did not occur owing to a de-coupling of the hydraulic and biomass dilution rates. Biofilm growth on the carbon fibers was clearly visible, demonstrating biomass retention.

Comparison of performance across reactor configurations

The performance in each of the different reactor configurations can be compared by considering the volumetric sulfate reduction rate relative to the volumetric sulfate loading rate. At a feed sulfate concentration of 1 g/L, the performance was similar at HRTs from four days down to one day, with a sulfate reduction efficiency of between 85-95%. Significant divergence in performance was observed at lower HRTs, where washout of a portion of the sulfate reducing community occurred in the stirred tank reactors as the dilution rate exceeded the maximum specific growth rate. The two systems that were characterized by either recycling of the biomass (BSR reactor coupled to membrane filtration unit) or efficient retention of the biomass (carbon microfiber channel reactor) maintained higher VSRRs, owing to the requisite decoupling of the MCRT and HRT. At the HRT at which washout is first observed in the CSTR (0.5 day), for the channel reactor the VSRR was approximately 20% higher than the baseline study, while for the membrane system it was over 50% higher, despite the challenges associated with elemental sulfur formation. Maree and co-workers (2004) achieved very efficient sulfate reduction by recycling sludge from a clarifier back to a well mixed primary reactor, although the clarifier volume was equal to that of the reactor, which has capital cost and process footprint implications.

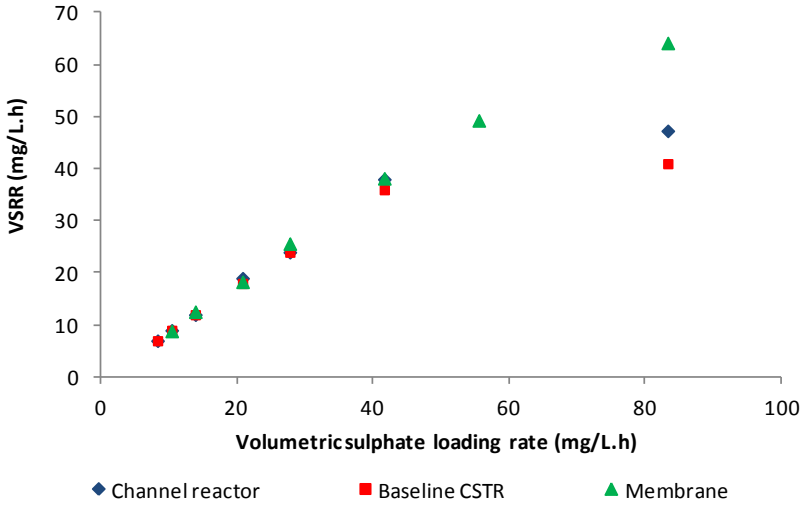

Figure 4 Comparison of the VSRRs across the three reactor configurations at a feed sulfate concentration of 1 g/L

CONCLUSION

Decoupling of mean cell and hydraulic retention times was achieved successfully in both the LFCR, where biofilm formation on the carbon microfibers was very efficient and ensured biomass retention and the reactor fitted with the microfiltration membrane, where the membrane permeate was consistently cell free, demonstrating biomass recycle. The maintenance of the biomass within the reactor resulted in significantly improved performance at low HRTs, with the volumetric sulfate reduction rate in the channel and membrane coupled reactors being 20% and 50% higher respectively than the baseline CSTR data at a HRT of 0.5 days.

In both systems, the complete elimination of oxygen was not possible, resulting in the partial oxidation of a portion of the sulfide formed to elemental sulfur. In the channel reactor this occurred primarily in a floating biofilm, similar to that observed in the dedicated sulfide oxidation reactor, with some sulfide oxidation also occurring in the effluent pipe. This suggests that sulfide oxidation and sulfur recovery could be coupled with sulfate reduction in this configuration.

The sulfur formation presented more of a problem in the membrane system as particulate sulfur blocked the permeate drainage line and peristaltic pump tubing, restricting permeate flow, as well as forming a layer on the outer surface of the membrane, reducing transmembrane flux. As a consequence, a significant amount of the accumulated biomass was lost as overflow from the reactor. Despite this, the membrane coupled system resulted in the most efficient sulfate reduction. Subsequent experiments have shown that active pumping of permeate is not required and this has eliminated the problem.

ACKNOWLEDGEMENTS

The authors gratefully acknowledge the financial support of the Water Research Commission of South Africa. Sue Harrison and Tynan Marais acknowledge the financial support from the South African Research Chairs Initiative (SARChI) of the Department of Science and Technology (DST) and National Research Foundation (NRF) in South Africa.

REFERENCES

APHA (American Public Health Association) (2005) *Standard Methods for the Examination of Water and Wastewater,* 21st Edition. American Public Health Association, Washington, D.C.

Gazea, B., Adam, K. & Kontopoulos, A. (1996) 'A review of passive systems for the treatment of acid mine drainage', *Minerals Engineering*, vol 9, pp 23—42.

Harrison, S.T.L., van Hille, R.P., Mokone, T., Motleleng, L., Smart, M., Legrand, C. & Marais, T. (2014) Addressing the challenges facing biological sulphate reduction as a strategy for AMD treatment: Analysis of the reactor stage: raw materials products and process kinetics, Water Research Commission, Pretoria, South Africa.

Hedin, R.S., Nairn, R.W. & Kleinmann, P.L.P. (1994) *Passive Treatment of Coal Mine Drainage*. US Bureau of Mines Information Circular 9389, US Department of the Interior, Bureau of Mines, Pittsburgh, PA., pp 1—35.

Heimann, A.C., Friis, A.K. & Jakobsen, R. (2005) 'Effects of sulfate on anaerobic chloroethene degradation by an enriched culture under transient and steady-state hydrogen supply' *Water Research*, vol 39, pp 3579—3586.

Janssen, A.J.H., Sleyster, R., van der Kaa, C., Jochemsen, J., Bontsema, J. & Lettinga, G. (1995) 'Biological sulphide oxidation in a fed-batch reactor', *Biotechnology and Bioengineering*, vol 47, pp 327—333.

Johnson, D.B. & Hallberg, K.B. (2005) 'Acid mine drainage remediation options: a review', *The Science of the Total Environment*, vol 338, pp 3—14.

Maree, J., Greben, H. & de Beer, M. (2004) 'Treatment of acid and sulphate-rich effluents in an integrated biological/chemical process', *Water SA,* vol 30, pp 183—190.

Molwantwa, J.B. & Rose, P.D. (2013) 'Development of a Linear Flow Channel Reactor for sulphur removal in acid mine wastewater treatment operations', *Water SA*, vol 39, pp 649—654.

Moosa, S., Nemati, M. & Harrison, S.T.L. (2002) 'A kinetic study on anaerobic reduction of sulphate, Part 1: Effect of sulphate concentration', *Chemical Engineering Science*, vol 57, pp 2773—2780.

Moosa, S., Nemati, M. & Harrison, S.T.L. (2005) 'A kinetic study on anaerobic reduction of sulphate. Part II: Incorporation of temperature effects in the kinetic model', *Chemical Engineering Science*, vol 60, pp 3517—3524.

Oyekola, O.O., Harrison, S.T.L. & van Hille, R.P. (2012) 'Effect of culture conditions on the competitive interaction between lactate oxidizers and fermenters in a biological sulphate reduction system' *Bioresource Technology*, vol 104, pp 616—621.

Oyekola, O.O., van Hille, R.P. & Harrison, S.T.L. (2009) 'Study of anaerobic lactate metabolism under biosulfidogenic conditions' *Water Research*, vol 43, pp 3345—3354.

Oyekola, O.O., van Hille, R.P. & Harrison, S.T.L. (2010) 'Kinetic analysis of biological sulphate reduction using lactate as carbon source and electron donor: Effect of sulphate concentration', *Chemical Engineering Science*, vol 65, pp 4771—4781.

van Hille, R.P. & Mooruth, N. (2013) Investigation of carbon flux and sulphide oxidation kinetics during passive biotreatment of mine water. Research report no. 2139/1/13, Water Research Commission, Pretoria, South Africa.

Zagury, G.J., Neculita, C.M. & Bussière, B. (2007) 'Passive treatment of acid mine drainage in bioreactors using sulfate-reducing bacteria: critical review and research needs', *Journal of Environmental Quality*, vol 36, pp 1—16.

Permeable Concrete with Bio-Reactive Layers to Target Heavy Metals and Sulfates in Acid Mine Drainage

Steven Zaal[1, 2] and Craig Sheridan[2]
1. Aurecon South Africa Pty Ltd
2. Industrial and Mining Water Research Unit, University of Witwatersrand, South Africa

ABSTRACT

The aim of this research is to reduce heavy metal and sulfate content of acid mine drainage (AMD) through the methods of passive filtration by combining permeable concrete and organic materials to achieve a low cost, yet effective temporary treatment method for rural/poor communities who are affected by AMD. The acids are filtered through layers of alternating pervious concrete and biological composting layers. The concrete layers target removal of heavy metals such as iron, manganese, potassium, magnesium, etc. through precipitation as well as reduce sulfate content to a small degree along with total dissolved solids. The concrete layers aid in raising the pH of the AMD to more acceptable levels. The biological layers achieve sulfate reduction through the metabolism of sulfate- reducing- bacteria (SRB) - this process however will require time and the organic layer thus will be thicker and less permeable than the concrete layers in order to allow seepage to take place at a reduced rate. A wide variation of composting layers were tested including cow manure, chicken manure, sawdust, straw, zoo manure, leaf compost, grass cuttings and river mud to find an optimum mix of materials which allows for the greatest sulfate reduction through SRB's. Long-term testing and effectiveness of the rigs will be undertaken to establish limitations and lifespan of the filtration system. AMD from the Witwatersrand gold fields and Mpumalanga coal fields with exceptionally high sulfate content were used to test effectiveness of the organic materials over a short period of time with long term testing being conducted with a synthetic AMD due to limited supply of the reagent. The short term testing yielded reductions of sulfates in the region of 56% when using kraal manure as the biological reagent mixed with sawdust for added organic carbon. The filter also successfully raised the pH to 8 while removing a significant portion of heavy metals. The results show promise for using the technology as a low cost, temporary measure to protect locally impacted groundwater, especially for isolated and/or rural communities.

Keywords: AMD, SRB, permeable concrete, remediation

INTRODUCTION

Acid Mine Drainage (AMD) is the name given to outflows of water that contain high levels of acidity and heavy metals due to the reaction and oxidation of geological layers which consist of sulfide containing minerals, especially pyrite(FeS_2). The amount and rate at which AMD is generated is a function of the rock mineralogy and degree of exposure/presence of oxygen and water. The sulfides in the rock oxidise when in contact with these substances to create a highly acidic, sulfate rich mixture with characteristically low pH and often a high content of heavy metals in soluble form.

This acid generating phenomenon is a naturally occurring process resulting from the weathering and erosion of sulfide carrying minerals in exposed rocks weathering on hills and valleys or through ground water seepage. This however creates AMD at a slow rate due to the relatively small exposed surface area; and in the case of ground water seepage the lack of excess oxygen; therefore allowing the surrounding alkaline rocks to neutralise the AMD, and water bodies to dilute it sufficiently before it has a chance to significantly impact the environment (Durand, Meeuvis, & Fourie, 2010).

Mining activities however; such as deep pit excavation, crushing, quarrying, mine waste rock pilling, tailings and tunnelling; result in massive volumes of rock being exposed, which when weathered creates excessive amounts of acid mine drainage. This AMD has greatly adverse effects on the environment, its biodiversity, as well as long-term damage to waterways, aquifers and ultimately our drinking water (Coetzee et. al, 2010). AMD can also cause damage to structures such as culverts and bridge abutments exposed to waterways that have a high concentration of AMD as the high acidity and sulfate levels have an accelerated corrosion effect on steel reinforcing (Gurdeep, 2006). More importantly, AMD carries a health risk to human settlements, especially those of the mining communities often living in low cost, slum/squatter camp type environments adjacent or nearby mine dumps/tailings. Some of the Heavy metals contained in AMD can be extremely harmful if consumed in elevated consecrations and in some cases AMD has been found to be carcinogenic.

Extent of the problem in South Africa

AMD is an extensive problem with coal and gold mining, as marcasite and pyrite (or "fools gold" as it is often known) is highly prevalent in the mine wastes and surrounding mineralogy. South Africa has notably large deposits of these sulfur rich natural resources. The AMD problem faced by the mines in Johannesburg is being further accentuated with the gold mining operations ceasing and mines not being maintained after closure. This is resulting in uncontrolled amounts of AMD welling up inside the mine voids left from deep excavations as the ground water level is no longer being drawn down and controlled to allow for mining along the reef. To put things into perspective , the potential volume of AMD produced by the Witwatersrand Goldfields alone amounts to an approximated 350ML/day which is around 10% of the daily supply of potable water by Rand Water according to Hobbs et al (2009).

There is huge concern regarding the state of the water level at the central basin in Witwatersrand as ground water with high concentrations of AMD has been rising at an average rate of 0.59 metres

per day (m/d) since July 2009 which translates to approximately 15m/month (Akcil and Koldas, 2006).

If this rising water level is not treated and controlled it would threaten to flood the low lying tourist areas of the mine at Gold Reef City and of more consequence, pollute and compromise the shallow ground water resources along with causing damage to the dolomitic strata. This will ultimately affect the dolomites ability to sustain loadings in the southeast part of Johannesburg according to Coetzee et al. (2010). One of the largest concerns of AMD is the accelerated karstification of dolomite (which is soluble in acid) resulting in potentially large sinkholes and soil subsidence coupled with the consequential contamination of aquifers and decanting into waterways. This ultimately pollutes and impacts all types of biodiversity including with time our drinking water. This same threat is faced by the cradle of humankind in Krugersdorp and is of huge concern as the structural stability of the surrounding areas are in question threatening the heritage site and the artefacts contained within its soil as the dolomitic aquifers carry more and more highly acidic AMD into the area (Durand et al. 2010).

According to Case studies done by Hochmann et al. (2010) on coal mining in South Africa, an account of the mining community living at the Maguqa township near an open cast coal mine in the Brugspruit valley was given, where AMD carrying toxic heavy metals is flowing into the Brugspruit stream and from there into the Olifant's river system. The children of the township play soccer on the flat white surfaces of sulfate salt precipitates left by the AMD, oblivious to the potential health risks. Therefore there is a need for a rapid temporary solution which has the potential to reduce the risk to such impacted communities whilst a long term solution is sought.

Treating AMD

Treatment of AMD is complex, costly and requires a fairly large amount of capital and infrastructure to be put in place for the treatment methods to be implemented (Hobbs et al., 2009). There are a number of effective treatment techniques, all of which can be broadly characterised as either active or passive. Active treatments are those treatments which involve ongoing and continual input and often involve electrical and mechanical implementations that are highly sophisticated and engineered which make use of chemical dosing or similar techniques to ensure the remediation of the contaminated water [Shabalala (2013) , Skousen et al. (2000)]. Passive treatment techniques are those which can operate with little to no input over the long term and often require longer periods of time/processing in order to reach the same level of effectiveness as an active system and don't often involve chemicals or mechanical equipment (Jennings and Blicker 2008). Some of the more commonly used passive methods are discussed further below.

Anaerobic wetlands

This system is a modification of an aerobic wetland and incorporates a bed of limestone with a thick layer of organic rich medium above it to promote bacterial growth. This system creates anaerobic conditions when the AMD permeates through the organic material due to microbial activity leading to high oxygen demand. It is thus described as a sub-surface treatment method as it requires sub surface flow of the AMD to be effective unlike the aerobic wetlands where the AMD can flow along the surface. This system can thus treat highly acidic AMD through the dissolution of the fluid due to a limestone layer. This system however requires a large surface area and extended residence time

within the ponds for effective treatment with low/slow flow rates [Skousen et al. (2000), Zipper et al. (2011)].

Experiments conducted by Sexstone et al. (1993) involving anaerobic wetland setups resulted in good pH reduction resulting in almost neutral levels upon exiting the wetland (pH of 6.5) which was largely attributed to the limestone. The tests were run for a period of four years over which it was observed the systems became less and less effective with metal retention and pH reduction due to the system having a finite capacity and thus highlight the need for larger areas as smaller setups are less effective and have a shorter life span than respectively larger setups. Wieder (1992) documented that the performance of wetlands are different depending on the season and age of the wetland which was attributed to factors such as bacteria activity, current loading of the wetland and ability of the aquatic plants to absorb precipitated heavy metals.

Permeable reactive barriers (PRBs)

Permeable reactive barriers are essentially a permeable obstruction placed typically below surface which intersects the AMD plume as it flows along with ground water and treats the influent as it passes through the barrier. The treatment is achieved in the majority of cases through the use of Iron metal and silica sand, with some instances using organic matter to treat nitrate and sulfates depending on the AMD that is to be treated (Powell et. al, 1998). According to work done by Blowes et al. (2000) the use of solid organic matter such as wood chips, sawdust, compost and leaves have positive effects on sulfate reduction in AMD due to the proliferation of sulfate reducing bacteria which reduce sulfate to sulfide which in turn leads to the formation of insoluble metal sulfides. However one of the most important considerations of using a PRB for treatment is the fact that sulfides have low solubility in anaerobic conditions and thus if oxidation occurred metals could be released by the barrier (Blowes et al., 2000). Another drawback is the Installation of a PRB is quite costly as often impermeable structures are constructed to channel the AMD to the Barrier and these can be quite large and long such as a slurry piled wall.

One of the limiting factors according to Taylor et al. (2005) is the finite amount of reactive substrate available and the need for the AMD to have low oxygen content upon entering the system to prevent clogging. The organic substrate is consumed in the treatment process which creates void spaces that are then filled with the metal precipitates - compaction and the filling of these void spaces can lead to reduced porosity and effectiveness of the system.

Bioreactors and (SRB) Sulfate reducing bacteria

Most passive treatments that target AMD with a high sulfate content will make use of sulfate reducing bacteria (SRB). The bacteria consume organic forms of carbon (CH_20) under anaerobic conditions to produce bicarbonate; which promotes neutralization of the AMD; and H_2S which creates an environment where low solubility metals will precipitate out as shown in the Equation 1 [Shabalala (2013), Younger et al. (2002)]:

$$SO_4^{2-} + 2CH_2O \rightarrow H_2S + HCO_3^- \quad (1)$$

This process is highly dependent on the availability of an organic feedstock for the bacteria to proliferate and become increasingly effective. Temperature also plays a role with the bacterial activity where they become increasingly more active at higher temperatures and less so at lower temperatures [Akcil & Koldas (2006), Younger et al. (2002)].

Bioreactors essentially create a concentrated carbon rich environment where these SRBs can thrive and proliferate in order to effectively remove sulfates and heavy metals of fluids that pass through them. Bioreactors are commonly used with most sludge and waste water treatment facilities. The problem with some bioreactors arises where they become inundated with metal precipitations and lose their effectiveness. Replenishment of the carbon source is sometimes needed and removal of the heavy metal rich sludge can be costly and expensive to dispose of.

Use of Concrete in AMD treatment

The use of concrete in the treatment of AMD has not been extensively tested and its use in conjunction with biological layers is novel. There has been some experimental work done by Ekolu et al. (2013) with concrete in the removal of heavy metals, where it was shown that removal of iron content in the order of 95-99% was achieved through a single pass through a concrete cube. It was also found to have effectiveness in reduction of other such heavy metals and approximately 30% removal of sulfate content. It is also expected that the lime within the Portland cement will react to increase the pH of the AMD solution. Permeable concrete is most effective for the purposes of the research presented here as it will allow AMD fluids to pass through the cube while retaining heavy metals within its macro porous structure. The concrete cube will have a finite life much like the Alkali Limestone Drains solutions due to armouring and preferential flow paths forming through the cube.

METHODOLOGY

Filters were constructed out of permeable concrete and organic material in an attempt to combine the benefits of anaerobic wetland conditions, permeable reactive barriers, along with the benefits of heavy metal reducing concrete to achieve a low cost yet effective remediation system aimed at the local communities such as those in Johannesburg that are hard hit by rapidly proliferating AMD. Two phases of testing were undertaken. The first phase was aimed at finding a suitable medium for SRB proliferation and tests were conducted over a 2-3 week period to determine effectiveness of the biological layers. Once an effective medium was found, phase one testing was stopped and a long term filtration system was setup for phase 2. These long term setups have a drip system to pass AMD through them continuously and sulfate reduction levels will be monitored over time for a period of 3-6 months in order to gauge/quantify the effectiveness and ability to perform over the short to medium term. These phase 2 experiments are currently underway and are ongoing.

Permeable concrete

Concrete cubes and cylinders for the filters were batched using Sure build Afrisam 42,5 PPC cement, no fines and 9.5mm dolerite aggregates. Dolerite aggregates were chosen due to their hardness and resistance to acidity which is expected to increase the lifespan of the concrete in AMD remediation. Research conducted by Ekolu et al. (2013) showed that greater sulfate reduction was obtained with dolerites as opposed to granite and limestone. The mix design proportions used for the research are given in the table below:

Table 1 Mix design proportions

Material	**Quantities Used**
Portland Cement	325 kg/m^3
Fine Aggregates	0 kg/m^3
Coarse Aggregate (9.5mm aggregates)	1500kg/m^3
Water/Cement Ratio	0.3

These values are based on the need for greater permeability to allow movement of the AMD through the concrete while still maintaining workability and ease of placement along with maintaining suitable concrete strength. Once the concrete had been cast it was immediately covered to prevent any moisture loss and allowed to set for 24 hours. Thereafter casts were submerged and allowed to cure for 28 days as per standard cement curing processes.

Filtration systems

Filters for the first phase were constructed out of Perspex sheets and were rectangular with an internal dimension of 105mm in order to accommodate a standard 100x100x100mm concrete cube and have a length of 450mm in order to allow for sufficient space for two concrete cubes and a 200mm thick composting layer in between them. The experimental rigs were placed vertically and AMD was passed through the filter under gravitational force. The base plate as well as the midpoint of the filter has a nozzle to allow samples to be taken during filtration. An example of the phase one setup can be seen in Figure 1.

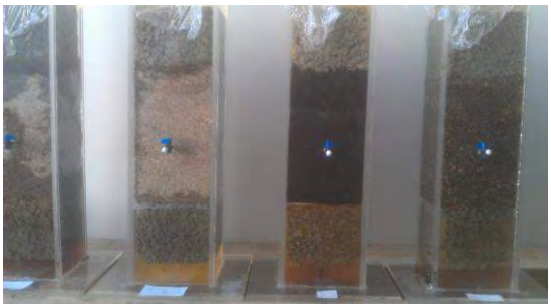

Figure 1 Short term experimental rigs in operation

An AMD taken from coal mine tailings in Mpumalanga with exceptionally high sulfate content (8200ppm) was used to test the effectiveness of the phase one setups. The composting layers used were varied in order to ascertain an effective medium which maximized SRB population growth and activity while not adding any adverse chemicals or metals to the system. The layers tested consisted of leaf compost, wood chips, kraal manure, chicken manure, zoo manure, elephant dung,

sawdust and straw. Combinations of the above along with additions of lime were also tested once an effective medium had been established.

Samples and testing

For the short term experiments samples were taken at 3, 7, 10, 14 and finally at 21 days. These preliminary phase 1 tests were stopped after 21 days as results were showing trend lines of favourable (or otherwise) at this point. Samples were extracted from the bottom, midpoint as well as the top of the filter during phase 1 testing. The samples were tested for sulfate concentration through the use of barium chloride, standard solutions and a spectrograph as per the test methodology stipulated in the sulfate testing methods IS:3025 (Part 24) - Reaffirmed 2003 and ASTM D516 methods.

RESULTS AND DISCUSSION

The results presented are an average of the three samples taken from the top, middle and bottom of the filters. The pH of the samples was checked and it was found that the concrete cubes were very effective at raising the pH of the AMD from 3 to an average of 7.68. The test setup with only permeable concrete cubes in them had a pH of 11 after 21 days.

In Figure 2, the data presented indicates that a mixture of kraal manure with sawdust in the proportions 80%:20% had the most significant remedial effect (a kraal is a South African word for an enclosure normally used to house cattle). The manure sourced from the Johannesburg zoo also had a significant effect on sulfate removal but is hard to come by and in short supply. Chicken manure and a mixture of zoo leaf compost with sawdust had the least effect.

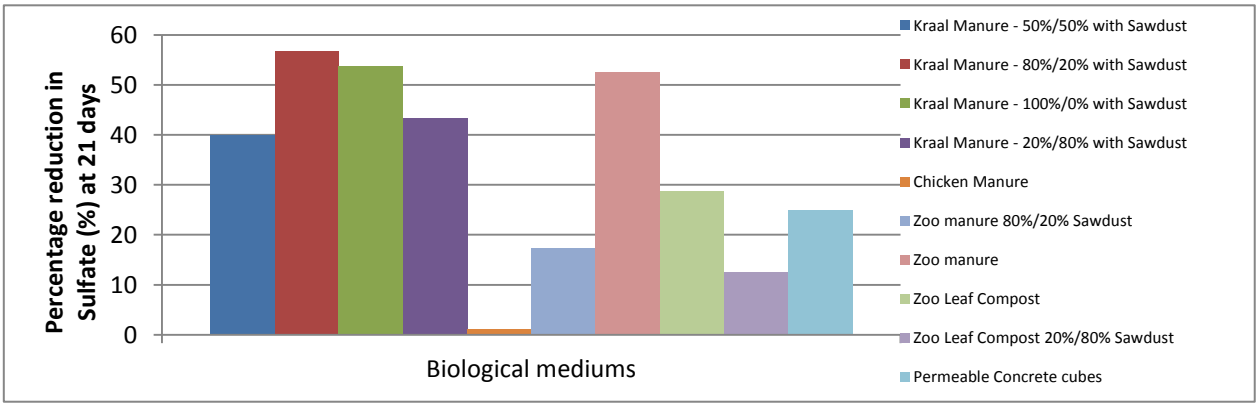

Figure 2 Sulfate removal after 21 days of operation for different organic feedstocks

The effect of residence time on the removal of sulfate for 5 selected scenarios is presented in Figure 3. Similarly to the data shown in Figure 2, kraal and zoo manure were the fastest removers of AMD with chicken manure having almost no effect after 7 days. This could be as a result of the ruminant bacteria which would occur in cattle, elephant, buffalo, and other herbivorous animal dung (which would not be present in the chicken manure). The sharp initial drop in sulfate concentration at the

start of the experiment (shown as the difference between AMD and the series) is attributed to the absorption of sulfates into the permeable concrete and organic materials. This effect, however, is short lived as the filter quickly becomes saturated and sulfate concentrations rise before DSR (Dissimilatory sulphite reductase) begins.

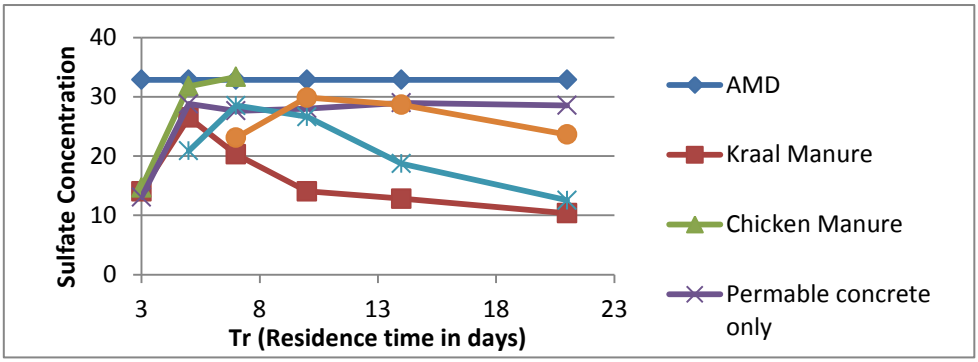

Figure 3 Effect of residence time on sulfate reduction

The permeable concrete cubes were able to reduce sulfates by 25% which is regarded as significant, as well as being effective at raising the pH of the passing AMD. The kraal manure was selected as the best performer and candidate for long term testing due to is ease of sourcing across Southern Africa, especially within the rural mining communities and areas, and is considered the best biological medium for the filters. As can be seen the organic medium typically becomes more effective at sulfate removal with time which correlates to the proliferation of SRBs and the curves typically represent a steady growth rate resulting in accelerated sulfate removal with time. The permeable concrete setups also show the initial drop in sulfates but show steady reduction of approximately 25% throughout the testing cycle which correlates well with the sulphate reductions found by Ekolu et al. (2013) in their experiments.

CONCLUSION

From the results of the research it is concluded that kraal manure is the most effective and readily available on a large scale of the organic feedstocks and when coupled with permeable concrete is able to effectively remove sulfates in a relatively short time frame (favourable results in 2-3 weeks) while raising the pH to almost neutral. The costs of the materials needed to construct these filters is significantly lower than other current passive solutions, and thus the filter system shows great promise as a low cost temporary solution to communities such as those like Maguqa township and others in Johannesburg where AMD is proliferating at high rates.

Due to the promise shown by the research over the short term it will be test further to ascertain the ability of the system to provide favourable remediation over longer periods, while quantifying limitations, capacities and performance of the filter system. The authors have already commenced with this long term testing, and it is ongoing.

Permanent long term solutions in South Africa more often than not require enormous capital outlay and infrastructure from government or mining bodies, and may take a number of years to be implemented. The hope is that the proposed filter system would be able to offer some short term relief to heavily affected receptors, especially in poor and/or rural communities.

REFERENCES

Akcil, A. & Koldas, S., (2006). Acid Mine Drainage (AMD): causes, treatment and case studies. Journal of Cleaner Production, 14(12-13), pp.1139–1145.

Blowes, D.W. et al., (2000). Treatment of inorganic contaminants using permeable reactive barriers. Journal of Contaminant Hydrology, 45(1-2), pp.123–137.

Chimuka, L., Ogola, O. & Matshusa-Masithi, M., (2009). Use of compost bacteria to degrade cellulose from grass cuttings in biological removal of sulfate from acid mine drainage. Water SA, 35(1), pp.111–116.

Coetzee, H. et al., (2010). Mine water management in the Witwatersrand Gold fields with special emphasis on acid mine drainage, DWAF : Report to inter-ministarial comittee on Acid Mine Drainage under the co-ordination of the council of Geosciences, December 2010

Durand, J., Meeuvis, J. & Fourie, M., (2010). The threat of mine effluent to the UNESCO status of the Cradle of Humankind World Heritage Site. TD: The Journal for Transdisciplinary Research in Southern Africa, 6(July 2010), pp.73–92.

Ekolu, S ;Azene , A; Diop, S., (2013). A concrete reactive barrier for acid mine drainage treatment. ICE - Water Management Journal, 167(7), pp.373–380.

Geraldine Hochmann, Mathews Hlabane, S.L., (2010). The Social and Enviromental Consequences of Coal Mining in South Africa, SA Green revolutionary council and Eviromental monitoring group January.

Gurdeep, S., 2006. A survey of Corrosivity of underground mine water. International Mine Water Journal 2006, pp.21–23.

Hobbs, P., Godfrey, L. & Dr Manders, P., (2009). Acid Mine Drainage in South Africa. CSIR Briefing Notoe 2009/02 August, (August), pp.1–2.

Jennings, S. & Blicker, P., (2008). Acid mine drainage and effects on fish health and ecology: A review. Reclamation Research Group (2008), 1(June).Anchorage, Alaska, 99501

Powell, R., Puls, R. & Blowes, D., (1998). Permeable reactive barrier technologies for contaminant remediation. EPA/600/R-98/125, EPA/600/R-(125), pp.30–49.

Sexstone, A.J. et al., (1993). Iron removal from Acid Mine Drainage by wetlands.pdf. National meeting of the American Society of Surface mining and reclaimation, 1(1), pp.609–620.

Shabalala, A., (2013). Assessment of locally available reactive materials for use in permeable reactive barriers (PRBs) in remediating acid mine drainage. Water SA, 39(2), pp.251–256.

Skousen, J. & Ziemkiewicz, P., (1996). Acid mine drainage control and treatment, Book section, Reclamation of Drastically Disturbed Lands. American Society for Surface Mining and reclaimation. Agronomy No. 41

Wieder, R.K., (1992). A field study to evaluate man-made wetlands for acid coal mine drainage treatment. Report to the US Office of Surface Mining.

Younger, P., Banwatt, S. & Hedin, R., (2002). Mine Water; Hydrology, Pollution and Remediation, Kluwer Academic Publishers, London, UK.

Ziemkiewicz, P.F., Skousen, J.G. & Simmons, J., (2003). Long-term Performance of Passive Acid Mine Drainage Treatment Systems. Mine Water and the Environment, 22(3), pp.118–129.

Zipper, C. & Skousen, J., (2011). Passive treatment of acid mine drainage. Reclaimation Guidl*ines for Surface Mined Land 460-133*, 460-133, pp.1–13.

10th ICARD IMWA 2015 | 10th International Conference on Acid Rock Drainage & IMWA Annual Conference

Bioreactor and *In Situ* Mine Pool Treatment Options for Cold Climate Mine Closure at Keno Hill, YT

Jim Harrington[1], Joe Harrington[1], Eric Lancaster[1], Andrew Gault[2] and Kai Woloshyn[2]

1. *Alexco Environmental Group, USA*
2. *Alexco Environmental Group, Canada*

ABSTRACT

Biological treatment systems can offer relatively low cost and minimal maintenance closure options for metal-rich adit discharge waters compared to conventional chemical-based water treatment facilities, however, sustaining the biological activity required to successfully treat the mine water in northern, cold climates has impeded its wider adoption. As part of an ongoing program to assess the potential of harnessing microbial sulfate-reduction to remove metals from mine water, a pilot bioreactor was built and operated at the Galkeno 900 adit in the Keno Hill Silver District (KHSD), located in central Yukon. The bioreactor operated year round at test flow rates between 0.5 and 1 L/s, achieving sustained removal of zinc (>99% removal; 5 – 6 mg/L reduced to 0.01 mg/L) and cadmium (0.0015 mg/L reduced to below detection limit (<0.0001 mg/L)), the primary contaminants of concern. Reductions in arsenic, antimony, and nickel loads of >80% were also observed under optimized flow rates, and the technology is being developed for closure of various adits across the KHSD.

Stimulation of sulfate-reducing conditions in underground mine pools that feed adit water discharge has also been advanced as the preferred option for water treatment for several underground mines in the KHSD. Such *in situ* treatment has been successfully piloted at the Platoro mine (CO, USA), where soluble organic carbon (molasses, methanol) was injected into the mine pool, which created sulfate-reducing conditions, causing >90% removal of zinc and arsenic. Annual injections of organic carbon were enough to maintain the low metal(loid) concentrations. Similar *in situ* treatment at the Schwartzwalder mine (CO, USA) lowered uranium concentrations by ~90%, from 22.8 mg/L to 1.8 mg/L, and the technology is currently being tested at the Silver King mine in the KHSD. Such relatively inexpensive and low maintenance options show great promise to the reliable closure of remote, cold climate mining sites.

Keywords: Bioreactor, mine pool treatment, zinc, uranium, cold climate

INTRODUCTION

Bioremediation of metal(loid) contaminated waters has garnered increasing interest in the past three decades as a relatively low cost tool to clean up former mining and industrial complexes, and provide closure options for operational sites. In particular, the semi-passive nature of many bioremediation systems, often requiring minimal maintenance and low power requirements, make them attractive treatment options in remote, cold climate settings which have limitations regarding power supply and year-round access. A number of bioremediation technologies harness the activity of sulfate-reducing bacteria (SRB), which are capable of coupling the oxidation of organic matter to the reduction of sulfate, to produce sulfide which reacts with many metals (e.g. zinc, cadmium, lead, nickel) to precipitate low solubility metal sulfide minerals. SRB are ubiquitous, thus simple addition of a soluble source of organic carbon to the contaminated waters, such as alcohol or molasses, is often enough to stimulate their activity.

Alexco Environmental Group has embarked on a multipurpose program to assess the potential of adding an organic substrate to mine adit water to support metals removal, whether within a constructed bioreactor or an underground mine pool, for use as a closure option for various historic adits in the Keno Hill Silver District (KHSD; Yukon, Canada). Although a number of bioreactor studies have been performed in cold climate settings (e.g. Ness, Janin & Stewart, 2014), there is a need for evaluating such technology on a site-specific basis, particularly under the challenging conditions of cold climate sites such as Keno Hill, which has a mean annual temperature of -3.3 °C. Treatment of subsurface metal-rich waters *in situ* by injection of soluble organic carbon to stimulate microbial activity has also received significant attention in recent years, showing promise for the removal of chalcophile metals (Saunders et al., 2005, 2008) and uranium (Anderson et al., 2003; Watson et al., 2013). Both such technologies have undergone (bioreactor) or are in the initial stages (*in situ* injection treatment) of testing at Keno Hill to evaluate their suitability as treatment options for the closure of historic adits in the District. This paper presents an overview of:

- The Galkeno 900 bioreactor trial at Keno Hill; and
- Case studies of *in situ* injection treatment of mine pools at Platoro (CO) and Schwartzwalder (CO) mines as an analogue for treatment at Keno Hill

METHODOLOGY

Bioreactor

The pilot bioreactor was constructed to treat a portion of water leaving the Galkeno 900 adit in Keno Hill. The adit water was circumneutral and the primary contaminant of concern was zinc, which typically ranged between 5 and 7 mg/L in the untreated adit water over the duration of the pilot test.

Construction

The bioreactor was approximately 90 feet by 100 feet and had a liquid-filled portion that was 10 feet deep. It was dug partially into the native ground with an excavator, and the remaining depth was created by forming a berm around the excavated area. The bermed/excavated area was lined with 60 mil HDPE liner to form a pond, and then filled with waste rock recovered from a local placer

mine. A geofabric was laid across the bioreactor, and soil from the excavated area and hillside was used to provide a 4 foot soil cover over the bioreactor, which acted as an insulating layer. All inlet and outlet piping was similarly buried to reduce the possibility of freezing. Water entered the bioreactor through an inlet valve and influent sump where it was pumped into a perforated distribution pipe, and the mine water then flowed through the bioreactor to a 0.75 inch hole perforated collection pipe on the far side of the bioreactor. Baffling was installed in two locations to create a tortuous flow path and increase the contact time of the water with the media within the bioreactor (Figure 1).

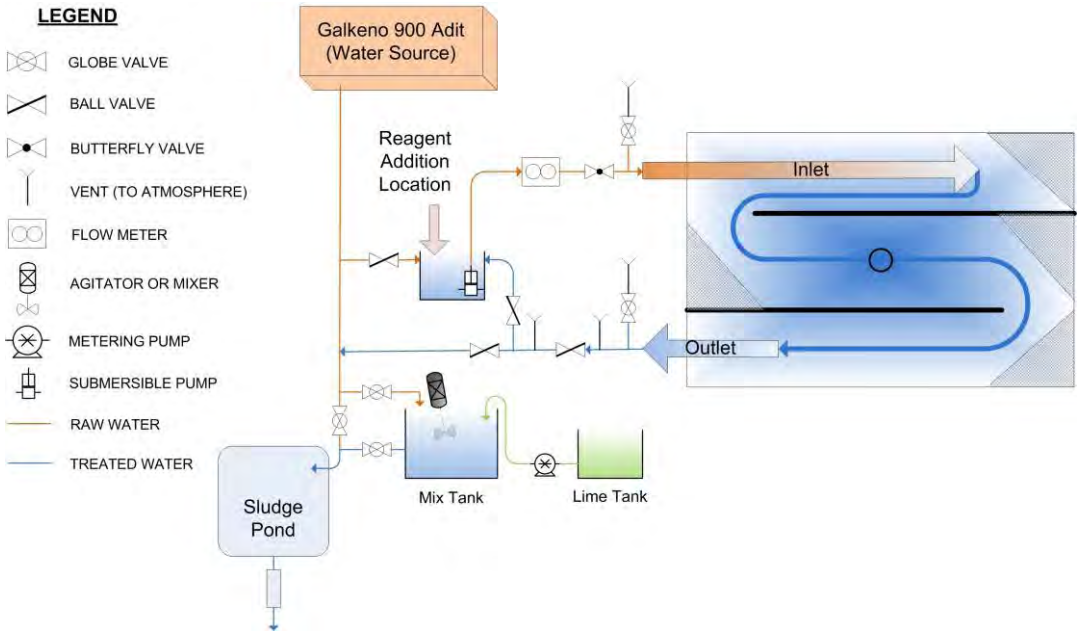

Figure 1 Pilot bioreactor layout

Operation

Following construction in October 2008, the bioreactor was filled with adit water, which was initially supplemented with sucrose (182 kg), methanol (416 L) and dried milk solids (1.8 kg) to stimulate indigenous microbial activity. Over the subsequent year, water was recirculated within the bioreactor to allow reducing conditions to develop. Further batches of methanol (416 L in January 2009) and sucrose (20 kg in July 2009) were added to promote the transition to sulfate-reducing conditions, assisted by the continuous addition of methanol via a metered pump (1 L/day, initiated in May 2009). Once sulfate-reducing conditions were established, the bioreactor began flow-through operation at 0.5 L/s in October 2009, transitioning to 1 L/s in December 2009, then to 0.75 L/s in August 2010. The pilot bioreactor was terminated in March 2011.

Overview of *in situ* mine pool treatment

In situ mine pool treatment is accomplished by delivery soluble organic carbon into the mine workings. Depending on the mine geometry and setting, the organic carbon can be injected in an upgradient area of a mine and the treatment is accomplished in the mine along the flow path.

Alternatively a recirculation approach can be taken, where water is pumped up from the mine workings from a shaft or other access location, amended with soluble organic carbon by mixing at the surface, then returned to the mine via a second pipe placed down another shaft. This recirculation loop allows for mixing of the subsurface water, while the injected organic carbon stimulates indigenous microbial activity. Prior to, or during, organic carbon addition, a tracer is injected (salt or organic dye) to determine the residence time of the mine pool. The form of organic carbon selected is dependent on the residence time; alcohol-based reagents (e.g. methanol) are preferred for short residence times (few weeks) or for sustaining treatment after initial phases of application, whereas slower degrading sugars or starch-based reagents (e.g. molasses) are employed for mine pools with longer residence times (few months or longer) or in the initial growth phase. Injections of organic carbon are typically spaced a few months to as long as years apart, depending on the extent and longevity of the water quality improvements observed, and the rate of recharge of oxygenated water or oxidized constituents (metals, sulfate, or nitrate).

Mine pool treatment can also be enhanced by the addition of ferric oxyhydroxide-based precipitates generated from water treatment plants (WTP). Application of the treatment sludge back into the mine is done by blending the sludge with starches and cellulosic matter to provide a slow release organic carbon source, which supports microbial transformation of the sludge and the subsequent formation of iron sulfide which tends to coat the subaqueous surfaces in the mine. Furthermore, density differences (e.g. sugar syrups are denser than water, alcohols (methanol/ethanol) are less dense than water) are used to target deep zones in mine pools that would not otherwise be accessible to mixing by recirculation.

Platoro, CO

The Platoro underground gold-silver mine is located at 10,000 feet elevation in the remote San Juan mountains of southern Colorado. Adit discharge water (pH 2.7), supplied by an underground mine pool, contains elevated concentrations of arsenic (*ca.* 50 mg/L) and zinc (*ca.* 17 mg/L), which a conventional lime-based WTP had difficulties in reliably treating to meet local discharge standards. *In situ* mine pool remediation was piloted in 2000 (single injection of soluble organic carbon in September) as a pre-treatment step which would lower the metal load exported by the adit and allow for more effective metal removal by the existing WTP. Annual treatment was initiated in August 2006 in which an alcohol and a molasses-based carbon source was injected into the mine pool to again drive the system towards microbially-mediated sulfate-reducing conditions. In August 2009, July 2010 and July 2012, a total of 15,000 m^3 of waste metal hydroxide sludge produced by the WTP was also injected into the mine pool to raise the pH. As the sludge was injected into the mine, potato and/or corn starch was blended into the sludge while soluble carbon addition continued. Throughout the sludge reinjection process the ratio of soluble carbon (sugars and alcohols) to insoluble carbon sources (starches) was carefully modulated based on observation of the redox of the mine pool. Also, the selection of the potato starch vs the corn starch was varied in response to both pricing variations and to target the optimal average particle size of starch to settle in the mine pool water at the same rates as the sludge particles.

Schwartzwalder, CO

The Schwartzwalder uranium mine is located in Jefferson County, CO. Prospecting and mining at Schwartzwalder started as recently as 1953 and was developed as a multi-level, hard rock underground mine. The mine was placed into closure in 2000. Since 2010, alluvial groundwater

around the mine has been collected and treated via ion exchange (IX). De-watering and treatment via reverse osmosis (RO) has also occurred to treat the elevated uranium concentrations (23 mg/L) present in the circumneutral mine pool/groundwater. *In situ* mine pool treatment was initiated in May 2013 as a pre-treatment step to the RO system in which molasses and methanol were injected into the mine pool. Three further monthly injections of methanol followed, and a second injection of molasses and methanol was made six months after the start of operations. Water quality was monitored biweekly.

RESULTS AND DISCUSSION

Galkeno 900 Bioreactor

During the initial nine months of bioreactor recirculation and organic carbon amendment, the concentrations of zinc, cadmium and arsenic declined (Figure 2), however, sulfate-reducing conditions were not yet established. Metal(loid) removal during this period is primarily ascribed to co-precipitation with, and adsorption on manganese and iron (oxyhydr)oxides that likely formed within the bioreactor during recirculation. Lower manganese and iron levels observed in the bioreactor compared to the adit water support this premise, as does the presence of manganese and iron-bearing (oxyhydr)oxide phases around the Galkeno 900 adit, and other adits elsewhere in the KHSD. A sharp increase in bioreactor concentrations of arsenic and cadmium (and a moderate rise in zinc) was observed in August 2009. This was coincident with sequential spikes in manganese and then iron concentrations in the bioreactor discharge, suggesting that the bioreactor had transitioned from oxic to manganese- and iron-reducing conditions, causing solubilization of the iron and manganese (oxyhydr)oxides that had been deposited earlier, and release of their sorbed and co-precipitated metal(loid) inventory. The subsequent rapid fall in zinc and cadmium concentrations in the bioreactor discharge from August 2009 onwards is interpreted as the onset of sulfate-reducing conditions and the associated precipitation of zinc and cadmium as sulfide minerals (Jong & Parry, 2004). Indeed, mineralogical analyses of material collected from the bioreactor interior at the end of the pilot by electron microprobe and synchrotron-based techniques indicated sequestration of zinc as biogenic sphalerite (ZnS). Arsenic concentrations declined more slowly, related to continued supply from dissolution of iron (oxyhydr)oxide hosts, but were still considerably lower than adit levels (Figure 2), likely adsorbed on, or incorporated into other biogenic metal sulfide phases such as mackinawite and pyrite (Omoregie et al., 2013; Saunders et al., 2008).

That it took almost one year to reach sulfate-reducing conditions in the bioreactor is partly a reflection of the slow growth rate of psychrophilic SRB at the temperature range of the adit water (1 – 10°C over the year). Based on the bioreactor volume, and the mass of sulfate removed from the bioreactor at a flow-through rate of 1 L/s, the sulfate reduction rate (SRR) was calculated to be 45 $mM/m^3/day$. This is in line with the SRR observed in arctic ocean sediments by Kostka et al. (1999), which was generally in the range 60 – 100 $mM/m^3/day$, suggesting that the bioreactor had a similar SRR as natural systems that have long term adaptation to cold environments.

Following the recirculation period and onset of sulfate-reducing conditions, the bioreactor operated year round in flow-through mode at various test flow rates. It achieved sustained removal of zinc (>99% removal; 5 – 6 mg/L reduced to 0.01 mg/L) to levels well below the site effluent quality discharge standard (0.5 mg/L) at flow rates of 0.5 and 0.75 L/s. Concentrations of cadmium, another constituent of concern at Keno Hill, were typically lowered from *ca. 0*.0015 mg/L to below detection

limit (<0.0001 mg/L) at all flow rates tested. Reductions in arsenic, antimony, and nickel loads of >80% were also observed at flow rates of 0.5 – 0.75 L/s. Changes in the flow-through rate in the bioreactor had little impact on the removal of cadmium and arsenic from the influent adit water, however, a switch from 0.5 L/s (21 day residence time) to 1 L/s (10.5 day residence time) impacted the treatment efficiency for zinc. The lower hydraulic residence time at the high flow rate limits the extent of zinc sulfide precipitation, and the higher flow rate restricts the ability for the particulate zinc sulphide formed to physically fall out of solution. Indeed, the majority of zinc leaving the bioreactor was in particulate form (>0.45 μm), suggesting that the coarse rock in the bioreactor was unable to filter out the zinc sulphide formed, in line with observations from other bioreactors studies (Gammons & Frandsen, 2001).

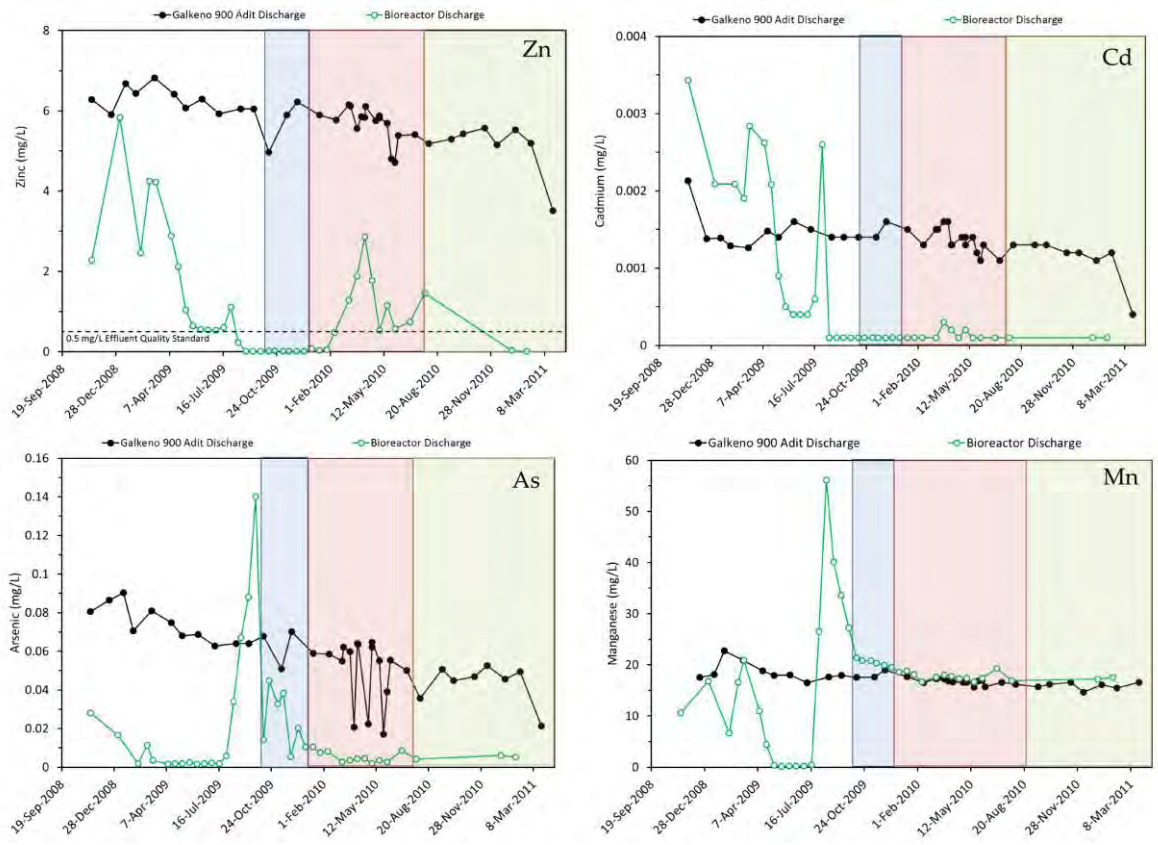

Figure 2 Concentrations of selected parameters in untreated adit water and bioreactor discharge water. Flow-through operation at 0.5 L/s, 1 L/s and 0.75 L/s, indicated by blue, red, and green shaded boxes, respectively

In situ mine pool treatment

Platoro, CO

The initial injection of soluble organic carbon into the subsurface mine pool at Platoro in September 2000 caused a rapid diminution in zinc and arsenic concentrations (Figure 3). The decline in zinc and arsenic levels was mirrored by a drop in total organic carbon (TOC) and sulfate. This points toward the oxidation of organic carbon by SRB, resulting in the precipitation of zinc sulfide (likely

sphalerite) and incorporation of arsenic into arsenic sulfide and co-precipitation with, and sorption on other authigenic metal sulfide minerals (Saunders et al., 2005, 2008; Omoregie et al., 2013; Kirk et al., 2010). Within three months of injection, arsenic concentrations had declined by >90%, reaching peaks of >99% removal over the following 6 – 18 months. The rate of zinc removal was slightly lower, reaching >90% removal seven months after treatment began, and also peaked at >99% sequestration 14 – 18 months after the injection of soluble organic carbon. Slight rises in zinc and arsenic concentrations were observed during freshet as oxidizing surface waters were introduced to the mine, however, substantially diminished concentrations of arsenic and zinc (>80% lowered) persisted for thirty months before a rebound was observed (Figure 3). It is interesting to note that the zinc and arsenic concentrations did not fully recover, and instead oscillated between 30% and 60% lower than their pre-treatment levels, suggesting some longer-term sequestration potential.

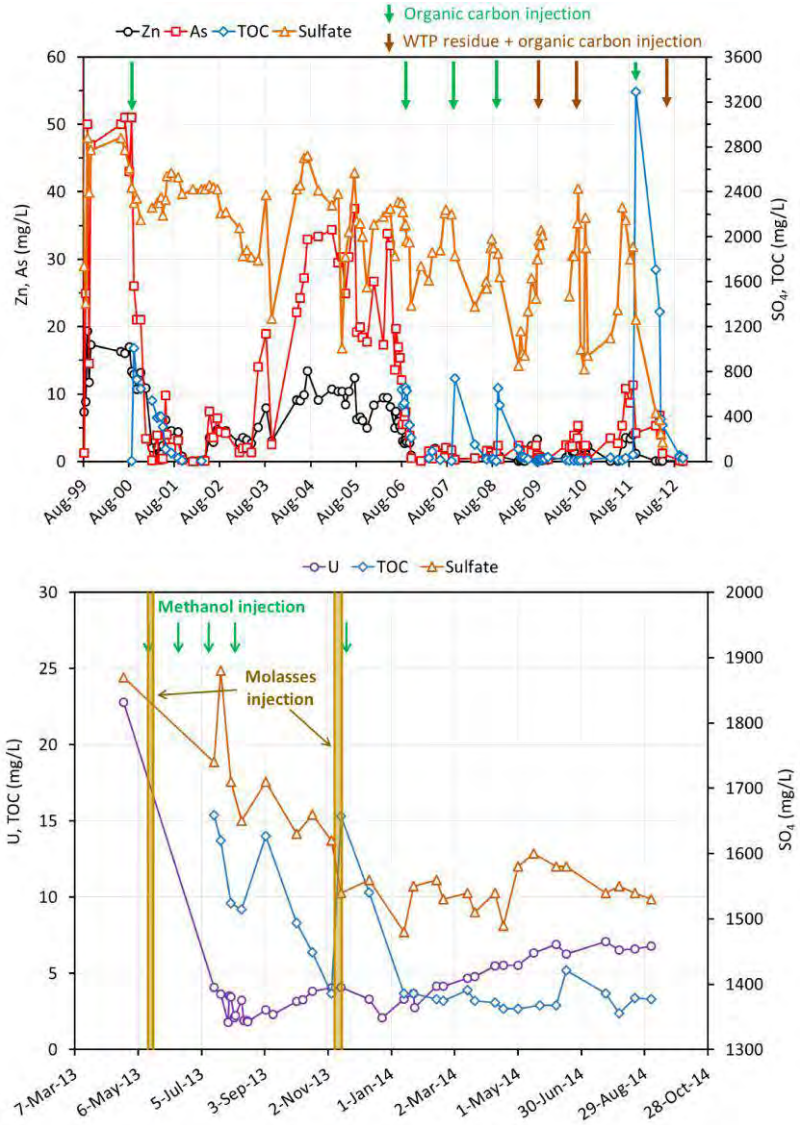

Figure 3 Change in mine pool concentrations of selected constituents at Platoro (top) and Schwartzwalder (bottom) during *in situ* mine pool treatment

A program of single, annual treatment injections was initiated at Platoro in August 2006. This maintained lowered arsenic and zinc concentrations with average removal efficiency of 97% and 93%, respectively, enabling the existing WTP to meet regulatory discharge requirements. Recycling of metal hydroxide sludge produced by the WTP into the mine pool caused the mine pool pH to rise from 2.7 to 8 within six weeks of the onset of sludge transfer to the mine workings. This further reduced the strain on the downstream WTP by reducing the amount of lime required to raise the pH and minimizing the amount of sludge requiring disposal.

Schwartzwalder, CO

Within three months of injection of molasses and methanol into the Schwartzwalder mine pool, the uranium concentration dropped by 90%, from 22.8 mg/L to 1.8 mg/L (Figure 3). This was accompanied by a decline in the concentration of sulfate and sulfide mineral-forming elements such as molybdenum, indicating that a sulfate-reducing environment was rapidly established in the mine pool. This was supported by the appearance of black suspended particulates and the development of a sulfurous odor in the mine pool water within the first few weeks of treatment. Numerous field-based studies (e.g. Anderson et al., 2003; Watson et al., 2013) have documented that such conditions are conducive to the reduction of soluble U(VI) to insoluble U(IV), resulting in the decline in uranium concentrations observed in the mine pool. Scanning electron microscope (SEM) analysis of the black suspended particulates revealed abundant microbial cells encapsulated in iron sulfide and uranium (Figure 4), the latter likely present as uraninite (UO_2) and/or monomeric uranium (Bargar et al., 2013).

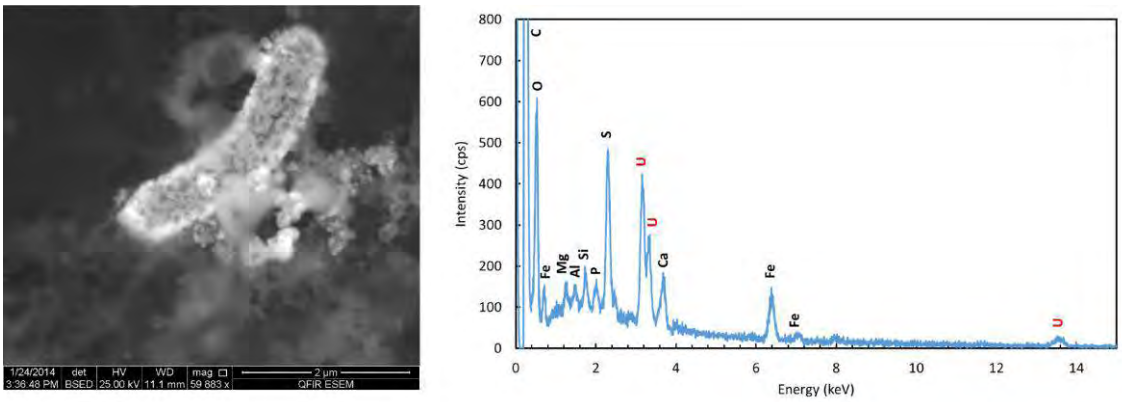

Figure 4 SEM image (left) and elemental analysis (right) on mineral encrusted microbial cell present in suspended particulates collected from Schwartzwalder mine pool a few weeks after treatment was initiated

U(VI) reduction can be mediated by direct, enzymatic activity by a range of metal- and sulfate-reducing microorganisms (Kostka & Green, 2011), or indirectly by the products of microbial sulfate-reduction (Gallegos et al., 2013), with a coupling of abiotic-biotic pathways likely (Barger et al., 2013). Indeed, the pool of iron sulfide (likely mackinawite) minerals formed can serve as a buffer to retard re-oxidation and re-solubilization of uranium (Dullies et al., 2010; Gallegos et al., 2013). Thus, although uranium concentrations in the Schwartzwalder mine pool started to rise three months after the last molasses/methanol treatment (Figure 3), the increase was likely slowed by the presence of reduced mineral phases that tempered the impact of any oxygenated water that

migrated into the system. Furthermore, ferric (oxyhydr)oxide minerals produced from the oxidation of iron sulfide phases can limit the release of oxidized uranium via sorption processes (Gallegos et al., 2013).

The low metal(loid) concentrations that were sustained in the Platoro adit discharge are likely due to the higher concentration of organic carbon that was injected (creating a large electron donor source to maintain ongoing sulfate reduction) compared to the Schwartzwalder site. The in-situ treatment of the Schwartzwalder mine pool was interrupted by a 0.5 m rainfall event which destroyed access to the site by large tanker trucks. Only 60% of the target carbon addition was achieved due to this disruptive event. It was important that dosage of the mine pool not exceed the overall targeted stoichiometry and that the rate of addition be carefully controlled because the RO membranes are susceptible to fouling with organic matter and because of the regulatory requirement that RO system operation commence with the organic carbon dosage of the mine pool.

CONCLUSION

When continuous flow was maintained to the Galkeno 900 bioreactor at acceptable flow rates, effective treatment was maintained, meeting discharge requirements for zinc, and reducing arsenic and cadmium levels to close to detection limits. The removal efficiency of zinc and nickel suffered at higher flow rates, likely due to a combination of reduced hydraulic residence time and poor filtration of the particulate metal sulfide phases formed due to the coarse nature of the rock used to construct the bioreactor. Design improvements for future bioreactors at Keno Hill include:

- Use of smaller fill material in the bioreactor to improve filtration and removal of metal sulfides within the bioreactor (Tsukamoto, Killion & Miller, 2004);
- Creation of longer, narrower flow paths to increase residence time and limit "dead zones" where little sulfate-reduction occurs; and
- Incorporation of solid phase carbon (e.g. sawdust, wood chips) into the bioreactor during construction to provide a secondary source of carbon in the event that addition of soluble organic carbon is temporarily suspended

In situ injection treatment at the Platoro and Schwartzwalder mine pools resulted in >90% removal of zinc, arsenic and uranium within a few months of the treatment injection. The low metal(loid) concentrations were sustained over many months, allowing further treatment injections to be made on an infrequent basis (annual in the case of Platoro), which is suited to remote mine sites. This treatment may be used as a stand-alone technology for sites where metal concentrations are within an order of magnitude of discharge standards, or as a pre-treatment option to reduce metal loads (and associated maintenance costs) entering more conventional downstream treatment systems. Based on these results, *in situ* injection is currently being piloted at the historic Silver King mine in Keno Hill.

ACKNOWLEDGEMENTS

The authors would like to acknowledge the assistance of Jim Lancaster and Joe Lister in the construction of the Schwartzwalder treatment/mine pool dewatering and reinjection system, and Krystal Truax in data collection and management at the Schwartzwalder mine treatment project. Jim Lancaster and Jim Muntzert are also thanked for their support in the sludge transfer and treatment process at the Platoro project.

REFERENCES

Anderson, R.T., Vrionis, H.A., Ortiz-Bernad, I., Resch, C.T., Long, P.E., Dayvault, R., Karp, K., Marutzky, S., Metzler, D.R., Peacock, A., White, D.C., Lowe, M., Lovley, D.R. (2003) Stimulating the in situ activity of *Geobacter* species to remove uranium from the groundwater of a uranium-contaminated aquifer, Appl. Environ. Microbiol., 69, 5884-5891.

Bargar, J.R., Williams, K.H., Campbell, K.M.,,Long, P.E., Stubbs, J.E., Suvorova, E.I., Lezama-Pacheco, J.S., Alessi, D.S., Stylo, M., Webb, S.M., Davis, J.A., Giammar, D.E., Blue, L.Y., Bernier-Latmani, R. (2013) Uranium redox transition pathways in acetate-amended sediments, Proc. Nat. Acad. Sciences, 110, 4506-4511.

Dullies, F., Lutze, W., Gong, W., Nuttall, H.E. (2010) Biological reduction of uranium – From the laboratory to the field. Sci. Total Environ., 408, 6260-6271.

Gallegos, T.J., Fuller, C.C., Webb, S.M., Betterton, W. (2013) Uranium(VI) Interactions with mackinawite in the presence and absence of bicarbonate and oxygen, Environ. Sci. Technol., 47, 7357-7364.

Gammons, C.H., Frandsen, A.K. (2001) Fate and transport of metals in H_2S-rich waters at a treatment wetland, Geochem. Trans., 2:1

Jong, T., Perry, D.L. (2004) Heavy metal speciation in solid-phase materials from a bacterial sulfate reducing bioreactor using sequential extraction procedure combined with acid volatile sulfide analysis, J. Environ. Monit., 6, 278-285

Kirk, M.F., Roden, E.E., Crossey, L.J., Brealey, A.J., Spilde, M.N. (2010) Experimental analysis of arsenic precipitation during microbial sulfate and iron reduction in model aquifer sediment reactors, Geochim. Cosmochim. Acta, 74, 2538-2555.

Kostka, J.E., Thamdrup, B., Glud, R. N., Canfield, D.E. (1999) Rates and pathways of carbon oxidation in permanently cold Arctic sediments, Mar. Ecol. Prog. Ser., 180, 7–21.

Kostka, J.E., Green, S.J. (2011) Microorganisms and processes linked to uranium reduction and immobilization, In: *Microbial Metal and Metalloid Metabolism: Advances and Applications*, Stolz, J.F., Oremland, R.S. (Eds.), ASM Press, pp. 117–138.

Ness, I., Janin, A., Stewart, K. (2014) Passive Treatment of Mine Impacted Water In Cold Climates: A review. Yukon Research Centre, Yukon College. http://www.yukoncollege.yk.ca/research

Omoregie, E.O., Couture, R.M., Van Cappellen, P., Corkhill, C.L., Charnock, J.M., Polya, D.A., Vaughan, D., Vanbroekhoven, K., Lloyd, J.R. (2013) Arsenic bioremediation by biogenic iron oxides and sulfides, Appl. Environ. Microbiol., 79, 4325–4335.

Saunders, J.A., Lee, M-K., Wolf, L.W., Morton, C.M., Feng, Y., Thomson, I., Park, S. (2005) Geochemical, microbiological, and geophysical assessments of anaerobic immobilization of heavy metals, Bioremed. J., 9, 33-48.

Saunders, J.A., Lee, M-K., Shamsudduha, M., Dhakal, P., Uddin, A., Chowdury, M.T., Ahmed, K.M. (2008) Geochemistry and mineralogy of arsenic in (natural) anaerobic groundwaters, Appl. Geochem., 23, 3205-3214.

Tsukamoto, T.K., Killion, H.A., Miller, G.C. (2004) Column experiments for microbiological treatment of acid mine drainage: low-temperature, low-pH and matrix investigations, Wat. Res., 38, 1405-1418.

Watson, D.B., Wu, W., Mehlhorn, T., Tang, G., Earles, J., Lowe, K., Gihring, T.M., Zhang, G., Phillips, J., Boyanov, M.I., Spalding, B.P., Schadt, C., Kemner, K.M., Criddle, C.S., Jardine, P.M., Brooks, S.C. (2013) In situ bioremediation of uranium with emulsified vegetable oil as the electron donor, Environ. Sci. Technol., 47, 6440-6448.

Investigation of Microbial In-Situ Remediation of Uranium Mine Site Pollutants in the Flooded Mine Königstein

Andrea Kassahun, Ulf Jenk and Michael Paul
WISMUT GmbH, Germany

ABSTRACT

Mining activities in the former uranium mine Königstein left acidic, highly oxidized drainage waters with pollutant concentrations (e.g. uranium) of several milligrams per litre. In the current process of mine flooding, pump and treat prevents pollution spreading. Since acid mine drainage will be generated over long periods of time, possibilities of in-situ pollutant retention within the pollutant plume are under investigation as cost saving alternative to decades of pump and treat.

A novel reactive zone technology for retention of inorganic mine site pollutants based on the stimulation of autochthonous sulphate reducing bacteria and a sequence of mineral forming processes was developed. The key process is the microbial mediated precipitation of iron sulphides, which bind pollutants and act as redox buffers under gradual transformation of their surface bound iron oxy(hydr)oxides when exposed to oxygen containing groundwater.

The stimulation of autochthonous sulphate reducing bacteria, whose existence in the mine sediments was previously shown, was tested in column experiments using a novel reactive material. It consists of silicate foam glass and zero-valent iron powder. In contact with AMD, the reactive material emits molecular hydrogen and serves as pH-buffer. Microbial colonization, precipitation of pyrite and other mineral species and pollutant accumulation to several weight percent (e.g. 1 to 3 wt.% for uranium, arsenic and zinc) were analysed at the surface of the reactive material after contact with mine waters and sediments for about one year. At redox transition to oxic conditions, iron oxyhydroxide crystallization was observed as coatings around reduced mineral formations ensuring a long term stable pollutant immobilization. Effluent pollutant concentrations during the column experiments remained beneath 150 µg/l.

Keywords: bioremediation, microbial sulphate reduction, biofilm, pollutant bonds

INTRODUCTION

From 1946 to 1990, SDAG WISMUT in former East Germany was the major foreign uranium supplier to the Soviet Union. During that period, around 215,000 tonnes of uranium were produced from more than 20 deposits. The Königstein deposit provided around 10 % of the total amount. Around 6,000 tonnes of U from the Königstein deposit were mined by acidic in-situ leaching. Mining activities caused primary uranium ores as well as sulphidic co-mineralisation to oxidize and shift to water soluble forms. The mine's inventory of mobile uranium prior to flooding was estimated 2,000 tonnes.

The Königstein mine is situated in the deepest of four sandstone aquifers. Groundwater would seep through the mine at natural flow conditions. At mine flooding, pump-and-treat prevents pollutant spreading into adjacent aquifers. Within the first fifteen years of flooding, 25 – 50 tonnes of uranium were discharged from the mine every year. Presuming constant mass flow rates, removal of the estimated amount of mobile uranium would last 40 to 80 years. Declining pollutant concentration with time will even prolong the period of potential pollution of adjacent aquifers.

In order to find cost saving alternatives to decades of pump and treat, the in-situ retention of mine site pollutants within a reactive zone was investigated. The aimed key process within the reactive zones is reductive precipitation of pollutants and thus their transfer back to water insoluble forms.

METHODOLOGY

For initiation of reductive pollutant precipitation, reducing geochemical conditions and a surplus of sulphide ions is required. Therefore, microbial sulphate reduction by autochthonous SRB is to be stimulated within the reactive zone. Microbial screening of mine drainage water, sandstone and iron hydroxide sludge samples was carried out to assess the presence of autochthonous SRB. DNA extractions were performed and 16S rDNA clone libraries were constructed [Seifert et al, 2008].

Batch tests were used to stimulate and quantify microbial sulphate reduction and to identify pollutant fixation at sulphate reducing conditions. Mine drainage water (1.07 l) was added to a mixture of milled sandstone (50 g) and milled iron hydroxide sludge (17.5 g) in gas tight glass bottles. Stimulation of SRB was performed by addition of ZVI (3 g cast iron powder) releasing H_2 as substrate for autotrophic microbes and iron ions to stimulate the formation of reduced pollutant precipitates. The headspace of the test bottles was first flushed with N_2 and later with a mixture of H_2/CO_2 after each water sampling. Tests were conducted for 240 d. Sulphate reduction rates were obtained from $^{32/34}S$ isotope analysis at dissolved sulphate ions (Helmholtz Centre for Environmental Research). Pollutant fixation was investigated by ICP-OES analysis of mine water solutes and XPS (X-ray photoelectron spectroscopy) analysis of pollutant coordination within the sediment (SGS Institute Fresenius).

To induce autotrophic sulphate reduction and pollutant precipitation within the flooded mine, a reactive material was developed. It consists of silica covered foam glass. The silica cover contains cast iron powder. The granules (1-3 cm diameter) float at mine typical pressures. They provide substrates that favour microbial growth and mineral precipitation. The reaction sequence of microbial sulphate reduction and mineral precipitation induced by the reactive material was investigated in column experiments. 25 kg of sandstone (< 3 mm), 4.5 kg of iron hydroxide sludge and 2.4 kg of reactive material were place in horizontal glass columns equipped with water in- and outlets as well as sample ports for water, gas and solids. The columns were filled with 8 l of mine water and exposed to continuous mine water flow-through at ~250 ml / d for 250 days. Pollutant fixation was investigated by

ICP-OES analysis of mine water solutes and REM-EDX analysis (TU Bergakademie Freiberg) of reactive material surfaces. For identification of pollutant bonds, sequential extractions were used [Graupner et al., 2007 for method description]. Microbial colonization was investigated by DNA extraction and classification using the clone bank constructed. Furthermore, $^{32/34}S$ isotope analysis of dissolved sulphate ions (Helmholtz Centre for Environmental Research) and GC-analysis of dissolved permanent gases were performed.

RESULTS AND DISCUSSION

Microbial screening

The mine drainage water was dominated by acidophilic iron oxidizing *Betaproteobacteria* (abundance of sequences related to *Ferribacter polymyxa*; second major sequence group with similarities to *Acidithiobacillus ferroxidans*), and heterotrophic acidophiles in minor parts.

A dominance of the sulfate-reducing bacteria *Desulfovibrio* (ca. 70%) in association with other members of the *Deltaproteobacteria*, members of the *Alpha-*, *Beta-* and *Gammaproteobacteria*, *Actinobacteria,* and *Firmicutes* was obtained for the analysed iron hydroxide sludge sample. The sandstone sample revealed a high bacterial diversity. About 20% of the analysed clones could be classified as sulphate-reducing bacteria, others were similar to aerobic and anaerobic bacteria with various physiological properties.

Fig. 1 depicts the frequency of the bacterial classes obtained by sequence analyses of clone libraries constructed with DNA of the sludge and the sandstone sample. The phylogenetic tree (Fig. 2) shows the distribution of sequenced clones belonging to the classes of *Firmicutes* and *Deltaproteobacteria* from the two clone libraries. Both harbor genera described as sulphate, sulphite, thiosulphate, and sulphur reducing bacteria. The obtained clones were used to create a fragment library for T-RFLP. This database was used to investigate further samples from the mine site, in which sulfate-reducing bacteria, like *Desulfovibrio* and *Desulfosporosinus* were detected [Seifert et al., 2008].

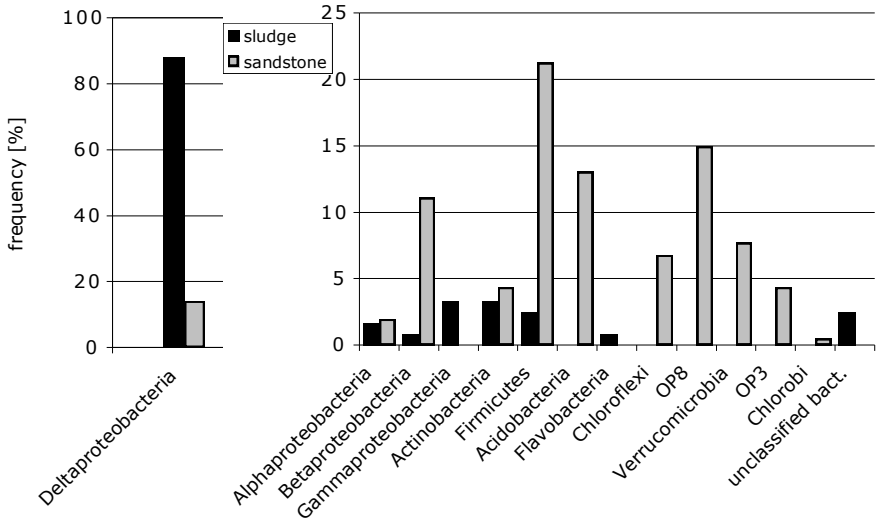

Figure 1 Frequency of bacterial classes obtained from DNA extracted from mine sandstone and mine iron hydroxide sludge [Seifert et al, 2008]

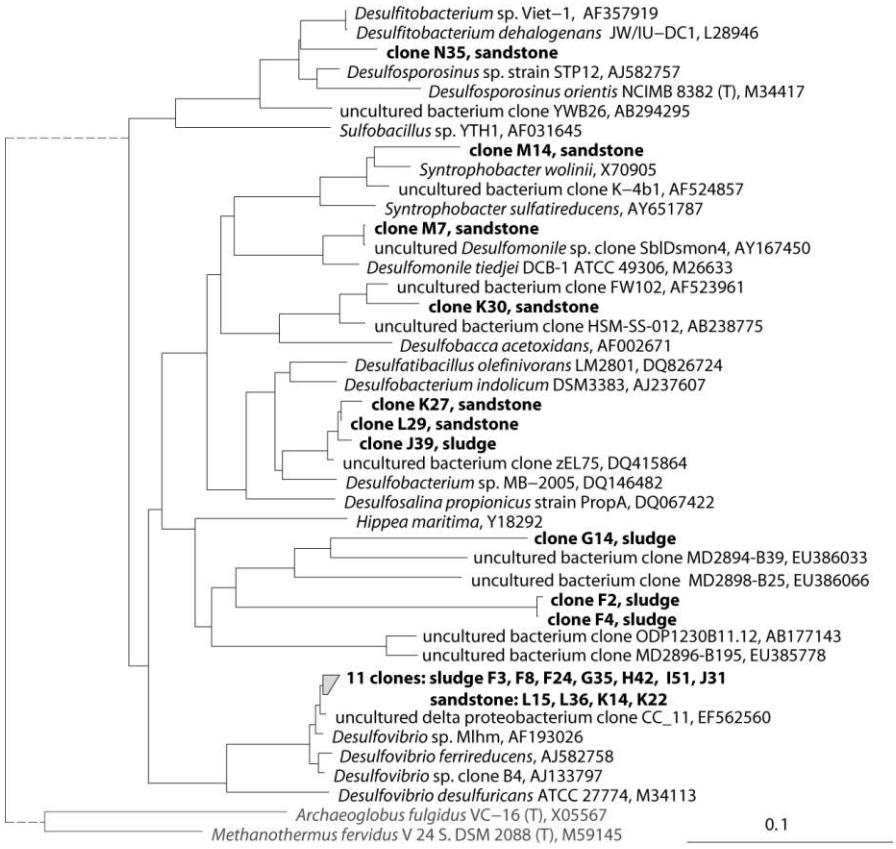

Figure 2 Phylogenetic tree of 16S rDNA sequences of *Deltaproteobacteria* and *Firmicutes* from the sludge and the sandstone sample (the sequence group within the *Desulfovibrionales* branch consists of 11 sequences from both samples; Seifert et al, 2008)

Batch tests

Tab. 1 contains the average mine water composition used for pollutant removal batch tests.

Table 1 Selected chemical parameter of mine water

pH	E_H [mV]	EC [mS/cm]	SO_4 [mg/l]	Fe [mg/l]	Ca [mg/l]	U [mg/l]	Zn [mg/l]	Ni [mg/l]	Pb [mg/l]	Cd [mg/l]	As [mg/l]
2.8	640	3	1,500	120	300	15	15	0.5	0.5	0.1	0.05

Resulting from anaerobic iron corrosion (eq. 1), redox potential decreased to -35 mV after 7 days while H_2 was detected in the bottles headspace and the concentration of iron ions increased by a factor of 3.5. After 35 days, redox potential further dropped to – 120 mV causing pollutant concentrations to fall below 200 µg/l. At the same time, pH increased to > 6.5 (Fig. 3 - upper graph).

$$Fe^0 + 2H_2O \rightarrow Fe^{2+} + H_2 + 2OH^- \quad (1)$$

Sulphate reduction was observed after a lag-phase of about 40 days in all batch tests. At first it was verifiable by a complete blackening of the bottles, which indicates iron sulphide precipitation. Because of excess of ferrous iron, no dissolved sulphide was detectable. Simultaneous decrease of iron and sulphate concentrations was measured from day 40 onwards until the end of the tests (Fig. 3 - lower graph). With decreasing SO_4 concentration in solution, the heavy isotope ^{34}S enriched within the remaining dissolved sulphate (Fig. 4). This serves as indicator of microbial sulphate reduction, since the light isotope ^{32}S is favoured in metabolism of sulphate reducing bacteria. T-RFLP investigations of batch tests aqueous phase (day 130) showed, that the microbial community was dominated by *Desulfovibrio sp.* and *Desulfosporosinus sp.*. Autochthonous sulphate reducing bacteria were stimulated successfully. The microbial sulphate reduction rate was 1-5 mg / l ·d.

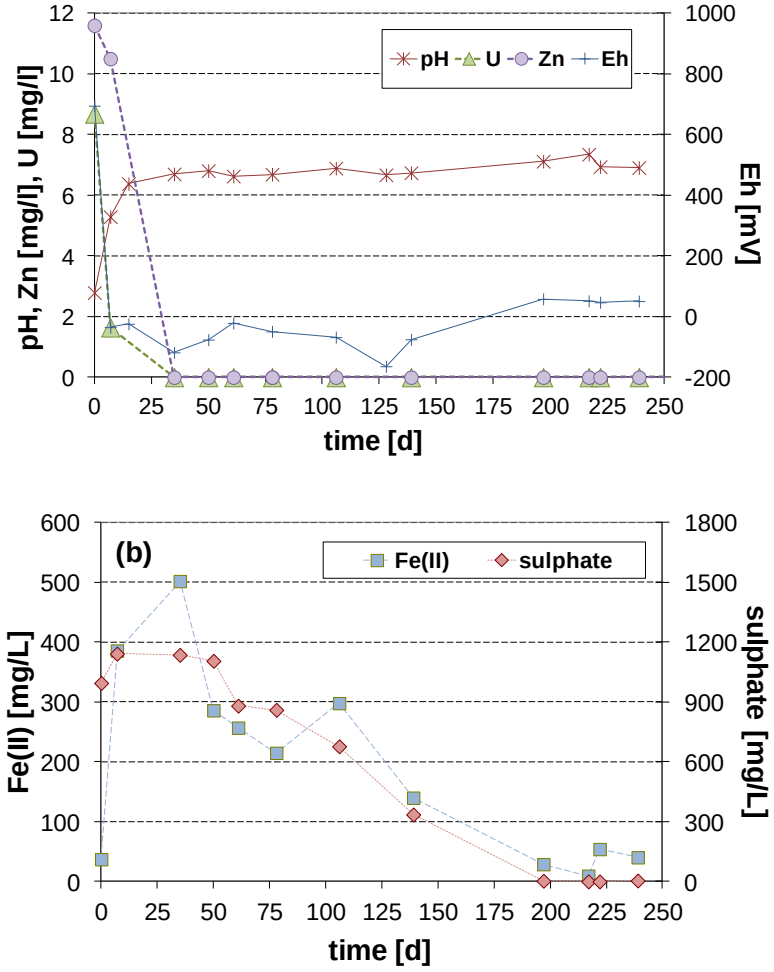

Figure 3 Selected solution parameter (above: pH, E_H, U, Zn; below: Fe, SO_4) during batch tests

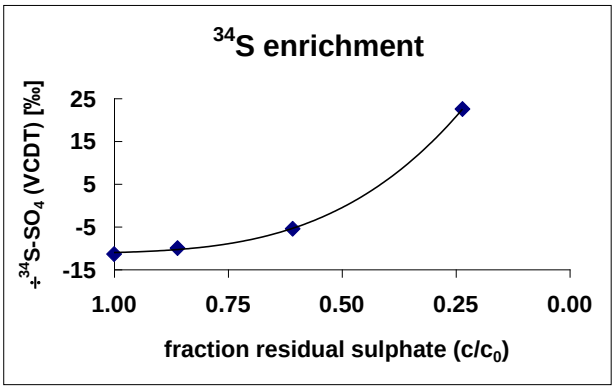

Figure 4 ^{34}S isotope enrichment in the residual dissolved sulphate of the batch test aqueous phases

XPS analysis of the solid phase (day 240) identified sulphur to occur completely reduced in monosulphide (50.9%) and disulphide phases (49.1%). This implies complete sulphate reduction and partly alteration of the initially precipitated iron monosulphide within the time period of the test. Iron was shown to be bond to sulphides (19.9%) and oxides (80.1%). The high percentage of iron oxides is related to the iron hydroxide sludge used in the test systems. Moreover, XPS analyses revealed uranium to be nearly complete immobilized in reduced mineral phases. It occurs predominantly tetravalent (80.1% UO_2) and partially in polysulphide phases (9.1% US_x (x>1)). 10.8% of the sediment bonded uranium remained hexavalent, most probably adsorbed to the iron hydroxide phase. Zn was found in ZnO coordination, which may result from $Zn(OH)_2$ precipitation with subsequent phase transformation. The test results indicate pollutant precipitation and iron sulphide formation as independent processes. Pollutant precipitation occurs prior to iron sulphide formation and is related to changes in pH and pe resulting from anaerobic iron corrosion. Microbial sulphate reduction is stimulated by H_2 evolving at anaerobic iron corrosion. Sulphide precipitates with ferrous iron to iron monosulphide, which in turn transformed partly to iron disulphide.

Column tests

The initial composition of the column feed is summarized in Tab. 2. Selected chemical parameter of the column effluents are depicted as function of test duration in Fig. 5 (above: U and Zn; below: pH, redox potential, dissolved H_2, H_2SiO_3). The pollutant concentrations[1] of the column effluent remained beneath 150 µg/l over the entire test period. Column passage caused a rise in pH from pH=3 to pH>8 and a drop in redox potential from Eh=770 mV to Eh≤250 mV due to immediate silica dissolution at the surface of the reactive material.

Table 2 Initial concentrations of column feed

pH	E_H [mV]	EC [mS/cm]	SO_4 [mg/l]	Fe [mg/l]	Ca [mg/l]	U [mg/l]	Zn [mg/l]	Pb [mg/l]	As [mg/l]	H_2SiO_3 [mg/l]	TIC [mg/l]
2.9	770	1.5	625	65	110	8.9	6.7	0.5	0.03	25	3

[1] also for Pb, As, Cd and Ni (not depicted in Fig. 5)

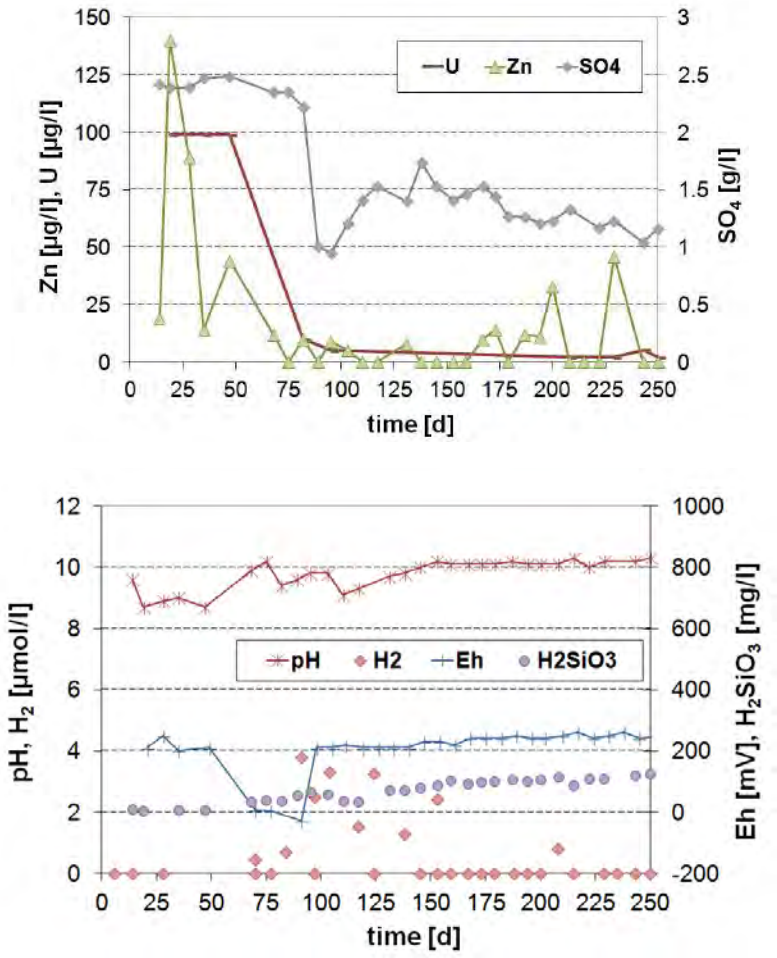

Figure 5 Selected parameter of column effluent (above: U, Zn, SO_4; below: pH, E_H, H_2, H_2SiO_3)

Around 70 days after the experiment started, anaerobic oxidation of the silica embedded ZVI set in as indicated by H_2 formation and redox potential decrease. At the same time, dissolved silica concentrations of the column effluent increased (Fig. 5 - lower graph). Dissolution of reactive material silica coatings led to pH buffering and exposure of the embedded ZVI. H_2 was detectable in water and gas samples sporadically until the end of the experiments (gas phase data not shown). Due to high pH, mine water iron precipitated within the column immediately and the effluent did not contain any dissolved iron. At the beginning of the experiments, sulphate concentrations multiplied by factor 4 during column passage because of sulphate leaching from the rock material (Fig. 5 - upper graph). At day 90, effluent SO_4 concentrations declined sharply, while anaerobic iron oxidation and H_2 supply was ongoing already. Because SO_4 feed concentrations stayed constant (data not shown) and microbial sulphate reduction counts for a maximum concentration decrease of 160 mg/l only (32 days residence time within the column; 5 mg/ l · d maximum SO_4 reduction rate), sulphate leaching rates and mineral reactions affect the effluent sulphate concentrations significantly. This prevents clear evidence for microbial sulphate reduction from concentration decrease and ^{34}S enrichment in the residual sulphate. ^{34}S isotope data of the effluent sulphate show only a slight enrichment of the heavy isotope (Fig. 6).

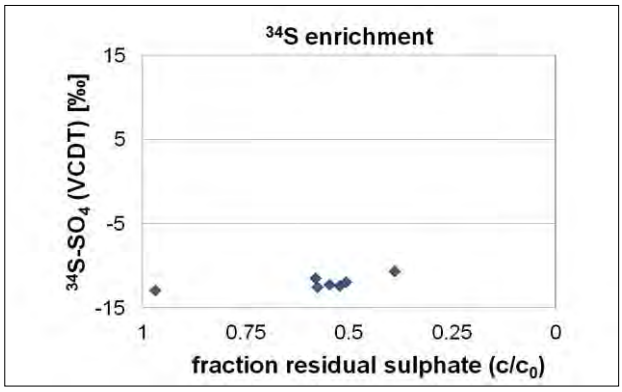

Figure 6 ^{34}S isotope enrichment in the residual dissolved sulphate of the column test effluent

The presence of sulphate reducing bacteria in the column effluent at the end of the experiment was confirmed by T-RFLP investigations. 35 % of the identified microbial DNA was assigned to sulphate reducers. Iron and sulphur oxidizing bacteria and nitrogen fixing bacteria were also identified. Next to species which were detected before in mine water and sandstone samples, the column effluent also contained typical soil bacteria (*Bosea thiooxidans sp.*, *Solirubrobacter soli sp.*).

After the experiment, the reactive material was sampled from the column for investigation of pollutant content and mineralization. Fig. 7 shows REM photographs of the reactive material surfaces, which were found to be extensively colonized by microbes (A). Within the biofilm, pollutant enrichments were identified by EDX-analysis. The bright particles (B - strong backscattering in BSE mode of heavy elements) contain U, Pb, Fe, S and C and are interpreted as sulphidic and reduced mineralization. The smaller spheres are iron (hydr)oxides (C). Their EDX spectra contain U, As, Fe, C and lack S. The coexistence of reduced and oxidized minerals is possible due to their embedding in the biofilm matrix which allows for redox niches.

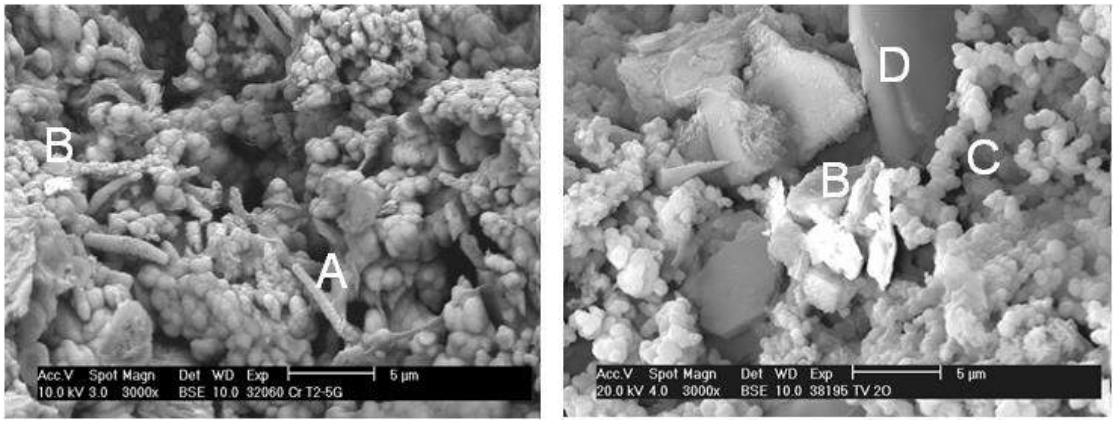

Figure 7 REM photographs of reactive material surfaces after the experiment (left: biofilm remnants and microbial structures with cell wall mineralisation (A) and heavy element accumulations (light coloured particle B); right: heavy element accumulation (light coloured particles B), iron (hyr)oxides spheres (C) and silica sheets (D)

The coexistence of oxidized and reduced minerals also occurred in a larger scale. The left photograph in Fig. 8 shows a glass column segment after the experiment with blackening of iron hydroxide sludge (orange) and sandstone dust (grey) in contact with reactive material. The right photograph shows the alteration of the reactive material (originally grey granules), on which mineral coatings precipitated (orange and blackish-red granules). Sequential extractions of the blackish-red coating revealed the highest pollutant content within the reduced mineral fraction, followed by the fraction content of amorphous iron hydroxides and biofilm organic substances (Fig. 8 – upper bar chart). In contrast, most iron is bond to amorphous iron hydroxides, followed by biofilm organic substances (Fig. 8 - lower bar chart). The reduced phases contain ~1 wt% iron, which equals 1.6 wt% iron monosulphide or 2.15 wt% iron disulphide, respectively.

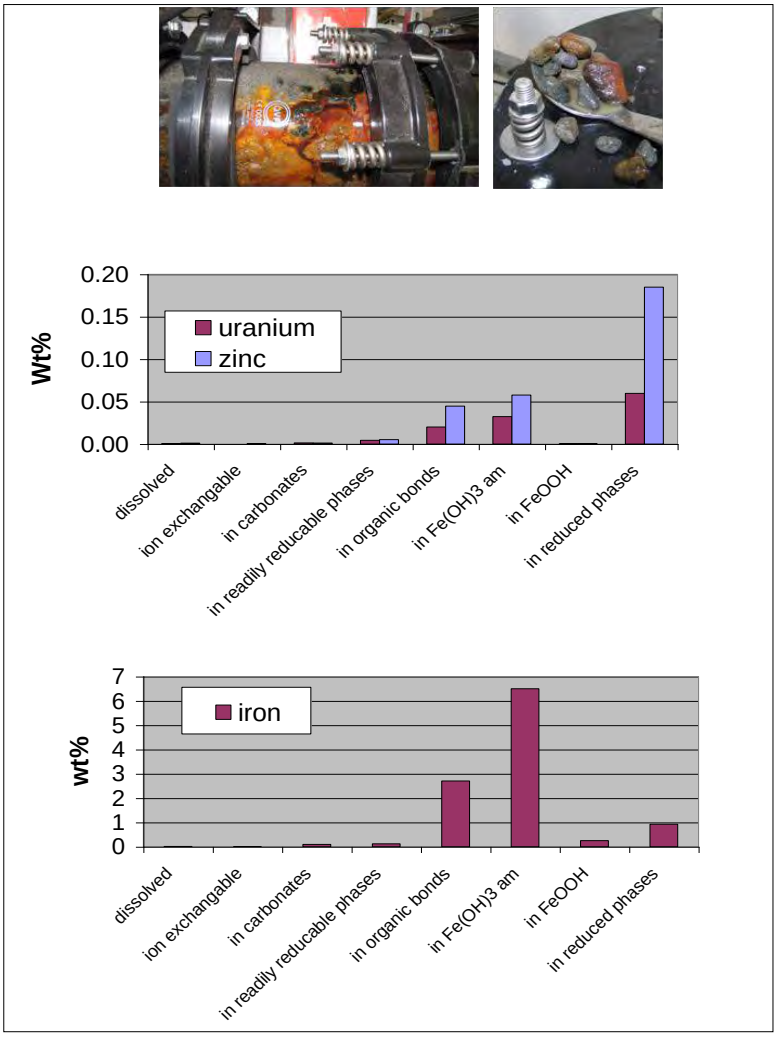

Figure 8 Photographs of glass column segment and reactive material after the experiment and bar charts on uranium, zinc (upper graph) and iron contents (lower graph) in different binding forms as extracted from the blackish-red reactive material coating after the experiment (sequential extraction)

CONCLUSION

The flooded mine Königstein hosts a diverse autochthonous microbial biocenosis. Its autotrophic growth can be stimulated by anaerobic iron corrosion products (OH^-, H_2). At anaerobic oxidation of cast iron powder in mine water, autochthonous sulphate reducing bacteria form sulphide ions at rates of 1 – 5 mg / l · d. The presence of sulphide facilitates pollutant immobilization by direct precipitation (e.g. lead, zinc, uranium) and by iron monosulphide formation, which in turn transforms to iron disulphide. Iron disulphide surface reactions reduce oxidized solutes and cause pollutant reduction comparable to ZVI (e.g. for uranium). Pollutant immobilization from acid mine water in contact with ZVI depends on sorption and reduction at ZVI surfaces, sulphidic precipitation, sorption and reduction at iron sulphides and its ferrous iron hydroxide surface layers as well as on redox buffering. The latter is based on the oxidant scavenger effect of elemental and ferrous iron oxidation with subsequent ferric iron hydroxide formation. If ferric hydroxide formation occurs in close vicinity to the reduced minerals, it may form coatings that protect them from re-oxidation. That is of special importance for preventing future pollutant remobilization in contact with dissolved oxygen upon completion of microbial activity stimulation.

A reactive material designed to carry ZVI, microbes and precipitates by floating in mine water is suited for in-situ-application of ZVI induced pollutant retention. Comparable to cast iron powder, the reactive material is able to emit H_2, to stimulate autochthonous sulphate reducers, to buffer pH and to induce pollutant and iron sulphide precipitation. Moreover, the material provides dissolved silica and serves as microbial growth support and biofilm carrier. This facilitates sustainable pollutant retention considerably. Biomolecules promote mineral formation by serving as precipitation templates. Biofilm matrices provide niches that allow for different redox conditions and thus for coexistence of reduced and oxidized minerals in very close spatial vicinity. Incorporation of silica in mineral precipitates decreases their water solubility. If exposed to mine water flow, mineral coatings form on the reactive material. They contain both reduced and oxidized pollutant bonds. Their iron hydroxide coatings encapsulate mine water pollutants also under oxidizing conditions.

Based on the investigation of underlying processes, microbial in-situ remediation seems feasible to inhibit the discharge of uranium mine site pollutants from the flooded mine Königstein.

REFERENCES

Graupner, T., Kassahun, A., Rammlmair, D., Meima, J.A., Kock, D., Furche, M., Fiege, A., Schippers, A., Melcher, F. (2007) Formation of sequences of cemented layers and hardpans within sulphide-bearing mine tailings (mine district Freiberg, Germany). *Applied Geochemistry*, vol 22, pp. 2486-2508.

Seifert, J., Erler, B., Seibt, K., Rohrbach, N., Arnold, J., Schlömann, M., Kassahun, A., Jenk, U. (2008). Characterization of the microbial diversity in the abandoned uranium mine Königstein. In: Merkel, B., Hasche-Berger, A. (eds.) *Uranium, Mining and Hydrogeology*, Springer, pp. 733-742

10th ICARD IMWA 2015 | 10th International Conference on Acid Rock Drainage & IMWA Annual Conference

Heavy Metal Removal and Partitioning in Sulfate-Reducing Bioreactors Treating Mine Influenced Water

Benjamin Uster[1], Mark Milke[1], Aisling O'Sullivan[1], James Pope[2], Dave Trumm[2] and Jennifer Webster-Brown[3]

1. *Civil and Natural Resources Engineering, University of Canterbury, New Zealand*
2. *CRL Energy Ltd., New Zealand*
3. *Waterways Centre for Freshwater Management, University of Canterbury, New Zealand*

ABSTRACT

Four upward flow sulfate-reducing bioreactors (SRBRs) were tested in duplicate for two hydraulic retention times (HRT; 3 and 10 days) to treat mine influenced water (MIW) over a 10 month period. Locally available organic materials (bark, compost and bark mulch) as well as two alkalinity generating materials (limestone or waste mussels shells) were used as SRBR substrates. Following the flow-through treatment period, the spent substrate mixtures were analyzed using a combination of wet chemical and mineralogical analyses, including a sequential extraction procedure (SEP), X-ray diffraction, X-ray fluorescence and scanning electron microscopy equipped with X-ray energy dispersion spectrometer (SEM-EDS). Results from the SEP indicated that (1) Al, Fe, Cu and Ni are mostly retained in the residual, sulfide or organic-bound fractions, (2) Mn is mainly concentrated in the exchangeable and carbonate fractions, and (3) Zn and Cd are predominantly associated with the reducible, sulfide or organic bound fractions. While Mn partitioning was influenced by the HRT (a longer HRT resulted in more Mn associated with the carbonate fraction), all other metals seemed to behave independently from it. Furthermore, the HRT had an influence on the localization of the metals within the substrate, as the short HRT resulted in larger concentrations of Fe and Al in the top part of the reactors compared to the long HRT which resulted in similar concentrations for both the top and the bottom parts. SEM-EDS microanalyses identified Fe, Cu and Zn associated with sulfur. These combined analyses allowed us to assess metal removal mechanisms in SRBRs as well as potential metal mobility during management of spent substrates used in MIW passive treatment systems.

**There is no full article associated with this abstract.*

Evaluation of Biological Diffusive Exchange System Prototypes for Acid Mine Drainage Treatment

Norma Pérez, Gustavo Chaparro and Alex Schwarz
Centre of Water Resources for Agriculture and Mining (CRHIAM), Universidad de Concepción, Chile

ABSTRACT

Acid mine drainage is a pollution problem affecting mining, and chemical and/or biological remediation are used to solve it. The use of biological treatment is restricted to low toxicity of the acid drainage; at low pH and/or high metal load, chemical treatment steps must be applied prior to biological treatment. This investigation works on a new biological treatment, the diffusive exchange bioreactor, which incorporates the principle of transverse diffusion and uses fine organic material as reactive substrate, to minimize negative effects of toxicity, clogging, passivation and inefficient use of space. Our goal is to optimize a diffusive exchange system. Organic substrate source, method of inoculation, operation with toxic drainage and three bench scale prototypes were evaluated.

The sulfate reduction potential of several organic substrate mixtures was assessed in batch reactors for three synthetic acid drainages of increasing strength. Then, we test three diffusive exchange reactor prototypes using the optimum substrate mixture, and compare their performance with a conventional homogeneous biochemical reactor. The design goals were to protect microbial communities from toxicity and avoid clogging while allowing means for valuable metals recovery. The organic substrate mixtures had high sulfate reduction rates between 700 and 1500 mmol/m^3/day. The mixtures with cellulose fibers presented the highest rates. The reactors removed over 99% of influent metals (528 mg Cu/L, 85 mg Zn/L, and 95 mg Al/L) and between 28 and 33% of the sulfate. In the diffusive exchange systems, metal precipitation was mainly due to biological activity, and higher sulfate reduction rates were obtained with screened tubes of smaller diameter. In the homogeneous reactor, on the other hand, sulfate reduction was detected only after 44 days. Because hydraulic loads were low, all reactors performed well. In the future, however, under much higher hydraulic loads, we expect the diffusive systems to perform better.

**There is no full article associated with this abstract.*

CHAPTER 7

MINE WATER DRAINAGE COLLECTION AND TREATMENT – PASSIVE TREATMENT

10th ICARD IMWA 2015 | 10th International Conference on Acid Rock Drainage & IMWA Annual Conference

Passive Treatment of ARD Using Mussel Shells – Part I: System Development and Geochemical Processes

Paul Weber[1], Chris Weisener[2], Zach DiLoreto[2] and Mark Pizey[3]

1. *O'Kane Consultants Ltd., New Zealand*
2. *Great Lakes Institute for Environmental Science, University of Windsor, Canada*
3. *Solid Energy New Zealand Ltd.*

ABSTRACT

The passive treatment of acid rock drainage (ARD) impacted waters using waste mussel shells utilises vertical flow successive alkalinity producing system (SAP) technology, with considerable industry acceptance in New Zealand. This paper discusses the seven year R&D pathway for this technology. The process is attractive to the mining industry as the shells are free-to-site in some instances, and the installation process is relatively straightforward.

Sulfate Reducing Bioreactors (SRB's) and oxic and anoxic treatment of ARD impacted waters are common passive treatment technologies employed by the mining industry. Mussel shells have significant advantages over these systems, being negative value (and thus free-to site, or even delivered for profit), having a high acid neutralisation capacity (> 80 wt% $CaCO_3$ equivalent), good hydraulic conductivity (~$1x10^{-3}$ m/s), and sufficient organics to support sulfate reducing bacteria catalysts for metal removal. This means that processing costs are reduced and the shells can be placed directly into the reactor.

Down-flow bioreactors using shells have been investigated to encourage the calcium carbonate induced neutralisation of ARD followed by SRB alkalinity generation and trace metal removal. Details are presented of two systems (fresh and weathered shells) that were established at the Solid Energy Stockton Coal Mine, West Coast, New Zealand. Results show the formation of an upper zone dominated by sediment transitioning into underlying Fe then Al precipitate zones that is eventually replaced by a deeper sulfate reducing zone. Metal removal efficiencies range from 96 – 99% for Fe, Al, Ni, and Zn. The longevity of the system is linked to permeability, which is controlled by layers of sludge that develop during treatment.

INTRODUCTION

Acid Rock Drainage (ARD) is typically, the greatest long-term environmental and financial liability for the mining industry where acid-forming waste rock is disturbed. It can result in a project 'hangover' after closure that requires water treatment in perpetuity. Hence other projects and new mines are required to support the cost of legacy treatment. The goal for many companies at closure is to implement passive treatment as a final, lower cost ARD treatment option compared to active treatment.

For remote locations, the use of convention media (compost, bark, sawdust, limestone, etc) for passive treatment is expensive and transport costs can be significant. In New Zealand, research into passive treatment of ARD has been ongoing for a number of years (e.g., Trumm et al., 2008; McCauley et al., 2009; Trumm, 2010; Mackenzie et al., 2011). More recently, since 2007 research investigating the benefits of waste mussel shells for passive treatment of ARD impacted waters has been completed in New Zealand (e.g., Weber et al., 2008; Crombie et al., 2011., Uster et al., 2014; Weisener et al., 2015; Trumm et al., 2015)

BACKGROUND

The green-lipped mussel (*Perna canalicuta*), known as the New Zealand Mussel is an endemic shellfish occurring along most New Zealand coast lines. More than 95,000 tonnes of mussels were harvested from farms in 2011 and greater than 80% of these mussels were exported as half-shells generating considerable shell waste (Uster et al., 2014). Significant cost are associated with the disposal of these shells, which means that any beneficial reuse option becomes a win-win outcome for both suppliers and end-users.

In 2007, a trial was conducted at the Stockton Coal Mine to determine the benefits of the addition of a 300 mm layer of shells beneath 5 m of potentially acid forming (PAF) waste rock (Weber et al., 2008). The trial involved 10 tonnes of mussel shells in a 4 m by 10 m lysimeter that was then covered with 3 m of PAF. A control lysimeter containing only acid-forming overburden was set up adjacent in the same manner. Leachate from the lysimeter treated with mussel shells had a pH of 6.7; acidity of 2 mg/L $CaCO_3$; 0.5 mg/L Fe and 0.2 mg/L Al versus pH 3.3 for the control; acidity of 350 mg/L $CaCO_3$, 8.5 Fe mg/L and 54.7 mg/L Al.

Subsequent work investigated the use of mussel shells as an alternative ARD neutralisation source in vertical flow sulfate reducing bioreactors (SRB) (e.g., McCauley et al., 2009; McCauley, 2011). Laboratory trials indicated that the shells provided significant alkalinity compared to limestone (McCauley, 2011; Uster et al., 2014) confirming the use of shells as an alkalinity source in a SRB type systems.

Key components of any material blend to be used within an SRB are a source of alkalinity, a source of organic matter suitable for bacteria, bacteria, and good porosity. Generally for SRBs this requires the use of materials such as sawdust, bark, compost, limestone, etc, which can be expensive. Mussel shells, as provided from the processing factory, have been chipped to reduce particle size and have a porosity of 0.72 (McCauley, 2011); an acid neutralisation capacity (ANC) or carbonate content of 786 - 894 kg $CaCO_3$/tonne as determined by the ANC test; and an organic (meat) content for fresh shells of 5 – 12 wt% (Crombie et al., 2011). In addition to this 'meat' the shells contain significant protein and chitin.

MANCHESTOR STREET PILOT SCALE MUSSEL SHELL BIOREACTOR

The Manchester Street Mussel Shell Bioreactor, a pilot scale trial, was constructed in June 2009 to treat the Manchester Street Seep (pH 2.8; 422 mg $CaCO_3$/L Acidity; 29 mg/L Fe; 51 mg/L Al) derived from acid forming waste coal overburden. Fresh shells were chipped to < 30 mm in diameter to enable full-weight loads for transport and were typically delivered within 24 hrs. Odour associated with the decomposing meat residue present in the shells was a key issue along the transport route and for onsite stockpiling.

A simple system was planned to minimise costs, which involved a downwards flow reactor design (Figure 1). Manchester Seep influent entered the bioreactor and formed a pond over the shells. This was created by having a riser on the outflow pipe that created a 200 mm water cover over the shells to control odour and ensure saturation of the shells. Water then flowed from this pond down through the shells into a drainage network, which then discharged to Ford Creek, a stream impacted by ARD. A total of 160 t of shells was placed in the reactor to produce a layer 2 m deep and 35 m by ~ 5m wide (range 2.7 -10.2 m).

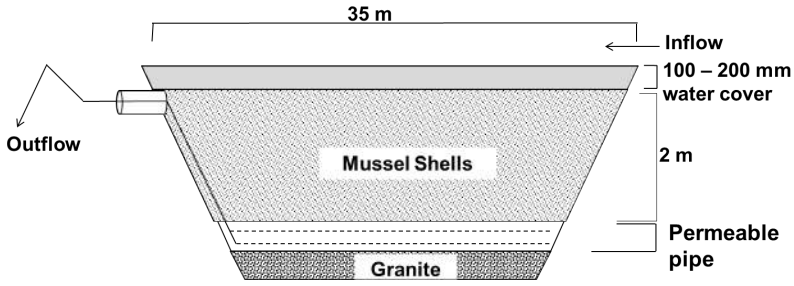

Figure 1 Manchester Street mussel shell bioreactor design.

Water samples from the influent and effluent were collected daily for 28 days and thereafter weekly. Field-based analysis included temperature, pH, EC, DO, odour, and flow. Laboratory analysis included acidity (mg $CaCO_3$/L), ammoniacal nitrogen, and dissolved Al, Fe, Ni, and Zn (Ni and Zn were selected to due being elevated in ARD impacted waters at site). Typical flows for the system were 0.04 – 0.59 L/s with a mean of 0.3 L/s. Often during higher flow (> ~1L/sec) the capacity of the mussel shell reactor was exceeded.

Monitoring results indicated that the mean pH (based on [H+]) of the seep increased from pH 2.8 to pH 6.9 after treatment, and for 59 out of 84 days the effluent pH was ≥7. The mean acidity recorded in the influent was 422 mg $CaCO_3$/L, which is significantly above the mean effluent of 0.3 mg $CaCO_3$/L. Metal removal efficiency was 96-99% for Al, Fe, Ni, and Zn (Crombie et al., 2011). Ammoniacal nitrogen and carbonaceous biochemical oxygen demand ($CBOD_5$) were initially elevated at 46 mg/L and 200 g O_2/m^3 respectively on day 16 before, decreasing steadily to a mean of 3.4 mg/L and 58.44 g O_2/m^3 respectively.

An autopsy of the mussel shell bioreactor was completed by draining the pond (and diverting the inflow) and digging several 300 mm square holes through the sludge layer into the shells (Figure 2). It was observed that the reactor had an upper sludge-sediment layer, a lower thinner orange layer, a white precipitate layer beneath that changed into a lower layer of black shells, which continued to the base of the reactor. It was expected these zones reflected a change from a low pH, high DO, high acidity, high metal ARD to a circum-neutral pH, low DO, low acidity, low metal environment. Samples were sent for laboratory analysis.

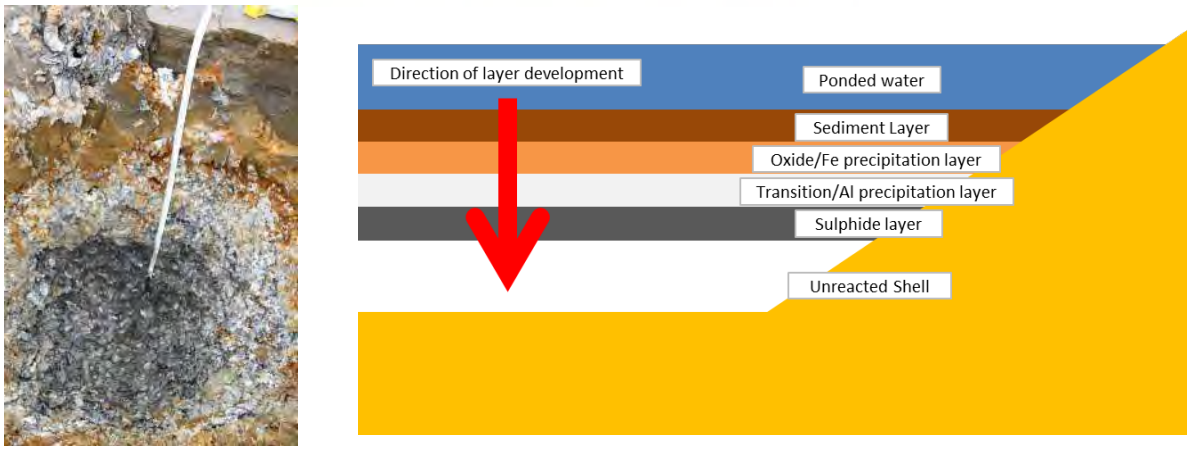

Figure 2 Manchester Street Mussel Shell Bioreactor (photo and schematic). Autopsy test pit (photo) showing sediment (TSS) sludge layer; Fe precipitate layer; Al precipitate layer; and at depth black unreacted shells. The tape measure is 800 mm from the surface to the base of the hole.

The red-brown sludge layer (~200 mm deep) forming on top of the mussel shells is likely to be a combination of road dust, sediment (TSS) transported into the reactor from the seep, and mineral precipitates derived from the AMD. Based on the depth of the sludge and pond dimensions 5 m^3 of sludge was calculated to have accumulated after one year. The median TSS for the seep that drains into the reactor is 18.8 mg/L, although intensive events can range up to 2,960 mg/L (McCauley et al., 2009). Analysis indicated that the Fe layer contained predominantly Fe (24,000 mg/kg) with minor Al (1,620 mg/kg) and less Si (32 mg/kg). Analysis of the white precipitate on the shells below the Fe layer confirmed it was a precipitate high in Al (~70% of the sample or 14,000 – 28,000 mg/kg).

Testing indicated that the neutralization capacity of the shells in the upper white precipitate layer had decreased compared to the black underlying shells. This was determined by flooding shells from the different layers with influent AMD in a sealed container and measuring the time to reach pH 7.0. Results (Crombie et al., 2011) indicated that significant buffering occurred at pH 4 - 5, most likely due to $Al(OH)_3$ precipitation (and acidity buffering). Acidity was neutralized in 1 day for the black shells and 3 days for the white Al layer shells suggesting its neutralization capacity was diminished. ANC testing of the shell from different layers showed that ANC increased with depth and the upper layers are providing significant carbonate neutralization as indicated by reduced ANC (Table 1). Weathered shells have a higher ANC again (956 kg $CaCO_3$/t), which is likely to be a function of less organics due to decomposition.

Table 1 Manchester Street mussel shell bioreactor autopsy results.

Layer	Mean Depth (mm)	ANC (Diloreto, 2013)	Rinse pH	Dominant region of metal removal	Metal removal mechanism
Sediment Sludge Layer	160	8.76	3.01		
Orange Fe Layer	340	288	6.86	Fe, As, Cr	As – Adsorbed Cr- co-precipitated
White Al layer	420	499	6.84	Al (peak), Cu	Cu - sorbed

White Al Layer	550	825	7.54	Al, Zn, Ni	Ni- Co-precipitated with Al Zn - sulfides
Black Shell Zone	1050	846	8.64		Sulfides: wurtzite
Weathered shell from stockpile	Stockpile	956	8.77	-	-

Table 1 indicates that rinse pH increases with depth with a significant increase in pH from the sediment sludge layer to the orange Fe oxide layer. This suggests that the dominant zone of carbonate neutralization is within the orange Fe oxide layer raising the pH to > 6. The system can be divided into five layers if the Al-rich layer is divided into two zones based on the redox gradient and that together with pH this controls the metal removal mechanisms. Key observations from selective extractions (Table 1) indicate a variety of removal processes as shown in Table 1 (Diloreto, 2013).

The longevity of the bioreactor is compromised by the low permeability ferruginous-sediment rich sludge. The autopsy pits that were dug allowed ponded water to drain quickly indicating the higher permeability of the underlying shell layers. Therefore sludge management will be an important component of successful operation of down flow reactors using mussel shells.

Results indicated that ~0.035 tonnes of acidity were neutralised by the mussel shell bioreactor per day. The cost of water treatment for the site in 2011 was ~$320 per tonne of acidity. The cost of installing the mussel shell reactor was approximately $5,300, thus if the system neutralised ~17 tonnes of acidity, the payback of the capex to construct the mussel shell reactor had been achieved. Based on a neutralisation rate of 0.035 tonnes of acidity per day the reactor would achieve pay back after 480 days. This initial trial suggested that the technology had merit and a larger operational trial was planned.

WHIRLWIND STREAM OPERATIONAL MUSSEL SHELL BIOREACTOR

The Whirlwind Stream, towards the southern end of the Stockton Coal Mine and impacted by ARD was selected as a site for the construction of an operational mussel shell bioreactor capable of treating up to 6 L/sec flow, although expected flow rate for the site was ~1 L/s. Results indicated that the seep has less concentrated ARD chemistry compared to the Manchester Seep having pH = ~3.3; dissolved Al = 7.3 mg/L; dissolved Fe = 1.1 mg/L; acidity = 71.5 mg $CaCO_3$/L. In this system the Whirlwind seep flows into an upstream settling pond prior to entering the mussel shell bioreactor (see Weisener et al., 2015 this volume for schematics of the system). It was expected this would reduce the suspended sediment load significantly. Design data is provided in Table 2.

Table 2 Whirlwind Mussel Shell Bioreactor design specifications. Calculations are based on a shell density of 990 kg/m3 and a mussel shell ANC of 800 kg/t.

Parameter	**Rough size**
Average Plan Dimensions (m) (Shell layer)	14.0 x 21.5
Average Plan Area (m^2) (Shell layer)	302
Average Shell depth (m)	1.2
Ponding depth (m)	0.2 - 0.6
Freeboard (m)	0.8 - 0.4

Volume of shells (m^3)	366
Mass of Shells (T)	362
Pore volume (m^3)	192
Residence time (days) (@ 1 - 6 L/s)	2.2 - 0.44
Total ANC (T $CaCO_3$)	290

The pond height in the Whirlwind bioreactor was controlled by a riser from an underdrainage network providing 200 mm ponding depth above the shells. An overflow spillway was constructed at 600 mm above the shells. This provided 400 mm of storm water buffer until overflow to the spillway occurred. Based on the average plan dimensions (Table 2) this provided 120,400 L of capacity. Often after larger rainfall events the spillway was running and the discharge pipe from the mussel shell bioreactor was running at full capacity (6 L/s being the capacity of the drainage network).

One different aspect of this mussel shell bioreactor compared to Manchester Street was that weathered shells were used. As shown in Table 1 the ANC was higher, and the organic content was lower. It was the expectation of the authors that sufficient organic matter remained and little carbon was needed for the sulfate reducing bacteria. Results (Weisener et al., 2015) indicate that a similar geochemical gradient has occurred after 18 months although the thickness of the layers is smaller due to the lower ARD loadings per square meter. Carbon longevity still needs to be considered for this system and trials are in progress.

The treated water from the Whirlwind bioreactor was typically pH 7 and then entered the Whirlwind tributary at compliance water monitoring point S4 together with additional AMD impacted drainage. A significant increase in pH was observed at the S4 monitoring point within the Whirlwind stream after the mussel shell bioreactor was installed (Figure 3).

A key limitation for the longevity of down-flow passive treatment systems using mussel shells is the formation of a low permeability sludge layer. In June 2014, 18 months after the Whirlwind bioreactor was started a double ring infiltrometer was used to measure infiltration rates through the sludge layer that had formed on top of the reactor (22 mm thick). Results indicates that infiltration was in the order of 1.87×10^{-5} m/s, which based on the average plan area (Table 2) generated a flow of 5.7 L/sec for the system. This is within the design specifications of the system and ongoing monitoring will be undertaken every 6 months to measure any further decrease. It is proposed that the system has failed when permeability reduces such that treated flow is < 1 L/sec, or an infiltration rate of $<3.3 \times 10^{-6}$ m/s. At this point the sludge layer would be removed and additional mussel shells placed back in the bioreactor.

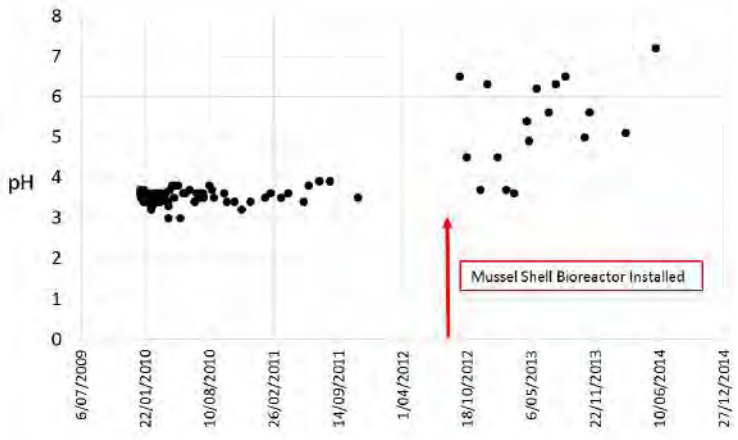

Figure 3 pH versus time profile for the S4 compliance monitoring point (affected by additional AMD impacted mine water) in the Whirlwind Tributary downstream of the Whirlwind Mussel Shell Bioreactor.

The Whirlwind bioreactor has been operating since September 2012. Ongoing research continues to investigate the bio-geochemical reactions occurring within the reactor (e.g., Diloreto, 2014; Weisener et al., 2015) and other research groups are considering other options for the use of mussel shells for passive treatment of AMD impacted waters (e.g., Trumm et al., 2015). A number of issues such as longevity; changing redox fronts, waste management, etc for mussel shell bioreactors still require consideration.

SUMMARY

A significant issue for passive treatment systems is longevity and surety that upfront capex costs will be a favourable use of resources for the treatment of AMD impacted waters in the long term. The short term performance of passive treatment systems are often well quantified, however, their long-term effectiveness is still poorly understood. Carbon exhaustion and hydraulic malfunctions are often amongst the most frequent reasons reported for system failure. As a summary, a risk analysis is presented for mussel shell bioreactors as a passive treatment technology for AMD impacted waters, based on the experience obtained from Stockton Coal Mine. The observations and approach developed is likely to transfer directly to other calcium carbonate shell waste from aquiculture (oyster shells, abalone, cockles, scallops, etc) as their physicochemical attributes are likely to be similar.

Table 3 Summary of key issues for down-flow mussel shell bioreactors. Traffic light classification is green for positive benefits or the process is understood and can be managed; red is negative aspects; and orange components are either indeterminate or need further investigations.

Component	Comment	Traffic Light
Material Characteristics		
Supply	• Limited by location of shells and reasonable transport distance. • Other shells may also be suitable (e.g., oyster, zebra mussels).	
Cost	• Low- or no-cost dependant on transport distance and commercial negotiations.	
Preparation	• No preparation costs as suppliers generally chip shells to increase density for transport to landfill.	
Blending	• No blending of shell with other materials required as it is a stand-alone product.	
Carbonate Neutralisation	• ANC values of > 800 kg $CaCO_3$/tonne expected with high surface area. • Carbonate alkalinity better than limestone based products on a weight basis.	
Organic Matter	• Greater organic matter content in fresh shells; unweathered shells contain less. • Longevity of organic matter unknown, although bacterial recycling may provide additional carbon. **Further investigations are underway.**	
Porosity	• Measured hydraulic conductivities of 1 x 10^{-3} m/s for fresh shells. • Porosity better than limestone for the same quantity of ANC / surface area	
Odour	• Can be a key issue for community and workforce. • Burial under a water cover removes the issue of odour; fine limestone application to the stockpile can also reduce the odour.	

Component	Comment	Traffic Light
Lifecycle Analysis	• Mussel shells are a waste stream and beneficial reuse of such materials provides a win-win for both the supplier and end-user. • $CaCO_3$ is not fossil CO_2 and can be considered renewable.	
Operational Performance		
Construction	• Shells can be placed directly into the reactor without further processing. • The system should be constructed such that excavators can access the site and remove any sludge as required.	
Start-up	• AMD impacted waters were fed in directly (no need to equilibrate system) • Sulfate reducing bacteria quickly populate the low DO high pH zones.	
Permeability	• Measured infiltration rates of 1.87×10^{-5} m/s determined; although this may decrease with time. **Further investigations are underway.**	
Longevity	• Such systems are expected to last 10-20 years and will be a function of cycling organic C, acidity and metal load. **Further investigations are underway.**	
Transitional pH, Eh profiles	• With maturity the defined geochemical layers may change resulting in the release of metals. Monitoring effluent discharge will provide early warning signs of such changes and system failure. **Further investigations are underway.**	
Maintenance	• It is expected regular maintenance is required to remove the formation of sludge on the surface of the reactor. Timeframes for this will be site specific. • Removal of the sediment sludge and Fe-oxide sludge in down-flow reactors could provide additional space in the reactor for upper shell layer replenishment.	
Sludge Disposal	• Oxidised materials from the upper layers can be disposed of in a "high and dry' environment. • Reduced materials need to be disposed in a structure that prevents oxidation of any sulfide minerals formed (e.g., permanently submerged, disused underground workings, etc)	
Health and Safety Concerns	• Potential for bacteria associated with rotting shellfish. • SRB reactors can produce H_2S and CO_2 and risks should be managed appropriately. • H_2S can create odour issues.	

ACKNOWLEDGEMENTS

This work was supported by Solid Energy New Zealand Ltd. Additional funding was provided by the Ministry for Business, Innovation and Employment, Contract CRL1202. The authors would like to thanks Fiona Crombie and William Olds for help with field trials and early reporting. Thanks to James Pope for reviewing the draft paper.

REFERENCES

Diloreto, Z.A., Weisener, C.G., Weber, P.A., (2014, in prep) Geochemical dynamics of a mussel shell bioreactor for the treatment of ARD, Stockton Coal Mine New Zealand. Applied Geochemistry.

Diloreto, Z.A., 2013. Characterisation of a mussel shell bio-reactor for the treatment of mine waste: Stockton Coal Mine New Zealand. Hons Thesis, University of Windsor.

Crombie, F.M., Weber, P.A., Lindsay, P., Thomas, D.G., Rutter, G.A., Shi, P., Rossiter, P., and Pizey, M.H. (2011) Passive treatment of acid mine drainage using waste mussel shell, Stockton Coal Mine, New Zealand. In: Proceedings of the Seventh Australian Workshop on Acid and Metalliferous Drainage, pp. 393–405.

Mackenzie, A., Pope, J., Weber, P., Trumm, D., and Bell, D. (2011) Characterisation of Fanny Creek catchment acid mine drainage and optimal passive treatment remediation options. *In:* Proceedings of the 43rd annual conference, New Zealand Branch of the Australasian Institute of Mining and Metallurgy.

McCauley C.A., O'Sullivan A.D., Milke M.W., Weber P.A., Trumm, D.A., 2009. Sulfate and metal removal in bioreactors treating acid mine drainage dominated with iron and aluminium. Water Research 43: 961-970.

McCauley, C.A., 2011. Assessment of passive treatment and biogeochemical reactors for ameliorating acid mine drainage at Stockton Coal Mine. Ph.D. Thesis University of Canterbury.

Trumm, D., Watts, M., Pope, J. and Lindsay, P. 2008. Using pilot trials to test geochemical treatment of acid mine drainage on Stockton Plateau. New Zealand Journal of Geology and Geophysics, 51:175-186.

Trumm D 2010. Selection of active and passive treatment systems for AMD - flow charts for New Zealand conditions. New Zealand Journal of Geology and Geophysics 53:195-210.

Trumm D, Ball J, Pope J, Weisener C, West R 2015. Passive treatment of ARD using mussel shells – Part III: Technology improvement and future direction. To be presented at 10th International Conference on Acid Rock Drainage, April 20-25, 2015, Santiago, Chile.

Uster, B., O'Sullivan, A.D., Ko, S.Y., Evans, A., Pope, J., Trumm, D., Caruso, B., (2014, in press). The use of mussel shells in upward-flow sulfate reducing bioreactors treating acid mine drainage. Mine Water Environment, accepted, DOI 10.1007/s10230-014-0289-1

Uster, B., Trumm, D., Pope, J., Weber, P., O'Sullivan, A., Weisener, C., Diloreto, Z., 2014. Waste mussel shells to treat acid mine drainage: A New Zealand Initiative. Reclamation Matters, Fall 2014. Official Publication of the American Society of Mining and Reclamation, p 23 – 27.

Weber, P.A., Lindsay, P., Hughes, J.B., Thomas, D.G., Rutter, G.A., Weisener, C.G., Pizey, M.H., 2008. ARD minimisation and treatment strategies at Stockton Coal Mine, New Zealand. In "Proceedings of the Sixth Australian Workshop on Acid and Metalliferous Drainage", Burnie, Tasmania. 15-18 April 2008. (Eds LC Bell, BMD Barrie, B Baddock, and RW MacLean) pp. 113 - 138 (ACMER: Brisbane).

Weisener C, Diloreto Z, Trumm D, Pope J, Weber P 2015. ARD passive treatment using waste mussel shells – Part II: System autopsy and biogeochemical investigations. To be presented at 10th International Conference on Acid Rock Drainage, April 20-25, 2015, Santiago, Chile.

10th ICARD IMWA 2015 | 10th International Conference on Acid Rock Drainage & IMWA Annual Conference

ARD passive treatment using waste mussel shells- Part II: System autopsy and biogeochemical investigations

Christopher Weisener [1], Zach Diloreto[1], Dave Trumm[2], James Pope[2] and Paul Weber[3]

1. *Great Lakes Institute for Environmental Science, University of Windsor, Canada*
2. *CRL Energy Ltd, New Zealand*
3. *O'Kane Consultants, New Zealand*

ABSTRACT

Acid rock drainage (ARD) impacted waters are a worldwide concern for the mining industry; both active and passive technologies are employed for the treatment of such waters. System autopsy and biogeochemical investigations are presented here for a novel, fully operational, mussel shell bioreactor used to treat low pH effluents elevated in Al, Fe, Ni, and Zn. This bioreactor is within the Whirlwind catchment at the Stockton Coal Mine, located on the West Coast of New Zealand. The Whirlwind bioreactor utilizes a mussel shell matrix, which is similar in concept to a vertical flow successive alkalinity producing system (SAP), for the passive treatment of an ARD seep derived from acid-forming overburden. The bioreactor has been in operation since September 2012; since construction it has effectively treated ≈99% of metals and continues to neutralize the influent acidity resulting in a circum-neutral effluent.

To understand the performance and functionality of the bioreactor a systematic approach has been undertaken to investigate the bio-physico-chemical dynamics of the system. An autopsy was performed in May 2013 (after 8 months operation) and in June 2014 to better understand the contributing biogeochemical mechanisms occurring. Within the bioreactor exists a complex redox gradient controlled by first order reaction kinetics, which are defined by both its physico-chemical environment (adsorption & precipitation) and microbiology (*i.e.* Complex Fe and S cycling). A horizontal and vertical grid pattern was used for sampling across, and within, the bioreactor. Bio-physico-chemical investigations to date indicate homogenous treatment across the bioreactor with no restrictions to vertical flow even with continued sediment loads to the system.

The work describes a comprehensive investigation of the chemistry, microbiology, and functionality of this novel passive treatment approach and sheds light on the functionality and performance for global technology transfer.

Keywords: geomicrobiology, mussel shell bioreactor, passive treatment, Acid rock drainage, metals.

INTRODUCTION

Acid Rock Drainage (ARD) within the mining industry is associated with the oxidation of sulfide minerals within exposed overburden and other waste rock sources including tailings. Unfortunately it remains an ongoing legacy for some mining operations worldwide. In the United States approximately 200,000 ARD sites exist; in Europe there are over 5000 km of watersheds impacted by direct ARD effluents some predating 1000 years (Lieβmann, 1992; Hochella *et al.,* 1999; Bakers and Banfield 2003; Schippers et al. 2010). The exposure of sulfide minerals to water and oxygen in the presence of bacteria (*e.g. Thiobacillus ferrooxidans*) will result in solutions with increased loads of dissolved metals, sulfate, and net acidity. The Brunner Coal Measures (BCM) associated with the Stockton opencast coal mine in New Zealand has a legacy of ARD which is well documented (*e.g.,* McCauley *et al*., 2010) (Figure 1).

Figure 1 The Stockton Coal Mine located on the West Coast of the South Island of New Zealand

The BCM were formed as part of a marginal marine setting consisting of carbonaceous mudstones, sandstones and coal containing elevated pyritic sulfide sequences (Flores & Sykes 1996; Black et al. 2005; Pope *et al.,* 2006). The sequence can result in significant acid generation and Fe, Al, and S release during the oxidation of pyritic overburden (Weisener & Weber 2010). Studies by McCauley *et al.,* (2010) have provide valuable baseline chemical data on the seep effluent chemistry associated with the Stockton Coal Mine, which has resulted in several viable remediation solutions for passive treatment of ARD impacted waterways. ARD control using passive treatment systems, some referred to as vertical flow wetlands (VFW), or biochemical reactors (BCR), have proven to be effective options to treat isolated geographically confined ARD seeps. These systems contain a porous media, which can range from organic mulch blended with crushed limestone, or systems unique to this particular study that utilise weathered mussel shells. The latter provides exceptional permeability and reactive surface area with extensive neutralization capacity and ability to remove 99% metals (McCauley *et al.,* 2010).

To gain a better understanding of the performance and functionality of the bioreactors using mussel shells, a systematic approach was used to investigate the bio-physico-chemical dynamics of the system. Physical sampling of an existing full-scale treatment cell was performed in May 2013 (after 8 months operation) and again in June 2014 to better understand the contributing biogeochemical mechanisms occurring within the system. Within the bioreactor exists a complex redox gradient

controlled by first order reaction kinetics, which are defined by both its physico-chemical environment (adsorption & precipitation) and a succession of microbial communities (*i.e.,* complex Fe and S cycling). Investigations to date indicate that homogenous treatment across the bioreactor with no restrictions to vertical flow even after continued sediment load to the system.

METHODOLOGY

Sample Collection

Samples for both bacterial and geochemical analysis were collected from the Whirlwind bioreactor (Figure 2) at 8 and 18 months after the system commenced treatment. Acid neutralization capacity (ANC) and metal distributions were performed on material collected at 8 months, while bacterial analysis was performed on 18 month samples. The samples were collected both horizontally and vertically from several pits within a square grid. Subsequent samples were collected at a 18 month time period in areas undisturbed by the previous 6 month sampling. Four vertical layers where targeted; the allochtonous overlying sediment, the iron precipitate layer, the aluminum precipitate layer, and the underlying unreacted shell layers. In addition to porewater and geochemical solid phase characterization, sub samples were also collected for molecular studies (*e.g.,* total DNA and RNA functional analyses). These samples were flash frozen using liquid nitrogen at site to preserve DNA and RNA for shipment to the laboratory.

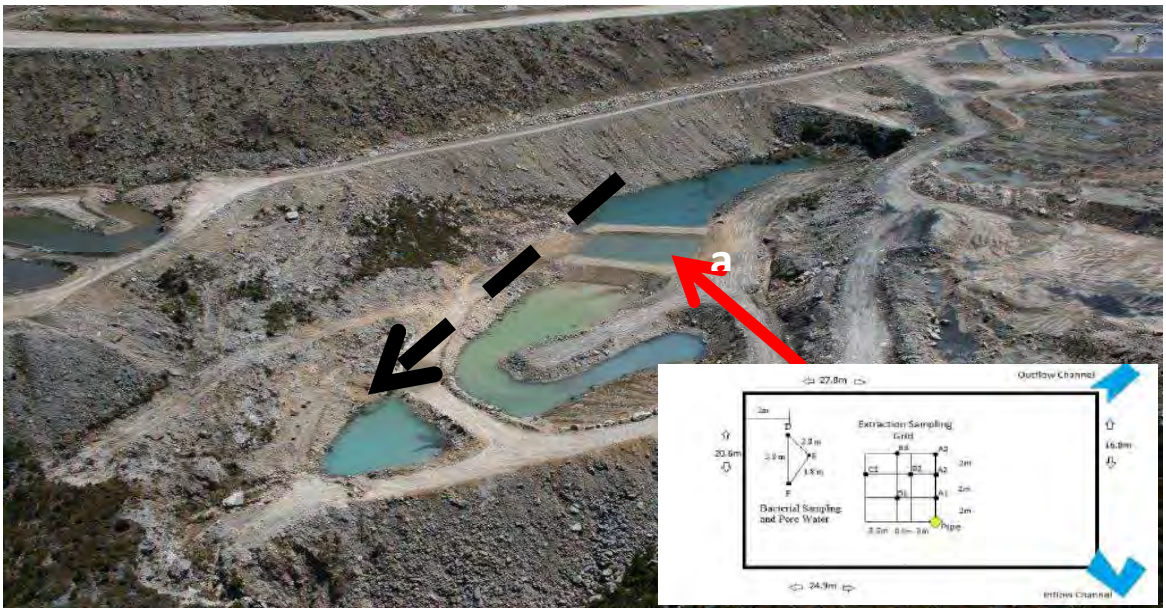

Figure 2 Emplacement of mussel shell bioreactor (location a); dashed line denotes direction of flow from the upper sediment pond, through the bioreactor and then two sediment ponds before discharge

Geochemical Characterization

The ANC test was used to evaluate the acid neutralization capacity of the bioreactor material from the different vertical sampling zones. This test was modified after Sobek *et al.* (1978), and the AMIRA ARD Test Handbook (AMIRA, 2002). Values from ANC testing are presented in kg of H_2SO_4 equivalent and as a percentage of $CaCO_3$ present. All Fe (total), pH and Eh values were measured from pore water collected from the bioreactor based on horizontal and vertical location and are shown averaged including statistical error. Approximately 100 ml of pore water were extracted from different depths within the bioreactor using rhizon pore water samples (Rhizosphere Research Products). Both pH and Eh determined from collected pore water was measured using Orion 8102BN probe by Thermo Scientific for pH and an Orion 01301MD (Duraprobe 4) by Thermo Scientific for Eh. Total iron concentrations were determined using ICPOES.

Bacterial Characterization

Three growth media were used to enrich the acidophilic iron oxidizers, neutrophillic iron oxidizers, and sulfate reducing bacteria (SRB). The media and method used for the enrichment of iron oxidizing bacteria was done using a modified 9K media described in Silverman & Lundgren (1958). Neutrophillic iron oxidizing bacteria were enriched using the Wolfe's media and methodology described in Emerson & Moyer (2002). The SRB were enriched using the Postgate media C and the methodology described in Postgate (1979). A Hucker's gram stain method (Gephardt *et al.*, 1981) was performed on samples extracted from bacterial enrichments. The bacteria were then examined using an Olympus BX61 petrographic microscope coupled with a Lumenera Infinity 1 digital video camera to determine relative abundances of gram (+) and gram (-) bacteria as well as examine their morphologies. Further characterization was performed using a FEI Quanta 200 FEG (Field Emission Gun) Variable Pressure Scanning Electron Microscope (SEM) with an EDAX® SiLi detector for bacterial morphology characterization. DNA extractions were performed using MoBio PowerSoil DNA isolation kit, following the manufacturer's instructions, and three sets of primers, which were used for amplicon targeting (PCR_1) within the 16S rRNA region for each sample. The thermocycling profile for PCR_1 conformed to the following parameters: initial denaturation for 5 min at 95°C followed by 34 cycles of 15 sec at 94°C, 15 sec at 48/55°C (bacteria/archaea), and 30 sec at 72°C, and a final extension of 1 min at 72°C. A second PCR was then performed for barcoding each of the samples (PCR_2), using a unique barcode for each sample as the forward primer and a universal reverse primer known as UniB-P1 (Table 1). The samples were diluted to a final concentration of 25 ng/μL and combined together in preparation for next generation sequencing using Ion Torrent platform (Life Technologies).

RESULTS AND DISCUSSION

Pore water and Solid Phase Characterization

A cross-section autopsy of the bioreactor shows a transitional environment dominated by geochemically distinct reactive layers of mineralization (Figure 3).

Figure 3 Geochemical gradient based on downward vertical flow within the mussel shell bioreactor

A summary of the average ANC profiles, Fe(III) distribution, pH and Eh from the bioreactor is provided in Figure 4. The ANC determinations, in terms of kg of H_2SO_4 (Figure 4a), as well as the distribution of Fe (III) within the vertical transect is shown in (Figure 4b). Both pH (Figure 4c) and Eh (Figure 4d) measurements show dramatic changes along the vertical depth suggesting a defined redox gradient. This assumption is supported by the physical appearance of distinct geochemical zones of precipitation observed in Figure 3. The top layer (0 – 10 mm thick) has a Eh of +199 mV and a measured pH of 3.6. This location correlates to ANC values of <5 kg H_2SO_4/t (<0.5 wt% $CaCO_3$) for ANC potential within the top sediment horizon. The capping allochthonous sediments is both oxidized and acidic with little, if any, capacity to neutralize incoming AMD effluent. The subsequent underlying iron oxide layer is dominated by reactive iron oxyhydroxides that extended from 11 to 40 mm depth and shows a rapid change in both porewater Eh and pH. Eh descreases to +26 mV and pH increases to 5.3 from 3.6. The ANC capacity within this layer increases to ~100 kg H_2SO_4/t (~10 wt% $CaCO_3$). The hydrolytic reactions involving iron observed within this layer are very characteristic of iron hydrolysis reactions that lead to its insolubility as pH increases above ~3.5. Below this reactive iron layer exists a thin zone dominated by white precipitates, which have been identified as amorphous aluminum hydroxide (unpublished data). The layer extends from a vertical depth of 40 to 62 mm with the reactor. Both Eh and pH continue to change with Eh from +26 mV to more reducing conditions of -33 mV and a subsequent pH increase from 5.2 to 6.5. The measured ANC values for the porewater collected within this layer is ~700 kg H_2SO_4/t (70 wt%

$CaCO_3$). The aluminum layer is characterized as a moderately reducing, circumneutral environment with high acid neutralization capacity. The bottom layer which extends from ~62 mm to 1655 mm (the base of the bioreactor) represents the unreacted mussel shell matrix. Porewater collected from within this layer shows low Eh values of -55 to -60 mV with an average pH of 7.2. The measured ANC values are slightly higher at 800 kg H_2SO_4/t (70 – 85 wt% $CaCO_3$). The unreacted shell layer represents a reduced environment with circum-neutral pH and a significant capacity to neutralize incoming acidic effluent. The redox reactions, which dominate the bioreactor, are controlled by a series of abiotic chemical and biotic catalyzed reactions, which give rise to favoured mineralogical phases, as well as direct influence to dominant microbial species present. Soluble Fe(III) (Figure 4b) correlates well with the observed iron oxyhydroxide interface noted in the profile.

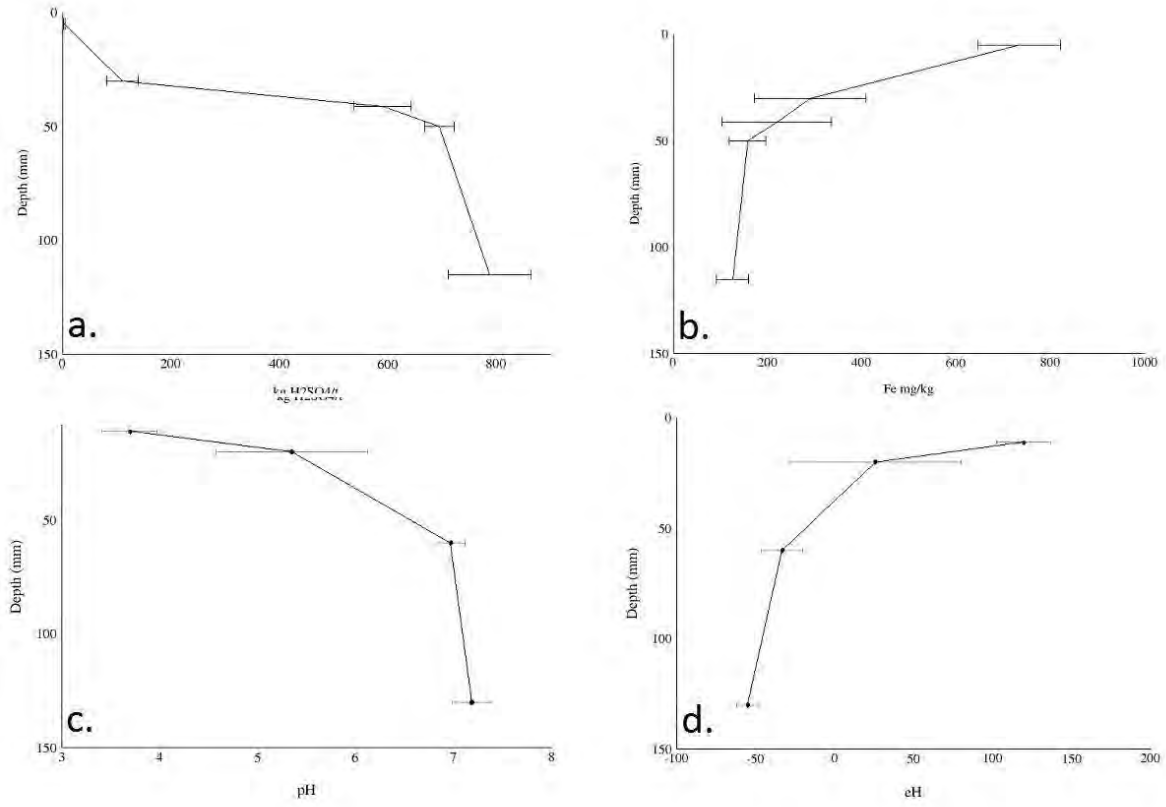

Figure 4 A summary of the of the neutralization capacity, iron distribution pH and Eh as a function of depth for the bioreactor (a) Acid Neutralization Capacity (ANC) at different depths (mm) within the bioreactor is based on kg H_2SO_4/T of material (b) Distribution of total Fe(III) within the vertical depth of the bioreactor (c) and (d) show pH and Eh profiles as a function of depth in the bioreactor

Bacterial Enrichment and Geochemical Conditions

The iron and sulfur dominant bacterial species were assessed using iron and sulfur enrichment cultures and molecular genomics (e.g. next generation sequencing- Ion torrent platform) to assess

the geochemical layers (Figure 5 & 6). This approach was used to differentiate prospective bacteria as a function of geochemical environments. A modified 9K media (Silverman & Lundgren, 1958) was used to target both iron and sulfur bacteria within the allochtonous sediment layer. This approach was successful allowing the enrichment of acidophilic iron oxidizers. The most common species at sites with similar effluent and geochemical conditions include *Thiobacillus ferrooxidans, Ferrobacillus ferrooxidans, Acidothiobacillus ferrooxidans, Aciothiobacillus thiooxidans, Leptospirillum ferrooxidans,* and *Ferrimicrobium spp.* (Silverman & Lundgren, 1958; Johnson 1998; Hallberg & Johnson, 2003; Johnson & Hallberg, 2003; Baker & Banfield, 2003; Hallberg, 2010; Schippers *et al.*, 2010). Based on the molecular characterization the dominant acid tolerant species identified was *Acidovorax sp*. This species is capable of metabolizing iron by coupling iron oxidation in the presence of nitrate and acetate. The dominant iron metabolizing species within the iron oxyhydroxide layer consisted of *Sideroxydans lithotrophicus* along with an increase in abundance of *Desulfotomacculum acetooxidans* a strict sulfate reducing anaerobe. The presence of *Sideroxydans lithotrophicus* within the iron oxide layer is interesting as this species is an neutrophillic aerobic oxidizer of Fe (II), and is capable of growing on other reduced mineral precipitates (e.g. siderite and pyrrhotite) at oxic–anoxic interfaces (Liu et al. 2012, Hedrich et al. 2011). Although suitable substrates within the reactor are possible other vectors should be determined considering the available HCO_3^- and Fe(II) in the transition zone making it possible for other enzymatic electron transport systems (EETS) to operate freely. No iron metabolizing bacteria were detected within the deeper profiles of the reactor including the aluminum oxide layer and the reduced unreacted shell matrix. A combination of both SRB enrichments and molecular investigation confirm the presence of *Desulfotomacculum acetooxidans* which is a spore forming SRB bacteria, and is more resistant to extreme environmental change (*e.g.,* periods of desiccation and oxic conditions) (Castro *et el.,* 2000). Postgate media C (Postgate, 1979) was used to enrich all SRBs present within the layers sampled from the bioreactor. In all layers positive growth was observed. Material collected below the sediment cap showed the fastest growth within the first 24 h compared to 2 - 3 week lag period for the cap sediment. This is likely due to oxygen stress at the top of the profile. Of note is the increased abundance of Archaea (e.g. methanogens) detected within the unreacted zone in Figure 5.

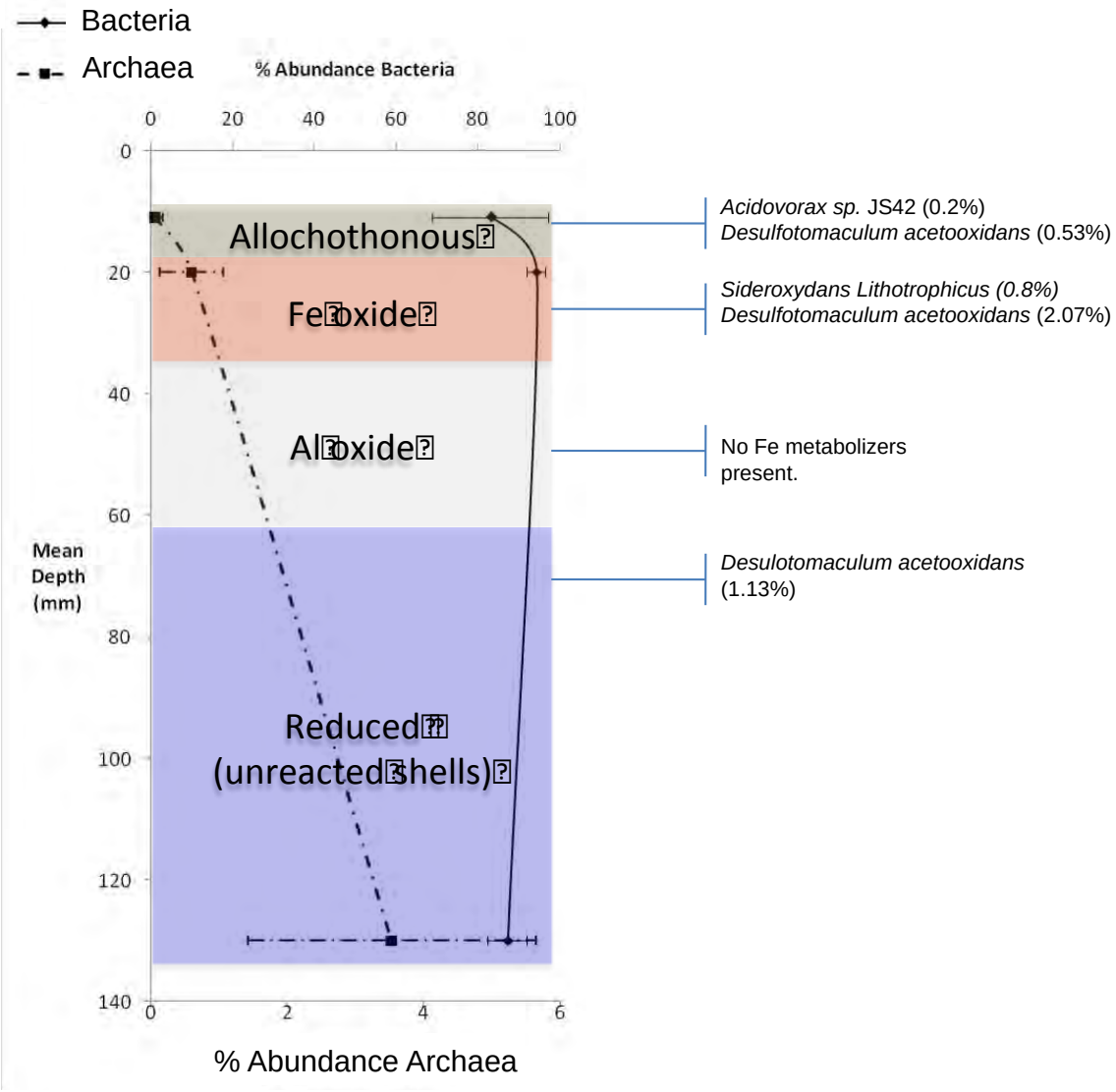

Figure 5 Correlation of iron and sulfur metabolizing bacteria and archaea within the bioreactor profile as a function of depth.

CONCLUSION

The formation of the geochemical profile within the mussel shell bioreactor and its influence on the development of microbial species is in part controlled by a series of abiotic chemical reactions that form during *in-situ* treatment of the ARD effluent. The rate of Fe(II) oxidation at pH values above 5 can be described by the following equation:

$$d[Fe^{2+}]/dt = k_1[Fe^{2+}][OH]^2 P_{O2} \quad (1)$$

where $k_1 = 8.0 \times 10^{13}$ min $^{-1}$ atm^{-1} mol^{-2}

It is noted that a 100-fold increase in the reaction rate occurs for every unit increase in pH (Gazea *et al.,* 1996). Given this situation the most important role of the *in-situ* reaction process would be adequate retention time for the dissolved constituents (Fe, Al) to oxidise and precipitate within the system. It should be noted that under these conditions the oxidation is slow, thus the contribution from iron oxidizing bacteria becomes increasingly important. The presence of acidophilic *Acidovorax sp.* and neutrophilic species such as *Sideroxydans lithotrophicus* and other chemoautotrophic species such as *Desulfotmacullum acetooxidans* (*e.g.*, SRB) which tolerate pH values 2-3 and 5-7 respectively will serve as key electron facilitators thus increasing the rate of iron oxidation or sulfur reduction by several orders of magnitude. Bacterial sulfate reduction in some respects is limited to very specific environmental conditions, which function best at pH >4 in the absence of other oxidising agents such as O_2 and Fe^{3+}(Postgate, 1984). The increase in SRB activity noted in the subsequent layers below the precipitated iron oxide layer confirms this fact. Additionally the abundance of amorphous zinc sulfide proximal to organic matter (data not shown) within this reduced zone (unreacted shells) is further testimony and results directly after iron is removed via oxidation and precipitation from waters flowing down through the reactor. These rapid precipitation fronts characterised by Fe, Al, and reduced metals contribute to the change in SRB activity and pH gradients. Preliminary investigations of the sulfur reducing consortia suggest a range of species able to capitalize on this, characterized by facultative acid tolerant species (gram + and -) near the surface of the reactor with a succession of species dominated by strict anaerobic chemotrophic neutrophilic SRBs within the reduced zones of the bioreactor. The SRB process involved in this case can be considered the reverse of pyritic sulfide oxidation with the end result contributing to the net consumption of acidity by the sulfate reduction process. In addition, considering that metal oxidation and hydrolysis reactions are not effective for removal of metals such as Zn, Tl, and Mn at pH values below 8 compared to bacterial produced hydrogen sulfide which readily reacts with metals above pH 3 forming insoluble metal sulfides in a reduced setting.

ACKNOWLEDGEMENTS

The authors wish to thank Solid Energy (SENZ) Ltd for permission to publish this work and their original and ongoing support of the research programme.

NOMENCLATURE

F(x)	cumulative probability density function
e	natural logarithm
α	scale parameter
β	shape parameter
x	random variable

REFERENCES

AMIRA, (2002) ARD Test Handbook, Ian Wark Research Institute, vol. 1, pp. 26-28.

Baker, B.J., and Banfield J.F. (2003) Microbial Communities in Acid Mine Drainage, *FEMS Microbiology Ecology*, vol. 44, (2) 139–52.

Black, A., Trumm, D.A, Lindsay, P. (2005) Impacts of coal mining on water quality and metal mobilization: case studies from West Coast and Otago, *Metal contaminants in New Zealand: sources, treatments, and effects on ecology and human health.* Christchurch New Zealand, Resolution Press, pp. 247-260.

Castro, H.F., Williams, N.H., and Ogram, A. (2000) Phylogeny of Sulfate-Reducing bacteria, *FEMS Microbiology Ecology*, vol. 31, (1) pp. 1–9.

Gephardt, P., Murray, R.G.E., Costilow, R.N., Nester, E.W., Wood, W.A., Kreig, N.R., and Phillips G.B. (1981) Manual of Methods for General Bacteriology American Society for Microbiology, vol. 1, pp. 415-416.

Emerson, D., and Moyer, C.L. (2002) Neutrophilic Fe-Oxidizing Bacteria Are Abundant at the Loihi Seamount Hydrothermal Vents and Play a Major Role in Fe Oxide Deposition, *Applied and Environmental Microbiology*, vol. 68, (6) pp. 3085–93.

Flores, R., Sykes, R. (1996) Depositional controls on coal distribution and quality in the Eocene Brunner Coal Measures, Buller Coalfield, South Island, *New Zealand, International Journal of Coal Geology*, vol. 29, pp. 291-336.

Gazea B., Adam K., (1996) A review of passive systems for the treatment of acid mine drainage, *Minerals Engineering*, vol. 9, (1) pp. 23-42.

Hedrich S., Schlomann, M. and Johnson B. (2011) The iron oxidizing proteobacteria. *Microbiology*, vol 157, pp. 1551-1564.

Hochella, M.F.Jr., Moore, J.N., Golla, U., and Outnis, A. (1999) A TEM study of samples from acid mine drainage systems: Metal-mineral associations with implications for transport, *Geochimica et Cosmochimica Acta*, vol. 63, pp. 3395-3406.

Ließmann, W. (1992) Historischer Bergbau im Harz: ein Kurzführe, Sven von Loga, vol. 1, pp.1-320.

Lui , J., Wang, Z., Belchik, S.M., Edwards, M.J., Liu C., Kennedy, D.W., Merkley, E.D., Lipton, M.S. Butt, J.N., Richardson, D.J. Zachara, J.M., Fredrickson, J.K., Rosso, K.M., Shi, L. (2012) Identification and characterizationb of MtoA: a decaheme c-type cytochrome of the nuetroplic Fe(II)-oxidizing bacterium *Sideroxydans lithotrophicus* ES-1. *Frontiers in Microbiology*, vol. 3 (37). pp. 1-11.

McCauley, C.A., O'Sullivan, A.D., Weber, P.A., and Trumm, D. (2010) Variability of Stockton Coal Mine Drainage Chemistry and Its Treatment Potential with Biogeochemical Reactors, *New Zealand Journal of Geology and Geophysics*, vol. 53, (2–3) pp. 211–26.

Norris, P. R., Clark, D.A., Owen, J.P., and Waterhouse, S. (1996) Characteristics of Sulfobacillus Acidophilus Sp. Nov. and Other Moderately Thermophilic Mineral-Sulphide-Oxidizing Bacteria, *Microbiology* (Reading, England), vol. 142, (4) pp. 775–83.

Pope, J., Newman, N., and Craw, D. (2006) Coal mine drainage geochemistry, West Coast, South Island a preliminary water quality hazard model, *Proceedings of the 39th Annual Conference of the New Zealand Branch of the Australasian Institute of Mining and Metallurgy*, Waihi, New Zealand, pp. 12.

Postgate, J.R. (1979) The Sulphate-Reducing Bacteria, *CUP Archive*, vol. 1, pp. 8-23.

Postgate J.R. (1984) The Sulfate Reducing Bacteria, Cambridge Univ. Press. NY, vol. 2, pp. 208.

Schippers, A., Breuker, A., Blazejak, A., Bosecker, K., Kock, D., and Wright, T.L. (2010) The Biogeochemistry and Microbiology of Sulfidic Mine Waste and Bioleaching Dumps and Heaps, and Novel Fe(II)-Oxidizing Bacteria, *Hydrometallurgy*, 18th International Biohydrometallurgy Symposium, Bariloche-Argentina, vol. 104, (3–4) pp. 342–50.

Silverman, M.P., and Lundgren, D.G. (1959) Studies on the chemoautotrophic iron bacterium ferrobacillus ferrooxidans: I. An Improved Medium and a Harvesting Procedure for Securing High Cell Yields, *Journal of Bacteriology*, vol. 77, (5) pp. 642.

Sobek, A. A. (1978) Field and Laboratory Methods Applicable to Overburdens and Minesoils, Industrial Environmental Research Laboratory, Office of Research and Development, U.S. Environmental Protection Agency, vol. 1, pp. 1-203.

Weisener, C.G. and Weber, P.A. (2010) Preferential oxidation of pyrite as a function of morphology and relict texture, *New Zealand Journal of Geology and Geophysics* , vol. 53, (1) pp. 22-33.

Passive Treatment of ARD Using Mussel Shells – Part III: Technology Improvement and Future Direction

Dave Trumm[1], James Ball[1], James Pope[1] and Chris Weisener[2]

1. *CRL Energy Ltd, New Zealand*
2. *Great Lakes Institute for Environmental Science, University of Windsor, Canada*

ABSTRACT

Green-lipped mussel is the largest seafood export from New Zealand, producing large amounts of shell waste which ends up in landfills. These shells, and waste mussel meat, provide a novel passive treatment approach for acid rock drainage (ARD). The shells provide a source of alkalinity and the meat provides a carbon source for sulfate-reducing bacteria. Until recently, these systems have been constructed with vertical downward flow. Dissolution of the shells results in precipitation of iron hydroxides on the top of the reactor, while reducing reactions deeper in the system form metal sulfides. The iron hydroxides on the top, however, can eventually reduce permeability.

In this study, three mussel shell reactors were constructed in series to treat ARD. Each reactor was constructed with an up-flow configuration in an attempt to establish reducing conditions throughout the reactor and prevent the formation of iron hydroxides. Inlet chemistry averaged: Fe (108 mg/L), Al (28 mg/L), Zn (6.3 mg/L), Ni (1.4 mg/L), and sulfate (2100 mg/L). The pH was raised from 2.9 to 8 through the reactors and alkalinity was produced. Metal removal rates ranged from 95 % to >99 %. Sulfate concentrations decreased by up to 500 mg/L, dissolved sulfide increased by approximately 60 mg/L, and dissolved oxygen concentrations decreased from near saturation to less than 1 %, all suggesting that reducing conditions were achieved throughout the systems. Microbiology work shows the systems to be dominated by sulfate-reducing bacteria. It is likely that Fe, Zn, and Ni were removed as sulfides. These results suggest that up-flow configurations may be a useful construction technique for mussel shell reactors, especially for ARD with elevated Fe.

Future work includes studies of permeability changes in down-flow reactors as hydroxides accumulate, biogeochemical investigations on both down-flow and up-flow reactors, and the installation of full scale systems using both techniques.

Keywords: Mussel Shells, Passive Treatment, Bioreactor

INTRODUCTION

The green-lipped mussel *(Perna canalicula)* is the largest seafood export from New Zealand. The aquiculture industry produces over 140 000 tons of shells annually (Aquaculture New Zealand, 2010). Native to New Zealand, much of the export is fully shelled mussels, which produces a large amount of shell waste. Although some of the waste is used as a lime amendment by the agricultural industry, much of it ends up in landfills.

Since 2007, various researchers have used waste mussel shells to treat acid mine drainage (AMD) in laboratory experiments, small-scale field trials, and large-scale systems in New Zealand. Mussel shells provide a source of alkalinity, and the associated waste mussel meat and other sea life (about 10 % by mass) provide organic material for sulfate-reducing bacteria (SRB). In the initial early laboratory experiments, the mussel shells were used as a replacement for limestone in typical sulfate-reducing bioreactors containing other sources of organic matter, such as compost, bark chips, and post peel waste strips (McCauley et al., 2009; Mackenzie, 2010; Mackenzie et al., 2011).

Later, large-scale field reactors were constructed with only mussel shells and their associated waste mussel meat. These reactors perform well, removing 96 to 99 % of iron, aluminum, nickel, and zinc and restoring pH from <3 to >7 (Crombie et al., 2011). Autopsy work by Diloreto et al. (in press, 2014) show that the metals are sequestered in distinct zones and in distinct forms within the reactors. The upper layer is dominated by a thick iron hydroxide precipitate, followed by a transition zone, below which is an aluminum hydroxide layer. Zinc sulfides and nickel sulfides are present below the aluminum layer. Mussel shells are nearly completely dissolved away near the surface, becoming more abundant with depth. Redox potential measurements (Eh) show a change with depth, from oxidizing conditions in the upper layers changing to reducing conditions within and below the aluminum hydroxide layer. The pH increases with depth, reaching neutral where shells are most abundant.

Performance of the mussel shell reactors over time is largely unknown. It is likely that the transition zone where conditions change from oxidizing to reducing migrates downward with time as the mussel shells are dissolved. If so, zinc and nickel sulfides precipitated in these layers may be oxidized and the metals released as the oxidation and dissolution front migrates downward. The iron oxide and aluminum layers would likely dominate the system with time, potentially reducing permeability and the system could fail once all the mussel shells have been dissolved.

All the previous systems (laboratory and field trials) were constructed with down-flow configurations. In our current study, we have constructed field-trial mussel shell reactors with an up-flow configuration to determine if reducing conditions would predominate over oxidizing conditions throughout the reactors, and if iron would precipitate as a sulfide rather than as a hydroxide. In addition, increased bicarbonate alkalinity generation in a fully reducing system may slow shell dissolution rates, increasing the lifespan of the systems.

METHODS

Three passive treatment systems were constructed using 1000 L plastic tubs (standard intermediate bulk containers) with PVC piping, alkathene piping and associated valves, and were installed at an active coal mine to treat AMD. Each system was filled with waste mussel shells from the fishing company Sandford Limited. The mussels were freshly harvested and shelled. The waste shells

contained approximately 10 % waste mussel meat, which included remnants of the green-lipped mussels, whole black-shell mussels, and miscellaneous sea life attached to the shells. Most shells were broken into pieces approximately 5 cm long (Figure 1).

Figure 1 Mussel shells in completed mussel shell reactor prior to filling with water

The systems were installed in series with an up-flow configuration, such that the inlet was at the base of each system and the water flowed upwards through the shell bed driven by sufficient hydraulic head. Sampling ports were located at the inlet to the three systems, between systems one and two, between systems two and three, and at the outlet from system three. Each system was covered with a tarp to exclude rainfall and sunlight.

The systems operated for a period of 141 days. Flow rates were varied to determine metal removal for different hydraulic residence times (HRTs). Inlet and outlet samples were collected fortnightly from each system and analyzed for dissolved iron (Fe), aluminum (Al), manganese (Mn), nickel (Ni), zinc (Zn), and calcium (Ca), nitrogen species, dissolved reactive phosphorous, sulfate, and dissolved organic carbon at a New Zealand laboratory using inductively coupled plasma mass spectrometry, colorimetry, ion chromatography, catalytic oxidation, and cadmium reduction techniques. Field measurement included pH, dissolved oxygen, and sulfide. Solid and liquid samples were collected from the top 10 cm of each system for microbiological analysis using Next-Generation Sequencing technologies.

RESULTS

Flow rates ranged from 40 to 660 ml/min through the system train, equating to HRTs ranging from 14 hours to 232 hours in each of the first two systems. The third system had slightly fewer mussel shells, resulting in a 9 % lower residence time compared to that in each of the first two systems.

The inlet AMD chemistry is dominated by sulfate (2100 mg/L), Fe (108 mg/L), Al (28 mg/L), and Mn (24 mg/L), with low concentrations of Zn (6.3 mg/L) and Ni (1.4 mg/L). The pH ranges from 2.9 to 3.1. Typically, Fe(II) comprises 5 % of the total Fe, dissolved oxygen is near saturation, and no dissolved sulfide is present.

As the water passes through the systems, the following metal removal rates are achieved: Fe (96 to >99 %), Al (>99 %), Ni (95 to >99 %), Zn (98 to >99 %), and Mn (0 to 22 %) (Figure 2).

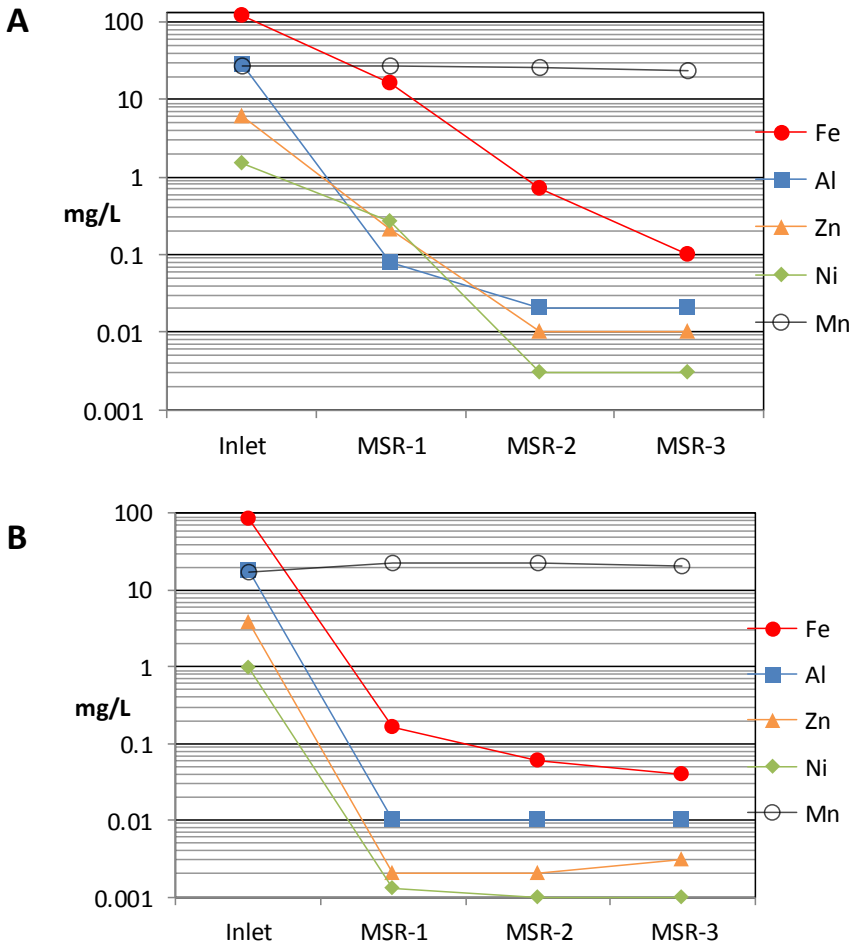

Figure 2 Concentrations of metals through treatment system. **A** HRT of 28 hours. **B** HRT of 95 hours. MSR-1, mussel shell reactor 1; MSR-2, mussel shell reactor 2; MSR-3, mussel shell reactor 3

Several parameters suggest that reducing conditions are being achieved in the systems. Sulfate concentrations decrease through the systems (by up to 500 mg/L) while dissolved sulfide concentrations increase (by approximately 60 mg/L) (Figure 3). Dissolved oxygen concentrations decrease from near saturation to below 1 % in the first reactor and ammoniacal nitrogen (reduced nitrogen) concentrations increase linearly through the three systems. The pH increases from 3 to 7.5 in the first reactor and shows some increase to near 8 through the second and third reactors (Figure 4). Concentrations of calcium (Ca) increase predominantly in the first reactor, while alkalinity follows a linear trend through the three systems.

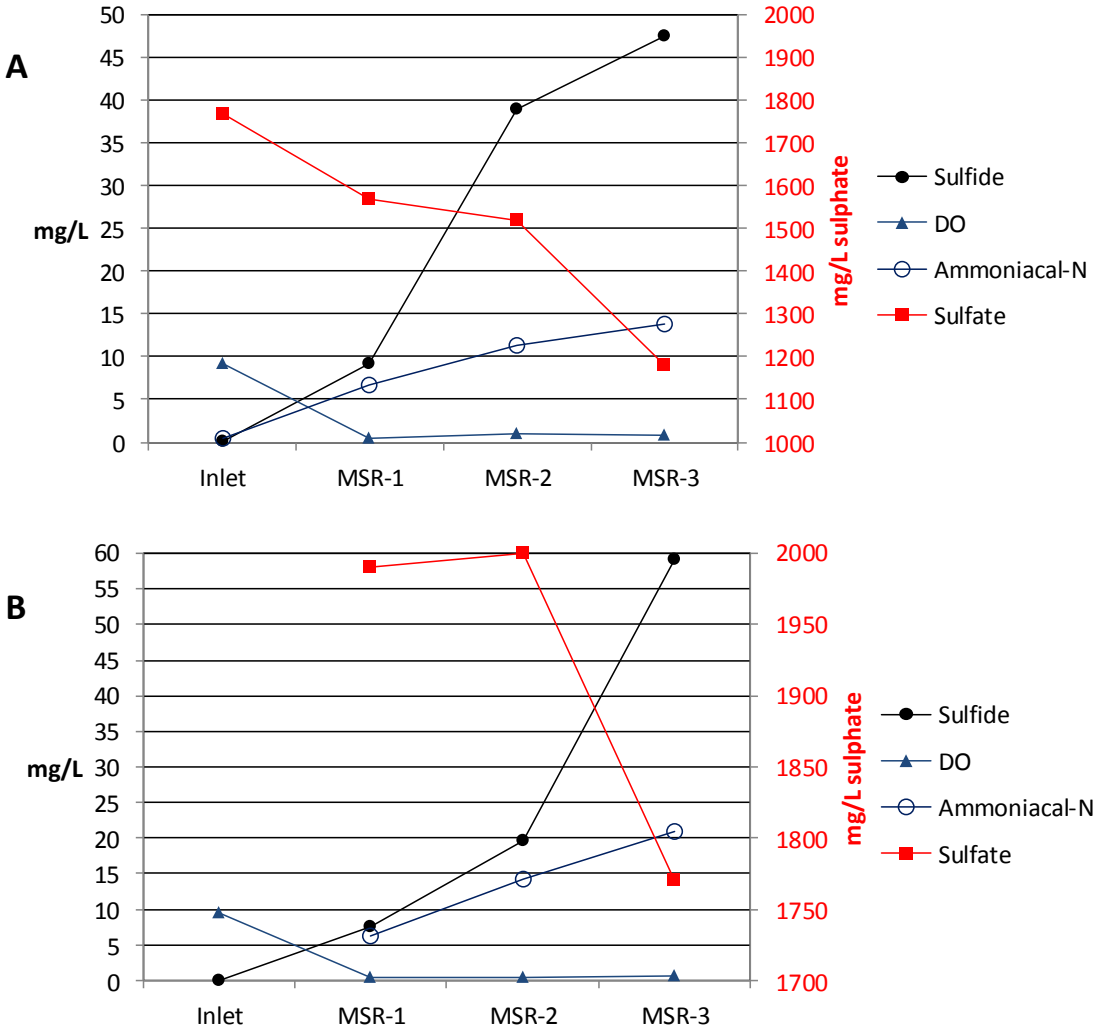

Figure 3 Sulfur species, DO, and ammoniacal nitrogen through treatment system. **A** HRT of 56 hours. **B** HRT of 95 hours. MSR-1, mussel shell reactor 1; MSR-2, mussel shell reactor 2; MSR-3, mussel shell reactor 3

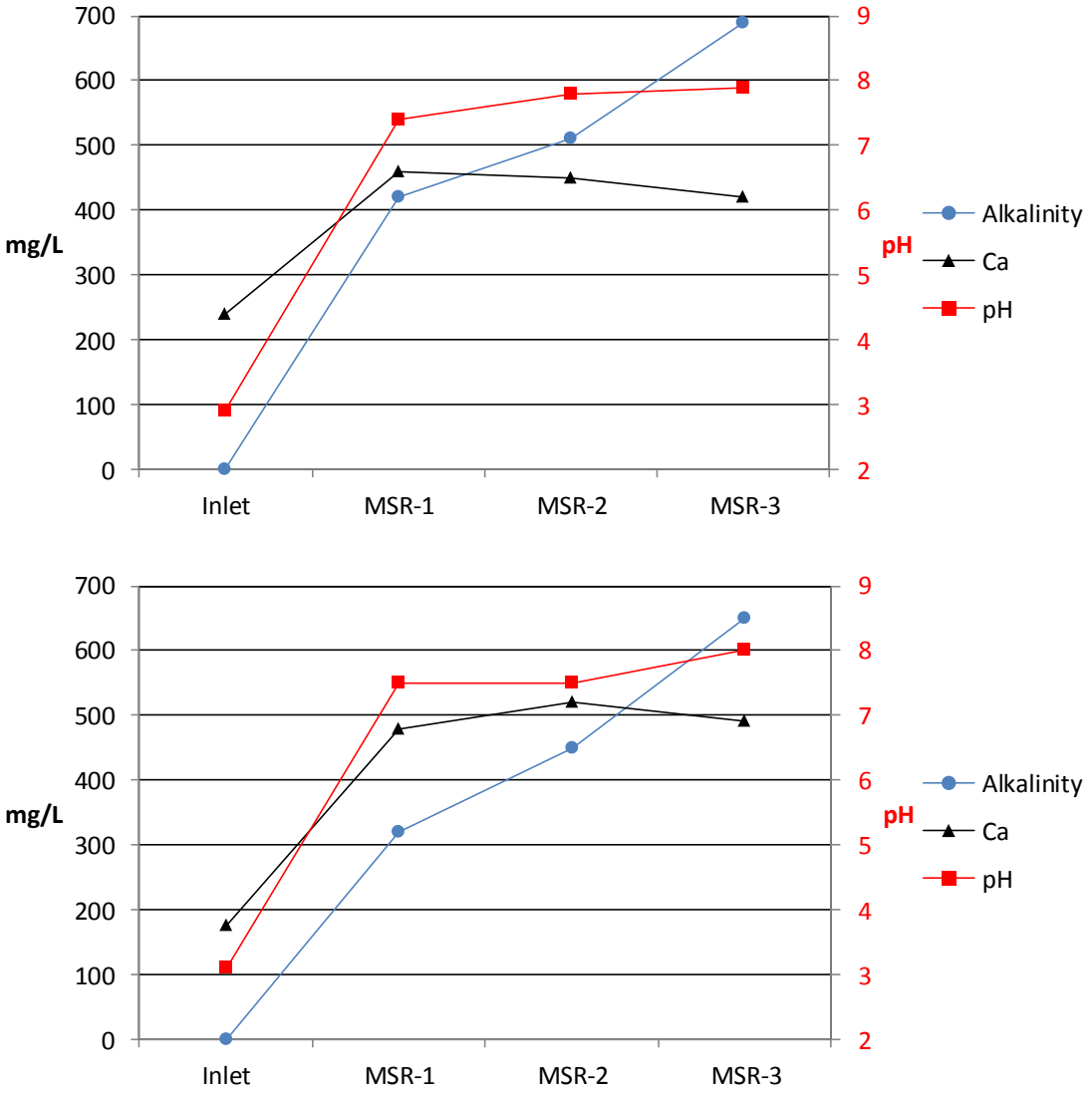

Figure 4 Alkalinity, calcium, and pH through treatment system. **A** HRT of 56 hours. **B** HRT of 95 hours. MSR-1, mussel shell reactor 1; MSR-2, mussel shell reactor 2; MSR-3, mussel shell reactor 3

Preliminary genomic DNA and RNA-Seq molecular analysis of the substrate shows a succession of bacterial communities through the three reactors. In the first reactor, the microbial community is comprised of bacteria (90 %) and archaea (10 %). The bacteria community is dominated by SRB (such as *Desulfotomaculum* and *Desulfovibrio*) but also contains many methanotrophs (methane-oxidizing bacteria). The second reactor contained some SRB but no methanotrophs. Compared to the first reactor, the SRB only comprised a minor proportion of the entire community. The third reactor did not contain any SRB or methanotrophs, but rather had very generic species such as bacterial halophiles of marine origin, and Firmicutes, such as soil bacteria of the Clostridia class (obligate anaerobes).

After the systems had operated for several months, precipitates were noted on the surface of the water in all three reactors (Figure 5). In the first two, this precipitate exhibited a vein-like and

crystalline-like texture with various colors of grey and tan. In the third reactor it was dominated by yellowish-white crystalline and amorphous material.

Figure 5 Precipitates on the water surface of mussel shell reactors

DISCUSSION

Neutralization of the AMD and generation of bicarbonate alkalinity is likely occurring through both dissolution of the mussel shells and sulfate reduction by SRB. Almost all of the metal removal by the systems and pH increase is accomplished in the first reactor, with the exception of Mn which shows removal (albeit minimal) in the second and third systems. Changes in dissolved oxygen, ammoniacal nitrogen, and sulfate show that reducing conditions are established in the first reactor, and are enhanced in the second and third reactors, suggesting that the transition metals Fe, Ni, and Zn are likely being removed as sulfides. The presence of SRB in the first two reactors confirms that sulfate reduction is occurring. The presence of methanotrophs in the first reactor show that methane is being produced, which only occurs under strong reducing conditions with an Eh below -150 mV (Wang et. al., 1993).

Aluminum, however, does not form a sulfide in these systems, but rather precipitates as a hydroxide. Manganese also does not form a sulfide in these systems, but rather can precipitate as oxides, hydroxides (Stumm & Morgan, 1996), and carbonates (Bamforth et al., 2006) and can be removed through adsorption onto iron hydroxides. It is unlikely that manganese oxides are forming under these reducing conditions and unlikely that Mn is being adsorbed onto iron hydroxides if most of the Fe is being removed as sulfide. It is possible that the minimal removal of Mn through these systems is occurring through the formation of manganese carbonates, similar to rhodochrosite ($MnCO_3$) or kutnahorite ($CaMn(CO_3)_2$. The formation of these minerals typically requires a pH of greater than eight, which is approached in the third system.

In the second and third reactors, additional alkalinity is produced, the pH is raised slightly higher, and sulfate concentrations are lowered significantly while dissolved sulfide concentrations increase. Minimal dissolution of mussel shells occurs in the second and third reactors, as evidenced by relatively stable, and even decreasing, Ca concentrations. Therefore, the increase in bicarbonate alkalinity in the second and third systems may be due in part to sulfate reduction by SRB. The presence of SRB in the second reactor confirms that sulfate reduction is occurring in that cell,

however, no SRB were detected in the third reactor. The microbiological samples were collected near the top of the reactors. It is possible that SRB may be present in the third reactor at depth.

The precipitates forming on the surfaces of the reactors may be elemental sulfur, since more sulfate is removed from these systems than can be accounted for by dissolved sulfide and the formation of metal sulfides. It is also possible that gypsum is forming on the surfaces, which could explain the decrease in both Ca and sulfate in the third reactor.

The construction of these three systems in series creates a true plug flow reactor (Schmidt & Lanny, 1998). Although short-circuiting is possible within each individual component, short-circuiting through the entire system train is prevented by having three distinct parts to the system. Since sampling can be conducted between each component of the system, the performance and removal mechanisms in each component can be analyzed separately and extrapolated to the potential performance of a full scale system. Construction of trial passive treatment systems in series can provide useful information on treatment performance and metal removal mechanisms.

The up-flow configuration likely contributes to the successful establishment of reducing conditions and likely will lead to minimal formation of iron hydroxides. It is preferable to avoid the formation of iron hydroxides, as this would lead to a decrease in permeability with time, as was noted in a large-scale mussel shell reactor constructed at Stockton Mine, West Coast, New Zealand (Crombie et al., 2011).

Additional up-flow mussel shell reactors have been constructed at the Bellvue abandoned coal mine AMD site on the West Coast of New Zealand (West et al., 2013). Along with mussel shell reactors, a bioreactor containing compost, bark chips, post peel strips, and mussel shells is operating at the Bellvue site to compare the performance of mussel shells with and without an organic matrix. The results from Bellvue and from this study will be used to optimize mussel shell reactor design for other sites in New Zealand.

Future work on mussel shell reactors includes permeability studies, biogeochemical investigations, and installation of full-scale systems. The permeability studies currently underway aim to measure the change in permeability in down-flow reactors as hydroxides accumulate. Biogeochemical investigations are currently underway for both up-flow and down-flow reactors, and several full-scale system are planned to be installed at AMD sites using both techniques.

CONCLUSIONS

1. Three small-scale mussel shell reactors were constructed in series at an active coal mine to treat AMD. Unlike previous mussel shell reactors, these were constructed in an up-flow configuration.
2. Inlet water chemistry to the system train had a pH of 2.9 to 3.1, and metal concentrations as follows: Fe (108 mg/L), Al (28 mg/L), Mn (24 mg/L), Zn (6.3 mg/L), and Ni (1.4 mg/L). Sulfate concentrations were 2100 mg/L.
3. Residence times in each of the three reactors ranged from 14 to 232 hours, over an operating period of 141 days.
4. The pH increased to 7 through the first reactor and near 8 through the second and third reactors and the effluent water had net alkalinity.
5. Metal removal rates were as follows: Fe (96 to >99 %), Al (>99 %), Ni (95 to >99 %), Zn (98 to >99 %), and Mn (0 to 22 %). With the exception of Mn, these metals were mostly removed in the first reactor.

6. Sulfate concentrations were lowered by up to 500 mg/L, dissolved sulfide increased by approximately 60 mg/L, DO concentrations decreased from near saturation to less than 1 %, and ammoniacal nitrogen increased through the systems, all suggesting that reducing conditions were achieved in the systems by means of SRB.
7. Sulfate-reducing bacteria were present in the first two reactors, confirming that sulfate reduction is occurring.
8. It is likely that Fe, Zn, and Ni were removed in the system as sulfides, Al as hydroxides, and Mn as carbonates.
9. A crystalline and amorphous precipitate forming on the surface of the reactors may be elemental sulfur with or without gypsum.
10. An up-flow configuration through mussel shell reactors may help to establish and maintain reducing conditions and remove Fe as sulfides rather than hydroxides, thereby maintaining permeability and extending the longevity of these systems.

ACKNOWLEDGEMENTS

This research was financed by the Ministry for Business, Innovation and Employment, Contract CRL1202. The mussel shells were donated by Sanford Limited, Christchurch. We acknowledge the anonymous mining company which allowed the systems to be constructed at their mine site. Preparation of graphs was completed by Patrick Turner of CRL Energy.

REFERENCES

Aquaculture New Zealand 2010. *New Zealand aquaculture farm facts.*

Bamforth, S.M., Manning, D.A.C., Singleton, I., Younger, P.L., and Johnson, K.L. (2006) Manganese removal from mine waters - investigating the occurrence and importance of manganese carbonates. *Applied Geochemistry* 21, 1274–1287.

Crombie, F.M., Weber, P.A., Lindsay, P., Thomas, D.G., Rutter, G.A., Shi, P., Rossiter, P., and Pizey, M.H. (2011) Passive treatment of acid mine drainage using waste mussel shell, Stockton Coal Mine, New Zealand. *In:* Proceedings of the Seventh Australian Workshop on Acid and Metalliferous Drainage. Pp. 393–405.

Diloreto, Z., Weber, P., and Weisener, C.G. (In Press 2014) Passive treatment of acid mine drainage using bioreactors: Investigating redox gradients and metal stability. *Submitted to Applied Geochemistry.*

Mackenzie, A. (2010) *Characterization of Drainage Chemistry in Fanny Creek Catchment and Optimal Passive AMD Treatment Options for Fanny Creek,* Unpublished M.Sc. thesis, University of Canterbury, Department of Geological Sciences.

Mackenzie, A., Pope, J., Weber, P., Trumm, D., and Bell, D. (2011) Characterisation of Fanny Creek catchment acid mine drainage and optimal passive treatment remediation options. *In:* Proceedings of the 43rd annual conference, New Zealand Branch of the Australasian Institute of Mining and Metallurgy.

McCauley, C.A., O'Sullivan, A.D., Milke, M.W., Weber, P.A., and Trumm, D.A. (2009) Sulfate and metal removal in bioreactors treating acid mine drainage dominated with iron and aluminum. *Water Research* 43, Issue 4, 961–970.

Schmidt and Lanny, D. (1998) *The Engineering of Chemical Reactions*, Oxford University Press, New York.

Stumm, W. and Morgan, J.J. (1996) *Aquatic chemistry: Chemical equilibria and rates in natural waters,* Third Edition, Wiley-Interscience. 470 p.

Wang, Z.P., Delaune, R.D., Masschelegn, P.H., and Patrick, Jr. W.H. (1993) Soil redox and pH effects on methane production in flooded rice soils. *Soil Sci Soc Am J*, 57: 382–385.

West, R. Trumm, D., Nobes, D., and Pope, J. (2013) Trialling passive remediation systems for treatment of severe AMD: A case study from Bellvue Mine, West Coast, New Zealand. *In:* Proceedings of the New Zealand Geological Society Conference, Christchurch, 25-27 November 2013.

The Sequential Experiments of Passive Treatment System Using Bioreactor for Acid Mine Drainage in Japan

Takaya Hamai[1], Takuya Kodera[1], Yuki Sato[1], Kousuke Takamoto1, Manami Ikeda[1], Kazunori Hatsuya[1], Kentaro Hayashi[1], Hiroko Tendo[1], Kazuya Sunada[1], Mikio Kobayashi[1], Masatoshi Sakoda[1], Takeshi Sakata[2] and Nobuyuki Masuda[2]

1. *Japan Oil, Gas and Metals National Corporation*
2. *International Center for Research and Education of Mineral and Energy Resources, Akita University, Japan*

ABSTRACT

Japan Oil, Gas and Metals National Corporation (JOGMEC) has been researching a low-cost microorganism-based passive treatment system for acid mine drainage (AMD). This system consists of the aerobic reactor and the following anaerobic one that utilizes iron-oxidizing bacteria and sulfate-reducing bacteria, respectively.

The aerobic reactor is filled with iron scales including iron-oxidizing bacteria from the aqueduct of drainage treatment facilities, and iron ions have been oxidized by iron-oxidizing bacteria and removed as iron oxides. In the anaerobic reactor, which is filled with rice husk, limestone, soil, and rice bran, various metal ions (copper, zinc, lead, cadmium, etc.) have been removed as sulfides by the action of sulfate-reducing bacteria. The materials used to be filled in the reactors are either free or very inexpensive to be got in Japan.

Since 2013, the field tests have been carrying out at abandoned mine site. The concentrations of solved metals in the targeted AMD are 35–40 mg/L iron, 18 mg/L zinc, and 8 mg/L copper, and the value of pH is 3.5. The results of field tests showed that 80% of the iron ion has been removed with the retention time of approximately 2 hours in the aerobic reactor, while almost of the other metal ions have been removed with the retention time of 50 hours in the anaerobic reactor. The tests have been running for approximately a year until at present, June 2014. The metals have been continuously removed without another maintenance and addition of materials and reagents during the test period. Moreover, in the reactors, which were not temperature-controlled, the metals continued to be removed even in winter, although the internal temperature dropped to approximately 5°C during the winter.

It is expected that this passive treatment system for AMD can be scale-upped and realized to be a cost-saving and energy-saving treatment system.

Keywords: Passive treatment, Sulfide reducing bacteria, Acid mine drainage, Iron-oxidizing bacteria

INTRODUCTION

Japan Oil, Gas and Metals National Corporation(JOGMEC) has conducted research on the passive treatment of mine drainage since 2007, and has focused on drainage treatment methods that remove metal ions as sulfides using sulfate reducing bacteria (SRB). For neutral pH mine drainage, field tests have been carried out using an anaerobic bioreactor filled with "rice husk" as an organic carbon source. The successful removal of metal ions had continued for approximately 1100 days under the appropriate conditions (retention time: 50 h, water temperature: over 15 °C). For acid mine drainage, with pH 3.0, containing several types of metal ions, the field tests are being performed using an anaerobic bioreactor filled with "rice bran" and "rice husk" as the organic carbon sources.

In many cases, acid mine drainages contains iron ions, which are difficult to be removed as sulfides because of their relatively high solubility. Therefore, in these field tests, iron oxide bacteria were employed separately to remove the iron ions from the mine drainage, prior to removing the non-ferrous ions as sulfides.

In this paper, the results of these tests are presented.

METHOD

Equipment

A prefabricated testing hut was built on the premise of the mine-drainage treatment plant of the mine site. Test equipment was installed in the prefabricated room. The aqueduct for mine drainage was introduced into the prefabricated hut to guide the drainage to the test apparatus.

Apparatus

A schematic diagram of the bioreactors used for the tests is shown in Fig. 1. For the test apparatus, an aerobic (iron oxidation-removal) bioreactor (left, Fig. 1) and an anaerobic bioreactor (center and right, Fig. 1) were prepared. A multistage process was configured to remove iron in the mine drainage by an aerobic bioreactor, and other metal ions by an anaerobic bioreactor. Both bioreactors are made of vinyl chloride. The iron oxidation-removal bioreactor is a rectangular parallelepiped with a bottom area of 900 cm^2 and a height of 45 cm. The anaerobic bioreactor is a cylinder with a diameter of 25 cm and a height of 110 cm. For the anaerobic bioreactor, four sampling ports (called the 1st, 2nd, 3rd, and 4th ports) were provided, in addition to an output port.

The iron oxidation-removal bioreactor was filled with approximately 15 kg in wet weight of iron scales that had been precipitating in, and sticking to the drainage aqueduct from the mine drainage treatment plant on the mine site (provided free of charge). Once filled with iron scales, the bioreactor was further filled with 20 L of mine water.

The anaerobic bioreactor, on the other hand, was filled with the following materials. Soil collected from the surface layer around the mine site was used as a source of bacteria, including SRB. Rice husk was used as a base material of the column and as a carbon source for bacteria. In addition, rice bran was added because it is more easily decomposed by bacteria than rice husk, due to its high levels of protein and lipids. Limestone (5 to 10 mm) was used as a structural material for securing cavities and for buffering the pH value. These materials are either free or very inexpensive to obtain in Japan and were easily collected. The column was filled with these materials to a height of 100 cm.

The weight of each material is as follows: approximately 4.5 kg of rice husk, approximately 1.5 kg of rice bran, 1 g of soil, and 18 kg of limestone. In this case, rice husk, limestone, and soil were combined and evenly distributed throughout the entire column. Rice bran, on the other hand, was filled intensively in the upper portion of the column (described later). The capacity of the column, to a height of 100 cm, is 50 L, and the volumetric composition of the content was approximately 95% rice husk, 3% limestone, and approximately 2% rice bran. In conjunction with the volume of solids, 35 L of mine water was used to fill the water level to 100 cm.

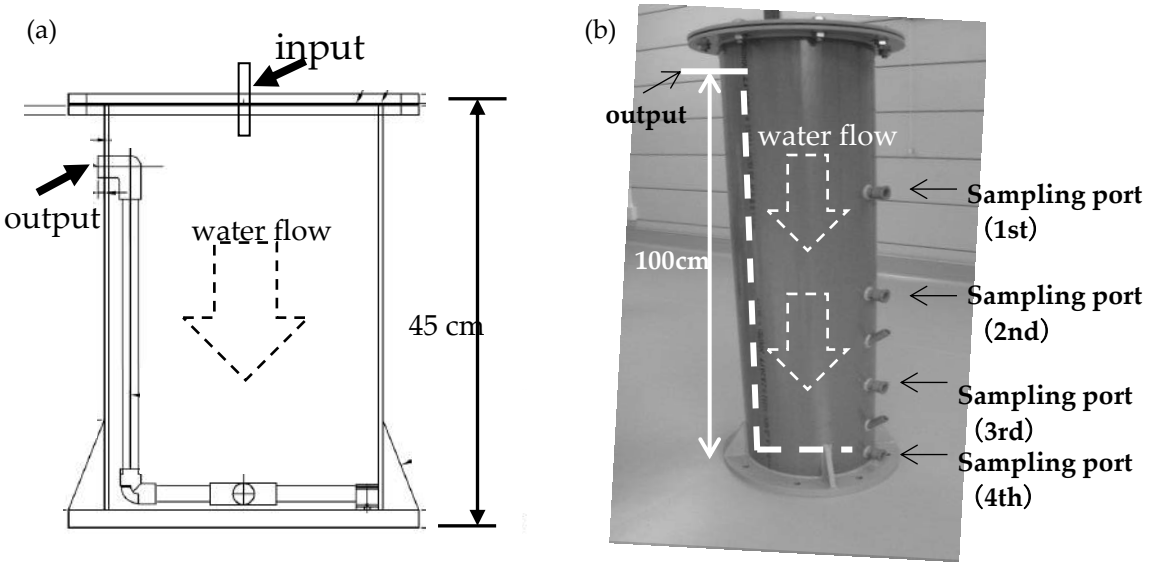

Figure 1 Bioreactor equipment.
Iron oxidation-removal reactor, (b) anaerobic bioreactor

Process

Acclimation of SRB in the anaerobic bioreactor

The anaerobic bioreactor was filled with the above-mentioned mixture of rice husk, limestone, and soil to the height of 100 cm. The contents were water sealed with 35 L of mine water as the sulfate ion source, and the SRB were acclimated under room temperature for approximately 10 days. In this case, rice bran was added to the top of the anaerobic bioreactor after acclimation of the SRB, and immediately before continuous feeding of the mine water. This was done because in laboratory tests it was observed that if bacteria are acclimated with added rice bran, microorganisms other than SRB ferment excessively, and eventually the sulfate reduction activity of SRB becomes non-detectable. Approximately 10 days after starting acclimation, the SRB became active, and the oxidation-reduction potential (ORP) of the water in the bioreactor became approximately -200 to -300 mV.

Water feeding method

After acclimation of the SRB, mine water was gravity-fed to the iron oxidation-removal bioreactor, with the flow rate adjusted to approximately 125 ml/min. Air was fed into the iron oxidation-removal bioreactor with an air pump so that the concentration of dissolved oxygen was

approximately 3 to 4 mg/L. The mine water passing though the iron oxidation-removal bioreactor was guided to the upper part of the anaerobic bioreactor with a pump. The flow rate was adjusted to 11.7 ml/min so that it passed through the anaerobic bioreactor as gravitational flow.

Quality of treated water

The mine drainage for the continuous test was sampled at the abandoned mine in Akita Prefecture, located in the northern part of Japan. The concentrations of zinc, copper, and iron in the drainage are shown in Table 1. These values exceed the national effluent standard; therefore, the drainage was selected as the sample in this investigation. Most of the iron was removed from the drainage after passing through the iron oxidation-removal bioreactor, and contained only 6 to 8 mg/L of iron (almost all the volume is ferric), while the pH value decreased to about 3.0. The concentrations of other metal ions in the mine water did not change after passing through the iron oxidation-removal bioreactor.

The temperature of treated water did not fluctuate very much throughout the year; it exited at a temperature of 12 to 14 °C.

Table 1 Water quality of the drainage and the national effluent standard values.

	pH	**Zn (mg/L)**	**Cu (mg/L)**	**Fe (mg/L)**	**SO_4^{2-} (mg/L)**
Mine drainage (min–max)	3.3–3.8	15–18	3–10	33–38	350–400
National effluent standard	5.8–8.6	2.0	3.0	10	

Analysis of items

Samples were collected periodically from the raw mine water, the treated water of the iron oxidation-removal bioreactor, as well as from the outlet and water sampling holes at each height of the anaerobic bioreactor. The samples were subjected to analysis, which included temperature, pH, ORP, metal ion concentrations (iron, copper, zinc, and cadmium), sulfate ion concentration, sulfide ion concentration, and COD. Concentrations of metal ion were determined using ICP and sulfate ion was determined using ion chromatography. Sulfide ion concentration was colorimetrically measured as hydrogen-sulfide ion and COD value determined titration method.

Retention time

The retention time for the raw mine water to pass through the iron oxidation-removal bioreactor was adjusted to approximately 1.5 to 2 h. The time to pass through the anaerobic bioreactor was set to 50 h.

Temperature conditions

Neither of the bioreactors was subjected to temperature control with a heater or air conditioner. Although no heating or cooling was applied, minimal heat insulating material (glass wool) was used to protect the test equipment from the elements, thus ensuring that the tests were conducted under natural temperature conditions. In addition, in the prefabricated hut, air conditioning was not employed, but minimal ventilation and lining of walls with heat insulating material was applied.

RESULTS AND DISCUSSION

Iron oxidation-removal bioreactor

Figure 2 shows the changes in the concentration of iron (total iron concentration, T-Fe) from the raw mine water (input) to the water that was treated with the iron oxidation-removal bioreactor (output) during the field test. The iron ion concentration in the bioreactor decreased gradually over the first 20 days, but it became steady at a low concentration after 50 days. The performance of the treatment did not change, even in the winter. Throughout the year, the iron concentration in the treated water was approximately 20% of that in the raw mine water. Moreover, there was no need for maintenance, such as replacement or replenishment of iron scales or other agents.

Anaerobic bioreactor

Changes in temperature in the anaerobic bioreactor

Figure 3 shows the changes of the temperature inside the anaerobic bioreactor in the field test and that of the mine water used for the test. The temperature inside the bioreactor was measured at the lateral center, at a depth of 40 cm from the top of the bioreactor. Figure 3 shows that the mine water used in this test entered at a constant temperature (12 to 14 °C) throughout the year. In contrast, the temperature inside the column exceeded 20 °C in the summer (September) and decreased to approximately 5 °C in the winter.

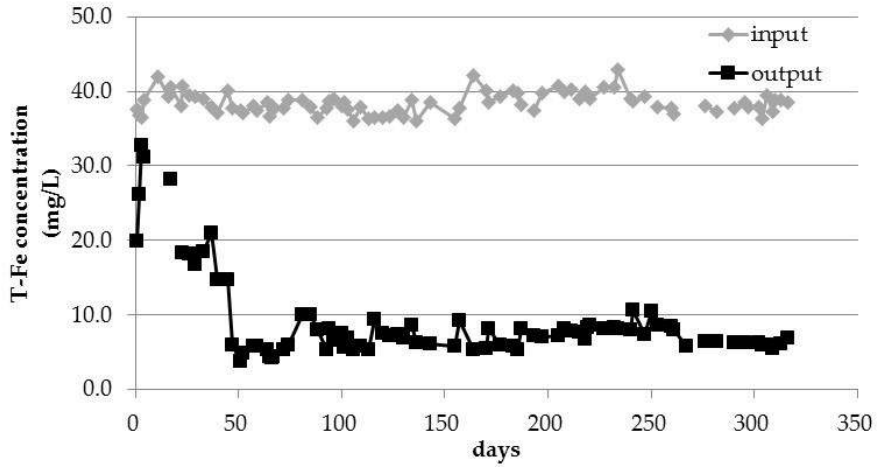

Figure 2 Changes in the concentrations of T-Fe in the mine drainage before and after treatment in the iron-oxidation removal bioreactor.

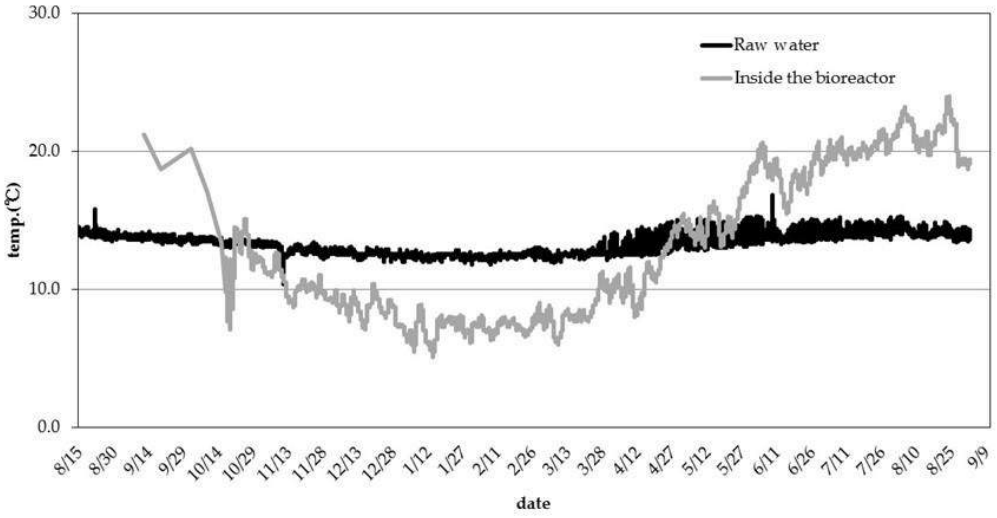

Figure 3 Changes in temperatures of raw mine water and inside the anaerobic bioreactor throughout the year.

Changes in pH and ORP values in the anaerobic bioreactor

Figure 4 shows the changes of the pH values in the anaerobic bioreactor. In the first port (1st) of the bioreactor, although the pH value was slightly lower in the winter, it was raised in the spring due to the rising atmospheric temperature. In the second (2nd) and subsequent (3rd and 4th) ports of the bioreactor, the neutral pH values remained steady, regardless of the fluctuations in the temperature. Figure 5 shows the changes in ORP values in the anaerobic bioreactor. The ORP in the first stage of the bioreactor was slightly unstable in the winter, sometimes exceeding -100 mV. In the second and subsequent stages of the bioreactor, the ORP was stably maintained below -200 mV. It is commonly said that the appropriate ORP for SRB is -200 to -300 mV. Accordingly, the ORP in this process remained within the above-mentioned range for one year after starting the test.

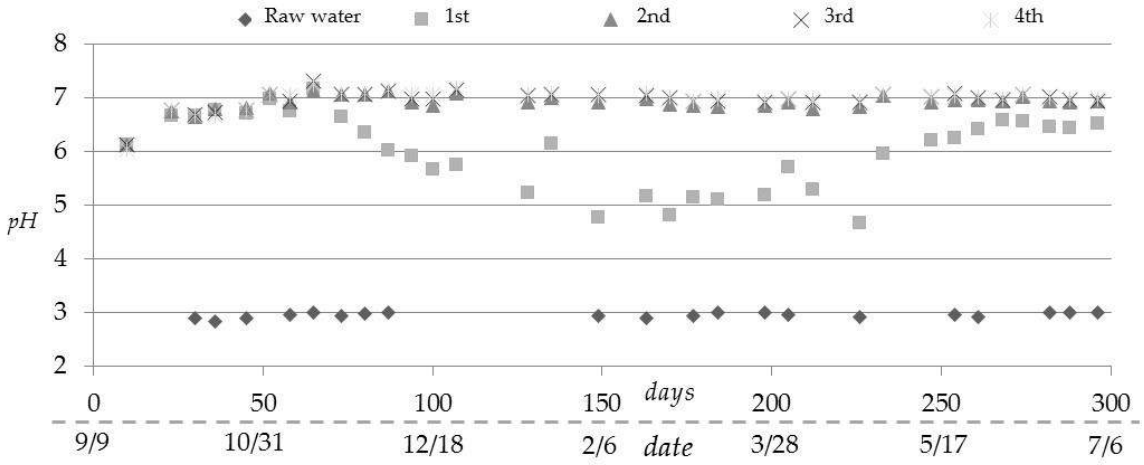

Figure 4 Changes in the pH values over time in the anaerobic bioreactor."1st, 2nd, 3rd, and 4th denote the location at which the sample was drawn"

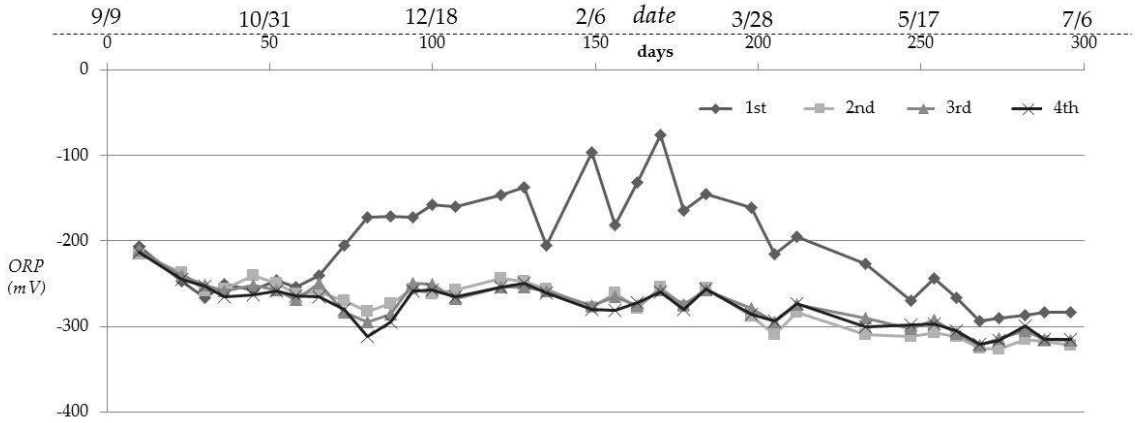

Figure 5 Changes in the ORP values over time in the anaerobic bioreactor.

Removal of metal ions in the bioreactor

Figure 6 shows the changes in the concentration of sulfate ions before and after treatment with the anaerobic bioreactor. In accordance with the fluctuations of the ORP values in Figure 5, the concentration of sulfate ion in the treated water did not be stabilized until 60 days from the start of the water feed. In the spring and summer seasons, after passing winter, the concentration of sulfate ion greatly decreased due to the high performance of sulfate reduction by the SRB in the bioreactor.

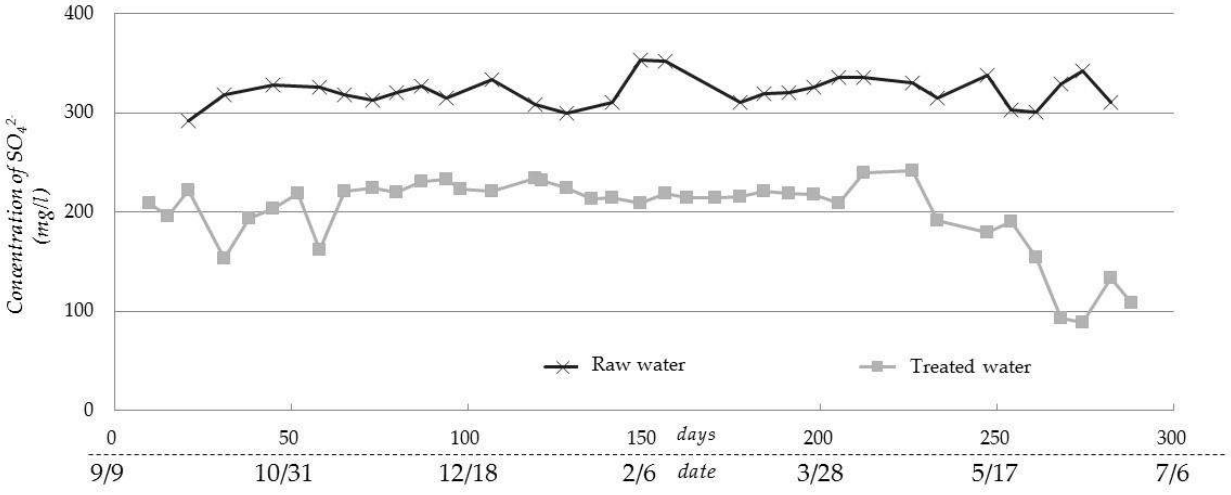

Figure 6 Concentration of sulfate ions in the mine drainage before and after treatment with the anaerobic bioreactor.

Figure 7 shows the changes in the concentration of zinc ions before and after the treatment with the anaerobic bioreactor. The concentration of zinc ions in the raw mine water was approximately 17 mg/L, with no large fluctuations throughout the test period. The water quality therefore always exceeded the national effluent standard in Japan. After the treatment with this process, the

concentration of zinc in the treated water was very low, indicating that the treatment had stably cleared the national effluent standard of 2 mg/L for one year. Other metal ions (copper, and cadmium) were also almost completely removed in the bioreactor. Although the temperature inside the bioreactor was as low as about 5 °C in the winter (as shown in Figure 5), no deterioration of the treatment performance was observed.

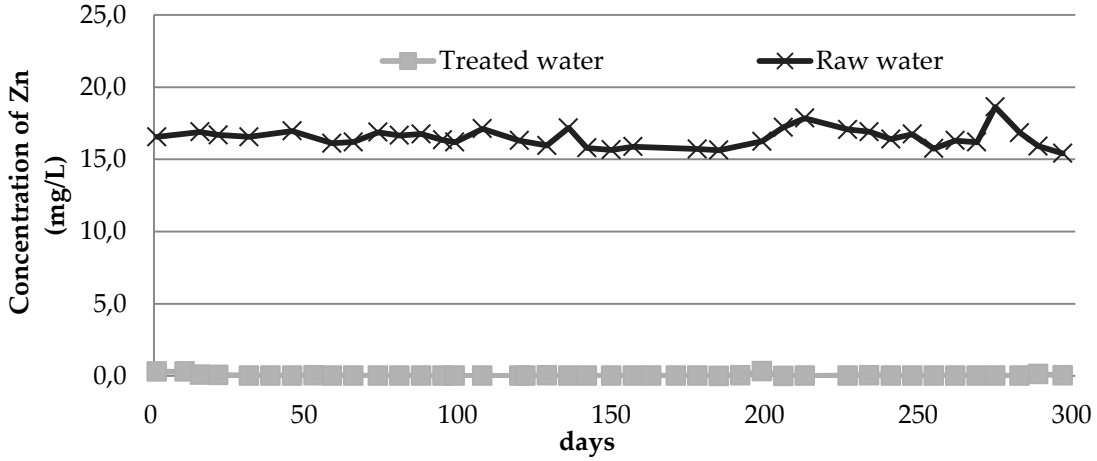

Figure 7 Concentration of zinc ions in the mine drainage before and after treatment with the anaerobic bioreactor.

Degree of pH, ORP, and sulfate ion reduction in the winter

Figure 4 and Figure 5 show that the pH decreased in the 1st stage of the anaerobic bioreactor and the ORP increased in the winter, respectively. The cause of the increase of pH in this process might be considered to be the neutralization effect of limestone and the progress of the sulfate ion reduction reaction of SRB. In the winter, the performance of sulfate ion reduction by SRB in the anaerobic bioreactor was lower than in other seasons, as shown in Figure 6, and so, it could be considered that the pH value in the 1st stage of the bioreactor was lower because the pH increasing effect of the sulfate ion reduction action was weakened. In the 2nd and subsequent stages of the bioreactor, it could be considered that the pH value was maintained stably even in the winter, mainly due to the neutralizing effect of limestone.

In the 1st stage of the anaerobic bioreactor, the observed increase in the ORP during the winter likely resulted from the decrease in activity of SRB due to the drop in the temperature. Moreover, the ORP tended to increase gradually because the raw mine water, which was always in an oxidation environment at the water channel from the mine site, was supplied in the 1st stage of the bioreactor. Therefore, generally the reduction condition was already weakened and the activity of the SRB was decreased, as mentioned above. Then, it could be conjectured that a stable reducing condition was revived in the 1st stage of the bioreactor and the activity of SRB increased again thereafter due to the temperature rise in the spring.

Treatment performance on metal ions (zinc, copper, and cadmium) in the winter

It is generally considered that the capability of sulfate ion reduction by SRB is weakened with a decrease in temperature. However, Figure 7 shows that almost all of the zinc ions contained in the raw mine water was removed after passing through the anaerobic bioreactor. Consequently, it could be considered that a sufficient volume of hydrogen sulfide ions, which were used for

precipitating metal ions in the raw mine water as sulfides, were generated in the anaerobic bioreactor. It was so far confirmed that this test apparatus could remove metal ions stably over a long period at a temperature of 15 °C. Furthermore, it was confirmed in the field test at this time that metal ions could be removed over a long period, even in an environment with low and seasonal temperature changes.

CONCLUSION

During the field tests in approximately one year, at the mine drainage treatment plant, iron was removed with the iron oxidation removal bioreactor, and other metal ions were removed with the anaerobic bioreactor stably and successfully without additional maintenance, such as replacement or replenishment of some materials. The materials used to be filled in both reactors are either free or very inexpensive to obtain.

Although the reaction temperature changed in the range of twenty degrees and it lowered to 5 °C in the winter, the sufficient reduction of sulfate ions occurred and the removal of metal ions continued very stably. This field test suggested that this process was applicable in low temperature environments, as low as approximately 5 °C, and therefore, it was probably applicable in environments with a wide range of temperatures.

For practical use of this passive treatment system, it is important that metal ions are removed stably for a long period, without any maintenance and even in the low temperature conditions. In our field tests, it was confirmed that metal ions were removed over a long period, even in the environment with lower temperatures and changing temperatures. Furthermore, in the case that mine drainage contained iron ions, it was confirmed that placing the iron oxidation-removal bioreactor before the anaerobic bioreactor during the treatment process was very useful. To develop a new cost-saving and energy-saving process, JOGMEC is now continuing the researches to make this multistep bioreactor process (“JOGMEC PROCESS”) more useful and durable.

Antimony Passive Treatment by Two Methods: Sulfate Reduction and Adsorption onto AMD Precipitate

Dave Trumm[1], James Ball[1], James Pope[1] and Chris Weisener[2]

1. *CRL Energy Ltd, New Zealand*
2. *Great Lakes Institute for Environmental Science, University of Windsor, Canada*

ABSTRACT

Two different passive water treatment methods to remove antimony from mine water were tested in field trials at a gold mine in New Zealand. In one method, antimony was removed through adsorption onto iron oxyhydroxides. The oxyhydroxides were collected from precipitate within an acid mine drainage discharge at a nearby coal mine. In the other treatment method, antimony was removed through precipitation as antimony sulfide (stibnite) in a sulfate-reducing bioreactor. Each system consisted of a 1000 liter plastic tub, filled with the treatment media. The loading ratio of iron oxyhydroxide in the adsorption chamber was 253 grams of precipitate per liter of water. The bioreactor contained equal parts of post peel, bark and compost. Inlet antimony concentrations ranged from 0.3 to 2.3 mg/L. Hydraulic residence times ranged from three minutes to 14 hours (adsorption chamber) and two hours to 30 hours (bioreactor). Removal rates in the adsorption chamber were 14 % at residence times of only three minutes and were up to 95 % at residence times greater than 2.5 hours. As the experiment progressed, removal rates by the adsorption chamber decreased over time, suggesting that adsorption capacity was being approached. Removal rates in the bioreactor were greater than 80 % at residence times above 15 hours. The greatest removal rate was 98 % at a residence time of 30 hours. Quantitative analysis using a scanning electron microscope confirmed the presence of stibnite in the bioreactor. Bioreactor performance continued to improve over time when compared to the adsorption chamber. This difference is possibly due to multiplication of sulfate-reducing bacteria. These results show that passive treatment can be a successful treatment method for antimony at gold mine sites, and that treatment through sulfate reduction and precipitation as stibnite is a favorable long-term treatment method over a treatment method using adsorption onto iron oxyhydroxides.

Keywords: Antimony, Passive Treatment, Adsorption, Sulfides

INTRODUCTION

The metalloid antimony (Sb) is often associated with gold mines, typically in the form of the sulfide mineral stibnite (Sb_2S_3) (Nesbitt et al., 1989; Williams-Jones & Normand, 1997). Removal techniques for Sb from solution are similar to those for arsenic (As) and include coagulation with ferric chloride, ion exchange, membrane filtration, and adsorption onto ferric hydroxide (Kang, 2003; Cumming et al., 2007; Klimko et al., 2008; Nokes, 2008). Other workers have documented potential removal of Sb through sulfate reduction and formation of stibnite. Biswas et al. (2009) conducted an experiment in a test tube to show that Sb can be removed as a sulfide in the presence of sodium sulfate. Wilson & Webster-Brown (2009) suspected that precipitation of stibnite could be occurring naturally at the bottom of Lake Ohakuri along the Waikato River where concentrations of hydrogen sulfide and Sb approach stibnite saturation conditions.

Trumm & Rait (2011) conducted a laboratory column leaching experiment to test removal of Sb from mine water in New Zealand by two different passive treatment methods. In one method, Sb was removed through adsorption onto iron oxyhydroxides. The oxyhydroxides were collected at two different coal mines where precipitate was forming within acid mine drainage (AMD). In the other treatment method, Sb was by removed through sulfate reduction and precipitation as stibnite in a sulfate-reducing bioreactor. Both techniques were effective in reducing the concentration of Sb in the mine water and X-ray powder diffraction analysis of the bioreactor substrate showed that stibnite had formed.

In this work, we extend the results of Trumm & Rait (2011) by installing small-scale passive treatment systems at the OceanaGold Globe Progress Gold Mine near Reefton on the West Coast of New Zealand to field test removal of Sb by two different techniques:

- Adsorption onto AMD precipitates in an adsorption reaction chamber
- Precipitation and formation of stibnite in a sulfate-reducing bioreactor

METHODS

Two passive treatment systems were constructed using 1000 L plastic tubs (standard intermediate bulk containers) with PVC piping, alkathene piping, and associated valves. The adsorption chamber was filled with a mixture of gravel and AMD precipitate from a nearby abandoned coal mine, composed primarily of goethite and ferrihydrite (Rait et al., 2010). The loading ratio of iron oxide in the adsorption chamber was 253 g precipitate per liter of water. The bioreactor was filled with equal proportions of post peel, bark chips, and compost. Each system was constructed in an up-flow configuration, such that the inlet was at the base of each system and the water flowed upwards through the treatment media driven by sufficient hydraulic head (Figures 1 and 2).

The systems operated for a period of 71 d. Flow rates were varied to determine Sb removal for different hydraulic residence times (HRTs). Inlet and outlet samples were collected approximately three times per week from each system, or more often for very short HRTs, and analyzed for dissolved As, dissolved Sb, and sulfate by inductively coupled plasma mass spectrometry using APHA method 3125-B (for metalloids) and by ion chromatography using APHA method 4500-PG (for sulfate) (APHA, 2005). Solid samples were collected from the top 10 cm of the bioreactor for mineralogical analysis by scanning electron microscopy (SEM) with energy dispersive X-ray spectrometer (EDS) and also for microbiological analysis.

Figure 1 Adsorption chamber prior to being filled with treatment medium

Figure 2 Adsorption chamber (on left) and bioreactor (on right) prior to being filled with water

RESULTS AND DISCUSSION

Adsorption chamber

Inlet concentrations to the adsorption chamber ranged from 0.3 to 2.3 mg/L. The system removed as much as 95 % of the inlet Sb concentrations (to as low as 0.09 mg/L) (Figure 3). The greatest percentage removal was noted at the beginning of the experiment, with removal effectiveness decreasing over time. A drop in treatment effectiveness with time likely indicates that adsorption capacity of the treatment media was being approached. Since HRT varied, it is possible to analyze the effectiveness of similar HRTs over the duration of the experiment. In general, the effectiveness of each HRT dropped with time (Figure 4). This suggests that if a consistent removal rate is required, HRT must be increased over time.

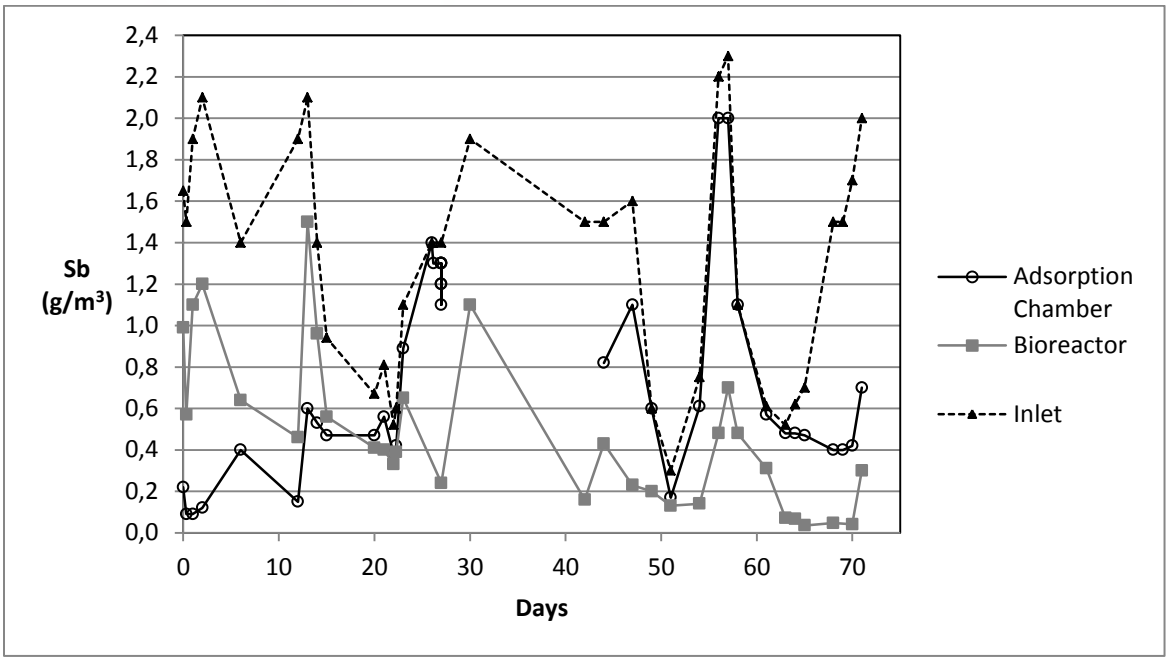

Figure 3 Inlet and outlet Sb concentrations for adsorption chamber and bioreactor over the duration of the field trials

At the very short HRT of 3 min, Sb removal in the adsorption chamber was 14 %, lowering Sb concentrations from 1.4 to 1.2 mg/L (Figure 5). Removal increased to 95 % at an HRT of 2.4 h (lowering Sb concentrations from 1.9 to 0.09 mg/L). For HRTs longer than 10 h, however, Sb removal was only 65 to 75 %. This is likely because Sb removal at these low flow rates were tested at the end of the experiment, after much of the adsorption capacity of the material had been exhausted and removal efficiency had declined.

Bioreactor

Antimony removal in the bioreactor was as low as 29 % near the beginning of the experiment, increasing to 98 % at the end of the experiment (Figure 6). Unlike the adsorption process where removal was initially good and decreased with time, Sb removal in the bioreactor was lower initially and improved with time, possibly due to growth and establishment of the sulfate-reducing bacteria population.

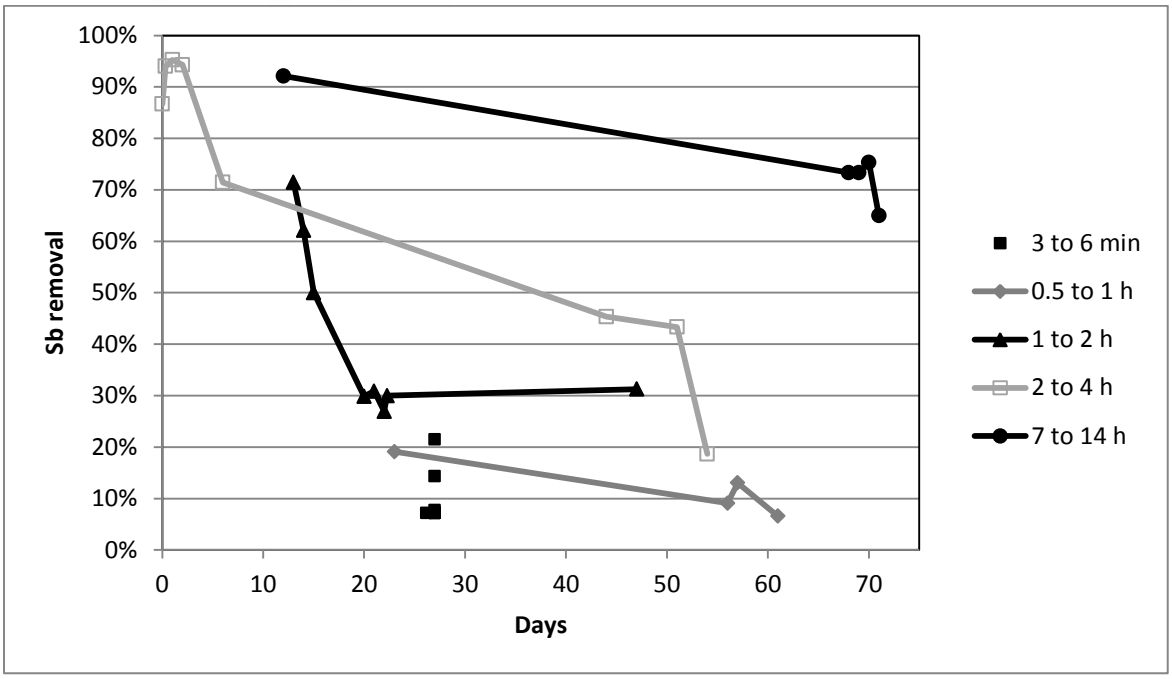

Figure 4 Antimony removal by adsorption chamber grouped according to HRT in the system to show trends

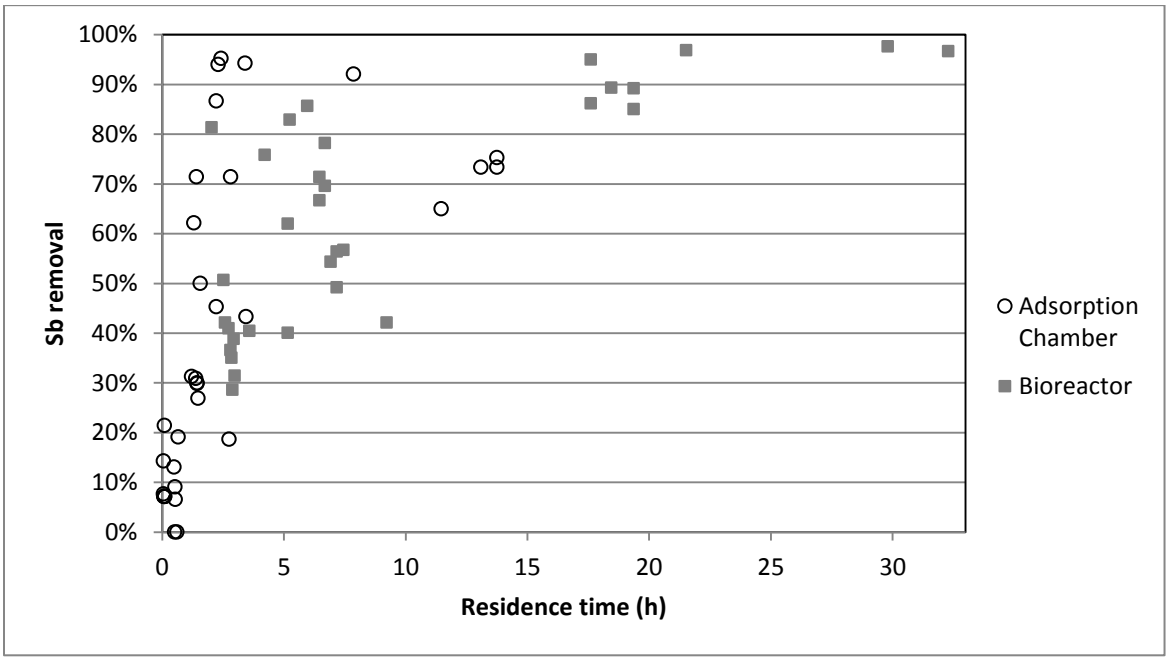

Figure 5 Antimony removal by adsorption chamber and bioreactor according to HRT

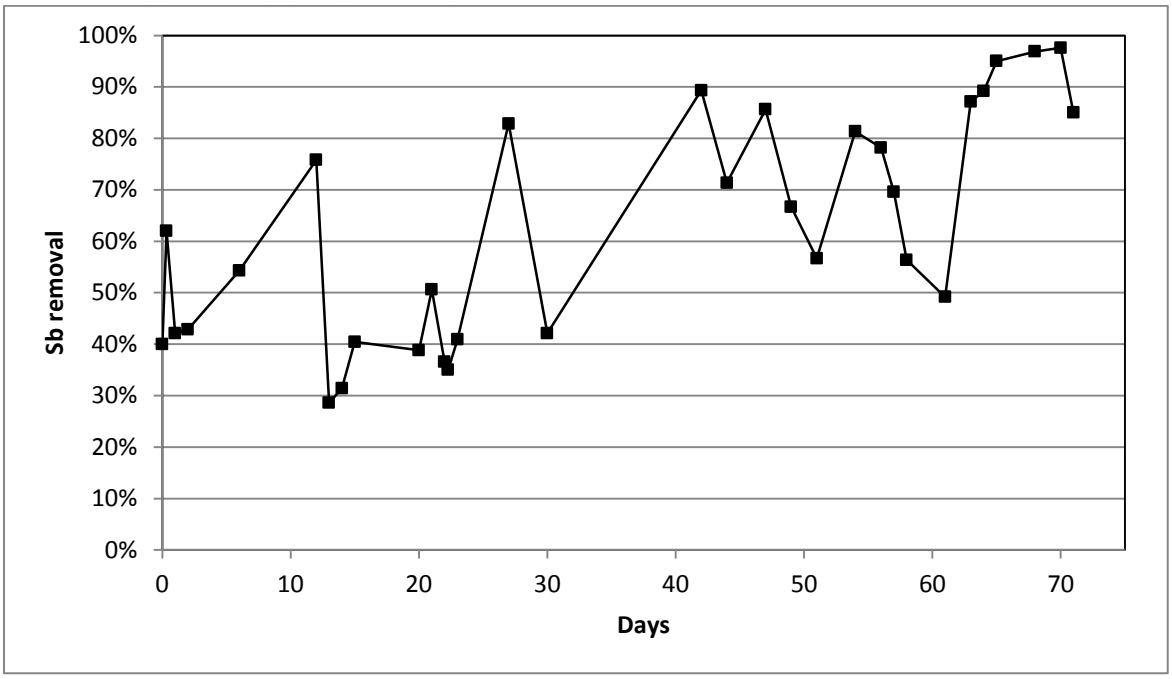

Figure 6 Antimony removal by bioreactor over the duration of the field trials

At HRTs below ~5 h, Sb removal was ~40 %, and at HRTs between 20 and 30 h, Sb removal was up to 98 % (Figure 5). Antimony removal rates ranged from 0.002 moles/m^3/d to 0.034 moles/m^3/d and are correlated with HRT. Solid samples from the bioreactor analyzed by SEM with EDS confirmed the presence of stibnite, suggesting *in situ* sulfate reduction was occurring (Figure 7). Preliminary genomic DNA and RNA-Seq molecular analysis of the substrate shows a complex community of sulfate-reducing bacteria along with species capable of metabolizing intermediate sulfur compounds, such as *Dethiosulfovibrio peptidovorans.*

Removal of Sb with a sulfate-reducing bioreactor may be a better long-term treatment technique than removal through adsorption onto iron oxyhydroxide precipitate. Preliminary work here shows that for similar sized systems, a bioreactor will outperform an adsorption chamber over time.

It should be noted that the duration of this experiment (71 d) was relatively short, and that the bioreactor had likely not reached steady-state conditions. It is possible that, over time, bacteria may reach a rate-limiting phase due to a condition such as complete lignocellulose hydrolysis (Brown, 1983) which could then compromise performance. To determine long-term performance of a bioreactor removing Sb (as well as long-term performance of an adsorption chamber), both systems were restarted and have been operating continuously for nearly two years. Complete data analysis will be presented in another publication, however, preliminary results show generally good performance over this time (Figure 8). Poor performance between days 124 and 162 and between days 405 and 483 coincide with cold winter conditions, which could affect the activity of sulfate-reducing bacteria.

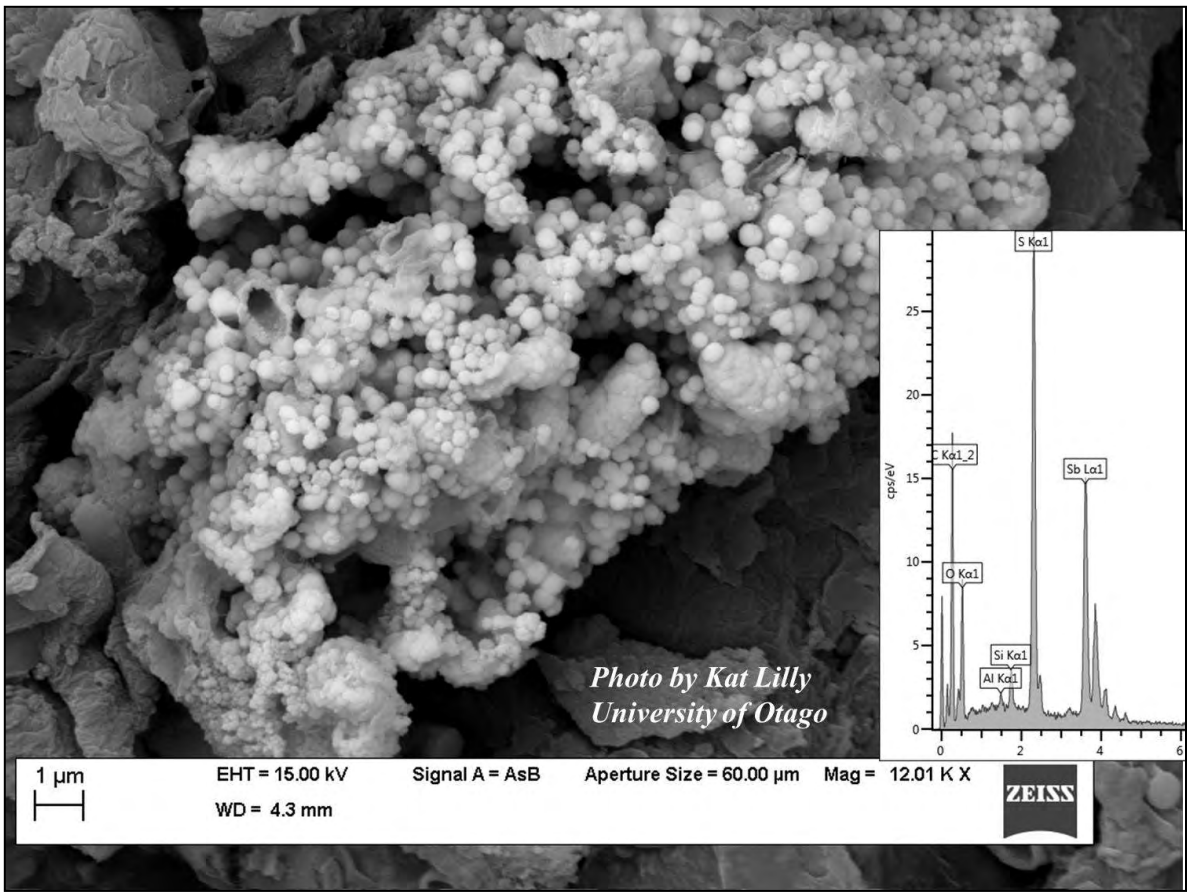

Figure 7 SEM microphotograph and EDS scan of antimony sulfide (stibnite) in substrate from the bioreactor

CONCLUSIONS

These results show that Sb dissolved in mine water can be removed through adsorption onto ferric hydroxide precipitates sourced from coal mine AMD. This study also shows that Sb can be removed through sulfate reduction in a sulfate-reducing bioreactor. For treatment by adsorption, Sb concentrations can be lowered by 14 % at HRTs of only 3 min and by 95 % at HRTs above 2.5 h. Performance declines in an adsorption chamber as the adsorption capacity of the treatment media is approached, therefore, HRT must be extended over time to compensate.

In a bioreactor, treatment of Sb occurs through sulfate reduction and formation of stibnite. Antimony concentrations can be lowered by 81 % at HRTs of only 2 h and by 98 % at HRTs above 20 h. Treatment performance increases with time as the microbial population expands and sulfate reduction improves. Therefore, HRTs should be longer initially and can be lowered as treatment performance improves.

Although this trial was only 71 d in duration, a second trial is underway (now nearly two years in duration) to measure long-term performance of a bioreactor and to determine if a rate-limiting phase may develop as steady-state conditions are approached. Preliminary results show good performance except during cold winter months when biological activity may be suppressed.

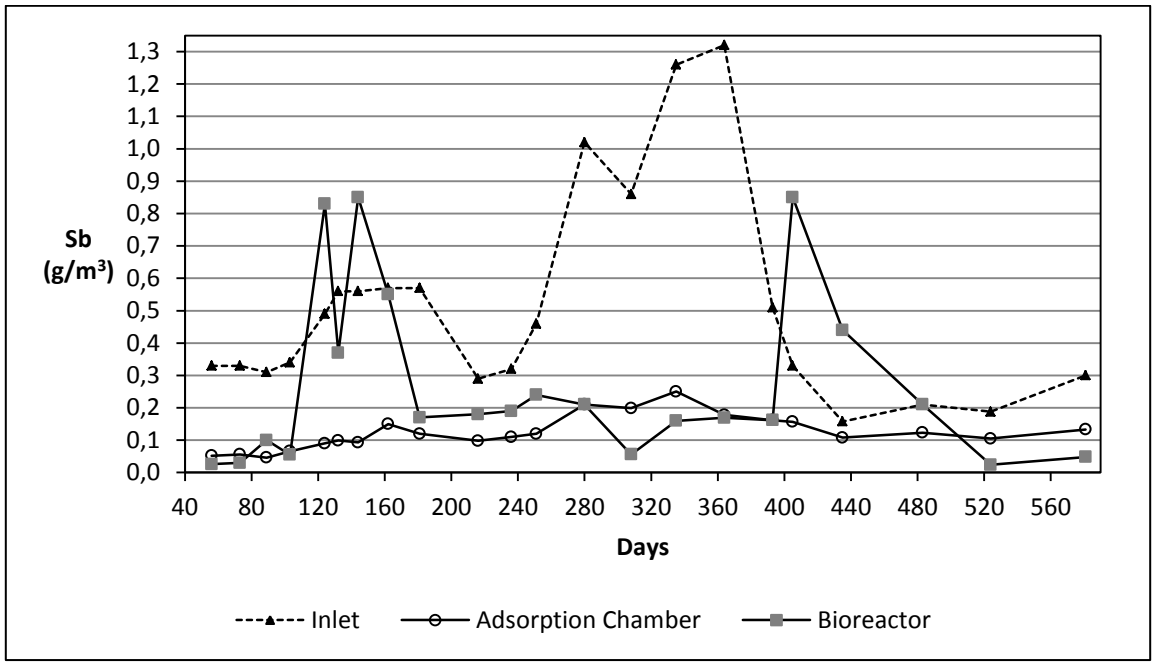

Figure 8 Inlet and outlet Sb concentrations for adsorption chamber and bioreactor over the duration of the second field trial

ACKNOWLEDGEMENTS

This research was financed by OceanaGold and by the Ministry for Business, Innovation and Employment (Contract CRL1202). Katherine Olsen of OceanaGold and Daya Gautam of CRL Energy assisted with sampling.

REFERENCES

American Public Health Association (APHA) (2005) *Standard methods for the examination of water and wastewater*, American Public Health Association: Washington, DC, 21st edition.

Biswas, B.K., Inoue, J., Wakakita, H., Ohto, K., and Inoue, K. (2009) Effective removal and recovery of antimony using metal-loaded saponified orange waste. *Journal of Hazardous Materials* **172**, 721–728.

Brown, D.E. (1983) Lignocellulose hydrolysis. *Phil. Trans. R. Soc. Lond.* B300, 305–322.

Cumming, L.J., Wang, L. and Chen, A.S.C. (2007) *Arsenic and Antimony Removal from Drinking Water by Adsorptive Media,* US EPA Demonstration Project at South Truckee Meadows General Improvement District (STMGID), NV Interim Evaluation Report EPA/600/R-07/081.

Kang, M., Kamei, T. and Magara, Y. (2003) Comparing polyaluminum chloride and ferric chloride for antimony removal. *Water Research* **37**, 4171–4179.

Klimko, T., Lalinská, B. and Šottník, P. (2008) Antimony Removal by Zero-valent Iron: Implications for Insitu Groundwater Remediation. *In:* Proceedings of the International Mine Water Association. Karlsbad, Czech Republic. 2–5 June 2008.

Nesbitt, B.E., Muelenbachs, K. and Murowchick, J.B. (1989) Genetic implications of stable isotope characteristics of mesothermal Au deposits and related Sb and Hg deposits in the Canadian Cordillera. *Economic Geology* **84**, 1489–1506.

Nokes, C. (2008) *An Introduction to Drinking Water Contaminants, Treatment and Management,* Environmental Science and Research Ltd, Prepared for the New Zealand Ministry for the Environment.

Rait, R., Trumm, D., Pope, J., Craw, D., Newman, N. and MacKenzie, H. (2010) Adsorption of arsenic by iron rich precipitates from two coal mine drainage sites on the West Coast of New Zealand. *New Zealand Journal of Geology and Geophysics* **53**, 179–195.

Trumm, D. and Rait, R. (2011) Passive treatment of antimony using AMD precipitates and through sulfate reduction. *In:* Proceedings of the 44th annual conference, New Zealand Branch of the Australasian Institute of Mining and Metallurgy. Queenstown, New Zealand. 27–30 August 2011.

Williams-Jones, A.E. and Normand, C. (1997) Controls of mineral parageneses in the system Fe–Sb–S–O. *Economic Geology* **92**, 305–324.

Wilson, N. and Webster-Brown, J. (2009) The fate of antimony in a major lowland river system, the Waikato River, New Zealand. *Applied Geochemistry* 24, 2283–2292.

10th ICARD IMWA 2015 | 10th International Conference on Acid Rock Drainage & IMWA Annual Conference

Use of Anaerobic Reactors for AMD Passive Treatment from a Waste Pile–Jacobina Mine

Luíz Lourenço Fregadolli[1], Flávio Vasconcelos[2] and Thomas Wildeman[3]

1. *Yamana Gold, Brazil*
2. *Hidrogeo Assessoria Ambiental Ltda, Brazil*
3. *Department of Chemistry and Geochemistry, Colorado School of Mines, USA*

ABSTRACT

Acid mine drainage (AMD) generation is one of the greatest challenges for mine water management and treatment. An alternative treatment for AMD is the application of passive systems that include the use of sulfate-reducing bacteria. This study aimed to evaluate the applicability of anaerobic bench-scale reactors to remove the presence of aluminum in the effluent from a waste pile of a gold exploration. Five anaerobic reactors were applied in parallel with different proportions of substrates composed by limestone, sugar cane bagasse, a leguminous species, manure and sawdust. A source of iron was also added into two of the studied reactors. The results suggest an aluminum removal higher than 99 % for all reactors. The pH of the reactors effluents was naturally kept over 6.0 during the whole study.

Keywords: AMD effluent treatment, anaerobic reactors

INTRODUCTION

Jacobina mine is a complex of underground gold mine located in the town of Jacobina in Bahia state Brazil and it belongs to YAMANA GOLD INC. Now a days this mine process 6,500 tons of ore per day in activated carbon pulp processing plant, this production started in 2005.

The occurrence of acid mine drainage (AMD) has been reported in the extraction of commodities such as gold, coal, copper, zinc and uranium. Sulphide minerals are formed under reducing conditions and therefore in the absence of oxygen. These minerals, when exposed to atmospheric oxygen due to excavation and deposition of tailings, they can become unstable and oxidize.

AMD is therefore the result of natural oxidation of sulphide minerals such as pyrite (FeS_2) and pyrrhotite ($Fe_{(1-x)}O$) when exposed to water and oxygen, and this chemical reaction action can be accelerated in the presence bacteria. AMD usually has a low pH (1.5 to 3.5) and high levels of dissolved sulphate and metals.

The passive treatment systems refer, in general, processes which do not require human intervention to regulate the activities of operation. Such systems are usually constructed from locally found materials (soils, clays and rock fragments), natural materials (crop residues such as straw, wood shavings, manure) to promote the growth of natural vegetation or to promote an environment where effluent treatment can occur through microbial activity.

Typically passive systems can be characterized by promoting water flow by gravity, by having long operation years without demanding equipment that requires electrical power supply.

The passive treatment has been applied to the detriment of several alternatives due to their low cost of deployment and maintenance processes. However, passive wastewater treatment is only possible to be applied in cases where the triad, effluent quality, flow and availability of area allows your application with greater probability of success.

The aim of this study is to present the results of the implementation of a passive system of anaerobic bench scale, applied to the treatment of acid mine water produced in the waste dump known by the name of João Belo and located at Jacobina Mining Corporation (JMC) that belongs to Yamana GOLD INC.

METHODOLOGY

Study area

The study area is comprised by the JMC mine, located in the town of Jacobina in Bahia State Brazil and belongs to YAMANA GOLD INC. The experimental apparatus is located downstream from the waste dump João Belo after the flooded area formed by the drain from the battery.

Characterization of DAM and early treatment

The characterization of the effluent from the mine waste dump was obtained from a sampling campaign conducted in August 2011, where the chemical of interest for treatment were determined. The mine effluent results were compared with the maximum concentration limits (MCL) of Brazilian water surficial water quality criteria (CONAMA 357/2005) for class 2 over the limits for effluent discharge.

Table 1 presents the results of this campaign, which also reports the results of detection, the legal concentration limit of the Brazilian regulation CONAMA 357/2005 for Class 2 water bodies and the analytical method employed. All components were dissolved and analyzed for their overall shapes.

Table 1 Characterization of acid drainage from the waste dump.

Chemical	DL(mg/L) (1)	JMC-03-tot (2)	JMC-03-dis(2)	MCL (mg/L) (3)	Chemical of interest	Analytical Method(4)
Al	0.0078	20.120	20.002	0.1	Yes	ICP-AES
As	0.0366	BDL	BDL	0.01	No	ICP-MS
Cd	0.0011	0.004	0.003	0.001	Yes	ICP-MS
Co	0.0023	0.203	0.199	0.05	Yes	ICP-AES
Cr	0.0026	0.127	0.127	0.05	Yes	ICP-AES
Cu	0.0005	0.123	0.122	0.009	Yes	ICP-AES
Fe	0.0021	1.789	1.753	0.3	Yes	ICP-AES
Mn	0.0003	1.171	1.150	0.1	Yes	ICP-AES
Ni	0.0017	0.223	0.219	0.025	Yes	ICP-AES
P	0.1043	BDL	BDL	0.02	No	Ion chrom
Pb	0.0176	BDL	BDL	0.01	No	ICP-MS
Sb	0.0133	BDL	BDL	0.005	No	ICP-MS
Se	0.0393	BDL	BDL	0.01	No	ICP-MS
SO_4	0.1200	186.640	184.366	250	No	ICP-AES

(1) DL: detection limit of the parameter;
(2) Metal Concentration in Total and Dissolved Forms
(3) Maximum Concentration Level for Water Bodies Class 2 According to CONAMA 357/2005.
(4) ICP-AES: Inductively Couple Plasma – Atomic Emission Spectroscopy
(4) Ion chrom: Ion Chromatograph

As noted, the main constituents of interest were those whose concentration is found above the legal limits for class 2 rivers, especially aluminum, whose concentration was 20 mg / L or approximately 1.0 x 10^{-3} mol / L.

The principle of treatment is guided by the fact that 0.3 moles of sulfide will be produced per cubic meter per day in the reactors. Each reactor contains about 150L to 200L of substrate and, consequently, each reactor should be capable of generating 0,045 moles of sulfide according to the following reaction.

$$2\ H^+ + SO_4^{=} + 2\ \text{“}CH_2O\text{”} \dashrightarrow H_2S + 2\ HCO_3^- \quad (1)$$

In the reaction, "CH2O" generically represents the organic matter present in the reactors. The contaminants are removed by two geochemical mechanisms. The H_2S generated by the reaction above reacts with Fe, Zn, Cu, Cd and Pb metals generating precipitated sulfides (secondary sulfides).

$$H_2S + Zn^{2+} \dashrightarrow ZnS + 2\ H^+ \quad (2)$$

Furthermore, HCO_3 increases the pH and form metal hydroxide precipitates, which will be important process for removing aluminum and chromium.

$$Al^{3+} + 3\ HCO_3^- \dashrightarrow Al(OH)_3 + 3\ CO_2 \quad (3)$$

According to the reactions as shown and the aluminum concentration found in the effluent, 2 moles of HCO_3^- are released for every mole of H_2S and 3 moles of HCO_3^- are necessary to 1 mol of aluminum be removed. Consequently, 0.045 mol of sulfide is generated in the reactors 0.030 mole of aluminum can be removed. Thus, 30L of water a day can be processed in reactors containing 150L to 200L of substrate, which corresponds to a rate of 20,5mL / min.

Experimental apparatus

The passive system deployed on the site consists of five anaerobic pilot scale with volume of 250L, which in turn receive the effluent from the mine waste dump. The effluent distribution system consists of a feed tank of 1,000L which forwards the effluents by gravity to five tanks/ of 50L, which in turn feed the reactors. The feed rate of each reactor is 30L / d. Figure 1 below shows a schematic of the system implementation.

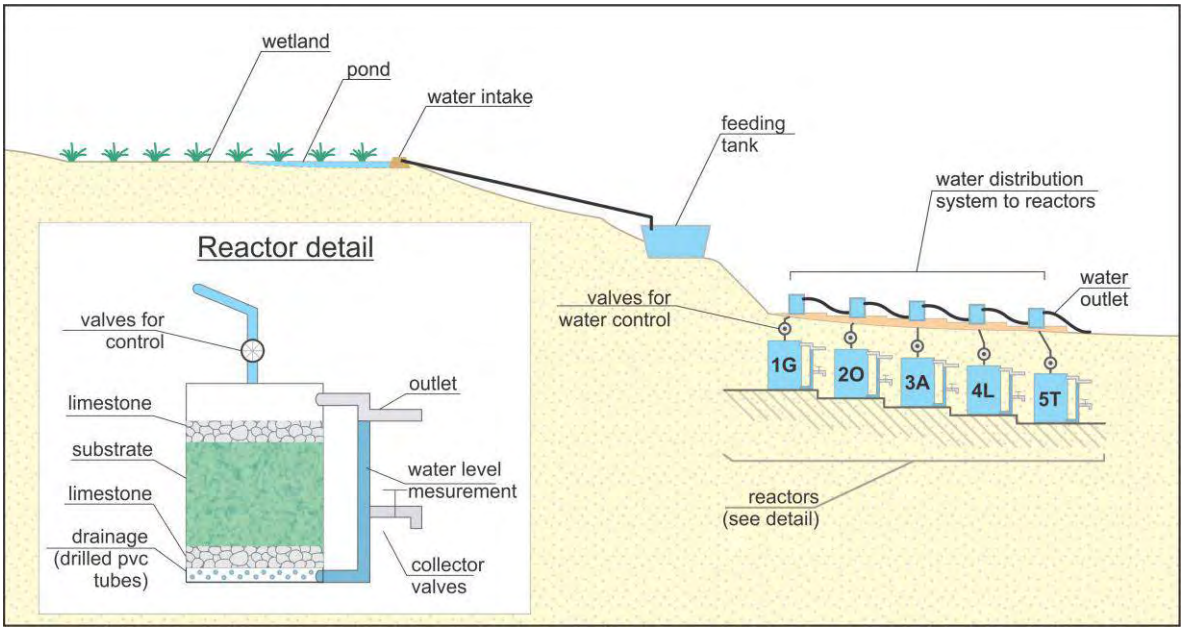

Figure 1 Bench scale passive treatment system developed in the Jacobina mine, belonging to Yamana Gold

The five reactors were sized to receive a limestone layer disposed on top of the substrate and a layer on the bottom of the reactor. The composition of the substrate comprises carbon sources, nitrogen, and an inoculum (manure), and a source of iron was added in two reactors. Table 2 below shows the composition of the substrates used in each reactor. The percentage of substrate used is relative to the working volume of the reactors (150L).

Table 2 Materials used for the substrate filled in each reactor.

Substrate	Reactors				
	1 G	2 O	3 A	4 L	5 T
Wood dust	40%	20%	30%	35%	40%
Limestone	30%	30%	25%	30%	30%
Sugarcane bagasse	-	10%	10%	15%	20%
Legume vegetation	20%	15%	15%	10%	-
Steel dust	-	10%	10%	-	-
Manure	10%	10%	10%	10%	10%

Monitoring and start-up system

After the implementation of the reactors on the site, the substrate was inserted into each reactor composition as indicated in Table 2. The start-up of the system was performed by maintaining the water level of the reactor above the substrate for a period of one week, so that the community of sulfate-reducing bacteria could be established in the system. For monitoring system, samples of effluent from the waste dump and effluents from the treatment of the five reactors were collected monthly between the months of October 2011 to March 2012. The monitored parameters were: temperature, pH, electrical conductivity and alkalinity. For monitoring the efficiency of the system, the concentrations of sulfate and metals aluminum, manganese and iron, in its dissolved form, were analyzed. The parameters of interest were analyzed according to Standard Methods for the Examination of Water and Wastewater. Metal concentrations in the influent and effluent of the system were analyzed through atomic emission spectrometry (ICP-AES) techniques.

RESULTS AND DISCUSSION

Table 3 shows the results of the concentrations of dissolved aluminum dissolved iron dissolved manganese sulfate, and pH from monitoring the influent and effluent produced by the five reactors.

Table 3 Results in mg/L of passive monitoring system for treatment of AMD.

Parameter	Average concentration (Parameter reduction - %)					
	In take	1G	2O	3A	4L	5T
Al	20,7	0,02 (99,9)	0,02 (99,9)	0,02 (99,9)	0,02 (99,9)	0,03 (99,8)
Fe	1,44	0,01 (99,6)	0,05 (96,4)	1,41 (2.17)	0,32 (77,3)	0,01 (99,3)
Mn	1,95	2,21 (25.1)	2,23	3,15	2,48	1,26 (35,5)
SO_4	209.21	75,7(63.8)	32,4 (84.5)	27,9 (86.6)	23.07 (88.9)	134,5 (35.7)
pH	3,03	7,47	7,14	6,89	6,98	7,39

As noted in Table 3, the average concentration of aluminum in the tributary system is 20,7mg / L and the effluent of the reactors yielded concentrations below 0.04 mg / L. The average efficiency for all reactors was greater than 99.8% removal of aluminum.

In the characterization of AMD produced on site, the main element of interest was the treatment of aluminum metal. The iron was introduced into the substrate only to promote coprecipitation of metal, so the high concentration observed in the effluent of reactor 3A is a consequence of the removal of iron present in the substrate. As noted, 10% by volume of the reactors of the substrate 2O and 3A is constituted of iron filings. Although the same amount of iron has been added in the substrate from both reactors, the reactor effluent showed 2O average concentration of 0.05 mg / L, and the effluent from the reactor had an average concentration 3A iron 1,41mg / L. Regarding other reactors, lower average concentrations to 0.4 mg / L was observed.

As noted, the increased manganese concentrations in the effluents of the reactors. The average concentration of manganese was 1,95mg / L and the influent was noted that the effluent from the reactors had concentrations above the value observed for influent. Due to the fact that manganese may be present in the crystal structure of carbonate minerals (e.g., rhodochrosite - $MnCO_3$), the increase in the average concentration in the effluent of the reactors can be attributed to solubilization of manganese present in the limestone.

With respect to pH, it was noted that the composition of the substrate was able to raise the pH of the effluents from all reactors. The average concentration of the effluent was pH 3.03 (in take) and the average concentrations of the effluent of the reactors were maintained pH between 6 and 8.

Efficiency in removing sulfate above 60% for all reactors except reactor 5T, whose average efficiency was 35.7% although the goal of treatment has not been the removal of sulfate, this was observed.

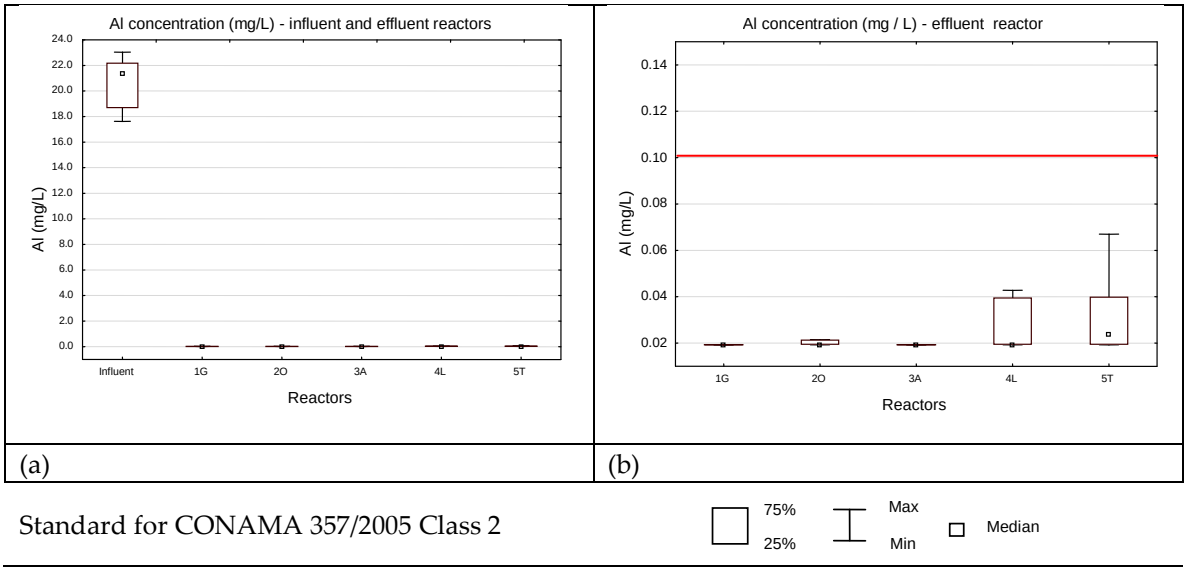

Graph 1 Concentrations of aluminum in the influent and effluent of the reactors.

The graphs (Figure 1) show the different aluminum concentrations in the influent and effluent of the reactors. Plot (a) shows the inflow concentrations compared to the effluent quality of the system. The graph (b) shows the effluent concentrations of the reactors and the limit for aluminum according to CONAMA No. 357 of 2005 for class 2 [4] water bodies.

It is observed that the average aluminum concentration in the influent of the reactor is between 20 and 22 mg / l. For effluent concentrations, we note that the maximum, minimum and median values have little variability for 1G, 3A and 2O reactors, while for the other reactors, 4L and 5T, concentrations were more variable, with maximum values exceed 0.04 mg / l. In fact, the effluent concentrations of aluminum were often below the detection limit of the analytical method in order to justify the stability of the observed values. It is seen that the concentrations of the effluent from reactor consistently met the threshold practiced 0.1mg / l.

Chart 2 below shows the concentrations of iron and manganese influent and effluent of the reactors.

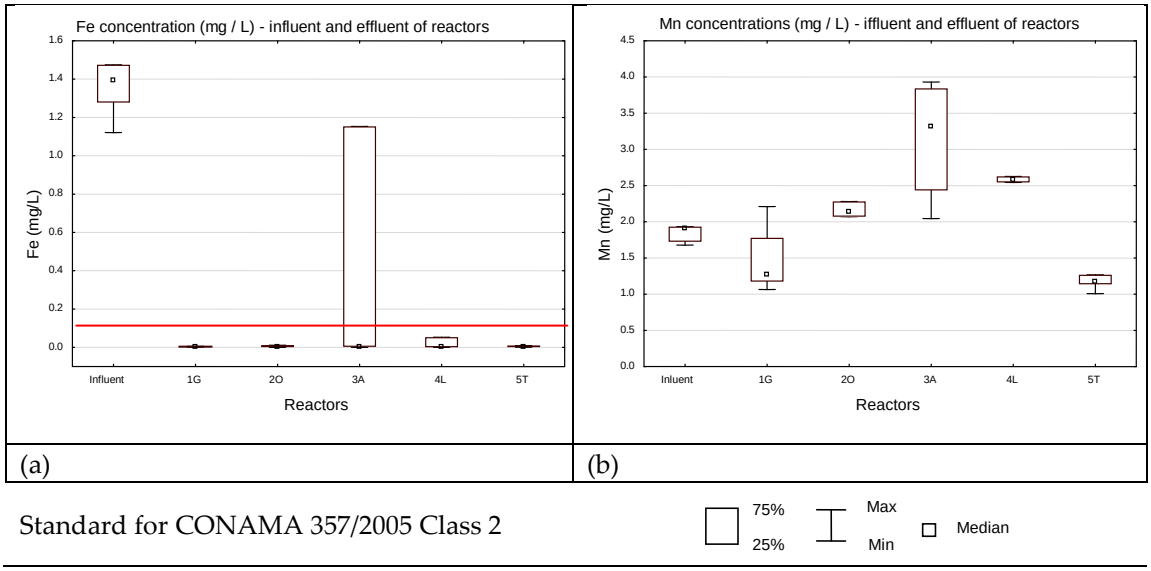

Graph 2 Concentrations of iron (a) and manganese (b) in the influent and effluent of the reactors.

The graphs show the concentrations of iron (a) and manganese (b) in the influent and effluent of the reactors. The iron concentration in the influent have a median value of 1.4mg / l and the effluent have median values below 0.1 mg / l. As previously mentioned, the source of iron present in the substrate may have contributed to the increase in concentration in the reactor effluent 3A. With respect to the concentrations of manganese, there is greater variability in the distribution of concentrations from reactor 3A, whose median was approximately 3,4mg / L.

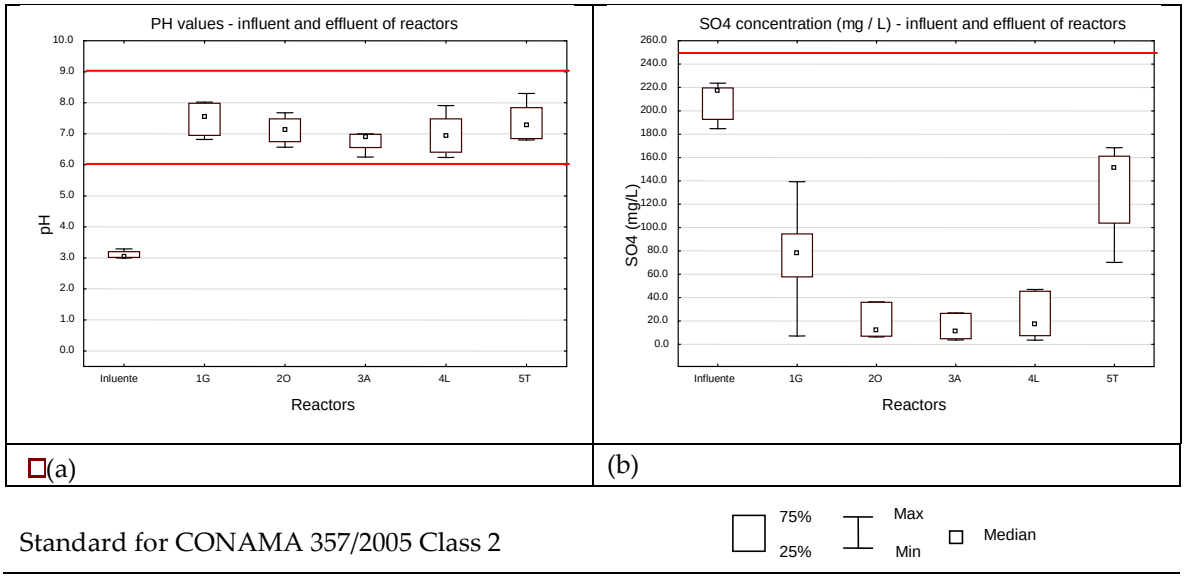

Graph 3 Values of pH (a) sulfate and (b) in the influent and effluent of the reactors.

As noted, the pH values consistently complied with the environmental laws, whose values should be between 6.0 and 9.0. Given that the median pH of the influent was approximately 3.0, the limestone used as the substrate alkalinity produced by anaerobic activity in the system was able to elevate and maintain the pH of the reactors to values above 6.0.

According to the graph (b) of the figure, we note that the sulfate median concentrations in the reactors 2O, 3A and 4T, were below 20,0mg / L. In comparison with the inflow concentrations, the removal of sulfate in the reactor was 63.4%, 84.5%, 86.6%, 88.9% and 35.7% for the 1G 2O, 3A, 4L reactor and 5T respectively. It is also noticed that the effluents did not exceed the maximum concentrations of 250 mg / L of sulfate, as pointed out by environmental legislation.

Regarding other metals characterized in acid drainage from the waste dump of João Belo, it was noted that their concentrations were below the detection limit of the analytical method used in all analyzes.

CONCLUSIONS

In accordance with the observed results, it can be concluded that all reactors are capable of complying with the procedure outlined for treatment of acid drainage from the waste dump John Belo, mine JMC main objective. It was observed that all reactors were able to reduce aluminum concentrations below the limit of 0.1 mg / l recommended by law. The mechanism for aluminum reduction is due to the precipitation of this metal as hydroxides, as it was mentioned before.

The production of alkalinity caused by anaerobic activity, as well as limestone applied to the substrate, greatly increased the pH of all reactors applied in passive treatment so that the effluent met the minimum and maximum limit recommended by law.

With respect to iron and manganese in the effluent of the reactors analyzed, it was noted that their concentrations exceeded the limits prescribed by law due possibly to the fact that these metals are present in the chemical composition of the substrate applied.

Considering the low cost of the ingredients and this stage of this effluent treatment study it was not necessary to develop cost estimation among the different reactors for a full scale implementation. Once this project moves to the next phase, a cost evaluation for the implementation of the different reactors will be developed. So the mine company would have the best cost / return ratio for this effluent treatment system.

REFERENCES

APHA; AWWA;WEF (2005): Standard Methods for the Examination of Water and Wastewater. 21th Baltimore, Maryland: United Book Press, Inc.

CONAMA (2005): Resolução n° 357 de 17 de Março de 2005. Dispõe sobre a classificação dos corpos de água e diretrizes ambientais para o seu enquadramento, bem como estabelece as condições e padrões de lançamento de efluentes, e dá outras providências. Brasília. Conselho Nacional de Meio Ambiente – CONAMA.

MELLO, J.W.V; ABRAHÃO, W.A.P (1998): Geoquímica da drenagem ácida. In: Recuperação de áreas degradadas. Viçosa, p. 45-57.

PINHEIRO, A. C.; GAIDZINSKI, R.; SOUZA, V. P., (2008): Utilização de Bactérias Redutoras de Sulfato para o tratamento biológico de efluentes provenientes da indústria da mineração de carvão. In: XVI JORNADA DE INICIAÇÃO CIENTÍFICA. CETEM/MCT.

SINGER,P.E.; STUMM, W (1970): Acid mine drainage: the rate determining step. Science, v. 167, p. 1121-1123.

WILDEMAN, T., D. UPDEGRAFF: Passive bioremediation of metals and inorganic contaminants. In: Perspectives in Environmental Chemistry, D.L. Macalady, Ed. Oxford University Press, New York, p. 473-495.

Start-Up of a Passive Remediation Bioreactor for Sulfate and Selenium Removal from Mine Tailings Water

Susan Baldwin[1], Parissa Mirjafari[1], Maryam Rezahdebashi[1], Gaurav Subedi[1], Jon Taylor[1], Luke Moger[2], Katie McMahen[2] and Art Frye[2]

1. *Chemical and Biological Engineering, University of British Columbia, Canada*
2. *Mount Polley Mine, Canada*

ABSTRACT

Before tailings pond water can be discharged to the environment it must meet the very stringent local water quality requirements. In British Columbia, selenium must be below 1μg/L and sulfate, depending on the hardness of the receiving water, must be as low as 100mg/L. To meet this challenge, in anticipation of future mine expansion, Mount Polley Mine commissioned a pilot-scale passive treatment system to remove selenium and sulfate from their tailings pond water. The design was based on laboratory column tests with wood chips and hay that verified removal of selenium and sulfate to the required levels. This paper describes the design and construction of a sub-surface flow wetland and its evolution over several years into a passive remediation system. Regular monitoring and troubleshooting led to upgrades and modifications that improved performance. The subsurface layer of woodchips, hay and manure provides microorganisms with carbon sources. As part of a genomics project, material from this layer was shown to contain many different species of sulfate-reducing bacteria. Additional carbon inputs come from plants and filamentous algae that are beginning to populate the periphery and surface of the wetland. The genomics work also showed that planktonic algae were plentiful in the water column. This pilot-scale process shows that passive remediation can be used to improve the water quality of mine tailings pond water.

Keywords: Biochemical reactors, metals, mining, bioremediation, microbial ecology, selenium, sulfate

INTRODUCTION

The mining industry in British Columbia was valued at C$8.3billion in 2012 (The Mining Association of Canada, 2012) and is therefore a great contributor to employment and prosperity in the Province. Almost every mine has a tailings storage facility into which process effluents consisting of finely ground rock and water are placed. These are very large (squares of kilometers in size). Mount Polley had been investigating several ways of treating their tailings pond water so that they could discharge some of it so as to ease the demand for additional storage capacity. One of the approaches under consideration included a passive treatment process for metal and sulfate removal.

Passive treatment means that natural biological and geochemical processes are harnessed in specially constructed sub-surface and/or surface flow wetlands. The purpose of each cell in the process is to provide the best environmental conditions to encourage the growth of biological organisms that promote metal immobilization and, in cases where needed, sulfate reduction. Since some engineering is usually required they are more accurately referred to as biochemical reactors (BCRs), and a variety of configurations have been used at mine sites to successfully remediate metal-contaminated water (Khoshnoodi et al., 2013; Mattes et al., 2011; Blumenstein and Gusek, 2008; Gusek, 2008).

The main constituents of interest that needed to be reduced in the Mount Polley tailings water in order to meet discharge requirements were sulfate, selenium, copper, molybdenum, phosphorus and nitrate. Sulfate can be reduced by sulfate-reducing bacteria, which are anaerobic organisms that grow in most natural terrestrial and oceanic sediments devoid of oxygen. Sulfate replaces oxygen as an electron acceptor in respiration of these organisms thereby producing the product sulfide. Metal removal occurs concomitantly as metal ions such as Cu^{2+} combine with S^{2-} to make sparingly soluble metal sulfide precipitates (Jalali, 2000). Metalloids such as selenate and selenite can be reduced directly by bacteria to produce elemental forms that precipitate and are immobilized (Stolz et al., 2006;Baldwin and Hodaly, 2003). To achieve metal and sulfate removal the microbes involved are encouraged to grow by being provided with nutrients and anoxic conditions. In BCRs this is achieved through using organic materials obtained from forestry, agricultural and other wastes available nearby the mine site. Within close proximity of the Mount Polley Mine, wood chips, hay and cattle feed lot manure were obtained and shown to support growth of sulfate-reducing bacteria in proof-of-concept laboratory reactors that successfully removed sulfate and selenium to below the required concentrations. Based on these results, a pilot-scale BCR was constructed at the mine site in 2009. This paper describes the configuration of this BCR, the results of water quality and microbial community monitoring carried out over the ensuing years and subsequent modifications that were made to improve performance.

METHODOLOGY

Proof of concept laboratory experiments

Plexiglas columns (I.D.: 11.43 cm, Length: 50.8 cm) with a mixture of 50%dw hay, 20%dw woodchips and 30%dw cow manure were used as up-flow BCRs. These organic materials were pre-soaked in water overnight and adjusted to pH 8.0 before being added to the columns together with laboratory cultures of sulfate-reducing and cellulose-degrading bacteria as inocula as well as

crushed limestone for pH control. For the first few weeks, the columns were fed with a Postgate-B growth medium (Postgate, 1983) to allow a healthy sulfate-reducing bacteria population to build up. Thereafter, simulated tailings water containing 600mg/L sulfate and 15µg/L selenium, plus 52mg/L Iron (Fe) and sources of nitrogen (N), phosphorus (P) and potassium (K) was fed to the BCRs. Iron was required as a source for excess sulfide precipitation. Accumulation of sulfide in the BCR would have inhibited the bacteria from growing, and therefore it had to be removed. The columns were set up so as to prevent any oxygen from getting in (since sulfate-reducers are obligate anaerobes). Over the period of operation, concentrations of sulfate and selenium were measured in the effluent using the turbidimetric barium sulfate American Water Work Association method 4500-SO_4^{2-}, and inductively coupled plasma mass spectroscopy (ICP-MS), respectively. Dissolved oxygen, pH and oxidation-reduction potential were monitored regularly so as to check that optimal conditions were being maintained in the BCRs.

Construction of the field-based pilot-scale BCR

A field-based pilot-scale BCR was constructed at the mine site in December 2009. After experimenting with smaller scale systems, a 100 gallon per minute sub-surface flow BCR with a water cover was constructed using the same organic material mixture composition as was used in the laboratory column experiments. The Figures below show the BCR during construction and immediately after commissioning.

Figure 1 Construction of the field-based BCR showing the perforated feed pipes, organics (brown) and rock (right-hand side) layers.

Figure 2 View of the completed BCR looking down from the top of the tailings storage facility.

Water from the tailings storage facility toe drain flows into the bottom of the BCR through a series of parallel, perforated pipes, percolates upwards through the organic material and then flows out. A layer of rocks on top of the organics keeps them in place. A 3-4m deep water cover acts as an oxygen barrier. The treatment area is approximately 50m by 70m. An island was included in the centre of the pond for aesthetics.

BCR monitoring

Water quality data were collected regularly from the influent and effluent to determine the effectiveness of metal and sulfate removal. The inside of the BCR was sampled once a year by the University of British Columbia team. Since samples from within the organic matrix could not be accessed easily due to the rock layer covering them, water samples from just above the

sediment/water interface were taken. If the BCR was performing as expected then the water percolating out of the sediments into the water column would be anaerobic with evidence of sulfide as an indication of active sulfate-reducing bacteria in the sediments. The microbiology of the water just above the sediments was assessed to see if any sulfate-reducing bacteria were entrained by the water flowing out of the sediments, and to see what other microbes were colonizing the water column. Microbiological analysis was done by extracting DNA and subjecting it to sequencing of the small subunit ribosomal ribonucleic acid (SSU rRNA) gene, which is a barcode that is used to identify microbes. In 2012, the BCR was shut down and drained. At this time, solid samples were taken from within the organic matrix and frozen to preserve the microbial community for later analysis. The BCR was modified based on monitoring results, adding a berm to increase hydraulic retention time and replenishing with fresh organics. Further modifications in 2013 included installation of booms to reduce wind mixing so that anaerobic conditions could be better maintained. One year after reconstruction (August 2013), samples taken from the sediment layer were used for metagenomics, which is a new technique for measuring both the microbes present as well as their function.

RESULTS AND DISCUSSION

Proof of concept laboratory experiments

Even though the pH was adjusted to 8.0 before starting the BCRs, additional NaOH needed to be added to maintain the pH above 6.5. Organic acids leaching from the wood, or produced due to fermentation of organic matter, contributed to pH decrease. Since the desired bacteria require a circum-neutral pH in which to grow, pH adjustment was needed. The pH of the laboratory BCR feed was 8.0, similar to that of the Mount Polley effluent. After 114 days, the pH stabilized above 6.0 and it was only necessary to add NaOH sporadically thereafter. Throughout their operation, conditions remained optimal for sulfate-reducers with dissolved oxygen below 1mg/L except until day 374, when it suddenly increased to 4.7-5.7mg/L. The ORP was below -300mV and the pH was steady between 6.0 and 7.0. Sulfide levels inside the BCR were always below 100mg/L, which is much lower than those known to cause inhibition of sulfate-reduction (Utgikar et al., 2002).

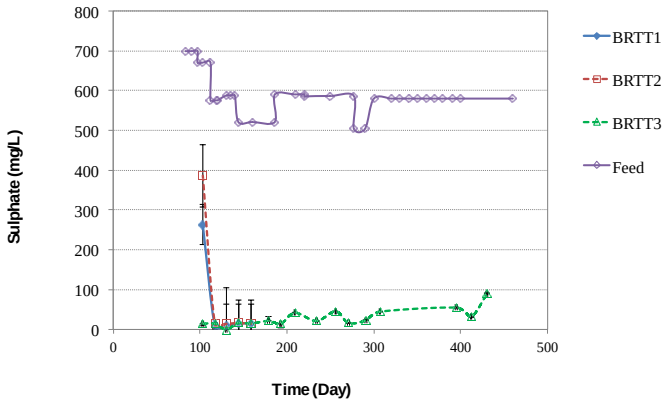

Figure 3 Plot of sulfate concentration versus time for the influent and effluents from all three of the laboratory BCRs. BRTT1, BRTT2 and BRTT3 are triplicate columns run under identical conditions. Sulfate concentration measurements were performed in triplicate with the average values plotted and the whiskers representing the standard deviation.

Two of the BCRs were stopped after approximately 100 days after starting feed of the simulated tailings pond water so as to examine the nature of the microbial population associated with successful performance. The third BCR was run for a total of 430 days to see if and when it would fail. Performance was consistently successful for the entire period (Figure 3). For all BCRs the sulfate concentrations in the effluent were below 100mg/L, the level desired for discharge. The selenium concentrations in the effluent were below the detection limit (< 0.0001mg/L). The proof-of-concept experiment demonstrated that sulfate and selenium can be removed from the Mount Polley tailings water to the required levels using these organic materials in a BCR, provided that the pH is maintained near neutral, no oxygen is allowed to enter the bioreactor and that enough metal ions be present to keep sulfide levels low.

Initial performance of the field-based pilot-scale BCR

Initially, the field-based BCR successfully removed nitrite- plus nitrate-N and selenium to below detection levels (Table 1). Twenty three percent of the sulfate coming in was removed, but the final sulfate concentration was still well above the desired concentration of 100mg/L. Molybdenum concentrations decreased slightly and copper concentrations increased a little. During the 17 June 2010 field trip, 1-3mg/L sulfide was found at the sediment water interface of the BCR at all of the four locations sampled. This indicated that sulfate-reducing bacteria were active in the sediments as expected. Over the course of the following year, performance of the BCR was similar with the exception that sulfate-reduction was less. During the second University field trip in August 2011, no sulfide was detected at three of the sampling locations in the BCR. Some, 4.3mg/L, was measured at only one of the locations, indicating that only parts of the BCR were active for sulfate-reduction. Also, at that time, the sulfate concentrations at the sediment/water interface (464-599mg/L) were not significantly different from those in the influent.

Table 1 Water quality parameters for the field-based pilot-scale BCR

Sampling date	Nitrite + Nitrate-N		Sulfate		Cu (dissolved)		Mo (dissolved)		Se (dissolved)	
	In	Out	In	Out	In	Out	In	Out	In	Out
04/15/2010	3.98	<0.0050	499	384	0.00317	0.00454	0.185	0.121	0.0239	<0.0020
04/15/2010-05/31/2011 *	1.901	0.037	478	416	0.0031	0.0038	0.1650	0.1185	0.0031	0.000917
06/9/2011-07/5/2012 *	1.114	0.123	434	452	0.0030	0.0011	0.1786	0.1237	0.0025	0.0009
09/15/2012-08/8/2013 *	1.613	0.075	498	406	0.0030	<0.0006	0.203	0.081	0.0053	0.00064
09/5/2013-08/8/2014 *	1.975	0.0725	518	475	0.0030	0.0011	0.208	0.109	0.0066	0.0020

* average values

Microbial community analysis from 2010 to 2012

Samples taken during the first two field trips in 2010 and 2011 from the sediment/water interface were analysed for microbial community composition, and in particular the types of sulfate-reducers present was determined (Figure 4). Sulfate-reducers were detected in the BCR in 2010 consistent with presence of sulfide, but they were absent from the sediment/water interface in 2011. Even though sulfate-reducers were not detected just above the sediment surface, they may still have been present inside the organic matrix. Nevertheless, the lack of detection of sulfate reducers coincided with declining performance of the treatment system (Table 1). In 2012, the BCR was drained and it became possible to take samples directly from the organic matrix. When these samples were analysed for microbial community composition, many sulfate reducers were found (Figure 4). The presence of sulfate-reducers suggested that the organic matrix and conditions inside the BCR were suitable for hosting these organisms. But, contrary to expectations, sulfate-reduction rates through the BCR were low. One possible explanation was that sulfate may be reducing to sulfide within the organics, but low metal ion concentrations were not enough to precipitate all soluble sulfide and it was re-oxidized to sulfate upon contact with oxygen diffusing down through the water column. Such a phenomenon was observed in the laboratory bioreactors before Fe^{2+} was added to the column bioreactor feed (Mirjafari et al., 2011).

Performance since 2012 modifications

Recharging of the BCR organics and increasing of the retention time resulted in improved performance (Table 1). The BCR was again visited in August 2013 and sampled for microbial community analysis.

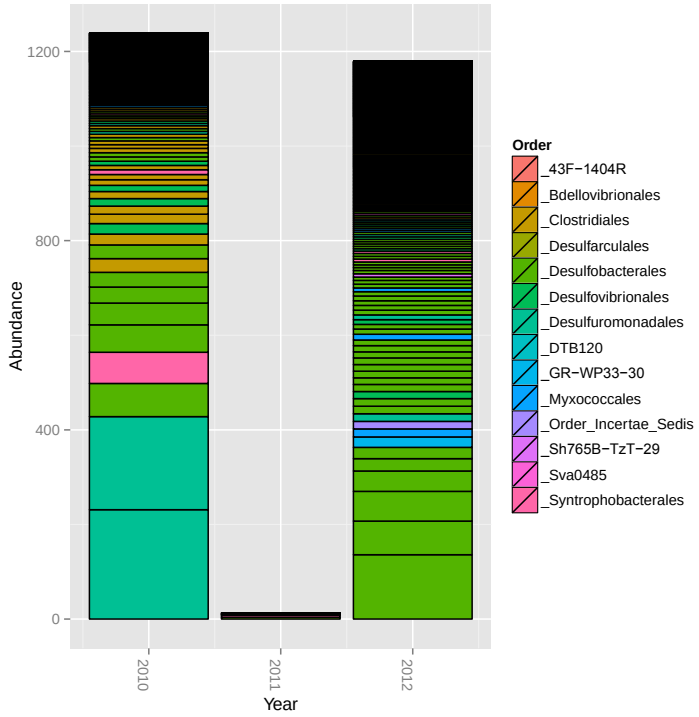

Figure 4 Sulfate-reducing micro-organisms detected in the BCR. Each bar on the plot represents one type of microbe. They are colored according to the Order in which they are classified. Bacteria are classified in taxonomic groups at different levels: Phylum;Class;Order;Family;Genus;Species. Abundance refers to the number of sequences out of a total of 12000, 8000 and 12000 for samples taken in 2010, 2011 and 2012, respectively.

Microbial community composition in 2013

A new technique was used called metagenomics. Instead of amplifying the SSU rRNA gene, which introduces possible biases, whole DNA was sequenced. From this we identified genes involved in sulfate metabolism, such as sulfate-reduction, and the types of bacteria that they came from, thus tying function to taxonomy. The results revealed that a psychrophilic organism, *Desulfotalea psychrophilia*, was the most prevalent sulfate-reducer in the BCR. Interestingly, this type of sulfate-reducer was first found in permanently cold Arctic marine sediments (Rabus et al., 2004), and even can survive at temperatures below 0°C. As before, the *Desulfobacterales*, *Desulfovibrionales* and *Desulfuromonadales* were sulfate-reducing bacteria taxa that were present in the BCR sediments. Presence of a healthy population of sulfate-reducers and detection of sulfide at the sediment/water interface (Table 2) coincided with active sulfate reduction and metal removal; although final sulfate concentrations were not meeting the 100mg/L discharge requirement.

A very interesting phenomenon was noted by the operators during the colder months of 2013, when the BCR was covered with ice and snow. Higher concentrations of sulfide and lower concentrations of BCR effluent sulfate were measured in Spring than in Summer (Table 2). This suggested that sulfate-reduction was active even though temperatures of the BCR water were between 2.1 and 7.7°C. The cover of ice and snow on the surface of the BCR prevented oxygen from getting into the water layer as dissolved oxygen profiles with depth revealed (Figure 5). Improved anaerobic conditions correlated with improved sulfate-reduction. The average BCR influent sulfate

concentration in 2013 was 498mg/L. Sulfate-reduction was highest (35%) in April. Metal removal was also greatly improved in the Spring compared with the rest of the year (percent removal: Se (86%); Cu(56%); Mo(44%)). Presence of cold-adapted sulfate-reducers in the BCR, and active sulfate-reduction and metal removal supports the use of biological treatment in cold climates

Table 2 Sulfate and sulfide concentrations measured in the BCR effluent over 2013

Parameter	14-Mar-13	4-Apr-13	1-May-13	6-Jun-13	10-Jul-13	8-Aug-13	5-Sep-13	3-Oct-13	5-Nov-13	3-Dec-13
Sulphate (SO_4) (mg/L)	383	323	365	434	446	486	488	469	481	493
Sulfides (mg/L) - Preserved with Zn-Acetate	31.6	14.5	0.71	1.23	0.085	0.01			0.106	5.1

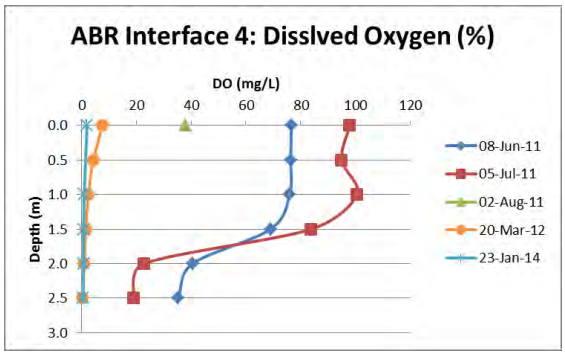

Figure 5 Dissolved oxygen concentrations versus depth below the BCR water surface during winter and summer months.

The BCR in 2014

During the most recent (26 August 2014) sampling of the sediment-water interface in the BCR, sulfide concentrations were higher than were measured in 2013 (August) (Table 2). The locations with higher sulfide concentrations coincided with lower sulfate concentrations. The North East side of the BCR (locations 3 and 4) was more active in terms of sulfate-reduction. Influent sulfate concentrations were 509mg/L. An extimated 15.6% sulfate is being reduced by the system.

Table 2 Concentrations of sulfate and sulfide in the Mount Polley BCR in 2013 and 2014.

	2013		2014	
Location	SO_4^{2-} (mg/L)	S^{2-} (mg/L)	SO_4^{2-} (mg/L)	S^{2-} (mg/L)
1	458	5	471	0
2	458	5	451	60
3	395	9	400	180
4	453	9	426	40-50
Average:	441		437	

Plants (*Typha latifolia*) and filamentus algae successfully colonized the sides and surface of the BCR (Figure 5). At other sites algae have been found to host many microbes, such as sulfate-reducers, and their presence adds organic carbon to the BCR plus they can directly improve water quality (Das et al., 2009;Larratt et al., 2007). Sequencing revealed many types of unicellular algae, such as *Dunaliella*, in the water column. Sub-aqueous plants could be seen growing on the bottom near the edges (Figure 6).

Figure 5 Photograph of the BCR looking South West.

Figure 6 Growth of aquatic plants

CONCLUSION

A laboratory proof-of-concept test demonstrated that removal of sulfate and selenium to below the required levels for discharge was possible. The field-based BCR constructed at Mount Polley Mine using a woodchip, hay and manure organic mixture was found to successfully support an active sulfate-reducing microbial community and some removal of nitrite/nitrate, metals and sulfate was occurring. The system worked best immediately after the addition of fresh organics but thereafter appeared to decline in performance. Rapid depletion of readily available organic material may be a limiting issue for passive treatment and is it recommended that an upstream surge pond be included in future designs into which fresh organics can be added. The BCR was more successful in the colder months when ice and snow covered the water and improved anaerobic conditions inside the BCR. Thus, addition of a more impermeable cover may improve performance throughout the year.

ACKNOWLEDGEMENTS

Genome British Columbia, the Natural Sciences and Engineering Research Council of Canada, Imperial Metals and Teck are acknowledged for providing funding for this work. Mine personnel are thanked for their assistance with the fieldwork and sampling.

REFERENCES

Baldwin, S.A., Hodaly, A.H., 2003. Selenium Uptake by a Coal Mine Wetland Sediment. Water Qual. Res. J. Canada 38, 483–497.

Blumenstein, E.P., Gusek, J.J., 2008. Designing a biochemical reactor for selenium and thallium removal, from bench scale testing through pilot construction, in: Young Taylor, PR, Anderson, CG and Choi, Y, C.A.

(Ed.), Hydrometallurgy: Proceedings of the Sixth International Symposium. Society for Mining, Metallurgy, Exploration Inc., Phoenix, AZ, pp. 117–129.

Das, B.K., Roy, A., Koschorreck, M., Mandal, S.M., Wendt-Potthoff, K., Bhattacharya, J., 2009. Occurrence and role of algae and fungi in acid mine drainage environment with special reference to metals and sulfate immobilization. Water Res. 43, 883–94. doi:10.1016/j.watres.2008.11.046

Gusek, J.J., 2008. Passive Treatment 101: An Overview of the Technologies, in: U.S. EPA/National Groundwater Association's Remediation of Abandoned Mine, Lands. Denver, CO, pp. 1–13.

Jalali, K., 2000. The role of sulphate reducing bacteria in copper removal from aqueous sulphate solutions. Water Res. 34, 797–806. doi:10.1016/S0043-1354(99)00194-3

Khoshnoodi, M., Dipple, G., Baldwin, S., 2013. Mineralogical Study of a Biologically-Based Treatment System That Removes Arsenic, Zinc and Copper from Landfill Leachate. Minerals 3, 427–449. doi:10.3390/min3040427

Larratt, H., Freburg, M., Hamaguchi, R., 2007. Developing Tailings Ponds and Pit Lakes as Bioreactors and Habitat Cost-Effective Successes at Highland Valley Copper, in: B.C.'s 31st Annual Mine Reclamation Symposium The British Columbia Technical and Research Committee on Reclamation (TRCR), Squamish, British Columbia.

Li, W., Baldwin, S. A., 2011. A UASB bioreactor using silage as a carbon source to reduce sulfate. Water Sci. Technol. Water Supply 11, 229. doi:10.2166/ws.2011.046

Mattes, A., Evans, L.J., Gould, D.W., Duncan, W.F.A., Glasauer, S., 2011. The long term operation of a biologically based treatment system that removes As, S and Zn from industrial (smelter operation) landfill seepage. Appl. Geochem. Sources, Transp. Fate Trace Toxic Elem. Environ. -IAGS 2009 26, 1886–1896.

Mirjafari, P., Moger, L., Martel, R., Baldwin, S.A., 2011. Factors affecting the start-up, operation and decline of a laboratory-based passive treatment system for selenium and sulphate removal, in: proceedings of Conference of Metallurgists. October 2011, Montreal, Canada.

Postgate, J.R., 1983. The Sulphate-Reducing Bacteria, 2nd ed. Cambridge University Press, Cambridge, England.

Rabus, R., Ruepp, A., Frickey, T., Rattei, T., Fartmann, B., Stark, M., Bauer, M., Zibat, A., Lombardot, T., Becker, I., Amann, J., Gellner, K., Teeling, H., Leuschner, W.D., Glöckner, F.-O., Lupas, A.N., Amann, R., Klenk, H.-P., 2004. The genome of *Desulfotalea psychrophila*, a sulfate-reducing bacterium from permanently cold Arctic sediments. Environ. Microbiol. 6, 887–902. doi:10.1111/j.1462-2920.2004.00665.x

Stolz, J.F., Basu, P., Santini, J.M., Oremland, R.S., 2006. Arsenic and selenium in microbial metabolism. Annu. Rev. Microbiol. 60, 107–30. doi:10.1146/annurev.micro.60.080805.142053

The Mining Association of Canada, 2012. Facts and Figures of the Canadian Mining Industry 2013, http://mining.ca/documents/facts-figures-2013.

Utgikar, V.P., Harmon, S.M., Chaudhary, N., Tabak, H.H., Govind, R., Haines, J.R., 2002. Inhibition of sulfate-reducing bacteria by metal sulfide formation in bioremediation of acid mine drainage. Environ. Toxicol. 17, 40–8.

10th ICARD IMWA 2015 | 10th International Conference on Acid Rock Drainage & IMWA Annual Conference

Metal Retention Mechanisms in Pilot-Scale Constructed Wetlands Receiving Acid Mine Drainage

Karine Dufresne[1,3], Carmen Neculita[1], Jacques Brisson[2] and Thomas Genty[3]

1. *Institut de recherche en mines et en environnement, Université du Québec en Abitibi-Témiscamingue, Canada*
2. *Institut de Recherche en Biologie Végétale, Université de Montréal, Canada*
3. *Centre technologique des résidus industriels, Canada*

ABSTRACT

Mining and metallurgical industries are critical to world's economy; however, their socio-environmental impacts are not negligible. Often, they have to deal with acid mine drainage (AMD), which is generated by sulfide oxidation in waste following the prolonged exposure to oxygen and water, if neutralizing minerals are insufficient. The AMD is characterized by low pH and high concentrations of dissolved metals and sulfates.

Environmental impacts of AMD can be minimized by passive treatment systems such as constructed wetlands (CWs). They represent an interesting approach, from technological, economic, environmental and regulatory points of view, for the efficient treatment of AMD impacted waters.

Wetlands have the capacity to increase pH and alkalinity, to remove dissolved iron and other metals, and to reduce sulfate concentration in AMD. Water treatment is accomplished by various physical (e.g. sedimentation, flocculation), chemical (e.g. sorption) and biological processes (e.g. sulfate reduction, phytoextration) acting independently, in some cases, or interactively, in others. However, cold climate could be challenging for CWs efficiency.

For the purpose of the present study, small-scale laboratory tests using cattail (*Typha latifolia*) were designed and carried out in 0.2 m^2 reactors filled with reactive mixtures, including substrates. The AMD, pH 4.2, contained an average 38.0 mg/L Fe, 2.6 mg/L Mn, 0.4 mg/L Ni, and 9.0 mg/L Zn, at pH 4.2. The AMD flow rate is 1.5ml/min.

CWs efficiency was evaluated during a 3 months period. Water chemistry analysis, as well as sequential extraction procedure (SEP) and microwave digestion of solids and plants were performed. Removal efficiency of Fe and Zn after treatment was up to 99%, at neutral pH. However, the removal of Mn and Ni, as well as of sulfate was negligible. The results of SEP performed on solids proved to be efficient tools for assessing metal fractionation and their potential mobility.

Keywords: Constructed wetlands (CWs), acid mine drainage (AMD), metal fractionation.

INTRODUCTION

Acid mine drainage (AMD) is one of the most significant environmental challenges faced by the mining industry worldwide. Its low pH and the high concentrations of dissolved metals and sulfates can severely impact surface and ground water making it harmful to human and aquatic life (Champagne *et al.*, 2005). AMD is formed by a series of complex biogeochemical reactions that occur when sulfide minerals are oxidized in the presence of water and oxygen to form acidic, sulfate- and metal-rich drainage (Neculita *et al.*, 2008; Genty, 2012). Passive systems, such as constructed wetlands (CWs), represent an interesting approach for the efficient treatment polishing of AMD. The CWs for secondary treatment of effluent are engineered systems specially designed to employ natural processes (vegetation, soil, and microbial activity), in order to treat the AMD (Vymazal, 2010). These systems are low-cost and low-maintenance, and are capable of removing heavy metals, nutrients, organic matters, and micropollutants (Neculita et al., 2007; Rötting *et al.*, 2008; Yeh, 2009;). The CWs increase pH and alkalinity, remove the dissolved metals, and reduce sulfate concentration in AMD.

Water treatment is accomplished by a variety of physical (sedimentation, flocculation), chemical (oxidation, hydrolysis, reduction) and biological (sulfate reduction, phytoextration) processes acting independently, in some cases, or interactively, in others (Matagi *et al.*, 1998; Stottmeimeister *et al.*, 2003). However, the mechanisms governing the removal of metals (plants versus reactive mixture) are not well understood, hence the need to elucidate these processes in order to ensure treatment effectiveness and system sustainability (Stottmeimeister *et al.*, 2003). In CWs, metals could exist in various particulate or dissolved forms (which can absorb onto particles), as complexes with inorganic and organic ligands or as free ions in water (Yeh et *al.*, 2009). The toxicity of a given trace metal is largely controlled by its speciation, thus evaluation of metal partitioning (operational speciation), as well as the becoming and availability under conditions simulating natural processes (e.g. pH variation, reduction and oxidation) is crucial (Ryan *et al.*, 2008). Sequential extraction procedure (SEP) is an important and widely applied tool for gaining information on potential mobility (hence, potential bioavailability and toxicity) of toxic elements in the environment (Bacon and Davidson, 2008). Basically, the ranking of metal mobility in SEPs is based on their concentrations in the water-soluble and exchangeable fractions, as well as the fractions that are reducible, bound to carbonate, and bound to organic matter or sulfides (Neculita *et al.*, 2008). Assuming that bioavailability of heavy metals decreases with each successive extraction step in the SEP, consistent with the decreasing order of solubility, then the following ranking is obtained: water soluble > exchangeable > carbonate bound > Fe-Mn oxides bound > organic matter/sulfides > residual (Jong and Parry, 2004). In fact, bioavailability is a complex and evolving concept, but has recently been defined as the degree to which chemicals present in the soil may be absorbed or metabolized by a human or ecological receptor or is available for interaction with biological systems (Bacon and Davidson, 2008).

The main objective of this study is to design a CW, which can be used in the polishing step of a multi-units passive system for the treatment of AMD contaminated by Fe, Mn, Ni, and Zn. The evaluation of removal mechanisms and of metal speciation in the reactive mixture and the plants of the CW is also performed. For this purpose, small-scale laboratory tests were carried out. The overall results improved the understanding of the processes governing the treatment and the evaluation of design criteria for a CW. This knowledge would allow the transfer of this technology on active, closed or abandoned mine sites, contaminated by the AMD. The research focuses also on hydrology, effect of plants, substrate or filter media that should not be neglected, since they are key elements, especially in a northern climate such as Abitibi-Témiscamingue.

METHODOLOGY

Bench-scale testing of CWs for AMD treatment

Bench-scale CWs were built in polypropylene (48 x 33 x 33 cm). Two different support media and two configurations (vertical and horizontal flow) were tested. Limestone (up to 20 mm in size) was

placed on the bottom of the vertical flow cells and was covered then with a mixture of gravel (8-16 mm) and peat, whereas free surface flow cells were filled with a mixture of sandy soil (0-4 mm), cattle manure, peat and granular dolomitic limestone. Once filled with the reactive mixture, 45 five month old *Typha latifolia* (cattail) were planted in tested wetland modules at a density of 2,84/m^2.

In parallel, unplanted CWs (control) were also set-up. The testing was carried out for a 3-month period (July to October, 2013).

Tap water was added to the plants for 3 weeks, before starting the artificial AMD feed. Continuous flow of AMD was then applied to the CWs, at a flow rate of 1.5ml/min, for a 5-day retention time. The artificial AMD, at pH 4.2, was constituted with Fe, Mn, Ni and Zn sulfates salts, at average concentrations of 38.1, 2.6, 0.4 et 9 mg/l, respectively.

Water sampling and analysis

Influent and effluent samples were collected from each wetland daily for the 3 months duration. The following parameters were measured in the laboratory: pH, redox potential (Eh) and sulfate. For the dissolved metal analysis, 10 ml of filtered samples were preserved using 2 % (by volume) of 70 % nitric acid and then analyzed (ICP-AES type: Vista AX CCO Simultaneous ICP-AES - Palo Alto) with detection limits of 0.39, 0.006, 0.004 and 0.008 mg/l, for Fe, Mn, Ni and Zn, respectively.

Media sampling and analysis

In addition to water samples, solid media from the top (0-5 cm) and middle (15 cm, for vertical-flow only) layers were collected from each CWs, toward the end of the testing. Sediments (solid media) were dried in an oven at 70 ºC and digested (0.200g) via microwave digestion by HNO_3:HCl (7:1) solution for the analysis of total metal concentration. The fractionation of heavy metals was evaluated using the SEP developed by Jong and Parry (2004), which is based on the classical method of Tessier *et al.* (1979). The SEP was performed to evaluate the partitioning of four heavy metals (Fe, Mn, Ni and Zn) into six operationally defined fractions. Dried sediment samples were used for the separation of the following metal fractions: soluble (extracted with water), exchangeable (extracted with 1 M $MgCl_2$, pH 7.0), carbonate bound (extracted with 1 M NaOAc buffered with HOAc, pH 5.0), reducible or bound to Fe–Mn oxides (extracted with 0.04 M NH_2OH-HCl in 25% (v/v) HOAc), oxidable or bound to organic matter (digested by HNO_3, H_2O_2, and 3.2 M NH_4OAc in 20% (HNO_3), and residual fraction (dissolved by acid attack with HNO_3 and HCl).

The SEP was conducted with 1 g of solid accurately weighed in 50 mL polypropylene centrifuge tubes. Between each two extraction steps, the supernatant was separated from the solid-phase residue by centrifugation (Thermo Scientific Sorvall ST-16) at 1000 rpm for 30 min. The supernatant was then carefully removed, filtered through a 0.45 μm filter and preserved in 50 mL vials. The remaining residue was washed twice with 8 mL deionized water, centrifuged for 30 min, and the filtered supernatant mixed with the initial extract and stored at 4°C before analysis for metal concentrations by ICP-AES.

RESULTS AND DISCUSSION

Evolution of pH and sulfate concentration

Results showed the effectiveness of CWs for increasing the pH, all along the 3-month testing period (Fig. 1). The data indicate that there was a significant increase in the pH at the outlet of both configurations. The effluent had, in average, pH of 8.0, for vertical-flow, and pH of 7.6 for surface-flow wetlands. The processes responsible for pH increase were probable (1) the dissolution of carbonate substrate materials, which generate alkalinity and consume protons, and (2) bacterially-mediated sulfate reduction producing carbonate alkalinity in anoxic conditions (Mayes *et al.*, 2009).

As a result, SO_4^{2-} concentration in VSS-flow planted and unplanted and HS-flow CWs halved over the time (292-138; 377-193; 309-146 mg/l), excepting for HS unplanted one (320-301 mg/l). It is reasonable to assume that SO_4^{2-} were released from the substrate material after the start-up (Zagury et al, 2006; Song et al., 2012).

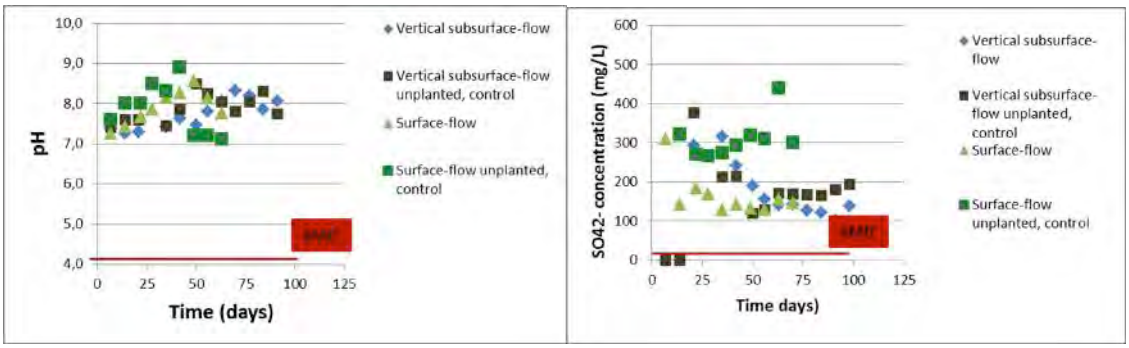

Figure 1 Evolution of pH and sulfate concentration over time in CWs

Metal removal efficiency

Results on bench-scale testing showed that CWs are efficient for Fe and Zn removal in AMD, with values up to 98.6%. The VSS-flow were more efficient than the HS-flow wetlands for contaminant removal (probable due to larger surface of contact), as well as the planted test cells. However, the removal of Mn and Ni was negligible, especially for HS-flow wetlands. Noteworthy, Mn is among the most difficult metals to remove due to the complexity of the interactions governing its solubility (Karathanasis *et al.*, 2009; Song *et al.*, 2012). Kinetics of Mn chemical oxidation are slow, whereas due to the high reduction potential of Mn(IV), parallel reactions, such as organic matter and Fe^{2+} oxidation, induce excessive oxidant consumption. Therefore, iron removal is required prior to manganese oxidation (Sylva *et al.*, 2010).

Table 1 Removal of Fe, Mn, Ni and Zn in AMD by CWs

Wetland design	Removal of metals (%)			
	Fe	Mn	Ni	Zn
Vertical subsurface-flow planted	98.6	75.5	88.5	96.7
Vertical subsurface-flow unplanted	92.7	23.1	46.4	95.7
Horizontal surface-flow planted	89.8	-20.3	58.1	96.3
Horizontal surface-flow unplanted	86.9	-35.2	-6.0	91.2

Fractions that contain most of Fe (5.01-5.04 mg/l) and Zn (1.01-4.43 mg/l) in planted and unplanted subsurface were bound to Fe-Mn oxides, whereas most of the Mn (0.84-0.47 mg/l) and Ni (0.28-0.27 mg/l) were found bound to carbonates. In surface-flow wetlands substrate, Fe was concentrated mostly to Fe-Mn oxides (4.43-3.95 mg/l) and residual fraction (6.57-6-40 mg/l) in planted and unplanted cells respectively, Zn to organic matter and sulfides (0.01-0.01 mg/l), Mn was found bound to carbonates (1.16-0.47 mg/l) and in the residual fraction (0.39-0.39 mg/l) and Ni was essentially found in the residual fraction (0.97-1.31 mg/l). These results indicated that metals were successfully immobilized in the microcosms. However, the availability of heavy metals within sediments can change over time, as a result of changes in redox potential, pH, organic material content (Yeh et al., 2009). Low pH could increase metal solubility, while low redox potential (more reducing conditions) could dissolve iron and manganese oxides, resulting in the mobilization of oxide-sorbed metals. On the contrary, increasing the redox potential (more oxidizing conditions) could mobilize metals by oxidation of metal sulfides (Hodda and Alloway, 1998).

CONCLUSION

The efficiency of bench-scale laboratory CWs was evaluated during a 3-month period for the treatment of AMD contaminated by Fe, Mn, Ni, and Zn. Results showed that the wetland test cells have the capacity to increase pH, to remove Fe and Zn, whereas they proved inefficient for Mn and Ni treatment. However, metals were immobilized in the substrate of CWs. The findings of the study include also the fact that the design and the substrate have no significant influence on the treatment effectiveness in laboratory.

Results from microcosm experiments must be interpreted with care due to edge and container effects but they are especially useful in determining broad patterns and investigating mechanisms. In order to investigate the "patterns" found in this bench-scale study and to understanding the processes governing the treatment of AMD, the overall results will be used to evaluate landscape-scale design criteria.

This knowledge would allow the transfer of this technology on active, closed or abandoned mine sites, contaminated by the AMD.

ACKNOWLEDGEMENTS

The authors of this study would like to thank their industrial and government sponsors, including Centre Jardin Lac Pelletier, Hecla Mining Company, Iamgold Corporation, Mine Canadian Malartic, Technosub, l'OBVT, CRIBIQ, CRSNG, and FQRNT.

Stability of metal precipitates and their potential mobility

As mentioned, the SEPs are currently used to assess the geochemical fractionation of metals in soils (Claff *et al.*, 2010). Partitioning patterns of heavy metals in CWs are shown in Table 2.

Table 2 Partitioning of Fe, Mn, Cd, Ni, and Zn in spent reactive mixtures from bench-scale CWs

Wetland design	Fraction	Fe (mg/g)	Mn (mg/g)	Ni (mg/g)	Zn (mg/g)
	F4	4.43 ± 022	0.26 ± 0.22	<LDD	<LDD
	F5	0.44 ± 0.00	0.01 ± 0.00	0.01 ± 0.00	0.01 ± 0.00
Vertical subsurface-flow planted	F1	<LDD	<LDD	<LDD	<LDD
	F6	6.57 ± 0.01	0.39 ± 0.01	0.97 ± 0.65	<LDD
	F2	<LDD	0.05 ± 0.00	<LDD	<LDD
	Sum	11.47	1.83	1.29	0.01
	F3	<LDD	0.84 ± 0.08	0.28 ± 0.02	<0.14
	MT	10.12	0.22	0.00	0.00
	F4	5.01 ± 4.21	0.41 ± 0.07	<LDD	1.01 ± 0.08
Horizontal surface-flow unplanted	F1	<LDD	<LDD	<LDD	<LDD
	F5	0.50 ± 0.07	0.03 ± 0.00	0.04 ± 0.00	0.04 ± 0.00
	F2	<LDD	<LDD	<LDD	<LDD
	Sum	5.51	1.34	0.33	1.05
	F3	<LDD	0.47 ± 0.18	0.27	<LDD
	MT	5.95	0.79	0.00	0.34
	F4	3.95 ± 0.00	0.11 ± 0.00	<LDD	<LDD
Vertical subsurface-flow unplanted	F1	<LDD	<LDD	<LDD	<LDD
	F5	0.40 ± 0.23	0.01 ± 0.00	0.01 ± 0.00	0.01 ± 0.00
	F2	<LDD	0.03 ± 0.00	<LDD	0.00
	F6	6.40 ± 2.41	0.39 ± 0.05	1.31 ± 1.25	<LDD
	F3	<LDD	0.47 ± 0.19	0.27	0.00
	Sum	10.75	0.99	1.59	0.01
	F4	5.04 ± 0.13	0.28 ± 0.06	<LDD	1.43
	MT	8.41	0.13	0.00	0.00
	F5	0.38 ± 0.03	0.03 ± 0.00	0.04 ± 0.00	0.04
	Sum	5.42	0.81	0.31	1.47
	MT	2.88	0.6075	<LDD	0,32
Horizontal surface-flow planted	F1	<LDD	<0.0063	<LDD	<LDD
	F2	<LDD	<0.06	<LDD	<LDD
	F3	0.02 ± 086	1.16 ± 0.86	0.31 ± 0.02	<LDD

REFERENCES

Bacon, J.R., Davidson, C.M. (2008) *Is there a future for sequential chemical extraction?* Analyst, Vol. 133, pp. 25–46.

Brisson, J. & F. Chazarenc. (2009) *Maximizing pollutant removal in constructed wetlands: Should we pay more attention to macrophyte species selection?* Science of the Total Environment, Vol. 407, pp. 3923-3930.

Champagne, P., Van Geel, P. and Parker, W. (2005) *A bench-scale assessment of a combined passive system to reduce concentrations of metals and sulphate in acid mine drainage*, Mine Water and the Environment, Vol. 24, pp. 124–133.

Claff, S.R., Sullivan, L.A., Burton, E.D. and Bush, R.T. (2010) *A sequential extraction procedure for acid sulfate soils: Partitioning of iron*, Geoderma, Vol. 155, pp. 224–230.

Hooda, P. S. & Alloway, B. J. (1998) *Cadmium and lead sorption behaviour of selected English and Indian soils*, Geoderma, Vol. 84, pp. 121–134.

Genty, T. (2012) *Comportement hydro-bio-géo-chimique de système passifs de traitement du drainage minier acide fortement contaminé en fer*, Thèse de doctorat, Institut de recherche en mines et en environnement, UQAT, QC, Canada, 270p.

Jong, T., Parry, D.L. (2004) *Heavy metal speciation in solid-phase materials from a bacterial sulfate reducing bioreactor using sequential extraction procedure combined with acid volatile sulfide analysis*, Journal of Environmental Monitoring, Vol. 6, pp. 278–285.

Karathanasis, A. D., Edwards, J. D. and Barton, C. D. (2010) *Manganese and sulfate removal from a synthetic mine drainage through pilot scale bioreactor batch experiments*, Mine Water Environment, Vol. 29, pp. 144–153.

Matagi, S.V., Swai, D. et Mugabe, R. (1998) *A review of heavy metal removal mechanisms in wetlands, African*, Journal for Tropical Hydrobiology and Fisheries, Vol. 8, pp. 23–35.

Neculita, C.M., Zagury, G.J. and Bussière, B. (2008) *Effectiveness of sulfate-reducing passive bioreactors for treating highly contaminated acid mine drainage: II. Metal removal mechanisms and potential mobility*, Applied Geochemistry, Vol. 23, pp. 3545–3560.

Neculita, C.M., Zagury, G.J.and Bussiere, B. (2007) *Passive treatment of acid mine drainage in bioreactors using sulfate-reducing bacteria: critical review and research needs*, Journal of Environmental Quality, Vol. 36, pp. 1–16.

Rötting, T.S, Ayora, C. and J. Carrera. (2008) *Improved passive treatment of high Zn and Mn concentrations using caustic magnesia (MgO): particle size effects*, Environmental Science and Technology, Vol. 24, pp. 9370–9377.

Ryan, P.C., Hillierb, S. and Wall, A.J. (2008) *Stepwise effects of the BCR sequential chemical extraction procedure on dissolution and metal release from common ferromagnesian clay minerals: A combined solution chemistry and X-ray powder diffraction study*, Science of the Total Environment, Vol. 4 0 7, pp. 6 0 3 – 6 1 4.

Silva, A.M., Cruz, F.L.S., Lima, R.M.F., Teixeira, M.C. and Leão, V.A. (2010) *Manganese and limestone interactions during mine water treatment*, Journal of Hazardous Materials, Vol. 181, pp. 514–520.

Song, H., Yim, G.J., Ji, S.W., Neculita, C.M. and Hwang, T.W. (2012) *Pilot-scale passive bioreactors for treatment of natural acid mine drainage: efficiency of mushroom compost vs. mixed substrates for metal removal*. Journal of Environmental Management, Vol. 111, pp. 150-158.

Stottmeister, U., Wiessner, A., Kuschk, P., Kappelmeyer, U., Kastner, M., Bederski, O., Muller, R.A. and Moormann, H. (2003) *Effects of plants and microorganisms in constructed wetlands for wastewater treatment*, Biotechnology Advances, Vol. 22, pp. 93-117.

Vymazal, J. (2010) *Constructed Wetlands for Wastewater Treatment: A review*, Water, Vol. 2, pp. 530-549.

Yeh, T.Y., Chou, C.C. and Pan. C.T. (2009) *Heavy metal removal within pilot-scale constructed wetlands receiving river water contaminated by confined swine operations*, Desalination, Vol. 249, pp. 368-373.

Zagury , G. J., Kulnieks, V.I. and Neculita, C. M. (2006*) Characterization and reactivity assessment of organic substrates for sulphate-reducing bacteria in acid mine drainage treatment*, Chemosphere, Vol. 64, pp. 944-954.

Performance of a 16 ha Engineered Wetland for the Treatment of Neutral-pH Gold Mine Effluent (Ontario, Canada)

Alan Martin[1], Connor McNee[1], James Russell[2] and David Gelderland[2]

1. *Lorax Environmental Services Ltd., Canada*
2. *Goldcorp Inc., Red Lake Gold Mines, Canada*

ABSTRACT

The Campbell Complex (Goldcorp Inc.), located in northwestern Ontario, Canada, has been the site of gold-ore milling operations since 1949. As part of water management measures for the site, an engineered surface-flow wetland was commissioned in 2002 to facilitate final polishing of neutral-pH effluents prior to discharge. The wetland is 16 ha in area, accommodates flows of ~10,000 m^3/day, and affords a mean hydraulic retention time (HRT) of 6-7 days. Vegetation consists predominantly of transplanted cattails (*Typha spp*.) with substrates comprised of inert mining waste-rock overlaid by organic topsoil containing *Typha* rootstock and native flora. The system operates during the ice-free period only (May through October), and serves as the final point of discharge for the mine. The wetland serves as a net sink for ammonia (NH_3), cyanide (CN), arsenic (As) and copper (Cu). Over the period 2011-2013, NH_3-N showed a pronounced decrease in concentration through the wetland, from a mean influent value of ~11 mg/L to a mean of 1.2 mg/L in the wetland discharge (overall reduction of 89% by mass). Over the same period, CN exhibited a mean loading reduction of 78%, with average influent and effluent concentrations of 0.14 mg/L and 0.07 mg/L respectively. Arsenic (primarily as dissolved species) showed a mean loading reduction of 56%, with concentrations being reduced from approximately 0.09 to 0.04 mg/L through the wetland system. Cu loading reductions averaged 33% (2011-2013), with values decreasing from a mean influent concentration of 0.01 mg/L to an outflow mean of 0.007 mg/L. In contrast to Cu and As, Ni shows evidence of remobilization within the wetland complex, with concentrations in the outflow (mean = 0.065 mg/L) exceeding those at the inflow (2011-2013 mean = 0.047 mg/L). Factors likely to contribute to variations in wetland performance include seasonal changes in HRT, redox-controlled processes, metal-CN complexation, and temporal variability in influent chemistry. Overall, the data demonstrate that constructed wetlands can be used effectively for the treatment of gold-mill effluents in cold-interior climates. This is particularly relevant for mine sites that have sufficient water storage capacity upstream of the wetland to allow for seasonal treatment during the warmer months when wetland performance is maximized.

Keywords: bioremediation, *Typha*, ammonia, arsenic, copper

INTRODUCTION

The use of bioremediation in the form of constructed wetlands for the treatment of mine-influenced wastewater has been widely used since the 1980's (Hammer, 1992). The potential utility and performance of constructed wetlands depend on several factors, including climate, the parameters of interest, parameter concentrations, vegetation type, wetland substrate, and the physical characteristics of the wetland itself, such as surface area, water depth, and hydraulic retention time (HRT). The following paper examines a surface flow constructed wetland in northwestern Ontario, Canada, designed for the bioremediation of effluents at an operating gold mine. This study specifically examines the data for the 2011, 2012, and 2013 treatment seasons, which extend from May to October in each year. The primary objectives of this paper are to: (a) quantify the magnitude of contaminant removal, (b) delineate the biogeochemical controls governing contaminant removal within the wetland complex, and (c), provide a general prognosis for the use of wetlands for the treatment of gold mill effluents in cold-interior climates.

SITE SETTING

The Campbell Complex (51º03'43"N and 93º44'40"W) comprises part of Goldcorp's Red Lake Gold Mines, and is located in Balmertown, Ontario, 7 km northeast of the town of Red Lake. The mine has been in continuous operation since 1949, following discovery of the deposit in the 1940's gold rush in the region. The project is located within the cold-interior region of North America, with mean monthly temperatures ranging from -19.3°C (January) to 18.3°C (July) (annual daily temperature of 0.9°C). The site receives an average of 644 mm of precipitation per year, with rainfall accounting for approximately 73% of the total. Snow cover generally persists from November until late March.

Ores are processed using a combination of grinding, flotation, pressure oxidation and carbon-in-pulp processing. Tailings slurry is sent to an SO_2/Air treatment circuit for CN destruction prior to discharge to the Main Pond. From the Main Pond, water is recycled back to the process plant and treated with lime to further precipitate dissolved metals. The treated effluent is then conveyed to the Settling/Polishing Ponds which afford 750,000 m^3 of storage for the polishing of treated effluent from the Main Pond. During warmer months (May through October) this polished effluent is conveyed to a 16 ha constructed wetland, which allows for further removal of NH_3, CN and trace elements. The wetland complex is divided into 34 cells, separated by internal dykes to maximize the length of the flow path and water retention time. All cells host transplanted cattails (*Typha spp*.) in a substrate composed of inert waste rock overlain by *Typha* rootstock, organic matter, and soil/loam. Water depths range from 15 to 70 cm (mean ≅ 45 cm). A mean flow of 10,000 m^3/day, a total surface area of 16 ha, and a mean water depth of 45 cm, translate to a HRT of ~7 days.

Effluents from the Polishing Pond are conveyed to two distinct inputs to the wetland (WET-IN and WET-IN2). These flows are treated in parallel wetland circuits, with the flows merging prior to discharge to Balmer Lake. The discharge from the wetland to Balmer Lake (WET-OUT) serves as the final point of discharge for the mine, and where Ontario compliance standards apply with regards to water quality and toxicity. The system of water management and storage upstream of the wetland facilitates the removal of total suspended sediments (TSS) prior to entry into the wetland (TSS <3 mg/L in wetland inflow). Accordingly, the performance of the wetland relies solely on processes

that remove dissolved species from solution. Inflows to the wetland are circumneutral in pH (6<pH<7).

METHODOLOGY

This study focuses on the treatment seasons of 2011, 2012 and 2013. These years correspond to the period of maximum wetland area (expanded to 16 ha in early 2011) and implementation of a new SO_2/Air treatment system (commissioned in late 2010). The latter had a significant effect in reducing the concentrations of CN and trace metals in inflows to the wetland complex. The 2011 and 2013 treatment seasons extended from late May to the end of October in each year. A shorter treatment season was implemented in 2012 (May through August).

This paper focuses on parameters (NH_3, CN, As, Cu, and Ni) although other parameters were examined to elucidate contaminant behaviour (*e.g.*, Fe, Mn, Se and U). Temporal resolution of the data varies by location and parameter. At WET-OUT, samples of all five major parameters as well as sulfate, were collected three times per week through the treatment period. In contrast, influent data (WET-IN) were collected once per week for NH_3, As, Cu, Fe, and Ni, and once per month for CN and sulfate. Flows are measured continuously at WET-OUT using an OCM III Ultrasonic flow meter. For loading calculations, inflow rates to the wetland were assumed to be equal to those at WET-OUT. Specifically, the influences of precipitation and evapotranspiration were assumed to be negligible given the magnitude of flow through the wetland system. HRT was calculated based on wetland dimensions and flow, and supported with analysis of lag times inferred from the timing of water quality changes between WET-IN and WET-OUT.

To provide additional insight in the role of redox controls within the wetland, high-resolution vertical profiles of dissolved oxygen (DO), temperature, pH, ORP and conductivity were collected from 7 locations within the wetland (July 2014). At these same 7 sites surface (0-3 cm) sediments were collected and analyzed for grain size, organic carbon, major elements and minor elements.

RESULTS AND DISCUSSION

Hydrology and Retention Time

Mean daily flow rates through the wetland for 2011, 2012 and 2013 were 11,200 m^3/day, 10,600 m^3/day and 7,200 m^3/day (Figure 1), translating to total volumes of 1.9 million m^3, 1.1 million m^3, and 1.1 million m^3, respectively. Wetland HRT typically varied between 6-7 days depending on the discharge rate from the Polishing Pond, with an overall 2011-2013 mean of 6.4 days. Estimates of HRT are supported by lag times observed between WET-IN and WET-OUT for changes in concentration of conservative parameters such as sulfate.

Water Quality

Ammonia

NH_3 originates from the degradation of CN compounds (*e.g.*, cyanate hydrolysis) as well as from the leaching of residual blasting residues used in underground mining. Influent concentrations of NH_3-N were variable, with values typically ranging between 10 and 15 mg/L (Figure 2). Concentrations at WET-OUT were greatly reduced compared to WET-IN, with the majority of

values in 2012 and 2013 being <0.5 mg/L. Removal rates ranged from 60 to 1,200 mgN/m²/day (2011-2013 mean = 482 mgN/m²/day), with mass removal showing a general decrease from 2011 to 2013 (overall mass removal efficiency of 89%)

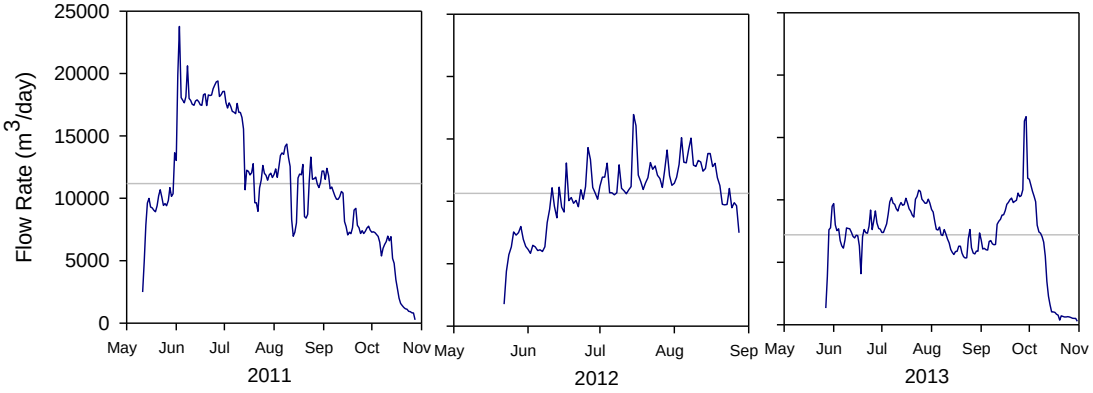

Figure 1 Daily flow rates (measured at WET-OUT) for the 2011, 2012 and 2013 wetland treatment periods.

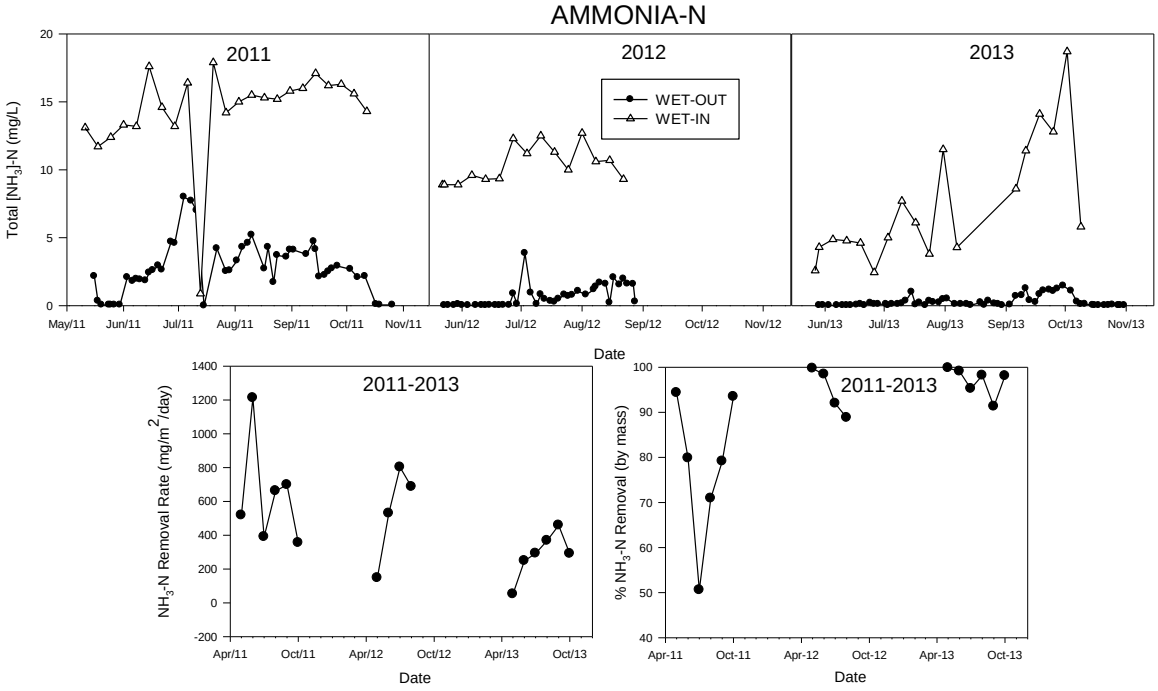

Figure 2 (Top) Time-series of NH_3-N concentration in the influent (WET-IN) and effluent (WET-OUT) of the wetland complex (May to October of 2011, 2012, and 2013). (Bottom left) Wetland removal rate for NH_3-N as monthly means for May to October of 2011, 2012, and 2013. (Bottom right) NH_3-N percent removal efficiency (by mass) as monthly means for May to October of 2011, 2012, and 2013.

(Figure 2). The decrease in removal rate from 2011-2013 is largely due to the general decline in influent NH_3 concentration over the study period. In contrast, removal efficiency generally increased over time, with % removal in 2013 ranging from 91 to 99% (Figure 2). Mechanisms of NH_3 removal include biological uptake (macrophytes, algae), adsorption to substrates and microbially-mediated nitrification (oxidation to nitrate). At the influent pH range (6<pH<7)

ammonia will be predominantly present as ammonium (NH_4^+); therefore, volatilization of $NH_3(g)$ is not predicted to be significant (Reddy and Patrick, 1984).

Wetland removal efficiency for NH_3 was seasonal, with maximum efficiency observed at the beginning of the treatment season, and efficiency decreasing to minima in July/August. Comparison of removal efficiency (by mass) as a function of HRT suggests NH_3 percent removal is dependent on flow rate to some degree (Figure 3). Specifically, NH_3 removal efficiency shows an asymptotic relationship with HRT, whereby the two parameters show a positive correlation up to a HRT value of 10 days, beyond which removal efficiency does not improve. The decrease in removal efficiency during the warmer months may also be linked to the remobilization of NH_3 associated with the degradation of organic matter within the wetland, which is expected to be at a maximum during the warmer period. Increased temperatures and rates of organic matter decomposition are also more likely to sustain low oxygen conditions in the water column, which are more conducive to the persistence of NH_3. Indeed, dissolved oxygen (DO) measurements in the wetland at the end of July 2014 revealed zones of low DO, with values as low as 1 mg/L at some locations. Dunne *et al*. (2013) also showed that releases of NH_3 were greatest during warm periods, and liked this to anoxia in the water column due to increased temperatures and rates of organic matter decomposition.

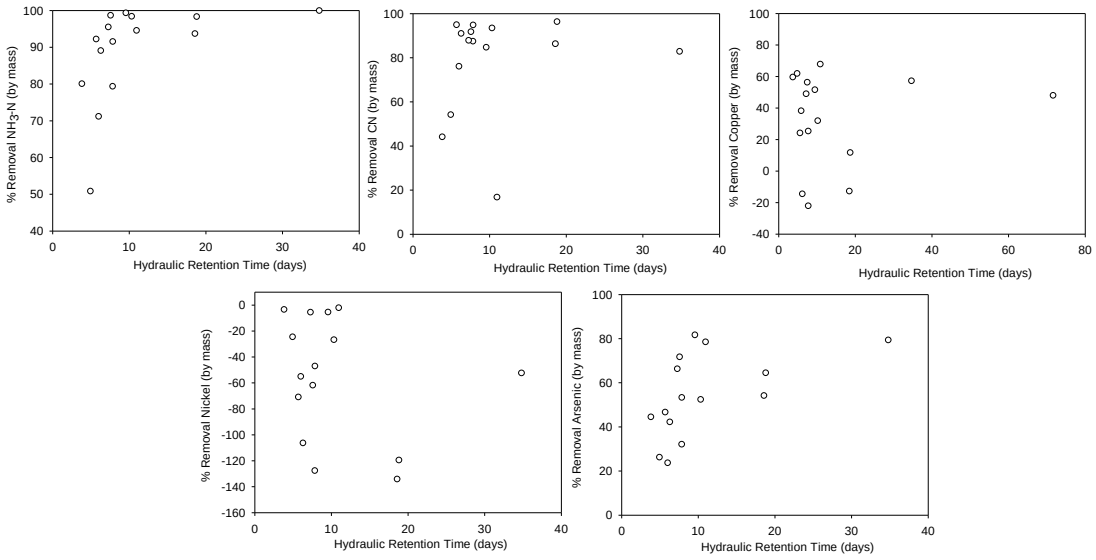

Figure 3 Wetland removal rates for NH_3-N, CN, Cu, Ni and As (as monthly means) as a function of hydraulic retention time (monthly means) for the period 2011-2013.

Cyanide

CN originates from the use NaCN in gold extraction during ore processing. Treatment using SO_2/Air methods reduced CN to values well below compliance limits prior to entry into the wetland. Values for total CN in the wetland inflow were low and variable (0.02 to 0.1 mg/L) (Figure 4). CN levels were reduced through the wetland system, with most values at WET-OUT in 2012 and 2013 being <0.01 mg/L. Such concentration reductions equate to a mean removal rate of 2.8 mg/m^2/day (range from 0.2 to 6.4 mg/m^2/day). Rates of CN removal are variable (17 to 95%; 2011-2013 mean = 78%), and increase over the course of each treatment season in 2011, 2012 and 2013 (Figure 4). For 2012 and 2013, the increases over time in removal efficiency can be explained by the

progressively increasing CN values at WET-IN in combination with the low and invariant values at WET-OUT. Similar to NH_3, CN removal efficiency shows a weakly-positive relationship to HRT (Figure 3), suggesting flow rate also affects CN removal efficiency.

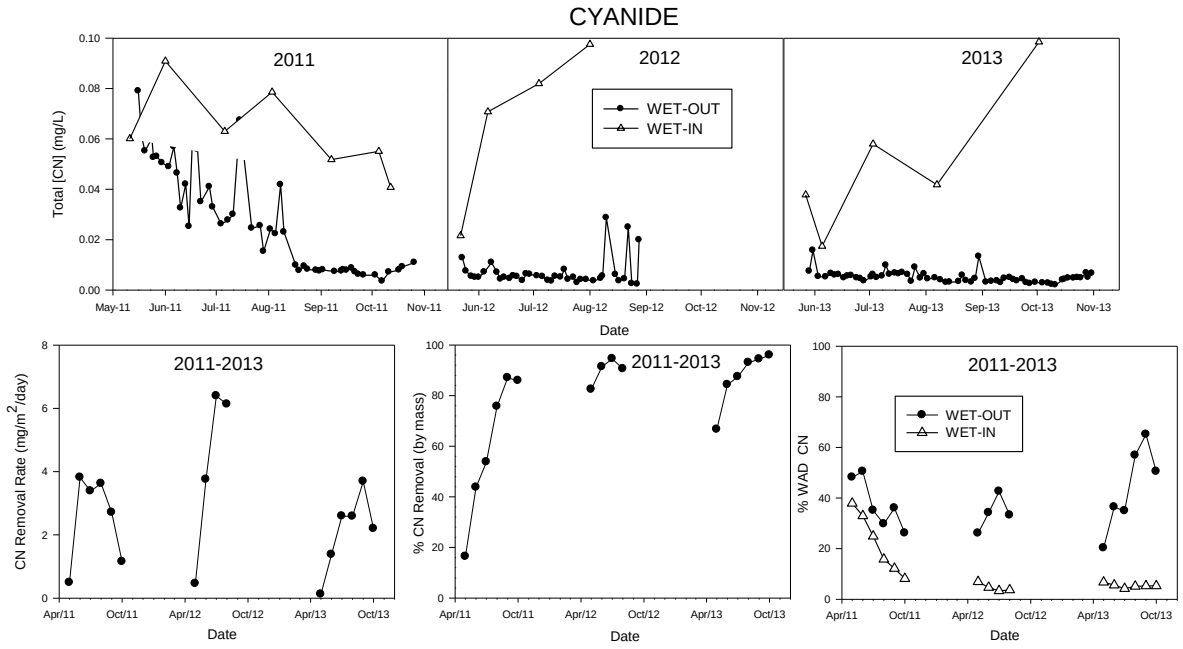

Figure 4 (Top) Time-series of total CN concentration in the influent (WET-IN) and effluent (WET-OUT) of the wetland complex (May to October of 2011, 2012, and 2013). (Bottom left) Wetland removal rate for total CN as monthly means for May to October of 2011, 2012, and 2013. (Bottom centre) CN percent removal efficiency (by mass) as monthly means for May to October of 2011, 2012, and 2013. (Bottom right) Ratio of WAD CN to Total CN in influent (WET-IN) and effluent (WET-OUT) as monthly means for May to October of 2011, 2012, and 2013.

Mechanisms for CN removal in wetland systems may include volatilization of HCN, UV-catalyzed oxidation, hydrolysis to NH_3 and precipitation of insoluble metal-CN complexes (Gasper and Beck, 1983). Insight into CN behaviour can also be garnered from the proportion of weak-acid-dissociable (WAD) CN in the wetland inflow and outflow (Figure 4). Specifically, in both 2012 and 2013, the %WAD-CN at WET-OUT increases during each treatment season, while the %WAD-CN in the inflow remains constant. These data indicate that either: 1) strong acid dissociable CN compounds (*e.g.*, ferri/ferro CN complexes) are preferentially removed within the wetland complex; and/or 2) WAD-CN complexes are increasingly remobilized into solution over the treatment period. These considerations also have relevance to the interpretation of Ni and Cu behaviour (discussed below).

Copper

Total Cu concentrations in the wetland inflow were variable, ranging from 0.001 to 0.022 mg/L (mean = 0.011 mg/L) (Figure 5). Over the course of each treatment season, inflow Cu concentration generally declined, which reflects processes occurring upstream in the tailings management area (TMA). Concentrations of Cu were significantly reduced by the wetland, with a mean outflow value of

0.0065 mg/L (range of 0.001 to 0.02 mg/L) (Figure 5). Cu removal rates range from -0.12 to 1.5 mg/m²/day.

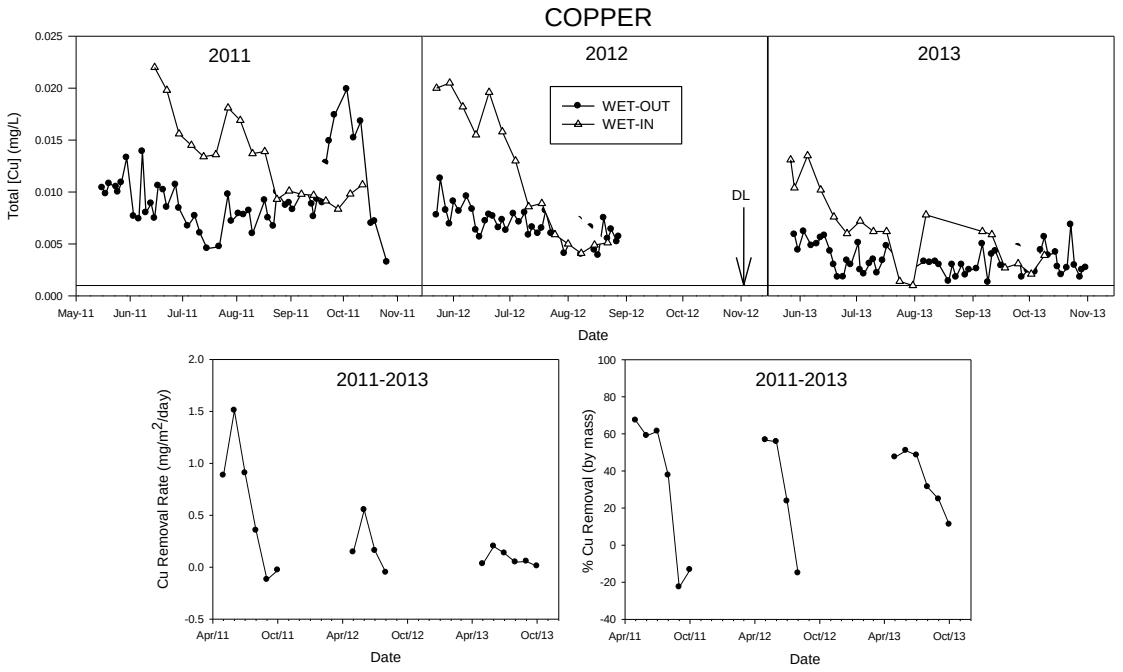

Figure 5 (Top) Time-series of total Cu concentration in the influent (WET-IN) and effluent (WET-OUT) of the wetland complex (May to October of 2011, 2012, and 2013) DL = detection limit (0.002mg/L). (Bottom left) Wetland removal rate for total Cu as monthly means for May to October of 2011, 2012, and 2013. (Bottom right) Total Cu percent removal efficiency (by mass) as monthly means for May to October of 2011, 2012, and 2013.

Removal rates declined over the course of each treatment season (May – October), possibly related to the decreases that occurred to inflow concentration (*i.e.*, decreased removal efficiency with decreasing influent concentration). Cu removal efficiency ranged between -23% to 68% (mean = 33%), indicating that in some months, the wetland served as a source of Cu rather than a sink (Figure 5). Cu removal efficiency was weakly proportional to HRT, suggesting flow rate is not a dominant variable with respect to percent removal (Figure 3).

Possible sinks for Cu in wetland systems include adsorption (*e.g.*, Fe oxides, organic matter, clays), biological uptake (bacteria, algae, biofilms, macrophytes), and precipitation as secondary phases (*e.g.*, Cu sulfides) (Sobolewski, 1999). As a means to assess the nature of Cu removal, elemental data for the near-surface substrates were examined. Cu concentrations in surface sediments were variable, and ranged from 17 to 504 mg/kg (mean = 136 mg/kg) (Figure 6). Most values greatly exceeded the local background (22 mg/kg) for sediments collected in a nearby reference wetland, demonstrating that the sediments are serving as a pronounced sink for Cu. Sedimentary Cu showed strong correlations (r^2>0.7) with parameters indicative of organic matter enrichment, including T-N and TOC (Table 1). Cu also shows strong correlations with parameters that preferentially accumulate in reducing sediments, including S and Se. In particular, the observation of Se enrichment in zones of high organic carbon provide strong evidence to indicate redox controls are important, given the tendency of dissolved Se to accumulate in organic-rich reducing sediments (Martin *et al.*, 2011). This is also supported by observations of low DO values in the wetland water

column (as low as 1 mg/L in some locations). Overall, the data suggest that Cu accumulation in sediments is in part tied to sedimentary organic matter abundance, which may reflect Cu uptake by macrophytes/algae and/or precipitation of Cu as secondary sulfides.

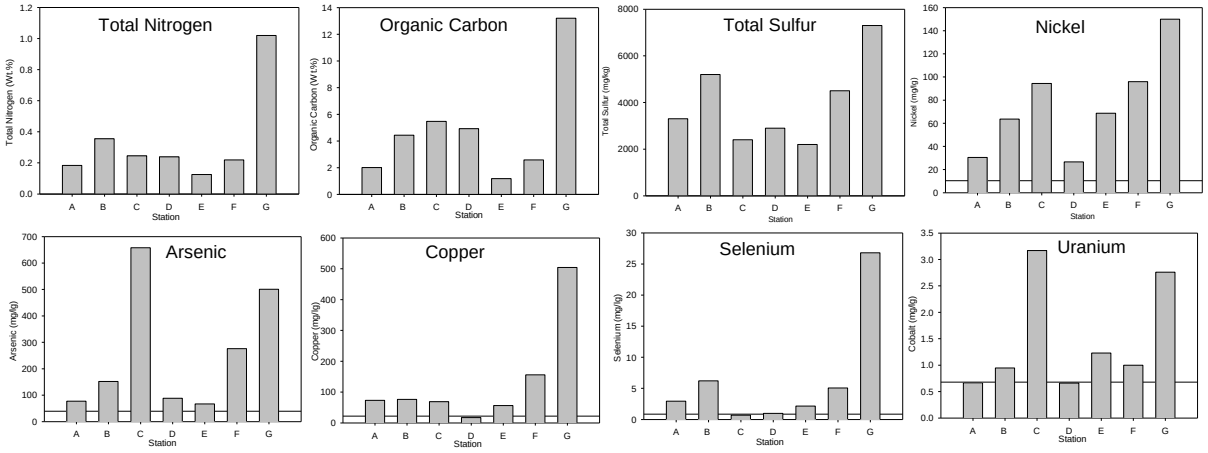

Figure 6 Solid-phase concentrations of total nitrogen, organic carbon, total sulfur and select trace elements (Ni, As, Cu, Se and U) in the upper 3 cm of wetland substrate at seven locations in the wetland complex. Horizontal lines for trace elements represent background values for a control wetland in the local area.

Table 1 Coefficients of determination (r^2) for correlations between total nitrogen (T-N), total organic carbon (TOC), sulfur (S) and select trace elements (As, Cu, Fe, Mn, Ni, Se and U) in the upper 3 cm of wetland sediments (n=7). R^2 values >0.7 are shaded.

Parameter	T-N	TOC	As	Cu	Fe	Mn	Ni	Se	S	U
T-N	1	0.92	0.24	0.90	-0.02	-0.019	0.57	0.95	0.77	0.29
TOC		1	0.38	0.74	-0.01	0.01	0.52	0.77	0.57	0.42
As			1	0.24	0.31	0.38	0.57	0.15	0.08	0.89
Cu				1	-0.03	-0.05	0.72	0.96	0.74	0.28
Fe					1	0.77	0.11	-0.05	-0.10	0.40
Mn						1	0.03	-0.08	-0.21	0.46
Ni							1	0.61	0.44	0.58
Se								1	0.82	0.20
S									1	0.20
U										1

Nickel

Ni concentrations in the inflow to the wetland showed a strong decline during the 2011-2012 period, from approximately 0.17 mg/L (June 2011) to 0.02 mg/L (August 2012), after which time values remained relatively invariant (Figure 7). This decrease in Ni may in part reflect implementation of a new SO_2/Air CN destruction circuit at the end of 2010, which would be expected to lower Ni solubility in response to reducing the potential for CN-Ni complexation. In contrast to Cu, Ni concentrations at the outflow are consistently higher than those at the inflow, demonstrating that the wetland behaved as a net source for Ni during 2011, 2012, and 2013 (Figure

7). Mean loading to the outflow was 0.9 mg/m²/day (2011-2013), translating to a mean increase of 54% (by mass) over the same period (Figure 7).

The source of Ni within the wetland complex is not clear. Possible reasons include the leaching of Ni from Ni-bearing waste rock used in wetland construction, or more likely, the remobilization of Ni through desorption processes. With respect to the latter, the remobilization of Ni through CN complexation may play a role. As described in the discussion of CN, the removal of CN appears to be linked to the preferential removal/destruction of strong-acid-dissociable species (*e.g.*, Fe-CN). This process may allow for secondary complexation of liberated CN- with other trace elements (*e.g.*, Ni) within the wetland complex. The strong correlation between Ni and Cu removal efficiencies (Figure 7, bottom right) implies that similar factors may apply to Cu.

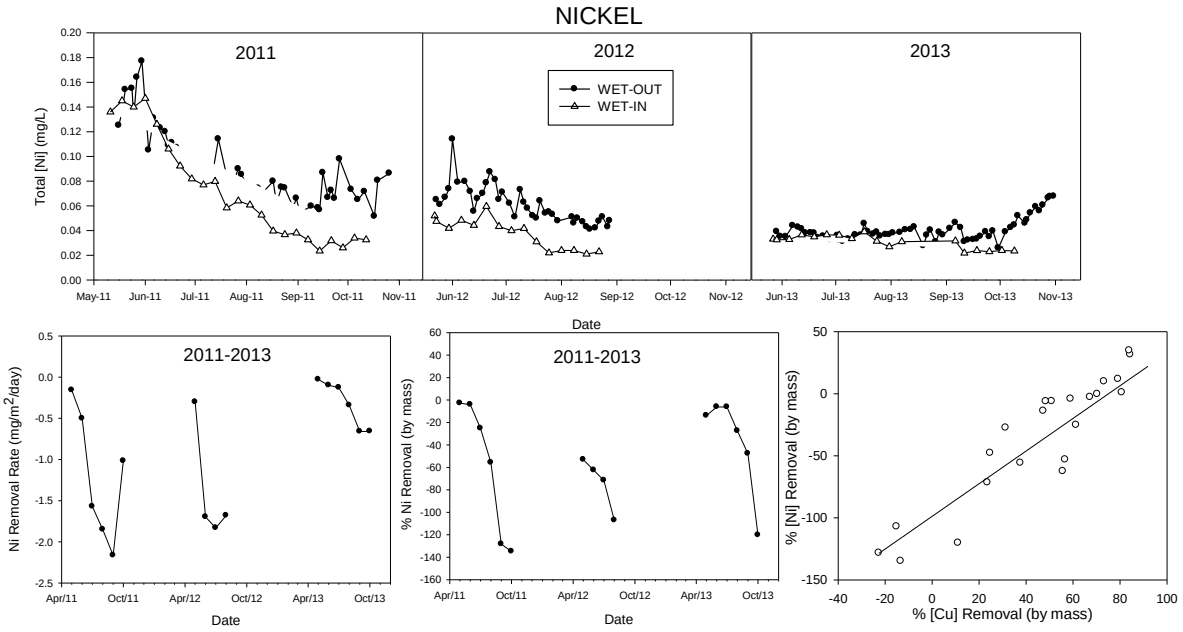

Figure 7 (Top) Time-series of total Ni concentration in the influent (WET-IN) and effluent (WET-OUT) of the wetland complex (May to October of 2011, 2012, and 2013). (Bottom left) Wetland removal rate for total Ni as monthly means for May to October of 2011, 2012, and 2013. (Bottom centre) Total Ni percent removal efficiency (by mass) as monthly means for May to October of 2011, 2012, and 2013. (Bottom right) Relationship between Ni and Cu percent removal efficiencies (regression of monthly means for period 2011-2013).

Alternatively, the remobilization of Ni from within the wetland complex may be related to the decline in Ni influent values during 2011-2012, which was likely the result of improved CN treatment upstream. Specifically, the pronounced decline in Ni concentrations in the wetland inflow may have promoted desorption of Ni from binding sites on particle/organic surfaces. Metal concentrations in solution that are governed by sorption reactions can be described in terms of a distribution coefficient (K_d) (Tessier, 1989), which is the ratio of sorbed metal concentration (expressed in mg metal per kg sorbent) to the dissolved metal concentration (expressed in mg/L) at equilibrium (Equation 1).

$$\square_{\square} = \frac{\square\square\square\square\square\square\ \square\square\square\square\square\ \square\square\square\square\square\square\square\square\square\square\square\square\ (\square\square/\square\square)}{\square\square\square\square\square\square\square\square\square\ \square\square\square\square\square\ \square\square\square\square\square\square\square\square\square\square\square\square\ (\square\square/\square)} \qquad \text{(Equation 1)}$$

According to this equation, if the dissolved metal concentration decreases, the sorbed concentration must also decrease to maintain a constant K_d value. This mechanism, which relies on the assumption of adsorptive equilibrium, provides a possible explanation of the remobilization of Ni from the wetland complex.

Arsenic

In the wetland inflow, As concentration consistently declined between June and October in each of 2011, 2012 and 2013, with values ranging from 0.43 to 0.16 mg/L (mean = 0.095 mg/L) (Figure 8). The decrease in As concentration in the wetland influent within each season likely relates to seasonal redox-related processes in the TMA upstream. Arsenic values were consistently lower at the wetland outflow (mean = 0.039 mg/L), indicating that the wetland served as a sink for dissolved As. Mean monthly As removal rates ranged from 0.6 to 6.9 mg/m2/day (mean = 2.3 mg/m2/day), translating to a mean removal efficiency of 56%. Arsenic removal efficiency showed a positive correlation with HRT (Figure 3), suggesting flow rate affected wetland performance to some degree. Within each treatment year, removal efficiency showed a seasonal decline to minima typically occurring in July or August. Removal efficiency increased late in the season (September) despite the influent concentration continuing to decrease. Such behaviour may relate to redox-controlled processes in the wetland. Specifically, higher rates of Fe-oxide reductive dissolution may be expected during the peak summer period, when rates of bacterially-mediated organic matter oxidation are at a seasonal maximum. This, combined with lower DO values in the water column, may promote the recycling of As into surface waters (Martin and Pedersen, 2002).

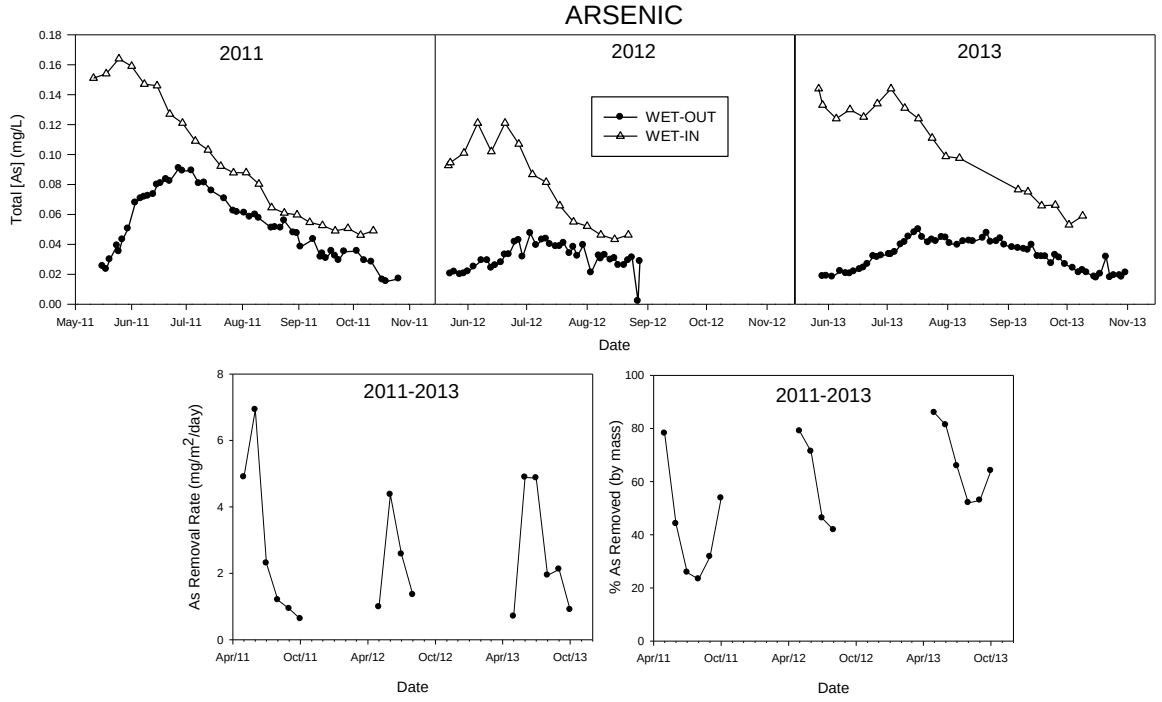

Figure 8 (Top) Time-series of total As concentration in the influent (WET-IN) and effluent (WET-OUT) of the wetland complex (May to October of 2011, 2012, and 2013). (Bottom left) Wetland removal rates for total As as monthly means for May to October of 2011, 2012, and 2013. (Bottom right) Total As percent removal efficiency (by mass) as monthly means for May to October of 2011, 2012, and 2013.

Arsenic showed significant solid-phase enrichment over background values in reference wetland substrates, indicating that the sediments are serving as a sink for As. Possible accumulation pathways include sorption to Fe/Mn oxides, adsorption of arsenite (As^{+3}) to particles, and precipitation of secondary As sulfides. Correlations of As with Fe (r^2=0.31) and Mn (r^2=0.38) are relevant, and suggest some degree of As adsorption with Fe and/or Mn oxides (Table 1). In contrast, As was poorly correlated with S (r^2=0.08), suggesting secondary As-sulfide formation is not a dominant accumulation pathway. Interestingly, As showed the strongest relationship with U (r^2=0.89) (Table 1). Like As, U is redox sensitive and tends to accumulate as discrete U phases in anoxic sediments (Lovely *et al*., 1991). The strong link of As to U, and weak correlations of As with S, Fe and Mn, may suggest that As adsorption as arsenite (*e.g*., to clays and/or organics) may play a significant role in governing As uptake within the wetland complex.

CONCLUSIONS

The results of this study demonstrate the successful utility of constructed wetlands for the treatment of neutral-pH gold mill effluents in cold interior climates, with parameters including NH_3, CN, Cu and As showing robust removal efficiencies. The data suggest that contaminant removal relates to a combination of biological uptake as well as redox-related processes that result in the sequestration of trace elements under conditions of suboxia. The successful application of wetland treatment at the Campbell Complex is strongly tied to the water management system, which facilitiates sufficient storage within the TMA to allow all mine waters to be discharged through the wetland during the ice-free period (May through end of October). The data also illustrate the effect of several processes that can influence wetland performance on seasonal and inter-annual scales, including changes to influent composition, variability in HRT, and biogeochemical processes that may promote contaminant remobilization.

REFERENCES

Dunne, E.J., Coveney, M.F., Marzolf, E.R., Hoge, V.R., Conrow, R., Naleway, R., Inglett, P.W. (2013). Nitrogen dynamics of a large-scale constructed wetland used to remove excess nitrogen from eutrophic lake water. Ecological Engineering, 61, Part A, 224–234. doi:10.1016/j.ecoleng.2013.09.039

Gaspar, V. and Beck, M.T. (1983) Kinetics of the photoaquation of hexacyanoferrate(II) ion, Polyhedron, 2, 387.

Hammer, D.A. (1992). Designing constructed wetlands systems to treat agricultural nonpoint source pollution. Ecological Engineering, 1(1–2), 49–82.

Lovely, D.R., Phillips, E.J.P., Gorby Y.A., Landa E.R. (1991) Microbial reduction of uranium. Nature 350:413-416.

Martin, A.J., Pedersen, T.F. (2002) Seasonal and interannual mobility of arsenic in a lake impacted by metal-mining. Env. Sci. Tech. 36:1516-1523.

Martin, A.J., Simpson S., Fawcett S., Wiramanaden C.I.E., Pickering I.J., Belzile N., Chen Y.-W., London J., Wallschläger D. (2011) Biogeochemical mechanisms of selenium exchange between water and sediments in two contrasting lentic environments Environ. Sci. Technol. 45:2605-2612.

Reddy, K.R., Patrick, W.H. (1984) Nitrogen transformations and loss in flooded soils and sediments. CRC Crit. Rev. Environ. Control.13:273–309

Sobolewski, A. (1999) A review of processes responsible for metal removal in wetlands treating contaminated mine drainage. Internat. J. Phyto. 1:19-51.

Tessier, A., Carignan, R., Dubreuil, B., Rapin, F. (1989) Partitioning of Zn between the water column and the oxic sediments in lakes. Geochim. Cosmochim. Acta. 53:1511-1522.

Passive Removal of Iron from AMD Using VFRs

Devin Sapsford[1], Kay Florence[1], James Pope[2] and Dave Trumm[2]
1. *School of Engineering, Cardiff University, United Kingdom*
2. *CRL Energy Ltd / University Canterbury, New Zealand*

ABSTRACT

This paper presents data on treatment trials of three low pH mine waters and one circumneutal mine water in the UK and New Zealand using Vertical Flow Reactors (VFRs) - mine water treatment systems where mine water is directed through an unreactive gravel bed to encourage metal removal under aerobic conditions. Previous VFR studies have demonstrated their efficacy at iron removal at circumneutral pH; this study demonstrates that significant removal of iron (as high as 85%) can be achieved at low pH (~3), within a practicable treatment area using the VFR system. The iron removal rate varies between the four study sites. The difference is attributed to the mechanism of removal which is suspected to be the agglomeration and filtration of nanoparticulate colloidal-sized ferric iron precipitates in addition to microbial Fe(II) oxidation and heterogeneous precipitation. The use of VFRs represents an inexpensive option for removing the majority of iron from low pH mine water without the requirement for any pH adjustment. The study also confirms the VFR's applicability to iron removal from circumneutral mine water.

Keywords: vertical flow reactors, nanoparticulate iron, filtration

INTRODUCTION

Passive mine water treatment involves a number of physicochemical and microbiological strategies for the removal of dissolved species of concern. Removal of metals is either achieved via harnessing of naturally occurring physicochemical and microbiological processes, for example the manipulation of solubility via changes in pH (e.g. by reaction with limestone) or redox conditions (through contact with organic matter) or through sorption processes. Removal of iron (Fe) is the focus of the present study.

In general, at pH below 9, the divalent Fe(II) species are highly soluble and do not readily form salts or hydroxide precipitates. Fe(III) solubility is such that under oxic conditions numerous Fe(III)-bearing phases precipitate (hereafter termed $Fe(III)_{(s)}$) over the pH spectrum. In acid mine drainage (AMD) environments it is common for the Fe hydroxy-sulfate mineral schwertmannite to form (e.g. Bigham et al, 1996)as well as jarosite-alunite minerals. Ferrihydrite and goethite dominate at higher pH (> 4). It is difficult to predict the exact solubility because of the heterogeneity of mineral products and the corresponding paucity of unanimity in thermodynamic data for Fe in the literature. Fe(II) is meta-stable under acidic oxidizing abiotic conditions due to slow oxidation kinetics but is widely reported to be microbiologically catalyzed (e.g. Kirby et al,1999), with the production of aqueous Fe(III) species or Fe(III) phases depending on the pH.

Iron is often the principal contaminant of concern from coal mine AMD and generally the approach to treatment is to contact the mine water with reagents to raise the pH to circumneutral pH or higher to accelerate Fe(II) oxidation and minimize Fe solubility. The reagents include lime, limestone, caustic soda, slag,. in different configurations depending on whether the treatment is active or passive or semi-passive. In active treatment schemes the resultant particulate Fe(III) will either be removed by polymer dosing and clarification; in passive systems a limestone drain, slag bed or RAPS will be used to raise pH ahead of settling ponds and/or aerobic wetlands which are used to settle and filtrate the suspended particulate Fe(III). In passive systems the rise in pH also accelerates the oxidation of Fe(II) to precipitate $Fe(III)_{(s)}$ and may be augmented by the addition of hydrogen peroxide or other oxidants in semi-passive treatment schemes.

Vertical Flow Reactors

Dey et. al (2003), Sapsford et. al (2008), and Sapsford and Williams (2009) and related publications detail a vertical flow system which operates under aerobic conditions to remove Fe from circumneutral coal mine water by (self)filtration of $Fe(III)_{(s)}$ supported by a gravel support bed and also heterogeneous Fe(II) oxidation and precipitation. This was based on earlier observations in the literature as well as observations from the field concerning the ubiquity of Fe(III) precipitates forming on vertical flow RAPS. There are a number of related publications concerning heterogeneous Fe(II) oxidation harnessed for treatment (e.g. Best and Aikman, 1983, Jarvis and Younger, 2001). Some authors have investigated harnessing low pH microbial Fe(II) oxidation (e.g. Burgos et al, 2004). This paper examines the application of VFRs to AMD. The specific aims of this study are to: (i) present data from field trials of VFRs operating at a low pH abandoned lead (Pb) – zinc (Zn) metal mine site in the UK and two AMD sites and one neutral mine drainage site in New Zealand (South Island), and (ii) to highlight the removal chemistry of iron in these systems.

Study Sites

Cwm Rheidol

The Cwm Rheidol former Pb/Zn mine was operated between 1848 and1917 and is located within the mid-Wales Orefield approximately 12 km east of Aberystwyth north of the river Rheidol. The mine is part of a big mine complex situated just below the village of Ystumteum, on the steep southerly face of the Rheidol Valley which runs ESE to WNW. The AMD issues from two adits. Cwm Rheidol is classified as one of the top 50 polluting metal mines in Wales and put forward as a priority site for remediation in the Metal Mines Strategy for Wales report by Johnston (2004).

Despite this mine complex having been abandoned for almost a century, AMD is still contributing almost half the Zn and Pb loading to the River Rheidol (Edwards and Potter, 2007).

Bellvue Mine

Bellvue Coal Mine is and underground mine located on the West Coast of the South Island of New Zealand approximately 15 km northeast of Greymouth. It operated from 1928 until 1964 and is currently abandoned. The entrance to the mine is on a hillside approximately 100 m above a nearby creek. An AMD water pool at the entrance drains to a cascade which flows down the slope to the creek. The water in the pool is in a reduced state, with the majority of iron as Fe(II) and very low dissolved oxygen (DO) concentrations, and a pH of approximately 2.5. As the AMD flows down the cascade, DO concentrations increase and Fe(II) oxidises to Fe(III) and some Fe hydroxides precipitate. The Fe and aluminum (Al) concentrations are some of the highest recorded at NZ mines.

Active Mine Site with AMD, New Zealand

The second AMD site in New Zealand is an active opencast coal mine. The AMD at the site issues from overburden waste rock dumps and contains relatively high concentrations of Fe, Al, and Mn and low pH.

Active Mine Site with neutral drainage, New Zealand

The neutral drainage site in New Zealand is an underground active coal mine. The neutral drainage issues from an old adit on the site and contains relatively low concentrations of Fe and a neutral pH.

METHODOLOGY

UK VFR

The system (see Figure 1) was adapted from the original design used in initial field trial at the Taff Merthyr site in South Wales (Dey et al, 2003), using a 1 m^3 intermediate bulk container (IBC) adapted to become a VFR treatment tank. A 100 mm gravel bed layer (of unreactive siliceous 5 mm chips), supported by a layer of 30 mm chips of the same material was used in the base of the tank upon which ochre is allowed to accumulate. IBCs have an outlet at the bottom of the tank which has a standard fitting which can be opened and closed manually. Inside the tank, underneath the gravel bed a length of coiled slotted drainage pipe was attached to the outlet valve which allowed the treated water to be collected and directed up through a swan neck outlet. A length of hose was fitted to that outlet valve to act as a swan neck mechanism so that the driving head within the container could be adjusted; the head was set to 200 mm. Monitoring of the influent and effluent mine water was conducted as follows: Samples for total iron (Fe-Tot) including suspended particulate Fe and dissolved Fe were taken directly from the mine water using a disposable Plastipak syringe and stored in a sample bottle and acidified with 0.1 ml of 20% (v/v) HNO_3. Samples for filtered Fe (Fe-Filt) were taken in the same way except that first they were filtered using disposable 0.2 µm syringe filters. These samples were analyzed by ICP-OES. Samples for Fe(II) were either measured in the field using a portable Merck SQ NOVA60 spectrophotometer with appropriate Spectroquant® Fe test cells or acidified with HCl and placed immediately into a dark cool box and stored at 4° C until analysis in the laboratory by the 2'2-bipyridyl solution method using a Hitachi U1900 spectrophotometer. All field pH/DO measurements were taken using Hanna combination meters, calibrated at each site visit. Influent and effluent flow measurements were taken by timing the length of time to fill a measuring cylinder.

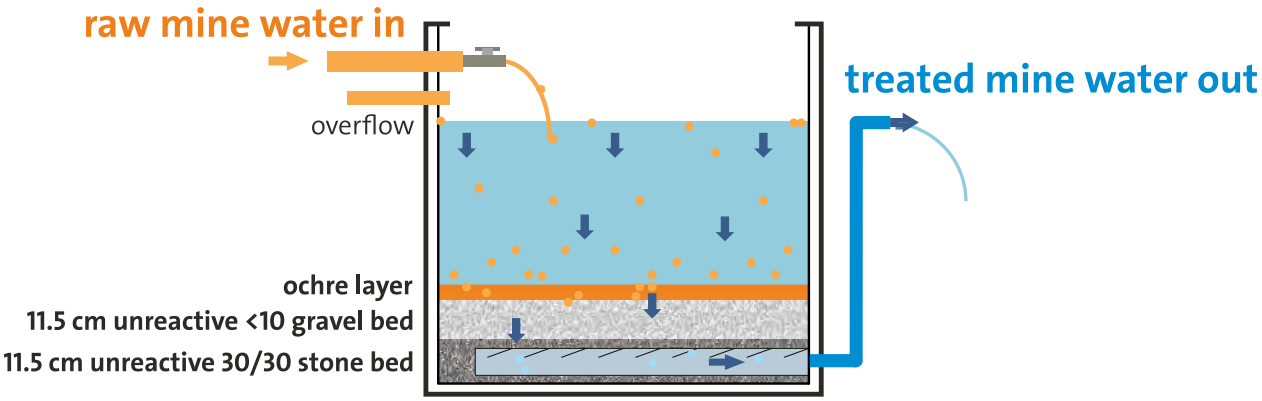

Figure 1 Schematic of Cwm Rheidol VFR

New Zealand VFRs

The systems installed in NZ used the same configuration as the one installed at Cwm Rheidol in the UK. Monitoring of the influent and effluent for the systems was conducted as follows: Samples for total iron (Fe-Tot) including suspended particulate Fe and dissolved Fe were taken directly from the mine water using a disposable Plastipak syringe and stored in a sample bottle and acidified with 0.1 ml of 20% (v/v) HNO_3. Samples for filtered Fe (Fe-Filt) were taken in the same way except that first they were filtered using disposable 0.45 µm syringe filters. These samples were analyzed by ICP-OES. Samples for Fe(II) were measured in the field immediately upon collection using Hach Method 8146 (1,10 Phenanthroline Method) and concentrations determined through absorbance using a Hach DR/2400 Portable Spectrophotometer. All field pH/DO measurements were taken using a portable YSI 556 multi-probe system, calibrated against known standards in the field. Influent and effluent flow measurements were taken by timing the length of time to fill a measuring cylinder.

RESULTS AND DISCUSSION

The results for iron removal are given in Figures 2 – 5. Further explanation of the bar charts presented is required with respect to the meaning of the reported breakdown of iron. Fe-Tot (total iron) is the sum of dissolved iron (both $Fe(II)_{(aq)}$ and $Fe(III)_{(aq)}$) + particulate iron suspended in the water. Fe-Filt (filtered iron) is the concentration of iron in all its forms that has passed a 0.2 μm filter (0.45 μm for New Zealand data) and Fe(II) is the spectrophotometrically determined aqueous Fe(II) concentration. Presented in the stacked format it can be seen what proportion of the total iron exist in each category, and how each form of iron is changing through the VFRs. Images of the VFR beds are given in Figure 6.

UK VFR

The Cwm Rheidol (UK) VFR was monitored 21 times between August 3, 2011 and July 4, 2012; of this data, ,Fe(II) analyses were included 11 times, and so the data set presented here is for these 11 monitoring occasions. For these times the mean data (± Stdv) was as follows: flow rate = 0.34 ± 0.29 L/min; Influent pH = 2.97 ± 0.63; Effluent pH = 2.98 ± 0.67; Influent DO = 7.69 ± 1.34 mg/L; Effluent DO = 6.45 ± 1.39 mg/L. The mean total Fe removal was 70% with a high of 85% and a low of 36%. The mean Fe removal rate was 30 g/m^2/d with a high of 87 g/m^2/d and low of 3.7 g/m^2/d. Iron accumulated on the VFR bed after 11 months of continuous operation is shown in Figure 6 (a).

A summary of the Fe removal (in various forms) is given for the Cwm Rheidol VFR in Figure 2. It can be seen that there is always Fe removal observed in the VFR, but the first thing to note is that removal of particulate Fe > 0.2 μm is not solely responsible for the observed removal of Fe in the system, nor is there a substantial change in pH which would explain Fe removal. Where Fe(II) is

present in the influent it is seen to dramatically decrease on passage through the VFR indicating the presence of active acidophilic Fe(II) oxidizers (this was in fact confirmed by a concurrent microbial study by Prof B Johnson, Bangor University, UK) which probably oxidize Fe(II) and precipitates the resultant Fe(III) as schwertmannite. However, it is interesting to note that on all occasions (except for '1') the decrease in Fe(II) between inlet and outlet is not sufficient to explain the observed decrease in Fe-Filt.

Excluding $Fe(II)_{(aq)}$ which is accounted for analytically, the other species that could be reasonably expected to be present and pass a 0.2 μm filter are $Fe(III)_{(aq)}$ and nanoparticulate $Fe(III)_{(s)}$. The definition of what is truely 'dissolved' and 'particulate' is largely operationally defined, but Waychunas et al (2005) have reported nanoparticles in mine water. The removal of dissolved/nanoparticulate Fe seems to be occurring within the VFR. PHREEQC modelling (not shown) indicates that a range of Fe(III) minerals (including schwertmannite) are oversaturated and able to precipitate. It is possible that the residence time (mean 39 hrs) in the VFR allows time for kinetically constrained hydrolysis of Fe(III) to occur, however, according to Combes et al., (1989) precipitation of Fe can be viewed as Fe(III) phases forming from solution begining as small clusters of octahedral $Fe(O, OH, OH_2)_6$ units that evolve into larger polymeric units with time, eventually reaching colloidal sizes. It is also feasible that heterogeneous nucleation is important in the VFR system.

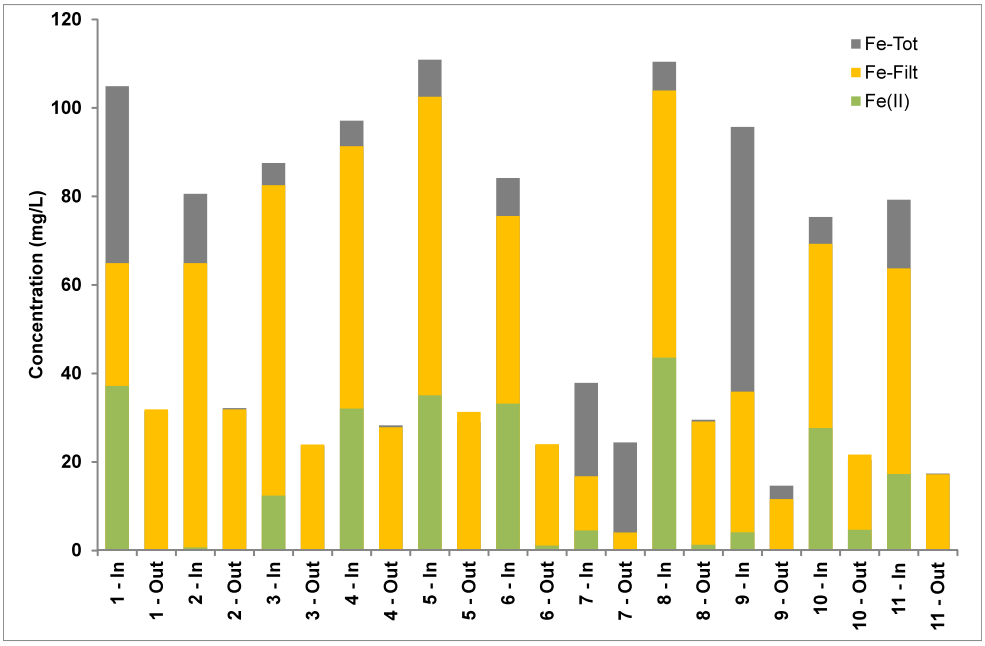

Figure 2 Cwm Rheidol (UK) iron concentration data for VFR influent (in) and effluent (out) on sampling occasions 1 - 11

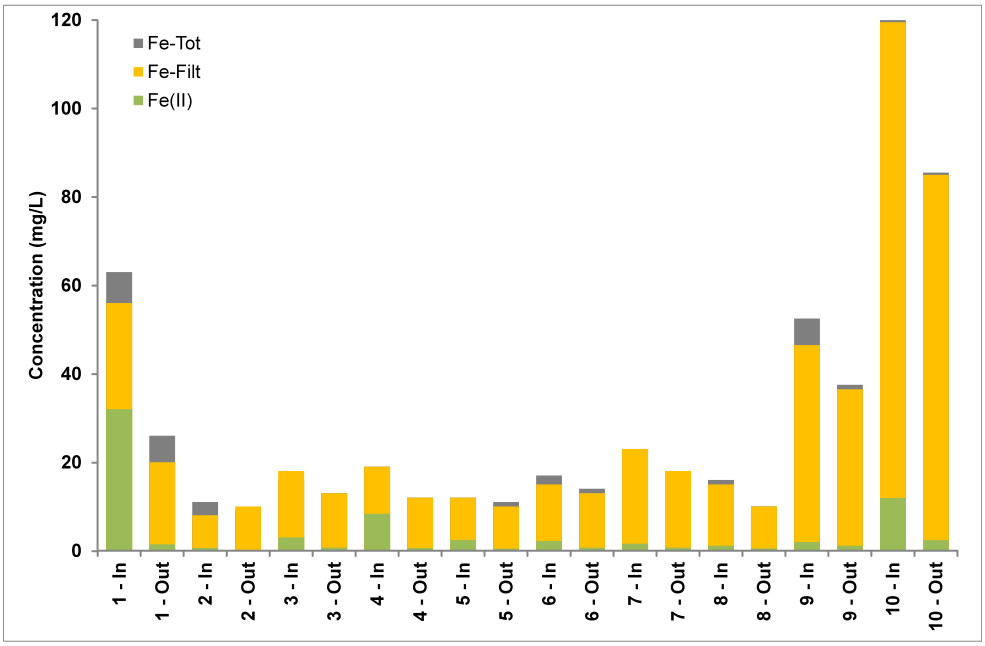

Figure 3 Active mine site with AMD (NZ) iron concentration data for VFR influent (in) and effluent (out) on sampling occasions 1 – 10

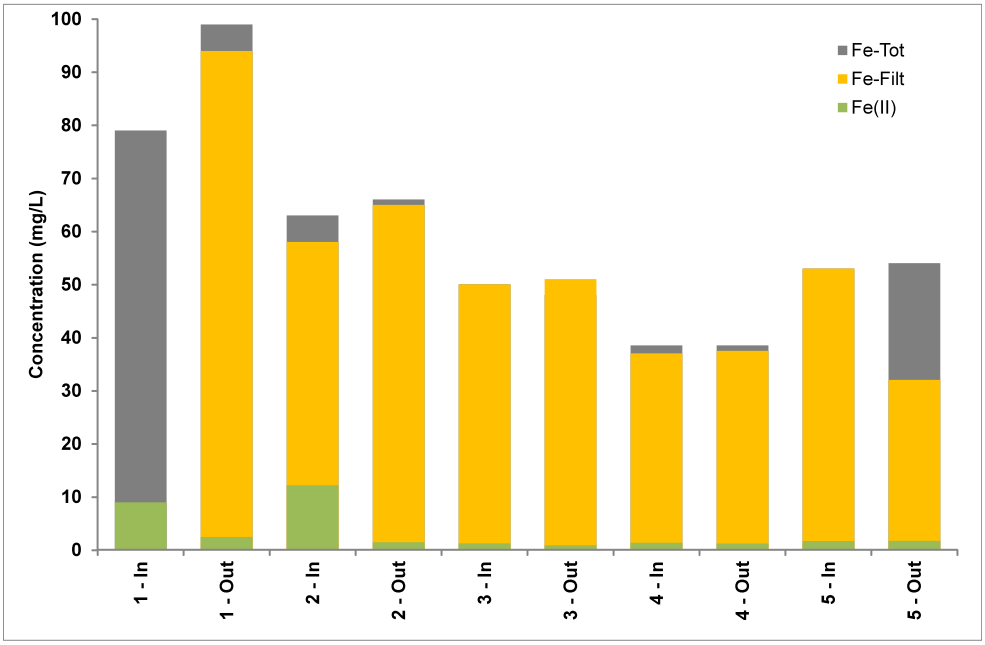

Figure 4 Bellvue (NZ) iron concentration data for VFR influent (in) and effluent (out) on sampling occasions 1 - 11

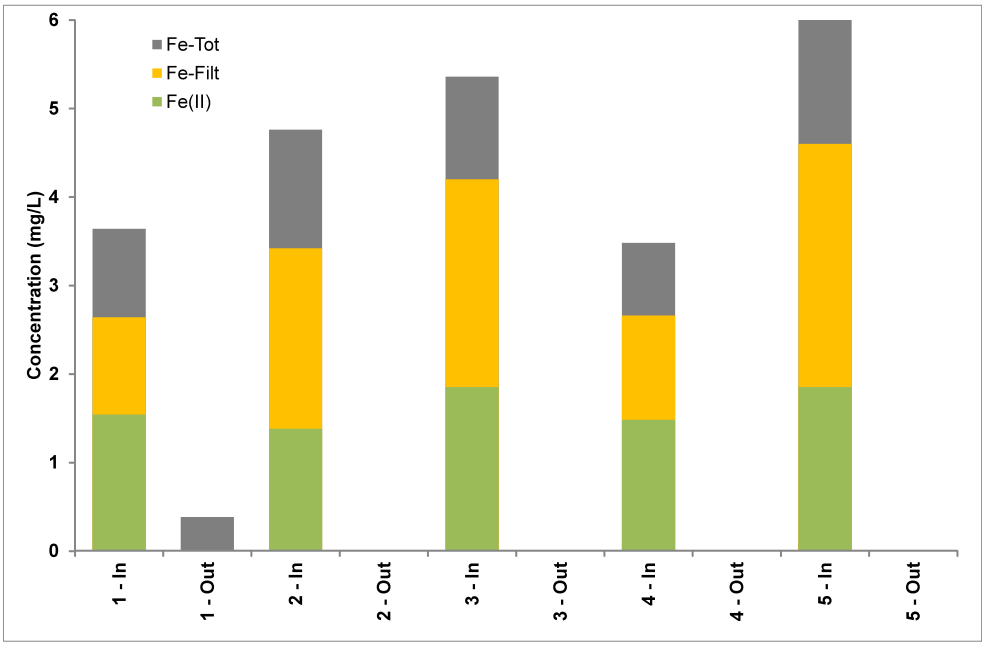

Figure 5 Active mine site with neutral mine drainage (NZ) iron concentration data for VFR influent (in) and effluent (out) on sampling occasions 1 – 10

Regardless of the removal mechanism (which warrants further research) the data show that the VFR is effective at removing a large proportion (70%) of the iron from the discharge. The full mine water discharge at Cwm Rheidol is circa 10 L/s. Based on an average flow of 0.34 L/min going through the 1 m^2 bed of the VFR, a VFR of 1765 m^2 (e.g. dimensions 50 m x 35 m) could remove circa 70% of the iron from the full discharge continuously for at least one year without the need for maintenance.

New Zealand VFRs

Active mine site with AMD

The VFR at the active mine site with AMD was monitored on 10 occasions between April 30, 2014 and September 11, 2014. The mean data (± Stdv) was as follows: flow rate = 0.47 ± 0.06 L/min; Influent pH = 3.19 ± 0.14; Effluent pH = 3.06 ± 0.11; Influent DO = 8.03 ± 0.66 mg/L; Effluent DO = 8.77 ± 0.89 mg/L. The mean total Fe removal was 28% with a high of 59% and a low of 8.3%. The mean Fe removal rate was 8.2 $g/m^2/d$ with a high of 26 $g/m^2/d$ and low of 8.3 $g/m^2/d$. Iron accumulated on the VFR bed after six months of continuous operation is shown in Figure 6 (b).

Despite being a slightly higher pH mine water than Cwm Rheidol in the UK, the Fe removal is consistently less for this VFR, however significant Fe removal is still occurring Figure 3. Fe(II) is generally a small proportion of the influent Fe, meaning that the Fe-Filt is likely either Fe(III)(aq) or nanoparticulate to colloidal $Fe(III)_{(s)}$. As with the Cwm Rheifol VFR, Fe(II) when present is seen to decrease through the VFR indicating the presence of active Fe(II) oxidizing microbes.

Unlike Cwm Rheidol, the decrease in Fe(II) through microbial oxidation and precipitation could explain the overall decrease in Tot-Fe between in and out for many of the observed sampling occasions, but not always, suggesting that there is another mechanism responsible for removing Fe-Filt as was observed at Cwm Rheidol. All of the removal could be accounted for by accumulation of particulate and nanoparticulate Fe(III). The pH at here is higher than at Cwm Rheidol, yet removal is lower suggesting the controls on Fe solubility are slightly different between sites. In summary

despite these differences with Cwm Rheidol the VFR at the New Zealand active mine site with AMD is effective at removing a proportion (28%) of the Fe from the discharge.

Bellvue

The Bellvue VFR was monitored on five occasions between May 7, 2014 and September 2, 2014. The mean data (± Stdv) was as follows: flow rate = 0.46 ± 0.06 L/min; Influent pH = 2.58 ± 0.06; Effluent pH = 2.57 ± 0.03; Influent DO = 8.55 ± 3.22 mg/L; Effluent DO = 9.98 ± 1,07 mg/L. It can be seen from Figure 4 that removal of Fe was not observed in this VFR. Figure 6 (c) shows that after four months of operation the gravel showed no signs of ochre build up (Note 1-In data for Fe-Filt is missing). Interestingly, it can be seen that despite the lack of removal of Fe, Fe(II) decreases across the VFR indicating, as with the other sites, an active Fe(II) oxidizing microbial community, although in this case the resultant Fe(III) is clearly not precipitating in the VFR.

New Zealand active mine site with neutral mine drainage

The VFR at the New Zealand active mine site with neutral mine drainage was monitored on five occasions between June 27, 2014 and September 1, 2014. The mean data (± Stdv) was as follows: flow rate = 0.46 ± 0.05 L/min; Influent pH = 7.46 ± 0.03; Effluent pH = 7.52 ± 0.10; Influent DO = 10.56 ± 0.19 mg/L; Effluent DO = 10.51 ± 0.38 mg/L. The mean total Fe removal was 98% with a high of 100% and a low of 90%. The mean Fe removal rate was 1.2 $g/m^2/d$ with a high of 5.3 $g/m^2/d$ and low of 2.0 $g/m^2/d$. Note that these are seemingly low but actually these are relatively high given the very low Fe concentration.

Overall Fe removal was excellent. Note that the pH is circumneutral and as such, Fe(II) should be rapidly oxidized either homogeneously or heterogeneously within the VFR and particulate Fe(III) removed by filtration/accretion. This observed performance is in line with earlier VFR studies (see references above) conducted at circumneutral pH. It is noteworthy in Figure 5 that Fe(II) ≠ Fe-Filt, despite the circumneutral pH suggesting that colloidal Fe(III) precipitates are passing the filter. On four of the five sampling occasions Fe was removed to below the detection limit of the spectrophotometer. This demonstrates that the VFR can be used to polish Fe levels down to very low levels as a last stage in treatment, and can replace wetlands in this function, which has the commensurate benefits for waste management of the arising ochre.

(a) Cwm Rheidol VFR, 11 months operation

(b) New Zealand active mine site with AMD VFR, 5 months operation, contours caused by underlying gravel

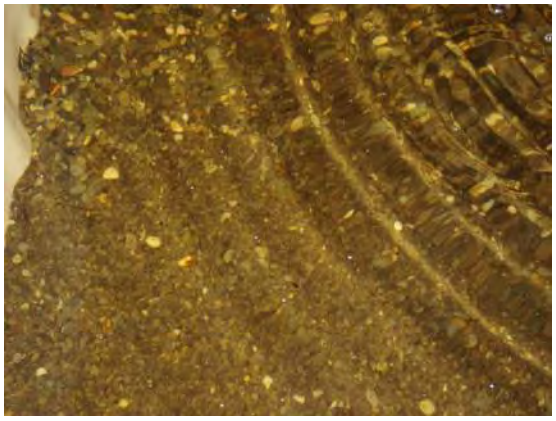

(c) Bellvue VFR, 4 months operation, note no precipitate in evidence.

Figure 6 Photographs of gravel bed after operation of the VFRs

CONCLUSION

In conclusion, the findings of this study were as follows:

- Where Fe is present as particulate Fe(III) it can be effectively filtered out in a VFR. Even at a low pH of circa pH 3, depending on the phase controlling Fe solubility, significant proportion of Fe can be in particulate form (albeit nanoparticulate) and/or supersaturated and able to be removed in a VFR where (self)filtration and precipitation occurs. This means that for many acid mine waters, significant removal of the principal contaminant can be achieved by a simple filtration-type system. This is of particular significance to coal mine AMD where Fe is the principle contaminant. Even slight pH change should be enough to remove much of the Fe.
- The precipitate and/or the gravel substrate hosts Fe(II) oxidizing microbes resulting in demonstrable Fe(II) oxidation. The activity of Fe(II) oxidizers is important in AMD treatment, but the data presented here shows removal of what appears to be 'dissolved' Fe may not always be due to Fe(II) oxidizers.
- An example scale up for the Cwm Rheidol mine water suggests that 70% of the Fe from the full discharge at that site of 10 L/s could be treated continuously for at least one year without removing the precipitate by a VFR of 42 m × 50 m.

ACKNOWLEDGEMENTS

The authors wish to thank the Coal Authority and the EPSRC for funding the UK part of this research and to CRL Energy Ltd for assisting with the research on the mine water in New Zealand.

REFERENCES

Bigham, J. M., Schwertmann, U., Traina, S. J., Winland, R. L., & Wolf, M. (1996). Schwertmannite and the chemical modeling of iron in acid sulfate waters. Geochimica et Cosmochimica Acta, 60(12), 2111-2121.

Burgos, William D., John M. Senko, and Mary Ann Bruns.(2008). Low pH Fe (II) oxidation incorporated into passive treatment. WV Surface Mine Drainage Task Force Symp. 2008.

Dey, Matthew, Piers JK Sadler, and Keith P. Williams.(2003). A novel approach to mine water treatment. Land Contamination & Reclamation 11.2 (2003): 253-258.

Kirby, C. S., Thomas, H. M., Southam, G., & Donald, R. (1999). Relative contributions of abiotic and biological factors in Fe (II) oxidation in mine drainage. Applied Geochemistry, 14(4), 511-530.

Jarvis, A. P., & Younger, P. L. (2001). Passive treatment of ferruginous mine waters using high surface area media. Water research, 35(15), 3643-3648.

PIRAMID Consortium (2003) Engineering Guidelines for the Passive Remediation of Acidic and/or Metalliferous Mine Drainage and Similar Waste Waters, A Research Project of the European Commission 5th Framework Programme.

Sapsford, D., Barnes, A., Dey, M., Williams, K., Jarvis, A., & Younger, P. (2007). Low footprint passive mine water treatment: field demonstration and application. Mine Water and the Environment, 26(4), 243-250.

Sapsford, D. J., & Williams, K. P. (2009). Sizing criteria for a low footprint passive mine water treatment system. Water research, 43(2), 423-432.

Waychunas, G. A., Kim, C. S., & Banfield, J. F. (2005). Nanoparticulate iron oxide minerals in soils and sediments: unique properties and contaminant scavenging mechanisms. Journal of Nanoparticle Research, 7(4-5), 409-433.

Characterization of Passive Treatment System Substrates and Potential for Zinc Recovery

Matthew Bailey, Adam Jarvis and Catherine Gandy
School of Civil Engineering and Geosciences, Newcastle University, United Kingdom

ABSTRACT

Treatment of mine drainage, during operation and following abandonment, can represent a substantial cost to mine operators and governing authorities. Recovery of valuable metals from mine drainage as part of the treatment process may offset costs, yet this is rarely seen in practice. Industrial-scale metal recovery from mine waters are the preserve of active treatment systems, where reactor conditions are carefully controlled to ensure consistent quality of product. In many circumstances passive treatment is the preferred approach, but close process control is not feasible in these systems. Analysis of substrate from a pilot-scale compost-based passive treatment system, which operated for two years, has been conducted. The treatment system, which harnessed bacterial sulfate reduction to remove metals as their sulfides, showed that under UK regulations used substrate was within the worst-case 'hazardous' category due to accumulated zinc, and required pre-treatment due to high total organic carbon. Typical costs for disposal are estimated at 1104 US$/tonne, excluding removal and transport. The majority of zinc accumulates in the upper substrate layer. Greatest zinc concentration of 14,050mg/kg (1.4%w/w) was observed in the 0–230mm depth layer; whereas in the corresponding lower layer, 230–460mm, zinc was 808mg/kg (0.08%w/w). This suggests that selective 'harvesting' of upper substrate layers may reduce waste volumes generated, and higher zinc concentrations may be more amenable to metal recovery. Batch-scale leaching tests have also been undertaken, demonstrating recovery in excess of 83 - 96% of zinc from the upper-layer substrate, depending on acid strength used (20; 100; 500mol/m^3 sulfuric acid), within a 100 hour leach test. The results are discussed in the context of the possible economic benefits of metal recovery for passive treatment systems at larger scale.

INTRODUCTION

Pollution of surface waters by drainage from long abandoned metal mines, often sourced from orphan sites, is extensive in the UK (Mayes, Potter and Jarvis, 2010). A national programme of remediation has recently been embarked upon, funded by the UK Government. The programme has the focus of improving water quality in both an effective and cost efficient way. Recovery of metals may offer a way to both reduce costs of waste disposal, and generate revenue for treatment system operators.

Active mine water treatment systems may be amenable to metal recovery, producing potentially valuable metal ores rather than the comparatively voluminous wastes of passive treatment alternatives (Johnson and Hallberg, 2002; Johnson *et al.*, 2006). However, the capital and operational costs of active treatment are high, and they may be visually intrusive. In many cases in the UK, abandoned metal mines are located within centres of significant heritage and ecological importance, and in areas of high recreational amenity, such as the Lake District National Park. In these settings, passive treatment systems, harnessing natural processes and having a minimal impact upon the landscape, tend to be favoured. For the removal of divalent metals such as zinc, the most prevalent contaminant in UK metal mine waters, bacterial sulfate reduction based systems have been shown to be effective (Gandy and Jarvis, 2012; Jarvis *et al.*, 2013). In 2014 the first large-scale metal mine water treatment system of this type (a Vertical Flow Pond; VFP) was built in the UK (see: Jarvis *et al.*, In press). The compost substrate of such VFPs is the main reactive ingredient, providing the reducing conditions and nutrients required to sustain bacterial communities. Sulfate reducing bacteria provide a critical role within the systems, converting dissolved sulfate to sulfide, which reacts with metal ions to form insoluble metal sulfides. This process has been cited as an important mechanism for metal removal within compost-based treatment systems (Machemer and Wildeman, 1992; Jong and Parry, 2004; Pereyra *et al.*, 2008), although some studies suggest that this is not always the case (Matthies, Aplin and Jarvis, 2010).

While there is a significant body of research into the performance of passive treatment systems, there has been little work considering the character of wastes generated, and their amenability to resource recovery. In a review of resource recovery options for passive treatment systems, Gray, Gandy and Jarvis (2012) suggest that further research should be conducted to characterise wastes from treatment systems, and to investigate processes to recover metals from them. In particular, the use of chemical and biological leaching processes should be considered.

METHODOLOGY

Study site

Mine water treatment trials came to an end at Nenthead in Cumbria, UK, in August 2012 after two years of operation. Here, a flow of circum-neutral mine water with zinc concentrations of 2 – 2.5mg/l was treated within a pilot-scale VFP system, as depicted in Figure 1 (photo taken during spring 2012). The system comprised a tank 2.5m x 1.5m x 1.0m (height) configured so that mine water passed vertically down through a 500mm deep substrate of mixed compost (45% v/v); wood chips (45%v/v); activated sewage sludge (10%). Below the substrate, a 200mm deep layer of limestone gravel facilitated underdraining. The compost substrate was completely submerged in water, with water level controlled by the invert height of the raised outlet pipe.

Sample collection

Compost samples were collected at the time the system was decommissioned in August 2012. Figure 2 shows the sample positions within the treatment tank in plan. The system was uncoupled from the mine water feed and allowed to partially drain, such that substrate samples could be collected from just below the water surface. Compost samples were collected from two layers: upper layer (approximately 0 – 230mm depth below compost surface) and lower layer (approximately 230 – 460mm, the base of the compost), which were denoted with postscripts A and

B. For example, a compost sample from the upper layer at position A2 (Figure 2) would be denoted A2A. Bulk samples were immediately placed into sealed polyethylene bags before being transported to Newcastle University where they were stored at -20°C until analysis.

Figure 1 Nenthead pilot treatment system

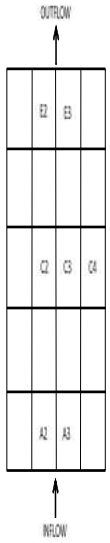

Figure 2 Sample plan of pilot tank

Geochemical analysis of VFP substrate

Relationship between particle size and zinc content

Wet and dry sieving of substrate was conducted on a single sample (C4B), followed by sequential extraction procedures of sieved and bulk samples, in order to determine the relationship between particle size and metal speciation and concentrations. Compost samples were removed from frozen storage and allowed to defrost within their airtight sample bags at room temperature. They were then quartered to obtain suitable subsamples which were oven dried overnight at 105°C, excepting one quartile for wet-sieving. Sieves of 2mm and 212μm were selected, as these provided a relatively even split between particle sizes during preliminary sieving of a test sample. In order to assess the impact of the use of a deionised water flush for wet sieving, compared to dry sieving, the two methods were conducted on quartiles of sample C4B. De-ionised water wash was sampled to determine any solubilised metal. Additional extractions in triplicate were conducted on the remaining two quartiles of the bulk sample in order to test reproducibility of results. Sieved and un-sieved fractions were all ground to less than 212μm and subsampled for sequential extraction. Figure 3 illustrates the quartering and sieving sample preparation procedure.

Spatial distribution of zinc

In addition to determination of the metal distribution in relation to particle size from a single sample location (and the impact of sieving methods on results), investigations were also conducted to assess the spatial variation in metal availability throughout the treatment system. The following twelve samples were investigated from the upper substrate layer: A2A, A3A, C2A, C3A, E2A, E3A; the lower substrate layer: A2B, A3B, C3B, E2B, E3B; plus a blank sample of substrate which had not been exposed to mine water.

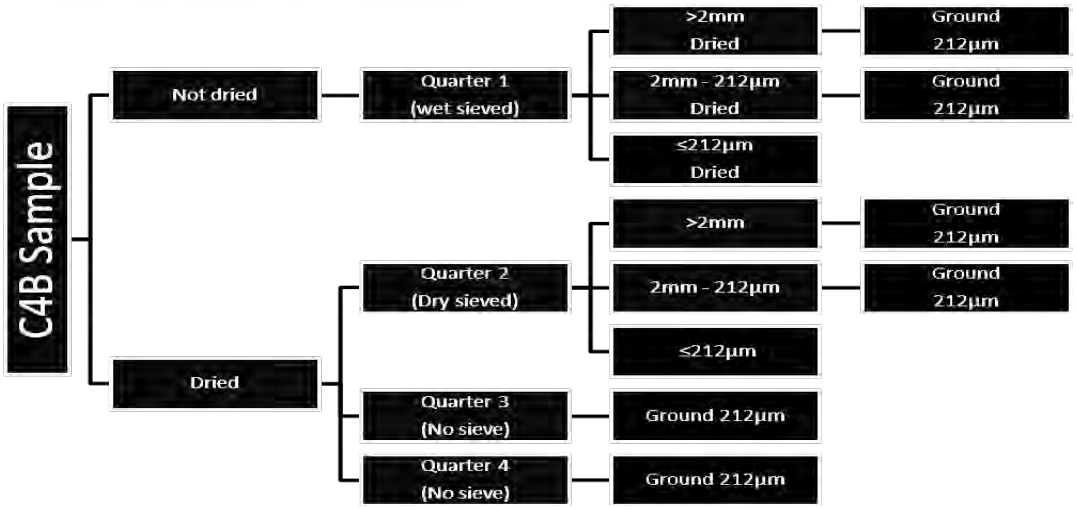

Figure 3 Flow chart showing sieving process

Masses of sieved fractions from sample C4B quartiles were determined and are specified in Table 1.

Table 1 Mass of compost fractions following sieving

Sample	Mass (g)
≤0.212mm dry sieved	1.17
2mm - 0.212mm dry sieved	4.58
>2mm dry sieved	7.04
Dry sieved total	**12.79**
≤0.212mm wet sieved	4.56
2mm - 0.212mm wet sieved	3.05
>2mm wet sieved	5.11
Wet sieved total	**12.72**

Sequential extraction procedure

Sequential extractions using procedures developed by Tessier, Campbell and Bisson (1979) were performed on 1.00g of homogenised sample, sieved to ≤212μm. The method (herein referred to as the 'Tessier' method) consists of five operationally defined extraction steps performed in the following order: 1: Exchangeable; 2: Bound to carbonates; 3: Bound to Fe and Mn oxides; 4: Bound to organic matter and 5: Residual. Solutions were recovered following each step by centrifugation for 30 minutes at 10,000rpm and removed using a glass pipette. Between the five steps, samples were washed with 8ml of deionised water, agitated and separated within the centrifuge for 30 minutes. The wash fluid was then discarded. All reagents were made up either from salts or concentrated solutions, diluted with 18.2MΩ/cm deionised water. Samples from step 1 were acidified with one drop of concentrated nitric acid to preserve metals in solution.

Analysis of extraction solutions was undertaken for iron, zinc, lead, manganese, cadmium, copper, cobalt and nickel in accordance with the Tessier method, although only zinc data are presented here.

Acid leaching of VFP substrate

Substrate used for the acid-leach tests was a composite of the upper layer samples from the treatment system (A2A, A3A, C2A, C3A, E2A, E3A) which were sieved to remove fragments greater than 2mm, and homogenised. Batch leaching tests were conducted over 100 hours at room temperature, with lixiviant sampling and measurements of pH, Eh, conductivity and temperature undertaken intermittently throughout the first day, then daily for the following four days. Lixiviant samples of approximately 10mL were collected and passed through 0.45μm syringe filters to remove any suspended material. Batch cells were operated in duplicate and comprised 2L plastic bottles containing 1.2L of lixiviant and 22.5g of substrate, providing a pulp density close to 2%. This ratio was experimentally determined to be effective by Bayat and Sari (2010) during similar leach-tests. Lixiviants were made up from analytical grade sulfuric acid (H_2SO_4) and distilled water. Compressed air was injected into the pulp continuously at a rate of 1 L/min (±0.07L) in order to maintain oxic conditions, and to promote mixing of substrate and lixiviant. Table 2 shows the starting pH of the various lixiviants.

Table 2 Batch leach test variables

Lixiviant	Distilled water		20 mol/m^3 H_2SO_4		100 mol/m^3 H_2SO_4		500 mol/m^3 H_2SO_4	
Sample	DWa	DWb	0.02Ma	0.02Mb	0.1Ma	0.1Mb	0.5Ma	0.5Mb
pH at start	6.63	6.75	1.99	1.96	1.37	1.35	0.93	0.84

Following completion of the leach tests, residues were collected, dried, subsampled and subjected to an aqua regia digest procedure in order to determine residual metal concentrations. The British Standard method ISO11466:1995 was adopted in duplicate, with addition of extra nitric acid to account for elevated Total Organic Carbon, (TOC) above 20% (BSI, 1995).

Lixiviant samples and aqua regia solutions were analysed for iron, zinc, lead, manganese, cadmium, copper and nickel, although only zinc data are presented.

All experimentation was conducted using laboratory grade reagents and acid washed glassware. Metals analysis was conducted using a Varian Vista MPX Inductively Coupled Plasma Optical Emission Spectrophotometer (ICP-OES),

RESULTS AND DISCUSSION

Zinc is the sole focus of the discussion, as it is both the most significant contaminant metal in the mine water discharge treated, and it is due to zinc that the substrate from the Nenthead pilot system has been classified as Hazardous Waste by independent laboratory testing. Hazardous Waste requires special treatment under UK waste regulations.

Relationship between particle size and zinc content

Figure 4 depicts zinc data from wet sieved and dry sieved fractions of substrate sample C4B. Note that in addition to a breakdown of the five extraction steps, the amount of zinc lost from the wash solution (included in ≤212μm wet sieved fraction) is depicted on this bar as 'Loss in wash'.

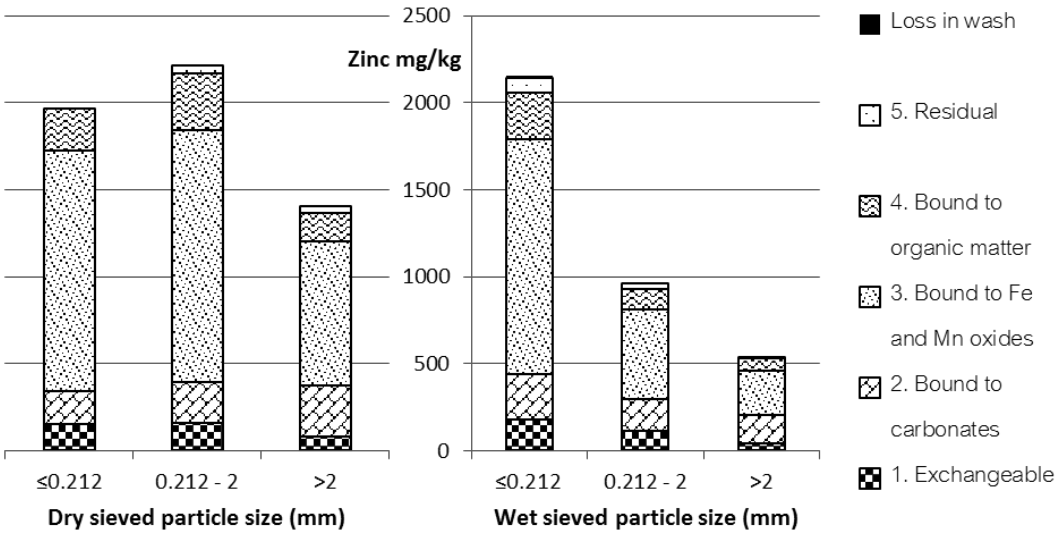

Figure 4 Zinc concentrations in sieved substrate samples

A distinct trend in total metal content was apparent within the wet sieved fraction, with highest zinc concentration in the finest fraction: wet sieved fraction ≤212μm contained 2,158mg/kg of zinc, in contrast to the >2mm fraction that contained just over a quarter of this amount at 541mg/kg. In fact, this trend is apparent for all extraction steps, excepting 2 (bound to carbonates). Dry sieving, however, did not yield such clear results: the ≤212μm fraction contained 2014mg/kg of zinc, in comparison to >2mm which had 1403mg/kg, while the intermediate size fraction contained the greatest amount (2214mg/kg). Such a distinct contrast between sieving methods is thought to be due to the behaviour of materials within the sieves: dry sieved compost, that was pre-dried to remove moisture, was composed of loosely cemented fragments bound to, and together with, fine grained material. Sieving only shows some success in separating these fragments, evidenced in part by the recovery rate of fine grained material (see table 1): just 1.17g passing ≤212μm, compared to 7.04g of material retained on the 2mm sieve. In contrast, 4.56g of material passed the 212μm sieve and 5.11g was retained on the 2mm sieve during the wet sieving operation. From observations during the sieving process, the deionised water wash appeared to aid the separation of compost fragments. It was not unexpected that wet sieving would assist the separation of particles during sieving, but it was recognised that the deionised water wash had the potential to both mobilise weakly-bound metals, and also potentially facilitate geochemical reactions that might alter speciation. Although it was not possible to assess whether metal speciation was influenced by the deionised water, a sample of the deionised water wash solution was analysed by ICP-OES (in parallel with a blank), and revealed that just 13.76mg/kg equivalent of zinc was leached from the compost (see 'Loss in wash' on Figure 4 for relative significance). In order to demonstrate reproducibility of the sequential extraction procedure, triplicate samples were run for the two un-sieved quartiles. Statistically, the standard deviation is less than 7% of the mean for all extraction steps across all sample quartiles, demonstrating good reproducibility.

Spatial distribution of zinc within treatment system

The degree of spatial variation of zinc concentration in the substrate was investigated in a second round of sequential extractions using the methods previously described. Particle size separation was not undertaken as part of these tests, which were conducted to assess the variation (if any) between metal species and their availability throughout different parts of the Nenthead pilot treatment system. Eleven bulk samples in total were analysed, plus a substrate blank. Figure 5 depicts zinc concentrations, and a breakdown of the steps by which they were extracted.

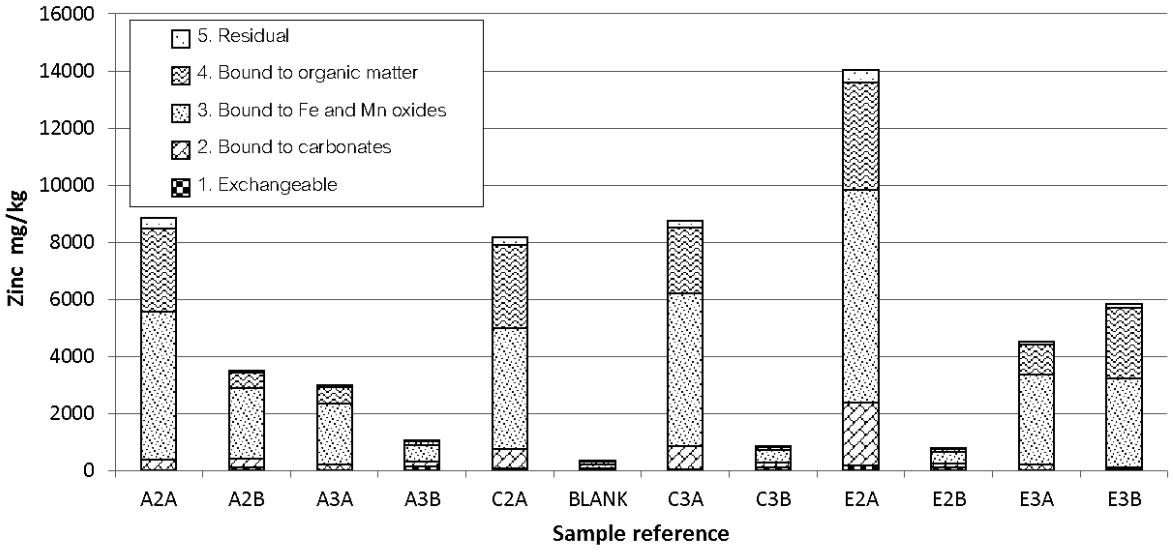

Figure 5 Zinc concentrations from a range of sample locations within the pilot treatment system

In all but one case (samples E3A/B), compost from the upper layer contained substantially more zinc than samples taken from the respective lower layer. Greatest zinc concentration was seen in sample E2A (14,050mg/kg) and the lowest seen in the corresponding lower layer sample (E2B; 808mg/kg). 340mg/kg zinc was measured in the blank substrate. No discernible trend in zinc concentration was evident either laterally or longitudinally.

Exchangeable zinc (step 1) provides perhaps the most pronounced difference between samples, from upper and lower levels, as significant exchangeable zinc is only shown at depth (although it is recognised that this is difficult to see in Figure 5). E3B does not show this clear trend, however this sample was previously identified as a possible outlier. In the upper layer, zinc species are dominated by Fe/Mn oxide and organically bound fractions (steps 3 and 4), with very small concentrations of exchangeable zinc and zinc bound to carbonates (steps 1 and 2 respectively). Residual zinc comprises a small fraction throughout, up to 5% in E2B; whereas most zinc is recovered during step 3: all in excess of 50%, other than C3B where 49% was extracted. Data for the 'blank' sample showed a similar pattern: almost half (46%) zinc was attributed to the Fe/Mn oxide fraction, with significant amounts of zinc extracted during step 2 and 4, and a lesser amount (5%) associated with step 1. Residual zinc in the blank was 8%, which in percentage terms was greater than all residual fractions in the samples from the treatment tank, but was less in absolute terms than all other compost samples. Several samples (A2A, C2A, E2A) had in excess of ten times the absolute amount of residual zinc, compared to the blank. Percentage residual zinc for these samples was 4%; 4% and 3%, respectively for A2A; C2A and E2A.

Neculita, Zagury and Bussière (2008) presented data from extractions using a modified Tessier method on compost from laboratory scale column based bioreactors. Mine water chemistry, treatment configuration and scale all differ from the work conducted here, however some general comments can be made on how both sequential extraction data compare. Samples were taken from both the top and the base of the column – analogous in some ways to the sampling of top and bottom layers of the Nenthead tank. Neculita, Zagury and Bussière (2008) found that, with duplicate columns treating mine water for a 7.3 day residence time, the greatest zinc fraction (37 – 50%) was associated with step 3, comparable with Nenthead data. In contrast, substantial zinc concentrations were associated with steps 4 and 5: specifically 4 in the top layers (36 – 46%) and 5 in the lower (28 – 36%) (Neculita, Zagury and Bussière, 2008). What is of significance is that substantial amounts of zinc appear more tightly bound in the 2008 study compared to Nenthead data, specifically at depth. Furthermore, while data from the Nenthead tank showed typically very low exchangeable zinc (step 1) in the surface layer, Neculita, Zagury and Bussière (2008) found that

this was where most exchangeable zinc occurred (8 – 12%). A second duplicate set of columns were investigated, with an increased hydraulic residence time of 10 days. These columns yielded similar results, though there was a slight increase in residual zinc in the bottom layers of the columns: 33 - 41%. The other trend of interest in relation to data from the study of Neculita, Zagury and Bussière (2008) is the higher proportion of exchangeable zinc being identified in the upper part of the column, rather than the bottom in the case of the Nenthead data. It is not clear what this could be attributed to, and the comparison is limited due to modifications of the Tessier method made by Neculita, Zagury and Bussière (2008).

Acid leaching of VFP substrate

Zinc recovery from the substrate is presented in Figure 6, which shows both zinc concentration in the leachate and zinc concentration in substrate residues, determined by aqua-regia digestion. Extraction was shown to be effective with moderately weak strength acids, with extraction efficiencies of over 80% in all acid-leach tests after 100 hours. Zinc recovery of 93.9% and 95.1% was achieved with 100mol/m^3 sulfuric acid, whereas the most concentrated acid (500mol/m^3) achieved extraction efficiencies of 95.1% and 96.0%. There appears to be only a marginal gain in efficiency for a fivefold increase in acid concentration. It is considered that under the conditions of these batch tests, the 100mol/m^3 acid represents the optimum balance between concentration and extraction efficiency.

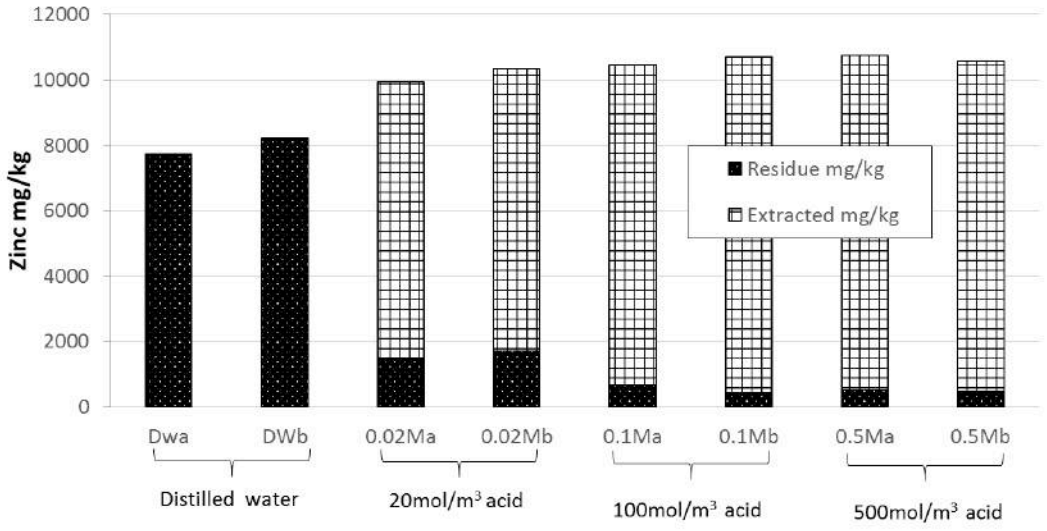

Figure 6 Zinc concentrations from leachate and residue after batch leaching

Batch leach data for zinc show good replication between duplicate columns; less than ±5% variation for all four experimental pairs, and less than ±2.5% variation between the sulphuric acid duplicates. Aqua regia digest duplicates were within 5% for distilled water blank samples and 500mol/m^3 acid, but duplicates for 20mol/m^3 and 100mol/m^3 had 7% and 20% discrepancies, respectively. This is perhaps attributable to heterogeneity of sample residues exposed to aqua regia.

CONCLUSIONS

Geochemical analysis was undertaken on substrate taken from a pilot-scale mine water treatment system following sieving by both wet and dry methods. Samples were also collected and analysed from 11 different positions within the treatment system. In addition, batch-leach tests were conducted on a composite substrate sample, to determine extraction efficiencies for a range of sulphuric acid concentrations.

Wet sieving suggested that substantially more zinc was associated with the fine grained fraction of substrate (≤212μm fraction). This trend was not seen in the dry sieved sample analyses, and these results may have been affected by cementing of substrate fragments during drying. Significantly more zinc was found in the upper layer of the substrate than at depth within the treatment tank. Moreover, zinc in the surface layer was more tightly bound, whereas some zinc at depth was recoverable by ion exchange. Sequential extractions to the Tessier method suggest that in both substrate layers, most zinc is bound with moderate strength and associated with Fe/Mn oxides; however, it should be noted that sample preparation and exposure to oxygen may have influenced speciation (Rapin *et al.*, 1986). Leach tests demonstrated that dilute sulfuric acid was effective at removing zinc from the compost substrate, with 100mol/m^3 providing the optimum balance between concentration and extraction performance. Further experimentation to test the absolute capacity of the acid for metal recovery is planned, in order to assess the feasibility of large-scale metal recovery operations (i.e. how much metal could be solubilised for a given acid volume).

Data presented in this paper indicate that zinc-laden mine water treatment substrates may be de-contaminated by: a. separation on the basis of particle size, and b. leaching with dilute acids. Additionally, spatial sampling identified that metals accumulated more rapidly within the surface layers of the treatment system, which may facilitate selective recovery: it may be that periodic removal and replenishment of surface substrate layers may offer a means of effectively extending the life of a given system, as suggested in a review by Gray, Gandy and Jarvis (2012). These processes may offer mechanisms of decreasing whole-life costs by extending system lifetimes, reducing waste and recovering metals. Further research is required to consider the practicalities and costs of substrate decontamination at a large scale, and options for concentrating metals within lower-volume materials to levels at which they might have a commercial value.

ACKNOWLEDGEMENTS

M T Bailey's PhD research is funded by the UK Coal Authority. The original Nenthead pilot-scale treatment system research was funded by the UK Government Department for Environment, Food and Rural Affairs and the Environment Agency (Project No.: SC090024/1). Technical assistance and advice in the lab and field was gratefully received from Jane Davis and Patrick Orme at Newcastle University, UK.

REFERENCES

Bayat, B. and Sari, B. (2010) 'Comparative evaluation of microbial and chemical leaching processes for heavy metal removal from dewatered metal plating sludge', *Journal of Hazardous Materials*, 174(1-3), pp. 763-769.

BSI (1995) 'Soil Quality, Part 3, Chemical Methods' *Section 3.9: Extraction of trace elements soluble in aqua regia*. International Organization for Standardization.

Gandy, C. and Jarvis, A. (2012) 'The Influence of Engineering Scale and Environmental Conditions on the Performance of Compost Bioreactors for the Remediation of Zinc in Mine Water Discharges', *Mine Water and the Environment*, 31(2), pp. 82-91.

Gray, N.D., Gandy, C.J. and Jarvis, A.P. (2012) 'Mitigation of pollution from abandoned metal mines. Part 2, Review of resource recovery options from the passive remediation of metal rich mine waters', *Environment Agency Publication, Project SC090024/1*.

Jarvis, A.P., Gandy, C.J., Bailey, M.T., Davis, J.E. and Orme, P.H.A. (In press) *Proceedings of the 10th International Conference on Acid Rock Drainage*. Santiago, Chile.

Jarvis, A.P., Gray, N.D., Davis, J., Gandy, C.J. and Orme, P.H.A. (2013) 'Mitigation of pollution from abandoned metal mines: Investigation of passive compost bioreactor systems for treatment of abandoned metal mine discharges', *Environment Agency Publication, Project SC090024/1*.

Johnson, D.B. and Hallberg, K. (2002) 'Pitfalls of passive mine water treatment', *Reviews in Environmental Science and Biotechnology*, 1(4), pp. 335-343.

Johnson, D.B., Sen, A.M., Kimura, S., Rowe, O.F. and Hallberg, K.B. (2006) 'Novel biosulfidogenic system for selective recovery of metals from acidic leach liquors and waste streams', *Mineral Processing and Extractive Metallurgy*, 115(1), pp. 19-24.

Jong, T. and Parry, D.L. (2004) 'Heavy metal speciation in solid-phase materials from a bacterial sulfate reducing bioreactor using sequential extraction procedure combined with acid volatile sulfide analysis', *Journal of environmental monitoring : JEM*, 6(4), pp. 278-285.

Machemer, S.D. and Wildeman, T.R. (1992) 'Adsorption compared with sulfide precipitation as metal removal processes from acid mine drainage in a constructed wetland', *Journal of Contaminant Hydrology*, 9(1–2), pp. 115-131.

Matthies, R., Aplin, A.C. and Jarvis, A.P. (2010) 'Performance of a passive treatment system for net-acidic coal mine drainage over five years of operation', *Science of the Total Environment*, 408(20), pp. 4877-4885.

Mayes, W.M., Potter, H.A.B. and Jarvis, A.P. (2010) 'Inventory of aquatic contaminant flux arising from historical metal mining in England and Wales', *Science of the Total Environment*, 408(17), pp. 3576-3583.

Neculita, C.-M., Zagury, G.J. and Bussière, B. (2008) 'Effectiveness of sulfate-reducing passive bioreactors for treating highly contaminated acid mine drainage: II. Metal removal mechanisms and potential mobility', *Applied Geochemistry*, 23(12), pp. 3545-3560.

Pereyra, L.P., Hiibel, S.R., Pruden, A. and Reardon, K.F. (2008) 'Comparison of microbial community composition and activity in sulfate-reducing batch systems remediating mine drainage', *Biotechnology and Bioengineering*, 101(4), pp. 702-713.

Rapin, F., Tessier, A., Campbell, P.G.C. and Carignan, R. (1986) 'Potential artifacts in the determination of metal partitioning in sediments by a sequential extraction procedure', *Environmental Science & Technology*, 20(8), pp. 836-840.

Tessier, A., Campbell, P.G.C. and Bisson, M. (1979) 'Sequential extraction procedure for the speciation of particulate trace metals', *Analytical Chemistry*, 51(7), pp. 844-851.

Metal Removal and Secondary Contamination in a Passive Metal Mine Drainage Treatment System

Adam Jarvis[1], Catherine Gandy[1], Matthew Bailey[1], Jane Davis[1], Patrick Orme[1], John Malley[2], Hugh Potter[3] and Arabella Moorhouse[4]

1. *School of Civil Engineering & Geosciences, Newcastle University, United Kingdom*
2. *National Trust, United Kingdom*
3. *National Land & Water Quality, Environment Agency, United Kingdom*
4. *The Environment Department, The Coal Authority, United Kingdom*

ABSTRACT

In March 2014, the UK's first full-scale passive treatment system for metal mine drainage was commissioned. The treatment system harnesses bacterial sulfate reduction (BSR) to immobilise the main contaminant metal, zinc, within the compost substrate of two parallel 'Vertical Flow Ponds' (VFPs), each of which has a treatment area of approximately 800 m^2. The final discharge from the treatment system enters a nutrient-sensitive upland river. Appropriate infrastructure was designed and installed to enable close control and monitoring of flow-rate and water quality. Such features include open channel flow with sharp-crested weirs for flow measurement, and an innovative penstock arrangement for fine adjustment of flow into the VFPs.

Effluent quality from the treatment system has evolved during early operation. Over the first 3 months of operation mean influent zinc concentration was 3.74 mg/L compared to 0.12 mg/L in the effluent (mean zinc removal of 97%; n = 15). Strongly reducing conditions are evident, with sharp decreases in sulfate concentration between influent (mean of 31.7 mg/L) and effluent (< 10 mg/L within approximately 2 months of commissioning) suggesting that BSR is an important metal attenuation mechanism. However, water first emerging from the VFPs had up to 82 mg/L ammonium, Biochemical Oxygen Demand (BOD) of up to 100 mg/L, and Chemical Oxygen Demand (COD) of up to 3084 mg/L, resulting in secondary contamination of the receiving watercourse. The issue was short-lived, with organics concentrations decreasing sharply. Within 4 months of commissioning the system the river was back to acceptable standards with respect to ammonium, BOD and COD concentrations. In this instance there were no downstream water users impacted by the secondary contamination. In other settings, mitigation measures may be required to address such issues during early operation of passive mine drainage treatment units of this type.

Keywords: passive treatment, secondary contamination, zinc, compost

INTRODUCTION

In March 2014 the UK's first full-scale passive treatment system for metal mine drainage treatment was commissioned, and at the time of writing has been operational for 6 months. The treatment system is located at the abandoned Force Crag mine in the Lake District National Park, north west England. The mine site lies at an elevation of 275 m.a.s.l. (above sea level), though the abandoned mine workings extend west by a horizontal distance of approximately 1 km, to an elevation of 600 m a.s.l. The mine operated intermittently for 157 years, but was finally abandoned in 1992 following a collapse in the lower workings. The mine is hosted in Ordovician-aged mudstone and lithic-wacke sediments (Kirk Stile Formation) (Barnes *et al.*, 2006). The vein-hosted mineralization present at Force Crag is dominated by galena (lead-ore) and sphalerite (zinc-ore) with barite and quartz gangue (Tyler, 2005). A series of nine individual levels form the workings at Force Crag, with Level 0 being the lowest level. Two adits currently drain the workings at Force Crag, namely Level 1 (the primary discharge) and Level 0.

Despite the occurrence of diffuse mining pollution, originating from the processing and mining waste located at the site, long-term monitoring demonstrated that the Level 1 discharge was the main point source of metal contamination to the receiving waters at Force Crag. Pollution from the mine site enters the Coledale Beck. Whilst the Coledale Beck is contaminated with metals due to both point and diffuse source pollution from the mine site, it is also a nutrient sensitive stream, with very low concentrations of both nutrients and organic compounds.

Table 1 illustrates that the main source of metals pollution to the Coledale Beck, the Level 1 discharge, is circum-neutral drainage (pH 5.6 – 7.7). The discharge is poorly mineralized, with low concentrations of all major ions, including sulfate, which has a concentration in the range 16.0 – 39.5 mg/L. The main metal of concern is zinc, which is present at concentrations in the range 1 730 – 4 660 μg/L. This concentration of zinc, and also the pH of the discharge, is typical of many discharges around England and Wales. The Level 1 discharge has a variable flow-rate (8.5 – 24.4 L/s) which is influenced by rainfall events (there is a clear inverse correlation between flow-rate and zinc concentration, indicating a dilution effect).

The installation of a treatment system for the Level 1 discharge was an initiative of the UK Coal Authority, the Environment Agency for England and Wales, the National Trust (the site owner) and Newcastle University. The treatment system was funded by the UK Department for Environment Food and Rural Affairs (Defra).

In this paper we discuss the design and early performance of the treatment system. However, whilst the main concern in relation to treatment performance is typically metal removal, an important consideration at the Force Crag site was the possibility of secondary contamination due to organic substances leached from the treatment media (see below). Therefore this paper focuses also on the evolution of treatment system effluent quality with respect to some of the more important organic constituents.

TREATMENT SYSTEM DESIGN AND LAYOUT

The passive treatment system at Force Crag is a downwards flow compost bioreactor, or Vertical Flow Pond (VFP). The treatment principle is to harness bacterial sulfate reduction (BSR) to attenuate divalent metals (Zn in particular) within the compost as their sulfides, as shown in Reactions (1) and (2).

$$2CH_2O + SO_4^{2-} \rightarrow H_2S + 2HCO_3^- \quad (1)$$

$$H_2S + Zn^{2+} + 2HCO_3^- \rightarrow ZnS(s) + 2H_2O + 2CO_2 \quad (2)$$

This is a widely reported approach to passive mine water treatment (e.g. Mayes et al., 2011; Neculita et al., 2007; Sheoran and Sheoran, 2010). However, a key issue in the UK is to keep

absolute system size to a minimum due to land constraints at many of the upland sites at which metal mine water discharges occur. On the basis of lab-scale (Mayes et al., 2011) and pilot-scale experiments (Gandy and Jarvis, 2012) the VFP units at Force Crag were therefore designed to have a hydraulic residence time of 15 – 20 hours, which is substantially shorter than typical designs.

As shown in Figure 1, the treatment system comprises two VFPs operating in parallel. Each VFP is lined with HDPE to prevent leakage. At the base of each VFP is a perforated pipe network. There are 4 separate perforated pipe networks in each VFP, each covering an equal area of the base of each VFP. There are also therefore 4 effluents from each VFP. Each pipe passes through the HDPE liner to a manhole chamber, where the pipes are raised to ensure that there is a 350 mm water cover over the compost substrate i.e. water level in the VFPs is controlled by the invert level of the effluent pipes in the manhole chambers. The pipe networks are overlain by a 200 mm layer of carboniferous limestone. Over the limestone is a 500 mm layer of compost substrate, which comprises 45% v/v PAS100 compost (see below), 45% v/v woodchips, and 10% v/v dried activated sewage sludge from a local municipal wastewater treatment plant. For this treatment system the limestone was used purely for the purposes of maintaining good permeability around the perforated pipe network, rather than being a requirement for generating alkalinity and elevating pH. BSI PAS100 compost meets certain agreed standards with respect to safety (British Standards Institute, 2011), and was therefore selected given that water draining through it would be entering a watercourse. The composition of the treatment media was based on successful pilot-scale trials reported by Gandy and Jarvis (2012).

Each VFP has a treatment substrate area of 760 m^2, and the volume of substrate in each VFP is 400 m^3 (each VFP is a trapezoidal basin, with internal slopes of 1:2.5). This volume of substrate was based on a design flow-rate of 6 L/s (3 L/s to each VFP, to give hydraulic residence time of 15 – 20 hours in each VFP). It will be apparent from the range of flow-rate for the Level 1 discharge (Table 1) that not all of the Level 1 discharge is treated by the system. This was due primarily to land constraints. As shown in Figure 1, excess water therefore discharges to the Coledale Beck untreated. However, during low flow conditions in the Coledale Beck, when the impact of the Level 1 discharge was historically greatest, the Level 1 flow-rate is typically at the lower end of the range reported in Table 1, and therefore the majority of the water is treated under such conditions.

Effluent from both VFPs drains to a small aerobic wetland, from where it is discharged back to the Coledale Beck (Figure 1).

Table 1 Summary water quality data for the Level 1 mine water discharge from the Force Crag mine, 2011 to 2014 (unpublished data of Environment Agency and Newcastle University)

Variable	Range	Mean	n[A]
Flow (L/s)	8.5 – 24.4	14.8	21
pH	5.6 – 7.7	6.8	25
HCO_3^- (mg/L)	8.5 – 26.8	16.7	28
Cl (mg/L)	4.7 – 7.6	5.7	28
SO_4 (mg/L)	16.0 – 39.5	26.6	28
Ca (mg/L)	5.1 – 14.5	9.5	28
Mg (mg/L)	1.95 – 5.00	3.30	28
Na (mg/L)	2.40 – 3.60	2.95	28
K (mg/L)	0.32 – 0.62	0.46	28[C]
Fe (mg/L)	0.26 – 1.08	0.52	28
Mn (mg/L)	0.29 – 0.76	0.51	28
Al (mg/L)	0.05 – 0.20	0.08	28
Zn (total) (μg/L)	1 730 – 4 660	2 997	28
Zn (filt.) (μg/L)[B]	1 710 – 4 550	2 950	28
Pb (μg/L)	25.0 – 87.9	43.6	28[D]
Cu (μg/L)	1.80 – 8.57	5.11	28[E]
Cd (μg/L)	5.00 – 20.00	14.24	28[F]
Ni (μg/L)	10.00 – 20.00	16.09	28

[A] number of samples
[B] Concentrations reported are after filtering through 0.45 μm filter

[C] 5 samples measured by ICP-OES below detection of 1.00 mg/L; value of 0.50 mg/L used for calculation of summary statistics
[D] 6 samples measured by ICP-OES below detection of 50 μg/L; value of 25 μg/L used for calculation of summary statistics
[E] 13 samples measured by ICP-OES below detection of 10 μg/L; value of 5 μg/L used for calculation of summary statistics
[F] 2 samples measured by ICP-OES below detection of 10 μg/L; value of 5 μg/L used for calculation of summary statistics

METHODS

Since commissioning of the treatment system flow and water quality monitoring has typically been undertaken on a weekly basis (fortnightly occasionally). The primary objective of monitoring has been to evaluate (a) the performance of the VFP system for Zn removal and (b) the improvement and / or impact of the treatment system effluent on the Coledale Beck downstream.

Flow-rate is measured via sharp-crested 20° V-notch weirs located at the influent of the system and the final effluent from the treatment system (at the effluent from the effluent from the aerobic wetland; see Figure 1). Flow-rate from the effluent pipes from the VFPs is measured by bucket-and-stopwatch (mean value of 3 measurements for each effluent pipe). Flow-rate in the Coledale Beck is measured with a flat V weir installed and operated by the England and Wales Environment Agency.

Because a primary objective of the Force Crag treatment system is to gain an improved understanding of the rate of removal of metals in the system, having the facility to accurately control flow-rate to the treatment units was a key consideration. For this system, a novel downwards-opening penstock arrangement was designed i.e. water is allowed to escape over the top of the penstock. Adjustment of the penstocks (one for each VFP) upwards or downwards controls water level in an open channel that is hydraulically connected to the penstock chamber. At the end of each channel is a sharp-crested 20° V-notch weir. Adjustment of the penstocks therefore controls depth of water over the V-notch weirs, and hence the flow-rate to the VFPs. This open channel arrangement is preferable to a system of pipes and valves, as the latter are prone to clogging where iron concentrations are even slightly elevated (Table 1).

Water quality samples are routinely collected and analysed by Newcastle University. Sampling and analysis is undertaken in strict accordance with methods documented in APHA (2005). Blanks and standards are run routinely, and triplicate samples are collected for analysis periodically.

There are 4 individual effluents from each of the VFPs. To evaluate overall performance of each VFP a composite sample is taken, as well as individual samples from each effluent pipe. The composite sample is made up of a volume of water from each individual pipe that is proportional to its contribution to the overall effluent flow-rate. For brevity, only composite analysis results are reported here.

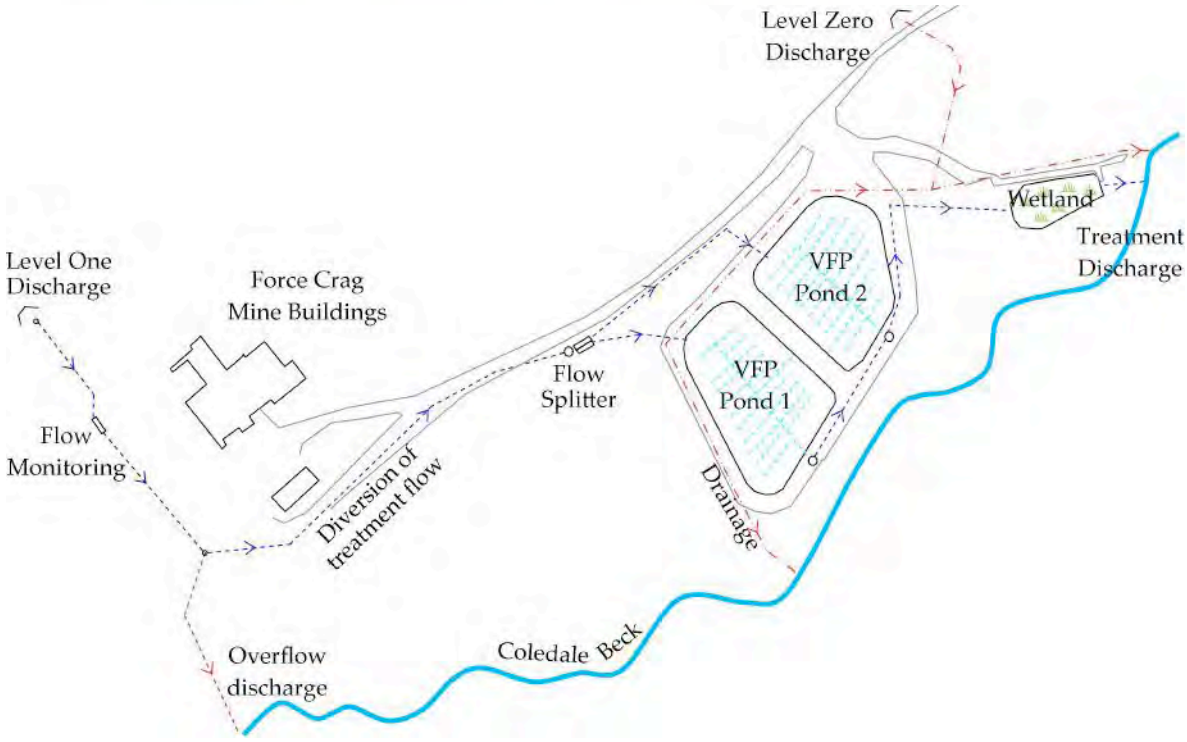

Figure 1 Layout of the Force Crag VFP passive treatment system (figure courtesy of the Coal Authority)

RESULTS AND DISCUSSION

Zinc removal

Figure 2 shows Zn removal by the treatment system for the first 6 months of its operation. Mean Zn removal efficiencies for VFP 1 and VFP 2 were 98.7% and 94.1% respectively for the period from 1 April 2014 to 23 September 2014. Overall treatment efficiency (Final effluent in Figure 2) was 96.8%. Sorption reactions, and precipitation of zinc as phases other than its sulfide, have been noted as possible sinks for zinc in previous investigations (e.g. Gibert et al., 2005; Neculita et al., 2008). At the Force Crag system it is too early to undertake detailed analyses of solid phases in the compost substrate. However, after elevated sulfate concentrations in the effluent waters for the first week of operation, sulfate concentrations decreased substantially between influent and effluent. Mean influent sulfate concentration to VFP 1 and VFP 2 was 30.4 mg/L (range: 19.3 – 38.2 mg/L) for the first 6 months of operation, whilst mean effluent concentrations were 10.1 mg/L for VFP1 (range: 0.4 – 27.8 mg/L) and 8.1 mg/L for VFP 2 (range 0.8 – 23.2 mg/L). Strong odours of hydrogen sulfide are also evident in the vicinity of the effluent manhole chambers.

Both total and filtered samples (0.45 μm) are collected for zinc analysis, and since June 2014 aliquots of both influent and VFP effluent waters have also been filtered through a 0.10 μm filter. For both VFPs, effluent filtered zinc concentrations were lower than effluent total zinc concentrations. For VFP 2 (which performed slightly less well than VFP 1), these data are illustrated in Figure 3. 0.45 μm filtered Zn concentration was, on average, 35.8% lower than total effluent concentration. 0.10 μm filtered Zn concentration was consistently below the 0.010 mg/L detection limit of the ICP-OES used for analysis (and are therefore shown as half this value – 0.005 mg/L – on Figure 3). The pattern was the same for VFP 1. This suggests that the zinc present in the VFP effluent waters is in colloidal phase. Future analyses will be undertaken to establish whether the colloidal zinc is sulfide or some other solid phase, with a view to investigating possible improvements to final water quality via additional treatment.

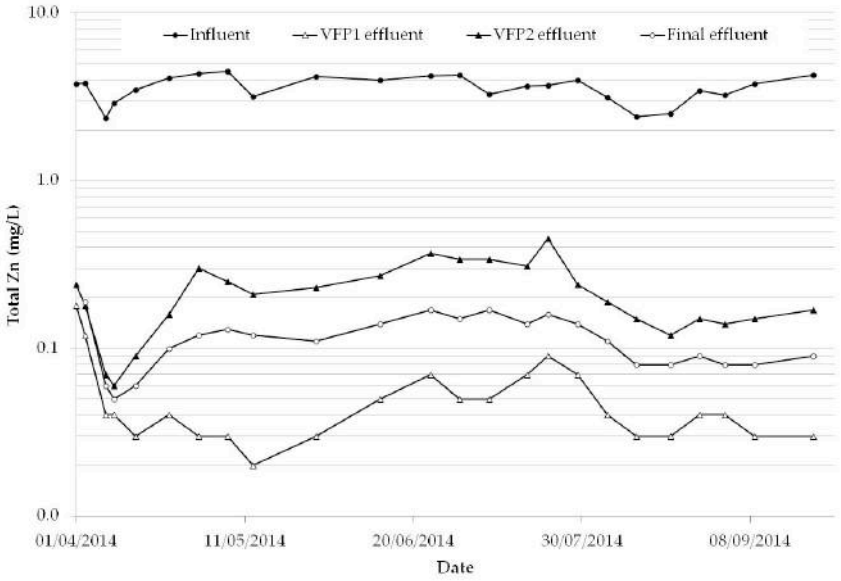

Figure 2 Zn removal at the Force Crag treatment system for the first 6 months of operation

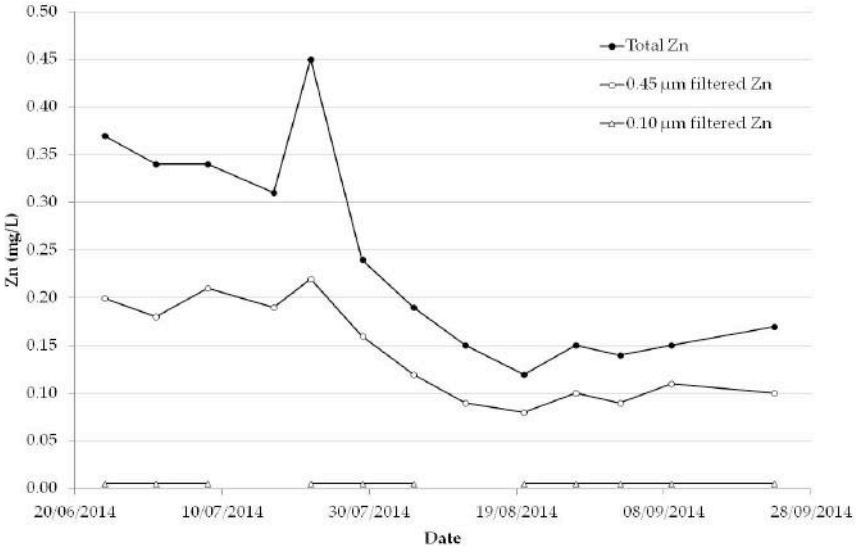

Figure 3 Differences in VFP 2 effluent total zinc concentration and effluent 0.45 μm and 0.10 μm filtered concentrations

Secondary contamination

The potential for secondary contamination from passive mine water treatment systems is rarely considered. As noted previously, the Coledale Beck is a nutrient-poor watercourse, with very limited organic enrichment. Concentrations of Biochemical Oxygen Demand (BOD), Chemical Oxygen Demand (COD), ammonium, nitrate and phosphate were therefore determined as part of the monitoring program for the Force Crag treatment system. A specific requirement of the

environmental regulator, the Environment Agency, was that ammonium concentrations in the Coledale Beck should not exceed 0.2 mg/L on a long-term basis.

Concentrations of BOD, COD, ammonium and nutrients, for both the Level 1 discharge itself, and the Coledale Beck upstream of the treatment system, are shown in Table 2, and illustrate the low concentrations in both. Effluent water from the treatment system was initially monitored twice weekly following commissioning. Final effluent nutrient concentrations, BOD, COD and ammonium are shown in Figure 4. Concentrations for the same variables for the Coledale Beck downstream of the treatment system are shown in Figure 5 (nitrate concentration is not shown in Figures 4 and 5 as it was consistently < 0.2 mg/L in the treatment system effluent).

Table 2 Nutrient and organic concentrations in the Level 1 discharge and Coledale Beck upstream of the treatment system (all concentrations in mg/L; range shown where relevant; n = 9)

Variable	Level 1 discharge	Coledale Beck upstream of treatment system
COD	< 1.0	< 1.0
BOD	< 1.0	< 1.0
NH_4	< 0.01	< 0.01
NO_3	< 0.2 – 0.3	< 0.2 – 0.8
PO_4	< 0.2 – 5.9	< 0.2 – 3.4

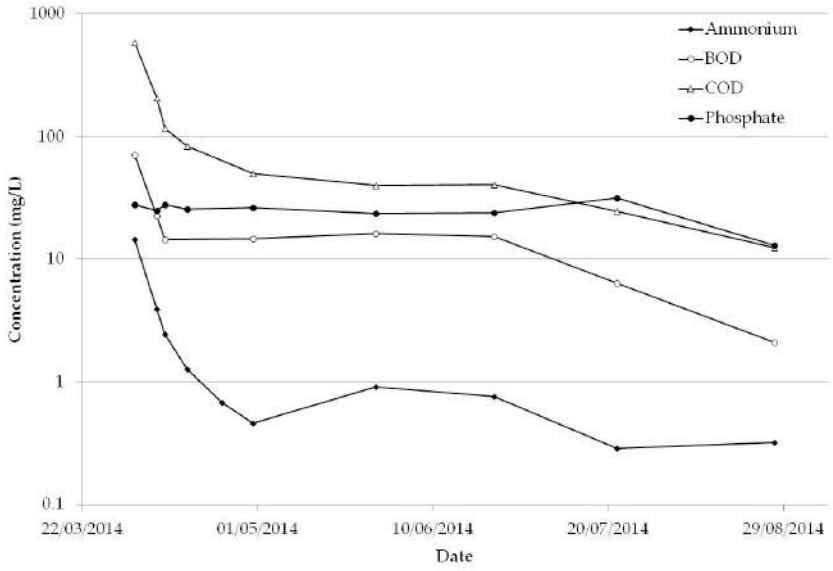

Figure 4 Concentrations of BOD, COD, NH4 and PO4 in the final effluent from the treatment system following commissioning in March 2014

There was a clear pattern of elevated concentrations of BOD, COD, PO_4 and NH_4 in the effluent water (Figure 4) compared to the Coledale Beck and Level 1 discharge (Table 2). In the final effluent water to the Coledale Beck initial concentrations of BOD, COD, PO_4 and NH_4 were 71 mg/L, 587 mg/L, 28 mg/L and 14.6 mg/L respectively. In the effluent directly from the VFPs concentrations were much higher: 82 mg/L NH_4, BOD of up to 100 mg/L, and COD of up to 3084 mg/L. However, these concentrations have dropped rapidly since water first emerged from the treatment system. These elevated concentrations were also reflected in the Coledale Beck downstream from the treatment system effluent (Figure 5), albeit absolute concentrations were lower due to dilution effects. Figure 4 illustrates that BOD, COD and NH_4 dropped rapidly within 5 – 10 days of commissioning, suggesting a 'flushing' effect through the compost substrate. NH_4

concentration in the Coledale Beck was also below the 0.2 mg/L value requested by the Environment Agency within 5 – 10 days.

The exception to this trend of rapidly decreasing concentrations was PO_4, which remained elevated in the effluent from the treatment system (Figure 4). Over the 6 month monitoring period, the mean PO_4 concentration was 4.3 mg/L in the Coledale Beck downstream of the treatment system effluent, compared to a mean of 1.8 mg/L upstream of the treatment system. The treatment system substrate therefore continues to act as a source of phosphate to the Coledale Beck. The downstream monitoring location on the Coledale Beck is only 70 m downstream from the final treatment system effluent point (this is below the mixing zone of treatment system effluent with the Coledale Beck). Additional dilution further downstream likely results in a decrease in PO_4 concentrations, and therefore in this instance the impact of elevated PO_4 is probably spatially limited. Nevertheless, the potential for elevated concentrations of nutrients, BOD, COD and NH_4 is an important consideration in the planning of passive, compost-based, treatment systems, especially where final discharge is to sensitive watercourses.

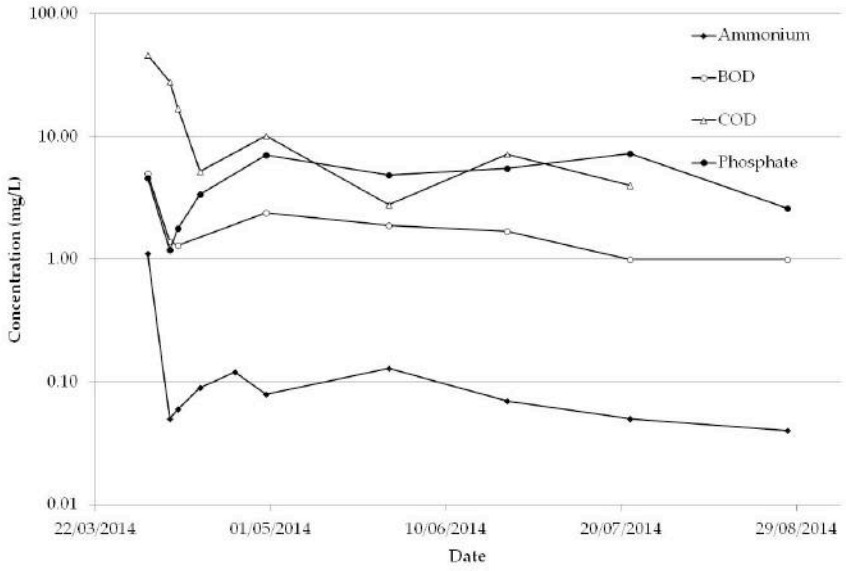

Figure 5 Concentrations of BOD, COD, NH4 and PO4 in the Coledale Beck downstream of the treatment system following commissioning in March 2014

CONCLUSIONS

The Force Crag mine water treatment system is the first full-scale passive treatment scheme for metal mine drainage in the UK. The system comprises two parallel Vertical Flow Ponds, which contain a compost substrate to encourage attenuation of zinc via bacterial sulfate reduction. The VFPs have a short hydraulic residence time for units of this type: 15 – 20 hours. For the first 6 months of operation the two VFPs consistently removed in excess of 90% of the zinc from the Level 1 discharge water at Force Crag, and overall treatment efficiency of the system for zinc removal was greater than 95%. Sulfate concentrations have consistently decreased across the treatment system, suggesting that bacterial sulfate reduction was an important attenuation mechanism. However, solid phase analyses of the compost substrate need to be undertaken to confirm this.

Over the first 6 months of operation secondary contamination was a concern. Concentrations of BOD, COD, NH_4, and PO_4 were initially elevated in the effluent water from the system, but rapidly decreased in all cases with the exception of PO_4. In the case of Force Crag, there are no downstream water users that could have been affected by these elevated concentrations, but in other situations measures may need to be put in place to deal with elevated organics / nutrients concentrations

from passive mine water treatment systems, especially if there are abstractions in close proximity to the effluent point from the treatment system.

ACKNOWLEDGEMENTS

The Force Crag treatment system was funded by the UK Department for Environment Food and Rural Affairs (Defra), and was an initiative of a partnership comprising the UK Coal Authority, Environment Agency, National Trust and Newcastle University. Construction of the system was managed by the Coal Authority. The consulting firm Atkins undertook the civil engineering design of the scheme, and the construction contractor was Bentleys. The views expressed in this paper are those of the authors only, and not necessarily any of the organizations mentioned herein.

REFERENCES

APHA. (2005) Standard Methods for the Examination of Water and Wastewater, 21st Edition. American Public Health Association, American Water Works Association and the Water Environment Federation: Washington, DC.

Barnes, R.P, Brenchley, P. J., Stone, P. and Woodcock, N.H. (2006). The Lakesman Terrane: the Lower Palaeozoic record of the deep marine Lakesman Basin, a volcanic arc and foreland basin. In: The Geology of England and Wales, 2nd Edition, P. J. Brenchley, and P. F. Rawson (Eds.), London, The Geological Society of London, pp 103-129.

British Standards Institution (2011) PAS 100: 2011 Specification for composted materials. ISBN 978 0 580 65307 0.

Gandy, C.J., Jarvis, A.P. (2012) The influence of engineering scale and environmental conditions on the performance of compost bioreactors for the remediation of zinc in mine water discharges. Mine Water and the Environment. 31, 82-91.

Gibert, O.; Pablo, J. de; Cortina, J.L.; Ayora, C. (2005) Municipal compost-based mixture for acid mine drainage bioremediation: Metal retention mechanisms. Applied Geochemistry. 20, 1648-1657.

Mayes, W.M., Davis, J., Silva, V., Jarvis, A.P. (2011) Treatment of zinc-rich acid mine water in low residence time bioreactors incorporating waste shells and methanol dosing. Journal of Hazardous Materials. 193, 279-287.

Neculita, C.-M.; Zagury, G.J.; Bussière, B. (2008) Effectiveness of sulfate-reducing passive bioreactors for treating highly contaminated acid mine drainage: II. Metal removal mechanisms and potential mobility. Applied Geochemistry. 23, 3545-3560.

Neculita, C-M.; Zagury, G.J., Bussière, B. (2007) Passive treatment of acid mine drainage in bioreactors using sulfate-reducing bacteria: Critical review and research needs. Journal of Environmental Quality. 36, 1-16.

Sheoran, A.S., Sheoran, V., Choudhary, R.P. (2010) Bioremediation of acid-rock drainage by sulfate-reducing prokaryotes: A review. Minerals Engineering. 23, 1073-1100.

Tyler, I. (2005). Force Crag: The history of a Lakeland mine. Blue Rock Publications, Keswick, pp. 130

Passive Treatment of Toe Drain Discharges from a Tailings Storage Facility using an Oxic Granite Bed

Robert Hedin[1], Jeffery Millgate[2], Brian Authurs[2], Ron Nunn Pattrick[2], Vinath Khamsana[2] and Neil Wolfe[1]

1. *Hedin Environmental, USA;*
2. *Phu Bia Mining Company, Lao Peoples Democratic Republic*

ABSTRACT

PanAust Limited (PanAust), through its Laos-registered subsidiary Phu Bia Mining (PBM), owns and operates the Phu Kham Copper-Gold Operation in the Lao Peoples Democratic Republic (Laos). The operation includes a flooded tailings storage facility that discharges through two toe drains installed in the facility's earthen dam. The toe drain discharges are alkaline with pH 6-7 and contain 2-10 mg/L iron and manganese. In May 2013, a passive system was installed to treat the toe drain discharges. The system consists of an oxidation pond followed by an oxic aggregate bed that is constructed with granite aggregate manufactured on-site. The system has treated, on average, 187 m^3/hr of flow to an effluent containing pH 7.2, 6.5 mg/L dissolved oxygen, 176 mg/L alkalinity ($CaCO_3$), 0.01 mg/L dissolved iron, and 0.14 mg/L dissolved manganese. The project demonstrates the feasibility of treating large toe drain discharges passively and the suitability of non-calcareous aggregate as a reactive media where the mine water is alkaline and contaminated with moderate concentrations of iron and manganese.

Keywords: copper mining, tailing storage facility, acid rock drainage, passive treatment

INTRODUCTION

The management of mine tailings in wet climates often includes their permanent subaqueous disposal in constructed storage reservoirs. The earthen dams that create the storage reservoirs are typically constructed with one or multiple internal seepage collection systems that collect infiltration into the dam and discharge through toe drains. During the years or decades over which the dam is raised and tailings are disposed of in the tailings disposal facility (TSF), the primary discharge is through the toe drains. As the toe drain effluent is often a final discharge point from the TSF, its quality is subject to discharge criteria defined in the mine permit. Mine operators typically attempt to maintain good quality water in the tailings reservoir (alkaline with low metals) so that the toe drain discharges are also good quality. Not uncommonly, however, the toe drain discharges contain elevated concentrations of iron (Fe) and manganese (Mn) that exceed the permit limits, requiring treatment during and after the mine's operation.

The Phu Kham Copper-Gold Operation in Laos includes a TSF created by a large earthen dam that contains two toe drains. The toe drains discharge alkaline water with concentrations of Fe and Mn ranging between 2 and 10 mg/L. In 2013, a passive treatment system was installed that receives the full flow from the toe drains. The system's construction is innovative in its use of granite aggregate instead of limestone aggregate for removal of Mn. This paper describes the construction of the treatment system in 2013, an investigation of the condition of the aggregate in 2014, and its treatment performance over its first 1.5 years of operation.

METHODOLOGY

Water samples were collected by PBM staff. Flow rates were measured at V-notch weirs located 10-20 metres below each of the two toe drain discharges. Water samples were collected at the weirs, within the treatment system, and at the final effluent channel. Analyses were made in the field for pH, DO, temperature, specific conductivity, and oxidation-reduction potential. Water samples were collected daily and transferred within 4 hours to the on-site laboratory where alkalinity was measured by titration, and concentrations of dissolved (<0.45 micron) Ag, As, Cu, Fe, Pb, Ca, Mg, Mn, Mo, Ni, Na and Zn were measured by atomic emission spectroscopy. A separate set of samples were collected approximately monthly from the toe drains and submitted to ALS Environmental laboratory in Bangkok for analysis of total concentrations of a much wider suite of elements.

Project site

The Phu Kham Copper-Gold Operation in Xaysomboun Province in Laos is located in a challenging mountainous environment subject to high monsoonal rainfall. The main rock types in the project area are red bed (korat group), limestone, andesite ash flow tuff (metamorphosed to schist), cataclastite and granite. The host sequence forms the upper plate of a thrust fault with red bed siltstone making up the foot wall. The Phu Kham deposit is sericitic-altered porphyritic igneous and magmatite - chalcopycite skarn clasts. The mineralisation shows a trend along north-north-west which is mainly hosted in highly foliated schist between red bed as the foot wall and cataclastite, limestone and granite as the top of the hanging wall. The sulphide mineral assemblage is predominantly pyrite, chalcopyrite, chalcocite, bornite, and covellite.

Before the Phu Kham operation commenced, acid rock drainage (ARD) was identified as the single most significant environmental risk. Potentially acid-forming waste rock and tailings were identified as by-products of the mining and processing of ore as part of the Environmental and Social Impact Assessment process. As a result, a detailed acid rock management plan was formed prior to mining and processing commencing.

PanAust has developed an integrated life-of-mine approach accounting for the entire 182 million tonnes of potentially acid forming (PAF) waste (Miller et al., 2012). The overall objective has been to prevent any ARD legacy from waste rock and tailings during the mine's construction, operation and after closure. To implement the plan, detailed operational guidelines incorporate ARD management practices into daily operating activities.

The ARD management plan is based on the fundamental strategy of isolating sulphidic mine waste from atmospheric oxygen. This essentially places the material within a pH and oxidation regime similar to the original ore body where pyrite is thermodynamically stable. This is the most geochemically secure option for ARD control.

Engineering options for achieving isolation from atmospheric oxygen include placing sulphidic material under a permanent water cover or construction of an engineered seal that essentially reduces oxygen transfer to geological rates. At Phu Kham, both strategies have been adopted with the higher sulphidic acid-generating waste rock and tailings reporting to the tailings impoundment (which maintains a minimum two metres of water cover) and the lower sulphidic acid-generating waste isolated in cells and zones (PAF cells) within the downstream portion of the tailings storage facility embankment.

RESULTS AND DISCUSSION

Toe drain characterisation

The primary toe drain (#1) has discharged since 2008. The effluent has always been alkaline. Table 1 shows the average total metal concentrations between 2008 and 2012. Concentrations of all hazardous metals are very low and well below effluent targets. The only metals that exceed effluent targets are Fe and Mn.

Table 1 Average pH and total metal concentrations for Toe Drain #1, Feb 2008 – May 2012. Analyses by ALS Environmental (Bangkok).

	pH	Al	As	Cd	Cu	Fe	Pb	Mn	Ni	Zn
	s.u.	mg/L	mg/L	mg/L	mg/L	mg/L	mg/L	mg/L	mg/L	mg/L
Average	6.8	0.38	<0.01	<0.002	0.007	2.3	0.003	3.0	0.006	0.018
Count	44	50	50	50	50	50	50	49	50	50
Limit	6-9	-	0.1	0.03	0.3	1.0	0.2	0.5	0.2	0.5

Passive system construction

The design of the treatment system is shown in Figure 1. The system includes a settling pond followed by a bed of aggregate. The design follows US Bureau of Mines guidance provided in 1994 (Hedin, Nairn & Kleinmann, 1994) and more recent advances in the use of limestone aggregate in mine water treatment (Hedin et al., 2013). The intention of the design is to oxidize and settle Fe solids in the pond and to oxidize and trap Mn solids in the aggregate bed. The two toe drains are combined into a single piped flow that discharges into the pond through a horizontal fountain. The Fe pond has a surface area of 1,800 m^2 and a depth of 2 m. The pond contains three geotextile curtains that spread flow across the pond and promote solids settling. Water flows from the pond through a wide shallow channel in to the aggregate bed. The bed has a surface area of 4,200 m^2, is 2 m deep, and contains 10,100 tonne of material.

The bed was constructed with granite aggregate produced on-site. Limestone, which is commonly used in Mn systems such as this, was not available. Figure 2 shows the particle size distribution of the aggregate used in the treatment system.

The elevation of water in the system is controlled by the final effluent. The design intended that the water elevation in the aggregate bed should be 10-15 cm below the aggregate surface. This feature was expected to minimise short circuiting of flow on top of the aggregate and also limit plant growth in the system.

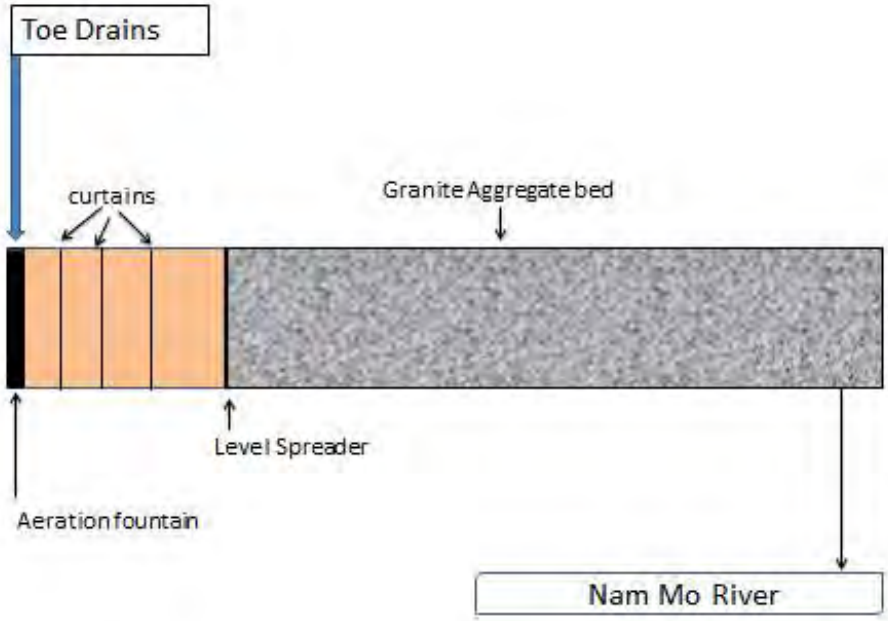

Figure 1 Design of the passive treatment systems

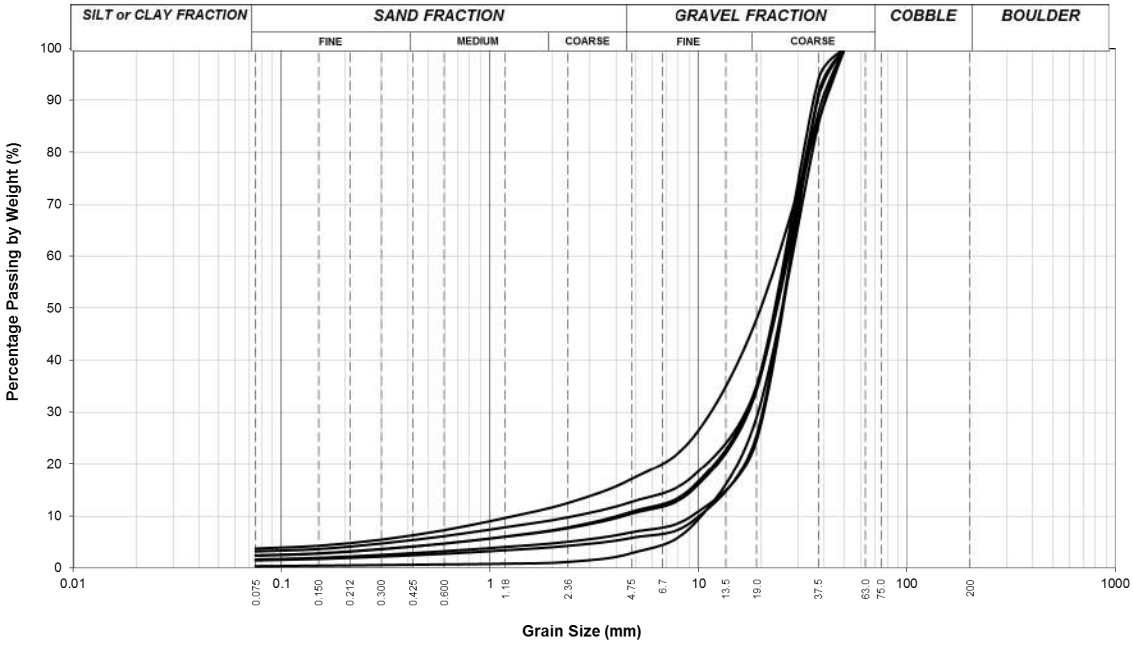

Figure 2 Particle size distribution for aggregate used in the passive system. The lines represent multiple samples collected from the bed after its construction.

Passive system treatment effectiveness

Table 2 shows the average chemistry of the treatment system influents, the calculated influent to the pond, the influent to the aggregate bed, and the final system discharge. All elemental concentrations shown are dissolved. Flow through the oxidation pond decreased Fe^D to from 2.1 mg/L to less than 0.1 mg/L and Mn^D from 4.0 mg/L to 2.6 mg/L. Flow through the aggregate bed decreased Fe^D below 0.01 mg/L and Mn to 0.07 mg/L.

Figure 3 shows concentrations of Mn^D between June 2013 and October 2014. Final effluent concentrations of Mn^D did not consistently meet the 0.5 mg/L target until July 9, 2013; 27 days after the system was first put into operation. Since that date, the discharge has contained less than 0.5 mg/L on every sampling occasion.

Table 2 Average flow and chemistry for the passive treatment system, Jun 2013 – Oct 2014. Flow rates are measured at weirs at Toe Drains #1 and #2. Other stations by addition.

	Flow	pH	DO	Alk	Ca^D	Mg^D	Na^D	Fe^D	Mn^D
	m^3/hr	s.u.	mg/L	mg/L	mg/L	mg/L	mg/L	mg/L	mg/L
Toe Drain #1	34.4	6.4	2.7	142	109	21	7.0	3.0	4.9
Toe Drain #2	17.8	6.5	2.8	244	137	34	8.1	0.3	2.4
Into pond*	52.2	6.4	2,7	177	119	25	7.4	2.1	4.0
Into granite bed	52.2	6.9	6.4	183	122	25	6.5	<0.1	2.6
Final	52.2	7.2	6.5	176	116	25	6.4	<0.1	0.1

** calculated mixture of Toe Drain #1 and #2*

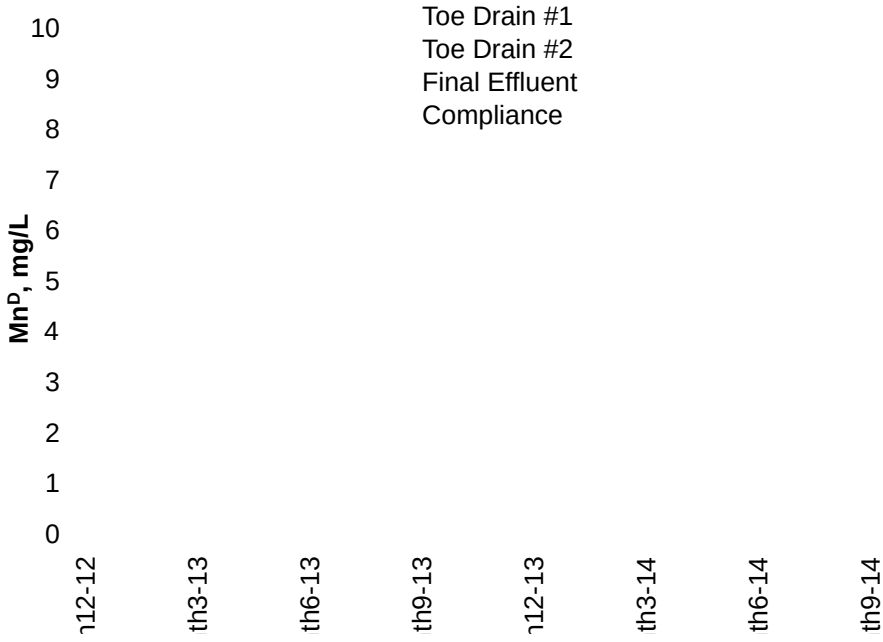

Figure 3 Concentrations of dissolved Mn at the toe drains (system influents) and the aggregate bed final effluent.

Table 3 Average loads (kg/d) of major water constituents at the treatment system stations, Jun 2013 – Oct 2014. % removal is the loss between the sum of the two influents and the final.

	Alk	Ca^D	Mg^D	Fe^D	Mn^D	Na^D
	kg/d	kg/d	kg/d	kg/d	kg/d	kg/d
Toe Drain #1	422	324	62	8.9	14.6	21
Toe Drain #2	375	211	52	0.5	3.7	12
Into granite bed	825	550	113	0.2	11.6	29
Final	794	523	113	0.0	0.6	29
% removal	0%	2%	2%	99%	96%	13%

Table 3 shows calculated loads of major constituents through the passive system. The system has negligible effect on alkalinity, calcium (Ca) and magnesium (Mg). A modest removal of sodium (Na) is indicated. The major effect of the system is removal of 96-99% of the Fe and Mn loading.

In mid-2014 water was observed flowing on top of a portion of the aggregate bed. In October 2014 an excavator was mobilised to investigate the change in hydraulics and also to investigate the condition of the aggregate. Flow on the top of the aggregate was limited to the first 25% of the bed. The investigation found algal growth on top of the stone that had created a dense biofilm that promoted flow of water on top of it. When the algal growth was disrupted by mixing the stone, water flowed into the aggregate and no longer flowed on the surface. The cause of the algal growth was suspected to be due to settling of the stone in the first portion of the bed, which allowed water on the surface during high flow conditions. During these conditions, algae growth was enabled. As a result of this observation, the effluent of the bed was lowered by 50 cm so that water would never flow on the surface and growth of algae would be inhibited.

The aggregate in the bed was inspected for signs of Mn removal. The raw granite is grey. Mn oxides form a black coating on the rocks. The aggregate in the final 25% of the bed did not have any black coloring, indicating that little Mn removal is occurring in this section (Figure 4a). As the investigation moved forward into the bed, stones stained black became visible (Figure 4b). In the first quarter of the bed, most of the stone in the top 30 cm was black (Figure 4c). The Mn staining was limited to the top 50 cm of the bed. Beneath 50 cm the aggregate retained its original grey color. These observations indicate that little Mn removal is occurring in the bottom 1.5 m of aggregate. When combined with the observations from the end of the bed, it was apparent that only 15% of the aggregate was involved in Mn removal. This condition likely has two explanations. First, removal of Mn is so effective in the first half of the bed that there is little Mn left for removal in the second half of the bed. This explanation suggests there is a large excess capacity for Mn removal in the second half of the bed which will be useful should Mn loadings increase. The observation that there is little visible Mn removal occurring below 50 cm suggests that flow is not well distributed through the bed. As the influent and effluent structures are both at the surface, there is an apparent preference of flow in the top 50 cm of the bed. This condition could be partially corrected by reconstructing the effluent as a perforated pipe placed on the bottom of the bed. There are no plans to make this change at this time.

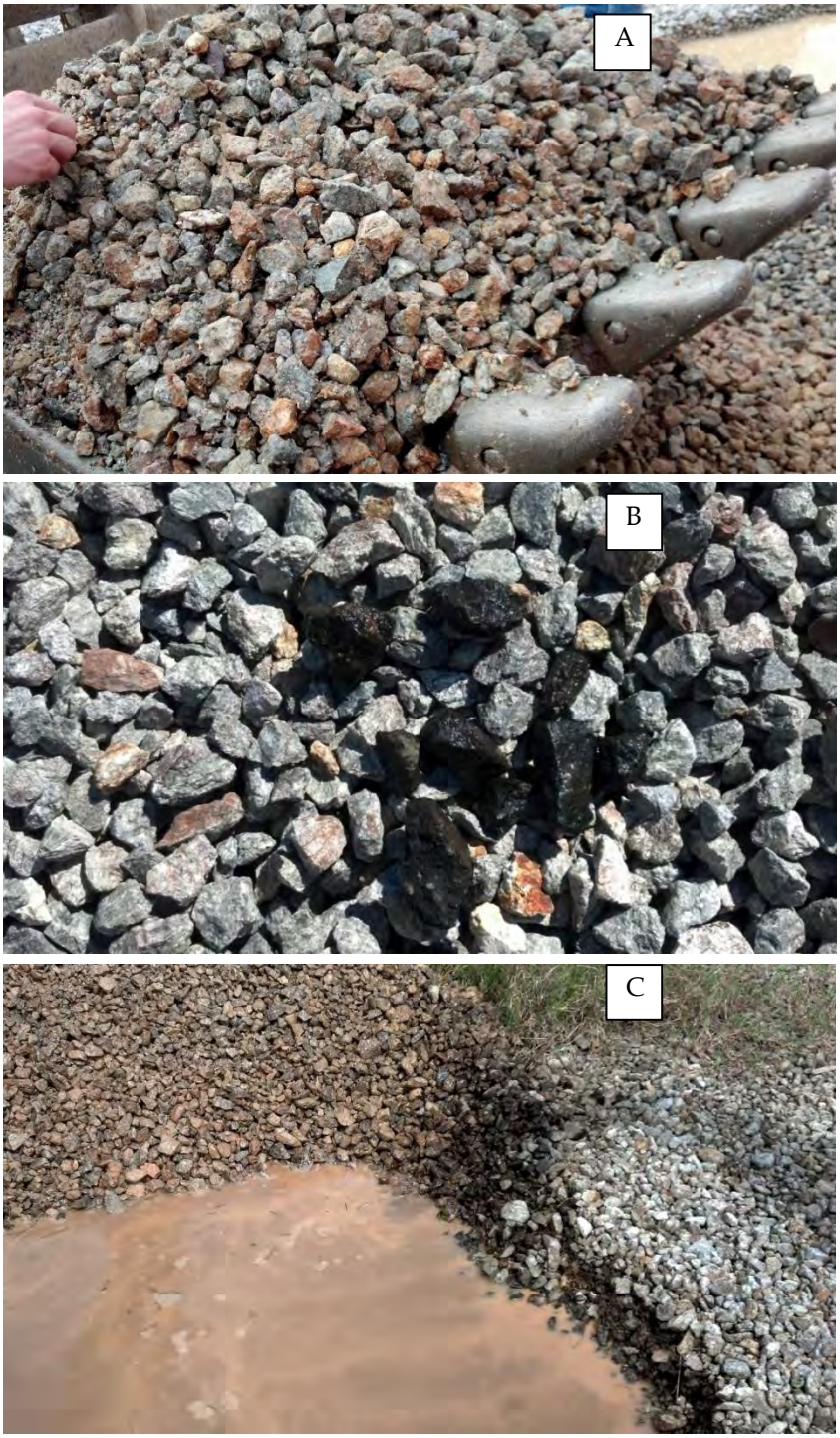

Figure 4 Aggregate encountered during system investigation. A) clean granite aggregate at the end of the system. B) black Mn-coated granite placed on clean stone to show contrast; C) layer of Mn-coated stone found in the first half of the bed.

This project demonstrates the feasibility for passive treatment of toe drain discharges when their chemistry is alkaline and the contamination is limited to moderate concentrations of Fe and Mn. These conditions are not uncommon as the primary author has observed similar chemistry at

tailings facility toes drains in Brazil and Tasmania. Mine planners should recognise that toe drains may need long-term treatment and reserve adequate land for placement of passive treatment systems below the toe drain discharges.

This project demonstrates that the passive removal of Mn from alkaline mine water does not require a limestone substrate. In the coalfield of eastern USA, where passive treatment technologies have been developed, limestone aggregate is preferred because it is readily available and its acid-neutralising capacity is considered a benefit. The very effective Mn removal in this system suggests that that the removal of Mn is dependent on physical aspects of the substrate, not chemical aspects. This finding should be of benefit in areas where mine waters are naturally alkaline and limestone aggregate is not available.

REFERENCES

Miller, S, Rowles, T, Millgate, J, Pellicer, J, Morris, L, Gaunt, J (2012) Integrated Acid Rock Drainage Management at the Phu Kham Copper Gold Operation in Lao PDR. In W Price, C Hogan, G Trembley (eds) 9th International Conference on Acid Rock Drainage, May 20-26, 2012, Ottawa Canada, pp615-627

Hedin, R, Nairn, R, Kleinmann, R (1994) Passive Treatment of Coal Mine Drainage. US Bureau of Mines Information Circular 9389, Washington DC.

Hedin, R, Weaver, T, Wolfe, N, Watzlaf, G (2013) Effective Passive Treatment of Coal Mine Drainage. In Proceedings of the 35th Annual National Association of Abandoned Mine Lands Programs Conference, Sept 23 2013, Daniels WV USA.

10th ICARD IMWA 2015 | 10th International Conference on Acid Rock Drainage & IMWA Annual Conference

Mechanisms of Iron Removal during Passive Treatment of AMD in a Vertical Flow Reactor

Kay Florence[1], Devin Sapsford[1] and Christian Wolkersdorfer[2]
1. *Cardiff School of Engineering, Cardiff University, United Kingdom*
2. *Tshwane University of Technology (TUT), South Africa; Lappeenranta University of Technology (LUT), Finland*

ABSTRACT

This paper presents data from a field trial for the passive removal of Fe from circa pH 3 metal mine water. In a 1 m^3 intermediate bulk container (IBC) converted into a vertical flow reactor (named here the VFR), mine water was passed through in a downward direction through an unreactive reactive gravel bed under aerobic saturated conditions. The VFR was deployed for a period of 414 days at the Cwm Rheidol mine, an abandoned historic Pb/Zn mine in Wales, UK that discharges circa pH 3 AMD with average Fe concentrations of 95 mg/L. Removal of iron, as high as (85%) was shown with an average of 65% achieved over the trial period from an average flow of 0.38 L/min. Results were encouraging, a very simple system providing an option to treat acidic coal mine drainage where iron is the principal contaminant or pre-treat 'metal mine' water by removing the bulk of the Fe as an iron-rich sludge to help prevent clogging of subsequent treatment stages for more environmentally toxic elements. The Fe removal mechanism is thought to be predominantly by the crystal growth and/or aggregation and filtration of nanoparticulate Fe(III) in the VFR. Centrifugation of influent water samples from site indicated that 80 – 90 % of the Fe in the inflow water is present as $Fe(III)_{(s)}$ particles < 35 nm. Microbial Fe(II) oxidation is suspected to be important along the flow path before water enters the VFR and to a small extent within the VFR. Analysis of the sludge indicates that schwertmannite is the dominant mineral phase.

Keywords: mine water, passive treatment, vertical flow reactor, Wales/UK

INTRODUCTION

Historically, north and south Wales, Cornwall and the midlands were extensively mined for base metal sulphides and coal. It is estimated that there are tens to thousands of abandoned mining facilities including onshore mining and quarrying sites (Palumbo-Roe and Colman, 2010). The clean-up of water from abandoned coal mines is the responsibility of the UK Coal Authority, but since the introduction of the Water Framework Directive in 2006, the Coal Authority and Natural Resources Wales have been working closely together to find long-term, low cost treatments options for the clean-up of the metal mines.

National Resources Wales (formerly known as the Environment Agency Wales) published the Metal Mines Strategy for Wales (Johnston, 2004) which lists the top fifty most polluting sites in Wales that were identified, following the monitoring of 5042 km of river stretches, 108 km of which failed ecosystem objectives as a direct consequence of pollution from abandoned mines (Jarvis et al., 2007). 38 of those top 50 sites are located in the Mid-Wales district of Ceredigion.

Metal mine water is commonly treated by active means, where chemicals are added to raise the solution pH and precipitate metals and metalloids. This tends to form a high volume of sludge, which, if containing metals other than Fe, for example, Zn, Pb, Cd may be classified and disposed of as hazardous waste, further adding capital and operational costs. Consequently, active treatment might be impractical, bearing in mind that the Coal Authority is a governmental organisation and mine water can continue to pollute for tens to hundreds of years. As such, active treatment is not currently considered for application to the majority of discharges in former UK mining regions. Furthermore, the metal mining areas tend to be concentrated in remote steep sided valleys, where access is difficult and a lack of basic infrastructure, such as power, exists. For this reason, the adoption of passive treatment is favoured. However, passive treatment options for metal mine drainage are not well developed in the UK.

Looking outside of the UK many countries have developed and deployed a host of these passive technologies (*e.g.* anoxic limestone drains) for treating metal-rich AMD (Brodie et al., 1991, Hedin et al., 1991, Skousen, 1991). Passive mine water treatment is commonly achieved via harnessing of naturally occurring physiochemical and biological processes, for example the manipulation of solubility via changes in pH by reaction with limestone (Blowes et al., 2003), altering the redox conditions through the use of organic matter (Lottermoser, 2007, Wildeman et al., 1993), the addition of high surface area materials used to provide sorption sites (Jarvis and Younger, 2001, Younger, 2000) or the use of low cost reactive materials (Warrender et al., 2011). The longevity of these treatments can be compromised by clogging due to the Fe (or Al) precipitates formed during the neutralisation of AMD with limestone or other alkalinity producing systems (Younger et al., 2002). This study considers these treatment methods with a modular approach, whereby a system such as a VFR could be used to remove Fe (as the bulk contaminant) from AMD. Such a technology could be deployed where Fe alone is the contaminant of concern (*e.g.* acidic coal mine drainage) or as a pre filter for Fe removal where Fe and other solubilized metals such as Zn occur together, thus allowing prolonged longevity for the second metal removal stage. The benefits of this would be the reduction of the volume of the 'hazardous' waste and the production of a clean (in terms of free of organics) iron-rich sludge that could have reuse value. The focus of this study is therefore to test the VFR as an Fe removal pre-treatment system for AMD.

On its course through the system, mine water passes down through the gravel bed support media. The vertical flow design reduces the footprint compared to more traditional systems that require large areas of land. Sapsford et al. (2007) detailed the testing of a VFR achieving 50% Fe removal from circum-neutral (pH 6–7) coal mine drainage with Fe concentrations of 8–10 mg/L. Iron removal occurred via filtration of iron hydroxide particles (formed in the water column) and surface-catalysed oxidation of Fe(II) (and precipitation) of Fe(III) hydroxide surfaces. This paper reports the results and possible Fe removal mechanisms of a VFR trialled for removal of Fe from pH 3 mine water.

METHODOLOGY

The system was adapted from the original design used in the initial field trial at the Taff Merthyr site in South Wales (Dey et al., 2003), using a modified 1 m³ intermediate bulk container (IBC, see fig. 1 in Sapsford, Florence, Pope and Trumm, these proceedings). A length of coiled, slotted drainage pipe was placed in the bottom of the tank. 30 mm angular coarse grained siliceous chips were added to the container to secure the pipe and provide a stable base on top of which a 200 mm depth layer of 5–10 mm grain size siliceous gravel was added (Fig. 2). A down flow of mine water was then maintained through the water column and through the ochre bed. Driving head was set via a swan neck mechanism through which the treated water was discharged. The VFR was set up alongside the River Rheidol to take a proportion of the flow from the lower number 9 adit discharge pipe of the Cwm Rheidol mine located at the base of the mine. Water was piped to the VFR under gravity from the adit discharge pipe (Fig. 1).

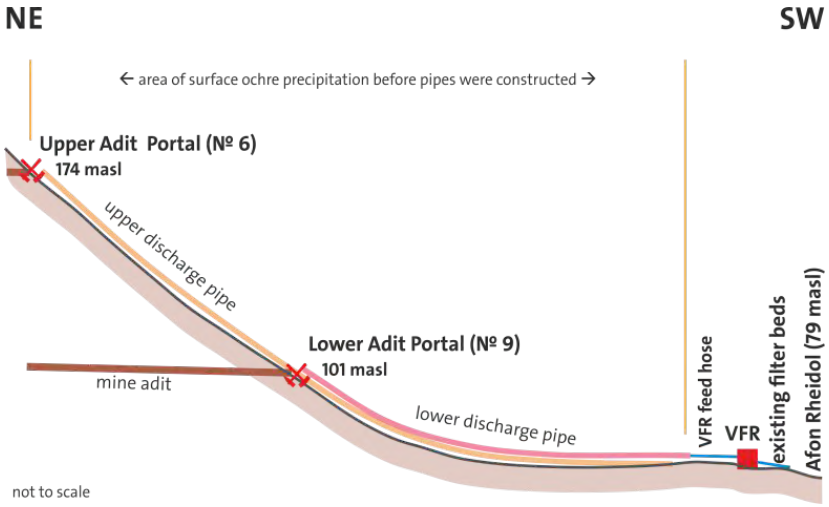

Figure 1 Schematic cross section of the upper number 6 adit and the lower number 9 adit and the location of the VFR at Cwm Rheidol. masl: meters above sea level.

Field data and water sampling

All field measurements of pH, EC, ORP and temperature were taken using Hanna combination meters HI-9828. The dissolved oxygen (DO), electrical conductivity and pH probes were calibrated at each site visit using the manufacturer's calibration procedure set out in the operator's manual. Flow rates were measured using the bucket-and-stop-watch-method.

At each of the 34 site visits between 2011-05-17 to 2012-07-04, filtered and unfiltered water samples were collected from the inflow and outflow. For the filtered samples, 0.2 μm Acrodisc PF syringe filters fitted to Plastipak syringes were used. In this study, the term filtered is used to describe samples that pass a 0.2 μm filter and is not a definition used to describe 'dissolved' species. All water samples were collected in 30 mL containers and rinsed with the sample and acidified with HNO_3 to stabilize the water chemistry. Samples collected on site were placed immediately into a dark cool box and stored at 4 °C until analysis was possible. Samples were analysed using a Perkin Elmer Optima 2100DV ICP-OES. Filtered unacidified inflow and outflow samples were also collected for sulphate analysis using a Dionex® ICS-2000 Ion Chromatography System Whilst samples for Fe total and Fe filtered were collected and analysed from each sample visit, Fe(II) was only measured on 11 of the sampling intervals. On the occasions that Fe(II) was measured in the field, filtered samples were analysed using a potable Merck NOVA60 spectrophotometer with appropriate Merck Fe test cells. Samples collected for Fe(II) analysis in the laboratory using a Hitachi U1900 spectrophotometer, were filtered and acidified with 20% (v/v) HCl. Samples for Fe(II) that could not be analysed on the same day were frozen until analysis was possible.

Centrifugation

A centrifugation method adapted from Hüttig and Zänker (2004) was used to determine the Fe particle size distribution in the unfiltered inflow water. In this context, truly dissolved relates to a particle size of less than 50 nm, which is close to the 20 nm cut off between "truly dissolved" and colloids suggested by Shiller (2003). 20 tubes of fresh mine water were collected in the field (10 × 2 to duplicate the experiment). Parallel centrifugation of each 2 × 50 mL of raw water was carried out at rotor speeds calculated as per Table 1 at rotor speeds of 300, 500, 700, 1000, 3000 and 5000 over a period of 1 h and 3500 rpm (rounds per minute) over a period of 2 h due to the limitation of the centrifuge instrument speed. Equivalent RCF values (relative centrifugal force, which is equivalent to the *g*-force used in table 1) at a given point in the centrifuge tube were calculated according to the equation 1:

$$RCF = 11.18 \times r \times U1000 \quad [1]$$

Where *r*: distance between the rotation axis and the particle in the centrifuge tube in cm and *U*: rpm rounds per min. After centrifuging, the supernatant was syringed from the centrifuge tube using a pipette. The sample was transferred to a new sample container, acidified with 20% nitric acid and the total unfiltered Fe concentration analysed by ICP-OES.

Table 1 Centrifuge parameters and calculated values

RPM	*t*, h	*g'*, -	*d*, nm
raw	-		
0	1		
300	1	283	683
500	1	474	417
700	1	659	293
1000	1	945	207
2000	1	1889	101
4000	1	4181	50
5000	1	5254	39
3500	2	3913	35

The maximum size of the particles still present in the supernatant was calculated with an assumed density of the colloids and under the assumption of a spherical form of the particles in accordance with equation 2:

$$d = 18\eta \ln r1 r0 (\rho 2 - \rho 1) \omega 2 t \quad [2]$$

with d diameter of particle in cm, ρ_2 density in g cm^{-3} (3.96 g cm^{-3} for ferrihydrite), r_0 distance of water level in vial to rotation axis before taking sample in cm, r_1 distance of water level in vial to rotation axis after taking sample in cm, t duration of centrifuging in s, η viscosity of water at 25 °C (0.008941 g cm^{-1} s), ρ_1 density of water at 25 °C (0.997 g cm^{-3}) and ω angular velocity in s^{-1} = U × $2\pi 60$.

PHREEQC Modelling

A full water analysis was used for chemical thermodynamic modelling with PHREEQC interactive Version 3.1.1.8288 (2013-12-05) and the WATEQ4F database (6895 2012-08-21 18:10:05Z) extended with kinetic data of schwertmannite.

Sludge analysis

Samples for XRD analysis were dried overnight at 60 °C, finely ground and placed in a slide window covered by glass plate, amorphous samples were scanned for 12 h. Settling velocities of the Cwm Rheidol sludge from within the VFR were calculated by measuring the distance at which the particles settled over time.

RESULTS AND DISCUSSION

Fe inflow and outflow concentrations

The data for iron show that average removal for Fe(total) is 65% on the sampling occasion across the 13 months period (Table 2). Fe removal rates remained consistent throughout the trial period and the flow rates stabilised between days 33 and 387 averaging 0.39 L/min (Fig. 3), which shows that after the initial drop, the permeability of the bed did not decrease significantly over time. On average, about 85% of the Fe in the influent is Fe-filtered (*i.e.* passing a 0.2 μm filter) and on average 99% of the effluent iron passes a 0.2 μm filter. The removal of Fe-Filtered is on average 53 mg/L (Table 1). This demonstrates that the VFR removes Fe(III) of < 0.2 μm, where the Fe could either be particulate (smaller than 0.2 μm, *i.e.* colloidal or nanoparticulate) or truly dissolved. Likely candidates for the removal of Fe-Filtered are (i) Microbial Fe(II) oxidation and precipitation of a Fe(III) solid phases (ii) Filtration of particulate-$Fe(III)_{(s)}$ which is < 0.2 μm and/or (iv) adsorption of dissolved Fe(III) to HFO followed by precipitation (self-seeding crystal growth). These are discussed in more detail below.

Figure 2 Left, initial stages of filling the VFR; centre: Ochre inside the VFR (after draining tank); right: ochre precipitates taken directly from the VFR.

Table 2 VFR field parameter measurements.

Date	Flow rate (L/min)	pH	pH	D.O (mg/L)	D.O (mg/L)	ORP (mV)	ORP (mV)	Temp (°C)	Temp (°C)	Fe-Tot (mg/L)	Fe-Tot (mg/L)	Fe-Tot Removal %	Fe-Filt (mg/L)	Fe-Filt (mg/L)	Fe (Filt) Removal %	Fe(II) (mg/L)	Fe (II) (mg/L)	Δ Fe-Filt (mg L)	RT (hrs)
	E	I	E	I	E	I	E	I	E	I	E		I	E		I	E	I/E	
2011-06-21	0.71	2.98	3.01	8.47	7.33	684	716	13.54	14.14	126	60.81	51.74	126.59	65.3	48.42	na	na	61.29	16
2011-07-11	0.46	3.29	3.38	7.54	7.81	670	742	15.41	18.01	23.25	17.1	26.45	16.45	15.8	3.95	na	na	0.65	24
2011-07-20	0.38	3.33	3.26	9.51	4.12	670	764	14.37	16.04	119.6	41	65.72	116.2	41.16	64.58	na	na	75.04	31
2011-08-03	0.25	3.03	3.09	5.83	4.38	678	763	16.97	16.26	104.9	31.37	70.10	64.87	31.82	50.95	37.1	<0.2	33.05	47
2011-08-11	0.11	2.58	3.05	6.49	5.89	758	776	17.88	19.64	80.56	32.09	60.17	64.87	31.82	50.95	0.58	<0.2	33.05	85
2011-08-22	0.3	3.42	3.58	6.9	4.30	673	710	15.27	14.48	146.2	53.34	63.52	138.7	52.45	62.18	na	na	86.25	48
2011-08-30	0.2	3.03	3.02	8.35	6.66	673	762	12.02	12.64	155.1	53.9	65.25	135.5	51.18	62.23	10.2	na	84.32	59
2011-09-19	0.2	3.05	3.00	5.66	5.55	767	678	12.88	12.19	87.54	23.63	73.01	82.5	23.86	71.08	12.3	<0.2	58.64	70
2011-09-25	0.29	3.04	3.06	8.85	5.40	663	757	12.28	14.05	101	20.75	79.46	77.17	20.19	73.84	na	na	56.98	30
2011-09-26	0.24	2.83	2.63	7.66	4.08	668	728	16.01	19.67	84.91	18.13	78.65	72.2	17.76	75.40	na	na	54.44	58
2011-10-04	0.26	2.5	2.41	9.20	6.31	664	718	12.40	12.26	97.09	28.19	70.97	91.31	27.78	69.58	32	<0.2	63.53	60
2011-10-07	0.24	2.65	2.68	7.19	6.73	741	724	15.08	15.38	110.9	28.91	73.93	102.5	31.23	69.53	35	<0.2	71.27	52
2011-10-21	0.31	3.01	3.15	7.70	10.02	638	648	10.44	11.46	84.13	23.64	71.90	75.53	23.92	68.33	33.1	1	51.61	40
2011-11-04	0.19	2.88	2.59	9.32	6.10	662	727	10.52	9.47	37.82	24.35	35.62	16.68	3.97	76.20	4.44	<0.2	12.71	50
2011-11-18	0.2	2.77	2.63	9.16	7.75	359	722	11.14	10.96	110.4	29.45	73.33	103.93	29.05	72.05	43.5	1.18	74.88	72
2012-01-02	0.1	2.45	2.37	9.13	6.83	718	726	6.75	6.74	95.67	14.56	84.78	35.83	11.53	67.82	4	<0.2	24.3	112
2012-03-18	0.23	2.38	2.32	7.07	6.45	773	741	9.18	10.81	79.15	23.51	70.30	72.32	24.74	65.79	na	na	47.58	38
2012-06-07	1.1	3.08	2.54	8.30	7.20	476	448	13.04	14.09	102.1	24.28	76.22	91.17	24.49	73.14	na	na	66.68	6
2012-06-30	1.1	4.86	4.94	6.60	5.54	505	492	14.37	13.63	75.3	20.37	72.95	69.26	21.6	68.81	27.6	4.6	47.66	10
2012-07-04	0.75	2.87	2.92	7.42	5.89	485	516	13.40	12.51	79.2	17.31	78.14	63.69	17.1	73.15	17.2	<0.2	46.59	15
Mean	0.38	2.83	2.77	7.8175	6.217	646	693	13.15	13.72	95.04	29.33	67.11	80.86	28.33	63.4	21.42	0.69	52.53	46

Filt: filtered, Tot: total, I: influent, E: effluent

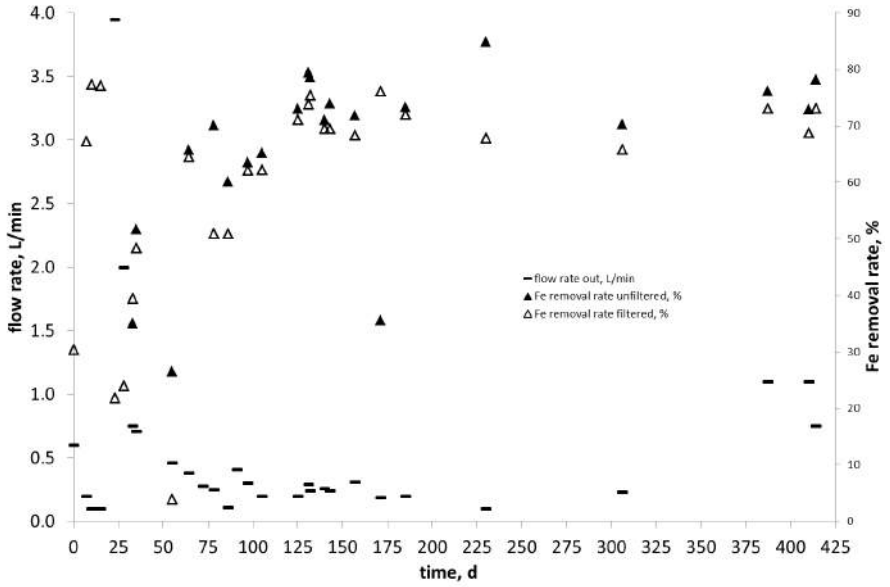

Figure 3 Filtered and unfiltered Fe(total) removal rate and flow rate of the VFR over time

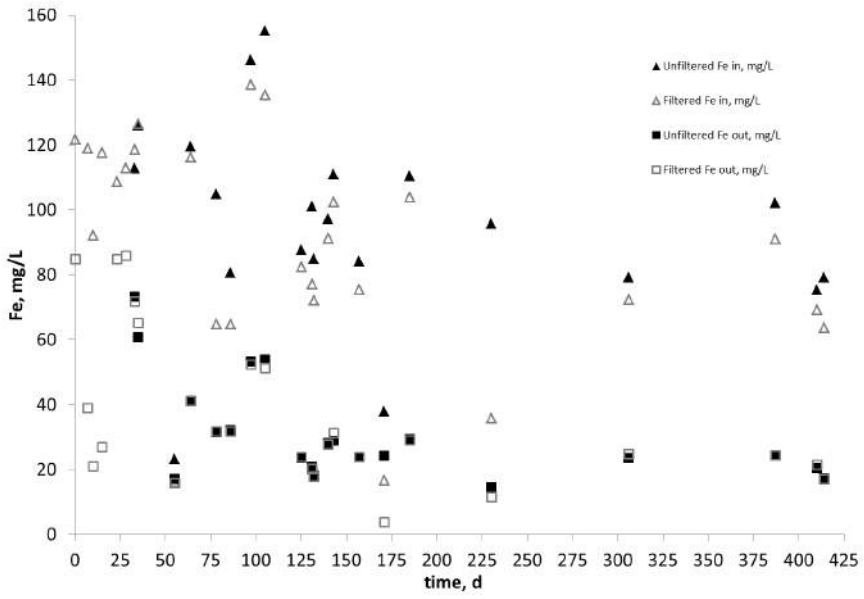

Figure 4 Filtered and unfiltered VFR inflow and outflow Fe(total) concentrations over time

Oxidation of Fe(II) and precipitation of Fe(III)(s)

Where Fe(II) analyses were performed in the field, it was apparent that Fe(II) only made up a small proportion of the influent Fe (highest observed was 42 % of the influent Fe-Filtered on 18-11-11). Fe(II) was removed in the VFR, with 7 of the 11 sampling occasions falling below the detection limit of the spectrophotometric method used (0.2 mg/L). The minimum removal of Fe(II) was 83 % on 30-06-12 (note: with only a short residence time of 10 h). Thus it is clear that despite Fe(II) being variable, it was typically a small component of the Fe-Filtered and that it was removed effectively in the VFR. Based on the microbial analyses (Florence, 2014) and the published rates for abiotic and biotic Fe(II) oxidation at low pH, the proposed mechanism for the observed results is microbial Fe(II) oxidation.

However, the change in filtered Fe between the influent and effluent cannot be simply explained by the oxidation of Fe(II), and in all of the cases observed during sampling the removal of filterable influent iron that initially passes a 0.2 μm filter cannot be explained by oxidation of iron (II) to an insoluble Fe(III) product. Thus the dominant removal for filterable iron must involve changes in dissolved Fe(III) or colloidal to nanoparticulate Fe(III) that passes the 0.2 μm filter.

Iron removal mechanism: Precipitation versus filtration of nanoparticulate-Fe(III)(s

70% of the Fe in the inflow passing a 0.2 μm filter is retained in the VFR (Fig. 4). On average, the remaining 30% of the inflow Fe is still present in the outflow. Water at Cwm Rheidol is typically well oxidised. The remaining 30% of the Fe that is not being removed was Fe(III) in either truly dissolved form (single solvated Fe(III) ions) or particulate $Fe(III)_{(s)}$ of < 200 nm. A centrifuge study was used to examine the size distribution for possible particulate Fe(III). The Fe data showed that Fe does decrease as centrifugation speed increases, however 87% of the iron measured in the raw mine water was still present after centrifugation for 2 h at 3500 rpm which corresponds to a stokes diameter of 35 nm. This means that on the sampling occasion, the Fe present in the mine water sample was less than 35 nm in size. This suggests that the Fe removal mechanism in the VFR involves either (i) precipitation and filtration of dissolved Fe(III) as it grows from molecular clusters to larger sizes range precipitates or aggregation and filtration of nanoparticulate Fe(III) < 35 nm in size that was present in the VFR influent.

At this scale, given the very small size of the particles involved, it becomes somewhat arbitrary what the operational definition of dissolved and particulate iron is. There is no general consensus in

the literature, under which threshold size particles can be considered "truly dissolved", and the distinction between the two is analytically challenging (Mudashiru, 2008). Commonly, 1–1000 nm are called colloids, 1–100 nm are nanoparticles and several authors call particle sizes under 30–50 nm "truly dissolved" (Daughney et al., 2004). Yet, 1 nm is still larger than the size of a molecule which is in the range of several Ångstroms but in the range of hydrated ions (Ranville and Schmiermund, 1999). As such, it could be viewed as the removal mechanism working in the system is providing retention time for the growth of ferric iron from truly dissolved state to particles large enough to be filtered out in this the VFR. Based on the results of the centrifuging and this definition of colloid ranges, it can therefore be suggested that the removal mechanism occurring in the VFR is one or a combination of nanoparticle filtration or precipitation and aggregation of truly dissolved (*i.e.* originally molecular-scale) Fe. The role of heterogeneous 'seeding' by the precipitated solids in the system is also potentially very important but it is not possible to distinguish this mechanism from the field data collected.

Sludge Composition and settling behaviour

The consistency of the sludge that accumulated within the tank was unusual and noteworthy: The sludge looked like it had been polymer dosed. Settling velocity experiments showed that the VFR precipitates had comparable settling rates to polymer dosed HDS sludge yet remained permeable throughout the field trial (Fig. 5, left). Bacterial presence is thought to be responsible for the unusual consistency of the flocs in the VFR (Fig. 2, right), which was supported by a supporting microbiological study (Florence, 2014). Sulphur analysis of the VFR sludge showed the sample to contain 4.4% sulphur which is an indication of that schwertmannite was formed. This is also consistent with XRD analysis (Fig. 5, right) that showed peaks of an amorphous Fe(III) (hydroxy) oxide that is characteristic of aged schwertmannite (Peretyazhko et al., 2009).

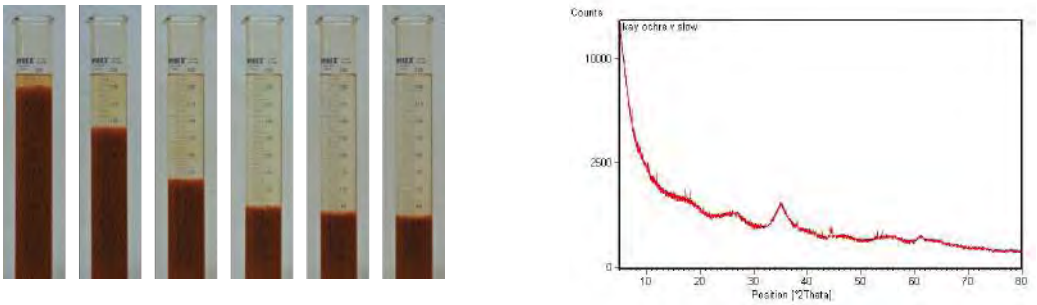

Figure 5 Left, settling properties of the precipitates that formed in the VFR at 15, 60, 120, 194, 240 and 284 s settling time. Right, XRD analysis of VFR ochre. The peaks at around 15, 35 and 45°2θ are characteristic for schwertmannite.

PHREEQC modelling

In support of the field and laboratory analyses of Fe speciation, PHREEQC modelling, suggests that Fe predominantly exists as Fe(III) (91%) and to a lesser degree of Fe(II) (9%) in the influent. The dominating Fe(III) an Fe(II) species are $FeSO_4^+$ (81%) and $FeSO_4^0$ (9%) respectively. Likely important phases that were predicted oversaturated for the mine water were K- jarosite and schwertmannite.

Iron removal in the context of the study site

Studying the layout of the mine is important as this helps to depict the chemical reactions responsible for the site being a producer of AMD (Fig. 1) and how the VFR is removing Fe from the mine water. Hydrolysis and oxidation of Fe(II) to Fe(III) occurs in the extended adits and mine workings prior to reaching the VFR. The adit length (600 m), flow rate (3 L/min) and a convex channel (0.5–1 m wide and 0.05 deep) results in a flow of approx. 0.10 m/min; data which is used to calculate the distance at which particles > 0.2 μm will settle based on Stoke's law. This was found to be 300–500 m. The first reaction occurring is the partial ochre precipitation in the adits (reaction 3):

$$Fe^{3+} + H_2O \rightarrow FeOOH\downarrow + H^+ + 2e^- \quad [3]$$

Mine water is further aerated and agitated during the pipe transport and more ochre forms in the pipe. The mine water that is now collected from the adit dicharge pipe and drained to the VFR contains the following aqueous components (based on PHREEQC results):

$$[Fe^{2+}] << [FeOH^{2+}] < [Fe^{3+}]$$

Solubility calculations and the chemical analysis at the discharge pipe shows, that part of the iron remains truly dissolved (and passes through the VFR), but that the water is still oversaturated with iron phases and able to precipitate iron, potentially as (nano-)particles < 0.2 μm in the acid mine water according to equation 3. In the VFR, due to the slow flow, prolonged residence time and intimate contact with precipitates compared to the adit and pipe flow, the (nano-)particles and/or dissolved Fe are removed. Yet, some of the dissolved Fe(III) remains in solution according to the solubility of the controlling Fe-phase at this pH (schwertmannite) and passes through the VFR without being removed.

CONCLUSION

The VRF trial at the abandoned Cwm Rheidol mine was effective at removing a large proportion of the Fe from low pH AMD. Whilst further work is required to understand the precise mechanisms of Fe removal in the VFR, where chemical, environmental and biological conditions are conducive, the VFR system has excellent potential as a Fe removal system for 'pre-treatment' (to remove a bulk of the iron) at metal mines such as Cwm Rheidol or to remove Fe from acidic coal mine drainage. Based on the results of the 13 month trial, a 50 m × 35 m VFR could remove approximately 70% of the Fe from the number 9 adit at Cwm Rheidol for at least a year without maintenance.

ACKNOWLEDGEMENTS

The authors thank the Coal authority, EPSRC and Cardiff University for their financial support.

REFERENCES

Blowes, D. W., Ptacek, C. J., Jambor, J. L. & Weisener, C. G. 2003. The Geochemistry of Acid Mine Drainage. *In:* Heinrich, D. H. & Karl, K. T. (eds.) *Treatise on Geochemistry.* Oxford: Pergamon, 149-204.

Brodie, A., G., Britt, C. R., Tomaszewski, T. M. & Taylor, H. N. 1991. Anoxic Limestone Drains to Enhance Performance of Aerobic Acid Drainage Treatment Wetlands – Experiences of the Tennessee Valley Authority. *In:* Wildeman T., B. G., Gusek J (ed.) *Wetland Design for Mining Operations.* Pensacola.

Daughney, C. J., Châtellier, X., Chan, A., Kenward, P., Fortin, D., Suttle, C. A. & Fowle, D. A. 2004. Adsorption and precipitation of iron from seawater on a marine bacteriophage (PWH3A-P1). *Marine Chemistry,* 91**,** 101-115.

Dey, M., Sadler, P. J. K. & Williams, K. P. 2003. A novel approach to mine water treatment. *Land Contamination and Reclamation,* 11**,** 253-258.

Florence, K. 2014. *Mechanisms of the Removal of Metals from Acid and Neutral Mine Water under varying Redox Systems*. Cardiff, unpub. PhD-Thesis Cardiff University.

Hedin, R. S., Nairn, R. W. & Watzlaf, G. R. 1991. A Preliminary Review of the Use of Anoxic Limestone Drains in the Passive Treatment of Acid Mine Drainage. *Proceedings, West Virginia Surface Mine Drainage Task Force Symposium 12.*

Hüttig, G. & Zänker, H. 2004. Kolloidgetragene Schwermetalle im Entwässerungsstollen einer stillgelegten Zn-Pb-Ag-Grube. *Wissenschaftlich-Technische Berichte,* FZR-403**,** 1-33.

Jarvis, A., Fox, A., Gozzard, E., Hill, S. & Mayes, W. M. 2007. Prospects for Effective National Management of Abandoned Metal Mine Water Pollution in the UK. *International Mine Water Association* Italy.

Jarvis, A. P. & Younger, P. L. 2001. Passive treatment of ferruginous mine waters using high surface area media. *Water Research,* 35**,** 3643-3648.

Lottermoser, B. 2007. *Mine Wastes – Characterization, Treatment and Environmental Impacts,* Heidelberg, Springer.

Mudashiru, L. K. 2008. *Electrochemical Determination of Dissolved and Particulate Iron in Mine-waters,* Newcastle, unpubl. PhD Thesis Univ. Newcastle upon Tyne.

Palumbo-Roe, B. & Colman, T. 2010. The nature of waste associated with closed mines in England and Wales.**,** 82.

Peretyazhko, T., Zachara, J. M., Boily, J. F., Xia, Y., Gassman, P. L., Arey, B. W. & Burgos, W. D. 2009. Mineralogical transformations controlling acid mine drainage chemistry. *Chemical Geology,* 262**,** 169-178.

Ranville, J. F. & Schmiermund, R. L. 1999. *General Aspects of Aquatic Colloids in Environmental Geochemistry,* Littleton, Society of Economic Geologists.

Sapsford, D., Barnes, A., Dey, M., Williams, K., Jarvis, A. & Younger, P. L. 2007. Low Footprint Passive Mine Water Treatment: Field Demonstration and Application. *Mine Water and the Environment* 26**,** 243-250.

Shiller, A. M. 2003. Syringe Filtration Methods for Examining Dissolved and Colloidal Trace Element Distributions in Remote Field Locations. *Environ. Sci. Technol.,* 37**,** 3953-3957.

Skousen, J. G. 1991. Anoxic limestone drains for acid mine drainage treatment. *Green Lands* 21**,** 30-35.

Warrender, R., Pearce, N. J. G., Perkins, W. T., Florence, K. M., Brown, A. R., Sapsford, D. J., Bowell, R. J. & Dey, M. 2011. Field Trials of Low-cost Reactive Media for the Passive Treatment of Circum-neutral Metal Mine Drainage in Mid-Wales, UK. *Mine Water and the Environment,* 30**,** 82-89.

Wildeman, T., Gusek, J., Dietz, J. & Morea, S. 1993. *Handbook for Constructed Wetlands Receiving Acid Mine Drainage,* Golden, Colorado School of Mines.

Younger, P. 2000. The adoption and adaptation of passive treatment technologies for mine waters in the United Kingdom. *Mine Water and the Environment,* 19**,** 84-97.

Younger, P., Banwart, S. A. & Hedin, R. S. 2002. *Mine Water Hydrology, Pollution, Remediation,* Dordrecht, Kluwer.

Passive Limestone Treatment of Mining Influenced Water with Low PH and High Concentrations of Ferric Iron

Linda Figueroa
Civil and Environmental Engineering, Colorado School of Mines, USA

ABSTRACT

Mining influenced water (MIW) with low pH and high ferric iron concentrations is typically treated in active systems by hydroxide addition. Limestone is an attractive reagent for neutralization and iron precipitation because it equilibrates at a neutral pH and thus is more amenable to lower operation and maintenance treatment systems. Existing design guidance is limited to passive limestone treatment of MIW with low ferric iron concentration or active limestone treatment of MIW with high ferric iron concentration. Extrapolation of current passive limestone bed design guidance has led to design failure for high ferric iron concentrations. Experimental and modelling analysis suggests that passive limestone reactors can be used for treatment of low pH and high ferric iron MIW.

Characteristics of passive limestone systems that will accommodate low pH and high ferric iron concentrations differ from conventional passive design guidance. Significantly smaller limestone aggregate sizes are needed to promote faster rates of limestone dissolution to minimize the reactor footprint. The limestone aggregate must be dispersed within a support matrix to provide pore space to collect iron hydroxide precipitates and maintain limestone reactivity. A multiple reactor approach is required to facilitate replacement of spent reactor media while maintaining treatment capacity.

Passive limestone treatment systems are underutilized for MIW with high ferric iron concentrations but they can be successfully designed using a modified strategy. This paper will present experimental and theoretical analysis to support a design strategy for passive limestone reactors for low pH and high ferric iron MIW.

Development of a Linear Channel Reactor for Simultaneous Sulfate Reduction and Sulfide Oxidation

Robert van Hille, Tynan Marais and Susan Harrison
Centre for Bioprocess Engineering Research, University of Cape Town, South Africa

ABSTRACT

Acid rock drainage from diffuse sources, such as waste rock dumps and coal spoils, poses a significant environmental threat to water resources in South Africa. Passive or semi-passive treatment systems are appropriate for these types of discharge. This research describes the development of a novel reactor unit that achieves simultaneous sulfate reduction and partial oxidation of the sulfide to elemental sulfur that can be recovered as a valuable resource.

The hydrodynamics within the linear channel reactor ensure the majority of the reactor remains anaerobic. Carbon microfibers are provided as a substrate for attachment of the sulfate reducing community and are rapidly colonized. The efficient biomass retention allows for operation at low hydraulic residence time, without cell washout. Sulfide is delivered to the air-water interface, where a floating biofilm containing sulfide oxidizing species develops. The biofilm restricts oxygen penetration, creating the necessary pH and redox environment for partial Sulfide oxidation.

The reactor was fed a synthetic solution containing 1 g/l sulfate, with lactate as the electron donor and carbon source at a COD to sulfate ratio of 0.7. Sulfate reduction efficiencies of over 90% were achieved at hydraulic residence times as low as 1 day. Complete conversion of the Sulfide occurred in the biofilm layer. The biofilm was harvested by collapsing onto a mesh screen 5 mm below the surface. A complete biofilm reformed within 24 hours. After 3-5 cycles the screen was removed and the sulfur recovered. A sulfur mass balance confirmed sulfur recoveries of over 70% of the reduced sulfate, or over 13.5 g/m^2.day. The reactor unit shows good potential as part of an integrated semi-passive process for ARD treatment.

**There is no full article associated with this abstract.*

10th ICARD IMWA 2015 | 10th International Conference on Acid Rock Drainage & IMWA Annual Conference

Bio-Remediation of Acid Mine Drainage Using Charcoal-Based Constructed Wetlands

Ileshree Moodley[1], Craig Sheridan[1], Karl Rumbold[2] Peter Kuschk[3] and Cindy Bartsch[3]

1. *Industrial and Mining Water Research Unit, School of Chemical and Metallurgical Engineering, University of the Witwatersrand, South Africa*
2. *Industrial and Mining Water Research Unit, School of Molecular and Cell Biology, University of the Witwatersrand, South Africa*
3. *Department of Environmental Biotechnology, Helmholtz Center for Environmental Research – UFZ, Germany*

ABSTRACT

Acid mine drainage (AMD) has long been considered to be an environmental hazard worldwide. South Africa faces a significant threat due from AMD, owing to its mining industry. Conventional methods of treating AMD are not always applicable. Constructed wetlands minimize some of these problems. These CWs rely mainly on microbial dissimilatory sulfate reduction (DSR) to treat AMD and a good carbon source is essential for the efficacy of this process. In South Africa, charcoal is known to be cheap, readily available and affords many chemical properties, which could be used to construct low-cost, low maintenance, efficient treatment CWs.

Although charcoal-based CWs can remediate AMD, the mechanisms are still not completely known and in this study we begin to quantify them. For this laboratory-scale study, three batch experiments in anaerobic bottles were conducted. All bottles were filled with a mineral medium containing 400 mg L^{-1} sulfate, the first bottle contained charcoal and glucose, the second contained glucose only and the third contained charcoal only. All three bottles were inoculated with an enrichment culture of sulfate reducing bacteria and the long-term incubation was realized under strict anaerobic conditions.

During the one year monitoring the sulfate concentrations decreased in all three experiments. In experiment I (bottle with charcoal and glucose) and experiment II (bottle with only glucose) sulfate concentrations decreased by an almost identical amount. Both, experiment I and II showed a much greater decline of sulfate concentration than experiment III (bottle without glucose). Thus it was concluded that the sulfate reducing bacteria were quite tolerant to the formed hydrogen sulfide (about 100 mg L^{-1} by calculation) and that the charcoal did not contain any bioavailable carbon source for DSR. Further experiments will test the appropriateness of charcoal to buffer/equalize high toxic heavy metal concentrations in continuous flow-through systems with highly varying concentrations.

**There is no full article associated with this abstract.*

CHAPTER 8

MINE WATER AND DRAINAGE COLLECTION AND TREATMENT – IMPACT ASSESSMENT AND MITIGATION

10th ICARD IMWA 2015 | 10th International Conference on Acid Rock Drainage & IMWA Annual Conference

Manganese Mining Impacts on Water Quality in the Caucasus Mountains, Republic of Georgia

Brian Caruso[1], Merab Mirtskhulava[2], Michael Wireman[3], William Schroeder[3], Boris Kornilovich[4] and Susan Griffin[3]

1. *University of Canterbury, New Zealand*
2. *National Center for Disease Control and Public Health, Republic of Georgia*
3. *US Environmental Protection Agency, USA*
4. *Technical University of Ukraine*

ABSTRACT

One of the world's richest manganese (Mn) deposits and largest Mn mining areas lies in the foothills of the Caucasus Mountains, near the city of Chiatura in the Republic of Georgia. This study was an initial evaluation of the effects of Mn mining on water quality in the Chiatura region. Seven river and stream locations (three on the Kvirila River and four on tributaries), five untreated drinking water supplies (four springs and one groundwater well), and one untreated industrial wastewater discharge (Mn processing) were sampled and analyzed for field indicator parameters, anions, cations, and metals. Five river bed sediment sites (co-located with river water sites) were also sampled and analyzed for metals. Three of the public water supplies were contaminated by coliform bacteria, and concentrations of dissolved Mn, Fe, and Ni exceeded Georgian drinking water criteria in the groundwater supply well. The Kvirila River had very high concentrations of total Mn and Fe relative to an upstream location, especially downstream of the industrial discharges. Several tributaries also had elevated concentrations due to nonpoint source pollution from mine waste near the streams. Mn and Fe loads in the Kvirila River and tributaries were primarily in the particulate form. The river bed sediments at all five sampled river sites contained elevated metal concentrations. Mn and Ni, in particular, were very high in the Kvirila River near the discharges compared to background soil levels. Although Mn and Fe oxide solids in sediment can increase adsorption and attenuation of other metals from the water column, the contaminated sediments can also serve as a long-term residual source of metal contamination of river water, with potentially significant adverse ecological and human health effects.

Keywords: Georgia, manganese, metals, mining, water quality

INTRODUCTION

Numerous former Soviet Union (FSU) nations have diverse mining industries that account for a relatively large percentage of their economic output. The Republic of Georgia's output of ferrous and nonferrous metals, ferroalloys, industrial minerals, and fuels is second only to agriculture in terms of gross national product (Levine and Wallace 2004). The country has more than 300 explored mineral deposits, only about half of which (copper, iron ore, barite, lead, zinc, arsenic, clay, sand, gravel, and a range of secondary metals, including gold and silver) have been brought into production. Georgia has been a major producer of high-grade manganese (Mn) for about a century. It has one of the world's richest Mn deposits and largest Mn mining areas in the foothills of the Caucasus Mountains, centered around the city of Chiatura, in the Imereti region of western Georgia.

The Mn ore deposits near Chiatura, first discovered in 1849, have been exploited since 1879. The ores include pyrolusite and psilomelane (oxide ores) and rhodochroisite (carbonate ore). The country's largest producer, Chiaturmarganets, mines Mn ores from open cast and underground operations in Chiatura, which are supplied to the nearby Zestafoni ferroalloys plant. The Chiatura deposit was estimated to be 215 metric tons of Mn ore, of which about half has been depleted since mining began. Following the dissolution of the Soviet Union, mineral production in Georgia declined sharply. However, Mn has become a critical component in metallurgy, where it has a twofold application: it scavenges impurities such as oxygen, sulfur, and other elements during the steel-making process, and imparts toughness, hardness and abrasion resistance as an additive to steel. Approximately 90% of the Mn consumed in the world is used in Mn ferroalloys. The rest is used to produce nonferrous products, such as aluminum alloys, fertilizers, bricks, and paint, and for water purification.

Although the mining and processing industries in FSU nations have provided many economic and societal benefits, they also have caused significant environmental impacts, including acid mine drainage (AMD) in some areas and contamination of groundwater, surface water, and soils. The degree and significance of AMD and metal contamination of water and soils are affected by complex biochemical reactions in the disturbed ore bodies and associated mine waste materials (tailings and waste rock; Caruso and Bishop 2009; Church et al. 2007; Nimick et al. 2004). Microbes in soils and water help to oxidize the sulfide minerals and catalyze acid- and dissolved metal-generating reactions. However, in Mn deposits, AMD generation is often not the major problem.

Mn is a redox sensitive metal that can exist in water as the manganous ion (Mn^{2+}), or in the oxidized state (Mn^{4+}). Most Mn salts are very soluble in water, but Mn oxides arenot and can easily form solid oxy-hydroxide precipitates that can coat streambeds where concentrations are high. Mn speciation is governed by pH and redox conditions, with Mn^{2+} dominating at lower pH and redox potential, and an increasing proportion of colloidal Mn oxy-hydroxides above pH 5.5 (Scott et al. 2002). Dissolved concentrations undergo diel variations in streams (Brick and Moore 1996; Filipek et al. 1987). Toxic metals and nutrients can co-precipitate with or sorb to Mn oxides (MnOx) on the streambed. Surface catalyzed oxidation and photoreduction can be important processes with regard to fate and transport, particularly in mountain streams (Scott et al. 2002). Light promotes oxidation, precipitation of MnOx, and removal from streams through photosynthetically enhanced oxidation processes (Scott et al. 2002).

Mn in water can be significantly bioconcentrated by aquatic biota at lower trophic levels. Uptake by aquatic invertebrates and fish greatly increases with temperature and decreases with pH, but is not significantly affected by dissolved oxygen (DO). Dissolved Mn concentrations of about 1 mg/L can cause toxic effects in aquatic organisms, and many countries have adopted 0.2 mg/L for protection of 95% of species with 50% confidence (Howe et al. 2004). Mn can be toxic to humans through exposure routes that include ingestion, dermal exposure, and inhalation of particulate forms in air. Inhalation of particulates, especially by workers at Mn mines and processing plants as well as nearby residents, is one of the primary exposure mechanisms and human health risks in the Chiatura mining region. Ingestion of contaminated water or soils/waste material and dermal exposure of residents are also major risks. These risks can be particularly high given the lack of regulations and pollution control, and the high density of poor communities interspersed with the mines, processing facilities, and waste piles, as well as downstream. Mn compounds are well known neurotoxic substances that may cause manganism in humans, a severe neurological disorder characterized by disturbances of movement, as well as Parkinson's disease (Howe et al. 2004; Olanow 2004).

The primary objective of this study was to evaluate the extent and significance of metal contamination, in particular Mn, in waters in the Chiatura region and potential risks to human health from operational and abandoned mines and mine facilities. The study was conducted in collaboration with the Science and Technology Center of the Ukraine, Georgia National Center for Disease Control and Public Health, and the Technical University of Ukraine through the US State Department and US Environmental Protection Agency's Biochemical Weapons Redirect Program. The goal of this program is to aid FSU states in redirecting their biochemical research institutes and scientists to peaceful objectives.

METHODOLOGY

Study Area

Chiatura is located in the Imereti region of western Georgia in a canyon of the Racha Mountains, in the southern foothills of the Greater Caucasus Mountains, 180 km west of Tbilisi, the capital and largest city (Fig. 1). The mines, main factory, and other industrial facilities are situated over an area of 50 km^2. The city lies in a mountain valley along the Kvirila River (named because of its yellow color); the main Chiatura Mine is also located in the valley adjacent to the city (Fig. 2). The city and its ore-enriching plants cluster in the narrow valley, with mines in the surrounding hills linked by cable railways and aerial carriers. The smelter receiving Mn concentrate from mines in Chiatura is located in the city of Zestafoni, 30 km to the southwest. The primary Mn factory (owned and operated by the Chiatura Manganese Company) is located adjacent to the left bank of the river in the village of Perofi in the Darkveti area. There is a railway connection between Chiatura and Zestafoni.

The Chiatura Mn deposits are situated in the north periphery of the Dzirula crystalline massif, in the middle reach of the Kvirila River. The area represents an almost horizontal plateau, divided by the Kvirila River and its tributaries. The ancient rocks are Palaeogene formations overlain by Jurassic rocks. These are overlain by Cretaceous sediments. Oligocene rocks are in upper layers with Mn beds, topped with middle-upper Miocene and ancient– modern Quaternary alluvial formations. The deposits are confined by major faults to the southwest. Within the boundaries of the deposit, Quaternary, Tertiary, Upper Cretaceous, Jurassic, and Palaeozoic hydrogeological

complexes can be delineated. Alluvial water-bearing horizons generally have high concentrations of Mn. Waters of the Sarmatian water-bearing horizons are used for water supply by the settlements on the left bank of the Kvirila River. The average hydraulic conductivity of these formations is

approximately 0.8–0.9 m/day; the depth to water is 6–8 m and the water is dominantly calcium bicarbonate, with 0.6–0.8 g/L of total dissolved solids and 9.8 mg-eq of hardness.

The climate in Chiatura is humid; the winters are moderately cold and the summers are hot and dry. Due to its location in the foothills of the Greater Caucasus Mountains, the Chiatura region receives a significant amount of precipitation, including a high snowpack with peak seasonal snowmelt in spring. The average annual precipitation is 1,100–1,200 mm, with greater depths at higher elevations and a maximum in autumn and winter. This water can drive the mobilization and transport of pollutants, including metals, from source areas such as tailings and waste rock piles to ground and surface waters in the form of nonpoint source pollution. Drinking water in the area is supplied primarily by four springs with headworks and one communal groundwater well; no water treatment or chlorination occurs.

There are approximately 20 Mn mines in the Imereti District and Chiatura region. Eleven mines are open pit and nine are underground mines. Sixteen of the 20 mines are located in tributary watersheds north of the Kvirila River and four are located south of the river. It is not known how many of these mines are currently operating because this type of information is not readily available from Georgian authorities or from the mining company. The Kvirila River flows through the center of themain ChiaturaMn deposit and is a tributary of the Rioni River, which flows west to the Black Sea. Numerous small mountain rivers and streams discharge to the Kvirila River, and several villages are located in the canyons of these tributaries. Mn mines are also located near some of these villages. Tailings and slag waste is present in large quantities above ground throughout the area. The waste contains primarily Zn, Pb, Ni, Co, Mn, and other potentially toxic substances based on preliminary information from the mining company. Industrial wastewater is also directly discharged untreated from the Chiatura Mn factories (including the peroxide enrichment factory (PEROF) and the ‘‘central keeping facility’’ (CKF), which is the main ore processing facility) to the Kvirila River. The environmental conditions, the proximity of the mines, tailings, and discharges to the river and human settlements, and the lack of adequate management or regulation of operations cause significant environmental and human health risks not only to the Chiatura region, but to all territories that the river flows through on its way to the Black Sea.

Figure 1

Figure 1 Location map of the Republic of Georgia, Caucasus Mountains, and Chiatura

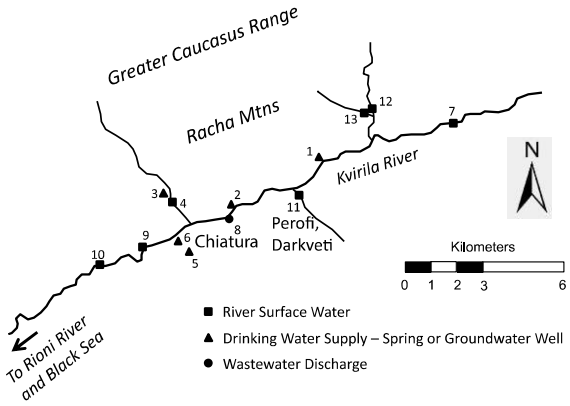

Figure 2

Figure 2 Sampling location map for Chiatura. Sites numbers refer to locations in Table 2

Sampling and Analysis

Water quality samples were collected at seven river and stream locations and five drinking water supply locations (four springs and one groundwater well) throughout the Chiatura study area (Fig. 2; Table 1). One sample was also collected directly from the industrial wastewater discharge from the main Mn factory (Perophi peroxide enrichment factory). Samples were collected as part of three synoptic sampling events during spring (April high flow) and late summer/autumn (September low flow) 2009, and early summer (June high flow) 2010.

Field indicator parameters included temperature, pH, DO, and specific conductivity (SC). Laboratory analytes included alkalinity, chloride (Cl), sulfate (SO_4), nitrate (NO_3), 5-day biochemical oxygen demand (BOD_5), chemical oxygen demand (COD), E. coli, metals (Na, K, Ca, Mg, Al, Cd, Co, Cu, Fe, Mn, Ni, Pb, and Zn), and As. All water quality-sampling tasks followed USEPA Region 8 standard operating procedures (SOP) for field sampling protocols (USEPA 2002). Field meters were calibrated according to the USEPA Region 8 SOP for the HydroLab multiprobe (USEPA 2003). Precision and accuracy for field indicator parameters were based on the USEPA field sampling protocols (USEPA 2002), or the manufacturer's specifications. Total carbonate hardness was estimated from Inductively Coupled Plasma Mass Spectrometry measurements of dissolved calcium and magnesium as $CaCO_3$. Samples for hardness, alkalinity, SO_4, NO_3, and Cl were collected in 250 mL HDPE containers and chilled to 4°C for preservation. A minimum of 125 mL of sample was collected for both dissolved and total metals analysis. Dissolved metals samples were filtered within 15 min of collection using a 0.45 μm filter (USEPA 2002). Total and dissolved metals were only sampled and analyzed during the first sampling round in April 2009. Only dissolved metals were sampled and analyzed during the other two sampling events. All metals samples were collected into HDPE or LDPE containers and preserved with 0.5 mL nitric acid in the field. Samples were analyzed by either a privately contracted laboratory (GAMMA), the Georgia Ministry of Environment Protection and Natural Resources, or the Technical University of Ukraine. Chain-of-custody procedures followed the USEPA field sampling protocols (USEPA 2002).

Table 1 Summary of Chiatura area water quality sampling locations

Table 1. Summary of Chiatura area water quality sampling locations

Site	Location	Description	Type
1	Grudo water supply	Near village of Grudo	Drinking water supply/Spring
2	Monasteri water supply	Water collecting reservoir near Fasknara	Drinking water supply/Spring
3	LeJubani water supply	Near village of LeJubani	Drinking water supply/Spring
4	Rgani stream	Right bank tributary	Tributary
5	Gagarin groundwater well water supply	On Gagarin Street	Drinking water supply/Well
6	Sakurdglia water supply	Near village of Sakurdglia	Drinking water supply/Spring
7	Kvirila River upstream	Near village of Sareki upstream of most mines	Main stem river
8	PEROF	Peroxide enrichment factory	Industrial wastewater discharge
9	Kvirila River upstream of CKF	Near administation building and village of Tiri	Main stem river
10	Kvirila River downstream of CKF	Downstream of most mines	Main stem river
11	Shuqruti Stream	Left bank tributary	Tributary
12	Jruchula River	Right bank tributary	Tributary
13	Darkveti Stream	Right bank tributary	Tributary

Dissolved As, Pb, and Zn were not sampled or analyzed after the first sample round in April 2009 because neither the total or dissolved forms of these metals were detected at any locations during that round. This was also partly the result of our limited budget for analysis, a typical issue in FSU countries. It is believed that these metals are only present at very low concentrations in the ore and the Chiatura environment, but the reason for their low levels is not known. Ca and Mg, alkalinity, sulfate, Cl, NO_3, BOD_5, and COD were also not sampled or analyzed during the last sampling round (June 2010) due to funding limitations. E. coli was only sampled and analyzed once during the first sampling round at the drinking water supply locations.

River bed sediment samples were collected at five locations during the three water quality sampling events. These were co-located with five of the surface water sampling sites: the Kvirila River upstream of Chiatura, the Kvirila River upstream and downstream of the CKF, Shuqruti stream, and the Jruchula River.

Field and analytical results were evaluated over time/between high and low flow sampling events and across locations and water types (river surface waters, spring or groundwater drinking water supply, and wastewater discharge). Results were also compared to applicable water quality standards and criteria. Georgian Ministry of Labour, Health and Social Affairs (2007a) maximum allowable concentrations (MACs) for drinking water were used for most analytes. Georgian regulations do not include MACs for toxic substances (including metals) in river bed sediments. Therefore, representative reference or 'background' values for Georgian soils (Ministry of Justice of Georgia 2003a, b) were used for comparison.

RESULTS AND DISCUSSION

The focus of the results here is on dissolved and total metals. With regard to indicator and other analytes, however, pH ranged from 6.5 to 8.8 across the 13 locations and three sampling events, reflecting circumneutral or slightly alkaline conditions. SC values were greatest in the Darkveti Stream samples (up to 1,869 µS/cm). Alkalinity was low and within the guidelines, with a range of 1.9–5.4 mg/L. Sulfate was above 100 mg/L in several stream samples, although all values were below the criterion of 250 mg/L, and concentrations at other sites were low. Alkalinity and sulfate values indicate that AMD is not a problem in this area. In April 2009, E. coli values exceeded the criterion (1 cfu/100 mL) at three locations (up to at 12 cfu/100 mL at the Grudo water supply).

With the exception of Mn and Fe, few samples had dissolved or total metal/semi-metal concentrations that exceeded drinking water MACs, and even the frequency of detection was rather low. In surface waters, the only dissolved or total metals that exceeded drinking water MACs were Mn and Fe at numerous locations and Ni in Darkveti Stream. Darkveti Stream generally had the highest concentrations of most metals, but values in the Kvirila River upstream and downstream from the CKF, and in Jruchula, Shuqruti, and Rgani streams, also sometimes exceeded criteria. As expected, the PEROF industrial (peroxide enrichment factory) discharge from the enrichment factory, which is untreated, had the highest levels of total Mn and Fe, but relatively low levels of dissolved Mn and Fe. Concentrations of dissolved and total Al, As, Cd, Pb, and Zn were all below detection limits.

For total metals sampled and analyzed in April 2009, Mn and Fe concentrations exceeded the MACs in most surface water samples. Total Mn concentrations were also very high upstream of the CKF, and in the Darkveti and Shuqruti stream samples. In the PEROF discharge, total Mn concentrations ranged from 0.85 to 7.62 mg/L. Total Fe concentrations increased to 18.4 and 22 mg/L in September 2009 and June 2010. These increases were likely due to increased mining and processing operations during this time period.

With regard to dissolved metals, Mn concentrations were very high in the Darkveti September 2009 (2.4 mg/L) and June 2010 (6.65 mg/L) stream samples relative to the MAC (Fig. 3). Only two other locations exceeded the MAC: the Shuqruti April 2009 stream sample and the Gagarin water supply well in both April and September 2009. Dissolved Mn concentrations in the PEROF discharge ranged from <0.2 to 0.34 mg/L. Mn loads in most surface waters are dominated by suspended Mn.

Dissolved Fe was only detected above the MAC in the PEROF discharge during the second sampling round in September 2009, and in the Rgani stream and Gagarin water supply samples in June 2010 (Fig. 4b). Similar to Mn, dissolved and total Fe data also indicate that Fe loads in the Kvirila River are dominated by particulate Fe.

All drinking water supply samples met the criteria for metals, except for the Gagarin groundwater supply well, where dissolved Mn, Fe, and Ni exceeded the MACs on at least one occasion. The June 2010 Mn and Fe concentrations were higher than in the previous sampling events in the Gagarin groundwater supply. Dissolved Co and Cu were only occasionally detected below the MACs. Total and dissolved metal concentrations were very similar between the other four public drinking water supplies.

Evaluation of temporal changes showed that concentrations of dissolved Mn increased in Darkveti Stream from April 2009 to June 2010. Increases of Na, K, Ni, and Co were also observed in 2010. These increases are generally attributed to greater inputs from metal sources and concentrations over time, rather than correlation with season or river flows. Both Mn and Fe concentrations were greater in the PEROF discharge in 2010 compared to previous years. Total Mn increased to 34 mg/L in the PEROF discharge in 2010, which was much higher than previous values.

Mn oxides do not readily dissolve and can easily form solid oxy-hydroxide precipitates that can coat streambeds where high concentrations occur, or can be transported as suspended particles under adequate hydraulic conditions (Scott et al. 2002). Other metals and nutrients can co-precipitate with or sorb to Mn oxides (MnOx) on the streambed (Butler and Caruso 2009; Gadde and Laitinen 1974). This adsorption can increase significantly with an increase in pH (Gadde and Laitinen 1974). Therefore, hydrous Mn oxides can play an important role in the fate and transport of other metals in rivers, such as Cd, Cu, and Zn, and should be considered in modeling and remediation (Butler and Caruso 2009). Adsorption of metals to bed sediment is also a function of

the percent of fine particles and clay, as well as organic matter/carbon (Caruso and Bishop 2009). The physical and chemical characteristics of the bed sediment and form of solid Mn and Fe on the river bed in the study area should be analyzed further.

The oxides and hydrous oxides of both Mn and Fe dissolve under reducing conditions that can occur with burial or mixing below surface layers of sediments beneath oxygenated waters (Van Cappellen and Wang 1996). Fe^{2+} and Mn^{2+} in pore water generated in the anaerobic zone can adsorb onto sediment, co-precipitate as a number of mineral phases, or move (by pore water diffusion and dispersion) back to the sediment-water interface. Redox of Fe and Mn is complex and can occur through a number of pathways, including benthic microbial and macroinvertebrate activity (Van Cappellen and Wang 1996). Biotic oxidation is an important process for removal of Mn^{2+} onto Mn oxides in the hyporheic zone and is directly proportional to Mn^{2+} concentration and pH (Fuller and Harvey 2000; Harvey and Fuller 1998; Marble 1998). Surface catalyzed oxidation and photoreduction can also be important with regard to fate and transport, especially in mountain streams (Scott et al. 2002).

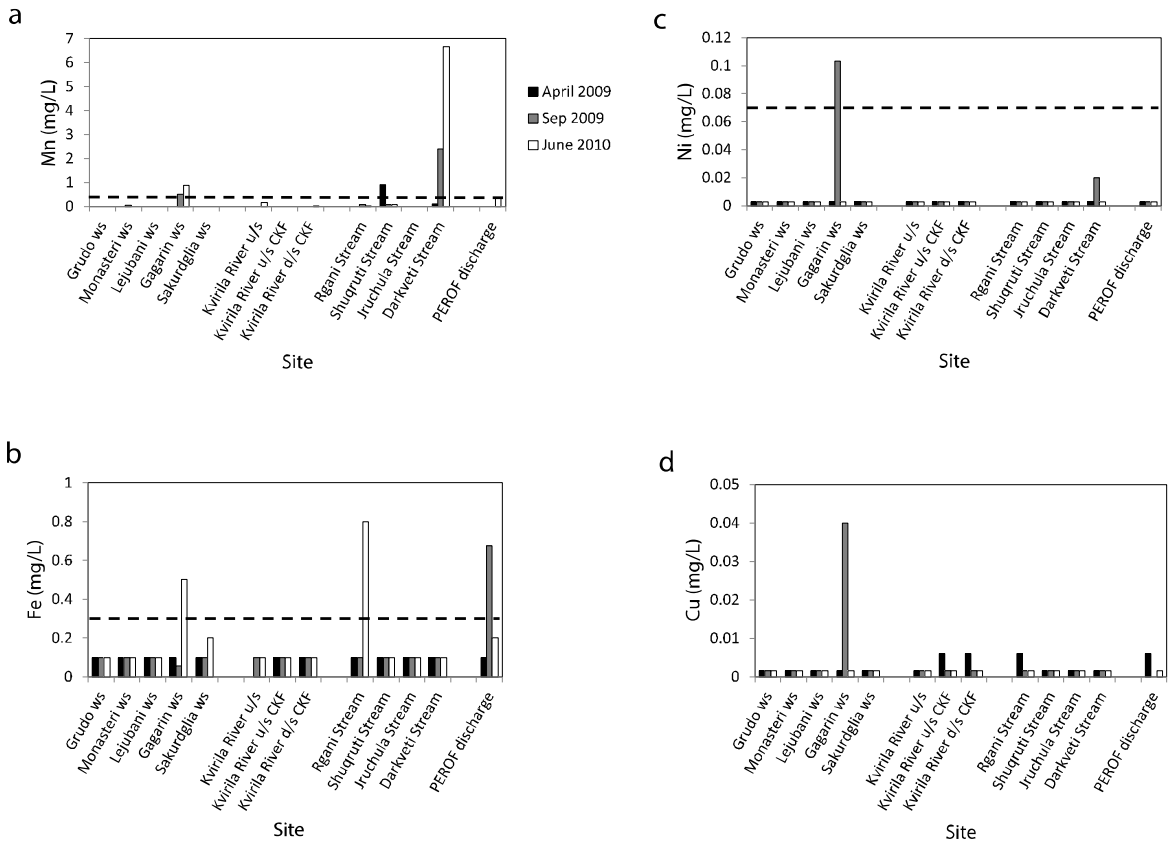

Figure 3 Chiatura dissolved metals results in water for a Mn, b Fe, c Ni, and d Cu. Dashed line is Georgian maximum allowable concentration (MAC). All MACs are for drinking water; MAC for Cu is 2.0 mg/L (not shown); ws water supply; u/s upstream; d/s downstream

River bed sediment metals concentrations were elevated at all five surface water sites. Background concentrations from Georgian estimates for soils were not available for Al and Fe, but Al values

ranged from 3.9% in the Kvirila River upstream of the CKF to 6.7% in the Jruchula Stream. Cd concentrations exceeded the background value of 0.5 mg/kg at all five locations, and were highest in the Kvirila River upstream and downstream of the CKF (3.2–4.5 mg/kg). Cu values followed a similar pattern, exceeding the background concentration of 3 mg/kg and having the greatest values at those two locations (44–70 mg/kg). Mn concentrations in the Kvirila River upstream and downstream of the CKF were very high and exceeded the background value for soils of 1,500 mg/kg (in the range of 80,000–95,000 mg/kg or 8–9.5%). Mn values also exceeded the background value at the other sites. Fe concentrations ranged from 1.5% in the Kvirila River upstream of the CKF to 3.9% for the furthest upstream Kvirila River sample). Fe concentrations were also elevated in the Kvirila River upstream and downstream of the CKF during some sampling rounds (2.4–3.6%).

The Kvirila River bed sediment metal concentrations generally were higher in 2010 than in 2009 with the exception of two locations (upstream and downstream of the CKF) where Mn concentrations in 2010 decreased (5.35 and 4.8%) compared to 2009 (9.5–8.0 and 8.5–8.0%, respectively). Cu values also decreased somewhat at these two locations. The reason for these decreases is not known, but transport and flushing of sediment from high flows could be a factor, as could dissolution of metal oxides or adsorbed metals to the water column. No other temporal trends were apparent in sediment concentrations at other locations. Although MACs for metals in river bed sediments have not been established by the Georgian government, comparison of Mn and Fe concentrations in sediment samples from the Kvirila River upstream and downstream of the CKF with Georgian background values for soils indicates that the sediments meet the criteria for ''highly-polluted soils''; sediment samples from the Jruchula and Shuqruti streams meet the criteria for ''low-polluted soils'' (Georgia Ministry of Labour, Health and Social Affairs 2007b).

CONCLUSION

Drinking water samples taken from three of the public water supplies (Grudo, Monasteri, and LeJubani) in the Chiatura mining area were contaminated by coliform bacteria. E. coli concentrations exceeded the criterion of 4 cfu/100 mL in samples from the Grudo and Monasteri supplies. Concentrations of dissolved Mn, Fe, and Ni exceeded the drinking water MAC in the Gagarin groundwater supply well.

Simple water treatment systems should be installed for the Grudo, Monasteri and LeJubani water supplies. The water should not be used for drinking without disinfection due to the risk of water-borne infectious and viral diseases. Drinking water in the catchment reservoirs of the Grudo, Monasteri, and LeJubani water supply systems should also be routinely disinfected. Drinking water quality in Chiatura's central water supply lines should be monitored based on Georgian government requirements and standard international practice to protect public health.

The communal Gagarin Street groundwater supply well should be cleaned and disinfected in accordance with Georgian government regulations and standard practices. Long-term consumption of this water may damage the digestive tract. The well should be re-sampled and analyzed for Mn, Fe, and Ni on a routine basis. If these metals continue to occur at levels above the MACs, the use of well water for drinking should be discontinued.

The Kvirila River is contaminated with Mn and Fe relative to the upstream location. Total Mn levels were almost 15 times the MAC downstream of the discharge from the CKF. Concentrations of total Mn were 2–12 times the MAC in Darkveti, Shuqruti, and Rgani streams, and total Fe values were 8–

55 times the MAC in these tributaries. Mn and Fe loads in the Kvirila River and most tributaries are primarily in the particulate form. Concentrations of dissolved metals in samples from the seven surface water locations were below the MAC except for dissolved Mn in Darkveti Stream and the Kvirila River upstream and downstream of the CKF. The primary sources of Mn and Fe in the Kvirila River are the untreated industrial wastewater discharged from the CKF, tailings and waste rock associated with the Mn ore disposed of on the Kvirila River floodplain, and the main tributaries (primarily Darkveti and Shuqruti streams).

Concentrations of all metals, including Mn and Fe, in river bed sediments were elevated at all seven river sites. Mn and Ni, in particular, were very high compared to background soil levels in the Kvirila River upstream and downstream of the CKF. Although Mn and Fe oxide solids in sediment can increase adsorption and attenuation of other metals from the water column, contaminated sediments can also serve as a long-term residual source of metal contamination of river water with significant adverse ecological and potential human health effects.

Use of the Kvirila River before and after the CKF, as well as Darkveti Stream, for drinking, economic, cultural, and household purposes should be prohibited. Based on Mn concentrations, these areas are extremely highly polluted water, according to Georgian regulations. Use of these rivers may result in increased exposure to Mn and associated diseases and symptoms. Water in Shuqruti and Rgani streams meets the criterion for moderately polluted water. Water from these rivers may be used as a drinking and economic water supply source only if the pollution level is reduced through end-of-the-pipe treatment.

Solid mine waste (tailings and waste rock) have been disposed of on the floodplain surface along the Kvirila River and some tributaries. This waste material is a significant source of metals that will continue to impact the water quality and ecological health of the Kvirila River and some tributaries. Industrial mine waste from the enrichment and processing plants should be managed in a way that isolates the material from the rivers and groundwater. The specific pollution sources in the Kvirila River should be identified and evaluated, and routine sampling of the river should be conducted at key locations. Discharge of untreated wastewater from the peroxide enrichment factoryinto surface waters should be discontinued as soon as possible and treatment facilities should be installed at the plant.

ACKNOWLEDGEMENTS

We thank Iryna Tomashevska and Victor Korsin of the Science and Technology Center in Ukraine, and Bill Freeman (Office of International Affairs) and Doug Steele (Office of Research and Development) of the US Environmental Protection Agency for administrative and logistical support, and overall direction of the project. We also thank several anonymous reviewers for very helpful comments on the original paper.

REFERENCES

Brick CM, Moore JN (1996) Diel variation of trace metals in the Upper Clark Fork River,Montana. Environ Sci Technol 30(6):1953–1960

Butler BA, Caruso BS (2009) Reactive transport modeling of remedial scenarios to predict cadmium, copper and zinc in the North Fork of Clear Creek, Colorado. Remediation 19(4):101–119

Caruso BS, Bishop M (2009) Seasonal and spatial variation of metal loads from natural flows in the upper Tenmile Creek Watershed, Montana. Mine Water Environ 28:166–181

Church SE, von Guerard P, Finger SE (eds) (2007) Integrated investigations of environmental effects of historical mining in the Animas River Watershed, San Juan County, Colorado. USGS Prof Paper 1651, Washington DC, pp 417–495

Filipek LH, Nordstrom DK, Ficklin WH (1987) Interaction of acid mine drainage with waters and sediments of West Squaw Creek in the West Shasta Mining District, California. Environ Sci Technol 21:388–396

Fuller CC, Harvey JW (2000) Reactive uptake of trace metals in the hyporheic zone of a mining-contaminated stream, Pinal Creek, Arizona. Environ Sci Technol 34:1150–1155

Gadde RR, Laitinen HA (1974) Studies of heavy metal adsorption by hydrous iron and manganese oxides. Anal Chem 46(13): 2022–2026

Georgia Ministry of Labour, Health and Social Affairs (2007a) Technical regulations for drinking water—order #349/n

Georgia Ministry of Labour, Health and Social Affairs (2007b) Sanitary rules and norms for surface water protection against pollution, SanRandN 2.1.5. 001–01

Harvey JW, Fuller CC (1998) Effect of enhanced manganese oxidation in the hyporheic zone on basin-scale geochemical mass balance. Water Resour Res 34:623–636

Howe PD, Malcolm HM, Dobson S (2004) Manganese and its compounds: environmental aspects. Concise international chemical assessment doc 63. World Health Org, Geneva

Levine RM, Wallace GJ (2004) The Mineral Industries of the Commonwealth of Independent States. Armenia, Azerbaijan, Belarus, Georgia, Kazakhstan, Kyrgyzstan, Moldova, Russia, Tajikistan, Turkmenistan, Ukraine, and Uzbekistan. USGS Minerals Yearbook, Reston

Marble J (1998) Biotic contribution of Mn(II) removal at Pinal Creek, Globe, Arizona. Unpubl MS thesis, Department of Hydrology and Water Resources, University of Arizona, Phoenix

Ministry of Justice of Georgia (ed) (2003a) Hygienic evaluation of soil in residential areas. Guideline 2.1.7.003–02, Georgian Official Juridical Journal Macne, #16 6.03.2003

Ministry of Justice of Georgia (ed) (2003b) On the assessment of the hazard related to soil contaminated by chemicals. Guideline 2.1.7.004–03, Georgian Official Juridical Journal Macne, #166.03.2003

Nimick DA, Church SE, Finger SE (eds) (2004) Integrated investigations of environmental effects of historical mining in the Basin and Boulder Mining Districts, Boulder River Watershed, Jefferson County, Montana. USGS Prof Paper 1652, Washington DC

Olanow CW (2004) Manganese-induced Parkinsonism and Parkinson's disease. Ann NY Acad Sci 1012:209–223. doi:10.1196/ annals.1306.018

Scott DT, McKnight DM, Voelker BM, Hrncir DC (2002) Redox processes controlling manganese fate and transport in a mountain stream. Environ Sci Technol 36:453–459

USEPA Region 8 (2002) Standard operating procedure #720. EPA Region 8 field sampling protocols. US Environmental Protection Agency, Denver

USEPA Region 8 (2003) Standard operating procedure #710: setup, calibration, maintenance, and use of the hydrolab multiprobe. US Environmental Protection Agency, Denver

Van Cappellen P, Wang Y (1996) Cycling of iron and manganese in surface sediments: a general theory for the coupled transport and reaction of carbon, oxygen, nitrogen, sulfur, iron, and manganese. Am J Sci 296:197–243

Best Available Technologies Economically Achievable (BATEA) to Manage Effluent from Mines in Canada

Kristin Pouw, Kathryn Campbell and Lisa Babel
Hatch, Canada

ABSTRACT

Hatch was commissioned by the Canadian Mine Environment Neutral Drainage (MEND) Program to complete a study to identify best available technologies economically achievable (BATEA) for the augmentation of existing effluent treatment systems, to improve effluent quality from mines in Canada. The study was commissioned in order to provide reference information to policy makers, industry, and civil society organizations for use in evaluating potential forthcoming changes within the Canadian *Metal Mining Effluent Regulations* (*MMER*) to the types of regulated mining facilities (addition of diamond and coal mines), the list of regulated parameters, and the authorized limits of regulated parameter concentrations in effluent discharged to the environment. This paper presents the overall objectives and methodology of the study and the participatory process used to gather and validate information, an overview of the various Canadian mining subsectors examined (metal mining: base metal, precious metal, iron ore, and uranium; diamond mining, and coal mining), a summary of technologies considered to be best available technologies (BAT) for Canadian mine effluent treatment, and incremental costs of implementing and operating BAT. BAT are defined as those technologies which have been demonstrated through full scale operation to achieve the present *MMER* regulated parameter limits via treatment of mine effluent under representative Canadian climate conditions. Finally, the paper presents Hatch's findings on best available technologies economically achievable (BATEA) for augmentation of effluent treatment systems, interpreted as technologies that can improve effluent quality through upgrades to existing treatment systems for a given subsector, within reasonable incremental capital and operating costs, as compared with previous capital expenditures and current operating cost expenditures. The study largely focuses on the improvement of effluent quality at existing operations; however, some BATEA suggestions for greenfield operations are also made. Parallels between the Canadian mining jurisdiction and other major international mining jurisdictions are drawn.

INTRODUCTION

Environmental regulations for the mining industry are becoming more stringent in many jurisdictions, amplifying the need for effective and efficient effluent treatment systems that are also economically viable. In Canada, the quantity and quality of mining effluent discharged to the environment are regulated at the federal and provincial/territorial levels. Potential forthcoming changes to the federal *Metal Mining Effluent Regulations* (*MMER*) generated a need to examine conventional approaches to effluent treatment at mining and mineral processing operations, with a focus on concentrations demonstrated by conventional technologies and which technologies are economically and operationally viable at Canadian operations, considering site conditions such as remote location and seasonal climatic variability.

The proposed changes to the *MMER* are outlined in the Environment Canada 2012 discussion paper, "10-Year Review of Metal Mining Effluent Regulations," and include:

- The addition of total ammonia, aluminum, iron, and selenium to list of regulated parameters for metal mines (base metal, precious metal, uranium, iron ore).
- The reduction in authorized limits of regulated parameter concentrations in effluent for metal mines.
- The addition of diamond and coal mines to the types of regulated mining facilities[1], and,
  - the introduction of authorized limits for pH, chloride, phosphorus, total suspended solids (TSS), and total ammonia as regulated parameters for diamond mines,
  - the introduction of authorized limits for pH, aluminum, arsenic, iron, manganese, selenium, TSS, and total ammonia as regulated parameters for coal mines (Environment Canada, 2012).

Environment Canada is undertaking the review of the *MMER* within a context of multi-stakeholder consultation, whereby stakeholders including industry, industry associations, regulators, non-governmental organizations, and First Nations organizations are engaged in working groups in order to provide feedback on the proposed changes through a series of meetings and workshops. As part of this multi-stakeholder consultation process, Hatch was commissioned by the Mine Environment Neutral Drainage (MEND) Program, on behalf of regulatory and industry stakeholders, to complete a study of water management and treatment practices at mining operations in Canada and to identify best available technologies economically achievable (BATEA) for the augmentation mining effluent treatment.

Hatch's study identifies and describes best available technologies (BAT) employed at metal, diamond, and coal mine operations in Canada and proposes BATEA for each sector. BAT were identified and characterized via extensive questionnaires issued to mining operations and technology vendors, as well as independent research. BATEA were selected based on a comparative assessment of the benefits in terms of effluent quality improvement against the incremental implementation and operating costs for each applicable BAT. BATEA selections are generic, in that they are based on the augmentation of a sector model effluent treatment system and do not consider site-specific factors not captured by the model. BATEA selections are also neutral, in that

[1] The diamond mining and coal mining sectors are presently not regulated by the *MMER*.

Hatch is not a water treatment technology supplier and has no vested interest in technology selection.

METHODOLOGY

Establishing Sector Models

A base case model for each sector representing the most commonly utilized water management practices and treatment process was established based on information collected from mine and mill operations. This model was utilized to identify and evaluate potentially augmentative technologies to improve effluent quality. To identify the most common practices, Hatch prepared a list of Canadian metal (i.e., base metal, precious metal, iron ore, and uranium), coal, and diamond mines. This list included the company, operation name, subsector classification by primary commodity, the location, and the operational status of the mine. After extensive revision and refinement of this list with the assistance of provincial, territorial, and federal industry associations, an operations contact list was generated. A comprehensive operations questionnaire was distributed to the contact list in order to solicit information on factors that impact treated effluent quality (i.e., mining, processing, and waste disposal practices, water management and effluent treatment systems, and untreated and treated effluent quality), as illustrated in Figure 1.

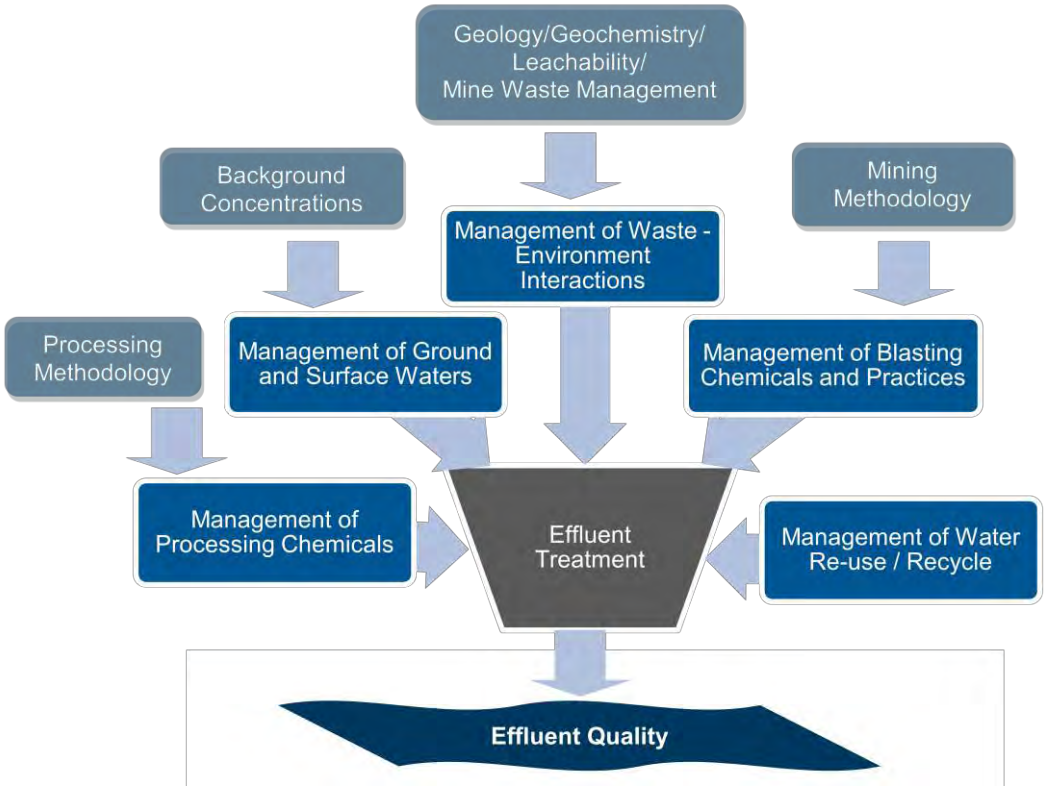

Figure 1 Factors of mine effluent quality

The questionnaire had an overall completion rate of 45% on an operations basis (i.e., 45% of individual operations identified as relevant to the study submitted completed questionnaires). This corresponds to 75 of the 164 operations contacted. By sector, the questionnaire completion rate varied between 32% and 75%. A more detailed summary of the questionnaire completion status by sector is provided in Table 1.

Table 1 Operations questionnaire completion by sector

Sector/Subsector	Number of Companies	Number of Operations Contacted	Number of Questionnaires Submitted
Metal			
Base Metal	31	57	31 (54%)
Precious Metal	33	56	18 (32%)
Iron Ore	4	6	2 (33%)
Uranium	4	16	7 (44%)
Diamond	4	4	3 (75%)
Coal	12	30	13 (43%)

Questionnaire responses were processed into a database format so the data could be easily compared and analyzed. Where necessary, follow-up inquiries were made with questionnaire respondents to clarify information provided prior to inclusion in the database and study report, in order to limit interpretation bias.

The database was compared with regulatory reporting information provided by Environment Canada, which included effluent discharge volume and quality data for all of the operations subject to *MMER*, as well as effluent discharge volume and quality data for the diamond sector, and a summary of effluent treatment technologies employed by operations in Ontario. Similar data for the coal sector was provided by the Coal Association of Canada, however discharge volumes were not provided. Additionally, because the coal sector data was anonymous, effluent quality data could not be related to operational practices and other effluent-influencing factors.

Later, a short follow-up survey was distributed to collect additional information from operations about effluent treatment system flow rates, final discharge point names used in *MMER* reporting, treatment system process unit operations, mechanism of removal of targeted contaminants, and influent and effluent quality data.

In combination with the questionnaires and resources described above, Hatch also undertook independent research to collect supplemental information about mining operations. This independent research drew from in-house knowledge and publicly available information concerning mining operations and effluent treatment processes (e.g., environmental compliance approvals, certificates of authorization, permits, etc.).

Based on the information collected, Hatch established a generic effluent management and treatment base case model for each mining sector. Each base case consists of a model water management block flow diagram, a model water treatment block flow diagram, nominal and design treatment flow rates, and treated effluent quality produced by model or model-like effluent treatment systems. The effluent treatment model developed for the base metal subsector of the metal mining sector is provided as an example in Figure 2. The models represent the most common practices and treatment systems for the sector described to Hatch by industry via the information provided in the

questionnaires, as illustrated in Figure 3. While more technologically advanced systems may be employed at Canadian mines, the model serves to exemplify the most common system as reported by industry.

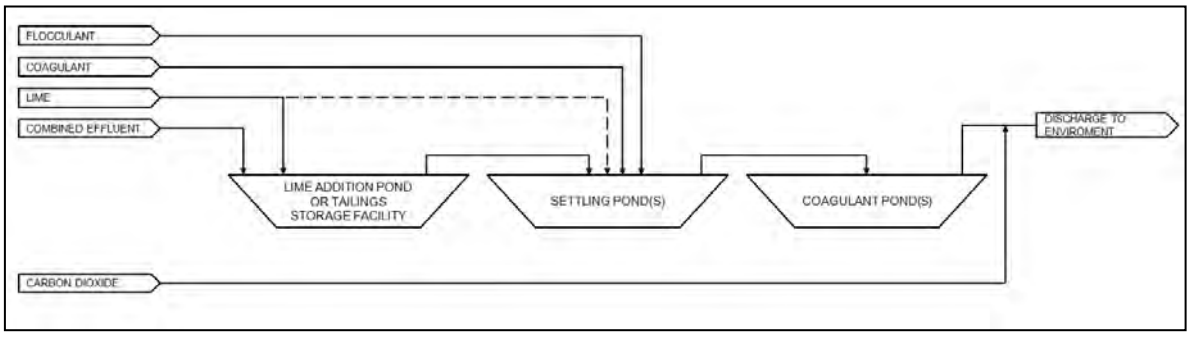

Figure 2 Base metal subsector effluent treatment model

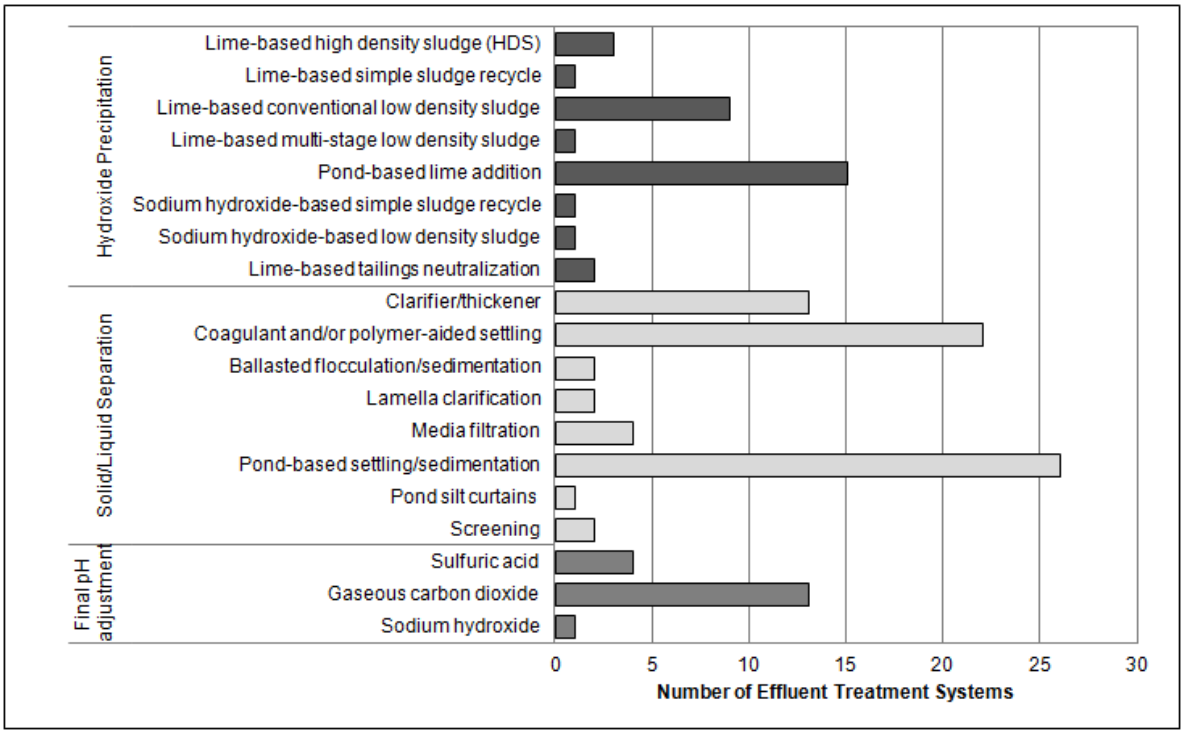

Figure 3 Distribution of hydroxide precipitation, solid/liquid separation, and final pH adjustment technologies for the base metal subsector

Model nominal and design treatment flow rates were generated from effluent discharge volume data and operations questionnaires, using a number of analytical approaches to generate statistical information and then applying judgment to select mid-range values. Model treated effluent concentrations for each current and proposed *MMER* parameter were determined by generating statistical treated effluent quality values for operations that employ model and model equivalent

treatment systems and also self-identify as targeting the parameter for removal with treatment. This was done to minimize the statistical influence of operations that do not employ model or model-equivalent treatment systems and that do not target the specific parameter being analyzed for treatment (i.e., treatment is not required for parameter compliance with discharge limits).

Identifying BAT Technologies

To identify best available technologies, Hatch first compiled a list of treatment technologies currently available on the market, both active and passive, that are applicable to the control of effluent quality for those contaminants that are currently or potentially regulated by the MMER. A questionnaire was distributed to vendors to solicit input concerning proprietary technologies, including existing case studies of their use, and capital and operating cost information.

The technologies included in the preliminary technologies list were then screened against the following criteria questions:

1. Can this technique achieve current MMER discharge limits?
2. Has this technique been demonstrated at full scale on mining effluent?
3. Has this technique been demonstrated under representative Canadian climate conditions?

Technologies that met all three criteria were carried forward in the study as best available technologies (BAT) for the treatment of Canadian mining effluent. BAT technologies are summarized in Table 2.

Table 2 Best available technologies and targeted (X) and synergistically removed (+) contaminants

Best Available Technologies	pH	Al	As	Cl	Cu	CN	Fe	Pb	Mn	Ni	P	Se	Zn	Ra-226	TSS	NH_3/ NH_4^+
Neutralization and Hydroxide Precipitation	X	X	+		X		X	X	+	X	+		X		+	+
Sulfide Precipitation			X		X		X	X	X	X		X	X		+	
Ferric Iron or Aluminum Salt Co-Precipitation			X								X	X			+	
Barium Chloride Co-Precipitation														X	+	
Metal Oxidation							X		X							
Reacidification	X															+
Solid/Liquid Separation		+	+		+		+	+	+	+	+	+	+	+	X	
Enhanced Coagulation and Settling		+	+	+	+		+	+	+	+	+	+	+	+	X	
Cyanide Destruction (SO_2/Air and/or H_2O_2)						X										
Air Stripping																X
Ion Exchange	+	X	X	X	X	+	X	X	X	X	+	X	X	+		X
Adsorption																
Zero Valent Iron			+				+	+	+			X	+			
Biological Oxidation/Reduction																
Aerobic Biological Oxidation						X										X
Active Anoxic/Anaerobic Biological Reduction			+		+		+	+	+	+		X	+			
Membrane Size/Charge Exclusion – Nanofiltration		X	X		X		X	X	X	X	X	X	X	X		
Membrane Size/Charge Exclusion – Reverse Osmosis		X	X	X	X	X	X	X	X	X	X	X	X	X		X
Passive Treatment																
Natural Degradation						X					+					X
Aeration Cascades							X		X							

For each best available technology, the following aspects of implementation and operation were elaborated: incremental capital and operating costs, removal efficiencies and/or achievable concentration levels, applicability to Canadian mining effluent treatment, and the synergies and challenges resulting from the application of the technology for the control of effluent quality.

For each sector, the list of BAT was assessed to identify which technologies could augment the model effluent treatment system and improve treated effluent quality. Order of magnitude capital equipment and installed cost and operating cost estimates were then prepared for each augmentative BAT technology for each sector. Cost estimates were generated through the use of in-house capital and operating cost information, vendor and operations questionnaires, and cost data reported in literature. It is acknowledged that actual costs could vary significantly from the presented figures, depending on numerous site-specific factors. Augmentative BAT that could improve treated effluent quality from existing treatment systems at a reasonable incremental cost were designated best available technology economically achievable (BATEA). For some subsectors, the model flowsheet was designated to be BATEA since BAT would either not improve treated effluent quality or could not be implemented at a reasonable cost.

RESULTS AND DISCCUSION

Review of the **base metal subsector** included a total of 43 operations. The model effluent treatment system for the subsector, as determined by the prevalence of questionnaire responses, consists of hydroxide precipitation for metals removal and pond-based settling for bulk TSS removal. Coagulant and flocculant are dosed to facilitate metal precipitate and TSS sedimentation. The pond-based system also enables passive natural degradation of ammonia which does not readily occur in reactor based lime addition/clarification systems. The pH of the settling pond decant is adjusted, most commonly with carbon dioxide to meet *MMER* pH limits and/or meet un-ionized ammonia/toxicity requirements prior to discharge to the environment. The design and nominal flow rates selected to estimate capital and operating costs for system augmentation for the model treatment system were 2 000 m^3/h and 870 m^3/h, respectively. Based on an evaluation of improvement in effluent quality relative to incremental capital and operating cost, BATEA was selected as sulfide precipitation with polymeric organosulfide chemicals for dissolved metals polishing and the model effluent management and treatment system for total ammonia, bulk metals, and TSS removal. The incremental capital cost and operating cost for augmenting the model flowsheet with the BATEA were estimated to be C$550/$m^3/h$ and C$0.33/$m^3$, respectively. The incremental cost to implement this augmentative technology considers infrastructure not included in the model treatment system. Further details on the basis of the cost estimates are available in the full report.

Review of the **precious metal subsector** included a total of 40 precious metal operations. The model effluent treatment system for the subsector, as determined by the prevalence of questionnaire responses, consists of SO_2/air cyanide destruction on tailings and low density sludge lime hydroxide precipitation for bulk metal removal from effluent from tailings, mine, and waste rock areas. The design and nominal flow rates selected to estimate capital and operating costs for system augmentation for the model treatment system were 600 m^3/h and 180 m^3/h, respectively. Using the methodology outlined previously for the base metal subsector, BATEA was selected as sulfide precipitation with proprietary polymeric organosulfide chemicals for dissolved metals polishing, active aerobic biological oxidation for total ammonia removal, and the model effluent management

and treatment system for cyanide, bulk metals, and TSS removal. The incremental capital cost and operating cost for augmenting the model flowsheet with the BATEA were estimated to be C$50/m^3/h and C$0.20/m^3, respectively, for the polymeric organosulfide chemicals, and C$32,670/m^3/h and C$0.60/m^3, respectively, for active aerobic biological oxidation. The incremental cost for implementation of this augmentative technology is less than for the base metal model system, as the precious metal model treatment system infrastructure is better suited for the use of this technology and thus less additional equipment is required. Further details on the basis of the cost estimates are available in the full report.

Review of the **iron ore subsector** included all 6 operating iron ore operations. The model effluent treatment system for the subsector, as determined by the prevalence of questionnaire responses, consists of pond-based settling for bulk TSS removal with flocculant dosing to aid settling. The design and nominal flow rates selected to estimate capital and operating costs for system augmentation for the model treatment system were 7 000 m^3/h and 3 900 m^3/h, respectively. Using the methodology outlined previously for the base metal subsector, BATEA was selected as the model effluent management and treatment system for TSS, metals, and total ammonia removal. Hatch expects that with proper design and operation of water management infrastructure, a TSS concentration of 15 mg/L or lower can be achieved by the sector.

Review of the **uranium subsector** included a total of 12 operations. The model effluent treatment system for the subsector, as determined by the prevalence of questionnaire responses, consists of 2 stages: a high pH stage for precipitation of metals that precipitate in basic conditions and a low pH stage for metals and other parameters that precipitate or co-precipitate in acidic conditions. Between and after these pH stages, clarification and filtration are employed to separate precipitates from treated water. The design and nominal flow rates selected to estimate capital and operating costs for system augmentation for the model treatment system were 500 m^3/h and 350 m^3/h, respectively. Using the methodology outlined previously for the base metal subsector, BATEA was selected as active aerobic biological oxidation for total ammonia removal and the model effluent management and treatment system for metals and TSS removal. The incremental capital cost and operating cost for augmenting the model flowsheet with the BATEA were estimated to be C$31,800/m^3/h and C$0.45/m^3, respectively. Further details on the basis of the cost estimates are available in the full report.

Review of the **diamond sector** included a total of 4 operations. The model effluent treatment system for the sector, as determined by the prevalence of questionnaire responses, consists of settling pond(s), clarification, and media filtration for TSS removal. Coagulant is dosed into the clarifier. Prior to discharge to the environment, pH is adjusted using sulfuric acid to meet un-ionized ammonia/toxicity limits. The settling and polishing ponds enable passive natural degradation of ammonia and phosphorus. The design and nominal flow rates selected for the model treatment system were 3 000 m^3/h and 2 000 m^3/h, respectively. These flow rates were used to estimate capital and operating costs for system augmentation. Using the methodology outlined previously for the base metal subsector, BATEA was selected as the model effluent management and treatment system for chloride, bulk metals, ammonia, and TSS removal.

Review of the **coal sector** included a total of 16 operations. In the model effluent treatment system for the sector, as determined by the prevalence of questionnaire responses, bulk TSS is removed via pond-based settling and polishing which may be aided by the addition of flocculant. The settling and polishing pond(s) enable passive natural degradation of ammonia. The design and nominal flow rates selected for the model treatment system were 3 000 m^3/h and 1 000 m^3/h, respectively.

Using the methodology outlined previously for the base metal subsector, BATEA was selected as the model effluent management and treatment system for metals, total ammonia, and TSS removal.

It is important to note that BATEA cannot be applied universally to every mine in each subsector due to site-specific considerations. Factors such as feed water quality, flowrate, location, site conditions, legacy conditions, regulatory constraints, etc. will impact the cost of implementation and operation and may make these BATEA selections economically unattractive or their effluent concentrations technologically unachievable.

Hatch cautions that the use of polymeric organosulfide reagents should only be considered BATEA for operations that are capable of and dedicated to careful control of operating regimes to prevent effluent toxicity, as well as, careful control of residuals storage conditions to prevent long term instability and the potential generation of acid through sulfide oxidation and metals remobilization.

Table 3 provides a summary description of the model effluent treatment flowsheet, proposed BATEA, and achievable treated effluent quality with the proposed BATEA for each subsector. In the "Treated Effluent Quality" column, for those parameters not removed by the model treatment processes, the values presented are based on the 95th percentile of the final effluent concentrations for the entire subsector. The BATEA treated effluent concentrations are based on case study data and actual operating site data provided by vendors and industry as part of this study. Further details on the basis of treated effluent concentrations are available in the full report. These concentrations may not be achievable at every site due to local site conditions or operational factors which could affect the efficiency of the process. A pragmatic approach should be taken when assessing the probability of achieving these effluent target values under site-specific conditions.

CONCLUSION

For each subsector, utilizing the methodology presented herein to assess information compiled on the subsector and on effluent treatment technologies, Hatch selected BATEA for the removal of current and proposed contaminants under the Canadian federal *Metal Mining Effluent Regulations.* The study also provided valuable reference information to regulatory and industry stakeholders regarding subsector water management and treatment practices, the treated effluent quality achieved by model water management and treatment practices for each subsector, and effluent treatment technologies.

The study was published by MEND as Report 3.50.1 on their website at: ***mend****-nedem.org/wp-content/uploads/****MEND_3.50.1****_BATEA.pdf*

ACKNOWLEDGEMENTS

The authors of this study would like to extend their sincere thanks to MEND for sponsoring the study and to the industry associations, operations, technology vendors, and reviewers who provided invaluable inputs to this study.

REFERENCES

Please refer to the report for a complete listing of references (***mend****-nedem.org/wp-content/uploads/****MEND_3.50.1****_BATEA.pdf*).

Environment Canada (2012) *10-Year Review of Metal Mining Effluent Regulations Discussion Paper.*

Canada. *Metal Mining Effluent Regulations* (SOR/2002-222).

Table 3: Summary of proposed BATEA

(sub)Sector	Model Effluent Treatment Flowsheet	Proposed BATEA	Effluent Quality
Base Metal	• hydroxide precipitation for metals • coagulant and flocculant dosing and pond-based settling for TSS • natural degradation of ammonia • pH adjustment with CO_2	model +: polymeric organosulfide reagents for metals polishing	Al < 0.79 mg/L As <0.01 mg/L Cu <0.03 mg/L Fe <0.30 mg/L Pb <0.02 mg/L Ni <0.05 mg/L Se <0.04 mg/L Zn <0.02 mg/L TSS <10 mg/L NH_3/NH_4^+ <4 mg/L
Precious Metal	• SO2/air cyanide destruction on tailings effluent • reactor-based hydroxide precipitation for metals from tailings, mine, and waste rock • natural degradation of ammonia	model +: polymeric organosulfide reagents for metals polishing and active aerobic biological oxidation for ammonia	Al < 0.05 mg/L As <0.05 mg/L Cu <0.03 mg/L CN <0.1 mg/L Fe <0.30 mg/L Pb <0.01 mg/L Ni <0.05 mg/L Se <0.05 mg/L Zn <0.02 mg/L TSS <12 mg/L NH_3/NH_4^+ <2 mg/L
Iron Ore	• flocculant dosing and pond-based settling for bulk TSS • natural degradation of ammonia	model – no economically achievable augmentative technology	Al < 0.80 mg/L As <0.001 mg/L Cu <0.005 mg/L Fe <5.50 mg/L Pb <0.003 mg/L Ni <0.003 mg/L Se <0.005 mg/L Zn <0.04 mg/L TSS <62 mg/L[2] NH_3/NH_4^+ <8 mg/L
Uranium	• high pH hydroxide precipitation for metals • low pH hydroxide precipitation and co-precipitation for metals and metalloids • inter-stage clarification and filtration for TSS	model +: active aerobic biological oxidation for ammonia	Al < 0.70 mg/L As <0.06 mg/L Cu <0.04 mg/L Fe <0.50 mg/L Pb <0.002 mg/L Ni <0.20 mg/L Se <0.02 mg/L Zn <0.04 mg/L Ra-226 <0.11 Bq/L TSS <2 mg/L NH_3/NH_4^+ <2 mg/L
Diamond	• pond-based settling, clarification (with coagulant), and media filtration for TSS • pH adjustment with sulfuric acid	model – no economically achievable augmentative technology	Cl^- <1 240 mg/L P <0.1 mg/L TSS <7 mg/L NH_3/NH_4^+ <2.35 mg/L
Coal	• flocculant dosing and pond-based settling for bulk TSS • natural degradation of ammonia	model – no economically achievable augmentative technology	Al < 0.90 mg/L As <0.001 mg/L Fe <0.82 mg/L Mn <0.13 mg/L Se <0.38 mg/L TSS <77 mg/L NH_3/NH_4^+ <0.37 mg/L

[2] Proper design and operation of water management infrastructure can achieve TSS ≤ 15 mg/L.

Minimizing Life Cycle Costs at High Flowrates

Joseph Tamburini and H.C. Liang
Tetra Tech, USA

ABSTRACT

Open pit mining can require large dewatering operations at high flowrates. When this dewatering water is required to be treated prior to discharge back to the environment or reinjection, the resulting life cycle costs can be significant and can impact mine operations. A confidential mine in Nevada, USA was faced with such a problem, requiring it to treat greater than 8,500 m3/hr (37,500 gpm) of water from dewatering wells to remove arsenic. Typical arsenic treatment technologies such as adsorption, ion exchange and coagulation/microfiltration have been shown to be effective removing arsenic; however, the associated capital costs would be prohibitive at such high flowrates. Therefore a conventional ferric hydroxide precipitation followed by clarification process was selected as a capital cost-effective alternative; at approximately 50% the cost of other arsenic removal technologies.

Several process configurations were investigated, but the two main configurations considered involved either settling ponds or clarifiers for solid/liquid separation. Additionally, two different site locations were considered, and due to the high flowrates, small differences in elevation resulted in vastly different pumping conditions. In order to determine the "best" configuration, the design team performed a Life Cycle Value Analysis that included monetary factors such as capital and operating costs; but also included non-monetary factors such as Reliability, Complexity, Flexibility, Land Requirements, Risk, Maintenance, among others. This approach allowed all factors that were important to the mining company to be considered appropriately.

Interestingly, this approach yielded a result that the clarifier alternative was preferred over settling ponds, despite it having a higher capital cost. Operational costs over the life of the facility tilted the analysis toward the site location at a higher elevation despite the need to build a 2,150 m^3/hr (9,500 gpm) pump station in order to get some of the water to that elevation.

Keywords: Life Cycle, Water Treatment, Arsenic

INTRODUCTION

A large combination open-pit and underground mine in Nevada, USA has a sophisticated dewatering well system surrounding the mine works to allow extraction of ore from both the pit and the underground mine. Currently, this equates to 6,400 m^3/hr (28,200 gpm) of water in the dewatering system. After a thorough analysis of current dewatering water the current arsenic levels in the mine complex were determined to be approximately 0.020 mg/L. Future wells will increase the total dewatering flowrate to 8,500 m3/hr (37,500 gpm) and likely will have higher arsenic concentrations. These concentrations exceed the Nevada Division of Environmental Protection (NDEP) Profile I arsenic reference value of 0.010 mg/L. Since the arsenic concentration is similar from well to well, the mine will be required to treat arsenic from all of the water prior to infiltration and irrigation. A new Water Treatment Plant (WTP) must be constructed and be able to achieve high reliability of treatment.

To determine the WTP design requirements, the dewatering flowrate was modelled based on the water production from different well production zones as shown in Figure 1.

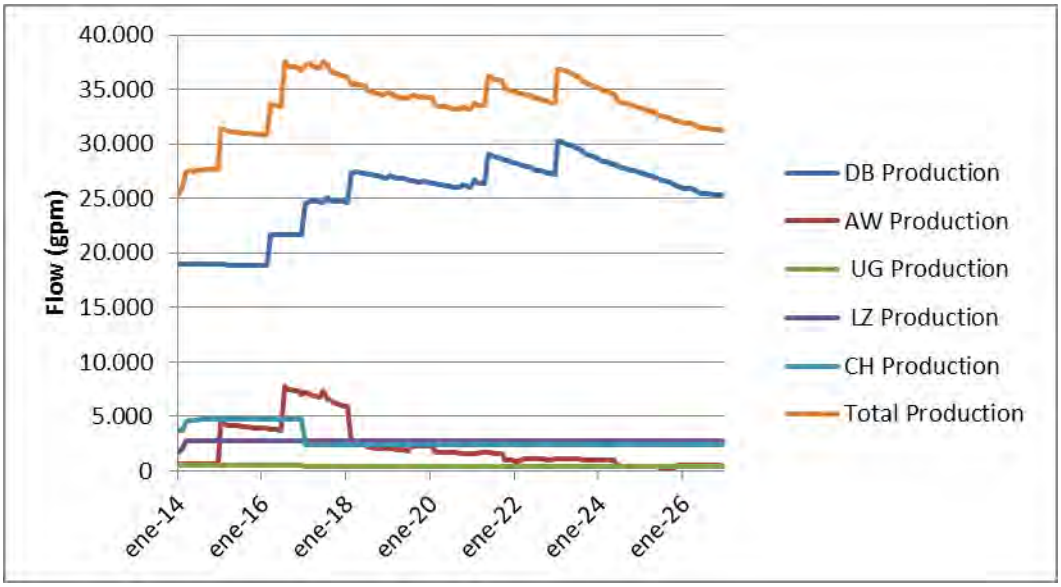

Figure 1 Dewatering Flowrate Projection by Production Zone

Finally, arsenic concentrations from each dewatering well were flow weighted to create a total projected arsenic concentration (mg/L), as presented in Figure 2. Average arsenic loading is important to understand for long-term chemical consumption when determining the operating costs; but peak arsenic values are also important for sizing chemical feed equipment and determining sludge handling alternatives. Therefore, three different sets of arsenic loading values were determined, the average, 85th percentile and the 95th percentile.

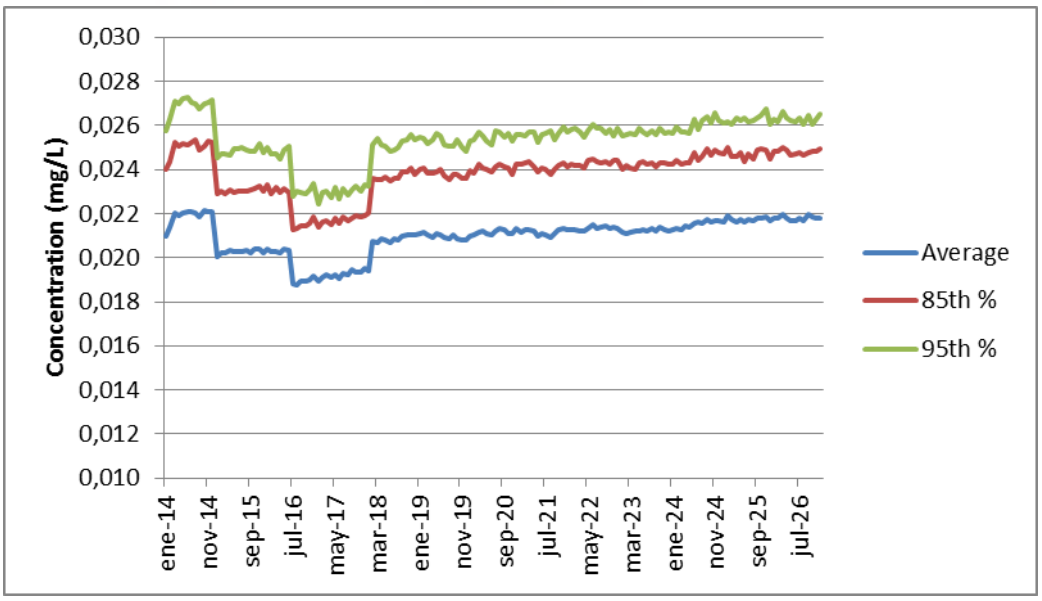

Figure 2 Projected Arsenic Concentration into the new WTP

Due to the high flowrates at the new WTP, mine staff's familiarity, and the cost effective nature of treatment, it was determined to utilize ferric hydroxide precipitation as the preferred method for arsenic removal. This process works by adding a ferric iron source (typically, ferric sulphate or ferric chloride) which forms a ferric hydroxide floc particle, as shown in Equation 1, which has an overall positive charge.

$$Fe_2(SO_4)_3 + H_2O \leftrightarrow Fe(OH)_2^+ \qquad (\text{at } pH < 7.3) \qquad (1)$$

Dissolved arsenic (V), or arsenate, has a net negative charge under most all pH conditions and adsorbs to the ferric hydroxide to form a precipitant that can be removed from the water solution.

$$H_2AsO_4^- + Fe(OH)_2^+ \rightarrow \text{Precipitant} \qquad (2)$$

During bench-scale testing, it was found that a portion of the arsenic present in the dewatering source was in the arsenic (III), or arsenite, form. Dissolved arsenic (III) has no net charge associated with it, and hence, cannot be removed via ferric hydroxide precipitation. Approximately 1.8 mg/L of hypochlorite bleach was added to oxidize all the arsenic to the arsenic (V) state so that it could be removed in the ferric precipitation step.

The project team desired to compare the life cycle costs of constructing a WTP utilizing settling ponds versus using clarifiers to settle this precipitant.

Additionally, there were two different site locations to evaluate. The "boneyard" site was at the bottom of a valley and allowed all the water from the dewatering wells to flow to that site without any modifications to any wells or without any additional booster pump stations. The second site, the "waste rock" site, was at a higher elevation on an old waste rock pile. Most of the dewatering zones could be pumped to the waste rock site without any additional modifications; however, one production zone required a booster pump for 2,150 m^3/hr (9,500 gpm) to get all the water to the WTP.

In order to evaluate which of the two different WTP processes and which of the two different site locations was best for this project, the team performed a Life Cycle Value Analysis (LCVA) on the alternatives. This paper will discuss how the LCVA process was used to quantify both monetary and non-monetary factors to make the best decision for this particular application.

METHODOLOGY

The LCVA approach combined monetary factors such as Capital Cost and Operation Cost (both Level 4 cost estimates at this stage of the project) as well as non-monetary criteria. The "non-monetary" criteria are summarized in Table 1. Monetary factors are easy to quantify; however, non-monetary factors are much more difficult to quantify. In order to accomplish this, each factor was given a weighting factor to determine how important each criterion was to that particular mine, which helped engage mine staff in the decision process. The "non-monetary" criteria developed by the mine were weighted as shown in Table 1.

Table 1 Non-Monetary Criteria Weighting Factors

Non-Monetary Criteria	Weighting Factor (1-4)
Reliability	4
Operational Complexity	2
Flexibility / Adaptability	3
Maintenance Requirements	1.5
Labour Requirements	2
Land Requirements	1
Risk / Liability	3
Truck Traffic	1
Redundancy	2

These criteria and weighting factors were input into the LCVA tool and each of the alternatives were scored on these particular "non-monetary" criteria on a scale of 1 to 5 with a score of one meaning that the particular alternative was not well suited for that particular criterion. The alternative score was then multiplied by the weighting factor to determine an overall score for each alternative for each non-monetary criterion. The scores for all non-monetary criteria were then added together to determine an overall "non-monetary" score for each alternative. These scores were used to quantify how well each alternative performed on criteria that were important to the mine other than just costs.

Finally, the monetary costs were normalized by dividing each cost by the lowest cost alternative, and the "non-monetary" scores were normalized by dividing each score by the lowest score. A simple monte-carlo analysis was conducted to compare the alternatives based on the scenarios in Table 2.

Table 2 LCVA Scenarios

Scenario	Monetary Weighting	Non-Monetary Weighting
1	30%	70%
2	50%	50%
3	70%	30%
4	100%	0%

RESULTS AND DISCUSSION

Solid / Liquid Separation Process

The two solid/liquid separation processes that were evaluated were double-lined earthen settling basins and standard circular clarifiers. The results of the non-monetary criteria for the solid/liquid separation process are summarized in Figure 3.

		Basins	Clarifiers
Weighting Factor		IS / WS	IS / WS
Reliability	4	2.0 / 8.0	4.0 / 16.0
Operational Complexity	2	3.5 / 7.0	3.5 / 7.0
Flexibility/Adaptability	3	1.5 / 4.5	3.0 / 9.0
Maintenance Requirements	1.5	2.0 / 3.0	4.0 / 6.0
Labor Requirements	2	3.0 / 6.0	3.0 / 6.0
Land Requirements	1	1.0 / 1.0	3.0 / 3.0
Risk/Liability	3	2.0 / 6.0	4.0 / 12.0
Truck Traffic	1	3.0 / 3.0	3.0 / 3.0
Redundancy	2	3.0 / 6.0	3.0 / 6.0
Overall Score		44.5	68.0
Alternative Ranking		**2**	**1**
Relative Ranking		1.55	1.00

Figure 3 Non-Monetary Evaluation for the Solid / Liquid Separation

The biggest "non-monetary" differences between the two alternatives in this study were Reliability, Flexibility and Risk. Settling basins, as configured for this project, were designed for sludge to be continuously removed from the basins with a stationary sludge pump. Many people on the design team expressed concern that this may not effectively remove sludge from everywhere else; leading to excessive buildup of sludge elsewhere in the pond. Therefore, there was an inherent Risk associated with the settling basin alternative. There were also questions about how clear the effluent water from the settling ponds would be if/when sludge build-up in the pond began to increase, so the system's Reliability to treat water consistently throughout the year came into question.

The simple monte-carlo analysis for the solid/liquid separation is summarized in Table 3.

Table 3 Final LCVA Analysis for the Solid / Liquid Separation Process

Alternative	Cost Rank	Weighted Cost Rank	Process Rank	Weighted Non-monetary Rank	Total Weighted Rank	Final Rank
Weighting		**30%**		**70%**		
Settling Basins	1.05	0.31	1.55	1.08	1.40	2
Clarifiers	1.16	0.35	1.00	0.70	1.05	1
Weighting		**50%**		**50%**		
Settling Basins	1.05	0.52	1.55	0.77	1.30	2
Clarifiers	1.16	0.58	1.00	0.50	1.08	1
Weighting		**70%**		**30%**		
Settling Basins	1.05	0.73	1.55	0.46	1.20	2
Clarifiers	1.16	0.81	1.00	0.30	1.11	1
Weighting		**100%**		**0%**		
Settling Basins	1.05	1.05	1.55	0.00	1.05	1
Clarifiers	1.16	1.16	1.00	0.00	1.16	2

At the start of the project, the mine operations and the engineering team felt that settling basins would be significantly less expensive and that the clarifier option would be prohibitively costly. Much to the team's surprise, when the LCVA process was completed it turned out that the clarifier option was the preferred alternative when the non-monetary criteria were weighted at 30% of the decision or higher, as shown in Table 3. The more weight the "non-monetary" criteria were given, the greater the LCVA analysis favored clarifiers.

Site Location Selection

The two different site locations that were evaluated were the "boneyard" site and the "waste rock" site. The results of the non-monetary criteria for the site location selection are summarized in Figure 4.

Weighting Factor		Boneyard IS / WS	Waste Rock IS / WS
Reliability	4	3.0 / 12.0	3.0 / 12.0
Operational Complexity	2	4.0 / 8.0	4.0 / 8.0
Flexibility/Adaptability	3	3.0 / 9.0	3.0 / 9.0
Maintenance Requirements	1.5	4.0 / 6.0	4.0 / 6.0
Labor Requirements	2	3.0 / 6.0	3.0 / 6.0
Land Requirements	1	3.0 / 3.0	3.0 / 3.0
Risk/Liability	3	4.0 / 12.0	3.0 / 9.0
Truck Traffic	1	3.0 / 3.0	3.0 / 3.0
Redundancy	2	3.0 / 6.0	3.0 / 6.0
Overall Score		65.0	62.0
Alternative Ranking		**1**	**2**
Relative Ranking		1.00	1.05

Figure 4 Non-Monetary Evaluation for the Solid / Liquid Separation

There was little difference in the non-monetary criteria between the two different site locations. The only real difference was that the waste rock site sat on an old waste rock pile that had settled over time, and a geotechnical evaluation of the site indicated that certain engineering design measures had to take place to account for differential settling across the site. Therefore, there was some associated Risk with this site over the virgin ground at the bone yard site. The engineering measures necessary to account for differential settling were taken into account in cost of building at that site.

The simple monte-carlo analysis for the site location selection is summarized in Table 4.

Table 4 Final LCVA Analysis for the Site Location

Alternative	Cost Rank	Weighted Cost Rank	Process Rank	Non-monetary Rank	Total Weighted Rank	Final Rank
Weighting		**30%**		**70%**		
"Boneyard"	1.05	0.31	1.00	0.70	1.01	1
"Waste Rock"	1.00	0.30	1.05	0.74	1.04	2
Weighting		**50%**		**50%**		
"Boneyard"	1.05	0.52	1.00	0.50	1.02	1
"Waste Rock"	1.00	0.50	1.05	0.53	1.03	2
Weighting		**70%**		**30%**		
"Boneyard"	1.05	0.73	1.00	0.30	1.03	2
"Waste Rock"	1.00	0.70	1.05	0.32	1.02	1
Weighting		**100%**		**0%**		
"Boneyard"	1.05	1.05	1.00	0.00	1.05	2
"Waste Rock"	1.00	1.00	1.05	0.00	1.00	1

Overall, the LCVA analysis showed very little difference between the two site locations. It indicated that the waste rock site was preferred when non-monetary criteria were weighted 50% or less, but not by a wide margin; and conversely, the bone yard site was preferred marginally higher when non-monetary criteria were weighted over 50%.

CONCLUSION

The Life Cycle Value Analysis procedure was proved to be a helpful tool for the mine team to make a decision regarding the preferred solid / liquid separation processes and the preferred site location. This procedure quantified everything that the mine felt was important to them, including monetary and non-monetary factors. The selected alternative from this analysis was to design the clarifiers for the solid / liquid separation process because it was decided that the non-monetary factors accounted for at least 30% of the decision with all the uncertainly related to the settling pond implementation. The waste rock site was selected as the best location since the LCVA showed that there was little difference between the alternatives based on the non-monetary criteria, so this decision could be made based on which alternative offered the most cost-effective approach.

The LCVA process can be applied to many different types of decisions at a mine site, especially when non-monetary criteria weigh heavily, such as with environmental measures. Through this process, it was critical that the appropriate team members are engaged in the process from the beginning.

ACKNOWLEDGEMENTS

Joel Migchelbrink, EIT, a former Tetra Tech employee performed some of the LCVA analysis.

10th ICARD IMWA 2015 | 10th International Conference on Acid Rock Drainage & IMWA Annual Conference

Assessment of Acid Neutralization Rates from Site Rock for AMD Control

Roger Smart[1], Joseph Ciccarelli[1], Shengjia Zeng[1], Rong Fan[1], Jun Li[1], Nobuyuki Kawashima[1], Andrea Gerson[1] and Russell Schumann[2]

1. *Minerals and Materials Science and Technology, Mawson Institute, University of South Australia*
2. *Levay & Co Environmental Services, University of South Australia*

ABSTRACT

In principle, a sustainable approach to acid mine drainage (AMD) management and final closure should be to reduce the acid generation rate (AGR) sufficiently that the acid neutralization rate (ANR) can match the AGR from rock and tailings disposal. This approach has not yet been fully designed or achieved although some parts of the overall strategy, including surface passivation of sulfide minerals to reduce AGR, have been implemented. Most mine sites have non-value minerals capable of providing some neutralization of AMD. They are often not considered or surveyed in primary site ore assessment. Standard site assessment methods define total potential acidity (AP) or alkalinity (NP) of these materials, *e.g.* NP/AP ratio, but do not consider the **rates** at which acid generating and neutralising reactions may take place. It is these relative rates in disposal of rock and tailings wastes that determine whether acid and metalliferous drainage occurs. Methods are now available to assess the rates at which neutralization can be supplied from reactive silicate minerals (additional to carbonates) in on-site waste rock types. Knowledge of both the amount and the rates of acid generation and neutralization can be used to assess future acid rock drainage liabilities but, more importantly, to plan greenfield or operating disposal to make maximum use of these on-site materials. The complete definition of geochemistry and mineralogy of site materials can provide more effective and reduced-cost management of these mining wastes. The application of this approach is particularly pertinent for use with emerging waste emplacement construction techniques. Definition of ANR in non-acid forming wastes used for encapsulating acid generating wastes during controlled placement storage can potentially be used to define oxygen flux and moisture targets to achieve matching AGR. Examples where neutralising waste rocks have been identified and assessed at three sites in the AMIRA P933A project are discussed.

Keywords: acid neutralization; kinetics; silicates; site mineralogy

INTRODUCTION

A sustainable approach to acid mine drainage (AMD) management in pre-planning or in operation should be to use, where possible, geochemical resources available at the mine site to reduce the acid generation rate (AGR) sufficiently that the acid neutralization rate (ANR) can match the AGR from rock and tailings disposal before final rehabilitation. This matching of acid generation and neutralization rates in kinetically controlled processes is, in principle, the only sustainable option for long-term closure. This has not yet been fully designed or achieved, but this paper will describe this approach with case studies illustrating some parts of the overall strategy that have been implemented to date. There are real opportunities for improved practice using full geochemical and mineralogical assessment of site materials.

In principle, AMD management involves strategies, at any scale from molecular to site storage, to minimise the interaction of reactive sulfide surfaces with air and/or water. At the site engineering scale, minimisation and control strategies selected are influenced by a range of factors including climate, topography, hydrology, mine geology, geochemistry and mineralogy of waste rock, tailings and available neutralising materials. Our focus is on the geochemical and mineralogical part of this control. Implementation of this geochemical strategy requires, firstly, treatments to reduce the AGR sufficiently that the ANR can match the AGR (Gerson et al., 2014). Reduction of AGR (50-90%) by formation of silicate-stabilised iron hydroxide layers on pyrite has been addressed in other publications (*e.g.* Miller et al. 2009; Schumann et al. 2009; Zeng et al., 2013; Gerson et al., 2014). The addition of carbonates in covers and layers, where available as limestone or dolomite on site, is recognised as the primary geochemical method of AMD control in acid rock dumps (GARD Guide). Studies, both laboratory (Schumann et al. 2009; Huminicki and Rimstidt 2009; Nicholson et al. 1990) and field (Li et al., 2012; Li et al., 2011; Miller et al., 2009), have shown that under neutral pH conditions maintained by added carbonates, pyrite oxidation rates, *i.e.* AGR, can be reduced by more than one order of magnitude. The mechanism for the reduction in sulfide oxidation rate is found to be through formation of continuous, coherent iron oxyhydroxide coatings which develop on the surface of the reacting sulfide and reduce oxygen diffusion rates to the surface (Huminicki and Rimstidt 2009; Nicholson et al. 1990). The nature and stability of these surface passivating layers has been extensively investigated in our research (Smart et al. 2010; Schumann et al. 2009). Under conditions of pH>6, multi-layered coatings of amorphous iron oxyhydroxide develop notably as stable, thin, continuous and conformal coatings often overlaid with a thicker (1-2 μm) coating of (semi)-crystalline goethite-like material. In field samples, the amorphous oxyhydroxide pyrite-passivating layer normally contains significant (5-10 mol%) silicate content. Where clay minerals are present in the waste, strongly adhering particles with micaceous texture can form a further external armouring layer (Miller et al., 2009).

The roles of pH and dissolved silicate in stabilising these passivating layers are critical. Pyrite oxidation rates are reduced when the pH is maintained above 6 and when the surrounding solution contains dissolved silicate (10–20 mg/L as Si) (Zeng et al. 2013). In the presence of dissolved silicate, the iron oxyhydroxide layer formed during pyrite oxidation retains its amorphous, conformal structure, while in the absence of silicate, conversion of this layer to the more-crystalline and less-passivating, separate goethite-like crystals occurs. These differences are illustrated in Figure 1. If initial alkaline amendments are made so that these passivating layers are formed and maintained then, for wastes with low to moderate AGR containing some reactive silicates, AGR may be sufficiently reduced (more than 90%) to enable matching by silicate ANR in the long-term. This sulfide passivation, with the use of reactive silicates from site rocks, forms the first part of the geochemical strategy for sustainable AMD management.

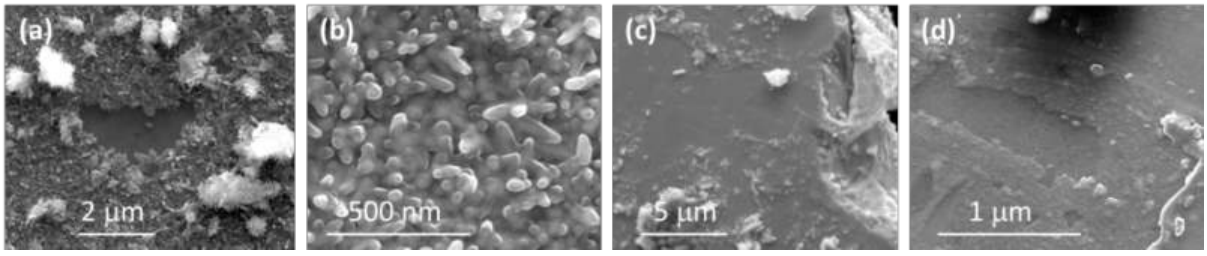

Figure 1 Evidence of the effect of the presence of silicate on pyritic surface layers at neutral pH. (a) and (b) pyrite surfaces immersed in calcite saturated water for 160 days showing clear crystalline overgrowths; (c) and (d) pyrite immersed under the same conditions with added silicate (20 mg/L Si) showing clear difference in surface layer morphology and significantly reduced pyrite oxidation (Zeng et al., 2013).

A specific example of the use of on-site alkaline materials for amelioration of AMD from previous rock dump fills has been provided by Cook et al. (2008). Re-mining of the Buffalo Creek coal seam site (Virginia, USA) to obtain coal from lower in the geologic column exposed new overburden, including an alkaline sandstone, that was used to add covers to the existing valley-fill AMD rock dumps. Drainage from the fills had resulted in high acidity/high metal (pH 3.5–4.5 with 100–200 mg/L $CaCO_3$ acidity) in the sub-watersheds. Addition of the sandstone covers improved water in the main stream of each drainage area from the fills. The water quality in the tributaries of Laurel Creek dramatically improved to pH 6.2 and acidities of <1 mg/L. Placement of alkaline material, recognised in the new mineralogy, into the extended valley fills eliminated the need for chemical treatment. With more than 10 years of data, it is apparent that there is high probability for the long-term success of the amendments.

A second example is the successful implementation and testing of on-site amendments to AMD from the historic B-Dump in the Savage River Rehabilitation Program (SRRP), a cooperative arrangement between the Tasmanian Government and current operators Grange Resources. Studies at this site have already been fully documented in previous ICARD meetings (Hughes et al., 2009, Hutchison et al. 2009, Li et al., 2011, Li et al., 2012). This used a water-shedding compacted top cover (from graded material) with over-dumped side covers and a base-dumped flow-through barrier comprised of chlorite-calcite schist waste material from the site. The covers have effectively reduced the overall AGR within the dump by about 43% over the past five years. Alkalinity from the covers has been migrating down into the acid-forming waste and forming passivating layers of silicate-stabilised iron oxy-hydroxide verified on pyrite grains (Li et al. 2011). Sulfate, Al and Cu flux in Main Creek have decreased by 50% after B-dump was capped. The discharge from Main Creek to the river has neutral pH, low sulfate (218 mg/L) and metal concentrations, *e.g.* Al 200 µg/L and Cu 30 µg/L, that are now below the SRRP fish target (Hughes et al. 2009).

In the context of requirements for implementation of the geochemical approach, a critical second requirement remains, however, to recognise, **measure** and control relative rates of acid neutralization from different waste mineralogies available on site. One of the significant inputs employed for the SRRP remediation is a comprehensive report (Thornett, 1999) on the rock types and mineralogy of the site prepared for the previous owners Australian Bulk Minerals. This identified a large variety of potentially neutralising mineralogy including the abundant chlorite-calcite schists with some dolomite, magnesite, talc-carbonate schist, dolerites and reactive silicates in mafic rocks, amphibole-chlorite-albite schists, serpentinites and possibly tonalite. This was recognised by site personnel and Rumble (2005) in planning of the amendments and provided the basis for the successful remediation.

Hence, there are two requirements that can potentially improve current practice in AMD control. The first is the need for detailed mineralogy, additional to standard AMD classification testing, of all site lithology, not just value lithology, preferably in greenfield assessment but also in operating and legacy sites. This enables a first-level estimate of both AGR and ANR for different lithologies based on the mineralogy alone (Ciccarelli et al., 2009, Miller et al. 2010). The AGR from the waste rock in passivated form at pH 6 can be estimated from well-established oxygen consumption and sulfate release methods (*e.g.* Hollings et al., 2001; Sracek et al., 2006). Associated with this should be

ANR carbonate and ANR non-carbonate (ANRnc; mainly reactive silicates) testing of potentially neutralising rock types using the dissolution cell and mineralogical methods to be described. These estimates can provide a reasonable basis to assess whether the ANR can match the reduced AGR at source. The second requirement is to plan to use these materials in layer dumping with AMD wastes and in cover design together with the engineering considerations. Short-term costs of this approach are likely to be greater than current practice but with the very high costs of closure and on-going management and liability in retained capital (*e.g.* several hundred million dollars at Newmont, Dowd, 2005), it may ultimately be more cost-effective. This comparison has not yet been fully evaluated but is clearly worthy of further development for sustainable AMD control.

METHODOLOGY

Current AMD test methods use static acid base accounting (ABA) assessment of potential acidity and neutralization together with long-term kinetic leach columns (KLC) usually requiring years to give reliable data (AMIRA/EGi ARD Test Handbook, 2002; MEND, 2009). The methodology required to use the our kinetic approach is a combination of AGR and ANR measurements (both in total mg H_2SO_4/kg/week or g H_2SO_4/tonne/week) on a time scale that allows snap-shot assessment of the ARD dump or tailings material prior to and during evolution of the AMD profile. The well-established oxygen consumption and sulfate release methods (*e.g.* Hollings et al., 2001; Sracek et al., 2006) on representative samples can provide reliable cross-checks and estimates of AGR at any point in this evolution. The requirement for short-term cross-checks and estimates of ANR can be met by a combination of dissolution rates from the sample mineralogy with dissolution cell measurement of released cations at the measured sample pH.

The mineralogical ANR estimates combine mineralogical assessment (Rietveld XRD, QEMSCAN or MLA) with dissolution rate data of individual minerals. The non-iron carbonate content of the mineralogy can be assumed to provide ANR for the equivalent AGR, *i.e.* at the same mg H_2SO_4/kg/week since their reaction rates exceed pyrite oxidation rates (Blodau, 2006). It is the additional neutralization from reactive silicate minerals that requires assessment. Eary and Williamson (2006) combined mineral dissolution rate data from Palandri and Kharaka (2004) with solution speciation modelling to examine dissolution of a number of theoretical rocks, with silicate mineralogy ranging from silicic through to mafic and containing 0–3 wt.% pyrite. Their results suggested that anorthite feldspar and some mafic minerals such as forsterite, augite and hornblende may dissolve quickly enough to neutralise acidity from pyrite oxidation. For instance, anorthite gives measurable short-term neutralization in the ABA Sobek test with estimated ANC of 10 kg H_2SO_4/t (AMIRA/EGi, 2002; MEND, 2009). Abundant chlorite minerals have also been shown to mediate acidity in both the Waite Amulet (Jambor et al., 1999) and Savage River (Li et al. 2012) examples. A similar mineralogical approach was used by Miller et al. (2010), wherein silicate ANR derived from mineral dissolution rates were compared with rates calculated from leachate analysis of solutions obtained from long-term kinetic leach column tests from which any carbonates had been previously exhausted. They found good agreement between the rates derived from mineralogy and those obtained from leach column tests when the pH was below 3. However at pH>4, ANR values calculated from mineralogy generally exceeded those derived from leach column testing (over 2-10 years) based on assays for metal cations (Na, K, Ca, Mg and Al) released in neutralization reactions as in the method of Paktunc (1999).

The amounts (mmol) of each cation in the 4-weekly leachate are determined from the assayed concentrations and the leachate volume. Thus (static) non-carbonate acid neutralising capacity ANCnc (mg H_2SO_4/kg) was determined from equation (1) with *Na, K, Mg, Ca* and Al in mmol; the factor 49 converts mmol H^+ ions to mg H_2SO_4; *m(kg)* is the mass of the sample in the column. *e.g.*

$$ANCnc = [(Na + K) + ((Mg + Ca) \times 2) + (Al \times 3)] \times 49 / m(kg) \quad (1)$$

For solution assays collected over specific time periods, usually 4 weeks, this can be represented as a rate, *i.e.* ANRnc in mg H_2SO_4/kg/week (or kg H_2SO_4/t/yr) for comparison with AGR measurement from sulfate release. The reason for the lower ANRnc measured by this method at pH>4 is likely to be due to the removal of some of these ions by secondary mineral formation particularly gypsum.

To improve the comparison with mineralogy, a short-term kinetic dissolution cell test to measure the ANRnc was developed using an initial pH-controlled flow-through method from which assays for metal cations (Na, K, Ca, Mg and Al) can be obtained after a steady-state dissolution rate is attained (usually 2 weeks) and ANRnc calculated as in Eq 1. This experimental procedure has been previously described in Ciccarelli et al. (2009). A summary is given here. The sample is first reacted with pH 2 HCl to remove all carbonates (verified with XRD and carbonate assay). The reaction cell is connected to an input reservoir at the pH of the original site sample and this solution is pumped through the reaction cell by a peristaltic pump with the sample in a holder with 0.45 μm filter papers placed above and below the sample to restrict sample loss. Leachate discharged from the exit port near the top of the reaction chamber is collected in output reservoirs for analysis of dissolved metals. Each of the collected effluent solutions is daily transferred into a sealed bottle pre-purged with Ar gas. The continuous flow-through tests are run under standard temperature (25°C) and atmospheric pressure conditions at an effective flow-rate of 40-50 mL per day, calibrated daily.

An example of this procedure applied to a fresh Savage River chlorite-calcite schist after carbonate removal is shown in Figure 2. This delivered an ANRnc of 480 mg H_2SO_4/kg/week at influent pH 4 and 90 mg H_2SO_4/kg/week at pH 5 both with effluent pH 7 at steady state. In the dump, the effective pH (as free proton concentration) close to the pyrite surfaces is likely to be below that in the bulk solution generating faster dissolution of reactive silicates adjacent to the pyrite. This can be compared with sulfate AGR from the B dump, to which this schist was added, of 10 mg H_2SO_4/kg/week in the seep at the toe of the dump (Li et al., 2012). The initial fast dissolution of Mg and later K may be due to ion exchange at high energy surface sites in silicate fines, *i.e.* chlorite and minor anorthite (Brantley and Chen, 1995) remaining after the pH 2 pre-treatment to remove carbonates. This initial greater reactivity can roughly double the effective initial ANRnc. More detail and other examples can be found in Ciccarelli (2012).

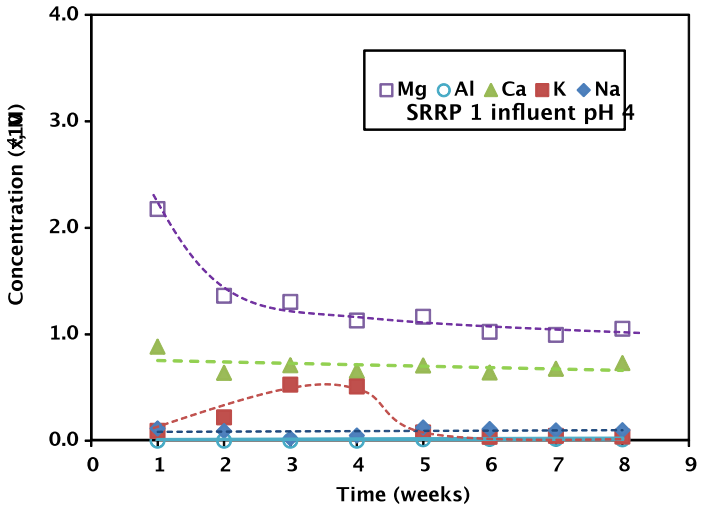

Figure 2 Major cation concentrations from the kinetic dissolution cell test of a Savage River chlorite schist waste sample at a flow rate of 4 L/kg/day and an influent solution pH of 4.

RESULTS AND DISCUSSION

Two other examples of the recognition and measurement of ANRnc in waste rocks potentially offering site treatment options not previously envisaged are discussed here.

BHP Billiton Iron Ore (BHPBIO)

A BHPBIO case study investigated the strategy of pyrite passivation and AMD reduction through the use of on-site ANR-generating wastes to minimise AGR in overburden storages at Mt.

Whaleback, Pilbara, Western Australia (Gerson et al., 2014). A Jeerinah shale and the highly reactive Mt. McRae shales were used as AGR-generating materials in kinetic leach columns (KLC). For ANR generation, a Jeerinah dolerite gave promising results. The mineralogy (determined from Rietveld XRD, QEMSCAN, bulk assay and carbon analysis) contains low carbonates (calcite 2-3 wt.%, ankerite 0.5-1 wt.%) with abundant reactive silicates including chlorite >30 wt.% (≈20 wt.% poorly crystalline not seen in QEMSCAN but not in XRD), anorthite 5 wt.%, tremolite 9 wt.% with a large amorphous fraction, 54 wt.%, in XRD probably consisting of chlorite-like material (from bulk assay reconciliation). The ANC of the carbonates from assay is around 30 kg $CaCO_3$/t but the measured ANC (modified Sobek test, AMIRA/EGi, 2002) of the dolerite is 47 (pH 2.4) to 84 (pH 1.2) kg $CaCO_3$/t depending on the final pH after the acid aliquot choice. Calcium concentrations were independent of initial pH suggesting that calcite and ankerite were quantitatively dissolved in each case with the remaining silicates (principally clinochlore chlorite) present in the dolerite contributing between 17 and 54 kg $CaCO_3$/t, depending on the *in situ* reaction pH. This initial characterisation is valuable for short-term neutralization but, given the abundance of silicates in most mine waste materials, it is the **rate of dissolution** rather than total concentration which determines the ability of silicates to buffer acidity resulting from sulfide oxidation. The ANRnc estimate from the mineralogy at pH 4 is 395 mg H_2SO_4/kg/week and at pH 5 is 81 mg H_2SO_4/kg/week suggesting significant neutralization as well as potential AGR reduction via pyrite passivation.

Blending 10 wt.% dolerite into the Jeerinah shale resulted in leachates characterized by neutral pH and a slight excess of alkalinity with low dissolved metal concentrations (not detectable in most cases). These results indicate that co-disposal of Jeerinah shale with Jeerinah dolerite, will substantially reduce the risk of drainage containing elevated levels of metals emanating from waste emplacements in which these materials are stored. Initially, dolerite was evaluated as a cover material for Mt. McRae shale. Results demonstrated that Jeerinah dolerite failed to supply sufficient alkalinity to keep the pH high enough to bring about pyrite passivation. However, leachates from the column tests in which Jeerinah dolerite was added to Mt. McRae shale as a base layer or as a vertical interlayer were characterized by: pH>7 effluent; no acidity (slight excess of alkalinity); low salinity (conductivity ≈100-200 μS/cm); low dissolved metal concentrations (non-detectable in most cases) and unexpectedly low sulfate, Ca and Mg concentrations. It appears that, under these test conditions, dolerite provides a preferential flow path for solution in the presence of Mt. McRae shale and could potentially be used in waste rock emplacements to channel acidic water flowing from ARD waste and to treat the seepage by removing both acidity and salinity.

Using the analyses for AGR and ANR, the evolution of W39 Terrace Dump at Mt. Whaleback has been characterized using water monitoring data collected at the AMD dam. The water samples had an average pH of 4.2 with high Mg (273 - 1210 mg/L), Al (up to 98 mg/L) and Si (up to 96 mg/L) concentrations suggesting that dissolution of (Mg, Al, Si)-containing chlinochlore has been the major buffering mechanism within the dump. The calculated AGR/ANRnc (ANR non-carbonate) data estimated from each of the AMD dam water samples fall within the values measured for long-term KLC tests, suggesting that the estimates made for the dump are quite reasonable. The average ratio of AGR/ANR of 1.02 indicates that the AGR was fairly close to the ANR provided by silicate minerals within the dump in 2008-2009 and that further reduction in AGR from the dump should give increased water pH in the AMD dam.

Hidden Valley Joint Venture (PNG)

A review of all previous reports on Hidden Valley (HV) waste rocks including waste classifications, site and consultants' KLC tests was completed (Gerson et al., 2014). The lithologies of the main rock types at the site are granodiorite (GD) and metasediment (MS) (the latter hosting most of the ore). The metasediment lithologies are all AMD-generating. Both lithologies can contain significant pyrite, but the HV granodiorite (HVGD) mineralogy contains calcite (11 wt.%) with the majority silicates as reactive plagioclase (anorthite with albite), chlorite, muscovite, orthoclase and quartz as well as significant pyrite content (4 wt.%). The overall ANC of the HVGD is high, *i.e.* 133 kg H_2SO_4/tonne and the ANRnc estimate from this mineralogy at pH 4 is 128 mg H_2SO_4/kg/week and at pH 5 is 30 mg H_2SO_4/kg/week delivering significant neutralization.

To test whether passivation of pyrite and AGR-ANR matching can be achieved with HVGD, KLC tests of a composite metasediment sample (2 wt% pyrite) with HVGD surface layers or in recycle from flow-through HVGD sub-columns were set up. The ANR (from effluent analysis) of the HVGD surface-layer column is initially about 50% of the AGR but the ANR matched the rapidly decreasing AGR at around 70 weeks, as the fine pyrite was depleted, but with pH still near 2.5. In the water recycle system, the effluent subsequent to both the MS composite column and the sub-column containing HVGD maintained neutral drainage and provided alkalinity up to 56 weeks. In recycle of this effluent to the MS composite column, the pH of the main recycle MS composite column in this system was only slightly increased but the acidity of the effluent was significantly lower (≈50 %) than for the MS composite control column after 16 weeks. Although recycle from the HVGD sub-column was not able to provide sufficient ANC to match the AGR of the MS composite main column, the results showed that the HVGD sub-column neutralised the acidity from the MS composite effluent in low–flow conditions. This suggested that HVGD may be useful as a flow-through reactive barrier (similar to that used at the Savage River Mine) for low-flow seeps to reduce current lime additions. To test this proposition, the effluent from a 2 kg batch of MS composite was used to flush a 1 kg HVGD sub-column in standard KLC flush conditions. The pH of the effluents from the HVGD sub-column maintained neutral to slightly alkaline pH across 60 weeks. Most of the toxic metal ions were precipitated and were below detection in the HVGD effluent except Mn. The ANR (derived from effluent concentrations) of the HVGD sub-column was slightly greater than the AGR of the MS composite up to 16 weeks but became slightly less than the MS AGR beyond 16 weeks. However, HVGD ANR is underestimated due to precipitation of gypsum (*i.e.* loss of Ca) in the HVGD sub-column, so that it is likely that the actual ANR of the sub-column exceeds the AGR of the MS column across more than 80 weeks. SEM analysis confirmed that the pyrite in the HVGD sub-column was passivated under these conditions.

This sample of HVGD had relatively high pyrite content (≈4 wt.%), twice as much as the MS composite material. However, the neutralization rate of the calcite/anorthite/chlorite in the HVGD was sufficient to enable formation of passivated pyrite surfaces within the HVGD reducing the pyrite oxidation rate. These results suggest that testing to locate HVGD lithology with lower pyrite content outside the MS areas may provide greater ANR for potentially matching AGR from MS wastes in co-disposal or layer dumping.

CONCLUSION

Most mine sites have non-value minerals capable of providing some neutralization of acid mine (rock or tailings) drainage often not considered or surveyed in primary site ore assessment or AMD dump construction. Standard assessment methods define only total acidity potential (AP) or neutralization potential (NP) of these materials, *e.g.* NP/AP ratio. This does not consider the **rates** at which acid generating and neutralising reactions may take place, although it is these relative rates in disposal of rock and tailings wastes that determine whether acid and metalliferous drainage actually occurs. Methods are now available to assess both AGR and ANR from both carbonates and reactive silicate minerals in on-site waste rock lithologies. The ratio of AGR/ANR can be followed using these assessments. These short-term, snap-shot methods can be applied at any point in the evolution of the dump or tailings from greenfield planning to operating dumping to assess current and future acid rock drainage liabilities and to make maximum use of these on-site materials. The complete definition of geochemistry and mineralogy of site materials can provide more effective and reduced-cost management of these mining wastes. Examples where neutralising waste rocks have been identified and assessed at Savage River (Tasmania), BHP Billiton Mt. Whaleback and Hidden Valley (PNG) have illustrated the value of this approach.

ACKNOWLEDGEMENTS

A Linkage Grant from the Australian Research Council, the assistance of Gray Bailey (Project Coordinator) and sponsors of the AMIRA P933A project (BHP Billiton Iron Ore, Savage River Rehabilitation Project, Hidden Valley Services PNG, Rio Tinto, Teck Metals) and permission to

publish the results from SRRP, BHPB Iron Ore and Hidden Valley Services are gratefully acknowledged.

REFERENCES

AMIRA/EGi. (2002). ARD Test Handbook (Smart R, Skinner W, Levay G, Gerson A, Thomas J, Sobieraj H, Schumann R, Weisener C, Weber P, Miller S, Stewart W, *AMIRA International*, http://www.amira.com.au/web/documents/downloads/P387AProtocolBooklet.pdf.

Blodau C, (2006). A review of acidity generation and consumption in acidic coal mine lakes and their watersheds. *Sci. Total Environ*. 369:307–332.

Brantley, A.F, Chen, Y., (1995). Chemical weathering rates of pyroxenes and amphiboles, in: *Chemical Weathering Rates of Silicate Minerals* (Eds White A.F., Brantley S.L.),. Mineralogical Society of America; ISBN 0-939950-38-3, pp. 119-172.

Ciccarelli JM, (2012). *Neutralization potential of silicate materials in the long-tern control of acid rock drainage*. PhD Thesis. University of South Australia, Adelaide, Australia.

Ciccarelli JM, Weber PA, Stewart WS, Li J, Schumann R, Miller SD, Smart R StC (2009). Estimation of long-term silicate neutralization of acid rock drainage. In *Proc. 8th Int. Conf. Acid Rock Drainage* (8 ICARD), June 22–26, 2009, Skellefteå, Sweden. website http://www.proceedings-stfandicard-2009.com. pp.1–12.

Cook, C., Skousen, J., Hilton, T. (2008). Covering pre-existing, acid-producing fills with alkaline sandstone to control acid mine drainage, *Mine Water Environ*., 27:259–264.

Dowd, P.J. (2005). The Business Case for Prevention of Acid Drainage. In *Proceedings of the Fifth Australian Workshop on Acid Drainage*, Fremantle, Western Australia. (Australian Centre for Minerals Extension and Research: Brisbane). Free download: www.inap.com.au/public downloads/Whats New/PD Keynote Speech 23 August 2005.doc.

Eary, L.E., Williamson, M.A. (2006). Simulations of the neutralizing capacity of silicate rocks in acid mine drainage environments. In *Proc. 7th Int. Conf. Acid Rock Drainage (7 ICARD)*, 27–30 March, St. Louis, MO, USA. Redhook, NY, USA: Curran Associates, Inc. pp. 564–577.

GARD Guide, *http://www.gardguide.com*.

Gerson, A.R., Smart, R.St.C., Li, J., Kawashima, N., Fan R., Zeng, S., Schumann, R., Levay, G., Dielemans, P., Mc Latchie, P., Huys, B., Hughes, A., Kent, S., Hutchison, B. (2014). Mineralogy Of Mine Site Neutralising Materials: A Missing Link In AMD Control Planning, Proc. Eighth Australian Workshop on Acid and Metalliferous Drainage (Eds. H. Miller and L.Preuss), ISBN: 978-0-9924856-0-3, Publ. JKTech Pty Ltd, Indooroopilly, Qld, Australia, 313-324.

Hollings, P., Hendry, M.J., Nicholson, R.V., Kirkland, R.A. (2001). Quantification of oxygen consumption and sulphate release rates for waste rock piles using kinetic cells: Cluff lake uranium mine, northern Saskatchewan, Canada. *App. Geochem*. 16:1215–1230.

Hughes, A., Dineen R., Kent S. (2009). Environmental performance of the Savage River rehabilitation project. In *Proc. 8th Int. Conf. Acid Rock Drainage* (8 ICARD), Skellefteå, Sweden. website http://www.proceedings-stfandicard-2009.com. pp.1–12.

Huminicki, D.M.C., Rimstidt, J.D. (2009). Iron oxyhydroxide coating of pyrite for acid mine drainage control. *App. Geochem*. 24:1626–1634.

Hutchison, B., Brett, D., Kent, S., Ferguson, T. (2009). Acid rock drainage management and remediation through innovative waste rock management techniques and mine planning at Savage River. In *Proc. 8th Int. Conf. Acid Rock Drainage (8 ICARD),* Skellefteå, Sweden. website http://www.proceedings-stfandicard-2009.com. website http://www.proceedings-stfandicard-2009.com/. pp. 1–10.

Jambor, J.L., Nesbitt, H.W., Blowes, D.W. (1999). Role of silicates in the compositional evolution and neutralization in the evolution of Fe- and Mg-sulfate waters in Waite Amulet tailings, Canada. in *Analytical Technology in the Mineral Industries, Min. Met. Mat. Soc. Canada.* Editors L.J. Cabri, C.H. Bucknam, E.B. Milosavlijevic, S.L. Chryssoulis and R.A. Miller. Warrandale PA, USA: The Minerals, Metals, and Materials Society (TMS). pp. 223–226.

Li, J., Kawashima, N., Schumann, R., Hughes, A., Hutchison, B., Kent, S., Kaplun, K., Ciccarelli, J.M., Smart, R.St.C. (2011). Assessment of alkaline cover performance for abatement of ARD from waste rock dumps at Savage River Mine. In *Proc. Seventh Australian Workshop on Acid and Metalliferous Drainage,*

Emerging Trends in Acid and Metalliferous Drainage Management. Indooroopilly Qld, Australia: JKTech Pty Ltd, Indooroopilly. pp. 241–253.

Li, J., Kawashima, N., Kaplun, K., Schumann, R., Smart, R.St.C., Hughes, A., Hutchison, B., Kent, S., (2012). Investigation of alkaline cover performance for abatement of ARD from waste rock dumps at Savage River Mine. In *Proc. 9th Int. Conf. Acid Rock Drainage (9 ICARD)*, 21–25 May, 2012 Ottawa, Canada. www.mend-nedem.org.

MEND, (2009). *Prediction Manual for Drainage Chemistry from Sulphidic Geologic Material, Report 1.20.1*, www.mend-nedem.org.

Miller, S., Schumann, R., Smart, R., Rusdinar, Y. (2009). ARD control by limestone induced armouring and passivation of pyrite mineral surfaces. In *Proc. 8th Int. Conf. Acid Rock Drainage (8 ICARD)*, Skellefteå, Sweden. http://www.proceedings-stfandicard-2009.com. pp.1–12.

Miller, S., Stewart, W., Rusdinar, Y., Schumann, R., Ciccarelli, J., Li J., Smart, R.St.C. (2010). Methods for estimation of long-term non-carbonate neutralization of acid rock drainage. *Sci. Total Environ*. 408:2129–2135.

Nicholson, R.V., Gillham, R.W., Reardon, E.J. (1990). Pyrite oxidation in carbonate-buffered solution: 2. Rate control by oxide coatings. *Geochim. Cosmochim. Acta* 54:395–402.

Palandri, J.L., Kharaka Y.K. (2004). *A compilation of rate parameters of water-mineral interaction kinetics for application to geochemical modelling*. Menlo Park, CA, USA: US Geological Survey. Open-File Rep.2004-1068.

Paktunc, A.D., (1999). Mineralogical constraints on the determination of neutralization potential and prediction of acid mine drainage. *Environmental Geology* 39 (2), 103-12.

Rumble C., (2005). Conceptual cover design for ARD control of the B Dump at the Savage River Mine, Geo-Environmental Management, B. Hutchison, private communication, Grange Resources.

Schumann, R., Kawashima, N., Li, J., Miller, S., Smart, R., Stewart, W.S. (2009). Passivating surface layer formation on pyrite in neutral rock drainage. In *Proc. 8th Int. Conf. Acid Rock Drainage* (8 ICARD), Skellefteå, Sweden. website http://www.proceedings-stfandicard-2009.com. pp.1–12.

Smart, R.St.C., Miller, S.D., Stewart, W.S., Rusdinar, Y., Schumann, R.C., Kawashima, N., Li, J. (2010). In situ calcite formation in limestone-saturated water leaching of acid rock waste. *Sci. Total Environ*. 408:3392–3402.

Sracek, O., Gélinas, P., Lefebvre, R., Nicholson, R.V. (2006). Comparison of methods for the estimation of pyrite oxidation rate in a waste rock pile at Mine Doyon site, Quebec, Canada. *J. Geochem. Exploration* 91:99–109.

Thornett J.R. (1999). *Report on the structural and lithological mapping of North Pit and South Lens Pit, Savage River Magnetite Mine*, Department of Environment, Tasmanian Government, Australia. e-mail: alison.hughes@environment.tas.gov.au.

Zeng, S., Li, J., Schumann, R., Smart, R. (2013). Effect of pH and dissolved silicate on the formation of surface passivating layers for reducing pyrite oxidation. *Computation Water, Energy Environ. Eng*. 2:50–55.

Acid Rock Drainage (ARD) Inhibition by Sulfite Used as Part of the Inco Process for Cyanide Removal

Leslie Hardy and Paul Morton
AMEC Foster Wheeler Environment & Infrastructure, Canada

ABSTRACT

Calcium sulfite ($CaSO_3$) has been used as an ARD inhibitor at coal ash sites for over a decade. Sulfite is considered a redox buffer and oxygen scavenger because it readily oxidizes to sulfate. Site history at a gold mine in Canada indicates sulfite can persist for decades in saturated mine tailings and inhibit the onset of ARD.

Sodium metabisulfite (SMBS, $Na_2S_2O_5$) was used as part of the Inco process to treat cyanide in 300,000 tonnes of tailings. A mass balance was developed for nitrogen, sodium, calcium and sulfur. The mass of reagents used is consistent with the mass discharging in water from the tailings, and the percentage of nitrogen discharged is lower than the other elements. Most of the nitrogen added as cyanide remains sorbed to the tailings as strong acid dissociable cyanides such as iron-cyanide complexes, and nitrogen gas is formed by biodegradation of cyanide and ammonia.

This paper discusses why the mine tailings have not become acidic as expected based on acid-base accounting or humidity cell results. The mill used approximately 270 tonnes of SMBS to treat 100,000 tonnes per year of tailings, giving a concentration of approximately 900 mg/kg as sulfur or 2,250 mg/kg as sulfite. Sulfite readily oxidizes to sulfate on exposure to air, and the ion chromatography laboratory method does not routinely distinguish sulfite from sulfate. The water concentrations reported as sulfate may actually be a combination of sulfite and sulfate. Sulfite contributes to titratable alkalinity, and the measured alkalinity versus total inorganic carbon indicates the continued presence of sulfite. Calcium sulfite has a much lower solubility than SMBS, and calcium from the lime used in the Inco process prevents depletion of sulfite from the tailings. Field observations and humidity cell results indicate that calcium sulfite in the tailings inhibits the onset of acid rock drainage.

Keywords: sulfite, sodium metabisulfite, INCO process, cyanide, acid rock drainage

INTRODUCTION

A gold mine in Canada used sodium cyanide and a carbon in pulp process to recover gold and the Inco process to remove cyanide from the effluent. The mine processed 100,000 tonnes of ore per year for three years, and the resulting 300,000 tonnes of tailings is impounded on permafrost ground behind a tailings dam constructed across a creek bed. Based on the 2% sulfide content of the tailings and some of the humidity cell test results, the tailings are predicted to create acid rock drainage. Mining and milling activities ceased in the 1990s, and most of the tailings porewater continues to have a high pH, with only preliminary indications of acid rock drainage.

Groundwater and surface water monitoring commenced in 1999, including the flow rate and chemistry of the toe seepage and decant water from the tailings impoundment. In recent years, the flow rate has increased and a conceptual remediation plan has identified that tailings relocation could be required. Based on recent monitoring data and information presented in previous reports, a revised interpretation of the mine tailings geochemistry was developed.

The hypothesis presented in this paper is that the onset of acid rock drainage is inhibited by sulfite which was added to the tailings at a concentration of 2,250 mg/kg as part of the Inco process to remove cyanide from the tailings. The inhibition of the onset of ARD by calcium sulfite was first reported by Hao and Dick (2000) who completed laboratory experiments to evaluate the geochemical mechanism. This paper presents field evidence for ARD inhibition, and is apparently the first reported observation of sulfite inhibiting the onset of ARD at a mine site.

INCO PROCESS DESCRIPTION

The mill used the Inco SO_2/Air process to oxidize cyanide in the tailings and tailings water prior to storage in the tailings pond. The following discussion about the Inco process is primarily based on Mudder, Botz & Smith, 2001, and Breuer, Jeffery & Meakin, 2011. This process description leads to an accounting of the mass of reactants used at the mill versus measured values in the tailings decant and toe seepage water.

The Inco process is based upon conversion of free cyanide and weak acid dissociable (WAD) cyanide complexes to cyanate using a mixture of sulfur dioxide (SO_2) and air in the presence of a soluble copper catalyst at a controlled pH. The specific amounts of reagents used vary between mine sites, and this mine used sodium metabisulfite ($Na_2S_2O_5$) in a liquid solution.

When the Inco process is applied to tailings liquids (i.e. homogeneous systems in chemistry terminology) all of the free cyanide and WAD-cyanide is converted to cyanate (i.e. it is stoichiometrically converted; see Breuer, Jeffery & Meakin, 2011). However, cyanide reacts very strongly with iron on tailings solids to form strong acid dissociable (SAD) iron-cyanide complexes which are not affected by the Inco process. When the Inco process is applied to tailings slurries (i.e. heterogeneous systems), most of the cyanide remains sorbed to the tailings solids as SAD-complexes. Residual metals liberated from the WAD-cyanide complexes are precipitated as hydroxides. Therefore, the Inco process oxidizes free cyanide and WAD-cyanides to the less toxic form of cyanate, but most of the cyanide remains complexed onto iron in the tailings as SAD-cyanides.

Table 1 summarizes the annual reagent usage listed in a design document for the mine.

Table 1 Design reagent usage at mill

Reagent	Formula	Design Consumption Rate (kg/tonne)	Mine Lifetime Usage (tonnes)
Sodium Cyanide	NaCN	1	300
Lime	CaO	4.6	1,400
Sodium Hydroxide	NaOH	0.18	54

Hydrochloric acid	HCl	0.18	54
Copper Sulfate	$CuSO_4*5H_2O$	0.27	81
Sodium Metabisulfite	$Na_2S_2O_5$	2.7	810

The design usage of sulfur dioxide (3.6 g/g CN), lime (8.7 g/g CN) and copper (0.13 g/g CN) is consistent with the average data presented for twelve mine sites in Mudder, Botz & Smith, 2001. The average usage is: sulfur dioxide (4.8 g/g CN), lime (3.7 g/g CN), and copper (0.1 g/g CN). The theoretical usage of SO_2 in the process is 2.46 grams of SO_2 per gram of WAD-cyanide oxidized, but in practice the actual usage ranges from about 3.0 to 5.0 grams of SO_2 per gram of WAD- cyanide oxidized. Based on the design document for the mill and the reviewed literature, the amount of reagents used at the mine is consistent with other mine sites.

Sulfite

The Inco process has been described as using sulfur dioxide, although Breuer, Jeffery & Meakin, 2011 state that the active reagent is actually sulfite which forms when SO_2 hydrates as shown in equation 1.

$$SO_2 + H_2O \text{ -----> } SO_3^{2-} + 2\ H^+ \qquad (1)$$

Sulfite (SO_3^{2-}) is a redox buffer and oxygen scavenger because it readily oxidizes to sulfate according to equation 2.

$$SO_3^{2-} + 0.5\ O_2 \text{ -----> } SO_4^{2-} \qquad (2)$$

As presented by Hao and Dick, 2000, sulfite consumes oxygen by the oxidation to sulfate according to equation 2, and this prevents the aerobic oxidation of pyrite which is the first step in the formation of acid rock drainage. Warren Dick (personal communication, 2013) stated that sulfite recovered from flue gas desulfurization at coal fired power plants has been co-disposed with pyrite bearing coal ash at several sites in the Ohio, USA, region, and more than a decade of monitoring data indicates that the sulfite is inhibiting the onset of acid rock drainage. The oxidation of sulfite to sulfate occurs slowly at low termperatures, high pH and water saturated conditions (which limits oxygen influx to the tailings), and the continued presence of sulfite in the tailings after two decades would be expected under the site conditions. However, sulfite in water samples cannot be preserved, and would be expected to readily oxidize to sulfate according to equation 2.

The source of sulfite used in the Inco process can be gaseous or liquid SO_2, sodium sulfite, or sodium metabisulfite (SMBS). This mine used SMBS based on cost and reagent handling considerations. Solid SMBS is made by evaporating a sodium sulfite solution, and when added to water, the bisulfite ion converts to sulfite. Table 2 summarizes the approximate aqueous solubility of various forms of sulfite.

Table 2 Aqueous solubility of various sulfites

Form of sulfite	Aqueous solubility (mg/L)
Sodium metabisulfite	450,000
Sodium sulfite	270,000
Magnesium sulfite	5,000
Calcium sulfite	54

SMBS and sodium sulfite are highly soluble in water, but calcium sulfite is orders of magnitude less soluble. Therefore, in the presence of high calcium concentrations in groundwater, sulfite will tend to precipitate as calcium sulfite and this is a constraint on the concentration of sulfite in water at the mine. In the tailings area, calcium is primarily derived from the 'lime' (CaO, also known as quicklime) used to control the pH for the Inco process. If calcium was not present in the tailings

water, the concentration of sulfite in the discharge would have been much higher, and the source would have been depleted more quickly.

High concentration aqueous sulfite solutions have a pH of about 9, and unlike sulfate (SO_4^{2-}), sulfite (SO_3^{2-}) can contribute to acid titrable alkalinity. The equilibrium pH point between SO_3^{2-} and HSO_3^- (i.e. the pKa) is 7.17, and when titrated to the standard alkalinity titration endpoint of pH = 4.5, sulfite buffers the addition of acid and contributes to the measured total alkalinity. Sulfate does not contribute to measurements of alkalinity because the pKa of SO_4^{2-} and HSO_4^- is 1.99 and alkalinity titrations only extend to an endpoint pH of 4.5. Therefore, in addition to carbonate alkalinity, as measured separately by total inorganic carbon (TIC), sulfite also contributes to total alkalinity. The potential contribution of sulfite is not explicitly recognized in textbook definitions of alkalinity, although weak acids such as sulfurous acid (H_2SO_3) can contribute to total alkalinity.

METHODOLOGY

Surface water and groundwater sampling commenced at this mine in the 1990s.. Tailings decant and toe seepage water samples have been collected approximately every three weeks (271 samples in 14 years) and analyzed for a comprehensive suite of analytical parameters including pH, alkalinity, chloride, sulfate, sulfide, metals, ammonia, nitrate, nitrite, and cyanides (free cyanide, WAD-cyanide, SAD-cyanide, thiocyanate, and cyanate). Groundwater has been sampled less frequently, with most locations being sampled five times since 2009. In 2013, some additional parameters and modified sampling protocols were used in conjunction with the standard parameters and methods. These modifications included the collection of unpreserved dissolved metals samples, and field measurements of sulfide in water. Additional parameters added in 2013 included total inorganic carbon (TIC), total organic carbon (TOC), and monitoring of the well headspace for biogenic gases (oxygen, carbon dioxide, and methane) using a landfill gas meter. Field parameters measured during the water sampling included pH, conductivity and dissolved oxygen.

Groundwater under flowing the tailings impoundment dam is collected by the seepage pond and the seepage is then continuously released to surface water. This seepage flow rate was measured daily using calibrated flow meters, and is consistent with water balances completed for the mine site. There appears to be minimal groundwater underflow from the tailings dam beyond that accounted for by the seepage meter because of the presence of permafrost ground. The observed seepage flow rate was approximately 50 L/min from 1999 to 2008, and has since increased to approximately 200 L/min.

Solid phase tailings samples were previously analyzed for standard acid base accounting, humidity cell testing, and field kinetic testing. The average sulfide content of the tailings was 2%, and the neutralization potential ratio of 0.5 indicates that the acid generating potential is greater than the neutralization potential. Based on these results, the tailings would be expected to generate acid rock drainage.

Sampling and analysis for sulfite in both soil and water is difficult due to the oxidation to sulfate by atmospheric oxygen and environmental analytical laboratories often cannot distinguish sulfite and sulfate when analyzing water samples by ion chromatography. The measurement of sulfite in water is also apparently limited by the formation and potential loss of SO_2 gas from water samples. There are analytical methods to measure sulfite in solids samples, although these methods are limited by the presence of sulfide minerals which can prevent the accurate measurement of sulfite.

RESULTS AND DISCUSSION

Reagent Mass Balance

The mass of a water quality parameter discharged is calculated as the volume of water times the concentration. The total mass for an element can be determined based on the various water quality parameters, and these values can then be compared to the mass of reagents used at the mill. For the

reagents listed in Table 1, water quality parameters are available to quantify the amount of sodium, calcium, sulfur and nitrogen discharged from the tailings area into the creek.

The volume of tailings water released was determined using a 10 day moving average centered on a date with water chemistry data. Graphs of the water discharged and corresponding water chemistry are presented on Figure 1 and the results are summarized on Table 3.

Inorganic nitrogen data is often reported by laboratories as mg/L-N to allow direct comparison between nitrogen species, and the total cyanide concentration as mg/L-N is calculated as shown on equation 3.

Total Cyanides as N = (14.01 g/mol) * [(CN-)/26.02+(SAD-CN)/26.02 + (OCN-)/42.02 + (SCN-)/58.08] (3)

By calculating total cyanides as N, a direct comparison with the breakdown products (ammonia, nitrate, and nitrite) can be completed as presented on Table 3. Total N is the sum of the various cyanide species (free cyanide, SAD-cyanide, cyanate, thiocyanate) and the measured inorganic nitrogen species (ammonia, nitrate, nitrite) formed by the degradation of the cyanides. WAD-cyanide is not included in this calculation as this cyanide fraction is included in the SAD-cyanide fraction reported by the laboratory as total cyanide. Note also that the measured WAD-cyanide values are higher than can be accounted for by the measured concentrations of metals that form WAD-cyanide complexes (e.g. copper) which indicate that in this case the WAD-cyanide test is actually measuring organic-cyanide complexes (Dzombak, Ghosh and Wong-Chong, 2006).

The total cyanide mass discharged reached an inflection point in about 2002 when the concentrations decreased to near non-detect levels; however, the concentration of the nitrogen breakdown products (ammonia, nitrate, and nitrite) has remained steady since monitoring began. This observation is consistent with the continued breakdown of the SAD-cyanide complexes on the tailings.

Mass balance calculations for the data presented on Figure 1 versus the mass of mill reagent chemicals used are presented on Table 3. Most (57%) of the sulfur added at the mill as sodium metabisulfite and copper sulfate is accounted for by the mass of sulfur measured in the discharge. For comparison, only 6.2% of the nitrogen added at the mill as cyanide is accounted for by the various nitrogen compounds analyzed (ammonia, nitrate, nitrite, free cyanide, SAD-cyanide, cyanate, thiocyanate). The lower value for nitrogen is consistent with the fact that most of the cyanide remains sorbed to the tailings as iron-cyanide complexes, and some nitrogen would also be lost as nitrogen gas (N_2) from the biodegradation of cyanide and ammonia. The higher percentage for sulfur may be due to the observation that this measurement is dominated by "sulfate" which is likely a combination of sulfate and sulfite, and also due to oxidation of sulfide minerals in the tailings.

Groundwater and Soil Gas Chemistry

Sample data and the calculations used to infer the presence of sulfite are presented on Table 4. The data presented is categorized as Well Series A to D, and sample data from a monitoring well representative of these categories is presented. There are approximately 30 groundwater monitoring locations.

Monitoring well headspace gas measurements show methane at percent level concentrations at four monitoring wells on the upgradient side of the tailings, and oxygen at (or above) atmospheric concentrations in the other monitoring wells within the tailings. The highest oxygen concentration measured was 23.9% using a calibrated GEM 2000 Plus. Well headspace gas monitoring was repeated three times using four different landfill gas meters. Reproducable results show the presence of methane at four wells, and that at most monitoring well locations oxygen is present at near atmospheric concentrations. These results are consistent with the presence of dissolved oxygen and lack of detectable sulfide in the water.

For monitoring wells classified as Well Series A (two wells on upgradient side of tailings), the pH is near 9, and sulfite was identified (but not quantified) in the ion chromatograms for the 2013

samples. These samples were not preserved to prevent oxidation of sulfite to sulfate, and the calculations on Table 4 show that slightly more than half of the total alkalinity expressed as $CaCO_3$ would be from sulfite, and this would represent approximately 10% of the total sulfur in the water sample.

Well Series B represent approximately 20 locations primarily within the mine tailings, and along a creek downgradient of the tailings dam. For Well Series B, the pH remains near 7.5, and the calculated sulfite concentration needed to provide the missing alkalinity ranges from 5 mg/L to 170 mg/L, with most locations having a calculated sulfite concentration of less than 80 mg/L. These calculated sulfite concentrations are consistent with the low solubility of calcium sulfite as shown on Table 2. Furthermore, the calculated concentrations of sulfite are consistent with the missing sulfur fractions when comparing the reported sulfate and total sulfur concentrations.

For monitoring wells classified as Well Series C (two wells on downgradient side of tailings dam), acid rock drainage is apparently starting in 2014. Since 2013 the sulfate concentration tripled, the pH decreased to slightly below 6, and the total alkalinity decreased to 35 mg/L. The reported 1990 mg/L of sulfate represents 651 mg/L of sulfur, and the measured total dissolved sulfur was 634 mg/L. This indicates that essentially all of the sulfur in the sample is present as sulfate. At both of these locations in 2013, acid rock drainage had not yet started, and the calculated sulfite concentration was consistent with Well Series B. At these two locations, it appears that the available sulfite has been depleted, and oxidation of the mineral sulfides has started.

For monitoring wells classified as Well Series D (four locations on or immediately downgradient of the tailings dam), the sulfate and total sulfur concentrations are low, and the amount of sulfite that would be required to provide the missing alkalinity is comparable to Well Series B. The water chemistry shown for Well D on Table 4 includes 583 mg/L of sulfate (measured on an unpreserved sample, and later confirmed by the laboratory), but only 1.6 mg/L of dissolved sulfur as measured in the acidified dissolved metals sample. In 2013, duplicate samples had reported sulfate concentrations of <5 mg/L and the dissolved sulfur concentration in duplicate samples was 1.6 mg/L. These samples are from water table monitoring wells, and the low sulfur concentration at these locations immediately downgradient of the tailings dam appears to indicate that sulfur is being lost from the water as sulfur dioxide gas.

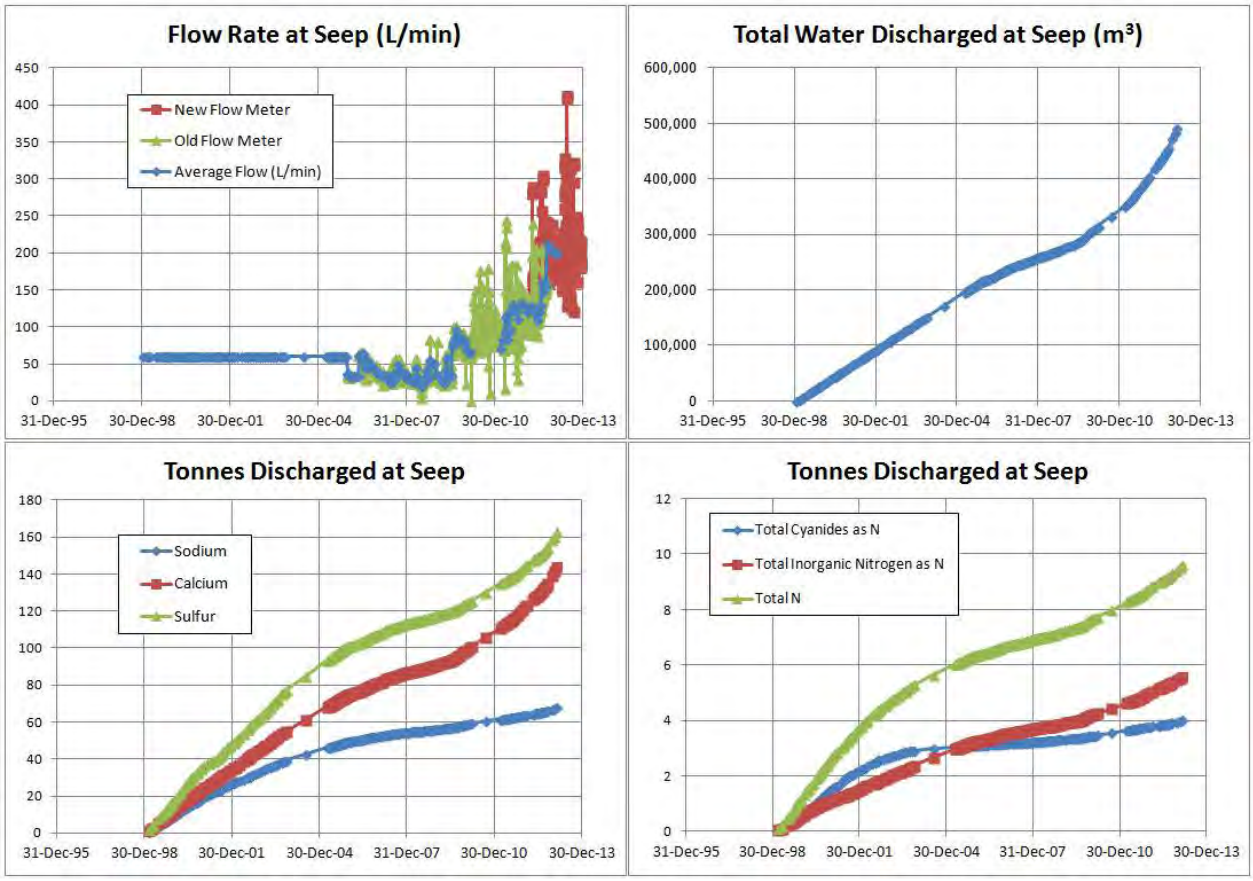

Figure 1 Graphs showing flow rate and total volume of water released from the tailings, and the total mass of sodium, calcium, sulfur and nitrogen compounds discharged

Table 3 Mass balance for mill reagents released from tailings 1999-2013

Parameter	Sodium	Calcium	Sulfur as S	Cyanides as N	Total Inorganic Nitrogen as N
Flow Weighted Average Concentration (mg/L)	139	294	331	8.7	11.3
Tonnes Discharged at Seep	68.0	144	162	4.3	5.6
Tonnes of Reagents Added at Mill	270	990	285		159
Tonnes Discharged as Percentage of Reagents added at Mill	25.2%	14.6%	57.0%		6.2%
Total water discharge from tailings from 1999 to 2013 was 490,800 m^3					

Like carbon dioxide (CO_2), when sulfur dioxide (SO_2) degases from water samples, acid is removed from the water and the pH rises. This effect is consistently seen in the monitoring data (with the exception of the two wells in Well Series A) where the field measured pH is lower than the laboratory measured pH. When CO_2 degases from a water sample, the pH rises but the total alkalinity in the sample bottle is unchanged due to the precipitation of calcite ($CaCO_3$). However, when SO_2 degases from a sample, the pH rises and sulfur is lost from the water sample as a gas. The loss of SO_2 usually occurs under acidic conditions, but several water samples collected

downgradient of the tailings dam have minmal amounts of both total sulfur and sulfate (i.e. Well Series D). This lack of sulfur in the water samples from this area could indicate that sulfur is either being precipitated as a solid, or lost as a gas.

The groundwater gradient steepens below the tailings dam, and this creates a larger surface area of water within the capillary fringe above the water table resulting in enhanced gas-water partitioning. Observations during groundwater sampling in 2013 indicate that the tailings porewater is charged with gas. This is likely to be nitrogen gas (N_2) created during the biodegradation of cyanide and ammonia. Nitrogen gas has a very high Henry's law constant (1540 L*atm/mol) and will partition from the water into the gas phase. Small amounts of nitrogen gas generated by the oxidation of cyanide and ammonia creates a high partial pressure of dissolved gas, and when the sum of the partial pressures exceeds the confining pressure, bubbles of gas can form (both in the tailings or in the sample bottle). Bubbles of gas were noted during the field sulfide testing and during the groundwater sampling. The presence of high partial pressures of dissolved gas provides a plausible mechanism to account for the lack of sulfur downgradient of the tailings dam despite the neutral pH and the high aqueous solubility and low Henry's law constant (0.8 L*atm/mol) for sulfur dioxide. Samples were flown from the mine on commercial jet aircraft, and the lower air pressure at altitude may have allowed bubbles to form which could effectively partition sulfur dioxide from the water into the gas phase.

Due to analytical limitations, there are only indirect measurements of sulfite in the soil and groundwater at this site. The presence of sulfite is indicated by the mass balance of the mill reagents, and measurements of pH, sulfate, total sulfur, total alkalinity, total inorganic carbon (TIC), and electrical charge balance. The lack of iron oxidation noted in unpreserved water samples for metals analysis collected in 2013 also indicates the potential presence of an oxygen scavenger such as sulfite. Additional calculations can also account for the alkalinity consumed by the oxidation of some of the Fe^{2+} in the unpreserved metals sample bottles. By accounting for this loss of alkalinity, the charge balances shown on Table 4 can be improved. The low dissolved sulfur and sulfate concentrations measured at locations downgradient of the tailings dam indicate the loss of sulfur from the water samples as SO_2 gas. Finally, the observation that sulfide oxidation did not occur in the humidity cell testing of untreated tailings samples even after two years, despite the 2% sulfide content, is indicative of the presence of sulfite on the tailings. Humidity cell samples that had been pre-treated with acid to accelerate the testing process produced acid rock drainage as expected, and this is consistent with the loss of sulfite from the acidified tailings samples as SO_2 gas.

CONCLUSIONS

A former gold mine in Canada used sodium metabisulfite (SMBS) as the source of sulfite (SO_3^{2-}) in the Inco process to remove cyanide. Documents for the mine show that the rate of reagent usage at the mine was consistent with other mines. A mass balance shows that approximately 57% of the sulfur added at the mine mill can be accounted for in the water discharge from the tailings, but only 6% of the nitrogen can be accounted for as the various measured nitrogen compounds. These results indicate that most of the cyanide remains on the tailings solids as strong acid dissociable (SAD) complexes such as iron-cyanide; however, biodegradation of these cyanide complexes is continuing.

As shown on Table 2, the aqueous solubility of calcium sulfite is orders of magnitude lower than for SMBS or sodium sulfite. The use of lime (CaO) to stabilize the pH in the Inco process has resulted in high calcium concentrations in the tailings, and the low solubility of calcium sulfite has limited the leaching of sulfite from the tailings. The oxidation of sulfite to sulfate (SO_4^{2-}) is slow under the site conditions (i.e. low temperature, high pH, water saturated) and the continued presence of sulfite in the tailings under these conditions would be expected. However, sulfite in water samples cannot be preserved, and would be expected to readily oxidize to sulfate according to equation 2. Furthermore, laboratory analysis typically does not distinguish sulfite from sulfate, and the reported concentrations of sulfate are likely a combination of these two sulfur species.

Calcium sulfite recovered from flue gas desulfurization inhibits the onset of ARD in pyrite bearing coal ash waste and this process has been documented in the scientific literature. The observations at this mine site are consistent with the inhibition of the onset of ARD due to the presence of calcium sulfite on the mine tailings. This paper presents field evidence for ARD inhibition, and is

apparently the first reported observation of sulfite inhibiting the onset of ARD at a mine site. If monitoring shows that sulfite is being depleted, SMBS could be injected into the mine tailings to maintain the soil and water concentrations of calcium sulphite needed to inhibit the onset of ARD.

REFERENCES

Breuer, Paul, Coby Jeffery and Rebecca Meakin (2011), *Fundamental Investigations of the SO2/Air, Peroxide and Caro's Acid Cyanide Destruction Processes*, ALTA conference, Perth, Australia.

Dzombak, D., Rajat Ghosh and George Wong-Chong (2006), *Cyanide in Water and Soil: Chemistry, Risk and Management*, CRC Press.

Hao, Y. and Warren Dick, (2000), *Potential inhibition of acid formation in pyritic environments using calcium sulfite byproduct,* Environmental Science and Technology, American Chemical Society.

Mudder, T.I., Michael M. Botz, and Adrian Smith (2001), *Chemistry and Treatment of Cyanidation Wastes*, Second Edition, 2001, Mining Journal Books, London.

Table 4 Example data and calculations

Parameter	Units	Well A	Well B	Well C	Well D
Date Sampled		27-Jun-14	27-Jun-14	28-Jun-14	29-Jun-14
Measured Values					
pH - Field	pH	9.66	7.54	5.82	7.10
pH - Lab	pH	8.74	8.14	6.52	8.20
Dissolved oxygen - field	mg/L	0.25	0.37	2.58	0.66
Oxygen (well headspace)	%	20.9	19.7	20.5	21.0
Carbon dioxide (well headspace)	ppm	520	830	950	520
Methane (well headspace)	%	nd	31	4	nd
Calcium	mg/L	77.6	112	587	143
Magnesium	mg/L	0.81	49.8	57.5	55.5
Sodium	mg/L	22.7	21	82.0	19.7
Potassium	mg/L	8.18	8.22	5.92	3.5
Iron	mg/L	0.40	11.7	87.4	20.1
Manganese	mg/L	0.06	4.15	17.9	4.87
Ammonia-N	mg/L	4.12	5.03	2.27	2.9
Alkalinity, Total (as CaCO3)	mg/L	80.2	581	35.7	204
Chloride	mg/L	2.5	<5.0	<0.4	<5.0
"Sulfate" as SO4	mg/L	136	31	1990	583
Sulfide	mg/L	<0.10	0.03	0.023	<0.02
Sulfur (S)-Dissolved	mg/L	132	11.9	634	1.6
Total Organic Carbon (TOC)	mg/L	28.3	48.4	10.8	74.3
Total Inorganic Carbon (TIC)	mg/L	9.2	89.1	4.9	19.7
Calculated Values					
"Sulfate" as S (32.06/98.06)	mg/L	44.5	10.2	651	191
Difference (Dissolved S - "Sulfate" as S)	mg/L	87.5	1.7	-16.6	-189.0
Cation Sum	meq/L	5.5	11.7	41.7	13.8
Anion Sum Using "Sulfate" and Total Alkalinity	meq/L	4.4	12.3	43.0	16.2
Balance (Cations/Anions)	%	123%	96%	97%	85%

Alkalinity from Carbon (TIC*4.17) where 4.17 = 50.04/12.01	mg/L	38.4	372	20.4	82.1
Excess Alkalinity (Total - TIC*4.17)	mg/L	41.8	209	15.3	122
Sulfite Concentration Needed to Provide Excess Alkalinity (40.03/50.04)	mg/L	33.5	168	12.2	97.5
Sulfite as S (32.06/80.06)	mg/L	13.4	67.0	4.9	39.0
% of Dissolved S as Sulfite	%	10.1%	563%	0.8%	2422%
Anion Sum - Using TIC*4.17 and Sulphite Alkalinity	meq/L	5.34	16.4	42.5	18.7
Balance (Cations/Anions)	%	102%	71%	98%	74%

Geochemical Study of the Interaction of Acid and Alkaline Mine Drainage with $BaCO_3$

Julio Castillo[1], Alba Gomez-Arias[1], Jan Posthumus[1], Megan Welman-Purchase[2], Esta van Heerden[1]

1. *Department of Microbial, Biochemical and Food Biotechnology, University of the Free State, South Africa*
2. *Department of Geology, University of the Free State, South Africa*

In this study the geochemical behaviour of $BaCO_3$ was investigated and the optimization of its use in acid (pH 2.93) and alkaline (pH 8.2) mine drainage (AMD) with high concentrations of sulfate (1250-1400 mg/L) and moderate to low metal concentrations (mainly Fe^{2+}> Al^{2+}> Mn^{2+}> Zn^{2+}) was determined. Batch experiments were conducted using a series of four interactions with $BaCO_3$:AMD ratios of 1:400 (0.1g:40mL), 1:57 (0.7g:40mL) and 1:160 (0.25g:40mL), 1:80 (0.5g:40mL) with $AMD_{alkaline}$ and AMD_{acid}, respectively. Each series of the experiments were composed of 15 sub-samples in which the reactions were stopped at different time intervals (0', 5', 15', 40', 2h, 6h, 12h, 24h, 36h, 48h, 72h, 96h, 120h, 144h and 168h). The neutralization process increased the pH (to 8.3 and 9.98 for $AMD_{acid/alkaline}$, respectively) through alkaline additive dissolution. The metal solubility decreased with the precipitation of $BaSO_4$ and divalent metals (Mn^{2+} and Zn^{2+}) as carbonates and poorly crystallized Fe-Al oxy-hydroxides. These precipitates acted as a sink for trace elements to the extent that the solutions reached the pre-potability requirements of water for human consumption. In all the experiments, the reactions achieved steady state conditions between 6h to 24h. The results showed 100% SO_4^{2-} removal in AMD_{acid} with an initial concentration of 1250 mg/L within a residence time of 6 hours. While in the $AMD_{alkaline}$ with an initial concentration of 1400 mg/, 86% SO_4^{2-} removal was obtained within 24 h with lower residual barium than 0.1 g:40 mL $AMD_{alkaline}$ interaction. The results showed that this ratio was optimal and could be used in the future for remediation systems. In addition, the treatment of $AMD_{acid/alkaline}$ with $BaCO_3$ removes up to 50% salinity and conductivity. The final product was $BaSO_4$ sludge with moderate to low metal concentrations, which could even be recycled and used by other industries.

Keywords: acid alkaline mine drainage, $BaCO_3$

INTRODUCTION

The Acid Mine Drainage (AMD) generated from pyrite's oxidative dissolution, typically contains high concentration of anions (SO_4^{2-}) and metal (mostly Fe^{3+}>Al^{3+}>Cu^{2+}>Zn^{2+}>Mn^{2+}) which makes it a significant environmental problem for South Africa, as well as for other mining countries (Bell et al., 1998; McCarthy, 2011).

The South African AMD is characterized by a wide pH range from acid (2.6) to alkaline (8). The main reason for this fact is that the host rock contains mainly pyrite and carbonates (such as dolomite). Therefore the AMD is characterized by having high salinity (Ca>Mg>Na), hardness and heavy metal concentrations such as Fe^{3+} > Al^{3+} > Mn^{2+} and moderate to low trace metal concentrations such as Ni^{2+} > Zn^{2+} > Cu^{2+} (Durand, 2012).

Therefore, the conventional passive chemical systems based on a $CaCO_3$ or MgO neutralization process are not completely effective for these leachates, because: (1) the acid mine drainage treatment by $CaCO_3$ or MgO allows the neutralization and removal of heavy metals. However, it increases the salinity and hardness in the treated effluent. (2) The low solubility of $CaCO_3$ at high pH limits its use in treating acid and not alkaline drainages (Maree et al., 2004; Caraballo et al., 2011; Bologo et al., 2012). Also the active systems, such as reverse osmosis or GYP-CIX, can remove salinity and hardness. However, the high maintenance costs and the brine generated by the treatment decreases the viability of these systems (INAP, 2003).

Based on hydrogeochemical characteristics of this type of leachate, many treatment systems have been showcased that are generally based on sulfate-reduction bioreactors. This technology, despite having been optimized in recent years, has not been able to completely remove the high concentration of SO_4^{2-} and it did not decrease salinity and hardness in these leachates (Du Preez et al. 1992; Moosa et al., 2002; 2005).

$BaCO_3$ was tested in simple batch experiments in the 70's due to its dissolution in a wider range of pH (0-9) and due to its capability to precipitate sulfate as $BaSO_4$, but it was not considered viable because the dissolution rate was very low at pH values of 7-10 (Kun, 1972). In the 80's, 90's and again in 2006, $BaCO_3$ was tested as a step in an active process to remove sulfate (Trusler et al., 1991; Hlabela et al., 2006). However, these studies did not optimize the $BaCO_3$ concentration, residence time nor provided relevant information about the geochemical behaviour of this compound and its use in AMD treatment.

Current studies have shown that $BaCO_3$ has a good dissolution rate between pH values of 0-6.5 and that the dissolution rate decreases when pH increases. In addition, it was also shown that $BaCO_3$'s dissolution rate increases with increasing temperature because of its endothermic nature. Moreover, previous studies showed variations between theoretical thermodynamics and experimental results regarding the dissolution of the $BaCO_3$ (Li & Jean, 2002).This knowledge is extended in this research which focused on addressing these issues by conducting a geochemical study with $BaCO_3$ and AMD that could explain both its behaviour as well as its potential to remediate these leachates. Understanding these processes will allow the optimization of $BaCO_3$ usage for sulfate removal and its contribution in removing salinity and hardness from acid and alkaline AMD.

METHODOLOGY

Starting materials

Acid and alkaline mine drainage

Two drainages with different hydrogeochemical characteristics from active and abandoned mines were collected from the South African provinces of Mpumalanga (25°42'20.4"S 29°59'28.4"E) and Gauteng (25°50'10.0"S 29°14'03.7"E) which were used as natural reagent solutions for batch experiments. The first drainage was an alkaline mine drainage (AMDE), whose hydrogeochemical characteristics conforms to the average of typical coal mine drainages (high sulphate, salinity and hardness concentration). The second drainage was acid mine drainage collected from an abandoned

mine (AMDK), which is characterized by high acidity and pollutant concentration (Bell et al., 1998; McCarthy, 2011). Each sample was taken on site in polyethylene tanks (ca. 260 L) for further experiments and part of each sample (1L/AMD) filtered through a 0.45 μm filter within 24 h for chemical analysis.

Alkaline material

Alkaline material used in this experiment was $BaCO_3$ (Protea Chemicals Company SA). $BaCO_3$ have a purity of 88.6%. These materials contain impurities including Fe and S as SO_4^{2-}, in negligible concentrations. Finally, a representative and homogeneous sample of 1 g was taken, which has been chemically and mineralogically analysed.

Batch experiment

Batch experiments were conducted to test the interaction of alkaline material with AMDE and AMDK at different time intervals (0min, 5min, 15 min, 40 min, 2 h, 6 h, 12 h, 24 h, 36h, 48 h, 72h, 96 h, 120 h, 144h and 168 h) in falcon tubes (50 mL) under continuous mixing in a rotary mixer at 12 rpm and room temperature. Four series of interactions were carried out using solid:liquid (w/w) ratios of 1:400, 1:57 and 1:160, 1:80 for experiments with AMDE and AMDK, respectively. Each interactions will be identified throughout the paper as E1 that refers to the interaction between 40mL of AMDE and 0.1 g $BaCO_3$; E2 to the interaction between 40mL of AMDE and 0.7 g of $BaCO_3$; K1 to the interaction between 40mL of AMDK and 0.25 g of $BaCO_3$ and K2 to the interaction between 40mL of AMDK and 0.5 of $BaCO_3$. At the end of each time interval, the tubes were removed from the rotary mixer and the supernatant was separated from the solid product by centrifugation at 4000rpm for 3min. Finally, the supernatant solutions were filtered through a 0.45μm filter and the solid product was dried at 40°C.

Chemical analysis

The following parameters were analysed on site from the collected samples to avoid the dissolution effects of the CO_2 (g) and O_2 (g): pH, Electrical Conductivity (EC), salinity (Sal), redox potential (Eh) and temperature (T). The pH, EC, Sal and T were measured with the ExStix®II multi-probe, while Eh was with ExStix®II ORP (Pt and Ag/AgCl electrodes) probe. The Eh measurements were then corrected to standard hydrogen electrode (SHE). Samples were filtered and acidified to pH < 2 with HNO_3 (2%) and stored at 4°C for further chemical analysis at the Institute for Ground Water Studies, University of the Free State. Sulfate concentrations were analysed by a portable Hach spectrophotometer (model DR/900 colorimeter) according to the turbidimetric method described in the Hach Procedures Manual-Method Sulfate 608. Fe^{2+} and Fe_{Total} were determined after filtration (0.45 μm) with a Hach spectrophotometer (model DR/900 colorimeter) according to the colorimetric method described in the Hach Procedures Manual-Method Ferrous iron 255 and FerroVer 265. All these chemical analysis also were carried out on site.

The neutralization potential of $BaCO_3$ was determined by treating a sample with a known excess of standardized hydrochloric acid subjected to heat treatment (95°C). Finally, the amount of neutralizing bases expressed in tons $CaCO_3$ equivalent/thousand tons of material was determined from the amount unconsumed acid by titration with standardized sodium hydroxide (Jackson, 1958).

The $BaCO_3$ was digested by an *aqua regia* solution (1HCl:1HNO_3:1H_2O) at 90°C for 1 h up to its complete dissolution (Pérez-López et al., 2010). Total Element Concentration (TEC) from the digestion, as well as the sub-samples, were analysed by inductively coupled plasma-atomic emission spectroscopy (ICP-AES; Jarrel Ash Atom comp 975). The mineralogical characterization of the final experimental products was carried out by X-ray diffraction (XRD, powder method) using a Panalytical Empyrean diffractometer under following conditions: slit fixed at 10mm, Cu/ Kα monochromatic radiation, 40mA and 45 kV. Samples were run at a speed of 2˚θ /min (5-70˚). The spectrum was obtained by Highscore software. In addition, solid samples were also studied using a scanning electron microscope equipped with an energy dispersive system (SEM–EDS; JEOL model GSM 6610).

Geochemical modelling

Precipitation of newly formed solid phases by the $BaCO_3$ dissolution could control the fate of the metal concentrations in both the acid and alkaline mine drainage, studied by the batch experiment. The results of the hydrogeochemical analysis from supernatant of each reaction (sub-sample) were modelled by PHREEQC-2 geochemical speciation model (Parkhurst and Appelo, 2005) using MINTEQ thermodynamic database (Allison et al., 1991) to predict the aqueous speciation of leachates and saturation indices of solid phases in the experiments [SI=log(IAP/KS) where IAP is the ion activity product and KS is the solubility constant]. Zero, negative or positive SI values indicate that the solutions are saturated, undersaturated and supersaturated, respectively, with respect to a solid phase.

RESULT AND DISCUSSION

Characterization of the starting materials

Acid and alkaline mine drainage (AMD)

Results of hydrogeochemical characterization of the AMDs are reported in Table 1. The main difference between the two mine water samples is the pH. The pH values of AMDE and AMDK were 8.2 and 2.93, respectively. In the case of AMDK, low pH values were related to the low carbonate concentration in the host rock, which contain high sulphide concentration. Its intense oxidation and subsequent dissolution of pyrite, produces a large amount of acidity. In the case of the AMDE it had circum-neutral to alkaline pH-values due the low content of sulphide minerals and the presence of carbonate or basic silicate minerals (Banks et al., 2002). The carbonate dissolution also contributes to lowering the water quality by increasing the hardness and salinity, which also affects the ecosystem.

Table 1 Significant physicochemical parameters of the acid and alkaline mine drainages

	AMDE	AMDK
pH	8.2	2.93
EC (mS m^{-1})	209	170
Redox potential (mV)	295	415
Ca (mg/L)	256.0	169.84
Mg (mg/L)	138.9	66.34
Na (mg/L)	12.18	41.30
Ba (mg/L)	0.040	0.028
Fe (mg/L)	0.042	34.24
Al (mg/L)	0.019	44.89
Sulfate (mg/L)	1250.0	1400
Mn (mg/L)	0.023	10.11
Zn (mg/L)	0.016	1.31

Alkaline materials

The neutralization potential of $BaCO_3$ obtained was 525 tons $CaCO_3$ equivalent / thousand tons of material. The neutralization potential of $BaCO_3$ is lower than calcite which has a high neutralizing capacity of 937.5 tons $CaCO_3$ equivalent / thousand tons of materials. However, the calcite is scarcely soluble at circum-neutral pH (6-7), while $BaCO_3$, despite having a low solubility at circum-neutral pH (6-7) is able to dissolve at pH values of up of 8-9. Total Element Concentration (TEC) confirmed the product data from Protea Chemicals, which indicated that the most significant impurities were S and Fe with values of 0.30% (total sulfur as SO_4^{2-}) and 0.004% (Fe total). The average particle size was 1-3 μm.

Preliminary batch experiments were carried out to test the dissolution capacity of the $BaCO_3$ in alkaline and acid mine drainage. The results obtained in these experiments showed a sulfate removal percentage of 90% on average and an increase to pH of 9. The $BaCO_3$ had a higher dissolution at lower pH such as 4-5, whereas, at higher pH such as 8.9 the dissolution of $BaCO_3$ was slower. However, the dissolution of $BaCO_3$ after 24 h showed the same behaviour in both AMDK and AMDE, indicating that the pH does not decrease the dissolution of $BaCO_3$ after 24 h

Hydrogeochemical study of BaCO3 dissolution with AMD

The hydrogeochemical evolution as a function of time of the physicochemical parameters such as pH, Eh, EC, Sal, as well as sulfate concentration in the four ratio (w/v) interactions are shown in Figure 1. The neutralization potential of $BaCO_3$ allowed the pH to increase from 2.93 to 8.27 for the K1 and K2 interactions (0.25 and 0.5 g of $BaCO_3$), and from pH 8.2 to 9.98 on average for the E1 and E2 interactions (0.1 and 0.7 g of $BaCO_3$), respectively. The Eh values decreased from 295 to 67 mV and from 415 to 128 mV on averages, whereas EC decreased to 942 μS/cm and 1091 μS/cm (variation ±5%), for the E1-E2 and K1-K2 interactions, respectively. The decrease in EC values reflects an improvement in the quality of AMDs that was confirmed by the decrease in sulfate concentration in the solution. In the experiments with AMDK all these parameters achieved a steady state in 6 h in both interactions (K1 and K2). The behaviour of $BaCO_3$ was different for the interactions with AMDE (E1 and E2), where a steady state was achieved after 24 h. The sulfate concentrations decreased slowly after 24 h (E 1 and E2 reached 280 and 120 ppm after of 168 h) without achieving a steady state, while in the K1 and 2 interactions, the sulfate concentration was completely removed after 24 h. $BaCO_3$ dissolution was faster in the K2 interaction where the pH increased from pH 2.93 to 6.79 and the interaction was almost immediate. However the Sal and EC evolution was slower.

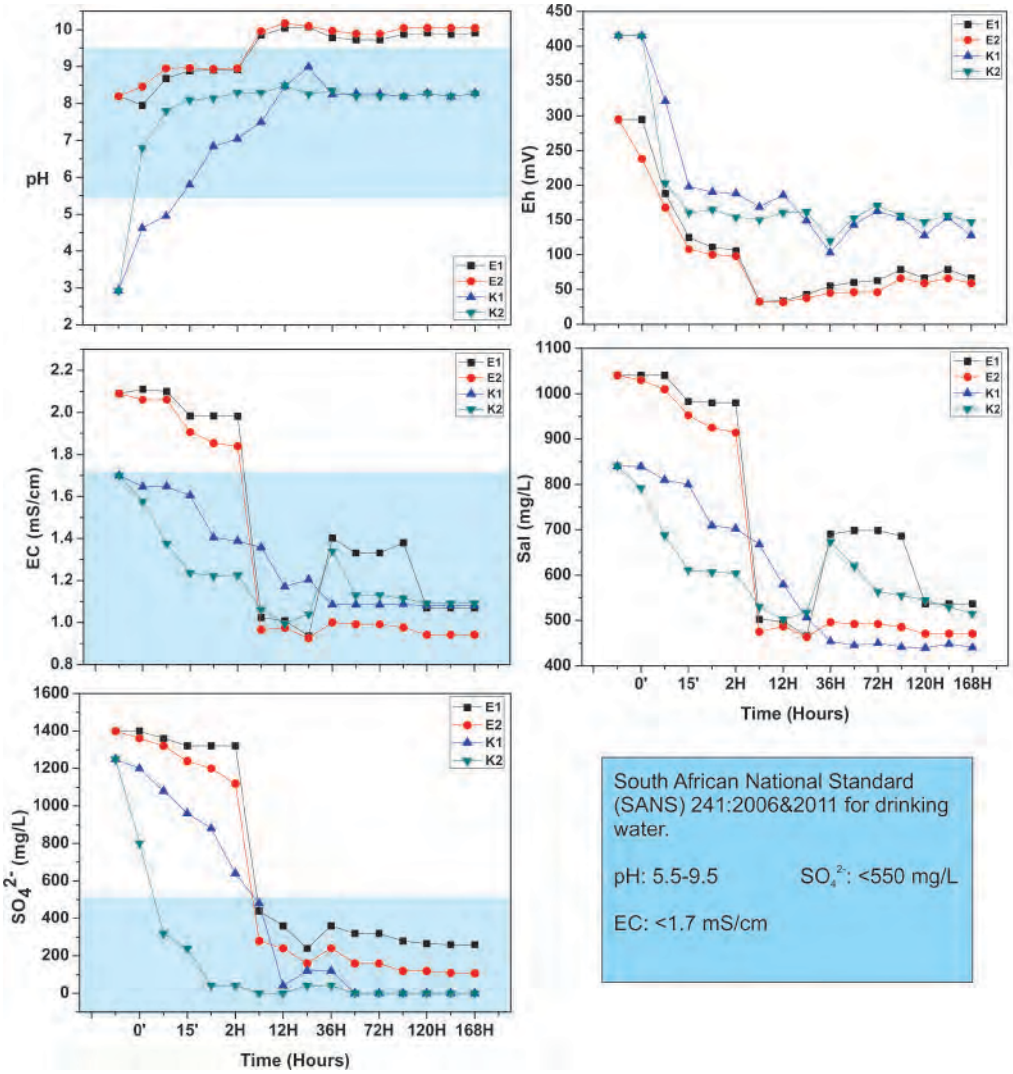

Figure 1 Temporal evolution of the physicochemical parameters from 0 to 168 h and its relation with drinking water standard (SANS 241)

The evolution of metals and sulfates are closely related to the dissolution rate and the concentration of $BaCO_3$ (Figure 2). Therefore, optimization and understanding of its behaviours is vital to assess its remediation potential. The interaction with a concentration of $BaCO_3$ larger than 0.1g (E1) showed higher concentration of dissolved Ba^{2+} at the end of the experiment (0.33, 6.7, 4.1 mg/L in E2, K1 and K2, respectively) which did not react during the experiment. Therefore, the concentration of $BaCO_3$ used in E1 can be considered as the optimum to be used in passive and active systems with a residence time of 24 hours, at most, to get an 86% sulfate removal rate.

The hydrogeochemical behaviour of the cations, such as Ca^{2+}, Mg^{2+} and Na^{+} over time was similar, between E1 and E2, as well as between K1 and K2. Ca decreased drastically within 6h, the removal reached 97 % in the E interactions, but in K interactions took 120 h to reach 51% of Ca^{2+} removal. The concentration of Na^{+} only decreased 18 % in K interactions.

The evolution of metals during the experiment will only be described and discussed with regards to the K interactions, due to the insignificant concentration of metals in AMDE. The concentration of metals in AMDK was as follow, $Al^{3+} > Fe^{3+} > Mn^{2+} > Zn^{2+}$ (44.89 > 34.24 > 10.1 > 1.3, respectively). The removal of Fe^{3+}, Al^{3+} and Zn^{2+} were 100%. However the removal of Mn was 66% in 24 h and 86% in 120 h.

Parameters such as EC, Sal and hardness decreased in all the interactions to values below the allowable limits for drinking water (SANS 241, 2006; 2011) (Figure 1). The removal of SO_4^{2-}, Ca^{2+} and heavy metals was the main reason for those parameters to decrease. Most of the passive systems are not able to remove Ca^{2+}, but increase its concentration (such as the systems based on $CaCO_3$), however this system has demonstrated its effectiveness in removing anions (SO_4^{2-}) and cations (mainly Fe^{3+}, Al^{3+}, Mn^{2+}, Zn^{2+} and Ca^{2+}) which is also reflected in the concentration of Sal and EC of the drainage.

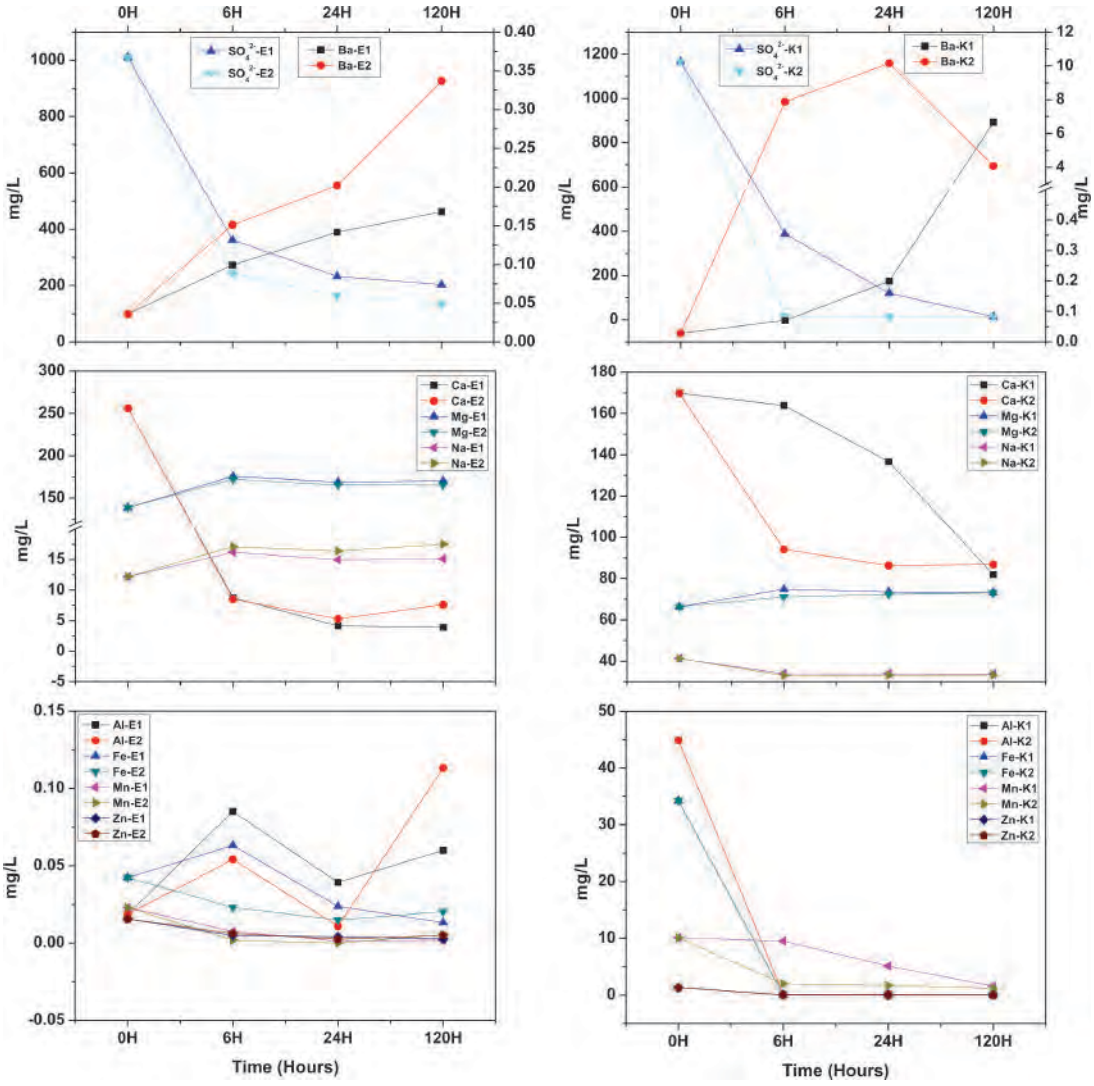

Figure 2 Temporal evolution of cations and anions from 0 to 168 h

The precipitates collected at the end of the experiment from E1 and K1 interactions, were analysed by XRD (Figure 3). The analyses showed mainly mineral phases related to the dissolution of $BaCO_3$ as well as to the precipitation of sulfate and Ca^{2+}. The geochemical processes involved in the increased of pH, as well as the sulfate, Ca^{2+}, Mg^{2+} removal, including Fe^{3+}, Al^{3+}, Mn^{2+} and Zn^{2+} has been represented by the following equations:

1. Representation of dissolution of $BaCO_3$ in AMD:

$$BaCO3s \rightarrow Ba2+(aq)+CO32-(aq) \quad (1)$$

2. pH values were increased by releasing OH^- radicals and formation of CO_2 that could act as a buffer to control the increase of pH .

$$CO32-aq+ H2Ol \rightarrow HCO3-aq+ OH-aq \quad (2)$$

$$HCO32-aq+ H2Ol \rightarrow H2CO3-aq+ OH-aq \quad (3)$$

$$H2CO32-aq \rightarrow CO2aq+ H2O(l) \quad (4)$$

3. The increased pH values would allow the trivalent and divalent metals precipitation as oxy-hydroxides and/or oxy-hydroxysulfate of Fe^{3+} and Al^{3+} and carbonates of Mn^{2+} of Zn^{2+}, respectively. In addition, the presence of carbonates and bicarbonates in solution would promote the Ca^{2+} and Mg^{2+} removal as carbonates and thus reduce the hardness of these AMDs.

$$Me+HCO3- \rightarrow MeCO3+H+ \quad (6)$$

$$Me+H2CO3- \rightarrow MeCO3+2\ H+ \quad (7)$$

The estimated percentage of those mineral phases were, according to the contact time (0h, 6h and 168 h), as follow: E1: 0h: witherite (71.2%) > calcite (15.9%) > barite (12.9%); 6h: barite (63.8%) > witherite (26.5%) > calcite (9.7%); 168h: barite (65.7%) > calcite (19.2%) > witherite (16.9%). K1: 0h: witherite (76.2%) > barite (13.5%) > calcite (10.3%); 6h: witherite (71.4%) > barite (18.9%) > calcite (9.6%); 168h: witherite (53%) > barite (28.5%) > calcite (18.5%).

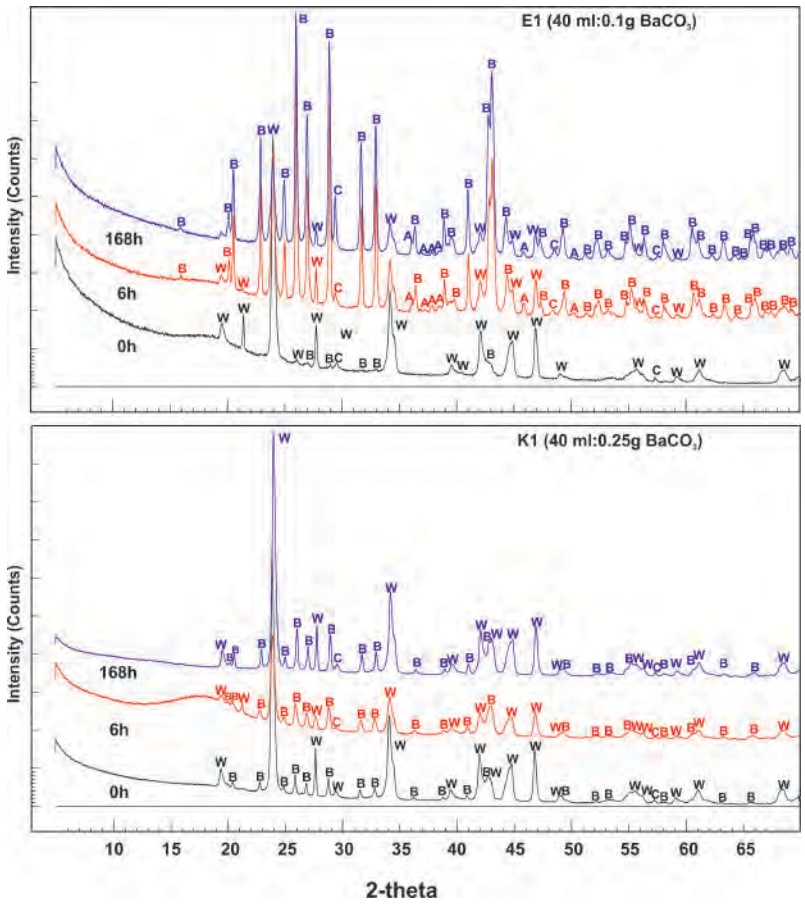

Figure 3 Difractograms of E1 and K1 at 0, 6 and 168 h. W: witherite, B: barite, C: calcite and A: aragonite

However these mineral phases could be masking other sub-idiomorphic or amorphous crystals, mainly in the K interactions, where the metal concentrations were high. This was corroborated by SEM-EDS analyses, where Fe^{3+}, Al^{3+} and Mn^{2+} were detected in the precipitates (Figure 4). The thermodynamic simulation with PHREEQC also supported this hypothesis by predicting the precipitation of Fe^{3+} and Al^{3+} as oxy-hydroxysulfate, poorly crystallized according to XRD analyses. This acted as a sink for trace elements and contributed to reaching the requirements for drinking water. The minerals phases of Mn^{2+} and Zn^{2+} were not predicted to be saturated by PHREEQC, however both metals were 100% removed from the AMDs. This again demonstrated that there are several discrepancies between the theoretical thermodynamic fundaments and the real geochemical data acquired throughout the experiment. Finally, the improvement of the quality of the AMDs used in the four interactions has been so effective that the final concentration of the sulfates was within the limit allowable for drinking water (South African National Standard 241, 2006; 2011).

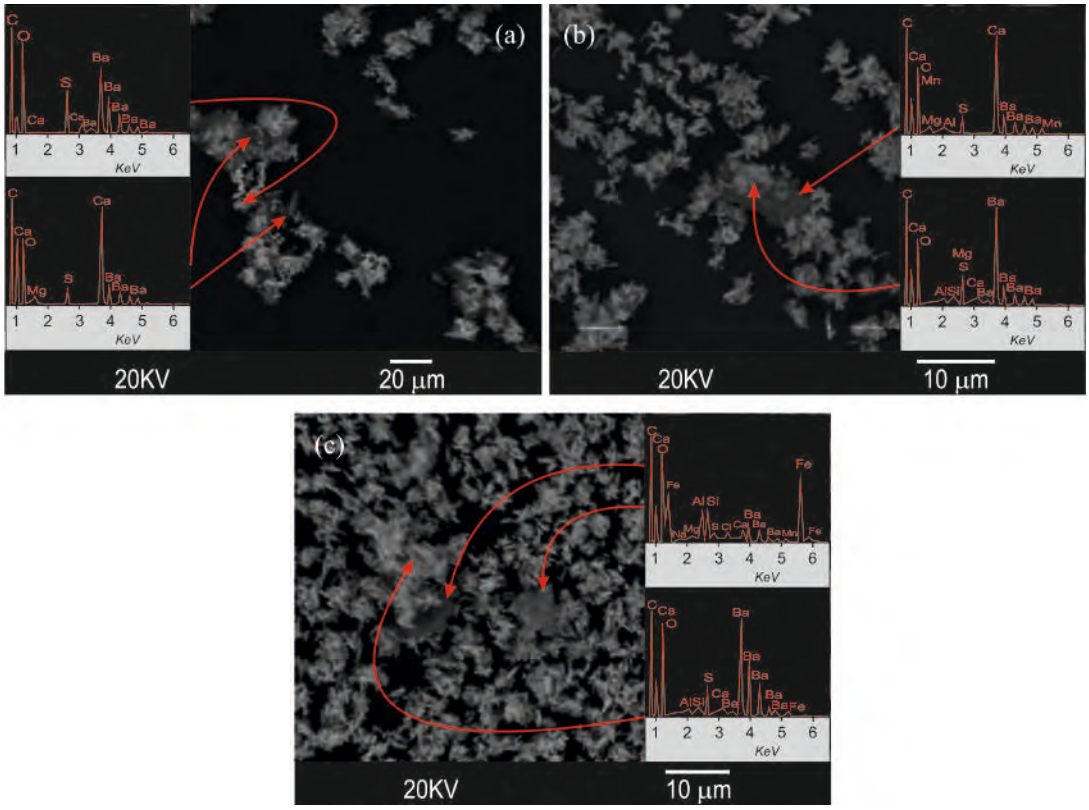

Figure 4 SEM-EDS images of minerals phase neoformed poorly crystallized

CONCLUSIONS

Batch experiments were conducted with the aim to study the behaviour and optimize the use of $BaCO_3$ in AMD remediation. Four interactions were carried out with two different AMDs and four different ratios (w/w) $BaCO_3$: AMD (1:400 and 1:57 with AMDE (alkaline) and 1:160 and 1:80 with AMDK (acid)). Each interaction was composed of 15 sub-samples, each of them with different contact time between AMD and $BaCO_3$ (from 0 to 168 h). All the samples achieved a steady state between 6 and 24 h. However the low solubility of the $BaCO_3$ at high pH slowed down the dissolution in E interactions, where the pH reached up 9.98 and the dissolution continued after 168 h. Nevertheless, E1 interaction reached a sulfates removal of 86% between 6 and 24 h. The sulfates and Ca removal were the most meaningful results in E interactions. Moreover, the total metal removal in K interactions was the determining factor for the improvement of the water quality. According to these results, the ratio used in the E1 interaction can be considered as the optimum to be used in systems with a residence time of 24 hours.

XRD and SEM-EDS analyses corroborated the sulfates and metals evolution over time by the identification of crystalline and amorphous mineral phases. The modelling also predicted the precipitation of mineral phases such as barite, calcite and Fe/Al oxy-hydroxides. However there were discrepancies between the predictions and the data acquired from the experiments, such as the removal of Zn and Mn that probably were precipitated as carbonates. Therefore the $BaCO_3$ dissolution varies according to the pH and the composition of the AMD. However, at the end of each experiment the water was within the South African National Standard for drinking water.

ACKNOWLEDGEMENTS

The authors would like to thank the Technology Innovation Agency (TIA) for funding the project, Kairos Industrial Holding Ltd. and Exxaro Resources Ltd. for samples and site access, as well as the Department of Geology and the Institute for Groundwater Studies, both at the University of the Free State, for the technical and analytical support.

REFERENCES

Allison, J.D., Brown, D.S. & Novo-Gradac, K.J. (1991) MINTEQA2/PRODEFA2, A geochemical assessment model for environmental systems. Version 3.0 User's Manual, Environmental Research Laboratory, Office of Research and Development, US Environmental Protection Agency, EPA/600/3-911021, Athens, Georgia.

Banks, D., Parnachev, V.P., Frengstad, B., Holden, W., Vedernikov, A.A. & Karnachuk, O.V. (2002) 'Alkaline mine drainage from metal sulphide and coal mines: examples from Svalbard and Siberia', *Geological Society*, London, Special Publications, vol. 198, pp. 287–296.

Bell, F.G., Bullock, S.E.T. & Marsh, C.A. (2001). 'Acid Mine Drainage: Two South African Case Histories', *International Journal of Coal Geology*, vol. 45, no. 2-3, pp. 195–216.

Bologo, V., Maree, J.P. & Carlsson, F. (2012) 'Application of magnesium hydroxide and barium hydroxide for the removal of metals and sulfate from mine water', *Water SA* vol. 38, pp. 23–28.

Caraballo, M.A., Macías, F., Nieto, J.M., Ayora, C., Castillo, J. & Quispe, D (2011) 'Hydrochemical performance and mineralogical evolution of a dispersed alkaline substrate (DAS) remediating the highly polluted acid mine drainage in the full scale passive treatment of Mina Esperanza (SW, Spain)', *American Mineralogist*, vol. 96, pp.1270–1277.

Du Preez, L.A., Odendaal, J.P., Maree, J.P. & Ponsonby, M., (1992) 'Biological Removal of Sulfate from Industrial Effluents using Producer Gas as Energy Source', *Environmental Technology*, vol. 13, no. 9, pp. 875–882.

Durand, J.F. (2012) 'The impact of gold mining on the Witwatersrand on the rivers and karst system of Gauteng and North West Province, South Africa', *Journal of African Earth Sciences*, vol. 68, pp. 24–43.

Hlabela, P., Maree, J. & Bruinsma, D., (2006) 'Barium Carbonate Process for Sulfate and Metal Removal from Mine Water' *Mine Water and the Environment*, vol. 26, no. 1, pp. 14–22.

INAP (2003) Treatment of Sulfate in Mine Effluents, International Network for Acid Prevention. LORAX Enviromental, Inc., October 2003 < http://www.inap.com.au [Accessed 6/9/2011]>

Jackson, M.L. (ed) (1958) Soil Chemical Analysis, Prentice-Hall, Englewood Cliffs, N.J.

Kun, L.E. (1972) A Report on the Reduction of the Sulfate Content of Acid Mine Drainage by Precipitation With Barium Carbonate, Anglo American Research Laboratories.

Li, C. Jean, J. (2002) 'Dissolution and Dispersion Behavior of Barium Carbonate in Aqueous Suspensions' J*ournal of American Ceramic Society*, vol. 85, no. 12, pp. 2977–83.

Maree, J.P., Hlabela, P., Nengovhela, R., Geldenhuys, A.J., Mbhele, N., Nevhulaudzi, T. & Waanders, F.B. (2004) 'Treatment of mine water for sulfate and meta removal using barium sulphide', *Mine Water and the Environment*, vol. 23, no. 4, pp. 195–203.

McCarthy, T. (2011)'The impact of acid mine drainage in South Africa', *South African Journal of Science*, vol. 107, no. 5-6, pp. 1–7.

Moosa, S., Nemati, M. & Harrison, S.T.L. (2002) 'A kinetic study on anaerobic reduction of sulfate, Part I:Effect of sulfate concentration', *Chemical Engineering Science*, vol. 57, pp. 2773–2780.

Moosa, S., Nemati, M. & Harrison, S.T.L. (2005). 'A kinetic study on anaerobic reduction of sulfate, part II: incorporation of temperature effects in the kinetic model', *Chemical Engineering Science*, vol. 60, pp. 3517 –3524

Parkhurst, D.L., Appelo, C.A.J. (2005) PHREEQC-2 version 2.12: A hydrochemical transport model, http://wwwbrr.cr.usgs.

Pérez-López, R., Castillo, J., Quispe, D., & Nieto, J.M. (2010) 'Neutralization of acid mine drainage using the final product from CO2 emissions capture with alkaline paper mill waste', *Journal of Hazardous Materials*, vol. 177, pp. 762–772.

Trusler, G.E., Edwards, R.I. & Buckley, C.A., (1991) 'Sulfate, Calcium and Heavy Metal Removal from Industrial Effluents using Barium Carbonate', *Water S.A.*, vol. 17, no. 2, pp. 167–172.

Recovery of River Systems Affected by the Hungarian Bauxite Processing Residue (Red Mud) Spill

William Mayes[1], Áron Anton[1], Viktória Feigl[2], Orsolya Klebercz[2], Katalin Gruiz[2], Ian Burke[3] and Adam Jarvis[4]

1. CEMS, University of Hull, United Kingdom
2. Budapest University of Technology and Economics, Hungary
3. University of Leeds, United Kingdom
4. Newcastle University, United Kingdom

ABSTRACT

The largest ever release of bauxite processing residue (red mud) into the surface water environment occurred in western Hungary in 2010 and left large areas of floodplain and river channel contaminated with a range of metals and metalloids such as Al, As, Cr, Co, Fe, Na, and V. Fluvial sediments provide an important sink, and potential secondary source for such contaminants, so there monitoring is key to assessing the health of the affected river environment. This study provides a comparative assessment of fluvial sediment quality in the Marcal-Rába catchment between post-disaster surveys (November 2010) and follow up surveys at the same locations in September 2013. The metal-rich signature of red mud apparent in initial surveys was much limited in extent in the recent surveys. These affected reaches amount to <1 km of stream, compared to the >20 km length of contaminated river in 2010. Concentrations of red mud-derived contaminants are predominately associated with fine fractions of the red mud (<8 □m). This fine-grained material has been preferentially transported out of the river system and in to the larger Danube system. These physico-chemical characteristics of the spill material, along with remedial efforts (primarily dredging), have substantially limited the within-channel inventory of potentially ecotoxic metals. As such, the legacy of the Hungarian red mud spill on the Torna-Marcal system appears to be largely overcome in a relatively short timescale since the disaster.

**There is no full article associated with this abstract.*

CHAPTER 9

COVER DESIGN AND PERFORMANCE

Incorporating Climate Variability into Cover System Design

Lindsay Tallon, Mike O'Kane, Jason Song and Amy Heidman
O'Kane Consultants, Canada

ABSTRACT

Climate is the ultimate determinant of cover system performance. Typical cover system design efforts apply average climate values as model inputs, resulting in an over-simplification of what is inherently a very complex system. The purpose of this work was to demonstrate a novel technique for separating the inherent scales of variability within a given climate signal. Long term air temperature and precipitation data from Fort McMurray, Canada were used. Air temperature averaged 0.3 °C, while the long term average precipitation was 412 mm. A moving average was used to reveal a long-term warming trend of 0.03 °C yr^{-1}. Determination of the cumulative departure from the mean for precipitation showed qualitatively periods where the annual average values departed substantially from the mean, suggesting the presence of wet and dry climate cycles. Unfortunately both techniques still operate under the assumption of data stationarity, or the assumption of a constant mean and variance, which by definition does not incorporate small scale cycles and long-term trends. Empirical mode decomposition (EMD) was used as a means of dealing with a non-linear, non-stationary dataset. The EMD technique works directly in the time domain to separate out the scales of variability inherent in the input signal, as well as to determine the contribution to the total measurement variance of each inherent scale. Air temperature was found to be dominated by the annual scale of variation, accounting for 76% of the total variance; a finding that is not surprising. However, the EMD technique was also able to demonstrate the long-term warming trend, while also uncovering high frequency variations from five to seventeen days. Precipitation had a more even contribution of high, medium, and low frequency cycles of variation. A major contribution to the total variance of the precipitation signal was at the 3 and 7 year scales, which are postulated to correspond to El Niño / La Niña cycles, and the Pacific Decadal Oscillation, respectively.

Keywords: Climate, cycles, variability, cover system

INTRODUCTION

Climate is the primary determinant governing cover system performance (MEND or INAP reference). The climate at a mine site will set the basic performance constraints, within which the cover system designer must work to achieve the design outcomes. Expected precipitation volumes and the evaporative capacity of a given location are two major design considerations that will ultimately dictate the success or failure of the entire closure landform. Given the risks involved should a closure landform not perform as designed, it is not surprising that climate data represents a critical model input during early design efforts.

Typical design approaches supply a long-term average precipitation value as a modelling input to predict future performance. However, using a single average value does not account for changing mean and variance in a climate dataset. Furthermore, applying a single average value does not allow for changes in antecedent conditions within the cover system. All periodic processes will have a range of scales of variation, from small, high-frequency changes on the order of minutes to hours, to large, low-frequency trends that can take decades to move through a single cycle. Failing to account for the many scales of variation in a climate dataset will ensure that the underlying complexities of the interactions at the soil atmosphere interface are not fully understood.

There are a number of methods for describing a climate dataset that range from very basic to extremely sophisticated. At its most basic, a characterization of the mean and variance will begin to describe the inherent qualities of the climate dataset. However, measurements of the central tendency and data dispersion soon become inadequate to properly characterize the variability of the climate model inputs. Geostatistical techniques are often employed to better understand the natural cycles of variability contained within a climate data time series. In addition, to the mean and variance, geostatistics only requires the probability distribution and the similarity between values at different temporal scales to be determined.

Geostatistics operate under the fundamental assumption that measurements made close together in time (space) tend to be more similar than those made further apart (Goovaerts, 1997). Geostatistics are used to analyze the distribution of data in a time series, and help to quantify patterns and structures within the dataset by describing the relationship between two points in time. The temporal (or spatial) structure, or the covariance, as a function of the separation, or the scale, helps to identify patterns in the dataset and major repeating processes (Si et al., 2007). Having an understanding of the structure of spatial or temporal variability in a dataset allows for better design of monitoring networks, proper data interpretation, and better assessments of simulation and uncertainty analyses (Si et al., 2008).

Whereas many common geostatistical techniques take advantage of the similarity of adjacent data points, spectral analysis transforms values from the spatial or temporal domain to the frequency domain. The result of analyzing data in the frequency domain is that the data are now partitioned wherein the total variation of the data are separated into different frequency scales. Spectral techniques then make it easy to identify dominant processes at discrete temporal or spatial scales, by simply identifying prominent spikes in frequency.

A drawback of spectral methods is that the mean and variance of the dataset do not change over time; a condition known as stationarity. For the cover system designer analyzing a climate dataset, this is problematic. Not only is it the cycles of variation within the dataset, it is the overall trend that in climate that can be of major concern. Using a single mean value for precipitation or temperature

ignores the implications of climate change in the cover system design. Spectral methods such as wavelet analysis (Torrance and Compo, 1998), Hilbert spectral analysis (Biswas et al., 2013), including empirical mode decomposition (Biswas et al. 2009) are methods that can account for nonstationary datasets. Thus, the methods are ideally suited for analyzing climate datasets when designing soil cover systems. Not only do the methods analyze high frequency, small scale climate cycles, but can also account for long term trends that span the entire dataset.

Application of geostatistics and spectral analysis to the investigation and design of unsaturated soil cover systems represents an excellent potential opportunity to define the dominant controls on performance. Too often the analysis of climate data inputs is reduced to using one mean value for the entire duration of the simulations, without consideration of the wider context of shorter term climate cycles and longer term trends. The objective of this manuscript is to demonstrate the utility of analyzing climate data inputs using geostatistical techniques.

METHODOLOGY

Dataset

The climate dataset in this analysis is the long-term Environment Canada data recorded at Fort McMurray, in the Athabasca region of Alberta, Canada. Records of precipitation extend from 1908 to 2012, while air temperature records begin in 1924 and continue to 2012. The Environment Canada data are freely available at http://climate.weather.gc.ca/. Data were initially analyzed by calculating the mean, variance, and standard deviation. Further analysis involved estimation of a 365 day moving average, and a cumulative departure from the mean (CDM). The CDM is simply calculated by summing the cumulative difference between the average value for a year, and the average value for the entire dataset.

Empirical Mode Decomposition

Geostatistical analysis was performed using empirical mode decomposition (EMD). The EMD method separates the variation in the temporal series into discrete component characteristic scales. The EMD method works directly with the dataset, rather than transforming the data into the spectral domain, as is the case with wavelet analysis. The method assumes that the temporal signal is composed of multiple components, all varying at their own specific scales of variability. The sum of all the components is equal to the dataset itself. Empirical mode decomposition is then used to sift out the component scales of variation into intrinsic mode functions (IMF) and determine their overall contribution to the total variance (Biswas et al., 2009).

The EMD method is adaptive and works directly with the data, without the need to rely on a mathematical function to transform the data, as is the case with wavelet analysis (Biswas and Si, 2011). For a complete treatment of the EMD process used to separate out the component IMFs the reader is referred to the examples shown by others (Huang et al., 1998; Biswas and Si, 2011; and Sang et al., 2012). In the present analysis, we are most concerned with the contribution of a particular temporal scale to the overall variance of the dataset.

$$\%Contribution = \left(\frac{Variance\ of\ IMF_i}{\sum Variance\ of\ all\ IMFs}\right) \times 100 \quad (1)$$

Examination of the amount of contribution of a particular IMF to the total variance allows for an estimation of the relative dominance of a particular spatial scale. The average scale of an IMF is calculated by counting the number of oscillations present in the IMF in question. For example, if over the 105 year dataset a particular IMF exhibits 5 oscillations, then the average scale of that IMF will be 105 / 5 = 21 years. This was the method used for reporting average temporal scales in the subsequent analysis. Oscillations of the IMFs can vary locally, and as such, reporting of temporal scales represents an average range for the particular scale. Therefore, the temporal scales of each IMF will be reported as a range, rather than a discrete value.

RESULTS AND DISCUSSION

Initial Data Analysis

Air temperature at Fort McMurray over the entire study period averaged 0.3 °C with a standard deviation of 1.4 °C (Figure 1). Precipitation averaged 412 mm with a standard deviation of 116 mm (Figure 2). Note that precipitation data are missing for 1911 through 1913, as well as 1947.

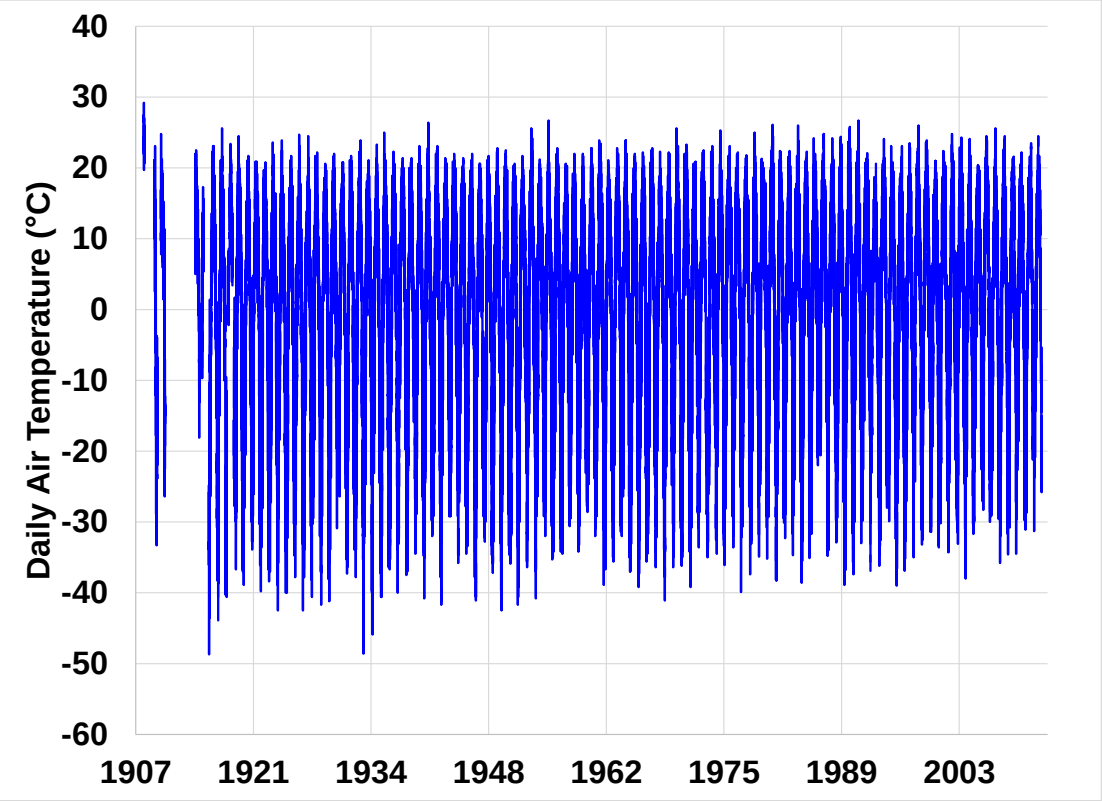

Figure 1 Average annual air temperature at Fort McMurray, 1908 to 2012.

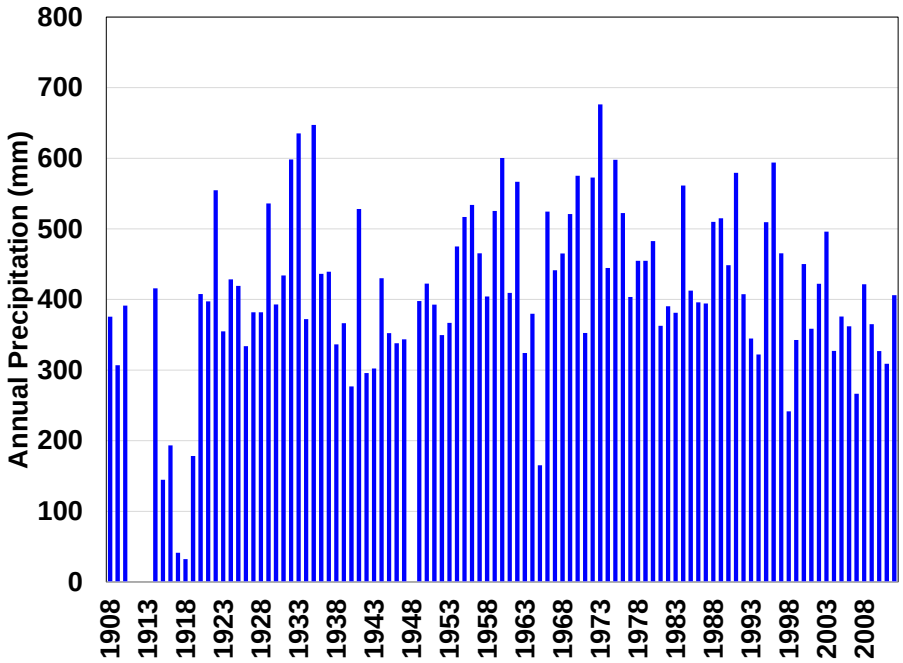

Figure 2 Average annual precipitation at Fort McMurray

Trends and cycles in the air temperature and precipitation data are not readily apparent from Figures 1 and 2. Without further investigation, the cover system designer could be satisfied that there a general annual average value for both air temperature and precipitation would be sufficient for use in modelling analyses. As will be further explored, the assumption of stationarity (constant mean and variance) may not be applicable.

A simple calculation of the average annual air temperature begins to suggest an overall trend in long term average air temperature (Figure 3). While it appears that temperatures have climbed above the mean value of 0.3 °C after 1970, the values are still within two standard deviations of the mean (± 2.8 °C).

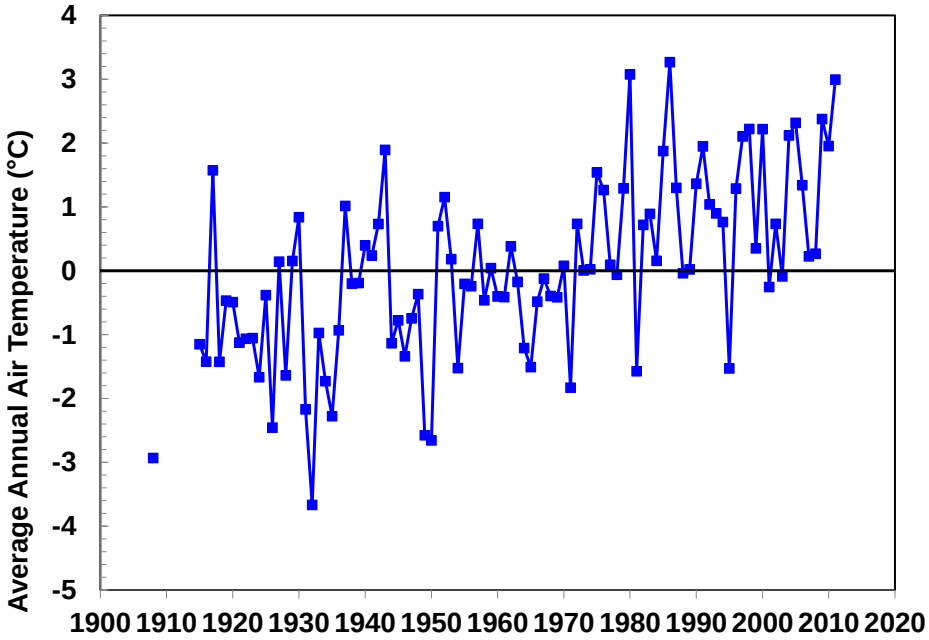

Figure 3. Average annual air temperature recorded at Fort McMuray, 1908 to 2012.

Moving Average

A common method to visualize long term trends in a dataset is to calculate a long term moving average. Three hundred sixty five day moving averages were calculated for air temperature (Figure 4).

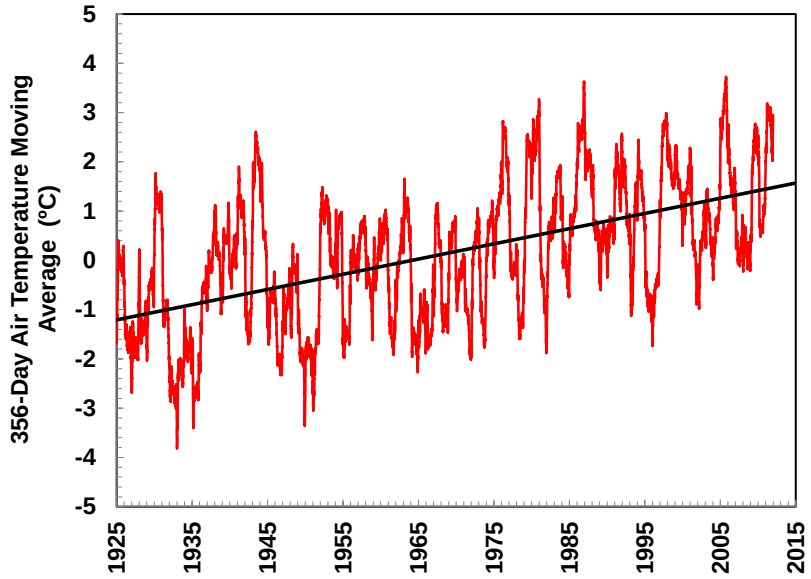

Figure 4 One year air temperature moving average.

A trend of increasing temperature is clearly evident from Figure 4. The slope of the trend line indicates a warming rate of 0.03 °C yr^{-1}. While the long term trend of the data is important, calculation of a moving average does not provide any additional information about the higher frequency, shorter duration cycles of variability within the dataset.

Cumulative Departure from the Mean

The cumulative departure from the mean of non-frozen precipitation (April through October) was calculated to demonstrate the variability of the precipitation dataset (Figure 5).

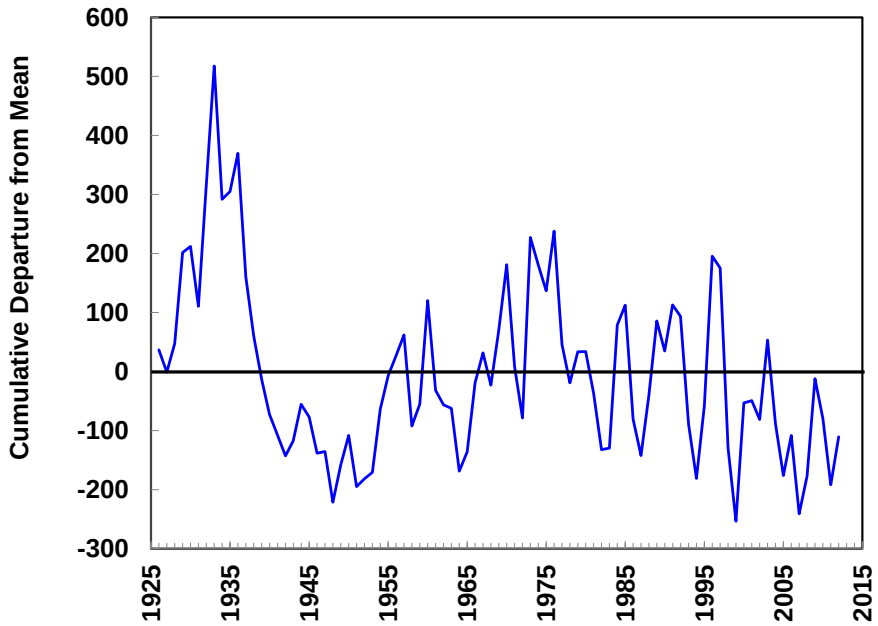

Figure 5 Cumulative departure from the mean for non-frozen precipitation.

The CDM technique is useful for demonstrating variability in a general sense. However, the technique still suffers from an assumption of data stationarity, in that the data are always compared to a single mean value. Furthermore, there is no means by which internal cycles of variability within the dataset can be elucidated.

Empirical Mode Decomposition

Empirical mode decomposition (EMD) works directly within the time domain to separate out scales of variation. The method results in a series of intrinsic mode frequencies that identify the scales of temporal variation buried within the data, as well as that scale's contribution to the total variance. Thus, an intuitive means of examining both low and high frequency variations results. Temporal variations of air temperature are dominated by the annual temperature signal (Figure 6).

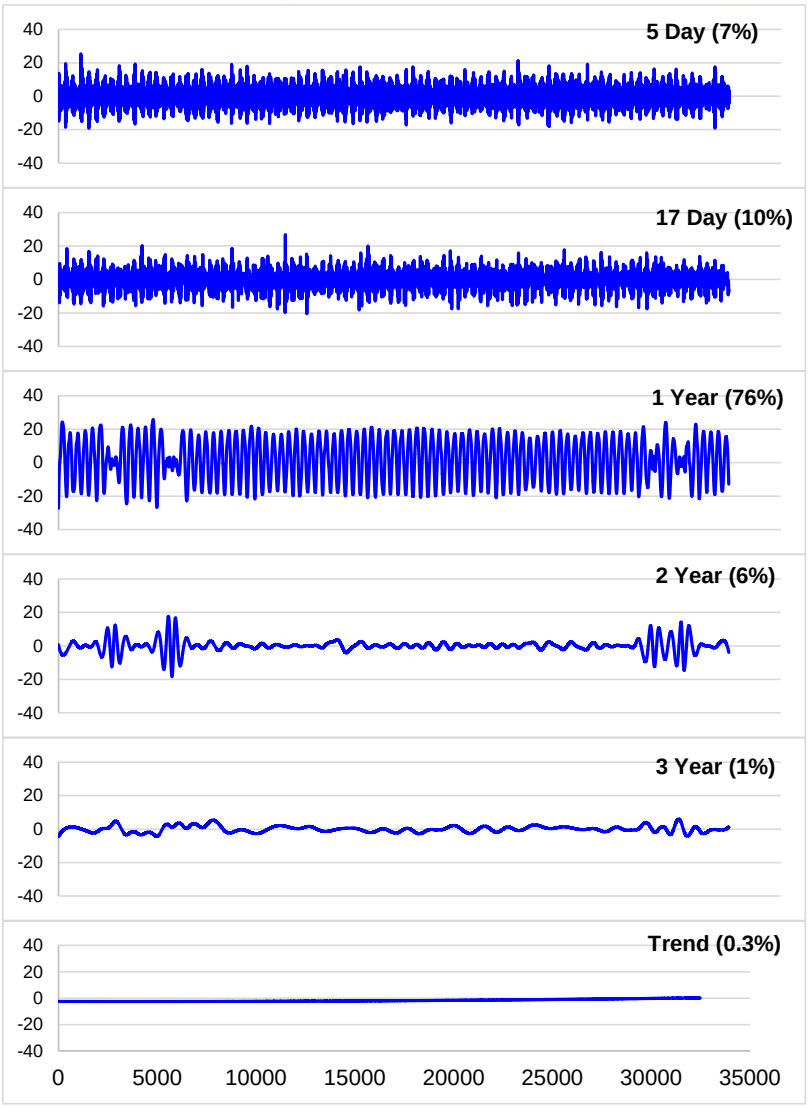

Figure 6. Temporal scales of variation intrinsic within the 1924 to 2012 Fort McMurray air temperature record.

It is clear from Figure 6 that temporal variations in air temperature are dominated by the annual signal and higher frequency signals between five and seventeen days. Also of note is the long term trend. Although the overall trend contributes very little to the total variance (0.3%), the trend is nonetheless present, thus verifying the trend that was identified earlier in the analysis. In fact, the overall trend increases at a rate of 0.03 °C yr^{-1}, providing further credence to the method.

Precipitation exhibits a more even distribution of scale contribution, relative to air temperature (Figure 7). Roughly a third of the scale dominance is contributed by the three year scale, suggesting that high frequency cycles of alternating wet and dry are to be expected in the region. It is possible that the three year cycles of variability could correspond to alternating El Niño / La Niña events.

Another major contributor to the total variance is the 7 year scale. It is interesting to note that the 7 year scale may roughly correspond to the Pacific Decadal Oscillation, another major determinant of Western Canadian weather patterns. Finally trend towards decreasing precipitation accounts for 23% of the total variance. While the EMD technique does not forecast into the future, it does elucidate the dominant cycles of variation over the timespan of the dataset. In the case of Fort McMurray for more than 100 years, the trend has been towards decreasing precipitation.

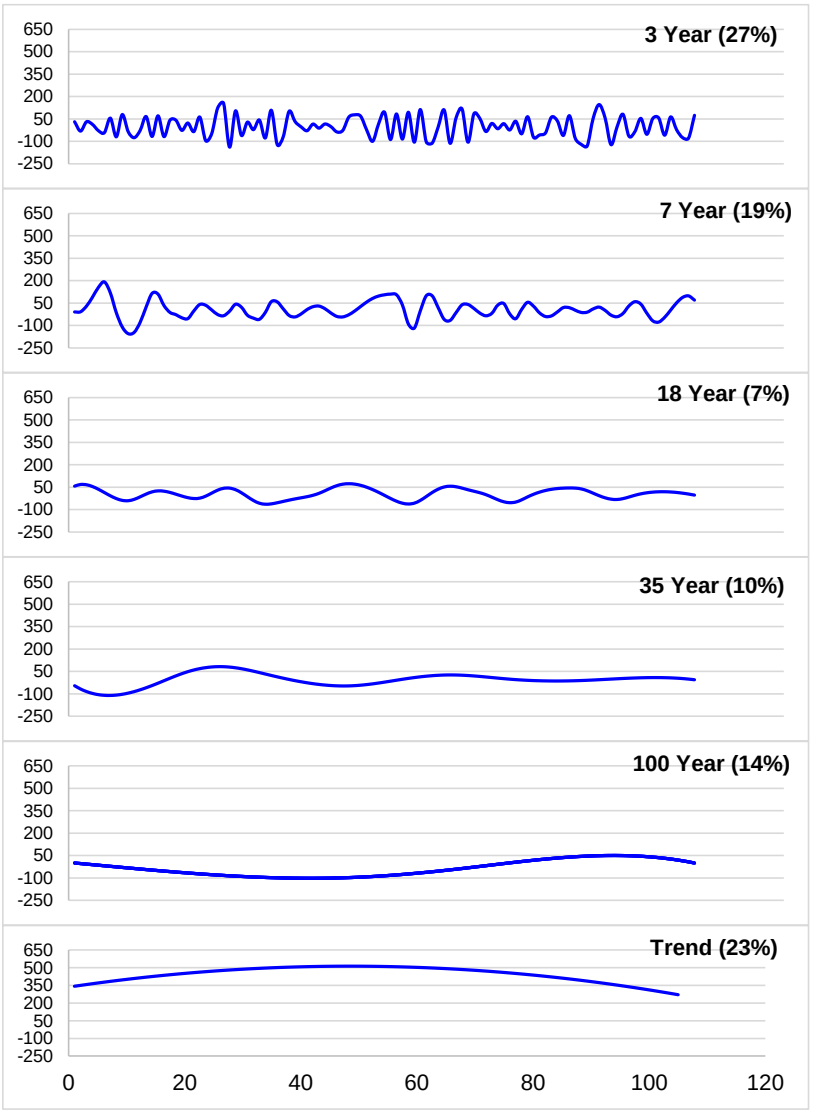

Figure 7. Temporal scales of variation intrinsic within the 1908 to 2012 Fort McMurray precipitation record.

CONCLUSION

Climate is the ultimate governor of cover system performance at a mine site. While certain cover system design parameters can be adjusted to certain degrees, the climate at a site cannot be controlled. Therefore, it is imperative that the designer understands the dominant climate at a site to the fullest extent possible. However, all too often a simple average of climate parameters is used as an input into the models used during the cover system design process. Not only does an average value of precipitation or air temperature result in an unrealistic generalization of site conditions, it fails to account for the cycles of variation that are inherent within all climate signals. Failure to examine the scales of variability within a climate dataset necessarily results in a spurious simplification of what is a very complex system.

The examples used in this manuscript demonstrate the need to have a greater understanding of the cycles of variability within a climate dataset, when designing a cover system. Long term temperature signals are not surprisingly dominated by the annual signal, but also contain a long term trend that indicates consistently rising temperatures. While the trend was not dominant, it explains why the recognition of changing temperatures is difficult to perceive. The signal of the warming trend is buried within more dominant, smaller scale / higher frequency signals.

Precipitation demonstrated that a number of scales of variation contribute to the total variance of the system. While no one signal was dominant, it goes to demonstrate that the cover system designer must be aware of all of the cycles of variation when designing the system. Determination of the cycles of variability underscores the importance of understanding where in a wet / dry cycle the system is being designed. If an average precipitation value is used from a dataset that doesn't capture the dominant scales of variability, the design of the cover system cannot be fully optimized. For instance, if a ten year average precipitation value is used to determine the optimal cover system thickness for supporting vegetation, and the average was taken from a wet cycle, the system may not be able to support vegetation throughout the entire life of the cover system. Conversely, when designing upland / wetland reclamation systems, it is critical to have a good understanding of long term climate in order to ensure that the watershed will have sufficient water supply to support wetland functions. If the watershed designer does not incorporate an analysis of precipitation trends and cycles of variability, the system will be less likely to be resilient to the cyclical changes in water supply.

REFERENCES

Biswas, A., L.K. Tallon, and B.C. Si. 2009. Scale-specific relationships between soil properties: Hilbert-Huang Transform. Paedometron. 28:17-20.

Biswas, A., H.P. Cresswell, H.W. Chau, R.A. Viscarra Rossel, and B.C. Si. 2013. Separating scale-specific soil spatial variability: A comparison of multi-resolution analysis and empirical mode decomposition. Geoderma. 209-210:57-64.

Goovaerts, P. 1997. Geostatistics for natural resources evaluation. Oxford University Press, Oxford.

Si, B.C. 2008. Spatial scaling analyses of soil physical properties: a review of spectral and wavelet methods. Vadose Zone J. 7:547-562.

Si, B.C., R.G. Kachanoski, and W.D. Reynolds. 2008. Analysis of soil variability. p. 1163-1192. In Soil sampling and methods of analysis. 2nd ed. Carter, M.R. and E.G. Gregorich (eds.) CRC Press, Boca Raton, FL.

Efficacy of Cover Systems in High Elevation Andean Climates

Michael Milczarek[1], Jason Keller[1], Tzung-mow Yao[1], Ernesto Prieto[2], Carlos Venegas[2], William Ludwick[2], Raul Orellana[2], Francisco Quevedo[2] and Guosheng Zhan[3]

1. *GeoSystems Analysis, Inc, USA*
2. *Minera Barrick Misquichilca, Peru*
3. *Barrick Gold Corporation, USA*

ABSTRACT

A number of mining properties are present in the high-elevation (> 4 000 m) tropical Andes. The environmental conditions at these properties present challenges for mine closure. Precipitation is typically characterized by wet and dry seasons: in Peru wet season precipitation can exceed1 000 mm over a six-month period. Conversely, average potential evaporation rates are typically 60 to 80% of precipitation on an annualized basis. This precipitation and potential evaporation imbalance precludes the control of infiltration and percolation into mine waste solely via evapotranspiration cover systems.

To evaluate the efficacy of different cover systems in controlling infiltration and net percolation, cover system trials and studies have been initiated by Minera Barrick Misquichilca at their Pierina and Lagunas Norte properties. Large-scale test panels have been constructed over waste rock and heap leach facilities to evaluate different multi-layer cover systems to include the use of variable clay and topsoil depths and the use of drainage layers. Study results indicate that infiltration and net percolation is highly variable and greatly affected by surface water channeling and topographic depressions. In addition, the hydraulic properties of the cover system change over time.

The presence of a drainage layer can reduce the amount of net percolation; however drainage layers require high drain rock permeability and low permeability of the underlying layer, and are equipment and labor intensive to construct, and hence costly.

Keywords: Evapotranspiration, unsaturated flow, waste rock, ore, clay, hydraulic conductivity, drainage layer

INTRODUCTION

Peru is the leading gold-producing country in Latin America and second only to Chile in copper production. Many of the Peruvian mining properties are located in the high tropical Andes at elevations in excess of 4 000 meters above mean sea level (amsl). The climate at these locations is characterized by a bimodal precipitation pattern, cool temperatures, and high relative humidity. Precipitation is typically greater than 1 200 mm/yr, with over 80% of precipitation occurring during the rainy season which characteristically occurs between the months of October and April. Average potential evaporation rates are typically 60 to 80% of precipitation on an annualized basis.

Mines are increasingly using evapotranspiration (ET) soil cover systems to control infiltration and percolation into mine waste. ET cover systems function by storing infiltrated precipitation in the soil cover overlying the waste until it is removed by either plant transpiration or evaporation. These systems require that ET be in excess of precipitation to be effective. However, the precipitation and PET imbalance in the Peruvian Andes precludes the sole use of ET cover systems for this purpose.

In the wet environment of the Peruvian Andes, a multi-layer cover system that includes a low-permeability clay layer underneath the ET soil layer is an alternative to the single-layer ET cover system. To alleviate build-up of soil pore pressures, high-permeability drainage materials or perforated drainage pipes (suction breaks) can be placed above the clay layer on sloped surfaces to remove infiltrated water. Drainage tends to reduce pore pressures and percolation into the underlying material.

Cover system trials and studies have been initiated by Minera Barrick Misquichilca at their Pierina and Lagunas Norte properties to evaluate the efficacy of different multi-layer cover systems in controlling infiltration and net percolation. Large-scale test panels have been constructed over waste rock and heap leach facilities to evaluate cover systems comprised of variable clay and topsoil thicknesses and with or without subsurface flow manipulation. In this paper we examine the performance of the clay layer and different subsurface drainage configurations in reducing net percolation.

Site Conditions

Minera Pierina

The Pierina mine is located on the eastern flank of the Cordillera Negra, about 10 km northwest of the City of Huaraz in the Ancash Region of Peru. Elevations of the Pierina mine facilities range between 3 800 m and 4 200 m amsl. Test panels were constructed in late 2005 and monitored through 2009. Temperatures at the site rarely fall below 0° C and do not change significantly month by month; the average annual temperature is about 6° C. The recorded average annual precipitation during the 2006 to 2009 monitoring period was approximately 1 290 mm. Recorded pan evaporation and estimated reference crop evapotranspiration (ETo) averaged approximately 935 mm/yr and 745 mm/yr, respectively, for the four year monitoring period.

Two test panels, approximately 20 m by 55 m, were constructed on a 2.5(H):1(V) heap leach pad side-slope to test different clay layer construction methods. Each test panel had clay/silt borrow material placed over the waste, followed by 30 cm of topsoil material for an ET soil layer. The clay/silt material in Panel 3 was roller compacted after placement to approximately 90% of maximum Proctor density (2.07 g/cm^3) with a final approximate thickness of 35 cm. In Panel 4, only equipment traffic compaction occurred on the clay/silt material, resulting in a final approximate thickness of 55 cm. The Pierina cover system used a network of perforated drainage pipes placed at regular 10-m intervals in the topsoil layer to act as suction breaks. Surface water runoff was routed to a geomembrane-lined canal. Test panels were installed in December, 2005 and subsequently seeded with a mix of native and non-native grasses and sedges. After plant establishment, vegetative ground and canopy cover generally approached or exceeded 100%.

A cover performance monitoring system was installed and brought online in February 2006 to develop a better understanding of the capability of the cover systems to minimize net percolation into the heap leach material after closure. Monitoring nests were installed at four locations in each

panel. Monitoring system sensors included soil water potential sensors (heat dissipation sensors (HDS), and advanced tensiometers, (ATs)); soil moisture content sensors (ECH_2Os); water flux meters (WFMs); oxygen content sensors (Figaros); and surface water flumes (H-Type flumes). Drainage from the suction breaks was monitored manually on a weekly basis. Instrument cross-sections are provided in Orellana et al. (2010).

Soil water potential (HDS and AT) and water content (ECH_2O) sensors monitored the wetness of the soil cover and the removal of water through drainage and evapotranspiration. WFM measurements provided a small-scale point measurement of deep flux at each location. Oxygen sensors monitored the efficiency of the clay/silt layer in minimizing oxygen flux into the leach ore. Finally, the H-flumes provided a very precise measurement of surface water runoff. A detailed discussion of the monitoring system and installation procedures is presented in Zhan et al. (2007).

In January 2010, a test panel decommissioning program was conducted at Pierina to excavate monitoring instruments and check for functionality, conduct in-situ bulk density and saturated hydraulic conductivity (K_{sat}) tests; collect cores for laboratory testing, and, conduct a rooting survey to measure root density and thickness. Excavation trenches were typically two meters in depth.

Minera Lagunas Norte

The Lagunas Norte mine is located approximately 175 kilometers north of the Pierina mine, in the La Libertad Region. Elevations at the Lagunas Norte facilities range between 4 000 m and 4 260 m above mean sea level. Average temperatures at Lagunas Norte are slightly cooler compared to Pierina, though temperatures at the site rarely fall below 0° C. The recorded average annual precipitation during the 2009 to 2013 monitoring period was approximately 1 420 mm; estimated ETo was approximately 775 mm/yr.

Two test panels were installed in late 2008 and have since been monitored continuously. The two test panels, each approximately 42 m by 100 m were constructed on a 2.5(H):1(V) waste rock facility side-slope to test dual- and triple-layer cover systems with suction breaks. The South Panel dual-layer cover system consists of approximately 30 cm of a topsoil ET layer above approximately 60 cm of clayey material. The North Panel triple-layer cover system consists of approximately 30 cm of topsoil over approximately 30 cm of coarse-textured drainage material (gravel) overlying approximately 30 cm of clayey material. Placement of the drainage layer on top of the clay layer is intended to facilitate lateral subsurface flow through the drainage layer. In both panels a series of suction breaks consisting of gravel filled trenches were placed at the base of the topsoil (South Panel) and drainage layer (North Panel) at approximately 10-m spacing. Test panels were installed in December, 2008 with subsequent seeding using a mix of native and non-native grasses and sedges.

A cover performance monitoring system similar to that at Pierina was installed at Lagunas Norte in December 2008 and included four sensor nests for each panel. Cross-sections of Lagunas Norte monitoring nest installations for the triple layer (North) test panel are presented on Figure 1.

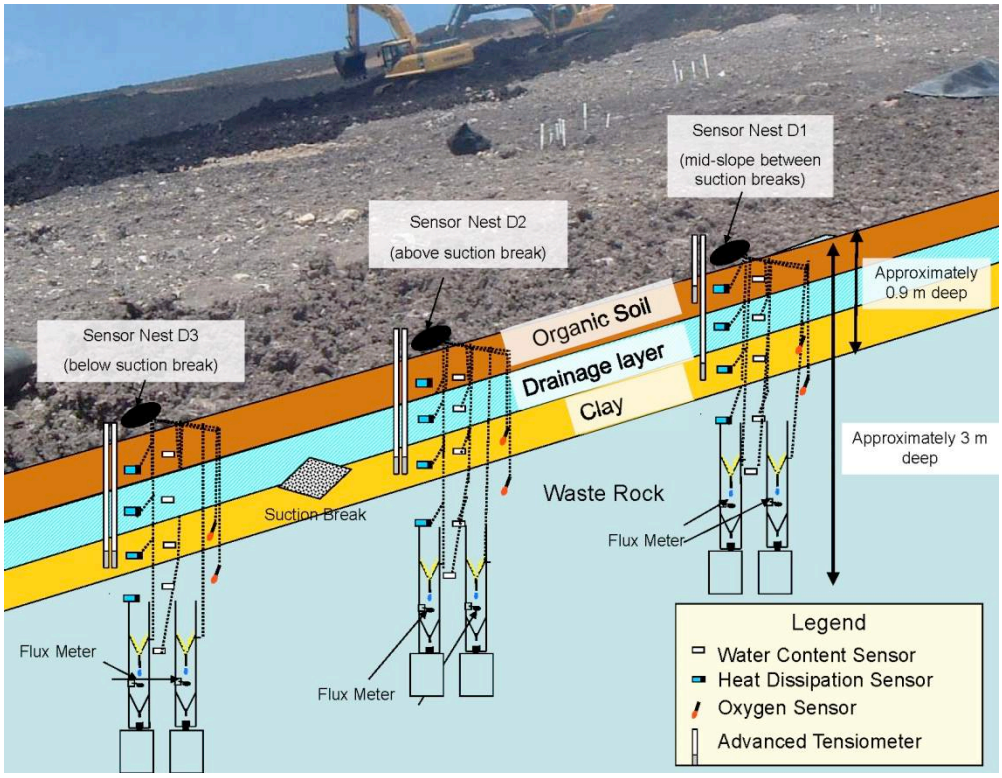

Figure 1 Cross-section of North Panel monitoring nest installation

RESULTS

For both sites the lowest precipitation rates were observed in July. Therefore, the water year was defined as the 12-month period from July 1 to June 30, and is designated by the calendar year in which it ends. For example, the water year starting July 1, 2012 and ending June 30, 2013 is called "Water Year 2013".

Surface Water Runoff and Subsurface Drainage

Measured stormwater runoff rates at the Pierina test panels were approximately 15% of precipitation (194 mm/yr). Similarly, the test panel runoff at Lagunas Norte has averaged approximately 18% of precipitation (256 mm/yr). For both sites, the observed stormwater runoff was simulated using the U.S. Soil Conservation Service (SCS) model (SCS, 1986) to estimate the approximate amount of runoff from a rainfall event in a defined area. Curve numbers (CNs) of 91 and 93 were needed to simulate the measured average panel runoff for Pierina and Lagunas Norte, respectively. Both CNs are much greater than what would be estimated using standard SCS method assumptions for hydrologic soil type and vegetative cover. These data indicate that stormwater runoff estimates using SCS curve numbers in this climate and soil types may need to be adjusted upwards to account for steep slopes and the hydrophobicity of the topsoil surface.

At Pierina, only minor amounts of drainage were recorded from the suction breaks at both panels (less than 1% of total precipitation). High topsoil and clay water content values were observed in the monitoring data. However, saturation of the topsoil is required for significant seepage from the suction breaks to occur. Low topsoil, or high clay, hydraulic conductivities could have reduced suction break efficiency. In addition, rooting around and into the geotextile material surrounding the suction break pipes could have resulted in reduced efficiency.

At Lagunas Norte, subsurface layer/suction break drainage was approximately 12% of precipitation (170 mm/yr) at the North Panel and 1% of precipitation (14 mm/yr) at the South Panel. Greater suction break flow from the North Panel indicates that the presence of a gravel drainage layer resulted in increased subsurface drainage efficiency.

Water Fluxmeter Data

WFM-measured flux at Pierina averaged 26% of precipitation (336 mm/yr) for Panel 3 and 16% of precipitation (207 mm/yr) for Panel 4. Panel 3 WFMs generally showed increasing fluxes over time.

Average WFM-measured flux greater than 250% of precipitation was recorded at the Lagunas Norte test panels during the first water year of monitoring (water year 2009), due primarily to several WFMs measuring flux in excess of 1 000% of precipitation. The high measured flux was believed to be due to topographical depressions resulting from ground settlement after sensor installation. These depressions were filled with topsoil in August 2009. The WFM-measured flux in the subsequent water years (water years 2010 – 2013) decreased, although not to rates consistent with other measurements of surface and subsurface flow.

Continued high WFM-measured flux after water year 2009 may be due to: 1) subsidence of the clay layer at the sensor nests resulting in accumulation of subsurface flow at these points, or 2) convergence of soil water flow into the WFM because of soil water potential conditions in the WFM being more negative (i.e. drier) than surrounding conditions. Based on AT data recorded during the rainy season, the soil water potential conditions are generally greater (i.e. wetter) than -30 cm, indicating that water potential conditions may be converging water into the WFM.

Water Content Data

Changes in water content over time indicate how the cover responds to seasonal climatic processes (precipitation and ET) and of the overall effectiveness of the cover system. At both sites water contents increased in response to the rainy season and decreased throughout the dry season (April through September) due to drainage and ET demand (Figure 2 and Figure 3). Wetting and drying occurred at all depths, in all panels, indicating that percolation occurs through the cover system. Water content in the topsoil layers generally decreased throughout the study period. This general drying trend is likely due to increasing vegetation and root density over the course of monitoring.

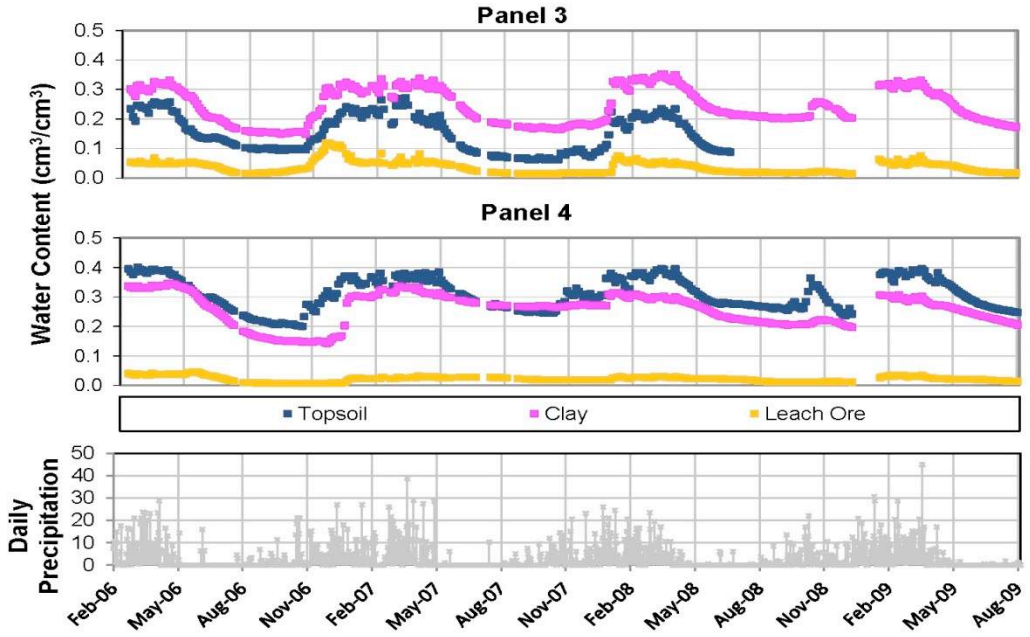

Figure 2 Pierina Mine Panel 3 and Panel 4 water content data

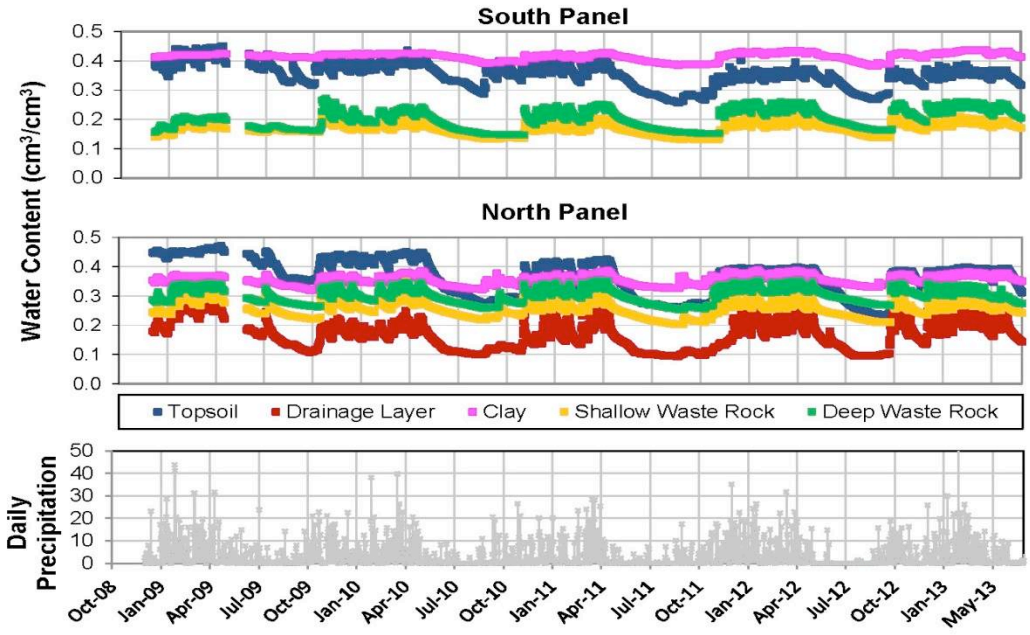

Figure 3 Lagunas Norte Mine South Panel and North Panel water content data

Clay layer wetting occurred within a short period after observed wetting in the overlying topsoil or drainage layer. Shallow and deep waste rock sensors immediately responded with little lag

compared to wetting of the overlying clay, indicating that the clay is allowing water to quickly percolate through that layer.

At Pierina, the clayey layer significantly dried out in both panels during the dry season and the ability of the clay to limit net percolation may therefore have been greater in Panel 4 due to its greater thickness (55 cm versus 35 cm). Additionally, the earlier wetting front arrival and greater water content in the leach ore in Panel 3 during each rainy season indicate that greater net percolation occurred in Panel 3.

At Lagunas Norte, topsoil sensors in the North Panel consistently recorded greater seasonal changes in water content than those in the South Panel, indicating that the North Panel drainage layer is removing water from the upper soil profile and accelerating the drying process. North Panel drainage layer sensors also showed rapid response to precipitation and subsequent drainage, which correlates with topsoil water content trends for North Panel. In general, the water potential (HDS and AT) wetting and drying trends were similar to water content sensor trends.

Estimated Net Percolation

A cover system water budget can be formulated as follows:

$$R = P - SR - AET - SB - \Delta S \quad (1)$$

where R is net percolation, P is precipitation, SR is surface runoff, AET is actual evapotranspiration, SB is suction break drainage and □S is soil storage change.

Precipitation, runoff, and suction break drainage were monitored at both sites; AET is calculated by solving Equation 1 and directly measuring or estimating net percolation. Estimated water budgets for each of the test panels are provided on Figure 4.

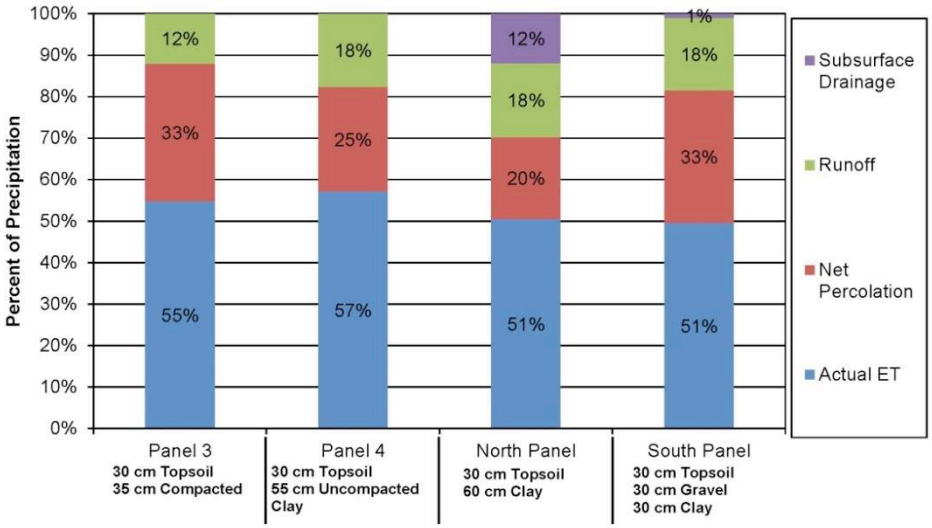

Figure 4 Estimated Pierina and Lagunas Norte test panel water budgets

Pierina Mine

At Pierina, the clay soil water potential data were used to approximate net percolation by applying the closed-form analytical solution by van Genuchten et al. (1980) to solve Darcy's law. Laboratory and field observed saturated hydraulic conductivity (K_{sat}), water content, and water potential relationships were combined to estimate van Genuchten parameters with a best fit. These parameters were further refined by comparing the predicted net percolation fluxes to the WFM-measured data and modifying the K_{sat} value until relative agreement was achieved. Additional details about the Pierina net percolation approximation are available in Orellana et al. (2010).

The Pierina test panel water budgets are shown on Figure 4. The Pierina approximated net percolation was 33% of precipitation (427 mm/yr) for Panel 3 and 25% of precipitation (324 mm/yr) for Panel 4. Applying these net percolation values and measured precipitation, surface runoff and suction break drainage in Equation 1 produced calculated AET values of 55% of precipitation (712 mm/yr) for Panel 3 and 57% of precipitation (738 mm/yr) for Panel 4.

The calculated AETs are approximately 95% to 99% of the calculated ETo for Panel 3 and 4 respectively. The high predicted AET values indicate that test panel vegetation had sufficient soil water during the dry season and/or had higher ET rates than ETo during the growing season. During Pierina test panel decommissioning extensive rooting was observed within the circum-neutral heap leach material to a depth greater than 2 m below ground surface (Orellana et al., 2010). It should also be noted that the development of vegetation in Panel 4 appeared to be more robust than in Panel 3. Consequently, the Panel 4 calculated AET would be expected to be greater than Panel 3, with potentially less net percolation.

Lagunas Norte

For estimation of Lagunas Norte net percolation the average estimated ratio of AET to ETo at the Pierina mine cover system test panel was adjusted to represent likely rooting conditions at the Lagunas Norte test panels. A numerical water balance model calibrated to the Pierina test panel monitoring data (Keller et al., 2012) predicted an approximately 5% reduction in AET to ETo when limiting the rooting depth to above the waste material compared to scenarios in which rooting was simulated within the waste material. Based on the model results and assuming rooting at Lagunas Norte is limited to above the waste material, AET at the Lagunas Norte test panels was estimated to be 92% of ETo, equivalent to 51% of precipitation (724 mm/yr).

The Lagunas Norte test panel water budgets are shown on Figure 4. Predicted water year average net percolation is 20% of precipitation (284 mm/yr) for the North Panel and 33% of precipitation (469 mm/yr) for the South Panel. The greater measured suction break drainage at the North Panel than the South Panel and lower water contents indicates that the drainage layer is contributing to increased drying of the topsoil and removal of infiltrated water.

Compared to the average net percolation measured by WFMs, the ratio of North Panel to South Panel WFM-measured flux (55%) and South Panel to North Panel water budget calculated net percolation (61%) are similar.

Hydraulic Property Measurements

The decommissioning tests at Pierina indicated a 6X and 8X increase in K_{sat} over the four-year test period in the uncompacted (Panel 4) and compacted (Panel 3) clay liners, respectively (Orellana et al., 2010). These data indicate that differences in K_{sat} values achieved via clay compaction diminish over time. Similar and even greater increases in clay K_{sat} have been observed due to wetting/drying processes and root development (e.g. Albright et al., 2006; Waugh, 2004; Taylor et al., 2003; Wilson et al., 2003). Rooting was extensive into the clay layers and heap leach materials to depths of at least 180 cm. The extensive rooting is most likely aided by the increase in clay K_{sat} and is also likely responsible for the predicted high AET rates.

CONCLUSIONS

The Pierina Mine and Lagunas Mine cover test panels tested the performance of multi-layer and low-permeability clay liner systems in reducing net percolation. Cover system performance monitoring data collected from both sites indicate that net percolation rates range from 20% to 33% of annual precipitation rates, and that the cover system performance is dynamic over time. The following trends were observed:

- Average surface runoff from the Pierina and Lagunas Norte test panels ranged from 15% to 18% of precipitation and can be modeled using the SCS equation with a CN of 91 to 93.

- At Pierina, suction breaks installed within the topsoil layer collected 1% or less of the total precipitation; relatively high clay Ksat for both the compacted and uncompacted clay liners is likely to have reduced the effectiveness of the suction breaks.
- The long-term estimated percolation through the Pierina Panel 3 compacted clay cover was 33% of precipitation; net percolation through Panel 4 uncompacted clay cover was 25% of precipitation, which indicates greater efficiency was achieved from using a thicker clay layer.
- WFM measured percolation at Pierina Panel 3 increased over time, suggesting that the effect of compaction in decreasing clay permeability decreased over time. This conclusion is further supported by observed increases in measured clay Ksat during panel decommissioning.
- The estimated net percolation through the Lagunas Norte North Panel cover, containing a drainage layer, was 20% of precipitation and net percolation through the South Panel cover system without a drainage layer system was 32% of precipitation.
- Suction break drainage averaged 12% of precipitation from the Lagunas Norte North Panel and reduced the estimated net percolation by about 40% compared to the South Panel cover system without the drainage layer.
- Numerical modeling indicates that the hydraulic conductivity of the clay layer largely influences the effectiveness of the drainage layer systems.
- Numerical modeling also indicates that, with extensive rooting into the underlying waste material, increasing cover thickness only nominally decreases predicted net percolation.

Based on these data, we conclude the following:

- There is no long-term advantage to roller-compacting a thin (30 cm) clay liner at these sites compared to a 50 cm clay layer compacted solely by the equipment used to place the clay.
- Drainage layers and/or suction breaks can significantly increase the efficiency of the cover system if there is high-drain rock permeability and low permeability underlying clay.

ACKNOWLEDGEMENTS

We thank staff and management at Minera Barrick Misquichilca S.A., for their support of these projects.

REFERENCES

Albright, W.H., Benson, C.H. Gee, G.W., Abichou, T., Mcdonald, E.V., Tyler, S.W. and Rock, S. (2006) Field performance of a compacted clay landfill final cover at a humid site, Journal of Geotechnical and Geoenvironmental Engineering 132(11), pp. 1393-1403.

Keller, J., Milczarek, M., Banerjee, M., Orellana, R., Ludwick, W., and Zhan, G. (2012) Evaluation of alternative cover systems in high precipitation environments using unsaturated flow modeling, Proceedings of the 9th International Conference on Acid Rock Drainage, May 20-25, Ottawa, Canada.

Orellana, R., Ludwick, W., Zhan, G., Bauman, W., Milczarek, M., Rice, R.C., Yao, T-M., and Keller, J. (2010) Final results of the cover system test panel trials at the Pierina Mine. Proceedings Mine Closure 2010, November 23-26, Viña del Mar, Chile.

SCS – See U.S. Soil Conservation Service

Taylor G., Spain, A., Timms, G., Kuznetsov, V. and Bennett, J. (2003) The medium-term performance of waste rock covers – Rum Jungle as a case study, Proceedings of the 6th International Conference on Acid Rock Drainage, July 12-18, Cairns, Australia.

U.S. Soil Conservation Service (SCS) (1986) Urban hydrology for small watersheds, Tech. Release 55, Washington, D.C.

van Genuchten, M Th (1980) A closed form equation for predicting the hydraulic conductivity of unsaturated soils, Soil Sci Soc Am J 44, pp. 892-898.

Waugh, W.J. (2004) Design, performance, and sustainability of engineered covers for uranium mill tailings, Proceedings of Long-term Performance Monitoring of Metals and Radionuclides in the Subsurface:

Strategies, Tools, and Case Studies. U.S. Environmental Protection Agency, U.S. Department of Energy, U.S. Geological Survey, Nuclear Regulatory Commission, April 21-22, 2004, Reston, VA.

Wilson, G.W., Williams, D.J. and Rykaart, E.M. (2003) The integrity of cover systems – An update, Proceedings of the 6th International Conference on Acid Rock Drainage, July 12-18, Cairns, Australia.

Zhan G., Baumann, W., Milczarek, M.A., Yao, T-M. and Rice, R.C. (2007) Cover system design and testing for Pierina Mine, Ancash, Peru. II International Seminar on Mine Closure, Santiago, Chile, October 16-19, 2007.

Integration of Climate Analysis into a Framework for Cover Design

Thomas Baumgartl, Andrea Farioli and Sven Arnold
Centre for Mined Land Rehabilitation, The University of Queensland, Australia

ABSTRACT

Successful performance of soil cover systems depends on both physical properties (including water retention characteristics, depth, and number and arrangement of materials), which define the soil cover design, and climatic conditions. While the physical properties can be addressed by site-specific selection or completion criteria and through technical means, climatic conditions are out of anthropogenic control. Climate parameters are commonly used in the first instance to plan the cover design. However, for some climates commonly used climate indices such as the rainfall to evaporation ratio or annual means of meteorological parameters oversimplify the complexity of variable and partly erratic rainfall patterns.

In this paper we present a climate-based planning framework for soil cover systems that explicitly considers climate variability. We demonstrate our approach based on a case study using historical rainfall and evaporation data from semi-arid Mount Isa (Queensland, Australia), where highly variable rainfall events are driven by monsoonal weather situations or intense convective storms. We use Hydrus-1D to simulate the seepage from two contrasting soil materials – a unimodal silt and a bimodal waste rock material. We run the model with a number of generated climate data based on the historical climate observations, and compare the seepage patterns for the two selected soil materials with uniform distributions of rainfall and evaporation.

As hypothesised, maximum seepage events and number of large seepage events were several orders of magnitude higher for the waste rock material. Interestingly, under some climatic conditions (mainly determined by its variability) the average seepage was higher for silt material. In any case, climate variability had a great impact on the seepage patterns; i.e., the median seepage, the maximum seepage events. The number of large seepage events was several orders of magnitude higher when including the variability of events compared with the control model, where rainfall and evaporation distributions were uniform. This indicates the critical role climate variability plays for the performance of soil cover systems, and the need to implement a similar approach into post-mining planning schemes.

Keywords: soil cover systems, climate variability, planning tool, soil water modeling, waste rock material

INTRODUCTION

The objective of soil cover systems, also referred to as monolithic alternative covers or phytocaps, is to minimise drainage into the underlying hazardous wastes by maximising intercepted rainfall by vegetation, soil water storage, and evapotranspiration (ET) and thereby minimising surface runoff and seepage (Salt et al., 2011). After rainfall events cease, the loss of stored soil water through ET increases the soil water storage capacity for future rainfall events (Hauser et al., 2001; Rock, 2010). Soil cover systems are increasingly accepted for the closure of mining waste facilities (Arnold et al., 2014; Gwenzi et al., 2013). Cover materials as well as cover designs vary greatly in their characteristics and complexity and may incorporate geotextile liners, multiple soil layers with selected hydrological properties, and compacted clay layers, depending on local climate and material availability (Benson et al., 2002). While the physical soil properties can be addressed by site-specific selection or completion criteria and through technical means, climatic conditions are out of anthropogenic control. Climate parameters such as long-term average rainfall or the ratio between rainfall and evaporation (aridity index) are commonly used in the first instance to design covers. However, for some climates these climate indices oversimplify the complexity of variable and partly erratic rainfall patterns (Audet et al., 2013). Consequently, the risk of performance failure of a soil cover; i.e., deep drainage and occurrence of contaminated water, is underestimated or even ignored.

In this paper we present a climate-based planning framework for soil cover systems that explicitly considers climate variability. We demonstrate our approach based on a case study using historical rainfall and evaporation data from semi-arid Mount Isa (Queensland, Australia), where highly variable rainfall events are driven by cyclonic events or intense convective storms, and the long-term average rainfall and aridity index are 423 mm and 0.13, respectively (Halwatura et al., 2014). We use Hydrus-1D (Simunek et al., 2005) to simulate the seepage from two contrasting soil materials – a silty substrate with a uni-modal pore size distribution and a waste rock dominated substrate with a bi-modal pore size distribution. Uniform, i.e., non-structured silty substrates, are classified with medium to low values of hydraulic permeabilities (Hillel, 2004), while rock containing substrate is characterized by some proportion of coarse pores, which are highly continuous and lead to high hydraulic permeabilities (Schneider et al., 2010). The water sorption capacity of substrates is used in cover design to mitigate the impact of rainfall by designing a cover around its substrate specific water storage capacity. While the storage capacity for water may be the same or similar for different materials, the intensity parameter, like hydraulic conductivity may be greatly different (Horn et al., 2002). The objective of this paper is to investigate the consequence of different values for functional parameters to realistic climatic situations and test the performance of a cover design in respect to risk and magnitude of deep drainage. For this purpose, we run the model with a number of generated climate data based on the historical climate observations, and compare the seepage patterns for the two selected soil materials with uniform distributions of rainfall and evaporation.

METHODOLOGY

We generated 35 time-series, each of 100 years length, using the LARS-WG stochastic weather generator (Semenov, 2008) and based on historical rainfall and evaporation data from Mount Isa, Australia (Bureau of Meteorology, 2014) (Fig. 1). Then we run Hydrus-1D (Simunek et al., 2005) with two soil materials (Table 1) and using the generated weather time series (Fig. 2) as atmospheric boundary condition (Appendix B). We assessed the frequency distributions of seepage for the two soil materials and compared them with the control scenario that ignored climate variability and was based on uniform distributions of rainfall and evaporation.

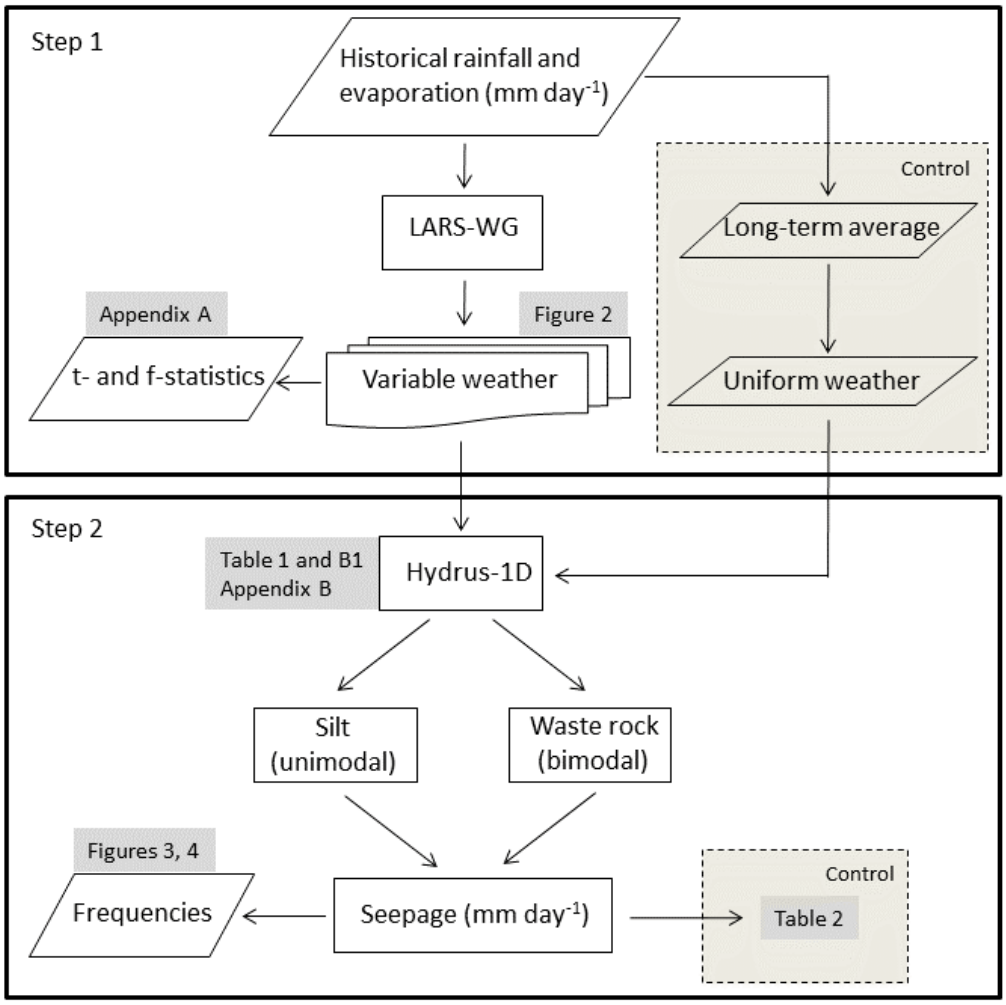

Figure 1 Schematic diagram of a climate-based planning framework for cover systems. Step 1 generates time series of rainfall and evaporation based on historical observations. Step 2 uses the generated weather data to assess frequency distributions of seepage based on selected soil materials. In total, we generated 35 time-series, each of 100 years length.

Generated rainfall and evaporation values (step 1)

The LARS-WG stochastic weather generator generates time-series of daily weather at a single site (Semenov, 2008). Here we used 100 years of historical rainfall observations from Mount Isa, Australia, to generate 35 time-series of rainfall that have the same statistical properties (mean and variance) as the empirical observations. Likewise, we generated time-series of evaporation based on 25 years of historical records. While the generated and observed rainfall values were not significantly different (Appendix A), the generated evaporation was underestimated (Fig. 2b). Therefore we corrected each generated time-series i of evaporation as:

$$E^{corr}_i = (E^s_i)^{1.22}, \quad (1)$$

where E^{corr}_i (mm day^{-1}) is the corrected evaporation used for further simulations, and E^s_i (mm day^{-1}) is the evaporation generated by LARS-WG. The ensemble mean and standard deviation of all E^{corr}_i values were 4% higher and 5% lower than the observed values.

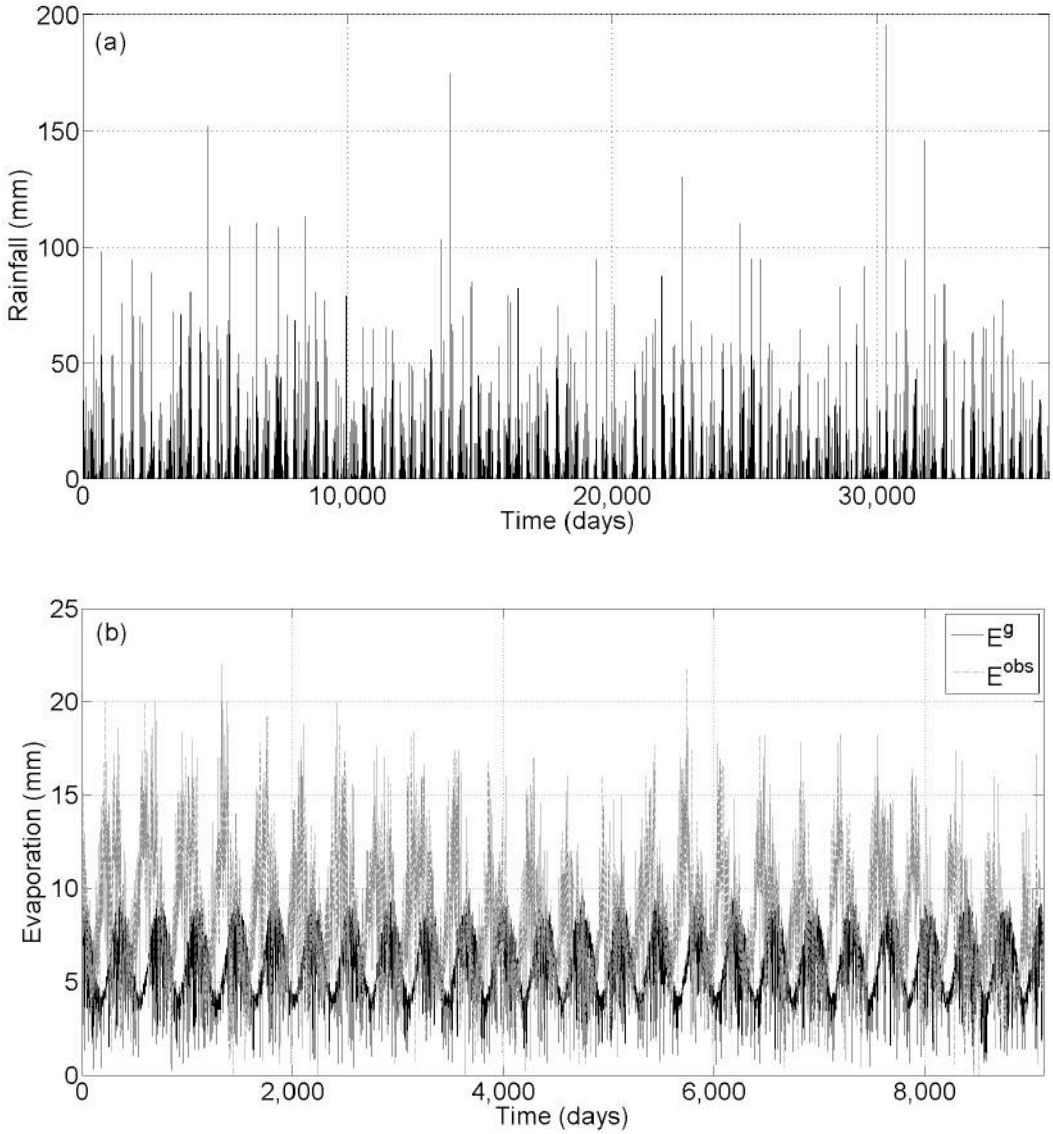

Figure 2 Examples of generated time-series of daily (a) rainfall and (b) evaporation values based on historical weather observations in Mount Isa. The generated evaporation values E^g underestimated the observed evaporation values E^{obs}.

Soil water modeling (step 2)

We used the generated time-series of rainfall and evaporation values as atmospheric boundary condition in the water flow and solute transport model Hydrus-1D (Simunek et al., 2005). We ran the model with two contrasting soil materials – a unimodal silt material reflecting a substrate with a very high water storage capacity and a bimodal waste rock material, representing a substrate with pronounced coarse and continuous pores (Table 1) – to assess the seepage patterns over a simulation period of 100 years at daily time steps. Further, we ran a control model with uniform distributions of rainfall and evaporation based on the long-term average daily records to assess the impact of climate variability on the seepage patterns of the two soil materials. For the control model, the daily rainfall and evaporation were 1.16 and 8.36 mm day^{-1}, respectively. More details on the configuration of the Hydrus-1D model are provided in Appendix B1. For each soil material

and each generated weather situation (i.e., expressed through rainfall and evaporation values), we calculated the median seepage, and recorded the maximum seepage as well as the number of seepage events greater than 1 mm day^{-1}, which occurred over 100 simulated years.

Table 1 Hydraulic parameters of selected soils, based on (van Genuchten, 1980).

Soil Parameter	Silt	Waste rock (dual porosity)
θ_r (m^3 m^{-3})	0.034	0.05
θ_s (m^3 m^{-3})	0.46	0.28
α (cm^{-1})	0.016	(1) 1, (2) 0.01
n (-)	1.37	(1) 6, (2) 1.15
K_s (cm day^{-1})	6	1000
w_2 (-)	-	0.4

RESULTS AND DISCUSSION

Impact of climate variability on seepage

For both soil materials, climate variability had a great impact on the seepage patterns. While under uniformly distributed rainfall and evaporation the median seepage ranged between 2.84 10^{-5} and 1.42 10^{-4} mm day^{-1} (Table 2), the median seepage was several orders of magnitude higher when climate was variable, and ranged between 0.01 and 0.05 mm day^{-1} (Fig. 3). Likewise, the maximum seepage events were several orders of magnitude higher under climate variability and ranged between 0.5 and 200 mm day^{-1} (Fig. 4) compared with 2 10^{-4} to 0.06 mm day^{-1} under uniform weather conditions (Table 2). Finally, the impact of climate variability was most dramatic when comparing the number of seepage events greater than 1 mm day^{-1} between uniform and variable distribution of rainfall and evaporation. While no such events occurred under uniform conditions (Table 2), under climate variability their number increased up to 1750 events within 100 years of simulation (Fig. 5). These distinct patterns are the consequence of the different daily rainfall amounts, which are only 1.16 mm day^{-1} under uniform conditions, but can be up to 200 mm day^{-1} under variable conditions (Fig. 2a) as observed over the last 100 years (Bureau of Meteorology, 2014).

Table 2 Seepage of the control model with uniform rainfall and evaporation of 1.16 and 8.36 mm day^{-1}, respectively.

Soil material Seepage	Silt	Waste rock
Median (mm day^{-1})	2.84 10^{-5}	1.42 10^{-4}
Maximum (mm day^{-1})	0.06	2 10^{-4}
Number of event greater than 1 mm day^{-1}	0	0

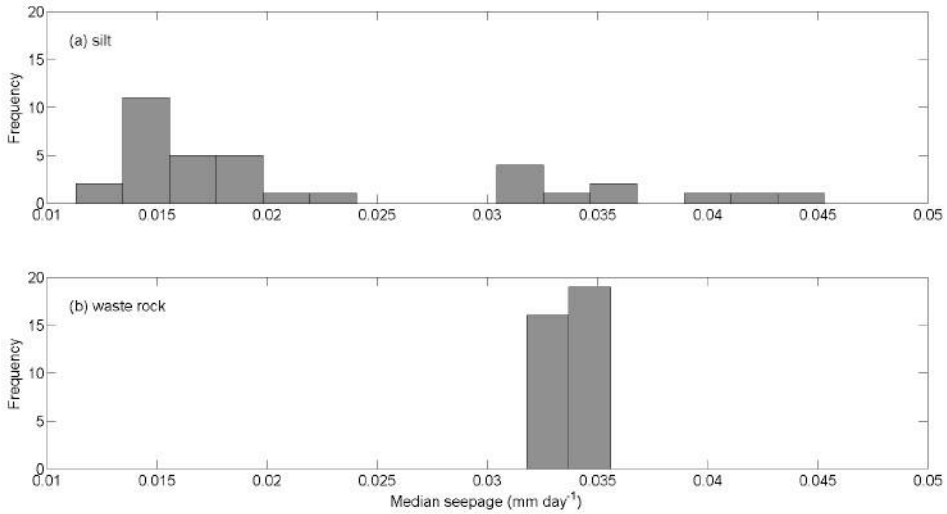

Figure 3 Frequencies of median seepage for (a) unimodal silt and (b) bimodal waste rock material and variable climatic conditions (based on 35 generated time-series, each of 100 years length).

Seepage patterns of two contrasting soil materials at variable climatic conditions

In general, seepage was lower for silt than for waste rock material. While for most of our simulations the maximum seepage for silt material was less than 1 mm day^{-1} (Fig. 4a), for waste rock material the maximum seepage ranged between 140 and 200 mm day^{-1} (Fig. 4b). Consequently, the frequency of seepage events greater than 1 mm day^{-1} ranged from 10 to 70 for silt (Fig. 5a), and from 1450 to 1750 for the waste rock material over the period of simulated 100 years of variable rainfall (Fig. 5b). The high number of seepage events >1 mm in the waste rock is a consequence of the bimodal pore system, consisting of a small proportion of wide and continuous pores and a majority of pores of medium to fine size. Water flow in coarse pores may only occur at rainfall events, which are sufficiently intensive to saturate these pores. For the majority of rain events these pores will not be filled and may not participate to downward flow because they function as a capillary barrier. Only if the soil is saturated or close to saturation, these pores will participate in the water flow. When averaging rainfall events across a large time scale, high intensive rainfall situations will be overlooked. For pore structures with a bimodal pore system and macro-pore flux, the consequences of water flow at saturated conditions will be ignored (i.e., higher maximum seepage events for silt rather than waste rock material (Table 2)).

At annual time scale, the median seepage ranged from 7 to 23 mm year^{-1} for silt (2-5 % of annual rainfall), and 175 to 229 mm year^{-1} for waste rock (44-50 % of annual rainfall). Interestingly, at a daily time scale, the median seepage ranged from 0.01 to 0.05 mm day^{-1} for silt (Fig. 3a), and 0.03 to 0.35 mm day^{-1} for the waste rock (Fig. 3b). That is, on a daily time scale and under same climatic conditions (variability), the average long-term seepage was higher for silt than for waste rock material. This finding is critical for the planning of soil cover systems and underpins the importance of using well-defined target parameters or closure criteria; i.e., whether average seepage or single seepage events should not exceed threshold values. In this regard, our case study of the climate in Mount Isa depicts that silt material much better reduces the probability of large seepage events (Figs. 4 and 5) at the expense of potentially higher average long-term seepage (Fig. 3).

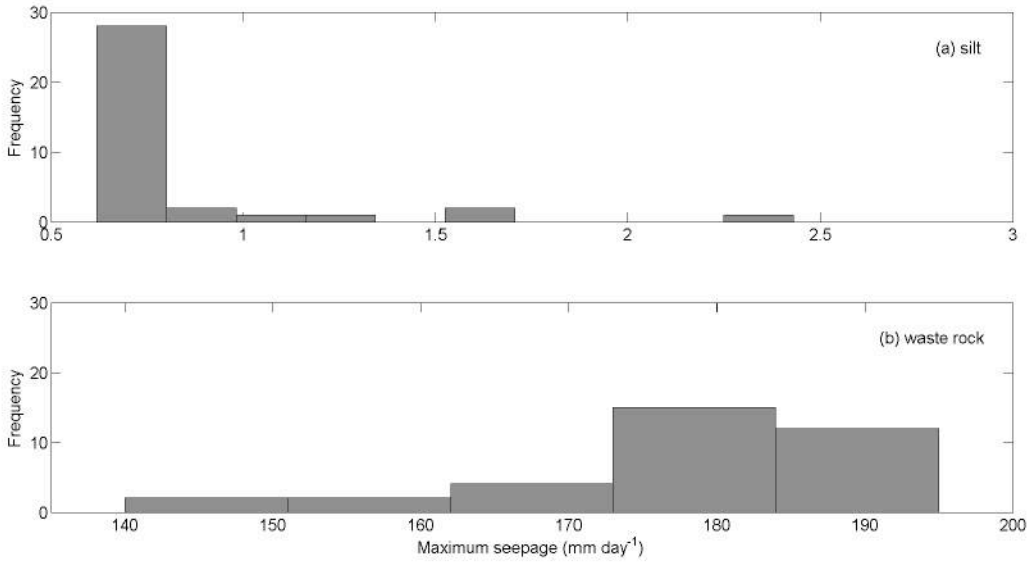

Figure 4 Frequencies of maximum seepage for (a) unimodal silt and (b) bimodal waste rock material and variable climatic conditions (based on 35 generated time-series, each of 100 years length). Note the scale differences.

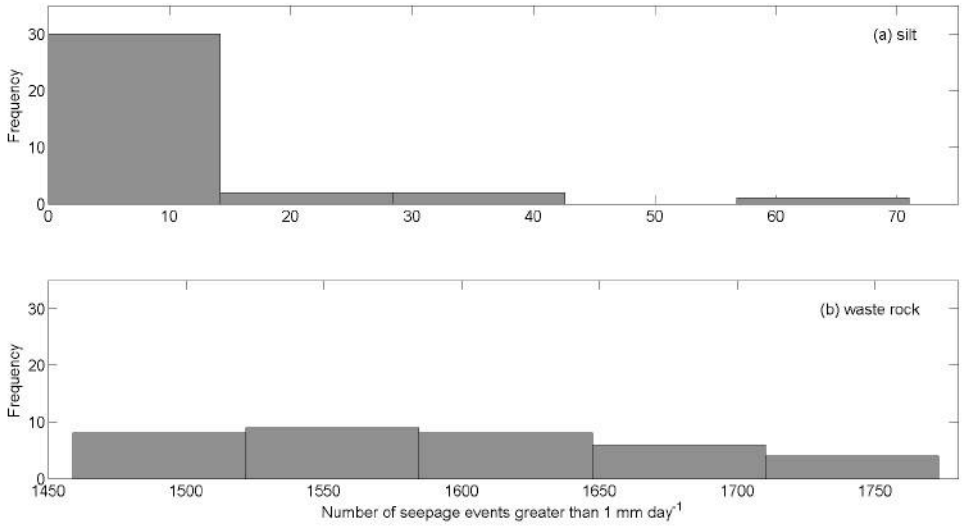

Figure 5 Frequencies of number of events with seepage greater than 1 mm day^{-1} for (a) unimodal silt and (b) bimodal waste rock material and variable climatic conditions (based on 35 generated time-series, each of 100 years length). Note the scale differences.

CONCLUSION AND FURTHER DIRECTIONS

A main consideration of our analysis is that the regional intensity, seasonality, and extremity of rainfall should represent a primary determinant of the design of soil cover systems. Our case study of climate in Mount Isa, Australia, indicates the critical role climate variability plays for the performance of soil cover systems, and the need to implement a similar approach into post-mining planning schemes (Audet et al., 2013). Based on our approach (Fig. 1), the strategy of: (i) using historical rainfall and evaporation data to generate statistically identical weather time-series, and

(ii) assess soil cover designs regarding seepage patterns when being forced to climate variability could be readily applied to other locations that are similarly affected by variable/erratic rainfall events and used to guide initial cover design planning.

ACKNOWLEDGEMENTS

This work was kindly supported by the Early Career Research Grant of The University of Queensland to Sven Arnold.

NOMENCLATURE

E^{corr}_i corrected evaporation used for further simulations (mm day^{-1})
E^{s}_i evaporation values generated by LARS-WG (mm day^{-1})

APPENDIX A

Table A1 Statistics of the generated rainfall time-series. The t-test compares the mean values and the associated p-values indicate the probability that the observed and generated mean values are derived from the same population. Likewise, the F-test tests whether the observed and generated rainfall are from normal distributions with the same variance.

Test	Average monthly p-value											
	Jan	*Feb*	*Mar*	*Apr*	*May*	*Jun*	*Jul*	*Aug*	*Sep*	*Oct*	*Nov*	*Dec*
t-test	0.620	0.515	0.628	0.357	0.587	0.664	0.607	0.572	0.546	0.616	0.573	0.418
F-test	0.063	0.448	0.242	0.366	0.199	0.230	0.225	0.206	0.264	0.499	0.332	0.553

APPENDIX B

Table B1 Configuration of the Hydrus-1D model for all selected soils.

Attribute	Value
Soil profile	
Depth (cm)	200
No. of layers	1
No. of nodes	300
Nodal density	200 (upper), 1 (lower)
Hydraulic model and boundary condions	
Single porosity model (silt)	van Genuchten-Mualem
Dual porosity model (waste rock)	Durner, dual van Genuchten-Mualem
Hysteresis	N/A
Upper boundary	Atmospheric (rainfall and evaporation data) with surface runoff
Lower boundary	Free drainage
Iteration criteria and time information	
Maximum No. of iterations	10
Water content tolerance	0.001
Pressure head tolerance (cm)	1
Lower [upper] optimal iteration range	3 [7]

Lower [upper] time step multiplication factor	1.3 [0.7]
Lower [upper] limit of the tension interval (cm)	10^{-6} [10^{4}]
Initial [final] time (day)	1 [36500]
Initial time step (day)	0.001
Minimum [maximum] time step (day)	10^{-8} [1]

REFERENCES

Arnold, S., Schneider, A., Doley, D., and Baumgartl, T.: The limited impact of vegetation on the water balance of mine waste cover systems in semi-arid Australia, Ecohydrology, n/a-n/a, 10.1002/eco.1485, 2014.

Audet, P., Arnold, S., Lechner, A. M., and Baumgartl, T.: Site-specific climate analysis elucidates revegetation challenges for post-mining landscapes in eastern Australia, Biogeosciences, 10, 6545-6557, 10.5194/bg-10-6545-2013, 2013.

Benson, C. H., Albright, W. H., and Roesler, A. C.: Evaluation of final cover performance: field datafrom the Alternative Cover Assesment Program (ACAP), Proc. Waste Management 02, Tuscon, AZ, 2002.

Bureau of Meteorology: Climate data online: http://www.bom.gov.au/climate/data, access: 03 September, 2014.

Gwenzi, W., Hinz, C., Bleby, T. M., and Veneklaas, E. J.: Transpiration and water relations of evergreen shrub species on an artificial landform for mine waste storage versus an adjacent natural site in semi-arid Western Australia, Ecohydrology, n/a-n/a, 10.1002/eco.1422, 2013.

Halwatura, D., Lechner, A. M., and Arnold, S.: Design droughts as planning tool for ecosystem establishment in post-mining landscapes, Hydrol. Earth Syst. Sci. Discuss., 11, 4809-4849, doi:10.5194/hessd-11-4809-2014, 2014.

Hauser, V. L., Weand, B. L., and Gill, M. D.: Natural covers for landfills and buried waste, J. Environ. Eng.-ASCE, 127, 768-775, 10.1061/(asce)0733-9372(2001)127:9(768), 2001.

Hillel, D., 2004. Introduction to Environmental Soil Physics. Elsevier, Amsterdam. 494p.

Horn, R., Baumgartl, T.: Dynamic properties of soils. In Warrick, A: Soil Physics Companion, 2002.

Rock, S. A.: Evapotranspiration covers for landfills, in: Application of Phytotechnologies for Cleanup of Industrial, Agricultural, and Wastewater Contamination, edited by: Kulakow, P. A., and Pidlisnyuk, V. V., NATO Science for Peace and Security Series C - Environmental Security, Springer, Dordrecht, 189-198, 2010.

Salt, M., Lightbody, P., Stuart, R., Albright, W. H., and Yeates, R.: Guidelines for the assessment, design, construction and maintenance of phytocaps as final covers for landfills, United States Environmental Protection AgencyREF No. 20100260RA3F, 99, 2011.

Schneider, A., Baumgartl, T., Doley, D., Mulligan, D., 2010. Evaluation of the Heterogeneity of Constructed Landforms for Rehabilitation Using Lysimeters. Vadose Zone Journal 9, 898–909. doi:10.2136/vzj2009.0172

van Genuchten, M.T., 1980. A closed form equation for predicting the hydraulic conductivity of unsaturated soils. Soil Sci. Soc. Am. J. 44, 892–898.

Semenov, M. A.: Simulation of extreme weather events by a stochastic weather generator, Climate Research, 35, 203-212, DOI: 10.3354/cr00731, 2008.

Simunek, J., Van Genuchten, M. T., and Sejna, M.: The HYDRUS-1D software package for simulating the one-dimensional movement of water, heat, and multiple solutes in variably-saturated media., University of California-Riverside Research Reports, 240 p., 2005.

Design, Construction and Preliminary Results for an Inclined Store-and-Release Cover Experimental Cell Built on an Abandoned Mine Site in Morocco

Jihane Knidiri[1], Bruno Bussière*[1], Rachid Hakkou[2], Mostafa Benzaazoua[1], Etienne Parent[1] and Abdelkabir Maqsoud[1]

1. *Université du Québec en Abitibi-Témiscamingue, Canada*
2. *Faculté des Sciences et Techniques, University Cadi Ayyad, Morocco*

ABSTRACT

In arid and semiarid climates, acid mine drainage (AMD; also called acid rock drainage, ARD) generated by mine tailings can be controlled by reducing water percolation. The use of store-and-release (SR) covers with capillary barrier effect is emerging as the most effective way to prevent water percolation through tailings under these climates. Four instrumented experimental cells made of phosphate wastes, as SR covers, were constructed on top (flat surface) of the abandoned Kettara mine site (near Marrakech, Morocco). Results confirmed the potential of phosphate mine waste as SR cover material to control water percolation. However, significant uncertainties remain about the influence of inclined conditions on the hydrogeological behavior of a SR cover at the mine, as the mine wastes at Kettara mine site are retained by dykes that reach a height of 10 m. Due to the slope inclination, water can accumulate above the tilt interface during extreme precipitation events, which could create a breakthrough of the capillary barrier; at this location, the cover is no longer effective to control water infiltration into the mine wastes. A field investigation was conducted to evaluate the influence of the slope on the Kettara SR cover's performance. An experimental field cell (10 m wide by 8 m long) inclined at an angle of 14.5 degrees was constructed on-site. The SR cover retained is made of 0.8 m of phosphate waste, placed over a capillary break layer made of coarse-grained materials. Cover performance was monitored using lysimeters, Tensiometers, suction and soil moisture sensors installed at four stations and at different depths. The paper presents the design, the construction and the instrumentation of an inclined SR covert. Preliminary results of the monitored parameters under natural conditions are also included. The field test showed that the slope influences water distribution in the cover with more water at the bottom of the slope. The inclined SR cover still effectively limited water percolation under natural conditions.

Keywords: Acid mine drainage -Experimental cell- inclined store-and-release- design and construction-mine site reclamation

INTRODUCTION

Acid mine drainage (AMD) from mine wastes is the main environmental problem facing the mining industry. It is a common practice to construct single or multi-layered engineered cover systems to control AMD from waste rocks and tailings. In dry climates, where the potential evaporation rate exceeds the annual precipitation, these cover systems are usually used to limit water percolation into mine waste disposal (e.g., Albright et al., 2004; Hauser, 2008). These covers use the physical process of evaporation or evapotranspiration to control water percolation into the reactive wastes (e.g., Morris and Stormont, 1997; Albright et al., 2004; Rock et al., 2012, Bossé et al., 2013). These cover systems are known as alternative covers, evapotranspiration (ET) covers, water balance, or store-and-release (SR) covers; this terminology (SR cover) will be used throughout this paper. The technology of SR covers has been applied with success to several mine sites such as Kidston Gold Mines (Australia) and Barrick Goldstrike Mines (Nevada, US) to control acid mine drainage (AMD) generation from sulfidic mine wastes (Zhan et al., 2001, 2006; Williams et al., 2006). The concept of this approach is to control water percolation by using a moisture-retaining layer (MRL) that acts as a sponge or a reservoir by storing water during precipitation events, and then releasing it back to the atmosphere by evaporation (e.g., Rock et al. 2012, Bossé et al., 2013). The water storage capacity in the MRL can be increased by the implementation of a capillary break layer (CBL) below the MRL. If the hydrogeological contrast between the two materials (MRL and CBL) is sufficient, capillary barrier effects (CBE) will control the water flow at the layers interface and increase the water storage capacity of the MRL. More details on CBE can be found in Morel-Seytoux, (1992) and Bussière (1999).

The abandoned pyrrhotite mine site, Kettara, is one of several abandoned AMD-generating mine sites in Morocco. The site is located in an arid climate (Bossé, 2014) approximately 35 km north-northwest of Marrakech (31°52'15"N–8°10'31"W). The region's climate is characterized by a bi-modal precipitation pattern with wet (October-April) and dry (May-September) seasons. The annual cumulative rainfall and the potential evapotranspiration (PET) are estimated at 334 mm and 2,178 mm respectively. The tailings pond area contains approximately 1,800,000 tons of mine wastes (Lghoul et al., 2012). These wastes were deposited at the surface without any concern about the environment (Hakkou et al., 2008, Bossé, 2014). This mine waste is considered as highly acid-generating, with negative net neutralization potential (NNP) values ranging from -453 to -22.5 kg $CaCO_3$/t (more information on Kettara mine waste characterization can be found in Hakkou et al., 2008). Indeed, this contaminated drainage is a source of pollution in this region that affects the surrounding ecosystems as well as the people living nearby the mine site (e.g. Khalil et al., 2013). One of the most promising reclamation options to control AMD generation at this Kettara mine site is the use of a SR cover system that integrates CBE. A very helpful factor facilitating the mine rehabilitation is the availability of alkaline mine wastes, generated by phosphate mines located nearby to be used for the MRL.

Four instrumented experimental cells (1D), made of phosphate wastes as SR covers, were constructed on top of the Kettara mine site to evaluate the use of the phosphate mine waste as MRL in the SR cover (Bossé, 2014). Results confirmed, for 1D conditions, that the phosphate limestone has the appropriate properties to become part of an efficient SR cover to reduce rainfall percolation and control AMD. However, uncertainties remain about the influence of inclined conditions on the hydrogeological behavior of a SR cover at the mine, as mine wastes at the Kettara mine site are retained by dykes (coarse mine wastes) that can reach a height of 10 m. Due to slope inclination, water can accumulate above the tilt interface during precipitation events, which would increase the water pressure at this location. When the pressure exceeds the water-entry value of the coarse-grained material, a breakthrough of the capillary break can occur at the interface, and the cover becomes no longer effective to control water percolation into the AMD-generating mine wastes (e.g., Ross, 1990; Steenhuis et al., 1991; Bussière, 1999; Aubertin et al., 2009; Maqsoud et al., 2011). In order to investigate the slope effect for the SR cover at the Kettara site, an experimental inclined SR cover was constructed. The objective of this article is to present the design and construction in the field of an instrumented inclined SR cover, and the preliminary results accumulated during the first months of monitoring. As mentioned earlier, one of the originalities of this work is mainly related

to the use of phosphate limestone wastes generated by a sedimentary phosphate mine, located close to the abandoned Kettara mine site, to construct the cover system.

FIELD EXPERIMENTAL CELL DESCRIPTION AND MATERIALS CHARACTERIZATION

Design and construction

The work was initiated during March 2014 at the Kettara mine site to evaluate the slope effect on the hydrological behavior of a SR cover system. The tested SR cover is made of two layers: a MRL made of 0.8 m of phosphate mine waste placed over CBL made of Kettara's coarse grained mine waste. The slope is approximately 14.5 degrees and the field cell area is about 10 × 34 m (Fig 1). A 3D schematic representation of the inclined field instrumented SR cell is presented in Fig 1.

The field experimental cell was constructed directly on the retention dyke. The dyke is 8 meters high and made of the reactive coarse-grained material at Kettara mine site (Fig 1).

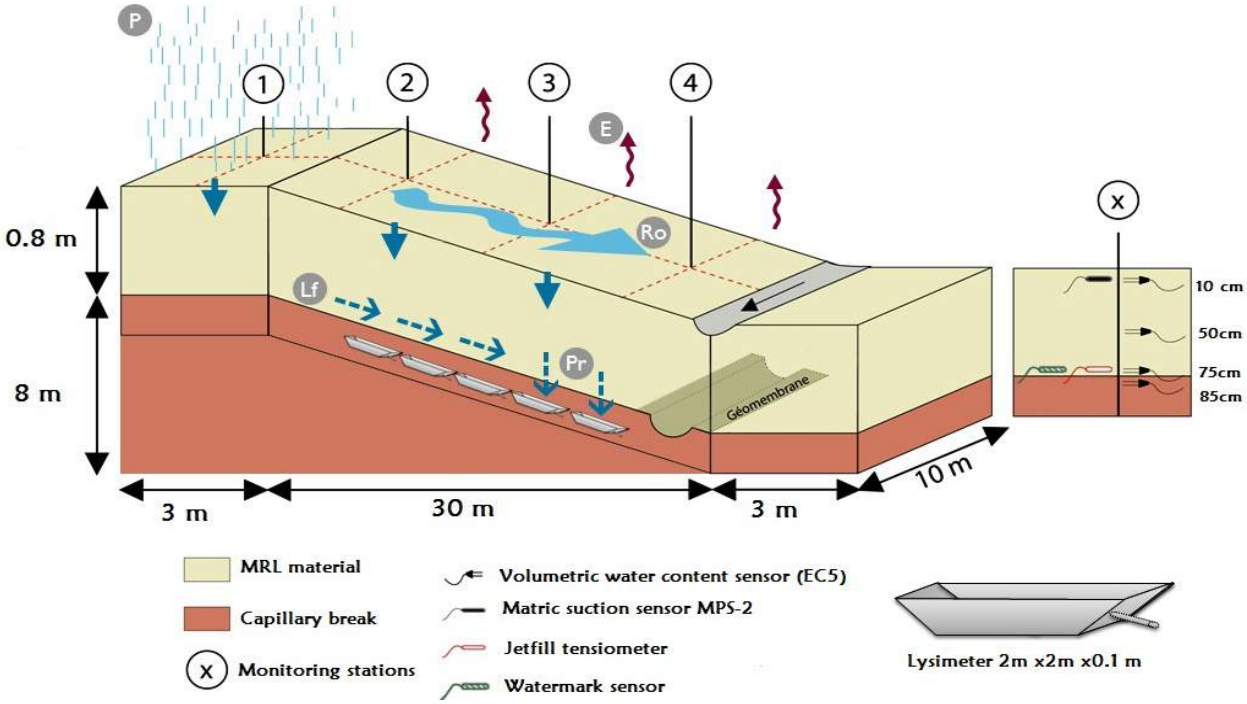

Figure 1 3D schematic representation of the field instrumented cell (E: evaporation; P: precipitation; R0: runoff; Pr : percolation; Lf: lateral flow); locations 1 to 4 on the slope are the monitoring stations

The MRL material was placed and compacted with a manual compactor to a dry unit weight of 15 kN/m^3. The experimental cell was constructed in different steps. The slope was first flattened and compacted (Fig 2-step 1) to a targeted porosity (n) of approximately 0.37 m^3/m^3 (dry unit weight = 18.3 kN/m^3). Five lysimeters were installed in the CBL material to monitor water percolation at the base of a cover system (Fig 2-step-2). The water collected may drain out of the lysimeters through a pipe by gravity. The phosphate limestone wastes were then placed and compacted at their natural water content (w ≈ 4%) to a porosity of approximately 0.41 m^3/m^3 (Fig 2–step-3). The material was compacted in successive lifts of about 20 cm thick to ensure a uniform density. Surface and lateral drainage systems were installed at the toe of the slope (Fig 1). The lateral drainage consists of the water that flows at the interface between the CBL and MRL due to the capillary barrier effects

(Fig 3.e). The surface drainage collector was installed to quantify the runoff water and to facilitate the calculation of the water balance (Fig 3.f).

Field instrumentation and monitoring

Field performance of the tested inclined SR cover is monitored by measuring the percolation through the CBL, the changes in moisture conditions (ΔS) within the cover layers, the internal lateral flow, run off and climatic conditions. Five lysimeters (2 m x 2 m x 0.1 m) were installed to measure water percolation into the underlying mine wastes at a depth of 90 cm from the cover surface (fig. 2 step 2). Daily precipitation (rainfall) i measured using an automated weather station (HOBO U30-NRC) installed at the Kettara mine site (fig 5.c; see Bossé, 2014 for more details). Changes in ΔS are estimated using ECH2O volumetric water sensors (EC5) (fig 3.a) and measured indirectly by matric suction sensors (MPS-2) (fig 3.b). Tensiometers and Watermark sensors are also used to measure matric suction in the inclined SR layers (fig 3.d). Tensiometers can measure suction between 0 and 80 kPa with an accuracy of 1 kPa, while the suction range of Watermark sensors is from 0 to 200 kPa (Bussière, 1999). The MPS-2 can measure suction between 10 kPa and 500 kPa (Bossé, 2014). Note that the three instruments (MPS-2, Tensiometers, and Watermarks) were soaked in water before installation to improve early measurements.

Before installation, EC5 sensors were calibrated for each material in the laboratory. The Tensiometers were inserted carefully at the required depth (75 below the surface) to ensure good contact between the high air-entry ceramic cups of the Tensiometers and the MRL material. Four EC5 sensors were placed at depths of 10, 50, 75 and 85 cm into the cover system, and a matric suction sensor (MPS-2) was placed at depth of 10 cm. To be able to compare measurements, JetFill tensiometers and Watermark sensors were placed beside each other at each monitoring station at a depth of 75 cm (close to the interface between the MRL and CBL). All monitoring stations were placed near the central axis of the cell. Manual monitoring of the Tensiometers and Watermark sensors is done three times per week while the monitoring frequency for the EC5 and MPS-2 sensors is a measured every 30 minutes

Materials characterization

The main properties of the inclined SR cover components (the phosphate limestone wastes, and Kettara coarse-grained mine) used in the experimental cell are summarized in Table 1. Material particle size distribution was determined using a Malvern Mastersizer laser particle size analyzer and by sieving (ASTM D 6913-04 2009). The specific gravity (Gs) was estimated with a Micromeritics Accupyc 1330 helium gas pycnometer (ASTM D5550-06 2006). The liquid limit (w_L), plastic limit (w_p) and plasticity index (PI) of materials were determined by Bossé et al., (2013) using ASTM standards (ASTM 4318-10-2010).

Step 1 Step 2 Step 3

Figure 2 Photos illustrating the field inclined SR cover construction steps

The specific gravity (Gs) and the percentage of fines (< 80 µm) of the phosphate limestone wastes were respectively estimated at 2.85 and 15%. The liquid limit wasless than 50%, the plasticity index was estimated to be 0.8 and the material is categorized as a non-plastic sandy silt according to the USCS classification (e.g., McCarthy 2007). The air-entry values (AEV- pressure at which the material starts to drain) of the phosphate and coarse tailing were-40 kPa and -0.1 kPa respectively. The water-entry values (WEV-pressure at which the water starts to enter) were -2000 kPa for the MRL material and -0.4 kPa for the CBL material (Bossé et al., 2013). The saturated hydraulic conductivity (k_{sat}) of the coarse-grained material (5.9 cm/s) was substantially greater than the one of the fine-grained material (5.7×10^{-6} cm/s; see tab 1). This important contrast in hydraulic properties between the two materials with different textures restricts water flow at the interface and enhances the water storage capacity of the fine grained layer (e.g., Khire et al., 1999). More information on phosphate limestone waste characterization can be found in Bossé, (2014)

PRELIMINARY RESULTS

After the construction of the experimental field cell, an important wetting event was simulated using drip irrigation tubes connected to a pump and installed on the inclined SR cover surface. Approximately 100mm of water over a period of 48 hours was applied to the tested area, to assess the behavior of the water diversion capacity of the cover. The hydrogeological behaviour of the inclined SR cover after the wetting event was also monitored.

Hydrogeological behaviour of the inclined SR cover during the wetting event

This section presents the behavior of the experimental cell test during the simulated wetting event. Figure 4 shows the fluctuation of volumetric water content (θ) within the inclined SR cover at 75 cm depth (fig 4.a) and 50 cm depth (fig 4.b) for the four monitoring stations (station 1 is located at the top and station 4 at the bottom; see fig. 1). The fluctuations of matric suction (ψ) measured with the watermark sensors (fig 4.c) and JetFill tensiometers (fig 4.d) are presented and compared for the 75 cm depth (close to the interface of the CBL and MRL). Note that a significant rainfall event occurred during construction which led to an increase in the moisture content in station 1, especially at the depth of 75 cm. The observed θ results at 50 cm and 75 cm depth are quite similar. During the wetting event, it took about 2 days to notice an increase in volumetric water content at station 2, 3 and 4 with a water arrival first at station 2, followed by station 3 and 4.

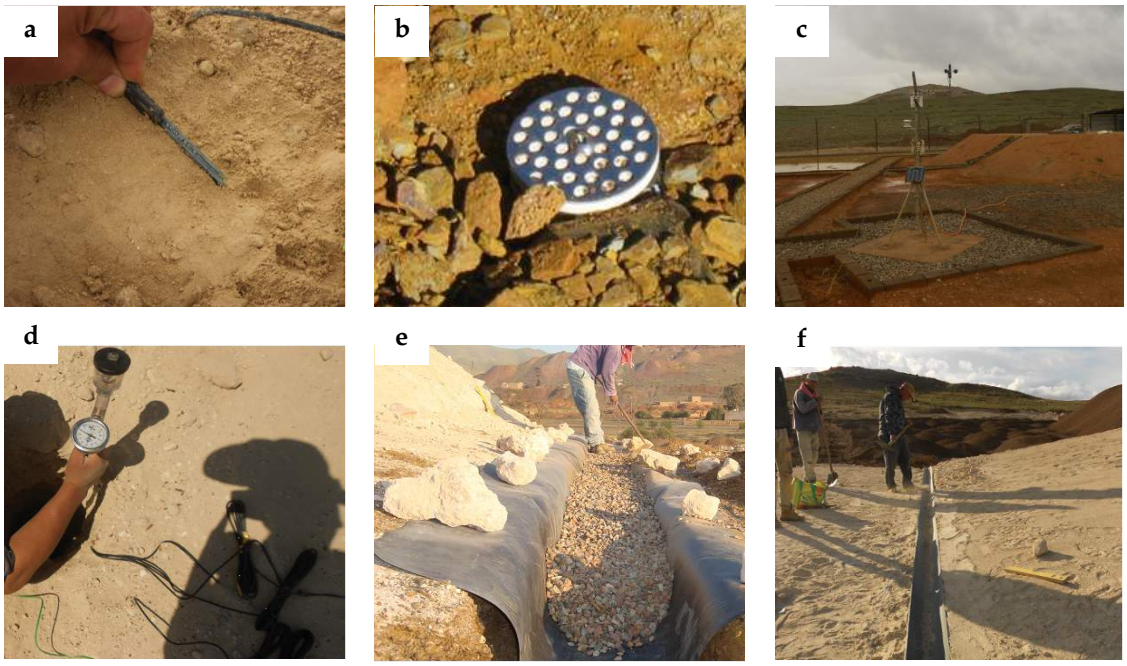

Figure 3 Photos illustrating the instrumentation used for the monitoring of the inclined SR cover: (a) Volumetric water content sensors (EC5) (b) Matric suction sensors (MPS-2) (c) Weather station (d) JetFill tensiometers (e) Lateral drainage collector (f) Surface drainage collector

Table 1 Basic properties of MRL (Phosphate limestone waste) and CBL (Kettara coarse-grained waste) materials

Parameter	Phosphate limestone waste	Kettara coarse-grained waste
Specific gravity	2.85	2.90
D_{60} [mm]	0.31	6.3
D_{10} [mm]	0.07	1.13
Fines content (< 80µm) (%)	15	7
w_L(%)*	26.4	-
w_p (%)*	25.6	-
*PI (%)**	0.8	-
k_{sat} (cm/s)*	5.7×10^{-6}	5.9
AEV (kPa)*	-40	-0.1
WEV(kPa)*	-2000	-0.4
Classification (USCS)*	Sandy silt	Poorly graded gravel with sand
Mineralogy by order of importance**	Calcite/fluoapatite/ Dolomite/quartz	Pyrite/pyrrhotite/ chlorite-serpentine, quartz, talc

* Values from Bossé et al., (2013); ** Values from Hakkou et al., (2009)

The wetting event did not have an impact on θ values at station 1 because water accumulates above this elevation; this behavior was also observed by Bossé, (2014) in a similar cover built on a flat surface. The magnitude of the volumetric water content increase is more pronounced at 50 cm than 75 cm depth but the MRL material didn't reach the saturation value (= porosity) of 0.41. It can also be observed that, as expected, the θ values are usually higher close to the bottom of the slope

(station 3 and 4; typically between 0.30 and 0.35) than close to the top. This behavior is due to the diversion capacity of the inclined SR cover; theoretically, water flows along the interface between the MRL and CBL until the MRL become nearly saturated and the pressure at the interface reaches the water entry value of the CBL material (e.g. Steenhuis et al., 1991; Aubertin et al., 2009). Note that no water flow was observed in the different lysimeters and no change in terms of θ in the CBL was detected; confirming that the tested inclined SR cover was able to divert the water during the wetting event. Field lysimeter is a very important tool to evaluate the performance of cover systems. The design involves different parameters such as the geometry of the lysimeter, hydraulic properties of the backfill material, and boundary conditions (Bew et al., 1997). Suction inside and outside the lysimeter must be similar to avoid preferential outward flow. It is worth mentioning that during another wetting event of 155mm/48h simulated in November 2014, water percolation was detected in the 5 lysimeters (Knidiri, 2015). These results prove that even if the height of the lysimeters is small (0.1 m), the lysimeters function well enough to detect a breakthrough of the capillary barrier.

The trend of ψ evolution during the wetting event close to the interface between the CBL and MRL is similar for the four stations. After the wetting event, the ψ value starts to decrease from values between 40 and 85 kPa to values below 20 kPa due to water accumulation. The lowest values were observed near the bottom of the slope where θ increased the most (station 3 and 4). It is interesting to note that both equipments tested (Watermark sensors and Jetfill tensiometers) gave similar trends even if the absolute values can be slightly different.

The hydrogeological behaviors of the inclined SR cover during summer 2014

Figure 5 illustrates hydrogeological behavior of the tested inclined SR cover exposed to natural climatic conditions after the wetting event; rainfall measured during this period is presented in red. Results indicate a decrease of the θ few days after the wetting event due to evaporation during the dry summer conditions. The daily air temperature during this period ranged from 15°C to 33°C with an average of 23.5°C. The fluctuation of θ is more pronounced at 10 cm depth than at 50 cm and 75 cm depth; this is due to atmospheric forcing that affects essentially the surface of the inclined SR cover. However, the effect of evaporation is also present at 50 and 75 cm, particularly for stations located close to the bottom (station 3 and 4) where a constant decrease of the volumetric water content is observed. Hence, the inclined SR cover is presently regaining its full capacity to store further precipitations by transferring water to the atmosphere via evaporation.

In summary, preliminary results show that the hydraulic behavior of the inclined SR cover is influenced by the inclination of the slope. θ in the inclined SR cover is greater at station 3 and 4 which are located in the lower slope positions of the inclined cover. No lateral flow and no percolation were observed during this wetting event. Water accumulated and was diverted by the capillary barrier effects at the interface of the two layers (CBL and MRL) to the bottom of the slope. The suction results indicate that the breakthrough of the capillary barrier (or the Down Dip Limit (DDL), Ross, 1990) was nearly reached at the bottom of the tested inclined SR cover with suction value close to 0 at station 4. These preliminary results also indicate that the cover is presently releasing the water stored during the wetting event to the atmosphere via evaporation.

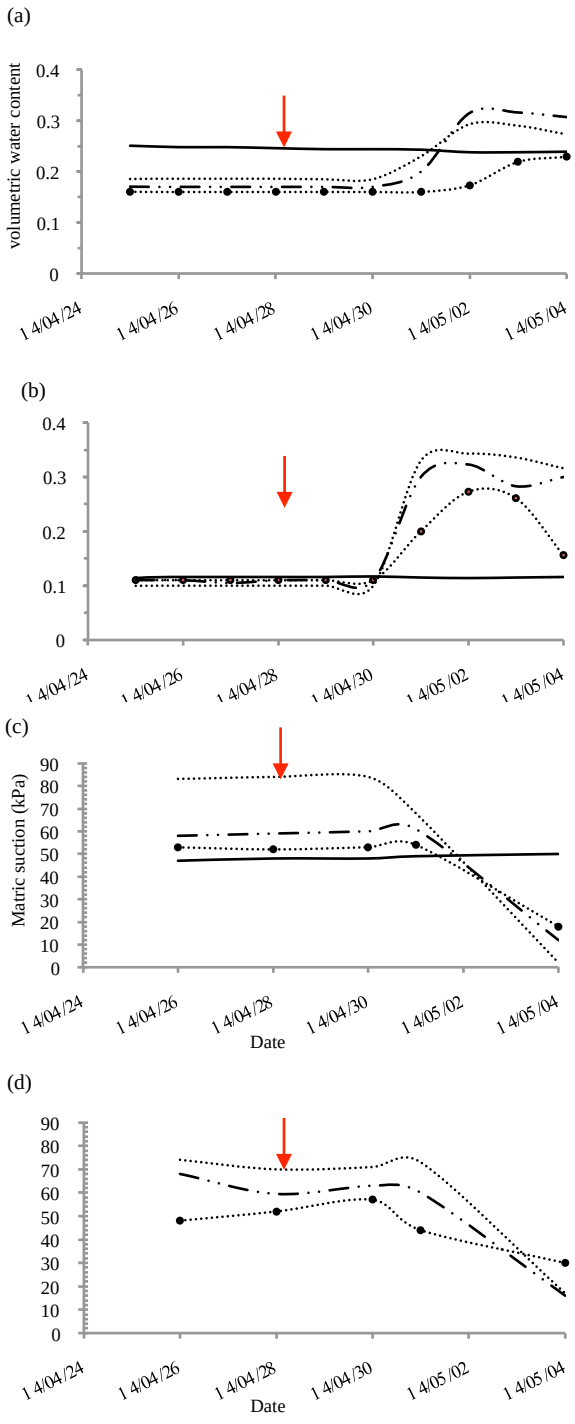

Figure 4 Measured volumetric water content at depths of 75 cm (a) and 50 cm (b) and measured matric suction at the depth of 75 cm with Watermark (c) and Jetfill (d) stations (the arrow in the figure indicates the wetting event)

FINAL REMARKS

The construction of an inclined SR cover in Kettara (Morocco) designed to investigate its slope effect was completed successfully and preliminary results confirm that the SR cover system is working properly to control water percolation. At this stage, measurements indicate that:

- Volumetric water content and suction obtained during the wetting event show that the sensors at 10, 50, 75 cm were affected by this event but the inclined SR cover was able to divert the water flux applied at inclined SR cover surface (100 mm per 48h) where no water percolation was collected in the lysimeters.
- Water was successfully diverted and stored within the phosphate limestone wastes, and is being presently released to the atmosphere during the dry summer period.

The hydrogeological monitoring of the system is underway. In addition, other wetting tests will be performed to investigate the diversion capacity of the tested inclined SR cover. A particular attention will be put on the DDL of the system. Numerical modelling will be also performed to better understand the hydrogeological behavior of inclined SR cover exposed to arid conditions.

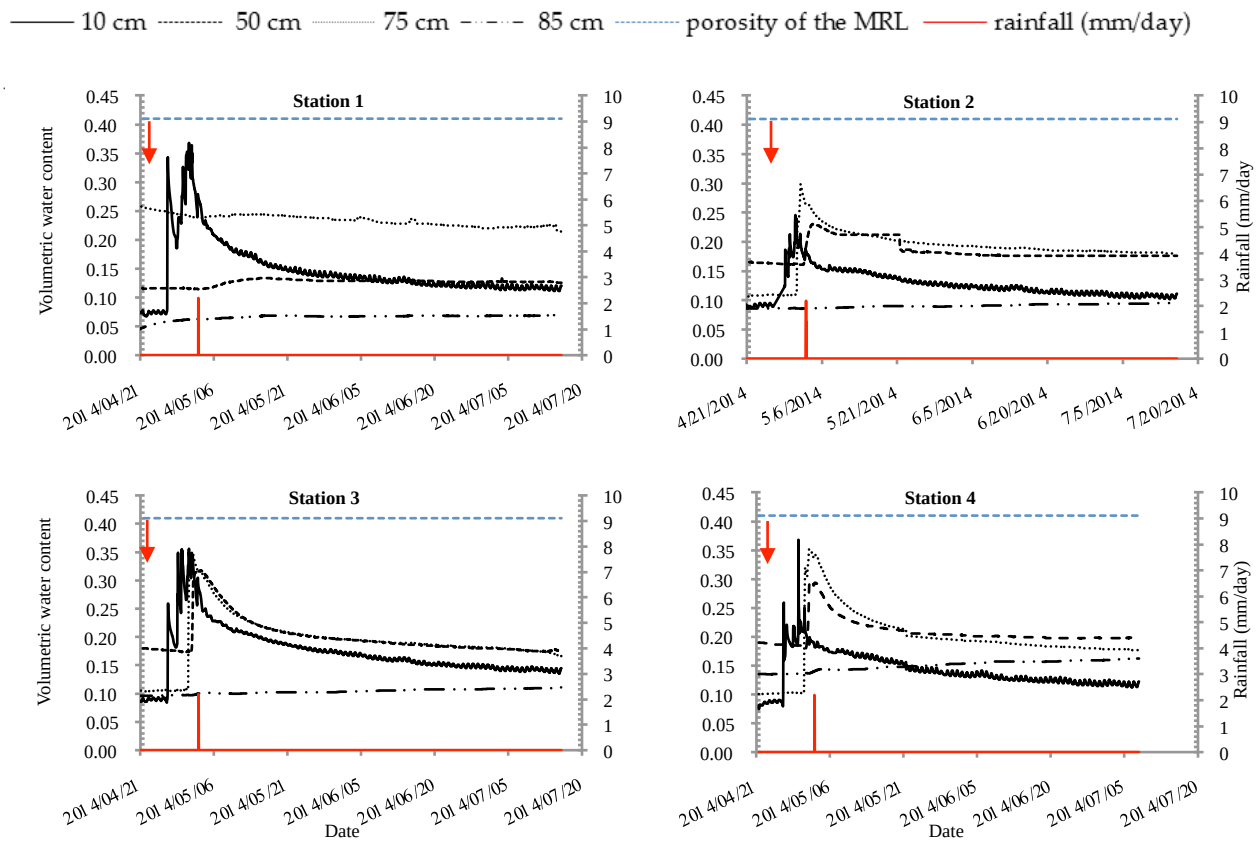

ACKNOWLEDGEMENTS

This study was funded by the International Research Chairs Initiative, a program funded by the International Development Research Centre (IDRC) and the Canada Research Chair program, and the Canada Research Chair on the rehabilitation of abandoned mine sites.

REFERENCES

Albright, W.H., Benson, C.H., Gee, G.W., Roesler, A.C., Abichou, T., Apiwantragoon, P., Lyles, B.F., Rock, S.A., (2004) 'Field water balance of landfill final covers' J. Environ. Qual. 33, 2317-2332.

Aubertin, M., Cifuentes, E., Apithy, S.A., Bussière, B., Molson, J., Chapuis, R.P., (2009) 'Analyses of water diversion along inclined covers with capillary barrier effects. Can. Geotech. J. 46, 1146-1164.

ASTM, (2006b). D5550-06 Standard test method for specific gravity of soil solids by gas pycnometer. Annual Book of ASTM Standards, Vol. 04.08.

ASTM, (2009). D 6913-04: Standard test methods for particle-size distribution (gradation) of soils using sieve analysis. Annual Book of ASTM Standards Vol. 04.09.

ASTM, (2010). D 4318-10: Standard test methods for liquid limit, plastic limit, and plasticity index soils. Annual Book of ASTM Standards Vol. 04.08.

Bews, B E., Barbour, S L., Wilson, G W., and O'Kane, M., 1997.'The design of lysimeters for a low flux cover system over acid generating waste', Canadian Geotechnical Golden Jubilee Conference, Pre-print Vol 1, pp 26-33 (The Canadian Geotechnical Society: Alliston).

Bossé, B., Bussière, B., Hakkou, R., Maqsoud, A., Benzaazoua, M., (2013) 'Assessment of phosphate limestone wastes as a component of a store-and-release cover in a semiarid climate' Mine Water and the Env. 32(2), 152-167.

Bossé, B., (2014).'Évaluation du comportement hydrogéologique d'un recouvrement alternatif constitué de rejets calcaires phosphatés en climat semi-aride à aride' Ph.D. Diss., UQAT, Rouyn-Noranda, Canada.

Bussière, B., (1999) 'Étude du comportement hydrique de couvertures avec effets de barrières capillaires inclinées à l'aide de modélisations physiques et numériques' Ph.D. Diss., École Polytechnique de Montréal, Canada.

Hakkou, R., Benzaazoua, M., Bussière, B., (2008a) 'Acid mine drainage at the abandoned Kettara mine (Morocco): 1 environmental characterization'. Mine Water Environ. 27, 145-159.

Hakkou, R., Benzaazoua, M., Bussière, B., (2009) 'Laboratory evaluation of the use of alkaline phosphate wastes for the control of acidic mine drainage' Mine Water Environ., 28(3), 206-218.

Hauser, V.L., (2008) 'Evapotranspiration covers for landfills and waste sites' CRC Press.

Khalil, A., Hanich, L., Bannari, A., Zouhri, L., Pourret, O., Hakkou, R., (2013) 'Assessment of soil contamination around an abandoned mine in a semi-arid environment using geochemistry and geostatistics: Pre-work of geochemical process modeling with numerical models' J. of Geochemical Exploration, 125, 117-129.

Khire, M.V., Benson, C.H., Bosscher, P.J., (1999)' Field data from a capillary barrier and model predictions with UNSAT-H' J. of geotechnical and geoenvironmental engineering, 125(6), 518-527.

Knidiri, J., 2014 'Évaluation de l'effet de pente sur le comportement hydrogéologique de recouvrements alternatifs type stokage-relarguage à l'aide de modélisations physique et numérique' Mémoire de maîtrise, École Polytechnique de Montréal, Canada

Lghoul, M., Teixidó, T., Pena, J.A., Hakkou, R., Kchikach, A., Guérin, R., Jaffal, M., Zouhri, L., (2012) 'Electrical and seismic tomography used to image the structure of a tailings pond at the abandoned Kettara mine, Morocco' Mine Water Environ., 31(1), 53-61.

Maqsoud, A., Bussière, B., Aubertin, M., Chouteau, M., Mbonimpa, M., (2011) 'Field investigation of a suction break designed to control slope-induced desaturation in an oxygen barrier' Can. Geotech. J. 48, 53–71.

McCarthy, D.F., (2007) Essentials of soil mechanics and foundations: basic geotechnics, 7th Ed. Pearson Prentice Hall, Upper Saddle River, NJ.

Morel-Seytoux, H., (1992) 'L'effet de barrière capillaire à l'interface de deux couches de sol aux propriétés fort contrastées' Hydrol Continent 7(2), 117-128.

Morris, C.E., Stormont, J.C., (1997)'Capillary barriers and subtitle D covers: estimating equivalency' J. Env. Eng. 123(1), 3-10.

Rock, S., Myers, B., Fiedler, L.,(2012) 'Evapotranspiration (ET) Covers' Inter. J. of Phyto. 14(S1), 1-25.

Ross, B., (1990) 'The diversion capacity of capillary barriers' Water Resources Research, 26, 2625-2629.

Steenhuis, T.S., Parlange, J-Y. and Kung, K-J.S.,(1991)'Comment on "The diversion capacity of capillary barriers' by Benjamin Ross. Water Resources Research, 27(8), 2155-2156.

Williams, D.J., Stolberg, D.J., Currey, N.A., (2006) 'Long-term monitoring of Kidston's "Store/Release" cover system over potentially acid forming waste rock piles'Proc. 7th ICARD, St Louis, MO, USA, p 26-30.

Zhan, G., Aubertin, M., Mayer, A., Burke, H., McMullen, J., (2001) 'Capillary cover design for leach pad closure'SME Annual Meeting, Denver, Colorado, 1-9.

Zhan, G., Schafer, W., Milczarek, M., Myers, K., Giraudo, J., Espell, R., (2006) 'The evolution of evapotranspiration cover systems at Barrick Goldstrick Mines' Proceedings of the 7th Intern. Conf. Acid Rock Drainage (ICARD), St. Louis, MO, USA, 2585–2603.

Evaluation of Cover System Field Trials with Compacted Till Layers for Waste Rock Dumps at the Boliden Aitik Copper Mine, Northern Sweden

Matt McKeown[1], David Christensen[1], Tami Taylor[2] and Seth Mueller[2]
1. *O'Kane Consultants Inc., Canada*
2. *Boliden Mineral AB, Sweden*

ABSTRACT

The Boliden Aitik copper mine is located outside Gällivare, northern Sweden. Since mining started in 1968, more than 500 Mt of waste rock have been deposited in waste rock dumps (WRDs). In the 1990s, a dry cover system was designed to reduce oxygen diffusion to the underlying waste rock and limit the subsequent formation of metal leaching and acid rock drainage (ML/ARD). The original cover system (applied to WRD5 and parts of WRD2) consists of 1.0 m compacted till placed in two lifts covered by 0.3 m organic material. Recent studies concluded that predicted annual diffusion flux estimates based on calibrated soil-plant-atmosphere modelling were similar in magnitude, but greater than, rates predicted in the 1996 design. Therefore, to increase the level of water retention within the compacted till and reduce oxygen ingress to the underlying waste rock, increased compaction from the current practice is required.

Multiple field and laboratory studies were completed to evaluate the cover system design and performance. Field compaction trials conducted in 2012 confirmed that increased compaction would enhance water retention characteristics within the cover system. A field study of freeze / thaw effects on the compacted till highlighted frost penetration to the compacted layer as an area of concern for long term performance of the cover system. Cover system trials implemented in 2013 were instrumented with monitoring instrumentation that will allow performance to be evaluated over time under site-specific conditions, providing essential insight into cover system response to climatic variations in terms of temperature and water storage dynamics.

Keywords: field performance monitoring, water retention capability, oxygen ingress

INTRODUCTION

The Boliden Aitik copper mine (Aitik) is located outside Gällivare, in northern Sweden. Since mining started in 1968, more than 500 Mt of waste rock have been deposited in waste rock dumps (WRDs). The Aitik site is located in a seasonally humid environment, subjected to frozen conditions for approximately half the year. Major seasonal weather events include spring snow melt and heavy rains in the late fall. In the 1990s, a dry cover system was designed to reduce oxygen diffusion to the underlying waste rock and limit the subsequent formation of metal leaching and acid rock drainage (ML/ARD). The original cover system consists of 1.0 m compacted till placed in two lifts covered by 0.3 m organic material. As part of ongoing reclamation activities at Aitik, this dry cover system design has been applied to WRD5 and parts of WRD2.

Recent studies found that predicted annual diffusion flux estimates based on calibrated soil-plant-atmosphere modelling were similar in magnitude, but greater than, rates predicted in the 1996 design. It was hypothesized that increased compaction from the current practice was a feasible option to increase the water retention capability of the compacted till layer, and reduce oxygen ingress to the underlying waste rock. To test this hypothesis, a compaction field trial program was completed to evaluate the relationship between compaction methods and achievable water retention characteristics (as determined by measurements of *in situ* dry density and hydraulic conductivity). Based on this relationship, an improved cover system design was developed. To improve understanding of the *in situ* performance of this cover system, cover system trials were designed, constructed, and instrumented.

METHODOLOGY

Methodology for this study involved compaction field trials, completed in September 2012, to measure achievable *in situ* dry density and hydraulic conductivity. A follow up testing program was completed in May 2013 to determine the effect of a freeze / thaw cycle on the compacted till layers. Cover system field trials were then designed using results of the compaction field trial program to determine optimum compaction methodology for the compacted till layers. Instrumentation installed in the cover system field trials allow for assessment of the cover system performance under site-specific conditions.

Compaction field trials

Compaction field trials were conducted in September 2012 for the purpose of determining the optimal method of construction and achievable level of compaction in terms of *in situ* dry density and minimum field permeability for a compacted till layer at Aitik. The previous methodology for constructing compacted till layers at Aitik consisted of compacting six passes with a 6 ton smooth-drum roller over ~50 cm lifts. The purpose of the compaction trials was to replicate and assess the level of compaction achieved for a compacted till layer using the previous construction methodology and evaluate the level of compaction achieved on a 50 cm lift compared to that achieved on a thinner 30 cm lift. Additional testing evaluated alternative compaction equipment (a 10 ton smooth-drum roller, and 6 ton pad-foot roller) on the 30 cm lift.

The compaction trials were established in an area approximately 60 m x 40 m wide on a surface of compacted, relatively smooth, waste rock that included both a relatively flat and a sloped surface. Each trial pad was approximately 60 m in length and 10 m in width, which accommodated the compaction equipment to create at least a three-pass-wide compacted surface.

For the reason that a significant potential exists for the permeability of a compacted layer to increase as a result of freeze / thaw cycling, a follow-up test program was implemented in the spring of 2013 to assess the effect of one freeze / thaw cycle on *in situ* density and field permeability of the compacted layers. Following completion of the compaction trial test program in 2012, the trial area was covered with a geotextile fabric and a layer of overlying till approximately 0.5 m thick. The fabric was placed immediately over top of the compacted layers to allow for differentiation between the overlying till and the compacted till layer.

Sampling and Laboratory Analyses

Two large samples (~40 kg) of till were collected from each compaction trial pad. Laboratory analyses included determination of particle size distribution (SS-EN 933-1, 2012), compaction testing (SSEN 13286-2, 2010), Atterberg limits (ASTM, 2010), and determination of specific gravity (ASTM, 2010). Distributions of particle sizes larger than 75 µm were determined by sieving, while the distributions of particle sizes less than 75 µm were determined by a sedimentation process using a hydrometer. Standard Proctor and Modified Proctor compaction tests were conducted on each sample to determine compaction characteristics.

In Situ Testing

A nuclear densometer was used to measure *in situ* density and water content (ASTM D 2922, 2005). During the 2012 compaction trials, 86 nuclear densometer measurements were taken at the surface (from a depth of 0 – 20 cm), while 12 nuclear densometer measurements were taken at depth on the 50 cm trial (20 – 40 cm). Small samples of till were collected throughout the testing program for laboratory determination of gravimetric water content (ASTM D2216, 1992); the primary purpose of this sampling effort was to use gravimetric water content results to correct *in situ* dry density measurements taken with the nuclear densometer. A total of 32 additional nuclear densometer tests were completed during the 2013 testing program (after freeze / thaw). Three techniques were used to measure *in situ* permeability, or field saturated hydraulic conductivity (K_{fs}) of the compacted layers: a Guelph permeameter (described in Mohanty et al., 1994) a pressure infiltrometer (described in Reynolds and Elrick, 1990), and borehole permeameters (ASTM, 2011).

Cover system field trial design and construction

Two cover system trials were constructed in the summer of 2013 over waste rock on WRD6. Based on results obtained during the compaction field trial program, a maximum till lift thickness of 0.3 m was implemented for construction of the compacted till layers, compacted at 1 – 2% wet of optimum water content to increase dry density through the lift profile and minimize hydraulic conductivity. In terms of methodology, a minimum of six passes with a 10 ton smooth-drum roller (using maximum vibratory action) was used. Cover System Field Trial # 1 was constructed using the 'preferred' design alternative: 0.3 m compacted till, overlain by 1.0 m non-compacted till, overlain by 0.3 m till and organic mixture. Cover System Field Trial #2 is the 'conservative' design alternative, consisting of 0.3 m compacted till, overlain by 1.5 m non-compacted till, overlain by 0.3 m till and organic mixture. Both trials are comprised of relatively flat plateau sections approximately 50 m wide by 50 m in length, and sloped areas (~3H:1V). The total footprint of the cover system field trials is approximately 1 ha.

The purpose of the cover system field trials is to track the evolution of the cover systems in response to site-specific processes (physical, chemical, and biological) to enhance understanding of key characteristics and processes that control cover system performance, and to assess and compare performance of the two cover system design alternatives. Cover system performance will be assessed in terms of susceptibility of the compacted till layer to freezing, the degree of saturation through the cover system profile, and net percolation to the underlying waste rock. To evaluate cover system performance, the cover system trials were instrumented with:

- A meteorological station, including:
  - a tipping bucket rain gauge for continuous monitoring of rainfall at the site;
  - a net radiometer to record daily totals of net solar radiation;
  - a sonic ranging sensor for continuous monitoring of snowpack depth; and
  - an air temperature sensor.
- Automated monitoring stations for measuring *in situ* volumetric water content, matric suction (i.e. negative pore-water pressure), temperature, and oxygen concentration in the cover system / upper waste rock profile every six hours.
- Manual gas sampling stations for monitoring the oxygen content within the cover system and upper waste rock materials using a portable gas detector.

RESULTS AND DISCUSSION

Laboratory test results

Results of particle size distribution testing indicate that the till used for the compaction trial program was generally well-graded from 1 to 30 mm and deficient in the range of particles smaller than 1 mm. The samples collected contained a range of 30 - 50% gravel, 33 - 52% sand, 15 - 20% silt, and less than 1% clay (Figure 1). The till material was screened to a maximum particle size of 100 mm. Atterberg Limits testing indicated that the till material is non-plastic.

Both Standard and Modified Proctor tests were employed for determining the compaction characteristics of the till material. The average maximum dry density and corresponding optimum water content as determined by the Standard Proctor test were 2.13 t/m^3 and 6.8%, respectively. The higher compaction energy of the Modified Proctor compaction test resulted in an average maximum dry density of 2.20 t/m^3 and a corresponding optimum water content of 6.2%. Density testing during the field program indicated that the higher compaction energy of the Modified Proctor test is more representative of the level of compaction achieved in the field.

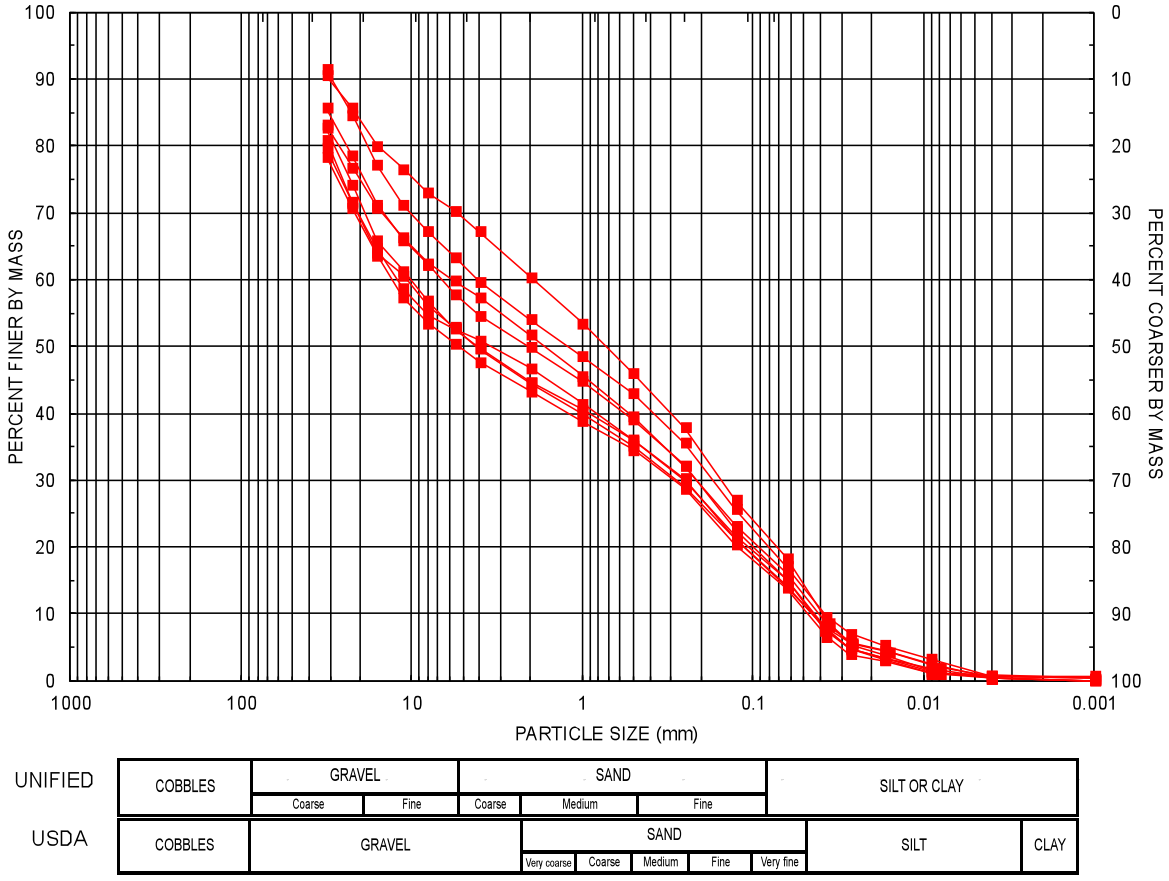

Figure 1 Particle size distributions for till used in compaction trial test program

Evaluation of compaction methodology

Results of compaction testing are summarized in Table 1. Six passes were sufficient to reach a maximum dry density for each test pad. Average dry density and water content values are

presented for each test surface. Unless otherwise noted, nuclear densomer measurements were taken at the surface (0 to 20 cm depth).

Table 1 Average in situ nuclear densometer measurements after various compaction treatments

Lift thickness	Compaction treatment	Plateau ρ_d (t/m³)	W.C. (%)	Slope ρ_d (t/m³)	W.C. (%)
(~50 cm)	6 t smooth-drum roller	2.09 ±0.03	9.1±1.0	2.10±0.05	8.4±1.0
	6 t smooth-drum roller (20 - 40 cm depth)	2.03±0.07	8.6±1.0	2.01±0.07	7.7±1.5
(~30 cm)	6 t smooth-drum roller	2.18±0.07	9.2±1.5	2.13±0.04	9.1±0.7
(~30 cm)	6 t pad-foot roller	2.14±0.05	8.8±0.9	2.18±0.03	7.9±0.7
(~30 cm)	10 t smooth-drum roller	2.23±0.09	8.2±1.3	No data	

Dry density in the 50 cm compacted layer was found to decrease with depth (Figure 2); this is attributed to the dissipation of compaction energy over the thicker lift. Results show that a higher dry density was achieved on a 30 cm lift compared to a 50 cm lift when subjected to the same compaction methodology (six passes with a 6 ton smooth-drum roller). It follows that the bottom 20 – 25 cm of material in the 50 cm compacted layer would not add any value in terms of increased cover system performance, and would therefore be more beneficial as part of the overlying till layer.

Evaluation of alternative compaction equipment on 30 cm lifts showed that compaction with a pad-foot roller was not beneficial in terms of achieving a higher dry density. The highest average dry density was achieved with a 10 ton smooth drum roller on the 30 cm lift (Figure 3).

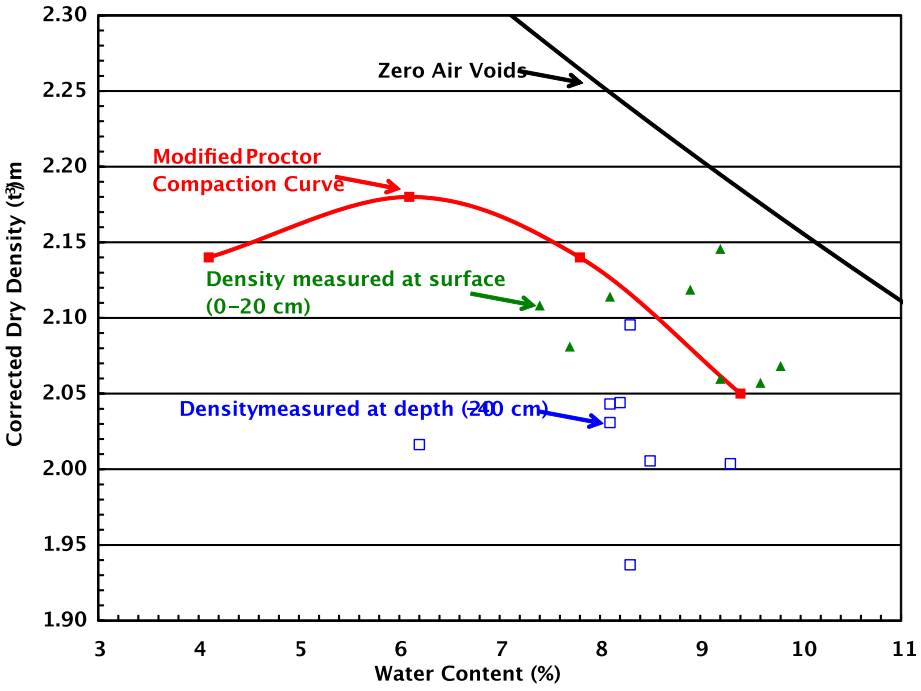

Figure 2 Comparison of in situ density measurements at surface – 20 cm and 20 – 40 cm depth within 50 cm lift

The zero air void line shown in Figure 2 and Figure 3 represent the theoretical line at which the till layer is 100% saturated (i.e. pore space is occupied by water). The zero air voids line is an approximation based on a specific gravity value of 2.74 (based on laboratory results), but it is still useful for illustrating trends. It is apparent from Figure 3 that compaction of a 30 cm lift resulted in reduced porosity (void ratio), and thus would potentially result in a higher degree of saturation and be more beneficial to performance of the cover system.

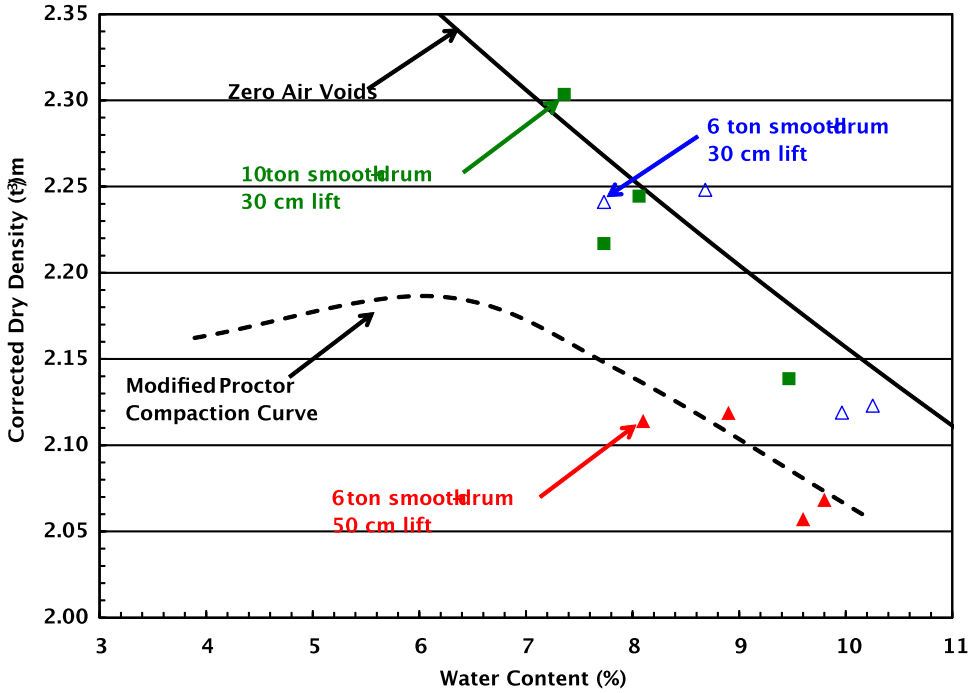

Figure 3 Comparison of dry density measurements on plateau surfaces

K_{fs} measured on the 30 cm thick test pads were in the range of 3 – 5 x 10^{-6} cm/s, while values measured on the 50 cm thick test pad were in the range of 6 – 8 x 10^{-6} cm/s. The lower K_{fs} values measured on the 30 cm test pads compared to the 50 cm test pad were expected because of the higher density measured on the thinner lift. Compaction increases material dry density by decreasing void space within the compacted material. Decreased void space within the compacted till layer increases the tortuosity and, as a result, there are fewer open paths for water (or gas) to move through. For a compacted soil layer, an inverse relationship exists between the capacity to retain and transmit water (i.e. a lower K_{fs} will generally result in higher levels of saturation). Thus, increased compaction achieved on the 30 cm lift leads to increased levels of water retention (degree of saturation) and lower rates of oxygen ingress.

Follow-up testing on compaction field trials to assess effect of one freeze / thaw cycle

A follow up test program in the spring of 2013 evaluated how the compacted layers were affected by a single freeze / thaw cycle. Results of density testing showed that average dry density did not substantially increase or decrease after one freeze / thaw cycle for any of the compaction trial test pads. Results of K_{fs} testing showed that the mean K_{fs} did increase for each test pad, and maximum K_{fs} increased by more than an order of magnitude for each test pad. Figure 4, a histogram (cumulative percentage) of K_{fs} measurements before and after the freeze / thaw, shows that before the freeze / thaw, 100% of measured K_{fs} measurements were lower than 6 x 10^{-6} cm/s, while in 2013, 0% were lower than 6 x 10^{-6} cm/s. The measured increase in K_{fs} is attributed to the effects of freeze / thaw processes on internal structure of the compacted layer.

Svensson and Knutsson (2012) investigated how hydraulic conductivity in till at Aitik changes upon freezing and thawing in a laboratory setting. Results showed little change in hydraulic conductivity after four to eight freeze / thaw cycles for samples that were well compacted prior to freezing, and hydraulic conductivity never exceeded 2×10^{-5} cm/s. When soils are subjected to freeze / thaw cycling, layers of soil are separated by volumetric expansion of ice lenses that form during freezing. In a cohesive soil these fractures may not close fully during thawing; however, in a non-cohesive soil, some degree of self-healing will take place and hydraulic conductivity can be re-established. Therefore, a smaller increase in hydraulic conductivity is expected to result from freeze / thaw cycling in non-cohesive soils compared to cohesive soils (Eigenbrod, 1996; Viklander, 1998). Viklander (1998) found that the hydraulic conductivity of initially dense silty till generally increased by a factor of less than two when subjected to repeated freeze / thaw cycling. Viklander notes, however, that if the till includes stones there is a potential for the soil structure to be affected by movements of the stones during the freeze / thaw cycling.

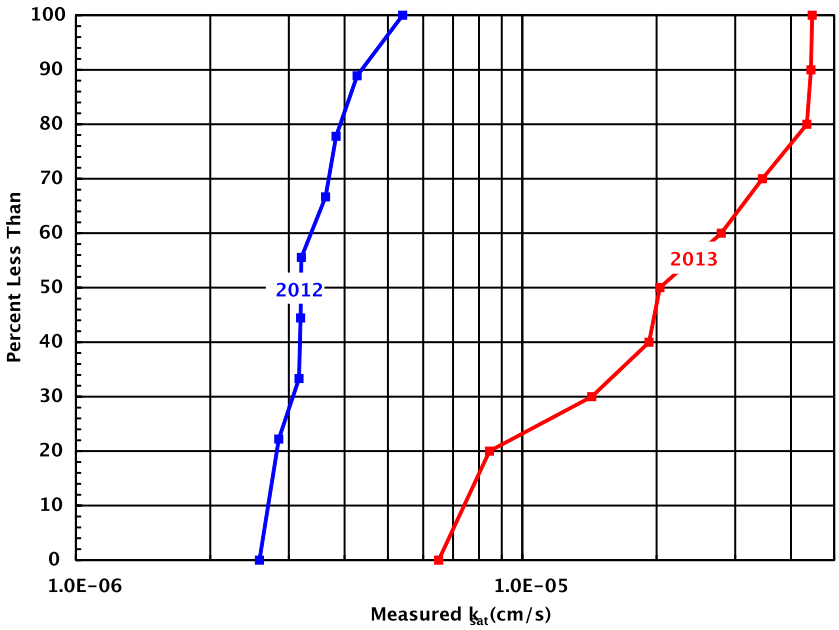

Figure 4 Cumulative histogram of Kfs values measured on compacted till layers in 2012 and 2013

In a compacted layer composed of non-cohesive till (such as that at Aitik) with stone inclusions, there is a potential for a single freeze / thaw cycle to result in an increase in hydraulic conductivity that would not have otherwise occurred in the same soil without stone inclusions (Viklander and Eigenbrod, 2000). Till used for the compaction trial study included stones of varying sizes; results of particle size distribution testing indicate that materials greater than 30 mm comprised, on average, 16% (by mass) of the till material. The presence of stones and the subsquent alteration of structure within the compacted layer caused by freeze / thaw processes was identified as a contributing factor to the measured increase in hydraulic conductivity on the compaction trial pads. Susceptibility of the compacted till layer's hydraulic conductivity to increase as a result of a single freeze / thaw cycle should be highlighted as a potential area of concern for the long-term performance of the cover system.

Depth of freezing front

Findings from the compaction trial study highlight the importance of designing appropriate overlying layers and construction sequencing to complete construction of the cover system before freezing temperatures can alter the structure of the compacted layer. Temperature monitoring of the WRD6 cover system trials using profiles of thermal conductivity sensors show *in situ* temperatures within the cover system and waste rock profile for the first year of monitoring (Figure 5 and Figure 6). Data shows that the freezing front did not reach the compacted layer of either of the cover system trials during this period. While neither compacted layer was affected by frost penetration in this scenario, it is evident that there is an increased buffer zone for Cover System Trial #2 provided by the additional covering layer thickness compared to Cover System Trial #1.

The average air temperature for the winter of 2013-14 (November to April) was -5.4°C, which is significantly ($p > 0.05$) higher than the 5 year site average measured at the WRD5 monitoring station (-6.9°C). It should be noted, however, that penetration of freezing temperatures for a given soil is not dependent solely on air temperature. Additional factors include, vegetative cover, snow cover, and antecedent water content within the cover system profile. The cover system trials were completed in the summer of 2013, providing time for the overlying layers of the cover system to wet up in response to climatic events, and for some vegetation to become established. The compacted layer is likely to be particularly susceptible to freeze / thaw cycling in the first year following construction as vegetation coverage will not be fully established before winter. Snow is an effective insulator, inhibiting the transfer of energy out of the cover system that would be necessary to decrease temperatures within the cover system profile. Lack of vegetative cover during the first winter following installation of monitoring instrumentation, and consequent lack of snowpack would contribute to lower temperatures within the cover system profile. High water contents within the cover system profile may result in a greater amount of energy required to be released for the cover system profile to freeze. If the cover system performs as designed, water content within the profile will remain high, resulting in higher *in situ* temperatures for a longer period of time relative to a cover system with a lower water content. Monitoring of *in situ* water storage dynamics and thermal regimes as well as meteorological parameters at site is necessary to confirm the cover system is performing as designed.

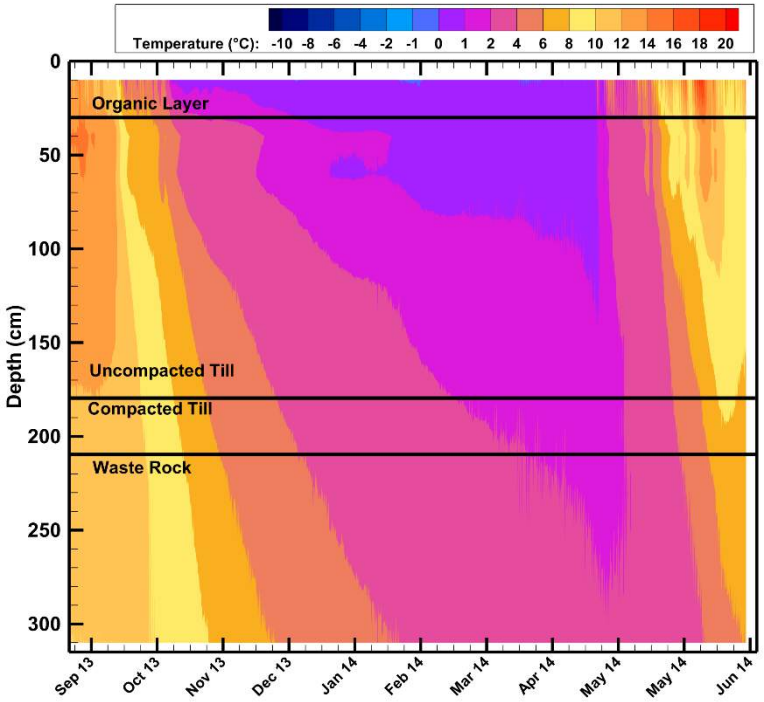

Figure 5 In situ temperature measured within the cover system and waste rock profile of cover system field trial #1.

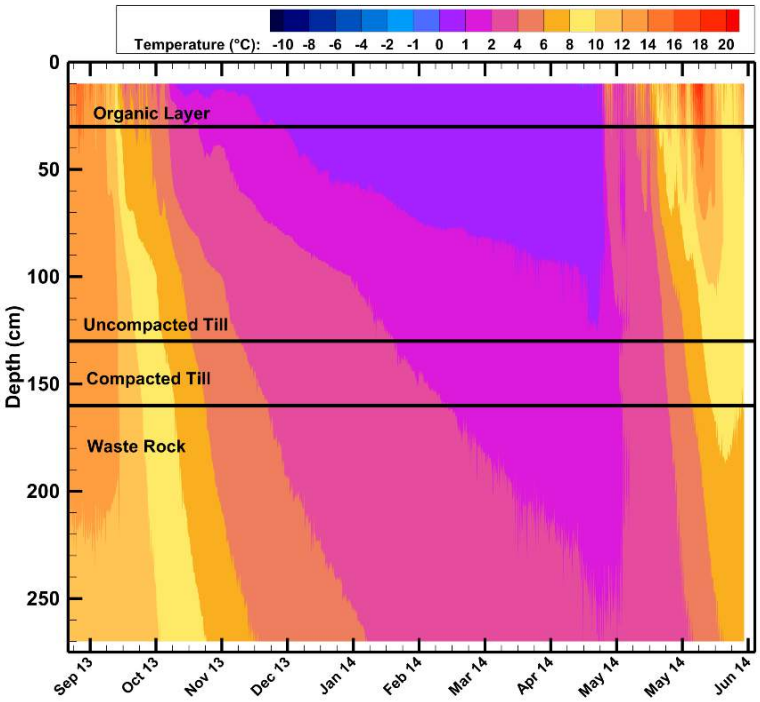

Figure 6 In situ temperature measured within the cover system and waste rock profile of cover system field trial #2.

CONCLUSIONS

Multiple field and laboratory studies have been completed at Aitik to achieve the overall objective of developing a reclamation design for the WRDs that will provide the necessary control on oxygen diffusion rates to waste rock material over the long term. Recent studies found that predicted annual diffusion flux estimates based on calibrated soil-plant-atmosphere modelling were similar in magnitude, but greater than, rates predicted in the 1996 design. It was hypothesized that by improving the methodology of compaction for the compacted till layer within the cover systems at Aitik, increased levels of water retention (degree of saturation) could be achieved, reducing potential oxygen ingress into the underlying waste rock. This hypothesis was tested by completing compaction field trials in 2012. Findings from this study confirmed the hypothesis; results showed that dry density was higher and K_{fs} was lower in a 30 cm layer when compared to a 50 cm layer when subjected to simliar compaction energy.

Two cover system field trials were designed based on results of the compaction trial testing. The cover system trials included various monitoring instrumentation that allow the performance to be evaluated over time under site-specific conditions, providing essential insight into cover system response to climatic variations in terms of temperature and water storage dynamics., thus providing greater confidence in full-scale cover system design.

Results of a field investigation in 2013 showed that increased K_{fs} as a result of freeze / thaw processes should be highlighted as a possible area of concern for the long term performance of the cover system. The potential for the freezing front to penetrate to the compacted layer is dependent on factors such as air temperature, snowpack, antecedent water content, thickness and composition of the overlying layer, and vegetative cover. First year monitoring data from the cover system field trials show that the freezing front did not reach the compacted till layers. Continued monitoring of meteorological and water balance components is necessary to determine an accurate representation of *in situ* cover system performance.

REFERENCES

ASTM (American Society for Testing and Materials) (1992) Standard test method for laboratory determination of water (moisture) content of soil and rock (D2216-92). Annual book of ASTM standards, vol. 04. 08.

ASTM (American Society for Testing and Materials) (2005) Standard test method for in-place density and water content of soil and soil-aggregate by nuclear methods (shallow depth) (D 2938-05). Annual book of ASTM standards vol. 04.09.

ASTM (American Society for Testing and Materials) (2010) Standard test methods for specific gravity of soil solids by water pycnometer (D854-10). Annual book of ASTM standards, vol. 04.08.

ASTM (American Society for Testing and Materials) (2010) Standard test methods for liquid limit, plastic limit, and plasticity index of soils (D4318). Annual book of ASTM standards, vol 04.08.

ASTM (American Society for Testing and Materials) (2011) Standard test method for field measurement of hydraulic conductivity using infiltration from a borehole (D6391-11). Annual book of ASTM standards, vol 04.09.

Eigenbrod, K.D. (1996) Effects of cyclic freezing and thawing on volume changes and permeabilities of soft fine-grained soils. Can. Geotechnical J. 33, pp 529-537.

Mohanty, B.P., Kanwar, R.S., and Everts, C.J., (1994) Comparison of saturated hydraulic conductivity measurement methods for a glacial till soil. Soil science society of America journal vol. 58.

Reynolds, W.D., and Elrick, D.E. (1990) Ponded infiltration from a single ring: I Analysis of steady flow. Soil science of America journal vol. 54.

Swedish Standards Institute (2010) Unbound and hydraulically bound mixtures – part 2: Test methods for laboratory reference density and water content – Proctor compaction. Swedish standard SSEN 13286-2.

Swedish Standards Institute (2012) Tests for geometrical properties of aggregates – part 1: determination of particle size distribution – sieving method. Swedish standard SS-EN 933-1.

Svensson, J., and Knutsson, S. (2012) *Hydraulisk konduktivitet i en morän* – Inveran av frys – och tiningscykler vid olia överlaster och packningsgrader.

Viklander, P., (1998) Permeability and volume changes in till due to cyclic freeze-thaw. Can. geotechnical journal 35. pp 471-477.

Viklander, P., and Eigenbrod, D. (2000) *Stone movements and permeability changes in till caused by freezing and thawing*. Cold Regions Sci. Technol. 31, pp 151162.

A Field-Scale Performance Evaluation of Erosion Control Measures for Slopes of Mine Tailings Dams

Francis Amponsah-Dacosta
Department of Mining & Environmental Geology, University of Venda, South Africa

ABSTRACT

Erosion is a serious problem at mine tailings disposal sites, particularly if the surface is left unprotected. Dust from the tailings dams can be harmful to human, animal, and plant life. Water erosion of the slopes of tailings dams is a considerable and costly maintenance and pollution problem. At present, erosion prevention and control in the short term is very often a process of trial and error and very little information exists on performance of erosion protection measures for long periods. The purpose of this study was to conduct a field-scale investigation into effectiveness of different erosion control measures. This involved creating erosion control panels on a typical slope of tailings dam with surface treatments ranging from simple vegetative techniques to fairly civil engineering erosion protection covers using fragments of rock. A series of measurement of erosion rates were made using measurement of sediment trapped in catchment paddocks and measurement by means of steel pegs to provide a quantitative basis for identifying effective and more economical erosion protection measures. Results of the erosion measurement have shown that erosion from the unprotected slope for the period of the experiment ranged from 257 to 316 tons/ha/year. These losses are alarmingly high and the surface loses its aesthetic appeal with time. On the other hand, any forms of vegetative and physical stabilization of the slopes can significantly reduce erosion of tailings and minimize environment problems at the tailings storage facility. The results of the field experiment have demonstrated that a protective treatment for slope surface takes a number of years to show its value. It has been shown that non-vegetative treatments such as fragments of rock are very effective in resisting erosive forces of nature, providing long-term stability and keeping maintenance to minimum.

Key words: Mine waste, tailings dams, erosion protection, rock fragments, vegetative techniques

INTRODUCTION

Mining and mineral processing result in generation of large quantities of waste such as overburden, waste rock, and tailings. These large volumes of mine waste are expensive to manage, and are frequently cited as an obstacle in the environmental sustainability of mining. Tailings are finely ground rock and mineral waste products of mineral processing operations. The tailings are usually mixed with water to form slurry which is then transported hydraulically into tailings ponds or dams.

Mine tailings are potentially subject to wind and water erosion, acid generation and the release of heavy metals. Dust generated from tailings dams on windy days can be a major problem especially where such dams are located near population centres (Fahey & Newson, 1997). Besides the visual impact of such dust clouds, there are also many potential public health and environmental problems associated with dust. Erosion of the slopes of tailings dams by rainwater runoff is a considerable and costly maintenance and pollution problem (Blight & Steffan, 1979). Cumulative and subsequent erosion down the slope of waste deposits results in gullies that can damage embankment and subsequently lead to instability of part of a slope (Bromhead, 1986). Gullies are also difficult to control and arrest and are not aesthetically pleasant, especially for unprotected slopes. The cost of repairing damages caused by erosion processes can be very high and of great concern to the mining industry.

A major environmental issue facing the mining industry is the rehabilitation options for tailings dams. Successful rehabilitation of mine waste deposits is a major problem, particularly in arid and semi-arid climates, and cannot be attained without substantial outlays of effort, money and innovative techniques (Stiller, Zimpfer & Bishop, 1980). Experience has shown that, of all the rehabilitation purposes, stabilising the impoundment against long-term wind and water erosion is often the most technically problematic and difficult to achieve (Vick, 1983). The need to prevent pollution, improve safety and the appearance of the environment has led to the use of various control and stabilisation techniques.

In South Africa, establishment of grass cover is by far the most common and usually the preferred stabilisation option for tailings impoundments. Vegetation not only serves to reduce wind and water erosion, it also stabilises slopes and results in improvement in the aesthetics of a tailings area. However, mine tailings are generally inhospitable medium for growth and are difficult to vegetate due to their characteristics such as the presence of acid and metals, deficiency in nutrients, lack of agglomerating material and extremes of moisture content (Gorber *et al*., 1978). In arid climates and for tailings having high concentrations of heavy metals or salts, establishment of vegetation may be a lengthy, difficult, and costly process.

It should be possible to identify potential rehabilitation options for a particular site well before the actual rehabilitation programme is implemented based on experience of long-term monitoring of alternatives and comparing their performance. This approach to rehabilitation assessment will provide more assurance that the rehabilitation programme will be successful. In this regard, a large-scale field experiment was designed and constructed to monitor the performance of various slope protection options.

RESEARCH METHODS

Experimental design

The experimental site was a south-facing slope with a slope angle of 16^{o} over the lower two-thirds of the slope length of 20 m and 28 ^{o} over the upper one-third. The slope was divided into 11 panels each measuring 20 m long (upslope) by 10 m wide. Each panel was separated from its neighbour by means of a 0.5 m metal sheet partly dug into the tailings surface to form a low vertical wall. The toe of each panel terminates in a catchment paddock to capture and hold solids removed from the slope by water erosion. Figure 1 shows a plan of part of the experiment.

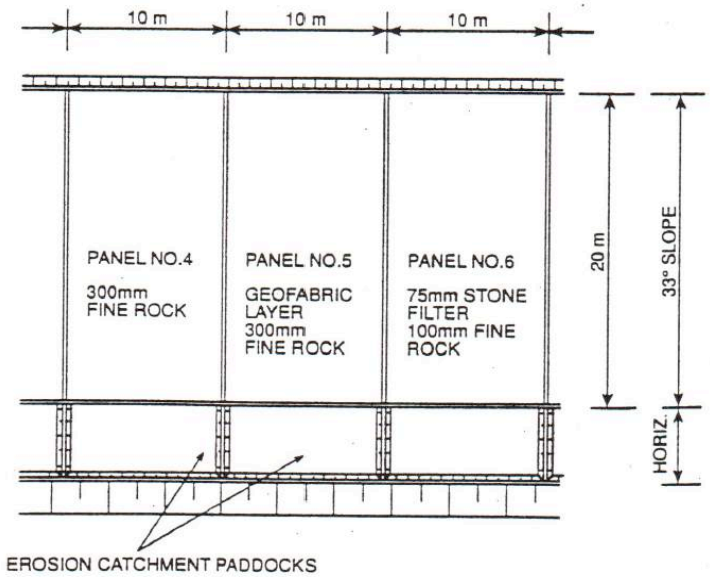

Figure 1 Part layout of erosion protection experiment

Design considerations of slope protection methods

The major design objectives were to utilise simple and low-cost control measures that prevent wind and water erosion, provide long-term stability, and require minimal maintenance to assure performance. A number of options identified for this experiment were rock armouring, revegetation and a combination of these two to take advantage of the benefits of each approach. These erosion protection methods range from very simple changes in vegetative methods to fairly civil engineering works. For any alternative surface treatment to be accepted, it will have to be demonstrated to have long-term durability.

Vegetation is by far the most common and usually the preferred stabilisation option for tailings impoundments. Vegetative stabilisation involves establishment of vegetation on top of a deposit, either by planting directly into the tailings material or by first covering the surface with a layer of top soil of suitable thickness. According to Blight (1989), where continuously maintained, fertilised and watered as needed, a good growth can establish. Physical stabilization involves covering the top and slopes of embankment of tailings dams with suitable thickness of soil, sand or broken waste rock or other restraining material to prevent and control erosion. The use of soil often has a dual advantage in that effective cover is obtained and a habitat is provided for local vegetation to encroach. Crushed rock for stabilisation purposes may be readily available at many mine sites in the form of mine waste or stripped overburden.

Cost estimation of erosion control options

The cost of erosion protection methods was determined only in terms of initial capital outlay without any maintenance cost component. This was to enable the most resilient surface treatment over the long-term without any maintenance to be determined. The cost components considered were: raw materials, direct labour and earthwork activities such as levelling and compacting. Raw materials (such as grass seed, rocks, soil fertiliser, and geofabric) are those materials that actually become part of the product which is the control measure. The cost of labour is the straight wages paid to the employees during construction of the control measure. Some of the surface treatments required levelling and compacting whilst others needed levelling only.

Erosion assessment of slope protection methods

Two methods were used for determination of erosion rates from the erosion protection panels. These were measurement of sediment trapped in catchment paddocks and measurement by means of steel pegs. Each panel was originally equipped with a sprinkler irrigation system to simulate rain, 3 rain gauges and a set of 10 surface pegs. Simulated rain was used to obtain initial results and for the next five years the slopes were exposed to natural weather. It should be noted that the erosion rates were measured differently for phases I to 2 and 3 to 5 of the experiment.

Phase 1 involved a five-week period of simulated rain during the dry winter season of the first year of the experiment. The sprinkling periods were carefully controlled by observation of the rain gauges, thereby ensuring an equal distribution of simulated rain on each of the panels. At the end of the five-week period, all eroded material captured in the catchment paddocks was extracted and weighed. Phase 2 comprised of measurements taken for two wet seasons. At the end of each wet season all eroded material accumulated in the catchment paddocks was measured by determining the in situ volume and unit weight of the captured material.

During phase 3 (cumulative erosion for 4 wet seasons), an unusually heavy rainstorm caused tailings to be washed onto the test slopes from above, thus rendering the origin of the mass of caught material questionable (Blight & Amponsah-Dacosta, 1999a). For this reason, erosion for phases 3 to 5 was assessed by measuring the retreat of the slope surface against the surface level pins. According to Toy (1983), this erosion pin technique is the most extensively used erosion measurement technique. It is also a more reliable method of measurement of soil losses from constructed slopes and gives an indication of the distribution of the soil loss from the slope. From the average measured surface retreat on the selected slopes and measured dry density of the material of the slope surface, the annual rate of erosion in tons/ha was determined. It should be noted that phase 4 and phase 5 represent cumulative erosion for 6 wet seasons and 8 wet seasons respectively.

Cost-effective evaluation of erosion control alternatives

The erosion control measures were assessed in terms of cost and likely effectiveness. This assessment is based on combination of considerations, including reported experience gained and relevant work undertaken by the contractors.

RESULTS AND DISCUSSION

Table 1 records the type of surface protection and its relative cost, actual erosion rates in tons/ha/year, relative erosion rates and a cost effectiveness number represented by the product of relative cost (C) and relative erosion rate (E). The most cost-effective treatment would be the one with the least value of the cost-effective number.

Table 1 Cost-effectiveness evaluation of slope protection methods

Panel Number	Treatment	Level & compact	Level only	Relative Cost/ha C %	Erosion Rate (tons/ha/year)			
					Phase 2	Phase 3	Phase 4	Phase 5
1	Conventional grassing	√	—	100	164	164	164	192
2	100 mm ballast (50 mm size)	√	—	67	105	32	35	23
3	300 mm coarse rock	√	—	62	170	12	23	23
4	300 mm fine rock	√	—	62	38	96	70	63
5	Geofabric + 300 mm fine rock	√	—	120	22	15	70	65
6	75 mm of 6mm stone + 100 mm fine rock	√	—	66	42	82	61	69
7	300 mm fine rock	—	√	54	118	75	67	53
8	250 mm open pit overburden	—	√	64	203	161	175	175
9	250 mm soil + Ag Lime +grass sods	—	√	120	19	72	78	74
10	100 mm soil + Ag Lime +grass sods	—	√	96	21	15	36	10
11	Zero control (no treatment)	—	—	0	276	257	316	261

Table 2 Cost-effectiveness evaluation of slope protection methods (continued)

Panel No.	Relative Erosion Rate E (%)				Cost-Effectiveness C X E (%)				Cost-Effectiveness Ranking			
	Phase 2	Phase 3	Phase 4	Phase 5	Phase 2	Phase 3	Phase 4	Phase 5	Phase 2	Phase 3	Phase 4	Phase 5
1	59	64	52	72	59	64	52	72	10	10	10	10
2	38	12	11	9	25	8	7	6	7	4	2	2
3	62	5	7	9	38	3	5	6	8	1	1	2
4	14	37	22	24	9	23	14	15	3	7	6	5
5	8	6	22	25	10	7	27	30	4	3	7	7
6	15	32	19	26	10	21	13	17	4	6	5	6
7	43	29	21	20	23	16	11	11	6	5	3	4
8	74	63	55	67	47	40	35	43	9	9	9	9
9	7	28	25	28	8	34	30	34	2	8	8	8
10	8	6	11	4	7	6	11	4	1	2	3	1
11	100	100	100	100	0	0	0	0	11	11	11	11

Rates of erosion from unprotected slopes of tailings dams can be frighteningly large. Erosion from the unprotected slope for the period of the experiment ranged from 257 to 316 tons/ha/year. According to COMSA (1996), losses of tailings from unprotected gold tailings dams in South Africa of over 500 tons/ha/year are quite common. Blight & Amponsah-Dacosta (1999b) have also recorded erosion exceeding 1000 tons/ha/year on some unprotected slopes of tailings dams in South Africa. Results of the erosion measurement also shows that protecting the slope, by armouring it with crushed rock or covering it with vegetation, increases the surface shear strength and this helps to reduce erosion considerably by dissipating the energy of the erosive forces of wind and water.

On the basis of cost-effectiveness for phase 2, conventional grassing ranks just above no treatment at all and a soil layer covered with grass sods (Panel 10) rated top. However, the grass sods have visibly deteriorated with time and most of the grass has now died. Only the presence of the grass roots has maintained the effectiveness of the treatment. Although establishment of grass cover is the most common means of stabilising tailings disposal sites in South Africa, there are several situations where vegetation is relatively or completely ineffective in protecting a slope from erosion. An important factor, which must be considered in any vegetation programme, is the related equipment necessary to neutralise, fertilise and seed the tailings. According to Gober et al. (1978), the finer fractions of the tailings when wet, is not capable for supporting the heavy equipment normally used for these purposes, and special techniques are required to vegetate these areas. Blight (1989) has also pointed out that grassing does reduce wind erosion but has much less effect on water erosion.

On panel 9, which has a thicker soil layer, and was expected to perform better than Panel 10, the grass has died and the panel rating has dropped from 2 to 8. The conditions of the surface of the various panels after six years are shown in Figures 2 to 4.

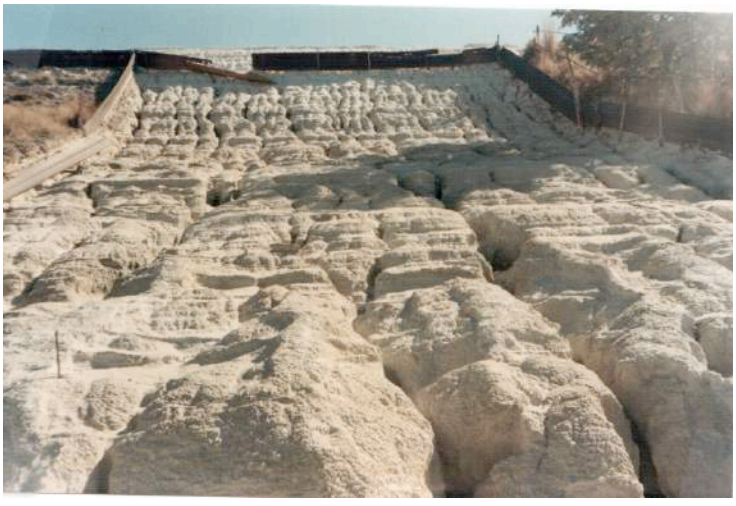

Figure 2 Devastating effect of erosion on unprotected slope (Panel 11)

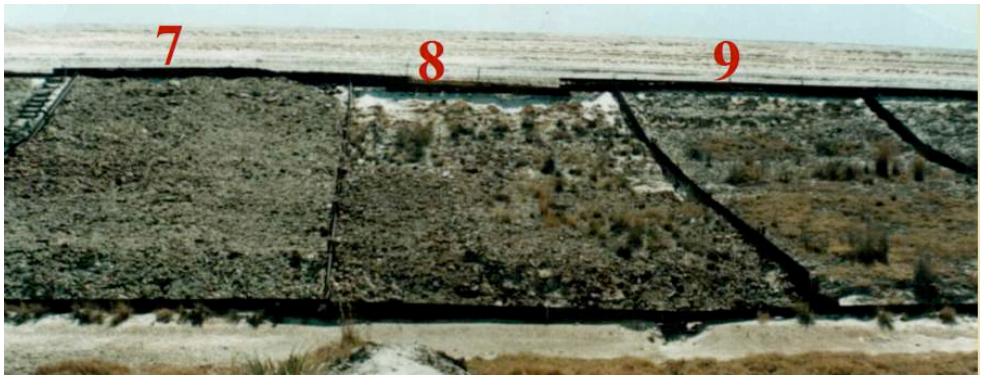

Figure 3 Slope protection panels 7 – 8

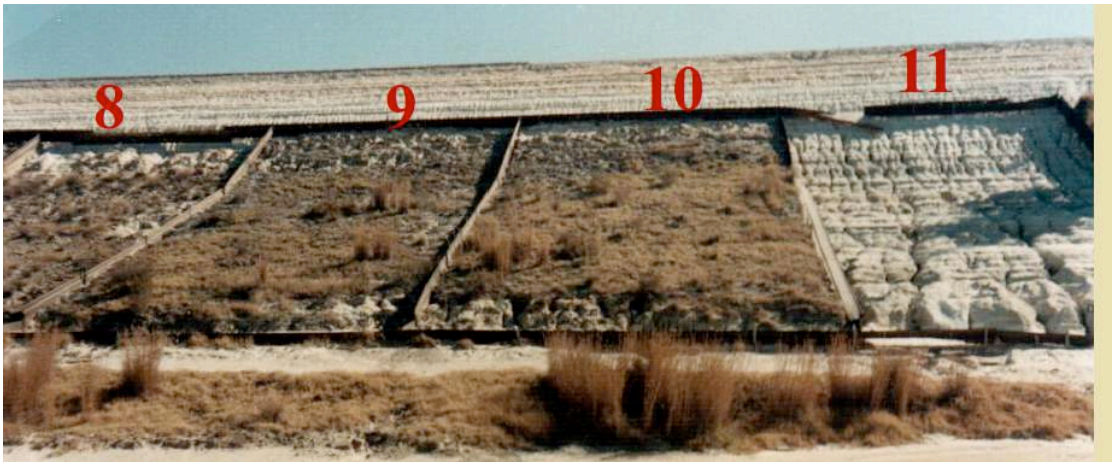

Figure 4 Slope protection panels 8 – 11

It is observed that unprotected panel shown in Figure 2 is highly eroded compared to the other panels which have some form of surface cover. Thus, physical roughness in the form of vegetation and crushed rock play an extremely important role in controlling erosion. Bare slopes of tailings dams experience accelerated erosion whilst any measure that provides cover significantly retards tailings loss and minimise erosion. These qualitative results reinforces the results of the quantitative erosion assessment by repeated measurements of surface elevation using pins driven into the slope surface as reference points and by sediment collection from paddocks that surface cover plays an extremely important role in controlling erosion from slopes of tailings dams.

Table 1 shows that non-vegetative treatments occupy 6 of the first 9 places in the ranking, and should therefore be seriously considered for use in future. The presence of riprap, coarse fragments of rock, on the tailings surface act as mulch. The size and mass of the riprap material absorbs the impact energy of rain drops, while the gaps between the riprap traps and slows the flow of water, lessening its ability to erode the tailings. Rock mulches significantly reduce erosion potential when a large percentage of the tailings surface is covered but this can be an expensive undertaking. The effectiveness of riprap to stabilise soil against erosion is evidenced in nature by the development of a desert pavement, a surface layer of pebbles that forms an effective erosion-resistant surface for long periods of time (Vick, 1983).

This experiment has demonstrated that a protective treatment for a slope surface takes a number of years to show its true value. According to Waugh & Richardson (1995), when earthen materials are

placed in an environment that is not harmonious with the surrounding system, rapid changes in characteristics of the placed material occurs as nature begins to bring the entire system into equilibrium. This point is further illustrated by Figure 5 which shows how the performance of six of the panels has changed with time, with the performance of some remaining relatively static, some improving and others deteriorating with time. It should be noted that season 1 represents application of irrigation and 100% corresponds to erosion of unprotected panel.

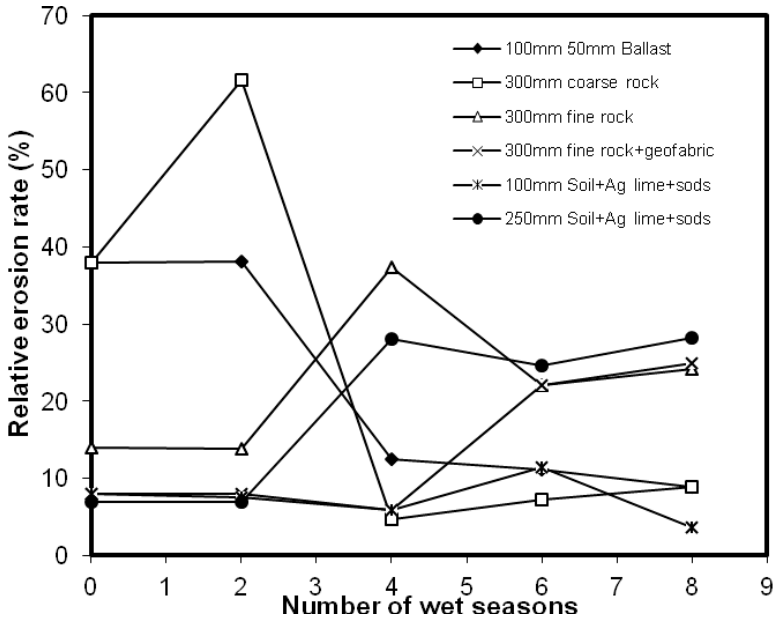

Figure 5 Variation of erosion rate with time (in wet seasons)

The successful long-term stabilization of mine tailings dams is a difficult and complicated process. Erosion prevention and control measures selected must be based on a thorough understanding of the characteristics of the tailings, site-specific properties, how they will react to various treatments, and how the erosion protection covers will change with time. The fundamental principle currently used associates erosion control of tailings dams with revegetation. However, erosion control of tailings dams by means of grassing or revegetation alone has indeed proved challenging to the mining industry. The actual amount of vegetation cover required for adequate erosion protection depends on several factors, including the amount and intensity of rainfall, length and angle of the slope to be stabilized, and erodibility of the tailings material.

This field experiment has shown that rock fragments over slopes of tailings dams are very effective in resisting erosive forces of wind and water. Tailings covers designed with crushed rock, gravel/cobble mixtures, or riprap have several advantages over vegetative covers. Large particle sizes are more resistive to movement by water and wind and have higher shear strengths compared with the smaller soil particles required for revegetation. However, the rock to be used for erosion protection should be geochemically analysed to ensure that it does not cause environmental pollution and evaluated to determine its suitability for providing the necessary long-term erosion protection.

CONCLUSION

Tailings and other mine residues are potentially subject to wind and water erosion. Unprotected surfaces of tailings dams offer little or no resistance to erosive forces and therefore experience accelerated erosion with time. Slope surfaces without cover are aesthetically unpleasant. From

mechanics of the detachment and transport of tailings by rainsplash, runoff and wind, it follows that the best way to minimise the potential adverse effect of tailings erosion on the surrounding environment and hasten the restoration of the area is to cover the surfaces of the tailings dams to protect it from raindrop impact and increase surface roughness to reduce the velocity of the runoff and the near-surface velocity wind.

The need to prevent pollution, improve safety and the appearance of the environment has led to the use of various control and stabilisation techniques. Observation of the various erosion protection panels indicates that nature is attempting to alter some panels in the short time they have been in existence. Some of the panels intended to protect tailings for long time periods experienced severe deterioration over only six years of the cover performance monitoring. Nevertheless, the experiment has enabled continual performance data to be compiled.

It is evident from the results that cost-effective slope protection can be achieved using non-vegetative methods. The rock fragments have potential field applications to mitigate erosion on tailings dams for longer-term period. However, guidelines need to be developed for system design and potential applications, taking into consideration the size of the fragments, the thickness of the cover and the durability of the material. Research to determine the optimum percentage of materials such as boulders, cobbles, gravels, and coarse sands for erosion resistance for a given slope gradient and length also need to be conducted.

REFERENCES

Blight, G. E. (1989) Erosion losses from the surfaces of gold tailings dams, Journal of South African Inst. Mining and Metallurgy, 89 (1), 23 - 29.

Blight, G. E. and Amponsah-Dacosta, F. (1999a) In search of the 1000 year tailings dam slope, Civil Engineering, Oct. 1999.

Blight, G. E. and Amponsah-Dacosta, F. (1999b) Improving the erosional stability of tailings dam slopes, Tailings and Mine Waste '99, 6th International Conference on Tailings and Mine Waste, Balkema, Fort Collins, Co. USA, 197 – 206.

Blight, G. E. and Steffen, K. H. (1979) Geotechnics of gold mining waste disposal, in Current Practice in Mine Waste Disposal, Committee on Embankment Dams and Slope of the Geotechnical Engineering Division, ASCE, New York, pp. 1- 52.

Bromhead, E. N. (1986) The Stability of Slopes, Blackie & Sons/Surrey University Press, London.

COMSA (1996) The Design, Operation and Closure of Metalliferous and Coal Residue Deposits, Handbook of Guidelines for Environmental Protection, Vol.1., Chamber of Mines of South Africa.

Fahey, M. and Newson, T. A. (1997) Aspects of the geotechnics of mining wastes and tailings dams, in Proceedings of the 1st Australia-New Zealand Conference on Environmental Geotechnics – GeoEnvironment 97, Bouazza, A., Kodikara, J. and Parker, R. (eds.), Melbourne/Victoria, Australia, 26 – 28 November, pp. 115 - 134.

Gorber, D. M., Ibbotson, B. G. and Knapp, R. A. (1978) Trends in uranium mining waste management, in Proceedings of the International Symposium on Waste Treatment and Utilisation, University of Waterloo, Waterloo, Ontario, Canada, July 5 – 7.

Stiller, D. M., Zimpfer, G. L. and Bishop, M. (1980) Application of geomorphic principles to surface mine reclamation in the semiarid West, Journal of Soil and Water Conservation, Nov./Dec., pp. 274 - 277.

Toy, T. J. (1983) A linear erosion/elevation measuring instrument (LEMI), Earth Surface Processes and Landforms, 8, 313 – 322.

Vick, S. G. (1983) Planning, Design, and Analysis of Tailings Dams, John Wiley & Sons Inc., New York, USA.

Waugh, W. J., and Richardson, G. N. (1995) Ecology, design, and long-term performance of waste-site covers: Applications at a uranium mill tailings site, in Proceedings of National Academy of Sciences Workshop on Barriers for Long-Term isolation, 13 Aug. 1995, Denver, Colorado.

Improving Till by Adding Green Liquor Dregs in Sealing Layers to Control AMD – A Pilot Study

Maria Mäkitalo[1], Josef Mácsik[2], Christian Maurice[1,3] and Björn Öhlander[1]

1. *Department of Civil, Environmental and Natural Resources Engineering, Luleå University of Technology, Sweden*
2. *EcoloopAB, Sweden*
3. *Ramböll Sverige AB, Sweden*

ABSTRACT

A common solution to minimize the formation of acid mine drainage (AMD) in sulphide-bearing mine waste is to use a conventional cover. The cover is usually constructed by using natural soils, in the boreal zone often till. Shortage of fine-grained till close to mines suitable as sealant material is often an issue. In the last years, considerable research has been carried out to use residual products from other industries in the control of AMD. Green liquor dregs (GLD), an alkaline and inorganic residual product generated by the sulphate pulp and paper mills, has shown desirable properties such as low hydraulic conductivity, high water retention capacity as well as long term sustainability, to be a candidate for constructing sealing layers in cover system designs. However, the geotechnical strength of the material is insufficient for engineering applications. If this issue can be overcome, developing a cover system with GLD would be possible. The challenge remains of finding a solution that is viable in regards to logistics and transport economics. To reduce transportation costs but take advantage of the physical properties of the residual product, GLD was blended with two types of till in a pilot scale study with the aim to optimize the use of GLD in a sealing layer application. 5-15% (wet weight) GLD was found sufficient to take full advantage of the physical properties of the residual product and to minimize transportation costs. Different mixing techniques were also evaluated. The results show that the quality of the till in regards to hydraulic conductivity and water holding capacity could be improved with the addition of only 5% GLD. A short and efficient mixing was preferred since mixing the material too vigorously released the bounded water resulting in increased water content and a reduction of the compaction efficiency. It results in a material that is difficult to apply and use in sealing layer constructions. Transportation, mixing and application costs are comparable or lower than of fine-grained till.

Keywords: Acid mine drainage, Sealing layer, Dry cover, Green liquor dregs

INTRODUCTION

Mining generates mainly two types of residues: waste rock and tailings. Waste rock is the material that lacks economic amounts of mineral and is removed to access the ore, while tailings are finely ground material that has been processed in the mill. Mine waste from sulfide ores has the potential for a significant environmental impact because it often contains iron sulfides such as pyrite and pyrrhotite. Acidification caused by oxidation of these minerals occurs when they are exposed to atmospheric oxygen (Höglund et al. 2004). If no alkaline material is present to consume this acidity, water entering the waste transports the oxidation products. This leachate is called acid rock drainage (ARD) and often contains high levels of heavy metals. ARD is one of the most significant challenges when dealing with sulfidic, pyrite rich mine waste. One common technique to mitigate the formation of ARD is to apply a barrier made of soil (in Sweden often till) on top of the mine waste that has a high degree of water saturation to limit oxygen diffusion and a low hydraulic conductivity to reduce water percolation. A protective layer is placed on top of the barrier to protect its integrity. Using till in barriers, or so-called sealing layers, is often associated with large costs due to the long distances that the material has to be transported, as finding till of suitable quality that can function in sealing layers and is located close to the mine is seldom possible. If the costs can be kept low, modifying the till available at the mining area may, therefore, be an alternative. To achieve a till that complies with the qualifications of a sealing layer (a highly saturated layer with a low hydraulic conductivity $<10^{-8}$m/s) to reduce oxygen ingress. One way to reduce the heterogeneity and increase the sealing properties of the till is to adjust the particle size distribution and change the porosity. It can be done by removing bigger rocks and adding a fine-grained material of suitable quality.

One potential candidate is the non-hazardous industrial residual waste Green liquor dregs (GLD) that has been characterized previously (Mäkitalo et al. 2014). GLD is the largest waste fraction retrieved in the chemical recovery cycle at sulfate pulp and paper mills and the production in Sweden is ~240 000 t per year. The material has small particle size (clay-silt fraction) and high porosity (>75%). In addition, it showed favorable qualities such as low hydraulic conductivity and high water retention capacity for use in sealing layers to reduce oxygen ingress in the prevention of AMD (Mäkitalo et al. 2014). However, GLD has low shear strength (Mäkitalo et al. 2014) making it difficult to use in engineering applications. It would also be expensive to transport GLD due to the large quantities needed per m^2 and its high water content. However, adding GLD to modify and improve the till to a grade where it can be used as a sealing layer could be an economically viable solution.

Mixing large volumes of **material** poses the risk of inadequate **mixing, therefore,** the mixing of selected proportions of till/GLD was conducted under both laboratory and field conditions. In the field, two different techniques, a loader with a crushing bucket and a mobile asphalt plant, were used in the frame of a pilot scale experiment. The aim was to find a mix that had decreased hydraulic conductivity and increased water retention capacity compared to till to decrease the oxygen influx through the material. The ability to be compacted under field conditions was also an important criterion.

METHODOLOGY

Material

GLD was obtained from the Smurfit Kappa sulphate pulp and paper mill in northern Sweden. Till was excavated at the Ragn-Sells waste management site at Brännkläppen, Sweden, referred to as Till A herein. The till was screened for a particle size of <20mm and had a content of 30% of particles <0,063mm. Another till, from BDX Material, Sweden, with the same maximum particle size, but with the content of <10% of particles <0,063mm was obtained and used to compare the tills. The till is referred to as Till B.

Method

Compaction properties such as maximum dry density, porosity and the optimum water content of till/GLD mixes blended in the laboratory with the proportions 90/10, 80/20, 70/30 and 50/50 were carried out by an accredited laboratory (MRM, Luleå, Sweden) with a standard procedure (EN 13286-2, 2010). Eight mixes of Till A or Till B blended with 5-15% GLD using either a Loader with a crushing bucket (Allu Group Inc.) (Figure 1) or a Mobile Asphalt Plant (Figure 2) were prepared. Total volumes of 10-60 tons were mixed to evaluate the ability to obtain a homogenous product and the production efficiency. The composition of the different mixes and the total amount mixed are shown in Table 1. The production speed of the machineries was recorded to get an estimation of the production costs. Compaction properties of till/GLD blended in the field, and 95/5, 90/10 and 85/15 blends carried out in the lab was determined using standard proctor compaction test. The compaction energy was 2.65 J*cm-3 according to the Swedish Standard SS 027109 (SIS, 1994) and was obtained by filling the column with three layers of material, compacting each layer with 25 blows with a Proctor hand hammer.

Figure 1 Loader with a crushing bucket

Figure 2 Mobile Asphalt Plant

A hydraulic conductivity test was carried out according to the Swedish standard (SIS, 1989) using Darcy's equation. Water was pressed through the column from below and collected in sampling bottles using constant water head. The amount of the permeated water was monitored by weighing. The density was calculated by weighing and water content could be calculated after the material was dried at 105°C for 24h. Water retention capacity (WRC) was measured on sample 4:3 (n=3) and on sample 1 (n=1). The samples were compacted in cylinders and saturated from below. The cylinders were then placed on a ceramic plate, and pressure was applied using a pressure plate apparatus (Soilmoisture Corp., Goleta, CA, USA).

RESULTS AND DISCUSSION

To identify the required amount of GLD that may improve the properties of till without losing the compaction properties, proctor experiments were carried out. A maximum of 20% GLD could be mixed with till. At higher additions of GLD, the plastic behavior prevented compaction by proctor. GLD has a water content of 120 - 150 % (by weight %). Its liquid limit, w_L, is ~132 %. It means that GLD at higher water content than 132 % will transform from a plastic to a liquid consistency. Based on this, 5-15% GLD was mixed with till for further analysis. The composition of the mixes is summarized in Table 1. The productions speed of the asphalt plant was 90 tonnes/h using a mixing time of 45s. The speed could be increased. The loader's capacity was 180 tonnes/h (mixed one time).

Table 1 The composition of the blends, mixing equipment, mixing time and the total amount generated are shown as well as the hydraulic conductivity (k), density (ρ) and water content. The results are given as mean ± SE (n=3).

Mix nr	Composition, mixing equipment, time	Total amount (tonne)	k (10^{-9} m/s)	ϱ (g/cm^3)	Water content (%)
1	10% GLD/Till A, asphalt plant, 45s	60	10.4 ± 9.4	2.0 ± 0.0	N/A
2	15% GLD/Till A, asphalt plant, 45s	30	12.5 ± 4.9	1.9 ± 0.0	21.4
3	10% GLD/Till A, asphalt plant ,2x45s	10	9.8 ± 3.2	2.0 ± 0.0	18.4
4 1	10% GLD/Till A, Loader, 1 run	30	61.4 ± 51.6	2.0 ± 0.0	19.1
4:2	10% GLD/Till A, Loader, 2 runs	30	4.9 ± 3.9	2.1 ± 0.0	N/A
4:3	10% GLD/Till A, Loader, 3 runs	30	4.8 ± 3.5	2.1 ± 0.0	N/A
4:4	10% GLD/Till A, Loader, 4 runs	30	32.7 ± 13.1	2.0 ± 0.0	19.1
4:5	10% GLD/Till A, Loader, 5 runs	30	55.7 ± 29.5	2.1 ± 0.1	16.1
5	5% GLD/Till A, asphalt plant ,45s	30	30.9 ± 31.7	2.1 ± 0.0	13.1
6	5% GLD/Till A, asphalt plant, 2x45s	30	13.7± 3.2	2.0 ± 0.0	16.4
7	10% GLD/Till B, asphalt plant, 45s	30	21.2± 26.7	2.1 ± 0.0	13.6
8	10% GLD/Till B, asphalt plant, 2x45s	30	8.17± 3.6	2.1 ± 0.1	13.8

A large difference in porosity and density of GLD and till was observed. GLD had substantially higher porosity, 83±3% vs. till 36±1%. The density of GLD and till was 1.21±0.05 g/cm^3 and 1.80±0.04 g/cm^3 respectively. The density for all blends was 1.9-2.1 g/cm^3. The average hydraulic conductivity of the blends was $3x10^{-8}$ m/s. It is a substantial decrease compared to till without additives that generated a hydraulic conductivity of $3.9x10^{-7}$ m/s (Table 1). The results indicate that longer mixing time may decrease the hydraulic conductivity. Only for Mix 4:4 and 4:5, the opposite applies. It is hypothesized that the multiple mixing times resulted in the inclusion of coarser till material from the ground in the blends due to the mixing technique (loader) causing the increased hydraulic conductivity. A decreased particle size of a material is usually correlated to a decreased hydraulic conductivity (Sivapullaiah et al. 2000; Benson & Trast 1995). Mixing 10% GLD with till having a silt content of 30% is sufficient to achieve a hydraulic conductivity of 10^{-8} -10^{-9} m/s (Table 1).

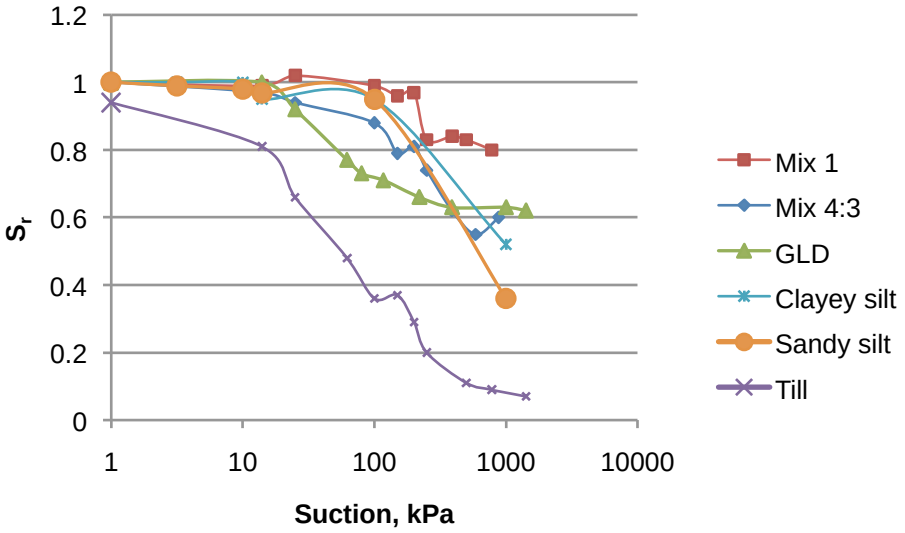

Figure 3 Water retention curves of Mix 1, Mix 4:3, GLD, clayey silt, sandy silt and till.

The water retention capacity for both the tested mixes was high (Fig. 3). Mix 1 and Mix 4:3 were of the same composition (10% GLD) but were blended with different techniques (asphalt plant respectively crushing bucket). Mix 1 blended with the asphalt plant had higher water content (*w)* and lower dry density compared to Mix 4:3, blended with the crushing bucket. It also had higher porosity. One hypothesis is that Mix 1 has undergone more intensive mixing resulting in different physical/geotechnical properties compared to the less disturbed Mix 4:3. The results indicate that intensive mixing of GLD releases bounded water. It increases the porosity and the *w* whilst the dry density decreases. A greater WRC can then be achieved. It has previously been shown that water content at field capacity (-10 or -33 kPa) is affected by macroporosity and structure (Sharma and Uehara, 1968). On the other hand, the water content at the wilting point (-1500kPa) is not dependent on the structure since the majority of the water is held with adsorption (Aina and Periaswamy, 1985). This may be the reason for the difference in WRC between Mix 1 and 4:3 decreases at this suction.

To enable the use of GLD as an additive, the factors affecting the retrieval of the finished product should be understood. Sufficient mixing could be achieved with both the loader and the Mobile Asphalt Plant. Comparing the compaction properties of the tested samples, it shows that the amount of GLD influences the degree of compaction. The 5% GLD blend achieved the highest degree of compaction, i.e. the mix that could achieve the highest dry density and lowest porosity and water content. The amount of GLD in the mix and the mixing energy/time that is applied to the samples are negatively correlated to the degree of compaction (Figure 4). The water content is dependent on mixing technology of the material and is negatively correlated to dry density. The mixing time may affect the properties of the blends and is correlated to the water content and silt content of the till/GLD mixtures. A longer mixing time increases the porosity of blends with high silt content whilst the opposite is noted for blends with low silt content. Using a till with high silt content can, therefore, increase the production process speed and efficiency. To obtain a product suitable for sealing layer purposes, the observed variations of the feed materials (GLD and till) has to be taken into account and the proportions and mixing energy should be adjusted thereafter. A guidance manual for end users is currently under construction.

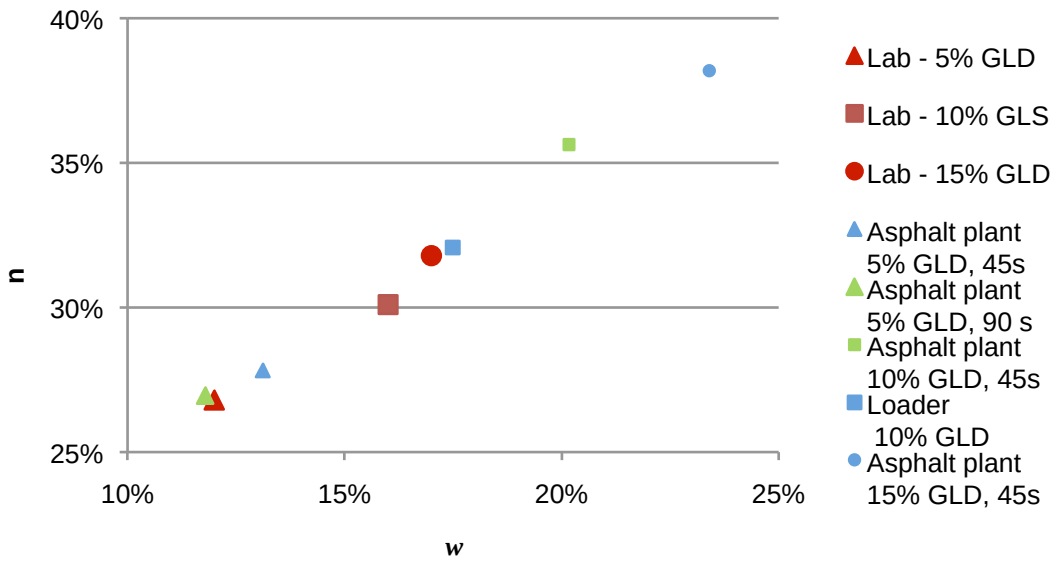

Figure 4 Correlation between water content and porosity of till/GLD samples.

GLD addition as a remediation method is a viable option and may generate decreased costs, better result or both compared with traditional remediation solutions. An assessment of transport economics, transport logistics, handling and management and other surrounding cost have been published (Mácsik and Maurice, 2014). The largest costs are concerned with transportation distances and the mode of transportation. The report showed that using GLD as an additive (addition of 10%) to till available close to the remediation site, is an economical alternative to consider if the distance to till that fulfill the requirements for sealant material is larger than ~10 miles and assuming GLD can be obtained within a reasonable distance (maximum ~500 miles).

CONCLUSION

The aim of the project was to produce mixes of till and GLD, with a hydraulic conductivity lower than 10^{-8} m/s and a high water retention capacity. This study shows that it is possible to produce homogenous mixtures under field conditions and achieve a material that can qualify as a sealing layer. Till blended with 10% GLD by using an asphalt plant showed a higher water retention capacity than till without addition of GLD, but also higher than sandy silt and even clayey silt. This is partly due to highly water saturated conditions in the compacted till/GLD mixtures. Water retention capacity and hydraulic conductivity are related to the mixtures porosity/dry density. Thereby the compacted Till/GLD blends dry density is a good measure of their function as a liner. The quality of the till, such as particle size and water content, as well as the quality of the GLD, such as water content and liquid limit, are important factors influencing the compaction and the hydraulic conductivity of the Till/GLD mixture. The amount of GLD and the mixing energy should be adjusted depending on the geotechnical properties, mainly particle size and water content.

ONGOING RESEARCH

This pilot-scale experiment creates the basis for the remediation of a part of a former mine (4.5 hectares) with a sealing layer made of GLD/till that will take place in 2015. A guide on how to design a sealing layer of till and GLD including mixing techniques, recipes, economics, etc. is currently under process and will be published during 2015. Another pilot scale experiment has been set up where the selected proportion (10%) of GLD/till has been used (based on this current

study) to construct a dry cover system to simulate the mine aimed for remediation. The cover system will be monitored during the next five years and is funded by Boliden Minerals and Vinnova.

ACKNOWLEDGEMENTS

Financial support from SP Processum, Swedish Research Council for Environment, Agricultural Sciences and Spatial Planning (FORMAS), Norrbottens Forskningsråd (NoFo), Ragn-Sells AB, Ramböll Sverige AB, Ecoloop AB and the Center of Advanced Mining and Metallurgy (CAMM) at Luleå University of Technology are gratefully acknowledged. Smurfit Kappa paper mill is acknowledged for providing Green liquor dregs. Gunnar Westin, Per Odén, Josefine Lampinen, Nadia Sandström, Johannes Pettersson, Alexandra Wikström and all the involved personnel at the Brännkläppen deposit are all gratefully acknowledged for taking part of the execution of this project.

REFERENCES

Aina, PO., Periaswamy, SP. (1985) *Estimating available water-holding capacity of western Nigerian soils from soil texture and bulk density, using core and sieved samples.* Soil Science. 1985;140:55–58. doi: 10.1097/00010694-198507000-00007.

Benson, CH., Trast, JM. (1995) *Hydraulic conductivity of thirteen compacted clays..* Clays Clay Miner. 43, 669-681

EN 13286-2. *Part 2: Test methods for the determination of the laboratory reference density and water content – Proctor compaction. Unbound and hydraulically bound mixtures*: ICS 93.080.20 (Road construction materials); 2010. p. 34.

Höglund, L-O., Herbert, R., Lövgren, L., Öhlander, B., Neretniks, I., Moreno, L., Malmström, M., Elander, P., Lindvall, M., Lindström, B. (2004) *MiMi – Perfromance assessment, Main report.* ISBN 91-89350-27-8.

Mácsik, J., Maurice, C. (2014) *Use of pulp and paper mills residual products in the remediation of mine waste- a technical and economic assessment. (Återbruk av massaindustrins restprodukter vid efterbehandling av gruvavfall- teknisk och ekonomisk potential).* (in Swedish) Available SP Processum

Mäkitalo, M., Maurice, C., Jia, Y., Öhlander, B. (2014) *Characterization of Green Liquor Dregs, Potentially Useful for Prevention of the Formation of Acid Rock Drainage.* Minerals. 4(2):330-344.

Makitalo, M., Lu, J., Stahre, N., Maurice, C., Öhlander, B. (2012) *Assessment of the effect of aging on Green liquor dregs cover for tailings deposits - Field investigation.* Proceedings of the 8th International Conference on the Environmental and Technical Implications of Construction with Alternative Materials. Wascon 2012, Goteborg, Sweden 30 May - 1 June 2012

Sharma, ML., Uehara, G. (1968) *Influence of soil structure on water relations in low humic latosols: I. Water retention.* Soil Science Society of America Journal. 1968;32:765–770. doi: 10.2136/sssaj1968.03615995003200060021x.

SIS. (1989) Swedish Standard (Svensk Standard) SS 027111, *Geotechnical Tests – Determination of Permeability (Geotekniska Provningsmetoder – Bestämning av Permeabilitet)* (in Swedish), Stockholm.

SIS. (1994) Swedish Standard SS 027109, *Geotechnical tests-Compaction properties-Laboratory (in Swedish).* SIS-Standardiseringskomissionen i Sverige, Stockholm.

Sivapullaiah, PV., Sridharan, A., Stalin, VK. (2000*) Hydraulic conductivity of bentonite-sand mixtures*. Can. Geotech. J. 37, 406-413.

Evaluating the Benefits of Water Covers as a Rehabilitation Strategy in Temperate Climates: A Tasmanian Perspective

Laura Jackson[1], Anita Parbhakar-Fox[1], Dan Gregory[1], Alison Hughes[2], Janelle Agius[2], Tony Ferguson[3] and Daniel Lester[3]

1. *School of Physical Sciences, University of Tasmania, Australia*
2. *EPA Division, Department of Primary Industries, Parks, Water and Environment, Australia*
3. *Grange Resources Limited, Australia*

ABSTRACT

Environmentally safe disposal of reactive sulphidic tailings is one of the major management challenges facing the mining industry. Consequently, there are a broad range of tailings rehabilitation strategies suitable for a variety of climates. One option is placement of tailings under a water cover to reduce oxygen influx. However, for sites in Australia that lie in a cool temperate climate, the suitability of engineered water covers is not well documented. The Old Tailings Dam (OTD) located at the Savage River Mine, Tasmania provides a unique opportunity to evaluate water covers as a rehabilitation strategy. The OTD extends roughly 1500 m northeast to southwest and 170 m east to west at its widest point (Hassell, 2005). The northern end is submerged under water, as the OTD was constructed on a natural gradient. Therefore, up to 0.2 km^2 are permanently submerged under water (maximum depth of 10 m) with some seasonal variation. In contrast, the southern portion in contrast has been exposed since 1982. Tailings from 14 trenches and 11 sediment cores were collected across the OTD. Selected samples were subjected to geochemical testwork and also used in mineralogical studies whereby a modified sulphide alteration index was developed. Results revealed a complex, heterogeneous sediment architecture with ten facies observed. From this, four zones were defined (A, unsaturated and coarse-grained, B- unsaturated and fine-grained, C- intermediate saturation and D- saturated). Geochemically, Zone D was identified as the lowest risk, with Zones A to C classified as having a high to extreme acid forming nature, which concurred with bulk mineralogy evaluations showing relatively high quantities of unoxidised pyritic tailings (5 to 9 wt. %). Sulphide alteration index assessments allowed for oxidation to be observed on a micro-scale, and indicated that a minimum water cover depth of approximately 1 to 1.5 m would be sufficient to significantly retard oxidation. Ultimately, a phased rehabilitation strategy which requires geotechnical earthworks and installation of flow-through reactors in combination with a water cover should be developed to successfully reduce AMD from this site.

Keywords: acid mine drainage, rehabilitation, tailings, Australia, mineralogy

INTRODUCTION

Uncontrolled sulphide oxidation can lead to the generation of acid mine drainage (AMD) - characterised by metal-laden acid-sulphate waters (Jambor *et al.* 2003). Impacts of AMD on the environment can occur throughout the life of mine (LOM) with many examples published in the scientific literature; e.g., Harris *et al.* (2003), Edraki *et al.* (2005), Parbhakar-Fox *et al.* (2014) and Candeias *et al.* (2014). As lower grade ore deposits are now being exploited for a range of commodities (c.f. Mudd, 2007), the management challenges are ever increasing as a consequence of the increased volumes of waste (Lottermoser, 2010). In turn, the complexity of mine waste (i.e., tailings, waste rock) management increases, and remains the most significant environmental challenge facing the mining industry (Harries, 1997).

In order to prevent sulphide oxidation and AMD generation in tailings storage facilities, appropriate control strategies are needed. Widely used strategies aim to exclude one or more of the ingredients required for oxidation; e.g., water, iron, oxygen, bacteria and sulphide minerals. Lottermoser (2010) suggested that the most effective control on oxidation rate is specifically reducing oxygen availability. Generally, this is achieved by using wet or dry covers, with a summary given in the GARD Guide (2014). More technologically advanced and innovative strategies have recently been developed and involve induced hardpan formation, grouting or mineral surface treatments (e.g., Ahn *et al.* 2011; Quispe *et al.* 2013). Lottermoser (2010) concluded that no single technology is appropriate for all mine sites and in many cases a combination of technologies offer the best chance of success.

When dealing with historic/legacy tailings sites, a cost-effective management strategy is favoured as the funds available to the lease holder (typically the mine regulator; i.e., government) is likely limited. In such cases, the use of a water cover should be considered. Recent studies by Yanful *et al.* (2004), Bjelkevik (2005) and Kachhwal *et al.* (2010) demonstrate the use of shallow water covers in North America and Sweden. Such covers are effective as the maximum concentration of dissolved oxygen in water is greater than three orders of magnitude lower than that of the atmosphere, so AMD formation is significantly retarded (Lottermoser, 2010). However, a minimum water cover depth must first be established. Yanful *et al.* (2004) proposed two criteria to determine this: (i) hydrological forecasting of the probability of occurrence of a drought event; and (ii) the minimum depth necessary to prevent re-suspension of tailings. Generally, deep water covers are not favoured due to concerns regarding the engineering stability of the containment walls, with high associated capital expenditure. Published studies documenting the use of water covers in Tasmania are scarce. However, as this state experiences a cool temperate climate (~600 mm rainfall/year) it would be well-suited to this type of rehabilitation strategy (c.f. GARD guide, 2014).

At the Savage River Mine AMD is emanating from the OTD, where 38 million tonnes of pyritic tailings were deposited from 1967 to 1982. Consequently, the OTD accounts for 50% of Savage River Mine's AMD load (Williams *et al.* 2014). To manage this, the Tasmanian State Government established the Savage River Rehabilitation Project (SRRP) in co-operation with the mine operator (currently, Grange Resources). This study focussed on: (i) confirming the necessity for a water cover at the OTD, and (ii) establishing an appropriate minimum water depth, should this type of cover be used.

METHODOLOGY

Site description

The Savage River Mine is located on the Savage River 420 km from Hobart on the northwest coast of Tasmania (Figure 1). It consists of five open-cut workings exploiting a group of magnetite-rich lenses irregularly distributed within a series of highly metamorphosed rocks of marble, schist and metabasic rocks. Open-pit mining and processing has resulted in the formation of several large excavations, waste rock piles, and tailings dams (Hutchison and Brett, 2006; Kent, 2013). The concentrated magnetite is slurred by pipeline to Port Latta on Tasmania's northwest coast, before shipping to market. The presence of pyrite in the waste materials (i.e., tailings and waste rock) has

caused AMD to emanate from the mine operations, which is of primary concern to the SRRP (Kent, 2013).

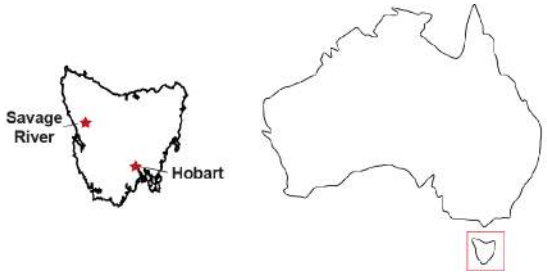

Figure 1 Location of the Savage River Iron Mine, Tasmania, Australia

Operations over the first 30 years of mine life caused environmental degradation to approximately 30 km of the Savage River, and downstream of the confluence with Main Creek exhibits the most severe degradation. This section was found in 1995 to have lost 90% of its invertebrate biodiversity and 99% of its invertebrate abundance. The OTD is located approximately 3 km from the township and 1.3 km from the processing plant. Pyritic tailings from Centre Pit South (CPS) and Centre Pit North (CPN) were deposited in the OTD (Kent, 2013). These were initially deposited behind the starter dam by end-of-pipe spilling into the southwest corner of the dam (Hassell, 2005). Subsequently, tailings were sprayed as slurry from the dam wall to allow it to be raised in lifts (Thompson and Brett, 1996). This deposition method has concentrated coarser, heavier and more permeable material against the dam wall (Kent, 2013). Consequently, the water table in the tailings has decreased proximal to the wall, resulting in extensive oxidation of the tailings in this area and AMD generation.

Sampling and sample preparation

In May 2014, an excavator was used to dig 12 trenches up to 1.5 m depth in the southern end of the OTD (Figure 2). At the northern end the tailings were saturated, so materials from locations 12, 13 and 24 were obtained by hand-dug trenches (c. 60 cm depth). From locations 14 to 23, a weighted piston corer was used, allowing the collection of samples below the northern pond under a varying water depth of 0.3 to 10 m. Samples to a maximum depth of 1.5 m were collected by the piston corer. All tailings samples were cooled and transported to the University of Tasmania (UTas). Cores were frozen to enable logging, and then oven-dried. Each sample (n= *144*) was split in two, with one portion milled to <63 μm for geochemical testwork, and the other used to prepare polished thin sections and grain mounts for mineralogical evaluations.

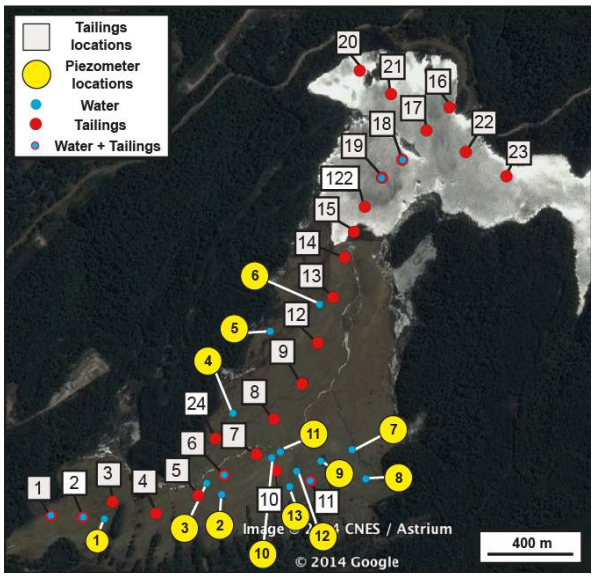

Figure 2 Plan view map of the Old Tailings Dam showing tailings sample locations (red; n=24), and water collection locations (blue). Established piezometer locations are shown in yellow circles (image from Google).

Geochemical testwork

Paste pH testing represents the most efficient manner by which to assess a sample's immediate acid forming characteristics, and was performed on all samples at UTas, according to ASTM D4972-01(2007) following the recommendations given in Noble *et al.* (2012). In addition, rapid and accurate measurement of total sulphur (wt. %) for calculation of maximum potential acidity (MPA) was performed on all samples using an Eltra C-S 2000 instrument at UTas. A sub-set of samples (*n=55*) was chosen for multi-addition NAG pH (UTas) and acid neutralising capacity (ANC) testing (Australian Laboratory Services, Brisbane, Australia). Pore water chemistry was assessed on 20 samples collected from established piezometers (Figure 2), the base of trenches, and the frozen waters in cores. These were analysed by solution ICPMS methods at UTas. Six samples were selected from across the OTD for laser-ablation ICPMS (LA-ICPMS) testwork to provide an indication of the pyrite chemistry. Appropriate sample blanks and standards and certified reference materials were used throughout all analyses, with the standard deviation for each data set calculated as <0.5.

Mineralogical evaluations

To determine their mineralogy, tailings samples were subjected to XRD analysis (*n=55*). A benchtop Bruker D2 Phaser X-ray diffractometer (XRD) instrument with a Co X-ray source was used to perform these analyses at UTas. Each sample was ground in an agate mortar and pestle, loaded into the sample holder and placed into the machine chamber. XRD analysis was performed for 1 hour at an operating voltage of 30 kV and 10 mA using a cobalt X-ray tube. A 0.6 mm (0.3°) fixed divergence slit, 2.5° soller slit and an iron-filter were also used. Each scan ranged from 5 to 120° (2θ) with a 0.02° step size and a measurement time of 0.6 seconds per step. Mineral phases were identified using the Bruker DIFFRAC.EVA software package with the PDF-2 (2012 release) powder diffraction file mineral database. Mineral abundances were semi-quantified by Rietveld analysis using TOPAS pattern analysis software. In general, bulk mineralogy is considered unable to confidently identify the presence of trace sulphide oxidation products (i.e., < 1 wt. %), so a modified sulphide alteration index (SAI) following Blowes and Jambor (1990) was established. Criteria for this SAI (Table 1) were established following the examination of select grain-mounted samples (*n=10*) using a Hitachi SU-70 field emission scanning electron microscope (UTas, Central Science Laboratory). Thin sections (*n= 55*) prepared from tailings samples were evaluated by reflected light

microscopy, with 20 pyrite grains ranked by this criteria and the values averaged to give a final SAI value.

Table 1 Modified sulphide alteration index (SAI) defined and used in this study.

Score (/10)	Features
0-1	Only a few grains of pyrite are weakly altered along edges and fracturing is minor; >95% of the grains have sharp, fresh margins.
2-4	Pyrite grains have rims emerging and fracturing is minor.
5-6	Pyrite grains have >narrow alteration rims with fracturing becoming predominant.
7-8	Appearance of secondary minerals, increase in abundance of fracturing and subsequent altering.
9	Pyrite <30% pyrite remaining, dominated by alteration around rims and fractures.
10	Only traces of pyrite remain.

RESULTS AND DISCUSSION

Tailings facies

Tailings within the OTD demonstrate a high degree of heterogeneity with ten facies identified, and four distinct zones defined: A - unsaturated coarse-grained (locations 1 to 3); B - unsaturated fine-grained (locations 4 to 6); C - intermediate (saturated/unsaturated; locations 7 to 14, 24); and D - saturated (locations 15 to 23). Oxidation of sulphide minerals in the tailings was indicated by a change in colour from grey to yellow, orange or red. The vertical extent of oxidation into the tailings varied throughout the OTD. For example, in Zone A, (proximal to the discharge) water percolation occurs due to the coarse nature of these tailings, therefore this zone is extensively oxidised (Figure 3a). In general, the oxidised hardpan layer thickness decreases towards the northern pond. Thin oxidised layers observed at depth (e.g., c. 10- 50 cm; Figure 3b) in trenches represent former hardpan surfaces, which have subsequently been covered with tailings. Some subsurface layers, particularly coarse sulphide sand layers, appeared to be undergoing some degree of oxidation (Figure 3c). This is likely caused by vertical fissures (occasionally observed) allowing water and oxygen ingress through the buried tailings. Re-sedimentation of hardpan material in the shallow pond area (e.g., Figure 3d) added complexity in determining the minimum depth of water cover required, as there may be a combined protective effect of both hardpan and water.

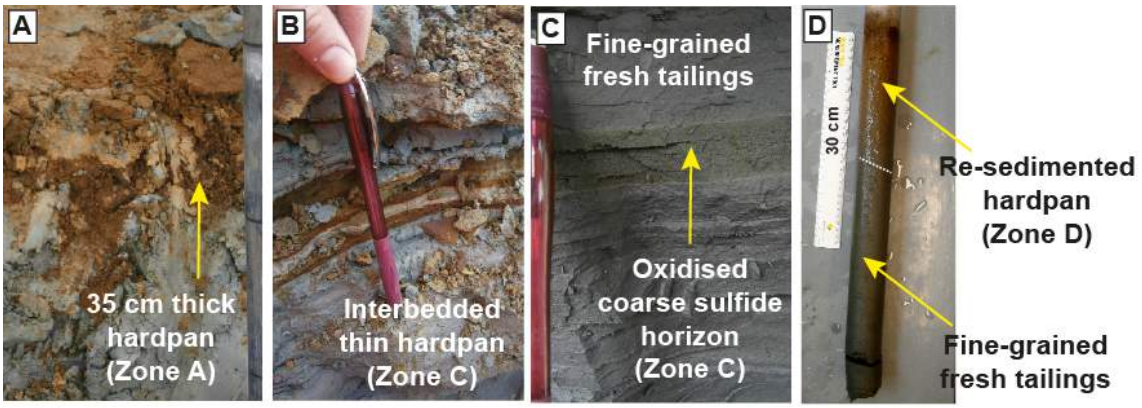

Figure 3 Examples of tailings oxidation observed in the OTD. A: Thick oxidised hardpan (30 to 35 cm depth) prevalent in Zone A; B: Thin hardpan layers interbedded within fresh tailings packages at depth (c.1 m; Zones B and C); C: Coarse oxidised sulphide horizon observed in Zones B and C; D: Re-sedimented hardpan seen in Zone D.

Tailings geochemistry

The assessment of lag-time to AMD and therefore risk (from high to low) was determined using the net acid generation (NAG) pH vs. paste pH classification scheme (Figure 4; Weber *et al.* 2006). The majority of samples from Zones A (unsaturated, coarse-grained), B (unsaturated, fine-grained) and C (intermediate zone) were classified as intermediate-high risk with acid formation rate predicted as rapid to immediate. This is new evidence that these tailings are severely acid forming at depth and require rehabilitation, as previously this has only been inferred from water chemistry and assessments of samples taken from the upper 30 cm (c.f. Hassell, 2005). The majority of Zone D samples fall into potentially acid forming (PAF)-low risk, inferring a potential relationship between permanent saturation and higher paste pH values. A net acid producing potential (NAPP) vs. NAG pH classification plot showed that the majority of OTD samples are PAF, with a NAPP range from -2.5 to 797 kg H_2SO_4/t (average: 187 kg H_2SO_4/t; median; 160 Kg H_2SO_4/t). Acid neutralising capacity (ANC) values were in the range from 0 to 41 kg H_2SO_4/t, with an average value of 15 kg H_2SO_4/t. Despite the presence of magnesite in the primary ore-mineral assemblage at Savage River, it was not reported by XRD (i.e., only trace amounts below the detection limit of 1% present). Therefore, ANC is likely sourced directly from chlorite, an effective silicate neutraliser (c.f. Craw, 2000; Jambor *et al.* 2002; 2007). Additionally, Hutchison and Brett (2006) and Gerson *et al.* (2014) have documented the use of the chlorite-calcite schist/amphibolite for AMD control at Savage River, from which both calcite and chlorite are thought to contribute to the net-neutralising potential.

Chemical analyses of pyrite (LA-ICPMS; *n= 180*) in six samples collected across the OTD indicated that generally the pyrite is enriched in Co and Ni (Figures 5a and 5c). Copper, which is elevated in the waters draining the site (c.f. Hassell, 2005), is also relatively high in these samples (average 620 ppm), with the highest concentrations measured in Zone A (Figure 5b). Zinc was generally low (average 10 ppm): however, its concentration steadily increased towards Zone D (Figure 5d), indicating that it has leached from Zone A; i.e., susceptible to meteoric water influx and under low pH conditions (average pore water pH: 2.7).

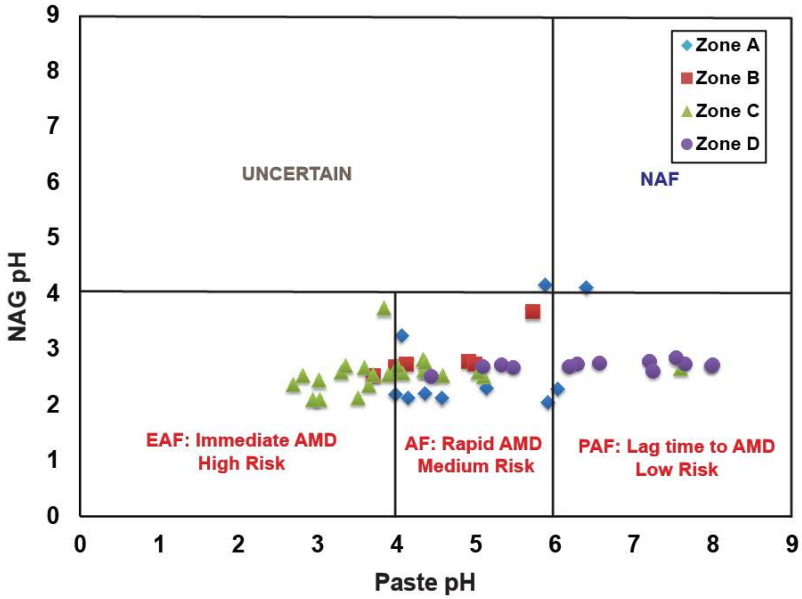

Figure 4 NAG pH vs. paste pH risk classification plot (after Weber et al. 2006) for tailings samples collected across the OTD (samples grouped by zones: A- unsaturated and coarse-grained; B- unsaturated, C- intermediate saturation and D- saturated). Abbreviations: EAF, extremely acid forming; AF, acid forming; PAF, potentially acid forming; NAF, non-acid forming.

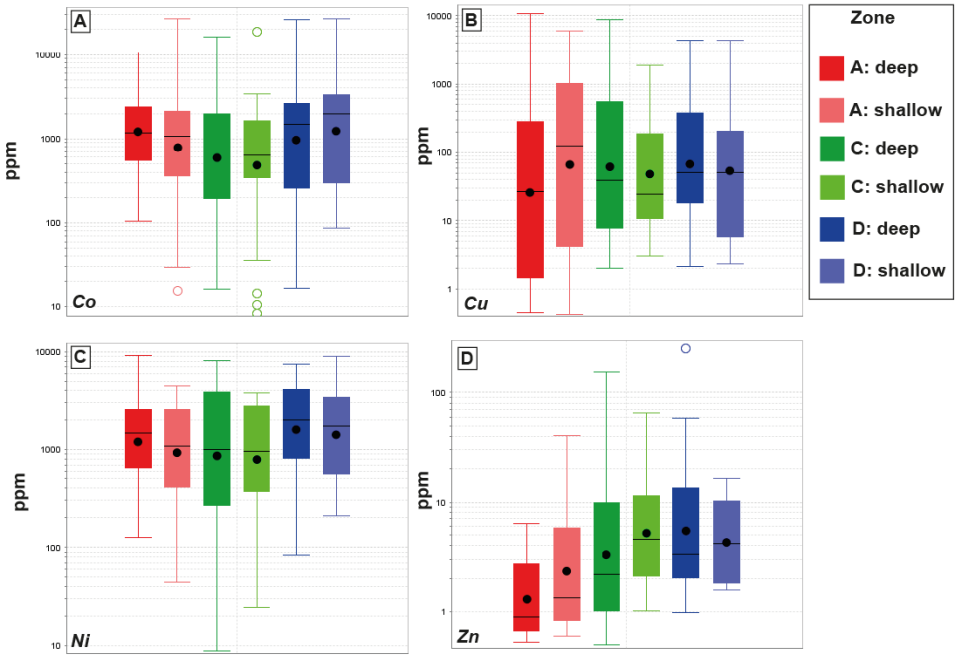

Figure 5 Tukey geochemical plots of select potentially deleterious elements (ppm) contained in pyrite (n=6) from the OTD: Co (A), Cu (B), Ni (C) and Zn (D). (NB/ black dots indicate average, solid black line the median, solid colour box ends indicate the interquartile range, whiskers include outliers (indicated by open circles and triangles) in the recalculated interquartile range).

Chemical analyses of tailings pore water showed high sulphate concentrations (max. 12,900 mg/L; Zone C) in the unsaturated and intermediate saturated zones, indicating active AMD formation. In Zone D concentrations below ANZECC (2000) drinking water guideline (DWG) values (500 mg/L) were measured (average 157 mg/L), confirming that the established natural water cover is effective at retarding AMD formation. Furthermore, average pH values of 4.5 were measured in this Zone. Across the OTD As, Cd, Ni, Sb, Pb and U were below ANZECC (2000) DWG values. Occasional exceedances of Al (max. 180 mg/L), Cu (max. 35 mg/L), Se (max. 0.1 mg/L) and Zn (max. 4.6 mg/L) relative to ANZECC (2000) DWG values were identified, predominantly in Zones B and C, but not in Zone D. In general, Fe was high across the OTD, with six locations reporting concentrations >1000 mg/L; however, no ANZECC (2000) DWG value is available for comparison. This is also the case for Co, with average concentrations of 5 mg/L measured.

Tailings mineralogy

The bulk mineralogy of the tailings across the OTD was dominated by albite, actinolite, antigorite, quartz, tremolite, talc and chlorite, as shown in Figure 6. In all zones the content of pyrite increased with depth, confirming the presence of fresh tailings at depth. In the upper most samples from Zone A and B trenches (0 to 30 cm), secondary minerals goethite, ferrihydrite, hematite and jarosite were observed, which are common hardpan minerals. The presence of goethite and jarosite indicated the latest stages of sulphide oxidation (c.f. Jambor, 2003). The highest jarosite concentrations were observed in Zone C (intermediate saturation), which concurs with the environment of its formation (c.f. Dutrizac and Jambor, 2000). In Zone D there was a notable decrease in the quantity of these secondary minerals, confirming that these materials are relatively fresh. Additionally, there is also a lower pyrite content, likely related to the distance from the discharge; although on average the grain size was finer. The bulk mineralogy confirms that the established water cover is effective in retarding oxidation, with very minor (< 2 wt. %) secondary minerals developed. Where these were observed (i.e., locations 15 and 18; Figure 2) it indicated re-sedimentation of hardpan materials from Zone C.

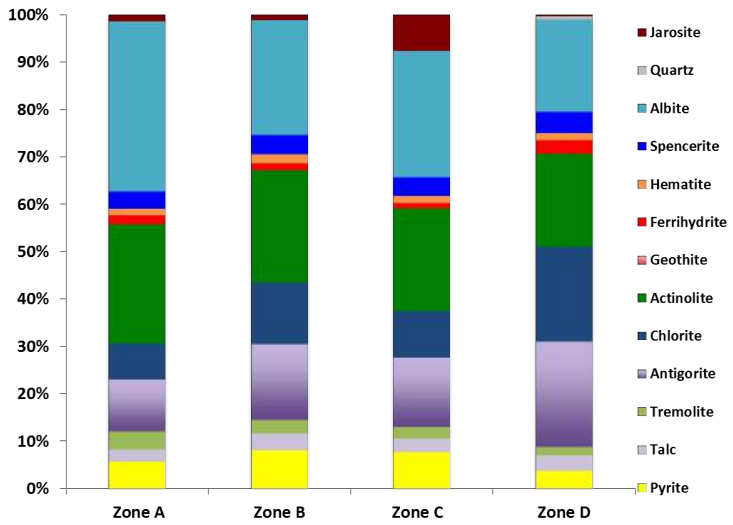

Figure 6 Summary of bulk mineralogy (measured by XRD semi-quantitative, modal abundance as a % shown) for Zones (A to D).

Sulphide alteration index (SAI) values calculated across the OTD are shown in Figure 7. The highest SAI values were measured in Zone A (6/10) in the upper horizons (c. 30 cm; Figure 8a). The lowest readings (1/10) were recorded in Zone D at depth (150 cm, under 430 cm water cover; Figure 8b). These results concur with the tailings geochemistry. From these values, the minimum depth of an effective water cover for retarding AMD formation is identified as 1 to 1.5 m.

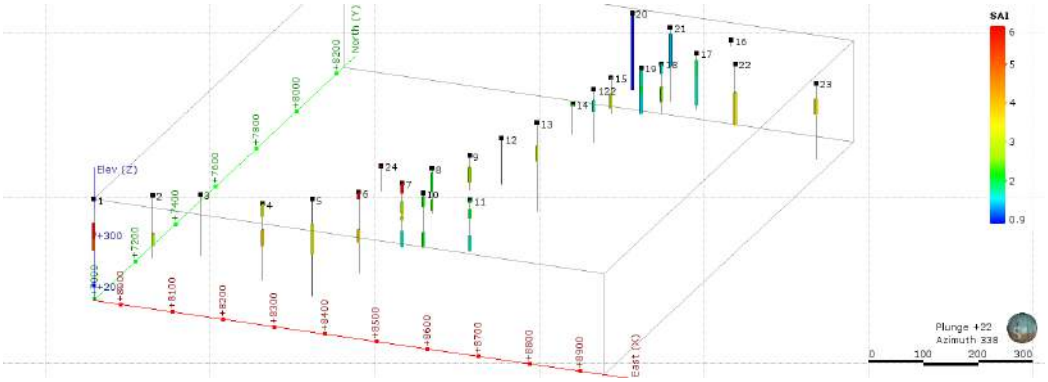

Figure 7 3D schematic diagram of the OTD showing sample locations and sulphide alteration index (SAI) values. Zones A to D are indicated (by thick black lines) and the northern pond is shown in Zone D.

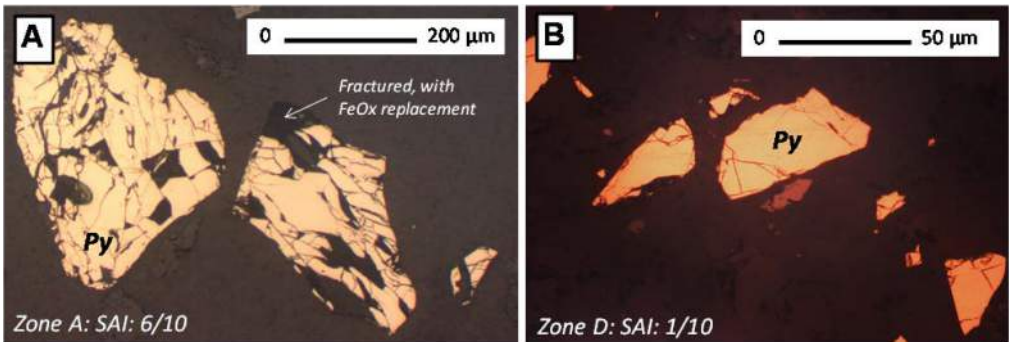

Figure 8 Photomicrographs (reflected light) of pyrite. A: Grains from Zone A (30 cm depth) showing extensive oxidation with a sulphide alteration index (SAI) score of 6/10 given; B: Grains from Zone D (45 to 75 cm depth, under; 100 cm of water) are comparatively smaller, and much less altered with a SAI score of 1/10 given, indicating this is an appropriate water cover depth.

CONCLUSION

The presence of a natural water cover in the northern portion of the OTD at the Savage River Mine provided the unique opportunity to evaluate the application of a total water cover as a cost-effective rehabilitation strategy. The OTD currently contributes 50% to the total AMD load from the Savage River Mine. As the OTD tailings are historic (managed by the SRRP), knowledge of the tailings geochemical and mineralogical characteristics at depth were limited, and therefore the nature of potentially reactive pyritic tailings remaining in the OTD unknown. This study has penetrated the OTD to depths of 1 to 1.7 m, revealing complex sediment architecture, with ten facies identified and four zones (A to D) defined based on grain size and degree of saturation. Geochemical results indicated that these tailings remain acid forming, with Zones A to C (unsaturated coarse-grained, unsaturated fine-grained, and intermediate, respectively) classified as high risk. Tailings in Zone D (saturated) were less reactive, and classified as low-risk. The sulphide alteration index (SAI) mineralogical assessment allowed for the oxidation front to be better approximated, and confirmed the natural water cover as effective for retarding oxidation. Furthermore, the results indicate that a minimum water cover depth of 1 to 1.5 m is required across the entire OTD. Predictions of re-suspension by wind or wave action have yet to be performed; however, observations of re-sedimented hardpan in the surface of core samples from Zone D show that at 1.5 m such sediments are not seen. Potentially, this more conservative depth of 1.5 m should be used.

Ultimately, a phased tailings rehabilitation management strategy which utilises a water cover will prove the best solution at the OTD. Phase one should focus on the removal of the upper most > 0.5

m of tailings (i.e., oxidised portion) in Zone A, followed by clay capping. This will leave this zone with characteristics similar to the remainder of the unsaturated portion of the dam (i.e., Zones B and C), allowing them to be managed together. Phase two involves the extension of the northern pond area to saturate tailings in Zones A (after clay-capping), B and C to 1.5 m depth in order to reduce sulphide oxidation rate. However, this should only be undertaken after geotechnical work to raise the dam walls has been completed. Phase three requires installation of flow-through reactors to neutralise any AMD emanating from the OTD. At least two alkaline flow through reactors should be installed, one at the north slot monitoring station where seepage is occurring, and the other at the former southwest spigot point in case the water in the OTD back flows as it is being filled. Phase four involves establishing a long-term monitoring programme, which focuses on identifying any additional seepage points, measuring water quality to test how effective the water cover is, measure water level fluctuations, and identifying if there has been any re-suspension of tailings. In several years, a follow up mineralogical study should be performed to evaluate the performance of the water cover by measuring the degree of oxidation using the SAI.

ACKNOWLEDGEMENTS

Financial support for this BSc. honours project was provided by the SRRP for which they are acknowledged. The authors would like to thank staff at the University of Tasmania (Dr. Nathan Fox, John Aalders, Sean Johnson, Dr. Paul Olin, Dr. Karsten Goemann, Dr. Sandrin Feig) for their analytical assistance. In addition, site personnel at Grange Resources past and present (Bruce Hutchison, Dr. Victoria Braniff) are acknowledged for initiating the project and providing additional information on the site.

REFERENCES

Ahn, JS, Song, H, Yim,GJ, Ji, SW, Kim, JG (2011) An engineered cover system for mine tailings using a hardpan layer: A solidification/stabilization method for layer and field performance evaluation, Journal of Hazardous Materials, vol. 197 pp.153-160.

ANZECC (2000) Australian guidelines for water quality monitoring and reporting. National Water Quality Management Strategy Paper No 7, Australian and New Zealand Environment and Conservation Council & Agriculture and Resource Management Council of Australia and New Zealand, Canberra.

Bjelkevik, A (2005) Water cover closure design for tailings dam: a state-of-the-art report, Lulea University, Sweden, pp. 103.

Blowes, DW, Jambor, JL (1990) The pore-water geochemistry and the mineralogy of the vadose zone of sulphide tailings, Waite Amulet, Quebec, Canada, *Applied Geochemistry*, vol.5 pp.327-346.

Candeias, C, Avila, PF, da Silva, EF.,Ferreira, A, Salgueiro, AR, Teixeira, JP (2014). Acid mine drainage from the Panasqueira mine and its influence on Zezere river (Central Portugal), *Journal of African Earth Sciences*, vol. 99 pp. 705-712.

Craw, D (2000) Water-rock interaction and acid neutralisation in a large schist debris dam, Otago, New Zealand, *Chemical Geology*, vol.171 pp.17-32.

Dutrizac, JE, Jambor, JL (2000) Jarosites and their application in hydrometallurgy, *Reviews in Mineralogy and Geochemistry*, vol.40 pp.405–453.

Edraki, M, Golding, SD, Baublys, KA, and Lawrence, M (2005) Hydrochemistry, mineralogy and sulfur isotope geochemistry of acid mine drainage at the Mount Morgan mine environment, Queensland, Australia, *Applied Geochemistry*, vol.20 pp. 789-805.

Fandrich, R, Gu, Y, Burrows, D, Moeller, K (2007) Modern SEM-based mineral liberation analysis, *International Journal of Mineral Processing*, vol. 84 pp. 310-320.

GARD (Global Acid Rock Drainage) guide (2014) The International Network for Acid Prevention (INAP), http://www.gardguide.com/

Gerson, A, Smart, R, Li, J, Kawashima, N, Fan, R, Zeng, S, Schumann, R, Levay,G, Dielemans, P, Mc Latchie, P (2014) Mineralogy of Mine Site Neutralising materials: A Missing Link in AMD Control Planning, *Proceedings of the Eighth Australian Workshop on Acid and Metalliferous Drainage* (Eds H Miller and L Press), pp.313-324.

Harries, JR (1997) Acid mine drainage in Australia: its extent and potential future liability, Canberra, Supervising Scientist, pp.94.

Harris, D.L., Lottermoser, B.G., Duchesne, J., 2003. Ephemeral acid mine drainage at the Montalbion silver mine, north Queensland, Australian Journal of Earth Sciences, vol. 50 pp.797-809.

Hassel, T (2005) Hydrogeological and geochemical characterisation of an abandoned tailings dam at Savage River Mine, Tasmania. BSc. Honours Thesis. Department of Environmental Geosciences Faculty of Science, Technology and Engineering La Trobe University Bundoora, Victoria.

Hutchison, BJ, Brett, D (2006) Savage river mine- practical remediation works. *7th International Conference on Acid Rock Drainage (*ICARD), March 26-30, 2006, St. Louis MO. R.I. Barnhisel (ed.) Published by the American Society of Mining and Reclamation (ASMR), 3134 Montavesta Road, Lexington, KY 40502 pp. 810-819.

Jambor, J.L., Blowes, D.W., and Ritchie, A.I.M. (Eds.), 2003. Environmental Aspects of Mine Wastes. Mineralogical Association of Canada, Short Course Series, vol. 31 p.436.

Jambor, JL (2003) Mine-waste mineralogy and mineralogical perspectives of acid-base accounting. In: Jambor, J.L., Blowes, D.W., and Ritchie, A.I.M. (Eds.), *Environmental Aspects of Mine Wastes*. Mineralogical Association of Canada, Short Course Series, vol. 31 pp. 117-145.

Jambor, JL, Dutrizac, JE, Groat, L, Raudsepp, M (2002) Static tests of neutralization potentials of silicate and aluminosilicate minerals, *Environmental Geology*, vol.43 pp.1-17.

Jambor, JL, Dutrizac, JE, Raudsepp, M (2007) Measured and computed neutralization potentials from static tests of diverse rock types, *Environmental Geology*, vol.52 pp.1019-1031.

Kachhwal LK, Yanful EK, Lanteigne L (2010) Water cover technology for tailings management: a case study of field measurement and model predictions, *Water Air Soil Pollution,* vol. 214 pp. 357–382.

Kent, S. (2013) Development proposal and environmental management plan, South deposit tailings storage facility, Grange Resources (Tasmania) Pty Ltd Savage River Mine. Caloundra Environmental Pty Ltd Report.

Lottermoser, BG (2010). Mine Wastes: Characterization, Treatment and Environmental Impacts, 3rd edition, Springer-Verlag, Berlin Heidelberg, pp. 400.

Mudd, GM (2007). An assessment of the sustainability of the mining industry in Australia, *Australian Journal of Multi-Disciplinary Engineering*, vol.5 pp.1-12.

Noble, TL, Lottermoser, BG, and Parbhakar-Fox, A (2012) Evaluating pH tests for mine water prediction, in *3rd International Congress on Water Management in the Mining Industry*, (eds: F Valenzuela, J Wiertz) pp. 504-512.

Ougrawa, M, Molson, J, Auberin, M, Bussiere, B, Zagury, GJ (2007) Predicting the performance of an elevated water table for preventing acid mine drainage, *Ottawa Geology Conference*, pp.1470-1478.

Parbhakar-Fox, A, Edraki, M, Hardie, K, Kadletz, O, and Hall, T (2014) Identification of acid rock drainage sources through mesotextural classification at abandoned mines of Croydon, Australia: Implications for the rehabilitation of waste rock repositories, *Journal of Geochemical Exploration*, vol. 137 pp. 11-28.

Quispe, D, Perez-Lopez, R, Acero, P, Ayora, C, Nieto JM, Tucoulou, R (2013) Formation of a hardpan in the co-disposal of fly ash and sulphide mine tailings and its influence on the generation of acid mine drainage, *Chemical Geology*, vol. 355 pp.45-55.

Vigneault, B, Campbell, PGC, De Vitre, R, Prémont, S (2001) Geochemical changes in sulfidic mine tailings stored under shallow water, *Water Research*, vol.35 pp.1066-1076.

Williams, DJ, Wilson, GW, Scott, PA, Hutchison, B, Kent, S, Hughes, A (2014) A review of the Savage River Rehabilitation Programme: 2002 to 2013. Proceedings of the Eighth Australian Workshop on Acid and Metalliferous Drainage (Eds H Miller and L Press) pp 21-36.

Yanful, EK, Samad, M, Mian, H (2004) Shallow water cover technology for reactive sulphide tailings management, *Geotechnical News*, September, pp.42-52.

Yanful, EK, Simms, P (1997) Review of water cover sites and research projects. MEND Project 2.18.1 Report, pp. 136.

Case Study of Geita Gold Mine: An Example of Proactive AMD Mitigation Performance

Bonnie Dobchuk[1], Peter Scott[2], Paul Weber[3], Dave Christensen[1] and Yusuph Mhando[4]

1. *O'Kane Consultants, Canada*
2. *O'Kane Consultants, Australia*
3. *O'Kane Consultants, New Zealand*
4. *Anglogold Ashanti (Geita Gold Mine), Tanzania*

ABSTRACT

Initial characterization at Geita Gold Mine (GGM) identified that ~38% of waste rock materials are potentially acid forming (PAF) and tailings are sulfidic (~4% pyrite). GGM has historical acid and metalliferous drainage from naturally-exposed sulfidic rocks and artisanal mining. Pre-mine groundwater studies indicated elevated concentrations of lead and iron, with bores in areas of known mineralization indicating elevated sulfate, arsenic, chromium and nitrate. During mine operation waste rock has contributed limited sulfate and metals. The mine's closure plan for the waste rock is to encapsulate the PAF waste rock within a buffer zone of non-acid forming (NAF) waste rock. The waste placement plan was developed prior to and in the early stages of mining based on geochemical characterization, mapping, and pit block modelling and is reconciled against the updated waste block model as mining progresses. The mine actively minimizes the infiltration of water into the waste rock materials using truck compaction of each dump lift and progressive reclamation.

This paper outlines the approach to designing cover systems and landforms suitable for final closure of the waste storage facilities. A detailed geochemical and geotechnical material characterization program of the current waste storage landforms, consisting of material sampling and field and laboratory testing was undertaken. The results of groundwater and surface water analyses indicated that the waste rock dumps are most likely constructed and behaving as designed with respect to PAF encapsulation. Thus, the conceptual model developed was that a cover system that resulted in moderate net percolation rate, coupled with a stable (geotechnical and geomorphologic) landform that properly managed surface water, was sufficient for reducing contaminants in downstream receptors to below discharge standards. The conceptual model was confirmed using soil-plant-atmosphere, groundwater flow, and contaminant transport numerical modelling to evaluate the predicted long-term water quality.

Keywords: PAF encapsulation, cover design, geochemical characterization, landform design, contaminant transport

INTRODUCTION

The modern Geita Gold Mine (GGM) owned by AngloGold Ashanti Ltd. and operated by Geita Gold Mining Ltd. is an open-pit mine situated in the Mwanza Region of north-western Tanzania, approximately 90 km from the regional capital of Mwanza and 20 kilometres south of Lake Victoria, in an area known as the Lake Victoria Goldfields.

GGM's broad reclamation objective is to leave the site in a condition that is safe, stable, and minimizes long-term environmental impacts as well as providing opportunities for alternative forms of business development. The project described in this paper was initiated to develop mitigation methods for the waste rock and tailings storage facilities that would result in GGM meeting or exceeding their stated reclamation objectives. GGM's closure criteria to meet these objectives for the waste storage facilities were the creation of stable landforms and the reduction of solute loading from the waste storage facilities to meet discharge standards at the downstream compliance points.

Prior to the onset of mining, GGM developed a waste placement plan for the waste rock storage facilities to proactively mitigate against AMD production. This involved detailed characterization of the future waste rock material into non-acid forming (NAF) and potentially acid-forming (PAF) categories (which are continuously updated during mining). The waste rock storage facilities were then designed to encapsulate the PAF materials.

It was hypothesized that a cover system and landform design using the locally-available borrow materials would reduce net percolation to a moderate level (10-15% of mean annual rainfall) in the waste rock and tailings materials and that this would be sufficient to reduce the solute loading at the downstream receptors to below discharge standards. This paper describes the support studies used to verify this hypothesis.

BACKGROUND

The modern Geita Gold Mine began to process ore mid-2000. The GGM operation comprises three mining areas: one centred on the old Geita Hill area (Geita Block) comprising several pits: Nyankanga, Geita Hill, Lone Cone and their associated waste rock dumps: WD1, WD5, WD6, WD14, WD15, the Nyamulilima Block is west of Geita Hill and comprises Star & Comet, Robert and Ridge 8 and waste rock dump WD16, and the third – Kukuluma Block, located ~20km away comprising the Kukuluma and Matandani pits and waste rock dumps WD7, WD8 and WD9. Tailings have been deposited in an historic TSF constructed prior to the current mining operation and referred herein as the Old TSF and a modern storage referred to as the New TSF (NTSF). The materials' composition in these landforms has the potential to generate acidic drainage from natural oxidation of contained sulfidic minerals and result in metal leaching. Previous characterization has shown up to 38% of waste rock materials as potentially acid forming (PAF), based on initial assessment in 2001 (Scott et al, 2014). Currently gold is mined from Nyankanga, Geita Hill and Star & Comet Pits. Kukuluma and Matandani pits and the Lone Cone pits are not operational. The current life of mine is planned until 2030.

Geology

GGM is located in the Geita Greenstones that form the northern arm of the regional Sukumaland Greenstone Belt of the Archaean Tanzanian Craton. Stratigraphically the Sukumaland Greenstone Belt belongs to the Neoarchaean Nyanzian Supergroup (Barth, 1990; Borg and Shackleton, 1997). The Geita deposits are hosted in Archaean-age rock Upper Nyanzian formations characterized by banded iron formation (BIF), felsic volcanics and andesite/diorite lithologies (Sibilski and Stephen, 2006). The BIF outcrops in all of the high ground in the area, while felsic volcanics occur in the lower flanks of the ridges and are either inter-bedded within the BIF or occur either side of it. The other main lithology in the Geita area is a trachyandesite, encompassing a suite of volcanic rock types, ranging from basalt to diorite in composition. The trachyandesite units are commonly interbedded and folded with the BIF. The volcanics, which host the gold mineralization, have been metamorphosed to lower greenschist facies. At Nyankanga the principal waste rocks are microdiorite and BIF. The Kukuluma host waste rock sequence is more variable and includes mafic to felsic volcanics, BIF and metasediments. The western section of the belt, in the GGM area, is cut by regional scale Proterozoic quartz-gabbro dykes with a strong north-east trend. The area is dominated by both NW and NE structural trends, with a weaker NNW trend occupied by Karoo dolerite dykes. The greenstone belts of the Tanzanian Craton are characterized by more localized and discontinuous structures.

Mineralogy

Gold mineralization is typically associated with quartz veins (inner belts) and disseminated sulfides (outer belt) in quartz-carbonate-chlorite shear zones replacing and crosscutting magnetite-rich BIF. Gold mineralization can also be associated with massive and disseminated sulfide bodies on contacts between felsic tuffs and BIF. The principal sulfide present in the shear and vein-hosted deposits is pyrite, with minor pyrrhotite and trace arsenopyrite, chalcopyrite, galena and sphalerite. Gold occurs as free native gold in quartz veins and as inclusions or surface adherents to iron sulfides. Carbonate minerals that are present in the mine sequence are dominated by calcite with accessory dolomite, ankerite and siderite. The carbonates occur as fine-grained pervasive mineralization in the altered BIF matrix and as coarser-grained calcite in veins. The supergene mineral assemblage is dominated by oxyhydrates of iron and aluminium.

Climate and Hydrology

The Geita District has a highland equatorial wet-dry weather pattern with a bimodal wet season (generally October to December and February to May) with a mean annual rainfall of ~980 mm. A distinct dry season extends from June to August/September with an average annual pan evaporation of ~1,300 mm. The areas annual minimum and maximum temperatures are between 14°C and 32°C. The average altitude is 1,180-1,350 m ASL for Nyankanga and Geita Hill-Lone Cone site, 1,550-1,620 m for Kukuluma-Matandani mine site and 1,450-1,500m ASL for Nyamulilima Star & Comet site to the west.

The main GGM operations (Geita Block) are located within the Mtakuja River catchment that drains to Lake Victoria 25 km to the northwest. Surface water enters the main Nyankanga and Geita Hill-Lone Cone site from the southeast via a dam diversion of the Nyankanga River, which diverts water and outlets to the Mtakuja River. The Mtakuja River runs through the main mine site between the NTSF and WD1 and continues northwest towards Lake Victoria. Surface water runoff from the upland ridges and ferricrete areas can be high, and under heavy rainfall conditions can produce fast response flows within surface water channels.

Two hydrogeological units have been identified in the main GGM site area that act to transmit the majority of groundwater seepage: transported ferricrete and saprock. The transported ferricrete acts as a shallow, unconfined aquifer, while a deep aquifer exists within the basement rock profile (saprock and fractured bedrock). The saprolite unit generally acts as an aquitard between the shallow and deep aquifers.

Waste Management Plan

The presence of sulfides in the host rocks to the GGM gold mineralization necessitated a set of waste management procedures be developed prior to commencement of mining to ensure effective waste rock storage facility (WRSF) design and correct placement of reactive (PAF and metal leaching) waste to minimize and manage AMD as outlined in Scott et al, 2014. These procedures included:

- Waste rock and tailings characterization using acid base accounting (ABA), metals analysis, and kinetic testing of representative waste rock and ore;
- Construction of the geological model of the waste;
- Block modelling of waste rock and merging with the ore resource model;
- Validating the waste model using in-pit geological mapping;
- Selective handling and placement of waste in designated areas of the WRSF and the NTSF embankments;
- Validating placement of waste within the WRSF and tailings dam embankment;
- Monitoring for success of placement using piezometers within the WRSF, tailings embankment and downstream of these facilities;
- Regular technical reviews monthly (internal), three to six monthly (external);
- Implementing these procedures for LOM.

The WRD design facilitates PAF encapsulation, with a NAF base layer 10-20 m thick, PAF placed in the middle of each dump lift, and an outer NAF layer between 80 and 100 m on each dump lift to complete the encapsulation. The basal layer is constructed by paddock dumping and then worked with a dozer to form the flattened base layer. Tipping of PAF material within the internal part of the dump is commonly undertaken by paddock dumping and worked continually by dozer to form the dump lift. Tipping of NAF material to form the outer layer is usually done at 35-37° batter angle depending on type of material (oxides to fresh), interspersed with 36 m wide berms at 20 m vertical increment lifts and the final batter angle is <20°.

METHODOLOGY

To verify the hypothesis, that a cover system and landform design that resulted in an average net percolation rate of 10-15% and a reduction in erosion would meet GGM's closure objectives, a number of studies were undertaken, including:

- Site visit and material characterization (geotechnical and geochemical);
- Surface and groundwater quality data assessment; and
- Soil-plant-atmosphere modelling, seepage and solute transport modelling, erosion modelling, and landform evolution modelling.

Site Visit and Material Characterization

A site visit and material sampling program was conducted at GGM in the fall of 2012. Samples of waste rock, tailings, topsoil, and laterite borrow material were sampled both for geochemical and geotechnical characterization. Material samples were sent to laboratories in both Australia and Canada for further detailed testing. The material characteristics were used refine the conceptual model and were used to develop input parameters for the numerical modelling. The geotechnical parameters measured were particle size distribution, gravimetric water content, Atterburg limits, specific gravity, saturated hydraulic conductivity, and the water retention curve. The geochemical testing included acid base accounting, metals geochemistry, and short-term leach testing.

Surface and Groundwater Quality Data Assessment

A review and compilation of the water quality monitoring data collected by GGM for the three distinct mining areas within the GGM licence area was undertaken to provide background in regards to water quality, hydrology, hydrogeology, the effects of AMD, and hence the information for a holistic approach to AMD management at the GGM.

Two mine pits (Matandani and Kukuluma) that have ceased operation and are filling with groundwater are impacted by AMD and contain significant acidity and metals. Downstream of WD7 and WD9 (Kukuluma/Matandani) the chemical signature is Ca, Mg, and HCO_3 dominated. This is typical of the background chemistry in the area indicating WD7 and WD9 are not significantly acid forming.

Another significant source of AMD is the toe seep derived from WD1 (SW37/SW37a). Treatment of the seep was implemented in 2010 and monitoring results suggest that water quality in the area has improved in recent years, which is represented by a drop in sulfate and TDS concurrent with an increase in pH.

The NTSF that was commenced in 2000 shows that a change in water quality has occurred with time for key indicators Ca, Na, sulfate, alkalinity, and TDS. While the concentrations for these analytes is above the concentrations recorded for upstream surface water monitoring sites they remain below the GGM discharge standards. Further, the concentrations vary over the year with higher concentrations occurring in the drier months of May to August and lower concentrations occurring in wetter months of October to April, a pattern that has remained consistent since 2005. The chemical signature of groundwater upstream and downstream of the NTSF is dominated by Na, K, Ca, Mg, SO_4 and HCO_3. Below the NTSF increases in sulfate concentration in groundwater occurs locally. Concentrations are below GGM discharge standards.

There are no surface water data for upstream of the WD1 facility, but it is expected to be similar to surface water quality upstream of the NTSF. Below WD1 surface water is low in major cations, chloride, sulfate and metals; above concentrations in waters upstream of the TSF; but below GGM discharge standards. Monitoring data for groundwater upstream of WD1 are not available; however, the chemical signature upstream of WD1 is expected to be similar to that upstream of the NTSF i.e. dominated by Na, K, Ca, Mg and HCO_3. Downstream of WD1 the groundwater is dominated by Ca and HCO_3, which suggests WD1 has minimal influence on groundwater.

Further down gradient, the groundwater compliance monitoring point has a similar chemical signature to the upstream NTSF suggesting WD1 has a minimal effect on groundwater chemical composition. Although it should be noted that the meq/L concentration at the groundwater compliance site is double the upstream NTSF concentration. Further down gradient, the surface water compliance monitoring point chemical signature is dominated by Na, K, Ca, and SO_4. This is consistent with influence from both the NTSF surface and groundwater.

From the data set available, the Star and Comet area appears to have been affected by artisanal workings, although the water quality appears to be improving. The Star and Comet groundwater has a chemical signature dominated by Ca and HCO_3. The surface water chemical signature is similarly dominated by Ca, Na, K, and HCO_3. This suggests mining at Star and Comet has a relatively minor effect on chemical signature.

Overall there is relatively little exceedance of discharge limits in groundwater across the GGM site. Sites that have generated AMD (including the Kukuluma Pit and Matandani Pit; and the toe of WD1 (SW37) up to 2011) have historically exceeded compliance limits for a number of trace metals, however ongoing data may show these metals are now compliant. Most other sites show evidence of sulfide oxidation in either elevated sulfate concentration and/or elevated Fe, Al, or trace metal concentrations. However typically these sites are circum neutral pH with relatively low acidities possibly driven by Fe^{2+} or residual Al.

Source-Term Development

Source terms were developed for sulfate (SO_4), chloride (Cl), and fluoride (F) as conservative analytes for modeling purposes. They were derived from results from short term leach tests on samples collected from WD1 and the new tailings storage facility as part of this study as well as from comparison with surface and groundwater monitoring data from 2000-2012. The waste materials were divided into three types for the development of source terms: WD1 NAF waste rock, WD1 PAF waste rock, and new tailings. Source terms for the waste materials, as well as discharge limits defined by the Tanzania Bureau of Standards (2006), ANZECC (2000, 2011), and GGM, are shown in Table 1.

Numerical Modeling Assessments

Numerical modeling tools were used to verify the conceptual model of the site and to evaluate various cover system and landform designs for the waste storage facilities. The evaluations included soil-plant-atmosphere modeling, seepage and solute transport modeling, and erosion and landform evolution modeling.

Table 1 Summary of source terms and water quality guideline values used in modeling.

Source	Sulfate (mg/L)	Chloride (mg/L)	Fluoride (mg/L)
WD1 – NAF Waste Rock	276	59	0.65
WD1 - PAF Waste Rock	960	59	0.65
Tailings - Base Case	588	41	0.65
Tailings - Elevated Sulfate	1590	41	0.65

Source	Sulfate (mg/L)	Chloride (mg/L)	Fluoride (mg/L)
Guideline Values			
ANZECC – Livestock	1000	n/a	2
ANZECC – Drinking water (health)	500	n/a	1.5
GGM discharge standards (Tanzania)	500	200	8

Cover Design Conceptual Model

A spectrum of achievable net percolation (NP) rates using a cover system was developed for GGM based on available materials and quantities, the vegetation potential, the local climate, and the landform. Four levels of NP rates were developed for the conceptual categories of "very low", "low", "moderate", and "high" NP. Table 2 summarizes these four levels, as well as the conceptual cover system designs that are anticipated to achieve each NP level at GGM.

The locally-available borrow materials at GGM are a laterite material (which is highly variable). Based on laboratory measurements, an appropriately-compacted layer, utilizing the laterite materials that contain a higher clay percentage, could achieve a saturated hydraulic conductivity (k_{sat}) of ~5 x 10^{-6} cm/s. A non-compacted layer of laterite material could achieve a k_{sat} in the range of 5 x 10^{-3} to 1 x 10^{-5} cm/s and act as a growth medium and to achieve store-and-release of infiltrating water.

Using a cover consisting of 0.3 m of compacted laterite overlain with a 0.5 m thick layer of non-compacted laterite, a low net percolation rate of 10% of mean annual rainfall could likely be achieved. Alternatively, using a cover consisting of a layer of non-compacted laterite between 0.5 m and 1.0 m thick, a moderate net percolation rate of 15% of mean annual rainfall could likely be achieved. The conceptual model assumes that water will be managed on the plateaus and slopes to prevent erosion and that there will be upland diversion to prevent upland water running onto the landform.

The production conceptual model assumed for AMD generation from the waste materials was a direct linear relationship between solute loading at the base and net percolation rate at the surface (i.e. a constant concentration model). The source terms developed based on the surface and groundwater quality assessment (Table 1) were used to complete the conceptual model for GGM.

Table 2 Spectrum of achievable net percolation (NP) rates for conceptual cover system design options for the GGM waste storage facilities.

NP Level	NP (%)	Conceptual Cover System Design	
		Plateau Areas	**Batter Slope Areas**
Very Low	< 5%	Geosynthetic product or 0.3 m compacted clay (10^{-7} cm/s) and 0.5 m non-compacted growth medium	0.3 m compacted clay (10^{-7} cm/s) and 0.5 m non-compacted growth medium

Low	5 to 10%	0.3 m compacted laterite (≤ $5x10^{-6}$ cm/s) and 0.5 m non-compacted laterite	0.3 poorly-compacted laterite and 0.5 m non-compacted laterite
Moderate	15 to 20%	0.5 non-compacted laterite	0.5 non-compacted laterite
	10 to 15%	1.0 m non-compacted laterite	1.0 m non-compacted laterite
High	>20%	<0.5 m non-compacted laterite	<0.5 m non-compacted laterite
	25 to 35%	Uncovered waste rock or tailings	Uncovered waste rock or tailings

Soil-Plant-Atmosphere Modeling

Soil-plant-atmosphere modeling using VADOSE/W was completed to confirm the conceptual model; in particular, this assessment was used to predict performance (in terms of net percolation) of various cover system designs for the waste materials. A 100-year climate database and estimates of key vegetation characteristics were developed for the modeling program. Material characteristics were developed from the results of the geotechnical characterization program.

The results of the soil-plant-atmosphere modeling confirmed the conceptual spectrum of cover performance shown in Table 2. The modeling indicated an improvement in performance when the non-compacted laterite thickness was increased from 0.5 m to 1.0 m but showed performance levelling off for thicknesses greater than 1.0 m. This result was due to the higher available water holding capacity in the thicker cover layer and greater volumes available for evapotranspiration (but this benefit tapers off in thicker layers when the water gets too deep for roots). The modeling also showed an increase in performance on the slopes for all cover types due to increased runoff rates. Thus a coarser-textured material could be used on the slopes, if required for erosion control, and performance of 10% net percolation could still be expected.

Seepage and Solute Transport Modeling

Both 3-D and 2-D seepage and solute transport modeling programs were completed to confirm the hypothesis that a cover system resulting in a net percolation rate of 10%, together with the assumed source terms and constant concentration production model, would reduce solute loading at the downstream receptors to below discharge limits.

A risk assessment conducted for GGM in 2012 highlighted an area of the main Geita Mine site including WD1, the NTSF, the OTSF, and the Mtakuja River as an area of highest risk owing to the potential for AMD from the waste storage facilities and their close proximity to surface water. This area is known as the Geita Triangle and was a particular focus for the 3-D seepage and solute transport investigation. The 3-D modelling of the Geita Triangle area was developed using the model Hydrogeosphere (HGS) (Brunner and Simmons, 2012).

The key outcomes from the seepage and solute transport analysis were to understand the long-term concentrations of solutes at the compliance points under various rehabilitation scenarios. An analysis of the dilution of solutes in the Mtakuja River was also completed to help inform on future diversion of water between the Nyankanga Pit and the river.

Six different solute transport scenarios were simulated with the 3-D model using the source terms shown in Table 1. Only the results of one scenario are presented in this paper: Scenario #1 used a

weighted average sulfate concentration of 500 mg/L (40% PAF (960 mg/L) and 60% NAF (276 mg/L)) applied to the entire WD1 and a sulfate concentration of 588 mg/L applied to the NTSF tailings, which was considered the base case. Source terms were applied to the waste materials as constant concentration values for the full 2000-year simulation as a conservative assumption. Each solute was evaluated to determine if water quality guidelines or discharge standards were exceeded at Mtakuja River, GW29 or GW56 (groundwater compliance locations). Figure 1 shows the predicted sulfate concentration plume 100 years post-closure for (a) uncovered and (b) covered (10% NP) (b).

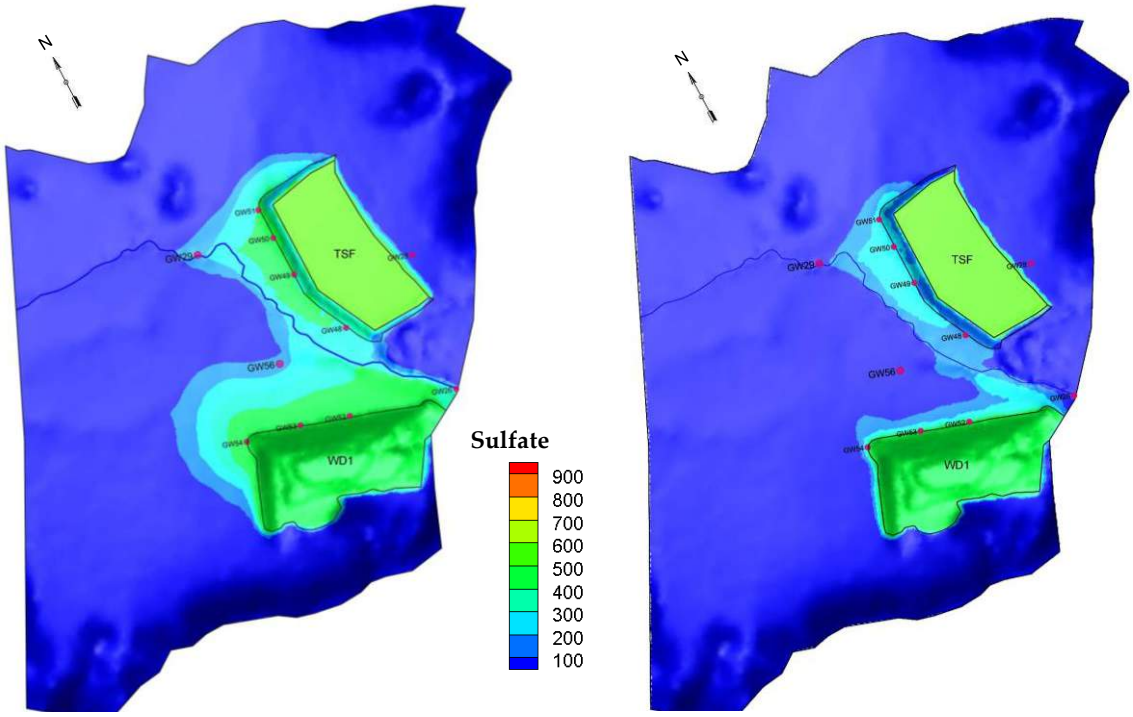

Figure 1 Predicted sulfate plume within Geita Triangle 100 years post-closure for (a) uncovered and (b) covered with net percolation of 10%. Groundwater compliance points GW29 and GW56 shown as well as Mtakuja River (surface water compliance).

Applying a cover system with an average NP rate of 10% is shown to significantly decrease the extent of the contaminant plume that develops from WD1 and the NTSF. Concentrations were predicted for the Mtakuja River based on the above model results. The mass loading predicted to report at the river included the predicted steady-state mass loading to the river from groundwater, WD1 and NTSF toe seepage, and upstream loading from the river. The Mtakuja river flow rate required to dilute loading to the river below the sulfate discharge standard (500 mg/L) for various NP rates was estimated. River concentrations were estimated for high and low river flow rates of 670 L/s and 50 L/s (based on both measured and estimated river flow rates). With high river flows (670 L/s), predicted sulfate concentrations in the river are diluted well below GGM discharge standards for all cover system scenarios. There is potential for river concentration to exceed GGM discharge standards if river flows are low (50 L/s) and cover system NP rates are 15% or higher,

indicating that the cover system and landform for WD1 and NTSF should reduce net percolation to 10% or less.

Erosion and Landform Evolution Modeling

Landforms at GGM are (generally) prone to erosion, owing to the local climate, the abundance of erodible lateritic soils, the presence of relatively steep landforms and the absence of water management structures in some locations. Erosion modeling and landform evolution modeling were conducted on various slope configurations for GGM's waste facilities to evaluate if the proposed mitigation measures would result in landforms that were safe, stable, and would meet expectations for business development opportunities. The main tools and information used in these analyses included LiDAR survey of the landforms, aerial imagery (Google Earth), the SIBERIA landform evolution model, the Water Erosion Prediction Project (WEPP) model, and material laboratory analysis results. A detailed discussion of these analyses can be found in Dobchuk et al. (2013) and Kemp et al. (2014).

Based on the results of the analysis conducted for this project, recommendations were made for a cover and landform design for each of the waste rock and tailings landforms at Geita Gold Mine (GGM) using a combination of specific strategies including:

- Re-vegetation strategies (seeding etc);
- Modification of soils to include a higher proportion of coarse NAF waste rock materials;
- Provision of drainage and bunding, especially to prevent plateau overtopping;
- Resloping the tops of each bench, during dump construction, towards a hard landform (natural hillslope) to direct surface water away from the crest areas of each lift; and
- Re-shaping landforms to profiles that resist erosion (final benched landforms on the outer slope of the waste rock dump are not recommended, linear or concave landforms are preferable).

DISCUSSION AND CONCLUSIONS

The project described in this paper was initiated to develop mitigation methods for the waste rock and tailings storage facilities at Geita Gold Mine (GGM) that would result in GGM meeting or exceeding their stated reclamation objectives including the creation of stable landforms and the reduction of solute loading from the waste storage facilities to meet discharge standards at the downstream compliance points. The conceptual model was that a cover system and landform design using the locally-available laterite material would reduce net percolation to a moderate level (10-15% of mean annual rainfall) and that this would be sufficient to reduce the solute loading at the downstream receptors to below discharge standards. This design was verified based on the results of the material characterization, the surface and groundwater quality assessment, and various numerical modeling analyses.

Based on the site visit and the results of the surface and groundwater quality assessment, it was determined that the PAF waste encapsulation as part of the GGM waste management plan was acting to reduce exposure of the PAF waste to oxygen and water and was leading to a reduced contaminant load to downstream receptors (versus non-encapsulated waste). The placement methodology, with trafficked layers of laterite material on top of each lift and the paddock-dumped base and PAF layers was likely acting to reduce the vertical infiltration of water and the advective movement of oxygen through the waste rock via preferential flow paths. Thus, with a lower

potential contaminant load within the waste facility, a cover system with only low to moderate reduction in net percolation (NP of 10-15%) was shown to be sufficient in reducing the solute concentrations at downstream receptors to below discharge limits. The cover system and landform design that met these requirements was also shown to be feasible using the locally-available laterite materials with only slight improvements to the landform design to increase stability—leading to rehabilitation options that were cost effective.

REFERENCES

ANZECC (2000) National Water Quality Management Strategy - Australian and New Zealand Guidelines for Fresh and Marine Water Quality, Volume 1, October.

ANZECC (2011) National Water Quality Management Strategy- Australian Drinking Water Guidelines 6, Volume 1, January. Barth H (1990) Provisional Geological Map of Lake Victoria Gold Fields, Tanzania 1:500000 (with explanatory notes). Geol. Jb. B 72, 59 pp.

Barth H (1990) Provisional Geological Map of Lake Victoria Gold Fields, Tanzania 1:500000 (with explanatory notes). Geol. Jb. B 72, 59 pp.

Borg, G and Shackleton, R M (1997) The Tanzania and NE Zaire cratons. In 'Greenstone Belts'. (Eds MJ de Wit and L D Ashwal) pp. 608–619. (Clarendon Press: Oxford, UK).

Brunner P and Simmons C T (2012) HydroGeoSphere: A Fully Integrated, Physically Based Hydrological Model, Ground Water, 50(2), 170-176

Dobchuk B, Scott P, Taylor I, Hancock G, Cooper H, Coulthard T. and Stephen R (2013) Landform Design for Geita Mine: Comparison of SIBERIA and CAESAR-Lisflood. In Proceedings of the 8th Australian Workshop on Acid and Metalliferous Drainage, Adelaide, Australia, April 29-May 2, 2014.

Kemp A, Taylor I R, and Dobchuk B (2014) Waste Landform Design: Applied Erosion Prediction and Validation. In Proceedings of the 9th International Conference on Mine Closure, Johannesburg, South Africa, October 2014.

Scott P, Phillip M, Stephen R, Mihayo E, Dobchuk B, Taylor (2014) Defining effective closure and reclamation measures for tailings and waste rock storages: an African case study. In Proceedings of the 8th Australian Workshop on Acid and Metalliferous Drainage, Adelaide, Australia, April 29-May 2, 2014.

Sibilski U and Stephen R (2006) ARD management at Geita Gold Mine. In 'Proceedings of 7th International Conference on Acid Rock Drainage'. St. Louis, MO, USA. 26-29 March 2006. pp. 2000-2010.

Tanzania Bureau of Standards (2006) Tanzania Water Quality Standards. Report TZS 860:2008, February.

The Diavik Waste Rock Project: Heat Transfer in a Large Scale Waste Rock Pile Constructed in a Permafrost Region

Nam Pham[1], Richard Amos[2], David Blowes[2], Leslie Smith[3] and Dave Sego[1]

1. *Department of Civil & Environmental Engineering, University of Alberta, Canada*
2. *Department of Earth and Environmental Science, University of Waterloo, Canada*
3. *Department of Earth, Ocean and Atmospheric Sciences, University of British Columbia, Canada*

ABSTRACT

Mining in permafrost regions of Canada has increased due to the rich natural resources, the offer of increased employment and revenue for the local people. However, Acid Rock Drainage (ARD) is also a major concern for the environment in the permafrost regions that are also being impacted by climate change and other industrial activities. In continuous permafrost regions, cold temperature provides an exceptional means to limit ARD using permafrost encapsulation of reactive waste rock. Oxidation of sulfide minerals in reactive waste rock decreases significantly in a sub-zero temperature environment, in addition, water in a frozen state limits transport of reactants and contaminants.

In this paper, thermal simulations of a full-size waste rock pile constructed in a continuous permafrost region with a Mean Annual Air Temperature (MAAT) of -9.1 °C are examined. Different cover thickness and climatic effects such as wind speed and warming air temperature are evaluated to determine their influences on the internal temperatures of the reactive waste rock stockpile. Under a warming of 5.6 °C/100 year, without a cover, the active layer in the waste rock is around 6 m, 5 m and 4.2 m at 10 %, 20 % and 30 % volumetric moisture content, respectively, after 100 years. However, with the pile covered by layers of 1.5 till and 3 m of a non-reactive rock, the active layer penetrates 3.3 m into cover layers after 100 years under this warming condition. At a permeability of the pile of 10^{-8} m^2, an average wind speed of 20 km/h has insignificant effects on thermal transport near the centre of the pile.

Keywords: Permafrost, Waste rock piles, Thermal modeling, Climate change, Active layer

INTRODUCTION

Mining involves the removal of significant quantities of waste rock to reach ore bodies and this waste is usually placed in engineered stockpiles. The stockpiles are often well above the water table; therefore they are generally unsaturated. In addition, waste rock usually contains some amount of sulfide minerals and the oxidation of sulfide minerals has the potential to produce acid rock drainage (ARD). Acidic drainage (low pH), high dissolved metal contaminants and other harmful components in leaching water from waste rock are a major concern for the receiving environments at and nearby the mine (Olson et al., 1979; Nordstrom and Alpers, 1999; Lefebvre et al., 2001). Based on the closure objectives of waste rock piles at a mine, engineered soil covers can be designed for different types of waste rock and they can be grouped into (MEND1.61.5b, 2010): "isolation covers", "barriers covers", "store and release covers", "water covers", and "insulation covers". However, in cold regions, cold temperatures are known to slow chemical and biological processes that are responsible for the oxidation of sulfide minerals and thus limit the generation of ARD (Jaynes et al., 1984; Langman et al., 2014). Therefore, to promote permafrost aggradation into reactive waste rock placed in a continuous permafrost region, insulation covers are a candidate as they transmit significant amounts of heat during the winter months and they serve as an insulation layer during the short summer (Arenson and Sego, 2007).

However, if climate change and warming occur, increasing air temperatures, changes of snow cover thickness and distribution, precipitation and other processes will significantly alter the subsurface thermal regime. The equilibrium between air temperatures and ground temperatures will change and cause a gradual increase in ground temperatures. The effects of warming in continuous permafrost regions would be a thickening of the active layer (the layer undergoing freeze and thaw near the surface) as a result of increases in temperatures. The impacts of warming would be more severe in discontinuous permafrost regions: such as thawing permafrost causing slope instability and loss of bearing capacity of infrastructure in these regions (Esch and Osterkamp, 1990). If a waste-rock pile is placed in a discontinuous permafrost area, the increase in ground temperatures due to warming could trigger the oxidation of sulfide minerals causing ARD. Various methods have been used to protect the underlying permafrost and to overcome the potential global warming in buildings and infrastructure,. These methods can also be used in waste-rock piles. Methods such as: ventilation pipes or ducts, thermosyphons and thermal piles, natural air convection embankments, foam insulation and other artificial ground freezing techniques (Goering and Kumar, 1996; Andersland and Ladanyi, 2004; Arenson and Sego, 2007).

SITE DESCRIPTION

The Diavik Diamond Mine is located on East Island, a 17 km^2 island in Lac de Gras, approximately 300 km northeast of Yellowknife, Northwest Territories in the Canadian Arctic (64°31′ N, 110°20′ W, el. 440 m). The site is located within the continuous permafrost region with an average precipitation of 283 mm including 60 % from snow (Neuner et al., 2013). Based on ground temperature measurements, the permafrost may extend to a depth of around 400 m and the active layer varies from 1.0 m in high moisture content soils to around 5.0 m in bedrock (Hu et al., 2003). Due to the cold and long winter season and relatively high evaporation at the site, water movement is limited to the active layer during the relatively short summer. Therefore, for the purpose of thermal modeling of the subsurface, convection associated with water flow is usually small and neglected; however, convective transport due to air is sometimes significant because of the high permeability of the waste rock.

Depending on the sulfur content, waste rock at Diavik is sorted into: Type I rock (< 0:04 wt % S), Type II rock (0.04 to 0.08 wt % S) or Type III rock (> 0:08 wt % S). Sorting the waste rock was used to classify between acid and non-acid generating waste rock. As a result, Type I rock is non-acid generating, Type II rock is low acid generating and Type III rock is potentially acid generating. At the end of the mine life, about 184 Mt of waste rock will be stockpiled in 60 to 80 m high piles covering about 3.5 km^2. Placement of an insulation cover is a closure concept for the Type II and Type III waste rock, including re-sloping the Type II and III areas to 18.4° (3H:1V) and covering the

stockpile with a 1.5 m low permeability layer of till, and a 3 m layer of Type I waste rock to act as an active freeze-thaw layer (Smith et al., 2013).

In this paper, ground temperatures were obtained using drill holes FD4 (39.8 m depth) and FD5 (77.4 m depth) from the top of full scale Type III waste-rock (Figure 1). Thermistor cables were installed into the drill holes at 5 m vertical spacing and ground temperatures are recorded on a 12 h interval. Ambient air temperature is measured hourly at the Diavik meteorological station, which is approximately 1 km from the waste rock dump. Numerical simulations of thermal transfer within the pile were also run under a predicted temperature warming over the next 100 years

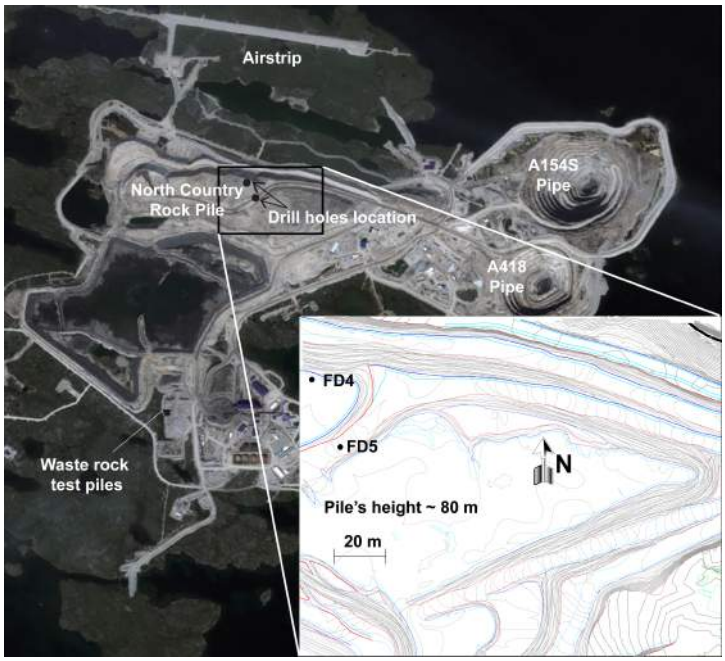

Figure 1 Drill holes location at Diavik diamond mine

Field data in 2013

Figure 2a indicates ground temperatures at depths between 45 m and 77.4 m (both holes) were constant throughout the year between -1.2 °C and -3.5 °C. Based on a thermistor near the ground surface the coldest and warmest temperatures were -28.5 °C and 13.5 °C, respectively. At a depth of 40 m, ground temperatures fluctuated and were much colder than nearby locations, which varied between -9 °C and -14 °C. This response occurs because the pile was built with 40m lifts and therefore permeability of the pile at locations near 40 m depth is higher, due to material segregation during tipping. Figure 2b shows that the thaw depth was at 4.8 m in August and September.

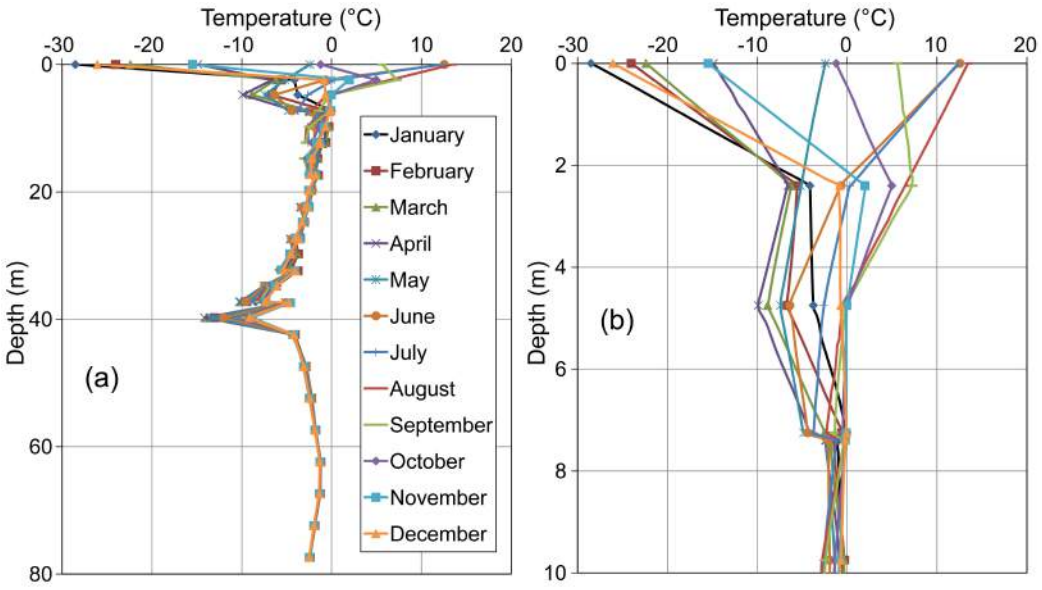

Figure 2 Measured ground temperatures in 2013, entire profile (a) and zoom-in the active layer (b)

NUMERICAL SIMULATIONS

In this section, the governing equations of heat conduction and convection due to moving air associated with density driven and wind effects were solved for temperature within the pile. The commercial Comsol Multiphysics software, which uses the finite element method, was used to solve the governing equations (Comsol, 2008). The mesh of the domain was refined near the surface to capture thaw depth due to the annual variation of air temperature.

Inputs to simulations

One cross section of the pile was chosen for the simulations because it is closely aligned with the dominant wind direction. The cross section is 2.5 km long and 80 m in height and the sides are at 3H : 1V (Figure 3). Furthermore, the bedrock foundation beneath the pile was placed at 100 m depth to complete the domain being analyzed. Air temperature measured at the site varies significantly throughout a year with the warmest and coldest temperatures in July with an average of 11.5 °C, and January with an average of -29.3 °C, respectively (Figure 4). Over the ten year period between 2000 and 2010, the MAAT is -9.1 °C, with 2004 air temperature being the coldest with MAAT of -12.1 °C and in 2010 the warmest with MAAT of -6.7 °C. The values of waste rock properties used in the simulations are listed in the Table 1 (Pham et al., 2013 and Neuner et al., 2013).

The initial in situ temperature profile was obtained using two thermistor cables installed from the top of the pile (FD4 and FD5) (Figure 5). Initial temperatures in bedrock between -15 m and -100 m were set to the same value as at -15 m. Surface temperatures of the pile were determined using measured temperature data from one thermistor near the surface which can be simulated using a sinusoidal function as:

$$T_s = A_s \sin\left(\frac{2\pi t}{365} - 4.34\right) - MAST + \frac{0.056t}{365} = 20.2\sin\left(\frac{2\pi t}{365} - 4.34\right) - 6.2 + \frac{0.056t}{365} \quad (1)$$

where t is time in days with the initial simulation time is January 1st, 2013, $A_s = 20.2$ is the amplitude, MAST (Mean Annual Surface Temperature) = -6.2 °C, which is different than MAAT

due to soil's surface conditions and local climate and the last term represents the predicted potential global warming of 0.056 °C/year (or 5.6 °C/100 years) for the site (Diavik, 2008).

Three scenarios were analyzed to evaluate the thermal behavior of the pile: Scenario 1: the pile was covered with 1.5 m till and 3 m Type I waste rock and no extrenal wind effect is assumed; Scenario 2: wind effects on temperature within the pile without a cover as air advection due to wind may change the thaw depth or active layer within the pile; Scenario 3: the pile without the covered layers and wind effects. All simulation scenarios include the effects of natural air convection, which will occur during winters as cold air sinks into the pile. All simulations were run for 100 years with the volumetric moisture contents of waste rock varying from 10 %, 20 % and 30 %.

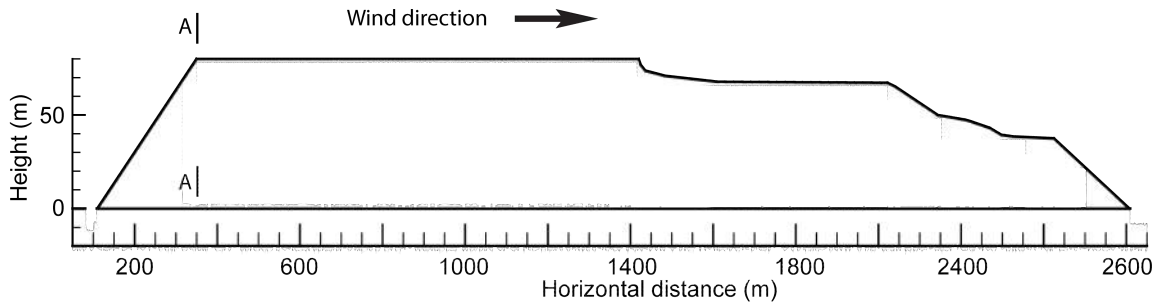

Figure 3 Geometry of the cross-section, the cut A-A is used to show temperature profiles in Figure 9.

Simulation results

Covered with 1.5 m till and 3 m Type I waste rock (scenario 1)

Figure 6 shows that the trumpet curves of ground temperatures at the center of the cross section indicate the waste rock beneath the till layer stays frozen year round. The till layer thaws down about 0.3 m between September and November each year and during the other months the till and Type III waste rock stay frozen (Figure 6). Depths below elevation 65 m are not shown because the temperature profiles remain constant between the elevation 65 m and 0 m. Due to the effects of latent heat in the till cover, ground temperatures in the Type III waste rock beneath the till after 100 years for various moisture contents are similar. Due to the till cover, the results indicate that conduction is dominant within the pile. The calculated pore air velocity beneath the till is on the order of 10^{-9} m/s, which is insufficient to effect heat transfer.

Pile with wind effects and no cover (scenario 2)

In this scenario, wind was assumed to be blowing at steady state at a velocity of 20 km/h, which is a little higher than an average wind speed at the site around 17 km/h (Chi et al., 2013) assuming that future wind speed will increase. Wind direction is from left to right as indicated in Figure 7. Air velocity within the pile was obtained by applying surface pressures around edges and top surface of the pile as boundary conditions. The surface pressures were obtained by solving the simplified 2-D representation of wind flow around the pile (Amos et al., 2009). Figure 7 shows that when using a permeability of waste rock of 10^{-8} m^2 the wind only affects the regions near the leading outer edge of the stockpile. Air velocities within the pile due to wind are also small with an average of about $2 \acute{} 10^{-4}$ m/s in the affected region around the edges.

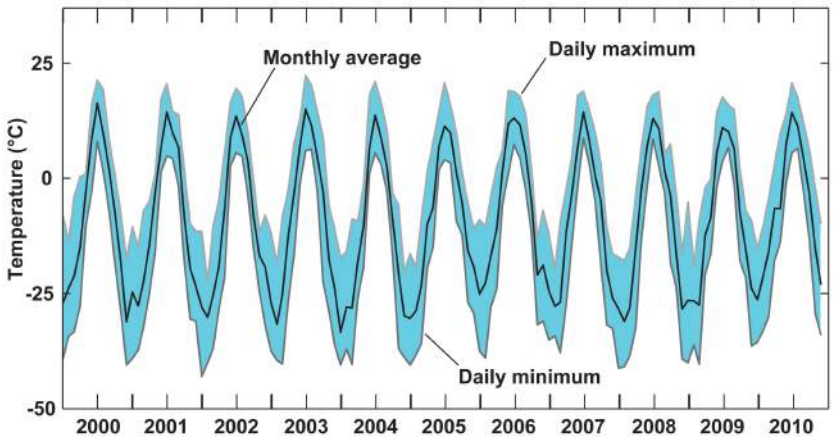

Figure 4 Monthly averaged air temperatures plotted with daily maximum and minimum air temperatures

Table 1 Material properties (data from Pham et al., 2013 and Neuner et al., 2013)

Property	Type I waste rock	Type III waste rock	Till	Bedrock
Porosity	0.25	0.25	0.2	0.003
Thermal conductivity (Frozen / thawed) (W/(m K))	1.7	1.8	3.2 / 2.9	3.0
Frozen bulk heat capacity (MJ/(m^3 K))	2.3	2.1	2.1	2.2
Thawed bulk heat capacity (MJ/(m^3 K))	2.4	2.3	2.5	2.2
Volumetric water content	0.1, 0.2, 0.3*	0.1, 02, 0.3*	0.18	0.0
Permeability (m^2)	10^{-8}	10^{-8}	$5 \cdot 10^{-16}$	0.0

* These values were assumed to examine the effects of moisture on ground temperatures within the pile

At this velocity, the effects of air convection on heat transfer within the pile would be insigficant due to the small specific heat of air. Therefore, the effects of wind on thermal regimes in the pile away from the edges will be negligible. Trumpet curves (Figure 8) show that the active layers are 6 m, 5 m and 4.2 m into the pile for 10 %, 20 % and 30 % volumetric moisture contents, respectively. The shallower active layer at higher moisture content is due to the effects of higher latent heat associated with the additional water. However, at 15 m below the surface, ground temperatures are constant of -2 °C regardless of moisture content.

Figure 9 shows the trumpet curves at 10 % volumetric moisture contents at the edge, 40 m offset and 80 m offset from the edge. The active layers are around 6.1 m and 6.3 m at the edge and 40 m

offset (Figure 9a and b) which are larger than at the centre of the pile (6 m). However, at 80 m offset from the edge at active layer is 6 m and the trumpet curve is similar to that of the centre location (Figure 8a and 9c).

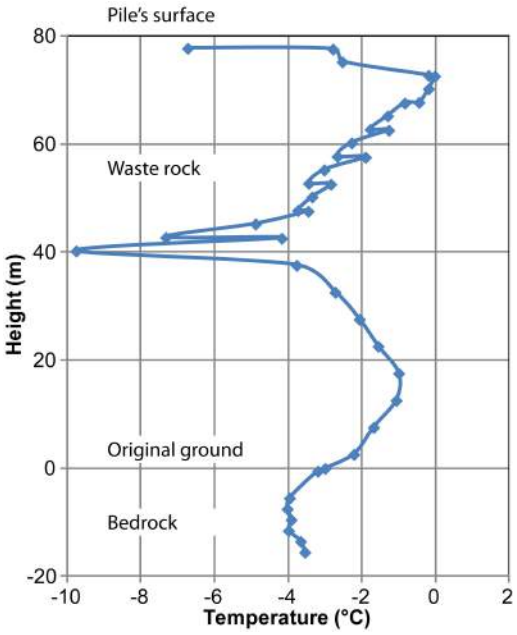

Figure 5 Initial temperature profile used in simulations, which is measured in January 1st, 2013.

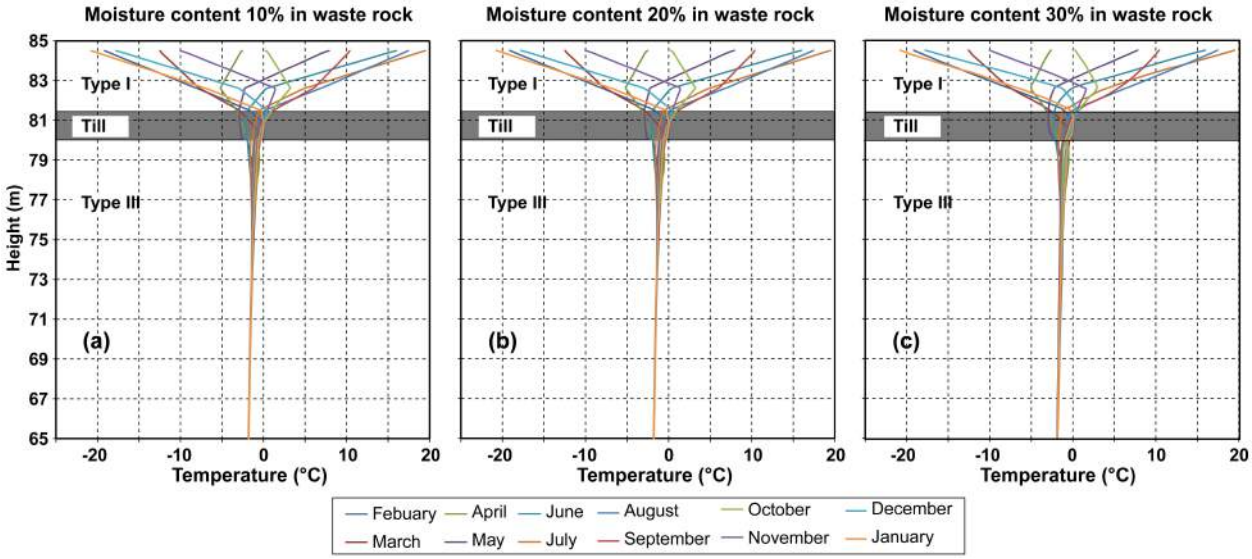

Figure 6 Trumpet curve of temperature profile in the pile for Scenario 1, with cover with 10 % (a), 20 % (b) and 30 % (c) volumetric moisture content in waste rock and no advective wind flow in year 100

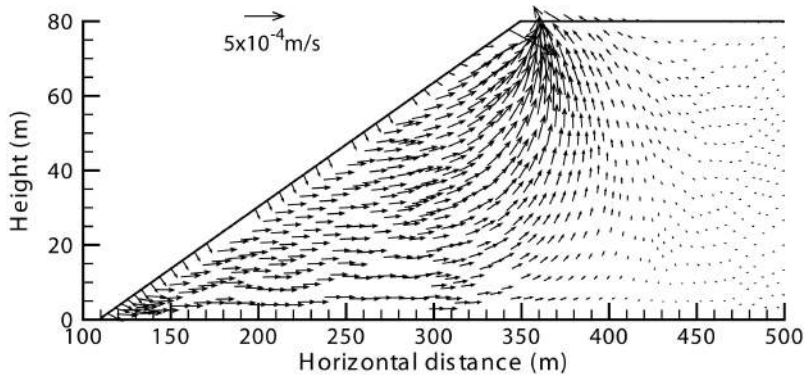

Figure 7 Air velocity within the pile due to wind

Pile without cover and wind effects (scenario 3)

As mentioned earlier, wind affects heat transfer only at the edges of the wind-facing side. Therefore, trumpet curves within the centre of the pile without and with wind effects are similar. The active layers are 6 m, 5 m and 4.2 m for the pile having 10 %, 20 % and 30 % volumetric moisture content, respectively (Figure 10). Figure 11 shows the isotherms during a winter after 100 years with warming and the thermal core with ground temperatures between -2 °C and -4 °C is the greatest in scenario 1 (Figure 11a) and smallest in scenario 3 (Figure 11c). Away from the edge, the thermal regimes between scenarios 1 and 2 are similar (Figure 11a and 11b).

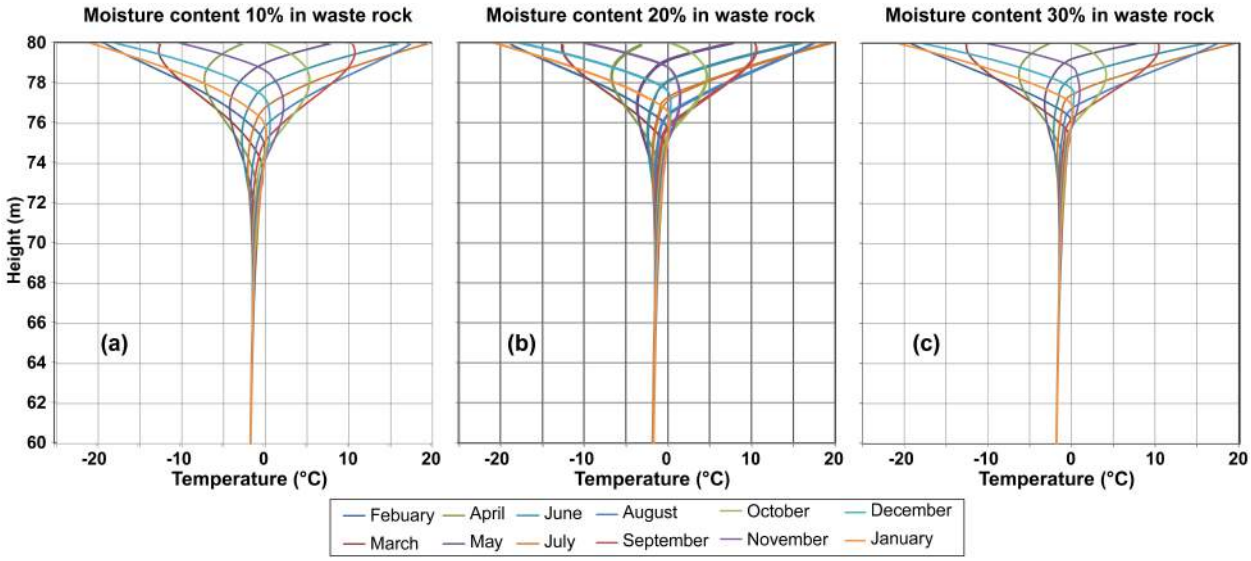

Figure 8 Trumpet curve of temperature profile in the pile for Scenario 2 with no cover, but with wind effects with 10 % (a), 20 % (b) and 30 % (c) volumetric moisture content in waste rock in year 100

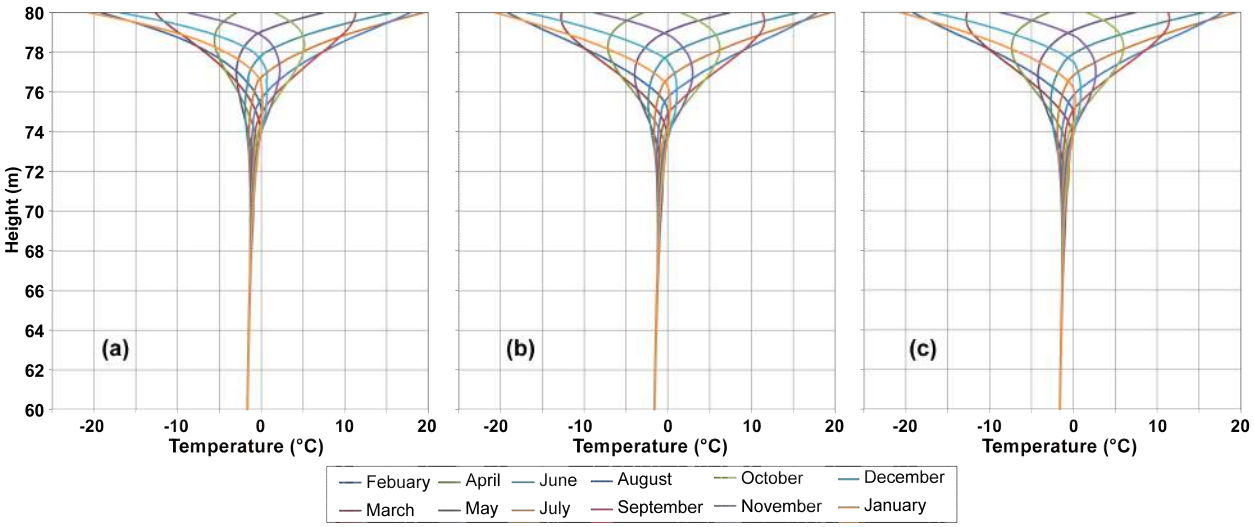

Figure 9 Trumpet curve of temperature profile in the pile with wind effects with 10 % volumetric moisture content in waste rock in year 100 at the edge, section A-A in Figure 3 (a), 40 m offset (b) and 80 m offset (c) from the edge

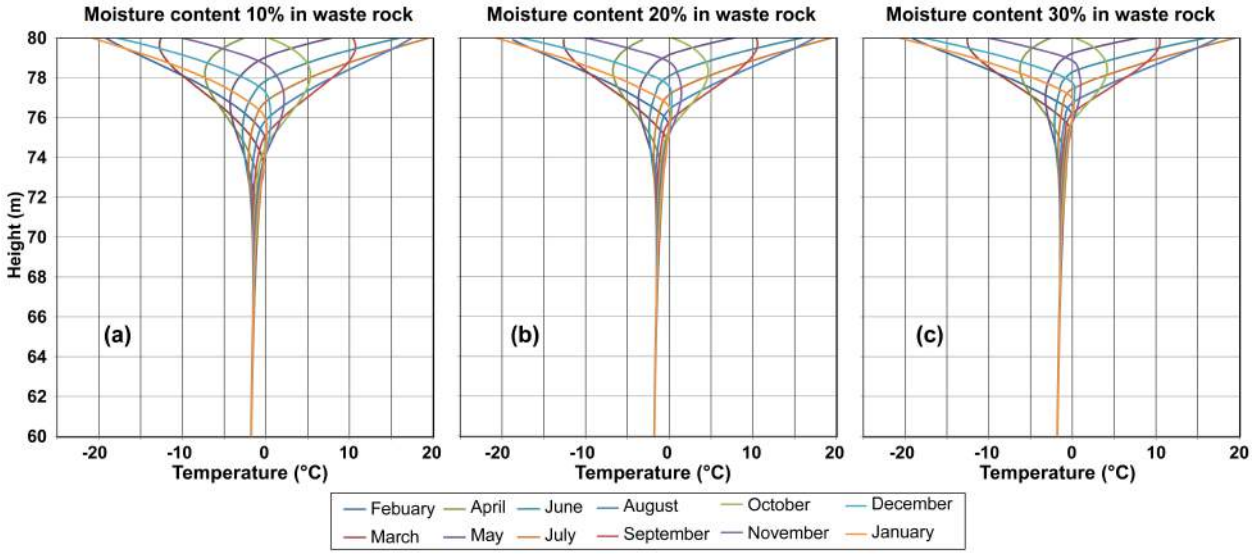

Figure 10 Trumpet curve of temperature profile in the pile for Scenario 3 without cover and wind effects with 10 % (a), 20 % (b) and 30 % (c) volumetric moisture content in waste rock in year 100

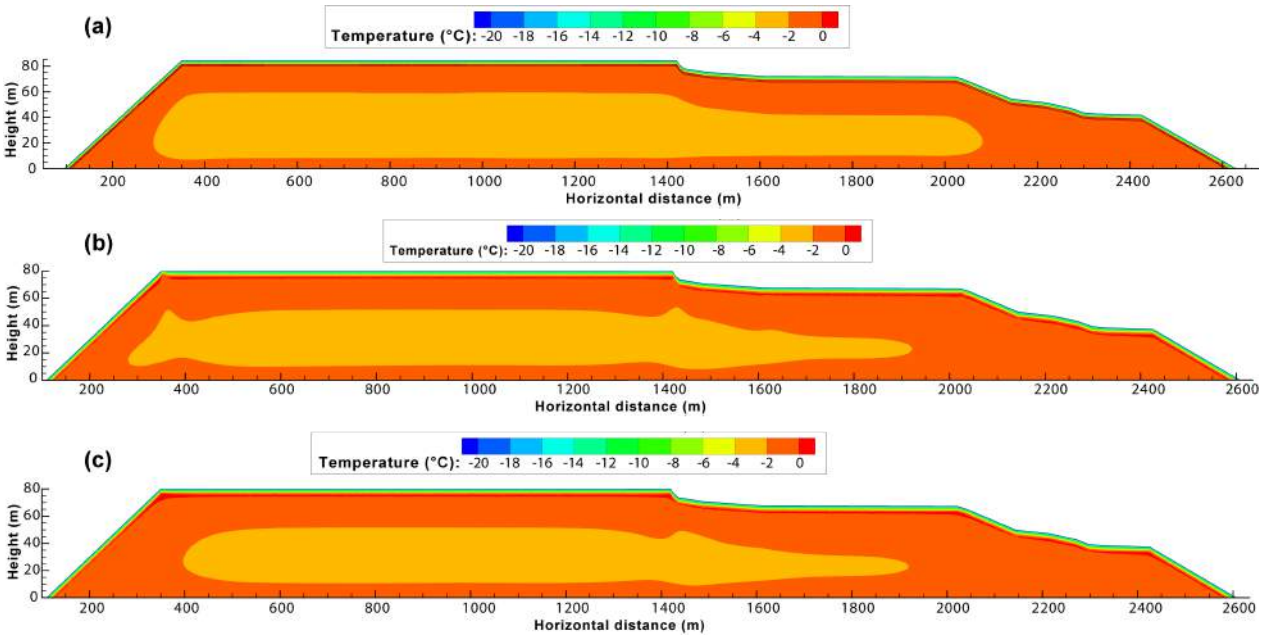

Figure 11 Temperature contours of the pile with cover (a) with wind effects and no cover (b) without cover and wind effects (c) after 100 years during winter at 10 % volumetric moisture content

CONCLUSION

Field temperatures from drill holes on top of waste rock pile indicate that the thaw depth was 5 m in 2013. However, under a warming of 5.6 °C/100 years and with the pile covered by layers of 1.5 till and 3 m of Type I rock, the active layer penetrates 3.3 m into cover layers after 100 years. Without a cover, the active layers will be 6 m, 5 m and 4.2 m at 10 %, 20 % and 30 % volumetric moisture content, respectively. The effects of wind on thermal regimes are insignificant near the centre of the pile. The region near the edge of the pile is affected by the wind with a permeability of the pile is 10^{-8} m^2 and a wind speed of 20 km/h. Therefore, under the predicted warming scenario, oxidation in waste rock may occur within a thin layer of active layer, of up to 6 m in the central portion of the waste rock pile.

ACKNOWLEDGEMENTS

Funding for this research was provided by a Collaborative Research and Development Grant from the Natural Sciences and Engineering Research Council of Canada (NSERC) awarded to D.W. Blowes, Principal Investigator; Diavik Diamond Mines, Inc.; the International Network for Acid Prevention; and the Mine Environment Neutral Drainage Program.

REFERENCES

Amos, R. T., Blowes, D. W., Smith, L., and Sego, D. C. (2009). Measurement of wind-induced pressure gradients in a waste rock pile. *Vadose Zone J*, 8(4):953–962.

Andersland, O. B. and Ladanyi, B. (2004). *Frozen Ground Engineering*. John Wiley & Sons.

Arenson, L. and Sego, D. (2007). Protection of mine waste tailing ponds using cold air convection. *Assessment and Remediation of Contaminated Sites in Arctic and Cold Climates*.

Chi, X.; Amos, R. T.; Stastna, M.; Blowes, D. W.; Sego, D. C. & Smith, L. The Diavik Waste Rock Project: Implications of wind-induced gas transport. *Applied Geochemistry*, 2013, 36, 246-255

Comsol Multiphsics (2008). COMSOL Inc, version 3.5a

Diavik Diamond Mine Inc (DDMI) (2008). Climate Change Adaptation Project Rio Tinto: Climate Change Impacts in the Diavik Region of Northern Canada.

Environment-Canada (2008). Climate Data Online. National Climate Data and Information Archive. Technical report, *Environment Canada*.

Esch, D. and Osterkamp, T. (1990). Cold Regions Engineering: Climatic Warming Concerns for Alaska. *Journal of Cold Regions Engineering*, 4(1): 6–14.

Goering, D. J. and Kumar, P. (1996). Winter-time convection in open-graded embankments. *Cold Regions Science and Technology*, 24(1): 57–74.

Hu, X., Holubec, I., Wonnacott, J., Lock, R., and Olive, R. (2003). Geomorphological, geotechnical and geothermal conditions at Diavik Mines. *In 8th International Conference on Permafrost. Zurich, Switzerland*.

Jaynes, D. B., Rogowski, A. S., and Pionke, H. B. (1984). Acid mine drainage from reclaimed coal strip mines: 1. Model description. *Water Resour. Res.*, 20:233–242.

Langman, J. B., Moore M. L., Ptacek C. J., Smith L., Sego D., Blowes D. W. (2014). Diavik Waste Rock Project: Evolution of Mineral Weathering, Element Release, and Acid Generation and Neutralization during a Five-Year Humidity Cell Experiment. *Minerals*. 4(2):257-278

Lefebvre, R., Hockley, D., Smolensky, J., and Gelinas, P. (2001). Multiphase transfer processes in waste rock piles producing acid mine drainage. 1: Conceptual model and system characterization. *Journal of contaminant hydrology*, 52(1-4): 137–164.

MEND1.61.5b (2010). Cold Regions Cover Research - Phase 2. Technical report, Indian and Northern Affairs Canada and Mine Environment Neutral Drainage (MEND).

Neuner, M., Smith, L., Blowes, D. W., Sego, D. C., Smith, L. J., Fretz, N., & Gupton, M. (2013). The Diavik waste rock project: Water flow through mine waste rock in a permafrost terrain. *Applied Geochemistry*, 36, 222-233.

Nordstrom, D. K. and Alpers, C. N. (1999). Negative pH, efflorescent mineralogy, and consequences for environmental restoration at the Iron Mountain Superfund site, California. *Proceedings of the National Academy of Sciences of the United States of America*, 96(7): 3455–3462.

Olson, G. J., Turbak, S. C., and McFeters, G. A. (1979). Impact of western coal mining–II.Microbiological studies. *Water Research*, 13(11): 1033 – 1041.

Pham, N. H., Sego, D. C., Arenson, L. U., Blowes, D. W., Amos, R. T., & Smith, L. (2013b). The Diavik Waste Rock Project: Measurement of the thermal regime of a waste-rock test pile in a permafrost environment. *Applied Geochemistry*, 36, 234-245.

Smith, L. J., Moncur, M. C., Neuner, M., Gupton, M., Blowes, D. W., Smith, L., and Sego, D. C. (2013). The Diavik Waste Rock Project: Design, construction, and instrumentation of field-scale experimental waste-rock piles. *Applied Geochemistry*, 36, 187-199.

CHAPTER 10

SCALING FROM LABORATORY TO FIELD STUDIES

10th ICARD IMWA 2015 | 10th International Conference on Acid Rock Drainage & IMWA Annual Conference

Waste Rock Dump Geochemical Evolution: Matching Lab Data, Models and Predictions with Reality

Steven Pearce, Peter Scott and Paul Weber

1. *O'Kane Consultants, Australia*
2. *O'Kane Consultants, New Zealand*

ABSTRACT

The prediction of how waste materials will evolve geochemically within waste rock storage facilities (WRSF) has been the subject of many hundreds of thousands of hour's research by geoscientists globally. Despite the quantity of research there are two significant areas of uncertainty that remain as partially resolved issues: (a) the majority of the research carried out has been at the laboratory not site scale (b) many predictions made using computer modelling have not, or are not normally able to be validated from site data.

OKC has had the opportunity to lead two large scale WRSF drilling programs at different sites in Western Australia where 12 historical waste dumps of around 10-30 years in age have been subject to detailed intrusive investigation. This has included approximately 2,000 m of sonic drilling, the recovery and detailed analysis of over 2000 samples of core material and the installation of over 150 sensors at depths between 5-140 m within the waste which have provided over 5 million points of monitoring data.

The extensive data gathered as part of the assessment has allowed OKC to determine the geochemical, hydrological and geophysical evolution of the waste rock facilities as a result of 10-30 years of exposure. This valuable site data has been used to both back test the results of predictive models made for the waste facilities, and to optimise predictive models for future scenarios. In addition the data has allowed the development of scaled up site specific kinetic leach columns.

Keywords: Kinetic testing, geochemical evolution, scale parameters, intrinsic oxidation rate

INTRODUCTION

The prediction of how waste materials will evolve geochemically within WRSFs has been the subject of many hundreds of thousands of hours of research by geoscientists globally. Despite the quantity of research there are two significant areas of uncertainty that remain as partially resolved issues: (a) the majority of the research carried out has been at the laboratory not site scale (b) many predictions made using computer modelling have not, or are not normally able to be validated from site date.

As part of a large scale investigation to improve the understanding of waste rock geochemistry at macro scale OKC has had the opportunity to lead two large scale WRSF drilling programs at different sites in Western Australia. 12 historical WRSFs of around 10-30 years in age have been subject to detailed intrusive investigation. This has included approximately 2,000 m of sonic drilling, the recovery and detailed analysis of over 2,000 samples of core material and the installation of over 150 sensors at depths between 5-140 m within the waste which have provided over 5 million points of monitoring data.

This paper focuses specifically on research carried out on sites within a semi arid climate and waste rock containing sulfidic black shale material taken from mines within the Pilbara in Western Australia.

LABORATORY TESTING AND THE ISSUE OF SCALABILITY

Laboratory testing methods have been developed and refined over many years for geochemistry assessment and AMD prediction which has resulted in a broad set of standardised testing methods being generally accepted internationally by the mine-geochemistry industry. This has been possible by and large because laboratory experiments are completed in a controlled environment with high degree of precision and accuracy. However a common factor and limitation to all laboratory assessments is that the scale at which these experiments are carried out.

Kinetic testing methods offer a good example of the issue of trying to determine how laboratory data should be used to extrapolate from the laboratory (micro) to site (macro) scale. Common kinetic tests such as humidity cells and leach columns utilise a few kilograms of material that has been crushed to a few millimetres in size that are then exposed to wetting and drying cycles with very high leaching rates. The concept of these kinetic tests is that by using small grain sizes and high leaching ratios the weathering processes (sulfide oxidation rates and carbonate dissolution) can be accelerated allowing the assessment of sulfide oxidation rates, acidity generation, neutralisation reactions, and leachate geochemistry to be assessed within a reasonable timeframe. It has been proven that these tests achieve the aim of simulating accelerated weathering. However, the precise method (and value) of how to utilise these results in a scaled up situation, for example in the extrapolation of data to predictions of field conditions such as oxidation rates or seepage quality has not yet been conclusively determined.

Table 1 outlines some scale factors that require consideration when using kinetic test data for "predictions" of field conditions, which will have a significant influence on the ability to predict field geochemical conditions and processes from laboratory data.

Table 1 Scale variables for laboratory kinetic tests compared to field conditions for medium to large size waste rock storage facility (>1 million tonnes)

Scale parameter	Laboratory test conditions	Typical Australian field conditions	Challenges extrapolating from lab to field
Grain size	PSD = 100% <6mm	PSD = 40% <6mm	Oxidation rates faster and dissolution of silicates/carbonates higher for smaller grain sizes. Lab tests may over estimate both sulfide oxidation rates and acidity buffering processes
Geochemical system	Open	Variable from open to closed	Open systems discharge acidity closed systems store acidity, lab tests are not reflective of field drainage geochemistry
Oxygen consumption measurement	Estimate from sulfate release	Estimate from in situ measurement	Using sulfate produced from leaching tests may not provide accurate prediction of oxygen consumption
Mass of material	1-2 kg	>1 Mt	Heterogeneity effects not accounted for in lab tests, bulk geochemistry of material in the field may not be well represented by material tested in the lab
Air flow (Oxygen supply)	Diffusion dominated unrestricted	Advection dominated potentially restricted	Lab tests assumed unlimited oxygen supply, field conditions may vary, generally significantly lower than lab conditions
Temperature	20-30 degrees	0-100+ degrees	Due to effect of thermal properties by total mass of material, field temperatures may be significantly higher than lab, this can effect geochemical reaction rates
Liquid : solid ratio	8:1 per year	0.001: 1 per year	Lab leachate is more dilute then field conditions due to high L:S ratio. No restriction on sulfide oxidation rates based on H_2O supply in lab, field reaction rates may be H_2O supply limited.

REACTION KINETICS IN CLOSED AND OPEN SYSTEMS: THE SUPPLY OF O_2 AND H_2O AS CRITICAL FACTORS

At the most basic level sulfide oxidation reaction kinetics are controlled by the relative supply of O_2 and H_2O. The commonly stated (simplified) reaction for iron sulfide oxidation in this case pyrite, to form sulphuric acid H_2SO_4 and ferrihydrite $Fe(OH)_3$ is (from Lottermoser, 2010):

$$FeS_2 + {}^{15}/_4\, O_2 + {}^{7}/_2\, H_2O \Rightarrow Fe(OH)_3 + 2\, H_2SO_4 \quad (1)$$

It is important to note that this reaction represents the interaction of O_2 with FeS_2 (pyrite) with H_2O thought to be acting as a catalyst. It is clear then that if either water or oxygen are not present then the reaction will not proceed, the kinetics of the reaction will therefore be determined by the relative supply of both. Lottermoser (2010) states that *"there is little consensus in the literature on the precise reaction mechanisms describing the oxidation of pyrite"*. Therefore it is not clear how the varying

supply of O_2 and H_2O will impact the pyrite oxidation reaction kinetics. It is however widely accepted that *"the transport of oxygen to the oxidation sites is considered the rate limiting process in dumps"* Lottermoser (2010). For example from equation (1) 7/2 moles H_2O are required for oxidation of 1 mole of FeS_2. However, in field conditions reactions take place in pore spaces of unsaturated waste rock where the pyrite mass is disseminated (at grades of a few percent) through the host rock. As a result this molar ratio of H_2O to Pyrite on a per kg rock mass basis will not be sufficient because at such low water contents the pore waters may not physically be in contact with sulfide mineral surfaces. The supply of O_2 and H_2O is in turn determined by the nature of the geochemical system as open or closed. In an open system there is a potentially unlimited supply of O_2 and H_2O into the system and a means for reaction products to exit the system. These systems are represented by laboratory free draining leach columns. A closed system in contrast is represented by either a restriction of supply of oxygen or water or a restriction on the means for reaction products to exit the system. With respect to field conditions the internal zones of WRSFs can vary between open and closed system conditions, and can often fluctuate between conditions on a seasonal basis.

Supply of H_2O, O_2 and the intrinsic oxidation rate (IOR)

The liquid to solid ratio (L:S) is a convenient way to express the relative supply of H_2O into the system, this simply reflects the weight for weight balance of water against the mass of the porous solid through which the liquid is passing. Free draining leach columns have very high L:S ratios in general, an AMIRA (IWRI and EGi, 2002) column has an annual L:S ratio of approximately 8:1 for example. In contrast WRSFs typically have low L:S ratios and annual ratios in the Pilbara are estimated to be around 0.001:1 (assuming a 40 m high WRSF has 400 mm of net percolation per annum).

Oxygen supply is dominated by the degree of saturation of the pore space within the material, and the process of air movement which can be driven by advective or diffusive processes. Within free draining leach columns the supply of oxygen is driven by diffusion as no advective forcing is applied. In WRSFs the supply of oxygen can be driven by advection or diffusion depending on site conditions. The work of Brown *et al*. (2014) indicates that convection of oxygen accounts for 90% of the oxygen transport into a WRSF and diffusion accounts for 10%. This is close to an order of magnitude difference between the two oxygen ingress processes.

The IOR is the oxidation rate where oxygen is freely available (Bennett *et al*., 1995). It has been reported that based on free draining leach column tests thast the IOR ranged from 1.6×10^{-8} to 3.3×10^{-6} kg $O_2/m^3/sec$ (EGI, 2001) for samples of pyritic shale materials (Mt. McRae shale) sourced form the Pilbara, Western Australia. Levay and Co (2013) report an acidity generation rate of ~1.5 kg H_2SO_4/t/week for a Mt. McRae shale sample having 3.2 wt.% S, which is equivalent to an IOR of 2.5×10^{-6} kg $O_2/m^3/sec$ and comparable to the EGi (2001) work.

Because an IOR of 2.5×10^{-6} kg $O_2/m^3/sec$ has been calcualted form a free draining leach column then it is assumed that given an unresticted oxygen supply that this is the minium oxygen requirement for the pyrite oxidation reaction not to be rate limited. On the same basis the amout of H_2O required for the reaction to not be rate limited can also be calculated. Based on reaction (1) and the produciton of 1.5 kg H_2SO_4/t/week requires a minmium of approximately 0.5 kg t/week of H_2O, which can be converted into an L/S ratio of 0.026 per year. Clearly given the L:S ratio is 8:1 in

column tests then there is a significant excess of H_20 for pyrite oxidation not to be rate limited, in fact there is approximately 300 times excess H_2O. It should be noted that the use of such excess H_2O in these tests will inevitably result in significant dilution of leachates, that is to say leachate strengths are unlikely to be representative of field conditions. For materials with low sulfide contents this is likely to be of particular concern as these tests will tend to significantly underestimate the concentration of contaminants of AMD leachates in the field

It is widely accepted in the industry that laboratory column leach tests and similar field based lysimeter trials provide elevated reaction rates compared to the field (Miller *et al*., 2003; Andrina *et al*., 2012). For example the calculated IOR for waste rock was an order of magnitude lower in trial dump experiments compared to a 500 tonne trial and lab columns in the work of Andrina *et al*., 2012. Most importantly, Andrina *et al*. (2012) notes that the trial dump was often well oxygenated with oxygen content often at 20%, which is comparable to atmospheric concentrations. Based on these studies when oxygen is generally freely available it may be proposed that the laboratory based IOR can be reduced by an order of magnitude due to scaling effects, which, for the purpose of this report is referred to as Laboratory to Field Conversion Factor (LFCF). However, as demonstrated by Table 1 there are many scaling effects that may impact the determination of field IOR rates, in addition the method of estimating IOR from sulfate production in these tests is subject to a degree of error that may be significant depending on the geochemistry of the situation.

WEATHERING PRODUCTS OF PYRITE OXIDATION: GEOCHEMICAL CONSIDERATIONS

Although a simple summary equation to represent the oxidation of pyrite (Equation 1), the weathering of metal sulfides in the environment do not often progress as shown in the direct production of H_2SO_4 and $Fe(OH)_3$. This is because interaction of the H_2SO_4, Fe^{x+}, H^+ or SO_4^{2-} with H_2O and O_2 results in the formation of many different compounds which are often meta-stable in the surface environment. Further interaction with H_2O and O_2 can occur depending on the pH/Eh of the geochemical environment. This simplified model of pyrite oxidation does not tell the whole story. Sulfide weathering has the potential to release all the acid 'potential' by the precipitation of hydroxides and oxides such as goethite or ferrihydrite:

$$Fe^{3+} + 3H_2O = Fe(OH)_3 + 3H^+ \quad (2)$$

This process does not store H^+ as stored metal acidity and releases maximum acidity. Hudson and Edwards *et al.* (1999) point out that even low concentrations of SO_4^{2-} in solution can suppress the formation of Fe hydroxides, and instead favours the formation of oxyhydroxysulfates. This alternative is the storage of acidity in secondary salts, which are only stable in oxidising acidic pH conditions. For example in the formation of jarosite:

$$3Fe^{3+} + K^- + 2SO_4^{2-} + 6H_2O = KFe_3(SO_4)_2(OH)_6 + 6H^+ \quad (3)$$

Often there is incomplete oxidation of the ferrous (Fe^{2+}) iron to ferric (Fe^{3+}) iron and ferrous salts such as melanterite, $FeSO_4$ (Equation 4) can form, which following any subsequent wetting can release the stored ferrous acidity (Equation 5). These acid salts are highly soluble.

$$FeS_2 + 7/2O_2 + H_2O \circledcirc FeSO_4 + SO_4^{2-} + 2H^+ \quad (4)$$

$$FeSO_4 + 1/2O_2 + 5/2H_2O \circledcirc Fe(OH)^3 + 2H^+ + SO_4^{2-} \quad (5)$$

However, if oxidation to ferric iron is complete yet the hydrolysis is incomplete, jarosite type secondary minerals can form. Jarosite type minerals form at pH values below 3.5 and release only $2H^+$ per Fe^{3+} incorporated into jarosite, not the associated $3H^+$ ions associated with complete Fe hydrolysis. Thus jarosite type minerals store acidity that can be released once pH increases (Equation 6). Jarosite is stable at pH values < 4 and above pH 4.7 it is soluble, dissolving slowly (Li et al., 2007), which has long term implications for the rebound of pH to circum-neutral conditions after sulphide exhaustion and/or for the treatment of AMD impacted waters.

$$KFe3(SO_4)2(OH)^6 + 3H_2O \circledcirc 3Fe(OH)^3 + 3H^+ + 2SO_4^{2-} + K^+ \quad (6)$$

The acid load associated with the dissolution of ferrous salts such as melanterite will occur immediately upon wetting. The precipitation and dissolution of these sulfate bearing minerals will exert a significant control on the sulfate produced in leachates and therefore the ability to accurately predict IOR rates from laboratory leaching experiments.

In semi-arid environments the precipitation of these secondary sulfate minerals as a result of low L:S ratios may therefore be a significant factor in determining how much acidity is released from the WRSF.

OPEN AND CLOSED GEOCHEMICAL SYSTEMS

Table 2 outlines the importance of consideration of the geochemical system being studied as open or closed. Laboratory methods are open systems and will generally have unlimited oxygen supply and very high L:S ratios so oxidation reaction rates are not rate limited. In addition these conditions will limit the potential storage of acidity as secondary sulfate minerals, which will also result in high output of dissolved phase oxidation reaction products. Field conditions in comparison represent a variable state system which may have a seasonal aspect as the system ranges from open to a closed state. It should be noted that contrary to widespread belief oxygen supply can still represent an unlimited condition in WRSFs as a result of advective air movements in coarser zones of waste. Whereas in semi-arid environments the supply of H_2O is likely to be the limiting factor with respect to formation of an open system due to low L:S ratios.

Table 2: Open and closed systems

Scenario	System	Oxygen supply	H_2O supply	Storage of acidity as meta stable minerals	Output of Fe^{2+}, Fe^{3+}, H^+ and SO_4^{2-} in leachate
AMIRA Leach column	Open	Diffusion controlled potentially unrestricted	Unrestricted. Annual LS ratio 8:1	Low	High due to high flushing rates (L:S ration 8:1)
Waste rock prior to "wetting up"	Closed	Advection controlled potentially unrestricted	Restricted: depth variable dependence,	Very high	Low due to very low flushing rates
Waste rock "wetted up"	Open	Advection controlled potentially unrestricted	Limited to net percolation rate, Annual LS ratio of 0.001:1 common	Variable	Variable due to seasonality of flushing rates. Annual L:S ratio of 0.001:1 common

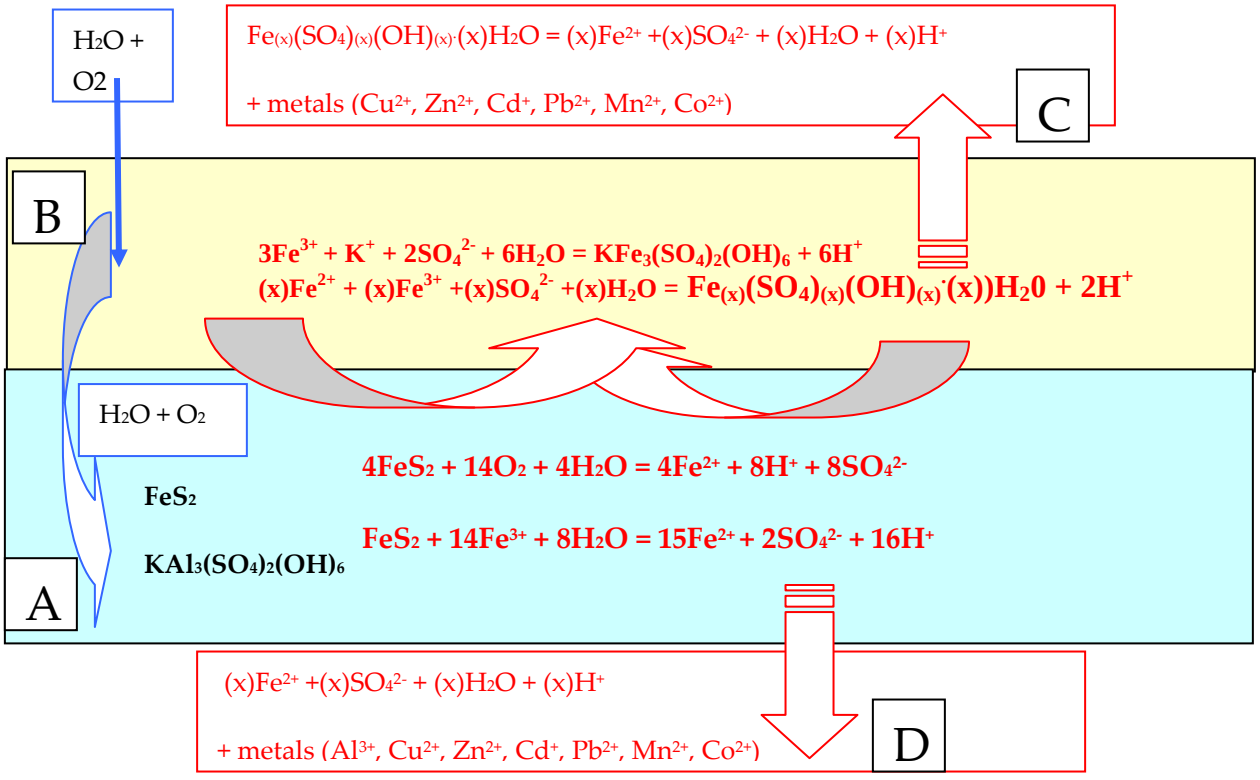

Figure 1 Simplified geochemical model of sulfide oxidation showing open and closed system pathways

Figure 1 shows the simplified geochemical model for initial stages of sulfide oxidation in an open system

- Box A indicates sulfide minerals that are undergoing oxidation in the presence of aluminium and potassium bearing silicate minerals and in contact with an unrestricted supply of oxygen and water resulting in production of Fe^{2+}, Fe^{3+}, H^{+} and SO_4^{2-}

- Box B indicates production of secondary oxyhydroxysulfates on mineral surfaces within pore spaces from dissolved phase species released from Box A. This process is likely to dominate in a closed system where L:S ratios are low and precipitation of these minerals exceeds losses from leachate discharges

- Box C indicates a situation where the precipitated oxyhydroxysulfates dissolve to form Fe^{2+}, Fe^{3+}, H^{+} and SO_4^{2-} and H_2O. This situation is representative of an open system where L:S ratios are high enough to dissolve any secondary minerals present that are soluble.

- Box D indicates the situation where the soluble products from Box A are directly discharged from the system. This is an open situation common to free draining laboratory kinetic tests where L:S ratios (flushing rates) are high. In this scenario secondary minerals (Box B) do not have much chance to form due to high dissolution rates caused by high L:S ratios.

CASE STUDY: INTRUSIVE WRSF INVESTIGATION

The presented study includes 12 WRSFs at various mine sites in the Pilbara, Western Australia. The mine sites are made up of multiple WRSFs which have been constructed by various techniques including end dumping. A proportion of the dumps contain pyritic black shale with some incorporating encapsulation techniques. OKC completed a drilling programme that resulted in 2,000 m of sonic drilling, the recovery and detailed analysis of over 2000 samples of core material the installation of over 150 instruments within 12 WRSFs up to a depth of 100 m. The WRSF monitoring systems were equipped with instrumentation to measure *in situ* moisture, oxygen pore-gas concentrations, pore-water pressure and *in situ* temperature within the WRSFs.

The Pilbara region consists of a climate classified as arid-tropical. Summers last from October to April and mild winters occur from May to September. Sporadic and intense thunderstorms are typical for the region from January to March, and tropical cyclones can result in daily rainfall amounts of up to 200mm over a 24hr period.

Presentation and analysis of the data collected from the instrumentation to date is beyond the scope of this paper and is reported in a separate paper published in Pearce and Barteaux 2014. A summary of the results is provided below which is important for understanding of field conditions within the WRSFs that are driving geochemical conditions:

- Wetting up of the WRSF's is not occurring uniformly throughout the waste. Generally the coarse cobble zones did not match the wetted-up model as moisture contents were lower than expected, whereas the finer textured materials had moisture contents closer to the wetted up model scenario.

- Based on responses of installed instrumentation the internal movement of water is considered to be governed by preferential flow paths predominantly within zones of coarser waste rock particle sizes. Fast responses to rainfall events are noted in these zones through the middle of the WRSFs, which can be tracked to basal zones of the WRSFs.

- The results of moisture content analysis indicates that water content varied between the borehole locations with the majority of results ranging from 3-15% by volume. If the moisture content is assumed to be on the upper end of the estimate at 10% on a mass basis this represents a current static L:S ratio of 0.1.

- Oxygen sensors installed indicate the WRSF's have high internal air flow rates and connectivity which is providing ample supply of oxygen to the whole waste rock profile with oxygen levels of between 16-20% being recorded through the whole profile of the waste in many WRSFs. In general oxygen concentrations increase with depth indicating convective supply source.

- Elevated internal dump temperatures (30-40 ^{o}C), high (and connected) internal air flows and supply of H_2O within preferential zones are postulated to be driving evaporative drying of pore waters which results in the transport and re distribution of water in the gaseous phase within the waste mass throughout much of the profile. This mechanism is considered to comprise a significant means of transfer of H_2O within the WRDs from zones of preferential flow to zones that do not receive much direct net percolation

Given the above observations it may be inferred that oxidation reactions within the WRDs studied may not be O_2 limited, but are more likely to be limited by the supply and movement of H_2O.

Geochemical analysis of drill core supports this conjecture as there is a significant presence of secondary sulfate minerals which are indicative of precipitation of sulfate bearing minerals as a result of stationary pore fluids (and therefore a very low L:S ratios). The geochemical system can therefore be best thought of as semi closed in that oxygen and H_2O (possibly supplied from internal evaporation rather than matrix pore water flow) can enter the waste but very limited leachate leaves the system. This results in a buildup of secondary sulfate minerals. Sulfur speciation results from analysis of black shale samples suggest a high degree of oxidation of sulfides for a large proportion of samples tested. From older WRSFs (30 yrs+) approximately 1500 samples were analysed from 49 boreholes, the average and median percentages of total sulfur that was in the form of sulfate was 80% and 72% respectively. The average proportion of total sulfur present as sulfate was 80%. At higher grades of >1% sulfur the sulfate ratio is slightly lower, around 60% average. It is assumed based on understanding of the mineralogy of the black shale that the material when deposited comprised sulfide as pyrite and little sulfate minerals. It is assumed therefore that the majority of sulfate present as measured represents secondary sulfate minerals that are the result of oxidation of the pyrite.

If it is assumed that the oxidation reactions have been occurring for approximately 30 years and no loss of sulfate from the system has occurred then IOR rates are determined as followed:

- IOR field = 3%S @ 60% oxidation over 30yrs = 0.04 kg H_2SO_4/t/week = 7.5^{-8} kg O_2/m^3/sec
- IOR field = 9%S @ 60% oxidation over 30yrs = 0.1 kg H_2SO_4/t/week = 1.9^{-7} kg O_2/m^3/sec

The field IOR rate calculated is considered a lower bound estimate as reaction rates may have declined with time as a result of fresh sulfide surfaces being smothered by secondary minerals. Laboratory calculated values lie in the range 4.9E-7 to 2.9E-6 kg O_2/m^3/sec. İn general the results of the case study assessment broadly agree with Andrina *et al*. (2012) where an order of magnitude difference in IOR was observed between field and lab IOR rates. It is interesting to note that even with the very low L:S ratios observed in the WRSFs that oxidation reactions have proceeded to 60% or greater completion. If it is assumed based on field monitoring data that oxygen is not the limiting factor, the main causes of the lower obsered field rates are likely to be:

- The impact of restricted water supply and time taken for "wetting up" to occur
- Formation of secondary sulfate mineral coatings around sulfide grains as a result of low matrix pore water flow and leachate "flushing"
- Larger particle sizes than laboratory tests

CONCLUSIONS

The use of laboratory leach column data for field estimates of IOR and seepage quality requires careful consideration as scaling factors will considerably impact the validity of the results. For WRDs in semi arid climates such as the Pilbara the low rainfall environment creates conditions of very low L:S ratios and geochemical systems within WRDs may remain in a quasi closed state for many years. High levels of oxygen ingress are indicated to occur as a result of high internal WRSF air temperatures and low waste rock saturation levels which means that sulfide oxidation reactions may become limited to a greater extent by net percolation rates than oxygen supply. It is noted that even with very low WRSF L:S ratios (0.1 or less), oxidation reactions have proceeded to 60% or greater completion. Storage ratios of acidity as secondary sulfate minerals are high during the period that the WRD remains as a quasi closed system. As a result future predictions of seepage quality must therfore consider the impact that future dissolution of these minerals will have if the WRD approches a "wetted up" state. Laboratory leach columns in comparrison to field conditions are charaterised by high L:S ratios and low levels of stored acidity. When extrapolating laboratory results to field conditions in semi arid envonrnments therefore it must be considered that leach columns data may overestimate IOR (by an order of magnitude), but likely significalty underestimate potential seepage quality compared to field conditions.

REFERENCES

Andrina, J., Wilson, G.W., Miller, S.D., 2012. Waste rock kinetic testing program: Assessment of the scale up factor for sulfate and metal release rates. In: Proceedings of the Ninth International Conference on Acid Rock Drainage (Ottawa, Canada 20-26 May 2012).

Bennett, J.W., Comarmond, M.J., Clark, N.R., Carras, J.N., Day, S., 1995. Intrinsic oxidation rates of coal reject measured in laboratory. In: Proceedings of Sudbury 1995: Conference on Mining and the Environment, Sudbury, Ontario, Canada, pp.9-17.

Brown, P.L., Logsdon, M.J., Vinton, B., Schofield, I., Payne, K., 2014. Detailed characterisation of the waste rock dumps at the Kennecott Utah Copper Bingham Canyon Mine – Optionality for Closure. Proceedings of the Eighth Australian Workshop on Acid and Metalliferous Drainage (Eds. H Miller and L. Preuss), Adelaide May 2014; pp 1-12.

IWRI and EGi (2002) ARD Test Handbook. AMIRA P387A Project: Prediction and Kinetic Control of Acid Mine Drainage. AMIRA International, Melbourne, Australia.

Li, J., Smart, R. St.C., Schumann, R.C., Gerson, A.R., Levay, G., 2007. A simplified method for estimation of jarosite and acid-forming sulphate in acid mine wastes. Science of the Total Environment 373: 391 – 403.

Lottermoser. B.G (2010) Mine Wastes Characterisation, treatment and Environmental Impacts, 3rd Edition, Springer

Miller, S. 2014. Leading practice solutions for acid rock drainage prevention and control: key to achieving a sustainable future for mineral resource development. In Proceedings of the Eight Australian Workshop on Acid and Metalliferous Drainage (Eds. H Miller and L. Preuss), Adelaide May 2014; pp 51-65.

Miller, S., Andrina, J., Richards, D., 2003. Overburden geochemistry and acid rock drainage scale-up investigations at Grasberg Mine, Papua Province, Indonesia. In Proceedings of the Sixth International Conference on Acid Rock Drainage, 12-18 July, 2003, Cairns, Queensland, pp 111-121.

Scaling Laboratory Sulfate Release Rates to Operational Waste Rock Piles

Kim Lapakko and Mike Olson
Minnesota Department of Natural Resources, USA

ABSTRACT

There is little agreement on scaling factors to be used for extrapolating laboratory dissolution test results for predicting solute release rates from proposed waste rock piles in the field. The scaling factor for a given solute is the ratio of its release rate in the field to that observed in the laboratory, and its magnitude is dependent on both the solute and site-specific variables. Scaling factors for sulfate release rates from Duluth Complex rock of moderate sulfur content were determined empirically by comparison of laboratory rates to field rates. The laboratory rates were calculated based on sulfate release during weeks 6 to 71 observed for 17 blast hole samples with sulfur contents of 0.18 to 1.64 percent. The samples were collected from the mine site from which comparative field data were generated. Annual field rates were determined over a period of 3 to 13 years for five waste rock piles, ranging in mass from 2,000,000 to 15,000,000 tons, with estimated sulfur contents of 0.24 to 0.97 percent. Laboratory and field rates were expressed per unit mass sulfur. Comparison of 17 laboratory rates and 42 annual field rates yielded in 714 distinct calculated scaling factors. These values were fit to a beta distribution for which the mean and standard deviation were 0.127 and 0.083, respectively.

Keywords: mine waste rock, mine drainage, environmental review, mine waste drainage quality prediction, laboratory scaling

INTRODUCTION

Environmental review for proposed operations requires predicting solute release from mine waste storage facilities. Such predictions can be informed by operational phase data from mine wastes of similar composition, disposed in similarly constructed facilities, and weathering under similar climatic conditions. Such information from "analog" sites is often not available. Consequently predictions are based on the scaling of laboratory data to field conditions. The magnitude of such scaling will depend on the solute being scaled, drainage pH, rock type, rock composition, method of laboratory rate generation (e.g. humidity cells vs. column tests), method of field rate generation (e.g. test plots vs. full scale storage facilities), and reaction environment variables in both the laboratory and field (e.g. temperature, leachate to rock ratio, oxygen availability). Consequently, it cannot be assumed that scaling factors quantified will be universal.

Previous Studies

Two approaches have been used for scaling laboratory rates to the field, the first of which applies scaling factors for individual mechanistic factors to account for differences such as rock composition, reaction environment, and solute transport. Considerable data and analysis for this approach was generated by studies focused on waste rock piles containing two varieties of both gneiss and schist in northern Sweden (Strömberg & Banwart, 1994; Strömberg et al., 1994; Strömberg & Banwart 1999a; Strömberg & Banwart 1999b). Apparent rates of pyrite, chalcopyrite, biotite, and plagioclase weathering in the field were found to be roughly 0.01 to 0.2 times those derived from laboratory batch tests on six different particle size fractions (Malmström et al., 2000). A "scale-dependence model" accounted for the differences between field and laboratory rates using quantitative contributions of particle size, temperature, pH, and hydrologic variables affecting solute transport.

Kempton (2012) included these factors as well as moisture content and pore gas oxygen concentration in a literature review of scaling factors for solute release from waste rock. This is less detailed consideration than that of scaling mineral dissolution rates but is adequate for application to predicting solute release from waste rock. He concluded that prediction of solute release rates based on reported ranges of scaling factors would have a high degree of uncertainty. For example, he stated that waste rock particle size distribution and its relationship to hydrologic factors affecting solute transport produced a scaling range covering a factor of 7.5.

A second approach is that of empirically determining scaling factor based on comparison of laboratory and field rates for the rock in question. Wagner et al. (2006) compared sulfate release rates from mafic and feldspathic gneiss in a northern Saskatchewan test pile (8 x 8 x 5 m high) to those derived from laboratory dissolution tests on five different size fractions of the rock (Hollins et al., 2001). Sulfate release rates (normalized for surface area) in the field were 0.3 times those observed in the laboratory, suggesting that factors such as temperature and solute transport limited sulfate release in the field. There were no humidity cell data for the typical -0.25-inch fraction used in humidity cell tests to calculate a scaling factor directly from this test to the test pile.

Shaw & Samuels (2012) conducted paired humidity cell and 30-gallon barrel tests on three porphyritic intrusive rocks and one metasedimentary rock. The particle size was similar in both tests and the average temperature and precipitation in the field were approximately 16 °C and 100 mm, respectively. Drainage pH from two of the field tests were 3.5 and 1 unit lower than the corresponding laboratory test, and values from the remaining two pairs were in fairly close agreement. Direct extrapolation of laboratory data yielded predicted sulfate concentrations that

were roughly 0.07 to 0.3 those observed in the field tests. The comparatively low laboratory rates were attributed to higher pH conditions resulting from the higher flushing rate in the laboratory. It was speculated that the higher flushing enhanced dissolution of neutralizing minerals and prevented development of acidic micro-environments in the laboratory tests.

Robertson, Barazzuol & Day (2012) compared sulfate release rates from 13 humidity cell tests on fresh drill core to field rates observed for 7.6 million tonnes of rock that had been weathering for 27 years in the field, roughly 200 km northeast of Timmons, Ontario. The rock was predominantly massive and pillowed basaltic rocks, some hydrothermally altered, and felsic and mafic intrusives. Comparison of the sulfate release rate for the median sulfur content rock (0.5 percent S) in the laboratory with that observed in the field yielded a scaling factor of 0.1. The corresponding factor assuming a 95 percentile sulfur content (1.46 percent) to be controlling release in the field yielded a scaling factor of 0.05.

Hanna & Lapakko (2012) determined scaling factors for sulfate release using data generated by 26-week humidity cell tests on seven drill core samples of finely laminated, fine-grained rock, referred to by miners locally as the lower slaty member of the Biwabik Iron Formation (Severson et al., 2010). Sulfate release rates, normalized for pyrite mass, calculated for roughly 50 million tonnes of this rock in northeastern Minnesota were generally equal to or greater than the corresponding rates in the laboratory.

Lapakko (1994) compared results from laboratory dissolution tests on fine noritic and gabbroic Duluth Complex rock (0.053 < diameter ≤ 0.149 mm) from the South Kawishiwi Intrusion to those generated by roughly 1000-tonne test piles of similar Duluth Complex rock from the Partridge River Intrusion in northeastern Minnesota. Rates in the field were compared to laboratory rates for rock of similar sulfur content and yielded scaling factors of roughly 0.1 to 0.3.

OBJECTIVE AND APPROACH

The objective of this report is to present scaling factors for sulfate release from operation scale stockpiles of Duluth Complex rock in the field relative to those that would be generated in humidity cell tests. The approach employed data that was generated in studies previously conducted by the Minnesota Department of Natural Resources (MN DNR) (Kellogg et al., 2014, MN DNR, 1996). Specifically, field data are from monitoring at the Dunka Mine and laboratory data are from dissolution tests on rock from that site. Those tests were conducted on rock with diameters in the range of 0.053 – 0.149 mm. Corresponding humidity cell rates were projected using data comparing results from the two methods.

METHODS

Field

Beginning in the 1960's, Duluth Complex rock was excavated at the Dunka taconite mine (Figure 1) and stockpiled at the site in order to access the underlying iron formation. In the mid-1970's it was discovered that sulfate and trace metal concentrations were elevated in Unnamed Creek, which drains the mining watershed, and the Duluth Complex rock was determined to be the source of these solutes. Due partly to concerns regarding water quality impacts from potential copper-nickel mining in the area, a program was

Figure 1 Location of Dunka Mine, Iron Formation and Duluth Complex in northeastern Minnesota

initiated to monitor the Duluth Complex rock seepage at the Dunka Mine. The following information was taken from a summary of waste rock composition, flow, and drainage quality data from the site (MN DNR, 1996).

The Duluth Complex rock mass within the individual seepage watersheds ranged from roughly 2 to 15 million tons, with average sulfur contents of approximately 0.2 to 1 percent (Table 1). Sulfur contents were determined based on analyses conducted on blast hole samples from 1980 to 1988. These analyses accounted for most of the rock in stockpiles 8018 and 8031, which drain to sites W1D and W4, respectively. Therefore, there is a relatively high degree of confidence in the sulfur contents and calculations based on these contents. In contrast, sulfur contents of stockpiles 8011, 8013, and 8014 were estimated based on analyses of roughly 19, 35, and 44 percent of the rock present. No sulfur analyses were submitted by the company for rock stockpiled after 1988.

Sulfate and metals are transported from the stockpiles in several well-defined seeps, as well as in diffuse flows. The seeps (and the associated stockpiles) discussed in the present report are designated EM8 (stockpiles 8011, 8014), Seep X (8013), Seep I (8013), W4 (8027, 8031), and WID (8018, 8031). Duluth Complex drainage quantity and quality data presented in this report were collected for periods of 3 to 13 years during the time span from 1979 to 1992. Since 1976, data have been collected on the drainage quality, quantity, and chemical mass release associated with stockpile drainages at the site. The Regional Copper-Nickel Study began the data collection and after 1980 monitoring was conducted by Erie Mining Company and LTV Steel Mining Company. The seasonal flow period typically extended from the middle of April to the end of November. Weirs and flow recording equipment were installed at all sites and flow was recorded automatically from roughly mid-May to mid-November. Beyond this time period flow measurements were conducted manually. Grab samples were typically collected 15 to 20 times per year for determination of pH, sulfate concentrations, and concentrations of other solutes that are not discussed in this paper.

Table 1 Duluth Complex stockpile and seep watershed characteristics

Seep	Stockpile	Deposition (start-end)	Mass in watershed,	%S	Area of pile in watershed, $ft^2 \times 10^6$	Watershed area,	Monitoring (start-end)
Seep X[1]	8013	1967-1991	8.44	0.24	1.3	1.7	1990-1992
Seep 1[2]	8013	1967-1991	1.86	0.24	0.50	0.65	1986-1992
EM8[3]	8011	1965-1986	12.92	0.23	3.6	7.7	1979-1991
W4[4]	8027[6]	1979-1979	0.14	0.12	0.12	7.5	1980-1991
W1D[5]	8018	1979-1985	2.18	0.98	0.75	1.9	1986-1992

[1] Weir and continuous flow recording equipment, installed in 1991
[2] Weir installed in 1977, recorder installed in 1980
[3] Weir and recorder installed in 1976
[4] Weir and recorder installed 1981 and 1983, respectively
[5] Weir and recorder installed 1981 and 1986, respectively
[6] Mass and composition reported by MN DNR, 1996

Laboratory

Seventeen samples were collected from blast holes at the Dunka mine (Figure 2a). These samples were characterized (chemistry, mineral content, mineral chemistry) and subjected to dissolution testing (Kellogg et al., 2014). For 15 of the 17 samples, particle size was reduced using a bucking maul, or mechanically, with a pulverizer. These samples were subjected to dissolution tests in duplicate. The remaining two samples (0.67, 0.82 %S) were stage crushed with a jaw crusher and were not replicated in dissolution testing. Particles with diameters from 0.053 to 0.149 mm (-100/+270 mesh) were retained for experimental use. For the crushed samples, sulfur content was determined by LECO furnace, metal concentrations were determined using ICP-AES, and mineral content and mineral chemistry were determined by microprobe analysis of 100 to 125 mineral grains for each sample.

Seventy-five grams of crushed rock were placed into the upper segment of a two-stage filter unit (Figure 2b). The solids were placed on a glass fiber filter that rested on a perforated plastic plate near the bottom of the reactor. At the inception of the experiment, each reactor was rinsed three times to remove any oxidation products that accumulated between sample crushing and onset of the experiment. Each week thereafter, two hundred milliliters of distilled-deionized water was added, and remained in contact with the solids for four to seven minutes, and then vacuum-pumped from the upper stage through a 0.45- micron filter on top of the lower stage of the filter unit. This procedure changed slightly beginning in July 2002. During weeks where no sample was collected, the reactors were filled with water as before, but were then gravity drained. The procedure remained the same as before for weeks during which samples were collected. Sample pH was determined weekly using either a Radiometer 29 or an Orion SA720 meter. Sulfate concentrations were determined biweekly (R1-R20) or monthly (R29-R43) at the MN DNR lab in Hibbing, MN using an HF Scientific DRT-100 nephelometer for the barium sulfate turbidimetric method (APHA et al., 1992). The sample volume was determined by weighing the sample collection flask containing the sample and subtracting the flask mass.

(a)

(b)

(c)

Figures 2a,b,c The first photo (a) depicts the weir at a site used for monitoring flow and water quality at the Dunka taconite mine in northeastern Minnesota, the second photo (b) depicts an MN reactor apparatus, and the third photo (c) depicts a typical humidity cell apparatus.

Between rinses, the solids remained within the reactors, allowing evaporation of retained rinse water and continuous oxidation. The reactors were stored in individual cubicles that formed a rectangular matrix within a topless housing with a perforated base; the housing was stored in a temperature and humidity controlled room (8.5 x 10.5 x 9.5 ft). Reactor experiments were initiated at three different times. For weeks 6-71 average temperatures for the three sets of samples ranged from 25.2-26.3 °C with standard deviations of 0.5-1.3 °C. Corresponding values for average relative humidity were 55.3-59.7% and 3.4-6.8%.

Calculations

For waste rock piles in the field, sulfate mass release was calculated for each day sulfate concentrations were measured. Flow data from the previous and subsequent measurements were used to determine the flow volume associated with the sulfate concentration (equation 1).

$$SO_4 \text{ mass release, } M(SO_4) = [SO_4]_i \left(\frac{Q_i+Q_{i-1}}{2}\right)\left(\frac{t_i+t_{i-1}}{2}\right) + [SO_4]_i \left(\frac{Q_i+Q_{i+1}}{2}\right)\left(\frac{t_i+t_{i+1}}{2}\right), \text{ where} \quad (1)$$

M (SO_4) = mass of sulfate associated with sample i, mg.

[SO_4] = sulfate concentration (mg/L),

Q = flow (liters/sec), and

t = time (seconds).

Cumulative sulfate mass release for the year was then divided by the product of the molecular weight of sulfate, annual mass of sulfur in the watershed and the time over which release occurred to determine annual average sulfate release rates (mol SO_4 (g S)$^{-1}$ s^{-1}) for each seep (Appendix 1, Table A1.1).

Annual rate of sulfate release was calculated as follows:

$(dSO4/dt)_A = \Sigma MSO4/(96.1*M(S)_{ws} * t)$, where (2)

$(dSO4/dt)_A$ = Average annual rate of sulfate release (mg/(gS*s)),

ΣMSO_4 = sum of mass sulfate release for individual sampling periods (mg), and

$M(S)_{ws}$ = mass of sulfur in the watershed (g).

The period over which flow and sulfate concentrations were determined typically extended from mid-April to the end of November. The calculation assumed that the sulfur content in each stockpile did not change over time (the final weighted average sulfur content was used), where in reality the sulfur content added to each pile varied each year.

For the 17 laboratory tests, the average sulfate release rate and associated standard deviation were determined for weeks 6 through 71 (Appendix 1, Table A1.2). The initial five weeks were omitted to eliminate contributions of sulfate generated during sample storage. Drainage pH values for most samples were circumneutral during this period, although minimum values as low as about 4.5 were observed for some of the higher sulfur sample. The mass sulfate release for each point at which sulfate concentration was determined was calculated as the product of that concentration and sample volume. For sulfate concentrations below detection (2 mg/L) a value of 1.0 mg/L was assumed. A total of 887 sulfate measurements were made for the 17 reactors (including the replicates), out of those 93 were below the detection limit. These typically occurred in the samples with S ≤ 0.41%. To determine the rate of release, normalized for sulfur content, the mass release was divided by the product of 604,800 seconds/week and the mass of sulfur present in the sample. Normalizing relative to the sulfur content allowed for direct comparison among laboratory and field rates.

Scaling factors were calculated to express the ratio of field rates to a laboratory rate from a humidity cell test (Figure 2c). This required scaling rates from the MN DNR reactors to humidity cells. This was done using data generated by subjecting Duluth Complex rock samples to testing in both reactors and humidity cells (seven and ten samples, respectively) (Lapakko, Olson, & Antonson, 2013). During weeks 6 through 71 (and throughout the first three years of testing) sulfate release rates as a function of sulfur content from the humidity cells were approximately one-third those from the reactors. Thus, the observed sulfate release rates for the reactors were divided by three to represent humidity cell rates.

A set of scaling factors was then calculated using the ratio of each of 42 annual field rates to each of the adjusted 17 laboratory rates. This generated a set of 714 distinct scaling factors (42 x 17 = 714) (Figure 3a). This data set was fit to normal, beta, and log normal distributions, and the associated mean and standard deviations were determined.

RESULTS AND DISCUSSION

The Duluth Complex rock mass within the individual seepage watersheds ranged from roughly 2 to 15 million tons, with average sulfur contents of approximately 0.2 to 1 percent (Table 1). Because lab samples were collected from blast holes at the site, it is assumed that the mineralogy is similar to those in the lab (see below). Sulfate concentrations in the field generally ranged from 600 to 1600 mg/L and geochem equilibrium modeling of 269 seepage samples indicated that the drainages were undersaturated with respect to gypsum in all cases except one.

Sulfate release rates in the field typically ranged from 0.8 x 10^{-12} to 4 x 10^{-12} mol (g S)$^{-1}$ s^{-1}, with a median value of 1.7 x 10^{-12} mol (g S)$^{-1}$ s^{-1} (Appendix 1, Table A1.1). These values were in good agreement with calculations by a slightly different method (MN DNR, 1996). Rates calculated for Seep 1 tended to be on the lower of the range and those from W4 on the higher end. Their respective mean rates were 1.2 x 10^{-12} and 3.3 x 10^{-12} mol (g S)$^{-1}$ s^{-1}. Rates for individual seeps showed no consistent temporal trend and values for each seep fell within a fairly consistent range over the period of record. The percent standard deviation of the mean value ranged from about 35 to 55 percent (Appendix 1, Table A1.1). Rates for Seep X, Seep 1 and EM8 were in reasonable agreement with those for W4 and W1D (Appendix 1, Table A1.1). Sulfur content of the rock in the watersheds of the last two sites was determined throughout the period of stockpiling (see Methods). The agreement among sulfate release rates suggests that estimations of sulfur content made for rock in the first three watersheds were not unreasonable. Minimum annual pH values for four of the five seeps reflected circumneutral pH conditions, typically ranging from 6.2 to 6.6. Values for Seep 1 were markedly lower, generally in the range of 4.6 to 4.8 (Appendix 1, Table A1.1).

Sulfur content of samples subjected to dissolution testing ranged from 0.18 to 1.64%. Pyrrhotite was the dominate sulfide mineral, followed by chalcopyrite, cubanite, and pentlandite. Cu and Zn sulfides were also observed in trace amounts. Plagioclase (36-65%), augite (3-17%), hypersthene (5-28%), and olivine (3-21%) contributed 65-97% of mineral content in Duluth Complex samples. Eleven samples contained the plagioclase species labradorite, while six samples contain the more sodium-rich species andesine (0.18 to 1.64%S). Unleached Duluth Complex silicate minerals had the following range of stoichiometric coefficients: plagioclase $(Ca_{0.40-0.63}Na_{0.32-0.55})Al_{1.44-1.66}Si_{2.35-2.57}O_8$, augite $((Ca_{0.76-0.95}Na_{0.01-0.03})(Mg_{0.36-0.79}Fe_{0.27-0.63}Ti_{0.01-0.02})(Si_{1.95-2.00}Al_{0.03-0.1})O_6)$, hypersthene $((Mg_{0.91-1.16}Fe_{0.78-1.66})2Si_{1.97-2.00}O_6)$, and olivine $((Mg_{0.72-1.00}Fe_{0.96-1.25})Si_{0.99-1.01}O_4)$ (Kellogg et al., 2014).

Laboratory rates typically ranged from 1.1 x 10^{-11} to 2.3 x 10^{-11} mol (g S)$^{-1}$ s^{-1} with three values in the range of 2.5 x 10^{-11} to 3.9 x 10^{-11} mol (g S)$^{-1}$ s^{-1} (Appendix 1, Table A1.2). Rates for six of the samples included estimations of sulfate concentrations for values reported as less than detection (Appendix 1, Table A1.2). For three samples with seven or fewer below detection values this introduced a maximum error not exceeding two percent. The maximum error increased to eight percent for 15 below detection values and 19 percent for 35 sulfate concentrations reported below detection. Median pH values for the period of record ranged from 4.3 to 6.6, and minimum pH values were generally 0.6 to 1.3 units lower. There was little dependence of these rates on pH, as indicated by a correlation coefficient of 0.062 for the regression of sulfate release rate against the median pH values.

The overall range of scaling factors was 0.019 to 0.687 with about two thirds of the values falling between 0.053 and 0.21 (Figure 3a). Fitting the set of scaling factors to a normal distribution yielded respective values for the mean, standard deviation, and skewness of 0.13, 0.09, and 1.69, respectively. Given the asymmetry of the data relative to a normal distribution (Figure 3a), a beta distribution was applied for dynamic systems modeling for scaling at a proposed mining operation in Minnesota. Scaling factors for probabilities of 5, 25, 50, 75, and 95 percent were 0.034, 0.064, 0.11, 0.17, and 0.30, respectively (Figure 3b). The respective mean and standard deviation for this distribution were 0.127 and 0.083; minimum, maximum, alpha, and beta values were 0.019, 0.687, 1.25, and 6.50, respectively. A log-normal distribution also fit the data well with mean and standard deviation for ln(x) of -2.25 and 0.675, respectively.

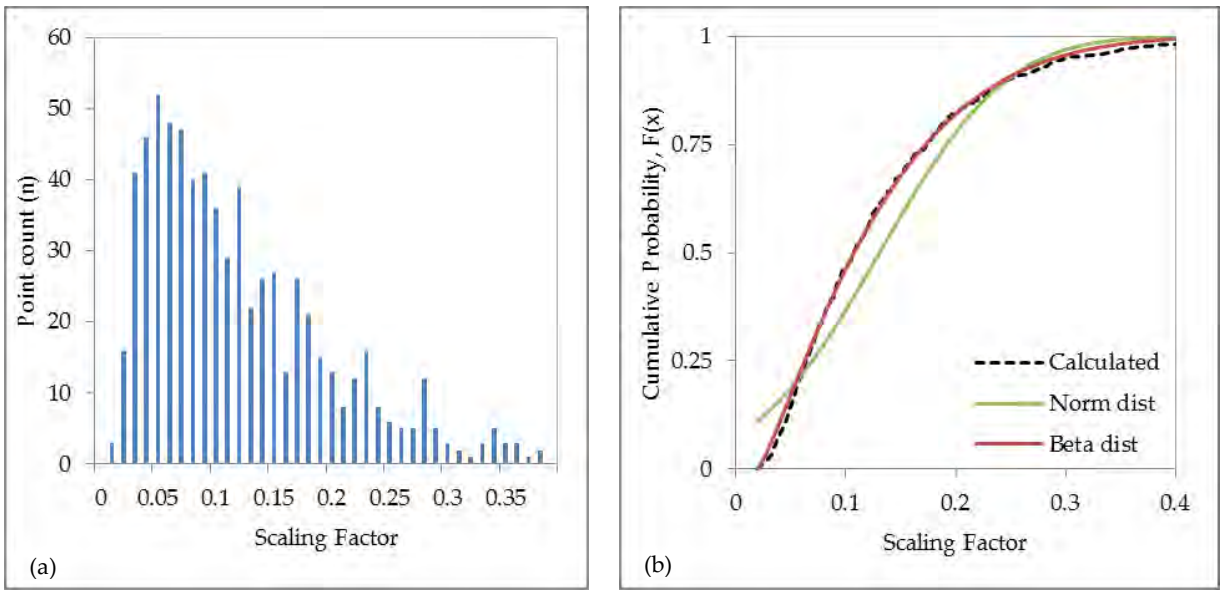

Figures 3a,b a) Calculated scaling factor histogram showing point counts and b) cumulative probability of composite scaling factors compared to normal and beta distribution fits. Omitted scaling factors > 0.40 to improve resolution.

The modeling used the distribution of scaling factors to generate a corresponding distribution of sulfate release rates for the field. Such distributions are recommended by the National Academy of Sciences (National Research Council, 2007) as opposed to a single value. They are deemed more appropriate for assessment of risk by regulatory agencies, an assessment that is essential to environmental review of proposed mining operations.

It should be noted that the scaling factors presented were calculated based on field rates determined during periods of open flow (roughly April through November) and ignored winter periods when ice covered seepage areas (roughly December through March). There were few data available to compare sulfate release rates during the winter to those during the remainder of the year. The best data available were from the outflow of the watershed, site EM1, roughly 1 to 3 km downstream of the seeps. From 1975 to 1998 average sulfate concentrations during the winter were 0.71 times the average during the summer (99 and 389 measurements, respectively). From 2000 to 2014, National Pollution Discharge Elimination System (NPDES) data indicated the monthly average flow during the winter was 0.46 times that during the open flow season (52 and 116 measurements, respectively). Using these ratios allowed estimation of yearly field rate (open flow and ice cover) as 84 percent of that during open flow alone. This would in turn yield scaling factors that were 84 percent of those calculated. For example, the mean value for the beta distribution would be reduced from 0.13 to 0.11. The lower scaling factor does not, however, imply a lesser potential for environmental impact. The lower field sulfate release rates estimated for the winter months actually yielded higher sulfate concentrations in the receiving stream due to lower input flows of unimpacted water.

Beyond the statistical description of uncertainty, specific variables in the calculation were considered. First, field rates were calculated based on sulfur contents of rock within seep watersheds. As discussed above, sulfate release rates for watersheds in which sulfur content was determined throughout stockpiling were in reasonable agreement with those for watersheds with less frequent rock analyses. Thus, it appears that such estimation did not introduce substantial error.

Second, the potential role of pH was investigated. As discussed above, the laboratory rates exhibited little dependence on pH for the period of record considered. Although most of the field seeps exhibited circumneutral pH, it is possible that acidic "hot spots" with elevated sulfate release rates could develop in isolated areas of piles. However, there were no indications suggesting such areas existed. That is, there were no sudden drops in pH and release rates of sulfate remained with constant ranges (Appendix 1, Table A1.1).

Indicators of acidification were observed at Seep 3 at the Dunka mine, a seep not included in the present calculation of scaling factors. From 1975 through1988 drainage pH at the seep was near 7.0, but declined to a minimum of 4.8 in 1989 (MN DNR, 1996). Despite pH values in the typical circumneutral range, the annual release rates for nickel, copper, cobalt, and zinc increased by factors of roughly 20 to 80 from 1986 to 1988, and the sulfate release rate increased by about a factor of nine during this period. Such increases are often associated with isolated acidic zones in waste rock piles generating circumneutral pH. In contrast, sulfate release rates from each of the seeps used for scaling calculations fell within a fairly constant range (Appendix 1, Table A1.1), as discussed above. Similarly, heavy metal concentrations from these seeps did not exhibit the radical changes observed at Seep 3. Thus, it seems unlikely that acidic zones within these piles influenced rates of solute release.

Acidic drainage pH was observed at Seep 1, where minimum values were between 4.6 and 5.2 (Appendix 1, Table A1.1), but the sulfate release rate for this site was the lowest of the five sites examined. This, in conjunction with the laboratory data, suggests there is not a strong dependence of sulfate release on pH in the range of roughly 4.5 to 7.

Third, the reliability of flow measurements was considered. Flow measurements were automated from roughly the middle of May to the middle of November and measurements were made manually beyond this period. To assess the reasonability of the annual flow volumes, these values were divided by total precipitation onto the seep watershed to quantify the annual fractional yields. The average annual yield coefficients for the periods of record for EM8, Seep 1, W1D and W4 were 0.28, 0.33, 0.36, and 0.37, respectively. These values do not suggest any substantial error in flow measurement.

The average annual yield coefficient for Seep X was notably higher at 0.74. At this site the yield coefficient decreased steadily from 1.03 to 0.56 over the three-year period of record and declined to 0.34 the following year. Visual observation of flow at the site was consistent with the high values reported. It is believed that release of stored water was responsible for the initial elevated flows, although the precise mechanism is unknown. The ultimate value of 0.34 is consistent with the annual averages from the other sites and is believed to reflect "typical flow" from the pile.

Finally, the scaling factors determined are in general agreement with values previously determined empirical scaling factors for Duluth Complex and Biwabik Iron Formation rock in northeastern Minnesota. Lapakko (1994) compared sulfate release rates from South Kawishiwi Intrusion rock tested in MN DNR reactors to rates observed for 1000 tonne test piles of Partridge River Intrusion rock. The approximate range of scaling factors reported was 0.1 to 0.3. The rates for the South

Kawishiwi rock in MN DNR reactors reported in the study can be converted to Partridge River rock in humidity cells. Subsequent research indicated that transforming these rates for influences of dissolution test type (MN DNR reactor rate/humidity cell rate ~ 3) and specific intrusion (South Kawishiwi rate/Partridge River rate ~ 0.5) (Lapakko, Olson, & Antonson, 2013). The resultant range of 0.15 to 0.45 represents that for scaling sulfate release rates from humidity cells to test piles, which is higher than the 0.127 mean for scaling humidity cell rates to operational scale piles. This seems reasonable considering, for example, that reaction product transport would likely be higher in the smaller test piles.

Hanna & Lapakko (2012) determined empirical scaling factors for waste rock piles from the lower slaty unit of the Biwabik Iron Formation waste rock piles in northeastern Minnesota. The more reliable of two methods reported yielded a range of 1.0 to 1.3, that is, field rates of sulfate release per gram pyrite were higher than those observed for drill core in the laboratory. This was largely attributed to laboratory rates determined for weeks 15 to 26 of humidity cell testing. Additional testing of weathered rock yielded rates that were roughly an order of magnitude higher than those for drill core. Using these rates for determination of scaling factors would have produced values near 0.1, which is in general agreement with the values determined in the present work. The values determined in the present work generally agree with those presented for operational scale piles by Robertson, Barazzuol, & Day (2012) and not extremely deviant from other literature values presented. However, as discussed previously, comparisons of scaling factors among different sites must be done with caution due to differences in site specific environmental conditions, rock characteristics, and test methods.

SUMMARY AND CONCLUSIONS

Sulfate release rates from Duluth Complex rock were determined for 17 laboratory tests and five operational waste rock seepages in northeastern Minnesota. The 714 scaling factors, representing the ratio of field rates to those in the laboratory, were fit to a beta distribution that yielded a mean of 0.127 and a standard deviation of 0.083. This empirically-based distribution forms a foundation on which laboratory rates can be scaled to develop a probability distribution of predicted operational rates for the purpose of environmental review, consistent with recommendations by the National Academy of Sciences (National Research Council, 2007). It should be noted that the results were generated based on dissolution of a specific rock type in the laboratory and under specific conditions of climate and waste rock stockpile design in the field. Consequently, care must be taken when applying these results to other conditions. It does provide an example for development of empirically based scaling factors. Further application of this approach to other rock types and field conditions will reduce uncertainty in the presently tenuous extrapolation of laboratory test results to the field conditions for proposed mining operations. Consequently, it is recommended that operations and regulatory agencies generate, compile and analyze data to develop additional distributions for empirical scaling factors.

ACKNOWLEDGEMENTS

Kathleen Smith of the U.S. Geological Survey provided constructive review of the draft submitted.

REFERENCES

American Public Health Association (APHA), American Water Works Association, Water Environment Federation. (1992) Standard Methods for the Examination of Water and Wastewater, 18th edition. American Public Health Association, Washington DC.

Hanna, B., Lapakko, K. (2012) Waste Rock Sulfate Release Rates at a Former Taconite Mine, Laboratory and Field-Scale Studies. 9th International Conference on Acid Rock Drainage (ICARD), May 20-26, 2012, Ottawa, Ontario, Canada.

Hollings, P., Hendry, M.J., Nicholson, R.V. and Kirkland, R.A. (2001) Quantification of oxygen consumption and sulphate release rates for waste rock piles using kinetic cells: Cluff Lake uranium mine, northern Saskatchewan, Canada. Applied Geochemistry 16, pp. 1215-1230.

Kellogg, C., Lapakko, K., Olson, M., Janzen, E. and Antonson, D. (2014) Laboratory Dissolution of Blast Hole Samples of Duluth Complex Rock from the South Kawishiwi Intrusion: Twenty-four year laboratory experiment. MN Dept. Nat. Resour. Div. Lands and Minerals, St. Paul, MN. 314 p. plus appendices.

Kempton, H. (2012) A Review of Scale Factors for Estimating Waste Rock Weathering from Laboratory Tests. 9th International Conference on Acid Rock Drainage (ICARD), May 20-26, 2012, Ottawa, Ontario, Canada.

Lapakko, K. A. (1994) Comparison of Duluth Complex rock dissolution in the laboratory and field. International Land Reclamation and Mine Drainage Conference and the Third International Conference on the Abatement of Acidic Drainage. 1, pp. 419-428.

Lapakko, K., Olson, M. and Antonson, D. (2013) Dissolution of Duluth Complex Rock from the Babbitt and Dunka Road Prospects: Eight-year laboratory experiment. MN Dept. Nat. Resour. Div. Lands and Minerals, St. Paul, MN. 88 p. plus appendices.

Malmström, M. E., Destouni, G., Banwart, S.A. and Stromberg, B. (2000) Resolving the scale-dependence of mineral weathering rates. Environmental Science and Technology 34, pp. 1375-1378.

Minnesota Dept. Nat. Resources (MN DNR), Div. Minerals. (1996) Dunka Data Summary: 1976-1993 (Draft). 46 pages.

National Research Council. (2007) Models in the Environmental Regulatory Decision Process. National Academy of Sciences. 286 pages.

Robertson, J., Barazzuol, L. and Day, S. (2012) Extraction of ARD/ML Information from a Brownfield Site for Development of an ARD/ML Plan at the Detour Gold Mine, Ontario, Canada. 9th International Conference on Acid Rock Drainage (ICARD), May 20-26, 2012, Ottawa, Ontario, Canada.

Severson, M., Ojakangas, D., Larson, P. and Jongewaard, P. (2010) Geology and stratigraphy of the central Mesabi Iron Range, *In* Field Guide to the Geology of Precambrian Iron Formations in the Western Lake Superior Region, Minnesota and Wisconsin. www.d.umn.edu/prc/workshops/Guidebooks. p. 15-52.

Shaw, S. and Samuels, A. (2012) An Empirical Comparison of Humidity Cell and Field Barrel Data to Inform Scale-Up Factors for Water Quality Predictions. 9th International Conference on Acid Rock Drainage (ICARD), May 20-26, 2012, Ottawa, Ontario, Canada.

Strömberg, B. and Banwart, S. (1994) Kinetic modelling of geochemical processes at the Aitik mining waste rock site in northern Sweden. Applied Geochemistry 9, pp. 583-595.

Strömberg, B. and Banwart, S. (1999a) Experimental study of acidity-consuming processes in mining waste rock: Some influences of mineralogy and particle size. Applied Geochemistry 14, pp. 1-16.

Strömberg, B. and Banwart, S. (1999b) Weathering kinetics of waste rock from the Aitik copper mine, Sweden: scale dependent rate factors and pH controls in large column experiments. Journal of Contaminant Hydrology 39, pp. 59-89.

Strömberg, B., Banwart, S., Bennett, J.W. and Ritchie, A.I.M. (1994) Mass balance assessment of initial weathering processes derived from oxygen consumption rates in waste sulfide ore. International Land Reclamation and Mine Drainage Conference and Third International Conference on the Abatement of Acidic Drainage 2 (U.S. Bureau of Mines Special Publication SP 06A-94), pp. 363-370.

Wagner, K., Smith, L. and Beckie, R. (2006) Hydrogeochemical characterization of effluent from mine waste rock, Cluff Lake, Saskatchewan. 7th Annual International Conference on Acid Rock Drainage (ICARD), March 26-30, 2006, St. Louis, Missouri, pp. 2207-2216.

APPENDIX 1. Field and laboratory release rates

Table A1.1 Annual precipitation, sulfate release rates (mol SO_4 (g S)$^{-1}$ s^{-1}), and minimum annual pH for the 5 seeps from 1979-1992

Year	Annual precip (cm)	Seep X[1]		Seep 1[2]		EM8[3]		W4[4]		W1D[5]	
		Rate	Min pH	Rate	Min pH	Rate	Min pH	Rate	Min pH	Rate	Min pH
1979	63	NA	NA	NA	NA	1.6E-12	6.6	NA	NA	NA	NA
1980	68	NA	NA	NA	NA	2.7E-12	6.8	8.4E-13	7.2	NA	NA
1981	70	NA	NA	NA	NA	1.5E-12	6.7	2.4E-12	6.6	NA	NA
1982	87	NA	NA	NA	NA	1.8E-12	6.4	4.1E-12	6.4	NA	NA
1983	78	NA	NA	NA	NA	1.2E-12	6.4	3.3E-12	6.2	NA	NA
1984	56	NA	NA	NA	NA	1.1E-12	7.0	4.0E-12	6.8	NA	NA
1985	84	NA	NA	NA	NA	8.6E-13	6.7	6.5E-12	6.5	NA	NA
1986	68	NA	NA	9.1E-13	5.1	7.8E-13	6.4	4.3E-12	6.4	1.5E-12	6.7
1987	56	NA	NA	7.5E-13	4.8	7.5E-13	6.5	2.8E-12	6.6	3.2E-12	6.9
1988	79	NA	NA	9.1E-13	5.2	2.0E-12	6.4	2.1E-12	6.7	1.7E-12	6.4
1989	66	NA	NA	2.5E-12	4.8	3.1E-12	6.3	3.3E-12	6.7	2.1E-12	6.8
1990	71	2.8E-12	6.2	8.5E-13	4.7	2.2E-12	6.9	2.9E-12	6.6	1.3E-12	6.9
1991	74	4.8E-12	6.2	1.6E-12	4.6	1.7E-12	6.8	3.1E-12	6.6	2.1E-12	6.8
1992	65	1.9E-12	6.5	8.2E-13	4.8	NA	NA	NA	NA	1.4E-12	6.7
Avg	70.4	3.2E-12	6.3	1.2E-12	4.9	1.6E-12	6.6	3.3E-12	6.6	1.9E-12	6.7
S.D.	9.3	1.5E-12	0.2	6.4E-13	0.2	7.3E-13	0.2	1.4E-12	0.2	6.6E-13	0.2

[1] Number of annual samples collected for analysis from 1990 to 1992 was 10, 23, and 10, respectively.

[2] Number of annual samples collected for analysis from 1986 to 1992 was 15, 15, 16, 14, 12, 14, and 7, respectively.

[3] Number of annual samples collected for analysis from 1979 to 1991 was 15, 13, 11, 15, 14, 14, 13, 15, 22, 20, 23, 18, and 24, respectively.

[4] Number of annual samples collected for analysis from 1980 to 1991 was 5, 15, 21, 15, 16, 14, 16, 15, 19, 23, 19, and 18, respectively.

[5] Number of annual samples collected for analysis from 1986 to 1992 was 16, 19, 15, 16, 16, 18, and 7, respectively.

Table A1.2 Summary of Dunka blast hole laboratory data (weeks 6-71). Average sulfate release rates (mol SO_4 (g S)$^{-1}$ s^{-1}) were determined for duplicated samples.

Reactor(s)	%S	Median pH	Minimum pH	Sulfate count	Avg dSO_4/dt
1,2[1]	0.18	6.55	5.97	65 (29<DL)	2.29E-11
3,4[1]	0.22	6.63	6.07	61 (15<DL)	1.79E-11
5,6[1]	0.40	6.30	4.86	64	3.89E-11
7,8[1]	0.41	5.32	4.48	64 (35<DL)	9.48E-12
9,10[1]	0.51	5.01	4.00	64 (7<DL)	1.70E-11
11,12[1]	0.54	5.17	4.10	64	2.32E-11
13,14[1]	0.57	5.34	4.09	64	2.28E-11
15,16[1]	0.58	4.69	4.04	64 (3<DL)	1.77E-11
40[3]	0.67	5.68	4.04	17	1.70E-11
17,18[1]	0.71	5.03	3.80	62 (4<DL)	1.35E-11
43[3]	0.82	5.42	4.49	17	1.19E-11
35,36[2]	1.12	4.30	3.51	43	3.01E-11
29,30[2]	1.16	4.61	3.63	44	1.36E-11
37,38[2]	1.40	4.84	3.55	44	1.42E-11
33,34[2]	1.44	4.43	3.42	42	1.15E-11
19,20[1]	1.63	4.38	3.61	64	1.60E-11
31,32[2]	1.64	4.40	3.64	44	2.54E-11
				Average	1.90E-11
				St Dev	7.52E-12

[1] Reactor initiated 2/14/89, average T = 26.25 ± 1.19, average R.H. = 57.77 ± 6.77.
[2] Reactor initiated 9/4/90, average T= 25.31 ± 1.32, average R.H. = 55.27 ± 5.79.
[3] Reactor initiated 8/12/97, average T= 25.23 ± 0.51, average R.H. = 59.65 ± 3.36.

Scaling Geochemical Loads in Mine Drainage Chemistry Modeling: An Empirical Derivation of Bulk Scaling Factors

Timo Kirchner and Bruce Mattson
Lorax Environmental Services Ltd., Canada

ABSTRACT

The development of water quality predictions for seepage from mine waste facilities is an integral component of the environmental assessment of minesites. Direct scaling of geochemical loads measured by laboratory kinetic tests such as humidity cells relative to the mass of a full-scale mine waste facility will lead to concentration predictions for mine drainage that are unrealistically high for many dissolved constituents. As a result, "scaling factors" are applied to account for discrepancies in parameters such as grain size, temperature and water/rock ratio between the laboratory experiments and the field scale waste rock facilities.

In this study, waste dump seepage chemistry data from two minesites are compared to upscaled, representative laboratory test cell leachate data in an attempt to better constrain bulk scaling factors. Additionally, larger scale field experimental data (field bins) were considered as an intermediate scaling step.

It was observed that geochemical loads for major ions from the sites are commonly more than two orders of magnitude lower than those predicted by direct scaling of laboratory kinetic test loads, yielding bulk scaling factors of <1%. In these models, many dissolved trace ions that may be of concern in mine drainage (*e.g.*, As, Cu, Cd, Se, *etc*.) may still be significantly overpredicted if the model is calibrated to major ions, likely as a result of solubility limits and other attenuation mechanisms. Unlike loading rates, concentrations in field bin and waste dump drainage were commonly found to be on the same order of magnitude for both neutral and acidic sites suggesting that geochemical equilibrium may be attained at relatively small scales in waste piles, highlighting the importance of intermediate-scale field experiments.

INTRODUCTION

One of the biggest environmental concerns related to modern mining is the release of acidity and metals into the surrounding environment in response to water-rock interaction occurring in sulfidic waste rock storage facilities. Drainage quality predictions conducted as part of geochemical studies incorporate small- to intermediate-scale kinetic experiments that are carried out on mine rock and tailings. These tests provide insight into the reaction mechanisms, lag time for onset of acid rock drainage (ARD), and metal leaching (ML) behavior. A major challenge associated with the application of kinetic test results is the extrapolation of leachate chemistry to predict full-scale minesite drainage chemistry even when waste rock compositions, tonnages and site water balance are constrained. A common approach is to convert laboratory kinetic test leachate concentrations into a geochemical loading rate (*e.g.*, mg/kgrock/week) which is then upscaled to the tonnage of the waste dump to predict drainage quality:

$$Predicted\ Concentration = \frac{HC\ Load\ x\ Time\ x\ Mass\ of\ Rock\ in\ Dump}{Volume\ of\ Infiltrating\ Water} \quad (1)$$

It has long been recognized that the resulting loads commonly strongly overestimate actual geochemical loads seen in drainage from waste dumps (Morin & Hutt, 1994; Malmström *et al.*, 2000). This is largely attributed to discrepancies in geochemical and physical conditions between laboratory kinetic reactors and full-scale waste dumps, including but not limited to:

- water-rock interaction (contact);
- gas transport and oxygen content;
- reactive grain size distribution (and associated occlusion of reactive minerals);
- temperature (both sulfide and carbonate dissolution reactions are temperature-dependent).

In an attempt to account for the variable geochemical regimes, many authors have begun introducing scaling factors based on theoretical assumptions and field observations (Malmström *et al.*, 2000; Neuner *et al.*, 2009; Kempton, 2012). In theory, a scaling factor (generally <100%) is assigned to each of the lab-to-field discrepancies identified and multiplied by the upscaled load. Understandably, depending on the type of waste material and the climatic conditions at a minesite, the sometimes inter-related individual scaling factors vary widely in practice (Kempton, 2012). A so-called bulk scaling factor, defined as the product of all individual scaling factors can be calculated empirically where laboratory kinetic and waste drainage chemistry data are available, however a comprehensive database for different deposit types and climate conditions is missing. Nevertheless, several studies have addressed this topic and bulk scaling factors on the order of 5 to 60% have been reported (*e.g.*, Andrina *et al.*, 2012; Hanna & Lapakko, 2012; Morin & Hutt, 1994).

This paper presents waste rock leachate and drainage chemistry results from reactors of various scales. The waste rock is associated with two minesites located in semi-arid regions, one with neutral and the other one with acidic drainage. The focus of this study is the dependence of geochemical loading rates on the scale as well as the variability of geochemical behavior between different species.

METHODOLOGY

Humidity cell experiments for materials from both sites were conducted according to the standardized method outlined in ASTM D5744 (2010) applying three days of dry air and three days of moist air flow to each 1 kg of waste rock followed by flooding with deionized water (500 mL) and leachate sampling on day seven. Column experiments on waste rock from Site B are made up of 5 kg of material with variable irrigation volumes (300-500 mL) applied as a trickle leach at 1 mL/min every two weeks. Between sampling cycles the cells were exposed to dry air allowing for a better representation of the mine-specific climate.

Field kinetic experimental procedures are consistent between the two minesites with field bins containing 150-200 kg of waste rock which are either flushed naturally by rain water or, in case of longer dry periods, are manually irrigated with deionized water. As the leachate sample is taken, the outflow volume is recorded to allow the calculation of geochemical loads.

RESULTS AND DISCUSSION

Static test results of the various waste rock materials and WRSA dimensions for Sites A and B are given in Table 1.

Table 1 Selected static test results and WRSA dimensions for the studied minesites

		Site A		**Site B**
		Oxide	*Sulfide*	*Diorite*
Total S	%	0.82	2.9	0.22
Sulfide S	%	0.020	2.5	0.030
NP	*kg CaCO3/t*	-1.0	-1.1	88
NPR		<0	<0	40
WRSA tonnage	*Mt*	57	38	2.7
WRSA footprint	*ha*	91		9.9

Notes: chemical results are median values; NP = bulk neutralization potential; NPR = net potential ratio.

Site A (acidic drainage)

Site A is a porphyry-gold deposit located in a semi-arid environment with an average annual precipitation of 550 mm. The waste rock storage area (WRSA) contains rock from volcanic intrusions and volcaniclastic sediments of intermediate to felsic composition. Sulfide S content and associated drainage chemistry is predominantly associated with the degree of natural weathering which led to the subdivision of waste rock into two main categories, namely Oxide and Sulfide materials. The former is generally devoid of sulfide minerals, but contains considerable amounts of acid-producing sulfate salts such as jarosite and alunite. Sulfide waste rock contains up to 7.6% of sulfide S with a median value of 2.5% (Table 1), mainly in the form of pyrite. Both material classes show little to no carbonate mineralization, and therefore have little capacity for acid-neutralization. All waste rock is stored within the same facility with Oxide rock used as cover material for the highly reactive Sulfide waste. Figure 1 shows a tertiary diagram of major elemental ratios in Site A WRSA drainage compared to Sulfide and Oxide humidity cell leachates. This plot illustrates the

mixed nature of the waste dump with the influence of Sulfide waste material becoming progressively more important over time. Due to the mixed nature of the WRSA, certain assumptions and data adjustments were made with respect to the calculation of geochemical loads:

- At the time of WRSA drainage collection the ratio of Oxide to Sulfide rock was set to 60% to 40%, consistent with the waste production schedule provided by the client;
- All flows contacting the WRSA are captured by the flow measurements at the seepage collection pond.

WRSA geochemical loading rates were calculated for a 64 week duration extending from September 2011 to December 2012 (construction of the WRSA began in 2010). Selected major ion and minor/trace ion loads are compared to the loading rates derived from kinetic experiments in Figure 2. In this plot, both field bin and humidity cell loads are normalized to the loads derived for the WRSA seepage to calculate an "exceedance factor":

Exceedance factor = Kinetic test load / WRSA load

The humidity cell exceedance factors range from 578 (Na) to ~52,000 (As), corresponding to bulk scaling factors of 0.17% to 0.002% (calculated as the inverse of the exceedance factor). These exceedance factors are greater than the field bin exceedance factors which range from 29 to ~24,000, for all parameters except arsenic. The latter is the only species showing a higher load in field bin versus humidity cell leachates. Greater exceedance factors for the humidity cells are consistent with

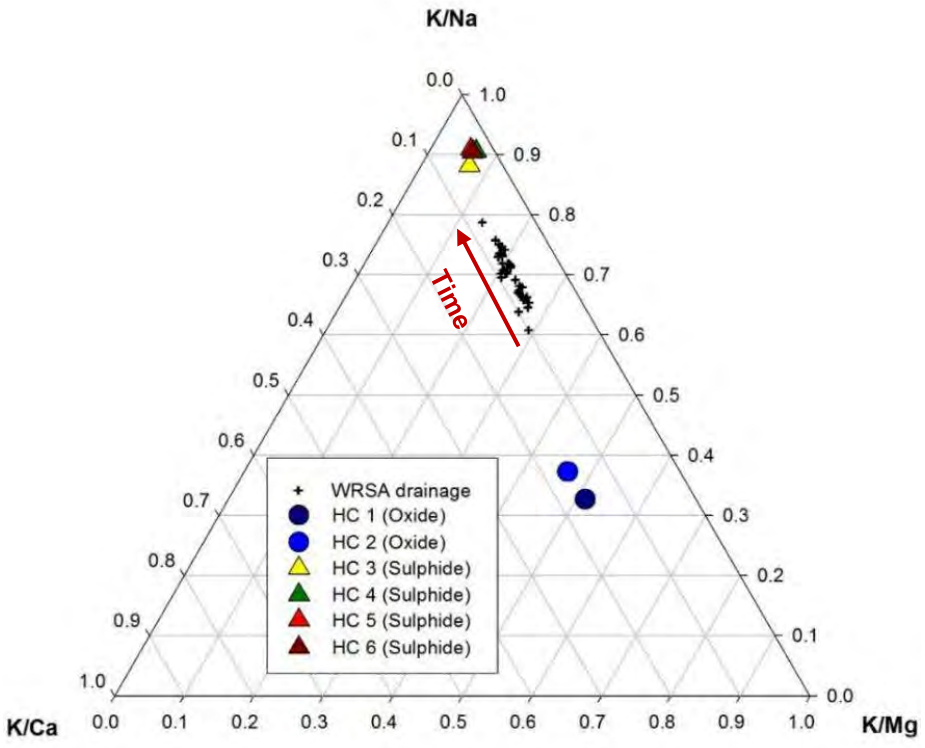

Figure 1 Ternary diagram showing the major elemental ratios in humidity cell leachates versus WRSA drainage for Site A

the greater scale differential between humidity cells and the WRSA compared to field bins versus WRSA.

Humidity cell exceedance factors for the major ions are typically lower than trace ion loads ranging from ~600 to ~1,000 (median bulk scaling factor of 0.15%) not including Fe and K (Figure 2). The latter species display higher exceedance factors around or greater than 5,000 indicating that they are being attenuated in WRSA drainage relative to humidity cell leachates. Under the pH conditions measured in the WRSA drainage, geochemical modeling using PHREEQC (Parkhurst & Appelo, 1999) suggests that the most likely solubility control for Fe and K is the mineral jarosite, which was also commonly identified in Oxide waste rock. The median humidity cell based bulk scaling factor for the shown minor and trace ions is 0.02%, almost an order of magnitude lower than that calculated for other major ions.

As a sensitivity analysis and to account for a conservative case in which the WRSA constantly produces a pH in the range of that seen in the latter stages of the Sulfide humidity cell experiments, the worst geochemistry (pH 3.2) recorded at the seepage collection pond was applied to the same drainage volume over the entire modeling period (64 weeks). In this scenario the median bulk scaling factor for major ions (SO_4, Na, K, Ca, Mg) increases to 0.41%, while the bulk scaling factor for minor and trace ions is 0.13%, still well below bulk scaling factors reported by other workers.

Several species in waste rock seepage can be expected to become saturated when a certain scale (or water/rock ratio) is reached. Therefore, in addition to assessing geochemical loads, it is crucial to also compare concentrations measured in leachate versus seepage waters. In Table 2, the range of field bin leachate concentrations is listed along with the median Site A WRSA drainage concentration for episodes of comparable pH (pH = 3.0 – 3.3). Of the presented parameters, only Al, Cd, and Cu exceed the maximum concentrations observed in field bin leachates but fall within a factor of three of the latter. The remaining species are within the range observed in field bin leachates suggesting that solubility limits control their concentrations.

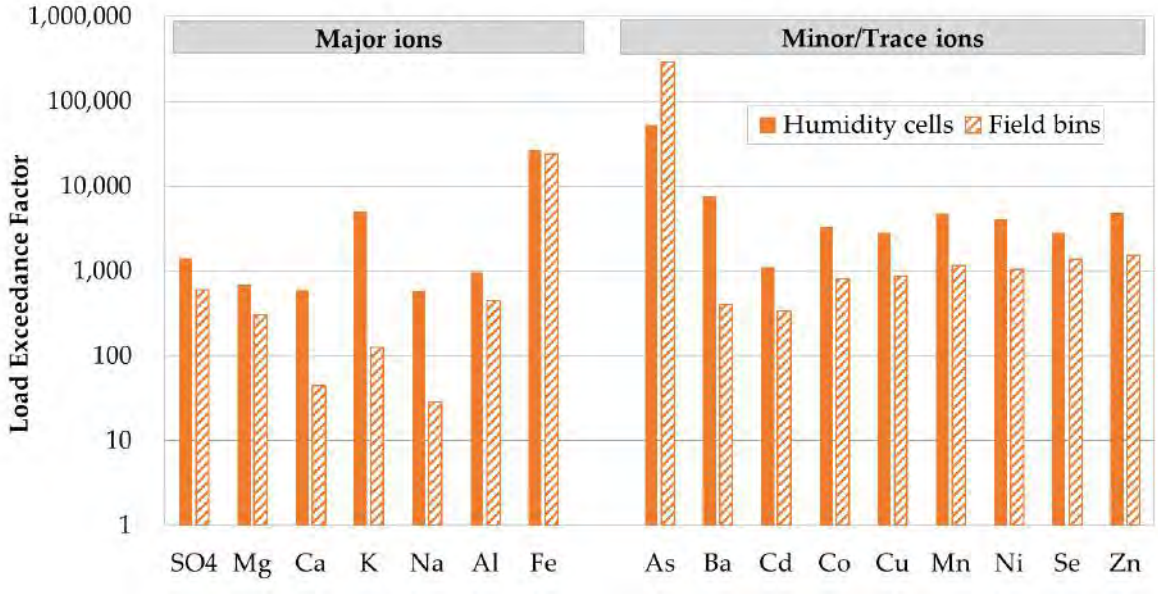

Figure 2 Exceedance factors (relative to WRSA drainage) in humidity cell and field bin leachates for acidic Site A

Table 2 Comparison of the range of field bin leachate concentrations with WRSA drainage chemistry at Site A

	SO_4	Mg	Ca	Na	K	Al	Fe	As	Ba	Cd	Co	Cu	Mn	Ni	Se	Zn
	mg/L	*mg/L*	*mg/L*	*mg/L*	*mg/L*	*mg/L*	*mg/L*	*mg/L*	*mg/L*	*mg/L*	*mg/L*	*mg/L*	*mg/L*	*mg/L*	*mg/L*	*mg/L*
FB (min)	628	34	66	12	10	32	22	0.083	0.070	0.19	3.3	0.33	18	3.2	0.0050	30
FB (max)	2140	168	238	29	13	67	59	0.19	0.19	0.53	4.2	1.5	38	4.7	0.013	89
WRSA	2080	111	194	19	7.1	**177**	55	0.029	0.067	**1.6**	1.2	**3.3**	12	1.1	0.0020	42

Notes: FB = field bin; WRSA drainage concentrations indicated in bold exceed the maximum field bin leachate concentration.

Site B (neutral drainage)

Site B represents a porphyry-copper deposit located in a semi-arid environment and hosted in a complex igneous system of mafic to intermediate plutonic and volcanic rocks. Several hybrid units comprising the major intrusions and volcanic rocks were identified near contacts. Compared to Site A, the sulfur contents at Site B are low with median sulfide sulfur concentrations of 0.22% (Table 1). Carbonate neutralization potential is abundant (median = 29 kg $CaCO_3$/t) and additionally it was identified that reactive silicate NP is present (median bulk NP = 88 kg $CaCO_3$/t; Table 1). Overall, waste rock from this site is not expected to generate net acidity, however species that form oxyanions under neutral conditions (*e.g.*, As, Se) may still be mobile in waste rock drainage. Geochemical loads released by humidity cells and their duplicate columns were compared against field bin leachate data (same lithology; no duplicates) and site pore-water from waste rock that is primarily made up of the same dioritic waste rock.

Seepage analyses from the WRSA were obtained through two monitoring wells that were installed at two different depths within a backfilled pit. Sampling depths are both below the water level, however geochemical analyses suggest that the water is sufficiently oxic to be representative of oxidizing pore-water chemistry. Geochemical loading from Site B WRSA was calculated based on the following assumptions:

- Tonnage: only the non-saturated rock (the upper 12 m) stored in the backfilled pit will contribute to sulfide oxidation, yielding a tonnage of 2.7 Mt;
- Flows: all infiltration into the waste pile (27 mm/yr) will be available for reaction.

Figure 3 shows the exceedance factors of geochemical loading rates calculated for humidity cells (1 kg), duplicate unsaturated columns (5 kg), and field bins (~150-200 kg) relative to the inferred loads from the WRSA at pH-neutral Site B. Loading rates from humidity cells are higher than or similar to those in column leachates. The discrepancy is highest for Al and Fe, suggesting that the attenuation of these two species under neutral conditions is already effective at small scales. The fact that geochemical loads calculated for several species in field bin leachates are similar to or even higher (exceedance factor < 1) than those in the WRSA pore-water suggests that assumptions made for WRSA loading calculations are conservative. This is likely a result of the poorly constrained water balance at this site and/or the fact that field bins were manually irrigated several times, likely increasing the overall load in this climatic setting. Consequently, exceedance and bulk scaling factors presented for Site B in the following should be considered semi-quantitative.

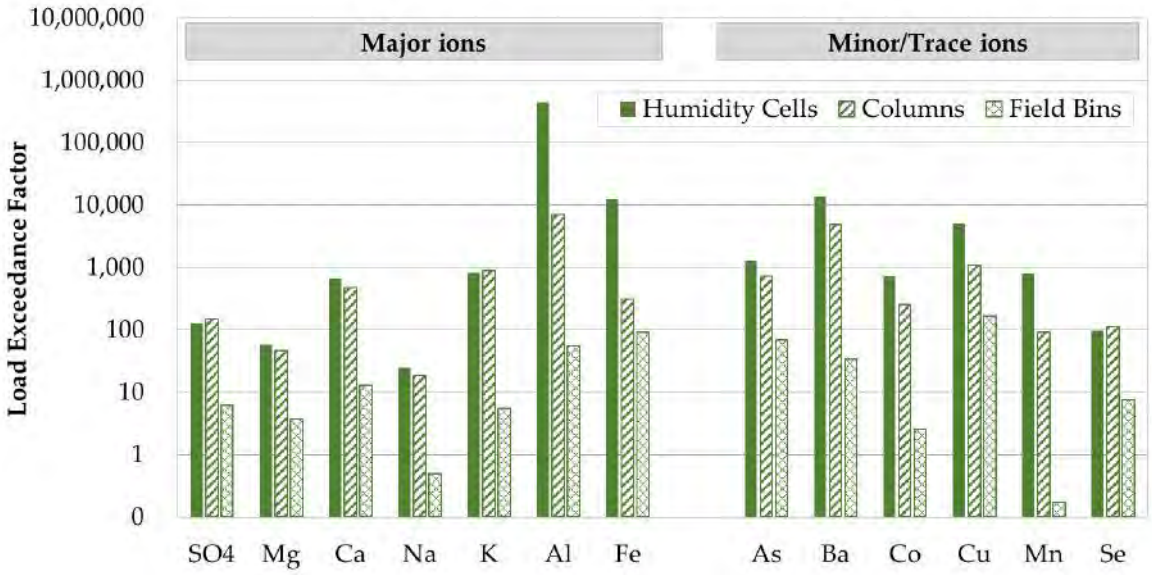

Figure 3 Exceedance factors (relative to WRSA drainage) in humidity cell, column and field bin leachates for neutral Site B

The discrepancy between major ions and trace ions is not as apparent as for Site A, which is likely a result of the different attenuation mechanisms occurring at neutral pH. For example, exceedance factors for laboratory kinetic experiments vary by more than three orders of magnitude for major ions ranging from 25 (Na) to ~444,000 (Al) (Figure 3). Excluding Fe and Al, which are known to be highly immobile under circum-neutral pH, a median bulk scaling factor of 0.8% was calculated. It should be noted that due to the high gypsum content observed in Site B waste rock, Ca and SO_4 are unlikely to behave conservatively. For the shown minor and trace ions, the calculated bulk scaling factor is 0.1% suggesting that, with few exceptions (*e.g.,* Se), scaling to major ions would generally overestimate predicted concentrations for these species in site drainage.

As for Site A, in addition to the geochemical load analysis, selected dissolved concentrations measured in field bin leachates are compared to the WRSA drainage chemistry in order to shed light on possible solubility controls occurring at different scales (Table 3). Na and Mn from the WRSA exceed five times the maximum concentrations in field bin leachates, while sulfate, Mg, K, and Co only slightly exceed the range of field bin leachate concentrations. The very high Na and Mn values may be explained by the impact of blasting residues and the development of suboxic conditions in the backfilled pit, respectively. The fact that many dissolved species fall within the range of field bin leachate concentrations suggest that attenuation mechanisms are active and equilibrium conditions are partly reached at relatively small scales.

Table 3 Comparison of the range of field bin leachate concentrations with WRSA drainage chemistry at Site B

	SO_4	Mg	Ca	Na	K	Al	Fe	As	Ba	Co	Cu	Mn	Se
	mg/L	*mg/L*	*mg/L*	*mg/L*	*mg/L*	*mg/L*	*mg/L*	*mg/L*	*mg/L*	*mg/L*	*mg/L*	*mg/L*	*mg/L*
FB (min)	42	6.9	15	1.2	4.2	0.0010	0.010	0.0016	0.0094	0.00010	0.0069	0.000050	0.0035
FB (max)	1030	92	277	4.4	21	0.015	0.030	0.047	0.067	0.00050	0.12	0.0089	0.042
WRSA	**1720**	**296**	239	**151**	**43**	0.0022	0.010	0.0081	0.031	**0.0014**	0.0046	**0.086**	0.041

Notes: FB = field bin; WRSA concentrations shaded indicated in bold and with a border exceed the maximum and five times the maximum field bin leachate concentrations, respectively.

CONCLUSIONS

Leachates from laboratory and field kinetic tests were compared to WRSA seepage at two different sites, one producing acidic and the other one with neutral drainage. The main findings from this study are summarized below:

- In order to predict WRSA seepage concentrations at Site A (acidic drainage) bulk scaling factors are <1% (based on humidity cell loads) would have to be applied. These scaling factors are significantly lower than those reported previously, commonly using major ion concentrations for model calibration purposes. Overall, bulk scaling factors for major ions tend to be higher than those calculated for minor/trace parameters, unless major ions are solubility-controlled under acidic conditions (*e.g.*, K and Fe by jarosite). This highlights the importance of differentiated water quality modeling for specific ions;
- Bulk scaling factors calculated for the neutral Site B, excluding Fe and Al, vary between 0.01% and 4% where major ion scaling factors are generally higher (median = 0.8%) than those calculated for minor/trace ions (median = 0.1%). Field bin loading rates that are on the same order of magnitude or even lower than calculated WRSA pore-water loads suggest that assumptions made for the calculation of WRSA loads are conservative and bulk scaling factors for this site are likely lower;
- For both sites, many species appear to be solubility-limited at a scale of field bin experiments (150-200 kg), which is a factor that should be accounted for in water quality prediction modeling.

-

REFERENCES

Amos, R. T., Blowes, D. W., Bailey, B. L., Sego, D. C., Smith, L., & Ritchie, A. I. M. (2014). Waste-rock hydrogeology and geochemistry. Applied Geochemistry.

Andrina, J., Wilson, G.W., & Miller S.D. (2012). Waste rock kinetic test program: Assessment of the scale up factor for sulfate and metal release rates. In Proceedings of the 9th International Conference on Acid Rock Drainage (ICARD), Ottawa, ON, Canada.

ASTM D5744 (2010). Standard test method for laboratory weathering of solid materials using a humidity cell. In Annual Book of ASTM Standards, ASTM International, West Conshohocken, PA, USA.

Hanna, B., Lapakko, K. (2012), Waste rock sulfate release rates from a former taconite mine, laboratory and field-scale studies. In Proceedings of the 9th International Conference on Acid Rock Drainage (ICARD), Ottawa, ON, Canada.

Kempton, H. (2012). A review of scale factors. In Proceedings of the 9th International Conference on Acid Rock Drainage (ICARD), Ottawa, ON, Canada.

Malmström, M. E., Destouni, G., Banwart, S. A., & Strömberg, B. H. (2000). Resolving the scale-dependence of mineral weathering rates. Environmental science & technology, 34(7), 1375-1378.

Morin, K.A., and N.M. Hutt (1994). An empirical technique for predicting the chemistry of water seeping from mine-rock piles. In Proceedings of the 3rd International Conference on the Abatement of Acidic Drainage, Pittsburgh, Pennsylvania, USA, April 24-29, Volume 1, p. 12- 19.

Neuner, M., Gupton, M., Smith, L., Pham, N., Smith, L., Blowes, D., and Sego, D. (2009). Diavik water rock project: unsaturated water flow. In Proceedings of the 8th International Conference on Acid Rock Drainage (ICARD), Skeleftea, Sweden.

Parkhurst, D. L., & Appelo, C. A. J. (1999). User's guide to PHREEQC (Version 2): A computer program for speciation, batch-reaction, one-dimensional transport, and inverse geochemical calculations.

Comparison of Leach Column Experiment from Laboratory Bench to Mine Site for Coal Mine Overburden

Rudy Sayoga Gautama[1], M. Sonny Abfertiawan[1], Ginting Jalu Kusuma[1] and Firman Gunawan[2]

1. *Department of Mining Engineering, Bandung Institute of Technology, Indonesia*
2. *Environmental Department, PT Berau Coal, Indonesia*

ABSTRACT

Column leach tests in the laboratory have been conducted for overburden samples from Lati coal mine in East Kalimantan, Indonesia. The samples consist of three different rock types, namely, potentially acid forming mudstone, non-acid forming mudstone and sandstone. Six columns were prepared for simulation of different layering scenarios between the rock types with one control column. This experiment was aimed to study the performance in controlling the acid mine drainage generation with different rock layer configuration and was conducted over 26 weeks.

The same simulation scenario was also implemented at the mine site with larger columns and sample grain size. The columns were placed in the open air area and exposed to the local climatic condition. An automatic rain gauge was also installed to continuously record the rainfall events.

The analysis was conducted by comparing the leachate collected from both the laboratory and field experiments of the different columns. Similar trends behaviour on the water quality, especially on pH parameter, have been observed in most of the columns except the column containing 100% PAF mudstone and 25% sandstone over PAF materials. Due to its water holding capacity as well as buffering capacity, NAF mudstone shows the potential for capping material.

Keywords: acid mine drainage, column leach test, laboratory experiment, on site experiment.

INTRODUCTION

Geochemical characterization that aims to classify a material as potentially acid forming (PAF) or non-acid forming (NAF) is an important step in the management of acid mine drainage (AMD). Static tests, which include acid base accounting and net acid generation tests, are the most common initial tools used to classify the geochemical conditions. However, static tests are uncertain in some cases and do not give the oxidation rate of sulfide minerals or the neutralization potential of the rock, which are very useful for the prediction of long-term water quality. Therefore, kinetic tests are often conducted to confirm the results of the static test and to get a picture of the quality of water that will leach from sulfide containing rocks that undergo oxidation.

Kinetic tests can be carried out both in the laboratory and in the field with various advantages and disadvantages. In laboratory tests, each input parameter (i.e. interval and volume of flushing water and temperature) and output (e.g. pH and metal content in the leachate water) that will affect each other, will tend to be more controlled when compared with the field test. The field test tends to be highly dependent on local weather conditions during the test. However, kinetic tests conducted in the field are believed to give a better picture of conditions on the ground, although this certainly requires a longer observation time and costs are relatively larger (Frostad et al., 2005).

Laboratory and field scale kinetic tests have been conducted with different layering scenarios between the rock types with one blank or empty column. The rock types include potentially acid forming (PAF) mudstone and non-acid forming (NAF) mudstone, and sandstone taken from Lati coal mine in Berau, East Kalimantan, Indonesia. The climate on Lati mine site is characterized as tropical, with rainfall in the range of 70.7 – 292.2 mm/month, temperature in the range of 21.2 – 35.8°C (average 26.68°C) and relative humidity in the range of 42 - 100% (average 87%).

The objectives of the current study were to compare the results obtained from the field kinetic tests with the laboratory kinetic tests based on the data of 6 columns (and 1 blank column) with similar configurations. They were conducted to provide more confidence in the use of laboratory data for the prediction of acid mine drainage generation of different rock layer configuration.

MATERIALS AND METHODS

Materials

Fresh rock samples consisting of two lithological types, namely mudstone and sandstone were taken from an active coal mine pit in Lati which lies in the late Eosen-middle Meosen Berau sub-basin, part of the Tarakan Basin. By considering the dominant existence of mudstone in Lati mine site, two samples were taken to represent the geochemical characteristics of PAF and NAF mudstone rock. While the sandstone, which exists as lenses between mudstone, is generally dominated by NAF rock type. Geochemical characteristics of the sample based on the static test results, which consist of acid base accounting (ABA) tests and the net acid generating (NAG) tests, are shown in Table 1. The MS-1 sample consists of 0.88% of total sulfur with no neutralizing capacity and produced low NAG pH (3.55), hence categorized as PAF material. On the other hand the NAF categorized MS-2 and SS samples consist of quite low total sulfur content (0.17% and 0.20%), with a small capacity to neutralize acid (5.74 and 1.51 Kg H_2SO_4/ton) and produce high NAG pH (8.72 and 6.63). Comparing with the geochemical characteristic databases of material in Lati Mine, these value were represent the general geochemical condition of this mine.

Table 1 Samples' Geochemical Characteristics

Rock Type	Tot. Sulfur*)	MPA**)	ANC**)	NAPP**)	Paste pH	NAG pH	NAG**)		ANC/MPA
							pH 4.5	pH 7	
MS-1(PAF)	0.88	26.93	0.00	26.93	6.80	3.55	3.85	2.25	0
MS-2(NAF)	0.17	5.20	5.74	-0.54	9.20	8.72	0	0	1.10
SS(NAF)	0.20	6.12	1.51	4.61	7.55	6.63	0	0.12	0.25

Note : MPA = Maximum Potential Acidity; ANC = Acid Neutralizing Capacity; NAPP = Net Acid Producing Potential; NAG = Net Acid Generating; MS = Mudstone; SS = Sandstone;
*) = in % ; **) = in Kg H_2SO_4/ton

Methods

Kinetic tests were conducted using free draining column leach test methods on transparent acrylic columns. Both laboratory tests and field kinetic tests used similar methods of sample placement in the column, with proportional consideration on column diameter and the initial grain size of samples. The C01 and C06 columns consisted of 100% PAF and NAF Mudstone, respectively. The C02 and C03 columns consisted of 75% and 50% PAF mudstone capped by 25% and 50% NAF mudstone, whereas C04 and C05 columns consisted of 75% and 50% PAF mudstone capped by 25% and 50% NAF sandstone, respectively (see Figure 1).

In the laboratory tests, columns with a diameter of 15 cm and a total height of 30 cm were used (Figure 2). The sample volume in the column was around 0.018 m^3, and the sample height in the columns was 25 cm. The sample grain size was in the range of 3 - 5 mm in diameter, which was obtained from crushing and sieving the bulk sample. A 60 watt light bulb was used to simulate solar radiation for 12 hours a day for 6 days in order to maintain the temperature in the range of 30-35 °C. Flushing was conducted with approximately 1,000 ml of de-ionized water in weekly cycles to simulate rainfall.

In the field tests, columns with a diameter of 30 cm and height 60 cm were used. The sample, with a grain size range of 3 – 18 mm after sieving, was placed in the column with a volume of 0.071 m^3 and the sample height in the column of 50 cm (Figure 3). An automatic rain gauge was installed on the experiment location to continuously measure the rainfall.

On both test scales, the leachate water in the collecting bottle/gallon was collected once a week and physical parameters such as pH, electric conductivity, oxidation-reduction potential and total dissolved solids were measured prior to further analysis of the ion and metal contents. In addition, rainfall water was also analyzed in a similar manner for comparison.

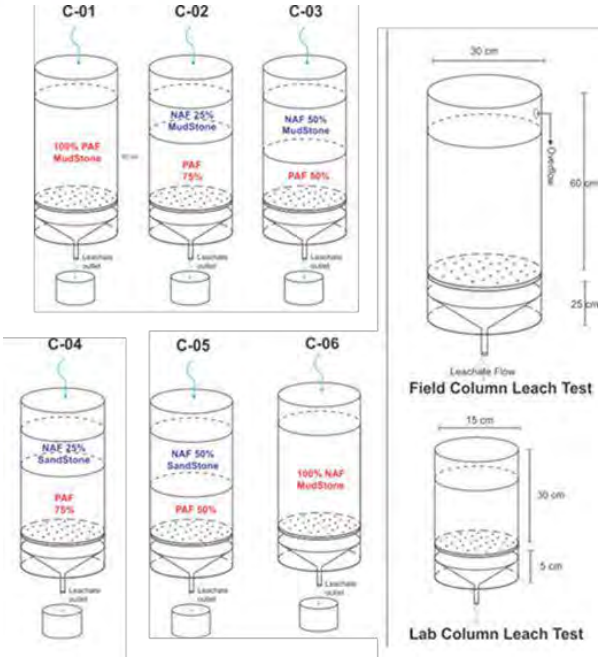

Figure 1 Scheme of kinetic test (left) and dimension of column (right)

Figure 2 Kinetic Test in Lab

Figure 3 Kinetic Test on Mine Site

RESULTS AND DISCUSSION

Inflow Characteristics

In the kinetic tests, one of the important factors that will control the acid formation characteristics of the sample is the wet and dry cycles; these are a result of the cycle of water flushing in the laboratory test, the occurrence of rainfall in the field test, and of course, the effects of evaporation. Wet and dry cycles simultaneously affect both physical and chemical processes that occur in the column sample. Physically, wet and dry cycles will initiate the occurrence of physical disintegration of the rock. Hence, the rock will experience deterioration and consequently the particle size of rock

matrix will decrease. This condition will increase the total area of reactive surface and will further accelerate the chemical process, both the oxidation rate of sulfide and also the neutralizing reaction (Davis and Ritchie, 1987). On the other hand, from a physical condition point of view, a finer-grained material, in addition to result in low permeability due to small pore size, also has a much higher water holding capacity than the coarse-grained rock (Desavahayam, 2006). The existence of water -as water content in pore space- will control the oxygen diffusion, slaking, and furthermore the reaction rate, both of sulfide oxidation and alkali dissolution, of minerals contained in the rock (Gosselin et al., 2007).

In the laboratory scale tests, the volume of water flushing was 1,000 ml, which represented a rainfall depth of 56 mm. The flushing interval was fixed at 1 week (7 days), which resulted in a fixed dry condition interval of 6 days for each cycle. In the field scale tests, the cumulative rainfall which infiltrated as the flushing water source varied in the range of 23.14 - 192.68 mm, with an average of 67.50 mm within a week (maximum daily was 50.8 mm/day), as shown in Figure 4. These rainfall events resulted in a dry condition interval in the range of 1 – 3 days. Moreover, if the net infiltration is assumed to only occur when the rainfall > 5 mm/day, the dry interval will be increased to 3 – 8 days.

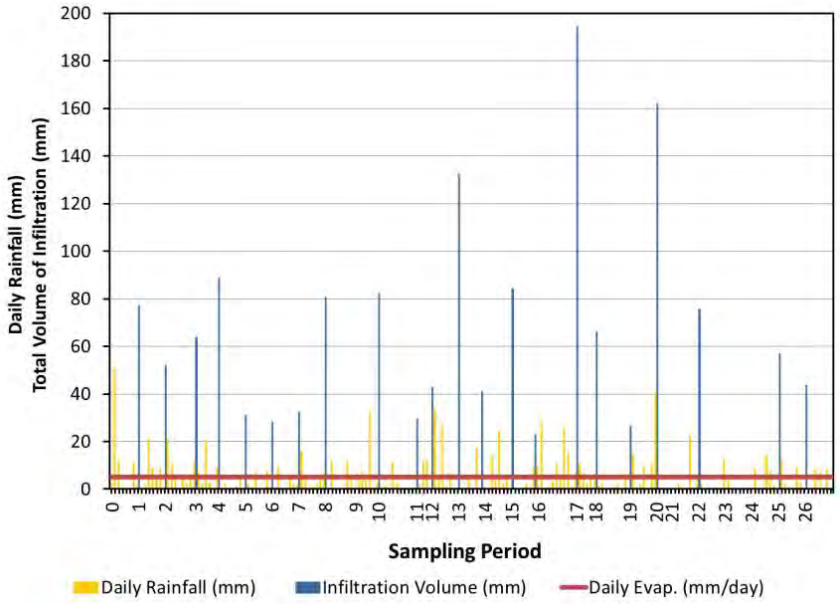

Figure 4 Daily rainfall characteristics during the field kinetic test and Total Infiltration Volume in the Blank Column

The leachate volume from each column throughout the test, and the ratio to rainfall or flushing volume, is summarized in Table 2. In the laboratory scale tests, the leachate volume is similar for each column; within the range of 300 – 800 ml/week, with ratios in the range of 27 – 87%. On the other hand, the field scale tests have various leachate volumes from each column with a minimum leachate volume ranging from 330 – 750 ml and the maximum volume in the range of 11.000 – 12.610 ml, with ratios of leachate volume to rainfall of 8 – 95 %. The column with mudstone in the upper layer tended to be more resistive in water infiltration compared to the column with the

sandstone layer, hence resulting in less leachate volume. However, for some cases in the cycle period with long intervals, the column with a thicker sandstone layer may produce less leachate volume due to the store and release effect (e.g. C05). This result has shown that in the field scale tests, the deep infiltration of water that will become leachate is very dependent on the physical properties of the sample (i.e. particle size, permeability, etc.), as they experienced similar weather conditions.

Table 2 Leachate volume and its ratio to Rainfall/Flushing volume

Column	Material Composition (%)	Type	Leachate Volume (ml)			Ratio to Rainfall/Flushing Volume (%)		
			Min	Max	Avg.	Min	Max.	Avg
C01	100 % PAF	Lab	332	869	764	33	87	76
		Field	415	11,000	3,474	8	89	64
C02	25% NAFms over 75% PAF	Lab	272	842	737	27	84	74
		Field	647	12,610	3,527	12	92	65
C03	50% NAFms over 50% PAF	Lab	290	830	723	29	83	72
		Field	715	12,570	3,498	16	91	65
C04	25% NAFss over 75% PAF	Lab	329	839	728	33	84	73
		Field	450	12,260	3,427	22	95	64
C05	50% NAFss over 50% PAF	Lab	334	836	703	33	84	70
		Field	330	12,530	3,176	11	95	58
C06	100% NAF	Lab	410	861	717	41	86	72
		Field	750	12,260	3,557	23	91	66

Note : ms : mudstone; ss = sandstone

Leachate characteristics

The summary of several water quality parameters (e.g. pH, Electric Conductivity and Sulfate content) for 26 weeks of monitoring is summarized in Table 3. In general, both laboratory kinetic and field kinetic tests resulted in similar time series trends in pH as seen in Figure 5 to Figure 7, with a slight difference in the occurrence period of acid formation among those kinetic test.

Table 3 pH, Electric Conductivity and Sulfate contents of column leachates

Column	Material Composition (%)	Test	pH		EC mS/cm		Sulfate (mg/L)	
			Min	Max	Min	Max	Min	Max
C01	100 % PAF	Lab	5.99	7.80	2.19	6.47	1198	5069
		Field	3.53	6.76	3.43	7.10	960	1340
C02	25% NAFms over 75% PAF	Lab	6.26	7.73	1.26	5.74	1176	4333
		Field	4.71	7.70	1.77	6.44	860	1320
C03	50% NAFms over 50% PAF	Lab	7.02	8.28	0.42	5.47	237	3749
		Field	7.20	8.01	1.20	5.91	600	1340
C04	25% NAFss over 75% PAF	Lab	2.20	7.12	1.82	9.52	3277	7392
		Field	3.32	8.26	2.11	7.14	900	1480
C05	50% NAFss over 50% PAF	Lab	2.63	7.96	1.49	6.09	1922	4846
		Field	3.59	8.87	1.86	6.62	1020	1380
C06	100% NAF	Lab	7.07	9.15	0.33	1.45	19	266
		Field	7.23	9.19	0.32	6.62	20	1260

Comparing the columns containing 100% PAF Mudstone, similar trends have been shown for the first eight weeks and the pH values are the neutral condition (see Figure 5 left). Afterward, the pH values in the field columns decreased significantly to below 5, indicating an acid formation. In the laboratory columns, the pH values remain neutral, probably because of the water holding capacity in the fine-grained sample is preventing oxidation during the dry cycle due to regular flushing. In the 100% NAF Mudstone column the pH values in the field test and in the laboratory are quite consistent with the results of NAG pH and paste pH, i.e. in the range of 7 to 9.

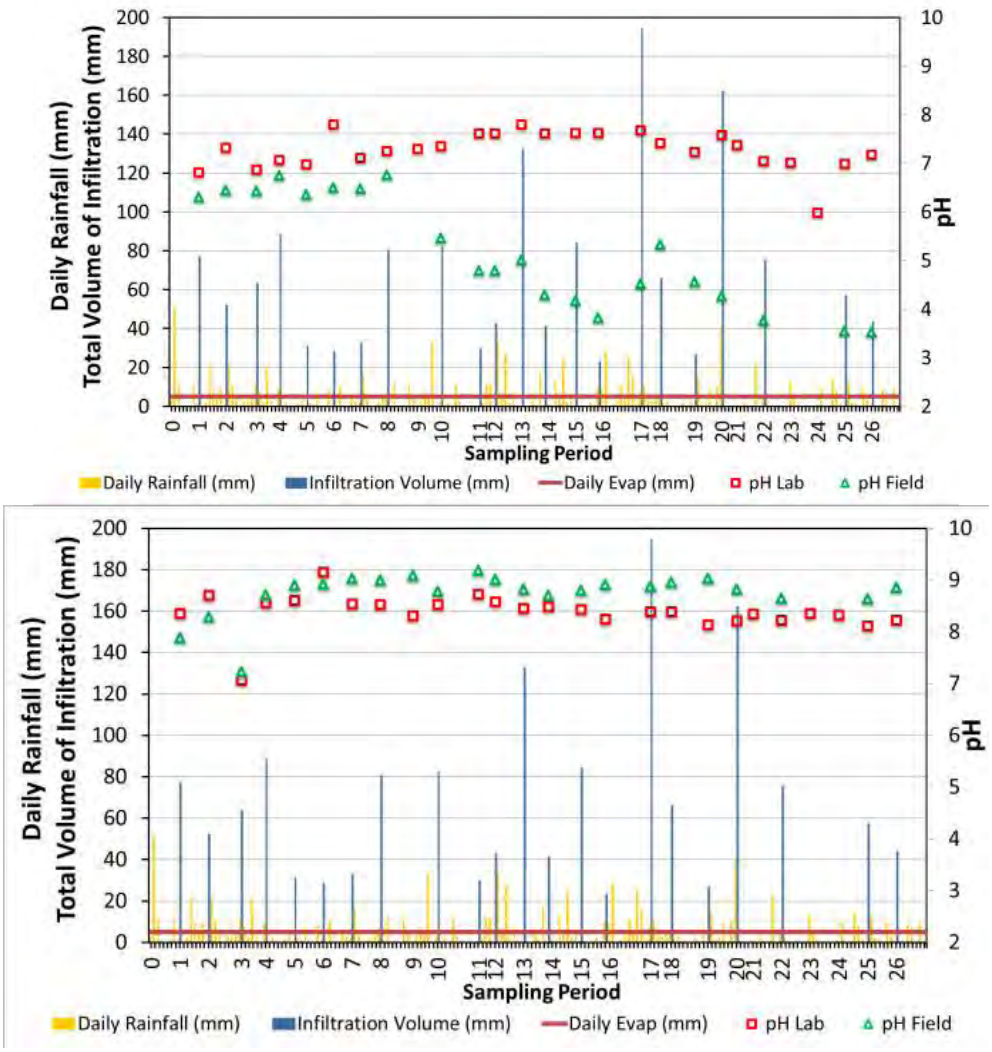

Figure 5 kinetic test result of the C01 column-100% PAF (left) and the C06 column-100% NAF (right)

Figure 6 shows the results of column C02 and C04 containing 75% of PAF material capped by 25% NAF Mudstone and 25% NAF Sandstone whereas Figure 7 shows the results of column C03 and C05 containing 50% of PAF material capped by 50% NAF Mudstone and 50% NAF Sandstone respectively. These columns are aimed to identify the capping characteristics of both NAF materials.

Fine-grained NAF Mudstone has the capacity to prevent oxygen diffusion into the PAF layer due to its water holding capacity but after 24 weeks the pH values decreased (see Figure 6 left). It seems that the thin NAF Mudstone layer is not sufficient for maintaining a consistent capping characteristic (as well as not enough in buffering capacity), compare with the capping performance of 50% NAF Mudstone which indicated no net-acid generation along the test period as shown in Figure 7 left.

On the contrary, acid formation in the laboratory column that had 25% and 50% of NAF Sandstone over the PAF material occurred starting in the 6th week, and the pH value decreased from around 7 to as low as 2.2 (see Figure 6 right and Figure 7 Right). Sandstone seems unable to prevent oxygen diffusion below the level where the acid product can be buffered by the low ANC (1.51 kg H_2SO_4/ton of rock). Similar trend of pH value

decreasing were also observed from field test, although had a lower decreasing rate compare with the laboratory test. An anomaly also can be observed where the pH value in the column with 25% NAF Sandstone started to decrease almost 13 week later than the column with 50% NAF Sandstone, which indicate a slower rate of acid formation. This anomaly is being observed along with the continuously monitored field kinetic test.

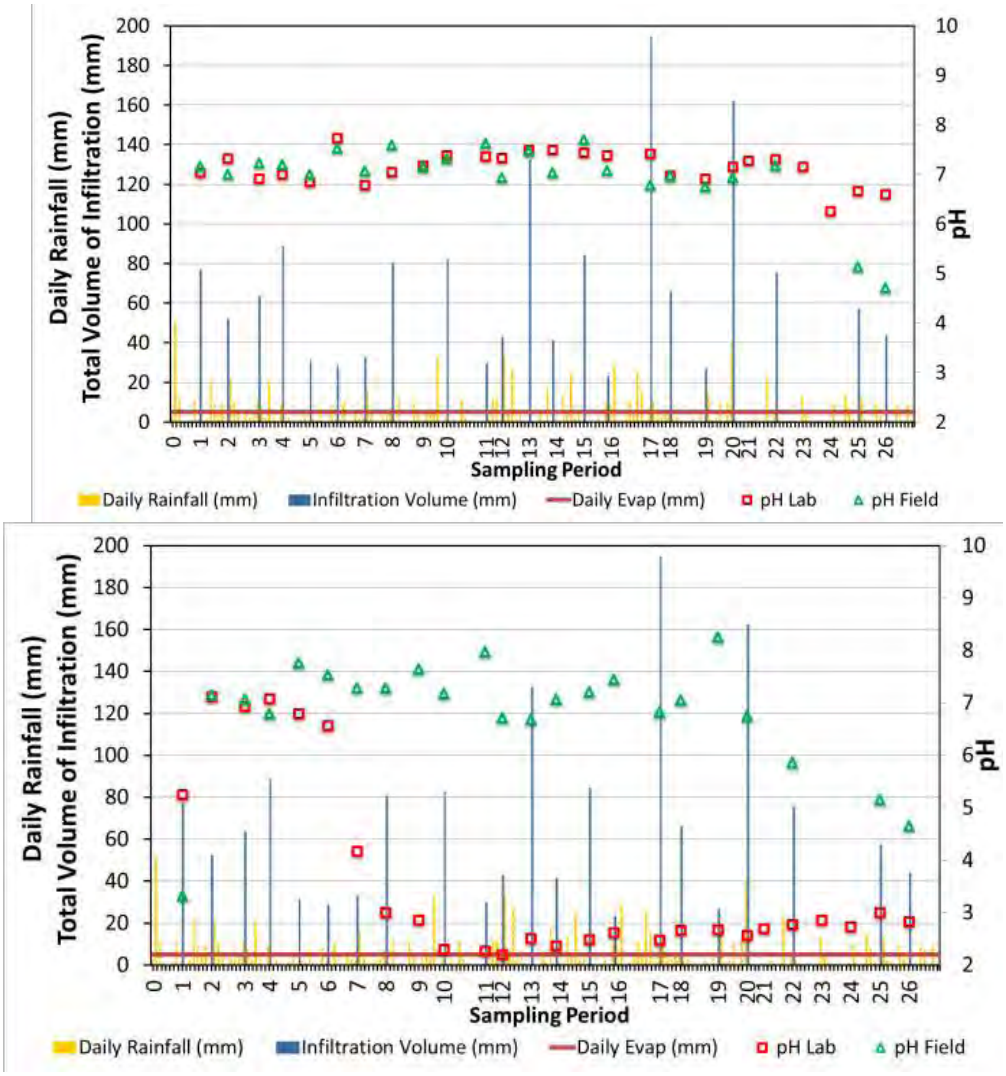

Figure 6 Kinetic test results of the C02 column with 25% NAF Mudstone (left) and the C04 column with 25% NAF Sandstone (right) over 75% PAF

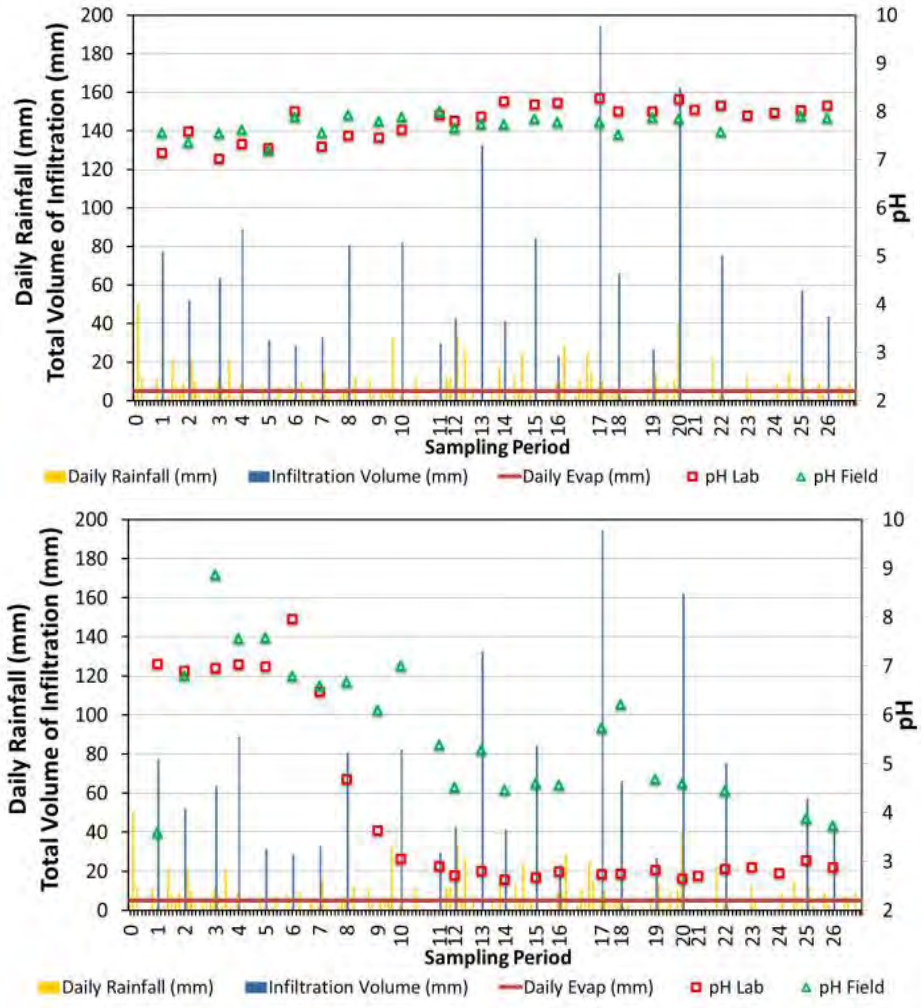

Figure 7 Kinetic test results of the C03 column with 50% NAF Mudstone over 50% PAF (left) and the C05 column with 50% NAF Sandstone over 50% PAF (right)

CONCLUSION

A kinetic test using free draining column leach tests has been conducted in the laboratory and on site using the samples taken from Lati coal mine in Berau, Kalimantan. Samples consisted of potentially acid forming mudstone and non-acid forming mudstone and sandstone. Columns with different configurations, namely 100% PAF mudstone, 100% NAF mudstone, 25% of NAF mudstone over PAF, 50% of NAF mudstone over PAF, 25% NAF sandstone over PAF and 50% NAF sandstone over PAF, were analysed in order to compare the results in the laboratory and on site. In general, similar trends were observed in the experiment, in the laboratory, and on site kinetic test.

The water inflow pattern, i.e. regular flushing versus natural rain condition, is playing an important role in characterizing the leachate chemistry. In fine grain material, the regular weekly flushing could retain water in the sample pores in a relatively saturated condition, and consequently prevent or minimize the oxygen diffusion in addition to the existence of acid buffering capacity of the

capping layer. These characteristics could be beneficial when using fine grain material as capping in PAF encapsulation prevention method.

Since the analysis is only conducted for 26 weeks, more interesting results are expected when longer monitoring data can be obtained, particularly from on-site experiments.

ACKNOWLEDGEMENTS

The authors would like to thank PT Berau Coal for their support in this research.

REFERENCES

Gautama R.S., Kusuma G.J, Lestari Iin, Anggana R.P., 2010, Weathering Behaviour of Overburden-Coal Ash Blending in Relation to Overburden Management for Acid Mine Drainage Prevention in Coal Surface Mine. – In: Wolkersdorfer, Ch. & Freund, A.: Mine Water & Innovative Thinking. – p. 417 – 421; Sydney, Nova Scotia (CBU Press).

Hideki SHIMADA, Ginting Jalu KUSUMA, Koh HIROTO, Takashi SASAOKA, Kikuo MATSUI, Rudy Sayoga GAUTAMA, Budi SULISTIANTO,Development of a New Covering Strategy in Indonesian Coal Mines to Control Acid Mine Drainage Generation: A Laboratory-scale Result,International Journal of Mining, Reclamation and Environment,Vol.26,No.1,pp.74-89,2012.03.

Mine Environment Neutral Drainage Program (MEND), 1998a. Blending and Layering Waste Rock to Delay, Mitigate or Prevent Acid Rock Drainage and Metal Leaching: A Case Study Review. Report 2.37.1, CANMET.

Frostad, S., Klein, B., & Lawrence, R. W. (2005). Determining the weathering characteristics of a waste dump with field tests. International Journal of Surface Mining, Reclamation and Environment, 19(2), 132-143.

Davis, G. B., & Ritchie, A. I. M. (1987). A model of oxidation in pyrite mine waste: part 3: import of particle size distribution, Appl Math Model. 11, pp. 417–422.

Devasahayam, S. (2006). Application of particle size distribution analysis in evaluating the weathering in coal mine rejects and tailings, Fuel Process Technol. 88, pp. 295–301

Gosselin, M., Mbonimpa, M., Aubertin, M., & Martin, V. (2007). An investigation of the effect of the degree of saturation on the oxygen reaction rate coefficient of sulphidic tailings, In Proceedings of ERTEP 2007 — First International Conference on Environmental Research, Technology and Policy, Accra, Ghana, July 17– 19, 2007.

Construction, Instrumentation and Preliminary Results of Field Leach Pads for Scaling Reaction Rates and Assessing Field Performance

Keith Mountjoy[1], Annetta Markussen-Brown[2], Vivian Ferrera[2] and Tyson Kaemffer[3]

1. *Klohn Crippen Berger, Peru*
2. *Klohn Crippen Berger, Canada*
3. *Site C Engineering, BC Hydro, Canada*

ABSTRACT

The construction of a large-scale hydroelectric project will result in the excavation of approximately 8 million cubic meters of sulfidic bedrock that will be permanently stockpiled. As part of a comprehensive geochemical characterization program, two Field Leach Pads were constructed to gain an understanding at a field scale of the relationship between physical and geochemical processes that may affect differences water quality between compacted and un-compacted material, during and after construction.

The Field Leach Pad 1 (West) is 2.4 meters high and was constructed in two 1.2 meter compacted lifts. Field Leach Pad 2 (East) is 2.1 meters high and was construction in two 1.05 meter uncompacted lifts. The sulfidic bedrock material used for Field Leach Pad construction was obtained from fresh excavated material. The lift height was selected based on engineering design at the time of Field Leach Pad construction. Both Field Leach Pads were instrumented with continuous multichannel tubing (CMT) multilevel systems (for oxygen and carbon dioxide monitoring and porewater sampling); temperature probes; water content sensors; and matric potential sensors. Information gained from the instrumentation will be used to evaluate site-specific factors and properties on sulfide oxidation rates and seepage chemistry.

This paper describes Field Leach Pad construction, instrumentation, and the preliminary results that includes: two leachate sampling events that (May 2013 and September 2013), one oxygen and carbon dioxide monitoring event that (September 2013), and the results from the sensors spanning the time period of August 2013 to April 2014. The preliminary results support the benefit of placing and compacting excavated shale. The gas concentrations and moisture content values suggest that the compacted Field Leach Pads should show lower reactivity over time and lower loading rates to the environment.

Keywords: Field Leach Pad, kinetic tests, instrumentation, scaling, loading rates, water quality

INTRODUCTION

The complexities of physiochemical processes that occur at the field-scale in waste rock piles and the scaling of laboratory reaction rates has been the subject of intensive and extensive research. At the 2012 ICARD conference, for example, many papers were focused on presenting on this subject (Andrina et. al., 2012; Kempton, H, 2012; Shaw and Samuels, 2012; Smith et. al., 2012a; Smith et. al., 2012b). While considerable debate remains on what methods are most appropriate for scaling, what is recognized is that field scale kinetic tests, at varying scales, can provide insights into key site-specific factors affecting the geochemical behavior of sulfidic waste materials and the subsequent loading rates and water quality.

A geochemical characterization program was established in 2009 to assess the potential for acid rock drainage and metal leaching (ARD/ML) from sulfide-bearing bedrock. As part of this program, Field Leach Pad (FLP) testing was undertaken as part of a larger effort to inform waste management strategies. Two FLPs were constructed in late 2012 using excavation sulfidic shale with minor siltstone (hereafter referred to as shale) with the objectives of:

- Assessment leachate quality generated under site-specific field conditions during the first year of operation,
- Comparison of leachate quality to kinetic tests at other scales,
- Gaining an understanding of the physical processes acting within the FLPs, and
- Asessment of the initial effectiveness of placing and compacting materials in 1 m lifts on oxygen ingress and water infiltration as an engineered management strategy to mitigate ARD/ML.

Preliminary results are presented for the FLPs that include:

- two leachate sampling events that occurred in May 2013 and September 2013,
- one oxygen and carbon dioxide monitoring/sampling event that occurred in September 2013, and
- data and results from the instrumentation sensors from August 2013 to April 2014.

METHODOLOGY

The types of sampling, measurements and testing carried out for the FLPs were: sampling and analysis of leachates; measurement, sampling and analysis of gases; measurement of changes in moisture content, and temperature measurements. Analytical testing of leachates and gases were carried out at Maxxam Analytical in Burnaby, British Columbia, Canada.

Field Leach Pad Construction and Instrumentation Installation

Field Leach Pad 1 (West) is 2.5 metres (m) high, and was constructed with sulfidic shale placed and compacted in two 1.25 m high lifts. Field Leach Pad 2 (East) is 2 m high and was constructed with the same material but uncompacted in two 1 m high lifts. Table 1 provides a summary of the instrumentation installed. Figure 1 shows a cross-section of each FLP and the location of the wells and instruments.

Continuous multichannel tubing multilevel piezometers (CMTs) were installed to monitor oxygen (O_2) and carbon dioxide (CO_2). Two CMT were installed in FLP 1 (West) with seven ports in each. Two CMTs were installed in FLP 2 (East) with six ports each. Temperature probes were attached to

the CMTs to monitor temperature. Three probes were installed per CMT and, where possible, were attached at the same depth as a CMT port. Campbell Scientific model CS650-L water content reflectometers were installed to measure the volumetric moisture content. A total of 10 reflectometers were installed in each FLP.

Table 1 Field Leach Pad Instrumentation Installation Summary

Instrument	Description	Supplier	Parameter
CS650-L	Soil water content reflectometer	Campbell Scientific	Volumetric water content
229-L	Water matric potential sensor	Campbell Scientific Canada Corp.; calibration O'Kane Consultants	Water flux
109-L	Temperature probe	Campbell Scientific	Temperature
CMT Multilevel System	Continuous Multichannel Tubing piezometer	Solinst Canada Ltd.	Porewater quality, O_2, CO_2
CR1000 Datalogger	Measurement and control system for data acquisition	R.S.T. Instruments Ltd./ Campbell Scientific.	-
Remote Multipexer	Increases number of sensor inputs.	R.S.T. Instruments Ltd.	-
Weather Station	Provides meteorological measurements	R.S.T. Instruments Ltd./ Campbell Scientific Canada Corp.	Precipitation, temperature, barometric pressure, wind speed/direction

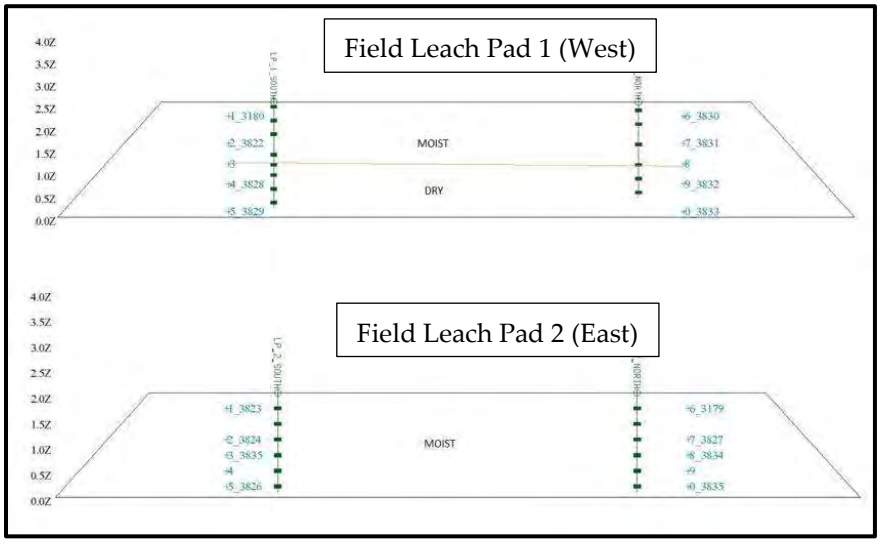

Figure 1 Field Leach Pad Sections: Green bars represent CMT ports. Blue crosses represent 650 and 229 sensors.

Surface Runoff and Infiltration Seepage Sampling

Leachate samples were collected from two locations: collection barrels (designed to collect infiltration seepage only) and collection ponds (designed to collect surface runoff and infiltration seepage). The following parameters were measured or analyzed: pH, electrical conductivity, oxidation-reduction potential, acidity, sulfate, total alkalinity, fluoride, chloride, total suspended solids, total dissolved solids, turbidity, and 54 total and dissolved metals suite. The CMTs were installed to collect porewater samples from within the FLPs; however, no porewater was present during the first year.

Instrumentation Monitoring and Data Logging

Instrumentation data logging commenced in August 2013 following installation and consisted of temperature, soil water content and soil matric potential. Monitoring data collected from August 2013 to April 2014.

Oxygen and Carbon Dioxide Sampling

The CMTs were used for the purpose of monitoring O_2 and CO_2. The first gas sampling/monitoring event took place from September 17th to September 18th, 2013. A GEM2000 gas monitor was used to take in-situ readings at each CMT port. Samples were also collected at select CMT ports to confirm in-situ readings. The samples were collected in Summa canisters and sent for analysis of gas composition.

RESULTS AND DISCUSSION

When sulfide minerals such as pyrite are exposed to water and oxygen; acidity, sulfate and elevated metals concentrations of are produced. Understanding the physical characteristics and processes acting on the material on site, can aid in scaling the laboratory water quality results and loadings to the field, and inform the waste management strategies. These physical processes include water infiltration, oxygen transport, multiphase flow and heat transfer (Lefebvre et. al., 1998; Wels et. al., 2003; Lahmira & Lefebvre, 2007).

The key parameters monitored by the instrumentation in the FLPs include oxygen, carbon dioxide, temperature, moisture content and matric potential. It is important to evaluate the relative influence of these parameters on sulfide oxidation and weathering reaction rates. For example, an oxygen supply is required for sulfide oxidation. Oxidation is an exothermic reaction and results in increased temperature. Changes in temperature and/or pressure may modify the oxygen transport mechanism from diffusion to advection (Wels et. al., 2003). Advection is more efficient at supplying oxygen and sustains higher oxidation rates at greater depths (Lahmira & Lefebvre, 2007).

Comparison of Cumulative Loadings

Precipitation that falls onto the FLPs eventually reaches the collection ponds either as infiltration or runoff. The collection ponds are open to the environment and, as a result, receive additional precipitation and also undergo evaporation. The leachate collection barrels are closed to the environment and only receive seepage that infiltrates through the FLPs.

The flows into the collection barrels and ponds were not measured therefore a number of methods for estimating output volumes for both the collection barrels and the sumps were investigated

based on measured and theoretical values. Loadings were calculated using the different outputs and compared. The most appropriate methods were selected and used to calculate the loadings presented here. The parameters presented here are based on previous shake flask extraction, humidity cell and Field Leach Barrel results for the shale unit.

The results show that the seepage loadings are up to one order of magnitude less than the runoff and seepage loadings combined. It can be inferred from this comparison that an increase of water volume from runoff will increase the loadings in the runoff and seepage combined while the concentrations will decrease.

As discussed earlier, the FLPs were constructed predominantly shale (Unit A) with minor siltstone (Unit B). Cumulative loadings for sulfate, calcium and magnesium over the first year of operation are presented for humidity cells, FLBs, and the seepage and combined seepage and runoff loadings from both FLPs in Figure 2. Overall, there was a clear decreasing sequence of cumulative loadings from humidity cells, to FLBs to FLP runoff and seepage to FLP seepage only (Figure 3 and Figure 4). Differences in cumulative sulfate loadings between humidity cells and FLPs were 4 to 7 times lower. Cumulative calcium loadings between humidity cells and FLPs were similar to sulfate and cumulative calcium magnesium loadings were up to 19 times lower (Figure 2a).

The differences in key metal cumulative loadings was more pronounced, with cumulative loadings up to more than one order of magnitude lower for aluminum, arsenic, cadmium, iron and zinc (Figure 2b).

This relative behavior is expected as the humidity cells have the smallest particle size (more surface area available for reacting), the highest water to solid ratio, and humidity cells are flushed weekly. The FLPs have the largest particle size overall, the lowest water to solid ratio, and are subject only to natural precipitation.

Both FLPs showed similar cumulative loadings. The compacted lifts of Field Leach Pad 1 (West) do not appear to have had a significant impact on cumulative loadings relative to Leach Pad 2 (East). However, it can be observed that seepage only cumulative loadings from Field Leach Pad 1 (West) were lower for sulfate, iron and aluminum.

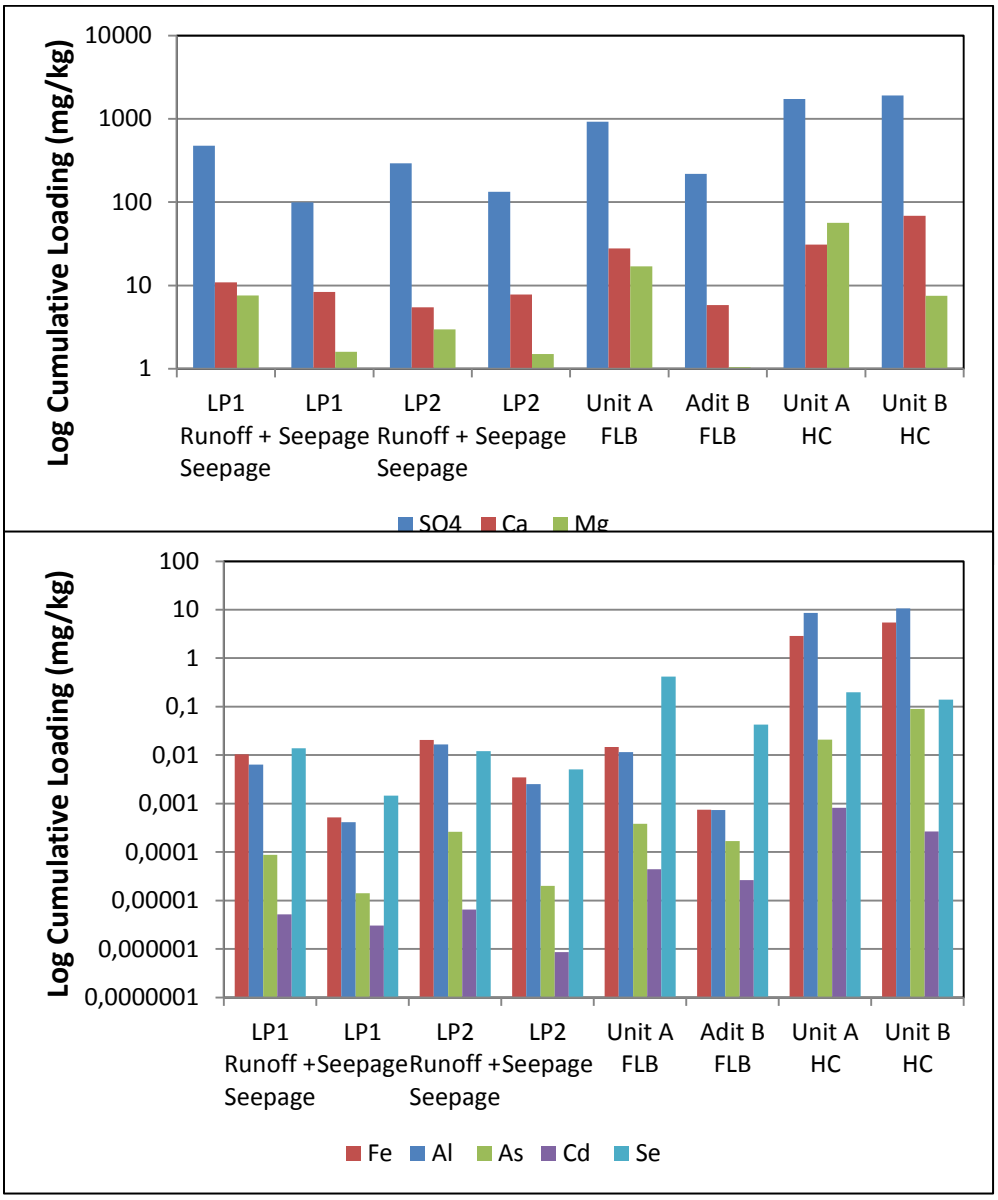

Figure 2 Summary Comparison of Kinetic Loading Rates: **a)** sulfate, calcium and magnesium **b)** iron, aluminum, arsenic, cadmium, selenium.

Notes: LP = Field Leach Pad, Unit A = shale, Unit B = siltstone, FLB = Field Leach Barrel, HC = Humidty Cell

Instrumentation

Oxygen and Carbon Dioxide

Sulfide oxidation consumes oxygen (O_2) and produces sulfuric acid, which can react with carbonate minerals, if present, to produce carbon dioxide (CO_2) gas.

There is a good correlation between O_2 and CO_2 readings (Figure 3). In 3 of 4 CMT's there was a corresponding decrease in O_2 with increasing CO_2. Overall, the FLPs represent an oxidizing ARD environment where O_2 is being consumed via pyrite oxidation, which produces acid that reacts with carbonate minerals to produce CO_2 gas.

The O_2 and CO_2 profiles for the north CMT of FLP 1 (West) suggest that compaction has not had a significant effect on oxygen infiltration. The O_2 and CO_2 concentrations at the bottom of the FLP may have been the result of oxygen flow through the dry zone located between 1.4 and 2.2 m depth. Overall, there was an increasing O_2 consumption and CO_2 production with depth to 1.8 m depth. The moist-dry contact observed during installation does not appear to have had any effect on the O_2 and CO_2 concentrations. Overall there was an O_2 consumption and CO_2 production to a depth of 0.8 m depth, below which concentrations remained constant.

The O_2 and CO_2 profiles for the north CMT of FLP 2 (East) suggests no compaction has not had a significant effect on limiting oxygen infiltration. Overall there was steady O_2 consumption and CO_2 production to a depth of 1.8 m depth, the maximum depth monitored. However, both profiles suggest that rapid surface weathering of the shale may have results in a weathered skin that may act as a cover at limiting O_2 consumption and therefore CO_2 production.

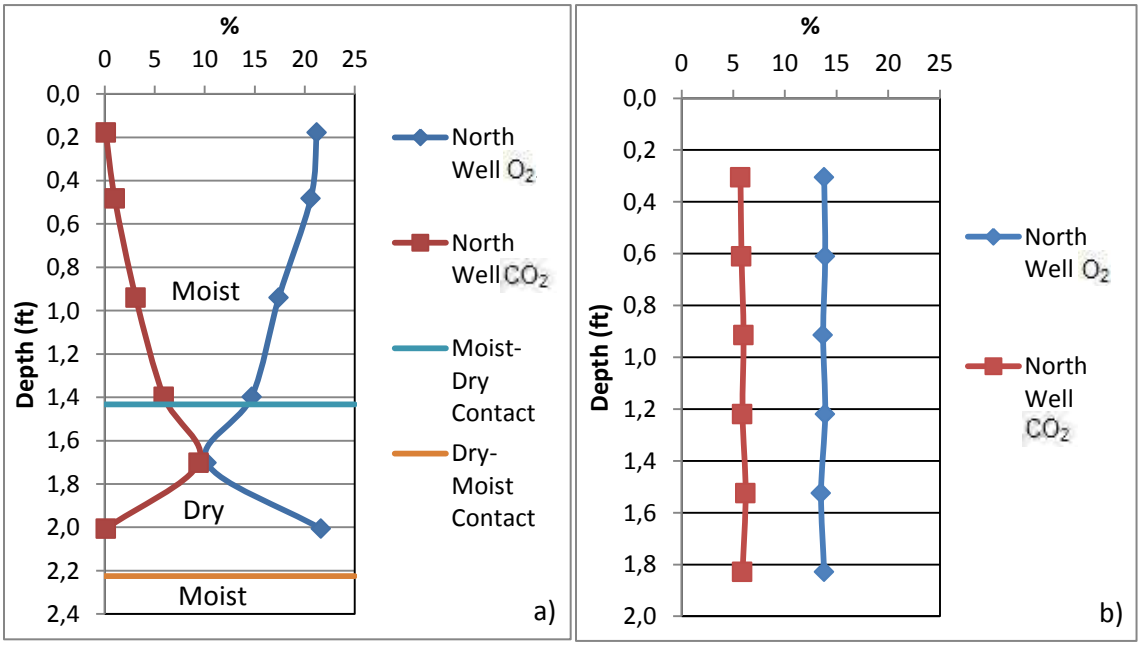

Figure 3 Oxygen (O_2) and Carbon Dioxide (CO_2) Profiles: **a)** Field Leach Pad 1 **b)** and Field Leach Pad 2

Notes: Moist and dry zones were observed at the time of installation and are included for reference only. It is unknown if they have changed.

Temperature

Temperature can be an indicator of sulfide oxidation. The temperature profile in a waste stockpile depends on the rate of heat produced from pyrite oxidation (an exothermic reaction), on ambient temperature changes at the surface of the waste stockpile and by heat diffusion (Ritchie, 1994; Lahmira et. al., 2007). If there are temperatures significantly higher than ambient within the waste stockpile, this suggests that rates of sulfide oxidation are high.

Figure 4**¡Error! No se encuentra el origen de la referencia.** shows an example of the monthly average temperature profiles within the FLPs. The temperatures within the FLPs were generally warmer than the ambient air temperatures at surface, primarily due to sulfide oxidation. In the summer months, temperatures decreased with depth, but overall were warmer than ambient air temperature. The highest temperatures within the FLPs occurred in August with a maximum of 20 °C. In the winter months, temperatures increased with depth with up to 20°C difference between the ambient air temperature and the base of the FLPs.

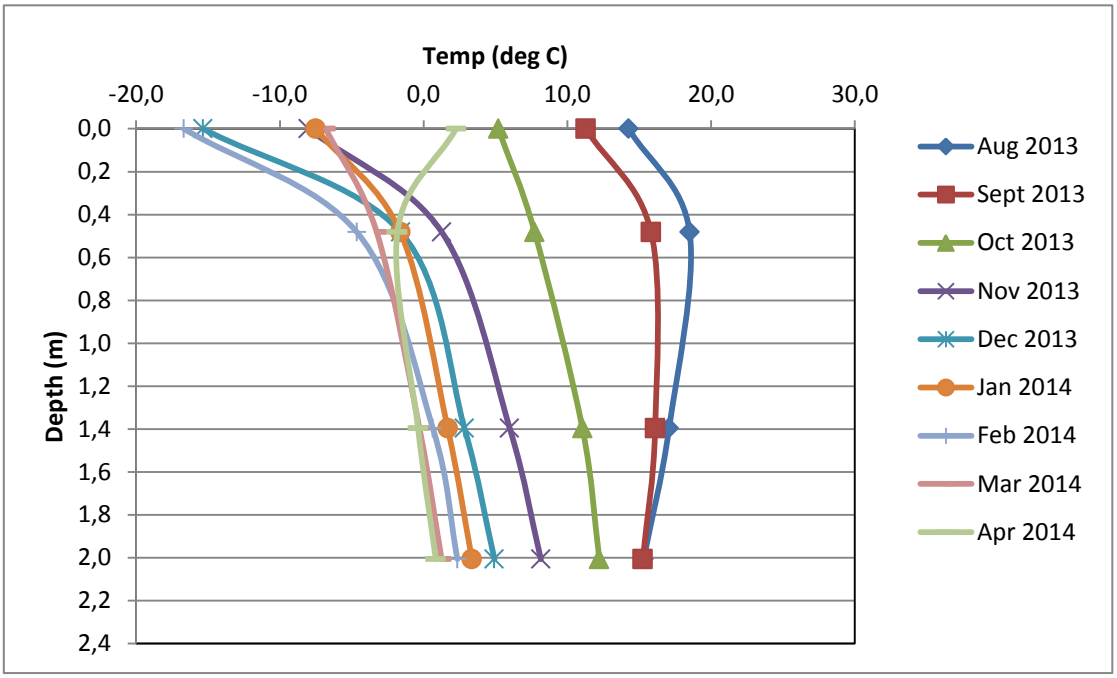

Figure 4 Average Monthly Temperature Profile for Field Leach Pad 1 (West) North CMT

Moisture Content

Moisture content can be used to evaluate the degree of saturation and the permeability of the material in response to precipitation events and seasonal variation.

Figure 5 shows the average monthly moisture content profiles. At the north end of FLP 1 (West), the water content increased with depth until the upper contact of the observed dry zone at 1.37m and then decreased slightly. In FLP 2 (East), water content increased with depth at both the north and south ends. In both FLPs, the uppermost sensors showed greater seasonal variability and the lower-most sensors were relatively stable throughout the year.

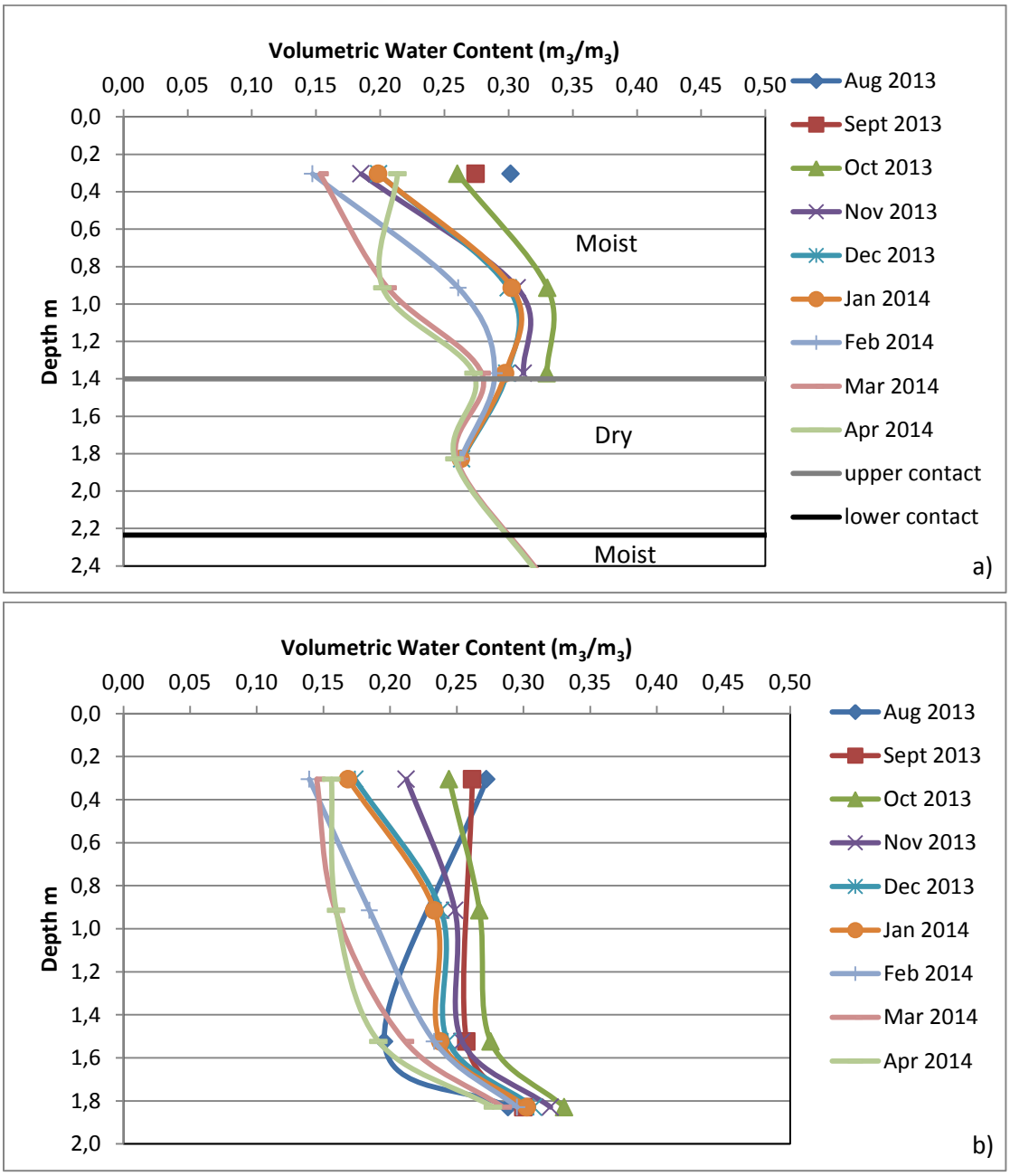

Figure 5: Average Monthly Volumetric Water Content Profile: a) Field Leach Pad 1 b) and Field Leach Pad 2

CONCLUSION

The compacted lifts of FLP 1 (West) does not appear to have had a significant impact on water infiltration or influenced corresponding water quality and cumulative loadings in the first year of monitoring. Both FLPs show similar water quality and cumulative loading rates, despite field observation of moist and dry zones at the time of instrumentation installation. However, the cumulative loadings of sulfate, iron and aluminum from FLP 1 (West) were notably lower than for

FLP 2 (East) Therefore there is some indication that compaction may result in measurable performance change over time.

The compacted cover of FLP 1 (West) may affect oxygen ingress. The north CMT showed oxygen gradually decreasing with depth as would be expected; but the south well shows a dramatic decrease at approximately 0.6m with a corresponding increase in carbon dioxide. This is likely attributable to the compacted cover or it may be the result of variability in grain size and material composition. In general, laboratory oxygen and field oxygen measurements were in agreement and support the observed field trends.

Both FLPs showed similar moisture content ranges, with greater seasonal variability near surface. However, the compacted lift in FLP 1 (West) may impact water content below the upper lift at approximately 1.2 m by impeding infiltration. This is seen by the decreasing trend in measured water content below 1.2 m. In addition, there were field observations of a dry zone at the time of instrumentation installation. FLP 2 (East) showed an overall increasing trend in measured water content with depth.

The preliminary results support the benefit of compaction and lifts. The gas concentrations and moisture content values suggest that the compacted FLPs should show lower reactivity over time and lower loading rates in seepage and surface runoff to the environment. The results also indicate that cumulative loadings are variable but more than one order of magnitude lower for aluminum, arsenic, cadmium and zinc than determined from humidity cells of the same material.

REFERENCES

Andrina J., Wilson G.W. Miller, S.D. 2012. Waste Rock Kinetics Testing Program: Assessment of the Scale Up Factor for Sulfate and Metal Release Rates. *In* Proceedings 9th International Conference on Acid Rock Drainage (ICARD) 20-26 May, 2012. Ottawa, Canada.

INAP, 2011. The Global Acid Rock Drainage (GARD) Guide. Available online http://www.gardguide.com/index.php/Main_Page Accessed January 2011.

Kempton, H. 2012. A Review of Scale Factors for Estimating Waste Rock Weathering from Laboratory Tests. *In* Proceedings 9th International Conference on Acid Rock Drainage (ICARD) 20-26 May, 2012. Ottawa, Canada.

Lahmira, B., Lefebvre, R., Aubertin, M., Bussière, B. 2007. Modeling the influence of heterogeneity and anisotropy on physical processes in ARD-producing waste rock piles. *In* Proceedings of 60th Canadian Geotechnical Conference and the 8th Joint CGS/IAH-CNC Groundwater Conference (pp. 21-24).

Lefebvre, R., Smolensky J., Hockley D. 1998. Modeling of Acid Mine Drainage Physical Processes in the Nordhalde of the Ronnenburg Mining District, Germany. *In* Proceedings of the TOUGH Workshop 1998. May 4-6, 1998, Berkeley, California (pp. 228-233).

MEND, 2009. Prediction Manual for Drainage Chemistry from Sulfidic Geologic Materials Mend Report 1.20.1. NRCan.

Ritchie, A.I.M., 1994. The waste-rock environment. In: Jambor, J.L., Blowes, D.W. (Eds.), Short Course Handbook Volume 22, The environmental geochemistry of sulfide mine-wastes. Waterloo. May 1994.

Shaw S., Samuels A. 2012. An Empirical Comparison of Humidity Cell and Field Barrel Data to Inform Scale-Up Factors for Water Quality Predictions. *In* Proceedings 9th International Conference on Acid Rock Drainage (ICARD) 20-26 May, 2012. Ottawa, Canada.

Smith L.J., Macdonald, G., Blowes D., Smith L., Sego D.C., Amos R.T. 2012a. Davik Waste Rock Project: Objectives, Construction, Current Conclusions and Implications. *In* Proceedings 9th International Conference on Acid Rock Drainage (ICARD) 20-26 May, 2012. Ottawa, Canada.

Smith L.J.D., Moncur M.C., Neuner M., Gupton M., Blowes D., Smith L., Sego D.C. 2012b. Davik Waste Rock Project: Design, construction and instrumentation of field-scale experimental waste rock piles. Applied Geochemistry. doi:10.1016/j.apgeochem.2011.12.026

Wels, C., Lefebvre, R., Robertson A. 2003. An Overview of Prediction and Control of Air Flow in Acid Generating Waste Rock Dumps. *In* Proceedings 6th International Conference on Acid Rock Drainage (ICARD) 12-18 July 2003. Cairns Australia (pp. 639-650).

10th ICARD IMWA 2015 | 10th International Conference on Acid Rock Drainage & IMWA Annual Conference

Up-Scaling from Trial to Operation: Practicalities of Construction and Permitting, Force Crag Mine

Arabella Moorhouse[1], Rachel Harris[1], Lee Wyatt[1], Stephen Hill[1] and Hugh Potter[2]

1. *Environment Department, The Coal Authority, United Kingdom*
2. *Land Contamination Management, Environment Agency, United Kingdom*

ABSTRACT

Following successful small-scale compost-based bioreactor (tank size 3.75 m^3; flow rate 1.1 L/min) metal mine treatability trials undertaken by Newcastle University, a full-scale vertical flow pond treatment system was constructed in 2014 at the abandoned Force Crag Mine (Cumbria, UK). Metal concentrations in the mine water are sufficiently high to cause the receiving water course, the Coledale Beck, to fail UK environmental quality standards. The innovative system remediates the baseflow of mine water (6 L/s), which contains elevated concentrations of zinc (3.8 mg/L) in a treatment area of 1250 m^2 with a target residence time of ~14 hours.

Force Crag is a remote site located within a National Park that is popular with tourists and walkers. The mine site, including the underground workings, buildings and mine surface, are owned and managed by the National Trust (a UK historical conservation charity). Construction of a treatment system in this isolated, open access, rugged area resulted in challenges that needed to be considered in the design process. The novel nature of the treatment technology deployed at the site required any scheme to be designed to enable rigorous scientific investigation of the system to prove the design concept. Furthermore, operational issues (*e.g.* quantities of gas release) that could result from the full-scale system also needed to be addressed.

All of these challenges were overcome, resulting in the successful delivery of a new treatment technology. This paper highlights the engineering and permitting aspects of up-scaling from a trial system to a full-scale novel treatment methodology.

Keywords: mine water, treatment, construction, full-scale, metal mines

INTRODUCTION

Novel mine water treatment technologies are continually being developed in both the academic and commercial sectors to tackle the problem of removing dissolved divalent metals from base metal mine discharges. Although well-established methods exist for the passive removal of iron, *i.e.* aeration cascades, settlement lagoons, aerobic reed beds and reducing alkalinity producing systems (RAPS) as described in the PIRAMID Guidelines (2000); passive techniques designed to remove other common contaminant metals such as zinc, cadmium, copper, lead etc., which are more difficult to precipitate from mine waters than iron, are less common. Active treatment methods, such as the lime dosing plant currently operating at Wheal Jane Mine in Cornwall, UK (Wyatt *et al.*, 2013), add an alkali to the water to increase the pH sufficiently to allow the formation of carbonate and/or oxy-hydroxide mineral species to precipitate, producing an ochre sludge. Systems such as these are expensive to operate however, requiring continuous staffing levels with high electricity consumption, in addition to the use of large quantities of chemical products. Furthermore, active systems often generate significant volumes of metal-rich sludge, which not only contain the metals themselves, but also the supplementary component of the chemical additions; which in the case of lime dosing, can be considerable. Consequently, active treatment systems, although a very successful option, often have both high capital and operational costs; the typical operational costs for the Wheal Jane mine water treatment facility for example, are £1.5M per year. For schemes that are in effect required for perpetuity, such systems are far from ideal. The desire to reduce high capital investment and high operational costs are two of the main drivers for researchers to develop alternative, more passive and accordingly more cost effective, treatment methodologies.

Laboratory scale trials are the first stage in the development process of any passive mine water treatment technology, which if proven successful, progress forwards to pilot-scale trials. However, for the often small-scale nature of pilot trials, important issues such as supply of materials, size of treatment areas, construction requirements, operational needs, variable or flashy flow rates, regulatory permits and local climatic variations are generally readily overcome. When attempts are made to scale-up a pilot-sized system to a full sized operational site however, these are factors that must be considered and addressed. Subsequently, although many successful pilot-sized treatment systems are described in the literature, the practicalities of the 'real world' can result in relatively few of these methodologies being successfully deployed in the field at the full-scale.

This paper discusses the challenges that can occur when a successful small trial passive system is up-scaled to a full sized, operational system situated in the natural environment.

Dealing with abandoned metal mining pollution in England

Throughout England, there has been historic mining of metals across many regions. However, in contrast to the legacy resulting from the coal mining industry, which is subject to legislation in the UK, there is no one single body responsible for metal mining pollution.

Following the transposition of the European Water Framework Directive (WFD) (2000/60/EC) in to UK national law in 2003, the Department of Environment, Food and Rural Affairs (Defra) has taken measures to establish a remediation program for water pollution from non-coal (predominantly metal) mines which affect up to 2 500 km of rivers in England. In 2012, a consortium published a report (NoCAM) identifying and prioritizing the principle non-coal mine water impacts present in England (and Wales) (Jarvis and Mayes, 2012). In 2011, Defra allocated funds to the Coal Authority (CA), based on the organization's *c.* 20 years experience in mine water remediation, in conjunction with the Environment Agency (EA), to deal with pollution from abandoned non-coal mines.

Force Crag Mine, Cumbria, UK

Force Crag Mine is an abandoned lead-zinc-barites mine located in the Lake District National Park in Cumbria (North West England), near the village of Braithwaite (Figure 1). Situated 7 km West of Keswick, in the headwaters of the Coledale Valley, the mine site covers an extent of approximately 1.2 km long from the banks of the Coledale Beck westwards towards the ridge of Grisedale Pike. Hosted in Ordovician siliciclastic sediments (Kirk Stile Formation), the east-west trending, vein-hosted mineralization present at Force Crag is a zoned ore body dominated by galena (lead-ore) and sphalerite (zinc-ore) with barite and quartz gangue (Tyler, 2005).

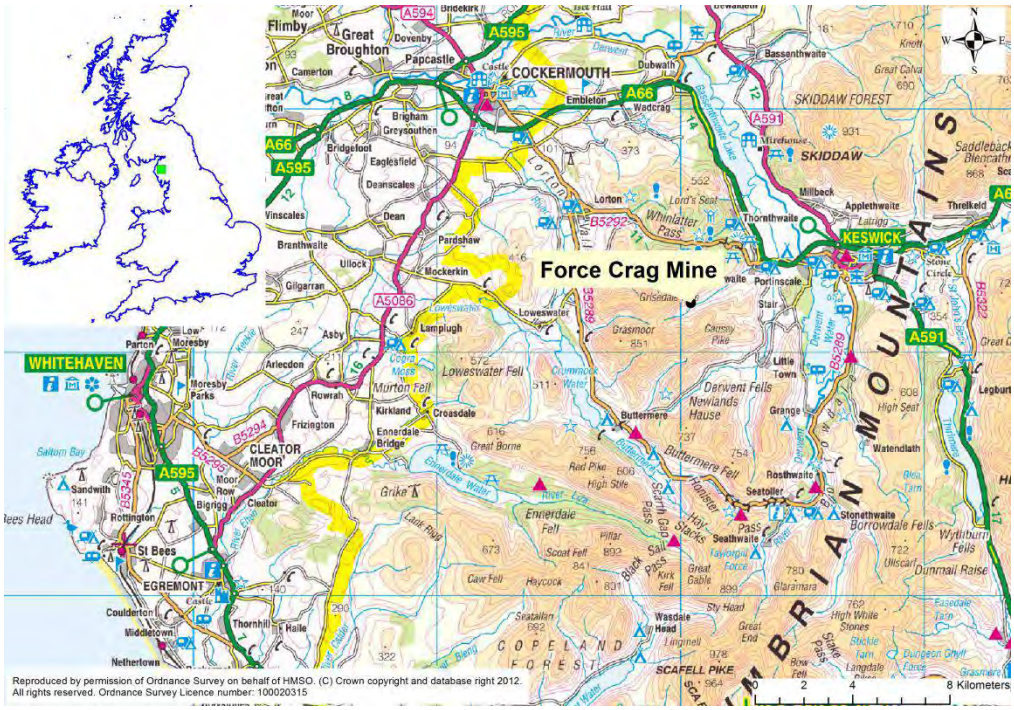

Figure 1 Location map for Force Crag mine and surrounding area

Mining has occurred at Force Crag since at least the 15th Century, although the most intensive period was during the 19th Century when the mine was worked intermittently for lead-ore and barite; operations finally ceased at the site when the mine closed in 1992 (Tyler, 2005).

Force Crag mine workings comprise of a series of nine individual levels driven into the mountainside. Level Zero forms the lowest level near the valley floor, and the workings are currently drained from both Level One and Level Zero. Despite the occurrence of some diffuse contamination originating from the processing and mining waste at the site, the Level One discharge has been have identified as the main point source of metal contamination in the Coledale Beck at Force Crag. The Coledale Beck is one of the main tributaries to the Newlands Beck and the impact of the pollution resulted in the Newlands Beck being ranked at number 16 in England and Wales (Jarvis and Mayes, 2012) on a priority list; in 2013, the EA raised Newlands Beck to rank 1 in England after collection of further data.

Mine Water Chemistry

The mine water at Force Crag is circum-neutral with elevated concentrations of zinc and cadmium, combined with relatively low concentrations of iron. Consequently, the receiving watercourses, the Coledale Beck and Newlands Beck, fail the UK environmental quality standards (currently classified as failing with moderate status under the WFD) for zinc (~12 µg/L) and cadmium (0.08 µg/L) for a reach of at least 10 km. A summary of the chemical characteristics of the mine water from Level One is provided in Table 1. The flow from Level One is relatively flashy in nature; on average, the flow rate is 8-10 L/s, although flow rates of >40 L/s have been recorded after storm events in 2014.

Table 1 Typical mine water chemistry (total metals) of the Level One discharge, Force Crag Mine (n=11 samples, data collected in 2014)

	pH	EC µs/cm	Alkalinity mg/L	Calcium mg/L	Magnesium mg/L	Iron mg/L	Zinc mg/L	Cadmium µg/L	Lead µg/L	Sulfate mg/L
Mean	7.1	150	25	13	5	0.63	3.8	18	40	31
Min	6.9	119	13	7	3	0.34	2.1	11	27	18
Max	7.4	270	56	15	5	0.80	4.9	22	66	38

Stakeholders

To facilitate the successful deployment of a novel mine water treatment system at the Force Crag mine site, a large number of stakeholders were required to work together. A group comprising of four organizations (CA, EA, Newcastle University and National Trust), formed the main body of stakeholders that collaborated closely to deliver the mine water treatment scheme. Overall however, a total of eleven different organizations (including 3 regulatory bodies) were involved in the project to differing extents. For further information on the methodology adopted by the CA on stakeholder management for this site, the authors direct the reader to Harris *et al.* (2014).

TREATMENT METHODOLOGY

The passive treatment methodology that has been deployed at Force Crag has been developed from laboratory and pilot scale trials undertaken by Newcastle University (NU) funded by Defra and published by the EA (Jarvis *et al.*, 2014). This technique employs an anaerobic compost bio-reactor where sulfate reducing bacteria are exploited to remove metals from circum-neutral mine waters. A key component of this methodology is to ensure that there is sufficient carbon present in the media to sustain the desired microbial community, without promoting competing methanogenic communities which would not attenuate the metals. Over a period of 40 months, the Newcastle team executed a series of simultaneous laboratory column experiments, laboratory-style field column experiments and pilot-scale reactors. One pilot-scale reactor which operated for 24 months, was deployed at Nenthead Mine; an abandoned lead-zinc mine in the North Pennines (Cumbria), located 7 km SE of Alston, with a circum-neutral mine water typically containing ~2 mg/L of zinc.

Pilot-scale systems installed in the field, particularly those which harness biological processes, often require time to allow the system to establish and reach a steady state. In addition, they must also be small enough to provide information on when the system reaches saturation, resulting in breakthrough of the metal contaminant. Important factors which require consideration when

building full scale treatment systems is the longevity of the system, in addition to the size of treatment area required. Consequently, it is crucial that pilot-scale systems provide the necessary data to address these important issues; the system deployed at Nenthead fulfilled these criteria.

Using a down-flow system, the Nenthead reactor treated an average flow of 1.1 L/min for a period of 24 months, successfully removing on average *c.* 70 % of the total zinc concentration, with a mean residence time of ~14 hours. Containing 2.25 m^3 of media mix, comprising of compost (PAS100 British Standards Institution), woodchips and activated digested sewage sludge with a limestone chip under drain, the Nenthead reactor was 2.5 m long, 1.5 m wide and 1.0 m deep (Jarvis *et al.*, 2014). Mixing of the four components, which were sourced locally, occurred on site to reduce heterogeneity in the media. Based on the success of the Nenthead reactor, and particularly the excellent zinc removal rates observed despite the short residence time, the full-scale vertical flow pond (VFP) system at Force Crag was proposed; however, the complexity of building a full-scale system presented a different set of challenges than those typically faced in small-scale systems.

DISCUSSION

Force Crag Mine site has a number of designations, including Site of Special Scientific Interest (SSSI), Special Area of Conservation (SAC) and Scheduled Monument; the site is also a popular tourist region in an area of open access (an area where free access is granted to the public). Furthermore, the Coledale Beck, which flows through the site, is a tributary of the Newlands Beck, which contributes to Bassenthwaite Lake and subsequently, the River Derwent; areas designated as SSSI, SAC and a National Nature Reserve. Contamination from abandoned metal mines has a negative impact on these environmentally sensitive areas; consequently, the remediation of the mine water discharge at Force Crag was identified as being able to deliver significant benefits to the whole catchment. Many of the challenges associated with constructing the system were related to the designations assigned to the site, in addition to the requirements for environmental permitting. This paper focuses on the issues pertaining to the construction and permitting of the scheme.

Construction

Some of the key challenges associated with the up-scaling from a pilot to a full-scale system are related to the construction, engineering and operational considerations for the scheme. This section focuses on some of these issues that occurred at the Force Crag site, and how they were addressed.

Mine water collection and scheme layout: the precursors to construction

Extensive investigations were undertaken by the EA, in conjunction with NU (funded by Defra), prior to construction of the treatment scheme, examining the point sources and diffuse pollution of the Force Crag site and the environmental impact on the Coledale Beck and Newlands Beck. This unpublished work identified the Level One discharge as the main point source of metal pollution at the site and concluded that remediation efforts should be focused on this primary source of cadmium and zinc. In 2013, a system of buried pipework was installed to take the Level One mine water from its original discharge point to the Coledale Beck; a flow measurement weir was also installed with the ability to allow diversion of water to the proposed treatment site.

Discussions with the National Trust and English Heritage were also ongoing during this period to finalize an agreement for the siting of the scheme within the site. Following negotiations between the CA, EA, National Trust and English Heritage, the area of the former tailings pond, located

between the old mine workings and the Coledale Beck, was chosen. This agreement was reached with the understanding that the remediation of the mine water discharge from Level One was part of the 'evolution' of the site from an area of active mining to one of environmental remediation.

Once the scheme location was established, plans were submitted to the local administrative authorities to obtain planning approval. When assessing the impact of a new development, planning officers need to understand the scale of the development and what the visual impact will be, especially in a sensitive region such as a National Park. At this point in time however, the trial at Nenthead was still ongoing; concept designs were therefore produced to provide the authorities with a high level plan using the layout and performance of the Nenthead reactor as a guide. Figure 2 shows the final layout of the scheme, which is not dissimilar from the plans originally submitted to the local planning authorities. The original plan envisaged a single treatment pond; however, a decision was subsequently taken to have two VFPs in parallel, to enable future variations in flow rates in each pond to investigate the influence of residence time on metal removal performance. At the time of engaging the local authority, some uncertainty still remained about the size of the new scheme and the amount of flow to be treated. Nominal guidelines were therefore provided to the CA by NU to size the scheme based on the results their team had obtained from the Nenthead trial. Furthermore, using the results obtained from the catchment monitoring undertaken by NU, a baseflow rate (6 L/s) for the scheme was also agreed that would result in a measureable improvement to the Coledale Beck while ensuring a consistent flow to the VFP. Further details of the Force Crag treatment scheme are provided in Jarvis *et al.* (2015).

Treatment Media

An important component of the VFP system is the treatment media. Following finalization of the system design, it was initially assumed by the design consultants that placement of the media (a mixture of PAS100 compost, woodchips and activated sewage sludge) into the ponds would be achieved by driving heavy plant machinery directly into the cells, using the media as a traversable surface. However, it became clear that this would have a detrimental impact on the material, reducing the porosity and permeability of the media by compaction and potentially damaging the under drain network. A key part of this system is the even down flow of water; any damage to the under drain or reduction in the porosity and permeability of the media, could result in water short circuiting, thereby decreasing residence times and reducing system performance. Discussions onsite with the contractor, design consultants and NU, resulted in the layout of the ponds being amended; the road way between the ponds was widened to facilitate the use of a long-reach excavator that could work from the pond edges.

Under drain

A complex under drain system, briefly mentioned above, is another key component of the system. This network of pipes divides each pond into four quadrants (each of which can be sampled individually at the discharge point), to facilitate the assessment of metal removal in each sector of the pond. The original under drain design drafted by NU included specific sizes for limestone chips and the number of perforations in the pipework. In preference to using customized products, it was decided to use commercially available pipes combined with larger limestone chips to achieve the same levels of permeability, whilst minimizing costs. Comprising of 770 m of standardized perforated drain pipes, the resulting network is encased in limestone gravel (20-40 mm), which protects the pipework and reduces the potential for the compost material to obstruct the system.

Initially it was proposed that the scree and spoil material readily available on site could be used for the gravel layer in lieu of limestone, as the only function of the drain was to facilitate the drainage of the treated water out of the system. However, this option was dismissed as this material would have introduced fresh metal contamination into the system following the removal of metals in the mine water by the media. It was therefore agreed that a limestone under drain would be installed. A local source of limestone was identified by the contractor, however on sampling by NU, it was found to contain slightly elevated concentrations of water-soluble sulfate. As some limestone dissolution is expected to occur, and it was important to be able to measure the amount of sulfate being removed by the system, a calcium carbonate limestone that contains fewer impurities was therefore imported from further afield.

Wetland

An aerobic wetland for the purpose of aerating the water exiting the anaerobic ponds and filtering any fine particulates that may remain in the water was required for the scheme. In preference to *Phragmites sp.* reeds that are typically used by the CA in constructed wetlands, it was decided to use metal-tolerant rushes (*Juncus sp.*) already established in the area to reduce the visual impact of the wetland. During construction, the plants were temporarily relocated before being placed in their final position in the wetland. There was some concern that although these plants prefer water-logged conditions, they would not survive submerged in a water depth of 300 mm; water levels were therefore lowered to 100 mm and to date, the plants are thriving in their new environment. It is intended to use similar wetland systems at future schemes employing this technology, although such wetlands will need to be larger in size compared to the small unit installed at Force Crag.

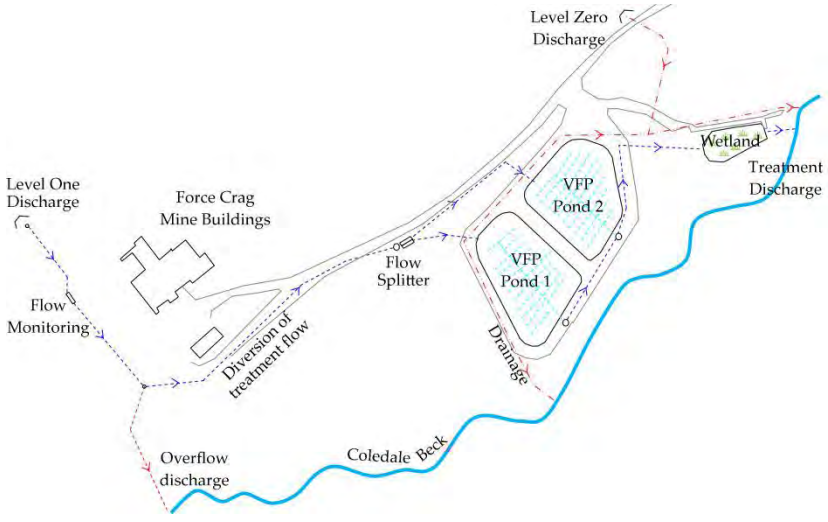

Figure 2 Schematic diagram of the treatment system at Force Crag mine (not to scale)

Flow rates

Low flow rates (typically L/min) in small scale systems are easily controlled and manipulated. In a full scale-system however, flow rates are less easy to regulate, yet in a trial setting it is vital to accurately control them to rigorously assess the performance of a system. The CA standard designs,

although adequate for coal mine water treatment schemes, do not provide sufficient control to accurately regulate flow rates through the ponds installed at Force Crag. A new system was therefore devised which can accurately capture a designated baseline flow from the Level One discharge, dividing the flow equally between the two ponds. This system also provides the ability to investigate effects on performance of increased flow rates and thus reduced residence times.

Gas

A potential by-product of harnessing sulfate reducing bacteria (SRB) is the generation of hydrogen sulfide (H_2S) gas. Although it was expected that some H_2S gas would be produced by the system (H_2S could be smelled at the Nenthead reactor and can also be smelt at the CA's RAPS unit installed at Tan y Garn in South Wales), it was unclear what the exact impact at the site would be. Force Crag is situated in a remote, upland, un-inhabited area, and although ramblers and walkers are frequently in the vicinity of the treatment system, it was decided that to install a cover would be prohibitively expensive and would not be aesthetically acceptable in the National Park. To mitigate the problem the following measures were taken; the water depth of the ponds was increased to ~400 mm (from 300 mm); open manhole covers were installed to limit gas build up in any confined spaces which require regular access; a rigorous gas monitoring regime has been instigated to examine gas production and where the 'hot-spots' are located; continuous gas monitors have been installed to assess the risk posed to maintenance operators and the public. Future treatment systems may be required to be sited in populated areas; the data collected from this pilot system will therefore be used to demonstrate the impact of H_2S gas and inform planning authorities about the risks associated with this type of system and the measures that can be taken to mitigate them.

Permitting

A second key challenge associated with the up-scaling from a pilot to a full-scale system in addition to the construction is the environmental permitting of a scheme. This section focuses on some of the permitting solutions that were implemented at the Force Crag site.

Treatment Media

In contrast to the small-scale reactor trial at Nenthead, where the bulk of the treatment media components were purchased from the local garden center and mixed on site in a bucket (A. Jarvis, 2013, *pers. comm.*), the importation and mixing of the media for the full-scale system deployed at Force Crag, caused obstacles which the CA needed to address. It quickly became apparent that in order to use a media containing activated sewage sludge, a waste permit would be required from the EA. Although PAS100 compost and woodchips are not individually classified as waste materials, the inclusion of activated sewage sludge within the mix results in the treatment media being classified as a waste material under EU law; and is therefore subject to the Environmental Permitting (England and Wales) Regulations 2010, which legislates for the movement, importation and placement of waste material(s).

To successfully achieve a homogenous mix of ~650 tonnes of media, large machinery were required to manage the volumes involved; as a suitable mixing area was not present at Force Crag, the materials were mixed off-site. Using a contractor with an existing waste permit to accept the sewage sludge (and willing to apply for the necessary extensions to their license to undertake the media mixing), removed the requirement to apply for these permits directly; saving both time and

reducing costs. Ultimately, the only regulatory requirements the CA were obliged to fulfill was to obtain the necessary permits to import and position the media into the VFP cells.

The long term placement of the media within the treatment ponds was an issue that the regulator was required to consider carefully, to ascertain under what conditions the CA could surrender the waste permit necessary for the placement of the media. It was desirable to surrender the permit upon completion of the construction work to ensure that the ongoing yearly obligations associated with holding waste permit were not incurred, thereby minimizing costs to the UK government. In order to accept the surrender of the permit, the EA had to be confident that the waste placement was a 'low' risk. Under normal circumstances this requires the waste material to be capped to prevent water ingress. At Force Crag, it was agreed that by preventing any mine water ingress into the surrounding ground from the ponds (through the use of impermeable liners), the capping of the treatment media by the overlying layer of water combined with the requirement for the water discharging from the treatment system being subject to monitoring under an environmental permit, the regulator agreed that the waste permit could be surrendered.

In addition to the waste permit requirements, the long term disposal of the spent metal-rich compost media also needed to be considered. Although some measures have been suggested which may increase the longevity of the system (*e.g.* 1. increase the working head of the water in the system to encourage the down flow of water if the permeability of the media reduces; 2. introduce a fresh carbon supply to replenish the food source for the bacteria), it is inevitable that eventually, the media will no longer be effective and require replacement. At some point in the future, the ~650 tonnes of material in the Force Crag VFPs will require permanent disposal, almost certainly off-site. At present, the precise chemical composition of the spent media is unknown. To compensate for this lack of knowledge, the material used in the Nenthead reactor has been used as a proxy to determine the most probable disposal route for the media used at Force Crag. The regulations pertaining to the disposal of waste requires that such material is categorized within a classification system that limits the disposal routes for certain types of wastes. Due to the high concentration of metals in the media, the material is likely to be classified as hazardous waste. However, the high organic content of the compost-based media limits the avenues for disposal; hazardous waste landfill sites within Europe are not permitted to accept wastes with an organic content in excess of 6 %. While there may be options to pre-treat the media prior to disposal the practicalities (both technical and financial) remain uncertain. Consequently, it was decided that a 'worst case' disposal option would be included in the whole-life cost of the system to ensure that future funds were available to dispose of the media at the end of its operational life should they be required.

Discharge Permit

It is recognized by the EA that there is a low risk of pollution from short-term pilot treatment systems at abandoned metal mines. Small-scale experimental mine water treatment plants can therefore be operated without an environmental permit provided the system is carefully monitored, the EA is notified of the trial and its duration and no pollution occurs. For full scale-systems however, environmental permits are required. In the UK, owners or operators of mines abandoned before 2000 cannot be held liable for permitting water pollution, and so public funds are being used to build and operate treatment systems at prioritized long-abandoned mines. Passive systems do not provide the same certainty of effluent quality as active systems, but should lead to significant improvements in river water quality. The EA has therefore decided that in specific circumstances, the numeric emission limits normally applied to effluents may not be appropriate for passive

treatment systems at abandoned metal mines. For the Force Crag system, the EA agreed to issue a permit that requires the CA to carry out detailed monitoring to demonstrate the performance of the VFP and to ensure that there is no increase in pollution, without numerical targets for metals.

CONCLUSION

This paper has focused on some of the construction and permitting issues that can result when taking a small-scale pilot system into the 'real world' as a full-scale operating scheme. Although challenging, these issues can often be overcome by being flexible with design and the sourcing of raw materials, in addition to engaging with numerous stakeholders to ensure a pragmatic approach is taken. In summary, the main challenges identified in this example are as follows:

- Provide local planning authorities with outline plans for designs whilst communicating the message that some modifications to the system may be required.
- Being flexible in the design process, as unforeseen problems will occur during the construction process.
- Clearly specify the materials and methods required and determine the detailed layout of the treatment system before construction commences.
- An adaptable operational monitoring program is required that can change to monitor unexpected issues (*e.g.* H_2S gas) that may arise in the first years of operation.
- Detailed discussions and agreement with the environmental regulator are required in the early stages of the project to ensure the correct permits can be attained.

REFERENCES

Environmental Permitting (England and Wales) Regulations 2010, No. 675.

Harris, R.A., Moorhouse, A.M.L., Hill, S. and Wyatt, L.M. (2014) Stakeholder Management: the key to successful metal mine discharge remediation. In "An interdisciplinary response to mine water challenges - Proceedings of the 12th Congress of International Mine Water Association 2014". Wanghau Sui, Yajun Sun and Changshen Wang (Eds.) pp 781-785.

Jarvis, A.P. and Mayes, W. (2012) *Prioritisation of abandoned non-coal mine impacts on the environment – The national picture.* SC03136/R2 Environment Agency, Bristol, UK. Available from https://www.gov.uk/government/publications/prioritisation-of-abandoned-non-coal-mine-impacts-on-the-environment (accessed 30 Sept 2014).

Jarvis A.P., Davis, J.E., Gray, N.D., Orme, P.H.A. and Gandy, C.J. (2014) *Mitigation of pollution from abandoned metal mines: Investigation of passive compost bioreactor systems for treatment of abandoned metal mine discharges.* Available from https://www.gov.uk/government/publications/treatment-of-pollution-from-abandoned-metal-mines (accessed 24 October 2014)

Jarvis A.P., Gandy C.J., Bailey M.T., Davis J.E., Orme P.A.H., Malley J., Potter H.A.B, Moorhouse A.M.L. (2015) Metal removal and secondary contamination in a passive metal mine drainage treatment system. 10th IMWA-ICARD 2015, Santiago, Chile.

PIRAMID Consortium. (2003) Engineering Guidelines for the Passive Remediation of Acidic and/or Metalliferous Mine Drainage and Similar Wastewaters. European Commission 5th Framework RTD Project no. EVK1-CT-1999-000021 "Passive in-situ remediation of acidic mine / industrial drainage (PIRAMID). University of Newcastle Upon Tyne, UK, pp. 166.

Tyler, I (2005) *Force Crag: The history of a Lakeland mine.* Blue Rock Publications, Keswick, pp. 130.

Wyatt L.M., Watson, I.A., Kershaw, S. and Moorhouse, A.M.L. (2013) An adaptable and dynamic management strategy for the treatment of polluted mine water from the abandoned Wheal Jane Mine, Cornwall, UK. In "Mine Closure 2013 – Proceedings for the Mine Closure Conference 2013". Eds Tibbett M., Fourie A.B. and Digby C. pp 69-78.

2000/60/EC The Water Framework Directive. (2000) *Directive of the European Parliament and of the council of 23 October 2000 establishing a framework for Community action in the field of water policy.*

10th ICARD IMWA 2015 | 10th International Conference on Acid Rock Drainage & IMWA Annual Conference

Using Oxygen Consumption Rates as a Guide to Scale Up Laboratory Kinetic Data to Field Conditions

L.E Eary
Hatch, USA

ABSTRACT

Field and modelling studies of sulfide oxidation in waste rock from the scientific literature indicate that O_2 penetration is typically less than about 50 m and commonly less than 20 to 30 m due to consumption by reactions with sulfide minerals. A compilation of data from a range of field and simulation modelling efforts indicates a consistent trend of increase in the intrinsic oxidation rate (IOR) with temperature over range of 2 to 57°C, yielding an activation energy of 91 kJ/mole. This value is consistent with the value of 92 kJ/mole determined for pyrite oxidation by ferric ion. This activation energy indicates an increase in IOR of about 3.7 times per increase in temperature of 10°C.

The O_2 consumption rate data provide a potential guide to scaling kinetic data collected in laboratory experiments to field conditions. A comparison of the field data to O_2 consumption rates for 594 laboratory tests from the International Kinetic Database (Morin et al. 1995) shows that ratios of the laboratory IOR to field IOR range from 23 at the 25th percentile to 58 at the 50th percentile to 206 at the 75th percentile or about one order of magnitude. If the potential exists for a waste rock to increase in temperature by 20°C due to exothermic oxidation reactions, the potential increase in IOR based on an activation energy of 91 kJ/mole is about 13.7 times. If this factor of temperature increase is considered in the scaling approach, the range in ratios of laboratory IORs to field IORs decreases to 1.7 to 15 at the 25th to 75th percentiles. With this scaling approach, no other scaling factors are needed because the IOR values here are based on field data and therefore include the various effects of particle size, water-rock ratio, and elemental content.

Keywords: oxygen, consumption, kinetics, waste rock

INTRODUCTION

One of the most common and often problematic tasks facing geochemists using predictive models of future water quality for mine wastes is developing approaches to extrapolate or scale up results from laboratory experiments conducted on small sample sizes (typically 0.5 to 1 kg of material) to represent reactivity in storage facilities that will contain tens of millions to billions of tons of material. Making this scale up effort especially difficult in many cases is the fact that the extrapolations for mine permitting are generally carried out prior to the placement of any material in the storage facilities, meaning that direct observations of reactivity are not available at the time of study.

In most cases, estimations of reactivity are focused on the rates of oxidation of sulfide minerals with respect to their potential to cause acid generation and metal leaching and thereby affect water chemistry. Even when leachates do not become acidic, sulfide mineral oxidation will produce some amount of metal leaching. Humidity and column leaching kinetic tests are the most common laboratory tests used to determine reactivity of mine waste materials. Different approaches have been used to scale up the laboratory kinetic tests to field conditions, such as water-to-rock ratios, water contact time duration, reaction kinetics for individual minerals comprising rock types, particle size, and surface area. The surface area approach may make the most technical sense in that reaction kinetics should be a function of surface areas of minerals and their degree of exposure to air and water; however estimating reactive surface areas for different minerals within a larger rock matrix of variable particle size often requires considerable estimation (Morin, 2013).

Scaling factors developed by various procedures indicate that laboratory rates may range anywhere from 2 to 8 times (Drever and Clow, 1995) to 100 to 1,000 times faster (Malmstrom et al., 2000; Smith and Beckie, 2003; Ritchie, 1994) faster than field rates. These ranges are very wide and difficult to apply with confidence to mine wastes containing sulfide minerals due to the many complicating factors of mineralogy, reactive surface area, particle size distribution, secondary mineral formation, and microbial activity. The purpose of this paper is twofold: 1) assess the effect of temperature on sulphide oxidation rate, and 2) provide a summary of oxidation rates interpreted to occur in existing waste rock storage facilities and compare those rates to laboratory rates in an effort to provide a narrower, statistically based range for typical scaling factors. It is important to note that while O_2 consumption rates provide an indication of the reactivity of sulfide minerals and potential for acid production, they are not necessarily a reliable indicator of leaching rates of all solutes that might be released from all mineral forms.

OXYGEN CONSUMPTION RATES IN WASTE ROCK

Intrinsic Oxidation Rate

A review of the literature shows a number of field-scale studies focused on deriving O_2 consumption rates in sulfidic waste rock (Table 1). The list in Table 1 is not meant to be exhaustive of all the geochemical literature, but is reflective of those found in peer-reviewed journals or easily found sources. Most of the studies in Table 1 involved the development of simulation models of complex air-water-mineral processes in waste rock where the rate of O_2 consumption is a key component for understanding reaction rates and in situ temperature. The rate of O_2 consumption is often referred to as the intrinsic oxidation rate (IOR) with units of kg O_2/m^3-yr where the m^3 term

indicates a cubic meter of waste rock. The IOR can be converted to an all mass set of units by dividing by the bulk density (kg/m^3).

In the simulation modelling studies cited in Table 1, the IOR is typically a parameter determined either through a calibration process by comparison of model results to temperature profiles, O_2 depth profiles, and/or rates of SO_4 production. Hence, in all cases, the IOR values in Table 1 are essentially empirical values that are indicative of sulfide mineral oxidation primarily in the outer portions of waste rock piles where sufficient O_2 is available to cause oxidation. For waste rock with high contents of reactive sulfides, O_2 penetration may produce heating and convective air flow, which may speed air transport into the pile, but the reactive nature also more rapidly consumes the O_2, limiting penetration depth. For waste rock with low sulfide content, O_2 may penetrate much farther before it is consumed. In addition, the method of dumping will affect O_2 penetration with end dumping more favourable to promoting air circulation than paddock dumping. For the most part, the results from the simulation models suggest that the depth of O_2 penetration will typically range from 5 to 50 m. This outer rim is the portion of the waste rock pile where oxidation occurs.

Table 1 Summary of waste rock studies focused on O_2 consumption rates

Source	IOR (kg O_2/ m^3-yr)	T* (°C)	Mean Pyrite (%)	O_2 Depth (m)	Max Air Velocity (m/s)	Notes
Molson et al. (2005)	0.04	10	6	NA	NA	Long term rate (20 years); simulation model (Doyon, Quebec)
Molson et al. (2005)	0.40	10	6	NA	NA	Initial rate (1 year); simulation model (Doyon, Quebec)
Linklater et al. (2006)	4.73	2	1.9	10-20	NA	Simulation model (Svartliden, Sweden)
Linklater et al. (2006)	1.58	2	0.6	5-20	NA	Simulation model (Svartliden, Sweden)
Linklater et al. (2006)	0.32	2	0.09	5-20	NA	Simulation model (Svartliden, Sweden)
Wels et al (Infomine)	0.06	16	1.5	~50	0.2	Simulation model (max temperature at 15 m) (Doyon, Quebec; Nordhalde, Germany; Questa, USA)
Wels et al (Infomine)	2.60	45	7	~50	50	Simulation model (max temperature at 12 m)
Wels et al (Infomine)	0.33	40	3.5	~30	100	Simulation model (max temperature at 20 m)
Sracek et al. (2006)	6.86	45	6.6	~30	NA	Interpretation of field depth profiles (Doyon, Quebec)
Sracek et al. (2006)	135.2	57	8.4	~30	NA	Interpretation of field depth profiles (Doyon, Quebec)
Harris & Ritchie (1985); Ritchie (1994)	1.44	45	2	5-15	NA	Interpretation of field depth profiles (Rum Jungle, Australia)
Lefebvre & Gelina (1995)	7.30	30	7	35-40	20	Simulation model (Doyon, Quebec)
Lefebvre et al. (2001a,b)	23.65	46	7	>20	50	Simulation model (Doyon, Quebec)
Lefebvre et al. (2001a,b)	0.32	16	3.1	~30	0.3	Simulation model (Doyon, Quebec)
Stromberg & Banwart (1998)	0.013	5	0.57	NA	NA	Simulation model; O_2 throughout entire 15-m height of waste rock (Aitik, Sweden)
Andrina et al. (2012)	2.27	45	2	NA	NA	Field measurements at trial dump (100 kt) (Grassberg, Indonesia)
Andrina et al. (2012)	2.58	45	4.6	NA	NA	Field measurements at trial dump (100 kt) (Grassberg, Indonesia)

*In-situ waste rock temperature not external air temperature

Effects of Temperature

The studies given in Table 1 show a wide range of IOR but they include both young and old waste rock located in a variety of climates some of which have sufficient sulfide mineral oxidation to

produce exothermic heating and elevated temperatures. The range of IOR from these various studies allows examination of the effect of temperature (Figure 1). The data in Figure 1 show a clear trend of increased rate with increased temperature with the exception of the rates derived from Linklater et al. (2006), which deviate significantly from other data for low temperature. The slope of the regression line implies an increase in IOR of 3.7 times per increase of 10°C, not including the IORs from Linklater et al. (2006).

If the same data are re-cast in an Arrhenius type plot, then it becomes possible to calculate an apparent activation energy. Figure 2 shows an Arrhenius plot of the logarithm of IOR as a function of the inverse of temperature. A regression of the data in Figure 2 results in a slope of –4,914.7 and an R^2 of 0.71, which yields an activation energy of 94 kJ/mol.

It should be noted that the regression analysis did not include three IOR values from Linklater et al. (2006) for 2°C because they appeared to deviate significantly from the trend established by the other data. The Linklater et al. (2006) IORs show there can be significant differences in rates, depending on conditions and mineralogy.

It seems reasonable to expect that IOR should be a function of the sulfide mineral content; hence, Figure 3 shows another Arrhenius plot but with IOR divided by the average pyrite content reported in the studies listed in Table 1. Linear regression of the data in Figure 3 produces an activation energy of 80 kJ/mole and a R^2 of 0.74, indicating that normalizing the IOR to pyrite content yields only a minimal improvement in the regression statistics.

The average of the two regression curves gives an activation energy of 87 kJ/mol. This average value is at the higher end of most of the values reported in experimental studies (Table 1). It is consistent with the activation energy of 92 kJ/mol determined by Wiersma and Rimstidt (1984) for pyrite oxidation by ferric ion, which is not surprising given the generally accepted concept that ferric ion is the primary oxidant in acidic systems with rapid enough sulfide mineral oxidation to produce an increase in temperature.

Table 2 Activation energies for sulfide mineral oxidation from various studies.

Source	Activation Energy (kJ/mole)	Notes
This study	87 (80-94)	Extrapolation of field-derived IORs
Linklater et al. (2006)	20	Estimate for field waste rock facility
Lowson (1982)	39-88	Experimental with pyrite
Schoonen et al. (2000)	48-86	Experimental with pyrite
Belzile et al. (2004)	34-100	Review of experimental pyrrhotite oxidation kinetics
Nicholson & Scharer (1994)	50 (pH 2-4)	
	100 (pH 6)	Experimental with pyrrhotite
McKibben & Barnes (1986)	56.9(±7.5)	Experimental with pyrite
Lu et al. (2005)	64.5(±8.1)	Experimental with pyrite
Rinker et al. (1997)	66-71	Experimental with marcasite
Nicholson et al. (1988)	88	Experimental with pyrite
Wiersma & Rimstidt (1984)	92	Experimental with pyrite; oxidation by ferric ion

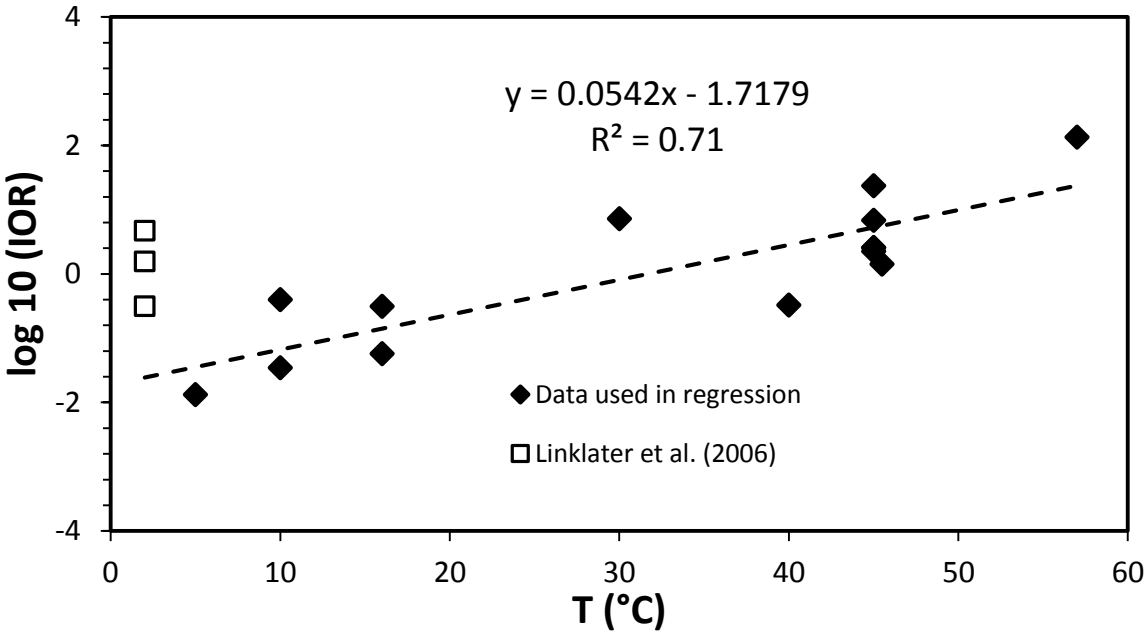

Figure 1 Effect of temperature on IOR

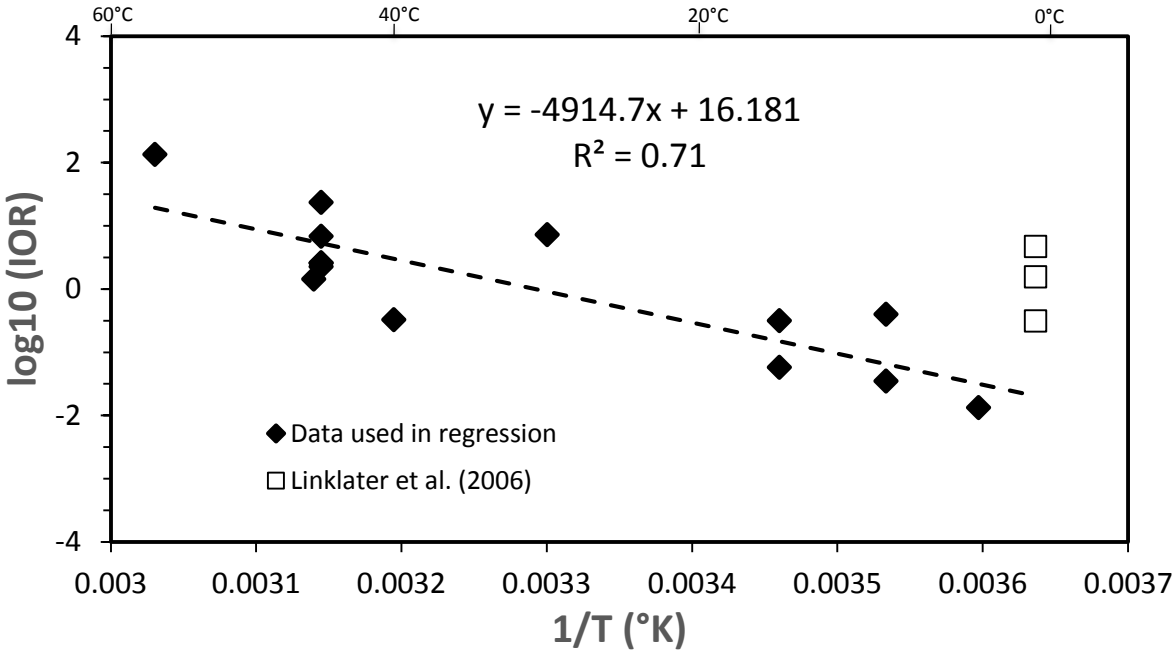

Figure 2 Arrhenius plot for IOR

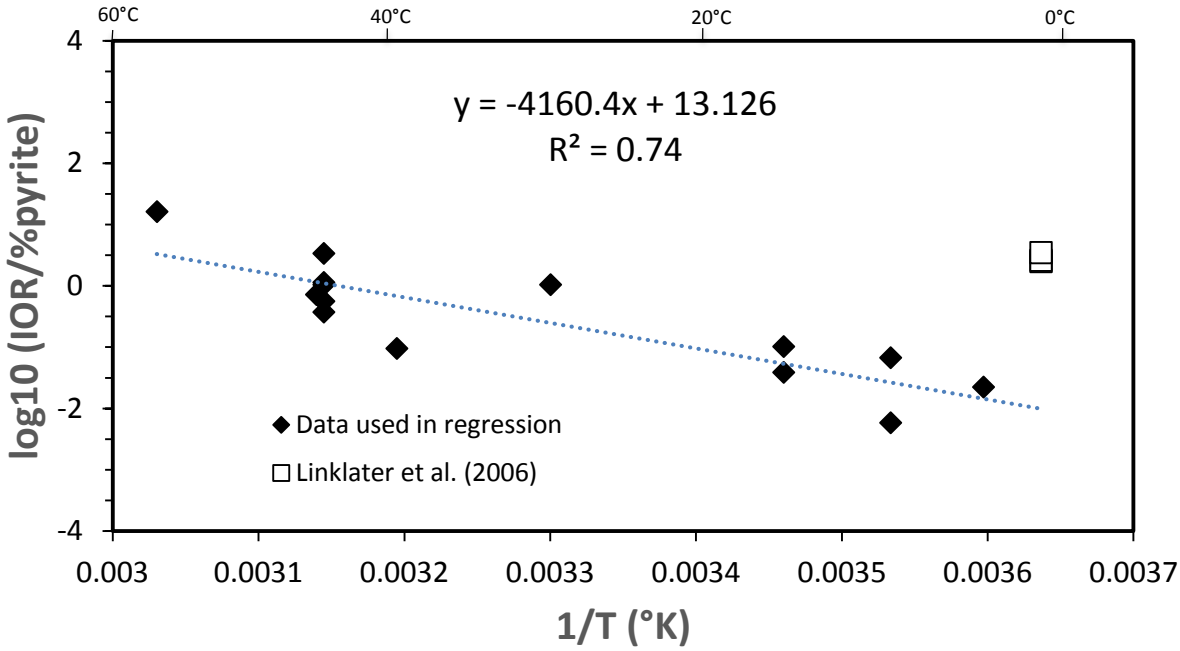

Figure 3 Arrhenius plot for IOR divided by percent pyrite

Comparison of Field and Laboratory IOR

The International Kinetic Database (IKD) from MDAG Publishing (Morin et al. 1995) contains a compilation of a kinetic leaching data from a large number of laboratory studies over a range of rock types and sulfide mineral contents. Figure 4 shows the distribution of IORs from the IKD where the IOR values were calculated from the rate of SO_4 production (mg/m^3-week), assuming a bulk density of 2000 kg/m^3, all sulfide-sulfur is FeS_2, and the following reaction stoichiometry:

$$FeS_2 + 7/2\ H_2O + 15/4\ O_2 \longrightarrow Fe(OH)_3 + 2\ SO_4^{-2} + 4\ H^+ \quad (1)$$

The distribution of IORs from the IKD data set range from 0.03 at the 5th percentile to 2.21 at the 95th percentile and median of 0.95 kg O_2/m^3-year/%Pyrite (Figure 4). The range of percentile values from the IKD is shown in Figure 5 relative to the field-derived rates from Table 1, assuming a laboratory temperature of 25°C. The ratios of the IKD laboratory IORs to field IORs range from 11 at the 5th percentile to 58 at the 50th percentile to 660 at the 95th percentile. The range in ratios from the 25th to 75th percentiles is 23 to 206 or about one order of magnitude. This range is greater than that observed in a series of laboratory to field scale tests conducted by Andrina et al. (2012), who found laboratory rates ranging from about 2 to 10 times field-scale measurements.

Generally, it is the intent and expectation that rates derived from laboratory tests should be significantly faster than field rates. The laboratory to field ratios discussed here based solely on IOR indicate that factors for extrapolating laboratory-derived oxidation rates to field scale can typically range from one to one and half orders of magnitude. However, it should be noted that if this approach is used for scaling up from laboratory to the field, then no other scaling factors are needed because the IOR values here are based on field data and therefore include the various effects of particle size, water-rock ratio, crystallinity, and elemental content.

Another consideration is for cases where kinetic testing data and numerical modelling predict that sulfide oxidation will be rapid enough to result in exothermic heating, then scaling factors should be reduced. For example, if the potential exists for a waste rock to increase in temperature by 20°C more than the temperatures of relevant laboratory tests, such as from 25°C to 45°C, the potential increase in IOR based on an activation energy of 91 kJ/mol is about 13.7 times. If this temperature effect is considered, the range in ratios of laboratory IOR to field IOR is reduced substantially from 1.7 (=23/13.7) to 15 (=206/13.7) at the 25th to 75th percentiles. The converse is also true for field conditions substantially colder than the relevant laboratory testing conditions, such as would be appropriate for northern or high altitude locations where average field temperatures are less than standard laboratory temperatures of 20 to 25°C.

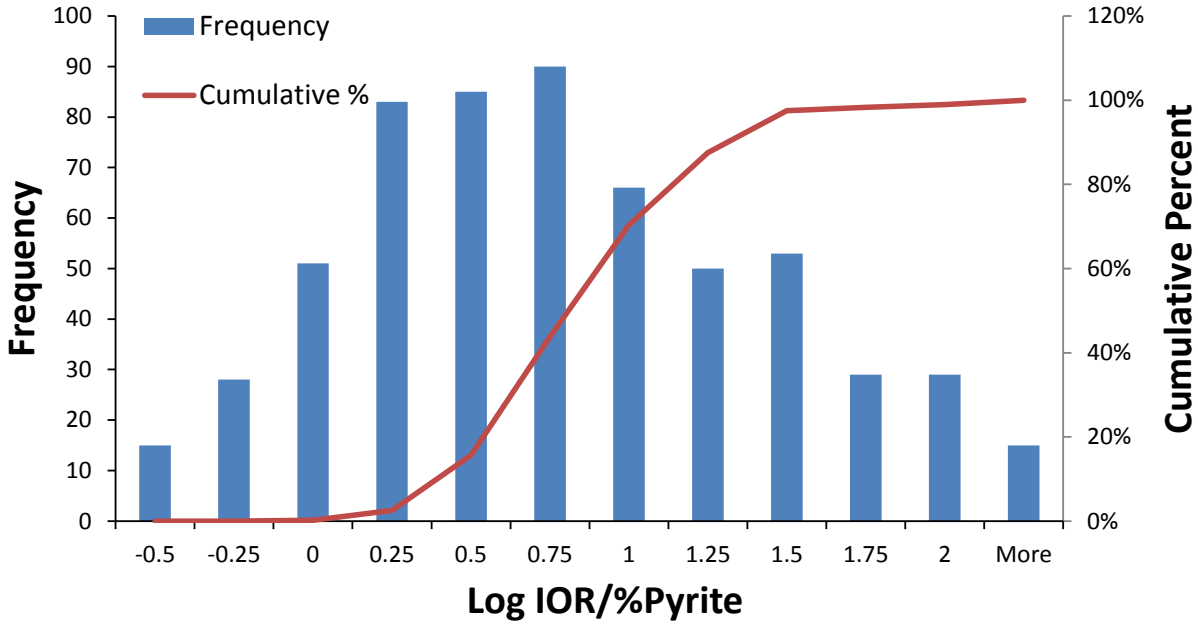

Figure 4 Frequency-cumulative probability for IOR/%Pyrite from the IKD (MDAG Publishing)

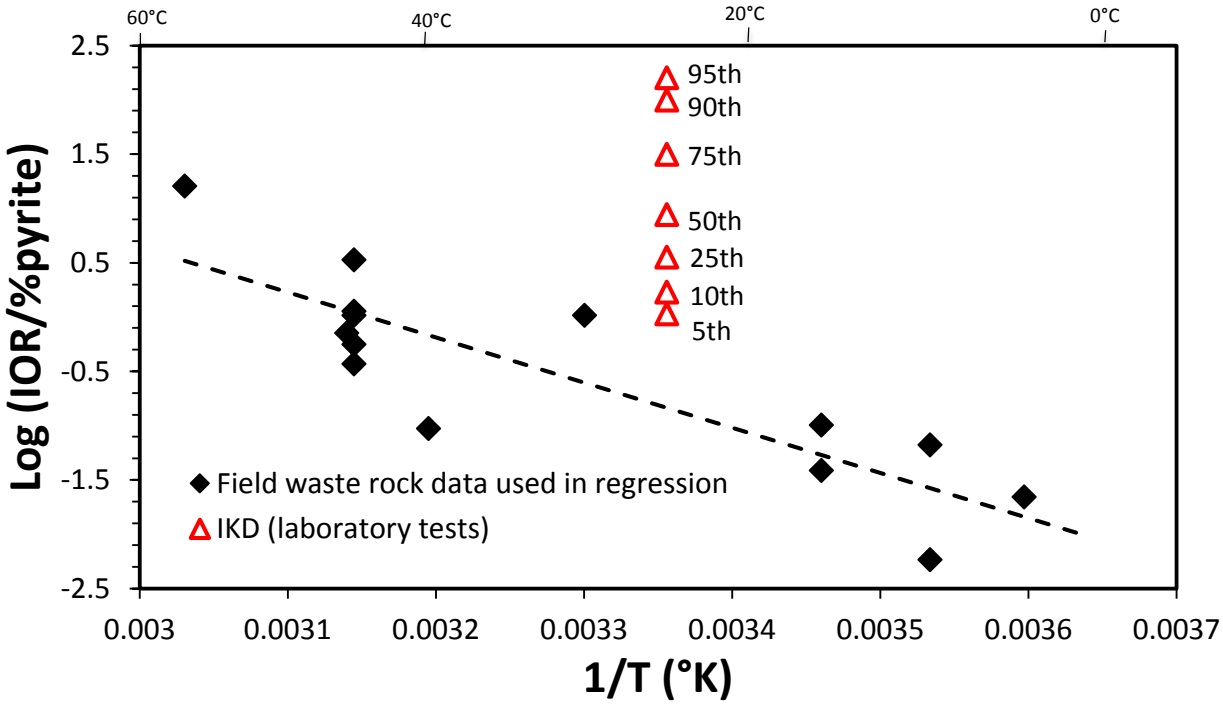

Figure 5 Comparison of IORs from laboratory tests (IKD) to field-derived IORs divided by percent pyrite

CONCLUSIONS

The validity of including temperature effects in approaches for scaling up results from laboratory tests to field scale for modelling oxidation processes in waste rock dumps has never been well established. The IOR data compiled here from a range of field and simulation studies show a consistent and significant effect of temperature, indicating temperature is a significant factor that should be included in scale up estimations. If field temperatures are expected to be substantially different than laboratory temperatures, perhaps greater than 10°, including a temperature factor in scale-up calculations is a reasonable approach. However, if a temperature factor is included as described in this paper, there is no need to add additional scaling factors because the temperature effects on IOR examined here inherently include many other water-rock reaction factors because they are based on observations and interpretations of field-scale systems,

NOMENCLATURE

IOR	intrinsic oxidation rate
kJ	kilojoule
m	meter
s	second
T	Temperature (°C or °K)
yr	year

REFERENCES

Andrina, J., Wilson, G.W., and Miller, S.D. (2012) Waste rock kinetic testing program: assessment of the scale up factor for sulphate and metal release rate. 9th International Conference on Acid Rock Drainage, May 20-26, 2012, Ottawa, Canada (W.A. Price, C. Hogan, G. Tremblay, Eds.) Curran Associates, Red Hook, NY, 882-893.

Belzile, B., Chen, Y.W., Cai, M.F., and Li, Y. (2004) A review of pyrrhotite oxidation. J. Geochem. Expl. 84, 65-76.

Drever, J.I. and Clow, D.W. (1995) Weathering rates in catchments. In Chemical Weathering Rates of Silicate Minerals (A.F. White and S. Brantley, Eds.) Reviews in Mineralogy 31, Mineral. Soc. Am., Washington, D.C., pp. 463-481.

Harris, J.R. and Ritchie, A.I.M. (1985) Pore gas composition in waste rock dumps undergoing pyritic oxidation. Soil Sci., 140, 143-152.

Lefebvre, R. and Gelinas, P.J. (1995) Numerical modeling and AMD production in waste rock dumps. Sudbury '95, Conference on Mining and the Environment Proceeding, 869-878.

Lefebvre, R., Hockley, D., Smolensky, J. and Lamontagne, A. (2001a) Multiphase transfer processes in waste rock pile producing acid mine drainage 2: Applications of numerical simulation. J. Contam. Hydr. 52. 165-186.

Lefebvre, R., Hockley, D., Smolensky, J. and Gélinas, P. (2001b) Multiphase transfer processes in waste rock pile producing acid mine drainage 1: Conceptual model and system characterization. J. Contam. Hydr. 52. 137-164.

Linklater, C.M., Bennett, J.W. and Edwards, N. (2006) Modelling of a waste rock dump design to control acid rock drainage at the Svartliden gold mine, Northern Sweden. 7th Intern. Conf. on Acid Rock Drainage, Mar 26-30, 2006, St. Louis, MO (R.I. Barnhisel, Ed.), Am. Soc. Min. Recl., Lexington, KY, 1079-1105.

Lowson, R.T. (1982) Aqueous oxidation of pyrite by molecular oxygen. Chem. Rev. 82, 461-497.

Lu, L., Wang,R., Xue,J., Chen, F., and Chen, J. (2005) Dependence of reaction rate of pyrite oxidation on temperature, pH, and oxidant concentration. Science China Earth Sciences 48, 1690-1697.

Malmstrom, M.E., Destouni, G., Banwart, S.A., and Stromberg, B. (2000) Resolving the scale-dependence of mineral weathering rates. Environ. Sci. Technol. 34, 1375-1378.

McKibben and Barnes (1986) Oxidation of pyrite in low temperature acidic solutions: Rate laws and surface textures. Geochim. Cosmochim. Acta, 50, 1509-1520.

Molson, J.W., Fala, O., Aubergin, M. and Bussiere, B. (2005) Numerical simulations of pyrite oxidation and acid mine drainage in unsaturated waste rock piles. J. Contam. Hydr. 78, 343-371.

Morin, K.A. (2013) Scaling factors of humidity-cell kinetics rates for larger-scale predictions. MDAG.com Internet Cast Study 38 (www.mdag.com/case_studies/cs38.html).

Morin, K.A., Hutt, N.M., and Ferguson, K.D. (1995) Measured rates of sulfide oxidation and acid neutralization in kinetic tests: statistical lessons from the database. Sudbury '95, Conference on Mining and Environment Proceedings, Sudbury, Ontario, May 28-June 1, 1995, 525-536.

Nicholson RV, Gillham RW, Reardon EJ (1988) Pyrite oxidation in carbonate-buffered solution: 1. Experimental kinetics. Geochim Cosmochim Acta, 52, 1077-1085.

Nicholson, R.V. and Scharer, J.M. (1994) Laboratory studies of pyrrhotite oxidation kinetics. In Environmental Geochemistry of Sulfide Oxidation (C.N. Alpers, and D.W. Blowes, Eds.) American Chemical Society, ACS Symposium Series, Vol. 550, Chapter 2, pp. 14-30.

Nicholson, R. V. (1994) Iron-sulfide oxidation mechanisms: laboratory studies. In Environmental Geochemistry of Sulfide Mine-Wastes (J.L Jambor and D.W. Blowes, Eds.) Mineralogical Association of Canada, Nepean, ON, vol. 22, pp. 164-183.

Rinker, M.J., Nesbitt, W.W., and Pratt,A.R. (1997) Marcasite oxidation in low-temperature acidic (pH 3.0) solutions: mechanism and rate laws. Am. Mineral. 82, 900-912.

Ritchie, A.I.M. (1994) Rates of mechanisms that govern pollutant generation from pyritic wastes. In Environmental Geochemistry of Sulfide Oxidation (C.N. Alpers and D.W. Blowes, Eds.). ACS Symposium Series 550, Am. Chem. Soc., Washington, DC, Chapter 9, pp. 108-122.

Schoonen, M., A. Elsetinow, M. Borda, and D. Strongin (2000) Effect of temperature and illumination on pyrite oxidation between pH 2 and 6, Geochem. Trans. 4-11.

Sracek, O., Gelinas, P., Lefebvre, R., and Nicholson, R.V. (2006) Comparison of methods for the estimation of pyrite oxidation rate in a waste rock pile at Mine Doyon site, Quebec, Canada. J. Geochem. Expl. 91, 99-109

Stromberg, B. and Banwart, S.A. (1994) Kinetic modelling of geochemical processes at the Aitik mining waste rock site in northern Sweden. Appl. Geoch. 9, 583-595.

Stromberg, B. and Banwart, S.A. (1998) Kinetic modelling of geochemical processes at the Aitik mining waste rock site in northern Sweden. Appl. Geochem. 9, 583-595.

Stromberg, B. and Banwart, S.A. (1999) Experimental study of acidity-consuming processes in mining waste rock: some influences of mineralogy and particle size. Appl. Geochem. 13, 1-16.

Wels, C., Lefebvre, R., and Robertson, A.M. (2014) An overview of prediction and control of air flow in acid-generating waste rock dumps. Technology.infomine.com/enviromine/publicat/Airflow_Wels_Lefebvre_Robertson.pdf (Accessed September 9, 2014).

Wiersma, C.L. and Rimstidt, J.D. (1984) Rates of reaction of pyrite and marcasite with ferric iron at pH 2. Geochim. Cosmochim. Acta 48, 85-92.

10th ICARD IMWA 2015 | 10th International Conference on Acid Rock Drainage & IMWA Annual Conference

Approach to Scaling Up from Laboratory Humidity Cells through a Field-Scale Unit to a Waste Rock Dump

Carla Calderón Rosas, María Carolina Soto, Natalia Farfán and Angela Oblasser
Fundación Chile

ABSTRACT

Humidity cells are kinetic tests designed to predict long-term weathering rates and the potential for mine waste and geologic materials to release discharges that may have impacts on the environment (GARD Guide, 2010). These tests are performed at the laboratory scale in a controlled environment. By developing humidity cell tests it is possible to determine the response of a given sample to cycles of moisture and flooding in terms of mine drainage generation and metal loading in laboratory conditions. However, laboratory conditions are very different from those that occur in a mining operation; in terms of volume of materials, granulometry, climatic conditions and time. Consequently the scaling up from laboratory results to real mining wastes facilities can become difficult.

Thus, in recent years, the medium and large scale field tests have become more common in mining operations around the world; nevertheless, no systematic analysis has been done in order to assess the improvement of the scaling challenge.

In this study, an initial analysis of development and comparison between standardized and modified humidity cells is presented, in order to find relevant information that allows a more realistic and close to the waste rock dump characteristics scaling approach in the future.

**There is no full article associated with this abstract.*

CHAPTER 11

RELIABLE MINE WASTE MANAGEMENT

The Canadian MEND Program – The First Twenty-Five Years

Gilles Tremblay and Charlene Hogan
Natural Resources Canada

ABSTRACT

Acidic drainage has long been recognized as the largest environmental liability facing the mining industry, and the public through abandoned mines. In 1989, provincial and federal governments, and the Canadian mining industry formed a consortium called Mine Environmental Neutral Drainage (MEND), to develop technologies and strategies to prevent and reduce acidic drainage.

The MEND program focussed the effort to develop technologies to reduce the effect of acidic drainage, and examined four key areas; prediction, prevention and control, treatment and monitoring. A toolbox of technologies was developed to plan for, operate and decommission mines in an environmentally acceptable manner. In 2002, a multi-year research strategy was put in place, based on regional priorities established by an extensive network of Canadian experts. On the world stage, through the Global Alliance, MEND has forged international partnerships among other organizations involved in acidic drainage research.

MEND's continued success lies in its collaborative multistakeholder approach, with members from two levels of government, the mining industry, and non-governmental organizations working on a common problem. Today, the MEND model of co-operation is copied in Canada and internationally to tackle both policy and science-based challenges.

Technology transfer remains central to MEND's activities. MEND has published over 200 technical reports and guidance documents; these are now all available on the MEND website. Workshops are considered the best route for timely and efficient transfer of technologies and case studies, and MEND has sponsored or co-sponsored over 40 workshops, including the hosting of three ICARDs. As a result of the efforts of MEND and other partners, our understanding of acidic drainage has greatly increased, and significant advances have been made in environmental stewardship.

Keywords: Multistakeholder, consortium, MEND

CANADA'S ROLE IN ACIDIC DRAINAGE AND THE MEND PROGRAM

Canada's research into acidic drainage technologies started in the 1970's and 1980's and focussed on tailings from metal mines. Canadian mining companies and the Government of Canada recognized the serious impacts of acidic drainage from mining activities on the environment, and the projected enormous liabilities for Canada and the mining industry. Extensive research was undertaken to develop methods to establish vegetative growth on tailings in an attempt to alleviate and prevent acidic drainage. These efforts were successful in revegetation of tailings sites, but did not improve water quality. There was a realization that this was not a sustainable solution – and the mining industry was left with few options to deal with acidic drainage, namely perpetual lime treatment. There was need for a better understanding of processes involved, and for new remedial technologies to be developed and demonstrated; a concerted effort was required.

The National Uranium Tailings Program (NUTP) (1983-1988) provided an early model for an acidic drainage program. NUTP's mandate was to develop predictive models to reduce liability for uranium mine tailings, the primary concern being the isolation of low levels of radioactivity. However, the research soon concluded, as it was realized that the real concern was acid generation from the residual sulphides in Ontario uranium tailings. This realization combined with the concerns of base metal and gold mining companies and government agencies led to the establishment of the Reactive Acid Tailings Stabilization (RATS) Task Force in 1986. One of the key lessons learned from NUTP was that more stakeholder involvement was necessary for any future multistakeholder program. The RATS Task Force was created with representatives from the mining industry, and federal and provincial governments. They produced a multi-year research plan and recommended that a coordinated approach be used to carry out the program. In addition to acidic drainage from tailings, it was quickly realized that waste rock was also a major source that had to be dealt with. Consequently, a new name was adopted, the Mine Environment Neutral Drainage (MEND) program. In 1988 the MEND consortium was launched and charged with the following two key objectives; (i) to provide a comprehensive information base to allow the mining industry and government agencies to establish long-term management requirements for reactive tailings and waste rock; and (ii) to establish techniques that permit the operation and closure of acid generating mine waste disposal areas in a predictable, affordable, and environmentally acceptable manner.

MEND (1987 - 1997)

Initially, a budget of $12.5 million Canadian over five years (1989-1994) was allocated for MEND research. MEND was a tripartite consortium that included the Canadian mining industry, 5 provincial governments and the Federal government of Canada. MEND was an unusual consortium, driven primarily by the 130 volunteer representatives of the different participating agencies; including regulators, mining company managers and engineers, and government officials and scientists who freely contributed their time and expertise. The program adopted an organizational structure that included a Board of Directors, a management committee and several technical committees, and a coordinating secretariat. Roles were simple. The Board of Directors provided vision and approval of annual plans and budgets; the management committee provided "hands-on" management of the program; and the technical committees addressed technological issues and solutions. The Secretariat was essentially the "hub" of the organization and ensured

coordination of the elements within, and external to MEND. NRCan, with a long history of mining R&D and mineral economic policy and an extensive network across Canada, was a natural fit for the Secretariat.

The research and development program focussed on four cornerstones: prediction, prevention and control, treatment and monitoring. The objectives for each area were:

Prediction: To develop better techniques to predict acid generation from mine waste material, as well as the rate and effect of acid generation, and to develop mathematical models to simulate acid generation processes.

Prevention and Control: To develop techniques to minimize or prevent acid generation, and to demonstrate these techniques in the field.

Treatment: To develop and demonstrate chemical and passive treatment systems, and to examine lime treatment sludge stabilization methods.

Monitoring: To develop new technologies to improve site monitoring of acid drainage, to develop field sampling methods and analytical reference standards, and to develop closure criteria.

In 1992, MEND revised its research plan to narrow its focus, solicit research on a competitive basis, increase its technology transfer and international liaison roles, and encourage innovation and the testing of new ideas. The plan extended MEND to a 9-year program, with an expanded budget of $18 million C$.

The Liability and the Results

In 1994, Natural Resources Canada surveyed mining companies and provincial databases to determine the amount of acid generating materials; an estimate of 1,900 Mt of tailings and 750 Mt of waste rock was obtained (MEND 5.8e, 1994). Geocon (MEND 5.8.1, 1995) estimated the associated liability at between $1.9 billion and $5.3 billion C$.

An evaluation of the MEND program was undertaken in 1996 by Young and Wiltshire (MEND 5.9. 1996). The survey concluded that liability had been reduced by $340 million C$ for five mine sites, alone. It was also acknowledged that the reduction in liability is significantly higher than this quoted value, with a minimum of $1 billion C$ commonly accepted by the mining industry. This was an impressive return on an investment of $17.5 million C$ over eight years. Other observations underline the value of the MEND program to Canadian science and policy:

- Increased diligence by regulators, public and industry
- Greater common understanding of issues and solutions
- Research has led to reduction in environmental impact
- Recognition of MEND as a model for industry-government co-operation
- The need to continue and strengthen international connections

As a result of MEND and associated research, technologies are in place to open, operate and decommission a mine property in an environmentally acceptable manner, both in the short and long term. This can have a major impact on new mine financing and development. Moreover, mining companies and consultants have acquired a great deal more capacity to deal with water contamination from mine wastes, including acid generation. Canada gained a reputation for expertise in dealing with acidic drainage issues, and that advisory expertise was sought internationally. MEND fostered working relationships with environmental groups, ensuring that they are an integral part of the process.

Over the first ten years, the two levels of government, together with the Canadian mining industry, spent over $17.5 million C$ within the MEND program to find ways to reduce the estimated liabilities. Planned funding for MEND was divided equally among the three major partners: the mining industry, the federal government and five provincial governments. When the first round of funding ended in December 1997, the federal government had contributed 37% of the funding, the provinces 24%, and industry 39%.

By 1997, about 200 MEND projects were completed across Canada. Some of the key technical results and observations are noted below; these are still important areas for MEND research today.

- Prevention is the best strategy. Once sulphide minerals start to react and produce contaminated runoff, the reaction is very difficult to stop.
- Prediction ensures that extraction of minerals occurs with minimal impact on the receiving environment. Chemical prediction methods, procedural manuals, and predictive models were developed and applied to predict the geochemical behaviour of wastes.
- In Canada, the use of water covers and underwater disposal are being confirmed as the preferred prevention technology for unoxidized sulphide-containing wastes. This technology is well suited to Canada geography and climate.
- Dry covers can be applied as effective oxygen and infiltration barriers. Innovative research has shown that a range of materials, including low cost waste materials from other industries (lime stabilized sewage sludge, paper mill sludge) may provide excellent potential for generating oxygen-reducing surface barriers. Non-acid generating tailings and membranes were also evaluated as covers.
- Studies verified that sludges will remain stable, if properly disposed. Concerns had been raised about the long-term chemical stability and the potential liability arising from dissolution of heavy metals contained in the sludge.
- In Canada, experience indicates that passive systems have niche applications for acidic drainage treatment. These range from complete systems for treating small seeps to secondary treatment systems, such as effluent polishing ponds.
- Several other disposal technologies were also investigated, including permafrost, using an elevated water table and in-pit disposal.

The MEND program cemented Canada's leadership in research into acidic drainage technologies applied to metal mines. Technology transfer activities were an important element of the 1987 – 1997 MEND program and were significantly expanded in its last few years. The dissemination of information on developed technologies to partners and the public is a major function of MEND and must continue.

MEND 2000 (1998 - 2000)

The MEND program concluded in 1997 and had achieved tremendous progress in reduction of liability. Partners agreed that additional work was needed to broadcast the research information, and to verify MEND-developed technologies in the field. A stream-lined program was established, funded by the Mining Association of Canada and Natural Resources Canada. The focus was on promoting technology transfer, monitoring and completing MEND-initiated projects, and providing an essential link among industry, governments and environmental organizations.

One of the key deliverables for MEND 2000 was the six-volume MEND Manual. This manual consists of a detailed summary volume, and five technical volumes addressing acidic drainage issues: sampling and analyses; prediction; prevention and control; treatment; and monitoring. The information from the more than 200 technical reports and workshop notes produced under MEND is compiled in this manual. The manual provides practitioners in the Canadian industry and government with a single reference on acidic drainage for the diverse and complex research undertaken during the MEND program. Given that acidic drainage is a highly technical area, where site-specific influences likely necessitate site-specific investigations and evaluations, the manual is not a "how to" document.

The transfer of information on developed technologies to partners and the public has always been an important part of MEND. A bilingual website http://mend-nedem.org was created in the 1990's and underwent several major updates as technologies advanced. For example, paper copies of MEND reports were originally ordered on-line; they are now all available electronically, for free, on the website. The website contains over 200 MEND reports and related publications, and features an advanced search function to enhance site accessibility.

Over its 25 years, MEND hosted over 40 workshops and conferences on key areas of technology at locations across Canada. These events were a successful and popular way to transfer current information. Each year the annual BC-MEND ARD/ML Workshop invites case studies and technical presentations from leading practitioners. In recent years, the workshop consistently attracted over 200 delegates. This workshop is regarded as one of best values for money events. Links were also established with international organizations involved in acidic drainage research, such as INAP (International Network on Acid Prevention), ADTI-USA (Acid Drainage Technology Initiative), and CETEM (Brazil).

MEND (2001 - 2015)

Sustainable development is a strong driving force for industry in dealing with environmental and societal issues such as water contamination from mine wastes. The MEND program focussed on developing technologies to reduce the effects of acidic drainage, and developed a toolbox of technologies to plan for, operate and decommission mine properties in an environmentally acceptable manner. Although the original MEND Program and its successor, MEND 2000, made major contributions to prevention and management of acidic drainage, it remained a significant environmental issue.

In 2001, funding was provided for a renewed MEND initiative focussing on regional and national needs. A Gap Analysis report (MEND 8.1, 2002) was completed to identify opportunities to advance acidic drainage research, along with a list of regional research needs. Subsequently, a multistakeholder expert Strategy Session was held in 2002, and a number of activities were proposed for a multi-year program (MEND 8.2, 2002). A questionnaire was distributed to the Canadian MEND network to help define research activities. The top-ranked priorities were closure management, verification of technologies, metal (neutral) leaching, passive treatment, early prediction, sludge management, cold temperature effects and paste backfill. Guidance documents and manuals, workshops and other technology transfer activities were identified as important issues that cut across all priorities.

Based on the widespread support from all stakeholders, a recommendation was made to move ahead with a renewed MEND with a research program that focused on these top priorities.

Funding was provided by the Mining Association of Canada, with support from other government departments and in-kind support from the project contractors.

Since 2003, the MEND Steering Committee developed an annual work plan to address many of the key research priorities. Many of these new projects re-examined issues and re-visited sites that were the subject of earlier MEND studies. Advances in technologies and knowledge made it timely to re-examine some of these issues. As well, several projects verified the full-scale application of MEND supported technologies, and investigated their long-term performance. There have been some shifts in priorities since 2003, with a greater interest in best management practices, cold temperature issues, guidance documents and more recently, regulatory concerns.

Several MEND reports, activities or project areas in the past five years are outlined below.

Accurate and timely prediction of acidic drainage and metal leaching is central to prevention of potential environmental impacts, and to minimize the high costs of mitigation. Prediction of drainage chemistry is a technically challenging subject, involving numerous methods, properties and processes. The *Prediction Manual for Drainage Chemistry from Sulphidic Geologic Materials* (MEND 1.20.1, 2009) provides a comprehensive document for use by technical experts or practitioners to conduct a prediction program and/or review the results. It is also a reference document for the public, educators or students studying or reviewing drainage chemistry.

With the large number of mines opening in Northern Canada, the effect of cold temperature on various technologies is of increasing importance. Research was conducted across a number of areas including dry covers. In 2004, MEND produced the *Dry Covers: Design, Construction and Monitoring of Covers Systems for Waste Rock and Tailings* (MEND 2.21.4), which integrated the best available technology for the design and construction of cover systems over mine wastes. One of the key gaps identified was the application of covers in the cold regions. Three projects were completed. The first, *Mine Waste Covers in Cold Regions* (MEND 1.61.1a, 2009), reviewed soil covers on mine waste in cold regions. Several dozen cold region processes were identified that could affect soil covers. In the second project, *Cold Regions Cover Research* (MEND 1.61.5b, 2010), cold region phenomena that could impact soil cover performance, including ground freezing, snow-distribution, and limits to revegetation were reviewed. The third report, *Cold Regions Cover System Design Technical Guidance Document* outlined the current state-of-knowledge of soil cover system design in cold regions, best practises on how a cover system design should be conducted, and a summary of information that should be provided during the design process (MEND 1.61.5c, 2012).

Climate change poses several risks to mining operations. MEND completed a high-level risk analysis on climate change, *Climate Change and Acid Rock Drainage – Risks for the Canadian* (MEND 1.61.7, 2011). It focuses on risks associated with acid rock drainage and metal leaching produced from mining activities. At mine sites, the prevention and management of acidic drainage includes the management of water, tailings and waste rock. Therefore, climate change risks related to acidic drainage arise from the impacts of a changing climate on water-management structures and activities, on waste-impoundment structures, and on the hydrologic/ hydrogeologic/ geochemical conditions affecting the flow of water and contaminants at mine sites. Previous studies on climate change impacts in Canada identified a range of potential impacts for the mining sector, including those on acidic drainage. This assessment builds on previous work by looking more closely at the impacts for specific infrastructure elements and determining which are most probable and significant for mining operations and for society.

Acidic drainage treatment and sludge management are important aspects of mine site environmental control practices. Sludge production is of increasing concern to industry, as the

inventory of sludge continues to grow from "perpetual pump and treat" operations. Several MEND projects were completed in sludge treatment and disposal, stability and re-use. The most recent is a survey of mine drainage treatment and sludge management practices titled *Acidic Drainage Treatment Operations in Canada – An Interactive Database* (MEND 3.43.1, 2013). Data on treatment practices and sludge management were collected on more than 100 Canadian and international sites. A comprehensive database, containing an extensive number of parameters, was developed to store the information. This report offers many potential uses and information for treatment processes with respect to planning and guidance.

MEND's latest report *Study to Identify BATEA for the Management and Control of Effluent Quality from Mines* identified the best available technologies economically achievable (BATEA) to manage and control effluent from metal, diamond, and coal mines in Canada (MEND 3.50.1, 2014). The study provided reference information for potential forthcoming changes to the Canadian mining effluent regulations. The study described the effluent management and treatment technologies and techniques currently employed at metal (base metal, precious metal, uranium, iron ore), diamond and coal mine operations in Canada. The study identified effluent treatment technologies that could be considered best available technologies (BAT) for the Canadian mining sector. The technologies were screened against a set of criteria, and those that satisfied them were carried forward for consideration as BATEA. Cost estimates were prepared based on capital and operating cost data from vendors and operations, in-house information and literature. Ultimately, BATEA for any given mining operation is site-specific. There are a multitude of geographic and operational factors to be considered that influence effluent quality, impact the technical feasibility of treatment technologies, and dictate financial constraints on capital and operating expenditures that can be borne by operations while still maintaining economic viability.

Another key and highly successful activity of the MEND program was hosting the 9th International Conference on Acid Rock Drainage (ICARD), in Ottawa in May 2012. The event attracted 526 delegates from 19 countries, and featured a conference program that was creative, thought-provoking and entertaining. The technical event covered eight pre-conference short courses (~ 250 participants), an exciting plenary session with experts representing industry, government and civil society, three-days of oral and poster paper presentations by world- leading practitioners (127 presentations and 43 posters), a trade show with 25 exhibitors and a two-day field trip to Northwest Quebec where four mine sites were toured. A social highlight was the banquet at the Museum of Civilization, with entertainment provided by the Painchaud Family assisted by several members of the audience. The proceedings and PowerPoint presentations are available on the MEND web site at http://mend-nedem.org/9th-icard/

CONSORTIUM APPROACH

In the 1980's, a collective approach for governments and industry to cooperate in technology development for advancing environmental management in the mining industry emerged in Canada. The MEND program was the first multistakeholder program to develop scientifically based technologies to reduce the effect of acidic drainage for metal mines. This approach allows policy decisions to be made based on sound science. Since then, this model of collaboration was used by both Canadian and international programs to address issues of national importance. For example, the National Orphaned and Abandoned Mines Initiative (NOAMI) adopted the MEND model to develop a policy-based program for remediation of orphaned and abandoned mine sites

in Canada (http://www.abandoned-mines.org). The success of these programs can be attributed to several factors.

- The partnerships developed among the two levels of government, the mining industry, and environmental groups working together to develop solutions to a major environmental problem.
- An extensive peer-review process, both formal and informal, resulted in enhanced credibility of the information base.
- A small dedicated secretariat that coordinated activities, managed the accounting, reporting and technology transfer, and served as the "glue" that held the program together.

GLOBAL ALLIANCE AND THE GARD GUIDE

Through the years, linkages with other international organizations were maintained by sharing information via conferences, workshops, reports and other publications. In 2002, INAP formally proposed an international model of interaction among organizations involved in acidic drainage research. In 2003, the Global Alliance (GA) partnership was launched. The GA brings numerous benefits to the partners, including minimizing research duplication, maximizing research dollars, worldwide links, and enhanced technology transfer capability.

One important example is the Global Acid Rock Drainage (GARD) Guide, which was published by INAP with support from the GA. The MEND Manual MEND 5.4.2 (2001), described earlier, was one of the key references used to develop the GARD Guide. The Guide described proven technologies to address ARD and ML, and considered climate, geographic and environmental factors and coverage for all stages of mine life. Another project is the Diavik Waste Rock Scale-up Study undertaken by three Canadian universities with support from the Canadian government, INAP and MEND. This project provides great value for Canada; many graduate students have completed their degree work at this site and a many publications have been produced.

CONCLUSION

MEND is a good example of a successful, multistakeholder initiative addressing a technical issue of national importance, and is a model for cooperation among industry, various levels of government and environmental groups. The MEND program provided a focus to develop solutions for environmental problems that face the mining industry across Canada and internationally. Through the 25 years of the MEND program, a significant reduction in environmental liability was achieved. MEND is now recognized world-wide for its contribution to the long-term sustainability of the industry and the environment. Although much progress has been made, new challenges are emerging that will require concerted efforts by MEND and other research organizations.

ACKNOWLEDGEMENTS

Thank you to the many dedicated volunteers who over the 25 years of the MEND program so generously contributed their time and expertise.

REFERENCES

MEND 1.20.1. (2009) Prediction Manual for Drainage Chemistry from Sulphidic Geologic Materials

MEND 1.61.5a. (2009) Mine Waste Covers in Cold Regions

MEND 1.61.5b. (2010) Cold Regions Cover Research

MEND 1.61.5c. (2012) Cold Regions Cover System Design Technical Guidance Document

MEND 1.61.7. (2011) Climate Change and Acid Rock Drainage – Risks for the Canadian

MEND 2.21.4. (2004) Design, Construction and Performance Monitoring of Cover Systems for Waste Rock and Tailings.

MEND 3.43.1. (2013) Review of Mine Drainage Treatment and Sludge Management Operations.

MEND 3.50.1 (2014) Study to Identify BATEA for the Management and Control of Effluent Quality from Mines.

MEND 5.4.2. (2001) MEND Manual.

MEND 5.8e (1994) Report of Results of a Workshop on Mine Reclamation. March 10-11, 1994, Toronto, ON

MEND 5.8.1 (1995) Economic Evaluation of Acid Mine Drainage Technology

MEND 5.9 (1996) Evaluation Study of the MEND Program.

MEND 8.1 (2002) Acidic Drainage Research and Technology Gap Analysis.

MEND 8.2. (2002). MEND3 Strategy Session, April 11-12, 2002, Ottawa, Ontario.

10th ICARD IMWA 2015 | 10th International Conference on Acid Rock Drainage & IMWA Annual Conference

Managing the Waste Rock Storage Design, Can We Build a Waste Rock Dump that Works?

Rebecca Barritt and Peter Scott
O'Kane Consultants, Australia

ABSTRACT

For a waste rock dump to be managed both during operations and at closure, a thorough understanding of the rock material properties to be stored is compulsory. This is facilitated by the preparation of a comprehensive waste block model, with an appropriate materials management and placement plan developed in conjunction with the mining schedule. However, a waste rock dump's success is hinged on such elements being regularly updated through ongoing materials characterization over the life of mine. Failure to undertake this may potentially result in inappropriate material placement, and unnecessary costs to the mine and surrounding environment.

This paper examines waste management process at different mine sites and compares the different approaches, and the opportunities and constraints that are placed on operation and closure of the facility by the management process adopted.

Keywords: characterization, planning, design

INTRODUCTION

The construction of waste rock dumps (WRDs) is a common requirement for most open pit mines across the globe. Historically many of these WRDs are deemed to have failed through the use of an inappropriate design or construction techniques, both being hinged on their appropriateness to the materials available and local conditions at the site. 'Failure' may be considered in terms of failure to understand the geochemistry of the mine waste leading to release of contaminants to the environment; failure to support vegetation or an eco-system, or geotechnical instability (Mitchell, 2012). The timing of the failure may be during operations or many years following any rehabilitation and closure of such facilities, and subsequent costs to rectify any damage caused (socioeconomic or environmental) can vary by several orders of magnitude.

It must be determined what is required of the site in order for a WRD to 'work'. This is an approach that requires a conceptual design to be developed and refined through initial mine feasibility and material characterization studies. The conceptual model must then revisited regularly, and refined as necessary, to ensure that the site is continuing to manage the onsite materials and achieve any closure criteria that have been initially determined. If this process is applied any alteration to the anticipated conditions, or misinterpreted geochemical data, can be managed as the mining life progresses, rather than at the end of operations when costs to rectify any issues will be far greater and availability of personnel and equipment fewer.

If a WRD 'works' it can be considered a success from its initiation through to a given time following closure. In terms of appropriate handling and placement for the materials present, should techniques and planning initially proposed lead to WRD 'failure' within a project this can be remedied. However this cannot be completed without a change in either the WRD design or materials handling processes employed.

At the start of a given project it is fundamental that the design is appropriate to the specific site considered. It is commonly seen that a design for Mine Site A is applied to Mine Site B because they have the same owners and it was previously considered to have 'worked' at A. However, little attention has been paid to the differences in equipment available, climate and terrain or more fundamentally differences in the waste rock materials.

Laboratory testing is often biased towards the ore being mined and the scenario is often that little information is obtained on the waste rock, or sampling and subsequent laboratory testing is sporadic and data gaps are common. Alternatively, enthusiasm is high during the initial stages of the venture, with full materials characterization completed and a thorough geological block model established, but as the project develops ongoing characterization through geotechnical and geochemical testing is absent. Here the mine site has failed to confirm that the anticipated conditions have been met, and as such there is potential that the initially appropriately designed facility cannot be constructed as conditions have changed.

This paper will discuss how the waste rock storage design can be developed from Day -1 of a venture and refined during the life of mine (LOM) to closure. The methodologies presented will be based on established experience in WRD design and construction, with relevant case study examples.

CONCEPTUAL DESIGN DEVELOPMENT

Standard practice allows a WRD to be designed at the start of a project, based on the initial geological block model. Once a site has an understanding of the materials anticipated to be recovered, and their respective volumes, a conceptual landform is proposed for regulatory and stakeholder review. The landform will normally have taken into account various initial laboratory test results, but essentially at this stage of the project any conceptual design can only be considered as good as the data that has been gathered for its development. At this stage no waste has been excavated and therefore the options for landform design are vast.

Any conceptual design where potentially geochemical problematic waste is considered should ensure that firstly sufficient volume of nonreactive waste is available at the appropriate time to construct the waste storage including for encapsulation or for use in a cover system. Secondly, that the nonreactive materials can be appropriately used within a design. For example, should a low permeability layer be constructed an understanding of the appropriate compaction required to achieve target values must be developed, or should erosive materials be known to the site it may be necessary to stabilize outer embankments with coarser grained rip-rap, recognizing this type of material does not readily support vegetation establishment.

Characterization and Availability of Materials

Understanding the materials present at the site is key for any mining project. The emphasis must be from the start on appropriately using the materials for the final WRD landform, in particular where reactive materials may be encountered and correctly placed within the facility.

During initial scoping studies exploration drilling often prevents sufficient sample size for most key geotechnical tests, for example particle size distributions (PSDs). In addition, the small sample collected may not be representative of the overall conditions, and flushing techniques can significantly alter the recovered material from its undisturbed, *in situ* position. Empirical equations can be used to further develop an understanding of the materials, however, these are often not referred to. Focus can be made on separating the anticipated stratigraphy into tens of individual units, some only 30 cm thick, whereas in terms of mining this becomes irrelevant as blasting or machine cutting may encounter several variations at once, and thus subsequent waste rock management and materials placement ignores initial characterization efforts.

In order to appropriately design and subsequently construct and close a WRD any materials characterization program should be completed with the geochemical and geotechnical test schedule focused on any potential issues that the anticipated waste materials may pose to the landform meeting prescribed closure criteria (Jasper *et al*, 2006). For example, if it is known that all waste rock is expected to be benign and geochemically non-reactive, but there is potential for it to be geotechnically unstable and erosive, then laboratory testing should be focused towards PSD analysis, specific gravity and development of erosion parameters such as rill and inter-rill. If materials are to be excavated from the fresh and un-weathered portion of a given stratigraphy geochemical testing should be focused on understanding the potential for acidity, sulfate and/or metals leachate to be generated.

Laboratory testing does not necessarily need to be expensive and timely. There are many low cost but comprehensive tests or procedures than can save time and budgets. Many WRDs have been designed with a limited number of tests completed, but having still developed an extensive

knowledge of the onsite materials. Field testing should also be completed to supplement any laboratory program, they provide great value and can assess any *in situ* conditions quickly and commonly at low costs. They may also present more accuracy when compared to laboratory tests that require the sample to be remolded, and thus representative of the *in situ* conditions. This is of particular relevance with permeability testing: multiple use of *in situ* testing across a range of locations at site allows for the heterogeneity of surface materials to be understood, of great importance if a cover system is required for WRD rehabilitation and subsequent closure, and for development of a revegetation plan. If on site clay materials are to be used as part of a low permeability sealing layer, or to limit atmospheric interactions with waste materials, it is prudent to compare laboratory hydraulic conductivity (K_{sat}) values with those that can actually be achieved on site with the equipment available. Often K_{sat} laboratory values are two orders of magnitude greater than can be achieved at site, if this is not addressed in terms of practicality and feasibility at an early stage then the project may be targeting an impossible design from the offset.

Once the materials available have been characterized it is paramount that their respective volumes and distribution within the material to be mined is determined. If reactive waste requires encapsulation, but the mining schedule has found that the nonreactive materials will all be recovered late in the operation then dump construction must be designed to minimise exposure of the reactive waste to uncontrolled oxidation. This practice will limit potential contamination during operations, in addition to reducing the requirement for material double handling. Understanding the total volume of materials required to be managed onsite allows for an appropriate conceptual landform design to be prepared. The marriage of material properties, respective available volumes and relative timing of materials extraction to the operation are key to appropriately designing a WRD.

Conceptual Design Modelling and Updating a Design

Once a thorough understanding of the materials expected to be encountered at site, and respective volumes, is determined the data should be used to develop a conceptual landform design. The design should be aimed at the final landform at its completion and closure, however, it is also important to it to be developed in 'workable' stages throughout the LOM.

Where initial materials characterization testing has identified potentially problematic materials expected to be encountered during operations it is paramount that they are appropriately considered and thus managed within the landform design. At this point it may be necessary to conduct numerical or analytical modelling to gain a perspective on how the facility may perform over a given timeframe. The use of modelling is a common tool to support a given design, however, it is often used to create the design. For example if a project requires PAF or reactive waste materials to be encapsulated the volume of available benign materials must be determined before any modelling commences. Without a basic understanding of the site conditions modelling simulations may determine that a much greater thickness of benign materials are required than is available, identifying a design which will either never be constructed or will require a separate mineable source of benign materials to what can be provided by the ROM operations. Where climate data is required for use within a model it must be site specific and preferably cover the timeframe that is modelled (O'Kane and Barbour, 2006). Often less than five years of data are compiled and then re-used for years 6-10 and so forth, potentially omitting any above or below average data, of which is key to understanding any WRD's limits in potential performance. If an appropriate range of climate data is not available then assessments relating to the probability of

exceedance must be made. It should be understood, however, that a model will never supply the final design and must only be used as a tool to help inform design decisions. There is a tendency to focus on model outputs and rely on values presented, without revisiting the conceptual design and questioning its feasibility, as previously mentioned.

Once a conceptual design has been approved by all relevant parties it is crucial that it is referred to and updated throughout the LOM. A change within the industry must be made whereby the development of a conceptual design is not just for regulatory approval to commence the operation, but it is something that must be regularly reviewed through the mine life. Should a variation be found (material properties, recoverable volumes and scheduling for example), a change to the WRD design is paramount. Failure to address such ongoing variations or problems may lead to incorrect waste placement, potential delays during operations and additional unnecessary costs.

If initial material characterization was poorly completed and conditions are found to vary during operations, but the conceptual design has not been updated, the relevant regulatory body may require further evidence that a facility can be constructed at site and will meet any prescribed closure criteria. This may also cause delays to the mining schedule and require costly drilling and investigation programs. At this stage a portion of the WRD will have already been completed, reducing the number of options available to the site for design and ultimate successful completion of the project, or requiring such materials to be moved.

DURING OPERATIONS: CONTINUE PLANNING AND CHARACTERIZING

Appropriate waste rock handling during operations is very important. Through the development of a mining schedule the characteristics and volume of materials excavated at any time within the LOM will be known. As such temporary works can be established as required. There may be a restriction on material movement at certain times of the year, for example within tropical regions the assessment of particularly reactive materials should be made and interim procedures proposed to limit rainfall infiltration into exposed reactive waste material during the wet or monsoon season. Materials that are proposed to be used within the outer portions of a landform should be appropriately stockpiled for use at a later date. However, an appropriate material movement register should be established documenting the type of material hauled and the date it occurred. Should operations cease at some point in the future, or the mine changes owners, records would be in place regarding the composition of the stockpiled waste/overburden. This register documents the location of potential rehabilitation materials to be utilized as intended, as well as reactive materials requiring encapsulation and management. It is not uncommon to find during the advanced stage of mine operations that the best materials for closure and rehabilitation of the WRD have been 'lost' as the control on material movement has been poor.

The dumping technique used for material placement must be appropriate to the waste. For example, short tip heads or paddock dumping should be considered for highly reactive materials that have the capability to spontaneously combust. Material segregation has previously been identified as a significant factor in PAF risk management. If preferential pathways exist for oxygen and water to easily move through the WRD it can be expected that oxidation of reactive materials will be accelerated (Pearce, 2014). This has the potential to generate significant issues to the mine site, in terms of personnel safety (from the production of harmful, toxic gasses and spontaneous combustion) and to the environment.

Wherever possible it is advisable to compact each lift as the WRD is progressed. This will assist in managing surface runoff and reducing net percolation. Compaction can be enhanced with the use of finer grained materials such as clayey silts. This process reduces waste rock atmospheric interactions and thus may prevent the generation of acid and metalliferous drainage (AMD) or hazardous gas formation. Compaction can be achieved by use of dedicated equipment or by truck compaction during routine haulage and dumping procedure. When haul trucks are dumping waste at a facility it is advisable to regularly vary the route across the facility that is taken, thus allowing the compaction force to be spread over the materials, rather than concentrating all efforts along the same, repetitive pathway.

It is important that appropriate quality assurance and control (QA/QC) measures are established at the start of any WRD construction project. Over time regulatory requirements are commonly becoming more stringent, and rather than just presenting a landform design for both operations and closure of a facility, organizations are requesting that the methods proposed regarding how such facility will be constructed and how it can be completed are presented. Based on the material characteristics developed QA/QC methods will promote the suitability of a material to its design. There are a vast range of QA/QC actions applicable to many materials and conditions, but very important to site utilizing a compacted clay layer (CCL) is ensuring that the compaction effort for each lift is consistent with the desired optimum water content and density values (as determined through the materials characterization and conceptual design process).

As a mine is progressed it is paramount that ongoing materials characterization is completed to ensure that the facility constructed is as per the designated design, and if this is not possible then the design must be amended to ensure that the designated closure criteria are achieved. Material testing frequency should be conducted at a high level during the initial stages of the mine venture in order to fully understand the strata encountered, and ensure it is as expected. As knowledge of a material is gained, and its characteristics understood, the testing frequency can be decreased. However, the frequency should be increased as materials change composition. Results should feed directly into the materials placement plan and allow for the landform model and design to be updated. There are international standards that discuss the frequency that bulk testing should be completed, for example INAP (2009), these should be best practice and would require consultation and referrence within mining and waste management procedures, as applicable.

CASE STUDY

The following section of this paper discusses relevant case study examples where efforts were made either prior to the excavation of any waste materials, or during the LOM, to appropriately design and construct a WRD that works. In other words, meet the designated closure criteria for the project and achieve regulatory and stakeholder approval.

Poly-Metallic Mine#1 Australia

A WRD landform design was recently developed to include encapsulation of PAF materials. A well-developed geological block model was presented prior to initiation of the mining venture, with comprehensive, and reliable geotechnical and geochemical data. Previously the mine site had been focused on several lithological units, of varying thickness and description. However, in terms of the conceptual landform design only three material types needed classifying: metasediments (heavily weathered sediments and volcanoclastic), dolerite and un-weathered mineralized host

rocks: termed mineralization. Geochemical testing had proven that materials within the weathered zone (upper 100 m deep) comprised entirely NAF waste. Below the zone of total oxidation some PAF material was identified within a transitional zone (active zone of weathering, some 15 m thick) and all fresh materials, unaltered by weathering processes, were PAF. Based on the understood mining schedule, and with reference to the mining equipment known to be utilized, a conceptual WRD design was prepared.

The design was developed based on the PAF waste reactivity and its relative timing in relation to the NAF materials required to encapsulate it and limit the ingress of atmospheric oxygen and incident water.

PAF encapsulation was to be achieved throughout the LOM, even though it would not be encountered until several months into the project. Fortunately, due to the proposed open-pit design PAF waste would be encountered concurrently with NAF materials. The initial design promoted moisture storage within the NAF waste following rainfall events, and its subsequent release to the atmosphere via evapotranspiration during dry periods, limiting rainfall infiltration to the underlying PAF. This moisture 'store-and-release' concept was deemed best suited to the arid to semi-arid climate that the mine site experiences. A second PAF waste management strategy was proposed that included a basal NAF layer to lift the PAF waste from the natural ground surface, thus eliminating the potential for lateral flow through the PAF waste and providing storage for seepage water from the overlying PAF waste (and potential adsorption of AMD products) if the upper NAF material are overwhelmed and seepage into the PAF waste occurs. Furthermore, additional geotechnical stability was provided.

The preferred final design comprised horizontal PAF and NAF layering of specified thicknesses (Figure 1). This option was chosen to be the most appropriate for several reasons, including concurrent placement of NAF and PAF waste at the facility thus preventing double handling or significant temporary works; allowing 'buffer' zones to exist should net percolation occur in extreme rainfall events; and reduction in the potential for differential settlement.

The outer WRD was designed based on the geotechnical properties of the available NAF materials and suitablity to the climate experienced. Perimeter embankments would be of sufficient width that PAF waste was not positioned beneath a sloping section and that PAF waste would not daylight the facility. In addition perimeter embankments utilized appropriate geometries whereby minimal surface erosion would occur and geometries appropriate to the materials and climate at the facility. NAF waste within the outer profile would be homogeneous, thus preventing the development of material segregation and preferential flow path establishment. Appropriate QA/QC measures were proposed in order to achieve the designated facility, in conjunction with an ongoing geotechnical and geochemical laboratory testing program. Finally, a surface water management plan was proposed that allowed individual catchment areas to be developed and minimize the potential for failure of the facility.

The success of this project came from 1) the initial extensive characterization of the materials present and their relative timing and 2) the use of ongoing materials sampling, laboratory testing and characterization to ensure that the facility constructed would perform as per the design.

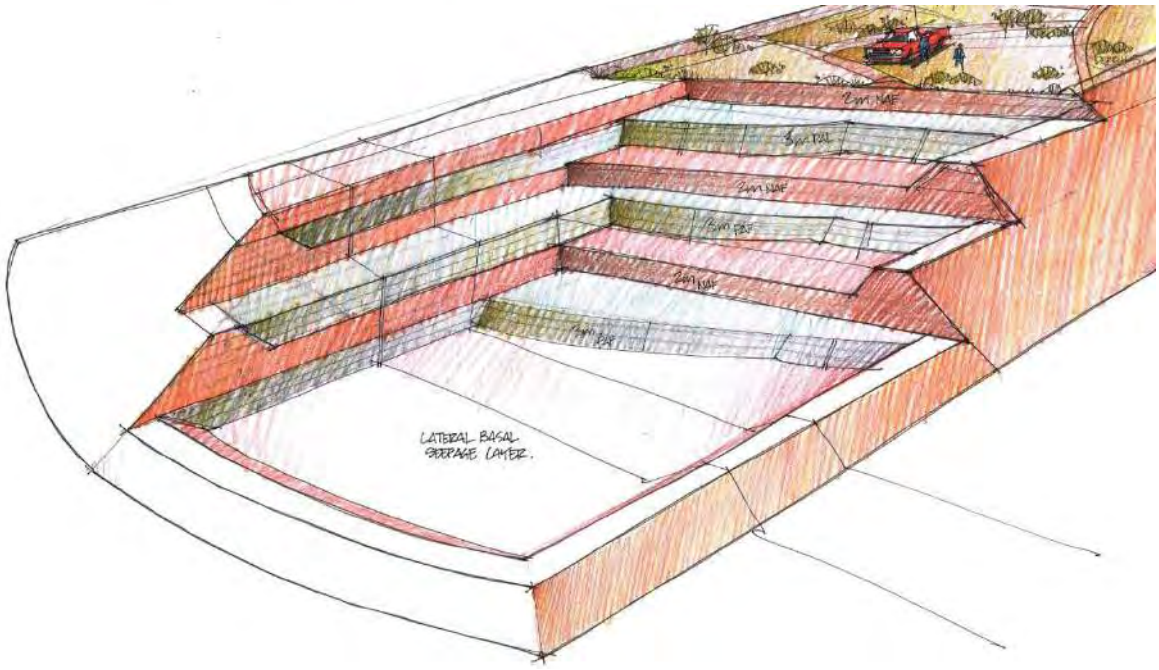

Figure 1 Schematic cross-section through the proposed WRD facility

Poly-Metallic Mine#2 Australia

A design was proposed for a large WRD that utilized NAF waste to encapsulate PAF material. The original geological block model was supported with geochemical data for a substantial (>15 m) unit of NAF waste, overlain by a CCL and finally growth medium. A second CCL was also proposed for between the PAF and NAF materials. As the project progressed it was determined that the waste materials had been incorrectly characterized. As such the design was amended with the NAF unit thickness decreasing. Further studies illustrated that portions of the NAF material were saline and metal leaching, and therefore could not be utilized as previously intended on the facility's outer embankment or plateau, in line with the regulatory requirements of the facility. As such the volume of 'clean' NAF was significantly reduced further and both the landform and cover system design required alteration to minimize any deleterious impact of the mine waste on the receiving environment in the short-term, and to facilitate recovery of the environment disturbed by mining over the long-term. A further complication was that the PAF waste had not been properly analyzed and it has been found to be highly reactive and capable of spontaneous combustion.

With this site efforts had been made to quantify the materials in-pit for WRD construction, however, the reactivity of the PAF material had not be fully understood. In addition, the geochemical characterization of the NAF waste had used the presence of sulfates and pH value as a discriminator for NAF vs. PAF, whereas the presence of salts and heavy metals had been overlooked. Furthermore, when the materials balance was initially amended the WRD construction techniques employed at site were not. As such the material placement measures promoted the materials' reactivity.

CONCLUSION

It is of utmost importance that all materials expected to be excavated are appropriately characterized and their available volume determined. With a thorough understanding of the waste rock both prior to initiation of a venture and confirmed or otherwise during operations, in addition to the climate and environment of a site efforts can be made in developing a conceptual landform design that will meet regulatory closure criteria and satisfy stakeholders. Failure to provide appropriate materials handling and construction techniques to a facility presents huge potential for WRD failure at some point during the LOM, thus leading to environmental issues and large costs in rectifying any damage made during operations.

REFERENCES

INAP. (2009) Global Acid Rock Drainage Guide (GARD Guide). Document prepared by Golder Associates on behalf of the International Network on Acid Prevention (INAP).

Jasper, D. A., Braimbridge, M. F., Lacy, H. W. B. and Russell, M (2006) Integrating waste characterization into landform design for low-risk and low-cost mine closure. Proceedings of the First International Seminar on Mine Closure, Brisbane, Australia.

Mitchell, I. C. (2012) Robust mine closure development and maintenance. Proceedings of the Seventh International Conference on Mine Closure, Perth, Australia.

O'Kane, M. and Barbour, S. L. (2006) Choosing representative climate years for predicting long-term performance of mine waste cover systems. Proceedings of the 6th International Conference on Acid Rock Drainage (ICARD).

Pearce, S. (2014) Beyond the PAF cell. Proceedings of the eighth Australian workshop on Acid and Metalliferous Drainage.

10th ICARD IMWA 2015 | 10th International Conference on Acid Rock Drainage & IMWA Annual Conference

On-Land or Submarine Tailings Disposal? – Pros and Cons

Bernhard Dold
SUMIRCO (Sustainable Mining Research & Consultancy), Chile

ABSTRACT

Mine tailings management is a major issue for the mining industry and a limiting factor due to competitive land use for example with agriculture or tourism. Most of mine tailings are stored today in constructed tailings impoundments on-land. This practise results in the exposure of sulfide minerals to oxidizing conditions and subsequent in acid mine drainage (AMD) formation in many cases. Due to the environmental and geotechnical stability problems of this tailings disposal practise, the mining industry is searching for alternatively tailings management options. Currently the deep marine tailings disposal is experiencing a revival as such an alternative option. After negative experiences of marine shore or shallow depositions around the world, the deep marine disposal (below the euphotic zone; i.e. < 150 m depth) is seen as a potentially save option in some sectors. The idea to deposit sulfide minerals in a reducing environment to prevent sulfide oxidation and the subsequent element and acid release is sound and appealing. However, the experiences from the past have shown that only the thorough mineralogical and geochemical characterization of the future tailings to be deposited can give the necessary information if the material is suitable for submarine disposal (The tailings can contain more soluble minerals, which are not stable in the marine environment). Then the disposal site has to be evaluated to ensure stable reducing conditions without currents and upwelling. This paper analyzes the pros and cons of each tailings management strategy and highlights the geochemical processes and characterization methodologies, which have to be considered in each case for decision-making.

Keywords: sulfide oxidation, acid mine drainage, prediction, waste management, reductive dissolution,

INTRODUCTION

Final waste management is a critical issue for mining operations, as around the world new legislations are in place for mine closure and environmental protection (e.g. new mine closure law 20.551 in Chile from November 2012). As nowadays metal mining focuses mainly on sulfidic ore bodies, the associated sulfide oxidation and formation of acid mine drainage in mine wastes like tailings are the mayor environmental issued of the on-land deposition of the mine tailings (Dold, 2010, 2014a). Mine tailings disposal is therefore a critical issue for any mine project and must be thoroughly studied before the most suitable solution of each case is found. Main problems associated to the tailings disposal are the geotechnical stability (Azam and Li, 2010; Rico et al., 2008a; Rico et al., 2008b) and the geochemical stability (Dold, 2010, 2014a).

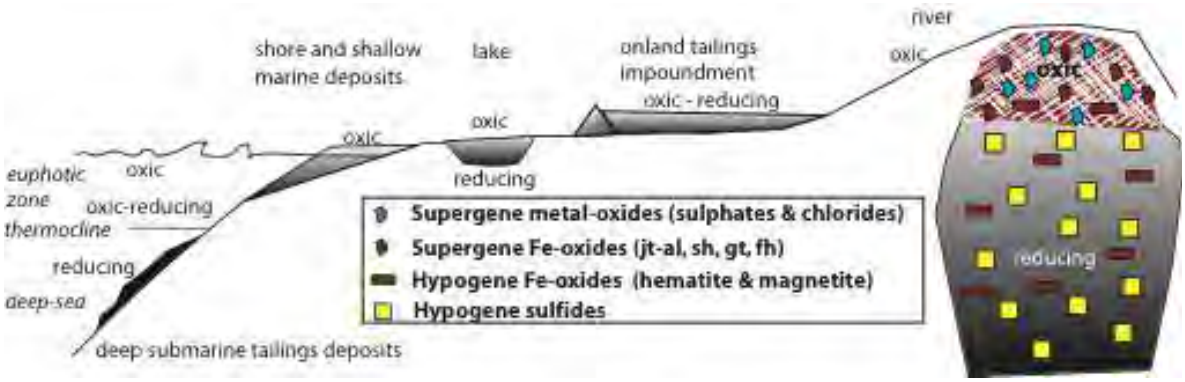

Figure 1: Overview over the different mine tailings disposal options (river, lake, sea and onland disposal (constructed impoundments) and the associated geochemical regimes. On the right the different main mineral assemblages from sulfide to oxide domination in an ore deposit are highlighted.

Historically, mine tailings were dumped first into close-by rivers (Fig. 1), lagoons or lakes (Dold, 2014b; Dold et al., 2009). In some cases the tailings reached the sea and formed so called shore tailings deposits, like at Chañaral/Chile (Bea et al., 2010; Dold, 2006; Korehi et al., 2013), Bahia de Ite/Peru (Diaby and Dold, 2014; Dold et al., 2011) y Bahia Portman/Spain (Benedicto et al., 2008; Martinez-Sanchez et al., 2008; Oyarzun et al., 2013). This practice led to a severe contamination of the associated aqueous systems.

In the years around 1970 at several place around the world, the so called deep submarine disposal of mine tailings started due to the visible problems of marine tailings deposition at the shore line and in the euphotic zone in the Atlas Mine, Filipinas, Island Copper Mine (50 m), Canada, Jordan River Mine, Canada and Black Angel Mine, Greenland. The cases of Island Copper Mine and Black Angel Mine have shown the difficulties of predicting the behavior of the oceanographic system and the importance of mineralogical and geochemical characterization of the tailings before marine deposition. In the latter case, soluble and oxide minerals liberated significant amounts of contaminants into the sea (Perner et al., 2010; Poling and Ellis, 1995), similar to the situation of Ensenada Chapaco (Dold, 2014b), and clearly showed that oxide minerals should not be deposited in a reducing environment.

As this historic overview shows, inappropriate tailings management and a lack of mineralogical, geochemical, and oceanographic characterization of the systems can lead to environmental damage, and has resulted in a shift by the mining industry back to on-land deposition in tailings impoundments.

However, also on-land tailings disposal has many severe problems (e.g. geotechnical and geochemical stability; AMD formation), receiving increasing pressures from society, and therefore, the submarine tailings disposal option is nowadays again being evaluated. This paper shows the factors to be considered for the final decision making for the best tailings disposal option.

METHODOLOGY

In order to be able to predict accurately the environmental long-term behavior of the tailings on-land or submarine, quantitative mineralogy is needed. This give the possibility to predict the behavior of the material in different geochemical conditions and for an accurate prediction of acid mine drainage formation (acid-base accounting). Today advanced technologies are available for automated mineralogical analysis like QEMSCAN® or MLA. If thoroughly calibrated with the ore mineralogy this give an accurate quantification of the complete mineral assemblage, degree of liberation, as well as grain size distributions, important information to increase the efficiency of the extraction process and to predict AMD formation and element release.

However, this methodology does not give detailed information on trace element association to specific minerals or mineral groups. This information is crucial in order to predict if a certain contaminant might be liberated from its host mineral. Therefore, the mineralogical data are combined with high-resolution geochemical data from a seven-step sequential extraction developed for the primary and secondary mineralogy present in typical porphyry copper deposits (Dold, 2003). The leach solutions are then analyzed by inductively coupled plasma–atomic emission spectroscopy. The sequential extractions data can additionally be used to perform a high-resolution ABA (Dold 2010) and should be correlated with the mineralogical data for quality control of the data, and in order to predict AMD formation and element liberation of any mined material. It is important to note that this extraction sequence might have to be adapted to the solubility of the specific minerals (primary and secondary) present in an ore deposit, as this might differ importantly in different ore deposit types.

In order to predict the kinetics of metal release to the environment, so-called kinetic tests are used (Weibel et al., 2011). The tests used in AMD prediction (e.g. ASTM D5744-96) are not suitable for prediction of the behavior of mine tailings in submarine environments, as they expose to an oxic environment. There is currently no kinetic test available to predict the behavior of mine tailings in a reducing environment. Therefore, efforts have to concentrate to develop such a test to simulate the geochemical conditions in the deep-sea environment.

DISCUSSION

Most of the mine tailings are deposited close to the mine site, or at least as close as possible in order to lower costs. However, there are examples were tailings are sent hundred kilometers to a suitable

disposal site. An overview of the principal pros and cons of both deposition strategies are given and then discussed in order to give assessment for decision making.

Pros and Cons of On-Land tailings disposal

Commonly Mentioned Advantages of On-Land tailings disposal are:

- Cheapest option, as lowest transport costs through close-by deposition;
- The economic value contained in the tailings might be exploited in future by new exploitations techniques;
- New dam construction techniques ensure geotechnical stability;
- New tailings impoundments contain an impermeabilization to prevent groundwater contamination and/or to recover water and dissolved metals (e.g. pregnant leach solutions; PLS) from the tailings.
- New tailings deposition techniques like dry stacking use less water and increase the geotechnical stability.

Commonly Mentioned Disadvantages and Risks of On-land tailings deposition are:

- Dam failures due to geotechnical instability (especially in seismic and high rainfall areas and for old tailings impoundments, which were not constructed in an appropriate and safe way);
- Formation of Acid Mine Drainage due to sulfide oxidation;
- Competition with other land-uses like agriculture and tourism;
- Groundwater contamination due to the lack of basal impermeabilization;
- Long-term maintenance and monitoring required
- Low social acceptance

Pros and cons of submarine tailings disposal (STD)

Commonly Mentioned Advantages of STD Are:

- Prevention of acid mine drainage: Reducing environment and lower concentrations of dissolved oxygen limit or prevent sulfide oxidation and any acidity produced through sulfide oxidation will be neutralized by the buffer capacity of marine water;
- Tailings are more geotechnically stable and the possibility of catastrophic failure of tailings dams (on land tailings dam heights may reach several hundred meters), especially in areas with high seismic activity and high rainfall is eliminated;
- Minimal land surface is used. This is a strong argument in Norway where, due to the Fjord topography, on-land space for the tailings deposition is very limited;
- Less long-term maintenance required after deposition compared to on-land disposals.

Commonly Mentioned Disadvantages and Risks of STD Are:

- Smothering benthic organisms and physical and geochemical alteration of bottom habitat;
- Reduced number of species and biodiversity of marine communities;
- Risk of liberation of toxic elements from the tailings to the seawater;
- Bioaccumulation of metals through the food chains and ultimately into fish consumed by Humans, with associated human health risks;
- The water content of the tailings cannot be recovered; this is especially critical in dry climates;
- The deposited tailings cannot be recovered (possible loss of valuable resources);
- Larger footprint on the seabed than on land;
- Potential toxicity of the flotation reagents used on the marine ecosystem;
- Plume sharing and dispersal of the fine particles throughout the sea;
- Relocation of the tailings in different compartments of the marine ecosystem due to upwelling and currents.
- If accidents happen it is nearly impossible to control them in the deep-sea environment.
- Low social acceptance

In the past, many mistake in mine tailings disposal have been done, which led to strong environmental contamination and threat through geotechnical instability. This led to an increasingly low acceptance by the public opinion and therefore difficulties in the permitting process. This is true for the on-land disposal as well as the submarine disposal. The main problems in both cases are the insufficient mineralogical and geochemical characterization of the tailings to be deposited and the characterization of the receiving environment. It is known, that when sulfidic tailings are exposed on-land to oxidizing conditions, acid mine drainage can form. In order to predict accurately if AMD will form, a thorough mineralogical and geochemical study has to be performed. Standard acid-base accounting tests and kinetic testing is not sufficient to address the complexity of the ore mineralogy. Additionally, most of the tailings impoundments do not have an impermeabilization in order to prevent the infiltration of the contaminated solution into the groundwater (Dold, 2014a), and the hydrogeology of the receiving environment is often poorly understood.

If the tailings are deposited into the sea, also a detailed study of the mineralogy and geochemistry of the ore is needed, as well as a detailed knowledge of the sea environment is needed. In this case a special attention has to be given to the oxide minerals (especially Fe-oxides like hematite, magnetite, goethite, ferrihydrite among others), which can contain important amounts of toxic elements (Nystroem and Henriquez, 1994) and might suffer reductive dissolution in the reducing environment of the deep sea (Dold, 2014b). Additionally, the long-term stability of the reducing conditions at the disposal site has to be proven by thorough oceanographic studies. These studies have also to show that at the site, there are no currents and upwelling, which could relocated the material into different geochemical conditions.

In the past on-land tailings disposal was done in very simple forms promoting the oxidation, and thus the AMD formation, mostly with direct contact with water bodies (river, lake, sea, or

groundwater), with the subsequent pollution of those. If on-land tailings disposal is done by best-practice, an impermeabilization and separation from the hydrological system is necessary (Dold, 2008). Also the formation of AMD might be prevented or controlled by different measures, in order to limit the impact on the receiving ecosystem. The geotechnical stability can be increased importantly by the use of state-of–the-art dam construction techniques. If all these factors are considered in the construction of an tailings impoundment on-land, most of the environmental and geotechnical problems from the past can be avoided, and the tailings are in condition for further exploitation with advanced technologies by future generations (Dold, 2008). However, the on-land tailings deposition still has to compete with other land-uses.

In case of submarine tailings disposal, it has to be proven that the material to be deposited is "inert inorganic geological material" following the London Protocol (Dold, 2014b). The objective of submarine tailings disposal is to deposit the sulfide containing minerals into a reducing environment, in order to prevent the sulfide oxidation. However it is often overlooked, that ore deposit often contain not only sulfide minerals, but also oxides like hematite and magnetite or other soluble minerals, which can contain also toxic trace elements. These minerals are not stable under the reducing, alkaline and organic matter rich environment of the deep-sea. Therefore, the mineralogical and geochemical characterization must be very thorough in order to ensure that the material is effectively "inert inorganic geological material".

CONCLUSION

Te above mentioned arguments show that both option have important pros and cons, and it has to be evaluated in each case, which might be the most suitable option. The examples show that only if we count on an accurate quantitative mineralogy and data on the association of trace elements to these minerals, a correct prediction of the behaviour of the material in the different geochemical compartments for the final deposition of the waste material can be given. This is crucial to ensure the long-term geochemical and geotechnical stability of the waste.

Due to the limitation for submarine tailings disposal that only "inert inorganic geological material" can be deposited into the sea, it can be predicted that only few sites might be suitable for this option. Instead, if on-land disposal uses best-practice methods for pollution prevention and geotechnical stability, this option ensures the possibility that future generation might be able to exploit these resources in the future by optimized exploitation techniques.

REFERENCES

Azam, S., and Li, Q., 2010, Tailings dam failures: A review of the last one hundred years: Geotechnical News, v. 28, p. 50-53.

Bea, S.A., Ayora, C., Carrera, J., Saaltink, M.W., and Dold, B., 2010, Geochemical and environmental controls on the genesis of efflorescent salts on coastal mine tailings deposits: A discussion based on reactive transport modeling: Journal of Contaminant Hydrology, v. 111, p. 65-82.

Benedicto, J., Martínez-Gomez, C., Guerrero, J., Jornet, A., and Rodriguez, C., 2008, Metal contamination in Portman Bay (Murcia, SE Spain) 15 years after the cessation of mining activities: Ciencias Marinas, v. 34, p. 389-398.

Cruz, J., Bustos, C., Martínez, C., and Suazo, H., 2012, Daily mineralogical control of Andina Division Concentrator CODELCO CHILE, Geomet2012.

Diaby, N., and Dold, B., 2014, Evolution of geochemical and mineralogical parameters during in-situ remediation of a marine shore tailings deposit by the implementation of a wetland: Minerals, v. 4(2) p. 578-602.

Dold, B., 2003, Speciation of the most soluble phases in a sequential extraction procedure adapted for geochemical studies of copper sulfide mine waste: Journal of Geochemical Exploration, v. 80, p. 55-68.

Dold, B., 2006, Element flows associated with marine shore mine tailings deposits: Environmental Science and Technology, v. 40, p. 752-758.

Dold, B., 2008, Sustainability in metal mining: from exploration, over processing to mine waste management: Reviews in Environmental Sciene and Biotechnology, v. 7, p. 275-285.

Dold, B., 2010, Basic concepts in environmental geochemistry of sulfide mine-waste management, *in* Kumar, S., ed., Waste Management, http://www.intechopen.com/books/show/title/waste-management, p. 173-198.

Dold, B., 2014a, Evolution of Acid Mine Drainage formation in sulfidic mine tailings: Minerals, v. 4(2), p. 621-641.

Dold, B., 2014b, Submarine Tailings Disposal – A Review: Minerals, p. 642-666.

Dold, B., Diaby, N., and Spangenberg, J.E., 2011, Remediation of a marine shore tailings deposit and the importance of water-rock interaction on element cycling in the coastal aquifer: Environmental Science & Technology, v. 45, p. 4876-4883.

Dold, B., Wade, C., and Fontbote, L., 2009, Water management for acid mine drainage control at the polymetallic Zn-Pb-(Ag-Bi-Cu) deposit of Cerro de Pasco, Peru: Journal of Geochemical Exploration, v. 100, p. 133-141.

Korehi, H., Blöthe, M., Sitnikova, M.A., Dold, B., and Schippers, A., 2013, Metal mobilization by iron- and sulfur-oxidizing bacteria in a multiple extreme mine tailings in the Atacama Desert, Chile: Environmental Science and Technology, v. 47, p. 2189-2196.

Martínez-Sanchez, M.J., Navarro, M.C., Perez-Sirvent, C., Marimin, J., Vidal, J., Garcia-Lorenzo, M.L., and Bech, J., 2008, Assessment of the mobility of metals in a mining-impacted coastal area (Spain, Western Mediterranean): Journal of Geochemical Exploration, v. 96, p. 171-182.

Nystroem, J.O., and Henriquez, F., 1994, Magmatic features of iron ores of the Kiruna type in Chile and Sweden; ore textures and magnetite geochemistry: Economic Geology, v. 89, p. 820-839.

Oyarzun, R., Manteca Martínez, J.I., López García, J.A., and Carmona, C., 2013, An account of the events that led to full bay infilling with sulfide tailings at Portman (Spain), and the search for "black swans" in a potential land reclamation scenario: Science of The Total Environment, v. 454-455, p. 245-249.

Perner, K., Leipe, T., Dellwig, O., Kuijpers, A., Mikkelsen, N., Andersen, T.J., and Harff, J., 2010, Contamination of arctic Fjord sediments by Pb-Zn mining at Maarmorilik in central West Greenland: Marine Pollution Bulletin, v. 60, p. 1065-1073.

Poling, G.W., and Ellis, D.V., 1995, Importance of geochemistry: the Black Angel lead-zinc mine, Greenland: Marine Georesources & Geotechnology, v. 13, p. 101-118.

Rico, M., Benito, G., and Díez-Herrero, A., 2008a, Floods from tailings dam failures: Journal of Hazardous Materials, v. 154, p. 79-87.

Rico, M., Benito, G., Salgueiro, A.R., Díez-Herrero, A., and Pereira, H.G., 2008b, Reported tailings dam failures. A review of the European incidents in the worldwide context: Journal of Hazardous Materials, v. 152, p. 846-852.

Weibel, L., Dold, B., and Cruz, J., 2011, Application and Limitation of Standard Humidity Cell Tests at the Andina Porphyry Copper Mine, CODELCO, Chile, SGA Biennal Meeting: Antofagasta, Chile.

Water Management in the Closure of Tailings Storage Facilities

Carlos Cacciuttolo[1] and Kathia Tabra[2]

1. *Delfing Ingeniería SpA, Chile*
2. *Pontificia Universidad Católica, Peru*

ABSTRACT

Tailings are the most visible remaining signs of mining activity, that together with mine waste rocks and open pit, are recognized as the "legacy" impacts of mining. In the past, the primary aim was to provide a well-engineered structure into which tailings can be deposited without a great deal of attention given to closure requirements or long term management of tailings storage facilities (TSF). Nowadays, the closure of TSF, must be planned at the beginning of the project so environmental, health and safety impacts do not remain in time after the closure. Not having a closure plan during the design stage may present serious economic consequences for the project, since closure costs without the planning at the end of mine life could threaten the project global economy. This implies that the closure concept must be included in the early phase of the TSF, to guarantee minor impacts in the future and ensure cost-effective closure activities considered in the global budget of the project.

This paper presents a guide to water management in the closure of TSF with focus on physical, hydrological and geochemical stability and its co-relation to improve closure activities for the long term waste and water management. Main impacts on water resources and TSF closure technologies are described like a methodology that needs to be engineered for closure during mine life by civil works and regular monitoring activities, so stability and environmental performance objectives can be achieved.

Successful TSF closure history cases are presented considering application in Chile and Peru, describing their design criteria, learned lessons, advantages/disadvantages, and technology performance under particular Andean region conditions.

Keywords: Contact/non-contact water management, TSF physical/hydrological/geochemical stability, seepage/infiltration control, covers, ARD mitigation

INTRODUCTION

Recently, there has been an increasing awareness for environmental and social sustainability of construction, operation and closure of mining projects. One of the main components that persist after closure is tailings storage facilities (TSFs). Whilst the engineering and geotechnical principles involved in the design of TSFs have been well developed in recent years, many attempts have been made, often on a trial and error basis, to ensure the long-term stability of TSF. Tailings are generally stored on the surface either within retaining structures (slurry or thickened tailings) or in the form of piles (paste or filtered tailings), but can also be stored underground in mined out voids (hydraulic fill or backfill tailings), or below water (lakes and sea) (Vick, 2001). In all cases TSFs host a residue that contain minerals, metallurgical reagents and water that can dissolve and transport contaminants to soil, groundwater and surface water. Also, site conditions may cause hydraulic erosion and soil liquefaction. For this reasons, water management of TSFs is an important issue to maintain physical, geochemical and hydrological stability after closure.

GEOCHEMICAL STABILITY ISSUES

Acid rock drainage (ARD) from mine waste is a worldwide environmental problem that can cause deterioration of downstream groundwater and surface water systems affecting aquatic biota. Weathering of sulphide minerals present in mine waste is responsible for generation of ARD. The quality of ARD is controlled by mineralogical and geochemical reactions in TSFs, and the outcome of these reactions is reflected in seepage waters surfacing through tailings dams, infiltration to soil and to groundwater. However, the design of tailings impoundment and tailings disposal technique ultimately determine whether sulphide minerals are exposed to weathering and whether mine drainage starts to form (Dold, 2014a).

Geochemical Considerations

Geochemical considerations for closure in TSFs depend on tailings disposal method. Most known disposal methods are surface, sub-aqueous and underground tailings disposal. Sub-aqueous (lake or submarine) tailings disposal has the advantage of eliminating air (oxygen) to minimize the oxidation of sulphides and prevent ARD with a low-cost closure and maintenance system. However, this method has been banned and restricted in several countries due to the high risk of environmental contamination. Historically, several cases of sub-aqueous tailings disposal has ended in final liberation of contaminants under reducing conditions, dispersion of chemicals from tailings and sediment contamination after decades of monitoring (Dold, 2014b). This has left impacts on aquatic biodiversity and risk of bioaccumulation of metals through food chains. The feasibility of sub-aquatic tailings disposal is dependent upon specific circumstances, extensive analyses of geochemical characteristics and its response under specific sub-aqueous conditions (Dold, 2014b). Monitoring of water quality, sediment quality and aquatic life is an important tool to control and evaluate sustainable closure.

Underground tailings disposal can prove viable for some of the tailings produced in mine life. In abandoned open pit mines, tailings material can be used to backfill the void, eliminating air (oxygen) and water contact with pit walls and water (groundwater, rainfall) decreasing closure costs associated with the tailings material at the same time as pit remediation. In underground mines tailings material can be used, after geochemical treatment and cement mixer, for structural

purposes on stopes. In this case, monitoring of groundwater and superficial water downstream is an important tool to control and evaluate sustainable closure.

Surface tailings disposal is the most common method, mainly because it is preferable to store tailings on the surface where potential negative impacts can be managed. However, the main problem with surface deposition is that it is very difficult to achieve a sustainable closure solution for surface TSFs since ultimately all materials decompose, erode and are transported to the oceans in geological time scale (Szymanski and Davies, 2004). Also, there is a constant risk of ARD generation by the contact of sulphide tailings with water (groundwater, rainfall) and oxygen (air). In surface tailings disposal, sulphide oxidation with subsequent metal release may occur in the unsaturated border zones close to the embankments (borrow, rockfill or cycloned tailings sand dams) and at the tailings beach surface in active impoundments (Chambers, 2012). Metals released in sulphide oxidation can be retained by secondary precipitates that had formed as a result of oxidation. This mechanism prevents the downward transport of metals in the circum-neutral conditions. However, in acidic conditions, metals are no longer retained in the precipitate and rather dissolved in ARD (Tabra and Lange, 2014). Is relevant to mention that not all metals will precipitate in neutral condition and even neutral drainage may be potentially contaminant.

TSF Site selection - tailings characterization and ARD prediction

Baseline information (seismic, geological, geotechnical, meteorological, hydrological, hydrogeological, biological, soil/sediment quality, flora, fauna, social, and economical) of potential sites for tailings disposal and geochemical characterization of tailings material, are important aspects to consider for the selection of tailings disposal site and disposal method. Land and water uses of populations, flora and animals near and/or downstream tailings disposal site must be considered. Some of these aspects are summarized in the following table.

Table 1 Environmental Aspects for TSF Disposal and Closure Water Management Systems

Environmental Aspects		Tailings disposal	Closure Water Management System
Weather	Rainy (Tropical or Highlands)	Thickened Tailings/sub aquatic disposal	Diversion ditches, spillway, channels, grout curtain, cut off trench, underdrain, drainage system, collection pond, passive or active effluent treatment
	Dry (Desert)	Dewatered tailings/ in pit tailings disposal or co-disposal with waste rock	Diversion ditches, spillway, channels, drainage system, collection pond, passive or active effluent treatment
Geomorphology	Steep terrain	Conventional disposal	Diversion ditches, spillway, channels, grout curtain, cut off trench, underdrain, drainage system, collection pond, passive or active effluent treatment
	Flat terrain	Thickened tailings/Filtered Tailings/ In pit tailings disposal or co-disposal with waste rock	Diversion ditches, spillway, channels, drainage system, collection pond, passive or active effluent treatment
Seismicity	High	Dewatered tailings	Diversion ditches, spillway, channels, drainage system, collection pond, passive or active effluent treatment
		In pit tailings disposal / backfilling mine stopes	Pumping wells, collection ponds, passive or active effluent treatment
	Low	Co-disposal	Diversion ditches, spillway, channels, drainage

Environmental Aspects		Tailings disposal	Closure Water Management System
			system, collection pond, passive or active effluent treatment
		Conventional disposal	Diversion ditches, spillway, channels, grout curtain, cut off trench, underdrain, drainage system, collection pond, passive or active effluent treatment
Hydrology	Rivers, creeks (at the proposed site)	Conventional disposal	Diversion tunnels and coffer dams (derivation of rivers and creeks), diversion ditches, spillway, channels, grout curtain, cut off trench, underdrain, drainage system, collection pond, passive or active effluent treatment
	Lake, sea	sub aquatic disposal	Aquatic flora and fauna monitoring, submarine flow monitoring
Hydrogeology	Unconfined aquifer, discharge zones, geological faults	Thickened tailings/Filtered Tailings	Diversion ditches, spillway, channels, grout curtain, cut off trench, underdrain, drainage system, collection pond, passive or active effluent treatment
	Confined aquifer, no discharge zones	Conventional Tailings / Dewatered tailings	Diversion ditches, spillway, channels, drainage system, collection pond, passive or active effluent treatment

Prevention of ARD

Prevention is the key to avoid negative environmental impacts and costly mining mitigation. ARD prevention may consider at least three basic options: pyrite removal, oxygen exclusion and water control. Pyrite removal from tailings prior disposal is an effective measure to prevent ARD. The residue with high content of pyrite may then be disposed in an anoxic or confined environment. The second option consists to dispose tailings with acid generation potential in an anoxic environment avoiding sulfide reactions, metal leaching and the subsequent migration of weathering products that result from sulfide oxidation. In the closure phase of TSF, this can be achieved by the development of an effective and durable barrier to oxygen, such as water covers, dry covers and/or geosynthetic membranes. Two types of covers are used to isolate wastes and prevent ARD: dry and wet covers techniques.

Dry covers

The dry cover approach aims to reduce the oxygen flux into the tailings, thereby minimizing sulphide oxidation. The amount of acid water formed is also reduced by limiting the water percolation into the tailings. A dry cover usually consists of a combination of drainage layers and sealing clay, inert or non-reactive tailings, geotextile and organic material. Dewatered and reagent-less tailings material is placed on top of the liner to act as an inert protective layer. A gravel and impermeable layer or waste overburden is placed on top of the inert tailings. This cover can be applied in surface and underground tailings disposal. Dry covers behave as a "water stock-release" structure that enhance evapotranspiration and minimize infiltration. The cover thickness will determine its water storage capacity and will be defined as a function of the local rain pattern. About quantitative criteria of water storage and release in dry covers, research should be oriented in that direction, requiring detailed studies and focused on this topic.

The main drawback with the dry cover technique is that it has a relatively high cost (earthworks and soil processing activities) that is difficult to get right.

Wet covers

Water covers are considered to be one of the most effective methods for the mitigation of potentially acid generating tailings. The water cover in man-made lakes and in situ flooded basins is generally shallow (less than 2m) to minimize the size of dams constructed. To limit metal transfer to the water cover, protective layers of sand or organic material are sometimes placed over the tailings to act as a diffusion and mass-flow barrier. A potential problem that should be mitigated is wind-induced mixing and re-suspension. Underwater disposal in natural water bodies is preferred since provides a deep water cover. However, as already mentioned, this method has been banned and restricted in several countries due to the high risk of environmental contamination (Dold, 2014b). A limitation to wet covers may also be the physical stability of TSF, particularly in seismic environments, with risk of water overtopping.

Liners

The use of liners is significantly less common in tailings facilities for mining closure activities. Synthetic materials, such as high density polyethylene (HDPE) are often used with compacted clays to form a composite lining system to prevent polluted seepage through the facility foundation. Liners are commonly used to facilitate the permitting process. This practice has however largely been avoided on cost grounds. New geosynthetic materials such as geosynthetic clay liners (GCL) need more exploration to study their behavior for mining closure activities for long term.

The third option basically consists on the derivation of runoff and collection of contact water, mainly infiltration. These methods are detailed in hydrological stability issues chapter.

Mitigation of ARD and monitoring

If ARD is generated, active and passive technologies are necessary increase pH and remove solutes to accomplish water quality standards for discharge or reutilization. This treatment involves passive and active closure criteria that largely increase closure costs. Improved methods of prevention and control substantially reduce ARD treatment. TSF design must consider the collection of this water, avoiding impacts on soil, groundwater and superficial water. After closure, monitoring of groundwater and superficial water downstream of TSF is an important issue to control possible flows of infiltration during operation and after final closure. However most monitoring plans don't last more than 10 years when the real effects of ARD can be noticed even after hundred years.

Ongoing laboratory testing of tailings and collection of supernatant pond and seepage water samples from TSF during operation and after closure of mine is needed to verify control methods and TSF geochemical stability.

PHYSICAL STABILITY ISSUES

Climate and seismic site conditions need to be considered for the closure of surface tailings disposal, focusing on provide robust structures against the following issues: (i) internal water erosion (piping), (ii) external water erosion (runoff), and (iii) wind erosion.

Erosion

In addition to influencing ecosystems (soil, water bodies, flora and fauna), dust emission can negatively affect human health through particulate matter (PM10) pollution. At TSF closure stage, a cover material is needed to manage runoff erosion and create an appropriate ground surface for project reclamation. Dust emission control play an important role in closure design and a proper implementation will provide the primary control mechanism to meet regulatory air quality requirements. Some other dust control alternatives are: soil cover, top soil/re vegetation cover, phytostabilization, binder material or chemical agglomeration, and wind mitigation civil work structures.

Dam Stability

The design of TSF embankment must consider the damage from repeated occurrences of extreme rainfall and earthquake events as well as progressive processes like internal erosion, which in conjunction degrade dam stability in the long term. For these reasons, a periodic inspection program is needed in the post closure stage (ICOLD, 2011), which includes the following activities:

- Evaluate dam stability, considering gentle slopes and benches.
- Evaluate geotechnical instrumentation (mainly piezometers, accelerometers, and underdrain collection sump).
- Evaluate the compaction of dam crest and slope benches.

However, it is important to consider that the potential for piping, filter clogging or creep deformations over hundreds of years cannot be appreciated by available dam safety evaluation methods (Szymanski, and Davies 2004) and designs need to consider long term civil works at TSFs beyond closure stage.

Geologic Hazards

In the indefinite future TSFs will be subject to the full suite of geomorphic processes operating at their sites. These include landslides and debris flows with river damming, characteristic of the Andes. Like the occurrence of these extreme events, the damaging effect of these processes is only a matter of time, and their recurrence rate is a factor particularly difficult to predict for large-scale geologic phenomena. Even benign processes of alluvial deposition will eventually fill water conveyance facilities unless they are continually cleared of sediment and debris. For these reasons, periodic surveillance programs need to be implemented for post closure stage at TSFs (ICOLD, 2011), to evaluate potential geologic risks and build rock falls and debris flow protection structures.

HYDROLOGICAL STABILITY ISSUES

TSF has to be designed for given annual hydrological conditions or more correctly for a range of conditions in which the storm events are statically included. Decants, pumping systems, spillways, piping, and treatment plants need to be sized for such criteria. However, TSF still has to able to cope with individual extreme runoff events, as they occur when the pond is at its maximum operating level. For closure design (long term) it is necessary to consider events that might come from an extremely heavy rainfall, snowmelt, debris/mud flows, climatic change, or a combination of them.

Freeboard

An adequate approach to closure design is to use two design floods: an environmental design flood (EDF) and a facility design flood (FDF). The EDF is typically from a storm with a finite return period of say 10 to 100 years, or it may be a rainfall/snowmelt event. It is the maximum storm event which still does not result in an unscheduled discharge of water to the environment. The flood from the EDF is retained at TSF, within a freeboard allowance below the invert of an emergency spillway, and managed within the normal operation of TSF basin. For this reason, a maximum operating water level (MOWL) should be specified in conjunction with the EDF. The MOWL should not be exceeded under normal operating conditions. The MOWL should provide for adequate freeboard to store the EDF without discharge over the emergency spillway. However, water storage within the TSF may be contradictory with dry cover integrity and may enhance water infiltration through the tailings deposit. This may result in consequent drainage with high sulfate and/or metal concentrations, for these reasons, is necessary to define dry cover zones (tailings beach against dam), wet cover zones (pond), and a maintenance dry cover program. Physical stability must be the primary objective of long-term closure. No means for controlling ARD can succeed unless the tailings are first made to stay in one place, and anything that violates this provision will necessarily compromise all others.

Spillway

The overtopping of a dam could result in a catastrophic failure, extensive erosion, loss of tailings to the environment, a very large uncontrolled spill of water, and even the complete emptying of the pond. For these reasons, an emergency spillway is a safety measure, which must be included in every TSF for closure, to handle unforeseen events and to protect the environment. Under any circumstance should tailings be allowed to escape from a basin or a dam is allowed to overtop. The FDF must be chosen to ensure that this does not happen. The routed FDF is used to size the emergency spillway. For a tailings basin, it is frequently based on the largest possible storm resulting from the probable maximum precipitation (PMP) which might or might not occur in conjunction with snowmelt. Robust spillways need to be designed and constructed. Floods in excess of the EDF are either allowed to spill unimpeded (very large storms) or to spill slowly with a reduced retention time through the emergency spillway. If spillage cannot be tolerated under any circumstances, then the EDF and the FDF have to be the same.

The following figures show the management of storm flow/freeboard concept and a spillway civil work.

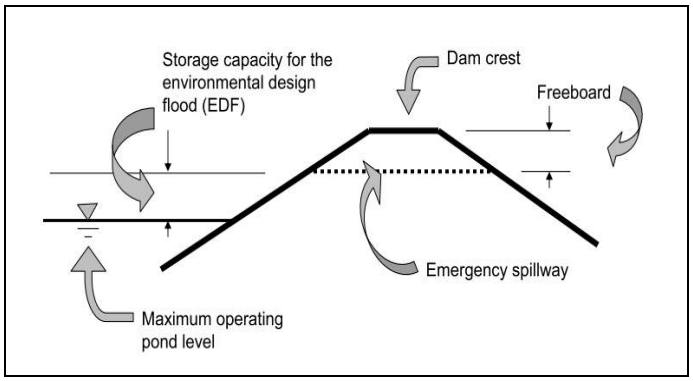

Figure 1 Management of Storm Flows (Golder, 1989)

Figure 2 Spillway and Energy Dissipators

Perimeter Diversion Ditches

Collection and diversion systems for non-contact water (runoff water), consisting of perimeter ditches is required as part of TSF design. For the closure and post-closure phases, it is important to provide lined diversion ditches with long term erosion-resistant materials such as geoweb/concrete solution, GCL liner, or reinforced concrete. Soil excavated ditches without liners are not recommended for TSF closure stage. A periodic inspection program needs to be carrying out for review the integrity of the diversion ditches.

Seepage Collection System – Collection/Polishing Pond

The seepage collection system consists of a cutoff trench and a robust underdrain system. Both systems convey the TSF contact water to collection geosynthetic lined ponds, where water quality is controlled. If the water quality meets the standards, it is possible to discharge it to natural courses. If it is not, water needs to be treated. The installation of downstream monitoring wells is recommended to control periodically the water quality on the TSF on post-closure phase. Polishing ponds or sedimentation ponds are designed to increase the environmental compatibility and quality of effluents from preceding treatments. The water in the reclaim pond is either sent to treatment/polishing ponds for discharge to the environment. Some reclaim water can be sent to evaporation ponds or sprays if the climate is suitable.

Water Storage Dams - Upstream of TSF

An adequate approach for closure design of TSF to control large floods and runoff is to manage water with a high dam storage capacity and a separate water-control dam located upstream of the TSF. Some advantages are: (i) buffering of probable maximum flood (PMF), (ii) controlled diversion, and (iii) promote non contact water.

TSF CLOSURE CASES

El Indio TSFs - Andean Region of South America - Chile

El Indio copper-gold mine is located in the Chilean Andes approximately, 180 km east of La Serena City. The climate is typical of Andes mountain region of dry conditions, with variable winter precipitations (May – September), mainly as snow. On the operation phase the mine had an open

pit and underground activities, with two waste rock dumps, three process/metallurgic plants, and three tailings storage facilities.

The mining company negotiated a voluntary agreement with the Chilean region IV regulatory authorities after 20 years mine lifetime to carry out the closure stage of El Indio Mining project, as there was no legislation yet in place in Chile focused on mine closure. One of the key components of the closure plan was surface water management works developed under the overall objective of "establish a physically and chemically stable drainage system with minimal maintenance and monitoring requirements" (Robledo and Meyer, 2007). As consequence of mining activities, Malo River stream was modified in several sectors with diversion civil works. The main closure activities were: (i) restoration of Malo River drainage system in the process plant area and on TSFs by the construction of engineered lined channels (lined with rockfill and cobblestones), and (ii) abandonment of the existing Malo river diversion system.

Tailings and waste facilities managed in El Indio Mine were: (i) Pastos Largos TSF, (ii) El Indio TSF, (iii) dry tailings modules (filtered tailings), and (iv) sedimentation pond (polishing pond). Specific closure works at the TSFs were considered including surface grading, placement of a cover to prevent hydraulic and wind erosion, and the construction of spillways to manage storm flows. The sedimentation pond is located at Malo River downstream of TSFs stored approximately 66,000 m^3 of sediments (As, Pb, and cyanide among others). Sediments were transported by haul trucks to Pastos Largos TSF for disposal. The pond was removed and the Malo River was restored in its natural stream.

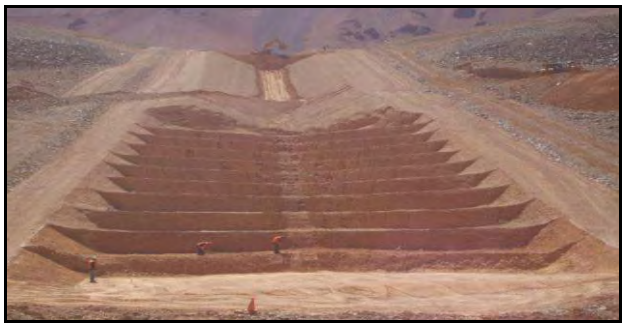

Figure 2 Malo river closure civil works construction (Saez, 2011)

Figure 3 Malo river closure civil works finished

(Saez, 2011)

Figure 4 Filtered TSF – Operating phase (Saez, 2011)

Figure 5 Filtered TSF – Closure phase (Saez, 2011)

Constructed diversion ditches were lined to reduce infiltration of surface water into mine tailings materials and to prevent capture by underground mine workings, with the intent to minimize chemical loading impacts to water. A geosynthetic clay liner (GCL) was selected for lining in most cases. The following pictures show some overall views of closure civil works at El Indio TSFs:

Figure 6 Filtered TSF – Closure construction phase – civil works (Saez, 2011)

Casapalca TSFs – Andean Region of South America - Peru

The Casapalca polymetallic mine is located in Peruvian highlands, approximately 113 km east of Lima city, Peru. The mine is composed by underground activities, and is near to the Rimac river, at an elevation of approximately 4,100 m above sea level. The climate is typical of Peruvian Andes conditions. Annual precipitation is approximately 700 mm with essentially this entire amount falling in the rainy season (November – March). To prevent and reduce the risks for human health and the environment, one of the key components of the closure plan was surface water management works developed under the overall objective of "establish a physically and chemically stable drainage system to Rimac River" (Estrella, 2008). As consequence of mining activities, the stream of the Tacpin creek was modified in several sectors by using a constructed diversion civil works. The main closure activities in the middle part of the Tacpin creek basin were: (i) restoration of Tacpin stream surface drainage channel in the land area and across tailings facilities by construction of engineered lined channels, and (ii) abandonment of the existing Tacpin stream diversion tunnel system.

The tailings waste facilities managed in the Casapalca Mine were: (i) Tablachaca I, and (ii) Tablachaca II. Specific closure works at the TSFs included surface grading and placement of a cover (organic soil layer + clay layer + gravel layer + HDPE layer) to prevent: (i) hydraulic and wind erosion, (ii) oxidation of sulphide tailings, and (iii) physical stabilization of TSF slopes. Hydraulic civil works constructed with reinforced concrete were: (i) diversion ditches to collect no contact water, (ii) diversion tunnel (rock wall reinforced), and (iii) Tacpin stream intake structure to divert runoff to diversion tunnel. Like a post closure activities revegetation was applied, with native plants from the site.

The following pictures show some overall views of closure civil works at Tablachaca TSFs:

Figure 6 Construction of closure civil works (Huaymanta, 2011)

Figure 7 Closure civil works finished (Huaymanta, 2011)

Figure 8 Tablachaca TSF before closure stage (Estrella, 2008)

Figure 9 Tablachaca TSF after closure stage (Estrella, 2008)

Figure 10 Tablachaca TSF closure overview (Estrella, 2008)

In both TSF closure cases the application of the concepts of closure, decommissioning, cover implementation, collection and diversion of non contact water and channeling of water streams are valuable issues. However, it is important to consider that tailings disposal on a riverbed is prone to geological and hydrological hazards on extreme flood events and geodynamic events. It is relevant to consider a periodic OMS program (operation, maintenance and surveillance) and ISR/DSR

programs (Inspection Safety Review/Dam Safety Review) after the closure activities to monitor and control the closure TSF performance at these study cases (ICOLD, 2011).

CONCLUSIONS

The main goal of long-term closure is to achieve "walk-away" conditions that assure physical, hydrological and chemical stability without the need of long-term monitoring and maintenance. This objective depend on the motivation and ability of authorities to deal with mining wastes after decades, and even centuries, avoiding to pass the burdens of today's resource extraction to future generations who will inevitably receive the impacts of these passives (Tabra and Lange, 2014).

One of the main challenges in closure design for TSF is probably their capacity to deal with extreme events (hydrological and seismic). For surface tailings disposal, water management related with high surface water flows should consider the rapid evacuation of water, minimizing erosion and instability, and temporal water storage that requires specific design to minimize infiltration. Civil works and control systems for TSFs must be designed in the early stages of a mining project with conservative criteria and robust structures, thinking about the perpetuity of this component and projecting a periodic schedule of maintenance and restoration in the post-closure stage (Cacciuttolo et al., 2014).

Geochemical stability is a relevant part of a TSF project, particularly if tailings contain acid-generating behavior, because these materials can degrade the strength properties of cycloned tailings sand dams and borrow dams, increasing dam failure risks and generating ARD. In general, mine residues that interact with the environment should be inert to materials and chemicals already in the same ecosystem. If mining wastes are not inert they should be isolated and in a form that is compatible with the adopted waste management technique, the sensitivity of ecosystem and social context.

In recent years, there have been significant advances in physical and hydrological stability of TSFs (investment effort and better decisions on site selection and use of technology for tailings management). However it still remains to devote more time to understand the action of tailings geochemistry and make greater efforts to prevent, control and mitigate ARD on TSF in the long term.

A long-term closure requires going beyond the usual engineering perspective, with an interdisciplinary approach taking in consideration all points of view in important decision making such as site disposal, method of disposal, TSF design, control methods, contingency plans, among others. In most cases, an initial high inversion is more rentable in the long term. Mining, mineral processing and waste management technologies, which offer improved environmental and social performance, and smaller surface footprint, should be preferentially adopted. Also, opportunities for re-use of waste material should be pursued when practicable.

REFERENCES

Cacciuttolo, C., Barrera, S., Caldwell, J., and Vargas, W., (2014). Filtered Dry Stacked Tailings: Developments and New Trends. *Proceedings of the 2nd International Seminar on Tailings Management TAILINGS 2014*, August 2014, Antofagasta, Chile.

Chambers, D. M. (2012). Long Term Risk of Releasing Potentially Acid Producing Waste Due to Tailings Dam Failure. *Proceedings of the 9th International Conference on Acid Rock Drainage ICARD*, May 2012, Ottawa, Canada.

Estrella, V., C. (2008), Remediación Ambiental Minera - Perspectivas y Oportunidades, Presentation at Jueves Minero, Instituto de Ingenieros de Minas del Perú IIMP, June 2008, Lima, Peru.

Dold, B. (2014a). Evolution on Acid Mine Drainage Formation in Sulphidic Mine Tailings, *Minerals Journal (Minerals 2014,* ISSN 2075-163X, July 2014, viewed at: www.mdpi.com/2075-163X/4/3/642/pdf

Dold, B. (2014b). Submarine Tailings Disposal (STD) – A Review, *Minerals Journal (Minerals 2014,* ISSN 2075-163X, July 2014, viewed at: www.mdpi.com/2075-163X/4/3/642/pdf

Dold, B. (2003). Aguas Ácidas: Formación, Predicción, Control y Prevención, *Revista Minería, 310, pp. 29-37.*

Franks, D. M., Boger, D. V., Cote, C. M., and Mulligan, D. R. (2011). Sustainable Development Principles for the Disposal of Mining and Mineral Processing Waste. *Resources Policy*, Elsevier, Ltd.

GARD Guide (2009). The Global Acid Rock Drainage Guide (GARD Guide), *International Network for Acid Prevention (INAP)*, 2009, viewed at http://www.gardguide.com

Golder Associates (1989). WATBAL – Tailings Basin Water Balance Model.

Huaymanta Webpage (2011) http://www.huaymanta.com/ pictures.

ICOLD (2011). Improving Tailings Dam Safety, Critical Aspects of Management, Design, Operation and Closure, Bulletin 139, *International Commission on Large Dams – United Nations Environmental Programme*, 2011.

Kauppila, P. M., Kauppila, T., Makinen, J., Kihlman, S., and Raisanen, M. L. (2011). Geochemistry in the Characterization and Management of Environmental Impacts of Sulfide Mine Sites, *Geoscience for Society 125th Anniversary Volume,Geological Survey of Finland* , 2011, Helsinki, Finland.

Mylona, E., Xenidis, A, Paspaliaris, I, Csovari,M, Nemeth, G, and Folding, G, (2004). Report Implementation and Improvement Closure and Restoration Plans for Disused Tailings Facilities, *Sustainable Improvement in Safety of Tailings Facilities TAILSAFE*, A European Reserch and technological Development Project, 2004.

Tabra, K., and Gaete, O., (2013) Ways to Deal with Mine/Plant Effluent Residues: A roadmap process. *Proceedings of the 142th SME Annual Meeting*, February 2013, Denver, Colorado, USA.

Tabra, K., and Lange, S., (2014). Active Treatment of Tailings Seepage with Focus on Sulphate and Manganese Removal. *Proceedings of the 2nd International Seminar on Tailings Management TAILINGS 2014*, August 2014, Antofagasta, Chile.

Robledo, M., and Meyer, J. (2007). El Indio Mine Closure – A Significant Environmental Accomplishment. *Proceedings of the 2nd International Seminar on Environmental Issues in Mining Industry ENVIROMINE 2007*, October 2007, Santiago, Chile.

Rotting, T., Amezaga, J., Younger, P., Jimenez, P., Talavera, C., Quintanilla, J., Oyarzún, R., and Soto, G., (2008). Cases Studies in Peru, Bolivia, and Chile on Catchment Management and Mining Impacts in Arid and Semi-Arid South America – Results from the CAMINAR Project. *Proceedings of the 10nd International Mine Water Association Congress IMWA 2008*, June 2008, Karlsbad, Czech Republic.

Saez, M., (2011), Experiencias de Movimientos de Tierra para Cierre de Faenas Mineras. *Presentation at 4th National Cierre de Faenas Mineras CIFAMIN 2011*, November 2011, Santiago, Chile. , viewed at http://www.cifamin.cl/neo_2011/pdf/2011/M3/2%20Marcelo%20S%E1ez.pdf

Szymanski, M., B., and Davies, M. P. (2004). Tailings Dams: Design Criteria and Safety Evaluations at Closure, *British Columbia Mine Reclamation Symposium*, 2004, Alberta, Canada.

Vick, S., G. (2001). Stability Aspects of Long –Term Closure for Sulfide Tailings, *Seminar on Safe Tailings Dam Constructions,European Commision*, 2001, Gallivare, Sweden.

10th ICARD IMWA 2015 | 10th International Conference on Acid Rock Drainage & IMWA Annual Conference

A Holistic Framework for Progressively Constructing Stable Waste Storage Facilities

Andrew Baisley[1], Mike O'Kane[1], Paul Weber[2], Peter Scott[3] and Steven Pearce[3]

1. *O'Kane Consultants, Canada*
2. *O'Kane Consultants; New Zealand*
3. *O'Kane Consultant, Australia*

ABSTRACT

Advective gas transport represents an important mechanism controlling internal geochemistry of waste rock dumps (WRDs). Advective transport into WRDs can result in increased contaminants of concern production or create potentially life threatening air quality conditions. Advective transport is a global concern; being the mechanism documented as contributing to the Sullivan Mine fatalities (British Columbia, Canada), and elevated radon emissions from Wismut Uranium mine (Saxony, Germany). Residual pore gas and diffusion across landform outer surfaces post construction contribute less to WRD legacy liability compared to advective transfer. Being advection is a mechanism of substantial liability, can WRDs be constructed economically while managing advective flow?

This paper investigates material controls that manage advective transport during construction. Beyond geochemistry, geotechnical properties are examined in relation to lift heights, material segregation and subsequent advective transfer rates. Waste rock has been characterized for its propensity to segregate based on tip height and dumping methodology, and classified according advective tendencies. Through comprehensive material characterization and scheduling, progressive management of waste material is possible when mine plans and waste rock management plans interface properly. Potential for larger waste rock lifts of reactive material may be possible if waste scheduling highlights that material is of adequate texture to reduce air permeability within larger cells or lifts, for example. Investigation results are compared using Net Present Value (NPV) analyses highlighting value in progressive management of mine wastes in regard to seepage water quality and quantity (and potential for treatment in perpetuity). This paper will present a framework for more comprehensive waste characterization, planning and scheduling, such that WRDs can be constructed economically over the long-term without a strong reliance on developing cover systems as "last minute" mitigation measures. Rather, cover systems be utilized as contributing seepage management mitigation tools, with appropriate WRD construction as the primary contributing management tool.

**There is no full article associated with this abstract.*

CHAPTER 12

RELIABLE MINE WATER OPERATION

Mine Water Balance for a Semi-Arid Climate: Overcoming Challenges to Maintain Operations

Scott Davidson and Emily O'Hara
New Gold Inc, Canada

ABSTRACT

Development of a mine water balance model (WBM) is an essential part of early permitting work and operational planning. New Afton is situated in a semi-arid climate, where its WBM predicted a zero-discharge and net loss facility. Challenges when situated in a semi-arid environment, include significant losses at various stages of the mining cycle and the requirement to supplement the process with freshwater. Water management onsite is essential for all mining operations, and minimizing water losses is essential for arid and semi-arid climates. Freshwater use is highly material to local communities of interest, in particular our First Nations partners. Another challenge that needed to be overcome was that New Afton's water license allows for 139m³/h of freshwater to be pumped from Kamloops Lake, although it had initially applied for 290 m3/hr.

Prior to full operation, two significant water losses were not completely understood. These included void loss in the Tailings Storage Facility (TSF) and ventilation losses from underground. Void losses account for on average 137m³/h when operating at 12,000 tonnes per day. This value was unable to be determined with accuracy until tailings had been produced from the mill, after operation had commenced. Ventilation losses were not expected to be significant, and thus weren't considered when the initial WBM was developed. Due to the extremely dry climate in Kamloops, ventilation losses were first monitored in 2013. Throughout the year, dry air that is pumped underground is vented as warm humid air due to equipment use and water sprays for dust control. Water losses through ventilation on average were found to range from 10 to 18 m³/h. Quantification of these losses was critical to being able to determine actual operation freshwater demands and allow New Afton to amend its permit.

Keywords: Mine, water, arid, climate

INTRODUCTION

New Afton is in its third year of operation, with commercial production reached in June 2012. The scheduled throughput for the mill was 11,000 tons per day, however, this throughput was exceeded early during commercial production. The mine currently operates at a rate of approximately 14,000 tons per day, with opportunity for increased throughput. It is currently licensed to withdraw 139m³/h, or 1,218,000m³ annually from Kamloops Lake.

Located in a semi-arid climate with on average 278mm of precipitation annually, water management is an essential part of New Afton's operating considerations. Water use at the mine site is a significant area of concern for local First Nations and the general community. Managing water quality is also of a very high interest. New Afton minimizes its water use through the following management strategies:

- Recycling of process water in the mill facilities
- Using chemical dust suppressant for dust control
- Recycling all water drawn from underground dewatering
- Maintaining a "zero discharge" water balance.

As part of permit applications prior to operation, New Afton completed a water balance model depicting pre-construction, construction, early operation, full operation and closure. Based on these water balance models, it was estimated that approximately 290m³/h of makeup water from Kamloops Lake would be required, to account for contingencies and increases in production. However, as part of regulatory applications, it was also mentioned that 139m³/h was required for base case, and thus this was the awarded withdrawal rate granted by the government. Following commencement of operations it was realized that the water balance developed for the permitting contained two significant omissions and that the permitted withdrawal rate was insufficient for continuous uninterrupted operations. In November 2013, an application was submitted to increase the licensed water withdrawal rate from 139m³/h to 212m³/h to ensure the operation has sufficient water for continuous operations.

METHODOLOGY

Following the commencement of operations, and as part of its Mines Act permit, New Afton was required to develop an operational water balance for the site. During the development of the operational water balance it was quickly noticed that tailings void losses had not been included along with ventilation system losses. The development of the operational water balance was conducted by BGC Engineering Inc. (BGC) and was based on a combination of process design details and operational data. In July 2013, BGC provided the following water balance based on actual inputs and estimated monthly averages from the first year of operations.

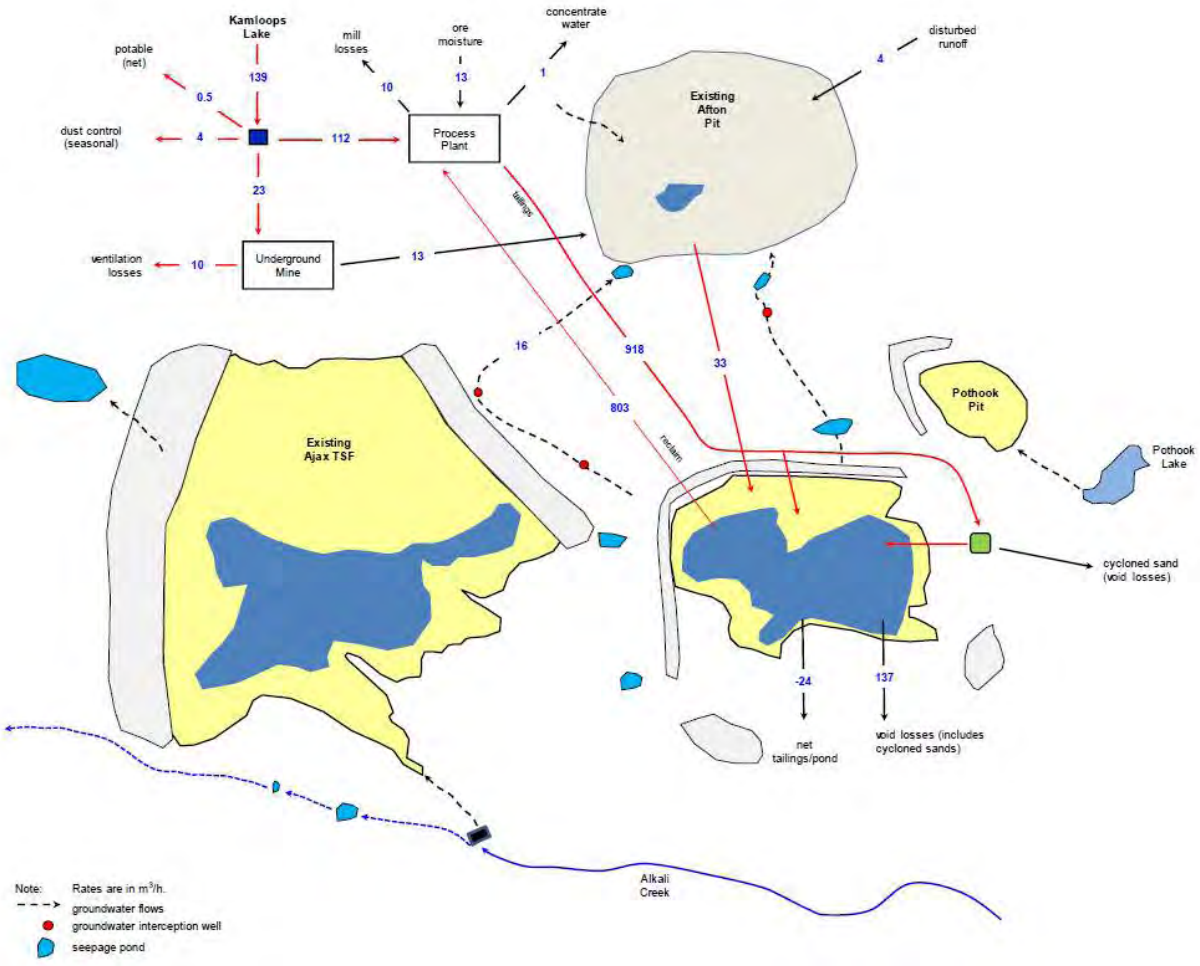

Figure 1 New Afton Average Annual Flows Life-of-Mine (BGC, 2013)

Tailings Void Losses

Tailings void losses is the volume of water that is lost in tailings voids during placement of tailings into the storage facility. Void losses are calculated through the following formula, which is derived from the dry unit weight equation (Budhu, 2007) (Nomenclature for all formulas can be found at the end of this publication):

$$void\ loss = \left(\frac{1}{\rho_s} - \frac{1}{SG}\right) \cdot tailings\ tonnage$$

The current assumption is that the final settled dry density of the tailings will be 1.47t/m³, however it is expected that realized final dry densities may range between 1.4t/m³ and 1.60t/m³ (BGC, 2013).

The settled dry density will vary throughout the life of the project due to ongoing consolidation, so estimating an average for the sake of developing a water balance needs to take this into consideration. Table 1 demonstrates the variation in void losses over the given range of settled dry densities at a production rate of 12 000 tonnes per day. It can be seen from this table that a relatively small change in the settled dry density of the tailings has a substantial impact on the volume of water being lost.

Table 1 Void Losses for Various Settled Dry Densities (BGC, 2013)

Settled Dry Density (t/m^3)	Void Loss (m^3/h)
1.40	176
1.47	159
1.55	141
1.60	131

Bathymetric surveys are carried out annually throughout the life of mine in order to provide data on the existing field settled dry densities and are used to update the water balance model. The surveys are conducted using a boat equipped with a GPS system and a sonar unit. The 2013 bathymetric survey resulted in an estimated settled dry density of 1.47 t/m^3 which matched the water balance value of 1.47 t/m^3.

Ventilation Losses

Ventilation losses were not calculated during the permitting process, as this was not expected to be a significant pathway for water loss. Operations personnel realized though that the ventilation system in the summer months was pushing warm to hot dry air underground while in the winter months the air was cold and dry. Exhaust from the underground was found to be warm humid air throughout the year. Table 2 demonstrates the monthly averages for temperature and relative humidity at the ventilation intake, exhaust and the Kamloops Airport weather station.

Table 2 Ventilation System Temperature and Relative Humidity

	Average Monthly Results				
	1981-2010	2013-2014			
Month	**Kamloops Airport Temp (°C)**	**Intake Temp (°C)**	**Intake RH (%)**	**Exhaust Temp (°C)**	**Exhaust RH (%)**
January	-2.8	-2.7	90.0	13.3	80.4
February	0.1	-6.8	72.3	12.5	76.8
March	5.2	2.9	64.8	12.9	78.7
April	9.9	7.6	55.4	13.9	81.2
May	14.6	12.8	59.6	16.1	86.3
June	18.4	16.1	53.9	17.7	85.5
July	21.5	21.9	42.3	20.0	83.7
August	20.9	20.3	53.8	20.2	90.4
September	15.6	13.7	58.1	18.7	84.9
October	8.5	-	-	-	-
November	2.1	-2.0	90.2	13.6	77.6
December	-2.7	-5.7	88.5	12.8	76.6

Ventilation losses are estimated through the monitoring of relative humidity and temperature at intake fans, exhaust fans and the portal. These readings are recorded hourly on a data logger and retrieved monthly. The water holding capacity for air is estimated based on the August-Roche-Magnus formula (Lawrence, 2005) as shown below:

$$e_s(T) = 6.1094e^{\left(\frac{17.625T}{T+243.04}\right)}$$

For this estimation, it is assumed that there is constant standard atmospheric pressure.

Figure 2 shows the calculated water losses that occurred throughout the monitoring period in 2014. This includes water loss from the ventilation fans only, with another 2m³/h approximately lost from the mine portal. Table 3 contains a monthly summary of the average calculated water losses from the ventilation system.

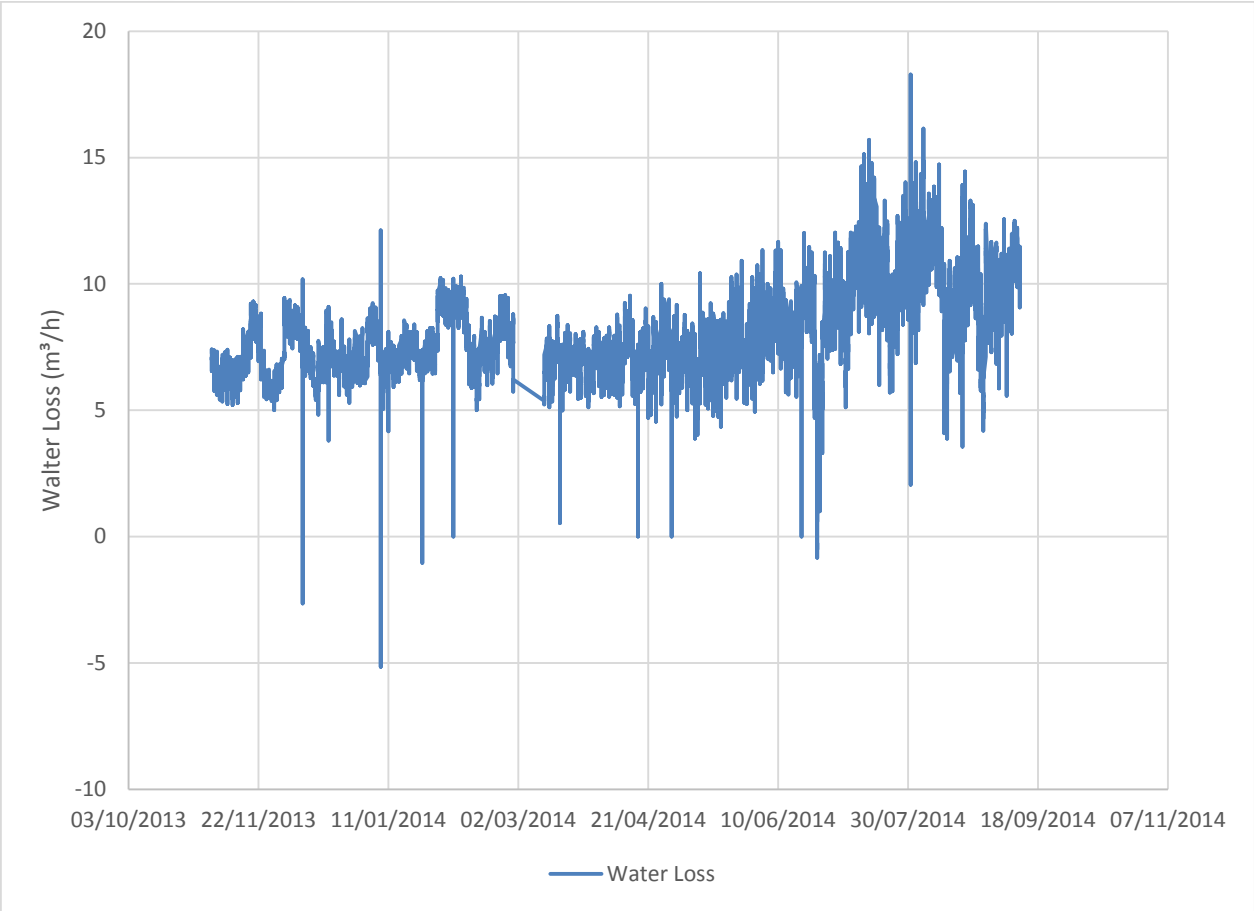

Figure 2 Calculated Ventilation System Water Loss

Table 3 Ventilation System Average Calculated Water Loss (m^3/hr)

Month	Average Calculated Water Loss (m^3/h)
January	9.2
February	10.2
March	9.6
April	9.9
May	9.8
June	11.1
July	12.9
August	12.8
September	13.5
October	-
November	8.5
December	9.1

Water Requirements

Fresh water is required throughout site for showers and bathrooms, underground dust suppression and mill operations. The semi-arid climate at New Afton requires the application of significant dust control measures. Often this would be the continual application of water to roads and bare surfaces, however New Afton has implemented the following controls to assist in the reduction of surface dust:

- Recycled asphalt application on high traffic areas
- Progressive reclamation to provide vegetative cover to bare surfaces
- Application of flocculant to exposed tailings sands during snow free period
- Application of Magnesium Chloride to roadways during dusty months.

The majority of makeup water is provided to the mill process, with on average $112m^3/h$ being used. Current testing is being completed to determine the effect of dissolved metals and salinity on gold and copper recovery, which could put further demands on the freshwater requirements within the mill.

The current major shortfall for water requirements is the ability to maintain a large enough pond volume on the Tailings Storage Facility (TSF). A sufficient volume of water within the pond is required in order to ensure sufficient settling time for fine particulate prior to being recycled back into the processing plant. Based on operating experience at New Afton, the minimum required tailings pond operating volume is approximately 1 Mm^3 at a throughput of 14,000 tpd. The original estimated minimum tailings pond volume for the design throughput of 11,000 tpd was 500,000 m^3, however, it was found even at volumes above this that there was insufficient settling time within the pond.

Figure 3 shows the estimated New Afton tailings pond free water volumes for different throughputs, based on the inclusion of measured ventilation system and tailings void losses. The figure shows the steep decline in free water within the tailings pond based on throughput.

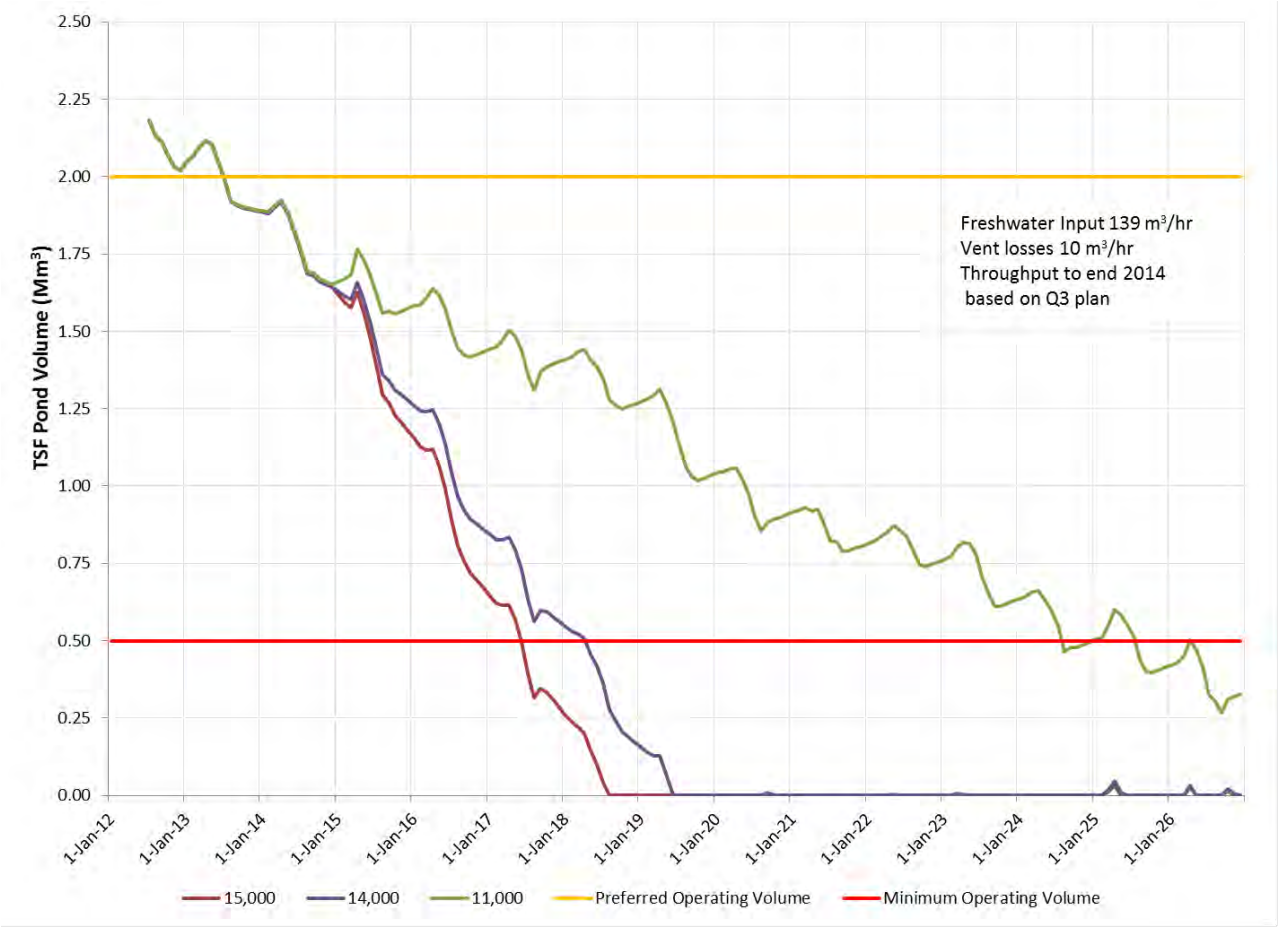

Figure 3 Estimated Tailings Pond Free Water Volume Based on Throughput

CONCLUSION

The reliability of water balances for mines operating in a semi-arid climate is critical to ensure uninterrupted operations. Water balances modelled prior to operation are often based on a variety of factors that can easily have significantly different results once operation commences. This can be due to a variety of reasons, and doesn't always imply that errors were made in the assumptions during the development of these models. As water balance models are an integral part of all levels of mine permitting, it is essential to have a level of confidence and that sufficient resources are made available to best develop this model. Errors or omissions in a water balance may have significant impacts on mine operations over the life of mine.

In the case for New Afton, insufficient care was taken to ensure all reports and applications had a single freshwater requirement and thus, the water volume allocated only accounted for the minimum requirements for an 11,000 tons per day operation, with no level of contingency. The omission of ventilation system losses and water contained within the tailings pores significantly

affect the estimated free water balance for the mine. New Afton has continued to increase its throughput above the original mine plan resulting in an additional shortfall of water volume. The mine has applied to increase its licensed water allocation, however this is an ongoing project that faces many delays through the regulatory process.

NOMENCLATURE

r_s	settled dry density
SG	specific gravity
$e_s(T)$	saturation vapor pressure (hPa)
T	temperature (degrees Celsius)

REFERENCES

BGC Engineering Inc. (2013) *BGC Project Memorandum – New Afton Water Balance Model,* July 5, 2013

Budhu, M (2007), *Soil Mechanics and Foundations,* John Wiley & Sons, Inc. 2nd Edition, pp. 36.

Lawrence, M. G. (2005), *The Relationship between Relative Humidity and the Dewpoint Temperature in Moist Air – A Simple Conversion and Applications,* American Meteorological Society, February 2005, pp. 226.

Rescan Environmental Services (2007) *Application for a Permit Approving the Mine Plan and Reclamation Program Pursuant to the* Mines Act *R.S.B.C. 1996, C. 293*, January 2007

Use of Cemented Paste Backfill Based on Arsenic – Rich Tailings from Cyanidation

Roger Hamberg, Christian Maurice and Lena Alakangas
Department of Civil, Environmental and Natural Resources Engineering, Division of Geosciences and Environmental Engineering, Luleå University of Technology, Sweden

ABSTRACT

Gold is extracted by cyanide leaching from inclusions in arsenopyrite from a mine in the north of Sweden. The major ore mineral assemblage consists of pyrrhotite and arsenopyrite-loellingite. Effluents from the gold extraction are treated with $Fe_2(SO_4)_3$, with the aim to form stable As-bearing Fe-precipitates (FEP). The use of cemented paste backfill (CPB) is one alternative suggested for management of tailings. In CPB, tailings are commonly mixed with water (typically 25%) and low proportions (3-7 %) of binders and backfilled into underground excavated areas. Tailings containing As (1000 ppm) mainly as As-bearing FEP:s were mixed with low proportions (1-3 %) of biofuel fly ash(BFA), ordinary cement (CE) and water for the formation of a monolithic CPB-mass. Two mixtures were blended; CE with 1 wt. % of cement and CE-FA consisting 2 wt. % of CE and 1 wt. % of BFA. Unmodified tailings and CPB-monoliths were submitted to a tank leaching test (TLT) for comparison of the leaching behavior of As in the tailings and CPB-masses respectively. Results from the TLT showed that the inclusion of As-rich tailings into a cementitious matrix increased leaching of As. In CPB-mixtures, small (> 1%) proportions of As desorbed from FEP:s and were subsequently incorporated into less acid-tolerant species (i.e. Ca-arsenates and As bonded to cementitious phases). CE was least effective in As-immobilization; the As-release was related to pH and the dissolution of Ca-arsenates. In CE-FA, As-release followed the behavior of Si suggesting the incorporation of As with Calcium-Silicate-Hydrates (C-S-H) in the cementitious matrix. Unmodified tailings generated an acidic environment in which As-bearing FEP: s was stable. As-leaching increased in CPB-mixtures on a short-term basis, but buffering minerals in CPB-mixtures could decrease the oxidation rate of pyrrhotite, which in turn, stabilizes pH and the As-bearing FEP: s.

Keywords: Arsenic, Cemented Paste Backfill, Cyanidation

INTRODUCTION

Gold ores and concentrates containing arsenic minerals (i.e. arsenopyrite) are often refractory in nature, meaning the minerals need to be dissolved in order to release the associated gold. Arsenopyrite usually co-exists with other sulphide minerals such as pyrrhotite and pyrite. Arsenic does not form stable complexes with cyanide, but it is very soluble during cyanidation. Consequently; the slurry produced in this process must be treated to immobilize As before discharge into tailings facilities. Cemented paste backfill (CPB) is a method where tailings are converted into a monolithic mass by the addition of low proportions (3-7 %) of binders. CPB focuses on the minimization and/or enhancement of the quality of percolating water. CPB offers moreover a geotechnical support to underground mine cavities increasing operational benefits for the mining industry (Coussy *et al*., 2011). CPB is also used for backfilling of non-load bearing constructions or tailings dams where strength of the CPB-material is of less concern, but aims for the prevention of metal release and reduction of Acid mine drainage (AMD) remains. Immobilization of As in CPB-materials have been attributed to the formation of stable As-precipitates, the entrapment of As in the cementitious matrix by sorption onto calcium-silicate-hydrates (C-S-H) or substitution within the crystal lattice of secondary cementitious minerals (Coussy *et al*., 2011). The most common binder material used in CPB is cement. As amounts of tailings often exceed millions of tonnes, the cost of cement becomes substantial and many studies have been done to promote the usage of alternate materials in CPB. Granulated blast furnace slag (GBFS) and biofuel fly ash (BFA) have successfully been used for partial replacement of cement in CPB due to their pozzolanic and alkaline properties (Kim & Jung, 2011; Coussy *et al*., 2011). GBFS and BFA could neutralize acidity arising from sulphide-rich tailings and prevent trace element spread (Coussy *et al*., 2011). However, Bertrand (1998) showed that low proportions (0.9-6.8 %) of slag and cement could be insufficient to mitigate Acid Mine Drainage (AMD)-production long-term. It is believed that alkaline materials (fly ashes, slags) increases the mobility of As, but some contradictory results have shown a reduced mobility by the possible formation of stable Ca-As complexes (Hartley *et al*., 2004; Randall, 2012).

Cyanidation tailings slurries from As-enriched sulphide ores are often treated with lime, H_2O_2 and O_2 and $Fe_2(SO_4)_3$ to co-precipitate As (V) with Fe forming stable As-bearing Fe-precipitates (FEP) and to increase the pH to prevent generation of AMD. Within these treatment processes, precipitates with varying Fe/As-ratios could form. As-bearing FEPs with a Fe/As < 4 are assumed to be stable under oxidized conditions when pH 4-7 (Riveros et al., 2001). The pH stability range of As-bearing FEPs is broadened with increasing Fe/As ratios and precipitates with Fe/As ratios $\geqslant 8$ are stable over a wide pH range (3-8).Raising pH to alkaline levels may increase the risk for destabilization of As-bearing FEP. Previously conducted studies (Benzaazoua *et al*., 2004, Coussy *et al*., 2011; Randall, 2012; Coussy *et al*., 2012) have focused on the stability of arsenopyrite, scorodite or spiked As in natural or synthetic CPB. The stability of As-bearing FEP:s in CPB-materials has gained less attention. The purpose of this study was therefore to investigate the behavior of As in a CPB-material using the tank leaching test (TLT).

MATERIALS AND METHODS

Tailings were collected from a gold mine in the north of Sweden. The major sulfide minerals are pyrrhotite(6.5 wt. %)and arsenopyrite-loellingite(0.2 wt. %). The gold occurred primarily as inclusions in arsenopyrite (Sciuba, 2013). Tailings were treated with $Fe_2(SO_4)_3$, H_2O_2, $CuSO_4$ and

lime in order to form stable As-bearing FEP:s, and detoxify residual cyanides. Samples were collected at depths of 0-30 cm from ten different locations on the tailings dam and mixed to form a bulk sample of approx. 15 kg. Two types of binders were tested for the preparation of various paste mixtures: Portland cement (Ordinary Portland Cement also named CE) and biofuel fly ash (FA) provided from a biofuel incineration plant located in Lycksele, Sweden. Main elements and total contents of As and S in tailings, CE and CE-FA are presented in table 1.

Table 1 Main elements, total content of S and As in tailings, CE and CE-FA (n = 3, ± SD)

	Unit	Tailings	FA	CE
SiO_2	% of TS	55.0 ± 4.9	34.6 ± 1.3	20.6 ± 0.8
Al_2O_3	″	4.69 ± 0.04	10.7 ± 0.6	5.61 ± 0.45
CaO	″	4.83 ± 0.25	14.1 ± 1.0	50.3 ± 1.8
Fe_2O_3	″	16.7 ± 0.6	13.9 ± 1.0	2.81 ± 0.05
K_2O	″	0.92 ± 0.03	2.89 ± 0.08	0.83 ± 0.05
MgO	″	3.24 ± 0.01	2.54 ± 0.08	4.00 ± 0.17
MnO	″	0.14 ± 0.01	0.92 ± 0.03	0.10 ± 0.01
Na_2O	″	0.82 ± 0.03	1.24 ± 0.08	0.65 ± 0.07
P_2O_5	″	0.24 ± 0.01	2.25 ± 0.05	0.06 ± 0.00
TiO_2	″	0.18 ± 0.00	0.34 ± 0.01	0.42 ± 0.02
As	mg/kg TS	1070 ± 30	124 ± 5	10.2 ± 0.2
S	″	20933 ± 493	13700 ± 200	9960 ± 219

Speciation of As and S in tailings was assessed using the modified sequential extraction scheme described by Dold (2003) and suggested that a majority (95 %) of As in the tailings of Svartliden was associated with the Fe (III)oxy-hydroxides-fraction (Table. 2). The majority of S was associated with the water-soluble fraction and the primary sulphides fraction.

Table 2 Speciation of As and S in tailings from Svartliden, extraction scheme adopted from Dold (2003) (values in % of total content).

Fraction	Water soluble	Exchangeable	Fe(III) oxy-hydroxides	Fe(III) – oxides	Secondary sulphides	Primary sulphides	Residual
As	0.00	0.81	94.6	1.81	0.02	2.75	0.03
S	35.0	10.8	6.99	5.36	4.41	37.5	0.00

Preparation of the CPB-material

Tailings were mixed with the binders, and distilled water was slowly added to reach a solid percentage about 73-74 %. A water content of 26-27% in the CPB-mixtures is required for paste transportation through a pipe network. CPB-mixtures of CE, FA, water and tailings were poured into plastic bottles with a diameter of 5 cm and a height of 10 cm. A small hole was drilled in the bottom of each bottle before filling for the drainage of excess water. After filling, the bottles were sealed and cured for 28 days in 22°C in a moist environment. Two mixtures were prepared: CE, with the addition of 1 wt % ordinary portland cement (OPC) and CE-FA, with an addition of 2 wt % OPC and 1 wt % biofuel fly ash. Proportions of binders and tailings were adjusted to achieve required hardened strength characteristics of 200 kPa with a minimal addition of binders. Tests of unconfined compressive strength (UCS, curing time of 28 days) on the CPB-materials showed that the mechanical strength of CE and CE-FA were 207 kPa and 179 kPa respectively.

Tank leaching test (TLT)

The Dutch standard (EA NEN 7375:2004) was implemented. TLT consists of the leaching of a monolithic block. CPB-samples were taken out of the bottles after 28 days of curing and rectified into regular cylinders. CPB-monoliths were applied on plastic supports at 2 cm from the bottom of the tanks. Distilled water was thereafter filled to reach a level that ensured a 2 cm water head surrounding the CPB-sample and a liquid/solid (L/S) ratio fixed to 10cm^3 of solution/cm^2 of exposed solid for all samples. A reference sample consisting solely of tailings was used for the comparison of cemented and unmodified tailings. Tailings (reference) were placed in paper filter bags (1μm) recessed in nylon filters. Nylon filters were then hung up in the lids of the tanks. Duplicates were realized for each CPB-sample, a total amount of 6 samples were leached at the same conditions. Leachate was removed and replaced after 6h, 1day, 2.25 days, 4 days, 9 days, 16 days, 36 days and 64 days. Leachate was stirred manually before collection and analysis. The same volume of leachate was used for each renewal. Leachates were filtered through a 0.45-μm membrane filter followed by measurement of pH, Eh and conductivity and analyzed for total content. The mass transfer of As in tailings and CPB-materials was calculated according to (EA NEN 7375:2004):

$$M_{ti} = (C_i \times V_i) / A \qquad \text{(eq. 1)}$$

M_{ti} (in mg/m^2) is the calculated as mass of As released during a leaching period, i, C_i (mg/l) is the As concentration in the period i, V_i (L) is the leachate volume in period i and A is the specimen surface area exposed to the leachate (m^2). The apparent diffusion coefficient of As was determined using the logarithm of cumulative M_t until the i-th period, plotted vs. the logarithm of time. Modelling was conducted using PHREEQC, adapting the database developed by Blanc et al., (2014). Element concentrations from the leachate in the TLT were used for the identification of arsenic species.

Sample analysis

Concentrations of 31 elements were determined for solid samples of tailings, cement and biofuel fly ash with triplicate samples. The modified EPA method 200.7 (ICP-AES) and 200.8 (ICP-SMS) (US EPA, 1991) were used and performed by an accredited laboratory (ALS Scandinavia, Luleå, Sweden). Water samples from the TLT were analyzed by an accredited laboratory (ALS Scandinavia, Luleå, Sweden) to determine their elemental composition. Elements (As, Cd, Cr, Cu, Mn, Ni, P, Pb and Zn) were determined by ICP-SFMS while Al, Ca, Fe, K, Mg, Na and S were determined by ICP-AES. ICP-SFMS and ICP-AES analyses were performed using modified versions of EPA methods 200.8 and 200.7 (US EPA, 1991), respectively.

RESULTS

In TLT, the highest As concentrations released during a leachate renewal cycle were 41.3 mg/m^2 observed for CE, 13.7 mg/m^2 for CE-FA and 1.6 mg/m^2 for tailings. The cumulative release of As is most pronounced in CE (101.5 mg/m^2), and least in tailings (5.3 mg/m^2). Leaching of As from tailings descends troughout the test but has an increasing trend in both CPB-mixtures (CE and CE-FA). The release of Fe was more than a 100-fold larger in tailings compared to that in the CPB-materials. The evolution of Si and As were closely related in CE-FA but showed less or no correlation in CE and tailings (Fig.1).

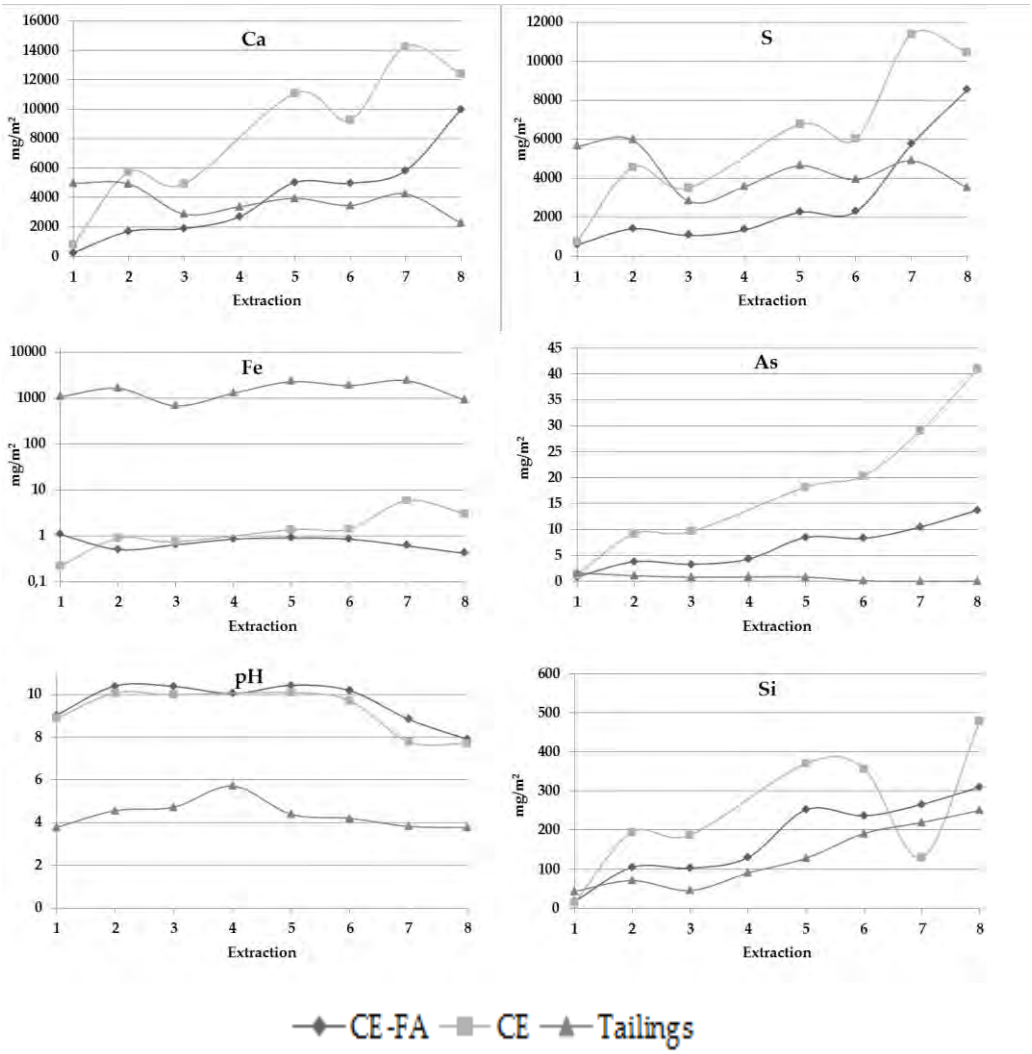

Figure 1 Evolution of pH, S, Ca, Fe, As and Si in tailings, CE and CE-FA during TLT.

For As dissolving from the surface and for the short initial release of surface-deposited As (surface wash-off), the graph slopes (r_c) are expected to be <0.4. In the case of a diffusion control mechanism, this plot is expected to be a straight line with a slope of 0.4–0.6 (EA NEN 7375:2004).

Table 3 Mass transfer mechanisms in tailings and CPB-materials during TLT

Mix	Cumulative As mg/m²	r_c	Mechanism
Tailings	5.5 ± 0.7	0.21 ± 0.09	Wash-off
CE	98 ± 4	0.62 ± 0.01	Diffusion
CE-FA	53 ± 0	0.46 ± 0.13	Diffusion

According to calculations based on the standard of (EA NEN 7375:2004), the mechanisms for As-leaching was a wash-off-effect in tailings and an effect of diffusion in the CPB-materials (Table. 3).

DISCUSSION

The cumulative release of As was highest in CE (98 ± 4 mg/m^2), followed by CE-FA (53 ± 0 mg/m^2) and comparatively less in tailings (5.5 ± 0.7 mg/m^2). Oxidized conditions prevailed in CE, CE-FA and tailings throughout the test and became more oxidizing with time.

As-leaching in tailings during TLT

The As-release was low in tailings during TLT and pH varied from 3.8-5.7. Previously conducted sequential extraction tests suggest that the majority of As was associated with FEP (Table. 2). Calculations in accordance to the TLT-standard suggested that leaching of As in tailings was predominately a wash-off-effect (Voglar and Leštan, 2013). In alkaline conditions during cyanidation, As-sulfides are oxidized to arsenite and arsenate in the presence of oxygen. The proportion of each species is dependent on solution composition, redox potential and pH. Release of As was initially higher from the tailings than from the CPB-materials. This could be due to the presence of As (III) in tailings pore water that was suggested by modeling. The presence of As (III) could be due to insufficient pre-oxidation of As (III) to As (V) during treatment processes.

FEP:s could become unstable at pH < 4, releasing adsorbed As into solution. The As-release was descending from the 2nd extraction in the TLT when pH was 5.7 -3.8 (Fig. 1). In the middle of the TLT-test, a reddish crust appeared on the tailings surface. This crust was assumed to be a Fe-precipitate that might decrease the permeability and weathering ability. The newly formed crust of Fe-precipitates could provide additional surfaces amenable for As-adsorption obstructing further As-release. The ability of FEP for adsorbing As (V) could be reduced due to competition of sorption surfaces by high concentrations of SO_4^{2-} in the leachate (Frau et al., 2010). The negative effect of SO_4^{2-} on the adsorption of As onto FEP could potentially be counteracted by the co-adsorption of Ca^{2+}, which may function as a multi-absorbent for As at pH values of 4-6 (Jia and Demopoulos, 2005).

As-leaching in CPB-materials (CE and CE-FA) during TLT

Initially, the cementation has decreased leaching of Ca, S, Fe, As and Si. According to modeling, As-release in the CPB-materials was governed by As (V) and Ca-arsenates. Initial release of As (III) in tailings could have been hindered by the addition of binder materials such as cement and fly ash which promotes the oxidation of As (III) to As (V) (Moon *et al*., 2008). Calculations in accordance to the TLT-standard suggested that leaching of As in CPB-materials is predominately an effect of diffusion (Table 3). A physical entrapment of As into the cementitious matrix could hinder the effect of As-diffusion in the CPB-materials. The hydration of pozzolanic additives under alkaline conditions forms secondary growths of calcium silicate hydrates (C-S-H). These C-S-H-products serve to improve the microstructure of CPB, leading to lower porosity and permeability mainly due to mineral precipitation (Benzaazoua *et al*. 1999; Hassani *et al*. 2001). The permeability of a CPB-material could increase due to a phenomenon called sulfate attack where sulfates react with Ca-ions forming swelling secondary phases such as gypsum. The volume of C-S-H: s could also be far in excess of the available pore volume and cause internal stress and subsequent micro-cracks increasing permeability in the CPB-material (Fall & Benzaazoua, 2005).

For CE-FA-samples, As release follows the behavior of Si. Arsenic may then have been incorporated into the matrix of (C-S-H) as suggested in Coussy *et al*., (2011). In CE-FA where pH varies from 10.5 to 8.0, all hydrated cement phases were assumed to have been dissolved (Ayora *et al*., 1998). The content of soluble S-species in tailings (approx. 11,000 ppm, Table. 2) increases the risk for a sulfate

attack to occur within the CPB-material (Fall & Benzaazoua, 2005). However, CE-FA includes BFA and Hassani *et al*. (2001) suggested that mixtures of fly ashes and cement in CPB-materials are more resistant to sulfate attack than cement alone.

The mechanisms of As-release in CE differed from the mixture of CE-FA. The As-release in CE was less correlated to the behavior of Si and increased more strongly as pH decreased from 10 to 8. The point of zero charge (PZC) for As-bearing FEP: s occurs at a pH≈8.3. Alkaline conditions (pH: 7.7-10.4) in CE suggested that As has been desorbed from FEP: s and re-precipitated as Ca-arsenates. In alkaline conditions observed in the CPB-materials, As (V)-species of $HAsO_4^{2-}$ and AsO_4^{3-} are the most probable As-species (Smedley & Kinniburgh, 2002). These anions could react with calcium ions in the pore water forming Ca-arsenates according to reactions 1 and 2 (Ahn *et al*., 2003):

$$HAsO_4^{2-} + Ca^{2+} + nH_2O \rightarrow CaHAsO_4 \cdot nH_2O \quad (1)$$

$$2AsO_4^{3-} + 3Ca^{2+} + nH_2O \rightarrow Ca_3(AsO_4)_2 \cdot nH_2O \quad (2)$$

Ca-arsenates formed in pH > 10, are highly soluble at lower pH (Benzaazoua *et al*., 2004). The presence of Ca-ions in the pore water could however increase the surface charge density of the FEP: s increasing their capacity for As (V)-adsorption. This effect is most evident at pH: s of 8-10 (Wilkie & Hering, 1996). The addition of binders lowered Fe-leaching, alkaline environments could enhance the precipitation of FEP: s forming crusts on the sulfide surfaces. These crusts form rapidly under alkaline conditions, creating a thin permeable coating obstructing the minerals' further oxidation (Belzile *et al*., 2004, Asta *et al*., 2013).

Leaching of As in the CPB-mixtures was most prominent when pH fell from 10 to 8 in the end of the TLT. This is probably due to a physio-chemical effect where cementitious phases sensitive to a pH-decrease have dissolved enabling more water to percolate through the monolith. More arsenic was released from CE. Increasing the binder-proportion will not necessary increase the strength of the material, but more swelling minerals could form and decrease the permeability.

Future aspects concerning the use of CPB on As-rich tailings from cyanidation

Most of the As in the tailings were present as As-bearing FEP: s which constituted approximately 95 % of the total As. Arsenic in these precipitates is sensitive to reductive, extreme acidic or alkaline environments. Arsenic dissolutions under reductive environment may contribute to the As release into solution when the management of tailings are not adequately designed. Although, results from the tailings TLT showed that As–bearing FEPs may be stable under acidic and oxidizing conditions common to the tailings piles, more extensive pyrrhotite oxidation generating extreme acidic conditions may increase As-leaching on a long term basis.

Results from TLT suggested that the addition of binders may increase As-leaching on a short term basis. However, the addition of binders increased the tailings' acid-neutralizing capacity and introduced more Ca-ions and Fe precipitates into the tailings matrix, both of which may facilitate the immobilization of As and reduce the potential for sulfide oxidation. Another positive effect originating from the formation of a monolithic mass is that the high degree of saturation in the material reduces the intrusion of oxygen and water percolation. Pyrrhotite oxidation is not obstructed, but in alkaline conditions, Fe may precipitate on the surfaces of sulfide grains retarding its further oxidation. The addition of binders may, therefore, have a positive effect on the stability of As-bearing FEP: s on a long term basis.

CONCLUSIONS

The inclusion of As-rich tailings into a cementitious matrix increased leaching of As. Alkaline conditions in CE and CE-FA during TLT caused a small proportion of As to desorb from As-bearing FEP: s. Desorbed As could then have been incorporated into the cementitious matrix and/or re-precipitated as Ca-arsenates. Leaching of As in CE-FA followed the behavior of Si, which implies that the dissolution of cementitious phases governed the As-release. The mechanism of As-leaching in CE differed from that in CE-FA. Leaching of As in CE increased more strongly as pH decreased from 10 to 8, suggesting the formation of Ca-arsenates. As-bearing FEP: s was stable in tailings where pH was 3.8-5.7, leaching of As was low and descended during TLT. The addition of binders could have a positive effect of As-leaching long-term due to increased acid-neutralizing capacity and higher proportions of FEP: s. This, in turn, could facilitate As-adsorption and decrease the sulfide oxidation capacity.

ACKNOWLEDGEMENTS

Financial support from Ramböll Sverige AB, Ramböll Foundation and the Center of Advanced Mining and Metallurgy (CAMM) at Luleå University of Technology are gratefully acknowledged. The personnel at Dragon Mining AB are also gratefully acknowledged for valuable information about the mining processes and for providing the tailings needed for this study.

REFERENCES

Ahn, J. S., Chon, C. -., Moon, H., & Kim, K. (2003). Arsenic removal using steel manufacturing by-products as permeable reactive materials in mine tailing containment systems. Water Research, 37(10), pp. 2478-2488.

Asta, M. P., Pérez-López, R., Román-Ross, G., Illera, V., Cama, J., Cotte, M. & Tucoulou, R. (2013). Analysis of the iron coatings formed during marcasite and arsenopyrite oxidation at neutral-alkaline conditions. Geologica Acta, 11(4), pp. 465-481.

Ayora, C., Chinchón, S., Aguado, A., & Guirado, F. (1998). Weathering of iron sulfides and concrete alteration: Thermodynamic model and observation in dams from central Pyrenees, Spain. Cement and Concrete Research, 28(9), pp. 1223-1235.

Bark, G., & Weihed, P. (2007). Orogenic gold in the new Lycksele-Storuman ore province, northern Sweden; the Palaeoproterozoic Fäboliden deposit. Ore Geology Reviews, 32(1-2), pp. 431-451.

Benzaazoua, M., Marion, P., Picquet, I., & Bussière, B. (2004). The use of pastefill as a solidification and stabilization process for the control of acid mine drainage. Minerals Engineering, 17(2),pp. 233-243.

Benzaazoua, M., Quellet, J., Servant, S., Newman, P., & Verburg, R. (1999). Cementitious backfill with high sulfur content physical, chemical, and mineralogical characterization. Cement and Concrete Research, 29(5), pp. 719-725.

Belzile, N., Chen, Y., Cai, M. & Li, Y. (2004). A review on pyrrhotite oxidation. Journal of Geochemical Exploration, 84(2), pp. 65-76.

Bertrand V.J. (1998)A study of the pyrite reactivity and the chemical stability of cemented paste backfill. Master Thesis, the University of British Colombia, Ottawa, Canada

Blanc, P., Lassin, A., Nowak, C., Burnol, A., Piantone, P., & Chateau, L. (2014) THERMODDEM: a thermo-dynamic database for waste materials. BRGM institute (french geological survey), Orléans, France.

Coussy, S., Benzaazoua, M., Blanc, D., Moszkowicz, P., & Bussière, B. (2011). Arsenic stability in arsenopyrite-rich cemented paste backfills: A leaching test-based assessment. Journal of Hazardous Materials, 185(2-3), pp. 1467-1476.

Coussy, S., Benzaazoua, M., Blanc, D., Moszkowicz, P., & Bussière, B. (2012). Assessment of arsenic immobilization in synthetically prepared cemented paste backfill specimens. Journal of Environmental Management, 93(1), pp. 10-21.

Coussy, S., Paktunc, D., Rose, J., & Benzaazoua, M. (2012). Arsenic speciation in cemented paste backfills and synthetic calcium-silicate-hydrates. Minerals Engineering, 39, pp. 51-61.

Dold, B. (2003). Speciation of the most soluble phases in a sequential extraction procedure adapted for geochemical studies of copper sulfide mine waste. Journal of Geochemical Exploration, 80(1), 55-68.

EA NEN 7375:2004, Leaching characteristics of moulded or monolithic building and waste materials, Determination of leaching of inorganic components with the diffusion test, The tank test, 2004.

Fall, M., & Benzaazoua, M. (2005). Modeling the effect of sulphate on strength development of paste backfill and binder mixture optimization. Cement and Concrete Research, 35(2), pp. 301-314.

Frau, F., Addari, D., Atzei, D., Biddau, R., Cidu, R., & Rossi, A. (2010). Influence of major anions on As(V) adsorption by synthetic 2-line ferrihydrite. Kinetic investigation and XPS study of the competitive effect of bicarbonate. Water, Air, and Soil Pollution, 205(1-4), pp. 25-41.

Hartley, W., Edwards, R., & Lepp, N. W. (2004). Arsenic and heavy metal mobility in iron oxide-amended contaminated soils as evaluated by short- and long-term leaching tests. Environmental Pollution, 131(3), pp. 495-504.

Hassani, F. P., Ouellet, J., & Hossein, M. (2001). Strength development in underground high-sulphate paste backfill operation. CIM Bulletin, 94(1050), pp. 57-62.

Jia, Y., & Demopoulos, G. P. (2005). Adsorption of arsenate onto ferrihydrite from aqueous solution: Influence of media (sulfate vs nitrate), added gypsum, and pH alteration. Environmental Science and Technology, 39(24), pp. 9523-9527.

Kim, J., & Jung, M. C. (2011). Solidification of arsenic and heavy metal containing tailings using cement and blast furnace slag. Environmental Geochemistry and Health, 33(SUPPL. 1), pp. 151-158.

Mollah, M. Y. A., Kesmez, M., & Cocke, D. L. (2004). An X-ray diffraction (XRD) and fourier transform infrared spectroscopic (FT-IR) investigation of the long-term effect on the solidification/ stabilization (S/S) of arsenic(V) in portland cement type-V. Science of the Total Environment, 325(1-3), pp. 255-262.

Moon, D. H., Wazne, M., Yoon, I. -., & Grubb, D. G. (2008). Assessment of cement kiln dust (CKD) for stabilization/solidification (S/S) of arsenic contaminated soils. Journal of Hazardous Materials, 159(2-3), pp. 512-518.

Randall, P. M. (2012). Arsenic encapsulation using portland cement with ferrous sulfate/lime and terra-bond™ technologies - microcharacterization and leaching studies. Science of the Total Environment, 420, pp. 300-312.

Smedley, P. L., & Kinniburgh, D. G. (2002). A review of the source, behaviour and distribution of arsenic in natural waters. Applied Geochemistry, 17(5), pp. 517-568.

US EPA (1991). Methods for the determination of metals in environmental samples. US Environmental Protection Agency, Office of Research and Development, Washington, DC, EPA/600/4-91/010

Voglar, G. E., & Leštan, D. (2013). Equilibrium leaching of toxic elements from cement stabilized soil. Journal of Hazardous Materials, 246-247, pp. 18-25.

Wilkie, J. A., & Hering, J. G. (1996). Adsorption of arsenic onto hydrous ferric oxide: Effects of adsorbate/adsorbent ratios and co-occurring solutes. Colloids and Surfaces A: Physicochemical and Engineering Aspects, 107, pp. 97-110.

10th ICARD IMWA 2015 | 10th International Conference on Acid Rock Drainage & IMWA Annual Conference

From Salt Balance to Contaminant Flux: Managing Water Quality Risk Using a Systems Approach

Terry Harck
Solution[H+], South Africa

ABSTRACT

We used a salt balance to describe contaminant transfer within a mine water system. The system included mine workings, mineral processing plants, water storages (both clean and dirty), and tailings storage facilities as components. Analysis of modelling results identified sub-systems associated with potential water quality risks. In particular, approximately 6 000 tonnes of dissolved salts associated with the tailings component could not be accounted for. Under the prevailing regulatory regime, this could be a significant water quality risk. However, the fragmented monitoring network and poorly characterised hydrogeology was not able to resolve the magnitude of the risk.

The cost of developing a tailings source term was significantly less than the cost of upgrading the groundwater monitoring network. Therefore, the tailings sub-system was characterised in detail. This involved collecting tailings process water and drain samples. We also collected tailings samples from various depths in the facility. Geochemical and hydraulic analysis of the tailings allowed an indicative source term to be developed. This quantified the contaminant flux through the tailings during deposition and after closure.

During the operational phase approximately 1 000 tonnes per year of dissolved salts actually leaves the tailings as seepage through the footprint. The residual salt mass leaves the tailings at the rate of approximately 250 tonnes per year once the tailings have desaturated.

The improved resolution of the tailings sub-system indicated that the tailings are a sink for dissolved salts in the mine water system. The fine particle size and low permeability of the tailings under compaction, is a natural mitigation that limits the rate of salt release. Therefore, the magnitude of the water quality risk was found to be moderate

Keywords: Salt balance, source term, tailings, water balance, drainage

INTRODUCTION

Two of the most important and fundamental tools of mine water management are water and salt balances (DWAF, 2006). Water distribution systems on mines are developed ad hoc in response to demand. Therefore, they include inherent inefficiencies, which lead to excessive water consumption and often unnecessary increases in dissolved solids. The goal of water and salt balances is to improve efficiency and water quality. However, the uncoordinated and independently led aspects of a mine water system overlap in a formidable way. As Ramo and St Clair (1998) put it: "it is like knitting with a tangled ball of yarn. It must be untangled before we try again to make the sweater".

The systems approach is a means of applying common sense (Ramo and St Clair, 1998). It is a tool for solving challenges in all spheres of human endeavour. Of course, the solutions typically involve interaction of previously self-directed groups of people and unprecedented flow of resources and information. Naturally, the solution is a considerable change from the present and past way of doing things.

A multi-disciplinary team has been assisting a South African platinum mining company in developing, refining and applying a detailed water balance. The team developed a water balance for a mine water system consisting of dozens of mine shafts and associated underground workings, multiple water storages (both clean and dirty), several mineral processing plants and associated tailings storage facilities (TSFs). The mining operation is located in the western limb of the Bushveld Igneous Complex. The team has "untangled the yarn" and assisted the mining company in "knitting a new sweater" out of their water distribution system. This paper describes one aspect of the work conducted. Specifically, it addresses the question of salt movement at TSFs.

METHODOLOGY

An annual water balance was developed for the operation by considering measured and estimated/calculated inflows and outflows from defined water management units (WMUs) according to the methodology of DWAF (2006). Each WMU is an individual sub-system of the larger mine water distribution system. To determine salt loads in circuit, chloride concentrations were obtained from four sources:

- The environmental monitoring programme, consisting of a database containing analytical results of samples collected from May 1995 to July 2012;
- Drinking water and service water quality analyses from March 2012 and June 2012;
- Tap water analyses from sampling conducted in May and June 2012; and
- Analyses from sampling conducted in June 2012.

Calculation of unmeasured chloride loads was conducted by determining the difference between input and output loads for each water management unit according to the methodology of DWAF (2006). Assuming that inputs equal outputs yielded the unmeasured chloride load by difference. Clearly, this is only valid for a chemical component that behaves conservatively within the mine water system.

Due to lack of data, seepage and interstitial water storage in TSFs were combined into one flow in the water balance. The salt mass balance calculated using water quality data and water balance flows revealed that the input salt load to most of the TSF sub-systems was greater than the output

load. To maintain salt mass balance a new output was added representing the salt load presumed to be lost in seepage (Figure 1).

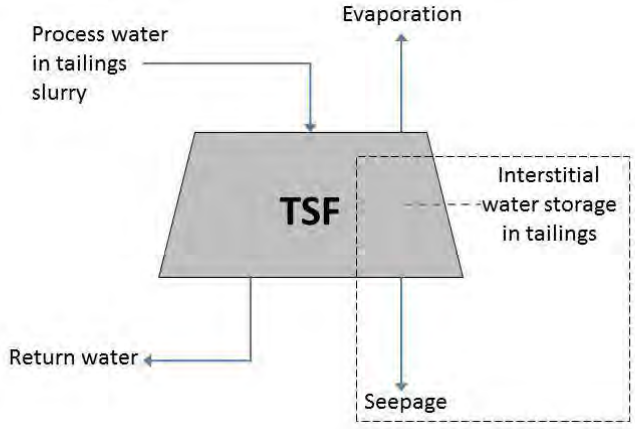

Figure 1 Schematic of the TSF water balance sub-system

The "seepage and interstitial" flow component was found to account for nearly half of chloride mass lost in the TSF sub-system (Table 1). However, the chloride mass of the seepage component could not be resolved from the available data. This was a question of considerable significance to the mining company. South African legislation makes it illegal to contaminate local water resources. Seepage from the TSFs could affect downstream water resources and potentially incur an environmental liability.

Table 1 Summary of water balance and calculated chloride mass balance for a selected TSF

Inputs	**Flow (m^3/a)**	**Cl mass (t/a)**	**Outputs**	**Flow (m^3/a)**	**Cl mass (t/a)**	**% diff**
Tailings slurry water from processing plants	3 670 038	1 703	Seepage, evaporation, interstitial losses	1 835 019	795	
			Return water	1 959 557	909	
Subtotals	**3 670 038**			**3 794 576**		**3.3**
		1 703			**1 704**	**0.1**

At the time, the mine was upgrading a fragmented water monitoring network and developing a more complete understanding of the local hydrogeology. Therefore, environmental monitoring data were unable to confirm the presence of a contaminant plume from the TSF, let alone its significance. Rather than incur the cost of additional monitoring wells, the mining company decided to establish a source term to resolve the seepage component of chloride losses from the TSF.

A source term describes the flux of contaminant mass emitted from a source. It is required for groundwater contaminant transport modelling and consists of a numerical description of the mass of contaminant emitted per unit time. The following tasks were conducted:

- Collect samples – augered from tailings, water samples
- Analyse samples – geotechnical characteristics, geochemical characteristics
- Develop source term from geochemical modelling of seepage quality coupled with estimates of seepage volume from the tailings

Sampling

Tailings samples were collected from auger holes bored into 12 locations on the top surface of the TSF using a portable, hydraulically-powered auger. Tailings samples were collected at 1.5 m intervals from each hole. Mixtures of tailings and distilled water at a ratio of 1:2 were made for each sample in the field and pH and EC measured using a calibrated Hanna HI98130 handheld meter. Twelve samples for laboratory analysis were selected based on the pH/EC profile results.

Water samples were collected from TSF drains 18, 32 and 54 on the perimeter of the TSF.

A drum was filled with slurry from a discharge point. The suspended tailings were allowed to settle and a sample of the tailings supernatant water was obtained. All water samples and the tailings supernatant were filtered by syringing the water through 0.45 μm polycarbonate membrane cartridges. A separate sub-sample for metals analysis was preserved with 2 mL of laboratory-grade nitric acid. All water samples were kept at 4°C from sampling to delivery at the laboratory. Samples were delivered to the laboratory the same day as collected.

Analysis

The analytical programme was conducted by a South African National Accreditation System (SANAS) certified laboratory.

Sixteen water samples were analysed including:

- Tailings drain samples (3)
- Tailings supernatant sample (1)
- Tailings sample leachates (12) obtained according to the modified ASTM D3987 method using deionised water at a liquid:solid ratio of 4:1.

All water samples were analysed for the following:

- Physico-chemical parameters (pH, Conductivity, Total dissolved solids (TDS), Alkalinity titration)
- Major anions (F, Cl, SO_4, NO_3)
- Cations (Na, K, Ca, Mg, Al, Fe, Mn, Cu, Pb, Zn, Cr, and others)

Twelve samples of tailings were analysed for the following:

- Mineral identification (by x-ray diffraction (XRD) or microscope petrography)
- Whole element analysis (by acid digestion and chemical analysis of the digest)
- Particle size distribution
- Saturated hydraulic conductivity
- Moisture content

Due to technical difficulties, unsaturated hydraulic conductivity was not measured. Generally, these results would inform numerical modelling of the long-term post-closure moisture content and seepage rate from the TSF. However, numerical seepage modelling was excluded from the scope of work due to time constraints.

Methodology

The analytical results were used to estimate tailings seepage quality during the operational phase of the TSF and post-closure. Interstitial water quality in the tailings during the operational phase, and hence seepage quality was estimated from the drain water quality. The post-closure seepage quality was estimated from the tailings leachates. PHREEQC (Parkhurst and Appelo 1999) was used to correct for dilution using the measured moisture content and mineralogy as inputs. Post-closure seepage rate were estimated from the saturated hydraulic conductivity results on the tailings samples.

RESULTS AND DISCUSSION

Water at Drain 18 appeared to be affected by local reducing conditions and is not considered to indicate the general quality of interstitial water in the tailings seepage (Table 2).

Table 2 Summary of water analysis results for the selected TSF

Parameter	DRAIN 18	DRAIN 54	DRAIN 32	SUPERNATANT
pH [s.u.]	10	8.1	8.1	7.4
EC [mS/m]	348	307	370	353
TDS	2400	2000	2600	2500
Alkalinity as $CaCO_3$	220	70	55	70
HCO_3	268.23	85.35	67.06	85.35
CO_3	66	0	0	0
Cl	564	530	481	352
NO_3	<0.1	6.5	<0.1	273
SO_4	1460	913	1440	835
F	0.26	<0.05	<0.05	0.09
Na	358	295	439	295
K	60	55	74	56
Ca	306	242	303	227
Mg	0.63	50	172	71
Al	0.27	<0.02	<0.02	<0.02
Fe	0.97	0.09	0.11	<0.05
Hg	0.0002	<0.0001	<0.0001	<0.0001

Chloride concentration in TSF seepage was estimated to be 433 mg/L based on the salt balance. This contrasts with the median chloride concentration of 506 mg/L in water from Drain 54 and Drain 32 (Table 2) and the chloride concentration of 352 mg/L in tailings supernatant. Equilibrium geochemical modelling of the water qualities indicates:

- Tailings supernatant is in equilibrium with calcium carbonate and aluminium hydroxide while being supersaturated with iron hydroxide.

- Water in contact with the tailings (Drain 54, Drain 32) becomes supersaturated with calcium carbonate, presumably from an increase in carbon dioxide partial pressure at depth in the tailings.
- Drain water is more concentrated than tailings supernatant and suggests a water loss of between 20% and 40% between the penstock pool and the drains.

Major ion proportions indicate that the supernatant and drain samples are compositionally similar (Figure 2). However, the compositions of the tailings leachates are significantly different (Figure 2 and Table 3).

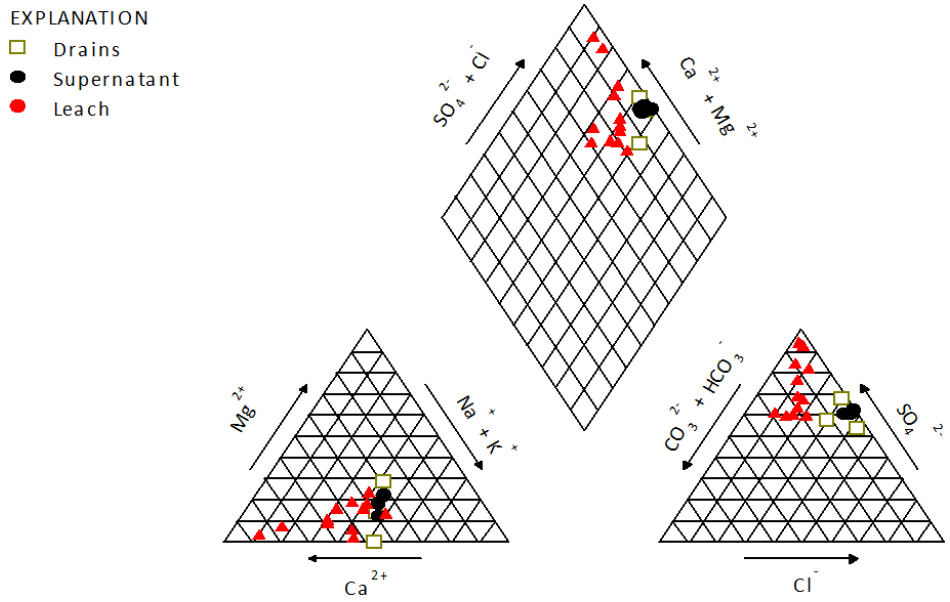

Figure 2 Piper diagram illustrating major ion composition of tailings leachates and water

Table 3 Summary of tailings leachate composition for the selected TSF

Parameter	T1	T2	T3	T4	T5	T6	T7	T8	T9	T10	T11	T12
pH	9.6	8.9	9.1	8.6	8.8	9	8.9	9.1	8.8	9.1	8.9	8.8
EC	27	30	22	114	40	22	31	19	34	22	35	134
TDS	132	150	104	844	250	134	178	88	202	114	192	1076
Alkalinity as $CaCO_3$	30	22	19	30	24	33	<12	27	30	27	33	43
HCO_3	20.3	22.6	17.1	31	25.2	33.5	12.0	26.4	32	25.8	34.1	41
CO_3	4.5	1.0	1.2	0.9	1.0	1.9	0.6	1.8	1.2	1.8	1.6	1.9
Cl	14	10	13	22	9.5	7.4	13	10	21	12	18	16
NO_3	<0.1	0.5	2.4	<0.1	3.2	5.9	2.5	<0.1	12.	1.4	<0.1	<0.1
SO_4	71	101	47	602	166	60	116	53	109	58	112	770
F	0.11	0.09	0.08	0.17	0.1	0.13	0.08	0.08	0.13	0.16	0.13	0.19
Na	15	15	12	26	16	9.1	11	7.1	17	11	18	20
K	3.9	5.3	6.4	15	6.8	4.1	6.1	3.3	8.5	5.2	7.8	14
Ca	18	15	10	135	32	13	24	13	20	12	24	189
Mg	0.39	5.6	2.2	7.8	2.7	3.1	2.4	2.3	4.3	3.2	1.6	3.6
Al	0.02	0.05	0.18	<0.02	<0.02	0.07	0.02	0.05	0.04	0.11	0.05	<0.02
Fe	0.09	0.08	0.22	<0.05	<0.05	0.06	<0.05	<0.05	0.06	0.11	<0.05	<0.05

Plagioclase, pyroxene, chromite are present in all samples which is consistent with the mineralogy of the platinum ore. Amphibole is also associated with the ore and is present in all but two samples.

Particle size distributions indicate that the tailings particles are in the range 0.001 mm to 0.85 mm (Figure 3). This classes the particles as silt or fine sand. The distribution for all samples is generally similar.

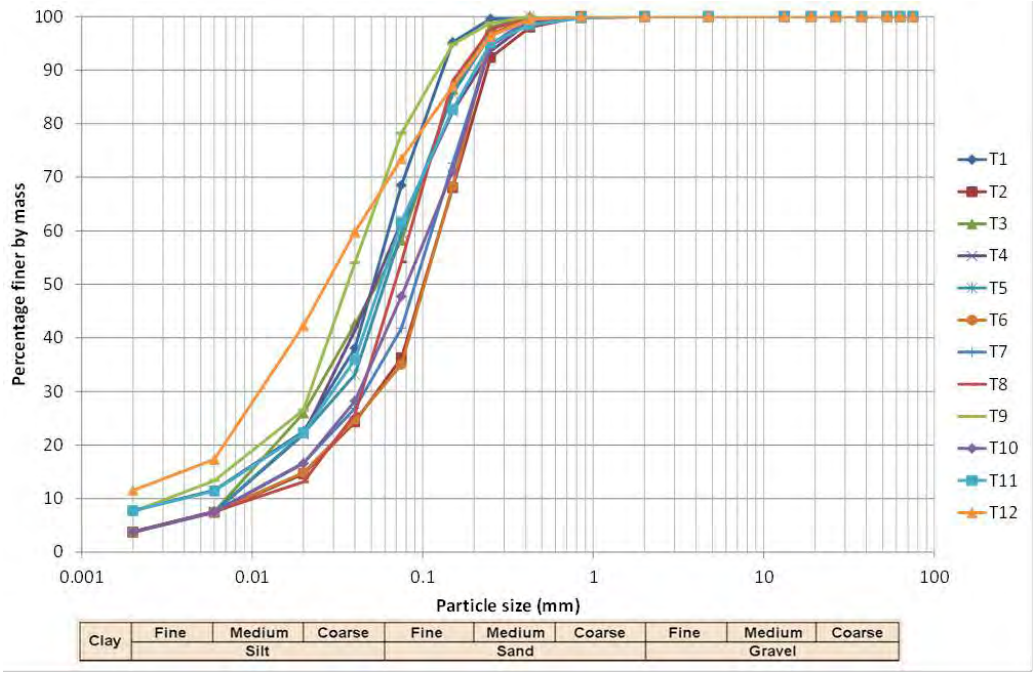

Figure 3 Tailings grain size

Saturated hydraulic conductivity of the tailings samples was directly measured by the laboratory at confining pressures of 50 kPa, 100 kPa, and 200 kPa. The median values were 1.15×10^{-7}, 5.85×10^{-8}, and 1.85×10^{-8} m/s respectively, showing a trend of decreasing hydraulic conductivity with increasing confining pressure. Median moisture content of the tailings samples was found to be 10%.

The TSF water balance indicates that seepage and interstitial losses in the tailings amount to 1 835 019 m^3 per year on average. Over a TSF footprint area of 119 ha this volume suggests that the effective hydraulic conductivity of the tailings is 5×10^{-8} m/s. This is consistent with the 10^{-8} to 10^{-7} m/s range in hydraulic conductivity expected in silt-sized material and is generally in agreement with the physical characterisation of the tailings conducted in this study.

Estimated confining pressure at the base of a 30 m column of saturated tailings ranges from 191 kPa to 272 Kpa with a median of 238 kPa. This is greater than the 200 kPa applied in the laboratory. Considering the trend of decreasing hydraulic conductivity with increasing confining pressure, a hydraulic conductivity of the order of 10^{-8} m/s or lower may prevail at the base of the tailings. Applied over the tailings footprint, this yields an annual seepage volume of 375 278 m^3.

After closure and draining of excess water, the tailings would eventually achieve equilibrium between the rate of rainfall recharge and moisture loss. Unsaturated conditions would prevail in the tailings and the actual rate of seepage through the footprint will be a function of tailings moisture content and the unsaturated hydraulic conductivity. As a rule of thumb, unsaturated hydraulic conductivity is one or more orders of magnitude less than saturated hydraulic conductivity. Therefore, for the selected TSF, unsaturated hydraulic conductivity would be at most 10^{-9} m/s. This yields an estimated post-closure seepage rate of less than about 37 528 m^3/year.

The TSF drain water is an indicator of seepage quality during the operational phase of tailings deposition. The median chloride concentration of samples DRAIN32 and DRAIN54 is 506 mg/L.

The leach tests on tailings samples indicate the results of interaction between the tailings and water. Therefore, they are a starting point for assessing the results of rainfall infiltrating the tailings after closure. However, the liquid to solid ratio in the TSF after closure is likely to be considerably lower than the 4:1 ratio used in the leach tests. Based on the laboratory moisture results, a liquid to solid ratio of 1:10 appears more likely.

The geochemical modelling code PHREEQC (Parkhurst and Appelo 1999) was used to simulate the removal of water from the test leachates in contact with the minerals gibbsite, barite, calcite, chromite and hematite (**¡Error! No se encuentra el origen de la referencia.**). A CO_2 partial pressure of 10^{-2} atm was applied to simulate conditions deep in the tailings.

Table 4 Summary of modelled post-closure seepage quality for the selected TSF

Parameter	Min	Median	Max
pH [s.u.]	6.8	7.2	7.4
Total dissolved solids	4 203	7 187	32 386
Alkalinity as $CaCO_3$	101	218	349
HCO_3	75	197	324
CO_3	0.05	0.33	0.87
Cl	308	540	915
NO_3	12	168	2 184
SO_4	1 490	3 051	12 557
F	1.80	3.37	5.51
Na	295	623	1 080
K	1 086	2 071	10 951
Ca	111	371	7 146
Mg	16	120	324
Al	0.56	0.88	1.32
Fe	nd	nd	nd

Graphical representation of the time varying seepage rate and seepage quality (as chloride concentration) from the TSF footprint is shown in Figure 4. The product of these two quantities yields the mass of chloride entering the groundwater system beneath the tailings. The duration of

the operational phase has been assumed to be 20 years, followed by approximately 20 years of dewatering.

Based on the outcome of this assessment, the chloride mass entering the groundwater is 190 tonnes/year during the operational phase. This decreases to 20 tonnes/year after closure (Figure 4). This contrasts with the combined seepage and interstitial estimates of 795 tonnes per year from the salt balance.

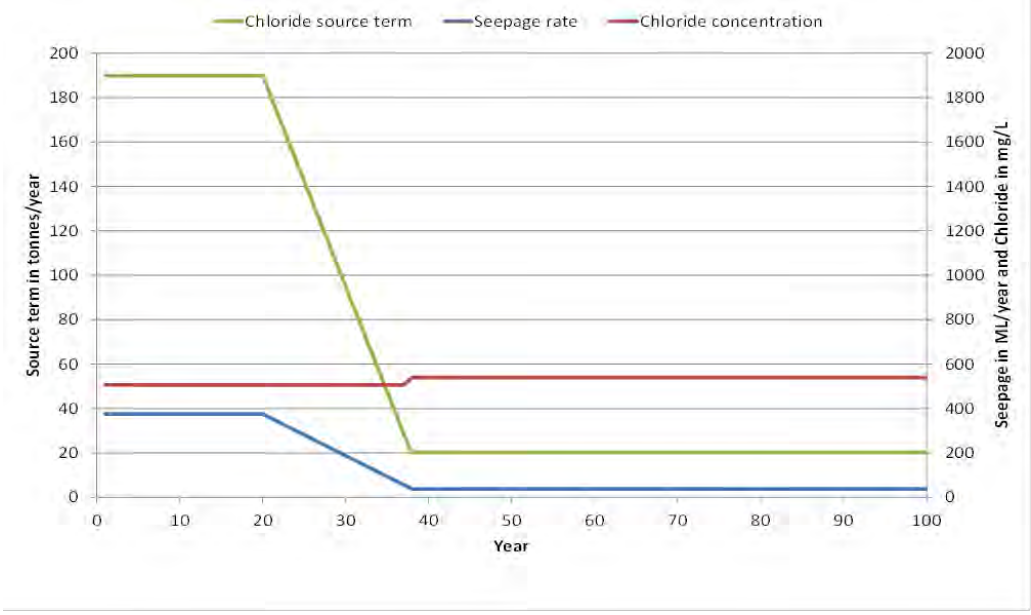

Figure 4 Source term for the selected TSF

CONCLUSION

Physical characterisation of tailings material from the selected TSF has allowed seepage through the TSF footprint to be estimated. This was calculated as 37 528 m^3/year during the operational phase, decreasing to 3 753 m^3/year after the tailings have desaturated post-closure.

Tailings seepage quality during post-closure can be geochemically modelled from drain water quality and leach test results. Considering the mineral assemblage in the tailings and the tailings moisture content, chloride concentrations vary from 506 mg/L during the operational phase to 540 mg/L after closure.

The source term combining the seepage rate and seepage quality indicates that the tailings are a sink for dissolved salts. During the operational phase 5 960 tonnes per year of dissolved solids are placed on the selected TSF. However, 1 117 tonnes per year actually leaves the tailings as seepage through the footprint. The residual salt mass leaves the tailings at the rate of approximately 262 tonnes per year once the tailings have desaturated. The fine particle size and low permeability of the tailings under compaction, is a natural mitigation which limits the rate of salt release.

Closer analysis of the TSF sub-system resolved water balance outputs from the mine water distribution system.

REFERENCES

DWAF (2006) *Best Practice Guideline G2: Water and Salt Balances.* South African Department of Water Affairs and Forestry (DWAF), *Best Practice Guidelines for Water Resource Protection in the South African Mining Industry*. August 2006.

Ramo S and St Clair RK (1998) *The Systems Approach: Fresh Solutions to Complex Problems Through Combining Science and Practical Common Sense*. KNI Incorporated, 150pp.

Parkhurst DL and Appelo CAJ (1999) *User's Guide to PHREEQC (Version 2) – A Computer Program for Speciation, Batch-Reaction, One-dimensional Transport, and Inverse Geochemical Calculations*. United States Geological Survey (USGS) Water-Resources Investigations Report 99-4259.

Innovative Mine Waste Management Planning at a Site with Multiple Waste Streams

Brent Johnson, Gary Parkison and William Cincilla
Hatch Consulting, USA

ABSTRACT

The Metates Project will exploit a large-scale, low-grade gold-silver-zinc deposit located in west-central Mexico in the states of Durango and Sinaloa. A total of 2.3 billion tonnes of ore and waste rock will be excavated at the mine site in Durango (the Metates site) over a mine life of 25 years. The ore will be crushed and sulfides floated, resulting in a concentrate that gets pumped about 120 km to the Ranchito site for additional processing. The concentrate will be pressure oxidized (POX) then cyanide leached to extract the gold and silver. The acidic solution generated in the POX circuit will be neutralized using limestone and lime, resulting in extractable zinc and a significant amount of residue. This process results in significant amounts of four primary waste streams: waste rock and flotation tailings at the Metates site and neutralization residue and cyanide tailings at the Ranchito site. An evaluation of these waste streams was conducted to develop environmentally sound and practical management strategies.

One testing program involved characterizing individual and blended neutralization residue and cyanide tailings. Testing included elemental analysis, acid-base accounting, net acid generation, rinse testing, mineralogy, and humidity cell testing. Additional testing was conducted on various engineered blends to optimize the pH to minimize metals and other constituent leaching from the blended waste material and to evaluate geotechnical stability of the blends.

Results indicate that a blend of neutralization residue, cyanide tailings, and limestone can be designed that has less leaching potential than either of the individual end-member waste materials. The blended residue also has the required characteristics to be geotechnically stable in a dry stack configuration, thereby reducing disturbance and aerial distribution of the waste material.

The resulting operational and closure waste management strategies are more protective of the environment and lower cost than conventional waste facilities for each waste material.

Keywords: closure, metals-leaching, tailings, treatment, blending

INTRODUCTION

The Metates Project is located in northwestern Mexico in the northwestern portion of Durango State, some 160 km northwest of the city of Durango and 175 km north of the coastal resort city of Mazatlan. The Project includes mining of an open pit for 19 years with an additional 6 years of processing, for a total operating mine life of 25 years. Ore will be milled and undergo flotation to produce a bulk sulfide concentrate. The concentrate will be transported via slurry pipeline to the processing site (Ranchito – Figure 1) where the sulfides will be oxidized in a pressure oxidation (POX) circuit prior to cyanidation to recover the gold and silver.

Four primary mine waste streams will be generated; waste rock and flotation tailings at the Metates site, and cyanide tailings (CNT) and neutralization residue (NR) at the Ranchito site. The flotation tailings and waste rock will be co-disposed in a single facility; with the flotation tailings being placed daily in layers, over exposed waste rock to limit oxidation of the waste rock during operations. At the Ranchito site, the two waste streams are to be blended together and placed as a paste in a tailings facility, taking advantage of the neutralizing capacity of the CNT to achieve an optimal paste pH such that metals (and other constituent) mobility is optimized. The blend will also take advantage of the geotechnical character of the NR to minimize infiltration and impacts to the environment.

This paper presents laboratory testing results from the CNT and NR materials which were conducted to identify management options including material blending opportunities.

METHODOLOGY

CNT and NR materials have been generated as part of ore processing development at various phases of feasibility to maximize recovery and reduce processing costs. As of September, 2014, two sets of materials have been generated, and a third set is proposed for early 2015. Results are presented for the first set of materials and some preliminary results for set 2.

The goal of the program is to develop a strategy to manage these waste streams to minimize the potential impacts to the environment while keeping operational costs low, and to design a system that will evolve seamlessly into a robust closure plan and design. Design objectives include:

- Using only a single facility for both waste streams
- Minimizing acid rock drainage and metals leaching
- Minimizing the footprint and disturbance
- Maximizing clean runoff and minimizing contact water quantity
- Minimizing infiltration of precipitation
- Maintaining the ability to execute concurrent reclamation
- Minimizing cost of construction, operations, maintenance, treatment, and closure.

Waste streams were evaluated separately and as a blended product to identify potential opportunities for improving the environmental and geotechnical behavior of the ultimate, placed material and to optimize the placement methodology. The waste material testing included:

- Acid base accounting (ABA) (ASTM D2492-02) (Sobek, 1978).
- Multi-element analysis (MEA) - EPA Method 3050 aqua regia digestion (USEPA, 1992a), and finish method 6010B (USEPA, 1994)

- Rinse testing including synthetic precipitation leaching procedure (SPLP - EPA Method 1312, USEPA, 1996), and shake flask extractions (SFE – ASTM D3987 – 85) and toxicity characteristic leaching procedure (TCLP – EPA Method 1311, USEPA, 1992b)
- Humidity cell tests (HCTs) - ASTM D5744-07 (2007)
- Lime titration
- Mineralogy

A CNT/NR blended tailings sample was titrated with lime (CaO) to raise the pH of the material in steps and develop a dosing curve for the material. A set of 11 samples was then generated at 0.2 pH shifts and sent for additional SPLP testing to evaluate the effect of material paste pH on constituent mobility. The resulting SPLP pH values suggested kinetic/aging effects. Based on this information, an additional blend was generated and analyzed at regular time intervals for mineralogy.

An additional blend of CNT and NR was generated and allowed to rest. A sub-sample of the blend was collected at selected time intervals and analyzed by x-ray diffraction (XRD) to determine the changes in mineralogy that occurs in the sample through time.

RESULTS AND DISCUSSION

Acid Base Accounting

The CNT have 5.5 percent total sulfur, of which 1.63 percent is sulfide. The paste pH value was 9.5. No NAG pH was tested on this sample. The neutralization potential (NP) to acid potential (AP) ratio (NPR) and the net neutralization potential (NNP) are reported well above the potentially acid generating (PAG) cutoffs suggesting the sample is non-PAG. HCT results indicate a pH of 7.44 after 28 weeks with measureable alkalinity (approximately 11 mg/L). 1,040 mg/L sulfate was being produced on the last week of the HCT.

The NR has 13.99 percent total sulfur, but the amount of sulfide sulfur is low at 0.35 percent. The paste pH is 7.9, but despite the low sulfide sulfur, both the NPR and NNP suggest the material may be PAG due to a low NP. Humidity cell data, however, indicate a steady pH of about 7.5 after 28 weeks and consistent production of alkalinity between 15 and 20 mg/L, indicating this sample is non-PAG.

Multi-element Analysis

Not surprisingly, the CNT are the most highly enriched with respect to metals (and other constituents). The CNT are, relative to crustal abundances, elevated in Mo, Pb, Cu, Ca, Cd, Bi, and As. Values of As, Sb, Bi and Pb are three orders of magnitude higher than average crustal values. These materials are depleted in Al, Mg, Na, K and Mn (up to two orders of magnitude compared to crustal values).

The NR is elevated in Cd, S, Ca, and Zn relative to the upper crustal values. Concentrations of As, Cd and S are over three orders of magnitude higher than crustal abundances. They are depleted in P, Na, Al, and K.

Rinse Testing

Results of the SFE tests are summarized in Table 1 and show the CNT, NR, and blended material rinsate chemistries (one test each). Data indicate that the major chemistries of the CNT and NR are very similar and that the blended material rinsate major ion concentrations are typically very similar to the end members; however, the metals and other ion concentrations tended to shift to be either greater or less than the range defined by the end member concentrations rather than in between. The orange cells in Table 1 are those constituent concentrations in the blend that are outside the range and higher, while the blue shaded cells represent those in the blend that are outside the range and lower.

The resulting blend pH is between the two end members, but the effect of this pH change is to shift constituents' solubility. This results in changes in constituent mobility with a relatively small change in the pH; some increasing, while others decreasing. Of those constituents with significant change, with a Mexican water quality standard, all decreased in the blend rinsate relative to the end members except for Cd.

Humidity Cell Tests

The NR HCT had an elevated first flush of sulfate from about 3,300 mg/L to just under 2,000 mg/L, at which point the sulfate concentration stabilized for about 8 weeks (Figure 1). Sulfate then declined to under 1,000 mg/L for about 6 weeks then rose and stabilized at 1,500 mg/L for the remainder of the test; likely in equilibrium with gypsum in the sample. The pH remained very stable, between 7 and 8 for the entirety of the test. Alkalinity was also stable at around 20 mg/L. No net acidity was generated during the test.

The HCT leachate for CNT indicated a relatively high initial sulfate concentration (8,160 mg/L), followed by a steady decline, asymptotically approaching 1,000 mg/L (Figure 2). The pH was in the 9 to 10 range during the first 12 weeks of the test and then declined to between 7.5 and 9 in the second half of the test. The alkalinity started at just above 200 mg/L and declined to stabilize between 10 and 20 mg/L through the test. No net acidity was generated.

Titrations and Mineralogy

Figure 3 shows the original titration results for the blended material from the bench measurements (bench paste pH). The titration curve shows a regular and linear trend. However when the subsequent individual samples were generated and sent for SPLP testing, the resulting pH values were much lower than the original pH values and much less linear.

Table 1 - SFE results summary

(orange shading indicates an increase in concentration relative to the end members; blue indicates a decrease)

Parameters	Units	Instrument/Method	Reportable Detection Limit	NR	CNT	NR/CNT Blend
Wt. of sample used	g	Weighing balance	0.01	50	70	50
Volume of DI water used	ml	Graduated Cylinder	0.01	1000	1400	1000
Final pH (18h)		pH Meter	0.5	7.90	9.7	9.09
Electric Conductivity (18h)	µS/cm	Conductivity Meter	0.5	3370.0	3380	2650.0
Acidity (pH 4.5)	mg/L	PC Titrator	0.5	<0.0005	<0.5	<0.0005
Acidity (pH 8.3)	mg/L	PC Titrator	0.5	3.2	<0.5	1.9
Alkalinity (Total)	mg $CaCO_3$/L	PC Titrator	0.5	28.9	29	14.1
Bicarbonate (HCO_3)	mg HCO_3/L	PC Titrator	0.5	35.2	21	17.3
Carbonate (CO_3)	mg CO_3/L	PC Titrator	0.5	<0.0005	6.8	<0.0005
Hydroxide (OH)	mg OH/L	PC Titrator	0.5	<0.0005	<0.5	<0.0005
Sulphate (SO_4)	mg/L	UV-Vis.	5	1710	1760	1530
Chloride (Cl)	mg/L	IC	0.5	4.3	7.0	1.8
Fluoride (F)	mg/L	SIE	0.01	0.10	0.10	1.50
Dissolved Analytes by ICP-MS						
Aluminum (Al)	mg/L	ICP-MS	0.001	0.005	0.007	0.099
Antimony (Sb)	mg/L	ICP-MS	0.0001	0.0169	0.0152	0.0013
Arsenic (As)	mg/L	ICP-MS	0.0001	0.118	0.130	0.004
Barium (Ba)	mg/L	ICP-MS	0.0001	0.0638	0.0736	0.0576
Beryllium (Be)	mg/L	ICP-MS	0.00005	<0.00005	<0.00005	<0.00005
Bismuth (Bi)	mg/L	ICP-MS	0.00003	<0.00003	<0.00003	<0.00003
Boron (B)	mg/L	ICP-MS	0.3	<0.3	<0.3	<0.3
Cadmium (Cd)	mg/L	ICP-MS	0.00003	<0.00003	<0.00003	0.00008
Calcium (Ca)	mg/L	ICP-MS	0.3	557	539	554
Cesium (Cs)	mg/L	ICP-MS	0.0003	0.0004	0.0005	0.0037
Chromium (Cr)	mg/L	ICP-MS	0.0005	0.0247	0.0272	0.0061
Cobalt (Co)	mg/L	ICP-MS	0.00003	0.00139	0.00139	0.00039
Copper (Cu)	mg/L	ICP-MS	0.0003	0.0085	0.0174	0.008
Iron (Fe)	mg/L	ICP-MS	0.005	0.207	0.248	0.032
Lanthanum (La)	mg/L	ICP-MS	0.0003	<0.0003	<0.0003	<0.0003
Lead (Pb)	mg/L	ICP-MS	0.00003	0.00004	0.00005	0.0001
Lithium (Li)	mg/L	ICP-MS	0.003	<.003	<0.003	14
Magnesium (Mg)	mg/L	ICP-MS	0.3	1.17	0.7	24.8
Manganese (Mn)	mg/L	ICP-MS	0.0003	<0.0003	<0.0003	2.2
Molybdenum (Mo)	mg/L	ICP-MS	0.0003	0.0176	0.0171	0.0223
Nickel (Ni)	mg/L	ICP-MS	0.0001	0.0001	0.0002	0.0007
Phosphorus (P)	mg/L	ICP-MS	0.01	0.028	0.02	0.043
Potassium (K)	mg/L	ICP-MS	0.3	172	168	46.7
Rubidium (Rb)	mg/L	ICP-MS	0.0003	0.301	0.274	0.137
Selenium (Se)	mg/L	ICP-MS	0.0002	0.0024	0.0025	0.0026
Silicon (Si)	mg/L	ICP-MS	0.5	5.73	5.9	0.688
Silver (Ag)	mg/L	ICP-MS	0.00003	0.00162	0.00265	0.00024
Sodium (Na)	mg/L	ICP-MS	0.3	163	165	41.6
Strontium (Sr)	mg/L	ICP-MS	0.0003	0.418	0.398	0.34
Tellurium (Te)	mg/L	ICP-MS	0.0001	<0.0001	<0.0001	<0.0001
Thallium (Tl)	mg/L	ICP-MS	0.00001	0.00251	0.00329	0.00127
Thorium (Th)	mg/L	ICP-MS	0.00003	<0.00003	<0.00003	<0.00003
Tin (Sn)	mg/L	ICP-MS	0.00005	<1	<0.00005	<1
Titanium (Ti)	mg/L	ICP-MS	0.003	<3	<0.003	<3
Tungsten (W)	mg/L	ICP-MS	0.00005	0.00024	0.00023	0.00014
Uranium (U)	mg/L	ICP-MS	0.00001	<0.01	<0.00001	<0.01
Vanadium (V)	mg/L	ICP-MS	0.001	<0.001	<0.001	<0.001
Zinc (Zn)	mg/L	ICP-MS	0.0005	<0.0005	<0.0005	0.0063

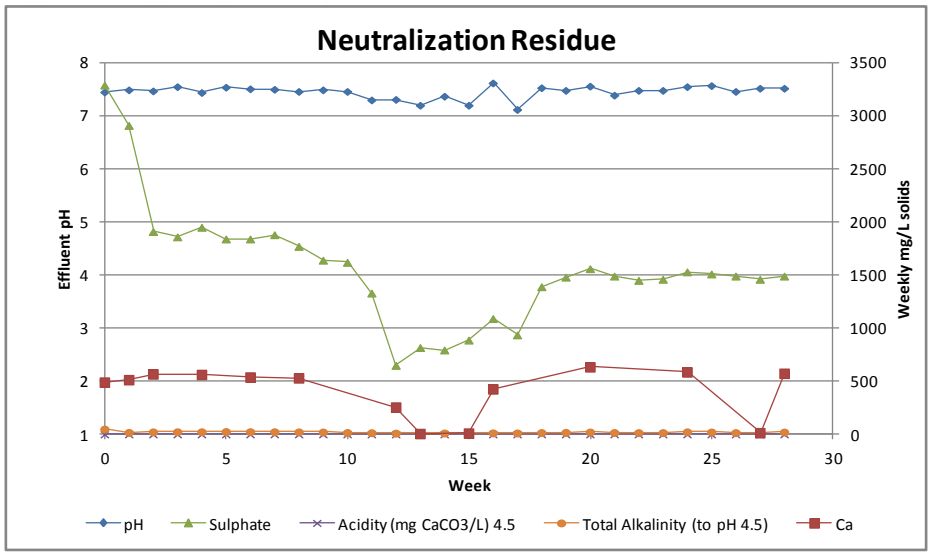

Figure 1 - NR HCT Results

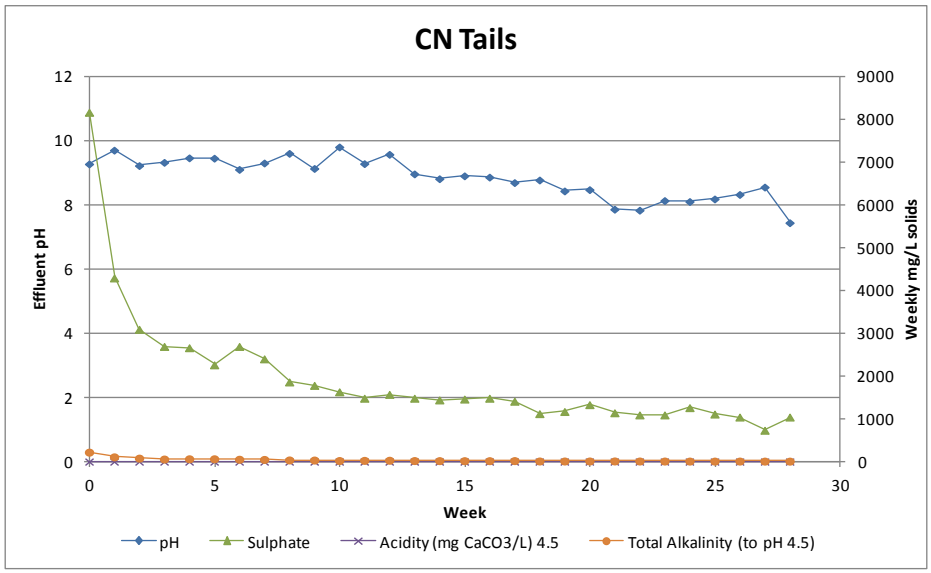

Figure 2 - CNT HCT Results

The difference noted between the bench titration and the SPLP suggests that the samples evolved chemically through time and consumed alkalinity, lowering the pH. Figures 4 and 5 show the major and trace analyte concentrations. Major ions were generally constant over the range of pH values tested in the SPLP except for aluminum concentration, which increased with increasing pH, and iron, which varied between 0.04 mg/L and 0.18 mg/L. Trace analytes were also largely below detection and somewhat insensitive to the relatively small change in pH tested by the SPLP. Arsenic increased slightly from 0.0046 mg/L to 0.0076 mg/L, likely reflecting the weaker sorption at higher pH values. Antimony and thallium decreased slightly with increasing pH.

The chemical changes suggested from the titration data were investigated further by aging a blended CNT/NR sample and analyzing samples' mineralogy at increments. Figure 6 shows the mineralogical composition through time. The results indicate that the majority of the material is gypsum, with lesser amounts of amorphous phases and silicates (predominantly mica and quartz). The quantity of amorphous material decreases from about 27 percent to about 10 percent over the course of 10 days, with a corresponding increase in gypsum content.

The geotechnical characteristics of the blended material that had been aged for only 12 days suggested significantly increased strength (compressive strength increased from 10 kPA to 440 kPa) and low hydraulic conductivity ($1x10^{-7}$ cm/s) is achieved.

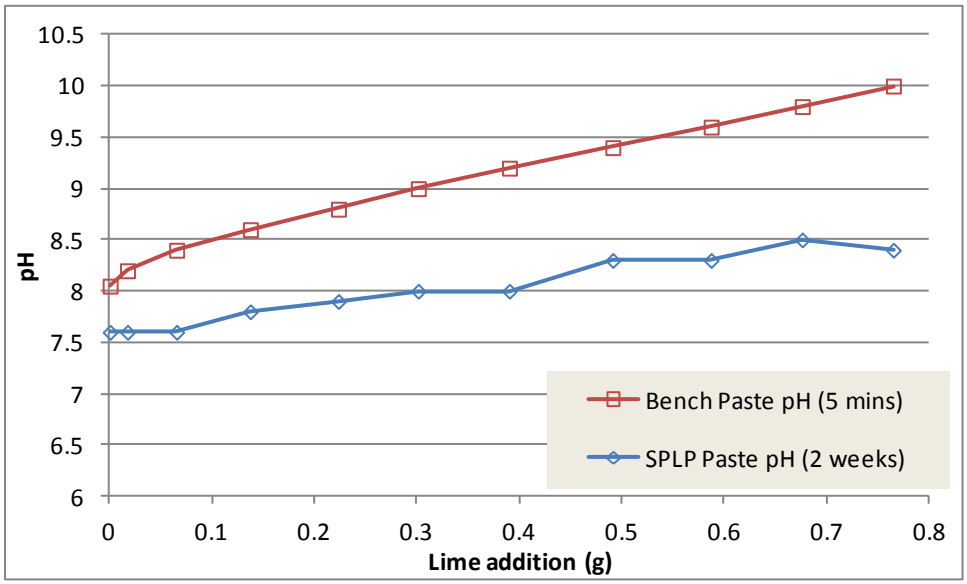

Figure 3 - Lime titration results

DISCUSSION AND IMPLICATIONS FOR MATERIAL MANAGEMENT

NR is a relatively inert material consisting predominantly of gypsum from the neutralization of sulfuric acid by lime in the process.

- NR is considered PAG by ABA because the net neutralization potential is -5.7 and NPR is 0.5, however sulfide sulfur is only 0.35 percent of the total 13.99 percent total sulfur so acid production is expected to be low or unlikely. Paste pH is 7.9.
- HCT data show that the final pH of the NR is 7.52 after 28 weeks with no acid generation. Elevated amounts of sulfate were generated, but this is likely due to the high gypsum content of the material.
- Multi-element analyses by aqua regia show this material is elevated in 9 metals over crustal abundances (at least four times crustal abundance) including sulfur.
- Rinsate chemistry has a circumneutral pH, and is a calcium-sulfate type with generally low-to moderate metal and metalloid concentrations.

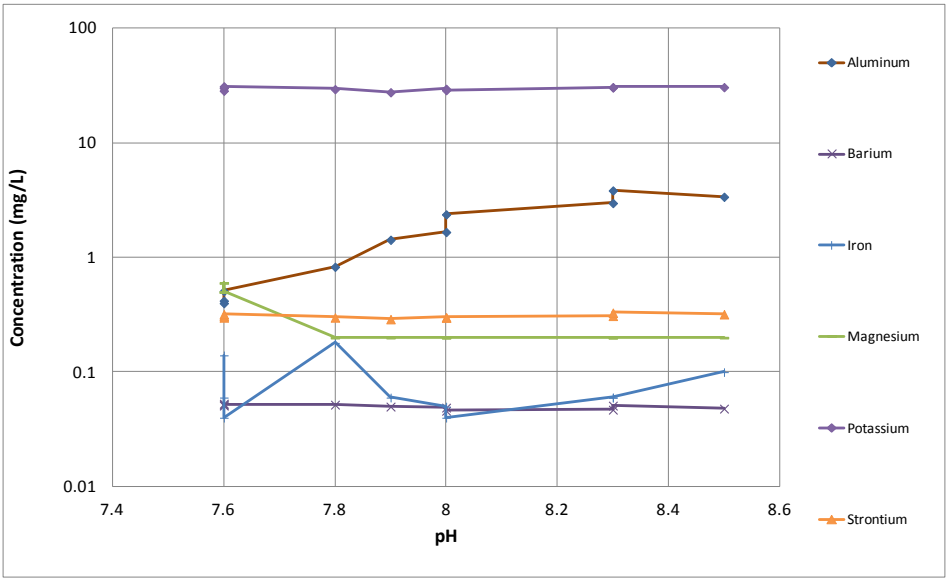

Figure 4 – Major analyte concentrations in SPLP extract

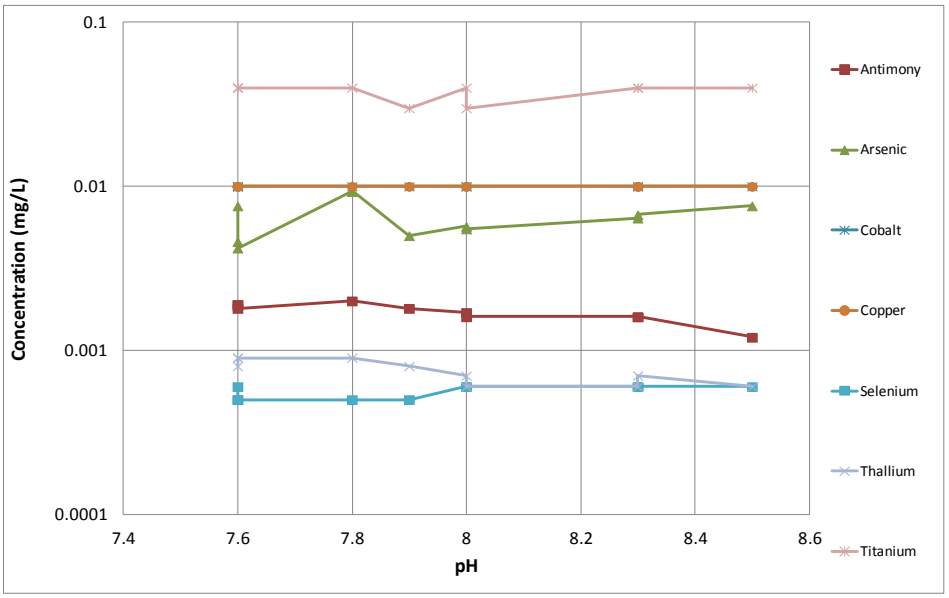

Figure 5 – Minor and trace analyte concentrations in SPLP extract

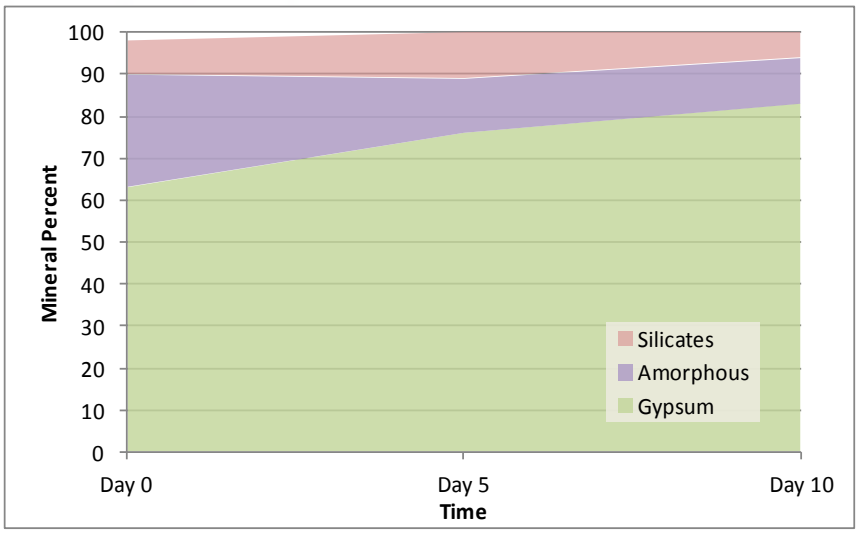

Figure 6 - Evolution of mineralogy through time of NCT/NR blend

CNT are generally alkaline due to the lime addition during the process, with some elevated metal and metalloid concentrations in leach and rinse testing. CNT have the following characteristics:

- CNT are considered non-PAG by ABA testing because NNP is 48.2 and NPR is 1.9. Paste pH is 9.5.
- While total sulfur is 5.5 percent and sulfide sulfur is 1.63 percent, the material does not exhibit acid production in HCT. Final pH was 7.44 after 28 weeks.
- Multi-element analysis indicates this material is elevated in 9 metals over crustal abundances (at least three times crustal abundance) including sulfur.
- Rinsate has an elevated pH (9.7) but a similar major ion chemistry as the CNT with a calcium-sulfate water type.

The CNT/NR blended material is geochemically stable with a circumneutral pH and low metal/metalloid leaching potential:

- Blended material had an NNP of 20.5 and an NPR of 3.2 which would categorize this material as non-PAG. Paste pH was 8.3.
- Total sulfur was 11.26 but the sulfide sulfur was 0.29. Because of this, acid generation is very low or negligible.
- Multi-element analyses by aqua regia show this material is elevated in 11 metals over crustal abundances (at least four times crustal abundance) including sulfur.
- Rinsate has an elevated pH (9.1) and was a calcium sulfate water type but constituent concentrations tended to shift (either up or down) compared to the CNT and NR.

Rinsate constituents from the CNT/NR blend generally show non-linear relationship (i.e., concentrations are not showing conservative behavior). For example, iron concentration declined to 0.032 mg/L from 0.21 and 0.25 mg/L (NR and CNT, respectively). Speciation modeling using PHREEQC (Parkhurst, 1995) indicates that all three waters are supersaturated with respect to various iron oxy-hydroxide phases (e.g., goethite), but that the blend was less supersaturated. This

suggests that iron oxy-hydroxide precipitation occurred in the blended material, providing sorption substrate for various other metals/metalloids in the process. Modeling results also suggests that the rinsate waters were kinetically unstable (relatively labile phases were indicated as being supersaturated) indicating that additional aging of the samples could result in significant mineralogical maturation and environmental behavior. These processes will continue to be investigated in ongoing studies.

Overall, data suggest the blended CNT/NR material will be a physically and chemically stable product that will be suitable for long-term storage. The blended material has physical and chemical properties that have environmental and geotechnical benefits which outperforms either end-member material. The material matures quickly resulting in a high-strength, low permeability material that is easily handled as a dry-stacked material, resulting in more streamlined operational management and lower risk environmentally both during operations and closure. Material can be blended at the run-of-mine production rates and placed in a single facility, with the high gypsum content acting to encapsulate and reduce metals mobility in the material. No acid generation and only minor metals leaching is expected from the material. Some elevated sulfate concentrations may require limited water management but will generally be suitable for reclamation using standard best engineering and closure practices.

ACKNOWLEDGEMENTS

Christian Kujawa and his staff and facilities at Paterson & Cooke in Golden, Colorado.

REFERENCES

Parkhurst DL, Appelo CAJ (2013). Description of Input and Examples for PHREEQC Version 3 – A Computer Program for Speciation, Batch-Reaction, One-Dimensional Transport, and Inverse Geochemical Calculations. US Geological Survey Techniques and Methods 6:1-497.

Sobek, A.A., Schuller, W.A., Freeman, J.R., and R.M. Smith. 1978. Field and Laboratory Methods Applicable to Overburdens and Mine soils. EPA-600/2-78-054.

USEPA. 1992a. Acid Digestion of Sediment, Sludges, and Soils. Method 3050.

USEPA. 1992b. Toxicity Characteristic Leaching Procedure. Method 1311

USEPA. 1994. Synthetic Precipitation Leaching Procedure. Method 1312

USEPA. 1996. Inductively Coupled Plasma-Atomic Emission Spectrometry. Method 6010B.

Groundwater in the Chilean North: A Brief Synopsis

Sven Renner[1] and Igor Aguirre[2]

1. *Federal Institute for Geosciences and Natural Resources, Germany*
2. *Senior Consultant on Geothermal and Groundwater Resources, Chile*

ABSTRACT

This paper synthesises information on the groundwater resources in the northern part of Chilean mainland, scattered to date.

The climate in the Chile increases in aridity towards the north and becomes extremely arid in coastal areas. North of 27ºS, precipitation ranges from less than 1 mm/y at the coast and in the Central Depression to 350 mm in the Andes. The lower, extremely arid parts make up the Atacama Desert.

This paper focuses on groundwater resources in the Chilean North, where water is scarce and a growing mining and agro industrial activity puts an increasing pressure on the resources. Ground water resources are found mainly in sedimentary basins. The geological evolution of the basins is always associated to the overarching process of the Andes Range uplift. There is however a great variety of different geological settings that produces different types of groundwater basins, with different dimensions and recharge mechanisms.

In order to give a general view on the hydrogeology of the Chilean North it was necessary to strongly simplify the often complex natural situations and to classify the groundwater basins. The main criterion for the classification was the geological setting as it controls much of the geographic location, hydraulic characteristics, size and geometry of the basins. Three types of groundwater basins are discussed in the paper. These basins host the biggest portion of the groundwater resources in the North. There is a brief description of the geology and groundwater characteristics for each.

Keywords: Hydrogeology, Chile, Groundwater, Resources, Management

INTRODUCTION

Chile's mainland stretches from 18°S to 56°S, approximately 4200 km along the west side of the Andes. The physical geography is characterized by a general subdivision of the country from West to East into a Coastal Area that quickly rises into the Coastal Mountain Range; farther to the East follows the Central Depression that separates the Coastal Mountain Range from the much larger Andes Mountain Range with volcanoes above 6000 m altitude (Fig. 1). This general pattern however varies, as the coastal range submerges into the Pacific Ocean in the northern and southern ends of the country.

The climate towards the North becomes arid to extremely arid. North of 27°S, precipitation ranges from less than 1 mm/y at the coast and in the Central Depression to 350 mm in the Andes. The lower, extremely arid parts make up the Atacama Desert. This paper focuses on groundwater resources in the north of the Chilean mainland, where water is scarce and a growing mining and agro industrial activity puts an

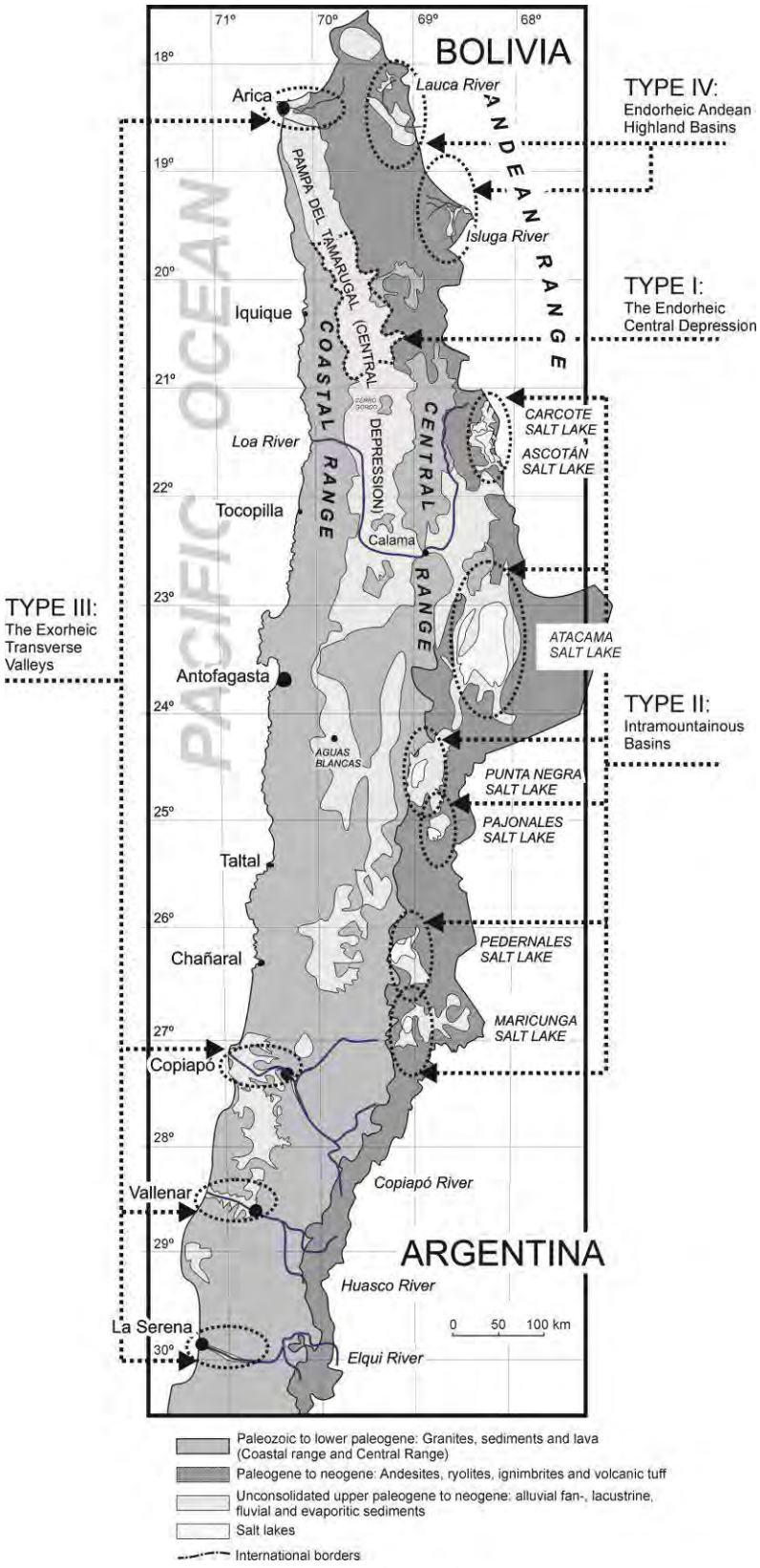

Figure 1 Groundwater basin types in northern Chile I through III as referred to in this paper. Type I is characterized by a clear division between coastal range, central depression and Andes Range. South of Cerro Gordo, the Andes Range splits into several horst and graben structures and develops a series of intramountainous basins (Type II) , where salt lakes can be found, like the *Atacama*, *Punta Negra*, *Ascotán* and *Carcote*. Type III is the E-W pointing river valley aquifer that drains into the Pacific Ocean.

increasing pressure on the resources. For the purpose of this paper, the Chilean North is defined as the part of the country located north of the capital. Groundwater is found mainly in sedimentary basins, the richest of them being located within the central depression. The geological evolution of the basins is always associated to the overarching process of the Andes Range uplift. There is however a great variety of different geological settings that produce different types of groundwater basins with changing geological and tectonic settings, dimensions and recharge mechanisms.

In order to give this brief overview on the hydrogeology of the Chilean North it was necessary to strongly simplify the often complex natural situations, highlight certain general patterns and omit other, less representative ones and to exclude areas that do not host major groundwater resources. It was further necessary to classify the groundwater basins. The main criterion for the classification was the geological setting as it controls much of the geographic location, hydrologic characteristics, size and geometry of the basins.

Three types of groundwater basins are discussed in the paper. They host the largest portion of the groundwater resources in the North (there are, however, other types of minor importance, like the endorheic highland basins in the far north, which are not considered in this paper). There is a brief description of the geology and groundwater characteristics for each.

THE GROUNDWATER BASIN TYPES OF THE CHILEAN NORTH

According to current knowledge, all major groundwater resources in the Chilean north are located in sedimentary basins. Sedimentation is occasionally interbedded with layers of ignimbrite or volcanic tuff. Aquifers of lesser importance are found in valley sediments of little extension and fractured rocks. The classification of groundwater basins in the Chilean North was based on structural and to lesser degree hydrographic criteria: Type I, The Endorheic Central Depression is a large sedimentary basin between the coastal mountain range and the Andes, roughly between 19°30´S and 21°S, known as the Pampa del Tamarugal, Type II, Intramountainous Basins: South of 21°S, the western flank of the Andes Range breaks up in a series of horst and graben structures that give way to the development of sedimentary basins of varying size, and Type III, Exorheic Transverse Valleys: This type includes river valleys with varying sedimentary deposits, which generally drain high Andean areas and flow from East to West. They occur in the extreme North of the territory.

TYPE I, THE ENDORHEIC CENTRAL DEPRESSION (PAMPA DEL TAMARUGAL)

Between 19°30'S and 21°S the Coastal Range rises parallel to the Andean Range and reaches 3000 m altitude, producing an Endorheic Central Depression (ECD) with a groundwater reservoir of unique importance (Fig. 1). North of it the Coastal Range dips below the Andean piedmont sediments and ignimbrites and allows the Andean Rivers to reach the Pacific Ocean. To the South, the ECD ends at the *Cerro Gordo* (Fig. 1), where the impermeable basement crops out.

The ECD in this area is named Pampa del *Tamarugal*, the *Tamarugo* Flatlands, after the prevailing vegetation of the area. It is a neogene and paleogene fluvial and alluvial basin, filled with sediment previously eroded in the Andes. The average altitude of the plane is 1200 m a.s.l.. The surface of the ECD is about 4000 km^2. (Fig. 2). Precipitation and direct groundwater recharge in the Pampa area is almost nil. Potential evaporation lies between 2000 and 2500 mm/a (Rojas & Dassargues, 2007).

Geology

Massive sedimentation into the ECD starts in the early to middle Oligocene (García, 2001) or early Miocene (Vogel et al., 1980). At the bottom lies the Azapa Formation, generally fluviatile in the east and clay rich, of lacustrian origin in the west (Karzulovic, 1979). During the Pliocene, volcanic activity in the Andes of northern Chile increases. Above the Azapa Formation lies the 60 to 200 m thick sequence of the Altos de Pica Formation, in which ignimbrites, rhyolites and volcanic tuff are frequently to be found between the terrestrial layers. Brüggen (1950) refers to it as *formación liparítica*.

Above the Altos de Pica Formation lies the Diablo-Formation, composed of up to 110 m of gravel, conglomerate, silt and clay. This formation, between parallels 19°45´S and the South end of the *Pampa del Tamarugal*, is in part overlaid by the Huaylas Formation series of ryolites and terrestrial sediments (Tobar et al. 1968, Vogel, 1972, Salas et al., 1966). In the ECD, the neogene sediments can be up to 450 m thick; together with the paleogene layers, the total thickness of the basin filling can reach 900 m.

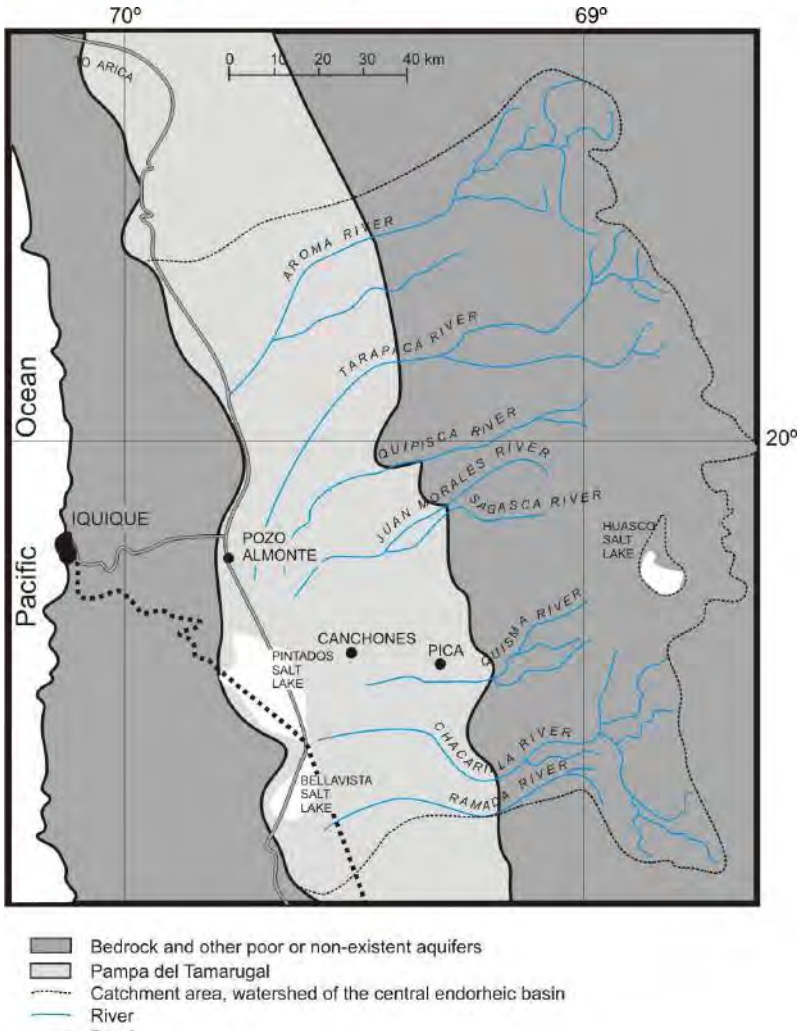

Figure 2 Catchment area and orography of the Basin Type I, the *Endorheic Central Depression – ECD – located in the Pampa del Tamarugal*.

Hydraulics, recharge and discharge

The pre-paleogene sedimentary, volcanic and metamorphic formations build the impermeable basement of the basin. The conglomerates and sandy layers of the upper 120 m of the Altos de Pica Formation provide the most important aquifers (Karzulovic, 1979). This formation is a series of layers that starts at the bottom with a generally thick layer of low permeability conglomerates, followed by volcanic tuff. They are covered by permeable sands and conglomerates, a layer of rhyolite and finally thick deposits of gravel and sand. As the volcanic layers thin out towards the West, sedimentary formations thicken. Their fluvial origin accounts for lateral and vertical hydraulic heterogeneities.

In the ECD, several rivers that come down from the Andes die in the alluvial fans of the Pampa. The most important are from North to South: *Aroma*, *Tarapacá*, *Quipisca*, *Sagasca / Juan de Morales*, *Quisma* and *Chacarilla* (Fig. 2). Their flow direction is generally North-East – South-West. Only the *Aroma* and *Tarapacá* are perennial. The rest is intermittent and infiltrates in the upper part of their hydrographic basin. Flow rates show a strong increase due to summer precipitation in the highlands.

Natural groundwater flows from North-East to South-West and into the *Bellavista Salt Lake* (Fig. 2), its natural point of discharge by evaporation. Groundwater depth decreases towards the point of discharge.

The upper aquifers (down to 20 m below surface) are generally unconfined or leaky. Lower aquifers are mostly confined. Billinghurst (1893) describes an artesian well near Pica in an aquifer 124 m below surface. Water levels however will most likely have dropped in the meantime due to intense water extraction from numerous wells in the basin.

Wells registered at the *Dirección General de Aguas* (DGA, 1988) show transmissivities between $6 \cdot 10^{-4}$ m^2/s and $1.5 \cdot 10^{-2}$ m^2/s with an almost normal distribution and a median of approximately $5 \cdot 10^{-3}$ m^2/s. This matches the average transmissivity of $5 \cdot 10^{-3}$ m^2/s, provided by Fritz et al. (1981).

A clear spatial zoning of hydraulic characteristics is not possible with the information at hand. Vertical permeability is generally low due to the numerous interbedded clay layers and the productivity of the aquifers usually decreases with depth. The deeper lying Paleogene aquifers have generally unfavorable hydraulic characteristics and are not used. Parts of these layered aquifers appear to have no present recharge but host water from humid periods in the Holocene (Fritz, 1981; Aravena, 1995). There is however a present recharge that has its origin in the higher Andes where precipitation is more abundant.

The infiltration of rivers flowing down from the Andes is by far the most important recharge mechanism in the ECD. Infiltration occurs mainly in the upper areas of the alluvial fans and ignimbrite outcrops on the West flank of the Andes (Karzulovic, 1979), which especially between 2500 and 3500 m a.s.l. are fractured by insolation weathering (at Canchones, temperature variations of up to 40°C within 10 hours have been recorded).

References for average groundwater recharge in the ECD vary between 500 l/s (Karzulovic, 1979) and 1000 l/s (DGA, 1988). Rojas & Dassargues (2007) calibrate their numerical flow model with the DGA (1995) calculations for the recharge rate of 975 l/s. The importance of storm runoff for ground water recharge has been a discussed subject. Houston (2001) claims strong influence of infiltrating flash floods after summer precipitations in the highlands and calculates its contribution in Quebrada de Chacarilla alone at over 200 l/s as an average over the year, which would considerably increase the estimates provided by DGA and Karzulovic. Peña et al. (1989) however, gave storm runoff much less importance based on isotope hydrochemistry in the Salar de Llamara, south of the Salar de Bellavista.

The ECD has its natural point of discharge in the *Bellavista* and *Pintados* salt lakes (Grilli et al. 1989, Falcón, 1966, Fig. 2), at the southern end of the basin, where the evaporation in 1980 was calculated at around 286 l/s (DGA, 1988). Since then, the increasing drawdown of the water levels must have diminished evaporation significantly. This assumption is confirmed by Rojas (2005), who calculates evaporation in the salt lake area at around 275 l/s in 1993 with a decreasing tendency.

To this, discharge through evapotranspiration of the *Tamarugo* trees must be added. Merino (1995) calculates this at around 1100 l/s for the whole basin. This value matches approximately the Rojas & Dassargues calculation (2007), which, based on the JICA (1993) and DGA (1988) studies, assume an increase of the evapotranspiration from 210 to 904 l/s between the years 1960 and 1993 due to forestation campaigns. Rojas & Dassargues (2007) suggest an additional discharge of 164 to 365 l/s of out-flowing groundwater at the southern edge of the basin, thus assuming this basin not to be completely endorheic.

In any event, groundwater pumping accounts for the highest withdrawal rates in the ECD. The utilization of the groundwater resources at an industrial scale started with the production of nitrate during the second half of the 19th century. The present pumping rate in the ECD is around 1,500 l/s, 700 of which are for drinking water and taken from the *Canchones* (Fig. 2) and El Carmelo deep wells. The use of groundwater for drinking purposes began in the 60´s. Today the total drinking water supply of Iquique (aprox. 250,000 inh.), *Pica*, *Pozo Almonte* and *Huara* is provided by the *Pampa del Tamarugal* groundwater.

The present groundwater extraction from the ECD aquifers plus the natural discharge of the system, according to all reports clearly exceeds recharge rates, even if there is an additional recharge from higher Andes regions via fractured base rock into the basin as suggested by Margaritz et al. (1990). Since the 60´s, the groundwater levels have fallen in almost all the DGA observation wells between 2 and 4 m (Rojas, 2005). According to Rojas & Dassargues (2007), by 2050, assuming an increasing pumping rate of 20%, water levels will have dropped another 2 m in average.

TYPE II, INTRAMOUNTAINOUS BASINS

South of the Cerro Gordo, the Central Depression continues (Fig. 1, Fig. 3), but not as an endorheic basin. Its ground water resources are generally poor and restricted to small areas, as described by Henríquez (1972) for the Pampa Unión area and Falcón & Henríquez (1968) for the *Baquedano* area, with high concentrations of TDS (Henríquez, 1977). The general lack of groundwater in the *Pampa del Tamarugal* south of the Loa River is due to a change in the geological setting: From the 21°S southwards. The Andes break up into numerous North – South oriented horst-and-graben structures, forming a chain of depressions: the *intramountainous basins* (Fig. 3). They trap water coming down from the Andes. Between the *Pampa del Tamarugal* and these basins rises a large horst structure called *Central Range* (*Cordón Intermedio* / *Cordillera Media*, Fig. 1), that hosts some of the worldwide most important copper deposits: *Chuquicamata*, *El Abra*, and further South *Escondida*.

The Atacama Salt Lake represents the biggest of these intramountainous basins. Combined with the Calama basin, it hosts around 90% of the groundwater resources of the Tarapacá region (Harza, 1978) with its capital Antofagasta (Fig. 3). The Calama tectonic basin as described by May (2005) is subdivided into the hydrographic units of the Middle and Upper Loa Basins plus the San Pedro and Salado basins, both tributaries to the Middle Loa basin (Fig. 3). The intramountainous basins further comprise the *Ascotán* and *Carcote* Salt Lake Basins in the North (21°30´S), the Punta Negra Salt Lake and Agua Verde Salt Lake Basins in the South, roughly at 25°S. This tectonic pattern continues to the South with the salt lakes of *Pajonales*, *Aguilar*, *Pedernales* and *Maricunga* at 27°S as described by Aguirre (2003), Iriarte et al. (1998) and Iriarte (1999). All but the Loa Basins and its tributaries are endorheic (Fig. 3).

Geology

The horst structure of the *Central Range* is called *Sierra de Domeyko* in the South and *Sierra Limón Verde* in the North (Fig. 3). The range is basically composed of low permeability Jurassic and Cretaceous folded granites and sediments (Zeil, 1964).

The neogene sedimentation processes in the intramountainous basins are equivalent to those described for the *endorheic Basin* of the Pampa del Tamarugal. Sedimentation occurs mainly from the Volcanic Andean range in the East and produces a generally several hundred meter thick sequence of paleogene and neogene alluvial fan deposits, fluvial, and in their western part often lacustrine or evaporitic sediments, interstratified occasionally with less permeable layers of ignimbrites and volcanic ash (Bravo, 1975). The main patterns of the intramountainous basins are therefore similar, consisting of large alluvial fans on one side (mostly in the east) and a gentle slope in the bottom area that ends in a salt pan.

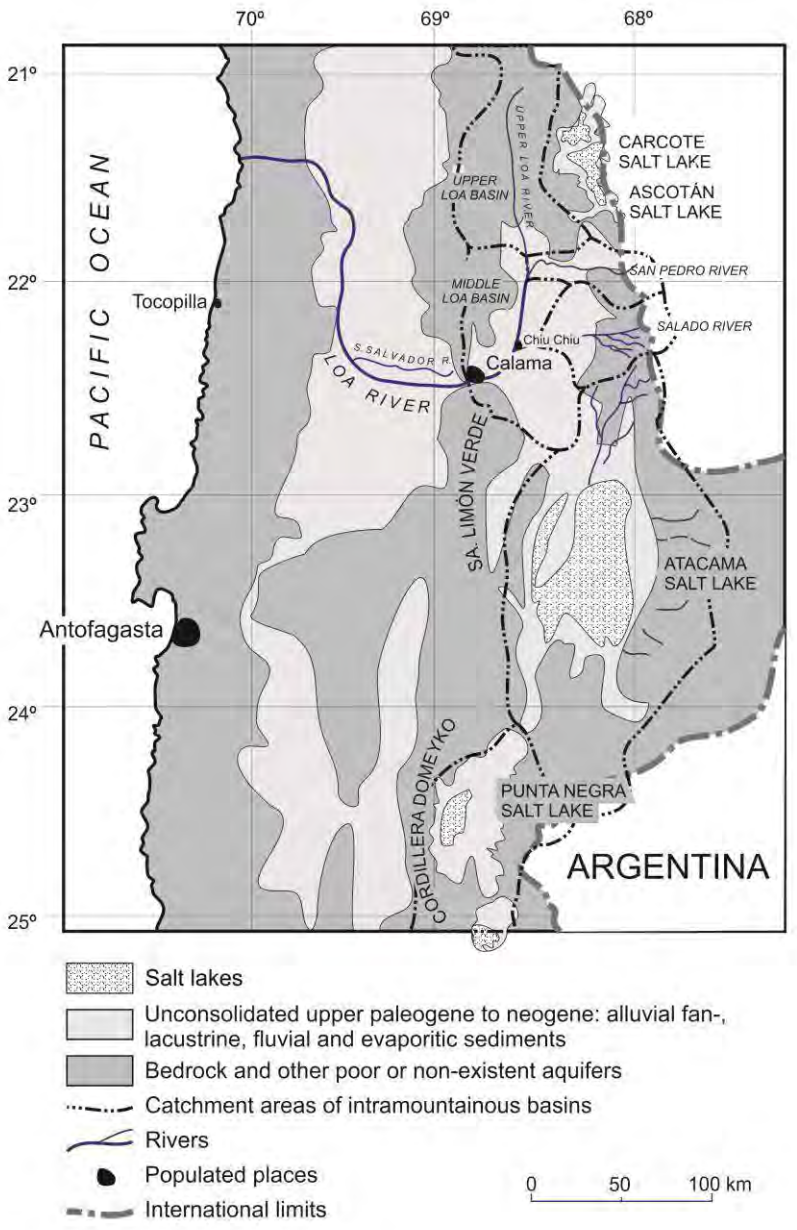

Figure 3 The intramountainous basins and their catchment areas. These depressions form a chain east of the Pampa del Tamarugal and trap the water coming down from the Andes.

Only the middle Loa Basin (Fig. 3) differs from this pattern and comprises aquifers in the 120 m thick Calama Formation and overlying Loa Formation, composed at the bottom of conglomerates and breccia and farther up of an unusual, 50 to 100 m thick series of lacustrine limestones. Naranjo & Paskoff, 1981, place the beginning of the Calama Formation in the Lower Miocene, while Marinovic & Lahsen (1984) place it in the Middle Miocene. This is contradicted by May et al. (2005), assuming the beginning of the Calama Formation during the lower Eocene. Both formations are overlain by the Pliocene Chiu-Chiu Formation. East of *Chiu Chiu*, the limestone shows evidence of karstification with a lake in a typical, large scale doline: The *Laguna Chiu Chiu* or *Inca Colla* (Hauser, 1999).

Hydraulics, recharge and discharge

Precipitation in the intramountainous basins depends largely on their geographical elevation and is generally higher than in the *Pampa del Tamarugal*. It reaches 25 mm/a at the *Salar the Atacama* (2300 m a.s.l.), 50 mm/y at the *Vega del Turi* (*Salado Basin* at 3000 to 3300 m a.s.l.), 40 mm/y at the *Ojos de*

San Pedro (3800 m) and 120 mm at the *Ascotán Salt Lake* (3700 m a.s.l.). Potential evaporation for all areas ranges between 1750 and 3500 mm/a (Harza, 1978).

Only in a few areas, such as *Aguas Blancas* (Fig. 1), South-East of Antofagasta, fresh water can be found (Henríquez, 1970). This is recharged by precipitation in the highest areas of the Central Mountain Range, at almost 5000 m, west of the *Punta Negra Salt Lake* (Fig. 3).

The general groundwater flow direction in the intramountainous basins is East-West, controlled by groundwater recharge from the Andes. Exceptions are found in the *Salar de Ascotán*, where a significant recharge occurs from the eastern flank of the *Aucanquilcha Volcano* (aprox. 6200 m a.s.l.), and in the *Atacama Salt Lake Basin*, where 80% of the recharge is provided by rivers that flow into the basin at its north-eastern end. Flow direction here is therefore predominantly NE-SW (Harza, 1978).

All basins host productive aquifers within the unconsolidated layers of neogene sand and gravel. Groundwater is found generally within an unconfined upper aquifer and a lower confined one, separated by one or several layers of ignimbrite or volcanic ash. Artesian fresh water springs were observed in the *Atacama Salt Lake*, in *Tebenquiche*, close to *San Pedro de Atacama* and *Tilopozo*, at the southern end of the salt lake by Galli (1955). Due to the tectonic setting and volcano activity thermal springs are frequent.

Groundwater depth generally decreases towards the salt pan. Transmissivity has been determined by Harza (1978) in all basins shown in Fig. 3 and ranges between $5 \cdot 10^{-2}$ and $7 \cdot 10^{-3}$ m^2/s. Specific yield ranges between 0.15 and 0.2.Depth of the unconsolidated, mostly saturated sediments reach 120 m in the Salado Basin, 350 m in the San Pedro Basin, 250 m in the Loa Basin, 160 m in the Ascotán / Carcote area and more than 400 m in the Salar de Punta Negra Basin (Harza, 1978).

The intramountainous basins are generally endorheic. Only the Loa basins and sub-basins differ, feeding the Loa River, the most important surface water of the Chilean North with a catchment area of around 34,000 km^2 (Fig. 3, Brinck, 1975). At the western edge of the Middle Loa Basin, where the impermeable bedrock crops out, ground water rises to the surface and forms the *Calama wetlands* (*bofedales*).

As a consequence of its geological features, the Middle Loa basin hosts two aquifers, the upper in the carbonate Loa formation and the lower in the granular Calama formation. The Loa Aquifer is fractured and unconfined. The lower aquifer is partly confined by a 30 to 120 m thick layer of clay (Hauser, 1999).

Groundwater recharge of the intramountainous basins is provided mostly by precipitation in the higher altitudes of the volcanic range of the Andes, where it reaches 300 mm/a. Water is led into the basins by mostly intermittent mountain rivers and creeks (during the rainy season between January and April) and subsequent base flow. Recharge rates are estimated by Harza (1978) in the various basins and yield at *Ascotán Salt Lake* (480 l/s), *San Pedro Basin* (700 l/s), *Rio Salado Basin* (1000 l/s), *Atacama Salt Lake Basin* (1600 l/s), *Punta Negra Salt Lake Basin* (800 l/s).

Groundwater recharge in the middle *Loa Basin* occurs through the inflowing rivers *Salado*, *San Pedro* and, first of all, *Loa* (Fig. 3), which gathers precipitation water from the *Miño Volcano* (5600 m a.s.l.). Precipitation in the basin itself is approximately 4 mm/a.

Groundwater discharge in the intramountainous basins occurs through evaporation at open water tables of wetlands and salt lakes, generally found at the western side of the basins (Fig. 3). Only the middle and upper Loa Basin have an important surface water discharge that drains the basin together with the evapotranspiration at the wetlands in *Chiu Chiu* and *Calama*.

The *Salado Basin* discharges through springs (*Baños del Turi* – 145 l/s) that flow into the Salado river (450 l/s) and evapotranspiration at the adjacent wetlands and salt lake (*Vega del Turi*). Harza´s (1978) estimation for the latter is of 400 l/s.

TYPE III, EXORHEIC TRANSVERSE VALLEYS

It was mentioned before, that the predominant geomorphological feature of the Chilean territory is the subdivision from West to East into a Coastal Mountain Range, the Central Depression and the Andes Mountain Range. This set of features, however, is discontinued in some areas and replaced by transverse valleys. In these areas, rivers run east-west in narrow valleys through the Andes and open up when approaching the pacific coast. Transverse Valleys can be found between 27°S and 33°S (from North to South: *Copiapó*, *Huasco*, *Los Choros*, *Elqui*, *Limarí*, *Choapa*, *Quilimarí*, *Petorca*, *La Ligua*, *Aconcagua*). It is only North of Santiago that the Coastal Range and the Central Depression reappears. Here it hosts the most fertile soils of the Chilean mainland. Another set of transverse Valleys are to be found in the northernmost part of the country, between 18°15´S and 18°40´S. It comprises the two major rivers *Lluta* and *San José* (called *Azapa* in its lower course) and their tributaries.

In what follows, the *Copiapó River* is picked out and described as a representative example for the Transverse Valleys between 27°S and 33°S. It appears to be representative not only in hydrogeological terms, but also with regard to its development as an important agricultural area, the mining industry that competes with it for water and the ever higher constraints of available water resources.

The Copiapó Valley

The *Copiapó River* begins with the confluence of its main tributaries, the *Río Jorquera* and the *Río Pulido*, with respective catchment areas of aprox. 4200 and 2000 km². From this point to the ocean, the river has a length of aproximately 162 km and drains a catchment area that extends over 18.400 km². Farther downstream, close to the village of La Junta, the *Copiapó River* is joined by the *Manflas River*. These are virtually the only superficial water courses. Approximately two thirds of the total catchment area does not feature superficial drainage (Fig. 4), except for occasional storm runoff.

Geology

The *Copiapó River* runs through a set of basement formations that contain folded sediment rocks, volcanic and volcanoclastic rocks, with a generally N-S oriented axial plane and varying slopes towards E and W. They constitue the base and the flanks of the river bed and are described in literature as *formación La Ternera*, *formación Lautaro*, *formación Punta del Cobre*, *formación Abundancia* and *Nantoco*, *formación Pabellón* and *Totoralillo*, *lavas and breccias of the Sierra La Indiana*, *formación Bandurrias*, *formación Cerrillos*, *Quebrada La Higuera*, *Lavas of the Sierra La Dichosa*, *Upper Cretacous Subvolcanic intrusives*, *Cretacous Granitoides* and *Paleocene intrusives*. These units are generally impermeable. Although some of them appear to be fractured, their hydraulic permeability and storage capacities are nil (Aguirre, 1999, y Troncoso, 2012).

River sediments are scarce above the confluence with the Manflas river (close to the Lautaro dam), at aprox. 1200m a.s.l. Downstream the confluence, quarternary fluvial and fluvioalluvial sands and gravel make up for thick and continuous confined and unconfined multilayered porous aquifers. Zones of lesser hydraulic permeability are found in old fluvial or fluvioalluvial mudflow sediments (Aguirre, 1999).

Hydraulics, recharge and discharge

In the findings and maps of Aguirre (1999) and Troncoso (2012) on the hydrogeology between the *Lautaro Dam* and *Piedra Colgada*, aprox. 10 km downstream of the city of Copiapó, hydrogeological units are grouped into four categories according to their relevance as a groundwater resource: high yielding, medium and low yield and those of nil relevance.

Aquifers that are relevant for groundwater storage and flow tend to be unconfined, but show local signs of confinement, especially between *Cerrillos* and *Valle Fértil*, as well as downstream the *Lautaro Dam*, between *San Antonio* and *Los Loros*. Between *Los Loros* and *Paipote*, wells yield between 1 and 150 l/s and groundwater levels vary between artesian and 135 m depth (Fig. 4) (Aguirre, 1999, Troncoso, 2012).

High yielding aquifers include those in fluvial deposits, especially fluvial deposits of present time river beds and some fluvial deposits that show interstratification with fluviolacustrine deposits (Fig. 4). These strata types are often interconnected and produce aquifer systems with relatively high storage coefficients and transmissivity values. Medium and low yield aquifers in the *Copiapó River Valley* are typically layers that contain a large interstitial fine sediment fraction, low porosity, low permeability and a certain degree of cementation. These layers generally receive their recharge through vertical infiltration during the meager rainfall events. They represent a relatively small share of the valley formations and can be found in some fluvioalluvial sediment bodies, mud flow deposits, ancient river terraces. There are, however, also high permeability layers like dunes and dejection cones, located at the flanks of the river bed, that produce low yields due to meager to nil vertical recharge.

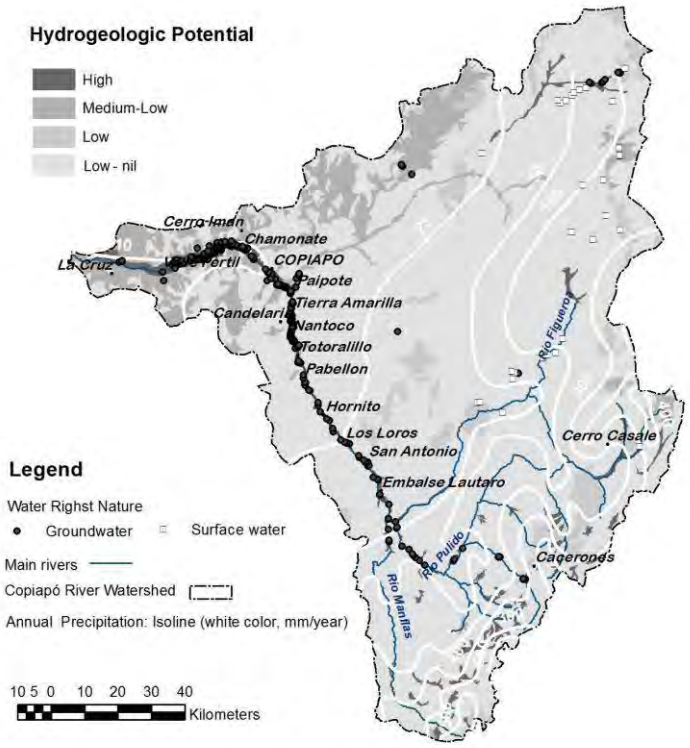

Figure 4 Hydrography of the Copiapó Valley (after Aguirre, 1999, SERNAGEOMIN, 2012, Hidromas, 2013)

The *Copiapó Valley* sediments are bedded in a basement of predominantly impermeable rocks with no relevant groundwater ocurrence. Exceptions can be found in fractured rock formations with locally interconnected flow paths but with a generally very limited recharge. A considerable number of intrusive rocks in the valley area form downright geological barriers, as for instance in La Puerta and Piedra Colgada (Fig. 4).

Hydrogeological properties (such as permeability, transmissivity, storage and specific yield) have been described extensively by DGA (1987), Aguirre (1999), SERNAGEOMIN-BGR (1999), SERNAGEOMIN (2012), DGA-DICTUC (2010) and HIDROMAS (2013).

Transmissivity of the valley sediments vary between $1 \cdot 10^{-3}$ and $2 \cdot 10^{-1}$ m^2/s. Highest values ($2 \cdot 10^{-1}$ m^2/s) can be found upriver, close to the *Lautaro Dam* and midway to Copiapó at *El Yeso* and *Totoralillo*. Lowest transmissivity values were measured in *Villa María*, *Hornitos*, *La Puerta* and *Los Loros* (Fig. 4). (DGA 1987a). Intermediate values of $5 \cdot 10^{-3}$ m^2/s are typically found where *Pulido River* joins the *Ramadillas River*. High variations are found close to *Iglesia Colorada* with values that range between $5 \cdot 10^{-3}$ and $4 \cdot 10^{-2}$ m^2/s.

Hydraulic permeabilities of the Copiapó River Valley aquifers typically range between $2 \cdot 10^{-4}$ and $2 \cdot 10^{-3}$ m/s, the lower end of this scale is often found perched aquifers. However, clay and silt-layers, located on the borders of the river bed and deposited mainly during occasional flooding, have permeability values as low as $1 \cdot 10^{-5}$ and $1 \cdot 10^{-6}$ m/s (SERNAGEOMIN-BGR, 1999).

There is only little information on storage coefficients. Data are provided by DGA (1987) indicate values between 0.016 and 0.11. Other studies (DGA, 1995) calculate averages of 0.05, 0.10 and 0.15 depending on the area. For resource estimation purposes, SERNAGEOMIN-BGR (1999) and DGA (1995 and 2003) assumed a storage coefficient of 0.1. Transmissivity values range between $1 \cdot 10^{-2}$ and $2 \cdot 10^{-1}$ m^2/s (DGA, 1987b, 1995).

Aquifer thickness varies strongly along the valley. Drillings proved maximum thickness of at least 180 m. However, geophysical campaigns (Aguirre, 1999 and SERNAGEOMIN, 2012) show fluctuating thicknesses between 100 and 200 m with local peaks of 250 and 300 m. These are supposed to be related to tectonic depressions produced by faults (Fig. 4) within the basement.

Recharge of the *Copiapó River* valley aquifers is produced by vertical infiltration of rainwater (especially in the higher catchment areas in years of high precipitation) and irrigation. In urban areas, losses of the potable water supply system as well as sewage play a major role. Discharge is dominated by groundwater pumping (in wells). A few points of natural spring discharge are left (such as *Los Loros-La Puerta*).

In general terms, there has been a continuous and marked overexploitation of groundwater resources in the aquifers of the Copiapó valley due to extraction rates that exceed recharge rates by far. The success of Chilean table grapes on the international market as of the 80's, led to a remarkable extension of Agricultural surfaces in the valley. Today, the valley is characterized my monoculture and irrigated surfaces are no longer restricted to the floodplain of the river but climb up the flanks.

In addition to this, mining industry and potable water supply of urban areas added another large portion to the demand. According to DGA-DICTUC (2010), natural and artificial recharge adds up to 3.6 m^3/s while estimated consumption is put at 5 m^3/s and therefore produces a deficit of aprox. 40%. These numbers are confirmed by the numerical modeling carried out by HIDROMAS (2013) that considers the time span between 1993 and 2012. The main conclusions are that the upper catchment system (down to *La Puerta* – Fig. 4) features a water surplus. Evidence is given by a large number of natural springs (e.d. in the vicinity of *Los Loros*). By way of contrast, the aquifers downstream of *La Puerta* suffer from a marked and continuous deficit of approximately 1.3 m^3/s, equivalent to 50% of the average recharge volume. This mismatch produces sustained and accelerating groundwater level drawdown since the 90's in several areas of the lower valley, especially between *Mal Paso* and the city of *Copiapó*.

REFERENCES

Aguirre, I. (1999). Hidrogeología del Valle del Río Copiapó entre El Tranque Lautaro y Piedra Colgada. Tesis, Universidad de Chile, Depto. de Geología; Depto. de Geofísica. 236 p. + anexos Santiago.

Aguirre, I. (2003): A hydrogeological, hydrochemical, isotopic and geophysical study on the Salar de Pedernales sub-basin, III región, Chile; Tesis, University of Tübingen, Institute of Geology and Paleontology; SERNAGEOMIN, Santiago.

Aravena, R. (1995): Isotope Hydrology and geochemistry of northern Chile groundwaters. Bull Inst. Frainçais Ëtudes Andines 24 (3): p. 495 - 503

Billinghurst, G., (1893): La irrigación en Tarapacá, Imprenta Ercilla, Santiago, Chile

Bobenrieth, L. (1980): Geología de los cuadrángulos Cerro Desamparado y Cerro Soledad, Regiones de Tarapacá y Antofagasta. Master thesis at the Universidad de Chile, Departamento de Geología, 171 p.

Bravo, N. (1975): Estudio hidrogeológico Salares Ascotán y Carcote, Provincia de Antofagasta, unpublished report, Instituto de Investigaciones Geológicas, Santiago, Chile

Brinck, G.,1975): Síntesis hidrogeológica del Norte Grande, unpublished report, Santiago, Universidad de Chile, Depto. de Geología

Brüggen, J.: Grundzüge der Geologie und Lagerstättenkunde Chiles, Heidelberg, Akademie der Wissenschaften, 1934.

DGA (1987a): Análisis y evaluación de los recursos hidrogeológicos valle del río Copiapó - III región: modelación de los recursos hídricos / MOP-DGA, Departamento de Hidrología, Alamos y Peralta Ingenieros Consultores; con la asesoría de : IPLA e HIDRELEC.

DGA (1987b): Prospección Geofísica y Mecánica Sistemas Acuíferos. DGA - Alamos y Peralta Ingenieros Consultores Ltda - Geoexploraciones Ltda. Autor del informe: Geoexploraciones Ltda. 2 v. Vol. 1, 16 p y Vol. 2, 224 p.

DGA (1988): Modelo de Simulación Hidrogeológico de la Pampa del Tamarugal. unpublished report, Centro de Recursos Hidráulicos, Departamento de Ingeniería Civil, Universidad de Chile

DGA (1989): Modelo de Simulación de Aguas Subterráneas del Valle de Azapa, Estudios Básicos y Modelo de Simulación, unpublished report by Ayala, Cabrera y Asociados LTDA on behalf of Dirección Nacional de Aguas de Chile (DGA)

DGA (1995): Análisis y evaluación de los recursos hídricos en el valle del río Copiapó, III región / Mario Cornejo S., inspector fiscal; Fernando Peralta T., jefe proyecto, MOP-DGA, Departamento de Estudios y Planificación, Alamos y Peralta Ingenieros Consultores.

DGA (1999): Política Nacional de Recursos Hídricos, published by Dirección Nacional de Aguas, Ministerio de Obras Públicas de Chile

DGA-DICTUC (2010): Análisis Integrado de Gestión en la cuenca del río Copiapó.

DMC (2010): Dirección Meteorológica de Chile, Dirección General de Aeronáutica Civil, http://www.meteochile.cl

Falcón, E. (1966): Salar de Pintados, Pampa del Tamarugal : determinación de dirección y velocidad de escurrimiento de agua subterránea, mediante isótopo yodo-131; unpublished report, Instituto de Investigaciones Geológicas, Santiago, Chile

Falcón, E., Henríquez, H (1968): Posibilidades de Aguas Subterráneas en Estación Baquedano, Provincia Antofagasta, unpublished report, Instituto de Investigaciones Geológicas, Chile

Fritz, P.; Suzuki, O.; Silva, C.; Salati, E. (1981): Isotope hydrology of groundwaters in the Pampa del Tamarugal, Chile. Journal of Hydrology 53 (1-2): 161-184.

Galli, C.; Dingman, R.J. 1962. Cuadrángulos Pica, Alca, Matilla y Chacarilla, con un estudio sobre los recursos de agua subterránea, Provincia de Tarapacá. Instituto de Investigaciones Geológicas, Carta Geológica de Chile, No. 7-10, 125 p.

Galli, C. (1955): Informe hidrogeológico preliminar acerca del bolsón de Atacama (Provincia de Antofagasta), unpublished report for Corporación de Fomento de la Producción (CORFO), Chile

García, M.; (2001): Evolution oligo-néogène de l'Altiplano Occidental (arc et avant-arc des Andes d'Arica, 18°-19°S). Tectonique, volcanisme, sédimentation, géomorphologie et bilan érosion-sédimentation. Thèse (Unpublished), Université Joseph Fourier, 178 p. Grenoble.

Grilli, A., Pollastri, A., Ortiz, J., Aguirre, E. (1989): Evaluación de tasas de evaporación desde salares, utilizando técnicas isotópicas - aplicación en el Salar de Bellavista, Chile, In: Isotope Hydrology Investigations in Latin America, Proceedings, IAEA TecDoc 502, Vienna (1989)

Harza Engineering Company International (1978): Desarrollo de los recursos de agua en el Norte Grande, Chile.-2 v, Report Harza Engineering Company International S.A.

Hauser, A. (1999): Hidrogeología segmento intermedio del Río Loa, Segunda región; unpublished report, SERNAGEOMIN, Santiago, Chile

Henríquez, H. (1970): Esquema hidrogeológico de la Provincia de Antofagasta; unpublished report, Instituto de Investigaciones Geológicas, Santiago, Chile

Henríquez, H. (1972): Hidrogeología de la cuenca de Pampa Unión, provincia de Antofagasta; unpublished report, Instituto de Investigaciones Geológicas, Santiago, Chile

Henríquez, H.; Falcón , E. (1975): Síntesis del potencial hidrogeológico de la I y II región; unpublished report, Instituto de Investigaciones Geológicas, Santiago, Chile

Henríquez, H. (1977): Esquema hidrogeológico de la II región; unpublished report, Instituto de Investigaciones Geológicas, Santiago, Chile

HIDROMAS, (2013). Actualización de la modelación integrada y subterránea del acuífero de la cuenca del río Copiapó. SIT N° 332.

Houston, J. (2001): The year 2000 storm event in the Quebrada Chacarilla and calculation of recharge to the Pampa Tamarugal aquifer. Rev. geol. Chile, Dec. 2001, vol.28, no.2, p.163-177. ISSN 0716-0208.

IMF (2014) Country information page - http://www.imf.org/http://www.imf.org/

Iriarte, S.; Ugalde, I.; Venegas M. (1998): Hidrogeología de la cuenca Laguna del Negro Francisco, Escala 1:100.000 Región de Atacama; Documentos de Trabajo n.10, Santiago, SERNAGEOMIN

Iriarte, S. (1999): Mapa hidrogeológico de la cuenca Salar de Maricunga: sector Salar de Maricunga, Escala 1:100.000, región de Atacama; Documentos de Trabajo n.13, Santiago, SERNAGEOMIN

JICA (1993): The study on the development of water resources in northern Chile, report by Pacific Consultants International, published by the Japan International Cooperation Agency

Jouravlev, Andrei (2001): Administración del agua en América Latina y el Caribe en el umbral del siglo XXI, Publicaciones CEPAL, Serie Recursos naturales, No. 3

Karzulovic, J.; García, F. (1979): Evaluación de recursos hídricos provincia de Iquique, I región Tarapacá; unpublished report, Iquique, Dirección General de Aguas

Marinovic, N.; Lahsen, A. (1984): Geología de la Hoja Calama. Escala 1:250.000. Servicio Nacional de Geología y Minería, Carta Geológica de Chile, No. 58, 140 p. Santiago.

May, Geoffrey, Hartley, Adrian J, Chong, Guillermo, Stuart, Fin, Turner, Peter, & Kape, Stephanie J. (2005): Eocene to Pleistocene lithostratigraphy, chronostratigraphy and tectono-sedimentary evolution of the Calama Basin, northern Chile. Revista geológica de Chile, 32(1), 33-58. Downloaded on January 12, 2015, from http://www.scielo.cl/scielo.php?script=sci_arttext&pid=S0716-02082005000100003&lng=es&tlng=en. 10.4067/S0716-02082005000100003

Merino, A. (1995): El desarrollo de los recursos hídricos en la parte Norte de Chile. En: Cuartas Jornadas de Trabajo, Programa Hidrológico Internacional, 01 al 03 de Agosto de 1995, Comité Chileno para el Programa Hidrológico Internacional.

Naranjo, J.A.; Paskoff, R. (1981): Estratigrafía de los depósitos cenozóicos de la región de Chiu-Chiu, Desierto de Atacama. Revista Geológica de Chile, N° 13-14; 79-85.

Naranjo, J.A. & Paskoff, R., (1984). Volcanisme, tectonique et réseau hydrographique sur le piémont Andin du désert du nord du Chili. Géographie Physique et Quatemaire, Vol. 2, p. 201-204

Peña, K., Grilli, A., Salazar, C., Orphanopoulos, D. (1989): Estudio de hidrología isotópica en el área del Salar de Llamara, Desierto de Atacama, Chile, In: Isotope Hydrology Investigations in Latin America, Proceedings, IAEA TecDoc 502, Vienna (1989)

Rojas, R. (2005): Groundwater flow model of Pampa del Tamarugal Aquifer – Northern Chile. MsC Thesis Water Resources Engeneering, Katholieke Universiteit Leuven and Vrije Universiteit Bruxelles, Belgium

Rojas, R. & Dassargues, A. (2007): Groundwater fow modelling of the regional aquifer of the Pampa del Tamarugal, northern Chile, Hydrogeology Journal, 15, pp. 537 – 551.

Salas, R., Kast, R.F., Montesinos, F. (1966): Geología y Recursos Minerales del Departamento de Arica, Provincia de Tarapacá. Instituto de Investigaciones Geológicas de Chile, Bol. N° 21, 114 pp.

SERNAGEOMIN (2002): Mapa Geológico de Chile escala 1:1.000.000.

SERNAGEOMIN-BGR (1999). Estudio hidrogeológico del valle del río Copiapó, segmento Embalse Lautaro - Piedra Colgada, región de Atacama. 186 p. + anexos Santiago. (Informe Registrado, IR-99-17); Autor del informe: Aguirre, I.; Hauser, A. y Schwerdtfeger, B.

SERNAGEOMIN (2012). Evaluación hidrogeológica de la cuenca del río Copiapó con énfasis en la cuantificación, dinámica y calidad química de los recursos hídricos superficiales y subterráneos.

Tobar, A., et al. (1968): Cuadrángulos Camaraca-Azapa. - Carta Geológica de Chile,19/20, Instituto de Investigaciones Geológicas de Chile, Santiago de Chile 20 pp.

Troncoso, R.; Espinoza, M.; Pérez, Y.; Castro, R.; Lorca, M.; Vega, N.; Feuker, P.; Arévalo, C.; Mercado, E.; Creixell, C.; Ortiz, M., Wall, R. (2012): Evaluación hidrogeológica de la cuenca del río Copiapó, con énfasis en la cuantificación, dinámica y calidad química de los recursos hídricos superficiales y subterráneos. Región de Atacama. Servicio Nacional de Geología y Minería. Informe Registrado IR-12-49, Santiago.

Vogel, S. (1972): Cuadrángulo Poconchile, Arica, informe no publicado, Arica, Instituto de Investigaciones Geológicas

Vogel, S.; Vila, T. (1980): Cuadrángulos Arica y Poconche: región de Tarapacá, escala 1:100.000; Carta geológica de Chile n.35; Instituto de Investigaciones Geológicas, Santiago, Chile

Zeil, W. (1964): Geologie von Chile, Borntraeger, Berlin

Building Better Waste Landforms for Reactive Waste: A New Level of Waste Assessment and Construction

Peter Scott, Ian Taylor, Paul Weber, Steven Pearce, Bonnie Dobchuk and André Kemp
O'Kane Consultants, Australia

ABSTRACT

Comprehensive waste characterisation and scheduling enables mines to design and construct waste landforms to manage acid and metalliferous drainage (AMD). Characterisation of wastes not only identifies problematic waste streams but also wastes with useful physical and geochemical properties that can be used to mitigate or neutralise AMD. However, optimising the placement of these beneficial materials whilst mirroring the mine schedule and avoiding double-handling requires planning from the outset.

Surface cover systems are often used in isolation at closure to manage water and oxygen ingress into waste rock storage facilities. Their effectiveness is generally limited by the type and availability of materials at that time, that is, there may be insufficient material, it may be degraded or otherwise lacking in its capacity to perform as wanted. Furthermore, the reliance on retro-active works may be complicated by competing demands for useful waste material and cost.

This paper outlines a holistic approach to designing and constructing mineral waste rock landforms based on a comprehensive understanding of the waste geochemical properties and schedule and integration with an appropriate landform design and cover system. The physical and geochemical properties of the waste, and interrelationships of key properties, including reactivity, hydraulic conductivity, moisture-holding capacity, erosion resistance is discussed. Consideration is given to construction and placement of wastes including tipping heights, selective placement of reactive waste, compacted intermediate low-permeability layers and surface water management.

The scope of this paper extends to the benefits of numerical modelling to provide a comprehensive understanding of materials placement and optimisation to reduce the reliance on only the final cover systems to manage net percolation and AMD generation. Specifically the ability to manage water seepage, oxygen ingress, acid generation rates and long-term surface erosion are fundamental.

Keywords: waste rock, geochemistry, landform, cover system, characterisation

INTRODUCTION

A continuing challenge to managing modern open-cast mining of deposits hosted in rocks that contain metal sulfides is the successful and "correct" disposal of reactive sulfidic and metalliferous waste rock within a landform that is geotechnical and geochemical stable, that is non-polluting and non-erodng. Waste rock containing metal sulfides when exposed to oxidising condtions will start to react and dissociate into more readily soluble and potentially deleteirous products (acidity, sulfate and metals) that may be released from their confining rock mass by meteoric waters, and are referred herein as reactive waste. Managing reactive waste rock during mining relies on a comprehensive understanding of the chemical and physical properties of the waste and an informed landform design. Only through better knowledge of materials characteristics and using this knowledge to effectively place mined waste in waste storage landform, considered in the context of the climate and environmental setting, can these objectives be reliably met. The presence of reactive waste necessitates a set of management procedures be developed to ensure effective waste rock landform design to minimise impacts of acid and metalliferous drainage (AMD). These procedures include those listed below and discussed in this paper:

- Construction of a geological model of the waste, based on the drillhole database;
- Waste chemical and physical properties characterisation using Static testing methods for waste rock, soil and subsoil;
- Block modelling of waste rock and merging with the ore resource model, to create the life of mine (LOM) waste mining schedule;
- Design and construction of waste landform for containment and management of reactive waste, including final batter design, and final cover system design, and erosion management;
- Design of water management for waste landform;
- Validating the waste model using in-pit geological mapping;
- Selective handling and placement of waste in designated areas of the waste rock landform;
- Validating placement of waste within the waste rock landform;
- Monitoring for success of placement using piezometers within the waste rock landform, and downstream of this facility;
- Regular technical reviews monthly (internal), three to six monthly (external);
- Implementing these procedures for Life of Mine.

MINE WASTE PROPERTIES

Geological model

The geological model of the potential waste associated the economic deposit is built from the exploration drillhole database of logged geological properties compiled during the exploration and resource evaluation phase. The drillhole database is the main source of geological information pertaining to the deposit and the potential waste, in the early stages of the project and will continue to be so through the life of the mine provided it is regularly updated with new data. A well-structured and comprehensive database makes it possible to define the range of waste rock types and their geological properties prior to undertaking the acid-base accounting testwork. The drill hole logging data that can be used to develop the sampling and to further classify waste include:

- Ore-waste boundaries;
- Lithology - major and minor (host rocks, cover rocks, construction material, soil, alluvium);
- Structural features - faults, shears, veins, fractures;
- Logged sulfide minerals quantity;
- Sulfide and carbonate mineralogy;
- Sulfide and carbonate texture and morphology;
- Spatial relationship of sulfides with acid consuming minerals in the host rocks;
- Depth of oxidation to include base of total oxidation (BOTO) and base of partial oxidation (BOPO);
- Depth of water table;
- Defining the transition waste areas to identify areas of partially oxidized PAF waste and flag these areas to be included in the waste model as reactive waste.

The drillhole database containing logged geological information is used to construct the 3D geological model. Using the geological model drill sections are constructed at regular grid spacing (e.g. 50 m or less for smaller deposits) through the proposed pit area and are used to derive the sampling plan. Each section has the drillhole trace and geological units plotted as well as logged data such as presence of sulfides, oxidation depths, structural data (faults and shears), ore and waste boundaries etc.

Sampling plan

All waste holes should be analysed for total sulfur, ideally at 1 m or 2 m interval widths up to a maximum interval width of 5 m and analysed for total sulfur. Total sulfur should also be analysed for each sample, waste as well as ore, collected for the exploration and resource drilling programs to build up the sulfur database for constructing the waste model.

Additionally representative samples of all lithological units related to the mine development need analysing. The sampling should cover all the areas of the mine plan, at least for the proposed Pit "Shell". This approach should aim to identify the geological units likely to provide an AMD problem, are acid neutralising, non-polluting waste, metal and sulfate saline leachate generating waste, as well as timing, destination and placement of the waste rock. The number and type of samples to be tested and evaluated is site specific and should reflect the complexity of the geology and the problem being addressed. Sampling interval widths should be a minimum of 1–2 m.

Samples of potential waste rock and ore selected in the sampling plan should be analysed for following chemical properties:

- total sulfur (LECO and portable XRF(field)) as a minimum, and ideally sulfate sulfur, and sulfide sulfur (CRS) to estimate maximum potential acidity (MPA);
- the drill holes sampled for the full pit profile (from surface to footwall to the ore) should be analysed for total sulfur as a minimum; these samples will provide the basis for construction of the waste block model;
- acid neutralising capacity (ANC); where
- net acid generation (NAG), including NAG pH;
- rinse pH, and field peroxide oxidation test;
- total and leachable metal concentrations; and
- overburden of subsoil and topsoil tested for soil nutrients, exchangeable cations, sodicity, salinity, and acidity.

Samples are typically classified as PAF (potentially acid forming), NAF (non-acid forming) based on the ABA results (Sobek *et al.*, 1978; Coastech, 1989; INAP, 2009), NAG (Miller *et al.*, 1997) and ANC:MPA or net potential ratio (NPR).

The development and understanding of physical material properties to be used within a landform construction are equally critical to its success as its chemical properties. Key physical properties to be derived and fully understood include:

- Characterizing the texture of the material, easily completed through particle size distribution (PSDs).
- Atterberg limits: important to understand the activity of a clay (potential to shrink/swell) and organic content.
- If clays are to be compacted to form a low permeability layer (CCL) it is critical that an understanding of the compaction effort, optimum moisture content and density required, through compaction testing (e.g. Standard Proctor).
- Target sampling and drilling is important to understand variation in material properties for different material types
- Erosion tests (slake durability, Emerson crumb, rill and inter-rill development);
- Moisture Retention Curves (MRCs) used to predict the soil/rocky mulch water storage, water supply to the plants (field capacity) and material aggregate stability
- Field and lab-based permeability tests (falling head, gain K_{sat}).

Assessment of waste rock properties doesn't end at the pre-mining stage but continues through the life of the mine to closure and decommissioning of the waste rock landform. The geological model and the waste block model must be regularly reviewed, reconciled and updated by in-pit mapping, sampling and testing of the in situ waste rock throughout the life of the mine. In-pit validation of waste by Mine Geologist involves:

- Checking the boundaries of the waste rock domains against exposed geology in the pit floor on the current mining bench; the pit geologist should utilise the geological information in the pit walls as well as the pit floor.
- Undertaking/supervising the waste validation sampling plan
- Checking domain classification is correct.
- Correcting the boundaries and classification, before and after blasting;
- Supervising/undertaking field testing of waste using field oxidation pH and rinse pH tests (Ahern *et al.* 2004) and sulfur by portable XRF.

A typical waste rock classification is summarised in Table 1.

WASTE BLOCK MODEL

Waste blocks commonly are larger in size (e.g. 20×20×5 m) external to the ore blocks, which may be 2.5×5.0×5.0 m in dimension. Block sizes used are governed by the geology of the ore and waste and the mining plan (Scott and Eastwood, 1998). The block model for waste is distinctively different from the sectional geological model used to identify waste types present and to design the sampling program. Block modelling for waste like ore resource modelling is used to calculate material volumes and hence tonnages. The block model calculates the volumes by defining and connecting adjacent cells with similar properties. The spatial properties of these cells are defined by x, y and z co-ordinates relative to a fixed reference point. Unlike the ore resource model, the amount of ana-

Table 1: Possible waste classes for sulfidic waste

Waste Type	Waste Class	Description
1	NAF	Non-reactive Waste comprising 100% NAF and negligible metals and is defined NAF non-metalliferous waste;
2	SD	Reactive Waste comprising rock material with excess acid neutralising capacity that will generate neutral to alkaline drainage with elevated sulfate and is defined as NAF sulfate saline (SD) waste;
3	MNAF	Reactive Waste comprising rock material with excess acid neutralising capacity and elevated metal concentration that will generate neutral to alkaline drainage with elevated sulfate and metals in leachate and is defined as mineralised NAF;
4	PAF	Reactive Waste that has limited acid neutralising capacity and elevated sulfide concentration and will generate acidic drainage with metals and sulfate and is classified as PAF waste.

lytical data concentration acquired from drilling for waste volume definition is commonly low. For some projects a large database for total sulfur has been compiled as part of the ore/waste definition and can be used to build the waste block model. For some project the deficiencies of analytical data in the waste database can be largely overcome through increasing the data density by integrating the acid base accounting (ABA) testwork with the drillhole database-derived geological model. This enables the testwork to be more effectively directed. It facilitates extrapolation of testwork data through association of test samples with like geology. It is advisable to keep the geological parameters simple, e.g. total pyrite, total carbonate, lithology, weathering, and fracture density etc. When interpolating static testwork data, it is important to use primary data such as ANC, MPA or sulfur values rather than ratios such as NPR or NAG.

Mine schedule

The waste schedule aims to identify waste units and their relative quantities to make use of their properties in different parts of the overall landform, including waste types suited for:

- NAF waste for basal layers and encapsulation of reactive waste, where exposure to oxygen, wind and water should be limited.
- Cover systems materials generally comprising inert material with properties that control the ingress of meteoric water into the landforms.
- The surface of landform embankments, comprising blockier units that resist erosion and or benign.
- Benign blocky material (rip-rap) waste for construction of drainage features, such as underdrainage, interflow drainage, drainage to intercept geological fracture flows (e.g. for in-pit or hillside landforms), diversion drains from upstream catchments, plateau catchment drains is required.
- Reduced permeability layers, typically comprising finer grained material, such as clays and oxide waste that can be suitably compacted.
- Use of natural alkalinity to neutralise acid salts: waste with excess ANC can be used in up gradient locations and in preferential flow areas to counter AMD.

- Growth medium to support vegetation, typically comprising stripped material from the landform (and pit) footprint, which generally is more suitable for revegetation.
- Layers forming capillary breaks, to limit the upward migration of salts.

WASTE LANDFORM CONSTRUCTION

Design and placement

The placement of PAF waste in the waste landform affects its reactivity by exposure to oxygen and seepage pathways. Consequently, the risk of gas production, AMD generation and the propensity for reactive material to self-heat and combust can be controlled via engineered placement.

In the waste rock landform and reactive waste and NAF are dumped separately, with the reactive waste encapsulated by the NAF waste. NAF waste is paddock dumped and then worked with a dozer to form the flattened and compacted base layer of the landform. Reactive Waste is placed in the middle each lift of the landform by paddock dumping and flattening with a dozer to reduce preferential pathways for air entry and net percolation. Finally, an outer NAF layer is constructed on each dump lift to complete the encapsulation. Compaction of materials occurs as dumping progresses, minimising infiltration of water into the dump. The tops of each lift are compacted and graded to slope away from the crest to manage runoff.

The key processes affecting pyrite oxidation are water seepage through the dump, thermal conductive heat transport and airflow through the dump mass. Numerical modelling and assessment at various mine sites has found that waste material texture and placement methodology is highly influential for both seepage rates and air flow rates (O'Kane *et al.*, 2012).

Most slopes in nature are characterized by a variety of shapes including convex and concave forms interspersed with ridges (spur ends) and swales (hollows), Carson and Kirkby (1972). Waste rock landform batter slopes should ensure geotechnical and erosional stability, aided by the coarse-texture and minimum length of slopes left at the angle of repose. Hence, low height slopes should be left at the angle of repose, and high slopes should retain the angle of repose for the upper part, retain intermediate benches or fill them, with the lower bench only pushed out to half the angle of repose (18° or 1 in 3). Reprofiled waste rock slopes should mimic natural concave slopes, which are stable geotechnically and erosionally (Ayres, 2006).

Erosion

Landform stability is related to erosion potential, and its assessment is a vital component of the landform design process. The greatest risk of failure of final rehabilitated mined landscapes is associated with gully erosion and failure of the re-established surface water drainage courses to adequately convey surface water flows McKenna and Dawson (1997). Erodibility and infiltration parameters are used to assess erosion potential for various batter slope options and overall landform shapes. Factors that should be considered include:

- selecting the least erodible materials for use in high erosion risk areas;
- modifying the erodibility of highly erodible materials, often through addition of rock or tree debris;
- batter gradient, slope length, and shape (linear, concave);
- additional inputs or design changes if required to manage risk of tunnel erosion;

- impact of increasing surface contact cover (rock, standing vegetation, tree debris etc.) and whether additional resources will be needed to stabilize batter slopes;
- impact of allowing flow from the landform top to discharge onto batters;
- impacts of concentrating flows (berms, rock drains); and
- Water infiltration and gas influx into the reactive mine wastes.

The Watershed Erosion Prevention Project (WEPP) modelling can be used to develop the indicative geometry of the variable concave landform at specific locations along the width of the landform and compares erosion along a series of transects that represent different longitudinal profiles (perpendicular to embankment contours) of a designed landform. In WEPP numerous slope configurations can be modelled and compared to develop a set of profiles that erode quite consistently along the modelled profile length. The slope configurations can then combined to form a 3D surface and modelled in SIBERIA to provide a quantitative assessment of erosion. The site survey can be interrogated using AutoCAD Civil 3D and together used to validate model predictions. The modelling is used to inform the engineering design.

Cover systems

The mine's primary strategy to manage reactive waste is to reduce the deep percolation of surface water through the waste material and thereby prevent AMD. This includes cover systems that limit advective gas transport into the waste pile and limit the flow of water (Cash *et al.*, 2014; Wilson *et al.*, 2014). Increasingly store and release covers are being provided to waste rock landforms as part of the closure design with the purpose of controlling percolation of rainfall runoff through these facilities. The focus in successful design is on the specification of the cover with respect to percolation performance and erosional stability facilitated by understanding cover material properties.

Construction of a cover system over reactive waste rock is a technique used at numerous mine sites around the world to control AMD over the long term. A cover for a waste landform located in a semi-humid or humid climate would typically include a reduced permeability layer of compacted fine-textured material (RPL) to reduce the ingress of atmospheric oxygen and net percolation of meteoric waters to the underlying waste material. A cover system with a RPL also requires an overlying layer to protect the integrity of the barrier layer and provide a medium for the growth of vegetation. This layer, referred to as the growth medium layer, also helps to reduce the percolation of meteoric waters to the underlying waste through storage and subsequent release of moisture to the atmosphere as a result of evapotranspiration. Where the site is subject to intense rain events there may be a need to install a drainage layer above the RPL and below the cover system to remove excess infiltration of meteoric water via interflow processes (O'Kane, 2012).

Over compaction of the growth medium layer, particularly in the root zone, should be avoided during construction. Soil compaction restricts root growth and reduces the available water holding capacity of the growth medium. Daniels & Amos (1981) found compaction was the major soil factor limiting long-term revegetation success at a re-claimed mine site in Virginia. Compaction between 80% and 85% of the standard Proctor maximum dry density provides many of the stabilizing benefits of soil compaction without jeopardizing the viability of vegetation development and growth (Gray, 2002).

WATER MANAGEMENT

The waste rock landforms must be able to provide drainage of surface water without significant erosion, limit net percolation of meteoric water to contained reactive waste rock and must retain sufficient moisture to support vegetation within the cover system. Options available in the landform design for managing meteoric water entering the landform catchment to minimise erosion and interaction with placed reactive waste rock include:

- Diverting clean water around the waste rock landform; limit run-on from external catchment to the landform;
- Diverting mine-affected water to holding dams for treatment prior to release or completed pits;
- Avoid shedding runoff from waste rock landform tops over slope crests which will result in erosion of the slopes; slope final and intermediate landform plateaus away from the slope crest and install crest bunding;
- Wherever possible divert runoff from waste rock landform tops to intercept natural gullies;
- Construct a cover system to handle incidental rainfall through increased storage capacity (e.g. store and release system);
- Construct cover system to handle excess water through providing drainage beneath the cover system (interflow) to reduce velocity and remove water excess to cover system capacity;
- Where reactive waste needs to be contained and managed the cover system must be designed to limit net percolation through the entire waste landform and may require a low permeability layer beneath the cover to assist in limiting net percolation;
- Avoid where possible contour banks and downslope drains as long term water management structures as they are prone to overtopping and piping; install these structures as temporary measures only (Williams *et al.*, 2012);
- Where possible avoid placement of reactive waste beneath final batter slope unless it can be adequately sealed to minimise interaction of reactive waste rock with meteoric water and discharge to receiving environment;
- Limit exposure of reactive waste to meteoric water during and post waste rock landform construction;
- Utilize compaction of intermediate waste rock landform surfaces to limit rainfall infiltration during landform construction; and
- Use cross-bunding and paddock dumping as part of the final cover system on the waste rock landform top surfaces to compartmentalise the landform catchment and contain incident rainfall, to encourage infiltration and reduce surface runoff.

MONITORING

The landform performance monitoring herein is referred to as initial (over a period of 1 – 2 years) and short-term (variable time frame) performance observation, investigation, and recording. The components of performance monitoring include erosion stability, vegetation establishment, weed and grazing control, and contaminant seepage rate from the wastes. The initial performance monitoring will provide inputs to the early remedial actions if the deficiency is identified in design and construction processes. During the short-term performance monitoring, the vegetation community develops and a range of soil processes continue to establish. As a result, landform stability should improve in response to the rehabilitated site evolution, and the contaminant leaching rate becomes

stable and acceptable to the receiving environment. At the end of the short-term performance monitoring, the landform should complete the transition from "newly rehabilitated land" to "established rehabilitated land".

Monitor key processes such as:

- Net percolation
- Heat transfer
- Vadose zone gas composition
- Oxygen migration
- Salt uptake
- Soil water characteristic curves

Cover system performance monitoring involving instrumentation includes:

- Meteorology
- Actual evapotranspiration (eddy covariance)
- Surface runoff
- Net percolation (lysimeter)
- Interflow or lateral sub-surface drainage
- Soil moisture
- Temperature
- Gas flux

CONCLUSION

The understanding of unsaturated zone hydrology and geochemistry is of key importance when considering the design of landforms containing mineral waste(s). Limited knowledge of waste material properties can lead to poorly designed and constructed landforms have the potential to cause unwanted environmental impacts, such as AMD, saline drainage, erosion, along with the inability to meet closure objectives and the desired final land use(s). Good environmental outcomes over long time scales is more likely with a thorough understanding of the waste materials properties, combined with early planning and design informed by in-situ data collection.

REFERENCES

Ahern CR, Sullivan LA, McElnea AE (2004) Laboratory Methods Guidelines 2004 — Acid Sulfate Soils, In Queensland Acid Sulfate Soil Technical Manual. Department of Natural Resources, Mines and Energy, Indooroopilly, Queensland, Australia.

Ayres B, Dobchuk B, Christensen D, O'Kane M and Fawcett M (2006) Incorporation of natural slope features into the design of final landforms for waste rock stockpiles, In Proceedings of 7th International Conference on Acid Rock Drainage', St. Louis, MO, 26-29 March 2006, 59-75.

Carson MA and Kirkby M (1972) Hillslope Form and Process, Cambridge University Press, Cambridge, UK, 475 p.

Cash, A., Wilson, G.W., Blowes, D.W., Amos, R.T., Robertson, J., and Turgeon, M.H., (2014) Characterisation of 26 year old waste rock stockpiles at the Detour Lake project, In Proceedings

of the Eighth Australian Workshop on Acid and Metalliferous Drainage (Eds H Miller and L Preuss); pp.197-210.

Coastech Research (1989) Investigation of Prediction Techniques for Acid Mine Drainage, MEND Project Report 1.16.1a, MEND, Ottawa, Ontario.DMP (Department of Mining and Petroleum) (2010), Draft Mine Closure Gudelines, State of Western Australia.

Daniels, W.L. & Amos, D.F. (1981) Mapping, characterization and genesis of mine soils on a reclamation research area in Wise County, Virginia. In Surface mining hydrology, sedimentology and reclamation; Proc. symp. Univ. of Kentucky, Lexington, KY: pp. 261-275.

Gray, D.H.(2002) Optimizing soil compaction. www.forester.net/ecm_0209_optimizing.html.

INAP (International Network for Acid Prevention), (2009) The Global Acid Rock Drainage Guide, Available at http://www.gardguide.com

McKenna GT and Dawson R (1997) Closure planning practice and landscape performance at 57 Canadian and US mines, In Proceedings of the 21st Annual British Columbia Mine Reclamation Symposium in Cranbrook, BC, 1997, pp. 74-87.

Miller, S., Robertson, A. and Donahue, T. (1997) Advances in acid drainage prediction using the Net Acid Generation (NAG) Test, Proc. 4th ICARD, Vancouver, BC, pp 533-549.

O'Kane, M. and Ayres, A. (2012) Cover systems that utilise the moisture store-and-release concept - do they work and how can we improve their design and perform, Proceedings of the Seventh International Conference on Mine Closure, September 25-27, 2012, Brisbane, Australia

Sobek, AA, Schuller, WA, Freeman, JR, and Smith, RM, (1978) Field and laboratory methods applicable to overburdens and minesoils, U.S. Environmental Protection Agency Environmental Protection Technology EPA-600/2-78-054, 203 p.

Scott, P.A, Eastwood, G., Johnston, G. and Carville, D., (1997) Early exploration and pre-feasibility drilling data for the prediction of acid mine drainage for waste rock, In McLean, R. & Bell, C. (Eds.) Proceedings of the 3rd Australian Workshop on Acid Mine Drainage, Australian Centre for Minesite Rehabilitation Research, Darwin NT, pp. 195-201.

Williams, D.J., Scott, P.A and Gerrard, J. (2012) Rehabilitation Commitments for Pits and Waste Rock Stockpiles at Frances Creek Iron Ore Mine, In W. A. Price, W, Hogan, C. and Tremblay, G (Eds) Proceedings of the 9th International Conference on Acid Rock Drainage (ICARD), Ottawa, Ontario, Canada, May 20-26, 2012.

Plugin Arcgis – FEFLOW – Case Study

Katty Barzola, Ezio Crestaz and Robin Dufour
DHI Peru

ABSTRACT

Numerical FEFLOW groundwater flow models are designed, evaluated and finalized according to the specific purpose of a study. Often following completion of a model it is necessary to make small changes to the model as new data is collected, and observe the effects these changes have. This would normally require a FEFLOW specialist. Arcgis-FEFLOW is a tool that has been developed with the purpose of allowing people with knowledge of Arcgis to make small changes to a completed flow model and assess the results including the automatic update of the figures for the report.
A simplified FEFLOW model developed to evaluate potential effects of a proposed mine expansion on the groundwater system was used to demonstrate a practical application of Arcgis-FEFLOW. The results of this model were presented in August of 2013, one year later this model required an update of water level information, pumping well rates and new values for recharge (boundary conditions). The results of the update were related to fluxes, flow direction water levels. These results were compared with the original for different scenarios created in FEFLOW. This process of edits and assessment was then re-created in Arcgis using the pluggin Arcgis-FEFLOW.
The advantage of this tool is that it is accessible by people who do not necessarily have years of experience in numerical modeling but are familiar with ArcGis and also allows the direct use of data from a database.
The main disadvantages of this plugin are the limited 3D visualization, which is standard when working directly in FEFLOW, also it is not recommended to try to perform a calibration with the Arcgis-FEFLOW plugin as it is not designed for this purpose.

Keywords: Feflow groundwater modeling, GIS technology.

**There is no full article associated with this abstract*

Mine Water Disaster Issues of Carboniferous and Permian Coalfields at Eastern China and Their Technical Countermeasures- A Case Study on Wanbei Mining Areas

YuhuaWu, Zhongwen Duan , BenkuiSun and Rongjie Hu
Wanbei Coal-Electricity Group, China

ABSTRACT

The coal bed of Eastern China coalfields is mainly composed of Carboniferous and Permian coal measures strata, where mining safety is threatened by a variety of water disasters especially at the Wanbei mining areas. In this study, we first introduce the main mine water disasters in the East China Coalfields such as Cenozoic loose stratum “bottom containing” water inrush, sandstone fracture water inrush, Carbonic and Ordovician limestone Karst water inrushes, Column collapse water inrush, water related environmental pollution and resource loss, and the like. We then expatiate on 1) several measures for water disasters prevention and control with Wanbei Coal-Electricity Group as an example, including in-advance rigorous problem explorations, and mine water inrush mechanisms and related forecast and early-warning technology, as well as key technologies, 2) eight-in-one water disaster prevention and control work system, 3) "water-control and green mining" concepts, and 4) the prospective of future development.

Keywords: East China; Wanbei Coal Mines; Mine water issues; Technical countermeasures

INTRODUCTION

The coal beds of coal mines in Eastern China are mainly composed of Carboniferous and Permian coal measures strata bounded by the Cenozoic loose layer at the top and Middle Ordovician carbonate rocks at the bottom. Because the former often contain multiple sand aquifers and the latter is the most water-rich regional aquifer, they are the main water sources causing mine water disasters. During the past two decades, water inrushes occurred in more than 220 mines in China, causing more than 8,000 deaths, and economic losses of more than 30 billion RMB[1]. These incidents occurred particularly in mines of the Carboniferous and Permian coalfields in Eastern China.

The Wanbei coal mining area is complicated because of geological, tectonic and hydrogeologic factors. It belongs to the Xuhuai region, Luxi subzone, Huabei stratigraphic zone and has bedrock covered by the Cenozoic loose layer and stratigraphic structure composed, in geologic time sequence, of Cambrian, Ordovician, Carboniferous, Permian, Tertiary and Quaternary rocks. The tectonics of the coal-mining area is well developed with a total of more than 50 faults with falls ≥100 m [2]. Most water inrushes are sourced directly from the roof and floor, with fracture water as the main source. Some floor inrushes from Karst water sources also occur to a lesser extent. In addition, the mining area has other features that present a potential water filling risk, such as water-conducting karst collapse columns, aquifers at the bottom of loose layers in the limestones of the Taiyuan group at coal bed's floor, and at sandstone fractures of the coal bed's roof and floor [3]. In the history of mining, all types of typical and representative water disasters and severe water disasters have occurred in this area.

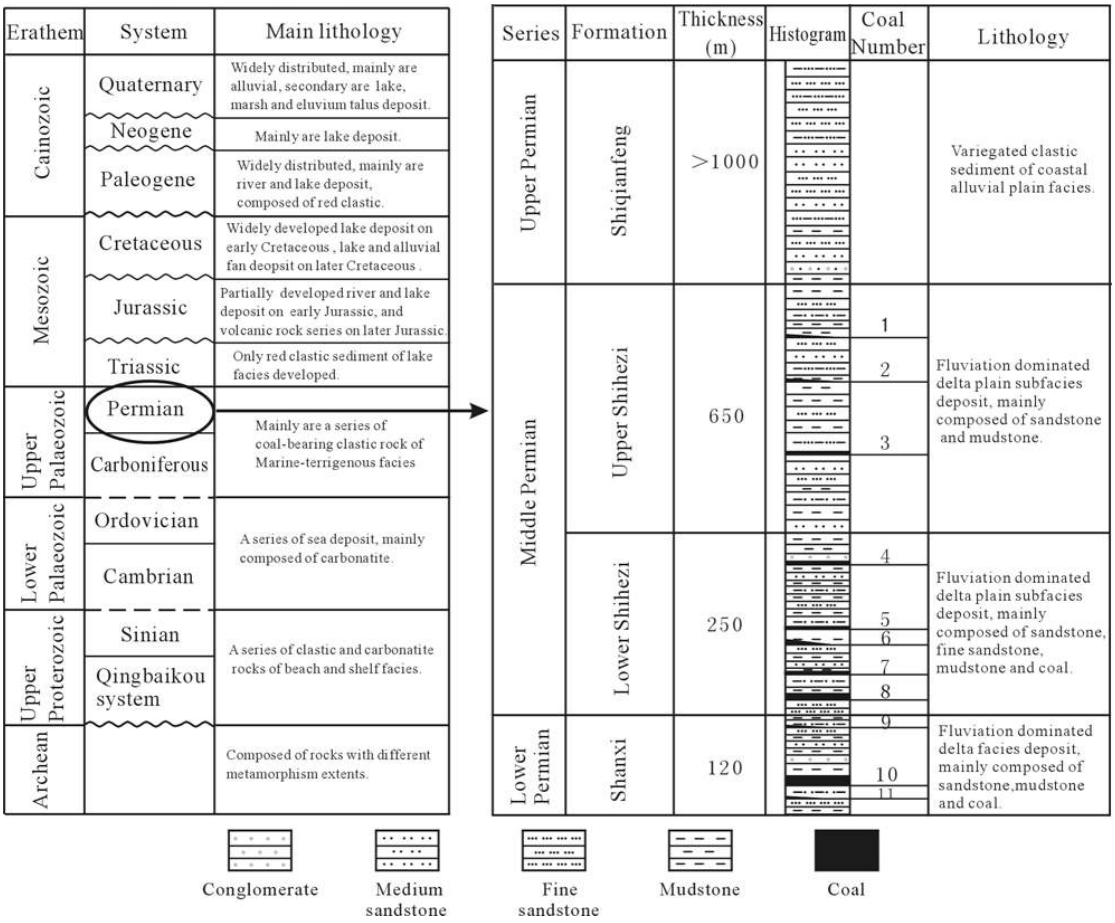

Figure 1 Stratigraphic integrated histogram

MAIN MINE WATER ISSUES IN WANBEI MINING AREA

The main mine water issues in Wanbei mining area include: 1) great threats to the mining faces positioned at shallow depth, caused by the well-developed Quaternary water-bearing strata located on the bottom of the Cenozoic loose layer and water-rich "ancient gullies" in some areas; 2) threats from abundant fracture water to the coal bed roof sandstones (faults), especially at new coal mine zones and faces; 3) threats from the confined aquifer to safely mining the No.10 coal bed floor, where the water inrush coefficient of high pressure limestone exceeds its critical value; 4) potential threats to safe production from many insidious karst collapse columns located near the coal-mining areas; 5) potential water hazards from goaf water in the mining areas; 6) potential environmental pollution from a large amount of mine water which flows in at an average rate of 310m^3/h and is highly mineralised, including high hardness, and some harmful elements if directly discharged [4]; and 7) a potential decrease in groundwater level, subsidence of the industrial complex located nearby, and the damage of mine shafts resulted from subsidence during coal production which consumes great amounts of municipal water mainly from the surface loose layer.

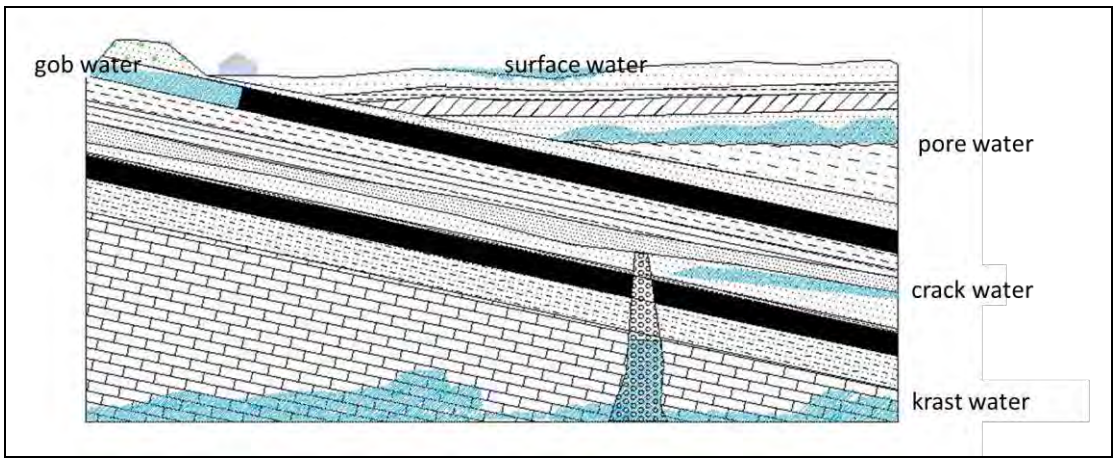

Figure 2 Schematic of coal mine water disasters

TECHNICAL COUNTERMEASURES AGAINST MAJOR MINE WATER ISSUES

Management System

It is necessary to establish 1) an effective three-in-one coal mine water disasters prevention and control system, consisting of a leadership subsystem, a technology management subsystem, and a technology, finance, and materials safeguard subsystem, 2) a sound eight-in-one coal mine water disasters prevention and treatment operation system of exploration, prediction, underground drilling, evaluation, measures, examination, monitoring, and protection, with the aim to form a complete mine water forecast and treatment pattern of "full members' attention, advanced equipment, leading technology and sound system.

Technical concept of water-controlling mining

The concept of water-controlling mining is proposed as 1) optimizing the rules for responding to catastrophes caused by sudden changes in rock and water coupling mining-induced rock fractures through the means of artificial and controllable factors such as pillar scale and mining sequels; 2) mastering the inherent and universal laws between catastrophe mechanisms and the natural/man-made controllable factors, i.e. understanding i) the enclosure conditions and control mechanisms of coal bed mining-induced fracture generation and propagation, as well as ii) the formation laws of channels connecting inrush water and collapsed sands; 3) proposing new water-controlling mining technical theory and engineering methods of coal seams subject to water inrush; 4) establishing and improving the water hazard prevention and treatment platform; and 5) completing the transition from passive water prevention and treatment to active water control. Overall, the following three objectives should be achieved: 1) water-protection and green mining; 2) safe and economic mining; and 3) clean production and resource conservation.

Exploration of advanced fine examination techniques of mine hydrogeological conditions

"Forecast and predict, explore when with doubt, investigate before digging, and mining after control" are not only the basic principles, but also the basic procedure of coal mine water disaster prevention and treatment. The exploration of mine hydrogeological conditions is based on forecasting and prediction [5]. In recent years, studies on the implementation of advanced fine examination techniques of mine hydrogeological conditions at Wanbei mine areas are mainly focused on the following areas:

1) High precision 3-D seismic exploration techniques: A series of processing techniques have been applied to achieve high precision 3D seismic exploration such as i) high-density, wide-azimuth 3D seismic data acquisition technology, ii) high-precision iterative static correction, pre-stack noise removal, amplitude maintaining, resolution improvement, pre-stack shifting processes, iii) forward modeling guidance, multi-character analysis, and comprehensive 3D visualization analysis [6].

2) Ground and underground collaborative, integrated advanced exploration techniques: Combined applications of the ground electric surveying, ground 3D seismic exploration, and dynamic data processing and interpretation with underground advanced geophysical exploration and advanced shield drilling exploration were implemented to accurately explore the hydrogeological tectonics, water-rich abnormal areas, and various water inrush risks for the purpose of safety production.

3) Underground multi-parameter monitoring and pre-warning and advanced exploration and treatment techniques of insidious water-bearing and -conducting karst collapse columns: Based on previous determination of insidious collapse columns, a management idea integrating "Geological pre-judgment, hydrological pre-warning, geophysical positioning, and drilling control" was implemented for active and preventive treatment. An online testing platform was established and studies on rapid identification of both water inrush sources and channels based on water quality, temperature, amount, and potential outflow points were conducted. Based on pre-judgment and following pinpoint positioning of collapse columns by integrated geophysical probing, both the underground roadway sealing-off and the ground, high-precision angle directional boreholes as well as multiple borehole combined dislocated grouting were jointly used for prevention of insidious collapse columns. Many such columns were found in advance and successfully treated, thus avoiding the occurrence of water inrush accidents.

4) Efficient, precise, and directional drilling exploration techniques: A series of techniques and measures such as borehole precise positioning and whipstocking branches, underground long-distance, nearly horizontal directional drilling, measurement while drilling, and safe and efficient construction in drilling and grouting were taken to achieve efficient, accurate, and directional drilling exploration.

5) Mixing water sources recognition techniques: The conventional water chemistry, trace elements, stable isotopes, and other means were applied to systemically study the primary control mechanisms of water chemistry in multiple aquifers. Combination of mathematical statistics, neural networks, and other measures was used to establish a water-sources identification model suitable for mine water prevention and treatment. An identification method for water source containing rare earth elements, a proportion calculation method for mixed water sources in mine were

proposed for the first time, which solved the technical difficulty in fast identification of mixing water sources at multiple water-bearing strata, and pioneered the studies on the mines' mixing water source.

6) Ongoing research projects include the seismic and electromagnetic method combined ground hydrogeophysical prospecting technique for mine water, the advanced exploration techniques integrated with roadway-borehole electromagnetic method, drilling and geophysical exploration, and the like.

Research on mine water inrush mechanisms and its forecast and pre-warning technology

Wanbei mining area is one of the earliest areas for studies and application of mine water inrush prediction and pre-warning technology. In this area, a series water hazards forecast and early warning techniques such as prevention and control of floor limestone water inrush, goaf water inrush, and roof's Cenozoic bedrock water inrush have been consecutively implemented, a mine water quality monitoring system and water chemistry information database of various water-filled and water-bearing strata were established, a water source identification model and calculation software were developed, and an effective early warning of mine water disasters was completed. In addition, researches in the mining area are focused on the deep-mining induced water hazard evaluation and prediction technologies as well as the real-time face water inrush forecast and early warning technologies. Considering the three prerequisites for the occurrence of mine water disasters (water sources, channels, and amount), a real-time, linear, and planar monitoring and early warning was implemented to achieve the goal of simultaneous monitoring and warning of mining-induced deformation and water inrush potentials. For example, a series of researches were conducted on water inrush prediction and early warning techniques of 1) floor limestone water at 6112 Face, II621 Face, and II615 Face of Hengyuan Coal Mine, 2) gob water from adjacent faces at 6131 Face of Qidong Coal Mine and 1018 Face of Wugou Coal Mine, and 3) Cenozoic roof and aquiferous floor at 7131 Face of Qidong Coal Mine. These researches on water inrush prediction and early warning techniques were effectively applied in water disaster prevention at mine faces.

Research and implementation of mine water disaster control technology

After years of research and innovation, Wanbei Coal Electricity Group co. Ltd. has solved a series mine water hazard control issues and constructed relatively complete and advanced coal mine water disaster prevention and treatment technology systems. Firstly, the insidious water-bearing and -conducting column collapse forecast and control technology has successfully detected insidious hazards in advance, thus avoiding many water inrush accidents in a timely manner. Secondly, the coal seams mining techniques under Cenozoic loose layer aquifers have been improved by using seam roof pre-split blasting and gangue backfill mining and implemented to effectively prevent and treat roof water inrush and sand downpour disasters. Thirdly, the coal seams mining technique on floor limestone confined water has been applied to perform a series of advanced face floors exploration, grouting reinforcement for ground floor ,and aquifer improvement, thus efficiently controlling limestone floor water inrushes. Fourthly, advanced

detection techniques of roof and floor sandstone fracture water were used to monitor and discharge water in a targeted manner, thus ensuring safe production. Below is an application example of presplit blasting technique for the face roof under confined water.

Qidong Mine coal measure stratum is covered by Cenozoic thick loose layers. Its bottom aquifer (the Quaternary aquifer) directly overlays the coal-bearing strata, and has characteristics of greatly varied lithologic composition, thickness, and water richness, as well as complicated ancient riverbed distribution condition, which directly threaten its safety exploitation. Since the operation of Qidong Coal Mine, its eight fully mechanized faces, Faces $3_2$22, $7_1$14, $7_1$12, $7_1$30, $7_1$21 and others, consecutively underwent 17 support failure accidents, among which, 15 ones were accompanied by water inrush. On November 25, 2001, both support failure and water inrush occurred at the first mined $3_2$22 Face, resulting in flooding the mine. The analysis of the Face data found that the development of damage to hard overburden stratum induced by fully mechanized mining was very large, the relationship between the maximum damage height of the overburden stratum and the mining depth didn't meet the general mining rules which complied by other mines in the hard overburden stratum exploitation. Under the conditions of Quaternary high water pressure and original fissures' great angle, longitudinal cracks development, the damaged height of overlying rocks sometimes increases significantly. Therefore, roof water disaster prevention and control for Qidong Coal Mine should focus on the determination of types and rational sizes of coal seam roof pillars and supports, the specific methods are as follows:

1) Roof's advanced pre-split blasting:

According to the physical characters of roof strata, advanced pre-split blasting of the face roof was taken. With the mining advancing, the construction blast parameters were constantly adjusted to reduce the periodic weighting step distance and the two-zone height of the roof. The measured two-zone height was 43 m, 10 m lower than that in the previous similar mining faces.

2) Comprehensive monitoring of roof water seepage physic field:

Through the monitoring of early warning boreholes in the face, the characteristics of ground electric field parameters of roof deformation and failure, as well as the migration of roof water seepage in its face mining process were measured to rightly forecast the face mining states.

3) Application of high resistance supports:

According to the combination of roof rock properties, high resistance supports were used to strengthen the face's supporting capacity for preventing support failure, water inrush, and roof caving, etc.

4) Ground monitoring and early warning:

Through long monitoring boreholes into the Quaternary strata, the level of water in the strata was real-timely tested; then, according to the relationship between the level of water and the cycle of

periodic weighting, face mining advanced scientifically under a reasonable wall pressure to avoid support failure.

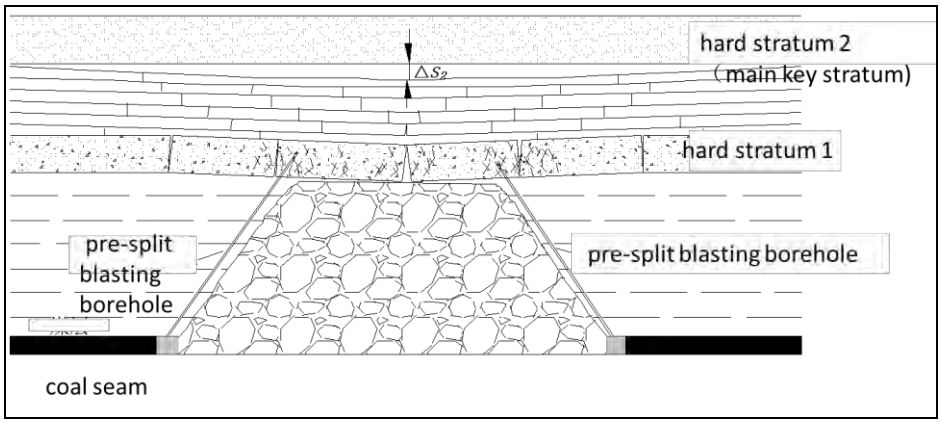

(a)

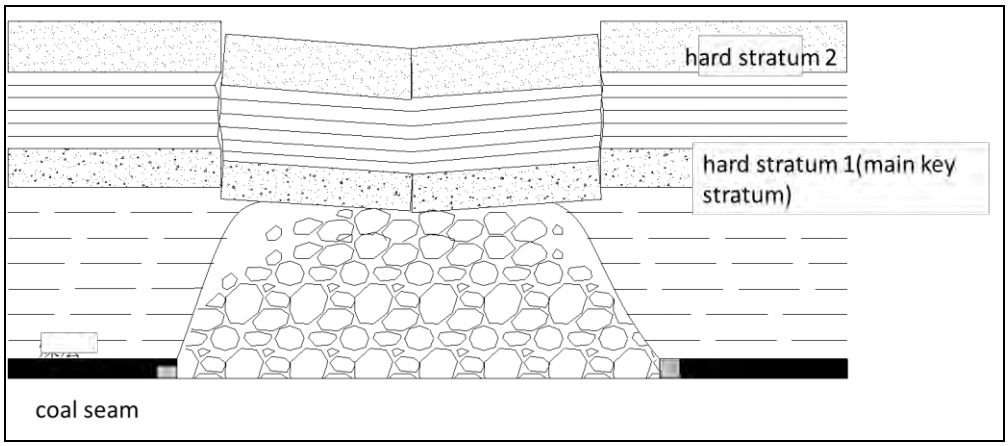

(b)

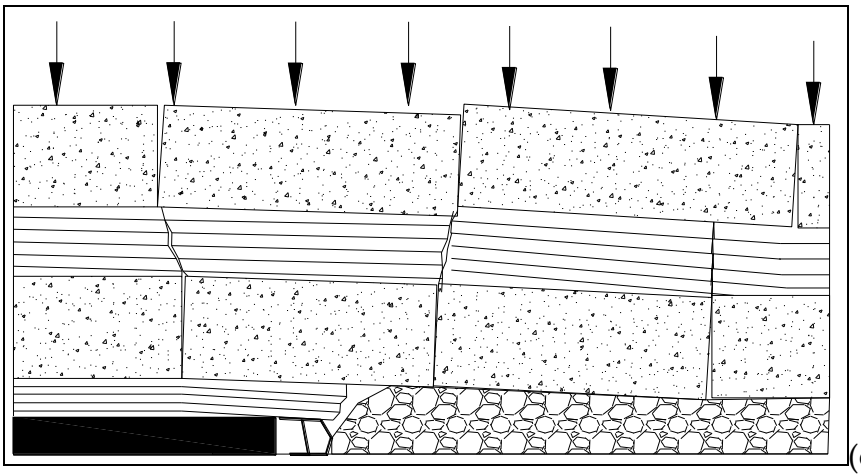

(c)

Figure 3 Schematic of face roof pre-split blasting

Mine water resources utilization technology

Wanbei mining area actively launches a series of researches on groundwater hydrogeochemistry, mining area water environment and quality assessments, mine water resources reclamation and utilization, forms the mine water drainage and supply combined technology, the reasonable mine surface water and underground water adjustment and distribution technology, the mine waste-water treatment and reclamation technology, and the three-in-one optimized management technology of mine water discharge, water supply, and eco-friendliness [7]. The mining area has installed the water treatment device to each mine in the area, and the treated mine water is used for mine coal production and living water, achieving 100% mine water process and utilization .At the same time, the utilization of mine water directly reduces the water withdrawal from the surface loose layer, and protects the natural balance of the surface phreatic water, thus avoiding sink age of surface water level, subsidence of the industrial squares, well-bore failure, and other issues caused by excessive water withdrawal from the surface loose layer and having very significant benefits to environments and society.

CONCLUSIONS

Wanbei Coal Electricity Group uses" water-controlling exploitation", safety and efficiency as its motto, prevention of mine water disasters as its focus, and with exploration, forecast, prevention and treatment, and comprehensive utilization of mine disasters as its main line. The group conducted a series of in-depth researches from the aspects of 1)mine water containing laws, 2) hydrogeologic precise exploration techniques, 3) water inrush mechanisms and forecast and early warning techniques, 4) water hazards prevention and treatment techniques,5) mine water resources utilization techniques, to develop and apply such key technologies as 1) the prevention and treatment of mine water disasters, 2) the comprehensive utilization of mine water resources, and 3) the protection of water environment, and takes a lot of measures to tackle the challenges of mine water issues and form a comprehensive prevention and treatment and management system to prevent and control mine water disasters and coordinate water resource and eco-environment protection with the hope to achieve harmonious development between human and nature.

Overall, Wanbei Electricity and Coal Group has formed a set of advanced coal water disaster prevention and treatment technologies and management patterns and ensured safe mining and production for consecutive 13 years. These techniques have been widely promoted and applied to North China Coal Mines located in the eastern China with significant benefits and achievements. In 2014, Wanbei Electricity and Coal Group established the National Engineering Technology Research Center for Coal Mine Water Disaster Prevention and Control to improve China's overall technological level, tackle coal mine water issues and promote safe, eco-friendly, and healthy development of the coal industry.

REFERENCES

[1] State Administration of Work Safety, State Administration of Coal Mine Safety. "China's Science and Technology Development Countermeasures for Prevention and Control of Coal Mine Water Disasters (draft)", 2013.12.

[2] Benkui Sun. Water Hazard Prevention and Control Approach to Safety. Chinese Journal of Coal Industry, 2008, 02, Total No. 252.

[3] Herong Gui and Luwang Chen. Study of Wanbei mines Main Water Inrush Sources Hydrogeologic Features. Journal of China Coal Society, 2004, 29 (3): 323-327.

[4] Jiwen Wu, Zhongwen Duan, and Benkui Sun, et al. Water Hazards Prevention and Control Measures of Coal-mining floor above High-pressure Confined Aquifer Karst water Body at Wanbei Mine Areas. Journal of North China Institute of Science and Technology, 04 2009.

[5] Yuhua Wu, et al. Study on Comprehensive Mine Water Hazard Prevention and Control Technology. China University of Mining and Technology Press, 2009.

[6] Qiang Wu, ShuninDong, and Zhilong Zhang. Prevention and Control of Coal Mine Water Disasters. China University of Mining and Technology Press, 2007.

[7] Qiang Wu and Zhanhua Shi. Research on Optimized Three-in-One Combination of Drainage, Supply, and Eco-friendliness for North China Type Coalfields. Science in China Series D. 1999, (6).

CHAPTER 13

MINE DEWATERING

Dewatering of Opencast Mines Using Model-Based Planned Horizontal Wells

Holger Mansel[1], Richard Eichler[2] , Marcel Nitz[1], Maik Biedermann[1], Rene Blankenburg[1] and Carsten Drebenstedt[2]

1. *Ingenieurbuero fuer Grundwasser GmbH, Leipzig, Germany*
2. *Technische Universität Bergakademie Freiberg, Germany*

ABSTRACT

As part of many mining and civil engineering projects that involve surface excavation, rock layers must be drained first to allow excavation, removal, and disposal of rock and soil. Today this drainage is mainly achieved by using vertical wells. Especially in thin aquifers the extractable water quantity by a single well is limited due to a very small length of the screen section. Since vertical wells may interfere with land use rights over the location of water catchments, horizontal drainage using Horizontal-Directional-Dewatering (HDD) is of increasing interest. There is a high potential to achieve the drainage capacity of many vertical wells by using fewer HDD wells. Furthermore, this allows for significant reduction in material and energy use, land use, and groundwater resources. Based on the results of the first phase of the project which dealt with the oncoming flow in HDD wells, the second phase addresses the hydraulic effects of the elements environmental impacts, cost effectiveness, and application on an industrial scale.

Keywords: PCGEOFIM, Groundwater modeling, horizontal wells, Horizontal-Directional-Dewatering (HDD)

INTRODUCTION

Dewatering of near-surface unconsolidated rock material is an important prerequisite for the technical implementation and safety of mining projects. The removal of water from the overlying rock is also a basic necessity for stable slopes and benches. For this purpose, considerable volumes of water are pumped annually in the construction and mining industries, about 1 billion cubic meters in Germany's open-cast lignite mines alone. Regarding the geological/hydrological conditions of deposits, particularly in basin structures, the piezometric pressure may also have to be reduced, and sometimes drained below the base of an excavation. Otherwise there would be a risk of footwall failure with water escaping from the ground. Higher residual water levels in overburden operations and out-of-control rising ground water levels could cause slides. A lot of negative experience has been gained through such hazards in lignite mining.

Nowadays vertical filter wells are commonly used on a large scale to lower the groundwater table and to relieve groundwater pressure. Depending on hydro-geological conditions, the lowering of ground water tables cannot usually be limited to the immediate mine area itself, even more so as this process must take place in advance to guarantee compliance with geotechnical and hydrological target values. This has a negative impact on the regional hydrological balance and must, therefore, be minimized.

METHODOLOGY

Based on the results of a successfully completed phase 1 the aim of the 2nd phase of the research project (both phases funded by the Deutsche Bundesstiftung Umwelt, DBU, [German Federal Foundation for the Environment]) is to develop the scientific and practical basis for the application of an alternative dewatering method , i.e., curved filter wells (Horizontal Directional Drilling - HDD) and to overcome the environmental drawbacks of the use of vertical filter wells as efficiently as possible.

Currently, the curved dewatering technique in lignite mining is limited to a few individual cases, but has great potential for easing the environmental burden of mining projects (Müller et al. 2009). Figure 1 shows how curved horizontal directional drilling can be performed with relatively little effort beneath an area that otherwise could only be accessed underground (with difficulty) or not at all.

Figure 1 Schematic presentation of horizontal drilling (Tracto-Technik 2010)

As a rule, installation of HDDS is divided into three successive steps – pilot bore, reaming(s) and pulling in pipes or filters.

A complete dewatering of the overlying rock, e. g., of an open-cast mine, or of the relieved aquifer of a footwall opens up a complete new range of applications for the curved filter well technique.

The basic principle is to let the water that is produced by the HDD filter wells discharge freely at the lowest point of the well.

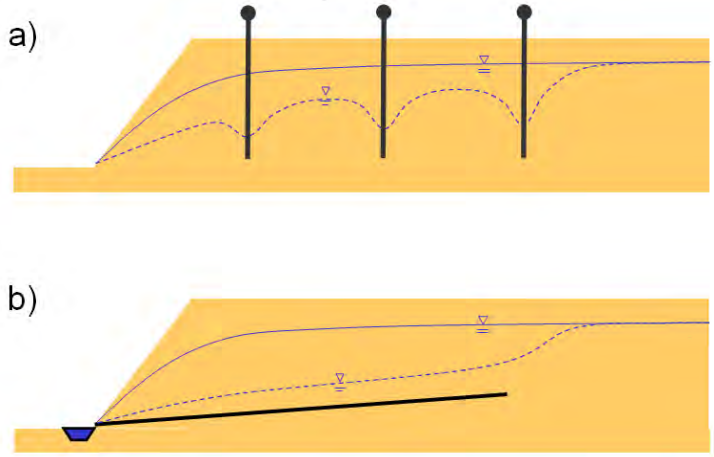

Figure 2 Drainage of overburden material at slopes of open-cast mines, a) using conventional vertical wells, b) using horizontal filter wells (Eichler 2013)

Figure 2b shows how the HDD well is installed in the rock formation next to the slope. Thus the water flows out by gravity continuously. Due to the mining progress material of the slopes is excavated and the end of the well will be cut time and time again. However, the water produced by the HDD flows out at the in-pit end of the well. The water will be collected by a trench on the bench and led to a central pumping station at the deepest point of the open-cast mine. By this means, there is no need for pumps or installations at every single well. Consequently, no pipelines are required to receive the water from the individual wells and to pipe it to a central water station as it is in the case of using vertical wells. The real field of an open cast mine is directly used only prior to the actual surface excavation when the HDD wells are installed. Furthermore, while the length of the effective filter section of vertical wells is reduced due to sinking water level, the effective filter length of horizontal wells remains constant. As a result, the number of required wells may be much lower due to the several times longer wetted filter screen compared to vertical wells.

The freely outflowing water will be collected at a central water station and pumped by large pumps whose efficiency is much higher than that of many small pumps that ought to be installed in the vertical wells. As a consequence power consumption will decrease. Such wells may be used in both, active slope systems and final and periphery slope systems.

Depending on geological and hydrological conditions and the geological structures, various modifications and designs respectively are possible due to the flexible installation of HDD filter wells. Based on preliminary studies, several options are conceivable.

Option 1: As illustrated in figure 3, a drill hole with an exit opening can be equipped with a submersible pump if the dewatering takes place close to the surface. Alternatively, a close-to-surface filter well can also be connected to a collection shaft (figure 4) allowing gravity flow from the HDD and extraction from the collection shaft as needed.

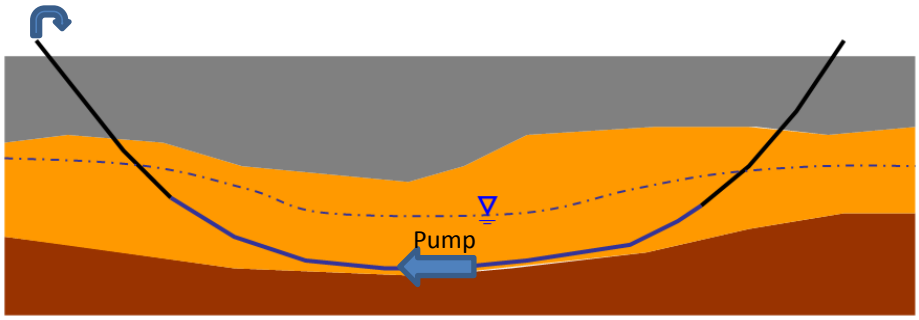

Figure 3 HDD well with submersible pump close to the surface with exit opening (Struzina 2012)

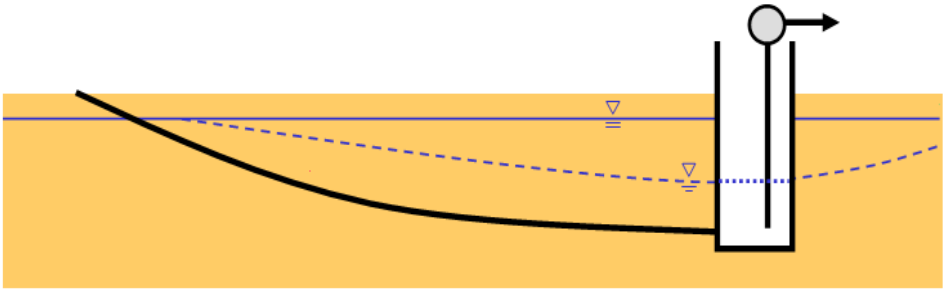

Figure 4 Close-to-surface HDD filter well with collection shaft

Option 2: In a mine's border slope system, HDD wells are drilled along the slopes. The water flows through their entry opening into water collection trenches put in place at the bottom of the slope from where the water is drained. Such a solution is illustrated in figure 5 whereas in certain cases several slopes can be dewatered by one HDD well.

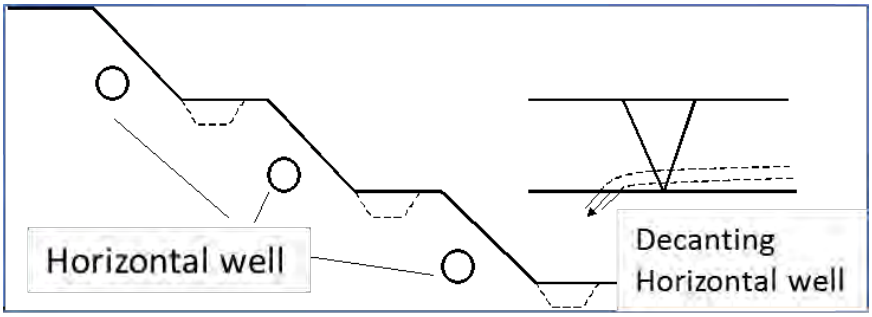

Figure 5 HDD filter well in a mine's border slope system

Option 3: The only alternative to vertical filter wells for dewatering projects with multiple aquifers are either HDD wells to be drilled in each aquifer or the connection of vertical infiltration wells with curved horizontal wells .

In addition to HDD drilling, which is comparably expensive, this option offers a cost-efficient alternative for continuous concentrated drainage of all horizons using one HDD well for all aquifers. For this purpose, all vertical injection wells are directly or indirectly connected with the horizontal filter train in the deepest aquifer to be drained. The water of low lying and hanging aquifers drained by injection wells flows to the bottom or deep-lying aquifer and is pumped through the HDD well wich has been put in place there (figure 6).

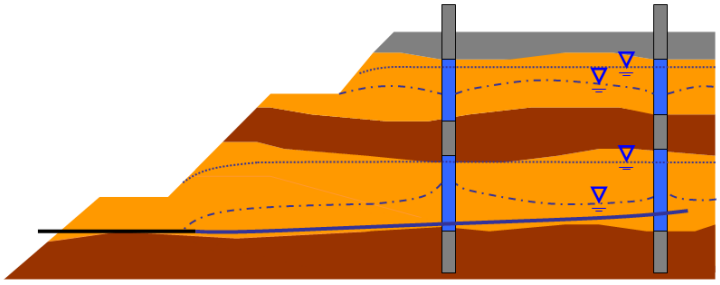

Figure 6 HDD well in connection with vertical injection well (Struzina 2012)

Further options and opportunities for the modification of HDD wells shall be examined and developed subject to the geological conditions and technological boundary conditions of construction sites and mining

Development of improved calculation methods and modeling

For planning and consulting engineering activities, the Ingenieurbüro für Grundwasser GmbH (IBGW) uses the PCGEOFIM® program (Sames et al. 2011) developed in house. This program was developed primarily for active mining and reclamation mining and is used for these purposes by other institutions as well, among them are the Mitteldeutsche Braunkohlengesellschaft mbH (MIBRAG), Lausitzer und Mitteldeutsche Bergbau-Verwaltungsgesellschaft mbH (LMBV), TU Bergakademie Freiberg, Vattenfall Europe Mining AG, Dresdner Grundwasserforschungszentrum e.V. (DGFZ) and more.

Based on the results from bench-scale and field tests and their model-aided monitoring in project phase 1, new knowledge was gained concerning the open channel pipe flow in the horizontal well as well as the pressure pipe flow by involving the pressure losses.

Figure 7 shows the impact of an HDD filter well on the groundwater flow when the well is fully flown and a pressure flow occurs in the filter pipe (left) and when the well is subject to a non-full flow and open channel flow in the filter pipe (right). Only the case of a full flow with pressure flow in the filter pipe has so far been correctly modeled and tested. Further possible are the case of full flow and open channel flow (this case was observed in a field test during project phase 1), the case of non-full flow and pressure flow and the case of no flow.

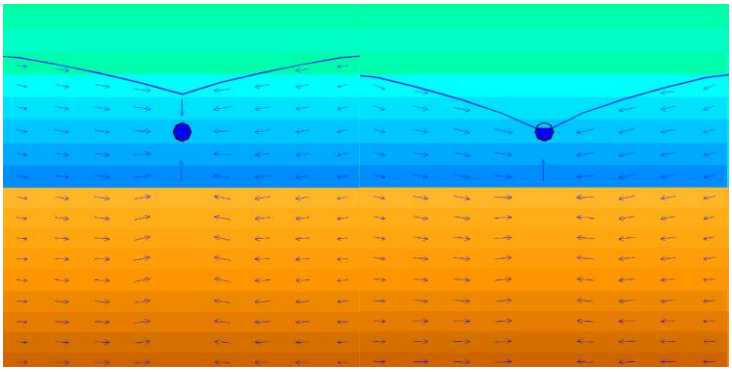

Figure 7 Full (left) and non-full flow (right) to a horizontal well with pressure pipe and open channel flow

On the basis of the results and knowledge gained from the tests performed in project phase 1, open channel pipe flow was realized in the groundwater model of the PCGEOFIM software system and

theoretical findings were made with regard to pressure loss behavior in pressure pipe flow scenarios.

For a comprehensive algorithmic presentation of the possible impact of HDD filter wells on the groundwater table, it will be necessary to develop further algorithms clearly describing the connection between the water level in the filter pipe and the water volumes flowing – in sections - into and out of the horizontal well. However, a solution has not been found for a case yet where both flows, i.e. open channel and pressure pipe flow, occur in the HDD filter well. The tipping point between open channel and pressure pipe flow shall be subject to further investigations in bench scale testing.

The capacity of an HDD filter well is limited by the pressurized water flow. Only a limited amount of water can be transported per time unit subject to length, diameter, pipe roughness and gradient. The formulas for pressure and open channel pipe flows are known. However, in phase 1 of this research project, new knowledge has been gained after considering open channel pipe flow in the model and findings were made with regard to the calculation of occurring pressure losses. The use of HDD filter wells as open channels with a free water surface following the conventional approach of Manning/ Strickler (pipe channel) enabled a more accurate representation in the model. Inflows to the individual HDD well sections are shown in figure 8.

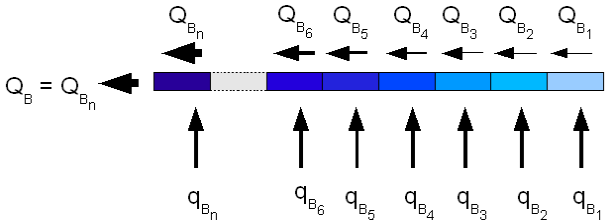

Figure 8 Calculation of the through flow in an HDD well used as an open channel

Fig. 9 shows a graph of water levels and pressure losses. Calculations follow the iterative method using an initial guess.

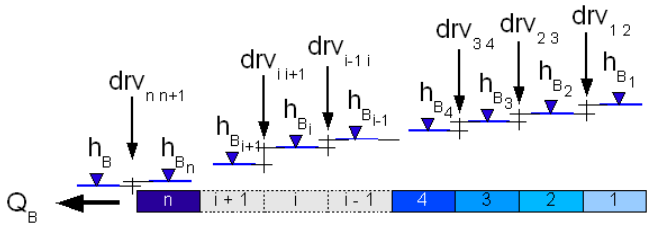

Figure 9 Calculation of pressure losses in a pressure pipe flow scenario

The theoretical knowledge gained in phase 1 with regard to the calculation of pressure, open channel pipe flows and pressure losses shall be implemented, verified and tested in the model algorithm within the scope of further research to be conducted in project phase 2.

Further work on the project will be focused on two parallel key subjects based on the results gained in the first project phase.

The first subject will include bench scale testing in order to evaluate the data for modeling. The focus will be on the extension of the data basis on one hand and on further investigation needs if identified as necessary from the results of the first project phase on the other hand. The second subject will be dedicated to a field test with a practical application of curved dewatering drilling in

a multiple aquifer scenario.Additionally, the investigations shall also include the exploration of opportunities for drainage modeling using curved horizontal drilling as a two-phase model.

RESULTS AND DISCUSSION

Within the scope of both the bench scale testing and field test to be done in the project phase, a geological structural model was created. Based on that model, a numerical groundwater model for the simulation suite PCGEOFIM was developed. By means of available measurement values, the groundwater model was calibrated for the startup time of an HDD-well to allow for prediction simulations. During the test phase, the model statement was continuously recalibrated on base of newly available observations (figure 10). The results obtained from both, the bench scale testing and the field test, were used to improve the knowledge of processes in the close range of HDD-wells. By means of accompanying research and mathematical model development, new algorithms were implemented into the groundwater simulation suite PCGEOFIM. A significant result is the consideration of head loss in the well pipe and its effects to the surrounding groundwater flow. The section below describes modeling results of the field scale test. It emphasizes the comparison of measured and computed values.

In Figure 10 the observed (red dots) and calculated (line) values of the outflow of an HDD-well are shown. The blue vertical bars depict the times of well development. Several well devleopments had to be conducted to achieve a good drainage. In general, the computed results show a very good agreement with the obervations.

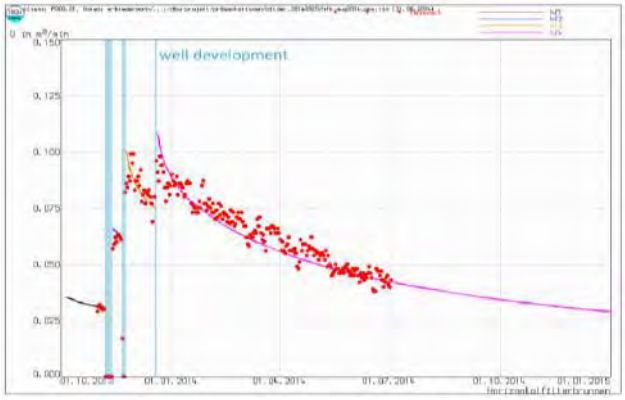

Figure 10 Simulation results (line) of an HDD-well including the head loss process.

Figure 11 a) and b) illustrates the situation in the groundwater at the startup time of the HDD-well. The thick blue line corresponds with the location of the HDD-well in the field test. Several observation points (black dots) are also drawn showing the results of the calibrated groundwater model.

In Figure 12 the groundwater situation is shown nearly 10 months after the startup of the HDD-well. The contour lines represent the groundwater level and show the draw down compared to Figure 11. The 2 circled observation wells are selected for a comparison of observed and calculated values over several months.

That comparison is shown in Figure 12. A very good overall agreement of simulated and measured groundwater levels can be stated.

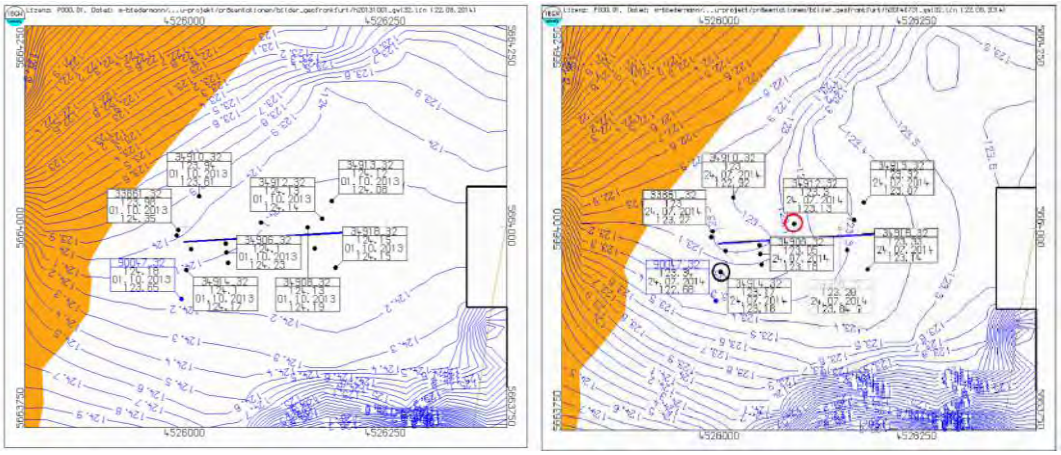

Figure 11a) Groundwater situation at startup of the HDD-well on 10/05/2013.
Figure 11b) Groundwater situation 10 months after startup. Colored circles show the position of 2 observation wells.

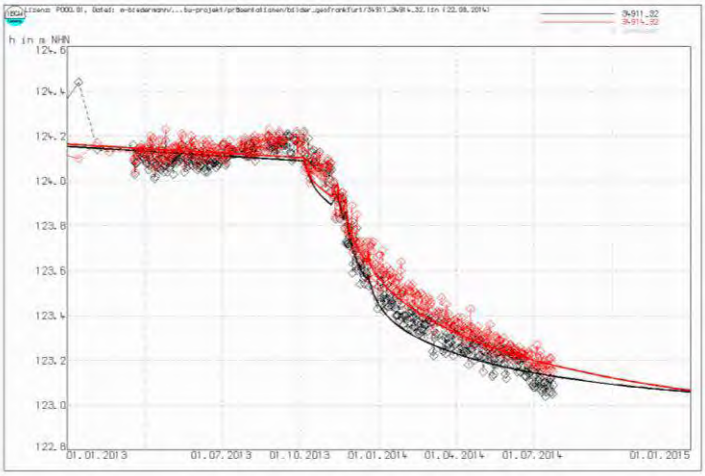

Figure 12 Comparison of observed (circles) and calculated values (line) at 2 different observation wells

CONCLUSION

Processing the data of the structural geological model, a groundwater flow model including a HDD was built up to enable the forecast of the dewatering. Therefore, the program PCGEOFIM, especially suited for mining drainage planning, was used. The calibration was conducted with the information of 28 monitoring wells. For the modeling, results of macroscale experiments regarding the incident flow of the HDD well, and differences between channel and pressure flow were taken into account. The results of several bench scale tests provide the possibility to forecast the dewatering of diverse HDD well configurations and different geological conditions.

Hence, the groundwater simulation suite PCGEOFIM is a tool to allow for the prognosis and planning of HDD-wells using groundwater models.

ACKNOWLEDGEMENTS

Thanks go to DBU (Deutsche Bundesstiftung Umwelt) Herr Heidenreich, Dr. Dietrich Sames and MIBRAG for their contributions to this document and supporting this work.

REFERENCES

Drebenstedt C (2010)
Use of environmental balance for selection of continuous or cyclic mining equipment on example of hard rock mining. In: Continuous Surface Mining, Freiberg, pages 390 – 406 (ISBN 978-3-86012-406-2)

Sames D, Blankenburg R (2013)
PCGEOFIM-Manual
Ingenieurbüro für Grundwasser GmbH, Leipzig, Germany

Müller M, Drebenstedt C, Struzina M, Mansel H, Preußler F, Bach F, Kretschmer T, Wagner S, Schramm R, Kummer S (2009)
Entwicklung eines umweltschonenden und effizienten Verfahrens zur Entwässerung oberflächennaher Lockergesteine im Bergbau und Bauwesen unter Nutzung der verlaufsgesteuerten Horizontalbohrtechnik. Ingenieurbüro für Grundwasser GmbH, project report, Leipzig, Germany

Struzina M (2012)
Beitrag zur Vorausberechnung der Wirkung verlaufsgesteuerter Horizontalfilterbrunnen (HDD-Brunnen) bei der Entwässerung von Lockergestein,
Ph.D. thesis, Fakultät für Geowissenschaften, Geotechnik und Bergbau der Technischen Universität Bergakademie Freiberg

Müller M, Jolas P, Mansel H, Struzina M, Drebenstedt C (2010): Dewatering of Multi-aquifer Unconsolidated Rock Opencast Mines – Alternative Solutions with Horizontal Wells. – In: Wolkersdorfer, Ch. & Freund, A.: Mine Water & Innovative Thinking. – p. 51 – 55; Sydney, Nova Scotia (CBU Press).

Mansel H, Drebenstedt C, Jolas P, Blankenburg R (2012): Dewatering of Opencast Mines using Horizontal Wells. – In: McCullough, C.D.; Lund, M.A.; Wyse, L.: International Mine Water Association Symposium. - p. 574 A – 574 I; Bunbury, Australia.

Nitz M, Biedermann M, Mansel H, Struzina M (2014)
Modellgestützte Planung eines verlaufsgesteuerten Horizontalfilterbrunnens zur Entwässerung von Muldenstrukturen in einem mitteldeutschen Tagebau; Proceedings of GeoFrankfurt 2014

Eichler R A, Drebenstedt C (2014)
Innovative Dewatering Concepts for Open Cast Mines Using Horizontal Wells (HDD-Wells) – In: Drebenstedt C, Singhal R (Eds.): Mine Planning and Equipment Selection, Proceedings of the 22nd MPES Conference, Dresden, Germany, 14th - 19th October 2013, Springer

Removing of High Flows of Acid Water from Disused Mines in Johannesburg

Axel Döring
ANDRITZ Ritz GmbH, Germany

ABSTRACT

South Africa is currently dealing with the problem of acid water because underneath the old gold mining city of Johannesburg is a lake containing heavily contaminated water, which spreads horizontally and vertically into the abandoned pits of the former gold mines.

Meanwhile, the water line has reached a critically high level. The corrosive sulphuric acids can in the worst case scenario, result in a pH value of 2, which is enough to cause lasting damage to humans and the environment.

Two state-of-the art pumps have been running since June 2014 in the middle of Johannesburg city centre with each pump capable of bringing 1,500 cubic meters (=1.5 million litres) of water to the surface per hour.

Because of this corrosive acid, these pumps are a customised construction. The design is based on a proven double-flow technology, which uses the concept of a double-suction pump. By the counter-rotating arrangement of the impellers the pumps run without axial thrust. With this design, delivery heads up to 1500 m can be reached. Due to the corrosive acid, the Johannesburg pumps were redesigned. Part of the new system is an encapsulation of the submersible motors. This technology enables the creation of an internal pressure higher than the external pressure, preventing the intrusion of the corrosive water and the components inside the motor being attacked and possibly destroyed. The water being drained is used to cool the motor and if required the motor can be extended by additional heat exchangers.

Keywords: Mine Dewatering, AMD Acid Mine Drainage, Pumps for Mine Dewatering, Water Management, Submersible Motor Pumps

INTRODUCTION

The city of Johannesburg located in South Africa was founded as a result of the Witwatersrand Gold Rush. Since 1886, when gold was discovered in the Central Basin, 40.000 metric tons – 30 percent of the gold of the world – have been extracted from the mines. The two deepest mines in the world are found in the Witwatersrand basin, extending nearly 4 kilometres below the surface.

While mining was operational, the inflowing ground water was pumped out of the mines by the ongoing infrastructure in place. But after the last mine closed down and pumping ceased altogether, the voids began to fill. The Western Basin filled and began to decant in 2002. Pumping ceased in the Central Basin in 2008 and in the Eastern Basin early in 2011.

These abandoned mine shafts of the former gold mines are gradually filling with water and need to be dewatered to avoid contamination of underground water and keep the water at an acceptable and safe level, or to bring this potentially contaminated water to surface for treatment.

Mine Drainage, has become an ecological issue and challenge. The metamorphic rock of the mining district contains abundant pyrite (iron disulphide) which reacts with oxygenated rainwater or groundwater resulting in elevated sulphate concentrations and eventually low pH values. With pH levels as low as two, the sulphuric acid mobilizes aluminium, potentially toxic metals and uranium from the rock and produces iron oxide as a by-product when the pH rises.

Figure 1 Map of South Africa (from http://superiormining.com/properties/south_africa; 13.11.2014)

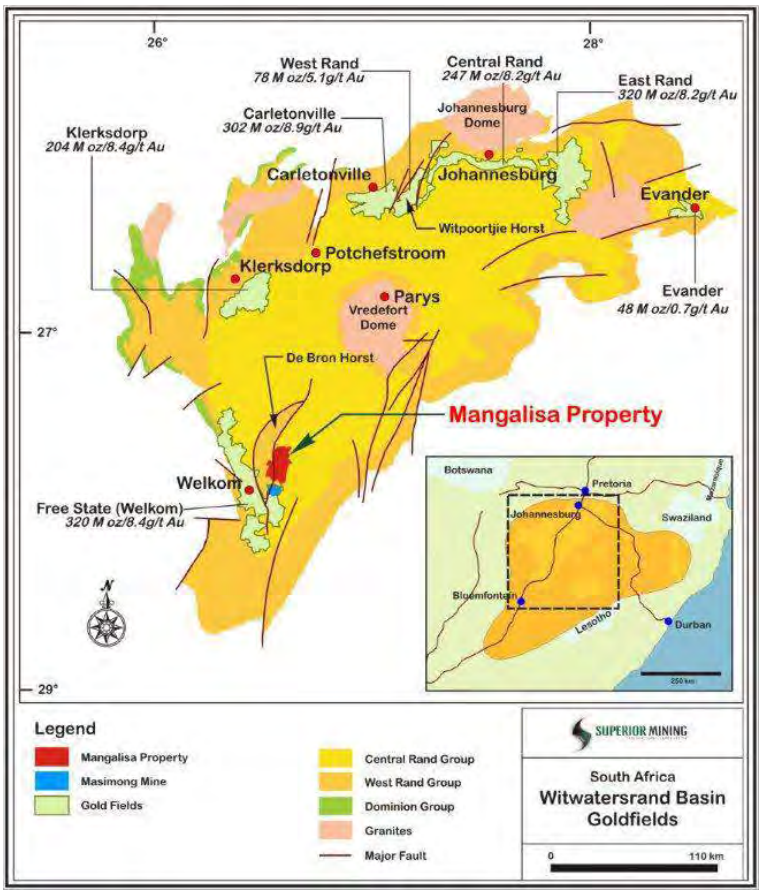

Figure 2 Landscape of Witwatersrand (from http://superiormining.com/resources/maps/20120213_witwatrand_basin.jpg; 13.11.2014)

RECOMMENDED MEASUREMENTS

Pumping out underground mine water to prevent reaching the environmentally critical level, controlling the ingress of water into mine shafts and in short term treating the contaminated mine water by neutralising the high acidity.

CHALLENGE – PUMP SOLUTION

The responsible technical experts looked for a long term draining solution to face the problem. Two main challenges had to be matched in this issue.

The materials which are in contact with the mine water – metals and elastomers – have to resist the medium for a long time. Therefore, the best material to face the medium and the mechanical properties had to be chosen. Multiple material options were taken into account and qualifying tests were necessary. Therefore, the renowned institute FEM (Forschungsinstitut für Edelmetalle) rebuilt artificial mine water based on the chemical analysis out of the mine and put test materials for a term of three months into this medium. Additionally by using higher temperatures, the reaction time gets

faster and a longer period of time could be simulated to get findings of the long-term behavior of the materials.

As a result of these tests, the material selection was refined. Out of the remaining materials the materials with the best mechanical properties for the parts of the pump unit were chosen to enable a compact design of the pump unit.

The used duplex steels combine the features of stainless chromium steels (ferritic or martensitic) and stainless chromium-nickel steels (austenitic). They have those rust and acid resistant properties which are necessary to resist the medium influences. Further they have the required mechanical properties.

Nevertheless, the water analysis may always only be counted as a snapshot of the current situation. As caused by environmental influences the water composition may change. But due to the selected high value materials absolute safety and resistance in operation can be expected.

As a further step and in order to protect the motor of the pump unit against the entrance of the contaminated medium it has been designed encapsulated. That means that the motor is packed into an additional casing to protect the motor materials against the acid medium.

The motor itself is filled with drinking water and put under overpressure. Fresh water is led to the motor through a long pipe from a quench placed on surface. The pressure is controlled constantly and in case of abnormal pressure signals, messages are displayed. Further, the filling level, the flow and the head (*Q* and *H)* are also monitored. The pump performance can be watched from all over the world by remote monitoring. Selected and qualified persons can also change parameters if it is necessary.

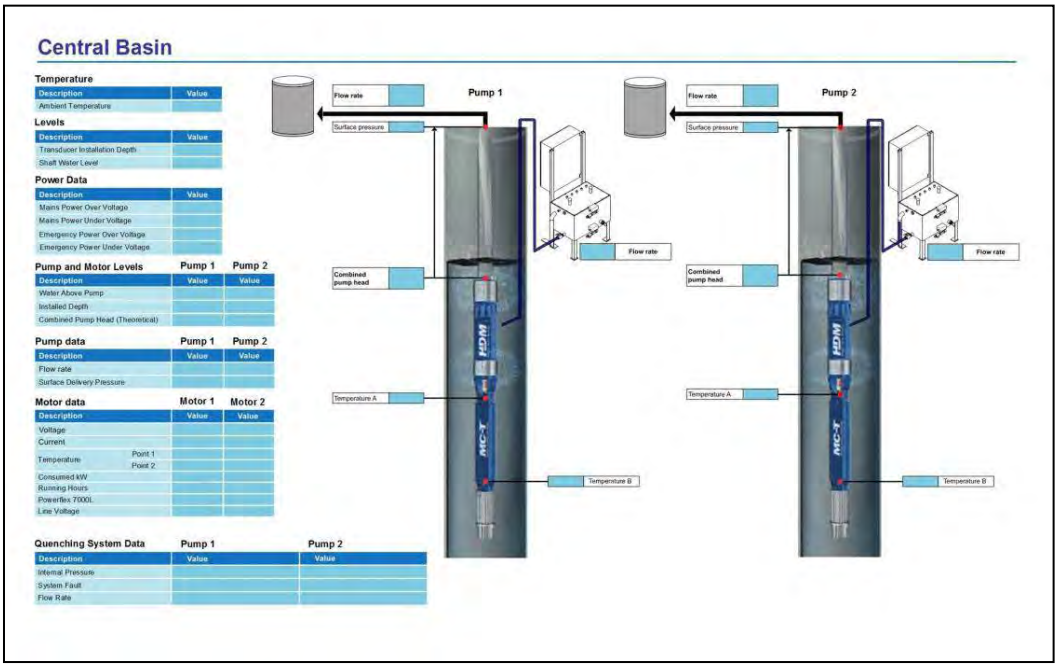

Figure 3 Monitoring scheme

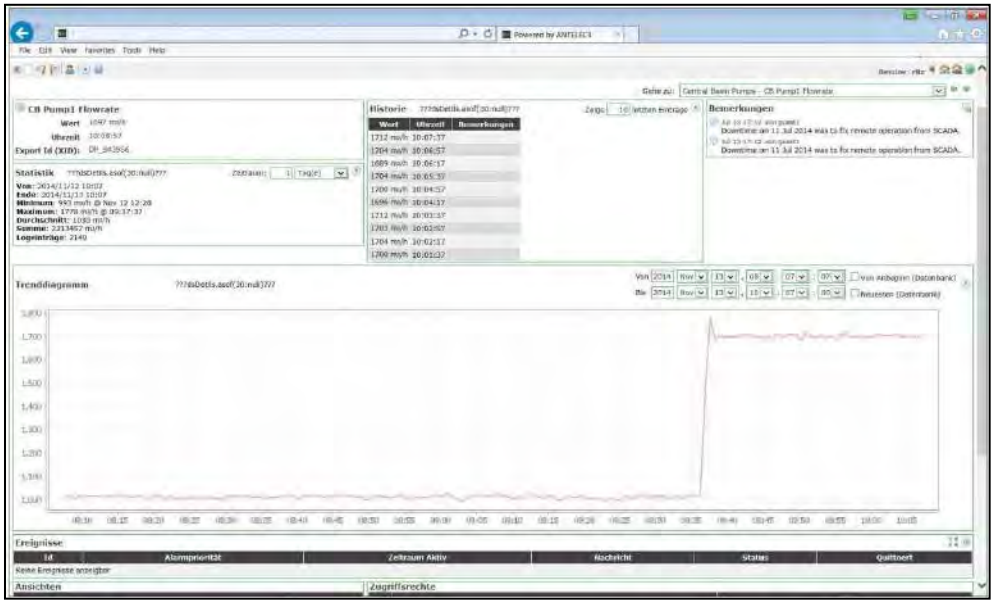

Figure 4 Remote monitoring display

The mechanical seal is tailored to the requirements of that special application. The sliding surfaces of the mechanical seal are specialized and all components are also matched up to the medium. A special construction of the mechanical seal guarantees absolute reliability and best operational characteristics. It is also charged with the inner pressure from a quench.

Weather conditions like rain influence the medium level as experienced with ground water all over the world. The changing water level requires a specific pump hydraulic to drain the water. Additionally, the level gets more or less steadily lower because of the dewatering. The more medium is pumped the lower is the level of the contaminated mine water. So the pump has to have a widely spread operation range.

The pump works with medium 70 m below the level of the contaminated water. When the level has reached the next lower marking, the pipe is enlarged with another pipe part. For the planning team it was important that the pipe can be enlarged easily and without loss of time. Therefore, quick snaps are used. Additionally to the quick assembly they score with their compact design, low weight and less effort in comparison to conventional screw connections.

With every step down, the pump has to manage a higher pumping head. This has also been considered in pump selection. Furthermore, the pump is equipped with a cooling shroud to guarantee the necessary cooling flow.

The used double-suction design of the pumps reduces any axial thrust nearly to zero. As a result, the pumps are extremely persistent and nearly maintenance free. Some pumps of that type had run in best performance up to 25 years without the need of maintenance. But considering the critical medium the terms of maintenance are shorter in this case. In case of maintenance the use of the quick snaps show their advantages. The pumps can be disassembled and reassembled in a comparably short time.

All pump units are identical, they have the same hydraulic. At least one complete pump unit is stored disassembled at site; which means that one set of parts is immediately available. Additionally a number of selected spare parts are stored at site, too.

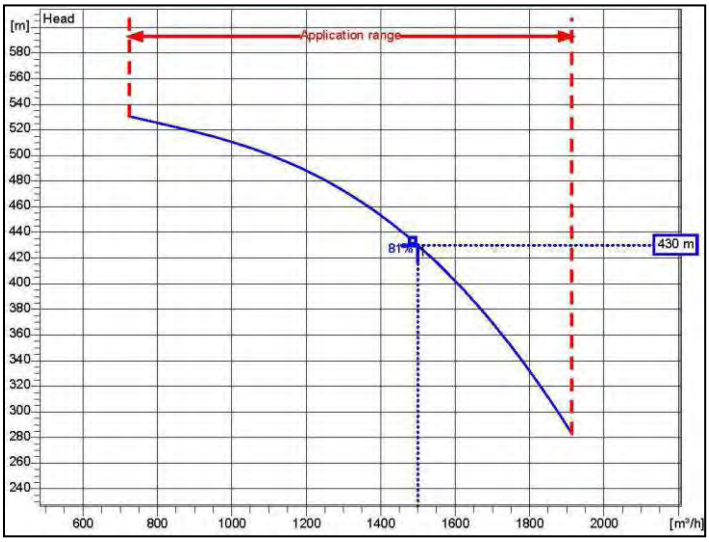

Figure 5 Performance curve of the pump

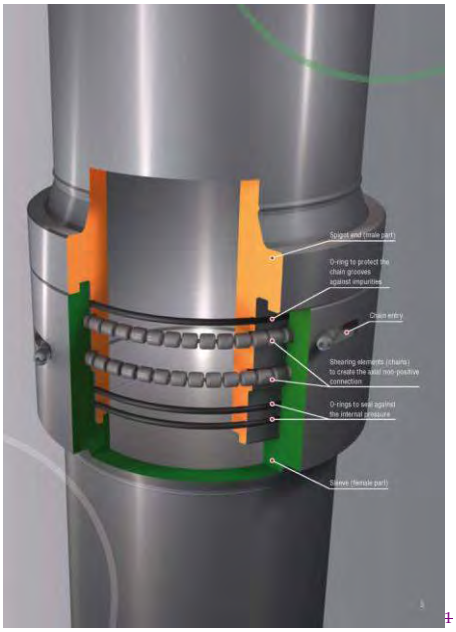

Figure 6 Quick snap connection (from Carl Hamm Pipesystems; ZSM-Connection Brochure English; issue 07/13)

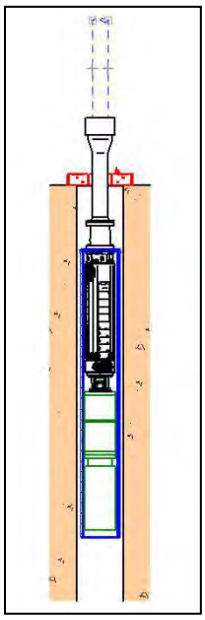

Figure 7 Assembly scheme

Figure 8 Assembly

CONCLUSION – ECOLOGICAL ASPECT

The mine water is being transported to the surface and onwards into an adjacent treatment plant. There, through the addition of lime, the pH value is raised, the acid is neutralised and the dissolved metals in the water are (co-)precipitated as hydroxides.

The South African authorities are planning a total of three pumping stations, which will each be developed at the mines' disused extraction shafts. In addition to the Central Basin in Johannesburg's city centre, pumping plants for the Eastern Basin and the Western Basin are currently in progress. The long term measurement is to force the water level in the flooded mines back from its current level of approx. 200 metres to a depth of 1000 metres and to keep it there, to then be able to begin mining gold and gold ore in the drained upper layers of the mines once again.

REFERENCES

McCarthy TS. The decant of acid mine water in the Gauteng city-region – analysis, prognosis and solutions. Provocations Series, Gauteng City- Region Observatory. Johannesburg: Universities of the Witwatersrand and Johannesburg; 2010.

Expert Team of the Inter-Ministerial Committee. Mine water management in the Witwatersrand Gold Fields with special emphasis on acid mine drainage. Report to the Inter-Ministerial Committee on Acid Mine Drainage. Pretoria: Department of Water Affairs; 2010.

Carl Hamm Pipesystems; ZSM-Connection Brochure English; issue 07/13

http://superiormining.com

10th ICARD IMWA 2015 | 10th International Conference on Acid Rock Drainage & IMWA Annual Conference

Dewatering of a Deep Shaft in a Complex Hydrogeologic Setting

Michael Gabora[1], Phillip Brown[2], Hank Ohlin[3], Korin Carpenter[3] and Greg French[3]

1. *Ausenco, USA*
2. *Independent Consultant, USA*
3. *Nevada Copper, Inc., USA*

ABSTRACT

The Pumpkin Hollow Project proposes to mine high-grade, Iron Oxide Copper Gold (IOCG) deposits within a porphyry copper and skarn district in the State of Nevada, United Sates. It is estimated that the district-wide mineral inventory is over 24 billion pounds of copper. As part of the Phase I underground mine, a 655 meter deep exploration shaft is being advanced to exploit a proven and probable reserve of 27.6 million tons of 1.5% copper with associated gold and silver. Existing hydrogeologic data suggested that substantial groundwater inflow would not occur until intersecting a low-angle fault at a depth of approximately 430 meters below ground surface known as the Flat Fault. A dewatering well and observation wells were initiated when water inflows were greater than the shaft excavator's grout program could mitigate. A 457 meter deep dewatering well (DW-1) and three multilevel vibrating wire piezometers (VWPs) were installed near the shaft as part of a staged approach to dewatering. Monitoring data from the first 40-days of DW-1 operation, in combination with the VWP and shaft inflow data, were used to calibrate a mine scale groundwater flow model. The model was used to locate a second dewatering well that was constructed to further minimize inflow and depressurize the Flat Fault during shaft construction. Subsequent testing and analysis of this second dewatering well (DW-2), additional packer testing and geophysical logging resulted in a significantly different hydrogeological conceptual model in the shaft area and as a result, different groundwater flow model results. The project highlights the utility of a well-designed, site specific hydrogeologic characterization program for major mine development.

Keywords: groundwater, dewatering

INTRODUCTION

The Pumpkin Hollow property is located 8 miles southeast of Yerington, Nevada. Four of the five known copper deposits on the project are currently in pre-development with drilling and engineering studies being conducted by Nevada Copper Corporation and an exploration shaft has been advanced in the East deposit (Figure 1). The Pumpkin Hollow Project is in the Basin and Range Province of western Nevada, just east of the Sierra Nevada. The site lies in eastern Mason Valley, bounded on the west by the Singatse Range and on the east by the Wassuk Range. The climate is arid, with hot summers, relatively mild winters, and mean annual precipitation ranging from approximately 101 millimeters at the lowest elevations to 406 mm at the highest.

Extensive hydrogeological studies were completed on the property and the immediate area of the proposed shaft was considered adequately characterized. In November 2013, significant groundwater inflows were encountered as the shaft excavation advanced beyond the static groundwater elevation in an andesite sill unit. Prior hydrogeologic characterization suggested that groundwater inflow through low permeability Tertiary volcanic rocks would be minimal until a low-angle normal fault (the Flat Fault) was encountered at approximately 430 meters (m) below ground surface (bgs). In order to mitigate groundwater inflow into the shaft a grouting program, a hydrogeologic characterization program and initial dewatering works were initiated.

This paper details the enhanced hydrogeologic understanding gained during dewatering and hydrogeologic studies to decrease inflow into the shaft and depressurize the Flat Fault. Additional characterization of the surrounding bedrock improved the ability to predict groundwater inflow into the Phase I underground mine and design appropriate dewatering infrastructure. This project demonstrates the necessity to elucidate hydrogeologic complexities in mine areas to effectively predict inflows and design appropriate dewatering and depressurization programs and explores variability in the effectiveness of two grouting programs.

Geologic Setting

At the project site, a thin veneer (0 to locally 150 feet) of Quaternary unconsolidated sand and gravel (Qal) covers most of the surface. Bedrock is exposed in the periphery of the site primarily as Tertiary volcanic rocks (tuffs) and underlying Mesozoic formations. The Mesozoic section is comprised of carbonaceous calcareous argillites, tuff, and limestone intruded by granitic dikes and sills. These rocks transition locally into skarn, marble, and hornfels with associated copper and iron mineralization forming the five separate but associated deposits; the North, South, Southeast, East, and E2. The deposits are blind with no outcrop and were discovered by aeromagnetic methods and subsequent drill delineation. A geologic model was developed from drill data without the advantage of projected surface geology.

A series of low-angle normal faults separate the Tertiary from Mesozoic rocks (Figure 2) and are zones of 15 to 50 m of enhanced fracturing, breccia development, and variable clay gouge. A pair of generally NNW-SSE trending normal faults bound a graben that down-drops the Tertiary and Mesozoic sections through the middle of the site.

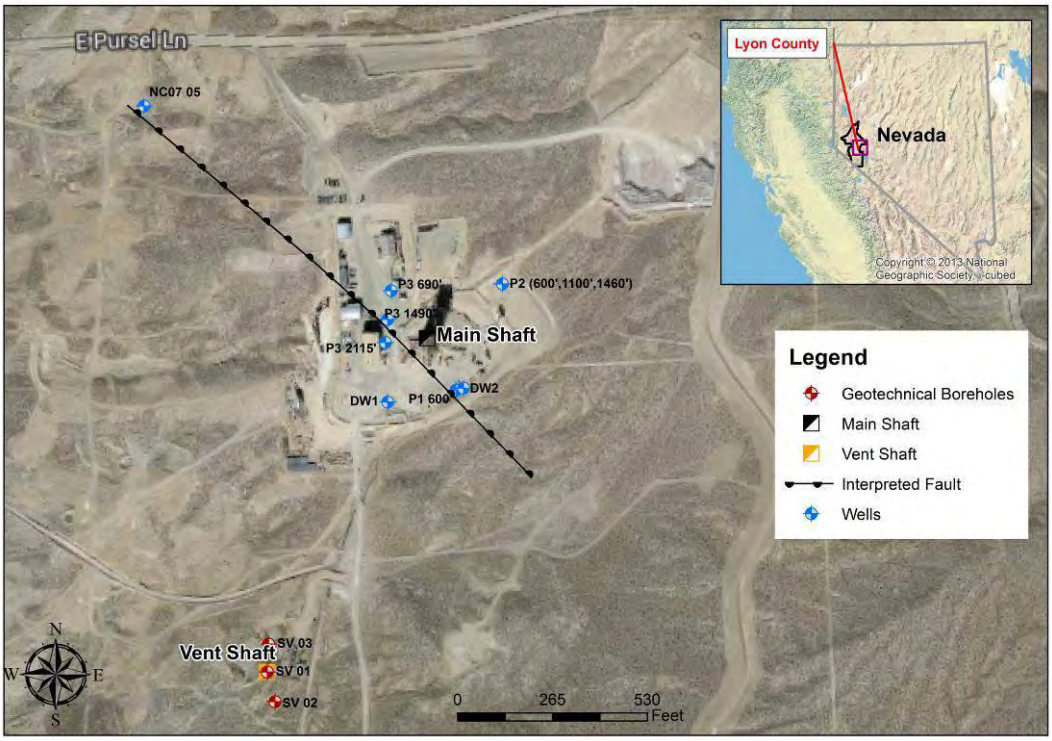

Figure 1 Project Location and Shaft Area Features

Mine Area Hydrogeology

An extensive hydrogeological characterization program was completed for the proposed mine including reviewing core data, testing of 34 boreholes to determine geothermal gradients, installation of monitoring wells and vibrating wire piezometers, packer testing in 3 boreholes, 5 injection tests, 3 slug tests and 2 air-lift drawdown and recovery tests and aquifer pumping tests on 2 wells. Groundwater occurs within the bedrock at a depth of approximately 100 m to 135 m bgs and flows toward the north and northwest, paralleling the flow of the Walker River valley. The bedrock is of generally low hydraulic conductivity except where fracture networks create secondary permeability and transmit groundwater.

Mean mine area estimates of bulk hydraulic conductivity for the Tertiary and Mesozoic bedrock are 1×10^{-2} m/d and 1×10^{-1} m/d, respectively. Tetra Tech (2012) reported that the Flat Fault had elevated hydraulic conductivity relative to the Tertiary and Mesozoic rocks with a mean of 4×10^{-1} m/d.

Calculations using the Maxey-Eakin method to estimate precipitation-derived recharge, based on precipitation estimates made by the USGS Precipitation Zone Method, indicate recharge is zero in the mine area (Tetra Tech, 2012). Stable isotope and 14C data suggest the last recharge to the Flat Fault occurred more than 30,000 years ago. Given the limited recharge potential, identifying lateral connectivity of the Flat Fault and other permeable horizons are considered critical to predicting groundwater inflow and related pore pressure responses in the bedrock. At property wide scales Tetra Tech (2012) used aquifer testing responses and geologic data to conclude that most faults are hydrologic boundaries interpreted to impede groundwater flow across the fault plane and thereby tend to act to compartmentalize the flow system.

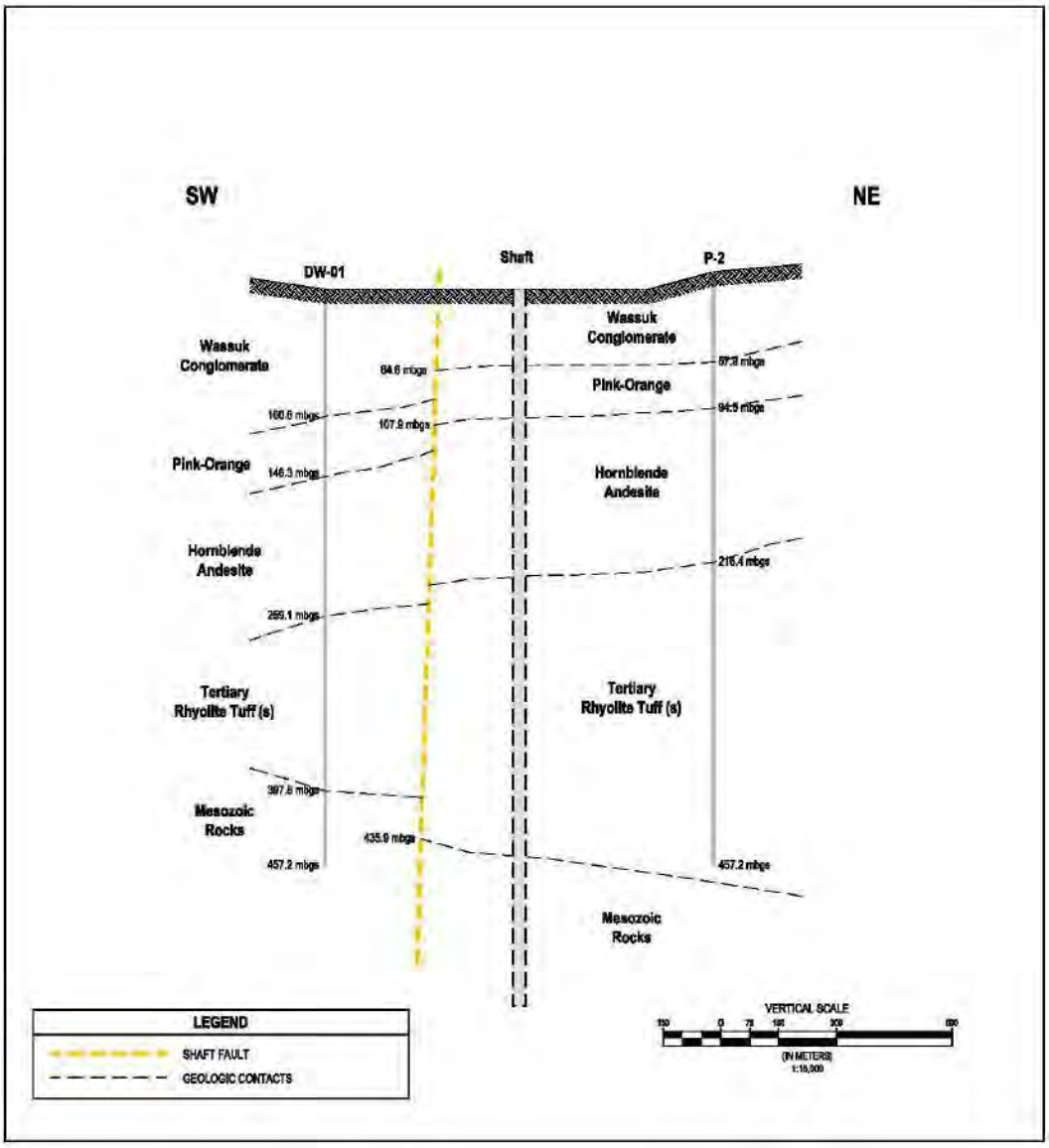

Figure 2 Geologic cross-section in the vicinity of the shaft

SHAFT DEWATERING STUDIES

Beginning in November 2013, the shaft excavation advanced into an andesite sill and below static groundwater elevation where inflow became significant. A grouting program was implemented to mitigate inflow and was only partially effective, groundwater continued to enter the shaft through bolt holes that penetrated the grout envelope and intersected fractures in the andesite. An initial dewatering well (DW-1, Figure 1) was advanced to a depth of 457 m with screen from 256 m to 457 m bgs. Three sets of nested vibrating wire piezometers were also installed at that time (Figure 1). An aquifer pumping test was performed on DW-1 at a rate of 28.4 liters per second (lps), the maximum achievable rate with the installed rental pump. The achieved drawdown in the pumping well was 76 m and 6 m was observed in VWP-01S at a distance of 130 m. The hydraulic

conductivity (*K*) was determined to be between 0.6 and 3.3 m/day, more permeable than mean site values. The storativity was estimated to be 1.2-percent. The time-drawdown data was indicative of a modest negative boundary condition, attributed to the perceived displacement of the Flat Fault between DW-1 and the shaft, P-2 and P3 piezometers by the Shaft Fault (Figure 2 and Figure 3). The test responses varied significantly with depth, with the greatest response in P3 445 m piezometer in the Flat Fault, suggesting the Flat Fault was yielding the most of the water to the well.

Significant available drawdown remained during the DW-1 pumping test (approximately 215 m). However, step-testing in April 2014 indicated that higher rates could not be sustained. As a result, initial DW-1 operations began pumping rates between 25.2 lps and 27.4 lps. Since that time, the operational pumping rate of DW-1 has steadily declined, likely the result of compartmentalization of the Flat Fault (Figure 4). Shaft inflow rates have also steadily declined as the andesite has dewatered, the shaft has advanced beyond the andesite, a new substantially more effective grouting program was implemented in late January 2014 and DW-1 began operating (Figure 4).

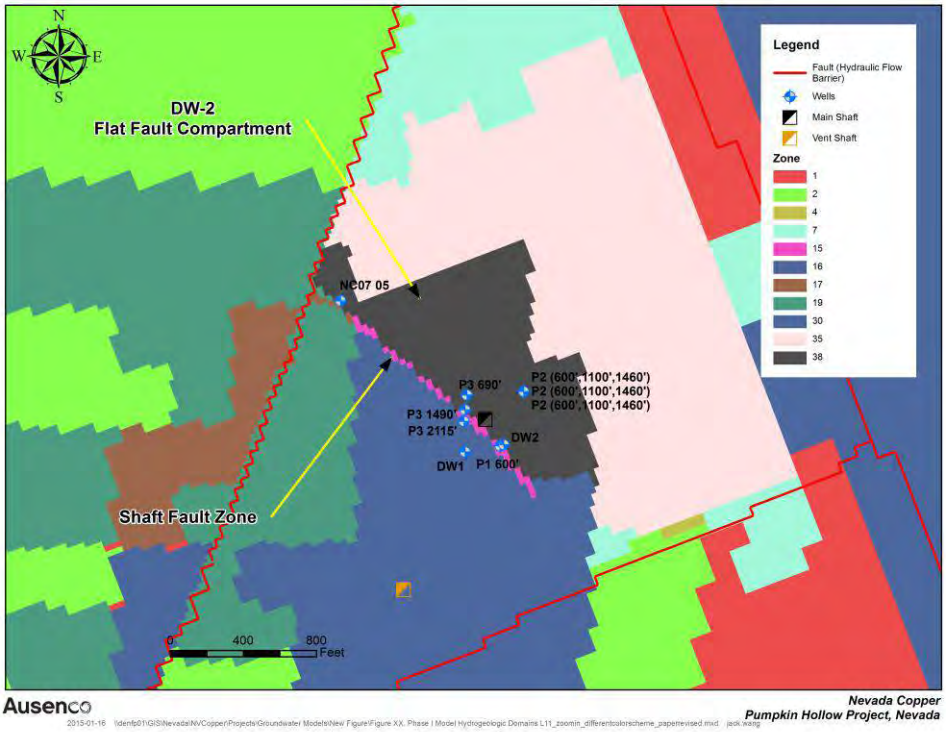

Figure 3 Geometry of the Flat Fault and Shaft Fault

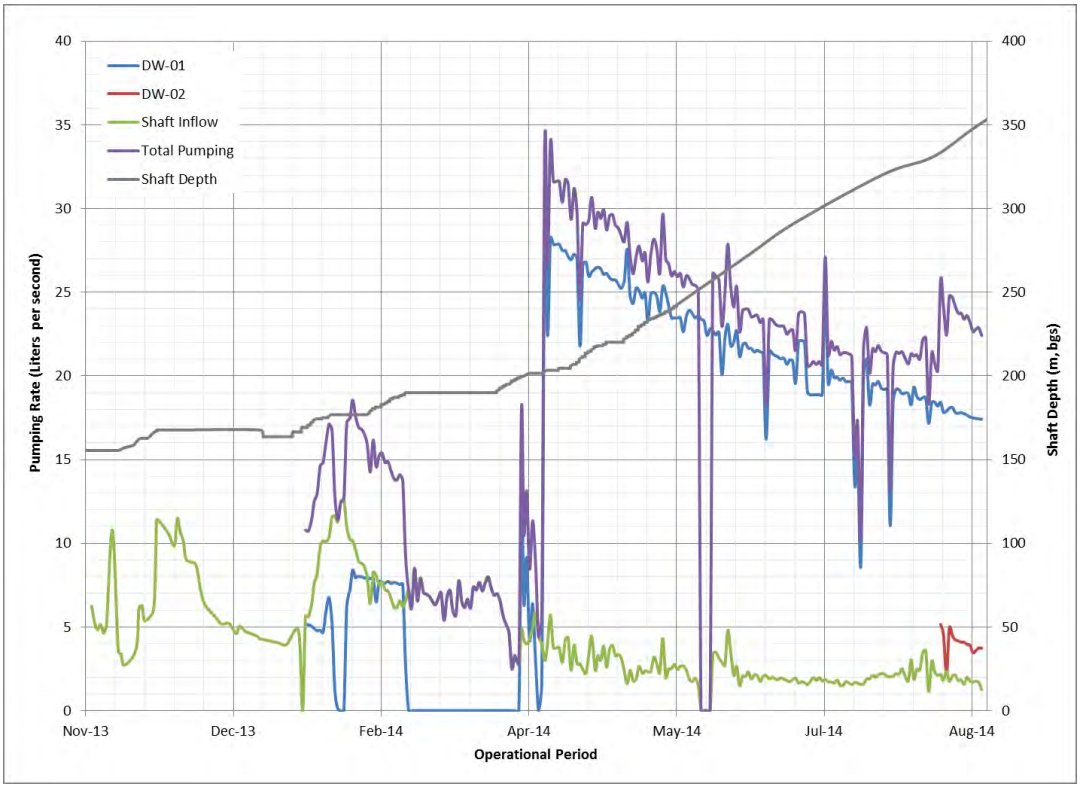

Figure 4 Operational Pumping Rates

A packer testing program and heat pulse flow meter testing were completed in geotechnical coreholes near a proposed vent shaft (Figure 1) to test the permeability of the deeper Mesozoic bedrock. Packer testing resulted in moderate *K* estimates for Mesozoic bedrock, between 2.0 x 10^{-4} m/day (746 - 759 ft bgs) and 4.9 x 10^{-1} m/day (609 – 624 m bgs) and heat pulse flow meter results yielded between 8.5 x10^{-3} m/day and 2.2 x10^{-1} m/day.

To further minimize groundwater inflow into the shaft, reduce pressure heads and reduce the need for costly grouting operations an additional dewatering well (DW-2; Figure 1) was installed upgradient of the shaft. DW-2 was completed to a depth of 632 m with screen between 198 m and 223 m bgs and 382 m bgs and 632 m bgs. DW-2 was commissioned August 16, 2014 pumping between 3.8 lps and 6.3 lps, much lower rates than what DW-1 (approximately 18 lps versus 4 lps) and numerical modeling suggested for DW-02.

Figure 5 presents the water level responses in vibrating wire piezometers at P3, including one in the Flat Fault (P3M 454 m), from the pumping of DW-1 and DW-2. Responses indicate the pumping of DW-1 in April impacted water levels in both the andesite and Flat Fault. It can also be seen that water levels within the Flat Fault were very sensitive to development and pumping at DW-2, despite the much lower pumping rate relative to DW-1. This is attributed to unforeseen geologic complexities, including compartmentalization of the Flat Fault by the Shaft Fault, the amount of clay gouge within the fault breccia and the discrete nature of the water bearing fractures in the Mesozoic rock beneath the fault gouge. These complexities result in a hydrogeological conceptual model (HCM) for the "DW-2 compartment" of the Flat Fault (Figure 3) that is significantly different than elsewhere on the property.

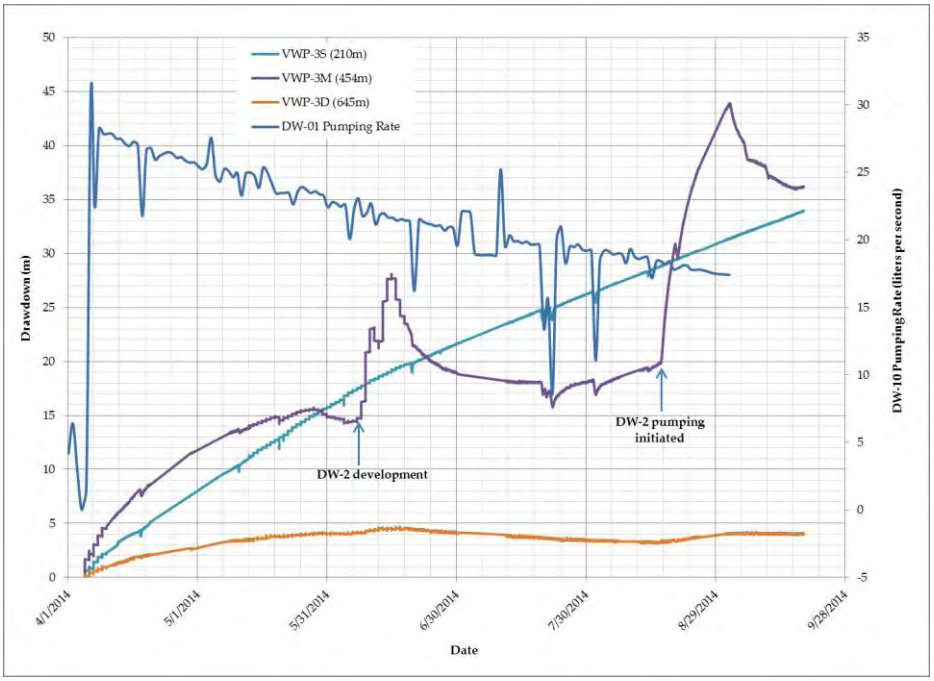

Figure 5 Measured drawdown and DW-1 pumping rates

Despite the lower pumping rate, considerable drawdowns occurred in the Flat Fault, Tertiary and Mesozoic bedrock. Accordingly, the seeps in the shaft walls dried up and inflows in the shaft appeared to decrease. Water levels within the Tertiary rhyolite tuff have also been significantly affected by pumping, with water levels in P2 (VWP at 335 m bgs) dropping by more than 90 m, since DW-2 began pumping.

GROUNDWATER FLOW MODELING

The objectives of the groundwater flow modeling were to develop a working tool to assist in improving our understanding of the hydrogeology in the area of the shaft and proposed East underground mine in order to predict the magnitude of groundwater inflow during shaft sinking, evaluate the effectiveness of the initial grouting program, evaluate pore pressures near the shaft and siting of dewatering wells and ultimately predict the groundwater inflow to the proposed East underground mine. An initial mine scale groundwater flow model (Hydro-Logic, 2014) was developed and calibrated using the 40-day DW-1 pumping test (initial model) and a second updated version of the model was calibrated using both the DW-1 (178 days) and DW-2 (15 days) transient calibration data sets and the updated hydrogeologic framework model (updated model) by Ausenco (2014). Both models also used the available shaft inflow data as part of the transient calibration. As a result of space limitations, some details of the models are not discussed here, instead the focus is on how incorporating the geometry and compartmentalization of the Flat Fault affected shaft inflow predictions and estimates of groundwater inflow.

Model Domain, Grid and Boundary Conditions

The Shaft Model domain (Figure 6) was extracted from the Regional Model (Tetra Tech, 2013) with the primary objective of having sufficient size to minimize boundary effects but also have an

appropriately small size to allow for refinement in the area of interest near the shaft (7.5 m^2 cells). The grid was rotated to be consistent with the direction of groundwater flow in the area (Figure 6) and to align the axis with the primary fracture network orientation. General Head Boundary (GHB) conditions were developed for the Shaft Model based on the heads from the steady-state Regional Model results. Faults are generally interpreted to be hydraulic barriers and included using the hydraulic flow barriers (HFB), based on updated structural modeling in the project area. The model utilized Groundwater Vistas Version 6 (Environmental Simulations Inc., 2011) as a pre- and post-processor and groundwater flow was simulated using MODFLOW-USG (USGS, 2013).

In addition to incorporating well pumping rates and piezometer water level responses, transient calibrations included calibrating the conductance of HFB and the drain cells used to simulate faults and grouted sections of the shaft. The simulated shaft inflows (Figure 6) during the 40-day calibration period of DW-1 testing are on the order of 3.8 lps and are relatively consistent over the 40-day calibration period (Figure 4).

The calibrated *K* values for grouted shaft cells indicate that grouting activities through January 2014, were minimally effective as evidenced by high calibrated effective *K* (0.12 m/d). This is a reasonable assertion because the preferred pathway of water through the grout was through bolt holes and not through the grout matrix or remaining ungrouted fractures. Inflow data suggest that revised grouting methods have been significantly more effective with a calibrated effective *K* of 0.02 m/d or between level 2 and level 3 grouting as defined by Wilson and Dreese (2003).

A predictive version of each model was developed to simulate the dewatering of the shaft from the end of the respective calibration period May 5, 2014 (initial model) or September 30, 2014 (updated model) to the terminal depth of the shaft, 590 m bgs and 660 mbgs, for the two models respectively. The assumed *K* values for grouted sections of the shaft also evolved between model versions as a result of changes to the HCM and hydraulic properties. Principal differences include achieving level 3 ($K = 8 \times 10^{-3}$ m/d) grouting the Flat Fault in the updated model (versus level 2 or $K = 8 \times 10^{-2}$ m/d in the initial model) based on lower pressure and permeability expectations within the "DW-2 compartment". The assumed dewatering well pumping rates for the predictive model differ as well evolving from 18.9 lps for both DW-1 and DW-2 in the initial Mine Model to 17.3 lps and 3.1 lps in the updated Mine Model.

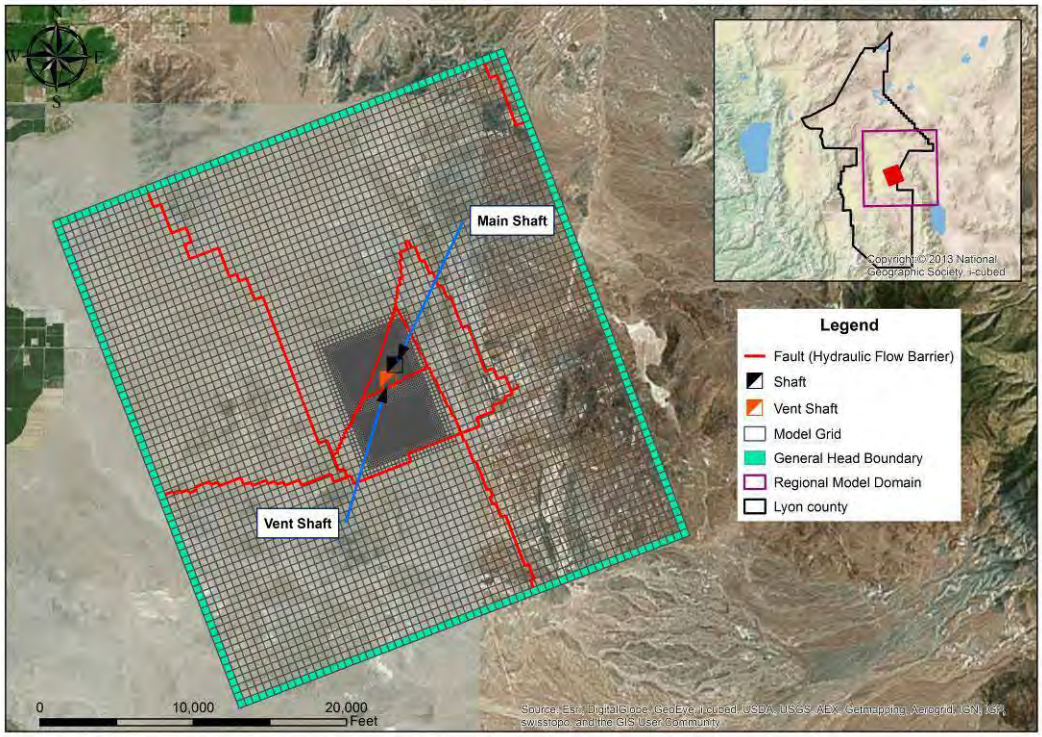

Figure 6 Shaft Model Grid, Boundary Conditions, Steady-State Groundwater Elevations

The calibrated *K* and storage parameters of the updated model were generally lower than in the initial model for both the Flat Fault and the Mesozoic bedrock. The calibrated Flat Fault response for the newly developed "DW-2 compartment" for the Flat Fault calibrated to a low specific storage, indicative of a discrete rock fracture response. Such values were required to mimic the hydraulic response at P3M to DW-2 pumping (Figure 5). This is consistent with an updated conceptual model of the Flat Fault in the "DW-2 compartment ", which suggests a discrete fracture confined by fault gouge, is able to rapidly transmit changes in pressure but dewaters rapidly due to limited transmissivity and storativity and the effects of compartmentalization. The expectation is that shaft probe holes may encounter high pressures but that the inflows in this zone will be short-lived.

Model Results

The model results were post-processed and examined as they related to the stated modeling objectives. Both models suggest that initial grouting performed in the shaft (up to February 2014) was relatively ineffective as the calibrated andesite *K* values (K_h = 0.6 m/d) are not reflective of overly permeable bedrock or values outside what would have been for such a rock type. Predicted inflows into the shaft have decreased in the updated model relative to the initial model (Figure 7), as the localized characterization (e.g. extent of clay gouge, lower *K* and storativity) and compartmentalized geometry of the Flat Fault have modified localized interpretations and calibrated hydraulic property values. Predicted mine inflow inflow through the Mesozoic rocks is lower than the initial model, as are the calibrated hydraulic properties. Available data suggest that, at most, periodic grouting will be required in higher yielding fracture zones of the Mesozoic bedrock.

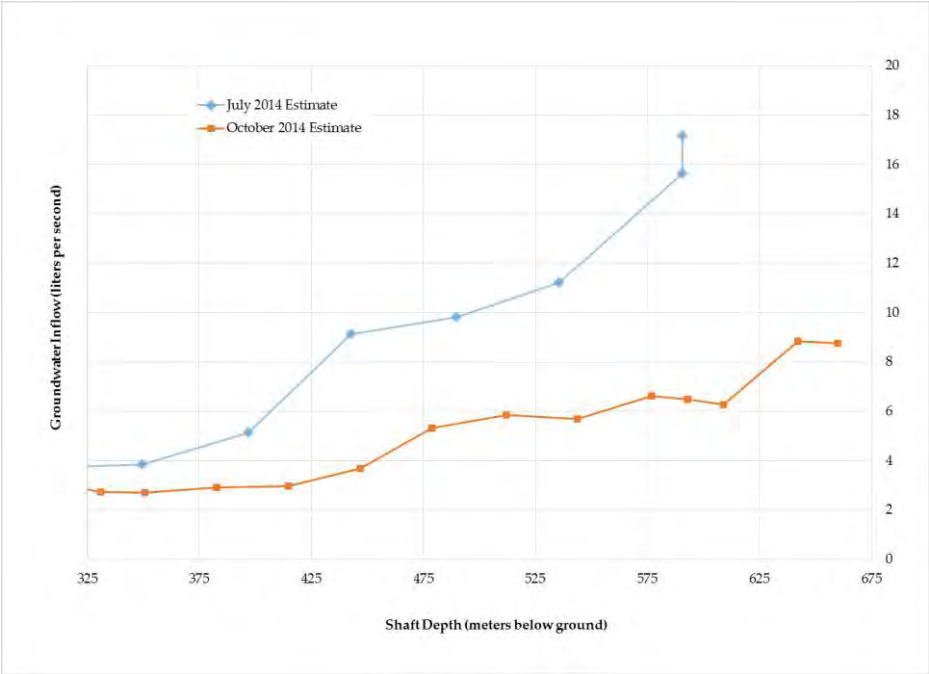

Figure 7 Predicted Inflow to the Shaft during Construction

The updated Mine Model was also used to predict groundwater inflow into the Phase I underground mine (first two years of mining). The base case estimated average monthly mine inflows for the first sixteen months are predicted to be 80 lps and for the last 12 months of operations the predicted monthly average is 120 lps. The Phase I mine simulation assumes that limited grouting will be completed and the groundwater inflow is governed by the native permeability of the surrounding bedrock.

CONCLUSIONS

The flow model results indicate that the calibrated *K* andesite sill (K_h=0.3 m/d) is greater than the range of values tested for Teritary Volcanic bedrock (2.0×10^{-4} m/d to 1.2×10^{-1} m/d) on the rest of the property, more than order of magnitude greater than the mean value (1.0×10^{-2} m/d) and two orders of magnitude greater than the median value of 1.8×10^{-3} m/d. This highlights the importance of not lumping hydraulic test results and HCMs in broad categories such as a 700 ft sequence of Tertiary volcanic rocks. The andesite sill in question was not being differentiated in the geologic model developed for quantifying ore reserves that was ultimately applied in geotechnical and hydrogeological assessments.

The inflow during shaft construction through the andesite was exacerbated by an initially ineffective grouting program. This assertion is supported by the decreasing shaft inflows and lower calibrated K values of the drains used to simulate grouted sections of the shaft. The revelation the DW-2 compartment of the Flat Fault and its differing hydraulic properties has led to a significantly different HCM than originally conceived. The depressurization of the DW-2 block of the Flat Fault

is expected to result in lower groundwater inflows and pore pressures during shaft construction. As a result grouting will be less frequently required during shaft advancement.

These findings highlight the need for having a well-designed, site specific hydrogeologic characterization program in place prior to shaft sinking or other major development. However, on sites such as Pumpkin Hollow, where groundwater is compartmentalized and the hydrogeologic characteristics of the water bearing units are highly variable, changes in inflow can occur rapidly and shaft sinkers should be prepared to meet such challenges. As the project moves towards the underground mine development, the hydrogeology-geology team will work to improve our understanding of the compartmentalization at depth and the hydraulic properties of the Mesozoic bedrock and identify any potential zones of concern.

ACKNOWLEDGEMENTS

The authors thank Nevada Copper for allowing for the insights gained as part of this project to be to be shared with mine water community.

REFERENCES

HydroGeoLogic, Inc. (2011) *MODLOW-SURFACT Software* (Version 4.0). Hendon, VA, USA.

Hydro-Logic (2014) *Technical Memorandum Preliminary Shaft Dewatering Model Results- Pumpkin Hollow Project*. Prepared for Nevada Cooper Inc., Hydro-Logic, March 6,2014.

Panday, S., Langevin, C.D., Niswonger, R.G., Ibaraki, Motomu, and Hughes, J.D., 2013. MODFLOW-USG Version 1: An Unstructured Grid Version of MODFLOW for Simulating Groundwater Flow and Tightly Coupled Processes Using a Control Volume Finite-Difference Formulation. U.S. Geological Survey Techniques and Methods, book 6, chap. A45, 66 p.

Tetra Tech (2012) *Hydrogeology and Dewatering - Pumpkin Hollow Project, Nevada USA*, Prepared for Nevada Copper Corporation. Report dated June 2012.

Wilson, D. and T. Dreese (2003) *Quantitatively Engineered Grout Curtains*, Grouting and Ground Treatment, Proceedings of the Conference sponsored by the Geotechnical Engineering Division of the American Society of Civil Engineers, New Orleans, LA, February 10-12, pp. 881-892.

Rumbaugh, J., & Rumbaugh, D. (2011) *Guide to using Groundwater Vistas, Version 6*.

10th ICARD IMWA 2015 | 10th International Conference on Acid Rock Drainage & IMWA Annual Conference

Comparison of Borehole Testing Techniques and Their Suitability in the Hydrogeological Investigation of Mine Sites

Michael Palmer and Houcyne El-Idrysy
SRK Consulting, United Kingdom

ABSTRACT

Analytical and numerical groundwater flow models are usually used to estimate groundwater inflows into mines and assess the need for dewatering and/or depressurisation of the rock formations around the mine. These models require various input parameters that have a defining control on the model results and the subsequent design of dewatering and/depressurisation systems. Therefore to increase confidence in model predictions and the efficiency of the mine water management design, it is essential to achieve accurate estimation of the hydraulic parameters.

Hydraulic parameters of geological formations are usually estimated from data obtained from borehole testing. There are five main hydraulic testing techniques commonly used in the hydrogeological investigation of mine sites: (1) Slug tests, (2) Airlift tests, (3) Flow logging (also called spinner tests), (4) Packer tests, and (5) Pumping tests.

In this paper the degree of suitability of the above borehole testing techniques is investigated, taking into consideration the data collection objectives, the expected water management challenges, and project stage. The paper also highlights the advantages and disadvantages of each of these tests, and compares ballpark cost and logistic requirements.

Keywords: Hydrogeology, borehole, hydraulic testing, techniques, mining.

INTRODUCTION

The type of hydraulic testing carried out in mine sites depends on the hydrogeological setting and geotechnical characteristics of the rock formations, and the mine project stage. At an earlier stage of a mine project (often called Scoping Study or Preliminary Economic Assessment), limited hydrogeological data collected from exploration boreholes or from an existing mine can provide enough information for the hydrogeological assessment of the project. However, as the project progresses toward advanced level (Preliminary Feasibility Study, Feasibility Study and Detailed Design Study) site specific data collected from specialist hydrogeological boreholes are necessary. This is particularly more relevant if the results of the initial study suggest significant challenges in the mine groundwater management. The degree of challenge and complexity of the water management aspect of a mine project usually depends on the project location and the hydrogeological and geotechnical setting of the mine, which may entail the followings:

- The proximity of the mine to surface and groundwater reservoirs and the hydraulic properties of the geological formations around the mine will have a significant control on the amount of groundwater inflows into the mine and dewatering requirements;
- The geotechnical and hydraulic parameters of non-aquifer saturated formations around the mine may have direct implication on mine stability and depressurization requirement;
- In cases where groundwater is the only potential water supply source for the project, investigations and borehole testing, possibly for a longer period of time, are required.

To assess the water management risk and challenges that a mine project may face, the hydraulic properties of the geological formations around the mine should be sufficiently investigated. This is usually achieved with the use of well positioned boreholes and testing techniques appropriate for obtaining the vertical and lateral variations of the parameters. The hydraulic parameters often obtained from borehole testing are: hydraulic conductivity (K), transmissivity (T), storativity and specific yield (S and Sy), conductance (C) and leakage coefficient, hydraulic boundaries, and anisotropy of aquifer response.

In this paper we compare five different types of borehole testing, namely: slug tests, airlift tests, flow logging, packer tests; and pumping tests. Other types of test, such as tracer test, exist but these are not widely used in the industry and usually carried out for specific purposes such as the delineation of contaminants and estimation of travel time. Laboratory testing of drill cores and grain size distribution of bulk samples are also sometimes used to estimate hydraulic conductivity when field tests are not possible. Therefore these are not considered in this paper.

Hydraulic test techniques are sometimes combined in one form or another depending on site characteristics and available equipment. For example packer tests can be combined with falling or rising head tests in a way that the target test zone is isolated with the packer and the borehole standpipe is either filled with water or pumped, and water level in the borehole measured subsequently for a certain time to obtain a drawdown-time curve that can be used to estimate the hydraulic parameters of the test zone. Water level in the borehole standpipe can also be kept constant in such configuration and the injection flow measured over time.

DISCUSSION

Slug tests

A slug test consists of displacing a known column of water instantly in a borehole and monitoring the subsequent water level recovery to the initial static state. Since water level recovery can be very fast in permeable formations, the use of a pressure transducer (or water level logger), is more suitable to achieve accurate and frequent measurements of water-level.

An appropriately sized slug should be selected that can produce enough displacement to provide a measureable change in water level. A water level change of 1 to 2m is adequate (Cunningham & Schalk, 2011). In high permeability formations a larger displacement is desirable due to the rapid recovery of water level towards equilibrium conditions.

In open coreholes falling head tests are not suitable because of interference with the unsaturated zone, contrary to rising head tests that can provide reliable results in such case.

Airlift Tests

Airlift testing can be conducted in exploration holes in order to provide an early estimate of permeability. Airlift tests can easily be implemented as part of early resource drilling programmes and are useful for projects where expensive hydrogeology programmes cannot be justified.

The most effective method for completing an airlift test in the early stage of a project is through the use of a drill rig that is equipped with a compressor (usually reverse circulation [RC] or rotary air blast [RAB]). In airlift tests using a drill rig, the drill bit can be removed and a bespoke airlift attachment threaded to the end of the rods. Subsequently air is injected down the drill rods into the hole and the air bubbles rise in the column of water, entraining and lifting water up the rods and out of the discharge hose (Howell, 2012). Careful consideration must be given to compressor capacity and dynamic submergence of the airline. The attachment diverts injected air and incorporates a chamber for a data logger at the base. The water level logger allows accurate measurements of drawdown and the recovery of water level during the test. More dedicated airlift testing outside a drilling programme involves the use of a drop pipe and air injection pipe, a compressor, and water discharge hose. The air flow is usually directed upward and the drop pipe ensures that water is flushed out of the hole with a smooth variation of water level and pressure, which can be measured using water level logger installed outside the drop pipe.

Airlift testing may also be conducted during drilling at pre-determined intervals in order to assess cumulative vertical permeability variations. If there are open holes located nearby then it is possible to monitor water level in these as in observation wells for a conventional pumping test (Beale & Read, 2013).

Spinner tests

Spinner flow logging is a well-documented technique used to determine vertical variation in hydraulic properties of geological formations (Molz et al 1989, Hill 1990, Paillet 1998). A rotating impellor is lowered at a constant low speed down the hole using a geophysical logging winch from which the impeller rotational velocity is measured and converted into a vertical flow profile. The analysis of spinner test data should preferably be completed in combination with caliper logging data (borehole diameter), acoustic televiewer (ATV) survey, and/or geotechnical core logging in order to improve the level of structurally-related interpretation (Pedder & El Idrysy, 2013).

The success of spinner testing is highly dependent on the condition of the hole that is being tested. Newly drilled diamond holes are suitable and commonly used for spinner testing since geotechnical core logging and ATV survey results, if available, yield useful validation data. However, it is imperative that the borehole design and drilling practices and procedures during planning stages take into account the subsequent use of the hole for flowmeter logging. This includes pre-collaring of any unstable overburden, drilling mud management and borehole cleaning/development techniques.

Flowmeter logging can either be conducted under ambient condition (i.e. water level is static; without pumping), or with a simultaneous pumping at a constant debit. The former is referred to in this paper as a static spinner test, and the later as a dynamic spinner test.

Typically, if vertical differences in hydraulic head exist between the geological formations in a borehole, groundwater inflow into the hole will not be uniform under ambient conditions and the flow will preferentially enter at permeable horizons (West & Odling, 2007). Ambient flow can be measured using static spinner tests. Non-detectable ambient flow during the test would suggest uniform hydraulic head or negligible hydraulic gradient. Detectable ambient flow would suggest vertical head differences.

Pumping of the borehole is necessary in order to sufficiently reduce the hydraulic head and induce flow from all permeable horizons. Assuming that the well is pumped with reasonable drawdown, the resulting hydraulic gradients should promote flow from all permeable horizons, with differing contributions based on permeability (Lloyd & Jeffery, 1983). This is an important consideration to ensure that the test result is representative of all permeable horizons. An open borehole with vertical head differences will exhibit a composite groundwater level and the level of drawdown during pumped spinner testing becomes of greater importance in order to draw water from all permeable horizons. The depth of the pump intake should not have a controlling effect on borehole inflows, providing that drawdown is sufficient. Instead of pumping, water injection (constant head/debit) can be used in some circumstances but the application of this method has more disadvantages and limitations.

Since pumping of an open borehole will initially draw water from borehole storage, it is important to achieve an appropriate flow regime prior to running the spinner test. Various authors (West & Odling, 2007; Paillet, 1998; and Molz et al, 1989) have cited that pumping should achieve a pseudo-steady state. This is achieved when all boundaries have been reached and pressure drop becomes proportional to time (Lu & Tiab, 2010, Bourdet, 2002 and Kruseman & De Ridder, 1994). Pseudo-steady state may take a long time to reach, particularly in unconfined aquifers and where multiple boundaries exist. This may be uneconomical when conducting spinner testing in line with other programmes (such as geotechnical drilling).

The outcome of dynamic spinner tests is a vertical profile showing cumulative reductions in inflow contribution. The relative reductions can be proportioned and analysed using established methods to calculate discrete fracture permeability. In numerical groundwater models for mine projects, fractured layers are often represented as “Equivalent Porous Mediums”. Consequently the availability of individual fracture estimates are of limited use. Instead, the test results will feed into a conceptual hydrogeological model to define the numerical model geometry and set-up. Also equivalent hydraulic conductivity for each model layer can be derived by incorporating fractured and non-fractured horizons into the analysis of spinner test results.

Packer Tests

Packer testing involves the use of an inflatable rubber packer to isolate an interval of a borehole for hydraulic testing. To conduct such a test, the packer is lowered down the hole and inflated using water (or compressible gas) that is injected and controlled from the ground surface. The packer tool channels the pumped water flow through a central pipe (the mandrel), which is blocked at one end by a blow-out plug, retained by a shear pin. When inflation pressure exceeds the shear pin rating, the blow out plug is ejected and the flow is directed into the test zone (rock formation), thus shutting down water flow into the packer element. Water is subsequently either injected or withdrawn from the test interval while flow rates and pressures are recorded. Once the injection/withdrawal of water and monitoring is complete the packer is deflated and removed. This process is repeated until the entire borehole is tested in a series of discrete or cumulative tests.

Packer tests can make use of either single or double (straddle) packers. The packer element can be inflated using either water or compressible gas. The former presents the advantage of being capable of testing borehole of much greater depths, and the approach is considered safer. In this paper the discussion relates mainly to water-inflated packer, specifically the Standard Wireline Packer System (SWiPS ®) manufactured by Inflatable Packers International.

Packer tests can be carried out during borehole drilling, whereby once drilling reaches the desired test depth, the drill string is pulled out to a certain level where the packer element needs to be set for the test. Once the test is completed drilling continues until it reaches the next packer designed depth. The next test is normally carried out covering the interval from the depth of the previous test to the current one. The advantage of such techniques is that it provides more accurate data compared to cumulative testing or straddle packer tests because it involves less risk of leakage, and all intervals are tested separately without the risk of masking that may happen if the hydraulic conductivity of the tested formations is low and anisotropic. The disadvantage of this, however, is that it causes delay of the drilling operation and additional cost, which may not be acceptable in some resource drilling programmes.

The alternative to testing while drilling is to test the borehole once the drilling is completed. This type of test requires either the use of double packers to isolate the test intervals or alternatively cumulative testing of the entire depth of the hole. The former presents the advantage of isolating and testing shorter intervals, however this may be time consuming and presents higher risk of leakage from around the double packer seals which translates into errors in the test results. Errors in packer test results related to leakage are especially more significant if the hydraulic conductivity of the tested formations is very low. Another risk involved in the use of double packer is the loss of the equipment due to borehole collapse because the length of the double packer configuration is very long, far beyond the protection of the drill string.

When packer testing is carried out using injection under several pressure steps, the procedure is called Lugeon test (Lugeon, 1933). The pressures used during an injection or Lugeon test must be high enough to force flow into the formation, but low enough to avoid artificially increasing the formation permeability. Lugeon test is the most widely used approach to packer testing, compared to water withdrawal or falling head tests. Lugeon tests have the advantage of being fast; 3-step pressure tests are usually carried out quickly compared to groundwater level recovery time if a withdrawal or falling head test is used. Attention should however be paid to pressure level and rock condition to avoid artificial fracturing, especially in shallow formations.

Pumping Tests

Pumping tests are an important and widely used method for characterising bulk-scale groundwater flow behaviour. Pumping tests usually involve the use of a submersible pump to pump water from a large diameter central well while monitoring groundwater level in the pumped well and nearby observation holes. Observation wells can be located up to hundreds of meters from the test well and should either be drilled or sought from existing exploration holes located nearby. Pumping tests are probably the most widely used hydraulic tests used in hydrogeological investigations and are therefore well known to all hydrogeologists. A full description of procedures is beyond the scope of this paper, so the reader is instead pointed towards literature such as Kruseman & De Ridder (1994) and Brassington (2006). The most commonly varieties of pumping tests are the calibration, step-drawdown test and the constant-rate discharge test.

The aim of the calibration test is to assess what the maximum short-term pumping rate might be, and to define the discharge control valve positions for the step test. Once the calibration test is complete and water levels have recovered, a formal step-test can be carried out.

The step-drawdown test is important to determine an appropriate pumping rate for the subsequent constant-rate test. It is equally important in order to account for head losses, the latter consisting of aquifer, linear and non-linear head losses (Rorabaugh, 1953, Jacob, 1947). Linear well losses are the most preventable and can be caused by the development of a well skin. A positive well skin may consist of drilling mud invading the formation that results in a low K skin. Conversely, negative skin can consist of a high K zone around the borehole, essentially caused by inadvertent hydraulic "fracking" due to poor drilling practices. If head losses are not properly accounted for, analysing the pumping test data may result in serious overestimation of S and underestimation of T (Agarwal et al, 1970; Jargon, 1976). The implications for mining projects might mean underestimated mine inflow estimates, which would lead to an under-designed dewatering system. It is therefore essential to design the constant-rate pumping test in conjunction with the step-test analysis. Once head losses have been calculated, the well performance can be expressed as a well efficiency percentage (Kruseman & De Ridder, 1994).

The constant-rate test should be carried out at the maximum sustainable pumping rate defined from the step-test results. The purpose of the constant-rate test is to obtain information on the hydraulic characteristics within the radius of influence of the pumping well (Beale and Read, 2013).

Criteria for Selecting a Hydraulic Technique

A guideline transmissivity range for selecting a hydraulic technique is proposed in Figure 1. These are based on the authors' test results and experience and input from various literature as shown in the list of references. The transmissivity is the criterion used in this paper since this parameter is more directly relatable to the overall capacity of a well, whereas the hydraulic conductivity alone is not enough.

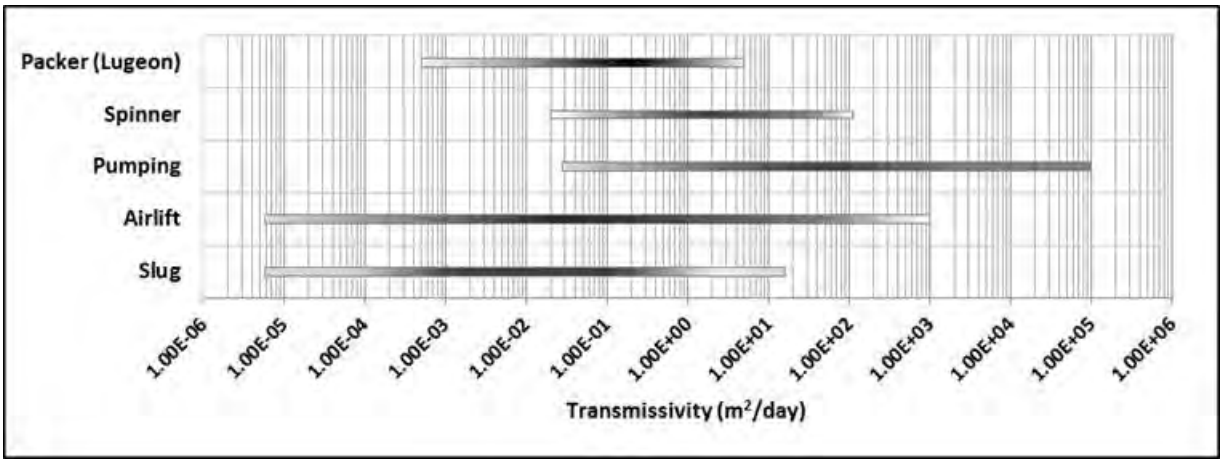

Figure 1: Approximate transmissivity range for the 5 hydraulic testing techniques

Hydrogeological investigations, and especially borehole testing, should be designed taking into consideration two criteria:

- The hydrogeological setting of the project and available logistics and resources;
- The level of confidence required in the mining study (PFS, FS, etc.). Usually each stage of mine development requires a certain level of design and justifies a commensurate investment.

Slug tests can be applied in a wide range of transmissivities, including very low permeability formations. Slug testing is limited to holes that are not highly transmissive due to rapid return of displacement towards original water level. This test becomes more reliable with decreasing permeability, however practical considerations (such as test time, seasonal impacts, etc.) may become relevant where measurement of displacement takes weeks or maybe months.

Airlift can be effective for a wide range of permeability conditions making this a very flexible test. Studies have shown (Howell, 2013) that conventional pumping test analysis of airlift tests that have produced less than approximately 0.1-0.2 L/s may result in unreliable estimation of permeability. Where airlift tests produce such yields they should be stopped early and the recovery data analysed as a rising-head test (e.g. Hvorslev, 1951).

Packer testing is applicable in a smaller range of transmissivity, from low to moderate. Previous packer testing programmes carried out by SRK in HQ boreholes suggest an upper limit of 3 m^2/d of transmissivity for packer testing results to be reliable. The results also suggest that packer testing can detect inflows for a transmissivity as low as 0.0005 m^2/d if the packer seal is placed within a non-fractured fresh rock section of the hole where the packer seal is effective to prevent leakage. It is less reliable at very low permeability because the accuracy of the data can be compromised by minor packer leaks, flow measurement, residual drill muds. The upper-limit is typically constrained by the maximum capacity of the packer equipment (pumps, compressor, etc.) and/or bore diameter.

Spinner tests can however be carried out in slightly larger range spreading especially toward the relatively higher transmissivities. The minimum start-up velocity of the spinner (velocity of water required) will vary depending on manufacturer and should be considered carefully. From the

authors' experience, spinner testing has yielded inconclusive results where the transmissivity of a tested formation is less than approximately 0.02m²/d.

Pumping tests can be used to test highly transmissive mediums, and the upper limit would depend only on the size of the submersible pump available and borehole diameters which is controlled by the available drill rigs capacity.

At the early stages of a mine project, hydrogeological investigations should attempt to utilise boreholes from resources drilling programmes and any existing historical drill holes. Rising head tests in such old boreholes may provide a coarse assessment of the hydraulic conductivity around the boreholes, although the results may be questionable. In newly drilled and cleaned boreholes with appropriate bentonite seal for the test zone, slug tests can provide useful data. Airlift testing may also be implemented very early in a project to test existing drill holes where the range in permeability is poorly understood. As part of exploration programmes, drill rigs often have the capacity to carry out airlift tests.

If it is necessary to characterise fracture flow or vertical variances in primary porosity, spinner tests may be considered. However, spinner tests are often not necessary at the early stages of the project, but rather at PFS or FS levels. Packer tests may be integrated into existing drilling programmes in consolidated and fractured rock. It is also important to consider the condition of the drill hole (packer seating) and experience of the driller.

Pumping tests provide the most reliable estimates of aquifer properties where groundwater management represents a high-risk to the project, and the required accuracy of the hydrogeological investigations has the potential to significantly affect the project engineering feasibility or economics. Given the associated high costs and required amount of resources, the justification for pumping tests should be based on existing data derived from integrated and retrospective programmes. Pumping tests are carried out in most of mining projects at PFS or FS stages, regardless of the level of risk of groundwater management. In fractured rock, when the control of groundwater is required, spinner or packer tests should be specified instead to define the vertical variation of rock mass and assess the dewatering requirement.

Cost and Logistical Comparison

The shipping of testing equipment into a project country requires consideration of cost, customs documentation (both departure and destination country) and insurance. Comparisons of these considerations are shown in Table 1. For simple hydrogeological tests (slug testing) there is no major cost or logistical issues. However, shipping equipment that is made up of numerous components (e.g. spinner, packer and pumping) increases the complexity of the process and can add significant time and cost. Therefore, the requirement for these tests needs to be considered carefully within the context of the investigation objectives in order to provide adequate justification for its use. Alternatively, good quality contractors should first be sought in-country where possible.

Table 1: Estimated Cost and Logistical Comparison of Common Tests

Test Equipment	Equipment Capital Cost (GBP)	Annual Maintenance Cost (GBP)	Shipping Cost (GBP)	Shipping Preparation Time
Slug	50 - 200	n/a	50-150	1 hour

Spinner	10,000 – 15,000	250 – 1,000	1,000 – 4,000	1-3 days
Packer	20,000 – 50,000		1000 – 8,000	
Pumping	8,000 – 20,000		1,000 – 6,000	

Advantages and disadvantages

Table 2: Advantages and disadvantages of various hydrogeological tests

Method	Advantages	Disadvantages
Slug Tests	-Quick and inexpensive. -Good for early-stage projects. -Good where permeability is low to moderate. -Can be used in polluted water wells because abstraction is not necessary -Very simple logistics and low cost -Maybe the only test suitable underneath a flowing-river bed to estimate conductance. -The stability of the borehole is not a problem.	-Less reliable where permeability is very high. -Less reliable than all other tests. -Only tests immediate area around the hole. -Sensitive to near-well conditions (low K skin, gravel pack, etc.) -No storage estimate. -Falling head test is not suitable for testing unconfined aquifers in open hole. The unsaturated zone requires bentonite seal.
Airlift Testing	-Cost-effective, if no significant rig standby time. -Good for early-stage projects and exploration hole testing. -Easily incorporated into existing drill programmes. -Covers wide permeability range. -Can use observation wells to estimate S and increase radius of characterisation.	-Less reliable than other tests. -Not good in polluted water due to abstraction -Becomes time-consuming at very low permeability where rig time is at a premium. -May cause erosion of borehole walls and cavitation in some circumstances. -The debit may not be stable enough to assume steady state condition for data analysis.
Spinner Tests	-Good for hydrogeological characterisation of bedrock fractures. -Provides vertical variation of hydraulic properties and accurate depth of flowing fractures (±10cm). -Can be easily compared with geotechnical, structural and geophysical data. -Static test can reveal natural flow between aquifers due to vertical hydraulic gradient. -Can be completed without a drill rig. -Can be easily combined with other downhole tools such as salinity, temperature or other surveys.	-Requires a clean, open hole at the test interval. -May require significant drawdown if large vertical head differences exist. -Risk of equipment loss due to hole collapse. -Not suitable for very low permeability formations. -Requires specialised equipment that may not exist in all countries. -To quantify the hydraulic conductivity in the tested borehole, spinner test results are not sufficient; a small scale pumping test is required in parallel with the spinner tests.

Method	Advantages	Disadvantages
Packer Tests	-Can easily be incorporated into existing drill programmes. -Can provide hydraulic input parameters readily incorporable into groundwater models. -Provides approximate location of groundwater flow zones, especially in fractured rock formations. -Can be carried out in vertical or inclined boreholes even in angles as low as 50 degree. -The test can be carried out in various small diameter holes (PQ, HQ or even NQ sizes). The packer equipment comes in various sizes to fit into specific borehole sizes.	-Experience is critical. -Unreliable in non-diamond holes (RC, rotary, etc.) due to potential poor packer seating risk. -Typically requires a wireline drill rig. -Not suitable in very high or very low permeability formations. -Require specialised equipment that may not exist in all countries. -Leakage around the packer can cause false interpretation of the test results. -Requires a relatively clean borehole. -In shallow, soft formations packer tests may induce hydrofracturing or hydro-jacking.
Pumping Tests	-Provide accurate and reliable estimations of more hydraulic parameters. -Wider aerial characterisation. -Many hydraulic parameters can be estimated (e.g. T,S, Sy, Kz/Kr, etc...). -Diagnose borehole efficiency. -Suitable to identify boundaries and flow regimes. -Comprehensive literature. -Tests can locally mimic dewatering operation. -Test wells can be used for dewatering and monitoring water level and quality.	-Time consuming and can be expensive. -Typically involves drilling of large diameter pumping wells and observation holes. -May not be suitable in polluted groundwater due to potential discharge permit. -Require more human resources and logistics than all other tests. -Not suitable in low permeability media, as low rate pumps may not be available. -Pumping tests are not suitable in fully open or steeply inclined boreholes.

CONCLUSIONS

Five hydraulic testing methods of boreholes for mine studies have been discussed in the present paper. A brief definition of each type of test has been presented, and their limitation and suitability discussed. Also the advantages and disadvantages of each of the tests have been highlighted. The material presented in this paper is mainly based on existing literature and the authors' work carried out using such techniques in various types of environments and hydrogeological settings.

At early stages of a mine study, slug tests and airlift tests are widely used; because these are simple and cheap and yet provide preliminary assessment of the hydraulic parameters of the rock formations around the mine. Further specialised testing is usually designed based on the results of these early stage testings and groundwater monitoring. At advanced feasibility studies pumping tests are usually carried out. Although such tests may be the most expensive option, they are usually carried out in most mine projects because they provide more representative values of the hydraulic parameters. Pumping tests usually require the use of contractors, but the availability of pumps and pipes in almost every country, however, justifies their use.

In projects where the vertical variation of the hydraulic parameters is predominant and the risk of groundwater inflow management is high, characterisation of the vertical profile of the hydraulic parameters is required. Pumping tests cannot provide such results, unless a very expensive investigation programme involving drilling many boreholes in various geological horizons is carried out. The alternative methods to pumping tests in this environment are the use of packer testing or flowmeter logging. The former can provide readily usable parameters for groundwater models if the tests are designed for such purpose. Spinner tests provide continuous profile of the hydraulic parameters thus accurately depicting the depths of open fractures and flow zones. The results of spinner tests however can be quantified for use in groundwater model only if a pumping test is carried out in the tested hole. Spinner tests and especially packer tests can be carried out in inclined and/or very deep boreholes. However, hole collapse and loss of equipment remain a major risk in packer testing and flowmeter logging. Also borehole cleaning is required prior to these tests to obtain more meaningful results.

REFERENCES

Agarwal, R.G, Al-Hussainy, R and Ramey Jr, H.J (1970) *An investigation of wellbore storage and skin effect in unsteady liquid flow*, Trans. Soc. Pet. Eng. vol. 249, pp. 279-290.

Beale, G and Read, J (2013) *Guidelines for evaluating water in pit slope stability*, CSIRO Publishing.

Bourdet, D (2002) *Well test analysis: The use of advanced interpretation models*, New York: Elsevier.

Brassington, R (2006) *Field hydrogeology, 3rd Edition. The geological field guide series,* John Wiley & Sons, Ltd.

Cunningham, W.L, and Schalk, C.W (2011) *GWPD 17—Conducting an instantaneous change in head (slug) test with a mechanical slug and submersible pressure transducer,* Groundwater technical procedures of the U.S. Geological Survey: U.S. Geological Survey Techniques and Methods, pp. 145-151.

Hill, A.D (1990) *Production logging – theoretical and interpretive elements: Richardson, Texas*, Society of Petroleum Engineers Monograph, vol.14.

Howell, R (2012) *Airlift testing in exploration coreholes,* IMWA 2013 "Reliable Mine Water Technology", Golden CO; USA.

Hvorslev, M.J (1951) *Time Lag and Soil Permeability in Ground-Water Observations,* Bull, No. 36, Waterways Exper. Sta. Corps of Engrs, U.S. Army, Vicksburg, Mississippi, pp. 1-50.

Jacob, C.E (1947) *Drawdown test to determine effective radius of artesian well.* Transactions, ASCE, vol. 223, paper 2321, pp.1047-1070.

Jargon, J.R (1976) *Effect of wellbore storage and wellbore damage at the active well on interference test analysis*, J.Pet.Tech., vol. 28, pp.851-858.

Kruseman, G.P, and De Ridder, N.A (1994) *Analysis and evaluation of pumping test data, 2nd Edition,* International Institute for Land Reclamation and Improvement, Publication 47.

Lloyd, J.W, and Jeffery, R.I (1983) *Deep aquifer testing methods and data interpretation,* Zeitschrift Deutschen Geologischen Gesellschaft Hydrogeologische Beitrage Nr. 8, Tubingen, vol. 134, pp.871-884.

Lu, J, and Tiab, D (2010) *Pseudo-steady state productivity formula for a partially penetrating vertical well in a box shaped reservoir.* Hindawi Publishing Corporation, Mathematical Problems in Engineering.

Lugeon, M (1933) *Barrage et Géologie. Dunod*, Paris Nielsen DM (1991), Practical Handbook of Ground Water Monitoring, Second Edition, CRC Press 1991.

Molz, F.J, Morin, R.H, Hess, A.E, Melville, J.G, and Güven, O (1989) *The impeller meter for measuring aquifer permeability variations: evaluation and comparison with other tests*, Water Resources Research, vol. 25:(7), pp.1677-1683.

Paillet, F.L (1995) *Using borehole flow logging to optimize hydraulic test procedures in heterogeneous fractured aquifers,* Hydrogeology Journal 3, vol. 3:, pp.4-20.

Paillet, F.L (1998) *Flow modelling and permeability estimation using borehole flow logs in heterogeneous fractured formations,* Water Resources Research 34, vol. 5, pp.997-1010.

Pandit, N.S, Miner, R.F (1986) *Interpretation of slug test data*, Ground Water, vol. 24, No.6, pp.743-749.

Pedder, R and El Idrysy, H (2013) *The combined use of spinner flow logging and geotechnical information to investigate the hydraulic properties of fractured rock mass*, IMWA 2013 "Reliable Mine Water Technology", Golden CO; USA.

Rorabaugh, M. I (1953) *Graphical and theoretical analysis of step-drawdown test of artesian well.* Proceedings Separate no. 362, ASCE, vol. 79, pp.1-23.

Sanders, L.L (1998) *A manual of field hydrogeology*. Prentice Hall, Upper Sattle River, NJ.

Spane, J.F, and Wurstner, S (1993) *DERIV: A computer program for calculating pore pressure derivatives for use in hydraulic test analysis,* Ground Water 31, Vol.5. pp.814-822.

Swason, E, and Titone, B (2013) *Packer testing program design and management*, IMWA 2013 "Reliable Mine Water Technology", Golden CO; USA.

Theis, C.V, (1935) *The relation between the lowering of the piezometric surface and the rate and duration of discharge of a well using groundwater storage*, Am. Geophys. Union Trans., vol. 16, pp. 519-524.

West, L, and Odling, N.E (2007) *Characterisation of a multilayer aquifer using open well dilution tests*. Ground Water 45, vol. 1, pp.74-84.

CHAPTER 14

MINE WATER MANAGEMENT FOR CLOSURE

Practices in Setting Sustainable Water Management Closure Performance Criteria

Henning Boshoff
ATC Williams, Australia

ABSTRACT

The processes and sources of acid rock drainage from mine wastes are well described, as is the definition of sustainability. However, the practices used to define closure performance criteria for mine water management do not always intersect with these definitions, nor does the water from operating mine sites or discharged from a closed mine site always meet sustainability criteria. The problem lays in that mine designers and planners develop initial mine water management objectives and criteria that are not always inherently linked with operational implementation. Furthermore, the same designers generally do not prepare these documents nor are they prepared at the same time creating further disparity. Setting suitable water management closure performance criteria are further complicated through not knowing definitively when closure related efforts will translate into a sustainable outcome.

It is recognised that appropriate and effective mine water management alone cannot ensure sustainable closure outcomes, which are made clear through environmental risk identification and the management thereof. However, experience shows that water management is key to achieving successful mine closure. Regulators require mining operations to closely manage mine effected water during and post mining, which are monitored through activities such as assessment of the receiving environment's water quality.

This paper provides perspective on the current guidelines and practices followed in setting mine water closure performance criteria and references current relevant Australian guidelines. Furthermore, it provides discussion on examples that are presented and recommendations to improve the current practices.

Keywords: Water Management, Closure, Performance Criteria

INTRODUCTION

Mine sites often face challenges to manage mine effected water, which vary from routine to the unexpected. Personnel responsible for mine water management will reference site procedures and guidelines when making some of these day to day decisions. However, in non-routine situations these decisions become difficult and more so, if the overall mine site water management objectives and performance criteria are unclear.

Those responsible for the planning and design of mine sites are not normally involved in the management of the mine site, and do not consider all management scenarios. Nor are they generally involved in closure planning or in implementing the closure and rehabilitation plans.

Various reports and planning documentation are developed during the feasibility and approval stage, during which high level mine management commitments are developed. These commitments include mine water management, which will provide the basis for setting mine water management objectives and criteria.

Significant work has been done in the field of assessing the potential and describing the formation of acid rock drainage with the aim prevent acid mine drainage. More strict legislation and setting better water management performance criteria aid in the drive to reduce the number of mine sites with acid mine drainage.

There is a lack of continuity in the design stage, and the operational and closure stages that results in developing mine water management criteria that are not sustainable. The paper highlights available the guidance, current practices and examples in setting sustainable water management criteria, and recommendations for further improvements.

METHODOLOGY

A desktop investigation was completed to identify relevant guidance documents and current practices followed in setting sustainable water management criteria. Information was compared to identify similarities and deficiencies to assist mine designers and planners to set sustainable water management criteria.

DISCUSSION

Mine water management is not the same for all mine sites, including the process followed to set sustainable mine water management closure performance criteria. The topic of mine water management is extensive and this paper will only focus on one aspect, which is believed to be pinnacle to the success of sustainable mine water management. Being, to identify and implement mine water management objectives and performance criteria.

Poorly defined performance criteria could lead to an anything-goes mentality. Unfortunately, this may result in long term closure liabilities such as acid rock drainage, saline drainage, erosion, flooding, etc. Furthermore, a lack of performance criteria will make assessment of closure performance nearly impossible.

What guidance is available for mine water management?

Regulators, scientific institutions and the mining industry develop many documents aimed at guiding the reader to undertake a specific activity. These documents are not developed by the same person or for the same purpose, and could duplicate information or contradict each other. Users of the information must therefore take care when using the information to ensure that it is applicable and of similar complexity to their situation.

The internet is a vast source of information and provides a multitude of relevant and irrelevant water management information. The following are some of the guidance information that are easily available:

- Water Management Leading Practice Sustainable Development Program- Australia (WMLPSDP, 2008);
- Managing Acid and Metalliferous Drainage Leading Practice Sustainable Development Program- Australia (MAMDLPSDP, 2007);
- Mine Rehabilitation Leading Practice Sustainable Development Program- Australia (MRLPSDP, 2006);
- Mine Closure and Completion Leading Practice Sustainable Development Program- Australia (MCCLPSDP, 2006);
- Guide to Leading Practice Sustainable Development in Mining- Australia (GLPSD, 2011);
- Managing mine water under extreme climate variability CSIRO project- Australia (CSIRO, 2013);
- Minesite Water Management Handbook- Australia (MWMH, 1997);
- Integrating the mining sector into water planning and entitlements regimes- Australia (Hamstead, 2012);
- Guidelines for Mining and Sustainable Development- International (UN, 2002);
- EU Water Framework Directive 2000/60- Europe (EU, 2000);
- Best Environmental Practices in Metal Ore Mining- Finland (Kauppila, 2013); and,
- Acid mine drainage prediction- United States (USEPA, 1994).

Other information that is not easily accessible on the internet, includes:

- Strategic Framework for Mine Closure 9 ANZMEC 2000. Strategic Framework for Mine Closure. Australian and New Zealand Minerals and Energy Council and Minerals Council of Australia (ANZMEC, 2000);
- Technical and Managerial Guidelines for Catchment Scale Management- United Kingdom (ERMITE, 2001);
- Checklists for sustainable mining- Australia (Barton, 2003); and
- Mining and the Environment from Ore to Metal- Australia (Spitz, 2008).

Guidance is also provided through legislation, licensing or policies. Mine sites identify site specific legislative requirements and manage these requirements. Not complying with relevant legislation or license conditions could result in legal action, under:

- The Environmental Protection and Biodiversity Act 1999 (EPBC Act), which protects and manages national and international important flora, fauna, ecological communities and heritage places. Notably, the EPBC Act on 22 June 2013 made water resources a matter of national environmental significance in relation to coal seam gas and large coal mining.

- The Queensland state government has released a number of environmental protection policies under the Environmental Protraction Act of 1994 (EP Act, 1994). The Environmental Protection Water Policy 2009 is one such policy relating to protection, monitoring and reporting of Queensland waters.

One common message was identified when reviewing the available guidance information. Being, that water management planning must be integrated at the beginning and throughout the project. Setting specific mine water management performance criteria gives focus to planning and design, and forms a common basis for setting related project objectives.

The guidance information is also clear on the importance of sustainability, which is well defined and discussed on many levels of society and industries. Water plays a vital role in the viability of economic activities (ATSE, 2012), such as mining and is one of the key resources assessed to ensure that a project is sustainable. This assessment includes both the reliance on water, as well as the potential risk to the water resource (NWI, 2011).

Guideline documents further identify the importance of setting water use regimes that support the mine water management performance criteria. A water use regime is set to ensure environmental and resource sustainability, while still allowing development. The 2011 National Water Initiative (NWI, 2011) identified the effect of mining on the sustainability of water resources, and raises concerns about the recognition and integration of the minerals industry in water reform. This is primarily due to historically treating the minerals and other extractive industries different to other water users, such as in the case of special water licenses giving mining operations the right to take and interfere with water (NWI, 2011).

Following the guidelines will assist in setting mine water performance criteria, however there are a number of issues to consider to ensure the sustainability of the mining project, these include:

- assuring an adequate water supply during the life of the project;
- ensuring that only water of an acceptable quality is discharged;
- providing infrastructure to prevent the flooding of mine workings and others;
- selecting a logical sustainability assessment process (Gasparatos, 2012); and
- considering project stakeholders and decision makers (RAC, 1992).

There are many sustainability assessment processes available (Gasparatos, 2012) however, selecting a suitable assessment process is not discussed in this paper.

Planning for effective mine water management in the initial design process

Mine water management has evolved over time and is a key focus area for many mining operations (Boshoff, 2014). Mine sites plan the mine water management layout based on the overall mine plan to ensure effective water management during all the stages of mining. Planning is generally based on modelling with limited verification of the assumptions and often no calibration of models, which could cause operational issues and redesign.

Mine designers also consider closure during this planning process and generally aim for a maintenance-free post mine closure water management system. Water management post closure will only be successful if supported through proper water and waste management during the life of the mine. This includes proper closure design for tailings and waste rock facilities. Integrating of closure requirements with the life of mine planning reduces the long term liabilities (Boshoff, 2014).

A water management plan is required for new mining projects seeking a license to operate. The Queensland government Department of Environment and Heritage Protection states that a water management plan must be developed by an appropriately qualified person and implemented by

the mine, as per the documented plan (EM944, 2013). Water management plans must further conform to guideline requirements (EM324, 2012), which include the following:

- study of the source of contaminants;
- a water balance model for the site;
- a water management system for the site;
- measures to manage and prevent saline drainage;
- measures to manage and prevent acid rock drainage;
- contingency procedures for emergencies; and
- develop a program for monitoring and review of the effectiveness of the water management plan.

Mine water management is not limited to the boundaries of the mine site, specifically in areas of high precipitation and for mine sites with an annual water excess that will most likely discharge frequently. Planning must include local and regional considerations to assess the impacts on water resources, including climate, topography, drainage and the receiving environment.

Mine planners and designers will assess the impacts, select objectives and develop cost effective mitigation strategies to ensure that the impacts post closure will be acceptable. Post mining water management performance criteria provides the basis for developing operational stage objectives. It will be difficult to meet more stringent closure performance criteria following an operational stage that had laxed performance criteria.

The mine designers involved during the feasibility stage of the mine are most likely not involved in operating of the mine (Bullock, 2011). Their objectives include cost effectiveness, which stems from pressures to make a mine feasible (McCarthy, 2013). The operating mine will also have an objective to keep overheads and production costs low, and the end result is a mine with inadequate water management considerations during the life of the mine and after closure.

Expertise and skill are required when planning, designing and implementing cost effective mine site water management that meet key cost effectiveness objectives. Even then, the water management plans should be considered living documents and altered as conditions change during mining or detecting unauthorised environmental impacts.

Setting effective mine site water management performance criteria

Will mine water management activities during mining and post closure result in sustainable outcomes? This is a question that cannot be answered qualitatively or quantitatively during the planning stage. Mine designers and planners consider project objectives and project design criteria during the design process (Elkington, 1997). The potential issues with project objectives and project design criteria includes:

- providing objectives that are not clear;
- selecting objectives that are general to the mining industry;
- selecting objectives prior to identifying environmental values;
- writing objectives as criteria or providing criteria as trigger limits;
- developing objectives that are not clear how and when it is relevant;
- quoting specific legislation or guidelines as objectives; and
- developing closure objectives not considering water management objectives and vice versa.

Below are some examples of water management objectives:

- General surface water management objectives (McArther River Mine, 2012):
    - **Separate** 'clean', 'dirty' and 'contaminated' water runoff as much as possible; and
    - **Minimise the area** of surface disturbance, thus minimising the volume of 'dirty' and/or 'contaminated' runoff.
- Site water management project operational and environmental objectives (RASP Mine, 2012):
    - **Prevent discharge** of potential contaminated surface waters from active mine areas off-site.
- Site water management principal objectives (Tarrawonga, 2006):
    - To ensure sufficient quantities of water can be obtained through the capture of "dirty" water, harvesting of "clean" water, and extraction/harvesting groundwater to meet the **requirements for dust suppression** on the mine site.
- Site water management objectives (Alpha Coal, 2011):
    - **Avoid** the need for **discharge** of contaminated water under normal operating conditions through preferential onsite reuse of contaminated water stores.

Similarities are observed, although planners and designers with different experiences and skills developed these objectives, of which the main similarities in the objectives consist of:

- meeting legislated mine site water management requirements;
- minimising the use of water from natural water resources on the surface and below;
- minimising the impact on surface water and groundwater flows and water quality;
- identify and control mine site erosion; and
- establishing a monitoring program to assess the actual impact on natural water resources.

Mine water management performance criteria, as with the objectives, are specific to the mine site. No one mine is the same or are located in exactly the same environmental setting resulting in different water management performance criteria. This is evident when comparing a number of environmental impact statements. The following are examples of water management performance criteria, of which the tabled water quality performance criteria were excluded:

- The characteristics of clean water are pH of 6.5 – 8.5 and suspended solids of **less than** 50 mg/l as well as hydrocarbons less than 10 mg/l (RASP Mine, 2012);
- Discharge **water quality will meet** the Australian and New Zealand Environment and Conservation Council Water Quality Guidelines for Fresh and Marine Waters (ANZECC, 2000);
- **Groundwater levels** in privately owned bore will **not exceed** more than 3 m sustained reduction over a 3 month period (RASP Mine, 2012);
- Long-term 'dirty' **runoff** drains that will be active for longer than 2 wet seasons **will be** constructed to **contain** the 1% Annual Exceedance Probability (100 year Average Recurrence Interval) design discharge (MacArthur River Mine, 2012);
- The performance of the water management plan in achieving the objectives and targets shall be **reviewed at least** quarterly (Ulan, 2014);
- Regularly **report environmental performance** to the environment and community manager (Ulan, 2014);
- **Runoff** from all disturbed areas across the mine site during the operational phase **is contained** by a mine water management system (Alpha Coal, 2011); and
- Mine closure runoff quality **meets** the water quality **objectives** for the identified surface water environmental values (Alpha Coal, 2011).

It was found that most of the water management performance criteria are focused on water quality and predominantly discharge water quality (as a lagging indicator), as required by the mine site license to operate. Regulators provide the discharge water quality requirements once the mine designed and approvals process are completed. The requirements are therefore based on the outcome of environmental studies, modelling and the mine's agreed/negotiated commitments. These commitments are therefore based on objectives, performance criteria and legislative requirements identified during the design and planning of the mine. More specifically, these commitments are specific to the environmental values relevant to the mine site and described in the key objectives to be enhanced or protected.

The main reason for selecting and describing water management performance criteria is to enable quantitative measurement of the effectiveness of the mine's water management activities.

Recommendations in setting mine water management performance criteria

Defining performance criteria for mine water management cannot be conducted by one person from a single engineering discipline (Gasparatos, 2012). This is due to the complexity of the issues associated with water management and closure objectives.

It is recommended to involve various disciplines; including civil engineering, mechanical engineering, structural engineering, environmental engineers, human resources, social and community studies in developing water management performance criteria.

Modelling of the water systems and assessing the potential effectiveness of various management options could provide early indications, however it is recommended that assumption must be verified once more tangible data becomes available.

A fully integrated planning and implementation process is recommended, which is broadly outlined as follows for all the stages in the life of the mine, including post closure:

- Identify surface water and groundwater environmental values relevant to the mining project;
- Set key closure objectives that will either enhance or protect the relevant surface water and ground water environmental values;
- Set water management performance criteria for the surface water and ground water relevant to the mining operations during;
- Undertake a risk assessment and identify the control measures, mitigation activities and responsibilities to ensure that closure objectives are met or exceeded;
- Set water management infrastructure design criteria relevant to the mining operations and key objectives;
- Plan, design and adequately cost the control measures and mitigation activities;
- Develop water management performance monitoring and reporting requirements;
- Develop a water management plan integrating closure;
- Obtain a social license to operate the mine committing to the water management plan;
- Verify all assumptions at the earliest possible stage of the design process; and
- Implement the water management infrastructure design and water management plan, as specified.

CONCLUSION

There are many freely available guidance documents that provide guidance in the development of water management performance and closure criteria. These objectives and performance criteria are best developed and agreed at the beginning of the planning and design process. Forward planning assist to ensure that selected water management objectives can be met during all stages of the mining project and after closure.

It can also be concluded that the development of objectives and the subsequent performance criteria needs input from individuals with experience and skill from a number disciplines. Site documentation must be linked back to the water management objectives and specific water management performance criteria. It is critical to develop effective objectives and criteria for water management performance and closure to ensure that site activities will drive to a common goal and that adequate budget is available during operations and after closure.

REFERENCES

Alpha Coal, (2011). *Alpha Coal Project Environmental Management Plan*, Alpha Coal Project, 2011.

ANZECC, (2000). *Australian and New Zealand guidelines for fresh and marine water quality*, Agriculture and Resource Management Council of Australia and New Zealand and the Australian and New Zealand Environment and Conservation Council, 2000.

ANZMEC, (2000). *Strategic Framework for Mine Closure 9 Strategic Framework for Mine Closure*, Australian and New Zealand Minerals and Energy Council and Minerals Council of Australia, 2000.

ATSE, (2012). *Sustainable Water Management: Securing Australia's future in a green economy*, Australian Academy of Technological Sciences and Engineering, 2012.

Barton, A (2003). *Checklists for sustainable mining: Best practice environmental management in mining series*, Environmental Australia, 2003.

Boshoff, H (2014). *Inadequate Water Management Planning Resulting in Long-term Closure Liabilities*, Life of Mine conference, Brisbane, 18 July 2014.

Bullock, R (2011). *Accuracy of Feasibility Study Evaluations Would Improve Accountability*, Mining Engineering, April 2011.

CSIRO, (2013). *Managing mine water under extreme climate variability*, CSIRO, April 2013

Elkington, J (1997). *Cannibals with Forks: The Triple Bottom Line of 21st Century Business*, 1997.

EM324, (2012). *Guideline for preparation of a water management plan for mining activities*, Department of Environment and Heritage Protection, 2 July 2012.

EM944, (2013). *Model mining conditions*, Department of Environment and Heritage Protection, 26 June 2014.

EP Act, (1994). *Environmental Protection Act 1994*, Queensland Government, Current as at 1 July 2014.

EPP Water, (2009). *Environmental Protection (Water) Policy 2009*, Queensland Government, Current as at 6 December 2013.

ERMITE, (2003). Environmental regulation of mine waters in the European Union, European Commission Framework Programme No. 5, July 2003.

EU, (2000). EU Water Framework Directive 2000/60, European Commission, December 2000.

Gasparatos, A (2012). *Choosing the most appropriate sustainability assessment tool*, Ecological Economics, Elservier, 20 May 2012.

GLPSD, (2011). G*uide to Leading Practice Sustainable Development in Mining: Leading Practice Sustainable Development Program for the Mining Industry*, Australian Government Department of Resources, Energy and Tourism, July 2011.

Hamstead, M, Fermio, S (2012). *Integrating the mining sector into water planning and entitlements regimes*, Waterlines Report Series No 77, March 2012

Kauppila, P, Räisänen, M, Myllyoja, S (2013). Best Environmental Practices in Metal Ore Mining, Finnish Environment Insitute, 2013.

MacArthur River Mine, (2012). *Draft Environmental Impact Statement, Phase 3 Development Project*, Glencore MacArthur River Mining, 2012.

MAMDLPSDP, (2007). *Managing Acid and Metalliferous Drainage: Leading Practice Sustainable Development Program for the Mining Industry*, Australian Government Department of Resources, Energy and Tourism, February 2007

McCarthy, P (2013). *Why Feasibility Studies Fail*, The Australasian Institute of Mining and Metallurgy Melbourne Branch, February 2013.

MCCLPSDP, (2006). *Mine Closure and Completion: Leading Practice Sustainable Development Program for the Mining Industry*, Australian Government Department of Resources, Energy and Tourism, October 2006

MRLPSDP, (2006). *Mine Rehabilitation: Leading Practice Sustainable Development Program for the Mining Industry*, Australian Government Department of Resources, Energy and Tourism, October 2006

MWMH, (1997). *Minesite Water Management Handbook*, Minerals Council of Australia, 1997

NWI, (2011). *The National Water Initiative—securing Australia's water future: 2011 assessment*, National Water Commission, September 2011.

RAC, (1992). *Multi-criteria assessment as a resource assessment tool, Resource Assessment Commission Research Paper No. 6*, Commonwealth of Australia, 1992.

RASP Mine, (2012). *Site Water Management Plan RASP Mine Broken Hill*, Broken Hill Operations, 30 April 2012.

Spitz, K, and Trudinger, J (2008). Mining and the Environment: From Ore to Metal, CRC Press, November 2008.

Tarrawonga, (2006). *Site Water Management Plan for the Tarrawonga Coal Mine*, Tarrawonga Coal Mine, February 2006.

Ulan, (2014). *Water Management Plan Ulan Coal Mine*, Umwelt Environmental Consultants, July 2014.

UN, (2002). *Guidelines for Mining and Sustainable Development*, United Nations, 2002.

USEPA, (1994). *Acid mine drainage prediction, Technical Document EPA 530-R-94-036*, U.S. Environmental Protection Agency, December 1994.

WMLPSDP, (2008). *Water Management: Leading Practice Sustainable Development Program for the Mining Industry*, Australian Government Department of Resources, Energy and Tourism, May 2008

Mine Water Management for Closure – Mine Reclamation and Surface Water Balances

Justin Straker[1], Mike O'Kane[2], Sean Carey[3], Dan Charest[4], and Lee Barbour[5]

1. *Integral Ecology Group, Canada*
2. *O'Kane Consultants, Canada*
3. *McMaster University, Canada*
4. *Teck Resources Limited, Canada*
5. *University of Saskatchewan, Canada*

ABSTRACT

Understanding reclamation effects on surface water balances in mine-affected watersheds is critical to both prediction of, and design for, water movement through the post-closure landscape, and for development of appropriate reclamation and revegetation treatments for mine closure. Substantial effort has been invested in increasing knowledge of the effects of mine-waste cover systems on key water-balance terms such as net percolation, but there is a lack of tools to extend that knowledge to effects of cover systems on vegetation establishment, and the subsequent effects of these vegetation-substrate interactions on water-balance terms. The concept of a "soil moisture regime" is used worldwide to understand edaphic conditions and plant communities. However, in most applications, soil moisture regime is a relative or unquantified parameter estimated from the presence of indicator plants or soil properties observed in natural ecosystems. Applications of these approaches to post-mining landscapes are challenging, because soils/surficial materials are reconstructed, and often reference plant communities are not fully re-established. Some quantitative approaches to estimation of properties that influence soil moisture regime (e.g., available water storage capacity) have been developed, but these are generally based on agricultural soil science, and have limited utility to many post-mining materials.

The authors propose new methods for estimating soil moisture regime on post-closure landscapes, using concepts from existing biogeoclimatic-ecosystem classification systems and new analyses of effects of particle-size distribution on soil water retention. Key variables in the proposed estimation model include regional and local climate, material particle-size distributions (including distributions typical of mine-waste materials) and organic-matter accumulation, and topography. This paper discusses methods development, application, and testing of this estimation approach across a number of mines, and presents suggestions for broader application of the approach for quantifying surface-water-balance components (e.g., net percolation) and for reclamation planning (e.g., revegetation species selection) in closure landscapes.

Keywords: reclamation, soil, moisture, regime, water

INTRODUCTION

One of the principal knowledge gaps in mine reclamation is that of characterizing soil water dynamics within surficial materials used in reclamation cover systems. The concomitant water balance in these materials is a dominant control on both ecosystem development and watershed performance, and better understanding of these water balances is critical for improved reclamation planning and projection of long-term characteristics of reclaimed ecosystems. It is also critical for improving our understanding of the hydrologic behavior of reconstructed mine-affected watersheds, including the role of net percolation on flushing of constituents of interest (CIs) from the mine wastes within these watersheds. Although substantial effort has been invested from an engineering perspective in investigating the effects of cover systems on rates of net percolation, this effort has generally not been coupled with understanding soil water dynamics within the same cover systems for the purposes of reclamation planning and execution. To date most ecological approaches used to address the above knowledge gap, where it has been addressed at all, have been borrowed from ecosystem classification systems, and are limited by some or all of the following factors:

- they are qualitative or semi-quantitative, and there is limited attempt to evaluate and demonstrate their hydrologic validity;
- they rely substantially on the presence of existing natural vegetation communities to provide information on edaphic conditions – these techniques are not applicable to mine-reclamation settings where vegetation communities are absent or introduced; and/or
- they have a narrow focus on a single aspect of the surface water balance, e.g., estimating water retention for revegetation planning. In these approaches, there is no attempt to provide a more comprehensive understanding of surface water balances, and of how water retention and use by vegetation may influence deeper percolation and the water balance of the underlying mine-waste landform.

This paper presents a quantitative method to relate the properties of landforms and cover-system materials to plant-available water and surface water balances, based on particle-size distributions and biogeoclimatic ecosystem classification.

BACKGROUND

Biogeoclimatic ecosystem classification

Biogeoclimatic ecosystem classification (BEC) is an ecological classification system developed primarily in the western Canadian province of British Columbia (B.C.) in which biogeoclimatic units ("zones") represent broad geographic areas of similar macroclimate, and are recognized as influencing biological characteristics of resulting ecosystems (Meidinger and Pojar, 1991). In the BEC system, biogeoclimatic zones can be subdivided into subzones, which can in turn be subdivided into variants, with each subdivision representing a reduction in climatic variability and geographic area (Lloyd et al., 1990). Within each subzone or variant, there are sequences of distinct ecosystems ("site series"), with associated vegetation communities reflecting differences in topography and soil depth, texture, drainage, moisture regime, and nutrient regime. In this system, soil water availability is believed to have the greatest influence on ecosystem development. This availability is in part determined by climate, but since climate is relatively uniform within a biogeoclimatic subzone or variant, variation in soil water availability at this level of classification

results from influences of soil and topography on surface water balances (Lloyd et al., 1990). These influences are manifested in resulting plant associations, i.e., each site series has an assemblage of plants that are adapted to its edaphic conditions – a fundamental principle of the BEC system is that sites with similar physical properties have similar vegetation potential (Meidinger and Pojar, 1990). A subset of plants on a site – "indicator plants" – are diagnostic of edaphic conditions due to their adaptation to narrow ranges of conditions, e.g., soil water availability.

Soil water availability

In the BEC system, soil water availability is estimated using a concept termed "soil moisture regime" (SMR), which reflects "the average amount of soil water annually available for evapotranspiration by vascular plants over an extended period of time (several years)" (Pojar, Klinka & Meidinger, 1985). The BEC system incorporates nine SMR classes ranging from driest (Class 0, or very xeric) to wettest (Class 8, or hydric) – this spectrum is referred to as a hygrotope (Pojar, Klinka & Meidinger, 1985; Meidinger and Pojar, 1990; Klinka et al., 1984). The most common classifications of hygrotope – and those that are used in the BEC system – are classifications of *potential* hygrotope, based on subjective inferences from site and/or vegetation features (e.g., source of water, rate of water removal, slope position, soil textural class), and represent relative ranking of sites in terms of potential soil water availability. A common example of this approach is provided by Meidinger and Pojar (1991), although more complex and semi-quantified examples exist in the BEC system (e.g., Lloyd et al., 1990). Actual hygrotopes integrate the above information with climate and surface-water-balance inputs and losses such as precipitation and evapotranspiration to provide estimates of absolute rather than relative water availability.

Quantified estimates of both potential and actual hygrotope or soil moisture regime are uncommon, and those that exist are limited in their application to specific geographic regions and/or ecosystems (e.g., Waring and Major, 1964). In B.C., Green et al. (1984, and summarized in Pojar, Klinka & Meidinger, 1985) used a water-balance approach to develop an actual hygrotope, but it is based on intra-annual duration of water deficits and on presence of water tables, and although the authors provide defining features for their classes, methods for classifying sites according to this system are not provided.

Various land-capability classification systems in Canada – beginning with agricultural land-capability systems – have used available water storage capacity (AWSC) as an index of potential soil-water availability. Available water storage capacity is defined as the volume of water per unit area held within the active or rooting zone of the soil profile between the volumetric water content at field capacity (FC) and the permanent wilting point (PWP). The field capacity is the volumetric water content at which the rate of gravitational drainage becomes negligible relative to the current rate of evaporation or evapotranspiration (Zettl, 2014). This water content is often taken to be the water content at negative pore-water pressures of 10-33 kPa, depending on soil texture. The permanent wilting point is the volumetric water content at which soil water is no longer available for plant uptake. Although this water content varies by plant species, by convention it is defined as the water content at a negative pore-water pressure of 1500 kPa.

AWSC is generally expressed as a depth of water (mm) over a specified soil depth, or as a depth of water per unit depth of soil (mm water/cm soil). A common practice has been to assign AWSC values based on soil texture: for example, the document *Land capability classification for agriculture in British Columbia* (B.C. Environment, 1983) provides AWSC values in mm water/cm of soil depth for soils of different textural classes. However, these systems, being initially focused on agriculture, do

not link AWSC to soil moisture regime, and to occurrence of typical natural ecosystems and/or larger hydrologic performance.

In northeast Alberta, the *Land capability classification system for forest ecosystems in the oil sands* (or "LCCS" – Cumulative Environmental Management Association, 2006; first published in 1996) attempted to use earlier concepts (and values) of assigning AWSC to textural classes for application to mine-reclamation and forest-ecosystem settings. The LCCS equates a potential hygrotope to numeric values calculated from texture-class-based AWSC, and some topography and surficial-material-depth modifiers such as slope position and depth to impermeable layers. This approach represents an advancement in producing an objective and quantified relative hygrotope, but still has a number of limitations for broader application. Consistent with conventional soil-science principles, calculation of AWSC in the LCCS is based solely on <2-mm particle-size fraction, with particles greater than 2 mm discounted on a volume basis. This has not been a substantial limitation in oil-sands reclamation applications due to relatively insignificant coarse-fragment contents, but it limits application of the LCCS approach to higher-coarse-fragment-content settings like hard- and soft-rock mine wastes. In addition, texture-based AWSC values in the LCCS apply uniformly across texture or material classes, and do not recognize or account for variation in particle-size distributions within these classes. For instance, the LCCS applies an AWSC value of 1.0 mm/cm to oil sands tailings, regardless of actual particle-size distribution and whether these tailings are complete, or are cyclone overflow or underflow products. Finally, although there has been substantial investigation and validation of the LCCS AWSC values (e.g., Barbour et al., 2010), and thus of their use as a relative hygrotope, there has been limited evaluation of the relationship between these values and actual soil water contents (i.e., the actual hygrotope), and of the relationship between these values and ecosystem development and landscape/watershed hydrologic performance.

The concept of soil moisture regime has been applied globally, based on duration or magnitude of growing-season water deficits, but typically involves relatively broad classes that can be mapped at a continental scale (e.g., Soil Survey Staff, 1999), versus application to differentiate between ecosystems and hydrologic behaviors at a local or regional scale.

METHODS DEVELOPMENT

Objectives of the proposed classification system

The classification system proposed here is substantially informed by the biogeoclimatic, hygrotope/SMR, and land-capability classifications described above, but is intended to derive estimates of plant-available water, surface-water-balance performance, and associated ecosystem characteristics from landscape, landform and surficial-material properties, using objective and quantified methods that can be consistently and easily applied. Further, the proposed system is designed to be broadly applicable to a range of climatic, physiographic, and surficial-material conditions (e.g., globally), yet have sufficient resolution to differentiate ecosystem characteristics and hydrologic performance at a local scale. Additional goals for the classification system are that it:

- be capable of derivation solely from information on material properties, topography and climate, and not rely on observations of intact above-ground ecosystems for diagnosis;

- be capable of evaluation and validation or adjustment through analysis of related empirical observations, including relationships with non-mine ecosystems classified through standard BEC methods; and
- provide useful interpretations for a range of mine-planning and reclamation-management considerations, including both cover placement/revegetation and understanding hydrologic behavior at the mine landform-landscape-watershed scale.

Classification framework

The proposed classification framework is based on three primary factors, with decreasing geographic scales of application (Table 1, adapted from Devito et al., 2005). For the first classification factor, AWSC is determined from particle-size distributions of materials in the upper one metre of surficial material. This determination can be applied globally, as it is based on universal principles of soil physics. The next classification factor involves modification of the profile AWSC estimate for topography-based energy regime – these modifications are specific to latitudinal ranges, and thus must be developed specifically at the continental to sub-continental scale. The final classification factor applies regional and local climate information to the potential hygrotope resulting from application of the first two factors to generate an actual hygrotope and identify ecosystems associated with this hygrotope. Thus application of the first classification factor (AWSC) requires only information contained in this paper; application of the second factor (topography/energy) may require modification of information contained in this paper, depending on latitude of application; and application of the third factor (climate) requires information on climate local to the application site and biogeoclimatic or similar classification information.

Table 1 Soil water regime classification framework

Factor	Range of factor		Scale of applicability	Classification outputs
1. PSD of surficial materials	High silt and clay contents, low sand, gravel and cobble contents: higher AWSC	High sand, cobble and gravel contents, low silt and clay contents: lower AWSC	Global	Profile AWSC in surface 1 m
2. Topography and energy	High latitude: slope and aspect significantly affect energy distribution	Tropical and sub-tropical: slope and aspect do not significantly affect energy distribution	Continental to sub-continental	Adjusted AWSC; relative SMR or potential hygrotope
3. Regional and local climate	Dry, arid to sub-humid (P < PET) • storage and ET dominant • runoff and NP may be reduced	Wet, humid (P > PET) • runoff and NP dominant	Regional to local	Actual SMR and hygrotope; identification of associated ecosystems

Determination of AWSC

A standard particle-size distribution (PSD) ternary diagram for engineering interpretations was used as a framework for generating PSD-based AWSC values. This framework (based on the Unified System of Soil Classification) was used both to allow evaluation of the contribution of particles >2 mm (as opposed to conventional soil-science approaches), and to facilitate communication between mine planners/engineers (who often use engineering PSD classification systems) and reclamation specialists (who often use soil-science PSD or texture classification systems). AWSC values were estimated from two databases of material characteristics[1] for all materials with measured PSDs and water-retention curves. The materials were separated into 100 textural groups corresponding to subdivisions of the PSD ternary diagram, based on gravimetric proportions of coarse (>4.75-mm), sand (0.075-4.75 mm), and finer (<0.075-mm) particles. The average AWSC for each group was used to populate the ternary subdivision position. If a textural group had little to no available AWSC data then an estimate was made from interpolation and/or extrapolation from surrounding positions. The resulting AWSC-populated ternary diagram is presented in Figure 1, where AWSC values are in mm water/cm material depth, and represent the center point of each subdivision. Values in this table are preliminary, in that they provide a framework and enable testing of the proposed system, but it is recognized that they require further refinement prior to broad application. In order to allow consistent and repeatable use of this tool, software has been developed that will take input PSD information and consistently interpolate an AWSC value from the center-point values, based on standard GIS interpolation algorithms. Input PSD information is based on all particles <100 mm. To facilitate more cost-effective and reliable

[1] Databases included an internal database from O'Kane Consultants Inc. (OKC), based on properties of mine-waste and cover materials observed by OKC at different client mining sites around the world, and the other internal to SoilVision Systems Ltd.'s numerical modelling software (www.soilvision.com).

classification, low-technology field equipment has also been developed to allow rapid determination of the cobble-and-gravel separate (>4.75 mm) based on a large volume of material, with subsequent determination of the sand and clay-and-silt separates based on laboratory analyses of smaller collected samples.

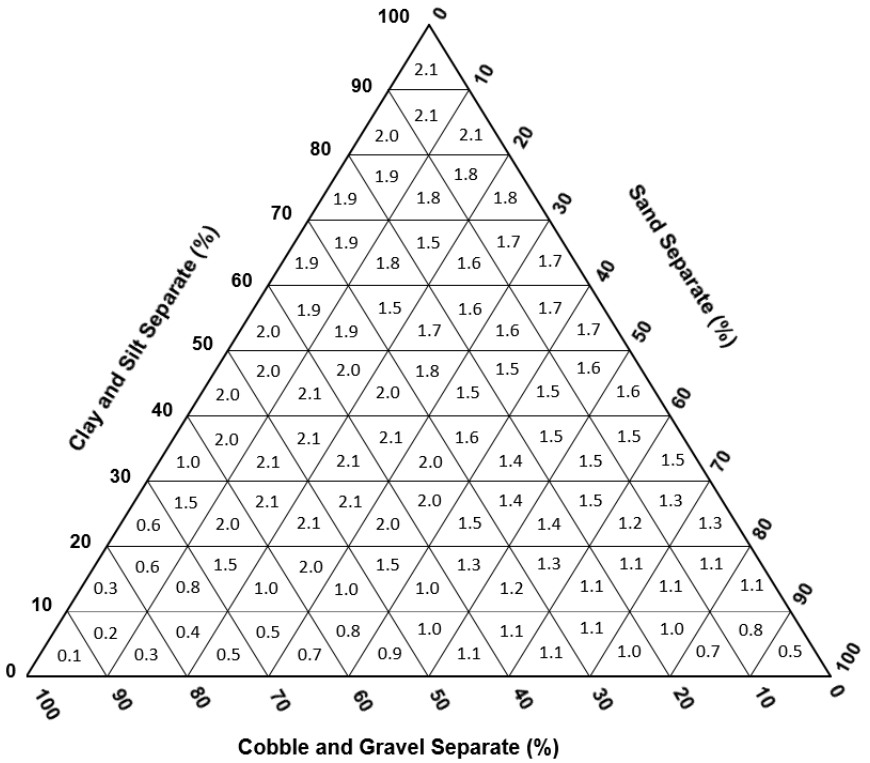

Figure 1 AWSC ternary diagram. AWSC values are in mm available water storage per cm of material depth, and represent the center point of each subdivision of the diagram

Values derived from Figure 1 are intended to represent a single material, and to be aggregated across a standard material profile or control section (typically 100 cm, but lesser sections could be used if stipulated). For instance, to estimate AWSC for a 50-cm soil cover placed on mining waste rock or tailings, one AWSC value is calculated for the cover material, another is calculated for the mine-waste material, and an aggregate AWSC is then generated by summing the values. If multiple layers are present within the soil cover (or mine waste), then an AWSC value is calculated for each layer corresponding to depth and PSD data. For natural soils, calculation is based on horizon depths and characteristics. In the case of shallow soils over non-rooting-zone materials, the AWSC for the control section is based only on the depth of the soil material, and thus is reduced compared to a 1-m potential rooting zone.

Modification of AWSC values for energy regime

In the British Columbia BEC system, the topographic effect on energy is recognized through "warm" and "cool" site modifiers. These modifiers are applied to slope angles >25% (14°), with warm aspects being southerly or westerly (135°-285°), and cool aspects being northerly to easterly

(285°-135°; Resources Inventory Committee, 1998). This approach was modified for the current classification system as presented below in Table 2 to include a neutral energy regime on southeast and southwest slopes. This modification is based on the fact that the shift in energy regime on slopes as aspects change is more accurately a continuous increase or decrease in insolation rather than a categorical shift – the modified classification still uses categories, but incorporates an intermediate neutral category instead of the immediate shift from cool to warm as implied by the BEC system. This modification is supported by evaluation of data on field-measured soil water-content profiles in comparison to estimated AWSC values, which indicates a better fit when southeast and southwest aspects are categorized as neutral than when they are classified as cool (southeast) or warm (southwest).

Modifiers in Table 2 are applicable to northern latitudes of approximately 48-60°. These magnitude of the modifiers could be increased for higher northern latitudes and decreased or eliminated for lower northern latitudes. For southern latitudes, the modifiers as presented or adjusted would be altered to reflect different warm and cool aspect relationships.

Table 2 AWSC energy modifiers

Energy class	Class definition	AWSC modifier
Neutral	Slopes <25% (<14°) Slope >25% (>14°); aspects 085-135° and 235-285°	none
Warm	Slope >25% (>14°); aspect 135-235°	Calculated AWSC – 30 mm
Cool	Slope >25% (>14°); aspect 285°-085°	Calculated AWSC + 30 mm

Equation of modified AWSC values to soil moisture regime[2]

Adjusted AWSC values (PSD-based AWSC from Figure 1 plus any applicable energy modifiers from Table 2) are used to determine soil moisture regime, as outlined in Table 3. This table uses the SMR classes of the BEC potential hygrotope, but replaces the relative ranking of various criteria with quantified ranges of adjusted AWSC. AWSC ranges for each SMR class are modified from the oil-sands reclamation land-capability classification system discussed above. The AWSC method for SMR determination applies only to upland (very xeric – mesic) SMRs, as wetter SMRs require input of seepage water or the presence of a water table within 100 cm of the soil surface, and are not dependent on soil storage. Thus determination of SMRs wetter than mesic in this system is based on observations of shallow groundwater seepage and/or the presence of a water table within the top 1 m of surficial materials. Note that these moisture regimes are intended to reflect dominant soil-water conditions over a multi-year period, consistent with the B.C. BEC-system hygrotope.

Table 3 Determination of SMR from adjusted AWSC

SMR	Primary water source	Water-table depth	Available water storage,

[2] The term "soil moisture regime" is applied in this paper both to soils and to surficial materials in reclamation landscapes due to its history of use and understood meaning. However, in mine reclamation, many of the materials for which SMR can be estimated are not soils, but are mine wastes and/or salvaged parent materials. Thus SMR should more properly be understood as a soil or surficial-material moisture regime.

		(cm below ground surface)	surface 1 m (mm)
Very Xeric (0)	Precipitation and soil storage	>100	<60
Xeric (1)	Precipitation and soil storage	>100	60-89
Subxeric (2)	Precipitation and soil storage	>100	90-119
Submesic (3)	Precipitation and soil storage	>100	120-149
Mesic (4)	Precipitation and soil storage	>100	>150
Subhygric (5)	Precipitation and seepage	>100	>150, seepage contributes to supply
Hygric (6)	Seepage	30-100	n/a
Subhydric (7)	Seepage or permanent water table	0-30	n/a
Hydric (8)	Permanent water table	Water table permanently at or above soil surface	n/a

METHODS TESTING

The methods discussed above were developed and tested at reclamation-monitoring sites at seven mining operations in 2012-2014: five metallurgical coal operations operated by Teck Resources Limited in southeastern B.C. and west-central Alberta; at the Teck Highland Valley Copper Partnership's Highland Valley Copper mine in south-central B.C.; and at Thompson Creek Metals' Endako molybdenum mine in central B.C. Of particular relevance to testing are the five Teck coal mines, as in 2011 Teck commenced development of an integrated, multi-year and multi-disciplinary applied research & development program focused on managing water quality in mining-affected watersheds. In 2012-13, this program included installation of soil and meteorological instrumentation and soils and vegetation assessments at 12 reclamation sites at these coal mines, to provide data on reclamation conditions co-located and concurrent with information on meteorological and soil-moisture variables at each study site. This instrumented-site network and the data it provides supports increased understanding of how surface water balances and soil moisture regimes are affecting reclamation responses over time, and *vice versa*, as well as how reclamation approaches affect reconstructed landform water balances and watershed hydrology.

Actual versus potential hygrotope

PSD data from 65 mine-reclamation and non-mine reference sites were plotted on the AWSC ternary diagram. Resulting AWSC values provide quantification of the potential hygrotope, as they indicate the *capacity* for soil water storage (and eventual release as evapotranspiration, interflow, and/or net percolation), not actual storage. Actual storage is a product of the interaction between the potential hygrotope and local climate, which delivers precipitation for storage and energy for evaporation and transpiration. To evaluate the relationship between potential (calculated) and actual hygrotope, analyzed volumetric-water-content (VWC) and matric-potential (ϕ_m) data collected by O'Kane Consultants from the Teck instrumented study sites were analyzed to derive mean growing-season *available* volumetric water contents (AWC) for each site. To do so, the VWC at permanent wilting point (PWP) was calculated for each material type (cover material, waste rock) from interpolated plots of VWC against ϕ_m for each sensor pairing. This gave each VWC

sensor a VWC-at-PWP value, which was then subtracted from each of its VWC measurements to calculate AWC (water content above PWP) for all sensors. To calculate mean AWC from all sensors over a profile depth, each sensor's AWC was mathematically weighted according to rooting patterns observed at vegetated sites, with weight assigned for both root abundance and root size. Where rooting data did not exist, mean root patterns from similar sites have been applied. Reported AWC values are means of all daily measurements made during the 2013 growing season, which was defined by site-specific meteorological data using the criteria of five consecutive days of average daily temperatures over and under 5°C as the beginning and end[3] of the growing season (Alberta Agriculture and Rural Development, 2009).

Predicted AWSC and SMR

SMR was assigned for each of the 65 study sites using the PSD-based AWSC estimates with energy modifiers as described above. For the Teck coal-mine research sites where AWC data are available, the AWSC-based SMR classification was evaluated using mean growing-season AWC (Figure 2Figure 2). These data show general support for the proposed classification system, with mean growing-season AWC increasing for every SMR class, despite differences in vegetation development across these sites. On average, very xeric sites have less than 30% of the plant-available water that mesic sites have during the growing season, while xeric sites have approximately 50% of the plant-available water of mesic sites. Research sites at Endako and Highland Valley Copper lack continuous measurement of soil water contents, and so cannot be added to this database, but reference sites in these studies provide some ability to evaluate system fit, as predicted SMR using methods proposed in this paper can be related to potential hygrotopic classification using standard subjective keys and the presence of indicator plants. All reference sites studied to date are zonal site series with mesic SMR – mean AWSC for these sites estimated with the proposed methods is 159 mm, which places them in the mesic SMR category according to the criteria presented in Table 3.

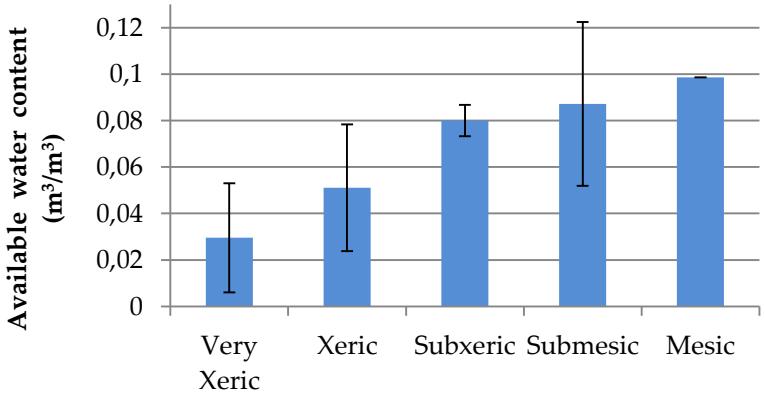

Figure 2 Mean AWC during the 2013 growing season at all sites classified by soil moisture regime – error bars show one standard deviation of the mean

[3] The end of the growing season cannot occur before August 1 regardless of temperature.

SUMMARY AND APPLICATIONS

This paper proposes a quantified and objective hygrotopic classification system that is broadly applicable to a range of ecosystems, including mine-waste-based landforms and mine-affected watersheds. Although the proposed classification system is initially based on potential hygrotope, the use of regional and local biogeoclimatic ecosystem classifications allows its translation into actual hygrotopes, based on regional and local climatic conditions. This translation from potential to actual hygrotope has been tested in two regions of western Canada on instrumented reclamation study sites. Initial results show promising relationships between predicted SMR using the proposed classification system and mean growing-season available water contents calculated from continuous measurement by *in situ* sensors, with increasing observed available water contents as SMRs predicted by the classification model progress from drier to wetter sites. In addition, the proposed classification system shows concordance with traditional ecosystem classification of non-mine reference sites where classification is based on indicator-plant presence and topographic/soil relationships.

The potential management applications of the classification system include:

- Reclamation and revegetation planning – using methods discussed above, soil moisture regime can be estimated for existing or planned landforms and covers, and locally appropriate candidate vegetation species adapted to these hygrotopic positions can be selected for reclamation.
- Assessment of pre- and post-development land capability – using estimated hygrotopic position and the BEC system or similar approaches allows comparison of anticipated post-closure ecosystems to pre-development inventories. These comparisons can then be used to evaluate the effects of mining on dependent values such as wildlife habitat, biodiversity, or land productivity, and can provide the basis for application for custodial transfer of reclaimed lands, or assessment of such applications.
- Quantification of the effects of surficial-materials management on landform surface water balances – when combined with information on local climatic conditions, the proposed classification system can be developed to provide relative estimates of surface-water-balance terms such as evapotranspiration and net percolation. This information can be used by reclamation practitioners to understand the effects of cover placement for reclamation on movement of water through the surface layers of the reclaimed landscape.

This proposed classification system and empirical approach to its evaluation represent a first attempt to populate the AWSC and modifier charts, and will continue to be updated and adapted as additional information is collected and as the classification system is refined.

REFERENCES

Alberta Agriculture and Rural Development (2009) Agricultural Atlas of Alberta: Agricultural Climate Elements. Alberta Ministry of Agriculture and Rural Development: Edmonton.

B.C. Environment (1983) Land capability classification system for agriculture in British Columbia. Province of British Columbia, Victoria.

B.C. Ministry of Energy, Mines and Petroleum Resources (2008) Health, safety and reclamation code for mines in British Columbia. Victoria, B.C.

Barbour L., D. Chanasyk, J. Hendry, L. Leskiw, T. Macyk, C. Mendoza, A. Naeth, C. Nichol, M. O'Kane, B. Purdy, C. Qualizza, S. Quideau, and C. Welham (2010) Soil capping research in the Athabasca Oil Sands Region, volume 1: technology synthesis.

Cumulative Environmental Management Association (2006) Land capability classification system for forest ecosystems in the oil sands, 3rd ed. Alberta Environment, Edmonton.

Devito, K., I. Creed, T. Gan, C. Mendoza, R. Petrone, U. Sillins and B. Smerdon (2005) A framework for broad-scale classification of hydrologic response units on the Boreal Plain: is topography the last thing to consider? *Hydrol. Process.* 19, 1705-1714.

Green, R., P. Courtin, K. Klinka, R. Slaco, and C. Ray (1984) Site diagnosis, tree species selection, and slashburning guidelines for the Vancouver Forest Region. Province of British Columbia, Victoria.

Lloyd, D., K. Angove, G. Hope, and C. Thompson (1990) A guide to site identification and interpretation for the Kamloops Forest Region. Province of British Columbia, Victoria.

Meidinger, D., and J. Pojar (1991) Ecosystems of British Columbia. Province of British Columbia, Victoria.

Pojar, J., K. Klinka, and D. Meidinger (1985) Biogeoclimatic ecosystem classification in British Columbia. Ministry of Forests, Victoria.

Resources Inventory Committee (1998) Standard for Terrestrial Ecosystem Mapping in British Columbia. Province of British Columbia, Victoria.

Soil Survey Staff (1999) Soil taxonomy. 2nd ed. Agriculture Handbook Number 436. United States Department of Agriculture, Washington, DC.

Waring, R., and J. Major (1964) Some vegetation of California coastal redwood regions in relation to gradients of moisture, nutrients, light, and temperature. Ecological Monographs 34: 167-215.

Zettl, J. (2014) Infiltration and drainage through coarse layered soil: a study of natural and reclaimed soil profiles in the Oil Sands Region, Alberta, Canada. M.Sc. thesis, University of Saskatchewan, Saskatoon.

Acid-Generating Waste Rock Encapsulation in a Subalpine Environment

Larry Breckenridge, Fred Bickford and Amy Livingston

Global Resource Engineering, USA

ABSTRACT

The Amulsar site, owned by Lydian International, is located at high elevations (2,500 m) in south-central Armenia. The site will produce two types of mine waste from an open pit gold mining operation: silicified andesite that is fully oxidized, and argillized andesite that contains sulfides. As a result, there is a risk that the mine waste will produce Acid Rock Drainage (ARD).

Global Resource Engineering (GRE) designed a Barren Rock Storage Facility (BRSF) that encapsulates the argillized andesite within envelopes of silicified andesite to isolate it from groundwater and surface water. Cell design included a degree of compaction to reduce the conductivity of the argillized waste.

Groundwater models were created to predict the following: infiltration and runoff into the BRSF during operations, the optimal design parameters of an evapotranspiration (ET) soil cover, and the impact of heavy spring snowmelt on the BRSF water balance. Geochemical models were then created to predict the quality of leachate and runoff during operations and postclosure.

The results of the groundwater models determined that the waste had sufficient storage capacity to absorb most of the operations-phase water, resulting in low volumes of ARD production during operations. The BRSF closure design included a three-layer soil cover 1.7 m thick, which was shown to provide excellent store-and-release performance, and greatly limited infiltration into the closed BRSF.

60-year-old mine waste piles exist on sites that have not produced severe ARD. Calibrating geochemical models to this data, GRE demonstrated that the region's cold climate and the argillized waste's low conductivity slowed sulfide oxidation reactions. The predicted water quality of BRSF leachate is suitable for passive treatment methods, thus saving the project millions of US dollars in active water treatment costs, and providing a path to clean closure.

Keywords: Mine waste encapsulation, predictive modeling

INTRODUCTION

Amulsar is an open-pit gold mining project being developed by Lydian International in the Lesser Caucasus Mountains of south-central Armenia. The deposit contains 94.9 million tonnes (Mt) of proven and probable reserves at an average gold grade of 0.75 g/t and average silver grade of 3.27 g/t. The life of the project is expected to be approximately 10 years, including two years of pre-mining construction. Ore mined from a series of coalescing pits near the top of Amulsar Mountain, at an elevation of approximately 2,500 m, will be crushed and then transported via a conveyer system to a heap leach facility.

The project will generate 283.1 Mt of waste rock. Disposal of some of that waste rock will be handled by backfilling early-mined portions of the pits, but 190.6 Mt will be disposed to the Barren Rock Storage Facility (BRSF). A portion of the waste rock has sulfide concentrations high enough to make production of Acid Rock Drainage (ARD) likely. Global Resource Engineering (GRE) was assigned the task of designing the BRSF to minimize ARD. This paper describes the waste rock and the methods used to characterize its ARD behavior, and explains the process used to generate a BRSF design that would minimize long-term postclosure ARD water production requiring treatment and optimize the quality of that water.

WASTE ROCK

The Amulsar deposit is hosted by an Eocene-Oligocene sequence of andesitic volcanic rocks that has been intruded by a sill-like porphyritic andesite intrusive. Waste rock that will be produced by the mining project can be divided into two lithologies. The Upper Volcanics unit (UV) is a strongly silicified variant of the andesitic volcanics. This rock type, which hosts the ore, is thoroughly oxidized, has low sulfide content, and has no appreciable neutralization potential. The Lower Volcanics unit (LV) forms a layer underlying the UV. The LV consists of alternating layers of andesitic volcanics and andesite sills. The sulfide content of the LV is variable, with sulfide contents of up to about seven percent. The LV is often argillized; most of the material observed through core drilling contains approximately 10% to 50% clay minerals.

Waste characterization

The waste rock was characterized using standard methodology of static geochemical testing followed by humidity cell tests (HCT). Results of the Acid-Base Accounting (ABA) testing can be seen in Figure 1.

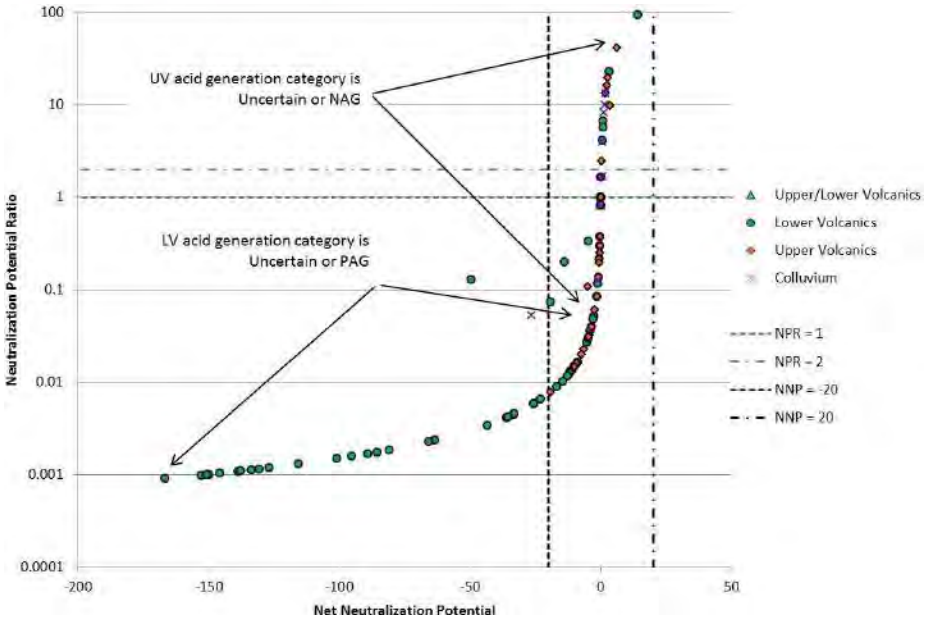

Figure 1 ABA test results

In Figure 1, samples that fall in the upper right-hand quadrant of the graph are non-acid-generating (NAG) based on accepted practice (INAP, 2009). No waste rock samples fall in this zone. Between the vertical dashed lines is a zone of uncertain ARD behavior. All samples of UV waste rock fall in this zone. In the quadrant to the lower left lie samples that are potentially acid-generating (PAG). Many LV samples and no UV samples lie in this zone, and no significant neutralization potential is present in either rock type.

Figures 2 and 3 show the graphs of pH over time and cumulative acidity over time for the HCTs.

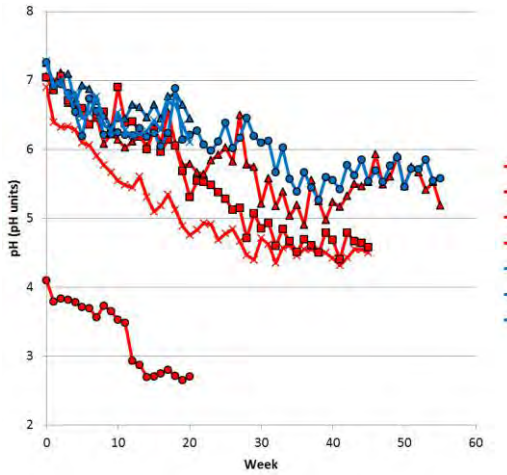

Figure 2 pH vs. time for HCTs

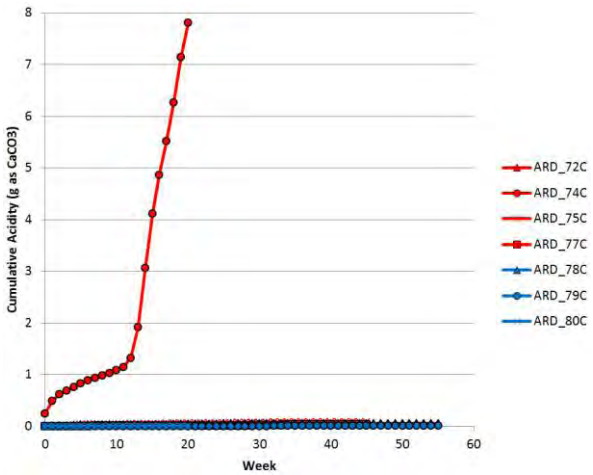

Figure 3 Cum. acidity vs. time for HCTs

No UV samples produced significant acidity, or produced elevated dissolved metals concentrations. LV samples showed variable behavior. Samples with high acid-generating potential (AP) produced acidic leachate, whereas many samples with lower AP did not produce significant acidity. One sample was oxidized prior to arrival to the lab. Two samples produced mild ARD for a full year, with the pH remaining above 4.5. One sample produced acidic leachate of significant quantity, and after 14 weeks exhibited the classic behavior of ferric iron oxidation catalysed by *Acidithiobacillus ferroxidan*s (biotic oxidation). However, in general, LV samples showed a remarkable resistance to biotic oxidation and strong ARD formation.

This behavior was reflected in LV waste piles left in the field by Soviet-era exploration activities on the Amulsar site. Two mine waste piles at the same elevation as the planned waste dump and from the same sulfidized LV formation have been in the field for sixty years. They generate ARD with ~100 mg/L total acidity, ~50 mg/L sulfate, and pH ranging between 4.0 and 3.3. Even after 60 years of exposure, these rocks have failed to undergo aggressive biotic oxidation despite the presence of abundant sulfides in the waste. Whether this behavior is primarily controlled by the cold climate (Sartz, 2011), the mineralogy of the rock, or the lack of microorganisms is uncertain at this stage in the investigation, but it is clear that the waste rock when exposed to the natural environment at this site displays some natural resistance to biotic oxidation. The ARD management plan will take advantage of this natural resistance to minimize the volume and intensity of ARD produced by mining activities.

BARREN ROCK STORAGE FACILITY

Waste rock that is not consumed in backfilling the pits will be disposed to the BRSF. The BRSF will occupy an upland topographic basin on the north flank of Amulsar Mountain, just north of the pit area (Figure 4).

BRSF basin characteristics

The southeast half of the upland basin that will host the BRSF is underlain by argillized LV and clayey alluvium and colluvium. The average hydraulic conductivity of surficial deposits in this area is low (~1x10^{-6} cm/s), which will limit the potential for seepage from the BRSF to impact groundwater beneath it. The remainder of the BRSF footprint is underlain by Cenozoic basalt flows with a higher average hydraulic conductivity. In places where the surface of the basalt is not already covered by an adequate thickness of low-permeability overburden, additional clay-rich material will be emplaced to minimize seepage from the BRSF into the foundation rock.

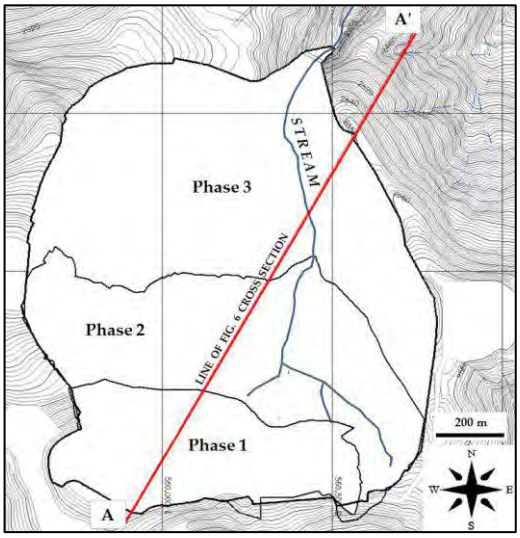

Figure 4 Map of BRSF basin

The north-facing southern slope of the basin hosts a set of springs. These mostly ephemeral springs largely drain perched water zones, whose recharge areas are on the mountain slopes upslope from the BRSF to the south. Springflows vary seasonally, with peak

measured flows of about 20 L/s corresponding to peak snowmelt flows in April and May. The BRSF will be built with an underdrain consisting of a five-meter-thick layer of crushed UV. The underdrain will allow unrestricted flow of the emerging springwater to the toe of the BRSF without coming into contact with the encapsulated LV cells. The water from the springs will mix with seepage from the BRSF, and the mixed water will be captured at a detention pond just below the BRSF toe.

Construction sequence

The BRSF will be built in three phases, Phase 1 occupying roughly the southern third of the ultimate facility footprint, Phase 2 built to overlie the northern slope of Phase 1 and extending northward to occupy the medial portion of the footprint, and Phase 3 overlying the northern slope of Phase 2 and extending to the footprint's northern extremity.

The phasing is required to establish an early platform for a low-grade ore stockpile on the south slope of the BRSF as it is being built up. The stockpile will be built during the first few years of mining, and at the end of the project's life the stockpiled ore will be processed.

An engineered evapotranspiration cover (ET Cover) will be placed over the final slopes of the BRSF concurrently with their completion. This will occur first over the Phase 3 northern slope. It will occur later on the slopes covered by the low-grade stockpile, as those slopes are exposed during removal of the low-grade ore. The BRSF is designed to encapsulate the LV waste such that it cannot easily come in contact with water or oxygen. The plan will benefit from the clay content in the LV waste, and the silicification of the UV waste. Cells of LV waste will be created through waste sorting. The LV will be contained in cells that are isolated from seeps, springs, and groundwater from below, and isolated from meteoric water from above. Once a final surface is achieved, the encapsulation will be completed with the placement of the ET Cover. Figure 5 shows the configuration of the final encapsulation cells down the axis of the BRSF in the interim between the completion of the BRSF and the processing of the LGS.

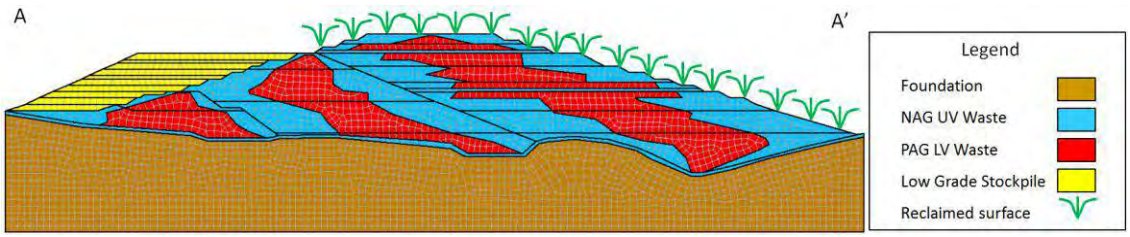

Figure 5 Cross section along axis of BRSF

PREDICTIVE MODELING OF BRSF LEACHATE AND RUNOFF

The BRSF encapsulation design is intended to minimize the quantity of mine waste leachate, and to isolate the LV formation from oxygen and water prior to the formation of biotic oxidation. Predictive modeling of moisture conditions within the BRSF was conducted to determine the quantity of leachate and surface runoff during operations and postclosure.

Numerical modeling of flow was done to generate a design that minimized seepage through the BRSF. The results of that modeling were then used as input to a geochemical model, which predicted the water quality of seepage. The flow modeling was done using Vadose/W (GeoStudio, 2014), a finite-element model that can comprehensively simulate the interaction of a range of

meteorological variables with the ground surface, and then simulate the flow of infiltrating water through both saturated and partially saturated material volumes.

Flow modeling approach

The flow modeling used a two-stage process. The first stage involved creating a series of one-dimensional transient column models, with each model representing a unique combination of materials and slopes. These models used daily variations in precipitation, temperature, wind speed, and relative humidity for a typical year, with the "typical year" based on several years of data from a nearby meteorological station representative of site conditions, to predict the variation of infiltration and runoff over time for each combination of material and slope for a single year. The typical year precipitation is ~680 mm, with half of the water content falling as snow. Summers are dry with rainfall occurring primarily in the spring or in October. The surfaces involved included LV waste, UV waste, and low-grade ore, as well as the various tested closure covers.

The second stage involved applying the infiltration predictions of the one-dimensional models to a transient two-dimensional model representing a cross section through the center of the BRSF (Figure 5). For the two-dimensional model, infiltration values determined for each combination of slope and surface material were set as prescribed boundaries, making it unnecessary to employ the computationally demanding climate functions for the larger two-dimensional model domain. Like the one-dimensional model runs, the two-dimensional runs included discretization of time into one-day increments, but the simulation covered the multi-year operations period and extended well into postclosure. The two-dimensional model dynamically tracked the development of the facility year by year, showing each phase's growth, the succession of phases, and the building and removal of the low-grade ore stockpile. Seepage rates were determined, and then those results were extrapolated to the third dimension to calculate the seepage flows that would report to the BRSF underdrain, and ultimately to the downgradient detention pond.

In addition to collecting seepage from the toe of the BRSF, the downstream detention pond also collects surface runoff from the facility. Runoff rates per unit area predicted by the one-dimensional models were used in conjunction with the scheduled change over time of areas of specified material and slope characteristics to predict the volume of ARD-impacted runoff water that would be received by the pond.

Predicted seepage rates

The modeling showed that seepage flow rates were comparatively small, both during the operations period and later during closure. This is largely a function of the climate. Essentially no infiltration occurs during the frozen-ground conditions of winter, and much of the year's precipitation total is lost either to sublimation of snow or to the spring runoff. Evaporative loss is also significant. During the operations period, when raw waste surfaces are exposed, the relatively dry waste has considerable ability to absorb such moisture as is available. However, the rapid growth of the waste pile means that any exposed waste surface has only limited time to take up additional moisture.

The cover consists of 0.2 m of soil over one m of compacted clay, above a capillary break layer 0.5 m thick. Because the crushed UV that will constitute the upper part of the encapsulation envelope is expected to have the hydraulic properties required for the capillary break, no separate layer is required.

Although infiltration of precipitation water into the accumulating waste is modest during the operations period, installation of the ET Cover further limits the amount of water that ultimately passes through the waste pile and emerges as seepage collected in the underdrain. This is not because the cover is impermeable; it is not. Instead, the cover functions as an effective store-and-release mechanism, allowing temporary storage of shallow-infiltrating water in the cover volume above the capillary break, but then yielding that water back to the atmosphere via evaporation in response to the high evapotranspiration potential that the site displays during much of the year. In the spring, the cover absorbs into storage to a maximum bulk moisture content of 20% (by volume). This storage is depleted by summer evapotranspiration.

Figure 6 shows the predicted flow of seepage from the base of the BRSF over time, subdivided according to the phase-footprint source of the water. The graph shows the gradual increase in total seepage flow as each phase is built, and as building of each succeeding phase begins. Seepage falls rapidly during the so-called "hiatus" period, when the flow of waste rock still being generated by ongoing mining is being diverted to backfill the early-mined pit volumes. Installation of the ET Cover takes place on the facility's completed final slopes (generally, those not occupied by the low-grade stockpile) at the beginning of that hiatus or earlier where possible, reducing infiltration rates over that area. When mining has been completed at the pits, removal of the low-grade stockpile begins. Concurrent installation of the ET Cover is done as the footprint of the stockpile recedes. After installation of the ET Cover is complete, seepage rates show a gradual decline in the early years of closure. The final predicted infiltration rate is ~1% of total precipitation. Field lysimeters will be installed to verify this modelled result.

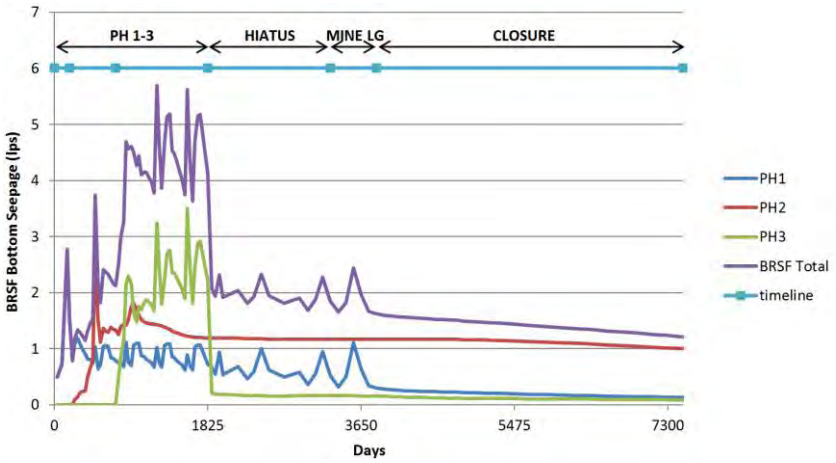

Figure 6 Predicted BRSF seepage flows vs. time

Maximum seepage rates of about five L/s are predicted during the three-year period that precedes the hiatus, with maximum rates around two L/s persisting through the end of removal of the low-grade stockpile. During operations all water is consumed, so that the cost of treatment is not an issue. From the beginning of the closure period onward, average seepage rates of less than two L/s are predicted, trending toward one L/s.

Moreover, the predicted seepage rates are small compared to the expected flow of water from the springs buried beneath the BRSF footprint. Although the spring-sourced flow rates will vary seasonally in a way that may not be synchronized with seepage from the BRSF, and the BRSF facility itself may cut off precipitation recharge to some of the source area of the springs, the water that ultimately reaches the toe of the facility will often be a mix of a small flow of ARD-impacted seepage with a larger flow of natural groundwater.

GEOCHEMICAL MODELING OF LEACHATE

In order to determine the effectiveness of encapsulation, the water quality in the BRSF was simulated using the PHREEQC geochemical model (Parkhurst & Appelo, 1999).

Oxygen penetration

Prior to geochemical modeling, it is necessary to simulate the depth to which oxygen can penetrate into the waste. This was done with Vadose/W, which has the capacity to calculate oxygen diffusion into materials based on pressure gradients, temperature gradients, and the degree of soil saturation. The oxygen consumption (from the production of ARD within the LV) and oxygen diffusion modeling showed that oxygen does not penetrate the ET Cover. It is assumed that the BRSF will always produce ARD and some oxygen consumption will occur within the LV. Figure 7 shows oxygen diffusion at its maximum extent in late summer, when moisture contents in the cover are at the lowest levels they reach prior to winter ground frost. As a conservative measure, it was assumed that the total depth of oxygen penetration was approximately 1.5 meters.

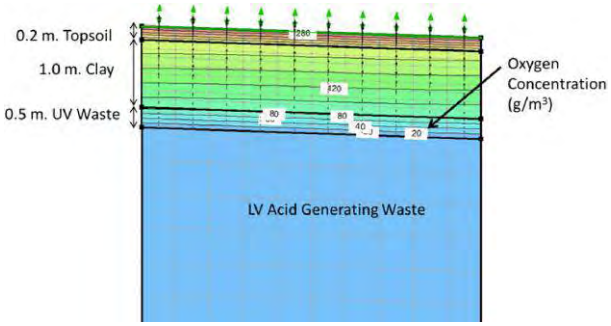

Figure 7 BRSF cover oxygen penetration

Conceptual model

The BRSF geochemical model determines the water quality of the BRSF basin discharge by determining the water quality of each of the flows that come together at the toe of the BRSF and by mixing the flows together in PHREEQC to come up with a resultant water quality.

Each flow is shown in Figure 8. Flows include: runoff from barren rock, runoff from unimpacted surfaces within the basin, seep and spring water, and seepage through the BRSF. The numerals shown in parentheses in Figure 8 represent the PHREEQC model solutions for the four designated water components discussed here.

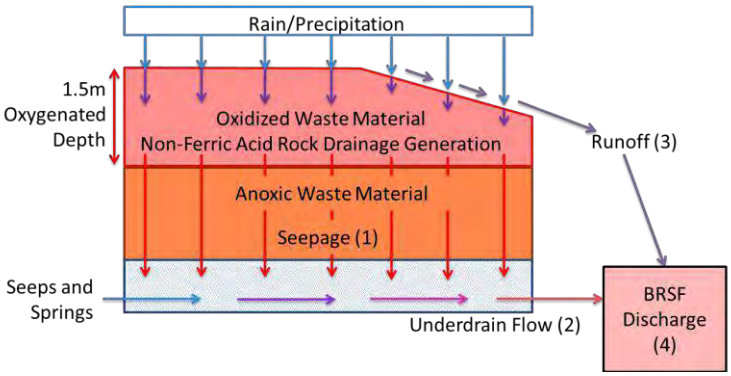

Figure 8 BRSF geochemical conceptual model

Seepage through the BRSF discharges into the BRSF underdrain (Solution 1 in Figure 8). Initial contact water solutions were compiled from weekly loading rates determined by the HCTs, total rock volume, and total seepage. Raw HCT results were used in order to provide a conservative ARD condition that reflects the ARD behavior of the samples tested. The loading rates were determined by first averaging the weekly concentrations of all constituents in the HCT leachate, then averaging each constituent's weekly averages. The rates were then applied to the total weight of rock within the oxygenated zone and the total seepage flow in order to simulate the initial seepage water quality (Solution 1). Solution 1 is then subjected to an oxygenated equilibrium followed by an anoxic equilibrium. These steps simulate the conditions in the top layer of the BRSF

(oxygenated) and deep within the BRSF (de-oxygenated), while allowing constituents to precipitate out in either condition.

Simulation of the underdrain water quality is derived by mixing the anoxic seepage mix (Solution 1) with the spring flow beneath the BRSF. The mix proportions are based on seep and spring surveys, and the seepage flows shown in Figure 6. BRSF seepage makes up from 16% to 37% of the mix. Spring water quality was based on samples taken during February, 2014. The mixture of spring water with the anoxic seepage greatly reduces the concentrations of metals and sulfate (Solution 2).

Runoff will also report to the BRSF pond, where it will mix with the toe discharge from the BRSF (Solution 2). Runoff water quality was determined by selecting a weighted average of the first eight weeks of the HCT results. Eight weeks is roughly the length of the Amulsar wet season (May and June), and therefore a reasonable contact time for runoff ARD reactions to occur. It is also important to note that rapid BRSF construction limits the potential contact time between runoff and LV mine waste. Runoff (Solution 3) mixes in the lined BRSF detention pond. During operations, this water is fully-consumed by the HLF. Upon closure, it must be treated prior to discharge. Figure 9 shows the predicted water quality. As a result of the LV waste encapsulation and the waste rock's natural resistance to biotic oxidation under site conditions, the modeling predicts that the Amulsar BRSF ARD seepage will be a moderate contamination source, with approximately 150 mg/L total acidity, 100 mg/L of sulfate, and pH of 3.8.

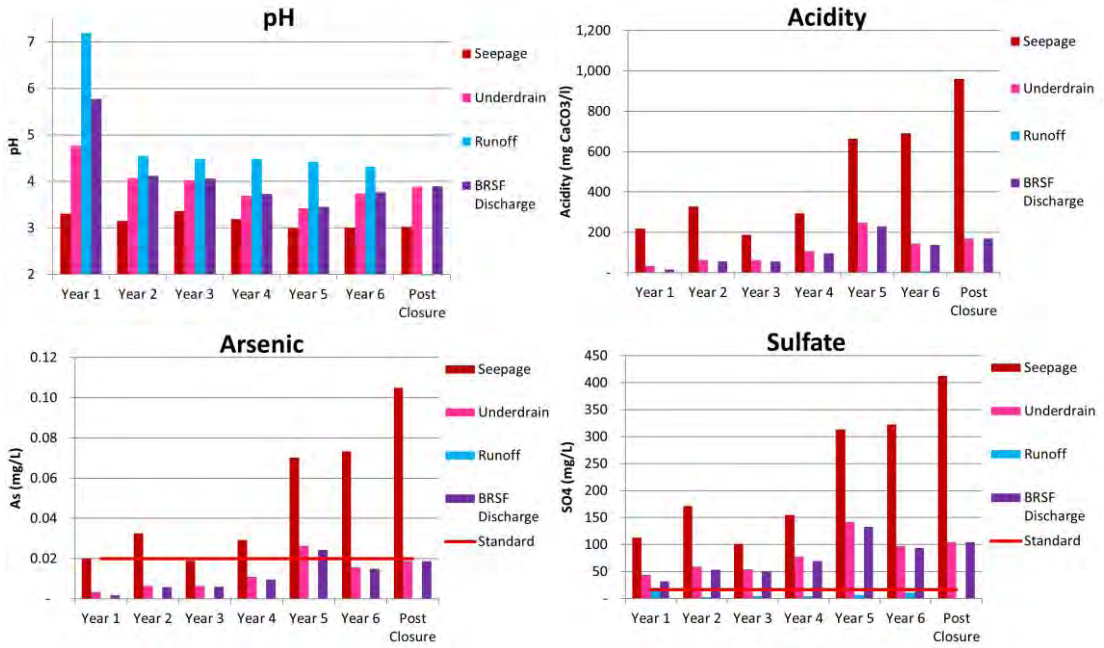

Figure 9 BRSF discharge water quality predictions

CONCLUSIONS

Characterization of Amulsar mine waste revealed that the LV formation has the potential to produce ARD. However, it is also apparent from mine waste exposed in the field that the waste has a resistance to the formation of the strongest level of ARD produced by sulfide-rich deposits. Biotic oxidation reactions catalyzed by *Acidithiobacillus ferroxidans* do not appear in the field, and only

occurred in two of eleven HCTs. The Project plans to take advantage of this natural resistance by encapsulating the LV mine waste within the BRSF in cells that isolate it from oxygen and water. Flow modeling confirmed that the mine waste maintains a low moisture content during construction, and when the waste is rapidly covered, flow through the mine waste can be reduced to a nominal one to two L/s. Oxygen also cannot penetrate the waste. Oxygen diffusion modeling showed that oxygen cannot penetrate the 1.2-meter-thick ET cover. Encapsulation is therefore feasible.

Geochemical modeling confirms that the encapsulation successfully controls and minimizes ARD. Not only is flow decreased, but the kinetics of geochemical reactions is sufficiently slowed to produce only mild ARD. Mild ARD makes passive treatment methods possible for long-term ARD management.

Prior ARD management plans, which did not consider the encapsulation option, required an active treatment system to control ARD. This would have necessitated construction of an active treatment plant for use during operations and continuing into postclosure, along with an extra clay under-liner in the BRSF. These factors resulted in a total project cost of US$101M for ARD management (net present value (NPV) calculated based on a three-percent discount factor).

The current plan, with the encapsulation and ARD mitigation measures described above, makes it possible for the mine to consume all ARD-impacted water during operations. In addition, the improvements in predicted water quality allow for passive treatment upon mine closure. These changes save the mine US$40M in capital and operating cost (adjusted for NPV). The resultant savings have a large positive impact on the NPV and IRR of the entire project while still meeting strict regulatory guidelines.

ACKNOWLEDGEMENTS

GRE would like to thank Lydian International Inc., for permitting us to present our work on this project.

REFERENCES

GeoStudio (2014) *Vadose/W: A Vadose Zone Modeling Program*, GEO-SLOPE International Ltd.

INAP (2009) *Global Acid Rock Drainage Guide*, International Network for Acid Prevention.

Parkhurst, D. L., and C. A. J. Appelo (1999) *User's guide to PHREEQC (Version 2): a computer program for speciation, batch-reaction, one-dimensional transport, and inverse geochemical calculations*, U. S. Geological Survey WRIR 99-4259.

Sartz, L. (2011) *Weathering of waste rock in different climatic conditions - a kinetic freeze/thaw and humidity cell experiment*, International Mine Water Association Congress.

Geophysical Tools to Delineate ARD and Sulfate in Groundwater at a Former Sulfuric Acid Plant

Jennifer Cole[1], Albert Stoffers[1] and Roy Angelow[2]
1. Golder Associates, Canada
2. Aboriginal Affairs and Northern Development Canada

ABSTRACT

During the operation of a former sulfuric acid plant located in Canada, sulfide minerals (e.g. pyrite, chalcopyrite), tailings and sulfuric acid were stockpiled on-site and imparted acidic solutions with high sulfate and metal concentrations to the subsurface. The topography is variable, from bedrock outcrops to 20 meters of overburden as clay, sand and gravel. Bedrock controls surface water and groundwater flows which include surface drainage ditches, marshes, an unconfined aquifer, and flow through fractured bedrock. After plant closure, historic remediation efforts included the removal of stockpiles, tailings and visually contaminated soil to the water table, lime amendment of soil at the water table, and importation of clean fill, which resulted in chemically heterogeneous subsurface conditions across the site. Most primary sulfide materials were removed except for sporadic zones that have the potential to generate acid rock drainage (ARD). Surface water and groundwater monitoring confirms near-neutral pH conditions with elevated concentrations of sulfate and metals at various locations throughout the site. Recent studies to delineate groundwater contamination and areas of active ARD included targeted soil and water sampling at select locations, which confirmed the heterogeneity of subsurface conditions. An electromagnetic geophysical survey was completed to minimize uncertainty and validate the results of previous investigations. It identified two zones of high conductivity, coinciding with high sulfate concentrations in groundwater and in static leaching tests on soil. Static test results confirm that soil collected from underneath the location of a former stockpile was depleted in buffering capacity, likely consumed by the infiltration of acidic drainage into the subsurface during plant operations. The results of the geophysical survey proved to be a cost-effective and efficient method to delineate the source and pathway of high sulfate in groundwater and thus demonstrated usefulness in assessing the environmental impact of high sulfide-containing mine wastes on groundwater quality.

Keywords: ARD, sulfate, conductivity, groundwater, geophysics

INTRODUCTION

The site is located on the north shore of Lake Huron (Aird Bay) in northern Ontario, Canada, near the community of Cutler. The 40 hectare site is the former location of the Cutler Acid Plant, a sulfuric acid production plant that was in operation from approximately 1956 to 1963. Iron sulfide minerals including pyrite and chalcopyrite were roasted to produce sulfuric acid, yielding a purple-red iron oxide/oxyhydroxide waste by-product. Historic facilities and structures on-site included the acid plant, pyrite unloading areas, sulfur stockpiles, acid storage tanks, fuel oil tanks, and a tailings storage facility and tailings pond. Site facilities are shown in FIGURE 1.

Figure 1 Site map showing operational facilities and site features

Plant operations resulted in subsurface contamination including the presence of sulfide minerals and acidic conditions in soil and elevated levels of sulfate and metals (Al, As, Cd, Co, Cr, Cu, Fe, Hg, Pb, Mn, Mo, Ni, Se, U, Zn) in groundwater and surface water . These contaminants were most likely introduced to the subsurface through sulfuric acid spills, leaking from acid storage tanks, and oxidation of sulfide minerals in the former stockpile areas and tailings pond.

In 1969, the acid plant and buildings on-site were demolished and debris was distributed across the site. Since then, the site has undergone several studies and remedial projects to address the presence of demolition debris and waste materials, as well as contamination related to the operation of the acid plant. Remedial efforts consisted of the excavation of building debris and visibly contaminated soils, after which both lime and clean imported fill was added in an effort to mitigate acidic conditions. These remedial efforts were limited to the depth of the fluctuating water table, leading to heterogeneous subsurface conditions observed presently on-site.

Past remediation efforts were not completely effective at removing all of the contamination associated with the former acid plant as localized areas of ARD potential in soil, high sulfate

concentrations in groundwater, and metal concentrations in soil and groundwater are still observed.

Various subsurface investigations have been completed in an attempt to delineate areas of contaminated soil in support of environmental site assessments (ESA), risk assessments, and remedial options analysis. Soil samples were recovered from test pits and boreholes to assess ARD and metal leaching potential through various static and kinetic test methods, and surface water and groundwater was also analyzed. Results of the various subsurface investigations confirmed the heterogeneous nature of the soil across the site. Local areas of ARD in the soil were identified, however it appears to be buffered locally as evidenced by neutral pH values in tested groundwater and surface water.

Due to heterogeneous conditions on site, a geophysical survey was conducted in lieu of an extensive drilling program in order to more efficiently delineate areas of subsurface contamination related to ARD and metal leaching, specifically those associated with historical plant operations and tailings storage. An electromagnetic geophysical survey well suited to mapping the apparent conductivity of the ground, including shallow buried metal objects, was completed on portions of the site. This approach has been used successfully at various other active and closed mine sites as documented by Gore & Olyphant (2010) and Schutts & Nicols (1991), Campbell & Fitterman (2000), and Paterson (1997). Areas selected for the geophysical survey were identified based on observed contamination and/or locations of historical operational infrastructure. The geophysical survey successfully identified areas of confirmed high sulfate in groundwater and was instrumental in delineating the probable sources and flow of high-sulfate groundwater on site.

SITE CONDITIONS

The site is located in an environment typical of the Canadian Shield with shallow bedrock, frequent outcrops, and poor drainage resulting in standing water. Undulating bedrock ranges from 16.5 meters below ground surface (mbgs) to surface outcropping. Three notable outcrops are present on site and control groundwater flow, including 1) the east shoreline bedrock outcrop, a large outcrop located at the shore of Aird Bay in the center of the site; 2) the west shoreline bedrock outcrop, a long and narrow outcrop on the west side of the site and on the shore of Aird Bay, and 3) the bedrock outcrop, a long and narrow outcrop in the southeast portion of the site perpendicular to the lake shore.

A large marsh is situated on the west boundary of the site and six streams and/or constructed ditches flow across the site and discharge into Aird Bay. The water table is shallow throughout most of the site; groundwater flows through both an unconfined aquifer and within fractured bedrock. Groundwater generally flows from northeast to southwest and discharges to Aird Bay between the west and east shoreline outcrops, as evidenced by downward vertical hydraulic gradients observed within all multi-level monitoring wells in this area. An area of up-ward groundwater flow (seep) exists between this zone of discharge to the lake and the adjacent marsh.

Overburden ranges from relatively coarse grained sand to a fine grained soil consisting of sand, silty sand, silt, and clay in varying proportions. Within the upper coarse grained layer, fill materials are largely comprised of sand similar in nature to that of native sand. Differentiation between native sand and fill materials is challenging unless obvious markers of fill material, such as an organic layer or anthropogenic debris, are present. Based on anecdotal information, it is understood

that fill materials of up to a thickness of two meters (m) have been placed over portions of the site. Field programs carried out to date have not identified any visible signs of lime in the soil.

Previous ESAs document metal concentrations above applicable provincial and federal guidelines in soil, groundwater, and surface water throughout the site (Ag, As, B, Ba, Cd, Co, Cr, Cu, Hg, Pb, Mo, Ni, Sb, Se, Sn, Tl, U, Zn). In soil, these elevated concentrations are clustered within several areas that generally correlate with previously identified and partially remediated contaminated areas and/or with former operational areas of the acid plant. Neutral to alkaline surface water and groundwater report various metal concentrations above guidelines at locations throughout the site; however metal concentrations are generally low and not observed to correlate with high sulfate above background concentrations. In Aird Bay near the east ditch discharge, the pH is neutral to alkaline and few parameters have been detected at concentrations above background concentrations and applicable guidelines.

METHODOLOGY

Subsurface Investigations and Soil Sampling

To date 105 test-pits and 33 boreholes have been completed in areas of previously identified contamination and near historic plant facilities to better delineate these zones. Test pits were excavated using a tracked excavator within and around previously identified areas of contamination as well as distributed in other areas of the site in an attempt to locate other previously unidentified areas of contamination.

Ten of the 33 boreholes were drilled using a hollow stem auger/rotary drill and a monitoring well was installed in each borehole. The remaining 23 boreholes were completed using a Geoprobe track-mounted drill rig and targeted areas of high conductivity identified in the geophysical survey. Of the 23 borehole locations, 11 were selected for the installation of monitoring wells screened within the overburden, two of which were multilevel wells. Boreholes were terminated after reaching refusal or to 1.8 m below the last visual sign of soil contamination. Sampling of overburden in each of the boreholes was carried out by the direct push of a 1.0 m long clear plastic Geoprobe sleeve into the subsurface at continual intervals. Geoprobe sleeves were inspected for any noticeable physical characteristics such as staining, evidence of lime or the presence of odors. Overall, 42 samples were collected for laboratory analysis on solid chemistry including sulfur speciation, acid base accounting (ABA), and soil leachate chemistry using the shake flask extraction (SFE) method.

Monitoring Well Installation and Sampling of Groundwater and Surface Water

Each monitoring well was constructed with threaded polyvinyl chloride (PVC) riser connected to a PVC well screen. The well screens were placed at depths intended to straddle the water table, and intersecting only a single overburden unit per screen where possible. Screen lengths were generally 1.5 m, however some subsurface conditions required a 3 m length.

Sampling of groundwater was conducted immediately following well development. Surface water was collected from identified monitoring locations in 4 streams / ditches. Samples were analyzed for general chemistry and total and dissolved metals; pH was measured in the field at the time of sampling.

Geophysical Survey

A geophysical survey was completed in order to further constrain localized ARD zones identified through the subsurface investigation, as well as areas between these zones that were not previously detected. This method was chosen because of its lower cost and short duration (two field days) compared with an extensive drilling program. The geophysical survey was completed using a Geonics EM31 and EM34-3, both of which are electromagnetic induction devices well suited to mapping apparent conductivity of the ground and shallow buried metal objects. The quadrature component measured by the EM31 system is sensitive to materials that have a low induction number, such as earth materials, or poorly conducting metallic targets. The EM31 quadrature response is calibrated to give a measure of the bulk apparent conductivity of the subsurface for a roughly hemispherical volume of radius 5 to 6 meters, centered at the measurement point. The in-phase component measured by the EM34-3 system is most sensitive to targets that have a high induction number and are good conductors, primarily larger surface and buried metal objects or very conductive groundwater such as brine. As such, the results provided by both the EM31 and EM34-3 are valuable in differentiating between buried metal objects and the apparent conductivity of the subsurface.

RESULTS AND DISCUSSION

Soil Chemistry

The soil chemistry of 81 samples was assessed through various static test methods. FIGURE 2 presents a frequency distribution diagram for pH values. A summary of select test results is provided in TABLE 1.

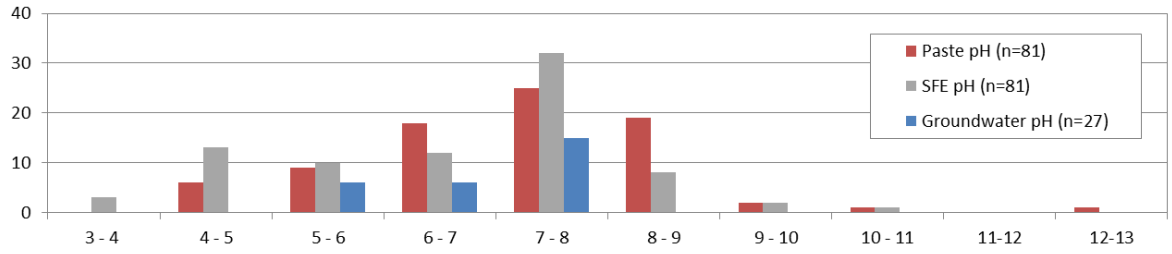

Figure 2 Frequency Distribution for paste pH, SFE pH, and groundwater pH

Table 1 Statistics for select static test results (n= 81 soil samples)

Parameter	Minimum	Maximum	Average
Total sulfur	<0.005%	5.4%	0.19%
Sulfide sulfur	<0.01%	5.3%	0.14%
Sulfate sulfur	<0.01%	1.3%	0.095%
NP	-7.8 t $CaCO_3$/1000t	166 t $CaCO_3$/1000t	13 t $CaCO_3$/1000t
CaNP	0.082 t $CaCO_3$/1000t	104 t $CaCO_3$/1000t	5.5 t $CaCO_3$/1000t
NNP	-164 t $CaCO_3$/1000t	166 t $CaCO_3$/1000t	10 t $CaCO_3$/1000t
NPR	-25	536	31
SFE Conductivity	24 µS/cm	2480 µS/cm	625 µS/cm
SFE Alkalinity	< 2 mg/L as $CaCO_3$	286 mg/L as $CaCO_3$	35 mg/L as $CaCO_3$
SFE SO4	2.1 mg/L	1800 mg/L	315 mg/L

Sulfate is the predominant form of sulfur in the tested soil, as indicated by high concentrations of sulfate compared with sulfide, resulting in low acid potential for most samples. Areas of high sulfide content are sporadically focused around the western part of the site near the former tailings pond, while the samples that dominantly contain sulfate sulfur are distributed throughout the site.

Mineral buffering capacity, defined as the neutralization potential (NP), is variable, with 72% of samples reporting low NP values between -7.8 and 11 tonnes $CaCO_3$/1000 tonnes. The buffering capacity of the samples is predominantly provided by alumino-silicate minerals with lesser carbonate minerals based on the lower calculated carbonate NP (CaNP).

Most tested samples (77%) have no potential to generate acid as indicated by net potential ratio (NPR) values greater than two (MEND, 2009) and neutral to alkaline paste pH values. Potentially acid generating (PAG) samples are sporadically located in the western half of the site around the former tailings pond area and were collected in shallow test pits (up to 3 m deep) above the water table.

Only a small portion of the tested soil samples (15%) were considered to be PAG under laboratory static test conditions. However, circum-neutral pH values in soil leachate and groundwater collected from within these areas suggest that there is sufficient buffering capacity in the system, possibly related to previous lime addition, to neutralize acid that may be generated from localized sulfide mineral oxidation. Therefore, ARD is not considered to be a dominant geochemical process on-site.

Short-term leach testing following the SFE method was used to assess the reactivity of the soil and its propensity to release metals to the receiving environment upon contact with water. Of the tested samples, 95% report circum-neutral SFE pH values. A handful of acidic pH values (3.0 to 4.3) were reported for soil from the eastern part of the site near the former acid storage tanks, but they were not associated with PAG areas and high sulfide content.

High sulfate concentrations in SFE leachate are documented from the following areas: former acid storage tanks, to the east of former process area, north and south of the former tailings ponds and around the former pump house. Samples from these areas also contain little to no buffering capacity (NP < 12 t $CaCO_3$/1000 t), yet report mostly circum-neutral leachate pH values between 4.5 and 8.0, suggesting no acid drainage is currently occurring in these areas. It is postulated that

previous sulfuric acid spills near the plant depleted the buffering capacity in the soil, resulting in a high sulfate charge and lower but not acidic pH values in the groundwater.

Groundwater Chemistry

In total 27 groundwater samples were analyzed for alkalinity, sulfate, conductivity, hardness and dissolved metals. A summary of the relevant parameters are presented in TABLE 2. A frequency distribution diagram for pH is presented in FIGURE 2.

Table 2 Select groundwater quality results (n= 27 water samples)

Parameter	Minimum	Maximum	Average
Conductivity	107 µS/cm	6150 µS/cm	1623 µS/cm
Alkalinity	<2 mg/L as $CaCO_3$	506 mg/L as $CaCO_3$	140 mg/L as $CaCO_3$
SO4	5.0 mg/L	5400 mg/L	886 mg/L

No correlation was identified between high sulfate concentrations in groundwater and the PAG conditions observed in soil samples from specific locations. Sulfate groundwater concentrations were measured above the maximum historical background groundwater concentration of 12 mg/L throughout most parts of the site (89% of samples), with average groundwater sulfate concentrations of 886 mg/L over three years of monitoring.

Anomalously high groundwater sulfate concentrations above 500 mg/L occurred in 56% of the samples. This correlated with high groundwater conductivity (>1500 µS/cm) and low alkalinity (<250 mg/L as $CaCO_3$) in the same samples. These trends were identified in the following locations: north of the west shoreline outcrop and south-southwest of the old Pow Wow grounds; east of the existing gravel parking lot; and northeast of the east shoreline bedrock outcrop in the area of the former acid storage tanks and sulfur stockpiles (FIGURE 3).

It is believed that historic plant activities in the northern part of the site introduced sulfate into the subsurface through sulfuric acid spills and leaks from the storage tanks, and/or infiltration from stockpiles where oxidation of pyrite was active.

These areas appear to be hydraulically connected to a zone of observed high groundwater sulfate (>1500 mg/L) in the southwestern portion of the site near the area of groundwater discharge (seep). In this area, the maximum concentration of sulfate in groundwater was observed (5400 mg/L). The high sulfate groundwater is believed to flow through fractured bedrock as evidenced by low sulfate concentrations in overburden groundwater between these two areas and higher concentrations of sulfate in bedrock wells (3300 mg/L) in the northeast area compared with adjacent overburden monitoring wells (470-1400 mg/L).

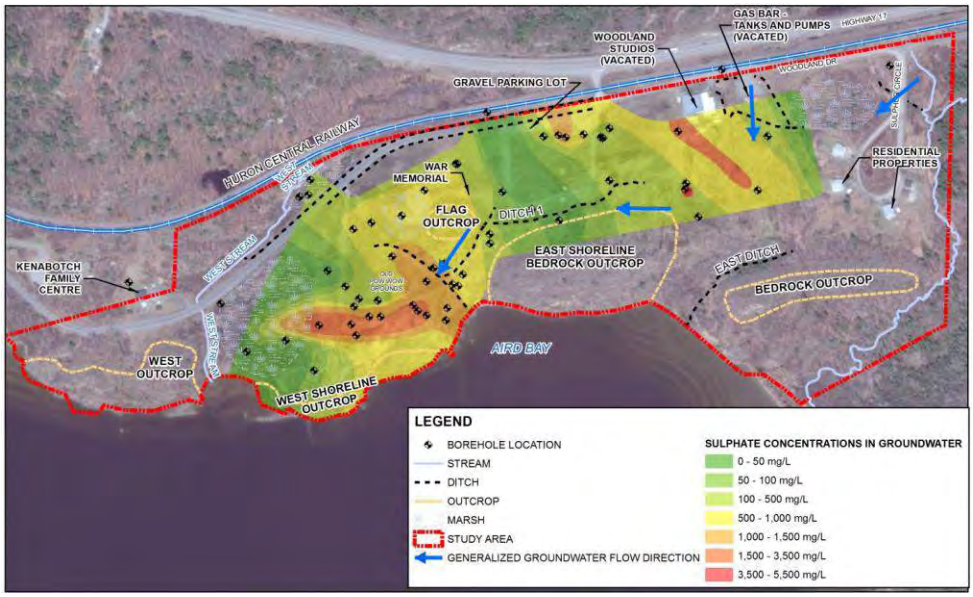

Figure 3 Sulfate concentrations in groundwater (mg/L)

Geophysical Survey

Geophysical survey results indicate that background terrain apparent conductivity values are between 10 and 20 millisiemens per metre (mS/m) in most soils and near 0 to 5 mS/m in the presence of bedrock outcrops or shallow bedrock. Anomalies above these ranges were observed in numerous areas on-site, with conductivity ranges between 75 to 115 mS/m. The results of the geophysical survey are presented in FIGURE 4.

Some of these high conductive areas are interpreted to have buried metal infrastructure from former and/or current site activities based on high in-phase results and documentation of historic remediation activities. The anomalous areas with elevated apparent conductivity readings that were not related to buried metallic objects are believed to be related to the occurrence of elevated sulfate concentrations in the groundwater or soil. These areas of high conductivity were targeted during a subsequent borehole program, with monitoring wells installed in some areas.

Sulfate concentrations measured within the bounds of the geophysical survey demonstrate strong correlation with the measured conductivity (Pearson correlation coefficient r=0.8 for n=15 samples). In the area where there is upward flowing groundwater (seep) in south west portion of the site, sulfate concentrations are greater than 1500 mg/L and up to 5400 mg/L. Conversely, in areas where the in-phase portion of the geophysical survey detected anomalies suggesting buried metallic objects, sulfate groundwater concentrations were in the 0-50 mg/L range (FIGURE 3 and FIGURE 4).

Figure 4 Electromagnetic geophysical survey results (mS/m)

CONCLUSION

During plant operations, sulfide minerals, tailings and sulfuric acid were stockpiled on-site and have historically imparted acidic and metal-loaded solutions to the subsurface through various processes. Site investigations to date identified that, despite remediation efforts, some soil remaining at site has the potential to generate ARD under laboratory conditions. However, sufficient buffering capacity maintains neutral pH conditions in groundwater in these areas.

The electromagnetic geophysical survey did not identify areas of active ARD but detected two conductivity anomalies that were found to correspond with areas of elevated sulfate concentrations in groundwater (500-5400 mg/L). The first anomaly is located in the northeast portion of the site where previous plant activities likely introduced sulfate into the subsurface. The second anomaly, which corresponds with the maximum sulfate concentrations detected across the site, is situated in the southwest portion of the site in the area of upward groundwater flow (seep) and is believed to be hydraulically connected to the first anomaly.

The strong correlation between the electromagnetic geophysical survey and measured sulfate concentrations suggests that geophysics is a useful tool to identify areas of high sulfate concentrations in the shallow subsurface. This tool could be an efficient method to monitor for acidic or neutral pH metal- and/or sulfate-rich waters that can migrate away from stockpiled waste rock and/or tailings storage facilities into the downstream environment.

ACKNOWLEDGEMENTS

This study is presented thanks to the Serpent River First Nation, Aboriginal Affairs and Northern Development Canada, and CLAW Environmental Services Inc. The authors thank the staff of CLAW Environmental Services Inc. and of Golder Associates Ltd., for their assistance in the studies described in this paper and the production of this article, especially Valerie Bertrand, Heather Fenton, Patrick Finlay, and Joel Campbell.

NOMENCLATURE

ARD	acid rock drainage
$CaCO_3$	calcium carbonate
CaNP	carbonate neutralization potential
ESA	Environmental site assessment
Kg	kilogram
L	liter
m	meters
mbgs	meters below ground surface
mg	milligram
mg/L	milligrams per litre
mS/m	millisiemens per meter
NP	neutralization potential
NPR	net potential ratio (neutralization potential/acid potential)
PAG	potentially acid generating
SFE	shake flask extraction test
SO_4	sulfate

REFERENCES

Campbell D.L. and D.V. Fitterman (2000) *Geoelectrical methods for investigating mine dumps,* Proceedings of the Fifth International Conference on Acid Rock Drainage, SME, Littleton, CO.

Gore, D.A. and G.A. Olyphant (2010) *Mapping the variability of groundwater quality in an abandoned tailings deposit using electromagnetic geophysical techniques,* National Meeting of the American Society of Mining and Reclamation, Pittsburgh, PA Bridging Reclamation, Science and the Community June 5 - 11, 2010.

MEND (2009) *Prediction Manual for Drainage Chemistry from Sulphidic Geologic Materials*, MEND Report 1.20.1, Mining Environment Neutral Drainage Program, Natural Resources Canada, December 2009.

Paterson, N. (1997) *Remote mapping of mine wastes*, Mapping and Monitoring the Mine Environment Paper 121, Proceedings of Exploration 97: Fourth Decennial International Conference on Mineral Exploration.

Schutts, L.D. and D.G. Nichols (1991) *Surface geophysical definition of ground water contamination and buried waste: case studies of electrical conductivity and magnetic applications*, Proceedings of the Fifth National Outdoor Action Conference on Aquifer Restoration, Ground Water Monitoring and Geophysical Methods.

Environmental Assessment for the Decommissioning of a Uranium Waste Rock Pile

Carolina Abreu[1], Peter Fleming[2], Dina López[3], Virginia Ciminelli[1] and Marcelo Mansur[1]

1. *Department of Metallurgical and Materials Engineering (PPGEM), Universidade Federal de Minas Gerais, Brazil*
2. *Nuclear Technology Development Center (CDTN), National Nuclear Energy Commission (CNEN), Brazil*
3. *Department of Geological Science, Ohio University, USA*

ABSTRACT

The Osamu Utsumi uranium mine (Minas Gerais, Brazil) operated between 1977 and 1995. Today, INB (Indústrias Nucleares do Brasil) and CNEN (Comissão Nacional de Energia Nuclear) work in an attempt to recover the areas impacted by mining and mineral processing activities. In this paper, acid effluents and surrounding waters from a uranium waste rock pile were characterized. Hydrochemical computer modeling (PHREEQC 2) and spectral analysis of transient data were used. Superficial and groundwater samples were collected from the massive waste rock, bedrock, and surrounding areas. Results indicate the existence of two oxidation patterns within the waste rock. At the western region, waters coming from the massive waste exhibit low pH, high total dissolved solids and high levels of sulfate, iron and aluminum, which are characteristic of acid drainage. These ions are supersaturated or close to the saturation limit. The waters of the wells located to the east exhibit characteristics of natural waters and are saturated in iron oxides. Transient data analysis showed that manganese, uranium, and sulfate in the effluent have a delay of three months with respect to the peak rainfall during the rainy season. Under conditions of supersaturation, acid drainage products precipitate in the porous medium, they are washed out during periods of peak flow and then transported to the output point. The pH has a prolonged effect until the next rainy season, explaining the slight variations from 3 to 4, over the hydrological year. Spatial variations in oxidation within the pile and the residence time of water and discharge of reaction products should be used in the remediation design of this pile.

Keywords: acid rock drainage, decommissioning, hydrogeochemical modeling, waste rock pile, uranium.

INTRODUCTION

Mineral oxidation of sulphide ores is the main mechanism to generate acid rock drainage. These minerals, once exposed to ambient weather conditions, Eh and pH, and biological agents can generate acidity. Chemical species containing sulfur are the primary source of acidity. The formation of acid effluent is commonly associated with the occurrence of sulfide minerals such as pyrite (FeS_2), chalcopyrite ($CuFeS_2$), arsenopyrite (FeAsS), sphalerite (ZnS) and galena (PbS) (MEND/CANMET, 2009).

The sulfate ion (SO_4^{2-}) is the most oxidized sulfur form in natural waters. Dissolution of sulfated minerals can reduce the pH of the medium. The formation of acid rock drainage from pyrite follows reaction 1, where 2 moles of protons (H^+) are produced for each mole of the mineral:

$$FeS_{2(s)} + 3{,}5O_{2(g)} + H_2O_{(l)} \rightarrow = Fe^{2+}_{(aq)} + 2SO_4^{2-}{}_{(aq)} + 2H^+_{(aq)} \quad (1)$$

The oxygen from the air can oxidize sulphide minerals within waste rock piles. Sulphide oxidation is favored as greater is the availability of oxygen at the surface of the mineral. The oxidation produces a variety of secondary mineralogical phases, changing the characteristics of the solid phases, which can be leached upon contact with the aqueous phase of the system.

This paper presents a geochemical characterization of the water circulating through a uranium waste rock pile and adjacent regions. The studied uranium waste rock pile, named Bota-Fora 4 (BF4), is located in the ore Treatment Unit of Caldas (UTM), under management of the Indústrias Nucleares do Brasil (INB), in the city of Poços de Caldas, Minas Gerais, Brazil. The region where the project is located is named Campo do Cercado. The activities of mining and ore processing were closed in 1995, and currently the area lies in decommissioning and implementation of a plan of reclamation process. Poços de Caldas plateau consists in a round caldera of approximately 33km in diameter along the axis northwest-southeast, and extends over around 800km², constituting the largest alkaline complex of South America. Outer ring that forms the caldera has altitude between 1500-1700m, and the inner mountains have an average altitude of 1300m. The ring structure of the caldera is Mesozoic origin, composed of volcanic rocks (alkaline) and plutonic rocks, containing significant amounts of U, Th and rare-earth elements (REEs) (Holmes et al., 1990; Schroscher and Shea, 1991).

Uranium mineralization has been classified into three distinct ore bodies, named A, B and E, according to the concentration of uranium. The body A presents average uranium content of 600ppm. Structurally, it has been described as a monogenic volcanic gap formed by enclosing angular rock fragments of tinguaite. The body B has average uranium content of 680ppm, and it has been described as a large mass of holes, arranged in a matrix tube. The matrix showed a tinguaite rock texture with minerals like pyrite, fluorite, uranium minerals, molybdenum and zirconium. In small amounts galena, sphalerite and barite were found. The Body E has an average grade of 1000ppm uranium, and it consists of a package of host rocks, non-brecciated, containing secondary mineral phases arising from the action of redox phenomena (Gerência da Minas de Caldas, 1988 apud Souza, 1995; Cipriani 2002).

The Bota-Fora 4 (BF4) was built on the valley of Consulta stream, adjacent to the pit mine area, burying natural drainage. The valley was previously prepared with deep drains to receive waste rock. A diversion channel (approximately 500m length) was excavated in natural terrain along the

left flank of the valley. The channel was covered with a compacted clay layer to prevent infiltration of water from the stream in the pile (Souza, 1995; Franklin, 2007). Upstream of Consulta stream deviation channel, a basin was constructed in order to regularize the flow. Downstream of the pile, Nestor Figueiredo basin (BNF) was built to catch the acidic effluents generated in BF4. The Bota-Fora 4 (BF4) has $12.4x10^6 m^3$ and occupies an area of $56.9x10^4 m^2$. The waste rock pile contains cover material of the mine and sterile sorting of body B (Figure 1).

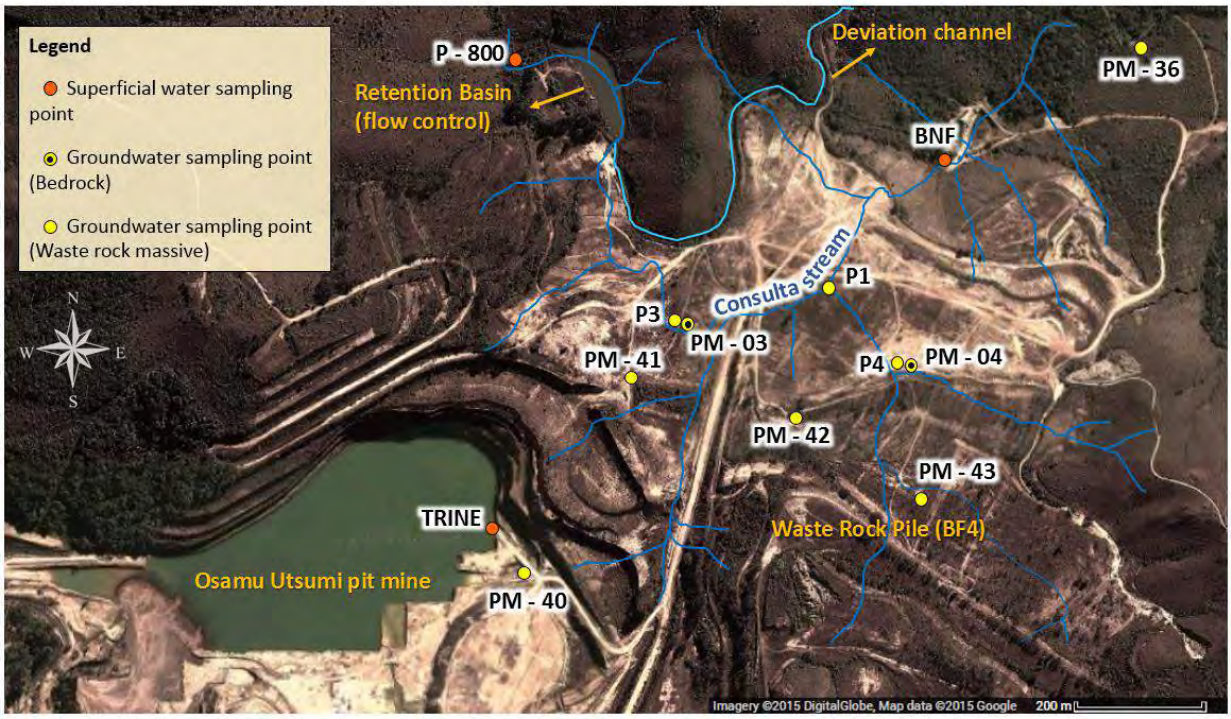

Figure 1 Partial view of the uranium exploration site with emphasis on Osamu Utsumi pit mine, waste rock pile (BF4) and water sampling points (adapted from Google maps, 2015).

METHODOLOGY

Water sampling and chemical analysis

Two sampling campaigns were carried out during the dry season, in August 2011 and July 2012. The sampling method used to collect the surface waters and the procedures for the preservation of the samples followed NBR 9898 standard (ABNT, 1987). Figure 1 shows the sampling points of surface and groundwater. For groundwater sampling, disposable bailers samplers produced in high-density polyethylene (HDPE) with 19:35 mm in diameter and 970mm in length were used. The following parameters were measured in all water samples: pH, total dissolved solids (TDS), redox potential (ORP), temperature and electrical conductivity (in situ, with the aid of a multiparameter meter manufacturer Myron L. Company, Ultrameter IITM model 6P). Table 1 shows the parameters and analytical methods used.

Table 1 Methods used in chemical analysis.

Ion	Analytical method	Ion	Analytical method
Na	Atomic Absorption	Al	ICP-OES
K	Atomic Absorption	Mn	Atomic Absorption
Mg	Atomic Absorption	F^-	Potentiometry
Ca	Atomic Absorption	SO_4^{2-}	EDXRF
Fe	Atomic Absorption	Alkalinity	Titration

Time series of discharge of acid drainage and its chemical composition, monitored monthly during 30 months from January 2007 to June 2009, were selected for spectral analysis (Fig. 2, Fig. 3 and Fig. 4). Time series for U, Mn, SO_4^{2-}, pH, acid discharge and precipitation (Fig. 5) were used. Selected chemical species have relevance for the treatment of effluents and for understanding the process generation of acid rock drainage.

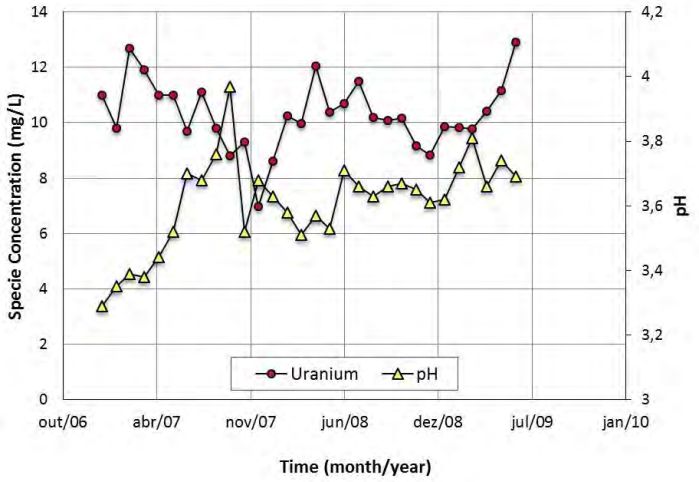

Figure 2 Time series of uranium and pH monitored from January 2007 to June 2009

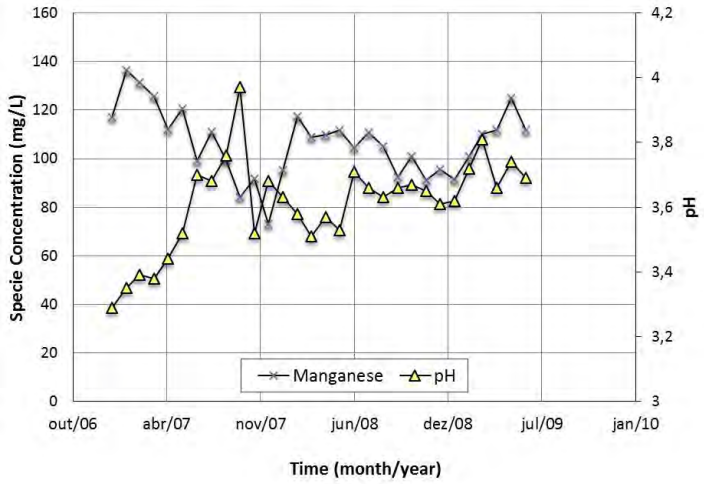

Figure 3 Time series of manganese and pH monitored from January 2007 to June 2009

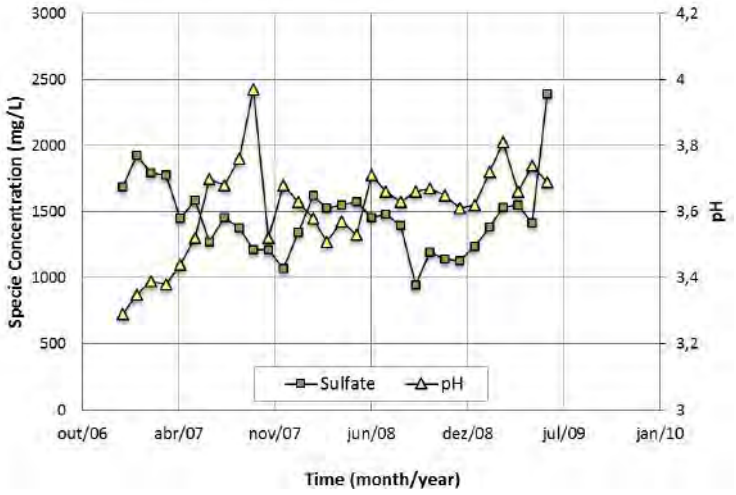

Figure 4 Time series of sulfate and pH monitored from January 2007 to June 2009

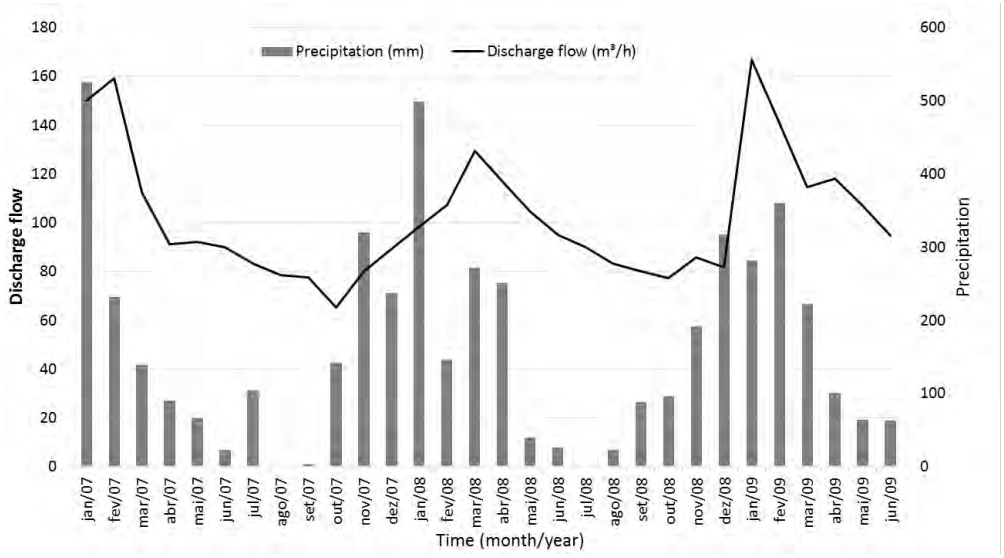

Figure 5 Time series of discharge flow of acid rock drainage and precipitation from January 2007 to June 2009

Data processing

The ionic concentration in the water is the product of geochemical reactions between the aqueous phase and the geological medium under certain environmental conditions. For evaluating the chemical evolution of water quality and the probable chemical reactions, a computational hydrogeochemical modeling was carried out using the software PHREEQC 2 (Parkhurst and Appelo, 1999).

Finally, the set of monitoring data of discharging acid drainage was analyzed by means of autocorrelation functions and cross-correlation. The former function considers the relationship between successive terms of a single time series and provides information on the duration of the

influence of an event in the system. The later function connects the sets of input and output, and indicates how they are correlated. The gap between zero and the maximum of the cross-correlation function, called delay, indicates how stress propagates thought the system.

RESULTS AND DISCUSSION

Computer modeling indicated a supersaturation of the samples of P1, P4 and PM-04 in chemical species containing iron (hematite, goethite and magnetite) and close to saturation limit of ferrihydrite. P1, P4 and PM-04 are also close to the saturation limit in relation to carbonated phase (calcite and aragonite). Non-precipitation of goethite in PM-41 and PM-43, unlike what happen in P1, P4 and PM-04, takes place at the higher pH, which favors the preferential formation of hematite (Tremocoldi, 2003). The preferential precipitation of magnetite compared to hematite takes place under reducing conditions, which is a characteristic of groundwaters.

Samples of the monitoring wells P3, PM-03, PM-40, TRINE and BNF are close to limit of saturation with respect to calcium sulfate (anhydrite or gypsum). PM-40 and P3 capture water from the bedrock of the terrain, below the BF4, have greater similarity in relation to the others. These samples are supersaturated in magnetite and close to the saturation limit in goethite and siderite. P3, PM-03, PM-40, TRINE and BNF are saturated in magnetite. This behavior highlights the trend of leach mineralogical phases containing iron, as expected in acid drainages. In addition, PM-03 and P3 samples, located side by side, are supersaturated in uranium, leading to precipitation of U_3O_8, U_4O_9 and uraninite. The sample of groundwater PM-36, located downstream of the waste rock pile did not show supersaturation in the evaluated phases. The control sample P-800 of surface water upstream of BF4, was supersaturated on hematite, goethite and magnetite.

Autocorrelation results presented similar buffer time, i.e., the duration of the influence of an event for all parameters analyzed, as showed on Table 3. Table 4 and 5 present the results for the cross-correlation. They present the response time of a phenomena (precipitation or discharge) and the signal propagation time in the system, i.e., how long the input phenomenon will affect the output phenomenon. According to the cross-correlation, the discharge on BNF (input parameter) is positively correlated to the chemical parameters (output). This implies that the increase in flow provides an increase in the concentration of U, Mn and sulfate, and a reduction of the pH (increase in H^+ concentration).

During the dry season, secondary phases are precipitated and/or adsorbed in the pores of the pile. With the onset of the rainy season, these species are leached and their peaks occur during this period. This period coincides with the seasonal dry and wet periods, explaining the formation of acid rock drainage throughout the hydrological year.

Such analysis allows us to infer on the hydraulic and geochemical behavior of the pile. After the onset of the rainy season, the pile will reflect an increased flow after 1.2 months. After three months, the pile will start to discharge the stored water in previous refills. The response of the system to the rainy season lasts about 4.8 months, i.e., nearly until the next rainy season. This explains the occurrence of discharge even during dry season. With the beginning of the discharge, the chemical species will be released after 3 months. It implies that these contaminants were leached and subsequently stored until their release in the medium. The release of contaminants

implies in a reduction of the pH. Contaminants as ferric ion is very effective to maintain low pH conditions due the low solubility of ferric hydroxide and to the release of protons by the hydrolysis reaction. It effect extends until the next rainy season.

Table 3 Autocorrelation function results.

	Buffer time (month)	**Correlation**
U	2.5	0.7
Mn	2.5	0.6
SO_4^{2-}	2.5	0.6
pH	3.0	0.7
Discharge flow	3.0	0.5
Precipitation	3.0	0.6

Table 4 Cross-correlation function and the time series of precipitation as the input parameter and the series of discharge as output parameters.

	Response to precipitation (month)	**Precipitation effect** (month)	**Correlation**
Discharge flow	1.2	4.8	0.7

Table 5 Cross-correlation function and the time series of discharge as the input parameter and the series of concentration of U, Mn, SO_4^{2-} and pH as output parameters.

	Response to discharge (month)	**Discharge effect** (month)	**Correlation**
U	2.5	5.4	0.7
Mn	2.5	5.8	0.6
SO_4^{2-}	2.5	5.4	0.6
pH	3.0	6.8	0.7

CONCLUSIONS

Two distinct hydrochemical patterns were identified. The western region of the cell, adjacent to the mine pit, preferably oxidizes and generates more acid effluent compared to the eastern region. The transient analysis of the discharges of Mn, U and sulfate in the acid mine drainage showed a positive correlation with flow, indicating that these species are precipitated and/or adsorbed in the pore media during dry periods and have their peak discharge after the beginning of the rainy season, indicating the occurrence of a leaching process. The pH has prolonged effect over 6 months, which explains the presence of acid drainage throughout the year hydrology.

The behavior of chemical species observed in the spectral analysis of monitoring data is corroborated by the results obtained by computational modeling. Acidic effluents are presented

supersaturated or near the saturation limit for Mn containing species, U and sulfate. It is highlighted by the occurrence of Mn concentrations close to saturation limits. The leaching process and subsequent saturation of aqueous species of Mn in the water appears as a phenomenon occurred independently of the formation of acid rock drainage.

ACKNOWLEDGEMENTS

The authors would like to thank the Comissão Nacional de Energia Nuclear (CNEN), particularly to Dr. Paulo Rodrigues and Dr. Carlos Alberto Carvalho. We would like to thank also the Conselho Nacional de Desenvolvimento Científico e Tecnológico (CNPq), Fundação de Amparo à Pesquisa do Estado de Minas Gerais (FAPEMIG), Coordenação de Aperfeiçoamento de Pessoal de Nível Superior (CAPES-PROEX), Instituto Nacional de Ciência e Tecnologia em Recursos Minerais e Biodiversidade (INCT–Acqua) and Indústrias Nucleares do Brasil (INB).

REFERENCES

ABNT - Associação Brasileira de Normas Técnicas (1987) *NBR 9898; Preservação e técnicas de amostragem de afluente líquidos e corpos receptores - Procedimento.*Rio de Janeiro, 22p.

Cipriani, M. (2002) *Mitigação dos impactos sociais e ambientais decorrentes do fechamento definitivo de minas de urânio.* Campinas: Instituto de Geociências, Universidade Estadual de Campinas, 332p. (Tese, Doutorado em Administração e Política de Recursos Minerais).

Franklin, M.R. (2007) *Modelagem numérica do escoamento hidrológico e dos processos geoquímicos aplicados à previsão da drenagem ácida em uma pilha de estéril da mina de urânio de Poços de Caldas – MG.* Rio de Janeiro: COPPE, Universidade Federal do Rio de Janeiro, 337p. (Tese, Doutorado em Engenharia Civil).

Gerência da Mina de Caldas. (1988) *Síntese dos trabalhos: Relatório Interno*. Indústrias Nucleares do Brasil.

Holmes, D.C.; Pitty, A.E.; Noy, D.J. (1990) *Geomorphological and hydrogeological features of the Poços de Caldas caldera and Osamu Utsumi mine and Morro do Ferro analogue study sites, Brazil.* Technical Report TR 90-14, Swedish Nuclear Fuel and Waste Management Co., 55p.

Mend/Canmet – Mining and Mineral Science Laboratory. (2009) *Prediction manual for drainage chemistry from sulphidic geologic materials.* MEND Report 1.20.1.

Parkhurst, D.L; Appelo, C.A.J. (1999) *User's guide to PHREEQC. Version 2. A computer program for speciation, batch-reaction, one-dimensional transport, and inverse geochemical calculations.*US Geological Survey, Denver.

Schorscher, H.D.; Shea, M.E. (1991) *The regional geology, mineralogy and geochemistry of the Poços de Caldas alkaline caldera complex, Minas Gerais, Brazil.* Technical Report TR 90-10, Swedish Nuclear Fuel and Waste Co., 36p.

Souza, V.P. (1995) *Drenagens ácidas do estéril piritoso da mina de urânio de Poços de Caldas: interpretações e implicações ambientais.* Dissertação de Mestrado, Universidade de São Paulo, Dept. de Engenharia de Minas. 141p.

Tremocoldi, W.A. (2003) *Silicate and iron oxide mineralogy of the clay fraction of soils developed from basic rocks in São Paulo state.* Taubaté: Rev. Biociênc. v.9, n.1, p15-22

Prediction of Drainage Water Quality from Mining Waste with Carbon Sequestration Potential

El-Hadji B. Kandji[1], Benoît Plante[1], Bruno Bussière[1], Akué-Sylvette Awoh[1], Bibi-Amiirah Ibrahim Saïb[1], Georges Beaudoin[2] and Pierre-Philippe Dupont

1. *Université du Québec en Abitibi-Témiscamingue (UQAT), Research Institute of Mines and Environment (RIME), Canada*
2. *Université Laval, Département de Géologie et Génie géologique, Canada*
3. *Royal Nickel Corporation, Canada*

ABSTRACT

Fixation of CO_2 by brucite or serpentine is widely recognized as a passive way to reduce carbon footprint. Ultramafic rocks are rich in minerals with high potential to sequester CO_2 in ambient conditions and are sometimes associated with base metals, such as Ni. Extraction of these base metals can lead to exposure of ultramafic wastes to atmospheric conditions, such as in the case of the Dumont deposit (Royal Nickel Corporation) near Amos, Quebec, Canada. The wastes of this future open pit mine are low in sulfide content (<1 %) and rich in ultramafic minerals with significant potential to trap atmospheric CO_2. This natural process, leading to the precipitation of stable carbonates, can influence the long term drainage water quality of the wastes. The aim of this study is to predict the geochemical behavior of such wastes, as well as the impact of CO_2 sequestration on drainage water quality. The five main lithologies found in the Dumont deposit were sampled, and a combination of these lithologies was studied as waste rock, whereas a tailings sample was produced by pilot scale metallurgical testing. All samples were submitted to laboratory kinetic columns tests and to CO_2 consumption tests. The results suggest that dissolution of Magnesium silicates and precipitation of secondary Magnesium carbonates are the main geochemical processes controlling Mg, Ca, and Si concentrations in the leachates, and generating high alkalinity values. The ultramafic lithologies, which fix CO_2, show alkaline drainage, with pH values varying from 9 to 10, versus 7.0 to 8.5 for non-ultramafic samples. These results help understand the mechanisms of CO_2 sequestration by mine wastes and its impact on water quality.

Keywords: mine wastes, ultramafic rocks, carbon sequestration, kinetic columns tests, alkaline drainage

INTRODUCTION

Ultramafic rocks are considered to be good candidates as an anthropogenic carbon sink. Many studies highlight the use of ultramafic rocks with high concentrations of serpentine (lizardite, chrysotile) and brucite to react with CO_2 (Goff & Lackner, 1998; Lackner et al., 1995). There are large amounts of mafic and ultramafic rocks scattered in the earth's crust. These rocks are sometimes associated with base metals, and their extraction leads to the exposure of mine wastes at the surface. Even though the fixation of CO_2 by magnesium silicates is a slow process, the exposure of significant quantities of mining wastes with high concentrations of serpentine minerals can reduce the carbon footprint of the mining activities (Harrison et al., 2013). Carbon sequestration by mine waste is very attractive because of the quantities that are produced during mining. Furthermore, these materials are often finely ground, which increases the exposed surface area.

Existing literature on carbon sequestration by mining wastes focuses mainly on the estimation of their sequestration potential or on the evaluation of factors that potentially affect their sequestration potential, such as temperature, surface passivation, or degree of saturation (Assima et al., 2014; 2012). Many research projects also focused on techniques to accelerate the process, in order to fix more Carbon and to move to the industrial scale (Larachi et al., 2010). Fixation of CO_2 by Mg or Ca silicates, also called mineral carbonation, likely occurs in the mine tailings in the following steps: (1) dissolution of CO_2 into interstitial water; (2) acid release is consumed by silicates which release Mg^{2+} or Ca^{2+}; (3) reaction between Mg^{2+} or Ca^{2+} with HCO_3^- or CO_3^{2-} to form stables carbonates under ambient conditions (Harrison et al., 2013; Wilson et al., 2009a). Processes leading to the formation of stables carbonates can impact the quality of mine drainage. As reported by Bea et al. (2012), Carbon sequestration by ultramafic tailings at Mount Keith (Australia) leads to alkaline drainage with pH varying from 8 to 10. Wilson et al. (2009b) suggest that precipitation of nesquehonite in kimberlite processing wastes could increase their neutralization potential by 1-2 %. Rollo and Jamieson (2006) also report that dissolution of chrysotile and precipitation of Magnesium carbonates are an important process affecting pore water composition at the same site. Thus, it is important to consider the Carbon sequestration potential of ultramafic mine wastes in order to predict the drainage water quality.

The wastes studied here are those of the Dumont project of Royal Nickel Corporation, an open pit project located 25 km west of Amos in the Abitibi-Témiscamingue region, Québec, Canada. The project intends to mine and process a deposit of Nickel mineralization which contains 2 types of mineralization: Nickel sulfides (pentlandite, millerite) and an Iron-Nickel alloy (awaruite). The operation plans to treat up to 105 tons/day of ore at an average grade of 0.27 % Ni, over a lifetime of 31 years. The deposit lies within a mineralized zone of serpentinized dunite, composed mainly of serpentine, and minor minerals including magnetite, brucite, chlorite, diopside, and chrysotile. Waste rocks are composed mainly of peridotite, gabbro and basalts containing serpentine, chromite, clinopyroxene, , quartz, and plagioclase (RNC, 2012). Previous work on the Royal Nickel wastes have highlighted their ability to fix Carbon (Plante et al., 2014; Awoh et al., 2013; Pronost et al., 2011), due to high serpentine concentrations in the wastes. (Pronost et al., 2011). Eudiometer tests

show that brucite and serpentine could react with CO_2 to form stable hydrated Magnesium carbonates (Pronost et al., 2011). The carbonates formed are dypingite $Mg_5(CO_3)_4(OH)_2$-$5H_2O$) and nesquehonite $Mg(HCO_3)(OH)$-$2H_2O$) (Pronost et al., 2011). Awoh et al. (2013; 2014) developed an innovative CO_2 consumption test in order to quantify the CO_2 flux sequestered by mine wastes. Results of the various laboratory and *in situ* CO_2 consumption tests suggest that the Dumont wastes sequester CO_2 fluxes of up to 1400 g/m^2/year in typical ambient conditions. These studies have also shown that the non-ultramafic lithologies of the Dumont deposit do not consume CO_2. CO_2 consumption tests also show that a specific water content is required for optimal carbonation (Assima et al., 2012; Awoh et al., 2013). Since CO_2 sequestration involves the precipitation of secondary carbonates that may affect water quality, the aim of this work is to predict water quality of the future Dumont wastes and the impact of Carbon sequestration on the quality of the drainage water from the Dumont wastes.

MATERIALS AND METHODS

Materials characterization

Different types of waste rocks from the Dumont project were sampled for the present study: one tailings sample, one ultramafic waste rock sample, and 5 samples of the main lithologies found in the Dumont project (low grade dunite, upper peridotite, footwall ultramafic (which is dominantly peridotite)gabbro, and volcanic basalt). The tailings sample was produced in a pilot-scale plant, while the ultramafic waste rock was taken from a bulk sample at the site consisting of dunite and peridotite. The five main lithologies were sampled from representative sections of drill core.

All samples were characterized physically and chemically. The chemical characterization was performed after an acid digestion (HNO_3-Br_2-HF-HCl) followed by ICP-AES analysis of over 20 elements. A whole-rock analysis of major elements of the Dumont samples was performed by X-ray fluorescence (XRF) following a Lithium borate fusion on pulverized sample aliquots (85 % < 200 mesh) by Acme Analytical Laboratories Ltd, Vancouver, Canada. The detection limits of the chemical characterizations of the oxides ranged between 0.001 and 0.1 %. Results of major elements are presented in Table 1. These results, combined with X-ray diffraction (XRD) analysis, allow identifying and quantifying minerals present in the samples. The tailings and ultramafic lithologies (low grade dunite, upper peridotite, footwall ultramafic) contain between 34.06 % and 42.68 % MgO. The gabbro and volcanic (which are not ultramafic materials) contain 9.96 % and 6 % MgO, respectively. All wastes contain significant amounts of SiO_2between34.17 (footwall ultramafic) and 49.27 % (gabbro). While the theoretical ratio of MgO/SiO_2 in serpentine equals 1.00, it is >1.00 for the tailings, low grade dunite, upper peridotite, and footwall ultramafic samples, suggesting an excess of Mg which can be attributed to brucite, $Mg(OH)_2$. Iron is present in all samples, with Fe_2O_3 concentrations between 5.82 % and 12.62 %. The gabbro and volcanic samples also contain more Al_2O_3 (13.41 and 14.07 %, respectively) and CaO (11.97 and 9.78, respectively) compared to the other samples (Al_2O_3: 0.22-3.08 %; CaO: 0.05-0.86 %), revealing the differences in mineralogical compositions between the non-ultramafic samples of gabbro and volcanic in comparison to the other materials. The initial total carbon and sulfur contents of samples were measured by a LECO carbon/sulfur analyzer (Maxxam Analytical, QC, Ca) with a reportable detection limit of 0.05 %.

The highest concentration of carbon was detected in the volcanic sample, due to the presence of calcite (0.8 %). The tailings, waste rock, low grade dunite, upper peridotite, gabbro, and footwall ultramafic contain similar carbon concentrations (between 0.12 and 0.17 %). The highest sulfur content was measured in the tailings sample with 0.2 %, while other samples contain less than 0.08 %.

X-Ray Diffraction results coupled with oxides and trace elements analysis indicate that the matrix of ultramafic samples such as tailings, waste rock, low grade dunite, upper peridotite, and footwall ultramafic is composed mainly of serpentine ($(Mg,Fe)_3Si_2O_5(OH)_4$). Other minerals are also, present such as brucite ($Mg(OH)_2$), magnetite (Fe_3O_4), and chlorite ($(Fe,Mg,Al)_6(Si,Al)_4O_{10}(OH)_8$). The waste rock sample also contains albite ($NaAlSi_3O_8$) and quartz (SiO_2). The gabbro and volcanic contain predominantly hornblende and epidote, with lesser quartz, albite, and diospide ($CaMgSi_2O_6$). The volcanic sample contains around 5 % calcite ($CaCO_3$). There is no serpentine detected in the gabbro and volcanic samples.

Table 1 Chemical composition (major elements) of the Dumont samples

	Ultramafic Waste rock	Tailings	Gabbro	Low Grade Dunite	Upper Peridotite	Volcanic (Basalt)	Footwall ultramafic
%SiO_2	41.40	35.10	49.27	34.53	35.83	47.93	34.17
%Al_2O_3	3.08	0.22	13.41	0.23	1.27	14.07	0.58
%Fe_2O_3	7.07	5.82	9.41	6.71	9.59	12.62	9.42
%CaO	0.86	0.05	11.97	0.15	0.69	9.78	0.16
%MgO	34.06	42.49	9.96	42.68	38.97	6.00	40.64
%Na_2O	0.74	<0.01	1.64	<0.01	<0.01	1.99	<0.01
%K_2O	0.25	<0.01	0.18	<0.01	<0.01	0.28	<0.01
%MnO	0.09	0.11	0.18	0.11	0.14	0.22	0.12
%TiO_2	0.13	<0.01	0.40	<0.01	0.05	0.87	0.02
%P_2O_5	0.02	0.05	0.03	<0.01	<0.01	0.08	<0.01
%Cr_2O_3	0.16	0.24	0.07	0.49	0.72	0.03	0.99
%LOI	12.31	16.15	2.72	15.41	12.94	5.30	14.11
total	100.18	100.23	99.22	100.30	100.20	99.18	100.21
MgO/SiO_2	0.82	1.21	0.20	1.24	1.09	0.13	1.19
% C	0.17	0.15	0.13	0.12	0.16	0.80	0.12
% S	0.04	0.17	0.02	0.04	0.03	0.06	0.02

The <2 cm fraction of the samples was selected for this study, and the grain size distribution was analyzed by sieving for the fraction between 2 cm and 355 µm. The tailings and the <355 µm fraction of the other samples was analyzed with a Malvern Mastersizer S laser grain size distribution analyzer. The main characteristics of the particle size distributions are shown in Table 2. The waste rock sample contains more fines (10% <355 µm) compared to the lithology samples (less than 4 %< 355 µm) because of the difference in the sampling method. This higher fine content in the waste rock sample could lead to a higher reactivity (due to the higher specific surface) compared to the lithology samples in the present study.

Table 2 Grain size distribution parameters of the samples

	% < 355 µm	D_{10} (µm)	D_{50} (µm)	D_{90} (µm)
	wt.%	wt.%	wt.%	wt.%
Tailings	99	2.2	32.4	191
Waste Rock	10	425	6700	13200
Low grade dunite	2	1400	9500	13200
Upper Peridotite	2	2800	11200	16000
Footwall ultramafic	2	1400	9500	16000
Gabbro	2	4750	11200	16000
Volcanic	2	2800	11200	16000

Kinetic column tests

Samples from the Dumont project were submitted to laboratory kinetic column tests. Approximately 20 kg of coarse material were deposited in plexiglass columns of 14 cm in diameter and 90 cm in height, while 8 kg of tailings were deposited in a column of the same diameter (14 cm) but lower height (60 cm). The interior of the tailings column was coated with vacuum grease in order to avoid preferential flow along the column wall. A porous ceramic plate was installed at the bottom of the tailings column in order to control the suction potential at a value of 1 m below the tailings. A volumetric water content probe and a dielectric water potential probe were installed 15 cm from the bottom of the tailings in the column. A geotextile was put at the base of the other columns in order to retain the fines within the column. The columns are flushed with 2 L of deionized water every two weeks for the waste rock and lithology samples, and once per month for the tailings column. The deionized water used has a pH between 5.5 and 6 and its carbonate content is negligible. The leachates were recovered after a contact time of a few hours. The column tests were run for over one year for coarse materials and for 2 years for tailings. Thermodynamical equilibrium calculations using Vminteq version 3.0 (USEPA, 307 1999) were performed on data from kinetic column tests in order to identify the different carbonates generated during kinetic tests. CO_2 consumption tests were performed on the columns each week. Detailed results of CO_2 consumption tests are not presented here, but they reveal that the gabbro and volcanic do not consume CO_2, while all other samples do (Plante et al., 2014; Awoh et al., 2014, 2013). The calculated fluxes for the tailings column vary between 50 and 800 g/m^2/year, depending on the interpretation method used and the water content. For coarse materials, the estimated fluxes reached up to 1400 g/m^2/year.

RESULTS AND DISCUSSION

Leachates recovered after each flush were analyzed for several parameters such as acidity, alkalinity, pH, electrical conductivity, and dissolved and total metals by ICP-AES and ICP-MS, and various anions by ionic chromatography. Only pH, sulfate, Mg, Si, and Ni are presented here. The pH of the leachates stabilized quickly for all materials and do not show a transitional phase, except for column tailings. The lithologies which do not sequester carbon (gabbro and volcanic) have a pH around 8.5, while other lithologies (low grade dunite, footwall ultramafic, upper peridotite) and the waste rock have a pH between 9.0 and 10. For tailings, the pH leachate remained near neutral (between 7.0 and 8.5) during the first 200 days, before gradually increasing and stabilizing between 9.0 and 9.5.

The lower pH observed during the first cycles for the tailings can be explained by the slower diffusion of CO_2 through the tailings than through the coarser waste rock and lithology samples, leading to a slower CO_2 sequestration and, therefore, a slower effect on leachate pH. The leachates of the ultramafic materials (tailings, ultramafic waste rocks, low grade dunite, upper peridotite, footwall ultramafic) contain high Mg concentrations (around 50-100 mg/L). In these types of wastes, Mg comes from the dissolution of serpentine and/or brucite with dissolved CO_2. For gabbro and volcanic, Mg in the leachates ranges from 1 to 5 mg/L, probably from the dissolution of gangue minerals such as hornblende and chlorite. The Si concentrations in the tailings leachates (which vary from 20 to 80 mg/L) are higher than in the other leachates. For gabbro and volcanic, Si varies from 1.7 to 5.7 mg/L. The other samples only show Si in some of the last leachates (0.1-1.0 mg/L) at the end of the kinetics test. The ratio of Mg/Si concentrations are very high, which suggest an incongruent dissolution of serpentine with a preferential release of Mg over Si and/or a fastest dissolution of brucite compared to serpentine (Assima et al., 2013; Harrison et al., 2013). All columns produce alkalinity and highest values were obtained for waste rock (275-300 mg $CaCO_3$/L) compared to other lithologies (<20 mg $CaCO_3$/L). The alkalinity in the tailings leachates increase with pH and stabilize around 200 mg $CaCO_3$/L after 400 days, probably due to the gradual buildup of secondary carbonates within the tailings. The metal concentrations remain very low during the column tests. For example, the Ni concentrations are shown in Figure 1; all leachates show very low Ni concentrations not exceeding 12 µg/l, and often below the detection limit (1 µg/L).

The sulfate release rates were calculated from the cumulative leached masses for the samples leaching regular detectable sulfate concentrations (Table 3). These results indicate an increase of sulfate release rate for tailings from 0.89 g/kg/d to 1.25 mg/kg/d at 290 days. Saturation indexes calculated indicate that a variety of calcium and magnesium carbonates may precipitate (Table 4). No carbonate is suggested to precipitate in the volcanic column and before day 290 in the tailings, when pH is near neutral. It suggests that carbonate precipitation occurs at alkaline pH values for tailings column. The most common magnesium carbonates to precipitate are magnesite and hydromagnesite.

At the end of the kinetics tests, all columns were dismantled and the final carbon content was determined for the first layer of the column, the first 5 cm for waste rock, tailings and footwall ultramafic, and for the first 10 cm of the others columns. The initial and final carbon contents are shown in Table 5. All materials show an increase in total carbon content except for the gabbro. The carbon enrichment for volcanic needs further investigation, since no CO_2 consumption is observed in that lithology. According to the carbon enrichment during the kinetic tests, the Dumont wastes can fix between 4 and 15 kg of CO_2 per ton of waste exposed at the surface, although the scale-up of these results to the large scale still needs to be investigated. Also, cementation was observed in the first 5 cm of the column for all samples that consume CO_2. Examples of cemented phases found in the columns are shown in Figure 2. The precipitation of secondary magnesium carbonates probably cemented the grains in the columns. The cementation of surface mining wastes due to mineral carbonation is already reported for chrysotile mine wastes in southern Québec, Canada (Beaudoin et al., 2008; Assima et al., 2012, 2013) and for ultramafic wastes of Cassiar and Clinton Creek in the Yukon Territory and British Columbia, Canada (Wilson et al., 2009a).

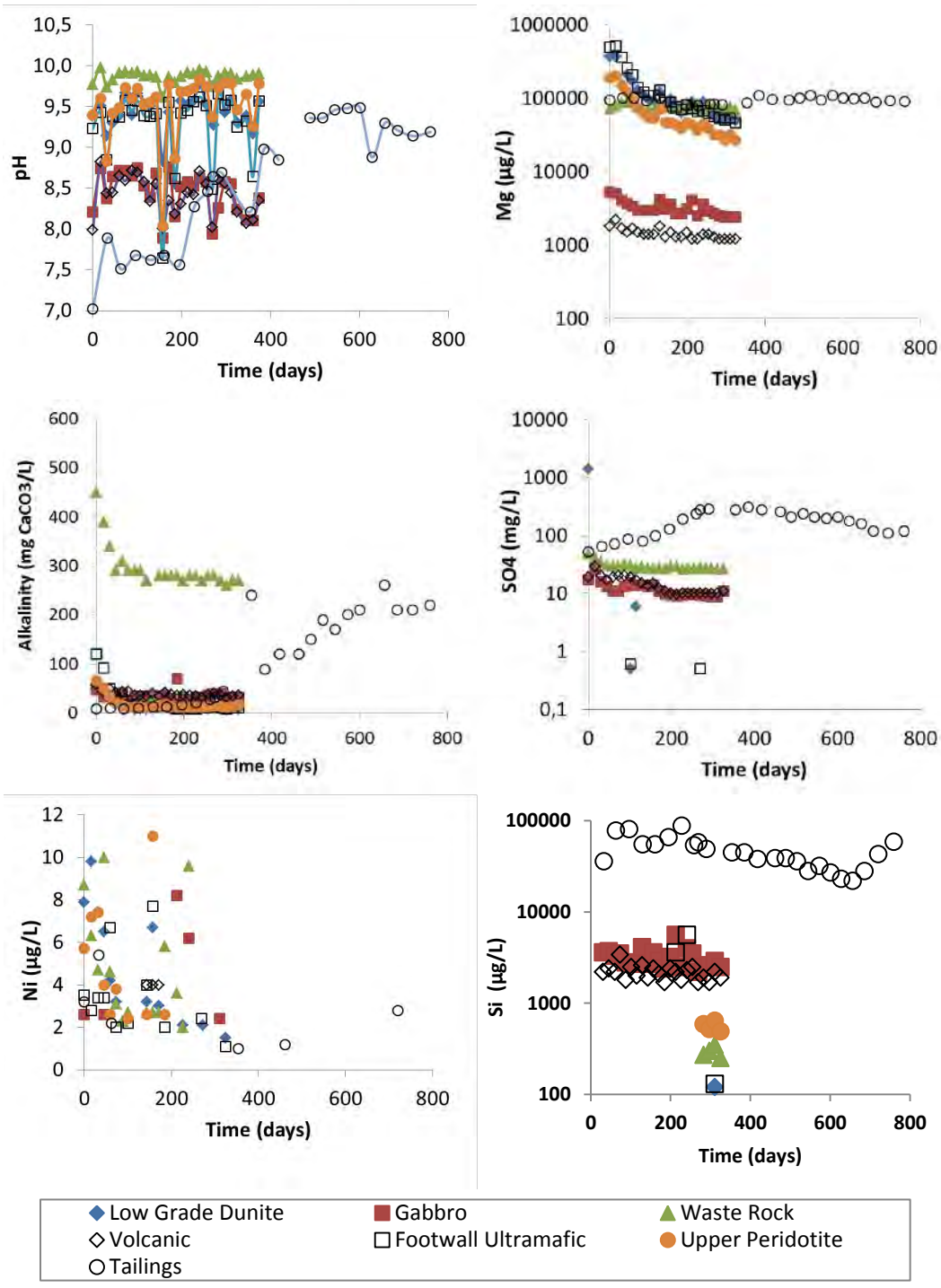

Figure 1 Evolution of pH, Mg, Alkalinity, Sulfates, Ni and Si concentration in kinetic column tests

Table 3 Sulfate release rates from kinetic column tests

	Ultramafic Waste Rock	Tailings (0 to 290 days)	Tailings (290 to 830 days)	Gabbro	Volcanic (Basalt)
Sulfate release rate (mg/kg/day)	0.204	0.894	1.252	0.083	0.099

Table 4 carbonates suggested to precipitate with Visual MINTEQ

	Low grade dunite	Footwall ultramafic	Upper peridotite	Ultra-mafic Waste rock	Tailings (0 to 290 days)	Tailings (290 to 830 days)	Gabbro	Volcanic (Basalt)
Magnesite	✓	✓	✓	✓		✓		
Hydromagnesite	✓	✓	✓	✓		✓		
Calcite	✓	✓		✓		✓	✓	
Dolomite	✓	✓	✓	✓		✓	✓	
Aragonite		✓	✓	✓		✓	✓	
Artinite	✓	✓	✓	✓		✓	✓	
Huntite	✓	✓	✓			✓		
Vaterite			✓	✓				
Magnesioferrite				✓				

Table 5 Initial and final carbon content of Dumont waste before and after kinetic column tests

	Tailings	Ultramafic Waste rock	Gabbro	Low Grade Dunite	Upper Peridotite	Volcanic (Basalt)	Footwall ultramafic
Initial % C	0.15	0.17	0.13	0.12	0.16	0.80	0.12
Final % C (first layer)	0.60	0.48	0.16	0.24	0.30	0.98	0.23

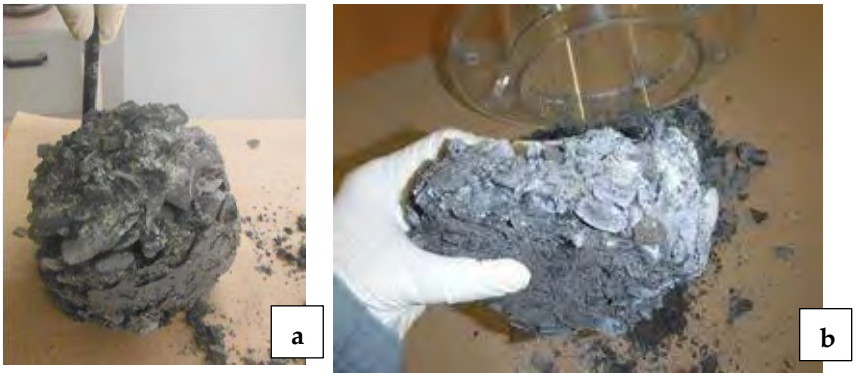

Figure 2 cementation on the first cm of columns a) Upper Peridotite, b) footwall ultramafic

CONCLUSION

Previous studies have confirmed the capacity of the Dumont wastes to sequester CO_2, and our investigations show that this process has an effect on the drainage water quality, as it leads to alkaline drainage with pH values up to 10. However, metal concentrations in the leachates remain low. The exact nature of the secondary carbonates formed will be investigated in the coming months. Cementation of the grains upon Carbon sequestration might reduce wind erosion and dust generation from the future waste rock piles and tailings ponds.

ACKNOWLEDGEMENTS

The authors thank Royal Nickel Corporation and NSERC for their contributions to a Research and Collaborative Grant, the RIME-UQAT and Royal Nickel Corporation staff, and the anonymous reviewers for their helpful and constructive insights.

REFERENCES

Assima, G., Larachi, F., Molson, J., & Beaudoin, G. (2014). Impact of temperature and oxygen availability on the dynamics of ambient CO2 mineral sequestration by nickel mining residues. *Chemical Engineering Journal*. Retrieved from http://www.sciencedirect.com/science/article/pii/S1385894713015830

Assima, G., & Larachi, F, Beqaudoin, Georges and Molson, J. (2012). CO2 Sequestration in Chrysotile Mining Residues: Implication of Watering and Passivation under Environmental Conditions. *Industrial & Engineering Chemistry Research*, 2–10. Retrieved from http://pubs.acs.org/doi/abs/10.1021/ie202693q

Assima, G. P., Larachi, F., Beaudoin, G., & Molson, J. (2013). Dynamics of carbon dioxide uptake in chrysotile mining residues – Effect of mineralogy and liquid saturation. *International Journal of Greenhouse Gas Control*, *12*, 124–135. doi:10.1016/j.ijggc.2012.10.001

Awoh, A. S., Plante, B., Bussière, B., & Mbonimpa, M. (2013). CO2 consumption test for the quantification of the mineral carbonation potential of mine waste rock. In *Canadian Geotechnical Conference*. Montreal, Quebec.

Awoh, A.S., Plante, B., Bussière, B. & Mbonimpa, M. (2014). Measurement and prediction of the CO2 effective diffusion coefficient in unsaturated media.

Bea, S. a., Wilson, S. a., Mayer, K. U., Dipple, G. M., Power, I. M., & Gamazo, P. (2012). Reactive Transport Modeling of Natural Carbon Sequestration in Ultramafic Mine Tailings. *Vadose Zone Journal*, *11*(2). doi:10.2136/vzj2011.0053

Beaudoin, G., Hébert, R., Constantin, M., Duchesne, J., Cecchi, E., Huot, F., Vigneau, S., and Fiola, R. (2008). Spontaneous carbonation of serpentine in milling and mining waste, southern Québec and Italy. In *Accelerated Carbonation for Environmental and Materials Engineering (ACEME2008)* (pp. 73–82). Rome (Italy).

Goff, F., & Lackner, K. (1998). Carbon dioxide sequestering using ultramafic rocks. *Environmental Geosciences*. Retrieved from http://archives.datapages.com/data/deg/1998/005003/89_deg050089.htm

Harrison, A. L., Power, I. M., & Dipple, G. M. (2013). Accelerated carbonation of brucite in mine tailings for carbon sequestration. *Environmental science & technology*, *47*(1), 126–34. doi:10.1021/es3012854

Lackner, K., Wendt, C., & Butt, DP, Joyce, E., Sharp, D. (1995). Carbon dioxide disposal in carbonate minerals. *Energy*, *20*(I), 1153–1170. Retrieved from http://www.sciencedirect.com/science/article/pii/036054429500071N

Larachi, F., Daldoul, I., & Beaudoin, G. (2010). Fixation of CO2 by chrysotile in low-pressure dry and moist carbonation: Ex-situ and in-situ characterizations. *Geochimica et Cosmochimica Acta*, *74*(11), 3051–3075. doi:10.1016/j.gca.2010.03.007

Plante, B., E.H.B. Kandji, B. Bussière, A.S. Awoh & B.A. Ibrahim-Saïb, G. Beaudoin, A. Gras & J. Molson, P. P. D. (2014). Geochemical behavior of carbon-sequestrating mine wastes: case of the Dumont project, Royal Nickel Corporation. In *Tailings and Mine waste* (p. 12).

Pronost, J., Beaudoin, G., Tremblay, J., Larachi, F., Duchesne, J., Hébert, R., & Constantin, M. (2011). Carbon sequestration kinetic and storage capacity of ultramafic mining waste. *Environmental science & technology*, *45*(21), 9413–20. doi:10.1021/es203063a

RNC. (2012). *Technical Report on the Dumont Project, Launay and Trécesson Townships, Québec, Canada. 2139-RPT-003* (p. 377). Quebec, Canada.

Rollo, H. a., & Jamieson, H. E. (2006). Interaction of diamond mine waste and surface water in the Canadian Arctic. *Applied Geochemistry*, *21*(9), 1522–1538. doi:10.1016/j.apgeochem.2006.05.008

USEPA. 1999. MINTEQA2, Metal speciation equilibrium model for surface and ground water, version 4.0. http://epa.gov/ceampubl/mmedia/minteq/index.html

Wilson, S. a., Raudsepp, M., & Dipple, G. M. (2009b). Quantifying carbon fixation in trace minerals from processed kimberlite: A comparative study of quantitative methods using X-ray powder diffraction data with applications to the Diavik Diamond Mine, Northwest Territories, Canada. *Applied Geochemistry*, *24*(12), 2312–2331. doi:10.1016/j.apgeochem.2009.09.018

Wilson, S., Dipple, G., & Power, I. (2009a). Carbon dioxide fixation within mine wastes of ultramafic-hosted ore deposits: Examples from the Clinton Creek and Cassiar chrysotile deposits, Canada. *Economic Geology*, 95–112. Retrieved from http://economicgeology.org/content/104/1/95.short

10th ICARD IMWA 2015 | 10th International Conference on Acid Rock Drainage & IMWA Annual Conference

A Management Plan towards the Flooding of an Open-Cast Mine with Adjacent Underground Sections

Eelco Lukas and Danie Vermeulen

Institute for Groundwater Studies, University of the Free State, South Africa

ABSTRACT

The colliery is situated in the Mpumalanga Coalfield, north of Trichardt in the Republic of South Africa. The opencast is already rehabilitated but still acts as an entrance to the underground sections of the mine. The *Life of Mine* indicates active mining until 2035. We were tasked to develop a mine closure plan. Two surface drainage systems are present, namely the Trichardt Spruit and the Steenkool Spruit. Both these systems have been diverted locally around the opencast with the necessary permission, to maximize coal extraction and protect the environment. Several passive treatment options were tabled to minimise the post closure environmental contamination. After careful consideration it was decided to develop a mine flooding plan to exclude oxygen from the mine thereby minimising the sulfate generation inside the opencast and underground sections. To start flooding as early as possible, sections of the underground mine were identified as natural or artificial compartments to store water. The rehabilitated opencast is flooded using recharge from rainfall only. The sulfate content of the decant water is expected to decrease and only passive treatment options will be needed to improve the water quality so that the decant water may be released into the streams.

INTRODUCTION

The colliery is situated in the southern portion of the Witbank Coalfield, being part of the larger Mpumalanga Coalfields in South Africa. The coal is extracted by opencast and underground mining methods. The opencast mining was done in virgin ground, hence dewatering of existing underground workings was not needed. During the mining operations the spoils (overburden) is placed back in the pit. The spoils are levelled according to a surface plan and covered with topsoil and seeded. The opencast mining has since ceased and the rehabilitation has been completed. The underground mining, which consists of four different sections and is connected to the opencast, is by bord-and-pillar method only (**Figure 1**). The life of mine plan does not include any high-extraction and is projected until 2035 after which the mine will apply for closure. Legislation in South Africa requires that water decanting from a mining environment needs to be treated before it may be released into a stream or canal.

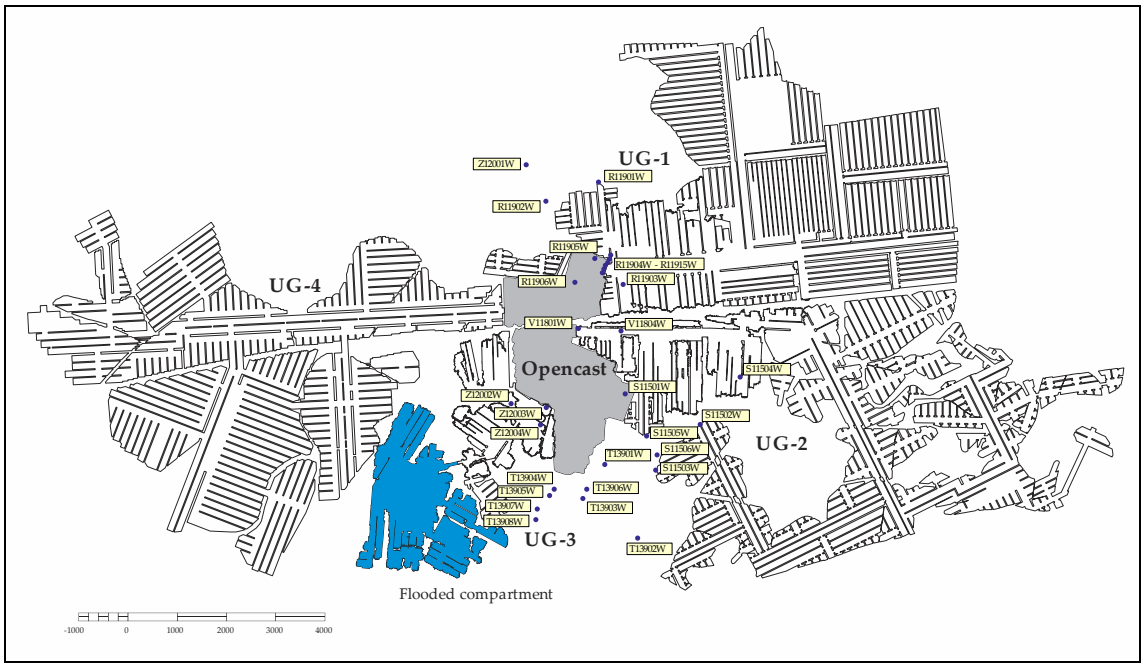

Figure 1 The opencast mine with the connected underground sections and monitoring boreholes.

METHODOLOGY

The underground workings are currently dry, except for one flooded compartment in the southern part of UG-3 (**Figure 1**). The opencast and all the underground sections have mined the same coal seam. This means that the floors of all the sections are connected. After mining has ceased the workings are allowed to be flooded. Water levels in the underground sections and opencast will rise together. The waterbody inside the workings will behave like a water table, or unconfined aquifer. Recharge in the opencast is much faster than in the underground. This means that the water level in the opencast will rise much quicker which in turn will lead to a water flow from the opencast into the underground sections. When the underground workings are completely filled, recharge to these workings will stop and only the opencast will continue to recharge. As the water table rises in the opencast sections so will the pressure in the connected underground and the waterbody in the underground will change into a confined

aquifer (the permeability of the roof is much lower than the permeability of the cavity). The water table will continue to rise until the system starts to decant. The decant position and elevation (meters above sea mean level, mamsl) was determined using the surface contours and opencast outline (**Figure 2**).

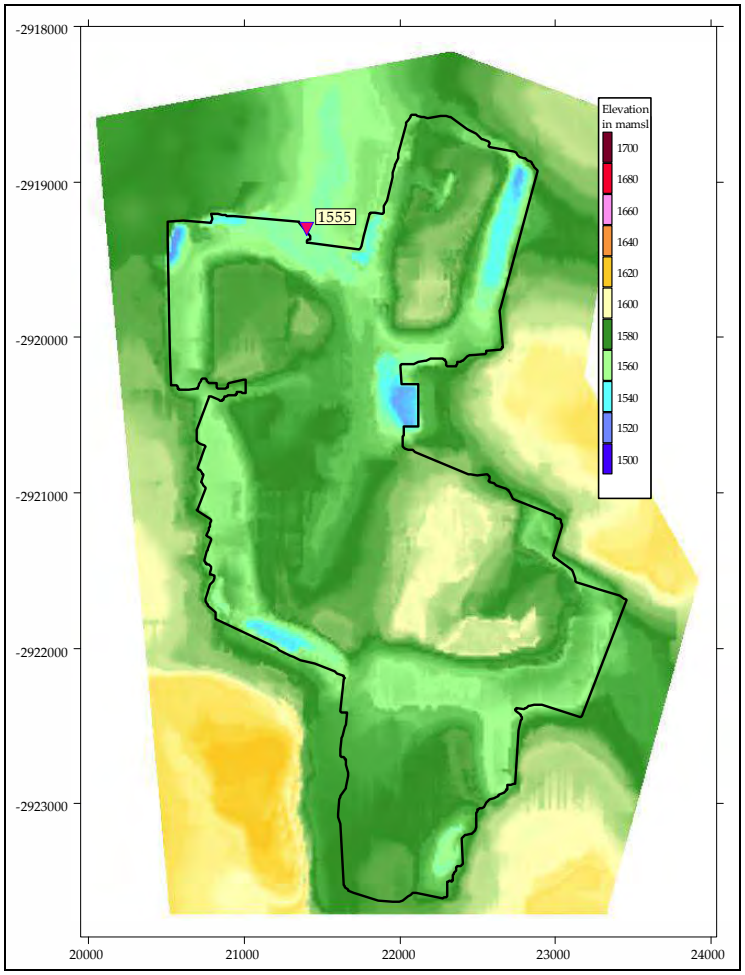

Figure 2 Opencast surface contours with decant point indicated

RESULTS AND DISCUSSION

Waterbalance

In terms of water make, the different mining methods have different recharge factors. Table 1 shows the recharge factors used in the Mpumalanga Area (Vermeulen, 2003). A fixed mining height of 4.60 m and the pillar-plan were used to determine the extraction factors for the four connected underground sections.

A stage-volume curve depicts the relationship between a water level elevation and the volume of water inside the opencast or underground workings. The water level is assumed to be horizontal. Using a stage-volume curve for the rehabilitated opencast pit with a void space of 25 % in the backfilled spoils, a volume can be determined at decant level. A management level

at 1 550 mamsl, five meters below the decant elevation, is suggested. This results in a 9 400 Mℓ buffer to be utilized in very wet seasons (**Figure 3**).

Table 1 Recharge values per mining methode

Mining method	Recharge as a percentage of the average rainfall
Bord-and-pillar	1 – 3%
Stooping	6 – 13%
Longwall and shortwall	15 – 20%
Opencast	20 – 30%

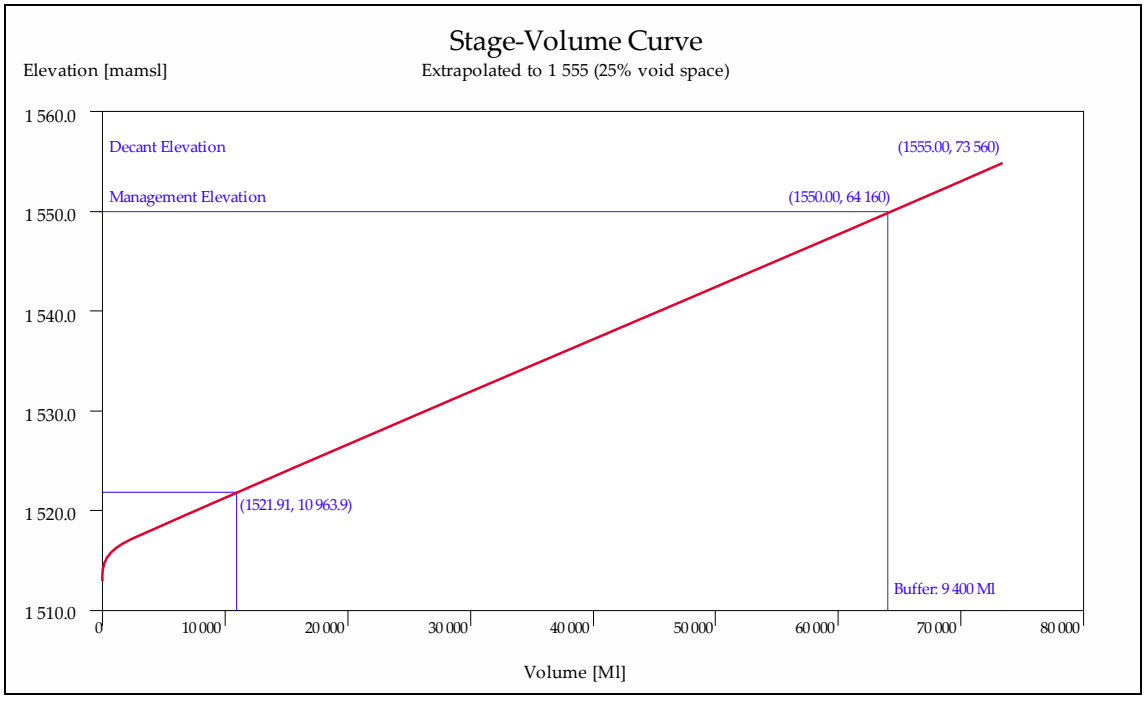

Figure 3 Stage-volume curve for the rehabilitated opencast

The stage-volume curve appears to be a mainly linear because the opencast does not have benches and the walls are almost vertical. The storage capacities for the separate workings were calculated using the outline pillar plan and a fixed mining height of 4.60 m. The opencast is currently not completely dry. Using two boreholes in the northern part of the pit, a water level elevation of 1 521.91 mamsl was determined (Table 2).

Table 2 Water storage capacity for separate working at the colliery

UG Section	Area (ha)	Mining Height (m)	Extraction factor (-)	Capacity (Mℓ)	Remaining Capacity (Mℓ)
UG-1	3 000	4.60	53.5	73 840	73 840
UG-2	2 848	4.60	53.5	70 051	70 051
UG-3	932	4.60	53.0	22 176	9 933
UG-4	3 173	4.60	55.0	80 279	80 279
OC @1550	780	-	25.0	64 160	53 196

Another factor that influences the inflow of water is the depth of mining. Natural permeability usually decreases with depth. This is because calcium carbonate, which is the binding material between the grains of sand (sandstone) and mud (shale), has to some degree been leached by circulating groundwater from the top 40 m of sediments. An empirical relationship between recharge and mining depth has been established through years of observation in the collieries as shown in Table 3 (Hodgson and Krantz, 1998).

Table 3 Bord-and-pillar recharge-values per depth of mining

Depth of mining (m)	Percentage recharge for average rainfall
10	3 – 10
20	2.5 – 5
30	2 – 3
40	1.5 – 2
>60	1 – 1.5

The depth of the underground workings at this colliery varies between 34 and 150 meters below ground level (**Figure 4**) and an average recharge rate of 1.5 % is suggested. Using the recharge rate the area of each section, a water make per section can be calculated, as well as the time it will take to flood the underground sections.

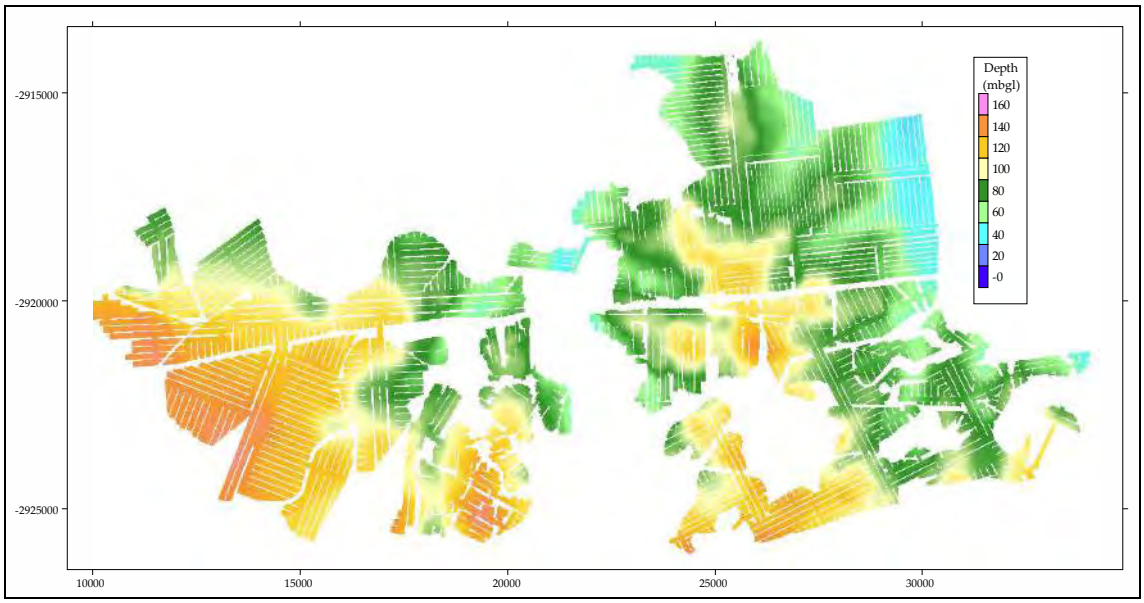

Figure 4 Depth of the coal floor in the current and future underground sections of the colliery

The recharge in the opencast is much higher than the recharge in the underground. Observations over the last twenty years have led to the values in Table 4 (Hodgson and Krantz, 1998). For the entire opencast a recharge value of 20 % is applied. Apart from the mining geometry, the other most important factor controlling water flow in a mine is the coal floor contours. As far as possible the provided peg data and mining height was used to generate a coal floor contour. Where gaps in the data exist, the coal floor was interpolated from exploration borehole information. The result is illustrated in **Figure 5**.

Table 4 Recharge values for opencast pits

Water source	Water into opencast [% rainfall]	Suggested average [% rainfall]
Rain onto ramps and voids	20 – 100	70
Rain onto not rehabilitated spoils	30 – 80	60
Rain run-off from levelled spoils	3 – 7	5
Rain seepage into levelled spoils	15 – 30	20
Rain run-off from rehabilitated spoils	5 – 15	10
Rain seepage into rehabilitated spoils	5 – 10	8
	[% of total pit water]	[% of total pit water]
Surface run-off from pit surroundings	5 – 15	6
Groundwater seepage	2 – 15	10

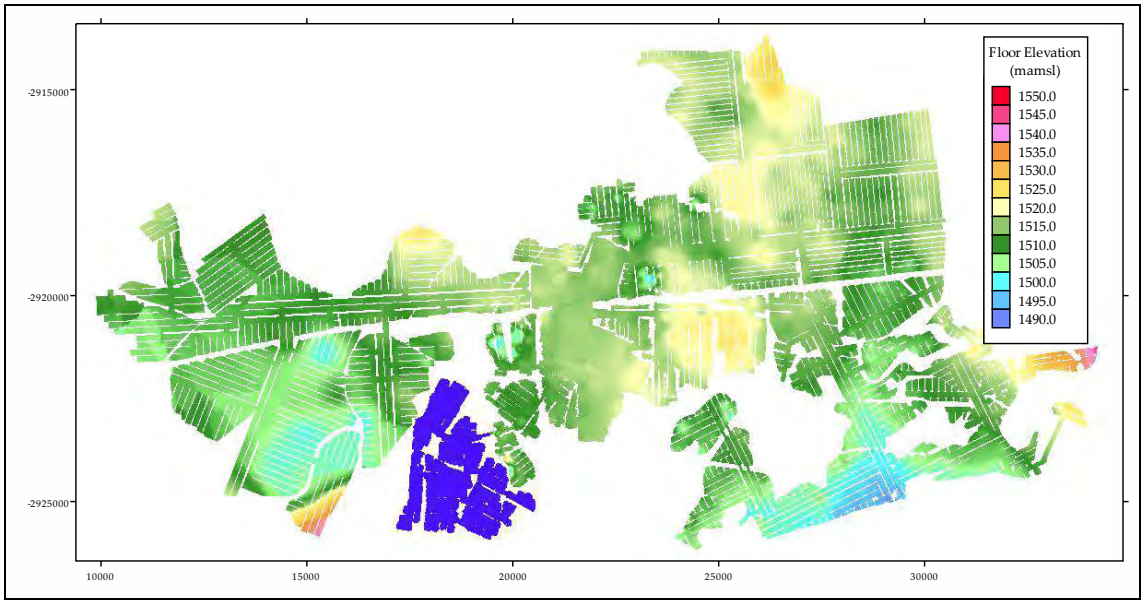

Figure 5 Coal floor contours for the current and future opencast and underground workings

Table 5 Recharge and time to fill values for each section

Section	Capacity Mℓ	Area ha	Rainfall m/a	Recharge %	Recharge Mℓ/a	Recharge m3/d	Time to fill years
UG-1	70 030	2 848	0.7	1.5	299	820	234
UG-2	73 840	3 000	0.7	1.5	315	863	234
UG-3 (Flooded)	0	534	0.7	1.5	0	0	0
UG-3	9 900	399	0.7	1.5	42	115	236
UG-4	80 280	3 173	0.7	1.5	333	912	241
OC @1550	53 196	780	0.7	20	1 092	2 992	49
TOTAL	**287 246**	**10 734**			**2 081**	**5 702**	

UG-3 is divided into a southern and northern part by the presence of a dolerite dyke. A downthrow of 10 m occurs on the southern part. The southern part has been flooded and does no longer partake in the water balance due to the fact that the artificial aquifer has changed from a water table to a confined aquifer.

The capacity of the opencast is calculated at the management elevation of 1 550.00 mamsl. As the opencast will recharge much faster than the connected underground, water will flow from the opencast into the underground sections. This will help the underground to fill up much faster and a total time of **139** years is calculated for the opencast and underground to be flooded to the management elevation of 1 550 mamsl. The management elevation is much higher than the highest points of the roof contours in each of the underground sections hence the underground will be flooded long before the whole system will start to decant. This also implies that when the water in the opencast is at its management elevation, water in the underground is under pressure and the water make in these sections will cease, resulting in a total water make, for the whole system, that is equal to the recharge of the opencast (1 092 Mℓ /a or 3 Mℓ /d).

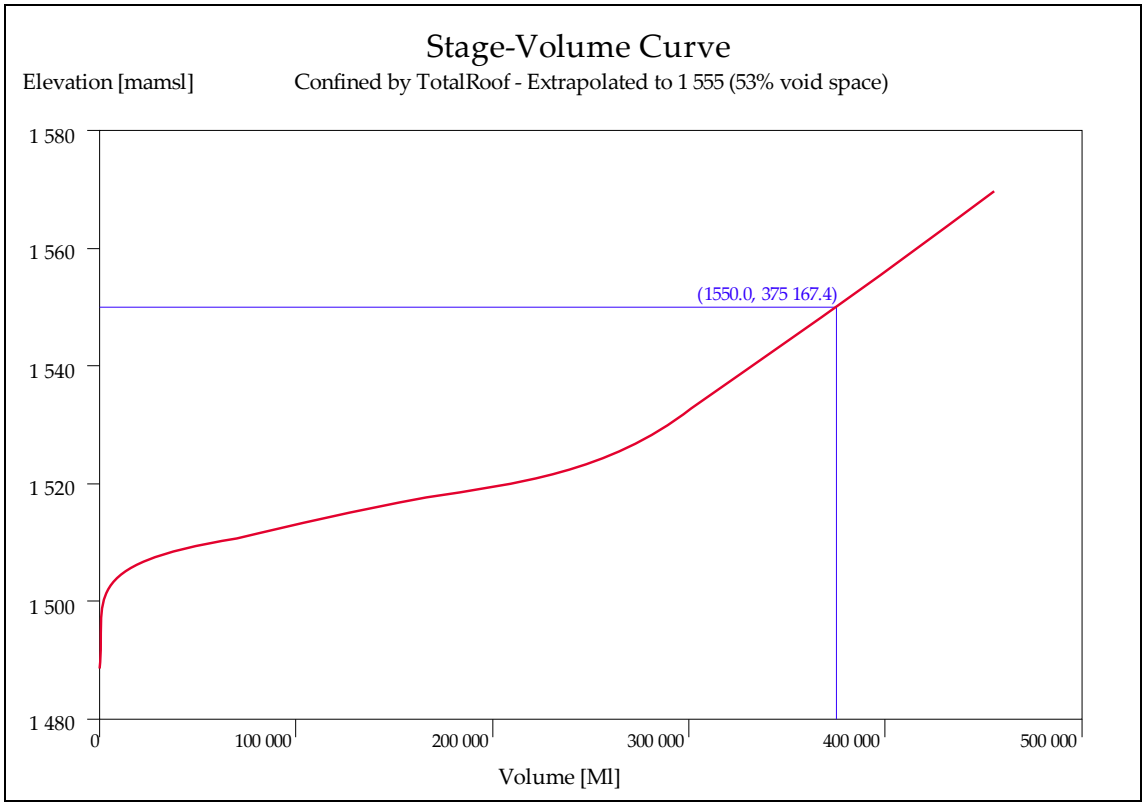

Figure 6 Stage-Volume curve for the combined opencast and underground workings

The recharge factor used in the calculations is the net gain of water in the pit. The gain of water is made up of the actual recharge minus evapotranspiration.

The colliery is situated in the quaternary Sub-Catchment A71H and has an annual evaporation of 1 550 mm (WRC Report: Surface Water Resources of South Africa, 1990).

To prevent future decant the complete water make of the opencast needs to be evaporated. A flooded area of 1 092 000 m^3 / 1.55 m = 70 ha is needed. This is above and beyond the existing final voids that have a combined wet footprint of 30 ha. A total flooded area (evaporation dams and final voids) of 100 ha is needed. Table 6 shows the flooded area on the surface of the rehabilitated opencast at different water level elevations together with the daily evaporation and the net recharge. The text at the decant elevation is in bold and the elevations above the

decant elevation are in red. Only at an elevation of 1 561 mamsl the flooded area is large enough to evaporate more than the water make, resulting in a negative recharge. (**Figure 7** & **Figure 8**)

Table 6 In-pit water level elevations with the size of the flooded areas

Elevation mamsl	Volume in Pit Ml	Flooded Area ha	Evaporating m³/d	Net Recharge m³/d
1 550	2 363	32.2	1 367	2 992
1 551	2 602	32.6	1 384	2 975
1 552	2 851	32.7	1 389	2 971
1 553	3 109	33.4	1 418	2 941
1 554	3 380	33.6	1 427	2 933
1 555	**3 689**	**34.8**	**1 478**	**2 882**
1 556	4 026	52.9	2 246	2 113
1 557	4 442	57.3	2 433	1 926
1 558	4 892	59.8	2 539	1 820
1 559	5 376	62.5	2 654	1 705
1 560	5 935	68.8	2 922	1 438
1 561	6 730	137.7	5 848	-1 488
1 562	7 823	153.4	6 514	-2 155
1 563	9 080	164.4	6 981	-2 622
1 564	10 476	173.6	7 372	-3 013
1 565	12 026	187.5	7 962	-3 603

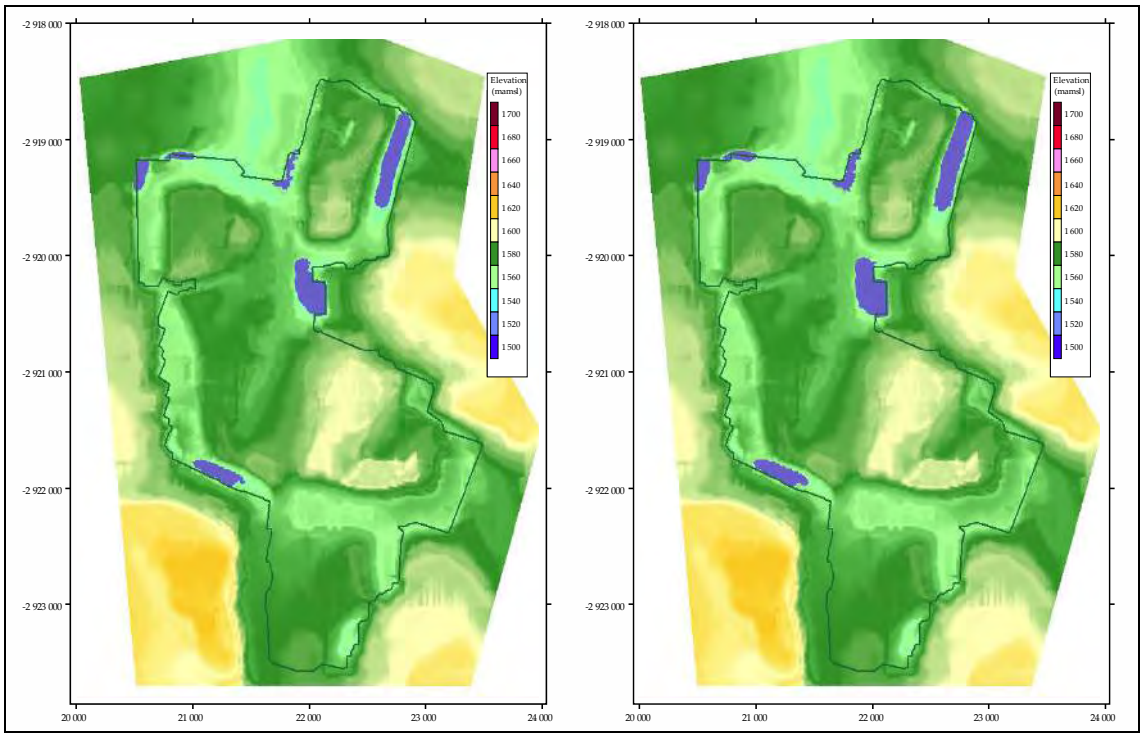

Figure 7 Flooded areas in the rehabilitated opencast - WL elevations at 1 550 & 1 555 mamsl

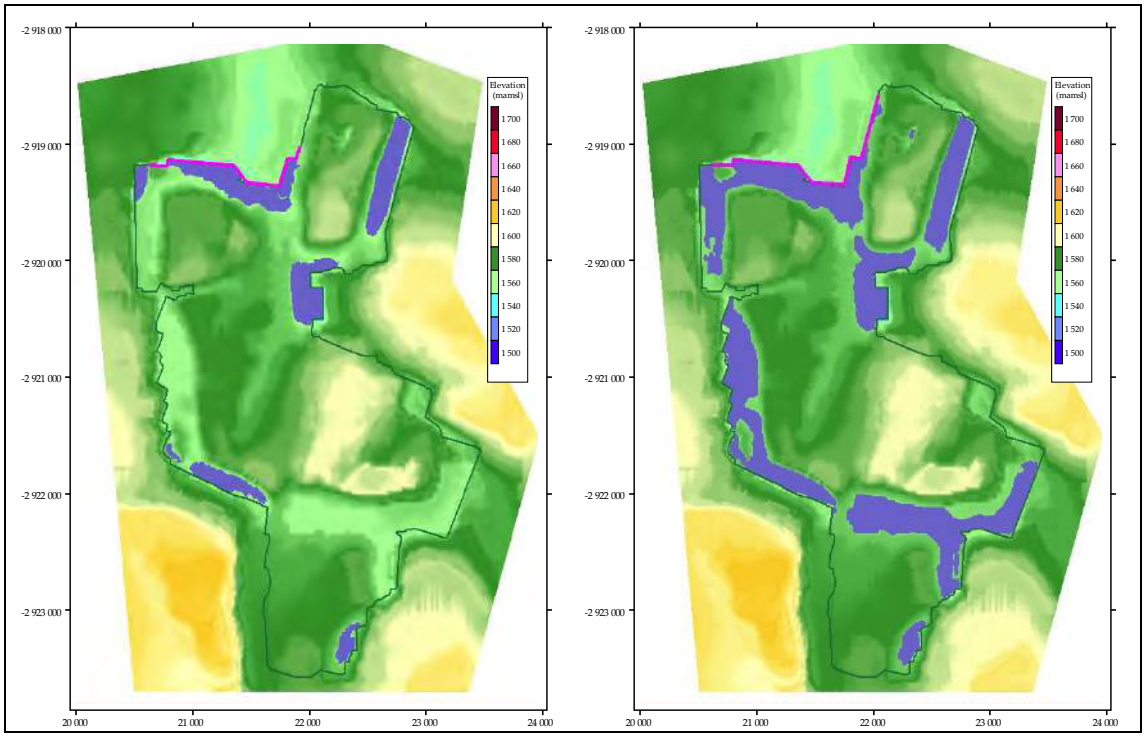

Figure 8 Flooded areas in the rehabilitated opencast - WL elevations at 1 560 & 1 565 mamsl

Sulfate generation

The remaining pillars in the underground as well as the spoils in the opencast will have a fair amount of pyrite. This in combination with the recharge water and oxygen will result in a sulfate generation that will continue until either the pyrite or the oxygen is depleted. The sulfate concentrations recorded during the last few years are erratic to say the least (**Figure 9**).

The expected long-term salinity of the opencast pit water can be calculated from the regional reaction rate within opencasts **7 kg/ha/d SO_4**. (Hodgson and Krantz, 1998). This rate appears to be fairly constant despite differences in degree of spoils saturation, age of spoils or regional impacts. It is therefore possible that the observed rates, as derived from flow and concentration calibration, reflect a maximum sulfate concentration with a consistent recharge. The maximum sulfate concentration is determined by the gypsum solubility (Usher, 2003). Hodgson has suggested that gypsum precipitation will play a role under low flow conditions (Hodgson, 2000). The sulfate generation in the underground is expected to be **1.2 kg/ha/d** (Vermeulen and Usher, 2006).

After mining has ceased the workings are allowed to be flooded. When the water level reach an elevation of 1 532 mamsl all the underground section, except for two little high parts in UG-2 and UG-4 will be flooded. The water volume will be 262 447 Mℓ and with a total recharge of 5.70 Mℓ/d (see Table 5) it will take 126 years to reach this stage.

The sulfate generated on a daily basis can be calculated:

For the opencast:	780 ha x 7 kg/ha/d	= 5 460 kg/d
For the underground:	9 420 ha x 1.2 kg/ha/d	= 11 304 kg/d
The average sulfate concentration:	16 764 kg/d ÷ 5 700 m^3/d	= 2.94 kg/m^3 (g/ℓ)

The opencast will continue to recharge with a 1092 Mℓ/d (see Table 5) with an expected sulfate concentration of: 5 460 kg/d ÷ 2 992 m^3/d = 1.82 kg/m^3 (g/ℓ)

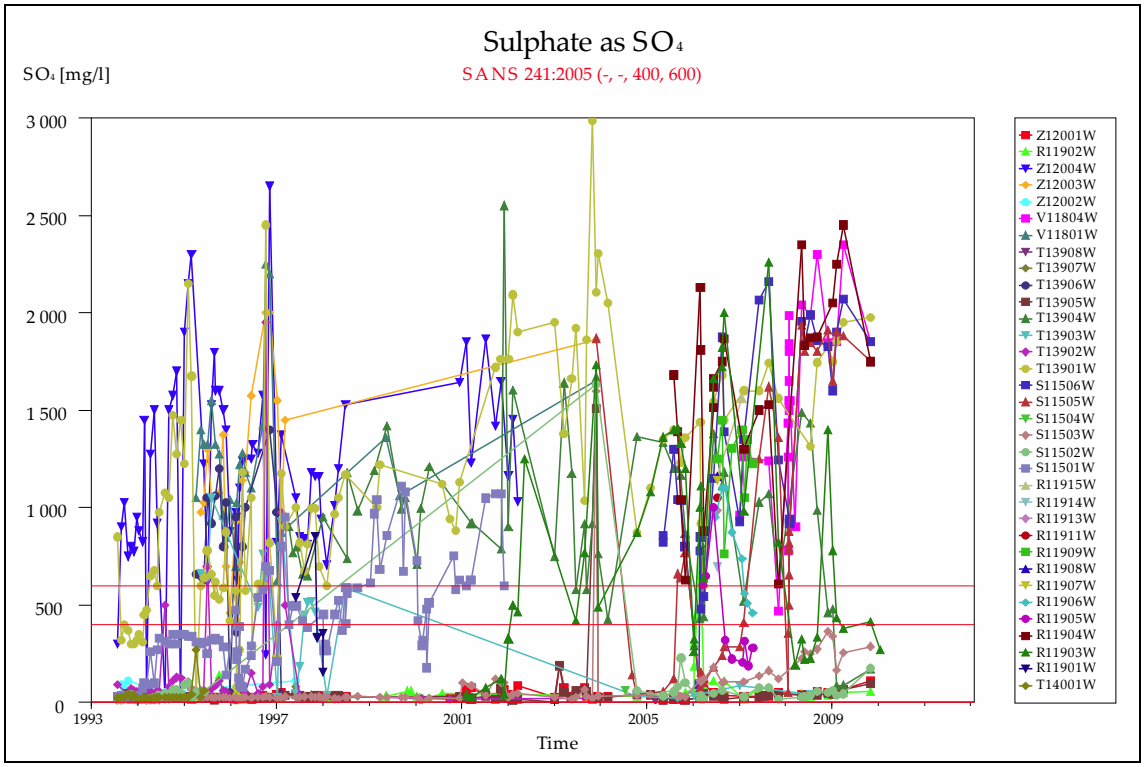

Figure 9 Recorded sulfate concentration at the colliery

CONCLUSION & RECOMMENDATIONS

To evaporate the excess water in the boundary of the opencast, three options may be considered:

1. Lower the current rehabilitated surface of the opencast, or at least some parts thereof in such a way that the flooded area at management level (1 550 mamsl) is 100 ha in size.
2. Raise the decant height to an elevation of 1 565 mamsl, a berm needs to be constructed at the northern part of the opencast allowing the water level to rise to 1 561 mamsl without the possibility of decanting. The berm needed will have to be 2.1 km long and 10 m high at places.

3. 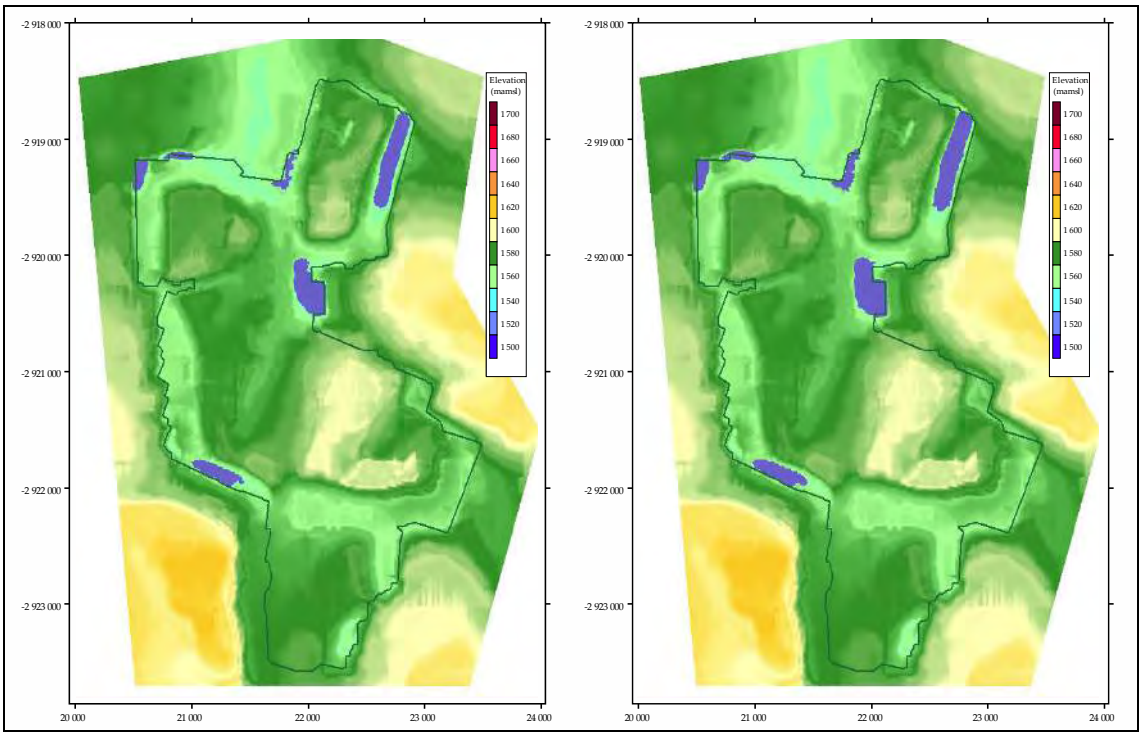

4. **Figure 7** rightmost picture shows the partly flooded surface of the opencast pit with the position of the dyke displayed in magenta.
5. A combination of the above options.

REFERENCES

Hodgson FDI and Krantz RM (1998). Groundwater quality deterioration in the Olifants river catchment above the Loskop Dam with specialized investigation in the Witbank Dam sub-catchment. WRC Report No: 291/1/95.

Hodgson FDI and Grobbelaar R (2000). Water and salt balance for Minnaar Colliery. Confidential Report to Ingwe S.A.

Midgley DC, Pitman WV and Middleton BJ (1994). Surface water resources of South Africa 1990. Book of Maps Volume II. WRC Report No: 298/2.2/94.

Usher BH (2003). The evaluation and development of hydrochemical prediction techniques for long-term water chemistry in South African coalmines. Unpublished PhD thesis. University of the Free State, South Africa.

Vermeulen PD (2003). Investigation of the water decant from underground collieries in Mpumalanga. Unpublished MSc thesis. University of the Free State, South Africa.

Vermeulen PD and Usher BH (2006). Sulphate generation in South African underground and opencast collieries - Environmental Geology. ISSN: 0943-0105 (Paper) 1432-0495 (Online)

Response to Increasing Rainfall and High Rainfall Events at Wheal Jane, Cornwall, UK

Lee Wyatt, Arabella Moorhouse and Ian Watson
Environment Department, The Coal Authority, United Kingdom

ABSTRACT

After the closure of Wheal Jane mine in 1991, and the associated mine water rebound, highly contaminated acidic mine water overflowed from the mine and discharged at surface. This caused a major pollution incident affecting the Fal Estuary and resulted in emergency pumping being undertaken at Wheal Jane to prevent re-occurrence. Investigations by the Environment Agency into future options, resulted in the treatment plant being constructed, becoming operational in 2000.

Management of the Wheal Jane plant was transferred to the Coal Authority in 2011 as a result of its expertise in managing coal mine waters. Prior to 2011, the primary objective focused on operating and maintaining the plant in order to comply with the permitted discharge limits; with limited emphasis placed on other factors such as regional context. The approach undertaken by the Authority is to maintain compliance with the permit, whilst endeavoring to make efficiency savings. Part of this strategy includes the assessment of treatment methodology, the regional context and long-term water management.

Two high rainfall events have occurred since 2011, which have necessitated the requirement for additional emergency pumping; thus stressing the treatment plant. These events, although atypical, are part of an on-going trend of increased pumping requirements to control water levels, particularly during winter months. It is unclear if climate change causes these observed changes. To aid management and understanding of these events and identify any trends, the Authority has undertaken assessments of rainfall, water levels, abstraction rates and hydrochemistry. The results show variable time delays in response to rainfall, changes in key metal parameters, and different regional trends in groundwater levels. These results indicate that a number of different pathways for water entering Wheal Jane are present. A dynamic strategy is therefore required, to manage any future high rainfall events or increases in annual rainfall.

Keywords: mine water, treatment, operation, rainfall, metal mine

INTRODUCTION AND HISTORY

Wheal Jane mine is located within a complex of interconnected mines in Cornwall, southwest England (Figure 1) and is a former tin mine (that also includes other ores for copper and zinc), which was worked from at least the early 18th Century until 1991, when the mine was abandoned. After the mine closed, de-watering pumping ceased and the water levels rose in the workings. Contingency plans were implemented to control the foreseen rises in contaminated mine water, which could result in a pollution incident. Despite this however, in January 1992, the plan was suspended, which resulted in a build-up of mine water underground (Hamilton, 1993). Consequently, in the same month the contaminated mine water started discharging at surface, releasing approximately 40 000 m^3 of water in to the River Carnon (a tributary of the River Fal) over a few hours with an iron concentration of 1 800 mg/L (Hamilton, 1993).

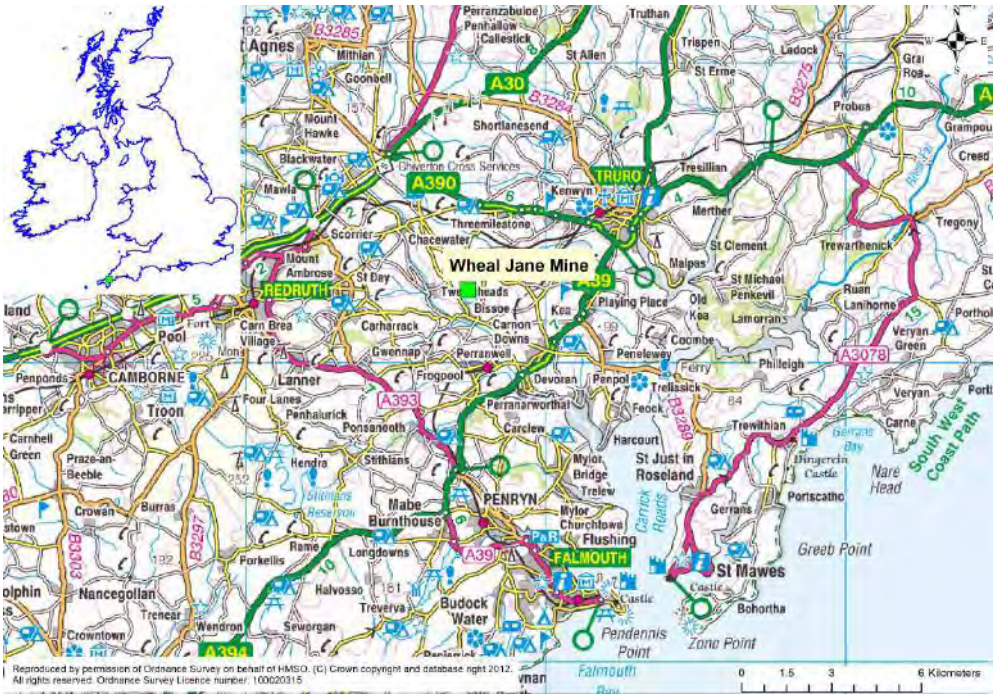

Figure 1 Location map for Wheal Jane mine and surrounding area

In the subsequent years, options for remediation of the mine water were considered, with a pilot passive treatment scheme being built in 1994, to undertake research in to long-term solutions. In 2000, the existing active (chemical treatment) plant was constructed and became operational. This plant remediates water pumped from Wheal Jane No.2 Shaft, using a high-density sludge approach, including aeration, pH adjustment (by lime dosing) and a clarifying (including polymer dosing) unit (Coulton *et al.*, 2003). Scheme capacity was originally designed for a flow of 440 L/s (Brown, Barley & Wood, 2000) with an environmental discharge consent of 350 L/s; this was later revised to the current discharge rate of 460 L/s. It should be noted that the discharge from the plant also includes a minor flow (*c.* 20 L/s) originating from the drain of the tailings lagoon.

GEOLOGY

Southwest England is dominated by late Carboniferous to early Permian Cornubian Granites, which intruded into predominantly Devonian-aged strata dominated by mudstones and siltstones, with occasional coarser-grained horizons; (Dines, 1956). A variety of different metal ores are found within the Cornish orefields including ores for tin, copper, lead, zinc and iron. These orebodies are typically zoned, following the order in which the minerals precipitated out of solution with increasing distance from the igneous intrusions. Typically tin-ores were the first to form, followed by copper-ore, zinc-ore, lead-ore and finally iron-rich minerals (Dines, 1956). At Wheal Jane the main mineralized lodes (or veins) occur in a ENE-WSW direction and recorded 19th Century returns are documented for tin, copper, lead, silver and zinc, with significant amounts of pyrite combined with smaller quantities of arsenic, ochre and iron-ore also being noted (Dines, 1956). These records suggest that a mineral assemblage containing ores such as cassiterite (tin-ore), chalcopyrite (copper-ore), arsenopyrite (source of arsenic contamination), sphalerite (zinc-ore), galena (lead-ore and also the source of silver) and pyrite (source of sulfur) are found at Wheal Jane. Assuming the ore deposit mined at Wheal Jane follows a similar zoning pattern to that found in other areas of the region, the cassiterite and chalcopyrite-rich sections of the mine will be concentrated in the deeper workings (i.e. nearer the emanative center, (Dines, 1956)), with the sphalerite-galena dominated assemblage situated in the shallower regions. Returns of ochre and iron-ore (situated in weathered gossans) (Dines, 1956), suggest that the ore body at Wheal Jane also contains a significant amount of pyrite. It is this mix of sulfide minerals which produces the acid mine drainage that occurs at Wheal Jane mine.

MINING CONTEXT

Wheal Jane Mine is located toward the southeast extent of a mining block including a series of interconnected abandoned mines, mine workings and drainage adits. Wheal Jane mine and its workings are connected to a number of other mines at depth and to at least three shallow drainage adits (Figure 2); including Janes Adit, Nangiles Adit and County Adit (or Great County Adit). The extent to which the river and streams in the area flow over shallow mine workings (lodes) and drainage adits, suggest that surface water ingress into the mine workings is common; in the catchment, this has been estimated at approximately 270 L/s (Wyatt *et al.*, 2013).

HIGH RAINFALL SETTING

In the southwest of England, the prevailing wind direction is from the southwest, resulting in Atlantic storms frequently buffeting the region, particularly over the autumn and winter months; although severe weather events can occur at any time of year. Some of these storm events can be localized in nature, being restricted to smaller individual catchment areas. For the purposes of this paper, rainfall data for the Wheal Jane area have been obtained from a number of locations within the catchment, spanning a variety of time periods.

Background rainfall

To undertake assessments of recent rainfall figures against the long-term background trends for the southwest of England, data from the rainfall gauge at Camborne (situated 14 km west of Wheal Jane Mine) was used to provide information commencing from 1979 to the present (Met Office,

2014). In addition to the rainfall gauge at Camborne, a separate gauge was installed in 2004 at Wheal Jane. A summary of these data are shown in Table 1.

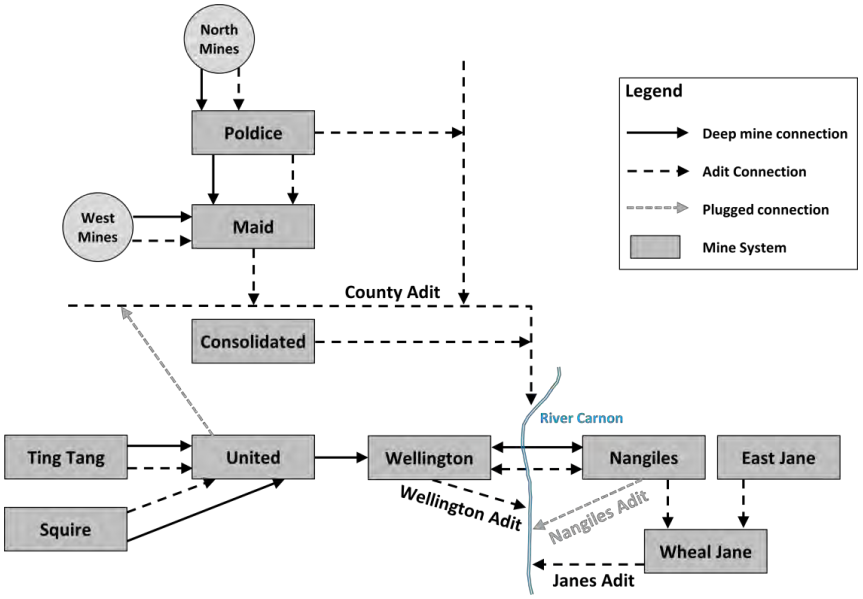

Figure 2 Conceptual diagram for Wheal Jane mine and connected mine (after Wyatt *et al.*, 2013)

Unprecedented high rainfall event in the UK

The time period between October 2013 and February 2014 resulted in exceptionally high rainfall throughout the UK, with the winter of 2014 (December 2013 to February 2014) being the wettest recorded (since 1766) in England and Wales (CEH, 2014a). Rainfall was especially high during the winter in southwest England with all months from December 2013 to February 2014 having higher than average rainfall. In December 2013, rainfall in the southwest of England was over 25% higher than the monthly average (CEH, 2013); in January 2014, the total rainfall was 63% (nearly two-thirds) higher than the monthly average (CEH, 2014b), whereas in February, double the monthly rainfall fell over the course of the month (CEH, 2014a).

Table 1 Summary table of rainfall for Camborne (C) and Wheal Jane (WJ) rainfall gauges (winter rainfall is 1st December to 28th February data)

Data set	Mean (mm)	Maximum (mm)	Period of Max Rainfall
C monthly rainfall 1979 to 2010	89	242	November 2002
C monthly rainfall 2010 to 2014	85	218	January 2014
WJ monthly rainfall 2004 to 2010	102	321	October 2005
WJ monthly rainfall 2010 to 2014	126	347	February 2014
C winter rainfall 1978 to 2010	348	561	1989/1990
C winter rainfall 2010 to 2014	345	584	2013/2014
WJ winter rainfall 2004 to 2010	305	501	2006/2007
WJ winter rainfall 2010 to 2014	467	876	February 2014

For the purpose of investigating the high rainfall events at Wheal Jane, comparisons of winter rainfall (*i.e.* 1st December to 28th February) have been assessed for both Camborne and Wheal Jane (see Table 1). Table 1 shows that the winter rainfall between 2010 and 2014, is higher than for the previous years; the winter of 2014 saw the highest volume of rainfall at Wheal Jane recorded. Furthermore, the weather patterns and uneven distribution of rainfall in the southwest of England (*i.e.* storm events) during this time period also resulted in the winter 2014 rainfall being significantly higher at Wheal Jane compared to that recorded at Camborne for the same time period (*i.e.* 876 mm at Wheal Jane compared to 584 mm at Camborne).

RESULTS

To manage the treatment plant effectively at Wheal Jane, regular measurements of water level, abstraction rates and chemical analysis are collated at Wheal Jane mine site; more recently regional monitoring of water levels around Wheal Jane has also been undertaken. The results from this wider monitoring program, in conjunction with rainfall and river stage data, have been used to analyze the Wheal Jane mine system and its surrounding environment.

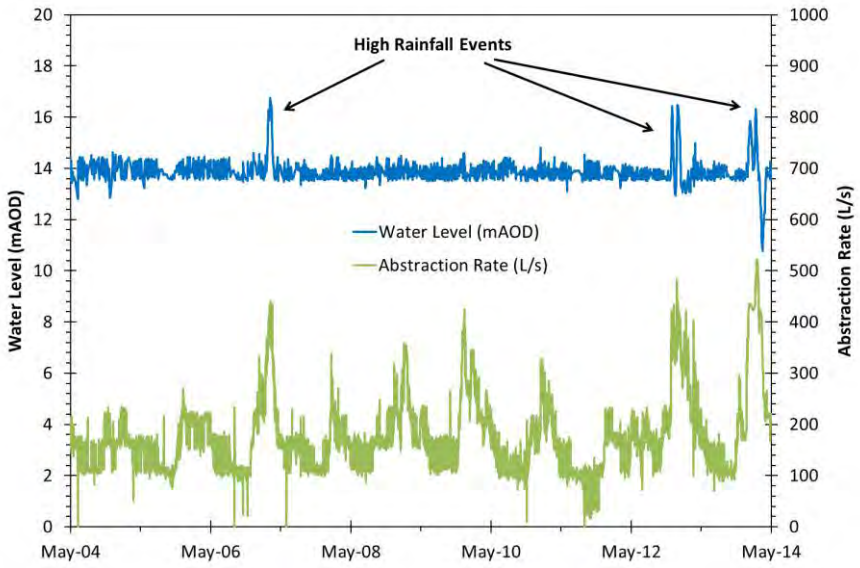

Figure 3 Plot of water level and abstraction rate at Wheal Jane

Water levels, abstraction rates and rainfall

Mine water levels have been measured on a daily basis concurrently with abstraction rates since the treatment plant became operational in 2000. A reasonably good correlation can be made between the data from the pumping shaft at Wheal Jane and the level of mine water in the shaft. Since 2011, datalogging systems have provided water level and pumping data at regular 15 minute intervals.

Results from the water level and abstraction rate data (Figure 3) show that under normal conditions, the pumping rate at Wheal Jane can be altered to maintain the water below an upper control level (i.e. 14.5 m above Ordnance Datum (AOD)); although on occasions the amount of

water in the mine workings is too great for the pumps; hence there are peaks in water level. Since 2004, the volume pumped and the number of pumps installed has increased; the pumping rate has increased from c. 300 L/s (six pumps) to the current position of c. 400 L/s (eight pumps), with an additional two emergency pumps (additional c. 100 L/s) kept on standby. Since 2004, when the current control bands were implemented, there have been three instances where pumping has been insufficient to control the water level within this designated operational band due to high rainfall events.

Chemistry

Routine daily measurements of key parameters are taken of the pumped mine water and treated effluent. Throughout some of the high-rainfall / high-water level events there have been some changes in the mine water quality observed. The results of selected parameters are summarized in Table 2. Figure 4 shows selected mine water chemistry data against water level since 2004. The chemistry data for the pumped mine water shows a trend of decreasing concentrations for some of the parameters over time; this is part of the 'first-flush' trend which has been on-going since 1991 (Wyatt *et al*., 2013).

Iron, calcium, sulfate and arsenic

Figure 4 shows that prior to 2007, the variation in the iron concentration over any 12 month period was greater compared to the differences demonstrated post 2007, as concentrations of iron have decreased over time. The trends for arsenic and sulfate (not displayed on Figure 4) follow the same pattern as iron, as do the seasonal variations shown by the calcium concentrations. Figure 4 shows that there is a reduction in concentration of iron and calcium during high rainfall events, which is echoed by reductions in concentrations of sulfate and arsenic (Table 2).

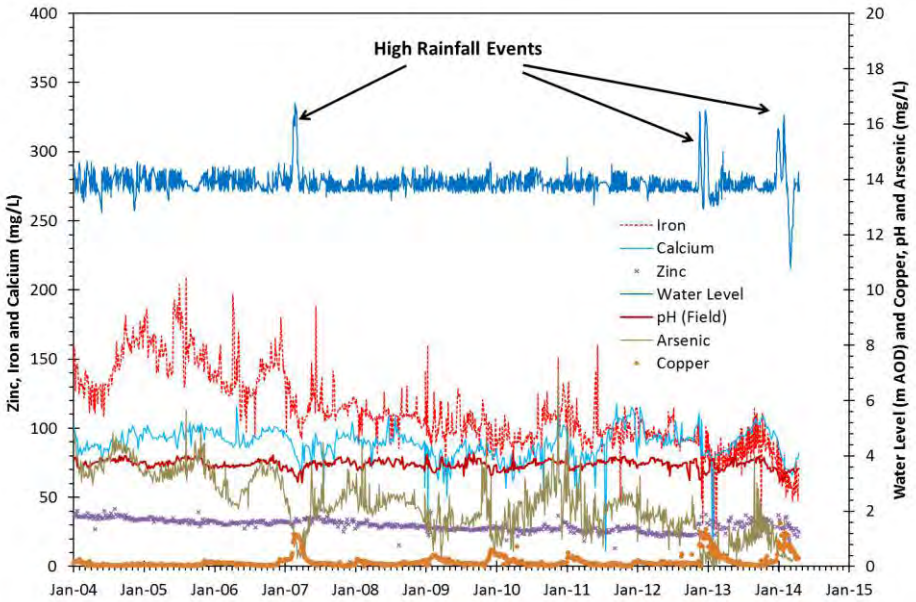

Figure 4 Plot of water level and selected chemistry parameters for the pumped water at Wheal Jane

Copper, pH and cadmium

Copper, pH and cadmium all show similar trends with respect to high rainfall and seasonal variations; with higher concentrations (decrease in pH) corresponding with high water levels and winter periods. However, the high water level peaks in cadmium are not as pronounced as copper.

Zinc, aluminum, manganese and nickel

Trends in zinc, aluminum, manganese and nickel concentrations do not appear to show any direct correlation with high rainfall or high water level events, and variations in concentrations throughout a season or during these events is very minimal or not present.

Table 2 Summary table of selected chemistry data for peak of each event and typical winter values

Parameter	Typical winter	2007 event	2012/2013 event	2014 event
Iron (Fe)	107 mg/L	118 mg/L	76 mg/L	70 mg/L
Zinc (Zn)	28 mg/L	32 mg/L	30 mg/L	31 mg/L
Sulfate (SO_4) *	624 mg/L / 457 mg/L	499 mg/L	401 mg/L	357 mg/L
Aluminum (Al)	10.6 mg/L	12.1 mg/L	9.6 mg/L	8.7 mg/L
Manganese (Mn)	3.7 mg/L	3.5 mg/L	3.3 mg/L	3.0 mg/L
Calcium (Ca)	91 mg/L	82 mg/L	87 mg/L	82 mg/L
Copper (Cu)	135 µg/L	1 044 µg/L	1 026 µg/L	863 µg/L
Nickel (Ni)	249 µg/L	267 µg/L	169 µg/L	177 µg/L
Cadmium (Cd)	15 µg/L	33 µg/L	41 µg/L	26 µg/L
Arsenic (As)	2,155 µg/L	932 µg/L	283 µg/L	443 µg/L
pH (in-situ)	3.7	3.3	3.3	3.2

* typical sulfate winter values are pre / post 2007 concentrations

DATA ANALYSIS

Analysis of the results presented above indicate a number of patterns and trends, these may represent different scenarios of the mine system during high rainfall events and high water levels.

Analysis of the rainfall data against water level (Figure 5) show that although the high water levels do correspond with high monthly rainfall, there are similar high monthly rainfall periods, which have not resulted in elevated water level. However, based on a seven day cumulative total rainfall (Figure 5) the peaks in water level do correspond more closely with the highest rainfall peaks (*e.g.* 5th to 6th February 2014). More detailed analysis of the rainfall data and water level data indicates that there is often a delay in response to rainfall, with the water level peaking approximately five to 10 days after a high rainfall event; although towards the end of the 2014 extreme event, this delay was only a few hours.

These data show that the Wheal Jane system is sensitive to rainfall; although the differences in water level responses suggest that there may be a variety of situations which affect the water flow paths and / or the residence of water in the mine workings. Given the complexity between the underground mine workings, available storage, rainfall volume, extent of saturated strata, surface conditions, river water levels and possible connections between surface and near-surface water to

the mine workings; the exact reasons for the different responses is complex and poorly understood. However, during the extreme rainfall event in 2014, which included a prolonged period of high rainfall, it could be seen that under fully saturated conditions, any rainfall impacted Wheal Jane almost instantaneously. Furthermore, evidence from previous high rainfall events indicate that as the ground becomes more saturated, the response time between rainfall and water make (*i.e.* water level and abstraction rate) generally becomes less.

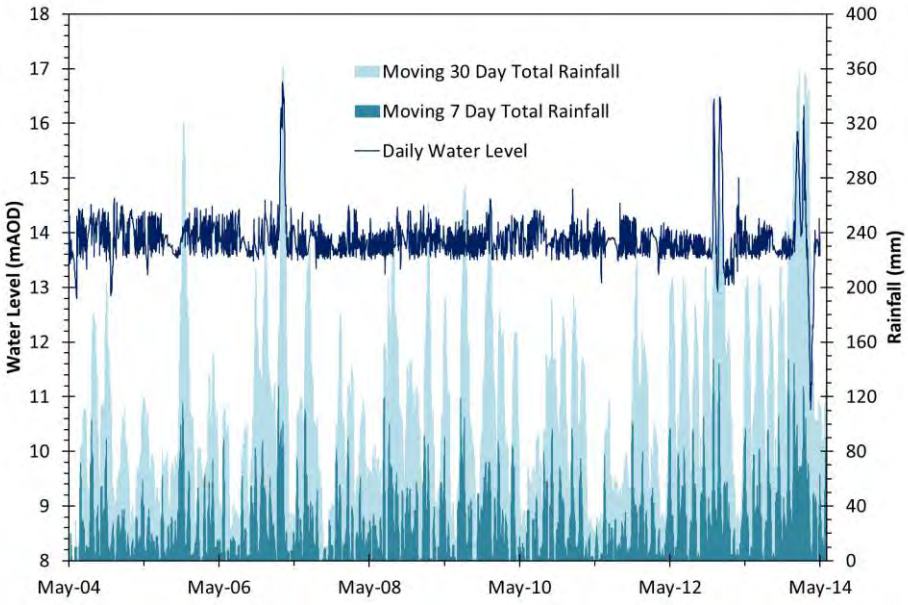

Figure 5 Plot of water level and rainfall as 30 day moving total

Chemistry

Throughout high rainfall events and high water level scenarios, there are changes in the mine water chemistry. Concentrations of some key metals and other parameters rise (*i.e.* Cu and Cd), some fall (*i.e.* As, Ca, SO_4, pH and Fe), whilst others remain steady (*i.e.* Ni, Zn, Al and Mn). These patterns in chemistry, although complex, suggest a different source of water during periods of high water level. Increases in certain metals, indicate that this water may not be all 'clean' shallow groundwater or surface water; moreover the results imply that water is passing through shallower mine workings (which are usually dry). However, from the geology and mineralization of the area, the copper ore (chalcopyrite) is often present in deeper workings, whereas the zinc ore (sphalerite) is commonly found in shallower workings; this trend is the opposite of those observed in the high water level scenarios. A possible explanation for this would be that secondary mineralization rich in Cu and Cd, potentially found in usually dry mine workings, tailing ponds and ore processing waste areas contribute a larger proportion of flow to the mine workings during these 'wet' periods.

To assess which mineral phases are saturated under normal and high flow conditions, the geochemical model PHREEQCi has been used. During normal flow conditions, iron and aluminum-rich phases such as gibbsite (SI=0.34), goethite (SI=1.82), alunite (SI=4.66) and hematite (SI=5.65) are supersaturated. In contrast, during high flow conditions the mineral phases are all under-saturated. This geochemical difference necessitates an increased level of treatment during high flow

conditions; i.e. extra alkali dosing to counter a lower initial pH. This increased operational demand is exacerbated by the increased flows occurring concurrently with worse water quality.

OPERATIONAL MANAGEMENT

At Wheal Jane, the primary purpose of the pumping and treatment is to prevent uncontrolled discharges of polluted mine water. Typically this is achieved through altering the pumping rate to maintain the water level within a control band (*i.e.* 13.5 mAOD to 14.5 mAOD). However, since the CA was awarded the management of Wheal Jane in 2011, key drivers have been to make efficiency savings whilst investigating alternative operational strategies (Wyatt *et al*., 2013).

The two most recent events have resulted in additional emergency pumping being required to prevent outbreak of mine water to the river; the latest event being in 2014 also resulted in the requirement to purchase additional pumps. However, this method of using emergency pumps (provided by the fire service) resulted in undesirable increases to the costs of managing Wheal Jane. These high rainfall events, in conjunction with the current conceptual model of the mining hydrogeology system, has led to some changes and recommended alterations to the management of Wheal Jane, especially during high rainfall / high water level events, which include:

- Purchase of additional pumps (in 2013) plus emergency pump and second back-up pump (in 2014) to give a total pumping capacity of *c.* 550 L/s; some 150 L/s greater than the rate in 2012.
- Drawdown test undertaken to assess the possibility of lowering the water level and acquire additional storage capacity in the mine workings ahead of predicted high rainfall events. This test also allowed assessments of any chemistry changes to be understood and specifically to confirm any improvements in water quality.
- Analysis of Wheal Jane mining and hydrogeological context to assess the impacts from pumping and to assess the influence on the surrounding environment on Wheal Jane. Required to confirm if changing the pumping control level will impact the surrounding area.
- Development of a high water level management strategy, including determination of any thresholds and triggers to develop a simple pragmatic system to manage the water level.

Investigation in to utilizing a controlled overflow (*i.e.* via Janes Adit) during high rainfall events; anticipated to be <50 L/s for <1 % of the time.

High water level management

A simple pragmatic system to manage the proposed water level is summarized below:

- Use up to six pumps to hold water level below 14.5 mAOD in normal conditions
- If water level rises, use all available pumps to lower water level to 11 mAOD
- Pump sufficient quantities of water to hold the level between 11 mAOD and 11.5 mAOD
- Continue to hold the water level at this band until only four pumps are required

Based on historical pumping data, this trigger level approach described above would only be implemented for up to 5 % of the time. Hence, such a trigger approach should not result in unwarranted extra pumping costs for an unacceptable number of false alarms.

SUMMARY AND CONCLUSIONS

Following work and investigations undertaken by the CA since 2011 in to various hydrogeological features of the Wheal Jane system, a variety of aspects have been observed, which include:

- Relatively quick response at Wheal Jane to high rainfall events suggests inputs from shallow groundwater and / or surface water. Thus, likely implying direct mining connections to the shallow drainage systems (*i.e.* County Adit) or to the surface (*i.e*. open stope workings)
- A quick response to rainfall suggests little available storage within the Wheal Jane mine system; especially in winter months when the ground storage is lower. To prevent risks of uncontrolled discharges to surface during high rainfall events, a lower water level could be maintained in drier periods for a lesser costs than at certain times in the winter
- High rainfall events which have high water levels, lead to a different hydrochemistry of the pumped mine water. This could reflect the influence of shallow water inputs, and / or different mineralogy in shallower mine workings
- A different approach in the management of high water levels could be implemented to create additional storage ahead of anticipated wet periods, this could also significantly reduce or remove the need for costly emergency pumping

The option of a controlled overflow reduces the current risks, however further investigations regarding flow and chemistry are required. In the medium to long-term and based on natural improvements to hydrochemistry of the mine water, this option (possibly with passive treatment) would be highly beneficial

REFERENCES

Brown, M, Barley, B and Wood, H (2002) Minewater Treatment Technology, Application and Policy, IWA Publishing, Dorchester, UK, pp 453.

CEH (2013) Hydrological summary for the United Kingdom, December 2013. Website http://www.ceh.ac.uk/data/nrfa/nhmp/hs/pdf/HS_201312.pdf Last accessed 18 September 2014

CEH (2014a) Hydrological summary for the United Kingdom, February 2014. Website http://www.ceh.ac.uk/data/nrfa/nhmp/hs/pdf/HS_201312.pdf Last accessed 18 September 2014

CEH (2014b) Hydrological summary for the United Kingdom, January 2014. Website http://www.ceh.ac.uk/data/nrfa/nhmp/hs/pdf/HS_201312.pdf Last accessed 18 September 2014

Coulton, R, Bullen, C, Dolan, J, Hallet, C, Wright, J and Marsden, C (2003) Wheal Jane tin mine, Cornwall: important construction and operation Land Contamination & Reclamation, 11(2), pp. 245 ¬252

Dines, H.G. (1956) The metalliferous mining region of South-West England, Economic Memoir of the Geological survey of Great Britain, British Geological Survey, Nottingham, pp 795.

Hamilton, R (1993) The impact of discharges from Wheal Jane and abandoned tin mine on environmental water quality in south west England, Proceedings of 1st SETAC World Congress, Lisbon, Portugal, pp. 213 ¬220.

Met Office (2014) website http://www.metoffice.gov.uk/pub/data/weather/uk/climate/stationdata/camborne data.txt Last accessed 18 September 2014

Wyatt, LM, Watson, IA, Kershaw, S and Moorhouse, AML (2013) An adaptable and dynamic management strategy for the treatment of polluted mine water from abandoned Wheal Jane Mine, Cornwall, UK, In Mine Closure 2013: Proceedings of the Eighth International Conference on Mine Closure 18–20 September 2013, Cornwall, England, Tibbett, M, Fourie, AB and Digby, C, (Eds), Australian Centre for Geomechanics, Nedlands, pp. 69 ¬78.

Simulation of Hydrological Processes in the Dump Slope of a Mining Pit for Landslide Forecasting

Jinxing Guo[1], René Blankenburg[2] and Peter-Wolfgang Graeber[1]

1. *Institute of Waste management and Contaminated Site Treatment, Technical University of Dresden, Germany*
2. *Ingenieurbuero fur Grundwasser - IBGW® Leipzig, Germany*

ABSTRACT

Dump slope in the open-cast mining pit is always a safety issue, as it can experience catastrophic destruction due to the slope failure caused by various factors, such as atmospheric conditions (especially precipitation), vegetation and so on. The precipitation has direct influence on the water content change with the infiltration water into the unsaturated slope especially during the heavy rainfall event. The significant effects of vegetation on the slope stability can be essentially contribute to two major aspects, water movement via the soil-plant-atmosphere continuum and soil reinforcement by the root system. The aim of this study is to investigate the hydrological regime in the dump slopes and the influence of the saturation degree on the stability of dump slopes under the consideration of precipitation and vegetation with the program PCSiWaPro® (by Technical University of Dresden).

Physical model tests of a sand slope at TU Dresden showed that it was the partial saturated condition that had already caused mechanical instabilities. Using the simulation program PCSiWaPro®, the distribution of the water saturation in the partial saturated slope area under transient boundary conditions can be simulated. It is based on solving the RICHARD's Equation in two spatial dimensions using the finite element method. The integration of a weather generator into PCSiWaPro® allows a transient flow calculation with respect to atmospheric conditions (precipitation, evaporation, daily mean temperature and sunshine duration) and removal of water by plant roots and leaves. With PCSiWaPro® a case study in an open-cast mining pit in Saxony (Germany) has been carried out to simulate the hydrological process in the dump slope especially for the unsaturated zone; then with the simulation results, the stability analysis models could be applied to verify how detailed water content and vegetation influence the stability of the dump slope.

Keywords: dump slope, water content, saturation, stability analysis,

INTRODUCTION

This study area locates between Leipzig and Bitterfeld with the City of Delitzsch in the center which has been shaped by the lignite mining activities for more than one century. Mining activities are always essential for the production of necessary minerals and then for the development of the modern society. However they also bring us lots of serious environmental and ecological problems, among which the dump slope landslide in the mining pit is one of the main concerns. Constantly appearing causes have a great weight on the issue of slope stability, like the heavy rainfall event and the change of the ground water level.

Surface erosion (surface runoff) and increase of water saturation in the dump slope body are the main causes of instability risk (Bonelli, 2013). There was an early assumption that the landslides and suffusion phenomenon can arise only in the fully saturated soil areas on the air side; however AIGNER (2004) indicated from a physical experiment (shown in Figure 1) that this can occur even in the partially saturated soil area of the slope. The surface erosion is relatively easy to be detected and avoided, while the soil moisture increase risk cannot be easily identified. Therefore, these geological structures are more sensitive and dangerous due to the flow from the ground water and rainfall water infiltration into the unsaturated zones (Bonelli, 2013).

Figure 1 A physical model slope with slides on the air side (Aigner, 2004)

In those unsaturated slope areas, various factors could influence the water balance and then the stability, for example, soil materials, geometry, atmospheric conditions (e.g. precipitation), and even vegetation (Tien H. Wu, 2013) (see Figure 2). The precipitation has direct influence on the water content change with the infiltration water into the unsaturated slope and then changes groundwater movement regime (especially in an extreme rainfall event). The significant influence of vegetation on slope stability can essentially be attributed to two major aspects: water movement via the soil–plant–atmosphere continuum (SPAC) (Coppin, Barker & Richards, 1990) and soil reinforcement by the root system (Gray, 1995). Vegetation is a major component of SPAC, responsible for the suction force of water against gravity. The absorbed soil water will subsequently be removed through the transpiration process into the atmosphere. Ultimately, this water cycle system would result in less saturated and more stable slopes. Concurrently, vegetation also contributes to mass stability by increasing the soil shear strength through root reinforcement (Gray, 1995). The frequency of slope failures tends to increase when vegetation is cut down and their roots decay (Abe, 1997).

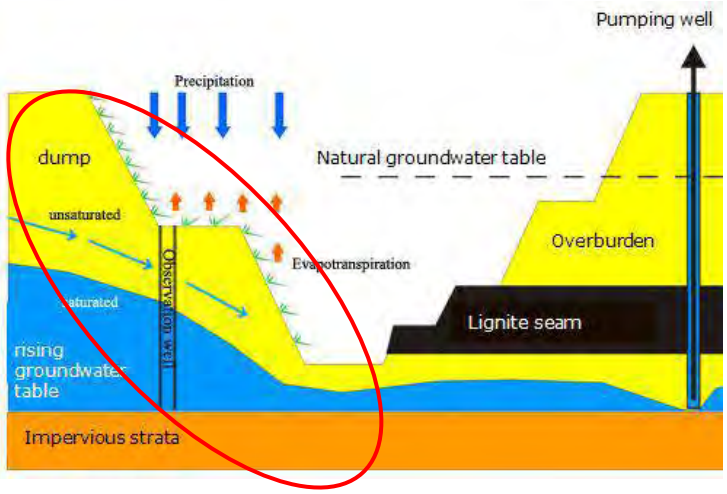

Figure 2 A simplified structure of the dump site

HYDROLOGICAL PROCESS SIMULATION PROGRAM

The hydrological process could be simulated by the Program PCSiWaPro® (developed at the Technical University Dresden, Institute of Waste Management and Contaminated Site Treatment) which could describe the distribution of water saturation under transient boundary conditions (Graeber et al., 2006). With PCSiWaPro® a 2D model of the dam could be built, incorporating information of geometry, soil properties, climate parameters and geohydraulic as well as time-dependent boundary conditions. To determine the effects of the factors mentioned above on the through-flow, water saturation and the geomechanical instabilities in the partially saturated region of the dump slope, the seepage line as the border between the fully saturated and partially saturated zones was used for validating the simulation results.

Theoretical Background of PCSiWaPro®

PCSiWaPro® simulates water flow and contaminant transport processes in variably saturated soils, under both steady-state as well as transient boundary conditions. The flow model can be described by the RICHARDS equation (equation 1).

$$\frac{\partial \theta}{\partial t} = \frac{\partial}{\partial x_i}\left[K\left(K_{ij}^{A} \frac{\partial h}{\partial x_j} + K_{iz}^{A} \right) \right] - S \qquad (1)$$

The equation contains the volumetric water content θ, pressure head *h*, spatial coordinates *xi* (x_1 = x and x_2 = z for vertically-plane simulation), time *t*, and K_{ij}^{A} as components of the dimensionless tensor of anisotropy K. S is a source/sink term, which can be partly characterized by the volume of water that is removed from the soil by plant roots. The effects described by this strongly nonlinear partial differential equation are subject to hysteresis, especially the relationship between water content and pressure head. This relationship can be described by the VAN-GENUCHTEN-LUCKNER equation (2).

$$\theta = \theta_r + \frac{\phi - \theta_{r,w} - \theta_{r,l}}{\left[1 + (\alpha h_c)^n\right]^{1-\frac{1}{n}}} \quad (2)$$

Φ is the porosity of the soil; h_c characterizes the pressure head difference between the wetting (water) and non-wetting phase (air); α (scale factor) and n (slope) are empirical VAN-GENUCHTEN parameters (Kemmesies, 1995). The simulation tool PCSiWaPro® implements this relationship and solves the RICHARDS equation in two vertically-plane dimensions with transient boundary conditions, using the numerical finite element approach. For the solution of the linear system of equation originating from discretizing the RICHARDS equation, an iterative preconditioned conjugate gradient solver is used.

Advantage of the Program PCSiWaPro®

There are some advantages of the program PCSiWaPro® in the field of the 2D simulation of hydrological processes. First of all, in PCSiWaPro® four kinds of Pedotransfer functions (Vereecken H. et al., 1989; Weynants, Vereecken & Javaux, 2009; Teepe, Dilling & Beese, 2003; Woesten, Pachepsky & Rawls, 2001) have been applied for the estimation of VAN GENUCHTEN-LUCKNER parameters α and n based of the corn-size-distribution-curves in the program operation interface shown in Figure 3 below.

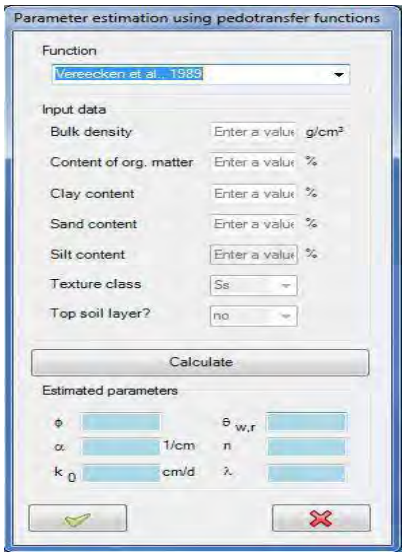

Figure 3 Operation interface of parameter estimation using pedotransfer function in PCSiWaPro®

Secondly, a further advantage of PCSiWaPro® is the coupling of a weather generator whose input data basis is real climatic data with the time frequency of one day, such as precipitation, daily average temperature and sunshine duration from the public weather data of the German Weather Service (DWD) (Figure 4); this generator allows for the generation of transient infiltration fronts with a temporal resolution up until 30 minutes with respect to those atmospheric conditions and removal of water by plant roots. In addition, it can be applied for the unknown location based on the method of the spatial interpolation and the method of the inverse distance with the geographic

coordinate of the surrounding climate stations. With these advantages, a much better resolution of the hydrological process simulation could be achieved in the dump slope either during a dry season or during a rainfall event. For example, variation of water content distribution in the slope could be simulated and predicted hourly especially during a wet season for the risk management of the possible landslide. However, when transferring this program to other countries (e.g. Poland, China, and Japan), the DWD data in this weather generator is no more suitable; instead, the local weather service data needs to be transferred to PCSiWaPro® in order to get high resolution time series for the local hydrological simulation work.

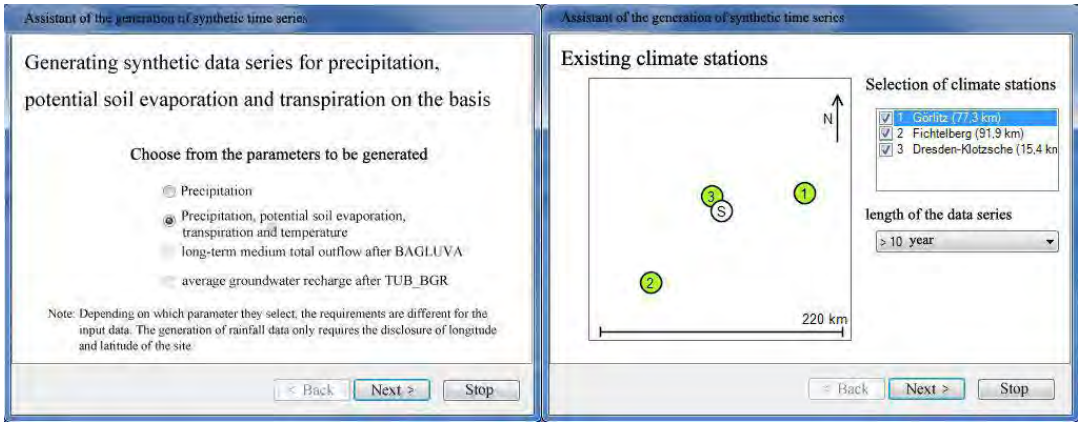

Figure 4 Operation interfaces of the weather generator for an example in the Dresden area

Thirdly, PCSiWaPro is coupled with soil parameter and chemical data bases for the estimation of the VAN GENUCHTEN-LUCKNER soil parameters and the transport parameters, respectively.

Lastly, PCSiWaPro® could provide us a strong calibration system between the simulation results and measured values from any observation point in the dump slope; with the pre-input of the measured data, this program carries out detailed calculation for different kind of values (e.g. pressure head, water content, concentration). This calibration system could also be taken as a test for the applicability and availability of the program PCSiWaPro® in our study area.

STABILITY ANALYSIS MODEL

Slope stability problems of the dump slope are among the most commonly encountered problems in geotechnical engineering. Numerous scientists conducted a large amount of research in this field and several numerical methods were developed for the slope stability analysis. The typical methods are Infinite Slope Equation, Ordinary Method of Slices, JANBU'S Simplified Method, MORGENSTERN-PRICE method and so on. Due to the close relationship between the water content (or saturation) and slope stability, the infinite slope equation is one of the most applicable equations to be used together with water flow simulation in unsaturated slope bodies (Hammond C. et al., 1992; Biondi G. et al., 2000); and it assumes identical conditions occur on any vertical section of the slope. The objective of the analysis is to produce estimates of the probability of infinite slope failure in form of the conventional factor of safety (Fs) which is defined as the ratio of shear strength to shear stress for a one-dimensional infinite slope under both saturated and

unsaturated conditions (Griffiths, Huang & Gordon, 2011; Duncan & Wright, 2005; Hammond et al., 1992); equation 3 and 4 are given for the Fs analysis within the root system as,

$$Fs_{(z)} = \frac{\tan\phi'}{\tan\beta} + \frac{2(c'+c_r)}{rz\sin 2\beta} + \frac{S_e}{rz}(u_a - u_w)(\tan\beta + \cot\beta)\tan\phi' \quad (3)$$

$$Fs_{(z)} = \frac{\tan\emptyset'}{\tan\beta} + \frac{2(c' + c_r)}{\gamma z \sin 2\beta} + \frac{S_e}{\gamma z}(u_a - u_w)(\tan\beta + \cot\beta)\tan\emptyset'$$

$$S_e = \frac{\theta - \theta_r}{\theta_s - \theta_r} \qquad S_e = \frac{\theta - \theta_r}{\theta_s - \theta_r} \quad (4)$$

where u_w is the pore water pressure; u_a is the pore air pressure; S_e is the saturation; θ is the volumetric water content; θ_r is the residual volumetric water content; θ_s is the saturated volumetric water content; $(u_a - u_w)$ is soil matric suction; z is vertical depth below the ground surface; Ø' is the angle of internal friction; c' is the soil cohesion; β is the slope angle and γ is the total soil and water unit weight (Lu & Godt, 2008); c_r is the root reinforcement (Tien H. Wu, 2013).

From the VAN GENUCHTEN-LUCKNER equation, the relationship between water content and matrix suction can be easily achieved, as shown below (equation 5):

$$u_a - u_w = \frac{\left[\left(\frac{1}{S_e}\right)^{\frac{n}{n-1}} - 1\right]^{\frac{1}{n}}}{\alpha} \quad (5)$$

α is scaling factor; n is slope factor. α and n could be achieved by the pedotransfer functions in PCSiWaPro®.

The root reinforcement c' should be neglected in equation 3 when the slope depth is below the root area. Generally, when the Fs value of a dump slope is reduced to less than one unit, landslides could be predicted and the necessary prevention is in need to reduce the landslide risk.

In the above three equations (3, 4 and 5), the values of all those parameters could be easily achieved from the local geo-data base except the volumetric water content θ which is variable depending on the local hydrological and atmospheric conditions. However, θ could be calculated or predicted by the program PCSiWaPro®.

DISCUSSION OF SIMULATION RESULTS

A real dump slope model has been selected from the mining area near the city of Leipzig for the practical application of the program PCSiWaPro® whose simulation results would play one of the key roles on the stability analysis. This study structure is totally 300m wide and 94m high with horizontally layered dump soils (e.g. 20m depth of clay layer in the middle with the hydraulic conductivity k_f of 10^{-8} m/s, 11m depth of sandy cover with the k_f value of $1.3 \cdot 10^{-5}$ m/s over the clay

layer) and sandy slope with the k_f value of $4.5 \cdot 10^{-5}$ m/s. Additional basic data, like groundwater water level change, have been obtained from the local agency and the company IBGW Leipzig.

After setup of the model in the program PCSiWaPro®, a simulation period of five years from Jan. 2000 to Jan. 2005 was selected. On the dump slope, atmospheric boundary condition has been defined, which means this slope would have additional input of rainfall water; after the formation of this dump slope, a constant groundwater level of 88m was detected during this simulation period, which supports the determination of the boundary condition of constant potential head on the left side of this model.

In order to better investigate the contribution of precipitation to the increase of water saturation in the slope and groundwater table, a simulation without input of rainfall water has been shown beforehand in Figure 5 which displays the saturation condition in different soil layers in this slope for the day of 30th June 2004. In the zoomed figure, the moderate increase of groundwater surface could be explained by the increasing capillary rise of water in the slope sand from the saturated clay soil which exhibits much higher water retention due to the much smaller particle size. Accordingly in Figure 6 the different blue colors below the groundwater surface indicate the different saturated water content of different dump materials; due to the larger porosity, the clay material with the darker blue color shows the higher saturated water content (0.52) compared with the sandy slope showing the lower water content (0.4). In addition, in PCSiWaPro® the implemented mesh generator for calculation depending on the finite element method uses the "Boundary Representation Modelling Technique" and therefore requires the specification of the model boundaries; in this simulation the structure of the model was discretized with medium finer (0.5 m) meshes, which results in a good representation of water content distribution. However the serrated lines between two different water content and water saturation layers could be even more smoothed with finer model structure meshes (e.g. 0.1 m).

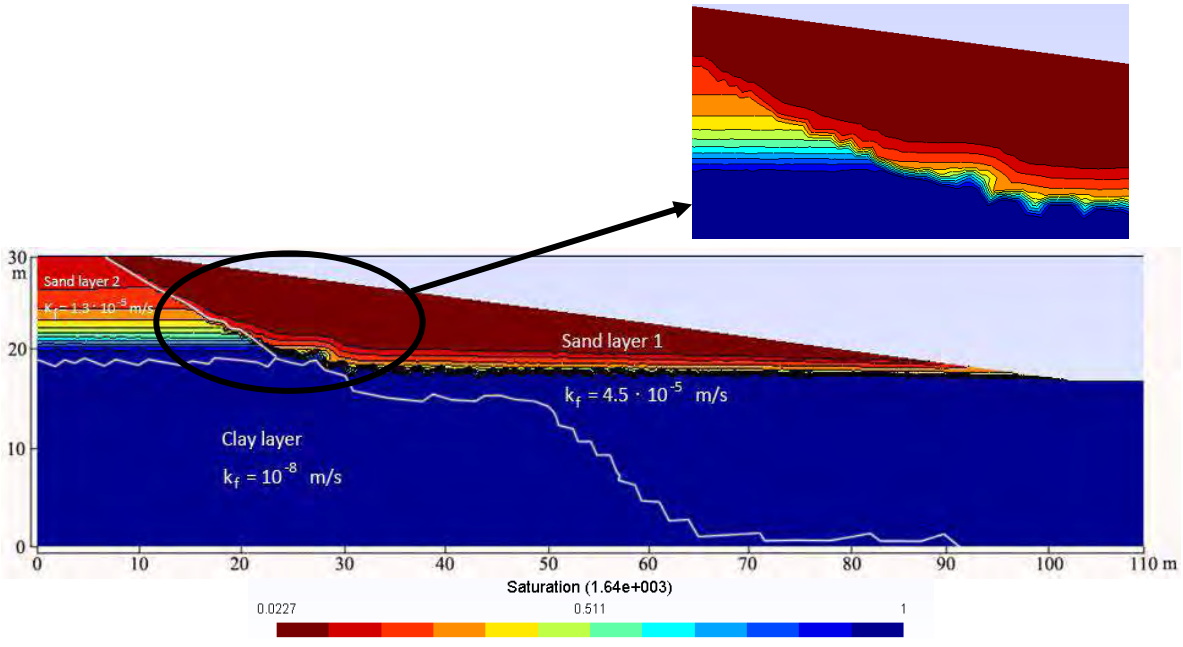

Figure 5 Water saturation simulation without input of precipitation on June 30th, 2004 (the white lines are the borders of different soil layers with different hydraulic conductivity)

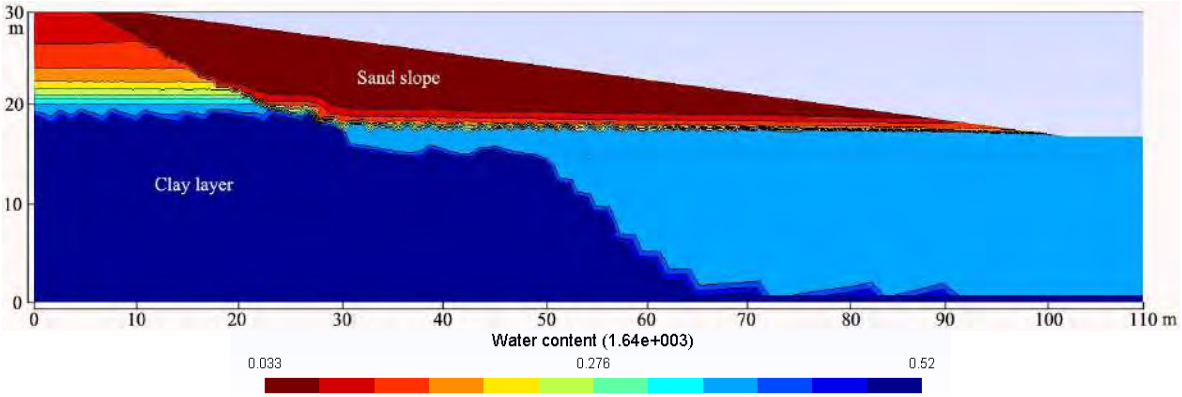

Figure 6 Water content simulation results without input of precipitation on June 30th, 2004

Figure 7 shows the precipitation data output from the weather generator in PCSiWaPro® for a typical year in the study area. As can been seen in this graph, the rainfall event mainly occurred in the summer between June and September, especially in the mid-June, early July and early September. In addition, although the rainfall season came every year from the mid-June, the ground-water level showed no change between the year of 2000 and 2005, which was mainly due to the manmade operation of pumping discharge from the groundwater during the mining activities in order to prevent the possible overload groundwater storage especially in the rainfall season and to prevent the possible geological and environmental disasters.

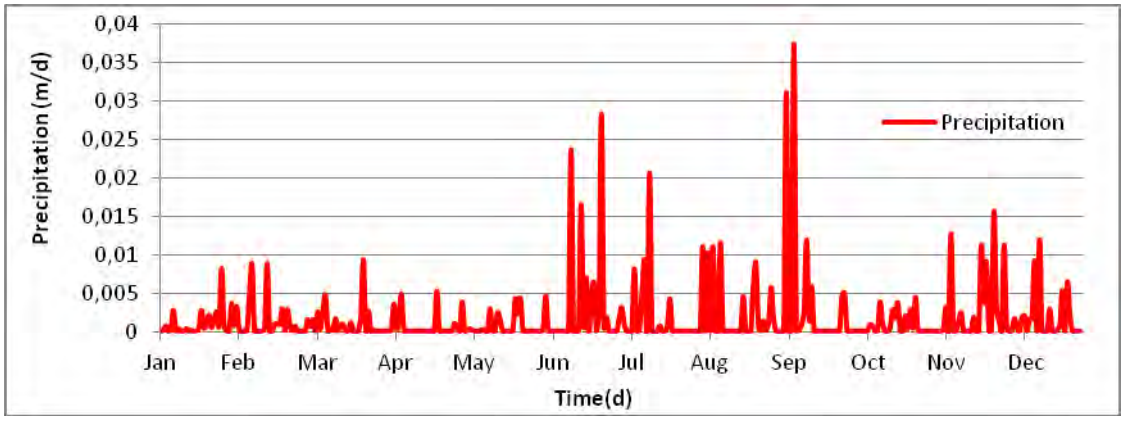

Figure 7 Typical daily precipitation data for one year in this area from the weather generator in PCSiWaPro®

Depending on the advantage of weather generator, the simulation result of water content was illustrated in Figure 8 for 30th June 2004 (during the rainfall season) considering both the groundwater flow and rainfall water infiltration. Rainfall water provided an additional flow into

the top and the right sand slope embankment, thereby increasing water content in this unsaturated slope. In addition, the rainfall water reaching the groundwater table in the slope has also performed as a complementary for the groundwater recharge.

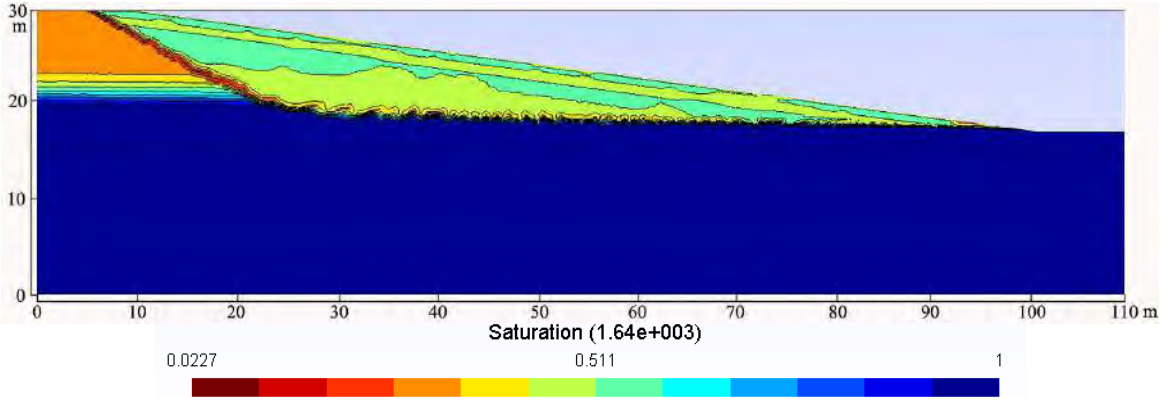

Figure 8 Simulation of water saturation distribution with input of precipitation on June 30th, 2004

In addition, due to the constant groundwater table after the year 2000, a stable value was achieved for the water level measurement from an observation well in this dump slope. A comparison between the measured and simulated water level has been carried out. The accordance between the measured and the computed values using the program PCSiWaPro® was good for our study area. However only a little bit deviation (0.3m) found in the comparison could be explained by the fact that our simulation was mainly based on the average values of those different dump soil parameters (e.g. average porosity, hydraulic conductivity); however the accuracy of the simulation could be improved with more field and laboratory investigation for soil parameters of the different dump slope soils.

CONCLUSIONS

1) The experiment results from the physical slope model in the laboratory indicated clearly that ground water flow had been already detected in the highly partial-saturated slope body; and due to the increasing of water saturation, the stability of this unsaturated slope was influenced with an already-happening surficial landslide.
2) With the Program PCSiWaPro®, water content and saturation distribution in the slope zone could be simulated and predicted dynamically within the whole study period, which is the preliminary work for stability analysis by the infinite slope model.
3) This study has also tested and calibrated the availability of PCSiWaPro® to simulate the groundwater level variation in an observation well within a continuous period.
4) The agreement between the measured groundwater level and the computed one using the program PCSiWaPro® was good for our study area; however there was a little deviation between those two values. These deviations could be caused by poorly estimated soil parameters (e.g. porosity, hydraulic conductivity).
5) With the simulation results, the stability analysis has been carried out and certified that this dump slope was stable (the minimum Fs value is 3, and the detailed calculation is not exhibited here); although the precipitation has contributed a lot for the decrease of the slope

stability, due to the manmade operation the groundwater table in this dump slope was always kept stably low between the year of 2000 and 2004, which resulted in a safe slope.

REFERENCES

Abe, K. (1997): A method of evaluating the effect of trees roots on preventing shallow-seated landslides, Bull. Forest. Forest Prod. Res. Inst. 1 (373), pp.1105–1181.

Aigner, D. (2004): Auswertung von Untersuchungen über den Einsatz einer Gummispundwand sowie einer Sickerleitung an einem durchströmten Modelldeich, Institut für Wasserbau und Technische Hydromechanik Dresden, Technische Universität Dresden.

Biondi, G., Cascone E., Magueri M., Motta E. (2000): Seismic response of saturated cohesionless slopes, Soil Dynam Earthquake Eng 2000; 20(1–4):209–15.

Bonelli S. (2013): Erosion in Geomechanics Applied to Dams and Levees, Wiley-ISTE, ISBN: 978-1-84821-409-5.

Coppin, N.J., Barker, D.H. & Richards, I. (1990): Use of Vegetation in Civil Engineering. Butterworths, Sevenoaks, Kent.

Duncan, J. M. & Wright, S. G. (2005): Soil Strength and Slope Stability, John Wiley, Hoboken, N. J., pp. 297.

Graeber, P.-W., Blankenburg R., Kemmesies O., Krug S. (2006): SiWaPro DSS - Beratungssystem zur Simulation von Prozessen der unterirdischen Zonen. [Buchverf.] Jochen Wittmann und Mike Müller. [Hrsg.] Mike Müller. Simulation in Umwelt- und Geowissenschaften. Leipzig: Shaker Verlag, 2006, pp. 225-234.

Gray, D.H. (1995): Influence of vegetation on the stability of slopes, In: Barker, D.H. (Ed.), Vegetation and Slopes Stabilisation, Protection and Ecology, Thomas Telford House, London, pp. 2–23.

Griffiths D.V., Huang Jinsong & Gordon A. Fenton (2011): Probabilistic infinite slope analysis, Computers and Geotechnics 38, pp. 577–584.

Hammond, C., Hall, D. E., Miller, S., Swetik, P. (1992): Level I Stability Analysis (LISA) Documentation for Version 2.0: U.S. Department of Agriculture, Forest Service, Intermountain Research Station; General Technical Report INT-285, Ogden, UT.

Kemmesies, O. (1995): Prozessmodellierung und Parameteridentifikation von Mehrphasenströmungsprozessen in porösen Medien, Dresdner Grundwasserforschungszentrum e.V., 1995, ISSN 1430-0176.

Lu, N., & J. W. Godt (2008): Infinite-slope stability under steady unsaturated conditions, Water Resour. Res., 44, W11404, doi: 10.1029/ 2008WR006976.

Teepe, R., Dilling, H. & Beese, F. (2003): Estimating water retention curves of forest soils from soil texture and bulk density, J. Plant Nutr. Soil Sci. 166, pp.111-119.

Tien H. Wu (2013): Root reinforcement of soil: Review of analytical models, test results, and applications to design, NRC Research Press.

Vereecken H., Maes J., Feyen J., Darius P. (1989): Estimating the soil moisture retention characteristic from texture, bulk density and carbon content, Soil Science. 1989, Vol. 148, No. 6, pp. 389-403.

Weynants, M., Vereecken, H. & Javaux, M. (2009): Revising vereecken pedotransfer functions: Introducing a closed-form hydraulic model, Vadose Zone Journal 8(1), pp.86-95.

Woesten, J. H. M., Pachepsky, Y. A. & Rawls, W. J. (2001): Pedotransfer functions: bridging the gap between available basich soil data and missing hydraulic characteristics, J. Hydrol. 251, pp.123-150.

10th ICARD IMWA 2015 | 10th International Conference on Acid Rock Drainage & IMWA Annual Conference

A Source Apportionment Methodology for South African Gold Mines

Ingrid Dennis[1], Rainier Dennis[1], Michael Eckart[2] and Christoph Klinger[2]

1. *Centre for Water Sciences and Management, North-West University, South Africa*
2. *DMT GmbH & Co. KG, Germany*

ABSTRACT

South Africa is faced with the legacy of environmental impacts due to gold mining activities which have taken place over 120 years in the Witwatersrand region. Over time, as economically exploitable gold ores have been depleted, progressive cessation of mining operations has taken place. Gold mining has caused considerable changes to the surface and subsurface water flow pathways. This is due to the influence of historical surface operations, shallow sub-surface mining and deep underground mine excavations. The generation of acid mine drainage as a result of the oxidation of pyrite and other metal sulphides associated with the gold ores has caused acidic mine water with a lowered pH, elevated levels of sulphate, and elevated concentrations of mobile toxic metals. The management of the acid mine drainage poses a major challenge. A vital question is: Who is responsible for the resultant environmental management and clean-up?

The approach adopted for the study is one that involves an integrated modeling methodology. The following elements and techniques are included: source identification, geochemical, solute mass and transport modeling, geochemical speciation and kinetic modeling. Use is made of environmental cost accounting so that the scientific source identification and apportionment findings can be expressed in terms of monetary values. The current study seeks to scientifically quantify the environmental risks associated with existing and historical gold mining activities, identify the parties whose activities are responsible for impairment of water resources, and to translate these in terms of responsible parties' respective contributions according to the "polluter pays" principle.

Keywords: Source Apportionment, Integrated Modeling Approach

INTRODUCTION

South Africa is faced with the legacy of environmental impacts due to gold mining activities which have taken place over 120 years in the Witwatersrand gold mining region. Over time, as economically exploitable gold ores have been depleted and progressive cessation of mining operations have taken place. Gold mining over this period has caused considerable changes to the surface and subsurface water flow pathways. This is due to the influence of historical surface operations, shallow sub-surface mining and deep underground mine excavations. The generation of acid mine drainage as a result of the oxidation of pyrite and other metal sulphides associated with the gold ores has caused acidic mine water with lowered pH, elevated levels of sulphate, and elevated concentrations of mobile toxic metals.

The management of the acid mine drainage poses a major challenge and a vital question is: Who is to responsible for the resultant environmental management and clean-up? The source apportionment methodology is underlain by an integrated modeling approach. The impact of identified pollution sources are simulated and quantified at selected downstream points.

BACKGROUND

The South African Inter-Ministerial Committee (IMC) on Acid Mine Drainage (AMD), comprising the Ministers of Mineral Resources, Water Affairs, Science and Technology, and the Minister in the Presidency: National Planning Commission, appointed a team of experts to report on the assessment and reappraisal of the situation with respect to acid mine drainage, focusing on the Witwatersrand goldfields (Inter-Ministerial Committee, 2010).

AMD has been reported in the Western, Central and Eastern Basins (South Africa) were identified as priority areas. These areas require immediate action due to the lack of adequate measures to manage and control the problems related to AMD. The urgency of implementing intervention measures is necessary before problems become more critical. Another concern is the proximity of these problems to densely populated areas.

Pumping of groundwater from Grootvlei Mine in the Eastern Basin ceased in 2011 and mine flooding commenced. The mine historically maintained the mine water level in this basin at a depth of ~700 mbgl by pumping 75–108 Ml/d. Treatment of the mine water has not occurred for some time and an early casualty of the situation is Blesbokspruit, including a Ramsar-listed wetland (Inter-Ministerial Committee, 2010).

The South African government is compelled to provide long-term water treatment facilities for the decanting mine water. Treatment plants could include desalinization, through one of several treatment methods involving chemical precipitation, membranes (such as reverse osmosis), ion exchange or biological sulphate removal. All methods produce clean, potable water, but are costly and produce waste products of their own (Pratt, 2011). Associated cost recovery of treatment plants will have to be conducted through the “polluter pays” principle and therefore it is necessary to formulate a source apportionment methodology.

Study Area

The study area is located in the Gauteng Province of South Africa and covers the East Rand area, including the towns of Boksburg, Germiston, Brakpan, Benoni, Heidelberg, Springs and Nigel. In Mining terms the area is referred to as the East Rand Basin. Mining in the Eastern Rand portion of the Witwatersrand Goldfields started in about 1888 at the Nigel Mines and in 1892 at Van Ryn Estates, slightly later than the mines on the Central Rand. The mine lease areas in the basin cover about 768 km^2 as shown in Figure 1. It is important to note that the East Rand Basin is geographically, hydrologically and hydrogeologically different from the other Witwatersrand mined basins (Scott, 1995).

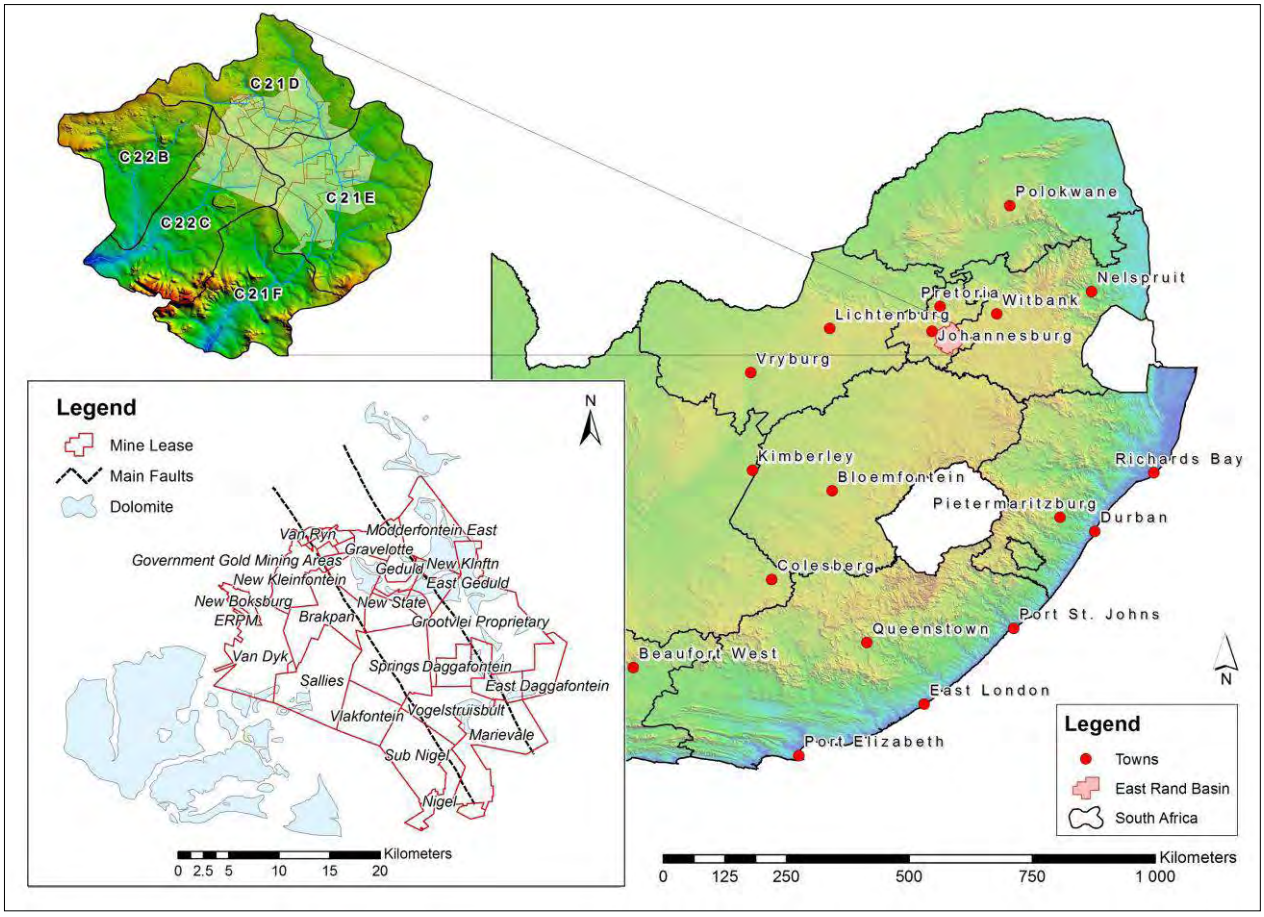

Figure 1 Locality map of the East Rand Basin

The surface catchment area considered comprises of five quaternary catchments (Figure 1): C21D, C21E, C21F, C22B and C22C. A summary of average hydrological values for each of the quaternary catchments are presented in Table 1. The two major drainage systems associated with the aforementioned catchments are the Blesbokspruit and the Natal/Rietspruit.

Table 1 Summary of average hydrological values for the study area (Middleton & Bailey (2005)

Quaternary	River	Catchment Area (km²)	MAP (mm/a)	MAR (mm/a)	MAE (mm/a)	Recharge (%MAP)
C21D	Blesbokspruit	446	698	36	1625	5.7
C21E	Blesbokspruit	628	691	35	1625	5.1
C21F	Blesbokspruit	426	704	38	1625	6.2
C22B	Natalspruit	392	692	32	1630	5.9
C22C	Rietspruit	465	684	31	1625	6.3

MAP – mean annual precipitation, MAR – mean annual rainfall, MAE – mean annual evaporation

Historic Mining

Mainly gold was mined in the area with selected coal deposits (mined via opencast pits). The gold reefs targeted were the Main, Kimberley and the Black Reef. The spatial extend of these mined-out reefs as well as a vertical profile is shown in Figure 2. Note the water level in the profile represents the shallow regional groundwater level and does not reflect the water level associated with the mine workings.

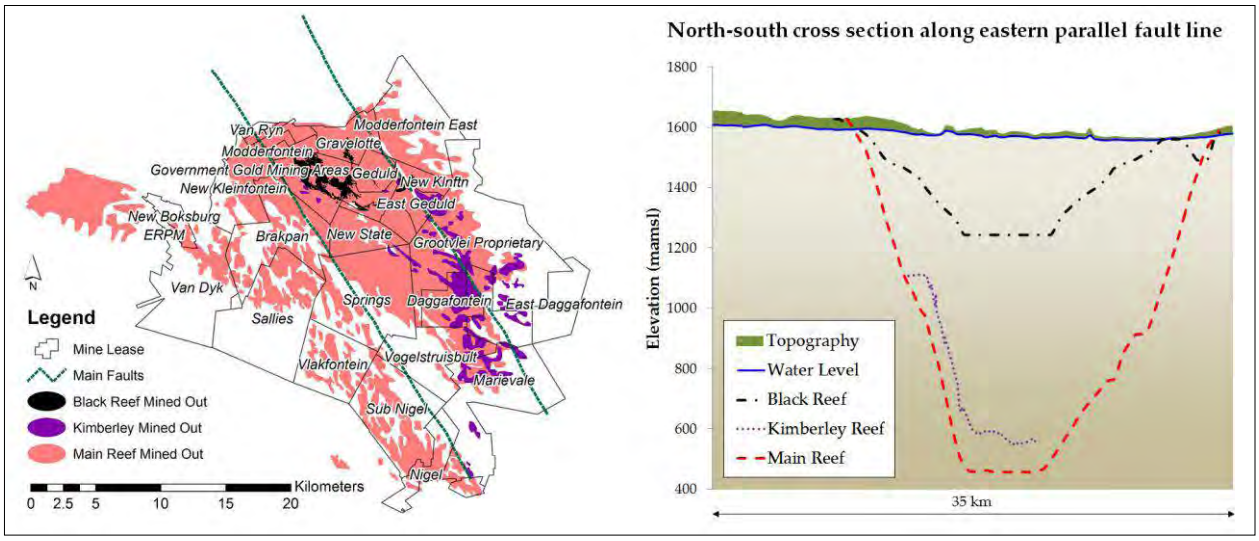

Figure 2 Mined out reefs of the East Rand Basin

METHODOLOGY

The source apportionment methodology relies on an integrated modeling approach between mine flooding, a regional groundwater model and a surface water model. Prioritization of sites and associated monitoring forms the bases of the aforementioned models. The methodology is discussed in more detail in the sections that follow.

Prioritization

A spatial approach was used to prioritize the different site types based on a site weighting given to each site. A regional model grid was used for this purpose and a layer was created for each site type e.g. tailing storage facilities (TSF), mines shafts, subsidence, dolomites, etc. A total of 13 different site types were used in the prioritization, where the resultant layer features were assigned a value of one. A zero value was assigned in the absence of these features. The priority for each grid cell was calculated as follows:

$$Priority = \left(\sum_{1}^{n} S_n W_n \right) \times DRASTIC \quad (1)$$

where n represents the number of sites types, S_n is the site value for the grid cell (zero or one) and W_n is the relative weight associated with the site type. The *DRASTIC* index (DWAF, 2006) is an index expressing the aquifer vulnerability between 1 and 200, where an index value of 200 expresses the highest aquifer vulnerability to possible groundwater pollution. Weights (W_n) applied in the prioritization is presented in Table 2. Note no weighting was assigned to the Dolomitic areas as these already form part of the DRASTIC index used.

Table 2 Summary of relative weights applied to site types in calculating priority

Site Type	W_n
Embankment	1
Pans	2
Dams, Reservoirs, Wetlands	3
Diggings, Excavations, Lineaments	5
Open Cast, Mine Shafts, TSF, Subsidence, Waste Water Treatment Works	10

The normalized prioritization map for the East Rand Basin is shown in Figure 3 together with selected pollution sources. Note that there are areas outside the mine lease area that received high prioritization. For the purpose of this study, the focus was on the prioritized areas within the mine lease area.

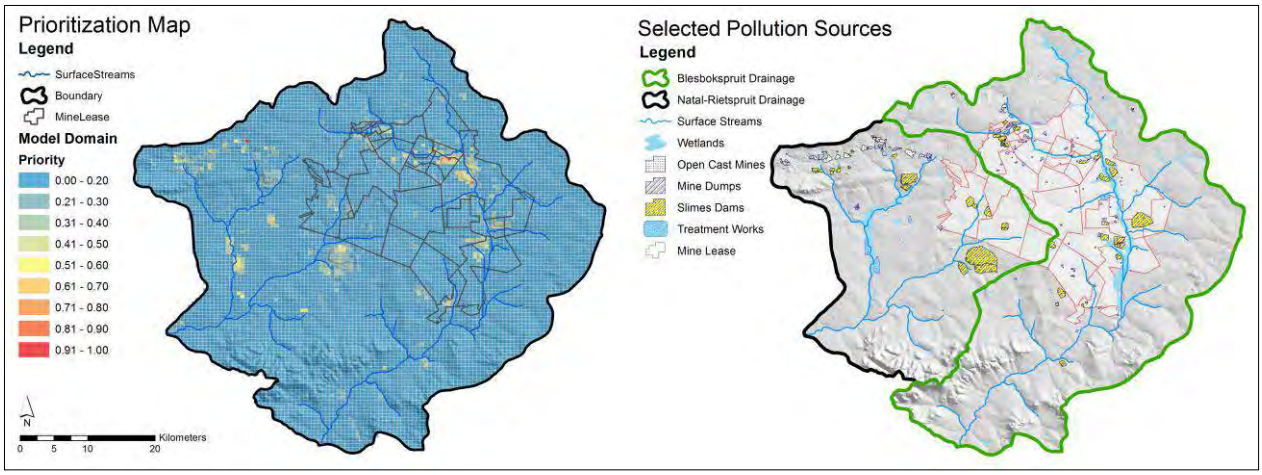

Figure 3 Normalized prioritization map and selected pollution sources of the East Rand Basin

Monitoring

A monitoring network for both the surface and groundwater had to be established due to the fact that all mining operations, with the exception of the reworking of selected tailings storage facilities (TSFs), ceased and no active monitoring was taking place. Historic datasets and reports were consulted to select monitoring points that coincide as far as possible with historic monitoring points. Physical access to sites and appropriateness of sites dictated the location of monitoring points. The final monitoring networks for both surface and groundwater are shown in Figure 4.

It is clear from the groundwater monitoring network that numerous boreholes were drilled into the dolomites for water supply. The groundwater monitoring network focused on the immediate mine lease area and only few boreholes were found that formed part of the monitoring network.

Only a single weir exists within the mine lease boundary which has data from 1977 to 2004 after which monitoring of the flow gauge stopped. Surface flow measurements were conducted through surveying cross sections and measuring stage and flow velocity. The existence of large areas comprising of wetlands (Figure 3), specifically in the Blesbokspruit, posed challenges in flow measurements as the wetland acts as a buffer to flow. Often zero flow velocities were recorded within the wetland itself.

Three sampling campaigns were conducted during the course of the study, which included both a wet and a dry season. Each sampling campaign recorded surface flow and quality as well as groundwater levels and quality.

Mine flooding water levels with selected water quality measurements were being monitored at selected mine shafts by the South African Government and this data were used to calibrate the mine flooding model.

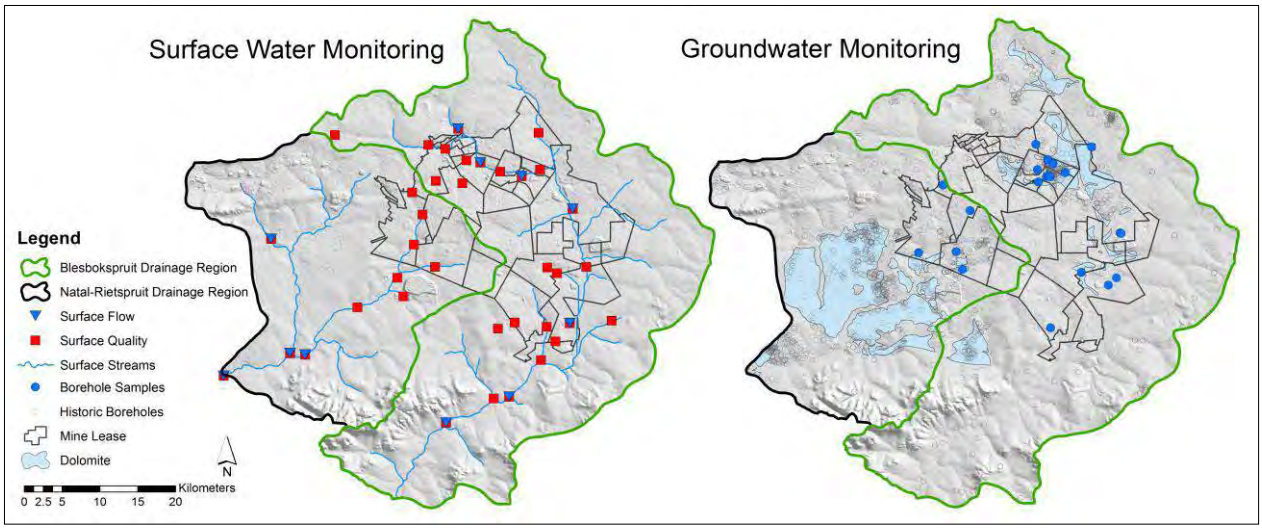

Figure 4 Surface and groundwater monitoring network

Source Term Determination

Material was sampled from the TSFs by making use of an auger. Samples were taken from the weathered and un-weathered zones. In storage facilities where the material is being reworked, samples were taken of the freshly exposed material. Samples were also taken from waste rock dumps.

In order to estimate the source terms that may impact on the study area, the risk sources were clustered based on their respective mineralogy. Geochemical models were developed for the various clusters types. Physical parameters of the heap that included geometry, particle size distribution, and saturation and oxygen concentration profiles formed part of the input to the geochemical models. In addition to this, the pore water composition was obtained through static leaching of the sampled materials. Humidity leach cell tests were performed in order to calibrate the numerical geochemical models.

A total of 18 TSFs and 12 waste rock dumps within the study area were sampled. A total of 9 source terms were determined for the nine cluster types determined for the TSFs and 8 source terms were determined for the waste rock dump clusters.

The spatial distribution of the TSFs and waste rock dumps are shown in Figure 3.

Model Concept

The mine hydrology, hydrogeology and surface hydrology of the area were modeled through the use of a surface run-off model, a regional groundwater model and a mine flooding model correspondingly. All three the aforementioned models are inter-connected to account for the total water balance and produce an aggregated system response. A graphic representation of the model framework is shown in Figure 5.

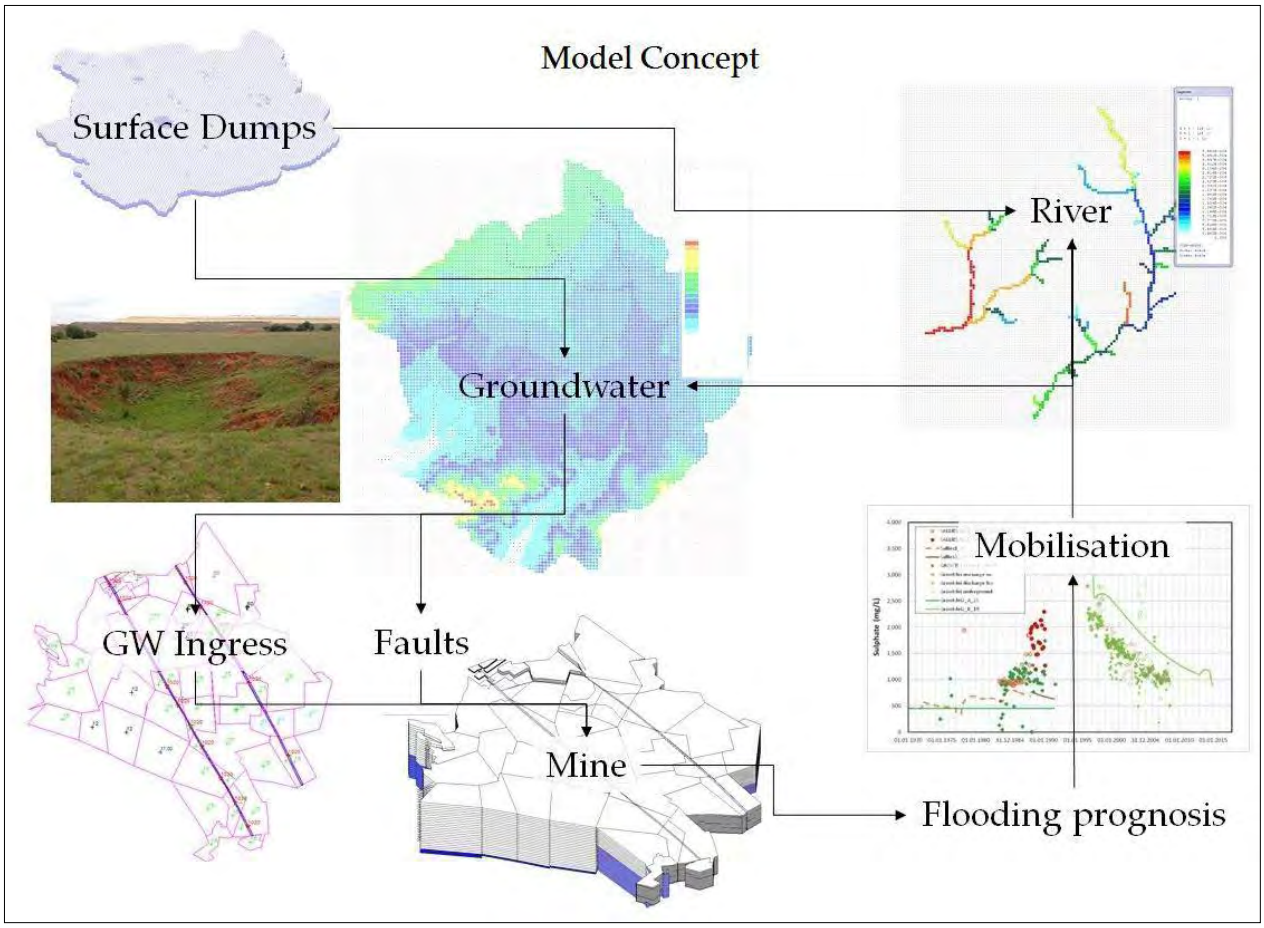

Figure 5 Source apportionment through an integrated modeling approach

The mine flooding model accounts for the two major fault lines running through the mine lease area (Figure 2) as well as areas of high ingress e.g. subsidence (Figure 5). The mine model is overlain by a multi-layer regional groundwater model onto which the surface pollution sources are added. The groundwater model grid size was chosen to ensure all TSFs and waste rock dumps were incorporated into the model.

The interface between the surface and groundwater model allows for surface-groundwater interaction which includes the decanting of mine water into the surface streams. The mine water decant to the streams can either be through surface runoff or via the shallow aquifer.

The source terms for the TSFs and waste rock dumps were included in the groundwater model.

Reactive mass transport modeling was applied in the mine flooding model and typical SO_4 results at the Grootvlei Shaft are shown in Figure 6.

In terms of the mass transport, the system was simplified to only consider sulfate as a conservative ion to track the pollution emanating from the various TSFs and waste rock dumps. The other major anion and cation movement can be modeled by making use of the associate geochemical modeling.

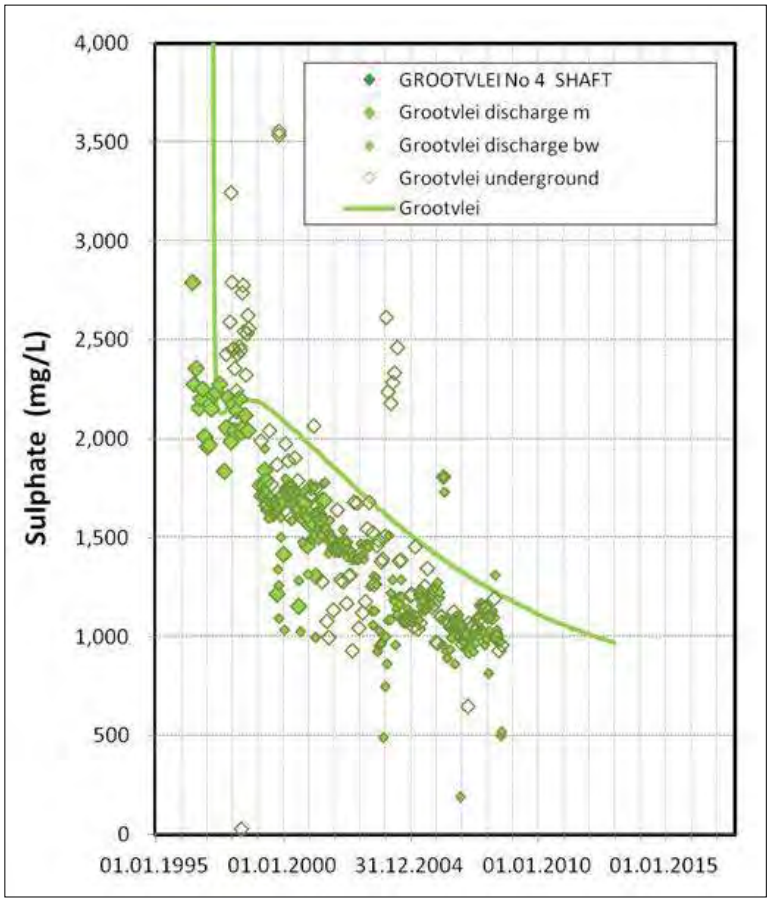

Figure 6 Model surface calibration points

Although the mine flooding model and the regional groundwater is calibrated individually, the surface water model calibration is representative of the integrated model calibration (Figure 7). The source apportionment is carried out at specified surface water points and the surface runoff model serves as a "water tree" routing all the contributions of pollution sources that report to surface water features downstream.

The groundwater model reports to the surface streams through surface-groundwater interaction and the mine flooding model reports to the surface streams through surface decant if it takes place.

The mine flooding model is also connected to the regional groundwater model and subsurface decant into the surrounding aquifer is accounted for where shafts are not hydraulically disconnected from the aquifer.

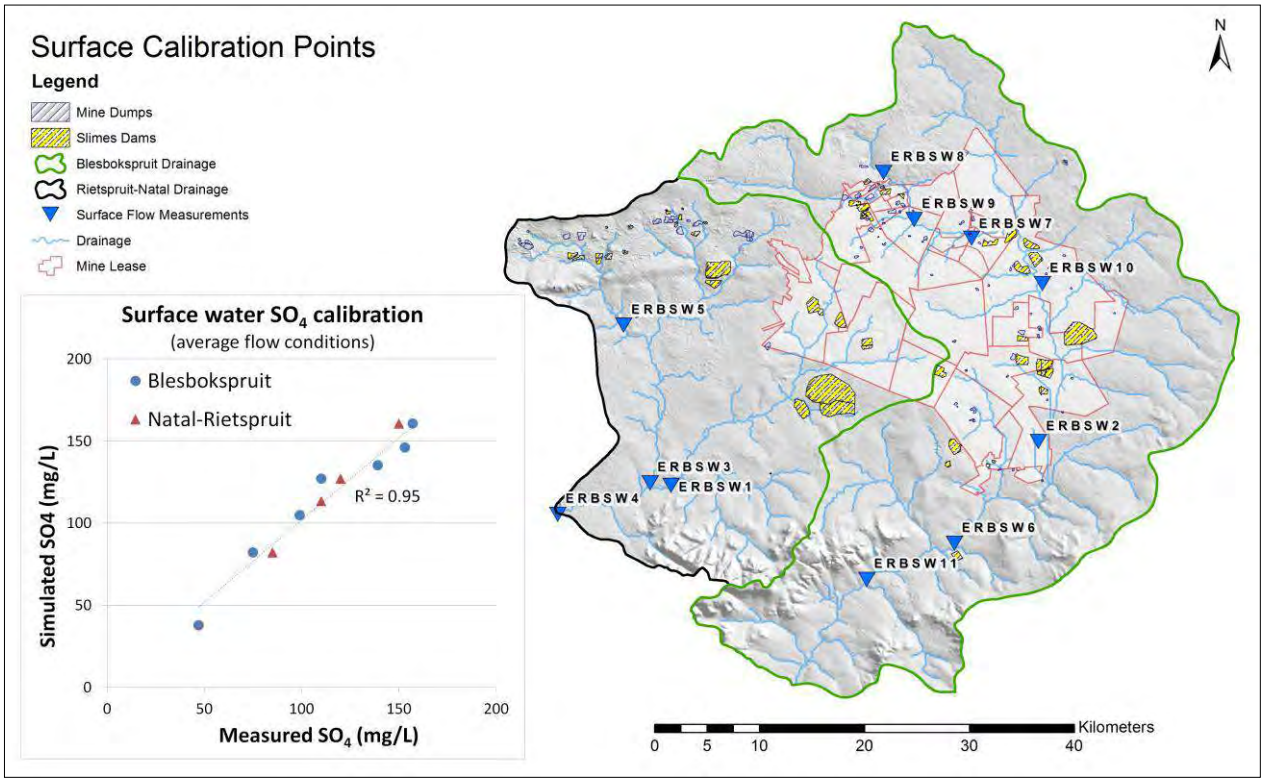

Figure 7 Integrated model surface calibration points and associated calibration

The surface water model only accounts for conservative mass transport as the surface water translates into a complex system with raw sewage (Figure 8) discharged into the water course due to faulty infrastructure or waste water treatment works running above designed capacity. Furthermore large wetlands (Figure 9) exist throughout the Blesbokspruit buffering flow and altering water chemistry.

Figure 8 Raw sewage discharged into the Blesbokspruit

Figure 9 Wetland in the Blesbokspruit

Mine Flooding Model

The mine flooding simulation was conducted using the DMT BoxModel. The BoxModel is a 3D finite volume program for modeling the flow of groundwater and mine water, heat transport and multi-component mass transport including sorption, microbial degradation and the reactions with minerals. A special feature is the highly flexible discretization, to model geological structures such as layers and faults as well as structural mining elements and mine excavations (DMT, 2011). The BoxModel also allows for interfacing to a regional groundwater model.

Regional Groundwater Model

MODFLOW was selected as choice of regional groundwater model for the study area. MODFLOW is the USGS's three-dimensional (3D) finite-difference groundwater model. MODFLOW is considered an international standard for simulating and predicting groundwater conditions and groundwater/surface-water interactions (Harbaugh, 2005).

Surface Water Model

The EPA SWMM (Storm Water Management Model) was used as primary rainfall-runoff model. The model is a dynamic and used for single event or long-term (continuous) simulation of runoff quantity and quality from primarily urban areas. The runoff component of SWMM operates on a collection of sub-catchment areas that receive precipitation and generate runoff and pollutant loads (Rossman, LA 2010). In general SWMM is not applicable to large-scale, non-urban watersheds, but Nakamura and Villagra (2009) has shown successful application of SWMM to a natural catchment. Calibration parameters from SWMM were used to setup the secondary surface water model which forms part of the DMT BoxModel.

Source Apportionment

The technical component of the source apportionment was conducted through the use of the interconnected model representing the study area. The effect of various sources described by the model could be quantified at specific points of interest through the use of a what-if analysis. The pollution sources in question are disconnected from the model and the net effect of the detached pollution sources is recorded at points of interest.

The financial modeling based on the interconnected model relies heavily on the confidence of the model output, which is difficult to quantify considering future scenarios. The status quo confidence of the model output is related to the calibration state of the model and associated data.

The legal part of the source apportionment, which falls outside the scope of this paper, is far more challenging than the technical part due to legacy mining concerns.

DISCUSSION

The interconnected modeling approach allows for a what-if analysis to quantify the impact of various pollution sources at specified points in the network.

A challenge in model output confidence exists for the East Rand Basin as the monitoring network established only reflect the system response for a single hydrological year. Very little historic monitoring data are available to validate the model calibration.

The change of water character entering the wetland areas is contributed to the existence of Sulphate Reducing Bacteria (SRB). The surface water model employed does not explicitly account for wetlands or the effect of SRB's and this mechanism is simulated with a "treatment plant" within the surface water model. A study is currently being carried out to characterize the wetland response function particularly for the use in the surface water model.

CONCLUSION

Source apportionment in a complex mining environment requires the use of an integrated modeling approach. Model confidence on both current and future scenarios is important for the purposes of financial modeling which is the final step in the apportionment study. Continued monitoring would be required to validate the model response before final apportionment studies can be carried out.

ACKNOWLEDGEMENTS

The authors would like to acknowledge the South African Council for Geoscience and the Department of Minerals and Resources who made this project possible.

REFERENCES

DMT GmbH & Co. KG (2011) *BoxModel Concept: ReacFlow3D,* Program description accompanying BoxModel documentation, Germany.

DWAF (2006) *Groundwater Resource Assessment II: Aquifer Vulnerability Map,* Department of Water Affairs, South Africa.

Harbaugh, AW (2005) *MODFLOW-2005, The U.S. Geological Survey Modular Ground-Water Model—the Ground-Water Flow Process,* U.S. Geological Survey, USA.

Inter-Ministerial Committee (2010) *Mine water management in the Witwatersrand Gold Fields with special emphasis on Acid Mine Drainage,* Council for Geoscience, South Africa.

Middleton, BJ and Bailey, AK (2005) *Water Resources of South Africa, 2005 STUDY (WR2005),* Water Research Commission, TT381/08, South Africa.

Nakamura, J and Villagra, N (2009) *Hydrologic Modeling of the Little Crum Creek Watershed with SWMM,* Swathmore College, USA.

Pratt, SE (2011) *Acid mine drainage: The toxic legacy of gold mining in South Africa,* Earth Magazine.

Rossman, LA (2010) *Storm Water Management Model User's Manual Version 5.0,* Environmental Protection Agency, EPA/600/R-05/040, USA.

Scott, R (2010) *Flooding of Central and East Rand gold Mines: an investigation into controls over the inflow rate, water quality and the predicted impacts of flooded mine,* Water Research Commission, WRC Report no 486/1/95, South Africa.

10th ICARD IMWA 2015 | 10th International Conference on Acid Rock Drainage & IMWA Annual Conference

Characterizing Abandoned Mining Dams by Geophysical Methods (ERI) and Sounding: La Carolina District (Southern Spain)

Julián Martínez[1], Javier Rey[2], María del Carmen Hidalgo[2], Jesús Garrido[3], Diego Rojas[2], Claus Kohfahl[4] and José Benavente[5]

1. *Department of Mechanical and Mining Engineering, Higher Polytechnic School of Linares, University of Jaen, Spain*
2. *Department of Geology, Higher Polytechnic School of Linares, University of Jaen, Spain*
3. *Department of Civil Engineering, Higher Technical School of Civil Engineering, University of Granada, Spain*
4. *IGME, Spain*
5. *Water Institute, University of Granada, Spain*

ABSTRACT

The mining exploitation of metallic sulphides in the Carolina district, together with the activities associated to the mineral treatment, when maintained through centuries due to the wealth of the ores, generate important accumulations of wastes in structures of different kind of tailing dams and ponds, for instance.

The objective of this study is, on the one hand, to check the applicability of geophysical prospecting internal structure of deposits of wastes on the other hand, the study also aims to apply such techniques to deduce some hydrological features of this waste deposits, a circumstance which must fit with their hydrogeological setting and with the results obtained of the hydrochemical survey of the selected site.

La Aquisgrana dam two profiles of 96 electrodes with the same configuration were made. Both were oriented in the NE-SW direction and were 285 m in length with spacing of 3 m between the electrodes. The profiles covered the dam from one end to the other to characterize the residue and the contact with the substrate. ERI has allowed us to obtain a model of the studied structure and has also permitted the selection of the best place to position borehole to control geochemical quality, which coincides with the preferential infiltration zones, the site where the water level and physico-chemical parameters are periodically measured.

**There is no full article associated with this abstract.*

Ten Years Later: The Ronneburg Waste Rock Relocation Project in the Light of Performance Monitoring and Sustainability Analysis

Michael Paul and Silvia Jahn
Division for Engineering and Radiation Protection, Wismut GmbH, Germany

ABSTRACT

A key project of the WISMUT remediation program, which is dedicated to the closure and remediation of the former East German uranium industry, is the Lichtenberg open pit remediation project at the former Ronneburg mine site (Thuringia, Germany). The project comprised the geochemically controlled relocation of about 133 Mm^3 of waste rock and associated contaminated material to the worked-out Lichtenberg open pit. Relocation started in 1990 and ceased in 2008. By 2014, cover construction and re-vegetation of the Lichtenberg backfill are complete at about 214 ha (95% of the total area), 100 ha have been reforested. Ongoing performance monitoring aims to measure the overall environmental impact and to prove successful implementation of the remedial work. Regular inspections confirm the physical stability of the 1.6 m thick two-layer soil cover. Re-vegetation is characterized by the establishment of 18 plant communities based on a 'controlled succession approach'. So far, the main root zone covers the uppermost 0.7 m of the soil profile. Water balance monitoring of the cover is carried out at five monitoring stations. For a mean hydrological year (710 mm precipitation) runoff rates were as follows: surface runoff 0…2 %, interflow 3…9 %, infiltration 8…13%. Further decrease of the infiltration rate is expected with progressive forest development. The mean radon exhalation rate through the soil cover is about 0.12 $Bq/(m^2s)$. Gas monitoring confirms the expected decrease of the oxygen concentrations vs. depth, with oxygen concentrations < 1% in depths below 3.5 m. Groundwater quality downstream the backfill area is characterized by significant pollution with uranium, heavy metals and sulfate, which partly results from the relocated waste material but mainly from flooding of the Ronneburg underground mine. In consequence, groundwater collection and treatment will be necessary for at least another two to three decades to come.

**There is no full article associated with this abstract.*

CHAPTER 15

MINE WATER GEOCHEMISTRY

Minewall Stations and Mass Loadings at an Epithermal High Sulfidation Deposit – What, No Scaling?

Claudio Andrade[1] and Keith Mountjoy[2]

1. *Barrick Gold Corporation, Canada*
2. *Klohn Crippen Berger, Peru*

ABSTRACT

A geochemical study was completed to determine in-situ loading rates from pit wall alteration types on a mass per unit area basis using Minewall wash stations. Surface water quality samples were also collected to determine the aqueous geochemical signature from acid rock drainage and metal leaching of the open pit and waste rock dumps. Secondary mineral precipitates were collected and analyzed to provide insight into metal controls. The study provided information for use in predictive water quality modeling of current and future pit and waste rock dump water quality.

Study results show that pit and waste rock dump water quality can be described as a Ca-Fe-Al-H-SO_4 system in an advanced state of pyrite oxidation and acid sulfate flushing. Surface water quality samples indicate there is a noticeable dry-wet cycle that stores and releases secondary acidic minerals of wide ranging solubilities. X-Ray Diffraction analyses identified alunite(?), calcite, gypsum, chalcanthite, paracoquimbite, coquimbite, ferricopiapite, zincocopiapite, bronchantite, antlerite, and posnjakite that can potentially store and release a host of major and trace ions.

Minewall loading rates are up to 100 to 1000 times higher than humidity cell loading rates on a mass per mass basis, and likely originating from both primary mineral weathering (sulfide oxidation) and secondary mineral dissolution. It is likely that the degree of secondary mineral storage and release changes throughout the year in response to dry- (storage) wet-season (release), compared to primary mineral weathering loading contributions. Implications of these Minewall station loading rates are that they do not require scaling factors for use in water quality modeling to avoid effectively underestimating modeling estimates.

Keywords: Minewall, epithermal, modeling, loading rates, water quality

INTRODUCTION

The ore deposit of interest is an economic Au-Ag high sulfidation epithermal type. The mine is an open pit heap leach operation and has been operating since the late 1990s. The mine classifies material in terms of alteration types summarized in Table 1 and Figure 1.

Table 1 Pit surface areas at end of mining

Final pit exposure surface areas				
Alteration	**Code**	**m²**	**km²**	**%**
Colluvium	CO	7,308	0.007	0.37
Argillic	AR	1,158,343	1.2	59
Quartz Alunite	QA	603,192	0.60	31
Vuggy Silica	VS	27,794	0.028	1.4
Siliceous Clay	SA	136,332	0.14	7.0
no information	-	24,080	0.024	1.2
Total		**1,957,048**	**2.0**	**100**

Notes: Argillic composed of argillic oxide (28.5%) and argillic sulfide (71.5%)

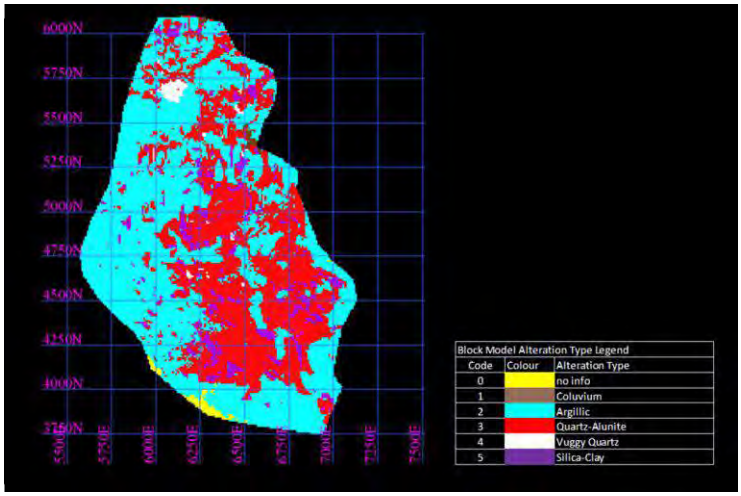

Figure 1 Pit alteration surface areas at the end of mining produced in Surpac

Table 2 summarizes the paragenetic minerals identified relevant to ARD-ML as sources of acidity and metal loadings to waste rock materials contact water quality. These minerals are termed as primary minerals in this study.

Table 2 Selected paragenetic minerals important to ARD-ML processes

Selected paragenetic minerals	Ideal formula
Alunite	$KAl_3(SO_4)_2(OH)_6$
Pyrite	FeS_2
Sphalerite	(Zn,Fe)S
Bismuthinite-stibnite	$Bi_2S_3 – Sb_2S_3$
Enargite	Cu_3AsS_4
Galena	PbS
Tennantite	$(Cu,Fe)_{12}As_4S_{13}$
Covellite	CuS
Native sulfur	S
Schwertmannite	$Fe^{3+}_{16}O_{16}(OH)_{12}(SO_4)_2$
Lepidocrocite	FeO(OH)
Goethite	FeO(OH)

The objectives of this study were to:

- Quantify site specific *in situ* loading rates of the various alterations types found on the open pit wall on a unit area basis [i.e., mass / (area * time)]
- Characterize surface water quality sampled directly downstream of the major mine components including pit walls and waste rock dumps
- Identify and quantify the secondary minerals controlling metal solubility, and
- Suggest modeling approaches to estimate closure water quality for mitigation purposes.

METHODOLOGY

International industry standard methods were employed throughout the desktop, laboratory and field scale studies consistent with MEND (2009) guidelines, the GARD Guide (INAP 2009) and Morin and Hutt (1997). Three types of sampling were carried out: surface waters, solid-phase secondary mineral precipitates and mine wall station leachate sampling within and directly downstream of the waste rock dumps (WRD) and pit walls. Analytical testing for the aqueous-phase was carried out at Certimin S.A., Lima (formerly CIMM) while solid-phase analyses were carried out at Mineral Services in North Vancouver, British Columbia, Canada.

Surface Waters

Surface water samples were collected within and directly downstream of the waste rock dumps and pits. The following parameters were measured or analyzed: pH (lab and field), electrical conductivity (lab and field), lab REDOX, acidity, sulfate, dissolved oxygen, alkalinity (carbonate, bicarbonate), cyanide (total, WAD), nitrogen (nitrate, nitrite, ammonia), fluoride, chloride, phosphate-phosphorus, total suspended solids, total dissolved solids, turbidity, and a 54 total and dissolved metals suite. Samples were collected in the field, split for total and dissolved metals analyses, preserved with standard high purity nitric acid after passed through standard 0.45 µm filters. Holding times were typically 24-48 hrs.

Secondary Mineralogy

Secondary mineral precipitates were identified in the field and collected for advanced mineralogical analyses. The objectives of the analyses was to identity and quantify the secondary weathering phases and associated metals of interest including Al, Fe, S, As, Cd, Cu, Pb, Sb, Zn and Hg. The mineralogical analyses consisted of X-Ray Diffraction with Rietveld-refinement, optical petrography, and scanning electron microscopy.

Thermodynamic Modeling

The geochemical thermodynamic modeling software Geochemist's Workbench (GWB) was used to model surface waters to determine potential secondary mineral controls on water quality (Bethke, 2008). Note that the data base thermo_minteq.dat was used for all modeling runs.

Minewall Stations

Established methodologies (Castendyk and Eary, 2009) for the prediction of closure pit lake water quality include mass-water balance approaches in parallel with thermodynamic geochemical modeling and water balance calculations. A prerequisite includes the quantification of elemental loading rates, typically sourced from standard humidity cells or larger-scale field kinetic tests (MEND, 2009) on a mass per unit mass basis over time [e.g., mg/(kg * week)]). Note that field based approaches are preferred for predictive water quality assessments as they include secondary mineral solubility controls under site-specific conditions of aged materials at advanced oxidation conditions (i.e., microbially mediated with pyrite oxidation by Fe^{3+}). Conversely, laboratory humidity cells are designed to estimate primary oxidation rates using a high liquid-to-solid leachate ratio (MEND, 2009) and are often the only source of elemental loading rate data available for predictive water quality modeling but require scaling from laboratory conditions to expected site-specific field conditions.

Another approach is the quantification of loadings rates on a mass per unit surface area basis [e.g., mg/(m^2*week)]. This later method, referred to as the Minewall approach, is a site-specific method and has been used successfully to bracket loading rates without the use of scaling factors (Morwijk Enterprises, 1995; Morin and Hutt, 2004). The method is particularly useful for active mines where reactive pit wall material is exposed and available for relatively easy leachate sampling. The method is designed for pit lake water quality predictions required for mine closure assessments.

Five Minewall stations were constructed on the main alteration types. Photo 1 shows an example station after construction. Between sampling events, a cover was placed over the station to allow:

- Mineral reactions to proceed aided only by humidity as the sole source of water, and

- Secondary minerals to precipitate and prevent flushing or hydraulic disturbance.

It is expected that the reactivity of a particular alteration type varies at different scales (mm to meters) and temporally as new materials is exposed on pit wall, however the size of the Minewall window (~1m), good understanding of typical alteration mineralogy and selection in the field results in reasonable representative sampling. Site-specific field-based calculations of material loading rates and reaction progress over time was subsequently generated.

Photo 1 Typical Minewall station prior to leachate collection (left) and with cover between sampling events (right). Note that the upper horizontal structure of the Minewall measures ~50cm for scale.

Minewall stations were sampled weekly for the first month and then monthly for eight months thereafter between November 7, 2011 and July 7, 2012. Sampling consists of gently flushing one litre of distilled water over the face of the exposed material and collecting the leachate in a clean HDPE sample bottle for analyses. Approximately 0.75 L of leachate was collected per sampling event. The following parameters were measured or analyzed: pH (lab), electrical conductivity (lab), REDOX, acidity, alkalinity, sulfate, and a 52 element total and dissolved suite. Full Minewall construction and sampling methodology can be found in Morin and Hutt (2004). Samples were collected in the field, split for total and dissolved metals analyses, preserved with standard high purity nitric acid after passed through standard 0.45 μm filters. Holding times were typically 24-48 hrs.

RESULTS AND DISCUSSION

Surface Water Quality (WQ)

These waste materials are highly acid generating; similar to other deposits types around the world, such as Pueblo Viejo, Dominican Republic and Summitville, Colorado. Waste rock dump and pit wall contact waters can be described by the Ca-Fe-Al-H-SO_4 system (Figure 1). The measured acidity over time indicates that there is a noticeable increase as the wet season begins, typically October or November. The mechanism for this temporal difference is due to the dissolution and flushing of soluble secondary acidic minerals, which have precipitated in the preceding dry season via evapo-concentration. This is a common climate driven process observed at other acidic mine sites controlling WQ (Nordstrom and Alpers, 1999). Such waters are often characterized by a Ficklin plot where the acidic system results in high dissolved trace metal concentrations, and in this case is an excellent predictive tool to determine bulk trace metal concentrations Figure 2. The pH shows a narrow acidic range less than pH 3.0 and can be considered to have high metals and high acidity originating from epithermal high sulfidation quartz alunite acid sulfate mine components (Plumlee et al, 1999).

Note that water treatment at site includes HDS + RO technology to meet national WQ regulations for users downstream. ARD has been calculated to continue and persist for several decades to hundreds of years after closure.

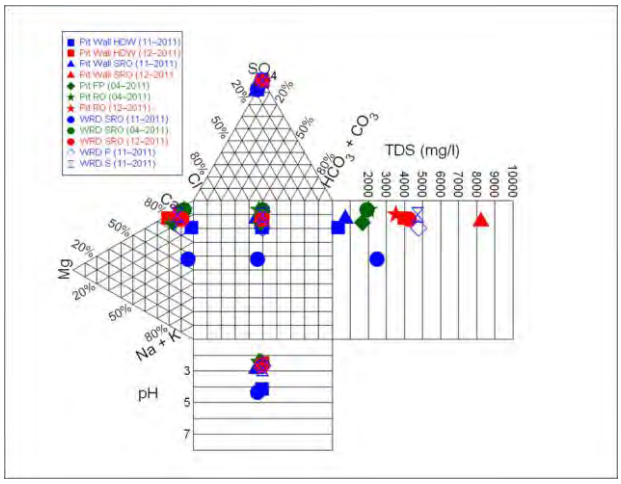

Figure 1 Durov diagram of waste rock dump and pit wall contact waters

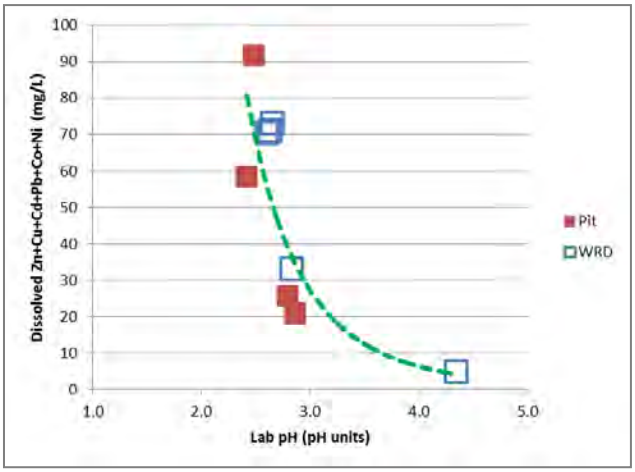

Figure 2 Ficklin Plot of waste rock dump and pit wall contact waters.

Thermodynamic Modeling

Sulfide oxidation and acid sulfate dissolution at Pierina are the main geochemical process impacting WQ. The paragenetic sequence of secondary Fe-SO4 minerals after pyrite oxidation has been documented by Bandy (1938), Buurman (1975) and Nordstrom and Alpers (1999) and is summarized by Jambor et al. (2000; Table 1). The mineral evolution can be regarded as an initial precipitation of hydrated Fe-SO4 minerals followed by progressive (de)hydration as the mineral crystal lattice matures. In an open system, such as WRDs and pits, the (de)hydration cycle will typically follow the seasonal climate trends (precipitation and evaporation). However, the entire or partial suite of hydrates may be present as moisture content or vapour pressure varies at the micro-scale within/on the WRD and pit wall materials.

Table 1 Paragenetic Secondary Mineral Sequence after Pyrite Oxidation (modified from Jambor et al, 2000)

Stage	Mineral	Formula
Early	Pyrite	FeS_2
	Melanterite	$FeSO_4 \cdot 7H_2O$
	Siderotil	$FeSO_4 \cdot 5H_2O$
	Rozenite	$FeSO_4 \cdot 4H_2O$
	Szmolnokite	$FeSO_4 \cdot H_2O$
	Copiapite	$Fe^{2+}Fe^{3+}_4(SO_4)_6(OH)_2 \cdot 20H_2O$
	Romerite	$Fe^{2+}Fe^{3+}_2(SO_4)_4 \cdot 14H_2O$
	Coquimbite	$Fe^{3+}_2(SO_4)_3 \cdot 9H_2O$
	Kornelite	$Fe^{3+}_2(SO_4)_3 \cdot 7H_2O$
	Rhomboclase	$(H_3O)Fe^{3+}(SO_4)_2 \cdot 3H_2O$
	Parabuttlerite/Voltaite	$K_2Fe^{2+}_5Fe^{3+}_4(SO_4)_2 \cdot 18H_2O$
Late	Jarosite/Halotrichite/Bilinite	$Fe^{2+}(Al,Fe^{3+})_2(SO_4)_4 \cdot 22H_2O$

Results of thermodynamic modeling of WRD and pit WQ are presented in Figure 3 through Figure 6. Modeling indicates dissolved Ca, K, Al and SO_4 may be controlled in the form of gypsum ($CaSO_4 \cdot 2H_2O$) and alunite precipitation [$(K, Na)_2Al_6(SO_4)_4(OH)_{12}$]. Additional potential controls on dissolved Cu and SO_4 include bronchanite [$Cu_4SO_4(OH)_6$] and antlerite [$Cu_3SO_4(OH)_4$], however the pH of the system would have to approach neutral conditions for bronchanite stability.

Other secondary minerals that may be theoretically controlling WRD and pit WQ are ferrihydrite [$Fe(OH)_3$], K-jarosite [$Fe^{2+}(Al,Fe^{3+})_2(SO_4)_4 \cdot 22H_2O$] and melanterite ($FeSO_4 \cdot 7H_2O$). Ferrihydrite is important as it is a common host for metal sorption in the aqueous systems (Dzombak and Morel, 1990). The latter two minerals are important as they bracket an important and common family of hydrated Fe-SO_4 minerals found in acid environments (Nordstrom and Alpers, 1999 and Jamieson et al, 2005) and may be additional controls on trace metals such as Zn.

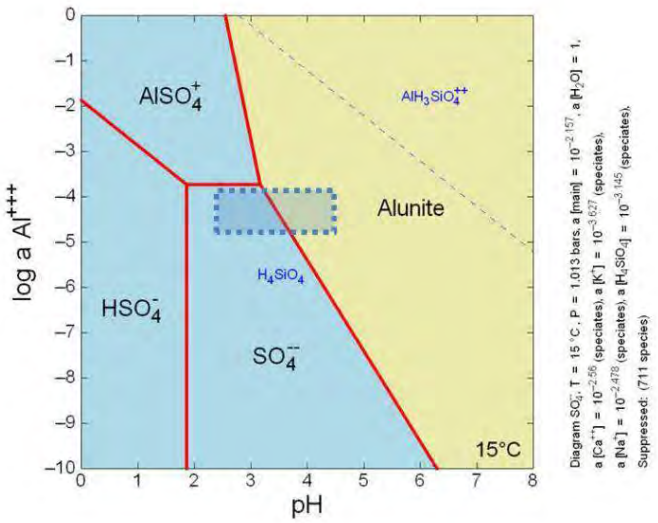

Figure 3 Log Activity of Al vs. pH Diagram (dashed box indicates WRD and pit waters)

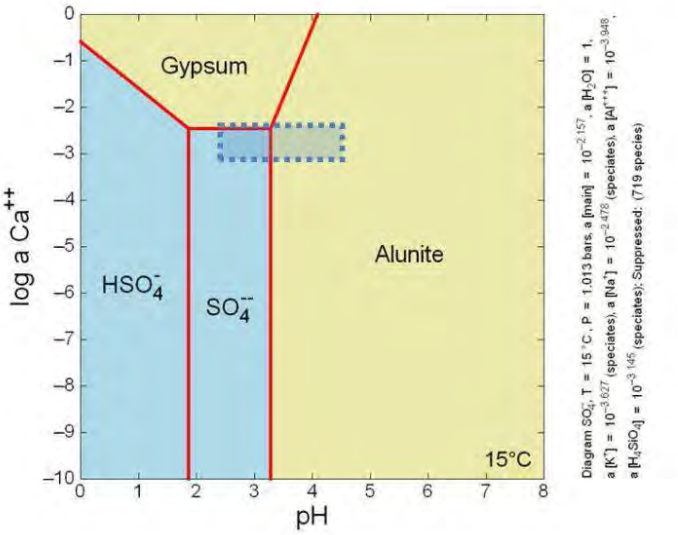

Figure 4 Log Activity of Ca vs. pH Diagram (dashed box indicates WRD and pit waters)

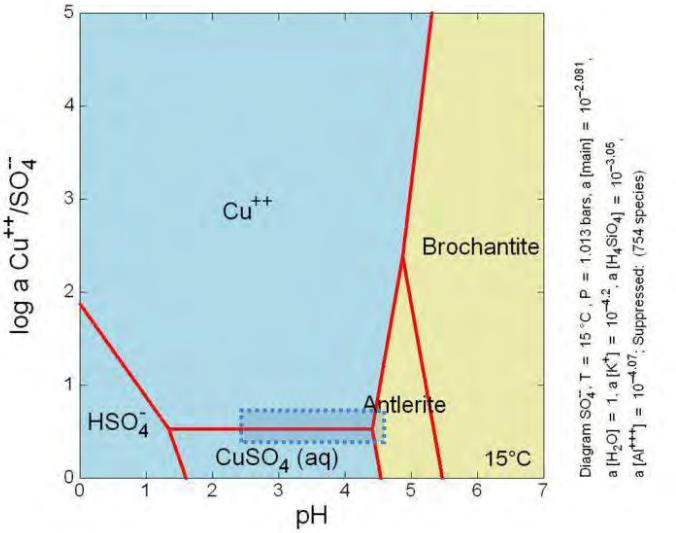

Figure 5 Log Activity of Cu/SO_4 vs. pH Diagram (dashed box indicates WRD and pit waters)

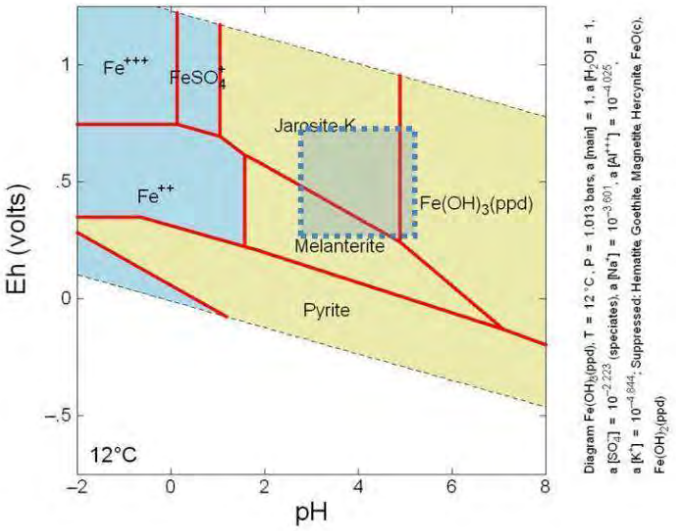

Figure 6 Eh-pH Diagram for the Fe-S-K System (dashed box indicates WRD and pit waters)

Secondary Mineralogy

Secondary mineral precipitates can be found at the centimetre to 10s of meter scale. Six of ten samples collected showed distinct morphological differences or were from distinct environmental locations (i.e., WRD and pit vs. Leach Pad) and were submitted for mineralogical analyses.

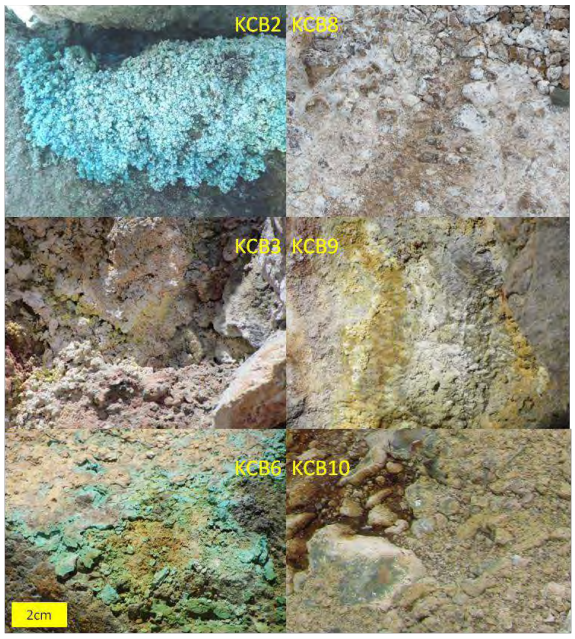

Figure 7 Secondary mineral sample locations

Table 2 summarizes the secondary minerals identified by XRD with Rietveld refinement. Note that primary alunite is present in several distinct morphologies and is ubiquitous. Furthermore, alunite is kinetically slow to precipitate at standard temperature and pressure likely requiring high ionic strengths in solution to overcome this barrier (Alpers et al, 1994). However, alunite has been observed in low P&T digenetic environments (Wray, 2011; Prietzel and Mayer, 2005; Goldbery, 1980 and Goldbery, 1978). The formation of alunite can be described as a result of the alteration of K-rich clays, such as kaolinte and/or illite in acidic environments. Although sample collection focussed on secondary minerals, "entrainment" of primary alunite in sample collection cannot be ruled out.

An unexpected result of the XRD analysis was the presence of calcite in the 6KCB sample. Calcite is extremely soluble in acidic conditions, such as those found within the pit and WRD environments. Analytical misinterpretation has been ruled out as this mineral was identified petrographically on several occasions. Carbonate is typically found as rims on lithic fragments and is thought to be either from the original paragenetic sequence or less likely, as a secondary precipitate forming at ambient conditions in the pit. In addition, calcite may be present at the core of particles, either through original paragenetic mineral encapsulation or subsequent secondary mineral armouring and unavailable for reactions. Neither of these possibilities can be ruled out at this time, and may be moot as there is nil buffering capacity evident in the highly acidic pit and WRD aqueous environment. However, the identification of bronchanite via XRD coupled with the theoretical thermodynamic modeling provides supporting evidence and a potential geochemical pathway for slightly acidic to near-neutral pH micro-environments. However, the pH of the pit on a macro-scale remains highly acidic.

Calcium, Cu, Fe, Zn and S attenuating mechanisms are evident through ideal crystal lattice structure formulas. This is especially important for the Cu-SO_4 phases where Cu contributes as much as 4 moles to the weight of the ideal minerals found at station 6KCB. Additional important trace elements associated by either substitution/co-precipitation into the lattice or sorption onto the

mineral include Cu, Co, Mn, S, Al, Si, Na, Pb, Mn. Note that no micro/nano mineralogical techniques were done to investigate these mechanisms and quantify concentrations.

Table 2 Secondary minerals identified by XRD with Rietveld refinement.

Selected Minerals	Ideal Formula	2KCB	3KCB	6KCB	8KCB	9KCB	10KCB
				Weight %			
Pyrite	FeS_2	2.6		4.2		5.7	3
Covellite?	CuS				0.2		
Alunite	$K_2Al_6(SO_4)_4(OH)_{12}$	6.9	6.3	7.6	1.2	9.8	1.4
Gypsum	$CaSO_4 \cdot 2H_2O$	0.5		35.3	1.1	19.5	13.5
Chalcanthite	$CuSO_4 \cdot 5H_2O$	78.1					
Paracoquimbite	$Fe_2(SO_4)_3 \cdot 9H_2O$		28.7 (Al, Si, Na)				
Coquimbite	$Fe_2(SO_4)_3 \cdot 9H_2O$		2.2				
Ferricopiapite	$Fe^{2+}_{0.66}Fe^{3+}_4(SO_4)_6O(OH) \cdot 20H_2O$		47.2 (Al, Si)				
Zincocopiapite	$ZnFe_4(SO_4)_6O(OH) \cdot 18H_2O$					11.7	
Calcite	$CaCO_3$			7.0(Cu, Co, Mn, S, Al, Si, Na)	0.5		
Bronchantite	$Cu_4(SO_4)(OH)_6$			14.1 (Al, Si, Fe)			
Antlerite	$Cu_3(SO_4)(OH)_4$			9.2 (Al, Si, Fe)			
Posnjakite?	$Cu_4(SO_4)(OH)_6 \cdot H_2O$			0.6 (Al, Si, Fe)			
Amorphous (SEM)	(Fe, Mn, Pb) - (hydr)oxide Fe – (hydr)oxide with As, Zn, P, Al						

Notes: Elements in parentheses identified in/on mineral structure by SEM.

Secondary minerals are both sinks and sources of the above mentioned elements. They are sinks as the dry season approaches and pit and WRD waters experience evapo-concentration and secondary mineral precipitation. Conversely, secondary minerals are sources of elemental loadings to surface waters as the wet season approaches and minerals dissolve due to their moderate to high solubility.

Mass Loadings per Unit Area

Minewall loading rates (Figure 8 to Figure 10), based on unit surface areas, were compared with humidity cell loading rates and show *in situ* field rates are potentially 100-1000 times higher than lab-based rates. This agrees with an extensive comparison of Minewall and humidity cell data done by Morin and Hutt (2004). The Minewall loading rates are believed to be originating from both primary mineral weathering rates (pyrite oxidation) as well as secondary mineral dissolution. The relative magnitude of each was not determined; however, it is likely that secondary dissolution contributions oscillate throughout the year being greater during the onset of the wet season compared to primary minerals weathering loading contributions. The humidity cells contained drill core reject (80% passing <2 mm) that was acid generating (Figure 8) and show initial high first flushes, but much lower than Minewall station average acid loading rates. Note that humidity cell material particles are assumed to have cubic surface areas as a reasonably conservative estimate (as opposed to a sphere) for each mesh size particle analysis and respective surface area calculations.

The above observations have important scaling implications to modeling. Scaling is defined as the factors used to estimate the climatic and physical factors in the field that require accounting for when loading rates are derived from laboratory-based kinetic experiments (e.g., humidity cells). Minewall stations are designed to produce site-specific in situ loading rates, meaning that climate and physical scaling factor products are equal to one. The Minewall station leachates are thus assumed to be at quasi-equilibrium (Morin and Hutt, 2007), meaning that the following factors are at a scale large enough not to require additional adjustments:

Mass – generally it is difficult to convert exposed Minewall station material to a mass basis, as the depth/thickness of mass contributing to active leaching cannot be accurately estimated. For example, if we assume a uniform 2.7 t/m^3 density of the minerals exposed at the QA Minewall station and either a 0.002 m or 0.01 m active leaching depth, the resulting calculations would yield 0.46 kg and 2.3 kg of active mass contributing to leaching, respectively. Field observations indicate that an estimated volume of <10% to 15% of the total flushing solution (~1 L) is initially taken up (i.e., sponge effect) by the wall material. Therefore, field observations would suggest that the depth of the active mineral layer is on the order of millimetres instead of cm. This estimate varies for the different alteration types (i.e., the AR material has a relatively higher sponge effect than the QA material), however the absolute differences between alteration types is not believed to impact concepts or interpretations materially. Note that inundation of large proportions of pit wall areas (i.e., pit lake formation) can result in water penetrating the wall to a significant depth as the pit lake develops and perhaps nullifying the small-scale observations at the Minewall station. Another important observation is that the ARG material shows continually increasing dissolved constituents and is likely associated with its friable nature. The advanced hydrothermal alteration inherent in the ARG material and subsequent chemical weathering at ambient conditions degrades this material physically into a fine-grained "muck" quickly after initial mining exposure. The potential suspended solids content is in the 1 g/m^2 to 10 g/m^2 range for all alteration types.

Area – at the Minewall station, the scale is believed to represent the alteration type average per unit area. In other words, alteration surface area in one part of the pit is equal to alteration surface area in another part of the pit (i.e., no scaling roughness factors according to fractures).

Surface Area Roughness – surface area roughness and/or fracturing is estimated to control loading rate estimates on a mass per unit area by 2-3 factors at most. This will not affect selection of base cases or upper bound loading rates for predictive WQ modeling.

Solid:Liquid ratio – over a one week period in April and November 2011, 5 L and 2 L of precipitation would have fallen on an average Minewall station surface area of 0.11 m^2, assuming

the Minewall surface was planar. In reality, the Minewall stations are inclined and if we assume a slope of 1:2.5 the resulting planar area of the average Minewall station would capture 2.2 L and 0.8 L for the month of April and November, respectively. In practicality, this is considered the same as the 1 L flushing and 0.75 L collection volumes during Minewall station sampling in the first month.

Reaction rates – reaction rates are assumed to be optimal (i.e., pH <3.5 and advanced enough that Fe^{3+} is the primary electron acceptor in pyrite oxidation likely mediated by microbial activity as shown in Equations 1). Note that no Fe speciation or microbial identification was carried out in this study; however, the low pH, high dissolved Fe, SO_4 and acidity in WQ samples and age of the pit wall material suggests this assumption is valid.

$$Fe^{2+}_{(aq)} + 0.25O_{2(aq)} + H^{+}_{(aq)} \rightarrow Fe^{3+}_{(aq)} + 0.5H_2O_{(l)}$$

$$FeS_{2(s)} + 14Fe^{3+}_{(aq)} + 8H_2O_{(l)} \rightarrow 15Fe^{2+}_{(aq)} + 2SO_4^{2-}{}_{(aq)} + 16H^{+}_{(aq)}$$

Equations 1 Ferrous Oxidation (upper) and Advanced Pyrite Oxidation (lower)

Conversely, humidity cell scaling factors typically -scale down loading rates for grain size based on the fact that the humidity cell is testing 80% <2 mm and is often assumed to typically represent 5% to 25% of the waste and pit wall grain size. Additionally, this is only one of several scaling factors that are applied to loading rates (Morin, 2013) translating into a typical factor product of 0.1-0.001. This effectively decreases the applied loadings rates and could underestimate WQ predictions. Note that the humidity cells operated for 25 and 60 weeks to near stable rates. The comparison between lab and field data strongly suggests the Minewall station data should be used for future pit inundation, flushing and pit lake predictions for closure WQ and mitigation assessments.

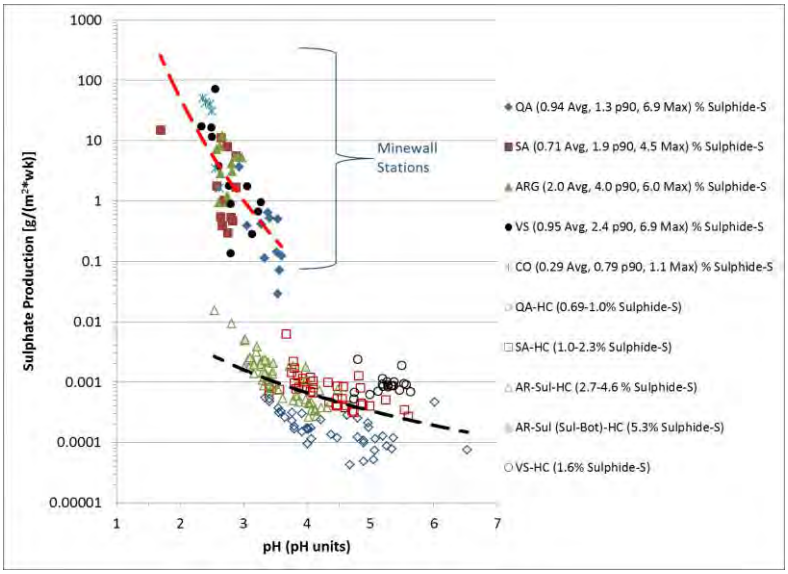

Figure 8 Minewall station and humidity cell leachate acidity loading rates versus pH.

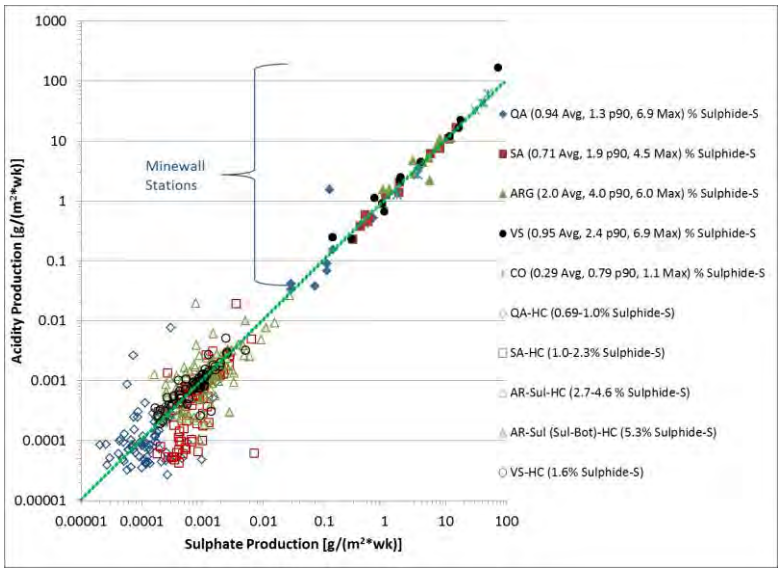

Figure 9 Minewall station and humidity cell leachate acidity versus sulfate loading rates.

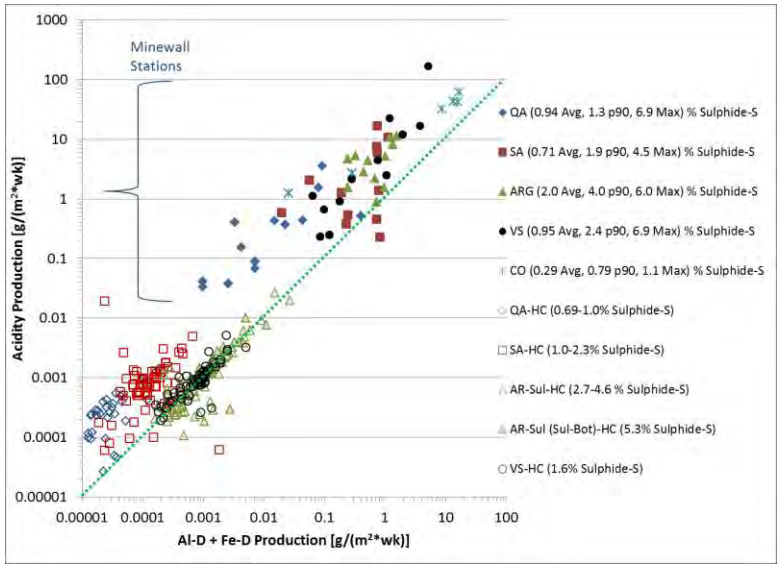

Figure 10 Minewall station and humidity cell leachate acidity versus Al-D + Fe-D loading rates.

CONCLUSION

Epithermal high sulfidation acid sulfate geology produces leachate water high in metal and acidity, consistent with other deposits of the same type. Field leaching studies were initiated on representative alteration types on aged pit walls at the meter scale known as Minewalls. Loading rates are up to 100 to 1000 times higher than humidity cell loading rates on a mass per unit area basis with both primary and secondary minerals contributing to loadings on a seasonal basis. Minerals of interest included pyrite, calcite, chalcanthite, paracoquimbite, coquimbite, ferricopiapite, zincocopiapite, bronchantite, antlerite, and posnjakite and possibly alunite. Minewall

station loading rates do not require scaling factors for use in water quality modeling and will avoid effectively underestimating estimates.

ACKNOWLEDGEMENTS

The authors wish to thank Alexandra Mauler-Steinmann for excellent and timely delivery of mineralogy reporting. Engaging discussions with Drummond "Dusty" Earley III were much appreciated. Data collection was facilitated by various dedicated and enthusiastic mine site and Klohn Crippen Berger personnel.

REFERENCES

Alpers, C.N., Blowes, D.W., Nordstrom, D.K., and Jambor, J.L., 1994. Secondary minerals and acid mine-water chemistry In: Jambor, J.L. and Blowes, D.W., (Eds.) Environmental Geochemistry of Sulfide Mine-Wastes, Short Course Mineral Association of Canada Vol. 22, 247-270.

Bandy, M.C., 1938. Mineralogy of three sulfate deposits of northern Chile. American Mineralogist, 23: 669-760.

Bethke, C.M., 2008. Geochemical and biogeochemical reaction modeling. New York, Cambridge University Press, 539 pp.

Buurman, P., 1975. In vitro weathering products of pyrite. Geolegie enMijnbouw, 54: 101-105.

Castendyk, D.N and Eary, L.E., 2009. Mine Pit Lake: Characteristics, predictive modeling and sustainability Management technologies for metal mining influenced waters, volume 3. Society for Mining Metallurgy and Exploration 304 pp.

Dzombak, D.A., and Morel, F.M.M, 1990. Surface complexation modeling: hydrous ferric oxide. Wiley and Sons, New York, 393 pp.

Goldbery, R., 1978. Early diagenetic, nonhydrothermal Na-alunite in Jurassic flint clays, Makhtesh Ramon, Israel. Bulletin of the Geological Society of America, 89: 687-698.

Goldbery, R., 1980. Early diagenetic, Na-alunite in Miocene algal mat intertidal facies, Ras Sudar, Sinai. Sedimentology, 27: 189-198.

INAP, 2009. The Global Acid Rock Drainage (GARD) Guide. Available online http://www.gardguide.com/index.php/Main_Page Accessed January 2011.

Jambor, J.L., Nordstrom, D.K. and Alpers, C.N., 2000. Metal-sulfate salts form sulfide mineral oxidation, In Alpers, C.N., Jambor, J.L. and Nordstrom, D.K. (Eds.) Sulfate minerals: Crystallography, geochemistry and environmental significance. Reviews in Mineralogy and Geochemistry, Vol 40, pp. 303-350.

Jamieson, H.E., Robinson, C., Alpers, C.N., McCleskey, R.B. Nordstrom, D.K., Peterson, R.C. 2005. Major and trace element composition of copiapite-group minerals and coexisting water from the Richmond mine, Iron Mountain, California. Chemical Geology 215, 387-405.

MEND, 2009. Prediction Manual for Drainage Chemistry from Sulphidic Geologic Materials Mend Report 1.20.1. NRCan.

Morin, K.A., and Hutt, N.M., 1997. Environmental Geochemistry of Minesite Drainage: Practical Theory and Case Studies. MDAG Publishing (www.mdag.com), Surrey, British Columbia. ISBN: 0-9682039-0-6.

Morin, K.A. and Hutt, N.M., 2004 The Minewall Approach for Estimating the Geochemical Effects of Mine Walls on Pit Lakes. Pit Lakes 2004; United States Environmental Protection Agency; Reno, Nevada; November 16-18, 2004.

Morwijk Enterprises Ltd., 1995. MINEWALL 2.0. Series of four reports (User's Manual, Literature Review, Application of MINEWALL 2.0 to three minesites and Programmer's notes and source code). MEND Report 1.15.2.

Nordstrom, D.K. and Alpers, C.N., 1999. Negative pH, efflorescent mineralogy and consequences for environmental restoration at the Iron Mountain Superfund site, California. Proceedings of the National Academy of Science, USA, 96: 3455-3462.

Plumlee, G.S., Smith, K.S., Montour, M.R., Ficklin, W.H., and Mosier, E.L., 1999, Geologic controls on the composition of natural waters and mine waters draining diverse mineral-deposit types, in Filipek, L.H., and Plumlee, G.S., eds., The Environmental Geochemistry of Mineral Deposits, Part B: Case Studies and Research Topics: Reviews in Economic Geology, v. 6B, p. 373-432.

Prietzel, J. And Mayer, B., 2005. Isotopic fractionation of sulphur during formation of basaluminite, alunite and natroalunite. Chemical Geology, 215, 525-535.

Wray, R.A.L., 2011. Alunite formation within silica stalactites from the Sydney Region, South-eastern Australia. International Journal of Speleology, 40(2), 109-116.

Establishing an Total Dissolved Solids: Electrical Conductivity Ratio for Mine Waters

Christian Wolkersdorfer[1] and Elena Hubert[2]

1. *Tshwane University of Technology, South Africa and Lappeenranta University of Technology, Finland*
2. *Technische Universität Bergakademie Freiberg, Germany*

ABSTRACT

Total dissolved solids (TDS) expresses the sum of all dissolved ions in water. In a given water, the TDS content in mg/L and electrical conductivity κ_{25} at 25 °C in µS/cm are related to each other by the equation $TDS = \kappa_{25} \times f$, where f is a constant, commonly referred to be in the range of 0.55 – 0.9. Mine water with elevated TDS contents rapidly causes scaling or corrosion, as high TDS values are often associated with lower pH-values. TDS is also used to calculate the potential amount of sludge in mine water treatment, which makes TDS a crucial parameter.

For accurate TDS determinations, filtered water samples are oven dried and the mass of the residue is the TDS-content. As this procedure is time consuming, the TDS is commonly estimated from EC measurements using the above equation and laboratory and field conductometers are manufactured with a programmable conversion factor. Normally TDS is reported without further considering the conversion factor or its way of measurement.

In this paper, we describe TDS/EC conversion factors for 45 South African, mining impacted waters. It can be shown that the conversion factor ranges from 0.25 to 1.34 with a mean of 0.86 and a standard deviation of 0.19. No correlation with other on-site parameters was found, though there is a tendency to higher conversion factors at lower pH-values and higher electrical conductivities.

Based on our work we conclude that prior to using the TDS/EC conversion equation, the conversion factor for the single mine water, not only site specific but also time depended, must be determined in the lab and the conductometer be programmed with this conversion factor. In addition, the conversion factor 0.65 recommended in the South African Water Quality Guidelines should no longer be used for mining impacted water.

Keywords: mine water, South Africa, electrical conductivity, total dissolved solids (TDS)

INTRODUCTION

When electrolytes or salts are dissolved in aqueous solutions their ions dissociate and increase both the amounts of dissolved solids in the solution and their conductivity (Hölting and Coldewey, 2013). Consequently, both parameters are relevant in characterizing the chemistry of aqueous solutions. Electrical conductivity (EC) and total dissolved solids (TDS) are commonly analysed in water samples to provide an indication for the waters' mineralization or salinity. Both parameters are related to each other, as each charged ion of the dissolved constituents contributes to the conductivity of the aqueous solution. EC measurements are therefore commonly used for estimating the TDS (Gustafson and Behrman, 1939).

Electrical conductivity is measured with a probe that determines the resistivity of the aqueous solution. Because the resistivity is the reciprocal of the conductance, the conductivity of the aqueous solution can be calculated based on the resistivity measurement (American Public Health Association et al., 2005, Hölting and Coldewey, 2013):

$$G = \kappa \frac{A_c}{l_c}$$

where G is the conductance in S, κ the electrical conductivity in S/cm, A_c the cross section of the conductor in m² and l_c the characteristic length in m. The electrical conductivity κ is calculated as follows:

$$\kappa = \frac{l}{A \cdot R}$$

where κ is the electrical conductivity in S/cm, l the distance between the electrodes in cm, A the cross section of the electrodes in cm² and R the electrical resistance in $\Omega = \frac{1}{S}$.

Because the electrical conductivity is temperature dependent (Smith, 1962), the measured value has to be temperature compensated, usually to 25 °C.

TDS is determined analytically by evaporating the aqueous solution and measuring the weight of the dry residue (Hem, 1985). Accurate determination of the total dissolved solids for filtered or unfiltered samples is achieved by evaporating the aqueous solution at predetermined temperatures, which are in the range of 105 to 110 °C and at 180 °C (American Public Health Association et al., 2005). When comparing the sum of all analysed ions and molecules with the analytically determined TDS, the latter frequently exceeds the sum of ions, as not all water constituents are usually included in the analysis (Howard, 1933).

Problems with this method occur when water contains considerable amounts of sulphate, as the minerals that precipitate during evaporation of the water are Ca, Mg or Na sulphates which contain water in their crystal structure (Howard, 1933). Even at a temperature of 180 °C, not all of the crystal water is released from the crystal and consequently, the determined TDS is greater than the sum of all analysed ions in the aqueous solution.

It can be shown that EC and TDS are related with each other by the following equation

$$\mathrm{TDS} = \kappa_{25} \cdot f \quad [\mathrm{mg/L}]$$

where TDS are the total dissolved solids in mg/L, κ_{25} the temperature compensated electrical conductivity in µS/cm at 25 °C and *f* a conversion factor in (10 g m)/(L S). Commonly, the value of this factor is given to be in the range of 0.55 – 0.9 (American Public Health Association et al., 2005, Wolkersdorfer, 2008) and many probes are pre-set to a factor in this range. If the water contains elevated concentrations of SiO_2, this relationship is no longer accurate and corrections for SiO_2 need to be applied (Day and Nightingale, 1984).

However, there are cases where those values can't be used to precisely calculate the TDS and as each aqueous solution contains different ions the factor *f* changes with the water's chemistry. Ali et al. (2012), for example, determined factors between 0.41 and 2.01 for industrial waste water in Korea and based on the data of Atekwana et al. (2004) for a contaminated aquifer in Michigan/USA a conversion factor of 0.50 to 1.21 can be calculated. For South African rivers, van Niekerk et al. (2014) determined factors between 0.48 and 0.86 (n = 144 643) and based on the data of Day and Nightingale (1984) the ratio for SiO_2-rich waters in California is between 0.56 and 0.82, while Weiner (2010) provides a range of 0.55 to 0.7 for surface and ground waters and 0.5 for seawater. Department of Water Affairs and Forestry (1996) recommends a single conversion factor of 0.65 for South African waters, while Hobbs (2013) inconsistently used 0.7 or 0.77 while he determined a factor of 0.73 from 1045 EC measurements and TDS lab analysis. In a personal communication, Hobbs reports TDS/EC ratios of 0.46 to 1.29 for a variety of surface, ground and waste waters with an average of 0.83 (n = 16).

Because high TDS values are often associated with lower pH-values, water with elevated TDS concentrations rapidly causes scaling or corrosion. Besides, TDS is used to calculate the potential amount of sludge in mine water treatment. Consequently, the effective and low cost evaluation of TDS becomes a crucial parameter. In this paper, we present first results of determining the TDS/EC-ratio for 45 South African mine water samples taken at various locations in the Witwatersrand gold fields, the Mpumalanga coal mines and various other locations in Gauteng, Mpumalanga and Limpopo.

METHODOLOGY

Unfiltered and unacidified water samples at 45 locations in the South African provinces Gauteng, Mpumalanga and Limpopo were taken in 1-L-PE bottles (Figure 1). On-site, the parameters temperature (Hach CDC401), pH (Hach PHC201), redox-potential (Hach MTC101), electrical conductivity (Hach CDC401) and oxygen saturation (Hach LDO101) connected to a Hach HQ40d were determined. pH was calibrated at the start of each sampling day with pH 4, 7, and 10 standard solutions. Electrical conductivity was calibrated with a 1413 µS/cm 0.01 M KCl standard solution. Samples were kept in a cooler box with cooling elements and stored in a cooling room at TUT until further analysis. Sample aliquots were allowed to warm to room temperature before each lab analysis.

TDS was determined in the lab using standard method 2540 (American Public Health Association et al., 2005) after filtering the sample through a 0.45 µm cellulose nitrate membrane filter. All samples were analysed in duplicates and if necessary in triplicates when the deviation of the duplicates was too high.

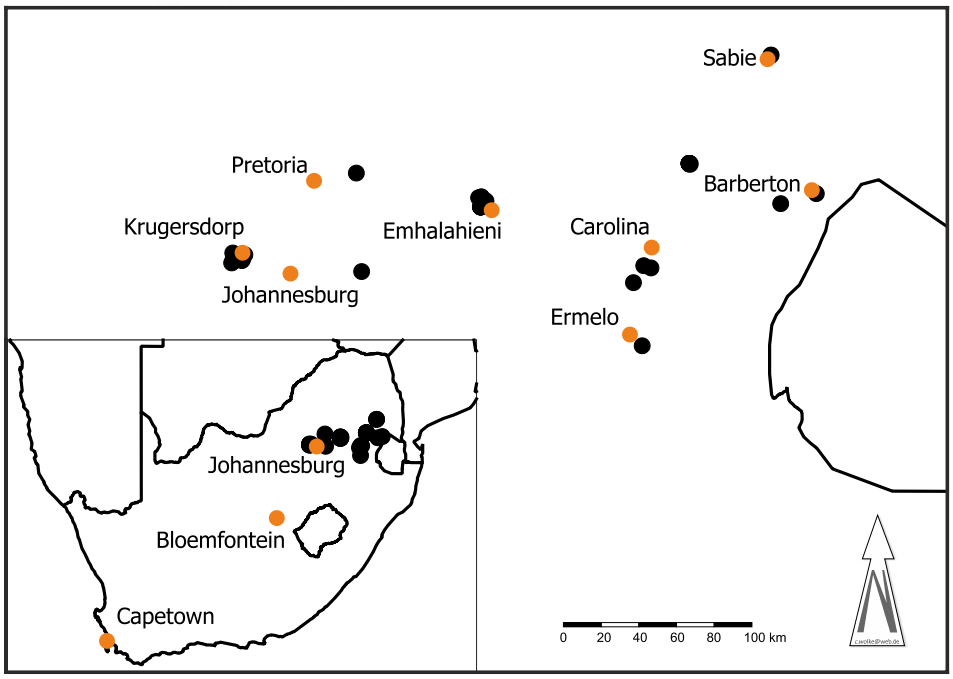

Figure 1 Map of the sampling locations (dark dots) within Nord-Eastern South Africa.

Electrical conductivity was measured in the lab with a daily calibrated EC probe (Hach CDC401) attached to a Hach HQ40d. All data was temperature corrected to 25 °C with a compensation factor individually determined for each sample from measurements of the EC while heating a cooled sample aliquot. This temperature correction factor ranged between 1.16 and 2.16 % with an average of 1.92 %. After measuring the EC and determining the TDS, the conversion factor was determined according to this equation:

$$f = \frac{\mathrm{TDS}}{\kappa_{25}}$$

where f is the correlation factor for EC and TDS in (10 g m)/(L S), TDS is the total dissolved solids in mg/L and κ_{25} the temperature compensated electrical conductivity in µS/cm at 25 °C. Then the averages of the correlation factors f determined for one sample by duplicate or triplicate measurements were calculated.

Both, the geological setting and the climatic conditions of the sampled sites vary. Geologically, the sites are located in the Karoo Supergroup (eMmalahleni, Carolina, Ermelo), the Transvaal Supergroup (Sabie, Krugersdorp, Edendale) and the Barberton Greenstone Belt (Barberton). Climatically, all the sites are within the humid subtropical climate zone (Köppen Climate Classification) with hot, rainy summers and cool dry winters and precipitation between 600 and 800 mm/a (Johnson et al., 2006, Lynch, 2004).

Results And Discussion

Field pH of the 45 samples ranged between 2.45 and 7.85 and the electrical conductivity between 45 and 16 369 µS/cm with average values of 3.92 and 5 091 µS/cm, respectively (Table 1). As can be

seen, most pH-values are in the range of the iron buffer, some in the aluminium buffer and those at higher pH-values in the carbonate buffer range (Figure 2).

Consequently, the water samples represent a wide range of mining impacted waters in South Africa from the low pH-values indicative for AMD, high pH-values for well buffered mine water and one surface water sample. As expected, the general trend of all samples is that lower pH-values often relate to higher electrical conductivities (Figure 2). Exceptions from the general trend are samples from the abandoned Transvaal and Delagoa Bay Colliery near eMalahleni, which show an exceptionally high electrical conductivity. Reason for this behaviour is that this mine was closed several decades ago, is very close to the surface, the coal was mined underground as well as strip mined and the pyrite oxidation is consequently higher than in the flooded mines with low pH-values. A similar situation occurred in the case of the Yorkshire № 1 and the Shoff mines in the US were the up-dip and strip mined Shoff mine also shows higher contamination loads than the down dip Yorkshire № 1 mine (Mentz et al., 1975).

Lab determined TDS ranged between 50 and 13 984 mg/L with an average of 4 279 mg/L and a standard deviation of 4 422 mg/L (Table 1). Using those analytically determined total dissolved solids concentrations, the calculated TDS/EC ratio is in the range of 0.25 to 1.34 with an average of 0.86 and a standard deviation of 0.19 (Figure 3). This result is unexpected as an e-mail poll revealed that most South African mine water researchers (n = 38) either use the factor 0.65 from Department of Water Affairs and Forestry (1996) or the factory programmed factor of the EC meters.

To identify which other on-site parameter can be used to estimate the TDS, statistical investigations were conducted. Yet, no dependency on another on-site parameter could be found for the 45 analysed samples. Most of the TDS/EC factors increase with increasing TDS of the sample, but the abandoned tailings dam and the Transvaal and Delagoa Bay Colliery samples deviate from this general trend (Figure 3).

Table 1 Field and lab parameters of the analysed mine water samples. Average of the pH calculated from the $\{H^+\}$ activity. TDS from lab analyses.

	pH, –	κ_{25}, µS/cm	TDS, mg/L
n	45	45	45
Minimum	2.45	67	50
Maximum	7.85	16 369	13 948
Median	3.76	3 059	2 832
Average	3.92	4 769	4 279
σ	1.93	5 091	4 422
σ, %	40	107	103

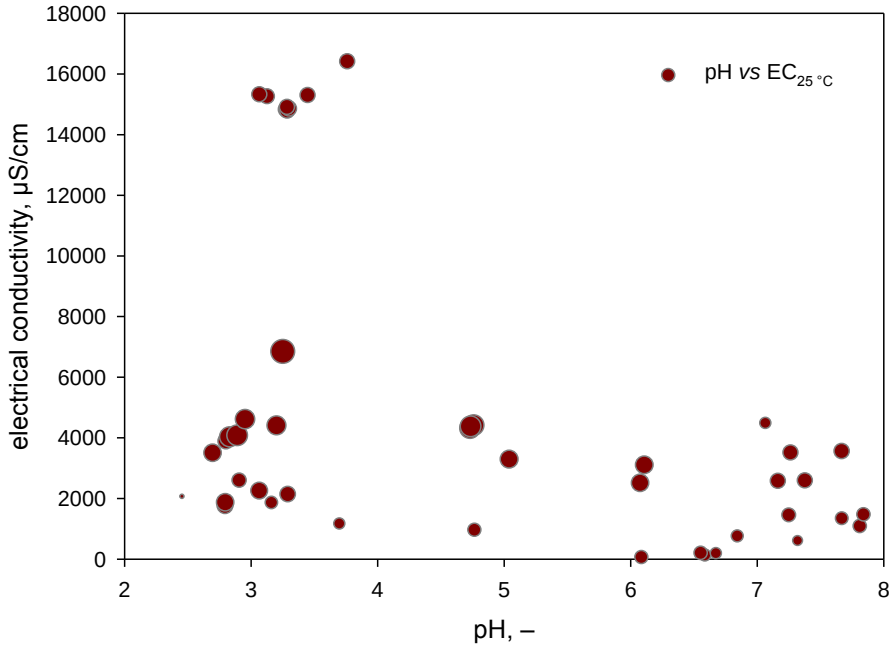

Figure 2 Scatter plot of the measured pH-values and electrical conductivities of all samples. The radius of the circles represents the TDS/EC ratio, $n = 45$.

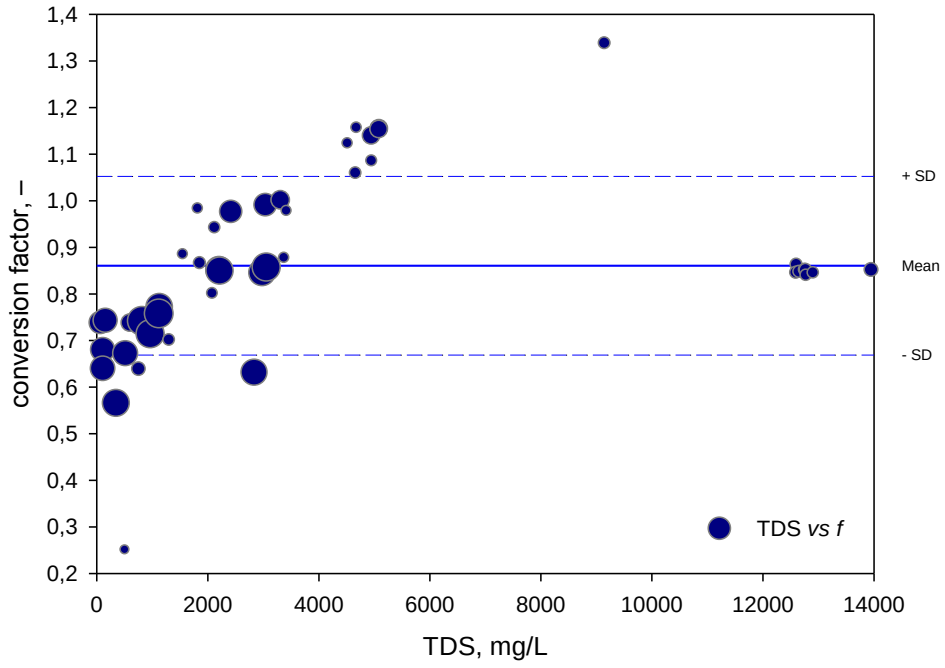

Figure 3 Scatter plot of the lab determined TDS and the TDS/EC ratios. The radius of the circles is proportional to the pH-value of the sample; $n = 45$.

CONCLUSIONS AND RECOMMENDATIONS

As can be seen from the above data, it is not possible to use a single conversion factor from EC to TDS to estimate the total dissolved solids of a mine water sample. The range of the ratio is too high to use it as a reliable tool for TDS estimations. Consequently, prior to using the TDS/EC conversion equation, the conversion factor for the single mine water, which might change with local, diel or seasonal variations, must be determined in the lab and the conductometer be programmed with this conversion factor. Together with the results, the applied conversion factors should be mentioned. In addition, the conversion factor 0.65 recommended in the South African Water Quality Guidelines (Department of Water Affairs and Forestry, 1996) should no longer be used for mining impacted water and the guidelines might need to be updated in this regard.

Future work will investigate a larger set of samples and will include chemical analyses as well. This shall determine how the TDS can be more reliably estimated from the EC without its lengthy lab determination.

ACKNOWLEDGEMENTS

We thank our colleagues at Tshwane University of Technology (TUT) who provided us with equipment and facilities for analysing the water samples and our colleagues at various mines and governmental institutions who provided us with locations, water samples and data. This work was financed by a SARChI (South African Research Chair Initiative) research grant of the NRF (National Research Foundation). Special thanks to Henk Coetzee who introduced us to the "heavily toxic" mine water situation in South Africa.

A more comprehensive paper with all the relevant data is currently under review in the Journal Water SA in will be available during the year 2015.

NOMENCLATURE AND ABBREVIATIONS

A	cross section of electrodes, [cm²]
A_c	cross section of conductor, [m²]
EC	electrical conductivity
f	conversion factor from EC to TDS, [(10 g m)/(L S)]
G	conductance [S]
l	distance of electrodes, [cm]
l_c	characteristic length of conductor, [m]
R	resistance, [Ω]
TDS	total dissolved solids
κ_{25}	electrical conductivity at 25 °C [S/cm, μS/cm]

REFERENCES

Ali, N. S., Mo, K. & Kim, M. 2012. A case study on the relationship between conductivity and dissolved solids to evaluate the potential for reuse of reclaimed industrial wastewater. KSCE J. Civ. Eng., 16, 708-713.

American Public Health Association, American Water Works Association & Water Environment Federation 2005. Standard methods for the examination of water and wastewate, Washington, American Public Health Association.

Atekwana, E. A., Atekwana, E. A., Rowe, R. S., Werkema Jr, D. D. & Legall, F. D. 2004. The relationship of total dissolved solids measurements to bulk electrical conductivity in an aquifer contaminated with hydrocarbon. Journal of Applied Geophysics, 56, 281-294.

Day, B. A. & Nightingale, H. I. 1984. Relationships Between Ground-Water Silica, Total Dissolved Solids, and Specific Electrical Conductivity. Ground Water, 22, 80-85.

Department of Water Affairs and Forestry 1996. South African Water Quality Guidelines – Volume 1 Domestic Use, Pretoria, Department of Water Affairs and Forestry.

Gustafson, H. & Behrman, A. S. 1939. Determination of Total Dissolved solids in Water by Electrical Conductivity. Ind. Eng. Chem. Anal., 11, 355-357.

Hem, J. D. 1985. Study and interpretation of the chemical characteristics of natural water. US Geological Survey Water Supply Paper, 2254, 263.

Hobbs, P. J. 2013. Pilot Implementation Of A Surface Water And Groundwater Resources Monitoring Programme For The Cradle Of Humankind World Heritage Site – Situation Assessment And Status Report For The Period April 2012 To March 2013. Pretoria: Council for Scientific and Industrial Research Natural Resources & the Environment.

Hölting, B. & Coldewey, W. G. 2013. Hydrogeologie – Einführung in die Allgemeine und Angewandte Hydrogeologie, Berlin Heidelberg, Springer.

Howard, C. S. 1933. Determination of Total Dissolved Solids in Water Analysis. Ind. Eng. Chem. Anal., 5, 4-6.

Johnson, M. R., Anhaeusser, C. R. & Thomas, R. J. 2006. The geology of South Africa, Pretoria, Council for Geoscience.

Lynch, S. D. 2004. The Development of a Raster Database of Annual, Monthly and Daily Rainfall for Southern Africa. WRC Report. Pretoria: Water Research Commission.

Mentz, J. W., Warg, J. B., Skelly & Loy, I. 1975. Up-dip versus down-dip mining – an evaluation. Environmental Protection Technology Series, EPA-670/2-75-047, 74.

Smith, S. H. 1962. Temperature Corrections in Conductivity Measurements. Limnol. Oceanogr., 7, 330-334.

van Niekerk, H., Silberbauer, M. J. & Maluleke, M. 2014. Geographical differences in the relationship between total dissolved solids and electrical conductivity in South African rivers. Water SA, 40, 133-137.

Weiner, E. R. 2010. Applications of Environmental Aquatic Chemistry – A Practical Guide, Boca Raton, CRC Press.

Wolkersdorfer, C. 2008. Water Management at Abandoned Flooded Underground Mines – Fundamentals, Tracer Tests, Modelling, Water Treatment, Heidelberg, Springer.

Arsenic Mobility under a Neutral Mine Drainage Environment in a Gold-Mine Tailings Dam

Leonardo Bissacot[1], Virginia Ciminelli[2] and Mark Logsdon[3]

1. *Yamana Gold, Brazil*
2. *Universidade Federal de Minas Gerais, Brazil*
3. *Geochimica, USA*

ABSTRACT

A geochemical assessment of a lined tailings deposit from an operating gold mine located in a semiarid climate was performed for this study. A total of 58 samples were collected, including surface and deep tailings as well as fresh tailings from the carbon-in-leach circuit. Several analyses were performed on these samples, including the modified acid-base accounting, NAG test, chemical and mineralogical characterization. Kinetic tests were also performed on two samples of fresh tailings. Both mineralogical characterization and the acid-base accounting showed that the neutralization potential in the tailings is at least two times higher than the acidification potential, confirming the current, slightly alkaline conditions of the reservoir, with pH value always higher than 7. The alkalinity trends monitored and gypsum detected in the mineralogical composition (1.3%) of the tailings collected in the reservoir suggest that acid neutralization and precipitation of sulphate salts are occurring. In the oxidizing environment within the tailings, the arsenic concentrations varied from below detection limit to 0.081 mg/L, always with a slightly alkaline pH. This concentration range can be related with the dissolution of amorphous ferric arsenate. The arsenic concentrations monitored in a slightly reducing environment (Eh=-12V) are much higher than the concentrations identified in the oxidizing environment. The Eh, pH, and dissolved iron concentrations (average 3 mg/L) suggest that the arsenic is being released by the reduction of Fe^{3+} to Fe^{2+}. Based on the results from this work, it was possible to establish a conceptual model of arsenic behavior in oxidizing and slightly reducing environments within the tailings, as well as recommend actions for a stable closure of the tailings dam to prevent the arsenic release in the long term to the environment.

Keywords: Arsenic, Neutral Drainage, Tailings Dam, Gold Mine

INTRODUCTION

In the semiarid climate of Brazil, a gold mine is operating since 1984. In 1988 the underground mining of sulphide ores started and since then, the tailings generated from processing this material (CIP circuit) are being deposited in a tailings dam.

The deposit has two of the ore occurrence of situations. The first one consists of sulfide ore bodies and the second one is consisting of quartz veins containing free gold, basically embedded in the levels of CAX (carbonate - actinolite - shale) of the intermediate package and corner sequence, northeast of Weber range. In the surface ten bodies of sulfide ore emerges of which eight are located in the first layer (thicker) and the two others in the second layer. The sulfide ore bodies are formed by a set of venules and veins , ranging from a few centimeters up to two meters thick. In the veins there are the occurrence of quartz, pyrite and arsenopyrite in different proportions. When the veins are in agreement with the foliation of the rock, the boundaries of the affected zone are regular and parallel to the edges of the veins.

Alteration zones bordering discordant veins are irregular and thicker, with a tendency to the appearance of jagged edges that penetrate laterally in the foliation planes of rock. In the affected zone there has been a decrease in the volume of chlorite, followed by an increase of albite and carbonates towards the vein. Magnetite is replaced by the sulfides and a small increase in biotite is observed. Carbonate and pyrite occur filling all the faults and fractures existing system in the mine, showing late barren hydrothermal event in gold, presented in many places cavities where well-formed crystals of carbonate and pyrite have been developed. The distribution of gold is very erratic, especially in quartz ore, where it is even possible to find visible particles, due to the gold on this type having a particle size larger than the one found in the sulfide ore.

A preliminary mineralogical characterization of the tailings was performed by X-ray diffraction indicating a significant presence of suphides and carbonates. The monitoring results along the years indicated that the tailings dam pond presents alkaline conditions and an increase of As and SO_4 concentrations with depth inside the dam. The arsenic concentrations in the lake are in the order of 10 mg/L while in the toe drain these concentrations are as high as 200 mg/L. All the effluent from the toe drains in recycled back to the reservoir resulting in no discharge to the environment. It is also possible to observe a variation in the Eh. The Eh conditions in the toe drain is -12 mV. This value is significantly lower than the ones monitored in the lake (265 mV). These conditions are expected since that in the toe drain, the water is not in contact with oxygen until it reaches the drain.

Differently from some other trace elements, As can be mobile under neutral to alkaline conditions, depending on the redox of the system (Craw et al., 2003). Since the operation is reaching its closure phase, it is important to evaluate the Acid Rock Drainage potential in the long term and understand the factors that are affecting the As mobility. This evaluation is important in order to establish mitigation actions for closure and post-closure and to immobilize and stabilize As concentrations.

A store and release cover system was designed based on field experiments that ran for 15 months. The objective of the designed cover is to avoid water to get in contact with the tailings. Since the

field experiments presented very good results, it is expected that once this cover is installed above the tailings in the closure stages, that the amount of water seeping at the toe drain decreases and eventually discontinue along the years, which would prevent elevated concentrations of arsenic from the anaerobic environment. This paper, documenting the site conditions and the ARD and As evaluations, is based on a Master of Science thesis presented in 2014 (Bissacot, 2014).

METHODOLOGY

Tailings Sampling

Tailings samples were selected for geochemical characterization beyond that of the standard protocols of the operation. The definition of the tailings sampling locations was carried out with the support of the mine's geology department. Twenty-one equidistant points on 150 meter centers were distributed along the tailings area and sampled at different depths (Figure 1). Two fresh CIL tailings samples and one composite sample of precipitated salts were also collected. For the deposited tailings, a cylindrical soil auger with 4.5 meters inches diameter and 39 cm length was used. The maximum depth achieved is 6 meters. A total of 55 samples of tailings were collected at different depths in the 21 points, totalizing 58 samples sent to the laboratory for further analyzes.

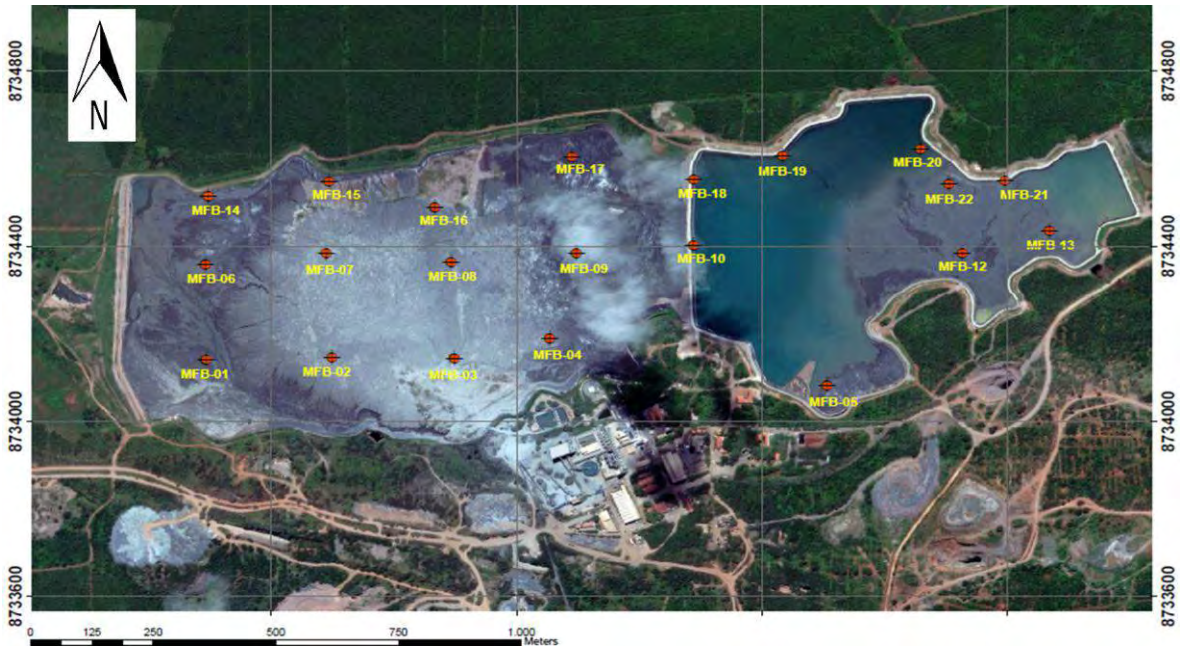

Figure 1 Sample Locations

Tailings Characterization

Several analyzes were performed for understanding the short and long term behave of these tailings and especially the arsenic mobility. The modified acid-base accounting (MABA) was performed in order to understand the potential of these samples for generating acidy. The Lawrence method (MEND, 1991) was selected for this analyzes. The Net Acid Generating test (NAG) was performed as an additional test according the procedure described by Stewart et al. in order to confirm the MABA results. The chemical composition of each sample was conducted by

digesting 0.500 g in aqua regia at 95°C for one hour. The extract was then diluted to 10.0 mL and analyzed for metals by combination of OES and MS using Optima 7300DV for ICP-OES and Elan 9000 for ICP-MS. These results were complemented by mineralogical analyzes by X-ray diffraction with Rietveld refinement and kinetic tests in leach columns according to the AMIRA (2002) procedure.

RESULTS AND DISCUSSION

Acid Rock Drainage Evaluation

The results of the MABA tests in the deposited tailings indicated an average sulfur concentration of 1.36% while the average sulfide sulfur was 1.09%, according to the figure 2 below.

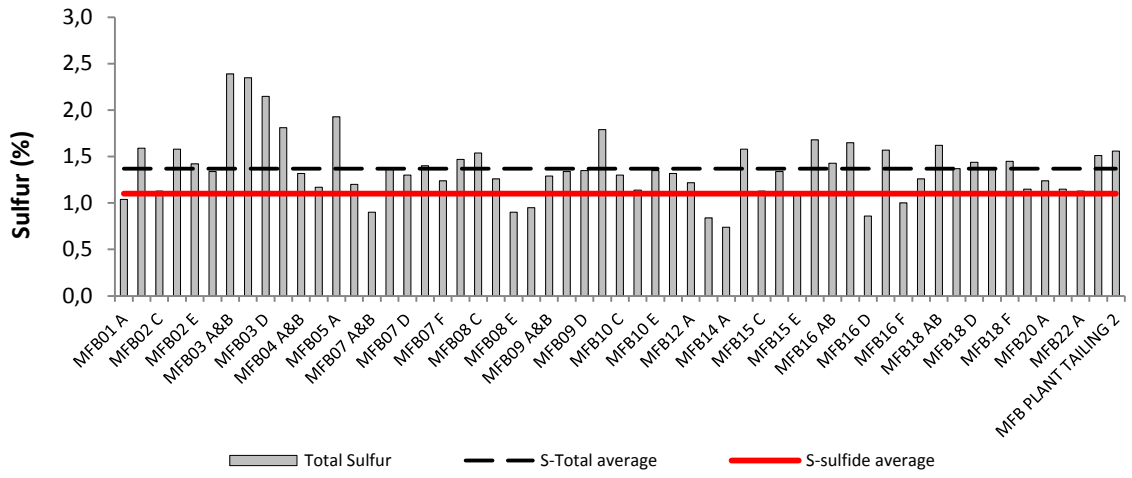

Figure 2 Comparison between S-total and S-sulfide

This can be related to the partial sulfur content that was oxidized into sulfates. In contrast, the fresh tailings collected after the CIL circuit presented an average concentration of 1.54% total sulfur and 1.48% sulfide sulfur. The composite sample collected of the precipitates presented 0.5% of total sulphur on its composition and 0.01% of sulfide sulfur. The average concentration of sulfur can be considered reasonably high, but the average neutralization potential (NP) was also elevated, with an average of 106 kgCaCO3eq/ton. In addition to these results, the NAG tests also indicated an elevated NAGpH for all the tailings tested. According to the NAG test procedure, a sample with a NAGpH greater than 4.5 can be considered as non-acid forming. The test results are summarized in Figure 2.

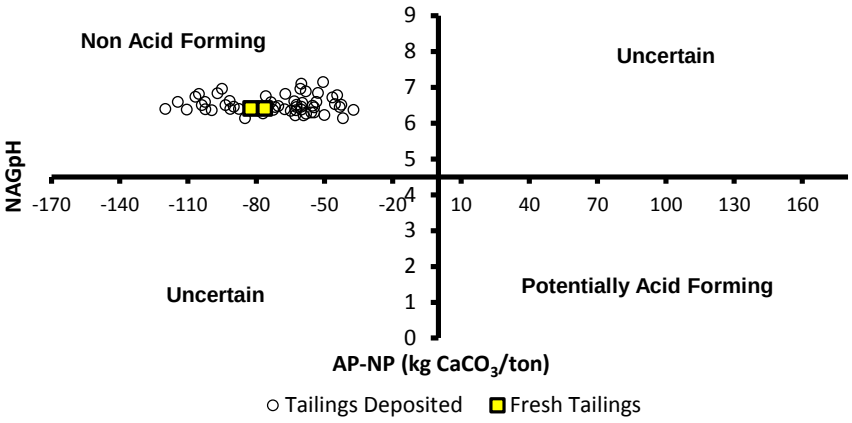

Figure 3 MABA x NAG diagram

Figure 2 combines the results of the MABA and NAG tests. The X-axis represents the MABA results as the difference of AP and NP. [Note that this is the Net Acid Producing Potential, the inverse of the Net Neutralization Potential typically used in North America. In the NAPP system values less than zero imply an excess of NP over AP.] The Y-axis represents the NAGpH. It is possible to observe that all samples were classified in the non-acid forming area of the diagram. In yellow it is possible to observe the fresh tailings and the circles represent the deposited tailings. Both deposited and fresh tailings presented similar characteristics in terms of ARD generation. The results indicated that acid rock drainage should not occur in the short and long term.

Chemical and Mineralogical Composition

The mineralogical characterization by X-ray diffraction with Rietveld refinement was carried out in all the samples. The advantages of this method are the quantitative nature of the method as well as the lower detection limits (Raudsepp & Pani, 2003). In terms of environmental relevance, the sulfides and carbonates are the most important. The silicates are relatively stable and do not significantly change the pH of the solution under most conditions in relevant time periods. The results presented a significant presence of pyrite (1%), arsenopyrite (0.5%) and pyrrhotite (0.7%). Regarding the carbonates, it was identified even higher concentrations of dolomite (3.7%), calcite (6.1%) and calcite/magnesian (2.9%). This may be explained by the limitations of the Rietveld method to identify arsenopyrite phase under at levels below 1%. The gypsum concentrations were detected in the deposited tailings with an average of 1.3%, while in the fresh tailings it was not detected. These concentrations of gypsum indicate that sulfate salts are being formed in the reservoir most like due to the sulfides oxidation. The presence of silicates represents around 80% of the minerals present in the samples, mostly present in the form of quartz and plagioclases. The mineralogy assessment summary is presented in Table 1:

Table 1 Average mineralogy composition - 58 samples

Mineral	Average %
Pyrite	1.0
Pyrrhotite	0.7
Arsenopyrite	0.5
Calcite	6.1
Ankerite – Dolomite	3.7
Calcite, magnesian	2.9
Gypsum	1.3
Silicates	80.3
Iron Oxides	3.6

In addition to these results, elevated grades of arsenic, with an average of 3860 mg/kg, were detected in all the 58 samples analyzed by ICP-MS. The average sulfur detected by ICP was 1.3%, confirming the results previously presented in the MABA.

Kinetic Tests

The kinetic tests are being performed in PVC columns according to the AMIRA 2002 procedure. The water addition is performed once a week in an entire cycle of four weeks. An amount of 200 mL of water is added in the first three weeks and in the fourth week, 800 mL is added. The leachate solution is collected and analyzed for pH, conductivity, sulfate and metals. The results of As and Fe are presented in Figure 3.

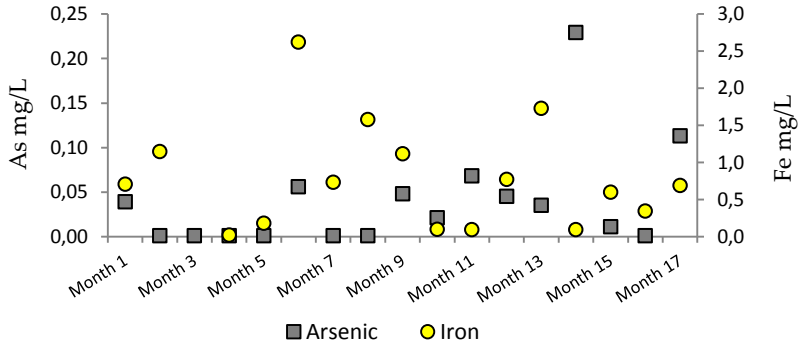

Figure 4 Arsenic and iron leaching after 17 months

It is possible to observe that after 17 months of water addition, the arsenic leached from below detection limit until concentrations of 0.229 mg L^{-1}. The iron concentrations varied from 0.09 to 2.6 mg/L. The concentrations of arsenic leached in the columns are significantly lower than the concentrations found deep in the lined tailings reservoir. According to the graph, it is possible to observe some correlation of the iron and arsenic concentrations in some of the cycles. Concentrations of iron on this order of magnitude are mainly in Fe^{2+} form since the Fe^{3+} would

precipitate quantitatively at pH 7 – 8.5. The low concentrations of As in the column can be related to the As co-precipitation with Fe^{3+} hydroxides that are stable under the pH-Eh conditions of the other months in the columns (Bissacot, 2014). These conditions are likely to be different from those conditions in the tailings pond water, where the redox varies from oxidizing to reducing conditions and concentrations of Fe of 5 mg L^{-1} are found at neutral pH. The results highlight the need to control the redox conditions to prevent arsenic mobilization and have important implications on environmental management in the industrial unit.

CONCLUSION

The mineralogical composition is consistent with both MABA results and current data available for the tailings dam, showing alkaline conditions. Arsenic mobility in the tailings water is mostly related to the presence and oxidation of arsenopyrite combined with the redox conditions variation along the tailings deposit (oxidizing to reducing). It is recommended that similar tailings with potential alkaline conditions and high concentrations of arsenic are disposed under oxidizing conditions and have the redox conditions controlled in order to avoid the long-term arsenic mobility. It is also important to avoid as much as possible seepage areas in the reservoir that creates reducing environments and potential discharges.

The oxidizing environment tested in the laboratory showed concentrations of leached As very low when compared to the ones observed in the anaerobic conditions of the toe drains. Also, as an alternative option, iron can also be added to the system in order to adsorb and decrease the dissolved arsenic concentrations but this action should be performed only when it is possible to maintain controlled redox conditions.

ACKNOWLEDGEMENTS

The authors thank the site personnel for the samples collection and preparation, Geochimica Company and INCT-Aqua institute for time in reviewing the text and Yamana Gold Corporation for the financial support in the research.

REFERENCES

AMIRA International. 2002. Ian Wark Research Institute and Environmental Geochemistry International Pty Ltd ARD Test Handbook. Australia. 41p,.

Bissacot LCG, 2014. Caracterização geoquímica de rejeitos de mineração de ouro como contribuição à gestão ambiental e ao projeto de fechamento da mina. Master's degree dissertation. Brazil.

Craw, D., Falconer, D. & Youngson, J.H. 2003. Environmental arsenopyrite stability and dissolution: theory, experiment and field observations. Chem. Geol. 199: 71-82.

Mend, 1991. Coastech Research, Acid Rock Drainage Prediction Manual, MEND Project Report 1.16.1b, Ottawa, Ontario.

Raudseep, M. & Pani, E. 2003. Application of Rietveld Analysis to Environmental Mineralogy - Chapter 8. In: J.L. Jambor, D.W. Blowes and A.I.M. Ritchie (eds.) Environmental Aspects of Mine Wastes. Mineralogical Association of Canada Short Course Series, volume 31.

Stewart, W.A., Miller, S.D. & Smart, R. 2003. Evaluation of the Net Acid Generation (NAG) Test for Assessing the Acid Generating Capacity of Sulfide Minerals. 6th ICARD. Cairns.

10th ICARD IMWA 2015 | 10th International Conference on Acid Rock Drainage & IMWA Annual Conference

Use of Oxygen Sensors and TDR Probes for In Situ Monitoring of Tailings Impoundments (Jaen, Spain)

María Carmen Hıdalgo[1], Diego Rojas[1], Claus Kohfahl[2] Javier Rey[1], Julián Martínez[3], María José de la Torre[1] and José Benavente[4]

1. Department of Geology, EPSL, University of Jaen, Spain
2. Instituto Geológico y Minero de España, Seville, Spain
3. Department of Mechanical and Mining Engineering, EPSL, University of Jaen, Spain
4. Water Research Institute, University of Granada, Spain

ABSTRACT

The objective of this study is to characterize former tailings impoundments from metallic sulfide ores exploited in the abandoned mining district of La Carolina (Spain). These fine grained tailings from flotation plants were built without any protection or isolation and, therefore, have a large interaction with the environment. Two selected sludge dams from La Aquisgrana and Apple mines were drilled to obtain continuous cores to subsequently perform sampling at different depths to analyze a series of variables (organic matter, pH, content of metal(oid)s and carbonates, among others). These boreholes were installed with fiber-optic oxygen sensors and TDR probes that determine humidity, temperature, electrical conductivity and oxygen partial pressure at different depths. Additionally, a piezometer was installed at each tailings disposal to allow the sampling of water from the saturated zone of the dams. Sediments analysis reveal elevated contents of Pb (8000 mg/kg), Zn (2200 mg/kg) and As (420 mg/kg), pyrite sulfur and organic carbon (up to 1,75% and 0,6%, respectively). Both sites present a large unsaturated zone of about 30 m with oxygen disappearing at 3-5 m depth due to high amount of electron donors. The monitored values decrease from 20% in surface to 0% below the first meters, indicating a shallow position of the oxidation front 30 years after closure. The water from the saturated zone presents an electrical conductivity of 3,3 mS/cm and a pH value of 6,5. The first results for TC, TOC and TIC show low values of these parameters (no more than 2% in any case) but that appear to be sufficient to have a buffering effect, since pH values are mostly alkaline.

Research funded by the Government of Junta de Andalucía (Project RNM 05959) and the Spanish Ministry of Economy and Competitiveness (Project CGL2013-45485-R, co-financed FEDER).

**There is no full article associated with this abstract.*

10th ICARD IMWA2015 | 10th International Conference on Acid Rock Drainage & IMWA Annual Conference

Electrical Resistivity Imaging in Abandoned Mining Dams: The Influence of Measurement Conditions (La Carolina District, Southern Spain)

Javier Rey[1], Julián Martínez[1], María del Carmen Hidalgo[1], Jesús Garrido[2], Diego Rojas[1], Claus Kohfahl[3] and José Benavente[4]

1. Higher Polytechnic School of Linares, University of Jaén, Spain
2. Higher Technical School of Civil Engineering, University of Granada, Spain
3. IGME, Spain
4. Instituto del Agua, Universidad de Granada, Spain

ABSTRACT

The metallogenic district of La Carolina (Southern Spain, Jaen province) is characterized by the presence of vein deposits, which are primarily composed of galena (PbS). The mineral industrial activity generated numerous gravimetric and flotation washing sites, that were deposited in spoil heaps and impoundments, which occupied relatively extensive areas in the vicinity of the concentration plants; no remediation was performed.

This study employed indirect geophysical prospecting techniques, particularly electrical resistivity imaging (ERI) to locating recharge-discharge zones and identifying the contact between the residue and the substratum of this mine.

During the dry season, a significant change in resistivity is detected across the boundary between the tailings dam and the substratum with higher values in the basement. Consequently, the previously mentioned geophysical prospecting method is an excellent tool for characterizing the basin morphology under these conditions. Conversely, the detection of this boundary during the rainy season is not feasible with this methodology because the electrical resistivity values for the deposits and the basement are similar. This similarity can be attributed to the finding that the base of the tailings dam and the upper part of the Palaeozoic substratum (highly altered) are saturated in water. However, during the rainy season, this methodology facilitates the identification of preferential groundwater flow zones and areas where groundwater tends to accumulate. The ERI profiles show how percolation of rainwater and infiltration through the mine tailings contribute to the drainage at the toe of the dam, which affects the water and soil in the surrounding area.

Research funded by the Government of Junta de Andalucía (Project RNM 05959) and the Spanish Ministry of Economy and Competitiveness (Project CGL2013-45485-R, co-financed FEDER).

**There is no full article associated with this abstract.*

CHAPTER 16

PIT LAKES

10th ICARD IMWA 2015 | 10th International Conference on Acid Rock Drainage & IMWA Annual Conference

Key issues in Mine Closure Planning Related to Pit Lakes

Jerry Vandenberg[1], Clint McCullough[2] and Devin Castendyk[3]

1. *Golder Associates, Canada*
2. *Golder Associates/ Edith Cowan University, Australia*
3. *Department of Earth & Atmospheric Sciences, State University of New York, USA*

ABSTRACT

Pit lakes form when surface mines close and open pits fill with water, either through groundwater recharge, surface water diversion or active pumping. Historically, the success in closing mines with pit lakes has varied tremendously: there are well known examples of legacy sites requiring perpetual treatment, whereas some other pit lakes have achieved various beneficial end uses. Although access to case studies is often limited, mining companies contemplating new open pit mines have a number of examples in both success and failure from which to draw "lessons learned" that can be used in future mine closure planning.

This paper discusses key issues that should be addressed in the mine planning process to increase the likelihood of successful mine closure. Examples of issues and potential management strategies to address them are given. The key issues examined in this paper include: determining potential risks and beneficial end use opportunities, developing closure objectives and criteria, which may include various water quality, riparian and littoral targets; anticipating and meeting stakeholder and regulator expectations; subaqueous disposal of liquid and solid mine waste; predicting and managing water balances; identifying contaminants of concern; historical reliability of model predictions; mitigating acid mine drainage; the importance of understanding long-term vertical mixing regimes; and health and safety issues.

Keywords: mine pit lakes; sustainability, AMD, closure, planning

INTRODUCTION

Pit lakes form when surface mines close and open pits fill with water, either through passive groundwater recharge, surface water diversion or active pumping. They often display poor water quality through Acid Mine Drainage/Acid and Metalliferous Drainage (AMD). Historically, the success in closing mines with pit lakes has varied tremendously: there are well known examples of legacy sites requiring perpetual treatment, whereas some other pit lakes have achieved various beneficial end uses. Although access to case studies is often limited, mining companies contemplating new open pit mines have a number of examples in both success and failure from which to draw "lessons learned" that can be used in future mine closure planning (Castendyk 2011).

This paper discusses key issues that should be addressed in the mine planning process to increase the likelihood of successful mine closure. Examples of issues and potential management strategies to address them are given with reference to previous experiences in North America, Australia and Asia.

KEY ISSUES

Determining Closure Objectives and Developing Closure Criteria

Discharge criteria applied to pit lakes are site-specific and dependent on the responsible regulatory agency. In most jurisdictions, there are no set guidelines for pit lake discharge. If pit lake water concentrations are below applicable generic water quality guidelines, then water quality would be deemed acceptable, but this will rarely be the case. More likely, site-specific objectives will need to be developed by the proponent of each pit lake. Site-specific objectives can be derived based on effects thresholds, technological limits, background concentrations, or combinations thereof.

Pit lakes are generally expected to be managed as closed-circuit waterbodies until they achieve water quality that will not cause adverse effects to aquatic life, at which time they can be reconnected to the receiving environment. If water quality in the pit lakes is not adequate by the time the lakes fill, active treatment may be required, as well as water diversions around the pit lake.

There are three nested "layers" that can be used to define and gauge success in pit lake closure:

1. **End use** – will the pit lake and associated watershed meet land use requirements for post-closure mine sites that are set regionally and nationally?

2. **Objectives** – will the pit lake meet functional targets that are achievable, desirable to stakeholders and acceptable to regulators?

3. **Criteria** – will the pit lake meet prescriptive criteria, such as site-specific water quality and toxicological thresholds?

There are several sources of information that can be used to define success, such as:

- Corporate sustainability goals and targets (MMSD 2002);
- Commitments made by the mining company in environmental impact assessments (EIAs) and other applications, which include commitments made by previous property owners;
- Numerical predictions that have been generated in EIAs and that have been used in ecological risk assessments;

- Stakeholder expectations;
- Regulatory requirements (Jones and McCullough 2011);
- Analogue lake studies (Van Etten et al. 2014);
- Observed water quality from existing pit lakes in similar geologic deposits (Johnson and Castendyk 2012)
- Leading, international mining-industry practice; and
- Prescriptive, site-specific objectives that are based on biological thresholds and ecological risk assessments.

The importance of developing closure criteria for pit lakes early in the planning process cannot be overstated, because all mine closure design and mitigation should be directed toward meeting these criteria.

Anticipating and Meeting Stakeholder and Regulator Expectations

As with the other components of mine operation and closure, all stakeholders should be identified early and consulted for their input on end of mine life quality and objectives, including objectives for pit lakes (Swanson 2011). Early engagement of stakeholders can lead to constructive input into the planning of pit lakes, reduced costs, fewer delays, and overall public/stakeholder/regulator acceptance.

Design for pit lakes is typically done by involving engineers and scientists, but not stakeholders (Swanson 2011). It is recommended to consult stakeholders on visions for pit lakes and potential beneficial end uses of pit lakes (McCullough and Lund 2006). Participation by communities in developing mine remediation targets leads to better decisions, and in some cases to lower overall costs for mine remediation (NOAMI 2003). This is because the major stakeholders were involved from the beginning in decisions that could affect their enjoyment/use of the landscape. Information presented to communities on pit lake predictions can be complex, and thus information should be presented in an easy-to-understand format in order to engage the stakeholders in constructive discussions (NOAMI 2003).

Predicting and Managing Water Balances

The time to refill pit lakes is site-specific and must be determined on a case-by-case basis. In cases with high rates of evaporation or highly permeable aquifers, the pit lakes can refill in a few years. In arid regions, some pit lakes will never refill passively, and are termed "terminal" pit lakes (McCullough et al. 2013) because they act as a groundwater sink. While not ideal, such lakes may be used as mitigation to prevent contaminated groundwater from migrating away from a mine site. In terminal lakes, evaporation is the only route through which water leaves a pit lake, so it can be expected (and readily predicted with mass balance models) that concentrations of solutes will increase over time (Castendyk and Eary 2009; Geller et al. 2013a). The ultimate concentrations may be controlled by solubility, which can be predicted using geochemical software.

In the sub-Arctic region of Canada, where net evaporation is low, it is expected that pit lakes will refill passively, but it is preferable to accelerate the filling process to reduce the closure management period. This option should be evaluated as part of the closure planning process, in consideration of regional surface hydrology and availability of water to be used for filling.

Connection of the pit lake to surrounding groundwater sources can play a large role in the water quality and hydrological cycle/budget of the pit lake; if a pit lake water surface is above the water

table, water will flow out of the pit to the groundwater and thus provide a pathway to transport potential contaminants to a larger area (Castendyk and Eary 2009).

Understanding Long-term Vertical Mixing Regimes

Compared to natural lakes, pit lakes are more prone to become meromictic (lower layers non-mixing) because they generally have smaller surface areas, larger depths and higher salinities. Vertical mixing in lakes is primarily driven by wind currents across the lake surface, and the smaller fetch of pit lakes provides less opportunity to translate wind energy into water currents that are necessary for lake turn-over.

In pit lakes, as in natural lakes, the frequency and depth of vertical mixing will affect many other variables. These parameters must be defined in advance of developing geochemical predictions of water quality so that accurate volumes for epilimnion, hypolimnion, and monimolimnion layers can be accurately represented and mixed at appropriate intervals. Vertical mixing transports oxygen to the lower portion of the lake, which in turn affects biological and chemical reactions. For example, oxidation state influences the mobilization of metals and cycling of nutrients. Of particular importance is the potential effect of oxidation state on sulfide minerals; under oxidizing conditions, sulfide minerals will react to form sulfuric acid and dissolved metals, whereas under reducing conditions, sulfide minerals will precipitate – a process that has been used to mitigate AMD in meromictic pit lakes (Pelletier et al. 2009). Given the influence of vertical mixing on these processes, the anticipated mixing behavior of a pit lake should be evaluated and understood as early as possible in the mine planning process.

There are a variety of guidelines that describe lake geometries that will affect lake mixing. The most common is the relative depth, defined as the maximum depth as a percentage of mean diameter. Natural lakes usually have relative depths of less than 2%, whereas pit lakes typically have relative depths of 10 to 40% (Doyle and Runnels 1997). While measures such as relative depth provide useful descriptors of pit geometries, they are not predictive measures because they do not account for other important variables, such as water density and wind speed. The most reliable method for predicting lake mixing is through the use of numerical models (such as CE-QUAL-W2 or DYRESM) that mechanistically account for these variables.

Identifying Contaminants of Concern

There are a wide range of contaminants of concern (COCs) in pit lakes. The most common COCs in hardrock pit lakes are low pH and elevated element concentrations caused by acidic mine drainage (AMD). AMD is a phenomenon that occurs when sulfur-bearing waste rock, tailings or other materials are weathered during mining and mine closure practices. Weathering of sulfide minerals can lead to release of acid and elevated concentrations of contaminants in runoff, groundwater or pit lake water. These acidic waters often carry a high load of elements that are more soluble at low pH. AMD is commonly associated with coal and hard rock mines

The COCs at a given mine are often, but not always, related to an obvious source such as the ore body or extraction chemicals. For example, the Berkeley Pit Lake in Montana, which is perhaps the most famous “worst-case” example of a pit lake, is a former copper mine pit that now contains levels of copper, zinc, and iron that exceed water quality guidelines by orders of magnitude (Gammons and Duaime 2006). Similar contamination has been observed at copper mines in California (Levy et al. 1997) and Sweden (Ramstedt et al. 2003).

Long-term water quality in a pit lake can be influenced by hydrochemical processes such as geoenvironmental characteristics, water balance, mineral solubility, and sediment biogeochemical processes (Geller et al. 2013a). Constituents that most often exceed guidelines are copper, cadmium, lead, mercury, nickel and zinc, followed by arsenic, sulfate, and cyanide (Kuipers et al. 2006). Blasting residues such as ammonia and nitrate are also often elevated in mine waters, and may persist into closure (Banks et al. 1997). In sub-Arctic Canadian mines, salinity and major ions are typical COCs (Environment Canada 2012) because of saline groundwater that must be dewatered for mining. The saline groundwater may be disposed of in pit lakes, or saline groundwater may flow passively into pit lakes at closure when dewatering ceases. In oil sands pit lakes, the COCs are primarily organic constituents such as naphthenic acids, phenolics and polycyclic aromatic hydrocarbons originating from process waters and tailings (CEMA 2012).

Less obvious COCs may be present as well. For example, at the proposed Gahcho Kué Diamond Mine (De Beers 2012), geochemical testing of pilot plant tailings identified phosphorus as a COC, which led to changes in the closure plan to mitigate runoff from mine wastes and to avoid eutrophication of closure waterbodies. Total suspended solids can be expected to be elevated during the early years of lake development, before vegetation becomes established in the littoral zone, but this should be a temporary phenomenon in a properly designed pit lake.

In summary, while there may be obvious COCs at a given mine, a full suite of metals, major ions, nutrients and organics should be evaluated to determine site-specific COCs prior to mine development.

Mitigating Acid and Metalliferous Drainage (AMD)

Poor water quality degraded by AMD is the single biggest environmental risk and cause of beneficial end use loss for pit lakes (McCullough 2008). Mine drainage may be acidic, neutral or even alkaline as constituents such as metals and metalloids may be in elevated concentrations in all. Once begun, the process of AMD is very difficult to stop. Hence, the emphasis on AMD management should always be first on preventing weathering of potentially acid generating (PAG) materials by exposure to water and oxygen (Castendyk and Webster-Brown 2007). This process begins by long-term geochemical characterization of all materials that may contact pit lake water or water sources including above ground sources, such as waste rock dumps and tailings impoundments, and below ground sources, such as backfill and fractured geologies.

Disposal of PAG materials above the water table is usually best suited to arid climates where AMD production will be limited by water availability. However, a strategy often considered to reduce pit lake AMD issues is subaqueous disposal of PAG occurring in tailings, waste risk and pit shell exposures (Dowling et al. 2004). However, subaqueous disposal of waste should not be thought of as a singular solution to PAG management. Rather it is merely one consideration of a broader closure strategy that, when used appropriately and in certain circumstances, may reduce AMD production and long-term environmental and social liability.

Where AMD has not been prevented, a number of active and passive treatments are available, although all of these treatments should be considered requiring ongoing attention and maintenance (Gammons et al. 2009; Geller et al. 2013b; Younger and Wolkersdorfer 2004). Active treatments may be simple limestone or lime putty additions to treat acidity, although the ongoing cost, particularly in remote areas once mine infrastructure is closed should not be under-estimated. The economic liability to the remaining responsible jurisdiction is likely to exceed the economic benefit from

mining with a few generations of treatment, which is why active treatment is only typically sought when there is a risk of off-site contamination exposure to social or environmental receptors.

Passive treatments may range from strategic catchment-scale diversions of inflows to attenuate and dilute pit lake waters (McCullough and Schultze 2015) to initial or ongoing treatment with biologically active materials such as nutrients and organic matter (Kumar et al. 2011).

Subaqueous Disposal of Liquid and Solid Mine Waste

The option to dispose of mine waste in pit lakes is often attractive to mining companies because it is more cost effective than other treatment or disposal technologies. Disposal of mine waste in pit lakes is an accepted practice in some industries and regions (Davé 2009; Dowling et al. 2004; Schultze et al. 2011). However, it is controversial and considered unproven until demonstrated at the field scale in the oil sands industry (OSTC 2012). If successful, several other companies in the region will likely apply water-capped tailings technology with a potential savings of billions of dollars for the industry as a whole compared to other disposal technologies. Deep pit disposal of fine tailings has also been approved for the diamond mining industry in Northern Canada (De Beers 2012).

If subaqueous disposal of tailings are contemplated, the following issues should be evaluated to reduce risks to closure water quality:

- **Tailings resuspension** – a hydrodynamic analysis should be completed to understand the potential for resuspension of fine particles, and the formation of buoyant plumes;
- **Metal leaching and AMD** – geochemical testing should be completed to predict the potential for acid generation and metal leaching, and to understand which oxidation state would minimize these effects on water quality; and
- **Sediment toxicity** – standard bioassays should be conducted to predict the toxicity to benthic organisms.

Health and Safety Issues

The most significant acute health and safety risks for persons in and around pit lakes relate to falls and drowning. Pit lake highwalls may often be unstable, particularly following rebounding groundwater pore pressures and decades of wave action. Unstable walls frequently result in slips that may endanger nearby structures and persons near the highwall (McCullough and Lund 2006). Where communities reside nearby, pit lakes may present risks for recreational swimmers where there is a risk of drowning with the steep lake margin typically of pit lake edges or by falls from high walls into water or submerged obstacles that have not been regraded (Ross and McCullough 2011).

Chronic health risks are not well understood, but there is potential for health issues for recreational users in AMD contaminated pit lake water; even in remote areas where pit lakes may be used as recreational opportunities. Low pH and elevated contaminant concentrations may lead to skin and eye damage and irritation, particularly for regular exposures in vulnerable groups such as children and the elderly (Hinwood et al. 2012).

There are also human health risks where end uses include fisheries; either planned or unplanned. Aquatic ecosystem foodchains have been found to accumulate contaminants such as selenium, mercury and cadmium. These metals bioconcentrate in keystone predator sportsfish and crustacea (McCullough et al. 2009b; Miller et al. 2013).

Historical Reliability of Model Predictions

The reliability and accuracy of mine water predictions was examined by Kuipers et al. (2006) in a comparison of water quality predictions made in environmental impact statements to operational water quality observed at hardrock mines. The mines that were examined included major mines across the Western USA, but the issues they identified are applicable to mines worldwide. They found that in the majority of cases, water quality predictions did not perform well, and impacts were often underestimated. They identified three main causes for the discrepancies:

- **Inadequate hydrologic characterization** – inaccuracies arose from overestimating dilution potential, poor characterization of the hydrologic regime and poor flood forecasting.
- **Inadequate geochemical characterization** – inaccuracies arose from inadequate sampling of geologic materials, lack of proper geochemical testing of materials such as metal leaching and AMD potential and improper application of test results to models.
- **Mitigation failure** – in many cases, mitigation was assumed to reduce concentrations, but the mitigation was either not effective or not implemented.

Although poor water quality prediction performance has been found at hardrock mines, present and future pit lake modelling efforts should be able to improve upon this record. Success in predicting water quality will be reliant on following leading modelling practices that were not adhered to in many of the case studies in Kuipers et al. (2006). Guidance for predicting pit lake water quality is provided in a companion document by Maest et al. (2005) as well as by Vandenberg et al. (2011).

In particular, a post-audit of water quality predictions is essential (Dunbar 2013) for identifying excursions from predictions early in the mine life and applying adaptive management strategies as soon as possible. Post-audits of modelling predictions should be available to stakeholders, reviewed by regulators, and ideally, disseminated to the wider modelling community so that they can learn from the strengths and weaknesses of past experiences and continually improve their methods.

CONCLUSIONS

Pit lakes are highly variable systems with a wide range of outcomes observed worldwide in terms of chemical characteristics and suitability for aquatic habitat. While there are examples of very unsuccessful pit lakes, these serve as "lessons learned" that can be followed to increase the likelihood of success in constructing future pit lakes (Castendyk 2011). The most important lessons learned are to develop a conceptual model of the pit lake and understand its processes as early as possible; engage stakeholders early in the process; begin environmental monitoring at the exploration stage and conduct a post-audit of predictions to guide adaptive management (Castendyk 2011; Gammons et al. 2009).

The key issues described above should be considered in each of the planning, designing, commissioning, and abandonment stages of a pit lake. The outcome of a decision made or an assessment completed during a previous stage of development may be found to be incorrect or no longer valid as environmental data or stakeholder or regulator requirements evolve. Or, the pit lake and its inflows may be altered by changing mine plans or mine closure plans in response to fluctuating commodity prices. Consequently, mining companies should anticipate an iterative process whereby assumptions and decisions are refined to reduce uncertainty related to the issues

above. This may involve reconsidering options and revisiting strategies discounted earlier under different circumstances such as understanding of the physico-chemical context and of regulatory and other social constraints and expectations. This iterative process of pit lake closure planning refinement should form an explicit part of mine closure planning for the broader site (McCullough et al. 2009a).

Guidance manuals (e.g., CEMA 2012; McCullough 2011) and compilations of pit lake experiences and research (Castendyk and Eary 2009; Gammons et al. 2009; Geller et al. 2013a) have been developed in the past five years, and these should be consulted throughout the planning, design, and construction process for additional details.

REFERENCES

Banks D, Younger PL, Arnesen R, Iversen ER, Banks SB (1997) Mine-water chemistry: the good, the bad and the ugly. Environmental Geology 32(3):157-174.

Castendyk DN (2011) Lessons learned from pit lake planning and development. In: McCullough CD, Mine Pit Lakes: Closure and Management. Australian Centre for Geomechanics, Perth, Australia. pp. 15-28.

Castendyk DN, Eary LE (eds) (2009) Mine Pit Lakes: Characteristics, Predictive Modeling, and Sustainability. Volume 3. Society for Mining, Metallurgy, and Exploration, Inc., Littleton, Colorado, USA. 304 p.

Castendyk D, Webster-Brown J (2007). Sensitivity Analysis in Pit Lake Prediction, Martha Mine, New Zealand 2: Geochemistry, water-rock reactions, and surface adsorption. Chemical Geology 244: 56-73.

CEMA (Cumulative Environmental Management Association) (2012) End pit lakes guidance document. Available online: http://cemaonline.ca/index.php/administration/doc_download/174-end-pit-lake-guidance-document.

Davé N (2009) Disposal of Reactive Mining Waste in Man-made and Natural Water Bodies; Canadian Experience. Marine and Lake Disposal of Mine Tailings and Waste Rock, Egersund, Norway. Sept. 7-10, 2009.

De Beers Canada Inc. (2012) Gahcho Kué Project Environmental Impact Statement. Supplemental Information Submission. Submitted to Mackenzie Valley Land and Water Board, April 2012. Available at http://www.mvlwb.ca/mv/registry.aspx, registry number MV2005L2-0015.

Dowling J, Atkin S, Beale G, Alexander G (2004). Development of the Sleeper Pit Lake. Mine Water and the Environment 23: 2-11.

Doyle GA, Runnells DD (1997) Physical limnology of existing mine pit lakes: Mining Engineering, 49, p. 76-80.

Dunbar DS (2013) Modelling of pit lakes. In: Acidic Pit Lakes - Legacies of surface mining on coal and metal ores, Geller, W.; Schultze, M.; Kleinmann, R. L. P. & Wolkersdorfer, C. (eds.) Springer, Berlin, Germany, 186-224 pp.

Environment Canada (2012) Diamond Mining Effluent. Appendix 3 to Metal Mining Effluent Regulations (MMER) Update. December 14, 2012.

Gammons CH, Duaime TE (2006) Long term changes in the limnology and geochemistry of the Berkeley Pit Lake, Butte, Montana: Mine Water and the Environment, 25, p. 76-85.

Gammons CH, HarrisLN, Castro JM, Cott PA, Hanna BW (2009) Creating lakes from open pit mines: processes and considerations - with emphasis on northern environments. Canadian Technical Report of Fisheries and Aquatic Sciences. 2826: ix + 106 p.

Geller W, Schultze M, Kleinmann R, Wolkersdorfer C (eds) (2013a) Acidic Pit Lakes: The Legacy of Coal and Metal Surface Mines. Springer-Verlag Berlin Heidelberg, Germany. 525 pp.

Geller W, Schultze M, Wisotzky F (2013b) Remediation and management of acidified pit lakes and outflowing waters. In: Geller W, Schultze M, Kleinmann R, Wolkersdorfer C (eds) Acidic pit lakes. Springer, Heidelberg, Germany. Pp. 225-264.

Hinwood A, Heyworth J, Tanner H, McCullough CD (2012) Recreational use of acidic pit lakes – human health considerations for post closure planning. Journal of Water Resource and Protection 4: 1,061-1,070.

Johnson E, Castendyk DN (2012) The INAP Pit Lakes Database: A novel tool for the evaluation of predicted pit lake water quality. In: W.A. Price, C. Hogan, and G. Tremblay (eds), Proceedings of the 9th International Conference on Acid Rock Drainage: Ottawa, Canada, May 20-26, 2012. Technical Paper 0037, p. 1-12.

Jones H, McCullough CD (2011) Regulator guidance and legislation relevant to pit lakes. In: McCullough CD, Mine Pit Lakes: Closure and Management. Australian Centre for Geomechanics, Perth, Australia. pp. 137-152.

Kumar NR, McCullough CD, Lund MA (2011) Bacterial sulfate reduction based ecotechnology for remediation of acidic pit lakes. In: McCullough CD, Mine Pit Lakes: Closure and Management. Australian Centre for Geomechanics, Perth, Australia. pp. 121-134.

Kuipers JR, Maest AS, MacHardy KA, Lawson G (2006) Comparison of Predicted and Actual Water Quality at Hardrock Mines: The reliability of predictions in Environmental Impact Statements. Available at http://www.earthworksaction.org/files/publications/ComparisonsReportFinal.pdf.

Levy DB, Custis KH, Casey WH, Rock PA (1997) The aqueous geochemistry of the abandoned Spenceville Copper Pit, Nevada County, California. Journal of Environmental Quality. 26:233-243.

Maest AS, Kuipers JR, Travers CL, Atkins DA (2005) Predicting water quality at hardrock mines: Methods and models, uncertainties and state-of-the-art. Kuipers and Associates, Butte, MT, USA. 89pp. Available at http://www.earthworksaction.org/files/publications/PredictionsReportFinal.pdf.

McCullough C D (2008) Approaches to remediation of acid mine drainage water in pit lakes. International Journal of Mining, Reclamation and Environment 22: 105-119.

McCullough CD (ed) (2011) Mine Pit Lakes: Closure and Management. Australian Centre for Geomechanics, Perth, Australia. 183 pp.

McCullough CD, Hunt D, Evans LH (2009a). Sustainable development of open pit mines: creating beneficial end uses for pit lakes. In: Castendyk DN, Eary LE (eds) Mine Pit Lakes: Characteristics, Predictive Modelling, and Sustainability: Society for Mining, Metallurgy, and Exploration, Inc., Littleton, Colorado, USA. pp. 249-268.

McCullough CD, Lund MA (2006) Opportunities for Sustainable Mining Pit Lakes in Australia. Mine Water and the Environment. 25: 220–226.

McCullough CD, Marchand G, Unseld J (2013) Mine closure of pit lakes as terminal sinks: best available practice when options are limited? Mine Water and the Environment 32: 302-313.

McCullough CD, Schultze M (2015). Riverine flow-through of mine pit lakes: improving both mine pit lake and river water quality values? Proceedings of the 9th International Mine Water Association (IMWA)/International Conference on Acid Rock Drainage (ICARD). Santiago, Chile.

McCullough CD, Steenbergen J, te Beest C, Lund MA (2009b) More than water quality: environmental limitations to a fishery in acid pit lakes of Collie, south-west Australia. Proceedings of the International Mine Water Conference. Pretoria, South Africa. 19-23 October, International Mine Water Association, 507-511pp.

Miller LL, Rasmusssen JB, Palace VP, Sterling G, Hontela A (2013) Selenium bioaccumulation in stocked fish as an indicator of fishery potential in pit lakes on reclaimed coal mines in Alberta, Canada. Environmental Management 52: 72-84.

MMSD (Mining, Minerals, and Sustainable Development). 2002. Breaking New Ground; Final Report of the Mining, Minerals, and Sustainable Development Project. London: Earthscan Publications.

NOAMI (National Orphaned/Abandoned Mines Initiative). (2003) Lessons Learned: On Community Involvement in the Remediation of Orphaned and Abandoned Mines; Case Studies and Analysis. A report of the National Orphaned/Abandoned Mines Initiative. February 2003. Available at http://www.abandoned-mines.org/pdfs/LessonsLearned.pdf.

OSTC (Oil Sands Tailings Consortium) (2012) Technical Guide for Fluid Fine Tailings Management. Technical guide prepared for OSTC and COSIA, August 2012. 131 pp. Available at http://www.cosia.ca/uploads/documents/id7/TechGuideFluidTailingsMgmt_Aug2012.pdf.

Pelletier CA, Wen ME, Poling GW (2009) Flooding pit lakes with surface water. In: Castendyk DN, Eary LE (eds) Mine Pit Lakes: Characteristics, Predictive Modelling, and Sustainability: Society for Mining, Metallurgy, and Exploration, Inc., Littleton, Colorado, USA. pp. 187-202.

Ramstedt M, Carlsson E, Lovgren L (2003) Aqueous geochemistry in the Udden pit lake, northern Sweden. Applied Geochemistry. 18:97-108.

Ross T, McCullough CD (2011) Health and Safety working around pit lakes. In: McCullough CD, Mine Pit Lakes: Closure and Management. Australian Centre for Geomechanics, pp. 167-181.

Schultze M, Boehrer B, Friese K, Koschorreck M, Stasik S, Wendt-Potthoff K (2011) Disposal of waste materials at the bottom of pit lakes. Mine Closure, 2011. Fourie AB, Tibbett M, Beersing A (eds) Australian Centre for Geomechanics, Perth, Australia. pp. 555-564.

Swanson SM (2011) What Type of Lake do We Want? Stakeholder Engagement in Planning for Beneficial End Uses of Pit Lakes. In: McCullough CD, Mine Pit Lakes: Closure and Management. Australian Centre for Geomechanics, Perth, Australia. pp. 29-42.

Van Etten EJB, McCullough CD, Lund MA (2014) Setting goals and choosing appropriate reference sites for restoring mine pit lakes as aquatic ecosystems: case study from south west Australia Mining Technology 123: 9-19.

Vandenberg JA, Lauzon N, Prakash S, Salzsauler K (2011) Use of water quality models for design and evaluation of pit lakes. In: McCullough CD, Mine Pit Lakes: Closure and Management. Australian Centre for Geomechanics, Perth, Australia. pp. 63-82.

Younger P, Wolkersdorfer C (2004) Mining Impacts on the fresh water environment: Technical and managerial guidelines for catchment scale management. Mine Water and the Environment 23:S2-S80.

Designing Meromictic Pit Lakes as a Mine Closure Mitigation Strategy in Northern Canada

Michael Herrell, Jerry Vandenberg and John Faithful
Golder Associates, Canada

ABSTRACT

Deep groundwater stored in the Canadian Arctic Shield is characterized by high salinity that increases by orders of magnitude with depth. Mining in these areas has the potential to upwell saline groundwater into the mine workings. Due to the pristine nature of the downstream receptors in Arctic Canada, treatment of saline water is often required prior to being discharged. Mitigation using conventional salinity treatment plants may not be economically feasible due to the remote nature of the northern Canadian mine sites and the harsh climates in this region. Furthermore, treatment of saline waters requires disposal of concentrated brine, rendering this strategy impractical for several mine sites.

An alternative mitigation strategy is to store saline waters on site and use them to create meromictic conditions in mined out open pits at closure. In this manner, the denser saline water is isolated from mixing with freshwater stored in the mixolimnion. This is the proposed strategy for the De Beers Gahcho Kué diamond mine, located in the Northwest Territories, Canada.

This paper focuses on the mine plan for the Gahcho Kué Project and the approach used to evaluate the likelihood of meromictic conditions developing and remaining stable in a flooded, mined-out, open pit. A discussion of the model results is presented to demonstrate the merits of the closure strategy.

Keywords: mine closure, mine water quality, pit lakes, meromixis

INTRODUCTION

Currently, there are three existing diamond mining operations (Diavik, Ekati, and Snap Lake) in the Northwest Territories (NWT), in Northern Canada. The Gahcho Kué mine is under construction, and others are being contemplated. Mining diamonds in the NWT can pose several challenges. The region is dominated by lakes, which can make access to the kimberlite pipes difficult and in the case of mines using open pit methods, often whole lakes, or a portion of a lake needs to be dewatered to facilitate access to the mine workings.

Open pit mining can also induce large volumes of groundwater that need to be managed during operations. Untreated discharge of these flows is not always feasible for the following reasons:

- Groundwater salinity in the Canadian Shield is known to increase by orders of magnitude with depth (Fritz and Frape, 1982);
- The remoteness, harsh weather conditions, and lack of roads during the open water season render all construction activities much more expensive than elsewhere;
- The mines are often located in regions of continuous permafrost limiting the amount of fresh lake water available to recharge the groundwater table during periods of draw down, promoting upwelling of deep seated saline groundwater and rapid increases in mine water salinity;
- Lakes in northern Canada are pristine with very low concentrations of total dissolved solids (TDS) (i.e. <20 milligrams per litre [mg/L]) with aquatic biota that are sensitive to changes in salinity; and,
- Conventional treatment of salinity is through reverse osmosis and disposal options of the treated brine are limited due to the remote nature of the mine sites.

Diamonds will be mined from three open pits at the Gahcho Kué Project (the Project), which will require the partial dewatering of Kennady Lake to access the mine workings. Water quality modelling (De Beers, 2012, Vandenberg et al. (in review)), indicates that mine-related activities at the Project is expected to increase salinity in mine site water during operations. To mitigate the discharge of saline water, De Beers Canada Inc. (De Beers) has developed a zero site water discharge water management plan after year three of operations (EBA 2013). At closure, saline water stored on site will be pumped to the bottom of a mined-out open pit and capped with natural local catchment runoff and supplemental freshwater from a nearby lake (Lake N11), promoting the development of meromictic conditions that will minimize the mixing of saline water with the overlying lake.

To demonstrate the feasibility of the proposed water management strategy to regulators and stakeholders, a numerical model was developed to evaluate the likelihood of meromixis occurring in the pit lake during post-closure. This paper presents the model development and results to illustrate the merits of this approach.

PROJECT DESCRIPTION

The Project is located approximately 280 kilometres (km) northeast of Yellowknife, NWT, Canada (Figure 1). Diamondiferous kimberlite will be mined from three open pits (5034, Hearne and Tuzo), located below Kennady Lake (Figure 2). Mining of the three open pits will take place over an

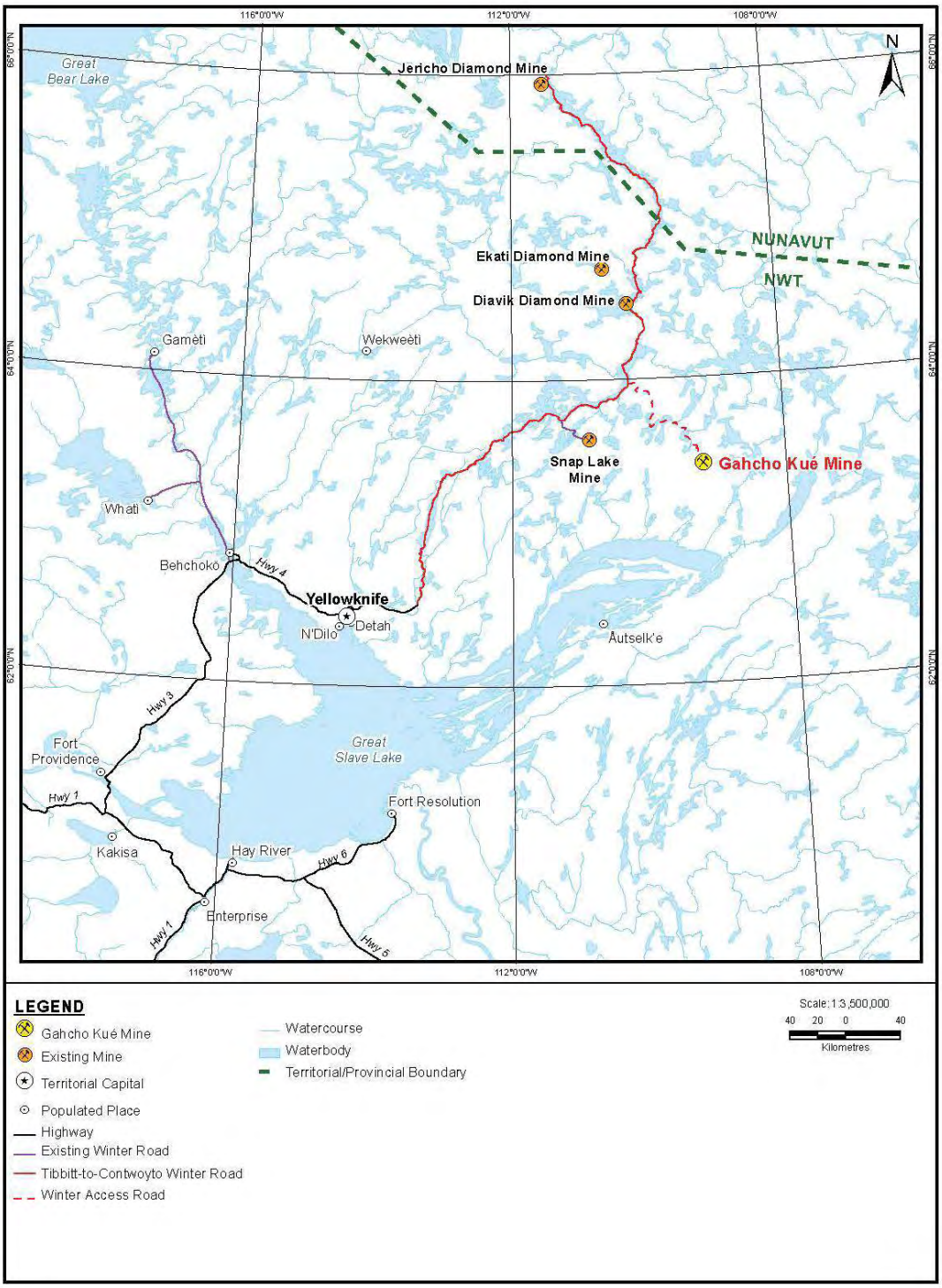

Figure 1 Location of the Gahcho Kué Project

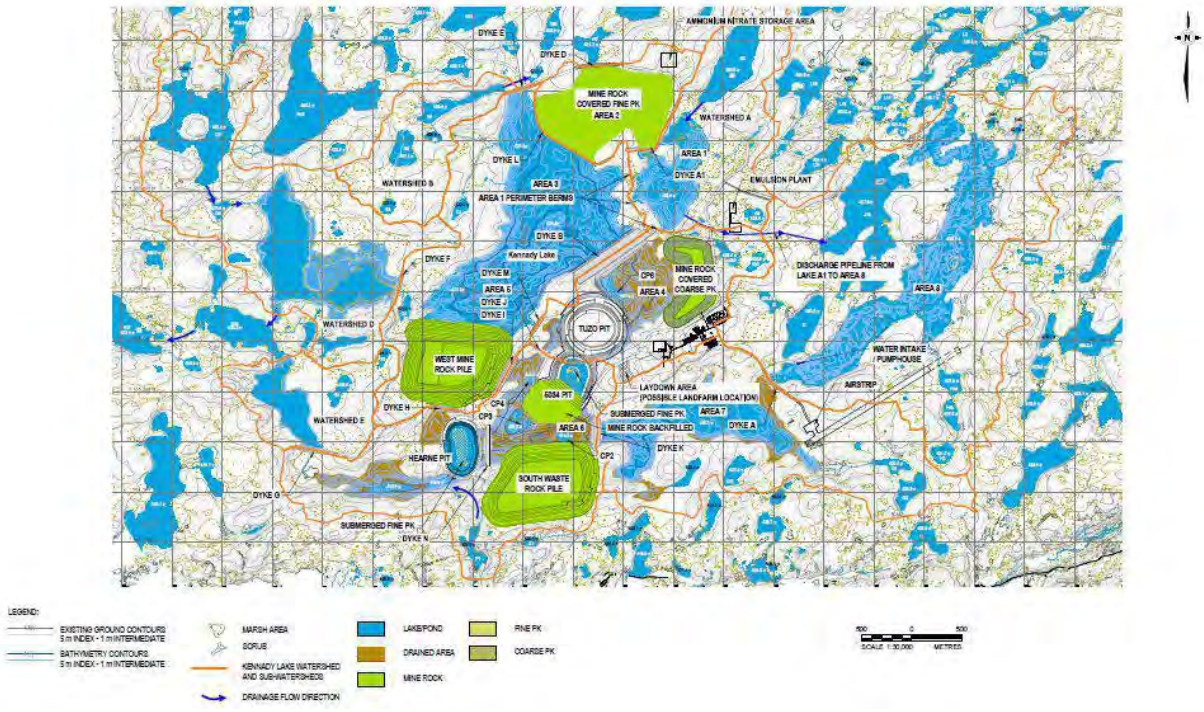

Figure 2 Gahcho Kué Mine Site Facilities

operational period of 11 years and produce 33.4 million tonnes [Mt] of ore, 300 Mt of mine rock, 10 Mt of fine processed kimberlite [PK] and 23.4 Mt of coarse PK (EBA 2013). The mine plan for the Project has been designed to minimize the surface disturbance and to facilitate progressive reclamation of mine site facilities during operations. The 5034 and Hearne pits will be mined first. During this period, fine PK will be stored in the Fine PK Containment (PKC) Facility in Area 2 and mine rock will be stored in the West and South Mine Rock Piles (Figure 2). Following the cessation of mining in the 5034 and Hearne pits, they will be used to store mine rock and fine PK, respectively, as well as process water and other mine site flows (e.g. pit groundwater inflows and natural runoff). Reclamation of the Fine PKC and mine rock piles will begin at this stage of the mine life. Mining of the Tuzo Pit will commence in Year 4 of operations. At completion it will remain an open void space.

The kimberlite pipes extend from near the bottom of the lake to approximately 300 metres (m) below the lake. To access the open pits, Kennady Lake will be segregated into six water management areas (2 to 7) separated by permeable and impermeable dykes. Area 2 is designated for deposition of fine PK. Areas 3 and 5 (referred to as Area 3/5) will be partially dewatered and converted into a water management pond (WMP) to settle solids in site discharges and to store process water during operations, open pit groundwater inflows, and natural catchment runoff from within the site area. All other areas (4, 6 and 7) will be fully dewatered to allow access to the mine workings.

The natural elevation of Kennady Lake is 420.7 metres above sea level [masl] with a total capacity of approximately 35 million cubic metres [Mm^3], in Areas 2 to 7 (EBA 2013). During the first year of dewatering, approximately 1 Mm^3 of water will be pumped from Area 7 to Area 8, a lake located

downstream of the mining disturbance (Figure 2). Subsequently, water stored in Area 7 will be pumped to Area 3/5 since it is expected that, at this point, total suspended sediment (TSS) concentrations will be elevated and preclude discharge from this area.

To maximize the operational storage capacity of the WMP, approximately 22 Mm^3 of water will be pumped from Area 3/5 to Lake N11 (located to the north of the Project) during the dewatering period, lowering the elevation of Kennady Lake to 418 masl. During the first three years of operations, 3.5 Mm^3 of water will be pumped annually from Area 3/5 to Lake N11. A total volume of 33.5 $Mm^3$of water will be discharged from the Project during dewatering and operations. Open pit groundwater inflows, process water, and natural catchment flows will be stored in the WMP and mined out open pits after the third year of operations.

At closure, the elevations in Area 3/5, Area 6 and Area 7 will be 422, 421.3, and 420.5 masl, respectively. The water level in these areas will be lowered to 417 masl and all the water stored above this elevation will be siphoned to the mined out Tuzo pit. Following the water transfer to the Tuzo pit, the available water storage capacity in the Tuzo pit and the overlying Kennady Lake will be filled primarily with natural catchment runoff and water pumped from Lake N11, a nearby lake in the adjacent watershed. Some residual groundwater flows will continue to report to the mined out Tuzo pit. Conceptually, this approach will promote the development of meromictic conditions in Kennady Lake, permanently isolating the high density saline water in the Tuzo pit (the monimolimnion) from interacting with the overlying low density water stored in Kennady Lake (mixolimnion). The phenomenon of meromictic conditions being established in pit lakes has been observed at several mines (Boehrer and Schultze, 2006).

Once Kennady Lake has re-established the natural lake elevation of 420.7 masl, and the water quality in the lake is of a suitable water quality and meets closure objectives, the lake will be reconnected to the downstream watershed. Water balance modelling (EBA 2013), indicates approximately eight years will be required to refill Kennady lake during the closure period of the Project.

METHODOLOGY

A site mass-balance water quality model was developed in GoldSim (GoldSim 2010) to assess the expected discharge concentrations during operations (from Area 3/5) and the average water quality in Kennady Lake following refilling. This model calculated the site water quality on a monthly basis using inputs from hydrology (EBA 2013, De Beers 2012), hydrogeology (De Beers 2012) and geochemistry (De Beers 2012). Details of the site water quality model are provided in De Beers (2012) and Vandenberg et al. (in press). As GoldSim does not have the inherent ability to simulate the hydrodynamic properties of water bodies, the stability of stratification in the Tuzo Pit was analyzed using two methods:

- hydrodynamic modelling of the first 100 years after refilling, using CE-QUAL-W2 (Cole and Wells 2008); and
- mass balance calculations over 15,000 years using a vertical slice spreadsheet model.

The spatial extent of the hydrodynamic model was Kennady Lake and Tuzo Pit. A model grid was developed based on GIS shapefiles of these connected water bodies. The grid was optimized to account for the full fetch of the lake with higher resolution near the pit.

CE-QUAL-W2 Model

The CE-QUAL-W2 (W2) model was used to compute TDS, temperature and density in Tuzo Pit. Near-surface layers were spaced at 1 m intervals, and deeper layers were spaced at 3 m intervals. The model also requires meteorological forcing data to drive currents and thermal behaviour in the lake. Meteorological data were obtained from weather stations at the nearby De Beers Snap Lake Mine and the Yellowknife, NWT Airport. Data were selected preferentially from the Snap Lake station because this station is closer to the Project, and data gaps were filled in using data from Yellowknife Airport. The required meteorological data were air temperature, dew point, wind speed and direction, and solar radiation.

In the W2 model, initial concentrations in the pit lake were determined by concentrations in Kennady Lake at closure, as simulated in the site mass balance water quality model. The 23 Mm^3 of water in the bottom of the pit was set equal to the concentration in the water storage areas Kennady Lake (e.g., the WMP) prior to refilling, because this volume will be drawn from the surface to fill the pit until Kennady Lake is lowered to 417 masl. 1.2 Mm^3 of groundwater is predicted to flow into the pit during the refilling period, so this was added as well, at time-varying constituent concentrations predicted by the hydrogeological model (De Beers 2012; Vandenberg et. al. in review). The upper portion of the lake was assumed to have a TDS concentration that was equal to the refilled Kennady Lake.

It is recognized that these layers will not form a sharp boundary due to turbulence caused by refilling and other factors. Therefore, the gradient was assumed to span a vertical transition depth of 40 m, and concentrations were calculated for the upper and lower portions respecting the mass of TDS in both layers and within the gradient.

It is not known exactly when the pit will be filled in terms of months of the year. Therefore, an average temperature of Kennady Lake was calculated based on samples that were skewed toward available site-specific, open-water sampling data. The resulting average temperature (5 degrees Celsius [ºC]) is anticipated to be reasonable, because refilling activities are also expected to be most intense during open water periods. The uniform temperature of 5ºC was used to initialize the pit lake water column. The temperature profile could be manipulated to increase the stability in the pit, but that manipulation was not examined as part of this modelling to conservatively assess pit lake stability.

Once the model was initialized, it was run for 100 years to predict the change in elevation of the pycnocline (i.e., the layer within the refilled pit where the density, or TDS gradient is greatest), and therefore the volume of water that will essentially be isolated from Kennady Lake. Groundwater discharge from the hydrogeological model was input to the hydrodynamic model at several vertical points according to time-varying volumes and constituent concentrations throughout the modelled time frame, and natural inflows to Kennady Lake were also included.

Vertical Slice Spreadsheet Model

To estimate the long-term stability of Tuzo Pit, long-term TDS profiles were calculated using a vertical slice spreadsheet model. A spreadsheet model was used because it was not feasible to run a hydrodynamic model for this length of time due to the computational limitations. The vertical slice spreadsheet model incorporated long-term inflows that were predicted by the hydrogeological model (De Beers 2012; Vandenberg et al. in review) to simulate TDS profiles over 15,000 years at 25 m vertical intervals in Tuzo Pit. This simplified approach is intended to evaluate directional

changes to TDS concentrations at depth over the very long-term and does not consider all processes influencing pit lake stability (e.g. climate change, diffusivity).

The main inputs used in the mass balance calculation were initial conditions in Tuzo Pit, which were the same as those used for the W2 model, and long-term groundwater inflows and outflows. Groundwater inflow volumes and constituent concentrations and outflow volumes were predicted for the first 1,000 years after Tuzo Pit is filled. After 1,000 years, the inflows were assumed to continue at constant volumes and concentrations.

To complete the calculations, inflow volumes and concentrations were directed to the appropriate 25 m interval within the pit. Within each interval, a mass-balance calculation was performed, and excess water (difference between inflow and outflow) was directed upwards to the next segment. The vertical slice spreadsheet model generated annual time series at 25 m intervals over a 15,000 year timeframe.

RESULTS AND DISCUSSION

The results of the W2 model are presented in Figure 3. The W2 model results indicate meromixis will occur in the Tuzo pit following refilling of Kennady Lake and remain permanently stratified; however, the model also indicates there will be some interaction between the monimolimnion and the mixolimnion during the 100-year model period (Figure 3). During the 100-year modelling period, the transition zone increases, reflecting an upward transfer of mass from the monimolimnion into the mixolimnion. This vertical movement is predicted to occur relatively rapidly after refilling, and gradually thereafter.

Concentrations of TDS decrease in the mixolimnion from approximately 170 mg/L to 60 mg/L (Figure 3). The gradual replacement of Kennady Lake waters with natural runoff will continue to reduce the TDS of the overlying water, thereby strengthening the stratification by increasing the density difference between the surface and deep water zones. A small influx of groundwater to the pits predicted by the groundwater modelling is not projected to increase TDS at depth over the modelled 100-year time frame and concentrations remained stable at approximately 915 mg/L.

The vertical slice mass-balance model projected a rising and strengthening stratification in Tuzo Pit in the long term (Figure 4). Although the hydrodynamic simulation indicated very little change in TDS in the monimolimnion in the first hundred years, the mass-balance slice model indicated that groundwater inflows would begin to change TDS at depth in the first thousand years. After 15,000 years, the model predicted that the monimolimnion would increase in TDS and expand upwards due to the slight net inflow (Figure 4). The deeper pit water will eventually, over the very long-term, take on the characteristics of the surrounding deep, high TDS groundwater.

While the general trend of increased TDS and upward expansion of the pycnocline is likely reliable, this model may over-predict the extent to which these phenomena may occur. The model did not account for upward diffusion due to a concentration gradient, and it extrapolated groundwater inflows beyond the timeframe modelled by hydrogeological modelling. Nevertheless, it may be concluded with some confidence from this modelling, that stratification in Tuzo pit, and hence its meromictic state, will strengthen with time.

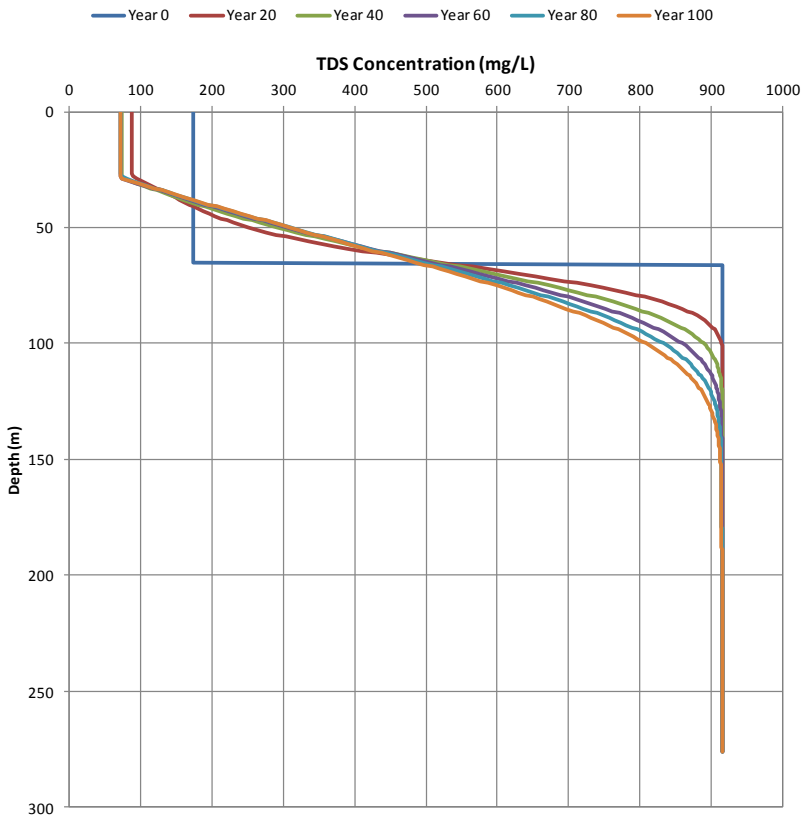

Figure 3 Hydrodynamic Model Results

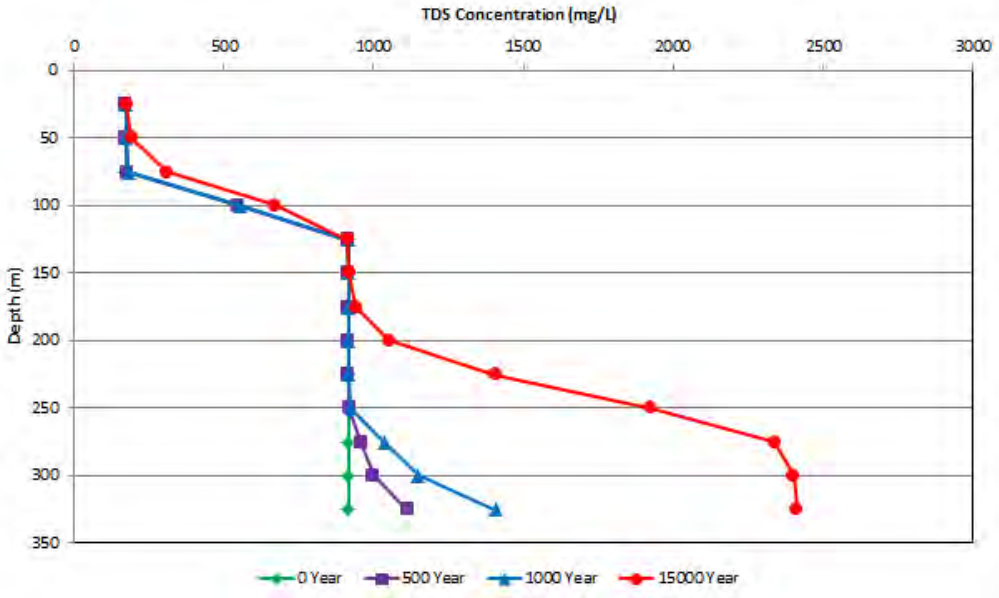

Figure 4 Vertical Slice Mass Balance Model Results

CONCLUSION

De Beers proposes to mine diamonds from three open pits (5034, Hearne, and Tuzo) at the Gahcho Kué Project. The mine waste and water management plan developed for the Project (EBA 2013), maximizes the use of mined out facilities for storage of mine waste and mine water to minimize the amount of discharge required from the Project during operations. In this manner, De Beers will only be required to discharge for the first three years of operations and water originating from natural runoff, groundwater inflows, or process water during the remaining years of operation can be stored on site.

Simulated water quality conditions in water storage facilities at the site, including the WMP and mined out Hearne pit during operations, indicate that TDS concentrations will increase (De Beers 2012; Vandenberg et al., in review). A pit lake hydrodynamic water quality model demonstrated that the transfer of the high TDS water stored in these areas during operations to the bottom of the Tuzo pit at closure will produce a density difference and meromictic conditions will be established following refilling, permanently isolating the high TDS water from interacting with the overlying freshwater stored in Kennady Lake after approximately 100 years (Figure 3). The vertical slice spreadsheet model indicates that as groundwater inflows increase TDS concentrations at depth in the long-term (i.e. >1000 years) in Tuzo pit, the continual replacement of Kennady Lake water with natural runoff and direct precipitation, lowers the concentrations near the surface, increasing the density difference and stratification stability of the pit lake (Figure 4).

In general, for mine sites where it can be demonstrated that density differences can be established and maintained over the long term, storage of mine waters in pit lakes is a viable option for permanent disposal of these solutions. This paper focused on the salinity (e.g. TDS) of the mine water to be produced at the Project; however, the Project water management strategy has the indirect benefit of managing elevated concentrations of other constituents of concern. For example, use of ammonium nitrate fuel oil (ANFO) can lead to elevated nitrogen concentrations in mine waters during operations. If it can be reasonably demonstrated that density differences can be used to segregate operational mine waters at closure, other constituents with elevated concentrations during operations can also be mitigated through being permanently stored in the pit lake monimolimnion.

It is recognized that the purpose of modelling is not to produce predictions of forecasts of future conditions, but rather to provide an estimate of the direction and magnitude of impacts from proposed mining operations, and to provide projections that are suitable for the assessment of effects. Therefore, mining projects that are relying on the use of pit lakes to mitigate the potential for effects of mine waters originating during operations to the surrounding environment (i.e., downstream waters), it is of utmost importance that the water quality model is periodically evaluated and updated in the context of field-based water quality monitoring during operations and closure to allow for calibration to existing conditions and to more accurately project future conditions. Furthermore, it is necessary to have alternate mitigation strategies available in the instance that the future performance of the modelled system does not behave as projected.

ACKNOWLEDGEMENTS

The authors of this paper would like to thank Ms. Veronica Chisholm of De Beers Canada Inc. for allowing Golder Associates Ltd. to publish results from the Gahcho Kué Project. The authors would

also like to thank George Wang of Golder Associates Ltd. for his assistance in developing the water quality model that was used for the current assessment.

REFERENCES

Boehrer, B and Schultze, M. (2006) On the Relevance of Meromixes in Mine Pit Lakes, poster paper presented at the 7th International Conference on Acid Rock Drainage (ICARD), March 26-30, 2006, St. Louis, MO.

Castendyk, D.N. and L.E. Eary. (2009). Mine Pit Lakes: Characteristics, Predictive Modeling, and Sustainability, Society for Mining, Metallurgy and Exploration Inc. Littleton, Colorado, 304 pp.

Cole, T.M. and Wells, S.A. (2008), CE-QUAL-W2: A Two-dimensional, Laterally Averaged, Hydrodynamic and Water Quality Model, Version 3.6 User Manual, August 2008.

De Beers Canada Inc. (De Beers) (2012) Environmental Impact Statement Supplemental Information Submission for the Gahcho Kué Project, Submitted to the Mackenzie Valley Environmental Impact Review Board, April 2012.

EBA (2013) Gahcho Kué Project, NT, Canada, Updated Water and Waste Management Plan, Issued for Review, December 2013.

Fritz, P, Frape, S.K., (1982) Saline Groundwaters in the Canadian Shield – a first overview, Chem. Geol. 36, 179-190.

GoldSim Technology Group (2010) Users Guide for GoldSim Version 10.5 in a Probabilistic Simulation Environment.

Vandenberg, J.A., Herrell, M.K., Faithful, J.W., Snow, A.M., Lacrampe, J., Bieber, S., Dayyani, S. and Chisholm, V. (in press) Use of Multiple Models for Assessing Mining Effects on Kennady Lake, Northwest Territories, Canada.

Variable-Density Transport Modeling in Hypersaline Pit Lakes

Guy Roemer, Colleen Burgers and Sonya Cadle
Tetra Tech, USA

ABSTRACT

In Western Australia there is the potential for many pit lakes to become point sources of hypersaline water. The low annual rainfall and high evaporation produces a rainfall deficit, contributing to the development of hypersaline pit lakes. The salinization of pit lakes can affect local and regional groundwater resources, as well as the broader natural environment. The extent of impact on the surrounding groundwater system is largely dependent on the local hydrogeology, which dictates whether the pit lake will act as either a terminal sink or a flow through system. A long-term concern is the downgradient movement of saline plumes from pit lakes, especially in flow-through systems.

In this study we perform variable-density transport modeling using SEAWAT to examine the potential for salinity migration from terminal sink pit lakes in Western Australia. As the pit lake water becomes denser over time due to evapoconcentration, the potential for migration into the groundwater system beneath the pit floor is more probable. SEAWAT model results are compared to constant-density transport results. The comparison indicates that failing to consider density changes in the pit lake water causes underestimation of the plume migration distance. Sensitivity analyses were also conducted to examine the sensitivity of model parameters, such as dispersivity, effective porosity, simulation time, and hydraulic conductivity. Results from this study show that given the low permeability of the bedrock beneath the pit floor, salinity migration from this pit will be limited and will not impact downgradient groundwater dependent ecosystems.

Keywords: salinity, pit lake, transport, density, groundwater

INTRODUCTION

The Cameco Corporation Australia in conjunction with Mitsubishi Development Pty. Ltd. is planning the Kintyre Uranium open-pit development in the East Pilbara region of Western Australia, approximately 80 km south of Telfer on the edge of the Great Sandy Desert. If the project was to eventually move forward utilizing the current mine plan, it could potentially run for approximately 14 years based on a total indicated resource of 55.2 million pounds of U_3O_8. The project is located immediately north of the Karlamilyi (Rudall River) National Park (Figure 1).

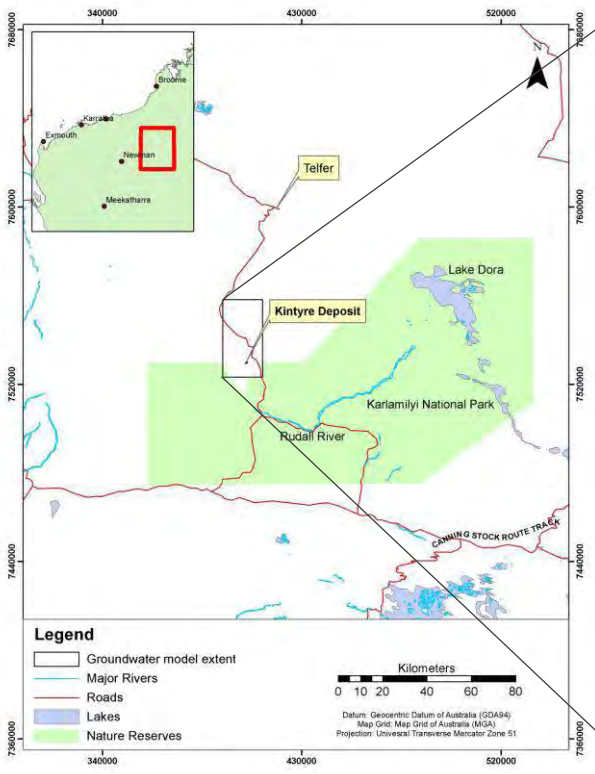

Figure 1 Kintyre Location Map

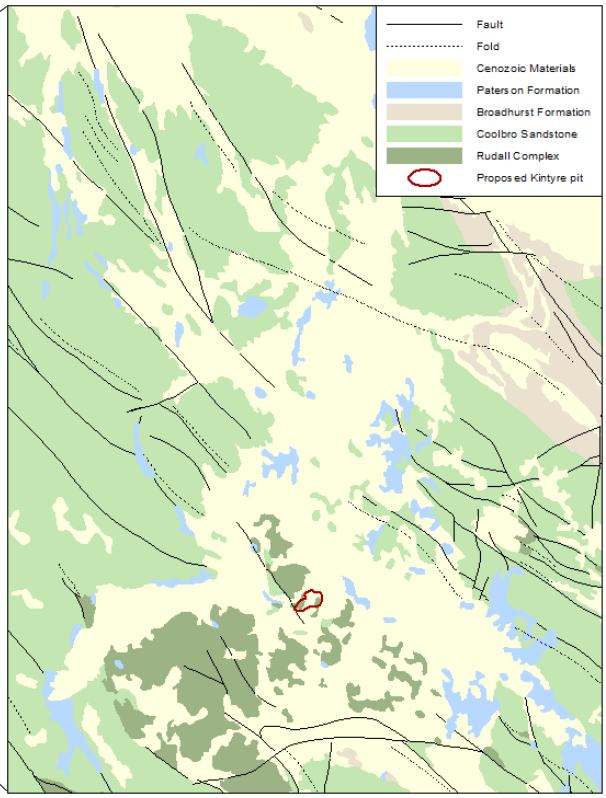

Figure 2 Regional Surficial Geology

The pit is required to be dewatered and, following closure, a pit lake is likely to form. As part of the Environmental Review and Management Program, groundwater, geochemical pit lake and salinity plume models were required to determine the potential for risk to downgradient receptors.

Geological environment

The site is located on a slight topographic high between two branches of the Yandagooge Creek. The creek flows toward the north-northeast between two nearby mountain ranges comprised of sedimentary Neoproterozoic rocks (Broadhurst Formation and Coolbro Sandstone) and metamorphic Paleoproterozoic rocks (Rudall Complex). Yandagooge Creek roughly follows the footprint of a Permian glacial valley that is incised into the Proterozoic rock. The glacial valley is mostly filled with Permian age glaciofluvial and glaciolacustrine sediments (Paterson Formation). The basal Permian is generally tillite and is overlain by

sandstone, siltstone, and claystone. Coarser-grained Cenozoic sediments overlie the Permian materials in most locations but tend to be unsaturated. Figure 2 illustrates the site layout and surficial geology.

Pit lakes

The pit shell used in the pit lake model was determined from the mining plan to be predominantly schist with areas of ore host rock, tillite and carbonate material (Figure 3).

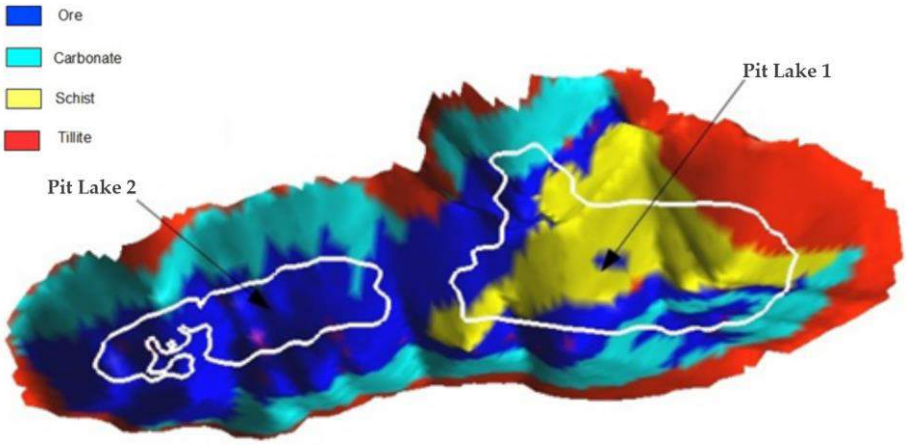

Figure 3 Cross section of pit showing locations of lakes and simplified geology

In semi-arid climates the dissolved constituents in water bodies become highly concentrated and there is an increasing concern that pit lakes will become point-sources of hypersaline groundwater. The Kintyre site occurs in the region with the highest average pan evaporation in Australia, at greater than 4 m per annum. This high evaporation coupled with a low mean rainfall of 372 mm per annum measured at Telfer (BOM, 2014) results in the pit lake becoming an evaporative, 'terminal' sink system (Figure 4) whereby the volume of water egress greatly exceeds ingress and the hydrogeological gradient is towards the pit. McCullough, *et al.* (2013) discusses the feasibility of allowing terminal sinks to form in order to reduce the impact to groundwater systems. The terminal sink draws all groundwater or leachate from tailings or waste rock material towards it, ensuring that it will not leave the footprint of the mine area and downgradient receptors will not be impacted by elevated uranium or other metals.

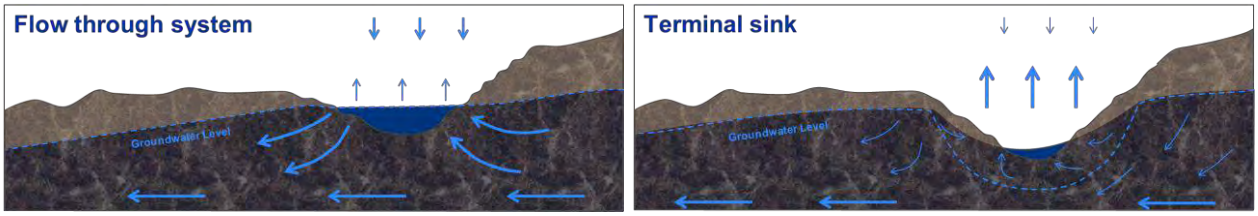

Figure 4 Illustration of pit lake systems

Despite the capture of any elevated element concentrations present in the groundwater by the pit lake evaporative sink, there was concern that a salinity plume could spread, against the flow gradient by diffusion and salinize the surrounding groundwater resources. In order to determine this risk the distance of likely diffusion was modelled.

The geochemical model integrated the pit lake volumes and dimensions to determine the limnological characteristics of the pit lakes. The dimensions of the pit lakes are shown in Figure 3 with the simplified geology used for the pit walls. If the depth of a lake relative to the area is greater than 20 percent, the lake is likely to be permanently stratified (Castendyk and Jewell, 2002). Table 1 shows the maximum depth, surface area, volume and the calculated relative depth. As the relative depth of Lake 1 is 38.6%, which is very much higher than the 20% point above which stratification is likely. It is estimated that Lake 1 will permanently stratify and not be subject to mixing while Lake 2 may not permanently stratify and will be subject to some mixing. Mixing will reintroduce oxygen into the deeper portions of the lake allowing chemical reactions to continue under oxygenated conditions.

Table 1 Pit lakes physical dimensions

Lake	Maximum lake depth (m)	Area (m^2)	Maximum volume (m^3)	Relative Depth %
Lake 1	139	1.02E+05	5.70E+06	38.6
Lake 2	58	8.69E+04	1.90E+06	17.4

The geochemical model was advanced to 1,000 years although chemical equilibrium was predicted to be reached within 10 years after closure. The final major ion, pH and total dissolved solids concentrations are given in Table 2.

Table 2 Pit lakes major ion concentrations predicted at 1,000 years

mg/L where applicable	Lake 1	Lake 2	mg/L where applicable	Lake 1	Lake 2
pH	7.58	7.52	Magnesium	4.66E+03	5.38E+03
Alkalinity as $CaCO_3$	219	243	Potassium	4.58E+03	5.26E+03
Calcium	432	439	Sodium	3.89E+04	4.49E+04
Chlorine	5.33E+04	6.15E+04	Sulfate	2.46E+04	2.82E+04
Fluorine	29.3	37.2	Total dissolved solids	1.27E+05	1.46E+05

METHODOLOGY

Groundwater flow models were developed and calibrated using MODFLOW-SURFACT to support permitting of the Kintyre project. Both regional and local-scale modelling were performed to assess the potential effects of mining on groundwater dependent flora and fauna (including subterranean) and to evaluate water supply availability. The local-scale model had identical properties to the regional model, but with finer discretization and smaller extents. The flow modelling predicted formation of terminal sink pit lakes. Geochemical models of the pit lakes' water quality using PHREEQC were developed next. The groundwater and geochemical models were used to develop a variable-density transport model using SEAWAT to examine the potential for salinity migration from the predicted terminal sink pit lakes.

Groundwater Flow Model

For modelling purposes, the geologic units were grouped into layers. The layer thicknesses were engineered such that the base of key layers corresponded to the base of the Cenozoic and Permian units

where these were present. Outside the vicinity of the paleochannel, the layers were flattened into a subdued representation of topography to maintain layer thickness. Hydraulic conductivity zones were used to represent the different geologic units. The ground surface was used to represent the top of the model.

The uppermost layer (Layer 1) of the model extends from ground surface to approximately 25 meters below ground. Layer 1 includes all Cenozoic materials; where the Cenozoic materials pinch out at the edges of the drainages, Layer 1 includes a portion of the uppermost bedrock unit (Permian or Proterozoic) to maintain layer thickness. Layer 2 includes the first 50 meters of the Permian units, which corresponds to the sandstone, siltstone, and claystone lithologies. Because the Permian units pinch out at the edge of the paleochannel, Layer 2 also includes a portion of the Proterozoic basement rock outside the channel to maintain layer thickness. Layers 3, 4, and 5 each include a 50-meter-thick section of the Permian tillite, with the lateral extent varying based on the paleochannel thickness at that depth. The remainder of each these layers is composed of Proterozoic basement rock to maintain layer thickness. The remaining layers represent the Proterozoic basement rock.

Model recharge was distributed by surficial geology, based on chloride balance data indicating approximate recharge rates. Model hydraulic conductivities and storage coefficients were distributed based on geologic unit.

Geochemical Model

A geochemical model of the final pit lake chemistry was developed using PHREEQC (Cameco Australia, 2013). The major conclusions were:

- The quality of the pit lake water is predicted to be hypersaline;
- Alkalinity is predicted to be moderate over the pit lake life;
- The pH ranges between approximately 7.5 and 8 and is not predicted to become acidic;
- Evaporative losses increase the concentrations of elements such as boron, fluorine, manganese, molybdenum, nickel and uranium over time;
- Salt inputs from the pit walls dissolved by direct rainfall increase the concentrations of arsenic, chromium, copper, lead, nickel, and selenium over time; and
- As a result of the alkaline pH, no iron is predicted to be in solution and aluminium concentrations are predicted to be low.

Variable-Density Flow Model

To simulate transport of salinity or any other solute, the initial concentration must be determined. For this study, the final equilibrium total dissolved solids (TDS) concentration calculated from the geochemical model PHREEQC was used as the initial salinity concentration for each pit lake (Lake 1 and Lake 2). Geochemical model results from PHREEQC do not explicitly calculate TDS concentrations, so the following equation (Csuros, 1997) was used to determine pit lake TDS values:

$$TDS = (0.6 \times Alk) + Na + K + Ca + Mg + Cl + SO_4 + SiO_2 + NO_3 + F \quad (1)$$

The components of this equation are the cations and anions that compose the TDS value. The calculated TDS of Lake 1 used in this model is 127,100 mg/L or 127.1 kg/m³ while the Lake 2 TDS is 146,400 mg/L or 146.4 kg/m³. Both lakes are considered to be hypersaline.

No manual activity corrections were made, beyond those adjustments that occur through the geochemical modelling associated processes. However, oversaturation of species was prevented by allowing chemical precipitation to remove chemical mass from the pit lake, and establish a limit on the maximum dissolved concentration for the associated components of that mineral. As a consequence, over the modelled evolution of both lakes, specific mineral species were predicted to precipitate, including phases containing chloride, sulfate, and fluorine as well as carbonate bearing species and silica.

Two other model parameters required to simulate solute transport are effective porosity and dispersivity. Effective porosity is defined as the ratio of volume of interconnected pore space to total volume of a rock sample. The bedrock units at Kintyre were assumed to have an effective porosity of 0.05 based on literature values for fractured crystalline rock that range between 0 to 0.10 (Freeze and Cherry, 1979).

Estimating dispersivity is challenging when there is no pre-existing solute plume. However, guidance exists regarding dispersivity in relationship to the model grid cell dimensions. The grid Peclet number is the grid spacing (25 m) divided by longitudinal dispersivity, and Peclet numbers should be five or less to minimize numerical errors or numerical dispersion during modelling (Delleur, 2006). For this study, therefore, longitudinal dispersivity is assumed to be 6.25 m, resulting in a Peclet number of 4.

SEAWAT includes a variable-density flow package that requires input values for minimum density, maximum density, as well as the slope of the linear equation of state, which relates fluid density to solute concentration. Density values were determined from standard values of sodium chloride solutions at different concentrations at 25°C (UCSD, 2014). The minimum density is estimated to be 1,075 kg/m³, which is slightly lower than the TDS concentration of Lake 1. The maximum density is estimated to be 1,100 kg/m³ which is slightly higher than the TDS concentration of Lake 2 to compensate for the simulated pit lake water temperature of 32°C. For reference, seawater has a density of 1,025 kg/m³. The slope of the linear equation of state is calculated to be 0.171.

Boundary conditions for the variable-density flow and transport model are identical to previous groundwater models (i.e., General-Head Boundaries around the model grid) except the pit lake cells are specified as either "no flow" for cells located above the water table or as constant head and constant concentration cells. The constant head pit lake cells are set to a hydraulic head equivalent to the final pit lake elevations from the previous groundwater flow model after 1,000 years. Lake 1 is set at 266.8 meters Australian Height Datum (mAHD) and Lake 2 is set at 268.82 mAHD. The constant concentrations at the pit cells are the final equilibrium TDS concentrations from the geochemical model.

Assumptions

Steady-state variable-density modelling was chosen for this study as previous groundwater and geochemical models predicted conditions to 1,000 years and showed that new steady-state conditions were achieved in approximately 100 years. Steady-state modelling was also chosen to reduce computational duration given the small time steps required to perform transport simulations. Assumptions for the variable-density modelling simulations are as follows:

- Precipitation of solids from pit lakes onto the pit lake floor (a process which would reduce permeability of the pit lake floor) is not simulated;

- TDS concentration and water-level elevation is constant in the pit lakes; and
- Salinity concentration of groundwater is zero.

Background salinity concentration of the groundwater was assumed to be zero instead of the mean concentration of 3,300 mg/L to assess only the effects of the pit lake on the groundwater system. This is a conservative assumption, as using zero for the surrounding salinity increases the concentration gradient from the pit lake water to the surrounding groundwater. Using the actual groundwater salinity concentration of 3,300 mg/L would potentially decrease the diffusion of pit-related salinity. Further, since the pit lake water-level elevations and salinity concentrations are held at their maximum simulated values and precipitation of solids from the pit lake are not included; this model is considered to be conservative.

RESULTS AND DISCUSSION

The groundwater flow model was calibrated to within 10% of observed data for both steady state and transient data sets. The calibration data set represented water levels measured in 2011 and 2012 when no onsite pump testing was occurring and as a consequence, the system was assumed to be at steady state. Multiple groundwater pumping tests were performed in a phased and overlapping sequence in six wells during 2011 and in three more wells during 2012. Monitoring data from nearly 50 wells monitored during the tests was used to calibrate the transient model.

Figure 5 summarizes the results of the hydrogeological and geochemical models as the recovery of the groundwater system to equilibrium after approximately 15 years and the achievement of a steady state in water quality after approximately 10 years. In the two pit lakes that are predicted to evolve at Kintyre, the total dissolved solids (TDS) of pit lake water will reach hypersaline concentrations of between 120,000 mg/L and 150,000 mg/L (Figure 5) and the pH will remain circumneutral to slightly alkaline.

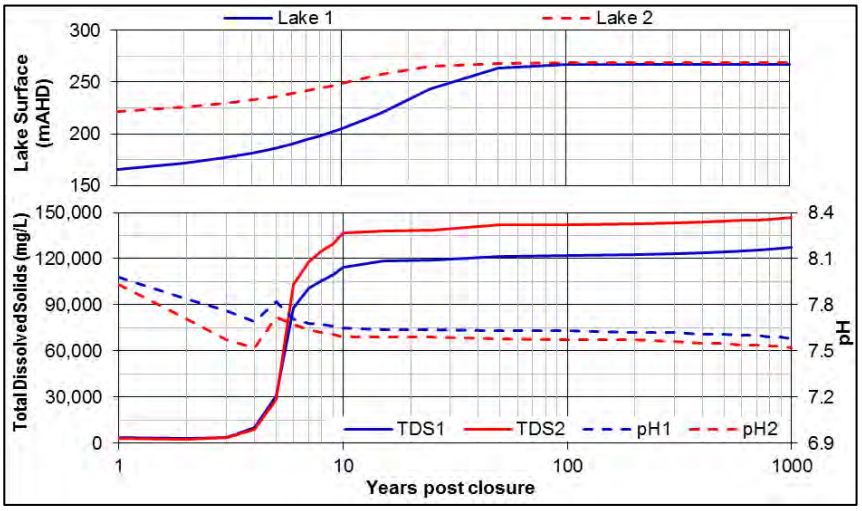

Figure 5 Pit lake level recovery with TDS and pH

Figure 6 shows the maximum extent of the salinity plume in the horizontal direction (from model layer 8 in the bedrock) for the constant-density case after 100 years. Contour intervals in Figures 6 through 9 are

1, 10, and 100 kg/m³, which are equivalent to 1,000, 10,000, and 100,000 mg/L, respectively. The mean TDS concentration of groundwater at the site is approximately 3,300 mg/L (i.e., brackish) so a minimum TDS contour of 1,000 mg/L was used. In Figure 6, salinity migrates less than 100 m horizontally from the pit lake as a result of dispersion because the pit lakes are terminal sinks.

Figure 8 shows the vertical extent of the salinity plume for the constant-density case through a west-east line indicated on Figure 6, over a distance of approximately 1 km after 100 years. Each model layer is approximately 25 m thick below the pit until a depth of approximately 320 m below ground surface (bgs). The lower model layers after a depth of approximately 320 m bgs are omitted from the vertical extent figures. Gray and blue cells represent no flow and pit lake cells, respectively. The blue and black contours represent the water table and the TDS concentration, respectively. Figure 7 indicates that a salt plume migrates approximately 50 m vertically before being indistinguishable from mean groundwater salinity.

Figures 7 and 9 show the horizontal and vertical extent of the salinity plume for the variable-density case after 100 years. In Figure 7, the horizontal extent is nearly identical to the constant-density case and the salinity plume does not move beyond the surface extent of the pit. In Figure 9, salinity migrates further vertically (approximately an additional 75 m) than the constant density case as a result of pit lake density effects, to a maximum depth of 150 m before it is indistinguishable from the salinity of the groundwater. There is no horizontal migration in the deeper model layers as a result of the low horizontal hydraulic conductivity (0.008 m/d) arising from decreased fracture density and aperture of the metamorphic rock at those depths, and consequently the salinity plume is not predicted to migrate offsite.

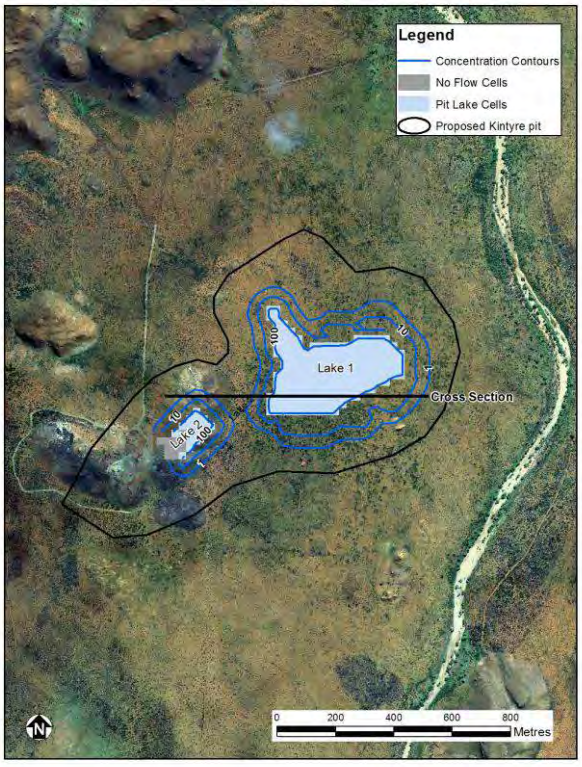

Figure 6 Constant-density salinity contours

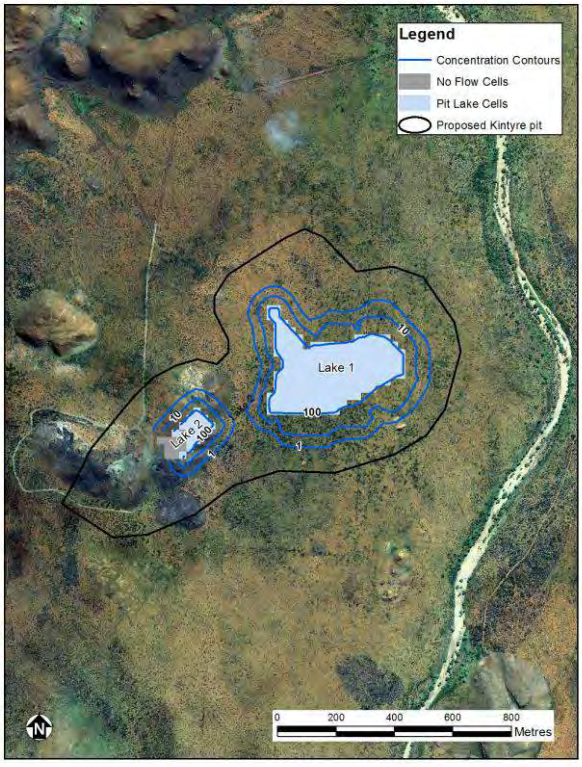

Figure 7 Variable-density salinity contours

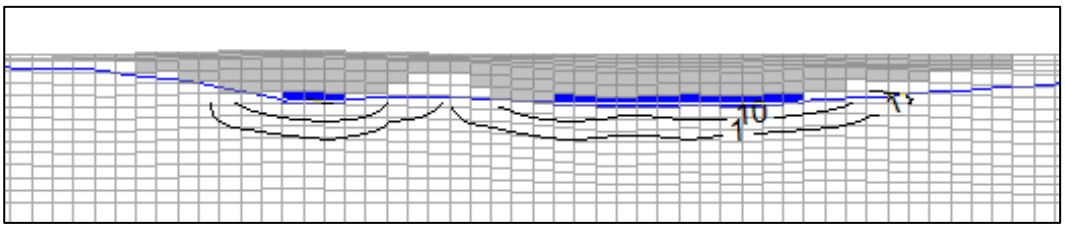

Figure 8 Vertical constant-density salinity contours along cross section from Figure 3. Contour interval is 1, 10, and 100 kg/m^3. Vertical grid spacing is 25m below the pit floor.

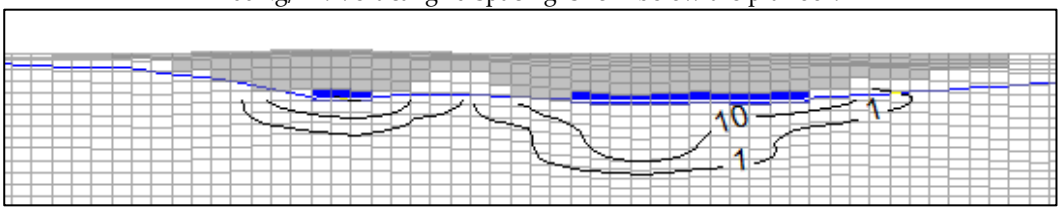

Figure 9 Vertical variable-density salinity contours along cross section from Figure 3. Contour interval is 1, 10, and 100 kg/m^3.Vertical grid spacing is 25m below the pit floor.

Given the uncertainty in dispersivity and effective porosity values, three sensitivity simulations were performed to bracket the salinity plumes horizontal and vertical extent:

- Dispersivity factor of four increase [Peclet Number (Pe) = 1];
- Dispersivity factor of 2.5 decrease (Pe = 10); and
- Effective porosity factor of 5 decrease (n = 0.01).

Table 3 provides the change in downgradient distance of the 1,000 mg/L concentration contour for each sensitivity simulation in the horizontal and vertical directions when compared to the variable-density case. Results show that increasing dispersivity could causes the 1,000 mg/L contour to reach the surficial pit shell boundary, but does not leave the site.

Table 3 Variable-density model sensitivity analysis results

Simulation	Horizontal Distance Change (m)	Vertical Distance Change (m)
Dispersivity factor increased (Pe = 1)	+100	+50
Dispersivity factor decreased (Pe = 10)	-25	-30
Effective porosity decreased (n = 0.01)	~0	~0

CONCLUSION

Detailed numerical analyses were conducted to assess if a salt plume originating from the Kintyre pit lakes could migrate offsite toward groundwater receptors. Results show that salinity does migrate horizontally and vertically from the pit lake, but the 1 kg/m^3 or 1,000 mg/L TDS contour progresses less than 100 m from the pit lake using base case parameters. Results from this study show that given the low permeability of the bedrock beneath the pit floor, salinity migration from this pit will be limited and will not impact downgradient groundwater dependent ecosystems.

ACKNOWLEDGEMENTS

We would like to thank David Maxton and Simon Williamson at Cameco Australia Pty Ltd for supporting this project. We also would like to thank the anonymous ICARD reviewers for their insightful comments and suggestions.

NOMENCLATURE

bgs	below ground surface
mAHD	meters Australian Height Datum
Pe	Peclet Number
TDS	Total Dissolved Solids

REFERENCES

BOM, (2014) *Climate statistics for Australian locations - Monthly climate statistics: Summary statistics TELFER AERO*. Australian Government Bureau of Meteorology, Last updated 28 August 2014, Accessed 1 September 2014. http://www.bom.gov.au/climate/averages/tables/cw_013030.shtml

Cameco Australia, Kintyre Uranium Project, Environmental Review and Management Programme, 2013.

Castendyk, Devin and Jewell, Paul, Turnover in Pit Lakes I. Observations of Three Pit Lakes in Utah, USA, Tailings and Mine Waste Conference Proceedings, 2002.

Csuros, M., (1997) Environmental Sampling and Analysis: Lab Manual, FL, CRC Press, 400 p.

Delleur, J.W. (2006) *The handbook of Groundwater Engineering*, 2nd Edition, FL, CRC Press, 1320 p.

Freeze, R.A., and Cherry, J.A. (1979) *Groundwater*, Englewood Cliffs, NJ, Prentice-Hall, 604 p.

McCullough, CD, Marchand, G & Unseld, J (2013) 'Mine Closure of Pit Lakes as Terminal Sinks: Best Available Practice When Options are Limited', Mine Water and the Environment, vol 32, no. 4, pp. 302 - 313.

University of California at San Diego (UCSD), Density (25°C) of NaCl solutions at different concentrations, accessed on 19 March 2014 at http://www.maelabs.ucsd.edu/mae171/Conc%20vs%20density.pdf.

Selecting Pit Lake Model Approaches Based on Data Availability

Jan Vanhooydonck[1], John Mahoney[2], Rebecca Stephen[3] and Gordon Maclear[4]

1. *Artois Consulting, Chile*
2. *Mahoney Geochemical Consulting, USA*
3. *African Barrick Gold, Tanzania*
4. *AngloGold Ashanti, Continental Africa*

ABSTRACT

Information on costs and environmental management strategies related to the closure of open pit mines requires results from comprehensive numerical hydrogeological and hydrochemistry models. Ideally, each model input parameter is defined by comprehensive field or laboratory tests.

Since closure assessments are now carried out earlier in the lifetime of a mine, it is rare that each input parameter can be accurately quantified prior to modelling. To compensate for data limitations, pit lake models increasingly incorporate additional, theoretical assumptions which are subsequently evaluated using sensitivity analyses.

Based on a study in equatorial Africa of three existing pit lakes (gold mines), we compare the water quality results of the initial water mixing models with the results of the more complex pit wall interaction models. The initial models only used water quality samples collected in the field while the more advanced models incorporated the results of the static and the kinetic leach tests for solids.

The differences between the model results are partially reduced by incorporating more laboratory data and by increasing the level of model complexity. But, additionally, for large operations where pits are in various stages of development, basic field sampling data facilitates a "calibration" to known conditions.

We recommend designing models based primarily on water balance components and available water quality data supported by the mineralogical and leaching characteristics of the wall rock. In circumstances where specific inflows dominate the water balance, simplified mixing models can provide defensible initial estimates with regard to the long term trends of the pit lake water quality.

Keywords: pit lake model, hydrogeology, hydrochemistry

INTRODUCTION

Financial, social and environmental obligations need to be met after the closure of a mining operation. As a result, the project developer, even at the earliest stages of an ore body's assessment, aims to incorporate the final closure conditions and determine their eventual impact on the planned development.

Due to the limited amount of data available at such early stages of a project, we increasingly rely on theoretical models to predict the future closure conditions. Specifically for pit lake studies, we use numerical hydrogeological and hydrochemistry models to simulate the pit lake rebound behavior and the pit lake quality, well before any excavation has taken place. In order to do so, ever more complex theoretical assumptions are made, which are then subjected to numerous sensitivity analyses.

In this paper, we compare the results of simple water mixing models with subsequent, more complex, mineral / water interaction models. We evaluate whether the increase in laboratory data and model complexity leads to a better understanding of the final closure conditions.

METHODOLOGY

The chemistry of pit lakes varies widely, ranging from circum-neutral or alkaline type waters with a low metal concentration to highly acidic waters with elevated metal concentrations. The type of lake chemistry is the result of physical and chemical interactions, namely (Bowell, 2002):

1. Geological controls: The composition of the host rock and the ore body determine the extent to which any geochemical reaction may occur (i.e. the source);
2. Geochemical controls: The types of minerals, the chemistry of the reactive water and the physical and chemical conditions determine the release and attenuation mechanisms;
3. Hydrological and hydrogeological conditions: The flow of water which, upon contact with the minerals, mobilizes the metals and mixes the different effluents; and
4. Limnological processes: Temperature and density variations related to the lake geometry influence the circulation and the stratification of the water inside the pit.

This paper focusses on the water balance calculations, the mixing of the different water qualities and the chemical reactions along the exposed pit wall. Many of the factors discussed by Castendyk et al. (in press) are included in the construction of the models. We compare these theoretical predictions with the actual lake rebound and water quality trends observed in three existing pit lakes.

Field sampling and laboratory tests

Since starting operations in 2000, the mine has collected and analysed approximately 1750 water samples, including surface water, groundwater, waste rock seepage and pit lake samples. The samples are collected quarterly in accordance with the environmental monitoring practices described by the US Geological Survey National Field Manual (USGS 2003) and the Standards Association of Australia (1998). The laboratory analyses are carried out in an accredited laboratory using standard techniques and protocols.

Mine safety regulations prohibited the collection of pit wall rock samples from the three closed open pits, "K", "M" and "L". Instead, 40 rock samples were collected from stockpiled materials on

site. The rock samples were subjected to a shake flask extraction (SFE) leachate test and a single addition net acid generation (NAG) test. These tests measure the composition of the contact water after the reagent (either distilled water for the SFE, or hydrogen peroxide for the NAG) has been in contact with the rock samples. The laboratory procedures recommended in the Acid Rock Drainage Prediction Manual (Coastech Research, 2008) and the ARD Test Handbook (AMIRA International, 2002) for these types of tests were followed.

Pit lake water balance

Open pit operations form depressions in the ground that collect rainfall, surface water run-off and groundwater (if the pit extends below the original groundwater table). The water body collecting inside the pit is also affected by losses, such as evaporation, pit rim overflow and seepage.

Therefore, a pit lake rebound calculation is essentially a water balance calculation to a terminal recipient (i.e. sink) or a through flow recipient (if overflow or seepage of lake water occurs). At specific time intervals (e.g. monthly or annually), the sum of the outflows is subtracted from the sum of the inflows to calculate the net gain or loss from the pit. The cumulative volume is then converted to the equivalent stage height and lake surface area using the pit geometry curves.

The following mathematical equations summarize the water balance calculation:

$$V_{tot}(t) = V_{tot}(t_0) + \int_{t_0}^{t} F_{in}(\tau).d\tau - \int_{t_0}^{t} F_{out}(\tau).d\tau \quad (1)$$

$$F_{in}(\tau) = F_{rain}(\tau) + F_{runoff}(\tau) + F_{runoff\_wall}(\tau) + F_{GWin}(\tau) \quad (2)$$

$$F_{out}(\tau) = F_{GWout}(\tau) + F_{evap}(\tau) + F_{discharge}(\tau) \quad (3)$$

The flow concepts are graphically shown in Figure 1.

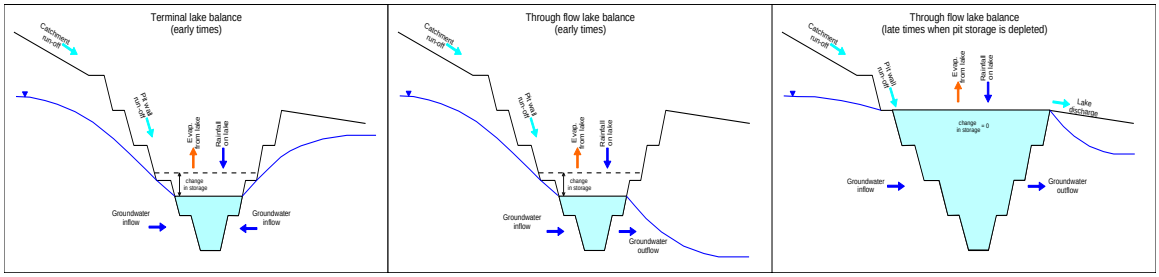

Figure 1. The dominant flow mechanisms during different stages of pit lake filling.

Pit lake chemistry

The pit lake geochemical model is a PHREEQCI Version 3 (Parkhurst and Appelo, 2013) model that represents a leaking beaker exposed to the atmosphere. The water inside the beaker is well mixed and is not stratified. Figure 2 shows the basic aspects of the two different models, including:

- Inflow of different water quality sources (such as rainfall, run-off and groundwater);
- Mineral / water interaction reproduced by an empirical formula. The incorporation or absence of this formula constitutes the main difference between the simple mixing model (A) and the more complex pit wall interaction model (B);

- The evaporation rate increases proportional to the expansion of the lake surface area, producing an evapo-concentration effect in the solution. At this site, the annual lake evaporation rate was approximately 1.3 times higher than the mean annual precipitation rate.
- Discharge is allowed via the seepage to the groundwater and/or discharge across the pit rim (the latter only occurring when the pit storage has been depleted);
- The model steps include the equilibration between carbon dioxide gas (CO_2) and oxygen gas (O_2). For the CO_2 gas, the partial pressure has been increased to $10^{-3.0}$ atmospheres to reflect the roll of biological activity in the lake (Cole et al., 1994);
- Finally, mineral precipitation and dissolution reactions may also take place inside the pit lake in accordance with a continuously stirred batch reactor.

This general approach has been used in other locations in Africa (Duthe et al., 2011) where it was originally set up for the removal of reactant phases. As minerals precipitate, the components are removed from the solution and the subsequent calculations, preventing the re-dissolution of the solids.

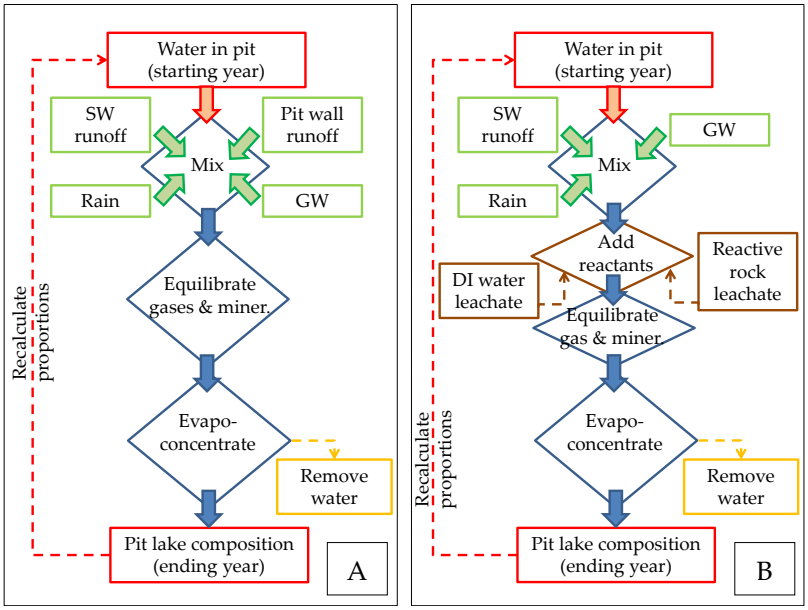

Figure 2. The PHREEQC water mixing model (A) and the pit wall interaction model (B).

RESULTS AND DISCUSSION

Water quality monitoring versus laboratory results

Figure 3 compares the results of 10 years of water quality monitoring at an acidic waste rock seep with the laboratory leach test results for 7 rock samples taken at the same acid forming waste rock dump. In contrast, Figure 4 compares the water quality monitoring data from a benign waste rock seep with the leach tests carried out on 3 rock samples taken from the same non-acid forming waste rock dump.

Based on a select number of signature parameters (such as pH, TDS, SO_4, Al, Mn and Fe), it is shown that the leach tests do not consistently identify the acid generation potential of the waste materials. For the acid forming materials, the laboratory tests overestimate the pH value and underestimate the sulphate and metal leaching effect. This is commonly observed when the rate of release of acidity and/or alkalinity is slower than the actual duration of the test.

Meanwhile, leach tests performed on the non-acid forming materials are generally similar to the water quality observed in the field.

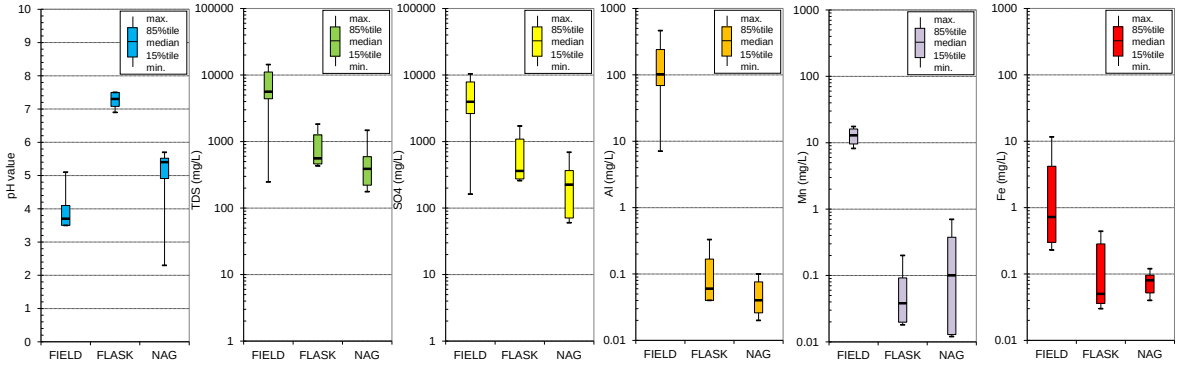

Figure 3. ARDML water quality field samples compared with leach test results for PAF materials.

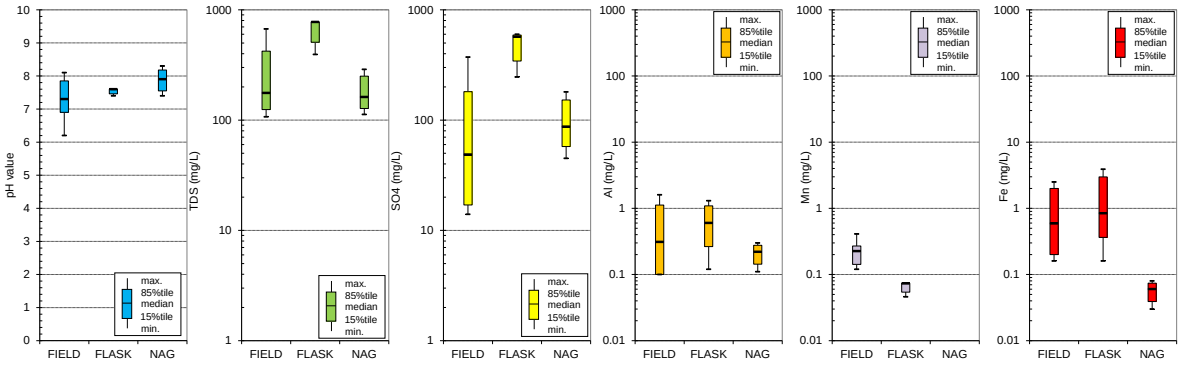

Figure 4. Benign water quality field samples compared with leach test results for NAF materials.

Pit lake water balance predictions

The mean annual precipitation (MAP) at the mine is in the order of 1000 mm/year and occurs mostly between November and April. The evaporation across open water bodies amounts to approximately 1300 mm/year. The surface water run-off and the groundwater infiltration rate are equal to 5% and 3% of MAP, respectively. The run-off from the exposed pit walls was set at 55% MAP after a calibration.

Figure 5 compares the predicted with the measured lake level rebound for the existing pit lakes "K", "M" and "L" during the 6 year monitoring period. The water balance conditions were

subsequently extrapolated using a statistical sequence based on 14 years of measured rainfall and evaporation records. The results are shown in Figure 6, indicating:

- A gradual filling of pit lake "K", eventually leading to overflow and groundwater seepage;
- A stabilizing condition at pit lake "M", maintaining a long term evaporative "sink"; and
- A relatively rapid rebound and overflow of pit lake "L", mainly due to a groundwater inflow contribution absent at "K" and "M".

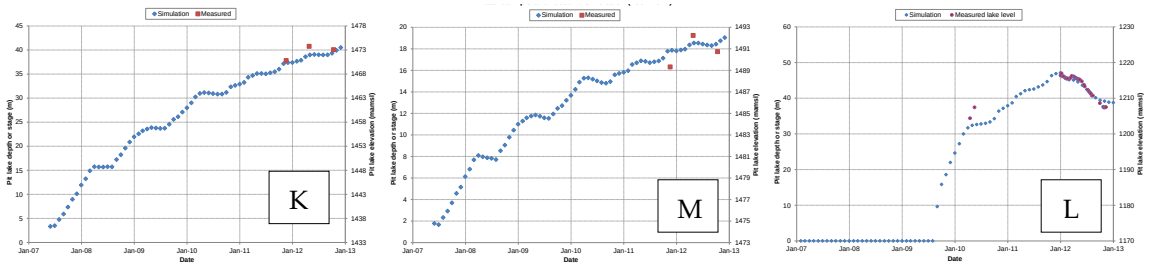

Figure 5. Predicted versus measured pit lake rebound behaviour at "K", "M" and "L".

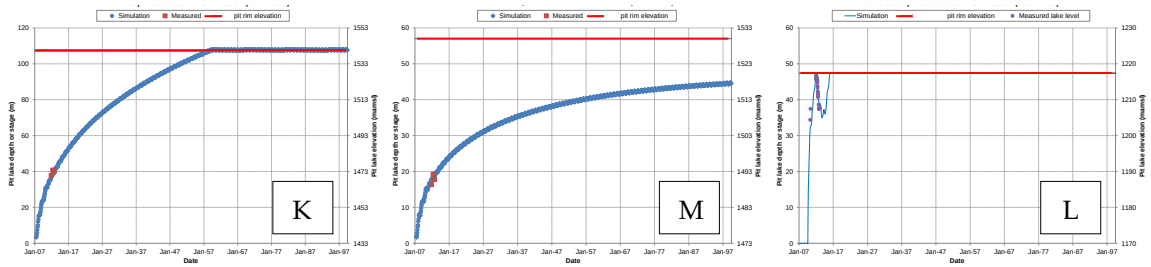

Figure 6. Long term predicted lake level rebound at "K", "M" and "L".

Pit lake chemistry predictions: water mixing models

The field samples of the "M" pit lake display a slight but apparently continuous improvement in water quality for indicators such as pH (increasing from 2.5 to 3.4), TDS (trending down to 400 mg/L) and sulphate (decreasing from 1800 to 200 mg/L).

Using this 6 year trend, an appropriate pit wall run-off composition was achieved by mixing 97% rainwater with 3% acid rock drainage / metal leaching (ARDML) type field water samples. The precipitation of minerals was allowed using the "Equilibrium_Phases"[1] option for calcite, alunite, jarositeK, malachite, ferrihydrite, gibbsite, magnesite and gypsum. If oversaturated, they precipitate and remove some concentrations of Al, Fe and SO_4 from the solution. This effectively meant that, upon precipitation along the pit floor, the solids became unavailable for further reactions.

[1] JarositeK formed in preference to ferrihydrite. So, although the model allowed for surface complexation onto the hydrous ferric oxide (HFO) surface, it did not take place due to the absence of ferrihydrite.

In particular the alunite and jarositeK phases had a slight, but not significant, effect on the modelled pH and SO_4 values. There was no significant impact on the trace metals concentrations due to the absence of hydrous ferric oxide (HFO) surfaces under these high SO_4 and low pH conditions.

The calibration and forward prediction results are shown in Figure 7, presenting an acceptable match between the modelled and measured signature parameters and trace metals, respectively.

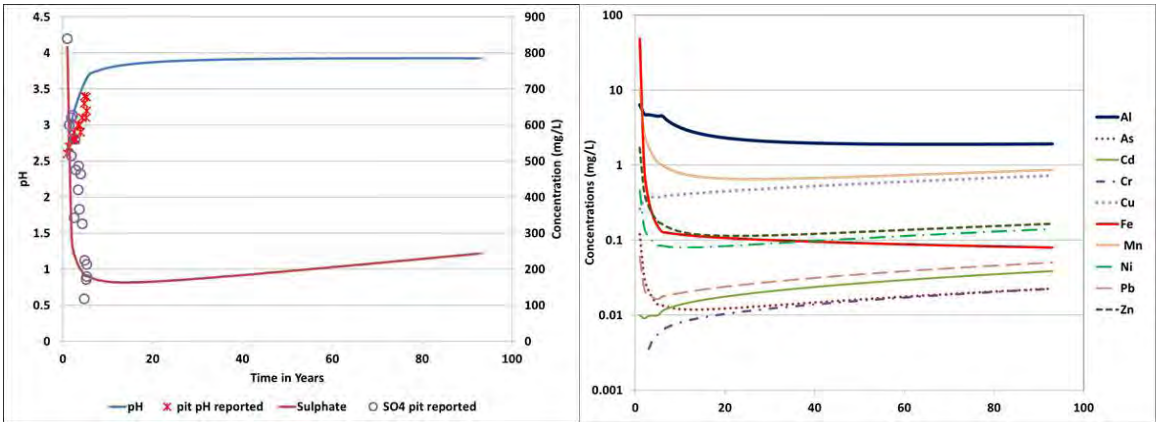

Figure 7. Long term predicted water quality at pit lake "M".

At pit lake "K" the 6 year field record indicated a downward trend from 1000 to 600 mg/L in SO_4, while the pH remained relatively constant at 2.71. Conventionally, when the pH of a pit lake remains relatively constant, the SO_4 is expected to increase or remain constant. The apparent contradictory behaviour of the measured pH and SO_4 complicated the calibration for the "K" pit lake.

The most representative wall rock runoff composition was achieved by mixing 70% rainwater with 30% ARDML type field water samples. It produced a reasonable fit to the SO_4 data, but the match with the pH data is poorer (even when considering the precipitation of jarositeK and alunite). The low pH values and the formation of jarosite phases will suppress the precipitation of ferrihydrite and, hence, prevent surface complexation and the sorption of trace metals.

The calibration and forward prediction results are shown in Figure 8, showing a slight over-prediction of sulphates and pH values. The trace metals are similar in order of magnitude.

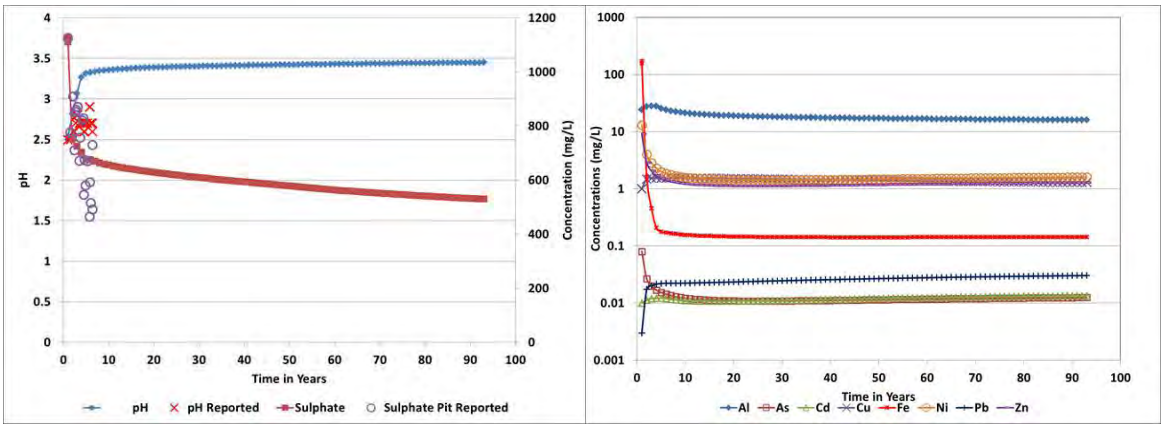

Figure 8. Long term predicted water quality at pit lake "K".

The "L" pit lake refilled quickly due to the storage of drained water from nearby operations, and natural groundwater inflow. The lake has a relatively good water quality with neutral to slightly alkaline pH values (7.3 – 8.1) and slightly elevated SO_4 (approximately 560 mg/L).

The results presented in Figure 9 rely on the inflow of a Ca-Mg / SO_4 type water with an average pH value of 7.7. Rapid filling prevented the generation of acidic pit wall run-off.

The simple mixing model confirms that relatively benign lake water qualities at "L" can be obtained over time if the dominant proportion of inflow is contributed by natural, alkaline groundwater rather than acidic pit wall run-off.

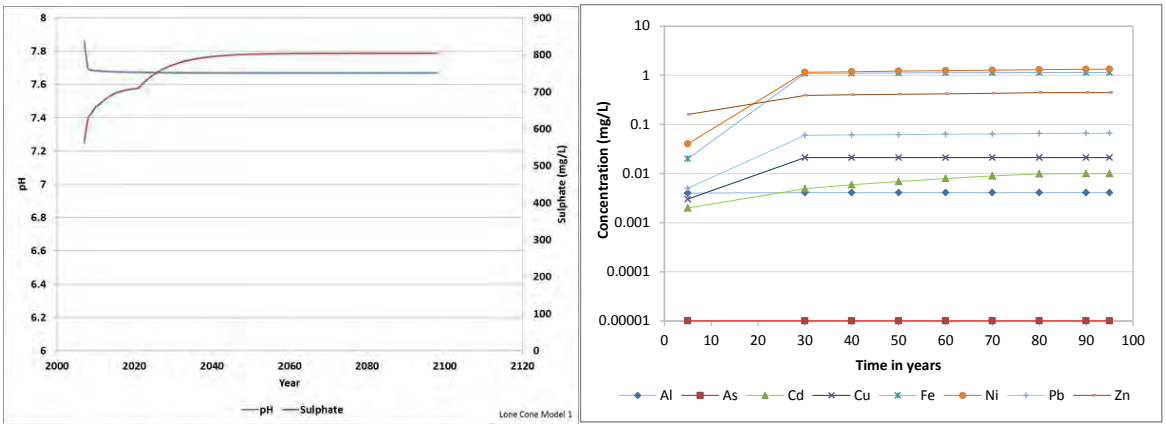

Figure 9. Long term predicted water quality at pit lake "L".

Pit lake chemistry predictions: pit wall interaction models

In the more complex models, rather than mixing two water types to obtain a representative pit wall run-off chemistry, we used the waste rock leach test results to calculate the following mineral / water reaction formula (partial representation):

(F)0.000474(Al2O3)0.000037(BaO)0.000004(CaCO3)0.324351(Fe2O3)0.000018(MgCO3)0.022222 …

… (ZnO)0.000015(As2O5)0.000004 PbO)0.000006(SeO3)0.000003(HgO)0.00000006

This partial formula represents a reactive leachate from a Banded Iron Formation, a common gold bearing horizon in central and southern Africa. As a check of the models, the formula was applied to reverse calculate the leachate composition of the NAG test for one specific sample, providing a calculated pH of 3.077 versus a measured pH of 2.3[2].

In addition to the reaction formula, the mineral amount that would potentially leach into the pit lake is also required for this type of simulation. We estimated this input parameter by multiplying the pit wall and pit floor surface area by a theoretical wall rock thickness. Based on the "M" and "K" pit lake water samples, the wall rock thickness would range from 5 mm to 20 mm, respectively.

Table 1 summarizes the results between the different simulations, indicating only minor differences in the pit lake composition predicted by the simple water mixing model and the more complex pit wall reaction model. The different years after closure are included for reference purposes.

Table 1. Current and predicted pit lake chemistry

Param.	Units	Pit Lake "K"			Pit Lake "M"			Pit Lake "L"	
		Field Chem.	Mixing Model	Reaction Formula	Field Chem.	Mixing Model	Reaction Formula	Field Chem.	Mixing Model
Years after closure		6	90	90	6	90	90	4	90
pH	pH unit	2.71	3.54	3.45	3.19	3.93	4.12	7.90	7.67
pe	pe units	-	17.10	17.16	-	16.68	16.48	-	12.94
Eh	Volts	-	1.01	1.01	-	0.99	0.97	-	0.76
Alk.(1)	mg/L	<1.0	-20.0	-24.4	<1.0	-7.4	-4.7	94.9	46.1
Al	mg/L	30.21	9.00	15.94	8.77	1.92	1.02	<0.20	0.0041
As	mg/L	0.03	0.01	0.01	0.032	0.023	0.020	<0.001	0.00001
Ca	mg/L	81	54	66	57	33	35	155	212
Cd	mg/L	0.01	0.03	0.01	<0.002	0.039	0.039	<0.002	0.01
Cl	mg/L	42.1	4.4	8.6	11.7	4.39	4.44	4.9	8.8
Cr	mg/L	0.09	0.01	0.05	<0.03	0.022	0.023	<0.03	0.06
Cu	mg/L	0.62	1.30	1.29	0.08	0.73	0.67	<0.003	0.021
F	mg/L	0.92	0.37	0.55	0.98	0.31	0.32	8.60	1.14
Fe	mg/L	38.45	0.10	0.14	2.43	0.08	0.07	<0.02	0.0015
K	mg/L	8.6	10.0	6.6	5.75	5.52	5.72	15.9	35.3
Mg	mg/L	70	79	89	22.5	39.85	39.39	61	82
Mn	mg/L	13.42	1.07	4.61	9.01	0.867	0.865	0.372	0.00001
Na	mg/L	4.6	6.3	13.9	7.29	6.36	6.34	25.5	55.0
Ni	mg/L	4.07	0.16	1.60	0.39	0.141	0.141	0.04	1.33
Pb	mg/L	<0.01	0.03	0.03	<0.01	0.050	0.048	<0.01	0.066
P	mg/L	<0.5	0.09	0.07		0.129	0.125	<0.005	0.068

[2] The difference is probably due to lower iron concentrations in the laboratory leach sample, whereby some ferric solid, ferrihydrite, $[Fe(OH)_3]$, schwertmannite $[Fe_8O_8(OH)_{4.8}(SO_4)_{1.6}]$ or jarosite formed and released more protons into the solution lowering the pH. It is likely that some acidity had been lost due to reaction with carbonate in the sample.

SO4	mg/L	585	508	530	261	243.92	240.37	562	804
Zn	mg/L	2.18	0.15	1.27	0.42	0.166	0.157	0.16	0.44

(1) Negative values calculated in PHREEQC

CONCLUSION

We recommend designing models based primarily on water balance components and available water quality data supported by mineralogical and leaching characteristics of the wall rock. Therefore, during the early stages of a mining project, the collection of site specific water monitoring data is as important as the more theoretical laboratory leach tests on solids.

Water mixing models to predict the pit lake chemistry behavior, when calibrated to known conditions measured in the field, can be acceptable substitutes for more complex mineral / water reaction models in circumstances where specific inflows dominate the water balance.

ACKNOWLEDGEMENTS

We extend our gratitude to AnglogoldAshanti who provided us with the data and the funding to develop the models presented in this paper. We also thank Dr. Dirk Vanhooydonck who reviewed the mathematical formulae used in the pit lake water balance.

NOMENCLATURE

V_{tot}: water volume inside pit [m^3]

F_{in}: Water inflow rate [m^3/s]

τ: time period [s]

F_{out}: Water outflow rate [m^3/s]

t_o: starting time [s]

t: end time [s]

F_{rain}: rainfall [m^3/s]

F_{runoff}: catchment runoff [m^3/s]

F_{runoff_wall}: pit wall [m^3/s]

F_{GWin}: groundwater inflow [m^3/s]

F_{GWout}: seepage [m^3/s],

F_{evap}: evaporation [m^3/s]

$F_{discharge}$: pit rim overflow [m^3/s]

REFERENCES

AMIRA International, 2002: *"ARD Test Handbook. P387A Project. Prediction and Kinetic Control of Acid Mine Drainage"*, Prepared by Ian Wark Research Institute & Environmental Geochemistry International.

Baron, D., and Palmer, C.D., 1996: *"Solubility of jarosite at 4-35°C"*, Geochimica et Cosmochimica Acta. Vol. 60, pp. 186-195.

Bowell, R.J., 2002: *"Mine water hydrogeology and geochemistry"*- In: Younger, P.L. and Robins N.S. (eds) Geological Society Special Publication no. 198, Geological Society of London, p. 159-185.

Castendyk, D.N., Eary, L.E., and Balistrieri, L.S., 2014, *"Modeling and management of pi lake water chemistry 1: Theory"* Appl. Geochem. *in press*.

Coastech Research Inc., 1991, electronic version 2008, *"Acid rock drainage prediction manual"* MEND Project 1.16.1 (b), prepared for Canmet-MSL Division, Department of Energy, Mines and Resources, Canada.

Cole, J.J., Caracao, N.F., King, G.W., and Kranz, T.K., 1994: *"Carbon dioxide supersaturation in the surface waters of lakes"* Science. Vol. 265, pp. 1568-1570.

Duthe, D. M., Mahoney, J.J., Shchipansky, A.A., and Terrell, C.L., 2011: *"Assessment of the Process of Pit Lake Formation and Associated Geochemistry in Open Pits – Mupane Gold Mine, Botswana"* – In: Rude, R.T., Freund, A. and Wolkersdorfer, Ch.: Mine Water Managing the Changes. p. 511-515. Aachen, Germany.

Dzombak, D.A., and Morel, F.M.M., 1990: *"Surface complexation modeling - hydrous ferric oxide"*, New York, John Wiley and Sons, 393 p.

Parkhurst, D.L., and Appelo, C.A.J., 2013: "*Description of input and examples for PHREEQC version 3: A computer program for speciation, batch-reaction, one-dimensional transport, and inverse geochemical calculations: U.S. Geological Survey Techniques and Methods"*, Book 6, chap. A43, 497 p., available only at http://pubs.usgs.gov/tm/06/a43.

Standards Association of Australia, 1998: *"Water Quality – Sampling Part 1, Part 4, Part 5, Part 6, Part 7, Part 8, Part 10, Part 11"*, AS/NZS 5667.4:1998, 5:1998, 6:1998, 7:1998, 8:1998, 10:1998, 11:1998.

USGS, 2003: *"National field manual for the collection of water quality data"*, US Department of the Interior, Version 2.

Predicting Pit Lake Formation and Water Quality

David Arcos, Jordi Guimerà, Salvador Jordana, Eduardo Ruiz and Jorge Molinero
Amphos 21 Consulting, Spain

ABSTRACT

Pit lakes form when open pit mining operations are discontinued and dewatering ceases. The resulting composition of the water within the lake is related to the geology and mineralogy of pit walls, water flow rates and climate conditions. In some cases, these lakes will develop acid sulphate conditions with high concentrations of metals, thus constituting an environmental concern. Preventing such conditions from the early stages of the mine project allows a proper planning for mine closure, yet conditions can be predicted, allowing taking informed decisions.

In this work, open pit flooding has been simulated using COMSOL Multiphysics, a well-known commercial FEM platform, and water quality can be calculated by coupling the geochemical code PHREEQC code with the Java interface iCP. In the implemented model the height of the lake depends on the relationships between the groundwater water inflow rate of the lake, the elevation of the spillway, the water volume of the lake as a function of the height of the water and the evaporation rate. In its turn, the height of the lake variable is used as a Dirichlet boundary condition at the bottom of the open pit in a realistic hydrogeological large-scale 3D aquifer. The water quality can be determined by considering the geochemical processes in the interaction of water with the pit walls, as well as by considering the contribution from rainwater and the evaporation effect.

The resulting model is able to recreate transient pit lake generation and water quality. The simulations predict the rise of water in the pit lake as a function of time, the maximum elevation of the lake and the flow rate of the creek that could appear by overflow if the lake reaches the pit boundary. In terms of water quality, the simulation is able to predict the composition evolution with time of both the water entering into the lake and the lake itself, even after reaching a hydraulic stationary state. Results obtained show a good agreement with currently available field data. It is worth mentioning that the model could also calculate lake stratification due to thermal and/or ionic strength effects, although it has not been implemented yet.

Keywords: Pit lake, mine closure, modelling, hydrogeology, geochemistry.

INTRODUCTION

Excavated pits can have several depths and sizes, but all of them require environmental reclamation. One possible reclamation endpoint could be the creation of pit lakes (Gammons et al., 1999). Pit lakes are created by filling by water the open pit left after the completion of mining operations. This water filling can be done by artificial flooding or natural hydrological processes such as rain or groundwater inflow (Castro and Moore, 2000).

The increase in open-pit metal mining since the 1970s will lead to the formation of numerous pit lakes over the next 50 years. Many of these lakes could develop acid sulphate conditions with high levels of dissolved metals. Recommended approaches for remediation of these conditions include the addition of lime or other alkaline materials and the stimulation of sulphate-reducing bacteria. However, prevention rather than remediation is probably the preferable approach. Measures, like filling the pits with water as fast as possible to promote anoxic conditions within the lake preventing the oxidation of sulphides present in the pit walls, thus minimizing the formation of acids and dissolved metals (Castro and Moore, 2000).

Local hydrogeology determines how fast an open pit lake is formed in natural conditions. A generalized water balance for a pit lake can be summarized as the change in water storage in the lake, which results from the addition of inflows (direct rain, surface water runoff and streams, and groundwater inflow) and the subtraction of the outflows (evaporation, groundwater outflow, surface water outflow as a creek from the lake). The rate of groundwater input depends on the site geology, topography and climate. A rough estimate of groundwater inflow can be obtained by looking at the amount of water that was pumped during active mining operations. This can provide a useful estimation during the early stages of flooding but the rate will change as the pit fills with water and the hydraulic gradient towards the lake will decrease. On this context, water quality will be the result of the interaction of groundwater with the pit walls, especially to a depth where atmospheric oxygen can penetrate. Considering that flow rates decrease as water level rises and that sulphide oxidation reactions are kinetically driven, the quality of the inflow water will be worst with time. Thus, the quality of the water in the lake is dependent on the velocity of lake formation. In addition, other aspects that may affect water quality are the surrounding groundwater composition, the amount of rainwater (and/or evaporation) and the characteristics of the pit walls (sulphide amount and distribution).

Once a pit lake has been filled to its ultimate surface elevation, there are many different hydrogeological scenarios for the lake, which can be considered important factors for “end use” decisions. For example, in an arid climate, it is very possible that evaporation will completely balance any water input terms. Such a lake is referred to as a “terminal” lake. A “flow-through” lake, on the other hand, will receive groundwater inputs from one side, but will lose groundwater to the other side. Flow-through lakes are especially common when the pit was excavated on a hillside with an initially sloping water table. Finally, if water inputs are high (such as in a wet climate, or where a stream is permanently diverted into the lake), then the final lake will probably have a surface water output. This could either be an engineered spillway or stream (Gammons et al., 2000). The effect on the water quality is also dependent on the behaviour of the lake once it reaches the ultimate surface elevation. In an arid climate, the excess evaporation will result in increasing the concentration of sulphate and metals in the water lake (Atkinson, 2002), resulting in the precipitation of sulphate minerals in the lakeshore. In “flow-through” lakes, the quality of the water will depend on the quality of entering groundwater, thus good quality groundwater will

result in improvement of the lake quality. Finally, in wet climate conditions, it could be expected that dilution result in increasing the quality of the water in the lake. Another aspect that must be considered is the role of emerged pit walls; if the amount of sulphides present is high, surface run-off can affect negatively the water quality in the lake, although tis effect needs to be assessed carefully.

To quantitatively approach pit lake formation and water quality, preliminary conceptual models are typically developed by: 1) compiling all available data (geologic, mineralogical, climatic, potentiometric, hydraulic testing, etc.); 2) evaluating the data to determine aquifer geometries, hydraulic boundaries, hydraulic parameters, groundwater movement, geochemical processes and other variables of interest; and 3) integrating this information into one or more working hypotheses that characterize the system.

Numerical simulations allow the validation of the conceptual models, as well as the quantification of the predicted effects on the pit lake, such as inflow and outflow rates, water quality and their dependency with time. To model this groundwater flow-lake system some specific modules as PITLAKE, LAKE, LAK2 (Moreno and Sinton, 2002) have been created for MODFLOW.

In this paper we will simulate this transient pit lake generation using COMSOL Multiphysics® (COMSOL, 2012). COMSOL provides generic partial differential equation (PDE) solvers and Algebraic Differential Equations (ADE) that are robust in handling coupled equations. COMSOL has developed several modules helpful for hydrologic applications, e.g., the Subsurface flow modules (COMSOL, 2012). However, singular implementations as the pit lake generation must be explicitly user defined. The geochemical processes are implemented with the PHREEQC code (Parkhurst and Appelo, 2013), which is coupled with COMSOL by means of iCP, a Java interface (Nardi et al., 2014).

METHODOLOGY

Groundwater system

The groundwater system is described by the flow equation (Bear, 1979), (nomenclature for all formulas can be found at the end of this publication):

$$S_e \frac{\partial p}{\partial t} = -\nabla q + Q \tag{1}$$

where the Darcy's flow (q) can be expressed by Darcy's law:

$$q = -K\left(\nabla p - \rho g\right) \tag{2}$$

Figure 1 shows a sketch of the hydrogeological system in the problem of interest.

The chemical part of the system is calculated through the code PHREEQC. One of the main aspects is related to the penetration depth of atmospheric oxygen ($10^{-0.67}$ bars partial pressure) into the rock in the unsaturated region, allowing the water to equilibrate with this oxygen pressure. In this zone sulphide oxidation can occur, so the primary minerals able to react are considered in the system allowing their dissolution following a kinetic rate. Secondary minerals are allowed to precipitate if they become supersaturated. Aqueous speciation is specifically considered in the code. Other geochemical processes such as sorption, cation exchange or solid solution precipitation can also be included in the calculations if needed. One important aspect is that mineral distribution in the rocks

around the pit is not uniform. Therefore, based on geochemical data and block model the mineral distribution in the system can be defined (Figure 2), allowing the definition of different mineral zones depending on their mineral content.

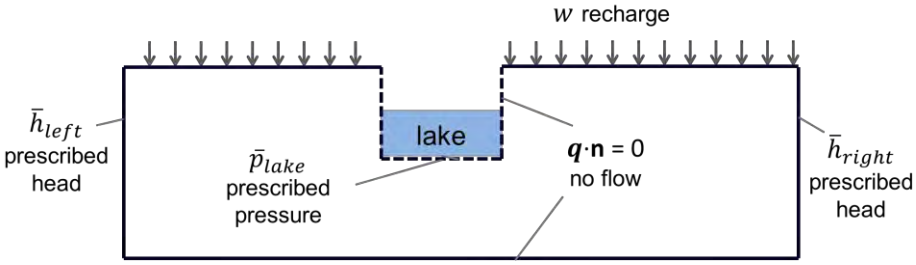

Figure 1 Sketch of the hydrogeological system in a synthetic problem

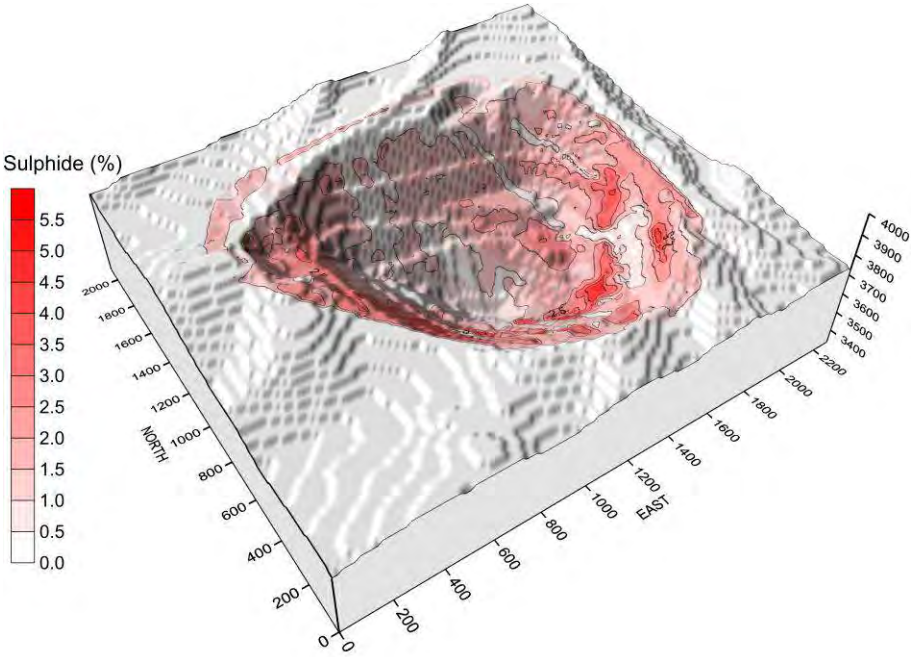

Figure 2 Sulphide distribution in the wall of a final open pit

Lake system

The volume water balance in the lake is described by:

$$\frac{d\left(V_{lake}\right)}{dt} = Q_{aq} - Q_{ev} + Q_r \tag{3}$$

The net groundwater flow rate from the aquifer to the lake is expressed by:

$$Q_{aq} = \int_{A_{\min}} \left(q \cdot n\right) dA \tag{4}$$

The evaporation outflow rate is calculated as:

$$Q_{ev} = E \cdot A_{lake} \tag{5}$$

The rain inflow rate is calculated as:

$$Q_r = w \cdot A_{lake} \tag{6}$$

Note that for simplicity here we only consider the rain that impacts straightforward to the lake surface, not the total of the lake hydrologic basin, but the model could also handle this condition with minor changes. Figure 3 shows the sketch of the lake system analysed in this problem.

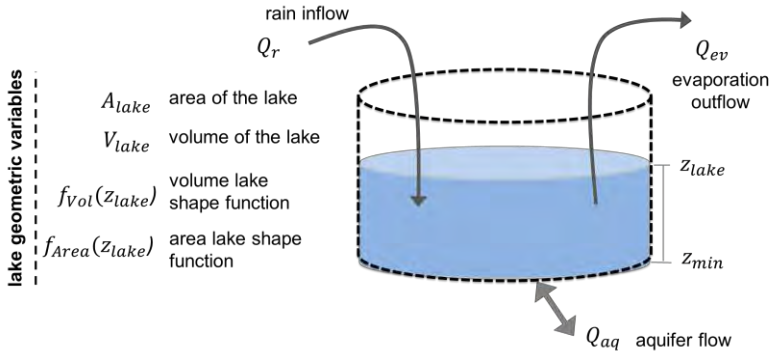

Figure 3 Sketch of the lake system in a synthetic problem

As in the case of the groundwater system, the interaction between lake water and mineral zones in the pit walls can occur. In this case the reactions are limited to the water in contact with the pit wall and sulphide oxidation is restricted to the near surface zone, where water with enough oxygen dissolved can be found. In addition to secondary minerals precipitated due to the water – rock interaction, they can also precipitate near the surface due to evaporation processes. However, this effect has not been implemented yet.

Analysis of the coupling used between underground and surface water

The groundwater and the lake system are coupled in both directions by the following terms (Figure 4):

- Equation 4 couples the lake system with the groundwater by means of the aquifer flow rate.
- The underground system is coupled by the Dirichlet boundary condition applied at the bottom of the lake,

$$\bar{p}_{lake} = \rho g z_{lake} \tag{7}$$

The natural evolution of the system tends to a steady state situation where the lake level is constant and the groundwater inflow rate is equal to the evaporation rate (Figure 5).

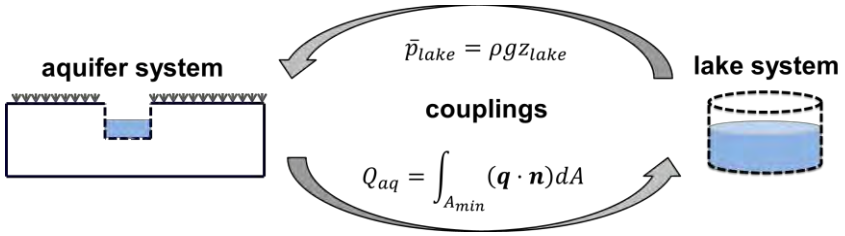

Figure 4 Couplings between the aquifer and the lake system

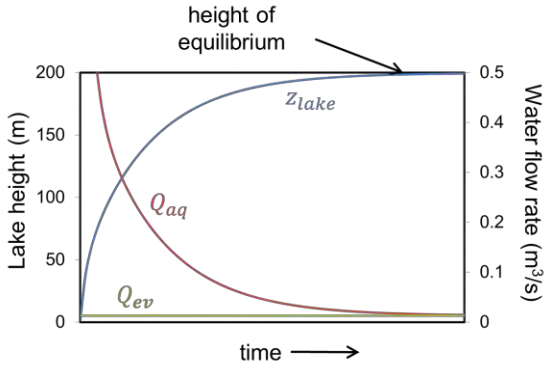

Figure 5 Expected behaviour of the system

This coupled problem has been solved by performing a Picard approach, solving the lake and the aquifer system iteratively until the solution has converged. The nonlinear system of equations of the lake has been solved by using a Newton-Raphson algorithm.

APPLICATION CASE

A pit lake generation in an open pit mine has been simulated using the abovementioned equation system. The mine, located in a temperate climate area, stopped the dewatering at the beginning of the 2000. Before that, the maximum dewatering flow rate was about 20 l/s.

The mine is placed onto a natural water divide and the topography has a gentle slope to both sides. The geology consists on a fractured crystalline rock with a significant alteration zone in the uppermost part. This shallow part formed mainly by sand, has a thickness of a few meters and constitutes the main aquifer (Figure 6).

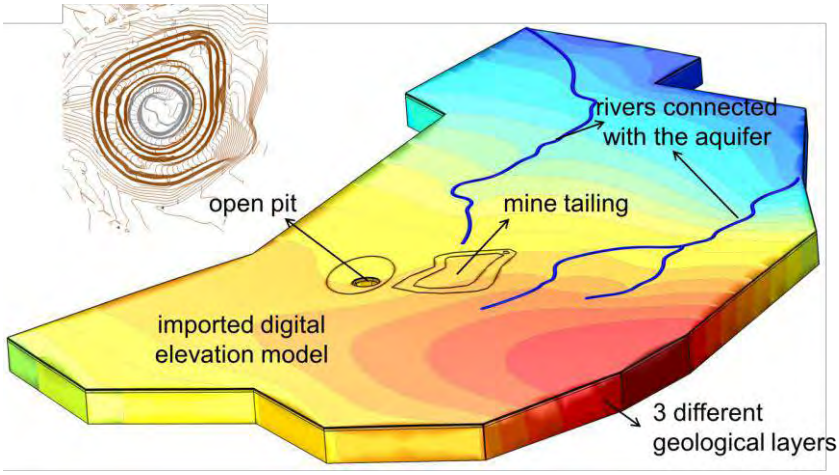

Figure 6 Hydraulic head distribution

Streams and creeks occur in the lowest areas. These streams flow permanently and have been set as fixed head (Dirichlet) boundary condition. Internal streams are ephemeral and they have been modelled by a mixed flow (Cauchy) condition. The upstream boundary, the highest one, has been considered as a prescribed head boundary, using available piezometric data. Remaining boundaries are considered impervious (no flow Neumann condition). Water recharge of 150 mm/y is prescribed on the top boundary, to account for infiltration of rainwater.

The final pit wall has been divided in geoenvironmental units (GEUs) according to the mineral contents, especially sulphides, and their geochemical behaviour based on previous geochemical tests (Table 1 and Figure 7). The primary minerals have been considered to dissolve following a kinetic rate. The reactive surface area of these minerals has been calculated based on rock porosity and assuming that water flows through fractures with a mean aperture of 0.02 mm. In this way, the rock surface in contact with a litre of water has been calculated, and then distributed between the different minerals according to their relative amount in the rock (Table 7). Secondary minerals are allowed to precipitate when they become supersaturated both in the rock (groundwater system) and in the lake (lake system). Other processes can be implemented, such as sorption or cation exchange, but they have not been considered in this case. In addition, the possibility of considering stratification of lake water due to ionic strength and temperature has not been considered. According to the COMSOL capabilities, it is possible to include this process in the model, but it has not tested yet.

Modelling stages were the following:

- Steady state flow model to simulate the conditions at the end of the period of activity of the mine. In this phase, the hydrodynamic parameters have been adjusted to fit site observations: the pumping dewatering rate and piezometer levels. During this stage the lake system is not active and a fixed head equals to the topographic value (zero pressure condition) has been considered at the bottom of the open pit.
- Transient model. The result of the steady state model of the previous stage has been used as initial conditions. At this stage the full system (lake and groundwater) is accounted to simulate the open pit lake generation.

In both stages the chemical composition of lake water depends on the geochemical processes occurring in:

- Pit walls: interaction of groundwater with defined GEUs; and
- Lake: water resulting from pit wall seepage and mixing with already existing lake water and rainwater, plus effects of evaporation.

Table 1 Mineral composition of the GEUs defined for the pit walls.

Minerals (wt %)	GEU 1	GEU 2	GEU 3	GEU 4
Pyrite	0.1	0.5	2.0	5.5
Chalcopyrite	0.0	0.02	0.1	0.7
Arsenopyrite	0.0	0.01	0.05	0.1
Sphalerite	0.0	0.01	0.03	0.2
Fe(III) oxides	0.1	0.5	0.5	2.5
Quartz	57	56	58	55
K-Feldspar	20	17	12	16
Biotite	0.8	0.8	0,5	0.8
Clay minerals	21	25	26	19

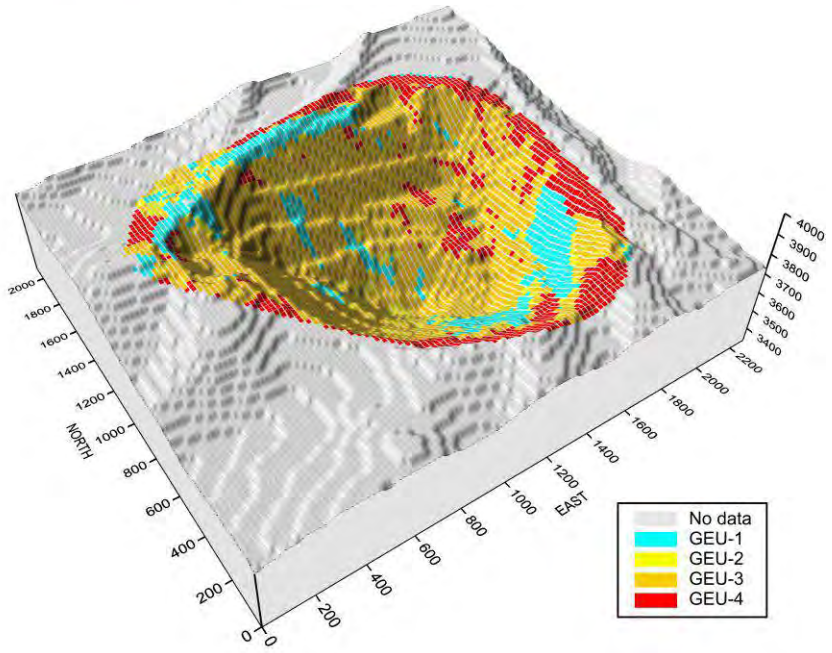

Figure 7 Distribution of geoenvironmental units (GEUs) in the final pit walls.

The domain has been meshed by means of nearly 700.000 tetrahedral quadratic elements. To improve the time and the accuracy of the non-linear calculation process the time steps and numerical convergence parameters has been adjusted for the transient simulation. In terms of chemical composition, it can be seen (Figure 9), that for the first 10 years of evolution (up to present) a major impact is not expected. However, after this time, it is expected that lake water became gradually more and more acidic and with higher metal concentrations.

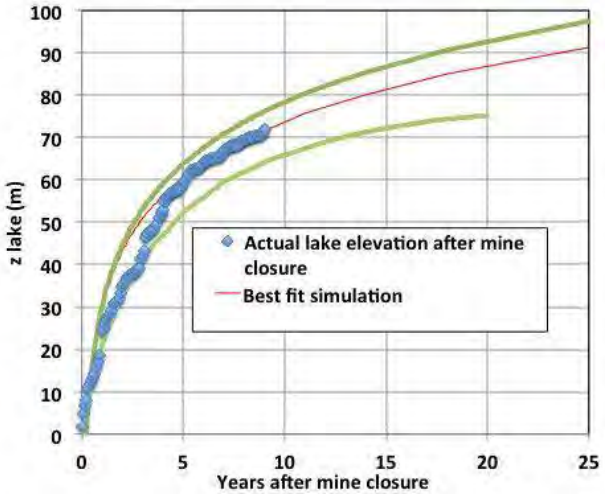

Figure 8 Sensitivity analysis (green lines) has shown permeability and storativity as most critical parameters for an accurate prediction

The mine operation counts with about 10 years of observation data available from the beginning of water rise in the open pit. These data have been used to calibrate the model and the best fit obtained reproduces satisfactorily the growth of the lake. A sensitivity analysis showed that the

response of lake level rise is very sensitive to the hydraulic parameters of the aquifer, to the recharge and evaporation rates and to open pit geometry (Figure 8).

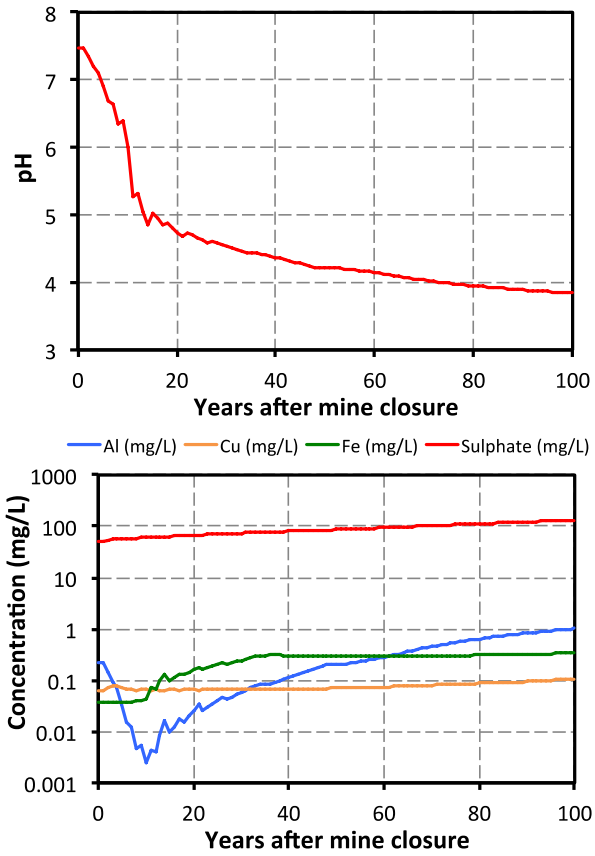

Figure 9 Predicted chemical evolution of the lake water.

For this particular mine, the computed results allows to conclude that at the final stages the lake will be a "flow-through" lake and also will eventually generate a stream through a spillway. All these results are very important for the management of effluents as they may be affected by old mining activities and may affect the environment.

CONCLUSION

The pit lake dynamics and quality can be modelled by the groundwater and lake coupled system developed in this work, as well as coupling hydrologic and geochmemistry processes. This system has been used in a real case and it reproduces satisfactorily the growth of the lake according the available data and predicts present and future water lake composition.

One of the most powerful aspects of the proposed formulation is its flexibility. The developed simulator admits all kind of open pit geometries since it is generalized for area and volume lake shape functions. In addition, other sources and sinks (even nonlinear ones) can be added easily in the lake water balance.

Important information that can be predicted by using this model is:

- The flow rate for dewatering and the lake height after closure,
- the time to generate a creek (if any) and its flow

- the lake and groundwater flow relationship: flow- through or terminal.
- the lake water composition, and its expected evolution with time.

The model presented in this paper constitutes a powerful pit lake prediction, especially when the environmental conditions claim for high accuracy.

NOMENCLATURE

A_{lake}	area of the lake (m^2)
A_{min}	minimum area of the lake (m^2)
E	evaporation rate ($m \cdot s^{-1}$)
g	gravity vector ($m \cdot s^{-2}$)
K	hydraulic conductivity tensor ($m \cdot s^{-1}$)
p	liquid pressure (Pa)
Q	source term ($m^3 \cdot s^{-1}$)
Q_{aq}	flow rate to the lake from groundwater ($m^3 \cdot s^{-1}$)
Q_{ev}	evaporation rate ($m^3 \cdot s^{-1}$)
Q_r	rain inflow rate ($m^3 \cdot s^{-1}$)
q	Darcy's flow ($m^3 \cdot m^{-2} \cdot s^{-1}$)
S_e	specific storage (m^{-1})
V_{lake}	Volume of the lake (m^3)
w	rain rate ($m \cdot s^{-1}$)
ρ	liquid density ($kg \cdot m^{-3}$)

REFERENCES

Atkinson, L.C. (2002) *The hydrology of pit lakes*. Southwest Hydrology, 1(3).

Bear, J. (1979) *Hydraulics of groundwater*. McGraw-Hill International Book Co., 1979 - 567 p.

Castro, J.M. and Moore, J.N. (2000) *Pit lakes: Their characteristics and the potential for their remediation*. Environ. Geol. 39, pp. 1254-1260.

COMSOL (2012) *COMSOL Multiphysics 4.3*. Viewed at www.comsol.com

Gammons, CH., Harris, L.N., Castro J.M., Cott, P.A. and Hanna, B.W. (2009) *Creating lakes from open pit mines: Processes and considerations – with emphasis on northern environments*. Can. Tech. Rep. Fish. Aquat. Sci. 2826: ix + 106 p.

Moreno, J. and Sinton, P. (2002) *Modeling mine pit lakes*. Southwest Hydrology, 1(3).

Nardi, A., Idiart, A., Trinchero, P., deVries, L.M. and Molinero, J. (2014) *Interface COMSOL-PHREEQC (iCP), an efficient numerical framework for the solution of coupled multiphysics and geochemistry*. Computers & Geosciences 6910–21.

Parkhurst, D. L. and Appelo, C. A. J. (2013) *Description of input and examples for PHREEQC version 3—A computer program for speciation, batch-reaction, one-dimensional transport, and inverse geochemical calculations*. USGS Techniques and Methods, book 6, chap. A43, 497 pp.

Riverine Flow-Through of Mine Pit Lakes: Improving both Mine Pit Lake and River Water Quality Values?

Clint McCullough[1] and Martin Schultze[2]

1. *Golder Associates/Mine Water and Environment Research Centre (MiWER), Edith Cowan University, Australia*
2. *UFZ Helmholtz Centre for Environmental Research, Department of Lake Research, Germany*

ABSTRACT

Coal mine pit lakes may form at mine closure when voids formed through mining extractions have extended below groundwater. Internationally, acid and metalliferous drainage (AMD) is a common problem for coal pit lake water quality. Even if not acidic, pit lake water quality may become degraded gradually through dissolution of contaminants and evapoconcentration.

Contaminated coal pit lake waters can present significant risk to both surrounding and regional communities and natural environments. Pit lake waters may discharge into surface and groundwater; or directly present risks to wildlife, stock and human end users.

Riverine flow-through is increasingly being proposed to mitigate pit lake water contamination. This paper presents the motivation for, and key processes and considerations regarding a flow-through final lake hydrology. International case studies as precedent and lessons for future application are also described from a review of literature describing pit lakes that use or propose surface water inflows and discharge as key components of their closure and pit lake management designs.

Chemical and biological processes such as dilution, absorption and flocculation and sedimentation reduce solute loads from river and lake. We conclude that riverine lake flow-through may often be a valid mine closure strategy for pit lakes with poor water quality. Although, we caution that maintenance of existing riverine system values must be maintained first and foremost, we further suggest that decant river water quality may, in some circumstances, be improved; notably in examples of meso-eutrophic river waters flowing through slightly acidic pit lakes.

Flow-through closure proposals for coal pit lakes must be scientifically justifiable and follow a risk assessment approach. Due to the high-uncertainty, biotic and physico-chemical attributes of both upper and lower river and lake should be well monitored. Monitoring should directly feed into an adaptive management framework approved by key stakeholders.

Keywords: pit lake, mine closure, flow-through, AMD, salinity

INTRODUCTION

Due to operational and regulatory practicalities, coal pit lakes will continue to be common legacies of many mine lease relinquishments. Weathering of potentially acid forming (PAF) materials in pit lake catchments, such as pit wall rock, waste rock dumps, and tailings storage facilities, may produce acid and metalliferous drainage (AMD) that reports to rivers and pit lakes (Younger, 2002). AMD-degraded water quality in pit lakes may reduce regional environmental values and may present practically perpetual risks to surrounding communities and environmental values (McCullough & Lund, 2006; Hinwood *et al.*, 2012). As a result, mine closure guidelines and regulations increasingly require low risk long-term to surrounding ecological and social environments for closure practices to be acceptable (McCullough *et al.*, 2009a). Many currently operating or planned mines do not have available options for AMD avoidance (e.g. Wisotzky (2013) in place for a variety of historical and contemporary socio-economic and regulatory reasons (Hilson & Haselip, 2004).

Increasingly, beneficial end uses are also required for pit lakes either through regulatory requirements, or through other stakeholder aspirations such as communities, or interest or non-governmental organisations (NGOs) (Swanson, 2011). As a result, sustainable pit lake management aims to minimise short- and long-term pit lake liabilities and maximise short- and long-term pit lake opportunities (McCullough & Lund, 2006). Such management may be very costly and difficult to achieve in remote mining regions (Kumar *et al.*, 2011).

The hydrological setting of lakes is well known as a key factor for water quality (Straskraba, 1999; Kratz *et al.*, 2006). Furthermore, lakes are usually storage elements in river networks, reactors transforming many of water constituents and sinks for particles and dissolved water constituents, but may act temporarily also as source. Accordingly, design and management of the connection of pit lakes to river systems and to the groundwater have been applied as management approach for controlling water quality both in pit lakes and in rivers e.g., (Schultze *et al.* (2011)).

This review presents the findings of a search for literature describing coal pit lakes that used surface water inflows and discharge as key components of their closure and pit lake management designs. The experiences documented in the found literature are summarised, evaluated and generalised.

PIT LAKE HYDROLOGY

The pit lake equilibrium water balance and final depth is defined by the net effect of all its hydrologic components. For example, groundwater intrusion and seepage, catchment and direct surface water inputs and evaporative losses (McCullough *et al.*, 2013b). This net effect will determine whether the final pit lake water balance is terminal as an evaporative sink (Figure 1a), source (surcharged) (Figure 1b) and perched above local groundwater levels or flow-through (Figure 1c,d) and directly to ground and surface waters. Terminal hydrology is most common for pit lakes in net negative rainfall areas due to their constrained catchment size relative to natural lakes (Niccoli, 2009) and surcharge or flow-through for lakes in net positive areas. However, in climates of marked rainfall seasonality, pit lakes may even demonstrate a combination of terminal and flow-through system depending on season.

Flow-through pit lakes distinctly show discharge of water to the greater catchment. These pit lakes have a relatively net nil water balance where water entering them exits as either a through-flow

groundwater (Figure 1c) hydrogeology (may or may not be expressed as surface water down-gradient) or a flow-through surface water hydrology (Figure 1d).

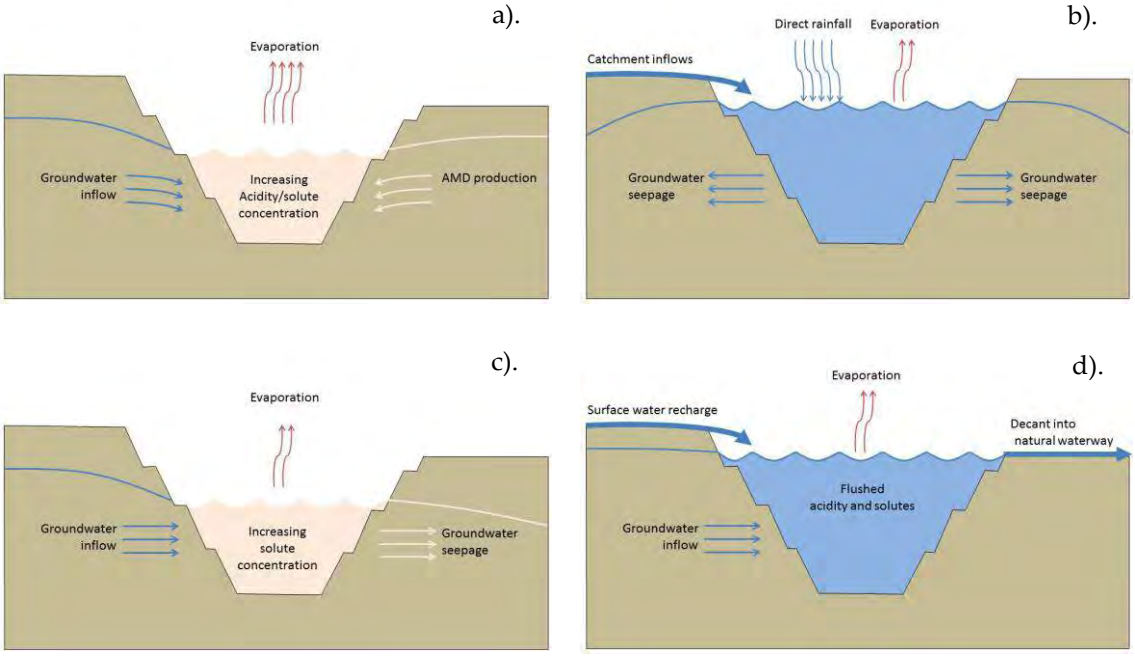

Figure 1: Conceptual equilibrium hydrogeological regimes for pit lakes. a) evaporative terminal sink, b) surcharged lake, c) groundwater through-flow system, d) surface water flow-through system

ENGINEERED PIT LAKE FLOW-THROUGH

There are a number of reasons for engineering a permanent diversion of river or other surface water into a pit lake, mostly related to maintaining or improving pit lake water quality:

a) because a surface drainage system was originally diverted around the pit void location and it is desirable that the system is diverted back into its 'natural' channel for mine closure for cultural or similar motivations;

b) the pit lake is proposed as a water reservoir, or for retaining and buffering high flows as flood protection for downstream;

c) higher quality (e.g., less acidic, lower salinity) river water is required to maintain a minimum pit lake water level or minimum water quality, or, conversely;

d) the pit lake is proposed as a treatment facility to improve water quality of the river.

Surface water flow-through processes

Pit lake water balance largely determines whether lake water quality reach equilibrium or continues to evolve over time. A pit lake water balance with evaporation as the primary water loss function will typically lead to increases in solute concentrations compared to a flow-through system

where incoming water can continue to replenish and dilute and solute concentration effects that are occurring/have occurred in previous dryer seasons (Niccoli, 2009).

For lakes affected by AMD, lake acidification can continue after initial rapid filling and neutralisation of acidity by alkaline waters e.g., from a river diversion. The major sources of both acidity and alkalinity are surface and, groundwater inflows, biogeochemical alkalinity generation inside the pit lake including its sediment and elution of side walls and shore material and final pH will reflect the net result of all geochemical contributions (Müller *et al*., 2011).

Solute and acidity concentrations are usually higher in pit lakes containing AMD (Banks *et al*., 1997) than in river waters (Meybeck, 2005). Consequently, flow-through by river water typically will result in dilution (likely to be insignificant for acidity, but potentially significant for salinity) and acidity neutralisation (which may be significant).

The reaction of river water bicarbonate with pit lake acidity is the most important chemical reaction removing lake acidification. It is accompanied by the precipitation of dissolved iron and aluminium as the main contributors to acidity. The success of metal removal may be limited since some metals require pH above 8 for removal (e.g., manganese, zinc). However, co-precipitation with iron and aluminium are also important mechanisms of the removal of substances from the lake water during neutralisation and in particular phosphorus and trace metals (Lee *et al.*, 2002; Kopacek *et al.*, 2005).

Acid pit lakes with high phosphorus loadings show increased algal biomass which may then lead to improvements in water quality through phytoremediation (Fyson *et al*., 2006) and sulfate reduction of decaying organic algal cells (Wendt-Potthoff *et al*., 2012). However, Totsche *et al.* (2006) demonstrated that artificial eutrophication, through stimulation of primary production, is limited by phosphorus fixation to iron minerals in the lake sediment. Although Schultze *et al.* (2011) considered the contribution of rapid river filling to phytoremediation to be small, in the case of ongoing lake flushing with river water, the contribution of primary production may become a much more important alkalinity-generating process over longer time scales.

In conclusion, flow-through pit lakes systems can contribute a number of important processes to improve and maintain pit lakes water quality over long-term scales (Table 1).

Table 1: Benefits and risks of flow-through pit lake closure strategy for pit lakes

Pit lake advantages	Limitations / Risks
Dilution of elevated solute concentrations in lake waters e.g., salinity, contaminants	Incoming flows may contribute solutes to the pit lake
Neutralisation of lake acidity by river water alkalinity	
Chelation and sorption of lake metals by river nutrients such as C and P (Fyson *et al.*, 2006; Neil *et al.*, 2009)	River water may introduce contaminants such as nutrients, organic pollutants and/or toxic metals (Klemm *et al.*, 2005)
Import of aquatic organisms through inflowing waters accelerating pit lake colonisation and establishment of a representative aquatic biotic community (Peterka *et al.*, 2011)	Aquatic communities may be riverine species and not representative of proposed lake ecosystems. Pest species may be established in pit lakes due to connectivity (Stich *et al.*, 2009; Kosík *et al.*, 2011)

River water can contribute much needed organic carbon and phosphorus to foodwebs of new pit lakes and especially for acid pit lakes (McCullough *et al.*, 2009b)	Lakes may become eutrophic following excess nutrient imports through river water (Hupfer *et al.*, 1998)
Acidity generation by interaction between lake water and lake sediment may be limited due to a fast accumulation of benthic sediment (Dessouki *et al.*, 2005)	Nutrients may be buried under inorganic sediments or in a monimolimnion and become unavailable (von Sperling & Grandchamp, 2008; McNaughton & Lee, 2010)
Provides nutrients stimulating primary production as an approach for pit lake neutralisation (Tittel & Kamjunke, 2004)	Only likely to be important over longer terms due to phosphorus fixation to iron and aluminium in water column and lake sediments (Kleeberg & Grüneberg, 2005; Kopacek *et al.*, 2005)
Inflows may provide a source of organic material which contributes organic carbon as a substrate for sulphate reduction in the lakes' sediment (Salmon *et al.*, 2008)	Only likely to be important over longer terms as sulfate reduction is a relatively weak alkalinity-generating process (Wendt-Potthoff *et al.*, 2012)
Meromixis may be stabilized (Boehrer & Schultze, 2006) allowing for save burial of hazardous mine waste and treatment of AMD (Pelletier *et al.*, 2009)	Meromixis may result in enrichment of hazardous substances (metals, H_2S, CO_2, methane) in the monimolimnion affecting the entire lake water body in the case of limnic eruption or other reasons for long-term instability of chemical stratification (Sanchez-España *et al.*, 2014)

Since diversion of river water is a substantial impact for the river, respective aspects have to be considered. Beside legal, economic and social aspects (e.g. existing rights for water use) there are also ecological advantages and risks as shown in Table 2.

Table 2: Benefits and risks of flow-through pit lake closure strategy to rivers

Advantages to rivers	**Limitations/risks to rivers**
Decreased suspended and dissolved contaminant loads, especially nutrients (McCullough *et al.*, 2013a)	Decreased pH and alkalinity. Increased solute contaminants such as heavy metals, ammoniacal nitrogen (McCullough *et al.*, 2012)
Extends riverine aquatic habitat	May form physical or chemical migration barrier to movements of aquatic life
Reduced flood incidence and extended base flow duration	Altered hydrological regime reducing flood peaks required for biology and for scouring and shaping river channels
	Reduced overall river flow volume as a result of greater seepage and evaporation

Although water quality in a river may benefit from diversion through pit lakes (Table 2), there may also be substantial risks for the river. They should be avoided by adequate management. Typically, impacts resulting from acidification of pit lakes will not affect the downstream river if flow-through is established following acidic pit lake water neutralisation and the precipitation/co-precipitation of metals. The amount of water diverted from a river into a pit lake can often be best managed by limiting diverted flow to the pit lake. This will depend on the hydrological situation in the river and should be directed to maintaining hydrological patterns downstream as necessary for sustaining river end uses. The barrier function of a pit lake for migrating organisms can be mitigated by

connecting the pit lake via bypasses to the river. This strategy may therefore allow for relatively simple management of flow-through, and, in this way, for balancing positive and negative effects of the flow through approach.

Lowest risk for downstream rivers will be presented when the river is already degraded. For instance, we do not recommend flow-through as leading practice for pit lake closures with high downstream river water quality and end uses. The strategy has worked particularly well in the Lake Kepwari pit lake situation (see EXAMPLES,) as the river channel was able to be maintained in its historical course and river water quality was already degraded (McCullough *et al.*, 2012; McCullough *et al.*, 2013a). This reduced risk of AMD on downstream river values. Similarly, the monitoring period has validated the closure approach.

Poor water quality could affect both the ecological communities that might come into contact with the surface water of the pit lake and the down-gradient groundwater system at flow-through pit lakes (McCullough *et al.*, 2013b). River flow timing such as hydroperiod of when water flow is elevated (or even available in seasonal/ephemeral rivers) may also be important for triggering biological responses such as fish spawning events.

Effects of climate change on flow-through hydrology

Climate is the single most important factor on the hydrologic processes associated with a pit lake (Niccoli, 2009). Changes in climate (e.g., temperature, rainfall, wind, precipitation amount and distribution) will affect the individual hydrologic components over a short period of time whilst ground water inflow responses are generally and ultimately generated from precipitation recharge. Pit lakes with significant interaction with a groundwater system will tend to be buffered against short-term climatic changes, however, long-term climatic changes will still be reflected in ground water inflows over the long-term.

The water balance may be affected so grossly in a dryer climate that reduced pit lake water levels lead to cessation of flow through and lakes then become terminal sinks. In comparison, a wetter climate will most likely result in elevated pit lake water levels leading previously terminal pit lakes to become flow-through to either ground or surface waters. However, it is difficult to make broad statements about how climate changes will affect the status of a pit lake (i.e., if it will change from a flow-through to a terminal pit lake or vice-versa) because climate changes will affect all the components of the hydrologic system. Because of this, the effect on water balance for each pit lake resulting from climate change must be evaluated on a case-by-case basis.

EXAMPLES

There are examples for beneficial application of pit-lake flow-through strategy in different countries. Lake Senftenberg (Germany) was neutralised and kept neutral (Werner *et al.*, 2001). Flushing of pit lakes will be the future strategy for many German pit lakes (Luckner *et al.*, 2013). To reach this goal, the connection of naturally separated river basins is already in practice and is discussed to be extended in Germany in future (Koch *et al.*, 2009). The Muldereservoir, a pit lake in Germany, traps considerable amounts of toxic trace elements (ranging from 16% for zinc to 90% for cadmium) from Elbe River and its tributaries into the North Sea (Zerling *et al.*, 2001; Klemm *et al.*, 2005). Moser and Weisser (2011) reported the successful neutralisation of a pit lake in Austria by diversion of river water. Lake Kepwari and Collie River (Western Australia) form a further example

for the successful application of the flow-through strategy (McCullough *et al.*, 2012; McCullough *et al.*, 2013a).

CONCLUSIONS

Flushing with river water has proved to be a very useful strategy for management of some pit lakes internationally. A fundamental prerequisite for the use of river water and mine water for filling and management of pit lakes is the water availability. Water scarcity may be a limiting factor for flow-through solutions to pit lakes that currently function as terminal lakes due to regional water availability. That is, the applicability of filling and flushing of pit lakes with river water and mine water strongly depends on the climate and the intensity of the use of water downstream the pit lakes. In the case of limited water availability, floods may be the only options for the filling of pit lakes under such arid conditions and this method may be evaluated similar to the practices in Germany. However, the ecological needs of the river system downstream the pit lakes have to be kept in mind, including the flow magnitude and variability of the flow rate under such conditions.

The water quality of the used river water also has to suit the requirements of the planned use of the pit lakes. Otherwise, treatment of the river water, the mine water or the pit lake may be necessary. Of more importance, priority should be given to river water quality and end uses and the maintenance, or improvement, of existing water values (McCullough & Pearce, 2014). River water quality should generally not be presented with risk of degradation by pit lake flow-through, which will limit opportunities to this strategy to pit lakes of early better water quality and/or rivers of relatively lower water quality. Ideally, hydrological and geochemical modelling will precede a trial period of flow-through which then validates the model expectations to stakeholders' satisfaction.

Some pit lakes can also be used as reactors under certain conditions for instance, removing nutrients from river water and in turn precipitating metals from lake water. Nonetheless, hydro-chemical processes will vary between operations and sites based on the specific geological, hydrological and climate characteristic of each lake and its inflow/outflow characteristics. Developing flow-through systems must be based upon reliable data and accurate predictions of water balance and water quality e.g., from deterministic models. Nevertheless, abatement of acidification and salinisation as the import of alkalinity and freshwater, is typically the key driver to use flow-through as a closure strategy for pit lakes.

REFERENCES

Banks, D.; Younger, P. L.; Arnesen, R.-T.; Iversen, E. R. & Banks, S. B. (1997). Mine-water chemistry: the good, the bad and the ugly. *Environmental Geology* 32: 157-174.

Boehrer, B. & Schultze, M. (2006). *On the relevance of meromixis in mine pit lakes*. Proceedings of the 7th International Conference on Acid Rock Drainage (ICARD). St Louis, Missouri, USA. Barnhisel, R. I. (ed.) American Society of Mining and Reclamation (ASMR), 200-213pp.

Dessouki, T.; Hudson, J.; Neal, R. & Bogard, M. (2005). The effects of phosphorus additions on the sedimentation of contaminants in a uranium mine pit-lake. *Water Research* 39: 3,055-3,061.

Fyson, A.; Nixdorf, B. & Kalin, M. (2006). The acidic lignite pit lakes of Germany - microcosm experiments on acidity removal through controlled eutrophication. *Ecological Engineering* 28: 288-295.

Hilson, G. & Haselip, J. (2004). The environmental and socioeconomic performance of multinational mining companies in the developing world economy. *Minerals and Energy* 19: 25-47.

Hinwood, A.; Heyworth, J.; Tanner, H. & McCullough, C. D. (2012). Recreational use of acidic pit lakes – human health considerations for post closure planning. *Journal of Water Resource and Protection* 4: 1,061-1,070.

Hupfer, M.; Fischer, P. & Friese, K. (1998). Phosphorus retention mechanisms in the sediment of an eutrophic mining lake. *Water, Air, and Soil Pollution* 141: 341-352.

Kleeberg, A. & Grüneberg, B. (2005). Phosphorus mobility in sediments of acid mining lakes, Lusatia, Germany. *Ecological Engineering* 24: 89-100.

Klemm, W.; Greif, A.; Broeckaert, J. A. C.; Siemens, V.; Junge, F. W.; van der Veen, A.; Schultze, M. & Duffek, A. (2005). A study on arsenic and the heavy metals in the Mulde River system. *Acta Hydrochimica et Hydrobiologica* 33: 475–491.

Koch, H.; Grünewald, U.; Kaltofen, M. & Kaden, S. (2009). Anpassungsstrategien für die Wasserbewirtschaftung auf den globalen Wandel im Einzugsgebiet der Spree. *Korrespondenz Wasserwirtschaft* 2: 600-605.

Kopacek, J.; Borovec, J.; Hejzlar, J.; Ulrich, K. U.; Norton, S. & Amirbahman, A. (2005). Aluminum control of phosphorus sorption by lake sediments. *Environmental Science & Technology* 39: 8784-8789.

Kosík, M.; Čadková, Z.; Přikryl, I.; Seďa, J.; Pechar, L. & Pecharová, E. (2011). *Initial succession of zooplankton and zoobenthos assemblages in newly formed quarry lake medard (Sokolov, Czech Republic)*. Proceedings of the International Mine Water Association (IMWA) Congress. Aachen, Germany. Rüde, T. R.; Freund, A. & Wolkersdorfer, C. (eds.), 517-522pp.

Kratz, T. K.; Webster, K. E.; Riera, J. L.; Lewis, D. B. & Pollard, A. I. (2006). Making sense of the landscape: Geomorphic legacies and the landscape position of lakes. In, *Long-term dynamics of lakes in the landscape,* Magnuson, J. J.; Kratz, T. K. & Benson, B. J. (eds.) Oxford University Press, New York, USA, 49-66pp.

Kumar, N. R.; McCullough, C. D.; Lund, M. A. & Newport, M. (2011). Sourcing organic materials for pit lake remediation in remote mining regions. *Mine Water and the Environment* 30: 296-301.

Lee, G.; Bigham, J. M. & Faure, G. (2002). Removal of trace metals by coprecipitation with Fe, Al and Mn from natural waters contaminated with acid mine drainage in the Ducktown Mining District, Tennessee. *Applied Geochemistry* 17: 569-581.

Luckner, L.; Raimann, S. & Koch, C. (2013). Teil 1: Herstellung und Nachsorge von Bergbaufolgeseen in Tagebaurestlöchern. In, *LMBV Flutungs, Wasserbehandlungs und Nachsorgekonzept Lausitz. Fortschreibung 10/2013,* Lausitzer und Mitteldeutsche Bergbau-Verwaltungsgesellschaft, Senftenberg, Germany, 58pp.

McCullough, C. D.; Ballot, E. & Short, D. (2013a). *Breach and decant of an acid mine lake by a eutrophic river: river water quality and limitations of use*. Proceedings of the Mine Water Solutions 2013 Congress. Lima, Peru. Infomine Inc., 317-327pp.

McCullough, C. D.; Hunt, D. & Evans, L. H. (2009a). Sustainable development of open pit mines: creating beneficial end uses for pit lakes. In, *Mine Pit Lakes: Characteristics, Predictive Modeling, and Sustainability* Castendyk, D. & Eary, T. (eds.) Society for Mining, Metallurgy, and Exploration (SME), Colorado, USA, 249-268pp.

McCullough, C. D.; Kumar, N. R.; Lund, M. A.; Newport, M.; Ballot, E. & Short, D. (2012). *Riverine breach and subsequent decant of an acidic pit lake: evaluating the effects of riverine flow-through on lake stratification and chemistry*. Proceedings of the International Mine Water Association (IMWA) Congress. Bunbury, Australia. 533-540pp.

McCullough, C. D. & Lund, M. A. (2006). Opportunities for sustainable mining pit lakes in Australia. *Mine Water and the Environment* 25: 220-226.

McCullough, C. D.; Marchand, G. & Unseld, J. (2013b). Mine closure of pit lakes as terminal sinks: best available practice when options are limited? *Mine Water and the Environment* 32: 302-313.

McCullough, C. D. & Pearce, J. I. (2014). *What do elevated background contaminant concentrations mean for AMD risk assessment and management in Western Australia?* 8th Australian Workshop on Acid and Metalliferous Drainage. Adelaide, Australia. 28 April - 2 May 2014, 147-158pp.

McCullough, C. D.; Steenbergen, J.; te Beest, C. & Lund, M. A. (2009b). *More than water quality: environmental limitations to a fishery in acid pit lakes of Collie, south-west Australia*. Proceedings of the International

Mine Water Conference. Pretoria, South Africa. 19-23 October, International Mine Water Association, 507-511pp.

McNaughton, K. A. & Lee, P. F. (2010). Water Quality Effects from an Aquaculture Operation in a Meromictic Iron Pit Lake in Northwestern Ontario, Canada. *Water Quality Research Journal of Canada* 45: 13-24.

Meybeck, M. (2005). Global occurrence of major elements in rivers. In, *Surface and ground water, weathering, and soil,* Drever, J. I. (ed.) Elsevier, Amsterdam, The Netherlands, 207-223pp.

Moser, M. & Weisser, T. (2011). The most acidified Austrian lake in comparison to a neutralized mining lake. *Limnologica* 41: 303-315.

Müller, M.; Eulitz, K.; McCullough, C. D. & Lund, M. A. (2011). *Model-based investigations of acidity sinks and sources of a pit lake in Western Australia*. Proceedings of the International Mine Water Association (IMWA) Congress. Aachen, Germany. Rüde, T. R.; Freund, A. & Wolkersdorfer, C. (eds.), 41-45pp.

Neil, L. L.; McCullough, C. D.; Lund, M. A.; Tsvetnenko, Y. & Evans, L. (2009). Toxicity of acid mine pit lake water remediated with limestone and phosphorus. *Ecotoxicology and Environmental Safety* 72: 2,046-2,057.

Niccoli, W. L. (2009). Hydrologic characteristics and classifications of pit lakes. In, *Mine Pit Lakes: Characteristics, Predictive Modeling, and Sustainability* Castendyk, D. & Eary, T. (eds.) Society for Mining, Metallurgy, and Exploration (SME), Colorado, USA, 33-43pp.

Pelletier, C. A.; Wen, M. & Poling, G. W. (2009). Flooding pit lakes with surface water. In, *Mine Pit Lakes: Characteristics, Predictive Modeling, and Sustainability* Castendyk, D. & Eary, T. (eds.) Society for Mining, Metallurgy, and Exploration (SME), Colorado, USA, 187-202pp.

Peterka, J.; Čech, M.; Draštík, V.; Jůza, T.; Frouzová, J.; Prchalová, M. & Kubečka, J. (2011). *Ten years of fish community succession in post-mining lake Milada-Chabařovice*. Proceedings of the International Mine Water Association (IMWA) Congress. Aachen, Germany. Rüde, T. R.; Freund, A. & Wolkersdorfer, C. (eds.), 535pp.

Salmon, S. U.; Oldham, C. & Ivey, G. N. (2008). Assessing internal and external controls on lake water quality: limitations on organic carbon-driven alkalinity generation in acidic pit lakes. *Water Resources Research* 44: W10414.

Sanchez-España, J.; Boehrer, B. & Yusta, I. (2014). Extreme carbon dioxide concentrations in acidic pit lakes provoked by water/rock interaction. *Environmental Science and Technology* 48: 4273-4281.

Schultze, M.; Geller, W.; Benthaus, F. C. & Jolas, P. (2011). Filling and management of pit lakes with diverted river water and with mine water – German experiences. In, *Mine Pit Lakes: Closure and Management,* McCullough, C. D. (ed.) Australian Centre for Geomechanics, Perth, Australia, 107-120pp.

Stich, H. B.; Hoppe, A. & Maier, G. (2009). Zooplankton composition in a gravel pit lake invadedd by the Ponto-Caspian mysid Hemimsis anomala G.O. Sars 1907. *Aquatic Invasions* 4: 697-700.

Straskraba, M. (1999). Retention time as a key variable of reservoir limnology. In, *Theoretical Reservoir Ecology and its Application,* Tundisi, J. G. & Straskraba, M. (eds.) International Institute of Ecology, Brazilian Academy of Science and Backhuys Publishers, Sao Carlos, 385-410pp.

Swanson, S. (2011). What type of lake do we want? Stakeholder engagement in planning for beneficial end uses of pit lakes. In, *Mine Pit lakes: Closure and Management,* McCullough, C. D. (ed.) Australian Centre for Geomechanics, Perth, Australia, 29-42pp.

Tittel, J. & Kamjunke, N. (2004). Metabolism of dissolved organic carbon by planktonic bacteria and mixotrophic algae in lake neutralisation experiments. *Freshwater Biology* 49: 1062-1071.

Totsche, O.; Fyson, A. & Steinberg, C. E. W. (2006). Microbial alkalinity production to prevent reacidification of neutralized mining lakes. *Mine Water and the Environment* 25: 204-213.

von Sperling, E. & Grandchamp, C. A. P. (2008). *Possible uses of mining lakes*. 33rd WEDC International Conference Accra, Ghana. Water, Engineering and Development Centre, Loughborough University, 75-380pp.

Wendt-Potthoff, K.; Koschorreck, M.; Ercilla, M. D. & España, J. S. (2012). Microbial activity and biogeochemical cycling in a nutrient-rich meromictic acid pit lake. *Limnologica* 42: 175–188.

Werner, F.; Bilek, F. & Luckner, L. (2001). Impact of regional groundwater flow on the water quality of an old post-mining lake. *Ecological Engineering* 17: 133-147.

Wisotzky, F. (2013). Avoidance and source treatment. In, *Acidic Pit Lakes - Legacies of surface mining on coal and metal ores,* Geller, W.; Schultze, M.; Kleinmann, R. L. P. & Wolkersdorfer, C. (eds.) Springer, Berlin, Germany, 258-264pp.

Younger, P. L. (2002). *Mine waste or mine voids: which is the most important long-term source of polluted mine drainage?* United Nations Environment Programme, Mineral Resources Forum: Current Feature paper 12pp.

Zerling, L.; Müller, A.; Jendryschik, K.; Hanisch, C. & Arnold, A. (2001). *Der Bitterfelder Muldestausee als Schadstoffsenke, Verlag der Sächsischen Akademie der Wissenschaften zu Leipzig*. 69pp.

Nucleation Seeding to Promote Chemical Precipitation of Hardness and Alkalinity from Mine Pit Lakes

Allison Haus and Mehgan Blair
BARR Engineering, USA

ABSTRACT

Several flooded taconite mine pits in northern Minnesota contain circum-neutral water with elevated concentrations of sulfate, hardness (dominated by Mg) and alkalinity, which together contribute to overall total dissolved solids and specific conductivity, and are of increasing local regulatory concern. Two of these mine pit lakes (pit lake "A" and pit lake "B") are meromictic, stratified both thermally and chemically. The deepest and densest water in the pits rarely, if ever, mixes with the overlying, more dilute water. Geochemical modeling suggests that both lakes are increasingly supersaturated with respect to calcite and aragonite with depth; it has been well documented that high concentrations of magnesium can act to kinetically inhibit precipitation of calcium carbonate. Reducing alkalinity and hardness via a passive strategy may be achieved by reducing the barrier to precipitation: nucleation. Nucleation seed crystal precipitation from concentrated bottom waters was initiated via four different processes, including evaporation, heating, lime addition, and salt addition. Precipitated seed crystals were then introduced to more dilute top water while alkalinity and hardness were monitored. Spontaneous precipitation of hardness and alkalinity was successfully achieved by heating deep pit water and exsolution of CO_2. This process is hypothesized to be responsible for the "white bathtub ring" that edges the pit lakes.

Keywords: hardness, carbonate, alkalinity, nucleation

INTRODUCTION

In some former taconite (iron ore) mine pits on the Mesabi Iron Range in northern Minnesota, oxidation products from trace sulfides are neutralized by relatively abundant carbonates, including siderite and ankerite. The resulting pit lake water quality has circum-neutral pH, but can contain elevated concentrations of sulfate, hardness and alkalinity. Together, these elevated salt concentrations increase total dissolved solids (TDS) and specific conductance, and are of increasing local regulatory concern. Sulfate, specifically, is strongly regulated in the state of Minnesota, where the water quality standard in water used for wild rice production is as low as 10 milligrams per liter (mg/L). The potential may exist to passively reduce salt concentrations by pairing strategies that promote sulfate-reducing bacteria (SRB) to reduce sulfate with strategies that reduce alkalinity and hardness. Non-mechanical strategies that result in reductions in alkalinity and hardness by encouraging chemical precipitation are explored herein.

BACKGROUND

Hardness and alkalinity in wastewater is typically removed via active processes such as ion exchange, membrane separation or chemical precipitation. Chemical precipitation occurs when the solubility product of calcite increases such that supersaturation occurs (Nancollas and Reddy, 1971). It may be possible to induce chemical precipitation of calcium carbonate in a relatively passive way in mine pit lakes by modulating solution parameters that directly influence saturation state.

The solubility expression and corresponding solubility product for calcite can be represented as:

$$CaCO_3 \leftrightarrow Ca^{2+} + CO_3^{2-} \quad K_{SP,\,calcite} = 10^{-8.48}$$

The driving force, or associated change in Gibbs free energy, of the calcite precipitation reaction is determined by the solubility constant of calcite (K_{SP}) and the ion activity product Q:

$$\Delta G = \Delta G^0 + RT \log (Q/ K_{SP}),$$

where R is the gas constant (8.314 J/mol K), and T is the temperature in Kelvin. The ion activity product, Q, is the product of the real concentrations of Ca and CO_3^{2-} in solution. When Q is greater than the K_{sp}, the solution is supersaturated, and precipitation of calcium carbonate is thermodynamically favorable. Several solution parameters can act to modify saturation state by increasing the carbonate concentration. For example, as pH increases, the carbonate equilibrium shifts to the right, meaning carbonate (CO_3^{2-}) concentrations increase, as does saturation state of calcite. Similarly, CO_2 influences saturation of calcite because of its control on pH. Finally, carbonates demonstrate retrograde solubility: as temperature increases, they are more likely to precipitate. Taking advantage of these relationships may facilitate passive chemical precipitation.

The water quality at several northern Minnesota taconite mine pit lakes is supersaturated with respect to carbonates, but there may not be adequate "driving force" to overcome the barrier to nucleation (Teng et al, 2000). The barrier to precipitation may be removed when a nucleation seed is presented to solution, thereby promoting precipitation in systems with lower driving force. This type of "nucleation seeding" strategy may result in alkalinity and hardness reductions in systems supersaturated with respect to carbonates. A form of this strategy has been used successfully to remove metals and TDS and to regulate pH for more than a decade at a 20-acre mine pit lake in Duck Town, Tennessee (Chermak, 2004). The pit lake water has elevated acidity and dissolved metals and is treated by adding lime to water highly concentrated in metals and TDS, such that nano-particulate iron-oxides begin to form. This water is then introduced to the more dilute pit lake, and metals within the pit lake water precipitate on the iron-oxide particulates, which then settle out at the bottom of the pit lake as sludge.

Precipitation of metals was kinetically limited in the Duck Town mine pit lake by a barrier to nucleation. Once the pit lake water was seeded with crystals that provided surface area, metals precipitated out. The following suggests that similar treatment might work at several of the flooded taconite mine pits to remove alkalinity and hardness:

- Water with the highest TDS occurs at the bottom of stratified pit lakes.
- Preliminary geochemical modeling of the quality of water in the mine pit lakes indicates that the water is supersaturated with respect to carbonates, both calcite and aragonite.
- Aragonite ($CaCO_3$) has been identified by X-ray diffraction (XRD) as an authigenic precipitate at the bottom of one of the mine pit lakes, and in the adjacent rock stockpiles.
- Occasional spontaneous formation of carbonates may be responsible for observed phenomenon within the pit lakes: the presence of a white "bathtub ring" surrounding several of the lakes, and periodic "whitings", when pit lake water color, which is normally dark blue, changes to a bright turquoise color.

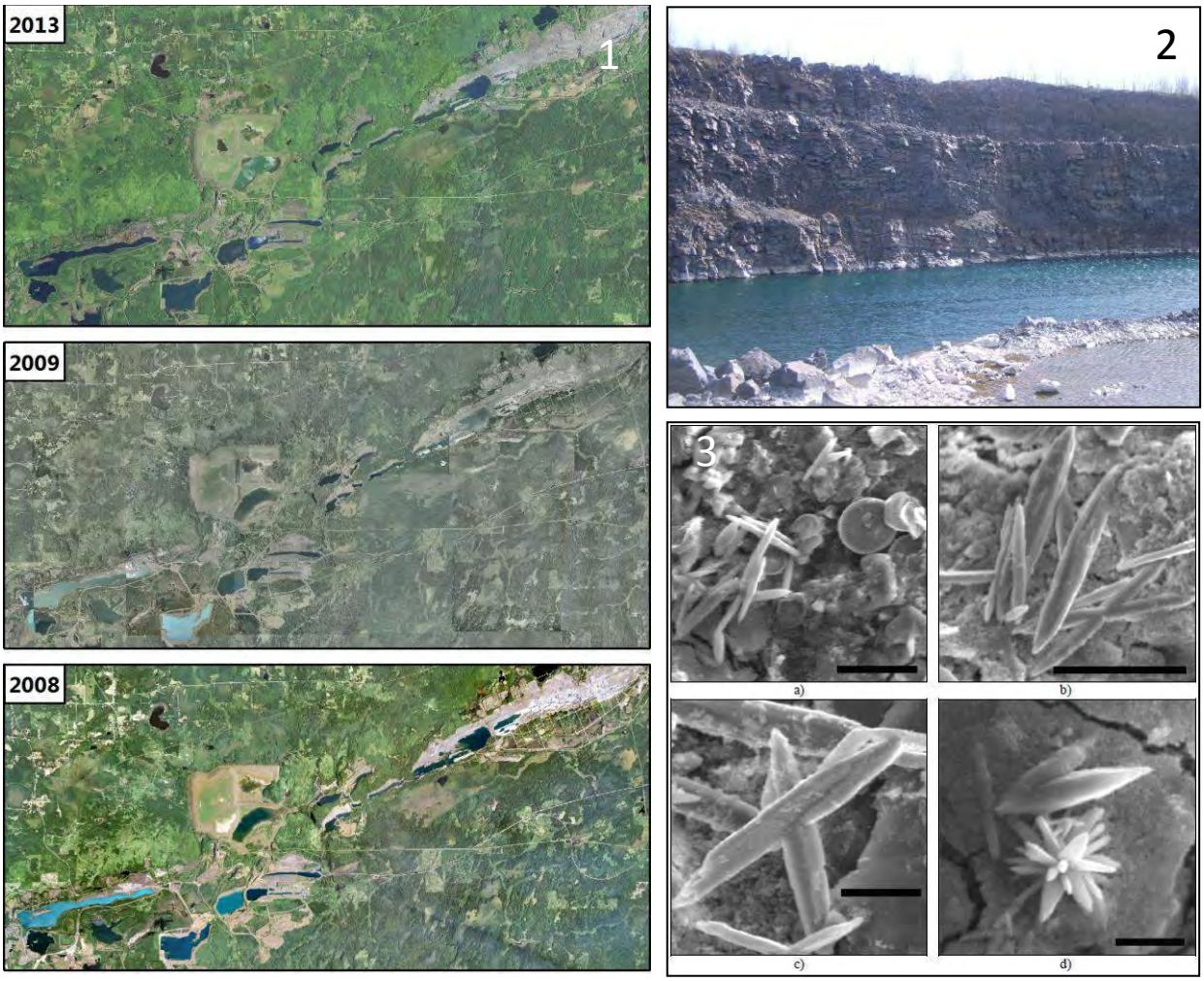

Figures 1, 2, 3 **1)** Aerial images of pit lakes during summer months (different years) capture color of individual lakes, normally dark blue, changing to turquoise during "whitings". Width of images above are approximately 40 km**. 2)** Top right picture shows Pit Lake "A", including the remnant highwall (approximately 37 meters high) and a white "bathtub ring" in foreground**. 3)** SEM Micrographs of aragonite crystals in a taconite mine pit lake sediment sample. a) and b) show single blades and clusters. c) a twinned crystal. d) single blades and a radiating cluster of aragonite crystals. SEM images- scale bar: a) 1,500X; 20 μm scale b) 4,000X; 12.5 μm scale c) 6,000X 5 μm scale; d) 3,500X; 10 μm scale.

We investigated, through modeling and bench-testing, whether it is possible to induce chemical precipitation of carbonates, thereby decreasing concentrations of hardness, alkalinity, and, by extension, TDS and specific conductivity from the pit lake water, with little mechanical input.

METHODOLOGY

The investigation consisted of two phases: experimental modeling in the geochemical software Geochemist's Workbench (Bethke, 2008) (GWB) and laboratory testing to explore a) if precipitation of $CaCO_3^{2-}$ from very concentrated pit water can be promoted, and, if successful, b) whether

alkalinity and hardness removal from the more dilute pit water will occur through precipitation onto seed crystals.

Water from Pit Lake "A" was collected from two depths (1 and 20 meters) corresponding to the two stratified regions of the meromictic lake: the mixolimnion, the uppermost portion of the water column that behaves as a holomictic or normally mixing lake, and the monimolimnion, or lower isolated portion of the lake. The monimolimnion is generally colder, more anoxic and saltier than the upper water column. The location of the chemocline was determined in the field, based on the temperature and salinity gradient. Chemical analyses of these water samples were conducted and the data are presented in Table 1.

Table 1 Initial Water Chemistry

Parameter	**Units**	**Pit A Deep-20 m**	**Pit A Shallow-1 m**
Calcium	mg/L	165	60.5
Iron		0.196	ND
Magnesium		293	171
Manganese		14.1	0.0211
Alkalinity, bicarb		474	205
TDS		2360	1230
Sulfate		1370	732
Temperature	°C	6.6	19.3
Conductivity	µS/cm	1870	1420
pH		7.52	8.7
Calcite Saturation	Log Q/K_{sp}	0.4198	1.0889
Aragonite Saturation	Log Q/K_{sp}	0.2844	0.9443

Phase 1: Reaction modeling in GWB

GWB was used to model reactions aimed at increasing saturation state with respect to calcium carbonate phases, based on the Pit Lake chemistry data (Table 1). The thermodynamic constraints

for mineral reactions were based on the Lawrence Livermore National Laboratory database provided within the GWB platform. Calculations of saturation were based on equilibrium state. The system was assumed open to atmosphere and the CO_2 endpoint was modeled at atmosphere (log $P_{CO2} = 10^{-3.4}$).

Phase 2: a. Promoting formation of calcium carbonate

In the laboratory, several clean jars (rinsed once with dilute acid, then 3 times with tap water, then 3 times with DI water) were filled with 500 mL of deep pit water (Pit A Deep – 20 m) and left open to atmosphere (some evaporation occurred). Carbonate precipitation was encouraged from concentrated pit water by 1) evaporation over three days and heating to room temperature (20 °C) (control), or 2) heating to 45 C. In the heated trials, jars were placed atop a hot plate. For the control, they were placed simply on the bench top. Neither trial was stirred. All of the tests were repeated 5 times, with concurring results.

b. Measuring removal of hardness and alkalinity through continued precipitation

When seed crystal formation was observed from the deep pit water trials, the precipitate was harvested using a screen sieve. Two quantities of this material was then introduced into 500 mL (each) of the more dilute shallow pit water: 1) 0.01 mol, and 2) 0.02 mol seed crystal (determined by dry mass) harvested from the deep pit water experiments. In comparable trials, small quantities of other materials that had the potential to either increase saturation state, or to act as seed crystals, were added to 500 mL (each) of shallow pit water: 1) 0.01 mol ground lime, and 2) 0.03 mol of commercially available fine-grained aragonite. These four trials were compared to a control trial which was subjected to evaporation and heating to room temperature (20 C).

During each trial, a multi-parameter water quality meter (YSI 556 Multi-Probe Meter) was used to measure specific conductivity, pH, dissolved oxygen, and oxidation-reduction potential. Alkalinity was measured using an alkalinity titration kit. At the conclusion of the experiments, six samples were selected for chemical analysis of hardness (Mg and Ca) and alkalinity. In the lime trial, where sludge formed at the bottom, the supernatant water was decanted off the top of the solid and sent for analysis. In trials where calcite crystals formed at the top, water for analysis was collected from below the floating crystals.

RESULTS AND DISCUSSION

The deep water (Pit A Deep – 20m) contained higher alkalinity, more dissolved constituents, and had a higher conductivity and TDS than the shallow pit water (Pit A Shallow – 1m), as shown on Table 1. Despite containing more than more than twice the concentration of alkalinity and approximately 2.5 times as much calcium as the shallow water, the geochemical equilibrium model predicted that the saturation state of calcite was lower in the deep pit water than it was in the shallow pit water. The solubility of CO_2 increased with decreasing temperatures; more CO_2 was

dissolved and the pH was lower in the deep pit water relative to the shallow pit water. Both temperature and pH exerted a strong influence on calcite saturation state (Figure 4).

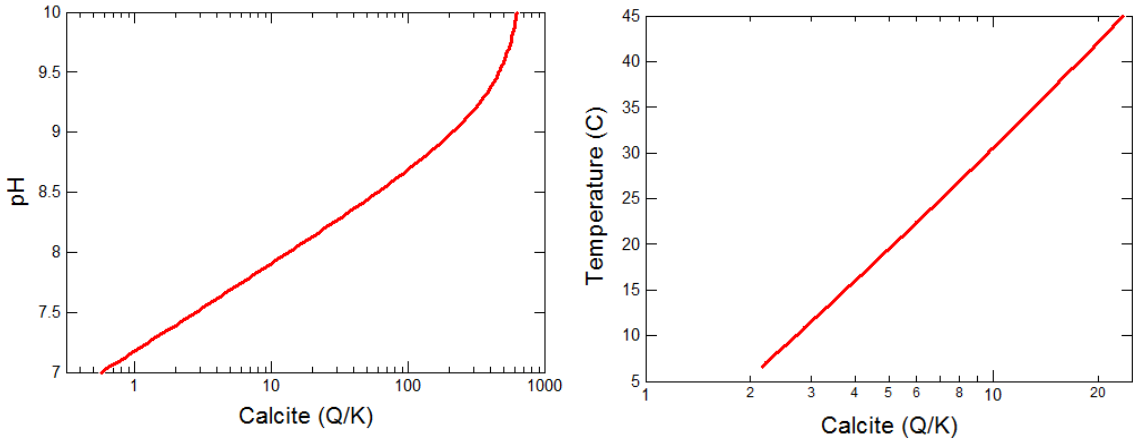

Figure 4 Predicted saturation state of Pit A Deep – 20 m water, as a function of A) pH, and B) temperature (°C).

The results of field and lab measurements from the laboratory experiments are presented in Table 2. Spontaneous precipitation of carbonate occurred with every test of Pit A Deep water (Figure 5). In the control experiment, as water equilibrated with atmospheric CO_2 and room temperature (~20 C), saturation state increased with increasing temperature and pH until precipitation of carbonate occurred after three days. Precipitation occurred more rapidly when Pit A Deep water was heated further: after four hours heating to 45 C. The increase in conductivity in the Pit A Deep water also reflected this temperature increase; conductivity of water increases by about 2-3% with every degree C. The precipitate formed at the water surface, coalesced into larger clumps with time (or application of heat), and settled to the bottom of water column with time (~2-3 days after formation in the control).

Little change in water quality was observed when carbonate seed crystals, precipitated from the Pit A Deep water, were introduced to the Pit A Shallow water. For example, conductivity remained fairly constant across almost all tests. Significant reductions in hardness, alkalinity, and specific conductivity were observed only in the lime addition test, which also experienced coincident increase in pH increase and saturation state. The formation of sludge at the bottom of the glass is also consistent with carbonate precipitation after the addition of lime.

Figure 5 A) Precipitate that formed from the deep pit water control over a period of 3 days. B) Groups of precipitated crystals that occurred at the surface during heating of the deep pit water.

Table 2 Experimental Results: Laboratory and Field Measurements, and Model Predictions

		Pit A Deep - 20 m			Pit A Shallow - 1 m					
Test	**Units**	**Start**	**Control**	**Heat to 45 C**	**Start**	**Control**	**0.01 mol lime**	**.03 mol Arag**	**.01 mol Seeds**	**.02 mol Seeds**
Calcium	mg/L	165	113	--	60.5	60.8	26.2	60	63.3	64.2
Magnesium	mg/L	293	321	--	171	164	166	170	171	172
Hardness, dissolved	mg/L as $CaCO_3$	1610	1600		852	824	746	847	859	866
Temperature	°C	6.6	20.35	45	19.3	19.51	19.53	19.42	19.51	19.73
Conductivity	uS/cm	1870	3111	3343	1420	1720	1467	1727	1716	1746
pH		7.52	8.43	8.02	8.7	8.53	9.08	8.4	8.39	8.4
Field alkalinity	mg/L as $CaCO_3$	860	780	640	540	520	280	400	400	480
Precipitate Evident		none	yes, see fig 3A	yes, fig 3B	no	no	sludge	few at surface	no	no
Calcite Saturation	Log Q/K	0.33	0.96	1.93	1.01	0.79	2.03	1.63	1.16	1.51
Aragonite Saturation	Log Q/K	0.19	0.82	1.79	0.87	0.65	1.89	1.48	1.30	1.37

Experimental results were modeled in GWB, and predicted saturation state post-reaction is plotted in Figure 6. The results indicate that precipitation of calcium carbonate occurred only during those tests during which the predicted saturation index increased by a factor of two or more (colored red in the figure. Tests in which no precipitate formed are colored blue). Though predicted saturation state is lower in the Pit A Deep control than it is in three of the Pit A Shallow tests, the relative change from the initial saturation state was greater in the Pit A Deep tests, and this change correlates with observed precipitation. All tests and controls were supersaturated with respect to calcite; only tests where the change in driving force was greater than 2 led to precipitation.

An additional factor that may explain the continued resistance to precipitation in the shallow pit water is inhibition due to high concentrations of Mg and sulfate in solution (Berner, 1975). Kinetic inhibition due to Mg can sometimes be overcome by a larger driving force (ΔG), such that precipitation can proceed. Generally, reactions with larger Gibbs free energies are more likely to proceed spontaneously than are those with smaller free energies (Langmuir, 1997). In either case, driving up saturation state to >2 via the addition of lime was the only test that successfully led to precipitation of calcite from the shallow pit lake water.

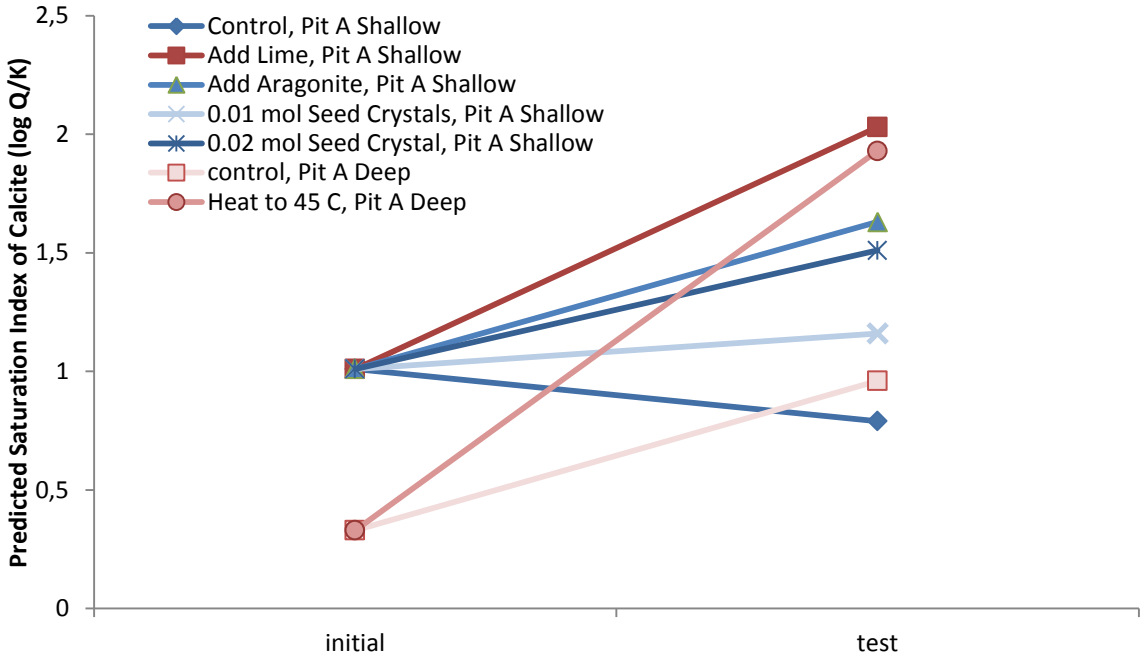

Figure 6 Predicted saturation with respect to calcite for Pit A Deep and Pit A Shallow, in initial waters and in each test. Precipitation of calcium carbonate was observed in tests shown in pink and red; precipitation did not occur in any of the tests colored blue. Precipitation occurred in both tests from the Pit A Deep water, during the control experiment and when the water was heated to 45 °C, and it occurred more rapidly and to a larger extent in the heated test. Lime addition was the only test that resulted in the precipitation of carbonate from the Pit A Shallow water.

CONCLUSION

Calcite precipitation occurred from the deep pit water in the control when it was removed from cold storage: changing temperature of deep pit water and allowing CO_2 to exolve increased saturation to the point of precipitation. This suggests that one potential treatment strategy to remove alkalinity and hardness is to pump the deep water to the surface and allow it to equilibrate with atmospheric conditions. The "whiting" events that have been observed at surrounding pit lakes demonstrate this process on a much larger scale, possibly due to turnover of the mixolimnion, which brings deeper, more saturated water to the surface. As saturated water equilibrates with atmospheric conditions, calcium carbonate precipitates, temporarily coloring the pit lakes a bright turquoise-blue. Test results predict that about 25% of the hardness and alkalinity

in the Pit A Deep water may be removed by pumping to the surface. The effect of pumping on pit lake hydrodynamics and stratification has not been investigated at this time.

Precipitation of hardness and alkalinity from shallow pit water was not achieved with the addition of nucleation seed crystals. It is possible that the quantity of seed crystals introduced to the dilute surface water didn't present enough surface area for additional precipitation to occur. Furthermore, adding a larger quantity of seed crystals could act to increase saturation state enough relative to the initial state to overcome the barrier to precipitation. Reductions in hardness and alkalinity in the shallow pit water was achieved by addition of a small amount of lime, a conventional wastewater treatment approach used to decrease water hardness.

ACKNOWLEDGEMENTS

Thanks to Barr Engineering Company for providing funding for this work.

REFERENCES

Bethke, C. (2008) *Geochemical and Biogeochemical Reaction Modeling*, Cambridge University Press, United Kingdom.

Berner, R. (1975) The role of magnesium in the crystal growth of calcite and aragonite from sea water, Geochimica et Cosmochimica Acta, 39:4, 489-504.

Chermak, J.A., B. Wielinga, E.G. Wyatt, and J. Taylor (2004) Cost-Effective Acid Rock Drainage Water Treatment Applied to Mining-Impacted Watersheds, ASMR.

Langmuir, D. (1997) *Aqueous Environmental Chemistry*, Prentice Hall, New Jersey, USA.

Nancollas, GH, and MM Reddy (1971) The crystallization of calcium carbonate. II. Calcite growth mechanism. *Journal of Colloid and Interface Science* 37:4; pp 824-830.

Teng, HH, Dove, PM, and JJ De Yoreo (2000) Kinetics of calcite growth: surface processes and relationships to macroscopic rate laws. *Geochmica et Cosmochimica Acta* 64:13; pp 2255-2266.

10th ICARD IMWA 2015 | 10th International Conference on Acid Rock Drainage & IMWA Annual Conference

Addition of Bulk Organic Matter to Acidic Pit Lakes May Facilitate Closure

Mark Lund[1] and Clint McCullough[1,2]

1. *Mine Water and Environment Research Centre (MiWER), Edith Cowan University, Australia*
2. *Golder Associates, Australia*

ABSTRACT

Macro nutrients (C, N, P) are essential for sustaining freshwater ecosystems. However, acidic pit lakes are often nutrient-poor as low pH levels and metal complexation (by Al, Fe and Mn) reduces dissolved P and C concentrations. In contrast, N is often not limiting as it is readily available from groundwater and blasting residues.

The Collie basin in Western Australia has a lake district of eleven acidic coal mine pit lakes (pH 3-7, low metals/metalloids and sulfate concentrations). Our previous researches at – microcosm, mesocosm and field scale demonstrated low C and P concentrations limit algal productivity. Addition of organic matter (in the form of terrestrial leaf litter) offered potential bioremediation benefits including habitat creation, sediment formation, the potential for sulfate reduction, and slow release of macronutrients to promote algal growth.

We tested the effect of organic matter additions of straw, lawn clippings and eucalypt leaves on acidic pit lake water and sediment in 1,200 L replicated mesocosms. We regularly measured water quality in each mesocosm over a year and concluded by measuring the development of macroinvertebrate communities. The highly labile C found in lawn clippings stimulated algal biomass, macroinvertebrate diversity and abundance, and improved water quality. Straw and eucalypt leaves did not alter water quality substantially but did increase abundance of macroinvertebrates.

Additions of nutrients, particularly as bulk organic matter increased macroinvertebrate abundance but also altered species composition from carnivorous highly mobile opportunists found in the controls to a range of herbivores/omnivores, while not necessarily altering water quality substantially. The presence of labile C (particularly in the grass) was able to increase algal biomass and improve pH. If conservation values are important for closure of pit lakes and eutrophication is not a risk, then addition of bulk organic matter (particularly labile forms) should be considered in closure plans. Organic matter could be actively added or passively through the catchment. As environmental improvements were seen in all treatments, adding many readily available organic matter types to pit lakes, may be helpful to achieving closure objectives associated with biodiversity.

Keywords: Macroinvertebrates, algae, ecosystem development, succession

INTRODUCTION

Natural lakes are increasingly degraded and lost through human activities. However, pit lakes resulting from the flooding of open-cut mine pits post-mining are creating new lakes (McCullough & Etten, 2011). Pit lakes can pose an environmental hazard to regional groundwater and surface waters, and nearby aquatic and terrestrial ecosystems (McCullough & Lund, 2006). Initially, pit lakes are geochemically controlled usually through acid and metalliferous drainage (AMD) from oxidation of sulfidic minerals in and around the lakes degrading water quality by increasing acidity, sulfate and metal/metalloid concentrations (Koschorreck & Tittel, 2007). Compared to natural aquatic systems, acidic pit lakes typically have greater depth, poor bankside stability, limited organic sediments, limited riparian vegetation cover and diversity, and low rate of allochthonous inputs (Van Etten, 2011; Lund *et al.*, 2013). The ecological development of pit lakes is poorly understood, but primary succession in terrestrial systems is largely driven by accumulations of organic matter and this is likely to be case in pit lakes. Poor water quality and low ecological values of acidic pit lakes may significantly reduce beneficial end use options for the lakes which might be otherwise possible.

Acidic pit lakes typically have low nutrient concentrations; especially of phosphorus and dissolved inorganic carbon, which may limit algal biomass (Nixdorf *et al.*, 2001). Although phosphorus is highly soluble under low pH conditions, it tends to co-precipitate with iron and aluminum in the water column or bind to the sediment (Kapfer, 1998). Dissolved organic carbon concentrations in the water are also often low due to limited allochthonous materials entering the lake from the catchment (Lund & McCullough, 2011). Acidic pit lakes often have adequate concentrations of nitrogen (left from blasting residue), but this nutrient predominantly exists as ammonia due to limited nitrification at low pH (Nixdorf *et al.*, 2001). Algal primary production is fundamental for lake ecological development leading to the establishment of a functional mature aquatic ecosystem (Kalin *et al.*, 2001; Lund & McCullough, 2011; McCullough & Etten, 2011). Additionally, algal biomass provides a substrate for in-lake alkalinity generation by microbes, and a binding site for metals (Dessouki *et al.*, 2005).

Carbon additions to a pit lake can also provide conditions and substrates suitable for the growth of sulfate reducing bacteria (SRB) (Frömmichen *et al.*, 2003). As SRB effectively reverse the AMD processes, they can substantially improve water quality in AMD affect pit lakes (McCullough & Lund, 2011). Furthermore, elevated metal ions may also be removed by direct sorption and complexation to internally-generated or added organic matter (Fyson *et al.*, 1998). Bioremediation by SRB activity shows some potential in the newer pit lakes in Collie which have higher sulfate concentrations (Read *et al.*, 2009). Readily available bulk organic materials such as mulch, hay, manure (cow) and sawdust have been found to be potentially useful for bioremediation in Collie (Thompson, 2000; Lund *et al.*, 2006). The comparatively low sulfate concentrations in Collie pit lakes ultimately limit the ability of SRB to improve the water quality of an entire pit lake but may produce local improvements within specific habitats within the lake (Lund *et al.*, 2006).

Closure criteria for pit lakes waters tend to focus on meeting water quality objectives for slightly disturbed environments (McCullough & Pearce, 2014). It is typically difficult to achieve such water quality closure criteria and active treatment of poor water quality is expensive and ongoing. In Collie pit lakes, there is a suggestion that additions of organic matter encourages algal growth and macroinvertebrate diversity and abundance despite little change in water quality (Lund *et al.*, 2006). We believe that with organic matter additions, there are broader opportunities for pit lakes to achieve biodiversity outcomes and ecological development trajectories to still meet closure criteria

defined by environmental values. Therefore, the aim of this project was to determine the effect of bulk organic material addition (straw, eucalypt leaves, and lawn clippings) on mine pit-lake water quality and aquatic biodiversity.

METHODS

Study site

The Collie pit-lake district is located within the Collie coal basin within the Collie River catchment. Collie township lies nearly 160 km south-southeast of Perth, and is the center of coal mining in Western Australia (Zhao *et al.*, 2009). The Collie Basin covers an area of approximately 225 km^2. Collie coal is a sub-bituminous coal with a relatively low sulfur content (0.3-0.9%), and low caking and ash (4–9%) properties (Le Blanc Smith, 1993). Low amounts of acidity are generated through pyrite oxidation, ferrolysis and secondary mineralization. This acidity is sufficient to generate low pH in pit lakes due to the low buffering capacity of the surrounding rock. There are currently 11 pit lakes in Collie; an overview of the entire lake district is provided in Lund *et al.* (2012). WO5H is one of the larger and more acidic lakes and was chosen as the source of water and sediment for this study.

Experimental Methods

In September 2012, SCUBA divers collected sediment from WO5H (top 0.2 m) in 20 L plastic containers at 2-3 m depth. In addition, a water tanker was used to collect ~12,000 L of WO5H water from the lake. Both water and sediment were taken to Perth within 24 h of collection and immediately transferred to mesocosms. The mesocosms were designed to mimic the littoral (<1 m deep) zone of WO5H. Twelve fiberglass mesocosms (diameter – 0.76 m and height – 0.80 m) with an individual capacity of 1,200 L were used for the experiment. Sediment was first added to all the mesocosms to a depth of 100 mm, followed by the WO5H water. Utilizing a randomized block design, three replicates of four treatments were randomly assigned. The treatments consisted of no additions (control), and additions of straw, eucalypt leaves and grass clippings. Grass clippings were obtained locally from a lawn mowing contractor, eucalypt leaves (*Eucalyptus* sp.) were obtained at Edith Cowan University, Joondalup campus during tree pruning operations, and straw was obtained from a pet supplier. All materials were allowed to dry in the sun for 2—3 days, before 3 kg was weighed and added to the appropriate mesocosm. This resulted in a layer approximately 50 mm deep for grass, and 0.3—0.4 m for eucalypt and straw across the bottom of the mesocosms (Figure 1). The mesocosm water volume was maintained at approximately 950 L, by rainfall and additions of reverse osmosis water to control for evaporation.

The mesocosms were monitored for changes in physico-chemical parameters initially every week for 6 months, then monthly until day 210, then at 3—4 month intervals for a total experimental duration of 421 days (18/9/2012—13/11/2013). A Datasonde 4a multi-parameter probe (Hydrolab, USA) was used to measure water temperature, pH, oxidation reduction potential (ORP), electrical conductivity (EC), dissolved oxygen saturation (DO), chlorophyll *a* and turbidity. Water samples were collected on five occasions (days 1, 38, 71, 113 and 421) from the surface (0.1 m deep) of each mesocosm. An aliquot of the water sample was filtered through 0.5 μm filter paper (Metrigard, Pall, USA), part of the filtered samples were acidified using analytical grade nitric acid (to achieve a pH of <2, approximately 1% w/v) for metal analysis (Al, Ca, Co, Cu, Fe, K, Mg, Mn, Na, Ni, and Zn) on

ICP–AES (Varian Vista-Pro, USA). Anions (SO_4^{2-} and Cl^-) were analyzed on filtered samples using ion chromatography (Metrohm 761 Compact, Switzerland). Ammonia/ammonium (NH_4-N), NOx-N (nitrate and nitrite) and filterable reactive phosphorus (FRP-P) in filtered and total nitrogen (TN-N) and total phosphorus (TP-P) on unfiltered samples were analyzed on an auto-analyzer (Skalar, USA). Dissolved organic carbon (DOC) was measured as non purgeable organic carbon and total organic carbon (TOC) in filtered samples using a TOC analyzer (Schimadzu TOC–V CSH, Japan). All analysis followed methods in APHA (1999).

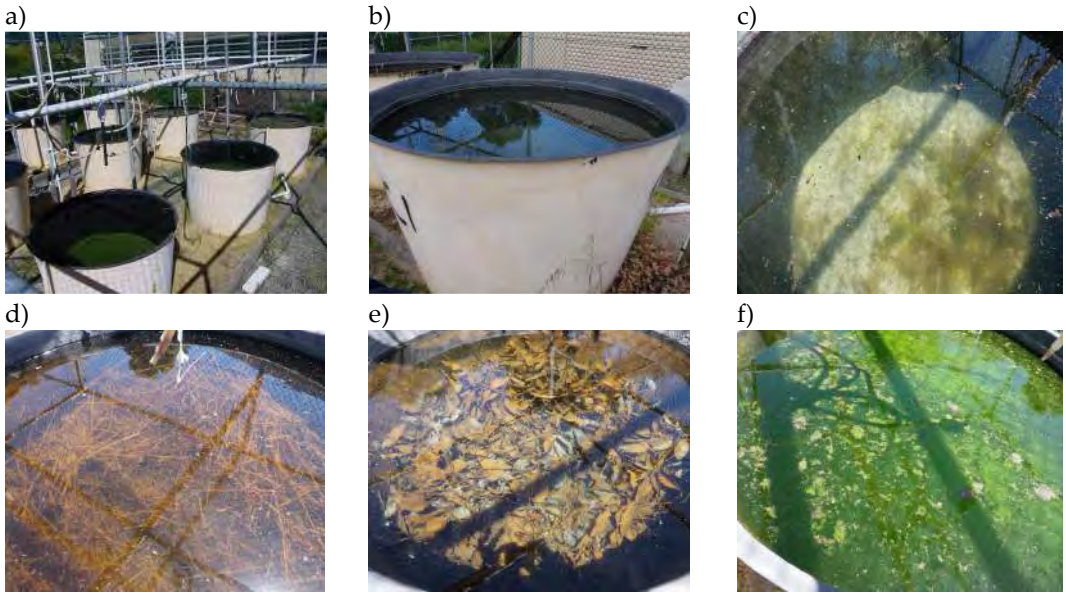

Figure 1. Photographs of the mesocosms in October 2012, showing a) experimental setup b) individual mesocosm, c) control, d) straw, e) eucalypt leaves and f) lawn clippings.

To avoid major disruption to the mesocosms, two surface small sweeps of the mesocosms for collection of macroinvertebrates were undertaken on days 38 and 86 using a small aquarium net (~500 µm mesh, 0.1 x 0.15 m). This was followed on day 421 by a sweep covering as much of each mesocosm as possible with a (0.22 x 0.22 m, 500 µm mesh) sweep net. Samples were preserved in 70% ethanol, sorted using a Bogarov trap and then counted and identified to broad taxonomic groups under a Olympus SZ-STU2 stereo microscope.

Water quality data from five water sampling occasions (days 1, 38, 71, 113 and 421), was ordinated using principal components analysis (PCA) in PRIMER (v6). We used a two-way ANOSIM on normalized data to determine if water quality was significantly different among treatments and times (excluding day 1, just after the treatments were added). We then analyzed treatments just for day 1 to establish that initial water quality parameters were similar across all mesocosms, regardless of treatment. Analyzed parameters included only those where more than half of the samples were above the detection limit – any values below detection were replaced with half the detection limit. Missing data were replaced by the average of any other data for that specific time and treatment, and auto-correlated parameters were reduced to a single parameter.

RESULTS AND DISCUSSION

Water Quality

At the beginning of the experiment (day 1), water quality among mesocosms was not significantly different (Global R = 0.145, P > 0.05), regardless of treatment (Figure 2). After day 1, treatments were significantly different overall (Global R=0.714, P<0.05) and between all treatment pairs (all P < 0.05, although straw x eucalypt R = 0.296, P = 0.04). Throughout the experiment, water quality among controls remained close to day 1 samples, with a slight divergence at the end of the experiment in day 71 (Figure 2). This shift is probably due to dilution by rainfall. The treatments separated from the controls on days 38 and 71, where grass generally was different to the other two treatments. On days 71 and 113, the treatments were similar to each other but distinct from the controls.

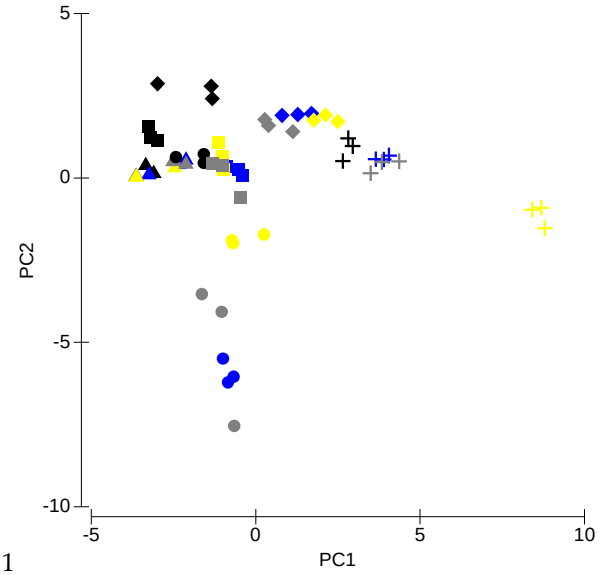

Figure 2. PCA of water quality data in mesocosms with acidic mine water over 14 months of incubation with bulk additions of carbon, 33.3% of the variability is associated with the first principal component axis (PC1) and 17% with PC2. *A priori* groups are time (by symbol) and treatment (by color). ▲ day 1, ● day 38, ■ day 71, ◆ day 113, + day 421, black = control, blue = straw, grey = eucalypt and yellow = grass)

There were significant differences (Global R=0.877, P<0.01) between all sampling times (excluding day 1). Temperature of the mesocosms followed seasonal trends peaking at just over 30 °C (summer) and dropping to just less than 16 °C (winter). There were no important differences in temperature between any of the mesocosms. No evidence was seen of stratification in the mesocosms, presumably due to the shallow depth and wind driven mixing. Conductivity (mean±SE, 1.5±0.01 mS cm^{-1}) follows a similar seasonal trend to temperature, reflecting largely evapoconcentration effects in summer (days 74-163) and dilution by rainfall in winter (days 256—347). Two notable trends were a slight increase in conductivity (of ~100 mS cm^{-1}) in the eucalypt treatment on days 60 and 64, and the lower conductivity from day 22 onwards in the grass treatment (of ~100 mS cm^{-1}) compared to the control and other treatments. No water samples were taken around days 60 and 64 so it is unclear what triggered the increase in conductivity for eucalypt leaves. The consistently lower conductivity seen for grass suggests binding of ions to leaves or ion precipitation may have been responsible.

The control remained aerobic (>60% saturation) throughout the experiment, but by day 20 dissolved oxygen in all treatments was less than 30% saturation (although grass by day 40 had started to return back to control levels). All treatments had returned to levels of dissolved oxygen similar to the controls after day 200. Biological oxygen demand caused by decomposition of the added organic matter was most likely responsible for reduced oxygen levels. Higher chlorophyll *a* concentrations in the grass-treated mesocosms are presumed to have increased oxygen concentrations as a result of photosynthesis. ORP follows the initial decline observed in dissolved oxygen for all the treatments, however by day 60 ORP in all treatments had returned to levels seen in the controls. On day 22, the mesocosms with straw had ORP of <-400 mV, the level at which methanogenesis (methane production) is possible, although by day 29 it had increased to >-103 mv.

pH was very stable at just over 3 for the entire experiment in eucalypt, straw and control treatments (Figure 3). Our previous mesocosm experiments using Collie pit-lake water have found pH has increased to circum-neutral in controls over the course of the experiment. At the time, we hypothesized that groundwater may be responsible for maintaining pH stability *in situ* (see Salmon *et al.*, 2008; Kumar *et al.*, 2011a). The current study used sediments collected from greater depths, 2-3 m compared to <1 m in the other studies, which may be more representative of lake sediment. It is possible that sediment processes in these sediments may be responsible for pH regulation (as per Peine *et al.*, 2000). Alternatively, the difference could be related to which lake the sediment was taken from i.e. WO5H compared to Lake Kepwari.

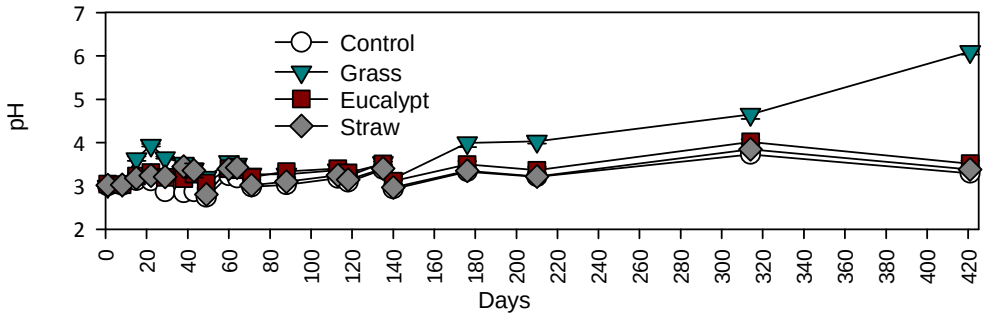

Figure 3. Mean (± SE) pH found in experimental mesocosms containing acidic mine-lake water collected from days 1 to 421.

Chlorophyll *a* concentrations were very low in the controls at <3 μg L^{-1}. Grass stimulated chlorophyll *a* production peaking at 332 μg L^{-1} more than the other treatments; however eucalypt and straw also increased chlorophyll *a* slightly between days 60 and 140 compared to the control. It is likely that alkalinity generation by algae was partially responsible for the lawn clippings after day 140 increasing pH to >6 by the end of the experiment.

Variation in Mn, K, Na, Mg, and Ca concentrations were minimal among treatments but declined slightly over the course of the experiment likely due to dilution with rainwater (Figure 4). Concentrations of Al, Co, Ni and Zn dropped by an average of >40% over the experiment in all treatments and control, although declines were lowest in the control and highest for the grass treatment (>95%). Copper was low in all treatments (mean = 0.755 mg L^{-1}) but appeared to increase slightly over the experiment in the control (peak = 5.5 mg L^{-1}), the most likely source being release from the sediments On day 38, Fe concentrations decreased for both controls and grass (mean = 0.9 mg L^{-1}) from an initial mean of 3.4 mg L^{-1}, and increased for eucalypt and straw (mean = 18.7 mg L^{-1}). By day 71, Fe concentrations were <1 mg L^{-1} in all treatments and control. The day 38 peaks are

not easily explained by ORP/anoxia induced release from the sediment and this suggests that the Fe might have been released directly from the eucalypt leaves and straw in these treatments.

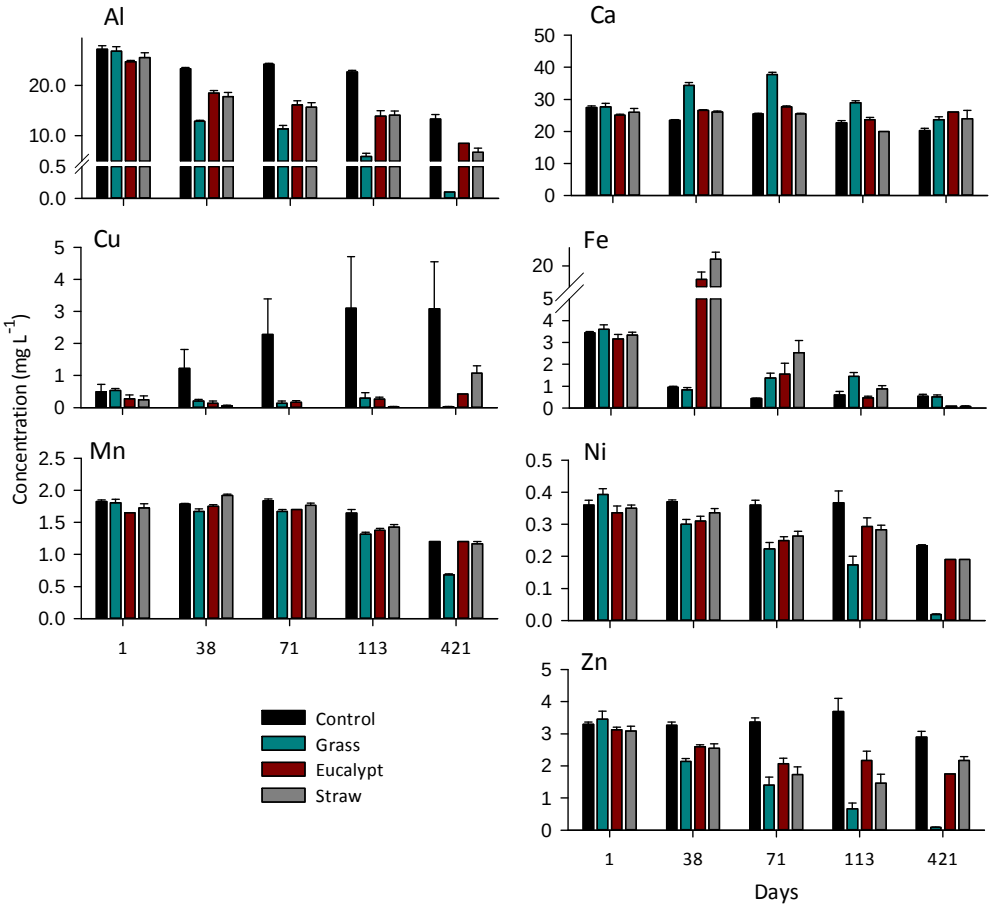

Figure 4. Mean (± SE) concentrations (mg L^{-1}) of select metals found in experimental mesocosms containing acidic mine-lake water collected from days 1 to 421.

Nitrification of ammonia to nitrate does not occur below pH 3 (Jeschke *et al.*, 2013) and initially the mesocosms were at pH 3. On day 1, NH_4-N was present at a mean concentration of 517 µg L^{-1}, with NOx-N concentrations at 68 µg L^{-1}. Ammonification from the likely rapid breakdown of the grass produced exceptional high NH_4-N concentrations in the grass treatment in days 38 and 71 exceeding 6000 µg L^{-1} (Figure 5). Over the course of the experiment, slight increases in pH appear to have allowed for nitrification of ammonia to NOx, evidenced by the overall decline in mean NH_4-N concentration to 69 µg L^{-1} and slight increase in NOx to 88 µg L^{-1} with differences between treatments probably dependent on algal and possible sediment uptake. Kumar *et al.* (2011b) has shown that algal growth in Collie pit lakes is limited primarily by P availability. Although bulk organic matter is not typically rich in P, it does provide a potential source. Initially in the mesocosms FRP concentrations were <14 µg L^{-1} and total P was below the detection limit of 20 µg L^{-1}. FRP remained very low throughout the experiment (<20 µg L^{-1}) with the exception of a mean of 63 µg L^{-1} recorded for eucalypt on day 38. As the experiment progressed, total P increased above detection limits for all treatments, however on days 71 and 113, reached over 3500 µg L^{-1} in the

grass treatments. As FRP concentrations in the grass treatments remained low, it is likely that algal biomass was responsible for the high total P values. The apparent ability of grass to release P is an important additional benefit of using this material within a pit lake. However, the decline in total P on day 421 to near start conditions, suggests that P release from the organic material was exhausted. The highest peak concentrations of DOC and TOC were from eucalypt and straw (mean of 30 and 40 mg L^{-1} for TOC respectively) on day 38, however these quickly dropped to <10 mg L^{-1}, with grass having the highest overall concentrations of DOC and TOC (mean 3.4 and 8.0 mg L^{-1} respectively) after day 38.

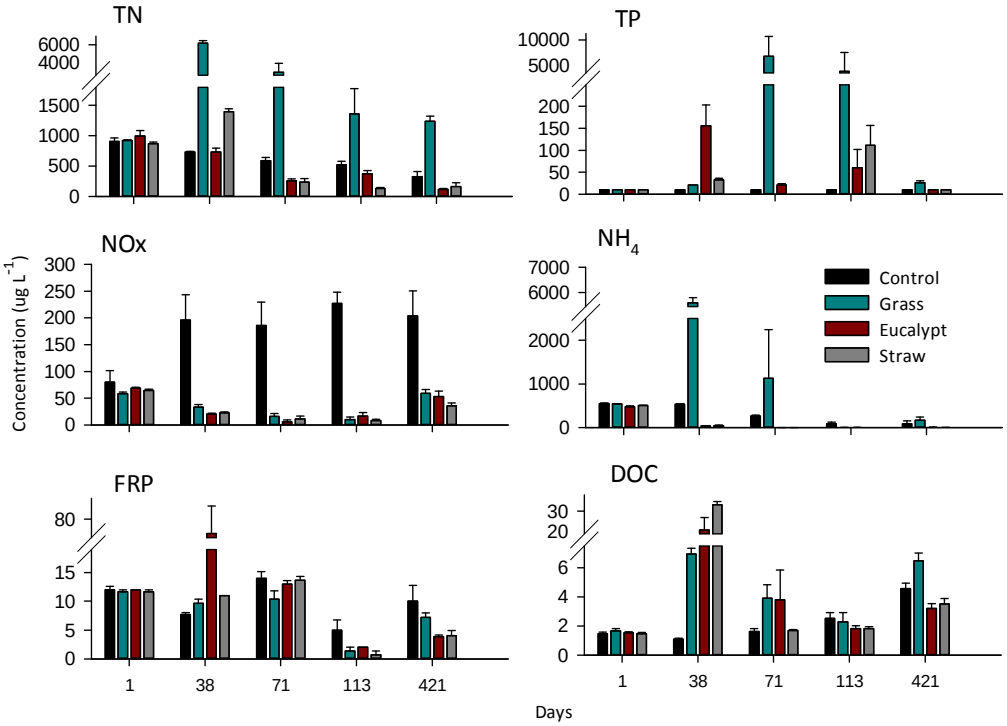

Figure 5. Mean (± SE) concentrations of nutrients in experimental mesocosms for days 1 to 421.

Chloride concentrations were consistent between treatments and as a conservative ion appeared to only change in relation to evapoconcentration and dilution by rainfall (Figure 6). Sulfate concentrations declined in all treatments and the control from mean of 830 µg L^{-1} on day 1, with the control only showing a slight decline (mean 422 mg L^{-1}) and the highest declines seen for grass (mean 112 mg L^{-1}) on day 421 (Figure 6). This suggests that sulfate reduction/secondary mineralization was occurring in all the mesocosms (Triantafyllidis & Skarpelis, 2005), but adding C enhanced SRB activity and that the more labile the C the stronger the effect. Algae were observed growing in all of the mesocosms, which would have contributed labile carbon to the sediment. The grass treatment produced a phytoplankton bloom, measured as chlorophyll *a*, but the controls only produced benthic algae.

Biota

On day 38, all the mesocosms were dominated at the surface by mosquito larvae (Culicidae), with similar abundances and species. By day 86, saw the mosquito larvae replaced by Chironomidae larvae and pupae and Ceratopogonidae larvae and pupae with the occasional Coleoptera adult. All

mesocosms were very similar in species and abundance, although this may be an artifact of the limited sampling that was possible at this time. At the end of the control contained a large proportion of Coleoptera and mites (~40%) compared to the treatments (<2%). The presence of these hardy predatory species is common in pit lakes (Proctor & Grigg, 2006). Eucalypt and straw in contrast were dominated by Chironomidae (>95%), which are also hardy and common to many pit lakes. Grass was different with approximately 15% of the taxa recorded being Culicidae. Total abundance of macroinvertebrates increased with the treatments, with increases over the control of four fold, eight fold and 48 fold for eucalypt, straw and grass respectively. All the taxa collected were most likely colonists from nearby water bodies rather than introduced with the organic material or present in the water or sediment.

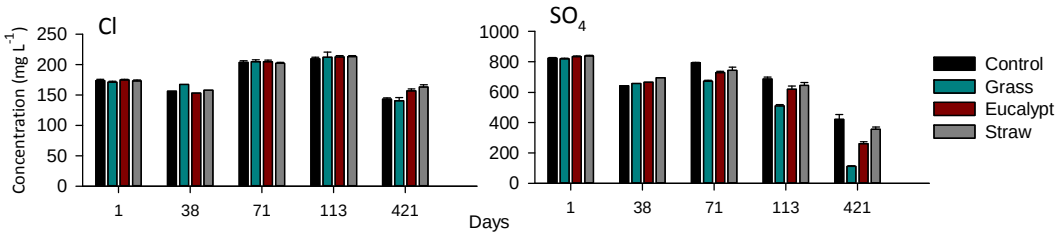

Figure 2. Mean (± SE) concentrations of Cl and SO_4 in experimental mesocosms from days 1 to 421.

CONCLUSIONS

Adding organic matter to highly acidic pit lake waters such as found at WO5H, resulted in no change in pH using more refractory C sources, but subtle improvements in other measured water quality parameters. Some of this improvement is likely due to secondary mineralisation and the sulfate reduction by SRBs. The more labile C produced by the grass treatment ultimately had the biggest impact on water quality and increased pH to 6. The grass also increased macroinvertebrate abundance. Although the taxa diversity (at this low level of taxonomic resolution) does not appear to have increased significantly in any of the treatments; there was a shift away from the predator dominated taxa seen in the control to more herbivorous/omnivorous taxa. Abundance of taxa also increased substantially in the treatments, particularly for the grass. These results suggest that when organic matter is added to pit lakes, more labile carbon sources may provide greater environmental value improvements. However, the results suggest that even refractory C sources such as straw have at least some environmental benefits. Although the quantities of organic material used in this study were very high (approximately 6 kg m^{-2} dry material) compared to what might be achievable in the field, benefits are still likely at lower levels. As these organic matter additions are targeting biodiversity rather than treatment of water quality per se, restricting the material to the littoral zone would likely achieve positive benefits without requiring unrealistic quantities of material. Using pit lake catchments to help supply organic matter to the lakes (see Lund *et al.*, 2013) may be one way to achieve sufficient inputs of carbon over long term to compensate for biotic/abiotic losses. This increasing carbon enrichment may allow even an acidic pit lake to develop ecological values, as an alternative to water quality-driven closure objectives.

ACKNOWLEDGEMENTS

This research has been funded by the Australian Coal Association Research Program (C21038) and Premier Coal Pty and Griffin Coal Pty. The support of Edith Cowan University in providing

infrastructure support is greatly appreciated. In particular, the authors wish to thank Dr Digby Short and Colm Harkin at Premier and Paul Irving at Griffin for their support. The invaluable assistance of Lorraine Wyse, Michelle Newport, Frazer McEnhill, Jay Gonzalez and Eddie Gazzetti with fieldwork is greatly appreciated.

REFERENCES

APHA (1999). Standard methods for the examination of water and wastewater. 20th edn, American Public Health Association, American Water Works Association, Water Environment Federation, Washington DC, USA. 1,220pp.

Chow, T. J. & Earl, J. L. (1970). Lead aerosols in the atmosphere: Increasing concentrations. *Science* 169: 577-580.

Dessouki, T. C. E.; Hudson, J. J.; Neal, B. R. & Bogard, M. J. (2005). The effects of phosphorus additions on the sedimentation of contaminants in a uranium mine pit-lake. *Water Res.* 39: 3055–3061.

Frömmichen, R.; Kellner, S. & Friese, K. (2003). Sediment conditioning with organic and/or inorganic carbon sources as a first step in alkalinity generation of acid mine pit lake water (pH 2-3). *Environ. Sci. & Technol.* 37: 1414-1421.

Fyson, A.; Nixdorf, B. & Steinberg, C. E. W. (1998). Manipulation of the sediment-water interface of extremely acidic mining lakes with potatoes: laboratory studies with intact sediment cores. *Water Air Soil Pollut.* 108: 353–363.

Jeschke, C.; Falagán, C.; Knoeller, K.; Schultze, M. & Koschorreck, M. (2013). No nitrification in lakes below pH 3. *Environ. Sci. & Technol.* 47(24): 14018-23

Kalin, M.; Cao, Y.; Smith, M. & Olaveson, M. M. (2001). Development of the phytoplankton community in a pit-lake in relation to water quality changes. *Water Research* 35: 3215-3225.

Kapfer, M. (1998). Assessment of the colonization and primary production of microphytobenthos in the littoral of acidic mining lakes in Lusatia (Germany). *Water Air Soil Pollut.* 108: 331-340.

Koschorreck, M. & Tittel, J. (2007). Natural alkalinity generation in neutral lakes affected by acid mine drainage. *J. Environ. Qual.* 36: 1163–1171.

Kumar, N. R.; McCullough, C. D. & Lund, M. A. (2011a). *Use and Water Quality Remediation of Acidic Coal Pit Lakes by Adjacent Aquaculture*. Unpublished Report 2011-10. Edith Cowan University, Perth, Australia. 103pp.

Kumar, N. R.; McCullough, C. D.; Lund, M. A. & Larranãga, S. A. (2011b). Evaluating the factors limiting algal biomass in acidic pit lakes of the Collie Lake District, Western Australia. International Mine Water Association (IMWA) Congress. Aachen, Germany. Rüde, T, Freund, A. & Wolkersdorfer, C. (eds), IMWA, 523-527.

Le Blanc Smith, G. (1993). *The geology and Permian coal resources of the Collie Basin, Western Australia*. Western Australian Geological Survey Report 38. 86pp.

Lund, M. A. & McCullough, C. D. (2011). Restoring pit lakes: factoring in the biology. In, *Mine Pit lakes: Closure and Management*, McCullough, C. D. (ed.) Australian Centre for Geomechanics, Perth, Australia, 83–90.

Lund, M. A.; McCullough, C. D. & Kumar, R. N. (2012). *The Collie Pit Lake District, Western Australia: An Overview*. International Mine Water Association Symposium. Bunbury, Australia. McCullough, C. D.; Lund, M. A. & Wyse, L. (eds.), IMWA, 287 - 294.

Lund, M. A.; McCullough, C. D. & Yuden (2006). *In-situ coal pit lake treatment of acidity when sulfate concentrations are low* 7th International Conference on Acid Rock Drainage (ICARD). St Louis, Massachusetts, USA, 1106-1121.

Lund, M. A.; Van Etten, E. J. B. & McCullough, C. D. (2013). *Importance of catchment vegetation and design to long-term rehabilitation of acidic pit lakes.* Reliable Mine Water Technology - International Mine Water Association. Denver, Co. Brown, A., Figueroa, L. & Wolkersdorfer, C. (eds.), Publication Printers, 1029-1035.

McCullough, C. & Etten, E. B. (2011). Ecological Restoration of Novel Lake Districts: New Approaches for New Landscapes. *Mine Water & Environ.*30: 312-319.

McCullough, C. D. & Lund, M. A. (2006). Opportunities for sustainable mining pit lakes in Australia. *Mine Water & Environ.* 25: 220-226.

McCullough, C. D. & Lund, M. A. (2011). Bioremediation of Acidic and Metalliferous Drainage (AMD) through organic carbon amendment by municipal sewage and green waste. *J. Environ. Manage.* 92: 2419-2426.

McCullough, C. D. & Pearce, J. I. (2014). What do elevated background contaminant concentrations mean for AMD risk assessment and management in Western Australia? 8th Australian Workshop on Acid and Metalliferous Drainage. Adelaide, Australia.

Nixdorf, B.; Fyson, A. & Krumbeck, H. (2001). Review: plant life in extremely acidic waters. *Environ. Exp. Bot.* 46: 203–211.

Peine, A.; Tritschler, A.; Kusel, K. & Peiffer, S. (2000). Electron flow in an iron-rich acidic sediment—evidence for an acidity-driven iron cycle. *Limnol. & Oceanog.* 45: 1077-1087.

Proctor, H. & Grigg, A. (2006). Aquatic macroinvertebrates in final void water bodies at an open-cut coal mine in Central Queensland. . *Aust. J. Entomol.* 45: 107-112.

Read, D. J.; Oldham, C. E.; Myllymäki, T. & Koschorreck, M. (2009). Sediment diagenesis and porewater solute fluxes in acidic mine lakes: the impact of dissolved organic carbon additions. *Mar. Freshw. Res.* 60: 660-668.

Salmon, S. U.; Oldham, C. E. & Ivey, G. N. (2008). Assessing internal and external controls on lake water quality: Limitations on organic carbon-driven alkalinity generation in acidic pit lakes. *Water Resources Res.* 44: W10414.

Thompson, S. (2000). *Managing the acidity of abandoned water filled coal mining voids in Collie (Western Australia) using organic matter,* M.Sc. thesis, Edith Cowan University, Perth. 205pp.

Triantafyllidis, S. & Skarpelis, N. (2005). Mineral formation in an acid pit lake from a high-sulfidation ore deposit: Kirki, NE Greece. *J. Geochem. Explor.* 88: 68-71.

Van Etten, E. J. B. (2011). The role and value of riparian vegetation for mine pit lakes. In, *Mine Pit Lakes: Closure and Management,* McCullough, C. D. (ed.) Australian Centre for Geomechanics, Perth, Australia, 91-105.

Zhao, L. Y. L.; McCullough, C. D. & Lund, M. A. (2009). *Mine Voids Management Strategy (I): Pit Lake Resources of the Collie Basin* Unpublished report to Department of Water 2009-10. Edith Cowan University, Perth, Western Australia. 215pp.

10th ICARD IMWA 2015 | 10th International Conference on Acid Rock Drainage & IMWA Annual Conference

Pit Lake Rebound Modeling, a Fully Integrated Approach Using FEFLOW

Alexia Carpentier and Robin Dufour

DHI Peru

ABSTRACT

An essential component of a mine closure plan is the prediction of the groundwater table rebound and the potential formation of a pit lake at the end of mine life. The time period over which the groundwater levels rebound needs to be estimated and the estimated inflows to the pit lake are needed for estimating the geochemistry and resulting water quality of the pit lake.

Pit lake formation is generally estimated using a simple water balance approach: the inflows to the pit lake are estimated from groundwater inflow or outflow, direct precipitation on the lake surface, runoff from the pit walls and direct evaporation from the lake surface. The water balance is dependent on the lake water level which controls the area of exposed pit wall and lake surface area. The rate of pit lake filling is therefore directly dependent on the pit lake water level. This internal dependency on the rate of pit lake filling is non-linear and complicates the modeling process in time varying (dynamic) models. This complex pit lake modeling challenge is difficult to solve using the general industry approach of simple spreadsheet based water balance calculation methods. Consequently the water balance is estimated by either splitting the pit rebound model process into various disconnected (independent) sub models or by simplifying the water balance process using separated groundwater and surface water models.

A more comprehensive and reliable approach is to couple the various ground and surface water models into a single integrated model where the feedback between pit level and water balance is inherent. DHI have developed a module (plug-in) for the FEFLOW model that combines the pit rebound model processes with the groundwater model. The plug-in allows for the continuous update of the pit lake level as a boundary condition (recharge) to the groundwater model on a time step basis. This paper describes the process of coupling the pit lake and groundwater models and demonstrates the application of such a model.

Keywords: Pit Lake, Rebound, Groundwater, Modeling, FEFLOW

**There is no full article associated with this abstract.*

10th ICARD IMWA 2015 | 10th International Conference on Acid Rock Drainage & IMWA Annual Conference

Use of Pit Lake Water Quality Prediction as a Tool to Support Management of Mine Closure Decisions

Luciano Santos
Pimenta de Ávila Consultoria e Projetos Ltda., Brazil

ABSTRACT

Current best practice dictates that all mines should be 'designed for closure'. This paper describes a water quality model approach used as a tool to predict a pit water quality in a future porphyry copper mine in southwest region of Brazil. The objective of the geochemical modeling effort was evaluating the future environmental impacts associated with water from the pit lake and also to assist in planning the rapid filling of pit lakes with other sources of water in the post-closure phase, in order to attempt the required quality levels for future use.

Based on the expected inflows to the pit lake (groundwater seepage, waste rock seepage and precipitation) in relation to the annual evaporation from the pit lake surface, a geochemical pit lake predictive model was developed using a PhreeqC approach. Precipitation of a large number of geochemically credible mineral phases was assessed by the mixing of all inputs to the pit lake. Also precipitation of ferrihydrite and adsorption onto this phase were simulated.

The predicted ranges of water qualities of pit lake, for the scenario without pumping from the rivers around the future mine to the pit (base case) are predicted to be moderately acid (pH ~4.5). All chemical parameters concentrations are expected to be bellowing the local effluent quality standards, with the exception of copper, and manganese. From all geochemically credible mineral phases included in the model, amorphous gibbsite, ferrihydrite, Schwertmannite, Barite and malachite were found as having the potential to precipitate.

Simulations considering rapid filling of the pit using the water from rivers around the future mine was also modeled. Four simulations were conducted using pumping rates of 1,500m^3/h, 2,000m^3/h, 3,000m^3/h and 5,000m^3/h. The results for rapid filling shown that this approach was a good one to achieve desired limit that is similar to water quality standards for all parameters using pumping rates higher than of 3,000m3/h. The final pH modeled for pumping rate of 3,000m^3/h is ~5.5.

Due to the use of many simplifying assumptions the pit lake water qualities necessarily cannot be considered highly quantitative. However, the model shows to be useful in evaluations of strategies for pit lake water quality management.

**There is no full article associated with this abstract.*